



PHYSICOCHEMICAL STUDIES ON
SPECTROSCOPIC CHARACTERIZATION,
PRECONCENTRATION, SEPARATION,
DETERMINATION AND/OR CHEMICAL
SPECIATION OF VARIOUS INORGANIC AND
ORGANIC COMPLEX SPECIES IN
DIFFERENT MEDIA

By

MOHAMMAD S. EL-SHAHAWI

A thesis and collection of the works submitted to Strathclyde University
in partial fulfillment for the degree of

DOCTOR OF SCIENCE

FACULTY OF SCIENCE

September 2013

This thesis and copy of collected works has been supplied in condition that anyone who consults it is understood to recognize that its copyright rests with the author and that no quotation from the thesis and no information derived from it may be published without the author prior consent.

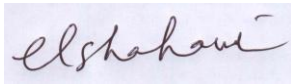
Table of Contents

	Page
Author's Declaration	1
Acknowledgements	2
Dedication	3
Major Scientific Accomplishments	4
Recognition and Merit Awards	15
Statement of the Achievements, Innovations, Novelty, and Impact	16
Submission Form	20
	24
List of Thesis Supervision	
Funded Research Projects	31
Curriculum Vitae Reviewed	44
Publications	70
	91
Citation Indices	
Publications	

Author's Declaration

At no time during the registration for the degree of Doctor of Science has the author been registered for any other University award without prior agreement of the Graduate Committee.

Work submitted for this research degree at Strathclyde Glasgow University has not formed part of any other degree, either at Strathclyde Glasgow University or at other establishment.

A handwritten signature in black ink on a light blue rectangular background. The signature is cursive and reads 'elshahawi'.

Mohammad S. El-Shahawi

June, 2015

Acknowledgements

The collection of works presented here was only possible through the dedication and support of my great professor (A.B. Farag) and many talented and dedicated researches, working for me, with me, and around me over the past thirty five years.

It to all these wonderful students an colleagues I must say thank you.

Dedication

This collection of work is dedicated to my lovely wife Azza E. Abdrabbo and my lovely daughters Ghada, Sara, Aya and Alaa.

“A heart is not judged by how much you love; but by how much you are loved by others”

L. Frank Baum, *The Wonderful Wizard of Oz*

Major Scientific Accomplishments by Prof.

M.S. El-Shahawi I. Academic qualifications:

1. PhD: Analytical Chemistry (1986) at Strathclyde University, Glasgow, UK
2. M.Sc: Analytical Chemistry, 1980, Mansoura University, Mansoura, Egypt
3. B.Sc: Special Chemistry, 1975, Mansoura University, Mansoura U, Mansoura, Egypt
4. Currently Professor of Analytical and Environmental Chemistry at King Abdulaziz University (KAU), Saudi Arabia since September, 2005.
5. I have held several academic posts at Mansoura University (Egypt, March 1986 –August 1991; September 1997- August 2005) and the University of the United Arab Emirates (September 1991-August 1997) and was appointed a series of research fellows at Strathclyde University (Glasgow, UK, JulySeptember 1993, C/O Prof W.E. Smith), Queens University of Belfast (Belfast, North Ireland, July 1995 –August 1995, C/O Prof D.T. Burns) ; Plymouth University (Plymouth, UK, July 1997-September 1997; July 2000 – August 2000; January 2003 –February 2003 C/O Prof E.P. Acterberg) and at Institute Für Chemie, Humboldt- Universtat Zu Berlin, (Berlin, Germany, August 2002 – October 2002, C/O W. Meritz) (see CV for details).

II. Professional experience

A. Consultant to:

1. The Federal Environmental Agency at United Arab Emirates 1997;
2. The Centre of Excellence in Environmental Studies at KAU 2009-2011.
3. Advisor for few Industrial chemical companies in Egypt e.g. Seperia and finally
4. Ministry of interior in Egypt and Saudi Arabia.

B. Research Projects: Good experience in project management and I have attracted over 4000,000 \$ US Dollars in research funds since 1992 via participation as PI and /or Co-author in a number of research projects as follows:

1. National Research Projects (Please see:

- i. At United Arab emirates University (1992-1996).
- ii. Ministry of Higher Education, Egypt “Quality Assurance and Accreditation Program (2004 - 2005)”, (QAAP) A/MAN/3/09“; iii. King Abdulaziz University (2006-2012), Jeddah, Saudi Arabia.

2. International Collaboration:

- i. **DFID link Project:** Research Project entitled: “Water Quality in River Nile” Funded by British Council in Egypt, (2000-2003) between Dr. E.P. Achterberg

"Plymouth University, UK" and Prof. M.S. El-Shahawi "Mansoura University, Egypt", 25000 British Pounds.

- ii. **GEOMAR, Germany:** In October 2012, I have participated effectively with Prof. Eric P. Achterberg at GEOMAR, Helmholtz Centre for Ocean Research, 24148 Kiel, Germany in getting a fund (1,150,000 \$ US Dollars) of the research proposal entitled: Investigation of Novel Pollutants e.g. silver nanoparticles, Gallium, Lead, Nickel, Vanadium and Nutrients in Jeddah Coastal Waters and

Their Biological Effects” between King Abdulaziz University, Saudi Arabia and Helmholtz Centre for Ocean Research, Kiel.

- iii. **Miami U:** In September 2012, I have participated effectively with Prof. Rogers M. Leblanc

(Cooper Fellow), Professor and Chair at the Department of Chemistry, Miami U, USA in getting a fund (1,350,000 \$ US Dollars) of the research proposal entitled: Detection of Hepatocellular Carcinoma (HCC) in AT-Risk Groups by using biomarker alfa-L-fucosidas (AFU) to screen and identify at risk groups for early tumors which will need treatment” between King Abdulaziz University, Saudi Arabia and Miami U, USA.

III. Research Interests:

1. Application of untreated and physically treated polyurethane foams (PUFs) and other solid phase extractor e.g. active carbon, local clay and date pits for separation, determination and chemical speciation of trace concentrations of toxic and non toxic metal ions and organic pollutants in complicated matrices using batch, flow and pulse modes of separation.
2. Application of nanosized solid phase extractor (SPE) and solid phase microextraction (SPME) e.g. nanosized Fe_3O_4 treated for PUFs, nanogold treated PUFs, nano ZnO treated PUF, and Fe_3O_4 chemically impregnated clay and clay minerals in batch, flow and pulse modes for separation, determination and chemical speciation of trace concentrations of toxic and non toxic metal ions and organic pollutants in complicated matrices.
3. Application of conventional liquid-liquid (LL) extraction, cloud point microextraction and dispersive liquid –liquid microextraction techniques (DLLME) techniques for separation, determination and chemical speciation of trace metal ions, food colors, biogenic amines and phosphorous pesticides in complex matrices.
4. Assessment of pollution level in fresh water (River Nile) and marine water (Red sea and Arabian Gulf post and after Gulf War I) and fish organs as bio indicators.
5. Determination, chemical speciation of trace metal ions and oxyions of Cr, Ru, Bi, W, As, Sb, Au, Pt, etc and for measuring the activity of the enzyme α - Lfucosidase as tumor marker employing:
 - i. High fold chemical amplification reactions involving KIO_4 ; ii. Extractive spectrophotometric; iii. Extractive and non- extractive spectrofluorometric techniques.
6. Developing of simple, selective and cost – effectiveness voltammetric methods for precise determination and speciation of ultra trace concentrations of metal ions, food colorants, co-enzyme Q_{10} , pesticides, anticancer drugs, β blockers drugs, steroids and persistent organic pollutants (POPs) in complex matrix e.g.

wastewater, pharmaceutical formulations, drug residue in wastewater, etc using glassy carbon electrode (GCE), hanging mercury dropping electrode (HMDE) and nano composite surface modified GCEs.

7. Developing Dual-wavelength β -correction spectrophotometric methods for analysis of trace concentrations of CN^- , Th, Bi and Hg ions in industrial wastewater effluents.

8. Total determination and speciation of trace metal ions and some selected inorganic ions e.g. F^- , Cl^- , SO_4^{2-} , NO_3^- , NO_2^- , Ca^{2+} , Mg^{2+} , Al^{3+} , K^+ , Na^+ , NH_4^+ in total suspended matter (TSP), PM_{10} and $\text{PM}_{2.5}$ in air aerosols.

9. Preparation and fully characterization of a series of optically active and non active transition complexes of biological and industrial applications using a series of spectroscopic (UV-visible, IR, NMR), electrochemical (Cyclic voltammetry, Coulometry), thermal analysis and elemental analysis.

10. Studying the spectroelectrochemical behavior using thin layer cyclic voltammetry, thin layer coulometry and optically transparent thin layer electrochemical cells (OTTEs) for characterization and quantification of a series of various redox systems e.g. metal complexes, anthraquinones, etc.

IV. Publications, Translated Books, Conferences and Meeting of Professional Societies:

A. Publications of Book Chapters (3 Entries)

1. **M.S. El-Shahawi**, E.A. Al-Harbi and H.M. Al-Saidi

“Speciation of Tellurium in soil, sediment and environmental samples” and “Speciation of Chromium in soil, sediment and environmental samples” A Book Chapter in Sezgin Bakirdere 'Chief Editor' Book entitled “Speciation Studies in Soil, Sediment and Environmental Samples” Science Publishers books, CRC Press/Taylor & Francis Group, 2013.

2. **M.S. El-Shahawi**^{1†}, A. A. Al-Sibaai¹, H.M. Al-Saidi² and E. A. Assirey

Fast, Selective Removal and Determination of Total bismuth (III) and (V) in Water by Procaine Hydrochloride Immobilized Polyurethane Foam Packed Column Prior to Inductively Coupled Plasma – Optical Emission Spectrometry in "Polyurethane", A Book Chapter 13 in Fahmina Zafar and Eram Sharmin “Chief Editor” ISBN 979-953-307-642-2. In Tech, Open Access publisher in the fields of Science, Technology and Medicine Published 2012.

3. M.S. El-Shahawi

Retention Profiles of Some Commercial Pesticides, Pyrethroid and Acaricide Residues and Their Applications to Tomato and Parsley Plants. Special Issue in Water pollution edited by E. Heftmann, Elsevier press, Special issue J. Chromatography A, 760 (1997) 179 -192.

B. Published and/ or revised research articles:

1. Published articles (131 Entries): 125 articles (Published) and 6 articles

(Published from M.Sc & Ph.D) in refereed papers published in internationally recognized Journals such as Trends in Analytical Chemistry, Anal. Chim. Acta, J. Chromatography, Analyst, Talanta, Analytical and Bioanalytical Chemistry, J. Hazardous Materials, Analytical Sciences, Electroanalysis etc.)

2. Submitted and / or revised articles: 6 Articles Revised and/ or submitted for publication.

C. Translated Books

Translated Books to Arabic language: 3 Translated books from English to Arabic. These Books

are:

1. J.N. Miller and J.C. Miller “Statistics and Chemometrics for Analytical Chemistry” 6th Edn. Prentice Hall Publisher, Pearson Education Limited, England, 2010 by: Y.Moustafa and M.S. El-Shahawi.

2. D.A. Skoog, F.M. Holler, S.R. Grouch “**Principles of Instrumental Analysis**” 6th Edn., Thomson Brooks Publisher, 2007 by Y.Moustafa and M.S. ElShahawi.

3. J.M. Reed “**Principles of Ceramics Processing**” 2nd Edn., John Wiley & Sons, Inc., 1995. by Y. M. Moustafa, M.S. El-Shahawi and A. Algamdy.

D. Conferences, Workshops and Meeting of Professional Societies

(Oral Presentation =28; Poster =32), Workshops (2) and Meetings of Professional Societies (4) 1. Oral presentations in National and International

Conferences: **28.**

2. **Poster presentations** in National and International Conferences and Symposium: **32**

3. Workshops: **2**

4. Meetings of Professional Societies: **4**

V. Prizes and Merit Awards

1. King Abdulaziz University Award for "Distinguished Scientist in Research of the Year" (Chemistry), Jeddah, Saudi Arabia, **2008, 2009, 2010, 2011, 212.**

2. Scopus Appreciation and Recognition for Excellence of Publishing in Elsevier Publishing Company (46 entries), King Abdulaziz University, Ryadah, Kingdom of Saudi Arabia, **2008. .**

3. "The Egyptian State Award of Recognition of the Year in “Chemistry” Awarded by the Academy of Scientific Research and Technology, Ministry of Higher Education, Cairo, Egypt, **2004.**

4. Shoman Award for "Young Scientist of the Year" (Chemistry) in the Arab World", Amman, Jordan, **1993.**

5. Perkin Elmer Award, 18th Intern. Symp. on Chrom., Amsterdam, the Netherlands, September 18-23, **1990..**

VI. Scholarships

1. British Council scholarships (British Council at United Arab emirates 1993, 1995, 1997).
2. DFID grants 2000, 2001 and 2003 at Plymouth University, Plymouth, UK.
3. Deutsche Forschungsgemeinschaft (DFG) Scholar Ship at Institute Für Chemie, Humboldt- Universtat Zu Berlin, Berlin (Belin, Germany, Humbltd, 2002). The grants covered traveling and living allowances.

VII. Supervisions for Ph.D, M.Sc thesis and research projects (B.Sc students) (1986-2012):

i. 32 M.Sc thesis's (**31** awarded and 1 in progress) **ii. 20** Ph.D thesis's (18 Awarded and 2 in progress) **iii.. 60** undergraduate students Final research projects for B.Sc graduation since 1986

VIII. Collaboration and editorial

A. National and international recognition:

1. Associate Editor of E-Journal of Chemistry, Hindawi Publishing Corporation, a peer reviewed, open access journal. (March 11, 2012).
2. Lead Guest Editor of an upcoming Special Issues for International Journal of Analytical Chemistry, Hindawi Publishing Corporation, November 2011.
3. Invited by Science Publishers books, CRC Press/Taylor & Francis Group, 2012 to write a book chapter entitled “**Speciation of Tellurium in soil, sediment and environmental samples**” and “Speciation of Chromium in soil, sediment and environmental samples” in Sezgin Bakirdere 'Chief Editor" Book entitled “Speciation Studies in Soil, Sediment and Environmental Samples” Science Publishers books, CRC Press/Taylor & Francis Group, 2012 (**Published January, 2013**).
4. Was invited by In Tech, Open Access publisher in the fields of Science, Technology and Medicine in writing a book chapter in "Polyurethane", A Book Chapter 13 in Fahmina

Zafar and Eram Sharmin “Chief Editor” ISBN 979-953-307-642-2. In Tech, Open Access publisher in the fields of Science, Technology and Medicine. **Published January, 2012).**

5. Was invited by Dr. S. A. Iqbal, Chief Editor (2009) to participate in writing a book chapter in the international book entitled “Pollution”: The Ugly Face of Environment”.

6. Acted as an advisor for the Federal Environmental Protection Agency, United Arab Emirates.

7. Member of the Experts Referee Panel “Promotion Committee”, Ministry of Higher Education, Egypt, 2002-2005.

8. Participated in writing a Book Chapter entitled: Was invited by E. Heftmann in writing a book Chapter entitled: “Retention Profiles of Some Commercial Pesticides, Pyrethroid and Acaricide Residues and Their Applications to Tomato and Parsley Plants in a Book entitled “Water pollution by hazardous materials” by E. Heftmann, Elsevier press, Special issue J. Chromatography A, Orinda 1997.

B. Collaboration with National and International Centers and Excellence of research

1. Was invited by Prof. O’Sullivan, Rovira I Virgili University (Spain) to be a member of the Referee Panel committee for the PhD student (Mr. H.M. Nassef).

2. Acted as a co-supervisor with Prof D.T. Burns in supervision on a PhD student (Mr. Salem A. Barakat, 1992).

3. Carried out joint research collaboration with Prof. Eric Achterberg group in DFID funded Project.

4. Carried out collaborative research with several research teams from UK, North Ireland, Saudi Arabia, and Germany.

5. Submitted a project with Prof O’Sullivan, Spain and another Project with Prof E. Achterberg, Southampton, UK to the Deanship of Scientific Research.

6. Acted as a sponsor on a “Workshop” "Demonstration of some Low Cost and Applicable Procedures for Detection and Semi quantitative Determination of Trace Metal Ions in Water.

C. Reviewing and services:

1. Reviewer in over 42 international Journals in Analytical and / or Inorganic Chemistry. Regularly referee papers (\approx 20-25 Articles /year) form a host of International Scientific Journals (>42 Journals) and Scientific Review Panels (Please see full CV).
2. Examiner for several MSc and PhD dissertations at National level (Egypt, UAE and Saudi Arabia).
3. Acted as a reviewer **for Arabic Translation** of “Oxford Book Series in Instrumental Analysis , Chromatographic separation and Electroanalysis”. The following **four books** were reviewed:
 - i. Christopher M.A. Brett and Ana M.O. Brett "**Electroanalysis**", Series sponsor: Zeneca, Oxford University Press, 2005.
 - ii. Ritchard P. Wayne "**Chemical Instrumentation**", Series sponsor: ZENECA, Oxford Science Publication, Oxford University Press Inc., New York, 1995.
 - iii. John R. Chipperfield "**Non – Aqueous Solvents**", Series sponsor: ZENECA, Oxford Science Publication, Oxford University Press Inc., New York, 2007.
 - iv. **Fisher, A.C. , ““Electrode Dynamics”** Series sponsor: ZENECA, Oxford Science Publication, Oxford University Press Inc., New York, 1996.

D. Research Collaboration in Service for Industry and Commerce

Consultancies for local and international industries:

1. Was invited on five occasions by the Modern Academy of Science (Department of Environmental Affairs, Prof H.M. Fahmy) to arrange for a one day workshop presenting to the General Directors of Environmental for industrial companies, Egypt.

2. Was involved with a consultancy on Rare Earth Elements (REEs) separation from Apatite ore.
3. Acted as consultant for the Damietta Port Authority, Drinking Water Supply Authorities and Ministry of Interior, Egypt.
4. Advisor for the wastewater treatment processes for an Egyptian-American company.

IX. Contribution to Teaching and Learning Activities

1. As a member of University Committees including Council for Graduate and Research Advisors.
2. Responsible for undergraduate teaching exam preparation and double marking responsibilities.
3. Participate in the student advisory scheme and placement visits for Chemistry students on annual bases.
4. Participated in curriculum design for MSc in Environmental Sciences.
5. Completed the staff development: Effective Supervision; Computer Aided Assessment; Assessment for Quality of Teaching.
6. Taught on various courses/modules related to analytical chemistry for both under and postgraduate students .

X. Involvement in Technology and Knowledge Transfer

1. Participated as a reviewer in the "National Promotion Committee" for academic staffs in Egyptian Universities.
2. Participated as an active staff member in the accreditation and Quality Assurance for BSc degree in Chemistry degree for at KAU, Saudi Arabia and Mansoura, Egypt Universities.
3. Internal reviewer for the Accreditation and Quality Assurance for the following three programs:
BSc of Environmental Science; BSc of Environmental Health; MSc in Environmental Sciences at Faculty of Meteorology, Environment and Arid Land Agriculture at King Abdulaziz U, Saudi Arabia.
4. Internal reviewer for the Accreditation and Quality Assurance for the following B.SC Chemistry programs at Faculty of Science at Hail U, Saudi

Arabia

- 5.** During 1994-1995 (United Arab Emirates, Ministry of Education) and 2003-2004 (Ministry of Education, Egypt) I became involved with other staff members in organizing several chemistry lectures for secondary school post teachers and teachers in various provinces in each country.
- 6.** Regularly involved in providing laboratory experience for Secondary School teachers and students within the different labs at Mansoura Universities.
- 7.** I have involved in organizing several scientific meetings to
- i.** Secondary school teachers in the province. A total of 4 one – day visits involving providing a laboratory experience within four different labs within the Department of Chemistry and organized presentations involving at least 6 members of staff and the head of the Department. This was my initiative in trying to promote the Department and enhance application from local student in Chemistry and other degree programmer.
 - ii.** Water Treatment chemists and technicians for demonstrating classical tests for most well known common organic and inorganic pollutants in water.

Recognition and Merit Awards:

- 1. King Abdulaziz University Award for "Distinguished Scientist in Research of the Year" (Chemistry), Jeddah, Saudi Arabia, 2008, 2009, 2010, 2011, 2012.**
- 2. Scopus Appreciation and Recognition for Excellence of Publishing in Elsevier Publishing Company (46 entries), King Abdulaziz University, 2008, Ryadah, Saudi Arabia. .**
- 3. "The Egyptian State Award of Recognition of the Year in "Chemistry" Awarded by the Academy of Scientific Research and Technology, Ministry of Higher Education, Cairo, Egypt, 2004.**
- 4. Shoman Award for "Young Scientist of the Year" (Chemistry) in the Arab World", Amman, Jordan, 1993.**
- 5. "Perkin Elmer Award", 18th Intern. Symp. on Chrom., Amsterdam, the Netherlands, September 18-23, 1990.**

Statement of the Achievements, Innovations, Novelty, and Impact

Among the 131 published papers, conferences, workshops and other scientific activities the following work stand out for it received great deal of interest from the scientific community, solved problems for the industry, and contributed to the health improvement of the community:

1. Analysis of oxyions:

This class of chemicals is well known species but their determinations are not well established. Thus, part of my work was focused on the development of new methods for the determination of oxyions e.g. chromate, selenate, selenite, permanganate, periodate, iodate, perrehanate, perruthanate, bismuthate, tungstate. This work has resulted in publishing over 12 papers in ISI international journals with good impact factor during 1990-2012. This work has received great attention from the scientific community and I believe it added to our understanding of these species and helped in a better detection and prevention of exposure from toxic ions. Our developed method for the determination of ReO_4^- was used by Imperial Chemical Industry (ICI), one of the largest chemical companies in the UK to measure the rehenium content in their alumina and carbon catalysts. Our work on chromate and manganese and periodate and iodate has successfully used by Quality Control Laboratories in analysis of manganese and chromium in British Steel and analysis of iodine in Table salt.

2. Removal of heavy toxic metal ions and cyanide ions:

One of the very promising and rapidly developing novel industrial applications of polymers is in the field of polymeric membrane separations employing polyurethane foams (PUFs) for the production of pure chemicals and clean effluents. Thus, part of my work was focused on the removal of heavy toxic metals and cyanide from industrial waste. This work has resulted in publishing over 30 papers in ISI international journals with good impact factor during 1990-2012. PUFs

are very effective and economical. The work has frequently cited in literature. This work has resulted in a complete procedure that was adopted by Speria Egypt (A chemical company). This work helped them to comply with Environmental Protection Agency (EPA) of Egypt (Law 4 for Year 1994) requirements. This also led to successful clearance of huge amounts of industrial liquid wastes which was treated using the methods developed for removing heavy and toxic metals. Piles of industrial wastes were cleared depending on this method.

3. Removal and determination of organic pollutants

Part of my work was focused on removal of preconcentration and removal of organic pollutants e.g. phenols, aromatic amines, carboxylic acids, chlorinated and phosphorous and chlorinated aromatic hydrocarbons from industrial applications employing PUFs for clean effluents. This work has resulted in publishing over 10 papers in ISI international journals with good impact factor during 1988-2008. The work has frequently cited in literature.

4. Recovery of gold from waste:

We developed new methods for the recovery of gold from the liquid and solid wastes of electroplating plant which was adopted by the gold industry in both Egypt and South Africa. This work resulted in publishing more than 5 papers.

5. Health related applications:

Hepatitis C is a severe liver condition that is considered an epidemic in Egypt, my work on the development of a diagnostic method for HCV was adopted by the largest hospital in our region and helped control this disease. Part of my work is focused on the separation of ^{90}Y from its parent ^{89}Sr by Zirconium-vanadate Gel Ion-Exchanger for medical use. Excellent radionuclidic purity and radiochemical purity of the eluted ^{90}Y were achieved. Part of the work was focused on analysis of a series of drugs in drug formulations and wastewater samples. The overall work resulted

in publishing 7 papers employing spectrofluormetry, voltammetry and neutron activation analysis. Most of these methods are low cost and proceed in short time.

6. Amplification Reactions (Determination and speciation of Metal ions: The use of high fold chemical amplification reactions involving periodate oxidation allowed us to develop new methods for the determination of many metal ions and their speciation. These methods received great attention from the scientific community and are now applied in many research labs and industry especially in places with limited funding. This work has resulted in publishing 6 papers.

7. Amplification of detection limits:

Many elements are very difficult to determine due to their very low concentrations and complex matrices they are present in. We developed many new preconcentration procedures involving low cost and effective solid sorbent polyurethane foams that are now adopted by many researchers for determinations and chemical speciation under these extreme conditions. This work resulted in publishing over 10 papers and is frequently cited. 8. Novel approach for detecting binuclear Cu species:

Our work on bulk cyclic voltammetry and thin layer cyclic voltammetry were the first to employ this technique for confirmation of bi-nuclear copper complex species. This work has resulted in publishing over 4 papers and is frequently cited. This work opened the door for many advances in electrochemistry field. This work resulted in publishing over 8 papers and is frequently cited. One of these papers was cited over 28 citations.

9. Work in metal accumulation in biological system:

My work on the interaction of hard toxic metal ions with liver methioproten in fish was first to shed light on how metal ions interact or bonded with body chemicals and accumulate in certain parts/ tissues. The paper resulted from this work is

frequently cited in the literature (over 300 citations). This kind of work was of great importance on assessing pollution of marine water by hard toxic metal ions and it can be used as bioindicators of marine water by metal pollution.

10. Catalytic activity: My work on preparation of Ru complexes resulted in publishing over 4 papers. Some of the complexes showed excellent catalytic activity towards oxidation of primary and secondary alcohols.

I believe that these highlights show many innovations that resulted in actual applications in industry, health, pollution control, and advancement of science



SUBMISSION FORM: DEGREE OF DOCTOR OF SCIENCE

1. Name in full: MOHAMMAD SOROR EL-SAEED EL- SHAHAWI

2. Full Postal Address: Department of Chemistry, Faculty of Science, King Abdulaziz

University, P.O. Box 80203, Jeddah 21589, Saudi Arabia. E-mail

address malsaeed@kau.edu.sa,

mohammad_el_shahawi@yahoo.co.uk

3. Complete either (a) or (b) below:

(a): Degrees of the University of Strathclyde, with dates of award

Doctor of Philosophy (Ph.D), 1986

(b): Offices held in the University of Strathclyde, or in an institution in association with the University of Strathclyde, with dates (If the status of your candidature is in respect of (b) above, state here the degree or equivalent qualifications which you hold, with dates of awards.)

4. Details of present employer and post held

Please see details of Employment and Administrative Experience, Recognition (Prize Merits), Reviewing, Community and University Services in the CV.

i. Professor of Analytical and Environmental Chemistry, Department of Chemistry, Faculty of Science, King Abdulaziz University, Jeddah, **September 2005- to present, Kingdom of Saudi Arabia.**

ii. Visiting Professor at the School of Environmental and Earth Sciences (c/o Prof. E.P. Achterberg **2000, 2001, 2002, 2003** at Plymouth U (School of Ocean & Earth Science) and Southampton University (National Oceanography

- Centre). **iii.** Visiting Professor at Institute Für Chemie, Humboldt- Universität Zu, Berlin (c/o Prof. W. Moritz), Berlin, **August – October 2002, Germany.**
- iv.** Chairman of the Department of Environmental Sciences, Faculty of Sciences at Damiatta, Mansoura University, Mansoura, **January –July, 2000.**
- v.** Consultant at the "Federal of Environmental Protection Agency", Abu-Dhabi, **September 5-26, 1999, United Arab Emirates.** **vi.** Professor of Analytical Chemistry, Mansoura University, Mansoura, **November 1996 – 2005, Egypt.**
- vii.** Honorary Senior Visiting Professor and Research Fellow at the Department of Environmental Sciences Sciences (c/o Prof. E.P. Achterberg), Plymouth University, Plymouth, **July - August 1997, UK.** **viii.** Professor of Analytical Chemistry United Arab Emirates. University, AlAin, November, **1996 – September, 1997, United Arab Emirates.**
- ix.** Honorary Senior Visiting Professor and Research Fellow at the School of Chemistry (c/o Prof. D. T. Burns), the Queen's University of Belfast, Belfast, **July-August 1995, Northern Ireland, UK.**
- x.** Honorary Senior Visiting Professor and Research Fellow at Pure and Applied Chemistry (c/o Prof. W.E. Smith), Strathclyde University, Glasgow, **JulyAugust 1993, UK,**
- xi.** Associate Professor of Analytical Chemistry, UAE. University, Al-Ain, **September, 1991 –November, 1996, United Arab Emirates** **xii.** Associate Professor of Analytical Chemistry, Mansoura University, Mansoura, **July 1991 - September 1991, Egypt.**
- xiii.** Lecturer of Analytical Chemistry, Mansoura University, Egypt, May 1986 - July 1991, Egypt; Research Assistant at Pure and Applied Chemistry, Strathclyde University, Glasgow, Scotland, UK, **(September 1982 - 1986);** Research Assistant at the Department of Chemistry, Royal Holloway College, London University, UK. (October 1981- April 1982); Demonstrator at the Department of Chemistry, Mansoura University, Egypt, **(December 1977 – 1981).**

5. Titles of works submitted published and/or unpublished.

(Published works should be listed chronologically, giving year and, in the case of books, place of publication.

Attach a separate list if necessary.)

Please see the List of publications in CV. The list of Publication includes the following items:

- A. List of Papers Submitted and / or Revised and/ or under Revision for Publication in International Journals (**5 Manuscripts**).
- B. Papers Accepted and/ or published in International Journals (**131 Full papers**): **125** articles for reviewing (**1-125**) and **6** from M.Sc & Ph.D (**125-131**)
- C. Conferences (**Poster =32, Oral Presentation= 28**), Workshops (**2**) and Meetings of Professional Societies (**4**).
- D. Book Chapters published (**Three Book Chapters are published in 1997, 2012 and 2013.**
- E. Three Books translated from English to Arabic (Under review for publication).
- F. Supervisions: List of Ph.D (20) & M.Sc (32) thesis and B.Sc (>70) students
- G. Funded Projects: Good experience in project management and I have attracted over 4000,000 \$ US Dollars in research funds since 1992 via participation as PI and /or Co-author in a number of research projects (Please see details in CV)
- H. Please see Research interest in the CV.

6. If you have already submitted any of the work to another Institution for a Higher Doctorate, state the name of the Institution and date of submission

None / not applicable

7. Declaration:

I hereby declare that the work specified in section 5 above has been composed by myself or, in the case of joint work (see note 2), that the attached statement concerning the extent of collaboration is true and correct.

Signature ...Mohammad Soror El-Saeed El-Shahawi Date

January 5, 2012

The work or works submitted in candidature should be deposited with the Secretary to Senate, together with this form, duly completed, and the fee of * (insert fee). (see notes overleaf)**

NOTES :

I. A candidate for the degree of Doctor of Science shall submit **three** sets of published works together with any additional unpublished work and **three** copies of a summary of not more than 1000 words outlining the contents thereof. **II.**

Candidates may submit work for which they have been jointly responsible provided that such work is accompanied by a signed statement clearly defining the extent of the candidate's contribution to such work.

III. A candidate who has previously submitted the material or any part of it for examination for a degree, including a Higher Doctorate, of the University or of any other institution must declare this on the submission form. A candidate should not submit material which has been presented for a lower degree unless it is considered that its omission would result in an inadequate representation of the candidate's research.

Published articles from Ph.D & MSc Degrees (6) (Numbers 125-131 entries) in the list of publication.

Published work for reviewing 125 articles (1-125 entries) in the list of publication.

List of Thesis Supervision

M. S. El-Shahawi

Professor of Analytical and Environmental Chemistry

Supervision of Thesis's and Dissertations (M. Sc. and Ph.D) i. **32**

M.Sc thesis's (**30** awarded and **2** in progress) ii. **20** Ph.D thesis's

(**18** Awarded and **2** in progresses)

I. Master of Science Theses

A. At King Abdulaziz University, Jeddah, Saudi Arabia

1. Name of the candidate: Mr. Adel A. Al-Malki (In progress)

Title of the thesis:

Retention Profile and Chromatographic Separation of Trace Concentration of Some Organic and Inorganic Contaminates in Industrial Wastewater and Other Matrices by Nanosized Solid Phase Extractors

2. Name of the candidate: Miss Rehab M. Al-Harbi (In progress)

Title of the Thesis:

"Biosorption of Some Selected Heavy Metal ions by selected Local Algae"

3. Name of the candidate: Mr. Waleed M. Al-Shawafi (Awarded, 2012)

Title of the Thesis:

" Retention Profile, Chromatographic Separation and Determination of some Water Soluble Inorganic Pollutants "

4. Name of the candidate: Miss Rania M. Bashamy (Awarded 2011)

Title of the Thesis:

"Spectroelectrochemical Behavior of Some Schiff Base Metal Complexes and their Analytical Applications"

5. Name of the candidate: Mr. Maged Ba Muslam (Awarded 2011)

Title of the Thesis:

"Determination of Antibacterial Activity in Relation to Antioxidant Power of Locally Produced Honey"

6. Name of the candidate: Miss. Wegdan T . Al-Saggaf (Awarded, 2009)

Title of the Thesis:

"Novel Methods for the Determination of Some Selected Persistent Inorganic and Organic Pollutants in Different Matrices"

7. Name of the candidate: Miss. Magdah R. Al-Otibey (Awarded, 2009)

Title of the Thesis:

"Novel Methods for the Determination of Trace Concentrations of Some Selected Biocomponent and Inorganic Species in Different Matrices" **8.**

Name of the candidate: Mrs. Tharawat N. Abdeljabbar (Awarded, 2008)

Title of the Thesis:

"Comparative Studies on the Chemical Constituents of Green Tea"

9. Name of the candidate: Mr. Hakeem Qaid Al-Ariqe (Awarded, 2007) Title of the Thesis:

"Novel Methods for Chemical Separation and Quantitative Determination of Titanium and Lead in Food Studies and Industrial Wastewater"

10. Name of the candidate: Mrs. Effat A. Bahiddra (Awarded, 2007) Title of the Thesis:

"Electrochemical and Voltammetric Determination of Sulfadiazine and Spironolactone Drugs in Their Pharmaceutical Preparations and Industrial Wastewater"

11. Name of the candidate: Mrs. Fatma M. Al-Shreef (Awarded, 2007) Title of the Thesis:

"Retention Profile, Chromatographic Separation and Chemical Speciation of Gold (I& III) Employing Polyurethane Foam Solid Sorbent"

B. At United Arab Emirates University, United Arab Emirates

12. Name of the candidate: Mr. Ali S. Al-Meqbali, (Awarded, 1998) Title of the Thesis:

"Pre-concentration and Voltammetric Behavior of Some Water Soluble Pesticides and their Determination in Water and Plant Samples"

13. Name of the candidate: Mr. Mehboob Hassan Saleh, (Awarded, 1996) Title of the Thesis:

"Collection and Chromatographic Separation of Some Inorganic and Organic Pollutants from Aqueous Media by Polyurethane Foams"

14. Name of the candidate: Mr. Rashed Saleh-Al-Mehrezi (Awarded, 1996) Title of the Thesis:

"Retention Profile and Chromatographic Separation of Some Inorganic and Other Water Pesticides Using Polyurethane Foams and Other Extracting Agents"

15. Name of the candidate: Miss. Mariam H. Al-Yousuf (**Awarded, 1995**) Title of the Thesis:

"Determination of Heavy Metals in Adult and Juvenile Emperors, *Lenthrinus Lentijan Fish* (Family: *Linthrinide Toelost*) from the Arabian Gulf in United Arab Emirates Coastal water"

C. At Al-Azhar University, Cairo, Egypt

16. Name of the candidate: Miss. Shreen K.H. Al-Zagzok, (**Awarded, 2008**) Title of the Thesis:

"Retention Profile and Chromatographic Separation of Some Inorganic Ions onto Polyurethane Foams and Other Extracting Agent"

17. Name of the candidate: Miss Dalia A.A. Al-Borsh, (**Awarded, 2007**) Title of the Thesis:

"Retention Profile and Chemical Speciation of Some Metal Ions Present in Water Employing Polyurethane Foams and Other Extracting Agent"

D. At Menofia University, Menofia, Egypt

18. Name of the candidate: Mr. Ahmad T. Talaat, (**Awarded, 2004**) Title of the Thesis:

"Preconcentration and Determination of Some Textile Dyes in the Industrial Wastewater"

E. At Mansoura University, Mansoura, Egypt

19. Name of the candidate: Miss. Naglaa E. Al-Brashly, (**Awarded, 2007**) Title of the Thesis:

"Environmental Studies on the Removal and Degradation of some Water Pollutants"

20. Name of the candidate: Mr. Wael M. Mamdoh (**Awarded, 2007**) Title of the Thesis:

"Spectroscopic and Electrochemical Characterization of Some Metal Complexes of *O, O* Donor ligands"

21. Name of the candidate: Miss Halla A. Saleh (**Awarded, 2006**) Title of the Thesis:

"Preparation, Spectroscopic and Electrochemical Characterization of Some Thio- semicarbazide Schiff –Base Metal Complexes"

22. Name of the candidate: Mr. Fadel A. H. El-Gandy (**Awarded, 2006**) Title of the Thesis:

"A Study on the Uptake of some Inorganic Pollutants Using Solid Sorbents"

23. Name of the candidate: Mr. Ahamed Abd El-Basser (Awarded, 2005) Title of the Thesis:

"Synergetic of Some 4- Phenylthiazole Derivatives on Preventing Dezincification of alfa- Brass in Acid Chloride Solutions"

24. Name of the candidate: Mr. Yasser A. Al-Ashwaih (Awarded, 2005) Title of the Thesis:

"Spectroscopic and Electrochemical Characterization of Some Copper (II) Complexes"

25. Name of the candidate: Mohammad A. Abdel Fadel (Awarded, 2004) Title of the Thesis:

"Novel Methods for the Separation and Determination of Some Inorganic and Organic Pollutants Present in the Industrial Wastewater".

26. Name of the candidate: Mr. Tamer A. El-Mogy (Awarded, 2004) Title of the Thesis:

"Electrochemical Behavior and Voltammetric Determination of Some Pharmaceutical Compounds in Aqueous Media"

27. Name of the candidate: Mr. Hossam M. Nassef (Awarded, 2004) Title of the Thesis:

"Spectroelectrochemistry of Some Redox Systems at Optically Transparent Thin Electrodes"

28. Name of the candidate: Mr. Mohammad Abdel –Hay (Awarded, 2003) Title of the Thesis:

"Kinetics, Retention and Thermodynamic Characteristics of Some Fission Products onto Titanium (IV) – Molybdate Ion Exchanger and Other Stationary Phases"

29. Name of the candidate: Mr. Hani A. Nassef, (Awarded, 2002) Title of the Thesis:

"Retention Profile and Determination of Some Water Soluble Organic and Inorganic Pollutants Employing Polyurethane Foams and Other Extracting Agents"

30. Name of the candidate: Mr. Hassan A. Hassan, (Awarded, 1993) Title of the Thesis:

"Physicochemical Studies of Some Conducting Polymers"

31. Name of the candidate: Mr. Abdelhamid M. Othman, (Awarded, 1993) Title of the Thesis:

"A Study on the Chemical Stability of Some Antibiotics"

32. Name of the candidate: Mrs. Iman I Askar (Awarded, 1991) Title of the Thesis:

"A Comparative Study on Some Methods of Chemical Analysis"

II. Doctor of Philosophy, Ph. D

A. At King Abdulaziz University, Saudi Arabia

33. Name of candidate: Mr. Ziab A. Al-Ariany (In progress) Title of the Thesis:

Novel Methods for Chromatographic Separation and Determination of Inorganic and Organic complex Species in Different Matrices

34. Name of candidate: Mr. Waqas A. Fadl Rabani (In progress) Title of the Thesis:

35. Name of candidate: Mrs. Amal M. Al-Baqawy (Awarded, 2015) Title of the Thesis:

Retention profile and Chromatographic Separation of Some inorganic Pollutants from Aqueous Media by nanosized solid sorbent and other extractors

36. Name of candidate: Mr. Nabeel H.A. Khraibah (Awarded, 2015) Title of Thesis:

Development of Novel Chemically Modified Electrodes for Electrochemical Determination of Trace Amounts of Complex Species of Biochemical Importance.

37. Name of candidate: Mrs. Gharam I. Mohammad (Awarded , 2015) Title of Thesis:

Novel Electrochemical and Spectrofluorimetric Methods for Analysis of Selected Organic and Inorganic Species in Complex Matrices

38. Name of candidate: Mrs. Zinab M. Seqil (Awarded, 2015) Title of the Thesis:

Novel Methods for Minimization, Determination and Chemical Speciation of Trace and ultra UltraTrace Concentrations of some Selected Heavy Metal ions and Chlorophenols in Industrial Wastewater and other Matrices

39. Name of Candidate: Miss Amal. A. Bahaffi (Awarded, 2013)

Title of the Thesis:

"Novel Methods for the Determination and Separation of Trace Concentrations of Some Inorganic Pollutants in Wastewater.

40. Name of Candidate: Mr. Hamed H. Alsadi (Awarded, 2010)

Title of the Thesis:

"Retention Profile, Chromatographic Separation and Quantitative Determination of Ultra Trace Concentrations of Some Inorganic Pollutants and Food Colorants in Aqueous Media and Food Stuffs"

41. Name of the candidate: Mrs. Einas H. Al-Ghany (Awarded, 2010)

Title of the Thesis:

"Novel Methods for the Chromatographic Separation and Voltammetric Determination of Selected Inorganic Pollutants and Food Colors in Industrial Wastewater"

42. Name of the candidate: Miss Iman A. Al -Harbyi (Awarded, 2010)

Title of the Thesis:

"Novel Methods for the Chromatographic Separation, Chemical Speciation and Determination of Some Inorganic and Organic Water Soluble Pollutants"

B. At Mansoura University, Mansoura, Egypt

43. Name of the candidate: Mrs. Neveen E. M. H. Eweda (Awarded 2009) Title of the thesis:

"Radiochemical Studies on the Separation of Yttrium-90 from Strontium-90 Relevant to Cyclotron Produced Radionuclide"

44. Name of the candidate: Mr. Khalid M. Moqbal (Awarded, 2006) Title of the Thesis:

"Physicochemical Studies of Some Novel Organic Compounds and Their Complexes"

45. Name of the candidate: Mr. Ali M. Dowidar, (Awarded, 2006) Title of the Thesis:

"Adsorption Behavior of Some Polyaromatic Hydrocarbons on Modified Activated Carbon"

46. Name of the candidate: Mr. Gamil A.A.M. Al-Hazmi, (Awarded, 2004) Title of the Thesis:

"Spectral and Electrochemical Studies on Thiosemicarbazone derivatives and Their Metal Complexes.

47. Name of the candidate: Mrs. Mervat A Abdel-Mageed (Awarded, 2004) Title of the Thesis:

"Novel Methods for the Removal of Some Inorganic Pollutants Present in the Industrial Wastewater"

48. Name of the candidate: Mrs. Nadia R. Abdel-Mouhty, (Awarded, 2003) Title of the Thesis:

"Radiochemical Studies on the Preparation and Evaluation of Radioimmunoassay Systems of Thymoglobulin for Monitoring Thyroid Status"

49 Name of the candidate: Mrs. Mai M.A. Shanab, (Awarded, 2003)

Title of the Thesis:

"Spectroscopic and Electrochemical Studies on Some Transition Metal Complexes of 1-Hydroxy-2-Acetonaphthone and its Schiff Bases" **50.**

Name of the candidate: Mr. Mahmoud El-Tawoosy, (Awarded, 2001)

Title of the Thesis:

"Developmental studies on radio iodination of some organic compounds and biomolecules"

51. Name of the candidate: Mr. Abdal Gawad A Radi, (Awarded, 1993)

Title of the Thesis:

"Inhibition of Corrosion of Semiconductors Conjunctions in Aqueous Electrolytes"

C. At the Queens University of Belfast, Belfast, UK

52. Name of the candidate: Mr. Salem A. Barakat (Awarded 1992)

Thesis Title: "Flow Injection Spectrophotometric Techniques for the Determination of Chromium and Manganese in British Steel"

Funded Research Projects

A. Research Projects under International Collaboration:

1. DFID Link project between Plymouth University –Mansoura University (2000-2003)

Local PI: " Water Quality in River Nile" DFID link project between Dr. E.P. Achterberg at "Plymouth University" and Prof. M.S. El-Shahawi at "Mansoura University", funded by DFID, British Council in Egypt, (2000-2003).

Duration	3 Years	Starting date:
June 2000-June 2003		Amount
Awarded	25,000 British Pounds	
Awarding Body	DFID and British Council, Egypt	

2. GEOMAR, Helmholtz Centre for Ocean Researc, Keil , Germany: In October 2012, I have participated effectively with Prof. Eric P. Acterberg at GEOMAR, Helmholtz Centre for Ocean Research, 24148 Kiel, Germany in getting a fund (1,150,000 \$ US Dollars) of the research proposal entitled: Investigation of Novel Pollutants e.g. silver nanoparticles, Gallium, Lead, Nickel, Vanadium and Nutrients in Jeddah Coastal Waters and Their Biological Effects" between King Abdulaziz University, Saudi Arabia and Helmholtz Centre for Ocean Research, Kiel.

3. Miami U, Miami, USA: In September 2012, I have participated effectively with Prof. Rogers M. Leblanc (Cooper Fellow), Professor and Chair at the Department of Chemistry, Miami U, USA in getting a fund (1,350,000 \$ US Dollars) of the research proposal entitled: Detection of Hepatocellular Carcinoma (HCC) in AT-Risk Groups by using biomarker alfa-L-fucosidas (AFU) to screen and identify at risk groups for early tumors which will need treatment" between King Abdulaziz University, Saudi Arabia and Miami U, USA.

B. National Research Projects at King Abdulaziz, Um-ALQRA, Taibah, Mansoura and United Arab Emirates Universities, Saudi Arabia (2011-2012)

1. PI : “Preparation and Characterization of Novel Schiff Bases and their complexes with some Precious Group Metals”

Duration: 9 moths, Starting date:
March 2012

Amount Awarded: **51,400 SR (Saudi Ryals)**

Awarding Body: Deanship of Scientific Research, King Abdulaziz University

2. Co author: “Superheated Water as Eluent in High-temperature High – Performance Liquid Chromatographic Separations of Steroids on a Bonded C18 Columns”

Duration: 9 moths, Starting date:
March 2012

Amount Awarded: **59,400 SR (Saudi Ryals) Awarding**

Body:

Deanship of Scientific Research, King Abdulaziz University.

3. Co author: "Determination of Essential Elements and Antibacterial Activity in Relation to Antioxidant Power of Locally Produced Honey in Kingdom of Saudi Arabia”

Duration: 9 moths Starting date:
March 2012

Amount Awarded: **62,000 SR (Saudi Ryals)**

Awarding Body: Deanship of Scientific Research, King Abdulaziz University.

4. Co author: "Soil Pollution Hazardous to Environment ": A Case study on the chemical composition and correlation to automobile traffic of the Roadside soil of Al_Madina Al_Monawarah City, Saudi Arabia”

Duration: 10 moths Starting date:
October 2012

Amount Awarded: **50,200 SR (Saudi Ryals)**

Awarding Body: Deanship of Scientific Research, Taibah University

5. Co author: " Retention Profile and Developing of Novel Electrochemical methods for the determination of Precious Group

Metals”

Duration: 10 months Starting date:

October 2012

Amount Awarded: **59,200 SR (Saudi Ryals)**

Awarding Body: Deanship of Scientific Research, Taibah University

6. PI : “Preconcentration, Removal and Chemical speciation of Chromium (III & VI) in wastewater”

Duration: 9 months, Starting date:

March 2011

Amount Awarded: **61,250 SR (Saudi Ryals)**

Awarding Body: Deanship of Scientific Research, King Abdulaziz

University.

7. Co author: "Chemical Speciation of Trace Concentrations of Inorganic Arsenic (III, V) Species in Different Matrices by Stripping Voltammetry”

Duration: 9 months,

Starting date: March 2011

Amount Awarded: **67,200 SR (Saudi Ryals)**

Awarding Body: Deanship of Scientific Research, King Abdulaziz

University

8. Co author:" Novel method for the Determination of bromate ion in ozonated drinking water”

Duration: 9 months, Starting date: May

2011

Amount Awarded: **67,200 SR (Saudi Ryals)**

Awarding Body: Deanship of Scientific Research, UM Al-Qra

University.

9. Co author:" Production of Sodium dichromate and extraction of PGEs from Saudi chromite

Duration: 9 months, Starting date: May

2011

Amount Awarded: **67,200 SR (Saudi Ryals)**

Awarding Body: Deanship of Scientific Research, King Abdulaziz University

10. Co author:" Comparative Studies of Chemical Constituents of Green Tea Part II1: Analysis and Chemical Speciation of some Selected essential, non essential metal ions and Phosphorous in Green Tea in the Local Market of Saudi Arabia by Spectrochemical Techniques”

Duration: 9 months, Starting date:
March 2011

Amount Awarded: **72, 200 SR (Saudi Ryals)**

Awarding Body: Deanship of Scientific Research, King Abdulaziz University

11. PI:" Chemical Separation of Some Toxic Metal ions Present in Industrial Wastewater by Solid Stationary Phases”

Duration: 9 months, Starting date:
March 2010

Amount Awarded: **63, 150 SR (Saudi Ryals)**

Awarding Body: Deanship of Scientific Research, King Abdulaziz University

12. PI: “Novel Methods for the Determination of Ultra Trace Concentrations of Some Selected Food Colorants in their Formulations”

Duration: 9 months, Starting date:
March 2010

Amount Awarded: **63, 150 SR (Saudi Ryals)**

Awarding Body: Deanship of Scientific Research, King Abdulaziz University

13. Co author: “Analysis of Some Selected Chlorinated Pesticides in Water and Food Stuffs by Differential Pulse – Cathodic Stripping”

Duration: 9 months, Starting date:
March 2010

Amount Awarded: **73, 600 SR (Saudi Ryals)**

Awarding Body: Deanship of Scientific Research, King Abdulaziz University.

14. Co author: “Comparative Studies of Chemical Constituents of Green Tea

Part II: Simultaneous Determination of Catechins and Caffeine in Green Tea in the Local Market of Saudi Arabia using High Performance Liquid Chromatography”

Duration: 9 months, Starting date:
March 2010

Amount Awarded: **67, 600 SR (Saudi Ryals)**

Awarding Body: Deanship of Scientific Research, King Abdulaziz University

15. Co author: “Preparation, Characterization of metal oxide nanoparticles-loaded on activated local clay samples: Application in purification of municipal and industrial wastewaters ”

Duration: 20 months, Starting date:
March 2010

Amount Awarded: **845, 000 SR (Saudi Ryals)**

Awarding Body: The Center of Excellence of Environ. Studies (CEES), King Abdulaziz U.

16. Co author: “Development of carbon nanotubes based nanosensors for monitoring the ultra trace concentration of carbon mono-oxide in air”

Duration: 20 months, Starting date:
March 2010

Amount Awarded: **746,000 SR (Saudi Ryals)**

Awarding Body: The Center of Excellence of Environ. Studies (CEES), King Abdulaziz U.

17. PI: “Radiochemical Pollution I: “Spectrophotometric and Voltammetric Studies for the Chemical Speciation of Thorium Ions in Water Employing Some Selected Azo Compounds

Duration 9 month, Starting
date: Feb., 2009

Amount Awarded **71,00 SR (Saudi Ryals)**

Awarding Body: Deanship of Scientific Research King Abdulaziz

University

18. Co-Author : Preparation, Spectroscopic and Electrochemical Characterizations of some Selected Schiff Bases and their Complexes with Transition Metal ions

Duration 9 moths, Starting date Feb. , 2009

Amount Awarded **66,500SR (Saudi Ryals)**

Awarding Body Deanship of Scientific Research King Abdulaziz University

19. Co-Author: "Designing and Synthesis of New Fluoroorganic Compounds Bearing Heterobicyclic Systems in Searching of New Biocidal Reagents and Chelating agents for Separation and Determination of Some toxic Elements in Industrial Liquid Waste"

Duration 10 moths, Starting date: Feb. , 2009.

Amount Awarded **79,900SR (Saudi Ryals)**

Awarding Body Deanship of Scientific Research, King Abdulaziz University

20. PI: "Separation and Chemical Speciation of Ultra Trace Concentrations of Some Selected Toxic Metal Ions Present in Industrial Wastewater Employing Novel Derivatives of Thiazolidinone"

Duration 9 moths, Starting date: Feb., 2009.

Amount Awarded 66,900 SR (Saudi Ryals)

Awarding Body SABIK International Company, Saudi Arabia

21. Co-Author: Comparative Studies of Chemical Constituents of Green Tea Part 1: Simultaneous Determination and Health Benefits of some selected Inorganic Anions in Green Tea in the Local Market of Saudi Arabia by Suppressed Ion Chromatography

Duration 9 moths, Starting date: February, 2009

Amount Awarded 90,900SR (Saudi Ryals)

Awarding Body Deanship of Scientific Research, King Abdulaziz University

22. Co –Author: Part I: “Polarographic and Voltammetric Studies on Some Novel Reactive Dye 4'-Tricyanovinyl-hydrazone and some of its Derivatives”

Duration 9 moths, Starting date: October, 2009.

Amount Awarded 81,900 SR (Saudi Ryals)

Awarding Body Deanship of Scientific Research, King Abdulaziz University

23. Principal Investigator: Proposal Title: Pre concentration, Determination and Chemical Degradation of some Selected Nutrients Part 1:

Preconcentration and Chemical Degradation of Inorganic and Organic Phosphate in Sea – and Industrial Wastewater

Duration 9 moths, Starting date: Feb., 2009

Amount Awarded 60,900SR (Saudi Ryals)

Awarding Body Deanship of Scientific Research, King Abdulaziz University

24. Principle Investigator: Environmental Chemistry IV: Novel

Preconcentration and Voltammetric Methods for the Determination of Titanium and Lead Ions in Selected Food Stuffs and Wastewater Samples".

Duration 9moths, Starting date: February, 2008.

Amount Awarded 71,800 SR (Saudi Ryals)

Awarding Body SABIK International Company

25. Co-Author: "Environmental Chemistry III: Retention Profile, Chromatographic Separation and Chemical Speciation of Gold (I & III) Ions from Liquid Wastes".

Duration 9moths, Starting date: Feb., 2008.

Amount Awarded 80,800 SR (Saudi Ryals)

Awarding Body Deanship of Scientific Research, King Abdulaziz University

26. Co-Author: "Synthesis, Specific and Voltammetric Studies on some Novel Spiro-Thiazolidinone Steroids Derived from Sulfa Drugs and their Analytical Applications in Industrial Wastewater".

Duration 10 moths, Starting

date: Feb., 2008

Amount Awarded 76,300 SR (Saudi Ryals)

Awarding Body SABIK International Company

27. Co-Author: "Analysis of Uranium in Local Phosphate Fertilizers in Kingdom of Saudi Arabia".

Duration 9 moths, Starting

date: Feb., 2008

Amount Awarded 75,100 SR (Saudi Ryals)

Awarding Body Deanship of Scientific Research, King Abdulaziz University

28. Co – Author: "Synthesis of some Novel 1- Acyl /benzoyl -1-anilido-4methyl-butadiene Derivatives as Trapping Chelating Agents for Trace Separation and Subsequent Determination of Heavy Metals in Industrial Wastewater"

Duration 9moths, Starting

date: Feb., 2008

Amount Awarded 71,800SR (Saudi Ryals)

Awarding Body SABIK International Company

29. PI: "Environmental Chemistry: Environmental Studies on Developing Novel Methods for the Determination of some Drug Residues in Pharmaceutical Formulations and Industrial Wastewater and Their Impacts Using Adsorption Voltammetry".

Duration 9moths, Starting date:
Feb., 2008

Amount Awarded 65,600SR (Saudi Ryals)

Awarding Body SABIK International Company

30. Co –Author: "Mineral Processing and Extraction of Rare Earth Elements from the Wadi Khamal Nelsonite Ore, northwestern Saudi Arabia.

Duration 6 moths, Starting date: May
2008

Amount Awarded 51,800 SR (Saudi Ryals)

Awarding Body Deanship of Scientific Research, King Abdulaziz
University

31. Co Author: Proposal title: "Spectroscopic Characterization,
Electrochemical and Catalytic Activity of Some Novel Schiff Bases and Their
Palladium (II), Ruthenium (II) and Rhodium (III) Complexes".

Duration 6 moths, Starting
date: May 2008

Amount Awarded 45,200 SR (Saudi Ryals)

Awarding Body Deanship of Scientific Research, King Abdulaziz
University

32. Co –Author: "Synthesis of Novel Heterocyclic Organic Compounds
Containing Sulfur Nitrogen, and Oxygen and their Metal Complexes as
Treatment reagents for Dengue Fever and their Applications Against Aedes
and Culex in Jeddah, Saudi Arabia

Duration 9moths, Starting date:
Feb., 2008.

Amount Awarded 51,800SR (Saudi Ryals)

Awarding Body
Deanship of Scientific Research, King Abdulaziz University

33. PI: "Spectroelectrochemical Studies on Some Redox Systems of Some
Organic and Inorganic Color Pigments".

Duration 9 moths, Starting date:
March,2007.

Amount Awarded 79,800SR (Saudi Ryals)

Awarding Body SABIK International Company

34. Co-Author: "Fertilizer Pollution Hazardous to Human Life: A Case Study on
the Analysis and Separation of Some Essential and Toxic Trace Metal
Ions Present in Selected Fertilizers in Jeddah Market, Kingdom of Saudi
Arabia"

Duration 9 moths, Starting
date: March, 2007

Amount Awarded 81,800SR (Saudi Ryals)

Awarding Body SABIK International Company

35. Co – Author: Proposal title: "Green Chemistry I: Synthesis of Novel Cyclic and Non-cyclic Organic Compounds Containing Nitrogen, Sulfur and Oxygen for Their use in the Separation and Subsequent Determination of some Toxic Trace Heavy Metal Ions in Industrial Treated Wastewater in Jeddah city".

Duration 9 moths, Starting date
March, 2007.

Amount Awarded 77,800SR (Saudi Ryals)

Awarding Body SABIK International Company

36. PI "Project entitled: Environmental Chemistry II: "Novel Methods for the pre-concentration, Separation and Determination of Some Trace Toxic Heavy Metal Ions in Coastal and Industrial Waste Water Samples in Jeddah".

Duration 9 moths, Starting date:
March, 2006.

Amount Awarded 78,200SR (Saudi Ryals)

Awarding Body SABIK International Company

37. Principal Investigator: Proposal title: "Quality Assurance and Accreditation Program (2004 - 2005)", (QAAP) A/MAN/3/09

Duration 3 years Starting date
January 2005

Amount Awarded 150,00 Egyptian Pounds

Awarding Body Ministry of Higher Education, Egypt

38. Co –Author:" Determination of Heavy Metals in Soil around Industrial Areas of the United Arab Emirates", UAE University, Research Council, United Arab Emirates, 1994-1995.

Duration 12 month Starting
date: October 1995 Amount Awarded

15,000 Dirham's,

Awarding Body Research Council at United Arab Emirates U

39. Co –Author: "Determination of Some Pharmaceutical Drug Containing Purine Derivatives Using Adsorption Stripping and Spectrophotometric Methods of Analysis"

40. Duration 10 month **Starting date:** October 1994 **Amount**

Awarded 10,000 Dirham's

Awarding Body Research Council at United Arab Emirates U

41. PI "Application of Spectroelectrochemical Techniques in Studying Various Redox Systems of Naturally Occurring Ligands and their Metal Complexes in vivo" UAE University, Research Council United Arab Emirates, 1992.

Duration 10 month **Starting date:** March, 1993 **Amount Awarded**

10,000 Dirham's,

Awarding Body Research Council at United Arab Emirates U

42. "Extraction, Recovery and Separation of Some Inorganic and Organic Pollutants by Chromatographic and Electrochemical Techniques"

Duration 10 month **Starting date:** October 1994

Amount Awarded 10,000 Dirham's

Awarding Body Research Council at United Arab Emirates U

43. Co – Author: "Electrochemical Studies of Polynuclear Copper Protein Model"

Duration 10 month **Starting date:** October 1992 **Amount Awarded**

10,000 Dirham's

Awarding Body Research Council of UAE University

44. Co –Author: "Determination of Heavy Metals in Soil around Industrial Areas of the United Arab Emirates", UAE University, Research Council, United Arab Emirates, 1994-1995.

Duration 12 month Starting date
October 1995 Amount Awarded
15,000 Dirham's

Awarding Body Research Council at UAE University

45. Co –Author: "Determination of Some Pharmaceutical Drug Containing Purine Derivatives Using Adsorption Stripping and Spectrophotometric Methods of Analysis",

Duration 10 month Starting date
October 1994 Amount Awarded
10,000 Dirham's,

Awarding Body Research Council at UAE University

46. PI "Application of Spectroelectrochemical Techniques in Studying Various Redox Systems of Naturally Occurring Ligands and their Metal Complexes in vivo" UAE University, Research Council United Arab Emirates, 1992.

Duration 10 month Starting
date March, 1993 Amount
Awarded 10,000 Dirham's,

Awarding Body Research Council of UAE
University

47. I "Extraction, Recovery and Separation of Some Inorganic and Organic Pollutants by Chromatographic and Electrochemical Techniques"

Duration 10 month Starting date Oct.,
1994
Amount Awarded 10,000 Dirham's,

Awarding Body Research Council of UAE University

48. Co – Author: "Electrochemical Studies of Polynuclear Copper Protein Model"

Duration 10 month Starting date

October 1992
10,000 Dirham's,
Awarding Body
University

Amount Awarded

Research Council of UAE

Curriculum Vitae

Professor M. S. El-Shahawi I:

Personal:

Birth date October 2, 1953.
Nationality Egyptian
Marital Status: Married with four
Home Tel/Fax.: Egypt: Home : 002 050-2230344; Work: 002-057 2403866;
Mobile: 002-01223238742
Saudi Arabia:, Home: 00966-6753772; Work 6952000/64422
Fax:009662-6952292

Contacts [Email:malsaeed@Kau.edu.sa](mailto:malsaeed@Kau.edu.sa); Mobile: 00966-0551691130
mohammad_el_shahawi@yahoo.co.uk

Permanent address Mansoura University Residence Staffs, Mansoura, Egypt

II. Education and Professional Qualifications:

- 1. D.Sc 2013:** Strathclyde University, Glasgow, U. K., Thesis title:
“Physicochemical Studies on Spectroscopic and Electrochemical
Characterization, Preconcentration, Separation, Determination and / or
Chemical Speciation of various Inorganic and Organic complex species
in Different Media
- 2. Ph. D. 1986:** Strathclyde University, Glasgow, U. K., Thesis title:
“Spectroscopic and Electrochemical Characterization of some Transition
Metal Complexes”.
- 3. M. Sc.1980:** Mansoura University, Egypt, Thesis title:
“Separation and Determination of some Inorganic and Organic Pollutants in
Aqueous Solutions Employing Polyurethane and Other Extracting Agents”.
- 4. B. Sc. 1975:** Special Chemistry, Mansoura University, Egypt

III. Employment and Administrative Experience:

A. Employment Experience

November 1996 – Present:

1. September 2005 – present:

Professor of Analytical and Environmental Chemistry, Department of Chemistry, Faculty of Science, King Abdulaziz University, Saudi Arabia and Mansoura University, Egypt.

2. September 1997 – August 2005:

Professor of Analytical Chemistry, Department of Chemistry, Faculty of Sciences at Damietta, Mansoura University, Mansoura, Egypt.

3. December 1999 - present:

In December, 1999, I have promoted to Professor of Environmental and Analytical Chemistry at the Department of Environmental Sciences, Faculty of Sciences at Damietta, Mansoura U, Mansoura, Egypt.

4. November 1996 –August 1997:

In **October 11, 1996**, I have promoted to Professor of Analytical Chemistry and I have continued my contract at the Department of Chemistry, Faculty of Science, UAE University, United Arab Emirates up to **September 7, 1997**.

5. September 1986 – October 1996:

i. August 1991 – October 1996:

Associate Professor of Analytical Chemistry, Department of Chemistry, Faculty of Science, UAE University, United Arab Emirates.

ii. April 1986 – July 1991:

Lecturer of Analytical Chemistry at the Department of Chemistry, Faculty of Sciences at Damietta, Mansoura University, Mansoura, Egypt.

6. December 1977 – March 1986:

i. September 1982 –March 1986:

Research Assistant at Pure and Applied Chemistry, University of Strathclyde.

Ph.D research was supported by the Egyptian Government (**September 1982 - 1986**). The research work was under the supervision of Prof. D.H.

Brown and Prof. W.E. Smith. Prof. W.E. Smith) thesis. **ii. October 1981 –**

September 1982:

- Research Assistant at Department of Chemistry (Bourne Haber Laboratory) , Royal Holloway College, University of London U, UK.. **iii.**

November 1980 –October 1982:

Teaching Assistant at Department of Chemistry, Faculty of Education, Mansoura U, Mansoura, Egypt.

iv. November 1977 – November 1980:

Demonstrator and research assistant at Department of Chemistry, Faculty of Education, Mansoura U, Egypt.

B. Administrative Experience:

Chairman of the Department of Environmental Sciences, Faculty of Sciences at Damietta, Mansoura University, Mansoura, Egypt, (**February – July 1999**).

C. Consultancies and Recognition:

1. Lead Guest Editing of one of upcoming Special Issues for International Journal of Analytical Chemistry, Hindawi Publishing Corporation.
2. M.S. El-Shahawi, A. A. Al-Sibaai, A.S. Bashammakh, H.M. Al-Saidi and E. A. Assirey
“Fast, Selective Removal and Determination of Total bismuth (III) and (V) in Water by Procaine Hydrochloride Immobilized Polyurethane Foam Packed Column Prior to Inductively Coupled Plasma – Optical Emission Spectrometry” A Book Chapter in Fahmina Zafar “Chief Editor” in "Polyurethane", ISBN 979-953-307-642-2. In Tech, Open Access publisher in the fields of science, technology and medicine.
3. Consultant at the Centre of Excellence in Environmental Studies (CEES), King Abdulaziz University, Jeddah, Saudi Arabia (2009 – present).
4. External Reviewer of Scientific merits of projects submitted to the Deanship of Scientific research, King Saud University, 2008 – present.
5. External Reviewer of Scientific merits of projects submitted to the Deanship of Scientific research, Taeif, Tibah (Al-Madinah Al- Minawara) and King Abdulaziz Universities, Saudi Arabia, **2007 -2011**.
6. Sponsor on a “Workshop” "Demonstration of some Low Cost and

Applicable Procedures for Detection and Semi quantitative Determination of Trace Metal Ions in Water "**Oral Presentation** and Experimental Evidences", The 15th International Conference of Chemical Education in Chemistry and Global Environmental Change", Cairo, August 9-14, 1998, Egypt.

7. Was invited as an external consultant and visiting professor to Federal Environmental Protection Agency (FEPA), Abu-Dhabi, United Arab Emirates during the period of February – March, 2004 and August – September, 1999.
8. Was invited by the Deputy Dean of Environmental Affairs, Modern Academy of Science and carried out a one day work shops (over 5) for the Directors and Environmental Directors of well known industrial companies in Egypt.
9. Member of the Experts of the "Reviewer Panel for Ministry of Higher Education", Higher Promotion Committee to Associate Professor and/ or Professor of Academy of Scientific Research and Technology, Ministry of Higher Education, **Egypt**.
10. Consultant for Damietta Port Authority, Damietta, Egypt **1999-2000** and the Egyptian Ministry of Interior **2001**.
11. Consultant for wastewater treatment at the Egyptian-American pigment company (SPREA MISR), Cairo, Egypt, 1999.
12. Consultant for treatment station of Drinking water supply at Damietta **1988-1990, 2001**, Egypt.
13. General Chemistry Advisor at Zaid II Military College, United Arab Emirates, **1992, 1993**.
14. Was invited to write a Chapter entitled” "Unloaded and Specially Treated Polyurethane Foams as Solid Extractor in Separation Sciences and their medical Applications" To be submitted in M.Y. Abdelaal ""Poly Functionalized Polymer and their Medical Applications" , Sign Post Publishers, **2009**.
15. Was invited by Prof. Dr. S. A. Iqbal, **Chief Editor and Publisher of the international research Journals: Oriental Journal of Chemistry, Materials Science Research India**, Current World Environment and Oriental Journal of Computer Sciences and Technology to contribute an article (write-up) entitled: "**Identification and Estimation of Pesticide in Water**" in the

international book entitled “**Pollution: The Ugly Face of Environment**”, Sign Post Publishers, **2009**.

D. Scholarships and Collaboration with International Research Activity

Scholarships:

1. Visiting Professor at the School of Environmental Sciences, University of Plymouth, Plymouth (January-February 2003) under DFID and British Council Fund, Cairo, Egypt.
2. Visiting Professor at Institute Für Chemie, Humboldt- Universtat Zu Berlin, Berlin, (**August – October 2002**) Under Deutsche Forschungsgemeinschaft (DFG)Fund, Germany.
3. Research follow at the School of Environmental Sciences, Plymouth University, Plymouth (**July - August 2001**) under DFID and British Council Fund, Cairo, Egypt.
4. Visiting Professor at the Department of Environmental Sciences, Plymouth University, Plymouth (**July- August 2000**) under DFID and British, Cairo, Egypt.
5. Honorary Senior Visiting Professor and Research Fellow at Department of Environmental Sciences, Plymouth University, Plymouth (**July- September 1997**) Funded by British Council, Abu-Dhabi, United Arab Emirates.
6. Honorary Senior Visiting Professor and Research Fellow at School of Chemistry, the Queen's University of Belfast, Belfast, Northern Ireland (**July- August 1995**) Funded by British Council, Abu-Dhabi, United Arab Emirates.
7. Honorary Senior Research Fellow at Pure and Applied Chemistry Strathclyde University, Glasgow, Scotland (**July – August, 1993**) Funded by British Council, Abu-Dhabi, United Arab Emirates.
8. The International Exchange of Fulbright and Peace Scholars ships Programs, University of Texas at Austin, **1991 (C/O A.J. Bard)**. These two scholar ships were canceled due to my contract with UAE University **1991**.
9. Research Assistant at the Department of Chemistry, Royal Holloway College, University of London (**October 1981-April 1982**) Funded by Ministry of Higher Education, Cairo, Egypt.

IV: Prizes: Recognition and Merit Awards:

- 1. King Abdulaziz University Award for "Distinguished Scientist in Research of the Year" (Chemistry), Jeddah, Saudi Arabia, 2008, 2009, 2010, 2011, 2012.**
- 2. Scopus Appreciation and Recognition for Excellence of Publishing in Elsevier Publishing Company (46 entries), King Abdulaziz University, 2008, Ryadah, Saudi Arabia. .**
- 3. "The Egyptian State Award of Recognition of the Year in "Chemistry" Awarded by the Academy of Scientific Research and Technology, Ministry of Higher Education, Cairo, Egypt, 2004.**
- 4. Shoman Award for "Young Scientist of the Year" (Chemistry) in the Arab World", Amman, Jordan, 1993.**
- 5. "Perkin Elmer Award", 18th Intern. Symp. on Chrom., Amsterdam, the Netherlands, September 18-23, 1990. V. Research Interest :**

The overall area of my research is focused on the following four categories:

1. Application of untreated and physically treated polyurethane foams (PUFs) and other solid phase extractor e.g. active carbon, local clay and date pits for separation, determination and chemical speciation of trace concentrations of toxic and non toxic metal ions and organic pollutants in complicated matrices using batch, flow and pulse modes of separation.
2. Application of nanosized solid phase extractor (SPE) and solid phase microextraction (SPME) e.g. nanosized Fe₃O₄ treated for PUFs, nanogold treated PUFs, nano ZnO treated PUF, and Fe₃O₄ chemically impregnated clay and clay minerals in batch, flow and pulse modes for separation, determination and chemical speciation of trace concentrations of toxic and non toxic metal ions and organic pollutants in complicated matrices.
3. Application of conventional liquid-liquid (LL) extraction, cloud point microextraction and dispersive liquid –liquid microextraction techniques (DLLME) techniques for separation, determination and chemical speciation of trace metal ions, food colors, biogenic amines and phosphorous pesticides in complex matrices.

4. Assessment of pollution level in fresh water (River Nile) and marine water (Red sea and Arabian Gulf post and after Gulf War I) and fish organs as bio indicators.
5. Determination, chemical speciation of trace metal ions and oxyions of Cr, Ru, Bi, W, As, Sb, Au, Pt, etc and for measuring the activity of the enzyme α -L-fucosidase as tumor marker employing:
 - i. High fold chemical amplification reactions involving KIO_4 ; ii. Extractive spectrophotometric; iii. Extractive and non- extractive spectrofluorometric techniques.
6. Developing of simple, selective and cost – effectiveness voltammetric methods for precise determination and speciation of ultra trace concentrations of metal ions, food colorants, co-enzyme Q_{10} , pesticides, anticancer drugs, β -blockers drugs, steroids and persistent organic pollutants (POPs) in complex matrix e.g. wastewater, pharmaceutical formulations, drug residue in wastewater, etc using glassy carbon electrode (GCE), hanging mercury dropping electrode (HMDE) and nano composite surface modified GCEs.
7. Developing Dual-wavelength β -correction spectrophotometric methods for analysis of trace concentrations of CN^- , Th, Bi and Hg ions in industrial wastewater effluents.
8. Total determination and speciation of trace metal ions and some selected inorganic ions e.g. F^- , Cl^- , SO_4^{2-} , NO_3^- , NO_2^- , Ca^{2+} , Mg^{2+} , Al^{3+} , K^+ , Na^+ , NH_4^+ in total suspended matter (TSP), PM_{10} and $\text{PM}_{2.5}$ in air aerosols.
9. Preparation and fully characterization of a series of optically active and non active transition complexes of biological and industrial applications using a series of spectroscopic (UV-visible, IR, NMR), electrochemical (Cyclic voltammetry, Coulometry), thermal analysis and elemental analysis.
10. Studying the spectroelectrochemical behavior using thin layer cyclic voltammetry, thin layer coulometry and optically transparent thin layer electrochemical cells (OTTLEs) for characterization and quantification of a series of various redox systems e.g. metal complexes, anthraquinones, etc.

Teaching (Institutions and Courses): A.

Undergraduate Courses:

At Egyptian (1986-1991; 1997-2005); United Arab Emirates (1991-1997) and Saudi Arabian (2005-2012) Universities:

1. General Chemistry (101, 102)
Chemistry for Engineering
2. General
3. Classical Analytical Chemistry
Analysis
4. Instrumental
5. Separation Methods
Topics in Analytical Chemistry
6. Selected
7. Industrial Analysis
8. Solid and Liquid Wastes
9. Electro analytical Methods
10. Research Projects I, II (Level 4) B.

Postgraduate Courses:

At Egyptian (1986-1991; 1997-2005); United Arab Emirates (1991-1997) and Saudi Arabian (2005-2012) Universities:

1. Advanced Chemical Methods of Analysis
Methods in Chemical Analysis
2. Chromatographic
4. Selected Topics in Analytical Chemistry
Chemistry
4. Environmental
5. Teaching and Education of Analytical Chemistry
6. Titrations in Nonaqueous
Solvents
7. Advanced Electrochemical Techniques

C. Conferences, Workshops and Meetings of Professional Societies

Posters: 32 Entries

Oral Presentations: 28 Entries

Workshops: 2 Entries

Meeting of Professional Societies: 6 Entries

1. 1st International Conference and Exhibition on Sustainable Water Supply and Sanitation, July 25-27, 2010, Cairo, Egypt
1. Determination of Trace Cyanide Ions Using the Novel Reagent 3-(2-oxoindolin-3-ylidenamino)-2thioxo-5-dihydro-1,3-thiazine-4,6-dione and the Dual-Wavelength \square Correction Spectrophotometry.

2. 1st International Symposium on Analytical Chemistry for a Sustainable Development, March 17-19, 2010, Mohammedia, Morocco.
3. Chemical Speciation of Arsenic (III & V) in Water Samples by Adsorptive Cathodic Stripping Voltammetry and Some Complexing Agents. 1st International Symposium on Analytical Chemistry for a Sustainable Development, 17-19 March 2010, Mohammedia, Morocco.
4. Retention Profile of Cadmium (II) onto Polyurethane Foam Physically Immobilized with Some Basic Dyes. 1st International Conference and Exhibition on Sustainable Water Supply and Sanitation, 25-27 July 2010, Cairo, Egypt.
5. Determination and Chemical Speciation of Ultra Trace Concentrations of Titanium with Some Selected Complexing Agents by Adsorptive Cathodic Stripping Voltammetry.
10th International Conference on Chemistry and Its Role in Development, 16-21 March 2009, Mansoura & Sharm El-Sheikh, Egypt.
6. 10th International Conference on Chemistry and Its Role in Development, March 16-21, 2009, Mansoura & Sharm El-Sheikh, Egypt
7. 8th International Symposium on New Trends in Chemistry and 2nd Congress of African Societies of Chemistry, 3-7 January 2009, Cairo, Egypt.
8. I. Ismail, M. Kadi and **M. El-Shahawi**
"Electrochemical Behavior of Uranium (VI) - arsine azo III chelate and its Analytical Application for the Analysis of Ultra Trace Concentrations of Uranium in Marine- and Underground water Samples" "**Poster Presentation**", the 216th ECS Meeting - Vienna, **October 4 - 9, 2009, Austria.**
9. Eman A. Al-Harbi[†], A. Hamza, A. S. Bashammakh, A. A. Alsibai and **M.S. El-Shahawi**
"Square Wave Stripping Voltammetric Determination of Malathion Pesticides in Different Matrices" "**Oral Presentation**", The 1st International Conference on Chemistry, Taibah University, Al-Madinah Al-Minawara, **March 22-25, 2009, Saudi Arabia.**

10. Hammed M. Al-Saidi[†], A. Hamza, A. S. Bashammakh, A. A. Alsibaai and

M.S. El-Shahawi

"Retention Profile, Kinetic Characteristics and Sequential Determination of Bismuth (III) Employing Unloaded – and Immobilized Procaine Hydrochloride -Polyurethane Foams"

"Poster Presentation ", The 1st International Conference on Chemistry , Taibah University, Al-Madinah Al-Minawara, **March 22-25, 2009, Saudi Arabia.**

11. Eman A. Al-Harbi[†], A. Hamza, T.A. Amirah, and **M.S. El-Shahawi**

"Chemical Speciation of Selenium (IV & VI) species by Adsorptive Cathodic Stripping Voltammetry " **"Oral Presentation"**, The 1st International Conference on Chemistry , Taibah University, Al-Madinah Al-Minawara, Saudi Arabia, **March 22-25, 2009, Saudi Arabia.**

12. Majdah R. Otaibi[†], A. S. Bashammakh, S.O. Bahaffi and **M.S. ElShahawi**

"Chemical Speciation of Arsenic (III & V) species by Adsorptive Cathodic Stripping Voltammetry and Some Complexing Agents"

"Poster Presentation ", The 1stInternational Conference on Chemistry , Taibah University, Al-Madinah Al-Minawara, **March 22-25, 2009, Saudi Arabia.**

13. Wejedan T. Al-Saggaf[†], A. Hamza, A. S. Bashammakh and **M.S. ElShahawi**

"Cathodic Stripping Voltammetric Determination of Some Persistent Organochlorinated Pollutants in Water and Sediments: An Interlaboratory Study"

"Oral Presentation", The 1st International Conference on Chemistry , Taibah University, Al-Madinah Al-Minawara, **March 22 -25, 2009, Saudi Arabia.**

14. A.G. Hamza, S.O. Bahhafi T.N. Abdul-Gabbar and **M.S. El- Shahawi**

"Simultaneous Analysis of Catechins and Caffeine in Green Tea by High Performance Liquid Chromatography" **"Poster Presentation "**, The 10th International Conference on Chemistry and its Role in Development, Mansoura-Sharm El-Sheikh, **March 16-21, 2009, Egypt**

15. M.W. Kadi[†], A. S. Bashammakh and **M.S. El-Shahawi**

"Determination of Trace Thorium using some Selected Azo Reagents and the

Dual - Wavelength β Correction Spectrophotometry" "**Poster Presentation**", The 10th International Conference on Chemistry and its Role in Development, Mansoura-Sharm El-Sheikh, **March 16-21, 2009, Egypt.**

16. S. Bashammakh, A.I. Al-Sibaai, H. K. Al-Ariqe and M.S. El- Shahawi
Determination and Chemical speciation of ultra Trace concentrations of Titanium with some Selected Complexing Agents by Adsorptive Cathodic Stripping Voltammetry. "**Poster Presentation**", The 10th International Conference on Chemistry and its Role in Development, Mansoura-Sharm ElSheikh, **March 16-21, 2009, Egypt.**

17. M. S. T Makki[†], R. M. Abdel-Rahman and M.S. El-Shahawi "Synthesis of Novel Cyclic and Non-cyclic Organic Compounds Derived from Dithioic Formic Acid Hydrazide and Thiocarbohydrazide and Analytical Applications" "**Poster Presentation** ", The 10th International Conference on Chemistry and its Role in Development, Mansoura-Sharm ElSheikh, **March 16-21, 2009, Egypt.**

18. A. Hamza, A. S. Bashammakh, A. A. Al-Sibaai, H.M. Al-Saadi and M.S. El-Shahawi

Part II "Determination of Trace Cyanide ions using the Novel reagent 3- (2-oxoindolin-3-ylidenamino)-2-thioxo-5-dihydro-1,3-thiazine-4,6-dione and the Dual - Wavelength β - Correction Spectrophotometry" "**Poster Presentation** ", The 8th International Symposium on New Trends in Chemistry and 2nd Progress of the Federation of the African Societies of Chemistry (FASC) and the Chemistry in the National Development, Cairo University, Cairo, **January 3-7, 2009, Egypt.**

19. M.W. Kadi and M.S. El-Shahawi

"Determination and Chemical speciation of ultra Trace concentrations of Uranium with some Selected Complexing Agents by Adsorptive Cathodic Stripping Voltammetry", "**Poster Presentation**", International Conference on Radioanalytical Chemistry, Lisbona, **September 7-12, 2008, Portugal.**

20. H. O. Al-Wael, A. S. Bashammakh and M. S. El-Shahawi

"Simple Liquid-Liquid Extractive Spectrophotometric Procedures for the Determination of the Thiocyanate Ions Employing the Ion Pair Reagent

Amiloride Monohydrochloride"

"Poster Presentation", The 9th International Conference on Chemistry and its Role in Development, Mansoura-Sharm El-Sheikh, **April 14-17, 2007, Egypt.**

21. A. S. Bashammakh and H. K. Al- Ariqe and M. S. El-Shahawi

Thoron I, a New Complexing Agent for Lead Speciation in Food Stuffs and Waste- and natural water Samples by Adsorptive Cathodic Stripping Voltammetry at The Hanging Mercury Drop Electrode" **"Poster**

Presentation ", The 9th International Conference on chemistry and its role in development Mansoura-Sharm El-Sheikh, **April 14-17, 2007, Egypt. 22.**

A. S. Bashammakh and H. K. Al- Ariqe and M. S. El-Shahawi

"ICP-AES Determination of Titanium (IV) in Marine and Wastewater Samples after Preconcentration onto Unloaded and Reagent Immobilized Polyurethane Foams Packed Columns",

"Poster Presentation ", The 13th B NNASS, Pasly, Glasgow, **July 10-13, 2006, Scotland, UK,**

23. Effat A. Bahaidarah,* Abdulaziz S. Bashammakh and M.S. El-Shahawi

"Adsorptive Cathodic Stripping Voltammetric Determination of Spironolactone drug in Pure Form and in Pharmaceutical preparation at the Hanging Dropping Mercury Electrode" **"Oral Presentation"**, The 1st International Conference on Chemistry and its Role in Development, Makka, **April 14-17, 2007, Saudi Arabia.**

24. M.S. El-Shahawi and H.M. Nassef

"Spectroelectrochemical Behaviour of Some Schiff Bases Metal Complexes Containing Benzoin Moiety and Their Complexes"

"Oral Presentation" The 8th International Conference on Chemistry and its Role in Development, Mansoura-Sharm El-Sheikh, **April 14-17, 2005, Egypt.**

25. M.S. El-Shahawi, M.A. Al-Sonbati

"Retention Profile, Kinetics and Sequential Determination of Selenium (IV) and (VI) Employing 4,4'-Dichlorodithizone Immobilized Polyurethane Foams".

"Oral Presentation", The 8th International Conference on Chemistry and its Role in Development, Mansoura-Sharm El-Sheikh, **April 14-17, 2005, Egypt.**

26. Workshop on Management and Monitoring of Quality Assurance and Accreditation System, Cairo University, Cairo, Egypt, September 3-4 and November 10, **2004.**

27. A.M.Othman N. M. H. Rizk and **M. S. EL-Shahawi**

Potentiometric Determination and Voltammetric Behavior of Dopamine in Pharmaceutical Preparations Based on a Crown Ether-PVC Membrane **"Oral Presentation"**, The 7th International Conference on Chemistry and its Role in Development Mansoura - Sharm El-Sheikh, **April 14-17, 2003, Egypt.**

28. M.S.El-Shahawi

"Speciation of Bismuth in Water by Adsorptive Cathodic Stripping Voltammetry Involving Pridyl-azo Resorcinol",

"Poster Presentation", Euroanalysis-12, Dortmund, **September 8-13, 2002, Germany.**

29. M.S.El-Shahawi

"Spectrophotometric Determination of Cadmium (II) in Water by Liquid-Solid Separation Involving 3-Fluorodithiazon Impregnated Polyurethane Foams",

"Poster Presentation" Leipzig, September 17-22, , 2002, Germany.

30. E. P. Achterberg, M. Gledhil and **M. S. El-Shahawi**

"Development of a Novel Voltammetric Method for Lead Speciation in Fresh and Estuarine Waters **"Oral Presentation"**, The 3rd International Conference on Electrochemistry and its Applications, Luxor, **February 13-15, 2001, Egypt.**

31. M. S. El-Shahawi and S.M. Saleh

"Spectrophotometric Determination of Cadmium in Water by Liquid-Liquid Extraction Employing Amiloride Monohydrochloride" **"Poster**

Presentation ", The 3rd Mediterranean Basin Conference on Analytical Chemistry, MBCAC, III, Antalya, **June 4-9, 2000, Turkey.**

32. M. S. El-Shahawi

“Retention profile and Spectrophotometric Determination of Uranyl ion in Aqueous Solution Employing Crown Ether Impregnated Polyurethane Foams”
"Oral Presentation", The 7th International Conference of Nuclear Science and Application, Cairo, **February 6-10, 2000, Egypt.**

33. A.B. Farag and M.S. El-Shahawi

Sponsor on a “Workshop” Title of the lecture" Demonstration of some Low Cost and Applicable Procedures for Detection and Semi quantitative Determination of Trace Metal Ions in Water

"Oral Presentation", The 15th International Conference of Chemical Education in Chemistry and Global Environmental Change", Cairo, **August 9-14, 1998, Egypt.**

34. M. S. El-Shahawi and S. M. Aldahaheer

“A Case Study on the Determination of Some Heavy Metal Ions in Soil around Al-Ain Cement Factory”,**"Poster Presentation "**, Euroanalysis 10, Basel, **September 6-11, 1998, Switzerland.**

35. M. S. El-Shahawi and S. M. Saleh

“Spectrophotometric Determination of Gold in Water by Liquid-Liquid Extraction using Amiloride Hydrochloride”**"Poster Presentation "**, Euroanalysis 10, Basel, **September 6-11, 1998, Switzerland.**

36. M. S. El-Shahawi and S. M. Saleh

“Spectrophotometric Determination of Tungsten and Iron in Water by Solvent Extraction of Their Anionic Thiocyanate Complexes with Amiloride Hydrochloride” **"Poster Presentation"**, Euroanalysis 10, Basel, **September 6-11, 1998, Switzerland.**

37. I.M. Banat, E.S. Hassan, M.S. El-Shahawi and A.H. Abu-Hilal "Post-Gulf War Assessment of Nutrients, Heavy Metal Ions, Hydrocarbon and Bacterial Pollution in the UAE Coastal Waters of the UAE." **"Oral Presentation"**, **Poster presentation**, International. Conference on Long - Term Environmental Effects of the Gulf - War, **November 18-20, 1996, Kuwait.**

38. M. S. El-Shahawi

"Reserved Phase HPLC Determination of Perrhenate, Perchlorate and

Periodate as their Amiloride Ion-Association Complexes", "**Poster Presentation**", 21st International Symposium on Chromatography, Stuttgart, **September 15-20, 1996, Germany.**

39. M. S. El-Shahawi and S. M. Aldhaheri

"Intercomparison Study on the Preconcentration of Trace Amounts of Aluminum (III) and Iron (III) in Natural Water Employing Polyurethane Foams and Amberlite XAD-2 Columns", "**Poster Presentation**", The 21st International Symposium on Chromatography, Stuttgart, **September 15-20, 1996, Germany.**

40. M.S. El-Shahawi

"Preconcentration and Separation of Water Organic Phosphorous Pollutants by Porous Polyurethane Foam Columns""**Poster Presentation**", The 20th International Symposium on Chromatography, Bournemouth, UK. **June 19-24, 1994.**

41. M.S. El-Shahawi

"Qualitative, Semi-quantitative and Spectrophotometric Determination of Ruthenium (III) Using Solid Phase Extraction with 3-Hydroxy-2-Methyl-1, 4 Naphthoquinone-4-Oxime Loaded Polyurethane Foam Columns" "**Poster Presentation**", The 20th International Symposium on Chromatography, Bournemouth, **June 19-24, 1994, UK.**

42. M.S. El-Shahawi and S.M. Al-Dhaheri

"Selective and Sensitive Spectrophotometric Determination of Bismuth (III, V) in Sea water After Ion-Pair Liquid-Liquid Extraction Using Tetrabutylammonium Chloride as a Counter Ion", "**Poster Presentation**", The 2nd Gulf Water Conference, Bahrain, **November 5-9, 1994, Bahrain.**

43. M.S. El-Shahawi and S.M. Aldhaheri

"Collection and Recovery of Some Organic Water Pollutants by Porous Polyurethane Foams", "**Oral Presentation**", Healthy Cities of Arabian Gulf Countries, Dubai, **November 26-28, 1994, United Arab Emirates.**

44. M. S. El-Shahawi, M. H. Al-Yousuf and S. Al-Ghais

"Biomonitoring of Heavy Metals in Different Organs of Adult and Juvenile Emperors (*Lethrinus lentjan*) Fish in Arabian Gulf Water Around the Western United Arab Emirates" **"Oral Presentation"**, The Regional Environmental Symposium on Ecosystem, Environmental Protection and Graduate Education in Environmental Sciences, UAE University, Al-Ain, **December , December 11-14, 1994, United Arab Emirates.**

45.M.S. El-Shahawi, A.M. Kiwan, S.M. Al-Dhaheeri and M.H. Saleh
"The Retention Behavior and Separation of Some Water Soluble Organo Phosphorous Insecticides on Polyester" **"Oral Presentation"**, The Regional Environmental Symposium, on Ecosystem, Environmental Protection and Graduate Education in Environmental Sciences, UAE University, Al-Ain, **December , December 11-14, 1994, United Arab Emirates.**

46. E.S. Hassan, I.M. Banat, **M.S. El-Shahawi** and A.H. Abu Hilal
"Pollution Levels Assessment along the Eastern Coastal Area of the United Arab Emirates"
"Oral Presentation", The Regional Environmental Symposium, on Ecosystem, Environmental Protection and Graduate Education in Environmental Sciences, UAE University, Al-Ain, **December , December 11-14, 1994, United Arab Emirates.**

47. M.S. El-Shahawi
"Preconcentration and Separation of Some Water Soluble Chlorinated Organophosphorous Insecticides on Polyether Based Polyurethane Foam"
"Oral Presentation", The Regional Environmental Symposium, on Ecosystem, Environmental Protection and Graduate Education in Environmental Sciences, UAE University, Al-Ain, **December , December 11-14, 1994, United Arab Emirates.**

48. M.S. El-Shahawi and W.E. Smith
"Spectroelectrochemical Studies of Some Nickel (II) Schiff Base Complexes Using an Optically Transparent Thin Layer Gold Mesh Electrode" **"Oral Presentation"**, The International. Symposium on Electroanalysis in Biomedical Environmental and Industrial Sciences, Loughborough, Leicestershire, **April 20- 23, 1993, UK**

49. M.S. El-Shahawi

"Iodometric Microgram Determination of Cysteine, Gultathione and Ascorbic Acid by High Fold Chemical Amplification Reactions" "**Poster Presentation**", Euroanalysis VIII, Edinburgh, **September 5-11, 1993, UK.**

50. M.S. El-Shahawi, and A.B. Farag

"Spectrophotometric Determination of Chromium (VI) by the Sorption of Chromium (III)-Diphenylcarbazone on Polyurethane Foam", "**Poster Presentation**", Euroanalysis VIII, Edinburgh, **September 5-11, 1993, UK.**

51. A.B. Farag and M.S. El-Shahawi

"Removal of Organic Pollutants from Aqueous Media". Part II. "Extraction, Separation and Preconcentration of Some Phenols by Polyurethane Foam", "**Poster Presentation**", The 1st Int. Confr. in Chemistry and its Applications, Doha, **December 13-15, 1993, State of Qatar.**

52. M.S. El-Shahawi and S.A. Metwally,

"Spectroelectrochemistry of 4-(Dicyano-methylene)-3-methyl-1-phenyl-2pyrazolin-5 one using an Optically Transparent Thin Layer Electrode (OTTLE)" "**Oral Presentation**", The 1st International Conference in Chemistry and its Applications, Doha, **December 13-15, 1993, State of Qatar.**

53. M.S. El-Shahawi

"Removal of Organic Pollutants from Aqueous Solutions, the Extraction, Recovery and Separation of Some Insecticides from Water with Untreated Porous Polyurethane Foams and Activated Carbon" "**Poster Presentation**", The 19th International Symposium of Chromatography, Aix-en-Provence, **September 13-18, 1992, France.**

54. M.S. El-Shahawi and A.B. Farag, and M.R. Mustafa,

"Collection and Chromatographic Separation of Some Phenols from Water by Untreated and Treated Foams" "**Poster Presentation**", The 19th International Symposium of Chromatography, Aix-en-Provence, **September 13-18, 1992, France.**

55. M.S. El-Shahawi and A.B. Farag

“A Comparative Study on the Extraction, Recovery and Chromatographic Separation of Some Organic Insecticides Using Unloaded Polyurethane Foam Column” **"Poster Presentation"**, The 18th International Symposium on Chromatography, Amsterdam, **September 22-27, 1990, The Netherlands.**

56. M.S. El-Shahawi

“Spectrophotometric Determination of Nickel (II), Cobalt (II) and Copper (II) with Some Schiff Base Ligands” **" Oral Presentation"**, The 2nd International Symposium on New Trends in Chemistry. The Role of Analytical Chemistry in National Development, Faculty of Science, Cairo University, Cairo, **January 13-15, 1989, Egypt.**

57. A.B. Farag, M.S. El-Shahawi and A.M. El-Wakil

“Removal of Organic Pollutants from Aqueous Solution: Part II: A Comparative Study of the Concentration of Some Phenols by Loaded and Unloaded Open Cell Polyurethane” **"Oral Presentation"**, The 2nd Conference on Chemistry and its Applications, Mansoura University, Mansoura, **September 27-28 (1988) 372 -379, Egypt.**

58. A.B. Farag, M.S. El-Shahawi, A.M.A. Helmy and S. Farrag

“The Extraction and Recovery of Some Organic Insecticides from Aqueous Media with Cellular Polyurethanes” **"Oral Presentation"**, The 2nd Conference on Chemistry and its Applications, Mansoura University, Faculty of Science, Mansoura, Egypt, **September 27-28, (1988) 351 -356.**

59. A.B. Farag, M.S. El-Shahawi A.M. Helmy and S. Farrag

“Sensitive Detection and Semi quantitative Determination of Molybdenum (VI) Using Unloaded and Specially Treated Polyurethane Foams”, **"Oral Presentation"**, The 2nd Conference on Chemistry and its Applications, Mansoura University, Faculty of Science, Mansoura, Egypt, **September 26-28, 1988, Egypt.**

60. A.B. Farag, A.M. El-Wakil, M.S. El-Shahawi and M.A. Mashaly

Collection and Separation of Some Organic Insecticides on Polyurethane Foam Columns”,

"Oral Presentation", The 1st First National Conference on Environmental

Studies and Research, Ain Shams University, Cairo, **April 11-14, 1988, Egypt.**

61. Participant at The First Conference on Chemistry and its Applications, Mansoura University, Faculty of Science, Mansoura, **June 6-9, 1986, Egypt.**

62. Active Member at the Electroanalytical Meetings, Rospriary Glasgow, Scotland, UK, October **1983, 1984** and **1985.**

63. Participant "**Oral Presentation**", "Strathclyde University Inorganic Chemistry" Meeting, Rospirary, Glasgow, **1985, UK.**

64. Active Member at Scottish Dalton Meeting, Edinburgh, **July, 1984, UK 65.**
Participant in the "Strathclyde University Inorganic Chemistry" Meeting, Rospirary, Glasgow, U K, **1984.**

66. Participant in the Strathclyde University Inorganic Chemistry (USIC) Conference, Galashiels, Glasgow, UK, **1983.**

D. Published Book Chapters (Authored) and Translated Books to Arabic

i. Translated Books to Arabic

1. Y. M. Moustafa, M.S. El-Shahawi

"Principle of Instrumental Analysis " by D.A. Skoog, D.M. West and R.N. Holler"

Translated from **English** to **Arabic** language. To be published by Umm AlQura University publisher, 2012, Makkah, Saudi Arabia after permission from the authors and Publisher.

2. Y. M. Moustafa, M.S. El-Shahawi, A. Algamdy

"Principles of Ceramics"

Translated from **English** to **Arabic** language. To be published by King Abdulaziz University publisher, 2012, Jeddah, Saudi Arabia after permission from the authors and Publisher.

3. S.T.I. Makki, R.M.Abdel-Rahman and M.S. El-Shahawi

"Water and Water Pollution" A General Chemistry Book in Arabic Language. **To be published by King Abdulaziz University Publisher, Jeddah, Saudi Arabia, 2011.**

E. Reviewing

A. Book Reviewer (Reviewed or Verified)

Acted as an External Reviewer **for Arabic Translation** of a series of "Oxford Book Series in Instrumental Analysis and Chromatographic separation".

The translated books are:

1. Christopher M.A. Brett and Ana M.O. Brett "**Electroanalysis**", Series sponsor: Zeneca, Oxford University Press, 2005.
 2. Ritchard P. Wayne "**Chemical Instrumentation**", Series sponsor: ZENECA, Oxford Science Publication, Oxford University Press Inc., New York, 1995.
 3. John R. Chipperfield "**Non – Aqueous Solvents**", Series sponsor: ZENECA, Oxford Science Publication, Oxford University Press Inc., New York, 2007.
 4. Fisher A.C. " Electrode Dynamics", Series sponsor: ZENECA, Oxford Science Publication, Oxford University Press Inc., New York, 1996
- Presented by The Electrochemistry Group of the Royal Society of Chemistry

B. Reviewer for Academic Journals:

Regularly referee papers (18-25) from a host of scientific journals including

- | | |
|--|--|
| 1. Analytica Chimica Acta | 2. Talanta, |
| 3. J. Chromatography | 4. J. Food Science and Nutrition |
| 5. J. Environmental Biotechnology | 6. Chemical Papers, Poland |
| 7. Bulletin of Solid State Electrochemistry | 8. J. Hazardous Materials |
| 9. J. Electroanalytical Chemistry | 10. Chemosphere |
| 11. Intern. J. Environ. Analytical Chemistry | 12. J. Molecular structure |
| 13. J. Environmental Management | 14. Chemical Engineering Communication |
| 15. Environmental Engineering Science | 16. J. Chem. Technol. Biotechnology |
| 17. Analytical Sciences of Japan | 18. Analytical Letters |
| 19. Ecotoxicology and Environmental Safety | 20. Process Biochemistry |
| 21. Environ. Engineering Communication | 22. Desalination |

- | | |
|---|---|
| 23. Letters in Drug Design & Discovery | 24. Sensors Letters |
| 25. Molecules
Chemistry | 26. South African J.
Chemistry |
| 27. Separation Science and Technology
Analytical Chemistry | 28. American J.
Analytical Chemistry |
| 29. European J. Chemistry
Environmental safety | 30. Ecotoxicology and
Environmental safety |
| 31. Arabian J. Chemistry (Elsevier Publisher)
Journal. | 32. Scientific Research
Journal. |
| 33. Bulletin of the Faculty of Science, King Abdulaziz University, Jeddah,
KSA | |
| 34. Bulletin of the Faculty of Science, UAE University, UAE | |
| 35. Bulletin of the Faculty of Science, Mansoura University, Egypt | |

Examiner of MSc and Ph.D Thesis':

Internal Reviewer

1. Internal Reviewer for **25** Master of Sciences at Egyptian and Saudi Arabian Universities.
2. Internal Reviewer for **15** Ph. D Thesis's in Analytical and Environmental Chemistry at Egyptian, Saudi Arabia (King Abdulaziz University) and United Arab Emirates Universities.

External Reviewer:

1. External Reviewer for **20** Master of Sciences at Egyptian and Saudi Arabian Universities
2. External Reviewer for **24 Ph. D** Theses in Analytical and Environmental Chemistry at Egyptian and Saudi Arabia (King Saud) Universities.

Reviewer of Research Projects:

At Taiba, Taif and King Abdulaziz Universities, Saudi Arabia:

1. **Research Project entitled** "Extraction and Characterization of Major Components in Almadinah Almunawarah Mint Species"
Research project Funded by Taiba University, Al-Madiah Al-Minwara, Saudi Arabia, **2009**.

2. Research project entitled "Removal of Heavy Metal ions from polluted Water Using Low cost Materials"

Research project Funded by Taiba University, Al-Madiah Al-Minwara, Saudi Arabia, **2008**.

3. Research project entitled "Fabrications and Characterization of Electrochemical Biosensors Modified with Layer – by-Layer Nanostructure Films for Biochemical and Biomedical Analysis"

Research project Funded by Taiba University, Al-Madiah Al-Minwara, Saudi Arabia, **2008**

4. Research project entitled "Analysis of Pharmaceutical Residues in Municipal Wastewater and Predicting Their Impact in the Human Environment"

Research project Funded by Taiba University, Al-Madiah Al-Minwara, Saudi Arabia, **2008**

5. Research project entitled "Biochemical Method for the Desulphurization of Petroleum Hydrocarbons"

Research project Funded by King Abdulaziz University, Jeddah, Saudi Arabia, **2008**

6. Research project entitled "Soil Pollution Hazardous to Human Life : A Case Study on the Determination of Some Heavy Metal Ions in Soil Around Al-Ain Cement Factory , United Arab Emirates", **1995**.

Research project Funded by Scientific Research Council, UAE University, Al-Ain, United Arab Emirates, **1995**.

7. Research project entitled "Analysis of Pharmaceutical Residues in Municipal Wastewater and Predicting Their Impact in the Human Environment.

8. Research project entitled "Biochemical Method for the Desulphurization of Petroleum Hydrocarbons"

At King Abdulaziz Research City, Saudi Arabia

1. Research project entitled "Removal of Phenolic Compounds from Water using Carbon Nanotubes (CNTs) and Activated Carbon (AC) Materials.

2. Research project entitled " Desulphurization of Petroleum Hydrocarbons".

Creative Research and Other University Activities:

A. Development

Development of certain flow modes for the Separation and complete removal of trace and ultra trace of toxic metal ions and cyanide ions from the industrial effluent employing Specially Treated Stationary Phases. **B.**

Training Courses:

1. Training course on Quality Assurance, Accreditation and Course Evaluation, **2006**, Mansoura University and King Abdulaziz University.
2. Training course in nuclear safety, Radioactive Isotopes and its Applications at Nuclear Authority, **1988**, Egypt.
3. Training course in glass blowing at Royal Holloway College, London University, **1981-1982**.
4. Training course in English at the Faculty of Education, Mansoura University, *1981*.

C. Course Developments and the Methods of Teaching:

1. Analytical Chemistry for Special Chemistry and Non-Chemistry Students
2. Instrumental Analysis for Under and Post Graduate Students
3. Industrial analysis
4. Practical contents in Analytical Chemistry at UAE, Mansoura and King Abdulaziz Universities.
5. Separation Methods of Analysis
6. Practical contents in Analytical Chemistry at UAE and Mansoura Universities.

Community Services:

A. Consultation:

1. Consultant for the Egyptian Ministry of Interior **2001**.
2. Consultant for the Damietta Port Authority, Damietta, Egypt **1999-2000**. 3. Consultant for wastewater treatment at the Egyptian-American pigment company (SPREA MISR), Cairo, Egypt, 1999.
4. Consultant for water treatment station at Damietta **1988-1990, 2001**, Egypt.

5. Consultant for the Federal Environmental Protection Agency (FEPA), Abu-Dhabi, United Arab Emirates (February – March, 2004 and August – September, 1999).

B. Teaching and Seminars for community:

1. General Chemistry at Zaid II Military College, United Arab Emirates, 1992, 1993.
2. Lecturing for senior secondary school teachers in chemistry at Mansoura, Damietta and Port Said, cities, November, 2000.
3. Training course for the chemists that are working in water treatment stations at Damietta, 2001.
4. Lecturing for senior secondary school teachers in chemistry at United Arab Emirates, 1995.
4. Presenting many seminars and articles of general interest on Pollution, preconcentration and determination of pesticides in soil and water and treatment of wastewater at Mansoura University, Egypt and UAE University, United Arab Emirates.
5. Participate in Undergraduate teaching exam preparation and double marking responsibilities
6. Participate in the student advisory scheme and placement visits for Chemistry students during the academic year on the annual bases (1991 1997).
7. Participated in curriculum design for MSc. Environmental Sciences
8. I completed the following staff development: Effective supervision, Computer Aided Assessment and Assessment for Quality of teaching.
9. I have taught a wide variety of courses in analytical chemistry to under- and postgraduate student.

Involvement in Technology and Knowledge Transfer

i. I have participated in the promotion of many academic staff members **ii.** I became involved in organizing the accreditation of the Chemistry degree. **iii.** I involved in providing a laboratory experience within different labs within the Faculty during several visits for preparative school students (13 – 14) in the Damietta Province **University Committees**

R. José Moreira Sobrinho, s/n CEP:45206-190, Jequiezinho, Jequié-BA, Brazil

Phone: +55 73 3528-9621/3528-9630 FAX: +55 73 3525 6683.

5. Prof. M.H. Abdel Kader

Professor of Analytical chemistry,

University President, German University in Cairo, New Cairo, Egypt.

Tel: +2 02 7589990-8, Fax: +2 02 E. Mail: university.president@guc.edu.eg

6. Prof. W.E. Smith

E. Mail: wsmith@st.ac.uk

Department of Pure and Applied Chemistry, Strathclyde University,

Glasgow, UK

Reviewed Publications with citations

Publications

A. Publications:

Published Book Chapters (3 Entries):

1. M.S. El-Shahawi, E.A. Al-Harbi and H.M. Al-Saidi

“Speciation of Tellurium in soil, sediment and environmental samples” and
“Speciation of Chromium in soil, sediment and environmental samples” A Book
Chapter in Sezgin Bakirdere 'Chief Editor" Book entitled “Speciation
Studies in Soil, Sediment and Environmental Samples” Science Publishers books,
CRC Press/Taylor & Francis Group, 2013.

2. M.S. El-Shahawi, A. A. Al-Sibaai, H.M. Al-Saidi and E. A. Assirey

Fast, Selective Removal and Determination of Total bismuth (III) and (V) in
Water by Procaine Hydrochloride Immobilized Polyurethane Foam Packed
Column Prior to Inductively Coupled Plasma – Optical Emission Spectrometry
in "Polyurethane", A Book Chapter 13 in Fahmina Zafar and
Eram Sharmin “Chief Editor” ISBN 979-953-307-642-2. In Tech, Open Access
publisher in the fields of Science, Technology and Medicine Published 2012.

3. M.S. El-Shahawi

Retention Profiles of Some Commercial Pesticides, Pyrethroid and Acaricide
Residues and Their Applications to Tomato and Parsley Plants. Special Issue in
Water pollution edited by E. Heftmann, Elsevier press, Special issue J.

Chromatography A, 760 (1997) 179 -192. **B.**

Published Articles (131 Entries):

Published article for reviewing (125 Entries, 1-125)

1. R. M. Ba-Shami, H. Gazzaz, A. S. Bashammakh, A. A. Al-Sibaai and M. S. El-Shahawi

Redox Behavior and a Sorptive Cathodic Stripping Voltammetric Determination of Nanomolar Levels of Palladium using a Novel Schiff Base Reagent Containing a Squaric Acid Moiety, *Anal. Methods*, 6 (2014) 69977005.

2. M.S. El-Shahawi, A.S. Bashammakh, M.I. Orief, A.A. Alsibaai, E.A. AlHarbi,
Separation and Determination of Cadmium in Water by foam Column Prior to Inductively Coupled Plasma- Optical Emission Spectrometry, *J. Industrial and Engineering Chemistry* 20 (2014) 308–314. **Cited 6**

3. M.S. El-Shahawi and R. Al-Hindi

Physicochemical Characteristics of Saudi Arabian Locally Produced Raw and Diluted Honeys and Their Relations to Antimicrobial Activity Submitted to *International J. Food Sciences and Nutrition*” *Journal of Advances in Chemistry*, 10 (6) (2014) 2766- 2774.

4. M. S. T. Makki, R. M. Abdel-Rahman and M.S. El-Shahawi

Voltammetric Behavior, Biocidal effect and Synthesis of some New Nanomeric Fused Cyclic Thiosemicarbazones and Their Mercuric (II) Salts”, *Arabian J. Chemistry* 7 (5) (2014) 793-799. **Cited zero**

5. M.S. El-Shahawi, A. Hamza, A. A. Al-Sibaai, A. S. Bashammakh and H.M. Al-Saidi,

A New Method for Analysis of Sunset Yellow in Food Samples Based on Cloud Point Extraction Prior to Spectrophotometric Determination, *J. Industrial & Engineering Chemistry* 19 (2) (2013) 529-535. **Cited 18**

6. M.S. El-Shahawi, A. S. Bashammakh, A.A. Al-Sibaai and E.A. Bahaidarah

Analysis of spironolactone residues in industrial wastewater and in drug formulations by cathodic stripping voltammetry, *J. Pharmaceutical Analysis*, 3 (2013) 137-143. **Cited 0**

7. M.S. El-Shahawi , M.S. Al-Jahdali, A.S. Bashammakh, A.A. Al-Sibaai and H.M. Nassef,

Spectroscopic and Electrochemical Characterization of some Schiff Base Metal Complexes Containing Benzoin Moiety, *Spectrochimica Acta Part A* 113 (2013) 459-465. **Cited 4**

8. M.S. El-Shahawi and H.M. Al-Saidi

Dispersive Liquid-Liquid Microextraction for Determination and Chemical Speciation of Ultra Trace Concentration of Metal ions, *TRAC- Trends in Analytical. Chemistry* 44 (2013) 12-24. **Cited 22**

9. M.S. El-Shahawi, M.W. Kadi, S.H. El-Khouly, A. Abd El-Mohty, S.M.Saad and N.E.A. Eweda

Retention Profile and Selective Separation of ^{90}Y from ^{89}Sr using Zirconiumvanadate Gel packed column *J. Radioanal. Nucl. Chem*, 295(3) (2013) 1873-1880. **Cited 1**

10. M.S. El-Shahawi, M.W. Kadi, S.H. El-Khouly, A. Abd El-Mohty , S.M.Saa and N.E.A. Ewed

Separation of Y from Sr by Zirconium-vanadte Gel Ion-Exchanger Sorbent: Kinetics and

Thermodynamic Study, *J. Radioanal. Nucl. Chem*, 295 (1) (2013) 15-22. **Cited 3**

11. M. S. T. Makki , **M.S. El-Shahawi** and R. M.Abdel-Rahmn

Synthesis and Voltammetric Study of some New Macrocyclic Sulfur Compounds for use as Chelating Agents for Separation of Arsenic in Wastewater and as Molluscicidal Agents, *Comptes Rendus Chimie C*. 15 (7) (2012) 617–626. **Cited 1**

12. Z.H. Khan, M. S. Ansari, N.A. Salah, S.S. Habib and **M.S. El-Shahawi**

Multi-Walled Carbon Nanotubes Film Sensor for Carbon Mono-oxide Gas” *Current Nanoscience* 8(2) (2012) 274 -279. **Cited zero**

13. M.S. El-Shahawi and L.A. Alkateeb

Spectrofluorometric Determination and Chemical Speciation of Trace Concentrations of Tungsten Species in Water using the Ion Pairing Reagent Procaine Hydrochloride” *Talanta* 88 (1) (2012) 587-592. **Cited 3**

14. M.S. El-Shahawi, A.G. Hamza, S.O. Bahaffi, A.A. Al-Sibaai, T.N. Abduljabbar

Analysis of some Selected Catechins and Caffeine in Green tea by High Performance Liquid Chromatography” Food Chemistry 134 (2012) 2268–2275.

Cited 34

15. M.S. El-Shahawi, A.S. Bashammakh, A.A. Al-Sibaai, M. Orief and F.M. AlShareef,

Solid Phase Preconcentration and Determination of Trace Concentrations of Total Gold (I) and / or (III) in Sea and Wastewater by Ion Pairing Impregnated Polyurethane Foam Packed Column Prior Flame Atomic Absorption Spectrometry”, Intern. J. Mineral Processing, 100 (2011) 110 -115. **Cited 12**

16. M.S. El-Shahawi, A. Hamza¹, A. A. Al-Sibaai¹ and H.M. Al-Saidi²

Fast and Selective Removal of Trace Concentrations of Bismuth (III) from Water onto Procaine Hydrochloride Loaded Polyurethane Foams Sorbent: Kinetics and Thermodynamics of Bismuth (III) Study”, Chemical Engineering Journal, 173 (2) (2011) 29 -35. **Cited 12**

17. Mohammad W. Kadi and M. S. El-Shahawi,

Selective Determination of Thorium in Water using Dual-wavelength β -Correction Spectro -photometry and the Reagent 4-(2-Pyridylazo)resorcinol” Radianalytical and Nuclear Chemistry, 294 (2011) 127 -234.

Cited 2

18. Z.H. Khan, M. S. Ansari, N.A. Salah, A. Nemic, S. Habib and M.S. El-Shahawi

Cobalt Catalyzed –Multi-Walled Carbon Nanotubes film Sensor for Carbon Mono-oxide Gas” Digest J. Nanomaterials and Biostructures, 6 (4) (2011) 1947 -1956. **Cited zero**

19. R. R. Al-Hindi, M. S. Bin-Masalam, M. S. El-Shahawi

Antioxidant and Antibacterial Characteristics of Phenolic Extracts of Locally Produced Honey in Saudi Arabia”, Intern. J. Food Science and Nutrition, 62

(5) (2011) 513 -517.

Cited 5

20. M. S. El-Shahawi, A. S. Bashammakh, and M. Abdelmageed,
Chemical Speciation of Chromium(III) and (VI) using Phosphonium Cation
Impregnated Polyurethane Foams Prior to Their Spectrometric Determination”
, Analytical Sci. (Japan), 27 (7) (2011) 757 -763.

Cited 4

21. M.S. El-Shahawi, A. Hamza, A. S. Bashammakh, A. A. Al-Sibaai and W. T.
Al-Saggaf,

Analysis of Some Selected Persistent Organic Chlorinated Pesticides in Marine
Water and Food Stuffs by Differential Pulse - Cathodic Stripping
Voltammetry”, Electroanalysis, 23 (5) (2011) 1175 – 1185.

Cited 3

22. H. M. Harbi †, A. EldougDoug, and **M.S. El-Shahawi**

Mineral Processing and Extraction of Rare Earth Elements from the Wadi
Khamal Nelsonite Ore, northwestern Saudi Arabia”, Arabian J. Geosciences, 4
(3 -4) (2011) 353 -363.

Cited zero

23. M.S.T. Makki, R. M. Abdel-Rahman, K.O. Alfooty and **M. S. El-
Shahaw**

Thiazolidinone Steroids Impregnated Polyurethane Foams as a solid Phase
Extractant for the Extraction and Pre concentration of Cadmium (II) from
Industrial Wastewater”, Electronic J. Chemistry, 8 (2) (2011) 887 -895.

Cited 2

24. M.S. El-Shahawi, A.A. Al-Sibaai, M.M. Al-Saidi, A.S. Bashammakh and
M.A. Abdelfadeel, “Spectrofluorometric Determination and Chemical
Speciation of Trace Concentrations of Chromium (III & VI) Species in Water
using the Ion Pairing Reagent Tetraphenyl phosphonium Bromide”, Talanta,
84 (1) (2011) 175 -180.

Cited 20

25. M.S. El-Shahawi, A.S. Bashammakh, A. A. Al-Sibaai, S.O. Bahaffi and
E.H. Al-Gohani

Chemical Speciation of Antimony (III & V) in Water by Adsorptive Cathodic
Stripping Voltammetry using the 4-(2- Thiazolylazo) – resorcinol”,

Electroanalysis, 23 (3) (2011) 747-754. **Cited 9**

26. M.S.T. Makki, R. M. Abdel-Rahman and M.S. El-Shahawi

“Synthesis of New Bioactive Sulfur Compounds Bearing Heterocyclic Moiety and Their Analytical Applications”, Intern. J. Chemistry, 3 (1) (2011) 181 - 192. **Cited 1**

27. M. S. T. Makki, R. M. Abdel-Rahman and M.S. El-Shahawi

Synthesis of Polyfunctional Organic Systems Containing 1- Acyl / aroyl - anilido-butadienes and Their Uses as Photochemical Probes and Chelating Agents for Removal of Bismuth (III) from Industrial Wastewater” J. Bioanalysis and Biomedicine, 2 (4) (2010) 85 – 90. **Cited 1**

28. A. Hamza, A.S. Bashammakh, A.A. Al-Sibaai, H.M. Al-Saidi, M.S. El-Shahawi

Part I. Spectrophotometric Determination of Trace Mercury (II) in Dental – Unit Wastewater and Fertilizer Samples using the Novel Reagent 6-Hydroxy3-(2-oxoindolin-3-ylideneamino)-2-thioxo-2H-1,3-thiazin-4 (3 H)-one and the Dual-wave β —correction spectrophotometry J. Hazard.Mater, 178 (2010) 287 -292. **Cited 22**

29. M.S. El-Shahawi, A. Hamza, A. S. Bashammakh and W. T. Al-Saggaf
An Overview on the Accumulation, Distribution, Transformations, Toxicity and Analytical Methods for the Monitoring of Persistent Organic Pollutants”, Talanta, 80 (5) (2010)1587 -1597. **Cited 116**

30. A. Hamza, A.S. Bashammakh, A.A. Al-Sibaai, H.M. Al-Saidi and M.S. El-Shahawi

Dual-wavelength β -correction spectrophotometric determination of trace concentrations of cyanide ions based on the nucleophilic addition of cyanide to imine group of the new reagent 4-hydroxy-3-(2-oxoindolin-3ylideneamino)-2-thioxo-2H-1,3-thiazin-6(3H)-one" Anal. Chim. Acta, 657 (1) (2010) 69-74. **Cited 17**

31. A.S. Bashammakh and M.S. El-Shahawi

Extraction Equilibrium and Simple Extractive Spectrophotometric Determination of Gold (I& III) in Water using the Ion - Pairing Amiloride Hydrochloride” Intern. J. Chemistry 2 (2) (2010)155 -163. **Cited zero 32.**
M.W. Kadi and **M.S. El-Shahawi**

Differential Pulse Cathodic Stripping Voltammetric Determination of Uranium with Arsenazo-III at the Hanging Mercury Dropping Electrode. Radiochim. Acta 97 (2009) 613 -619. **Cited 7**

33. M.S.El-Shahawi, A.M.Othman, M. E. El-Houseini, B. Nashed and M.S. Elsofy

Spectrofluorimetric Method for Measuring the Activity of the Enzyme α - L-Fucosidase using the Ion Associate of 2-Chloro-4-nitro phenol - rhodamine-B, Talanta, 80 (2009) 19 – 23. **Cited 5**

34. A. S. Bashammakh, S.O. Bahaffi, F. M. Al-Shareef and **M. S. El-Shahawi**

Development of an Analytical Method for Trace Gold in Aqueous Solution using Polyurethane Form Sorbents: Kinetic and Thermodynamic Characteristic of Gold (III) Sorption Analytical Sciences (Japan) 25 (2009) 413 – 418. **Cited 23**

35. E.M. Saad, R. A. Mansour, A. El-Asmy and **M.S. El-Shahawi**

Sorption Profile and Chromatographic Separation of Uranium (VI) Ions from Aqueous Solutions onto Date Pits Solid Sorbent, Talanta, 76 (2008) 1041-1046. **Cited 33**

36. M.S.El-Shahawi, S.S.M. Hassan, A.M.Othman and M.A.El-Sonbati

Retention Profile and Subsequent Chemical Speciation of Chromium (III) and (VI) in Industrial Wastewater Samples Employing some Onium Cations Loaded Polyurethane Foams" Microchemical J 89 (2008) 13 -319. **Cited 19**

37. A. M. Dowidar **M. S. El-Shahawi** and I. A. Ashour

Adsorption of Polycyclic Aromatic Hydrocarbons onto Activated Carbon from Non-Aqueous Media: Part 1. The Influence of the Organic Solvent

Polarity" Sep. Sci. Technol, 42 (16) (2007) 3609-3622. **Cited (14)**

38. A.B. Farag, M.H. Soliman, O.S. Abdel-Rasoul and M.S. El-Shahawi

Sorption Characteristics and Chromatographic Separation of Gold (I& III) from Silver and Base, Metal Ions using Polyurethane Foams" Anal. Chimica Acta , 601 (2007) 218 -229. **Cited 38**

39. M. S. El-Shahawi*, A. S. Bashammakh and S.O. Bahaffi

Chemical Speciation and Recovery of Gold (I & III) from Wastewater and Silver by Liquid-Liquid Extraction with the Ion Pair Reagent Amiloride Mono Hydrochloride and AAS Determination" Talanta, 72 (2007) 1494 -1499.

Cited 62

40. A. S. Bashammakh, S.O. Bahaffi, A. A. Al-Sibaai, H. O. Al-Wael and M. S. El-Shahawi

Extractive Liquid-Liquid Spectrophotometric Procedure for the Determination of Thiocyanate Ions Employing the Ion Pair Reagent Amiloride Monohydrochloride" Anal. Chimica Acta, 592 (2007)16 -23. **Cited 8**

41. M.S. El-Shahawi, S.O. Bahaffi and T.El-Mogy

Analysis of Domperidone in Pharmaceutical Formulations and Wastewater by Differential Pulse Voltammetry at Glassy - Carbon Electrode. Anal. Bioanal. Chem., 387 (2007) 719-725. **Cited 19**

42. I. M. Saad, M. S. El-Shahwai, H. Saleh and A.A. El-Asmy

Studies on Bismuth (III) Complexes of Ligands Containing Nitrogen/Sulfur and Extractive Procedure for Determination of Bismuth (III)" Transition Metal Chem., 32(2) (2007) 155 – 162. **Cited 27**

43. M. S. El-Shahawi, A.M. Othman, A.S. Bashammakh and M.A.El-Sonbati

Chemical Equilibria and Sequential Extractive Spectrophotometric Determination of Selenium (IV) & (VI) using the Chromogenic Reagent 4, 4⁻ Dichlorodithizone" International J. Environ. Anal. Chem.86 (12) (2006) 941 – 954. **Cited 10**

44. M.S.El-Shahawi, A.S. Bashammakh and T.El-Mogy

Determination of the Trace Levels of Disomin in Pharmaceutical Preparation by Adsorptive Stripping Voltammetry at Glassy Carbon Electrode Analytical Sciences (Japan), 22 (2006) 1351-1354. **Cited 17**

45. S.E. Ghazy, R.M. El-Shazly, **M.S. El-Shahawi**, G.A.A.Al-Hazmi and A.A.El-Asmy

Spectrophotometric Determination of Copper (II) in Natural waters, Vitamins and Certified steel scrap samples Using Acetophenone-*p*-Chlorophenylthiosemicarbazone". J. Iranian. Chem. Soc 1(2006)140- 150.

Cited 32

46. R.M. El-Shazly, G.A.A.Al-Hazmi, S.E. Ghazy, **M.S. El-Shahawi** and A.A.El-Asmy

"Synthesis and Spectroscopic Characterization of Cobalt (II) Complexes with Some Thiosemicarbazone Derivatives". J. Coord. Chem. 59 (2006) 845 -859.

Cited 23

47. A.M.Othman, **M. S. EL-Shahawi**, M. Abdel -Azeem and N.M. Rizk "A Novel Barium (II) polymeric Membrane Sensor for Selective Determination of Barium and Sulphate Ions Based on The Complex Ion associate of Barium (II) - Rose Bengal Neutral Ionophore" Anal. Chimica

Acta 555(2006) 322 -328.

Cited 13

48. **M. S. El-Shahawi** and M.A.El-Sonbati

Retention Profile, Kinetics and Sequential Determination of Selenium (IV) and (VI) Employing 4,4⁻Dichlorodithizone Immobilized Polyurethane Foams" Talanta 67 (2005) 800 -815. **Cited 31**

49. **M.S.El-Shahawi**, A.M.Othman, and M.A.Abdel-Fadeel

"Kinetics, Thermodynamic and Chromatographic Behavior of the Uranyl ions Sorption from Aqueous Thiocyanate Media onto polyurethane foams". Anal. Chimica Acta, 546(7) (2005) 221-228. **Cited 28**

50. S.S.M. Hassan, **M.S. El-Shahawi**, A.M. Othman and M.A Mosaad

A potentiometric Rhodamine-B Based Membrane Sensor for the Selective

Determination of Chromium Ions in Wastewater. Anal. Sci (Japan) 21(6)
(2005) 673 -678. **Cited 29**

51. G.A.A.Al-Hazmi, **M.S. El-Shahawi** I. M. Gabr and A.A.El-Asmy
"Spectral, Magnetic, Thermal, and Electrochemical Studies on New Copper
(II) Complexes Thiosemicarbazone Complexes". J. Coord. Chem.58 (2005)
713 -733. **Cited 47**

52. G. A. A. Al-Hazmi, **M.S. El-Shahawi** and A. A. El-Asmy
Ligand Influence on the Electrochemical Behavior of Some Copper (II)
Thiosemicarbazone Complexes". Transition Metal Chem., 30 (2005) 464 -470.
Cited 15 53.

M.S. El-Shahawi, A.M.Othman, H.A. Nassef and M. A.Abdel-Fadeel
An Investigation into The Retention Profile and Kinetics of Sorption of the
Ternary complex Ion Associate of the uranyl ions with Crown Ether and Picric
Acid by the Polyurethane Foams. Anal. Chimica Acta, 536 (1-2) (2005) 227 -
235. **Cited 12**

54. **M.S. El-Shahawi**, S.S.M.Hassan, A.M. Othman, M.A. Zyada and M.A. El-
Sonbati
Chemical Speciation of Chromium (III&VI) Employing Extractive
Spectrophotometry and Tetraphenylarsonium Chloride or
Tetraphenylphosphonium Bromidesss as Ion-Pair Reagent" Anal. ChimActa,
534 (2005) 319 -326. **Cited 31**

55. A. Radi, **M.S. El-Shahawi** and T. El-Mogy
Differential Pulse Voltammetric Determination of the Dopaminergic Agonist
Bromocriptine at Glassy Carbon Electrode". J.Pharm.Biomed.Analysis. 37
(2005) 195- 198. **Cited 14**

56. R.M. El-Shazly, G.A.A.Al-Hazmi, S.E. Ghazy, **M.S. El-Shahawi** and
A.A.El-Asmy
Spectroscopic, Thermal and Electrochemical Studies of some Nickel (II)
Thiosemicarbazone Complexes". Spectrochimica Acta part A, 61 (2004) 243-

57. A. M. Othman, N. M. H. Rizk and M. S. El-Shahawi

Polymer Membrane Sensors for Sildenafil Citrate (Viagra) Determination in Pharmaceutical Preparations. *Anal. Chimica Acta*, 515 (2004) 303 - 309".

Cited 46 58. A. M. Othman, N. M. H. Rizk and M. S. El-Shahawi

Potentiometric Determination of Dopamine in Pharmaceutical Preparation by Crown Ether –PVC Membrane Sensors" *Anal. Sci. (Japan)* 20 (2004) 651 - 655.

Cited 20**59. M. S. El-Shahawi and A. F. Shoair**

Synthesis, Spectroscopic, Characterization, Redox Properties and Catalytic Activity of Some Ruthenium (II) Complexes Containing Aromatic Aldehyde and Triphenylphosphine or Triphenylarsine *Spectrochimica Acta Part A* 60 (2004) 121-127.

Cited 59**60. M.M. Abu-Mesalam, I.M. El-Nagar, M.S. Abdel-Hai and M.S. El-Shahawi**

Use of Open-Cell Resilient Polyurethane Foam Loaded with Crown Ether for the Preconcentration of Uranium from Aqueous Solutions *Radiochem. Radioanal. Chem.* 258 (2003) 619- 625. **Cited 14**

61. M. S. El-Shahawi, G. El-Shaboury, M. A. M. Aly and M. El-Tawoosy
Chemical and Thermodynamic Characteristics of the Isotopic Exchange Reaction between Radioiodine and Iodohippuric Acid Isomers *Analytical Sciences (Japan)*, 19 (2003) 1331- 1334. **Cited 4**

62. M. S. El-Shahawi and H. A. Nassif

Kinetics and Retention Characteristics of Some Nitrophenols onto Polyurethane Foams" *Anal. Chim Acta*, 487 (2003) 249 -259. **Cited 16**

63. M. S. El-Shahawi and H. A. Nassif

Retention and Thermodynamic Characteristics of Mercury (II) complexes onto Polyurethane Foams" *Anal. Chim Acta*, 481 (2003) 29 - 39. **Cited 57**

64. S.M. Saleh, S.A. Sayd and **M. S. El-Shahawi**, Extraction and Recovery of Au, Sb and Sn from Electro refined Solid Waste Anal. Chimica Acta, 436 (2001) 69 -77. **Cited 21**

65. S.I. Mostafa, **M. S. El-Shahawi** and A. El-Asmy
Ruthenium (II) 2-Hydroxybenzophenone- N(4)- Substituted
Thiosemicarbazones Complexes Transition Metal Chemsitry, 25 (2000) 470 -
473. **Cited 30**

66. M. H. Al-Yousuf, **M. S. El-Shahawi** and S. M. Al-Gais
"Trace Metals in Liver, Skin and Muscle of *Lethrinus lentijan* Fish Species in
Relation to Body Length and Sex. The Science of the Total Environment, 256
(2000) 87- 94. **Cited 301**

67. **M. S. El-Shahawi** and M. H. Al-Yousuf
"Trace Metals in *Lethrinus Lentijan* Fish from the Arabian Gulf (Ras AlKhaimah,
United Arab Emirates): Metal Accumulation in Kidney and Heart
Tissues". Bull. Environ. Contam. Toxicology, 62 (1999) 293- 300. **Cited 11**

68. A.S.R. Al-Meqbali, **M. S. El-Shahawi** and M.M. Kamal
Differential pulse Polarographic Analysis of Chlorpyrifos insecticide
.Electroanalysis, 10 (1999) 784 -786. **Cited 13**

69. **M.S. El-Shahawi** and M.M. Kamal,
Determination of the Pesticide Chlorpyrifos by Cathodic Adsorptive Stripping
Voltammetry", Fresenius J. Anal. Chem., 362 (1998) 344 -347. **Cited 16**

70. **M.S. El-Shahawi** and A.Z. Abu Zuhri
Sequential Titrimetric and Spectrophotometric Determination of Trace
Amounts of Tin (II) and Tin (IV) by Amplification Reactions".*Bull. Chem.
Soc. Japan*, 71 (1998) 597 -601.**Cited 4**

71. **M. S. El-Shahawi** and M. H. Al-Yousuf
Heavy Metals (Ni, Co, Cr, Pb) Contamination in Liver and Skin Tissues of

Lethrinus Lentjan Fish (Family: *Lethrinidae (toelost)* from the Arabian Gulf".

Intern. . J. Food Sci. Nutrition, 49 (1998) 447- 451. **Cited 5**

72. I.M. Banat, E.S. Hassan, **M.S. El-Shahawi** and A.H. Abu Hillal. Post - Gulf-War Assessment of Nutrients, Heavy Metal Ions, Hydrocarbons and Bacterial Pollution Levels in the United Arab Emirates Costal Waters". Environ.Intern. 24 (1998) 109 -116. **Cited 41**

73. A.M. Kiwan, **M.S. El-Shahawi**, S.M. Aldhaheeri and M.H. Saleh Sensitive Detection and Semiquantitative Determination of Mercury (II) and Lead (II) in Aqueous Media Using Polyurethane Foam Immobilized 1, 5-di (2fluorophenyl)-3-mercaptoformazan" *Talanta*, **45 (1997) 203 -211. Cited 20**

74. M.S. El-Shahawi Extraction Equilibrium of the Ion-Associate of Periodate with Amiloride Hydrochloride and Simultaneous Spectrophotometric Determination of Periodate and Iodate by Liquid-Liquid Extraction" *Anal. Chimica Acta*, 356 (1997) 85 - 91. **Cited 23**

75. M.S. El-Shahawi, M.H. Abdel Kader and R.S. Al-Mehrezi Retention and Separation Behaviour of Some Organophosphorous and Pyrethroid Insectides on Polyurethane Faoms" *Analytical Sciences (Japan)* 13 (1997) 633 - 638. **Cited 4**

76. M.S. El-Shahawi and R.S. Al-Mehrezi Detection and Semiquantitative Determination of Bismuth (III) in Water on Immobilized and Plasticized-Polyurethane Foams with Some Chromogenic Reagents", *Talanta* 47 (1997) 483 - 489. **Cited 17**

77. M.S. El-Shahawi. Retention Profiles of Some Commercial Pesticides, Pyrethroid and Acaricide Residues and Their Applications to Tomato and Parsley Plants" *J. Chromatography A*, 760 (1997) 179 -192. **Cited 21**

78. E.S. Hassan, I.M. Banat, **M.S. El-Shahawi** and A.H. Abu-Hilal. Bacterial Nutrients and Heavy Metal Ions Pollution Assessment along the

Eastern Coastal Area of the United Arab Emirates". J. Aquatic Ecosystem Health 5 (1996) 73 -81. **Cited 5**

79. M.S. El-Shahawi and F.A. Al-Hashimi

Spectrophotometric Determination of Periodate or Iodate and Ions by Liquid-Liquid Extraction as an Ion-Pair with Tetramethylammonium Iodide. Talanta, 43 (1996) 2037 -2043. **Cited 37**

80. M.S. El-Shahawi and S.M. Aldhaheri

Spectrophotometric Determination of Bismuth (III and V) in Water after Ion-Pair Liquid-Liquid Extraction Using Tetramethylammonium Cation as Counter Ion". Fresenius Z. Anal. Chem., 354 (1996) 200 -203. **Cited 11**

81. D.T. Burns, M.S. El-Shahawi, M.J. Kerrigan and P.M.T. Smyth

Spectrophotometric Determination of Rhenium as Perrhenate by Extraction with Amiloride Hydrochloride". Anal. Chimica Acta 322 (1996) 107 – 109.

Cited 5

82. M.S. El-Shahawi and S.M. Aldhaheri

"Preconcentration and Separation of Acaricides by Polyether Based Polyurethane Foam". Anal. Chimica Acta, 320 (1996) 277 -287. **Cited 26**

83. M.S. El-Shahawi

"Spectroscopic and Electrochemical Studies of Chromium (III) Complexes of Naturally Occurring Ligands Containing Sulphur" Spectrochimica Acta, 52 A (1996) 139 -148. **Cited 16**

84. M.S. El-Shahawi and S. A. Barakat.

"Chemical Amplification Methods for the Sequential Determination of Trace Amounts of Ruthenium by Titrimetric and Spectrophotometric Procedures" Talanta, 42 (1995) 1641- 1649. **Cited 9**

85. M.S. El-Shahawi, A.M. Kiwan, S.M. Aldhaheri and M.H. Saleh.

"The Retention Behaviour and Separation of Some Water Soluble

Organophosphorous Insecticides on Polyester-Based Polyurethane Foams". *Talanta*, 42 (1995) 1471-1478. **Cited 20**

86. M.S. El-Shahawi and A.B. Farag.

"Iodometric Determination of Gold and Platinum by 168- and 126- Fold Chemical Amplification Reactions". *Analytica Chimica Acta*, 307 (1995) 139-144. **Cited 17**

87. M.S. El-Shahawi and S.A. Barakat.

"Spectral and Electrochemical Studies of D- Tartaric and DL- Mandelic Acids with Different Chromium Ions". *Spectrochimica Acta*, 51A (1995) 171-175.

Cited 1

88. M.S. El-Shahawi.

Chromium (III) Complexes of Some Naturally Occurring Lignans, *Spectrochimica Acta*, 51A (1995) 161-170.

Cited 15

89. M.S. El-Shahawi and M. Almehdi.

"Qualitative, Semi-Quantitative and Spectrophotometric Determination of Ruthenium (III) by Solid Phase Extraction with 3-Hydroxy-2-methyl-1,4-naphthoquinone-4-oxime Loaded Polyurethane Foam Columns". *J. Chromatography*, 679 (1995) 185-190. **Cited 19**

90. M.S. El-Shahawi and M.M. Kamal

"Microgram Determination of Bismuth by Sequential High Fold Chemical Amplification Reactions".

Analytical Sciences (Japan), 11 (1995) 323-326.

Cited 3

91. M.S. El-Shahawi, and W.E. Smith

"Spectroelectrochemistry of Nickel (II) Complexes of N, N'-bis(salicylaldehyde)-*o*-phenylenediamine and N,N'-bis(2-hydroxy-1-naphthaldehyde)-*o*-phenylenediamine Using an Optically Transparent Thin Layer Electrode" *Analyst (London)*, 119 (1994) 327-331. **Cited 18**

92. M.S. El-Shahawi, A.Z. Abu Zuhri and S.M. Aldhaheri.

Spectrophotometric Determination of Ruthenium after Extraction of Perruthenate and Benzyl tributyl -ammonium Chloride, *Fresenius J. Anal.*

Chem., 350, (1994) 674-677. **Cited 7**

93. M.S. El-Shahawi, A.Z. Abu Zuhri and M.M. Kamal

Adsorptive Stripping Voltammetric Measurements of Trace Amounts of Platinum(II) and Ruthenium(III) in the Presence of 1-(2-Pyridylazo)-2-naphthol" *Fresenius Z. Anal. Chem.*, 348 (1994) 730-735. **Cited 14**

94. H. Doweidar, A.A. Megahed, S.A. Almaksoud, **M.S. El-Shahawi** and Y. El-Fol

Properties and Structure of ZnO-PbO-B₂O₃ Glasses" *Physics and Chemistry of Glasses*, 35 (1994) 187-192. **Cited 6**

95. A.A. El-Asmy, E.M. El-Saad and **M.S. El-Shahawi**

"Electrochemical Synthesis, Magnetic, Spectral and Cyclic Voltammetric Studies on Lactic Acid Complexes" *Transition Metal Chemistry*, 19 (1994) 406-408. **Cited 7**

96. A.B. Farag, **M.S. El-Shahawi** and S. Farag.

The Sorption Behavior and Separation of Some Metal Thiocyanate Complexes on Polyether - Based Polyurethane Foam". *Talanta*, 41 (1994) 617-623. **Cited 12**

97. M.S. El-Shahawi

"Retention and Separation of Some Organic Water Pollutants with Unloaded and Tri -n-Octyl -amine Loaded Polyester - Based Polyurethane Foam" *Talanta*, 41, (1994) 1481-1488. **Cited 27**

98. M.S. El-Shahawi, A.B. Farag and M.R. Mostafa

Pre-concentration and Separation of Phenols from Water by Polyurethane Foams, *Sep. Sci. Technol*, 29 (1994) 289-299. **Cited (18)**

99. A.Z. Abu Zuhri, A.H. Rady, **M.S. El-Shahawi** and S.M. Aldhaheeri.

Spectrophotometric Determination of Ampicillin by Ternary Complex Formation with 1,10-phenanthroline and Copper (II)., *Microchemical. J.* 40 (1994) 111-115. **Cited 4**

- 100.** A.Z. Abu Zuhri, **M.S. El-Shahawi**, M.M. Kamal and M.Hannoun
Spectrophotometric and Polarographic Studies of Di-2-pyridyl ketone
2thienoyl-hydrazone".
Analytical Letters, 27 (1994) 907-1919. **Cited 6**
- 101. M.S. El-Shahawi**
Chromium (III) Complexes of Naturally Occurring Amino Acids, Transition
Metal Chemistry, 18 (1993) 385-390. **Cited 9**
- 102.** A.B. Farag, **M.S. El-Shahawi** and E.M. El-Nemma.
Iodometric Microdetermination of Arsenic and Antimony in Organic
Compounds by Use of Amplification Reactions" Fresenius Z. Anal. Chem.,
346 (1993) 455-455. **Cited 6**
- 103.** A.Z. Abu Zuhri, **M.S. El-Shahawi** and M.M. Kamal
"Adsorptive Stripping Voltammetric Behaviour of Gold (III) at a Hanging
Mercury Drop Electrode in the Presence of 1-(2'-Pyridylazo)-2-Naphthol,
Anal.Chimica. Acta.,282 (1993)133-137 **Cited 6 104.**
- M.S. El-Shahawi,**
"Pre- concentration and Separation of Some Organic Water Pollutants with
Polyurethane Foam and Activated Carbon" Chromatographia., 36 (1993)318-
322. **Cited 10**
- 105. M.S. EL-Shahawi** and A.A. El-Bindary
"Chromium (III) Complexes with Some Optically Active α -Hydroxy Acids, Z.
Naturforsch., 48B (1993) 282-286. **Cited 10 106.**
- D.T. Burns, S.A. Barakat , M. Harriott , **and M.S. El-Shahawi**
Flow Injection Extraction Spectrophotometric Determination of Manganese
(VII) with Benzyl tributylammonium Permanganate" Analytica Chimica Acta,
270 (1992) 213-215. **Cited 13**
- 107. M.S. El-Shahawi** and S.E. Ghazy
Chromium (III) Complexes of D (-) Tartaric and L (-) Mandelic Acids,
Transition Metal Chemistry, 17 (1992) 543 -546. **Cited 3**
- 108.** D.T. Burns, S.A. Barakat, **M.S. El-Shahawi**, and M. Harriott
Flow-injection Extraction Spectrophotometric Determination of Permanganate
with Triphenyl -sulphonim Cations, Fresenius J. Anal. Chem., 344 (1992) 131-

132. **Cited 9**
- 109.** A.M. Abdallah, **M.S. El-Shahawi**, M.M. El-Defrawy and E.E. Askar
Removal of Heteropolyanions Interferences in the Atomic Absorption
Determination of Silver and Gold, *Chemia Analityczna*, 37 (1992) 589-598.
Cited 14
- 110.** D.T. Burns, M. Harriott, S.A. Barakat and **M.S. El-Shahawi**. "Flow-
injection Extraction Spectrophotometric Determination of Manganese in Steel
as Triphenylsulfonium or Benzyltributyl-ammonium Permanganate"
Analytical Proceedings, 29 (1992) 369, PG 5. **Cited 0 111.**
- A.B. Farag, **M.S. El-Shahawi**, A.M.A. Helmy and S. Farrag.
"The Extraction and Recovery of Some Organic Insecticides from Aqueous
Media with Cellular Polyurethanes, *Bull. Soc. Chem. (France)*. 128 (1991)
641-643. **Cited 0**
- 112. M.S. El-Shahawi**
"Spectrophotometric Determination of Nickel (II) with Some Schiff Base
Ligands, *Analytical Sciences (Japan)* 7 (1991) 443 - 446. **Cited 13**
- 113.** A.B. Farag and **M.S. El-Shahawi**
Removal of Organic Pollutants from Aqueous Solution V. A Comparative Study
of the Extraction, Recovery and Chromatographic Separation of Some Organic
Insecticides Using Unloaded Polyurethane Foam Columns, *J.*
Chromatography, 552 (1991) 371-379. **Cited 24**
- 114.** A.M. El-Wakil, **M.S. El-Shahawi** and A.B. Farag.
"Trace Analysis by Direct Spectrophotometric Measurements on Polyurethane
Foam, Determination of Chromium (VI) as Blue Perchromic Acid with
Unloaded & Tri-n-Butyl Phosphate Loaded Foam". *Analytical Letters*, 23
(1990) 703 -717. **Cited 12**
- 115.** A.M. El-Wakil, A.B. Farag and **M.S. El-Shahawi**
Iodometric Microdetermination of Thallium in Aqueous Media and in Organic
Compounds Via Chemical Amplification Reactions, *Fresenius J. Anal. Chem.*
337 (1990) 886 - 886. **Cited 6**
- 116.** H. Doweidar, **M.S. El-Shahawi**, F.M. Reicha, H.A. Silim and K. El-
Egaly

Phase Separation and Physical Properties of Sodium Borosilicate Glasses with Intermediate Silica Content". J. Phys. D: Appl. Phys. 23 (1990) 1441-1446.

Cited 10

117. M. Mashaly, **M.S. El-Shahawi** and P. P. Sandra

"Domestic Indoor Pollution: CGC and CGC/MS Investigation of the Exhaust Particulate Matter Deposited on the Inside Wall of Kerosene Lamp, Bull. Fac. Sci. Mans. Univ. 17 (1990) 45 – 56, Accepted also in Asian J. Chemistry, 1989.

Cited 0

118. A.M. El-Hendawy and **M.S. El-Shahawi**

Complexes of Ruthenium (III) Derived from *o,o*-Donor Ligands" Polyhedron, 8 (1989) 2813 - 2816.

Cited 35

119. A.M. El-Wakil, A.B. Farag and **M.S. El-Shahawi.**

Iodometric Microgram Determination of Mn (II) in Aqueous Media by an Indirect Chemical Amplification Reactions Talanta, 36 (1989) 783 -785.

Cited 12

120. A.B. Farag, A.M. El-Wakil and **M.S. El-Shahawi**, M.Mashaly

"Extraction and Recovery of Some Organic Insecticides on Polyurethane Foam Columns"

Analytical Sciences (Japan), 5 (1989) 415 - 417.

Cited 9

121. A.B. Farag, A.M.A. Helmy, **M.S. El-Shahawi** and S. Farrag

"Sensitive Detection and Semi quantitative Determination of Molybdenum (VI) Using Unloaded and Specially-Treated Polyurethane Foams" Analusius, 17 (1989) 478 - 480. **Cited 8**

122. A.B. Farag, **M.S. El-Shahawi** and A.M. El-Wakil and M.N. Abbas

The Extraction and Recovery of Some Organic Amines from Aqueous Solution by Polyurethane Foam, Bull. NRC, Egypt, 14 (1) (1989) 39 - 46.

Cited 0

123. A.B. Farag, A.M. El-Wakil, **M.S. El-Shahawi** and and M.N. Abbas

Collection and Recovery of Some Mono- and Di-carboxylic Acids on Polyurethane Foam, Bull. NRC, Egypt, 14 (1) (1989) 29 - 37. **Cited 0**

124. A.B. Farag, **M.S. El-Shahawi** and A.M. El-Wakil

"Removal of Organic Pollutants from Aqueous Solution. Part II: A

Comparative Study of the Concentration of Some Phenols by Loaded and Unloaded Open Cell Polyurethane Foams". Proc.2nd. Chemistry Conference, Faculty of Science, Mansoura University, Egypt II (1988) 372-378. **Cited (0)**

125. M. Mashaly, P. P. Sandra, M. Sofan and **M.S. El-Shahawi** CGC and CGC/MS Investigation of the Aliphatic Hydrocarbon Fraction of Street Dust Giza Square, Egypt. The First National Conference on Environmental Studies and Research, Jan, Cairo, Egypt (1988) 405 - 413. **Cited (0)**

Articles Published from MSc and Ph.D Thesis (Not for evaluation) (6

Entries)

126. D.H. Brown, W.E. Smith, **M.S. El-Shahawi** and M.F. K. Wazier Chromium (III) Complexes with Sugars". Inorg. Chim. Acta, 124 (1986) L25 –L 26. **Cited (17)**

127. A.B. Farag, A.M. El-Wakil and **M.S. El-Shahawi** Collection and Separation of Some Organic Insecticides on Polyurethane Foam Columns". Fresenius Z Anal. Chem. 324 (1986) 59 -60. **Cited (18).**

128. A.B. Farag, A.M. El-Wakil and **M.S. El-Shahawi.** Separation of Cadmium (II), Iron (III), Nickel (II) and Copper (II) in Aqueous Solution Using Adogen-foam Columns". Bull. Soc. Chim. Belg. 94 (1985) 631- 633. **Cited (3).**

129. A.B. Farag, A.M. El-Wakil and **M.S. El-Shahawi.** Detection and Semiquantitative Determination of Nickel with Dimethylglyoxime Loaded Foam". Talanta, 29 (1982) 789 -790. **Cited (6)**

130. A.B. Farag, A.M. El-Wakil and **M.S. El-Shahawi.** "Qualitative and Semiquantitative Determination of Iron (III) in Aqueous Thiocyanate Solution Using Tricaprylylamine Foam Annali. di Chimica. (Rome), 72 (1982) 103 -106. **Cited (4)**

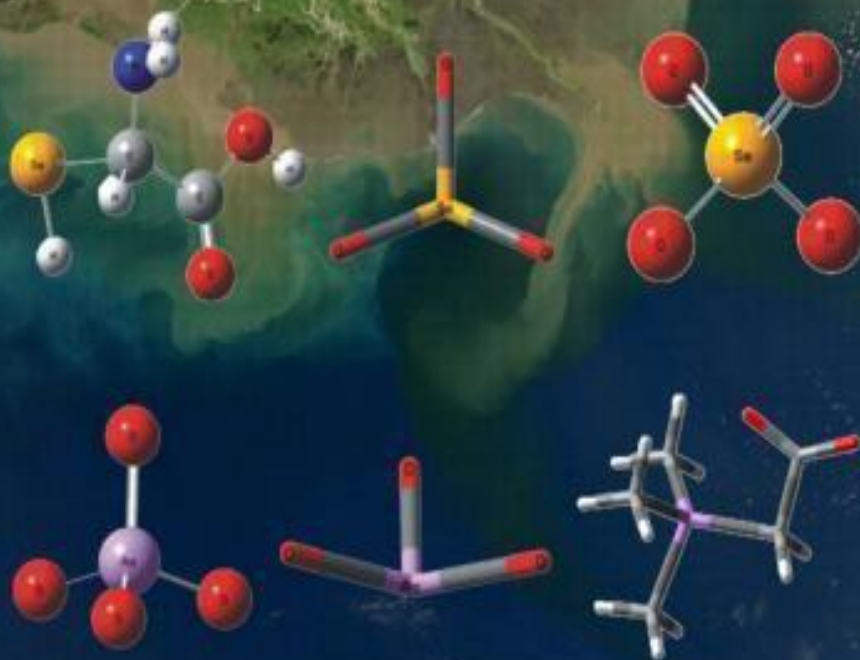
131. A.B. Farag, A.M. El-Wakil and **M.S. El-Shahawi.** "Qualitative and Semiquantitative Determination of Chromium (VI) in Aqueous Solution Using 1, 5- Diphenylcarbazide Loaded Foam" *Analyst (London)*, **106 (1981) 809 -812.** **Cited (18)**

Citation Indices:

Paper no	No Citation						
1	-	42	27	83	16	124	-
2	6	43	10	84	9	125	-
3	-	44	17	85	20	126	17
4	-	45	32	86	17	127	18
5	18	46	23	87	1	128	3
6	-	47	13	88	15	129	6
7	4	48	31	89	19	130	4
8	22	49	28	90	3	131	18
9	1	50	29	91	18		
10	3	51	47	92	7		
11	1	52	15	93	14		
12	-	53	12	94	6		
13	3	54	31	95	7		
14	34	55	14	96	12		
15	12	56	64	97	27		
16	12	57	46	98	18		
17	2	58	20	99	4		
18	-	59	59	100	6		
19	5	60	14	101	9		
20	4	61	4	102	6		
21	3	62	16	103	6		
22	0	63	57	104	10		
23	2	64	21	105	10		
24	20	65	30	106	13		
25	9	66	301	107	3		
26	1	67	11	108	9		
27	1	68	13	109	14		
28	22	69	16	110	-		
29	116	70	4	111	-		
30	17	71	5	112	13		
31	-	72	41	113	24		
32	7	73	20	114	12		
33	5	74	23	115	6		
34	23	75	4	116	10		
35	33	76	17	117	-		
36	19	77	21	118	35		
37	14	78	5	119	12		
38	38	79	37	120	9		
39	62	80	11	121	8		
40	8	81	5	122	-		
41	19	82	26	123	-		

Total Citation= 2211
h-index =24 i
10-index =72

Speciation Studies in Soil, Sediment and Environmental Samples



Editor
Sezgin Bakirdere

 **CRC Press**
Taylor & Francis Group
A SCIENCE PUBLISHERS BOOK

Table of Contents

Aspects of speciation, *Emrah Yildirim and Lütfiye Sezen Yildirim*

Sample Pre-treatment Methods for Organometallic Species Determination, *Antonio Moreda-Piñeiro, Jorge Moreda-Piñeiro, and Pilar Bermejo-Barrera*

Separation Techniques for Elemental Speciation in Soil, Sediments, and Environmental Samples, *Márcia F. Mesko, Carla A. Hartwig, Cezar A. Bizzi, Edson I. Müller, Fábio A. Duarte, and Paola A. Mello*

Role and Importance of Hyphenated Techniques in Speciation Analysis, *Rajmund Michalski, Magdalena Jabłońska, and Sebastian Szopa*

Speciation of Arsenic in Soil, Sediment and Environmental Samples, *Selin Bora, Işıl Aydın, Ersin Kılınç, and Firat Aydın*

Speciation of Chromium and Vanadium in Soil Matrices, *Khakhathi L. Mandiwana and Nikolay Panichev*

Selenium Speciation in the Environment, *Rodolfo G. Wuilloud and Paula Berton*

Speciation and Solubility of Thallium in Low Temperature Systems: Additional Aqueous and Solid Thallium Species Potentially Important in Soil Environments, *Yongliang Xiong*

Fractionation and Speciation Analysis of Antimony in Atmospheric Aerosols and Related Matrices, *Patricia Smichowski*

Methods for Mercury Speciation in Environmental Samples, *Zhenli Zhu, Qian He, and Zhifu Liu*

Zinc Speciation Studies in Soil, Sediment and Environmental Samples, *Todd P. Luxton, Bradley W. Miller, and Kirk G. Scheckel*

Speciation Analysis of Tin in Environmental Samples, *Valderi Luiz Dressler, Clarissa Marques Morreira dos Santos, Fabiane Goldschmidt Antes, Erico Marlon de Moraes Flores, and Dirce Pozebon*

Speciation and bioavailability of Iodine in Edible Seaweed, *Vanessa Romaris Hortas, Antonio Moreda Piñeiro, and Pilar Bermejo Barrera*

Speciation and Determination of Tellurium in Water, Soil, Sediment and Other Environmental Samples, *M.S. El-Shahawi, H.M. Al-Saidi, E. A. Al-Harbi, A.S. Bashammakh, and A. A. Alsibbai*

Trace Elements and Health, *Mehrdad Gholami*

Speciation and Determination of Tellurium in Water, Soil, Sediment and other Environmental Samples

M.S. El-Shahawi,^{1,2,} H.M. Al-Saidi,³ E.A. Al-Harbi,⁴
A.S. Bashammakh¹ and A.A. Alsibbai¹*

1. Introduction

In the past, the determination of total element concentrations was considered to be enough for clinical and environmental analyses. However, the knowledge of chemical speciation has primary importance because the toxicity, mobility, bioavailability and bioaccumulation of elements largely depend on their chemical species (Ebdon et al. 2001). Chemical species are specific forms of an element defined as isotopic composition, electronic or oxidation state and/or complex or molecular structure (Templeton et al. 2000). Tellurite, Te (IV) is 10 times more toxic than tellurate, Te (VI) (Huang and Hu 2008). Therefore, speciation studies are important for the accurate evaluation of pollution levels in a wide variety of samples such as water, soil and sediment.

¹ Department of Chemistry, Faculty of Science, King Abdulaziz University, P.O.Box 80203, Jeddah 21589, Saudi Arabia.

² Email: malsaeed@kau.edu.sa, mohammad_el_shahawi@yahoo.co.uk

³ Department of Chemistry, University College, Umm Al Qura University, Makkah, Saudi Arabia.

⁴ Department of Applied Chemistry, College of Applied Science, Taibah University, Al-Madinah Al-Munawarah, P.O. Box: 3193, Saudi Arabia. *Corresponding author

Speciation analyses have been widely used to identify the metal species that have adverse effects on living organisms (Cava-Montesinos et al. 2004). The interaction of metal ions with biota is highly dependent on their oxidation state and/or organic or inorganic structure rather than to their total concentration. Due to its wide applications as alloying additives in steel, copper, lead alloys, vulcanizing agent and accelerator in the processing of rubber, and the component of catalysts for synthetic fiber production, the level of exposure of tellurium has largely increased in the last years (Jain and Ali 2000). Therefore, an overview on distribution, toxicity and chemical speciation of tellurium will be presented in this chapter. The recent developments in the analytical techniques frequently used for chemical speciation of tellurium will be discussed in detail.

2. Occurrence, Uses and Toxicity of Tellurium

Tellurium was discovered in 1782 by the Austrian mineralogist Baron Franz Joseph Muller (Nordberg et al. 2007, Bragnall 1966). The element seldom occurs in its pure state in nature. However, it is usually found as a compound in ores of gold, silver, copper, lead, mercury or bismuth (Cava-Montesinos et al. 2004, Jain and Ali 2000). The most well-known ores containing tellurium are the ores of gold and silver, e.g., Calaverite (AuTe_2), Sylvanite (AgAuTe_4) (Tsai and Jan 1993, Emsley 2002). Tellurium is considered one of the rarest stable solid elements on the Earth's crust even in comparison with some lanthanides and it is usually associated with selenium at trace and ultra trace levels (Cooper 1971, Sadeh 1987). The level of Te in soil ranges from 0.05 to 30 $\mu\text{g kg}^{-1}$, while in sea Te level is about 0.15 ng L^{-1} (Emsley 2002).

Tellurium exists in the environment in elemental (Te), inorganic–telluride (Te^{2-}), Te (IV), Te (VI) and organic (dimethyl telluride (CH_3TeCH_3)) forms (Cooper 1971), oxyanions are more stable and common than the elemental state (Summers and Jacoby 1977). Many Te compounds are redox-active, with the formal oxidation states of Te in these compounds range from -2 to $+6$ (Yosef et al. 2007, Cunha et al. 2009). Chemical and physical properties of tellurium are largely similar to those of selenium (Cooper 1971). At physiological pH, Te is less soluble than Se and its oxidation states (IV), e.g., TeO_3^{2-} , and (VI), e.g., TeO_4^{2-} or TeO_2 occur easily. Tellurium has many stable isotopes involving ^{130}Te , 34.48%; ^{128}Te , 31.79%; ^{126}Te , 18.71%; ^{125}Te , 6.99%; ^{124}Te , 4.61%; ^{122}Te , 2.46%; ^{123}Te , 0.87%; ^{120}Te , 0.089% (CRC Handbook 1975).

Tellurium has been used in metallurgic industry to improve the mechanical properties of steels and other ferrous alloys. It is also employed in the form of alloys with copper and lead, used in welding and chemical equipment. Tellurium is utilized in the rubber industry to improve heat resistance and as a catalyst in many industrial applications. Thermo electrical devices used in power plants and

refrigeration are based on the Seebeck effect, for current production when heating up a junction of two different metals, and in the Peltier effect that consists of heat transfer by means of an electrical current flow through a metallic junction (Geological Survey 2011). Due to relatively high conductivity, Te is used in semiconductors and other electronic devices. Tellurium also finds application in “daylight lamps and ceramics. Photographic and pharmaceutical industries also utilize some quantities of this element (Kabata-Pendias 2011). Tellurium found historical applications in the treatment of microbial infections prior to the discovery of antibiotics. Early documentation in 1926 reports its use in the treatment of syphilis and leprosy (De Meio and Henriques 1947).

The oxyanion tellurite has been used in microbiology since the 1930s when Alexander Fleming reported its antibacterial properties (Fleming 1932, Fleming and Young 1940). In 1984, it was suggested that TeO_2^{3-} could be a potential antisickling agent of red blood cells in the treatment of sickle cell anemia (Asakura et al. 1984). While in 1988, tellurium-containing immunomodulating drugs were proposed as treatment agents for AIDS (Jacobs 1989). On the other hand, Te compounds, especially organo-tellurium compounds, have been found to exhibit probable antioxidative and anticancer properties (Bagnall 1966, Jacob et al. 2000, Engman et al. 2002).

The toxicology of tellurium has received less attention compared to selenium. However, toxicity of tellurium compounds largely depends on the chemical form and the quantity of the element consumed. Tellurium showed acute toxicity in young children when ingestion of metal-oxidizing solutions containing significant concentrations of Te (Yarema and Curry 2005, Taylor 1996). Tellurium can be accumulated in the kidney, heart, liver, spleen and muscle and its content in liver and the kidney in excess of 0.002 g kg^{-1} (Chai and Zhu 1994). The occurrence of Te in mammalian tissues is at the level of $20 \mu\text{g kg}^{-1}$ (Chai and Zhu 1994). Tellurium slowly leaches out and its half-time is estimated to be 600 d (Hollins 1969). Tellurium level in human urine concentration is reported $< 1 \mu\text{g l}^{-1}$ (Reimann and Caritat 1998), whereas in blood it is less than $0.3 \mu\text{g l}^{-1}$. Tellurium toxicity is associated with impaired neurotransmission that affects saliva and sweat secretion in humans. The daily dietary intake of Te by adults from food has been estimated at around $0.1 \text{ mg kg}^{-1} \text{ BW}$ (Kobayashi 2004).

3. Analytical Methods for Chemical Speciation and Determination of Tellurium

Many analytical techniques such as voltammetry, flame atomic absorption spectrometry (FAAS), electrothermal atomic absorption spectrometry (ET-AAS), inductively coupled plasma-mass spectroscopy (ICP-MS), inductively coupled plasma-optical emission spectroscopy (ICP-OES), X-ray fluorescence, spectrophotometry, and electrophoresis have been used for Te determination in various environmental matrices (Table 14.1). Among these techniques, AAS and ICP coupled with a suitable hydride generation system have been widely used for

the chemical speciation of Te in various samples due to their high sensitivity. However, the direct determination of Te using most detection techniques mentioned above is still a difficult task due to its occurrence in trace and ultra trace levels and strong interference of the sample matrices. Therefore, a preconcentration step becomes necessary to get accurate results. Below, we will discuss some different analytical techniques widely used for the estimation of Te in detail.

3.1 Determination of Te in water

3.1.1 Speciation of Te using hydride generation

Hydride generation (HG) using tetrahydroborate (THB) at present is considered to be one of the most widespread derivatization procedures for the determination of trace and ultra-trace amounts of chemical vapor forming elements, in combination with various atomic spectrophotometric techniques (Xi et al. 2010). Tellurium (IV) is most often determined by HG followed by atomic absorption spectrometry (AAS) or atomic fluorescence (AFS) (El-Hadri et al. 2005), while, tellurium (VI) concentration is obtained by the difference between the total tellurium and Te (IV) contents. Thus, both HG-AAS and GH-AFS techniques have found wide applications in chemical speciation of Te (IV) and Te (VI) in various matrices.

3.1.2 Determination of Te using liquid-phase microextraction

Atomic spectrometric techniques, e.g., AAS, ICP-OES, atomic fluorescence spectrometry and ICP-MS in combination with an efficient preconcentration technique have been successfully used for the chemical speciation of tellurium (El-Hadri et al. 2005). Most of these methods are based upon selective extraction of the Te (IV) complexes. Therefore, Te (II) or Te (0) have to be oxidized to Te (IV), while, Te (VI) must be reduced to Te (IV) for determination of total Te species (Cava-Montesinos et al. 2004).

Table 14.1 List of some analytical methods used for tellurium determination in variety of samples.*

Analytical features Ref.	
LOD=3ngL ⁻¹ ; Linearity=0-5.0µgL ⁻¹	Yu et al. 2003
LOD=600ngL ⁻¹ (Te ⁴⁺); 700ngL ⁻¹ (Te ⁶⁺); Linearity=2-100µgL ⁻¹	Viñaset al. 2005
	Huang and Hu 2008
ngL ⁻¹ ; Linearity(23.0-400ngL ⁻¹); (XAD) LOD=66ngL ⁻¹ ; Linearity	Pedro et al. 2008
	Ghasemi et al. 2009
µgL ⁻¹ ; Linearity=	Ghasemi et al. 2010
	Najafi et al. 2010
	Lu et al. 2011
	Urbánková et al. 2011
	Fathirad et al. 2012
MIBK extraction—Hubert and Chao	1985)
LOD=0.1 µg g ⁻¹	Donaldson and Leaver 1990
	Holland and Pelchat 1997

Table 14.1 contd....

technique	octadecyl(C18)sorbent
	complexingagent
	γ -MPTMSLOD=0.079ngL
GF-AASTapwaterDowexX8andXADresins(Dowex1X8)LOD=7ngL	
GF-AASWaterVoltammetryLOD=2.0ngL	
GF-AASNaturalwatersHF-LPMELOD=4.0ngL	
GF-AASNaturalwaterDLLMELOD=4.0ngL	
HG-CLNaturalwaterLOD=2000.0ngL	
	edsilicasorbentsLOD<10 μ g/L
GF-AASNaturalwaterUSAE-SFODMELOD=3.0ngL	
extraction	
	HG-ICP-MSGeologicalmatricesLOD=1.0mgKg

	Technique Sample type Pre-concentration
	ICP-MS Freshwater Non-polar silica-based
	LC-HG-AFS Wastewater Anion-exchange-
ICP-MS Seawater	
	ICP-MS water Modifi
FAAS Geological and sediment	
	GF-AAS Ores and sediments Iron collection and xanthate

technique
CSV Geological matrices SPE by chelating resin LOD <math>< \mu\text{g Kg}</math>
HG-AFSTealeaves-LOD=0.0022 μgg
HG-IAT-FAASFlyash; Garlic LOD=900.0ngL
D-HGAAASUrine LOD=260.0ngL
sonication
Solvent extraction LOD=7.0ngL

	Technique	Sample type	Pre-concentration
	HG-AFS	Air	Extraction with aquaregia LOD = 6×10^{-6}
	HPLC/ICP-MS	Water; urine;	
			fish and soil
			HG-AFS Milk
	Differential oscillopolarography		Leaching of slurries by Heart, Liver, Kidney, Spleen and Lung

There are many studies describing the use of liquid-phase microextraction techniques in combination with AAS for the chemical speciation of Te in different environmental samples.

Recently, excellent pre-concentration techniques before the measurement step by AAS have been reported for the chemical speciation and total determination of various tellurium species in complicated matrices (Ghasemi et al. 2010, Najafi et al. 2010, Fathirad et al. 2012). The method of Ghasemi et al. 2010 was based upon extraction of Te (IV) complex species with ammonium pyroldine dithiocarbamate (APDC) by hollow fiber liquid phase microextraction (HF-LPME), while dispersive liquid-liquid microextraction (DLLME) and ultrasound-assisted emulsified cation solidified floating organic drops microextraction (USAESFODME) have been reported by Najafi et al. 2010 and Fathirad et al. 2012, respectively. In these methods Te (VI) was first reduced to Te (IV), and then the microextraction technique was then applied before AAS determination of total Te.

3.1.3 Determination of Te using Solid Phase Extraction

The applications of solid-phase extraction (SPE) were more common than those of liquid phase extraction for Te speciation analysis. In general, SPE is based on the utilization of a major constituent as the bonded stationary phase immobilized different ligand or functional group (Marahel et al. 2011). Mercapto-modified silica microcolumn was used as an effective stationary phase for developing a novel and sensitive method for the determination of trace amounts of Te (IV) in waters by HG-AAS (Körez et al. 2000). This method offered the limit of detection of less than 0.04 ng ml⁻¹ in sea water.

Yu et al. 2003 have described a procedure for the speciation of tellurium (IV, VI) by SPE-ICP-MS. In this method, Te (IV) complex with APDC was completely retained on a nonpolar silica-based octadecyl (C18) sorbent-containing SPE cartridge, while the uncomplexed Te (VI) passed through the cartridge and remained as a free species in the solution prior to its determination by ICP-MS. The Te (IV) concentration was calculated as the difference between total tellurium obtained by ICP-MS and Te(VI) concentrations. Simultaneous determination of Te, As, Sb, and Se by ICP-MS after pre-concentration of analytes using modified silica sorbent was described Urbánková et al. (Urbánková et al. 2011). The analytes were retained on modified silica in the form of ion associates with cationic surfactants in the presence of the presence of 4-(2-pyridylazo) resorcinol, 2-pyrrolidinedithioate and 8-hydroxyquinoline-5-sulfonic acid as chelating agents. The quantitative retention occurred at pH 7 ± 0.2 and the mixture of acetone with ethanol in ratio 1:1 in the presence of 0.1 mol L⁻¹ HCl was used for the quantitative elution. Organic solvents and the excess of acid were removed by evaporation prior to the determination by ICP-MS.

Tellurium is present in seawater in the form of tellurium (IV) and (VI) at trace level (ng L^{-1}), on the other hand, the high concentration of matrix ions in sea water causes instrumental drift, signal suppression and clogging of the sample introduction system of instrument. Therefore, pre-concentration and extraction of Te from the matrix of seawater becomes an important step prior to measurement. Huang and Hu used the magnetic nanoparticles (MNPs) as SPE adsorbent for the separation of inorganic tellurium species from seawaters prior to their determination by ICP-MS (Huang and Hu 2008). Within the pH range of 2–9, Te (IV) could be quantitatively adsorbed on γ -mercaptopropyltrimethoxysilane (γ -MPTMS) modified silica-coated magnetic nanoparticles (MNPs), while the Te (VI) was not retained and remained in solution. Like other magnetic separation techniques, tellurite loaded on MNPs could be separated easily from the aqueous solution by applying external magnetic field without filtration or centrifugation. Under the optimal conditions, the LOD obtained for Te (IV) was 0.079 ng/L, while the precision was 7.0 percent.

3.1.4 Determination of Te by chemiluminescence

HG technique coupled with chemiluminescence (CL) has been successfully used to minimize matrix interference during determination of tellurium (IV) in natural water (Luo et al. 2011). The developed method was based upon the strong CL emission obtained by the reaction between hydrogen telluride and luminol in basic medium. Under the optimized condition, excellent linear dynamic range of CL intensity vs. Te (IV) concentrations ($10\text{--}200 \mu\text{g L}^{-1}$) was achieved. The limits of detection and quantification by this method were found excellent compared to the reported methods in the literature.

3.1.5 On-line pre-concentration of Te in water

Two flow-injection graphite furnace atomic absorption spectrometry (FI-GFAAS) systems for the determination of Te in tap water have been reported by Pedro et al. (Pedro et al. 2008). Because Te (VI) is hydride inactive, this procedure is suitable for Te (IV) and if Te (VI) needs to be detected, the pre-reduction step is necessary. The first approach was based on the on-line pre-concentration of the analyte onto a strong anionic resin (Dowex X8) using as packaging material of a micro-column inserted in the flow system. The second approach was based on the co-precipitation of tellurium with $\text{La}(\text{OH})_3$ followed by retention onto adsorbent fillings (XAD resins). Although, the use of Dowex 1X8 as material filling fulfills the requirements for the on-line operation of the FI-GFAAS system, the low selectivity of the anionic exchange resin constrains its use in complex matrix like saline samples. On the other hand, amberlite XAD shows a higher level of tolerance to the presence of dissolved ions. But neither automatic operation nor

long-term use of the adsorbent resin is possible due to its severe compaction during the default sequence of washing of the GF auto sampler.

Pre-concentration of Te using selective electrodeposition with mercury-coated electrode was proposed for the chemical speciation of Te (IV) and Te (VI) in water samples by GF-AAS (Ghasemi et al. 2009). The method is based on the selective reduction of the Te (IV) at a controlled applied potential (2.0 V) on the mercury-coated electrode. In acidic media (1.0 mol L⁻¹ HCl solution), only Te (IV) can be electrodeposited onto the mercury electrode surface and separated, while, Te (VI) remained in solution. The electrode was withdrawn from the solution and the spent electrolyte containing Te (VI) was measured by GFAAS. Tellurium (IV) was calculated from the difference between the measured total Te and Te (VI) content.

3.1.6 The chromatographic determination of Te

According to our knowledge, the applications of chromatography for the determination of Te species are limited. As an example, Liquid Chromatography-Hydride Generation coupled Atomic Fluorescence Spectrometry (LC-HG-AFS) was used for speciation of Te (IV) and Te (VI) in wastewater (Viñas et al. 2005). Anion-exchange LC with multidentate complexing agents, e.g., EDTA and potassium hydrogen phthalate (KHP) in the mobile phase was used to improve column efficiency because such agents have very high complexing capacity and can transform the positive metal ion into negatively charged complexes.

3.1.7 Spectrophotometric methods of Te determination in water

Direct determination of Te using spectrophotometric methods is rarely used due to the low sensitivity of such methods. However, survey of the literature reveals that a few spectrophotometric methods were proposed for the determination of Te in the environmental samples. One of the most recent spectrophotometric methods was proposed for direct determination of Te in water, plant materials and soil (Prasad et al. 2007). The method is based on the oxidation of leuco methylene green (LMG) to its blue form by Te (IV) in acetate buffer medium (pH 3.0 to 5.0). Measurements were linear over the concentration range 0.4–2.5 µg mL⁻¹. The extractive spectrophotometric method with Bismuthiol II is highly sensitive and selective for the determination of Te in water and other environmental samples (Toshida et al. 1966). In acid media, the complexing agent bismuthiol II reacts with Te (IV) to form a neutral 1:4 (Te: reagent) complex which is extractable into CHCl₃. The unreacted (free) bismuthiol II is also extracted into chloroform and it absorbs in the same region with its Te (IV) complex. Excess bismuthiol II in the organic phase was stripped into the aqueous phase by shaking with buffer solution of pH ≈ 8. However, this method suffers from serious interference of Hg²⁺, Se⁴⁺

Fe³⁺ and Sb³⁺. From the view of sustainable methods, the method is not recommended because of the use of chloroform.

3.2 Tellurium in plants, soil and geological samples

3.2.1 Tellurium in plants

Te concentrations in plants varied from < 0.013 to 0.35 mg kg⁻¹ and do not exceed 1 mg kg⁻¹ in contaminated systems (Moreno et al. 2007). For uncontaminated systems Te concentrations less than 0.001 mg kg⁻¹ have been reported by Fathirad et al. 2012. Some plants, such as tea, accumulate Te because Te displaces Se and inhibits biological activities (Nordberg et al. 2007). Therefore, simultaneous determination of both Te and Se in plants samples is a worthwhile task. Studies concerned with development of new methods for the determination of Te in plants are still limited. Zhang et al. 2011 have designed a new multi-channel hydride generation atomic fluorescence spectrometry (HG-AFS) for determination of As, Bi, Se, and Te in tea plants (Zhang et al. 2011). After sample pre-treatment using HNO₃ and H₂O₂ and under optimal conditions, the detection limits for As, Bi, Te and Se in tea leaves were 0.0152, 0.0080, 0.0022, 0.0068 µg g⁻¹, respectively.

3.2.2 Tellurium in soils

Limited data are available on the occurrence of tellurium in soils. As a representative example, Te content in some types in USA is in the range 0.02 and 0.69 mg kg⁻¹ (Govindaraju 1994). Trace and ultra trace levels of tellurium in soil make the direct determination of Te element a very difficult task. Chemical speciation of Te and Se was carried out simultaneously using chelating resin combined with cathodic stripping voltammetry (Ferri et al. 1998). The developed method was found suitable for the determination of Te in soil at µg kg⁻¹ with good precision. Pre-treatment by microwave digest in the acid mixture of HCl, HNO₃, and HF has been reported as an effective digestion approach for Te in soil (Hubert and Chao 1985). Determination of Au, In, Te, and Th in geological materials by flame atomic-absorption spectrophotometry has been reported by Hubert and Chao 1985. In this method, the sample was decomposed by a mixture of hydrofluoric acid, aqua regia, and hydrobromic acid-bromine solution. The analytes were separated and pre-concentrated by two steps—MIBK extraction at two concentrations of HBr. First, gold and thallium were extracted from HBr (0.1 mol L⁻¹) medium, while Te and In were separated by HBr (3.0 mol L⁻¹).

Total concentrations of tellurium in dried mine tailings and in downstream waters and sediments have been reported (Wray 1998, Moreno et al. 2007). Moreno et al. 2007 found that Te and other base metals are mainly associated with the particulate inhalable fraction of the dry tailings, while, elevated levels of these

trace elements have been reported in waters and sediments downstream from the same tailings deposits (Kyle et al. 2011). Harada and Takahashi 2009 studied the distribution and speciation of Te and Se between the solid and aqueous phases in synthetic soil. Under oxic conditions both elements are mainly associated with iron (III) hydroxides, and Te (IV) and (VI) species were both found to inner-sphere complexes. Under reducing conditions, tellurium (0) species was formed in batch studies. Tellurium distribution between soil and water was much lower than Se under a wide range of redox conditions, likely due to higher affinities of Te (IV) and (VI) for iron (III) hydroxides.

3.2.3 Geological samples

Donaldson and Leaver described a method for quantifying Te down to $\sim 0.01 \mu\text{g g}^{-1}$ in ores, rocks, soils and sediments (Donaldson and Leaver 1990). After sample decomposition and evaporation of the solution to incipient dryness, Te is separated from $> 300 \mu\text{g}$ of copper by co-precipitation with hydrous ferric oxide from an ammonia solution and the precipitate is dissolved in HCl (1.0 mol L^{-1}). Tellurium in the resultant solutions is reduced to Te (VI) by heating and separated from iron, lead and various other elements by a single cyclohexane extraction of its xanthate complex from HCl ($\sim 9.5 \text{ mol L}^{-1}$) in the presence of thiosemicarbazide as a complexing agent for copper. After washing with HCl (10.0 mol L^{-1}) hydrochloric acid followed by water is used to remove residual iron, chloride and soluble salts, tellurium is stripped from the extract with nitric acid (16.0 mol L^{-1}) and finally determined in a 2% v/v nitric acid medium, by graphite-furnace atomic-absorption spectrometry at 214.3 nm in the presence of nickel as a matrix modifier. Small amounts of gold and palladium, which are partly co-extracted as xanthates if the iron-collection step is omitted, do not interfere. The method is directly applicable, without the co-precipitation step, to most rocks, soils and sediments.

The influence of pre-treatment type on Te determination in some geological samples by GH-ICP-MS was critically investigated (Hall and Pelchat 1997). The study was based on the change of HCl concentration in the mixture of pre-treatment (aqua regia and HF-HClO₄-HNO₃-HCl).

Arsenic (III and V) were also examined as a potential interference and it was found that As (V) severely suppressed the Te signal in both the 2 and 4 mol L⁻¹ HCl experiments. As (III) did not interfere and Ge, Sn and Pb were not measured, because formation of their hydrides at the concentration of HCl used (2–4 mol L⁻¹) would be negligible. 4 mol L⁻¹ HCl was determined to be the preferred acid medium because of reduced interferences and a shorter wash-out time between samples (i.e., decreased memory effect).

Hydride generation combined with an integrated atom trap (HGIAT) atomizer for flame AAS was proposed for the determination of Te in reference material

(GBW 07302 Stream Sediment), coal fly ash and garlic (Matusiewicz and Krawczyk 2007). The results confirm that the present hyphenated technique using a continuous mode hydride generation gas phase *in situ* trapping on an integrated silica tube trap, followed by atomization in acetylene–air flame with simultaneous direct thermal heating of the collector (atomizer), can be used for the determination of trace amounts of Te in samples and reference material. Following the trapping stage, the performance of the device and related problems are quite similar to the case of hydride generation-electrothermal atomization (*in situ* trapping) HG-GF-AAS. The detection limit of this HG-IATFAAS system for Te is considerably improved compared with those reported for measurements of Te by any flame AAS approach. High-performance liquid chromatography (HPLC) coupled with inductively coupled plasma mass spectrometry (ICP-MS) was presented for speciation analysis of Te in a variety of samples involving soil (Lindemann et al. 2000). Tellurium was almost quantitatively extracted from samples using CH₃OH and H₂O, while, recoveries after extraction with water and sulfuric acid (0.01 mol L⁻¹) were below 20 percent.

3.3 Tellurium in food, biological samples and air

3.3.1 Tellurium in food

Tellurium (VI) is hydride inactive; therefore, this oxidation state must be quantitatively reduced to Te (IV). The reduction is performed mostly by HCl or HBr at various concentrations, temperatures and reaction times (Ulivo 1997). The main problem with the reduction procedures is the low selectivity, since an undetermined fraction of other inorganic and organic species may be converted into Te (IV) during the reduction step, causing an over-estimation of Te (VI). Thus, reduction of Te (VI) to Te (IV) has been carried out in a microwave oven for Te speciation in milk using hydride generation, atomic fluorescence (HG-AFS) (Ródenas-Torralba et al. 2005). Batch leaching of Te has been performed by sonication at room temperature for 10 min using aqua regia (Ródenas-Torralba et al. 2005). The extract was treated by NaBH₄ in HCl medium to form the corresponding hydrides and finally AFS measurements were processed in front of external calibrations prepared and measured in the same way as samples. The proposed method provided a high sampling frequency of 24 hr⁻¹ for the determination of both, free Te (IV) ions and total Te, in a same sample. Hydride generation atomic fluorescence spectrometry (HG-AFS) after the microwave-assisted sample digestion procedure established for tellurium determination in milk. The method provides sensitivity values of 1591 and 997 fluorescence unit's ng ml⁻¹ with detection limits of 0.015 ng ml⁻¹ for Te.

Application of the methodology to the analysis of cow milk samples in the Spanish market gave evidence of the presence of concentration ranges from 1.04

to 9.7 ng ml⁻¹ for Te having found a good comparability with data obtained after dry-ashing of samples (Cava-Montesinos 2003). Trace Te from some food samples typically consumed by the French population was determined during the second French Total Diet Study (TDS). Among the main trace element analyzed by inductively coupled plasma-mass spectrometry (ICP-MS) after microwave-assisted digestion. The contents were compared using data from worldwide total diet studies. Data for tin in canned food and beverages were compared with European guidelines. The food groups with the highest levels of Te were “Sweeteners, honey and confectionery” with dark chocolate, “Fish and fish products” and particularly “Shellfish” (Te (0.003 mg kg⁻¹) and “Fat and oil” (Milloura 2012).

3.3.2 Tellurium in biological samples

Aggarwal et al. 1994 have developed a method for the determination of Te in urine. The method has been based upon conversion of Te(IV) into volatile compounds using a Grignard reagent [4-fluorophenyl] magnesium bromide] in dry diethyl ether to give the final product [Te(FC₆H₄)₂]. After removing the excess of Grignard reagent, Te derivatives were extracted by toluene. The extract was evaporated to dryness and the residue was reconstituted in methylene chloride. The method was found suitable for GC-MS isotope dilution determination of Te in urine using ¹²⁰Te as an internal standard.

Hydride generation atomic absorption spectrometry with derivative signal processing (D-HG-AAS) has been proposed for Te determination in urine (Ha et al. 2001). The method offered limit of detection less than 0.2 µg L⁻¹, recovery of 98 percent and excellent sensitivity and selectivity for Te estimation in urine samples. Differential oscillopolarography has been used for speciation analysis of Te in biological samples, e.g., heart, liver, kidney, spleen and lung (Li et al. 2000). The method was based upon the activation effect of Te (IV) on the slow Pd (II)-catalyzed reaction between sodium hypophosphite and methyl red and the analyte was extracted from samples by liquid-liquid extraction using MIBK.

3.3.3 Tellurium in air samples

The concentration of Te in air ranges from 0.35 to 50 ng m⁻³ (Kobayashi 2004). Because of the low level of Te in various matrices, few methods were found suitable for Te detection in air. The most widely used technique for the determination of Te in air is hydride generation coupled with AAS or AFS. A highly sensitive and simple method, based on HG-AFS has been developed for the determination of Te (IV) in aqua regia extracts from atmospheric particulate matter samples (Moscoso-Pérez et al. 2004). Atmospheric particulates were collected on glass fiber filters using a medium volume sampler (PM10 particulate

matter). Two-level factorial designs have been used to optimize the hydride generation atomic fluorescence spectrometry (HG-AFS) procedure. The effects of several parameters affecting the hydride generation efficiency (hydrochloric acid, sodium tetrahydroborate and potassium iodide concentrations and flow rates) were evaluated using a Plackett–Burman experimental design. The parameters affecting the hydride measurement, e.g., delay, analysis and memory times were also investigated. The significant parameters on using sodium tetrahydroborate and sodium tetrahydroborate at selected flow rate for Te(IV)) were optimized by using 2^n + star central composite design. Using a univariate approach these parameters were optimized. The accuracy of methods were verified using several certified reference materials: SRM 1648 (urban particulate matter) and CRM 1649a (urban dust). Detection limits in the range of 6×10^{-3} to 0.2 ng m^{-3} was achieved. The developed methods were applied to several atmospheric particulate matter samples corresponding to A Coruña city (NW Spain).

4. Conclusion

Determination of different chemical forms of tellurium in different matrices (water, food, biological and air samples) is important because of their various toxicological effects. In analysis of tellurium in environmental samples, the techniques used should be sensitive and selective. The inherent advantages and disadvantages of each method can be used to select the most appropriate method based on the type of sample matrix to be analyzed and the tellurium species and concentration levels to be determined.

References

- Aggarwal, S.K., M. Kinter, J. Nicholson and D.A. Herold. 1994. Determination of tellurium in urine by isotope dilution gas chromatography/mass spectrometry using (4-fluorophenyl) magnesium bromide as a derivatizing agent and a comparison with electrothermal atomic absorption spectrometry. *Anal. Chem.* 66: 1316–1322.
- Asakura, T., Y. Shibutani, M.P. Reilly and R.H. DeMeio. 1984. Anti sticking effect of tellurite: apotent membrane acting agent *in vitro*. *Blood.* 64: 305–307.
- Braggall, K.W. 1966. *The Chemistry of Selenium, Tellurium, and Polonium*. Elsevier Publishing Co., London, UK.
- Cava-Montesinos, P., A. de la Guardia, C. Teutsch, M.L. Cervera and M. de la Guardia. 2004. Speciation of selenium and tellurium in milk by hydride generation atomic fluorescence spectrometry. *J. Anal. Atom. Spectrom.* 19: 696–699.
- Chai, Z.F. and H.M. Zhu. 1994. *Introduction to Trace Element Chemistry*, Atomic Energy Press. Peking, China.
- Cooper, W.C. 1971. *Tellurium*. Van Nostrand Reinhold Co., New York, USA.
- CRC Handbook of Chemistry and Physics*. 1975. CRC Press. Cleveland, OH, US.
- Cunha, R.L., I.E. Gouvea and L. Juliano. 2009. A glimpse on biological activities of tellurium compounds. *An Acad Bras Cienc.* 81: 393–407.

- De Meio, R.H. and F.C. Henriques. 1947. Tellurium IV, excretion and distribution in tissues studied with a radioactive isotope. *J. Biol. Chem* 169: 609–623.
- Donaldson, E.M. and M.E. Leaver. 1990. Determination of tellurium in ores, concentrates and related materials by graphite-furnace atomic-absorption spectrometry after separations by iron collection and xanthate extraction. *Talanta*. 37: 173–183.
- Ebdon, L., L. Pitts, R. Cornelis, H. Crews, O.F.X. Donard and P. Quevauviller. 2001. Trace Element Speciation for Environment, Food and Health, The Royal Society of Chemistry, Cambridge, UK.
- Emsley, J. 2002. *Nature's Building Blocks: An A-Z Guide to the Elements*; Oxford University Press, New York, USA.
- El-Hadri, F., A. Morales–Rubio and M. de la Guardia. 2005. Determination of tellurium by continuous hydride generation and atomic fluorescence spectrometry. *Ciencia*. 13(2): 218–227.
- Engman, L., N. Al-Maharik, M. McNaughton, A. Birmingham and G. Powis. 2002. Thioredoxin reductase and cancer cell growth inhibition by organotellurium antioxidants. *Anticancer Drugs*. 14: 153–161.
- Fathirad, F., D. Afzali, A. Mostafavi and M. Ghanbarian. 2012. Ultrasound-assisted emulsification solidified floating organic drops microextraction of ultra trace amount of Te (IV) prior to graphite furnace atomic absorption spectrometry determination. *Talanta*. 88: 759–764.
- Ferri, T., S. Rossi and P. Sangiorgio. 1998. Simultaneous determination of the speciation of selenium and tellurium in geological matrices by use of an iron(III)-modified chelating resin and cathodic stripping voltammetry. *Anal. Chim. Acta*. 361: 113–123.
- Fleming, A. 1932. On the specific antibacterial properties of penicillin and potassium tellurite. *J. Pathol. Bacteria*. 35: 831–842.
- Fleming, A. and M.Y. Young. 1940. The inhibitor action of Potassium tellurite on coliform bacteria. *J. Pathol. Bacteriol*. 51: 29–35.
- Ghasemi, E., N.M. Najafi, S. Seidi, F. Raofie and A. Ghassempour. 2009. Speciation and Determination of Trace Inorganic Tellurium in Environmental Samples by Electrodeposition-Electrothermal Atomic Absorption Spectroscopy. *J. Anal. At. Spectrom*. 24: 1446–1451.
- Ghasemi, E., N.M. Najafi, F. Raofie and A. Ghassempour. 2010. Simultaneous speciation and preconcentration of ultra traces of inorganic tellurium and selenium in environmental samples by hollow fiber liquid phase microextraction prior to electrothermal atomic absorption spectroscopy determination. *J. Hazard. Mater*. 181: 491–496.
- Govindaraju, K. 1994. Compilation of working values and sample description for 383 geostandards. *Geostand Newsletters*. (Special Issue) 18: 1–158.
- Ha, J., H.W. Sun, J.M. Sun, D.Q. Zhang and L.L. Yang. 2001. Determination of tellurium in urine by hydride generation atomic absorption spectrometry with derivative signal processing. *Anal. Chim. Acta*. 448: 145–149.
- Hall, G.E.M. and J.-C. Pelchat. 1997. Analysis of Geological Materials for Bismuth, Antimony, Selenium and Tellurium by Continuous Flow Hydride Generation Inductively Coupled Plasma Mass Spectrometry. *J. Anal. At. Spectrom*. 12: 97–102.
- Harada, T. and Y. Takahashi. 2009. Origin of the difference in the distribution behavior of tellurium and selenium in a soil–water system. *Geochim. Cosmochim. Acta*. 72: 1281–1294.
- Hollins, J.G. 1969. The metabolism of tellurium in rats. *Health Phys*. 17: 495–505.
- Huang, C. and B. Hu. 2008. Speciation of inorganic tellurium from seawater by ICP-MS following magnetic SPE separation and Preconcentration. *J. Sep. Sci*. 31: 760–767.
- Hubert, A.E. and T.T. Chao. 1985. Determination of gold, indium, tellurium and thallium in the same sample digest of geological materials by atomic-absorption spectroscopy and two-step solvent extraction. *Talanta*. 32: 568–570.
- Jacob, C., G.E. Arteel, T. Kanda, L. Engman and H. Sies. 2000. Water-soluble organotellurium compounds: catalytic protection against peroxy nitrite and release of zinc from metallothionein. *Chem. Res. Toxicol*. 13: 3–9.
- Jacobs, J.L. 1989. Immunologic developments in AIDS. *Year Immunol*. 4: 276–285.
- Jain, C.K. and I. Ali. 2000. Arsenic: occurrence, toxicity and speciation techniques. *Water Res*. 34: 4304–4312.

- Kabata-Pendias, A. 2011. 21 Elements of Group 16 (Previously Group VIA). *In: Trace Elements in Soils and Plants*. Taylor and Francis Group, LLC, CRC Press New York, USA. p. 381.
- Kobayashi, R. 2004. Tellurium. *In: E. Merian, M. Anke, M. Ihnat and M. Stoeppler [eds.]. Elements and their compounds in the environment*. 2nd edn. Wiley-VCH. Weinheim. pp. 1407–1414.
- Körez, A., A.E. Eroğlu, M. Volkan and O.Y. Ataman. 2000. Speciation and preconcentration of inorganic tellurium from waters using a mercapto silica microcolumn and determination by hydride generation atomic absorption spectrometry. *J. Anal. At. Spectrom.* 15: 1599–1605.
- Kyle, J.H., P.L. Breuer, K.G. Bunney and R. Pleysier. 2011. Review of trace toxic elements (Pb, Cd, Hg, As, Sb, Bi, Se, Te) and their deportment in gold processing: Part II: Deportment in gold ore processing by cyanidation. *Hydrometallurgy*. 111–112: 10–20.
- Li, L., P. He and Y. Fang. 2000. Catalytic determination of ultra trace amounts of tellurium by 2.5-order differential oscillopolarography. *Fresenius J. Anal. Chem.* 366: 239–243.
- Lindemann, T., A. Prange, W. Dannecker and B. Neidhart. 2000. Stability studies of arsenic, selenium, antimony and tellurium species in water, urine, fish and soil extracts using HPLC/ICP-MS. *Fresenius J. Anal. Chem.* 368: 214–220.
- Luo, L., Y. Tang, M. Xi, W. Li, Y. Lv and K. Xu. 2011. Hydride generation induced chemiluminescence for the determination of tellurium (IV). *Microchem. J.* 98: 51–55.
- Marahel, F., M. Ghaedi, M. Montazerzohori, M.N. Biyareh, S.N. Kokhdan and M. Soylak. 2011. Solid Phase Extraction and Determination of Trace Amount of Some Metal Ions on Duolite XAD 761 Modified with a New Schiff Base as Chelating Agent in Some Food Samples. *Food and Chemical Toxicology*. 49: 208–214.
- Matusiewicz, H. and M. Krawczyk. 2007. Determination of tellurium by hydride generation with in situ trapping flame atomic absorption spectrometry. *Spectrochim. Acta. Part B.* 62: 309–316.
- Milloura, S., L. Noël, R. Chekri, C. Vastel, A. Kadar, V. Sirot, J. Leblanc and T. Guérin. 2012. Strontium, silver, tin, iron, tellurium, gallium, germanium, barium and vanadium levels in foodstuffs from the Second French Total Diet Study. *J. Food Comp. Anal.* 25: 108–129.
- Moreno, O., A., I. MacDonald and W. Gibbons. 2007. Preferential fractionation of trace metals–metalloids into PM10 resuspended from contaminated gold mine tailings at Rodalquilar, Spain. *Water, Air, and Soil Pollution*. 179: 93–105.
- Moscoco-Pérez, C., J. Moreda-Piñeiro, P. López-Mahía, S. Muniategui-Lorenzo, E. Fernández-Fernández and D. Prada-Rodríguez. 2004. Hydride generation atomic fluorescence spectrometric determination of As, Bi, Sb, Se(IV) and Te(IV) in aqua regia extracts from atmospheric particulate matter using multivariate optimization. *Anal. Chim. Acta.* 526: 185–192.
- Najafi, N.M., H. Tavakoli, R. Alizadeh and S. Seidi. 2010. Speciation and determination of ultratrace amounts of inorganic tellurium in environmental water samples by dispersive liquid–liquid microextraction and electrothermal atomic absorption spectrometry. *Anal. Chim. Acta.* 670: 18–23.
- Nordberg, G., B. Fowler, M. Nordberg and L. Friberg. 2007. *Handbook on the Toxicology of Metals*. 3rd edn. Elsevier.
- Pedro, J., J. Stripekis, A. Bonivardi and M. Tudino. 2008. Determination of tellurium at ultratrace levels in drinking water by on-line solid phase extraction coupled to graphite furnace atomic absorption spectrometer. *Spectrochim. Acta Part B: Atomic Spectroscopy*. 63: 86–91.
- Prasad, P.R., J.D. Kumar, B.K. Priya, P. Subrahmanyam, S. Ramanaiah and P. Chiranjeevi. 2007. Determination of tellurium(IV) in various environmental samples with spectrophotometry. *E-J. Chem.* 4: 354–362.
- Reimann, C. and P. de Caritat. 1998. *Chemical elements in the environment*. Springer-Verlag, Berlin Heidelberg.
- Ródenas-Torralba, E., A. Morales-Rubio and M. de la Guardia. 2005. Multicommutation hydride generation atomic fluorescence determination of inorganic tellurium species in milk. *Food Chem.* 91: 181–189.
- Sadeh, T. 1987. *In: S. Patai [ed.]. The Chemistry of Organic Selenium and Tellurium Compounds*. Wiley. Chichester. pp. 367–376.

- Stewart, D.A., P.M. Tyroler and S. Stupavsky. 1985. The Removal of selenium and tellurium from copper electrolyte at INCO's copper refinery electrowinning department. *In*: A.J. Oliver [ed.]. 15th Annual Hydrometallurgical Meeting. Vancouver, Canada. CIM Metallurgical Society. Paper No. 18.
- Summers, A.O. and G.A. Jacoby. 1977. Plasmid mediated resistance to tellurium compounds. *J. Bacteriol.* 129: 276–281.
- Taylor, A. 1996. Biochemistry of tellurium. *Biol. Trace Elem Res.* 55: 231–239.
- Templeton, D.M., F. Ariese, R. Cornelis, L.G. Danielsson, M. Muntau, H.P. van Leenwen and R. Lobinski. 2000. *Guidelines for terms related to chemical speciation and fractionation of elements. Definitions, structural aspects, and methodological approaches.* *Pure Appl. Chem.* 72: 1453–1470.
- Toshida, H., M. Taga and S. Hikime. 1966. Spectrophotometric determination of small amounts of tellurium with bismuthiol II. *Talanta.* 13: 185–191.
- Tsai, S.J. and C.C. Jan. 1993. Determination of trace amounts of thallium and tellurium in nickelbase alloys by electrothermal-atomic absorption spectroscopy. *Analyst.* 118: 1183–1191. U.S. Geological Survey. 2011. Mineral Commodity Summaries.
- Ulivo, A.D. 1997. Determination of Selenium and Tellurium in Environmental Samples. *Analyst.* 122: 117R–144R.
- Urbánková, K., M. Moos, J. Machát and L. Sommer. 2011. Simultaneous determination of inorganic arsenic, antimony, selenium and tellurium by ICP-MS in environmental waters using SPE preconcentration on modified silica. *Int. J. Environ. Anal. Chem.* 91: 1077–1087.
- Viñas, P., G.I. López-García, B. Merino-Meroño and M. Hernández-Córdoba. 2005. Ion chromatography-hydride generation-atomic fluorescence spectrometry speciation of tellurium. *Appl. Organometal. Chem.* 19: 930–934.
- Wray, D.S. 1998. The impact of unconfined mine tailings and anthropogenic pollution on a semi-arid environment—an initial study of the Rodalquilar mining district, south east Spain. *Environ. Geochem. Health.* 20: 29–38.
- Xi, M., R. Liu, P. Wu, K. Xu, X. Hou and Y. Lv. 2010. Atomic absorption spectrometric determination of trace tellurium after hydride trapping on platinum-coated tungsten coil. *Microchem. J.* 95: 320–325.
- Yarema, M.C. and S.C. Curry. 2005. Acute tellurium toxicity from ingestion of metal-oxidizing solutions. *Pediatrics.* 116: 319–321.
- Yosef, S., M. Brodsky, B. Sredni, A. Albeck and M. Albeck. 2007. Octa-O-bis-(R,R)-tartarate ditellurane (SAS)—a novel bioactive organotellurium(IV) compound: synthesis, characterization, and protease inhibitory activity. *Chem. Med. Chem.* 767: 1601–6. 768.
- Yu, C.H., Q.T. Cai, Z.X. Guo, Z.G. Yang and S.B. Khoo. 2003. Speciation analysis of tellurium by solid-phase extraction in the presence of ammonium pyrrolidine dithiocarbamate and inductively coupled plasma mass spectrometry. *Anal. Bioanal. Chem.* 376: 236–242.
- Zhang, N., N. Fu, Z. Fang, Y. Feng and L. Ke. 2011. Simultaneous multi-channel hydride generation atomic fluorescence spectrometry determination of arsenic, bismuth, tellurium and selenium in tea leaves. *Food Chem.* 124: 1185–1188.

POLYURETHANE

Edited by Fahmina Zafar and Eram Sharmin



Materials Science » Polymers

“Polyurethane”

Edited by Fahmina Zafar and Eram Sharmin, ISBN 978-953-51-0726-2, 480 pages,

The enchanting and worthy world of PU beckoned to bring forth the book titled "Polyurethane". The book is divided into three sections: structures, properties and characterization of PU, applications of PU and a separate section on Biobased PU, covering the research and development in these areas. Each contributed chapter handles new and interesting topics introducing the reader to the wider known and unknown applications of PU such as PU for grouting technologies, fuel binder, extraction of metals, treatment of industry wastewater, alkanolamide PU coatings and foams, and others. The book aims to cater a larger audience comprising of readers from polymer chemistry, materials chemistry, and industrial chemistry.

- Chapter 1 **Polyurethane: An Introduction** by Eram Sharmin and Fahmina Zafar
- Chapter 2 **New Liquid Crystalline Polyurethane Elastomers Containing Thiazolo [5,4d] Thiazole Moiety: Synthesis and Properties** by Mohammed Ahmed Issam and Hamidi Mohamed Rashidah
- Chapter 3 **The Modification of Polyurethanes by Highly Ordered Coordination Compounds of Transition Metals** by Ruslan Davletbaev, Ilsiya Davletbaeva and Olesya Gumerova
- Chapter 4 **Bottom-Up Nanostructured Segmented Polyurethanes with Immobilized in situ Transition and Rare-Earth Metal Chelate Compounds - Polymer Topology - Structure and Properties Relationship** by Nataly Kozak and Eugenia Lobko
- Chapter 5 **Thermal Analysis of Polyurethane Dispersions Based on Different Polyols** by Suzana M. Cakić, Ivan S. Ristić and Olivera Z. Ristić
- Chapter 6 **Polyurethane Flexible Foam Fire Behavior** by Ahmadreza Gharehbagh and Zahed Ahmadi
- Chapter 7 **Polyurethane in Urological Practice** by Valentina Cauda and Furio Cauda
- Chapter 8 **Polyurethane as Carriers of Antituberculosis Drugs** by Yerkesht Batyrbekov and Rinat Iskakov
- Chapter 9 **Use of Polyurethane Foam in Orthopaedic Biomechanical Experimentation and Simulation** by V. Shim, J. Boheme, C. Josten and I. Anderson
- Chapter 10 **Biocompatibility and Biological Performance of the Improved Polyurethane Membranes for Medical Applications** by Maria Butnaru, Ovidiu Bredetean, Doina Macocinschi, Cristina Daniela Dimitriu, Laura Knieling and Valeria Harabagiu
- Chapter 11 **HTPB-Polyurethane: A Versatile Fuel Binder for Composite Solid Propellant** by Abhay K. Mahanta and Devendra D. Pathak
- Chapter 12 **Synthesis of a New Sorbent Based on Grafted PUF for the Application in the Solid Phase Extraction of Cadmium and Lead** by Rafael Vasconcelos Oliveira and Valfredo Azevedo Lemos

- Chapter 13 **Fast, Selective Removal and Determination of Total Bismuth (III) and (V) in Water by Procaine Hydrochloride Immobilized Polyurethane Foam Packed Column Prior to Inductively Coupled Plasma - Optical Emission Spectrometry** by M.S. El-Shahawi, A.A. Al-Sibaai, H.M. Al-Saidi and E.A. Assirey
- Chapter 14 **Polyurethane Grouting Technologies** by Jan Bodi, Zoltan Bodi, Jiri Scucka and Petr Martinec
- Chapter 15 **On the Use of Polyurethane Foam Paddings to Improve Passive Safety in Crashworthiness Applications** by Mariana Paulino and Filipe Teixeira-Dias
- Chapter 16 **Polyurethane Trickling Filter in Combination with Anaerobic Hybrid Reactor for Treatment of Tomato Industry Wastewater** by Ahmed Tawfik
- Chapter 17 **Polyurethane as an Isolation for Covered Conductors** by Žiga Voršič
- Chapter 18 **Seed Oil Based Polyurethanes: An Insight** by Eram Sharmin, Fahmina Zafar and Sharif Ahmad
- Chapter 19 **Polyglucanurethanes: Cross-Linked Polyurethanes Based on Microbial Exopolysaccharide Xanthan** by Nataly Kozak and Anastasyia Hubina
- Chapter 20 **Biobased Polyurethane from Palm Kernel Oil-Based Polyol** by Khairiah Haji Badri

Fast, Selective Removal and Determination of Total Bismuth (III) and (V) in Water by Procaine Hydrochloride Immobilized Polyurethane Foam Packed Column Prior to Inductively Coupled Plasma – Optical Emission Spectrometry

M.S. El-Shahawi, A.A. Al-Sibaai, H.M. Al-Saidi and E.A. Assirey

Additional information is available at the end of the chapter

<http://dx.doi.org/10.5772/47962>

1. Introduction

Bismuth is found in nature in trivalent state as bismuthinite, Bi_2S_3 , bismite, Bi_2O_3 and bismuth sulfide-telluric, $\text{Bi}_2\text{Te}_2\text{S}$. It is also found as a secondary component in some lead, copper and tin minerals [1]. Bismuth (V) compounds do not exist in solution and are important in the view of pharmaceutical analytical chemistry [1]. In the Earth's crust, bismuth presents at trace concentration ($8 \mu\text{g Kg}^{-1}$) while, bismuth minerals rarely occur alone and are almost associated with other ores [2]. Bismuth appears to be environmentally significant because its physical and chemical properties have led it to be used in different areas of life. Pamphlett et al, 2000 [3] have reported that, bismuth compounds after oral intake enter the nervous system of mice, in particular, in motor neurons [3]. Hence, bismuth species are included in the list of potential toxins [3].

The development of selective, separation, pre-concentration and determination method for bismuth at sub-micro levels is a challenging problem because of its extremely low concentrations in natural samples and of its strong interference from the sample matrices. Several methods e.g. hydride generation atomic absorption spectrometry [4], electro thermal atomic absorption spectrometry [5], atomic fluorescence spectrometry [6], hydride generation atomic absorption spectrometry [7], and cathodic and anodic adsorptive stripping voltammetry [8 - 10] have been reported for bismuth determination. Most of these methods require preconcentration of bismuth for precise determination because most analytical techniques do not possess adequate sensitivity for direct determination.

Solvent extraction in the presence of co-extractant ligands e.g. bis (2, 4, 4-trimethyl pentyl) mono thiophosphinic acid [11], pyrrolidine dithiocarbamate [12] etc has received considerable attention. However, these methods are too expensive, suffer from the use of large volumes of toxic organic solvents, and time-consuming. Thus, recent years have seen considerable attention on preconcentration and/ or monitoring of trace and ultra trace concentrations of bismuth by low cost procedures in a variety of samples e.g. fresh, marine and industrial wastewater [13]. Solid phase extraction (SPE) techniques have provided excellent alternative approach to liquid – liquid extraction for bismuth preconcentration prior to analyte determination step [14 -18].

Polyurethane foams (PUFs) sorbent represent an excellent solid sorbent material due to their high available surface area, cellular and membrane structure and extremely low cost [19]. Thus, several liquid solid separation involving PUFs methods have been employed successfully for separation and sensitive determination of trace and ultra trace levels of metal ions including bismuth (III) [19-29]. The membrane like structure and the available surface area of the PUFs make it a suitable stationary phase and a column filling material [25, 27]. Thus, the main objectives of the present chapter are focused on: i. developing of a low cost method for the removal of bismuth(III) and (V) species after reduction of the latter to tri valence state employing PUFs impregnated $PQ^+.Cl^-$; ii. Studying the kinetics, and thermodynamic characteristics of bismuth (III) sorption by trioctylamine plasticized $PQ^+.Cl^-$ treated PUFs and finally iii. Application of the developed method in packed column for complete removal and / or determination of bismuth (III &V) species in wastewater by $PQ^+.Cl^-$ treated PUFs sorbent.

2. Experimental

2.1. Reagents and materials

All chemicals used were of A.R. grade and were used without further purification. Stock solution ($1000 \mu\text{g mL}^{-1}$) of bismuth (III) was prepared from bismuth (III) nitrate (Aldrich Chemical Co Ltd, Milwaukee, WC, USA). More diluted solutions of bismuth (III) ($0.1 - 100 \mu\text{g mL}^{-1}$) were prepared by diluting the stock solution with diluted nitric acid. Stock solutions of procaine [2-(diethylamino)ethyl 4 aminobenzoate] hydrochloride, $PQ^+.Cl^-$ (1.0 %w/v), Fig.1 and KI (10%w/v) were prepared by dissolving the required weight in water (100 mL). A stock solution (1%v/v) of trioctylamine (Aldrich) was prepared in water in the presence of few drops of concentrated HNO_3 . Sodium bismuthate

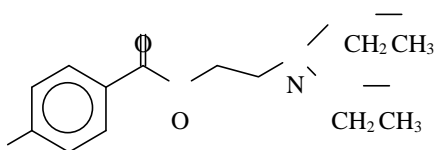




Figure 1. Chemical structure of procaine hydrochloride.

(NaBiO_3 , 85% purity) (BDH, Poole, England) was used for preparation of stock solution ($50 \mu\text{g mL}^{-1}$) of bismuth (V) in dark bottle [30] as follows: an accurate weight of NaBiO_3 was heated in a suitable volume of HClO_4 (20 mL, 0.5 mol L^{-1}) filtered and the solution was made up to 250 mL with deionized water and finally analyzed under the recommended conditions of bismuth determination by ICP-OES (Table 1). The measured concentration was taken as a standard stock solution of bismuth (V) in the next work. Bismuth (V) solution was finally stored in low density polyethylene bottles (LDPE) in dark. Stock solutions (0.1-1% w/v) of $\text{PQ}^+\cdot\text{Cl}^-$ (BDH) and trioctylamine (Merck, Darmstadt, Germany) abbreviated as TOA were prepared in deionized water containing few drops of concentrated HNO_3 . Sodium diethyldithiocarbamate (Na-DDTC) and $\text{PQ}^+\cdot\text{Cl}^-$ (1% w/v) were purchased from Fluka, AG (Buchs, Switzerland). Commercial white sheets of PUFs were cut as cubes (10 -15 mm), washed, treated and dried. The reagent $\text{PQ}^+\cdot\text{Cl}^-$ (1.0 % w/v) was dissolved in water, shaken with the PUFs cubes in the presence of TOA (1% v/v) with efficient stirring for 30 min, squeezed and finally dried as reported [21]. The certified reference material (CRM) i.e. trace metal in drinking water standard (CRM-TMDW) was obtained from High-Purity Standard Inc. Sulfuric acid (0.5 mol L^{-1}) was used as an extraction medium in the sorption process of bismuth (III) by the PUFs. Commercial white sheets of open cell polyether type polyurethane foam were purchased from the local market of Jeddah City, Saudi Arabia and were cut as cubes (10-15 mm). The PUFs cubes were washed and dried as reported [21, 27]. A series of Britton- Robinson (B-R) buffer (pH 2-11) was prepared as reported [31].

Parameter	
Rf power (kW)	1050 (900.0)
Plasma gas (Ar) flow rate, L min^{-1}	15 (15)
Auxiliary gas (Ar) flow rate, L min^{-1}	0.2 (1.2)
Nebulizer gas (Ar) flow rate, L min^{-1}	0.80 (0.93)
Pump rate, mL min^{-1}	1.5
Observation height, mm	15
Integration time, s	10
Wavelength, nm	Bi 223.061
*ICP-MS operational parameters are given in parentheses. Other parameters are: lens voltage =9.0; analog stage voltage 1750 V; pulse stage voltage =750 V; quadrupole rod offset std = =0.0; cell rod offset =-18.0; discriminator threshold =17.0; cell path voltage Std = -13.0 V and atomic mass 208.98 am.	

Table 1. ICP-OES operational conditions and wavelength (nm) for bismuth determination*

2.2. Instrumental and apparatus

A Perkin - Elmer (Lambda 25, Shelton, CT,USA) spectrophotometer (190 - 1100 nm) with 10 mm (path width) quartz cell was used for recording the electronic spectra and measuring the absorbance of the ternary complex ion associate $\text{PQ}^+\cdot\text{BiI}_4^-$ of bismuth (III) at 420 nm before and after extraction with the reagent $\text{PQ}^+\cdot\text{Cl}^-$ treated PUFs. A

Perkin Elmer inductively coupled plasma – optical emission spectrometer (ICP- OES, Optima 4100 DC (Shelton, CT, USA) was used and operated at the optimum operational parameters for bismuth determination (Table 1). A Perkin Elmer inductively coupled plasma – mass spectrometer (ICP – MS) Sciex model Elan DRC II (California, CT, USA) was also used to measure the ultra trace concentrations of bismuth in the effluent after extraction by the developed PUFs packed column at the operational conditions (Table 1). A Corporation Precision Scientific mechanical shaker (Chicago, CH, USA) with a shaking rate in the range 10 – 250 rpm and glass columns (18 cm x 15 mm i.d) were used in batch and flow experiments, respectively. De-ionized water was obtained from Milli-Q Plus system (Millipore, Bedford, MA, USA). A thermo Orion model 720 pH Meter (Thermo Fisher Scientific, MA, USA) was employed for pH measurements with absolute accuracy limits being defined by NIST buffers.

2.3. General batch procedures

2.3.1. Preparation of the immobilized reagent ($PQ^+.Cl^-$) polyurethane foams.

The reagent $PQ^+.Cl^-$ (1% w/v) in water was shaken with the PUFs cubes in the presence of the plasticizer TOA (1% v/v) with efficient stirring for 30 min. The loaded $PQ^+.Cl^-$ PUFs cubes were squeezed and dried between two filter papers [20, 21]. The amount of $PQ^+.Cl^-$ retained onto the PUFs sorbent was calculated using the equation [21]:

$$\bar{a} = \frac{(C_0 - C) \cdot v}{w} \quad (1)$$

where, C_0 and C are the initial and final concentrations (mol L^{-1}) of the reagent ($PQ^+.Cl^-$) in solution, respectively, v = volume of the reagent solution (liter) and w is the mass (g) of the PUFs sorbent. The reproducibility of $PQ^+.Cl^-$ treated PUFs is fine and the PUFs can be reused many times without decrease in its efficiency.

2.3.2. Batch extraction step

An accurate weight (0.1 ± 0.002 g) of unloaded- or $PQ^+.Cl^-$ immobilized PUFs was equilibrated with an aqueous solution (100 mL) containing bismuth ($10 \mu\text{g mL}^{-1}$) in the presence of KI (10% w/v), H_2SO_4 (0.5 mol L^{-1}) and ascorbic acid (0.1% w/v) to minimize the aerial oxidation of KI. The test solution was shaken for 1 h on a mechanical shaker. The aqueous phase was then separated out by decantation and the amount of bismuth (III) remained in the aqueous phase was then determined spectrophotometrically against reagent blank [32] or by ICP-OES at ultra trace concentrations. The amount of bismuth (III) retained on the foam cubes was then calculated from the difference between the absorbance of $[\text{BiI}_4]$ in the aqueous phase before (A_b) and after extraction (A_i). The sorption percentage (%E), the distribution ratio (D), the amount of bismuth (III) retained at equilibrium (q_e) per unit mass of solid sorbent (mol/g) and the distribution coefficient (K_d) of sorbed analyte onto the foam cubes were finally calculated as reported. The %E and K_d are the average of three independent measurements and the precision in most cases was $\pm 2\%$. Following these procedures, the influence of shaking time and temperature on the retention of bismuth (III) by the PUFs sorbents was fully studied.

2.3.3. Retention and recovery of bismuth (III)

An aqueous solution (100 mL) of bismuth (III) ions at concentration ($5 - 100 \mu\text{g L}^{-1}$), KI (10%) and H_2SO_4 (1.0 mol L^{-1}) was percolated through the $\text{PQ}^+\cdot\text{Cl}^-$ loaded PUFs ($1.0 \pm 0.002 \text{ g}$) column at 2.0 mL min^{-1} flow rate. A blank experiment was also performed in the absence of bismuth (III) ions. Bismuth (III) sorption took place quantitatively as indicated from the analysis of bismuth species in effluent solutions by ICP- OES. After extraction, the ultra trace concentrations of bismuth (III) remained in the test aqueous solutions were estimated by ICP-MS. Bismuth (III) species were recovered quantitatively with HNO_3 (3.0 mol L^{-1} , 10 mL) at 2.0 mL min^{-1} flow rate.

2.3.4. Retention and recovery of bismuth (V)

An aqueous solution (100.0 mL) of bismuth (V) at concentration $< 10 \mu\text{g L}^{-1}$ was allowed to react with an excess of KI (10% w/v) - H_2SO_4 (1.0 mol L^{-1}). The solution was then percolated through $\text{PQ}^+\cdot\text{Cl}^-$ loaded PUFs ($1.0 \pm 0.002 \text{ g}$) packed column at 2.0 mL min^{-1} flow rate of 2.0 mL min^{-1} . The retained bismuth (III) species were recovered with HNO_3 (10.0 mL, 1.0 mol L^{-1}) at 2.0 mL min^{-1} flow rate and analyzed by ICP- OES.

2.3.5. Sequential determination of total bismuth (III) and (V)

An aqueous solution (100 mL) containing bismuth (III) and (V) at a total concentration $\leq 10 \mu\text{g L}^{-1}$ was analyzed according to the described procedure for bismuth (V) retention and recovery. Another aliquot portion (100 mL) was adjusted to pH 3 - 4 with acetate buffer and then shaken with Na-DDTC (5.0 mL, 1%w/v) for 2-3 min. Bismuth (III) ions were then extracted with methylisobutylketone (5.0 mL) as $\text{Bi}(\text{DDTC})_3$ after 2 min [24]. Bismuth (V) remained in the aqueous solution was reduced to bismuth (III) by an excess of KI (10% w/v) in the presence of H_2SO_4 (0.5 mol L^{-1}) and then percolated through the $\text{PQ}^+\cdot\text{Cl}^-$ loaded PUFs column at 2 mL min^{-1} flow rate at the optimum experimental conditions. The retained bismuth species were recovered and finally analyzed following the recommended procedures for bismuth (III). Thus, the net signal intensity of ICP- OES (or ICP-MS) at ultra trace concentrations of the first aliquot (I_1) will be a measure of the sum of the bismuth (III) and (V) ions in the mixture, while the net signal intensity of the of the second aliquot (I_2) is a measure of bismuth (V) ions. The difference ($I_1 - I_2$) of the net signal intensity is a measure of bismuth (III) ions in the binary mixture.

2.4. Analytical applications

2.4.1. Analysis of certified reference material TMDW

The TMDW water sample (2 mL) was digested with nitric acid (10 mL, 3.0 mol L^{-1}) and hydrogen peroxide (10 mL, 10% v/v), boiled for 5 min and diluted by an excess of KI (10% w/v) - H_2SO_4 (1.0 mol L^{-1}) to 100 mL. After cooling, the test solution was percolated through the $\text{PQ}^+\cdot\text{Cl}^-$ loaded PUFs column at 2 mL min^{-1} flow rate. The retained bismuth species were recovered with HNO_3 (10.0 mL, 1.0 mol L^{-1}) at 2.0 mL min^{-1} flow rate and analyzed by ICP- OES following the recommended procedures for bismuth (III).

2.4.2. Analysis of total bismuth in wastewater

Wastewater samples (1.0 L) were collected and filtered through a 0.45 μm membrane filter (Millex, Millipore Corporation). The test solution was digested with nitric acid (10 mL, 3.0 mol L^{-1}) and hydrogen peroxide (10 mL, 10% v/v), boiled for 5 min and spiked with different amounts (0.05- 0.5 μg) of bismuth (III) in presence of an excess of KI (10% w/v). After centrifugation for 5 min, the sample solutions were percolated through $\text{PQ}^+\cdot\text{Cl}^-$ loaded PUFs packed columns at 5 mL min^{-1} flow rate. The concentration of bismuth in the effluent solution was determined by ICP - MS. The retained bismuth (III) species on the PUFs were then recovered and analyzed as described above.

2.4.3. Analysis of total bismuth in seawater

The general procedure for the extraction and recovery of bismuth (III) ions from seawater samples onto $\text{PQ}^+\cdot\text{Cl}^-$ impregnated PUFs was performed as follow: A 100 mL of water samples were filtered through 0.45 μm membrane filter, adjusted to pH zero with H_2SO_4 (0.5 mol L^{-1}) in the presence of KI (0.1%w/v) and ascorbic acid. The sample solution was then passed through $\text{PQ}^+\cdot\text{Cl}^-$ impregnated PUFs (1.0 \pm 0.001 g) packed column (10 cm x 1.0 cm i.d.) at 5 mL min^{-1} . The retained bismuth(III) species were then recovered and analyzed as described above. The recovered bismuth (III) ions were then determined by ICP-OES.

3. Results and discussion

In recent years [28, 29], PUFs immobilizing some ion pairing reagents have received considerable attention for selective separation, determination and / or chemical speciation of trace and ultra trace metal ions. The non-selective sorption characteristic of the PUFs has been rendered and became more selective by controlling the experimental conditions e.g. pH, ionic strength, etc. Preliminary investigation has shown that, on shaking unloaded PUFs and $\text{PQ}^+\cdot\text{Cl}^-$ immobilized PUFs with aqueous solutions containing bismuth (III) ions, KI (10%w/v) and H_2SO_4 (0.5 mol L^{-1}), considerable amount of bismuth (III) species were retained onto $\text{PQ}^+\cdot\text{Cl}^-$ treated PUFs in a very short time compared to the untreated PUFs ones. Thus, in subsequent work, detailed study on the application of $\text{PQ}^+\cdot\text{Cl}^-$ immobilized PUFs for retention of various bismuth (III & V) species to assign the most probable kinetic model, sorption isotherm models, mechanism and thermodynamic characteristics of retention of bismuth (III) from the test aqueous solutions.

3.1. Retention profile of bismuth (III) from the aqueous solution onto PUFs

Bismuth (III) forms an orange – yellow colored tetraiodobismuthate(III) complex, $[\text{BiI}_4]^-$ [32] in aqueous solutions containing sulfuric acid (0.5 mole L^{-1}) and an excess of KI (10%w/v). Thus, the sorption profile of aqueous solutions containing bismuth (III) at different pH by $\text{PQ}^+\cdot\text{Cl}^-$ loaded foams was critically studied after shaking for 1h at room temperature. After equilibrium, the amount of bismuth (III) in the aqueous phase was determined spectrophotometrically [32]. The results are shown in Fig. 2. The %E and K_d of bismuth (III) sorption onto the PUFs markedly decreased on increasing solution pH and maximum uptake was achieved at pH zero. At pH >1, the sorption of bismuth (III) by $\text{PQ}^+\cdot\text{Cl}^-$ treated PUFs towards bismuth (III) decreased markedly (Fig.2). This behavior is most likely attributed to

the deprotonation of the ether oxygen (-CH₂ - O- CH₂ -) and/or urethane nitrogen (- NH-CO-) of PUFs, instability, hydrolysis, or incomplete extraction of the produced ternary complex ion associate of PQ⁺·[BiI₄]⁻ on/ in the PUFs sorbent.

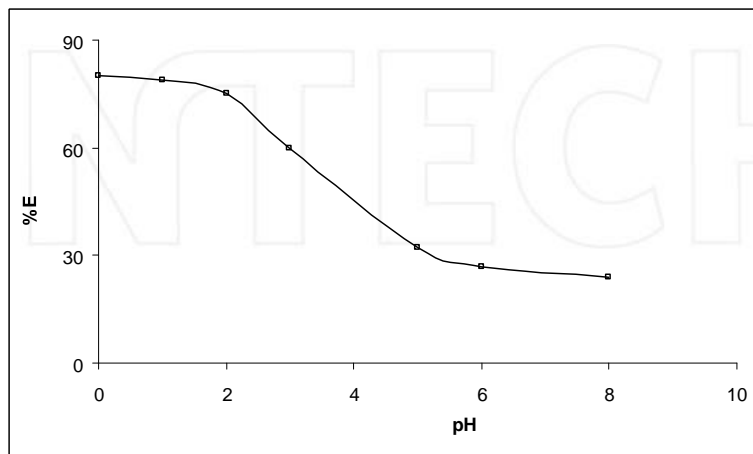


Figure 2. Effect of pH on the sorption percentage of bismuth (III) from aqueous solutions containing KI (10 % m/v) - H₂SO₄ (2.0 mol L⁻¹) onto PQ⁺·Cl⁻ immobilized PUFs (0.1 ± 0.002 g) at 25 ± 0.1°C.

The retention of bismuth (III) at low pH of aqueous media is most likely attributed to sorbent membranes. The pK_a values of protonation of oxygen atom of ether group (- CH₂ OH⁺- CH₂-)_{foam} and nitrogen atom of the amide group (- N⁺H₂ - COO-)_{foam} are - 3 and 6, respectively [32]. Thus, in extraction media containing H₂SO₄ (0.50 mole L⁻¹) and KI, the complexed species of bismuth [BiI₄]⁻ are easily retained onto the protonated ether group of the PUFs than amide group of PUFs sorbent. The stability constants of the binding sites of the PUFs with [BiI₄]⁻ were calculated using the Scatchard equation [33]:

$$\frac{n}{[Bi]} = K(i - n)$$

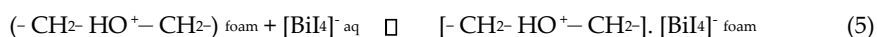
and n is given by the equation:

$$n = \frac{\text{weight of bismuth bound to foam (g)}}{\text{weight of foam (g)}} \quad (3)$$

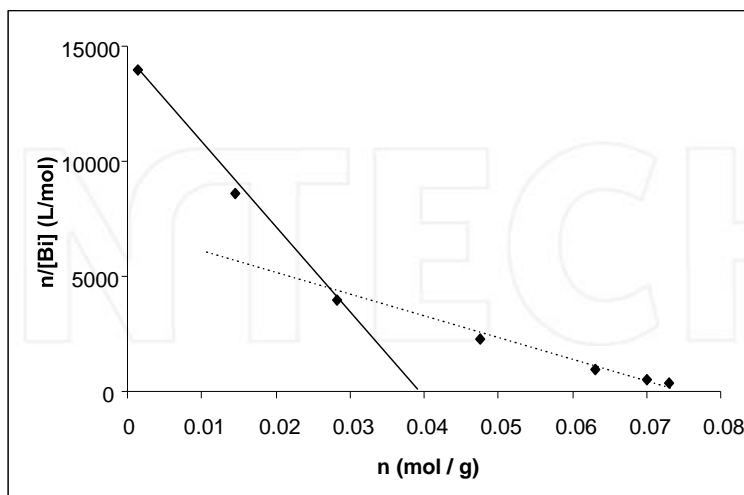
where, K = stability constant of bismuth (III) on PUF, n_i = maximum concentration of sorbed bismuth (III) by the available sites onto the PUFs, and $[Bi]$ is the equilibrium concentration of bismuth (III) in solution (mol L^{-1}). The plot of $n/[Bi]$ versus n is shown in Fig. 3. The curvature of the Scatchard plot demonstrated that more than one class of complex species of bismuth (III) has been formed and each complex has its own unique formation constant. The stability constants $\log K_1$ and $\log K_2$ for the sorbed species derived from the respective slopes were 5.56 ± 0.2 and 4.82 ± 0.5 , respectively. The values of n_1 and n_2 calculated from the plot were found equal 0.038 ± 0.005 and $0.078 \pm 0.01 \text{ mol g}^{-1}$, respectively. The values of the stability constants ($\log K_1$ and $\log K_2$) indicated that, the sorption of bismuth (III) species took place readily on site K_1 that most likely belong to the ether group. The fact that, ether group has a stability greater than the amide group (site K_2) as reported [32]. Moreover, the high values of K_1 and K_2 indicated that, both bonding sites of PUFs are highly active

towards $[\text{BiI}_4]^-$ species in good agreement with the data reported involving the extraction of the bulky anion $[\text{BiI}_4]^-$ by methyl isobutyl ketone and other solvents that possess ether linkages in their structures e.g. diethyl ether and isopropyl ether [34]. Based on these data and the results reported on the retention of AuCl_4^- and CdI_4^- by PUFs [29, 34], a sorption mechanism involving a weak base anion ion exchanger and/ solvent extraction of $[\text{BiI}_4]^-$ by the protonated ether oxygen or urethane nitrogen linkages of the PUFs as a ternary complex

Ether group, PUF:



Urethane group, PUF:



ion associate is most likely proceeded as follows:

Figure 3. Scatchard plot for the binding of $[\text{BiI}_4]^-$ species by $\text{PQ}^+ \cdot \text{Cl}^-$ immobilized PUF ($0.1 \pm 0.002 \text{ g}$) from aqueous media containing KI (10 % m/v) - H_2SO_4 (0.5 mol L^{-1}) at $25 \pm 0.1^\circ\text{C}$.

The distribution ratio of bismuth (III) onto $\text{PQ}^+ \cdot \text{Cl}^-$ immobilized PUFs showed high retention ($D = 6.17 \times 10^4 \text{ mL g}^{-1}$) compared to the unloaded PUFs ($3.05 \times 10^3 \text{ mL g}^{-1}$) due to the formation of the ion associate ($[(\text{PQ}^+) \cdot (\text{BiI}_4)]^-$) on/in treated PUFs. Thus, the solution pH was adjusted at pH 0.0 – 1.0 and $\text{PQ}^+ \cdot \text{Cl}^-$ treated PUFs was used as a proper sorbent in the subsequent work.

The influence of the plasticizer e.g. tri-n-octylamine (TOA, 0.5 -2.0 %v/v) and tri-n-butylphosphate (TBP, 0.01%v/v) on the retention of bismuth (III) from the aqueous solutions onto the $\text{PQ}^+ \cdot \text{Cl}^-$ loaded PUFs was studied. Bismuth (III) sorption onto the PUFs sorbent increased ($D = 6.6 \times 10^4 \text{ mL g}^{-1}$) in presence of TOA (1% v/v). The formation of the co ternary complex ion associates $\text{TOA}^+ \cdot \text{BiI}_4^-$ and $\text{PO}^+ \cdot \text{BiI}_4^-$ in acidic media may account for the observed increase.

3.2. Kinetic behavior of bismuth (III) sorption onto $\text{PQ}^+ \cdot \text{Cl}^-$ -TOA loaded PUFs

The influence of shaking time (0 – 60 min) on the uptake of bismuth (III) from the aqueous acidic media at pH zero was investigated. The sorption of bismuth (III) ions onto TOA plasticized $\text{PQ}^+ \cdot \text{Cl}^-$ immobilized PUFs was fast and reached equilibrium within 60 min of shaking time. This conclusion was supported by calculation of the half-life time ($t_{1/2}$) of bismuth (III) sorption from the aqueous solutions onto the solid sorbents PUFs. The values of $t_{1/2}$ calculated from the plots of $-\log C/C_0$ versus time for bismuth (III) sorption onto PUFs, where C_0 and C are the original and final concentration of bismuth(III) ions in the test aqueous solution, respectively. The value of $t_{1/2}$ was found $2.32 \pm 0.04 \text{ min}$ in agreement with $t_{1/2}$ value reported earlier [19]. Thus, gel diffusion is not only the rate-controlling step for $\text{PQ}^+ \cdot \text{Cl}^-$ immobilized PUFs as in the case of common ion exchange resins [19] and the kinetic of bismuth (III) sorption by $\text{PQ}^+ \cdot \text{Cl}^-$ immobilized PUFs sorbent depends on film and intraparticle diffusion step where, the more rapid one controls the overall rate of transport.

The sorbed bismuth (III) species onto PUFs sorbent was subjected to Weber–Morris model [35]:

$$q_t = R_d (t)^{1/2} \quad (8)$$

where, R_d is the rate constant of intraparticle transport in $\mu \text{ mole g}^{-1} \text{ min}^{-1/2}$ and q_t is the sorbed Bi (III) concentration ($\mu \text{ mole g}^{-1}$) at time t . The plot of q_t vs. time (Fig 4) was linear ($R^2 = 0.989$) at the initial stage of bismuth (III) uptake by TOA plasticized $\text{PQ}^+ \cdot \text{Cl}^-$ loaded PUFs sorbents was linear up to $10 \pm 1.1 \text{ min}$ and deviate on increasing shaking time. The rate of diffusion of $[\text{BiI}_4]_{\text{aq}}^-$ species is high and decreased on increasing shaking time. Thus, the rate of the retention step of $[\text{BiI}_4]_{\text{aq}}^-$ onto the used solid sorbent is film diffusion at the early stage of extraction [34, 35]. The values of R_d computed from the two distinct slopes of Weber – Morris plots (Fig.4) for bismuth(III) retention by the solid sorbent were found equal 3.076 ± 1.01 and $0.653 \text{ m mole g}^{-1}$ with correlation coefficient (R^2) of 0.989 and 0.995, respectively. The observed change in the slope of the linear plot (Fig.4) is most likely attributed to the different pore size [34, 35]. Thus, intra-particle diffusion step is most likely the rate determining step.

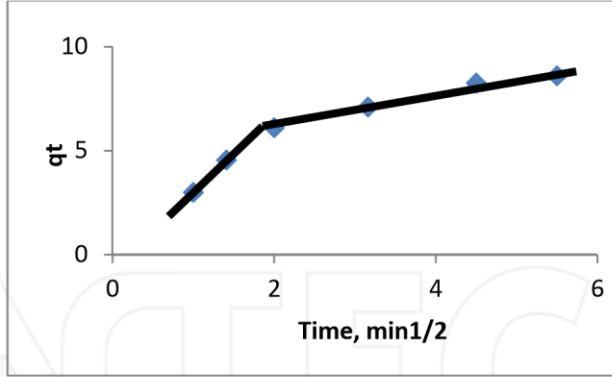
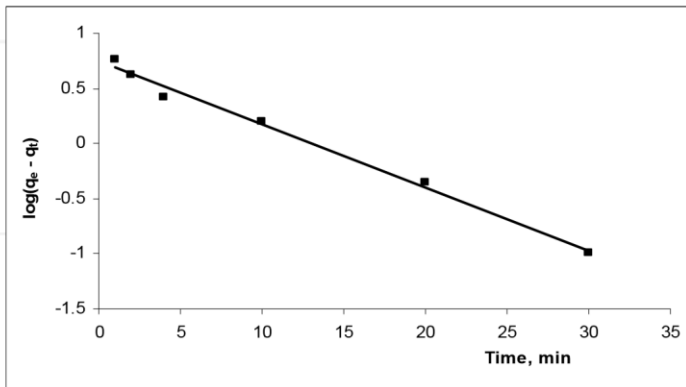


Figure 4. Weber – Morris plot of sorbed bismuth (III) onto PQ*.Cl immobilized PUFs vs. square root of time. Conditions: Aqueous solution (100 mL) containing KI (10 % m/v) and H₂SO₄ (0.5 mol L⁻¹), foam doze = (0.1 ± 0.002 g and 25 ± 0.1°C.

The retention step of the [BiI₄]⁻ species onto the loaded PUFs at 25 ± 1 °C was subjected to Lagergren model [28]:

$$\log (q_e - q_t) = \log q_e - \frac{K_{Lager}}{2.303} t \tag{9}$$

where, q_e is the amount of [BiI₄]⁻ sorbed at equilibrium per unit mass of PUFs sorbent (μmoles g⁻¹) ; K_{Lager} is the first order overall rate constant for the retention process per min and t is the time in min . The plot of $\log (q_e - q_t)$ vs. time (Fig.5) was linear. The computed value of K_{Lager} was $0.132 \pm 0.033 \text{ min}^{-1}$ ($R^2= 0.979$) confirming the first order kinetic model of sorption of [BiI₄]⁻ species onto the solid sorbent [29]. The influence of adsorbate concentration was investigated and the results indicated that, the value of K_{Lager} increased on increasing adsorbate concentration confirming the first order kinetic nature of the retention process and the formation of monolayer species of [BiI₄]⁻ onto the surface of the used adsorbent [26, 29].



(9)

Figure 5. Lagergren plot of bismuth (III) uptake onto PQ⁺.Cl⁻ PUFs from aqueous solutions containing KI (10 % m/v) - H₂SO₄ (2.0 mol L⁻¹) vs. time at 25 ± 0.1°C.]

The sorption data was also subjected to Bhattacharya- Venkobachar kinetic model [36].

$$-K_{\text{Bhatt}} \log (1 - U(t)) \propto t \quad (10)$$

$$\text{where, } U(t) \propto \frac{C_0 - C_e}{C_0 - C_e}$$

where, K_{Bhatt} = overall rate constant (min⁻¹), t = time (min), C_t = concentration of the bismuth (III) at time t in μg mL⁻¹, C_e = concentration of Bi (III) at equilibrium in μg mL⁻¹. The plot of log (1-U(t)) vs. time was linear (Fig.6) with R² = 0.987. The computed value of K_{Bhatt} (0.143 ± 0.002 min⁻¹) from Fig. 6 was found close to the value of K_{Lager} (0.132 ± 0.033 min⁻¹) providing an additional indication of first order kinetic of bismuth (III) retention towards PQ⁺.Cl⁻ loaded PUFs sorbent.

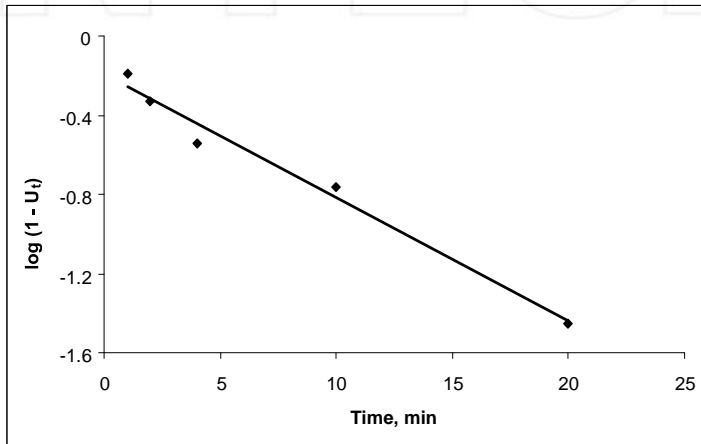


Figure 6. Bhattacharya-Venkobachar plot of bismuth (III) retention from aqueous media containing KI (10 % m/v) - H₂SO₄ (0.5 mol L⁻¹) at 25 ± 0.1°C onto the PQ⁺.Cl⁻ and TOA loaded PUFs.

The value of BT, which is a mathematical function (F) of the ratio of the fraction sorbed (q_t) at time t and at equilibrium (q_e) in μ mole g⁻¹ i.e. F = q_t / q_e calculated for each value of F employing Reichenburg equation [36].

$$BT \propto -0.4977 - 2.303 \log (1 - F)$$

$$C - C_0t$$

The plot of Bt versus time at 25 ± 1 °C for TOA plasticized $PQ^+.Cl^-$ PUFs towards bismuth (III) species was linear ($R^2 = 0.990$) up to 35 min (Fig. 7) . The straight line does not pass through the origin indicating that, particle diffusion mechanism is not only responsible for the kinetic of $[BiI_4]^-$ -sorption onto the $PQ^+.Cl^-$ treated sorbents. Thus, the uptake of $[BiI_4]^-$ onto the employed sorbents is most likely involved three steps: i- bulk transport of $[BiI_4]^-$ in solution, ii- film transfer involving diffusion of $[BiI_4]^-$ within the pore volume of TOA plasticized $PQ^+.Cl^-$ treated PUFs and/ or along the wall surface to the active sorption sites of the sorbent and finally iii- formation of the complex ion associate of the formula $[-CH_2- HO^+ - CH_2-].[BiI_4]_{Foam}$ or $[-NH_2 - COO^-].[BiI_4]_{Foam}$. Therefore, the actual sorption of $[BiI_4]^-$ onto the interior surface of PUFs was rapid and hence particle diffusion mechanism is not the rate determining step in the sorption process. Thus, film and intraparticle transport might be the two main steps controlling the sorption step. Hence, "solvent extraction" and/or "weak base anion ion exchanger" mechanism is not only the most probable participating mechanism and some other processes e.g. surface area and specific sites on the PUFs are most likely involved simultaneously in bismuth (III) retention [37].

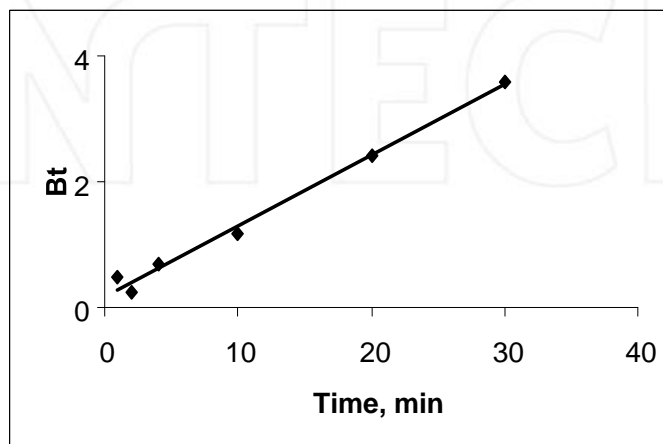


Figure 7. Reichenburg plot of bismuth (III) retention from aqueous media containing KI (10 % m/v) - H_2SO_4 (0.5 mol L^{-1}) at 25 ± 0.1 °C onto $PQ^+.Cl^-$ loaded PUFs.

3.3. Thermodynamic characteristics of bismuth (III) retention onto plasticized $PQ^+.Cl^-$ loaded PUFs

Bismuth (III) retention onto TOA plasticized $PQ^+.Cl^-$ PUFs was studied over a wide range of temperature (293-353 K) to determine the nature of bismuth (III) retention onto solid sorbent at the established experimental conditions. The thermodynamic parameters (ΔH , ΔS , and ΔG) were evaluated using the equations:

$$\ln K_c = \frac{\Delta H}{RT} + \frac{\Delta S}{R} \quad (12)$$

$$\Delta G = \Delta H - TS \quad (13)$$

where, ΔH , ΔS , ΔG , and T are the enthalpy, entropy, Gibbs free energy changes and temperature in Kelvin, respectively and R is the gas constant ($\approx 8.3 \text{ J K}^{-1} \text{ mol}^{-1}$). K_c is the equilibrium constant depending on the fractional attainment (F_e) of the sorption process. The values of K_c of bismuth (III) retention from the test aqueous solutions at equilibrium onto the plasticized $\text{PQ}^+ \cdot \text{Cl}^-$ PUFs were calculated using the equation:

$$K_c = \frac{F_e}{1 - F_e} \quad (14)$$

Plot of $\ln K_c$ vs. $1000/T$ (K^{-1}) for bismuth (III) retention was linear (Fig. 8) over the wide range of temperature range (293- 323 K). The value of K_c decreased on increasing temperature, revealing that, the retention process of $[\text{BiI}_4]$ -species onto the sorbents is an exothermic process [21, 22]. The numerical values of ΔH , ΔS , and ΔG calculated from the slope and intercept of the linear plot Fig. 8 were $-18.72 \pm 1.01 \text{ kJ mol}^{-1}$, $54.57 \pm 0.5 \text{ J mol}^{-1} \text{ K}^{-1}$

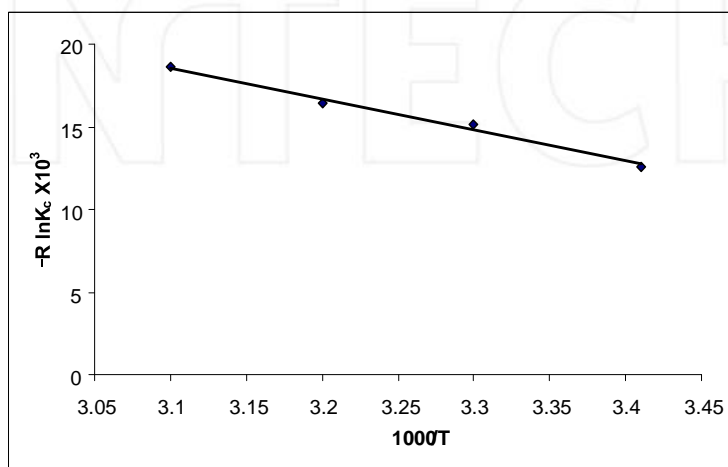


Figure 8. Plot of $\ln K_c$ vs. $1000/T$ (K^{-1}) of bismuth (III) sorption from aqueous media containing KI (10 % m/v) - H_2SO_4 (0.5 mol L^{-1}) onto $\text{PQ}^+ \cdot \text{Cl}^-$ treated PUFs.

The retention of bismuth (III) by plasticized $\text{PQ}^+ \cdot \text{Cl}^-$ loaded PUFs was also subjected to Vant Hoff model:

$$\log K_d = \frac{-\Delta H}{2.30 RT} + C \quad (15)$$

where, C is a constant. Vant - Hoff plot of $\log K_d$ vs. $1000/T$ (K^{-1}) of bismuth (III) uptake from the test aqueous media of KI (10 % m/v) - H_2SO_4 (0.5 mol L^{-1}) onto plasticized $\text{PQ}^+ \cdot \text{Cl}^-$ loaded PUFs sorbent was linear (Fig. 9). The value of ΔH calculated from the slope of Fig. 9 was $-20.1 \pm 1.1 \text{ kJ mol}^{-1}$ in good agreement with the values evaluated from equations 12 and 13. The ΔS of activation were lower than $T \Delta S$ at all temperature. Thus, the retention step is entropy controlled at the activation state. and $-2.46 \pm 0.1 \text{ kJ mol}^{-1}$ (at 298 K), respectively with a correlation factor of 0.998.

The negative value of ΔH and the data of D and K_c reflected the exothermic behavior of bismuth (III) uptake by the employed solid PUFs and non-electrostatics bonding formation between the adsorbent and the adsorbate. The positive value of ΔS proved that, bismuth (III) uptake are organized onto the used sorbent in a more random fashion and may also indicative of moderated sorption step of the complex ion associate of $[\text{BiI}_4]^-$ and ordering of ionic charges without a compensatory disordering of the sorbed ion associate onto the used sorbents. The sorption process involves a decrease in free energy, where ΔH is expected to be negative as confirmed above. Moreover, on raising the temperature, the physical structure of the PUFs membrane may be changing, and affecting the strength of intermolecular interactions between the membrane of PUFs sorbent and the $[\text{BiI}_4]^-$ species. Thus, high temperature may make the membrane matrix become more unstructured and affect the ability of the polar segments to engage in stable hydrogen bonding with $[\text{BiI}_4]^-$

species, which would result in a lower extraction. The negative of ΔG at 295 K implies the spontaneous and physical sorption nature of bismuth (III) retention onto PUFs. The decrease in ΔG on decreasing temperature confirms the spontaneous nature of sorption step of bismuth (III) is more favorable at low temperature. The energy of urethane nitrogen and/or ether oxygen sites of the PUFs provided by raising the temperature minimizes the interaction between the active sites of PUFs and the complex ion associates of bismuth (III) ions resulting low sorption via "Solvent extraction" [38]. These results encouraged the use of the reagent loaded PUFs in packed column mode for collection, and sequential

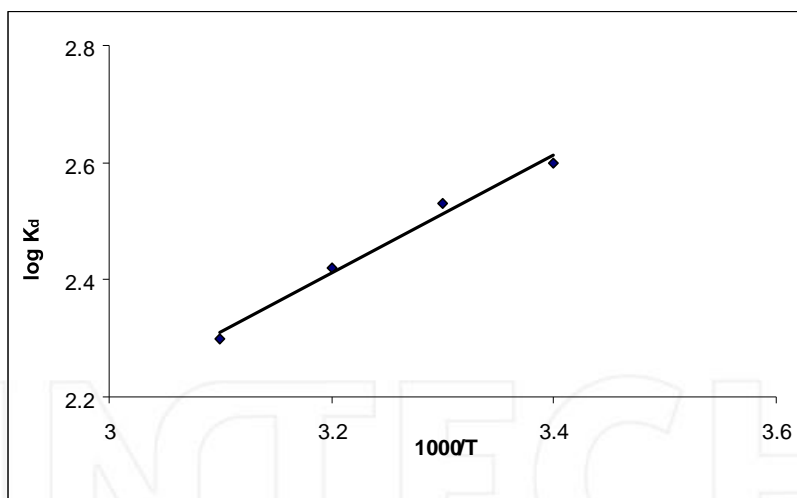


Figure 9. Vant - Hoff plot of $\log K_d$ vs. $1000/T$ (K^{-1}) of bismuth (III) retention from aqueous media containing KI (10 % m/v) - H_2SO_4 (0.5 mol L^{-1}) onto $\text{PQ}^+ \cdot \text{Cl}^-$ loaded PUFs. determination of bismuth (III) and (V) in water samples.

3.4. Sorption isotherms of bismuth (III) onto $\text{PQ}^+ \cdot \text{Cl}^-$ loaded PUFs sorbents

The development of a suitable preconcentration and/ or separation procedures for determination of trace concentrations of bismuth (III) in water is becoming increasingly

important. PUFs physically immobilized with a series of quaternary ammonium ion pair reagents e.g. tetraphenyl phosphonium chloride, amiloride hydrochloride, tetraheptyl ammonium bromide or procaine hydrochloride was tested for the separation of bismuth (III) from aqueous iodide aqueous media. The results revealed considerable retention of bismuth (III) onto $PQ^+ .Cl^-$ loaded PUFs compared to other onium cations. Thus, the retention profile of bismuth (III) over a wide range of equilibrium concentrations of bismuth (III) ions onto $PQ^+ .Cl^-$ loaded PUFs sorbent from aqueous KI (10%w/v) - H_2SO_4 (1.0 mol L^{-1}) solutions was investigated. The amount of $[BiI_4]^-$ retained onto the PUFs at low or moderate bismuth (III) concentration varied linearly with the amount of bismuth (III) remained in the test aqueous solution (Fig. 10). The equilibrium was approached only from the direction of

$[BiI_4]^-$ species-rich aqueous phase confirming a first-order sorption behavior [39]. The sorption capacity of bismuth (III) species towards $PQ^+ .Cl^-$ immobilized PUFs as calculated from the sorption isotherm (Fig.10) was $40.0 \pm 1.10 \text{ mg g}^{-1}$. The plot of distribution coefficient (K^d) of bismuth (III) sorption between the aqueous solution H_2SO_4 (0.5 mol L^{-1}) and KI (10% w/v) and $PQ^+ .Cl^-$ loaded PUFs sorbent is given in Fig. 11. The most favorable values of K^d of bismuth (III) sorption onto PUFs sorbent were also obtained from more diluted aqueous solutions (Fig. 11). The K^d values decreased on increasing the concentration of bismuth (III) ions in the aqueous phase and the PUFs membranes became more saturated with the retained $[BiI_4]^-$ species.

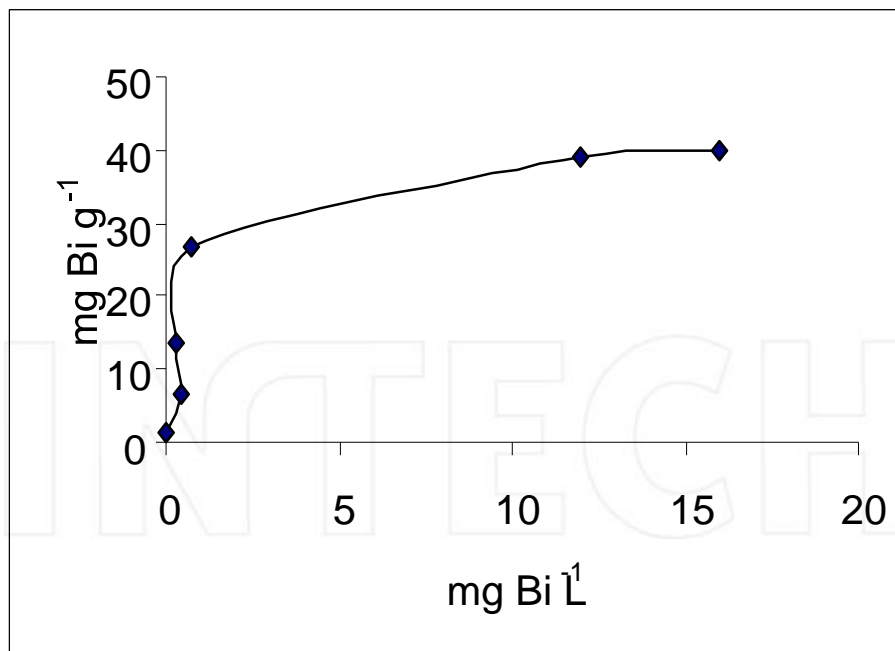


Figure 10. Sorption isotherm of bismuth (III) from aqueous solution of H_2SO_4 (0.5 mol L^{-1}) and KI (10% w/v) onto the $PQ^+ .Cl^-$ immobilized PUFs.



Figure 11. Plot of the distribution coefficient (K_d) of bismuth (III) sorption between the aqueous solution H_2SO_4 (0.5 mol L⁻¹) and KI (10% w/v) and $\text{PQ}^+\cdot\text{Cl}^-$ loaded PUFs

Sorption of bismuth (III) onto PUFs sorbent was subjected to Langmuir isotherm model expressed in the following linear form [40]:

$$\frac{C_e}{C_{ads}} = \frac{1}{Qb} + \frac{C_e}{Q}$$

where, C_e is the equilibrium concentration ($\mu\text{g mL}^{-1}$) of bismuth (III) in the test solution, C_{ads} is the amount of bismuth (III) retained onto PUFs per unit mass. The Langmuir parameter Q and b related to the maximum adsorption capacity of solute per unit mass of adsorbent required for monolayer coverage of the surface and the equilibrium constant related to the binding energy of solute sorption that is independent of temperature, respectively. The plot of C_e/C_{ads} vs. C_e over the entire range of bismuth (III) concentration was linear (Fig.12) with correlation coefficient of, $R^2 = 0.998$ indicating adsorption of the analyte by $\text{PQ}^+\cdot\text{Cl}^-$ treated PUFs sorbents followed Langmuir model. The calculated values of Q and b from the slope and intercept of the linear plot (Fig.12) were $0.21 \pm 0.01 \text{ mol g}^{-1}$ and $5.6 \pm 0.20 \times 10^5 \text{ L mol}^{-1}$, respectively.

(16)

Dubinin - Radushkevich (D - R) isotherm model [41] is postulated within the adsorption space close to the adsorbent surface. The D-R model is expressed by the following equation:

$$\ln C_{ads} = \ln K_{DR} - \beta Q^2$$

(17)

where, K_{DR} is the maximum amount of bismuth (III) retained, β is a constant related to the energy transfer of the solute from the bulk solution to the sorbent and ϵ is Polanyi potential which is given by the following equation:

$$\epsilon^2 = RT \ln (1+1/C_e) \tag{18}$$

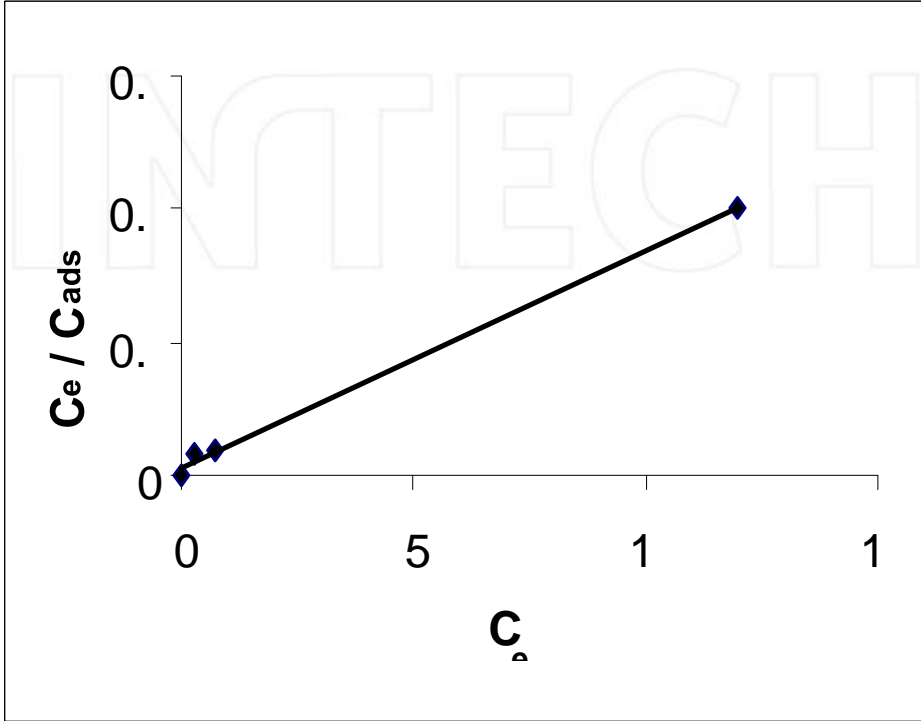


Figure 12. Langmuir sorption isotherm of bismuth (III) uptake from aqueous solution onto $PQ^+.Cl^-$ loaded PUFs at optimum conditions.

The plot of $\ln C_{ads}$ versus ϵ^2 was linear with $R^2 = 0.986$ (Fig. 13) for the $PQ^+.Cl^-$ immobilized PUFs indicating that, the D-R model is obeyed for bismuth (III) sorption over the entire concentration range. The values of β and K_{DR} computed from the slope and intercept were found $0.33 \pm 0.01 \text{ mol}^2 \text{ KJ}^{-2}$ and $171 \pm 2.01 \mu \text{ mol g}^{-1}$, respectively. Assuming that, the surface of PUFs is heterogenous and an approximation to Langmuir isotherm model is chosen as a local isotherm for all sites that are energetically equivalent, the quantity β can be related to the mean of free energy (E) of the transfer of one mole of solute from infinity to the surface of PUFs. The E value is expressed by the following equation:

$$E = \frac{1}{\sqrt{\beta}} \tag{19}$$

The value of E was found $1.23 \pm 0.07 \text{ KJmol}^{-1}$ for the $PQ^+.Cl^-$ loaded foam. Based on these results, the values of Q and b and the data reported [42, 43], a dual sorption sorption

mechanism involving absorption related to "weak – base anion ion exchange" and an added component for "surface adsorption" is the most probable mechanism for the uptake of bismuth (III) by the used PUFs. This model can be expressed by the equation:

$$C_r C_{abs} - C_{ads} - DC_{aq} = \frac{SKG_{aq}}{1 + KG_{aq}} \quad (20)$$

where, C_r and C_{aq} are the concentrations of bismuth (III) retained onto the PUFs and the aqueous solution at equilibrium, respectively. C_{abs} and C_{ads} are the concentrations of the absorbed and adsorbed bismuth (III) species onto the PUFs at equilibrium, respectively and S and K_L are the saturation parameters for the Langmuir adsorption model.

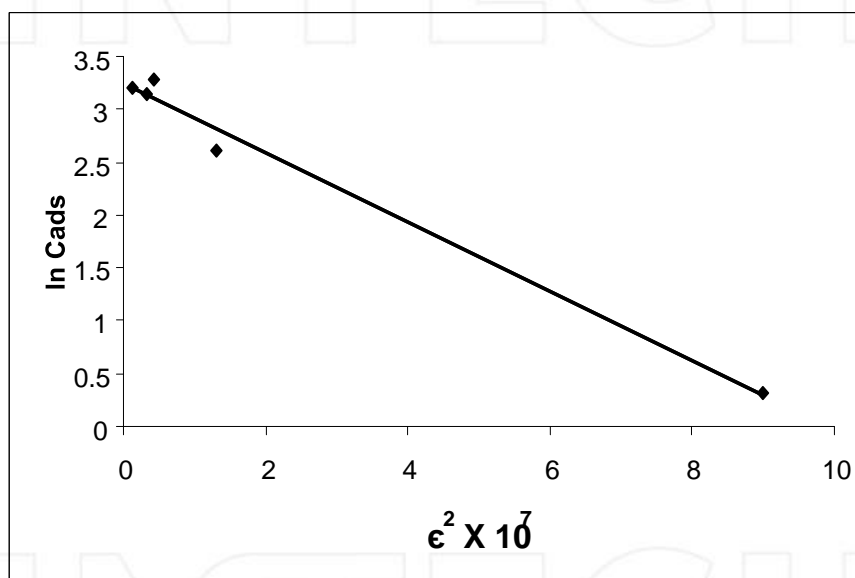


Figure 13. Dubinin-Radushkevich (D-R) sorption of bismuth (III) extraction from aqueous solution onto PQ+.Cl⁻ loaded PUFs at the optimum conditions

3.5. Chromatographic behavior of bismuth (III) sorption

The membrane like structures, the excellent hydrodynamic and aerodynamic properties of PUFs sorbent [42, 43], kinetics, capacity and the sorption characteristics of bismuth (III) retention towards plasticized PQ+.Cl⁻ PUFs sorbent [39] encouraged the use of the sorbent in packed column for quantitative retention of bismuth (III) from the test aqueous iodide solution. Thus, the test solutions (1.0 L) of the deionized water containing KI (10% w/v) - H₂SO₄ (1.0 mol L⁻¹) was spiked with various trace concentrations (5 -100 μg L⁻¹) of bismuth (III) and percolated through the PUFs packed columns at 5 mL min⁻¹ flow rate. ICP-OES measurements of bismuth in the effluent indicated complete uptake of bismuth (III). A series of eluting agents e.g. NH₄NO₃, HClO₄ and HNO₃ (1-5. mol L⁻¹) was tested for complete elution of the retained bismuth (III). An acceptable recovery (96.0 ± 2.1) of bismuth (III) was achieved using HNO₃ (10 mL, 3 mol L⁻¹) at 2 mL min⁻¹ flow rate. Therefore, HNO₃ (3 mol L⁻¹) was

selected as a proper eluting agent for bismuth (III) from the packed columns. With HNO₃, reproducibility data even at ultra trace concentrations (0.5 ng mL⁻¹) of bismuth (III) were successfully achieved. The data of pre concentration and recovery of various concentrations of bismuth (III) are summarized in Table 2. A recovery percentage in the range 98.0 ± 1.5 - 104.2 ± 2.3 was achieved confirming the performance of the developed of PQ⁺.Cl⁻ loaded PUFs.

Bismuth (III) taken, μg L ⁻¹	Bismuth (III) found, μg L ⁻¹	Recovery, %
98.5	98.0 ± 1.5	98.0 ± 1.5
52	52.10 ± 2.3	101 ± 1.1
104	104 ± 2.3	101 ± 1.1

* Average (n=5) ± relative standard deviation.

Table 2. Recovery percentage (%) of bismuth (III) ions from deionized water by the developed PUFs packed columns

The proposed PUFs packed columns was also tested for collection and recovery of bismuth (V) species (< 5 μg L⁻¹) from aqueous solutions after reduction to bismuth (III). A series of reducing agents e.g. H₂S, Na₂SO₃, and KI was tested and satisfactory results were achieved using KI. Thus, in the subsequent work, KI was selected as a proper reducing agent for bismuth (V) to bismuth (III) species. Reduction of bismuth (V) to bismuth (III) was found fast, simple and also form a stable [BiI₄]⁻ species. The solutions were then percolated through PUFs packed column following the described procedures of bismuth (III) retention. The results are summarized in Table 3. An acceptable recovery percentage of Bismuth (V) in the range 94.0 ± 2.1 – 95.0 ± 3.5 was achieved. The proposed PUFs packed column was also tested for chemical speciation and determination of total bismuth (III) and (V) species in their mixtures. An aqueous solution of bismuth (III) and (V) was first analyzed according to the described procedure for bismuth (V). Another aliquot portion was also adjusted to pH 3 – 4 and shaken with Na-DDTC for 2-3 min and extracted with chloroform (5.0 mL) as Bi (DDTC)₃ [33]. The remaining aqueous solution of bismuth (V) was reduced to bismuth (III) with KI (10%w/v) - H₂SO₄ (0.5 mol L⁻¹) and percolated through the PQ⁺.Cl⁻ loaded PUFs column. The retained bismuth species were then recovered and finally analyzed following the recommended procedures of bismuth (III) retention. The signal intensity of ICP- OES of the first aliquot (I₁) is a measure of the sum of bismuth (III) and (V) ions in the mixture, while the net signal intensity of the second aliquot (I₂) is a measure of bismuth (V) ions. The difference (I₁-I₂) of the net signal intensity is a measure of bismuth (III) ions in the binary mixture. Alternatively, bismuth (III) as Bi(DDTC)₃ in the methylisobutyl ketone phase was stripped to the aqueous phase by HNO₃ (1 mol L⁻¹) and analyzed by ICP-OES The results are given in Table 4. An acceptable recovery percentage in the 92.5 ± 3.01– 104.3 ± 4.5% of bismuth (III) and (V) ions was achieved.

Bismuth (V) added μg L ⁻¹	Bismuth (V) found, μg L ⁻¹	Recovery, %
100	95 ± 1.5	95.0 ± 3.5
250	235 ± 50	94.0 ± 2.1

*Average recovery of five measurements ± relative standard deviation.

Table 3. Recovery (%) of bismuth (V) ions from deionized water by PUFs packed columns

Bismuth (III) and (V) taken, $\mu\text{g L}^{-1}$	Total bismuth found $\mu\text{g L}^{-1}$		Recovery, % *
Bi (III)	Bi (V)		
20	25	47 ± 3.5	104 ± 4.5
25 100	118 ± 5	94.4 ± 2.9	10 ± 10
	18.5 ± 1.5	92.5 ± 3.01	

* Average recovery of five measurements \pm relative standard deviation.

Table 4. Recovery (%) of total bismuth (III) and (V) in their mixture from aqueous media

3.6. Capacity of the PQ⁺.Cl⁻ immobilized PUFs

The developed method was assessed by comparing the capacity of the used sorbent towards bismuth (III) sorption with most of the reported solid sorbents e.g. 2, 5- di- mercapto-1, 3, 4thiadiazol loaded on Silica gel [44] and amionophosphonic dithio-carbamate functionalized polyacrylonitrile [45]. The capacity of the used PQ⁺.Cl⁻ loaded PUFs sorbent ($40.0 \pm 1.10 \text{ mg g}^{-1}$) towards bismuth (III) retention was found far better than the data reported by other solid sorbents e.g. 2, 5- dimercapto-1, 3, 4-thiadiazol loaded on Silica gel (3.5 mg g^{-1}) [44] and amionophosphonic dithiocarbamate functionalized poly acrylonitrile (15.5 mg g^{-1}) [45] and some other solid sorbents.⁵

3.7. Analytical performance of the immobilized PUFs packed column

The performance of the PUFs packed column was described in terms of the number (N) and the height equivalent to the theoretical plate (HETP). Thus, aqueous solution (1.0 L) containing bismuth (III) at concentration of $100 \mu\text{g L}^{-1}$ at the optimum experimental conditions was percolated through the PUFs packed columns ($1.0 \pm 0.001 \text{ g}$) at 5 mL min^{-1} flow rate. Complete retention of [BiI₄⁻] was achieved as indicated from the analysis of bismuth in the effluent solution using ICP-MS. The retained bismuth (III) species were then eluted with HNO₃ (10 mL, 3 mol L^{-1}) and a series of fractions (2.0 mL) of eluent solution at 2.0 mL min^{-1} were then collected and analyzed by ICP-OES. The calculated values of N and HETP values from the chromatogram method (Fig. 14) using Gluenkauf equation [14] were equal to 90 ± 3.02 and $0.11 \pm 0.02 \text{ mm}$, respectively. The values of N and HETP were also computed from the breakthrough capacity curve (Fig. 15) by percolating aqueous solution (2.0 L) containing bismuth (III) at $100 \mu\text{g L}^{-1}$ under the experimental conditions through PQ⁺.Cl⁻ loaded PUFs column at 5 mL min^{-1} flow rate of. The critical and breakthrough capacities [42, 45] calculated from Fig.15 were 1.95 ± 0.1 and $31.25 \pm 1.02 \text{ mg g}^{-1}$, respectively. These HETP (97 ± 4) and N ($0.13 \pm 0.02 \text{ mm}$) values are in good agreement with the values obtained from the chromatogram method.

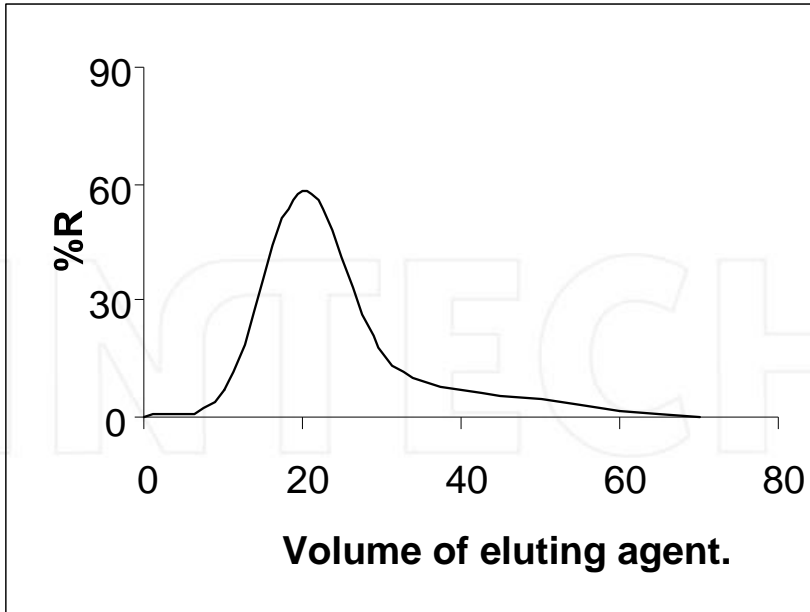


Figure 14. Chromatogram of bismuth (III) recovery from PQ+.Cl⁻ loaded PUFs packed column using nitric acid (5 mol L⁻¹) as eluting agent at flow rate of 2.5 mL min⁻¹.

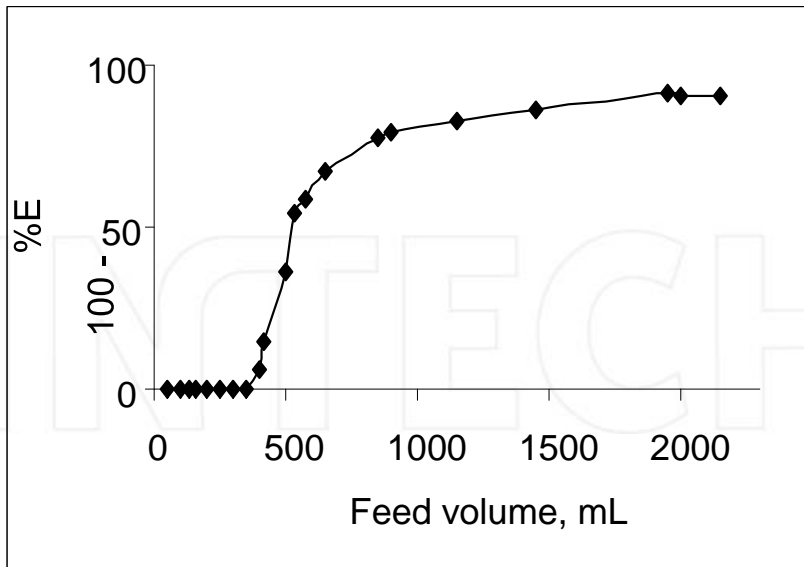


Figure 15. Breakthrough capacity curve for bismuth retention onto PQ+.Cl⁻ loaded packed column at the optimum conditions.

3.8. Figure of merits of the PQ⁺.Cl⁻ immobilize PUFs packed column

The LOD, LOQ, enrichment and sensitivity factors and relative standard deviation, (RSD) under the optimized conditions were determined. The plot of signal intensity of ICP- OES (I) versus bismuth (III) concentration (C) has the regression equation:

$$I = 4.19 \times 10^3 C \text{ (ng L}^{-1}\text{)} + 12.96 \text{ (r=0.9995)} \quad (21)$$

According to IUPAC [46, 47], the $LOD = 3S_{y/x}/b$ and $LOQ = 10S_{y/x}/b$ were 0.9 and 3.01 ngL⁻¹, respectively ($V_{\text{sample}} = 100 \text{ mL}$) where, $S_{y/x}$ is the standard deviation of y - residual and b is the slope of the calibration plot [46]. The LOD of the developed method is much better than direct measurement by ICP – OES (5.0 μg mL⁻¹). The enrichment factor ($F_c = V_{s,b} / V_{e,v}$) was defined as the ratio between the volume of analyte sample ($V_{s,b} = 1000 \text{ mL}$) before preconcentration and the eluent volume ($V_{e,v}$) after retention and recovery. An average value of F_c of 100 was achieved. The sensitivity factor (the ratio of the slope of the preconcentrated samples to that obtained without preconcentration) was 33.3. The RSD of the method for the determination of standard bismuth (III) solution (50 μg L⁻¹) was ± 2.5% (n= 5) confirming the precision of the method. The figure of merits of the developed method were compared satisfactorily to the reported methods e.g. ICP-OES [45], spectrophotometric [47] and electrochemical [49 -51] (Table 5) in water confirming the sensitivity and applicability of the proposed method. The LOD of the method could be improved to lower values by prior pre concentration of bismuth (III) species from large sample volumes of water (>1.0L). Thus, the method is simple and reliable compared to other methods [50 -52].

SPE	Technique	Linear range, μg L ⁻¹	LOD, μg L ⁻¹	Reference
Microcrystalline	UV – Vis	0 – 2 X10 ⁴	—	34 benzophenone
Microcrystalline	DPP	180 – 135x10 ²	55	35 naphthalene
Octylsilane (RP-8)	ASV	10.5 – 1000	0.73	36 cartridge
Amberlite XAD-7 resin	HG-ICP-OES	Up to 100	0.02	6
Modified Chitosan	ICP-MS		0.1*	15
PQ ⁺ .Cl ⁻ -loaded PUFs	ICP – OES	0.01 – 100	2.7*	Present work

Table 5. Figure of merits of the developed and some of the reported SPE coupled with spectrochemical and electrochemical techniques for bismuth determination in water

3.9. Interference study

The influence of diverse ions relevant to wastewater e.g. alkali and alkali earth metal ions Ca²⁺, Mg²⁺, Cl⁻, Zn²⁺, Mn²⁺, Cu²⁺, Hg²⁺, Fe²⁺, Fe³⁺, Pb²⁺, Al³⁺, Ni²⁺, Co²⁺ and nitrate at various concentrations (0.5 -1.0 mg/ 100 mL sample solution) on the sorption of 10 μg bismuth (III) from a sample volume of 100 mL at the optimum conditions was studied. The tolerance limits (w/w) less than ± 5% change in percentage uptake of bismuth was taken as free from interference. The tested ions except Pb²⁺ did not cause any significant reduction on the percentage (96 -102 ± 2%) of bismuth (III) sorption. Lead ions were found to interfere at higher

concentrations (> 0.5 mg/100 mL sample solution). Thus, it can be concluded that, the method could applied for the separation and / or determination of bismuth (III) and bismuth (V) after reduction of the latter to trivalence.

3.10. Analytical applications

The validation of the developed method was performed using the certified reference materials (CRM-TMDW). Good agreement between the concentration measured by the proposed method (8.9 ± 0.9 $\mu\text{g L}^{-1}$) and the certified value (10.0 ± 0.1 $\mu\text{g L}^{-1}$) of the total bismuth was achieved confirming the accuracy of the method for trace analysis of bismuth in complex matrices.

The method was also applied for the determination of bismuth in wastewater samples (1.0 L) after digestion and percolation through the PUFs packed columns as described. Complete retention of bismuth was achieved as indicated from the ICP-MS analysis of bismuth in the effluent. The retained $[\text{BiL}_4]$ species were recovered with HNO_3 (10 mL, 3.0 mol L^{-1}) and analyzed by ICP-OES. Various concentrations of bismuth (III) were spiked also onto the tested wastewater samples and analyzed (Table 6). Bismuth (III) determined by the method and that expected (Table 6) in the tested water samples revealed good recovery percentage ($98.4 \pm 2.3 - 104.3 \pm 2.8$ %) confirming the accuracy and validation of the method.

Bismuth (III) added, ($\mu\text{g L}^{-1}$)	Bismuth (III) found, ($\mu\text{g L}^{-1}$)	Recovery, %*
–	22	–
50	75	104.3 ± 2.8
100	120.5	98.4 ± 2.3

* Average recovery of five replicates \pm relative standard deviation.

Table 6. Recovery study applied to the analysis of bismuth in wastewater by the developed method

The selectivity of the procedure was further tested for the analysis of bismuth in Red sea water at the coastal area of Jeddah City, Saudi Arabia following the standard addition. as described..The results are summarized in Table 7. An acceptable recovery percentage of $107.01 \pm 3.5 - 108.1 \pm 2.7$ was achieved confirming the selectivity, accuracy and validation of the method.

Bismuth (III) added, ($\mu\text{g L}^{-1}$)	Bismuth (III) found, ($\mu\text{g L}^{-1}$)	Recovery, %*
–	0.07	–
0.30	0.40 ± 0.01	108.1 ± 2.7
0.5	0.61 ± 0.02	107.01 ± 3.5

* Average recovery of five replicates \pm relative standard deviation

Table 7. Recovery test for bismuth in sea water by the developed method

4. Conclusion

PQ⁺.Cl⁻ treated PUFs solid sorbent was successfully used for the pre concentration/separation procedures of bismuth (III) and bismuth (V) after reduction of the latter species to bismuth (III). The developed method minimizes the limitations related to sensitivity and selectivity for bismuth determination in various matrices. The intra-particle diffusion and the first order model of bismuth (III) retention onto the tested PQ⁺.Cl⁻ PUFs sorbent are confirmed from the kinetic data. PUFs packed column has shown itself to be a very useful and precise for the analysis of total bismuth (III) & (V) species in water at trace concentrations in water. The PUFs packed column can be reused many times without decrease in its efficiency. Work is continuing for calculating ligation capacity, influence of competitive agents and organic material present in water samples. The LOD of the method is quite close to the concentration of bismuth species reported in marine water. Work is still continuing on developing PQ⁺.Cl⁻ treated PUFs packed column mode for on line determination of bismuth (III) and/ or (V) species at ultra concentrations in aqueous media.

Author details

M.S. El-Shahawi

Department of Chemistry, Faculty of Science, King Abdulaziz University, Jeddah, Saudi Arabia

A.A. Al-Sibaai

Department of Chemistry, Faculty of Science, King Abdulaziz University, Jeddah, Saudi Arabia

H.M. Al-Saidi

Department of Chemistry, University College, Umm Al-Qura University, Makkah, Saudi Arabia

E. A. Assirey

Department of Applied Chemistry, College of Applied Science, Taibah University, Al-Madinah Al-Munawarah, Saudi Arabia

5. References

- [1] J. A. Reyes- Aguilera, M. P. Gonzalez, R. Navarro, T.I.Saucedo, M. Avila-Rodriguez, supported liquid membranes (SLM) for recovery of bismuth from aqueous solution, *J.Membrane Sci*, 2008, 310, 13.
- [2] N. Tokman, *Anal. Chim. Acta*, 2004, 519, 87.
- [3] R. Pamphlett, M .Stottenbery. J. Rungby, G. Danscher, *Neurotoxicol. Teratol*, 2000, 22, 559.
- [4] A . S. Ribeiro, M. A. Z. Arruda, S . Cadrore, *Spectrochim. Acta Part B*, 2002, 57, 2113.
- [5] O. Acar, Z. Kilic, A. R. Turker, *Anal. Chim Acta*, 1999, 382, 329.
- [6] L. Rahman, W. T. Corns, D. W. Bryce, P. B. Stockwell, *Talanta*, 2000, 52, 833.
- [7] Y. Zhang, S.B. Adeloju, , *Talanta*, 2008, 76, 724.
- [8] H. Guo, Y. Li, P. Xiao, N. He, *Anal. Chim. Acta*, 2005, 534, 143.
- [9] H.Y. Yang, W.Y. Chen, I.W. Sun, *Talanta*, 1999, 50, 977.
- [10] R. Hajian, E. Shams, *Anal Chim Acta*, 2003, 491, 63.
- [11] S. G Sarkar, P. M Dhadke, *Sep. Purif. Technol*, 1999, 15, 131.

- [12] J. M. Lo, Y. P. Lin, K. S. Lin, , *Anal. Sci (Japan)*, 1991, 7, 455.
- [13] M.A. Taher, E. Rezaeipor, D. Afzali, *Talanta*, 2004, 63,797.
- [14] Y. Yamini, M. Chalooosi, H. Ebrahimzadeh, *Talanta*, 2002, 56,797.
- [15] E. M. Thurman, M. S. Mills "Solid Phase Extraction, Principles and Practice" John Wiley and Sons, 1998.
- [16] B. Manadal, N. Ghosh, *J. Hazard. Materials*, 2010,182, 363.
- [17] M. Sun, Q. Wu, *J. Hazard. Materials*, 2010, 182, 543.
- [18] M.A. Didi, A.R. Sekkal, D. Villemin, *Collids and Surfaces A: Physicochemical and Engineering Aspects*, 2011, 375 (1-3), 169.
- [19] S. Palagyi and T. Braun "Separation and Pre-concentration of Trace Elements and Inorganic Species on Solid Polyurethane Foam Sorbents" In Z. B. Alfassi and C. M. Wai "Preconcentration Techniques for Trace Elements" CRC Press, Boca Rotan, FI, 1992.
- [20] G.J. Moody, J.D.R. Thomas, "Chromatographic Separation with Foamed Plastics and Rubbers" Dekker, New York, 1982.
- [21] M. S. El-Shahawi, M. A. El-Sonbati, *Talanta*, 2005, 67, 806.
- [22] M. S. El-Shahawi, M.A. Othman, M. A. Abdel-Fadeel, *Anal. Chim. Acta*, 2005, 546, 221.
- [23] M. S. El-Shahawi, R. S. Al-Mehrezi, *Talanta*, 1997, 44, 483.
- [24] M. S. El-Shahawi, H. A. Nassif, *Anal. Chim. Acta*, 2003,487, 249.
- [25] M. S. El-Shahawi, H. A. Nassif, *Anal. Chim. Acta*, 2003, 487, 249.
- [26] T. Braun, J. D. Navratil, A. B. Farag "Polyurethane Foam Sorbents in Separation Science" CRC Press Inc, Boca Raton, FL 1985.
- [27] D.D. Mello, S.H. Pezzin, S.C. Amico , The effect of Post – consumer PET particules on the performance of flexible polyurethane foams, *Polymer Testing*, 2009, 28, 702.
- [28] A.B. Farag, M.H. Soliman, O.S. Abdel-Rasoul, M.S. El-Shahawi, *Anal. Chim. Acta*, 2007, 601, 218.
- [29] A.B. Bashammakh, S.O. Bahaffi, F.M. Al-shareef, M.S. El-Shahawi, *Anal. Sci (Japan)*, 2009, 25, 413.
- [30] F. A. Cotton and G. Wilkinson"Advanced Inorganic Chemistry" Wiley, London. 1972.
- [31] A.I. Vogel "Quantitative Inorganic Analysis"^{3rd} edn. Longmans Group Ltd., England, 1966.
- [32] Z. Marczenko "Separation and Spectrophotometric Determination of Elements" 2nd edn. John Wiley and Sons,1986.
- [33] M. M. Saeed, M. Ahmed, *Anal. Chim Acta*, 2004,525, 289.
- [34] P. R. Haddad, N. E. Rochester, *J. Chromatogr*, 1988, 439, 23.
- [35] W. J. Weber, and J. C. Morris, , *J. Sanit. Eng. Div. Am. Soc. Civ. Eng.*, 1963, 89, 31.
- [36] A. K. Bhattacharya and C. Venkobachar, *J. Environ. Eng.*, 1984, 110, 1.
- [37] D. Reichenburg, *J. Am. Chem. Soc.*, 1972, 75, 589.
- [38] S. Zhi-Xing, P. Qiao-Sheng, L. Xing-yin, C. Xi-Jun, Z. Guang-Yao, R. Feng-Zhi, *Talanta*, 1995,42, 1127.
- [39] M.S. El-Shahawi, A. Hamza, A. A. Al-Sibaa and H.M. Al-Saidi, *Chem. Eng. J.* 2011, 173 (2), 255.
- [40] L. Langmuir, *J. Am. Chem. Soc*, 1918, 40, 136.
- [41] G.A. Somorjai" Introduction to Surface Chemistry and Catalysis" John Wiley& Sons, INC, 1994.

- [42] O. D. Sant'Ana, L. G. Oliveira, L. S. Jesuino, M. S. Carvalho, M. L. Domingues, R. J. Cassella and R. E. Santelli, *J. Anal. At. Spectrom*, 2002, 17, 258.
- [43] S. Palagyi and T. Braun "Separation and Pre-concentration of Trace Elements and Inorganic Species on Solid Polyurethane Foam Sorbent" in Z. B. Alfassi and C. Wai

4 edn., 1994.

- [48] C.Lin, H. Wang, Y. Wang, Z. Cheng, *Talanta*, 2010, 81,30.
- [49] D. Thorburn Burns, N. Tungkananuruk and S. Thuwasin, *Anal. Chim. Acta*, 2000, 419, 41.
- [50] A. Bhalotra and B.K. Prui, *J.AOAC Intern*, 2001,84, 47.
- [51] M.H. Pournaghi-Azr, D. Djozan, and H. A. Zadeh, *Anal. Chim. Acta*, 2001, 437, 217.
- [52] I. Kulaa, Y. Arslanb, S. Bak irdere, S. Titretir, E. Kenduzler and O. Y. Atamanb, *Talanta*, 2009, 80, 127.

"Preconcentration Techniques for Trace Elements" CRC Press, Boca Roton FL.1992. [44]

K. Terada, K. Matsumoto and Y. Nanao, *Anal. Sci. (Japan)*, 1985,1, 145.

- [45] W.X.Ma, F.Liu, K.A.Li, W.Chen and S.Y.Tong, *Anal.Chim.Acta*, 2000, 416, 191.
- [46] M. Filella, *J. Environ. Monitoring*, 2010, 12, 90.
- [47] J.C.Miller, J. N. Miller "Statistics for Analytical Chemistry" Ellis-Horwood, New York,

Retention profiles of some commercial pesticides, pyrethroid and acaricide residues and their application to tomato and parsley plants¹

M.S. El-Shahawi²

Chemistry Department, Faculty of Science, UAE University, P.O. Box 17551, Al-Ain, United Arab Emirates

Received 9 March 1996; revised 1 October 1996; accepted 9 October 1996

Abstract

This work deals with the preconcentration of some water soluble pesticides, pyrethroids and acaricides by polyurethane foams. The retention profiles of the tested species were found quickly and reached equilibrium in a few min. Various parameters – e.g. pH, extraction media, shaking time, salt effect, temperature and sample volume – affecting the preconcentration of the tested species by the unloaded foams and tri-*n*-octylamine and tri-*n*-methylphosphate treated foams were optimized. The unloaded foams were employed in a column mode to study the quantitative retention and recovery of the tested species. The sorption efficiency and recovery of the compounds by the unloaded foam column were found to be up to 99.5%±2.1. The height equivalent of a theoretical plate for the unloaded foam column was found to be in the range 1.9–2±0.2 mm. The sorption mechanisms of the tested compounds by the foams are discussed. Analysis of N, P, Na, K, Cu, Zn, Mn, Fe, humidity, wet and dry mass of tomato and parsley untreated and sprayed for different time intervals – i.e. 24, 72 and 120 h – with Chlorpyrifos, was carried out .

Keywords: Polyurethane foam; Sample preparation; Tomato; Parsley; Environmental analysis; Stationary phases, LC; Thermodynamic parameters; Water analysis; Pesticides; Pyrethroids; Acaricides

1. Introduction

In recent years industrial growth and the need to increase agriculture productivity have resulted in the presence of pollutants in water and air. Since these compounds are present at levels lower than ppb their determination causes problems [1]. Among these substances, pesticides, pyrethroids and acaricides must be watched with particular attention because of

their very low limits of tolerability. These compounds are deliberately directed against living organisms and show strong bioaccumulation [1,2].

The most common reported extraction procedures for the water pollutants are liquid–liquid extraction [3], adsorption on activated charcoal [4] and/or cellulose triacetate membrane filters [5], Tenax, Chromosorb 101 and Porapak as trapping materials [6]. Such preconcentration methods are not satisfactory with respect to their capacity for trapping pollutants present at very small amounts and their recovery, and they are also too extensive for routine analysis where many large sample volumes are concentrated on site prior to quantitative analysis [7].

¹ Paper originally submitted for the thematic issue on Pesticide Residues [J. Chromatogr. A, 754 (1996)].

² On leave from the Chemistry Department, Faculty of Science, at Damiatta, Mansoura University, Damiatta, Egypt.

Recently, porous polyurethane foam has been used as an inexpensive solid extractor and effective sorbent for the removal of water pollutants [8,9]. The membrane-like structure of the foam together with its efficient sorption properties offered higher concentrating ability and flow-rates compared with other solid granular supports [10]. The present study was aimed at investigating the retention profiles of some pesticides, pyrethroids and acaricides in water at low levels (ppb) by polyether-based polyurethane foams. The influence of Chlorpyrifos on the uptake of some essential elements, e.g. N, K, P, Na, Fe, Zn, Mn and Cu, and on the wet and dry mass and humidity percentage of tomato and parsley plants after different times of spraying was also studied.

2. Experimental

2.1. Reagents and materials

All chemicals used were of analytical reagent grade. Open pore polyether-type-based polyurethane foams were supplied by K.G. Schaum (Stoffwerk, Kremsmunster, Austria). Foam cubes of approximately 1 cm³ were cut from polyurethane foam sheets. The foam cubes were dried as reported previously [11]. The foam cubes were loaded with tri-*n*-octylamine (TOA) and tri-*n*-methylphosphate (TMP) by mixing the dried foam cubes with 5% TOA and 5% TMP separately in *n*-hexane (20 cm³/g dry foam) with stirring for 10 min, respectively, and drying as reported [11]. Stock solutions (1 M) of lithium, sodium, ammonium and potassium chlorides were prepared separately in distilled water. Britton–Robinson buffer (pH 2–12) solutions were prepared by mixing equimolar concentration (0.08 M) of boric, acetic and phosphoric acid in distilled water and adjusting the pH with sodium hydroxide (0.04 M).

The tested pesticides are Chlorpyrifos, *o,o*-diethyl-*o*-(3,5,6-trichloro-2-pyridyl) phosphorothioate (I); Parathion, *o,o*-diethyl-4-nitrophenyl phosphorothioate (II); Malathion, diethyl-[(dimethoxyphosphinothioyl)thio]butanedioate (III); the pyrethroid Cypermethrin, cyano(3-phenoxyphenyl)methyl-3-(2,2-dichloroethyl)-2,2-dimethylcyclopropanecarboxylate (IV); and the acaricides Dicofol, 2,2,2-trichloro-

1-bis(4-chlorophenyl)ethanol (V) and Bromopropylate, isopropyl-4,4-dibromobenzilate (VI). The structures of these compounds are given in Fig. 1.

A stock solution of each compound (100 µg/cm³) was prepared by dissolving the exact mass of the compound in ethanol. A series of various concentrations of these compounds was then freshly prepared by diluting their stock solutions with distilled or tap water and a few drops of ethanol whenever it was required to provide a clear solution. The solutions were stored in polyethylene bottles.

2.2. Apparatus

UV absorbance of the tested insecticides was obtained with a Pye Unicam UV-Vis SP8-400 spectrometer with 0.2- and 1-cm quartz cells. An Orion pH meter and glass columns (15 cm×15 mm I.D.) and a Lab-Line Orbit Environ-Shaker Model 35271-1 were also used. A Corning flame photometer (410) and a Pye Unicam SP-9 atomic absorption spectrometer were used to measure the concentration of Na, K, Fe, Mn, Zn and Cu. Calcium was determined by EDTA titration. The Kjeldahl method was used for the determination of the nitrogen content in plant (tomato and parsley) tissues. Hot Box oven Honda spray machine with high pressure and stoppered flasks (50 cm³ capacity) were used.

2.3. General procedures

2.3.1. Batch experiments

Influence of shaking time on the retention profiles of the tested compounds on the unloaded and loaded polyurethane foams

The unloaded and loaded (TOA or TMP) polyurethane foam cubes (0.3+0.004 g) were equilibrated with 100 cm³ aqueous solution at pH 4–6 of each compound at concentrations of 100 µg/cm³ in polyethylene bottles and shaken in a thermostated mechanical shaker at 20±0.1°C for various time intervals up to 2 h. After shaking, the foam cubes were separated and the amount of the compound remaining in the aqueous phase was determined from its absorbance measurements at the wavelength of maximum absorbance against a blank; the amount of the insecticide retained on the foam was calculated

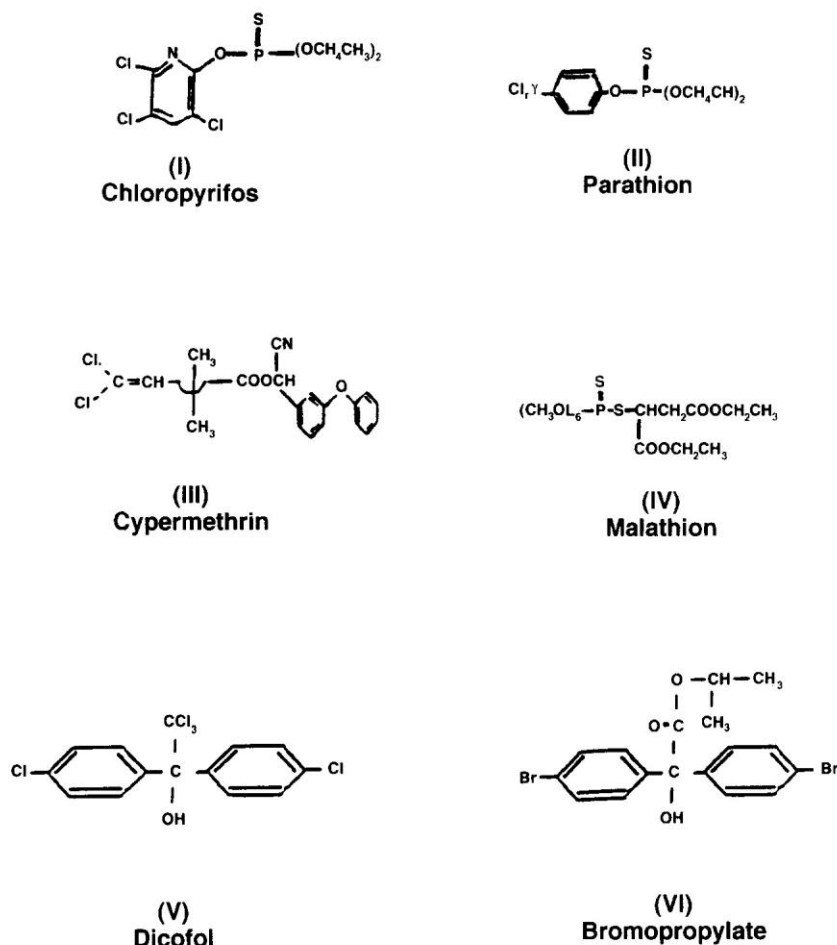


Fig. 1. The structure of the tested organophosphorous insecticides, pyrethroid and acaricides.

using this difference. The extraction efficiency (%*E*) and the distribution coefficient (*D*) of the tested species by the unloaded foams were determined employing the equations:

$$\% \text{Extraction } (E) = \frac{a_0 - a}{a} \times 100 \quad (1)$$

and

$$D = \frac{\%E}{100 - \%E} \times \frac{\text{Volume of solution (l)}}{\text{Mass of foam (kg)}} \quad (2)$$

or

$$D = \frac{\%E}{100 - \%E} \times \frac{\text{Volume of solution (cm}^3\text{)}}{\text{Mass of foam (g)}} \quad (3)$$

where a_0 = concentration of the tested compound in

solution before extraction and a = concentration of the solute in solution after extraction.

Following these procedures, the influence of solution pH, nature of extraction media, temperature, compound concentration and salt concentration ($\leq 0.1 M$) of different chloride salts (Li, Na, K and NH_4) on the retention profiles of the tested compounds by the unloaded, TOA- and TMP-loaded polyurethane foams were critically determined.

2.3.2. Column experiments

Chromatographic behaviour of the tested insecticides on a column packed with the unloaded foam

Quantitative retention and elution of the tested compounds on the unloaded foam columns were

carried out using the vacuum method of foam packing [11]. Tap or distilled water (0.1–6 dm³) samples containing 0.05 mg of the tested compound at the pH of maximum retention on the unloaded foams was percolated through the column packed with 3±0.006 g of the unloaded foam at 10 cm³/min. After squeezing water from the foam material, the compound was recovered from the foam with 100 cm³ acetone in a Soxhlet extractor for 6 h. The sample quantity was then determined from a pre-constructed calibration curve by measuring the absorbance of the extracted acetone solution against a blank.

2.3.3. Plant analysis

Sample preparation

Plant sample (leaves) of tomato and parsley were sprayed with 20 g of commercial Chlorpyrifos (40%, w/w) mixed with 20 dm³ water (4:1×10⁴, w/v) in the open field using a high-pressure sprayer. The treated plant samples were left for periods of 24, 72 and 120 h. Five samples each of untreated and treated leaves were then collected, washed with distilled water until all dust and sand were removed completely and finally dried with a napkin. The leaves were cut into small pieces, washed with water and spread for 24 h at room temperature for drying and grinding into powder form.

Determination of the total nitrogen content

A mass of the dry leaves (0.2–0.3 g) was accurately weighed and placed in a 800 cm³ Kjeldahl flask; 50 cm³ of concentrated sulphuric acid containing 1.65 g of salicylic acid were added. Five grams of sodium thiosulphate were added, the mixture was heated for 30 min, cooled and 10 g of a sodium hydrogensulphate–selenium mixture (100:1, w/w) were added and the mixture was digested in the Kjeldahl apparatus. After complete digestion, the mixture was cooled and 300 cm³ of water and 100 cm³ of concentrated sodium hydroxide were added. Then the distillate standard sulphuric acid was distilled and titrated and the nitrogen content was determined employing the equation:

$$\%N = \frac{14NV}{10W} \quad (4)$$

where N and V are the normality and volume in cm³ of sulphuric acid consumed in the titration and W is the mass of the dry leaves in g.

Determination of P, Na, K, Cu, Zn, Mn and Fe by wet ashing

An accurate mass (2–3 g) of the ground plant material was placed in 20 cm³ of a concentrated sulphuric–perchloric acid mixture (1:1, v/v). The reaction mixture was heated on a hot plate until the acid fumes were completely evolved; the volume of the reaction mixture was reduced to 3–5 cm³ by evaporation on a hot plate and 50 cm³ of distilled water were added to the mark. Calibration graphs for phosphorous and molybdenum were made by UV-visible spectrophotometry; for sodium and potassium flame photometry was used, and for copper, zinc, manganese and iron atomic absorption spectrometry was employed. The unknown sample concentration was then obtained from a calibration graph of each element employing the following equation:

$$\%M = \frac{C \text{ (ppm)} \times \text{solution volume (cm}^3\text{)}}{10^4 \times \text{sample mass (g)}} \quad (5)$$

where $M = P, Na, K, Cu, Zn, Mn$ or Fe and C is the concentration of the element to be determined in ppm.

Determination of the moisture or humidity content

The sample was spread in the container, rapidly weighed, dried in a circulation oven at 70–80°C to a constant mass, cooled in a desiccator, weighed. The humidity and dry matter percentages of the plant leaves were obtained by employing the equations:

$$\text{Moisture (\%)} = \frac{\text{Loss in mass on drying (g)}}{\text{Initial sample mass (g)}} \times 100 \quad (6)$$

$$\text{Dry matter (\%)} = \frac{\text{Oven dry mass (g)}}{\text{Initial sample mass (g)}} \times 100 \quad (7)$$

Ash content

The crucible in a muffle furnace was heated to about 500°C, cooled in a desiccator, weighed and an accurate mass of 1 g of oven-dried sample was transferred into the crucible. The crucible containing the dry sample was placed into a cool muffle furnace

and the temperature was increased to 500°C. After 3 h at 500°C the crucible was removed, allowed to cool in a desiccator, weighed and the ash content was determined by employing the equation:

$$\text{Ash (\%)} = \frac{\text{Ash mass (g)}}{\text{Oven dry mass (g)}} \times 100 \quad (8)$$

Dry ashing

A 0.2-g amount of air-dried ground sample was weighed into an acid-washed porcelain basin, ignited to 500°C for 3 h in a muffle furnace (refer to ashing procedure) and cooled; 5 cm³ of HCl (1:1, v/v) were added and the sample was covered with a watch glass and heated on a steam bath for 15 min. Then 1 cm³ of concentrated HNO₃ was added, the sample evaporated to dryness, and heating continued for 1 h; 2 cm³ of HCl (1:1, v/v) were added, the sample swirled to dissolve the residue, diluted to 20 cm³ with water and warmed to complete dissolution. Then the sample was filtered through a No. 44 filter paper into a 100 cm³ volumetric flask and diluted with distilled water to the mark. Blank determination was carried out in the same way.

3. Results and discussion

The use of unloaded polyurethane foams (PuF) in the separation and preconcentration processes led to observation of the potential of their spherical geometrical form (spherical membrane-shaped geometry) and to the proposal of their general use in column operations as a substitute for the traditional granular supports in extraction chromatography. The membrane-like structure of the foams together with the efficient sorption and mass-transfer properties offer higher concentrating abilities and flow-rate compared with other solid supports. Thus, in recent years, considerable progress has been made in the use of polyurethane foam as an inexpensive solid extractor and effective sorbent for the removal of water pollutants.

3.1. Retention behaviour of the tested compounds on the unloaded and loaded foams by batch experiments

Batch experiments using unloaded foams have

shown that the retention of Parathion, Malathion, Chlorpyrifos and Cypermethrin was rapid and the equilibrium was reached in less than 50 min, followed by a plateau. Hence, a minimum shaking time of 1 h was adopted in the subsequent work. The results obtained are summarized in Fig. 2. The average values of the half-life ($t_{1/2}$) of the sorption equilibrium calculated from Fig. 2 were found to be in the range 2–3 min.

Similarly, batch experiments using unloaded, TMP- and TOA-loaded polyurethane foams have shown that the extraction of the investigated acaricides Dicofol and Bromopropylate from aqueous solution at pH ≤ 3 is rapid and the equilibrium is reached in less than 1 h, followed by a plateau. A good extraction efficiency and rapid preconcentration of the tested acaricides from aqueous media were obtained with TOA-treated foam as compared to the unloaded and TMP-loaded foams. The average values of the half-life ($t_{1/2}$) of equilibrium sorption on the unloaded, TOA- and TMP-loaded foams were found to be in the range 3–5, 2.5–3 and 3–4 min, respectively. The tri-*n*-octylamine acts as a plasticizer on the polyether foam. Thus, the collection

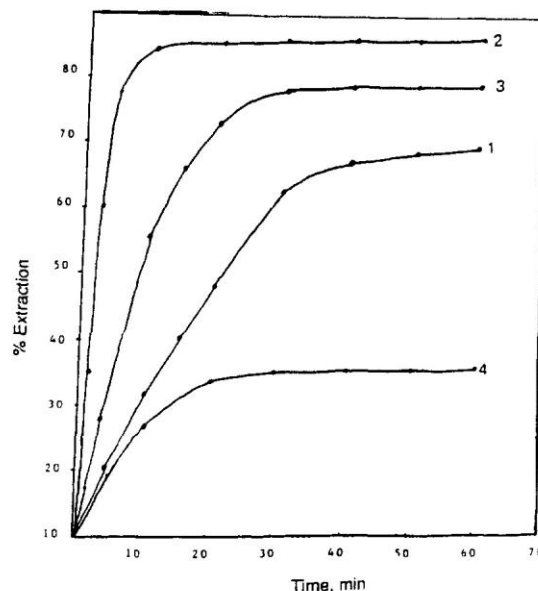


Fig. 2. Effect of shaking time on the sorption profiles of (1) Parathion, (2) Malathion, (3) Chlorpyrifos and (4) Cypermethrin at 100 mg/cm³ in aqueous solution (100 cm³) at pH 5–7 and 20 ± 0.1°C using the unloaded foam (0.3 ± 0.004 g).

rates of the compounds with plasticized TOA foams are generally better than with unplasticized ones. This can be attributed to the high mobilities and diffusion rates of the tested acaricides through the open pores and the quasi-spherical membrane structure of the plasticized TOA foam [11,12]. The plasticizer acts as an efficient nonvolatile solvent for the foam plastic itself. These results are in good agreement with the data reported by Braun et al. [13]. The foam membrane acts as a true sorbent where the diffusion rates of the chemical species in the membrane structure are considerably higher than those in bulky solids [14,15].

The influence of the pH on the extraction of each of the tested compounds by the unloaded foams at $100 \mu\text{g}/\text{cm}^3$ concentration was examined over the pH range 2–12. The sorption profiles of the investigated compounds by the unloaded foams increased markedly in the pH range 5–7 except for Chlorpyrifos which reached a maximum retention in the pH range 2–4. Malathion displays the lowest removal at pH 9 and the percentage removal slightly increased at higher pH. Lowering the pH tends to protonate the nitrogen atoms of the urethane linkage of the polyurethane foam, Fig. 3, as reported by El-Shahawi [16]. The percentage removal of Dicofol and bromopropylate by the unloaded foams decreased at moderate pH (5–7) and reaches a maximum at $\text{pH} < 3$ at which the compounds exist in the neutral form. Thus, the sorption of these compounds involves neutral species and this is consistent with a solvent extraction mechanism [16].

3.2. Sorption isotherms

The extraction isotherms of the tested compounds (I–IV) on the unloaded foams were developed over a wide range of equilibrium concentrations (10–100

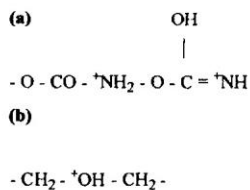
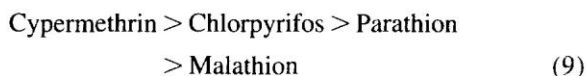


Fig. 3. (a) Protonated urethane, and/or (b) ether oxygen atoms of the polyurethane foam.

$\mu\text{g}/\text{cm}^3$) for each species at 100°C . The pH values of the aqueous solution were adjusted to a pH in the range 4–7, so that the compounds were predominately in the undissociated form. At low concentration the sorption isotherms exhibited a first-order behaviour and tended to plateau at higher bulk solution concentrations. Fig. 4 shows plots of the remaining concentration of the tested insecticides in the aqueous phase versus their concentration retained on the foam material. The sorption of the different species by the unloaded foams increased in the order:



Similar trends for the extraction of the tested

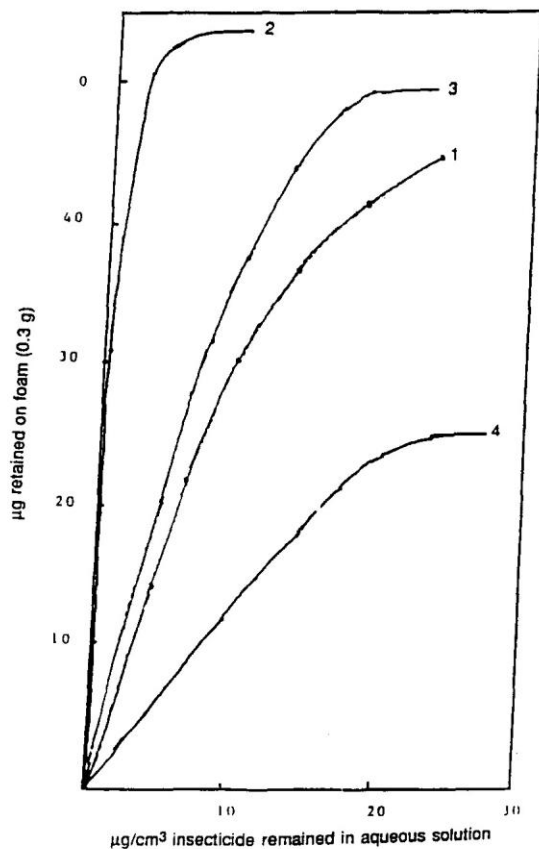


Fig. 4. Extraction isotherm of (1) Parathion, (2) Cypermethrin, (3) Chlorpyrifos and (4) Malathion at concentrations of 10–100 $\mu\text{g}/\text{cm}^3$ using the unloaded foams ($0.3 \pm 0.004 \text{ g}$) from a 100 cm^3 aqueous sample at pH 5–7 and $20 \pm 0.1^\circ\text{C}$ and 1 h extraction time.

compounds were obtained with diethyl ether and for other similar species retained on the polyurethane foams [16]. Therefore, 'solvent extraction' is the most probable mechanism for the sorption of the tested species by the unloaded polyurethane foam [7]. However, it is worth noting that the molecular masses (M_r) of Chlorpyrifos ($M_r=345.5$), Malathion ($M_r=230.3$), Parathion ($M_r=291.0$) and Cypermethrin ($M_r=419.6$) are also participating factors in the extraction step by the foam. These data are also consistent with the general understanding that the larger the molecular mass of the sorbate the larger the amount of the tested insecticides retained on the foam when the substances concerned are similar in nature [17].

The sorption behaviour of the investigated acaricides (Dicofol and Bromopropylate) from aqueous solution by the unloaded and TMP- and TOA-loaded foams was found also to depend on the concentration. Thus, the extraction isotherms were developed over a wide range of equilibrium concentrations ($10\text{--}200\ \mu\text{g}/\text{cm}^3$) for each compound at $20\pm 0.1^\circ\text{C}$. The pH values of the aqueous solution in these experiments were adjusted at $\text{pH}\leq 3$. A good linear correlation between the concentration of each compound extracted on the unloaded and TMP- and

TOA-loaded foams was achieved. The sorption profiles obtained using the unloaded and loaded foam increased in the order:

$$\text{TOA - foam} > \text{TMP - foam} > \text{unloaded foam} \quad (10)$$

The influence of various concentrations of alkali metal (Li^+ , Na^+ , NH_4^+ and K^+) chlorides at concentrations $\leq 0.1\ M$ on the sorption percentage of the tested compounds at $80\ \mu\text{g}/\text{cm}^3$ was studied at the optimum pH extraction. The results obtained on the sorption by the unloaded foams are summarized in Table 1. A significant increase in the distribution ratios of Malathion, Dicofol and Bromopropylate was observed with increasing LiCl or NaCl concentrations from 0.01 to 0.1 M and the following order of extraction was noted:

$$\text{Li}^+ > \text{Na}^+ > \text{NH}_4^+ > \text{K}^+ \quad (11)$$

This behaviour is characteristic of the 'solvent extraction mechanism' with the salt acting as salting out and the cation-chelation mechanism excluded [9,16]. The distribution ratios of Malathion increased with the amount of salt added from $\log D=3.43$ and 3.41 to 3.52 and 3.42 for Na^+ and Li^+ ions at 0.05 and 0.1 M (Fig. 5). The added salts (Li^+ , Na^+)

Table 1

Logarithm distribution coefficient (D) data for the sorption profiles of the tested compounds using the unloaded foams in the presence of different univalent cations

Cation concentration (M)	Insecticides			Pyrethroid	Acaricides	
	Malathion	Parathion	Cypermethrin	Chlorpyrifos	Dicofol	Bromopropylate
Li^+						
0.01	3.43	2.94	2.70	3.79	3.84	3.61
0.05	3.49	2.58	2.55	3.71	3.60	3.66
0.10	3.52	2.42	2.41	3.59	3.38	3.69
Na^+						
0.01	3.41	2.65	2.91	3.92	3.54	3.50
0.05	3.44	2.40	2.76	3.90	3.37	3.53
0.10	3.42	2.28	2.64	3.90	3.37	3.53
				3.88	3.30	3.55
K^+						
0.01	3.37	2.05	3.60	4.60	2.58	3.92
0.05	3.30	2.02	3.52	4.72	2.62	3.45
0.10	3.19					
NH_4^+						
0.01	3.35	2.03	2.61	4.40	3.37	3.62
0.05	3.32	1.98	2.50	4.45	3.35	3.58
0.10	3.23	1.92	2.42	4.52	3.40	3.54

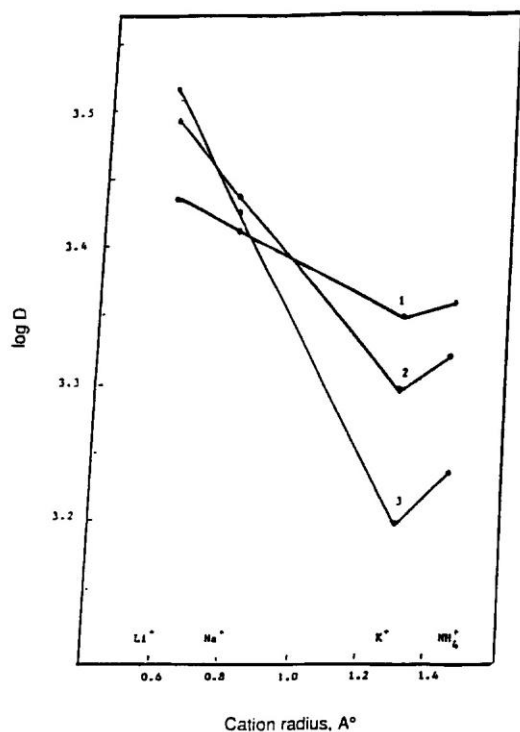


Fig. 5. Effect of extraction media on the sorption profile of Malathion using unloaded foam at 1 h shaking time, with (1) 0%, (2) 5% and (3) 10% of ethanol–water (v/v). Other conditions are as in Fig. 2.

increased the sorption profiles of the tested compound into the polyether foams by reducing the number of water molecules available to solvate the organic compound which would, therefore, be forced out of the solvent phase into the foam. In such cases some amount of the free water molecules are preferentially used to solvate the ions added [18]. Hence, the influence of these salts can be explained by the salting-out effect and 'solvent extraction' is the most probable mechanism [9].

The retention behaviour of Cypermethrin and Chlorpyrifos by the unloaded foams (Table 1) decreased with increasing concentration of the alkali metal Li^+ , Na^+ , K^+ and NH_4^+ chlorides, and the following order of sorption

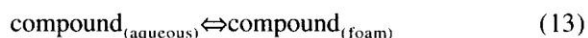
$$\text{K}^+ > \text{Na}^+ > \text{NH}_4^+ > \text{Li}^+ \quad (12)$$

was achieved at 0.1 M salt concentration. Therefore, the ion dipole interaction of NH_4^+ with the oxygen

sites of polyurethane foam might highly predominate in the sorption profiles of Cypermethrin and Chlorpyrifos.

According to the 'cation-chelation mechanism' the presence of K^+ ions should facilitate the extraction of Cypermethrin and Chlorpyrifos by the foam more than the other alkali metal ions (NH_4^+ , Na^+ or Li^+) because of the better fit of this ion into the central cavity of the oxygen-rich helix in the polyurethane foam. The sorption profiles of Cypermethrin and Chlorpyrifos are in good agreement with the data recently reported by Palagyi et al. [15]. Therefore, the 'cation-chelation mechanism' is the most probable mechanism for the sorption of these species. In accordance with this mechanism, the polyalkenoxy chains of the PuF sorbent form a clathrate with suitable simple cations [16].

In batch experiments the influence of temperature (35, 45 and 55°C) on the sorption profiles of the tested species (I–IV) by unloaded foams was determined at the pH of maximum extraction of each compound. The percentage extractions and the distribution ratios of the tested compounds increased slightly with increasing temperature and similar trends to that obtained at 20°C were achieved. Assuming no precipitation or chelation and the extracted species to be neutral, then the equilibrium constant K for the equation



is equivalent to the distribution ratio, D . Thus by plotting $\ln D$ vs. T and employing the equation:

$$\ln K = \frac{\Delta H^0}{RT} + \frac{\Delta S^0}{R}, \quad (14)$$

the values of the standard enthalpy change ΔH^0 and the standard entropy change ΔS^0 were obtained (Table 2). The ΔS^0 for Malathion and Parathion were found to be -20 ± 2 and -38 ± 4 J/mol deg, while for the Cypermethrin and Chlorpyrifos the ΔS^0 values were found to be -16 ± 1.8 and -19 ± 2 J/mol deg, respectively, for the sorption into the unloaded foam. The high molecular mass of the Cypermethrin ($M_r = 416.6$) may account for its higher value of ΔS^0 . The observed decrease in the ΔS^0 of Malathion and Parathion is possibly due to the presence of the P=S group which could reduce the

Table 2
Thermodynamic data for the sorption of the tested insecticides and acaricides by (a) unloaded, and (b) TOA-loaded foams

	ΔH^0 (kJ/mol)		ΔS^0 (J/mol deg ⁻¹)	
	a	b	a	b
Malathion	24±2		20±2	
Parathion	26±1.2		38±4	
Cypermethrin	28±1.8		16±1.8	
Chlorpyrifos	25±2.1		19±2	
Dicofol	20.12±2	22.7±2.3	27.9±2.9	33±2
Bromopropylate	23.2±2.6	27.2±3	30±3	42±3

Conditions: extraction from aqueous solution (100 cm³) at pH 3 and temperature range 20–55°C.

ion-dipole interaction with the oxygen sites of the polyurethane foam. This also would reduce the degrees of freedom of movement of the tested organic compounds in the polyurethane foam, as previously reported [18–20].

The polymeric nature and/or the different functional groups or heteroatoms in the foam may also take a part in the sorption process of both Malathion and Parathion. These data are also consistent with the solvent extraction mechanism and are in good agreement with the data previously reported by Schumack and Chow [19]. The values of ΔH^0 were found in the range 24–28±2.1 kJ/mol. Raising the temperature may facilitate the partition of the tested species through the polyurethane foam via urethane linkage and/or ether oxygen atoms.

The values of the standard entropy change ΔS^0 and the standard enthalpy change ΔH^0 for the tested acaricides on the unloaded and TOA-treated foams are also summarized in Table 2. The ΔS^0 for the Dicofol and Bromopropylate were found to be in the range –27–30±3 J/mol deg, for extraction into the unloaded foams and –33–42±3 J/mol deg, for sorption into the TOA foams. The decrease in the entropy change with the use of the TOA foam is believed to be due to the hydrogen bonding reducing the degree of freedom of movement of the organic compound in the polyether foam, as reported [20]. These results are consistent with the solvent-extraction mechanism. The bonding of the organic compound with the foam was estimated to be about 10 kJ/mol, which is lower than the intermolecular H-bonding (30 kJ/mol) [16,19]. Raising the temperature may facilitate the formation of intermolecu-

lar H-bonding between the hydrogen group of the tested acaricide and the polyurethane foam via nitrogen and/or oxygen atoms.

The influence of the sorption media on the pre-concentration of the tested compounds by the foams was examined at the optimum pH by the addition of various proportions of ethanol (0–10%). The sorption percentages of Malathion and Parathion were decreased by the addition of ethanol up to 10%. Representative results are summarized in Fig. 6. This behaviour is probably due to the formation of different association in the aqueous solution [20]. These data are also consistent with the fact that with a compound of low dielectric constant, the degree of extraction should increase with increasing polarity of the polar phase [16]. Thus the 'solvent extraction mechanism' is the most probable mechanism for the sorption of Malathion and Parathion. In contrast, the sorption profiles of Cypermethrin and Chlorpyrifos increased with increasing ethanol concentration.

The effect of ethanol (0–10%) on the sorption percentage of the tested acaricide by the unloaded and TMP-loaded foams was determined. The sorption profiles of compounds V and VI by the unloaded foams are given in Fig. 7. The extraction of the compounds by the unloaded foams increased by the addition of ethanol (up to 10%) to the aqueous solution. Similar trends were also obtained with TMP-loaded foams. Dicofol and Bromopropylate species in the aqueous solution are well solvated in the presence of ethanol and so it is difficult for these ions to form ion-pairs in the aqueous solution. Thus, the solvent extraction mechanism is the most probable mechanism.

3.3. Chromatographic behaviour of the tested insecticides on polyurethane foam columns

Static experiments on the sorption behaviour of the tested pesticides, pyrethroid and acaricides (I–VI) from the aqueous solution with the unloaded foams suggest the possible application of the foam in the column extraction mode. Distilled or tap-water samples (0.1–6 dm³) containing 0.05 mg of each compound were percolated separately through the foam columns at a flow-rate of 10–15 cm³/min at the pH of maximum extractibility. More or less complete retention of the tested compounds was

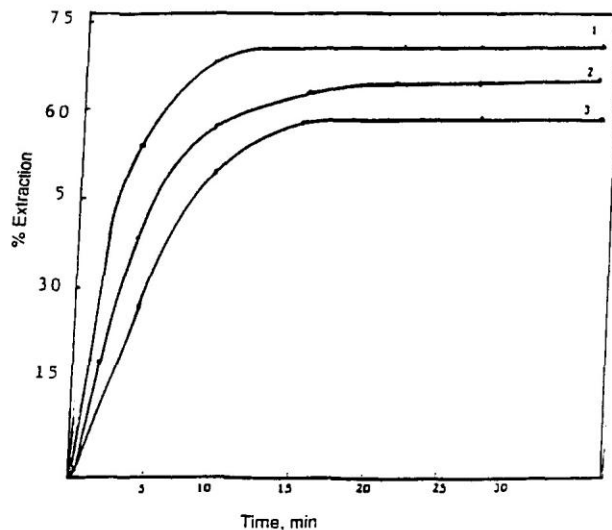


Fig. 6. Effect of extraction media on the sorption profile of Malathion using the unloaded foam at 1 h shaking time, with (1) 0%, (2) 5% and (3) 10% of ethanol. Other conditions are as in Fig. 2.

achieved by the foam column. After squeezing water from the foam, the retained compounds were recovered quantitatively from the foam material with 100 cm³ acetone in a Soxhlet extractor and determined spectrophotometrically at the optimum wavelength. Satisfactory recovery percentages (99.5% ± 2.1) of the tested compounds from the aqueous media by the proposed foam column method are summarized in Table 3.

The dependence of the sorption profiles of the tested species by the proposed unloaded foam column on the flow-rate (2–25 cm³/min) and sample volume (0.1–6 cm³) was investigated. An aqueous sample (2 dm³) containing 0.05 mg Parathion was percolated through the foam column at various flow-rates up to 25 cm³/min. Complete retention of Parathion was obtained at a flow-rate up to 15 cm³/min. The extraction efficiency decreased significantly to 76% at a flow-rate of 20–25 cm³/min from a 6 dm³ aqueous sample solution. On the other hand, on increasing the sample volume from 2 to 6 dm³ at a flow-rate < 15 cm³/min, no significant decrease on the retention percentage was observed.

To determine the performance of the untreated foam column by the chromatogram method a quantitative retention of Dicofol (0.01 mg) in 0.5 dm³ aqueous solution at optimum pH of extraction was

achieved followed by elution with 200 cm³ acetone–HCl (1:1, v/v) from the unloaded foam column at a flow-rate of 5 cm³/min. The height equivalent to a theoretical plate (HETP) was obtained from the elution curves using the equation [9]

$$N + \frac{L}{\text{HETP}} = \frac{8V_{\text{max}}^2}{w_e}, \quad (15)$$

where N = number of theoretical plates, V_{max} = volume of elute at the peak maximum, w_e = width of the peak at $1/e$ of the maximum solute concentration and L = length of the column foam bed in mm. The HETP values were found to be equal to 1.9 ± 0.2 and 2 ± 0.2 mm at flow-rates of 15 and 20 cm³/min, respectively.

The unloaded foam column performance was also calculated from the breakthrough capacity curve method for Parathion (Fig. 8). An aqueous solution (5 dm³) of Parathion (50 µg/cm³) was percolated through the column at 10 and 20 cm³/min and the height equivalent to the theoretical plates was calculated by employing the equation:

$$N = \frac{V_1 V_2}{(V_1 - V_2)^2} = \frac{L}{\text{HETP}}, \quad (16)$$

where V_1 = volume of the effluent at the centre of the

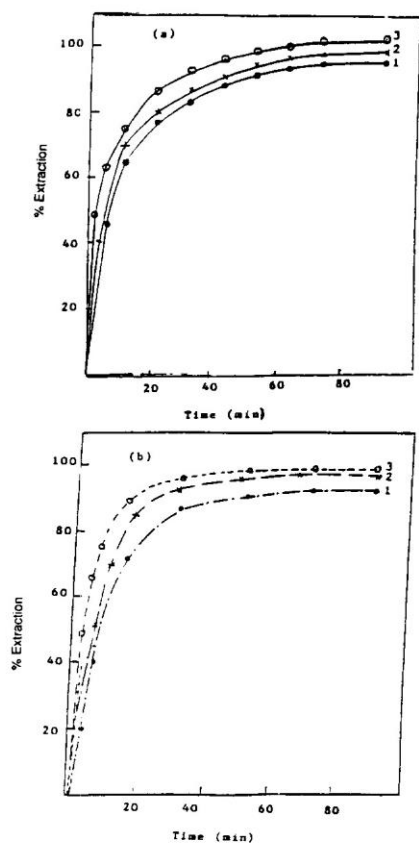


Fig. 7. Effect of extraction media on the sorption profile of (a) Dicofol and (b) Bromopropylate using unloaded foams at pH < 3 and 1 h extraction time. Ethanol concentrations are: (1) 0%, (2) 5% and (3) 10%. Other conditions are as in Fig. 2.

Table 3

Extraction and recovery of the tested compounds from 3 dm³ distilled and tap water by the proposed unloaded foam column^a

Compound	Recovery (%)		Wavelength (nm)
	Distilled water	Tap water	
Parathion	95.6 ± 0.4	95.9 ± 0.4	274
Malathion	93.5 ± 0.5	99.5 ± 2.1	206
Cypermethrin	94.2 ± 0.4	95.7 ± 0.7	273
Chlorpyrifos	96.5 ± 0.6	97.2 ± 0.4	206
Dicofol	97 ± 1.2	94.9 ± 2.1	248
Bromopropylate	97.2 ± 2.2	95.1 ± 1.7	242

^a Average ± S.D. for five measurements.

S-shaped part of the breakthrough capacity curve where the concentration is one-half of the initial concentration and V_2 is the volume at which the effluent has a concentration of 0.1578 of the initial concentration. The volume of HETP obtained by this method was found to be in the range 2.1 ± 0.2 mm at flow-rates of 10 and 20 cm³/min. These values are in good agreement with the data obtained from the chromatogram methods at a flow-rate of 10 cm³/min.

The proposed foam column method has been successfully employed for the separation of the binary mixtures Malathion–Cypermethrin and Parathion–Cypermethrin insecticides from different volumes (0.1–2 dm³) of the aqueous media. A mixture containing 0.05 mg Malathion (or Parathion) was separated from 0.05 mg of Cypermethrin at pH 1.5 and 0.1 M lithium chloride. Sorption of Malathion (or Parathion) took place while Cypermethrin was not retained on the foam column and collected quantitatively in the eluent. Malathion (or Parathion) was then recovered from the column by 100 cm³ acetone in a Soxhlet extractor, as described before.

3.4. Capacity

Break-through capacity was defined as the amount of the compound that could be retained on the column when the solution of the tested compound was allowed to pass through it at a reasonable flow-rate (5–10 cm³/min) until the compound was first detected in the effluent solution. Practically, this capacity was determined from the actual volume that was collected just before the appearance of the compound in the effluent solution minus the free-column volume. The resulting value was multiplied by the concentration of the marginal solution. After reaching the break-through volume, percolation of the test solution was continued until the effluent solution concentration reached that of the feed aliquot. The curves of Fig. 8 present the break-through volume and the volume needed to reach feed saturation for Parathion (50 µg/cm³) at the optimum pH at flow-rates of 10 and 20 cm³/min. The break-through and the overall capacities of the proposed column packed with 1 g dry foam for the retention of Parathion were 0.4 and 0.35 mg insecticide per g of

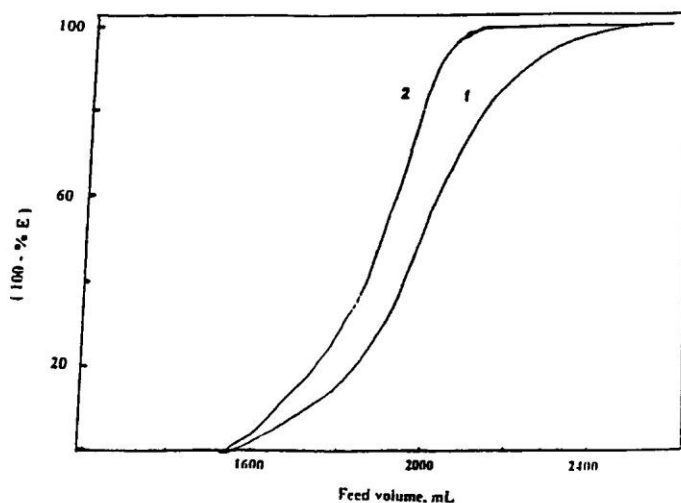


Fig. 8. Breakthrough capacity curves of the sorption profiles for Parathion at flow-rates of (1) 10 cm³/min and (2) 20 cm³/min using the unloaded foam column.

the unloaded foam at 10 and 20 cm³/min, respectively.

3.5. Effect of Chlorpyrifos treatment on tomato and parsley plants

Total trace-element analysis of tomato and parsley

plants was performed before (1) and after spraying with Chlorpyrifos in water for 24 (2), 72 (3) and 120 (4) h. The results are summarized in Tables 4 and 5 for tomato and parsley, respectively. The overall average concentration pattern of the essential elements N, K, P, Na, Fe, Zn, Mn and Copper in tomato is summarized in Table 4.

Table 4

Total trace element of tomato before and after spraying with Chlorpyrifos in water (0.04%, w/v)^a

S. No.	Type	Content (%)				Concentration (ppm)			
		N	K	P	Na	Fe	Zn	Mn	Cu
1	Tomato before spray	3.45±0.52	0.80±0.08	0.43±0.10	0.31±0.04	100.±3.40	12.0±2.40	55.5±2.80	41.0±3.10
2	Tomato after spray 24 h	3.16±0.60	0.86±0.12	0.46±0.26	0.36±0.05	110.±2.80	11.5±1.80	61.0±2.90	26.0±2.20
3	Tomato after spray 72 h	3.22±0.32	0.87±0.22	0.45±0.14	0.29±0.09	080.±4.00	12.0±1.20	45.0±2.10	30.0±2.80
4	Tomato after spray 120 h	3.36±0.40	0.75±0.11	0.46±0.10	0.32±0.07	055.±3.20	12.0±1.30	40.0±2.60	16.0±1.20

^a Average of three measurements.

Table 5

Total trace element of plant parsley before and after spraying with Chlorpyrifos in water (0.04%, w/v)^a

S. No.	Type	Content (%)				Concentration (ppm)			
		N	K	P	Na	Fe	Zn	Mn	Cu
1	Parsley before spray	3.10±0.29	1.90±0.07	0.39±0.20	1.50±0.10	72.5±3.20	30.5±2.90	31.0±2.40	07.0±1.20
2	Parsley after spray 24 h	3.67±0.29	1.97±0.07	0.43±0.34	1.48±0.07	70.0±2.80	32.5±1.60	33.5±1.90	07.0±1.10
3	Parsley after spray 72 h	3.81±0.30	2.60±0.08	0.43±0.50	0.92±0.08	60.0±2.10	34.0±3.00	35.0±1.80	08.0±1.10
4	Parsley after spray 120 h	3.75±0.24	2.52±0.10	0.50±0.60	1.05±0.06	65.0±1.80	34.0±2.20	35.0±2.10	08.0±0.90

^a Average of three measurements.

Table 6
Wet mass, dry mass and humidity of tomato before and after spraying with Chlorpyrifos in water (0.04%)^a

S. No.	Sample	Wet mass (g)	Dry mass (g)	Humidity (%)
1	Tomato before spray	11.78±0.70	02.13±0.11	81.90±6.22
2	Tomato after 24 h spray	14.81±0.90	02.08±0.07	86.10±4.90
3	Tomato after 72 h spray	17.78±0.40	07.53±0.60	81.00±5.20
4	Tomato after 120 h spray	17.57±0.42	03.43±0.10	78.40±3.20

^a Average of five measurements.

For iron (55–110±4 ppm), manganese (40–61±2.9 ppm) and copper (16–41±3.1 ppm), the concentration pattern follows the sequences 2>1>3>4, 2>1>3>4 and 1>3>2>4, respectively. The observed decrease of these elements is possibly attributed to the great ability of Chlorpyrifos and its modes of action [21] to penetrate through tomato plant tissues and complexing with these metal ions. Accumulation of Chlorpyrifos complex species may also decrease the uptake of these metal ions. No significant changes in the uptake of zinc (12±0.4 ppm) and nitrogen (3.2–3.4±0.6%) were observed.

In plant parsley (Table 5) the distribution of phosphorous (0.39–0.50±0.2%) and copper (7–9±1.2 ppm) before and after spray follows the sequence 4>3>2>1, while for nitrogen (3.1–3.8±0.3%) and potassium (1.9–2.6±0.1%) the uptake follows the order 3>4>2>1.

In the case of sodium (0.9–1.5±0.1%) and iron (60–72.5±3.9 ppm) the distribution follows the sequence 1>2>4>3, while for zinc (30.5–34±3 ppm) and manganese (31–35±2.4 ppm), the uptake follows the sequences 4>3>2>1 and 3>4>2>1, respectively. The uptake of phosphorous and copper increased with increasing spray time of Chlorpyrifos, while the uptake of sodium and iron decreased. These results may be attributed to the influence of Chlorpyrifos on the plant tissues.

Tables 6 and 7 show the effect of Chlorpyrifos on the percentages of humidity, wet mass and dry mass for tomato and parsley plants. In tomato (Table 6) the percentages of humidity (78.4–86.1%), dry mass (2.1–7.5%) and wet mass (11.8–17.8%) distribution patterns follow the sequences 2>1>3>4, 3>4>1>2 and 3>4>2>1.

In parsley plant (Table 7), a more or less similar observation on the humidity (78.4–81%), dry mass (2.3–3.8%) and wet mass (12.3–17.6%) was observed. The distribution patterns follow the sequences 2>3>1>4, 4>2>1>3 and 4>2>3>1.

These results suggest a similar mode of action of Chlorpyrifos on the humidity percentages of plant tomato and parsley. A more or less similar mode of action of Chlorpyrifos on the dry and wet mass was found for tomato and parsley tissues untreated and treated with Chlorpyrifos for different periods of time (0–120 h).

4. Conclusion

Loaded and unloaded foams in batch and column modes can be applied to trap trace amounts of insecticides, pyrethroids and acaricides from water. The retained species can be separated with an appropriate eluent, provided that there is a suffi-

Table 7
Wet mass, dry mass and humidity of parsley before and after spraying with Chlorpyrifos in water (0.04%)^a

S. No.	Sample	Wet mass (g)	Dry mass (g)	Humidity (%)
1	Parsley before spray	12.29±0.20	2.55±0.40	79.00±5.20
2	Parsley after 24 h spray	15.61±0.30	2.97±0.40	81.00±2.90
3	Parsley after 72 h spray	14.32±0.62	2.34±0.12	79.00±3.40
4	Parsley after 120 h spray	17.57±0.75	3.80±0.25	78.00±4.20

^a Average of five measurements.

ciently large difference in the optimum condition of extraction of each compound. The study of the tested compounds shows that Parathion, Malathion and acaricides are extracted in their neutral form by a simple solvent extraction mechanism. This conclusion is supported by the short time required for the extraction equilibrium and the salting-out phenomenon. The molecular mass of the sorbate and the strong hydrogen bonding between the tested acaricides with the polyether foam have also a great influence on the extraction process. Moreover, the plasticization of the foam with TOA offers a wider range of modifications than normal granular solids. The good hydrodynamic properties of the foam sorbents give unique advantages in rapidity, versatility and preconcentration of the tested compounds. The foam provides advantages because it is low cost, easily separable and non-polluting. The foam membrane offers unique advantages because of its high flow-rates, effective separations and preconcentrations of different species from fluid systems when large sample volumes are analyzed.

References

- [1] A.S.Y. Chan, B.K. Afghan and J.W. Robinson, *Analysis of Pesticides in Water, Significance, Principles, Techniques and Chemistry of Pesticides*, CRC Press, Boca Raton, FL, Vol. 1, 1982.
- [2] C.A. Edward, *Persistent Pesticides in Environment*, CRC Press, Boca Raton, FL, 2nd ed., 1973.
- [3] C.A. Edward, *Environmental Pollution by Pesticides*, Plenum Press, New York, 1981, p. 409.
- [4] J.P. Mieux and M.W. Dietrich, *J. Chromatogr. Sci.*, 11 (1973) 559.
- [5] B. Versino, M. DeGroot and F. Geiss, *Chromatographia*, 7 (1974) 302.
- [6] D.S. Walker, *Analyst*, 103 (1978) 397.
- [7] M.S. El-Shahawi, A.B. Farag and M.R. Mostafa, *Sep. Sci. Technology*, 29 (1994) 289.
- [8] S. Palagyi and T. Braun, in Z.B. Al-Fassi and C.M. Wai (Editors), *Preconcentration Techniques for Trace Elements*, CRC Press, Boca Raton, FL, 1992.
- [9] T. Braun, J.D. Navratil and A.B. Farag, *Polyurethane Foam Sorbents in Separation Science*, CRC Press, Boca Raton, FL, 1985.
- [10] M.S. El-Shahawi and S.M. Aldhaheeri, *Anal. Chim. Acta* 320 (1996) 277; I.L. Stewart and A. Chow, *Talanta*, 40 (1993) 1345.
- [11] T. Braun and A.B. Farag, *Anal. Chim. Acta*, 73 (1974) 301.
- [12] G.J. Moody and J.D.R. Thomas, *Chromatographic Separation with Foamed Plastics and Rubbers*, Marcel Dekker, New York, 1982.
- [13] T. Braun, *Z. Anal. Chem.*, 333 (1989) 85; T. Braun and A.B. Farag, *Anal. Chim. Acta*, 99 (1978) 1; and references cited in these.
- [14] S. Palagyi and T. Braun, *J. Radanal. Nucl. Chem.*, 163 (1992) 69.
- [15] S. Palagyi, T. Braun, Z. Homonny and A. Vertes, *Analyst*, 117 (1992) 1537.
- [16] M.S. El-Shahawi, *Talanta*, 41 (1994) 1481, and references cited therein.
- [17] A.W. Adamson, *Physical Chemistry of Surfaces*, Academic Press, New York, 2nd ed., 1967.
- [18] P. Fong and A. Chow, *Talanta*, 39 (1992) 497.
- [19] L. Schumack and A. Chow, *Talanta*, 34 (1987) 957; A.B. Farag, A.M. El-Wakil and M.S. El-Shahawi, *Fresenius Z. Anal. Chem.*, 324 (1986) 59.
- [20] T. Schafer, R. Sebastian, R. Laatikainen and S.R. Salman, *Can. J. Chem.*, 62 (1983) 326.
- [21] R.S. Al-Mehrezi, M. Sc. Thesis, UAE University, United Arab Emirates (1996).

Cite this: *Anal. Methods*, 2014, 6, 6997

Redox behavior and adsorptive cathodic stripping nanomolar levels of palladium using a novel Schiff base reagent containing a squaric acid moiety

R. M. Ba-Shami,^{5,6,7} H. Gazzaz,^a A. S. Bashammakh,^a A. A. Al-Sibaai^a and M. S. El-Shahawi^{†*ab}

The redox behavior of a palladium(II)-3,4-bis(2-hydroxyphenyl-imino) cyclobut-1-en-1,2-diol complex at Pt, Au and hanging mercury drop electrodes (HMDE) was studied for developing a low cost and precise method for determination of Pd concentration in road dust and other environmental samples. Hence, a controlled adsorptive accumulation of this complex on HMDE provided the basis for adsorptive cathodic stripping voltammetric (AdCSV) measurements of palladium at nanomolar levels at pH 9–10 and at 0.64 V vs. the Ag/AgCl reference electrode. The calibration plot was obtained in the range of 1.87×10^9 to 3.05×10^7 M (0.2 to 32.5 mg L⁻¹) Pd. The limit of detection was found to be 4.70×10^{10} M (0.05 mg L⁻¹), with a relative standard deviation (RSD) of 2.1% (n = 5) at 2.0 mg L Pd level. Common anions and cations did not interfere in the determination of Pd concentration. The method was applied to the determination of the concentration of Pd in pure authentic samples, roadside dust and water samples. The method offers a simple system coupled with good reproducibility, accuracy, ruggedness

Received 15th May 2014
Accepted 26th June 2014

DOI: 10.1039/c4ay01160k

voltammetric determination of

www.rsc.org/methods

and cost effectiveness.

Cu.¹In different areas of science and technology, Pd has been used in brazing alloys, petroleum, electrical industries, catalytic chemical reactions and in converters in motor vehicles.²Concentrations of Pd in fresh water, salt water, soil, sewage sludge and in ambient air levels in urban areas where Pd catalysts are used generally range from 0.4 to 22 ng L⁻¹; 19 to 70 pg L⁻¹; <0.7 to 47 mg kg⁻¹; 18 to 260 mg kg⁻¹ and below 110 pg m⁻³,³ respectively. Drinking water usually contains <24 ng L⁻¹ Pd; this metal is found in urine of adults in the concentration

1. Introduction

Platinum-group elements (PGEs) have low crustal abundance (21 ng g⁻¹). In the earth's crust, Pd usually occurs in its native form associated with one or more of the other PGEs as well as with Cr, Au, Fe, Ni, and

⁵ Chemistry Department, Faculty of Science, King Abdulaziz University, P. O. Box 6, Jeddah 21589, Saudi Arabia

⁷ Center of Excellence in Environmental Studies, King Abdulaziz University, Jeddah, Saudi Arabia. E-mail: malsaeed@kau.edu.sa; mohammad_el_shahawi@yahoo.co.uk; Fax: +966-2-6952292; Tel: +966-2-6952000

[†] Permanent address: Department of Chemistry, Faculty of Science, Damietta University, Damietta, Egypt.

range of 0.006 to <0.3 mg L⁻¹, while the average dietary intake of Pd for humans

appears to be up to 2 mg per day.³ Thus, the development of analytical techniques for analysis of PGEs including Pd is growing because of their applications in medicine, micromechanics and chemical engineering. Because of Pd toxicity,⁴ the frequency at which even trace levels of this metal are being monitored in surface waters, soil surfaces, plants and particulate matter has been rapidly increasing. The low level of Pd together with the high concentration of interfering matrix components often requires a preconcentration step combined with a matrix separation.⁵ Hence, it is necessary to develop a method to accurately and precisely determine the concentration of Pd in samples with very low analyte content, such as in airborne particulate matter, various water samples and urine.

A series of analytical methods, e.g., flame atomic absorption spectrometry (FAAS), graphite furnace-AAS, electrothermal AAS, AAS, inductively coupled plasma-optical emission spectroscopy (ICP-OES), ICP-mass spectrometry (MS) and electrospray ionization mass spectrometry (ESI-MS), have been reported for analysis of trace levels of Pd.^{4–18} The high costs of the instruments, complexity, preconcentration step and the need of some degree of expertise for their proper operation are the main disadvantages of these techniques. Thus, recent years have seen an upsurge of interest in the development of low-cost, easy-to-operate, highly sensitive and reliable methods for routine analysis of Pd, which is of prime importance.

Numerous adsorptive cathodic stripping voltammetry (AdCSV) methods have been reported for sensitive Pd concentration determination.^{19–29} To the best of our knowledge, the Schiff base 3,4-bis(2-hydroxyphenylimino)cyclobut-1-en-1,2-diol

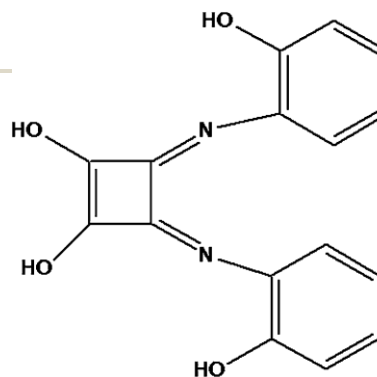
(SQ-OH) (Fig. 1) has so far not been used as a chelating agent for voltammetric and/or spectrometric determination of Pd and other platinum-group elements. Thus, this article is focused on: (i) studying the redox behavior of Pd with the SQ-OH; (ii) developing a low-cost and precise AdCSV method for Pd analysis; (iii) studying the interference by other metal ions and organic contaminants; and finally (iv) applying the proposed method to determine the concentration of Pd in various environmental samples. The developed method compares favorably with many spectrometric and electroanalytical methods in terms of better selectivity, precision, linear dynamic range (LDR), limit of detection (LOD), ease of use and less interference.

2. Experimental

2.1. Reagents and materials

Analytical reagent-grade chemicals were used as received. The reagent 3,4-bis(2-hydroxyphenylimino)cyclobut-1-en-1,2-diol was prepared from the condensation of squaric acid with oaminophenol in a molar ratio of 1 : 2 as reported.³⁰ A series of Britton–Robinson (BR) buffers (pH 2–11.9) was prepared from a mixture of acetic (0.08 M), phosphoric (0.08 M), and boric (0.08 M) acids after adjusting the pH to the desired pH value with NaOH (0.02 M), and these buffers were used as supporting electrolytes. A BDH stock solution (1000 mg L⁻¹)

Fig. 1
structure of



hydroxyphenylimino)cyclobut-1-en-1,2-diol Schiff base.

Chemical
3,4-bis(2-

of palladium(II) was used for the preparation of more diluted solutions in deionized water. A stock solution (1.2 × 10⁻³ mol L⁻¹) of SQ-OH was prepared in methanol, stored in a refrigerator, and employed within a week. Concentrated HF, HCl and HNO₃ acids (Merck, Darmstadt, Germany) were used for the digestion of the certified reference materials (CRM) IAEA-soil-7 and the geological standard sample (GBW07291). The influence of diverse ions commonly found together with palladium, e.g. ions of Al, Cu, Cr, Fe and Mg (1000 mg L⁻¹), was investigated. All glassware and electrochemical cells were pre-cleaned by soaking in HNO₃ (10% v/v), washed with de-ionized water and dried before use.

2.2. Apparatus

Adsorptive differential pulse cathodic stripping voltammetric (AdCSV) and cyclic voltammetry (CV) measurements were performed on a Metrohm 746 VA trace analyzer and 747 VA stand, using a three-compartment voltammetric cell (10 mL) composed of HMDE (0.38 mm²), Pt wire (BAS model MW-1032) and Ag/AgCl (3 M KCl) as working, counter and reference electrodes, respectively. A Perkin Elmer ICP-MS Sciex model Elan DRC II (California, CT, USA) was used as a reference material for method validation and palladium concentration determination at the operational parameters (Table 1). A Perkin-Elmer (model Lambda 25, USA)

spectrophotometer with a 10 mm (path width) quartz cell was used for recording the UVVisible spectra (190–1100 nm) and absorbance measurements. De-ionized water was obtained from a Milli-Q Plus system (Millipore, Bedford, MA, USA) and was used for preparation of the standard solutions. A Jenway pH meter (Model, 3505, UK) and a microwave system (Mars model, 907500, USA) were used respectively for pH measurements and sample digestion of the certified reference material.

2.3. Recommended AdCSV procedure

An accurate volume (10 mL) of the B–R buffer at pH 9–10 was transferred to the electrochemical cell, and a stream of pure N₂ gas was passed through the test solution for 15 min before recording the voltammogram. The scan was initiated in the negative direction of the applied potential from 0.0 V to 1.5 V vs. the Ag/AgCl reference electrode. After recording the voltammogram, an accurate volume (10.0 mL) of the SQ-OH reagent (5.1 × 10⁶ mol L⁻¹) was added. The solution was purged with N₂ gas for 5 min. Stirring was then stopped and, after 10 s quiescence time, the voltammogram was recorded again. Unless otherwise stated, the background voltammogram of the supporting electrolyte and the blank solution was recorded at pH 9–10 under the optimum operational parameters of deposition potential (0.2 V), accumulation time (300 s), starting potential (0.0 V), scan rate of 100 mV s⁻¹ and pulse amplitude of 60 mV of chelated Pd at the surface of the Hg drop of the HMDE. After recording the voltammogram of the blank solution, an accurate volume (10–100 mL) of Pd solution (1.2 × 10⁶ mol L⁻¹) was added and the solution was purged with N₂ gas for 5 min. Stirring was then stopped and, after 10 s quiescence time, the scan was initiated in the negative direction of applied potential from 0.0 V to 1.5 V vs. the Ag/AgCl electrode. The voltammograms were finally recorded again as described, under the same operational parameters.

2.4. Applications

2.4.1. Analysis of certified reference materials. Accurately weighed amounts (0.13–0.15 0.01 g) of the CRM sample (IAEAsoil-7) were placed in Teflon beakers (50.0 mL) containing HF (5 mol L⁻¹, 7.0 mL), concentrated HCl (2.0 mL), and concentrated HNO₃ (5.0 mL). Various amounts of standard Pd²⁺ were added to the samples at room temperature³⁰ to confirm the correctness of the method. The reaction mixture was heated at 100–150 C for 1 h. After NO₂ fumes had ceased, the reaction mixture was evaporated almost to dryness and re-dissolved in concentrated HNO₃ (5.0 mL). The process was repeated three times and the mixture was again evaporated to dryness. The solid residue was re-dissolved in dilute HNO₃ (5.0 mL, 1.0 mol L⁻¹) and the mixture was filtered through Whatman 41 filter paper, transferred to a volumetric flask (25.0 mL), and deionized water was added to the solution until the flask was filled to the mark. An accurate volume of the digested sample was adjusted to pH 9–10 (5.0 mL) and a few drops of NaOH (1.0 mol L⁻¹) and B–R buffer (4–5 mL) at pH 9–

10 were added to adjust the solution pH. The solution was transferred to the volumetric cell and the AdCSVs were recorded by applying a negative potential scan from 0.0 to 1.5 V vs. the Ag/AgCl electrode at the optimum conditions. The peak current at 0.64 V was measured and used for constructing a linear standard addition plot and the Pd content in the CRM sample was determined.

2.4.2. Analysis of palladium in samples of road dust. Homogenized samples of road dust were collected from the surface of the roadside dust of the busy streets of Jeddah City, from heavy and light traffic locations. The method of Narin et al.³¹ was applied for the digestion of trace metal ions from the road dust samples in the presence of various known Pd concentrations. Accurately weighed amounts (0.13–0.15 0.01 g) of the road dust sample were placed in Teflon beakers (25.0 mL) containing HF (5 mol L⁻¹, 7.0 mL), concentrated HCl (2.0 mL) and concentrated HNO₃ (5.0 mL), and various standard amounts of Pd²⁺ were added to the samples at room temperature.³¹ The samples were dried at 110 C for 2 h, ground through a 200-mesh sieve and homogenized for analysis. Accurately weighed amounts (0.13 to 0.16 g) of the roadside soil samples were digested in concentrated HCl–HNO₃ (3 : 1 w/v) in a conical flask (100 mL) and refluxed for 4 h. Each sample solution was centrifuged, filtered through a 0.45 mm membrane filter, transferred to the measuring flask (25.0 mL) and filled to the mark with HNO₃ (0.5 mol L⁻¹). The solution was adjusted to pH 10, transferred to the cell and AdCSVs were recorded from 0.0 to 1.5 V vs. the Ag/AgCl electrode at various additions of standard Pd solutions. The peak current at 0.64 V was measured and the change in peak current was used for constructing a linear plot of standard addition against a reagent blank.

2.4.3. Analysis of total palladium in water samples. A Red Sea water sample (100.0 mL) was collected from the coastal area of North Jeddah city, Saudi Arabia. Tap water samples in the laboratory, after allowing the water to flow for 5 min, were also collected. Water samples were filtered through a 0.45 mm cellulose acetate membrane filter and subjected to UV digestion at 254 nm in the presence of HCl (10% v/v) for 5 h. Palladium was then analyzed following the recommended AdCSV procedure. The Pd content was also determined by the standard ICPMS at the recommended instrumental parameters for

comparison.

3. Results and discussion

3.1. Electronic spectra of the reagent SQ-OH and its Pd²⁺ chelate

The reaction of the reagent SQ-OH with Pd(II) in aqueous solution revealed that the reaction is pH dependent. Detailed study of the pH revealed formation of a stable brown-colored complex species of Pd–SQ-OH at pH 9–10. At this pH, the reaction was fast, as indicated from the development of an intensely colored complex species in a very short period of time. An electronic spectrum of Pd(II)–SQ-OH complex showed four absorption peaks at λ_{max} 269, 294, 340 and 388 nm (Fig. 2) with molar absorptivities of 3.71 × 10⁴, 3.41 × 10⁴, 2.91 × 10⁴,

and $2.55 \times 10^4 \text{ L mol}^{-1} \text{ cm}^{-1}$, respectively. The spectrum of the free Schiff base showed three peaks at λ_{max} 275, 310 and 389 nm with molar absorptivities of $3 \times 1.40 \times 10^4$, 1.14×10^4 and $1.48 \times 10^2 \text{ L mol}^{-1} \text{ cm}^{-1}$, respectively. The color change and the observed bathochromic shift of λ_{max} of the reagent to a longer wavelength upon addition of Pd^{2+} confirmed formation of the Pd–Schiff base complex. The ratio of Pd(II) to SQ-OH in the complex was determined by continuous variation methods.³² Formation of a 1 : 2 molar ratio of Pd to SQ-OH was achieved, confirming formation of a complex with the formula $[\text{Pd}(\text{SQ-OH})_2]$. The complex was stable over 3 h, as noticed from the constancy of its absorbance at λ_{max} . The complex was crystallized from ethanol as brown crystals and it decomposed at 280 °C. The structure of the complex $[\text{Pd}(\text{C}_{24}\text{H}_{22}\text{N}_4\text{O}_4)]$ was also confirmed from its elemental analysis: analytical found: C % 54.42, H % 3.42, N % 7.67 and Pd % 15.54%; calculated: C % 55.14, H % 3.16, N % 11.74, S % 8.01 and Pd % 15.28%.

3.2. Redox behaviour of Pd(II)–SQ-OH complex

A detailed AdCSV investigation of the SQ-OH reagent in the absence and presence of Pd^{2+} ions at various pH values was carried out. Representative AdCSVs at various pH values are shown in Fig. 3. At $\text{pH} < 6.5$, no cathodic peaks were noticed, suggesting no Pd ion complex was formed and/or that any Pd complex species formed with the SQ-OH Schiff base was unstable. Poor adsorption of the reduced species, formation of hydrogen at the surface of the HMDE and the instability of the electrogenerated species may also account for this observation.³³ The Schiff base may also be reduced at a more negative potential than the allowed potential window of the HMDE.

In the pH range 6.5 to 7, two well-defined cathodic peaks at 0.04 V and 0.20 V vs. the Ag/AgCl electrode were observed and were safely assigned to the adsorption and/or formation of

the Hg–SQ-OH salt and reduction of the azomethine,³⁴ respectively. At pH 8–9, two peaks at 0.18 and 0.35 V and a new peak at 0.56 V were observed and attributed to reduction of the hydroxyl group of the Schiff base and the involvement of protons on the reduction steps.³³ Between pH values of 9 and 11, four well-defined peaks at 0.1, 0.27, 0.45 and 0.64 V were observed at more negative potentials compared to the peaks observed at $\text{pH} < 9$ (Fig. 3). At pH 11, the cathodic peak potentials shifted to more negative values indicating prior protonation in the region of the azomethine, leading to a decrease in the electron density on the electroactive functional group and facilitating the acceptance of an electron during the reduction step. Reduction of the two azomethines via direct exchange of 4 electrons in four successive one-electron/one-proton steps may have also occurred.^{33,35} The plot of the change of the cathodic peak potential at 0.56 V vs. pH is linear and best fits the following regression equation:

$$E_{p,c} \approx 0.124 \text{ pH} + 0.661, (R^2 \approx 0.9787) \quad (1)$$

The data suggest that B–R buffer with a pH value between 9 and 10 should be used in the development of a low-cost AdCSV method for determining the concentration of Pd.

Fig. 2 Electronic spectra of the Schiff base SQ-OH and its $\text{Pd}(\text{SQ-OH})_2$ complex in DMF. Palladium $\approx 3.0 \times 10^{-6} \text{ mol L}^{-1}$ and $[\text{SQ-OH}] \approx 1.0 \times 10^{-5} \text{ M}$.

Fig. 3 AdCSVs of palladium(II)–SQ-OH complex species in B–R mol L buffers at the HMDE vs. the Ag/AgCl electrode. Palladium $\approx 3.0 \times 10^{-6} \text{ mol L}^{-1}$ and pulse 10 ms , $[\text{SQ-OH}] \approx 1.0 \times 10^{-5} \text{ M}$; scan rate $\approx 100 \text{ mV s}^{-1}$ amplitude of 50 mV.

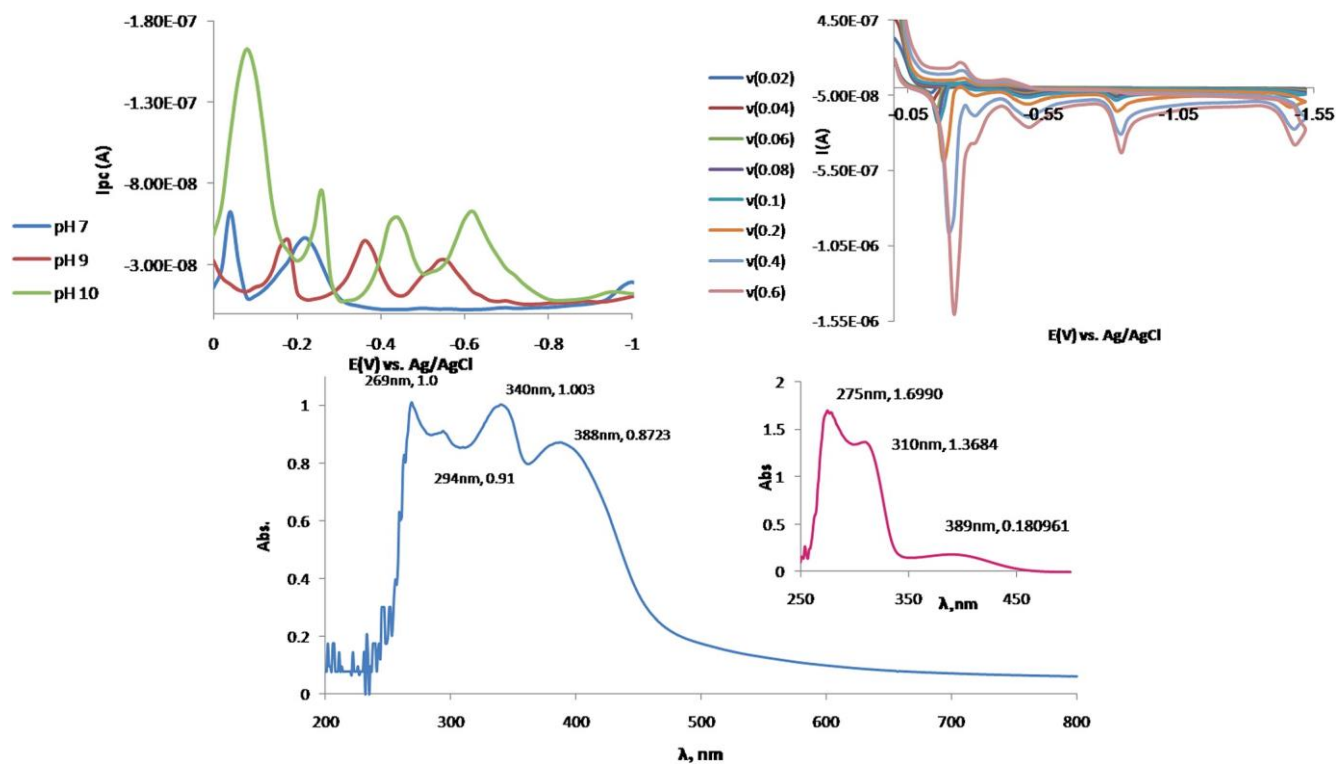


Fig. 4 CVs of Pd(II)-SQ-OH at various scan rates (20–600 mV s⁻¹) at pH 10 at the HMDE vs. the Ag/AgCl electrode.

Cyclic voltammograms (CV) of the Pd(II)-SQ-OH complex in the potential range of 0.0 to 1.5 V at the HMDE in B-R buffer of pH 9–10 were recorded at various scan rates (n). Representative CVs are shown in Fig. 4. At a scan rate in the range 20–600 mV s⁻¹, the CV showed four well-defined cathodic peaks at 0.16, 0.48, 0.82 and 1.46 V. On the reverse scan, two anodic peaks at 0.26 and 0.42 V with potential separation ($\Delta E_p > 100$ mV) were observed, suggesting the irreversible nature of the reduction steps. The peak potentials were shifted to more negative values upon increasing the scan rate, confirming the irreversible nature of the reduction.

The plots of $E_{p,c}$ of the first and second cathodic peaks at 0.16, 0.48 V vs. $\log n$ are linear (Fig. 5), with slope values proportional to an_a , where n_a is the number of electron transfers involved in the reduction steps and a is the corresponding charge-transfer coefficient of the adsorbed Pd species. These results added further support to the irreversible nature of the reduction process.^{35–37} The values of n_a and a of the adsorbed Pd species were calculated from the slope of the linear plots of $E_{p,c}$ vs. $\log n$ (Fig. 5) using the following equation:

$$\Delta E_{p,c}/\Delta \log(n) \approx 29.58/an_a \quad (2)$$

The number of electrons (n_a) transferred in the rate-determining step was found to be equal to 2 and the value of a was in

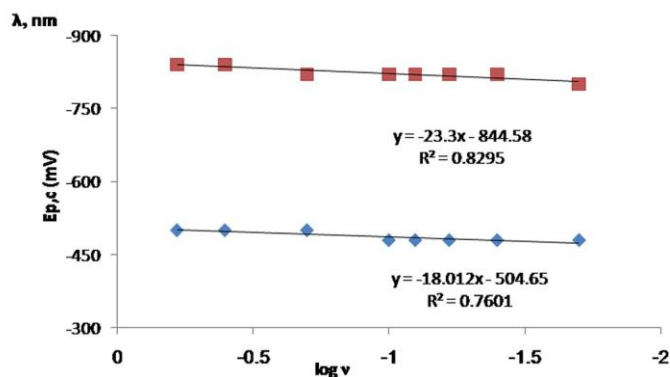


Fig. 5 Plots of the first (♦) and second (■) cathodic peak potentials vs. $\log(n)$ of the CVs of Pd-SQ-OH complex at the HMDE at pH 10 vs. the Ag/AgCl electrode.

the range 0.89–0.05 indicating the irreversible nature of the cathodic process at the surface of the HMDE. The value is somewhat close to the theoretical value (1.0) expected for an adsorption process at HMDE.^{36,37} In the CV, the irreversible nature of the electrode processes was also confirmed from the progressive shift of the $E_{p,c}$ to more negative values on rising the sweep rate.

The current functions ($i_{p,c}/n^{1/2}$) at 0.50 V and 0.82 V vs. Ag/AgCl increased upon raising the scan rate. Thus, the reduction process of the Pd(II)-SQ-OH favors chemical reaction of the EE type mechanism^{36,37} and the product of the reduction process also undergoes a very rapid follow-up chemical reaction.³⁷ The plot of $i_{p,c}$ vs. $n^{1/2}$ is linear, indicating that the reduction process is a diffusion-controlled electrochemical process.³⁷ The surface coverages (Γ) of Pd-SQ-OH at

the HMDE, Pt and Au working electrodes were also determined at various scan rates.^{35,37} The $i_{p,c}$ at 0.64 V is related to the surface concentration of the electroactive species by the equation:

$$i_{p,c} \approx n^2 F^2 A G n / 4RT \quad (3)$$

where n is the number of electrons involved in the electrode reaction, A is the geometric surface area of the working electrode (HMDE, Pt or Au), G (mol cm^{-2}) is the surface coverage and other symbols have their usual meaning.³⁷ The G values were calculated from the slopes of the linear plots of $i_{p,c}$ vs. scan rate. Assuming $n = 2$, the G values were found to be 4.2×10^{10} , 4.19×10^{11} and 3.08×10^{10} mol cm^{-2} at the HMDE, Au and Pt electrodes, respectively. The value of G at the HMDE suggests that this electrode should be used in the development of an AdCSV method for analysis of Pd in environmental samples. The cathodic peak at the HMDE was also well defined, sharp, and symmetric.

3.3. Analytical parameters

The redox behaviour of palladium(II)–SQ-OH chelate, the sensitivity of the developed $i_{p,c}$ at 0.64 V and at pH 10, and the high surface coverage of Pd at the HMDE suggests that the Schiff base SQ-OH should be used for developing a low-cost and convenient AdCSV method to determine Pd concentrations.

Thus, the effect of pH (2.5–11) on peak current at 0.64 V was studied. Maximum $i_{p,c}$ was achieved at pH 11. The SQ-OH reagent is most likely dissociated easily at $\text{pH} > 9$ and participated in complex formation with Pd^{2+} . However, in a solution of pH 9–10 (Fig. 6) the observed cathodic peak at 0.64 V was well resolved and reproducible. Thus, in the subsequent work, a solution of pH 9–10 was adopted as a convenient supporting electrolyte in the following experiments.

The AdCSV peak current intensity depends on the accumulation potential (E_{acc}) (0.0 to 0.8 V) in B–R buffer at pH 9–10 during the preconcentration step. Thus, the effect of accumulation potential on the $i_{p,c}$ at 0.64 V vs. the Ag/AgCl electrode was studied (Fig. 7). The $i_{p,c}$ was strongly influenced by the preconcentration potential and maximum $i_{p,c}$ was achieved at $E_{\text{acc}} = 0.2$ V. The AdCSVs also showed that at $E_{\text{acc}} = 0.2$ V, the $E_{p,c}$ at 0.64 V was much more developed, symmetric and sharp. Hence, an adsorption potential of Pd(II) was favoured at an accumulation potential of 0.2 V. At a potential more negative than 0.2 V, the $i_{p,c}$ decreased gradually and levelled off (Fig. 7). The accumulation potential of Pd(II)–SQ-OH could bear a negative charge at the employed pH. Thus, an accumulation potential of 0.2 V was chosen for subsequent

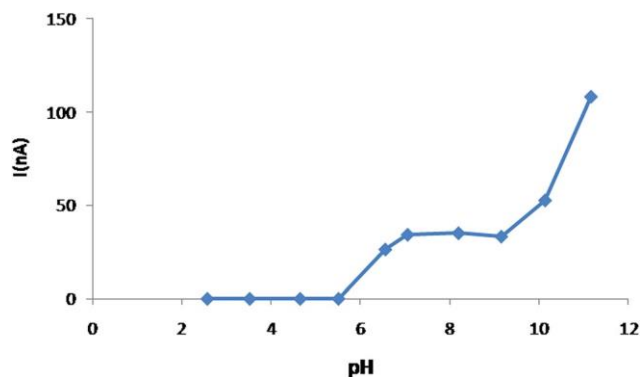


Fig. 6 Plot of $i_{p,c}$ vs. pH; deposition potential: 0.64 V. [SQ-OH] = 5.1 $\times 10^{-6}$ M; [Pd(II)] = 1 $\times 10^{-6}$ M.

scan rate: 100 mV s^{-1} ; pulse amplitude: 0.05 V and at 100 mV s^{-1} ; deposition time: 0.4 s.

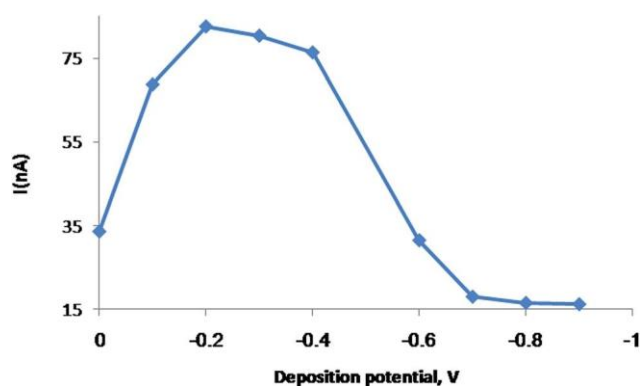
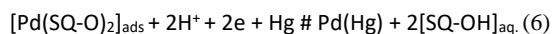
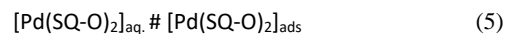
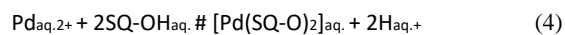


Fig. 7 Effect of deposition potential on $i_{p,c}$. Conditions: pH 10; [SQ-OH] = 180 μM ; [Pd(II)] = 1 $\times 10^{-6}$ M; [Ag/AgCl] = 0.05 M; scan rate: 100 mV s^{-1} ; pulse amplitude: 0.05 V; deposition time: 0.4 s.

the following reactions:



The choice of collection of the analyte is a compromise between surface coverage, sensitivity, the time required for an analysis, and the effect of competitive adsorption. The differential-pulse adsorptive cathodic peak current intensity of Pd(II)–SQ-OH in B–R buffer of pH 9–10 was found to be dependent on the preconcentration time period

(t_{acc}). Thus, the influence of t_{acc} (60–420 s) on the $i_{p,c}$ at 0.64 V was studied at a fixed SQ-OH concentration. The $i_{p,c}$ current at 0.64 V grew to a limited value upon increasing accumulation time up to 300 s (Fig. 8), suggesting that an equilibrium between the dissolved and adsorbed complex Pd species was reached. Thus, an accumulation time of 300 s was adopted in the subsequent AdCSV experiments of Pd.

The influence of scan rate (20–200 mV s^{-1}) on $i_{p,c}$ at 0.64 V was investigated. The $i_{p,c}$ increased steadily upon raising the scan rate up to 100 mV s^{-1} . However, the best signal to background current and peak symmetry were achieved at 60 mV s^{-1} . Hence, a scan rate of 60 mV s^{-1} was chosen for the present analytical stripping voltammetry study. The pulse amplitude has a pronounced effect on the AdCSV response of the Pd–SQOH species at pH 10. Thus, the peak current intensity of the AdCSV of Pd–SQ-OH in pH 9–10 buffer was studied. The $i_{p,c}$ was directly proportional to the pulse height up to 90 mV and the $i_{p,c}$ increased steadily upon increasing the pulse height from 10–60 mV. At a pulse amplitude of 70–90 mV, the $i_{p,c}$ increased due to the increase in the capacitive current, however, a sloping background current signal was observed. The strongest peak to background signal for the AdCSV peak current at 0.64 V was observed at 60 mV pulse height. Thus, in the subsequent work, a 60 mV pulse height was selected.

The influence of SQ-OH concentration on $i_{p,c}$ at pH 9–10 was studied. Upon increasing this reagent concentration to $1.0 \times 10^6 \text{ mol L}^{-1}$, the $i_{p,c}$ increased linearly and remained constant up to $5.1 \times 10^6 \text{ mol L}^{-1}$ (Fig. 9). At SQ-OH $> 5.1 \times 10^6 \text{ mol L}^{-1}$

L^{-1} , the $i_{p,c}$ leveled off and deteriorated due to competitive adsorption of free reagent. At the breakpoint, the reagent concentration ($5.1 \times 10^6 \text{ mol L}^{-1}$) was just close to the Pd^{2+} concentration, revealing a [Pd(SQ-OH)] structure for the adsorbed species. Thus, a concentration of $5.1 \times 10^6 \text{ mol L}^{-1}$ for SQOH was used in subsequent experiments.

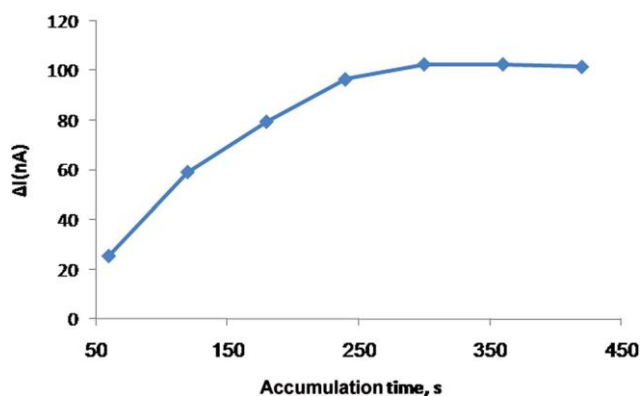


Fig. 8 Plot of deposition time vs. $i_{p,c}$ at 0.64 V. Conditions: [SQ-OH] $\approx 5.1 \times 10^6 \text{ M}$; [Pd] $\approx 1.0 \times 10^{-6} \text{ mol L}^{-1}$; deposition potential $\approx 0.2 \text{ V}$; pulse amplitude $\approx 0.05 \text{ V}$ and a scan rate of 0.1 V s^{-1} .

saturation.^{32–34} A regression equation of $i_{p,c}$ (nA) $\approx 1.2215 \text{ C} (\text{mg L}^{-1}) + 2.17$ was obtained with a correlation coefficient of 0.9967.

3.4. Interference study

Analyses of Pd ions at a concentration of 4.65 mM and in the presence of a relatively high excess concentration of foreign ions Mg^{2+} , Ba^{2+} , Ca^{2+} , Ni^{2+} , Pb^{2+} , Co^{2+} , Cu^{2+} , Zn^{2+} , Al^{3+} , Fe^{3+} , Co^{2+} , Si^{4+} , AsO_2 , VO_3 , SbO_2 and SeO_3 were carried out, for each of these foreign ions individually, by the developed method. The tolerance limit is defined as the concentration of foreign ion added causing a relative deviation within 5.0% in the magnitude of the peak current at 0.64 V. Most of these ions did not interfere with the palladium signal. Ca^{2+} and Al^{3+} decreased the stripping current of Pd(II)–SQ-OH, but their interference was masked by adding a few drops of EDTA and NaF, respectively. Fe^{3+} and Si^{4+} increased the stripping current by producing a diffusion-controlled peak-like shoulder on the cathodic side of the Pd(II) peak (0.64 V). Interference of Fe^{3+} and V^{5+} ions was masked by adding a few drops of triethanolamine. Cobalt(II) at 10-fold excess had no influence on the cathodic peak current.

3.5. Analytical performance

Under the optimized conditions of pH 9–10, an accumulation potential of 0.2 V, preconcentration time of 300 s, scan rate of 100 mV s^{-1} , pulse height of 60 mV and SQ-OH concentration of $5.1 \times 10^6 \text{ M}$, AdCSV voltammograms at various Pd concentrations were recorded. The results are shown in Fig. 10. The plot of $i_{p,c}$ at 0.64 V versus Pd^{2+} concentration is linear in the range 1.87×10^{-9} to $3.05 \times 10^{-7} \text{ M}$ (0.2–32.5 mg L^{-1}) Pd and leveled off at higher concentrations because of adsorption

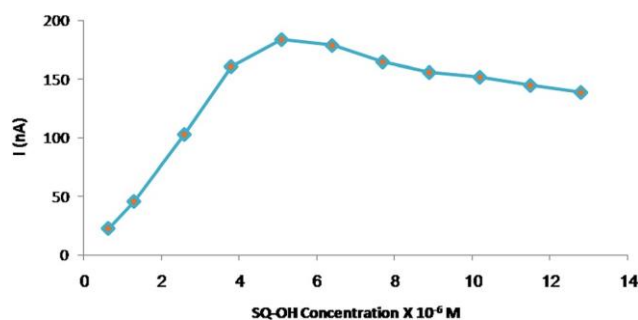


Fig. 9 Plot of SQ-OH concentration vs. $i_{p,c}$ at 0.64 V. Conditions: pH 9–10; deposition potential 0.2 V; deposition time $\approx 300 \text{ s}$; scan rate $\approx 0.1 \text{ V s}^{-1}$, pulse amplitude $\approx 0.06 \text{ V}$ and [Pd] $\approx 5.1 \times 10^{-6} \text{ mol L}^{-1}$.

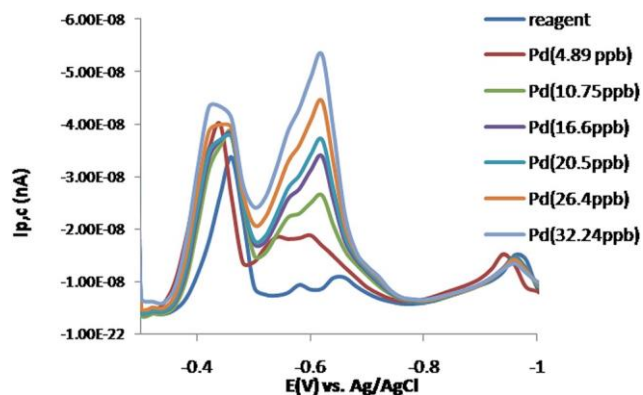


Fig. 10 AdCSV voltammograms of Pd²⁺ over the concentration range 21.87×10^9 to 3.05×10^7 M (0.2 – 32.5 mg L⁻¹) at pH 9–10 at the HMDE vs. the Ag/AgCl electrode.

The calculated values of LOD and limit of quantification (LOQ),³⁸ using the formulas $\text{LOD} \approx 3S_{y/x}/b$ and $\text{LOQ} \approx 10S/b$ where $S_{y/x}$ is the standard deviation of the y-residual and b is the slope of the calibration plot, were found to be equal to 4.70×10^{10} M (0.05 mg L⁻¹) and 1.55×10^9 M (0.16 mg L⁻¹), respectively. The analytical features (LOD, LOQ and linear dynamic range) of the developed method compare favorably with those of many spectrometric^{4–18,39–45} and electroanalytical methods.^{19–29,46,47} The developed method provides better LOD and LDR, ease of use and less interference (Table 2). Some of these other methods have shown high LOD and serious interference by halide ions. The LOD of the current method selectivity and these measures are better than and/or comparable with the previously reported methods. Most of the reported methods suffer from the need of technical expertise to carry them out and from the need for costly solvents. Likewise, good preconcentration, simple sample preparation, high selectivity, low LOD and low cost make the developed method suitable for measuring Pd in various environmental samples. The developed method could also be extended for analysis of Pd even at levels <ng mL⁻¹ or ng g⁻¹ after preconcentration of Pd from a large sample volume onto a solid sorbent-packed column.⁴⁹

3.6. Analytical applications

The developed AdCSV method was validated by analysis of total Pd in the CRM sample IAEA-soil-7. The $i_{p,c}$ at 0.64 V increased linearly as standard Pd was added to the CRM sample. Excellent agreement between the results of the AdCSV and the ICP-MS methods was achieved for Pd analysis (Table 3). The recovery of the AdCSV method was not significant in comparison with the reference ICP-OES method where $t_{\text{critical}} \approx 2.20 > t_{\text{exp}} \approx 1.81$ – 1.93 , at a 95% confidence. Thus, the developed AdCSV method was able to effectively analyze palladium in real samples.

The recommended AdCSV method was successfully applied for analysis of Pd in road dust, and the results are in good agreement with the ICP-MS data (Table 3). As can be seen, the added Pd was quantitatively recovered, indicating the validity of

Table 3 Analysis of palladium(II) in the CRMs and roadside dust samples by the developed DP-CSV and ICP-MS methods^aTable 4 Analysis of palladium(II) in various water samples by the developed DP-CSV and ICP-MS methods^a

Sample	Added, mg L ⁻¹		Found SD, mg L ⁻¹		Recovery RSD, %	
	0.0	19.66	nd	18.9 0.13 (19.2 0.3)	—	96.2 6.98
Drinking water	39.32	78.65	40.2 0.17 (39.7 0.3)	102.15 4.6		
	0.0	19.66	77.36 0.13 (79.5 0.5)	98.36 1.76		
	39.32	78.65	0.13 0.05 (0.14 0.01)	—	96.2 6.98	
	19.66	39.32	20.21 0.15 (19.8 0.22)	102.15 4.6		
	0.0	19.66	40.6 0.18 (5.5 0.23)			

the recommended AdCSV method for analysis of Pd in real samples. The method is as good as the standard method (critical $t_{0.05, 4} = 2.20 > t_{exp} = 1.71-1.83$, 95% confidence level). The proposed method effectively analyzed palladium in real samples.

Analysis of Pd in water samples was carried out by the standard addition method and the results are summarized in Table 4. According to the results in Table 3, the Pd content was below the LOD. The added Pd was quantitatively recovered as can be seen in Table 3. The

method compares favorably with LOD of GFAAS (0.4 mg L⁻¹) and FAAS (1.24 mg L⁻¹). A value of RSD of 2.1% (n = 5) was achieved at 2.0 mg L⁻¹ Pd. The LOD of the method is lower than the maximum allowable level of Pd in soil (<0.7 to 47 mg kg⁻¹) and solid sewage (18 to 260 mg kg⁻¹) according to the World Health Organization (WHO).^{3,48} The method compares favorably with other reported methods for Pd concentration determination (Table 2). Thus, the developed method shows very good limit of detection, wide linear dynamic range, good precision and

concentration of Pd²⁺ in a tap water (0.065–0.005 mg L⁻¹) sample was close to the measured value by ICP-MS (0.07–0.001 mg L⁻¹, RSD of 5.6%). Pd recoveries in three consecutive determinations ranged from 96.2–6.98 to 102.2–4.6 and are close to values achieved by ICP-MS (Table 4), confirming the suitability and validity of the present AdCSV method for Pd analysis in real samples. The developed method can be extended for Pd analysis in environmental samples where the analyte content is in its usual ng g⁻¹ or ng mL⁻¹ range. Such a type of analysis will require an enrichment step prior to AdCSV determination of Pd. This step can be achieved by preconcentration of Pd²⁺ ions from a large sample volume of water onto a polyurethane foam sorbent-packed column⁴⁸ followed by elution with HNO₃ (1.0 mol L⁻¹) and subsequent AdCSV determination.

4. Conclusion

The method developed in the current work was successfully applied for analysis of Pd in pure authentic and real samples. The method can be utilized readily for routine analysis of Pd in water and other matrices since most of the reported methods suffer from many drawbacks such as cost, multiple steps, being time consuming and the need for costly solvents (HPLC). The developed method offers a simple system with good reproducibility, ruggedness and cost

Sample	Added, mg L ⁻¹		Found SD, mg L ⁻¹		Recovery RSD, %	
	0.0	19.66	nd	18.9 0.13 (19.2 0.3)	—	96.2 6.98
IAEA-soil-7 (CRM)	10.0	20.0	9.9 0.10 (10.12 0.13)	20.6	99.0	1.01
	0.0	20.0	0.14 (19.6 0.4)	103.0	0.7	
Roadside dust	165.2	189.0	2.6 (169.3 2.1)	189.0	—	
	3.7	192.3	2.5	102.05	1.99	

^a ICP-MS data are given in parentheses.

Table 2 Analytical performance of the developed AdCSV and some of the reported methods^a

Method	LOD, ng mL ⁻¹	Linear range, ng mL ⁻¹	Reference	Remarks
DLIME coupled FAAS	90.0	100–2000	12	Sensitive, time consuming
Chemosensor	0.029	0.5–12	7	Time consuming
FI-spectrophotometry	0.1	10–10 000	8	2,2-Furyldioxime
USAE-SFODME/FI-FAAS	0.3	1.5–100	5	—
Spectrophotometry	31.95	106.4–1064.0	37	Polyethylenimine
AdCSV, HMDE	0.042	nd	18	DMG
ASV, GCE	169.6	nd	44	
SWAdSV	0.15	nd	45	DMG
SWAdSV	0.075	nd	22	DMG, HCl
AdCSV	0.05	0.2–32.5	This work	Simple, low cost

^a Abbreviations: AAS = atomic absorption spectrometry, FAAS = flame atomic absorption spectrometry, CPE = carbon paste electrode, DLIME = dispersive liquid–liquid microextraction, USAE-SFODME/FI = ultrasound-assisted emulsification-solidified floating organic drop microextraction, DMG = dimethylglyoxime, USAE-SFODME/FI-FAAS = ultrasound-assisted emulsification-solidified floating organic drop microextraction/injection flame atomic absorption spectrometry, FI = flow-injection.

effectiveness. The LOD is also lower than the maximum allowable level (MAL) of Pd by the World Health Organization (WHO) in water and favorably compared with the LOD of many spectrochemical (e.g. GFAAS, FAAS and ICP-MS) and electrochemical techniques. The method could also be extended to ultratrace (picomolar) analysis of environmental samples via prior on-line preconcentration from large sample volumes onto a polyurethane foam-packed column.

References

- J. Banham, Annual Report and Accounts, Johnson Matthey, 2008, pp.19–20.
- B. Dimitrova, K. Benkhedda, E. Ivanova and F. Adams, *Can. J. Anal. Sci. Spectrosc.*, 2004, 49, 347–352.
- Environmental Health Criteria 226, World Health Organization (WHO), Geneva, 2002.
- X. Dong, Y. Han, Q. Hu, J. Chen and G. Yang, *J. Braz. Chem. Soc.*, 2006, 17, 189–193.
- G. Asimellis, N. Michos, I. Fasaki and M. Kompitsas, *Spectrochim. Acta, Part B*, 2008, 63, 1338–1343.
- S. Dadfarnia, A. M. H. shabani and M. Amirkavei, *Turk. J. Chem.*, 2013, 37, 746–755.
- M. R. Jamali, Y. Assadi and R. Rahnama Kozani, *Journal of Chemistry*, 2013, 2013, 671743, DOI: 10.1155/2013/671743.
- G. Zhang, Y. Wen, C. Guo, J. Xu, B. Lu, X. Duan, H. He and J. Yang, *Anal. Chim. Acta*, 2014, DOI: 10.1016/j.aca.2003.10.054.
- S. Sacmaci and S. Kartal, *Talanta*, 2013, 109, 26–30.
- M. Mohamadi and A. Mostafavi, *Talanta*, 2010, 81, 309–313.
- B. Majidi and F. Shemirani, *Talanta*, 2012, 93, 245–251.
- P. Liang, E. Zhao and F. Li, *Talanta*, 2009, 77, 1854–1857. 13 T. A. Kokya and K. Farhadi, *J. Hazard. Mater.*, 2009, 169, 726–733.
- N. Kovachev, A. Sanchez, K. Simitchiev, V. Stefanova, V. Kmetov and A. Canals, *Int. J. Environ. Anal. Chem.*, 2012, 92(9), 1106–1119.
- C. Puls, A. Limbeck and S. Hann, *Atmos. Environ.*, 2012, 55, 213–219.
- P. G. Jaison, P. Kumar, V. M. Telmore and S. K. Aggarwal, *Rapid Commun. Mass Spectrom.*, 2012, 26(17), 1971–1979.
- Y.-Q. Ye, X.-Z. Yang, X.-S. Li, F.-Q. Yao and Q.-F. Hu, *Asian J. Chem.*, 2012, 24(11), 4967–4970.
- Z. Marczenko and M. Balcerzak, *Separation, Preconcentration and Spectrophotometry in Inorganic Analysis*, Elsevier, Amsterdam, 2000.
- C. Locatelli, *Electroanalysis*, 2007, 19, 2167–2175 and references therein.
- S. I. Kim and K. W. Cha, *Talanta*, 2002, 57(4), 675–679.
- Z. Zhao and Z. Gao, *J. Electroanal. Chem.*, 1988, 256, 65–75. 22 M. Georgieva and B. Pihlar, *Electroanalysis*, 1996, 8, 1155–1159.
- C. Locatelli, *Electroanalysis*, 2005, 17, 140–147. 24 C. Locatelli, D. Melucci and G. Torsi, *Anal. Bioanal. Chem.*, 2005, 382, 1567–1573.
- C. Locatelli, *Electrochim. Acta*, 2006, 52, 614–622.
- C. Locatelli, *Anal. Chim. Acta*, 2006, 557, 70–77.
- C. Locatelli, *Electroanalysis*, 2007, 19, 445–452.
- V. E. Sladkov, G. V. Prokhorova and V. M. Ivanov, *J. Anal. Chem.*, 2000, 55, 889–892.
- G. Raber, K. Kalcher, C. G. Neuhold, C. Talaber and G. Kolbl, *Electroanalysis*, 2005, 7, 138–142.
- O. E. Offiong, *Spectrochim. Acta, Part A*, 1994, 50, 2167–2171.
- I. Narin, M. Soylak and M. Dogan, *Fresenius Environ. Bull.*, 1997, 6, 749.
- D. Sawyer, W. R. Heinemann and J. Beebe, *Chemistry Experiments for Instrumental Methods*, John Wiley & Sons, New York, 1984.
- N. Menek, S. Basaran, G. Turgut and M. Odabasoglu, *Dyes Pigm.*, 2004, 61, 85.
- M. S. El-Shahawi and M. M. Kamal, *Fresenius. J. Anal. Chem.*, 1998, 362, 344.
- A. J. Bard and L. R. Faulkner, *Electrochemical Methods; Fundamentals and Applications*, John Wiley and Sons, New York, 1980.
- M. Sharp, M. Petersson and K. Edstrom, *J. Electroanal. Chem.*, 1979, 95, 123.
- R. S. Nicholson and I. Shain, *Anal. Chem.*, 1964, 36, 706. 38 J. C. Miller and N. Miller, *Statistics for Analytical Chemistry*, Ellis-Horwood, New York, 4th edn, 1991, p. 115. 39 A. Niazi, B. Jafarian and G. Ghasemi, *Spectrochim. Acta, Part A*, 2008, 71, 841–846.
- S. Tokalioglu, T. Oymak and S. Kartal, *Anal. Chim. Acta*, 2004, 511, 255–260.
- A. Niazi, A. Azizi and M. Ramezani, *Spectrochim. Acta, Part A*, 2008, 71, 1172–1177.
- I. Mori, T. Kawakatsu, Y. Fujita and T. Matsuo, *Talanta*, 1999, 48, 1039–1044.
- R. Ruhela, J. N. Sharma, B. S. Tomar, R. C. Hubli and A. K. Suri, *Talanta*, 2011, 85, 1217–1220.
- N. Shokouhi, F. Shemirani and M. Shokouhi, *Spectrochim. Acta, Part A*, 2009, 74, 761–766.
- A. Niazi, B. Jafarian and J. Ghasemi, *Spectrochim. Acta, Part A*, 2008, 71, 841–846.
- P. Abiman, G. G. Wildgoose, L. Xiao and R. G. Compton, *Electroanalysis*, 2008, 20, 1607–1609.
- A. Bobrowski, M. Gawlicki, P. Kapturski, V. Mirceski, F. Spasovski and J. Zarebski, *Electroanalysis*, 2009, 21, 36.
- G. F. Nordberg, B. A. Fowler, M. Nordberg and L. T. Friberg, *Handbook on the Toxicology of Metals*, Academic press, Elsevier, USA, 3rd edn, 2007.
- A. B. Farag, M. H. Soliman, O. S. Abdel-Rasoul and M. S. ElShahawi, *Anal. Chim. Acta*, 2007, 601, 218.

Provided for non-commercial research and education use.
Not for reproduction, distribution or commercial use.



This article appeared in a journal published by Elsevier. The attached copy is furnished to the author for internal non-commercial research and education use, including for instruction at the authors institution and sharing with colleagues.

Other uses, including reproduction and distribution, or selling or licensing copies, or posting to personal, institutional or third party websites are prohibited.

In most cases authors are permitted to post their version of the article (e.g. in Word or Tex form) to their personal website or institutional repository. Authors requiring further information regarding Elsevier's archiving and manuscript policies are encouraged to visit:

<http://www.elsevier.com/authorsrights>

M.S. El-Shahawi ^{a,*}, A.S. Bashammakh ^a, M.I. Orief ^b, A.A. Alsibai ^a, E.A. Al-Harbi ^c



Contents lists available at [SciVerse ScienceDirect](http://www.sciencedirect.com)

Journal of Industrial and Engineering Chemistry

journal homepage: www.elsevier.com/locate/jiec



Separation and determination of cadmium in water by foam column prior to inductively coupled plasma optical emission spectrometry



^a Department of Chemistry, Faculty of Science, King Abdulaziz University, P. O. Box 80203, Jeddah 21589, Kingdom of Saudi Arabia ^b Department of Marine Chemistry, Faculty of Marine Science, King Abdulaziz University, Jeddah, Saudi Arabia ^c Department of Applied Chemistry, College of Applied Science, Taibah University Al-Madinah Al-Munawarah, P. O. Box 3193, Saudi Arabia

ARTICLE INFO

ABSTRACT

Article history:

Received 21 August 2012
Accepted 24 March 2013
Available online 24 April 2013

The sorption profile of cadmium(II) ions from aqueous iodide media onto procaine hydrochloride (PQ⁺Cl⁻) treated polyurethane foams (PUFs) solid sorbent was studied. PQ⁺Cl⁻ treated PUFs solid sorbent was found suitable and fast for Cd²⁺ uptake as [CdI₄]_{aq}²⁻. Thus, removal of Cd²⁺ at trace levels by the sorbent packed columns was achieved. The sorbed Cd²⁺ species onto packed column were recovered

Keywords:

Cadmium(II)
Polyurethane foam
Determination
Sorption models
Foam packed column

spectrometry (ICP-OES). Plot of Cd²⁺ ions concentration was linear in the range 0.05–15 mg L⁻¹. The limits of detection and quantification of Cd²⁺ were found 0.01 mg L⁻¹ and 0.033 mg L⁻¹, respectively. Such limits could be improved to lower values by retention of Cd²⁺ species from large sample volumes of

the aqueous phase at the optimized conditions. The relative standard deviation of the packed column for the extraction and recovery of standard aqueous solutions (0.1 L) containing 1.0 and 5.0 mg L⁻¹ (n = 3) of

Cd²⁺ ions at flow rate of 5.0 mL min⁻¹ were 1.98 and 2.9%, respectively. The method was validated by

analysis of Cd in certified reference materials (CRMs) IAEA-Soil-7 and TMDW water and wastewater samples.

© 2013 Published by Elsevier B.V. on behalf of The Korean Society of Industrial and Engineering Chemistry.

with HNO₃ (10.0 mL, 1.0 mol L⁻¹) prior determination by inductively coupled plasma-optical emission

1. Introduction

Cadmium is considered as extremely toxic metal ions and environmentally is so important that a large number of studies devoted to clarify this element present in natural samples and their different degree and toxicity and availability [1–4]. World Health

Organization (WHO) established 3 mg L^{-1} as the maximum permissible limit for Cd in drinking water [5]. The limit established by Environmental Protection Agency (EPA) is 5 mg L^{-1} [5,6].

Cadmium is known to damage organs such as the kidneys, liver and lungs [5]. The International Agency for Research on Cancer classified cadmium as a human carcinogen.

The direct determination of the trace Cd in sea and wastewater samples and mineral waters by atomic absorption spectrometry (AAS) is very difficult due to its low level and also interference of main components of the water samples. Among the common

* Corresponding author. Present address: Department of Chemistry, Faculty of Science, Damietta University, Damietta, Egypt. Tel.: +96626952000; fax: +96626952292.

E-mail addresses: malsaeed@kau.edu.sa, mohammad_el_shahawi@yahoo.co.uk (M.S. El-Shahawi).

1226-086X/\$ – see front matter 2013 Published by Elsevier B.V. on behalf of The
<http://dx.doi.org/10.1016/j.jiec.2013.03.033>

to develop a precise low cost and selective separation and determination procedures for cadmium species in water. The mechanism of Cd retention by the PUFs sorbent is also properly assigned. PUFs packed column could also be reused more than 10 times without decrease in performance. 2. Experimental

2.1. Instrumental and apparatus

A Perkin Elmer inductively coupled plasma-optical emission spectrometer (ICP-OES, Optima 4100 DC (Shelton, CT, USA) was used and operated at the optimum operational parameters for Cd determination (Table 1). A Perkin Elmer ICP-mass spectrometry (ICP-MS) Sciex model Elan DRC II (California, CT, USA) was also used to measure the ultra trace concentrations of cadmium in the aqueous media at the operational parameters. The ICP-MS instrument is optimized daily before measurements and operated as recommended (Table 1). Cadmium and multi-element standard solutions were used for analytical verification. All samples were analyzed first using ICP-OES spectrometer. If the resulting concentration was below 1.0 mg mL^{-1} , ICP-MS was performed

for analysis of cadmium in the sample with greater accuracy. A Corporation Precision Scientific mechanical shaker (Chicago, CH, USA) with shaking rate in the range 10–250 rpm and glass columns (10.0 cm 15 mm i.d.) were used. A Milli-Q Waters Plus system (Milford, MA, USA) and a Thermo Fisher Scientific Orion model 720 pH Meter (Milford, MA, USA) were also used.

2.2. Reagents and materials

All chemicals and solvents used were of analytical reagent grade and were used without further purification. Milli-Q Water was used through the work. Cadmium

preconcentration techniques, solid phase extraction (SPE) is particularly proposed to preconcentrate trace elements from matrices that adversely influence atomic absorption spectrometric detection [6]. SPE offers a simple and rapid preconcentration technique and an enrichment factors in the range 100–500 for the recoveries of trace elements, alkali and alkaline earth elements while other techniques are time-consuming. A series of chelating e.g. 4-benzyl-3-methyl-1-phenyl-5-pyrazolone, quaternary ammonium salt, 2-thenoyltrifluoroacetone [7–9] and some solid sorbents such as Amberlite XAD-16 [10], Chromosorb-106 resin [11], octadecyl immobilized surface [12], chelating resin e.g. Chelite P with aminomethylphosphoric acid groups [13], thioacetamide chemically immobilized on silicagel [14], and green alga [15–17] has been reported for selective separation of cadmium in water. Some of these methods are not precise, expensive, and unselective and require careful experimental conditions and considerable time consuming.

Recently, the potentialities of PUFs for trace analysis and

speciation of metal ions are promising [18–24]. PUFs are the only sorbent types effective for metal speciation in water [25–27]. In continuation to our work on trace metal separation by PUFs sorbent, the present script reports the sorption profile of cadmium from aqueous media by PQ^+Cl treated PUFs sorbent in an attempt

Korean Society of Industrial and Engineering Chemistry.

(II) nitrate was purchased from Aldrich Chemicals Co. Ltd. (Milwaukee, WC, USA) and was used for preparation of stock solution (1000 mg mL^{-1}) of

cadmium (II). More diluted solutions (1.0 – 100 mg L^{-1}) of cadmi-

um (II) were prepared by suitable dilution of the stock with MilliQ Waters in presence of few drops of dilute H_2SO_4 (1.0 mol L^{-1}).

The measured cadmium concentration was taken as a standard stock solution for cadmium (II) and was stored in low density polyethylene bottles (LDPE) in dark. Stock solutions (0.1–1% (w/v)) of PQ^+Cl (BDH) and trioctylamine (Fig. 1), TOA (Merck,

Darmstadt, Germany) were prepared in water in presence of few

drops of dilute HNO_3 . White sheets of PUFs of polyether type were cut as cubes (10 – 15 mm), washed with HCl (1.0 mol L^{-1}),

distilled water and acetone and finally dried [17]. Trace metal in drinking water standard (CRM-TMDW) was obtained from High-Purity Standard Inc. The reagent PQ^+Cl immobilized PUFs

were prepared as reported [18].

Table 1
ICP-OES operational conditions and wavelength (nm) for cadmium determination.^a

Parameter	
Rf power (kW)	1050(900.0)
Plasma gas (Ar) flow rate, L min ⁻¹	15(15)
Auxiliary gas (Ar) flow rate, L min ⁻¹	0.2(1.2)
Nebulizer gas (Ar) flow rate, L min ⁻¹	0.80(0.93)
Pump rate, mL min ⁻¹	1.5
Observation height, mm	15
Integration time, s	10
Wavelength, nm	214.44

^a ICP-MS operational parameters are given in parentheses. Other ICP-MS parameters are: lens voltage=9.0; analog stage voltage 1750.0; pulse stage voltage=750; quadrupole rod offset std=0.0; cell rod offset=18.0; discriminator threshold=17.0; discriminator threshold=17.0; cell path voltage std=13.0 and more abundance atomic mass (112.41).

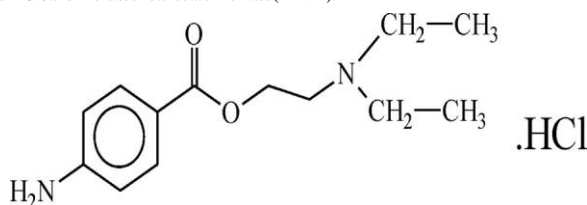


Fig. 1. Chemical structure of procaine hydrochloride.

2.3. General recommended procedures

2.3.1. Batch experiments

Accurate weights (0.1–0.002 g) of PQ⁺Cl immobilized PUFs

were equilibrated with aqueous solutions (100 mL) containing

cadmium (II) at various concentrations (1.0 × 10⁵ to 1.0 × 10³

g L⁻¹) in presence of KI (10% (w/v)) and H₂SO₄ (1.0 mol L⁻¹). After

equilibrium, Cd species remained in the aqueous phase were analyzed by ICP-OES.

Cadmium (II) retained onto the sorbent at equilibrium was calculated by difference between cadmium (II) concentration in the test solutions before (C_b) and after (C_a) extraction with PUFs. Cadmium (II) retained onto PUFs at equilibrium (q_e) per unit mass of solid sorbent (mmol g⁻¹), the sorption percentage (%E), and

the distribution ratio (D) of the analyte were finally calculated as reported [18].

2.3.2. Chromatographic separation of cadmium (II) by PUFs packed column

An aqueous solution (100 mL) of cadmium (II) ions at concentration (1.0–100 mg L⁻¹), KI (10%) and H₂SO₄ (1.0 mol L⁻¹)

packed) was percolated column at a through flow rate of 2.0 mL min⁻¹ loaded in PUFs A blank (1.0 experiment 0.002 g)

1

was also performed in the absence of cadmium (II) ions. Trace concentrations of cadmium (II) in the effluent were measured by ICPMS with the aid of calibration plot at the optimum condition. The retained cadmium (II) species were recovered with HNO₃ (10 mL, 3.0 mol L⁻¹) at flow rate of 2.0 mL min⁻¹ and analyzed. Cadmium

content in the effluent and in the recovered solution was determined by ICP-OES (or ICP-MS) vs. a reagent blank, respectively.

The influence of the ions Mg²⁺, Ca²⁺, Cu²⁺, Cd²⁺, Pb²⁺, Hg²⁺, Fe³⁺,

Al³⁺, Ni²⁺, Sb³⁺, Co²⁺, SO₄²⁻, NO₂⁻ and NO₃⁻ at 10- to 100-fold

excess was studied individually on the sorption of cadmium (II) (100 mg L⁻¹, 100 mL) by percolating the solution through PUFs

packed column. Cadmium in the effluent was determined by ICPOES (or ICP-MS) vs. a reagent blank.

2.4. Analytical applications

2.4.1. Analysis of lead in certified reference material (IAEA Soil-7)

The validity of the method was investigated by analysis of cadmium in the CRM (IAEA Soil-7) sample as follows: an accurate weight (0.20–0.300.001 g) of the CRM sample was transferred into a Teflon beaker (50.0 mL) containing HF (7.0 mL), concentrated HCl (2.0 mL), and concentrated HNO₃ (5.0 mL) at room temperature to digest the sample gradually and slowly. The mixture was heated for 1 h at 100–150 °C on a hot plate. After NO₂ fumes had ceased, the reaction mixture was evaporated to dryness and mixed again with concentrated HNO₃ (5.0 mL). The process was repeated three times and the mixture was evaporated to dryness. The residue was dissolved in dilute HNO₃ (10.0 mL, 1.0 mol L⁻¹), transferred to

volumetric flask (100.0 mL) and completed to the mark with deionized water. At the optimum experimental conditions of iodide, the test solution was percolated through the packed column at a reasonable flow rate (5 mL min⁻¹). The retained Cd species were then

recovered with HNO₃ (10 mL, 3.0 mol L⁻¹) and analyzed by ICP-OES

vs. a reagent blank.

2.4.2. Analysis of cadmium (II) in CRMs (TMDW by PQ⁺Cl) PUFs packed column

The TMDW water sample (2 mL) was digested with nitric acid (10 mL, 3.0 mol L⁻¹) and hydrogen peroxide (10 mL, 10% (v/v)),

boiled for 5 min and diluted to 100 mL with excess of KI (10% (w/v)) H₂SO₄ (1.0 mol L⁻¹). The test solution was percolated through PQ⁺Cl loaded PUFs column at flow rate of 5 mL min⁻¹.

The retained Cd species were recovered with HNO_3 (10 mL, 3.0 mol L⁻¹) at 2.0 mL min⁻¹ flow rate and analyzed by ICP-OES using the recommended procedures.

2.4.3. Analysis of cadmium (II) in wastewater and Red Sea water samples

Industrial wastewater samples (1.0 L) or Red Sea water samples (100 mL) collected from the Northern coastal area of Jeddah City, Saudi Arabia were collected, filtered through a 0.45 μm membrane filter (Millex, Millipore Corporation) and digested with nitric acid (10 mL, 3.0 mol L⁻¹) and H_2O_2 (10 mL, 10% (v/v)). The solutions

22

were boiled for 5 min, spiked with various amounts (0.05–0.5 mg) of cadmium (II) in presence of an excess of KI (10% (w/v)) and centrifuged for 5 min. The sample solutions were percolated through PQ⁺ treated PUFs packed columns at 5 mL min⁻¹ flow

Cl

rate. Cadmium (II) retained on PUFs were then recovered and analyzed.

3. Results and discussion

Preliminary investigation on shaking PQ⁺Cl loaded PUFs with

the test aqueous acidic solutions of cadmium (II) ions in the

presence of KI (10% (w/v)), has shown that, considerable sorption of cadmium (II) in a very short time compared to untreated PUFs. Thus, detailed investigation on the use of PQ⁺Cl loaded PUFs for

sorption of Cd ions has been carried out.

3.1. Retention profile of cadmium (II) onto the PUFs

The solution pH is one of the important parameters in the sorption characteristics of trace metal ions by SPE. It has a pronounced effect on preconcentration, and sensitivity. Thus, the sorption profile of Cd ions from aqueous KI solution (100 mL) at various pH onto PQ⁺Cl-loaded foams was critically studied after

shaking for 1 hr at room temperature. At equilibrium, the amount of cadmium (II) remained in the aqueous solution was determined by ICP-OES. The %E and D of Cd²⁺ onto PQ⁺Cl loaded PUFs

increased markedly on increasing the solution pH and reached maximum at pH 6–7. Representative data are shown in Fig. 2. At 6 < pH < 8, the observed increase in Cd uptake onto the reagent PUFs is most likely attributed to the ease of formation of the

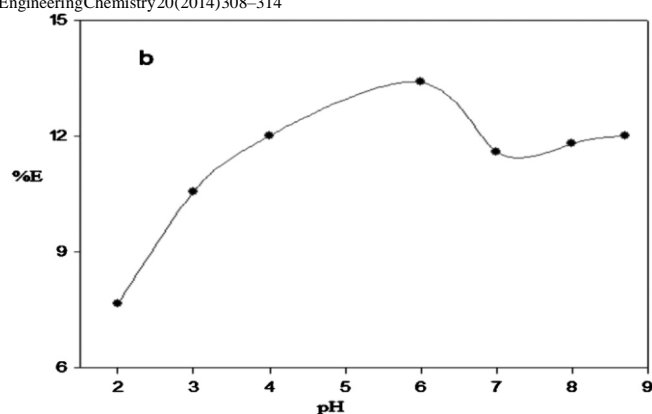


Fig. 2. Plot of pH vs. %E of cadmium (II) from an aqueous solution onto PQ⁺Cl loaded PUFs at 25 ± 1 °C.

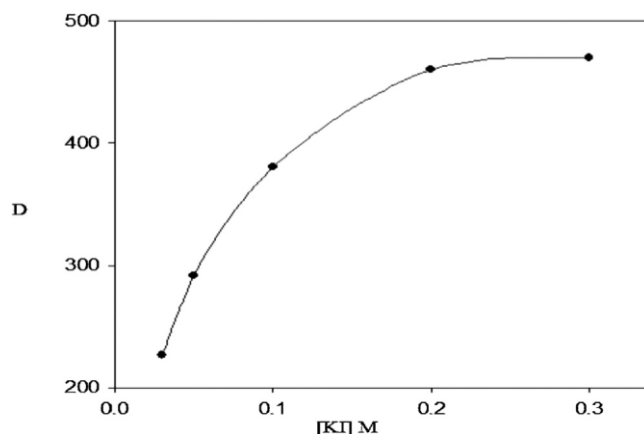


Fig. 3. Plot of the KI concentration on the sorption profiles of cadmium (II) from aqueous solutions of pH 6–7 onto the reagent treated PQ⁺Cl treated PUFs at 25 ± 1 °C.

complex anion $[\text{CdI}_4]_{\text{aq}}$. The observed decrease at pH > 8 is most likely attributed to the instability, hydrolysis or the incomplete extraction of the produced complex ion associate of $\{[\text{PQ}^+] [\text{CdI}]_2\}_{4 \text{ PUFs}}$. At pH < 6, the observed decrease in the

cadmium (II) uptake onto the reagent PUFs is most likely attributed to the incomplete dissociation of the complex species $\text{H}[\text{CdI}_4]$ which minimizes formation of the complex ion associate $\{[\text{PQ}^+] [\text{CdI}]_2\}_{4 \text{ PUFs}}$ onto PUFs sorbent. At pH 6–7, the available

binding sites (ether and/or urethane linkages) in the PUFs sorbent membrane may also participate in the retention step. Thus, in the next work, the solution was selected at pH 6–7.

Medium polarity may affect the retention step by the reagent immobilized PUFs. Thus, the influence of various concentrations (0–15% (v/v)) of ethanol on Cd uptake by the reagent treated

PUFs was tested. Cadmium (II) sorption decreased linearly on raising the ethanol content up to 10% (v/v) followed by a plateau. The change of the environment around the cadmium (II) ions makes the available binding sites of the PUFs more hydrophilic which further diminished the need for solvating water molecule and reduces cadmium (II) uptake onto the reagent immobilized PUFs to the added ethanol [24,25].

The influence of various cation (Li^+ , Na^+ , K^+ , Rb^+ and NH_4^+) size and their concentrations (0.01–0.2 mol L⁻¹) on cadmium (II)

uptake onto PUFs was studied. A slight increase (5–9%) in Cd²⁺

retention was observed in the presence of these ions. The uptake of Cd²⁺ retention followed the order:

$$NH_4^+ \delta \log D_{4\text{ PUFs}} : 2.42 > Rb^+ \delta \log D_{4\text{ PUFs}} : 2.24 > Li^+ \delta \log D_{4\text{ PUFs}} : 2.13 > K^+ \delta \log D_{4\text{ PUFs}} : 2.04 > Na^+ \delta \log D_{4\text{ PUFs}} : 2.00 \quad (1)$$

The reduction of the repulsive forces between adjacent sorbed $\{ [PQ^+] [CdI] \}^2$ [26,27] is most likely account for this trend.

The ion–dipole interaction of NH₄⁺ with the oxygen sites of the PUFs are not the predominating factors in the retention step of [CdI₄]_{aq} species onto PUFs and “solvent extraction” mechanism with the salt acting as salting-out agent participates on Cd uptake.

The added ions (Li⁺, Na⁺, K⁺ or NH₄⁺) reduce the number of water molecules available to solvate the [CdI₄]_{aq} species which would be forced out of the solvent phase onto the PUFs. The free water molecules are preferentially used to solvate the added cations [26–28].

The effect of the sorbent dose (w) and batch factor (v/w) on the cadmium (II) (10 mg mL⁻¹) retention onto the reagent treated PUFs

was investigated. Cadmium (II) sorption increased on increasing the sorbent dose up to 0.2 g of the PUFs. Therefore, a 0.2 g of the solid PUFs sorbent was adopted in the subsequent work. The

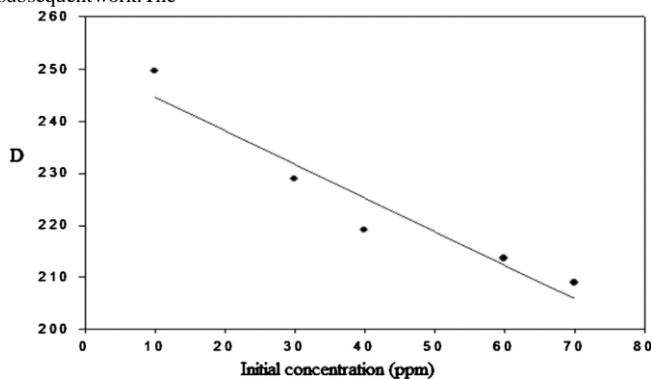


Fig. 4. Plots of D vs. initial cadmium (II) concentration from aqueous solutions of pH 6–7 onto PQ⁺Cl treated PUFs.

sorption percentage of cadmium (II) onto treated PUFs also decreased up to 60.3.5% on increasing the sample volume from

50.0 mL to 500 mL

The influence of the plasticizers TBP, NPO and TOA on the retention of cadmium (II) from the test solution by the unloaded and reagent immobilized PUFs was studied. The results indicated that, the %E of cadmium (II) followed the following order: unplasticized PQ⁺Cl-PUFs > TOA plasticized PQ⁺Cl-PUFs > TBP

TBP plasticized PQ⁺Cl-PUFs > NPO plasticized PQ⁺Cl-PUFs. The %E of cadmium (II) by the unloaded PUFs followed the following order: TOA treated PUFs > PUFs > TBP treated PUFs > NPO treated PUFs. Thus, on the subsequent work, PQ⁺Cl-PUFs were used.

The effect of surface active agents e.g. sodium dodecyl sulfate (SDS), Triton-X 100 (TX-100) and tributylhexyl-ammonium chloride (TBH⁺Cl⁻) on cadmium (II) uptake by the reagent PUFs followed the order:

$$TBH^+Cl^- \delta D_{406} > SDS \delta D_{101.2} > TX100 \delta D_{91} \quad (2)$$

The effect of KI concentration (0.03–0.3 M) on the Cd²⁺ sorption by PQ⁺Cl immobilized PUFs was investigated. Cadmium (II) uptake increased on increasing KI up to 0.2 M followed by a plateau and remained constant as shown (Fig. 3). Thus, in the next work, KI was adopted at 0.3 mol L⁻¹. Moreover, the use of PQ⁺Cl loaded PUFs in packed in column mode for complete separation and subsequent determination of trace concentrations of cadmium (II) in various water samples was critically investigated in the next work.

3.2. Sorption isotherms of cadmium (II) by PQ⁺Cl loaded PUFs sorbents

Low cost preconcentration and/or separation procedures for determination of ultra trace concentrations of cadmium (II) in water are becoming increasingly important in recent years. Thus, the retention profile of cadmium (II) over a wide range of equilibrium concentrations (1–100 mg mL⁻¹) from aqueous KI (0.3 M) solutions of pH 6–7 was investigated. The plot of D of cadmium (II) species retained onto the PUFs vs. corresponding concentration in the bulk aqueous solution is shown in Fig. 4. The amount of [CdI₄]²⁻ retained onto the PUFs at low or moderate Cd²⁺ concentration varied linearly with Cd²⁺ remained in the aqueous solution confirming the first order reaction. The most favorable D of bismuth (III) sorption onto PUFs sorbent was also achieved from more diluted aqueous solutions (Fig. 4). The D values decreased on increasing cadmium (II) concentration and the PUFs membranes became more saturated with the retained [CdI₄]²⁻ species. The sorption capacity of cadmium (II) species toward PQ⁺Cl immobilized PUFs calculated from the sorption isotherm demonstrated in Fig. 5 was found equal 41.0–1.10 mg g⁻¹.

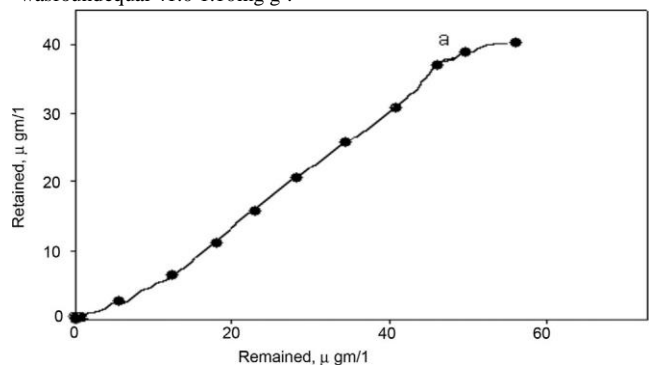


Fig. 5. Sorption isotherms of cadmium (II) uptake from aqueous solutions at pH 6–7 onto PQ⁺Cl treated (b) PUFs at 25.0, 18°C.

The retention of cadmium (II) onto PUFs sorbent was subjected to Langmuir isotherm model expressed in the following linear form [29,30]:

$$\frac{C_e}{C_{ads}} = \frac{1}{Qb} + \frac{C_e}{Q} \quad (3)$$

where C_e is the equilibrium concentration (mg mL⁻¹) of cadmium (II) in the test solution, C_{ads} is the amount of cadmium (II) retained onto PUFs per unit mass.

The constants Q and b are the Langmuir parameter related to the maximum adsorption capacity of solute per unit mass of adsorbent required for monolayer coverage of the surface and the equilibrium constant related to the binding energy of solute sorption that is independent of temperature, respectively. The plot of C_e/C_{ads} vs. C_e over the entire concentration range of cadmium (II) onto the reagent

immobilized PUFs was linear (Fig. 6) ($R = 0.998$) indicating that, the adsorption of the analyte onto

PQ⁺Cl immobilized PUFs sorbents followed Langmuir model. The values of Q and b as calculated from the slope and intercept of the linear plot were, respectively, found equal $0.92 \pm 0.01 \text{ mmol g}^{-1}$ and

$$0.27 \pm 0.02 \text{ L mol}^{-1}$$

The retention of cadmium (II) onto PUFs sorbent was subjected to Dubinin–Radushkevich (D–R) isotherm model [29,30] model expressed in the following linear form [29]:

$$\ln C_{\text{ads}} = \ln K + b C_{\text{DR}}^2 \quad (4)$$

where K_{DR} is the maximum amount of cadmium (II) retained, b is a constant related to the energy transfer of the solute from the bulk solution to the sorbent and e is Polanyi potential which is given by

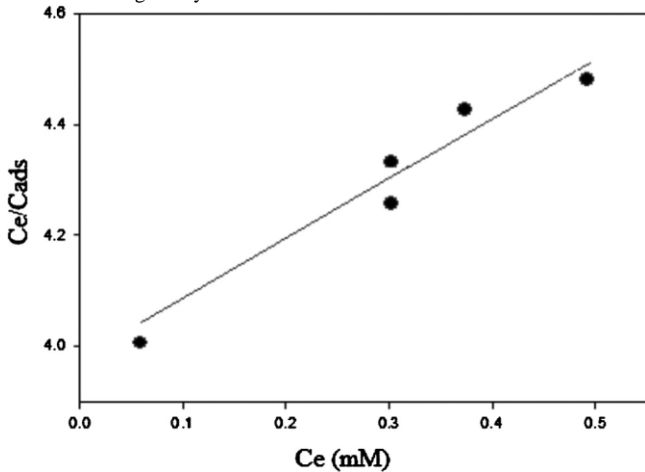


Fig. 6. Langmuir sorption isotherms of cadmium (II) uptake from aqueous solutions of pH 6 onto PQ⁺Cl immobilized foams at 298K.

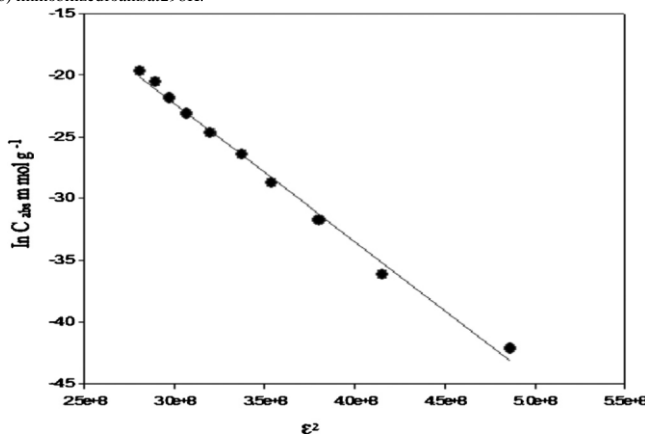


Fig. 7. Dubinin–Radushkevich (D–R) sorption isotherms of cadmium (II) retention from aqueous solutions of pH 6–7 onto PQ⁺Cl immobilized foams at 298K.

$$e^2 = \frac{RT}{C_e} \ln \left(\frac{C_0}{C_e} \right) \quad (5)$$

where R is gas constant in $\text{L J mol}^{-1} \text{ K}^{-1}$ and T is the absolute temperature in Kelvin. The plot of $\ln C_{\text{ads}}$ vs. e^2 was linear with $r = 0.986$ (Fig. 7) for the PQ⁺Cl immobilized PUFs indicating that, the D–R model is obeyed for cadmium (II) sorption over the entire concentration range. The values of b and K_{DR} computed from the slope and intercept were found equal $1.19 \times 10^{-8} \text{ mol}^2 \text{ kJ}^{-2}$ and $309.062 \text{ mmol g}^{-1}$, respectively.

Assuming that, the surface of PUFs is heterogenous and an approximation to a Langmuir isotherm model [30] is chosen as a local isotherm for all sites that are energetically equivalent, the quantity b can be related to the mean of free energy (E) of the transfer of one mole of solute from infinity to the surface of PUFs. The E value is expressed by Eq. (6):

$$E = \frac{1}{2} \ln \left(\frac{C_r}{C_{\text{abs}}} \right) \quad (6)$$

The value of E was found $64.82 \text{ kJ mol}^{-1}$ for the PQ⁺Cl loaded foam. Based on these results, b and K_{DR} parameters b and K_{DR} and the data reported [20], a dual sorption mechanism involving absorption related to “solvent extraction, ligand addition reaction and weak–base anion exchange” and an added component for “surface adsorption” is the most probable retention mechanism for cadmium (II) by the used PUFs. This model can be expressed by the equation:

$$C_r = C_{\text{abs}} \left(\frac{K_{\text{L}} C_{\text{aq}}}{1 + K_{\text{L}} C_{\text{aq}}} \right) \quad (7)$$

where C_r and C_{aq} are the concentrations of cadmium (II) retained onto the PUFs and the aqueous solution at equilibrium, respectively. C_{abs} and C_{ads} are the concentrations of the adsorbed and adsorbed cadmium (II) species onto the PUFs at equilibrium, respectively and S and K_{L} are the saturation parameters for the Langmuir adsorption model.

3.3. Chromatographic separation of cadmium (II)

The membrane structure of the PUFs [18] and the kinetics and thermodynamic characteristics of cadmium (II) uptake from aqueous iodide solutions into PQ⁺Cl treated PUFs suggested application of the sorbent PQ⁺Cl treated PUFs in packed column for separation of Cd^{2+} ions from aqueous solution. Thus, aqueous iodide solutions (0.5L) of deionized water containing Cd^{2+} at

Table 2
Recovery of analyte spikes from deionized water (n=5) by PUFs packed columns.^a

Cadmium (II)		Recovery, % ^b
Added, mg L ⁻¹	Found, mg L ⁻¹	
100	102.22	102.2
50	51.10	97.0
5	5.10	100.2

^a Cadmium was determined by ICP-OES using nitric acid as eluting agent. ^b Average recovery (n=5) relative standard deviation.

concentration 5.0–100.0 mg L⁻¹ were percolated through the PUFs

Eq. (5):

packed columns as described in Section 2. Analysis of the effluent vs. reagent blank indicated complete retention of $[Cd^{II}]^2$ onto

4

PUFs packed columns. A series of eluting agents e.g. $HClO_4$

2.4×10^{-1}

(1.0×10^{-1} molmol L^{-1}), and thiourea H_2SO_4 (1.0×10^{-1} molmol L^{-1}) was tested (0.1 mol for L cadmium^{II}), HNO_3

recovery. Complete recovery of Cd^{II} ions was achieved using HNO_3 (10 mL, 1.0 mol L^{-1}). Various concentrations (5 – 100 mg L^{-1} ,

100 mL) of cadmium ions spiked into deionized water were percolated at 5 mL min^{-1} flow rate through the packed column.

2+

The retained Cd^{II} species were then recovered with HNO_3 and the results are summarized in Table 2. An excellent recovery percentage of cadmium was achieved.

The effect of flow rate (2 – 15 mL min^{-1}) on Cd^{2+} uptake and

recovery was tested by percolating 100 mL of deionized water spiked with cadmium (10 mg L^{-1}). More or less complete retention

(> 96 %) of cadmium was achieved at flow rate < 10 mL min^{-1} . At flow rate higher than 10 mL min^{-1} , the sorption of Cd decreased and the width of the elution peak increased on increasing flow rate.

Thus, in the subsequent work a flow rate of 10 mL min^{-1} was

adopted. The effect of the sample volume (0.1 – 1.0 L) on the cadmium (II) recovery was also investigated at 10 mL min^{-1} flow

rate. Almost complete uptake and recovery ($96.04.5\%$, $n=5$) of 2+

Cd^{II} were achieved on the PUFs packed column with good reproducibility.

The performance of reagent immobilized PUFs packed column was determined by calculating the number (N), the height equivalent to theoretical plate of PUFs packed columns from the breakthrough capacity curve [18]. An aqueous solution (0.5 dm³)

containing Cd^{II} ions at 5.0 mg mL^{-1} was passed through $PQ+Cl$

treated PUFs packed column at 10.0 mL min^{-1} flow rate. The

results are displayed in Fig. 8. The rising portion of the S-shaped curve has large slope indicating a high transfer rate on/in the foam membranes and rapid attainment of equilibrium between the $[Cd^{II}]^2$ and the $PQ+Cl$ treated PUFs. The HETP and N were in the

4

range 1.25 – 0.05 mm and 80 – 1 , respectively. These values are in good agreement with the results obtained from the chromatogram

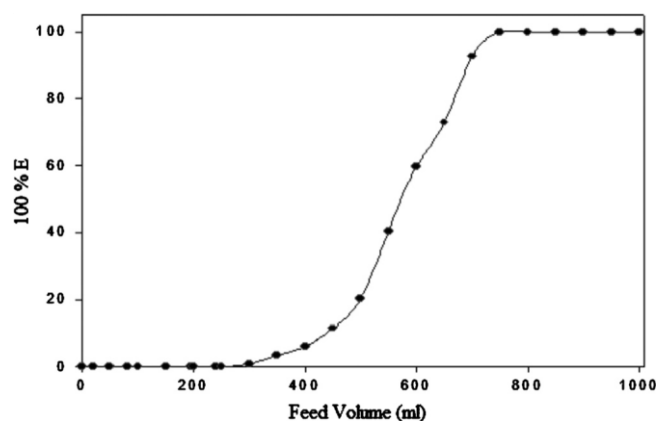


Fig. 8. Breakthrough capacity curves for cadmium(II) ions at 10 mg mL^{-1} onto $PQ+Cl$ immobilized PUFs packed columns at 15 – 20 mL min^{-1} flow rate.

method. The values of critical and breakthrough capacities [31] of cadmium retained onto the PUFs packed columns calculated from Fig. 8 were found equal 2.67 – 0.07 and 2.95 – 0.04 mg g^{-1} cadmium

(II) retention per gram of the solid sorbent.

3.4. Figures of merits

The lower limits of detection (LOD) and limit of quantification (LOQ) of cadmium(II) retention, recovery and subsequent determination were calculated for the $PQ+Cl$ packed column

Cl

using the equation [32]: $LOD = 3S/b$ and $LOQ = 10S/b$, where S is the standard deviation of the blank ($n=5$) and b is the slope of the calibration plot [32]. Under the optimal conditions of cadmium retention and recovery using treated PUFs packed columns, the linear calibration plot is given by the equation:

$$A = 0.0011 \rho + 0.47C \quad \sigma_n = 3; R^2 = 0.98 \text{ and } C = 0.0515 \text{ mg } L^{-1} \rho \quad (8)$$

The LOD and LOQ of 0.01 mg L^{-1} and 0.033 mg L^{-1} were

achieved, respectively. Such limits could be improved to lower values by collection of cadmium (II) species from large sample volumes of the aqueous phase at the optimum conditions. The relative standard deviation of the developed column for extraction 2+ and recovery of standard Cd from aqueous solutions (0.1 L)

containing 1.0 and 5.0 mg L^{-1} ($n=3$) of Cd^{2+} at 5.0 mL min^{-1} flow

rates were 1.98 and 2.9% , respectively. An enhancement and 2+ sensitivity factors of 100 and 33.3 for Cd by the developed packed column were achieved, respectively.

3.5. Effect of diverse ions

The uptake of cadmium (II) (5 mg mL^{-1}) from aqueous solution

by the reagent treated PUFs packed column was investigated in the presence of a relatively high excess (1 mg) of some diverse ions, e.g. Cu^{2+} , Al^{3+} , Ni^{2+} , Co^{2+} , Cd^{2+} , SO_4^{2-} , PO_4^{3-} , alkali and alkaline earth

metals relevant to waste water and are often accompanying cadmium (II) was examined under the optimal conditions. The amount of foreign ion causing an error 3% in the uptake of cadmium (II) is considered free from interference ratios (w/w) limit. Good extraction (>96.92%) for the cadmium (II) ions was achieved successfully in the presence of the diverse ions. In the presence of some other ions e.g. MnO_4^- , Fe^{3+} and VO_2^+ , 2 mL of NaNO_3 (0.1%) and

NaF (0.1%) solutions were introduced to the aqueous solution, respectively to obtain unambiguous and selective preconcentration.

NaF solution forms anionic complex species with both Fe^{3+} and VO_2^+ anions. The reagent NaN_3 was added to eliminate the interference of permanganate ions via reduction of manganese (VII) to manganese (II) ions. The tolerance limit of these interfering ions was improved to acceptable limit (97.62.2%) after employing these modifications. These results and the resilient characteristics of the PUFs also extend the use of the proposed reagent immobilized PUFs for the separation and sequential speciation of Cd ions.

3.6. Validation of analytical method

The method was validated by analysis of Cd in the CRM samples as described in Section 2. The results showed excellent agreement with the standard and ICP-MS 95% (1.3 confidence 0.02 mg interval g^{-1}) and (1.1 the-

(1.3 mg g^{-1}) certified value

2.7 mg g^{-1} , n = 18) [33].

3.7. Analytical applications

Validation of the method was successfully assessed by performing the extraction and recovery tests for cadmium (II) in

Table 3
Analytical determination of cadmium (II) spiked into various water samples by the proposed PQ^+Cl^- immobilized PUFs packed columns.

	Cadmium (II)		Recovery, % ^a
	Added, mg L^{-1}	Found, mg L^{-1}	
Tap-water	10	10.90.07	109.0W0.6
	100	108.50.9	108.5W0.8
	1000	995.1.5	99.5W0.2
Drinking water	1	0.0	0.0
	10	9.70.05	97W0.5
	50	50.00.12	100W0.2
	100	108.0W1.7	108.0W1.7
	500	108.01.8	102.0W0.5
		5102.5	

^a Average recovery (n=5) relative standard deviation.

tap-, drinking and industrial wastewater samples. The water samples were first acidified with phosphoric acid and filtered through a 0.45 mm cellulose membrane filter. An aqueous solution (0.5 L mL) of the water sample was then spiked with cadmium species at a concentration in the range 6–10 mg L^{-1} levels. The

sample solution was percolated through the packed column at 5 mL min^{-1} flow rate. The recovered cadmium species was

subsequently determined by ICP-MS. The results summarized in Table 3 (95.83.9 to 97.32.2) indicate that method is applicable to analyze the water samples containing trace amount of Cd after 100-fold preconcentration.

4. Conclusion

PQ^+Cl^- treated PUFs packed column has been successfully applied to the determination of trace amounts of Cd in water samples with acceptable accuracy and precision. PQ^+Cl^- treated

PUFs packed column provides a SPE approach for removal and

determination of cadmium species in water. Packed column was reused many times (n = 5) without loss in column performance. PUFs membranes are superior compared to the known rigid or granular solid sorbents and permit rapid separation at relatively high flow rate. Work is continuing for studying the influence of memory effect, organic material in fresh water samples, competitive complexing agents and on-line determination of Cd in water by cold vapor flame atomic absorption or other analytical techniques will be continued.

Acknowledgment

This project was funded by the Deanship of Scientific Research (DSR), King Abdulaziz University, Jeddah, under grant number 8-8/ 430. The authors, therefore, acknowledge with thanks DSR technical and financial support.

References

- [1] E. Merian, M. Anke, M. Ihnat, M. Stoepler, Elements and their Compounds in the Environment: Occurrence, Analysis and Biological Relevance, 2nd ed., Wiley, VCH Verlag GmbH & KGaA, Weinheim, 2004.
- [2] G.G. Briand, N. Burford, Chemical Reviews 99 (1999) 2601.
- [3] U. Forstner, G.T.W. Wittman, Metals Pollution in the Aquatic Environment, Springer-Verlag, Berlin, Heidelberg, Germany, 1981.
- [4] World Health Organization (WHO), Guidelines for Drinking Water Quality, Health Criteria and Other Supporting Information, vol. 2, 2nd ed., 1998.
- [5] E. Merin, M. Anke, M. Ihnat, M. Stoepler, Elements and Their Compounds in the Environment, Occurrence, Analysis and Biological Relevance, 2nd ed., Wiley-VCH Verlag GmbH & KGaA, Weinheim, 2004.
- [6] G. Doner, A. Ege, Analytica Chimica Acta 547 (2005) 14.
- [7] M. Soylak, I. Narin, Chemia Analityczna (Warsaw) 50 (2005) 705.
- [8] C. Xijun, Z. Ran, W. Sui, Chemia Analityczna (Warsaw) 50 (2005) 407.
- [9] H.A. Acevedo, F.A. Vazquez, R.G. Wuilloud, R.A. Olsina, L.D. Martinez, Chemia Analityczna (Warsaw) 46 (2001) 432.
- [10] M. Tuzen, K. Parlak, M. Soylak, Journal of Hazardous Materials 20 (2005) 79.

- 1093.
- [13] O. Muse, C.N. Carducci, J.D. Stripeikis, M.B. Tudino, F.M. Fernandez, *Environmental Pollution* 54(2005)234.
- [14] Z.H. Xie, F.Z. Xie, L.Q. Guo, X.C. Lin, G.N. Chen, *Journal of Separation Science* 28(5) (2005)462.
- [15] K. Miranda, A.G.C. Dionisio, O.D.P. Neto, M.S. Gomes, E.R. Pereira-Filho, Micro-Soylak, L. Elci, *Talanta* 59(2003)287.
- [16] P.K. Tewari, A.K. Singh, *Talanta* 53(2001)823. [29] M.M. Dubinin, L.V. Radushkevich, *Proceedings of the Academy of Sciences USSR - Physical Chemistry Section* 55(1974)133. (1995).
- [18] T. Braun, J.D. Navratil, A.B. Farag, *Polyurethane Foam Sorbents in Separation Science*, CRC Press Inc., Boca Raton, FL, 1985. [31] W.X. Ma, F.Liu, K.A.Li, W.Chen, S.Y. Tong, *Analytica Chimica Acta* 416(2000)191. [19] M.S. El-Shahawi, A.S. Bashammakh, S.O. Bahaffi, *Talanta* 72(2007)1492. [32] J.C. Miller, J.N. Miller, *Statistics for Analytical Chemistry*, 4th ed., Ellis-Horwood, New York, 1994p. 115.
- [21] M.S. El-Shahawi, A. Hamza, A.A. Al-Sibaai, H.M. Al-Saidi, *Chemical Engineering Soil-7: Trace Elements in Soil*, IAEA/RL 112, IAEA, Vienna, Austria, 1984. Journal 173(2)(2011)29.
- [24] M.S. El-Shahawi, M.A. Othman, M.A. Abdel-Fadeel, *Analytica Chimica Acta* 546(2005)221.
- [25] M.S. El-Shahawi, M.A. El-Sonbati, *Talanta* 67(2005)806.
- [26] J. Nakajima, Y. Hirano, K. Oguma, *Analytical Sciences* 19(2003)585.
- [27] U. Divrikli, L. Elci, *Analytica Chimica Acta* 452(2002)231. *chemical Journal* 100(2012)27. [28] S. Saracoglu, M. Sciences(Japan) 25(2009)413.
- [30] G.A. Somorjai, *Introduction to Surface Chemistry and Catalysis*, 2nd, John Wiley & Sons Inc., New Jersey, USA, 2010.
- [33] L. Pszonicki, A.N. Hanna, O. Suschny, *Report on the Intercomparison Run IAEA-*



Physicochemical Characteristics of Saudi Arabian Locally Produced Raw and Diluted Honeys and Their Relations to Antimicrobial Activity

M.S. El-Shahawi^{1†} and R. Al-Hindi²

¹Department of Chemistry, Faculty of Science, King Abdulaziz University, P.O. Box 80203, Jeddah 21589, Saudi Arabia,

² Biology Department, Faculty of Science, King Abdulaziz University, Jeddah, Saudi Arabia,

ABSTRACT

The physicochemical characteristics and antibacterial activity of Saudi Arabia honeys were studied for the first time. The levels of free and total acidity, pH, ash and moisture content were in the range 1.6 ± 0.17 - 15.1 ± 0.1 meq/kg, 2.77 ± 0.06 - 5.37 ± 0.04 , 1.1 ± 0.02 - 1.7 ± 0.03 % and < 18.0 %, respectively. Lovibond comparator color scale (P , mm) of samples was ranged from water white ($P=0.0-1.3$), extra light Amber ($P=38.14-46.57$), light Amber ($P=60.39-75.54$), Amber ($P=86.72-110.08$), dark ($P=142.39-348.44$) and very dark shade ($P= 541.84$). Dark honeys showed excellent inhibitory effect against bacterial growth. Excellent correlation between color of raw and diluted ($>10.0\%$ m/v) honey and antimicrobial activity was noticed. Honey species from different floral sources possess strong antioxidant and anti bacterial activities and are scavengers of active oxygen species.

Indexing terms/Keywords

Physicochemical characterization; Antibacterial activity; Total acidity; Lovibond comparator scale; Saudi Arabia honeys.

[†]Corresponding author: Email address: malsaeed@kau.edu.sa; mohammad_el_shahawi@yahoo.co.uk

On sabbatical leave from Department of Chemistry, Faculty of Science, Damiatta University, Damiatta, Egypt

Council for Innovative Research

Peer Review Research Publishing System

Journal: Journal of Advances in Chemistry



1. INTRODUCTION

Honey is the natural substance produced by honey bees, *Apis mellifera*, in almost every country of the world and it has been used since the earliest time [1]. (Blasa et al., 2006). It is widely appreciated as the only concentrated form of sugar available worldwide and is also used as a food preservative [2]. The antibacterial property of honey has long been recognized in vivo and in vitro as reported by Aljadi & Yusoff, 2003 [3]. The biological activities (antimicrobial and antibacterial properties) of the honey have been attributed largely to H₂O₂ and non-peroxide compounds of the samples [4]. The non-peroxide antibacterial activity of the honey has been associated with sugar concentration, antioxidant and proteinaceous compounds present in honey [3, 5-7].

Natural honey had enhanced the function of liver in treated animals with Doxorubicin (DOX) + honey and reduced the pathological effects of DOX on the morphological symptoms as well in the hepatocytes [8]. Honey also can act as a natural antioxidant which is important with the recent emphasis on decreasing the use of artificial preservation in food and perception of honey as a healthy sweetener [9]. Total phenolic content/antioxidant levels in honey including quercetin, catechin, gallic acid, caffeic acid and ferulic acid have been estimated by Al Lawati et al., 2014 [10]. The effect of formaldehyde and other enhancers on CL signal intensity was extensively investigated. The method was applied to honey samples. In this study, nine different honey samples have exhibited total phenolic/antioxidant levels of 41.2 to 765.4 mg kg⁻¹ with respect to gallic acid. The Folin–Ciocalteu (FC) assay results were well correlated with the chemiluminescence results.

Color and transparency of honey have been correlated with pigment content, antioxidant properties and suspended particles e.g. pollen [11]. The acidity of honey (pH 3.2 - 4.5) has been attributed to organic acids resulting from enzymatic action in the ripening nectar [6, 12]. Water content (<18 w/w %) of the honey has been correlated to weather, nectar conditions, humidity inside the hive and treatment of honey during its extraction and production, storage steps and other environmental factors [12].

The functional properties of honey species in foreign countries are well studied. However, the physicochemical properties of Saudi Arabia honey are not fully investigated. To the best of our knowledge, no study on the relationship between physicochemical properties and antibacterial activity of raw and diluted Saudi Arabian honeys was performed. Thus, in this study, the physicochemical properties (color, free and total acidity, pH, ash and moisture content) of raw and diluted honey species were evaluated. Honey species from different floral sources possess strong antioxidant and antibacterial activities and are scavengers of active oxygen species. Therefore, our results obtained are expected to be used as a reference for food composition and nutritional value of this mushroom.

2. EXPERIMENTAL

2.1. Apparatus and reagents

A Perkin – Elmer Lambda 25 (Shelton, CT, USA) spectrophotometer (190 – 1100 nm) and a Corporation Precision Scientific mechanical shaker (Chicago, USA) with a shaking rate of 10 – 250 rpm were used. A Milli-Q Plus deionized water system and an Orion pH meter model 720 (MA, USA), an incubator (Imperial III), oven (Daihan Lab-Tech Co.), autoclave, UV cabinet (Esco, Germany), centrifuge (Clay Adams) and water bath (Techné, England) were used. The brand of twenty natural honey samples and their commercial names were collected from Saudi Arabia beekeepers during the period 2007-2008 and stored in dark at 4 °C (Table 1). The *Staphylococcus aureus* ATCC 24213, *Micrococcus luteus* ATCC 49732 and *Escherichia coli* ATCC 25922 microorganisms were delivered from the Microbiology laboratory, King Abdulaziz University hospital [13].

**Table 1** Description of Saudi Arabian locally produced honey samples (personal name) collected from different regions

Sample No.	Trade name	Floral origin	Collection region
1	Rabea Alfayyadh	Multifloral	Al-qaseem (North of Kingdom)
2	Wadi Reeth	Unifloral (Sidr)	Gizan-Wadi Reeth (South of Kingdom)
3	Takhfa	Multifloral	Al-qaseem (North of Kingdom)
4	Alfagara	Multifloral	Al-Madinah Al-munawrah-Alfagara (North of Kingdom)
5	Albojaidi	Unifloral (Gatad)	Makkah Al-Mukarramah-Wadi Albojaidi (West of Kingdom)
6	Sidr Om Alasafeer	Unifloral (Sidr)	Makkah Al-Mukarramah (West of Kingdom)
7	Alnadheem	Multifloral	N.A.
8	Alhandhal	Unifloral (Handhal)	N.A.
9	Taba	Unifloral (Talh)	South east of Hail (North of Kingdom)

10	Alkorrath	<p>Unifloral (Korrath)</p>	South of kingdom
11	Rabea Algobbah	Multifloral	Al-qaseem, Al Gobbah (North of Kingdom)
12	Alsail Alkabeer	Unifloral (Somrah)	Alsail Alkibir (West of Kingdom)
13	Almeshaan	Multifloral	Hail (North of Kingdom)
14	Altenhat	Multifloral	North east of Riyadh (North of Kingdom)
15	Jabal Algahr	Multifloral	Giza (South of Kingdom)
16	Aba Alwrood	Multifloral	Al-qaseem Aba-Alwrood (North of Kingdom)
17	Wadi Daraa	Multifloral	Makkah Al-Mukarramah-Dehban (West of Kingdom)
18	Rabea Alsahra	Multifloral	Nufud desert



19	Motreba	Multifloral	North of Lina
20	Bani Kabeer	Multifloral	Al baha (Sout h of King dom)

2.2. Measurement of antibacterial activity

Antibacterial activity of honey samples was determined following the method reported by Patton *et al.*, 2006 [14] as follows: i. suspensions of bacterial isolates of *S. aureus*, *M. luteus* and *E. coli* were prepared by the reported turbidity standard McFarland 0.5 procedures [15]; ii An accurate volume (100 μ L) of the suspension was inoculated onto Muller Hinton agar by streaking plate method; iii six wells were made on the inoculated agar using sterile cork borer (diameter 6mm), iv a 90 μ L of honey sample solutions (10 - 100% m/m) was taken and transferred to the designated wells on the agar plates and inoculated plates and incubated at 37°C for 24h. The average (n=3) of inhibition zone's diameter (mm) was measured and the inhibition zone swabs were finally cultured on a nutrient agar and incubated for 24 h at 37 °C.

2.3. Measurements of total acidity, ash- and moisture content, pH and color

The acidity, ash and moisture contents, pH and color of the test honey samples were determined as reported [16, 17] as follows:

- Acidity measurement: An accurate weight (5- 10 \pm 0.06 g) of the homogenized honeys samples in deionized water (5075 mL) was titrated with standard carbonate-free NaOH (0.1 N) until the pH reached 8.5. The amount of consumed NaOH is equivalent to the acidity value.
- Ash content (% w/w) was determined by weighing an accurate weight (5-10 \pm 0.06 g) of the honey sample was placed in a porcelain crucible in a muffle furnace for 6 h at 550°C. The ash content was then computed from the difference of gram crucible weight before and after ignition.
- Moisture (%): Moisture content was determined by weighing an accurate weight (5 -10 \pm 0.06 g) of honey sample in a porcelain crucible. The sample was then placed in an oven at 120°C for 4 h. The moisture content (%m/m) finally calculated from the difference in weight before and after drying. iv. pH measurements: pH was determined by placing an accurate weight (5-10 \pm 0.06 g) of the homogenized honey in deionized water (50.0 mL) and read the pH directly by pH meter.
- Color measurements: Color of samples was determined by heating the honey samples to 50°C to dissolve sugar crystals and subsequent dilution with deionized water to 50% (w/v). The absorbance (Abs) of honey samples were measured at 635nm and based on P fund scale (mm), color of the honey samples was determined using the equation (Patton *et al.*, 2006):

$$P fund = - 38.70 + 371.39 \times Abs \quad (1) \text{ where}$$

P= Lovibond comparator color scale.

2.4. Statistical treatment of data

Data were expressed as means \pm standard deviations (SD) of three measurements and analyzed by SPSS V.13 (SPSS Inc., Chicago, USA). One way analysis of variance (ANOVA) and the Duncan's New Multiple-range tests were successfully used at $P < 0.05$.

3. RESULTS AND DISCUSSION

Phenols are important constituent of honey because of their scavenging ability by the available hydroxyl group [18]. Honey constituents also play an important role in stabilizing lipid oxidation [19].The high levels of phenolic compounds in honey extract reflect the radical scavenging activity.

3.1. Influence of physicochemical characteristics of raw honey on antibacterial activity

The total acidity varied between 2.0 \pm 0.17 (sample 10) and 13.1 \pm 0.46 meq/kg (sample 20). The average value (7.55 \pm 0.32 meq/kg) was found lower than the data of Finola *et al.* 2007 (20.65 \pm 0.12 meq/kg). At $P = 0.01$, significant correlation coefficients (R^2) between the total acidity and the inhibition zone (mm) for *S. aureus* ($R^2 = 0.93$), *M. luteus* ($R^2 = 0.62$) and *E. coli* ($R^2 = 0.74$) were noticed (Fig.1A).

The ash content (%) of the samples was varied between 1.1 \pm 0.02 – 1.7 \pm 0.03 % in agreement with Finola *et al.* 2007 (0.02 - 0.18 g %) [16] and Al-Doghairi, *et al.* 2007 (0.001-10.11 %) [20].The ash content is mainly dependent on the soil type and the nectar bearing plant [18]. At $P = 0.01$ significant, the ash content was poorly correlated with the inhibition zone (mm) ($R^2 = 0.41, 0.50$ and 0.37) for *S. aureus*, *M. luteus* and *E. coli*, respectively (Fig.1 B).

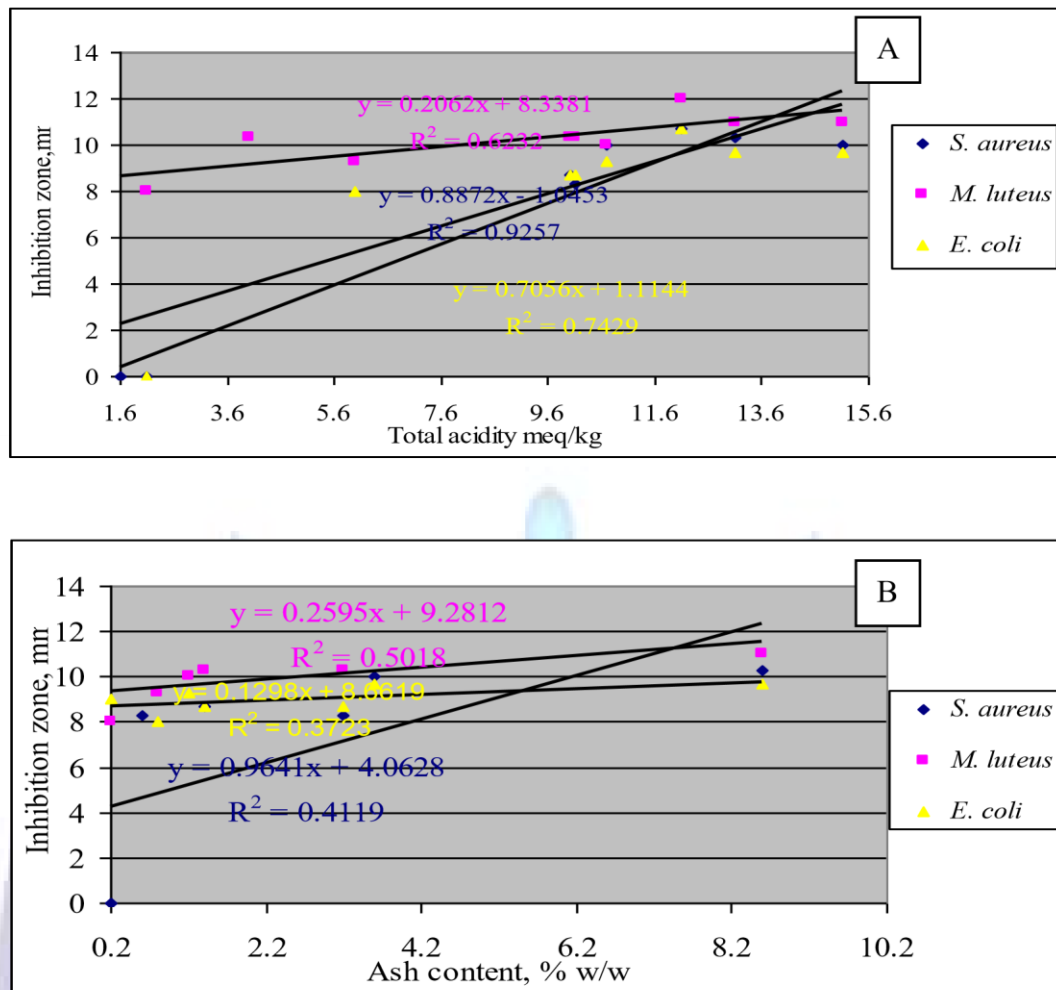


Fig.1. Plot of total acidity (meq/kg) (A) and ash content (%w/w) (B) of honey samples vs. inhibition zone (mm) of *S. aureus*, *M. luteus* and *E. coli*.

Moisture content (%) of the honey samples was in the range 6.6 ± 0.12 - 17.6 ± 0.05 %. The average value (12.1 ± 0.085 %) was lower than the average value reported (14.9 %) [20] and Anupama *et al.*, 2003 (19.8%w/w) [21]. The fermentation process is extremely low and guarantees the very long shelf- life of honey, without fermentation risk. The value of the moisture content is known to depend on the osmotic yeasts [22] and it is also responsible for the fermentation that occurred naturally in the honey. The moisture content was poorly correlated with the inhibition zone (mm) of *S. aureus* *M.*

The pH of honey samples varied from 2.77 ± 0.06 to 5.33 ± 0.09 in good agreement with the data reported (3.51-5.27) [18, 20]. Organic acids e.g. Gluconic acid and inorganic ions are most likely responsible for acidity (Kucuk *et al.*, 2007) of honey [6]. Samples of pH >5 are characterized by low purity and quality [6]. The pH values of the honey samples were inversely proportional with the inhibition zone, mm ($R^2 = 0.73$, 0.67 and 0.15) for the organisms of *S. aureus* *M. luteus* and *E. coli*, respectively (Fig.2 A, $R^2 = 0.73$).

E. coli, respectively (Fig. 2 B). The inhibition zones are comparable to pH values of the honeys from U.S. (pH range 3.46.1).

3.2. Influence of physicochemical properties of diluted honey on antibacterial activity

The inhibition of various diluted (10 -100% w/w) twenty honey samples vs. *S. aureus*, *M. luteus* and *E. coli* was investigated. The results are demonstrated in Table 2. Diluted honey content $\leq 10\%$ showed no significant effect, while diluted samples at concentrations $>10\%$ on nutrient agar medium showed grow in inhibition zones on increasing honey content. All samples showed bacterio -static effect against organisms. Some few samples at 80% and 100% (w/w) revealed bactericidal and clear antibacterial effects. The average diameters of inhibition zones (mm) of *S. aureus*, *M. luteus* and *E. coli* by raw honey samples were 33.9

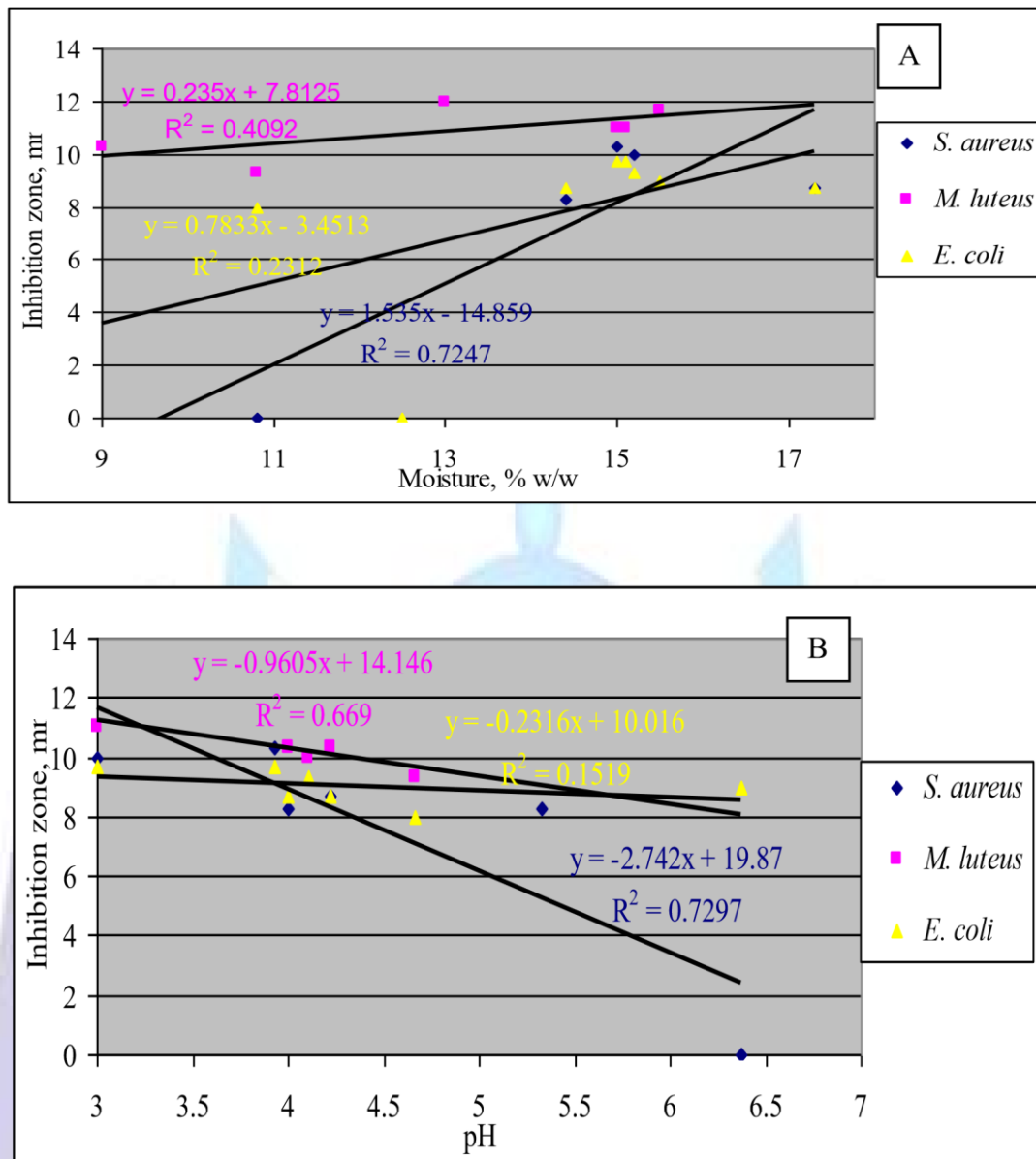


Fig.2 Plot of moisture content (%w/w) (A) and pH (B) of honey samples vs. inhibition zone (mm) of *S. aureus*, *M. luteus* and *E. coli*.

± 1.4 , 17.1 ± 1.5 and 31.0 ± 1.2 mm, respectively in agreement with the data reported earlier [5, 17]. Dark colored samples showed high antibacterial capacity in agreement with the data reported by Beretta *et al.* 2005 [5] and Estevinho *et al.* 2008 [23]. The differences in sample concentrations were significant in the antibacterial effect at $p = 0.05$. New strategies to treat wounds infected with *S. aureus* and the use of honey as a convenient and low cost option is of great importance. High antioxidant and antibacterial activity were detected in darkest honey. Phenols, flavonoids, ascorbic acid, betacarotene and sugars content in the dark honey samples account for the trend observed.

Table 2 Antimicrobial activities of diluted (10-100 %) honey samples vs. *S. aureus*^a



Sample No.	Inhibition zone diameter (mm) ^a					
	Concentrations (w/w) of diluted honey					
	10%	20%	40%	60%	80%	100%
1	0 ^a	22 ^b ±1.73	28 ^c ±1	32 ^{de} ±2	32 ^e ±1	37 ^f ±2
2	0 ^a	0 ^a	8 ^b ±1	12 ^c ±1	17 ^d ±1	21 ^e ±1
3	0 ^a	0 ^a	13 ^{bc} ±1	14 ^c ±1	19 ^{de} ±1	20 ^e ±1
4	0 ^a	0 ^a	12 ^b ±2	14 ^c ±1	17 ^d ±2	19 ^e ±1
5	0 ^a	24 ^b ±1	26 ^c ±1	32 ^d ±2	36 ^e ±1	34 ^f ±1
6	0 ^a	21 ^b ±1	28 ^c ±1	30 ^d ±1	32 ^e ±2	38 ^f ±1
7	0 ^a	0 ^a	28 ^{bc} ±1	28 ^c ±2.65	32 ^{de} ±2	32 ^e ±3
8	0 ^a	12 ^b ±2	24 ^c ±2	30 ^{def} ±1	30 ^{ef} ±1	32 ^f ±1
9	0 ^a	28 ^b ±1	34 ^{cde} ±1	36 ^{de} ±1	36 ^e ±1	40 ^f ±1
10	0 ^a	26 ^b ±1	30 ^{ce} ±1	32 ^d ±1.73	30 ^e ±1	34 ^f ±2
11	0 ^a	28 ^{bcd} ±1	28 ^{cde} ±1	28 ^{de} ±1	30 ^e ±1.73	34 ^f ±1
12	0 ^a	24 ^b ±3	34 ^{cd} ±1	32 ^{de} ±2	30 ^{ef} ±1	28 ^f ±3
13	0 ^a	24 ^b ±1	32 ^{cdef} ±1	32 ^{def} ±1	30 ^{ef} ±1	30 ^f ±1
14	0 ^a	20 ^b ±1	28 ^{cdef} ±1	28 ^{def} ±0	30 ^{ef} ±2	28 ^f ±1
15	0 ^a	18 ^b ±1	32 ^{cd} ±1	32 ^d ±1	38 ^{ef} ±1	38 ^f ±1
16	0 ^a	28 ^{bcd} ±1	30 ^{cd} ±1	32 ^{df} ±1.73	36 ^e ±2	30 ^f ±1
17	0 ^a	26 ^b ±1	32 ^{cd} ±1	32 ^d ±3	36 ^e ±1	40 ^f ±1
18	0 ^a	26 ^b ±1	30 ^c ±1.73	36 ^{de} ±1	36 ^e ±1	34 ^f ±1
19	0 ^a	22 ^b ±1	30 ^{cd} ±2	30 ^d ±1	35 ^{ef} ±2	33 ^f ±1
	20	23 ^b ±1	30 ^{cde} ±3	32 ^{de} ±1	32 ^e ±1	36 ^f ±2

^a Average (n=3) ± standard deviation. The mean difference is significant at the 0.05 level.

(0) means no antibacterial activity or inhibition.

Different superscripts denote significant differences at p <0.05.

3.3. Influence of physicochemical properties of raw honey on the Lovibond comparator scale

The effect of physicochemical parameters (total acidity, ash and moisture content, pH and color) of honey on *P* fund color scale, (*mm*) was studied. The results are summarized in Table 3. Based on *P* fund color scale, the color of samples ranged from water white (*P*=0.0-1.3) (sample numbers 10, 14 and 18), extra light Amber (*P*=38.14-46.57), light Amber (*P*=60.39-75.54), Amber (*P*=86.72-110.08), dark (*P*=142.39-348.44) and very dark shade (*P*= 541.84). The results reflect the pigment content e.g. carotenoids and flavanoids. Dark honeys contain more minerals than the lighter ones [21]. Good

² correlation between *P* fund color scale and inhibition zone (*R* =0.65- 0.68) of the organisms was noticed.

Table 3 *P* fund scale of colored honey samples

Honey sample no.	<i>P</i> fund scale	<i>P</i> fund Grader color	Honey sample	<i>P</i> fund scale	<i>P</i> fund Grader color
1	60.39	Light Amber	11	156.47	Dark
2	46.57	Extra Light Amber	12	41.30	Extra Light Amber
3	88.02	Amber	13	38.14	Extra Light Amber
4	66.03	Light Amber	14	0.00	Water White
5	142.39	Dark	15	348.44	Dark
6	212.77	Dark	16	58.75	Light Amber
7	549.84	Very dark	17	110.08	Amber
8	74.76	Light Amber	18	1.30	Water White
9	86.72	Amber	19	75.54	Light Amber
10	0.41	Water White	20	338.89	Dark

4. CONCLUSIONS

Uni floral samples showed “non-peroxide” anti-QS and antimicrobial activity does not correlated linearly with the total and individual phenolic compounds. Colors of honey samples varied from water white to very dark shade. pH, total acidity, moisture and ash content of the honey samples were comparable and / or equivalent to values reported for U.S. honey. Work is continuing to study which honey constituents are responsible for “non-peroxide” anti-QS activity.

REFERENCES

- [1] Balsa, M., Canddiracci, M., Accorsi, A., Piacentini, M.P., Albertini, M.C., Piatti, E. 2006 Raw Millefiori Honey is Packed Full of Antioxidants. *Food Chemistry* 97, 217-222.
- [2] Lambert, O., Piroux, M., Puyo, S., Thorin, C., Larhantec, M., Delbac, F., Pouliquen, F. 2012 Bees, Honey and Pollen as Sentinels for Lead Environmental Contamination. *Environmental Pollution* 170, 254-259.



- [3] Aljadi, A. M., & Yusoff, K. M. 2003. Isolation and Identification of Phenolic Acids in Malaysian Honey with Antibacterial Properties. *Turkish Journal of Medical Science*, 33, 229 -236.
- [4] Weston, R. J. 2000. The Contribution of Catalase and Other Natural Products to the Antibacterial Activity of Honey: *Food Chemistry*, 71, 235– 243.
- [5] Basualdo, C., Sgroy, V., Finola, M.S., Marioli, J.M. 2007. Comparison of the Antibacterial Activity of Honey from Different Provenance Against Bacteria Usually Isolated from Skin Wounds. *Veterinary Microbiology* 124 (3-4), 375–381.
- [6] Kucuk, M., Kolayl, S., Karaog̃lu, S.I., Ulusoy, E., Baltac, C., Candan, F.2007 Biological Activities and Chemical Composition of Three Honeys of Different Types from Anatolia. *Food Chemistry* 100, 526 –534.
- [7] Truchado,P., Lopez-Galvez,F., Gil,M.I. Tomas-Barberan, F.A., Allende, A. 2009 Quorum Sensing Inhibitory and Antimicrobial Activities of Honeys and the Relationship with Individual Phenolics. *Food Chemistry*, 115, 1337–1344.
- [8] Ganash,M.A., Mujallid, M.I., Al-Robai, A.A., Bazzaz, A.A. 2014 Cytoprotectivity of the Natural Honey Against the Toxic Effects of Doxorubicin in Mice. *Advances in Bioscience and Biotechnology* 5, 252-260.
- [9] Popova, M. P., Bankova, V. S., Bogdanov, S., Tsevetkova, I., Naydenski, C., Marcazzan, G. L. 2007 Chemical Characteristics of Poplar Type Propolis of Different Geographic Origin. *Apidologie*38, 306–311.
- [10] Al Lawati,H.A.J., Al Haddabi, B., FakhrEldin O. Suliman, F.O. 2014. A Novel Microfluidic Device for Estimating the Total Phenolic/Antioxidant Level in Honey Samples Using a Formaldehyde/Potassium Permanganate Chemiluminescence System. *Anal. Methods*. 6, 7243-7249.
- [11] Beretta, G., Granata, P., Ferrero, M., Orioli, M., & Facino, R.M. 2005 Standardization of Antioxidant Properties of Honey by a Combination of Spectrophotometric/Fluorimetric Assays and Chemometrics. *Analytical Chimica Acta*, 533, 185–191.
- [12] Gomes, S., Dias, L.G., Moreira, L.L., Rodrigues, P. Estevinho, L. 2010 Physicochemical, Microbiological and Antimicrobial Properties of Commercial Honeys from Portugal. *Food and Chemical Toxicology* 48, 544–548.
- [13] Al-Hindi, R.K., Bin-Masalam, M.S., El-Shahawi, M.S. 2011. Antioxidant and Antibacterial Characteristics of Phenolic Extracts of Locally Produced Honey in Saudi Arabia. *International Journal of Food Sciences and Nutrition*, 62(5), 513–517.
- [14] Patton, T., Barrett, J., Brennan, J., Moran, N. 2006 Use of a Spectrophotometric Bioassay for Determination of Microbial Sensitivity to Manuka Honey. *Journal of Microbiological Methods*, 64, 84– 95.
- [15] Bertoneelj, J., Doberšek, U., Jamnik, M. and Golob, T. 2007 Evaluation of the Phenolic Content , Antioxidant Activity and Color of Slovenian Honey. *Food Chemistry* 105 (2) 822-828.
- [16] Finola,M.S., Lasagno, M.C. and Marioli, J.M. 2007 Microbiological and Chemical Characterization of Honeys from Central Argentina. *Food Chemistry* 100 (4), 1649-1653.
- [17] Ferreira, I.C.F.R., Aires, E., Berreira, J.C.M., Estivenho, L.M. 2009 Antioxidant Activity of Portuguese Honey Samples: Different Contributions of the Entire Honey and Phenolic Extract. *Food Chemistry* 114 (4), 1438-1443.
- [18] Anklam, E. (1998). A Review of the Analytical Methods to Determine the Geographical and Botanical Origin of Honey. *Food Chemistry* 63 (4), 549-562.
- [19] Varshneya, C, Kant, V, Metha, M. 2012 Total Phenolic Contents and Free Radical Scavenging Activities of Different Extracts of Seabuckthorn (*Hippophae Rhamnoides*) Pomace Without Seeds. *International Journal of Food Sciences and Nutrition*, 63(2), 153-159.
- [20] Al-Doghairi, M.A., Al-Rehiayani, S., Ibrahim, G.H., Osman, K.A. 2007. Physicochemical and Antimicrobial Properties of Natural Honeys Aroduced in Al.Qassim Region. Saudi Arabia. *Metabolism of Environment of Arid Land Agriculture. Science*. 18 (2), 3-18.
- [21] Anupama, D., Bhat, K.K. and Sapna, V.K. (2003). Sensory and Physicochemical Properties of Commercial Samples of Honey. *Food Research International*. 36 (2), 183–191.
- [22] Lusby, P.E., Coombes, A.L. and Wilkinson, J.M. 2005 Bactericidal Activity of Different Honeys Against Pathogenic Bacteria. *Archives of Medical Research* 36 (5), 464– 467.
- [23] Estevinho, L., Pereira, A.P., Moreira, L., Dias, L.G., Pereira, E.2008 Antioxidant and Antimicrobial Affects of Phenolic Compounds Extracts of Northeast Portugal Honey. *Food and Chemical Toxicology* 46, 3774 – 3779.





King Saud University
Arabian Journal of Chemistry

www.ksu.edu.sa
www.sciencedirect.com



ORIGINAL ARTICLE

Voltammetric behavior, biocidal effect and  CrossMark synthesis of some new nanomeric fused cyclic thiosemicarbazones and their mercuric(II) salts

M.S.T. Makki ^{*}, R.M. Abdel-Rahman, M.S. El-Shahawi ¹

Department of Chemistry, Faculty of Science, King Abdulaziz University, P.O. Box 80203, Jeddah 21589, Saudi Arabia

Received 14 May 2011; accepted 22 July 2011

Available online 31 July 2011

KEYWORDS

Macrocyclization;
Nanomeric sulfur–metal
salts/complexes;
Molluscicidal agents;
Cyclic voltammetry;
Mechanism of electrode
reaction

Abstract New nanomeric 3-thioxo-5-methoxy-4,5-dihydro-6-methyl-9-unsubstituted/substituted 1,2,4-triazino[5,6-b]indoles (2a–c) and 3-thioxo-5-methoxy-4,5-dihydro-6,7-dihydroxy-1,2,4-triazino[5,6]-cyclobut-6-ene (3) were prepared via reaction of thiosemicarbazide with 5-unsubstituted and substituted-indol-2,3-diones and/or 3,4-dihydroxycyclobutane-1,2-dione in methanol–concentrated HCl at room temperature. A series of mercury(II)–ligand salts e.g. compound 4b and Hg(II) complexes 5a,b and 6 of cyclic Schiff base were prepared. Structures of these compounds were established by elemental analysis and spectral measurements. The redox characteristics of selected compounds were studied for use as chelating agents for stripping voltammetric determination of mercuric(II) ions in aqueous media. The compounds were also screened for their use as molluscicidal agents against *Biomphalaria Alexandrina* Snails responsible for Bilharziasis. © 2011 Production and hosting by Elsevier B.V. on behalf of King Saud University.

1. Introduction

In recent years (Mukkerjee and Sarker, 1988; Pasini and Casella, 1979; Offiong and Martelli, 1994; Zhong et al., 1998;

Beer et al., 1997; Hambley et al., 2001; Hunzenkamp et al., 2000; Yildiz et al., 2005) great attention has been directed toward designing macrocyclic compounds and their salts for several purposes e.g. as chelating agents for selective separation, removal and subsequent determination of trace and ultra trace heavy metal ions in complicated matrices. Electron-deficient moieties inserted within the back-bone of nanomeric macrocyclic complex species have opened the door on host/guest chemistry and electron transfer as supra-molecular chemistry (Bradshaw, 1997).

Calixarenes (1) are phenols metacyclophenanes having immense potential for developing molecular receptors for

^{*} Corresponding author. Tel.: +966 2 6952000; fax: +966 2 6952292.

E-mail address: mmakki@kau.edu.sa (M.S.T. Makki). ¹

Permanent address: Department of Chemistry, Faculty of Science at Damietta, Mansoura University, Mansoura, Egypt.

Peer review under responsibility of King Saud University.



<http://dx.doi.org/10.1016/j.arabjc.2011.07.028>

1878-5352 © 2011 Production and hosting by Elsevier B.V. on behalf of King Saud University.

added calix[n]arene is dependent upon the chain-length of appended alkyl groups (Foroughifar et al., 2009). The effect was more pronounced in calix[11]arenes compared to calyx[12]arenes and calyx arenes having the same function group R (Chandra, 2005). Condensation of sequearic acid and its esters with aliphatic or aromatic amines yielded the corresponding bis amide (Hamaue and Minami, 1999), while cyclocondensation of sequearic acid with amino guanidine in 1:1 molar ratio have afforded 2-alkylthio-4-chloro-5-methyl-N-(1,2-dihydroxycyclobuta[e][1,2,4]-triazin-3-yl) benzenesulfonamide (Pandey and Sengupta, 2006). These compounds have acted as potent inhibitors against HOP-62 non small cell lung cancer line (in vitro anti-tumor activity) (Pandey and Sengupta, 2006).

Recently, a series of nanomeric molecules and some of their metal salts have been reported (Xu et al., 2006; Ali et al., 2008). Thus, the present article is focused on: (i) The synthesis of new nanomers derived from cyclocondensation of squaric acid and cyclic bi-carbonyl compounds; (ii) evaluating the molluscicidal properties of the prepared compounds; and finally (iii) studying the redox characteristics of selected compounds for use as selective reagents in stripping voltammetry for mercury determination in wastewater samples.

2. Experimental

2.1. Apparatus

A Perkin Elmer (Lambda EZ-210) double beam spectrophotometer (190–1100 nm) with 1 cm (path width) quartz cell was used for recording the electronic spectra of the compounds. A Perkins Elmer model RXI-FT-IR system 55529 was used for recording the IR spectra. A Bruker advance DPX 400 MHz model using TMS as an internal standard was used for recording ^1H NMR and ^{13}C NMR spectra (Chemical shift in ppm) of the compounds on deuterated DMSO. A GC-MS-QP 1000-Ex model was used for recording the mass spectra of the compounds. Melting points were determined with an electro thermal Bibbly Stuart Scientific Melting Point SMPI (US). Molecular weights and elemental analysis of the compounds were preformed on Micro analytical center, Cairo University, Egypt. Cyclic voltammetric measurements were performed on a Metrohm 757 VA trace analyzer and 747 VA stand (Basel, Switzerland). The electrochemical data were recorded at room temperature and the peak current heights were measured using the “tangent fit method.”

2.2. Reagents and materials

Analytical reagent grade chemicals were used as received. Low density polyethylene (LDPE) bottles, Nalgene were used for collection of various water samples. LDPE bottles were carefully

recognition of ions and small organic molecules. Chawla and Pathak (2000) have reported that addition of calix[n]arenes to methylene blue markedly speeded sensitized photoxygenation of 4,5-diphenylimidozolones. The remarkable effect of

cleaned first with hot detergent, soaked in 50% HCl (Analar), HNO_3 (2.0 mol IPP^{1PP}), subsequently washed with dilute HCl (0.5 mol IPP^{1PP}) and finally rinsed with distilled water. In cyclic voltammetry, solutions were made in N,N-dimethylformamide (DMF) in the presence of tetramethyl-ammonium chloride as supporting electrolyte.

2.3. Organic syntheses

2.3.1. N-Methyl-indol-2,3-dione derivatives (1a–c) Equimolar amounts of methyl iodide and isatin, 5-nitro/5-fluoroisatin in ethanolic KOH (5% w/v) was stirred at room temperature for 4 h. The solution was left to cool overnight. The solid precipitates were filtered off, washed and dried to give 1a–c, respectively.

Compound 1a was crystallized from ethanol as pale yellow crystals. Yield = 75%, m.p. 180 C. Analytical data: Found: C, 66.69; H, 4.21, N, 8.39; Calculated for $\text{C}_9\text{H}_7\text{NO}_2$: C, 67.7; H, 4.34; N, 8.69.

Compound 1b was crystallized from ethanol as yellow crystals. Yield (71%), m.p. 226 C. Analytical data: Found: C, 51.82; H, 2.72; N, 13.44; Calculated for $\text{C}_9\text{H}_6\text{N}_2\text{O}_4$: C, 52.42; H, 2.91; N, 13.59.

Compound 1c was crystallized from ethanol as faint yellow crystals. Yield (69%), m.p. 212 C. Analytical data: Found: C, 59.67; H, 3.31; N, 7.73; F, 10.49. Calculated for $\text{C}_9\text{H}_6\text{NFO}_2$: C, 60.33; H, 3.35; N, 7.82; F, 10.61.

2.3.1.1. 3-Thioxo-5-methoxy-4,5-dihydro-6-methyl-9-unsaturated/substituted-1,2,4-triazino[5,6]indoles (2a–c). A mixture of compound 1a–c (1.0 mmol) in dry methanol (50 mL) and thiosemicarbazide (1.0 mmol) in concentrated HCl (10 mL) was stirred for 6 h at room temperature. The produced solids were filtered off, washed with methanol and dried to give 2a–c, respectively.

Compound 2a was crystallized from ethanol as yellow crystals. Yield = 55%, m.p. 220 C. Analytical data: Found: C, 52.64; H, 4.78; N, 22.33; S, 12.76. Calculated for $[\text{C}_{11}\text{H}_{12}\text{N}_4\text{SO}]$: C, 53.22; H, 4.83; N, 22.58; S, 12.90.

Compound 2b was crystallized from ethanol as yellow crystals. Yield = 58%, m.p. 305 C. Analytical data: Found: C, 44.55; H, 3.71; N, 23.62; S, 10.80; Calculated for $[\text{C}_{11}\text{H}_{11}\text{N}_5\text{SO}_3]$: C, 45.05; H, 3.75; N, 23.89; S, 10.92.

Compound 2c was crystallized from ethanol as yellow crystals. Yield = 65%, m.p. 250 C. Analytical data: Found: C, 49.07; H, 4.13; N, 21.05; S, 12.03; F, 7.14. Calculated for $[\text{C}_{11}\text{H}_{11}\text{N}_4\text{SFO}]$: C, 49.62; H, 4.13; N, 21.05; S, 12.03; F, 7.14. IR: m cm^{-1} 3200, 3140 (N^2H , N^4H), 1160–1130 (C,S), 1600, 1060–1049 (C,N, OMe); ^1H NMR (d ppm): d: 11.3, 9.3, and 3.4, 2.5 (N^4H , N^2H , OCH_3), ($\text{CH}_3\text{-N}$), 7.5, 7.18, 6.9 (3H of aromatic ring); ^{13}C NMR (d ppm): 178.19, 162.18, 158.47, 156.9, 138, 130.87, 130.85, 117.01, 111.55, 55.48, 38.51, 18.02. m/s (Int.%) 270 (M+4, 18.9, 149 (100), 95 (35) as $\text{C}_5\text{H}_4\text{F}$ radical.

2.3.1.2. 3-Thioxo-5-methoxy-4,5-dihydro-6,7-di-(hydroxy-1,2, 4-triazino[5,6]-cyclobut-6-ene) (3). Equimolar amounts of squaric acid and thiosemicarbazide in dry methanol (100 mL)–concentrated HCL (10 mL) was stirred at room temperature for 6 h. The solution was left to cool overnight and the resultant solid precipitate was filtered off, washed with methanol to give compound 3.

Compound 3 was crystallized from ethanol as yellow crystals. Yield = 82%, m.p. 178–180 C. Found: C, 35.39; H, 3.42; N, 20.87; S, 15.74; Calculated for $C_6H_7N_3SO_3$, (201). C, 35.82, H, 3.48, N, 20.89, S, 15.93. M/e: 202 (M+1 (12.35), 157 (5.18), 129 (23.15), 58 (100). IR: $m\text{ cm}^{-1}$ 3429, 3308 (2 OH), 2947, 1614 (Me, C,N), 1317, 1167 (NCS & C–S), 1046 (–O–Me); $^1\text{H NMR}$ (d ppm): d: 10.3 9 (2 NH), 6.085, 5.910 (2 OH) and 3.43(OCH₃); $^{13}\text{C NMR}$ (d ppm): 181.42 173.55, 55.46, 39.44, 38.76, 38.49, 18.01.

2.3.2. Synthesis of compound 4a and mercury(II) compounds (4b, 5a,b)

A mixture of compound 2b or 2c (2 mmol) in dry methanol (100 mL) and mercuric(II) chloride (1.0 mmol) was stirred at room temperature for 12 h. The solution mixtures were left to cool overnight and the resultant solid precipitates were filtered off, washed with methanol to give compounds of type 5a,b. On diluting the filtrates, yellow precipitates were isolated, washed and dried in vacuum to give type of compounds 4a,b, respectively.

Compound 4a was crystallized from ethanol as yellow crystals. Yield = 18%, m.p. 240 C. Found: C, 30.39; H, 1.19; N, 17.66; S, 8.05; Cl, 8.93; Calculated for $[C_{20}H_{12}N_{10}S_2O_4Cl_2Hg]$; C, 36.34; H, 1.51; N, 17.69; S, 8.09; Cl, 8.97. IR: $m\text{ cm}^{-1}$ 3215, 3170 (2 NH), 2880, 1485(CH₃), 1165 (C–S).

Compound 4b was crystallized from ethanol as yellow crystals. Yield = 48%, m.p. 238 C. Analytical data: Found: C, 31.94; H, 2.39; N, 14.90; S, 8.51, F, 5.05, Cl, 9.45. Calculated for $[C_{20}H_{12}N_8S_2F_2Cl_2Hg]$ (740, M+3) C, 32.56; H, 1.62; N, 15.19; S, 8.61; F, 5.11; Cl, 9.65. M/S: 740 (M+3, 15.21), 150 (100). IR: $m\text{ cm}^{-1}$ 3210, 3180 (N⁴H, N²H), 2920, 1440 (–CH₃), 1250 (C–F). $^{13}\text{C NMR}$ (d ppm): d: 161.83, 130–128, 110, 38.53 and 17.76 ppm.

Compound 5a was crystallized from ethanol as yellow crystals. Yield = 35%, m.p. 236 C. Analytical data: Found: C, 32.87; H, 2.19; N, 19.00; S, 8.44; Calculated for $C_{20}H_{16}N_{10}S_2O_4Hg$ (726, M+2); C, 33.81; H, 2.22; N, 19.33; S, 8.83. IR: $m\text{ cm}^{-1}$ lack of SH functional groups.

Compound 5b was crystallized from ethanol as pale yellow crystals. Yield = 48%, m.p. 270 C. Analytical data: Found: C, 35.58; H, 1.78; N, 16.06; S, 9.50; F, 5.59; Calculated for $C_{20}H_{16}N_8S_2F_2Hg$ (670, M), C, 35.82; H, 2.38; N, 16.70; S, 9.59; F, 5.69. IR: $m\text{ cm}^{-1}$ lacks of NH, SH. $^1\text{H NMR}$ (d ppm): d: 2.55 (3 H, s, CH₃–N), 7.2–7.6 (5 H, m-phenyl protons); $^{13}\text{C NMR}$ (d ppm): 170.48, 164.37, 162.74, 144, 123.65, 117.61, 113.63, 36.04.

2.3.3. Di[4,5-dihydro-6,7-di(hydroxyl-1,2,4-triazino[5,6]cyclobut-6-ene)-3-thioato]-mercuric chloride 6 A mixture of 3 (2 mmol) and mercuric(II) chloride in dry methanol (100 mL) (1.0 mmol) in 2:1 and 1:1 molar ratios was stirred for 12 h at room temperature. The mixtures were left to cool overnight and the resultant solid were filtered off, washed with methanol to give compounds of type 6.

Compound 6 was crystallized from ethanol as yellow crystals. Yield = 65%, m.p.225 C. Analytical data: Found: C, 19.42; H, 1.28; N, 13.59; S, 10.26; Cl, 11.38. Calculated for

$[C_{10}H_8N_6S_2O_4HgCl_2]$ (614, M+3). C, 19.63; H, 1.3; N, 13.74; S, 10.47; Cl, 11.62. IR: $m\text{ cm}^{-1}$ 3429, 3380 (2 OH), 3180, 3166 (2 NH), 1360 (CNS), 1155 (C–S); $^1\text{H NMR}$ (d ppm): d: 8.8 (1H s, NH), 5.7, 5.2 (each s, 2 OH) and 7.8 (s, 1H of C₅NHNH-1,2,4-triazine).

2.4. Cyclic voltammetric experiments

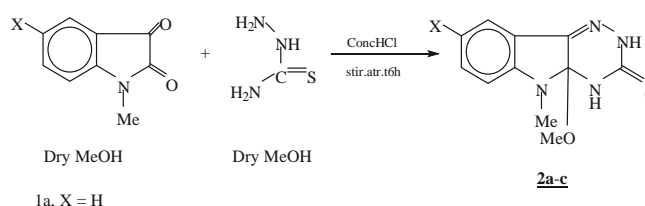
An accurate concentration (2.0 mmol) of the compound 3 or its mercury(II) salt or complex and the supporting electrolyte tetramethyl ammonium chloride (TEAC) (200 mmol) in DMF were transferred into the electrochemical cell composed of Pt working (small surface area), Pt (large surface area) and Ag/AgCl as working, counter and reference electrodes, respectively. The test solution was then stirred with nitrogen gas for 5 min to release oxygen and the voltammograms were then recorded at various scan rates (50–1000.0 mV/s) in the potential range 1.5 to +1.0 V vs. Ag/AgCl electrode.

3. Results and discussion

3.1. Chemical characterization

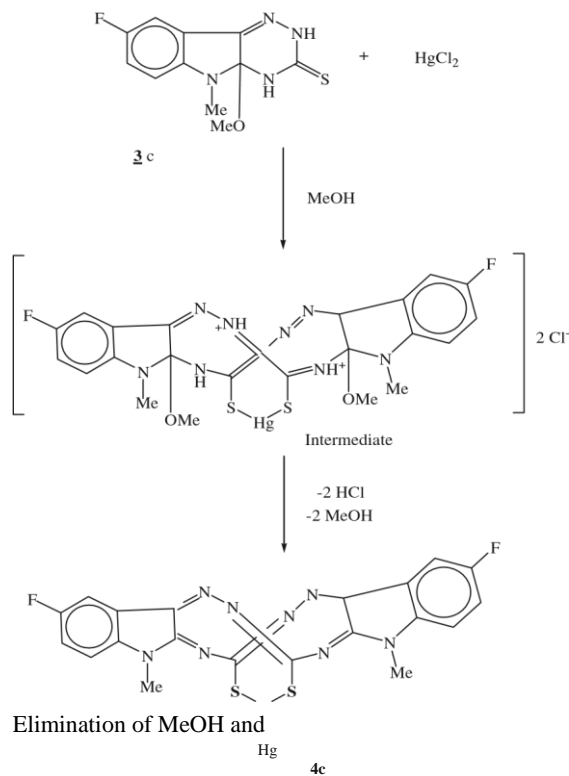
Preliminary investigations of coordination chemistry of the prepared organic ligands containing nitrogen and/or nitrogen–sulfur atoms, have shown that, heterocyclic ligands react with mercuric(II) chloride in a mono dentate or bi dentate fashion via SH or NH. Condensed 1,2,4-triazin-3-thiones are known heterocyclic thione exists in two thione and thiol tautomeric forms (Maya et al., 2000; Belloc et al., 2000; Singh and Patel, 2003; Rourk, 1999; Abdel-Monem, 2010; Nicholson and Shain, 1964). These compounds coordinate as neutral ligand via sulfur atom (Singh and Patel, 2003) or as bi dentate ligand (S, N), S, N bridging by loss of a proton (N–S). Interaction of cyclic dicarbonyl reagents as 1-methyl-indol2,3-diones (1a–c) and thiosemicarbazide in dry methanol– HCl (2.0 mol L⁻¹), yielded 3-thioxo-5-methoxy-4,5-dihydro6-methyl-9-unsubstituted/substituted-1,2,4-triazino[5,6b]indoles(2a–c) (Scheme 1).

Structures of 2a–c were established from their elemental analysis and spectral measurements. IR spectrum of 2c showed the stretching bands characteristics to NH, NH and C,S at 3200, 3140 and 1160–1130 cm^{-1} . The vibration modes at 1600 cm^{-1} and 1060–1040 cm^{-1} were observed and were safely assigned to C–N and OMe functional groups. $^1\text{H NMR}$ spectra recorded signals at d 11.3, 9.2, 3.48, and 2.5 ppm due to N²H, N⁴H, OCH₃ and Me–N protons with aromatic protons at 7.5, 7.18, and 6.9 ppm. $^{13}\text{C NMR}$ spectrum of 2c recorded resonated signals at 178.19, 111.55, 55.48, 38.51, and 18.02 ppm confirming the proposed structure. M/S spectrum of 2c showed m/z at 270 (M⁺+4) as molecular ion with a base peak at 149 assigned to C₉H₈NF (1-methyl-5-fluorindole) radical.



Cyclocondensation of squaric acid with thiosemicarbazide in dry methanol–HCl (2.0 mol L⁻¹) afforded 3-thioxo-5-methoxy-4,5-dihydro-6,7-dihydroxy-1,2,4-triazino (Beer et al., 1997; Hambley et al., 2001). Structure of 3 was established from their elemental analysis and spectral measurements. Mass spectrum of 3 showed mainly two peaks at m/z 202 (M+1) as molecular ion (C₆H₇N₃SO₃) and at m/z 58 as a base peak. IR spectrum recorded vibration bands at 3429 and 3388 cm⁻¹ of two hydroxy groups at 2947, 1614 cm⁻¹ of aliphatic CH₃ and C,N functional groups. Another vibrations at 1371, 1167 and 1046 cm⁻¹ attributed to CNS, C–S and O–Me functional groups. ¹H NMR spectrum showed resonated signals at δ: 10.3, 9.7, and 6.085 and 5.9 ppm attributed to two NH and OH protons with peaks at 3.43 ppm of OMe proton. ¹³C

Scheme 2



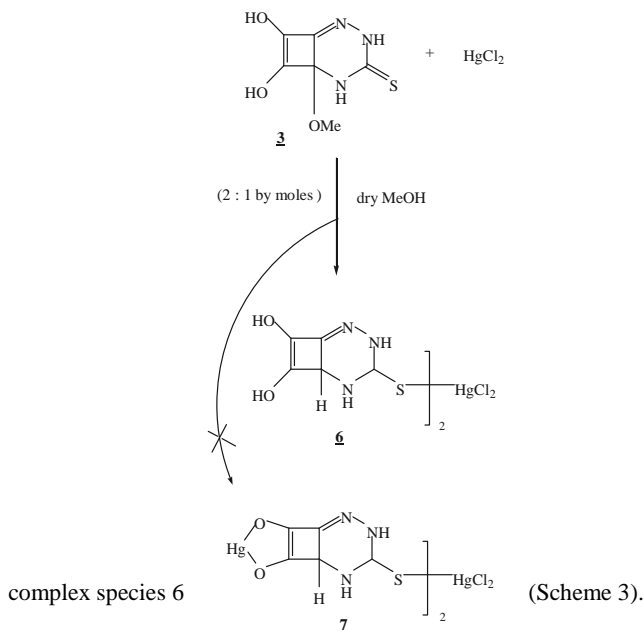
coordination of sulfur atom to mercury(II) ions as mono dentate was noticed. IR spectrum showed the presence of two hydroxy and NH groups indicating complexation with mercury is in a pseudo-tetrahedral environment with organic ligands bonded to the metal ion. ¹H NMR spectrum of 6 recorded signals δ:5.7, 5.2 ppm due to hydroxyl and C₅-H of 1,2,4-triazine with δ at 8.4, 8.8 ppm attributed to two NH and NH protons confirming the structure of complex 6 (Scheme 4).

3.2. Voltammetric behavior of selected compounds (3, 4c and 5)

Selection of the tested compounds 3, 4c and 5 was based on the influence of mercury(II) on the redox characteristic of the resulting species and also to see whether compound 3 or similar compounds can be used as effective chelating agents for trace metal determination employing stripping voltammetry. Cyclic voltammograms (CVs) of 3 and its nanomeric mercuric salts prepared in 1:1 (4c) and in 2:1 (5) molar ratios of 3 to mercury(II) in DMF–TEAC at Pt were carried out. The CVs of compound 3 versus Ag/AgCl reference electrode at various scan rates (50–500 mV s⁻¹) were carried out. Representative voltammograms are shown in Fig. 1. The CV at 50 mV s⁻¹ (Fig. 1) revealed one well-

Scheme 3 Formation of 4b from 2c on reaction with HgCl₂.

NMR spectrum showed resonated signals at 18.01, 38.49, 38.76, 39.44, 55.46, 173.55, 181.42 ppm confirming the proposed structure. Complexation of 3 with mercuric(II) chloride in dry methanol in 1:1 and 2:1 molar ratios gave only one



defined anodic peak at 0.75 V coupled with an ill defined cathodic peak at 1.2 V vs. Ag/AgCl electrode. At a scan rate >1000 mV s⁻¹, the anodic and cathodic peaks became ill defined suggesting the instability of the electrogenerated species at Pt working electrode i.e. slow kinetics and irreversible electrochemical process (Nicholson and Shain, 1964; Bowmaker et al., 1982; Bard and Faulkner, 1980).

The CVs of compound 4c at Pt working electrode versus Ag/AgCl reference electrode at various scan rates (100–3000 mV s⁻¹) were carried out and representative CVs at 100 and 300 mV s⁻¹ are shown in Fig. 2. The CV at 100 and 300 mV s⁻¹ revealed one well-defined anodic peak at 0.65 V and two ill defined anodic peaks at 0.3 and 0.80 V coupled with one well defined cathodic peak at 1.0 V. On increasing the scan rate from 400 to 3000 mV/s, one well defined electrode couple was noticed on the potential range from 1.3 to 0.3 V and the other anodic peaks disappeared suggesting slow kinetics electrochemical process (Bard and Faulkner, 1980). The observed cathodic and anodic shifts to more negative and positive potential, respectively, suggesting irreversible nature of the electrochemical process (Nicholson and Shain, 1964; Bowmaker et al., 1982; Bard and Faulkner, 1980). Plot of the square root of the scan rates versus anodic and cathodic

Scheme 4 Formation of 6 from 3 with HgCl₂.

peak currents increased linearly (Fig. 3)

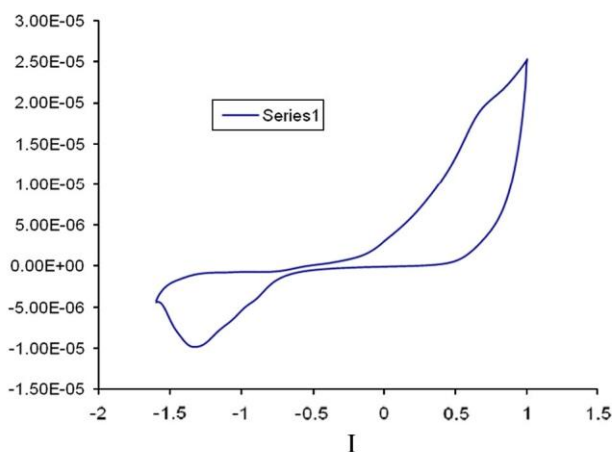


Figure 1 CV of compound 3 at 50 (I) and 200 (II) mV s^{-1} in DMF.

Figure 2 CV of compound 4c at 100 and 300 mV s^{-1} in the potential window 1.5 to +1 V versus Ag/AgCl reference electrode.

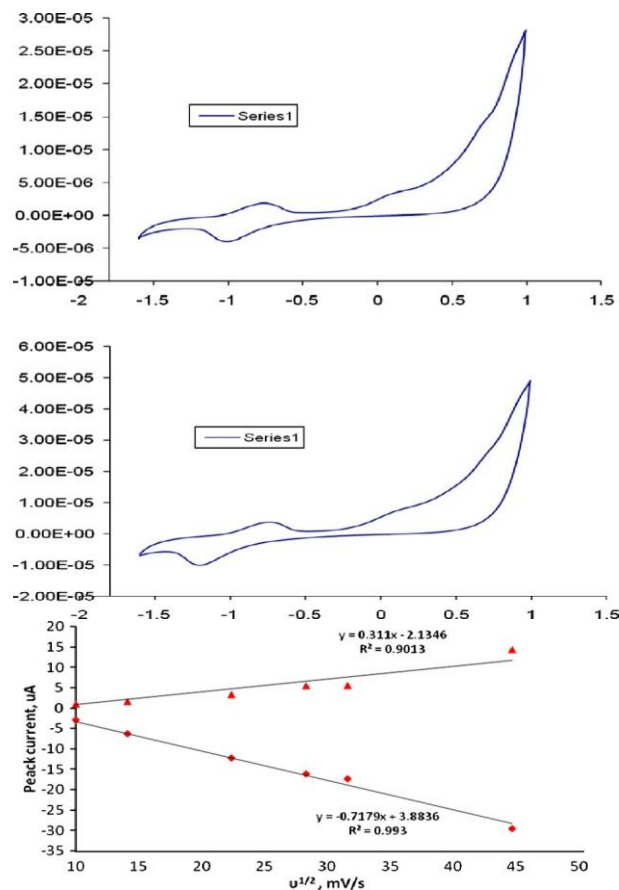
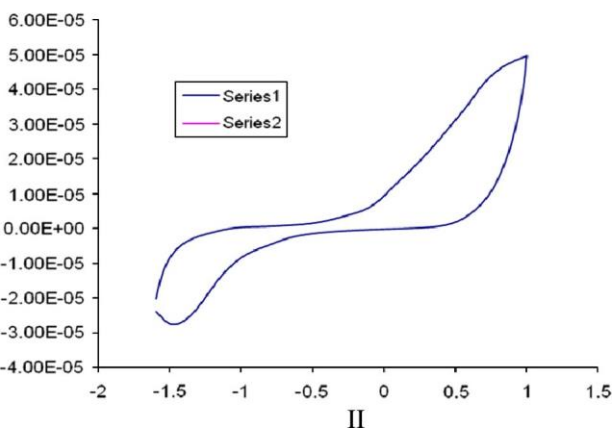


Figure 3 Plot of I_p , a and I_p , c vs. square root $t^{1/2}$ of the CVs of compound 4b at Pt working electrode.

indicating that the process is a diffusion controlled electrochemical process and favors electrode-coupled (EC) chemical reaction mechanism of the type EC (Bard and Faulkner, 1980). These data suggest the possible use of compound 4b in stripping voltammetric determination of mercury(II) in aqueous solution.

The CVs of compound 5 at various scan rates were recorded at various sweep rate 50–3000 mV/s . Representative CVs are shown in Fig. 4. The CV at 50 mV s^{-1} showed an ill defined (like a shoulder) anodic peak at 0.3 in addition to another peak at 01 V versus Ag/AgCl electrode. On the reverse scan, two well defined cathodic peaks were noticed at 0.3 and 0.6 V and are safely assigned to $\text{Hg}^{\text{II}}/\text{Hg}^{\text{I}}$ and $\text{Hg}^{\text{I}}/\text{Hg}^0$, respectively. Plots of the cathodic or anodic peak currents versus the square root were linear revealing that the reduction process is diffusion controlled process (Bard and Faulkner, 1980). The plot of the current function (cathodic peak current/square root of sweep rate) versus sweep rate decreased linearly indicating that the first reduction processes ($\text{Hg}^{\text{II}}/\text{Hg}^{\text{I}}$) proceeded according to the EC mechanism (Bard and Faulkner, 1980). Thus, compound 5 can be used in differential pulse cathodic stripping voltammetric determination of mercury(II) in wastewater. On raising the sweep rate from 500 to 1000 mV s^{-1} , the cathodic and anodic peaks are shifted to more negative values confirming the irreversible nature of the

electrochemical process. The cathodic peak current increased linearly on increasing the analyte concentration confirming the performance of

Table 1 Molluscicidal activity of the compounds against *Biomphalaria Alexandria* Snails

Compound. no.	Concentration/% killing		
	100 ppm	50 ppm	25 ppm
2a	20	10	0
2b	30	10	0
2c	40	10	0
3	20	10	0
4b	60	30	20
5	50	30	20
6	80	40	20
Reference standard, Baylucide	100	100	100

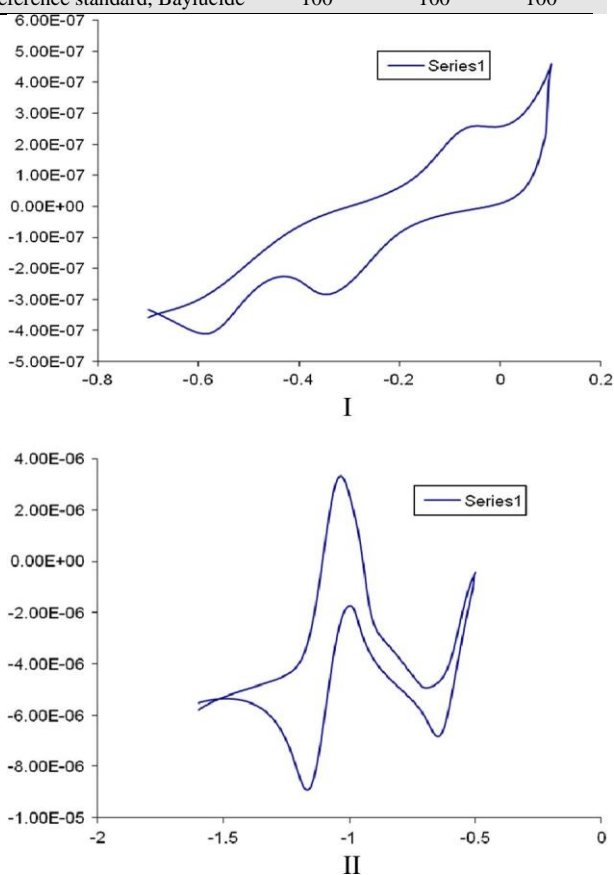


Figure 4 CVs of compound 5 at 50 (I) and 100 mV s⁻¹ versus Ag/AgCl reference electrode.

exposed to each concentration for 24 h followed by another 24 h as a recovery period in dechlorinated water (WHO, 1965). Snails *Biomphalaria Alexandria* (shell in diameter 9–11 mm) was tested. The intermediate host of *Schistosoma mansoni* which helps in causing intestinal Bilharzias the most common problem in Egypt was collected from the irrigation canals in Abu-Rawash, Giza Govern state. The snails were adapted to laboratory conditions for two weeks before use to be sure that the Snails are strong and healthy. Snails were kept in plastic aquaria containing de

chlorinated tap water at 25–27 C. The efficiency of the compounds against snails followed the order: 6 > 4b > 5 > 2 and 2c > 2b > 2a.

Molluscicidal activity

Recently, 1,2,4-triazine derivatives have been used as molluscicidal agents against snails responsible for Bilharzias (Abde-Rahman et al., 2010). In a similar manner, the prepared 1,2,4-triazine compounds and their mercury(II) complexes were screened. Solutions of the compounds (20–80 ppm) in dechlorinated tap water of pH 7–7.7 at 27 C were tested in the present study and their LC₅₀ were calculated (WHO, 1953; WHO, 1965). Exactly 10 snails were

chlorinated tap water at 25–27 C. The efficiency of the compounds against snails followed the order: 6 > 4b > 5 > 2 and 2c > 2b > 2a. The electron barrier of the molecular structure of the compound participated in the enzymatic inhibition of the living processes for the Snails thereby causing break of a vital cycle of Snails. Hg and F atoms in the compounds enhanced the mortality of snails due to the high toxicity of mercury(II) and a deposition of protein in the vital cell of Snails by the available fluorine atoms (Table 1).

Acknowledgments

The authors would like to thank the Deanship of Scientific Research (DSR), King Abdulaziz University, Jeddah for the financial support under grant number 33-97-430 H and the Chemistry Department for the facilities provided.

References

- Abdel-Monem, W.R., 2010. *Eur. J. Chem.* 1 (3), 168.
- Abde-Rahman, R.M., Makki, M.S.T., Ali, T.E., Ibrahim, M.A., 2010. *Eur. J. Chem.* 1 (3), 236.
- Ali, T.E., Abdel-Rahman, R.M., Hanafy, F.H., El-Defawy, S.M., 2008. *Phosphorous, Sulfur, Silicon and Related Compounds* 183, 2265.
- Bard, A.J., Faulkner, L.R., 1980. *Electrochemical Methods Fundamental and Applications*. John Wiley, New York.
- Beer, P.D., Szemes, F., Balzani, V., Sala, M., Drew, M.G.B., Dent, S.W., Maestri, M., 1997. *J. Am. Chem. Soc.* 119, 1864.
- Belloc, N., Montaban, A.G., Bradley, D., Williams, G., Cook, A.S., Anderson, M.E., Feng, X., Barrett, A.G.M., Hoffman, B.M., 2000. *J. Org. Chem.* 65, 1774.
- Bowmaker, C.A., Boyd, P.D.W., Campbell, G.K., Hope, J.M., Martin, R.L., 1982. *Inorg. Chem.* 21, 152.
- Bradshaw, J.S., 1997. *J. Inclusion Phenomena, Macrocycl. Chem.* 29, 221.
- Chandra, S., Gupta, L.K., 2005. *J. Indian Chem. Soc.* 82, 454.
- Chawla, H.M., Pathak, M., 2000. *J. Indian Chem. Soc.* 77, 98.
- Foroughifar, N., Mobinikhaledi, A., Ebrahimi, S., Moghanian, H., Fard, M., Kalhor, M., 2009. *Tetrahedron Lett.* 50, 836.
- Hamaue, N., Minami, M., Hirafujii, M., 1999. *CNS Drug Reviews* 5, 331.
- Hambley, T.W., Lindoy, L.F., Reimers, J.R., Tumer, P., Wei, G., Cooper, A.N.W., 2001. *J. Chem. Soc. Dalton Trans.*

- Hunzenkamp, F., Stucke, A.C., Cavolli, E., Godel, H.U., 2000. *J. Chem. Soc. Dalton Trans*, 251.
- Maya, E.M., Vazquez, P., Torres, T., Gobbi, L., Diederich, F., Pyo, S., Echegeyen, L., 2000. *J. Org. Chem.* 65, 823.
- Mukkerjee, G.N., Sarker, L., 1988. *Indian J. Chem.* 27A, 514.
- Nicholson, R.S., Shain, I., 1964. *Anal. Chem* 36, 709.
- Offiong, O.E., Martelli, S., 1994. *Farmaco* 49 (7–8), 513.
- Pandey, J.K., Sengupta, S.K., Pandey, O.P., 2006. *J. Indian Chem. Soc.* 83, 1073.
- Pasini, A., Casella, L., 1979. *J. Inorg. Nucl. Chem.* 36, 2133. Rourk, M.J., Iowa State Uni., 1999, 2nd Florida Heterocyclic Conference 3–7 2001.
- Singh, N., Patel, R.N., Sukla, K.K., 2003. *Indian J. Chem (A)* 42, 1883.
- WHO, Expert Committee on Bilharziasis, 65 (1953) 33. WHO, Snail Control Information of Bilharziasis Monograph Series 50 (1965) 124.
- Xu, H., Wang, D., Zhang, W., Wei, Z., Yamamoto, K., Jin, L., 2006. *Anal. Chim. Acta* 577, 207.
- Yildiz, M., Bulger, B., Cinar, A., 2005. *J. Indian Chem. Soc.* 82, 414.
- Zhong, C.F., Deng, J.C., Tong, J., Yao, X.H., Zhu, W.S., 1998. *Chem. J. Chin. Univ.* 19 (2), 174.

Provided for non-commercial research and education use.
Not for reproduction, distribution or commercial use.



This article appeared in a journal published by Elsevier. The attached copy is furnished to the author for internal non-commercial research and education use, including for instruction at the authors institution and sharing with colleagues.

Other uses, including reproduction and distribution, or selling or licensing copies, or posting to personal, institutional or third party websites are prohibited.

In most cases authors are permitted to post their version of the article (e.g. in Word or Tex form) to their personal website or institutional repository. Authors requiring further information regarding Elsevier's archiving and manuscript policies are encouraged to visit: <http://www.elsevier.com/copyright>



Contents lists available at SciVerse ScienceDirect

Journal of Industrial and Engineering Chemistry

journal homepage: www.elsevier.com/locate/jiec

A new method for analysis of sunset yellow in food samples based on cloud point extraction prior to spectrophotometric determination

M.S. El-Shahawi^{a,*}, A. Hamza^a, A.A. Al-Sibaai^a, A.S. Bashammakh^a, H.M. Al-Saidi^b

^a Department of Chemistry, Faculty of Science, King Abdulaziz University, P.O. Box 80203, Jeddah 21589, Saudi Arabia ^b University College, Department of Chemistry, Umm Al-Qura University, Makkah, Saudi Arabia

ARTICLE INFO

ABSTRACT

Article history:

Received 19 July 2012

Accepted 5 September 2012 Available online 19 September 2012

Keywords:

Micelle-mediated cloud point extraction
Sunset yellow
Sorption isotherm
Thermodynamics
Chemical equilibria Food stuffs

A simple new micelle mediated preconcentration method was developed for analysis of sunset yellow (SY) prior to its spectrophotometric determination. The method was based upon cloud point extraction of the ion associate of SY and trioctylamine (TOA) in HCl–Triton X-100. In the surfactant phase the SY species react with TOA yielding hydrophobic ion associate of SYTOA⁺. The distribution coefficient of SY

between surfactant-rich phase and aqueous phase was approximately 104. Validation was tested by comparing the results with standard HPLC. Isotherm and thermodynamic parameters, chemical equilibrium, extraction constants and stoichiometry of the associate were assigned.

© 2012 The Korean Society of Industrial and Engineering Chemistry. Published by Elsevier B.V. All rights reserved.

1. Introduction

Synthetic dyes are usually added to food stuffs and soft drinks not only to improve appearance, color and texture but also to maintain the natural color during processor storage. This class of compounds has been added legally into food since the 1880s to make food more attractive and appetizing for customers [1]. Western studies have found little evidence that sunset yellow possesses significant genotoxic potential either when given orally or by injection to rodents, in mammalian cells in culture, or in bacterial assays, including a large number of Ames tests [1]. The entrance of such azo dye compounds into the environment is a concern due to coloration of natural waters and also due to their toxicity, mutagenicity, carcinogenicity and their biotransformation products [1,2]. Many kinds of synthetic food colorants, e.g. sunset yellow, tartrazine, allura red are widely used over the world due to their low cost and stability [2]. The food colorant sunset yellow is one of the common food additives to food, drug and cosmetics.

Several methods e.g. bivariate calibration and derivative spectrophotometry [3,4], polarography and voltammetry [5–8],

* Corresponding author. Permanent address: Department of Chemistry, Faculty of Science, Damietta University, Damietta, Egypt. Tel.: +9662695200x54422; fax: +96626952292.

E-mail addresses: malsaeed@kau.edu.sa, mohammad_el_shahawi@yahoo.co.uk (M.S. El-Shahawi).

HPLC-MS [9], capillary electrophoresis [10], thin layer chromatography [11] and ion-pair liquid chromatography [12] have been reported for determination of food colorants. Some of these methods, e.g. chromatography and polarography are not considered as green analytical methods due to utilization of hazardous organic solvents and dropping mercury as in polarography. At trace level of SY, its determination by these techniques was not applicable without preconcentration step prior measurement.

Micelle-mediated extraction (MME) has been recognized as an alternative approach to the conventional liquid–liquid extraction (LLE) and solid-phase extraction (SPE) due to a number of advantages, e.g. low cost, environmental safety, short analysis time, high capacity and high recovery and concentration factors to concentrate a wide variety of analytes of widely varying nature [13,14]. The extraction of the analyte in CPE procedure can be accomplished by optimizing the conditions, e.g. temperature, the addition of salts, etc. [13,15]. SPE cartridges are quite expensive. The surfactant solution becomes turbid because it attains the cloud

point and the original surfactant solution separates into the two isotropic phases namely coacervate phase, i.e. the surfactant rich phase (SRP) of small volume containing the analyte trapped by micelle structures and bulk diluted aqueous phase (AQ) [15,16].

Clouding phenomena in solutions of nonionic surfactants, e.g. Triton X-100 or TX-114 is attributed to the ethyl oxide and polyethylene glycol segments in the micelles that repel each other at low temperature and attract at higher one [17,18]. After CPT, most of the analyte separates into the SRP [19]. In the aqueous solution of neutral surfactant, the solute is distributed between the two phases at CPT and

1226-086X/\$ – see front matter 2012 The Korean Society of Industrial and Engineering Chemistry. Published by Elsevier B.V. All rights reserved.
<http://dx.doi.org/10.1016/j.jiec.2012.09.008>

solubilization of non polar solubilizes increases in the SRP on raising temperature after CPT due to increase in the number of aggregated micelles. The solubilization of polar solutes also decreases owing to dehydration of the polyoxyethylene chains accompanied by coiling more tightly [20–25]. Surfactant molecules in water at concentrations above its critical micellar concentration (CMC) form micelles. At a certain temperature some micellar solutions can macroscopically phase separate into a micelles-rich phase and micelles-poor phase [20]. Micelles formation phenomenon has been widely used to extract organic and complex species from aqueous solutions [21–27].

As a sign of the wide use of CPE technique, a search in Science Finder returns 905 papers, 16 of them referring specifically to dyes determination based on CPE. A few numbers of them have provided detailed investigations about thermodynamic characteristics and chemical equilibrium of dye solubilization in the SRP. Thus, the present article reports a sensitive CPE spectrophotometric procedure for analysis of SY food colorant residues in food stuffs and in soft drinks using TOA and Triton X-100. The isotherm, thermodynamic characteristics and chemical equilibrium of SY solubilization in SRP will be also discussed. 2. Experimental

2.1. Instrumentation

A Perkin–Elmer (Lambda 25, Shelton, CT, USA) spectrophotometer (190–1100) with 2 mm (path width) quartz cell was used for recording the absorption spectra and absorbance measurements. An Orion pH meter was used for pH measurements with absolute accuracy limits at pH being defined by NIST buffer. A Sorvall RT 6000 B centrifuge (Du Pont, Wilmington, DE, USA) and a Precision Scientific thermostat water bath (Chicago, USA) were maintained at the desired temperature.

2.2. Chemicals and reagents

All reagents were of analytical reagent grade. Iso-octyl phenoxy polyethoxy ethanol (Triton X-100) was purchased from Aldrich Chemical Co. Ltd. (Milwaukee, WI, USA) and was used as received. An aqueous solution (0.03 mol L⁻¹) of Triton X-100 was prepared

by dissolving the required weight in deionized water. A stock solution (1000 mg mL⁻¹) of sunset yellow (1-sulfophenylazo-2-

naphthol-6-sulfonic acid disodium salt (E 110) FCF (Aldrich) was prepared by dissolving an accurate weight (0.1001 g) of SY in water (100 mL). A series of solutions (20–450 mg L⁻¹) of the SY was

prepared by dilution with deionized water. A stock solution of HCl (1 mol L⁻¹) was prepared by diluting the concentrated acid

(sp. gr. = 1.19 and 37%, w/v) with water in measuring flask (100 mL). A stock solution (3%, v/v) of trioctylamine (TOA) (Aldrich) was prepared by diluting the reagent (3.0

mL) with water containing drops of HCl in measuring flask (100 mL). Commercial soft drink (2153.0 ng mL⁻¹), sweet (80.5 1.2 mg g⁻¹) and orange gelatin

(443.2 5.8 mg g⁻¹) were purchased from the local market, accurate

weights of sweet and orange gelatin were dissolved in deionized water and filtered. The filtrates were completed with water in measuring flasks to get final solutions of 325 and 295 ng mL⁻¹,

respectively. The stability of the food colorant SY up to 100 °C was checked by recording its absorbance at 530 nm for up to 2 h. The food colorants tartrazine, allura red, ponceau 4 R and amaranth were purchased from Aldrich, France. Stock solutions (100 mg mL⁻¹) of the

food colorants in deionized water were prepared and used as interfering species. 2.3. Recommended procedure

In a typical CPE experiment, a known concentration of SY (20–452 mg L⁻¹) solution was added to Triton X-100 (4 mL of

0.03 mol L⁻¹) and TOA (3 mL, 3%, v/v) in a glass centrifuge tube

(10 mL) containing aqueous HCl (1 mL, 0.1 mol L⁻¹) and Na SO

(1 mL, 1.00 mol L⁻¹). The solution was completed to the mark with

deionized water and mixed by a vortex mixer for 1 min. The solution was then kept in an ultrasonicated thermostated water bath at 70 °C for 10 min and centrifuged at 3000 rpm for another 10 min to complete phase separation. The solution was kept in an ice bath for 10 min and the aqueous phase (upper part) was withdrawn and its volume was measured using a 10 mL syringe. The SRP (300–400 mL) was separated out, diluted with MeOH (100–200 mL) to decrease the viscosity of the solution before measurement. The absorbance of the diluted SRP was finally measured at 532 nm vs. reagent blank.

2.4. Adsorption study

In aqueous HCl medium (0.03 M), a series of solutions containing Triton X-100, TOA and various concentrations of SY (20–200 mg mL⁻¹) were mixed together and placed in a

thermostat bath at 70 °C for 10 min. After cooling the solutions and centrifugation for 10 min at 3000 rpm, separation of phases was carried out and the concentration of SY in diluted phase (C_d) was determined at 532 nm using the standard curve. The aqueous phase was diluted to minimize the effect of Triton X-100 micelles and to ensure that the concentration of the surfactant is lower than its critical micelle concentration and facilitating determination of SY in the coacervate phase (C_m) employing the equation:

$$C = \frac{C_0 V_0}{V_0 + V_d} \quad (1)^m$$

where, C_0 is the initial concentration of SY; V_0 and V_d are the volumes of the original solution and the dilute phase after CPE, respectively.

2.5. Analytical applications

2.5.1. Analysis of SY in soft drinks

Various samples of soft drinks were collected from the local market of Saudi Arabia and used without prior treatment. A certain volume (10 mL) of the drink was diluted with distilled water to the mark in a 50 mL measuring flask. An accurate volume (2.0 mL) of this solution was treated under the recommended procedure and the exact SY concentration in the original sample was then determined with the aid of a calibration curve.

2.5.2. Analysis of SY in sweet and gelatin stuffs

In conical flasks (50.0 mL), the sweet or gelatin samples were added and shaken well with distilled water (10 mL) for 5 min and filtered through Whatman No. 40 filter paper. The filtrate was transferred to measuring flask (25 mL), completed to the mark with deionized water and SY was analyzed under the optimum procedure and the content of SY in the original sample was then determined.

3. Results and discussion

3.1. Optimization of the cloud point extraction conditions

Preliminary investigation on the effect of acidity on the efficiency of CPE showed that the cloud point extraction of SY

from aqueous solution containing Triton X-100 and TOA is more effective in acidic media. The color of the dye is changed at higher pH values and becomes colorless. This behavior is probably due to the increase in the attractive forces involving the water molecules and the surfactant polar groups as the acidity increases. The influence of mineral acids HCl, HNO₃, and H₂SO₄ (0.01 mol L⁻¹) on

the absorbance (A) of the extracted SY species onto the SRP on CPE was investigated. The absorbance of SY in the SRP increased in the order: HCl (A = 0.25) > HNO₃ (A = 0.15) > H₂SO₄ (A = 0.13). The competition between the complex ion associates of TOA⁺ with Cl⁻,

NO₃⁻ or HSO₄⁻ and TOA⁺ with SY in the SRP may account for the observed trend. Thus, in the subsequent work, HCl was selected as a suitable extraction medium.

The influence of HCl concentration (0.005–0.04 mol L⁻¹) on the

CPE of SY was demonstrated in Fig. 1. The absorbance of SY in the SRP increased on raising HCl concentration up to 0.01 mol L⁻¹ and

remained constant. The phase separation was favorable and the hydrophobicity of the surfactant increases on raising HCl concentration [21]. It was observed that, as the CP increases, the volume of the SRP decreases, meaning that more surfactant remains in the aqueous phase and that, the extraction is less effective. So, in the subsequent studies, HCl concentration was adopted at 0.01 mol L⁻¹. It is well known that, most of the food

colorants showed high absorption at pH in the range of pH 3.0–5.5 [21]. Thus, the effect of pH (pH 0.0–6.0) on the CPE using HCl and/or NaOH (0.001 mol L⁻¹) was investigated. The data revealed that, at

pH 2, the extraction of the TOA⁺SY associate into the SRP is low,

> negligible and the absorbance was less than 0.04.

The effect of the Triton X-100 concentration (0.015–0.05 mol L⁻¹) on the extraction of SY (200 ng mL⁻¹) was

investigated in the presence of TOA (3 mL, 3%, v/v) and HCl (0.01 mol L⁻¹) at 70°C after 10 min centrifugation at room

temperature. The plot of the absorbance of SY in the SRP after CPE vs. Triton X-100 concentration was demonstrated in Fig. 2. The absorbance and volume of the SRP (V_{SRP}) increased linearly on increasing Triton X-100 concentrations up to 0.03 mol L⁻¹ and

remained constant. So, by increasing Triton X-100 concentration, the number of hydrophobic micelles increased and causes responsive increase of the extractability of Triton X-100 [28]. In all measurements, the V_{SRP} was in the range 300–400 mL while, the volume of bulk aqueous phase (V_{AQ}) was in the range 9.6–9.7 mL. The amount of SY in sample solution (10.0 mL) was measured after preconcentration onto a final volume of 0.4 mL by CPE after dilution with methanol (200–100 mL) to minimize the viscosity of the solution.

The enrichment factor (F_c = C_{SRP}/C_{AQ}) was defined as the ratio between the analyte concentration in the SRP (C_{SRP}) and the analyte concentration in the initial aqueous solution (C_{AQ}). The

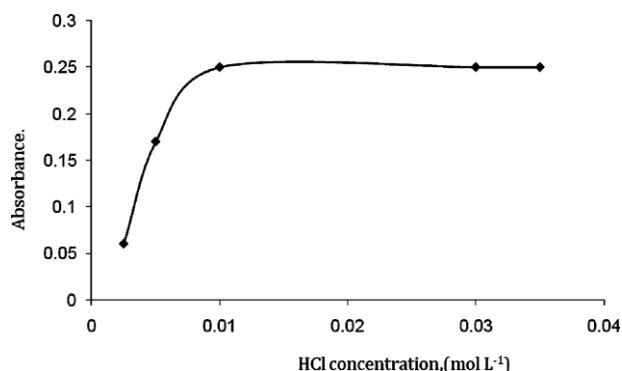


Fig. 1. Plot of the absorbance of SY (λ_{max} = 532 nm) in the SRP vs. HCl concentration. Conditions: Triton X-100 (0.03 mol L⁻¹); temperature = 70°C and 20 min shaking time.

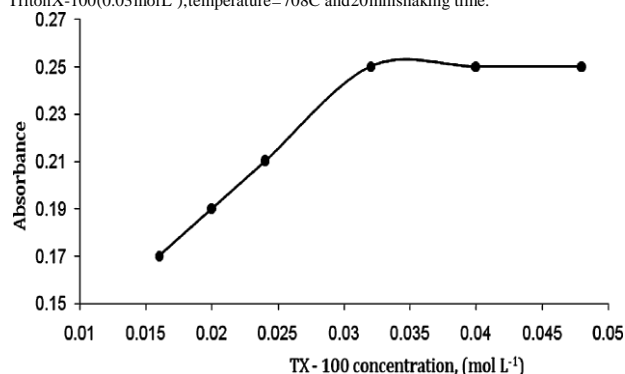


Fig. 2. Plot of absorbance of SY (λ_{max} = 532 nm) in the SRP vs. concentrations of Triton X-100. Conditions: SY = 200 mg mL⁻¹, temperature = 70°C and 20 min shaking time.

calculated value of F_c was found in the range 80.03–2. At Triton X-100 concentration < 0.03 mol L⁻¹, the volume of the SRP was very small (< 100 mL) and the analysis of SY become more difficult and not precise. So, to achieve maximum absorbance and extraction of SY Triton X-100 concentration was adopted at 0.03 mol L⁻¹.

The extraction of SY depends on the hydrophobic interaction between the ion associate of SY and TOA and the hydrophobic micelles in the test solution. Thus, the influence of TOA concentration was investigated at the optimal Triton X-100 concentration. The plot of the absorbance of the SRP vs. TOA concentration was shown in Fig. 3. Maximum absorbance of the SRP was achieved after adding 3 mL of TOA (3%, v/v) to achieve complete extraction of SY up to 450 ng mL⁻¹.

The dependence of extraction efficiency on the equilibrium time (5–30.0 min) was studied. The absorbance of the SRP reached a maximum at 10 min equilibrium time. Such equilibration time is much shorter than the time required to attain equilibrium on using solid adsorbents [28]. The influence of equilibration temperature (25–80 °C) on the CP extraction was also tested. The absorbance reached a maximum value above 70 °C, hence in the next work, an equilibration temperature of 70 °C was adopted.

It is well known that, addition of electrolytes (salting-out effect) has a pronounced effect on the phase separation of analyte and decreases cloud point (CP) temperature of surfactant, resulting in a more efficient extraction [29,30]. Thus, the effect of NaCl, CaCl₂ and Na₂SO₄ on CPE of SY was investigated in the concentration range 0.02–0.2 mol L⁻¹. The absorbance of SY increased on increasing

electrolyte concentration according to the following order:

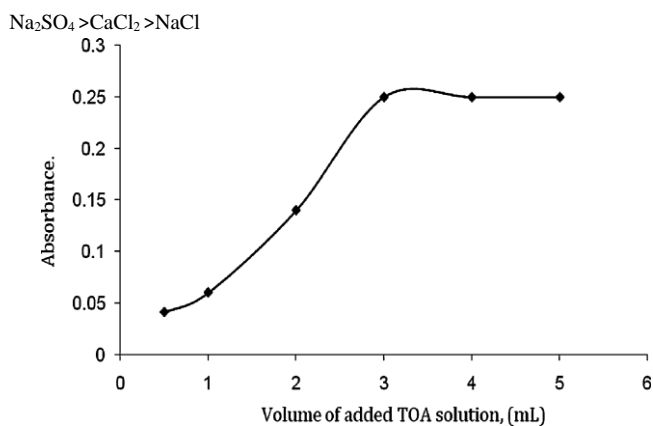


Fig. 3. Plot of absorbance of SY ($\lambda_{max} = 532 \text{ nm}$) in the SRP vs. volume of TOA added. Conditions: SY = 1.0 mg mL⁻¹; Triton X-100 = 0.03 mol L⁻¹, temperature = 70°C and 20 min shaking time.

The absorbance of the SRP reached a maximum value at concentration of 0.1 mol L⁻¹ Na₂SO₄ and remained constant. The

2 4

fact that, addition of Na₂SO₄ electrolyte increased the size of the micelles and aggregation number, thus, enhancing the analyte to be more soluble in the SRP [15] so, more water goes to the dilute phase because of the salting-out effect. The added sulfate ions also decrease the self-association of water molecules, hydration of the polyoxyethylene chain and the surfactant solubility in water, causing a decrease in CPE [31]. Thus, a concentration of 0.1 mol L⁻¹

of Na₂SO₄ was adopted in the subsequent work. Although addition of Na₂SO₄ decreases the CP of Triton X-100 to 57.8°C, the equilibration temperature was adopted at 70°C since; the CPE methodology requires raising the temperature higher than the CPT of the surfactant to achieve the optimum temperature [30,31]. The SRP undergoes dehydration on increasing temperature equilibration; however, this does not mean that the increase in temperature decreases the efficiency of extraction [31].

3.2. Adsorption isotherm

Distribution of various concentrations of SY between the SRP and AQ at equilibrium vs. initial concentration (Fig. 4) can be explained by adsorption of the solute into the interior or outer palisade layers of micelles. Thus, assuming a homogeneous monolayer adsorption, the linearized Langmuir sorption model can be applied using the equation [32]:

$$\frac{1}{q} - \frac{1}{q_m} = \frac{1}{m n C_e} \quad (2)$$

where, q is the amount of SY solubilized per unit mass of surfactant and m and n are constants representing the maximum solubilization capacity and energy, respectively and q is defined by the equation:

$$\frac{1}{q} = \frac{C_m}{C_s} \quad (3)$$

where, C_s is the surfactant concentration in the SRP and it is given by the equation:

$$C_s = \frac{C_{os} V_o - C_{ds} V_d}{V_o + V_d} \quad (4)$$

where, C_{os} and C_{ds} are the surfactant concentrations used in the feed solution and diluted phase after CPE, respectively. Because C_{ds} is close to the critical micelle

concentration (CMC) that is always much less than the feed concentration of surfactant [33], i.e. the value of C_{ds} V_d can be neglected and Eq. (4) is simplified as:

$$C_s = \frac{C_{os} V_o}{V_o + V_d} \quad (5)$$

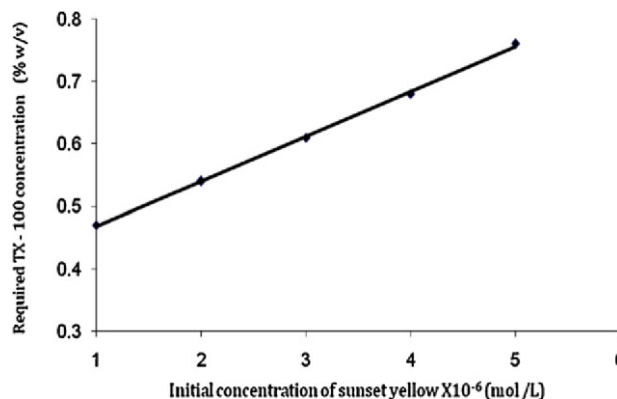


Fig. 4. Plot of D of SY in the SRP vs. initial SY concentrations.

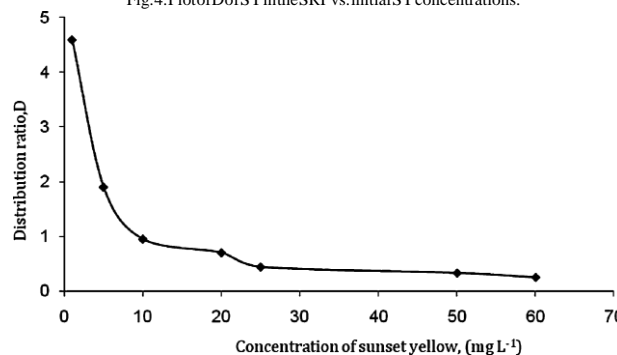


Fig. 5. Theoretical concentrations of Triton X-100 required for achieving quantitative extraction of SY at various surfactant concentrations.

Plot of 1/q vs. 1/C_e over the entire SY concentrations was linear with a correlation coefficient of 0.998. Thus, the solubilization of SY in the SRP obeys the Langmuir adsorption model. The calculated values of Langmuir parameters m and n from the slope and intercept of the linear plot of 1/q vs. 1/C_e were found equal to 1.1 × 10³ and 2.69 × 10⁵ L mol⁻¹, respectively. The feed surfac-

tant concentration (C_{os}) required for achieving the desired level of recovery of SY was estimated using the equation [30]:

$$C_{os} = \frac{E C_o}{1 - E} \quad (6)$$

where, E is the extraction percentage of the solute. The plot of the theoretical extraction of SY as 95%, vs. Triton X-100 concentrations needed for the uptake of SY at different feed concentrations is shown in Fig. 5. Thus, SY can be concentrated using relatively low concentrations of Triton X-100. The favorable distribution ratio, D of SY solubilization in the SRP was achieved from more diluted solutions of SY (Fig. 5) confirming saturation of SRP with SY.

3.3. Thermodynamic characteristics

At cloud point temperature (CPT), aqueous solution of a nonionic surfactant separates into two phases namely SRP which has small volume and contains a high

concentration of surfactant and SY and the AQ phase containing low surfactant concentration. In the aqueous solution of non-ionic surfactant, the solute molecules are distributed between the two phases above CPT. Thus, the influence of temperature on the solubilization of SY in Triton X-100 was studied in absence of electrolytes over the range 343–364 K of temperature at the optimum experimental conditions. The thermodynamic parameters (DH, DS, and DG) of the solubilization process were recalculated using the following equations [33,34]:

$$q = \frac{DS}{DH} \log \frac{C_e}{C_0} \approx \frac{2.303RT}{p} \quad (7)$$

$$\frac{DG}{RT} = \frac{DH}{T} - \frac{DS}{R} \quad (8)$$

where, the ratio of q_e is the mole of SY solubilized per mole of nonionic surfactant, C_e is the equilibrium concentration of dye (mol L⁻¹) before the completion of two phases, q/C_e is the solubilization affinity and DH, DS, DG, T and R are the enthalpy, entropy, Gibbs free energy changes, temperature in Kelvin and gas constant (R=8.315 J K⁻¹ mol⁻¹), respectively. The plot of $\log(q/C_e)$

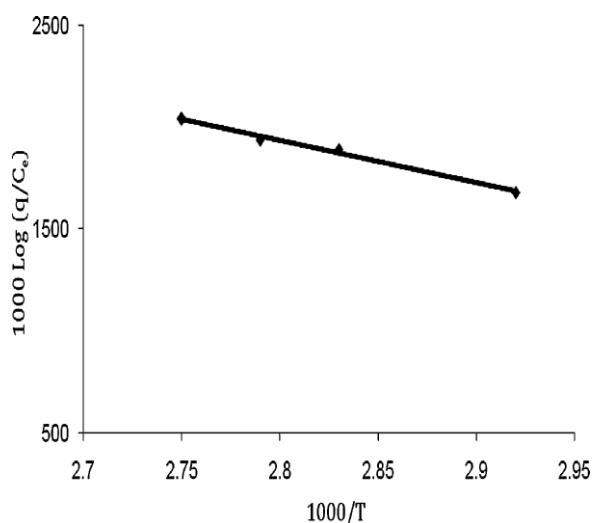


Fig. 6. Plots of 1000 log q/C_e of SY sorption vs. 1000/T (K⁻¹) from aqueous HCl solution.

vs. 1000/T of the extraction of SY by CPE was linear (Fig. 6) with R² = 0.997. The values of DH and DS were found equal

39.77 1.34 kJ mol⁻¹ and 148.39 3.54 J mol⁻¹ K⁻¹, respectively.

The value of DG increases on increasing temperature. The negative value of DG (10.99 1.95 kJ mol⁻¹ at 343 K) indicated that, the SY

solubilization process is spontaneous and thermodynamically favorable. The observed decrease in DG on raising temperature revealed great driving force of solubilization as indicated from the great extent of SY extraction on increasing temperature [33,34]. The positive value of DH reflects the endothermic nature of the solubilization affinity of SY in the SRP. Thus, the number of hydrophobic micelles in the SRP becomes more, while, the critical micelle concentration of

non-ionic surfactant decreased by increasing temperature, causing an increase in the extraction percentage of Triton X-100 [33]. The polarity of SY also decreased on raising temperature and it shows preferentially hydrophobic nature at higher temperature. The positive value of DS reflects the good affinity and organization of the dye molecules in a more random fashion in the SRP [33] in agreement with the data reported for azo dyes solubilization in Triton X-100 [17]. The negative value of DG indicates spontaneous physico-solubilization nature of SY in Triton X-100.

3.4. Figure of merits

The performance of the developed method was tested by determining the molar absorptivity (l_{max} = 532 nm), linearity, limit of detection, and reproducibility. The effective molar absorptivity (e) calculated from Beer-Lambert's plot was 9.110⁵ L mol⁻¹ cm⁻¹. The calibration plot was linear in the

concentration range 20–452 ng mL⁻¹ of SY in the feed solution and the following linear regression equation was achieved:

$$A = 1.5 \cdot 10^{-3} C_x + 0.036 \quad (9)$$

where, A is the absorbance of SY in the SRP after CPE; C_x is the initial analyte concentration, ng mL⁻¹. The plot of A vs. SY concentration,

i.e. C_x was linear with a good correlation coefficient (R = 0.999, n = 5). The precision and accuracy of the developed procedure were evaluated by the recovery studies of five measurements of SY at 50 mg L⁻¹. The values of RSD at 50 mg L⁻¹ and the relative error of

the method were 1.49% and 1.2%, respectively. The limits of detection (LOD = 3 S_{y/x}/b) and quantification (LOQ = 10 S_{y/x}/b) [35,36]

Table 1
Analytical characteristics of the developed CPE-Triton X-100-TOA (A) and direct spectrophotometric at pH 3–4 (B) methods.

Parameters	A	B
Linear concentration range, ng mL ⁻¹	20–452	2000–30,000
Molar absorptivity, L mol ⁻¹ cm ⁻¹	9.110 ⁵	2.710 ⁴
Regression equation	A = 1.5 · 10 ⁻³ C _x + 0.036	A = 5 · 10 ⁻⁵ C _x + 0.005
Correlation coefficient, r	0.999	0.996
LOD, ng mL ⁻¹	0.5	620
Preconcentration factor	33.3	–
Enrichment factor	80.03.2	–

were 5.0 and 16.0 mg L⁻¹, respectively where S_{y/x} is the standard deviation of y-residual and b is the slope of the calibration plot [35]. Without CPE direct spectrophotometry at l_{max} = 530 nm and pH 3–4, the calibration plot was linear in the range 2–30 mg mL⁻¹ SY with LOD of 0.6 mg mL⁻¹.

The LOD of the developed CPE could be improved to lower values by increasing sample volume of the aqueous of SY at the optimum conditions. The improvement factor (the ratio of slopes of calibration plots with and without CPE) was 39.824. The analytical characteristics (molar absorptivity, linearity, limit of detection and reproducibility) of the developed method with and without CPE are summarized in Table 1. A preconcentration factor (V_{AQ}/V_{SRP}) of 33.3 was achieved confirming the sensitivity of the developed CPE method. A comparison between the figure of merits of the proposed method and some of the reported chromatographic methods [2,25,33–37], spectrophotometric [38] and stripping voltammetric [39,40] methods (Table 2) revealed the precision and accuracy of the present method. The value of LOD of Zhou et al. method [33] is lower than the value of LOD in the present study, but it is

suffered from interferences by halides ions. So, the developed method provides simple, sensitive and selective approach for SY determination.

3.5. Extraction equilibrium

Assuming no dimerization of the extracted species and formation of poly anion ion associates is negligible, the equilibrium constants K_{ex} , b and K_d of the TX-100 micellar solution containing SY and the ion-pairing reagent TOA⁺Cl in HCl medium were calculated using the following extraction equilibrium:

(i) Formation of the ion associate according to the equation:

$$SY^{2-} + TOA^+ \rightleftharpoons SY^{2-} TOA^+ \quad (10)$$

with a corresponding ion associate equilibrium constant, b

$$b = \frac{[SY^{2-} TOA^+]_{aq}}{[SY^{2-}]_{aq} [TOA^+]_{aq}} \quad (11)$$

(ii) Distribution of the associate between SRP and aqueous phase with a corresponding distribution coefficient, K_d :

$$K_d = \frac{[SY^{2-} TOA^+]_{SRP}}{[SY^{2-} TOA^+]_{aq}} \quad (12)$$

$$K_d = \frac{[SY^{2-} TOA^+]_{SRP}}{[SY^{2-}]_{aq} [TOA^+]_{aq}}$$

$$K_d = \frac{[SY^{2-} TOA^+]_{SRP}}{[TOA^+]_{aq} [SY^{2-}]_{aq}} \quad (13)$$

(iii) The overall extraction process is then described by the equation:

$$D = \frac{[SY^{2-} TOA^+]_{SRP}}{[SY^{2-}]_{aq} [TOA^+]_{aq}} \quad (14)$$

Table 2
Figure of merits of the developed CPE and some of the reported chromatographic and stripping voltammetric methods.

Method	LOD, ng mL ⁻¹	Linear range ng mL ⁻¹	Remarks	Reference
Ion chromatography with UV–Visible detector	143.0	2000–4000	Less sensitivity, need expertise for instrument	[2]
HPLC with C18 modified by TX-100	160.0		RSD is high, time consuming	[22]
Extraction by Adogen-464	4.41	Upto 3600	Sensitive but required toxic organic solvents	[31]
Reversed phase HPLC-DAD	8.0	13–5500	Expensive and required large volumes of toxic organic solvents	[34]
Stripping voltammetry	1.0	5–90	Use of hanging mercury dropping electrode	[35]
Gold nanoparticle carbon paste electrode	13.5	45–905	Severe interferences of some dyes	[36]
Salting-out assisted liquid–liquid extraction	70	400–15,000	Less sensitivity and uses large volume of toxic organic solvent	[37]
CPE by TX-100 and TOA	5.0	20–452	Sensitive, simple, low cost, and friendly to environment	Present work
Direct spectrophotometry ^a	620.0	2000–30,000	High LOD	Present work

^a Spectrophotometry.

The corresponding equilibrium constant, i.e. extraction constant, K_{ex} , is given by the equation:

$$K_{ex} = \frac{[SY^{2-} TOA^+]_{SRP}}{[SY^{2-}]_{aq} [TOA^+]_{aq}} \quad (15)$$

The distribution ratio, D , can be expressed by the equation:

$$D = \frac{[SY^{2-} TOA^+]_{SRP}}{[SY^{2-}]_{aq} [TOA^+]_{aq}} \quad (16)$$

At low concentrations of TOA⁺Cl, i.e. $[SY^{2-}] : [TOA^+Cl]$, the association in the aqueous phase $[TOA^+SY^{2-}]_{(aq)}$ is negligible. Thus, Eq. (16) transforms into:

$$D = \frac{[TOA^+]_{SRP} [SY^{2-}]_{SRP}}{[SY^{2-}]_{aq} [TOA^+]_{aq}} \quad (17)$$

Substituting Eq. (16) into Eq. (17) and taking the logarithms, yields Eq. (18)

$$\log D = \log K_d + b \log [TOA^+]_{aq} \quad (18)$$

The values of the equilibrium (b and K_d) and extraction (K_{ex}) constants of the extracted ion associate were then determined

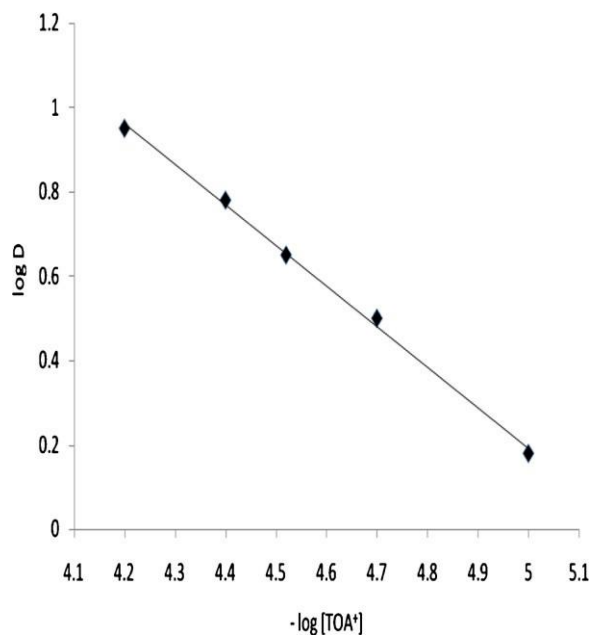


Fig. 7. Plot of log D of SY in the SRP vs. log [TOA] concentration.

graphically from the linear plot of log D vs. log [TOA] (Fig. 7). The

plot of the experimental data in the same coordinates of equation (18) yielded a straight line with a slope of 0.96 close to unity confirming the proposed chemical model of the ion associate. The values of b , and K_d and $K_{ex} = b K_d$ constants of the associate computed from Fig. 6 were found equal 2.09, 0.02, 12.99, 0.7 and 3 2.0 0.3 10, respectively. The distribution ratio, D was experi-

mentally obtained from the normalized absorbance values using the equation:

$$\frac{1}{4} \frac{D A_c - A_0}{A_1 A_c} \quad (19)$$

$A_1 A_c$

where, A_0 is the absorbance of the SRP when TOA is absent, A_c is the absorbance for a certain concentration C of the TOA and A_1 is the absorbance of maximum extraction. Satisfactory agreement

between the experimental and the theoretical data was achieved at 1:1 molar ratio of TOA to SY in the associate.

3.6. Selectivity

The influence of a relatively high excess (0.05–1.0 mg) of some diverse ions or compounds present in the foodstuffs, e.g. Na^+ , Li^+ ,

NH_4^+ , K^+ , Ca^{2+} , Mg^{2+} , SO_4^{2-} , Cl^- , I^- , NO_2^- , NO_3^- , PO_4^{3-} citrate,

tartarate ions, tartrazine, ascorbic acid, and glucose on the analysis of SY (100 ng mL^{-1}) was studied. The tolerance limit (w/w) was

defined as the concentration of the added diver's species causing a relative error of 5% of SRP absorbance. At 1:1000 tolerable concentrations of SY to the foreign species, the tested ions, ascorbic acid, and glucose showed no significant changes in the absorbance of the SRP. In the presence of the food additives tartrazine (427 nm), allurared (507 nm), ponceau 4R (508 nm) and amaranth (520 nm), a tolerance limit of 1:80 was achieved, confirming the accuracy of the method on analysis of SY in a variety of food samples. A tolerance limit over 1:80 of SY to food additives, an observed increase in the SY absorbance (15–20%) of the SRP was noticed.

3.7. Analytical applications

The proposed method was successfully applied for the analysis of SY in food stuffs, e.g. soft drinks, sweets and orange gelatin in the local market of Saudi Arabia as described in the experimental section. Five replicates determinations were performed and satisfactory results were obtained (Table 3). The percentage recovery was always higher than 95% confirming the accuracy, precision and the independence of the method from the matrix interference. The method was validated successfully by comparing the obtainable results in Table 3 with that measured using the standard ion-pair liquid chromatography [12] and HPLC methods [24] by performing t-test. No significant differences were noticed

Table 3

Analysis of sunset yellow colorant in soft drink and food samples by the developed CPE.

Sample	SY, added, ng mL^{-1}	SY, found, ng mL^{-1}	Recovery, %
Soft drink ^a	35	208.1	96.79
	92	38.05	95.86
Sweets ^b	–	88.20	–
	92	327.31	106.41
Orange gelatin ^c	–	292.20	–
	40	9438.51	96.25

^a The level of SY in the soft drink = 215 3.0 ng mL^{-1} .
^b The concentration of SY in commercial sweets sample = 80.51 2 mg g.
^c The concentration of SY in commercial orange gelatin = 443.2 5.8 mg g.

between the two results at 95% confidence level. The method was also validated by analysis of standard concentrations of SY spiked to the tested food samples. Good agreement between the recovery percentage obtained by the developed CPE (96.79 0.72) and the standard ion-pair liquid chromatography (98.83 1) [12] and HPLC [27] (97.54 2) methods indicating the accuracy of the proposed method. In this study, the developed methods with and without CPE could also be extended for analysis of SY in nonalcoholic drinks (50.0 mg L^{-1}) and in bitter soda (100.0 mg L^{-1}) set by EC regulations

after dilution to be within the linear dynamic range of the developed methods.

4. Conclusion

CPE technique offers several advantages, e.g. low cost, sensitivity, selectivity and safety with good extraction efficiency. To the best of our knowledge this is the first report on the use of TOA as an ion pairing on the CPE for SY. The CPE has great potential to be explored in improving the LOD and other analytical characteristics over spectrochemical methods. Surfactants used in CPE make the micellar extraction procedure simple and economical. Thus, micellar extraction is a fertile and promising for the development of effective analytical methods applied to several matrices.

Acknowledgement

The authors would like to thank the Deanship of Scientific Research, King Abdulaziz University, Jeddah, Saudi Arabia for the financial support of the research proposal number 3-109-430.

References

- [1] V.M. Ghorpade, S.S. Salunkhe, in: J.A. Maga, A.T. Tu (Eds.), *Food Additives Toxicology*, Marcel Dekker, New York, 1995, p. 179.
- [2] Q.C. Chen, S.F. Mou, X.P. Hou, J.M. Riviello, Z.M. Ni, *Journal of Chromatography A* 827 (1998) 73.
- [3] P.L. López-de-Alba, L.I. Michelini-Rodríguez, K. Wrobel, J. Amador-Hernández, *Analyst* 122 (1997) 1575.
- [4] N. Pourreza, Sh. Elhami, *Analytica Chimica Acta* 596 (2007) 62.
- [5] N. Pourreza, S. Rastegarzadeh, A. Larki, *Talanta* 77 (2008) 733.
- [6] N. Pourreza, S. Rastegarzadeh, A. Larki, *Food Chemistry* 126 (2011) 1465.
- [7] Y. Ni, J. Bai, *Talanta* 44 (1997) 105.
- [8] A.A. Barros, J. Antó'nio, M. Rodrigues, *Electroanalysis* 3 (1991) 243.
- [9] M.R. Fuh, K.J. Chia, *Talanta* 56 (2002) 663.
- [10] M.P. Urquiza, R. Ferrer, J.L. Beltrán, *Journal of Chromatography A* 883 (2000) 277.
- [11] R.A. Hoodles, K.G. Pitman, T.E. Stewart, J.M. Thompson, J.E. Arnold, *Journal of Chromatography A* 54 (1971) 393.
- [12] M.P. Urquiza, M.D. Part, J.I. Beltrán, *Journal of Chromatography A* 871 (2000) 227.
- [13] M. de Almeida Bezerra, M.A.Z. Arruda, S.L.C. Ferreira, *Applied Spectroscopy Reviews* 40 (2009) 269.
- [14] L.L. Wang, J.Q. Wang, Z.X. Zheng, P. Xiao, *Journal of Hazardous Materials* 177 (2010) 114.
- [15] A. Santalad, S. Srijaranai, R. Burakham, J.D. Glennon, R.L. Deming, *Analytical and Bioanalytical Chemistry* 395 (2009) 1307.
- [16] C.O. Rangel-Yagui, A. Pessoa-Jr, D. Blankschein, *Brazilian Journal of Chemical Engineering* 21 (4) (2004) 531.
- [17] M. Corti, C. Minero, V. Degiorgio, *Journal of Physical Chemistry* 88 (1984) 309.
- [18] H.I. Ulusoy, R. Gurkan, S. Ulusoy, *Talanta* 88 (2012) 516.
- [19] L. Ana, J. Denga, L. Zhou, H. Li Fei, H. Wang, Y. Liua, *Journal of Hazardous Materials* 175 (2010) 883.
- [20] M.K. Purkait, S.S. Vijar, S. Dasgupta, S. De, *Dyes and Pigments* 63 (2004) 151.
- [21] J.H. Clint, *Surfactants Aggregation*, Hardbound edn., Springer, 1992.
- [22] C.P. Sanz, R. Halko, Z.S. Ferrera, J.J. Santana Rodríguez, *Analytica Chimica Acta* 524 (2004) 265.
- [23] C.G. Pinto, J.L.P. Pavon, B.M. Cordero, *Analytical Chemistry* 66 (1994) 874.
- [24] Z. Shi, J. He, W. Chang, *Talanta* 64 (2004) 401.
- [25] E.C. Vidotti, W.F. Costa, C.C. Oliveira, *Talanta* 68 (2006) 516.
- [26] F. Capitan, L.F. Capitan-Vallevey, M.D. Fernandez, I. de Orbe, R. Avidad, *Analytica Chimica Acta* 331 (1996) 141.
- [27] L.F. Capitan-Vallevey, M.D. Fernandez, I. de Orbe, R. Avidad, *Analyst* 120 (1995) 2421.
- [28] W. Lia, W. Zhao, J. Chen, M. Yang, *Analytica Chimica Acta* 605 (2007) 41.
- [29] Y.S. Ho, G. McKay, *Chemical Engineering Journal* 70 (1998) 115.
- [30] M.K. Purkait, S. Banerjee, S. Mewara, S. DasGupta, S. De, *Water Research* 39 (2005) 3885.
- [31] C. Kukusamude, A. Santalad, S. Boonchiangma, R. Burakham, S. Srijaranai, O. Chailapakulb, *Talanta* 81 (2010) 486.
- [32] G.A. Somorjai, *Introduction to Surface Chemistry and Catalysis*, John Wiley & Sons, Inc., New York, 1994.
- [33] Z. Zhou, D. Zhao, J. Wang, W. Zhao, M. Yang, *Journal of Chromatography A* 1216 (2009) 30.
- [34] M.K. Purkait, S.D. Gupta, S. De, *Desalination* 244 (2009) 130.
- [35] M.K. Purkait, S.D. Gupta, S. De, *Journal of Hazardous Materials* 137 (2006) 827.
- [36] J.C. Miller, J.N. Miller, *Statistics for Analytical Chemistry*, 4th edn., Ellis Horwood, New York, 1994, p. 115.
- [37] K.S. Minioti, C.F. Sakellariou, N.S. Thomaidis, *Analytica Chimica Acta* 583 (2007) 103.
- [38] R.S. Razmara, A. Daneshfar, R. Sahrai, *Journal of Industrial and Engineering Chemistry* 17 (2011) 533.
- [39] S.M. Ghoreishi, M. Behpour, M. Golestaneh, *Food Chemistry* 132 (2012) 637.
- [40] J.J.B. Nevado, J.R. Flores, M.J.V. Llerena, *Talanta* 44 (1997) 467.



ORIGINAL ARTICAL

Analysis of spironolactone residues in industrial wastewater and in drug formulations by cathodic stripping voltammetry

M.S. El-Shahawi*, A.S. Bashammakh, A.A. Al-Sibaai, E.A. Bahaidarah

Department of Chemistry, Faculty of Science, King Abdulaziz University, P.O.Box 80203, Jeddah 21589, Saudi Arabia

Received 18 February 2012; accepted 13 October 2012
 Available online 23 October 2012

KEYWORDS

Spironolactone drug residue;
 Cathodic stripping voltammetry;
 Wastewater;
 Aldactone® tablets;
 Electrode mechanism

Abstract The redox behavior of spironolactone (SP) drug in Britton–Robinson (BR) buffer of pH 2–11 was investigated by differential pulse cathodic stripping voltammetry (DPCSV) and cyclic voltammetry (CV) at hanging mercury dropping electrode (HMDE). At pH 9–10.5, the DPCSV of SP drug showed two cathodic peaks at -1.15 and -1.38 V at the HMDE vs. Ag/AgCl reference electrode. In the CV, at pH 9–10, the dependence of the cathodic peak current, I_{pc} and peak potential, $E_{p,c}$ of the second peak ($E_{p,c2}$) on the scan rate (ν) and on the depolarizer (SP) concentrations was typical of an electrode coupled (EC) chemical reaction type mechanism. The plot of I_{pc} at -1.380 V of the DPCSV vs. SP concentration at pH 9 was linear over the concentration range of 1.2×10^{-10} – 9.6×10^{-7} M. The lower limit of detection (LLOD) and limit of quantification (LOQ) of the drug were 1.1×10^{-11} and 4.14×10^{-11} M, respectively. The method was successfully applied for the analysis of SP residues in industrial wastewater, in pure form ($98.2 \pm 3.1\%$) and in drug formulations e.g. Aldactone® tablet ($98.35 \pm 2.9\%$). The method was validated by comparison with HPLC and the official data methods.

© 2013 Xi'an Jiaotong University. Production and hosting by Elsevier B.V. All rights reserved.

1. Introduction

Many drug residues have been found in water and the analysis of drug residues is the recent area and increasing its importance day by day [1,2]. Spironolactone (SP) chemically named as 7α -acetylthio-3-oxo-17 α -pregn-4-ene-21,17 β -carbolactone acid- γ -lactone is a steroid that acts as a competitive antagonist of the potent endogenous mineral-corticosteroid, aldosterone. It is a drug in a class of drugs called potassium-sparing diuretics (water pill). Such drug is widely used to treat high blood pressure, and fluid retention caused by various conditions, including heart disease. SP is indicated in the treatment of essential hypertension, edema associated with congestive heart failure, hepatic cirrhosis with

*Corresponding author at: Department of Chemistry, Faculty of Science, Damiatta University, Damiatta, Egypt. Tel.: +966 2 6952000; fax: +966 2 6952292.

E-mail addresses: malsaeed@kau.edu.sa, Mohammad_el_shahawi@yahoo.co.uk (M.S. El-Shahawi)

Peer review under responsibility of Xi'an Jiaotong University.



Production and hosting by Elsevier

ascites, the nephritic syndrome, idiopathic edema, and in diagnosis of primary aldosteronism [3–6].

Numerous methods e.g. chromatographic [7,8], spectrofluorimetric [9,10], spectrophotometric methods using univariate and multivariate calibration [11] and partial least-squares, multivariate calibration [12] have been reported for the analysis of SP in drug formulations, its metabolite canrenone, pure form human serum and urine. Most of these methods have insufficient sensitivity and selectivity for the trace levels of the drug in human serum and urine [11,12]. The low level of SP residues in wastewater samples was also not compatible with the detection limits of most of these methods [9–12]. Some of these methods are un-selective and require careful experimental conditions and time consuming [11,12].

Polarographic [13] and square-wave adsorptive cathodic stripping voltammetric (SW-AdSV) [14] have been developed for SP determination in drug formulations at dropping mercury electrode (DME) and hanging mercury drop electrode (HMDE) at pH 2–3, respectively. The selectivity and detection limit of polarographic method [13] are not compatible with the low level of SP residues in wastewater. On the other hand, in SW-ACSV method [14], peak resolution and selectivity of the observed cathodic peak at -1.15 V were also not compatible for analysis of SP residues in wastewater. In continuation to our previous work on analysis of drug residues in wastewater [15], this paper reports the redox behavior of SP drug in an attempt to develop a low cost and selective differential pulse cathodic stripping voltammetry (DPCSV) method for analysis of SP residues in wastewater and drug formulations. HMDE not only exhibited a strong adsorption towards SP but also provided remarkable stable and quantitatively reproducible analytical results. HMDE is safe as long as storage and its disposal is undertaken in a safe manner. HMDE is the only electrode type sensitive enough for metal speciation and drug residues in complex matrices e.g. natural water and wastewaters [16,17].

2. Experimental

2.1. Apparatus

A Metrohm 746 VA trace analyzer and 747 VA stand were used for recording the voltammetric measurements. A three-compartment (Metrohm) voltammetric electrochemical cell (10 mL) incorporating HMDE (0.38 mm^2) as a working electrode, double-junction Ag/AgCl, KCl (3.0 M) as a reference electrode and platinum wire (BAS model MW-1032) as a counter electrodes was used. Deionized water was supplied from Milli-Q Plus system (Millipore, Bedford, MA, USA). A digital pH-meter (model MP 220, Mettler Toledo) and a digital-micro-pipette (Volac) were used for pH measurements and sample solutions.

2.2. Reagents

All chemicals used were of analytical reagent grade (BDH, Poole, England). Deionized water was used throughout. SP drug was obtained from Amriya Rhone-poulenc Pharmaceutical Industries Co. (Alexandria, Egypt). Stock solution of SP (2.4×10^{-3} M) was prepared in a minimum volume of ethanol and completed to the mark with deionized water. More diluted

concentrations were prepared by diluting the stock solution with water. A series of BR buffers (pH 2.3–11.5) were used as supporting electrolytes. Aldactone® tablets (25 mg/tablet) were obtained from High Wycombe, England. Low density polyethylene (LDPE) bottles, Nalgene were used for storage of wastewater samples from municipal discharge station, Jeddah, KSA and stored at -20 °C in a refrigerator. The LDPE bottles were cleaned with hot detergent, HNO_3 (2.0 M) and HCl (0.5 M), and finally rinsed with water.

2.3. General DPCSV procedures

An accurate volume (10.0 mL) of an aqueous solution containing BR buffer at the required pH (2.1–11.5) was placed in the voltammetric cell. The solution was stirred and purged with N_2 gas for 10 min before recording the voltammograms. The stirrer was then stopped and after 10 s quiescence time, the DPCSV of the buffer was recorded by applying a negative going potential scan from 0.0 to -1.5 V vs. Ag/AgCl at a deposition potential of -0.45 V, accumulation time 60 s, starting potential 0.0 V, scan rate 60 mV/s and pulse amplitude -50 mV. After measurement of the blank solution, an accurate concentration (4.8×10^{-7} M) of SP was placed into the cell. The solution was stirred, purged with N_2 gas for 5 min and the voltammogram was recorded under the same experimental conditions of the supporting electrolyte. The influence of scan rates ($v=500$ – 1000 mV/s), pH and SP concentration on the cyclic voltammeteries (CVs) was also recorded at HMDE and Pt working electrodes.

2.4. Analytical applications

2.4.1. Analysis of SP in Aldactone® tablets

Ten tablets of Aldactone® (25 mg SP/tablet) were pulverized in a mortar, homogenized, accurately weighed and the average mass per tablet was then determined. An appropriate portion of the finally ground material was accurately weighed and dissolved in the minimum volume of ethanol in a sonicator for 20 min. The test solution was shaken for 15 min in a mechanical shaker to achieve complete dissolution of the active material and accurately transferred to a 25 mL measuring flask. The solution was completed to the mark with ethanol and an accurate volume ($20.0 \mu\text{L}$) of the clear supernatant liquor was transferred to the cell containing 10 mL of BR buffer at pH 9. The amount of the unknown SP drug in the test solution was then determined with the aid of standard curve constructed at $E_{p,c} = -1.4$ V. Alternatively, the spiking method was also used as follows: An accurate volume ($20 \mu\text{L}$) of the supernatant liquor was transferred to the cell containing 10 mL of BR buffer at pH 9. Under the optimum conditions, the DPCSVs of the test solution before and after addition of various volumes of standard SP (10 – $50 \mu\text{L}$ in ethanol) were recorded. The current displayed at -1.40 V by the solution before and after addition of SP was measured and the unknown SP concentration was then computed from the linear plot of the standard addition.

2.4.2. Analysis of SP in water samples

Wastewater samples (200–300 mL) were collected from municipal discharge station samples, Jeddah city, KSA using a battery powered, peristaltic pump and immediately filtered through

0.45 μm cellulose membrane filters and stored in LDPE sample bottles (500 mL). An accurate volume (2.0 mL) of the test solution was transferred to the cell and the solution was completed to 10.0 mL with BR buffer (pH 9). The DPCSVs of the test solution before and after addition of standard SP (10–50 μL , 0.3 $\mu\text{g}/\text{mL}$ in ethanol) were recorded. The current displayed at -1.38 V vs. Ag/AgCl electrode was measured and the concentration of the unknown sample was then determined from the linear plot of the spiked concentrations of SP vs. the corresponding cathodic peak current.

3. Results and discussion

3.1. Electrochemical behavior of SP drug

In BR buffer over a wide range of pH (2.1–11.5), the DPCSVs of SP (5×10^{-7} M) at the HMDE vs. Ag/AgCl electrode were investigated. Representative DPCSVs are shown in Fig. 1. The

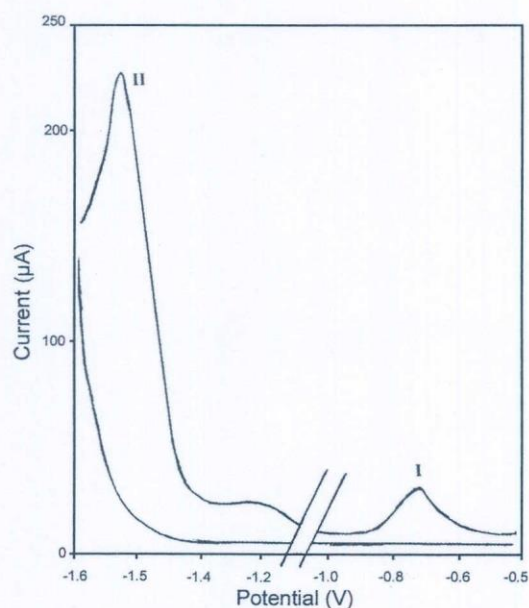


Fig. 1 DPCSVs of SP (4.8×10^{-6} M) at pH 3(1), pH 9 (2) and pH 7 (3) at the HMDE vs. Ag/AgCl reference electrode. $E_{acc} = -0.25$ V; $t_{acc} = 100$ s; scan rate = 60 mV/s and pulse amplitude of -50 mV.

DPCSVs of the SP drug solutions at pH lower than 7.0 displayed one reduction peak at -1.05 V ($E_{p,c1}$) assigned to the reduction of the carbonyl group of pregn-4-ene-21-carboxylic acid, 7-(acetylthio)-17-hydroxy-3-oxo, γ -lactone (7 α , 17 α)-, aldactone to pregn-4-ene-21-carboxylic acid, 7-(acetylthio)-17-hydroxy-3-hydroxy-, γ -lactone (7 α , 17 α)-, aldactone in two electrons reduction step ($2\text{H}^+/2\text{e}^-$) [13] (Scheme 1). In solutions of $7 < \text{pH} < 10$, the DPCSVs of SP drug showed two peaks in the range from -1.11 to -1.20 V (peak I, $E_{p,c1}$) and from -1.36 to -1.46 V (peak II, $E_{p,c2}$) and were safely assigned to successive reduction of the SP drug in two consecutive reduction steps (H^+/e^-) [18,19]. On increasing the solution pH ($7 < \text{pH} < 10.5$), the values of $E_{p,c1}$ and $E_{p,c2}$ were shifted cathodically and the plot of pH vs. $E_{p,c1}$ or $E_{p,c2}$ was linear confirming direct exchange of one H^+ /one e^- in two successive single-electrochemical steps leading to the conversion of $\text{C}=\text{O}$ group to $-\text{CH}-\text{OH}$ group [16]. At $\text{pH} > 10.5$, peak I disappeared and peak II was ill defined and affected by adsorption.

The dependence of CV of SP drug at HMDE on pH was critically investigated. Representative CV at pH 9 at 200 mV/s scan rate at HMDE vs. Ag/AgCl electrode is shown in Fig. 2.

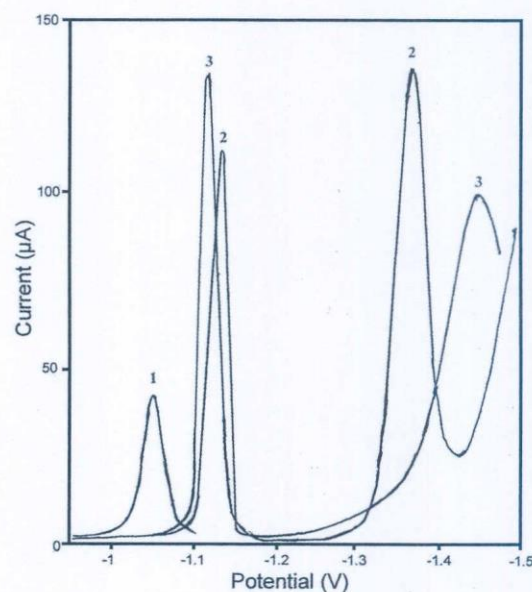
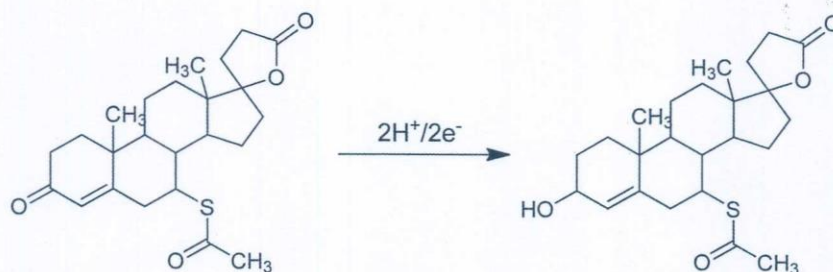


Fig. 2 CVs of SP (1.2×10^{-4} M) at pH 9.0 at HMDE vs. Ag/AgCl electrode at 200 mV/s scan rate.



Scheme 1 Proposed electrochemical reduction of spironolactone in BR buffer at $\text{pH} < 7$.

In solutions of $\text{pH} < 7$, one reduction peak was observed in the range from -1.38 to -1.42 V, while in solutions of $7 < \text{pH} < 10.3$, two cathodic peaks were noticed. On raising the solution pH ($7 < \text{pH} < 10.5$), the potential of $E_{p,c1}$ or $E_{p,c2}$ of SP drug at 200 mV/s was shifted to more negative potential confirming the irreversible nature of the process and the electrode reaction involves hydrogen ions [18,19]. On the reverse scan, no anodic peaks were noticed confirming the irreversible nature of the process.

The influence of the scan rate, ν (50 – 2000 mV/s) on the CV of SP at pH 9 was studied at HMDE. Two peaks I and II were observed and were assigned to two H^+/e^- consecutive reduction steps of $\text{C}=\text{O}$ to $-\text{CH}-\text{OH}$ group. No anodic peaks were noticed on the reverse scan indicating the irreversible nature of the reduction process [19]. On increasing the scan rate, $E_{p,c1}$ and $E_{p,c2}$ at pH 7–9 were shifted cathodically confirming the irreversible nature of the reduction steps [19]. The plots of $I_{p,c2}$ vs. ν increased linearly confirming the adsorption process of SP at HMDE [19].

The variation of the current function ($I_{p,c}/\nu^{1/2}$) with scan rate is an important diagnostic criterion for distinguishing between the ECE (chemical reaction coupled between two charge-transfer processes) and EE (two successive one-electron charge-transfer processes) [19] type mechanisms. The plot of $I_{p,c}/\nu^{1/2}$ vs. ν of peak I increased linearly on raising the ν indicating that the observed behavior does not favor the EC mechanism. This finding may be taken as an indication of the CE mechanism with an irreversible reduction step of the drug [19,20]. The observed behavior may possibly be explained by considering that the protonation reaction is very fast or virtually complete, so that, the electrode reaction appears to be of the ECE type at the scan rates used in the present investigation. In the CV, a small reduction peak current at high ν corresponding to peak I was noticed. Thus, it can be concluded that, the reduction step undergoes a very rapid follow-up chemical reaction [13,14]. The dependence of the CV response on analyte concentration at pH 9.0 showed no significant changes on the cathodic current of the observed cathodic peak at -1.20 V, indicating that the electrochemical process is a typical of ECE type electrochemical mechanism [19].

The value of the electron transfer coefficient (α) involved in the rate determining step was calculated employing the following equation [21]:

$$\Delta E/\Delta \log \nu = -29.58/\alpha n_{\alpha} \quad (1)$$

where n_{α} is the number of electron transfer in the rate determining step. Assuming n_{α} is equal 1 or 2, the computed values of α from the linear plots of $\log \nu$ vs. $E_{p,c1}$ of peak I and $\log \nu$ vs. $E_{p,c2}$ of peak II were found higher than 0.6 confirming the irreversible nature of the observed reduction steps [13,20]. This trend is also indicative of kinetic complications in the electrode process and the reduction process comprises several reactions including adsorption [13,19].

The surface coverage (Γ) of the electroactive species was calculated from the CVs using the following equation [21]:

$$I_{p,c} = n^2 F^2 A \Gamma \nu / 4RT \quad (2)$$

where, n = number of electron, A = area of the electrode surface, cm^2 , T is the absolute temperature and R is the gas constant. For $n=2$, a value of Γ was found equal 77×10^{-6} M encouraging application of the DPSCV for SP determination.

3.2. Analytical parameters

Preliminary DPSCV investigation has shown that, the current of peak I was independent from the SP concentration; however, the $I_{p,c2}$ of peak II is dependent. The high degree of surface coverage of SP onto the HMDE and sensitivity of cathodic peak II towards SP concentration encouraged studying the analytical parameters that control the peak current of peak II using DPSCV procedures. Thus, peak I was not selected in the next work, while the influence of analytical parameters that control cathodic peak current of peak II was critically studied. The plot of pH vs. $I_{p,c2}$ (Fig. 1) revealed that, $I_{p,c2}$ reached the maximum at pH 9–10.3 and in this pH range, the cathodic peak was sharp and symmetric. Thus, in the subsequent work, the solution pH was adopted at pH 9–10.

The effect of the adsorption time (t_{ad}) on the collection and stripping procedure of SP drug at the HMDE was tested in the range of 30–180 s. The maximum peak current was achieved at t_{ad} of 60 s (Fig. 3) for SP solution (5×10^{-7} M). At accumulation time greater t_{ad} than 180 s, the peak current leveled off because of adsorption saturation of SP drug at the HMDE (Fig. 3). Because of the strong adsorption of SP drug at the surface of the HMDE at the equilibrium time, the plot of t_{ad} vs. $I_{p,c}$ of peak II did not pass through the origin [19,20].

The effect of deposition potential (E_{ad}) on the peak current of peak II (-1.38 V) at HMDE vs. Ag/AgCl reference electrode was studied. The maximum peak current was achieved at $E_{ad} = -0.45$ V. At deposition potential < -0.45 V, the background current gradually deteriorates (Fig. 4). Thus, a deposition potential of -0.45 V was selected in the next work. The effect of ν (10 – 60 mV/s) at pH 9–10 on the $I_{p,c2}$ of peak II at the HMDE was tested at the optimum t_{ad} and E_{ad} . At scan rate of 60 mV/s, the $I_{p,c2}$ increased steadily on raising the ν and best background, sensitivity and peak resolution were achieved. Thus, a 60 mV/s scan rate was adopted in the next work.

The effect of pulse amplitude (-90 to 100 mV) on the DPSCV peak under the optimal conditions was studied. The peak current increased steadily on decreasing pulse amplitude

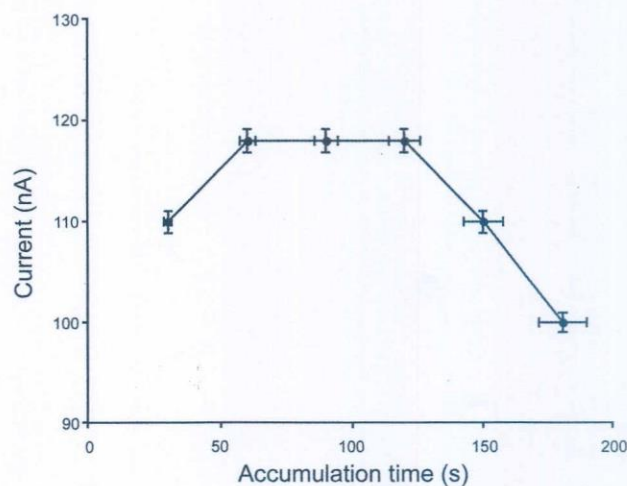


Fig. 3 Influence of deposition time on the $I_{p,c2}$ of SP (4.8×10^{-7} M) at pH 9 at HMDE vs. Ag/AgCl electrode.

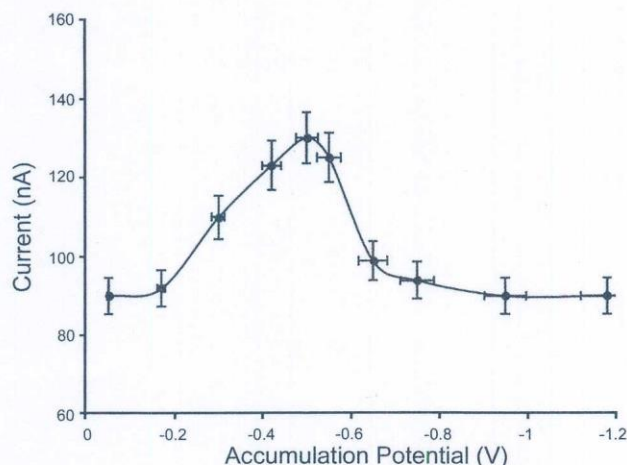


Fig. 4 Influence of deposition potential on the $I_{p,c2}$ of SP (4.8×10^{-7} M) at pH 9 at HMDE vs. Ag/AgCl electrode.

down to -50 mV. At this value, best sensitivity and peak current were achieved. Thus, in the next work a pulse amplitude of -50 mV was chosen. The influence of varying the starting potential (0.0 to -1.0 V) on the DPCSV peak current at 1.40 V was evaluated at HMDE. At starting potential < 0.0 V, the value of $I_{p,c2}$ decreased due to the prior reduction of SP drug at a starting potential close to -0.2 V. The maximum peak current was achieved at 0.0 V, hence, a starting potential of 0.0 V was selected in the next work.

3.3. Figure of merits

Under the optimum experimental conditions of pH 9–10, deposition time 60 s, deposition potential -0.45 V, pulse amplitude -50 mV, starting potential -0.0 V and scan rate 60 mV/s, the DP CSV of SP showed that, the $I_{p,c1}$ at -1.1 V was not sensitive and independent on SP concentration, while the $I_{p,c2}$ at -1.40 V vs. Ag/AgCl increased linearly on increasing the drug concentration in the range from 1.2×10^{-10} to 9.6×10^{-7} M (Fig. 5). Above 9.6×10^{-7} M, the $I_{p,c2}$ tended to level off because of the adsorption saturation with the following a regression equation:

$$I_{p,c2}(\text{nA}) = 1.71C(\mu\text{M}) + 3E^{-14} \quad (R^2 = 0.995)$$

According to International Union of Pure and Applied Chemistry (IUPAC) [22], the lower limit of detection (LOD = $3S_{y/x}/b$) and limit of quantification (LOQ = $10S_{y/x}/b$), where $S_{y/x}$ is the standard deviation of y -residual and b is the slope of the calibration plot of SP, were found equal 1.1×10^{-11} and 4.14×10^{-11} M. A relative standard deviation (RSD) of SP at 8.5×10^{-7} M was found equal 2.39% ($n=5$). The main analytical features of the proposed method were compared with the reported CdSe quantum dots as luminescent probes [9], polarographic [13] and square wave DP CSV [14] methods for SP determination. The figures of merits (linear dynamic range, LOD, LOQ and RSD) of the developed DPCSV method are better than those of the HPLC [7], polarographic [13], SW-AdSV [14] and official [23] methods. Although the present method requires higher overvoltage (-1.4 V) which is more liable to be interfered by other redox

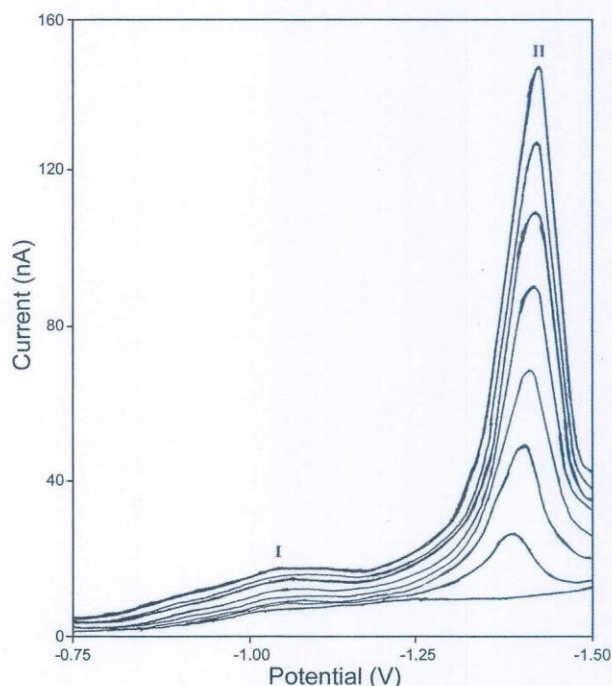


Fig. 5 DPCSVs of SP in BR buffer of pH 9 at HMDE vs. Ag/AgCl reference electrode at various SP concentrations. Conditions: $E_{acc} = -0.45$ V, $t_{acc} = 60$ s, $v = 60$ mV/s, pulse amplitude -50 mV and 0.0 V starting potential.

species than the SW-AdSV (-1.0 V) [14], the present method is selective, rapid, and shows excellent figures of merits.

3.4. Selectivity

The selectivity of the DPCSV method was estimated by adding various excipients, diluents and active ingredients e.g. magnesium stearate, talcum powder, sodium lauryl sulfate, sucrose, glucose, lactose maltose, starch and mannitol used in pharmaceutical formulations. Each excipient (0.4–0.6 g) was added according to the manufacturer's batch formula to known concentration of SP (9.6×10^{-7} M). The tolerable limit was defined as the concentration of the excipient causing a deviation in the range $\pm 3.0\%$ of the peak current at -1.45 V vs. Ag/AgCl of SP solution under the optimum condition. No significant changes on the magnitude of $I_{p,c2}$ (nA) by more than $\pm 3.0\%$ were noticed. Thus, the method is free from the tested excipients. A series of SP solutions (9.6×10^{-7} M) containing atenolol, metoprolol, amiloride, aspirin, or quinine individually at concentration of 9.6×10^{-7} M were also tested. Amiloride drug interfered seriously at a concentration of amiloride 100 times SP. This behavior is most likely attributed to the competitive adsorbability of amiloride with SP drug on the surface of the HMDE at the optimum pH.

3.5. Analytical application

3.5.1. Analysis of SP in pure- and dosage form

The method was applied to the analysis of SP in pure form and in pharmaceutical preparations via calibration plot and

Table 1 Determination of SP ($n=3$) in pure form and in dosage form (Aldactone, 25 mg/tablet) by direct calibration (A) and the standard addition (B) of the DPCSV method, HPLC (C) and the official titrimetric (D) procedures.^a

Drug product	A	B	C	D
Pure drug (%)	97±2	101±2	98±2	98±3
RSD(%)	2.56	2.1	2.3	3.1
<i>t</i> -Value ^a			1.63 (2.31)	1.54 (2.31)
<i>F</i> -value ^b			1.29 (2.31)	1.75 (2.31)
			2.20 (6.39)	2.7 (6.39)
			1.18 (6.39)	2.64 (6.39)
Aldactone tablet	98±2	101±2	99±2	99±2
RSD	–	±3.66	±2.93	±3.85

^aAverage recovery \pm ts/ $n^{1/2}$; $n=3$.

^bThe theoretical figures of *t*- and *F*-values at $P=0.05$ are given in parentheses.

standard addition method. The results are summarized in Table 1. These results were validated by comparison with the standard HPLC [7] and the official methods [23] data following the method of validation [24]. A recovery of $97.35 \pm 2.2\%$, with RSD of ± 2.56 in pure drug was achieved via direct linear plot in good agreement with the results obtained via the standard addition procedure ($101.4 \pm 2.4\%$, RSD = ± 2.10). These results were successfully validated by comparison with standard HPLC ($97.9 \pm 1.7\%$, RSD = ± 2.3) and the official ($98.4 \pm 2.9\%$, RSD = ± 3.1) [7,23,24] methods. The *F* and student *t*- tests showed no significant difference between the developed and these methods [7,23–25].

The results of analysis of SP in Aldactone (Searle) tablet (25.0 mg/tablet) by the developed method via calibration plot and standard addition are given in Table 1. The results of the present method (24.46 ± 0.9 mg/tablet, $n=3$) are in agreement with the claimed value (25.0 mg/tablet), HPLC (24.6 ± 0.72 mg/tablet) [7] and the official (25.2 ± 0.97 mg/tablet) [23,24] methods. At the 95% probability, the Student's *t*- and *F* tests showed no significant differences between the developed DPCSV, HPLC [7] and the official [23,24] methods (Table 1).

3.5.2. Analysis of drug in wastewater

The sensitivity of the developed DP CSV encourages determination SP residues in tap and industrial wastewater samples by the spiking method. Various volumes (10–50 μ L) of standard SP (0.3 μ g/mL in ethanol) were added to wastewater sample and analyzed as described in the experimental section. The recovery percentage of the developed method ($101.80 \pm 2.9\%$) was close to the results obtained by the official titrimetric method ($98.6 \pm 2.7\%$) [23,24] for SP drug added. The *t*- (1.78) and *F*- (1.25) tests at 99% confidence levels did not exceed the theoretical ones 2.31 and 6.39, respectively, confirming the accuracy of the DP CSV method.

4. Conclusion

The developed method provides an excellent alternative approach for the determination of SP in comparison with HPLC, polarographic and voltammetric and the official methods. The sensitivity and selectivity of the developed procedures for the determination of SP in various matrices

could be improved by the preconcentration from large sample volumes onto solid sorbent packed column followed by elution and subsequent analysis. Work is continuing for the application of on-line stripping analysis of SP in serum, blood and environmental samples.

Acknowledgments

This project was funded by the Deanship of Scientific Research (DSR), King Abdulaziz University under grant number 172/428. The authors, therefore, acknowledge with thanks DSR technical and financial support. The authors would like also to thank the quality control laboratory and the municipality of Jeddah City, Saudi Arabia the loan of pure SP and wastewater samples provided, respectively.

References

- [1] I. Ali, V.K. Gupta, P. Singh, et al., Screening of domperidone in wastewater by high performance liquid chromatography and solid phase extraction methods, *Talanta* 68 (2006) 928–931.
- [2] K. Kummerer, Drugs in the environment: emission of drugs, diagnostic aids and disinfectants into wastewater by hospitals in relation to other sources: A review, *Chemosphere* 45 (2001) 957–969.
- [3] M. Ouzounian, A. Hassan, J.L. Cox, et al., The effect of spironolactone use on heart failure mortality: a population-based study, *J. Card. Failure* 13 (2007) 165–169.
- [4] J.J. Bradstreet, S. Smith, D. Granpeesheh, et al., Spironolactone might be a desirable immunologic and hormonal intervention in autism spectrum disorders, *Med. Hypotheses* 68 (2007) 979–987.
- [5] C.S. Rigsby, D.M. Pollock, A.M. Dorrance, Spironolactone improves structure and increases tone in the cerebral vasculature of male spontaneously hypertensive stroke-prone rats, *Microvasc. Res.* 73 (2007) 198–205.
- [6] P.K. Singh, D.P. Singh, Effect of spironolactone on acid and alkaline phosphatase in the testes of albino rat, *Indian J. Clin. Biochem.* 20 (1) (2005) 115–116.
- [7] A. Jankowski, A.S. Jankowska, H. Lamparczyk, Simultaneous determination of spironolactone and its metabolites in human plasma, *J. Pharm. Biomed. Anal.* 14 (1996) 1359–1365.
- [8] R. Herraizhernandez, E. Sorianovega, P. Campinsfalco, High-performance liquid chromatographic determination of spironolactone and its major metabolite canrenone in urine using ultraviolet detection and column-switching, *J. Chromatogr. B Biomed. Appl.* 658 (1994) 303–310.

- [9] J.G. Liang, S. Huang, D.Y. Zeng, et al., CdSe quantum dots as luminescent probes for spironolactone determination, *Talanta* 69 (2006) 126–130.
- [10] O. Hernandez, E. Martin, F. Jimenez, et al., Use of partial least-squares regression for multicomponent determinations based on kinetic spectrofluorimetric data. Simultaneous determination of canrenone and spironolactone in urine, *Analyst* 125 (2000) 1159–1165.
- [11] M.L. Luis, J.M. Garcia, F. Jimenez, et al., Simultaneous determination of chlorthalidone and spironolactone with univariate and multivariate calibration: wavelength range selection, *J. AOAC Int.* 82 (1999) 1054–1063.
- [12] E. Martin, O. Hernandez, A.I. Jimenez, et al., A partial least-squares multivariate calibration method for the simultaneous spectrophotometric determination of spironolactone, canrenone and hydrochlorothiazide, *Anal. Lett.* 31 (1998) 1857–1877.
- [13] F. Belal, Polarographic behaviour and determination of spironolactone, *Acta Microchim.* 107 (1992) 11–17.
- [14] A.H. Al-Ghamdi, A.F. Al-Ghamdi, M.A. Al-Omar, Electrochemical studies and square-wave adsorptive stripping voltammetry of spironolactone drug, *Anal. Lett.* 41 (1) (2008) 90–103.
- [15] M.S. El-Shahawi, S.O. Bahaffi, T. El-Mogy, Analysis of domperidone in pharmaceutical formulations and wastewater by differential pulse voltammetry at a glassy-carbon electrode, *Anal. Bioanal. Chem.* 387 (2007) 719–725.
- [16] E. Fischer, C.M.G. Van Den Berg, Determination of lead complexation in lake water by cathodic stripping voltammetry and ligand competition, *Anal. Chim. Acta* 432 (1) (2001) 11–20.
- [17] K. Yokio, A. Yamaguchi, M. Mizumachi, et al., Direct determination of trace concentrations of lead in fresh water samples by adsorptive cathodic stripping voltammetry of a lead–Calcein Blue complex, *Anal. Chim. Acta* 316 (3) (1995) 363–369.
- [18] N. Abo-el-Maali, Voltammetric analysis of drugs, *Bioelectrochemistry* 64 (2004) 99–107.
- [19] A.J. Bard, L.R. Faulkner, *Electrochemical Methods: Fundamentals*, John Wiley & Sons, New York, 1980 218.
- [20] Z. Galus, *Fundamentals of Electrochemical Analysis*, Ellis Harwood, Ltd., New York, 1976.
- [21] D.T. Sawyer, W.R. Heinemann, J.M. Beebe, *Chemistry Experiments for Instrumental Methods*, John Wiley & Sons, New York, 1984.
- [22] J.C. Miller, J.N. Miller, *Statistics for Analytical Chemistry*, 4th Ed., Ellis-Horwood, Limited, New York, 1994 115.
- [23] *U.S. Pharmacopeias*, 27th Ed. US Convention, Rockville, MD, 2004.
- [24] *The British Pharmacopoeia*, Her Majesty's Stationary Office, London, 1988, pp. 531, 1003.
- [25] J. Ermer, J.H. McB. Miller, *Method Validation in Pharmaceutical Analysis*, 1st Ed., Wiley – VCH Pub., Germany, 2005.

Provided for non-commercial research and education use.
Not for reproduction, distribution or commercial use.



This article appeared in a journal published by Elsevier. The attached copy is furnished to the author for internal non-commercial research and education use, including for instruction at the authors institution and sharing with colleagues.

Other uses, including reproduction and distribution, or selling or licensing copies, or posting to personal, institutional or third party websites are prohibited.

In most cases authors are permitted to post their version of the article (e.g. in Word or Tex form) to their personal website or institutional repository. Authors requiring further information regarding Elsevier's archiving and manuscript policies are encouraged to visit:

<http://www.elsevier.com/authorsrights>

Spectrochimica Acta Part A: Molecular and Biomolecular Spectroscopy 113 (2013) 459–465



Spectroscopic and electrochemical characterization of some Schiff base metal complexes containing benzoin moiety^q



M.S. El-Shahawi [†], M.S. Al-Jahdali, A.S. Bashammakh, A.A. Al-Sibaai, H.M. Nassef

Department of Chemistry, Faculty of Science, King Abdulaziz University, P.O. Box 80203, Jeddah 21589, Saudi Arabia

highlights

A series of complexes of Rh, Ru, Pd and Cu complexes of selected Schiff bases of benzoin was prepared.

The electrode potential of the couple

M^{2+}/M^{3+} of complexes is correlated to the nature of the d orbital's involved. The orbital's are HOMO consisting of $d_{x^2-y^2}$ and while LUMO consisting of the p orbital of ligand.

The high value of Rh^{2+}/Rh^{3+} and Ru^{2+}/Ru^{3+} couple can be explained in terms of the higher energy of $d_{x^2-y^2}$ compared to Pd.

3+ 2+

article info

Article history:

Received 15 September 2012

Received in revised form 16 April 2013

Accepted 24 April 2013 Available online 7 May 2013

Keywords:

Schiff bases

Chelates

Bond length

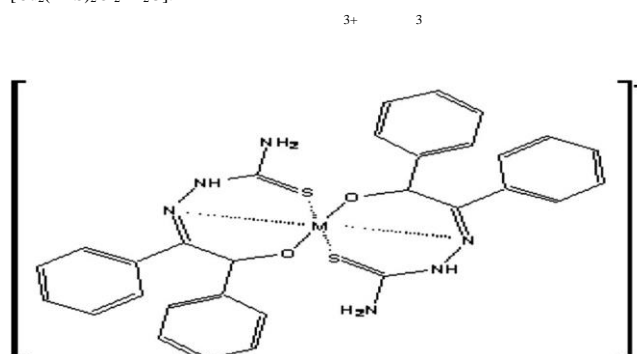
Rach parameters

Electrode mechanism

Thin layer voltammetry

graphical abstract

A series of benzoin Schiff bases and their complexes with Rh^{3+} , Ru^{3+} , Pd^{2+} , Cu^{2+} and Ni^{2+} . The prepared and fully characterized. The proposed chemical structure of Rh^{3+} , or Ru^{3+} complexes are shown in Scheme I. Based upon the 10Dq values of the aforementioned O_h BTS complexes, the stability of the complexes followed the order: $[Ru(BTS)_2]Cl > [Rh(BTS)_2]Cl > [Cu_2(BTS)_2Cl_2 \cdot 2H_2O]$.



Scheme I: Proposed structures of Rh or Ru complexes of Schiff base BTS.

abstract

The ligation behavior of bis-benzoin ethylenediamine (B₂ED) and benzoin thiosemicarbazone (BTS) Schiff bases towards Ru^{3+} , Rh^{3+} , Pd^{2+} , Ni^{2+} and Cu^{2+} were determined. The bond length of M–N and spectrochemical parameters (10Dq, b, B and LFSE) of the complexes were evaluated. The redox characteristics of selected complexes were explored by cyclic voltammetry (CV) at Pt working electrode in non aqueous solvents. Au mesh (100 w/in.) optically transparent thin layer electrode (OTTLE) was also used for recording thin layer CV for selected Ru complex. Oxidation of some complexes occurs in a consecutive chemical reaction of an EC type mechanism. The characteristics of electron transfer process of the couples M^{2+}/M^{3+} and M^{3+}/M^{4+} ($M = Ru^{3+}$, Rh^{3+}) and the stability of the complexes towards oxidation and/or reduction were assigned. The nature of the electroactive species and reduction mechanism of selected electrode couples were assigned.

© 2013 The Authors. Published by Elsevier B.V. All rights reserved.

⁹ This is an open-access article distributed under the terms of the Creative Commons Attribution-NonCommercial-No Derivative Works License, which permits non-commercial use, distribution, and reproduction in any medium, provided the original author and source are credited.

† Corresponding author. Permanent address: Chemistry Department, Faculty of Sciences, Damietta University, Damietta, Egypt. Tel.: +966 2 695200x64422.

E-mail addresses: malsaeed@kau.edu.sa, mohammad_el_shahawi@yahoo.co.uk (M.S. El-Shahawi).

Schiff base compounds are well known to exhibit a wide range of applications in pharmaceutical, antimicrobial, anticarcinogenic reagents, industrial and analytical uses [1–4]. Thus, in the last few years Schiff base macrocyclic ligands and their complexes have received considerable interest [5–15]. The introduction of a transition metal ion into molecules containing a chromophore which is

influence of the chromopheres in many types of metal complexes [21–25]. The redox behavior of benzoin Schiff bases and their transition metal complexes has special interest [26–28]. Little informations on the redox properties of their coordination compounds are known.

The influence of metal ions in the spectroscopic and electrochemical behavior of Schiff bases metal complexes containing benzoin moiety is not well known. Thus, this article is focused on the spectroscopic and electrochemical characteristics of benzoin thiosemicarbazone, BTS and N,N-bis benzoin-ethylenediamine, B₂ED Schiff bases (Fig. 1) and some of their Ru³⁺, Rh³⁺, Pd²⁺, Cu²⁺ and Ni²⁺ complexes. Nature of the electrode couples were also assigned.

Experimental

Reagents and materials

Analytical reagent grade chemicals were used as received. Tetrabutylammonium chloride (TBA⁺Cl) and tetrabutylammonium hexafluorophosphate TBA^b F₆P (BDH Ltd., Poole, England) were used as supporting electrolyte in N,N-dimethylformamide (DMF). BDH RhCl₃, RuCl₃·3H₂O, PdCl₂, CuCl₂ and Ni(CH₃COO)₂ were used. DMF was chosen as a proper solvent, since it is easily purified and its functions as a better Lewis base. The Schiff bases and their metal chelates have significant solubility in DMF.

Apparatus

A Perkin–Elmer infrared (IR) model RXI-FT-IR system 55529 spectrometer (4000–200 cm⁻¹) was used for recording the spectra of the Schiff bases and their complexes in KBr disc. ¹H NMR spectra in d₆-DMSO were recorded on a Bruker advance DPX 400 MHz model using TMS as an internal standard. A Unicam UV₂₋₁₀₀ Spectrometer was used for recording electronic spectra of the compounds. A Perkin Elmer TGA 7 FT thermogravimetric analyzer (0.0–1400 C) coupled with thermal analysis controller TAC 7/DX were used for recording the thermogravimetric measurements in a nitrogen atmosphere (25–900.0 C) at 5 C min rate using Al₂O₃ as a reference. A Portable Potentiostat wave generator model PP2 (Oxford Electrodes) coupled with a Phillips 8043 X-Y recorder. The electrochemical cell assembly consists of Pt wires (0.5 mm id, BAS model MW-1032) as working and counter electrodes and a double-junction Ag/AgCl, KCl(3.0 mol L⁻¹) as a reference electrode. The reference electrode was separated from the bulk solution by a fritted-glass bridge filled with the solvent/supporting electrolyte mixture. Bioanalytical system Pt mesh (100 w/in.) was used in the fabrication of OTTLE cell as reported [29]. Thin layer cyclic voltammetry experiments were performed on a home-built OTTLE that utilized a light transparent Pt mesh (BAS, 100 w/in.) working electrode [29]. Molar conductance (K_m) in DMF was carried out YSI-conductometer, Model-32. Magnetic data were measured on a Jhonson–Matthey magnetis susceptibility balance.

Preparation of the Schiff bases and their complexes

1386-1425/\$ - see front matter 2013 The Authors. Published by Elsevier B.V. All rights reserved.
<http://dx.doi.org/10.1016/j.saa.2013.04.090>

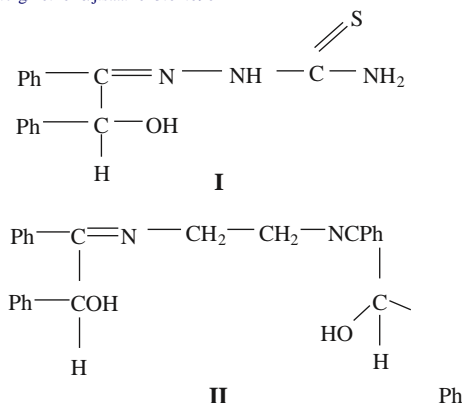


Fig. 1. Chemical structures of benzoin-thiosemicarbazone (BTS), I and benzoin ethylenediamine (B₂ED), II Schiff bases.

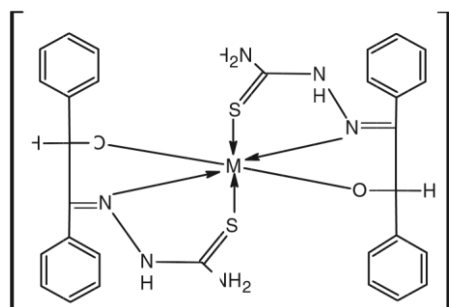


Fig. 2. Proposed structure of Rh³⁺ or Ru³⁺ complex of Schiff base BTS. M = Ru or Rh.

based on the Schiff base group in many cases produces low color strength [16–20].

The redox properties include oxidation and reduction of the central metal ion and various oxidation and reduction of the ligands, and the process involve both the central atom and the ligand [21,22]. The spectroscopic and electrochemical techniques provide an excellent approach for studying the redox behavior and the

The Schiff bases BTS and B₂ED (Fig. 1) were prepared by the method of Offiong [2,3]. To a hot solution of benzoin (2.0 mmole) in ethanol (10 mL), two drops of glacial acetic acid and thiosemicarbazide (2.0 mmole) or ethylenediamine (1.0 mmole) in hot ethanol (10 mL) were added. The reaction mixtures were refluxed for 2 h under constant stirring. The produced pale yellow solid precipitates of B₂ED and BTS were separated out, filtered off, washed with hot ethanol, recrystallized from ethanol and finally dried at 110 C. ¹

¹HNMR spectrum of BTS showed signals at δ 3.7, 7.05, 8.6, 7.94 ppm due to OH, NH, NH₂ and benzylidenimin protons, respectively [25]. ¹HNMR spectrum of B₂ED showed signal at δ 5.4 ppm and was assigned to OH proton. Signals at δ 7.02, 7.54, 7.66 and 8.54 ppm were attributed to benzylidenimin protons [15]. Azomethine proton signal was observed at δ 8.02–8.7 ppm as a multiplet in both BTS and B₂ED ligands.

Metal complexes were prepared by mixing an accurate weight (4.0 mmole) of the Schiff base in hot ethanol (10 mL) with RhCl₃, RuCl₃·3H₂O, PdCl₂, CuCl₂ or Ni(CH₃COO)₂ (2.0 mmole) in ethanol (25 mL) for 2 h with constant stirring. The precipitates were filtered off, washed with hot ethanol, ether and dried under vacuum at 70 C.

Results and discussion

The prepared Schiff bases and their metal complexes are listed in Table 1 together with their elemental analyses and colors. The complexes are red, brownish black, brownish green, green, blue and buff and have high melting points >200 C owing to their inherent stability. The complexes are stable in air, insoluble in common organic solvents and are easily soluble in DMF. The structures of the complexes are in agreement with their stoichiometries (Table 1). Rh(BTS)₂Cl and Ru(BTS)₂Cl have molar conductances in the range 47–58 X¹ indicating formation of complexes of 1:1 electrolytic nature [30]. [Pd(BTS)Cl], [Cu(BTS)Cl·2H₂O], [Cu(B₂ED)], [Ni(B₂ED)] have molar conductance in the range 2.6–4.3 X¹ confirming formation of non-electrolyte complex species [30].

Table 1
Physical properties and analytical data (%) of the Schiff bases and their metal chelates. (For interpretation of the references to color in this figure legend, the reader is referred to the web version of this article.)^a

Compound No.	Compound	Color	Calculated (Found) (%)			
			C	H	N	M
1	BTS	Yellow	63.86 (64.20)	5.58 (5.71)	14.41 (14.23)	–
2	B ₂ ED	Yellow	80.88 (81.21)	6.47 (6.60)	6.35 (6.42)	–
3	[Rh(BTS) ₂]Cl	Red	49.61 (49.96)	3.54 (3.46)	11.30 (11.26)	
4	[Ru(BTS) ₂]Cl	Brownish black	50.40 (50.72)	3.97 (4.10)	11.90 (11.80)	14.38 (14.50)
5	[Pd(BTS)Cl]	Brownish green	42.30 (42.90)	3.36 (3.42)	9.84 (9.42)	25.70 (25.80)
6	[Cu(BTS)Cl H ₂ O]	Green	36.36 (36.42)	3.20 (3.12)	8.05 (7.9)	20.98 (21.20)
7	[Cu(B ₂ ED)]	Blue	70.73 (70.85)	5.11 (5.24)	5.50 (5.67)	12.37 (12.7)
8	[Ni(B ₂ ED)]	Buff	70.48 (70.60)	4.85 (4.70)	5.36 (5.20)	11.38 (11.20)

^a Theoretical values are given in parentheses.

Table 2
Significant IR frequencies (cm⁻¹) and bond length of MAN (r, Å) of metal chelates with relevant bands of the free Schiff bases in brackets.^a

Complex No.	m _s NH	m _n NH	d NH	mC@N	mCN + d NH	mCN + mMAN	mC@S	mMAO	mMAN	mMAS	mMACl	Dm	r(Å)
3	3274 s (3420s)	3169 s	1610	1605 (1635)	1530	1085	840	520	474	362		35	2.6
4	3260 (3420s)	3170 s (3165)	1595 (1610)	1600 (1635)	1575 m (1505)	1120 (1125)	860 m (900)	545 m	480	369		30	2.73
5	3270 m (3420) s	3185	1610	1595 (1635)	1530	1130	895	510	465		330, 290	32	2.69
6	3285 m	3190	1612	1603 (1635)	1520	1139	760	495 s	450	342	345	55	2.27
7				1590 (1620)				490	430			30	2.73
8				1570 s (1620)				480 s	390 w			50	2.44

^a s = strong, m = medium and br = broad, m_{OH} = 3420–3452 cm⁻¹.

Infrared studies

The IR spectra of the Schiff base BTS and its metal complexes suggest that, the ligand BTS bind to metal ions in a mononegative tridentate fashion through C@S, C@N and OH groups with deprotonation of OH. This behavior was achieved for Ru³⁺, Rh³⁺, Pd²⁺ and Cu²⁺ complexes based upon the following evidence: (i) the m(C@S) and m(C@N) bands are shifted to lower frequency by 10–35 and 30–40 cm⁻¹, respectively and (ii) the third coordinating site m(OH) at 3420 cm⁻¹ is shifted by 15–20 cm⁻¹ to lower frequency (Table 2) suggesting involvement of azomethine nitrogen in coordination of ligand with Ru³⁺, Rh³⁺, Pd²⁺ and Cu²⁺ ions [31,32]. The bands observed at 495–545, 450–480 and 342–369 cm⁻¹ are assigned to m(MAO), m(MAN) and m(MAS) [31,32], respectively. The two bands in the range 310–300 cm⁻¹ in the spectra of [Pd(BTS)Cl], and [Cu(BTS)ClH₂O] are assigned to mMACl vibration [31].

The significant IR frequencies of most relevant bands of the free Schiff base B₂ED and its [Ni(B₂ED)] and [Cu(B₂ED)] complexes with their probable assignments are also given in Table 2. The IR spectrum of B₂ED showed characteristic vibrations of C@N and OH groups at 1620 and 3452 cm⁻¹ [31,32], respectively. In the spectra of Ni²⁺ and Cu²⁺ complexes, the azomethine band (mC@N) was shifted to lower wavenumber (1595–1605 cm⁻¹) whereas, the m(OH) is shifted by 10–15 cm⁻¹ to lower frequency upon

complex formation suggesting involvement of C@N and OH groups in coordination [30]. Bands in the range 480–490, 390–430 and 330–345 cm⁻¹ of Ni²⁺ and Cu²⁺ complexes are assigned to mMAN and mMAO [31], respectively.

The frequency shift (Dm) in the IR data (Table 2) is dependent on the nature of the transition metal ion and/or ligand involved in chelation and change in the electrostatic field of the metal ions and the vibrational dipoles of ligand [31]. The metal ions (Ru³⁺, Rh³⁺) or (Ni²⁺, Pd²⁺, Cu²⁺) have the same charge, therefore the distance between the metal ion and the coordinating center would be the main factor affecting band shifts. Thus, the magnitude of frequency shifts between metal ion and the coordinating group (mC@N) was used for determining bond length (r) employing the equation [32]:

$$Dm \propto \frac{32\pi^2 a^2 m_{\text{ligand}}}{m_{\text{complex}}} \frac{1}{r^3} \exp \left[\frac{2\pi^2 f^2}{r} \right] \quad (1)$$

where a is the bond polarisability, Dm the shift in the oscillator frequency (m_{ligand}–m_{complex}), a the lattice constant of the metal ion used [33], m_{x@y} the frequency of the oscillator with single bond, m_{x@y} the frequency of the oscillator with double bond, and l is the length of the oscillator coordinated to the metal ion. The plot of log Dm vs. (r)^{1/2} was linear. The values of (r) and MAN of the complexes are given in Table 2. The m(C@N) shift and the calculated bond length (MAN) of the C@N group upon coordination of BTS Schiff base follow the order:

Cu₂p < Pd₂p > Rh₃p > Ru₃p

The MAN frequencies decreased in the same order as the azomethine vibrations, revealing thereby decreasing in the strength of the metal nitrogen bond in the same order. The low value of r CuAN is attributed to increase in the strength of electrostatic field of the Cu²⁺ as a result of the small ionic radius of copper (II) ion.

Electronic spectra

The electronic spectra of the Schiff bases BTS and B₂ED showed one p?p transition at 35,570 cm⁻¹ and two n ?p bands at 32,700 and 29,800 cm⁻¹. These bands were shifted to higher wavenumbers on complex formation. The spectra and positions of the absorption bands of the complexes in DMF and in solid state at ambient temperature are not significantly different, showing no electronic or geometric changes and the compositions of the chromophores of the complexes are the same in DMF and in solid state and are stable [34]. The spectra of the complexes in DMF with their probable assignments and ligand field parameters (10Dq, b, B and LFSE) [34] are given in Table 3.

In the spectrum of [Rh(BTS)₂]Cl, three absorption bands at m₁ = 16,790, m₂ = 28,620 and m₃ = 39,420 cm⁻¹ were observed with low molar extinction coefficients (Table 3). The complex was diamagnetic and it is consistent with O_h symmetry of N and S atoms producing strong field. ¹H NMR spectrum in d₆-DMSO showed signals at δ 7.07, 8.6, and 7.94 ppm assigned to NH, NH₂ and benzylideneimin protons, respectively [29]. The azomethine proton (CH@N) signal showed downfield shift at δ 8.16–8.7 ppm indicating involvement of azomethine in coordination. Thus, the first two bands were assigned to spin-allowed transitions for t_{2g}⁵ e_g¹ state in O_h symmetry around Rh. Hence, the two peaks were assigned to ¹A_{1g} ? ¹T_{1g} and ¹A_{1g} ? ¹T_{2g} and charge transfer ¹A_{1g} ? b, ¹T_{1u} transitions, respectively.

The interelectronic repulsion parameter B of [Rh(BTS)₂]Cl was about 59% of the free ion (B = 720 cm⁻¹) (Table 3) indicating considerable orbital overlap with a strongly covalent metal–ligand bond character [34]. The low value of B is associated with a reduction in the effective nuclear charge (Z) on Rh³⁺ ion [34]. The variation of B of 4 d metal ions with ionic charge (Z), and the number of d-electrons in the partially filled d-state (q) is given by the equation:

$$B \approx 742 \cdot p \cdot 28q \cdot \frac{1}{50} \delta Z \cdot p \cdot 1p \cdot 500 = \delta Z \cdot p \cdot 1p \cdot \delta 2p$$

The value of Z of Rh in [Rh(BTS)₂]Cl complex was 0.75 below the formal value of trivalent metal ions. The nephelauxetic parameter b (0.58) of the complex indicated that, the ligand BTS lies in the middle of the nephelauxetic of other nitrogen donor series indicating participation of BTS in a tridentate fashion (SNO) to Rh³⁺.

The spectrum of [Ru(BTS)₂]Cl displayed three bands at m₁ = 13,700, m₂ = 21,320 and m₃ = 23,600 cm⁻¹. The I_{eff} of the complex was 1.94 BM, indicating a one electron paramagnetic of a low spin t_{2g}⁵ (S = 1/2) O_h symmetry around Ru (III) ion. Hence, the ground state ²T_{1g} of Ru (III) in an O_h environment is arising from t_{2g}⁵ configuration [34]. The order of increasing energy of the first excited doublet levels is ²A_{2g} and ²T_{1g} arising from t_{2g}⁵ e_g¹ configuration. Hence, the first (m₁) and third (m₃) bands are assigned to the spin forbidden ²T_{1g} ? ²E_{2g} and ²T_{1g} ? ²A_{1g} whereas, the band at 21,320 cm⁻¹ is due to the spin allowed transitions ²T_{2g} ? ²A_{2g} of low spin d⁵ Ru³⁺ in O_h geometry, t_{2g}⁵ [27–29]. B value was about 443 cm⁻¹ and 70% of the free ion (B = 630 cm⁻¹) indicating considerable orbital overlap with a strongly covalent metal–ligand bond character [25]. The low values of 10Dq and B for Rh³⁺ and Ru³⁺ complexes (Table 3) may be attributed to

participation of S in coordination [25]. The nephelauxetic parameter, b₃₅ of Rh³⁺ and Ru³⁺ BTS complexes was 0.58 and 0.64, respectively. The 10Dq values (Table 3) are close to the range for RuN₂O₂S₂ [25]. Thus, the ligand BTS lies in middle range of the spectrochemical series. The decrease in B values of the two complexes compared to the free ions suggests strong covalent bonding between the donor site and the metal ions. The increase in the 10Dq, was associated with considerable electron delocalization in the complex [29–31]. A representative structure of Rh³⁺ or Ru³⁺ complex is proposed in Fig. 2.

The electronic spectrum of [Pd(BTS)Cl] showed peaks at 20,449, 21,929 cm⁻¹, 24,043 and 26,666 cm⁻¹ (Table 3) with low extinction coefficient. The complex was diamagnetic and its ¹H NMR spectrum in d₆-DMSO showed proton signals at δ 7.07, 8.6, 7.94; 8.4–

8.9 ppm and were assigned to NH, NH₂, benzylideneimin and CH@N protons, respectively [29] indicating participation of OH and the CH@N groups. Thus, the two peaks at 20,449 and 21,929 cm⁻¹ were assigned to spin allowed transitions ¹A_{2g} ? ¹B_g and ¹A_{1g} ? E_g in square planar-geometry [34]. Bands at 24,043 and 26,666 cm⁻¹ are assigned to CT or ligand bands [34].

The spectrum of [Cu(BTS)Cl H₂O] showed three bands around 12,820 (br.), 25,440 and 34,366 cm⁻¹ (Table 3). I_{eff} was 1.8 B.M concluding formation of paramagnetic copper complex. Thus, broad band at 12,820 cm⁻¹ was assigned to ²E_g ? ²T_{2g} transition in Oh symmetry [34]. The band at 25,440 cm⁻¹ was assigned to S ? Cu (II) LMCT, whereas the band at 34,366 cm⁻¹ was assigned to O ? Cu (II) LMCT and intraligand (n ?p) charge transfer [34].

Thermal analysis of the complex showed well defined peak at 160 C due to loss of water molecule suggesting water coordination to central copper (II). Based upon the 10Dq values (Table 3) of the aforementioned O_h BTS complexes, the stability of the complexes followed the order [28]:



In the spectrum of [Cu(B₂ED)], the broad bands at 14,700 cm⁻¹ (log ϵ = 1.6) and 16,650 cm⁻¹ were assigned to spin allowed ²B_{1g} ? ²A_{1g} (m₁) $\delta d_{x^2-y^2} \rightarrow d_{z^2}$ (10Dq) and ²B_{1g} ? E_g (m₃) $\delta d_{x^2-y^2} \rightarrow d_{xz}; d_{yz}$ transitions in square-planar geometry [34]. I_{eff} of the complex was 1.76 B.M. and close to the spin moment for one un-unpaired electron confirming the proposed structure. The spectrum of [Ni(B₂ED)] showed two bands at 21,270, 27,170 and 33,120_(sh) cm⁻¹. The complex was diamagnetic and its ¹H NMR spectrum showed signals at δ 7.02, 7.54, 7.66, 8.54 and 8.8 ppm confirming deprotonation of OH group upon coordination. The bands at 21,270, 27,170 and 33,120 (sh) cm⁻¹ are assigned to ¹A_{1g} ? A_{2g} (m₃) and ¹A_{1g} ? B_{2g} (m₂) and a CT transitions in a square-planar geometry [34], respectively.

Redox behavior of metal complexes

The CV data of selected complexes vs. Ag/AgCl electrode at 50 mV s⁻¹ sweep rate (m) are summarized in Table 4. Representative CV of [Rh(BTS)₂]Cl complex in DMF-TBA⁺Cl is shown in Fig. 3. In the CV of [Rh(BTS)₂]Cl, one cathodic peak (E_{p,c}) at 0.86 V coupled with one anodic peak (E_{p,a}) at 0.2 V with potential–potential separation (DE_p = E_{p,a} - E_{p,c}) of 0.66 V were observed. The number of electron transfer was calculated from charge–time curve of controlled potential coulometry (CPC) at the potential of the limiting current plateau of cathodic peak under N₂ atmosphere at Pt net electrode under the same experimental conditions. The complex was reduced by a potential step from 0.2 V to 0.9 V and the number of electron transfer was calculated using the equation:

$$Q_F \approx Q_T \cdot Q_B \approx nFVc$$

where Q is the charge in coulomb, Q_F the faradic charge required for complete electrolysis of the complex in solution, Q_T the faradic charge required for complete electrolysis of the test solution which was measured by extrapolating the linear of the curve to zero time, Q_B the faradic charge required for complete electrolysis of the supporting electrolyte only, V the volume of the test solution in the cell in liter, C the concentration of the test solution, mol L⁻¹ and F is the Faraday's number, 96,485 C/equiv. A value of one electron transfer was computed from charge–time curve. One electron nature of this couple was also established by comparing the displayed current height with similar analogous of Rh (III) complexes [24]. The irreversible nature of the couple was confirmed from the observed increase in DE_p on rising scan rate.

The product of the number of electron transfer involved in the reduction step ($n\alpha$) and the corresponding charge transfer coeffi-

Table 3
Electronic spectral data (cm⁻¹) of the complexes with band assignments and ligand field parameters (Dq) in DMF.

Complex	Band position (cm ⁻¹) 10 ³	Assignments	10Dq 10 ³ cm ⁻¹	B (cm ⁻¹)	b ₃₅	LFSE (cm ⁻¹)
[Rh(BTS) ₂]Cl	16.79 (m ₁) 28.62 (m ₂) 39.42 (m ₃)	¹ ₁ A _{1g} ? T _{1g} ¹ ₁ A _{1g} ? T _{2g}	24.260	424.8	0.58	10.62
[Ru(BTS) ₂]Cl	13.700 21.32 24.86	¹ ₁ A _{1g} ? b, T _{1u} ² ₂ T _{1g} ? E _{2g}	27.342	443	0.70	16.67
[Pd(BTS)Cl]	20.449 21.929 24.043 26.664	² ₂ T _{2g} ? A _{2g} ² ₂ T _{1g} ? A _{1g}				
[Cu(BTS)Cl H ₂ O]	12.82 25.44 34.36	¹ ₁ A _{1g} ? A _{2g} ¹ ₁ A _{1g} ? B _{1g}	12.820			
[Cu(B ₂ ED)]	14.70 16.65 27.47 (sh) 28.65	¹ ₁ A _{1g} ? E _g ² ₂ T _{2g} S? Cu n?p	14.700			
[Ni(B ₂ ED)]	21.27 27.17 33.12	² ₂ B _{1g} ? A _{1g} ² ₂ B _{1g} ? E _g CT, d?p IL (CT) ¹ ₁ A _{1g} ? E _g ¹¹ A _{1g} ? B _{2g} IL (CT)				

Table 4

Complex	Amperometric data of selected complexes at 100 μA vs. Ag/AgCl reference electrode ^a									
	Couple I			Couple II			Couple III			
	E _{p,c}	E _{p,a}	DE _p	E _{p,c}	E _{p,a}	DE _p	E _{p,c}	E _{p,a}	DE _p	
[Rh(BTS) ₂] Cl	0.86 (0.5)	1.22	0.2 (0.06) 0.24	0.66 (0.44) 0.98	0.04 (0.02)	1.5 (0.5)	1.46 (0.48)	1.3		
[Ru(BTS) ₂]Cl	0.71 (0.54)	0.41	0.13 (0.22)	0.58 (0.32)		1.68				
[Ru(BTS) ₂]Cl				0.21	0.29	0.73 (0.68)	0.44			
[Cu ₂ (BTS)Cl H ₂ O]	0.32		0.2	0.21		0.55		1.14		
[Cu(B ₂ ED)]			0.11		0.5	0.85	0.35	1.13	1.56	2.7

^a Electrochemical data of OTTLE experiments are given in parantheses.

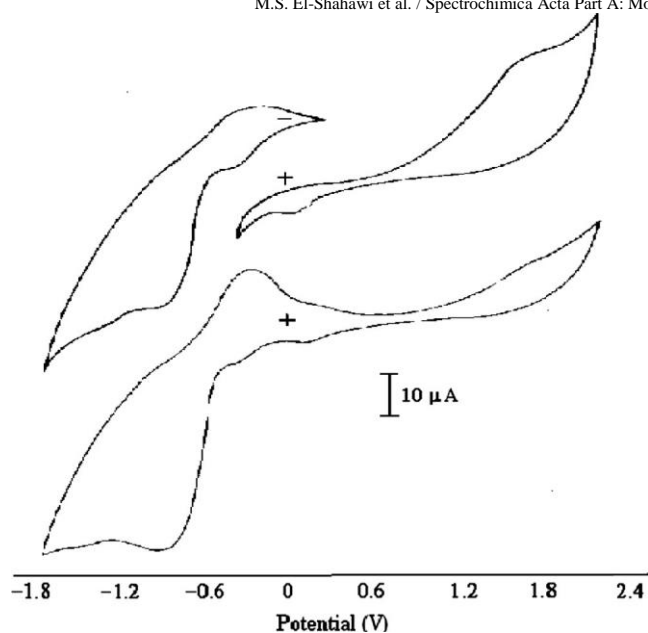


Fig. 3. CV of $[Rh(BTS)_2]Cl$ ($1 \times 10^{-3} \text{ mol L}^{-1}$) in DMF-TBA⁺Cl ($1 \times 10^{-2} \text{ mol L}^{-1}$) at 50 mV s^{-1} scan rate at Pt electrode vs. Ag/AgCl electrode.

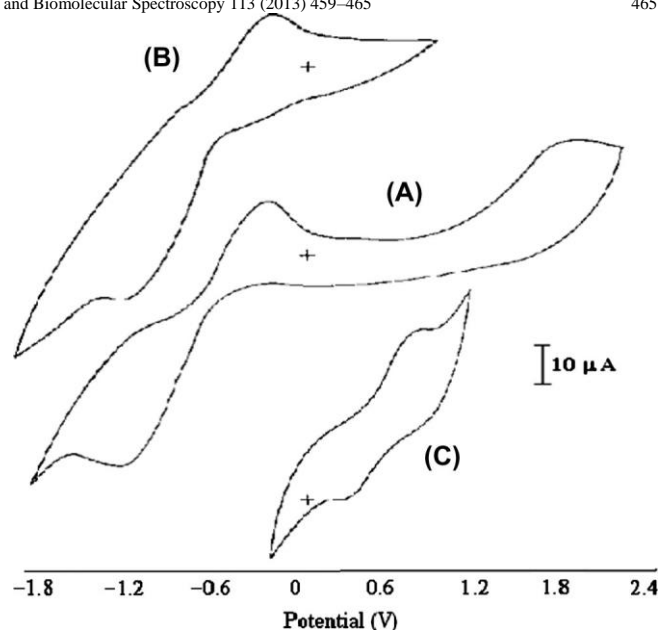


Fig. 5. CV of $[Ru(BTS)_2]Cl$ ($1 \times 10^{-3} \text{ mol L}^{-1}$) in DMF TBA⁺Cl (A, B) and DMFTBA PF₆ (C) at 100 mV/s at Pt electrode vs. Ag/AgCl electrode.

cient (a) was calculated from the linear dependence of cathodic peak potential ($E_{p,c}$) vs. $\log m$ (Fig. 4) using the equation:

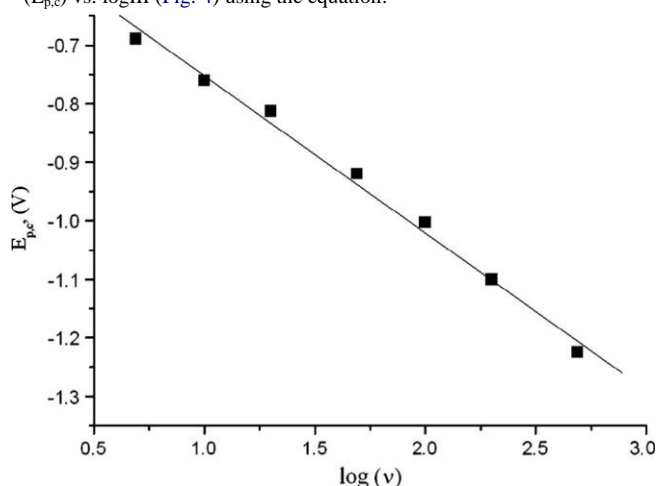


Fig. 4. Plot of $E_{p,c}$ of the redox couple Rh^{3+}/Rh^{2+} vs. $\log m$ of $[Rh(BTS)_2]Cl$ ($1 \times 10^{-3} \text{ mol L}^{-1}$) in DMF-TBA⁺Cl ($1 \times 10^{-2} \text{ mol L}^{-1}$) at Pt electrode vs. Ag/AgCl electrode.

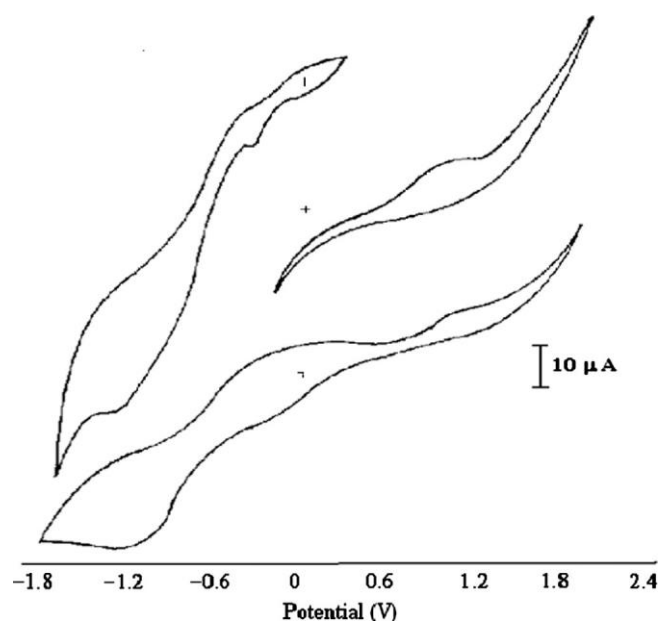


Fig. 6. CV of $[Cu(B_2ED)]$ ($1 \times 10^{-3} \text{ mol L}^{-1}$) in DMF TBA⁺Cl at 100 mV/s at Pt electrode vs. Ag/AgCl electrode.

$$DE_{p,c} = D \log \frac{m}{\nu} \quad \text{29:58} = a n_a \quad \delta 4p$$

Assuming $n = 1$, the value of a was found 0.56 in the range expected for irreversible one-electron transfer step [35,36]. Thus, electron transfer nature of the complex can be expressed by the irreversible metal-based reduction (Rh^{3+}/Rh^{2+}) couple [37,38] as given in the following equation:



The reduction peak current, ($i_{p,c}$) of the couple increased on increasing the scan rate from $m = 10$ to 100 mV s^{-1} and the anodic/cathodic peak currents ratios ($i_{p,a}/i_{p,c}$) were less than unity and gradually increases to unity on increasing scan rate. Plot of $i_{p,c}$ vs. $m^{1/2}$ was linear indicating diffusion-controlled electrochemical process [36]. The current function ($i_{p,a}/m^{1/2}$) approximately remains constant along the whole range of scan rate indicating that a coupled chemical reaction of EC mechanism type takes place [38,39]. Based on the CV of other analogous of Rh (III) complexes [35], the observed couple with an ill defined $E_{p,c}$ at 0.04 V, $E_{p,a} =$

+1.5 V and $DE_p = 1.46$ V was tentatively assigned as metal based oxidation of Rh^{3+}/Rh^{4+} . The plot of the current ratio ($i_{p,a}/i_{p,c}$) vs. $m^{1/2}$ was linear and parallel to the X axis ($m^{1/2}$), suggesting a negligible adsorption on the electrode surface [35].

The CV of $[Ru(BTS)_2]Cl$ in DMF-TBA⁺Cl at Pt electrode at 100 mV s⁻¹ showed $E_{p,c}$ at 1.22 V coupled with an $E_{p,a} = +1.5$ V at 0.24 V with $DE_p = 0.98$ V (Fig. 5A and B). CPC under N₂ at a Pt net electrode at the same experimental conditions showed one electron transfer. On increasing the scan rate > 200 mV s⁻¹, the $E_{p,c}$ was shifted cathodically, while $E_{p,a}$ shifted anodically confirming irreversible nature of the couple. At a scan rate < 200 mVs⁻¹, the dE_p values between the two counter peaks ($E_{p,a}$, $E_{p,c}$) decreased on lowering the scan rate. Thus, the couple was assigned to the irreversible reduction couple Ru^{3+}/Ru^{2+} [39,40]. Plot of $i_{p,c}$ vs. $m^{1/2}$ was linear indicating that, the electrode reaction is diffusion controlled process and mass transfer is limited [38]. Based on CPC of $E_{p,a}$ at 1.68 V and comparison with other analogs of Ru^{3+} complexes [37,38], the couple was assigned to irreversible Ru^{3+}/Ru^{4+} .

Thin layer CV using OTTLE cell of $[Ru(BTS)_2]Cl$ (Fig. 5C) showed two $E_{p,c}$ at 0.71 and 0.29 V coupled with two $E_{p,a}$ at 0.13 and 0.73 V with $DE_p = 0.58$ and 0.44 vs. Ag/AgCl electrode (Table 4), respectively. $E_{p,c}$ at 0.71 V was assigned to Ru^{III}/Ru^{II} couple as follows:



CPC under N₂ gas at a Pt electrode on the limiting current plateau of the second couple revealed one electron transfer. Thus, the couple of $E_{p,c} = 0.29$ V and $E_{p,a} = 0.73$ V (Fig. 5C) was assigned to Ru^{3+}/Ru^{4+} couple [27,28].

The CV data of $[Cu(B_2ED)]$ and $[Cu(BTS)Cl] \cdot H_2O$ at 100 mV s⁻¹ are given in Table 4 and representative CV of $[Cu(B_2ED)]$ is shown in Fig. 6. CV showed one $E_{p,c} = 0.32$ V, $E_{p,a} = 0.11$ V and $DE_p = 0.21$ V (Table 4) and CPC of this couple revealed one-electron transfer step. On increasing the scan rate, a slight shift on the potentials of $E_{p,a}$ and $E_{p,c}$ was noticed, while $i_{p,a}$ became smaller relative to $i_{p,c}$ on decreasing scan from 100 to 10 mV s⁻¹. Analysis of $i_{p,c} = f(m^{1/2})$ and $E_{p,c} = f(\log m)$ is consistent with diffusion-controlled electrochemical process. Thus, the couple was assigned to Cu^{2+}/Cu^+ with CE mechanism [40]. Based on CPC data, the couple with $E_{p,c} = +0.5$ V, $E_{p,a} = +0.85$ V and $DE_p = 0.35$ V was safely assigned to irreversible Cu^{2+}/Cu^{3+} couple [41]. Change from Cu(II) to Cu(III) state (d^8 low spin) involves a drastic reduction of the metal ion radius and no changes in the geometries of Cu^{2+}/Cu^{3+} complexes in solution. The more positive values of $E_{p,a}$ (Table 4) the more difficulty in stabilizing Cu (III) state for both copper (II) complexes. The values of $E_{p,c}$ for Cu^{2+}/Cu^+ couple (Table 4) revealed the difficulty in reducing Cu(II) ion in both complexes.

The potential of the redox couples of Rh^{3+} , Ru^{3+} , Pd^{2+} and Cu^{2+} of BTS complexes may be related to the nature of the orbitals involved in the redox processes. These orbitals are HOMO consisting predominately of the $d_{x^2-y^2}$ and LUMO consisting of $2z^2-3x^2$ p orbital of $2z^2-3x^2$ BTS. The high positive value of the couple Rh/Rh or Ru/Ru (Table 4) compared to the corresponding couples was explained in terms of the higher energy of $d_{x^2-y^2}$ in Pd than in Rh or Ru [42]. Thus, the changes in $E_{1/2}$ are strongly related to changes in the electrophilic properties of the metal ions. Within the context of ligand field theory, the correlation between $E_{1/2}$ of these couples and the size of the metal ion involved has been attributed to the spherical potential generated by the electron density of the donor atoms in the antibonding d-orbitals as reported by Lintvedt and Fenton [43].

4. Conclusion

BTS complexes with Rh^{3+} , Ru^{3+} and Cu^{2+} are six-coordinate octahedral. The M (II) and M (III) complexes may be used as one-electron redox reagents, since the former is a strong reducing agent and the latter is strong oxidizing

agent. The low DE_p in the OTTLE cell for the redox couples favor reversibility as compared to bulk CV.

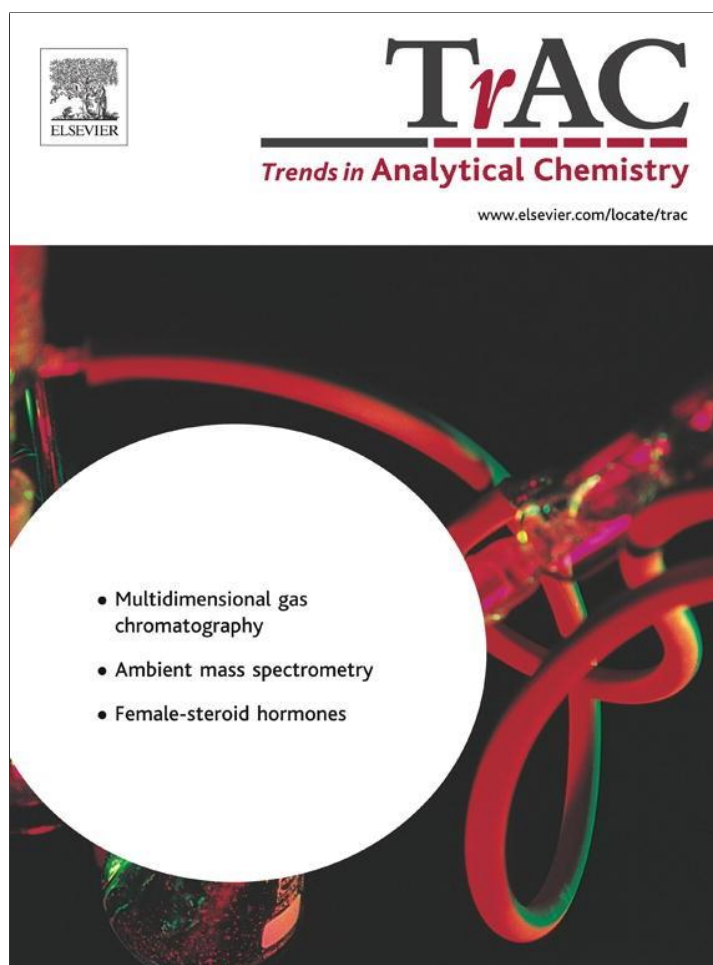
Acknowledgements

This project was funded by the Deanship of Scientific Research (DSR), King Abdulaziz University, Jeddah, under Grant no. 3-083/429. The authors, therefore, acknowledge with thanks DSR technical and financial support.

References

- [1] R.H. Holm, W.G. Everett Jr., A. Chakravorty, *Progress. Inorg. Chem.* 7 (1966) 83.
- [2] A.D. Garnovskii, A.L. Nivorozhkin, V.I. Minkin, *Coord. Chem. Rev.* 126 (1-2) (1993) 1.
- [3] H. Molina, R.A. Mederos, in: A.B.P. Lever (Ed.), *Comprehensive Coordination Chemistry II*, vol. 1, Elsevier-Pergamon Press, Amsterdam-Oxford-New York, 2003, pp. 411–446.
- [4] O.E. Offiong, *Spectrochim. Acta Part A* 50 (1994) 2167.
- [5] P.A. Vigato, S. Tamburini, L. Bertolo, *Coord. Chem. Rev.* 251 (11–12) (2007) 1311.
- [6] P.A. Vigato, S. Tamburini, *Coord. Chem. Rev.* 252 (18–20) (2008) 1871.
- [7] I. Yilmaz, H. Temel, H. Alp, *Polyhedron* 27 (2008) 25.
- [8] P. Souza, A.I. Matesanz, C. Pastor, *Inorg. Chem. Commun.* 5 (2002) 344, and references cited therein.
- [9] P.A. Vigato, S. Tamburini, *Coord. Chem. Rev.* 248 (17–20) (2004) 1717.
- [10] W. Jiangtao, W. Hedong, *Int. J. Biol. Macromol.* 48 (2011) 523.
- [11] I.M. Saad, M.S. El-Shahawi, H. Saleh, A.A. El-Asmy, *Transition Met. Chem.* 32 (2) (2007) 156.
- [12] R.M. El-Shazly, G.A.A. Al-Hazmi, S.E. Ghazy, M.S. El-Shahawi, A.A. El-Asmy, *J. Coord. Chem.* 59 (2006) 84.
- [13] G.A.A. Al-Hazmi, M.S. El-Shahawi, I.M. Gabr, A.A. El-Asmy, *J. Coord. Chem.* 58 (2005) 713.
- [14] R.M. El-Shazly, G.A.A. Al-Hazmi, S.E. Ghazy, M.S. El-Shahawi, A.A. El-Asmy, *Spectrochim. Acta Part A* 61 (2005) 243.
- [15] G.A.A. Al-Hazmi, M.S. El-Shahawi, A.A. El-Asmy, *Transition. Met. Chem.* 30 (2005) 464.
- [16] A.A. El-Asmy, E.M. Saad, M.S. El-Shahawi, *Transition Met. Chem.* 19 (1994) 406.
- [17] R.P. John, A. Sreekanth, R. Maliyackal, P. Kurup, *Spectrochim. Acta Part A* 59 (2003) 1349.
- [18] D.K. Demertzi, M.A. Demertzi, J.R. Miller, C. Papadopoulou, C. Dodorou, G. Filousis, *J. Inorg. Biochem.* 86 (2001) 555.
- [19] M.S. El-Shahawi, W.E. Smith, *Analyst* 119 (1994) 327.
- [20] G. Wolfbauer, A.M. Bond, G.B. Deacon, D.R. MacFarlane, L. Spiccia, *J. Electroanal. Chem.* 490 (1–2) (2000) 7.
- [21] A.Y. Kim, W.K. Seok, Y. Dong, H. Yun, *Inorg. Chim. Acta* 319 (1-2) (2001) 194.
- [22] E. Franco, E. Lopez-Torres, M.A. Mendiola, M.T. Sevilla, *Polyhedron* 19 (2000) 441.
- [23] M.L.P. Santos, I.A. Bagatin, E.M. Pereira, A.M.D. Ferreira, *J. Chem. Soc. Dalton Trans.* 6 (2001) 838.
- [24] B.S. Parajon-Costa, A.C. Gonzalez-Baro, E.J. Baran, Z. Anorg. Allg. Chem. 628 (2002) 1419.
- [25] A.A. El-Asmy, O.A. El-Gammal, H.S. Saleh, *Spectrochim. Acta Part A* 71 (2008) 39.
- [26] A. Garoufis, S.K. Hadjikakou, N. Hadjiliadis, *Coord. Chem. Rev.* 253 (2009) 1384. [27] S.B. Padhye, G.B. Kaffman, *Coord. Chem. Rev.* 63 (1985) 127.
- [28] S.I. Mostafa, A.A. El-Asmy, M.S. El-Shahawi, *Transition Met. Chem.* 25 (2000) 470.
- [29] D.T. Sawyer, W.R. Heineman, J.M. Beebe, *Chemistry Experiments for Instrumental Methods*, John Wiley & Sons, 1984, p. 93.
- [30] W. Geary, *Coord. Chem. Rev.* 7 (1971) 81.
- [31] K. Nakamoto, *Infrared and Raman Spectra of Inorganic and Coordination Compounds*, vol. 222, Wiley Interscience, New York, 1971.
- [32] R.K. Parashar, R.C. Sharma, A. Kumar, G. Mohan, *Inorg. Chim. Acta* 151 (1988) 201.
- [33] *Selected Powder Diffraction Data for Education & Training*, International Centre for Diffraction Data, USA, 1988.
- [34] A.B. Lever, *Inorganic Electronic Spectroscopy and Theory and Applications*, Elsevier, Amsterdam, 1984.
- [35] M.L.P. Santos, I.A. Bagatin, E.M. Pereira, A.M.D. Ferreira, *J. Chem. Soc. Dalton Trans.* 6 (2001) 838.
- [36] M.B. Armando, R.R. Lena, M.E. Rafael, D.J. Federico, *J. Coord. Chem.* 29 (1993) 359.
- [37] L.D. Field, B.A. Messerie, L. Soler, I.E. Buys, T. Hambley, *J. Chem. Soc. Dalton Trans.* (2000) 1959.
- [38] J.M. Pingarrón, I.O. Hernández, A.G. Cortés, P.Y. Sedeño, *Anal. Chim. Acta* 439 (2001) 281.
- [39] A. Cinquantini, R. Seeber, R. Cini, P. Zanello, *J. Electroanal. Chem.* 134 (1982) 65.
- [40] V.J. Catalano, R.A. Heck, C.E. Immoos, A. Öhman, M.G. Hill, *Inorg. Chem.* 37 (1998) 2150.
- [41] Y. Sulfab, S. Al-Mousawi, A. Hussain, *Transition Met. Chem.* 11 (1986) 356.
- [42] K. Sui, S.M. Peng, S. Bhattacharya, *Polyhedron* 18 (1999) 631.
- [43] R.L. Lintvedt, D.E. Fenton, *Inorg. Chem.* 19 (1980) 569.

Provided for non-commercial research and education use.
Not for reproduction, distribution or commercial use.



(This is a sample cover image for this issue. The actual cover is not yet available at this time.)

This article appeared in a journal published by Elsevier. The attached copy is furnished to the author for internal non-commercial research and education use, including for instruction at the authors institution and sharing with colleagues.

Other uses, including reproduction and distribution, or selling or licensing copies, or posting to personal, institutional or third party websites are prohibited.

In most cases authors are permitted to post their version of the article (e.g. in Word or Tex form) to their personal website or institutional repository. Authors requiring further information regarding Elsevier's archiving and manuscript policies are encouraged to visit: <http://www.elsevier.com/copyright>

Dispersive liquid-liquid microextraction for chemical

speciation and determination of ultra-trace concentrations of metal ions

M.S. El-Shahawi, H.M. Al-Saidi

Available online 7 December 2012

Recent years have seen an upsurge of interest in developing a low-cost, easy-to-operate, reliable preconcentration technique for precise determination of ultra-trace concentrations of metal ions in aqueous matrices. Dispersive liquid-liquid microextraction (DLLME) is a novel sample-preparation technique offering high enrichment factors from low volumes of water samples.

We compare DLLME, cloud-point extraction and other microextraction techniques. We also highlight the current best practices for analysis and chemical speciation of metal ions in highly salted media.

We strongly recommend the stripping voltammetric technique at modified electrodes coupled to DLLME and other microextraction techniques to develop low-cost, precise methods for ultra-trace concentrations of metal ions in biological and environmental samples.

Crown Copyright © 2012 Published by Elsevier Ltd. All rights reserved.

Keywords: Chromatography; Dispersive liquid-liquid microextraction (DLLME); Metal ion; Microextraction; Miniaturization; Preconcentration; Sample preparation; Speciation; Spectrochemistry; Ultra-trace concentration

1. Historical overview

Traditional methods for sample preparation {e.g., liquid-liquid extraction (LLE), Soxhlet extraction, chromatography, distillation, and absorption [1–3]} usually suffer from the following disadvantages: time consuming, tedium, use of large amounts of toxic organic solvent, and, to some extent, difficulty in automation. In recent years, it has therefore been important to develop less time-consuming, more effective, faster, lower cost and accurate methods that require smaller amounts of organic solvents, and provide precise data with reasonable limits of quantification (LOQs). Dispersive liquid-liquid microextraction (DLLME) represents one of the most attractive techniques for preconcentration of organic and inorganic analytes from various matrices [3].

tration of organic and inorganic analytes from various matrices [3].

In the past few years, comprehensive reviews have been published on microextraction and DLLME [2,4–19]. However, most of these reviews [4–6,8–10,12,14] are descriptive rather than critical and are not independent in discussing the DLLME technique. Other reviews [2,15,16] include applications of DLLME for preconcentration and determination of organic and inorganic species. These reviews did not discuss the use of auxiliary solvent to adjust the density of the extraction mixture and displacement–DLLME (D–DLLME). Also, in the past three years, the number of papers devoted to the application of DLLME for trace-metal analysis has grown rapidly. The recent review by AlSaidi and Emara [19] is incomplete because they did not discuss a lot of recent

M.S. El-Shahawi*
Department of Chemistry,
Faculty of Science, King Abdulaziz
University, P.O.
Box 80203, Jeddah 21589,
Saudi Arabia (On leave from the
Department of Chemistry,
Faculty of Science, Damiatta
University, Damiatta, Egypt)

H.M. Al-Saidi
Department of Chemistry,
University College in Makkah,
Umm AlQura University,
Makkah 21955, Saudi Arabia *

Corresponding author.

Tel.: +966 0551691130; Fax:

+966 2 6952292.;

E-mail: malsaeed@kau.edu.sa,

mohammad_el_shahawi@yahoo.co.uk,

0165-9936/\$ - see front matter Crown Copyright © 2012 Published by Elsevier Ltd. All rights reserved.

doi:<http://dx.doi.org/10.1016/j.trac.2012.10.011>

Trends in Analytical Chemistry, Vol. 44, No. , 2013

developments and applications of DLLME, so the chemical literature still needs an independent review discussing the use of DLLME in the analysis of trace and ultra-trace metal ions in various matrices.

The present review focuses on recent developments and applications of DLLME for preconcentration, sequential determination and/or chemical speciation of trace and ultra-trace metal ions in variety of samples. Thus, we focus on improvements in DLLME since its introduction in 2006. We

focus great attention on the use of DLLME with simultaneous derivatization of analytes and the connection of DLLME to other samplepreparation techniques for preconcentration and subsequent determination and/or chemical speciation of several groups of inorganic analytes in various matrices. We give a brief description of exchange of toxic chlorinated solvents with low toxic hydrocarbons, alcohols and ionic liquids (ILs). We discuss many more modifications of newly developed techniques for DLLME. Finally, we predict some of the future trends and limitations of DLLME and other microextraction techniques. We also

aim to highlight current best practices for the analysis and chemical speciation of metal ions. A major focus on DLLME technique has revealed the need for low-cost, precise techniques that can be implemented easily in developing countries (e.g., stripping voltammetry at surface-modified electrodes).

2. Analytical parameters controlling the extraction efficiency of DLLME

In DLLME, extraction solvent, disperser solvent, extraction time and electrolyte added are the main parameters that control performance. These components must meet certain requirements to obtain high extraction efficiency. Although, several review articles have stated that the extraction solvent must have a density higher than that of water, some applications of lower density solvents have also been proposed [15]. For less dense extractant, the recovery step is relatively tedious. Hitherto, several methods have been developed for this purpose, including solidification of the floating organic drops [20,21], adsorption by nanoparticles [22], centrifugation and collection of organic phase in special apparatus [23,24]. However, when the density of extraction solvent is lower than that of water, an auxiliary solvent has been used to make the density of the mixture higher than that of water [25].

In auxiliary solvent-based DLLME, a quaternary system including an aqueous sample, an extraction solvent, an auxiliary solvent, and a disperser solvent is employed instead of a ternary-component solvent system. The auxiliary solvent that has to be miscible with both the extraction solvent and the disperser solvent plays an important role in adjusting the density of the extraction

Trends

mixture, so phase separation can be performed by centrifugation without the use of special apparatus similar to those mentioned in [23,24]. The unique physical and chemical properties of ILs {e.g., negligible vapor pressure, non-flammability and good extractability for various organic compounds and metal ions as neutral or charged complexes [26]} enhanced the use of ILs as replacement organic solvents in DLLME. A series of extraction solvents {e.g., 1-hexyl methyl- imidazoliumhexafluorophosphate ([HMIM][PF₆]), 1-octyl-3-methylimidazolium-bis(trifluoromethylsulfonyl)imide [Omim] [TF₂N], 1-hexyl-3-methyl imidazolium- bis(trifluoromethylsulfonyl), ([Hmim][TF₂N])} and fatty alcohols has been successfully used for enrichment and determination of many inorganic species [27–30]. Toxic organic solvents have been replaced by fatty alcohols {e.g. 1-decanol [30]} to minimize side effects in the environment.

Disperser solvents [e.g. acetone, methanol, acetonitrile, tetrahydrofuran (THF) and ethanol] play an important role in decreasing the interfacial tension between water and the

extraction solvent and producing smaller droplet size. Disperser solvent in a few cases may also serve as terminating solvent {i.e. as demulsifier to break up the oil-water (O/W) emulsion and end the extraction process without centrifugation [31,32]}. After a few minutes of injecting the extraction mixture containing disperser solvent, another amount of disperser solvent is then injected into the top surface of the bulk aqueous phase to break up emulsion formed rapidly. This technique was named solvent-terminated DLLME (ST-DLLME) and has been applied with lowdensity extraction solvent. The methodology does not require centrifugation for the separation phase because the solution forms two phases quickly after the addition of de-mulsifier. Low volumes of disperser solvent could not disperse the extraction solvent properly, so the cloudy solution cannot be formed completely. By contrast, on increasing the volume of the disperser solvent at high temperature, the solubility of analytes in water increases and the extraction process is incomplete [33].

The extraction time in a DLLME technique is defined as the time between injecting the mixture for extraction and centrifugation [34]. Many investigations have shown that the extraction is accomplished a very short time after formation of the cloudy solution and the equilibrium state is achieved rapidly [35,36]. The very short time of DLLME was attributed to the infinitely large surface area between the extraction solvent and the aqueous phase [35–37]. The solubilities of the target analyte and the organic extraction solvent in aqueous phase are usually decreased with the increase of ionic strength due to the salting-out effect [38]. The volume of organic phase increases on raising salt concentration, so analyte concentration and enrichment factor decrease

Trends

[38,39]. In a few cases, electrolyte addition does not influence the efficiency of extraction.

3. Analytical application of DLLME in trace-metal analysis

The novel sample preparation of the DLLME technique can be combined with spectrochemical techniques [e.g., flame atomic absorption spectrometry (FAAS), graphite furnace AAS (GF-AAS), inductively-coupled plasma optical emission spectrometry (ICP-OES), ICP-mass spectrometry (ICP-MS) and ultraviolet-visible spectrophotometry (UV-vis)] and other techniques [e.g., gas chromatography (GC) and high-performance liquid chromatography (HPLC)]. The DLLME technique has therefore been widely applied for the preconcentration and subsequent determination of organic and inorganic compounds in complex matrices [37,38]. Applications of DLLME to the analysis of metals represent the second most popular group after pesticides. However, almost half the papers on DLLME published in 2011 were devoted to analysis of metals, so this review focuses on only the recent applications of DLLME for preconcentration, sequential determination and/or chemical speciation of trace and ultra-trace metal ions in variety of samples. Table 1 shows the versatility of DLLME combined with different analytical techniques for the extraction of inorganic compounds from various matrices.

3.1. Spectrochemical techniques coupled with DLLME
Simple ions do not tend to dissolve in organic solvents, so they should be converted into complex ions or compounds that have strong tendency to dissolve in organic media before applying DLLME. Two ways are known for the application of conventional DLLME for preconcentration of simple metal ions:

- (1) addition of chelating agent to the sample solution followed by the appropriate extraction solvent and disperser solvent (Fig. 1A); and,
- (2) simultaneously inject the chelating agent, extraction solvent, and disperser solvent into the sample solution containing metal ion (Fig. 1B).

After shaking, a cloudy mixture is formed, and the metal ions react with the chelating agent and are extracted into the fine droplets of extraction solvent.

3.1.1. Atomic absorption spectrometry coupled to DLLME.
AAS has been widely used in combination with DLLME for the preconcentration and subsequent determination of several inorganic analytes. AAS requires only a few mL of sample, so it is well suited for combination with DLLME [39]. Because DLLME is well suited for monitoring trace and ultra-trace levels of metal ions, the first applications of DLLME coupled with AAS were for monitoring very low

Trends in Analytical Chemistry, Vol. 44, No. , 2013

concentrations of the most toxic metal elements {e.g., cadmium in water [34,40], and lead in water [41] and human urine [33]}. The methods developed were sensitive, simple, accurate, low cost and suitable for monitoring such elements, even at sub-ng/L levels in samples under investigation. A high preconcentration factor has been easily achieved using small volumes of samples (Table 1).

Since 2008, conventional DLLME-AAS has been successfully applied for extraction and preconcentration of a wide variety of metal ions, mainly from water samples. However, many metal ions in solid samples were also analyzed using conventional DLLME-AAS. Examples of such applications are the determination of gold in silicate ores, soil and river sediments [42,43]. Analysis of silver in certified reference materials of human hair, bush twigs, and leaves employing DLLME has been reported [44]. In all applications mentioned, the analytes were pre-extracted from the solid matrix and the extract was used for DLLME. Transferring these analytes into the extraction solvent was based upon different methodologies; in the case of gold determination in silicate ores, its complex with Victoria blue B was transferred to extraction solvent, while, the complex ion association formed between AuCl_4 and $[\text{CH}_3(\text{CH}_2)_3\text{N}^+]$ was used for the analysis of gold in soil and river sediments. However, DDTc has been successfully used as a suitable chelating agent for formation of CCl_4 -soluble complex with Ag.

Metalloids and non-metals (e.g., arsenic, antimony, tellurium, and selenium) occur in the environment as various chemical species. Since the toxicity of As, Sb, Te, and Se depends mainly upon their chemical forms and oxidation states, chemical speciation of these elements become necessary for accurate characterization of pollution levels. There are many papers describing the use of conventional DLLME-AAS for the chemical speciation of As and Sb(III) and Sb(V) [45,46], Te(IV) and Te(VI) [47] and Se [48] in different environmental samples. In all methods, the lower oxidation state of the element under investigation was converted to complex by APDC and then extracted by DLLME, while, the higher oxidation state of elements remained in the aqueous phase. The total inorganic content of the element was determined after reduction of the higher oxidation state to the lower oxidation state using a suitable reducing agent and performing DLLME, and the difference was then calculated. In Se determination, a pyrolytic graphite platform was used to avoid Se loss since the Se-APDC complex is highly volatile.

Since the first configuration proposed for DLLME, many improvements have been introduced to increase extraction efficiency, and expand the range of applications. DLLME evolution focused on the following main factors:

- (1) type of extraction solvent;
- (2) improvement of dispersion;
- (3) simplification of procedure; and,

Table 1. Figure of merits of the reported dispersive liquid-liquid microextraction (DLLME) methods

Analyte [Ref]	Technique	Dynamic linear range (lg/L)	LOD (lg/L)	EF	Chelating agent	Extraction solvent	Matrix
Co [27]	FAAS	0.4–120	0.1	118	PAN	[Hmim], [PF ₆] ⁻	Water and salen samples
Pb [33]	GF-AAS	0.1–20	0.04	78	PMBP	CCl ₄	Biological and water samples
Cd [33]	GF-AAS	0.002–0.02	0.0006	125	APDC	CCl ₄	Water
Cd [40]	GF-AAS	0.002–0.02	0.0005	122	Salen	CCl ₄	Water
Au [42]	GF AAS	0.03–0.5	0.002	388	Victoria Blue R	Chlorobenzene	Water and silica ore
As ³⁺ & As ⁵⁺ [45]	GF-AAS	0.1–10	0.036	45	APDC	CCl ₄	Water
Te ⁴⁺ & Te ⁶⁺ [46]	GF-AAS	15–1000	4	125	APDC	CCl ₄	Water
Ag [44]	GF-AAS	0.1–10	0.012	132	Na – DDTC	CCl ₄	Human hair, Water, bush twigs, leaves
Pb [41]	GF AAS	0.05–1	0.02	150	DDTP	CCl ₄	Water
Cr ⁶⁺ [49]	GF-AAS	0.5–8.0	0.07	300	APDC	[Hmim], [PF ₆] ⁻	Natural water
Cd [50]	GF-AAS	2 x 10 ⁻⁴ –1.5 x 10 ⁻⁵	7400	67	DDTC	[Hmim], [PF ₆] ⁻	Water
Tl ⁺ , Tl ³⁺ [51]	GF-AAS	0.0033–4	0.0033	100	KI	[Hmim][PF ₆]	Water
Au [43]	GF-AAS	–	0.0084	220	[CH ₃ (CH ₂) ₃] ₄ N ⁺ . [AuCl ₄] Associate	Chlorobenzene	Water, soil, river sediments
Ag [52]	GF-AAS	0.1–5	0.02	72	DDTC	CCl ₄	CRM
Cu, Pb [53]	FAAS	Cu: 0.16–12 Pb: 2.3–160	Cu: 0.04 Pb: 0.54	Cu: 560, Pb: 265	ADDP	Xylene	Water
Cu [54]	FAAS	0.5–500	0.1	122	HOX	1-Dodecanol	cereals
Tl ⁺ , Tl ³⁺ [55]	FAAS	6–900	2.1	42.7	PAN	1-Dodecanol	hair
Se ⁴⁺ , Se ⁶⁺ [48]	Modified GF-AAS	0.1–3	0.05	70	APDC	CCl ₄	water
Cu [56]	FAAS	50–2000	3	42	HOX	CHCl ₃	Water
Pd [57]	GF-AAS	0.02–0.6	0.007	350	ACDTA	CCl ₄	Water, and soil samples
Pd [58]	FAAS	100–2000	90	45.7	Thioridazine - HCl	CHCl ₃	Water
Mo ⁶⁺ [59]	GF-AAS	0.04–0.8	0.007	362	Na – DDTC	CCl ₄	Water
As ₃₊ , As ₅₊ , Sb ₃₊ , Sb ₅₊ [47]	GF-AAS	As: 0.06–2 Sb: 0.05–5	As: 0.01 Sb: 0.05	115	APDC	CCl ₄	Water
Cr, Cu, Ni, Zn [61]	ICP-OES	Cr: 1–750 Cu, Ni, Zn: 1–1000	Cr: 0.27 Cu: 0.23 Ni: 0.4 Zn: 0.55	Cr: 8 Cu: 9 Ni: 8 Zn: 9	Na-DDTC	CCl ₄	Water
Al [37]	ICP-OES	1.0–250	0.8	128	Morin	1-Undecanol	Water
Cd, Pb, Bi [62]	ICP-OES	0.01–1	Cd: 0.005 Pb: 0.0016 Bi: 0.0047	Cd: 460 Pb: 900 Bi: 645	Na-DDTC	CCl ₄	Water
Cr ⁶⁺ [63]	ICP-OES	–	⁵² Cr: 0.11 ⁵³ Cr: 0.31	–	APDC	CCl ₄	Water
Co [64]	Spectrophotometry	–	0.5	125	PAN	CHCl ₃	Water
Fe ²⁺ [65]	Spectrophotometry	25–1000	7.5	70	o-Phenanthroline	CHCl ₃	Water
Cd, Cu [66]	Spectrophotometry	Cd: up 0.025 Cu: up 200	Cd: 1 x 10 ⁻⁴ Cu: 0.5	Cd: 3458 Cu: 10	Cd: H ₂ Dz Cu: DDTC	CCl ₄	Water
Cu ²⁺ [67]	FO-LADS	2–70	0.34	–	BPDC	CCl ₄	Water

(4) increase of the selectivity.

Pd, Co [68]	FO-LADSPd:2-100	Pd:0.20	PANDCBWater
Se ⁴⁺ and Se ⁶⁺ [74]	Co:1-70 GC-ECP0.015-100.005-4-Nitro-	Co:0.25	BrPADAP1-DodecanolWastewater phenyl endiamine ChlorobenzeneWater 2N]Water
Rh [29]	FAAS4-5000.37-BPADP[Omim][TF		
Ni(II), Co(II), Pb(II) and Cr(III) [38]	GF-AAASCr:0.0002	Co, Ni, Pb:0.0013	
Cu [70]	Spectrophotometry20-905.0-DIDCAmylacetateWater		
B [71]	Spectrophotometry220-1870015-AstraPhloxineAmylacetateWater		
MeHg ⁺ and Hg ²⁺ [75]	HPLC-ICP-MSMeHg	MeHg ⁺ :0.0076 Hg ²⁺ :0.0014	DDTCCI 4 Water

Abbreviations: ADDP, Ammoniumdiethyldithiophosphate; APDC, Ammoniumpyrolidinedithiocarbamate; DDTP, Diethyldithiophosphoric acid; DDTTC, Diethyldithiocarbamate; Salen, N,N-Bis(Salicylidene)-ethylenediamine; HOX, 8-Hydroxyquinoline; PAN, 4-(2-Pyridylazo)-2-naphthol; PMBP, 1-Phenyl-3-methyl-4-benzoyl-5-pyridylthiocarbonyl acid; H₂Dz, Dithizone; BPDCA, 4-benzylpiperidinedithiocarbamate; BPADP, 2-(5-bromo-2-pyridylazo)-5-diethylaminophenol; DCB, Dichlorobenzene; CRM, Certified reference material; FAAS, Flame atomic absorption spectrometry; GF-AAAS, Graphite-furnace atomic absorption spectrometry; ICP-OES, Inductively coupled plasma-optical emission spectrometry; ICP-MS, Inductively coupled plasma-mass spectrometry; FO-LADS, Fiber optic-linear array detection spectrophotometry; GC-ECP, Gas chromatography-electron-capture detection; HPLC-ICP-MS, High-performance liquid chromatography-inductively coupled plasma-mass spectrometry.

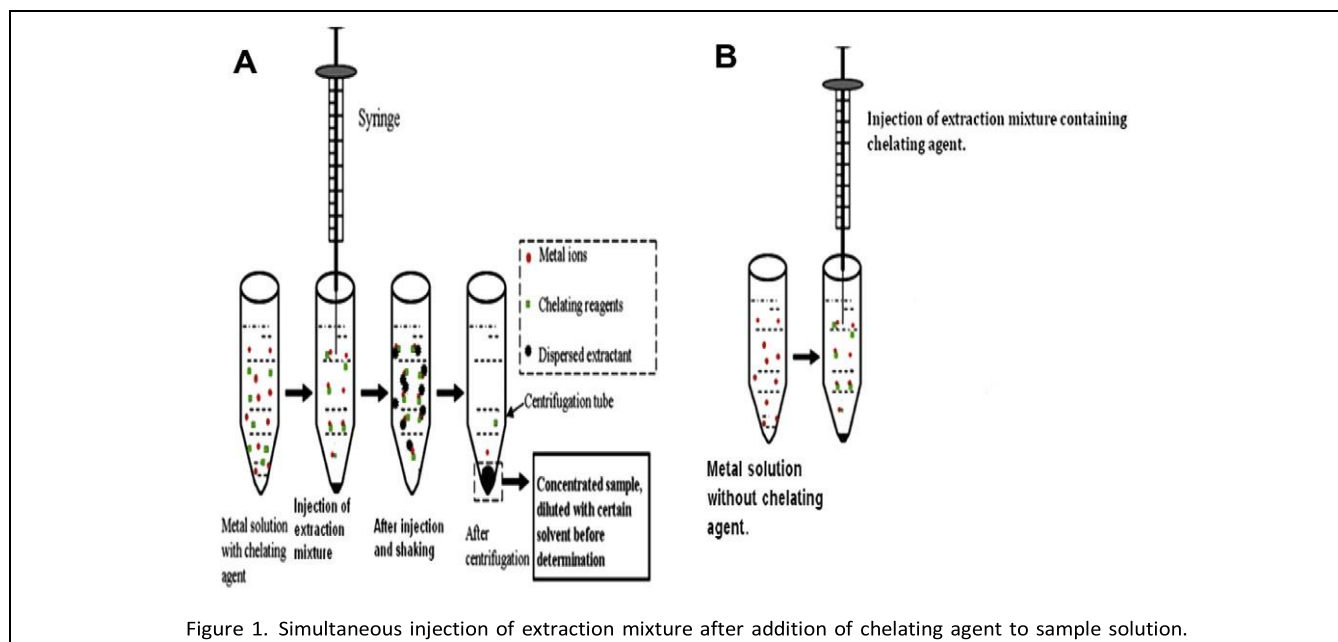
After these improvements, DLLME became completely free of toxic organic solvents and undesirable interferences from metal ions co-existing with the analyte, so DLLME was found suitable for combination with the different analytical techniques.

The most common improvement to DLLME is the usage of ILs as extraction solvents instead of toxic organic solvents (e.g., chlorinated hydrocarbons). The performance of IL-based DLLME decreases significantly in the presence of a high concentration of salts. On increasing the ionic strength of the aqueous solution, the solubility of ILs in aqueous media increases [27]. Further increasing the salt concentration enhances the solubility of ILs completely in aqueous medium and the cloudy solution is not formed. Thus, IL-based DLLME cannot be applied for extraction and preconcentration of analyte(s) from samples containing a high concentration of salt [27].

Recently, Yousefi et al. [27] successfully introduced an IL-based DLLME technique for preconcentration of inorganic species even at high salt concentration {up to 40% (m/v) [27]}. The proposed robust IL-based DLLME technique was based upon the use of 1-hexyl-3-methylimidazolium hexafluorophosphate {[Hmim][PF₆]}, NaPF₆ and ethanol as extraction solvent, common ion and disperser solvent, respectively. The solubility of ILs {e.g., [Hmim][PF₆]} in aqueous media largely decreases in the presence of common ion (PF₆), according to the common-ion effect, even at the high ionic strength, so robust IL-based DLLME has been applied for aqueous samples containing high salt concentrations {e.g., saline water [27]}.

The development of IL-based ultrasound-assisted DLLME (IL-based USA-DLLME) technique makes DLLME completely free of volatile organic solvents. In IL-based USA-DLLME, the ultrasonic probe is employed, rather than disperser solvent, to disrupt the IL (i.e. the extraction solvent). New IL-based USA-DLLME methods have been proposed for the determination of chromium (VI) [49] and cadmium [50] using GF-AAS, and rhodium(III) by FAAS [29]. The hydrophobic chelates of chromium(VI) with APDC, and cadmium with DDTc have been extracted into the fine droplets of [Hmim][PF₆], while the rhodium(III)-2-(5-bromo-2-pyridylazo)-5diethylamino phenol complex formed was transferred into the IL {[Omim][TF₂N]}.

Instead of using disperser solvent, all ILs employed were dispersed into the aqueous sample solution by an ultrasonic probe. Table 1 has more details about the figures of merits of these methods. The solubilization of anionic complexes of metal ions in a hydrophobic IL phase can be improved by using two ILs. In this methodology, one IL serves as an ion-pairing reagent, while the other is the extraction solvent. Escudero et al. [51] proposed using this technique for



chemical speciation of thallium in water. Tl^+ was complexed by an iodide ion at pH 1 in diluted sulfuric-acid solution, then tetradecyl(trihexyl)phosphonium chloride IL (CYPHOS IL 101) was used as ion-pairing reagent to form an ion-associate with TlI^4 . The complex ion-pair formed was extracted using [HMIM][PF₆] dissolved in ethanol.

An efficient, novel approach to DLLME namely displacement DLLME (D-DLLME), has been developed for eliminating undesirable interferences due to the competition

of co-existing metal ions with the analyte. The DDLLME technique was proposed for the selective determination of silver in environmental and geological samples [52]. The principle of this technique is based upon the difference in the stability of metal complexes. The targeted metal (M_1) with higher complex stability (M_1L , L is the ligand) can be replaced by another metal (M_2) with lower complex stability from its complex (M_2L), whereas the reverse reaction cannot occur. Through the displacement reaction, interferences from

Trends

the co-existing ions due to competition for the ligand could be greatly eliminated. In the D-DLLME technique proposed for determination of silver ions, DDTC was selected as a chelating agent. According to the order of the stability constants of DDTC complexes, Cu^{2+} ions were selected as a pre-extraction metal ion for selective preconcentration of silver because the only metal ions that can replace copper (II) ions from Cu-DDTC complex are Hg^{2+} , Pd^{2+} , and Ag^+ [52]. According to the scheme given in Fig. 2, the DLLME procedure was carried out twice during a single sample pretreatment process, as follows:

- (1) Cu^{2+} was complexed with DDTC and subjected to DLLME process;
- (2) After removal of the aqueous phase, the sedimented phase was dispersed into the sample solution containing silver ion by methanol and another DLLME process was carried out.

Because the stability of Ag-DDTC is greater than that of Cu-DDTC, Ag^+ can replace Cu^{2+} from the pre-extracted Cu-DDTC complex and enter the sedimented phase. Then, the sedimented phase was subjected to GFAAS for Ag determination.

Recently, the most important improvement of DLLME was the use of an automatic on-line hydrodynamic analytical system using microcolumns as an alternative to centrifugation to collect the hydrophobic droplets containing analyte [53]. Automation and on-line coupling of DLLME to analytical instruments seems to be more efficient before using the same type of column.

Anthemidis and Ioannou [53] recently developed an on-line sequential injection DLLME system coupled to FAAS for the sequential determination of copper and lead in water samples [53]. The xylene droplets, containing the metal complexes, were retained on the PTFE turnings into the microcolumn. In this experiment, isobutyl methyl ketone (MIBK) segment (300 μL) was pumped through the microcolumn as eluting agent for the analyte. The eluent was then forwarded to the nebulizer for atomization and measurement. Table 1 shows the figures of merit of the method. In 2011 [30], the same authors developed a microcolumn packed with a novel hydrophobic sorbent polyetheretherketone (PEEK) turning to separate the extractant as fine droplets from aqueous solution. Fatty alcohols (e.g., 1-undecanol) in

<http://www.elsevier.com/locate/trac> 17

methanol were employed for the extraction of Ag-DDTC complex. The fine droplets of extractant retained in the microcolumn were quantitatively eluted by MIBK and transported directly to the FAAS nebulizer. Under the optimized conditions, a limit of detection (LOD) of 0.15 $\mu\text{g/L}$, a relative standard deviation (RSD) of 2.9% at 5.00 $\mu\text{g/L}$ Ag(I) concentration level and an enhancement factor of 186 were obtained.

Trends in Analytical Chemistry, Vol. 44, No. , 2013

Despite many benefits of conventional DLLME, the choice of extraction solvent is its main drawback. In conventional DLLME, solvents with the densities higher than water are required and, further, they are not often compatible with some detection techniques (e.g., ICPOES and reversed-phase HPLC).

DLLME based on solidification of floating organic droplet (DLLME-SFO) developed by Leong and Huang in 2008 [104] uses solvents with densities lower than water

(3) speciation of Tl(III) and Tl(I) in hair samples [55].

In all applications, 1-undecanol was selected as extraction solvent due to its low melting point (13°C), so solidification

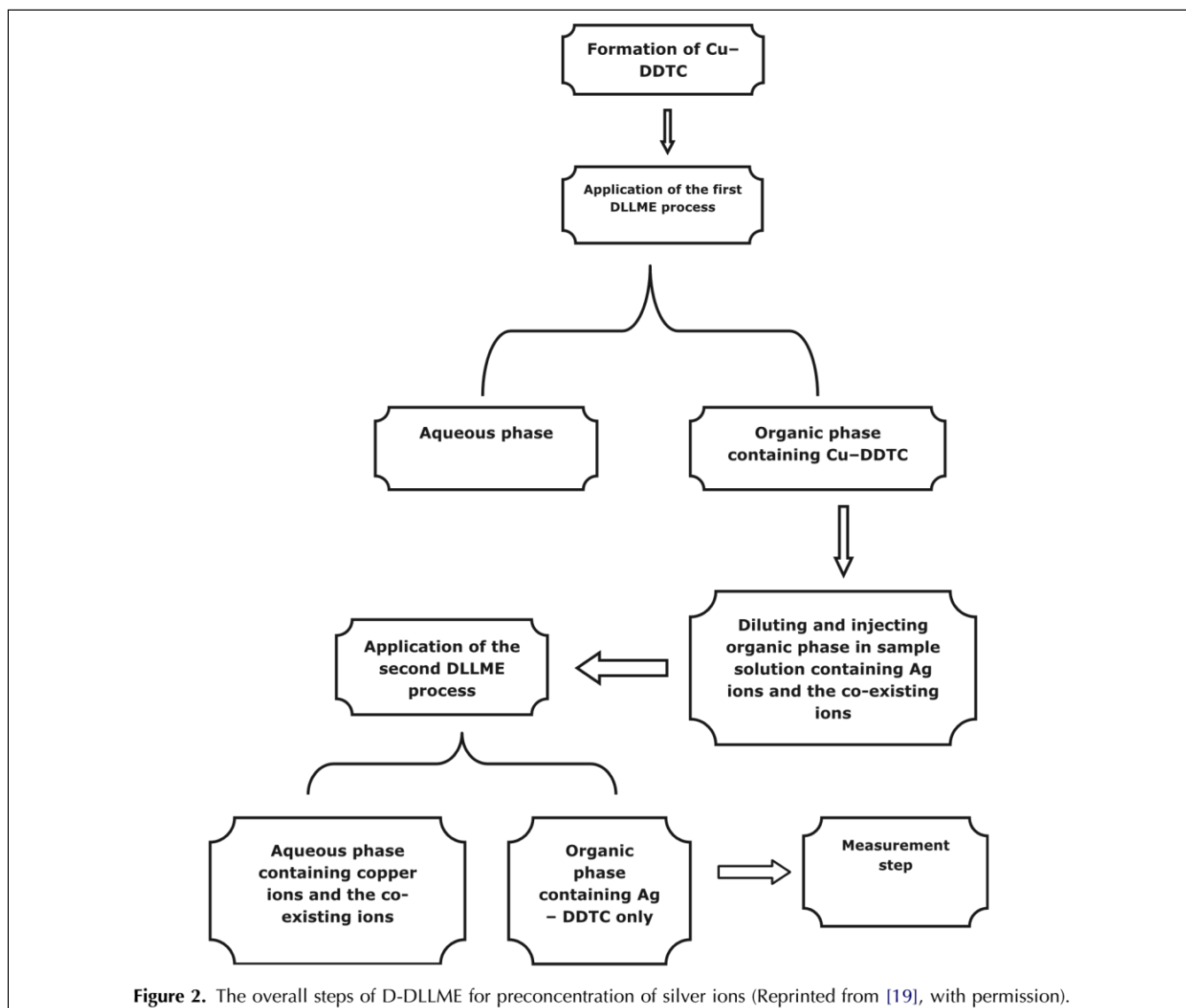


Figure 2. The overall steps of D-DLLME for pre-concentration of silver ions (Reprinted from [19], with permission).

and lower toxicity, so the version of DLLME developed was suitable for coupling to more detection techniques, and has few side effects on the environment. However, the solvents used in DLLME-SFO must have melting point near room temperature (in the range 10–30°C) to solidify the floated extractant droplet quickly [53]. In DLLME-SFO, an extraction solvent is dissolved in a water-miscible disperser solvent, and is then rapidly injected into an aqueous sample by syringe. The analytes in the sample are extracted into the fine droplets, which are further separated by centrifugation. The floating droplet of extractant on top of the test tube is rapidly solidified in an ice bath and can be easily collected. Three applications of DLLME-SFO coupled with AAS were described

- (1) pre-concentration of copper ions in cereal samples [54];
- (2) simultaneous determination of Ni(II), Co(II), Pb(II) and Cr(III) in wastewater [38]; and,

was rapid. The solidified solvent was transferred into the cup of an AAS autosampler by a simple glass spatula, and there it started to melt at room temperature. Table 1 shows the type of chelating agent and figures of merit of both methods.

Last, but not least, Table 1 lists other applications of conventional DLLME combined with AAS for:

- (1) determination of copper in water samples (FAAS) [56];
- (2) pre-concentration of palladium in water and soil samples (GF-AAS) [57];
- (3) selective determination of trace amounts of palladium (FAAS) [58]; and,
- (4) determination of molybdenum in water samples (GF-AAS) [59].

3.1.2. Inductively-coupled plasma coupled to DLLME. At the beginning of DLLME development, ICP was rarely employed as the detection technique, most probably because of the use of extraction solvents with densities higher than water, which are not often compatible with ICP [15].

Trends

Evaporation of the extraction solvent becomes a necessary but time-consuming step before sample introduction into the ICP spectrometer. Following this methodology, Mallah et al. [60] introduced an excellent, novel preconcentration DLLME method for simultaneous determination of samarium, europium, gadolinium and dysprosium using chloroform and PAN as extraction solvent and chelating agent, respectively. However, simultaneous determination of chromium, copper, nickel, and zinc using ICP-OES [61], and cadmium, lead and bismuth using ICP-MS [62] in water samples was performed by conventional DLLME after evaporation of CCl_4 and dissolving the residue in a suitable solvent. The metal ions were complexed by Na-DDTC, and then the complexes formed were extracted into CCl_4 . Table 1 shows the figures of merit for both methods.

Drying the extraction solvent prior to its injection into the ICP-MS spectrometer provided with a laser-ablation (LA) unit for sample introduction was necessary for the determination of ultra-trace amounts of Cr(VI) in water samples [63]. In this procedure, dried microdroplets (7 IL) of CCl_4 were ablated from a polystyrene substrate and analyzed by ICP-MS. External calibration was used in combination with platinum (^{195}Pt) as internal standard. The proposed methodology yields sufficiently low LODs (0.11 $\mu\text{g/L}$ and 0.31 $\mu\text{g/L}$ for ^{52}Cr and ^{53}Cr , respectively) with precision of 4–8%. The method was applied to determine Cr(VI) in tap-water and river-water samples. The spike recoveries showed the performance of the method was acceptable.

Trends

Applications of DLLME-ICP may become more popular after the introduction of different modes of DLLME, which use solvents with densities lower than water. Such solvents are compatible with ICP and evaporation or drying of extraction solvent becomes unnecessary. However, the applications of modern modes of DLLME with ICP are still limited. Rezaee et al. used one of these modes (DLLME-SFO) for preconcentration and determination of aluminum in water samples by ICP-OES [37]. An appropriate mixture of acetone and 1-undecanol was injected rapidly into the aqueous sample containing an aluminum-morin complex and, as a result, a cloudy mixture formed. After centrifugation, the test tube was cooled for 5 min. The solidified 1-undecanol on top of the solution was transferred into a suitable vial and then dissolved in 100 IL of 1-propanol to decrease the viscosity and increase the nebulization efficiency in the ICPOES instrument. The enhancement factor of 128 was obtained for only 20.0 mL of the water sample. The calibration graph was linear in the range 1.0–250.0 $\mu\text{g/L}$ with an LOD of 0.8 $\mu\text{g/L}$.

3.1.3. UV-visible spectrophotometry coupled to DLLME. Because the phase remaining after DLLME is in IL, the use of special apparatus like cylindrical micro-cells with internal capacity less than 100 IL to hold extract during

Trends in Analytical Chemistry, Vol. 44, No. , 2013

measurement become necessary. However, some researchers used micro-cells with capacity greater than 500 IL after suitable dilution of organic phase [64–66]. The dilution would affect the ratio of volumes between water phase and organic phase, so leading to poor enhancement factors, so selection of dilution solvent plays an important role in increasing the sensitivity of the method. The most widely-used dilution solvents are acetone, methanol, and ethanol.

Another problem in coupling DLLME to UV-vis spectrophotometry is focusing light for studying IL volumes obtained after DLLME. This problem was solved using fiber optic-linear array detection spectrophotometry (FOLADS), which found wide applications with DLLME for the determination of many metal ions {e.g., copper (II) [67], palladium and cobalt [68], and molybdenum (VI) [69]}. In FO-LADS, the light passed through the optical fiber is focused to the sample cell by a special lens to obtain sensitive, reproducible measurements.

Of the different extraction solvents proposed for DLLME-UV-vis spectrophotometry, the most frequently used were chlorinated solvents [64–68]. However, ILs {e.g., [Hmim][TF₂N]} were proposed as extraction solvents for the determination of molybdenum(VI) [69], and mercury [29]. The adjustment of the density of the extraction mixture using an auxiliary solvent was proposed in some applications of DLLME coupled to UV-vis spectrophotometry {e.g., the determination of gold [25], copper [70], and boron [71] in variety of samples}. As mentioned above, this approach is based on adding an

<http://www.elsevier.com/locate/trac> 19

auxiliary solvent to the extraction solvent in order to ensure that the resulting mixture of solvents has a density higher than that of water, thus allowing simple phase separation by centrifugation.

Many organic solvents with a density significantly higher than water were tested as auxiliary solvents. CCl_4 was preferred in most applications of DLLME coupled with UV-vis spectrophotometry because it offered a minimal blank test. To obtain maximum analytical signal, the ratio of solvents must be optimized well. The optimization can be carried out by two kinds of procedure:

- (1) the ratio of extraction solvent to auxiliary solvent is kept constant, while, the proportion of disperser solvent was altered; or,
- (2) the ratio of auxiliary solvent and disperser solvent is fixed, while the proportion of extraction solvent is changed.

Most papers published on DLLME coupled to UV-vis spectrophotometry were devoted to the analysis of one oxidation state of the same element, but DLLME-SFO coupled to UV-vis spectrophotometry was proposed for simultaneous determination of Fe(II) and Fe(III) in water

samples [72]. The iron species interacted with the 2-thenoyltrifluoroacetone (TTA) and then extracted into the 1-undecanol. Because of the overlap of the complex spectra, chemometric analysis was used to improve the selectivity.

3.2. Chromatographic techniques coupled to DLLME Applications of DLLME coupled to GC for the determination of inorganic species are very limited so far, most probably because very few inorganic compounds are volatile and thermally stable. However, the simple inorganic ions do not tend to be extracted by organic solvents due to their low solubility in organic media, but the conversion of such compounds to volatile and thermally stable species can be carried out by derivatization reactions. Examples of such conversion are the determination of calcium stearate in a polymer matrix after its conversion to stearic acid [73], and Se(IV) in surface water after conversion to piaszelenol [74], and the chemical speciation of some organotins (e.g. monobutyltin, dibutyltin, tributyltin, monophenyltin, diphenyltin and triphenyltin) in water samples after derivatization with sodium tetraethylborate [75].

The first use of HPLC with DLLME required the evaporation of chlorinated extraction solvents before injection of the extract into the HPLC instrument [16]. Since then, most researchers have used direct injection of chlorinated solvents into HPLC operated in reversed phase mode [16]. DLLME coupled to HPLC-ICP-MS was employed for mercury speciation (MeHg^+ and Hg^{2+}) in tap water, snow, and lake water using direct injection of extract without the tedious solvent-evaporation step [76]. Only the extract of complexes of MeHg^+ and Hg^{2+} with DDTC was diluted by mobile phase then directly injected into the HPLC system. The direct injection of the sedimented phase without heating prevented the mercury species from being lost.

Another application of DLLME-HPLC in metal-ion analysis is the method proposed for the simultaneous determination of Cu(II) and Zn(II) ions in water samples [77]. In this method, experimental and central composite designs coupled with response-surface methodology were used to optimize the experimental parameters. The calibration graphs were linear in the range of 10–4000 $\mu\text{g/L}$ with an LOD of 3.0 $\mu\text{g/L}$ for both analytes

[77].

3.3. Miscellaneous coupling of DLLMEDLLME combined with digital colorimetry was proposed for determination of trace nitrite in water samples [78]. After application of DLLME, the settled organic phase was spotted into the silica-gel thin-layer chromatography (TLC) plate and then directly imaged by a digital camera. The integral value of the gray scale of the spot was proportional to nitrite concentration. The proposed method was simple and sensitive, since it offered a linear response in the range 2.0–80 $\mu\text{g/L}$, while the LOD was 0.22 $\mu\text{g/L}$.

Shokoufi and Hamdamali [79] designed a new method combining laser induced-thermal lens spectrometry (LITLS) and DLLME for determination and preconcentration of trace amounts of lead in liquid samples. A single laser TLS instrument was designed by two investigators in the laboratory. DLLME-LI-TLS is favorable because TLS is suitable for IL volumes of the phase remaining after DLLME. Also, organic solvents greatly enhance the thermal lens effect in the phase remaining after DLLME, in comparison with aqueous media. Under optimal conditions, the calibration graphs were linear in the range 0.1–75 $\mu\text{g/L}$ with the LOD of 0.01 $\mu\text{g/L}$. The enhancement factor of 1000 was obtained from a sample volume of 10.0 mL and determination volume of 25 μL . The DLLME-LI-TLS method was applied to the analysis of human blood serums and real water samples.

4. Advantages of DLLME

Simplicity of operation, rapidity, low cost, high recovery, high preconcentration factor and environment friendliness are the main advantages of DLLME. The problems of contamination and loss of analytes are significantly less than in classical LLE, since only one operational step is required. In general, DLLME and conventional LLE methods exhibit similar separation efficiency in recovery and precision. However, in DLLME, the LOD is much better than the conventional extraction methods. In DLLME, high enrichment factors could be achieved easily. DLLME has many advantages {e.g., short total

Table 2. Comparison of dispersive liquid-liquid microextraction (DLLME) with cloud -point extraction (CPE)

Analyte	Detection technique	Chelating agent	CPE						DLLME					
			Dynamic range ($\mu\text{g/L}$)	LOD ($\mu\text{g/L}$)	EF	Acidity or pH	Heating time (min)	Ref.	Linear dynamic range ($\mu\text{g/L}$)	LOD ($\mu\text{g/L}$)	EF	Centrifugation time (min)	Extraction mixture	Ref.
Pb	GF-AAS	DDTP	–	40	18	0.32 mol/L HCl	20	[80]	0.05–1	0.02	150	2	CCl_4 , Acetone	[41]
Sb(III&V)	GF-AAS	APDC	0.1–3	0.02	–	pH 5.0	15	[81]	0.05–5	0.05	115	2	CCl_4 , Methanol	[47]
As	GF-AAS	APDC	0.1–20	0.04	36	pH 4.2	9	[82]	0.06–2	0.01	115	2	CCl_4 , Methanol	[47]
Cu	Spectrophotometry	BPDC	5–200	1.6	–	pH 6	–	[83]	2–70	0.34	–	–	–	[67]
Co	Spectrophotometry	PAN	0.6–30	0.2	198	pH 6	10	[84]	1–70	0.2	165	2	DCB, Ethanol	[68]
Hg	Spectrophotometry	TMK	5–80	0.83	33.3	pH 3	15	[85]	–	–	–	–	3.9 [TF ₂ N], 18.8 [29] acetone	5 [Hmim]

TMK, 4,4^o-
Bis(dimethylamino)thiobenzophenone.

Table 3. Comparisons between dispersive liquid-liquid microextraction (DLLME), solid-drop microextraction (SDME) and hollow-fiber liquid-phase microextraction (HF-LPME)

Analyte	SDME					HF-LPME					DLLME			
	Technique	Reagent	EF	LOD (lg/L)	Ref.	Tech.	Reagent	EF	LOD (lg/L)	Ref.	Technique	Reagent	LOD (lg/L)	Ref.
Pb	GF-AAS	PMBP	16	0.025	[94]	GF-AAS	ADTP	66–22	0.007	[99]	GF-AAS	PMBP	0.04	[33]
Se	ETV-ICP-MS	APDC	–	Se ⁴⁺ 0.0027 Se ⁶⁺ 0.003	[98]	ETV-ICP-MS	APDC	480	0.005	[95]	Modified GF-AAS	APDC	0.05	[48]
MeHg	HPLC-PDA	Dithizone	27	1	[94]	GF-AAS	–	55	0.1	[101]	HPLC-ICP-MS	DDTC	0.0076	[76]
Cu	Spectrophotometry	DDTC	33	0.150	[95]	FAAS	HOX	551	4	[102]	ICP-OES	DDTC	0.23	[61]
V	DRS-FTIR	HDPBA	–	40	[96]	ETV-ICP-OES	APDC	74	86	[103]	GF-AAS	BPHA	0.007	[92]

ADTP, Ammonium o,o^o-diethyldithiophosphate; ETV-ICP-MS, Electrothermal vaporization-inductively-coupled plasma-mass spectrometry; DRS-FTIR, Diffuse reflectance Fourier transform infrared spectroscopy; HDPBA, N¹-hydroxyl-N¹,N²-diphenylbenzamide; PDA, Photodiode array.

ex-
tit-
at-
tio-
n
ti-

Author's personal copy

Trends

me, cost, and feasibility compared to other liquid-phase microextraction techniques [e.g., solid-drop LLME (SDLLME), homogeneous LLME (HLLME), single-drop microextraction (SDME), and hollow fiber-based liquid-phase microextraction (HF-LPME)]}.

Addition of an acid, base, or salt for conversion to biphasic system is inevitable in HLLME, so some analytes may be affected or decomposed by changing conditions [67]. The problem of drop dislodgment is common in SDME, due to the use of a syringe as the drop holder during the extraction process, while the syringe in DLLME is employed for collection and injection of the extract, so such problems are avoided.

Careful comparison of the DLLME and cloud-point extraction (CPE) techniques for some applications using the same detection techniques and chelating agents [80–85] has revealed that both techniques have similar efficiencies in terms of sensitivity and recovery (Table 2). DLLME is much faster than CPE since, in a few cases, CPE requires aqueous solutions to be heated for long periods to achieve the cloud-point temperature. Moreover, in CPE, extraction efficiency may also decrease in the presence of more than 3% of a water-miscible organic solvent (e.g., THF). This solvent is usually used to decrease the viscosity of surfactant-rich phase and it facilitates sample handling due to dissolution of the surfactant-rich phase and decrease in the volume of this phase [86]. DLLME can also be used as a clean-up procedure.

The injection of a mixture of “extraction and dispersion” solvents, which already contain the target analytes in an aqueous solution, may be developed successfully (recovery values are maintained and cleaner extracts are obtained). The figure of merits of DLLME have been successfully compared with SDME and HF-LPME (Table 3).

5. Expected developments in DLLME

The present review has focused on the recent developments in DLLME and its applications in conjunction with different analytical techniques for preconcentration and chemical speciation of inorganic species in different samples. DLLME has been mostly applied to the analysis of the simplest matrices, mainly water and more rarely urine (Table 1), while its efficiency is relatively low in complex matrices (e.g., biological samples). The combination of DLLME with dispersive solid-phase extraction (dSPE) may extend its applications to more complex matrices. This combination would lead to higher levels of selectivity and sensitivity because DLLME is more focused on sensitivity improvement, while the aim of dSPE is selectivity enhancement.

However, applications of DLLME are still limited in the analysis of inorganic compounds. One of the main disadvantages of DLLME is the consumption of relatively

Trends in Analytical Chemistry, Vol. 44, No. , 2013

large volumes (i.e. mL) of disperser solvents, which usually decrease the partition coefficient of analytes into the extractant solvent [31,87]. To avoid this problem, some improvements have been suggested (e.g., ultrasonic energy or cationic surfactant to disperse the extraction solvent instead of disperser solvent) [47,88,89]. To improve the enrichment factor and to enhance the method to be more environmental friendly, two new techniques based on DLLME with little solvent consumption (DLLME-LSC) have been developed by Cruz-Vera et al. [90]. In this technique, a few IL of a binary mixture of disperser/extraction solvents were proposed [90]. However, DLLME-LSC has not so far been used for preconcentration of inorganic analytes. Although D-DLLME has effectively minimized some of interferences due to the low selectivity of some ligands towards metal ions, it takes some time and consumes reagents. Further research in this area is still needed to eliminate such interferences in less time and at low cost.

6. Outlook on the future work and the limitations of DLLME

Conventional DLLME is unsuitable for routine, on-line, preconcentration procedures, since it usually requires phase separation by centrifugation. The application of microcolumns packed with suitable sorbents as an alternative to centrifugation may open the door to automation and on-line coupling of DLLME to analytical instruments. We believe that DLLME has several disadvantages (e.g., the necessity to use a microcolumn and the use of several hundred IL of solvents for elution). As an alternative to this approach, Andruch et al. [91] have developed novel miniaturized SDME and DLLME techniques, which have attracted a great deal of interest from analytical chemists. An amyl acetate-CCl₄-acetonitrile 1:1:2 (v/v/v) mixture used in this system as a carrier was aspirated at high flow rate, resulting in formation of cloudy state and the extraction of analyte. The mixture of extraction and auxiliary solvent is immiscible with water and has a density higher than that of water, so the resulting fine droplets in the mixture, which contain the extracted analyte, self-sediment in a short time at the bottom of conical tube. Thus, centrifugation and use of a microcolumn are not required for separation of the extraction phase. Afterwards, the extracted analyte is aspirated and transferred to a 1L Z-flow cell and the absorbance is measured.

The complexity of the procedure presented is far from the simplicity of the technique originally proposed by Asadollahi et al. [92], so further research is necessary to complete experiments in this area. When performed in manual mode, DLLME is time consuming due to the centrifugation step. However, this time-consuming step

Trends in Analytical Chemistry, Vol. 44, No. , 2013

can be avoided by ST-DLLME, described above in detail. In spite of that, applications of this technique in the field of inorganic analysis remain few. The only application of ST-DLLME to metal-ion determination is the method proposed by Majidi and Shemirani [93] for estimating Pd in water.

In most investigations, experimental parameters affecting the extraction efficiency of DLLME are usually optimized by employing a step-by-step approach, in which each factor is varied sequentially. This approach is unsuitable when the number of influential factors is relatively large, and a step-by-step approach does not show the interaction among experimental parameters, so use of experimental designs is highly recommended in order to achieve the best extraction conditions quickly and in a relatively small number of experiments.

The number of detailed investigations in this field is still very limited. The number of the applications of DLLME combined with spectrofluorimetry for the determination of inorganic species is still very limited, so we expect that this hot research area will attract considerable interest due to the suitability of combining DLLME with spectrofluorimetry. Electrochemical techniques, in particular stripping analysis, have no applications with DLLME. Application of voltammetric techniques for monitoring trace and ultratrace concentrations of inorganic species in different matrices provides an efficient, low-cost, selective and excellent approach. However, further work continues on the possible application of on-line DLLME combined with stripping voltammetric analysis of such chemicals in various biological and environmental samples.

7. Conclusion

DLLME is a novel sample-preparation technique offering several advantages (e.g., high enrichment factors from low volumes of water samples, simplicity, low cost and ease of method development), which have made it available to virtually all analytical laboratories. In DLLME, toxic chlorinated solvents can be replaced by low toxic hydrocarbons (e.g., alcohols and ILs). We gave a detailed literature survey and compared DLLME with other preconcentration techniques {e.g., CPE [76–81], SDME [94–98] and HF-LPME [99–103]} on enrichment, subsequent determination and/or chemical speciation of ultra-trace concentrations of inorganic species in different types of samples.

DLLME provides the advantages of simplicity of operation, speed, low cost and high enrichment factors. DLLME may also be utilized for green analytical chemistry, since it reduces consumption of hazardous chlorinated organic solvents. DLLME is a highly versatile sample-preparation method, because not only can it be used for practically all classes of analytes, but also it is compatible, directly or after solvent replacement, with a wide range of final detection techniques. DLLME com-

petes with most of the enrichment techniques (e.g., SPE, SPME and SDME) in the extraction of analytes from various aqueous samples.

The review also highlighted the current best practice for analysis of ultra-trace metal ions in various matrices. A major focus revealed the need for low-cost methods that can easily be coupled with DLLME and implemented.

References

- [1] A. Rios, A. Escarpa, B. Simonet, *Miniaturization of Analytical Systems*, John Wiley and Sons, Chichester, UK, 2009. [2] Z. Xiaohuan, W. Qiu-Hua, Z. Mei-Yue, X. Guo-Hong, W. Zhi, *Chin. J. Chem.* 37 (2009) 161.
- [3] M. Rezaee, Y. Assadi, M.R. Hosseini, E. Aghae, F. Ahmadi, S. Berijani, *J. Chromatogr., A* 1116 (2006) 1.
- [4] C.D. Stalikas, Y.C. Fiamegos, *Trends Anal. Chem.* 27 (2008) 533. [5] A. Sarafraz-Yazdi, A. Amiri, *Trends Anal. Chem.* 29 (2010) 1.
- [6] F. Pena-Pereira, I. Lavilla, C. Bendicho, *Trends Anal. Chem.* 29 (2010) 617.
- [7] A.V. Herrera-Herrera, M. Asensio-Ramos, J. Hernandez-Borges, M.A. Rodríguez-Delgado, *Trends Anal. Chem.* 29 (2010) 728.
- [8] F. Pena-Pereira, I. Lavilla, C. Bendicho, *Spectrochim. Acta, Part B* 64 (2009) 1.
- [9] C. Ner'in, J. Salafraña, M. Aznar, R. Batlle, *Anal. Bioanal. Chem.* 393 (2009) 809.
- [10] A.N. Anthemidis, M. Miro', *Appl. Spectrosc. Rev.* 44 (2009) 140. [11] A.N. Anthemidis, K.I.G. Ioannou, *Talanta* 80 (2009) 413.
- [12] F. Pena-Pereira, I. Lavilla, C. Bendicho, *Anal. Chim. Acta* 669 (2010) 1.
- [13] E.M. Martinis, P. Berton, R.P. Monasterio, R.G. Wuilloud, *Trends Anal. Chem.* 29 (2010) 1184.
- [14] S. Dadfarnia, C. Haj, A.M. Shabani, *Anal. Chim. Acta* 658 (2010) 107.
- [15] M.Rezaee, Y. Yamini, M.Faraji, *J.Chromatogr., A* 1217(2010)2342.
- [16] A. Zgoła-Grzeskowiak, T. Grzeskowiak, *Trends Anal. Chem.* 30 (2011) 1382.
- [17] L. Kocu'rova', I.S. Balogh, J. S'andrejova', V. Andruch, *Microchem. J.* 102 (2012) 11.
- [18] M. Jiping, L. Wenhui, C. Lingxin, *Curr. Anal. Chem.* 8 (2012) 78.
- [19] H.M. Al-Saidi, Adel A.A. Emara, J. Saudi Chem. Soc. (2011) (in press) (DOI: <http://dx.doi.org/10.1016/j.jsocs.2011.11.005>).
- [20] Z.D.H. Xu, D.S.L. Lv, F. Yu-Qi, *Anal. Chim. Acta* 636 (2010) 28.
- [21] M.R.K. Zanjani, Y. Yamini, S. Shariati, J. Jonsson, *Anal. Chim. Acta* 585 (2007) 286.
- [22] Z.G. Shi, H.K. Lee, *Anal. Chem.* 82 (2010) 1540.
- [23] A. Saleh, Y. Yamini, M. Faraji, M. Rezaee, M. Ghambarian, *J. Chromatogr., A* 1216 (2009) 6673.
- [24] M.A. Farajzadeh, D.B.R. Djozan, *Talanta* 81 (2010) 1360.
- [25] L. Kocurova, I.S. Balogh, J. Skrlíkova, J. Posta, V. Andruch, *Talanta* 82 (2010) 1958.
- [26] T.P.T. Pham, C.W. Cho, Y.S. Yun, *Water Res.* 44 (2010) 352. [27] S.R. Yousefi, S.J. Ahmadi, *Microchim. Acta* 172 (2011) 75.
- [28] E. Molaakbari, A. Mostafavia, D. Afzali, *J. Hazard. Mater.* 185 (2011) 647.
- [29] M. Gharehbaghi, F. Shemirani, M. Baghdadi, *Int. J. Environ. Anal. Chem.* 89 (2009) 21.
- [30] A.N. Anthemidis, K-I. G. Ioannou, *Talanta* 84 (2011) 1215.
- [31] W.C. Tsai, S.D. Huang, *J. Chromatogr., A* 1216 (2009) 5171.
- [32] H. Chen, R. Chen, S. Li, *J. Chromatogr., A* 1217 (2010) 1244.
- [33] P. Liang, H. Sang, *Anal. Biochem.* 380 (2008) 21.
- [34] J.E. Zeini, A. Bidari, Y. Assadi, M.R.M. Hosseini, M.R. Jamali, *Anal. Chim. Acta* 585 (2007) 305.

Trends

- [35] R.E. Rivas, I. Lo'pez-Garc'ia, M. Hern'andez-Co'rdoba, *Microchim. Acta* 166 (2009) 355.
- [36] D. Nagaraiu, S.D. Hang, *J. Chromatogr., A* 1161 (2007) 89.
- [37] M. Rezaee, Y. Yamini, A. Khanchi, M. Faraji, A. Saleh, *J. Hazard. Mater.* 178 (2010) 766.
- [38] M. Mirzaei, M. Behzadi, N.M. Abadi, A. Beizaei, *J. Hazard. Mater.* 186 (2011) 1739.
- [39] C.B. Ojeda, F.S. Rojas, *Chromatographia* 69 (2009) 1.
- [40] A. Moghimi, *J. Chin. Chem. Soc.* 55 (2008) 369.
- [41] M.T. Naseri, M.R.M. Hosseini, Y. Assadi, A. Kiani, *Talanta* 75 (2008) 56.
- [42] M. Shamsipur, M. Ramezani, *Talanta* 75 (2008) 294.
- [43] I. De La Calle, F. Pena-Pereira, N. Cabaleiro, I. Lavilla, C. Bendicho, *Talanta* 84 (2011) 109.
- [44] P. Liang, L. Peng, *Microchim. Acta* 168 (2010) 45.
- [45] P. Liang, L. Peng, P. Yan, *Microchim. Acta* 166 (2009) 47.
- [46] R.E. Rivas, I. Lopez-Garcia, M. Hernandez-Cordoba, *Spectrochim. Acta, Part B* 64 (2009) 329.
- [47] N.M. Najafi, H. Tavakoli, R. Alizadeh, S. Seidi, *Anal. Chim. Acta* 670 (2010) 18.
- [48] A. Bidari, E.Z. Jahromi, Y. Assadi, M.R.M. Hosseini, *Microchem. J.* 87 (2007) 6.
- [49] H. Chen, P. Du, J. Chen, S. Hu, S. Li, H. Liu, *Talanta* 81 (2010) 176.
- [50] S. Li, S. Cai, W. Hu, H. Chen, H. Liu, *Spectrochim. Acta, Part B* 64 (2009) 666.
- [51] L.B. Escudero, P. Berton, E.M. Martinis, R.A. Olsina, R.G. Wuilloud, *Talanta* 88 (2012) 277.
- [52] P. Liang, L. Zhang, E. Zhao, *Talanta* 82 (2010) 993.
- [53] A.N. Anthemidis, K.I.G. Ioannou, *Talanta* 79 (2009) 86.
- [54] W.X. Wu, Q.H. Wu, C. Wang, Z. Wang, *Chin. Chem. Lett.* 22 (2011) 473.
- [55] S.Z. Mohammadi, A. Sheibani, F. Abdollahi, E. Shahsavani, *Arab. J. Chem.* (2012) (in press) (DOI: <http://dx.doi.org/10.1016/j.arabjc.2012.03.008>).
- [56] M.A. Farajzadeh, M. Bahram, B.G. Mehr, J.A. Jonsson, *Talanta* 75 (2008) 832.
- [57] M. Shamsipur, M. Ramezani, M. Sadeghi, *Microchim. Acta* 166 (2009) 235.
- [58] T.A. Kokya, K. Farhadi, *J. Hazard. Mater.* 169 (2010) 726.
- [59] M. Shamsipur, A. Habibollahi, *Microchim. Acta* 171 (2010) 267.
- [60] M.H. Mallah, F. Shemirani, M.G. Maragheh, *J. Radioanal. Nucl. Chem.* 278 (2008) 97.
- [61] H. Sereshti, V. Khojeh, S. Samadi, *Talanta* 83 (2011) 885.
- [62] X. Jia, Y. Han, Y. Liu, T. Duan, H. Chen, *Microchim. Acta* 171 (2010) 49.
- [63] I. Razmislevicien, A. Padarauskas, B. Pranaityt, E. Naujalis, *Current Anal. Chem.* 6 (2010) 310.
- [64] M. Gharehbaghi, F. Shemirani, M. Baghdadi, *Int. J. Environ. Anal. Chem.* 88 (2008) 513.
- [65] A.B. Tabrizi, *J. Hazard. Mater.* 183 (2010) 688.
- [66] X. Wen, Q. Yang, Z. Yan, Q. Deng, *Microchem. J.* 97 (2010) 249.
- [67] M. Ezoddin, F. Shemirani, M.R. Jamali, *J. Anal. Chem.* 65 (2010) 153.
- [68] N. Shokoufia, F. Shemirani, Y. Assadi, *Anal. Chim. Acta* 597 (2007) 349.
- [69] M. Gharehbaghi, F. Shemirani, *Food Chem. Toxicol.* 49 (2011) 423.
- [70] J. S'kr'l'ikova', V. Andruch, I.S. Balogh, L. Kocu'rova', L. Nagy, Y. Bazel, *Microchem. J.* 99 (2011) 40.
- [71] L. Rusna'kova', V. Andruch, I.S. Balogh, J. S'kr'l'ikova', *Talanta* 85 (2011) 541.
- [72] M.R. Moghadam, A.M.H. Shabani, S. Dadfarnia, *J. Hazard. Mater.* 197 (2010) 176.

Trends in Analytical Chemistry, Vol. 44, No. , 2013

- [73] A. Ranji, M.G. Ravandi, M.A. Farajzadeh, *Anal. Sci.* 24 (2008) 623.
- [74] A. Bidari, P. Hemmatkhan, S. Jafarvand, M. Reza, M. Hosseini, Y. Assadi, *Microchim. Acta* 163 (2008) 243.
- [75] A.P. Birjandi, A. Bidari, F. Rezaei, M.R.M. Hosseini, Y. Assadi, *J. Chromatogr., A* 1193 (2008) 19.
- [76] J. Xiaoyu, H. Yi, L. Xinli, D. Taicheng, C. Hangting, *Spectrochim. Acta, Part B* 66 (2011) 88.
- [77] M.A. Farajzadeh, M. Bahram, M.R. Vardast, *Clean Soil, Air, Water* 38 (2010) 466.
- [78] Z.Q. Ding, G.D. Liu-Chin, *J. Anal. Chem.* 37 (2009) 119.
- [79] N. Shokoufi, A. Hamdamali, *Anal. Chim. Acta.* 681 (2010) 56. [80] T. de A Maranh'õ, D.L.G. Borges, M.A.M.S. da Veiga, A.J. Curtius, *Spectrochim. Acta, Part B* 60 (2005) 667.
- [81] X. Jiang, S. Wen, G.J. Xiang, *Hazard. Mater.* 175 (2011) 146.
- [82] T. Anna, D. Guo-sheng, Y. Xiu-ping, *Talanta* 67 (2005) 942.
- [83] F. Shemirani, M.R. Jamali, R.R. Kozani, *Chem. Anal. (Warsaw)* 52 (2007) 327.
- [84] N. Shokoufi, F. Shemirani, F. Memarzadeh, *Anal. Chim. Acta* 601 (2007) 204.
- [85] A. Niazi, T. Momeni-Isfahani, Z. Ahmari, *J. Hazard. Mater.* 165 (2009) 1200.
- [86] J.L. Manzoori, G. Karim-Nezhad, *Anal. Chim. Acta* 484 (2003) 155.
- [87] S.Z. Mohammadi, D. Afzali, Y.M. Baghelani, L.J. Karimzadeh, *Braz. Chem. Soc.* 22 (2011) 104.
- [88] J. Regueiro, M. Llompert, C. Garcia-Jares, G.C. Garcia-Monteagudo, R.J. Cela, *J. Chromatogr., A* 1190 (1-2) (2008) 27.
- [89] M. Moradi, Y. Yamini, A. Esrafil, S. Seidi, *Talanta* 82 (2010) 1864.
- [90] M. Cruz-Veru, R. Lucena, S. Cardenas, M. Valcarcel, *Anal. Methods* 3 (2011) 1719.
- [91] V. Andruch, C.C. Acebal, J. S'kr'l'ikova', H. Sklena'r'ova', P. Solich, I. Balogh, F. Billes, L. Kocu'rova', *Microchem. J.* 100 (2012) 77.
- [92] T. Asadollahi, S. Dadfarnia, A.M. Shabani, *Talanta* 82 (2010) 208.
- [93] B. Majidi, F. Shemirani, *Talanta* 93 (2012) 245.
- [94] P. Liang, R. Liu, J. Cao, *Microchim. Acta* 160 (2008) 135.
- [95] L.-B. Xia, B. Hu, Z.-C. Jiang, Y. Wu, R. Chen, L. Li, *J. Anal. At. Spectrom.* 21 (2006) 362.
- [96] F. Pena-Pereira, I. Lavilla, C. Bendicho, L. Vidal, A. Canals, *Talanta* 78 (2009) 537.
- [97] X. Wen, Q. Deng, J. Guo, *Spectrochim. Acta, Part A* 79 (2011) 1941.
- [98] D. Verma, M.K. Deb, *Int. J. Environ. Anal. Chem.* 91 (2011) 1. [99] J.S. Carletto, E. Carasek, B. Welz, *Talanta* 84 (2011) 989.
- [100] E. Ghasemi, N.M. Najafi, F. Raofie, A. Ghassempour, *J. Hazard. Mater.* 181 (2010) 491.
- [101] H. Jiang, B. Hu, B. Chen, W. Zu, *Spectrochim. Acta, Part B* 63 (2008) 770.
- [102] Z. Eshaghi, R. Azmoodeh, *Arab. J. Chem.* 3 (2010) 21.
- [103] L. Li, B. Hu, *Talanta* 72 (2007) 472.
- [104] M.-I. Leong, S.-D. Huang, *J. Chromatogr., A* 1211 (2008) 8.

*Retention profile
and select 90Y
from 89Sr using
zirconium packed
column*

*ive
separation
of
um-vanadate
gel*

M. S. El-Shahawi,

M. W.

**Khouly, A. Abd El-
Mohty**

N. E. A. Eweda

**Journal of Radioanalytical and
Nuclear Chemistry**

An International Journal Dealing with
All Aspects and Applications of Nuclear
Chemistry

ISSN 0236-5731

Volume 295

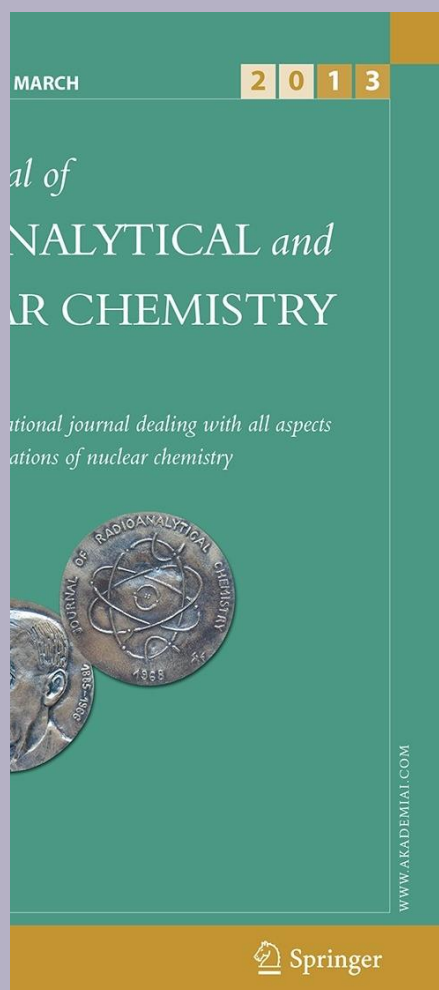
Number 3

J Radioanal Nucl Chem (2013)

295:1873-1880

DOI 10.1007/s10967-012-2262-4

Kadi, S.
H. El, S.
M. Saad &



123

Your article is protected by copyright and all rights are held exclusively by Akadémiai Kiadó, Budapest, Hungary. This e-offprint is personal use only and shall not be self-archived in electronic repositories. If you wish to self-archive your work, please use the accepted author's version for posting to your own website or your institution's repository. You may further deposit the accepted author's version on a funder's repository at a funder's provided it is not made publicly until 12 months after publication.

**request,
available**

123

Retention profile and selective separation of ^{90}Y from ^{89}Sr using zirconium-vanadate gel packed column

M. S. El-Shahawi · M. W. Kadi · S. H. El-Khouly ·
A. Abd El-Mohty · S. M. Saad · N. E. A. Eweda

Received: 23 July 2012/Published online: 28 September 2012
Akadémiai Kiadó, Budapest, Hungary 2012

Abstract A low cost and selective method has been developed for the separation of trace concentrations of ^{90}Y from its parent ^{89}Sr .

The proposed procedure is based upon complete retention of $^{90}\text{Y}^{3+}$ onto zirconiumvanadate (Zr-V) gel ion exchanger packed column from aqueous solutions containing HCl ($1.0 \times 10^{-5} \text{ mol dm}^{-3}$). Under these conditions, $^{89}\text{Sr}^{2+}$ species were not retained onto Zr-V sorbent. The retained $^{90}\text{Y}^{3+}$ species were then recovered with HCl. The performance of Zr-V sorbent packed column was determined via the height equivalent to the theoretical plates (HETP) and the number of plates (N). Validation of the developed method was checked by calculating the radionuclidic purity in terms of purification factor ($P_f = A/A_0$) and radiochemical purity of the eluted

N. E. A. Eweda—deceased

M. S. El-Shahawi (&)
Department of Chemistry, Faculty of Science,
Damiatta University, Damiatta, Egypt e-mail:
mohammad_el_shahawi@yahoo.co.uk;
malsaeed@kau.edu.sa

M. S. El-Shahawi M. W. Kadi
Department of Chemistry, Faculty of Science, King Abdulaziz
University, P.O. Box 80203, Jeddah 21589, Kingdom of Saudi
Arabia

S. H. El-Khouly A. Abd El-Mohty
Department of Radioactive Isotopes and Generators, Hot Labs
Center, Atomic Energy Authority, Inshas, P.O. Box 13759,
Cairo, Egypt

S. M. Saad N. E. A. Eweda

^{90}Y from the column. Zr-V sorbent packed column offers unique advantages of retention and quantitative separation of ^{90}Y from retention over conventional solid sorbents in rapid and effective separation of trace concentration of $^{90}\text{Y}^{3+}$ from $^{89}\text{Sr}^{2+}$ in their aqueous equilibrium media.

Keywords Separation ^{90}Y generator

Zirconiumvanadate (Zr-V) gel ion exchanger Column chromatography Radiochemical and radionuclide purity

Introduction

^{90}Y is an important radioisotope that has found useful applications in nuclear medicine. Site-specific monoclonal antibody labeling with ^{90}Y isotope has been used in radioimmunotherapy including cancer treatment [1–3]. Zevalin, a drug that incorporates ^{90}Y was approved by the US food

Cyclotron Project, Nuclear Research Center, Atomic Energy Authority, Inshas, P.O. Box 13759, Cairo, Egypt and drug administration fueling more interest in ^{90}Y research [4]. ^{90}Y is a pure β -emitter that decays to the stable ^{90}Zr daughter. Properties of ^{90}Y such as its relatively short half-life ($t_{1/2} = 64.2 \text{ h}$), suitable β -particles energy ($E_{\text{max}} = 2.28 \text{ MeV}$), and high complex formation constants of Y^{3+} with chelating ligands make it valuable in preparing radiopharmaceutical reagents [5–7].

The major issue concerning ^{90}Y production is the quantitative separation of ^{90}Y from ^{90}Sr for radiopharmaceutical preparations [8]. The most common routes in producing ^{90}Y are from its readily available parent ^{90}Sr [4] and from neutron activation of ^{89}Y . For an effective use of

^{90}Y

Y in radiotherapy, issues like chemical form of the product nuclide, stability of the column and radio purity of the eluant has to be solved [8, 9]. Numerous methods have been reported for the separation of Y from Sr. These methods include cation ion exchanger resin-732 [10] pyridyl azo naphthol (PAN)/zeolite composite [11], silica gel coated with crown ether, Teflon grain solid support and di(2-ethyl hexyl) phosphoric acid (D₂EHPA) as a liquid phase, di(2-ethyl hexyl) phosphoric acid-dodecane [12, 13], ion exchanger Dowex-50 and EDTA [14], cerium(IV) iodotungstate cation exchanger [15].

Separation of carrier-free ⁹⁰Y from high level waste by chromatographic techniques e.g. Dowex 50WX8 [16], Aminex A-5 resin [17–19] has shown some success. ⁹⁰Y generator system comprised of two extraction columns for selective separation of ⁹⁰Y from ⁹⁰Sr [20] and the application of sec-octylphenoxy acetic and tri-n-butyl phosphate as a modifier in kerosene for extraction and separation of ⁹⁰Y from the rare earths [21] have been reported. A ⁹⁰Sr/⁹⁰Y generator that produces ⁹⁰Y eluate free of ⁹⁰Sr with elution efficiency [90 % has been constructed [22]. A preferential separation of ⁹⁰Y from ⁹⁰Sr by solvent extraction using N,N,N,N-tetraoctyl diglycolamide, N,N,N,N-tetra-2-ethylhexyl diglycolamide and N,N,N,N-tetra-2-ethylhexyldiglycolamide (T2EHDGA) as extractants has been reported [5–7, 23]. Most of these methods suffer from complexity, high cost, and the need of some degree of expertise for proper operation. Inorganic ion exchangers such as clinoptilolite, potassium titanosilicate pharmacosiderite, sodium titanosilicate, sodium nonatitanate, cerium (IV) iodotungstate, zirconium oxide in multiple steps have been reported for selective separation of

⁹⁰Y from ⁹⁰Sr [15, 24–26]. A radiochemical separation scheme for the ⁹⁰Y daughter from its ⁹⁰Sr parent using zirconium vanadate ion exchanger has been developed by Roy et al. [27]. Efforts are still ongoing in the quest of development of an optimal ⁹⁰Y generator. In continuation to our previous on Zr-V ion exchanger [28], the present manuscript reports the retention profile of ⁹⁰Y and ⁸⁹Sr on new zirconium-vanadate (Zr-V) gel ion-exchanger sorbent. A low cost, simple and selective ⁹⁰Y

separation method using Zr-V gel packed column is presented.

Experimental

Apparatus

A high purity germanium (HPGe) (crystal active volume of 137.8 cm³) coupled to a calibrated multichannel gamma analyzer (Silena, Milan, Italy) was employed to check impurities in irradiated targets. The detector's resolution (FWHM) is 0.77 and 0.63 keV at 122 and 1,332 keV, respectively. NaI(Tl) detector was used for ⁸⁹Sr c-ray measurements. Calibration was performed using a mixed source of ¹⁵⁵Eu (86.5, 105.3 keV) ⁵⁷Co (122.1, 136.5 keV), and

¹³⁷

CS (661.6 keV). Beta activity was measured with a window type Geiger-Muller counter. A thermostated mechanical shaker (Corporation Precision Scientific, Chicago, USA) with 10–250 rpm shaking rate and a centrifuge Chermle Z 230 A of 5,500 rpm speed was used in batch experiments. A tight glass Jar chromatography (40 cm L and 5 cm id) of Whatman paper No 1 (3 cm 9 30 cm) was used. Atomic absorption spectrometer (AAS) (model 200 Buck scientific, USA) was used for analysis of V and Zr. A Shimadzu thermogravimetric analyzer (Model DT40) at 10 C min⁻¹ heating rate under N₂ gas fitted with a DGC 40 balance type, weighing a platinum pan and a heating device were also used. X-ray diffraction (Philips model DX-DI series type) with a Ni filter and a Cu-K_α radiation (Japan) and a pH meter (Hanna model HI 8418) with microprocessor electrode for pH measurements with absolute accuracy limits being defined by NIST buffers were used. De ionized water was obtained from Milli-Q Plus system (Millipore, Bedford, MA, USA). Glass columns (10.0 cm length) of various internal diameters (0.6–0.8 mm) were used in chromatographic separation of ⁹⁰Y.

Reagents and materials

All chemicals used were of analytical reagent grade and were used without further purification. Low-density polyethylene (LDPE) sample bottles, Nalgene and reagent containers were precleaned by soaking in hot 5 % (v/v) BDH DECON micro detergent (Poole, England) for 24 h, followed by 50 % HCl (A.R, Merck BDH) for 1 week, soaked in HNO₃ (2.0 mol

J Radioanal Nucl Chem (2013) 295:1873–1880
 dm^{-3}), and subsequently in HCl (2.0 mol dm^{-3} , 1 week), then they were rinsed with deionized water and finally dried in an oven. BDH stock solutions ($1.0 \text{ g } 10^{-5}$ to 1.0 mol dm^{-3}) of HCl, HNO_3 , NaCl and NaNO_3 (Poole, England) were prepared by dissolving the appropriate volume (or mass) of the respective compound in deionized water. Zirconyl chloride ($\text{ZrOCl}_2 \cdot 8\text{H}_2\text{O}$) and Sodium monovanadate NaVO_3 were purchased from BDH chemicals. Stock solution (1 mg mL^{-1}) of zirconium (IV) was prepared by dissolving the required mass (3.90 g) of $\text{ZrOCl}_2 \cdot 8\text{H}_2\text{O}$ in HCl (10 mL , 2.0 mol dm^{-3}) and the solution was diluted to one liter with deionized water. Standard vanadium solution (1 mg mL^{-1}) was prepared by dissolving NaVO_3 (1.22 g) in one liter of deionized water. The radio tracers ^{90}Y and ^{89}Sr were obtained by irradiating Y_2O_3 and SrCO_3 targets. ^{89}Sr tracer was used as a surrogate for ^{90}Sr . Gamma ray associated with ^{89}Sr decay (0.908 MeV) was used to check the separation efficiency via ^{89}Sr measurements. Purity of the recovered ^{90}Y was ascertained by monitoring the decay curve of ^{90}Y over a period of 3 half lives and calculating the half-life of the nuclide.

Preparation of radioactive ^{90}Y and ^{89}Sr tracer radionuclide's

Accurate weight (100 mg) of the target materials Y_2O_3 and SrCO_3 were wrapped in pure Al foil pre-cleaned with acetone and dried in air before use. Al foil was placed in another outer layer of Al foil to prevent leaks. Target compounds (Y_2O_3 and SrCO_3) were irradiated for 48 h in the vertical channel of 2 MW water cooled research reactor ERR-1 research center at Inshas, Egypt. The average thermal neutron flux density was $1.3 \text{ g } 10^{13} \text{ neutrons/cm}^2/\text{s}$. The irradiated targets were left to cool for a period of 1 day before use. The HPGe detector was used to check the purity of the irradiated targets and an accurate weight of each irradiated target was dissolved in HCl (2.0 mol dm^{-3}). The produced solutions of $^{90}\text{YCl}_3$ and $^{89}\text{SrCl}_2$ were heated gently to dryness and redissolved in deionized water. Purity of the product

$^{90}\text{YCl}_3$ was checked by monitoring the decay profile over a period of at least 3 half lives and calculating the $t_{1/2}$ from the slope of the semi-log plot ($t_{1/2} = 0.301/\text{slope}$). The specific

activity (S) was calculated using the following equation [29]:

$$S = \frac{I_0}{M} \left(1 - \exp^{-\lambda t} \right) \left(1 - \exp^{-\lambda t_{1/2}} \right)$$

where, S = number of disintegrations per second; I = flux (unit of surface) $^2/\text{s}$; r = excitation cross-section in (barns) 10^{-24} cm^2 ; M = number of target atoms of bombarded element t = irradiation time and $t_{1/2}$ is the half-life of the radionuclide.

Preparation of zirconium-vanadate gel

An aqueous solution of NaVO_3 (100 mL , 1.0 mol dm^{-3}) was added slowly to $\text{ZrOCl}_2 \cdot 8\text{H}_2\text{O}$ solution (50 mL , 1.0 mol dm^{-3}) under stirring for 30 min at 2:1 molar ratio at room temperature (Roy, et al.). The solution pH was adjusted to pH 5–6 with drops of concentrated ammonia solution and left for 24 h. A pale yellow solid precipitate was separated out by centrifugation, washed with deionized water to a constant pH and dried at 50 C for 24 h until constant weight. In the sorption batch experiment, the dried solid was crushed and sieved to 100–200 μm fractions. Zirconium-vanadate (1:2 molar ratios) gel was washed several times with deionized water, filtrated, washed with hot water and re-dried at room temperature [30]. After wet digestion, Zr and V contents in the exchanger were analyzed by AAS. Water content was determined via weight loss of the gel sample at 150 C . The gel was stable in various solutions ($0.5\text{--}2 \text{ mol dm}^{-3}$) of HCl, HNO_3 and NaNO_3 .

Separation procedures

Batch extraction step

In a penicillin bottle (20 mL), an accurate weight ($0.1 \pm 0.002 \text{ g}$) of the Zr-V ion-exchanger gel was equilibrated with solution of HCl (20 mL , $1.0 \text{ g } 10^{-5} \text{ mol dm}^{-3}$) in penicillin bottles (20 mL) containing $^{90}\text{YCl}_3$ solution ($10^{-3} \text{ mol dm}^{-3}$) and $^{89}\text{SrCl}_2$ ($10^{-3} \text{ mol dm}^{-3}$). The solutions were shaken for various time intervals up to 10 days. After phase separation, 1 mL of the test aqueous phase was pipetted out and the corresponding radioactivity of ^{90}Y and ^{89}Sr was measured. At equilibrium, the sorption percentage (%E), distribution ratio (D) and the amount of

^{90}Y or ^{89}Sr sorbed at equilibration (q_e) per unit mass of Zr-V (mol/g) exchanger were determined via measuring

Y and Sr activity before and after shaking [31, 32]. The influence of extraction media (HCl, HNO₃, NaCl or NaNO₃), temperature, sorbent doze, particle size, preparation step and stoichiometry of the sorbent was investigated. The %E and D are the average of three independent measurements and the precision in most cases was ±3.1 %.

Chromatographic separation of ⁹⁰Y from ⁸⁹Sr by Zr-V packed column

An accurate weight (1.0 ± 0.002 g) of Zr-V sorbent was equilibrated with an aqueous HCl solution (1.0 × 10⁻⁵ mol dm⁻³) and transferred to a glass column (10 cm × 0.8 mm i.d.). After the exchanger had settled down, quartz wool was put at the top of the exchanger to prevent its disturbance during percolation through Zr-V sorbent packed column. The column was washed with deionized water and the test solution (20 mL) of ⁹⁰Y and ⁸⁹Sr or ⁸⁷Rb in HCl (1.0 × 10⁻⁵ mol dm⁻³) as a suitable adsorbing medium was passed through the column at 1.0 mL min⁻¹. Complete retention of ⁹⁰Y was achieved, while ⁸⁹Sr or Rb species were passed through the column without any sorption as indicated from the measured radioactivity of ⁹⁰Y and ⁸⁹Sr in the effluent. The retained ⁹⁰Y was recovered from Zr-V packed column with HCl (8.0 mL, 0.1 mol dm⁻³) at 1.0 mL min⁻¹ flow rate. Fractions (1.0 mL) of the eluate were collected and counted for ⁹⁰Y. The percent yield of ⁹⁰Y was calculated from the ratio of ⁹⁰Y activity in the total eluate to initial ⁹⁰Y on the column multiplied by 100. The influence of particle size (0.2, 0.4 and 0.6 mm), flow rate, column diameter (0.5–2.0 cm) was also studied.

Radiochemical purity

The radiochemical purity of ⁹⁰Y was assigned via ascending paper chromatography where, a drop of 5 μL of the recovered ⁹⁰Y was put onto the lower end of one strip of chromatographic Whatman paper No. 1 and dried. The strip was immersed at its lower end in 0.1 M tris buffer at pH 7 as a solvent without reaching the spot. The paper was left to develop for 5 min, taken out the solution, and was allowed to dry. The paper was divided into equal parts, counted for β activity and the retention factor (R_f) was then calculated. Radionuclidic purity of ⁹⁰Y eluate was determined by monitoring the

decay profile curve over a period of at least 3 half lives and calculating t_{1/2}. The decay curve for ⁹⁰Y was plotted by observing β activity at 24 h time intervals for 10 days after elution.

Results and discussion

Retention profile of ⁹⁰Y, ⁸⁹Sr, Rb onto Zr-V

The influence of shaking time (0.0–10.0 days) on the sorption of ⁹⁰Y(III) ions from aqueous HCl solution (1.0 × 10⁻⁵ mol dm⁻³) onto Zr-V ion exchanger prepared at various molar ratios (1:1; 1:2 and 1:3 molar ratios) was investigated. The uptake of ⁹⁰Y(III) ions reached maximum at short time on using Zr-V ion exchange prepared at 1:2 molar ratio. Representative data using Zr-V (1:2 molar ratio) ion exchange are demonstrated in Fig. 1. The uptake of ⁹⁰Y increased rapidly and steadily at the initial shaking time and reached equilibrium after 7 days using the ion exchanger prepared at 1:2 molar ratio of Zr-V. Thus, in subsequent work, a shaking time of 7 days was adopted.

The uptake of the cationic complex species [Y(H₂O)₆]³⁺ onto the sorbent Zr-V ion exchanger can be represented by the following equation [6, 15]:

$\frac{1}{2}Y(H_2O)_6^{3+} + nHR_{(s)} \rightleftharpoons nH^+ + \frac{1}{2}Y(H_2O)_6^{3+}R_n$ where, nHR_(s) is the exchanger phase. For simplicity, H⁺ ion can be omitted and the metal ion proton exchange constant (K^{M_H}) at equilibrium constant K^{M_H} is given by:

$$K_{HM} = \frac{1}{2} \frac{H^+ R_n}{M R_n} = \frac{1}{2} \frac{HR_n}{M} \quad (3)$$

Since the metal ion concentration experimentally is less than the hydrogen ion and the [HR]ⁿ can be considered constant, the distribution ratio (K_d) of the metal ion at equilibrium is given by the equation:

$$K_d = \frac{1}{2} \frac{HR_n}{M} \quad (4)$$

Substitution Eq. (2) in Eq. (3) gives

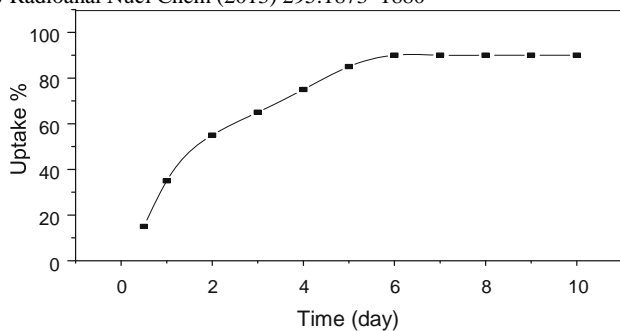


Fig. 1 Effect of shaking time on % uptake of ⁹⁰Y(III) from aqueous HCl medium

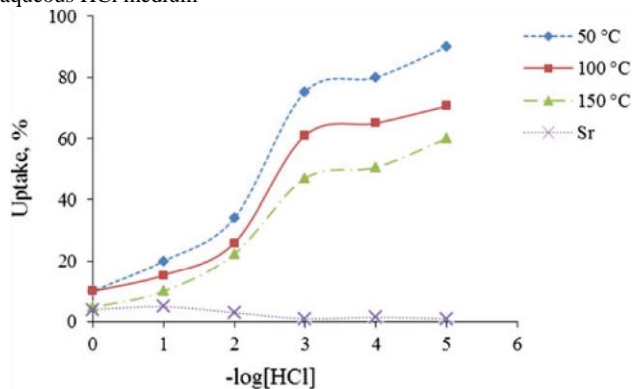


Fig. 2 Influence of drying temperature of the sorbent Zr-V gel on % uptake of ⁹⁰Y(III) and ⁸⁹Sr(II) from aqueous media containing various concentrations of HCl

$K_d \propto K_{MH} \frac{1}{2} H R_n = \frac{1}{2} H_{pn} \propto K = \frac{1}{2} H_{pn}$

δ5P

Thus, on increasing hydrogen ion concentration with HCl concentration [1.0×10^{-5} mol dm⁻³, the values of K_d for the cation exchanger process decreased. The influence of drying temperature (50–150 C) of Zr-V (1:2 molar ratio) ion exchanger on the retention of ⁹⁰Y and ⁸⁹Sr from aqueous HCl solution (1.0×10^{-5} to 1.0 mol dm⁻³) was investigated after a shaking time of 7 days. Maximum retention of ⁹⁰Y was achieved at 50 C drying temperature (Fig. 2) at pH 5 of the gel and HCl concentration of 1.0×10^{-5} mol dm⁻³. Under these conditions Sr or Rb showed no retention at all by the ZrV sorbent.

The sorption of Y in the presence of various concentrations (1.0×10^{-5} to 1.0 mol dm⁻³) was studied over a wide range of temperatures (298–333 K). The sorption of Y decreased on increasing temperature from 298 to 333 K confirming the exothermic nature of the retention process and the uptake of Y is more favorable at low temperature. Raising temperature may

affect the physical structure of the sorbent and weaken the strength of intermolecular interactions between the Zr-V membrane and Y(III) species. The membrane matrix could become more unstructured affecting the ability of polar segments to be engaged by forming stable hydrogen bonding with Y(III) species.

To probe the effect of extraction medium upon extraction of yttrium from strontium ions by Zr-V ion exchanger, the sorption profile of ⁹⁰Y and ⁹⁰Sr from aqueous solutions (20.0 mL) containing HCl, HNO₃, NaCl and NaNO₃ at various concentrations (1.0×10^{-5} to 1.0 mol dm⁻³) was studied after shaking at room temperature. The amount of

⁹⁰Y and ⁸⁹Sr remaining in the aqueous solution after equilibrium was then determined. Representative results are demonstrated in Fig. 3. The distribution ratio of Y uptake increased on decreasing HCl or HNO₃ from 1.0 to 1.0×10^{-5} mol dm⁻³ (Fig. 3a), while the uptake of Y

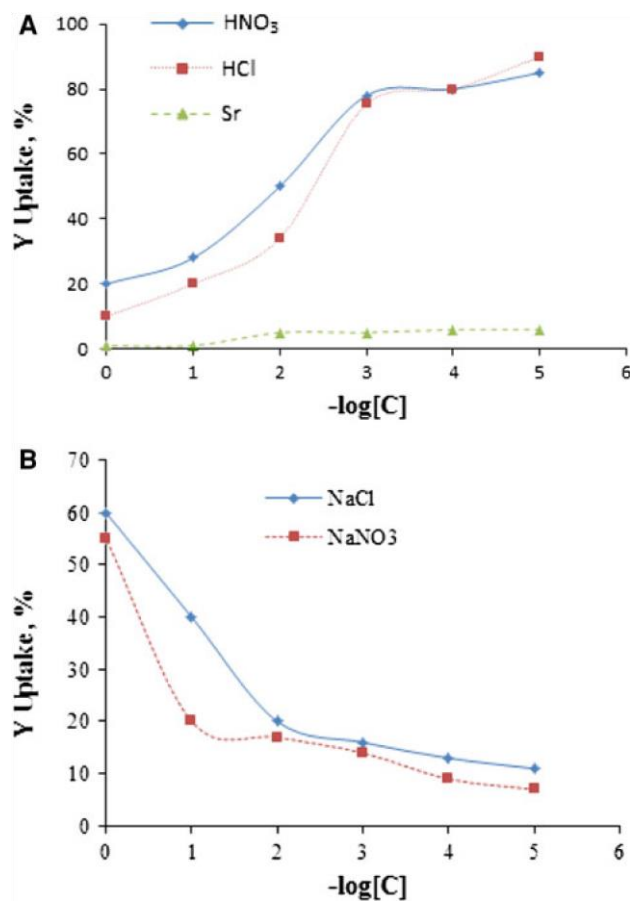
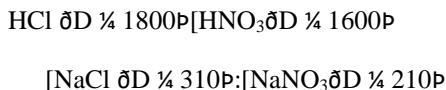


Fig. 3 Influence of various concentrations of HCl and HNO₃ (a) and NaCl and NaNO₃ (b) in the extraction media on the uptake of ⁹⁰Y(III) and Sr

increased on increasing NaCl or NaNO₃ from 1.0 × 10⁻⁵ to 1.0 mol dm⁻³ (Fig. 3b). The general sorption selectivity ordering for ⁹⁰Y sorption onto Zr-V sorbent in the presence of HCl, HNO₃, NaCl and NaNO₃ at 1.0 × 10⁻³ mol dm⁻³ followed the sequence:



Under these conditions, ⁸⁹Sr species are not retained even in the presence of high concentrations of acid or salt added. Therefore, in the subsequent chromatographic separation was carried out in the presence of HCl (1.0 × 10⁻⁵ mol dm⁻³) as proper extraction medium in subsequent work.

Chromatographic separation of ⁹⁰Y(III) onto Zr-V (1:2 molar ratios) packed column

Preliminary batch experiments on the use of Zr-V (1:2 molar ratios) for retention of ⁹⁰Y and ⁸⁹Sr from aqueous HCl media have suggested the application of Zr-V ion-exchanger in column for chromatographic separation of ⁹⁰Y species from

⁸⁹Sr from aqueous HCl (1.0 × 10⁻⁵ mol dm⁻³). Thus, percolation of an aqueous solution (100.0 mL) of HCl (1.0 × 10⁻⁵ mol dm⁻³) containing ⁹⁰Y(III) and ⁸⁹Sr species (10⁻⁵ mol dm⁻³) through Zr-V packed columns at 1.0 mL min⁻¹ flow rate was performed as described. Complete sorption of

⁹⁰Y(III) species took place as indicated from analysis of effluent solution against reagent blank under the same experimental conditions. ⁸⁹Sr species were passed through the column without any retention. A series of eluting agents e.g. HNO₃, HClO₄, H₂SO₄ and acetic acid

(0.1 mol L⁻¹) were investigated to recover ⁹⁰Y(III) species. Quantitative recovery of ⁹⁰Y(III) was achieved with HNO₃ (1.0 mol dm⁻³) from Zr-V packed column (99.7 ± 3.1 %).

The effect of flow rate (0.5–3 mL min⁻¹) on the uptake and recovery of ⁹⁰Y(III) by Chelex-100 packed column was also examined by percolating 100 mL of deionized water spiked with ⁹⁰Y(III) species at 10⁻⁵ mol L⁻¹. Complete retention of ⁹⁰Y(III) species was achieved quantitatively (99.7 %) at flow rate of 2 mL

min⁻¹. At higher flow rate, the sorption performance decreased and the width of the elution peak increased. The effect of internal diameter (0.8, 1.5 and 2 cm) of Zr-V packed column was also investigated at 2 mL min⁻¹ flow rate. Excellent separation was achieved using column of 0.8 cm, while at larger internal diameter [0.8 cm, the chromatogram became broader. Hence, a column of internal diameter of 0.8 cm is the best for effective separation and was used in the subsequent work. The effect of sample volume (0.025–100.0 mL) on ⁹⁰Y(III) retention was also investigated at 2 mL min⁻¹ flow rate. Almost complete retention (99.0 ± 4.5 %, n = 5) of ⁹⁰Y has been achieved successfully on the packed columns with good reproducibility. Performance of the developed Zr-V packed column

An aqueous solution (25 mL) containing ⁹⁰Y(III) (1.0 × 10⁻⁵ mol dm⁻³) and HCl (1.0 × 10⁻⁵ mol dm⁻³) was passed through Zr-V gel (0.6 mm particle size) packed column at 1.0 mL min⁻¹. Complete retention of ⁹⁰Y(III) took place, while Sr species are not retained at all. The retained species of ⁹⁰Y(III) were then recovered with HNO₃ (10.0 mL, 1.0 mol L⁻¹). Fractions (1.0 mL) of the eluant solution at 1.0 mL min⁻¹ were collected and analyzed for ⁹⁰Y(III). The results are demonstrated in Fig. 5. The performance of Zr-V packed column was determined via the number (N) and the height equivalent to the theoretical plate (HETP) from the elution curves employing equation (6) [31]

$$N = \frac{8V_{\text{max}}}{W^2} = \frac{L}{\text{HETP}}$$

where, V_{max} = volume of eluate at peak maximum, W = width of the peak at 1/e times the maximum solute

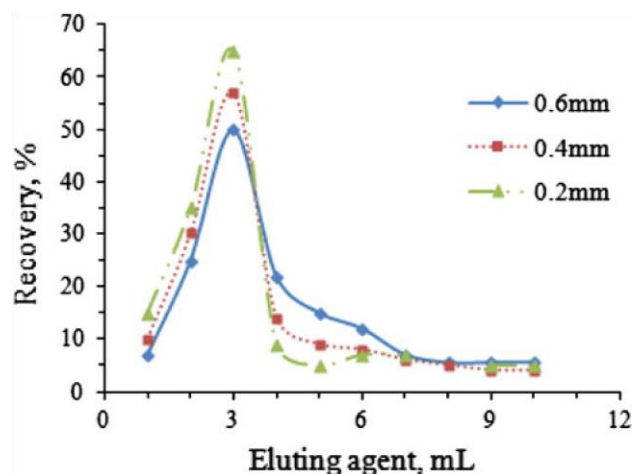


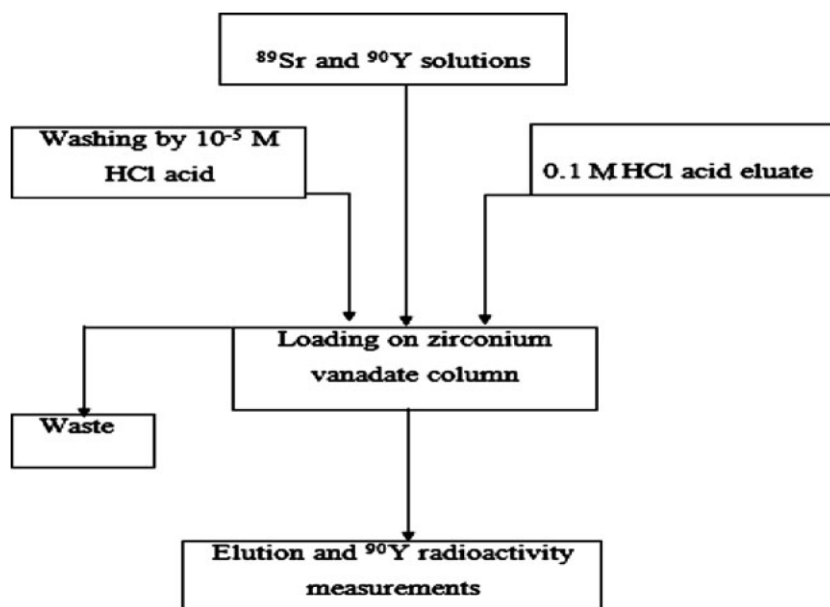
Fig. 4 Influence of particle size of Zr-V (1:2 molar ratio) gel sorbent packed column (10.0 cm \times 0.8 cm id), on the chromatogram of

^{90}Y (III) elution using HCl at 1.0 mL min⁻¹ flow rate

concentration and L is the length of the foam bed in mm.

The HETP and N were in the range 0.84 ± 0.04 mm and $91.0.0 \pm 3$, respectively. These values are in good agreement with the results obtained from the chromatogram method employing Zr-V cation ion exchanger.

Fig. 5 Proposed flow chart for separation of ^{90}Y from ^{89}Sr based on Zr-V sorbent packed column



The particle size of Zr-V (1:2 molar ratio) gel played an important role on the separation step of Y from Sr. Thus, the influence of particle size (0.2–0.6 mm) of Zr-V gel on the performance of gel packed column was investigated. The results of elution curves of Y by HNO₃ (1.0 mol dm⁻³) are demonstrated in Fig. 4. The value of HETP for Zr-V gel of size 0.20 mm was found smaller than the sorbent of size 0.4 and 0.6 mm. The N values for sorbent of small particle size (0.2 mm) was found higher than the corresponding values for sorbent of 0.4 and

0.6 mm particle size. Thus, a proposed flow sheet for production of ^{90}Y from ^{89}Sr by the developed Zr-V ion exchanger is demonstrated in Fig. 5. The data in the flow sheet (Fig. 5) revealed that, on percolating solution of ^{90}Y from ^{89}Sr , only ^{90}Y species were retained while

^{89}Sr was not retained at all. The retained ^{90}Y species were recovered quantitatively with HCl (0.1 mol L⁻¹) and used successfully in the subsequent work.

Radiochemical validation of the developed separation procedure

The validation of Zr-V packed column for separation of ^{90}Y from ^{89}Sr was tested by measuring the radiochemical purity of the eluted ^{90}Y from the column by HNO₃ (1.0 mol L⁻¹). The recovered ^{90}Y species was checked by developing Whatman filter No. 1 in Tris buffer (pH 7.0) as a developer. After a reasonable distance of solvent travels, the strip was

dried and cut into 1.0 cm sections where each section was counted for ^{90}Y . In the test solution ^{90}Y -HNO₃ moved with the front and the free ^{90}Sr stayed at the start. The radiochemical purity (%E) and retardation factor (R_f) were determined from the radio-chromatogram of ^{90}Y constructed by plotting radioactivity versus distance, cm. The percentage of radiochemical purity and R_f calculated from the radiochromatogram were found equal to 99.0 and 10 cm (the major activity travel), respectively in good agreement with the data reported [32] by confirming the performance of the developed procedures.

Radionuclide purity of the developed method purity

Validation of the developed method was also checked by calculating the radionuclide purity in terms of purification factor ($P_f = A/A_0$) where, A = ^{89}Sr activity in the recovered solution and A_0 is the activity of ^{89}Sr in the loaded solution.

1880

The calculated value of P_f was found less than 1.0×10^{-6} confirming purity of ^{90}Y from ^{89}Sr [33]. The purity was also checked from $t_{1/2}$ value calculated from the decay curve of ^{90}Y . A satisfactory value of $t_{1/2}$ of 64.4 h was achieved confirming purity of ^{90}Y from Sr or Rb by the developed procedures [33].

Conclusion

The prepared Zr-V ion exchanger at 1:2 molar ratio at pH 5 and dried at 50 C was successfully used as solid sorbent in packed column for complete separation of ^{90}Y from ^{90}Sr with excellent purity. A proposed flow sheet for production of ^{90}Y from ^{89}Sr by the developed ion exchanger is demonstrated. The uptake of the cationic complex species $[\text{Y}(\text{H}_2\text{O})_6]^{3+}$ onto the sorbent Zr-V ion exchanger can be properly assigned. The exchanger Zr-V sorbent packed column could be reused many times for separation of ^{90}Y from ^{90}Sr without decrease in column performance. Work is still continuing on developing on-line separation method of ^{90}Y from complicated matrices.

References

- Govindan SV, Goldenberg DM (2010) New antibody conjugates in cancer therapy. *Sci World J* 10:2070–2089
- Schmidt GP, Paprottka P, Jakobs TF, Hoffmann RT, Baur-Melnyk A, Haug A (2012) FDG-PET-CT and whole-body MRI for triage in patients planned for radiobolisation therapy. *Eur J Radiol* 81:269–276
- Matthews KM, Bowyer TW, Saey PRJ, Payne RF (2012) The workshop on signatures of medical and industrial isotope production -WOSMIP; Strassoldo, Italy, 1–3 July 2009. *J Environ Radioact* 110:1–6
- Theuer CP, Leigh BR, Multani PS, Allen RS, Liang BC (2004) Radioimmunotherapy of non-Hodgkin's lymphoma: clinical development of the Zevalin regimen. *Biotechnol Annu Rev* 10: 265–295
- Dutta S, Mohapatra PK, Raut DR, Manchanda VK (2011) Preferential extraction of ^{90}Y from ^{90}Sr using N,N,N,N-tetra-2-ethylhexyl diglycolamide (T2EHDGA) as the extractant. *J Radioanal Nucl Chem* 288:389–394
- Dutta S, Mohapatra PK, Manchanda VK (2011) Separation of ^{90}Y from ^{90}Sr by a solvent extraction method using N,N,N', N'-tetraoctyl diglycolamide (TODGA) as the extractant. *Appl Radiat Isot* 69:158–162
- Dutta S, Mohapatra PK, Raut DR, Manchanda VK (2011) Chromatographic separation of carrier free ^{90}Y from ^{90}Sr using a diglycolamide based resin for possible pharmaceutical applications. *J Chromatogr A* 6483–6488:2011
- Bonardi ML, Martano L, Groppi F, Chinol M (2009) Rapid determination of ^{90}Sr impurities in freshly "generator eluted" ^{90}Y for radiopharmaceutical preparation. *Appl Radiat Isot* 67: 1874–1877
- Castillo AX, Perez-Malo M, Isaac-Olive K, Mukhallalati H, Gonzalez EC, Berdeguez MT, Diaz NC (2010) Production of large quantities of ^{90}Y by ion-exchange chromatography using an organic resin and a chelating agent. *Nucl Med Biol* 37:935–942
- Yusan S, Erenturk S (2012) Adsorption characterization of strontium on PAN/zeolite composite adsorbent. *World J Nucl Sci Technol* 1:6–12
- Chuang JT, Lo JG (1996) Extraction chromatographic separation of carrier-free yttrium-90 from strontium-90/yttrium-90 generator by crown ether-coated silica gels. *J Radioanal Nucl Chem* 204:83–93
- Hsieh BT, Tinga G, Hsieh HT, Shen LH (1993) Preparation of carrier-free yttrium-90 for medical applications by solvent extraction chromatography. *Appl Radiat Isot* 44:1473–1480
- Bray LA, Wheelwright EJ, Western DW, Carson KJ, Elovich RJ, Shade EH, Alexander DL, Culley GE, Atkin SD (1992) Production of ^{90}Y at Hanford. *Radioact Radiochem* 3:22–25
- Chinol M, Hnatowich DJ (1987) Generator-produced yttrium-90 for radioimmunotherapy. *J Nucl Med Soc Nucl Med* 28:1465–1470
- Dhara S, Sarkar S, Basu S, Chattopadhyay P (2009) Separation of the ^{90}Sr - ^{90}Y pair with cerium(IV) iodotungstate cation exchanger. *Appl Radiat Isot* 67:530–534
- Achuthan PV, Dhami PS, Kannan R, Gopalakrishnan V (2000) Separation of carrier-free ^{90}Y from high level waste by extraction chromatographic technique using 2-ethylhexyl-2-ethylhexyl phosphonic acid (KSM-17). *Sep Sci Technol* 35:261–270
- Malja S, Schomacker K, Malja E (2000) Preparation of ^{90}Y by the ^{90}Sr - ^{90}Y generator for medical purpose. *J Radioanal Nucl Chem* 245:403–406
- Chuvilin DY, Khvostionov VE, Markovskij DV, Pavshook VA, Ponomarev-Stepnoy NN, Udovenko AN, Shatrov AV, Vereschagin YI, Rice J, Tome LA (2007) Production of ^{89}Sr in solution reactor. *Appl Radiat Isot* 65:1087–1094
- Chakravarty R, Pandey U, Manolkar RB, Dash A, Venkatesh M, Pillai MR (2009) Development of an electrochemical ^{90}Sr - ^{90}Y generator for separation of ^{90}Y suitable for targeted therapy. *Nucl Med Biol* 35:245–253
- Lewis RF, FU-Mins S, Lane TA, Olewine KR, and Holton PS (2004) In: USPTO (ed) Method and apparatus for separating ions of metallic elements in aqueous solution, G21G1/02 ed. Bristol Myers Squibb Pharma Company, Princeton
- Li W, Wang X, Meng S, Li D, Xiong Y (2007) Extraction and separation of yttrium from the rare earths with sec-octylphenoxo acetic acid in chloride media. *Sep Purif Technol* 54:164–169
- Chinol M (2006) New designed ^{90}Sr / ^{90}Y generator and ^{90}Sr breakthrough determination, development of generator technologies for therapeutic radionuclides. European Institute of Oncology, Milan, pp 65–67
- Dutta S, Raut DR, Mohapatra PK (2012) Role of diluent on the separation of ^{90}Y from ^{90}Sr by solvent extraction and supported liquid membrane using T2EHDGA as the extractant. *Appl Radiat Isot* 70:670–675
- Sylvester P (2005) In: USPTO (ed) Ion exchange materials for the separation of ^{90}Y from ^{90}Sr . Lynntech, Inc., College Station
- Hui-Bo G, Hong-Sheng B, Xiao-Hai J, Wei Y, Liang-Ge H, Hong-Qiang F (2006) Preparation of a new kind of inorganic adsorbent

- J Radioanal Nucl Chem (2013) 295:1873–1880
for ^{90}Y , development of generator technologies for therapeutic radionuclides. European Institute of Oncology, Milan, pp 21–25
26. Castillo AX (2006) Development of a reproducible methodology for the production of ^{90}Y from $^{90}\text{Sr}/^{90}\text{Y}$ chromatographic generator, development of generator technologies for therapeutic radionuclides. European Institute of Oncology, Milan, pp 26–34
 27. Roy K, Mohapatra PK, Rawat N, Pal DK, Basu S, Manchanda VK (2004) Separation of ^{90}Y from ^{90}Sr using zirconium vanadate as the ion exchanger. *Appl Radiat Isot* 60(5):621–624
 28. El-Shahawi MS, Kadi MW, El-Khouly SH, Abd El-Mohty A, Saad SM and Eweda NEA (2012) Separation of Y from Sr by zirconium-vanadate gel ion-exchanger sorbent: kinetics and thermodynamic study. *J Radioanal Nucl Chem*. doi:[10.1007/s10967-012-1892-x](https://doi.org/10.1007/s10967-012-1892-x)
 29. Helus F (1983) Radionuclides production. CRC Press, p 39
 30. Roy K, Pal DK, Basu S, Dalia N, Susanta L (2004) Synthesis of a new ion exchanger, zirconium vanadate, and its application to the separation of barium and cesium radionuclides at tracer levels. *Appl Radiat Isot* 57:471–474
 31. Braun T, Navratil JD, Farag AB (1985) Polyurethane foam sorbents in separation science. CRC Press, Inc, Florida
 32. Malja S, Schomacker K, Damani G (1997) Preliminary results on labelling antibody Mab B72.3 with ^{90}Y . *J Radioanal Nucl Chem* 218:255–257
 33. Cheng Z, Li M, Cao Z, Yang W, and Shengting Z (1995) Studies on the preparation of medical ^{90}Y generator, China Nuclear Information Centre, Atomic Energy Press, document No. SINRE-0151

Separation of Y from Sr by zirconium vanadate gel ion-exchanger sorbent: kinetics and thermodynamic study

M. S. El-Shahawi · M. W. Kadi · S. H. El-Khouly ·
A. Abd El-Mohty · S. M. Saad · N. E. A. Eweda

Received: 5 December 2011/Published online: 3 July 2012
Akadémiai Kiadó, Budapest, Hungary 2012

Abstract A new zirconium vanadate (Zr–V) ionexchanger was synthesized and characterized for fast and selective separation procedure of ^{90}Y from ^{89}Sr . The method was based on $^{90}\text{Y}(\text{III})$ sorption from aqueous HCl solution containing $^{89}\text{Sr}(\text{II})$ onto Zr–V gel exchanger. The kinetics of Y(III) sorption from HCl solution by Zr–V exchanger was subjected to Weber–Morris, Lagergren, Bhattacharya and Venkobachar, and Bt models. Initially, the uptake of Y(III) onto the exchanger was fast followed by kinetically first-order sorption with an overall rate constant, $K_{\text{Lager}} = (3.55 \pm 0.03) \times 10^{-4} \text{ min}^{-1}$. Film and intraparticle transport are the two steps that might influence Y(III) sorption. The negative values of DG of ^{90}Y retention dictate that, the process is a spontaneous. The negative values of DH and DS reflect the exothermic nature of

N. E. A. Eweda—Deceased.
This article is dedicated to the memory of Dr. N. Eweda.

M. S. El-Shahawi · M. W. Kadi

Department of Chemistry, Faculty of Science, King Abdulaziz University, P.O. Box 80203, Jidda 21589, Saudi Arabia

M. S. El-Shahawi (&)

Department of Chemistry, Faculty of Science at Damiatta, Mansoura University, Mansoura, Egypt e-mail: mohammad_el_shahawi@yahoo.co.uk

S. H. El-Khouly · A. Abd El-Mohty

Department of Radioactive Isotopes and Generators,

$^{90}\text{Y}(\text{II})$ sorption and the random uptake of $^{90}\text{Y}(\text{III})$ onto Zr–V sorbent. Zr–V exchanger offers unique advantages of

$^{90}\text{Y}(\text{III})$ retention over conventional solid sorbents in rapid and effective separation of traces of $^{90}\text{Y}(\text{III})$ from Sr. The exchanger was successfully packed in column for an effective separation of ^{90}Y .

Keywords Yttrium(III) Strontium(II) Zirconium vanadate ion-exchanger Retention Kinetic models Thermodynamic Column

Introduction

^{90}Y radionuclide has been used widely in radiotherapy [1, 2]. The favorable properties of ^{90}Y such as short half-life (64.2 h), pure β radiation with maximum energy of 2.28 MeV, and a non-radioactive daughter product ^{90}Zr , allow an efficient use of ^{90}Y -compounds as radiopharma-

Hot Labs Center, Atomic Energy Authority,
P.O. Box 13759, Inshas, Cairo, Egypt

S. M. Saad · N. E. A. Eweda

Cyclotron Project, Nuclear Research Center, Atomic Energy Authority, P.O. Box 13759, Inshas, Cairo, Egypt
ceuticals [3–6]. ^{90}Y can be produced by neutron irradiation of ^{89}Y , but the presence of large quantities of inactive ^{89}Y hinders the effective use of any prepared radiopharmaceuticals. Another route in producing ^{90}Y is from its

readily available parent nuclide ^{90}Sr however this route requires efficient separation of the Sr–Y pair [7, 8]. Electrochemical ^{90}Sr – ^{90}Y generator, similar to the famous Mo/ ^{99}Tc cow, for ^{90}Y separation suitable for targeted

thereby has shown slight success [8, 9]. However many issues e.g. radio purity of the eluant, stability of the column and chemical form of the product nuclide remain to be solved [10].

Various methods have been developed for preparation of antibodies labeled with generator produced ^{90}Y for human using Dowex-50 cation exchange resin and EDTA [11], di(2-ethyl hexyl) phosphoric acid–dodecane [12], di(2ethyl hexyl) phosphoric acid (D_2EHPA) extracting agent as a liquid phase [13], silica gel coated with crown ether [14] and cation ion exchange resin (732 resin) [15]. Solvent extraction using N,N,N,N-tetraoctyl diglycolamide and N,N,N,N-tetra-2-ethylhexyl diglycolamide as extractants have been employed for the separation of ^{90}Y [16, 17]. Separation of carrier-free ^{90}Y from high level waste by Dowex 50Wx8) and Aminex A-5 resin organic ionexchangers has been developed [18, 19]. ^{90}Y generator system comprised of two extraction columns has been used for selective separation of ^{90}Y [20]. Separation of ^{90}Y from rare earth elements in chloride media using sec-octylphenoxy acetic, tri-n-butyl phosphate as modifier has been reported in kerosene [21].

Recently, several radiochemical separation and determination methods have been reported for separation of ^{89}Y and ^{89}Sr employing ion exchange materials [22–25], tributylphosphate (TBP) and TBP impregnated Amberlite XAD-4 [26], co-precipitation followed by microfiltration [27], cationic ion-exchanger IR-120 in presence of alcohols and subsequent Cherenkov counting [28], sodium hydroxide fusion method and a streamlined column separation process with stacked TEVA, TRU and DGA resin cartridges [29], HCl-benzo-15-5 (B 15 C5)-hydrogen dicarbollylcobaltate in the two-phase water–nitrobenzene system [30, 31], and Sr and DGA resins for Sr and Y separation [32], respectively. A series of inorganic ionexchangers e.g. clinoptilolite, potassium titanosilicate pharmacosiderite, sodium titanosilicate, sodium nonatitanate, cerium(IV) iodotungstate, ZrO_2 in multiple steps and Dowex-50 column has been reported for ^{90}Y separation [22–24, 33–35]. Thus, the overall objectives of the present article are focused on separation of Y from a mixture of Y–Sr by Zr–V gel using ^{90}Y and ^{89}Sr to follow the kinetics and thermodynamic processes.

Experimental

Reagents and materials

All chemicals used were of analytical reagent grade and were used without further purification. Stock solutions (1.0×10^{-5} – 1.0 mol L^{-1}) of hydrochloric acid, nitric acid, NaCl and NaNO_3 , were prepared by dissolving the appropriate volume or amounts of the respective compound in deionized water. Zirconyl chloride ($\text{ZrOCl}_2 \cdot 8\text{H}_2\text{O}$) and Sodium monovanadate NaVO_3 were purchased from BDH chemicals. Standard solution (1.0 mg mL^{-1}) of zirconium(IV) was prepared by dissolving the required mass of $\text{ZrOCl}_2 \cdot 8\text{H}_2\text{O}$ (3.9 g) in HCl (10.0 mL, 2.0 mol L^{-1}). The solution was then diluted to one liter with deionized water. Standard vanadium solution (1 mg mL^{-1}) was prepared by dissolving NaVO_3 (1.22 g) in one liter of deionized water. The radiotracers ^{89}Sr and ^{90}Y were obtained by irradiating SrCO_3 and Y_2O_3 targets in the ERR-1 research reactor at Radioactive Isotopes and Generators Department, Atomic Energy authority, Inshas, Egypt. ^{89}Sr tracer was used as a surrogate for ^{90}Sr . The 0.908 MeV gamma-ray associated with the decay of ^{89}Sr allow examination of separation efficiency.

Apparatus

Beta activity was measured with a window type Geiger–Muller counter. A high purity germanium (HPGe) and NaI(Tl) detectors were used for gamma-ray measurements. Calibration was performed using a mixed source of ^{155}Eu (86.5, 105.3 keV) ^{57}Co (122.1, 136.5 keV), and ^{137}Cs (661.6 keV). A tight glass Jar chromatography (40 cm L and 5 cm id) of Whatmann paper No. 1 (3 9 30 cm^2) was used. A Centrifuge Chermle Z 230 A of 5,500 rpm speed and a thermostated mechanical shaker (Corporation Precision Scientific, Chicago, USA) with 10–250 rpm shaking rate were used in batch experiments. Atomic absorption spectrometer (AAS) (model 200 Buck scientific, USA) was used for analysis of Rb, V and Zr. A Shimadzu UV–Visible spectrophotometer (Model UV 160 A, Japan) was also used for the analysis of vanadium and zirconium [36]. Infrared (IR) spectra were recorded on a Broker FT-IR (model IFS 66, USA) spectrophotometer, electric oven Memmert, temperature (30–200 C) and a Shimadzu thermogravimetric analyzer (Model DT40) at 10 C/min heating rate under nitrogen gas fitted with a balance type DGC 40, weighing platinum pan and heating device were also used. X-ray diffraction (Philips model DX-DI series type) with a Ni filter and a Cu- K_α radiation (Japan) and glass columns (10.0 cm length 9 0.6 i.d) were used in chromatographic separations of ^{90}Y . A pH meter (Hanna model HI 8418) with

microprocessor electrode for pH measurements with absolute accuracy limits being defined by NIST buffers was used. De ionized water was obtained from Milli-Q Plus system (Millipore, Bedford, MA, USA).

Preparation of zirconium vanadate gel inorganic ion-exchanger

The ion-exchanger was prepared following the method of Roy et al. [35] as follows: An aqueous solution of NaVO_3 (100 mL, 1.0 mol L^{-1}) was added slowly to an acidic solution of pH 2–3 of $\text{ZrOCl}_2 \cdot 8\text{H}_2\text{O}$ (50 mL, 1.0 mol L^{-1}) at room temperature under constant stirring for 30 min. The reaction mixture was adjusted to pH 5–6 with few drops of concentrated NH_4OH solution and left for 24 h. The produced pale yellow solid precipitate was separated out by centrifugation, washed with deionized water to constant pH and dried in an automatic furnace at 50 C for 24 h until constant weight. The dried product was crushed and sieved to 100–200 μm fractions for sorption studies. The zirconium vanadate (1:2 molar ratios) gel was washed several times with deionized water, filtrated and again washed with hot water and re-dried at room temperature to a constant weight for batch and column experiments [35]. Zirconium and vanadium were determined spectrophotometrically [36]. Water content was determined via weight loss of the gel sample at 150 C. The resultant gel was found stable in various solutions of HCl, HNO_3 and NaNO_3 (0.5–2 M) and no dissolution of Zr and V.

Preparation of ^{90}Y or ^{89}Sr

An accurate weight of the target material SrCO_3 (100 mg) Y_2O_3 (100 mg) was wrapped in highly pure aluminum foil to preserve the material from any contamination through the reactor cooling circuit. The aluminum foil was introduced into another outer leak proof of aluminum and the target materials. The target was irradiated for 48 h in the vertical channel of 2 MW water cooled research reactor ERR-1 at Inshas, Egypt. The average thermal neutron flux density was $1.3 \times 10^{13} \text{ n/cm}^2\text{s}$. The irradiated target was left to cool for a period of 1 day before use. An accurate weight of each irradiated target SrCO_3 (100 mg) and Y_2O_3 were dissolved in HCl (2.0 mol L^{-1}). The solutions of

89

90

SrCl_2 and YCl_3 were heated gently to near dryness and redissolved in deionized water. Gamma-ray

spectroscopy was used to check for impurities in the irradiated product. The specific activity (S) was calculated employing the equation:

$$S = \frac{h}{M} \exp(-\lambda t) \quad (1)$$

where S is the number of disintegrations per second; h is the flux (unit of surface) $^2/\text{s}$; r is the excitation cross-section in (barns) 10^{-24} cm^2 ; M is the number of target atoms of bombarded element; t is the irradiation time and $t_{1/2}$ is the half-life of the radionuclide.

Batch extraction step

In a penicillin bottle (20 mL), an accurate weight ($0.1 \pm 0.002 \text{ g}$) of the Zr–V ion-exchanger gel was equilibrated with various solutions of HCl, HNO_3 , NaCl or NaNO_3 , (20 mL, $1.0 \times 10^{-5} \text{ mol L}^{-1}$) containing $^{90}\text{YCl}_3$ solution ($10^{-3} \text{ mol L}^{-1}$) and $^{89}\text{SrCl}_2$. The solutions were shaken for various time intervals up to 10 days. The phases were allowed to settle down and 1 mL of the aqueous phase was pipetted out and the corresponding radioactivity of ^{90}Y and ^{89}Sr in 1.0 mL solution was measured. The uptake percentage (%E), distribution ratio (D) and the amount of ^{90}Y or ^{89}Sr sorbed at equilibrium (q_e) per unit mass of Zr–V (mol/g) exchanger were determined via measuring ^{90}Y and ^{89}Sr activity before and after shaking [37]. Following these procedures, the influence of extraction media and temperature was investigated. The %E and D are the average of three independent measurements and the precision in most cases was $\pm 2 \%$.

Recommended procedure for solid phase extraction packed column of real samples

The separation and recovery of ^{90}Y from ^{89}Sr and/or Rb onto Zr–V exchanger was performed as follow: a 20 mL of sample solution containing, Sr and/or Rb was percolated through Zr–V sorbent ($1.0 \pm 0.001 \text{ g}$) packed column (10 cm long and 0.8 cm i.d.) containing glass wool at the end at 0.6 mL min^{-1} . Sr(II) and/or Rb species were passed through the column in the effluent solution without retention, while Y(III) species were completely retained. The column was then washed with HCl ($1.0 \times 10^{-5} \text{ mol L}^{-1}$) to remove any traces of physically retained ^{89}Sr . The sorbed Y(III) species were then recovered from the column with HNO_3 (10.0 mL, 1.0 mol L^{-1}) at 1.0 mL min^{-1} .

Results and discussion

Due to the excellent stability of solid inorganic ionexchangers against high temperatures and radiation, this class of materials has received considerable interest in the field of radio analytical chemistry for separation of carrierfree daughter radio nuclides from their respective parents [27, 30]. Recently, generators based on ion-exchanger have received considerable attention for routine and selective separation of ^{90}Y – ^{90}Sr [27, 30, 31]. Ion-exchangers can be made more selective by controlling the experimental conditions such as pH and ionic strength. Preliminary investigations have shown that, on shaking Zr–V with an aqueous solution of HCl ($1.0 \times 10^{-3} \text{ mol L}^{-1}$) containing Y(III) ions ($1.0 \times 10^{-3} \text{ mol L}^{-1}$) considerable amount of Y(III) was retained onto the exchanger in a short time compared to the cerium(IV) iodotungstate and other ionexchangers [35, 38, 39]. Thus, a detailed study was carried out to assign the kinetics, thermodynamics, and the most probable retention mechanism of ^{90}Y (III) from test aqueous solutions by Zr–V solid sorbent.

Characterization of Zr–V ion exchange

In this study a pale yellow zirconium vanadate ionexchanger was prepared as a gelatinous precipitate by mixing Zr(IV) and V(V) at 1:2 molar ratios' at room temperature and a pH of 5–6. The percent content of Zr and V in the exchanger varied within the ranges 25.8–26.02 and 30.01–30.41 % (m/m), respectively. The percent water content measured via weight loss of the sample after heating to 150 C was found to be in the range 15–15.1 % (m/m).

The chemical stability of Zr–V gel was investigated individually at various concentrations (1.0×10^{-5} – 4.0 mol L^{-1}) of HCl, HNO₃, NaCl and NaNO₃ solutions. Results revealed excellent stability of the Zr–V gel at concentrations up to 2.0 M of the tested mineral acids or salts in good agreement with the data reported by Roy, et al. [35]. Powdered X-ray diffraction pattern of the ionexchanger Zr–V gel confirmed the amorphous structure of the gel.

Infrared spectrum of Zr–V exchanger showed strong and broad bands in the region 3,000–3,600 cm^{-1} of the stretching vibration of the bonded O–H groups of the water molecules with inter molecular hydrogen bonding. The sharp peak at 1,612 cm^{-1} was assigned to H–O–H bonding. The broad band in the region 830–

500 cm^{-1} revealed the presence of vanadate and metal oxide [40].

Thermogravimetric (TG) and differential thermal analysis (DTA) of Zr–V gel were critically investigated. The thermograms of Zr–V gel exchanger at 1:2 molar ratios are shown in Fig. 2. The TG thermograph (Fig. 1a) shows continuous irreversible water loss (11.8 % m/m) up to 200 C and was safely assigned to the loss of interstitial and crystallization water. The observed loss (7.1 % m/m) at 600 C is attributed to loss of coordinated water. Thus, the total loss (18.9 %) of the exchanger proves the stability of the exchanger at temperatures ≤ 600.0 C. DTA thermograph curve (Fig. 1b) displayed two ill defined endothermic peaks at 105.90 and 560.4 C confirming the loss of free water molecules. Another well defined exothermic peak around 600.0 C was observed and were safely assigned to a crystallization process.

Kinetic behavior of Y(III) sorption onto Zr–V ionexchanger

The influence of shaking time (0–10 days) on the uptake of Y from HCl solution ($1.0 \times 10^{-5} \text{ mol L}^{-1}$) was investigated. Sorption of Y(III) by the ion exchange Zr–V occurs in one step (Fig. 2), i.e., gel diffusion is not the rate controlling step as in the case of common ion exchange resins [27, 41]. The rate of Y sorption was fast and reached equilibrium within a shaking time of 6 days. The half-life ($t_{1/2}$) of equilibrium sorption as calculated from the curves of the plot of $-\log C/C_0$ versus time (Fig. 2) is 24 h. This value is comparable to the value of $t_{1/2}$ reported for iodotungstate ion exchange [34]. The kinetics of ^{90}Y sorption onto the Zr–V sorbent depends on film and intraparticle diffusion where, the slower step controls the overall rate of transport.

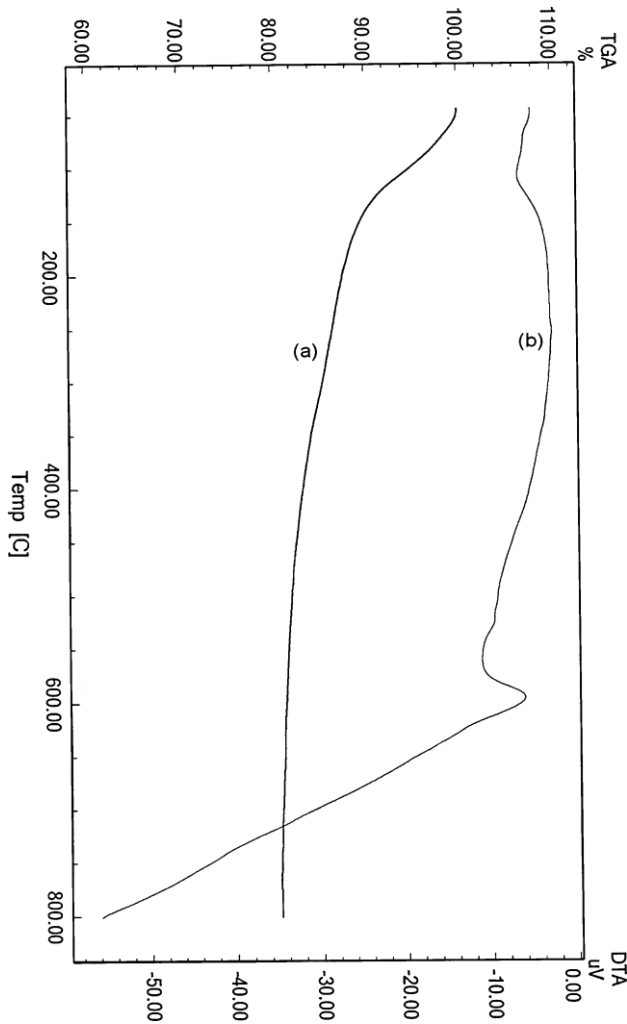


Fig. 1 TG (a) and DTA (b) of zirconium vanadate ion-exchanger

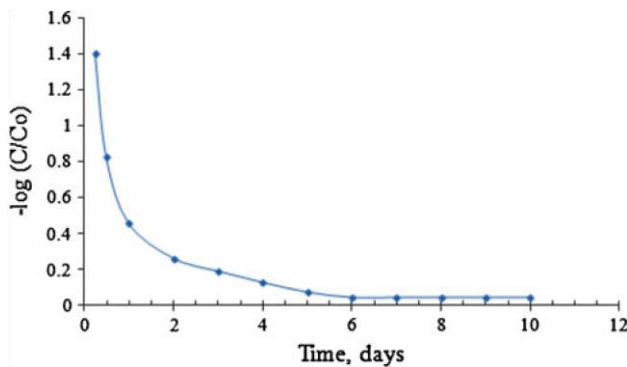


Fig. 2 Rate of retention of ⁹⁰Y(III) on Zr-V ion-exchanger at room temperature from aqueous HCl solution (1.0 9 10⁻⁵ mol L⁻¹)

A Weber–Morris model was applied on the sorption process. In this model Eq. (2) is applied [42]:

$q_t \approx R_d \sqrt{t}$ $\frac{\partial q}{\partial t} = \frac{R_d}{2\sqrt{t}}$ Fig. 3 Weber–Morris plot of the sorbed ⁹⁰Y(III) onto zirconium vanadate gel ion-exchanger versus square root of time. Conditions: aqueous HCl solution (20 mL, 1.0 9 10⁻⁵ mol L⁻¹); sorbent doze = 0.1 ± 0.002 g and 25 ± 0.1 C where R_d is the rate constant of intraparticle transport in l mol g⁻¹ min^{-1/2} and q_t is the sorbed ⁹⁰Y concentration (l mol g⁻¹) at time t. The values of R_d computed from the two distinct slopes of Weber–Morris plots (Fig. 3) for the Zr–V sorbent were found equal 0.025 and 0.23 mmol g⁻¹ with R² = 0.989 and 0.995, respectively. The observed change in the slope of the linear plot (Fig. 3) is most likely attributed to the different pore size [43, 44]. Thus, intra-particle diffusion step is most likely the rate determining step. The retention step of the Y species onto Zr–V sorbent at 25 ± 1 C was subjected to Lagergren model:

$$\log(q_e - q_t) \approx \log q_e - K_{Lager} t \quad (3)$$

where q_e is the amount of ⁹⁰Y sorbed at equilibrium per unit mass of sorbent (l mol g⁻¹); K_{Lager} is the first order overall rate constant for the retention process and t is the time in min. The plot of log (q_e - q_t) versus time (Figs. 4, 5) is linear and the calculated value of K_{Lager} = 3.55 9 10⁻⁴ ± 0.073 min⁻¹ (R² = 0.979) confirming the first order kinetics of the sorption process [45]. The increase of K_{Lager} values with ⁹⁰Y concentration confirms

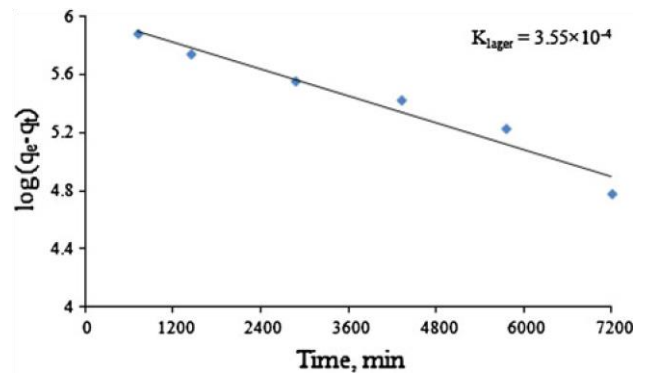


Fig. 4 Lagergren plot of ⁹⁰Y(III) uptake onto zirconium vanadate ion-exchanger from aqueous HCl solution (1.0 9 10⁻⁵ mol L⁻¹) versus time at 25 ± 0.1 C

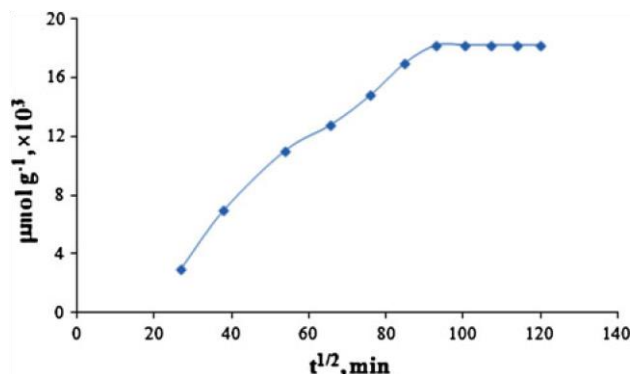


Fig. 5 Bhattacharya–Venkobachar plot of $^{90}\text{Y}(\text{III})$ retention onto zirconium vanadate gel ion-exchanger from aqueous HCl solution ($1.09 \times 10^{-5} \text{ mol L}^{-1}$) versus time at $25 \pm 0.1 \text{ C}$

the first order kinetic nature of the retention process and indicates the formation of monolayer species of ^{90}Y onto the surface of the used adsorbent [43, 44]. The sorption data was also subjected to Bhattacharya–Venkobachar kinetic model represented by Eq. (3) [46].

$$\log(1 - U_{(t)}) = -K_{\text{Bhatt}} t^{1/2} \quad (3)$$

where $U_{(t)} = (C_o - C_t)/(C_o - C_e)$, K_{Bhatt} is the overall rate constant, t is the time (min), C_t is the concentration of Y at time t in lg mL^{-1} , C_e is the concentration of ^{90}Y at equilibrium. The plot of $\log(1 - U_{(t)})$ versus time is linear (Fig. 6) with a correlation coefficient of $R^2 = 0.987$. The computed value of K_{Bhatt} ($2.859 \times 10^{-4} \text{ min}^{-1}$) is close to K_{Lager} value ($3.559 \times 10^{-4} \text{ min}^{-1}$) providing an additional indication of first order kinetic of Y retention.

The value of Bt , which is a mathematical function $F = q_t/q_e$ calculated for each value of F employing Reichenberg equation [47].

$$Bt = 0.4977 - 2.303 \log \delta F \quad (4)$$

A plot of Bt versus time at $25 \pm 1 \text{ C}$ for uptake of Y by the Zr-V sorbent is linear ($R^2 = 0.990$) up to 90 h and

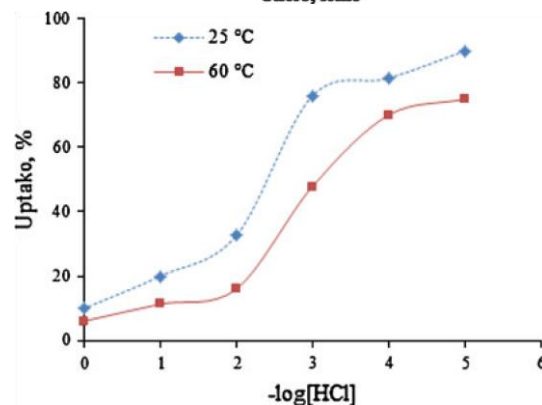
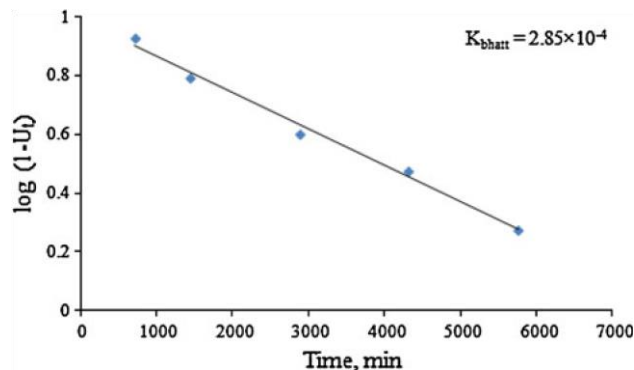


Fig. 6 Plot of %E of $^{90}\text{Y}(\text{III})$ versus HCl concentrations (1.09×10^{-5} – 1.0 mol L^{-1}) onto zirconium vanadate ion-exchange at 298 and 333 K does not pass through the origin revealing that particle diffusion mechanism is not the only process responsible for the kinetics of ^{90}Y sorption. The sorption of ^{90}Y is most likely involves three steps: bulk transport of ^{90}Y in solution, film transfer involving diffusion of ^{90}Y within the pore volume of Zr-V and/or along the wall surface to the active sorption sites of the sorbent, and finally formation of complex species of $^{90}\text{Y}(\text{III})$ onto the sorbent. The actual sorption of ^{90}Y onto the interior surface is rapid and hence it is not the rate determining step in the sorption process leaving film and intraparticle transport the two main steps controlling sorption. This means that “solvent extraction” or “weak base anion ionexchanger” is not the most probable participating mechanisms. Thus, other processes such as surface area and specific sites on the sorbent are possibly involved simultaneously in the retention step of ^{90}Y [48].

Thermodynamic characteristics of Y retention

The sorption of Y was studied over wide range of temperatures (298–333 K) to determine the nature of Y retention at the established experimental conditions. The thermodynamic parameters (ΔH , ΔS , and ΔG) can be calculated employing Eqs. (5) and (6).

$$\ln K_c \approx \frac{DH}{RT} + \frac{DS}{R} \quad (6)$$

$$DG \approx DH - TDS \quad (7)$$

K_c is the equilibrium constant depending on the fractional attainment (F_c) of the sorption process. K_c values of Y ions retention from test aqueous solutions onto Zr–V exchanger were calculated using Eq. (7)

$$K_c \approx \frac{F_c}{1 - F_c} \quad (8)$$

The plots of uptake percentage of Y sorption versus HCl concentrations (1.0×10^{-5} – 1.0 mol L^{-1}) at 25 and 60 C are demonstrated in Fig. 6. The extraction percentage of Y decreased on raising temperature from 25 to 60.0 C revealing the exothermic nature of the sorption process. The numerical values of DH, DS, and DG were calculated using Vant-Hoff equation:

$$\ln K_c \approx \frac{DH}{T} - \frac{DS}{RT} + \frac{2.303RT_1T_2}{T_1T_2} \quad (9)$$

where $K_c = D_1/D_2$, D_1 and D_2 are the distribution ratios of Y(III) retention at T_1 and T_2 , respectively. The average values of DG, DS and DH, calculated using Eq. (8) were found in the range -2.1 to $-2.4 \text{ kJ mol}^{-1}\text{K}^{-1}$, -3.5 to $3.90 \text{ J mol}^{-1}\text{K}^{-1}$ and -3.6 kJ mol^{-1} , respectively with correlation factors in the range 0.995–0.998. The negative value of DH and the data of D and K_c reflect the exothermic nature of Y uptake by the sorbent and non-electrostatic bond formation between the adsorbent and Y. The negative value of DS proves that Y uptake takes place in a random fashion and may be also indicative of moderated sorption process. The DS of activation were also lower than TDS at 298 and 333 K indicating that the reorientation step is entropy controlled at the activation state.

When the temperature was increased from 298 to 333 K, the value of DG shifted from -3.9 to $-3.5 \text{ kJ mol}^{-1}\text{K}^{-1}$, indicating that, the sorption process is spontaneous and the retention process is more favorable at low temperature. Temperature increase may affect the physical structure of the sorbent weakening the strength of intermolecular interactions between the Zr–V membrane and Y(III) species. The membrane matrix could become more unstructured affecting the ability of polar segments to be engaged by forming stable hydrogen bonding with Y(III) species. The energy of the active sites of the Zr–V sorbent provided by increasing the temperature minimizes the interaction between the active sites of the sorbent towards Y(III) resulting in a lower sorption related to

“Solvent extraction” in agreement with data for polyurethane foams [43, 44].

The obtainable results suggest the use of Zr–V sorbent in column mode for extraction and separation of Y(III) from coexisting strontium and/or rubidium. In fact the validation of the developed procedures was primarily tested by separation of ^{90}Y from ^{89}Sr and/or Rb species in their aqueous HCl ($1.0 \times 10^{-5} \text{ mol L}^{-1}$) solution mixtures by Zr–V sorbent packed column. Complete retention of ^{90}Y

was achieved, while Sr and Rb were not sorbed at all as indicated from the analysis of ^{90}Y and ^{89}Sr activity and Rb by AAS at 780.02 nm in the effluent solution. The retained ^{90}Y

was recovered quantitatively by elution with the eluting agent HNO_3 (1.0 mol dm^{-3}) from Zr–V packed column (10 cm, 0.6 mm i.d) as indicated in the elution curve (Fig. 7). A satisfactory recovery percentage of $99.7 \pm 3.1 \%$ of ^{90}Y ions was achieved.

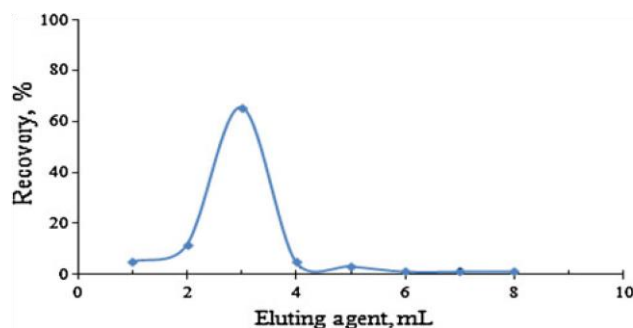


Fig. 7 Elution curve for Y on a Zr–V inorganic ion exchange packed column of 10 cm bed height at room temperature using nitric acid (10.0 mL , 1.0 mol L^{-1}) as eluting agent at flow rate of 1.0 mL min^{-1}

Conclusion

The prepared solid gel Zr–V ion-exchanger showed excellent chemical stability in mineral acids (HCl, HNO_3) and salts, (NaCl and NaNO_3) solutions at concentrations up to 2.0 M. The exchanger provides good selectivity for separation of ^{90}Y from ^{89}Sr in their matrices. The intraparticle diffusion and the first order model of ^{90}Y retention onto Zr–V solid sorbent are confirmed from the kinetic data. The retention process of Y is spontaneous and more favorable at low temperature. Moreover, on raising the temperature, the physical structure of the sorbent membrane may be changing, thus affecting the strength of the intermolecular interactions between the Zr–V sorbent membrane and Y species. The interaction between the active sites of the sorbent towards Y(III) resulting in a lower

sorption related to “Solvent extraction” in agreement with data for polyurethane foams [42, 43]. However, work is still continuing for: (i) fully characterization of the ion-exchanger in terms of textural specific area, pore volume, ion exchange capacity and comparison with other ionexchangers and (ii) developing a Zr–V sorbent packed column mode for selective separation and complete in aqueous media.

References

- Qaim SM (2001) Therapeutic radionuclides and nuclear data. *Radiochim Acta* 89(4–5):297–302
- Kampen WU, Voth M, Pinkert J, Krause A (2007) Therapeutic status of radiosynoviorthesis of the knee with yttrium [90Y] colloid in rheumatoid arthritis and related indications. *Rheumatology (Oxford)* 46(1):16–24
- Wike JS, Guyer CE, Ramey DW, Phillips BP (1990) Chemistry for commercial scale production of yttrium-90 for medical research. *Int J Radiat Appl Instrum A* 41(9):861–865
- Knapp FF Jr, Mirzadeh S (1994) The continuing important role of radionuclide generator systems for nuclear medicine. *Eur J Nucl Med* 21(10):1151–1165
- Wang SJ, Lin WY, Lui WY, Chen MN, Tsai ZT, Ting G (1996) Hepatic artery injection of yttrium-90-lipiodol: biodistribution in rats with hepatoma. *J Nucl Med* 37(2):332–335 (Official Publication, Society of Nuclear Medicine)
- DeNardo SJ, Kramer EL, O'Donnell RT, Richman CM, Salako QA, Shen S, Noz M, Glenn SD, Ceriani RL, DeNardo GL (1997) Radioimmunotherapy for breast cancer using indium-111/ yttrium-90 BrE-3: results of a phase I clinical trial. *J Nucl Med* 38(8):1180–1185 (Official Publication, Society of Nuclear Medicine)
- Theuer CP, Leigh BR, Multani PS, Allen RS, Liang BC (2004) Radioimmunotherapy of non-Hodgkin's lymphoma: clinical development of the Zevalin regimen. *Biotechnol Annu Rev* 10:265–295
- Bonardi ML, Martano L, Groppi F, Chinol M (2009) Rapid determination of (90)Sr impurities in freshly “generator eluted” (90)Y for radiopharmaceutical preparation. *Appl Radiat Isot* 67(10):1874–1877
- Chakravarty R, Pandey U, Manolkar RB, Dash A, Venkatesh M, Pillai MR (2008) Development of an electrochemical 90 Sr–90 Y generator for separation of 90 Y suitable for targeted therapy. *Nucl Med Biol* 35(2):245–253
- Castillo AX, Perez-Malo M, Isaac-Olive K, Mukhallalati H, Gonzalez EC, Berdeguez MT, Diaz NC (2010) Production of large quantities of 90Y by ion-exchange chromatography using an organic resin and a chelating agent. *Nucl Med Biol* 37(8):935–942
- Chinol M, Hnatowich DJ (1987) Generator-produced yttrium-90 for radioimmunotherapy. *J Nucl Med* 28(9):1465–1470 (Official Publication, Society of Nuclear Medicine)
- Bray LA, Wheelwright EJ, Western DW, Carson KJ, Elovich RJ, Shade EH, Alexander DL, Culley GE, Atkin SD (1992) Production of ⁹⁰Y at Hanford. *Radioact Radiochem* 3:22–25
- Hsieha BT, Tinga G, Hsieha HT, Shen LH (1993) Preparation of carrier-free yttrium-90 for medical applications by solvent extraction chromatography. *Appl Radiat Isot* 44(12):1473–1480
- Chuang JT, Lo JG (1996) Extraction chromatographic separation of carrier-free yttrium-90 from strontium-90/yttrium-90 generator by crown ether-coated silica gels. *J Radioanal Nucl Chem* 204(1): 83–93
- Cheng Z, Li M, Cao Z, Yang W, Shengting Z (1995) Studies on the preparation of medical ⁹⁰Y generator
- Dutta S, Mohapatra PK, Manchanda VK (2011) Separation of ⁹⁰Y from ⁹⁰Sr by a solvent extraction method using N,N,N',N'-tetraoctyl diglycolamide (TODGA) as the extractant. *Appl Radiat Isot* 69(1):158–162
- Dutta S, Mohapatra PK, Raut DR, Manchanda VK (2011) Preferential extraction of ⁹⁰Y from ⁹⁰Sr using N,N,N',N'-tetra-2ethylhexyl diglycolamide (T2EHDGA) as the extractant. *J Radioanal Nucl Chem* 288:389–394
- Achuthan PV, Dharmi PS, Kannan R, Gopalakrishnan V, Ramanujam A (2000) Separation of carrier-free ⁹⁰Y from high level waste by extraction chromatographic technique using 2-ethylhexyl-2-ethylhexyl phosphonic Acid (KSM-17). *Sep Sci Technol* 35(2):261–270
- Malja S, Schomacker K, Malja E (2000) Preparation of ⁹⁰Y by the ⁹⁰Sr-⁹⁰Y generator for medical purpose. *J Radioanal Nucl Chem* 245(2):403–406
- Lewis RE, Fu-Min S, Lane TA, Olewine KR, Holton PS (2004) Method and apparatus for separating ions of metallic elements in aqueous solution
- Li W, Wang X, Meng S, Li D, Xiong Y (2007) Extraction and separation of yttrium from the rare earths with sec-octylphenoxy acetic acid in chloride media. *Sep Purif Technol* 54(2):164–169
- Sylvester P (2005) Ion exchange materials for the separation of ⁹⁰Y from ⁹⁰Sr. USA Patent
- Castillo AX (2006) Development of a reproducible methodology for the production of ⁹⁰Y from ⁹⁰Sr/⁹⁰Y chromatographic generator. Development of generator technologies for therapeutic radionuclides. European Institute of Oncology, Milan
- Chinol M (2006) New designed ⁹⁰Sr/⁹⁰Y generator and ⁹⁰Sr breakthrough determination. Development of generator technologies for therapeutic radionuclides. European Institute of Oncology, Milan
- Chuvilin DY, Khvostionov VE, Markovskij DV, Pavshook VA, Ponomarev-Stepnoy NN, Udovenko AN, Shatrov AV, Vereschagin YI, Rice J, Tome LA (2007) Production of ⁸⁹Sr in solution reactor. *Appl Radiat Isot* 65(10):1087–1094
- Aardaneh K, Saal D, Swarts G, Dewindt SC (2008) TBP and TBP impregnated amberlite XAD-4 resin for radiochemical separation of ⁸⁸Y from Sr and Al. *J Radioanal Nucl Chem* 275(3):665–669
- Cao J-G, Gu P, Zhao J, Zhang D, Deng Y (2010) Removal of strontium from an aqueous solution using co-precipitation followed by microfiltration (CPMF). *J Radioanal Nucl Chem* 285:539–546
- Grahek Z, Ivsic A-G, Krljan N, Nodilo M (2011) Separation of Sr combination of ion exchange and Sr resin with alcohol–nitric acid solution and rapid determination of ⁹⁰Sr in wine and soil samples. *J Radioanal Nucl Chem* 289(2):437–449

29. Sherrod L, Maxwell III, Culligan B-K, Noyes G-N (2010) Rapid separation of actinides and radiostrontium in vegetation samples. *J Radioanal Nucl Chem* 286:273–282
30. Vanura P, Makrlik E (2006) Mathematical modeling of separation of microamounts of strontium from yttrium in the water–HCl–15-crown-5-hydrogendicarbolylcobaltate extraction system. *J Radioanal Nucl Chem* 268(2):437–439
31. Makrlik E, Vanura P (2008) Mathematical modeling of separation of microamounts of strontium from yttrium in the water–HCl–15-crown-5-hydrogendicarbolylcobaltate extraction system. *J Radioanal Nucl Chem* 275(3):673–675
32. Groska J, Molnar Z, Bokori E, Vajda N (2011) Simultaneous determination of ^{89}Sr and ^{90}Sr : comparison of methods and calculation techniques. *J Radioanal Nucl Chem* 287(2):459–467
33. Hui-Bo G, Hong-Sheng B, Xiao-Hai J, Wei Y, Lian-Ge H, Hong-Qiang F (2006) Preparation of a new kind of inorganic adsorbent for ^{90}Y . Development of generator technologies for therapeutic radionuclides. European Institute of Oncology, Milan
34. Dhara S, Sarkar S, Basu S, Chattopadhyay P (2009) Separation of the ^{90}Sr – ^{90}Y pair with cerium(IV) iodotungstate cation exchanger. *Appl Radiat Isot* 67(4):530–534
35. Roy K, Mohapatra PK, Rawat N, Pal DK, Basu S, Manchanda VK (2004) Separation of ^{90}Y from ^{90}Sr using zirconium vanadate as the ion exchanger. *Appl Radiat Isot* 60(5):621–624
36. Marczenko M (1986) Separation and spectrophotometric determination of elements. Wiley, New York
37. El-Shahawi MS, Hamza A, Al-Sibaai AA, Al-Saidi HM (2011) Fast and selective removal of trace concentrations of bismuth(III) from water onto procaine hydrochloride loaded polyurethane foams sorbent: kinetics and thermodynamics of bismuth(III) study. *Chem Eng J* 173(1):29–35
38. Dimova N, Burnett WC, Horwitz EP, Lane-Smith D (2007) Automated measurement of ^{224}Ra and ^{226}Ra in water. *Appl Radiat Isot* 65(4):428–434
39. Nour S, El-Sharkawy A, Burnett WC, Horwitz EP (2004) Radium-228 determination of natural waters via concentration on manganese dioxide and separation using diphonix ion exchange resin. *Appl Radiat Isot* 61(6):1173–1178
40. Nakamoto K (1970) Infrared spectra of inorganic and coordination compounds, 2nd edn. Wiley, New York
41. Braun T, Navratil JD, Farag AB (1985) Polyurethane foam sorbents in separation science. CRC Press, Boca Raton, pp 132–133
42. Weber WJ, Morris JC (1963) Kinetics of adsorption on carbon from solution. *J Sanit Eng Div Am Soc Civ Eng* 89:31–60
43. Pala'gyi S, Braun T, Homonnay Z, Ve'rt'es A (1992) Mossbauer spectroscopic investigation of the sorption of iron by polyether type polyurethane-foam sorbents. *The Analyst* 117(10):1537–1541
44. El-Shahawi MS, Nassif HA (2003) Kinetics and retention characteristics of some nitrophenols onto polyurethane foams. *Anal Chim Acta* 487(2):249–259
45. Ma WX, Liu F, Li KA, Chen W, Tong SY (2000) Preconcentration, separation and determination of trace Hg(II) in environmental samples with aminopropylbenzoylazo-2-mercaptobenzothiazole bonded to silica gel. *Anal Chim Acta* 416(2):191–196
46. Bhattacharya AK, Venkobachar C (1984) Removal of cadmium(II) by low cost adsorbents. *J Environ Eng* 110(1):110–122
47. Reichenburg D (1953) Properties of ion exchange resins in relation to their structure III. Kinetics of exchange. *J Am Chem Soc* 75:589–597
48. Su Z-X, Pu Q-S, Luo X-Y, Chang X-J, Zhan G-Y, Ren F-Z (1995) Application of a macroporous resin containing imidazoline groups to preconcentration and separation of gold, platinum and palladium prior to ICP-AES determination. *Talanta* 42(8): 1127–1133



Full paper/Mémoire

Synthesis and voltammetric study of some new macrocyclic sulfur compounds for use as chelating agents for separation of arsenic(III) in wastewater and as molluscicidal agents against *Biomphalaria Alexandrina* Snails

M.S.T. Makki *, R.M. Abdel-Rahman, M.S. El-Shahawi ¹

Department of Chemistry, Faculty of Science, King Abdulaziz University, P.O. Box 80203, 21589 Jeddah, Kingdom of Saudi Arabia

ARTICLE INFO

ABSTRACT

Article history:

Received 11 May 2011

Accepted after revision 3 May 2012

Available online 29 June 2012

Keywords:

Nanomeric sulfur compounds

Molluscicidal activity

Voltammetry

Removal of arsenic

Wastewater

A series of some new nanomeric molecules of cyclic 5-methoxy-5,6-diaryl-4,5-dihydro-2H-1,2,4-triazin-3-thiones (1–3) has been synthesized. The interaction of compounds 1–3 with HgCl_2 in 1:1 and 1:2 molar ratios was used for the synthesis of the macrocyclic Schiff base [5,6,11,12-tetraaryl-1,2,4,7,8,10-hexa-aza cyclododeca-4,6,10,12-tetraene-3,9-dithione] (4), macrocyclic thioethers 5 and/or complex 6. Chemical structures of the compounds were determined from elemental analysis and spectral measurements. The compounds were screened as molluscicidal agents against *Biomphalaria Alexandrina* snails which cause Bilharziasis. Cyclic voltammetry of selected compounds showed well-defined irreversible electrode couple suggesting application of these compounds as chelating agents for separation of arsenic in industrial wastewater samples. Compound 1 was physically immobilized on polyurethane foams (PUFs) and was successfully used for complete removal of arsenic (III) & (V) species from wastewater.

2012 Académie des sciences. Published by Elsevier Masson SAS. All rights reserved.

1. Introduction

Synthesis of macrocyclic molecules and their applications as chelating agents for separation and/or determination of toxic metal ions have been reported [1–4]. These systems also possess bacteriostatic properties *in vitro* and facilitate the iron mobilization from Fe labeled reticu-

locytes [5]. Nanomers, e.g. macrocyclic ligands allow selective complexation and extraction of metallic cations and anions of environmental importance [6–11].

Recently, nanomeric molecules and macrocyclic transition metal complexes in which structural changes have made to the basic crown ethers in an attempt to enhance the selectivity of such class of compounds towards metal

ions and catalysis [12–14]. Crown ethers of Schiff bases and their complexes (Fig. 1) have great potential to generate novel metabolites and act as fungitoxic than free ligands [14]. These compounds could also be used as selective agents for the maintenance of animal or human health from infections [15–17].

Nanomeric systems as strain allowed have been synthesized from heterocyclization of aryl-1,3-dicarboxaldehyde with 2-acetylpyridine in ethanolic sodium hydroxide. The resultant compound was refluxed with ammonium acetate-glacial acetic acid afforded 1,3-biscompound 1 [17]. Reaction of compound 1 with $\text{RuCl}_3 \cdot x\text{H}_2\text{O}$ in successive steps has produced a type of nanomer (Fig. 2) [17].

The compounds 3-thioxo-1,2,4-triazines and their macrocyclic Schiff bases have great importance as

*Corresponding author.

E-mail address: mmakki@kau.edu.sa (M.S.T. Makki). Permanent address:
Department of Chemistry, Faculty of Science at

medicinal and pharmacological agents [18–21]. Blanco et al., 2002 [22] have reported the nanomers derived from thiosemicarbazide and acyclic bicarbonyl compounds.

Therefore, the present article is focused on:

Damiatta, Mansoura University, Mansoura, Egypt.

1631-0748/\$ – see front matter 2012 Académie des sciences. Published by Elsevier Masson SAS. All rights reserved.
<http://dx.doi.org/10.1016/j.crci.2012.05.004>

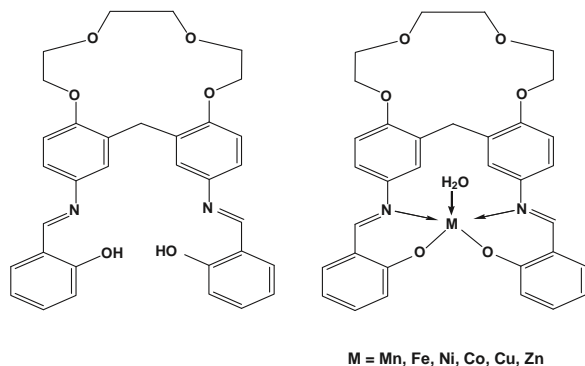


Fig. 1. Macrocyclic transition metal complexes.

synthesis of some new nanomeric sulfur compounds derived from thiosemicarbazide and acyclic bicarbonyl

compounds;

testing their toxicity properties as molluscicidal agents against

Biomphalaria alexandrina snails;

studying the redox behavior of selected compounds for use as chelating agents in stripping voltametric analysis of arsenic;

application of compound 1 for separation of arsenic (III) & (V) species from industrial wastewater.

2. Results and discussion

2.1. Chemistry

In continuation to our previous work on the preparation of sulfur organic compounds [18–21] to be used as excellent biocidal reagents, the present investigation reports the preparation and spectroscopic characterization of macromolecules as nanomer systems to be used as molluscicidal agents against *Biomphalaria alexandrina* snails responsible for bilharzias. Thus, treatment of methanolic acyclic 1,2-bicarbonyl compounds such as benzil, 4,4'-dimethoxybenzil and 4,4'-difluorobenzil with methanolic thiosemicarbazide in hot concentrated HCl with stirring afforded 5-methoxy-5,6-diaryl-4,5-dihydro-1,2,4-triazine-3-thiones (1-3) (Scheme 1). The compounds were characterized by elemental analysis and spectral measurements.

IR spectra of compound 1 in solid state and in chloroform showed the disappearance of NH and/or SH groups in the solution suggesting formation of a type of oxidation and/or complex formation products on treatment with HgCl_2 . Structure of compound 1 was deduced from elemental analysis and spectral data as given below:

UV absorption spectrum in DMF recorded I_{max} at 325, 280 and 210 nm assigned to $\pi \rightarrow \pi^*$ and $n \rightarrow \pi^*$ transitions;

IR spectrum showed characteristic bands at IR: ν cm^{-1}

3180 (NH), 2946 and 2835 (aliphatic CH), 1488 and 1446 (deformation of CH), 1056 (C-O-Me), 976 and 886 cm^{-1}

(phenyl groups);

Mass spectrometry recorded the molecular ion M^+ at m/z

298 (12.5), $M+1$ at 299 (3.8) with base peak at m/z 77 (Scheme 2).

Treating 5-methoxy-5,6-diaryl-4,5-dihydro-2H-1,2,4-triazine-3-thiones (1-3) with HgCl_2 in methanol at 1:2 molar ratio at room temperature under stirring, produced a type of macrocyclic thioether Schiff base 4

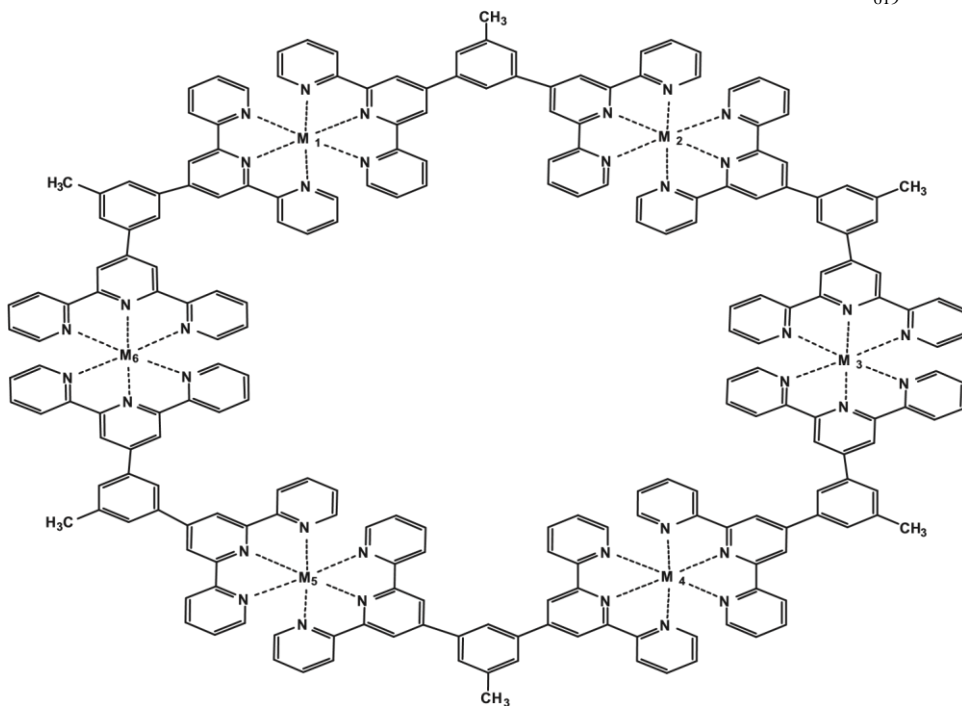
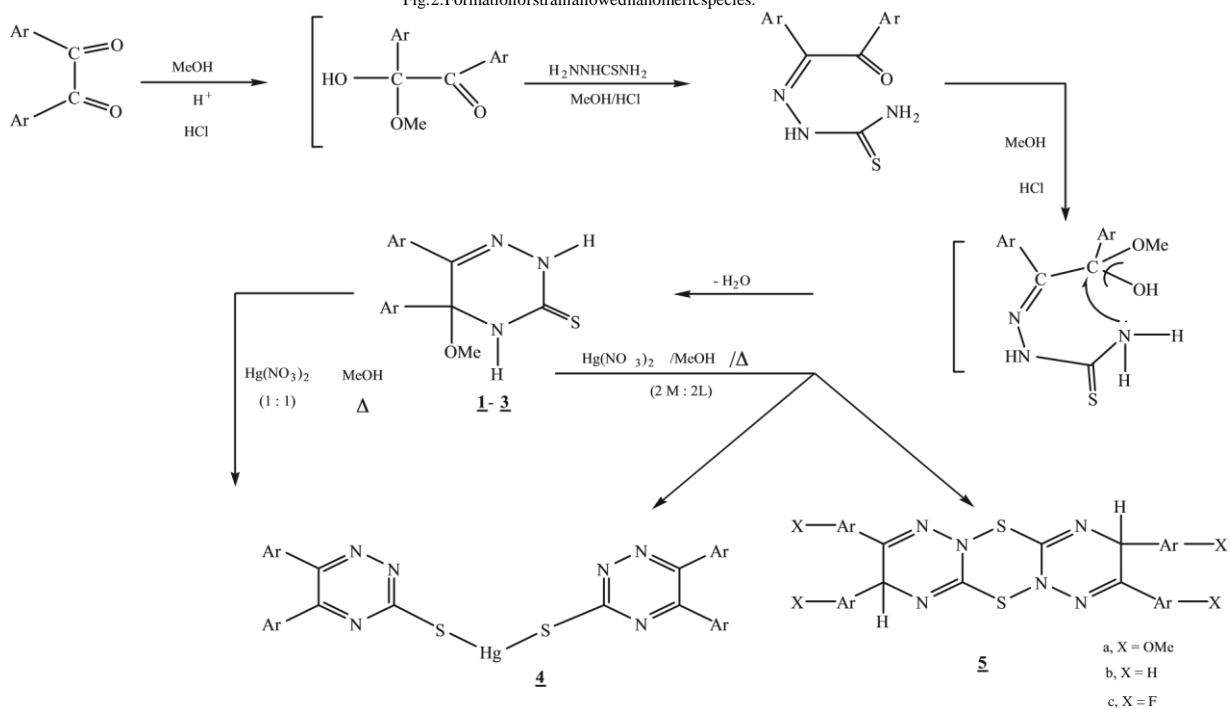
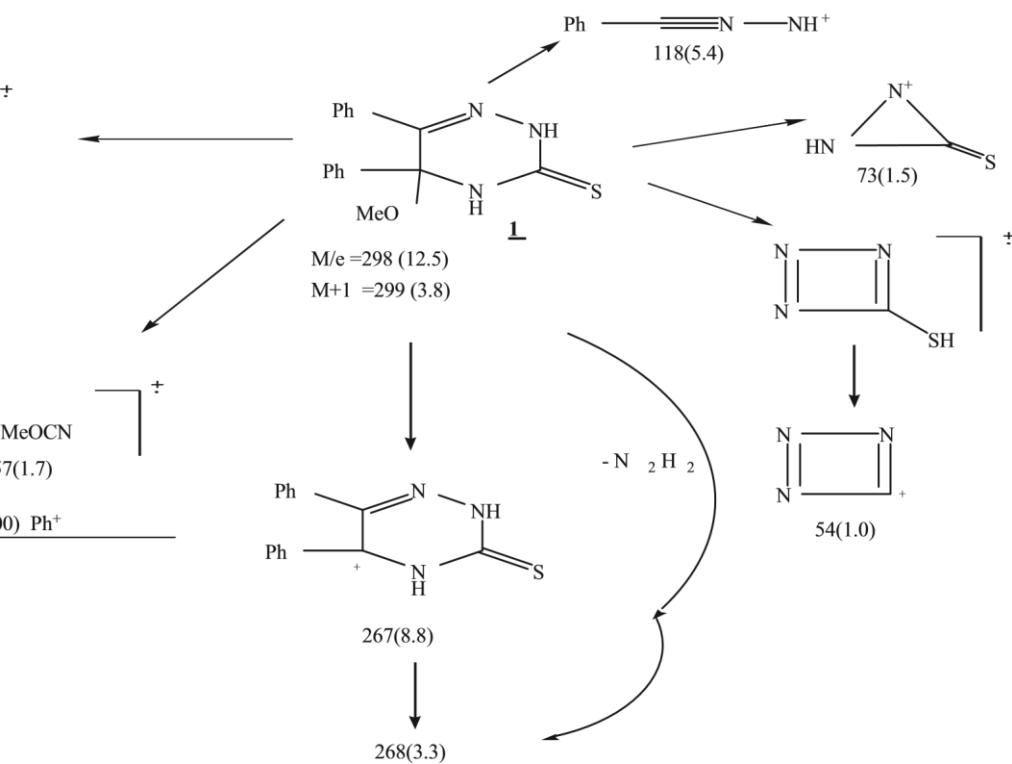


Fig.2. Formation of strain allowed nanomeric species.



Scheme 1. Formation of 1–5.

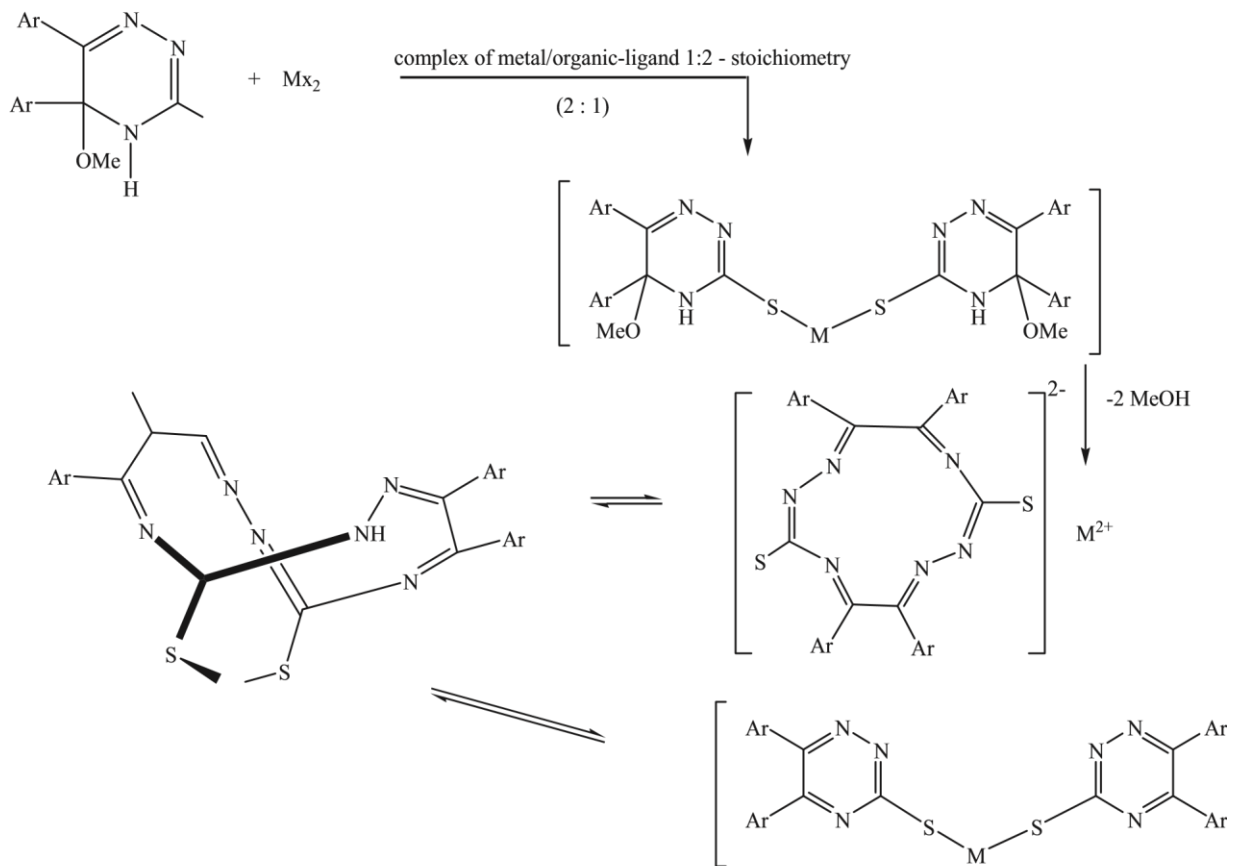


Scheme 2. Mass fragmentation of compound 1.

as [5,6,11,12-tetraaryl-1,2,4,7,8,10-hexa-aza-cyclododeca-4,6,10,12-tetraene-3,9-dithione] (Scheme 3).

Mass spectrum of compound 4 showed two peaks which are assigned to $[\text{C}_{34}\text{H}_{28}\text{N}_6\text{S}_2\text{O}_4]\text{Hg}$ fragment and to the molecular ion of selective

ligand $\text{C}_{34}\text{H}_{28}\text{N}_6\text{S}_2\text{O}_4$, respectively. IR spectrum of $[\text{Hg}(\text{ligand})_3(\text{Cl})_2]$ recorded lack of both NH and SH functional groups, suggesting hydrogen bonding between the ligand molecules in the



SH

Ar

M 1 formed complex. H NMR spectra of the isolated complex 8.8 and 8.5 ppm afforded to four NH with a

signals due to

species showed the absence of amine nitrogen's and OMe aromatic protons at 7-7.3, 7.5-7.7 in addition at 3.45 ppm groups through complexation. C NMR spectrum of the 3.25 ppm of 4-OMe. On the other hand, compounds 1-3

formed complex also showed lacks of carbons of OCH₃ and with HgCl₂ gave the corresponding complexes of metal two imino carbons confirming the proposed structure. ligand in 1:2 stoichiometry.

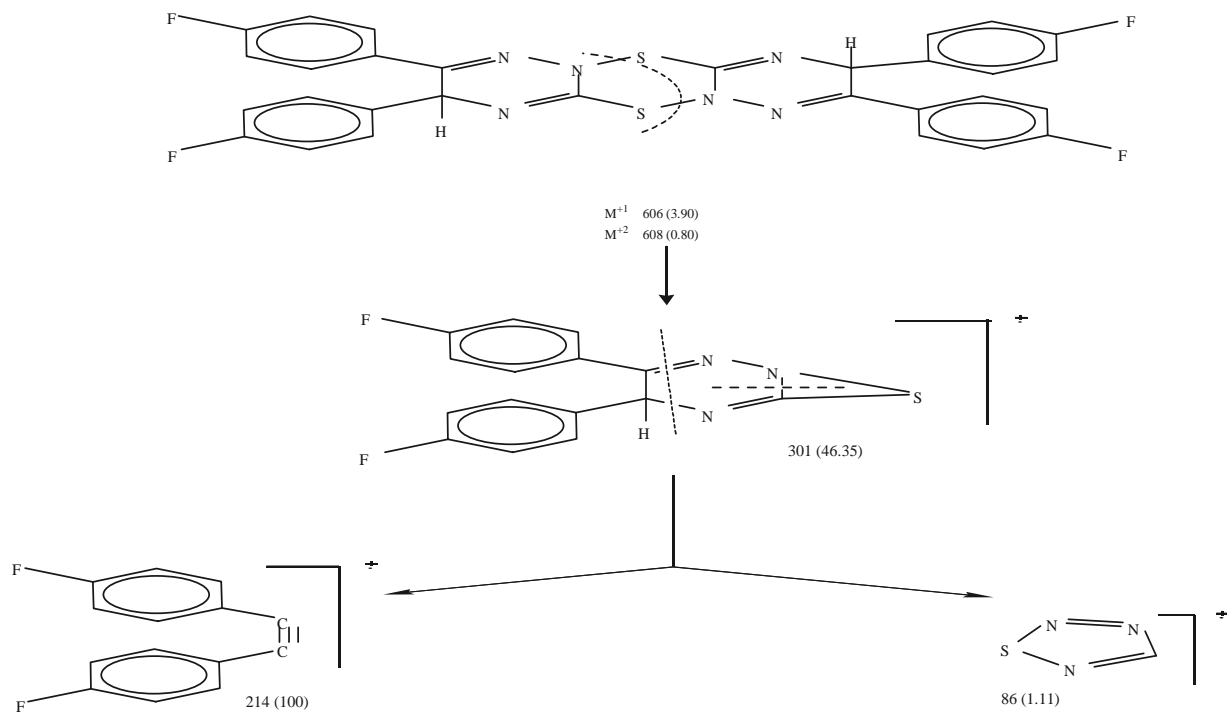
On treatment compounds 1-3 with HgCl₂ in 1:1 molar ratios in methanol at room temperature, compounds 5a-c 2.2. Molluscicidal activity were isolated. Formation of these compounds may take place via simple oxidation through mercuric ions. IR Based upon the earlier work by Ali et al. [23] on the spectrum of compound 5c showed lacks of both NH and SH synthesis of phosphono-3-substituted-5,6-diphenyl functional groups as well as M/z recorded M+2, M+1 and 1,2,4-triazine derivatives and their molluscicidal activities + M at 608, 606 and 602 with a base peak at 214 (Scheme 4). against Biomophalaria Alexandrina Snails responsible for

It is interesting to note that, on treating compound 3 Bilharziasis diseases, the prepared compounds were tested with HgCl₂ in 1:1 molar ratio in methanol and stirring at room temperature, bis(5,6-diaryl-5-methoxy-2,4-dihydro-1,2,4-triazin-3-thiato)mercury was separated out as Sohistosomamausoni in Giza Governorate that was not solid complex 6, while complex 5c was soluble in the treated with molluscicides. The snails were adapted to filtrate. A possible mechanism of formation of the complex laboratory conditions for two weeks before being used in 6 was suggested via addition of metal salts on C₃=N₄ of toxicity tests to be sure that the snails are strong and 1,2,4-triazine (Scheme 5), while complex 5c was formed healthy. Snails were kept in plastic aquaria filled with de
oxidation of mercapto group followed by elimination of chlorinated tap water at room temperature (25–27 °C).
via

methanol molecules. IR spectrum of compound 6 recorded Stock solutions (500 mg mL⁻¹) of the tested compounds

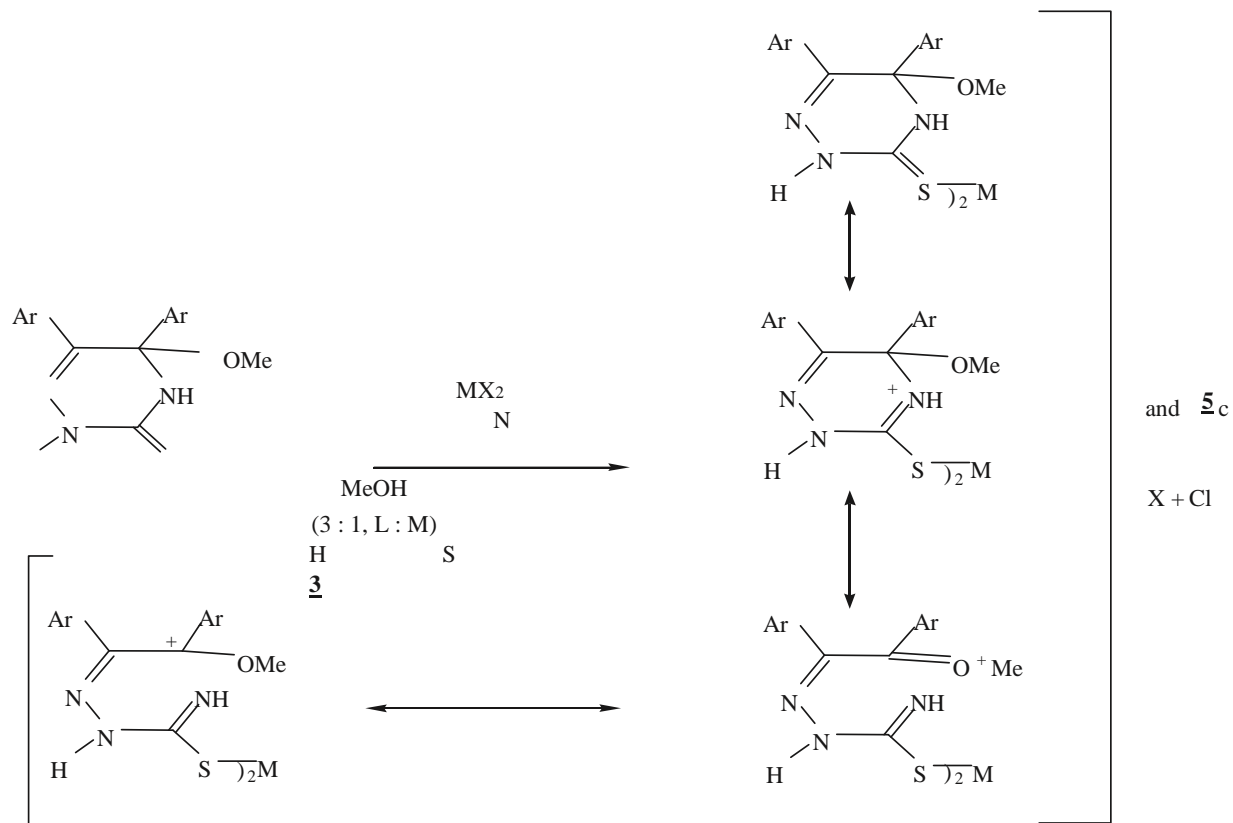
peaks at ν cm⁻¹ 3210, 3165 cm⁻¹ of two NH, in addition at were prepared in the least volume of ethanol and

1507, 1372, 1158 and 1039 cm⁻¹ due to presence of completed to the required volume with de-chlorinated tap water on the basis of weight/volume. A series of more thiocarbamide, -C-OMe functional groups. H NMR spectrum in DMSO recorded resonated signals at: δ : 12.5, 10.7, diluted solutions were then prepared following the



Scheme 4. Mass fragmentation pattern of compound 5c.

$\underline{5c}$, M^+ 602 (5.15)



Scheme 5. Mechanism of formation of compound 6 from 3.

Table 1
The Molluscicidal activity of the prepared systems.

Compound N°			Mortality of Snails at various concentrations, ppm		
1			50		100
2			20	100	
3			50	100	
	4a	40	40	100	
			80	4a	70
5b			30		100
Reference standard, Baylucide			100		100

instructions given by WHO organization [24,25]. The results given in Table 1 revealed high activity towards snails and the following sequences:

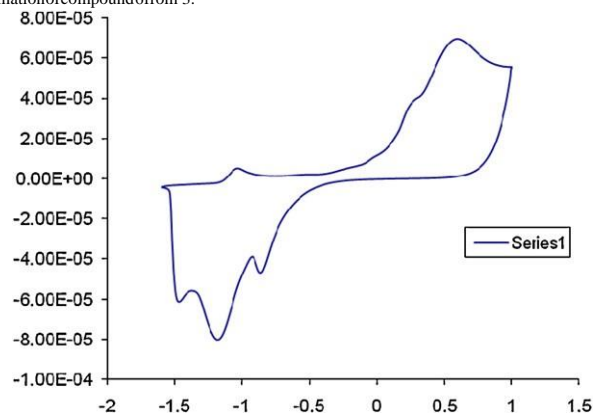
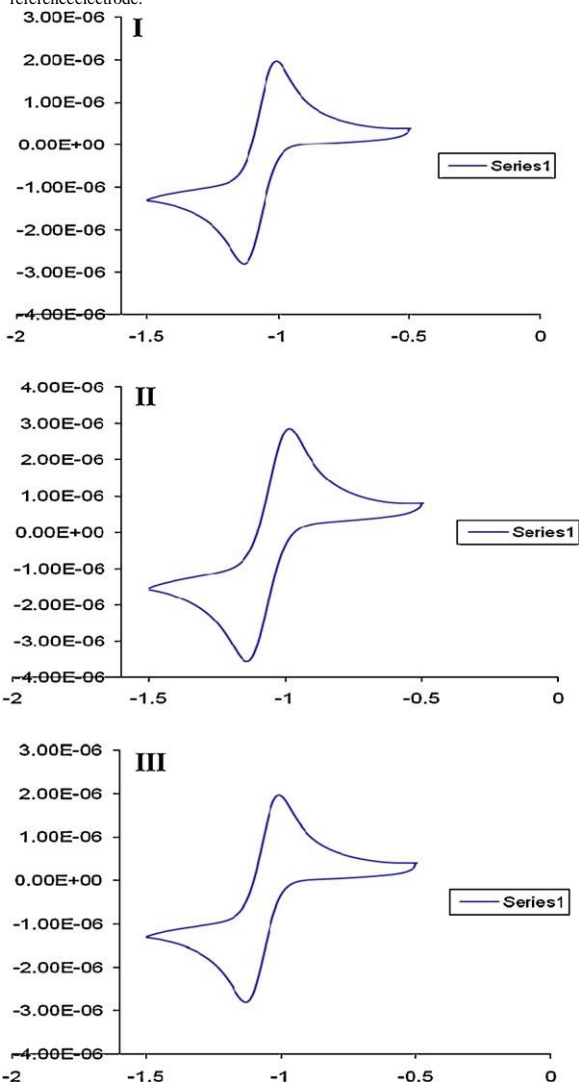
$4a > 5b > 5a$ and $3 > 2 > 1$ were achieved. Total electron barrier of molecular distribution of the evaluated systems led to inhibition of enzymatic effect on the living processes for the tested Snails thereby causing break of a vital-cyclic of snails. The presence of Hg and/or F atoms in system 4 enhanced the toxicity and a deposition of protein $2+$ in the vital-cell of snails. The fact that Hg ions are most

likely able to react with protein containing sulfur forming stable chelate causing deposition of the vital-cell of the snails.

2.3. Voltammetric behavior

Compounds 1 and 4 were selected for cyclic voltammetric studies as representative for organic macromolecule 1 and its mercuric (II) complex. The choice of the two compounds was based upon the influence of mercury (II) on the redox characteristic of the resulting species. The CVs of compound 1 in DMF–tetramethylammonium chloride (TMA⁺.Cl) as supporting electrolyte at Pt working electrode vs. Ag/AgCl reference electrode at various scan rates are demonstrated in Fig. 3. Two well-defined anodic peaks at -1.0 and $+0.75$ V coupled with two cathodic peaks at -1.25 and -0.75 V were noticed. An ill-defined anodic peak at -0.55 V was also noticed at 100 mV s⁻¹ (Fig. 3)

suggesting the irreversible nature of the observed electrode couples. On increasing the scan rates from 100 to

Fig. 3. CVs of compound 1 at 100 mV s⁻¹ in the potential window -1.5 to $+1.5$ V vs. Ag/AgCl reference electrode.Fig. 4. CVs of compound 1 at 50 (I), 100 (II) and 1000 (III) mV/s 500 mV s⁻¹ in the potential window -2 to 0.0 V vs. Ag/AgCl electrode.

1000 mV s⁻¹, the cathodic and anodic peaks were shifted

cathodically and anodically, respectively (Fig. 4). These results confirmed the irreversible nature of the electrode couples [26,27]. Continuous scan of the CV significantly decreased the peak current and the signal was hardly discernible from the baseline, indicating passivity of the surface of the Pt working electrode via formation of polymeric oxidation product or fouling of the electrode by the reduction products.

The CVs of compound 4a in DMF-TMA+Cl at various scan rates (Fig. 5) showed one well-defined cathodic and anodic peaks in the range 1.2–0.8 V with peak–peak potential separation (60 mV) suggesting reversible electrochemical process [26]. The plot of anodic (at -0.91 V) or cathodic (-0.97 V) peak current vs. square root of the scan rate increased linearly on increasing the scan rate, indicating that, the electrochemical reduction process is diffusion controlled electro-chemical process [26,27]. The

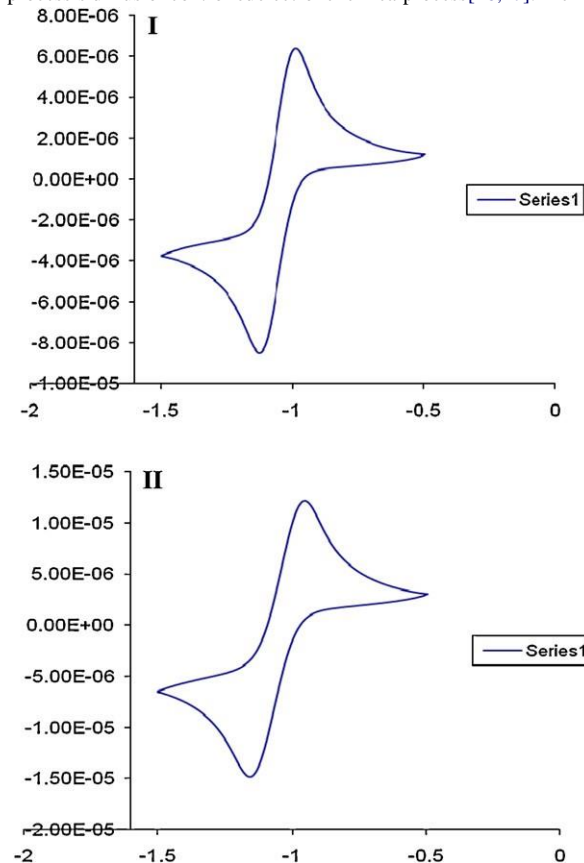


Fig. 5. CVs of compound 4a at 50 (I) and 200 (II) mV s⁻¹ V vs. Ag/AgCl electrode.

plot of the cathodic peak potential vs. log scan rate was also linear on raising the scan rate. The current function (i_p , c/v^{α}) decreased on raising the square root of the scan rate continuously. Thus, the first reduction processes of the compound preceded according to the well-known electrode-coupled chemical reaction mechanism of type EC [26,27]. These results suggested the possible use of compound 1 and its derivatives as complexing agent in stripping voltammetric determination and also in solid phase extraction for separation of arsenic (III, V) ions in industrial water.

2.4. Retention profile of arsenic (III) by reagent 1 immobilized polyurethane foams

Polyurethane foams (PUFs) sorbent represent one of the most effective solid sorbent due to its high available surface area, aerodynamic, cellular and membrane structure and extremely low cost [28,29]. A recent literature survey revealed no data on the use of compound 1 or its derivatives as chelating agents for metal separation and/or determination in different matrices. Thus, considerable attention was focused on preconcentration of trace and ultratrace concentrations of arsenic (III) ions in water by compound 1 physically immobilized onto PUFs prior its determination by inductively coupled plasma-optical

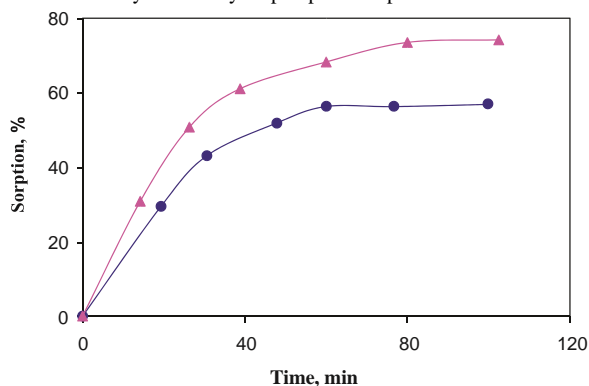


Fig. 6. Influence of shaking time on arsenic (III) sorption from aqueous solution onto the unloaded (-) and compound 1 immobilized (-) PUFs from aqueous solutions of pH 3-4.

emission spectrometry (ICP-OES). Preliminary investigation revealed considerable retention of arsenic (III) species onto compound 1 treated PUFs). Therefore, the influence of shaking time, pH and acidity on arsenic (III) uptake by PUFs was investigated. The sorption profile of an aqueous solution of arsenic (yyy) at pH 3 by untreated PUFs and compound 1 loaded PUFs at room temperature was studied. Arsenic (yyy) in the aqueous phase after equilibrium was determined by ICP-MS. The extraction percentage (%E) and the distribution ratio (D) of arsenic (yyy) reached maximum within 90 minutes (Fig. 6). Thus, a shaking time of 90 min was adopted in the subsequent work.

The sorption profile of arsenic (III) ions at 10.0 mg mL⁻¹

concentration level from the aqueous solutions (50 mL) at different pH by the immobilized PUFs (0.20.01 g) was investigated after 90 min shaking time. The sorption profile of arsenic (III) by the immobilized PUFs decreased on increasing the solution pH and maximum sorption percentage was achieved at pH 3. At pH > 3, the decrease in the uptake of arsenic (III) by the loaded PUFs is most likely due to the instability or the hydrolysis of the produced complex species formed between arsenic (III) and the reagent immobilized PUFs. The retention of arsenic (yyy) in pH 2-3 is most likely attributed to the protonation of the ether (

CH₂ OH CH₂) and/or urethane linkages group (-NH₂ COO-) available in the PUFs sorbent membrane. Thus, the retention of analyte proceeded via "solvent extraction and/or weak base anion exchange mechanism" [28,29]. The K_a of

the protonated ether group (CH₂ OH⁺ CH₂)_{foam} and amide

group(-NH₂-COO-) foam are 3 and 6, respectively [28,29]. Thus, the uptake of arsenic(III) is easily proceeded via ether group of the PUFs than the protonated amide group of the PUFs.

2.5. Performance of the reagent I treated polyurethane foams packed column

The performance of compound 1 loaded PUFs packed column was determined via critical (CC) and breakthrough capacities (BC) [31,32]. The CC was defined as the amount of arsenic(III) that could be retained on the PUFs column at 2 mL min⁻¹ flow rate until the arsenic (III) was first

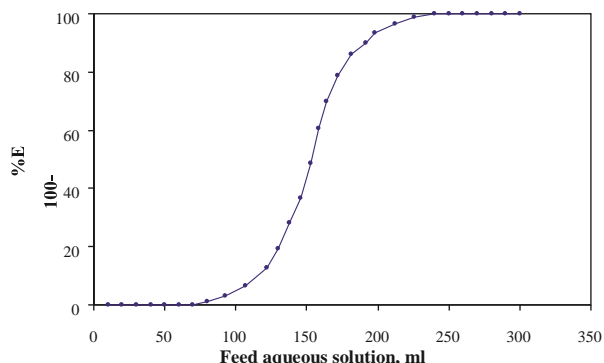


Fig. 7. Breakthrough curve of arsenic(III) uptake on compound 1 loaded PUFs (1.00.01 g) packed columns at 5.0 mL min⁻¹.

detected in the effluent. Practically, this value equal the actual volume of the effluent collected just before first appearance of arsenic (III) in the effluent minus the free column volume. The calculated values of CC and BC of arsenic(III) ions from the breakthrough (S-shaped) curve (Fig. 7) were found equal 0.55 and 0.88 mg g⁻¹ to be at a

flow rate of 2 mL min⁻¹ [28,29].

The reagent PUFs packed column was tested for retention and recovery of arsenic (III) from wastewater samples (1.0 L). The sample was spiked with arsenic (III) (5–10 mg) and percolated through PUF column at 2.0 mL min⁻¹ flow rate. Complete recovery of the retained

arsenic(III) species was achieved by percolating acetone (10 mL) at 2.0 mL min⁻¹ flow rate as indicated from the

ICP-OES analysis of arsenic before and after extraction. Arsenic(V) can also be preconcentrated by the developed treated PUFs packed column after reduction with SO₂ gas to arsenic(III) in water. 3. Experimental

3.1. Apparatus

The following apparatuses were afforded by the Chemistry Department, Faculty of Sciences, King Abdulaziz University. A Perkin Elmer (Lambda EZ-210) double beam spectrophotometer (190–1100 nm) with 1 cm (path width) quartz cell was used for recording the electronic spectra of the compounds. A Perkin Elmer model RXI-FTIR system 55529 was used for recording the IR spectra of the compounds. A Bruker advance DPX 400 MHz model using TMS as an internal standard was used for recording the ¹H NMR and ¹³C NMR spectra (Chemical shift in ppm) of

the compounds on deuterated DMSO. AGC-MS-QP1000Ex model was used for recording the mass spectra of the compounds. Melting points were determined with an electro thermal Bibby Stuart Scientific Melting Point SMPI (US). Molecular weights and C, H, N analysis of the compounds was performed on Micro analytical center, Cairo University, Egypt. Cyclic voltammetric measurements were carried out on a Metrohm 757 VA trace analyzer and 747 VA stand (Basel, Switzerland). A digital micro-pipette 10–100 mL (Volac) was used for transferring sample solutions to the electro-chemical cell. The data were recorded at room temperature and the peak current heights were measured using the “tangent fit method”.

3.2. Reagents and materials

Analytical chemicals and reagents grade quality were purchased from BDH chemicals. Low density polyethylene (LDPE) bottles, Nalgene were used for the collection of the different water samples. LDPE bottles and electrochemical cell were carefully cleaned first with hot detergent, soaked in 50% HCl (Analar), HNO₃ (2.0 mol IPP^{BB}), subse-

quently washed with dilute HCl (0.5 mol IPP^{BB}) and

finally rinsed with distilled water. The sample solution was stored in LDPE bottles and stored at -20°C. Stock solutions (0.1% w/v) of the reagent were prepared in the appropriate solvent. A stock BDH stock solution of metal ion to be analyzed (1.0 mg/mL) in dilute nitric acid was used. Commercial white sheets of open cell PUFs based polyether type were used as solid sorbent for the separation of the tested metal ions. The foam cubes were then washed with acetone in a Soxhlet extractor for 6 hours, and dried at 80°C in an oven for 2 hours. The dried foam cubes were then stored in dark low density polyethylene bottles.

3.3. Organic preparation

3.3.1.5-Methoxy-5,6-diaryl-4,5-dihydro-2H-1,2,4-triazine-3-thiones (1-3)

A solution of thiosemicarbazide (12.50 mmol) in dry methanol (150 mL) was added drop wise to a solution of benzil and 4,4-di(methoxy/fluoro) benzil (12.5 mmol) in absolute methanol with concentrated HCl (25 mL, 2 mol L⁻¹) with constant stirring for 8 hours. The solution

was left to cool overnight. The formed precipitates were filtered off, washed and dried to give 1-3, respectively. Compound 1 was crystallized from methanol as yellow

C. Analytical data: Found: 0 crystals. Yield = 75%, m.p. 190

C=64.39,H=4.99,N=13.98,S=10.53%;Calculatedfor

$C_{16}H_{15}N_3SO$:C=64.64,H=5.05,N=14.14,S=10.77%;m/z

298 (C H N SO +1, 35%) IR: cm^{-1} = 3184, 3131 (NH),

16 15
3
n
1

1608 (C = N), 1550, 846 (thioamide I & II). ^1H NMR (DMSO):

d: 12.0 (1 H, s, NH), 10.0 (1 H, s, NH), 7.5 (2 H, m, 5- H), 7.77.2 (8 H, m, diphenyl), 3.1 (3 H, s, OCH_3). Compound 2 was crystallized from methanol as yellow

0 crystals. Yield (65.2%), m.p. 183 -185 C. Analytical data:

Found: C = 59.49, H= 5.85, N = 11.74, S = 8.97%; Calculated for $C_{18}H_{19}N_3SO_3$:C=60.14,H=5.35,N=11.74,S=8.97%; m/z 359 (C H N SO +2, 15%) IR: n cm^{-1} = 3210, 3190

18 19 3 3

(NH), 1610 (C=N), 1560, 860 (thioamide I & II), 1050 (C-O-

Me). ^1H NMR (DMSO): d: 12.3, 10.8 (each 1 H, s, NH), 7.8 -

7.3 (8 H, m, aryl protons), 3.55 (6 H, s, two OCH_3), 3.35 (3 H, s, $-\text{OCH}_3$), ^{13}C NMR 29.35 – 30.39, 55.74 – 56.25, 106.94, 115, 125.91 – 133.09, 146.72, 160.39, 166.01, 180.37 and 194.48 and 197.64.

Compound 3 was crystallized from methanol as faint 0 yellow crystals. Yield (82%), m.p. 225-226 C. Analytical

data: Found: C = 57.25, H = 3.85, N = 12.46, S = 9.49; F = 11.27%. Calculated for $C_{16}H_{13}N_3SF_2O$:C=57.61, H=3.95,N=12.94,S=9.67;F=11.41%;m/z334.

(C H N SF O +1, 26%) IR: n cm^{-1} = 3250 – 2850

16 13 3 2

(b, NH, aromatic & aliphatic CH), 1610 (C=N), 1485 (deformation CH_3), 1530, 880 (thioamide I, II), 1200 (C=S),

1060 (C-O-Me), 680 (C-F). ^1H NMR (DMSO): d: 11.2, 10.8

(each 1 H, s, NH), 7.8–7.2 (8 H, m, aryl protons), 3.35 (3 H, s, $-\text{OCH}_3$), ^{13}C NMR 29.58, 31.09, 36.23, 40.85, 162.86 and 206.45.

3.3.2.5,6,11,12-Tetraaryl-1,2,4,7,8,10-hexaaza-cyclododeca-4,6,10,12-tetraene-3,9-dithiones (4)

A solution of mercuric chloride (0–70 mmol) in methanol (50 mL) was added to a solution of compound 2 (1.4 mmol) in absolute methanol (50 mL). The reaction mixture was stirred for 4 h at room temperature. The solid precipitate was filtered off, washed with methanol and dried to give 4. Dilution of the filtrate yielded the cyclic thioether 5. The solution was

filtered and crystallized from methanol. This compound was crystallized from methanol

0 as yellow crystals. Yield (45%), m.p. 110 C. Analytical data:

Found: C = 47.52, H = 3.26, N = 9.78, S = 7.45%, Calculated for $[C_{34}H_{28}N_6S_2O_4]Hg$: C=48.5, H=3.29, N=9.95, S =7.53%; IR: n cm^{-1} lacks of both NH, SH; ^1H NMR (DMSO):

d: 3.15, 10.8 (4s, OCH_3), 7.07, 7.1, 7.2, 7.3, 7.5, 7.6, 7.7 and 7.8 (eachs, 8H, 8 Haryl protons).

3.3.3. Cyclichthioether 5a

A solution of mercuric chloride (0–70 mmol) in methanol (50 mL) was added to a solution of compound 2 (0–70 mmol) in absolute methanol (50 mL). The reaction was stirred for 4 hours at room temperature and the solid precipitate was filtered off, washed with methanol and dried.

Compound 5a was crystallized from ethanol as pale yellow crystals. Yield (35%), m.p. 130 Analytical data: Found: C = 62.29, H = 4.56, N = 12.79, S = 9.49%. Calculated, for $(C_{34}H_{30}N_6S_2O_4)$ C=62.76, H=4.61, N=12.92, S=9.84%.

IR: n cm^{-1} lacks of both NH, SH with peaks at 1620 (C = N),

1180 (C-S), 1055 (C-O-Me); ^1H NMR (DMSO): d: 8.8 (2 H,

s < H-C₅ of 1,2,4-triazine), 7.7-7.0 (16 H, m, aryl protons), 3.65-3.55 (12 H, s, 4- OCH_3).

3.3.4. Cyclichthioether, 5b

Compound 5b was prepared as mentioned using compound 1 and mercuric chloride salt in 1:1 molar ratio and crystallized from ethanol as yellow crystals. Yield (80%), m.p. 120. Analytical data: Found: C=67.37, H=4.10, N=15.67, S=11.94%. Calculated for $C_{30}H_{22}N_6S_2$: C=67.9, H=4.15, N=15.84, S=12.07%. IR: n cm^{-1} 2704 (N-S-N), 1525, 1329 (cyclic amide I, II),

1024 (C-S-N), 867, 807 (phenyl CH), ^1H NMR (DMSO): d:

7.3-7.8 (22 H, m, phenyl & H-C₅ of 1,2,4-triazine), ^{13}C NMR 167 (CS), 156, 1, 156.0 (C-N), 131.31 and 128.84 (carbon-phenyls).

3.3.5. Bis[5,6-di(4-fluorophenyl)-5-methoxy-2,4-dihydro-1,2,4-triazin-3-thiato]-mercury, 6 and cyclichthioether, 5c

A methanolic solution of mercuric chloride (0.01 mmol) in methanol (50 mL) was added to a solution of compound 3 (0.03 mmol) in absolute methanol (50 mL). The reaction mixture was stirred for 8 hours at room temperature. The solid precipitate was filtered off and dried to give type of complex 6. On diluting the filtrate, a solid compound was separated out, filtered off, washed with methanol and dried to give 5c.

Compound 5c was crystallized from THF as pale yellow

crystals. Yield (45%), m.p. 280 °C. Analytical data: Found:

C=59.50, H=2.90, N=13.70, S=10.35, F=12.45%. Calculated for $C_{30}H_{18}N_6S_2F_4$, C=59.80, H=2.99, N=13.95, S=10.63, F=12.62%. M/z 602 (M, 5.15), 606 (M+1,

3.901, 608)(M+2, 0.80), 301(46.35), 214(100) and 86 (1.11).

Compound 6 was crystallized from methanol as yellow crystals. Yield (40%), m.p. 190 °C. Analytical data: Found: C=40.90, H=2.84, N=8.18, S=6.09, F=8.31%, M/z=938.

Calculated for $C_{32}H_{26}N_6S_2F_4O_2HgCl_2$, C=40.93, H=2.87, N=8.95, S=6.82, F=8.39%. IR: ν cm⁻¹ 3210, 3165 (NH,

NH), 1507, 1372 (thiocarbamide), 1156 (C=S) and 1039 (C-O-Me); ¹H NMR (DMSO): δ : 12.5 (1H, s, NH), 10.7 (1H, s,

NH), 8.8 & 8.5 (1H, each, s, NH), 7.7–7.5 (4H, m, aryl), 7.3–

7.0 (4H, m, aryl) and 3.45 (6H, each, s, O-CH₃); CNMR 29.35, 30.39 (O-CH₃); 116.45, 116.71 (C-N), 131–134 (aryl carbons), 206.19 (C=S).

3.4. Analytical applications

3.4.1. General cyclic voltammetry

The general procedure for recording cyclic voltammetric at differential sweep rates was carried out as follows. An accurate concentration (10 mmol) of the test compound and supporting electrolyte tetra methyl ammonium chloride (100 mmol) in DMF were transferred into the voltammetric cell. The solution was stirred with nitrogen for 15 minutes to release oxygen. The voltammograms were then recorded in the potential ranges -1.5 to 1.5 V at Pt working electrode versus Ag/AgCl reference electrode.

3.4.2. Preparation of polyurethane foam packed column

Compound 1 was physically immobilized onto PUFs as follows: PUFs cubes (1.0 cm) were shaken well with

compound 1 for 10 minutes as reported [28]. An accurate weight (1.00–0.1 g) of the reagent 1 immobilized PUFs was packed in a column (1000 × 10 id mm) using the vacuum method of foam packing [28, 29]. The aqueous solutions (0.1 L) containing arsenic (III) at concentrations 10 g mL⁻¹ were

percolated through the PUFs packed column at 5 mL min⁻¹

flow rate after adjustment the solution to pH = 2–3 with B-R buffer. The sample and blank PUFs packed columns were then washed with 100 mL of B-R buffer solution at the same pH. Quantitative retention of arsenic (III) took place on the immobilized PUFs as indicated from the ICP-AES measurement of arsenic in the effluent solutions. The retained arsenic

(III) species were then recovered quantitatively from the foam column with acetone 910 mL at 5 mL min⁻¹ flow rate.

Acknowledgement

The authors would like to thank the Deanship of Scientific Research, King Abdul Aziz University, Kingdom of Saudi Arabia for the financial support under the grant number MX/11/20 and the Chemistry Department for the facilities provided.

References

- [1] G.N. Mukkerjee, L. Sarker, Indian J. Chem. 27A (1988) 514.
- [2] A. Pasini, L. Casella, J. Inorg. Nucl. Chem. 36 (1979) 2133.
- [3] O.E. Offiong, S. Martelli, Farmaco 49 (7–8) (1994) 513.
- [4] C.F. Zhong, J.C. Deng, J. Tong, X.H. Yao, W.S. Zhu, Chem. J. Chin. Univ. 19 (2) (1998) 174.
- [5] P.D. Beer, F. Szemes, V. Balzani, M. Sala, M.G.B. Drew, S.W. Dent, M. Maestri, J. Am. Chem. Soc. 119 (1997) 11864.
- [6] J. Costa, R. Delgado, M.G.B. Drew, V. Felix, J. Chem. Soc. Dalton Trans. (1998) 1063.
- [7] Y. Al-Shihadeh, A. Benito, J.M. Leoris, R.M. Manez, T. Pardo, J. Soto, M.D. Marcos, J. Chem. Soc. Dalton Trans. (2000) 1199.
- [8] I.A. Atkinson, J.D. Chartres, G.E. Everett, X.-K. Ji, L.F. Lindoy, O.A. Mathews, G.V. Meehan, B.W. Skelton, G. Wei, A.N. White, J. Chem. Soc. Dalton Trans. (2000) 1191.
- [9] C.W. Rogers, M.O. Wolf, Chem. Commun. (1999) 2297.
- [10] P.D. Beer, P.A.G. Gale, Z. Chen, J. Chem. Soc. Dalton Trans. (1999) 1897.
- [11] I.A. Shihadeh, A. Benito, J.M. Lforis, R. Martinez Manez, T. Pardo, J. Soto, M.D. Marcos, J. Chem. Soc. Dalton Trans. (1999) 2000.
- [12] T.W. Hambley, L.F. Lindoy, J.R. Reimers, P. Tumer, G. Wei, A.N.W. Cooper, J. Chem. Soc. Dalton Trans. (2001) 614.
- [13] F. Hunzenkamp, A.C. Stucke, E. Cavolli, H.U. Godel, J. Chem. Soc. Dalton Trans. (2000) 251.
- [14] M. Yildiz, B. Bulger, A. Cinar, J. Indian Chem. Soc. 82 (2005) 414.
- [15] N. Foroughifar, A. Mobinikhaledi, S. Ebrahimi, H. Moghanian, M. Fard, M. Kalhor, Tetrahedron Lett. 50 (2009) 836.
- [16] J.K. Pandey, S.K. Sengupta, O.P. Pandey, J. Indian Chem. Soc. 83 (2006) 1073.
- [17] Newkome G. University of South Florida, USA. 2001, 2nd Florida Heterocyclic conference, 3–7 March 2001.
- [18] Z. El-Gendy, J. Morsy, H. Allimony, W.R. Abdel-Monem, R.M. AbdRahman, Phosphorous, Sulfur, Silicon and Related Compounds 178 (2003) 2055.
- [19] M.A. Ibrahim, R.M. Abdel-Rahman, A.M. Abdel-Halim, S.S. Ibrahim, H.A. Allimony, Arkivoc XVI (2008) 202.
- [20] M.A. Ibrahim, R.M. Abdel-Rahman, A.M. Abdel-Halim, S.S. Ibrahim, H.A. Allimony, J. Braz. Chem. Soc. 20 (2009) 1275.
- [21] R.M. Abde-Rahman, M.S.T. Makki, T.E. Ali, M.A. Ibrahim, Eur. J. Chem. 1 (3) (2010) 236.
- [22] M.A. Blanco, E.L. Torres, M.A. Mendiola, E. Brunet, M.T. Sevilla, Tetrahedron 58 (2002) 1525.
- [23] T.E. Ali, R.M. Abdel-Rahman, F.H. Hanafy, S.M. El-Defawy, Phosphorous, Sulfur, Silicon and Related Compounds 183 (2008) 2265.
- [24] W.H.O., Expert Committee on Bilharziasis 65 (1953) 33.
- [25] W.H.O., Snail control information of Bilharziasis monograph series 50 (1965) 124.
- [26] R.S. Nicholson, I. Shain, Anal. Chem. 36 (1964) 709.
- [27] C.A. Bowmaker, P.D.W. Boyd, G.K. Campbell, J.M. Hope, R.L. Martin, Inorg. Chem. 21 (1982) 1152.
- [28] M.S. El-Shahawi, M.A. Othman, M.A. Abdel-Fadeel, Anal. Chim. Acta. 546 (2005) 221.
- [29] M.S. El-Shahawi, H.A. Nassif, Anal. Chim. Acta. 481 (2003) 33.

Multi-Walled Carbon Nanotubes Film Sensor for Carbon Mono-Oxide Gas

Zishan H. Khan^{1,*,#}, Numan A. Salah¹, Sami S. Habib¹, Ameer Azam¹ and M.S. El-Shahawi²

¹Center of Nanotechnology, King Abdulaziz University, Jeddah, Saudi, Arabia; ²Center of Excellence in Environmental Studies, King Abdulaziz University, Jeddah, Saudi Arabia

Abstract: This paper reports the fabrication of a carbon nanotubes based carbon mono-oxide gas sensor. Initially, iron catalyzed carbon nanotubes were grown on silicon oxide grown silicon substrate using low pressure chemical vapor deposition. Morphology and microstructure of these CNTs were studied by field emission scanning electron microscopy (FESEM) and high resolution transmission electron microscopy (HRTEM). Morphological analysis shows the formation of multi-walled carbon nanotubes (MWNTs) with an average diameter of 30 nm. Typical response of MWCNTs gas sensor in the presence of CO gas has been studied. It was observed that this MWNTs gas sensor gives a quick response to CO gas and the recovery time of this sensor is also fast. The sensitivity of this sensor was found to decrease with an increase in the CO gas concentration. At a particular gas concentration, the responsiveness of this sensor increases with the increase in temperature. Electrical transport properties of this MWNTs film sensor have also been explained on the basis of temperature dependence of conductivity. On the basis these properties, it is suggested that this MWNTs-based gas sensor has potential to be used as a novel CO gas sensor.

Keywords: Multi-walled carbon nanotubes, gas sensor, carbon mono-oxide, sensitivity, responsiveness.

INTRODUCTION

Carbon nanotubes (CNTs) can be understood as one or more graphite sheets rolled up into a seamless cylinder. CNTs have gained much attention and scientific interest due to their unique properties [1] and potential applications [2-6] since their discovery in 1991 [7]. In general, electrical properties of nanotubes depend on the structure and the chirality [8-10]. Depending on the arrangement of carbon atoms, CNTs can be either metallic or semiconducting [8-10]. For semiconducting CNTs, the bandgap is normally inversely proportional to the diameter [8,9]. Thus, structure control of the CNTs is important in controlling the electrical properties of the CNTs. Furthermore, CNTs are excellent electrical candidates for nanoscale devices [11-15]. Due to high conductivity and the high current density, multiwall carbon nanotubes (MWNTs) in particular have been considered for the use in wiring leads in future LSI circuits [16]. For this novel electronic system, there are many interesting properties expected in future. Some of the devices such as nano-scale diodes [11,14], field effect transistors [12] and single electron transistors (SETs) [13] using CNTs have been already demonstrated and characterized. Due to their unique inherent morphologies and properties, the progress and application in CNTs-related technology has been extraordinary within a short span of time. Gas sensors based on both SWNTs and MWNTs have been developed. These sensors have demonstrated huge potential and found their application in various areas. Both theoretically and experimentally, it has been proved that the electrical resistance, thermoelectric power, and local density of states of CNTs can be significantly changed by exposure to certain gases/vapours. The gas sensing FET or resistors that measure the resistance change of CNTs as the transducer is the most commonly used sensor structures. However, this limits the range of the gases that CNTs sensors can detect, especially for the sensing of inert agents. Compared with the resistance sensors, CNTs enhanced ionization chambers allow the detection of gas molecules with low adsorption energy, hence a wide range of vapours can be detected. With CNTs integrated, the breakdown voltage can be lowered significantly.

[#]Also at the Department of Applied Sciences & Humanities, Jamia Millia Islamia (Central University), New Delhi-110025 (India).

Other promising methods to improve the sensing characteristics include the functionalization of CNTs and nanocomposites of CNTs with various polymers, which can broaden the sensing range or enhance the sensitivity. Although CNTs have demonstrated their great potential for gas sensing experimentally, there are still several practical challenges such as stability of the CNTs-based devices, degradation of the devices and slow response and recovery. However, it is believed that, with the increased interests and development of related technologies, CNTs based gas sensors have promising future and will bring huge changes to the current industries and our everyday life. In the present work, a multi-walled carbon nanotubes based sensor has been fabricated and the carbon mono-oxide gas sensing properties of this sensor has been studied.

EXPERIMENTAL

Initially, nanocrystalline film of iron to be used as catalyst was deposited by RF Sputtering technique on silicon substrate with thick oxide layer on it under an ambient argon pressure of 5 Torr. The thickness of film was kept at 10 nm. Multi-walled carbon nanotubes (MWNTs) were grown on the catalyst film using low pressure chemical vapour deposition system. These CNTs were produced by the catalytic deposition of C₂H₂ at 800°C, at a chamber pressure of 200 Torr and the growth time was kept fixed at 10 minutes. Initially, nitrogen gas was passed for 10 mins. at a temperature of 800°C, just after this process, the etching gases NH₃ and H₂ with flow rates of 100 sccm and 50 sccm respectively were passed through reactor for 20 mins using mass flow controllers (MFCs). At the final stage, the hydrocarbon gas C₂H₂ with flow rate 25 sccm was added for 10 minutes. Therefore, the final gas mixtures of NH₃:C₂H₂:H₂ with flow rates 100:50:25 sccm respectively, were used to grow the carbon nanotubes. The morphology of these catalyst films as well as multi-walled carbon nanotubes (MWNTs) were studied using Field Emission Scanning Electron Microscope (FESEM). High Resolution Transmission Electron Microscope (HRTEM) was employed to study the microstructure of these as-grown MWNTs. We have recorded the Raman spectra of as-grown CNTs using DXR Raman Microscope, Thermo Scientific with 532 nm laser as an excitation source at a power of 8 mW to verify the structure of as-grown CNTs. We have used a specially designed gas sensing set-up to study the gas sensing properties of the present MWNTs based sensor. To evaluate the gas sensing properties of the as-prepared MWNTs films, MWNTs gas

*Address correspondence to this author at the Department of Applied Sciences & Humanities, Jamia Millia Islamia (Central University), New Delhi 110025, India; Tel/Fax: +966-2-6951597; E-mail: zishan_hk@yahoo.co.in

sensor was placed inside a stainless steel chamber and the resistance was measured using a Keithley 4200 I-V measurement system. An electrode pattern of

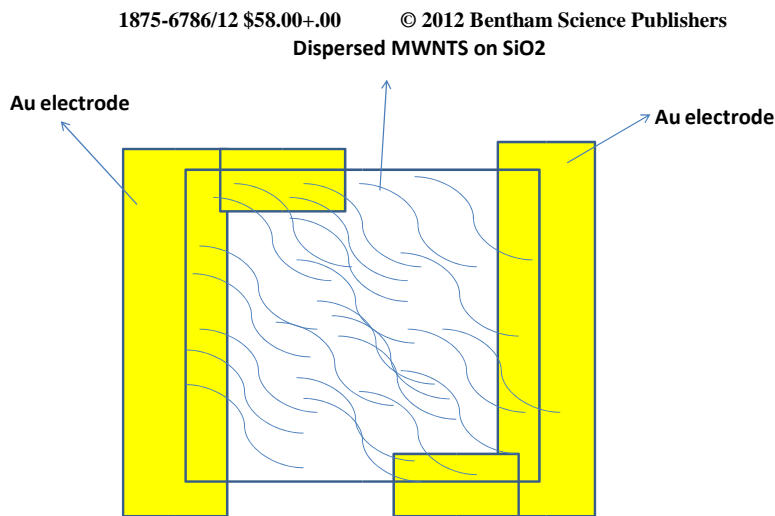
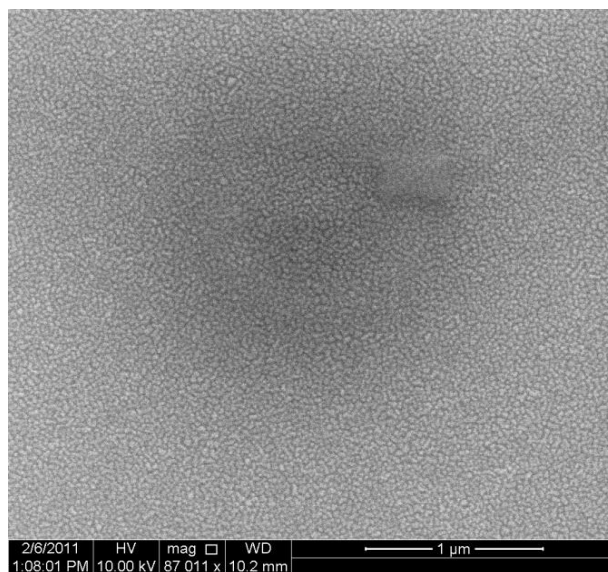


Fig. (1). Electrode pattern of MWNTs film sensor.

gold as shown in Fig. (1) was evaporated using thermal evaporation. This electrode pattern was directly evaporated on MWNTs film for measuring the real time resistance of the MWNTs based sensor. This sensor was annealed at 600 °C for 5 mins. in air to remove the unwanted carbon from the surface of the sensing film. The sample was examined in a chamber with the detecting gases flowing through. The mass flow controllers were used to control the concentration of detecting gas. The Ag-Pt heater was used to heat and control the operation temperature of the sample. Initially, the MWNTs based sensor was mounted inside the sample holder and probes were connected to sample. The system was evacuated up to 10^{-6} Torr with the help of turbo molecular pump. After attaining the required degree of vacuum, the turbo and rotary pump valves were closed and air was purged with the flow rate of 2 l/min for 5 mins. The real time resistance was measured to obtain a baseline resistance. Once a baseline resistance was obtained, the detecting gas i.e. carbon mono-oxide with the set concentration was introduced into the sample holder. This gas was purged for 1-2 minutes to measure the change in resistance with time up to 2 minutes and after the time was over, we stopped the flow of detecting gas in to the sample holder and measured recovery time of the sensor. We

coated Si substrate

repeated these cycles for different concentrations of carbon monooxide in pure air to study the response of this CNT sensor for detecting carbon mono-oxide (CO). The gas sensing measurements were made within a dynamic flow system with control of sensor operating temperatures (300–500K) under variable gas concentrations (100–500 ppm) of carbon mono-oxide. The sample gas flow time and the clean air reference flow time were fixed at 2 minutes and 5 minutes, respectively. It should be noted that these switching interval was selected so that the resistance change is at least 90% of the saturated value. The sensor resistance was sampled and recorded every second for subsequent analyses. The electrical properties of sample were also measured at various temperatures from room temperature up to 500K, and at various concentrations of CO gas (100, 200 and 500 ppm CO in pure air). The relative changes in the electrical parameters of the film are considered as sensor output.



RESULTS AND DISCUSSION

Fig. (2) represents the morphology of the catalyst nanocrystalline film of the iron deposited on silicon oxide grown silicon substrate. The size of these nanoparticles varies from 5-10 nm. Figs. (3a&b) show the FESEM images of CNTs grown on iron catalyst films. The diameter of these nanotubes varies from 20-60 nm and length of these CNTs is of the order of several tens of micrometers. Fig. (4) shows the HRTEM image of these as grown iron catalyzed CNT. It is clear that the nanotube is multi-walled with a diameter of

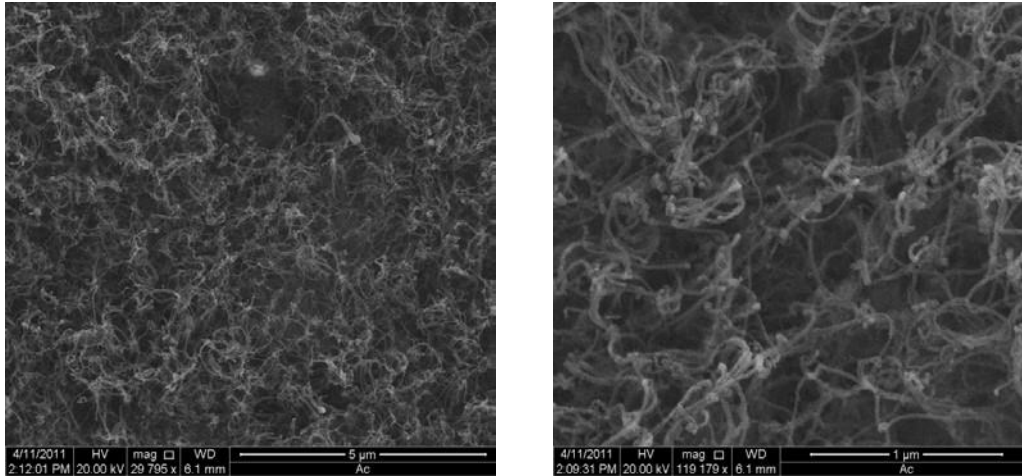


Fig. (3). (a&b) FESEM images iron catalyzed MWNTs.



Fig. (2). FESEM image of iron nanocrystalline film.

30 nm. The diameter of the center hollow portion of the MWNT is about 20 nm with the wall thickness of about 6 nm.

Fig. (5) shows the Raman spectrum of as-grown MWNTs. The spectrum Fig. (5) clearly shows strong peak at 1580 cm^{-1} (G-band), indicating the formation of more graphitized MWNTs. The D band (the disorder band), located between $1330\text{-}1360\text{ cm}^{-1}$ is generally observed in CVD grown MWNTs. The less intense peak observed at 1320 cm^{-1} (D-band) suggests that the less quantity of amorphous carbonaceous particles adhered to MWNTs walls. Fig. (6) presents the typical responses of MWCNTs gas sensor in the presence of CO gas. The changes experienced in the resistance of the sensing materials after their exposure to successive concentrations of CO can be observed. It is also found that response time ($t_{res.}$) of the sensor changes from 14.6 sec. to 17.4 sec. for different concentration of CO gas (100, 200 & 500 ppm), whereas the recovery time ($t_{rec.}$) changes from 18.5 sec. to 26.3 sec. The fast recovery time may be due to the low binding energy between MWNTs and CO. This MWNTs gas sensor has fast response and recovery time due to the fast adsorption/desorption process of gas molecules on MWNTs. This fast response may also be due to weak bonds and less partial electron transfer between MWNTs and CO molecules.

Temperature dependence of resistance for the Fe-catalyzed multi-walled carbon nanotubes (MWNTs)-based film sensor in air and 100, 200, & 500 ppm CO gas in the temperature range 300K-500K is shown in Fig. (7). It is evident from Fig. (7) that the resistance of MWNTs film decreases with the increase in temperature. The resistance of MWNTs film sensor increases on exposing the sensor to CO gas and it also increases with increase in concentration of CO gas from 100 ppm to 500 ppm. The sensitivity of this MWNTs gas sensor was calculated using the following relation;

$$\text{Sensitivity} = R_{\text{air}}/R_{\text{gas}}$$

where R_{air} is the sensor resistance in air and R_{gas} is the sensor resistance in the presence of a toxic species.

Fig. (8) presents the sensitivity versus temperature plot. It is observed that the sensitivity of these MWNTs based sensor decreases as the temperature increases from room temperature to 500K for all the studied concentration of CO gas. The sensitivity of MWCNTs gas sensor changes from 99.84% to 99.22% when 100 ppm, 200 ppm and 500 ppm CO gases are introduced in the test chamber at room temperature, suggesting thereby a decrease in the sensitivity with an increase in the CO gas concentration. It means the process of CNTs-hybridization reduces the gas sensitivity toward CO gas.

In order to quantify the performance of a given sensor, its responsiveness (SR) can be defined as the ratio of the resistance change due to the exposure to the test gas and the sensor's baseline resistance in air:

$$SR = (R_{\text{air}} - R_{\text{gas}})/R_{\text{air}}$$

The responsiveness of this sensor calculated at different temperatures and for different CO concentration is presented in Table 1. The results indicate that the MWNTs gas sensor could detect CO at room temperature and for the gas concentration as low as 100 ppm. At a particular gas concentration of 500 ppm, the responsiveness increases from 0.78% to 12.09% as the temperature increases from 300K to 500K. During the temperature range (300-500K), it is suggested that thermal energy enhances the reactions involved to overcome their respective activation energy barriers, which results in an increase in responsiveness of the present sensor with the increases in temperature [15,16]. This responsiveness also shows an increasing trend with the CO concentration. Therefore, it is suggested that this MWNTs sensor gives a good response to the different gas concentration within a temperature range of 300-500K.

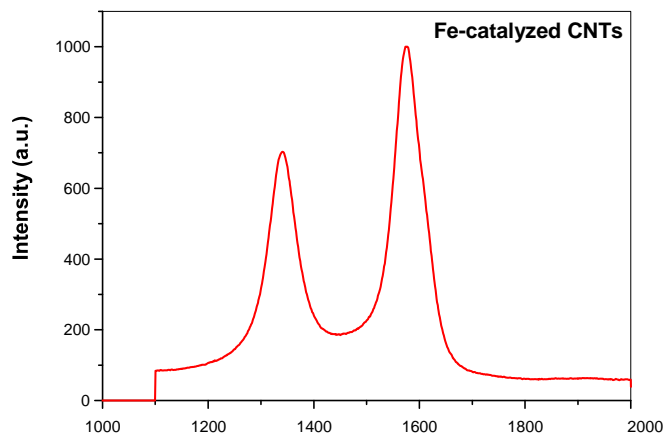


Fig. (5). Raman spectra of iron catalyzed MWNTs.

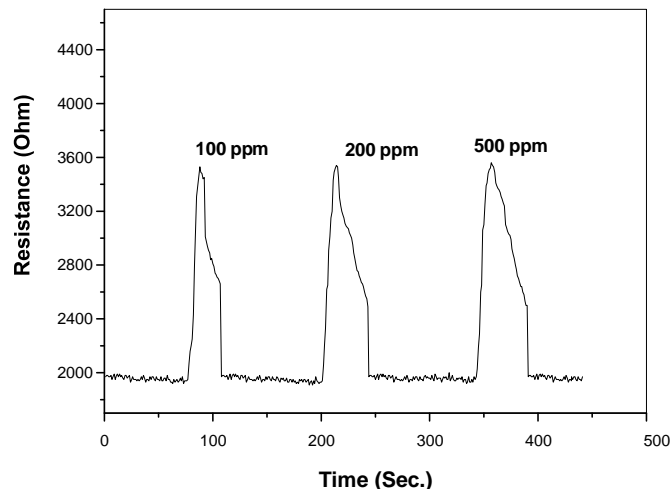


Fig. (6). Typical responses of MWCNTs gas sensor for different concentration of CO gas (100, 200 & 500 ppm).

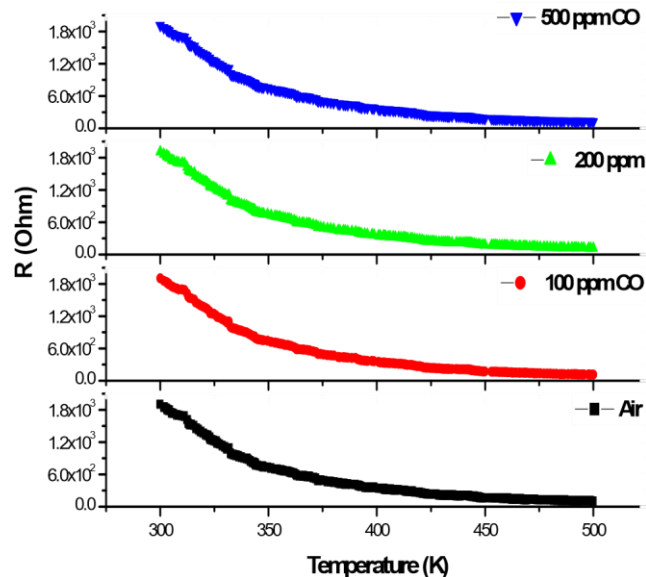


Fig. (7). Temperature dependence of resistance for the Fe-catalyzed MWNTs-based film sensor in air and 100, 200, & 500 ppm CO gas for the temperature range of (300-500K).

MWNTs to form an MWNT-molecule-MWNT junction. This will result in a hopping kind of mechanism for intertube charge transfer between nanotubes. Therefore, an intertube modulation of the CNTs network may be responsible for the conductivity change. This

Khan et al.

Table 1. Electrical Parameters for the Fe-catalyzed MWNTs-based Film Sensor at 500K

CO Concentration (ppm)	Resistance (Ω)	Responsiveness [$(R_{air}-R_{gas})/R_{gas}$]	Sensitivity (R_{air}/R_{gas})	Activation Energy (E) (eV)	Pre-exponential Factor (σ_0) ($\Omega^{-1}\cdot\text{cm}^{-1}$)
100	112	0.0268	0.9732	0.187	87.79
200	116	0.0603	0.9397	0.180	67.76
500	124	0.1209	0.8790	0.169	45.61
Air	109	-----	-----	0.192	103.96

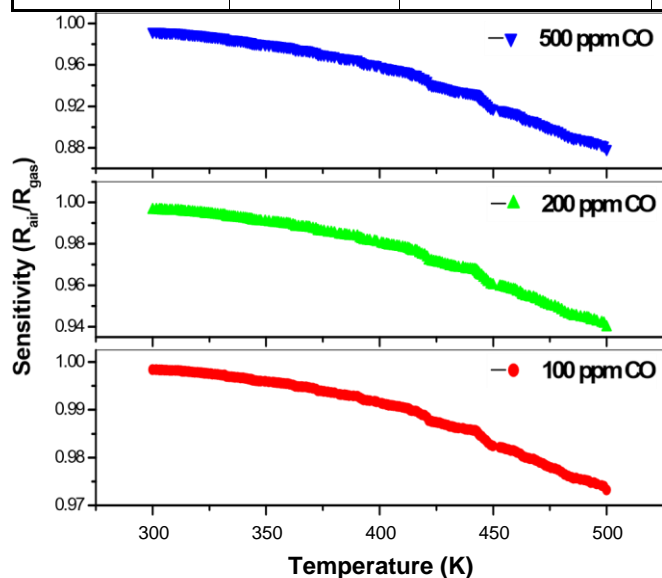


Fig. (8). Temperature dependence of sensitivity for the Fe-catalyzed MWNTs-based film sensor in air and 100, 200, & 500 ppm CO gas for the temperature range of (300-500K).

The results of carbon mono-oxide absorption into MWNTs film indicated that the carbon nanotubes samples were sensitive to CO gas. Upon exposure to CO gas, the resistance of carbon nanotubes increased significantly. The maximum resistance detected was 1990 ohm at 500 ppm concentration CO, which is almost 5% higher than the resistance measured in air. Carbon monoxide is a reducing gas and its absorption resulted in injection of electrons to the CNTs and reduced number of holes in the material. Holes are the main charge carrier for p-type semiconductor, holes depletion will result in an increase in resistivity or a decrease in conductivity of the sample.

Here, we may suggest two possible sensing mechanisms for the electrical response to molecular adsorption in MWNTs. The first mechanism involves the adsorption resulting in direct charge transfer between a donor or acceptor type of molecule and MWNTs. This will lead to the shift in Fermi level in the semiconducting tubes (intratube modulation), resulting in a change in conductivity [17]. In other mechanism, the adsorption occurs in the interstitial space between

phenomenon is common for all types of molecules and for both metallic and semiconducting CNTs. This kind of modulation is similar to that of the interaction between semiconductor metal oxides and donor or acceptor types of molecules, showing a nonlinear (power law) response [18].

Fig. (9) shows the plots of $\ln \sigma$ Vs $1000/T$ for the temperature range of (300-500K). It is observed that the plots of $\ln \sigma$ Vs $1000/T$ are straight line, suggesting that the conduction in this system is through thermally activated process. The conductivity is expressed by the usual relation

$$\sigma = \sigma_0 \exp(-E/k_B T) \quad (1)$$

where E is the activation energy, σ_0 is pre-exponential factor and k_B is Boltzman constant. The value of E is calculated using slope of Fig. (9) and the value of pre-exponential is estimated from the intercept. These calculated values are presented in Table 1. It is found that the value of both the activation energy and pre-exponen-

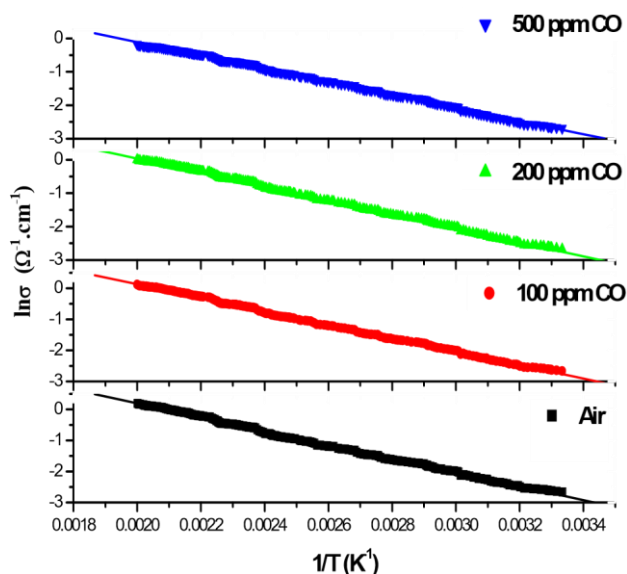


Fig. (9). Temperature dependence of conductivity for the Fe-catalyzed MWNTs-based film sensor in air and 100, 200, & 500 ppm CO gas for the temperature range of (300-500K).

tial factor (ϕ) decreases on increasing the CO concentration. The value of pre-exponential factor (ϕ) is estimated to be 1.04×10^2 when air is purged in to sample holder, which decreases to $0.88 \times 10^2 \text{ ohm}^{-1} \cdot \text{cm}^{-1}$ on introducing CO gas in the sample holder. This value further, decreases to $0.46 \times 10^2 \text{ ohm}^{-1} \cdot \text{cm}^{-1}$ on increasing the CO gas concentration from 100 ppm to 500 ppm. On the basis of the calculated values of E and ϕ , it is therefore, suggested that conduction takes place in localized states through a thermally activated process for the present system [19,20].

Table 1 also presents the calculated values of thermal activation energy (E) of multi-walled carbon nanotubes for air and different concentration of carbon mono-oxide gas. For individual metallic and semiconducting SWNTs, the thermal activation energy (E) values of approximately 5 meV and 29 meV at high temperature (70–300 K) are reported [21]. On the basis of this work, it can be suggested that the resistance of CNT networks increases due to the presence of large number of semiconducting CNTs which lead to high value of thermal activation energy [22]. Various others reports suggested that the value of activation energy for CNTs based composites is in the range of 160–280 meV [23]. In our case, the activation energy of MWNTs sensor film decreases from 192 meV to 169 meV after the exposure to air and different CO gas concentration (100 ppm, 200 ppm and 500 ppm), which may be correlated to the increase in resistance of MWNTs sensor film. It is also reported that an increase in conductivity was also associated with a decrease in thermal activation energy. Our results are in good agreement with the results reported in literature [23].

CONCLUSION

A MWNTs-based CO gas sensor was fabricated and its resistive response to CO was studied. From the typical responses of MWNTs gas sensor in the presence of CO gas, it was observed that response time ($t_{res.}$) and the recovery time ($t_{rec.}$) are very short and show a significant change for different gas concentrations. The fast recovery time may be due to the fast adsorption/desorption process of gas molecules on MWNTs. At room temperature, the sensitivity of MWNTs gas sensor changes from 99.84% to 99.22%. At a particular gas concentration of 500 ppm, the responsiveness increases from 0.78% to 12.09% as the temperature increases from 300K to 500K. It also shows an increasing trend with the CO concentration. On the basis of electrical transport properties, it is suggested that conduction takes place in localized states through a thermally activated process for the present system of MWNTs film sensor.

CONFLICT OF INTEREST

None.

ACKNOWLEDGEMENT

Authors are thankful to Center of Excellence in Environmental Studies, King Abdulaziz University, Jeddah, Saudi Arabia for providing financial support in the form of Research Project (No. 1/H/2).

REFERENCES

- [1] Iijima, S. Helical microtubules of graphitic carbon. *Nature*, **1991**, *354*, 56.
- [2] Iijima, S.; Ichihashi, T. Single-shell carbon nanotubes of 1-nm diameter. *Nature*, **1993**, *363*, 603.
- [3] Bethune, D.S.; Kiang, C.H.; de Vries, M.S.; Gorman, G.; Savoy, R.; Vazquez, J.; Beyers, R. Cobalt-catalysed growth of carbon nanotubes with single-atomic-layer walls. *Nature*, **1993**, *363*, 605.
- [4] Kroto, H.W.; Heath, J.R.; O'Brien, S.C.; Curl, R.F.; Smalley, R.E. C₆₀: Buckminsterfullerene. *Nature*, **1985**, *318*, 162.
- [5] Charlier, J.C.; Issi, J.P. Electrical conductivity of novel forms of carbon. *Phys. Chem. Solids*, **1996**, *57*, 957.
- [6] Ajayan, P.M.; Zhou O.Z. *Applications of carbon nanotubes* In: Springer Topics in Applied Physics, Dresselhaus, M.S., Dresselhaus, G., Avouris, P.H. (Berlin: Springer), **2001**, vol. 80, p. 391.
- [7] Saito, Y., Hamaguchi, K., Uemura, S., Uchida, K., Tasaka, Y., Ikazaki, F., Yumura, M., Kasuya, A., Nishina, Y. Field emission from multi-walled carbon nanotubes and its application to electron tubes. *Appl. Phys. A*, **1998**, *67*, 95.
- [8] Valentini, L., Lozzi, L., Cantalini, C., Armentano, I., Kenny, J.M., Ottaviano, L., Santucci, S. Effects of oxygen adsorption on gas sensing properties of carbon nanotube thin films. *Thin Solid Films*, **2003**, *436*, 95.
- [9] Ong, K.G., Zeng, K., Grimes, C.A. A wireless, passive carbon nanotubebased gas sensor. *IEEE Sensors J.*, **2002**, *2*, 82.
- [10] Philip, B., Abraham, J.K., Chandarsaker, A., Varadan V.K. Carbon nanotube/PMMA composite thin films for gas sensing applications. *Smart Mater. Struct.*, **2003**, *12*, 935.
- [11] Dillon, A.C., Jones, K.M., Bekkedah, T.A., Kiang, C.H., Bethune, D.S., Heben, M.J. Storage of hydrogen in single-walled carbon nanotubes. *Nature*, **1997**, *386*, 377.
- [12] Li, J. In *Carbon Nanotubes: Science and Applications*, Meyyappan, M. Ed., CRC Press, Boca Raton, Fla, USA, **2005**.
- [13] Rittersma, Z.M. Recent achievements in miniaturised humidity sensors-a review of transduction techniques. *Sens. Actuators A*, **2002**, *96(2-3)*, 196.
- [14] Fener, R., Zdankiewicz, E. Micromachined water vapor sensors: a review of sensing *IEEE Sensors J.*, **2001**, *1(4)*, 309.
- [15] Shinde, V.R., Gujar, T.P., Lokhande, C.D. LPG sensing properties of ZnO films. *Sens. Actuators B Chem.*, **2007**, *120*, 551.
- [16] Zeng, Y., Zhang, T., Wang, L., Kang, M., Fan, H., Wang, R., He, Y. Enhanced toluene sensing characteristics of TiO₂-doped flowerlike ZnO nanostructures. *Sens. Actuators B Chem.*, **2009**, *140*, 73.
- [17] Zhao, J., Buldum, A., Han, J., Lu, J.P. Gas molecule adsorption in carbon nanotubes and nanotube bundles. *Nanotechnology*, **2002**, *13*, 195.
- [18] Gardner, J., Bartlett, P.N. *Electronic Nose: Principles and Applications*; Oxford University Press: New York, **1999**.
- [19] Mott, N.F. Conduction in non-crystalline systems IV; Anderson localization in a disordered lattice. *Phil. Mag.*, **1970**, *22*, 7.
- [20] Mott, N.F., Davis E.A. Conduction in non-crystalline systems V. Conductivity, optical absorption and photoconductivity in amorphous semiconductors. *Phil. Mag.*, **1970**, *22*, 903.
- [21] Skakalova, V., Kaiser, A.B., Woo, Y.S., Roth S. Electronic transport in carbon nanotubes: From individual nanotubes to thin and thick networks. *Phys. Rev. B*, **2006**, *74*, 085403.
- [22] Lim, J-H., Phiboolsirichit, N., Mubeen, S., Rheem, Y., Deshusses, M.A., Mulchandani, A., Myung, N. V. Electrical and gas sensing properties of polyaniline functionalized single-walled carbon nanotubes. *Nanotechnology*, **2010**, *21*, 075502.
- [23] Singh, R., Arora, V., Tandon, R. P., Chandra, S., Mansingh, A. Charge transport and structural properties of polyaniline. *J. Mater. Sci.*, **1998**, *33*, 2067.



Spectrofluorometric determination and chemical speciation of trace concentrations of tungsten species in water using the ion pairing reagent procaine hydrochloride

M.S. El-Shahawi*, L.A. AlKhateeb

Department of Chemistry, Faculty of Science, King Abdulaziz University, P.O. Box 80203, Jeddah 21589, Saudi Arabia

article	info	
Article history: Received 20 September 2011 Received in revised form 13 November 2011 Accepted 14 November 2011 Available online 19 November 2011		determination of trace concentrations of tungsten (VI) in water. The method was based upon solvent extraction of the developed ion associate $[(PQH^+) \cdot WO_4^{2-}]$ of the fluorescent ion-pairing reagent [2-(diethylamino)ethyl 4 aminobenzoate] hydrochloride namely procaine hydrochloride, $PQH^+ \cdot Cl^-$ and tungstate (WO_4^{2-}) in aqueous solution of pH 6–7 followed by measuring the resulting fluorescence enhancement in n-hexane at $\lambda_{ex/em} = 270/320$ nm. The fluorescence intensity of $PQH^+ \cdot Cl^-$ increased linearly on increasing tungstate concentration in the range 25–250 $g L^{-1}$. The limits of detection (LOD) and quantification (LOQ) of tungsten (VI) were found 7.51 and 24.75 $g L^{-1}$, respectively. Chemical composition of the developed ion associate and the molar absorptivity at 270 nm were found to be $[(PQH^+) \cdot WO_4^{2-}]$ and 2.710 ⁴ $L mol^{-1} cm^{-1}$, respectively. Other oxidation states (III, IV, V) of tungsten species could also be
Keywords: Spectrofluorometry Tungsten (VI) Chemical speciation Certified reference material (IAEA Soil-7) Procaine hydrochloride Water		

abstract

A highly selective and low cost extractive spectrofluorimetric method was developed for I. Introduction

Due to various processes of remobilization, heavy metals may be released and moved into the biological or food chain and concentrate in fish and other edible organisms, thereby reaching humans and causing chronic or acute diseases [1,2]. These chemicals are introduced into aquatic environment through, dumping wastes, effluents from runoff of terrestrial system and geological weathering [2]. Heavy metals are very harmful to plants and animals [3,4] and are not bio- or photodegradable and once they enter the environment, their potential toxicity depends to a large extent on their chemical forms [5–8]. Thus, the analyses of biologically essential or toxic metal ions present in the environment are of prime importance [8].

Tungsten is the elemental metal with the highest melting/boiling points, tensile strength at high temperature and a density of 19.1 $g cm^{-3}$. Tungsten occurs naturally in soils and

sediments usually in small concentrations, e.g. in the lithosphere

determined after oxidation with H_2O_2 in aqueous solution of tungsten (VI). The method was applied for analysis of tungsten in certified reference material (IAEA Soil-7) and wastewater samples. The results were compared successfully (>95%) with the data of inductively coupled plasma-mass spectrometry (ICP-MS).

* Corresponding author. Permanent address: On leave from the Department of Chemistry, Faculty of Science at Damietta Mansoura University, Mansoura, Egypt. Tel.: +966 2 6952000x64960; fax: +966 2 6952292.

E-mail addresses: malsaeed@kau.edu.sa, mohammadelshahawi@yahoo.co.uk, mohammadelshahawi@hotmail.com (M.S. El-Shahawi).

0039-9140/\$ – see front matter © 2011 Elsevier B.V. All rights reserved.
doi:10.1016/j.talanta.2011.11.039

© 2011 Elsevier B.V. All rights reserved.

the average concentration values are in the range 0.2–2.4 mg/kg [9]. W also occurs in the oxidation states III, IV, V and VI, however, oxidation state VI represents the most stable one of tungsten species. These properties make tungsten suitable for a wide variety of industrial and military uses [9,10]. In spite of its extensive uses, biological and biochemical effects of tungsten and tungsten compounds are not well known [10]. Due to the resilience and biocompatibility of tungsten, it has also become very popular as a constituent of metal alloys in medical implantable devices, e.g. prostheses in orthopaedic and maxillofacial surgery, dental implants, intravascular mobilization coils, and mechanic heart valves [11,12]. However, tungsten effects on environmental systems have not been investigated extensively and published data are fragmentary. Thus, developing of novel and sensitive methods for its determination are of great importance.

A series of extractive liquid–liquid spectrophotometric methods has been reported [13–16]. Numerous analytical techniques involving the use of benzoinoximate, tributyl-phosphate, thiocyanate and dithiol and Amberlite XAD-1180 has been used effectively for the separation and/or spectrophotometric determination of tungsten(VI) species from aqueous media and industrial wastewater [13–16]. Most of these methods are not precise, expensive, and unselective and require careful experimental conditions and considerable time consuming.

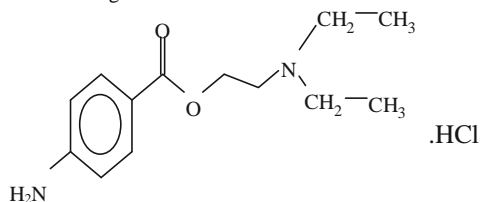


Fig. 1. Chemical structure of procaine hydrochloride (PQH⁺·Cl⁻).

Recently, the common analytical techniques for tungsten determination are graphite furnace atomic absorption spectrometry (GFAAS) [13], energy dispersive X-ray fluorescence [18], inductively coupled plasma-atomic emission spectroscopy (ICP-OES) or ICP-mass spectrometry (ICP-MS) [19] and adsorptive stripping voltammetry [20]. The main disadvantages of these techniques are the complexity and the high cost of the instruments, and the need of some degree of expertise for their proper operation. Hence, the development of low cost method, easy to operate, highly sensitive and reliable for routine analysis, e.g. spectrofluorometry or spectrophotometry is still of great concern. The former technique is better than the later due to its high sensitivity and selectivity. To our knowledge, there has been no study on the use of the title reagent PQH⁺·Cl⁻ (Fig. 1) on liquid–liquid extractive spectrofluorimetric determination and chemical speciation of trace amounts of

tungsten species in industrial wastewater. Therefore, the present article reports the use of the reagent PQH⁺·Cl⁻ for developing a

simple and low cost spectrofluorimetric method for determination and/or chemical speciation of tungsten species in water.

2. Experimental

2.1. Reagents and materials

All chemicals and solvents were of analytical reagent grade and were used without further purification. Stock solutions (1000 g mL⁻¹) of tungsten (VI), AsO³⁻, ClO₃⁻, BrO₃⁻, IO₃⁻, Li⁺, Ni²⁺, Cu²⁺ and H₂O₂ were prepared from the BDH chemicals (Poole, England) Na₂WO₄, Na₃AsO₄, KCN, KMnO₄, NaNO₂, KClO₃, KBrO₃, KIO₃, LiCl, NiSO₄, CuSO₄ and H₂O₂ (30% v/v) in water (100.0 mL), respectively. Solutions of other metal ions were prepared from their nitrate or chloride salts in deionized water. A series of Britton–Robinso (BR) buffer of pH (2–11) and acetate buffer (pH 2.3–5.7) were prepared as a stock solution (0.1/0% m/v) of procaine hydrochloride (Sigma–Aldrich) chemically named as 4-aminobenzoic acid 2-diethylamino ethylester hydrochloride, Fig. 1 was prepared by dissolving the required weight in deionized water (100 mL) mark with water.

2.2. Apparatus

Fluorescent measurements were recorded on a Perkin-Elmer (Norwalk, CT, USA) LS 55 spectrofluorimeter, equipped with a xenon lamp and a 10 mm quartz cell. A Perkin-Elmer (model Lambda 25, USA) spectro-photometer with 10 mm (path width) quartz cell was used for recording the UV–visible spectra (190–1100 nm) and absorbance measurements. A digital micropipette (Volac) and an Orion pH-meter (model EA 940) were used for the preparation of diluted tungsten (VI) solutions and pH measurements, respectively. De-ionized water was obtained from Milli-Q Plus system (Millipore, Bedford, MA, USA) and was used for preparation of solutions. A Perkin Elmer ICP-MS Sciex model Elan DRC II (California, CT, USA) was used as a reference method for tungsten determination at the operational parameters (Table 1).

Table 1
ICP-MS operational conditions for tungsten determination.

Parameter	
ICP RF power (W)	1100
Nebulizer gas flow (L min ⁻¹)	0.94
Plasma gas (Ar) flow rate (L min ⁻¹)	15
Auxiliary gas (Ar) flow rate (L min ⁻¹)	1.2
Lens voltage (V)	0.9
Analog stage voltage (V)	-1750.0
Pulse stage voltage	800
Quadrupole rod offset std	0.0
Discriminator threshold	22 Cell path voltage std (V) -13
Cell rod offset (V)	-18.0
Atomic mass (am)	52.9407 Sample flow rate, mL 093

2.3. Recommended procedure

2.3.1. Recommended spectrofluorimetric procedures for tungsten (VI) determination

An appropriate concentration (25–200 g L⁻¹) of tungsten (VI)

in aqueous solution of pH 6–7 was transferred to a separating funnel (50.0 mL) containing the reagent (PQH⁺·Cl⁻) (2.0 mL). The test solu-

tion was completed to the mark with deionized water (25.0 mL) and

the reaction mixture was shaken twice with n-hexane (2 × 2.5 mL) for 3 min. After separation of the layers, the organic phase was subjected to the fluorescence measurement at the excitation and emission wavelengths of 270 and 320 nm, respectively against reagent blank. The enhanced fluorescence intensity of the reagent PQH⁺·Cl⁻ by tungsten (VI) added was represented by the equation:

$$I = \frac{I_0 - I_f}{I_0} \times 100 \quad (1)$$

where I₀ and I_f are the fluorescence intensity of the PQH⁺·Cl⁻

reagent before and after addition of tungsten (VI), respectively. A blank experiment was also carried out under the same experimental conditions.

2.3.2. Recommended procedure for tungsten (V) determination

Aqueous solution (100.0 mL) containing tungsten (V) ions prepared as reported [13] at concentration in the range $0.05\text{--}100\text{gL}^{-1}$ was transferred to a conical flask (250mL). The

solution was oxidized to tungsten (VI) by adding few drops of concentrated nitric acid– H_2O_2 (2mL, 10% w/v) and boiling for 10min. After cooling, the test solution was adjusted to the required pH 6–7 with few drops of dilute HCl and/or NaOH and analyzed following the recommended procedures for tungsten (VI) determination against reagent blank.

2.3.3. Chemical speciation of inorganic tungsten (V) & (VI)

An aqueous solution (0.5L) containing the binary mixture of tungsten (V) and tungsten (VI) species at a total concentration of tungsten species $\leq 100\text{gL}^{-1}$ was first analyzed following the rec-

ommended procedures for tungsten (VI) determination. Another aliquot sample (0.5L) was oxidized to tungsten (VI) and analyzed as mentioned for tungsten (V) determination. The fluorescence intensity of the first aliquot ($I_1, \%$) is equivalent to tungsten (VI) ions, while the fluorescence intensity of the second aliquot ($I_2, \%$) is a measure of the sum of tungsten (V) and (VI) ions in the mixture. Thus, the fluorescence intensity ($I_2 - I_1$) is a measure of tungsten (III) ions in the binary mixture (Fig. 3).

2.4. Applications

2.4.1. Analysis of tungsten in certified reference material (IAEA Soil-7)

The validation of the developed procedure was investigated by determination of chromium in CRM (IAEA Soil-7) as follows: an accurate weight ($0.20\text{--}0.30 \pm 0.001$ g) of the CRM sample was transferred into a Teflon beaker (50.0 mL) containing HF (7.0mL), concentrated HCl (2.0mL), and concentrated HNO_3 (5.0 mL) at room temperature to digest the sample gradually and slowly. The reaction mixture was heated slowly for 1 h at $100\text{--}150^\circ\text{C}$ on a hotplate. After evolution of NO_2 fumes had ceased, the reaction mixture was evaporated almost to dryness and mixed again with concentrated HNO_3 (5.0mL). The process was repeated twice and the solid residue was re dissolved in dilute HNO_3 ($10.0\text{ mL}, 1.0\text{molL}^{-1}$), transferred to volumetric flask (25.0mL) and com-

pleted to the mark with deionized water. An accurate volume of the sample solution (10.0 mL) was adjusted to pH 6–7 with few drops of dilute HCl and/or NaOH and analyzed following the procedures of tungsten (V) determination. The change of the fluorescence intensity of the reagent $\text{PQH}^+\text{-Cl}^-$ by tungsten added was evaluated and

used for tungsten determination via the linear plot of the standard

addition method. Blank sample was analyzed following the same digestion and analytical procedures.

2.4.2. Analysis of total and chemical speciation of tungsten in wastewater

Wastewater samples were collected from the industrial effluent collection points in the industrial zones of chemicals, tanning, and dyes industries (Jeddah city, KSA). The water samples were filtered, condensed 100-folds with rotary

evaporator and finally digested with concentrated nitric acid to remove the coexisting organic substances. The solution was adjusted to the required pH and analyzed following the recommended procedures of tungsten (III) determination. For the chemical speciation of tungsten (III & VI), the sample solution was oxidized to tungsten (VI) by H_2O_2 (0.5 mL, 30%, w/v) in alkaline solution (pH ~ 9) adjusted with drops of KOH and heated for 10 min to assure complete oxidation of tungsten (III) and to remove excess H_2O_2 . An accurate volume (10 mL) of the sample after centrifugation and filtration was analyzed following the recommended procedure of tungsten (VI) determination against blank. Tungsten (III) species was obtained by subtracting the measured tungsten (VI) from the total tungsten content.

3. Results and discussion

Preliminary study has shown that, on mixing tungsten (VI) with the ion pairing reagent $\text{PQH}^+\text{-Cl}^-$ (Fig. 1) in aqueous solution of

pH 6–7 and shaking with n-hexane, a colorless – complex species

was developed. In the absence of tungsten (VI), the absorption UV spectrum of the reagent $\text{PQH}^+\text{-Cl}^-$ (1×10^{-5} M) showed no absorp-

tion bands in n-hexane. Similar trend was also obtained on shaking tungsten ions with n-hexane. The electronic absorption spectra of the developed ion associate of $\text{PQH}^+\text{-Cl}^-$ (1×10^{-5} M) and tungsten

(VI), $\text{PQH}^+\text{-Cl}^-$ and tungstate ions in n-hexane are shown in Fig. 2.

The spectrum of the developed associate in n-hexane showed two bands at 280 nm (like shoulder) and 270 nm confirming the associate formation. The value of the molar absorptivity (ϵ) at λ_{max} 270 nm of the associate formed was found equal $2.7 \times 10^4 \text{ Lmol}^{-1} \text{ cm}^{-1}$ in

n-hexane suggesting the possible use of the title reagent for spectrofluorimetric determination of tungsten. The composition of the produced ion associate was determined by Job's continuous variation and molar ratio methods at λ_{max} 270 [21]. The results revealed that, the ratio of tungstate: $\text{PQH}^+\text{-Cl}^-$ was 1:2 molar ratio. Thus,

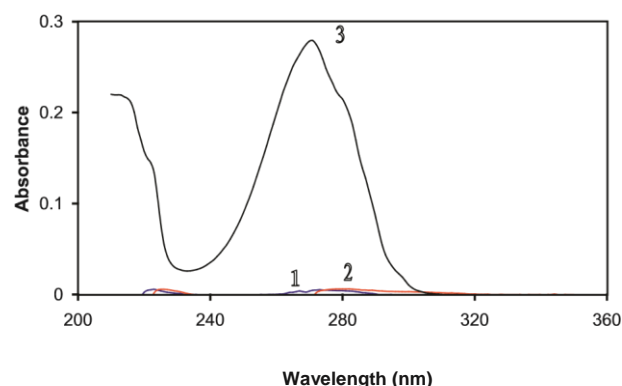


Fig.2.Electronic spectraofPQH⁺·Cl⁻ (1),tungstate(2)andthedevelopedionassociate[(PQH⁺)₂·WO₄²⁻] in n-hexane (3). Aqueous phase (10 mL) of pH 6–7 containing tungsten (100 g L⁻¹) 0.2 mL PQH⁺·Cl⁻ (0.01% w/v) and n-hexane (10 mL).

the most probable composition of the extracted species [(PQH⁺)₂·WO₄²⁻].

2
WO₄²⁻].

In the absence of tungsten (VI), the reagent PQH⁺·Cl⁻ has

no fluorescence at $\lambda_{ex/em} = 270/305$ nm in n-hexane. The fluorescence intensity of PQH⁺·Cl⁻ was enhanced on raising tungsten (VI)

concentration with negligible shift in the wavelength confirming

the formation of the complex ion associate in the ground electronic state. Representative results are demonstrated in Fig. 3. The absence of new emission band in the spectrum indicates that, the formed ion associate in the excited state does not exist under the experimental conditions [12]. The developed enhancement in the fluorescence intensity was successfully used for developing a new spectrofluorimetric method for determination of tungsten (VI) and total inorganic tungsten (V) and (VI) species in water.

3.1. Influence of analytical parameters

The effect of pH on the enhancement of the fluorescence intensity of the developed ion associate in n-hexane was tested at various pH ranges employing BR buffer (2–11) and acetate (2.3–5.7). The results revealed the interference of the BR buffer on the signal therefore it was excluded. Maximum and constant fluorescence

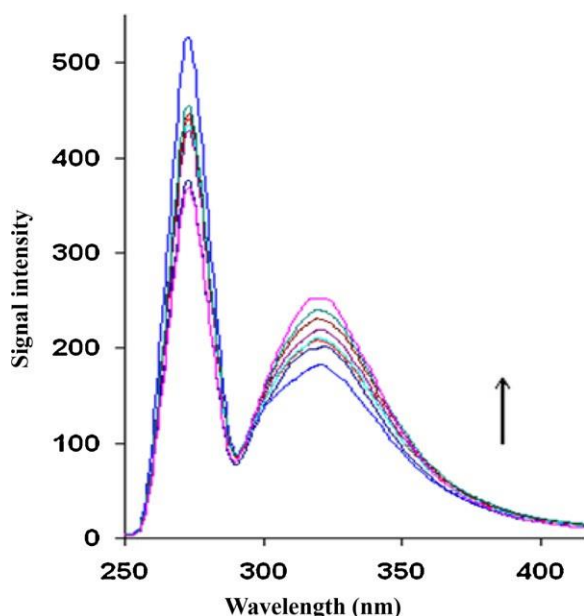


Fig.3.EmissionspectraofPQH⁺·Cl⁻inn-hexaneuponadditionofvariousconcentrations(25–100g L⁻¹)of tungsten(VI).

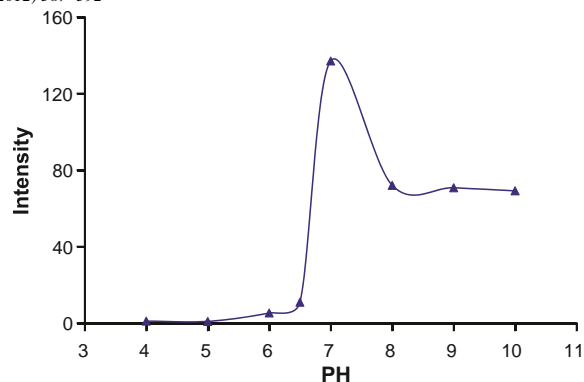


Fig.4.InfluenceofpHonthefluorescenceenhancementofthedevelopedionassociate[(PQH⁺)₂·WO₄²⁻] inn-hexane.

enhancement was achieved in acetate media in the pH range 6–7. Representative results are shown in Fig. 4. Therefore, in the subsequent work, the solution pH was adjusted to pH 6–7 using few drops of dilute HCl and/or NaOH.

The influence of shaking time on the fluorescence quenching intensity of the reagent PQH⁺·Cl⁻ by the developed ion associate

in the organic phase was investigated. Maximum and constant

quenching intensity was achieved at 3 min shaking with n-hexane (Fig. 5). Thus, a shaking time of 3 min was selected in the next work.

The influence of the reagent PQH⁺·Cl⁻ concentration on the

fluorescence intensity was investigated. The results are demon-

strated in Fig. 6. Maximum and constant fluorescence intensity was achieved using 2.0 mL of the reagent (0.1% w/v). High concentration of PQH⁺·Cl⁻ makes the fluorescence quenching so small that it

cannot be detected.

The extraction performance of the ion associate [(PQH⁺)₂·WO₄²⁻]

was tested in a series of organic solvents, e.g. n-hexane, dichloromethane, carbon tetrachloride, toluene, chloroform and methyl isobutyl ketone. The extraction of the ion associate increased in the following order: n-hexane > toluene > dichloromethane > chloroform > methyl isobutyl ketone in agreement with the order of lowering the dielectric constant. Maximum extraction and constant fluorescence signal intensity was achieved in n-hexane. Therefore, in the subsequent work n-hexane was chosen as a preferred solvent.

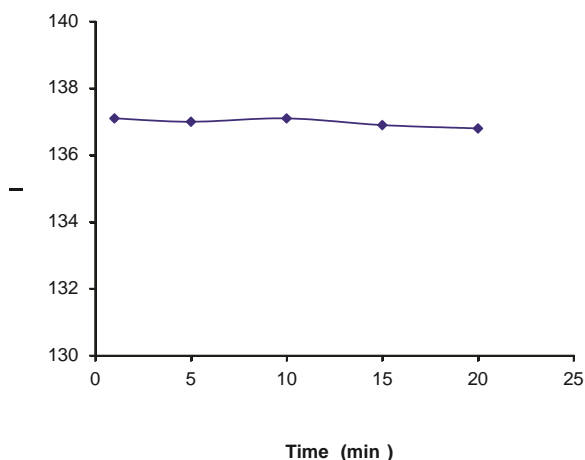


Fig. 5. Effect of shaking time on the fluorescence enhancement of PQH⁺·Cl⁻ in the presence of tungsten (VI) (100.0 g L⁻¹) in a aqueous solution of pH 6–7.

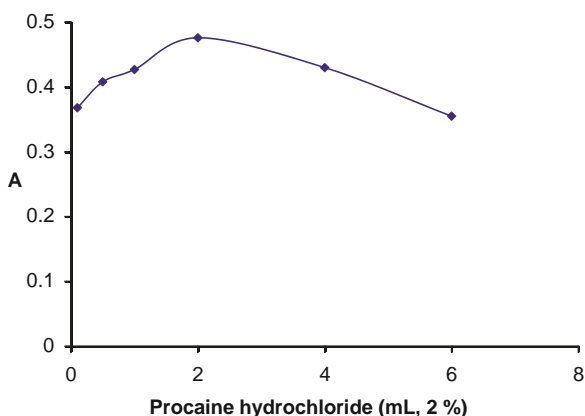


Fig. 6. Influence of reagent PQH⁺·Cl⁻ concentration on the signal of fluorescence intensity of the developed ion associate with tungsten (VI).

3.2. Selectivity

The selectivity of the developed method was examined in the presence of a series of foreign ions under the established conditions. The tolerance limits (w/w) less than ±4% change in the fluorescence intensity of tungsten (VI) was considered as free from interfering species. Solutions containing 1.0 g L⁻¹ of tungsten (VI) and the

interfering species in different ratios were subjected to complete analysis. The results are summarized in Table 2. Complete extraction of tungsten (VI) was achieved as indicated from the ICP-MS and fluorescence measurements. The anions BrO₃⁻, IO₃⁻, and MnO₄⁻, CN⁻ and Cu²⁺ interfered seriously with the fluorescence intensity

of the PQH⁺·Cl⁻ reagent and tungsten (VI) determination. The inter-

ference of cyanide and copper was eliminated by adding few drops

of, KOH (0.1% mL V) –H₂O₂ and sodium thiosulphate, respectively. The interference of MnO₄⁻ was eliminated by the addition of few drops (0.1% m/v) NaN₃ to reduce manganese (VII) to manganese (II) and the tolerance was improved to acceptable limit (98 ± 2%). The results denoted that, the method has good selectivity even in the presence of high concentration of tungsten (III) species. Thus, the method was found suitable for the chemical speciation of tungsten (V, VI) in a variety of environmental water samples.

3.3. Figure of merits

Under the optimized experimental conditions, the plot of tungsten (VI) concentration vs. fluorescence enhancement by the developed ion associate PQH⁺·Cl⁻ was linear in the concentration

range 25–250 g L⁻¹. A regression equation

of:

$$I = 636.51 C (\text{g L}^{-1}) + 1.5179 \quad (2)$$

with a correlation coefficient of 0.998 (n=6) were achieved. Based on the IUPAC [13], the values of LOD and LOQ of tungsten (VI) species were 7.51 and 24.75 g L⁻¹, respectively. The LOD

Table 2

Tolerance limits of interfering species in tungsten (VI) (1.0 mL⁻¹) determination by the developed method.

Interfering species	Interfering to analyte ratio
As ³⁺ , Ni ²⁺ , Bi ³⁺ , Li ⁺ , Na ⁺ , K ⁺ , Ca ²⁺ , Mg ²⁺ , Al ³⁺ , Ag ⁺ , CO ₃ ²⁻ , SO ₄ ²⁻ , NO ₃ ⁻	1000:1
Fe ³⁺ , Hg ²⁺ , Pb ²⁺ , Mn ²⁺ , Co ²⁺ , Cu ⁺ , Cr ³⁺ , Cl ⁻ , F ⁻ , NO ₂ ⁻ , H ₂ O ₂	100:1
MnO ₄ ⁻ , and BrO ₃ ⁻	50:1
IO ₃ ⁻	0.5:1
CN ⁻	10:1 ^a

^a Interference was minimized by adding few drops of diluted KOH (0.1%) and hydrogen peroxide. (7.51 g L⁻¹) lower than the instrumental detection limits of flame

(750 μ AAS g L⁻¹), ICP-OES radial (17.0 g L⁻¹) and energy disper-

sive X-ray fluorescence spectrometry (157.51 g mL) for tungsten determination. The method provides LOD lower than the maximum allowable level (<15.0 g L⁻¹) of tungsten recommended by

WHO [9]. The present method has a limit of detection lower than some of the reported methods of tungsten determination and ICPOES [13–15, 18]. The LOD of the developed was found higher than the reported method [12]. The relative

standard deviation at concentration 50 g L^{-1} tungsten (VI) was $\pm 3.6\%$ ($n=5$). The figures of

merits of the proposed method were compared successfully with many of the published electrochemical, chromatographic and spectrometric methods [12,13,17–20]. Thus, the method presents an effective approach in pre concentration and separation of tungsten from natural waters. The method could be extended to be on-line for the pre concentration of ultratrace concentrations of tungsten (VI) from sea water samples. However, most of the reported methods [12,17–20] suffered from time consuming, selectivity and reproducibility. The fluorescence enhancement of the reagent by tungsten (VI) added under the optimum experimental conditions suggested use of the $\text{PQH}^+\text{-Cl}^-$ reagent for the pre concentration

and determination of tungsten (VI) from large sample volumes

of deionized water. Thus, aqueous solutions (0.5 L) of deionized water samples containing various concentrations ($5.0\text{--}50.0 \text{ g L}^{-1}$)

of tungsten (VI) at pH 6–7 were shaken with n-hexane as described above. Analysis of aqueous solutions by ICP-MS against reagent blank has revealed complete extraction ($96\text{--}98 \pm 1.6$) of tungsten (VI). The concentration of tungsten (VI) species in the organic phase was quantitatively determined ($94\% \pm 3.6$) by measuring the enhancement in the fluorescence of $\text{PQH}^+\text{-Cl}^-$ in n-hexane at opti-

mum $_{\text{ex/em}}$. Tungsten (III) species in aqueous solutions (0.1 L) in the concentrations range $0.05\text{--}50 \text{ g mL}^{-1}$ was also determined by

the $\text{PQH}^+\text{-Cl}^-$ reagent after oxidation to tungsten (VI) species as

described. Satisfactory extraction percentage ($96 \pm 2.7\text{--}102 \pm 1.9\%$, $n=5$) of tungsten (V) species was also achieved.

3.4. Analytical applications

3.4.1. Analysis of tungsten in the certified reference material (IAEA Soil-7)

The validation of the developed method was performed by the analysis of tungsten in the certified reference materials (IAEA Soil7). Good agreement between the total tungsten content added and analyzed by the developed spectrofluorimetric, and ICP-MS methods based on dry weight in the range of 95% confidence interval. These data demonstrated the accuracy and precision of the developed method for trace analysis of tungsten in complex matrices.

3.4.2. Analysis of tungsten in water

The proposed method was applied for the chemical speciation of tungsten (V & VI) in tap and wastewater samples. Total tungsten content in water samples was determined via the developed spectrofluorimetric (A) and ICP-MS (B) methods (Table 3).

Table 3

Analysis of tungsten (g L^{-1}) species in water by the developed spectrofluorimetric (A) and ICP-MS (B) methods (mean \pm standard deviation, $n=5$).

Sample	Tungstate added	Tungstate found	Total tungsten	
			A	B
Wastewater	–	6.92 ± 0.7	7.1 ± 0.34	6.24 ± 0.57
	50	59.3 ± 2.4	60.7 ± 4.1	60.34 ± 1.9
Tapwater	–	nd	nd	2.4 ± 1.2
	10	10.8 ± 2.6	11.3 ± 1.1	10.93 ± 2.1

Good agreement between the percentage recovery determined by the developed spectrofluorimetric and ICP-MS methods was achieved and always higher than 95% confidence confirming the precision of the independence of the method from matrix interference. Statistical treatment of data using F test [21] revealed that, no significant differences between the two variances of the developed and the ICP-MS methods. The calculated value of F (2.78) is lesser than the tabulated F value (6.39) for five replicate measurements. The student t test [21] was also applied to the analytical data of the developed and ICP-MS methods. No significance difference between the two methods. The tabulated value at 95% confidence limit was 2.306 and the calculated value by applying Student's t test to the results of wastewater sample was found lesser (0.79) for five measurements.

4. Conclusion

The analytical merits of the proposed method were successfully compared with some of the reported spectrofluorimetric methods. The method provides LOD lower than the maximum allowable level ($50.0 \text{ } \mu\text{g L}^{-1}$) of tungsten recommended by WHO [12]. The reagent $\text{PQH}^+\text{-Cl}^-$ appear to be promising as the basis of a sensitive and clean spectrofluorimetric procedure for tungsten speciation.

The LOD of the method could be improved to lower value by prior pre concentration onto $\text{PQH}^+\text{-Cl}^-$ immobilized polyurethane

packed column before determination. Most of reported methods

exhibited a relatively high LOD ($10.0\text{--}50.0 \text{ g L}^{-1}$), and serious

interferences of Ag^+ , Hg^{2+} , Pb^{2+} , Cr^{3+} , and Ni^{2+} [18–20]. The

method could be applied easily for the analysis of polytungstic acids, and other oxo after digestion in alkaline solution [2]. Work is continuing for on-line determination and speciation of inorganic tungsten and different polyoxotungstate such as heteropoly acids, paratungstate A $[\text{W}_6\text{O}_{20}(\text{OH})_2]^{6-}$ and $[\text{W}_7\text{O}_{24}(\text{OH})_2]^{9-}$

and paratungstate B $[\text{H}_2\text{W}_{12}\text{O}_{42}]^{10-}$ and $[\text{H}_3\text{W}_{12}\text{O}_{42}]^{9-}$, and metatungstate, e.g., Keggin ion isomers B $[\text{HW}_6\text{O}_{21}]^{7-}$, 12 40

6 6 conditions of pH 8–9 [2].

$[\text{H}_2\text{W}_{12}\text{O}_{40}] - [\text{W}_7\text{O}_{24}(\text{OH})_2]$ - after decomposition in alkaline

Acknowledgements

The authors would like to thank the Deanship of Scientific Research, King Abdulaziz University, Kingdom of Saudi Arabia for the financial support under the grant number 17-21/430 and the Chemistry Department for the facilities provided.

References

- [1] G.N. Mukherjee, L. Sarker, *Indian J. Chem.* 27A (1988) 514.
- [2] N. Strigul, *Ecotoxicol. Environ. Saf.* 73 (2010) 1099.
- [3] O.E. Offiong, S. Martelli, *Farmaco* 49 (1994) 513.
- [4] C.F. Zhong, J.C. Deng, J. Tong, X.H. Yao, W.S. Zhu, *Chem. J. Chin. Univ.* 19 (1998) 174.
- [5] P.D. Beer, F. Szemes, V. Balzani, M. Sala, M.G.B. Drew, S.W. Dent, M. Maestri, *J. Am. Chem. Soc.* 119 (1997) 11864.
- [6] J. Costa, R. Delgado, M.G.B. Drew, V. Felix, *J. Chem. Soc. Dalton Trans.* (1998) 1063.
- [7] Y. Al-Shihadeh, A. Benito, J.M. Leoris, R.M. Manez, T. Pardo, J. Soto, M.D. Marcos, *J. Chem. Soc. Dalton Trans.* (2000) 1199.
- [8] E. Lassner, W.D. Schubert, *Tungsten Properties, Chemistry, Technology of the Element, Alloys and Chemical Compounds*, Kluwer Academic/Plenum Publishers, Boston, 1999.
- [9] A. Koutsospyros, W. Braidia, C. Christodoulatos, D. Dermatas, N. Strigul, *J. Hazard. Mater.* 136 (2006) 1.
- [10] Y. Tajima, *J. Inorg. Biochem.* 94 (2003) 155.
- [11] G.S. Guandalini, L. Zhang, E. Fornero, J.A. Centeno, V.P. Mokashi, P.A. Ortiz, M.D. Stockelman, A.R. Osterburg, G.G. Chapman, *Chem. Res. Toxicol.* 24 (2011) 488.
- [12] R. Piech, A. Bugajna, S. Bas, W.W. Kubiak, *J. Electroanal. Chem.* 644 (2010) 74.
- [13] Z. Marczenko, *Separation and Spectrophotometric Determination of Elements*, 2nd ed., John Wiley and Sons, 1986.
- [14] S.P. Masti, *Anal. Sci. (Jpn.)* 18 (2002) 913.
- [15] B.F. Quin, R.R. Brooks, *Anal. Chim. Acta* 58 (1972) 301.
- [16] S. Li, N. Deng, F. Zheng, Y. Huang, *Talanta* 60 (2003) 1097.
- [17] M. Soylak, L. Elci, M. Dogan, *Talanta* 42 (1995) 1513.
- [18] S. Uskokovic-Markovic, M. Todorovic, U.B. Mioc, I. Antunovic-Holclajtner, V. Andric, *Talanta* 70 (2006) 301.
- [19] A.J. Bednar, W.T. Jones, M.A. Chappell, D.R. Johnson, D.B. Ringelberg, *Talanta* 80 (2010) 1257.
- [20] D.T. Sawyer, W.R. Heinemann, J.M. Beebe, *Chemistry Experiments for Instrumental Methods*, John Wiley & Sons, 1984.
- [21] J.N. Miller, J.C. Miller, *Statistics and Chemometrics for Analytical Chemistry*, 5th ed., Pearson Education Limited, Prentice Hall, New York, 2005.



Analytical Methods

Analysis of some selected catechins and caffeine in green tea by high performance liquid chromatography

M.S. El-Shahawi [†], A. Hamza, S.O. Bahaffi, A.A. Al-Sibaai, T.N. Abduljabbar

Department of Chemistry, Faculty of Science, King Abdulaziz University, P.O. Box 80203, Jeddah 21589, Saudi Arabia

article

info

abstract

Article history:

Received 6 February 2011

Received in revised form 16 February 2012

Accepted 7 March 2012 Available

online 28 March 2012

Keywords:

Green tea water extract

Catechins

Gallated catechins

Caffeine

HPLC

Antioxidant

Green tea seems to have a positive impact on health due to the catechins—found as flavanols. Thus, the present study was aimed to develop a low cost reversed phase high performance liquid chromatographic (HPLC) method for simultaneous determination of flavanol contents, namely catechin (C), epicatechin (EC), epigallocatechin (EGC), epicatechin 3-gallate (ECG) and epigallocatechin 3-gallate (EGCG) and caffeine in 29 commercial green tea samples available in a Saudi Arabian local market. A C-18 reversed phase column, acetonitrile–trifluoroacetic acid as a mobile phase, coupled with UV detector at 205 nm, was successfully used for precise analysis of the tested analytes in boiled water of digested tea leaves. The average values of N (No. of theoretical plates), HETP (height equivalent of theoretical plates) and R_s (separation factor) (at $10 \text{ } \mu\text{g ml}^{-1}$ of the catechins EC, EGC, EGCG and ECG) were $2.6 \times 10^3 \pm 1.2 \times 10^3$, $1.7 \times 10^3 \pm 4.7 \times 10^4 \text{ cm}$ and $1.7 \pm 5.53 \times 10^2$, respectively. The developed HPLC method demonstrated excellent performance, with low limits of detection (LOD) and quantification (LOQ) of the tested catechins of $0.004\text{--}0.05 \text{ } \mu\text{g ml}^{-1}$ and $0.01\text{--}0.17 \text{ } \mu\text{g ml}^{-1}$, respectively, and recovery percentages of 96–101%. The influence of infusion time (5–30 min) and temperature on the content of the flavanols was investigated by HPLC. After a 5 min infusion of the tea leaves, the average concentrations of caffeine, catechin, EC, EGC, ECG and EGCG were found to be in the ranges 0.086–2.23, 0.113–2.94, 0.58–10.22, 0.19–24.9, 0.22–13.9 and 1.01–43.3 mg g^{-1} , respectively. The contents of caffeine and catechins followed the sequence: EGCG > EGC > ECG > EC > C > caffeine. The method was applied satisfactorily for the analysis of (+)-catechin, even at trace and ultra trace concentrations of catechins. The method was rapid, accurate, reproducible and ideal for routine analysis.

2012 Elsevier Ltd. All rights reserved.

1. Introduction

Tea is one of the most widely consumed beverages in the world (Cheng, 2004; Goncalves, Paterson, & Lima, 2006; Jian, Xie, Lee, & Binns, 2004; Peres, Tonin, & Tavares, Rodriguez-Amaya, 2011; Vinson, 2000; Yang, Maliakal, & Meng, 2002). All tea types come from the leaves of the “*Camellia sinensis*” plant, which is a member of the aceae family (Gutman & Ryu, 1996). Based upon the degree of fermentation, tea is classified into green tea (unfermented), oo-long tea (semi-fermented), and black tea (fully fermented) (Chen, Zhao, Chen, Lin, & An Zhao, 2011; Fujiki, Suganuma, Imai, & Nakachi, 2002; Haslam, 2003; Singh, Akhtar, & Haqqi, 2010; Yanagida et al., 2006; Ye, Zhang, & Gu, 2011; Zhao et al., 2011; Zhu, Hackman, Ensunsa, Holt, & Keen, 2002). Green tea is more popular among the Chinese and Japanese (Koo & Cho, 2004), whereas black tea is preferred more in India, Europe, North America and North Africa (Chow & Kramer, 1990; Chung, Schwartz, Herzog, & Yang, 2003;

Mackay & Blumberg, 2000) and they account for approximately 23% and 75% of the global production, respectively.

Tea infusion not only gives specific taste and flavour, but also many essential dietary compounds for human health (Cabrera, Artacho, & Gimenez, 2006), such as polyphenols, caffeine, amino acids, vitamins, carbohydrates and trace elements (Horie & Kohata, 2000; Ramos, 2007; Steinberg, Bearden, & Keen, 2003). The main green tea catechins (GTCs) are epigallocatechin 3-gallate (EGCG), epicatechin 3-gallate (ECG), epigallocatechin (EGC) and epicatechin (EC) (Dalluge, Nelson, Thomas, & Sander, 1998). Epigallocatechin 3-gallate, the “signature” compound in green tea, represents over 60% of the total catechins which have major effects in prevention of most diseases (Yang & Koo, 1997). Tea catechins are wellknown natural powerful antioxidant (Koo & Cho, 2004; Rietveld & Wiseman, 2003) and recent studies have reported that they play an important role in the prevention of cardiovascular diseases (Cheng, 2006; Yang & Koo, 2000) and cancers of several types

0308-8146/\$ - see front matter 2012 Elsevier Ltd. All rights reserved.

<http://dx.doi.org/10.1016/j.foodchem.2012.03.039>

(Chen & Zhang, 2007; Jian et al., 2004). Tea catechins and caffeine have diverse pharmacological effects, including: anti-hypertensive

[†]

Corresponding author.

E-mail address: mohammad_el_shahawi@yahoo.co.uk (M.S. El-Shahawi).

(Yang, Lu, Wu, Wu, & Chang, 2004), anti-inflammatory (Cheng, 2003; Mutoh et al., 2000), anti-obesity (Chantre & Lairon, 2002; Dulloo et al., 1999), hypocholesterolemic (Yang & Koo, 1997), antidiabetic (Waltner et al., 2002; Zeyuan, Bingying, Jiming, & Yifeng, 1998), anti-bacterial, anti-viral (Cross, 2002), improving alertness and reaction time, and mitigating tiredness (Griffiths & Griffiths, 2005), anti-aging effects (Esposito et al., 2002) and inhibition of α -glucosidases and glycogen phosphorylase (Kamiyama et al., 2010). The component EGCG in green tea could reduce the risk of becoming infected by human immunodeficiency virus (HIV) (Williamson et al., 2007; Singh et al., 2010).

Many methods have been reported for the analysis of catechin contents in green tea (Friedman, Levin, Choi, Kozukue, & Kozukue, 2006; Kodamatani, Shimizu, Saito, Yamazaki, & Tanaka, 2006; Yang, Ye, Xu, & Jiang, 2007; Yao, Caffin, Ndarcy, Jiang, & Shi, 2005): capillary electrophoresis (CE) (Kotani, Takahashi, Hakamata, Kojima, & Kusu, 2007; Lee & Ong, 2000), thin-layer chromatography (Vovk, Simonovska, & Vuorela, 2005), near infrared spectrometry (Chen, Zhao, Zhang, & Wang, 2006; Dou, Sun, Ren, Ju, & Ren, 2005), Fourier transform near infrared spectrometry (Chen, Zhao, Chaitep, & Guo, 2009; Chen, Zhao, & Lin, 2009; Sinija & Mishra, 2009), reflectance spectroscopy, centrifugal precipitation chromatography (Baldermann, Fleischmann, Watanabe, Winterhalter, & Ito, 2009), potentiometric flow injection (Koutelidakis et al., 2009; Niehetal., 2009) high-speed counter-current chromatography (Kumar & Rajapaksha, 2005; Yanagida et al., 2006), multivariate calibration techniques (Schurek, Portolés, Hajslova, Riddellova, & Hernández, 2008).

Recent studies (Chen et al., 2011; Singh et al., 2010; Ye et al., 2011) have reported that, theaflavin-3,3-gallate and green tea polyphenol EGCG are good inhibitors of tyrosine receptor kinase. Thus, the increasing interest in green tea polyphenols and their anticarcinogenic effects has led to many analytical developments for their determination. The present work was aimed at: (i) developing low cost HPLC procedures for simultaneous determination of five catechins and caffeine (using HPLC) in green tea water extract; (ii) characterization of 29 commercial green tea samples available in the local market of Saudi Arabia in respect to catechin and caffeine contents in infusion of green tea (in boiled water extract) and, finally, (iii) Correlation of the total average contents of catechins and epigallocatechin 3-gallate and EGC markers in green tea with tea prices in the Saudi Arabian market.

2. Materials and methods

2.1. Reagents and materials

All chemicals and solvents used were of analytical reagent grade quality and were used as received. Doubly deionized water was used throughout. Standards of the analytes: (+)-catechin (C, puriss P 99%), (+)-epicatechin (EC, purum P 95%), epicatechin-3 gallate (ECG, purum P 98%), epigallocatechin (EGC, purum P 90%), and epigallocatechin-3-gallate (EGCG, purum P 97%) and caffeine were purchased from Fluka (AG, USA). The catechins and caffeine were used as received. Boric acid, acetonitrile and trifluoroacetic acid (HPLC-grade) were purchased from Sigma (ST. Louis, MO, USA). Sodium chloride, absolute methanol, sodium dihydrogen and potassium hydrogen phthalate were obtained from Merck (Darmstadt, Germany). Other chemicals, e.g. HNO_3 and H_2O_2 (Aldrich Chemical Company, Milwaukee, WI, USA), were also used without further purification. Twenty-nine green tea samples of different origins (China, Japan, Indonesia, Sri Lanka and Taiwan) of different prices were randomly collected and purchased from the Saudi Arabian local market. The origin, numbering and the commercial names of the

investigated tea leaves and their prices, in Saudi Arabia currency (Saudi Ryals/100 g tea stuff), are shown in Table 1. Ultrapure water of resistance 18 MO cm^1 obtained from a Milli-Q purification device (Millipore Co., Bedford, MA, USA).

Distilled and deionized water was used for the preparation of standard solutions and samples.

2.2. Apparatus

A Perkin–Elmer (Analyst – TM 200, USA) HPLC, equipped with UV–Visible detector, column oven, quaternary pumping system and chromatography interface (Perkin–Elmer model 600), auto injector (Villiers-1e-Bel, France) and IRIS Spectral Processing software for peak identification and integration (Milford, MA, USA), was used for peak purity determination. The chromatographic separation was performed on a guard and analytical cartridge system (Partisphere 5 C_{18} , 5 μm , 250 mm and 4.6 mm I.D.) (Whatman) with column temperature set at 32 C. A Whatman solvent IFD disposable filter device was used for on-line filtration and degassing of the mobile phase. In gradient HPLC elution, the two mobile phases (A&B) employed for gradient HPLC elution, composed of: (A) 5% (v/v) acetonitrile containing 0.035% (v/v) trifluoroacetic acid and (B) 50% (v/v) acetonitrile containing 0.025 (v/v) trifluoroacetic acid (Lee & Ong, 2000), were used at 1.0 ml min^{-1} flow rate. The gradient elution profile started with A–B (90:10), B was gradually increased to 20% at 10 min, and back to 40% at 30 min. The column was then re-equilibrated with the initial conditions for 3 min before the next injection. A 20 μl injection volume was used in recording the chromatograms and concentration levels of caffeine and catechins in the tea sample infusions in boiled water for different time intervals (5–30 min). The UV spectrum of each catechin or caffeine, after subtraction of the corresponding UV base spectrum, was normalized automatically by the computer and the plots were superimposed. Peaks were considered to be chromatographically pure when their spectra showed exact coincidence. Twenty-nine green tea types were analysed, with UV detection at 205 nm.

2.3. Standard preparation

The main stock solutions (5 mg ml^{-1}) of caffeine and catechins were prepared by dissolving 5 mg of the respective compound in 0.2 ml of ethanol, followed by 0.8 ml of distilled water. The main stock solutions of the other ingredients were prepared individually from 5 mg of the respective compound in 1.0 ml of 20% (v/v) acetonitrile. Working standards for calibration were prepared with concentrations ranging from 0.01 to 500 $\mu\text{g ml}^{-1}$ of analytes.

2.4. Recommended procedures

2.4.1. HPLC analysis of the standard mixtures of the catechins and caffeine

Stock solutions (1000 $\mu\text{g ml}^{-1}$) of catechin, epicatechin, epicatechin-3 gallate, epigallocatechin, epigallocatechin-3-gallate and caffeine were prepared individually by dissolving the required weight of each compound in acetonitrile–water (1:5 v/v). More diluted solutions (10.0 $\mu\text{g ml}^{-1}$) of each catechin or caffeine were also prepared individually in acetonitrile–deionized water (1:5 v/v). Various mixtures containing all catechins and caffeine at concentrations of 1, 5, 10 and 20 $\mu\text{g ml}^{-1}$ of each compound, were prepared in acetonitrile–deionized water (1:5 v/v) and used as standard mixtures for the calibration curves. Working standard solutions (5–20 $\mu\text{g ml}^{-1}$) for each catechin or caffeine were injected into the HPLC machine and the corresponding peak area was recorded and measured. A standard calibration plot for each catechin or caffeine was constructed by plotting concentration (X-axis) versus peak area at the same retention time and

the quantification was also carried out from the integrated peak areas of the green tea samples and the corresponding standard graph.

Table 1
Local names, origin and prices (Saudi Ryals/100 g of green tea samples randomly purchased and collected from the local market of Saudi Arabia).

Local names of green tea samples	Price/100 g Saudi Ryals	Country	Number of samples
Sample(1): Al-Deafa	3.33	China	18
Sample(2): Twinings	13.25		
Sample(3): Green Tea Wadi al Nahil	6		
Sample(5): China Green Tea	1.67		
Sample(6): Unknown	Unknown		
Sample(9): China Green Tea Camel	4.4		
Sample(11): Badraiq Green Tea	3.16		
Sample(12): Bafart Green Tea	9.9		
Sample (14): Camel Green Tea.	3.4		
Sample(15): Beoko Green Tea	25		
Sample(16): Kudin Green Tea Long Leaves	14		
Sample(17): Kudin Green Tea Buds Leaves	16		
Sample(18): Alishan Green Tea	28		
Sample(19): Lung Ching	28		
Sample(20): Yaiqua Yeen Green Tea	10		
Sample(22): White Needle Green Tea	20		
Sample(23): Al-Afea Chines Green Tea	9.50		
Sample(24): Chines Green Tea (Al Margalani)	4.65		
Commercial name of green tea samples	Price/100 g	Country	Sample numbers
Sample(7): Sencha Green Tea 1	110	Japan	5
Sample(21): Sencha Green Tea 2	8		
Sample(25): Sencha Green Tea 3	26		
Sample(26): Kukicha	10		
Sample(27): Hirabancha	14		
Sample(10): Green Tea Abu Sheba	9.50	Indonesia	2
Sample (4): Lipton Green Tea	3.75		
Sample(8): Rabea Green Tea	3.8	Sri Lanka	2
Sample(13): Maatouq Green Tea	10.53	Taiwan	
Sample(28): Gao Shan Alishan			
Samples(29): High Mountain Green Tea	400		
	450		

2.4.2. Analysis of caffeine and catechins in green tea samples

As the catechins were photo-sensitive, the sample preparation was carried out in a dim lighting working environment. An accurate weight ($0.25\text{--}0.26 \pm 0.01$ g) of green tea sample was individually placed into boiled water (100 ml) and incubated at 90 C for 5 min. This condition was similar to an actual brewing condition for a cup of tea. After cooling, each sample solution was filtered through medium (No.1) and slow (No.5) Whatman filter papers, respectively. The filtrate and the washing solutions were then transferred to the volumetric flask (100 ml). Immediately, an appropriate volume (10.0 ml) of the tea water extract was filtered through a disposable 0.45 μm cellulose membrane filter and injected into the HPLC under the optimum operational conditions of the machine described (Lee & Ong, 2000) at 205 nm of the UV detector with some modifications described below. The mean concentration ($\mu\text{g g}^{-1}$) of the unknown caffeine and catechins in the water tea extract of the tea sample was determined from the standard curve at the retention time of the required component, employing the equation:

$$\frac{1}{m} \frac{A_C - B}{V} = \frac{C}{m}$$

Average total concentration; $\mu\text{g g}^{-1}$

m

where, C is the average total compound concentration in sample solution ($\mu\text{g ml}^{-1}$) of tea infusion; B is the blank reading; V is the volume (ml) of the sample solution and m is the mass (g) of the tea. Quantification was carried out from peak areas of the sample with the aid of the corresponding standard graph. Similarly, the influence of infusion time (5–30 min) of selected tea samples (No. 5) in boiled water was also investigated.

3. Results and discussion

3.1. Chromatographic performance of the tested catechins and caffeine

Nakagawa and Miyazawa (1997) have reported the most sensitive HPLC method for analysis of catechins in green tea using chemiluminescence detection, with a limit of detection of $\mu\text{g ml}^{-1}$. This level of sensitivity is not required for analysis of major tea polyphenols. Dalluge et al., (1998) have reported that, the presence of trifluoroacetic acid is essential for high resolution and efficient chromatography of catechins in tea. A detection sensitivity of $0.5\text{--}1.0 \mu\text{g ml}^{-1}$ of different catechins in green tea, using UV absorbance at 280 nm, has been reported by Harms and Schwedt (1994). Lee and Ong (2000) reported that the use of acetonitrile, instead of methanol, as eluent provided a higher UV absorbance and easy detection of trace and ultra concentrations of catechins or caffeine at 205 nm instead of 275 nm. In the present study, our preliminary investigation on the analysis of catechins in the various green tea leaves has revealed that, the two mobile phases used in the gradient separation composed of different proportions of acetonitrile and trifluoroacetic acid, provided excellent chromatographic separation (at UV 205 nm). The HPLC chromatograms of the standard solutions ($10.0 \mu\text{g ml}^{-1}$) of the five catechins (catechin, epicatechin, epigallocatechin, epigallocatechin gallate and epicatechin gallate) and caffeine were recorded individually under the recommended experimental procedures. The retention times of the tested species are given in Table 2. HPLC chromatograms of each catechin and caffeine were also recorded individually at various concentrations ($5.0\text{--}20 \mu\text{g ml}^{-1}$) to construct the calibration plot for each component under the optimum operational conditions.

HPLC chromatograms of the five catechins and caffeine in their standard mixtures at various concentrations ($5.0\text{--}20 \mu\text{g ml}^{-1}$) were recorded. A representative chromatogram, at $10.0 \mu\text{g ml}^{-1}$ of each component in their mixture, is shown in Fig. 1. The catechins, EGC, EC, EGCG and ECG, showed well defined peaks at retention times at 9.57; 15.87; 16.56 and 21.06 min, respectively. The observed shift in the retention times of these catechins in their standard mixture (Fig. 1) compared to each individual component (Table 2) is most likely attributable to the electrostatic interaction of their hydroxyl groups, in addition to the possible formation of inter- or intra-molecular H-bonding. On the other hand, caffeine

Table 2

Retention time of the five catechins and caffeine.

Compound	Retention time (min)
EGC	7.3
Caffeine	10.95
C	11.16
EC	15
EGCG	15.8
ECG	20.6

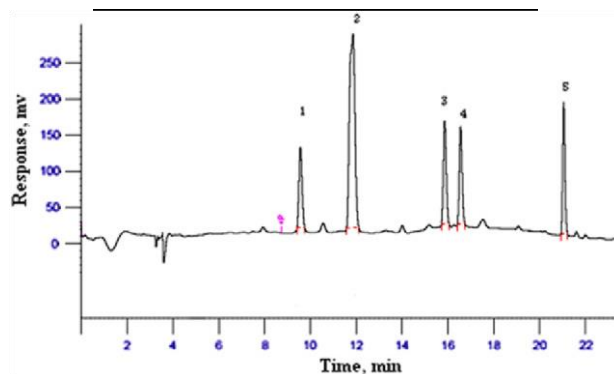


Fig. 1. HPLC chromatogram of the standard solution mixture containing EGC (1); Caff.+ C; (2) EC (3); EGCG (4); and ECG (5) ($10.0 \mu\text{g ml}^{-1}$ of each component) at 205 nm under the experimental conditions.

and catechin peaks are overlapped since their retention times are close under the developed HPLC procedures (Table 2). This behaviour was confirmed by the HPLC chromatogram of the standard solution mixture of catechin and caffeine ($10.0 \mu\text{g ml}^{-1}$ of each component) shown in Fig. 2. This may be due to the fact that analyses using HPLC are generally more complex and conditions sometimes are more difficult to optimize for complete separation of numerous polyphenols, e.g. catechins, caffeine and other tea components. Preliminary investigation on the separation of caffeine from catechin has revealed that components of the running buffer are of great importance and it is essential to maintain boric acid in the mobile phase. Boric acid, in the concentration range 150–250 mM, was found suitable to achieve an efficient separation of caffeine and catechin in the presence of acetonitrile (20–30% v/v).

3.2. Merits of the developed HPLC procedure

The average values of the number of the theoretical plates (N) and the height equivalent of the theoretical plates (HETP) for the catechins EC, EGC, EGCG and ECG at $10 \mu\text{g ml}^{-1}$ were in the range

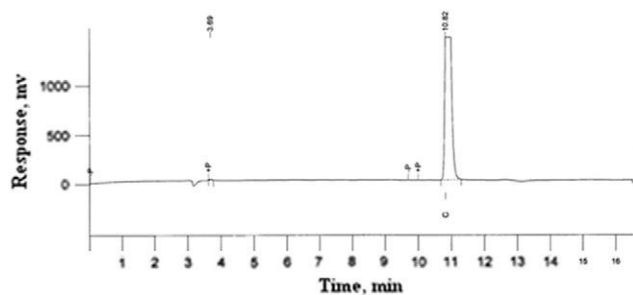


Fig. 2. HPLC chromatogram of solution mixture of caffeine and catechin (10.0 lg ml⁻¹) under the experimental conditions.

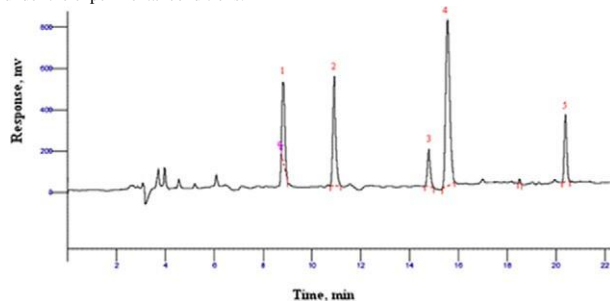


Fig. 3. HPLC chromatogram of water extract of green tea sample number 11 under the experimental conditions.

$2.6 \cdot 10^4 \pm 1.2 \cdot 10^3$, and $1.7 \cdot 10^3 \pm 4.7 \cdot 10^4$ cm, respectively. The value of the separation factor (R_s) calculated from the chromatogram for EGCG and EC, was $1.7 \pm 5.53 \cdot 10^2$. These values revealed excellent performance of the employed C-18 column and the employed HPLC procedure. The column performance was also evaluated from the values of the asymmetry (A_s) and capacity factors (k_0). The average values of the symmetry and capacity factors for the four catechins, EGC, EC, EGCG and ECG, were 1.0 and 2.97, respectively. The data revealed good performance of the modified HPLC procedures for analysis of catechins in the green tea leaves. According to IUPAC (Miller & Miller, 1994), the $LOD = 3S_{y/x}/b$ and $LOQ = 10S_{y/x}/b$ were calculated, where $S_{y/x}$ is the standard deviation of y-residual and b is the slope of the calibration plot. The values of LOD of the catechins EGC, EC, EGCG and ECG, were 0.05, 0.004, 0.03 and 0.006 lg ml^{-1} , respectively. The calculated values of LOQ of the same catechins were 0.17, 0.012, 0.08 and 0.02 lg ml^{-1} , respectively. The RSD of the method for determination of standard catechins solutions (10 lg l^{-1}) was in the range $\pm 3.5\%$ ($n = 3$), confirming precision of the method. The coefficients of correlation (r) for analysis of catechins by the developed method exceeded 0.988. Merits of the method compared satisfactorily with the reported methods for the analysis of catechins and caffeine in green tea water extracts (Harms & Schwedt, 1994; Lee & Ong, 2000; Nakagawa & Miyazawa, 1997).

3.3. Reliability and quantification of catechins and caffeine

The developed HPLC method was successfully used for the analysis of 29 commercially available green tea samples in boiled water for 5 min. Analysis of five selected catechins and caffeine, under the recommended experimental conditions, revealed the presence of reasonable amounts of all catechins and caffeine in the investigated green tea samples. Representative chromatograms of selected green tea water extracts of samples 11 and 21 are shown in Figs. 3 and 4. The average content (mg g⁻¹) of catechins and

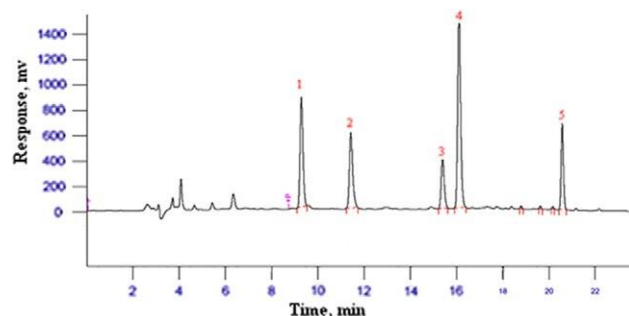


Fig. 4. HPLC chromatogram of water extract of green tea sample number 21 under the experimental conditions.

Table 3

The average content of catechins and caffeine (mg g⁻¹) on the water extracts of dry green tea samples infusion in boiled water for 5 min.

Sample No.	EGC	C	Caffeine	EC	EGCG	ECG
1	1.23	2.48	1.89	2.62	7.77	4.98
2	0.877	1.90	1.44	5.08	4.05	6.63
3	4.58	2.16	1.65	3.34	14.4	5.87
4	3.96	1.80	1.37	3.84	10.8	6.46
5	3.12	1.86	1.41	3.69	6.34	3.48
6	18.8	2.58	1.96	7.90	24.7	6.91
7	0.453	1.57	1.20	2.55	4.26	3.36
8	ND	2.01	1.53	2.66	5.84	3.22
9	ND	2.01	1.53	2.66	5.84	3.22
10	ND	1.29	0.978	1.66	2.01	3.78
11	10.1	2.45	1.87	5.17	30.8	6.97
12	11.0	2.31	1.76	3.21	22.3	4.93
13	23.2	2.94	2.23	10.2	30.7	10.8
14	7.03	2.33	1.77	1.78	12.3	2.18
15	10.4	1.52	1.16	4.91	12.5	3.97
16	ND	0.113	0.0859	ND	ND	0.501
17	ND	ND	ND	ND	ND	1.15
18	5.23	0.734	0.558	1.31	3.56	0.387
19	1.76	2.15	1.63	1.76	16.6	3.19
20	2.82	0.985	0.750	0.644	1.91	ND
21	24.9	2.58	1.97	9.50	43.3	13.9
22	ND	2.29	1.74	0.689	3.51	1.06
23	7.27	2.06	1.57	2.45	11.2	2.01
24	7.52	2.28	1.73	2.36	13.9	3.35
25	20.0	2.82	2.14	5.10	24.2	4.22
26	ND	0.464	0.353	ND	ND	ND
27	0.196	0.830	0.631	0.577	1.01	0.216
28	8.48	1.19	0.904	1.60	4.67	0.751
29	4.12	0.370	0.282	1.37	ND	ND

caffeine in the investigated green tea samples were then calculated from their calibration plots and also from the peak area of each standard. The results are summarized in Table 3. The levels of catechins in green tea samples were found to be in the range 0.113–43.3 mg g⁻¹ dry tea leaves. These results are in good agreement with the fact that green tea generally has higher concentrations of catechin such as EC, ECG, EGC and EGCG. Epi-gallocatechin gallate had the highest concentration (1.01–43.3 mg g⁻¹) in all water extracts of green tea samples, while catechin had the lowest. Significant differences between all green tea catechins and caffeine composition were noticed in all tea samples (Table 3), indicating that all the investigated tea samples are comparably good sources of these catechins. The overall sequence of the catechins and caffeine in the green water extracts followed the order:

EGCG > EGC > ECG > EC > C > Caffeine

δ2P

The overall average percentage (%) of the five catechins and caffeine in the water extracts of the green tea leaves' infusion (in boiled water for 5 min) are given in Fig. 5. The observed differences in the average

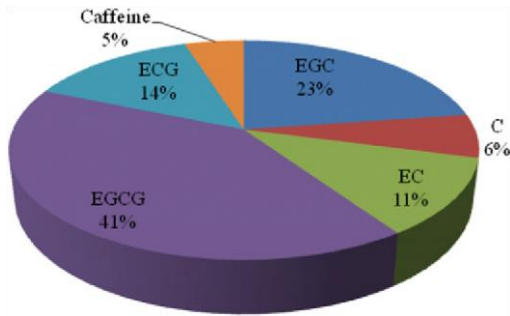


Fig. 5. The average percentages (%) of the analyzed catechins and caffeine on GTWs extract for five min infusion on boiled water.

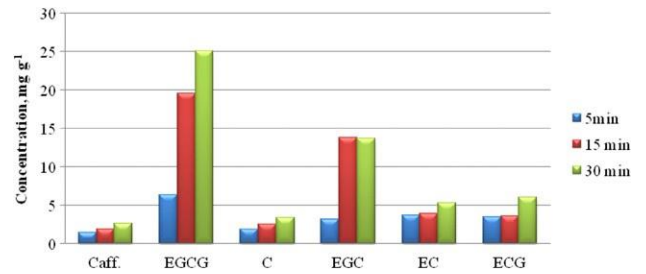


Fig. 8. Histogram representing the influence of infusion time (5–30 min) on the release of green tea catechins and caffeine into boiled water.

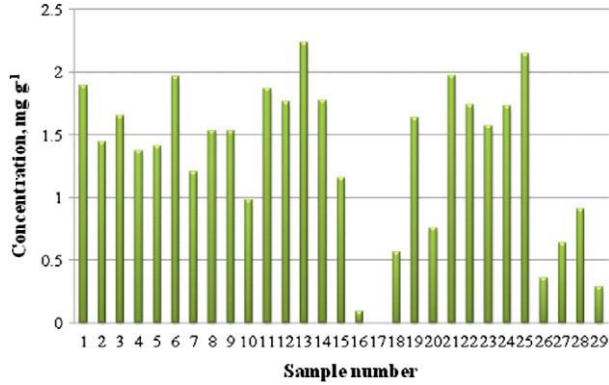


Fig. 6. Distribution pattern of caffeine in the different types of tea.

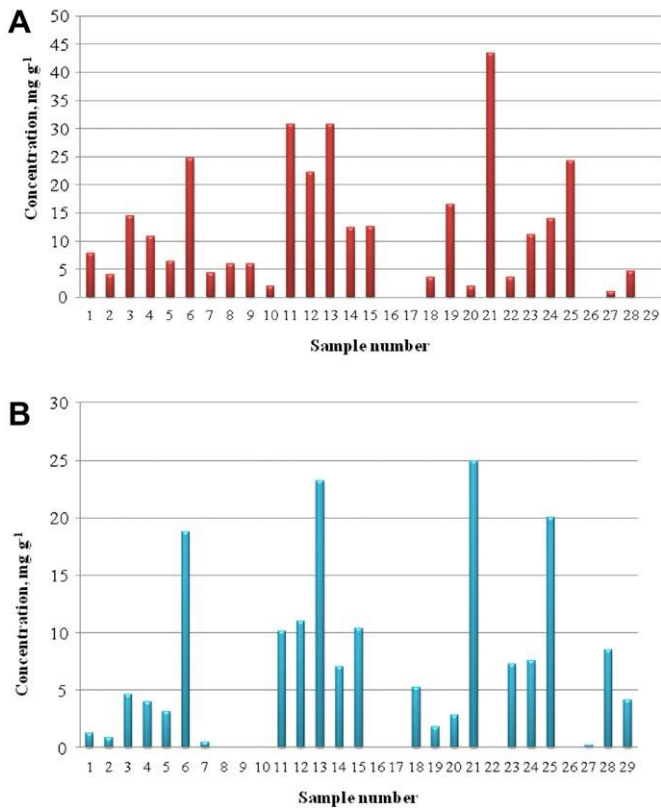


Fig. 7. Distribution pattern of EGCG (A) and EGC (B) in the different green tea samples.

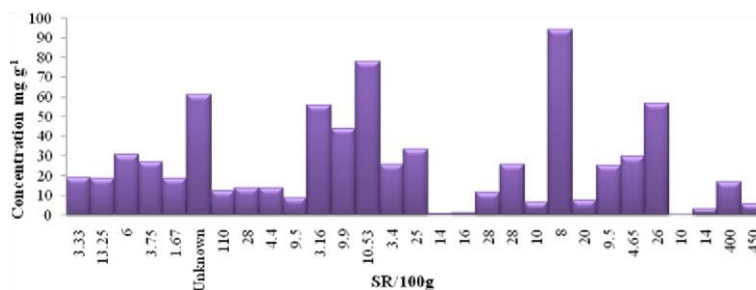


Fig. 9. Variations of the average content of catechins with the prices of green tea samples.

content of catechins and caffeine (Table 3) of the investigated GTs samples are most likely attributable to the differences in the geographical origins and tea processing (Beilenson, 1995). Green tea processing, e.g. plucking, storing, fermentation stopping, rolling and heating (roasting, steaming or boiling) of tea leaves, may also participate in the observed trend. Heating (roasting, steaming or boiling) of fresh tea leaves, deactivates polyphenol oxidase inside the tea leaves that links together polyphenols with oxygen producing new types of chemicals (theaflavins and thearubigins). The chemical process

involving polyphenols combining with oxygen is called fermentation.

Polyphenol oxidase, like other proteins and enzymes, can be damaged by heat (Beilenson, 1995).

The anti-oxidative activity of green tea water extract greatly depends on the total amounts of catechins and their relative distribution. The two catechins EGCG and EGC are the most abundant catechins in the GTWs and they also exhibit the highest antioxidant activity. A representative histogram, showing the average content of caffeine, is given in Fig. 6. The average contents of EGCG and EGC catechins in green tea water extracts are shown in Fig. 7A and B, respectively. The average content of EGCG in water extracts of sample numbers 16, 17, 26 and 29 was very low or not detected. The procedure of processing of green tea most likely plays an important role in the observed trend. The sample numbers 21 and 13 have the highest concentration (compared to other tea samples).

The influence of infusion time (5, 15 and 30 min) (of green tea leaves in boiled water) on the amount of catechins and caffeine released was critically investigated. The results indicated that, on rising the infusion time of green tea leaves in boiled water from 5 to 30 min, the average content of caffeine, EGCG, C, EC and EGC increased from 1.93 to 2.59, 19.5 to 25.0, 2.54 to 3.40, 3.87 to 5.34 and 3.60 to 6.03 mg g⁻¹ of dry green tea leaves, respectively. A representative histogram, showing the influence of infusion time on the release of the GTCs and caffeine, is shown in Fig. 8. In general, the data indicate that the rate of release of green tea catechins and caffeine into boiled water increased on increasing infusion time (Fig. 8). However, EGC showed no significant changes in the average content after a 15 min infusion time. The amount of EGCG released from tea leaves into boiled water showed significant increase on increasing infusion time in boiled water. The observed trend of the catechins and caffeine released from green tea leaves into boiled water is most likely attributable to the stability constants of the complexes formed between these phenolic compounds with the most abundant and available transition metal ions present in the tea leaves. The possible hydrolysis of phosphate esters of these species may also influence the observed trend (Beilenson, 1995). The flavonoid content of one cup of tea depends on two main factors: the composition of the green tea leaves itself, and the brewing characteristics. The tea itself is influenced by tea type and the processing method.

The brewing characteristics of the green tea leaves are also affected by the strength and type of tea infusion, e.g. green tea particle size, surface area, weight; the rate of release of flavonoid, efficiency i.e. the smaller particle size compared to the loose tea used in tea balls or pots, and finally brewing conditions. Of all of these parameters, the types and weights of the tea leaves have the greatest effects on the flavonoid content in a cup of tea (Lakenbrink, Lapczynski, Maiwald, & Engelhardt, 2000). A comparison between the green tea samples indicated that, the amount catechins and caffeine released from the tea samples into hot water depends on the particle size of the tea samples. The results also revealed that, the average contents of catechins and caffeine released from ground green tea bags were slightly higher than that released from green tea leaves (Beilenson, 1995).

The quantitative data reported in this study (Table 3) show that consumption of just one cup of GTWs (assuming the volume of a cup as 100 ml) contributes approximately 1.04–212 and 0.19–5.04 mg of total catechins and caffeine, respectively to the diet (Table 3). Based on these results, consumption of 2–3 cups per day of moderate green tea may provide significant amounts of catechins and caffeine, which are potentially beneficial compounds. The antioxidative activity of the GTWs mainly depends on the total amount of catechins and in particular EGCG and EGC catechins. EGCG and EGC are the most abundant catechins in GTWs and both exhibit the highest antioxidant activity (Chen, Schell, HO, & Chen, 1998). Ferrara, Montecioce, and Senatore, (2001) have shown that, the polyphenols, in particular catechins, in GTWs decrease the risk of cancers of several types, stimulate the production of several immune system cells and have antibacterial properties, even against the bacteria that cause dental plaque.

Detailed investigations involving correlation between the average contents of EGCG and EGC catechins and caffeine, of significant health benefits, in the green tea water extracts and their prices (Saudi Ryals per 100 g), have been reported. The results are shown in Fig. 9. The total average concentrations of the biologically active catechins, and the markers epigallocatechin 3-gallate and EGC, in the investigated GTs samples revealed no clear correlation with their prices in the local market of Saudi Arabia. Thus, there is a need to protect buyer and seller by developing analytical methods that can be used to identify and quantify the provenance of teas (Ye et al., 2010).

4. Conclusion

This work, although limited by the number of samples available and origins, clearly shows that the differentiation and classification of tea samples is possible using analytical techniques and applying pattern recognition techniques. The developed HPLC method for analysis of catechins and caffeine in green tea is ideally, rapid, reproducible and accurate. Significant differences in GTCs composition in water extracts of various tea samples were noticed. The level of catechins followed the order: EGCG > EGC > ECG > EC > C > Caffeine. The anti-oxidative activity of GTWs greatly depends on the total amount of catechins and their relative presence. It could be suggested to utilize one or two catechins (EGCG and/or EGC) as markers of the major quality of green tea extracts. Quantitative data revealed that, consumption of approximately 100 ml of brewed GTWs contributes approximately 1.04–212 and 0.19–5.04 mg of total catechins

and caffeine to the diet. Moderate tea consumption (2–3 cups/day) is likely to provide significant amounts of the potentially beneficial antioxidant catechins in particular epigallo catechin gallate. It is very useful for adults to drink higher volumes (200–300 ml) of green tea beverages. Work is continuing on the influence of various additives on the tea infusion in boiled water e.g. phosphate buffers, ascorbic acid and citric acid, lemon juice in various amounts and pH, antioxidative, and chelating agents.

Acknowledgements

The authors would like to thank the Deanship of Scientific Research, King Abdulaziz University, Jeddah, Kingdom of Saudi Arabia for the Grant number 3-107-430. Thanks also go to the Chemistry Department, Faculty of Science; King Abdulaziz University for the provided facilities.

References

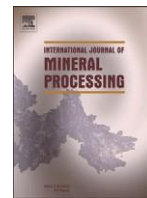
- Baldermann, S., Fleischmann, P., Watanabe, M. B. N., Winterhalter, P., & Ito, Y. (2009). Centrifugal precipitation chromatography, a powerful technique for the isolation of active enzymes from tea leaves (*Camellia sinensis*). *Journal of Chromatography A*, 1216(19), 4263–4267.
- Beilenson, J. P. (1995). *The book of tea. Processing and marketing of tea*, New York, USA: Peter Pauper Press [chap. 13].
- Cabrera, C., Artacho, R., & Gimenez, R. (2006). Beneficial effects of green tea. *Journal of American College of Nutrition*, 25, 79–99.
- Chantre, P., & Lairon, D. (2002). Recent findings of green tea extract AR25 (Exolise) and its activity for the treatment of obesity. *Journal of Phytomedicine*, 9, 3–8.
- Chen, A. P., Schell, J. B., HO, C. T., & Chen, K. Y. (1998). Green tea epigallocatechin gallate shows a pronounced growth inhibitory effect on cancerous cells but not on their normal counterparts. *Cancer Letters*, 129, 173–179.
- Chen, O., Zhao, J., Lin, H. (2009). Study on discrimination of roast green tea (*Camellia sinensis* L.) according to geographical origin by FT-NIR spectroscopy and supervised pattern recognition. *Spectrochimica Acta Part A*, 72(4), 845–850.
- Chen, L., & Zhang, H. Y. (2007). Cancer preventive mechanisms of the green tea polyphenol ()-epigallocatechin-3-gallate. *Molecules*, 12, 946–957.
- Chen, Q., Zhao, J., Chaitep, S., & Guo, Z. (2009). Simultaneous analysis of main catechins contents in green tea (*Camellia sinensis*) by Fourier Transform Near Infrared Reflectance (FT-NIR), spectroscopy. *Food Chemistry*, 113(4), 1272–1277.
- Chen, Q., Zhao, J., Chen, Z., Lin, Z., & An Zhao, D. (2011). Discrimination of green tea quality using the electronic nose technique and the human panel test, A comparison of linear and nonlinear classification tools. *Sensors and Actuators B*, 159, 294–300.
- Chen, Q., Zhao, J., Zhang, H., & Wang, X. (2006). Feasibility study on qualitative and quantitative analysis in tea by near infrared spectroscopy with multivariate calibration. *Analytica Chimica Acta*, 572(1), 77–84.
- Cheng, T. O. (2003). Why did green tea not protect against coronary artery disease but protect against myocardial infarction. *American Journal of Cardiology*, 91, 1290–1291.
- Cheng, T. O. (2004). Will green tea be even better than black tea to increase coronary flow velocity reserve? *American Journal of Cardiology*, 94(9), 1223–1224.
- Cheng, T. O. (2006). All teas are not created equal the Chinese green tea and cardiovascular health. *International Journal of Cardiology*, 108, 301–308.
- Chow, K., Kramer, I. (1990). *All the tea in China*. San Francisco: China Books and Periodicals, Beijing, China: Agricultural Academic press.
- Chung, F. L., Schwartz, J., Herzog, C. R., & Yang, Y. M. (2003). Tea and cancer prevention: Studies in animals and humans. *Journal of Nutrition*, 133, 3268–3274.
- Cross, M. L. (2002). Microbes versus microbes: Immune signals generated by probiotic lactobacilli and their role in protection against microbial pathogens. *FEMS Immunology Medical Microbiology*, 34, 245–253.
- Dalluge, J. J., Nelson, B. C., Thomas, J. B., & Sander, L. C. (1998). Selection of column and gradient elution system for the separation of catechins in green tea using high performance liquid chromatography. *Journal of Chromatography A*, 793, 265–274.
- Dou, Y., Sun, Y., Ren, Y. Q., Ju, P., & Ren, Y. L. (2005). Simultaneous non-destructive determination of two components of combined paracetamol and amantadine hydrochloride in tablets and powder by NIR spectroscopy and artificial neural networks. *Journal of Pharmaceutical and Biomedical Analysis*, 37, 543–549.
- Dulloo, A. G., Duret, C., Rohrer, D., Girardier, L., Mensi, N., Fathi, M., et al. (1999). Efficacy of a green tea extract rich in catechins polyphenols and caffeine in increasing 24-h energy expenditure and fat oxidation in humans. *Journal of Clinical Nutrition*, 70, 1040–1045.
- Esposito, E., Rotilio, D., Di, M. V., Di, G. C., Cacchio, M., & Algeri, S. (2002). A review of specific dietary antioxidants and the effects on biochemical mechanisms related to neurodegenerative processes. *Journal of Neurobiology*, 23, 719–735.
- Ferrara, L., Montenioco, D., & Senatore, A. (2001). The distribution of minerals and flavonoids in the tea plant. *II Farmaco*, 56, 397–401.
- Friedman, M., Levin, C. E., Choi, S. H., Kozukue, E., & Kozukue, N. (2006). HPLC analysis of catechins, theaflavins and alkaloids in commercial teas and green tea dietary supplements: Comparison of water and 80% ethanol/water extracts. *Journal of Food Science*, 71, 328–337.
- Fujiki, H., Suganuma, M., Imai, K., & Nakachi, K. (2002). Green tea: Cancer preventive beverage and/or drug. *Cancer Letter*, 188, 9–13.
- Goncalves, A. B., Paterson, R. R., & Lima, N. (2006). Survey and significance of filamentous fungi from tap water. *International Journal of Hygiene and Environmental Health*, 209(3), 257–264.
- Griffiths, R. R., & Griffiths, J. W. (2005). *Caffeine, grolier multimedia encyclopedia*. Danbury, CT: Scholastic Library Publishing Inc..
- Gutman, R. L., & Ryu, B. H. (1996). Rediscovering tea. An exploration of the scientific literature. *Herbal Gram*, 37, 30–33.
- Harms, J., & Schwedt, G. (1994). Applications of capillary electrophoresis in element speciation analysis of plant and food extracts. *Fresenius Journal of Analytical Chemistry*, 350, 93–100.
- Haslam, E. (2003). Thoughts on thearubigins. *Phytochemistry*, 64, 61–73.
- Horie, H., & Kohata, K. (2000). Analysis of tea components by high performance liquid chromatography and high performance capillary electrophoresis. *Journal of Chromatography A*, 881, 425–429.
- Jian, L., Xie, L. P., Lee, A. H., & Binns, C. W. (2004). Protective effect of green tea against prostate cancer: A case-control study in south east China. *International Journal of Cancer*, 108, 130–135.
- Kamiyama, O., Sanae, F., Ikeda, K., Higashi, Y., Minami, Y., Asano, N., et al. (2010). In vitro inhibition of α -glucosidases and glycogen phosphorylase by catechin gallates in green tea. *Food Chemistry*, 122, 1061–1066.
- Kodamatani, H., Shimizu, H., Saito, K., Yamazaki, S., & Tanaka, Y. (2006). High performance liquid chromatography of aromatic compounds with photochemical decomposition and tris (2,20-bipyridine) ruthenium(III) Chemiluminescence detection. *Journal of Chromatography A*, 1102, 200–205.
- Koo, M. W., & Cho, C. H. (2004). Pharmacological effects of green tea on the gastrointestinal system. *European Journal of Pharmacology*, 500, 177–185.
- Kotani, A., Takahashi, K., Hakamata, H., Kojima, S., & Kusu, F. (2007). Catechins determination by capillary liquid chromatography with electrochemical detection. *Journal of Analytical Science*, 23, 157–163.
- Koutelidakis, A. E., Argiri, K., Serafini, M., Proestos, C., Komaitis, M., Pecorari, M., et al. (2009). Green tea, white tea, and pelargonium purpureum increase the antioxidant capacity of plasma and some organs in mice. *Nutrition*, 25(4), 453–458.
- Kumar, N. S., & Rajapaksha, M. (2005). Separation of catechin constituents from five tea cultivars using high-speed counter-current chromatography. *Journal of Chromatography A*, 1083(1–2), 223–228.
- Lakenbrink, C., Lapczynski, S., Maiwald, B., & Engelhardt, U. H. (2000). Flavonoids and other Polyphenols in Consumer Brews of Tea and other Caffeinated Beverages. *Journal of Agricultural and Food Chemistry*, 48, 2848–2852.
- Lee, B. L., & Ong, C. N. (2000). Comparative analysis of tea catechins and theaflavins by high-performance liquid chromatography and capillary electrophoresis. *Journal of Chromatography A*, 881, 439–447.
- MacKay, D. L., & Blumberg, J. B. (2000). The role of tea in human health: An update. *Journal of American College Nutrition*, 21, 1–13.
- Miller, J. C., Miller, J. N. (1994). *Statistics for Analytical Chemistry* (4th ed.), New York: Ellis-Horwood.
- Mutoh, M., Takashi, M., Fukuda, K., Komatsu, H., Enya, T., Masushima-Hibiya, Y., et al. (2000). Suppression by flavonoids of cyclooxygenase-2 promoter-dependent transcriptional activity in colon cancer cells: Structure–activity relationship. *Journal of Cancer Research*, 91, 686–791.
- Nakagawa, K., & Miyazawa, T. (1997). Chemiluminescence high performance liquid chromatographic determination of tea catechin, ()-epigallocatechin-3-gallate at picomole levels in rat and human plasma. *Analytical Biochemistry*, 248, 41–49.
- Nieh, C., Hsieh, B., Chen, P., Hsiao, H., Cheng, T., & Chen, R. (2009). Potentiometric flow-injection estimation of tea fermentation degree. *Sensors and Actuators B: Chemical*, 136(2), 541–545.
- Peres, R. G., Tonin, F. G., Tavares, M. F. M., Rodriguez-Amaya, D.B. (2011). Determination of catechins in green tea infusions by reduced flow micellar electrokinetic chromatography. *Food Chemistry*, 127, 651–655.
- Ramos, S. (2007). Effects of dietary flavonoids on apoptotic pathways related to cancer chemoprevention. *Journal of Nutritional Biochemistry*, 18(7), 427–442.
- Rietveld, A., & Wiseman, S. (2003). Antioxidant effects of tea: Evidence from human clinical trials. *Journal of Nutrition*, 133, 3285.
- Schurek, J., Portolés, T., Hajslova, J., Riddellova, K., & Hernández, F. (2008). Application of head-space solid-phase microextraction coupled to comprehensive two-dimensional gas chromatography–time-of-flight mass spectrometry for the determination of multiple pesticide residues in tea samples. *Analytica Chimica Acta*, 611(2), 163–172.
- Singh, R., Akhtar, N., & Haqqi, T. M. (2010). Green tea polyphenol epigallocatechin-3-gallate: Information and arthritis. *Life Sciences*, 86, 679–684.
- Sinjia, V. R., & Mishra, H. N. (2009). FT-NIR Spectroscopy for caffeine estimation in instant green tea powder and granules. *LWT – Food Science Technology*, 42(5), 998–1002.
- Steinberg, F. M., Bearden, M. M., & Keen, C. L. (2003). Cocoa and chocolate flavonoids implications for cardiovascular health. *Journal of the American Dietetic Association*, 103, 215–221.
- Vinson, J. A. (2000). Black and green tea and heart disease. *BioFactors*, 13, 127–132.

- Vovk, I., Simonovska, B., & Vuorela, H. (2005). Separation of eight selected flavan-3-ols on cellulose thin-layer chromatographic plates. *Journal of Chromatography A*, 1077, 188–194.
- Waltner, M. E., Wang, X. L., Law, B. K., Hall, R. K., Nawano, M., & Granner, D. K. (2002). Epigallocatechin gallate, a constituent of green tea, represses hepatic glucose production. *Journal of Biological Chemistry*, 277, 34933–34940.
- Williamsonof, M. (2007). Green Tea May Keep HIV at Bay. BBC NEWS (International Version).
- Yanagida, A., Shoji, A., Shibusawa, Y., Shindo, H., Tagashira, M., Ikeda, M., et al. (2006). Analytical separation of tea catechins and food-related polyphenols by high-speed counter-current chromatography. *Journal of Chromatography A*, 1112(1–2), 195–201.
- Yang, X. R., Ye, C. X., Xu, J. K., Jiang, Y. M. (2007). Simultaneous analysis of purine alkaloids and catechins in *Camellia sinensis*, *Camellia piliphyll* and *Camellia assamica* Var. *Kucha* by HPLC. *Journal of Food Chemistry*, 100, 1132–1136.
- Yang, T. T. C., & Koo, M. W. L. (1997). Hypocholesterolemic effects of Chinese tea. *Pharmacological Research*, 35(6), 505–512.
- Yang, T. T. C., & Koo, M. W. L. (2000). Inhibitory effect of Chinese green tea on endothelial cell-induced LDL oxidation. *Atherosclerosis*, 148, 67–73.
- Yang, Y. C., Lu, F. H., Wu, J. S., Wu, C. H., & Chang, C. J. (2004). The protective effect of habitual tea consumption on hypertension. *Archives of Internal Medicine*, 164, 1534–1540.
- Yang, C. S., Maliakal, P., & Meng, X. (2002). Inhibition of carcinogenesis by tea. *Annual Review of Pharmacology and Toxicology*, 42, 25–54.
- Yao, L., Caffin, N., Ndarcy, B., Jiang, Y., Shi, Singanusong, R., Liu, X., Datta, N., Kakuda, Y., Xu, Y. (2005). Seasonal variations of phenolic compounds in Australia – grown tea (*Camellia sinensis*). *Journal of Agriculture and Food Chemistry*, 16, 6477–6483.
- Ye, N., Zhang, L., & Gu, X. (2011). Classification of Maojian teas from different geographical origins by micellar electrokinetic chromatography and pattern recognition techniques. *Analytical Science (Japan)*, 27, 765–769.
- Zeyuan, D., Bingying, T. X. L., Jinming, H., & Yifeng, C. (1998). Effect of green tea and black tea on the blood glucose, the blood triglycerides, and antioxidation in aged rats. *Journal of Agriculture and Food Chemistry*, 46, 875–878.
- Zhao, Y., Chen, P., Lin, L., Harnly, J. M., Yu, L., & Li, Z. (2011). Tentative identification, quantitation, and principal component analysis of green pu-erh, green, and white teas using UPLC/DAD/MS. *Food Chemistry*, 126, 1269–1277.
- Zhu, Q. Y., Hackman, R. M., Ensunsa, J. L., Holt, R. R., & Keen, C. L. (2002). Antioxidative activities of oolong tea. *Journal of Agriculture and Food Chemistry*, 50, 6929–6934.



Contents lists available at ScienceDirect

International Journal of Mineral Processing

journal homepage: www.elsevier.com/locate/ijminpro

Solid phase preconcentration and determination of trace concentrations of total gold (I) and/or (III) in sea and wastewater by ion pairing impregnated polyurethane foam packed column prior flame atomic absorption spectrometry

M.S. El-Shahawi ^{a,*}, A.S. Bashammakh ^a, A.A. Al-Sibaai ^a, M.I. Orief ^b, F.M. Al-Shareef ^a^a Department of Chemistry, Faculty of Science, King Abdulaziz University, P. O. Box 80203, Jeddah 21589, Kingdom of Saudi Arabia ^b

Department of Marine Chemistry, Faculty of Marine Sciences, King Abdulaziz University, Kingdom of Saudi Arabia

article

info

abstract

Article history:

Received 15 February 2011

Received in revised form 23 April 2011

Accepted 8 May 2011 Available

online 14 May 2011

Keywords:

Gold (I & III)

Determination

Ion-pairing

Foams packed column

Wastewater

A low cost solid-phase extraction based protocol for the preconcentration and subsequent determination of gold (I) and (III) in various complex matrices was developed. The method was based upon the use of the ion pairing reagent tetraheptylammonium bromide (THA⁺.Br⁻) immobilized polyurethane foams (PUFs) sorbent in packed column for retention of ultra trace concentrations of gold (III) from aqueous chloride medium of pH 3–4 at 5 mL min⁻¹ flow rate. The retained gold (III) species were recovered (98.5±2.7) by thiourea–HCl at 5 mL min⁻¹ flow rate. Gold (I) ions after oxidation to gold (III) with Br₂ water–HCl were also retained onto the reagent packed PUFs column and recovered (96.5±2.1). A linear plot of gold (III) concentration in the range 0.0–20 ng mL⁻¹ and a limit of detection of 0.06 ng mL⁻¹ were achieved. The method was applied satisfactorily (N95%) for the analysis of total inorganic gold (I) and/or gold (III) ions in wastewater samples and anodic slime.

© 2011 Elsevier B.V. All rights reserved.

1. Introduction

Gold is one of the most important noble metals due to its wide application in industry and economic activity. Gold occurs on Earth in very low natural contents and its concentration in natural water is extremely low, in the range of 0.05–0.2 ng mL⁻¹ (Pal et al., 2006). In the Earth crust, gold is widely distributed at a background level of 0.03 mg kg (Pal et al., 2006; Merian et al., 2004). Hydrothermal ore deposits of gold occur in metamorphic rocks and igneous rocks e.g. alluvial deposits (Merian et al., 2004). It is also found in-situ or at the original location of deposition from mineralizing solutions in lode deposits (Medved et al., 2004). The gold level is about 4.0 ng g⁻¹ and 1.0 ng g⁻¹ in basic rocks and soils, 0.05 and 0.2 ng mL⁻¹ in sea- and river water samples, respectively (Pourreza & Rastegarzadeh, 2005; Barecct & Van Loon, 1999). Thus, low cost, simple, and selective methods for the pre concentration and determination of traces of gold are of great importance.

Several articles have been published on the pre-concentration and subsequent determination of traces of gold (I) and gold (III) species in various matrices using capillary electrophoresis, solvent extraction, ion chromatography, selective transport through liquid membrane, activated carbon of apricot stones, modified multi-

¹ On leave from Department of Chemistry, Faculty of Science, Mansoura University, Mansoura, Egypt.

0301-7516/\$ – see front matter © 2011 Elsevier B.V. All rights reserved.

doi:10.1016/j.minpro.2011.05.004

walled carbon nanotubes, modified organo nanoclay sorbent, 2-carboxyl-1-naphthalthio-rhodanine, Spheron (R), (biphenyl) dimethane thiol, modified octadecyl silica membrane disks, Spheron (R) thiol 1000, Amberlite-2000 and co-precipitation with nickel(II)-5-methyl-4-(2-thiazolylazo) resorcinol complex (Corma et al., 2008; Haddad & Rochester, 1988; Oleschuk & Chow, 1996; Soylak et al., 2000; Behpour et al., 2005; Li, 2006; Ertas & Ataman, 2006; Zhao et al., 2006; Hu et al., 2006; Dasaram, 2006; Medved et al., 2006; Chen et al., 2006; Morales & Toral, 2007; Elci et al., 2007; Farag et al., 2007; El-Shahawi et al., 2007; Konečná & Komárek, 2007; Tuzen et al., 2008; Soleimania & Kaghazchi, 2008; Pyrzyrska, 2005; Liang et al., 2008; Bozkurt & Merdivan, 2008; Afzali et al., 2010a). Most of these methods are too expensive, unselective; require careful experimental conditions and not compatible with the limits of gold in natural samples.

The potentialities of PUFs for trace analysis and chemical speciation of metal ions are promising (Farag et al., 2007; Braun et al., 1985; Saeed & Ahmed, 2004; Portugal et al., 2010). The applications of ion exchange PUFs and untreated PUFs have been reported for the pre concentration of traces of gold (I) species (Farag et al., 2007). The kinetics and sorption characteristics of gold (III) retention from aqueous media onto PUFs immobilized with onium cations have shown good retention and rapid equilibrium of gold (Bashammakh et al., 2009). In this context, the present article is focused on

* Corresponding author. Tel.: +966 2 0551691130; fax: +966 2 6952292 E-mail addresses: malsaeed@kau.edu.sa, mohammad_el_shahawi@yahoo.co.uk (M.S. El-Shahawi).

studying the retention profile and the most probable sorption mechanism of gold (III) from aqueous media onto ion pairing reagent immobilized PUFs and finally developing a low cost method for the separation and subsequent determination of labile inorganic gold (I), gold (III) and total gold (I and III) in wastewater and anodic slime using the PUFs packed column.

2. Experimental

2.1. Apparatus

A Perkin-Elmer (Analyst TM 800, USA) atomic absorption spectrometer equipped with an HGA 500 graphite furnace was used for gold determination. A flame atomic absorption spectrometer (FAAS) equipped with deuterium background correction and hollow-cathode lamp at 242.8 nm with a 0.7 nm slit width, 10 mA lamp current, 7.5 burner height and air (9.4 L min⁻¹)-acetylene (2.0 L min⁻¹) flame were also used for gold determination according to the manufacturer's recommendation and were optimized daily before measurement. A mechanical Shaker (Corporation Precision Scientific, Chicago, USA) and glass columns (20 cm×10 mm i.d.) were used in batch and column modes for separation gold (III) and/or gold (I) species after oxidation of the latter to gold (III), respectively. Deionized water was delivered from a Milli-Q Plus system (Milford, MA, USA). A thermo Orion pH Meter (Model 720 Thermo Fisher Scientific, MA, USA) was used for pH measurements. At ultra trace concentrations of gold, few drops (0.1 mL) of the modifier Pd (NO₃)₃-Mg (NO₃)₂ were added according to the manufacturer's recommendation.

2.2. Reagents and materials

Analytical-reagent grade chemicals were used as received. A stock solution of gold (III) in de-ionized water was prepared from auric acid HAuCl₄ (Merk, Darmstadt, Germany). Potassium aurocyanide [KAu(CN)₂] was purchased from Fluka (Fluka AG, Switzerland). A stock solution (100 µg mL⁻¹) of KAu(CN)₂ was prepared in NaOH (0.1 mol L⁻¹). Tetramethylammonium perchlorate (TMA⁺.ClO₄⁻), tetrabutylammonium iodide (TBA⁺.I⁻) and THA⁺.Br⁻ were supplied from Sigma (St. Louis, MO, USA) and were freshly prepared in water (0.1 w/v). A stock solution (1000 µg mL⁻¹) of gold (III) was purchased from BDH chemicals (Poole, England) and was used for the preparation of more diluted and freshly solutions (0.01–100 µg L⁻¹) of gold in deionized water containing NaCl (2% w/v). Commercial PUFs plugs based polyether (30.0 kg m⁻³) type was cube as cubes (1.0 cm³) and stored in low density polyethylene (LDPE) bottles, Nalgene in dark. Glasswares were washed with a concentrated HCl-HNO₃ mixture (1:1 v/v) and water. The ion pairing reagent TMA⁺.ClO₄⁻, TBA⁺.I⁻ or THA⁺.Br⁻ (0.1% w/v) loaded PUFs were prepared as reported (Braun et al., 1985).

2.3. General batch experiments

An accurate weight (0.1±0.01 g) of the unloaded- or reagent TMA⁺.ClO₄⁻, TBA⁺.I⁻ or THA⁺.Br⁻ loaded PUFs cubes was shaken with an aqueous chloride solution (50.0 mL, pH 3–4) containing gold (III) at 10 µg mL⁻¹ in mechanical shaker at 200 rpm shaking rate for 1 h at 25±0.1 °C. The amount of gold (III) retained (q_e, mg g⁻¹) onto the PUFs at equilibrium was calculated by the equation:

$$q_e = \frac{V(C_b - C_a)}{m} \quad (1)$$

where C_b and C_a are gold concentration before and after extraction under the instrument's optimum settings with the aid of FAAS calibration curve of gold (III) ions, m and V are the mass in grams and volume (mL) of unloaded- (or reagent treated) PUFs and test solution, respectively. The extraction

percentage (% E), the distribution ratio (D) and sorption capacity of gold (III) uptake were calculated (Oleschuk & Chow, 1996; Farag et al., 2007).

2.4. Flow experiments

2.4.1. Retention and recovery of gold (III)

An accurate volume (0.5–1.0 L) of water containing NaCl (2% w/v) and gold (III) (0.01–15 µg L⁻¹) adjusted to pH 3–4 was permitted to flow through the THA⁺.Br⁻ loaded PUFs (1.0±0.01 g) column at 5 mL min⁻¹ flow rate using the method of foam packing (Farag et al., 2007). Sample and blank PUFs columns were then washed with aqueous solutions (50 mL) containing NaCl (2.0% w/v) and gold (III) retained ions were eluted with thiourea (0.5% w/v, 10 mL)-HCl (1.0 mol L⁻¹) at 5 mL min⁻¹ flow rate. Fractions (5.0 mL) of the eluate were collected and analyzed for gold. Further, an accurate amount (0.5–1.0 µg) of gold (III) were also spiked into water (1.0 L) sample and allowed to pass through the column at 10–15 mL min⁻¹ flow rate. The retained gold species were recovered with the same elution system and analyzed.

2.4.2. Retention and recovery of gold (I) species

Gold (I) species were oxidized to gold (III) (El-Shahawi et al., 2007) as follows: equal volumes (50.0 mL) of de-ionized water containing various amounts (5.0–10 µg) of gold (I) were transferred to conical flasks (50 mL) followed by adding 10 mL Br₂ water-HCl (1.0 mol L⁻¹) mixture. The solutions were left for 5 min to oxidize gold (I) to gold (III) and boiled for 5 min to remove excess Br₂. The solutions were allowed to cool, adjusted to pH 3–4, diluted with water (100 mL) containing NaCl (2% w/v) and passed through the THA⁺.Br⁻ loaded PUFs packed column at 10 mL min⁻¹ flow rate. The retained gold species were recovered with thiourea (0.5% w/v, 10 mL)-HCl (1.0 mol L⁻¹) at 5 mL min⁻¹ flow rate and analyzed for gold. The same procedures were also carried out by spiking known amounts (0.5–1.0 µg) of gold (I) onto water (1.0 L) and the retained gold species were recovered and analyzed as described.

2.4.3. Separation and recovery of total gold (I) and gold (III)

Aliquots (0.5 L) of gold (I) and (III) species at a total concentration ≤ 10 µg L⁻¹ were treated with Br₂ water-HCl (mol L⁻¹) system and boiled for 5 min. The solutions were then adjusted to pH 3–4 and percolated through the THA⁺.Br⁻ PUFs packed columns (1.0±0.01 g) at 5 mL min⁻¹ flow rate. The retained gold species were then eluted and analyzed as described.

2.5. Applications

2.5.1. Analysis of gold in tap and industrial wastewater

Tap- and wastewater samples of electroplating industry samples (0.5–1.0 L) were collected, filtered through a 0.45 µm membrane filter and adjusted to pH 3–4. Accurate amounts (0–15 µg) of gold (III) species were spiked individually into the test water samples (0.5–1.0 L). The solutions were percolated through the reagent -PUFs packed foam columns at 10 mL min⁻¹ flow rate. Gold (III) retained was recovered with thiourea-HCl (10 mL) at 5 mL min⁻¹ flow rate and analyzed by FAAS. On another experiment, an accurate amount (1.0 µg) of gold (III) ions was spiked to wastewater (1.0 L), allowed to percolate through the column at 10 mL min⁻¹ flow rate. The retained gold (III) species were finally recovered and analyzed.

2.5.2. Analysis of gold in anodic slime

An accurate weight (0.20±0.01 g) of the surface of the anodic slime was digested with aqua regia (10 mL), evaporated to dryness and cooled. A mixture (10 mL) of concentrated HNO₃-H₂O₂ (30% v/v) (5:1 v/v) was added to the residue and the suspension was filtered through filter paper. The contents of the reaction and the washing solutions (HNO₃, 10% v/v) of the insoluble residue were heated on a water bath for 20 min and diluted with distilled water in a calibrated flask (50.0 mL). The solution was adjusted to pH 3–4 and allowed to

pass through PUFs packed column at 5 mL min⁻¹ and analyzed against a reagent blank.

3. Results and discussion

3.1. Retention characteristics of gold (III)

The sorption of gold (III) from aqueous acetate solutions containing NaCl (2% m/v) onto the unloaded- or TMA.⁺ClO₄⁻, THA.⁺Br⁻ or THA.⁺I⁻ treated PUFs was pH dependent and reached maximum at pH 3–4 after 60 min shaking time. Sodium chloride was added to the test solutions to stabilize the complex anion AuCl₄⁻ in the aqueous solution and also to enhance the formation of the complex ion associate between AuCl₄⁻ and the ion pairing or the PUFs. The sorption profile of gold (III) ions by the unloaded PUFs and loaded PUFs followed the order: THA.⁺Br⁻ (90%) > Unloaded PUFs (75.3%) > N TMA.⁺ClO₄⁻ (66.9%) > NTBA.⁺I⁻ (50.5%). The ion pair THA.⁺Br⁻ able to form high molecular weight, stable and less soluble ternary complex ion associate of the formula {(THA.⁺ AuCl₄⁻)}. The complex anion AuCl₄⁻ may also able to form ion associate with the protonated ether and/or urethane of PUFs. The % E and D of gold (III) by the immobilized PUFs was better than the unloaded PUFs. Thus, in the next work, THA.⁺Br⁻ loaded PUFs were used. The stability constants of the binding sites of the PUFs with AuCl₄⁻ were calculated using the Scatchard equation (Saeed & Ahmed, 2004):

$$\frac{1}{2} \text{Au} \quad \delta \quad \rho \quad \delta \rho$$

and n is given by the equation:

$$n = \frac{\text{weight of gold bound to foam}}{\text{weight of foam } \delta \rho} \delta \rho^2$$

$$\frac{1}{n} = K n_i - n \quad 2$$

where, K=stability constant of gold (III) on PUF, n_i=maximum gold concentration retained by the PUFs sites and [Au] is the equilibrium concentration of gold (III) in solution (mol L⁻¹). The plot of n/[Au] vs. n demonstrated that more than one class of ternary gold (III) complex species are existed with unique formation constant. The values of log K₁ and log K₂ of the sorbed species derived from the respective slopes were 6.16±0.3 and 3.45±0.3, respectively. Thus, the sorption of gold (III) species took place readily on site K₁ that belongs to the ether group which has a greater stability than the amide group (site K₂) (Braun et al., 1985) in agreement with AuCl₄⁻ extraction by methyl isobutyl ketone and other ether solvents (Braun et al., 1985).

The effect of polarity of the extraction media on gold (III) retention by unloaded- and reagent THA.⁺Br⁻ treated PUFs was studied at pH 3–4 in the presence of various concentrations of ethanol (2.5–20% v/v) and shaking for 60 min. Maximum gold (III) sorption by the unloaded PUFs was achieved at 5% (v/v) ethanol and decreased at ethanol content 15% v/v. The value of log D at zero ethanol (log D=2.9) increased to log D=3.6 at 5% (v/v) ethanol. The THA.⁺Br⁻ treated PUFs showed maximum gold (III) retention at 2.5% (v/v) ethanol (log D=3.8) and decreased (log D=2.6) on increasing ethanol up to 10% (v/v). The change of the environment around gold (III) ions and the available binding sites of the PUFs became more hydrophilic and reduces the gold (III)

uptake onto the THA.⁺Br⁻ treated PUFs (Hayashita et al., 1992; Nambiar et al., 1996).

The influence of the competitive anions (Cl⁻, Br⁻, CN⁻) as NaCl, NaBr and NaCN at various concentrations up to 5.0% (m/v) on the gold (III) uptake was studied. Significant extraction of gold (III) was only achieved using NaCl and increased on raising NaCl concentration upto 2% (w/v). Thus, the retention of gold (III) may took place via a “weak anion ion exchange” mechanism (Hayashita et al., 1992).

The effect of monovalence cation (Li⁺, Na⁺, K⁺ and ⁺NH₄) size as salts (2% w/v) on gold (III) retention at 10 µg mL⁻¹ onto the unloaded and THA.⁺Br⁻ treated PUFs was studied. The sorption profiles of AuCl₄⁻ onto the unloaded PUFs increased in the order: Li⁺ > Na⁺ > NH₄⁺ > K⁺

while the sorption of gold (III) by the THA.⁺Br⁻ treated PUFs followed the sequence: Na⁺ > Li⁺ > NH₄⁺ > K⁺

$$D = 3:62 \rho \text{ N } \text{Li}^+ \delta \log D = 3:54 \rho \text{ N } \text{NH}_4^+ \delta \log D = 3:06 \rho \text{ N } \text{K}^+ \delta \log D = 3:04 \rho$$

The reduction of the repulsive forces between the adjacent sorbed ion associate of gold (III) complex may account for this trend (Cordoba et al., 1988; Halhouli et al., 1995). The ion–dipole interaction of NH₄⁺ with the oxygen sites of the PUFs is not the only predominating factor in the extraction step. Thus, “solvent extraction and/or a weak base anion ion exchange” mechanism with salt acting as a salting-out agent are not only the most probable mechanism and other process e.g. adsorption and specific sites on the sorbent are involved simultaneously on/in the [AuCl₄⁻] sorption. The added cations reduced the number of water molecules available to solvate gold ions which would therefore, be forced out of the solvent phase onto the PUFs. Free water molecules are also preferentially used to solvate the added cations (Palagyi et al., 1992).

3.2. Sorption isotherms

The retention profile of gold (III) over a wide range of equilibrium concentrations (4.1×10⁻⁶–2.58×10⁻⁴ mol L⁻¹) onto the unloaded and THA.⁺Br⁻ treated PUFs was studied. The amount of AuCl₄⁻ retained at low or moderate analyte concentration onto PUFs sorbent varied linearly with the amount of gold (III) remained in the aqueous phase. The sorption capacity of gold (III) ions toward the unloaded PUFs and THA.⁺Br⁻ immobilized PUFs sorbents was 17±0.7 and 19.5 ±0.65 mg g⁻¹, respectively. These values are better than the data reported (11, 21±1.8 and 5.29±0.9 mg g⁻¹) for other solid sorbents (Soylak et al., 2000; Aworn et al., 2005) and PUFs (El-Shahawi et al., 2007). Thus, gold (III) sorption onto the used sorbents was subjected to Langmuir isotherm model (Somorjai, 1994):

$$C_e = \frac{Q_b}{1 + \frac{C_e}{K_b}} \quad \delta 4 \rho$$

where, Q represents the Langmuir constant related to the maximum adsorption capacity of the solute per unit mass of adsorbent required for monolayer coverage of the surface and b is the binding energy of the solute adsorption that is temperature independent. The plots of C_e/C_{ads} vs. C_e give straight lines with a linear regression coefficient of 0.991–0.999 (Fig. 1) over the entire range of gold concentration confirming the Langmuir model. The Q and b were 0.103±0.02 mmol g⁻¹ and 50.83±1.2 L mol⁻¹ for the unloaded PUFs

and $0.101 \pm 0.02 \text{ mmol g}^{-1}$ and $282.2 \pm 6.4 \text{ mmol}^{-1}$ for $\text{THA}^+ \cdot \text{Br}^-$ treated PUFs towards gold (III) uptake, respectively.

Assuming the surface of the PUFs is heterogeneous and Langmuir model is chosen for all sites that energetically equivalent, the mean free sorption energy (E) for transfer of one mole of the solute from the infinity to the surface of PUFs was in range of $0.43\text{--}0.72 \pm 0.07 \text{ kJ/mol}$ for the unloaded-and $\text{THA}^+ \cdot \text{Br}^-$ immobilized PUFs. The low value of E indicates physisorption of gold (III) onto the PUFs.

The results were also subjected to the Dubinin–Radushkevich (D–R) isotherm model (Dubinin & Radushkevich, 1974) within the adsorption space close to the adsorbent surface. The D–R model can be expressed by the regression equation:

$$\ln C_{\text{ads}} = \ln K_{\text{DR}} - \beta M^2 \quad (5)$$

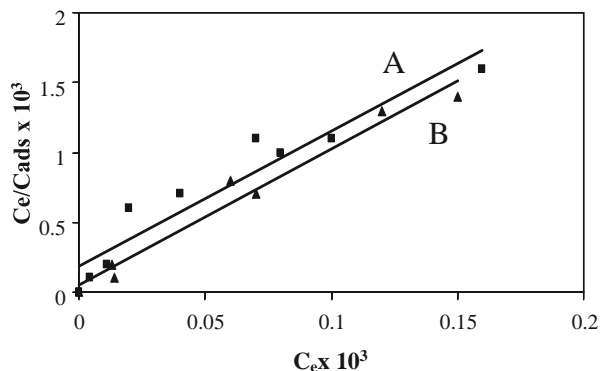


Fig. 1. Langmuir sorption isotherms of gold (III) uptake from the aqueous acetate solutions of pH 3–4 onto unloaded (A) and $\text{THA}^+ \cdot \text{Br}^-$ treated PUFs.

where K_{DR} = the maximum amount of gold (III) retained onto the solid sorbent, β is a constant related to the energy of transfer of the solute from the bulk aqueous solution onto the solid sorbent and is Polanyi potential. The plots of $\ln C_{\text{ads}}$ vs. M^2 were linear (Fig. 2) for the unloaded and treated PUFs indicating that the D–R isotherm model is obeyed for gold (III) sorption onto the unloaded- and loaded PUFs over the entire concentrations range. The β and K_{DR} values were $0.26 \pm 0.01 \text{ mmol}^2 \text{ kJ}^{-2}$ and $14.9 \pm 0.42 \text{ mmol g}^{-1}$ for the unloaded- and $0.091 \pm 0.001 \text{ mmol}^2 \text{ kJ}^{-2}$ and $73.6 \pm 1.9 \text{ mmol g}^{-1}$ for the loaded PUFs. Thus, a dual sorption mechanism involving “solvent extraction” and/or a “weak-base anion exchange” and an added component for “surface adsorption” are most probable model for gold (III) uptake by PUFs (Farag et al., 2007; Braun et al., 1985; Palagyi et al., 1992).

3.3. Chromatographic behavior of gold (III)

The sorption data in addition to the kinetic and thermodynamic results (Bashammakh et al., 2009) of gold (III) retention by $\text{THA}^+ \cdot \text{Br}^-$ loaded PUFs have suggested its use in packed column for the preconcentration and/or separation of gold (III). Thus, aqueous solutions ($0.5\text{--}1.0 \text{ L}$) containing gold (III) species at concentrations $\leq 10 \mu\text{g L}^{-1}$ were percolated through the $\text{THA}^+ \cdot \text{Br}^-$ loaded PUFs

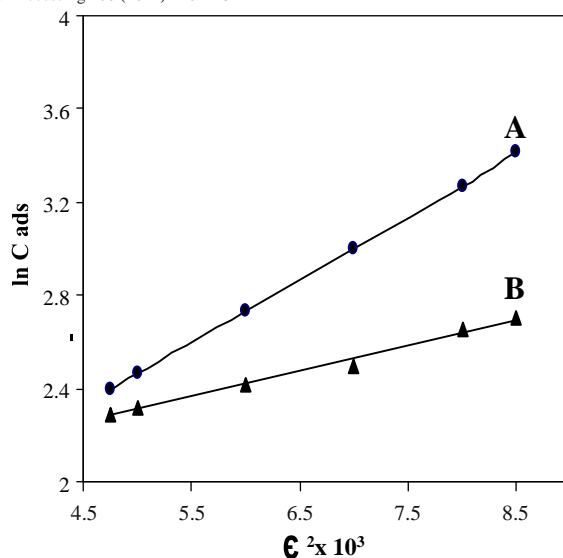


Fig. 2. D–R sorption isotherms of gold (III) extraction from the aqueous acetate solutions of pH 3–4 onto unloaded (A) and $\text{THA}^+ \cdot \text{Br}^-$ loaded PUFs at $25 \pm 0.1 \text{ }^\circ\text{C}$.

Table 1

Analytical data ($\mu\text{g L}^{-1}$) of the extraction and recovery of gold (III) ions from de ionized water by the $\text{THA}^+ \cdot \text{Br}^-$ loaded PUFs packed column.

Gold (III) added	Gold (III) found	Recovery, % ^a
5.0	4.9 ± 0.167	$98. \pm 3.4$
10.0	9.7 ± 0.21	97.0 ± 2.1
15.0	14.6 ± 0.37	97.3 ± 2.5

^a Average ($n=5$) \pm relative standard deviation.

packed columns as described before. Analysis of gold in the effluent against reagent blank indicated complete sorption of $[\text{AuCl}_4]^-_{\text{aq}}$ onto the PUFs packed columns. The eluting systems HClO_4 (1.0 mol L^{-1}), thiourea (1.0 mol L^{-1})– HCl (1.0 mol L^{-1} – 0.1 mol L^{-1}) and thiourea (1.0 mol L^{-1})– H_2SO_4 (0.1 mol L^{-1}) were tested to recover gold (III) species. Complete recovery ($97.0 \pm 2.1\text{--}98.0 \pm 3.4\%$) was achieved by thiourea (30 mL , 0.5% w/v)– HCl (1.0 mol L^{-1}) system at 2.0 mL min^{-1} flow rate. The results are summarized in Table 1. The procedure was also checked by spiking an amount ($1.0 \mu\text{g}$) of gold (III) to 1 l of water and allowed to pass through the column at 2 mL min^{-1} . The retained species were recovered (97.0 ± 3.4) with the same elution system (10 mL).

The $\text{THA}^+ \cdot \text{Br}^-$ loaded PUFs packed columns was also tested for the sorption and recovery of gold (I) species after oxidation (El-Shahawi et al., 2007) from the aqueous solutions. A satisfactory recovery percentage ($100.0 \pm 2.8\%$, $n=5$) of gold (I) species was achieved. The same experiment was also employed by spiking various amounts ($0.5\text{--}1.0 \mu\text{g mL}^{-1}$) of gold (I) in water and a recovery percentage (96 ± 2.5) was obtained. The PUFs packed column was tested for the extraction and recovery of the total inorganic gold (I, III) species in their aqueous mixtures at a total concentration $\leq 10 \mu\text{g mL}^{-1}$. The results are given in Table 2. A recovery of total gold in the range $96.5 \pm 3.9\text{--}98.3 \pm 32.2$ was obtained.

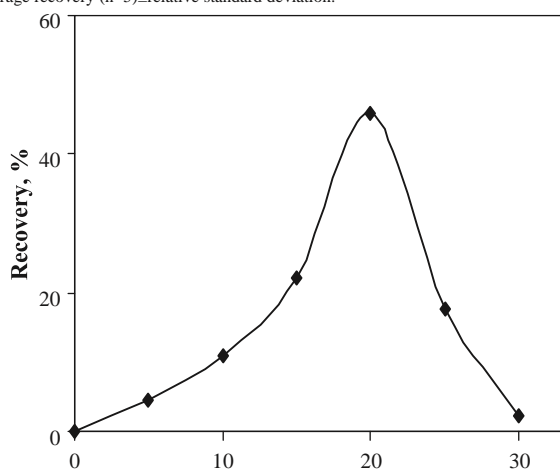
The effect of flow rate ($5\text{--}20 \text{ mL min}^{-1}$) on the uptake of gold (III) by the $\text{THA}^+ \cdot \text{Br}^-$ PUFs packed column was examined by percolating the water sample (100.0 mL) containing $10 \mu\text{g}$ gold (III). A recovery percentage ($N 96\%$) was achieved at a flow rate $\leq 15 \text{ mL min}^{-1}$. The sorption percentage decreased and the width of the elution chromatogram increased on raising the flow rate. The effect of sample volume ($0.1\text{--}1.5 \text{ L}$) was also studied by passing the test solution through the PUFs packed column at 10 mL min^{-1} flow rate. The retention of gold (III) species was not affected by sample volume below 1.0 L at 10 mL min^{-1} flow rate.

The efficiency of the THA⁺.Br⁻ treated PUFs packed column (1.0 g) was determined in terms of the number (N) and the height equivalent to the theoretical plate (HETP). The values of HETP and N were determined by passing an aqueous solution (1.0 L) containing gold (III) at 50 µg L⁻¹ through the column at 10 mL min⁻¹. Complete sorption of gold (III) was achieved. The retained gold (III) species were then eluted with thiourea (30 mL, 1.0% w/v)-HCl (1.0 mol L⁻¹) and the elution chromatogram is

Table 2
Analysis (µg L⁻¹) of total inorganic gold (I) and gold (III) in their binary mixtures by the developed THA⁺.Br⁻ packed columns.

Gold (I) and (III) added		Average of total gold found,	Recovery, % ^a
Au ⁺	Au ³⁺		
1.0	5.0	5.9	98.3 ±2.2
5.0	5.0	9.5	95.0 ±3.9

^a Average recovery (n=5)±relative standard deviation.



114

M.S. El-Shahawi et al. / International Journal of Mineral Processing 100 (2011) 110–115

Fig. 3. Chromatogram of the gold(III) retention and recovery at concentration of 50 µg L⁻¹ by THA⁺.Br⁻ immobilized PUFs packed columns.

shown in Fig. 3. The calculated values of N and HETP from Fig. 3 (Braun et al., 1985) were 83±2 and 1.12±0.07 mm, respectively. The N and HETP values were computed from the breakthrough capacity curve (Fig. 4) (Braun et al., 1985) constructed by passing an aqueous solution (0.7 L) containing gold (III) ions at 5 µg mL⁻¹ through the reagent loaded PUFs column at 10 mL min⁻¹ flow rate. The N and HETP values were 78±4 and 1.27±0.07 mm, respectively in agreement with the chromatogram method (Fig. 3). The critical and break through capacities of gold (III) retention computed from the S-curve (Fig. 4) (Ma et al., 2000) were 1.9 ±0.04 and 0.29±0.07 mg g⁻¹ PUFs, respectively. The S-shaped curve has a large slope indicating the high transfer rate of [Au Cl₄]⁻ on/in PUFs and rapid equilibrium between the [Au Cl₄]⁻_{aq} and the PUFs.

3.5. Figures of merits

Under the established conditions of gold (III) retention and recovery, a linear calibration curve was obtained with the following regression equation:

$$A = 0.021 + 0.32 C_n = 5; R^2 = 0.998$$

δ6P

where, C is the gold (III) concentration in the range 0–20 µg L⁻¹ and the intercept=0.021±0.0003. The value of LOD (based on LOD=3 σ_{y/x}/b) of

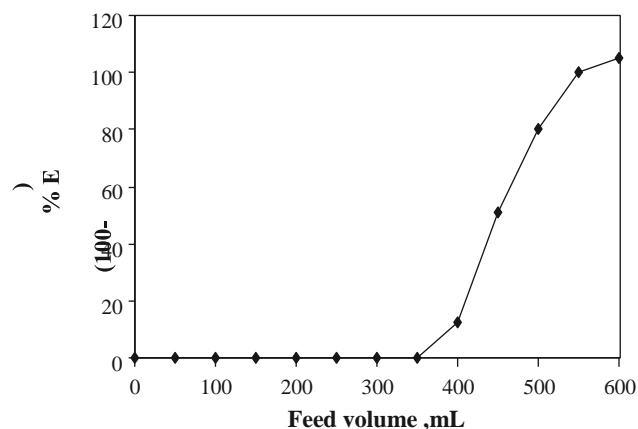


Fig. 4. Breakthrough capacity curves for gold (III) retention at 5 µg mL⁻¹ onto THA⁺.

Br⁻ PUFs packed column at 10 mL min⁻¹ flow rate.

the calibration plot (Miller & Miller, 1994) was 0.01 ng mL⁻¹, where, σ_{y/x} is the standard deviation of y-residual and b is the slope (0.32±0.001). A lower limit of quantification (LOQ=10 σ/b) of 0.05 µg L⁻¹ was achieved. The LOD value of the developed method below the gold content in sea (0.05 ng mL⁻¹) and river (0.2 ng mL⁻¹) water samples (Barectt & Van Loon, 1999; Corma et al., 2008). The relative standard deviation (RSD) of gold (III) based at 5 and 10 µg L⁻¹ gold concentrations were 2.7% and 2.2% (n=5), respectively confirming the precision of the proposed reagent treated PUFs packed column. The method provides LOD lower than the instrumental detection limits of FAAS (9.0 µg L⁻¹); ICP-OES (1.0 µg L⁻¹) and GFAA (0.15 µg L⁻¹) for gold. The figure of merits (Table 3) of the method was compared successfully with many of the preconcentration and subsequent determination methods [Table 3] (Farag et al., 2007; Afzali et al., 2010b; Carasek, 2000; Tunceli & Turker, 1997; Al-Merey et al., 2003; Du & Xu, 2001; Pm et al., 2003; El-Naggar et al., 2010). Some of the methods and other methods (Soylak et al., 2000; Behpour et al., 2005; Li, 2006; Ertas & Ataman, 2006; Zhao et al., 2006; Hu et al., 2006; Dasaram, 2006; Medved et al., 2006; Chen et al., 2006; Morales & Toral, 2007; Farag et al., 2007; El-Shahawi et al., 2007) are too expensive, unselective; and not compatible with the limits of gold in natural samples. Most of these methods exhibited a relatively high LOD (10.0–50.0 µg L⁻¹) and serious interferences by Ag⁺, Hg²⁺, Pb²⁺, Cr³⁺, and Ni²⁺.

3.5. Selectivity

The effect of diverse ions relevant to gold on wastewater was investigated by studying the sorption of gold (III) at 1.0 µg mL⁻¹ level of

Au from aqueous NaCl media (100 mL) by the THA⁺.Br⁻ PUFs packed column. The ions Cu²⁺, Al³⁺, Ni²⁺, Co²⁺, Cd²⁺, Hg²⁺, Fe³⁺, VO₃⁻, AsO₄²⁻, SO₄²⁻, and PO₄³⁻ ions at a high excess (0.1–0.5 mg) were added individually to the test solution and the preconcentration of gold was determined. The tolerance limit (w/w) of ±5% change in the gold (III) uptake is considered free from interference. The ions Fe³⁺ and VO₃⁻ were interfered seriously and were eliminated by adding few drops of saturated NaF (0.1% w/v). The interference of the MnO₄⁻ was minimized by adding drops of NaN₃ (1% w/v) to the solution to reduces Mn⁷⁺ to Mn²⁺ to get selective gold (III) separation and the tolerance was improved to acceptable limit (96.34±3%). The results also extended the

use of the PUFs column for separation of gold species from the industrial effluent. The developed method could be applied for samples which contain high amounts of other ions at mg L⁻¹ levels.

3.6. Analytical applications

The method was validated by performing the recovery tests of gold (I and/or III) spiked onto tap and/or wastewater samples of electroplating industry. The water samples (0.5–1 L) were percolated through the THA⁺Br⁻immobilized PUFs packed columns as described. The retained gold species were then quantitatively recovered with thiourea–HCl (10 mL) at 10.0 mL min⁻¹ (Table 4). Moreover, an accurate amount (1.0 µg) of gold (III) was spiked onto the wastewater sample (1.0 L) and percolated through the column at flow rate of 10–

Table 3

Figure of merits of the developed and some of the reported preconcentration methods for gold (µg L⁻¹) determination in water.

Chelating agent	Sorbent	LOD, µg L ⁻¹	Reference
Ammonium diethyldithiophosphate	Xylene	3	44
	Amberlite XAD-16	46	45
	Dowex	19	46
Diethyldithiocarbamate	NaBH ₄	24	47
2-Mercaptothiazole	Silica gel	10	48
Ion exchange PUFs	PUFs	0.01	20
Brilliant green	Triton-114	1.5	49
Ion pairing reagent	PUFs	0.01	Present work

Table 4

Analysis (µg L⁻¹) of gold (III) spiked onto wastewater samples by the proposed packed column.

Gold (III) added	Gold (III) found	Recovery, % ^a
5.00	5.1	102.±2.7
10.0	10.3	103.0±1.9
15.0	14.7	98.3±2.9

^a Average of five measurements±relative standard deviation.

15 mL min⁻¹. Complete retention and recovery were achieved confirming precision of the method for the analysis of gold in real samples.

The analysis of gold in anodic slime samples by the method was carried out. The recovered gold species was subsequently determined and a recovery percentage of 96±3.7 was obtained. Thus, the developed column is acceptable for gold separation and/or preconcentration from metallurgical samples.

4. Conclusion

The present method provides low cost procedures for the preconcentration and subsequent determination of inorganic gold (I), gold (III) and/or total inorganic gold from aqueous media at ultra trace concentrations. The reusability of the reagent loaded PUFs packed column was greater than 20 cycles without loss in its performance. The PUFs packed column could be extended to pre concentrate ultra traces of inorganic and organo gold (I), gold (III) from large volume of sea water samples by on line analysis. The method provides LOD lower than gold level in sea and river water and more selective than the method reported (Farg et al., 2007; Portugal et al., 2010).

References

- Afzali, D., Ghaseminezhad, S., Taher, M.A., 2010a. *J. AOAC Int.* 93, 1287.
 Afzali, D., Mostafavi, A., Mirzaei, M., 2010b. *J. Hazard. Mater.* 181, 957.
 Al-Meray, R., Hariri, Z., Abu-Hilal, J., 2003. *Microchem. J.* 75, 169.

- Aworn, A., Thiravetyan, A., Nakbanpote, W., 2005. *J. Colloid. Interface Sci.* 287, 394.
 Barect, R.R., Van Loon, J.C., 1999. *Talanta* 49, 1.
 Bashammakh, A.S., Bahhafi, S.O., Al-Shareef, F.M., El-Shahawi, M.S., 2009. *Anal. Sci. (Japan)* 25 (3), 413.
 Behpour, M., Attaran, A.M., Ghoreishi, S.M., Soltani, N., 2005. *Anal. Bioanal. Chem.* 382, 444.
 Bozkurt, S.S., Merdivan, M., 2008. *Environ. Mon. Assess.* 140, 2008.
 Braun, T., Navratil, J.D., Farag, A.B., 1985. *Polyurethane Foam Sorbents in Separation Science*. CRC Press, Inc, Boca Raton, FL.
 Carasek, E., 2000. *Talanta* 51, 173.
 Chen, Z.Y., Huang, Z.J., Chen, J., Yin, J.Y., Su, Q.D., Yang, G.Y., 2006. *Anal. Lett.* 3, 579.
 Cordoba, M.H., Navarro, P.N., Garcia, I.L., 1988. *Intern. J. Environ. Anal. Chem.* 32, 97.
 Corma, A., Domínguez, I., Ródenas, T., Sabater, M.J.J., 2008. *Catalysis* 259, 26. Dasaram, B., 2006. *Indian J. Mar. Sci.* 35, 7.
 Dasaram, B., 2006. *Indian J. Mar. Sci.* 35, 7.
 Du, X., Xu, S., 2001. *Presenius J. Anal. Chem* 370, 1065.
 Dubinin, M.M., Radushkevich, L.V., 1974. *Proc. Acad. Sci. USSR Phys. Chem. Soc.* 55, 133.
 Elci, L., Sahan, D., Basaran, A., 2007. *Environ. Monitoring. Assess.* 132, 331.
 El-Naggar, W.S., Lasheen, T.A., Nouh, E.A., Ghoniem, A.K., 2010. *Cent. Eur. J. Chem.* 8 (1), 34.
 El-Shahawi, M.S., Bashammakh, A.S., Bahaffi, S.O., 2007. *Talanta* 72, 1494.
 Ertas, G., Ataman, O.Y., 2006. *Appl. Spectros.* 60, 423.
 Farag, A.B., Soliman, M.H., Abdel-Rasoul, O.S., El-Shahawi, M.S., 2007. *Anal. Chim. Acta* 601, 218.
 Haddad, P.R., Rochester, N.E., 1988. *J. Chromatogr.* 439, 23.
 Halhouli, K.A., Darwish, N.A., Al-Dhoon, N.M., 1995. *Sep. Sci. Technol.* 30, 3313.
 Hayashita, T., Lee, J.H., Krzykawski, J., Bartsch, R.A., 1992. *Talanta* 39, 857.
 Hu, Q., Chen, X., Yang, X., Huang, Z., Chen, J., Yang, G., 2006. *Anal. Sci. (Japan)* 22, 627.
 Konečná, M., Komárek, J., 2007. *Spectrochim. Acta B* 62, 283.
 Li, Z.X., 2006. *J. Anal. At. Spectros.* 21, 435.
 Liang, P., Zhao, E., Ding, Q., Du, D., 2008. *Spectrochim. Acta B* 63, 714.
 Ma, W.X., Liu, F., Li, K.A., Chen, W., Tong, S.Y., 2000. *Anal. Chim. Acta* 416, 191.
 Medved, J., Bujdos, M., Natus, P., Kubova, J., 2004. *J. Anal. Bioanal. Chem.* 379, 60.
 Medved, J., Matus, P., Bujdos, M., Kubova, J., 2006. *Chem. Pap.* 60, 27.
 Merian, E., Anke, M., Ihnat, M., Stoeppler, M., 2004. *Elements and Their Compounds in the Environment, Occurrence, Analysis and Biological Relevance*, 2nd ed. WileyVCH Verlag GmbH & KGaA, Weinheim.
 Miller, J.C., Miller, J.N., 1994. *Statistics for Analytical Chemistry*, 4th ed. Ellis-Howood, New York, p. 115.
 Morales, L., Toral, M.I., 2007. *Miner. Eng.* 20, 802.
 Nambiar, C.H.R., Narayana, B., Rao, B., Mathew, R., Ramachandra, B., 1996. *Microchem. J.* 53, 175.
 Oleschuk, R.D., Chow, A., 1996. *Talanta* 43, 1545.
 Pal, B., Sen, P.K., Sen, K.K., Gupta, K.K., 2006. *Indian J. Chem. Soc.* 83, 762.
 Palagyi, S., Braun, T., Homonnay, Z., Vertes, A., 1992. *Analyst* 117, 1537.
 Pm, Q., Liu, P., Sun, Q., Su, Z., 2003. *Microchim. Acta* 45, 143.
 Portugal, F.C.M., Pinto, M.L., Pires, J., Nogueira, J.M.F., 2010. *J. Chromatogr. A* 1217, 3707.
 Pourreza, N., Rastegarzadeh, S., 2005. *Anal. Chem. (Warsaw)* 50, 695.
 Pyrzyńska, K., 2005. *Spectrochim. Acta B* 60, 1316 and reference cited in.
 Saeed, M.M., Ahmed, M., 2004. *Anal. Chim. Acta* 525, 289.
 Soleimania, M., Kaghazchi, T., 2008. *Bioresour. Technol.* 99, 5374.
 Somorjai, G.A., 1994. *Introduction to Surface Chemistry and Catalysis*. John Wiley & Sons, INC.
 Soylak, M., Elçi, L., Dogan, M., 2000. *Anal. Lett.* 33, 513.
 Tunceli, A., Turker, A.R., 1997. *Analyst* 122, 239.
 Tuzen, M., Saygi, K.O., Soylak, M., 2008. *J. Hazard. Mater.* 156, 591.
 Zhao, J.S., Li, J.S., Huang, Z.J., Wei, Q.Y., Chen, J., Yang, G.Y., 2006. *Indian J. Chem. A* 45, 1651.



Fast and selective removal of trace concentrations of bismuth(III) from water onto procaine hydrochloride loaded polyurethane foams sorbent: Kinetics and thermodynamics of bismuth(III) study

M.S. El-Shahawi^{a,*}, A. Hamza^a, A.A. Al-Sibaai^a, H.M. Al-Saidi^b

^a Department of Chemistry, Faculty of Science, King Abdulaziz University, P.O. Box 80203, Jeddah 21589, Saudi Arabia ^b Teachers College, Chemistry Department, Umm AL-Qura University, Makkah, Saudi Arabia

article	info	
		foams (PUFs). The rate of removal of bismuth (III) ions from aqueous solution by procaine hydrochloride (PQ ⁺ ·Cl ⁻) immobilized polyurethane foams (PUFs) were studied in batch conditions employing
Article history: Received 4 May 2011 Received in revised form 6 July 2011 Accepted 20 July 2011		Weber–Morris, Lagergren, Bhattacharya and Venkobachar, and Bt models. The rate of sorption of bismuth (III) was rapid initially within 5–15 min and reached a maximum in 30 min compared to other solid sorbent. Initially, the uptake of [Bi ³⁺] onto PQ ⁺ ·Cl ⁻ loaded PUFs was fast followed by kinetically
Keywords: Bismuth(III) Retention Kinetic models Thermodynamic Polyurethane foams		first-order sorption with an overall rate constant, $k = 0.132 \pm 0.033 \text{ min}^{-1}$. Thus, film and intraparticle transport are the two steps that might be influence bismuth(III) sorption. The negative values of G of the retention step of bismuth(III) dictate that the uptake of the analyte onto the used sorbent is spontaneous phenomena. Exothermic nature of bismuth(III) sorption is governed by the negative value of H . The positive value of S reflects the organized uptake of bismuth(III) on the used sorbent in a more random fashion. The PUFs offers unique advantages of [Bi ³⁺] _{aq} retention over conventional solid sorbents in rapid and effective separation of trace concentration of bismuth(III) from aqueous media. Thus, the developed PQ ⁺ ·Cl ⁻ treated PUFs sorbent could be packed in column for removal of bismuth (III) species
abstract		from industrial wastewater.

Bismuth (III) species are included in the list of potential toxins for motor neurons. Thus, fast and selective method for removal of bismuth (III) species has been developed. The method was based upon the formation of tetraiodobismuthate [BiI₄]⁻ in the test aqueous solution in the presence of KI-H₂SO₄ followed by subsequent extraction of [BiI₄]⁻ by procaine hydrochloride (PQ⁺·Cl⁻) immobilized polyurethane

Bismuth is found in nature in trivalent state as bismuthinite, Bi₂S₃, bismite, Bi₂O₃ and bismuth sulfide-telluric, Bi₂Te₂S. It is also found as a secondary component in some lead, copper and tin minerals [1]. Bismuth(V) compounds do not exist in solution and are important in the view of pharmaceutical analytical chemistry [1]. In the Earth's crust, bismuth presents at trace concentration (8 g kg⁻¹) while, bismuth minerals rarely occur alone

and are almost associated with other ores [2]. Bismuth appears to be environmentally significant because its physical and chemical properties have led it to be used in different areas of life. Pamphlett et al. [3] have reported that, bismuth compounds after oral intake enter the nervous system of mice, in particular, in motor neu-

* Corresponding author. Tel.: +96626952000; fax: +96626952292.

E-mail address: mohammad_elsahawi@yahoo.co.uk (M.S.El-Shahawi).

1385-8947/\$ – see front matter © 2011 Elsevier B.V. All rights reserved.
doi:10.1016/j.cej.2011.07.028

The development of selective, separation, pre-concentration, purification and determination methods for bismuth at sub-micro levels is a challenging problem because of the extremely low concentrations of bismuth present in natural samples and of its strong interferences from the sample matrices. Several methods, e.g. hydride generation atomic absorption spectrometry [4], electro thermal atomic absorption spectrometry [5], atomic fluorescence spectrometry [6], hydride generation atomic absorption spectrometry [7], and cathodic and anodic adsorptive stripping voltammetry [8–10] have been reported for the determination of bismuth (III). Most of these methods have required, pre-concentration of bismuth for precise determination because most analytical techniques do not possess adequate sensitivity for direct determination.

Solvent extraction in the presence of co-extractant ligands, e.g. bis (2,4,4-trimethylpentyl) mono thiophosphinic acid [11], pyridine dithiocarbamate [12], etc. has received considerable attention. However, these methods are too expensive, suffered

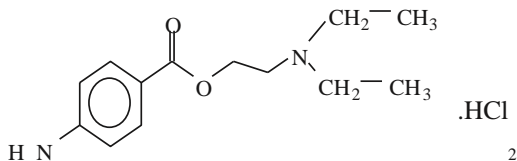


Fig. 1. Chemical structure of procaine hydrochloride.

from the use of large volumes of toxic organic solvents, and time-consuming. Therefore, recent years have seen considerable attention on pre-concentration and/or monitoring of trace and ultra-trace concentrations of bismuth by low cost procedures in a variety of samples, e.g. fresh, marine and industrial wastewater [13]. Solid-phase extraction, SPE, provides an excellent alternative approach to liquid-liquid extraction for the pre-concentration and purification of analyte prior to determination step [14–18]. Polyurethane foams (PUFs) sorbent represent an excellent solid sorbent material due to their high available surface area, cellular and membrane structure and extremely low cost [19]. Thus, several liquid solid separation involving PUFs methods have been successfully employed for the separation and sensitive determination of trace and ultra-trace concentrations of metal ions including bismuth (III) [19–29]. The membrane-like structure and the available surface area of the PUFs make it a suitable stationary phase and a column filling material [25,27]. Thus, the main objectives of the present article are focused on: (i) developing of a low cost method for the removal of bismuth (III) and (V) species after reduction of the latter to tri valence state employing PUFs physically impregnated with the ion pairing reagent PQ^+Cl^- ; (ii) studying the kinetics, and

thermodynamic characteristics of bismuth (III) sorption by trioctylamine plasticized PQ^+Cl^- treated PUFs and finally (iii). Application

of the developed method for the removal and/or determination of

inorganic bismuth (III & V) pollutant species in industrial wastewater by PQ^+Cl^- treated PUFs sorbent packed column.

2. Experimental

2.1. Reagents and materials

All chemicals used were of A.R. grade and were used without further purification. Stock solution (1000 gmL^{-1}) of bismuth

(III) was prepared from bismuth (III) nitrate (Aldrich Chemical Co Ltd., Milwaukee, WI, USA). More diluted solutions of bismuth (III) (0.1 – 100 gmL^{-1}) were prepared by diluting the stock

solution with diluted nitric acid. Stock solutions of procaine [2-(diethylamino)ethyl 4 aminobenzoate] hydrochloride, PQ^+Cl^-

(1.0% w/v), Fig. 1 and KI (10% w/v) were prepared by dissolving

the required weight in water (100 mL). A stock solution (1% v/v) of trioctylamine (Aldrich) was prepared in water in the presence of few drops of concentrated HNO_3 . Sulfuric acid (0.5 molL^{-1}) was used as an extraction medium in the sorption process of bismuth (III) by the PUFs. Commercial white sheets of open cell polyether type polyurethane foam were purchased from the local market of Jeddah City, Saudi Arabia and were cut as cubes (10–15 mm). The PUFs cubes were washed and dried as reported [21,27]. A series of Britton–Robinson (B–R) buffer (pH 2–11) was prepared as reported [30].

2.2. Apparatus

A Perkin–Elmer (Lambda 25, Shelton, CT, USA) spectrophotometer (190–1100 nm) with 10 mm (path width) quartz cell was used for recording the electronic spectra and measuring the absorbance of the ternary complex ion associate $PQ^+BiI_4^-$ of bismuth (III) at 420 nm before and after extraction with the reagent PQ^+Cl^- treated PUFs. A Perkin Elmer inductively coupled plasma-

optical emission spectrometry (ICP-OES, Optima 4100 DC Shelton,

CT, USA) was operated at the optimum instrumental parameters for bismuth determination. A mechanical shaker (Corporation Precision Scientific, Chicago, USA) with a shaking rate in the range of 10–250 rpm was used in batch experiments. De-ionized water was obtained from Milli-Q Plus system (Millipore, Bedford, MA, USA). A thermo Orion model 720 pH Meter (Thermo Fisher Scientific, MA, USA) was employed for pH measurements with absolute accuracy limits being defined by NIST buffers.

2.3. General batch procedures

2.3.1. Preparation of the immobilized reagent (PQ^+Cl^-) polyurethane foams

The reagent PQ^+Cl^- (1% w/v) in water was shaken with the PUFs

cubes in the presence of the plasticizer TOA (1% v/v) with efficient

stirring for 30 min. The loaded PQ^+Cl^- PUFs cubes were squeezed

and dried between two filter papers [20]. The amount of PQ^+-Cl^-

retained onto the PUFs sorbent was calculated using the equation [21]: v

$$a = (C_0 - C)W \quad (1)$$

where C_0 and C are the initial and final concentrations (mol L^{-1}) of the reagent (PQ^+-Cl^-) in solution, respectively, v = volume of the

reagent solution (L) and w is the mass (g) of the PUFs sorbent. The reproducibility of PQ^+-Cl^- treated PUFs is fine and the PUFs can be

reused many times without decrease in its efficiency.

2.3.2. Batch extraction step

An accurate weight (0.1 ± 0.002 g) of the reagent PQ^+-Cl^- immo-

bilized PUFs was equilibrated with an aqueous solution (100 mL) containing bismuth (10 mg mL^{-1}) in the presence of KI (10% w/v),

H_2SO_4 (0.5 mol L^{-1}) and ascorbic acid (0.1% w/v) to minimize the aerial oxidation of KI. The test solution was shaken for 1 h on a mechanical shaker. The aqueous phase was then separated out by decantation and the amount of bismuth (III) remained in the aqueous phase was then determined photometrically against the reagent blank [31] or by ICP-OES at ultra trace concentrations. The amount of bismuth (III) retained on the foam cubes was then calculated from the difference between the absorbance of $[BiI_4]^-$ in the aqueous phase before (A_b) and after extraction (A_f). The sorption percentage (%E), the amount of bismuth (III) retained at equilibrium (q_e) per unit mass of solid sorbent (mol g^{-1}) and the distribution coefficient (K_d) of sorbed analyte onto the foam cubes were finally calculated as reported. The %E and K_d are the average of three independent measurements and the precision in most cases was $\pm 2\%$. Following these procedures, the influence of shaking time and temperature on the retention of bismuth (III) by the PUFs sorbents was fully studied.

2.3.3. Recommended procedure for solid phase extraction of real samples

The general procedure for the extraction and recovery of bismuth (III) ions from real water samples onto PQ^+-Cl^- impregnated

PUFs was performed as follow: A 100 mL of tap-, well- or Red Sea

water samples were through 0.45 m membrane filter, adjusted to pH zero with H_2SO_4 (2.0 mol L^{-1}) in the presence of KI (0.1% w/v) and ascorbic acid was passed through PQ^+-Cl^- impregnated

PUFs (1.0 ± 0.001 g) packed column (10 cm long and 1 cm i.d.) at

5 mL min^{-1} . The retained bismuth (III) species were then recovered the

from the column with acetone (5 mL). The recovered bismuth (III) ions were then determined by ICP-OES.

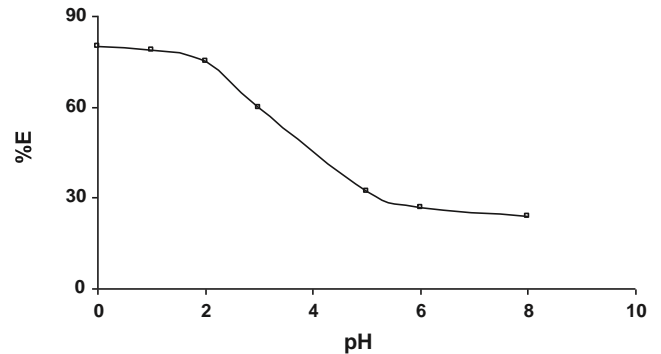


Fig. 2. Effect of pH on the sorption percentage of bismuth (III) from aqueous solutions containing KI (10% m/v)– H_2SO_4 (2.0 mol L^{-1}) onto PQ^+-Cl^- immobilized PUFs (0.1 ± 0.002 g) at 25 ± 0.1 °C.

3. Results and discussion

In recent years [28,29], PUFs immobilizing some ion pairing reagents have received considerable attention for selective separation, determination and/or chemical speciation of trace and ultra trace metal ions. The non-selective sorption characteristic of the PUFs has been rendered and became more selective by controlling the experimental conditions, e.g. pH, ionic strength, etc. Preliminary investigation has shown that, on shaking PQ^+-Cl^- loaded PUFs

with an aqueous solution of bismuth (III) ions containing KI (10%

w/v) and H_2SO_4 (0.5 mol L^{-1}), considerable amount of bismuth (III) retained onto treated PUFs in a very short time compared to the untreated PUFs ones. Thus, in subsequent work, detailed investigation has been carried out to assign the kinetics, thermodynamics and the most probable sorption mechanism of bismuth (III) from the test aqueous solutions by PQ^+-Cl^- treated PUFs solid sorbent.

3.1. Retention profile of bismuth (III) from the aqueous solution onto PUFs

Bismuth (III) forms an orange-yellow colored tetraiodobismuthate (III) complex, $[BiI_4]^-$ [31] in aqueous solutions containing sulfuric acid (0.5 mol L^{-1}) and an excess of KI (10% w/v). Thus, the

sorption profile of the aqueous solutions containing bismuth (III) at different acidity and pH by the PQ^+-Cl^- loaded foams was criti-

cally studied after shaking for 1 h at room temperature. The amount

of bismuth (III) in the aqueous phase after equilibrium was determined either photometrically [31] or by ICP-OES. The %E and the D of bismuth (III) sorption onto the PUFs decreased markedly on increasing the solution pH and maximum uptake was achieved at pH zero. Representative data are shown in Fig. 2. At $pH > 1$, the sorption performance of the unloaded PUFs and PQ^+-Cl^- treated PUFs

towards bismuth (III) decreased markedly (Fig. 2). This behavior

is most likely attributed to the deprotonation of the ether oxygen (–CH₂–O–CH₂–) and/or urethane nitrogen (–NH–CO–) of the PUFs, instability, hydrolysis, or incomplete extraction of the produced ternary complex ion associate of PQ⁺·[BiI₄]⁻ on/in the PUFs solid

and nitrogen atom of the amide group (–CH₂–OH⁺–CH₂–) and nitrogen atom of the amide group (–N⁺H₂–COO⁻) are –3 and –6, respectively [32]. Thus, in the extraction media containing H₂SO₄ (2.0 mol L⁻¹) and KI, the inter-

action of the complexed species [BiI₄]⁻ is easily proceeded with the protonated ether group of the PUFs than with protonated amide

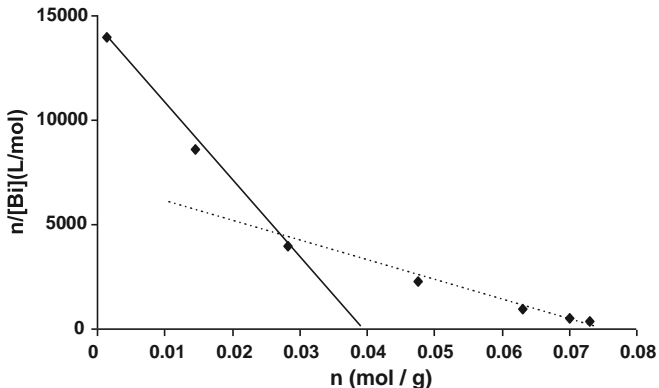


Fig. 3. Scatchard plot for the binding of [BiI₄]⁻ species by PQ⁺·Cl⁻ immobilized PUF (0.1 ± 0.002 g) from aqueous media containing KI (10% m/v)–H₂SO₄ (0.5 mol L⁻¹) at 25 ± 0.1 °C.

group of the PUFs. The stability constants of the binding sites of the PUFs with [BiI₄]⁻ were recalculated using the Scatchard equation [32]:

$$[BiI_4] = K(n_i - n) \tag{2}$$

and n_i is given by the equation:

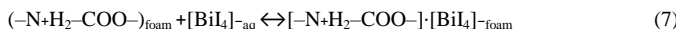
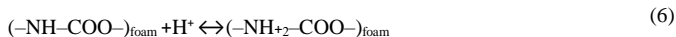
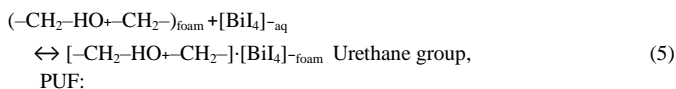
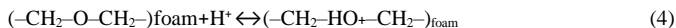
$$n_i = \frac{\text{weight of bismuth bound to foam (g)}}{\text{foam (g)}} \tag{3}$$

where K = stability constant of bismuth (III) on PUF, n_i = maximum concentration of bismuth (III) sorbed by the available sites on the PUFs, and [BiI₄]⁻ is the equilibrium concentration of bismuth (III) in solution (mol L⁻¹). The plot of n/[BiI₄]⁻

versus n is shown in Fig. 3. The curvature of the Scatchard plot demonstrates that more than one class of complexes has been formed and each complex has its own unique formation constant. The stability constants log K₁ and log K₂ for the sorbed species derived from the respective slopes were 5.56 ± 0.2 and 4.82 ± 0.5, respectively. The calculated values of n₁ and n₂ were found equal 0.038 ± 0.005 and 0.078 ± 0.01 mol g⁻¹, respectively. The values

of the stability constants (log K₁ and log K₂) indicated that, the sorption of species took place readily on site K₁ that most likely belong to the ether group because this group has a greater stability than the amide group (site K₂) as reported earlier [32]. Moreover, the high values of K₁ and K₂ indicated that, both bonding sites of PUF are highly active towards [BiI₄]⁻ species. These results are in good agreement with the data reported earlier [33] involving the extraction of the bulky anion [BiI₄]⁻ by methyl isobutyl ketone and other solvents that possess ether linkages in their structures, e.g. diethyl ether and isopropyl ether. Based on these data and the results reported on the retention of AuCl₄⁻ and CdI₄⁻ by PUFs [29,32], a sorption mechanism involving a weak base anion exchange and/solvent extraction of [BiI₄]⁻ by the protonated

ether (–CH₂–HO⁺–CH₂–) oxygen or urethane (–N⁺H₂COO⁻) nitrogen linkages of the PUFs as a ternary complex ion associate is most likely proceeded as follows: Ether group, PUF:



The distribution ratio of bismuth (III) onto PQ^+-Cl^- immobilized

PUFs showed high retention ($D = 6.17 \times 10^4 \text{ mLg}^{-1}$) compared to

the unloaded PUFs ($3.05 \times 10^3 \text{ mLg}^{-1}$) due to the formation of the

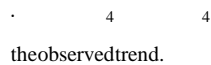
ion associate $[(PQ^+) \cdot (BiI)]_{4 \text{ foam}}$ on/in treated PUFs. Thus, in the subsequent work, the solution pH was adjusted in the pH range 0.0–1.0 and PQ^+-Cl^- immobilized PUFs was used as a proper sorbent.

The influence of the plasticizer, e.g. tri-n-octylamine, TOA (0.01% v/v), and tri-n-butyl phosphate, TBP (0.01% v/v) on the retention of bismuth (III) from the aqueous solutions onto the PQ^+-Cl^-

loaded PUFs was studied. Bismuth (III) sorption onto the PUFs sor-

bent dramatically increased ($D = 1.6 \times 10^4 \text{ mLg}^{-1}$) in the presence

of TOA (1% v/v). The formation of the ternary complex ion associates $TOA^+ BiI^-$ and $PO^+ \cdot BiI^-$ in acidic media may account for



the observed trend.

The proposed PUFs can be packed in columns for the collection of bismuth (V) species from aqueous solutions after reduction to bismuth (III). The solutions were then percolated through the PUFs packed column following the recommended procedures of bismuth (III) retention. Thus, the proposed PUFs packed column could be extended for the chemical speciation and determination of total inorganic bismuth (III) and (V) species in their mixtures. An aqueous solution of bismuth (III) and (V) was analyzed according to the after reduction of bismuth (V) to bismuth (III) by KI (10% m/v). Another aliquot portion was also adjusted to pH 3–4 and shaken with sodium diethyldithiocarbamate (Na-DDTC) for 2–3 min and extracted with methylisobutyl ketone, MIBK (5.0 mL) as $Bi(DDTC)_3$. The remaining aqueous solution of bismuth (V) was reduced to bismuth (III) with KI (10% w/v) – H_2SO_4 (0.5 molL⁻¹), and percolated

through the PQ^+-Cl^- loaded PUFs column. The retained bismuth

species were then recovered and finally analyzed following the

recommended procedures of bismuth (III) retention. The signal intensity of ICP-OES of the first aliquot (I_1) is a measure of the sum of bismuth (III) and (V) ions in the mixture, while the net signal intensity of the second aliquot (I_2) is a measure of bismuth (V) ions. The difference ($I_1 - I_2$) of the net signal intensity is a measure of bismuth (III) ions in the binary mixture.

3.2. Kinetic behavior of bismuth (III) sorption onto PQ^+-Cl^- and

TOA loaded PUFs

The influence of shaking time (0–60 min) on the uptake of bismuth (III) from the aqueous acidic media at pH close to zero was critically investigated. The sorption of bismuth (III) ions onto plasticized PQ^+-Cl^- immobilized PUFs sorbents with TOA was fast and

reached equilibrium within 60 min of shaking time. This conclusion

was supported by calculation of the half-life time ($t_{1/2}$) of bismuth (III) sorption from the aqueous solutions onto the solid sorbents PUFs. The values of $t_{1/2}$ calculated from the plots of $\log C/C_0$ versus time for bismuth (III) sorption onto PUFs. The values of $t_{1/2}$ was found to be $1.5 - 2.32 \pm 0.04$ min in agreement with the values of $t_{1/2}$ reported earlier [19]. Thus, gel diffusion is not only the rate-controlling step for PQ^+-Cl^- immobilized PUFs as in the case of

common ion exchange resins [19] and the kinetic of bismuth (III)

sorption onto the PQ^+-Cl^- immobilized PUFs sorbent depends on

film and intraparticle diffusion where, the more rapid one controls

the overall rate of transport.

The sorbed bismuth (III) species onto PUFs sorbent was subjected to Weber–Morris model [34]:

$$qt = R_d(t)^{1/2} \quad (8)$$

where R_d is the rate constant of intraparticle transport in $\text{moleg}^{-1} \text{ min}^{-1/2}$ and q is the sorbed Bi (III) concentration

(moleg^{-1}) at time t . The results are shown in Fig. 4. The plot of

q versus time were found linear ($R^2 = 0.989$) at initial stage of

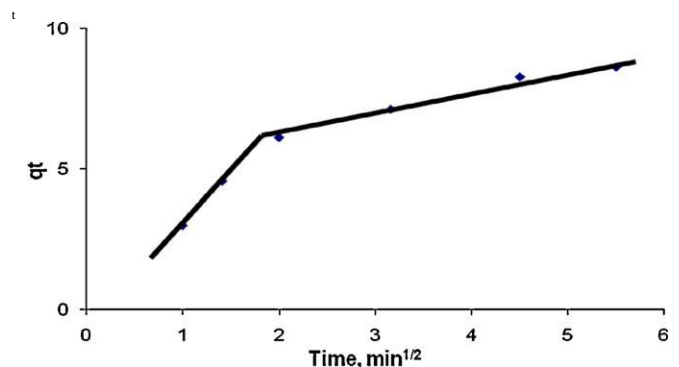


Fig. 4. Weber–Morris plot of the sorbed bismuth (III) onto PQ^+-Cl^- immobilized PUFs vs. square root of time. Conditions: aqueous solution (100 mL) containing KI (10% m/v) and H_2SO_4 (0.5 molL⁻¹), foam doze = $0.1 \pm 0.002 \text{ g}$ and 25 ± 0.1 °C.

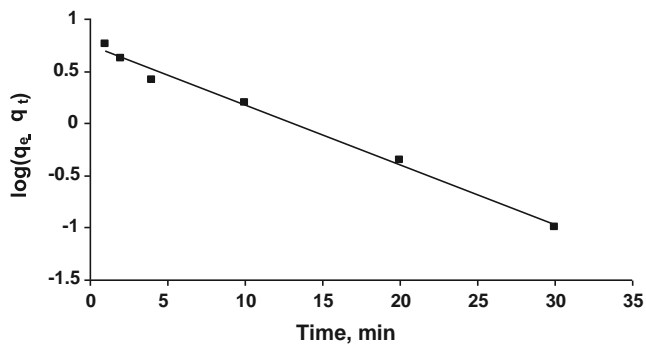


Fig. 5. Lagergren plot of bismuth (III) uptake onto PQ⁺-Cl⁻ PUFs from aqueous solutions containing KI (10% m/v)-H₂SO₄ (2.0 molL⁻¹) vs. time at 25±0.1 °C.

bismuth (III) uptake by the TOA plasticized PQ⁺-Cl⁻ loaded PUFs

sorbents up to 10±1.1 min and deviate on increasing the shak-

ing time. These results revealed that, the diffusion rate of [BiI₄]^{-aq} species is high and decreased on passage of the time. Thus, the rate of the retention step of [BiI₄]^{-aq} onto the used solid sorbent is film diffusion at the early stage of extraction [34,35]. The values of R_d computed from the two distinct slopes of Weber–Morris plots (Fig. 4) for the TOA plasticized PQ⁺-Cl⁻ loaded PUFs were found

equal 3.076±1.01 and 0.653 mmoleg⁻¹ with R = 0.989 and 0.995,

respectively. The observed change in the slope of the linear plot (Fig. 4) is most likely attributed to the different pore size [34,35]. Thus, intra-particle diffusion step is most likely the rate determining step.

The retention step of the [BiI₄]⁻ species onto the TOA plasticized PQ⁺-Cl⁻ loaded PUFs at 25±1 °C was subjected to Lagergren model

[28]:

$$\log(q_e - qt) = \log q_e - \frac{K_{Lager}}{2.303} t \quad (9)$$

where q_e is the amount of [BiI₄]⁻ sorbed at equilibrium per unit mass of sorbent (mole g⁻¹); K is the first order overall rate

constant for the retention process per min and t is the time in min. The plot of log(q_e - q_t) versus time (Fig. 5) was linear and the calculated value of K_{Lager} was found equal 0.132±0.033 min⁻¹

(R²=0.979) confirming the first order kinetics of the sorption of

[BiI₄]⁻ species onto the used solid sorbent [29]. The influence of adsorbate concentration was investigated and the results indicated that, the value of K_{Lager} increases on increasing adsorbate concentration confirming the first order kinetic

nature of the retention process and the formation of monolayer species of [BiI₄]⁻ onto the surface of the used adsorbent [26,29].

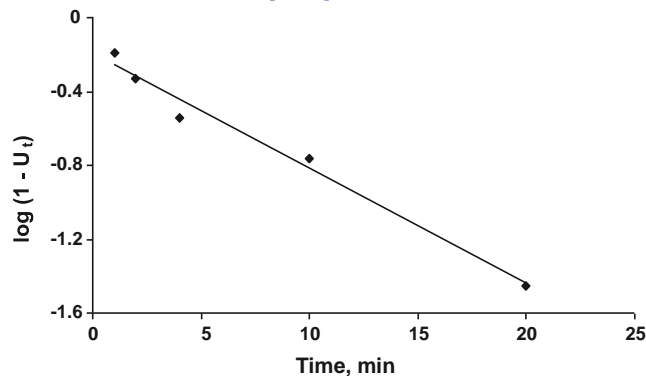


Fig. 6. Bhattacharya–Venkobachar plot of bismuth (III) retention from aqueous media containing KI (10% m/v)-H₂SO₄ (0.5 molL⁻¹) at 25±0.1 °C onto the PQ⁺-Cl⁻ and TOA loaded PUFs.

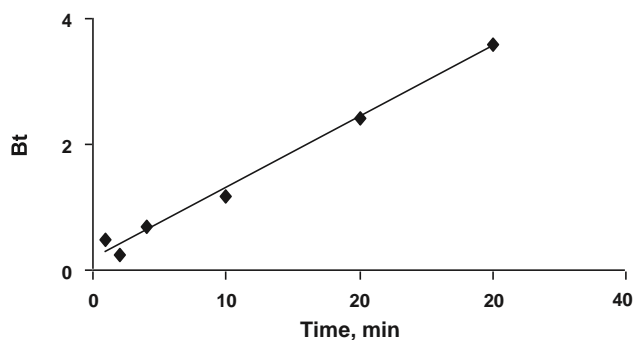


Fig. 7. Reichenburg plot of bismuth (III) retention from aqueous media containing KI (10% m/v)-H₂SO₄ (0.5 molL⁻¹) at 25±0.1 °C onto PQ⁺-Cl⁻ loaded PUFs.

The sorption data was also subjected to Bhattacharya–Venkobachar kinetic model [35].

$$\log(1 - U_{(t)}) = -\frac{K_{Bhatt}}{2.303} t \quad (10)$$

where U_(t) = (C₀ - C_t)/(C₀ - C_e), where, K_{Bhatt} = overall rate constant (min⁻¹), t = time (min), C_t = concentration of the bismuth (III) at time t in mL⁻¹, C_e = concentration of Bi (III) at equilibrium in g mL⁻¹. The plot of log(1 - U_(t)) versus time was linear (Fig. 6) with a correlation coefficient of R² = 0.987. The computed value of K_{Bhatt} (0.143±0.002 min⁻¹) from Fig. 6 is quite close to the value of K_{Lager} (0.132±0.033 min⁻¹) providing an additional indication of first order kinetic of bismuth (III) retention towards the sorbent.

The value of Bt, which is a mathematical function (F) of the ratio of the fraction sorbed (q_t) at time t and at equilibrium (q_e) in mole g⁻¹, i.e. F = q_t/q_e calculated for each value of F employing Reichenburg equation [36].

$$Bt = -0.4977 - 2.303 \log(1 - F) \quad (11)$$

The plot of Bt versus time at 25 ± 1 °C for plasticized PQ⁺-Cl⁻ PUFs towards bismuth (III) species was linear (R² = 0.990) upto 35 min (Fig. 7). The straight line does not pass through the origin revealing that, particle diffusion mechanism is not only responsible for the kinetic of [BiI₄]⁻ sorption onto the PQ⁺-Cl⁻ treated sorbents. Thus, the uptake of [BiI₄]⁻ onto the employed sorbents is most likely

involved three steps: (i) bulk transport of $[\text{BiI}_4]^-$ in solution, (ii) film transfer involving diffusion of $[\text{BiI}_4]^-$ within the pore volume of the $\text{PQ}^+\text{-Cl}^-$ and TOA treated PUFs and/or along the wall surface to the active sorption sites of the sorbent and finally (iii) formation of the complex ion associate of the formula $[-\text{CH}_2-\text{HO}^+-\text{CH}_2-] \cdot [\text{BiI}_4]^-_{\text{foam}}$ or $[-\text{NH}_2-\text{COO}^-] \cdot [\text{BiI}_4]^-_{\text{foam}}$. Therefore, the actual sorption of $[\text{BiI}_4]^-$ onto interior surfaces is

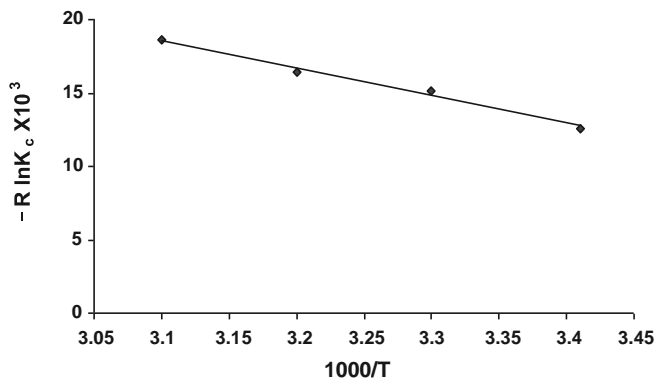


Fig. 8. Plot of $\ln K_c$ of bismuth(III) sorption from aqueous media containing KI (10% m/v)– H_2SO_4 (0.5 molL⁻¹) onto $\text{PQ}^+\text{-Cl}^-$ PUFs vs. $1/T$ (K⁻¹) onto $\text{PQ}^+\text{-Cl}^-$ treated PUFs.

rapid and hence it is not the rate determining step in the sorption process. Thus, film and intraparticle transport might be the two main steps controlling the sorption step. Hence, “solvent extraction” or “weak base anion ion exchanger” mechanism is not only the most probable participating mechanisms and some other processes, e.g. surface area and specific sites on the PUFs are possibly involved simultaneously in the bismuth(III) retention [37].

3.3. Thermodynamic characteristics of bismuth(III) retention onto plasticized $\text{PQ}^+\text{-Cl}^-$ loaded PUFs

The sorption of bismuth(III) onto the tested PUFs was critically studied over wide range of temperature (293–353 K) to determine the nature of bismuth (III) retention onto TOA plasticized $\text{PQ}^+\text{-Cl}^-$

loaded PUFs at the established experimental conditions. The ther-

modynamic parameters (H , S , and G) were evaluated using the equations:

$$\ln K_c = \frac{-\Delta H}{RT} + \frac{S}{R} \quad (12)$$

$$G = H - TS \quad (13)$$

where H , S , G , and T are the enthalpy, entropy, Gibbs free energy changes and temperature in Kelvin, respectively and R is the gas constant (8.3 JK⁻¹ mol⁻¹). K is the equilibrium constant

depending on the fractional attainment (Fe) of the sorption process. The values of K_c of bismuth(III) retention ions from the test aqueous solutions at equilibrium onto the $\text{PQ}^+\text{-Cl}^-$ loaded foam were

calculated using the equation:

Fe

the

$$K_c = 1 - Fe \quad (14)$$

Plot of $\log K_c$ versus $1000/T$ (Fig. 8) for the bismuth(III) retention onto $\text{PQ}^+\text{-Cl}^-$ loaded PUFs was linear over the temperatures

range (293–323 K). The value of the equilibrium constant decreased

on increasing temperature, revealing that, the retention process of $[\text{BiI}_4]^-$ species onto the used sorbents is an exothermic process. The numerical values of H , S , and G calculated from the slope and intercept of the plot (Fig. 7) were -18.72 ± 1.01 kJmol⁻¹,

54.57 ± 0.5 Jmol⁻¹ K⁻¹ and -2.46 ± 0.1 kJmol⁻¹ (at 298 K), respec-

tively with correlation factor 0.998.

The retention of bismuth (III) by $\text{PQ}^+\text{-Cl}^-$ loaded foam was subjected to Vant Hoff model employing the equation:

$$\log K_d = 2 - \frac{H}{RT} + C \quad (15)$$

where C is constant. The plot of $\log K_d$ versus $1/T$ for $[\text{BiI}_4]^-$ species retained onto the PUFs sorbents was linear (Fig. 9). The calculated value of H from the slope of the linear plot (Fig. 9) was -20.1 ± 1.1 kJmol⁻¹ in good agreement with the value evaluated

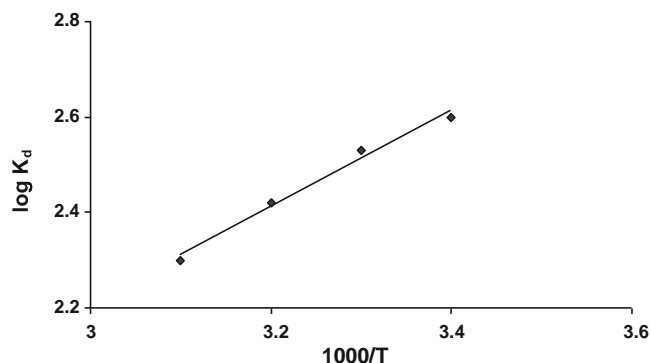


Fig. 9. Vant Hoff plot of bismuth(III) retention from aqueous media containing KI (10% m/v)– H_2SO_4 (0.5 molL⁻¹) onto $\text{PQ}^+\text{-Cl}^-$ loaded PUFs at various temperatures.

from Eqs. (14) and (15). The S of activation was lower than TS at all temperature. Thus, the orientation step is entropy controlled at the activation state.

The negative value of H and the data of D and K_c reflect the exothermic behavior of bismuth (III) uptake by the employed solid PUFs and non-electrostatics bonding formation between the adsorbent and the adsorbate. The positive value of S prove that bismuth (III) uptake are organized onto the used sorbent in a more random fashion and may be also indicative of the moderated sorption step of $[\text{BiI}_4]^-$ complex ion associate and ordering of ionic charges without a compensatory disordering of the sorbed ion associate onto the used sorbents. Since the sorption process involves a decrease in free energy, the H is expected to be negative as confirmed earlier. Moreover, on raising the

temperature, the physical structure of the PUFs membrane may be changing, thus affecting the strength of the intermolecular interactions between the PUFs membrane and the $[\text{BiL}_4]^-$ species. Thus, the high temperature may make the membrane matrix become more unstructured and affect the ability of the polar segments to engage in stable hydrogen bonding with $[\text{BiL}_4]^-$ species, which would result in a lower extraction. The negative of G_{at295K} implies the spontaneous and physical sorption nature of bismuth (III) retention onto PUFs. The decrease in G on decreasing temperature confirms the spontaneous nature of the sorption step and bismuth (III) uptake is more favorable at low temperature. The energy of urethane nitrogen and/or ether oxygen sites of the PUFs provided by raising the temperature minimizes the interaction between the active sites of PUFs and the complex ion associates of bismuth (III) ions resulting a lower sorption related to "Solvent extraction". These results suggest the use of the reagent loaded PUFs in column modes for collection, and sequential determination of bismuth (III) and (V) in water samples.

3.4. Interference study

The influence of diverse ions relevant to wastewater, e.g. alkali and alkali earth metal ions Ca^{2+} , Mg^{2+} , Cl^- , Zn^{2+} , Mn^{2+} , Cu^{2+} , Hg^{2+} ,

Fe^{2+} , Fe^{3+} , Pb^{2+} , Al^{3+} , Ni^{2+} , Co^{2+} and nitrate at various concentra-

tions (0.5–1.0 mg/100 mL sample solution) on the sorption of 10 g bismuth (III) from a sample volume of 100 mL at the optimum conditions was studied. The tolerance limits (w/w) less than $\pm 5\%$ change in percentage uptake of bismuth was taken as free from interference. The tested ions except Pb^{2+} did not cause any signif-

icant reduction on the percentage ($96\text{--}102 \pm 2\%$) of bismuth (III) sorption. Lead ions were found to interfere at higher concentrations (>0.5 mg/100 mL sample solution). Thus, it can be concluded that, the method could be applied for the separation and/or determination of bismuth (III) and bismuth (V) after reduction of the latter to trivalence.

Table 1

Recovery percentage (%) of bismuth (III) ions various water samples by the developed PUFs packed columns.

Sample	Bi(III) taken, g L^{-1}	Bismuth(III) found, g L^{-1}	Recovery, % ^a
Tapwater	0.0	nd	
Wealwater	10.00.0	9.8	98.0 ± 1.5
	100.0	9.9	99.0 ± 3.6
Seawater		0.3	
	10.0	10.5	102 ± 3.5

^a Average ($n=5$) \pm relative standard deviation. nd=not detected.

3.5. Analytical applications

The validation of the developed procedures was tested by separation and determination of bismuth (III) in tap and weal water and Red Seawater samples. The water samples were spiked with known (0.5–1 g) concentrations of bismuth (III). Complete retention of bismuth (III) was achieved as indicated from the analysis of the effluent. A satisfactory recovery percentage ($98\text{--}102$) of bismuth (III) ions was achieved, confirming the performance of the developed procedures. The results are summarized in Table 1. The data were also compared successfully

with the ICP-MS by performing t-tests. The results revealed no significant difference between the two results at 95% confidence level.

4. Conclusion

The use of $\text{PQ}^+\text{-Cl}^-$ treated PUFs solid sorbents for the pre con-

centration/separation procedures of bismuth (III) and bismuth (V)

after reduction of the latter species to bismuth (III) is able to minimize the limitations related to sensitivity and selectivity for bismuth determination in various matrices. The intra-particle diffusion and the first order model of bismuth (III) retention onto the tested $\text{PQ}^+\text{-Cl}^-$ PUFs sorbent are confirmed from the kinetic data.

Work is still continuing on developing $\text{PQ}^+\text{-Cl}^-$ treated PUFs packed

column mode for quantitative collection and recovery of bismuth (III) and/or (V) species at ultraconcentrations in aqueous media.

References

- [1] J.A. Reyes-Aguilera, M.P. Gonzalez, R. Navarro, T.I. Saucedo, M. Avila-Rodriguez, Supported liquid membranes (SLM) for recovery of bismuth from aqueous solution, *J. Membr. Sci.* 310 (2008) 13–19.
- [2] N. Tokman, *Anal. Chim. Acta* 519 (2004) 87–91.
- [3] R. Pamphlett, M. Stottenbery, J. Rungby, G. Danscher, *Neurotoxicol. Teratol.* 22 (2000) 559–563.
- [4] A.S. Ribeiro, M.A.Z. Arruda, S. Cadore, *Spectrochim. Acta B* 57 (2002) 2113–2120.
- [5] O. Acar, Z. Kilic, A.R. Turker, *Anal. Chim. Acta* 382 (1999) 329–338.
- [6] L. Rahman, W.T. Corns, D.W. Bryce, P.B. Stockwell, *Talanta* 52 (2000) 833–843.
- [7] Y. Zhang, S.B. Adeloju, *Talanta* 76 (2008) 724–730.
- [8] H. Guo, Y. Li, P. Xiao, N. He, *Anal. Chim. Acta* 534 (2005) 143–147.
- [9] H.Y. Yang, W.Y. Chen, I.W. Sun, *Talanta* 50 (1999) 977–984.
- [10] R. Hajian, E. Shams, *Anal. Chim. Acta* 491 (2003) 63–69.
- [11] S.G. Sarkar, P.M. Dhadke, *Sep. Purif. Technol.* 15 (1999) 131–138.
- [12] J.M. Lo, Y.P. Lin, K.S. Lin, *Anal. Sci. (Japan)* 7 (1991) 455.
- [13] M.A. Taher, E. Rezaeipour, D. Afzali, *Talanta* 63 (2004) 797–801.
- [14] Y. Yamini, M. Chalooosi, H. Ebrahimzadeh, *Talanta* 56 (2002) 797–803.
- [15] E.M. Thurman, M.S. Mills, *Solid Phase Extraction, Principles and Practice*, John Wiley and Sons, 1998.
- [16] B. Manadal, N. Ghosh, *J. Hazard. Mater.* 182 (2010) 363–370.
- [17] M. Sun, Q. Wu, *J. Hazard. Mater.* 182 (1–3) (2010) 259–265.
- [18] M.A. Didi, A.R. Sekkal, D. Villemin, *Colloids Surf. A: Physicochem. Eng. Aspects* 375 (1–3) (2011) 169–177.
- [19] S. Palagyi, T. Braun, Separation and pre-concentration of trace elements and inorganic species on solid polyurethane foams sorbents, in: Z.B. Alfassi, C.M. Wai (Eds.), *Preconcentration Techniques for Trace Elements*, CRC Press, Boca Raton, FL, 1992.
- [20] G.J. Moody, J.D.R. Thomas, *Chromatographic separation with foamed plastics and rubbers*, Dekker, New York, 1982.
- [21] M.S. El-Shahawi, M.A. El-Sonbati, *Talanta* 67 (2005) 806–815.

- [22] M.S.El-Shahawi, M.A.Othman, M.A. Abdel-Fadeel, *Anal. Chim. Acta* 546(2005) 221–228.
- [23] M.S.El-Shahawi, R.S.Al-Mehrezi, *Talanta* 44(1997) 483–489.
- [24] M.S.El-Shahawi, H.A.Nassif, *Anal. Chim. Acta* 487(2003) 249–259.
- [25] M.S.El-Shahawi, H.A.Nassif, *Anal. Chim. Acta* 487(2003) 249.
- [26] T. Braun, J.D. Navratil, A.B. Farag, *Polyurethane Foam Sorbents in Separation Science*, CRC Press Inc., Boca Raton, FL, 1985.
- [27] J.D. Mello, S.H. Pezzin, S.C. Amico, The effect of post-consumer PET particules on the performance of flexible polyurethane foams, *Polym. Test.* 28(2009) 702–708.
- [28] A.B. Farag, M.H. Soliman, O.S. Abdel-Rasoul, M.S. El-Shahawi, *Anal. Chim. Acta* 601(2007) 218–229.
- [29] A.B. Bashammakh, S.O. Bahaffi, F.M. Al-shareef, M.S. El-Shahawi, *Anal. Sci. (Japan)* 25(2009) 413–419.
- [30] A.I. Vogel, *Quantitative Inorganic Analysis*, 3rd ed., Longmans Group Ltd., England, 1966.
- [31] Z. Marzenko, *Separation and Spectrophotometric Determination of Elements*, 2nd ed., John Wiley and Sons, 1986.
- [32] M.M. Saeed, M. Ahmed, *Anal. Chim. Acta* 525(2004) 289–297.
- [33] P.R. Haddad, N.E. Rochester, *J. Chromatogr.* 439(1988) 23–36.
- [34] W.J. Weber, J.C. Morris, *J. Sanit. Eng. Div. Am. Soc. Civ. Eng.* 89(1963) 31–36.
- [35] A.K. Bhattacharya, C. Venkobachar, *J. Environ. Eng.* 110(1984) 1–299.
- [36] D. Reichenburg, *J. Am. Chem. Soc.* 75(1972) 589–597.
- [37] S. Zhi-Xing, P. Qiao-Sheng, L. Xing-yin, C. Xi-Jun, Z. Guang-Yao, R. Feng-Zhi, *Talanta* 42(1995) 1127–1133.

Selective determination of thorium in water using dual-wavelength b-correction spectrophotometry and the reagent 4-(2-pyridylazo)-resorcinol

Mohammad W. Kadi · M. S. El-Shahawi

Received: 29 January 2011/Published online: 11 May 2011
Akadémiai Kiadó, Budapest, Hungary 2011

Abstract A simple, fast, low cost, and precise direct b-correction spectrophotometric method was developed for thorium determination in water. The method is based on the reaction of Th(IV) with 4-(2-pyridylazo)-resorcinol (PAR) in aqueous solution of pH 5–6 and measuring the absorbance of the resulting red-colored complex at k_{\max} 497 nm. The effective molar absorptivity of the Th(IV)PAR complex was $2.52 \times 10^4 \text{ L mol}^{-1} \text{ cm}^{-1}$. Beer's law and Ringbom plots were obeyed in the concentration range 0.04–2.0 and 0.07–1.2 $\mu\text{g mL}^{-1}$ of thorium ions using b-correction spectrophotometry, respectively. The limits of detection and quantification of Th(IV) were 0.02 and 0.066 $\mu\text{g mL}^{-1}$, respectively. The developed method was applied for the analysis of thorium in certified reference material (IAEA-soil-7), tap-, underground- and Red-sea water samples. The validation of the method was also tested by comparison with data obtained by ICP-MS. The method is convenient, less sensitive to common interfering species and less laborious than most of published methods. The statistical treatment of data in terms of Student t-tests and variance ratio f-tests has revealed no significance differences. The structure of the Th(IV)-PAR complex was determined with the aid of spectroscopic measurements (UV-Visible and Fourier Transform Infrared Spectroscopy).

Keywords Thorium (IV) ions Natural radioactivity
Determination of thorium b-Correction spectrophotometry
ICP-MS

Introduction

Thorium occurs naturally in the earth's crust at an average lithosphere concentration of 8–12 $\mu\text{g g}^{-1}$. Thorium has excellent applications as an alloying element in magnesium for alloys used in aircraft engines, imparting high strength and creep resistance at elevated temperatures [1]. The common source of thorium is the rare-earth thoriumphosphate mineral monazite, which may contain up to 12% (w/w) thorium oxide. Thorium and its compounds are highly toxic and can cause progressive or irreversible renal injury and in acute cases may lead to kidney failure and death. Based on Gilman's studies, the tolerably daily intake of both thorium and uranium established by the World Health Organization (WHO) is 0.6 $\mu\text{g kg}^{-1}$ of the body weight per day [2, 3]. According to the WHO, Health Canada and Australian drinking water guidelines, the maximum thorium concentration in drinking water must be less than 20 $\mu\text{g L}^{-1}$ [3]. Pollution with radioactive elements has been a matter of great concern for human health and animals [4, 5]. Therefore, there is a need for low cost and reliable methods for the separation and pre concentration of thorium and other actinide ions from biodegradable, environmental, biological and nuclear waste samples for subsequent determination [6].

A series of techniques such as solvent extraction coupled with flame atomic absorption spectrometry (FAAS), inductively coupled plasma optical emission spectrometry (ICP-OES), inductively coupled plasma mass spectrometry (ICP-MS), stripping voltammetry, extraction chromatog-

Department of Chemistry, Faculty of Science, King Abdulaziz

University, P. O. Box 80203, Jeddah 21589,
Kingdom of Saudi Arabia e-mail:
mkadi@kau.edu.sa

raphy, PRIPYAT-2M gamma-ray coincidence spectrometer with six NaI (Tl) detectors, radiochemical neutron activation analysis, and spectrophotometry have been reported for thorium determination [7–20]. FAAS is an unfavorable method because of difficult atomization of thorium [9, 10]. The use of ICP-OES and ICP-MS improves the sensitivity but these techniques are timeconsuming and involve expensive instrumentation which is not available at several laboratories [17]. Visible absorption spectrophotometry represents the most popular technique because of the availability of the instrument, simplicity, speed, precision, accuracy and low cost. However, most of reported spectrophotometric methods lack sensitivity and/or selectivity due to the significant interference of the excess chromogenic reagent with the analyte at k_{\max} . This problem can be solved by employing b-correction spectrophotometric method to calculate the real absorbance of the complex [21–24].

Dual-wave b-correction spectrophotometry has successfully been used for the determination of toxic ions e.g. antimony (III), bismuth (III), mercury (II) and cyanide ions [23–25]. An up to date literature review has revealed that there is no study on the application of b-correction spectrophotometry involving the use of azo reagents for the determination of thorium. Therefore, the present article is focused on the use of PAR for developing a simple and precise method for thorium determination in water samples using b-correction spectrophotometry technique to minimize the interference of the excess PAR reagent.

Experimental

Reagents and materials

All chemicals and solvents used were of analytical reagent grade quality and were used without further purification. A stock solution of Th(IV) ($1000 \text{ } \mu\text{g mL}^{-1}$) was prepared from thorium nitrate. More diluted standard ($0.01\text{--}20 \text{ } \mu\text{g mL}^{-1}$) solutions were prepared by dilution of the stock solution and stored in low density polyethylene (LDPE) volumetric flasks. These flasks were pre cleaned with hot detergent, soaked in 50% HCl, HNO_3 (2.0 mol L^{-1}), washed with dilute HCl (0.5 mol L^{-1}) and finally rinsed with deionized water. Stock

solution ($1.9 \times 10^{-3} \text{ mol L}^{-1}$) of PAR was prepared by dissolving the required weight of the reagent in ethanol. A series of acetate buffers of pH 2.5–5.6 were prepared. Britton–Robinson (B–R) buffers of pH 2.0–10.0 were also prepared. LDPE bottles were used for the collection of water samples. A mixture of concentrated HF, and HNO_3 (Merck, Darmstadt, Germany) was used for the digestion of the certified reference material (IAEA-soil-7).

Apparatus

UV–visible (190–1100 nm) and IR (200–4000 cm^{-1}) spectra were recorded on a Perkin–Elmer (model Lambda 25, USA) and a Perkin Mattson 5000 FTIR spectrophotometers, respectively. Absorbance of reagents and their Th(IV) complexes were also measured with a Perkin–Elmer (Lambda 25, USA) spectrophotometer with 10 mm quartz cell. A digital micropipette (Volac) was used for the preparation of the standard and test solutions. Perkin–Elmer ICP-OES (model Optima 4100 DV) and ICPMS (Scienc model Elan DRC II, USA) were used as standard methods for the analysis of trace concentrations of Th(IV) at optimum operational conditions. Digital pHmeter (model MP220, Mettler Toledo) was used for pH measurements with accuracy limits of ± 0.1 pH unit defined by NIST buffers.

Recommended analytical procedure

An appropriate concentration ($0.05\text{--}2.0 \text{ } \mu\text{g mL}^{-1}$) of the Th(IV) solution was transferred to measuring flasks (10 mL) containing acetate buffer (pH 5–6) and PAR reagent (2 mL, 0.05% w/v). Solutions were completed to the mark with deionized water, shaken and were allowed to stand for 2 min. The absorbance of the produced red colored species was recorded at 413 (k_1) and 497 nm (k_2). The Th(IV) content was then determined from the calibration plot of Th(IV) concentration versus the corrected absorbance using dual-wavelength (k_1 , k_2) b-correction spectrophotometric method. The absorbance data were measured in triplicate.

Analytical applications

Analysis of thorium (IV) in certified reference material (IAEA-soil-7)

The developed procedure was validated by determination of thorium in the CRM (IAEA-soil-7) sample as follows: An accurate weight ($0.20\text{--}0.30 \pm 0.01 \text{ g}$, w/w) of the CRM sample was digested as reported earlier [26]. After cooling, the solid residue was redissolved in nitric acid (10.0 mL, 1.0 mol L^{-1}), transferred quantitatively to a volumetric flask

(25.0 mL) and was completed to the mark with acetate buffer of pH 5–6 in the presence of PAR (1.6 mL, 0.05% w/v) and few drops of EDTA (0.1% w/v). If the solid residue of the sample matrix was not dissolved in dilute HNO₃, the digestion step is repeated. The solution was then adjusted to pH 5–6 and analyzed following the recommended procedures of Th(IV) determination. A blank sample was digested and analyzed following the same digestion and analytical procedures.

Determination of thorium in tap, underground and Red Sea water samples

Tap-, underground (S₁–S₄)- and Red-sea water samples were collected from our lab at the chemistry department, different wells (from the western region of the country) and North of Jeddah city, respectively. Water samples were acidified with few drops of pure H₃PO₄, filtered through 0.45 μm cellulose membrane filters prior to analysis and stored in LDPE bottles (250 mL). The water samples (1000 mL) were subjected to UV radiation at 254 nm for 6 h in the presence of HCl (10%), adjusted to pH 3 and shaken initially with sodium diethyldithiocarbamate (5 mL, 1% w/v) for 3–5 min. The test solutions were then extracted with chloroform (5 mL) [19]. The extracted thorium in the chloroform phase was then stripped to the aqueous phase by shaking with nitric acid (5 mL, 1.0 mol L⁻¹), adjusted to pH 5 with acetate buffer and analyzed following the recommended b-correction spectrophotometry procedures. The absorbance of the test solution was then recorded and the Th(IV) concentration was determined from the standard calibration curve using the equation:

$$\text{Thorium concentration} \propto C_{\text{std}} \frac{A_{\text{samp}}}{A_{\text{std}}} \quad (1)$$

where C_{std} is standard thorium concentration and A_{samp} and A_{std} are the corrected absorbance of the Th(IV)-PAR complex species in the unknown sample and the standard, respectively. Alternatively, the method of standard addition was also carried out as follows: transfer known volume (5.0 mL) of water samples to the volumetric flask (25.0 mL) adjust to pH 5–6 with buffer (5 mL). An accurate volume (1.6 mL) of PAR solution and few drops of EDTA (0.1% w/v) were added to the test solution and the reaction mixture was made up to the mark with distilled water. The same procedures are repeated after adding various known concentrations (0.01–1.0 μg mL⁻¹) of thorium ions. The

true absorbance displayed by the test solutions before and after addition of the standard Th(IV) solution was measured by the developed method. The thorium content was then determined via the calibration curve of the standard addition procedure. The average of five independent measurements was taken and the precision in most cases was ±3%. Samples were also analyzed by ICP-MS. All chemical assays were carried out in triplicate and the data were expressed as means ± standard deviation.

Results and discussion

Spectroscopic characterization of the developed colored Th(IV)-PAR complex

In aqueous media, on mixing the reagent PAR with Th(IV) ions, a red orange colored complex was developed immediately. The electronic spectrum of the reagent PAR against water showed one absorption peak at 413 nm (k_1)

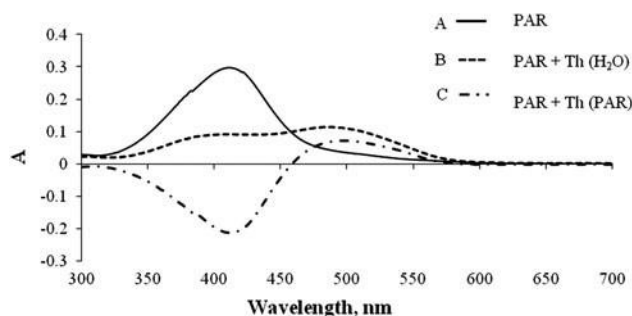


Fig. 1 Electronic spectra of PAR and its Th(IV) complex at pH 5–6, Curve A is the spectrum of the reagent blank (reference water); B is for Th(IV)-PAR complex (reference, water); and C is the spectrum of Th(IV)-PAR complex (reference reagent blank)

(Fig. 1) and was assigned the $n \rightarrow p^*$ transition [27]. In the reaction with Th(IV) ions at pH 5–6, significant changes were noticed where, a new absorption band at 497 nm (k_2) was observed on the electronic spectrum versus water (Fig. 1). The stoichiometry of the Th(IV)-PAR complex was determined via the mole ratio and continuous variation methods by measuring the absorbance of the colored complex at k_{max} 497 nm at various Th(IV) concentrations [27]. The results revealed formation of Th(IV)-PAR complex at 1:2 Th(IV) to PAR molar ratio. Thus, the structure of the proposed complex is most likely $\text{Th}(\text{PAR})_2^{2-}$ as reported earlier [19].

The characteristic infrared (IR) frequencies of the solid PAR reagent in KBr disk changed after the addition of Th(IV). The IR spectrum of PAR showed two bands at 3020

and 3080 cm^{-1} and are safely assigned to $\nu(\text{C-H})$. These bands are stable in position as well as in intensity when one goes from IR spectrum of PAR to the IR spectrum of its Th(IV) complex indicating that, the vibrations are purely $\nu(\text{C-H})$. Another broad and weak band appeared around 3290 cm^{-1} in the IR spectrum of PAR and was assigned to $\nu(\text{O-H})$ [27]. In the IR spectrum of Th(IV)PAR complex, this broad band was slightly decreased in intensity and shifted to 3240 cm^{-1} indicating complex formation via hydroxyl oxygen. In the Th(IV)-PAR complex, the vibration bands due to the azo group $\nu(\text{-N=N-})$ of the free PAR at 1401 and 1554 cm^{-1} are shifted to higher and shorter wave numbers at 1499 and 1360 cm^{-1} , respectively in the complex formation suggesting coordination of Th(IV) to one nitrogen of the azo group. Thus, the data obtained suggest that PAR coordinates to Th(IV) in a bi-dentate fashion (NO), presumably via one azo nitrogen and the hydroxyl oxygen.

Application of b-correction spectrophotometry

Most reported spectrophotometric methods for Th(IV) determination suffer from significant interference of the excess chromogenic reagent with the analyte at k_{max} . This problem was solved in the b-correction spectrophotometric method by calculating the real absorbance of the colored species [20–25]. The spectrum of $\text{Th}(\text{PAR})_2^{2+}$ against the reagent blank at pH 5–6 showed a well defined absorption peak (k_2) 497 nm with a molar absorptivity (ϵ) of $2.469 \times 10^4\text{ L mol}^{-1}\text{ cm}^{-1}$ (Fig. 1). These results suggest the possible application of the b-correction spectrophotometric technique to improve the sensitivity of the proposed complex $\text{Th}(\text{PAR})_2^{2+}$ for the determination of Th(IV) ions. The interference caused by the excess PAR in the reaction mixture will be eliminated. The real absorbance (A_c) and the spectrophotometric parameters a , b of the Th(IV) complex $\text{Th}(\text{PAR})_2^{2+}$ species in solution were calculated using Eqs. 3 and 4 as follows: [22, 23]

$$A_c = \frac{DA}{DA_0 - \delta_1} \quad \delta_2 = b \quad A_0 = A_0 \quad \epsilon_{kL_2} = \epsilon_{kL_1}$$

$$\delta_3 = a \quad A_{0a} = A_a \quad \epsilon_{kML_1} = \epsilon_{kML_2} \quad \delta_4 =$$

where DA^0

and DA , are the absorbance values of the produced Th(IV) complex $[\text{Th}(\text{PAR})_2^{2+}]$ versus reagent blank at k_1 and k_2 , respectively. The parameters A^0 and A_0 represent

the absorbance of the blank solution against water at k_1 and k_2 , and A_a^0 and A_a are the absorbances of the $\text{Th}(\text{PAR})_2^{2+}$ formed in the solution versus water at k_1 and k_2 , respectively. It should be noted that, the sensitivity of the developed dual b-correction method becomes better than that of the single wavelength method by selecting wavelengths k_1 and k_2 at the

valley and the peak of the electronic spectrum of the complex $\text{Th}(\text{PAR})_2^{2+}$ versus blank solution, respectively. Curve C in Fig. 1 shows the minimum and maximum absorption of $\text{Th}(\text{PAR})_2^{2+}$ at pH 5–6 at 413 nm (k_1), and 497 nm (k_2), respectively. The absorbance of the complex $\text{Th}(\text{PAR})_2^{2+}$ at k_2 versus reagent blank (ordinary single wavelength) was found to be less than the corrected absorbance by b-correction spectrophotometric technique. From curve A and Eq. 3, the parameter b was found to equal 0.13. The parameter a was also calculated from Eq. 4 and curve B (Fig. 1) and was found to equal 1.22.

Optimization of chemical variables

Preliminary investigations has revealed that, the formation and the color intensity of the Th(IV)-PAR chelate is pH dependent. Thus, the effect of pH employing acetate buffer (pH 2.2–5.7) and/or B–R buffer (pH 2–11) was carried out. The real absorbance of a suitable Th(IV) concentration (1.0 lg mL^{-1}) in the presence of PAR at various pH values was measured at 497 nm after 2 min of mixing. Representative results are illustrated in Fig. 2. Maximum absorbance of the produced colored complex was obtained at pH 5–6

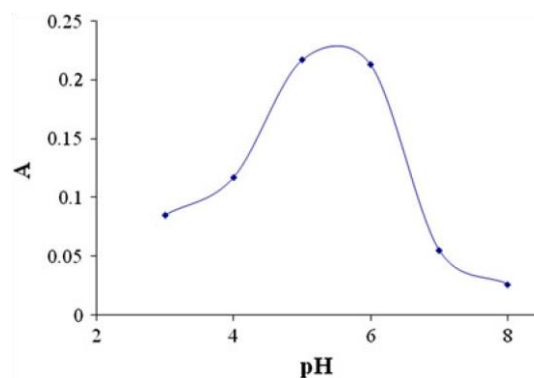


Fig. 2 Plot of the true absorbance of the Th(IV)-PAR complex versus pH of the test aqueous solution using acetate buffer employing acetate buffer. The stability and time required for the formation of the colored species in acetate buffer is much better than in the presence of B–R buffer. This behavior is most likely attributed to the ability of acetate ions to form as binuclear complex species of Th(IV) in which acetate ion acts as bidentate fashion ligand [28].

At pH B 4.5, the absorbance of the colored complex species was low since the reaction shifts to the left. Thus, the quantity of the dissociated species of PAR available to form complex species with Th(IV) decreases. In aqueous solutions of pH C 6, the absorbance of the colored species decreased dramatically on raising the pH. The hydrolysis of the complex and the formation of non-colored species of Th(IV) e.g. hydroxo complex species minimize the intensity of the colored complex and may account for the observed trend. Thus, aqueous solutions were kept at pH 5–6 using acetate buffer to ensure complete complex formation and color stability.

The influence of PAR concentration on the formation of Th(PAR)₂²⁺ complex species of Th(IV) ions at concentration of 1.0 lg mL⁻¹ was studied at pH 5–6. Various volumes of the reagent (0.05% w/v) solution were added to test solutions. A quantity of 1.6 mL of the reagent (0.05% w/v) was found sufficient to quantitatively determine Th(IV) up to 2.0 lg mL⁻¹ (10 mL) in the aqueous solution (Fig. 3). A large excess of the PAR decreased the absorbance because of lowering of the pH of the aqueous phase which minimizes formation of the Th(PAR)₂²⁺. The colored complex was stable after 0.5 min for up to 60 min. The absorbance of Th(PAR)₂²⁺ was generally measured within 20 min of mixing.

Interference study

Analysis of Th(IV) ions at concentration 1 lg mL⁻¹ in the presence of a relatively high excess (0.05–1.0 mg) of some interfering ions that are commonly relevant to water samples e.g. Ca²⁺, Mg²⁺, NH₄⁺, Li⁺, Al³⁺, Co²⁺, Cd²⁺, Fe³⁺,

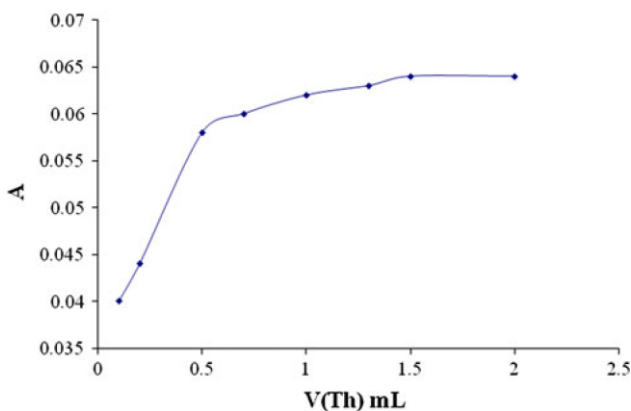


Fig. 3 Effect of reagent concentration on the true absorbance of Th(IV)-PAR complex

VO₃⁻, MnO₄⁻, AsO₂⁻, SO₄²⁻, and PO₄³⁻ ions was investigated following the recommended procedures in the experimental section. The tolerance limit (w/w) was defined as the concentration of the interfering ions added causing a relative error within ±3% in the true absorbance of Th(IV)-PAR complex. The ions: Ca²⁺, Mg²⁺, NH₄⁺, Li⁺, AsO₂⁻, SO₄²⁻, F⁻ and Cl⁻, I⁻, Br⁻ and NO₃⁻ did not cause any significant change in the corrected absorbance of the thorium complex even at 1:100 tolerable concentrations of Th(IV) to the foreign ions, respectively. The ions Pb²⁺ and Fe³⁺, Al³⁺, MnO₄⁻ at concentrations 50 times higher than those of the analyte interfered seriously. Addition of NaCl minimizes the interference caused by Pb²⁺ due to the formation of PbCl₂ precipitate while, the addition of NaF (0.1% w/v) to the test solution eliminates the interference caused by Fe³⁺, Al³⁺, due to the formation of colorless complex species [FeF₆]³⁻ and [AlF₆]³⁻, respectively. The interference of MnO₄⁻ was eliminated by the addition of NaN₃ and heating for few seconds [25]. Thus, the tolerance level of the interfering ions was improved to acceptable limits (96.6–97.4 ± 2.9%) extending the use of the method for Th(IV) determination in water samples.

Analytical performance

The utility of the developed method was determined in terms of the dynamic linear range, limits of detection (LOD), and limits of quantification (LOQ), repeatability, and specificity for Th(IV) determination under the established conditions. The effective molar absorptivity (ε) and the Sandell’s sensitivity index [19, 29] of Th(IV) with and without the use of dual-wavelength b-correction method were found to be 2.52 9 10⁴ and 2.2 9 10⁴ L mol⁻¹ cm⁻¹ and 0.004 and 0.006 lg cm⁻², respectively. The plot of the absorbance of the complex at 497 nm versus concentrations employing b-correction spectrophotometry obeyed Beer’s law in the concentration range 0.2–2.0 lg mL⁻¹.

The regression of the plot using b-correction spectrophotometry is given by the equation:

$$A = 0.0246C_x - 0.0225R + 0.995P \quad \delta 5P$$

The effective concentration range of Th(IV) ions lies within the range 0.2–0.96 lg mL⁻¹. The accuracy of the developed procedure was evaluated by recovery studies of four replicate measurements of Th(IV) in deionized water at concentration level of 1.0 lg mL⁻¹ using b-correction and the ordinary single-wavelength spectrophotometry methods. The relative standard deviation of the develop b-correction method was 1.5% while it was 3.7 for single wavelength

Table 1 Analytical features of the developed dual-wavelength b-correction spectrophotometry and some reported methods

Technique	LOD (lg mL ⁻¹)	LOQ (lg mL ⁻¹)	Dynamic range (lg mL ⁻¹)	Reference
Grafted SPE spectrophotometry	0.004	0.013	0.013–0.103	[12]
Optical sensor using Thorin	0.429	1.43	1.43–231.7	[32]
PLS modified Amberlite XAD-2000 SPE spectrophotometry	0.0005	0.002	0.002–0.08	[13]
Chromatographic separation ICP-MS and spectrophotometric detection	0.001	0.0033	0.0033–5.3	[11]
Dual-wavelength b-correction spectrophotometry	0.01	0.033	0.2–2	Present work

SPE Solid phase extraction, PLS Partial least square

Table 2 Analysis of Th (lg g⁻¹) in the CRM sample (IAEA-soil-7) by the developed (A), the standard ICP-MS (B) methods

Thorium, lg added	A (lg g ⁻¹) ^a	B (lg g ⁻¹)	Official method (NIST-SRM) (lg g ⁻¹)
0.0	6.48 ± 0.1	6.6 ± 0.2	5–8
1.0	7.56 ± 0.06		
5.0	11.49 ± 0.05		
	Average = 6.51 ± 0.07		

The concentration of thorium in the CRM was claimed to be on the range 6.5–8.7 lg g⁻¹

^a Average of three measurements ± relative standard deviation; standard addition technique was employed

spectrophotometry. This level of precision is suitable for routine analysis of Th(IV) in various water samples. The values of LOD and LOQ of the developed procedure calculated [30] for Th(IV) with single wave spectrophotometry were found to be 0.16 and 0.52 lg mL⁻¹ respectively. Such limits were improved to 0.06 and 0.2 lg mL⁻¹ employing the developed dual wave b-correction method. Such limits are comparable to most spectrophotometric methods involving pre concentration step onto solid sorbent [10, 15–17]. The main analytical features of the developed method

were compared with many of the recent electroanalytical and spectrometric methods (Table 1). Some of the reported methods exhibited high detection limit, serious interferences by halides ions, time-consuming [12, 13] and involve expensive instrumentation [31, 32]. Thus, it can be concluded that, the developed method is more selective and sensitive than reported methods. The present method is characterized by the availability of the instrument, simplicity, speed, precision and low cost.

Analytical applications

Analysis of thorium content in certified reference material (IAEA-Soil-7)

The method was validated by the analysis of thorium in the CRM IAEA-Soil-7. After digestion, the sample was analyzed by performing the recovery tests after addition of various known concentrations of Th(IV) in the 1–5 lg range by the developed and ICP-MS methods. Results obtained are summarized in Table 2. The certified and recommended values for IAEA-soil-7 are also given in Table 2. The thorium content determined by the developed method (6.48 ± 0.1 lg g⁻¹) is close to the value obtained by ICP-MS (6.6 ± 0.2 lg g⁻¹) and in the claimed range (5–8 lg g⁻¹) of thorium in the CRM determined by official methods. The t- and F-tests at 95% confidence levels did not exceed the tabulated (theoretical) ones and revealed no significant differences between the averages and the variances of the developed and ICP-MS methods in terms of

precision and accuracy. At 95% confidence, the calculated value of t = 2.61 and F = 2.33 are greater and lower than the

theoretical ones ($t = 2.31$) and $F = 6.38$, respectively. Therefore, the developed method is precise and applicable for the determination of low concentrations of thorium compared to other reported spectrochemical methods [32]. Analysis of thorium content in water samples

The developed method was used for the analysis of Th(IV) in tap- and well-water samples (S_1 – S_4) employing the standard addition procedures after digestion with UV irradiation at 254 nm. Water samples were spiked with various concentrations (0.01 – 1.0 $\mu\text{g mL}^{-1}$) of Th(IV). The test solutions were then analyzed as described in Sect. 2.4.2. The results for the analysis of underground water samples (S_1 – S_4) are summarized in Table 3. Samples were also analyzed by the ICP-MS method. The data of both methods revealed the absence of thorium in tap water confirming the precision of the proposed b-correction method for thorium determination. Measured concentration of thorium by the ICP-MS was found close to the results obtained by the proposed method.

The applicability of the method for the chemical speciation of Th(IV) in the tested well water samples was also tested. Analysis of thorium in the tested well water samples (S_1 – S_4) without UV digestion revealed that, the labile

Table 3 Level of Th ($\mu\text{g L}^{-1}$) in local underground- and Red-sea water samples by the developed (A) and the standard ICP-MS (B) methods

Sample no.	A ($\mu\text{g L}^{-1}$)	B ($\mu\text{g L}^{-1}$)
S_1	1.90 (1.4)	2.14
S_2	2.14 (1.34)	2.3
S_3	2.69 (2.45)	2.84
S_4	2.36 (2.16)	2.3
R_{a1}	2.49	2.7

Average of three measurements ($n = 3$) \pm relative standard deviation The values in parentheses represent the labile Th(IV) ions

^a R_1 Red sea water sample from the coastal area of Jeddah City

thorium content in samples S_1 , S_2 , and S_4 are high compared to sample S_3 confirming the applicability of the developed method for thorium speciation in the underground water samples.

A Red sea water sample was collected from the coastal water north of Jeddah city and analyzed according to the described procedures in the experimental section. The results are summarized also in Table 3. The discrepancy between the ICP-MS and the developed method is attributed to the amount of thorium bound to organic matter present in the Red sea water samples which are measured only by ICP-MS.

Conclusion

The analytical method described in this work for the determination of Th(IV) in water samples, involving dualwavelength b-correction spectrophotometry, has the advantage of virtual freedom from interferences from extraneous ions. Therefore it serves as an alternative to widely used methods for rapid and precise determination of trace amounts of thorium in natural waters and effluent samples. The color of the complex appears rapidly in less than 2 min and remains stable for up to 1 h.

Acknowledgment The authors would like to thank the Deanship of Scientific research King Abdul-Aziz University, Saudi Arabia for funding under the grant number 3-100-429.

References

- Rao TP, Metilda P, Gladis JM (2006) *Talanta* 68:1047–1064
- Jia G, Torri G, Magro L (2009) *J Environ Radioact* 100:941–949
- WHO (2004) Guidelines for drinking-water quality, 3rd edn. Geneva (Switzerland)
- Jain VK, Pandya RA, Pillai SG, Shrivastav PS (2006) *Talanta* 70:257–266
- Yang X, Feng Y, He Z, Stoffella PJ (2005) *J Trace Elem Med Biol* 18:339–353
- Tamborini G (2004) *Microchimica Acta* 145:237–242
- Nasab ME, Sam A, Milani SA (2011) *J Radioanal Nucl Chem* 287:239–245
- Alam LMN, Rahman N, Azmi SNH (2008) *J Hazard Mater* 155:261–268
- Welz JB, Sperling M (1999) Atomic absorption spectrometry. Wiley VCH, New York
- Ghasemi JB, Zolfonon E (2010) *Talanta* 80:1191–1197
- Gladis JM, Rao TP (2002) *Anal Bioanal Chem* 373:867–872
- Shimada A, Haraga T, Hoshi A, Kameo Y, Nakashima M (2010) *J Radioanal Nucl Chem* 286:765–770
- Antovic NM, Svrkota N, Antovic I (2010) *J Radioanal Nucl Chem* 283:313–318
- Hořlriegl V, Oeh U, Roßmuß M, Gerstmann U, Roth P (2005) *J Radioanal Nucl Chem* 266:441–444
- Guo GL, Luo MB, Xu JJ, Wang TX, Hua R (2009) *J Radioanal Nucl Chem* 281:647–651
- Fukuma T, Fernandes EAN, Nascimento MRL, Quinelato AL (2001) *J Radioanal Nucl Chem* 248:549–553
- Das SK, Kedari CS, Tripathi (2010) *J Radioanal Nucl Chem* 285:675–681

18. Rozmaric M, Ivsic AG, Grahek Z (2009) *Talanta* 80:352–362
19. Marczenko Z, Balcerzak M (2000) *Separation, preconcentration and spectrophotometry in inorganic analysis*. Elsevier, Amsterdam
20. Abbaspour A, Baramakeh L (2002) *Talanta* 57:807–812
21. Abbaspour A, Baramakeh L (2005) *Talanta* 65:692–699
22. Abbaspour A, Mirzajani R (2006) *Spectrochim Acta Part A* 64:646–652
23. Michalowski T, Baterowicz A, Wojtowicz A (2000) *Talanta* 52:337–340
24. Hamza A, Bashammakh AS, Al-Sibaai AA, Al-Saidi HM, El-Shahawi MS (2009) *Anal Chim Acta* 657:69–74
25. Hamza A, Bashammakh AS, Al-Sibaai AA, Al-Saidi HM, El-Shahawi MS (2010) *J Hazard Mater* 178:287–292
26. Kadi MW, El-Shahawi MS (2009) *Radiochim Acta* 97:613–619
27. Sawyer DT, Heineman WR, Beebe JM (1984) *Chemistry experiments for instrumental methods*. Wiley, New York
28. Nakamoto K (1978) *Infrared and Raman spectra of inorganic and coordination compounds*, 3rd edn. Wiley, New York
29. Sandell EB (1959) *Colorimetric method of analysis*. Wiley-Interscience, New York
30. Miller JC, Miller JN (1994) *Statistics for analytical chemistry*, 4th edn. Ellis Horwood, New York
31. Li, YR, Pradhan, NK, Foley, R, Low, GKC (2002) *Talanta* 57 (2002) 1143–1151
32. Rastegarzadeh S, Pourreza N, Saeedi I (2010) *J Hazard Mater* 173:110–114

COBALT CATALYZED-MULTI-WALLED CARBON NANOTUBES FILM SENSOR FOR CARBON MONO-OXIDE GAS

ZISHAN H. KHAN*, M. SHAHNAWAZE ANSARI, NUMAN A. SALAH,
ADNAN MEMIC, SAMI HABIB & M. S. SHAHAWI^a

Center of Nanotechnology, King Abdulaziz University, Jeddah, Saudi, Arabia

^a
*Center of Excellence in Environmental Studies, King Abdulaziz University, Jeddah,
Saudi Arabia*

The fabrication of cobalt (Co) catalyzed multi-walled carbon nanotubes (MWNTs) film sensor for the detection of carbon mono-oxide (CO) gas has been reported. Cobalt (Co) catalyzed carbon nanotubes have been synthesized on silicon oxide grown silicon substrate using low pressure chemical vapor deposition. The diameter of these multi-walled nanotubes (MWNTs) varies from 40-100 nm and the length is on the order of several tens of micrometers. To measure the gas sensing properties of this sensor, a typical pattern of gold electrodes has been thermally evaporated. The typical responses of MWCNTs gas sensor for different concentration (40, 100, 140 & 200 ppm) of sensing gas i.e. carbon mono-oxide (CO) have been studied. It is observed that this MWNTs gas sensor shows a quick response to CO gas with the fast recovery time. Temperature dependence of the resistance of this MWNTs-based film sensor has also been studied for a temperature range of 300-500K. It is found that the resistance decreases with the increase in temperature for all concentration of CO gas. The sensitivity and responsiveness has been estimated with respect to the time as well as temperature. The responsiveness increases whereas the sensitivity of this sensor decreases with the increase in temperature for all concentrations of CO gas. Some electrical parameters such as activation energy and pre-exponential factor have also been estimated to understand the electrical transport properties of this sensor.

(Received October 19, 2011; accepted

Keywords: sensor; carbon nanotubes; cobalt

1. Introduction

Recently, gas sensors, or chemical sensors, have drawn a lot of attention due to their widespread applications in industry, environmental monitoring, space exploration, biomedicine, and pharmaceuticals. The demand of today's sensing technology is the gas sensors with high sensitivity and selectivity, avoiding the leakage of explosive gases such as hydrogen, and allowing easy operation of real-time detection of toxic or pathogenic gases in industries. For monitoring and controlling our ambient environment, especially with the increasing concern of globe warming, we need highly sensitive gas sensors. Scientists at National Aeronautics and Space Administration (NASA) are seeking the use of high-performance gas sensors for the identification of atmospheric components of various planets.

The evolution of new materials and devices play a key role in the development of accurate and reliable devices such as sensors. During the last few decades, the technology of nanosensors has developed tremendously by joining many scientific achievements from various disciplines, offering challenges and opportunities. A lot of research work is focused on the fabrication of

smaller devices capable of molecular level imaging and monitoring of pathological samples and macromolecules, particularly for remote monitoring, due to the increasing need for environmental safety and health monitoring [1-2].

*Corresponding author: zishan_hk@yahoo.co.in

Several workers [3-6] used multiwalled carbon nanotubes (MWNTs) to sense polar as well as non polar gases such as carbon monoxide (CO), carbon dioxide (CO₂), ammonia (NH₃), water (H₂O), and ethanol (C₂H₅OH), helium (He) and nitrogen (N₂). In case of nanotubes, it is observed that the oxygen (O₂) molecules are electron acceptors with substantial adsorption energies and charge transference, whereas ammonia (NH₃), nitrogen (N₂), carbon dioxide (CO₂), methane (CH₄), water (H₂O), hydrogen (H₂) and argon (Ar) are electron donors [7]. The adsorption in nanotubes is determined by adsorption energy and availability of sites, with typically four different adsorption sites: external surface, grooves between carbon nanotubes on the bundle outside, pores inside carbon nanotubes, and interstitial channel between adjacent tubes inside the bundle [8-9]. Jhi et al. [10] reported that the electronic and magnetic properties of oxidized nanotubes and they concluded that the nanotubes have high potential for gas sensors. They further demonstrated that the sensing mechanism of as synthesized nanotubes is more related to oxygen doping than to intrinsic properties, and depends on the structural defects created during the synthesis of these nanotubes.

Many reports on different types of gas sensors are available in the literature [11-13]. These sensors generally operate on different principles and various gas sensing elements have been employed for these sensors, out of which resistive metal oxide sensors comprise a significant part. However, the metal oxide sensing elements typically operate at an elevated temperature for maximum performance, thereby, causing higher power consumption. This limits the application of these sensors in various fields such as wireless technology. Since their discovery [11], carbon nanotubes have drawn a lot of research interests due to their unique geometry, morphology, and properties. Their preparation, properties (such as electronic, mechanical, thermal, and optical properties), and applications on various fields are all studied intensely [12-17]. These properties make them potential candidates as building blocks of active materials in nanoelectronics, field emission devices, gas storage and gas sensors [18-20]. Among these, it has been reported [3, 21] that the carbon nanotubes show excellent room temperature gas sensing property for many applications. The large surface area provided by the hollow cores and outside walls in nanotubes gives them very large gas absorptive capacity. Interaction with any gas can change the electrical properties of CNTs at room temperature. Also, they have fast response and good reversibility [22]. Therefore, we set-out to study the carbon mono-oxide gas sensing properties of carbon nanotubes in the present manuscript. In the present work, a cobalt catalyzed multi-walled carbon nanotubes film sensor has been fabricated and the carbon mono-oxide gas sensing properties of this sensor has been studied.

2. Experimental

Carbon nanotubes (CNTs) were synthesized on cobalt catalyzed film using low pressure chemical vapour deposition system. These CNTs were grown by the catalytic deposition of C₂H₂ at 750°C, at a chamber pressure of 100 Torr and the growth time was kept fixed at 5 minutes. Initially, nitrogen gas was passed for 10 mins. at a temperature of 700°C, just after this process, the etching gases NH₃ and H₂ with flow rates of 100 sccm and 50 sccm respectively were passed through the reactor for 15 mins using mass flow controllers (MFC's). At the final stage, the hydrocarbon carbon gas C₂H₂ with a flow rate of 20 sccm was added for 5 minutes. Therefore, the final gas mixtures of NH₃:C₂H₂:H₂ with flow rates 100:50:20 sccm respectively, were used to grow the carbon nanotubes. The morphology of these carbon nanotubes (CNTs) were studied using Field Emission Scanning Electron Microscope (FESEM). Raman spectrum of as-grown CNTs was recorded using DXR Raman Microscope, Thermo Scientific with 532 nm laser as an excitation

source at a power of 8 mW. A specially designed gas sensing set-up was used to study the gas sensing properties of these as-synthesized carbon nanotubes (CNTs) based sensor. An electrode pattern of gold was thermally evaporated on this film. To study the gas sensing properties of the as-prepared CNTs film sensor, the gas sensor was kept inside a stainless steel chamber and the resistance was measured using a Keithley 4200 I-V measurement system. The mass flow controllers were used to control the concentration of detecting gas. The Ag-Pt heater was used to heat and control the operation temperature of the sample. For measuring the gas sensing properties, CNTs based sensor was kept inside the sample holder and probes were connected on the electrodes of CNTs film. The system was evacuated up to 10^{-6} Torr with the help of turbo molecular pump. After attaining the required degree of vacuum, the turbo and rotary pump valves were closed and air was purged with a flow rate of 2 l/min for 3 mins. Real time resistance was measured to obtain a baseline resistance. Once a baseline resistance was obtained, the detecting gas i.e. carbon mono-oxide with a set concentration was introduced into the sample holder. This gas was purged for 1-2 minutes to measure the change in resistance with time up to 2 minutes and after the time was over, the flow of detecting gas in to the sample holder was stopped and we measured the recovery time of the sensor. We repeated these cycles for different concentrations of carbon mono-oxide with respect to pure air to study the response of this CNT sensor for detecting carbon mono-oxide (CO). The sample gas flow time and the clean air reference flow time were fixed at 1 minute and 3 minutes, respectively. It should be noted that these switching intervals were selected so that the resistance change is at least 90% of the saturated value. The sensor resistance was sampled and recorded every second for subsequent analysis. The relative changes in the electrical parameters of the film were considered as sensor output. Typical response of this resistive sensor is measured with respect to time and temperature respectively.

3. Results and discussion

Figs. 1(a) & 1(b) represent the morphology of as-grown carbon nanotubes (CNTs). The diameter of these nanotubes varies from 40-100 nm and length of these carbon nanotubes (CNTs) is on the order of several tens of micrometers. TEM image of these CNTs is presented as Fig. 2. It is observed that these nanotubes are multi-walled and the diameter of inner and outer wall is 10 nm and 40 nm respectively. To verify the graphitic nature of as-grown carbon nanotubes, we have employed Raman Spectroscopy. Fig. 3 presents the Raman spectrum of as grown multi-walled carbon nanotubes (MWNTs). The presence of strong peak at 1580 cm^{-1} (G-band) in this spectrum clearly indicates the graphitized nature of these as-grown cobalt catalyzed multi-walled carbon nanotubes (MWNTs). The D mode (the disorder band) located between $1330 - 1360\text{ cm}^{-1}$, is generally observed in CVD grown MWNTs. Here, the D-band peak observed at 1320 cm^{-1} seems to be less intense, which predicts that the less quantity of amorphous carbonaceous particles is adhered to MWNTs walls. In the present work, we have studied the typical resistive response of the cobalt catalyzed multi-walled carbon nanotubes (MWCNTs) gas sensor with respect to time and temperature.

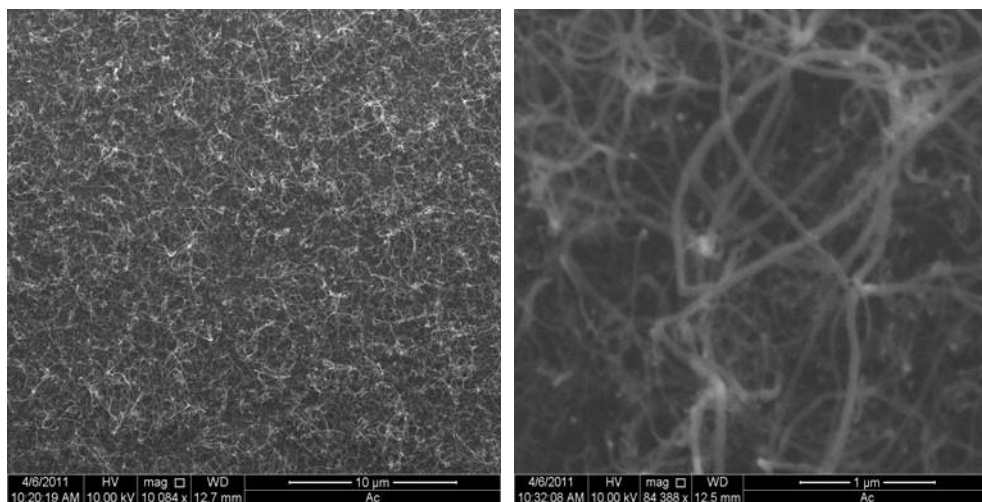


Fig. 1(a&b) FESEM images of Co-catalyzed CNTs.

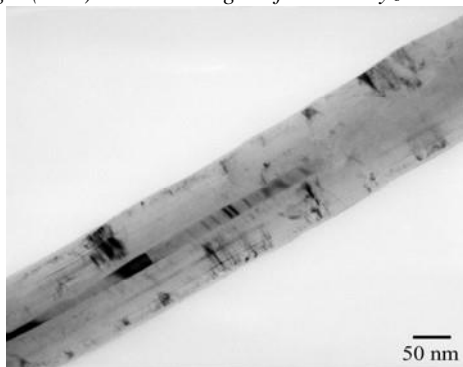


Fig. 2 TEM image of Co-catalyzed MWNT.

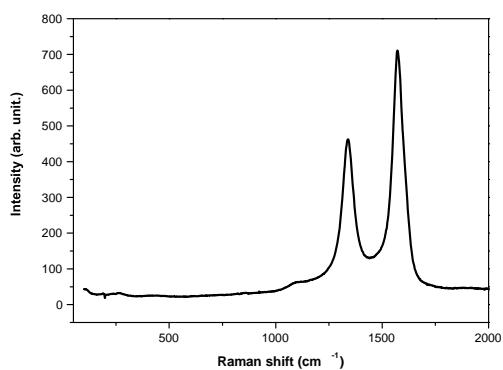


Fig. 3. Raman spectra of Co-catalyzed MWNTs.

4. Typical response on the basis of resistance versus time cycles

On the basis of resistance versus time cycles, typical response of this multi-walled carbon nanotubes (MWCNTs) gas sensor in the presence of carbon mono-oxide (CO) gas is presented in Fig. 4. It is observed that the resistance of the sensing materials increases on increasing the

concentration of CO from 40 ppm to 200 ppm. This suggests that the CO is identified as an electron acceptor. It is also reasonable to propose that this behavior in the present sample may be due to the adsorbed CO molecules on the wall of these carbon nanotubes. CO has an unpaired electron and is known as oxidizer. Upon CO adsorption, a charge transfer is likely to occur from MWNTs to CO due to the electron-acceptor character of CO molecules inducing the formation of electronic levels in the semiconducting nanotube gap, very near to the Fermi level. Further increase in CO concentration may result in the interaction of a large number of CO molecules with the defective sites on the wall of the nanotubes, causing an increase in the electrical resistance. It is also well known that the carbon mono-oxide is a reducing gas and its absorption will result in injection of electrons to the CNTs and reduction in the number of holes in the material. As holes are the main charge carrier for p-type semiconductor, the reduction in the number of holes will result in an increase in resistance of the sample on the exposure of CO gas.

On the basis of the dynamical response (resistance-time (R-t) cycles) of this MWNTs film sensor, the response and recovery time has been calculated and the calculated values are given in Table 1. It is seen that the response time ($\tau_{res.}$) first decreases from 39.78 seconds to 33.06 seconds and then, it increases to 37.50 seconds with the increase in the concentration of carbon monoxide (CO) gas, whereas the recovery time ($\tau_{rec.}$) changes from 31.38 seconds to 43.14 seconds. Here, it may be suggested that this increase in the recovery time with the increase in CO concentration may be due to the increase in binding energy between MWNTs and CO. This overall increase in the response and recovery time may also be due to the increase in the adsorption/desorption process of gas molecules on MWNTs.

Table-1. Typical sensor parameters for the Co-catalyzed MWNTs-based film sensor

CO Concentration (ppm)	Resistance (Ohm)	Responsiveness $[(R_{air}-R_{gas})/R_{gas}]$	Sensitivity (R_{air}/R_{gas})	Response Time (τ_{res}) (Sec.)	Recovery Time (τ_{rec}) (Sec.)	Activation energy (ΔE) (eV)	Preexponential factor (σ_0) ($ohm^{-1}.cm^{-1}$)
40	115.11	0.4645	0.8608	39.78	39.78	0.193	1.698
100	125.93	0.5094	0.8506	33.06	40.62	0.187	1.318
140	141.65	0.5645	0.7953	34.14	42.54	0.180	1.092
200	152.47	0.5949	0.7407	37.50	43.14	0.170	1.725
Air				-----	-----	0.190	3.196

To evaluate the sensitivity of this MWNTs gas sensor, we use the following relation;

$$\text{Sensitivity} = R_{air}/R_{gas} \quad (1)$$

Where, R_{air} is the sensor resistance in air and R_{gas} is the sensor resistance in the presence of a toxic species. The sensitivity of this gas sensor has been estimated for different gas concentrations. The sensitivity response with time for all the studied CO concentrations is shown in Fig. 5. The sensitivity of this MWNTs gas sensor decreases from 86.08% to 74.07% with the increase in gas concentration from 40 ppm to 200 ppm. This means the process of CNTshybridization reduces the gas sensitivity toward CO gas.

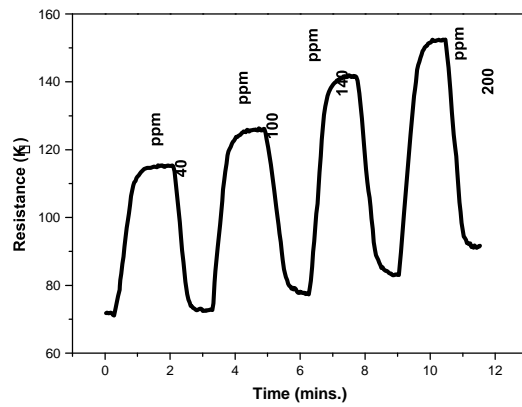


Fig. 4. Typical responses of Co-catalyzed MWCNTs gas sensor for different concentration of CO gas (40, 100, 140 & 200 ppm).

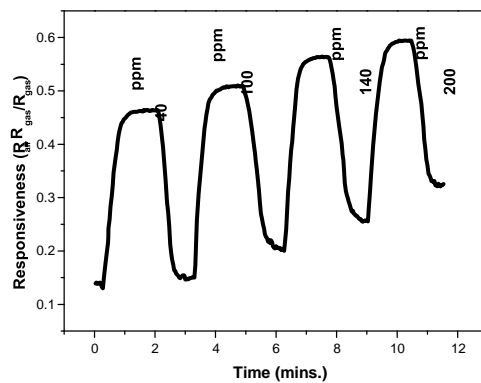


Fig. 5. Typical responsiveness of Co-catalyzed MWCNTs gas sensor for different concentration of CO gas (40, 100, 140 & 200 ppm).

For quantifying the performance of a given sensor, we use the following relation to calculate the responsiveness (SR) of the sensor;

$$SR = (R_{air} - R_{gas})/R_{air} \quad (2)$$

It is defined as the ratio of the resistance change due to the exposure to the test gas and the sensor's baseline resistance in air. Using above relation (eq.2), the responsiveness of the present MWNTs sensor is calculated at different CO concentration and the values are presented in Table 1. It is clear from this table that this MWCNTs gas sensor could detect gas concentration as low as 40 ppm of CO. From the responsiveness time cycles (Fig. 6), it is found that the responsiveness increases from 46.45% to 59.49% as the gas concentration increases from 40 ppm to 200 ppm. It is therefore, suggested that this MWNTs sensor gives a good response to the different concentrations of CO gas.

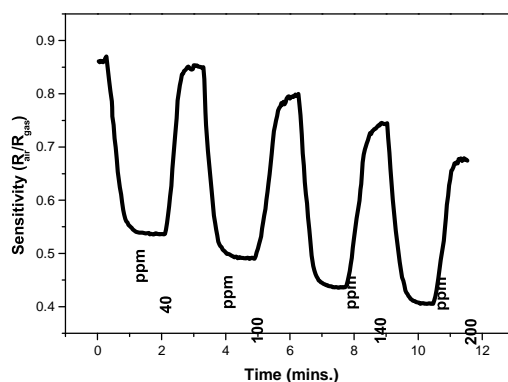


Fig. 6. Typical sensitivity of Co-catalyzed MWCNTs gas sensor for different concentration of CO gas (40, 100, 140 & 200 ppm).

In the present system, the electrical response to molecular adsorption in multi-walled carbon nanotubes (MWCNTs) may be explained on the basis of two sensing mechanisms namely (i) the adsorption resulting in direct charge transfer between a donor or acceptor type of molecule and MWNTs, which will lead to the shift in the Fermi level in the semiconducting tubes (intratube modulation), resulting in a change in resistance [23], (ii) the adsorption occurs in the interstitial space between MWNTs to form an MWNT-molecule-MWNT junction, which will result in a hopping kind of mechanism for inter-tube charge transfer between nanotubes. Therefore, an inter-tube modulation of the CNTs network may be responsible for the resistance change. This phenomenon is common for all types of molecules and for both metallic and semiconducting CNTs. This type of modulation is similar to that of the interaction between semiconductor metal oxides and donor or acceptor types of molecules, showing a nonlinear (power law) response [24].

5. Typical response on the basis of temperature dependence of resistance

Here, we have studied the variation of resistance with the temperature for different concentration of CO gas (40, 100, 140 & 200 ppm). Fig. 7 presents the temperature dependence of the resistance at different CO concentration for the present cobalt catalyzed MWNTs film sensor in the temperature range 300 to 500 K. It is observed that the resistance decreases exponentially with increasing temperature from 300 to 500 K, which suggests the semiconducting behavior of these MWNTs. At a particular temperature, the resistance is found to decrease with the increase in CO concentration. The variation of resistance with temperature for different concentration of CO (40, 100, 140 & 200ppm) is presented in Table 2.

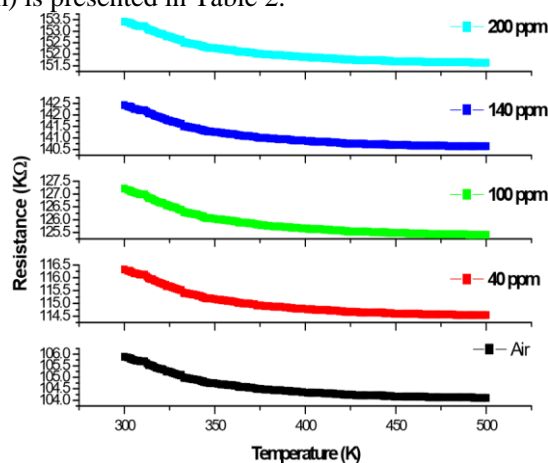


Fig. 7. Temperature dependence of resistance for the Co-catalyzed MWNTs-based film sensor in air and 40, 100, 140 & 200 ppm CO gas for the temperature range of (300-500K).

Table-2
Electrical parameters for the Co-catalyzed MWNTs-based film sensor

CO concentration	Resistance (k Ω) at different temperatures					Responsiveness $[(R_{air} - R_{gas}) / R_{air}]$ at different temperatures					Sensitivity (R_{air}/R_{gas}) at different temperatures					Activation energy (ΔE) (eV)	Pre-exponential factor (σ_0) (ohm ⁻¹ .cm ⁻¹)
	300K	350K	400 K	450 K	500 K	300K	350K	400 K	450 K	500 K	300K	350K	400 K	450 K	500 K		
40 ppm	116.33	115.17	114.77	114.60	114.54	0.0897	0.0906	0.0909	0.0910	0.0911	0.9103	0.9094	0.9091	0.9090	0.9089	0.193	1.698
100 ppm	127.21	126.05	125.65	125.47	125.41	0.1675	0.1690	0.1695	0.1698	0.1699	0.8325	0.8310	0.8305	0.8302	0.8301	0.187	1.318
140 ppm	142.43	141.26	140.87	140.69	140.63	0.2564	0.2586	0.2593	0.2596	0.2597	0.7436	0.7415	0.7408	0.7404	0.7403	0.180	1.092
200 ppm	153.43	152.27	151.86	151.70	151.64	0.3098	0.3121	0.3129	0.3133	0.3134	0.6902	0.6879	0.6871	0.6867	0.6866	0.170	1.725
Air	-----					-----					-----					0.190	3.196

It is found that the entire experimental data for the temperature region (300- 500K) gives a best fit to the thermally activated process. Therefore, we have applied the thermally activated process for the temperature region (300-500K) to understand the conduction mechanism in the present sample of Co catalyzed MWNTs film,. The plot of $\ln \sigma$ Vs $1000/T$ for the temperature range of (300-500K) is presented in Fig. 8. The plot is a straight line, indicating that the conduction in this system is through the thermally activated process. The conductivity, is therefore expressed by the usual relation

$$\sigma = \sigma_0 \exp(-\Delta E / kT) \quad (3)$$

where, σ_0 and ΔE represents the pre-exponential factor and activation energy respectively, K is Boltzmann constant.

We may write equation (1) as,

$$\ln \sigma = \ln \sigma_0 - (\Delta E / kT) \quad (4)$$

or
$$\ln \sigma = -(\Delta E / 1000 k) (1000/T) + \ln \sigma_0 \quad (5)$$

When we plot a graph between $\ln \sigma$ and $1000/T$, a straight line is obtained having slope $(\Delta E/1000 k)$ and intercept $\ln \sigma_0$.

We may calculate the activation energy (ΔE) and pre-exponential factor (σ_0) as follows,

$$\begin{aligned} (\Delta E) &= 1000 k \times \text{slope of straight line} \\ \sigma_0 &= \sigma / \exp(-\Delta E / kT) \end{aligned} \quad (6)$$

Using the above relations, the values of the activation energy and pre-exponential factor are calculated and these values are given in Table 2. On the basis of these calculated values, it is suggested that the conduction is due to thermally assisted tunneling of charge carriers in the localized states in band tails. The activation energy alone does not provide any indication as to where about of the conduction mechanism, whether it takes place in the extended states above the mobility edge or by hopping in the localized states. This is due to the fact that both of these conduction mechanisms can occur simultaneously. The activation energy in the former case represents the energy difference between mobility edge and Fermi level, $(E_c - E_f)$ or $(E_f - E_v)$. As

compared to the initial value, an overall decreasing trend is observed for conductivity of this system with the increase in CO gas concentration. This decrease in conductivity could be caused by the increase in the defect states associated with the CO gas molecules [25]. In order to obtain a clear distinction between two conduction mechanisms, Mott and Davis [26] have suggested that the pre-exponential factor in equation (4) for conduction in the localized states should be two to three orders lower than the conduction in the extended states, and should become still lower for the conduction in the localized states near the Fermi level. Thus, in the present system, the value of pre-exponential factor (σ_0) is of the order of unity. On the basis of this value of σ_0 , it is suggested that the conduction is taking place in the band tails of localized states. A significant change in the value of σ_0 is observed after exposing this MWNTs sensor to CO gas. This may be explained by using the shift of Fermi level after exposure to different concentration CO gas. Therefore, the change in the value of σ_0 may be due to the change in Fermi level with exposure of CO gas.

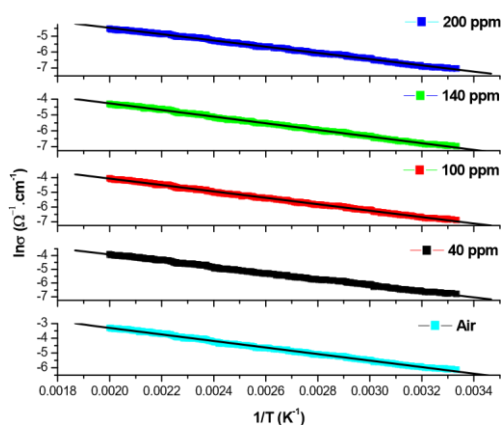


Fig. 8. $\ln \sigma$ versus $100/T$ for the Co-catalyzed MWNTs-based film sensor in air and 40, 100, 140 & 200 ppm CO gas for temperature range of (300-500K).

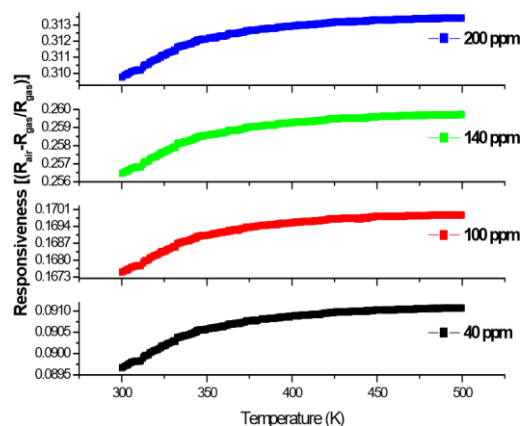


Fig. 9. Temperature dependence of responsiveness for the Co-catalyzed MWNTs-based film sensor in air and 40, 100, 140 & 200 ppm CO gas for the temperature range of (300-500K).

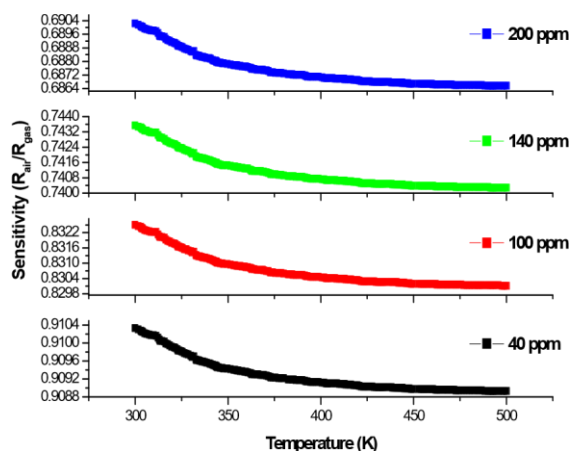


Fig. 10. Temperature dependence of sensitivity for the Co-catalyzed MWNTs-based film sensor in air and 40, 100, 140 & 200 ppm CO gas for the temperature range of (300-500K).

Fig. 9 presents the variation of responsiveness with temperature for different gas concentration. It is observed that the responsiveness of the presently studied sensor increases with the increase in temperature, suggesting that the sensor gives good response even at higher temperatures. Fig. 10 shows the variation of sensitivity with the temperature for different CO concentration. It is found that the sensitivity decreases with the increase in temperature. This indicates that the currently studied Co catalyzed MWNTs become more hybridized at higher temperature, thereby resulting in the decrease in sensitivity.

6. Conclusion

The dynamic response of electrical resistance with time suggests that the resistance of this cobalt catalyzed multi-walled carbon nanotubes (MWCNTs) sensor increases with the increase in the gas concentrations. An overall increasing trend is observed for the response time ($\tau_{res.}$) and the recovery time ($\tau_{rec.}$) with increasing gas concentration. This increase in response time ($\tau_{res.}$) and the recovery time ($\tau_{rec.}$) of this sensor with the increase in gas concentration may be due to the fast adsorption/desorption process of gas molecules on MWNTs. The sensitivity of multi-walled carbon nanotubes (MWCNTs) gas sensor decreases from 86.08% to 74.07% and the responsiveness increases from 46.45% to 59.49% as the gas concentration increases from 40 ppm to 200 ppm. Therefore, it is suggested that this MWNTs sensor gives a good response to the different gas concentration. From the temperature dependence of conductivity of this MWNTs sensor, it is observed that the conduction is though a thermally activated process in the band tails of localized states. The responsiveness of this sensor increases with the increase in temperature, whereas the sensitivity decreases for all the concentration of CO gas.

References

- [1] B. Ghaddab, J.B.Sanchez, C.Mavon, M.Paillet, R.Parret, A.A.Zahab, J.-L.Bantignies, V. Flaud, E.Beche, F.Berger, *Sensor and Actuators B : Chemical* (2011) Online version available.
- [2] Zishan H. Khan, Numan A. Salah, Sami Habib, A. Azam & M. S. Shahawi , *Current Nanoscience* (2011) (Accepted for publication).
- [3] K.G Ong, K.Zeng, and C.A. Grimes, *IEEE Sensors Journal*, **2** (2002) 82.

- [4] L. Valentini, C. Cantalini, I. Armentano, J. M. Kenny, L. Lozzi, and S. Santucci, *Diamond and Related Materials*, **13** (2004) 1301.
- [5] O. K. Varghese, P. D. Kichambre, D. Gong, K. G. Ong, E. C. Dickey, and C. A. Grimes, *Sensors and Actuators B: Chemical*, **81**, 32 (2001).
- [6] C. K. W. Adu, G. U. Sumanesekera, B. K. Pradhan, H. E. Romero, and P.C. Eklund, *Chemical Physics Letters*, **337**, 31 (2001).
- [7] J. Zhao, A. Buldum, J. Han, and J. P. Lu, *Nanotechnology*, **13**, 195 (2002).
- [8] G. Stan, and M. W. Cole, *Journal of Low Temperature Physics*, **110**, 539 (1998).
- [9] K. A. Williams, and P. C. Eklund, *Chemical Physics Letters*, **320**, 352 (2000).
- [10] S. H. Jhi, S. G. Louie, and M. L. Cohen, *Physical Review Letters*, **85**, 1710 (2000).
- [11] S. Iijima, *Nature*, **354**, 56 (1991).
- [12] A. C. Dillon, K. M. Jones, T. A. Bekkedah, C. H. Kiang, D. S. Bethune and M. J. Heben, *Nature*, **386**, 377 (1997).
- [13] J. Li, in *Carbon Nanotubes: Science and Applications*, M. Meyyappan, Ed., CRC Press, Boca Raton, Fla, USA (2005).
- [14] Z. M. Rittersma, *Sensors and Actuators A*, **96(2-3)**, 196 (2002).
- [15] R. Fenner and E. Zdankiewicz, *IEEE Sensors Journal*, **1(4)**, 309 (2001).
- [16] V.R. Shinde, T. P. Gujar, C. D. Lokhande, *Sens. Actuat. B Chem.*, **120**, 551 (2007). [17] Y. Zeng, T. Zhang, L. Wang, M. Kang, H. Fan, R. Wang, Y. He, *Sens. Actuat. B Chem.*, **140**, 73 (2009).
- [18] P.M. Ajayan and O.Z. Zhou, *Applications of carbon nanotubes Carbon Nanotubes (Springer Topics in Applied Physics vol 80) ed M S Dresselhaus, G Dresselhaus and Ph Avouris (Berlin: Springer) (2001) 391.*
- [19] Y. Saito, K. Hamaguchi, S. Uemura, K. Uchida, Y. Tasaka, F. Ikazaki, M. Yumura, A. Kasuya and Y. Nishina, *Appl. Phys. A*, **67**, 95 (1998).
- [20] L. Valentini, L. Lozzi, C. Cantalini, I. Armentano, J. M. Kenny, L. Ottaviano and S. Santucci, *Thin Solid Films*, **436**, 95 (2003).
- [21] B. Philip, J. K. Abraham, A. Chandarsaker and V. K. Varadan, *Smart Mater. Struct.*, **12**, 935 (2003).
- [22] A. C. Dillon, K. M. Jones, T. A. Bekkedah, C. H. Kiang, D. S. Bethune and M. J. Heben, *Nature*, **386**, 377 (1997).
- [23] J. Zhao, A. Buldum, J. Han, J. P. Lu, *Nanotechnology*, **13**, 195 (2002).
- [24] J. Gardner, P. N. Bartlett, *Electronic Nose: Principles and Applications*; Oxford University Press: New York, 1999.
- [25] S. Okano, M. Suzuki, K. Imura, N. Fukada, A. Hiraki, *J. Non-Crys. Solids*, **59-60**, 969 (1983).
- [26] N.F. Mott, E.A. Davis, *Philos. Mag.*, **22**, 903 (1970).

Antioxidant and antibacterial characteristics of phenolic extracts of locally produced honey in Saudi Arabia

RASHAD RIZK AL-HINDI¹, MAGED SALEM BIN-MASALAM¹, & MOHAMMAD SOROR EL-SHAHAWI²

¹ Department of Biological Sciences, Faculty of Science, King Abdulaziz University, Jeddah, Saudi Arabia, and Department of
² Chemistry, Faculty of Science, King Abdulaziz University, Jeddah, Saudi Arabia

Abstract

The antibacterial and antioxidant properties of 30 selected honey samples produced in Saudi Arabia have been studied. The inhibitory action of the total phenolic content of the honey samples has been tested against *Staphylococcus aureus*, *Micrococcus luteus* and *Escherichia coli*. The MIC values of the ten selected honey samples against *S. aureus*, *M. luteus* and *E. coli* were in the range 0.5 ± 0.2 to 3.6 ± 0.3 ; 0.45 ± 0.05 to 5.0 ± 0.6 and 0.6 ± 0.2 to 4.4 ± 0.4 mg/mL²¹. The antioxidant activities of the ethyl acetate extracts based on their anti-radical power using the 1,1-diphenyl-2-picrylhydrazyl scavenging assay and their ferric reducing antioxidant power were in the ranges $50.78 \pm 1.4\%$ to $99.52 \pm 0.2\%$ and 0.85 ± 0.13 to 1.167 ± 0.13 mg/ml, respectively. The total phenolic content was in the range 84.97 ± 0.57 to 317.39 ± 0.76 mg/100g.

Keywords: Saudi honey, total phenolic extract, antimicrobial and antioxidant activities

Introduction

Honey, like other saturated sugar syrups has an osmolarity sufficient to inhibit microbial growth (Chirife et al. 1983). Honey acidity (pH 3.2–4.5) is due to the presence of organic acids (White and Chiefe 1980, Kucuk et al. 2007). Honey contains a number of enzymes; for example, diastase, invertase, and so forth (Larson 1988, Al-Doghairi et al. 2007). Non-peroxide factors may also contribute to antimicrobial properties of honey (Weston et al. 2000, Snow and Harris 2004).

The phenolic compounds (e.g. caffeic and ferulic acids) are known to inhibit the growth of Gram-negative and Gram-positive bacteria (Davidson 1993). Flavanoids (Marcucci 1995) in nectar (Gil et al. 1995) and *Orthosiphon stamineus* Benth have also antioxidant activity. The total phenolic content (TPC) may be more beneficial than isolated constituents (Ho et al. 2010, Silici et al. 2010). The present article reports the antioxidant power of locally honey and the inhibitory action of the TPC on the growth of some types of bacteria.

Materials and methods

General experimental procedures

If not otherwise specified, reagents, materials and instrumentation are those previously reported (Prasad et al. 2009). Thirty samples of natural honeys (Table I) were purchased from the local market in Saudi Arabia. The *Staphylococcus aureus* ATCC 24213, *Micrococcus luteus* ATCC 49732 and *Escherichia coli* ATCC 25922 were obtained from the Microbiology Laboratory of King Abdulaziz University Hospital.

Extraction of total phenolic content

Honey solutions (10g/50ml) were acidified with HCl up to pH 2 and saturated with NaCl (3g/10ml) (Socha et al. 2009). The solution was extracted with ethyl acetate (3 × 25ml). The total extract was evaporated at 40°C under argon. The residues of extraction were redissolved in dimethylsulfoxide (DMSO) (5ml) and stored at 24°C in small sterile glass bottles.

Table I. Description of the locally produced honey samples collected from different regions of Kingdom of Saudi Arabia.

Sample	Trade name	Floral origin	Collection region
1	Rabea Alfayyadh	Multifloral	Al-qaseem (North of Kingdom)
2	Wadi Reeth	Unifloral (Sidr)	Gizan-Wadi Reeth (South of Kingdom)
3	Takhfa	Multifloral	Al-qaseem (North of Kingdom)
4	Alfagara	Multifloral	Al-Madinah Al-munawrah-Alfagara (North of Kingdom)
5	Albojaidi	Unifloral (Gatad)	Makkah Al-Mukarramah-Wadi Albojaidi (West of Kingdom)
6	Sidr Om Alasafeer	Unifloral (Sidr)	Makkah Al-Mukarramah (West of Kingdom)
7	Alnadheem	Multifloral	N.A.
8	Alhandhal	Unifloral (Handhal)	N.A.
9	Taba	Unifloral (Talh)	South east of Hail (North of Kingdom)
10	Alkorath	Unifloral (Korath)	South of Kingdom
11	Rabea Algobbah	Multifloral	Al-qaseem, Al Gobbah (North of Kingdom)
12	Alsail Alkabeer	Unifloral (Somrah)	Alsail Alkabar (West of Kingdom)
13	Almeshaan	Multifloral	Hail (North of Kingdom)
14	Altenhat	Multifloral	North east of Riyadh (North of Kingdom)
15	Jabal Algahr	Multifloral	Gizan (South of Kingdom)
16	Aba Alwrood	Multifloral	Al-qaseem Aba-Alwrood (North of Kingdom)
17	Wadi Daraa	Multifloral	Makkah Al-Mukarramah-Dehban (West of Kingdom)
18	Rabea Alsahra	Multifloral	Nufud desert
19	Motreba	Multifloral	North of Lina
20	Bani Kabeer	Multifloral	Al baha (South of Kingdom)
21	Om Aldiaba	Unifloral (Sidr)	Al-Artawia
22	Rabea Alhejaz	Multifloral	East of Makkah Al-Mukarramah (West of Kingdom)
23	Rabea Alqaseem	Multifloral	Al-qaseem (North of Kingdom)
24	Wadi Shawgab	Multifloral	South of Taif (West of Kingdom)
25	Alnokhba	Multifloral	Different regions in the Kingdom
26	Jabal Kabkab	Multifloral	East of Arafah, Makkah (West of Kingdom)
27	Sohail	Multifloral	Al-qaseem (North of Kingdom)
28	Wadi Aljorm	Unifloral (Gatad)	Makkah Al-Mukarramah-Om Aljorm (West of Kingdom)
29	Alheera	Unifloral (Sidr)	Northern borders
30	Wadi Debaa	Multifloral	Moda-Hafr Albatin

Measurement of antibacterial activity of phenolic extract of honey

The agar well diffusion method was employed (Estevinho et al. 2008). Ten selected extracts were dissolved in DMSO (5–20ml) to measure their minimal inhibitory concentrations (MICs, mg/ml). The MICs have been determined by the agar streak dilution method (Ferreira et al. 2004). The susceptibility of the tested organisms against DMSO was taken as a control and the plates were then

incubated at 37°C for 24h. The inhibition zone's diameter (mm) was measured and the swabs from the inhibition zones were cultured on nutrient agar plates and incubated at 37°C for 24h to test the inhibition effect. Various concentrations of penicillin–streptomycin in DMSO were used as standards.

Determination of TPC and antioxidant activities

Anti-radical power scavenging assay. The antioxidant activities of the honey samples were determined following the procedure described by Zamora (2006) and Turkmen et al. (2006) as follows: honey solutions (1g/5ml) were centrifuged at 4,350 g and filtered through filter papers. The test solutions (0.5ml) were mixed with 1,1-diphenyl-2-picrylhydrazyl (DPPH) (0.1N, 1.5ml) in methanol. A control test was made with distilled water instead of honey solution. The reaction mixtures were vortex-mixed and left in the dark at room temperature for an incubation period of 60min until stable absorbance value at 517nm against a reagent blank was measured. The blank was honey in methanol without DPPH under the same experimental conditions. The antioxidant activity (AA [%]) was expressed as the percentage inhibition of DPPH radical, and was calculated employing the equation:

$$AA\% = \frac{A_{\text{control}} - A_{\text{sample}}}{A_{\text{control}}} \times 100$$

where A_{control} is the absorbance of the DPPH solution and A_{sample} is the absorbance of the solution of the honey sample.

Ferric reducing antioxidant power assay. Antioxidant activities of the phenolic extracts of honey samples were carried out according to the reported methods (Estevinho et al. 2008, Prasad et al. 2009) with little modification. An accurate volume (2.5ml) of the 10 selected honey phenolic extracts concentrated in 12.5, 25 and 50mg extract/ml methanol were mixed with 2.5ml of 200mmol/l sodium phosphate buffer (pH 6.6) and 2.5ml of 1% potassium ferricyanide. After incubation of this mixture at 50°C for 20min, a volume of 2.5ml of 10% trichloroacetic acid (w/v) was added and the mixture was centrifuged at 1,000rpm for 87 minutes. An accurate volume (5ml) of the upper layer was diluted with deionized water (5ml) and 1ml of 0.1% of ferric chloride. After

homogenization of the mixture, the solution absorbance was measured at 700nm. All of the assays were carried out in triplicate. The extract concentration providing 50% inhibition (EC_{50}) was calculated from the curve of absorbance registered at 700nm against the correspondent honey extract concentration. The TPC of honey samples was determined by Socha et al. (2009).

Table II. Total phenolic content (gallic acid equivalent, mg/100g honey) of honey extract.

Sample	TPC	Sample	TPC
1	268.54 ± 0.786	16	282.86 ± 0.5
2	280.64 ± 3.5	17	317.39 ± 0.535
3	212.5 ± 3.57	18	204.46 ± 0.75

Statistical analysis

The data are expressed as mean ± standard deviation (n = 3). The difference between the honey samples were analyzed by one-way analysis of variance followed by least significant difference at 95% (P, 0.05).

Results and discussion

The honey samples differed in their contained phenolic amounts according to the type and source of flower (Weston et al. 2000). The results are summarized in Table II. Representative data are also shown in Figure 1. The TPC expressed as gallic acid equivalent (GAE) ranged from 84.97 ± 0.57 to 317.39 ± 0.535mg/100g in samples 10 and 30, respectively, with a mean of 211.7 ± 2.2mg GAE/100g using the standard curve (R = 0.9656). The value is higher than the values 56.32–246.21, 64–1,304, 93.5–144.94 and 21.7–75.3mg GAE/100g honey reported by Al-Mamary et al. (2002), Ouchemoukh et al. (2007), Bobis et al. (2008) and Socha et al. (2009), respectively.

Antibacterial activity of the total phenolic honey extract

The effect of the TPC on *S. aureus*, *M. luteus* and *E. coli* organisms revealed distinctive response susceptibility. The growth of *S. aureus* was inhibited by TPC of samples 1, 16, 17, 18, 20 and 30. The TPC of samples 1, 4, 5, 8, 11, 12, 13, 17, 20, 22, 28 and 30 effectively inhibited the growth of *M. luteus*, while the TPC of other samples showed moderate effect. The inhibition of TPC of all samples except 5, 6, 10, 20 and 21 on the *E. coli* growth was found lower than that of *M. luteus*. The TPC extracts of samples 4, 13, 17, 18 and 28 inhibited *E. coli* at higher levels. *M. luteus* is most sensitive than *S. aureus* and *E. coli*. The TPC extracts of samples 17 and 30 showed higher antibacterial activity against the three organisms. The MIC

Antioxidant and antibacterial properties of Saudi honey 515
of *M. luteus* (MIC = 0.45mg/ml) was lower than that of *S. aureus* (MIC = 0.5mg/ml). Thus, *S. aureus* organism was moderately sensitive to the antimicrobial activity in agreement with Mundo et al. (2004), Agbaje et al.

4	273.82 ± 3.21	19	195.93 ± 3.57
5	176.82 ± 2.89	20	225.5 ± 1.79
6	138.07 ± 3.036	21	265.11 ± 1.43
7	161.68 ± 0.43	22	115.75 ± 3.39
8	101.14 ± 0.46	23	96.29 ± 3.93
9	204.14 ± 2.5	24	206.46 ± 7.3
10	84.97 ± 0.57	25	292.32 ± 0.61

11	99.71 \pm 1.07	26	228.04 \pm 3.5
12	235.43 \pm 2.29	27	272.04 \pm 2.89
13	225.11 \pm 3.21	28	171.79 \pm 2
14	178.93 \pm 0.71	29	236.61 \pm 3.54
15	289.64 \pm 0.64	30	308.25 \pm 0.679

Average (n \pm 3) \pm standard deviation.

516 R. R. Al-Hindi et al.

Table IV. ARP of the tested honey samples.

Sample	ARP (%)	Sample	ARP (%)
1	92.28	16	98.39
2	92.71	17	99.52
3	93.67	18	95.98
4	93.24	19	94.53
5	95.17	20	92.76
6	94.85	21	94.53
7	95.82	22	76.84
8	75.98	23	94.53
9	93.41	24	96.84
10	50.78	25	98.34
11	79.57	26	96.46
12	95.39	27	88.42
13	95.17	28	96.62
14	95.98	29	98.45
15	94.75	30	97.96

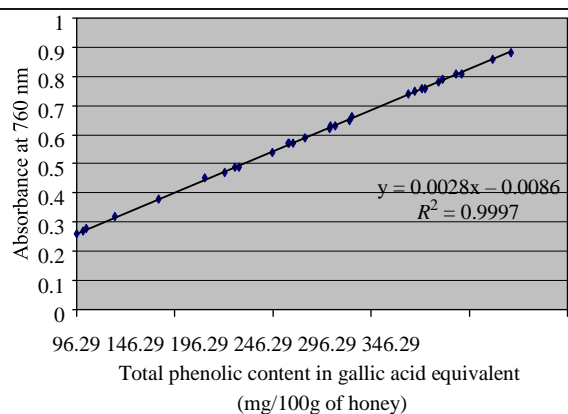


Figure 1. Plot of absorbance versus TPC expressed in gallic acid equivalent (mg/100g honey).

(2006) and Estevinho et al. (2008) (Table III).

Determination of antioxidant activity

The antiradical activity power (ARP) was determined by DPPH radical method (Zamora and Chirife 2006, Turkmen et al. 2006). The values of ARP were varied between 50.78% (sample 10) and 99.52% (sample 17). The antioxidant activity of honey extracts of samples 8, 10, 22 and 27 was the lowest (Table IV). The highest antioxidant activity was exhibited by the extracts of samples 16, 17 and 25. A linear and significant correlation between the ARP of samples and their TPC ($R^2 = 0.60$) were noticed at $P < 0.01$, indicating the responsibility and contribution of the TPC on the antioxidant activity and the ARP of the honey samples (Figure 2). A linear relationship between antioxidant

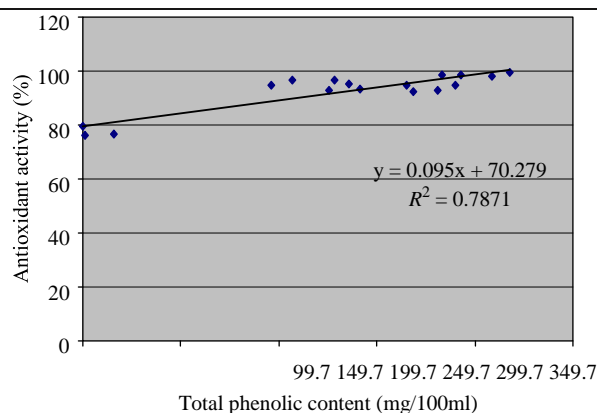


Figure 2. Correlation between the ARP of honey and its TPC (mg/100ml).

Table III. MIC of phenolic extract of honey samples against selected bacteria.

Sample	MIC (mg/ml)		
	S. aureus	M. luteus	E. coli
1	3.6 \pm 0.3	1.2 \pm 0.2	1.2 \pm 0.3
7	–	2.2 \pm 0.1	4.4 \pm 0.4
8	–	1.4 \pm 0.3	0.93 \pm 0.4
10	–	5.0 \pm 0.6	–
14	2.4 \pm 0.4	0.8 \pm 0.2	0.8 \pm 0.2
15	2.6 \pm 0.5	1.3 \pm 0.3	0.87 \pm 0.07
16	2.2 \pm 0.4	0.73 \pm 0.4	1.1 \pm 0.2
17	1.8 \pm 0.5	0.45 \pm 0.05	0.6 \pm 0.1
25	2.0 \pm 0.2	0.67 \pm 0.2	1.0 \pm 0.2
30	0.5 \pm 0.2	0.67 \pm 0.6	0.67 \pm 0.03

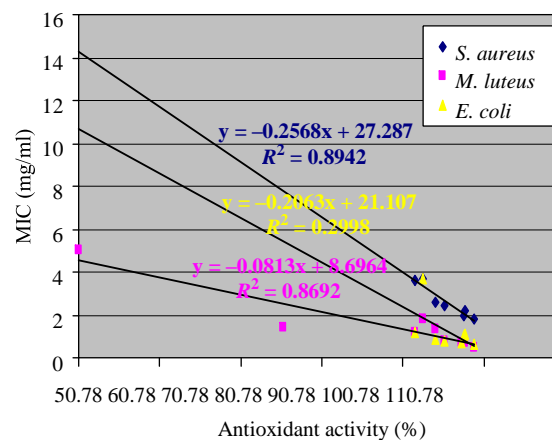


Figure 3. MIC of S. aureus, M. luteus and E. coli.

activity of TPC extracts and the corresponding MIC was achieved (Figure 3).

The antioxidant activity of the honey samples were also determined by the ferric reducing antioxidant power (FRAP) method (Prasad et al. 2009). The values varied from 0.85 ± 0.09 to 1.17 ± 0.09 in samples 10 and 30, respectively (Table V). The EC_{50} (i.e. 50% inhibition value) of the TPC extracts was in the ranges

Table V. Reducing power (FRAP) of phenolic honey extracts (2g/ml) honey in DMSO.

Sample	FRAP (extract of 2g honey/ml DMSO)	Sample	FRAP (extract of 2g honey/ml DMSO)
1	0.7429 ± 0.011	16	1.1341 ± 0.017
2	1.1185 ± 0.027	17	1.1675 ± 0.09
3	0.9505 ± 0.012	18	0.9059 ± 0.023
4	0.8847 ± 0.022	19	0.5926 ± 0.012
5	0.742 ± 0.03	20	0.6828 ± 0.003
6	0.3301 ± 0.0099	21	0.5958 ± 0.01
7	0.8568 ± 0.014	22	0.1851 ± 0.009
8	0.5412 ± 0.0199	23	0.411 ± 0.01
9	0.9016 ± 0.016	24	0.5692 ± 0.009
10	0.8528 ± 0.09	25	1.1441 ± 0.037
11	0.3079 ± 0.011	26	0.7532 ± 0.027
12	0.8318 ± 0.018	27	0.7806 ± 0.035
13	0.9166 ± 0.023	28	0.4833 ± 0.011
14	0.56 ± 0.007	29	0.7837 ± 0.009
15	1.1657 ± 0.009	30	0.9152 ± 0.041

Average ($n = 3$) \pm standard deviation.

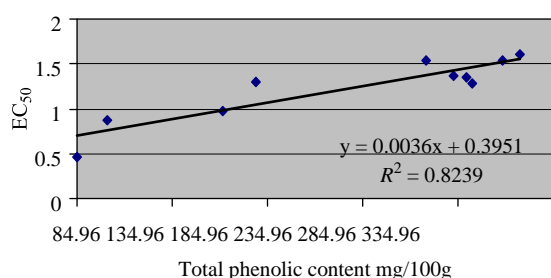


Figure 4. Plot of total antioxidant power (EC_{50}) versus TPC of the tested honey samples expressed in gallic acid equivalent (mg/100g honey).

24.04 ± 1.71 and 133.45 ± 4.83 mg/ml in samples 17 and 22, respectively. A positive linear correlation between FRAP and the TPC was noticed (Figure 4), indicating the predomination of TPC in the Total antioxidant power (TAP) of the samples in agreement with the previous findings (Blasa et al. 2006). Linear correlations between

the inhibition zone diameter versus TAP and MIC versus TAP determined by the FRAP method were also noticed.

Conclusion

The inhibitory activity of the locally honey samples against *S. aureus*, *M. luteus* and *E. coli* was comparable with the natural food preservatives. Honeys richest in TPC exhibited high antioxidant and antibacterial activities and low MIC. Efficient antioxidant and antibacterial activities were found for dark honey.

Acknowledgement

The authors would like to thank Abdulaziz City for Sciences and Technology (KACST), Saudi Arabia for the fund provided to one of the coauthors (M.S. Bin-Masalam).

Declaration of interest: The authors report no conflicts of interest. The authors alone are responsible for the content and writing of the paper.

References

- Agbaje EO, Ogunsanya T, Aiwerioba OIR. 2006. Conventional use of honey as antibacterial agent. *Ann Afr Med* 5:79–81.
- Al-Doghairi MA, Al-Rehiyani S, Ibrahim GH, Osman KA. 2007. Physicochemical and antimicrobial properties of natural honeys produced in Al-Qassim region, Saudi Arabia. *Met Env Arid Land Agric Sci* 18(2):3–18.
- Al-Mamary M, Ali A, Molham A. 2002. Antioxidant activities and total phenolics of different types of honey. *Nutr Res* 22: 1041–1047.
- Blasa M, Candiracci M, Accorsi A, Piacentini MP, Albertini MC, Piatti E. 2006. Raw Millefiori honey is packed full of antioxidants. *Food Chem* 97:217–222.
- Bobis O, Marghitas L, Rindt IK, Niculae M, Dezmirean D. 2008. Honeydew honey: Correlations between chemical composition, antioxidant capacity and antibacterial effect. *Lucr Stiint Zooteh Biotechnol* 41:2–3.
- Chirife J, Herszage L, Joseph A, Kohn ES. 1983. In vitro study of bacterial growth inhibition in concentrated sugar solutions: Microbiological basis for the use of sugar in treating infected wounds. *Antimicrob Agents Chemother* 23(5):766–773.
- Davidson PM. 1993. Parabens and phenolic compounds. In: Davidson PM, Branen AL, editors. *Antimicrobials in Foods*. 2nd ed. New York: Marcel Dekker. p 263–306.
- Estevinho L, Pereira AP, Moreira L, Dias LG, Pereira E. 2008. Antioxidant and antimicrobial effects of phenolic compounds extracts of Northeast Portugal honey. *Food Chem Toxicol* 46: 3774–3779.
- Ferreira ICFR, Calhelha RC, Estevinho LM, Queiroz MJRP. 2004. Screening of antimicrobial activity of diarylamines in the 2,3,5 trimethylbenzo(b) thiophene series: a structure-activity evaluation study. *Bioorg Med Chem Lett* 14:5831–5833.
- Gil MI, Ferreres F, Ortiz A, Subra E, Thomas-Barberian FA. 1995. Plant phenolic metabolites and floral origin of rosemary honey. *J Agric Food Chem* 43:2833–2838.
- Ho C-H, Noryati I, Sulaiman S-F, Rosma A. 2010. In vitro antibacterial and antioxidant activities of orthosiphon stamineus benth extracts against food-borne bacteria. *Food Chem* 122:1168–1172.

- Kucuk M, Kolayl S, Karaog̃lu SI, Ulusoy E, Baltac C, Candan F. 2007. Biological activities and chemical composition of three honeys of different types from Anatolia. *Food Chem* 100: 526–534.
- Larson RA. 1988. The antioxidants of higher plants. *Phytochemistry* 27:969–978.
- Marcucci MC. 1995. Propolis: chemical composition, biological properties and therapeutic activity. *Apidologie* 26:89–99.
- Mundo MA, Zakour OIP, Worobo RW. 2004. Growth inhibition of foodborne pathogens and food spoilage organisms by select raw honeys. *Int J Food Microbiol* 97(1):1–8.
- Ouchemoukh S, Louaileche H, Schweitzer P. 2007. Physicochemical characteristics and pollen spectrum of some Algerian honeys. *Food Control* 18:52–58.
- Prasad KN, Yang B, Dong X, Jiang G, Zhang H, Xie H, Jiang Y. 2009. Flavonoid contents and antioxidant activities from *Cinnamomum* species. *Innov Food Sci Emerging Technol* 10: 627–632.
- Silici S, Sagdic O, Ekici L. 2010. Total phenolic content, antiradical, antioxidant and antimicrobial activities of *Rhododendron* honey. *Food Chem* 121:238–243.
- Snow MJ, Harris MM. 2004. Analytical, nutritional and clinical methods on the nature of non-peroxide antibacterial activity in New Zealand manuka honey. *Food Chem* 84:145–147.
- Socha R, Juszczak L, Pietrzyk S, Fortuna T. 2009. Antioxidant activity and phenolic composition of herboneys. *Food Chem* 113:568–574.
- Turkmen N, Sari F, Velioglu YS. 2006. Effects of prolonged heating on antioxidant activity and colour of honey. *Food Chem* 95: 653–657.
- Weston RJ, Brocklebank LK, Lu Y. 2000. Identification and quantitative levels of antibacterial components of some New Zealand honeys. *Food Chem* 70:427–435.
- White JW, Jr, Chiefe. 1980. Honey, its composition and properties. Plant products laboratory. Eastern Utilization Research Service. p 56–64.
- Zamora MC, Chirife J. 2006. Determination of water activity change due to crystallization in honeys from Argentina. *Food Control* 17:59–64.

Chemical Speciation of Chromium(III) and (VI) Using Phosphonium Cation Impregnated Polyurethane Foams Prior to Their Spectrometric Determination

M. S. EL-SHAHAWI,⁹ A. S. BASHAMMAKH, and M. ABDELMAGEED

Department of Chemistry, Faculty of Science, King Abdulaziz University, P. O. Box 80203, Jeddah 21589, Saudi Arabia

Fast and selective sorptions of Cr(VI) species from aqueous media onto tetraphenylphosphonium bromide (TPP⁺·Br⁻) physically immobilized polyurethane foams (PUFs) sorbent were achieved. Based on the Scatchard model of binding sites of the PUFs and Langmuir and Dubinin–Radushkevich (D–R) adsorption models of Cr(VI) retention onto TPP⁺·Br⁻ immobilized PUFs, a dual retention mechanism involving absorption related to “weak-base anion ion exchange” and an added component for “surface adsorption” was proposed. Thus, the TPP⁺·Br⁻ loaded PUFs were successfully packed in column mode for preconcentration of trace and ultra trace concentrations of Cr(VI) as halochromates [CrO₃C]⁻_{aq} from aqueous HCl media. The retained [CrOCl₃]⁻_{aq} species were recovered with NaOH (1.0 mol L⁻¹) and analyzed by flame atomic absorption spectrometry. Cr(III) species after oxidation to Cr(VI) with H₂O₂ in aqueous KOH (1.0 mol L⁻¹) were also retained and could be recovered by the proposed method. The limits of detection (LOD) and quantification (LOQ) of Cr(VI) were 0.04 and 0.13 μg L⁻¹, respectively. The chemical speciation of Cr(III, VI) species in various water samples at trace and ultra trace levels were carried out by TPP⁺·Br⁻ loaded PUFs packed column. The enhancement factor and sensitivity factor of [CrO₃C]⁻_{aq} sorption were 80.0 and 30.0, respectively.

(Received February 22, 2011; Accepted May 10, 2011; Published July 10, 2011)

Introduction

Chromium is a metallic element usually found in aquatic systems in two oxidation states, Cr(III) and Cr(VI). Cr(III) appears to be an essential trace element species since it plays an important role in some metabolic processes and it is responsible for reducing blood glucose in addition to insulin,¹ while Cr(VI) is highly toxic and potentially responsible for carcinogenic effects in humans.² Thus, chemical speciation is one of the most interesting areas of research in the fields of environmental science, toxicology, nutritional sciences, environmental and occupational medicine and analytical sciences.^{1–3} Cr(III) and Cr(VI) species interact differently with living organisms. The guideline values set by World Health Organization (WHO) for Cr(VI) in ground and drinking water is 0.05 mg L⁻¹ for drinking water.^{4,5} Thus, the developing of effective, precise and accurate analytical methods for preconcentration and chemical speciation of Cr(III) and Cr(VI) species at trace level is extremely important.⁵

The two predominant forms of chromium in water *i.e.* Cr(III) and Cr(VI) have very different properties. The solution chemistry of chromium containing water plays an important role in the efficient removal of chromium by sorption/ion exchange.² Thus, preconcentration of chromium could be carried either as Cr(III) ions or as Cr(VI) ions.

Liquid–liquid^{6,7} and solid phase extraction (SPE) *e.g.* clay minerals, gelatin, biosorbent, and active carbon, synthetic polymers, C18-bonded silica, silica gel immobilized with Zr(IV) and Zr(VI) phosphate have been used for preconcentration and/or

separation of trace and ultra trace amounts of toxic metal ions from complex matrices.^{8–15} Determination and chemical speciation of Cr(III) and Cr(VI) at trace levels in welding fumes and in drinking water samples using strong anion ion-exchange,¹⁶ neutral alumina,¹⁷ mini-columns packed with resin immobilized with 8-hydroxyquinoline,¹⁸ activated carbon,¹⁹ leaching procedure with sodium carbonate⁵ and drawn and modified lingo cellulosic materials^{20,21} have been reported. However, some of these SPE methods^{10–15} are too expensive or unselective; they require careful experimental conditions, are time consuming and are not compatible with the detection limit of Cr(VI) in various matrices.

In the last three decades, polyurethane foam (PUF) sorbent has been used in extraction chromatography and in gas-solid and gas-liquid partition chromatography.^{22–24} The cellular structures of the PUFs in foamed and micro spherical forms make it a suitable and excellent filling material with good capacity for firmly retaining various extracting agents.^{25,26} Based on the resilience characters of the PUFs, El-Shahawi *et al.*²⁷ have used tetraphenylphosphonium bromide (TPP⁺·Br⁻) treated PUFs in medical syringes in pulse column for speciation of Cr(III) and Cr(VI) species in wastewater. The reagent TPP⁺·Br⁻ loaded PUFs sorbent survived the extraction and stripping process, its recycle ability was fine, it is safe as long as its storage and its disposal are undertaken in a safe manner. Thus, the present article reports the sorption mechanism of the halochromate species from the aqueous media onto the TPP⁺·Br⁻ loaded PUFs sorbent, the randomly distribution sites of energy in the PUFs sorbent and finally application of the treated PUFs

⁹ To whom correspondence should be addressed. E-mail: malsaeed@kau.edu.sa; mohammad_el_shahawi@yahoo.co.uk
On leave from the Department of Chemistry, Faculty of Science at Damietta, Mansoura University, Mansoura, Egypt.

column for preconcentration and subsequent speciation of Cr(III) and Cr(VI) species in wastewater.

Experimental

Reagents and materials

All chemicals used were of analytical reagent grade. Doubly deionized water was used throughout. BDH (BDH, Poole, England) diphenylcarbazine, DPC solution (0.1% w/v) was prepared by dissolving the required weight of the reagent in acetone-H₂SO₄ (0.01 mol L⁻¹). Stock solutions of BDH reagents TPP⁺·Br⁻, tetraphenylarsonium chloride (TPAs⁺·Cl⁻) (0.1% w/v), and K₂Cr₂O₇ (1 mg mL⁻¹) were prepared in deionized water. Foam cubes (10 – 15 mm edges) of commercial white sheets of polyether-type based PUFs were cut from the foam sheets, purified and finally dried.²³ Some immobilized reagent TPAs⁺·Cl⁻ or TPP⁺·Br⁻ immobilized PUFs foam cubes were prepared and homogeneously packed in the glass columns as reported.²⁵

Apparatus

A Varian Model AA-875 flame atomic absorption spectrometer (FAAS) was used at the optimum conditions of chromium determination at the optimum operational parameters for chromium. A single beam Digital Spectro UV-VIS RS Labomed, spectrophotometer (USA) with quartz cell (10 mm path length) was used for recording the absorbance of Cr(VI) species before and after extraction following the method reported by Sano.²⁸ A Lab-line mechanical Shaker (Corporation Precision Scientific, Chicago, USA) with a shaking rate in the range of 10 – 250 rpm and a glass column (18 × 10 mm i.d.) were used in batch and column experiments for chromatographic separation of Cr(VI), respectively. Deionized water was obtained from Milli-Q Plus system (Milford, MA). A Thermo Orion pH Meter Model 720 (Thermo Fisher Scientific, MA) was used for the pH measurements with absolute accuracy limits of pH defined by NIST buffers. A glass column of 18 mm length and 10 mm inner diameter was used in flow experiments.

Reagent foam preparation

The reagent foams were prepared by mixing the dried foam cubes with an aqueous solution containing TPP⁺·Br⁻ at 0.02% w/v (50 mL/g dry foam) with efficient stirring for 30 min. The immobilized reagent foam cubes were then squeezed and dried as reported earlier.²⁴

Batch experiment

An accurate weight (0.2 ± 0.01 g) of the reagent TPP⁺·Br⁻ or TPAs⁺·Cl⁻ treated PUFs was shaken with an aqueous solution (50.0 mL) containing Cr(VI) ions (10 µg mL⁻¹) and HCl (1.0 mol L⁻¹) at 25 ± 0.1°C in a low density polyethylene bottle for 2 h on a mechanical shaker. After phase separation, the aliquot solution was separated out and assayed by direct spectrophotometry at 545 nm²⁶ or by FAAS. At Cr(VI) concentrations lower than the lower limit of detection (LOD) of DPC,²⁷ AAS was used at the optimum operational conditions. The amount of Cr(VI) retained at equilibrium q_e on the PUFs cubes was determined from the differences between the absorbance of Cr(VI) solutions before (A_b) and after (A_a) shaking with the reagent PUFs cubes. The extraction percentage (%E) and the distribution ratio (D) of the Cr(VI) sorption onto the reagent loaded foam were then calculated as reported earlier.^{23,24}

Following these procedures, the influence of HCl concentration, polarity of the extraction medium, sample volume, cation size of mono valence ions and Cr(VI) concentration (0.05 – 80 µg mL⁻¹) on the retention step from the aqueous solutions onto the reagent loaded PUFs were examined. All experiments were performed in triplicate at ambient temperature (25 ± 0.1°C). The results of %E and D are the average of three measurements and the precision in most cases was ±2%.

Chromatographic separation of Cr(VI)

An aqueous solution (1.0 L) containing Cr(VI) at a total concentration in the range 0.05 – 5 µg mL⁻¹ in HCl (1.0 mol L⁻¹) was percolated through the TPP⁺·Br⁻ immobilized PUFs packed (4.0 ± 0.01 g) column at 10 mL min⁻¹ flow rate. The sample and the blank foam packed columns were then washed with an aqueous solution containing HCl (100 mL; 1.0 mol L⁻¹) at the same flow rate. Cr(VI) sorption took place on the PUFs as indicated from the analysis of Cr(VI) in the effluent solution. The sorbed Cr(VI) species were recovered from the foam column with NaOH (10 mL; 1.0 mol L⁻¹) at 3 mL min⁻¹ flow rate.

Retention of Cr(III)

An aliquot of the aqueous solution (100.0 mL) containing Cr(III) ions at a concentration in the range 0.05 – 50 µg mL⁻¹ was transferred to a conical flask (250 mL). The solution was oxidized to Cr(VI) in alkaline media (KOH, 1.0 mol L⁻¹) after boiling for 10 min with H₂O₂ (2 mL, 10.0% w/v). The solution was adjusted to the required acidity with HCl (1.0 mol L⁻¹) after cooling and was finally percolated through the reagent TPP⁺·Br⁻ loaded PUFs packed columns at 10 mL min⁻¹ flow rate as described for Cr(VI). The retained Cr(VI) species were then recovered from the foam column with NaOH (10 mL, 1.0 mol L⁻¹) at 3 mL min⁻¹ flow rate and determined *via* its standard curve.²⁹ Blank experiments were carried out under the same experimental conditions.

Chemical speciation of inorganic Cr(III) and Cr(VI)

An aqueous solution (0.5 L) containing the binary mixture of Cr(III) and Cr(VI) species at a total concentration of chromium species ≤15 µg mL⁻¹ was percolated through the TPP⁺·Br⁻ immobilized foam packed column at 5 mL min⁻¹ and analyzed according to the described procedure for Cr(VI) recovery. Another aliquot sample (0.5 L) was first oxidized to Cr(VI) and then analyzed as mentioned for Cr(III) retention. The absorbance of the recovered species of the first aliquot (A_1) will thus be a measure of Cr(VI) ions in the mixture, while the absorbance of the eluted species of the second aliquot (A_2) is a measure of the sum of Cr(III) and Cr(VI) ions. Therefore, the absorbance ($A_2 - A_1$) is a measure of the Cr(III) ions in the binary mixture.

Application

Fresh- or industrial wastewater samples (1.0 L) were first filtered through a piece of filter paper of Milpore type of 0.45 µm porosity. An aliquot (100 mL) of the sample that was adjusted with HCl of concentration 1.0 mol L⁻¹ and spiked with Cr(III) and/or Cr(VI) at a total concentration level ≤15.0 µg L⁻¹ was percolated through TPP⁺·Br⁻ immobilized PUFs packed column at 10 mL min⁻¹ flow rate as described for Cr(VI). The column was washed with an aqueous solution containing HCl (10 mL; 1.0 mol L⁻¹) at the same flow rate. The sorbed Cr(VI) species were recovered with NaOH solution (10 mL, 2 mol L⁻¹) at 3.0 mL min⁻¹ flow rate. The recovered Cr(VI) species was

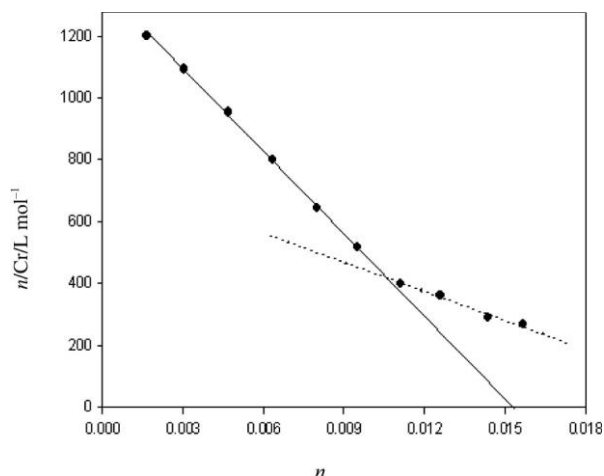


Fig. 1 Scatchard plot for the $[\text{CrO}_3\text{Cl}]^-$ retention from the aqueous solution onto PUFs in the presence of HCl (3.0 mol L^{-1}).

then analyzed with the aid of standard curve. Another aliquot sample (100 mL) was treated as described earlier for Cr(III) retention. The concentrations of Cr(VI) and total Cr(III, VI) were then determined from their standard curves constructed by FAAS.

Results and Discussion

Retention profile of Cr(VI) towards immobilized PUFs

A recent study²⁷ has revealed that, Cr(VI) sorption from aqueous solution by TPAs⁺·Cl⁻ or TPP⁺·Br⁻ loaded PUFs reached a maximum from HCl (3.0 mol L^{-1}) medium. These results and the data reported earlier²⁸ suggest that extraction of Cr(VI) by solvent extraction mechanism and the uptake will most likely proceed as follows:



Here, X = As or P.

The protonation of the ether oxygen ($-\text{CH}_2-\text{O}-\text{CH}_2-$)_{foam} and/or amide nitrogen ($-\text{NH}-\text{COO}-$)_{foam} linkages available in the PUFs sorbent membrane are -3 and -6, respectively.²⁹ Thus, in HCl extraction medium, the retention of the $[\text{CrO}_3\text{Cl}]\text{-aq}$ species that proceeded *via* the formation of ternary ion associates $[\text{CrO}_3\text{Cl}]\text{-aq}\cdot\text{PQ}^+\cdot\text{Cl}^-$ on/in the PUFs membrane was enhanced. The stability constants of the binding sites of the PUFs with $[\text{CrO}_3\text{Cl}]\text{-aq}$ were calculated using the Scatchard equation:

$$[\text{Cr}^n] = K n (1 - n) \quad (3)$$

$$n = \frac{\text{Weight of Chromium of foam (g) bound to foam (g)}}{\text{Weight of Chromium of foam (g) available to foam (g)}} \quad (4)$$

Here, K is stability constant of $[\text{CrO}_3\text{Cl}]\text{-aq}$ sorbed onto PUF, n_i the maximum concentration of $[\text{CrO}_3\text{Cl}]\text{-aq}$ sorbed onto the available sites of PUFs, and $[\text{Cr}]$ the equilibrium concentration of Cr(VI) in

solution (mol L^{-1}). The plot of $n/[\text{Cr}]$ versus n is shown in Fig. 1. It revealed formation of more than one class of complex species where each complex has its own unique formation constant. The stability constants ($\log K_1$ and $\log K_2$) of the sorption step of $[\text{CrO}_3\text{Cl}]\text{-aq}$ species onto PUFs took place readily on site K_1 belong to the ether group. This group has a greater stability than the amide group (site K_2) as reported.²⁹ The stability constants $\log K_1$ and $\log K_2$ for the sorbed species derived from the respective slopes were 4.95 ± 0.07 and $4.48 \pm$

0.09 , respectively. The calculated values of n_1 and n_2 were 0.015 ± 0.005 and $0.024 \pm 0.001 \text{ mol g}^{-1}$, respectively. The values of the stability constants ($\log K_1$ and $\log K_2$) indicated that the sorption of species took place readily on site K_1 or most likely belongs to the ether group because this group has a greater stability than the amide group (site K_2) as reported earlier.³⁰ The high values of K_1 and K_2 indicated that, both bonding sites of PUF are highly active towards $[\text{CrO}_3\text{Cl}]\text{-aq}$ species. The results are in good agreement with the data reported earlier involving the extraction of the bulky anion $[\text{CrO}_3\text{Cl}]\text{-aq}$ by methyl isobutyl ketone and other solvents that possess ether linkages in their structures *e.g.* diethyl ether and isopropyl ether.³¹ Based on these data and the results reported on the retention of AuCl_4^- and CdI_4^- by PUFs,^{25,30} a sorption mechanism involving a weak base anion ion exchange and solvent extraction of $[\text{BiI}_4]\text{-aq}$ by the protonated ether ($-\text{CH}_2-\text{HO}^+-\text{CH}_2-$) oxygen or urethane ($-\text{N}^+\text{H}_2\text{COO}-$) nitrogen linkages of the PUFs as a ternary complex ion associate will most likely proceed as follows.

The effect of ethanol content (1 – 15% v/v) *i.e.* solvent polarity upon Cr(IV) sorption by the reagent treated PUFs was investigated. The retention percentage ($\%E$) of Cr(VI) species onto PUFs increased linearly on raising the ethanol content from 0.0% ($E = 62\%$) and reached maximum at 2% ($E = 78.3\%$), followed by a plateau. The change of the environment around the Cr(VI) ions makes the available binding sites of the PUFs more hydrophilic which further diminished the need for solvating water molecules and reduces the Cr(VI) uptake onto the reagent immobilized PUFs to the added ethanol in the medium.³⁰

The effects of cation (Li^+ , Na^+ , K^+ and NH_4^+) size and concentrations (0.05 – 1% w/v) on the Cr(VI) uptake onto PUFs were studied. On increasing the salt concentration, one finds a slight increase ($\sim 5 - 9\%$) in the extraction percentage of Cr(VI) in the presence of LiCl, NaCl, KCl and NH_4Cl . The order of extraction followed the sequence: Li^+ ($\log D = 3.1$) > Na^+ ($\log D = 2.95$) ~ NH_4^+ ($\log D = 2.96$) > K^+ ($\log D = 2.7$).

This effect is most likely attributed to the reduction of the repulsive forces between adjacent sorbed species of $[\text{CrO}_3\text{Cl}\cdot\text{TPX}]\text{-foam}$.^{31,32} Thus, the ion-dipole interaction of NH_4^+ with the oxygen sites of the PUFs are not the predominating factors in the retention step of $[\text{CrO}_3\text{Cl}]\text{-aq}$ species and “solvent extraction” mechanism with the salt acting as salting-out agent participates on Cr(VI) uptake onto PUFs. The added ions (Li^+ , Na^+ , K^+ or NH_4^+) reduce the water molecules available to solvate the $[\text{CrO}_3\text{Cl}]\text{-aq}$ species which would be forced out of the solvent phase onto the PUFs. The free water molecules are preferentially used to solvate the added cations.³³

The influences of surfactant type and concentrations (0.0 – 2% m/v) *e.g.* tetraethyl ammonium chloride, sodium dodecyl sulfate (SDS) or Triton-X 100 on Cr(VI) uptake were investigated. The sorption percentage ($E = 62\%$) of Cr(VI) increased in the presence of SDS or Triton-X100 ($E = 86.7\%$) up to 0.1% (w/v) and leveled off at higher surfactant concentrations. The added surfactant increases the solution viscosity leading to a progressive change in the physical properties of the microenvironment of the associate

(CrO₃Cl⁻·TPX⁺) onto PUFs. It enhances the aggregation of the associate and also lowers the diffusion rate of the analyte within the PUFs membranes.³⁴ The competition between the excess surfactant and the ion pair reagent towards Cr(VI) may also predominate in the sorption step. Anionic surfactant may also interact directly with the ion pair reagent resulting in minimizing the retention of [CrO₃Cl⁻]_{aq} onto PUFs during the extraction process.

Sorption isotherms

The sorption profile of Cr(VI) from the bulk aqueous solution onto the reagent loaded foam over a wide range of concentrations (0.05 – 80 µg mL⁻¹) was determined. The amount of Cr(VI) retained onto the PUFs sorbent varies linearly at low or moderate analyte concentration in the aqueous test solution suggesting a first order behavior. On raising the Cr(VI), the values of *D* decreased rapidly and the most favorable *D* values were achieved for dilute solutions. Thus, film diffusion and intraparticle transport are the two steps that controlling the molecular diffusion at the macro pore of the PUFs.³⁵ Thus, the uptake of the analyte from the solution was subjected to Langmuir³⁶ and Dubinin–Radushkevich (D–R)³⁵ sorption models. The Langmuir sorption isotherm is expressed in the following linear form:³⁶

$$\frac{C_{\text{ads}}}{C_e} = \frac{Q}{b} + \frac{C_e}{Q} \quad (5)$$

where, *C_e* the equilibrium concentration (mol L⁻¹) of Cr(VI) in solution and *C_{ads}* the retained Cr(VI) concentration onto the loaded PUFs per unit mass of sorbent at equilibrium (mol g⁻¹). The Langmuir parameters *Q* and *b* are related to the maximum sorption capacity and to the binding energy of the solute sorption. Plots of *C_e/C_{ads}* versus *C_e* were linear over the entire concentration range of the analyte. The values of *Q* and *b* calculated from the slopes and intercepts of the linear plots were found 0.148 ± 0.05, 0.153 ± 0.03 mmol g⁻¹ and 12.2 ± 0.07, 11.12 ± 0.06 L mol⁻¹ for Cr(VI) sorption onto TPAs⁺·Cl⁻ and TPP⁺·Br⁻ loaded foams, respectively.

The D–R isotherm model³⁶ was postulated within the adsorption space close to the adsorbent surface. The linear form of D–R isotherm can be expressed as follows:

$$\ln C_{\text{ads}} = \ln K_{\text{DR}} - \beta \varepsilon^2 \quad (6)$$

where, *K_{DR}*, *β* and *ε* are constants related to the maximum amount of Cr(VI) retained onto the solid sorbent to the energy of transfer of the solute from the bulk solution to the solid sorbent, and the Polanyi potential, respectively. The value of *ε* is given by the equation:

$$\varepsilon = RT \ln \left[\frac{C_{\text{ads}}}{C_e} \left(1 + \frac{C_{\text{ads}}}{C_e} \right) \right] \quad (7)$$

where, *R* the gas constant (kJ mol⁻¹ K⁻¹) and *T* the absolute temperature in Kelvin. The plots of ln *C_{ads}* versus *ε*² are linear (Fig. 2) indicating that the D–R isotherm is applied for Cr(VI) sorption onto TPAs⁺·Cl⁻ or TPP⁺·Br⁻ loaded PUFs over the entire concentration. The *K_{DR}* and *β* values calculated from the intercepts and slopes are in the range 99 – 120 mmol g⁻¹ and 0.002 – 0.003 mol² kJ⁻², respectively, indicating that the surface adsorption of the analyte by the solid sorbent participates in the retention step. Based

on these results and the data reported,^{25,34} a dual retention mechanism model is proposed and can be expressed by the equation:

$$C_{\text{Cr}} = C_{\text{abs}} + C_{\text{ads}} = DC_{\text{aq}} + \frac{1}{S} K + K C_{\text{L}} C_{\text{L, aq}} \quad (8)$$

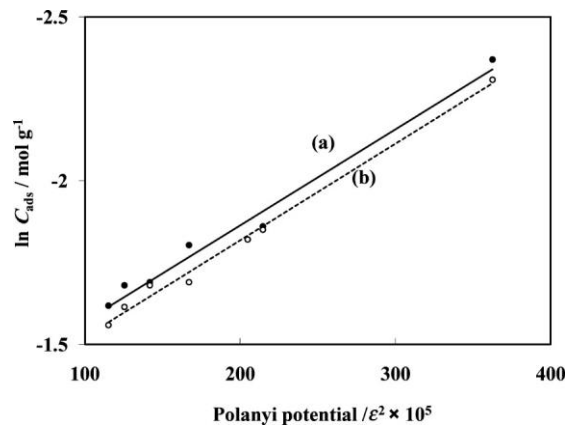


Fig. 2 Dubinin–Radushkevich (D–R) plots of Cr(VI) sorption (0.05 – 80 µg mL⁻¹) onto TPAs⁺·Cl⁻ (a) and TPP⁺·Br⁻ (b) immobilized foams (0.2 ± 0.01 g) at pH 0 and 298 K.

where *C_r* and *C_{aq}* are the equilibrium concentrations of Cr(VI) ions onto the solid sorbent and in aqueous solution, respectively.

C_{abs} and *C_{ads}* are the equilibrium concentrations of analyte retained onto the used solid sorbents as an adsorbed species and adsorbed species, respectively and *S* and *K_L* are the saturation values for the Langmuir adsorption model.^{24,36}

Chromatographic separation of Cr(VI)

The membrane like structures and the excellent hydrodynamic and aerodynamic properties of PUFs sorbent³⁷ enhanced Cr(VI) uptake onto the TPP⁺·Br⁻ treated PUFs packed columns. The kinetics and the sorption characteristics of TPP⁺·Br⁻ PUFs towards Cr(VI)²⁷ also suggested the use of the TPP⁺·Br⁻ treated PUFs in columns for the chromatographic separation of chromium. The sorption characteristics of Cr(VI) onto TPP⁺·Br⁻ immobilized PUFs suggested the use of reagent TPP⁺·Br⁻ loaded PUFs in column mode for the quantitative extraction, recovery and subsequent chemical speciation of Cr(III) and Cr(VI) from large sample volumes. Thus, distilled and/or tap water samples (1.0 L) containing HCl (1.0 mol L⁻¹) and various concentrations (0.2 – 5.0 µg mL⁻¹) of Cr(VI) were percolated through the PUFs packed column at the optimum experimental conditions and at various flow rates (5 – 20 mL min⁻¹). Analysis of the effluent solutions against the reagent blank have revealed complete (96 – 98 ± 1.6%) retention of Cr(VI) at 5 – 10 mL min⁻¹. The sorbed Cr(VI) species were then recovered quantitatively (97 ± 2.6%) from the PUFs packed column with NaOH (10 mL, 1.0 mol L⁻¹) at 3 mL min⁻¹ flow rate. The TPP⁺·Br⁻ packed column was also tested for the collection and recovery of Cr(III) ions. Aqueous solutions (0.1 L) containing Cr(III) at various concentrations (0.05 – 50 µg mL⁻¹) were oxidized to Cr(VI) using H₂O₂ in alkaline KOH (1.0 mol L⁻¹).²² They were then percolated through TPP⁺·Br⁻ PUFs packed column at 5 mL min⁻¹ flow rate against reagent blank at the optimum conditions of Cr(VI) retention. The resultant Cr(VI)

solutions were percolated through TPP⁺·Br⁻ PUFs packed column at 5 mL min⁻¹ flow rate against reagent blank. The retained Cr(VI) species were then recovered with NaOH (10 mL, 1.0 mol L⁻¹) at 5 mL min⁻¹ flow rate. A satisfactory recovery percentage (96 ± 2.7 – 102 ± 1.9%, *n* = 5) of Cr(III) species was achieved.

The TPP⁺·Br⁻ packed PUFs column was also used for the preconcentration and recovery of the binary mixture solution (0.5 L) containing Cr(III) and Cr(VI) at a total concentration ≤15.0 µg mL⁻¹ in HCl (1.0 mol L⁻¹). The test solution was first

Table 1 Recovery data of total inorganic Cr(III) and Cr(VI) in their binary mixture in the aqueous media by the developed PUFs packed column

Added/µg L ⁻¹		Average total chromium found/ -1	Recovery, % ^a
3+	6+		
Cr	Cr		µg L
10.0	5.0	15.9	106.0 ± 3.3
		5.0	5.0
		97.0 ± 3.2	
5.0	10.0	14.9	98.7 ± 4.5

a. Average recovery (*n* = 5) ± relative standard deviation.

percolated and recovered through the TPP⁺·Br⁻ packed PUFs column at 2 – 3 mL min⁻¹ flow rate against a reagent blank. It was then analyzed as described for Cr(VI). Another aliquot sample was analyzed following the recommended procedures for Cr(III) retention and recovery. Cr(III) ions were then determined from the difference (*A*₂ – *A*₁) between the absorbance of the first (*A*₁) and second (*A*₂) aliquots. Satisfactory recovery percentage of the total Cr(III) and Cr(VI) species was obtained in the range 97.0 ± 3.2 – 106.0 ± 3.3% (Table 1). The effect of flow rate (5 – 25 mL min⁻¹) on the retention of Cr(VI) by the TPP⁺·Br⁻ treated PUFs-packed columns was examined by percolating 0.5 L of distilled water spiked with 20 µg of Cr(VI) ions. Complete sorption of Cr(VI) ions from the test solutions was achieved quantitatively (~98.6 ± 2%) at a flow rate ≤15 mL min⁻¹.

Performance of the developed TPP⁺·Br⁻ PUFs packed column

The performance of the proposed TPP⁺·Br⁻ loaded PUFs packed columns for the Cr(VI) uptake at 10 mL min⁻¹ was determined from the elution curves of Cr(VI) with NaOH. Complete sorption of Cr(VI) onto the packed column took place at 5 mL min⁻¹. The retained Cr(VI) species were then recovered with NaOH (10 mL, 1.0 mol L⁻¹) and analyzed. The results are demonstrated in Fig. 3. The height equivalent (HETP) and the number (*N*) of the theoretical plates calculated from the elution curves³⁷ (Fig. 3) were 0.95 – 0.98 ± 0.1 mm and 138 – 141 ± 5, respectively. The HETP and *N* values computed from the breakthrough capacity curves (Fig. 4) were 0.97 ± 0.1; 131 ± 3 and 0.92 ± 0.13; 129 ± 4 (*n* = 5), respectively. The critical capacity of Cr(VI) ion sorption onto TPAs⁺·Cl⁻ and TPP⁺·Br⁻ loaded PUFs packed column calculated from Fig. 4 were 14.8 ± 1.2 and 15 ± 1 mg/g PUFs, respectively at 5 mL min⁻¹ flow rate. The breakthrough capacities³⁸ of Cr(VI) uptake onto the reagent TPAs⁺·Cl⁻ or TPP⁺·Br⁻ PUFs calculated from Fig. 4 were 19.0 ± 1.5 and 19.8 ± 1 mg g⁻¹, respectively. These values are quite good by comparison with other solid support such as Voltalef, silica gel and solid ion exchange in column modes.³⁷

Figure of merits of TPP⁺·Br⁻ treated PUFs packed method

Under the established conditions for the retention and recovery of various concentrations of Cr(VI) species from the test aqueous solutions (100 mL) onto TPP⁺·Br⁻ treated PUFs packed column, a linear calibration curve was obtained with the following regression equation:

$$A = 0.52C + 0.034 \quad (n = 5; R^2 = 0.98) \quad (9)$$

Here, *C* represents the analyte concentration (0 – 15 µg L⁻¹). According to the IUPAC,³⁹ the lower limits of detection (LOD = 3*S*_{y/x}/*b*) and quantification (LOQ = 10*S*_{y/x}/*b*) were found to be equal 0.04 and 0.13 µg L⁻¹, respectively where *S*_{y/x} is the

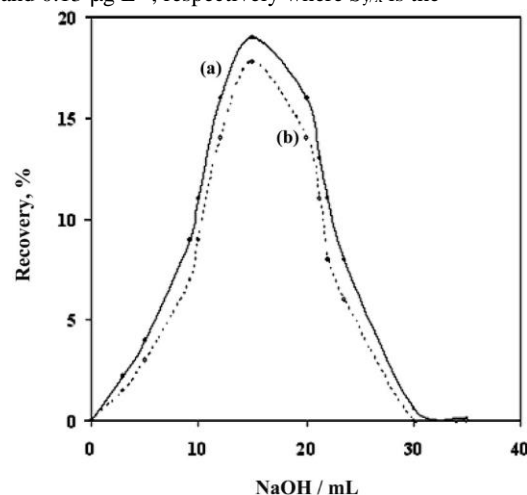


Fig. 3 Elution curves of Cr(VI) from immobilized TPAs⁺·Cl⁻ (a) and TPP⁺·Br⁻ (b) PUFs packed column (4 ± 0.01 g) at 3 mL min⁻¹ employing NaOH (1.0 mol L⁻¹) as an eluting agent.

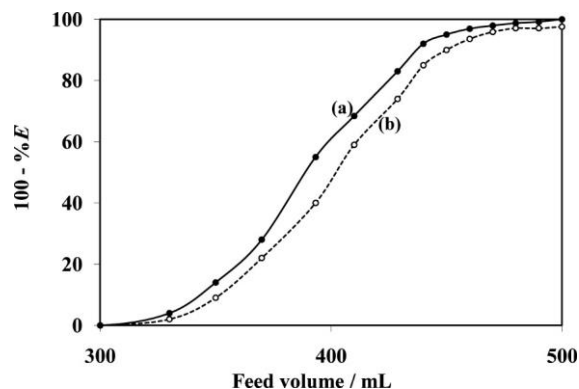


Fig. 4 Breakthrough curves for Cr(VI) at 10 µg mL⁻¹ sorption onto TPAs⁺·Cl⁻ (a) and TPP⁺·Br⁻ (b) impregnated PUFs (4 ± 0.01 g) packed column at 5 mL min⁻¹ flow rate.

standard deviation of *y*-residual and *b* the slope of the calibration plot.³⁷ The LOD is far below the permissible limit of chromium by most of the reported methods^{10–17} and the values of Cr(VI) at 0.05 and 0.2 ng mL⁻¹ in fresh and marine water samples, respectively. The LOD is sufficiently low as compared to those attained by AAS (9.0 µg L⁻¹) and ICP-OES (1.0 µg L⁻¹). Moreover, the LOD and LOQ could be improved to lower values by prior collection of ultra

trace concentrations of chromium species from large sample volumes at the optimum conditions. An enrichment factor of 50 was obtained ($V_{\text{sample}} = 1000$ and $V_{\text{eluent}} = 20$ mL). The sensitivity factor calculated from the ratio of slopes of the calibration plots with and without preconcentration step was close to 30. A relative standard deviation (RSD) of $\pm 3.4\%$ was achieved at a Cr(VI) concentration of $0.1 \mu\text{g mL}^{-1}$, $n = 5$, confirming the precision of the method. The analytical features of the proposed method were showed excellent performance compared with most of the reported methods.^{10,16} Some of these methods exhibited high detection limits in the range of $0.01 - 7.5 \mu\text{g L}^{-1}$.²³ Hence, the developed method is simple and less toxic, and provides an effective approach for the chemical speciation of Cr(III) and Cr(VI).

Table 2 Analysis of Cr(III) and Cr(VI) ions in industrial wastewater (1.0 L) by the proposed TPP⁺-Br⁻ foam packed column (A) and AAS (B) methods^a

Cr(III) added/ $\mu\text{g mL}^{-1}$	Cr(VI) added/ $\mu\text{g mL}^{-1}$	Cr found/ $\mu\text{g mL}^{-1}$		
		A	B	total chromium
5	5	5.54 ± 0.17	7.56 ± 0.14	12.9 ± 0.2
10	5	10.57 ± 0.16	7.33 ± 0.20	18.1 ± 0.2

a. Average ($n = 5$) \pm standard deviation.

Tolerance of electrolytes and diverse ions

The selectivity of the developed TPP⁺-Cl⁻ immobilized PUFs packed column for the preconcentration of Cr(VI) at $5 \mu\text{g mL}^{-1}$ concentration level from aqueous media (50 mL) was examined in the presence of a relatively high excess (1 mg) of the ions relevant to waste water e.g. alkali and alkaline earth metals, Cu²⁺, Al³⁺, Ni²⁺, Co²⁺, Cd²⁺, Hg²⁺, Fe³⁺, VO₃⁻, AsO₂⁻, SO₄²⁻, PO₄³⁻ and MnO₄⁻ ions which are often accompanying Cr(VI) ion. The tolerance less than $\pm 2\%$ change in the uptake of Cr(VI) is considered free from interference. The limit was set as the amount of foreign ion:analyte ratio (w/w) causing an error of $\pm 2\%$. Good extraction efficiency ($>98 \pm 2\%$) for the Cr(VI) ions was achieved in the presence of the investigated ions except Fe³⁺, VO₃⁻, MnO₄⁻, N₃⁻. The interference of Fe³⁺ and VO₃⁻ at 1:100 analyte to interfering ion was eliminated by adding 2 mL of NaF (1.0 mol L⁻¹) solution to the aqueous solution to obtain unambiguous and selective preconcentration and recovery of Cr(VI). In case of MnO₄⁻ ions, NaN₃ (1.0 mL, 0.1 % w/v) was added to the test solution to reduce Mn⁷⁺ to Mn²⁺ and an acceptable retention percentage of Cr(VI) of $98.02 \pm 2.12\%$ was achieved.

Applications

The TPP⁺-Cl⁻ treated PUFs packed column was applied for the determination of nanomolar concentrations of Cr(III) and/or Cr(VI) and total inorganic chromium in tap and/or industrial wastewater samples. A first aliquot (1 L) of tap water spiked (or without) with and/or Cr(VI) was percolated through the PUFs packed column at $3 - 5 \text{ mL min}^{-1}$ as described for Cr(VI) uptake. Cr(VI) was retained quantitatively, while Cr(III) species were passed through the column without sorption. The retained Cr(VI) species were then

recovered by NaOH (10.0 mL, 1.0 mol L⁻¹) at a 2 mL min^{-1} flow rate and analyzed by AAS. The results revealed the absence (not detectable) of Cr(III) and/or Cr(VI) in tap water; good extraction and recovery ($98 \pm 2\%$) of the spiked Cr(III) and/or Cr(VI) species were achieved. The chemical speciation of Cr(III) and Cr(VI) ions in industrial wastewater samples of an electroplating plant was carried by the standard addition. The results are given in Table 2. As it is seen, the results of the developed packed column and the data obtained by AAS are quite close. Cr(VI) sorption at concentration $\leq 0.01 \mu\text{g L}^{-1}$ was also tested for tap and wastewater samples (100 mL) and analyzed by FAAS as described.

Conclusion

The developed method allows continuous monitoring of Cr(VI) and

Cr(III) added/ $\mu\text{g mL}^{-1}$	Cr(VI) added/ $\mu\text{g mL}^{-1}$	Cr found/ $\mu\text{g mL}^{-1}$		
		A	B	total chromium
10	—	10.4 ± 0.12	2.4 ± 0.11	12.9 ± 0.1
5	10	5.43 ± 0.14	13.05 ± 0.26	17.9 ± 0.05

total Cr(III) and Cr(VI) species content in electroplating industry. The PUFs packed column was reused three times without decrease in its efficiency. The method could be applied even at ultra trace Cr(III) and/or Cr(VI) in the aqueous media. Work is still continuing for the speciation and sequential determination of organic and inorganic chromium species in environmental samples by on-site analysis.

References

- J. J. R. Frausto da Silva and R. J. P. Williams, "The Biological Chemistry of the Elements—The Inorganic Chemistry of Life", 1st ed., **1994**, Clarendon Press, Oxford, 541.
- G. P. Gallios and M. Vaclavikova, *Environ. Chem. Lett.*, **2008**, *6*, 235.
- J. O. Nriagu and E. Nieboer, "Chromium in Natural and Human Environment", **1988**, Wiley, New York.
- P. Metilda, K. Sanghamitra, J. M. Gladis, G. R. K. Naidu, and T. P. Rao, *Talanta*, **2005**, *65*, 192.
- P. Miretzky and A. F. Cirelli, *J. Hazard. Mater.*, **2010**, *180*, 1.
- E. O. Jorge, M. M. Rocha, I. T. E. Fonseca, and M. M. M. Neto, *Talanta*, **2010**, *81*, 556.
- M. S. Hosseini and M. Asadi, *Anal. Sci.*, **2009**, *25*, 807.
- R. A. Sanchez-Moreno, M. J. Gismera, M. T. Sevilla, and J. R. Procopio, *Sens. Actuators, B*, **2010**, *143*, 716.
- S. Gupta and B. V. Babu, *Chem. Eng. J.*, **2009**, *150*, 352.
- V. Camel, *Spectrochim. Acta, Part B*, **2003**, *58*, 1177.
- R. A. Gil, S. Cerutti, J. A. Gasquez, R. A. Olsina, and L. D. Martinez, *Talanta*, **2006**, *68*, 1065.
- A. E. Ofomaja, E. B. Naidoo, and S. J. Modise, *J. Environ. Management*, **2010**, *91*, 1674.
- I. Lopez Garcia, B. M. Merino, N. Campillo, and M. H. Cordoba, *Anal. Bioanal. Chem.*, **2002**, *373*, 98.
- H. F. Maltez and E. Carasek, *Talanta*, **2005**, *65*, 37.
- V. Orescanin, L. Mikelic, S. Lulic, and M. Rubcic, *Anal. Chim. Acta*, **2004**, *527*, 125.

16. R. Milacic, J. Scancar, and J. Tusek, *Anal. Bioanal. Chem.*, **2002**, 372, 549.
17. C. G. B. Bruhn, F. E. Pino, V. H. Campos, and J. A. Nobrega, *Anal. Bioanal. Chem.*, **2002**, 374, 131.
18. S. S. Samaratunga, J. Nishimoto, and M. Tabata, *Anal. Sci.*, **2005**, 21, 1073.
19. L. Elcl, U. Divrikli, A. Akdogan, A. Hol, A. Cetin, and M. Soylak, *J. Hazard. Mater.*, **2010**, 173, 778.
21. J. S. Wang and K. H. Chiu, *Anal. Sci.*, **2007**, 23, 1337.
22. M. S. El-Shahawi, S. S. M. Hassan, A. M. Othman, M. A. Zyada, and M. A. El-Sonbati, *Anal. Chim. Acta*, **2005**, 534, 319.
23. A. B. Farag, M. H. Soliman, O. S. Abdel-Rasoul, and M. S. El-Shahawi, *Anal. Chim. Acta*, **2007**, 601, 218.
24. A. M. El-Wakil, M. S. El-Shahawi, and A. B. Farag, *Anal. Lett.*, **1990**, 23, 703.
25. M. S. El-Shahawi and M. A. El-Sonbati, *Talanta*, **2005**, 67, 806.
26. V. A. Lemos, M. S. Santos, E. S. Santos, M. J. S. Santos, W. N. L. dos Santos, A. S. Souza, D. S. de Jesús, C. F. das Virgens, M. S. Carvalho, N. Oleszczuk, M. G. R. Vale, B. Welz, and S. L. C. Ferreira, *Spectrochim. Acta, Part B*, **2007**, 62, 4.
27. M. S. El-Shahawi, S. S. M. Hassan, A. M. Othman, and M. A. El-Sonbati, *Microchem. J.*, **2008**, 89, 13.
28. H. Sano, *Anal. Chim. Acta*, **1962**, 27, 398.
29. M. N. Sastri and T. S. R. Prasada Rao, *J. Inorg. Nucl. Chem.*, **1968**, 30, 1727.
30. M. M. Saeed and M. Ahmed, *Anal. Chim. Acta*, **2004**, 525, 289.
31. P. R. Haddad and N. E. Rochester, *J. Chromatogr.*, **2004**, 439, 23.
32. K. A. Halhouli, N. A. Darwish, and N. M. Al-Dhoon, *Sep. Sci. Technol.*, **1995**, 30, 3.
33. N. Condamines and C. Musikas, *Solvent Ext. Ion Exch.*, **1992**, 10, 69.
34. A. Aksoyoglu, *J. Radioanal. Nucl. Chem.*, **1989**, 134, 393.
35. G. A. Somorjai, "Introduction to Surface Chemistry and Catalysis", **1994**, John Wiley & Sons, Inc.
36. K. Rzeszutek and A. Chow, *J. Membr. Sci.*, **2001**, 181, 265.
37. T. Braun, J. D. Navratil, and A. B. Farag, "Polyurethane Foam Sorbents in Separation Science", **1985**, CRC Press Inc., Boca Raton.
38. W. X. Ma, F. Liu, K. A. Li, W. Chen, and S. Y. Tong, *Anal. Chim. Acta*, **2000**, 416, 191.
39. J. C. Miller and J. N. Miller, "Statistics for Analytical Chemistry", 4th ed., **1979**, Ellis-Howood, New York, 115.

Analysis of Some Selected Persistent Organic Chlorinated Pesticides in Marine Water and Food Stuffs by Differential Pulse Cathodic Stripping Voltammetry

M. S. El-Shahawi,^{a,*} A. Hamza,^a A. S. Bashammakh,^b A. A. Al-Sibaai,^a W. T. Al-Saggaf^a

^aDepartment of Chemistry, Faculty of Science, King Abdulaziz University, P. O. Box 80203, Jeddah 21589, Kingdom of Saudi Arabia ^bThe Centre of Excellence in Environmental Studies, King Abdulaziz University, P. O. Box 80203, Jeddah 21589, Kingdom of Saudi

Arabia ^cPermanent address: Chemistry Department, Faculty of Sciences at Damietta, Mansoura University, Mansoura, Egypt

*e-mail: mohammad_el_shahawi@yahoo.co.uk

Received: September 17, 2010;

Accepted: January 13, 2011

Abstract

Based on the redox characteristics of two selected organochlorine pesticides namely alachlor (ALC) and chlorfenvinphos (CHL) in Britton–Robinson (B–R) buffer at a hanging mercury drop, Pt and Au working electrode (HMDE), a fast, simple and selective differential pulse cathodic stripping voltammetric (DP CSV) method was developed for their determination. The cathodic stripping peak currents for ALC versus concentrations was linear in the range from 7.410^9 to 1.410^7 molL⁻¹ and in the range from 2.710^9 to 1.610^8 molL⁻¹ for CHL. The method was applied for the analysis of trace concentrations of ALC and CHL in fresh- and marine water (Atlantic and Red Sea) and sediment samples and food stuffs.

Keywords: Organochlorine pesticides, Stripping voltammetry, Determination, Marine water and sediment, Food stuffs

DOI: 10.1002/elan.201000581

1 Introduction

After the Second World War, scientists began to recognize that, certain chemical pollutants were capable persistent in the environment for long time, migrating in air, water, soil and sediments and accumulating to levels that could harm wildlife and human health. These chemical pollutants are called Persistent Organic Pollutants (POPs) [1]. POPs are typically “water-hating” and “fatloving” chemicals, i.e. hydrophobic and lipophilic. In aquatic systems and soils they partition strongly to solids, notably organic matter, avoiding the aqueous phase [1]. POPs are toxic chemicals, characterized by being subject to bioaccumulation potential and long-range transport capacity [2]. These contaminants are present at different concentrations in sewage sludge and are transferred to soil matrix, as soils have a high capacity to act as reservoirs of organic pollutants [2]. For agrochemical POPs the source is clear – the deliberate application to crops and soils. POPs are also entered our environment from a whole host of combustion sources, from metal refining and as impurities other, deliberately manufactured chlorinated compounds e.g. pentachlorophenol and organochlorinated pesticides (OCPs).

Organochlorine pesticides (OCPs) have been of great concern because of their harm effects, their deleterious effect on nontarget

organism, large production and usage, ubiquity, bioaccumulation and magnification in the food chain and persistence in our environment [3]. Herbicides or pesticides, define as a class of chemical substances used against organisms damaging humans, animals and plants, like insects, fungi, moulds, nematoda, and rodents. For their wide spread use and physical–chemical properties, these compounds represent an important class of pollutants for ground and surface water resources. The persistence of pesticides in the water environment depends upon doses, nature (that characterizes resistance to degradation process, dispersion and mobility), pedologic recipient soils and the hydrogeologic characteristics of the area involved. Contamination of ground waters may take a long time, even decades [4,5]. The concept of quality in analytical chemistry is mainly associated with the fact of reaching the maximum level of analytical properties for a given method [6].

Last decades have seen an upsurge of interest on developing precise methods for the determination of persistent organic pollutants (POPs) e.g. chlorinated pesticides, polychlorinated biphenyls in the environment [1]. The determination of pesticides and herbicides in many environmental matrices is generally determined by SPE-LC-ESI-

MS/MS [7], UPLC-MS/MS [8], HPLC [9], GC/MS

[10,11] and LC-MS/MS [12] and polarographic [15,16] and voltammetric [17–19] methods. Recent years have seen an upsurge of interest for rapid and sensitive analytical methods for

(Darmstadt, Germany) and stored in a refrigerator at 48C. Diluted solutions of each pesticide were prepared in water. A series of B–R buffer (pH 2.3–11) solutions was prepared [20] and

2011 Wiley-VCH Verlag GmbH & Co. KGaA, Weinheim



the determination of chlorinated pesticides in environmental samples e.g. water, sediment and air. A recent literature survey on the analysis of POPs has revealed little work [15–17] on the use of stripping voltammetry or any other electrochemical technique for the analysis of OCPs. Thus, the present manuscript reports the redox behavior of the pesticides alachlor and chlorfenvinphos at the hanging mercury drop, Pt and working electrodes in an attempt to develop a fast, simple, low cost and selective DP CSV method for their analysis in vegetables (spinach and carrot), cow cheese, tap and marine water (Red Sea and Atlantic Ocean) and sediment. On the other hand, the most probable reduction mechanism of the electrogenerated species was properly assigned.

was used as supporting electrolyte. Silica gel, anhydrous sodium sulfate, anhydrous magnesium sulfate, acetone and n-hexane were purchased from BDH (Poole, England).

2 Experimental

2.3 Recommended DP CSV Procedures

2.1 Apparatus

A Metrohm 757 VA trace analyzer and 747 VA stand (Basel, Switzerland) were used for recording the cyclic, linear and differential pulse cathodic stripping voltammetry. A three-compartment borosilicate (Metrohm) voltammetric electrochemical cell (10 mL) configuration incorporating hanging mercury drop electrode (HMDE, drop surface area 5 mm²) as a working electrode, double-junction Ag/AgCl,(3 M) KCl, as a reference and platinum wire (BAS model MW-1032) as counter electrodes, respectively. Platinum (Pt, surface area 2 mm²) and gold (Au, surface area 2 mm²) were also used as working electrodes. Pesticide was measured with a Shimadzu GC-17A, GC MS QP-5000 Mass spectrometer, Colum C18. The detector and the injector temperature were maintained at 2808C. The column was held isothermally at 508Cmin⁻¹, then the temperature was programmed at 258Cmin⁻¹ to 1508C and finally programmed at 108C min⁻¹ from 125 to 2808C with a holding time of 10.5 min and injection volume of 2 mL [18]. A digital micropipette 10–100 mL (Volac) was used for transferring the sample solutions to the electrochemical cell. A pH-meter (model MP220, Mettler Toledo) was used for pH measurements. A soxhlet extractor and a rotary evaporator were used for the extraction of the pesticides from the sediment or vegetables samples with n-hexane–acetone [19], respectively. An aqua wave Barnstead/Lab–Line ultrasonic bath (Model 9372) was used for the extraction of ALC and CHL compounds from the vegetable samples. Deionized water was obtained from A Milli-Q Plus water purification system (Milford, MA, USA) throughout the work.

The electrochemical cell was precleaned by soaking in nitric acid (10% v/v) and washed with de ionized water. The general procedures were preceded as follows: An accurate volume (10 mL) of an aqueous solution containing B–R buffer as supporting electrolyte of pH 2–3 was placed in the cell. The solution was stirred and purged with nitrogen gas for 10 min before recording the voltammogram. The stirrer was then stopped and after 10 s quiescence time, the background voltammogram of the supporting electrolyte was recorded by applying a negative going potential scan from 0 to 1.5 V vs. Ag/AgCl at a deposition potential of 0.35 V, accumulation time of 660 s and 750 s; scan rate of 50 mVs⁻¹ and pulse amplitude of 50 mV. After recording the voltammogram of the blank solution, an accurate concentration (8.3510⁻⁸– 11.110⁻⁸ molL⁻¹) of the chlorinated pesticide was placed into the electrochemical cell. The solution was stirred and purged with nitrogen gas for 5 min and the stirrer was then stopped. After 10 s quiescence time, the voltammogram of the pesticide was finally recorded by applying a negative going potential scan from 0.0 to 1.5 V vs. Ag/AgCl under the same experimental conditions as for the blank set up.

2.2 Reagents and Materials

Analytical reagent grade (A.R) chemicals were used except otherwise specified. Standard solutions of the chlorinated pesticide alachlor (ALC) and chlorfenvinphos (CHL) in methanol (10.0 mgmL⁻¹) were purchased from Merck

2.4 Applications

2.4.1 Analysis of the Chlorinated Pesticides in Fresh and Marine Water Samples

Tap- or Red Sea water samples collected from the coastal area of Jeddah City, Saudi Arabia and Atlantic Ocean (Elizabeth Port, South Africa) water were filtered through 0.45 mm cellulose membrane filter and stored in LDPE sample bottles. The recommended electrochemical procedures used for the standard curve of pesticides determination at pH 2–3 were finally followed. Alternatively, the standard addition method was used as follows: transfer known volumes (1.0–2.0 mL) of sample extract adjusted to pH 2–3 into the electrochemical cell. Measure the peak current displayed by the test solution before and after addition of various volumes of the standard ALC or CHL pesticide. The change in the peak current was then recorded and used for determining both pesticides.

2.4.2 Analysis of the Chlorinated Pesticides in Marine Sediment (Elizabeth Port, South Africa)

An accurate weight (5.00.001 g) of the marine sediment was extracted with n-hexane –acetone (1:1 v/v, 90.0 mL) for 8 h in a soxhlet extractor. The organic extract was then filtered through

the filter paper as reported [19]. The n-hexane–acetone extract and the washings were transferred to measuring flask (250 mL) and completed to the mark with the same solvent. An accurate volume (2.0 mL) of the n-hexane–acetone extract was transferred to the voltammetric cell and analyzed by the recommended DP CSV procedure in the presence of various volumes (10–60 mL) of the standard (1.0 mgmL⁻¹) pesticide. The pesticide concentration was then determined via the standard curve.

2.4.3 Analysis of the Chlorinated Pesticides in Vegetable Samples

Spinach and Carrot are the most common plants to be affected by the chlorinated pesticides [7]. Therefore, the edible part of spinach and carrot samples was first removed, freeze-dried and stored and analyzed according the method of Gonzalez-Rodriguez et al. [7] as follows: An accurate weight (20–25 g) of the shopped vegetable samples were placed in a 125 mL glass container and extracted with n-hexane–acetone (1:1 v/v, 60 mL). The glass container was vigorously homogenized in an ultrasonic bath for 10 min followed by NaCl (3 g) and anhydrous magnesium sulfate (12 g). The sample solution was then shaken vigorously with n-hexane–acetone for 5 min and left for equilibration for 10 min. The organic extract was separated out by filtration through filter paper and concentrated in a rotary evaporator [21,22].

2.4.4 Analysis of the Chlorinated Pesticides in Cheese of Cow Milk Sample

The extraction of the tested compounds from cheese of cow milk samples ((taken from animals grazing on polluted field) was carried out by matrix solid phase dispersion (MSPD) as reported earlier by Bordajandi et al. [22]. In this experiment, an accurate weight (5–10 g) of the cheese sample was mixed with 20 g of a solid mixture containing silica gel and anhydrous sodium sulfate (1:1 w/w). The solid mixture was homogenized, grounded to a fine powder and homogeneously packed onto the column accurately. The required compounds were then recovered from the column with n-hexane–acetone (150 mL) at a reasonable flow rate (7–10 mLmin⁻¹) and finally subjected to clean up process as described [21].

3 Results and Discussion

3.1 Electrochemical Behavior of the Tested Chlorinated Pesticides

The influence of the aqueous solution pH employing B–R buffer (pH 2.3–11) on the DP CSV behavior of the pesticides ALC and CHL species at the HMDE surface was critically investigated. Over the studied pH 2.3–6.0, the DP CSV of the two pesticides

displayed two well defined cathodic peaks in the range from 1.05 to 1.08 V (peak I) and 1.3 to 1.4 V (peak II) versus Ag/AgCl electrode. Representative results are given in Figure 2. In the DP CSVs of ALC and CHL pesticides at 2 < pH < 6, the first cathodic peak is most likely assigned to the reduction of the carbonyl group (C=O) and phosphate ester (+P=O) (Figure 1) in one step via 2 H⁺/2e electrochemical process forming CHOH and PHOH reduced species, respectively. A representative assignment is given in Scheme 1. The second cathodic peak is safely assigned to the reduction of the adsorbed hydrogen (H⁺+e⁻→H ads.) catalyzed by the pesticide. The second cathodic peak is safely assigned to the reduction of the adsorbed hydrogen. The assignment of this peak of ALC or CHL pesticide was confirmed by recording the residual current of the DP CSVs at the same pH 2–3 in the absence and in the presence of various concentrations of ALC or CH (Figure 3). The observed increase in the second peak on raising the pesticide concentrations confirms that, the reduction of hydrogen was catalyzed by ALC and CHL.

In the DP CSV, on raising the solution pH to pH 6, the potential of the cathodic peaks of both pesticides are shifted cathodically confirming the dependence of both peaks on the hydrogen ion concentration [22]. In solutions of pH > 6, no cathodic peaks for both pesticides were observed due to the difficulty of the reduction of C=O of ALC and the P=O phosphate ester of CHL and/or it may be reduced at more negative potentials outside the allowed potential window of the HMDE. The linear electrochemical processes for ALC and CHL can be expressed by the following regression equations:

$$E_{p,c1} \text{ } \mu\text{g} \text{ } 0:029 \text{ pH} 1:0074 \quad \delta R^2 \text{ } \mu\text{g} \text{ } 0:918 \text{ } \delta 1 \text{ } \mu\text{g}$$

$$E_{p,c1} \text{ } \mu\text{g} \text{ } 0:027 \text{ pH} 1:0416 \quad \delta R^2 \text{ } \mu\text{g} \text{ } 0:841 \text{ } \delta 2 \text{ } \mu\text{g}$$

with slopes of 0.029 and 0.027 mV/pH for ALC and CHL, respectively. These data confirmed the involvement of 2 H⁺/2e in the first cathodic peak of both pesticides. On raising the solution pH, the first cathodic peak potential was shifted to more negative values suggesting that the electrode reactions involved hydrogen ions [22,23]. These data added further confirmation of the direct exchange of 2H⁺/2e in one reduction processes converting the carbonyl and the phosphate ester groups in ALC and

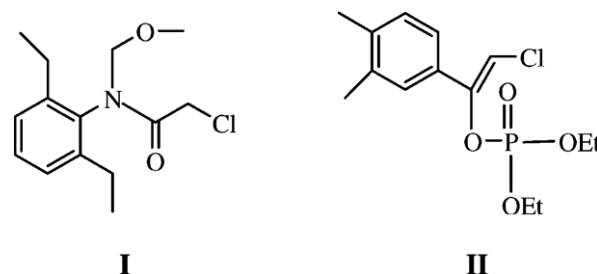


Fig. 1. Chemical structures of alachlor (I) and chlorfenvinphos (II).

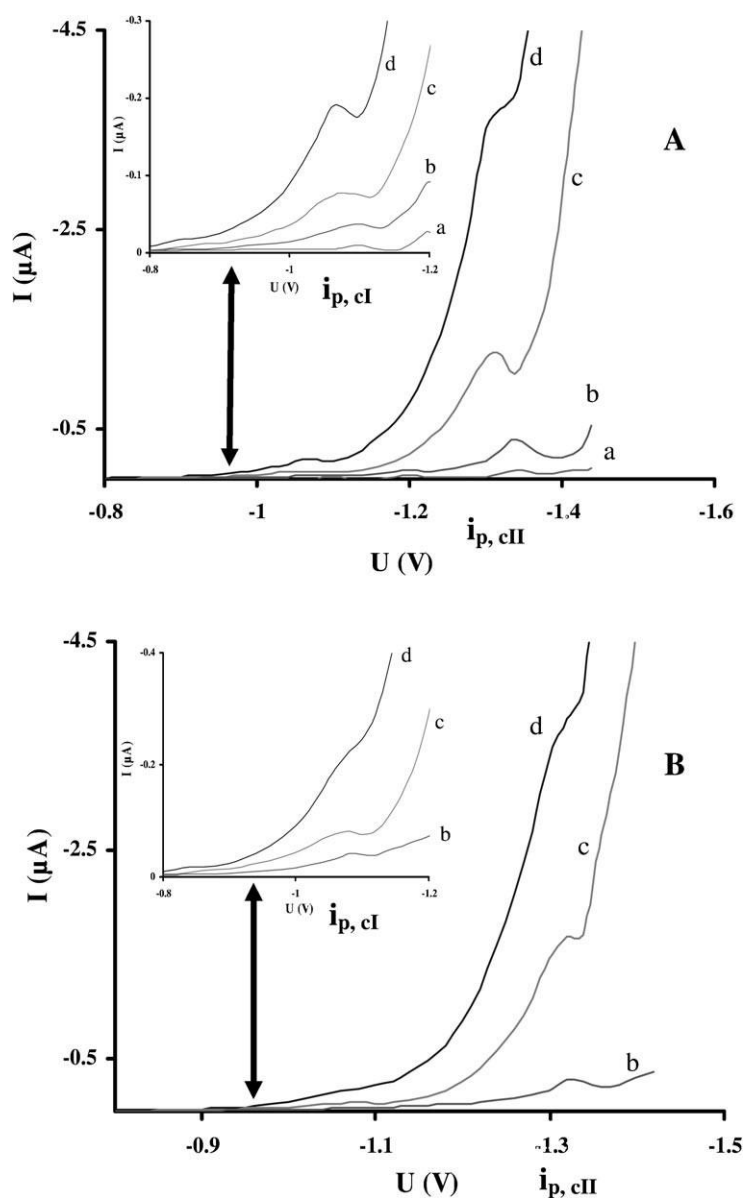
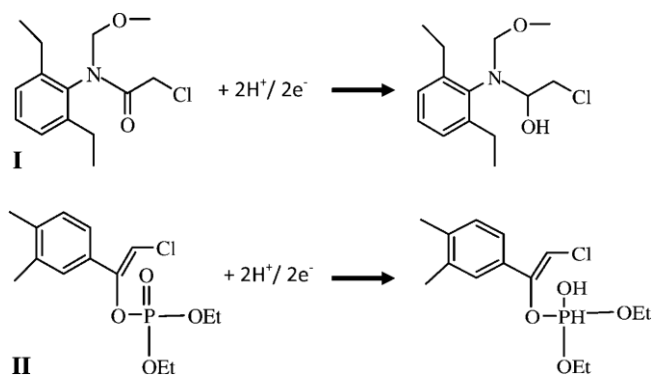


Fig. 2. DP CSV of alachlor (A) and chlorfenvinphos (B) in aqueous B–R buffer solution of pH 2.18 (a), 2.71 (b), 3.93 (c), and 5.08 (d) at the HMDE. Deposition time of 650 s; accumulation potential of 0.35 V; scan rate=50 mVs^{-1} and pulse amplitude of 50 mV vs. Ag/AgCl electrode.



Scheme 1. The proposed reduction mechanism of ALC (I) and therefore, it seems reasonable to assume from DP CSV CHL (II) at the HMDE. voltammograms in the acidic media that, the reduction of

CHL pesticides to CHOH and PHOH groups at $\text{pH} < 6$, respectively. Similar results were observed in previous studies [23]. At $\text{pH} > 6$, the reduction waves are ill defined and poorly resolved. The instability of the electrogenerated species, the fast electrode kinetics and the poor adsorption of the reduced species and hydrogen at the surface of the HMDE may account of the observed trend [24]. Also, in slightly and/or alkaline solutions, such compounds may be reduced at more negative potential than the allowed potential window of the HMDE. Thus, the cleavage of the C=O and P=O groups of ALC and CHL in acidic solution involves $2\text{H}^+ / 2\text{e}^-$ electrochemical process in one single step, respectively.

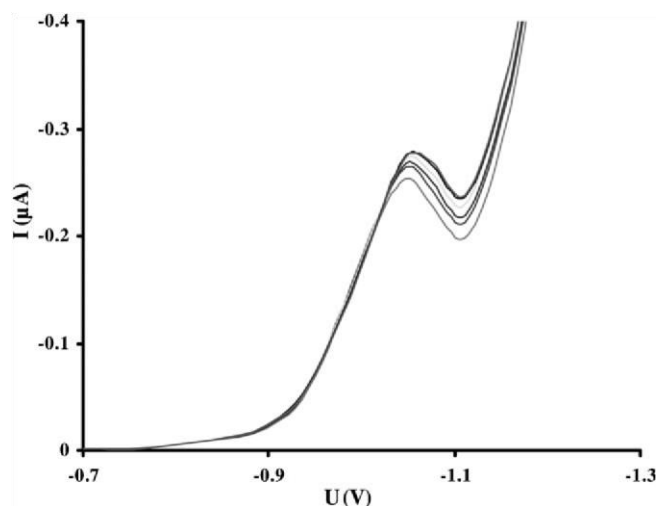


Fig. 3. DP-CSVs of chlorfenvinphos at pH 2–3 at HMDE vs. Ag/AgCl electrode at various concentrations. Deposition time of 650 s; accumulation potential of 0.35 V; scan rate=50 mVs⁻¹ and pulse amplitude of 50 mV vs. Ag/AgCl electrode.

the C=O and P=O groups for ALC and CHL is most likely involved two protons/two electrons (2 H⁺/2e⁻) reduction process. Figure 2. The DP-CSV of the complex showed a well-defined reduction peak in the range 0.1 to 0.55 V vs. Ag/AgCl reference electrode. At pH 2–3, well defined and symmetric cathodic peak was observed and the cathodic peak current ($i_{p,c}$) reached maximum. Thus, in subsequent work, the solution pH was adjusted at pH 2–3. At this pH, the cathodic peak was reproducible, sharp and symmetric with low background current.

The CVs of the ALC (1.1110⁶ molL⁻¹) and CHL (8.3510⁶ molL⁻¹) pesticides at pH 2–3 at different scan rates ($v=20$ –5000 mVs⁻¹) in the potential range 0.2 to 1.5 V were carried out at the HMDE, Pt and Au working electrodes vs. Ag/AgCl electrode. Representative CVs at HMDE are given in Figure 4. At the HMDE, the CVs of both pesticides at 0.4 V deposition potential displayed one well defined cathodic peak in the range 1.1 to 1.18 V assigned to the reduction of the C=O and P=O groups of ALC and CHL to CH-OH and PH-OH via

2 H⁺/2e⁻ reduction process, respectively. On reversing the scan, no anodic peaks were observed suggesting the irreversible nature of the electrochemical process of both pesticides. At low scan rate (<50 mVs⁻¹), the CVs of both pesticides showed no cathodic and/or anodic peaks indicating the poor adsorption and/or the instability of the reduced species at the HMDE.

In the CV, on raising the scan rate, the cathodic peak potential of both pesticides progressively shifted to more negative values and the plots of $E_{p,c}$ versus the scan rate (log v) were linear confirming the irreversible nature of the observed reduction processes and the surface reaction of the adsorbed pesticides [25]. Representative data are shown in Figure 5. The product of the number (N_a) of the electron transfer involved in the reduction

step and the corresponding charge transfer coefficient (α) i.e. a N_a of the surface reaction of the adsorbed pesticides were calculated from the slope of the linear plot (Figure 5) employing the equation:

Assuming $n=2$, the values of α were found in the range 0.16–0.2 confirming the irreversible nature of the observed cathodic processes at the surface of the HMDE [24]. The number of the electrons transferred in the rate-determining step (N_a) and the corresponding charge transfer coefficient (α) i.e. a N_a at the HMDE were also determined from the influence of the scan rate Sawyer et al., 1984 [26]. Assuming $N_a=2$, the values of α calculated from equations [26] was found <0.5 confirming the irreversible nature of the electrode process.

The variations of the cathodic peak current function ($i_{p,c}/v^{1/2}$) with the scan rate were investigated. The $i_{p,c}/v^{1/2}$ was decreased progressively on raising the scan rate. Thus, the reduction process of the pesticides favor the well known chemical reaction coupled between two charge-transfer processes) of the type EC mechanism [27]. In the EC mechanism with an irreversible chemical reaction, the $i_{p,c}/v^{1/2}$ should decrease continuously with increasing scan rate. Thus, the product of this reduction step undergoes a very rapid follow-up chemical reaction [27]. The observed behavior may possibly be explained by considering that, the protonation reaction is very fast or virtually complete in an acid medium [27,28].

The effect of the type of the working electrode (HMDE, Pt, Au) was studied on the absence and presence of various concentrations of ALC and CHL pesticides at pH 2–3 at a wide range of scan rate (20–500 mVs⁻¹) vs. Ag/AgCl electrode. In the absence of the pesticide, the residual current was negligible. Representative CVs of CHL at Pt working electrode are shown in Figure 6A. At scan rate 20–200 mVs⁻¹, the CV of CHL showed one ill defined cathodic peaks in the range from 0.7 to 0.86 V (Peak I). On reversing the scan rate, one well defined anodic peak in the range from 0.28 to 0.02 V was observed. Similar trends were also observed for ALC confirming the irreversible nature of the reduction process of both pesticides at Pt electrode. On increasing the scan rate, the cathodic was shifted to more negative values, while the anodic peak was shifted anodically confirming the irreversible nature of the observed electrode couple [27].

The CVs of CHL at Au electrode (Figure 6B) at various scan rate (20–500 mV) were also recorded. At scan rate <500 mVs⁻¹, two ill defined cathodic peaks (like shoulder) in the potential range 0.58 to 0.66 (peak I) and 0.7 to 0.8 (peak II) coupled with one well defined anodic peak in the potential range 0.2 to 0.14 V versus Ag/AgCl electrode (Figure 6B). A similar trend was noticed for the CV of ALC pesticide, too, where one cathodic peak in the range from 0.58 to 0.64 to 0.86 coupled with one anodic peak in the range from 0.22 to 0.14 V.

The dependence of the CV response on the analyte concentration was investigated at constant scan rate (200 mVs⁻¹). The results revealed no significant changes on the

cathodic peak current vs. Ag/AgCl electrode indicating that, the electrochemical process is typical of an electrode coupled chemical reaction mechanism (EC) in which an irreversible first-order chemical reaction is interposed between the charges [27,28]. A comparison of the redox potentials of the ALC or CHL at HMDE, Pt and Au working electrodes indicated that, the two pesticides are easily reduced on the following order of potential:

Pt > Au > HMDE

The electron donating nature of mercury compared to Au and Pt electrodes may account for the observed trend. The surface coverage (G) of the tested pesticides (ALC or CHL) onto the working electrodes HMDE, Pt and Au was determined from their CVs at various scan rate by adopting the method used by Sharp et al. [29]. According to this method, the cathodic peak current is related to the surface concentration of the electro active species by the following equation [30,31]:

$$I_{p,c} = n^2 F^2 A G v = 4RT \quad \delta 4p$$

where n represents the number of electrons involved in the reduction process, A is the geometric surface area of the working electrode (HMDE, Pt, Au), G (molcm^{-2}) is the surface coverage, v is the scan rate and other symbols have their usual meaning. Assuming $n=2$, the surface concentration (G) was calculated using the slopes of the linear regions of the $I_{p,c}$ versus scan rate plots. For ALC it resulted in 7.1410^5 , 3.8910^1 and 5.0810^1 molcm^{-2} while, for CHL it resulted in 9.2410^5 , 4.3110^1 and 4.6910^1 molcm^{-2} at HMDE, Pt and Au electrodes, respectively, suggesting the possible use of the DP CSV at HMDE for the analysis of ALC or CHL in various environmental samples. Also, at the HMDE, the cathodic peak was well defined, sharp and symmetric. On the other hand, HMDE is the only electrode type sensitive enough for in situ measurements in natural waters [32–34]. This electrode is safe as long as storage and disposal of Hg is undertaken in a safe manner. Thus, in the subsequent work, HMDE was selected.

3.2 Analytical Parameters

The results of the surface coverage of the analytes and the sensitivity of the developed cathodic peak of ALC or CHL using DP CSV at HMDE, suggest the application of this technique for developing an accurate procedure for the determination of ALC and CHL pesticides in fresh and marine water, sediment and food stuffs e.g. vegetable, cheese of cow milk samples. Therefore, a detailed investigation was carried out to study the influence of different parameters that control the peak current, sensitivity and selectivity of the observed cathodic peaks. The influence of the pH employing (B–R) buffer on the peak current at peak potential of 1.07 V (peak I) for ALC and 1.05 V (peak I) for CHL versus Ag/AgCl electrode was studied

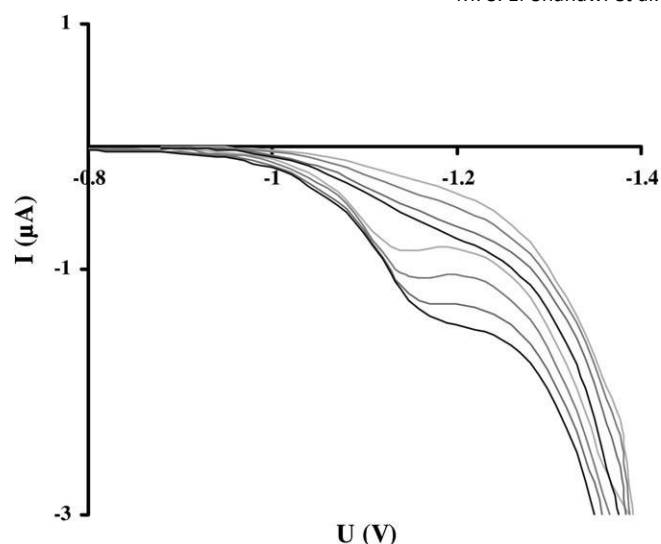


Fig. 4. Cyclic voltammograms of alachlor ($1.110^6 \text{ molL}^{-1}$) in B–R buffer (pH 2–3) at various scan rates: 500, 1000, 2000 and 3000 mVs^{-1} at the HMDE vs. Ag /AgCl electrode.

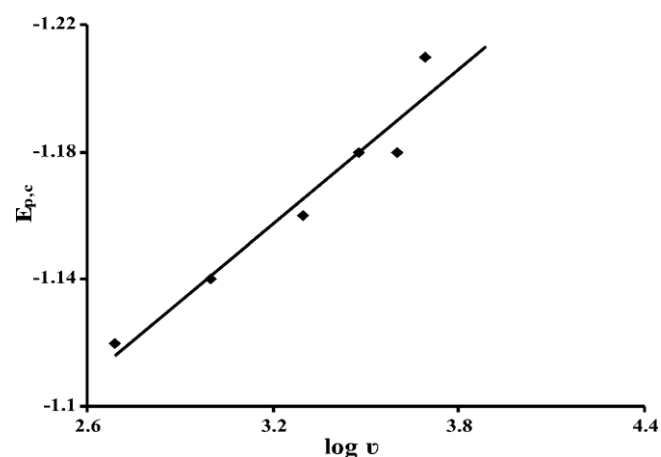


Fig. 5. Plots of $E_{p,c}$ vs. $\log v$ of alachlor in B–R buffer (pH 2–3) at HMDE vs. Ag/AgCl electrode.

over a wide range of pH 2.3–11.0 at the HMDE. At pH 2–3, maximum peak current and well defined; symmetric, excellent background of the blank reading and reproducible peak was achieved for both ALC and CHL (Figure 2). Thus, in the subsequent work, the pH of the aqueous solution was kept at pH 2–3.

Accumulation time (t_{acc}) is one of the most important parameters in stripping procedures that has a pronounced effect on sensitivity, linear range and lower limit of detection [35]. Maximum peak current, well defined and sharp peak were obtained for both ALC and CHL was achieved at a deposition time of 660 and 750 s for both ALC and CHL pesticides (Figure 7). At longer adsorption time, peak current began to decrease suggesting saturation of the electrode surface with the pesticides species.

The effect of deposition potential (0.0 to 0.6 V) on the cathodic peak current was evaluated at the HMDE.

The effect of scan rate on the $i_{p,c}$ of ALC and CHL was studied at pH 2–3 at the HMDE under the optimal accumulation time and potential. The $i_{p,c}$ was directly proportional to the scan rate over

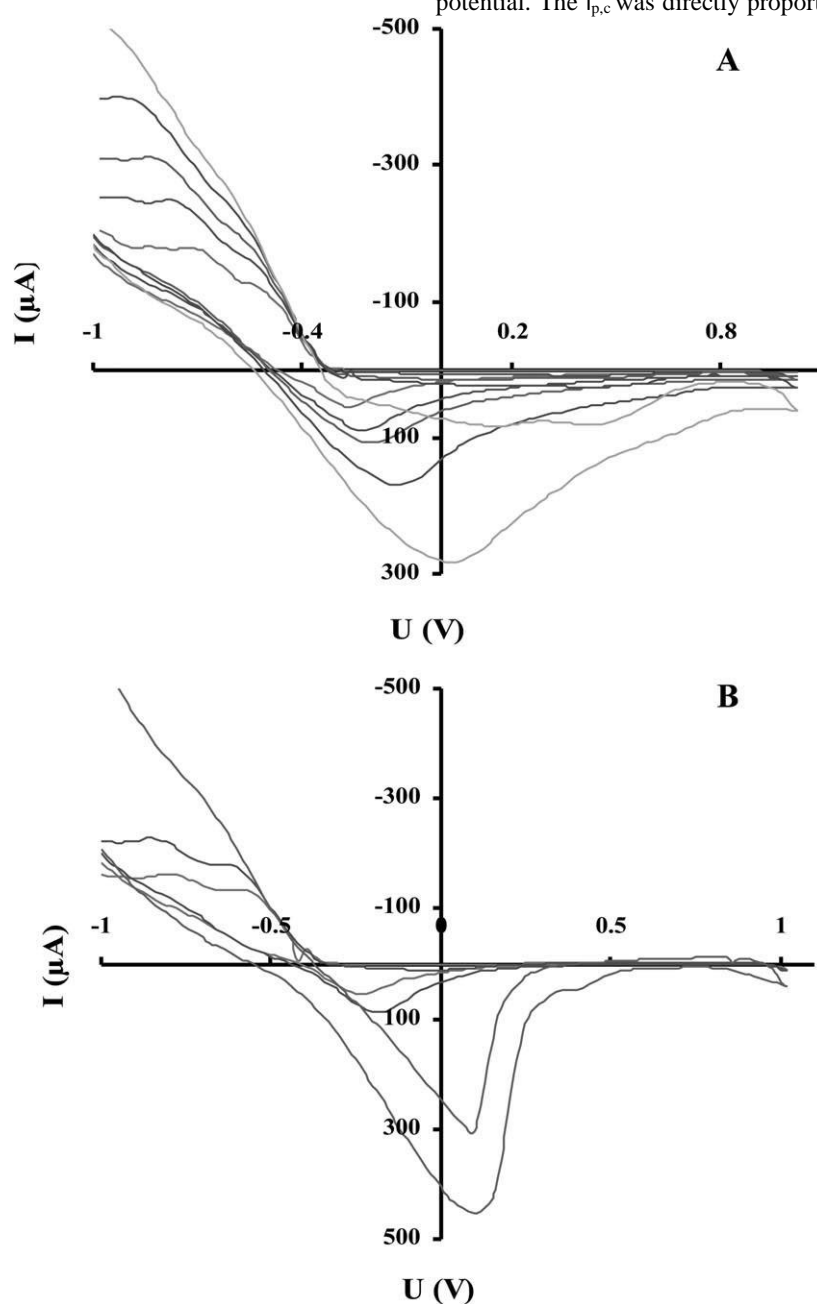


Fig. 6. Cyclic voltammograms of chlorfenvinphos in B-R buffer (pH 2–3) at Pt (A) and Au (B) electrodes vs. Ag/AgCl electrode at different scan rates: 20, 50, 100, 200 and 500 mVs^{-1} .

The plot of the deposition potential versus peak current for ALC and CHL pesticides is shown in Figure 8. Peak current reached maximum at an accumulation potential of 0.35 V. At a deposition potential <0.35 V, the peak current decreased gradually. Moreover, at a deposition potential of 0.35 V, the peak was symmetric and well defined. Thus, a deposition potential of 0.35 V was selected in the subsequent work.

at the range of 20 to 80 mVs^{-1} which suggested a surface-controlled process on the surface of the HMDE [27,28]. Good sensitivity, sharp and symmetric cathodic peak and excellent background was achieved at 50 mVs^{-1} scan rates. Thus, in the next work a scan rate of 50 mVs^{-1} was adopted. The influence of the pulse amplitude (10–100 mV) on the DP CSV peaks of ALC and CHL at pH 2–3 was tested at the optimal conditions. The peak current increased steadily on increasing the pulse amplitude. However, 60 mV pulse amplitude was selected in the next work, where good background and best sensitivity were achieved.

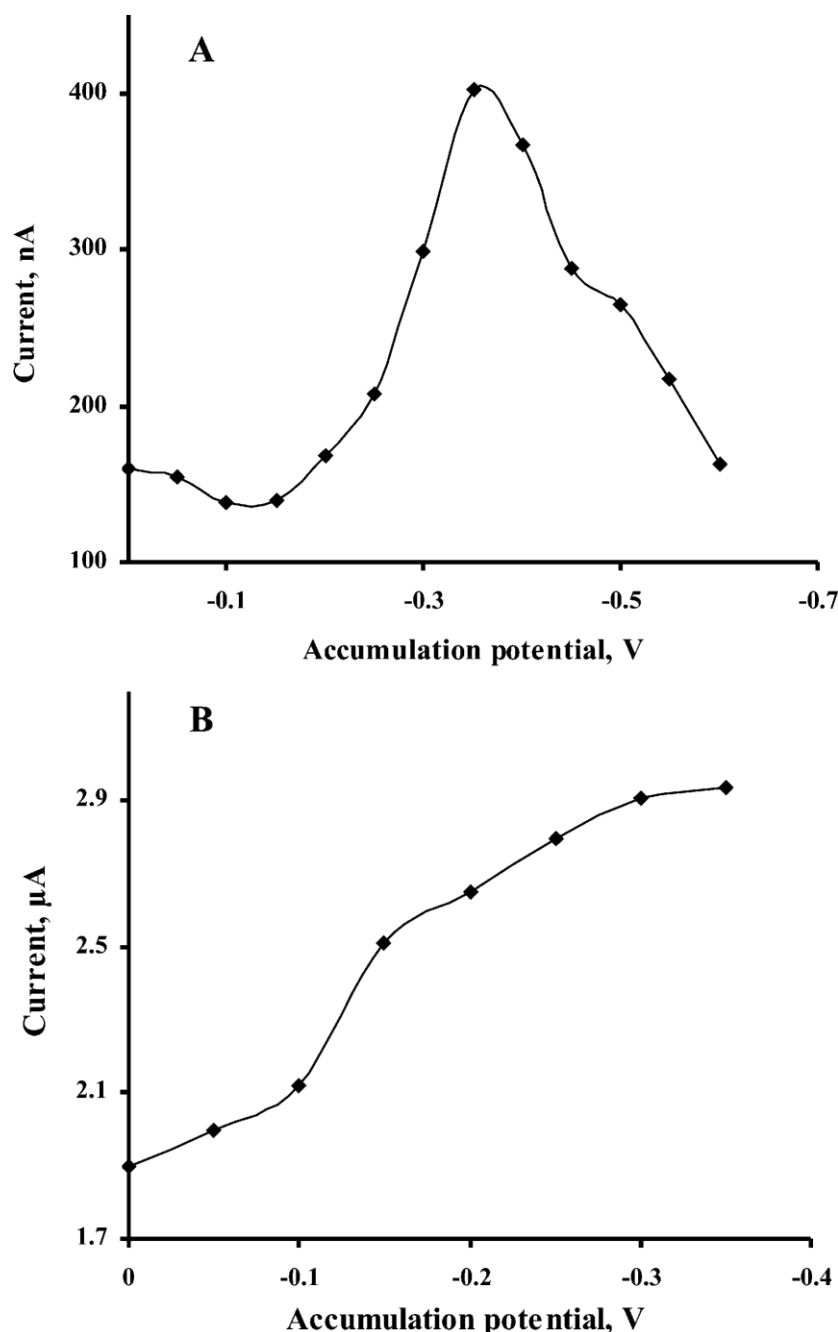


Fig. 7. Plots of the $i_{p,c}$ of alachlor (A) and chlorfenvinphos (B) vs. accumulation time at HMDE versus Ag/AgCl electrode. Deposition potential of 0.35 V; scan rate=50 mVs⁻¹ and pulse amplitude of 60 mV vs. Ag/AgCl electrode.

3.3 Figure of Merits of the Developed DP CSV Method

Under the optimum experimental conditions of pH, deposition time, accumulation and scan rate, the figure of merits (dynamic linear range, lower limit of detection and quantification, repeatability, recovery and specificity) of the developed DP CSV for the determination of ALC and CHL was determined. The DP CSVs of both chlorinated pesticides ALC and CHL pesticides at various concentrations (2.710^9 – 5.4110^7 molL⁻¹) of each pesticide were recorded individually at the HMDE. The plot of $i_{p,c}$ of peak II for ALC versus concentrations was linear in the range 7.410^9 (1.99 ppb)– 1.410^7 molL⁻¹ (37.73 ppb) (Figure 9), while for CHL

pesticide at peak I, the plot was linear in the range 2.710^9 (0.97 ppb)– $1.6 \cdot 10^8$ molL⁻¹ (5.75 ppb), respectively. At ALC concentration $>1.410^7$ molL⁻¹ and CHL $>1.610^8$ molL⁻¹, the calibration plots leveled off because of the adsorption saturation [27,28]. According to IUPAC [36], the values of LOD and LOQ for ALC were found equal 6.1810^{12} (1.67 ppt) and 2.0610^{11} (5.56 ppt) molL⁻¹, respectively, while, for CHL, the values of LOD and LOQ at peak I was found equal 4.3410^{12} (1.56 ppt) and 1.4410^{11}

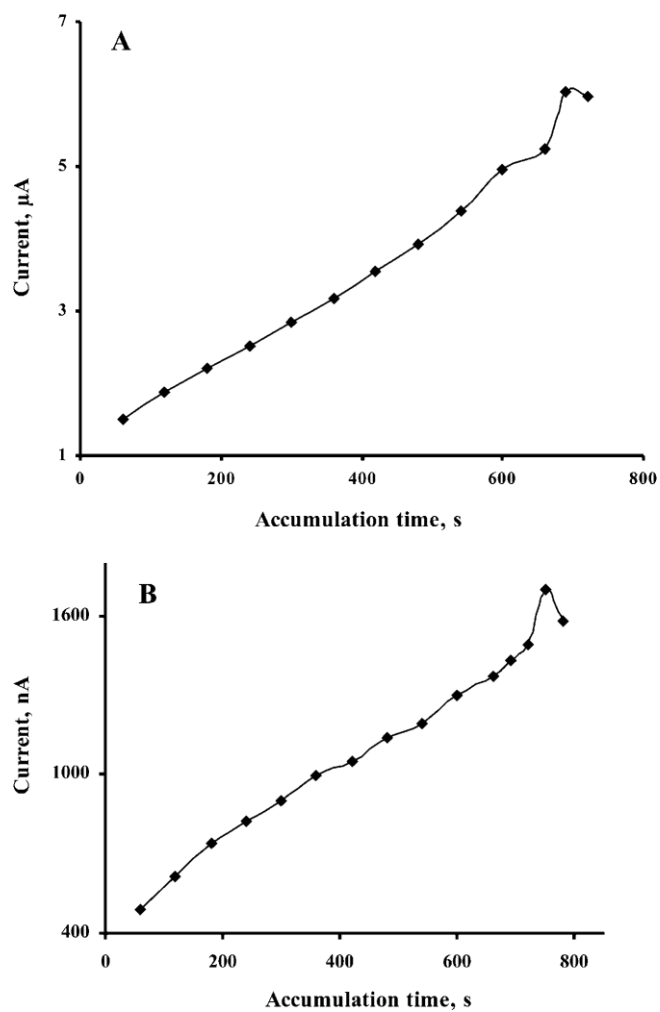


Fig. 8. Plots of $i_{p,c}$ of peak I (A) and peak II (B) of alachlor vs. deposition potential at HMDE vs. Ag/AgCl electrode. Alachlor concentration = 1.1610^{-7} molL $^{-1}$; sweep rate = 50 mVs $^{-1}$.

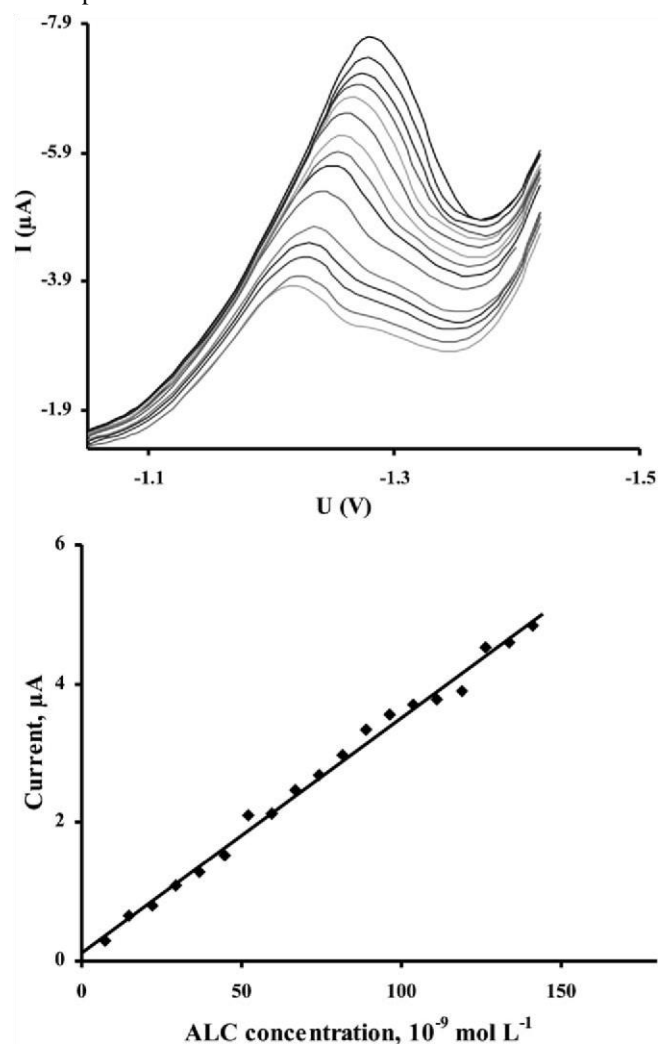


Fig. 9. DP-CSVs and calibration curve of alachlor at pH 2–3 at 1.3 V at HMDE vs. Ag/AgCl electrode. Deposition time of 660 s; accumulation potential of 0.35 V; scan rate=50 mVs⁻¹ and pulse amplitude of 60 mV vs. Ag/AgCl electrode.

(5.19 ppt) molL⁻¹, respectively. Both LOD and LOQ values confirmed the sensitivity of the proposed DP CSV procedure compared to most of the reported chromatographic methods e.g. SPE-LC-ESI-MS/MS [26], UPLCMS/MS [8], HPLC [9], GC/MS [10] LC-MS/MS [12] and polarographic [13,14] and voltammetric [15–17] methods. The main analytical features of the proposed method were compared successfully with many of the previously published chromatographic methods (Table 1). The relative standard deviation (RSD) of ALC and CHL based on five replicate measurements at concentrations 3.0 10⁸ and 8.010⁸ molL⁻¹ were found equal 2.9, 2.1, 2.76 and 2.39%, respectively confirming the precision and the performance of the developed DP CSV method for determination of the tested pesticides. Such limits could be improved to lower values by increasing the equilibrium and accumulation time at the optimized experimental conditions. Such level of precision is suitable for quality control analysis of pesticides in environmental samples.

3.4 Applications

3.4.1 Analysis of the Tested Chlorinated Pesticides in Water Samples

The proposed DP CSV method was used for the assay of ALC and CHL in various water samples (tap-, Red Sea and Atlantic Ocean close to Elizabeth Port, South Africa water). The water samples were processed as described. The results are summarized in Table 2. An acceptable recovery (970.02–1040.06) with a relative standard deviation (RSD) in the range 4.2–14.6% of the tested pesticides were successfully achieved (Table 2). The results are close to the values obtained by GC MS confirming the sensitivity and selectivity of the method for the analysis of the tested pesticides in complicated matrices compared to the highly cost chromatographic methods [7], GC/MS [10,11] and other methods [12].

Table 1. Figure of merits of the developed DP CSV and some of the reported methods [a].

Method	Pesticide	LOD (ngL ¹)	LOQ (ngL ¹)	Dynamic range (ngmL ¹)	Reference
SPE-LC-ESI-MS/MS	ALC	18	47	0.05–1	[37]
UPLC-MS/MS	ALC	6	17	0.02–0.5	[38]
HPLC	CHL	100000	333000	500–15000	[39]
GC/MS	ALC	75.1	250	25–200 200–10000	[40]
LC-MS/MS	ALC	6000	19980	0.1–2	[12]
	CHL	4000	13320	0.03–2	
GC/SQ-MS		400	1200		[41]
DP CSV	ALC	1.67	5.56	1.99–37.73	
	CHL	1.56	5.19	0.97–5.75	Present work

[a] SPE-LC-ESI-MS/MS: solid phase extraction – liquid chromatography – electrospray tandem mass spectrometry; UPLC-MS/MS: ultraperformance chromatography combined with tandem mass spectrometry; HPLC: high performance liquid chromatography; GC-MS: gas chromatography – mass spectrometry; MS/MS: liquid chromatography – tandem mass spectrometry; GC/SQMS: gas chromatography coupled to single quadrupole.

Table 2. Levels (ngmL¹) of the tested pesticides ALC and CHL in fresh-, Red Sea (coastal area of Jeddah City, Saudi Arabia) and Atlantic Ocean (Elizabeth port, South Africa) water determined by the developed DP CSV method [a].

Water sample	Pesticide added (ngmL ¹)		Found (ngmL ¹)		Recovery (%)	RSD (%)		
	ALC	CHL	ALC	CHL		ALC	CHL	ALC
Tap	0	0	–	–	–	–	–	–
	8	4.99	–	–	–	–	–	4.2
Red Sea	0	0	–	99	–	–	–	–
	8	5.99	–	0.003	–	–	–	7.4
	0	0	–	–	–	–	–	–
Atlantic Ocean	4	0.568.698.690.678.790.390.040.050.060.060.060.065.050.356.420.494.370.0020.0030.040.040.180.18	1010.05	101	–	–	–	14.6
			101	0.04	–	–	–	–
			0.06	970.18	–	–	–	–
			1040.06	–	–	–	–	–

[a] Average standard deviation (n=7).

Table 3. Analysis of ALC and CHL in Atlantic Ocean (Elizabeth port, South Africa) marine sediment by the developed DP CSV method [a].

Sample	Added (mgg ¹)		Found (mgg ¹)		Recovery (%)	RSD (%)	
	ALC	CHL	ALC	CHL		ALC	CHL
Sediment	0	0	–	–	–	–	–
	8	1.99	8.550.620.060.06	0.392.380.010.01	990.06	990.01	9.17 2.78

[a] Average standard deviation (n=5).

3.4.2 Analysis of Marine Sediment of Atlantic Ocean

The proposed DP CSV was used for the analysis of ALC and CHL in the marine sediment of Atlantic Ocean. In this experiment, an accurate weight (5.00.001 g) of the dry marine

sediment was extracted and analyzed as described before [19,20]. The results are summarized in Table 3. The content of ALC pesticide in the marine sediment sample was found 2.290.21 nM (0.620.06 mgL¹) with correlation coefficient of 0.98. The content of the CHL pesticide in the marine sediment was found 1.08¹ 0.03 nM (0.390.01 mgL) with a correlation coefficient of 0.98. An acceptable recovery percentage and relative standard deviation in the range from 990.01 to 99.006%

and 2.78 to 9.17%, were achieved, respectively. Thus, the developed DP CSV method compared favorably with the reported HPLC [9]. The method provides an alternative approach for the analysis of ALC and CHL pesticides in different matrices.

3.4.3 Analysis of the Chlorinated Pesticides in Food Samples

The high sensitivity of the developed DP CSV method for the analysis of the tested compounds in various water samples and solid sediment suggested the application of the method for the determination of trace concentrations of ALC and CHL residues in spinach, carrot and cheese samples. Various volumes of pesticides (10–50 mL) were added to the food samples and analyzed as described. The results (Table 4) of the analysis of ALC and CHL confirmed the sensitivity and precision of the method.

4 Conclusions

The developed DP CSV method for ALC and CHL determination is characterized by instrumental simplicity, economy, convenient, rapid, and accurate. The method

Table 4. Analysis of ALC and CHL in different food samples by the developed DP-CSV method [a].

Sample	OCs added (mg ^l)		FoundSD (mg ^l)	
	ALC	CHL	ALC	CHL
Spinach	0	0		
8		3.99		
Carrot	0	0		
8		2.01		
Cheese	0	0		
8		3.99	8.949.330.890.558.960.890.070.070.310.310.090.094.410.402.190.184.630.620.030.030.010.010.030.0	

[a] Average standard deviation (n=5).

compared favorably with the reported HPLC [7], GC/MS [10,11] and other methods [12] and provides an excellent alternative approach for the analysis of ALC and CHL pesticides in different matrices because of its sufficient precision. Work is still continuing for the possible application of on-line DP CSV determination in various environmental samples.

Acknowledgements

The authors would like to thank the Deanship of Scientific Research, King Abdul Aziz University, Jeddah, Saudi Arabia for the financial support under the Grant Number 3-106-430H and the Department of Chemistry for the facilities provided in terms of the laboratory facilities.

References

- [1] M. S. El-Shahawi, A. Hamza, A. S. Bashammakh, W. T. AlSaggaf, *Talanta* 2010, **80**, 1587.
- [2] R. Yang, A. Lv, J. Shi, G. Jiang, *Chemosphere* 2005, **61**, 347. [3] A. Passuello, M. Mari, M. Nadal, M. Schuhmacher, J. L. Domingo, *Environ. Internat.* 2010, in press.
- [4] J. Junior, N. Re-Poppi, *Talanta* 2007, **72**, 1833.
- [5] O. Fatoki, R. Awofolu, *J. Chromatogr. A* 2003, **983**, 225.
- [6] P. Richter, B. Sepulveda, R. Oliva, K. Calderon, R. Seguel, *J. Chromatogr. A* 2003, **994**, 169.
- [7] R. Gonzalez-Rodriguez, R. Rial-Otero, B. Cancho-Grande, J. Simal-Gandara, *J. Chromatogr. A* 2008, **1196**, 100.
- [8] C. Gervais, S. Brosillon, A. Laplanche, C. Helen, *J. Chromatogr. A* 2008, **1202**, 163.
- [9] M. Llasera, M. Reyes-Reyes, *Food Chem.* 2009, **114**, 1510. [10] M. Bruzzoniti, C. Sarzanini, G. Costantino, M. Fungi, *Anal. Chim. Acta* 2006, **578**, 241.
- [11] C. Lesuer, P. Knittl, M. Gartner, A. Mentler, M. Fuerhacker, *Food Control* 2008, **19**, 906.
- [12] L. Diaz, J. Llorca-Porcel, I. Valor, *Anal. Chim. Acta* 2008, **624**, 90.
- [13] P. Carrai, L. Nucci, F. Pergola, *Anal. Lett.* 1992, **25**, 163.
- [14] S. Screehar, *Talanta* 1997, **44**, 1859.
- [15] M. J. Ramalhosa, P. Paga, S. Morais, C. Delerue-Matos, M. Beatriz, *Anal. Lett.* 2007, **40**, 1085.
- [16] S. Morais, O. Tavaresa, C. Delerue-Matos, *Anal. Lett.* 2005, **38**, 1275.
- [17] M. Drevinek and V. Horak, *J. Electroanal. Chem.* 1997, **423**, 83.
- [18] X. Liu, Y. Shi, H. Wang, R. Zhang, *Forensic Sci. Int.* 2009, **192**, 14.
- [19] R. Bettinetti, C. Giarei, A. Provini, *Arch. Environ. Contam. Toxicol.* 2003, **45**, 72.
- [20] H. Britton, *Hydrogen Ions*, 4th ed., Chapman and Hall, London 1952, p. 113.
- [21] H. Gao, X. Jiang, F. Wang, D. Wang, Y. Bian, *Bull. Environ. Contam. Toxicol.* 2005, **74**, 673.
- [22] L. Bordajandi, G. Gomez, M. Fernandez, E. Abad, J. Rivera, M. Gonzalez, *Chemosphere* 2003, **53**, 163.
- [23] N. Menek, S. Basaran, G. Turgut, M. Odabasoglu, *Dyes and Pigments* 2004, **61**, 85.
- [24] N. Menek, S. Topcu, G. Turgut, *Bull. Electrochem.* 2003, **91**, 133.
- [25] B. Parajon-Costa, A. Gonzalez-Baro, E. Baran, *Anorg. Allg. Chem.* 2002, **628**, 1419.
- [26] D. Sawyer, W. R. Heinemann, J. Beebe, *Chemistry Experiments for Instrumental Methods*, Wiley, New York 1984.

- [27] A. J. Bard, L. Faulkner, *Electrochemical Methods: Fundamentals and Applications*, Wiley, New York 1980, p. 218.
- [28] R. Samuelsson, M. Sharp, *Electrochim. Acta* 1978, 23, 315. [29] M. Sharp, M. Petersson, K. Edstrom, *J. Electroanal. Chem.* 1979, 95, 123.
- [30] R. Nicholson, I. Shain, *Anal. Chem.* 1964, 36, 706.
- [31] C. van den Berg, *Anal. Chim. Acta* 1984, 164, 195.
- [32] M. J. Gomez Gonzalez, O. Dominguez Renedo, M. J. Arcos Martnez, *Talanta* 2007, 71, 691.
- [33] S. A. Bennett, E. P. Achterberg, D. P. Connelly, P. J. Statham, G. R. Fones, C. R. German, *Earth Planetary Sci. Lett.* 2008, 270, 157.
- [34] C. B. Braungardt, E. P. Achterberg, M. Gledhill, M. Nimmo, F. Elbaz-Poulichet, A. Cruzado, Z. Velasquez, *Environ. Sci. Tech.* 2007, 41, 4214.
- [35] E. Fischer, C. Van den Berg, *Anal. Chim. Acta* 2001, 432, 11.
- [36] J. Miller, N. Miller, *Statistics for Analytical Chemistry*, 4 th ed., Ellis Horwood, New York 1994.
- [37] M. Kuster, M. J. Lopez de Alda, C. Barata, D. Raldua, D. Barcelo, *Talanta* 2008, 75, 390.
- [38] G. Gervais, S. Brosillon, A. Laplanche, C. Helen, *J. Chromatogr. A* 2008, 1202, 163.
- [39] M. P. Garcia-de Llasera, M. L. Reyes-Reyes, *Food Chem.* 2009, 114, 1510.
- [40] M. C. Bruzzoniti, C. Sarzanini, G. Costantino, M. Fungi, *Anal. Chim. Acta* 2006, 578, 241.
- [41] C. Lesueur, P. Knittl, M. Gartner, A. Mentler, M. Fuerhacker, *Food Control* 2008, 19, 906.

Mineral processing and extraction of rare earth elements from the Wadi Khamal Nelsonite Ore, Northwestern Saudi Arabia

Hesham M. Harbi & Abdelmonem A. Eldougdoug & M. S. El-Shahawi

Received: 2 November 2008 / Accepted: 15 May 2009 / Published online: 13 August 2009
Saudi Society for Geosciences 2009

Abstract A technological sample (50 kg) from Wadi Khamal Nelsonite ore was subjected to magnetic and flotation concentration techniques. Excellent recovery percentages of 72.95% and 71.22% were achieved by the dry/ wet magnetic and flotation concentration techniques, respectively. The weight of the apatite concentrate reached a reasonable percentage of approximately 23.5% with an overall 40.23% P₂O₅ total content.

Analytical data of the apatite concentrate after digestion in concentrated sulfuric acid revealed that the total content of the rare earth elements (REE) constitutes about 0.2% of the total apatite content. The REE content (0.2%) was partitioned between phosphoric acid liquor (65%) and gypsum precipitate (36%). The extraction of the REEs from the phosphoric acid liquor using oxalic acid and sodium carbonate–bicarbonate mixture (1:10w/w) yielded the RE oxide cake which constitute about 1.2% (w/w). The produced rare earth oxide cake contains traces of various metal oxides, e.g., SrO, Na₂O, etc. in addition to rare earth oxides. Attempts to determine quantitatively the constituents of the cake will be considered in future work.

P.O. Box 80206, Jeddah, 21589, Kingdom of Saudi Arabia
Keywords Rare earth elements . Saudi Arabia .

Mineral processing . Phosphoric acid liquor.
Gypsum precipitate

Introduction

Last decades have seen an upsurge of interest on the potential use of REE and their extraction from ores and minerals. REE and compounds find application in many advanced materials of current interest, e.g., highperformance magnets, fluorescent materials, chemical sensors, high-temperature superconductors, magneto optical disks and nickel–metal hydride batteries. Trace concentrations of REE's are present as impurities in certain ores and minerals, such as apatite, columbite, tantalite, and others. Thus, information as to its actual contents in these is necessary in order for metallurgists to choose the most suitable separation technique for economic exploitation of metals, e.g., niobium, tantalum, and samarium.

Igneous apatite deposits that are rich in apatite, magnetite, and/ or ilmenite represent an economic source of phosphate, i.e., for the production of phosphoric acid, fertilizers, and iron and/or titanium for steel industries. These deposits are associated with different types of igneous rocks, e.g., alkaline-rich intermediate and ultramafic rocks and carbonatites such as Khibiny and Kovador complexes in the USSR (Notholt 1979), Palabora carbonatite complex in South Africa (Palabora Mining Company Limited Mine Geological and Mineralogical Staff 1976), alkaline and alkalinerich carbonatite from Brazil (Morbidelli et al. 1995; Ribeiro et al. 2005), apatite-magnetite ore associated with alkalirich volcanic rocks of Sweden (Frietsch 1973, 1978), Sokli and Siilinjärvi carbonatite complex of Finland

H. M. Harbi (*) : A. A. Eldougdoug
Department of Mineral Resources and Rocks,
Faculty of Earth Sciences,
King Abdulaziz University,
P.O. Box 80206, Jeddah, 21589, Kingdom of Saudi Arabia e-mail:
harbi-hesham@hotmail.com

M. S. El-Shahawi
Department of Chemistry, Faculty of Science,
King Abdulaziz University,

(Vartiainen 1975; Puustinen 1971), apatite-bearing Jacupirangite and related alkaline-rich basic igneous rocks at Kodal; Norway (Bergstol 1972), Fanshan alkaline ultramafic complex in China (Jiang et al. 2004), nelsonite (apatite-magnetite-ilmenite ore) associated with massif anorthosites (Philpotts 1967; McLelland et al. 1994; Mitchell et al. 1996; Dymek and Owens 2001), tholeiitic-layered intrusions (McCann et al. 1998; Ripley et al. 1998).

A recent study by Harbi et al. (2006) of Wadi Khamal mafic-ultramafic rocks, NW Saudi Arabia, led to the discovery of nelsonite deposits associated with Wadi Khamal gabbronorite-anorthosite complex. The nelsonite apatite content ranges between 20% and 40% with an average of 23% corresponding to an average of about 10% P_2O_5 while magnetite and ilmenite constitute about 75%. The apatite contains about 0.21% of rare earth metal oxides. According to BRGM, the ore reserves were roughly estimated to be at least about 10 million tons in Wadi Khamal (Chevremont and Johan 1981). Chevremont and Johan (1981) have reported the association of apatite with Fe–Ti oxides at Wadi Murattijah area which is located to the north of Wadi Khamal area. The igneous apatite is known for its richness in REEs which can be recovered as a byproduct (Jiang et al. 2004; Ribeiro et al. 2005; Kanazawa and Kamitani 2006). The apatite–nepheline ore bodies of the Khibiny Complex, USSR, generally contain 15–75% apatite (6–31% P_2O_5). The apatite concentrate contains $\approx 40\%$ P_2O_5 (Notholt 1979).

The potential use of ores and minerals depends mainly on the performance of the extraction techniques used to separate and/or preconcentrate the REEs. Trace concentrations of REEs are present as impurities in certain ores and minerals, e.g., apatite, columbite, tantalite, and others. Thus, information regarding the actual contents of REEs are necessary for metallurgists and to select the most suitable separation technique for economic exploitation of metals, e.g., niobium, tantalum, titanium, lanthanum, samarium, etc. (Chunhua, et al. 2006; Valls et al. 2001; Suvadhan, et al. 2006; Akl et al. 2006)

Based on the discovery of the Wadi Khamal nelsonite ore by Harbi et al. 2006 and the fact that Saudi Arabia imported phosphoric acid and sodium tri polyphosphate during the period 1994–1998 worth about 1.1 billion Saudi Riyal (Al-Shafei 1998); the overall goals of this article focused on:

1. Assessing the economic potentiality of the nelsonite ore from Wadi Khamal area, primarily as source for phosphoric acid production as well as magnetite–ilmenite and REEs as byproducts.
2. Acquisition of technological samples representing the ore (50 kg each) from Wadi Khamal area.
3. Selection of the most suitable technique, e.g., magnetic or floatation to get a concentrate with high apatite content.
4. Production of phosphoric acid from the apatite concentrates using sulfuric acid.
5. Studying the partitioning of REEs between the phosphoric acid liquor and gypsum produced from the treatment of the apatite ore with concentrated sulfuric acid.
6. Determination and recovery of the total content of REEs of the Wadi Khamal nelsonite ore, Saudi Arabia.

Experimental

Apatite concentration from nelsonite

Thirteen samples from different nelsonite lenses were analyzed for their P_2O_5 content which was found to range from 7.23% to 16.75% with an average of about 9.8% (Harbi et al. 2006). For the production of the apatite concentrate, a technological sample ≈ 50 kg was collected from one of the nelsonite lenses (Fig. 1). The sample was studied in polished thin section to define the grain size of the apatite and found to range between tens of microns and few millimeters (Fig. 2). Apatite crystals are either intergrown with or enclosed within ilmenite and magnetite. In order to get the best liberation, the sample (≈ 10 kg) was crushed and sieved using a set of sieves; two size ranges were produced: +40–300 and +30–150 μ m. The froth flotation and magnetic separation are the most widely used methods of beneficiating similar ores. Accordingly, the sample was subjected to both magnetic separation (dry, wet, and dry/wet) at different magnetic intensities and froth flotation using different chemical reagents. These studies were carried out at the Central Laboratories Sector, Egyptian Mineral Resources Authority, Cairo, Egypt.

Froth flotation

This method was conducted using the size ranges (+40–300 μ m) and at different conditions of chemical reagents. The fine fraction below –30 or –40 μ m was rejected because it causes some problems during flotation. The Denver instrument was used at 1,000 rpm. The flow sheet is presented in Fig. 3.

Experiment #1 This test was conducted using the following chemical reagents: Armac-T, H_2SO_4 (pH regulator), and

pine oil. Size range +30–150µm, P₂O₅ % of the head sample 12.96%.

The results of direct flotation where apatite ends up in the concentrate and the results of reverse flotation where



Fig. 1 A layered sequence of massive and disseminated nelsonite ores at sharp contact with anorthosite

apatite ends up in the tailing are given in the following table:

Product	Direct flotation		Reverse flotation	
	wt.%	P ₂ O ₅ %	wt.%	P ₂ O ₅ %
Concentrate	14.97	14.98	89.05	9.82
Tailing	84.22	11.01	10.94	29.62
Total	100	11.51	100	11.99

The results of the first experiment indicate that the experiment under these conditions was not efficient in separating apatite from magnetite and ilmenite.

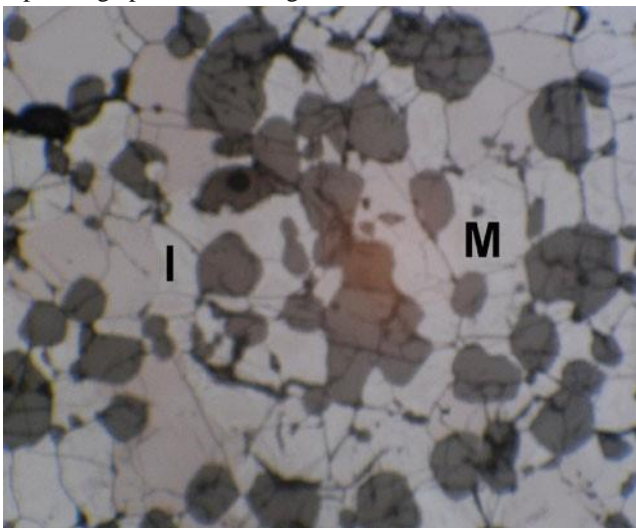


Fig. 2 Massive nelsonite ore consisting of rounded and subhedral apatite (dark gray) set in a ground mass of magnetite (M) and ilmenite (I). P.S., P.P.L., 30×

Experiment #2 This experiment was carried out on the size range (+40–300µm), the P₂O₅% of the head sample 9.93%. Five tests were conducted with different chemical reagents.

Test # 1: (Direct flotation)

Chemical reagents used were: NaOH, pH regulator at pH=8.5, olic acid suspended in kerosene 2:1 ratio at 1 kg/t, sodium silicate 200 g/t.

Product	wt.%	P ₂ O ₅ %	Recovery %
Conc.	24.56	20.31	49.72
Tail	68.81	5.79	39.71
Fine	6.63	16.00	10.57
Total	100	10.03	100

$$\text{Recovery\%} = \frac{\text{P}_2\text{O}_5\% \text{ Conc}}{\text{Total P}_2\text{O}_5\% \text{ headsample}} \times 100$$

The results indicate that the recovery is not acceptable at these conditions.

Test # 2: (Direct flotation)

Chemical reagents used were: NaOH as pH regulator at pH=9.5, olic acid suspended in ethylene glycol(1:1 ratio) 2 kg/t, soda ash, 200 g/t, sodium silicate, 200 g/t.

Product	wt.%	P ₂ O ₅ %	Recovery %
Conc.	40.61	20.95	85.07
Tail	52.72	0.81	4.27
Fine	6.67	16.00	10.66
Total	100	10.00	100

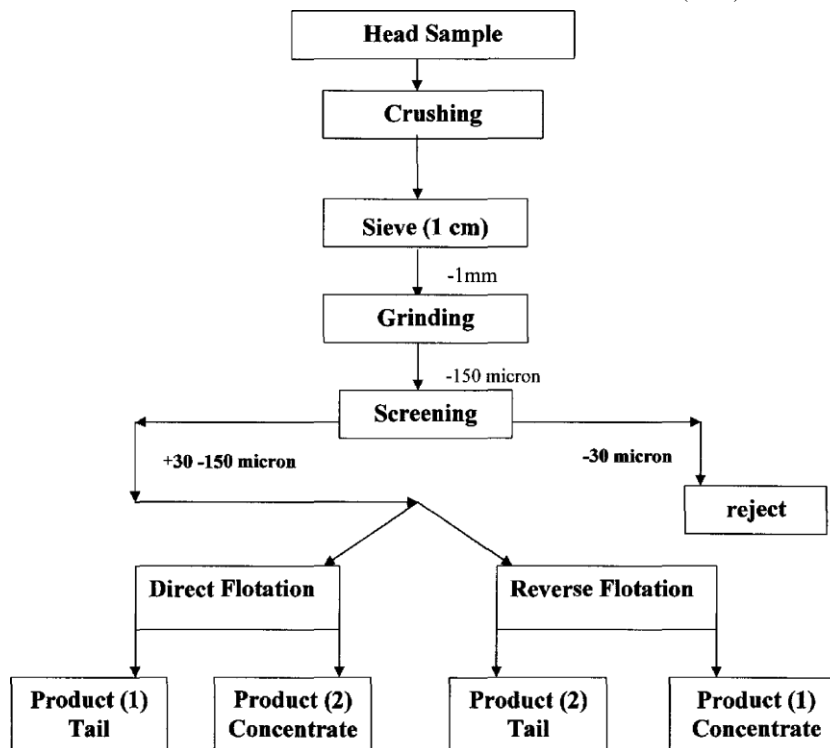
The results are satisfactory at these conditions and the test gives excellent separation and high recovery.

Test # 3: (Direct flotation)

Chemical reagents used were the same as in test #2 but the pH value was adjusted at 8 using NaOH to evaluate the effect of the pH value.

Product	wt.%	P ₂ O ₅ %	Recovery %
Conc.	40.17	20.66	82.98
Tail	53.18	1.20	6.38
Fine	6.65	16.00	10.64
Total	100	10.00	100

Fig. 3 Flow sheet for the froth flotation experiment



These results confirm the second test and show the importance of pH value where lowering the pH value from 9.5 to 8.0 led to the lowering of the recovery %.

Test # 4: (Direct flotation)

Chemical reagents used were: NaOH as pH regulator at pH=9.5, olic acid suspended in ethylene glycol (1:1) ratio, 2.5 kg/t, soda ash 200 g/t.

Product	wt.%	P ₂ O ₅ %	Recovery %
Conc.	33.42	22.00	73.54
Tail	59.98	2.65	15.90
Fine	6.60	16.00	10.56
Total	100	10.00	100

These results indicate that the increase of the amount of the collector led to the lowering of the recovery %.

Test # 5: (Reverse flotation) Chemical reagents used were:

- & NaOH as pH regulator at pH=8
- & Armac – C, 1 kg/t
- & Kerosene, 2 kg/t
- & Sodium and potassium tartrate

Product	wt.%	P ₂ O ₅ %	Recovery %
Conc.	42.10	11.92	50.74
Tail	51.35	7.40	38.50

Fine	6.64	16.00	10.76
Total	100	9.87	100

These conditions did not give a satisfactory recovery, and the test is not suitable for apatite separation. The above froth flotation tests indicate that the test #2 (Experiment #2) give the best recovery % (85.07%).

Magnetic separation

Magnetic separation experiments were conducted at different magnetic intensities: 500, 7000, 10,000, and 16,000 Gauss. LHEMS Corp. USA instrument was used for dry magnetic separation. BOXMAG RAPIDtype LI + WL England was used for wet magnetic separation. The samples were crushed, ground, and sieved; -63µm was used for wet magnetic separation, +40–200 and +63–200µm were used for dry magnetic separation.

First experiment, dry magnetic separation:

- Weight of the head sample: 1,000 g
- Grain size of the sample: -200µm
- Grain size of the sample to undergo dry magnetic separation (-200+40µm)
- Weight of the magnetite fraction: 322.3 g
- Weight of the ilmenite fraction: 190.3 g
- Weight of the middling: 36.4 g

Magnetic fractions

Weight of the apatite fraction: 169 g (Non magnetic) Weight of -40µm fraction: 282 g (slimes)

Material balance of dry magnetic separation:

Product	Grain size (µm)	Weight (g)	Weight (%)	P ₂ O ₅ (%)	Recovery %
Magnetic	-200+40	549	54.9	3.9	16.46
Nonmagnetic	-200+40	169	16.9	42.36	55.05
Slimes	-40	282	28.2	13.14	28.49
HS	-200	1,000	100	12.96	100

The flow sheet of the experiment is presented in Fig. 4. Second experiment, wet magnetic separation:

Weight of the head sample: 1,032 g

Grain size of the sample: -200µm

Grain size of the sample to undergo wet magnetic separation (-63µm)

Weight of the Magnetite fraction: 609.2 g Magnetic fractions

Weight of the Ilmenite fraction: 202.4 g

Weight of the Middling: 52.3 g

Weight of the Apatite fraction: 168.5 g (Nonmagnetic)

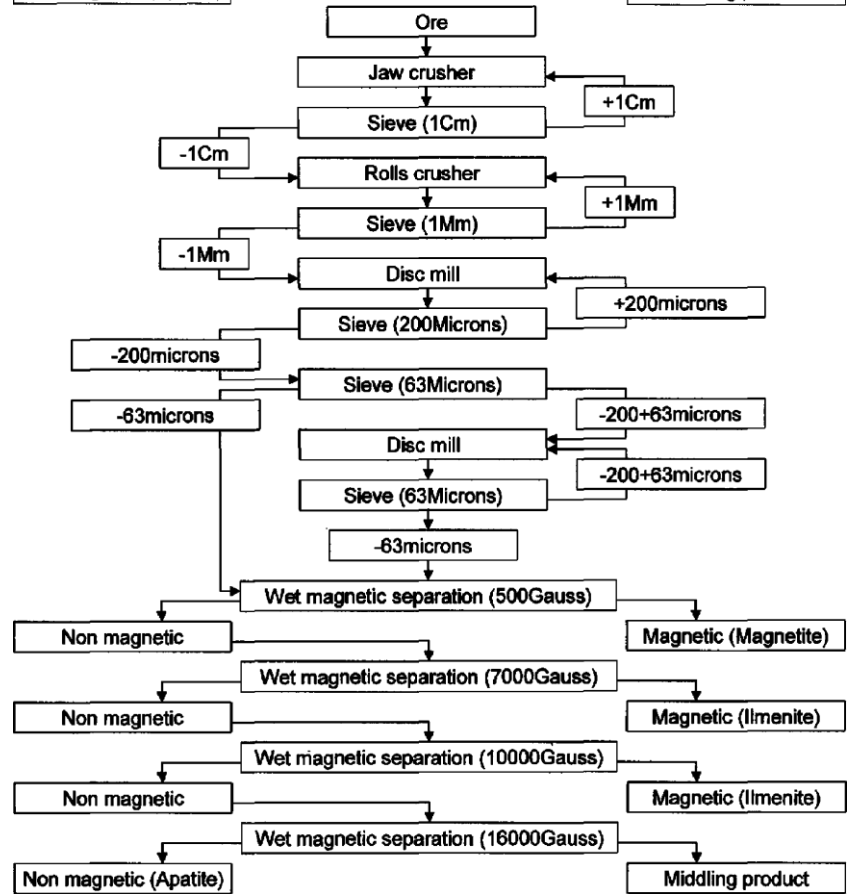
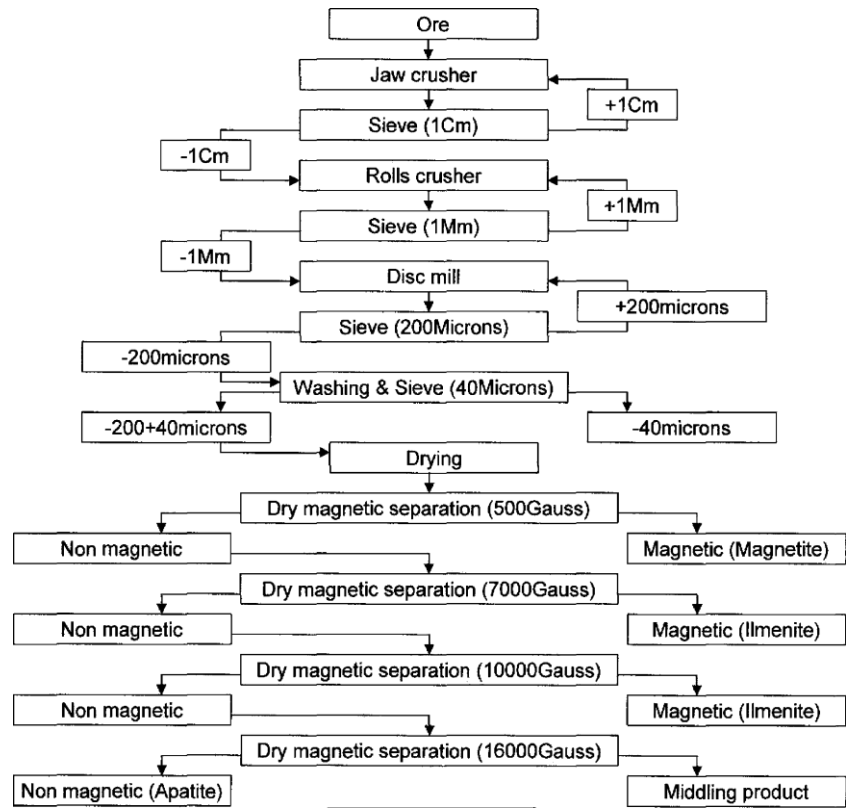
Material balance of wet magnetic separation:

Product	Grain size (µm)	Weight (g)	Weight (%)	P ₂ O ₅ %	Recovery %
Magnetic	-63	863.9	83.67	9.45	56.6
Nonmagnetic	-63	168.5	16.33	37.07	43.4
HS	-63	1,032	100	12.96	100

The flow sheet of the wet magnetic separation experiment is presented in Fig. 5.

Fig. 4 Flow sheet of dry magnetic separation experiment Fig. 5 Flow sheet of the wet magnetic separation experiment

Third experiment, dry, and wet magnetic separation:



Weight of the head sample: 2,100 g

Grain size of the sample: $-200\mu\text{m}$

Grain size of the sample to undergo dry magnetic separation ($-200+125\mu\text{m}$)

Weight of the magnetite fraction: 455.7 g

Weight of the ilmenite fraction: 241.9 g Magnetic

Weight of the middling: 138 g fractions

Weight of the apatite fraction: 254 g
(nonmagnetic)

Grain size of the sample to undergo dry magnetic separation ($-125+63\mu\text{m}$)

Weight of the magnetite fraction: 207.6 g Magnetic

Weight of the ilmenite fraction: 106.5 g fractions

Weight of the middling: 49.4 g

Weight of the apatite fraction: 126.1 g
(nonmagnetic)

Grain size of the sample to undergo wet magnetic separation ($-63\mu\text{m}$)

Weight of the magnetite fraction: 244.4 g Magnetic

Weight of the ilmenite fraction: 101.8 g fractions

Weight of the middling: 61.2 g

Weight of the apatite fraction: 113.4 g Nonmagnetic

Material balance of dry/wet magnetic separation:

Product	Grain size (μm)	Weight (g)	Weight (%)	P ₂ O ₅ (%)	Recovery %
Magnetic	$-200+63$	1,199.1	57.1	3.63	14.7
Nonmagnetic	$-200+63$	380.1	18.1	41.37	53.4
Magnetic	-63	407.4	19.4	12.92	17.9
Nonmagnetic	-63	113.4	5.4	36.41	14
HS	-200	2,100	100	12.96	100

The flow sheet of the dry and wet magnetic separation is presented in Fig. 6.

From the results of magnetic separation experiments, it appears that the dry and wet magnetic separation for the size range $+63-200$ and $-63\mu\text{m}$ gave the best recovery% (72.95%).

Separation efficiency

Concentrate grade and recovery are the most widely accepted measures of assessing separation performance.

4	83.58	26.90	56.68	40.17	20.66
5	74.04	21.00	53.04	33.42	22.00
Reverse flotation					
6	25.00	4.75	20.25	10.94	29.62
7	50.54	39.52	10.79	42.10	11.92

There have been many attempts to combine recovery and concentrate grade into a single index defining the efficiency of the separation process. Schulz (1970) reviewed these attempts and proposed the following definition:

Separation efficiency (S.E.)= $R_m - R_g$

Where $R_m = 100Cc/f$ $R_g = 100C(m-c)/(m-f)$

f assay of the feed (head sample) c
concentrate assay

C fraction of the total feed weight that reports to
conc. m percentage metal content of the valuable mineral.

In the present study, m is considered as P_2O_5 % of the mineral apatite which is equal to about 42.4%.

The values of R_m , R_g , and S.E. calculated for the different separation processes used in this study are listed in Table 1 along with the recovery %, concentrate weight %, and grade (P_2O_5 %).

The following conclusions can be extracted from the data in Table 1.

1. The inverse relationship between recovery and concentration grade.
2. The highest separation efficiency is achieved by the combined dry/wet separation (71.22%).
3. The wet magnetic separation is less efficient in separation because it needs more grinding.
4. The direct flotation (test #3) gives the second highest separation efficiency.
5. The reverse flotation is inefficient in separating apatite from magnetic and ilmenite.

Although the separation efficiency index can be useful in comparing the performance of different operating conditions on selectivity, it takes no account of economic factors. Since the purpose of mineral processing is to increase the economic value of the ore, the importance of recovery– grade relationship is in determining the most economic combination of recovery and grade which will increase the contained value of the ore. The latter depends

on the current price of the valuable products, costs of instruments, operation, and processing. The ore will be economic to work if: contained value/t > (total processing costs+other costs)/t

In order to decide whether the combined dry and wet magnetic separation or the direct flotation method is preferable, it is necessary to know the costs of the instruments, costs of operation, costs of processing (chemicals in case of flotation, price of the products, and byproducts (magnetite, ilmenite, apatite, REO)), and the costs of wet process to produce phosphoric acid.

Chemical studies

Apparatus

An inductively coupled plasma atomic emission spectrometry (ICP-AES) from Perkin–Elmer (USA) model Optima 4100DV was used for the determination of the rare earth elements in the tested aqueous solution under the optimum conditions given in Table 2. CEM microwave system (Mars model, 907500, USA) and digital pH meter (model MP220, Mettler Toledo) were used for sample digestion and pH measurements with absolute accuracy limits at the pH measurements being defined by NIST buffers, respectively. Reagents and materials

All chemicals and solvents used were of analytical reagent grade and were used without further purification. Doubly deionized water was used throughout. BDH stock solutions

(100 μ g mL⁻¹) of the investigated REEs La, Ce, Dy, Er, Eu, Ho, Lu, Pr, Sm, Tb, Tm, and Yb were used. The ICP-AES measurements of the elements La, Ce, Dy, Er, Eu, Ho, Lu, Pr, Sm, Tb, Tm, and Yb were carried out at the optimum wavelength of each element. Stock solutions (5.0% w/v) of each of the following compounds: sodium carbonate, sodium bicarbonate, sodium oxalate, and oxalic acid (BDH) was prepared in distilled water. All containers used were pre-cleaned by soaking in nitric acid (20% w/v) and rinsed with deionized water before use. Concentrated nitric acid

(HNO₃) and hydrogen peroxide (30% v/v; BDH) were used for the digestion of the phosphate samples. Low density polyethylene bottles, nalgene were used and were carefully cleaned first with hot detergent, soaked in 50% HCl (Analar), HNO₃ (2.0 mol L⁻¹), subsequently washed with dilute HCl (0.5 mol L⁻¹), and finally rinsed with water.

Recommended procedures

Digestion of the apatite sample in concentrated sulfuric acid: An accurate weight (0.77–5.01±0.01 g) of the apatite sample was transferred into a Pyrex conical flask (250 mL). To the solid sample, 20 mL of sulfuric acid (98%, w/v) were added to digest the sample. The reaction mixture was then boiled for 2–3 h at 100–120°C. After cooling, the precipitate was separated out by filtration through 0.45µm cellulose acetate membrane filter. The filtrate and the washing solution (5×5 mL hot water) of the precipitate were transferred to a volumetric flask (50.0 mL). The solution was completed to the mark with distilled water and finally analyzed using ICP-AES as described before (Table 2).

Moreover, an accurate weight (0.77–5.05±0.01 g) of the sample was mixed with 10.0 mL concentrated sulfuric acid (98%, w/v) in a Teflon digestion vessel (HP 500, maximum pressure=350 psi and temperature =100°C). The contents of the reaction vessel were then digested for 30 min. After cooling, the sample solution was then filtered after washing with water. The filtrate and the washing solutions were then transferred to the volumetric flask (50.0 mL), completed to the mark with water, and analyzed using ICP-AES. A blank experiment was digested and analyzed following the same digestion procedures.

Determination and extraction of the rare earth elements present in the phosphoric acid liquor: In this experiment, an accurate volume (50.0 mL) of the filtrate of another experiment was allowed to react with an approximate volume of oxalic acid (10.0 mL, 10% w/v) and boiling for 1 h. The solution was then concentrated to about 10 mL by solvent evaporation on a sand bath and filtered through 0.45µm cellulose acetate membrane filter. The produced oxalate precipitate was washed with hot water for three times and allowed to react with 20 ml of a mixture of sodium carbonate–sodium bi carbonate (10% w/v) with constant stirring and heating for half an hour. The produced precipitate was washed with hot water, filtered through

0.45µm cellulose acetate membrane filter and ignited in a muffle at 1,100°C for half an hour following the recommended procedures for the correct ignition. The produced residue was cooled and the percentage of the rare earth elements present as their oxides was then calculated after weighing.

Digestion of the gypsum precipitates (calcium sulfate) using concentrated HNO₃ and microwave digestion: An accurate weight (0.57–1.2±0.01 g) of the precipitate after drying was transferred into a conical flask (250 mL). To the solid sample, excess sodium carbonate was added followed by adding 20 mL of distilled water. The reaction mixture was heated for 1 h, and the produced precipitate was washed many times with hot water. The precipitate reaction mixture was then heated for 1 h at 100–120°C until dryness. Wash the produced precipitate with hot water, cool the solution, and filter through 0.45µm cellulose acetate membrane filter. Ignite the produced precipitate in a muffle at 1,100°C for half an hour. After cooling, the solid metal carbonate residue was then redissolved in dilute nitric acid (10.0 mL,

1.0 mol L⁻¹), transferred to a volumetric flask (50.0 mL), and the solution was completed to the mark with distilled water. The solution was then analyzed following the recommended experimental procedures for standard addition method described before (Table 2). A blank experiment was digested and analyzed following the same digestion and analytical procedures.

Digestion of the apatite sample in concentrated nitric acid: An accurate weight (0.77–5.01±0.01 g) of the apatite sample was transferred into a Pyrex digestion tube (250 mL). To the solid sample, 20 mL of nitric acid (65%, w/v) were added to digest the sample. The reaction mixture was then heated for 1 h at 100–120°C until dryness. After cooling, the solid residue was then redis-

solved in dilute nitric acid (10 mL, 1.0 mol L⁻¹), transferred to a volumetric flask (50.0 mL), and the solution was completed to the mark with distilled water. If the solid residue of the sample matrix not dissolved in dilute HNO₃, the digestion step was then repeated. The solution was then analyzed following the recommended experimental conditions for the standard addition method described before (Table 2).

Moreover, an accurate weight (0.77–5.01±0.01 g) of the sample was mixed with 8.0 mL concentrated HNO₃ (65% w/v) in Teflon digestion vessel (HP 500, maximum

pressure= 350 psi and temperature=210°C). The contents of the reaction vessel were then digested for 30 min. After cooling, the sample solution was then transferred to the volumetric flask (50.0 ml) and the solution was completed

Table 2 ICP-AES operational conditions for the measured elements

Parameter	
Rf power (kW)	1,050
Plasma gas (Ar) flow rate, L min ⁻¹	15
Auxiliary gas (Ar) flow rate, L min ⁻¹	0.2
Nebulizer gas (Ar) flow rate, L min ⁻¹	0.8
Pum rate, ml min ⁻¹	1.5
Observation height, mm	15
Integration time, s	10

dependent. The results revealed that heating the apatite ore with an excess of the sulfuric acid at 1:3 molar ratio for up to 8 h is sufficient for complete reaction. The results of the major elements concentration on the washing solution of gypsum with hot water determined by ICP-AEs showed the presence of low concentrations of most of the major elements. The data revealed the absence of tungsten, uranium, and thallium. An acceptable concentration of most major elements is present in the phosphoric liquor and also in gypsum as a side product. Gypsum has a great potentiality to adsorb the major and rare earth elements from the concentrated phosphoric acid liquor during leaching of the ore with concentrated sulfuric acid.

Distribution behavior of rare earth elements in apatite digested in concentrated nitric acid, phosphoric acid liquor, and gypsum digested with concentrated nitric acid

to the mark and analyzed as described above. A blank experiment was digested and analyzed following the same digestion and

analytical procedures.

Results and discussions

Major elements in the phosphoric acid liquor and the hot water washing solution of the produced gypsum from sulfuric acid leaching

Preliminary screening investigation on the local apatite ore involving its interaction with concentrated sulfuric acid revealed that the reaction is time- and temperature-dependent. The analysis of the total rare earth elements in apatite digest with concentrated nitric acid in microwave system is given in Table 3, column A. The distribution profiles (mg/kg) of the rare earth elements in the phosphoric acid liquor are summarized in Table 3, column B. An acceptable amount of rare earth elements are present in the phosphoric acid liquor and gypsum matrix (Table 3, column B). Approximately 36% of the rare earth elements is present in the gypsum, while in phosphoric acid liquor, the REEs constitutes about 65%.

Attempts to recover and/or separate the rare earth elements from phosphoric acid liquor were carried out as described in the experimental procedures after dissolution of the apatite with concentrated sulfuric acid and/ or sodium carbonate. The results revealed that, the total percent of the rare earth elements as their oxides in the phosphoric acid liquor varied between 1.1–1.2% (w/w). Attempts were also carried out to monitor the total rare earth metal after

dissolution of the apatite ore in concentrated nitric acid followed by gravimetric separation of the rare earth elements as their oxalates followed by their carbonate formation and subsequent an aerobic ignition revealed that 2.32% (w/w) of the rare earth metal oxides are present in concentrated nitric acid digest. The produced rare earth oxide cake contains traces of various metal oxide e.g. SrO, Na₂O, etc. in addition to rare earth oxides.

On comparison between the concentration of the REEs in the phosphoric acid liquor and gypsum leaching (Table 3, columns B, C) revealed that the partitioning of the rare earth

Magnetic and flotation techniques were used to get apatite concentrates from the nelsonite ore. It was found that the magnetic method led to the best recovery (72.95%) and the highest separation efficiency (71.22%). The apatite concentrate constitutes about 23.5% with 40.23% P₂O₅. The flotation method yielded an apatite concentrate which constitutes about 40.61% with 20.95% P₂O₅ at 85.68% recovery but with a less separation efficiency (58.85%). The constituents of the nelsonite ore could be concentrated by magnetic and froth flotation methods. The magnetic method ends up with concentrates of magnetite (43.3%), ilmenite

Table 3 Analysis of various rare earth elements (mg/kg) in apatite digested in concentrated nitric (A), phosphoric acid liquor (B), and in the digest of gypsum (C) in nitric acid with the aid of ICP-AES technique

Element	A	B	C
La	146.9	93.7	46.7
Ce	627.9	446	127.7
Pr	167.05	181	76.4
Sm	233.27	76.9	157
Eu	49.9	23.4	26.5
Tb	25.8	6.2	19.6
Dy	156.6	93.3	59
Ho	25.7	16.5	5.7
Er	104.2	57.2	47
Tm	6.2	1.9	4.6
Yb	42.7	34.6	1.96
Lu	8.9	6.3	5.4
Total	1,595.2	1,037 (65%)	572.0 (36%)

elements between the solid phase (gypsum) and the liquid phase (phosphoric acid) is most likely controlled by many contributing factors, e.g., ionic radii, ionic charge, and atomic weight. The results also revealed that, the percentage of the REEs in the phosphoric acid liquor is higher than that of gypsum digest. The data also revealed no significant differences between microwave and normal digestion of the apatite ore with nitric acid.

(21.4%), apatite (23.5%), and a waste (11.9%). Froth flotation ends up with an apatite concentrate (40.61%) and a mixture of magnetite and ilmenite (52.7%) and a waste fines (6.7%). The advantage of the magnetic separation is the production of a separate magnetite and ilmenite concentrates. It was found that about 4.3 t of the ore will produce 1.86 t of magnetite concentrate, 0.92 t from ilmenite concentrate, 0.51 t from middling (waste), and 1 t from apatite concentrate (40.23% P₂O₅). These results revealed that 1 t of the apatite concentrate will produce about 0.61 t

Conclusions

H₃PO₄ and about 1.28 t gypsum as a byproduct using 1.84 t concentrated sulfuric acid.

The apatite concentrate produced by the magnetic method was subjected to geochemical studies to determine the REEs after its dissolution in concentrated sulfuric acid.

The rare earth elements content of the apatite concentrate was found to be about 0.2%. The REEs content of the apatite concentrate was partitioned between the phosphoric acid liquor (65%) and the gypsum (36%) produced during the dissolution of apatite concentrate in concentrated sulfuric acid. The extraction of the REEs from the phosphoric acid liquor using oxalic acid and sodium carbonate–bicarbonate mixture (1:10w/w) yielded the RE oxide cake which constitute about 1.2% (w/w). The produced rare earth oxide cake contains traces of various metal oxide, e.g., SrO, Na₂O, etc. in addition to rare earth oxides.

The study provides a very useful set of data which will be helpful for conducting a pre-feasibility investigation to exploit the nelsonite ore components, namely, magnetite, ilmenite, and apatite. It is recommended to experiment the extraction of the rare earth elements from the phosphoric acid by liquid–liquid extraction or resins separation column separation techniques. Attempts to determine quantitatively the constituents of the REEs cakes will be considered in future work.

References

- Akl MA, Mori Y, Sawada K (2006) Solvent sublation and spectrometric determination of iron (II) and total iron using 3-(2-pyridyl)-5, 6-bis (4-phenylsulfonic acid)-1, 2, 4-triazine and tetrabutylammonium bromide. *Anal. Sci* 22:1169
- Al-Shafei AB (1998) National Resources and its Role in Industrial Development in Saudi Arabian Kingdom. El-Dar El Saudia for Consultancy Services, Riyadh (in Arabic)
- Bergstol S (1972) The Jacupirangite at Kodal, Vest fold, Norway. A potential magnetite, ilmenite and apatite ore: mineral. *Deposita (Berl.)* 7:233–246
- Chevremont P, Johan Z (1981) Wadi Khamal-Wadi Murattijah Ultramafic-Mafic layered complex. Saudi Arabian Deputy Ministry for Mineral Resources, Riyadh Open File Report BRGM-OF-01-36, 143 pp
- Chunhua Y, Jiangtao J, Chunsheng L, Sheng W, Guangxian X (2006) Rare earth separation in China, Tsinghua. *Sci Technol* 11:241
- Dymek RF, Owens BE (2001) Petrogenesis of apatite-rich rocks (Nelsonites and oxide-apatite gabbro-norites) associated with massif anorthosites. *Econ. Geol* 96:797–815
- Frietsch R (1973) The occurrence and composition of apatite with special references to iron ores and rocks in Northern Sweden. *Sveriges Geol. Undersokning, Ser. C* 624:32
- Frietsch R (1978) On the magmatic origin of iron ores of kiruna type. *Econ. Geo* 73:478–485
- Harbi HM, Hassanen MA, El-dougDoug AA, Al-Filali IY (2006) Economic Potentiality and Petrogenetic Evolution of the Maficultramafic Rocks in the Wadi Khamal Area, Northern Western Arabian Shield, Saudi Arabia. Final Report for Project No. (203/ 424). King Abdulaziz University, Institute of Research and Consultation, Jeddah, p 85
- Jiang N, Chu X, Mizuta T, Ishiyama D, Mi J (2004) A magnetic apatite deposit in the fanshan alkaline ultramafic complex, Northern China. *Econ. Geol.* 99:379–408
- Kanazawa Y, Kamitani M (2006) Rare earth materials and resources in the world. *J Alloys and Compounds* 408–412:1339–1343
- McCann AJ, Trzcienki W Jr, and Birkett TC (1998) The Soquem Septa-Iles Fe-Ti-P deposit (abs.), *Geol. Association of Canada: Mineralogical Association of Canada Program with Abstracts*, v. 23, p. A121
- McClelland J, Ashwal Z, Moore L (1994) Composition and petrogenesis of oxide-apatite rich gabbro-norite associated with Proterozoic anorthosites massifs: Examples from the Adirondack Mountains, New York. *Contrib Mineral Petrol* 116:225–238
- Mitchell JN, Scoates JS, Frost CD, Kolker A (1996) The geochemical evolution of anorthosite residual magmas in the laramie anorthosite complex, Wyoming. *J Petrol* 37:637–660
- Morbidelli L, Gomes CB, Beccaluva L, Brotzu P, Conte AM, Ruberti E, Traversa G (1995) Mineralogical, petrological and geochemical aspects of alkaline-carbonatite associations from Brazil. *Earth Science Reviews* 39:135–168
- Notholt AJG (1979) The economic geology and development of igneous phosphate deposits in Europe and the USSR. *Econ. Geol* 74:339–350
- Palabora Mining Company Limited Mine Geological and Mineralogical Staff (1976) The geology and the economic deposits of copper, iron, and vermiculite in the palabora igneous complex: a brief review. *Econ. Geol.* 71:177–192
- Philpotts AR (1967) Origin of certain iron-titanium oxide and apatite rocks. *Econ. Geol.* 62:303–315
- Puustinen K (1971) Geology of the Siilinjärvi carbonatite complex, Eastern Finland. *Comm. Geol. Finlande Bull* 249:3–43
- Ribeiro CC, Brod JA, Junqueira-Brod TC, Gaspar JC, Petrinovic IA (2005) Mineralogical and field aspects of magma fragmentation deposits in a carbonate-phosphate magma chamber: evidence from the catalao i complex, Brazil. *J. South American Earth Sciences* 18:355–369
- Ripley EM, Severson MJ, Hauck SA (1998) Evidence for sulfide and Fe-Ti-P rich liquid immiscibility in the Duluth Complex, Minnesota. *Econ. Geol* 93:1052–1062
- Schulz FF (1970) *Trans SME-AIME* 247:56
- Suvarthan K, Kumar KS, Rekha D, Jayaraj B, Naidu GK, Chiranjeevi P (2006) Preconcentration and solid-phase extraction of beryllium, lead, nickel and bismuth from various water samples using 2-propylpiperidine-1-carbodithioate with flame atomic absorption spectrometry. *Talanta* 68:735
- Valls, R.G., Hrdlicka, Perutka, J., Haval, J., Deorkar, N.V., Tavlarides, L.L., Munoz, M. and Valiente, M. (2001) Separation of rare earth elements by high performance liquid chromatography using a covalent modified silica gel column. *Anal Chem Acta* 439:247
- Vartiainen H (1975) Sampling in the assessment of the sokli phosphate ore. *Eripainos Vuoriteo-II isuus* 2:1–8



Thiazolidinone Steroids Impregnated Polyurethane Foams as a Solid Phase Extractant for the Extraction and Preconcentration of Cadmium(II) from Industrial Wastewater

MOHAMMAD S. TAWFIQ MAKKI*, R. MOHAMMADY ABDEL-RAHMAN,
K. OMMAR ALFOOTY and MOHAMMAD S. EL-SHAHAWI[§]

Department of Chemistry, Faculty of Science, King Abdulaziz University
P. O. Box 80203 Jeddah 21589, Kingdom of Saudi Arabia

[§]
Department of Chemistry
Faculty of Science at Damietta, Mansoura University, Mansoura, Egypt
mmakki@kau.edu.sa

Received 4 July 2010; Accepted 3 September 2010

Abstract: Two new thiazolidinone steroids namely sulfadiazino-imino- steroid (**I**) and 3-sulfonamoyl-phenyl-spiro[4-oxo-thiazolidin-2, 2']steroid (**II**) were prepared and characterized from their molecular weight determination and spectroscopic measurements. Compound **II** were physically immobilized onto polyurethane foams (PUFs) for the preconcentration of cadmium(II) from acidic aqueous media containing iodide ions. The kinetics of the retention step of cadmium(II) from aqueous solutions by compound **II** treated PUFs was studied. Particle diffusion was the most probable operating mechanism and did not control the kinetics of cadmium(II) retention by compound **II** immobilized PUFs. A preconcentration / separation procedure is presented for the solid phase extraction of trace cadmium(II) from aqueous media as its ternary complex ion associate with compound **II** in industrial wastewater samples onto compound **II** treated PUFs prior to determination by flame atomic absorption spectrometry (FAAS). Compound **II** treated PUFs sorbent was successfully packed in glass column for complete extraction and / or determination of trace concentrations of cadmium(II) in wastewater samples with satisfactory recovery (95 ±2.6). The cyclic voltammetry of compound **II** showed two well defined irreversible redox couples and suggested its possible use as complexing agent in stripping voltammetric determination of trace concentrations of toxic metal ions in wastewater.

Keywords: Cadmium(II), Thiazolidinone steroids, Removal, Determination, Polyurethane foam sorbent, Wastewater.

Introduction

Water pollution by cadmium species is of considerable concern, as this metal has found widespread use in various industries¹. The industrial effluents of many industries *e.g.* batteries, electroplating, leather tanning, nuclear power plant contain cadmium(II) at concentrations ranging from ten to hundreds of mg/L^{2,3}. It has been reported that, cadmium causes liver and lung cancer and kidney damage in humans and also it is toxic to other to other organism as well³.

Over the years, a variety of solid sorbent *e.g.* PUFs, cellulose, chromosorb-106 resin, Dowex 50 W-X4, *etc.* immobilized with various chelating agents have been developed and applied successfully for preconcentration and subsequent determination of trace and ultra trace concentrations of metal ions in water samples⁴. Thiazolidin -4-one derivatives have received considerable attention because their compounds have shown excellent biological and pharmacological activity as plant protection agents against bacteria and fungi^{5,6}. The basic properties of the thiazolidin -4-one derivatives increase in the orders: NH < S < =O. Thus, this class of compounds facilitates the formation of complexes with various toxic heavy metal ions even if they were present at trace and ultra trace concentrations of in wastewater^{6,7}.

Recent literature survey has revealed no use of the spiro-thiazolidinone reagents for separation and / or determination of trace concentrations of toxic metal ions in water and other complex matrices. Thus, in continuation to our previous work involving the use of PUFs sorbent⁸⁻¹⁴, the present article is focused on : i) synthesis of sulfadiazine-imino-steroid (**I**) and 3-sulfonamoylphenyl-spiro[4-oxo-thiazolidin-2,2' steroid (**II**); ii) studying the kinetics of the retention step of cadmium(II) from aqueous by the used solid PUFs sorbent in an attempt to develop low cost and effective preconcentration and / or determination method for trace and ultra trace concentrations of cadmium(II) in industrial wastewater samples using reagent physically treated PUFs in packed column and finally; iii) studying the voltammetric behavior of both steroids **I** and **II** (Figure.1) for suggesting cathodic stripping voltammetric procedures for determination of ultra trace concentrations of trace heavy metal ions in wastewater samples.

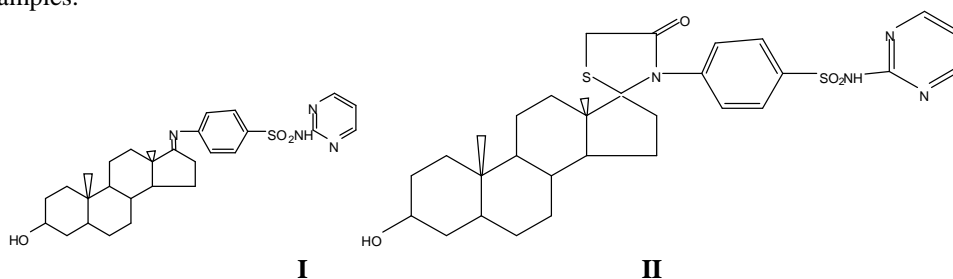


Figure 1. Chemical structures of sulfadiazine- imino- steroid (**I**) and spiro 4-thiazolidinone, 2-steroid (**II**)

Experimental

All chemicals used were of analytical reagent grade and were used without further purification. Most of the chemicals were provided by Merck (Darmstadt, Germany). Doubly de ionized water was used throughout the work. A.R grade sulfanilamide, tetraethyl ammonium tetra fluoroborate (TEAB), solvents and epiandrosterone (Fluka AG, USA) were used as received. The sample solution was stored in low density polyethylene (LDPE) bottles

and stored at $-20\text{ }^{\circ}\text{C}$ in a freezer. Stock solution (0.1% w/v) of the steroid compound **I** or **II** was prepared in ethanol. A stock solution of CdCl_2 (1 mg/mL) was prepared by dissolving an accurate weight (0.1630 ± 0.001 g) of the salt in doubly distilled water (100 mL).

Apparatus

A Perkin Elmer (Lambda EZ-210) double beam spectrophotometer (190-1100 nm) with 1 cm (path width) was used for recording the electronic spectra of the prepared solutions. A Perkins Elmer model RXI-FT-IR system 55529 was used for recording the IR spectra of the prepared compounds. A Bruker advance DPX 400 MHz model using TMS as an internal standard was used for recording the $^{10}\text{HNMR}$ spectra of the compounds on deuterated

DMSO. A GC- MS- QP 1000-Ex model was used for recording the mass spectra of the compounds. Mass spectra were recorded on Kartos (75 eV) M/S equipment. A Perkin-Elmer (Analyst TM 800, USA) atomic absorption spectrometer (AAS) was used for measuring the concentration of cadmium ions before and after extraction at 242 at the optimum operational parameters of the instrument. Deionized water was obtained from Milli-Q Plus system (Millipore, Bedford, MA, USA) was used for preparing all solutions. A pH meter (Orion EA940, MA, USA) was employed for the pH measurements with absolute accuracy limits at the pH measurements being defined by NIST buffers. An electrothermal Bibbly Stuart Scientific Melting Point SMPI (US) was used for recording the melting point. Molecular weights of the compounds were performed on Micro analytical center, Cairo University, Egypt. Digital pH-meter (model MP220, Metter Toledo) was used for pH measurements. A Metrohm 746 VA trace analyzer and 747 VA stand were used for recording the electrochemical experiments. A three-compartment borosilicate (Metrohm) voltammetric cell (10 mL) incorporating hanging mercury dropping electrode (HMDE, drop surface area 0.38 mm^2) as working, Ag/AgCl , (3M KCl), as a reference and Pt wire (BAS model MW-1032) as counter electrodes, respectively was used for recording the cyclic voltammetry of the tested compounds **I** and **II** in *N,N*-dimethylformamide solvent in the presence of TEAB.

Synthesis of sulfodiaziño-imino-steriod (**I**)

Compound **I** was prepared according to the following method. A mixture of sulfadiazine drug (0.01 mol) and the steroid epiandrosterone (0.01 mol) in DMF (50 mL) was refluxed for 2 h and the resultant reaction mixture was cooled, poured on an ice bath. The solid formed was filtered off, washed several times with methanol, re crystallized from tetrahydrofuran and dried *in vacuo* (yield 55%), m.p. $215\text{ }^{\circ}\text{C}$. Compound **I**, ($\text{C}_{29}\text{H}_{38}\text{N}_4\text{SO}_3$): molecular weight calculated 522, found 520; UV (DMF) λ_{max} (log ϵ): 305 nm (1.95); selected IR: ν 3520(OH), 3130 (NHSO_2), 2920, 2890, 2880 (stretching of CH_3 , CH_2 groups), 1640 ($\text{C}=\text{N}$), 1480, 1440 (deforming of CH_3 , CH_2 groups), 1350 (sulphonamido SO_2NH_2 group), 1255(exo C-N) and 810 cm^{-1} (p-substituted phenylz^{15,16}, $^1\text{H NMR}$ in d_6 -DMSO showed signals at δ : 0.8, 1.2, 3.5 (CH_3 of 18, 19 and 3 α -H of steroid), 2.8 (NH SO_2), 7.6 7.9 ppm (m, 4 H of aryl and of pyrimidine protons); M/S (m/z): 522 ($\text{M}^+ + 2$).

Synthesis of 3-sulfonamoylphenyl-spiro [4-oxo-thiazolidin-2, 2`steroid (**II**)

Compound **II** was prepared as follows: An accurate weight of the imino derivative (**I**), (0.01 mol) and thioglycolic acid (0.05 mol) in dry dioxan (100 mL) were refluxed for 8 h, left to cool and poured onto an ice- NaHCO_3 . The solid formed was washed several times with

¹⁰ HNMR in d_6 -DMSO showed signals at δ : 3.7 (2 H, S- CH_2), 0.8, 1.5, 3.5 (CH_3 of 18, 19 and 3 α -H of steroid), 3 (NH SO_2), 6.9 -7.9 ppm (m, 4 H, 3 H of pyrimidine and aryl protons); M/S (m/z): 593 ($\text{M}^+ + 2$).

methanol, re crystallized from tetrahydrofuran and dried *in vacuo* (yield 78 %), m.p. 185 °C to give **II**. Compound **II**, (C₃₁H₄₀N₄S₂O₄): molecular weight calculated = 596, found 593; UV (DMF) λ_{max} (log ε): 335 (0.5), 305 nm (1.5); selected spectroscopic data IR: ν 1660, 1330 (cyclic C=O NCS), 2950, 2880 (stretching of CH₃, CH₂ groups), 1200 cm⁻¹ (C-S)^{17,18};

Preparation of the compound II treated polyurethane foams

The compound **II** (1% w/v) in water was shaken with the PUFs cubes in the presence of the plasticizer TOA (1% v/v) with efficient stirring for 30 min. The loaded **II** PUFs cubes were squeezed and dried between two filter papers¹². The amount (a) of **II** retained onto the PUFs sorbent was calculated using the equation^{11, 12}:

$$a = (C_o - C) \frac{v}{w} \quad (1)$$

Where, C_o and C are the initial and final concentrations (mol L^{-1}) of the compound **II** in solution respectively, v = volume of the reagent solution (liter) and 'w' is the mass (g) of the PUFs sorbent.

Recommended batch extraction procedures

An accurate weight (0.1 ± 0.002 g) of the compound **II** immobilized PUFs was equilibrated with an aqueous solution (100 mL) containing cadmium ($5.0 \mu\text{g mL}^{-1}$) in the presence of KI (10% w/v), at various pH. The test solutions were shaken for 1 h on a mechanical shaker and the aqueous phases were then separated out by decantation. The amount of cadmium(II) remained in the aqueous phase was then determined by FAAS. The amount of cadmium(II) retained on the foam cubes was then calculated from the difference between the concentration of cadmium(II) in the test aqueous solutions before (C_b) and after extraction (C_f). The sorption percentage (%E), the amount of cadmium(II) retained at equilibrium (q_e) per unit mass of solid sorbent (mol/g) and the distribution coefficient (K_d) of sorbed analyte onto the foam cubes were finally calculated as reported. The %E and K_d are the average of three independent measurements and the precision in most cases was $\pm 2\%$. Following these procedures, the influence of shaking time and reagent concentration treated PUFs on the retention step of cadmium(II) by the tested PUFs sorbents was studied.

Recommended chromatographic separation

An aqueous solution (100 mL) containing cadmium(II) ions at concentration ($5, 10 \mu\text{g mL}^{-1}$), KI (10%) and H_2SO_4 (0.01 mol L^{-1}) was percolated through the $\text{PQ}^+ \text{Cl}^-$ loaded PUFs (1.0 ± 0.01 g) packed column at 5.0 mL min^{-1} flow rate. A blank experiment was also performed in the absence of cadmium(II) ions. Cadmium(II) sorption took place quantitatively as indicated from the analysis of cadmium species in the effluent solutions by FAAS. Cadmium(II) was quantitatively recovered with HNO_3 (25 mL, 1.0 mol L^{-1} , 10 mL) at 5.0 mL min^{-1} flow rate.

Results and Discussion*Spectroscopic characterization of compounds I and II*

Spiro-thiazolidinones have been reported to possess considerable pharmaceutical potentialities¹⁶⁻²⁰. Therefore, the present article is focused on the synthesis of two new compounds **I** & **II** derived from sulfadiazine drug for their use as suitable complexing agents for stripping voltammetric determination and separation of toxic metal ions in wastewater samples. Condensation of the sulfadiazine drug with ketonic steroid epiandrosterone in boiling DMF^{17,18} yielded **I**, which upon cycloaddition reactions with thioglycolic acid in dry dioxan¹⁷⁻¹⁹ led to the direct formation of **II**. The structure of obtained compounds was established from their molecular weight determination and spectroscopic data

Retention profile of cadmium(II) onto compound immobilized PUFs

Preliminary batch experiments employing the compounds **I** and **II** immobilized polyurethane foams (PUFs) for the uptake of trace concentrations of cadmium(II) ions from the aqueous solutions containing excess of KI (5% w/v) - H₂SO₄ (.0.01 M) revealed considerable retention of cadmium(II) by the latter reagent. Thus, the preconcentration of cadmium(II) ions from the aqueous KI - H₂SO₄ solutions onto the compound **II** immobilized PUFs as solid sorbent was critically investigated. The results revealed the dependence of cadmium(II) uptake from the test aqueous solution depends on the solution pH. Thus, the effect of the aqueous solution containing excess of KI (5% m/v) at different pH (pH 3-10) on the retention of cadmium(II) ions at reasonable concentration (5.0 µg mL⁻¹) by the immobilized PUFs was investigated. After shaking the test solutions of one hour, the amount of cadmium(II) remained in the aqueous solution was determined by flame atomic absorption spectrometry (FAAS). The results indicated that, the uptake of cadmium(II) onto the loaded PUFs decreased on raising the solution pH and maximum sorption percentage was achieved at pH ~ 3 (Figure 2). The retention of cadmium(II) by the immobilized compound **II** treated PUFs at pH ~ 3 is most likely attributed to the formation of the anionic complex species [CdI₄]⁻² in the aqueous phase and subsequent formation of ternary ion associate [(II⁺)₂.(CdI₄)⁻²] involving the steroid compound(II) and the anion [CdI₄]⁻² on / in the PUFs membrane. The protonation of the available binding sites in the PUFs *i.e.* ether and / or urethane linkages may also participate in the formation of an ion associate with the anion [CdI₄]⁻² at the solution of pH 3. The formation of the anion [CdI₄]⁻² and the protonation of the sorbent sites enhanced the retention of the ion associate [(II⁺)₂.(CdI₄)⁻²] on/ in the solid PUFs *via* a "solvent extraction" and /or weak base anion exchange mechanism". Similar trend has been reported for the retention of some anionic complex species of cadmium(II) by methyl isobutyl ketone and some other solvents that posses ether linkages in their structures *e.g.* diethyl ether, isopropyl ether and polyurethane ether -type foams^{20,21}.

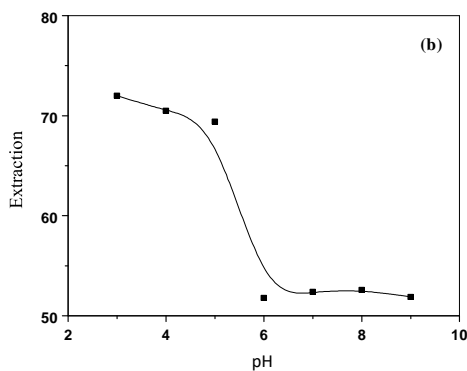


Figure 2. Effect of pH on the sorption profile of cadmium(II) from aqueous KI media (1% m/v) onto compound **II** treated PUFs after 1 h shaking time at room temperature.

The influence of the compound(II) concentration (0.01-0.05% w/v) immobilized PUFs on the extraction of cadmium(II) at pH 3 and shaken for 1 h showed a significance pre-concentration of cadmium(II) from aqueous media. Maximum cadmium(II) uptake was achieved at 0.02% (w/v) reagent immobilized PUFs cubes. The amount of the reagent immobilized is good enough to retain considerable concentration from the test aqueous solution. Therefore, on the subsequent work, the reagent loaded foams were adjusted at concentration of 0.01% (w/v).

Kinetics of cadmium(II) retention onto the compound II loaded PUFs

The sorption of cadmium(II) ions onto the steroid **II** immobilized PUFs sorbents was found to depend on shaking time and cadmium(II) uptake was fast and reached equilibrium at 20 min shaking time. This conclusion was supported by the values of the half-life time ($t_{1/2}$ ($t_{1/2} = 2$ min) of cadmium(II) sorption by the reagent immobilized PUFs (Figure 3). Thus, gel diffusion is not only the rate-controlling step for both sorbents as in the case of common ion exchange resins²⁰⁻²². Therefore, the kinetic behavior of cadmium(II) sorption onto the immobilized PUFs sorbents depends on film diffusion and intra particle diffusion and the more rapid one will control the overall rate of transport. The retention of cadmium(II) species onto the used immobilized reagent PUFs was subjected to Weber - Morris model²² as follow: $q_t = R_d (t)^{1/2}$ (2)

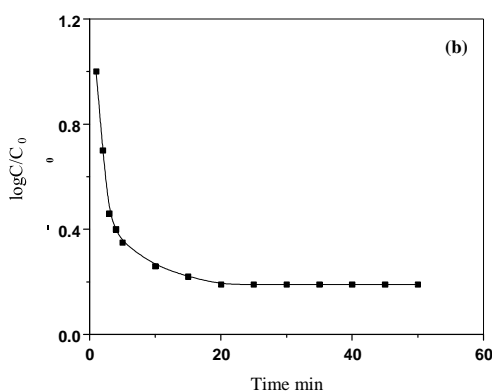


Figure 3. Rate of sorption of cadmium(II) onto reagent immobilized foams at 20 ± 0.1 °C.

Where, R_d is the rate constant of intra-particle transport in $\text{mmol g}^{-1} \text{min}^{-1/2}$ and q_t is the sorbed cadmium(II) concentration (mol.g^{-1}) at time t . The plots of q_t versus time were found linear with correlation coefficient in the range of $R^2=0.975-0.980$ in the initial stage of shaking time (up to 4-5 min) for cadmium(II) retention onto the reagent immobilized PUFs sorbents and deviate on increasing the shaking time. In the initial stage, the diffusion rate was high and decreased on passage of time indicating that the rate of the retention step is film diffusion at the early stage of extraction^{23,24}. The values of R_d were found equal $0.67 \text{ mol.g}^{-1}.\text{min}^{-1/2}$ for reagent immobilized PUFs in the initial stage up to 4.0 min of agitation time, respectively. Beyond 4-5 min shaking time, the values of R_d for immobilized PUFs towards retention of cadmium(II) from the aqueous solution reduced to $0.23 \text{ g}^{-1}.\text{min}^{-1/2}$, respectively. The change in the slope for the reagent immobilized polyurethane foams is most likely due to the existence of different pore sizes^{23,24} on the used solid sorbents and confirm that, the intra-particle diffusion step can be a rate controlling step.

The sorption of cadmium(II) onto the reagent loaded foams was also subjected to Lagergren kinetic model over the entire range of agitation time. The Lagergren model can be expressed by the following equation²⁵:

$$\log (q_e - q_t) = \log q_e - (kt/2.303) \quad (3)$$

Where, q_e represents the sorbed concentration of cadmium(II) onto the PUFs sorbent at equilibrium (mol.g^{-1}) and k is the over all first order rate constant. The plots of $\log (q_e - q_t)$ versus time up to 30 min were found linear. The values of the k calculated from the slopes of linear plot given was found equal 0.22 ± 0.0001 . These data confirm that, particle diffusion is

the most probable operating mechanism and does not control the kinetics of cadmium(II) sorption onto the immobilized foams. Thus, the retention of cadmium(II) onto PUF cubes involves three steps: i) bulk transport of cadmium(II) in solution; ii) film transfer involving diffusion of cadmium(II) species within the pore volume of PUF and/or along the pore wall surface to an active sorption site^{23,24} and finally; iii) formation of the ternary complex ion associate of the formula $[-CH_2-^+OH-CH_2] \cdot [CdI_4]^{-2}_{foam}$ and $[-CH_2-^+OH-CH_2] [CdI_4^{-2}R^+]_{foam}$ where R^+ = reagent. Therefore, the actual sorption of $[CdI_4^{-2}]$ onto the interior surface is rapid and hence it is not the rate determining step in the sorption process. Thus, one may conclude that, film and intra-particle transport might be the two main steps controlling the sorption step. Thus, "solvent extraction" or a "weak base anion ion exchanger" mechanism is not only the most probable participating mechanisms and most likely, some other processes like specific sites on the PUFs are possibly involved simultaneously in the cadmium retention from the bulk aqueous solution on the solid sorbent.

Analytical application

The validation of the compound **II** immobilized PUFs solid sorbent was successful assessed by using the compound **II** immobilized PUFs in packed column for collection of various concentrations (100 mL, 30-100 μgL^{-1}) of cadmium(II) in de ionized water. The sample solutions were percolated through the PUFs packed column at 5-10 mL min^{-1} flow rate. Complete retention of cadmium was achieved onto PUFs packed column as indicated from the absence of cadmium in the effluent by FAAS.

The retention of cadmium(II) from industrial wastewater was also carried out following the same procedures. The water samples of industrial wastewater (0.5 L) of electroplating industry after acidified with phosphoric acid was spiked with various concentrations (5, 10 $\mu\text{g mL}^{-1}$) of cadmium(II), acidified with phosphoric acid and filtered through a 0.45 μm cellulose membrane filter. The test water samples were percolated through the reagent packed column at 5 mL min^{-1} flow rate. The analysis of cadmium in the effluent solution by FAAS revealed complete retention of cadmium from the test solution. The results are summarized in Table 1. Cadmium was quantitatively recovered with nitric acid (25 mL, 1.0 M) and analyzed by FAAS. A satisfactory recovery percentage of total cadmium was achieved in the range 95.0 \pm 2.6.

Table 1. Analytical results for the preconcentration and recovery of cadmium(II) in wastewater samples by the compound **II** immobilized PUFs packed column

Cadmium(II) species		Recovery, %*
Added, $\mu\text{g/mL}$	Found, $\mu\text{g/L}$	
5.0	4.8	96.0 \pm 1.8
10.0	9.4	94.0 \pm 2.7

*Average \pm relative standard deviation Voltammetric

behavior of the tested compounds **I** and **II**

Cyclic voltammograms (CVs) of the two steroids **I** and **II** in DMF- TEAB at the hanging mercury drop electrode (HMDE) versus Ag/AgCl reference electrode at various scan rates were critically carried out. Representative CVs of **II** are shown in Figure 2. The CV of **II** (Figure 4) at various scan rates showed one well defined reduction wave in the range -0.32 – (-0.35) (Peak I) and two ill defined reduction peaks in the range -0.55- (-0.57) and -0.64 – 68

versus Ag/AgCl. On the reverse scan, no anodic peaks were observed suggesting irreversible nature of the electrochemical processes²⁷.

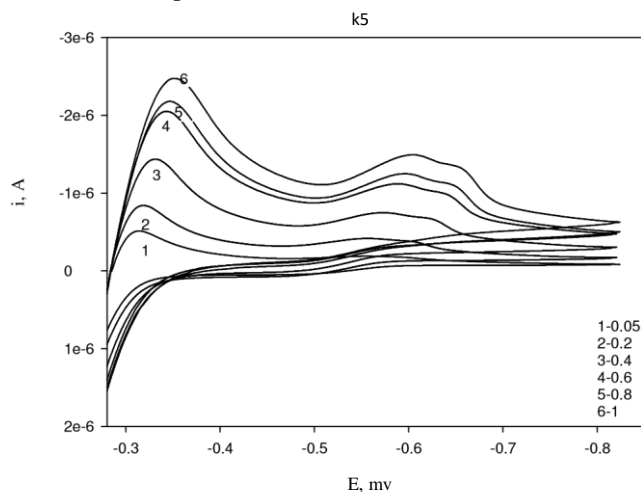


Figure 4. CVs of **II** in DMF-THAC at HMDE versus Ag/AgCl electrode at various scan rate.

The same observation was also confirmed from the progressive cathodic shift on increasing the scan rate confirming the irreversible nature of the reduction processes of the compound. The plot of the square root of the scan rate versus the corresponding cathodic peak current, $i_{p,c}$ of peak I increased linearly on increasing the scan rate, indicating that the electrochemical reduction process is a diffusion process. The CV of the steroid **I** in the potential range 0.0–(-1.0) V revealed one well-defined cathodic peak (peak I) in the potential range -0.34 – (-0.37) and another ill defined cathodic peak at -0.44–(-0.48) V versus Ag/AgCl electrode, while no anodic peaks were observed on the reverse scan, confirming also the irreversible nature of the two electrochemical reduction processes of the compound **I**. Continuous scan of the CV of compound **I** significantly decreased the peak current height and the signal is hardly discernible from the baseline, indicating passivity of the surface of the HMDE electrode via formation of polymeric oxidation product or fouling of the HMDE electrode by the reduction products²⁶. The overall results suggest the possible use of the **II** as complexing agent in cathodic stripping voltammetry for determination of cadmium(II) ions(II) in water.

Conclusion

The use of **II** for the minimization and separation of trace and ultra trace metal ions in drinking and wastewater samples represents a great challenge in recent years. The voltammetric behavior of the two compounds **I** and **II** suggested the use of the compound **II** as chelating agent for differential pulse - cathodic stripping voltammetry for the determination and chemical speciation of ultra trace concentrations of heavy metal ions. Thus, work is continuing for preparing a chemically modified glassy carbon electrode with the compound **II** to be used in stripping voltammetric mode for the determination and chemical speciation of trace metal ions in *e.g.* cadmium(II), arsenic(III), antimony(III) and bismuth(III) *etc.* in water as reported²⁷.

Acknowledgment

The authors would like to thank the Deanship of Scientific Research, King Abdul-Aziz University, Saudi Arabia for the financial support and funding under the grant number 9/11.

References

1. Forstner U and Wittman G T W, *Metals Pollution in the Aquatic Environment*, Springer-Verlag, Berlin, Heidelberg, Germany, 1981.
2. Mertz W, Ed., *Trace Elements in Human and Animal Nutrition*, Academic Press, London, 1986.
3. Merian E, "Metals and Their Compounds in The Environment, Occurrence, Analysis and Biological References" VCH, 1980.
4. Pohl P and Prusisz B, *Anal Chim Acta*, 2004, **502**, 83 and references cited therein.
5. Abdel-Rahman R M, *Bull Chimico Farmaceutico*, 2001, **140**, 410.
6. Zaki M T, Abdel-Rahman R M and El-Sayed A Y; *Anal Chim Acta.*, 1995, **307**, 127-138.
7. Kozlowski C A, Ulewicz M, Walkowiak W, Girek, T and Jablonska J, *Min Eng.*, 2002, **15**, 677-682.
8. El-Shahawi M S and Almehti M A, *J Chromatogr A*, 1995, **697(1-2)**, 185-190.
9. El-Shahawi M S and Nassif H A, *Anal Chim Acta*, 2003, **481**, 29-39.
10. El-Shahawi M S, Abou-Mesalam M M, Abdel-Hai M S and El-Naggar I M, *J Radioanal Nucl Chem.*, 2003, **258**, 619-625.
11. El-Shahawi M S, Othman M A and Abdel-Fadeel M A, *Anal Chim Acta*, 2005, **546**, 221-228.
12. Farag A B, Soliman M H, Abdel-Rasouland O S and El-Shahawi M S, *Anal Chim Acta*, 2007, **601**, 218.
13. El-Shahawi M S, Hassan S S M, Othman M A and El-Sonbati M A, *Microchem J* 2008, **89**, 13.
14. Bashammakh A S, Bahaffi S O, Al-Shareef F M and El-Shahawi M S, *Anal Sci Jpn.*, 2009, **25**, 413-418.
15. Mukherjee K S and Mukhopadhyay B, *J Indian Chem Soc.*, 2005, **82**, 936-937.
16. Duddeck H, Elgamal, M H A, Ricca G S, Danielli B and Palmisano G, *Org Magn Resonance*, 1978, **11**, 130-139.
17. Shafiullah S, Siddiqui I H, Ansari S A, Khan E H and Shafi S, *J Indian Chem Soc.*, 2000, **77**, 215.
18. Abdel-Monem W R, *Bull Chimico Farmaceutico*, 2004, **143(10)**, 239-247.
19. Talapatra S K, Polley M and Talapatra B, *J Indian Chem Soc.*, 1994, **71**, 527-532.
20. El-Shahawi M S, Othman A M, Bashammakh A S and El-Sonbati M A *Int J Environ Anal Chem.*, 2006, **86(12)**, 941.
21. Nambiar C H R, Narayana B, Rao B M, Mathew R and Ramachandra B, *Microchem J.*, 1996, **53**, 175.
22. Weber W J and Morris J C, *J Sanit Eng Div Am Soc Civ Eng.*, SA2, 1963, **89**, 31-60
23. Weber Jr W J and Morris J C, *J Sanit Eng Div Am Soc Civ Eng.*, SA3, 1964, **90**, 70.
24. Mukherjee K S and Mukhopadhyay B, *J Indian Chem Soc.*, 2005, **82**, 936-937.

25. Lagergren S and Sven B K, *Vatenskapsakad Handl*, 1898, 24.
26. Bard A J and Faulkner L R, *Electrochemical Methods, Fundamentals and Applications* Wiley, New York, 1980, 218-227.
27. Kadi M W and El-Shahawi M S, *Radiochimica Acta*, 2009, **97(11)**, 613-620.

Provided for non-commercial research and education use.
Not for reproduction, distribution or commercial use.



This article appeared in a journal published by Elsevier. The attached copy is furnished to the author for internal non-commercial research and education use, including for instruction at the authors institution and sharing with colleagues.

Other uses, including reproduction and distribution, or selling or licensing copies, or posting to personal, institutional or third party websites are prohibited.

In most cases authors are permitted to post their version of the article (e.g. in Word or Tex form) to their personal website or institutional repository. Authors requiring further information regarding Elsevier's archiving and manuscript policies are encouraged to visit: <http://www.elsevier.com/copyright>



Contents lists available at ScienceDirect

Talanta

journal homepage: www.elsevier.com/locate/talanta

Spectrofluorometric determination and chemical speciation of trace concentrations of chromium (III & VI) species in water using the ion pairing reagent tetraphenylphosphonium bromide

M.S. El-Shahawi^{a,*}, H.M. Al-Saidi^b, A.S. Bashammakh^c, A.A. Al-Sibaai^a, M.A. Abdelfadeel^a

^aDepartment of Chemistry, Faculty of Science, King Abdulaziz University, P.O. Box 80203, Jeddah 21589, Saudi Arabia ^bDepartment of Chemistry, University College, Umm Al-Qura University, Makkah, Saudi Arabia ^cThe Centre of Excellence in Environmental Studies, King Abdulaziz University, P.O. Box 80203, Jeddah 21589, Saudi Arabia

article

info

abstract

Article history:

Received 28 September 2010
Received in revised form
20 December 2010
Accepted 22 December 2010
Available online 8 January 2011

Keywords:

Spectrofluorimetry
Chromium speciation
Certified reference material (IAEA Soil-7)
Tetraphenylphosphonium bromide
Wastewater

A highly selective, and low cost extractive spectrofluorometric method has been developed for determination of trace concentrations of chromium (III & VI) in water samples using the fluorescent reagent tetraphenylphosphonium bromide (TPP⁺Br⁻). The method was based upon solvent extraction of the produced ion associate [TPP⁺CrO₃Cl⁻] of TPP⁺Br⁻ and halochromate in aqueous HCl and measuring the fluorescence quenching of TPP⁺Br⁻ in chloroform at $\lambda_{em} = 242/305\text{nm}$. The fluorescence intensity of TPP⁺Br⁻ decreased linearly on increasing the chromium (VI) concentration in the range of 1–114 gL⁻¹. The limits of detection (LOD) and quantification (LOQ) of chromium (VI) were 0.43 and 1.42 gL⁻¹, respectively. Chromium (III) species after oxidation to chromium (VI) with H₂O₂ in alkaline solution were also determined. Chemical speciation of chromium (III & VI) species at trace levels was achieved. The method was applied for analysis of chromium in certified reference material (IAEA Soil-7) and in tap- and wastewater samples and compared successfully (>95%) with the inductively coupled plasma-mass spectrometry (ICP-MS) results.

* Corresponding author. Permanent address: Department of Chemistry, Faculty of Science at Damietta Mansoura University, Mansoura, Egypt.

Tel.: +966 2 6952000x64422; fax: +966 2 6952292.

E-mail address: mohammad-el-shahawi@yahoo.co.uk (M.S. El-Shahawi).

0039-9140/\$ – see front matter © 2011 Elsevier B.V. All rights reserved.
doi:10.1016/j.talanta.2010.12.039

1. Introduction

Chromium occurs in the environment in two major valence states (III, VI).

Due to its wide use in electroplating, leather tanning, metal finishing, nuclear power plant, textile industries, and chromate preparation, chromium (VI) exists in air, soil, and aquatic systems [1]. It can also enter the drinking water distribution system from the corrosion inhibitors used in the water pipes [2]. Although the trivalent form is an essential nutrient, its disposal as liquid effluents in natural waters or as sludge in soils has to be avoided or controlled, because it may be oxidized, especially in soils, to the hexavalent form, which is highly toxic, carcinogenic and mutagenic in nature [3]. The ability of chromium (VI) to react with other elements and its high solubility in soil and aquatic systems makes it more toxic than other heavy metal ions [4,5]. Thus, total chromium measurement cannot be used to determine the actual environmental impact and chromium (III, VI) speciation in the environmental

samples is necessary to assess precisely the pollution levels [5].

The presence of chromium (VI) in the environment has resulted in the development of numerous analytical techniques for its preconcentration by solid phase extraction [6,7] and subsequent determination in different sample matrices. The most common analytical techniques for chromium determination are flow injection analysis [8], inductively coupled plasma mass spectrometry (ICPMS) [9], graphite furnace atomic absorption spectrometry (GFAAS) [10] and adsorptive stripping voltammetry [11]. The main disadvantages of these techniques are the complexity and the high cost of the

© 2011 Elsevier B.V. All rights reserved.

instruments, and the need of some degree of expertise for their proper operation. Therefore, the development of low cost method, easy to operate, highly sensitive and reliable for routine analysis e.g. spectrofluorimetry or spectrophotometry is still of great concern. The former technique is better than the later due to its high sensitivity and selectivity.

Recently, the complex ion associate of the halochromate (CrO_3Cl^-) and the ion pairing reagent tetraphenylphosphonium bromide (TPP^+Br^-) in chloroform has been used for the development of a simple and accurate extractive spectrophotometric procedure for speciation of chromium (III, VI) species in water [5]. Recent literature revealed no study on the use of the fluo-

176
Table 1
ICP-MS operational conditions for chromium determination.

M.S. El-Shahawi et al. / Talanta 84 (2011) 175–179

Parameter	
ICP RF power (W)	1100
Nebulizer gas flow (Lmin^{-1})	0.94
Plasma gas (Ar) flow rate (Lmin^{-1})	15
Auxiliary gas (Ar) flow rate (Lmin^{-1})	1.2
Lens voltage (V)	0.9
Analog stage voltage (V)	-17% 800
Pulse stage voltage	
Quadrupole rod offset std	0
Discriminat or threshold	22
Cell path voltage std (V)	-13
Cell rod offset (V)	-18 52.9 μ
Atomic mass (am)	
Sample flow rate, mL	93

rescent reagent TPP^+Br^- for spectrofluorometric determination of chromium (VI). Therefore, the present article reports the use of the produced non fluorescent ion associate [$\text{TPP}^+\text{CrO}_3\text{Cl}^-$] of TPP^+Br^- and chromium (VI) for developing a simple, convenient, and low cost spectrofluorometric method for determination and speciation of chromium (III, VI) species in water. 2. Experimental

2.1. Reagents and materials

All chemicals and solvents used were of analytical reagent grade and were used without further purification. Stock solutions (1000g mL^{-1}) of Cr (VI), Cr(III), As (V), MnO_4^- , NO_2^- , ClO_3^- , BrO_3^- , IO_3^- and H_2O_2 were prepared from the BDH chemicals (Poole, England) K_2CrO_4 , $\text{Cr}(\text{NO}_3)_3$, NaAsO_3 , KMnO_4 , NaNO_2 , KClO_3 , KBrO_3 , KIO_3 and H_2O_2 , (30%, w/v) in water (100.0mL), respectively. Solutions of other metal ions were prepared from their nitrate or chloride salts in deionized water. A stock solution (0.1%, w/v) of the reagent TPP^+Br^- (Merk, Darmstadt, Germany) was prepared by dissolving the required weight in ethanol (3.0mL) and the solution was completed to the mark with water.

2.2. Apparatus

All fluorescent measurements were recorded on a PerkinElmer (Norwalk, CT, USA) LS 55 spectrofluorimeter, equipped with a xenon lamp and a 10mm quartz cell. The UV-visible (190–1100nm) spectra were recorded on a Perkin-Elmer (model Lambda 25, USA) spectrophotometer with 10mm (path width) quartz cell.

A digital micropipette (Volac) and an Orion pH meter (model EA 940) were used for the preparation of more diluted chromium (VI) solutions and pH measurements, respectively. Deionized water was obtained from Milli-Q Plus system (Millipore, Bedford, MA, USA) and was used for preparation of solutions. A Perkin Elmer inductively coupled plasma–mass spectrometer (ICP–MS) Sciex model Elan DRC II (California, CT, USA) was used as a reference method for chromium determination at the optimum operational parameters (Table 1).

2.3. Recommended procedure

2.3.1. Recommended procedures for chromium (VI) determination

An appropriate concentration ($1\text{--}114\text{g L}^{-1}$) of chromium (VI) in aqueous HCl (0.5mol L^{-1}) solution was transferred to a separating funnel (50.0mL) containing the reagent TPP^+Br^- (2.0mL). The test solution was completed to the mark with deionized water (25mL) and the reaction mixture was shaken twice with chloroform ($2\times 2\text{mL}$) for 3min. After separation of the layers, the organic phase was subjected to the fluorescence measurement at the excitation and emission wavelengths of 242 and 305nm, respectively against reagent blank. The quenched fluorescence intensity of the reagent TPP^+Br^- by chromium (VI) added was represented by the equation:

$$I(\%) = \frac{I_0 - I_x}{I_0} \times 100 \quad (1)$$

where I_0 and I_f are the fluorescence intensities of the TPP^+Br^- reagent before and after addition of chromium (VI), respectively. A blank experiment was also carried out under the same experimental conditions.

2.3.2. Recommended procedure for chromium (III) determination

Aqueous solution (100.0mL) containing chromium (III) ions at concentration in the range $0.05\text{--}100\text{g L}^{-1}$ was transferred to a conical flask (250mL). The solution was oxidized to chromium (VI) in alkaline medium (KOH , 1.0mol L^{-1}) containing H_2O_2 (2mL , 10% w/v) [5] and boiling for 10min. After cooling, the test solution was adjusted to the required acidity with HCl (0.5mol L^{-1}) and finally analyzed following the recommended procedures for chromium (VI) determination against the reagent blank under the same experimental conditions.

2.3.3. Chemical speciation of inorganic chromium (III) & (VI)

Aqueous solution (0.5L) containing the binary mixture of chromium (III) & (VI) species at a total concentration of chromium species $\leq 100\text{g L}^{-1}$ was analyzed following the recommended procedures for chromium (VI) determination. Another aliquot sample (0.5L) was first oxidized to chromium (VI) and analyzed as mentioned for chromium (III) determination. The fluorescence intensity of the first aliquot (I_1 , %) is equivalent to chromium (VI) ions, while the fluorescence intensity of the second aliquot (I_2 , %) is a measure of the sum of chromium (III & VI) ions in the mixture. Thus, the fluorescence intensity ($I_2 - I_1$) is a measure of chromium (III) ions in the binary mixture.

2.4. Applications

2.4.1. Analysis of chromium in certified reference material (IAEA Soil-7)

The validation of the developed procedure was investigated by determination of chromium in CRM (IAEA Soil-7) as follows: An accurate weight ($0.20\text{--}0.30\pm 0.001\text{g}$) of the CRM sample was transferred into a Teflon beaker (50.0mL) containing HF (7.0mL), concentrated HCl (2.0mL), and concentrated HNO_3 (5.0mL) at room temperature to digest the sample gradually and slowly. The reaction mixture was heated slowly for 1h at $100\text{--}150\text{ }^\circ\text{C}$ on a hot plate. After evolution of NO_2 fumes had ceased, the reaction

mixture was evaporated almost to dryness and mixed again with concentrated HNO_3 (5.0mL). The process was repeated twice and the solid residue was re dissolved in dilute HNO_3 (10.0mL, 1.0molL^{-1}), transferred to volumetric flask (25.0mL) and completed to the mark with deionized water. An accurate volume of the sample solution (10.0mL) was adjusted to pH 0.0 with HCL and analyzed following the procedures of chromium (III) determination. The change of fluorescence intensity of the reagent TPP^+Br^- by chromium added was evaluated and used for chromium determination via the linear plot of the standard addition. A blank sample was analyzed following the same digestion and analytical procedures.

2.4.2. Analysis of chromium in wastewater

Wastewater samples were collected from the industrial effluent collection points in the industrial zones of chemicals, tanning, and dyes industries (Jeddah city, KSA). The water samples were filtered, condensed 100-fold with rotary evaporator and finally digested

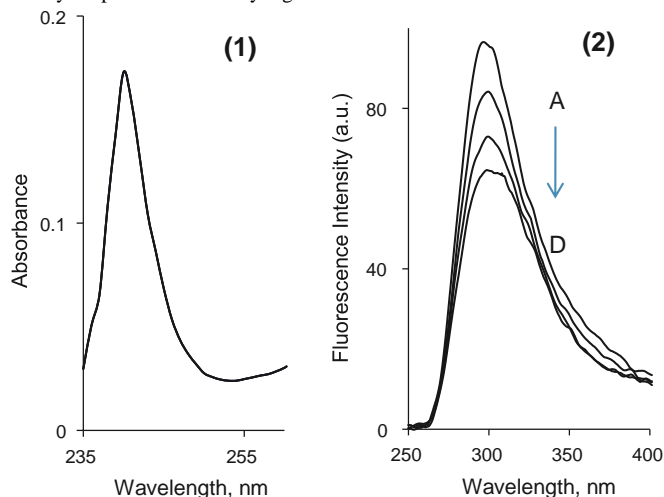


Fig. 1. UV-visible absorption spectrum (1) of TPP^+Br^- reagent and its emission spectra in chloroform (2) upon addition of various concentrations of chromium (VI): 0.00 (A); 5.0 (B), 20.0 (C) and $80.00\mu\text{gL}^{-1}$ (D) at $\lambda_{\text{ex/em}}=242/305\text{nm}$.

with concentrated nitric acid to remove the coexisting organic substances. The solution was adjusted to the required acidity and analyzed following the recommended procedures of chromium (III) determination. For the chemical speciation of chromium (III & VI), the sample solution was oxidized to chromium (VI) by H_2O_2 (0.5mL, 30%, w/v) in alkaline solution (pH ~9) adjusted with drops of KOH and heated for 10min to assure complete oxidation of chromium (III) and to remove excess H_2O_2 . After centrifugation and filtration, an accurate volume (10mL) of the sample was analyzed following the recommended procedure of chromium (VI) determination against a reagent blank. Chromium (III) species was obtained by subtracting the measured chromium (VI) from the total chromium content.

3. Results and discussion

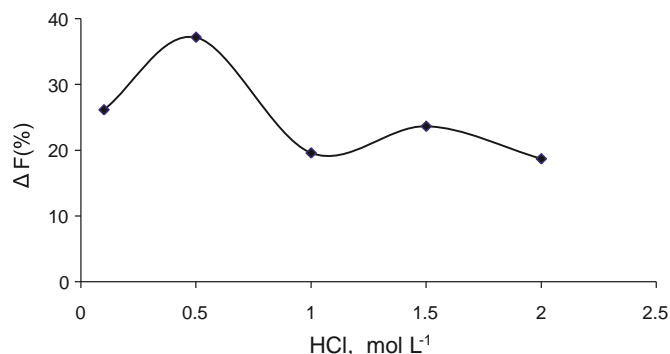
On mixing chromium (VI) with the reagent TPP^+Br^- in aqueous HCL solution and shaking with chloroform, a yellow-colored complex ion-associate of the formula $[\text{TPP}^+\text{CrO}_3\text{Cl}^-]$ was developed [5]. In absence of chromium (VI), the reagent TPP^+Br^- has intense fluorescence at $\lambda_{\text{ex/em}}=242/305\text{nm}$ in chloroform phase and the formation of the ion associate $[\text{TPP}^+\text{CrO}_3\text{Cl}^-]$ caused fluorescence quenching at the same wavelength (Fig. 1). The fluorescence intensity of TPP^+Br^- was quenched on raising chromium (VI) concentration with negligible shift in the wavelength confirming the formation of the associate $[\text{TPP}^+\text{CrO}_3\text{Cl}^-]$ [5] in the ground electronic state. The absence of new emission band in the spectrum (Fig. 1) indicates that, the formed ion associate in the excited state does not exist under the experimental conditions [12]. Hence, the developed quenching was successfully used for developing a new spectrofluorometric method for determination of chromium (VI) and total inorganic chromium (III) & (VI) species in water.

3.1. Influence of analytical parameters

The effect of acidity on the fluorescence quenching of the ion associate was tested in H_2SO_4 , HCL, HNO_3 or CH_3COOH (1.0molL^{-1}). Maximum and constant fluorescence quenching was achieved using HCL. Therefore, the effect of HCL concentration ($0.1\text{--}2.0\text{molL}^{-1}$) was critically studied. The results are shown in Fig. 2. Maximum and constant fluorescence quenching was achieved in HCL concentration in the range $0.4\text{--}0.6\text{molL}^{-1}$. Thus, HCL was adjusted at 0.5molL^{-1} in the subsequent work.

Fig. 2. Influence of HCL concentration ($0.1\text{--}2.5\text{molL}^{-1}$) on the fluorescence quenching of the ion associate.

The influence of shaking time on the fluorescence quenching intensity of the reagent TPP^+Br^- by the developed ion associate $[\text{TPP}^+\text{CrO}_3\text{Cl}^-]$ in the organic phase was investigated. Maximum and constant quenching intensity was



achieved at 3min shaking with CHCl_3 (Fig. 3). Thus, a shaking time of 3min was adopted in the in the next work.

The influence of the reagent TPP^+Br^- concentration on the fluorescence intensity was investigated. Maximum and constant fluorescence intensity was achieved using 2.0mL of the reagent (0.1%, w/v). High concentration of TPP^+Br^- makes the fluorescence quenching so small that it cannot be detected.

The extraction performance of the ion associate $[\text{TPP}^+\text{CrO}_3\text{Cl}^-]$ was tested in a series of organic solvents, e.g. n-hexane, dichloromethane, carbon tetrachloride, toluene, chloroform and methyl isobutyl ketone. The extraction performance of the ion associate increased in the following order: dichloromethane > chloroform > toluene > methyl isobutyl ketone > n-hexane ≈ carbon tetrachloride in agreement with the order of the dielectric constant. However, maximum extraction and constant fluorescence signal was achieved in chloroform. Therefore, chloroform was chosen as a preferred solvent.

3.2. Selectivity

The selectivity of the developed method was examined in the presence of a series of foreign ions under the established conditions. The tolerance limits (w/w) less than $\pm 4\%$ change in the fluorescence intensity of chromium (VI) was considered as free from interfering species. Solutions containing 50.0 g L^{-1} of chromium (VI) and the interfering species in different ratios were subjected to complete analysis. The results are summarized in Table 2. Complete extraction of chromium (VI) was achieved as indicated from the ICP-MS and fluorescence measurements. The anions BrO_3^- , IO_3^- ,

$[\text{TPP}^+\text{CrO}_3\text{Cl}^-]$ was linear in the concentration range $1\text{--}114 \text{ g L}^{-1}$ (1.9×10^{-8} to $2.19 \times 10^{-6} \text{ mol L}^{-1}$) with the regression equation: $I(\%) = 0.660C(\text{g L}^{-1}) + 5.56$

with a correlation coefficient of 0.998 ($n = 6$). Based on the IUPAC [13], the values of LOD and LOQ of chromium (VI) species were 0.43 and 1.42 g L^{-1} , respectively. The relative standard deviation at concentration 15 g L^{-1} chromium (VI) was $\pm 1.6\%$ ($n = 5$).

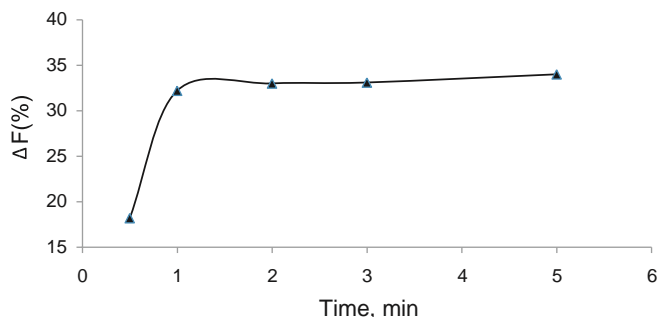


Fig. 3. Effect of shaking time on the fluorescence quenching of TPP^+Br^- in presence of chromium (VI) (100.0 g L^{-1}) in aqueous solution of HCl ($0.4\text{--}0.6 \text{ mol L}^{-1}$).

178 M.S. El-Shahawi et al. / Talanta 84 (2011) 175–179

Table 2
Tolerance limits of interfering species in chromium (VI) (50.0 ng mL^{-1}) determination by the developed method.

Interfering species	Interfering to analyte ratio
As^{3+} , Ni^{2+} , Bi^{3+} , Li^+ , Na^+ , K^+ , Ca^{2+} , Mg^{2+} , Al^{3+} , Ag^+ , CO_3^{2-} , SO_4^{2-} , NO_3^{2-} , CN^-	1000:1
Fe^{3+} , Hg^{2+} , Pb^{2+} , Mn^{2+} , Co^{2+} , Cr^{3+} , Cl^- , F^- , NO_2^- , H_2O_2	100:1
MnO_4^- , BrO_3^-	5:1
IO_3^-	0.5:1

and MnO_4^- interfered seriously with the fluorescence intensity of the TPP^+Br^- reagent and chromium (VI) determination. The interference of MnO_4^- was eliminated by the addition of few drops 0.1% , m/v NaN_3 to reduce manganese (VII) to manganese (II). After this modification, the tolerance of the interfering ions was improved to acceptable limit ($98 \pm 2\%$). The results denoted that, the method has good selectivity even in the presence of high concentration of chromium (III) species. Thus, the method was found suitable for the chemical speciation of chromium (VI & III) in a variety of environmental water samples.

3.3. Figure of merits

Under the optimized experimental conditions, the plot of chromium (VI) concentration vs. fluorescence quenching by the formation of the ion associate

Analysis of chromium species in water by the developed spectrophotometric (A) and ICP MS (B) methods (mean \pm standard deviation, $n = 5$).

Sample	Chromium added (g L^{-1})		Chromium found (g L^{-1})		Total chromium (g L^{-1})		Total recovery (%)	
	Cr^{3+}	Cr^{6+}	Cr^{3+}	Cr^{6+}	A	B	A	B
Wastewater	–	–	642 ± 8.1	39.8 ± 3.4	682 ± 10.1	684 ± 6.4	–	–
	50	50	794.3 ± 9	90.1 ± 4.1	785.2 ± 8	783 ± 10.1	100.4 ± 1.02	99.9 ± 1.3
Tap water	–	–	10.47 ± 1.6	ND	10.47 ± 1.6	11 ± 1.2	–	–
	10	10	20.50 ± 2.1	9.85	30.40 ± 1.1	32 ± 1.3	99.7 ± 3.6	103 ± 4.1

Table 4
Figure of merits of the developed and some of the reported spectrophotometric methods for chromium (g L^{-1}) determination in water.

Method	Disadvantages	Linear range	LOD (g L^{-1})	Reference
--------	---------------	--------------	---------------------------	-----------

Table 3

The fluorescence quenching of the reagent TPP^+Br^- by chromium (VI) added under the optimum experimental conditions suggested application of the TPP^+Br^- reagent for the pre-concentration and determination of chromium (VI) from large sample volumes of deionized water. Thus, aqueous solutions (0.5 L) of deionized water samples containing various concentrations ($20.0\text{--}50.0 \text{ g L}^{-1}$) of chromium (VI) and HCl (0.5 mol L^{-1}) were shaken with chloroform as described above. Analysis of aqueous solutions by ICP-MS against a reagent blank revealed complete extraction ($96\text{--}98 \pm 1.6$) of chromium (VI). The concentration of chromium (VI) species in the organic phase was quantitatively determined ($97\% \pm 2.6$) by measuring the fluorescence quenching of TPP^+Br^- in chloroform at optimum ex/em . Chromium (III) species in aqueous solutions (0.1 L) in the concentrations range $0.05\text{--}50 \text{ mg L}^{-1}$ was also determined by the TPP^+Br^- reagent after oxidation to chromium (VI) species as described. Satisfactory extraction percentage ($96 \pm 2.7\text{--}102 \pm 1.9\%$, $n = 5$) of chromium (III) species was also achieved.

3.4. Analytical applications

3.4.1. Analysis of chromium in the certified reference material (IAEA Soil-7)

The validation of the developed method was performed by the analysis of chromium in the certified reference materials (IAEA Soil7). Good agreement between the total chromium content determined by the developed spectrophotometric ($55.7 \pm 2.9 \text{ gg}^{-1}$), and ICP-MS ($58.4 \pm 1.3 \text{ gg}^{-1}$) methods and the recommended value (60 gg^{-1}) based on dry weight in the range of 95% confidence interval ($49\text{--}74 \text{ gg}^{-1}$). These data demonstrated that, the described method is accurate and precise for trace analysis of chromium in complex matrices.

3.4.2. Analysis of chromium in water

The proposed method was applied for the chemical speciation of chromium (III & VI) in tap and wastewater samples. Total

Cr ⁶⁺ – PTQA	Low sensitivity, interference of Ag ⁺ , Cr ³⁺ , Fe ³⁺ , Cu ²⁺	100–1.0×10 ⁴	50	[14]
Cr ⁶⁺ – 8-hydroxy quinoline-5-sulfonic acid benzophenone	Moderate sensitivity, low sensitivity with Pb ²⁺ , Hg ²⁺ , Ce ⁴⁺ , Sc ³⁺ , BrO ₃ ⁻	291–780	–	[15]
Magnetic Fe ₃ O ₄ /Py/PAM nanocomposite	Low sensitivity	100–14×10 ³	10	[16]
Cr ⁶⁺ – polyvinyl alcohol keto – derivatives nanoparticles	Low sensitivity	100–13×10 ³	20	[17]
Cr ⁶⁺ – rhodamine 6G	Interference of Cu ²⁺ , Ce ⁴⁺ , Sc ³⁺ , NO ₂ ⁻	8.0–80	0.8	[18]
Cr ⁶⁺ – quercetin	Interference of MnO ₄ ⁻ , BrO ₃ ⁻ , IO ₃ ⁻	5.2–104	0.47	[19]
Cr ⁶⁺ – 1,4-diaminoanthraquinone	Interference of MnO ₄ ⁻ , BrO ₃ ⁻ , IO ₃ ⁻	5.2–208	0.12	[20]
Diperoxo chromium–ethylacetate extract	Time consuming, expensive, interference of MnO ₄ ⁻ , BrO ₃ ⁻		0.2	[22]
Cr ⁶⁺ – TPP ⁺ -Br-	Interference of MnO ₄ ⁻ , BrO ₃ ⁻ , IO ₃ ⁻	1.0–114	0.42	Present work

M.S. El-Shahawi et al. / Talanta 84 (2011) 175–179

179

chromium content in water samples was determined via the developed spectrofluorometric (A) and ICP-MS (B) methods (Table 3). The recovery percentage of the developed method was in good agreement with the data obtained by ICP-MS data and always higher than 95% confidence level (Table 3). These data confirm the precision of the proposed method and its independence from matrix interference. Statistical treatment of data using F test [13] revealed that, no significant differences between the two variances of the developed and the ICP-MS methods. The calculated value of F (2.78) is lesser than the tabulated F value (6.39) for five replicate measurements. The Student t-test [13] was also applied to the analytical data of the developed and ICP-MS methods. The results revealed that, no significance difference between the two methods, since the tabulated t value at 95% confidence limit is 2.306, while the calculated t value by applying Student t-test to the results of wastewater sample was found lesser (0.79) for five measurements.

4. Conclusion

The reagent TPP⁺-Br- was successfully used for the chemical speciation of chromium (III, VI) species without previous separation step. The method has the following advantages: high selectivity, good reproducibility, stable fluorescence up to 4h, simple spectrofluorimeter and procedure. The analytical merits of the proposed method were successfully compared with some of the reported spectrofluorometric methods [14–20,22] (Table 4).

Most of the reported methods exhibited a relatively high LOD

(10.0–50.0 μg L⁻¹) [14,16,17], and serious interferences of Ag⁺, Hg²⁺, Pb²⁺, Cr³⁺, and Ni²⁺ [18–20]. The method provides LOD lower than the maximum allowable level (50.0 μg L⁻¹) of chromium recommended by WHO [21].

Acknowledgement

The authors would like to thank the Deanship of Scientific Research, King Abdul Aziz University, Kingdom of Saudi Arabia for the financial support under the grant number 3 -108 - 430 and Mr. Mr. O. N. Rathaw (Chairman of the Chemistry Department, University College, Umm Al-Qura University) for his support and excellent advices.

References

- [1] K. Umesh, M.P. Kaur, D. Sud, V.K. Gary, Desalination 249 (2009) 475.
- [2] A. Zhenga, J. Chenb, G. Wub, G. Wua, Y.G. Zhangb, H.P. Wei, Spectrochim. Acta A 74 (2009) 265.
- [3] M.M. Araujo, J.A. Teixeira, Int. Biodeteriorat. Biodegrad. 40 (1) (1997) 63.
- [4] P.K. Ghosh, J. Hazard. Mater. 171 (2009) 116.
- [5] M.S. El-Shahawi, S.S.M. Hassanb, A.M. Othman, M.A. Zyadaa, M.A. El-Sonbati, Anal. Chim. Acta 534 (2005) 319.
- [6] M. Narin, M. Soylak, K. Kayakirilmaz, L. Elci, M. Dogan, Anal. Lett. 35 (2002) 1437.
- [7] M. Tuzen, M. Soylak, J. Hazard. Mater. 129 (2006) 266.
- [8] P. Singer, A. Melissa, J.H. Aldstadt, Microchem. J. 74 (2003) 47.
- [9] Y.R. Li, N.K. Pradhan, R. Foley, G.K.C. Low, Talanta 57 (2002) 1143.
- [10] X.S. Zhu, B. Hu, Z.C. Jiang, M.F. Li, Water Res. 39 (2005) 589. [11] O. Dominguez, M.J. Arcos, Anal. Chim. Acta 470 (2002) 241.
- [12] P.M. Jayaweera, T. Sanjeevaa, K. Tennakone, Solar Energy Mater. Solar Cell. 91 (2007) 944.

- [13] J.C. Miller, J.N. Miller, Statistics for Analytical Chemistry, 4th Edn., Ellis Horwood, New York, 1994, p. p.115.
- [14] E.K. Paleologos, S.I. Lafis, S.M. Tzouwara-Karayanni, M.I. Karayannis, Analyst 123 (1998) 1005.
- [15] N.Q. Jie, J. Jiang, Analyst 116 (1991) 395.
- [16] S. Hong, H. Chen, L. Wang, Lun Wang, Spectrochim. Acta A 70 (2008) 449.
- [17] S. She, Y. Zhou, L. Zhang, L. Wang, L. Wang, Spectrochim. Acta A 62 (2005) 711.
- [18] N. Jie, Q. Zhang, J. Yang, X. Huang, Talanta 46 (1998) 215.
- [19] M.S. Hosseini, F. Belador, J. Hazard. Mater. 165 (2009) 1062.
- [20] M.S. Hosseini, M. Asadi, Anal. Sci. 25 (2009) 807.
- [21] WHO Guidelines for Drinking Water Quality, World Health Organization, Geneva, 2003.
- [22] A. Beni, R. Karosi, J. Posta, Microchem. J. 85 (2007) 103.

Chemical Speciation of Antimony(III and V) in Water by Adsorptive Cathodic Stripping Voltammetry Using the 4-(2-Thiazolylazo) – Resorcinol

M. S. El-Shahawi,^{*a, c} A. S. Bashammakh,^a A. A. Al-Sibaai,^a S. O. Bahaffi,^a E. H. Al-Gohani^b

^a Department of Chemistry, Faculty of Science, King Abdulaziz University, P. O. Box 80203, Jeddah 21589, Saudi Arabia ^b Department of Chemistry, Faculty of Applied Science, Omm-Al-Qura University, P. O. Box 3712, Makkah, Saudi Arabia ^c Permanent address: Department of Chemistry, Faculty of Science at Damietta, Mansoura University, Mansoura, Egypt *e-mail: mohammad_el_shahawi@yahoo.co.uk

Received: August 11, 2010;

Accepted: October 15, 2010

Abstract

A simple adsorptive cathodic stripping voltammetry method has been developed for antimony (III and V) speciation using 4-(2-thiazolylazo) – resorcinol (TAR). The methodology involves controlled preconcentration at pH 5, during which antimony(III) – TAR complex is adsorbed onto a hanging mercury drop electrode followed by measuring the cathodic peak current ($I_{p,c}$) at 0.39 V versus Ag/AgCl electrode. The plot of $I_{p,c}$ versus antimony(III) concentration was linear in the range 1.3510^9 – 9.5310^8 mol L⁻¹. The LOD and LOQ for Sb(III) were found $4.06 \cdot 10^{10}$ and 1.3510^9 mol L⁻¹, respectively. Antimony(V) species after reduction to antimony(III) with Na₂SO₃ were also determined. Analysis of antimony in environment water samples was applied satisfactorily.

Keywords: Antimony(III, V), 4-(2-Thiazolylazo)-resorcinol, Cathodic stripping voltammetry, Speciation, Certified reference material (IAEA Soil-7), Red sea water, Wastewater

DOI: 10.1002/elan.201000505

1 Introduction

Antimony and its compounds have many industrial uses e.g. manufacture of glass pottery and ceramics as well as in fire retardants and semiconductors [1]. Ultratrace level concentrations of antimony are commonly found in aquatic environment because of various human activities [2,3]. Antimony tends to accumulate in bottom sediments then releases into animal and vegetable tissues [4], thereby reaching humans and causing chronic diseases [5–8]. Antimony and its compounds are listed as priority pollutants by different international or government organizations [9]. Elemental antimony is more toxic than its salts and trivalent antimony compounds are generally more toxic than pentavalence form [10–12].

Numerous analytical techniques have been reported to measure antimony in environmental samples such as microwave induced plasma-atomic emission spectrometry (MIP-AES) [13,14], laser induced fluorescence [15,16], high performance liquid chromatography (HPLC) [17] and electroanalytical techniques [18–22]. Voltammetric methods are among the electrochemical techniques described for the analysis of antimony. These are relatively widespread and, due to their accuracy and sensitivity, have contributed greatly to its determination at trace level [22–24]. Adsorptive stripping

voltammetry has also been used for antimony determination using complexing agent such as Alizarin Red S [25].

The reagent 4-(2-thiazolylazo)-resorcinol, abbreviate as TAR (Figure 1) is the one of the popular chelating reagents. It forms either neutral or ionic stable chelates with high molar absorptivity with many metal ions according to the solution pH [26–28]. Recent literature survey has revealed no study of the reagent TAR for determination and/or chemical speciation of antimony. Thus, the present article reports a simple, accurate, convenient and low cost DP CSV procedures using the title reagent (TAR) for trace and ultra trace determination of antimony(III) and antimony(V) in water at a hanging mercury drop electrode. Mercury film and HMDE are the only electrode types sensitive enough for metal speciation measurements and in-situ metal measurements including antimony [29] and other metal ions [30,31] in natural waters. This electrode is safe as long as storage and disposal of Hg is undertaken in a safe manner. HMDE is widely used for ultra-trace metal speciation in natural waters.

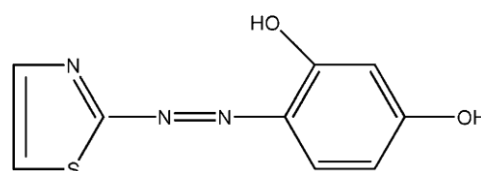


Fig. 1. Chemical structure of the reagent (4-(2-thiazolylazo)-resorcinol).

2 Experimental

2.1 Apparatus

The voltammetric measurements were performed on a Metrohm 797 VA trace analyzer and 747 VA stand (Basel, Switzerland). A three-compartment borosilicate (Metrohm) voltammetric electrochemical cell (10 mL) incorporating HMDE (5 mm²) as working electrode, double-junction Ag/AgCl, (3 M) KCl as a reference and platinum wire (BAS model MW-1032) as counter electrodes. A Perkin Elmer (Lambda EZ-210) double beam spectrophotometer (190–1100 nm) with 1 cm (path width) quartz cell was used for recording the electronic spectra of the reagent TAR and its antimony(III) complex. An ICP-MS (Sciex Elan DRC II, USA) Perkin-Elmer spectrometer was used as reference method for the analysis of antimony in the certified reference material, and water samples under the operational parameters recommended by the manufacturers. A Thermo Orion pH Meter model 720 (Thermo Fisher Scientific, MA, USA) was used for pH measurements with absolute accuracy limits of 0.1 pH unit defined by NIST buffers. Deionized water obtained from Milli-Q Plus system (Millipore, Bedford, MA, USA) was used to prepare all solutions.

2.2 Reagents and Materials

All chemicals used were of analytical reagent grade. Doubly deionized water was used throughout the work. Stock solution of TAR (110³ mol L⁻¹) was prepared in measuring flask (25 mL) in the least volume (2–3 mL) of ethanol and completed with deionized water to the mark. BDH stock solution of antimony(III) chloride (1000 mg mL⁻¹) was prepared in dilute HCl (10% w/v). More diluted solutions (1–12 mg mL⁻¹) of antimony(III) were freshly prepared in deionized water. A series of Britton–Robinson (B–R) buffers (pH 2.5–11.5) was prepared from the acid mixture (acetic-orthophosphoric and boric acids, 0.04 mol L⁻¹) adjusted to the required pH with NaOH (0.2 mol L⁻¹) and was used as supporting electrolyte.

2.3 General Procedures

2.3.1 Recommended DP CSV Procedures for Antimony(III)

An accurate volume (10 mL) of the B–R buffer at pH 5–6 was transferred into the electrochemical cell where the electrodes immersed in the test solutions through which pure nitrogen stream was passed for 15 min before recording voltammograms. The scans were initiated in the negative direction of the applied potential from +0.2 V to 1.3 V versus Ag/AgCl reference. After recording the voltammogram, an accurate volume (10.0 mL) of TAR reagent (2.2510⁸ mol L⁻¹) was added. The solution was stirred and purged with nitrogen gas for a period of 5 min. The stirrer was then stopped and after 10 s quiescence time, the voltammogram was recorded again. Unless otherwise stated the background voltammogram of the supporting electrolyte and the blank solution was recorded at the required pH under the optimum experimental conditions of deposition potential (0.5 V),

accumulation time (150 s); starting potential (0.25 V); scan rate of 60 mV s⁻¹ and 60 mV pulse amplitude. After recording the voltammogram of the blank solution, an accurate volume (10–100 mL) of antimony(III) solution (1.2 10⁶ mol L⁻¹) was added. The voltammogram was repeated with a new mercury drop under the same experimental conditions. The peak current of antimony(III) was measured at 0.39 V versus Ag/AgCl reference electrode. The influence of the scan rate (20–500 mV s⁻¹) and antimony(III) concentrations (10–100 mL; 1.010⁴ mol L⁻¹) on the cyclic voltammogram was carried out at pH 5.2 at HMDE and Pt working electrodes.

2.3.2 Recommended DP CSV Procedures for Antimony(V)

Antimony(V) was successfully reduced to antimony(III) following the work reported earlier by Feeney and Kounaves [32] as follows: an accurate weight (0.050.002 g) of sodium antimonite was allowed to react with an approximate weight (0.1 g) of sodium sulfite in the presence of HCl (2.0 mol L⁻¹). The solution was allowed to boil for 30 min to release the excess sulfur dioxide and was left to cool. The solution was finally diluted with deionized water and quantitatively transferred to volumetric flask. The solution was then analyzed following the recommended procedure for antimony(III) after adjusting the solution pH.

2.4 Applications

2.4.1 Analysis of Antimony in Certified Reference Material (IAEA Soil-7)

The validity of the developed procedure was investigated by the determination of antimony in CRM (IAEA Soil-7) as follows: An accurate weight (0.20–0.300.001 g) of the CRM sample was transferred into a Teflon beaker (50.0 mL) containing HF (7.0 mL), concentrated HCl (2.0 mL), and HNO₃ (5.0 mL) at room temperature to digest the sample gradually and slowly. The reaction mixture was then heated slowly for 1 h at 100–150°C on a hot plate. After the evolution of NO₂ fumes had ceased, the reaction mixture was evaporated almost to dryness and mixed again with concentrated HNO₃ (5.0 mL). The process was repeated thrice and the mixture was again evaporated to dryness. After evaporation, the solid residue was re dissolved in dilute HNO₃ (10.0 mL, 1.0 mol L⁻¹), transferred to volumetric flask (25.0 mL) and completed to the mark with deionized water. An accurate volume of the sample solution (5.0 mL) adjusted to pH 5–6 with B–R buffer (5.0 mL) was then transferred into the volumetric cell containing 10 mL (2.2510⁸ mol L⁻¹) of TAR reagent. The solution was then analyzed following the recommended experimental procedures and the standard addition method. Following the described procedure, the voltammograms were recorded and the change in the peak current was measured and used for antimony(III) determination via the linear plot of the standard addition. A blank sample was analyzed following the same digestion and analytical procedures.

2.4.2 Determination of Antimony in Water Samples

Red Sea (Jeddah site) and wastewater samples (1.0 L) were collected, and analyzed after a minor pretreatment as follows: the collected water samples were first filtered through Whatman no 1 and through cellulose membrane filters (0.45 μm) and stored in low density polyethylene (LDPE) bottles. An aliquot sample was analyzed for labile antimony(V) following the recommended procedure for antimony(III) determination.

Another aliquot was subjected to UV irradiation at 254 nm for 6 h in the presence of HCl (10%) to decompose organic matter including surface-active compounds and also to oxidise antimony(III) to antimony(V). The solution was then analyzed following the recommended procedures for antimony(V). Based on these bases, the $i_{p,c}$ of the first aliquot at 0.39 V versus Ag/AgCl reference electrode (i_1) will be a measure of labile antimony (III and V) species in the mixture, while the peak current of the second aliquot (i_2) is a measure of the sum of free and complexed antimony species. Therefore, the difference on the peak current (i_{21}) is a measure of the complexed antimony in the test samples.

3 Results and Discussion

Preliminary investigation involving the reaction of TAR with antimony(III) was critically investigated by UV-visible spectra. The electronic spectrum of TAR showed three absorption peaks at λ_{max} 302, 443 nm while the spectrum of the antimony(III)-TAR complex showed two well defined bands at λ_{max} 299 and 481 nm. The observed colour change and the shift in the electronic spectra in addition to the enhancement in the molar absorptivity of the

complex at 481 nm confirmed the complex formation of TAR with antimony(III). The stoichiometry of the antimony(III)-TAR complex, was determined via mole ratio method by measuring the absorbance of the complex at λ_{max} 481 nm at various concentrations of antimony(III). The FTIR spectrum of the reagent at 3290 cm^{-1} in the spectrum of TAR is assigned to ν (O H). This band was disappeared in the spectrum of the complex indicating participation of the OH in complex formation. The vibration bands due to the azo group ν (N=N) of the free ligand at 1401 and 1554 cm^{-1} are shifted to 1499 and 1360 cm^{-1} in the complex confirming coordination of antimony to nitrogen of the azo group. Thus, the reagent TAR coordinates to antimony in a bidentate fashion (NO) via azo and hydroxyl groups.

3.1 Electrochemical Behaviour of Antimony(III) – TAR Complex

In (B–R) buffer over a wide range of pH 2.2–11.2, the DP-CSV of antimony(III)-TAR complex ($4.310^7 \text{ mol L}^{-1}$) at the HMDE vs. Ag/AgCl reference electrode were critically recorded. The DP CSV of the supporting electrolyte i.e background, and the background with addition of TAR were recorded initially and the results revealed ill defined peaks. On the other hand, the DP CSV after addition of antimony(III) to the TAR solution at various pH (pH 2–11) well defined cathodic peaks were observed. Representative DP CSVs are shown Figure 2. The DP CSV of the complex showed a well-defined reduction peak in the range 0.1 to 0.55 V vs. Ag/AgCl reference electrode. The observed cathodic peak was most likely belong to the reduction of the azo group (N=N in the TAR reagent. The dependence of the cathodic peak po-

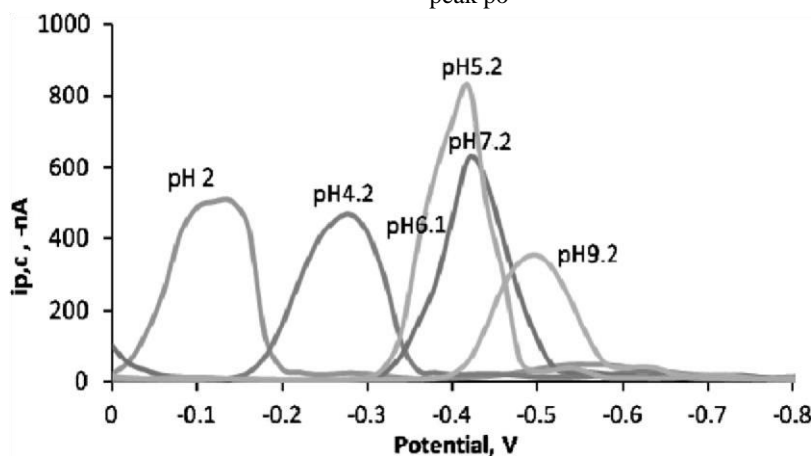


Fig. 2. DP CSV of TAR in presence of antimony(III) ions ($4.310^7 \text{ mol L}^{-1}$) at various pH at the HMDE. Scan rate=50 mV s^{-1} and pulse amplitude of 50 mV vs. Ag/AgCl electrode.

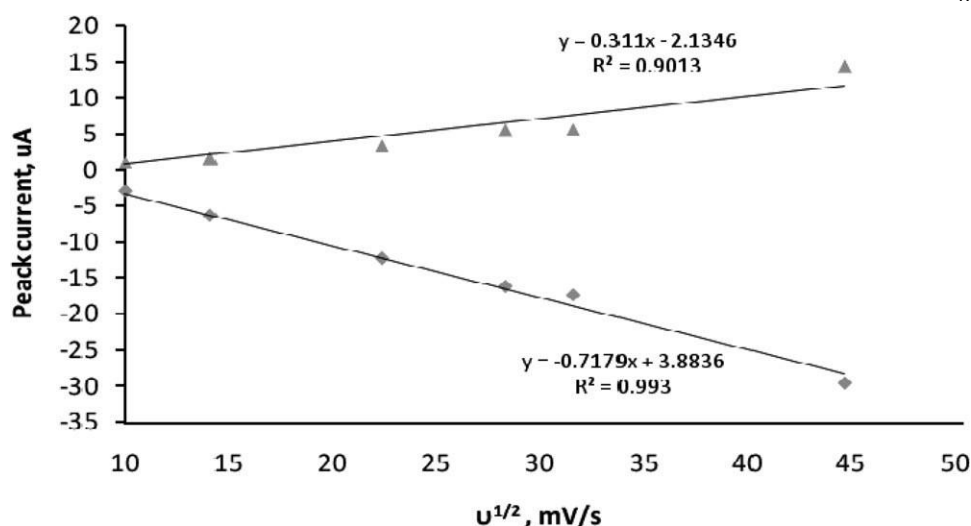


Fig. 3. Plot of ($I_{p,a}$) and ($I_{p,c}$) vs. $v^{1/2}$ of the cyclic voltammograms of antimony(III)-TAR ($1.210^6 \text{ mol L}^{-1}$) at HMDE vs. Ag/AgCl electrode at pH 5.2.

tential ($E_{p,c}$) on the pH was explained by a direct exchange of four electrons in one step. On increasing the solution pH, the $E_{p,c}$, at 0.35 was shifted to more negative potential confirming the irreversible nature of the process and the electrode reaction involves hydrogen ions [33,34]. The cathodic peak current ($I_{p,c}$) reached maximum at pH 5–6. Thus, in subsequent work, the solution pH was adjusted at pH 5.2.

The cyclic voltammograms for ($1.210^6 \text{ mol L}^{-1}$) of antimony(III) at pH 5–6 at HMDE vs. Ag/AgCl electrode at various scan rates (20–2000 mV s^{-1}) showed one well defined cathodic peak in the range $E_{p,c} = 0.34$ to 0.44 V. On the reverse scan, an anodic peak in the range $E_{p,c} = 0.07$ to 0.07 V was observed revealing the irreversible nature of the electrode process. The influence of the scan rate (20–2000 mV s^{-1}) on $E_{p,c}$ and $I_{p,c}$ of antimony(III)-TAR complex at pH 5.2 was investigated on a freshly drop of the HMDE. On raising the scan rate, the potential of the cathodic peak ($E_{p,c}$) was shifted cathodically confirming the irreversible nature of the electrochemical reduction process of Sb-TAR complex [33,34]. The $I_{p,c}$ increased linearly on raising the scan rate ($v^{1/2}$) indicating that, the reduction step is diffusion controlled electrochemical process (Figure 3) [34]. The plot of $\log I_{p,c}$ versus $\log v$ at pH 5.2 versus Ag/AgCl was linear with a slope close to 0.5 ($R=0.98$) confirming the irreversible nature of the electrochemical process. On the other hand, the current function ($I_{p,c}/v^{1/2}$) increased continuously on increasing the v (Figure 4). Thus, the reduction processes of antimony(III)-TAR complex do not favour the electrode-coupled chemical reaction mechanism of EC type [34]. The product of the number of the electron transfer (n) in the rate-determining step and the corresponding charge transfer coefficient (a) i.e. an at pH 5.2 were determined from the the linear plot of $E_{p,c}$ vs. $\log v$. Assuming $n = 2$, the value of a was then calculated from the slope of the linear plot using the equation:

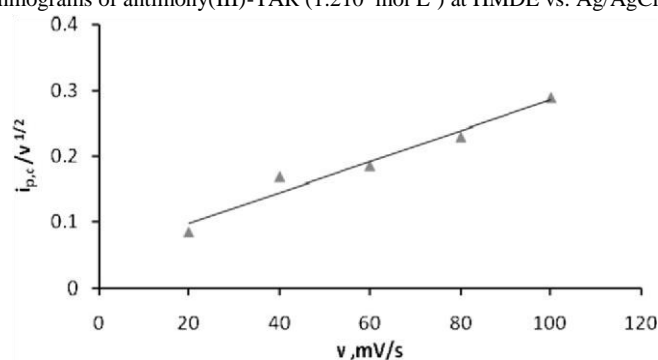


Fig. 4. Plots of the cathodic peak current function ($I_{p,c}/v^{1/2}$) of the cyclic voltammograms of antimony(III)-TAR ($1.210^6 \text{ mol L}^{-1}$) vs. scan rate at HMDE vs. Ag/AgCl electrode at pH 5.2.

$$DE_{p,c} = D \log v \quad \frac{29}{58} = a n \quad \delta 1 P$$

The computed value of a was found < 0.5 confirming the irreversible nature of the reduction step. The value of a was also calculated from the equations [35]:

$$E_{p,c} E_{p,c/2} \quad \frac{1}{57.5} \delta RT = a n F b \quad \delta^2 P$$

$$\delta E_{p,c/2} \delta E_{p,c} \quad \frac{1}{57.5} RT = a n F \ln \delta v_1 = v_2 b^{1-2} \quad \delta^3 P$$

where, $E_{p,c/2}$ is the cathodic peak potential at half height, T is the absolute temperature, F is the Faraday and R is the gas constant. The value of a ranged between 0.09– 0.16 confirming the irreversible nature of the reduction process. The surface coverage of the electroactive species (G) was calculated from the CV at the HMDE employing the equation [36]:

$I_{p,c} \quad \frac{1}{57.5} n^2 F^2 A G v = 4 R T \delta 4 P$ where, A = area of the electrode surface, cm^2 . Assuming $n=2$, a value of $1.06910^6 \text{ mol/cm}^2$ was obtained. These data suggested the use of the DP CSV for antimony(III) determination.

3.2 Analytical Parameters

The influence of the pH employing B–R buffer on the peak current height at the cathodic peak was studied over a wide range of pH 2.2–11.2 after 60 s pre-concentration time. Maximum enhancement of $i_{p,c}$ was observed in the pH range pH 5–6. Thus, on the next work, the solution pH was adopted between pH 5–6.

The effect of the accumulation potential (0.1 to –0.5 V) on the $i_{p,c}$ at 0.39 V versus Ag/AgCl electrode was examined over the potential range 0.0 to 1.05 V (Figure 5). The peak currents reached maximum at a deposition potential of 0.5 V, then the current were levelled off at more negative values. Therefore, in the subsequent work, a deposition potential of 0.5 V was selected.

The deposition time is one of the important parameters in stripping procedures that has a pronounced effect on sensitivity and dynamic linear range. Thus, the influence of the accumulation time (t_{acc}) over a wide range of time (10–200 s) was investigated at TAR (7.110^7) – antimony(III) (2.010^7 mol L⁻¹) concentrations. The plot of the resulting $i_{p,c}$ versus t_{acc} at cathodic peak potential of 0.39 V vs. Ag/AgCl electrode does not pass through the origin suggesting strong adsorption of the analyte at the electrode surface at the equilibrium time which was fixed at 10 s. Peak current was reached maximum at 150 s deposition time and it was levelled off at longer time, suggesting that the electrode surface was saturated with free TAR. Hence, an accumulation time of 150 s was applied for subsequent determinations of antimony(III).

The influence of the scan rate (10–100 mV s⁻¹) on the $i_{p,c}$ of antimony(III)-TAR complex was investigated under the above optimum experimental conditions at the HMDE. The $i_{p,c}$ increased steadily on raising the scan rate from 10 to 100 mV s⁻¹ then more slowly tending to levelled off, due to the hindering contribution of the capacitive background current on the total

measured current. However, at 60 mV s⁻¹ scan rate, well defined and symmetric, reproducible and sensitive cathodic peak was achieved.

The influence of the pulse amplitude on the DP CSV peak of Sb(III)-TAR complex was examined over a wide range (20 to 100 mV) under the above optimal conditions. The data revealed excellent, symmetric cathodic peaks and maximum peak currents were achieved at 70 mV. At pulse amplitude higher than 70 mV, the cathodic peak slightly displaced to the negative direction was obtained, revealing that, the charge transfer is predominantly controlling the reduction process. Therefore, in the present work, pulse amplitude of 70 was chosen as an optimum value. The influence of the reagent TAR concentration (2.210^8 – 1.310^7 mol L⁻¹) on the $i_{p,c}$ under the optimal experimental parameters was studied. The $i_{p,c}$ was increased on increasing the reagent TAR concentration and levelled off at 8.210^8 mol L⁻¹ TAR. Then the sensitivity of the cathodic peak current was decreased and deteriorated gradually at concentrations higher than $1 \cdot 10^7$ mol L⁻¹ of TAR. This trend is most likely attributed to the competitive adsorption of free TAR. However, the observed background, best sensitivity and cathodic wave resolution of the DP CSV peak vs. Ag/AgCl electrode was achieved at 60 mV s⁻¹ scan rate, 70 mV pulse amplitude, 0.5 V accumulation potential, 150 s accumulation time.

3.3 Figure of Merits

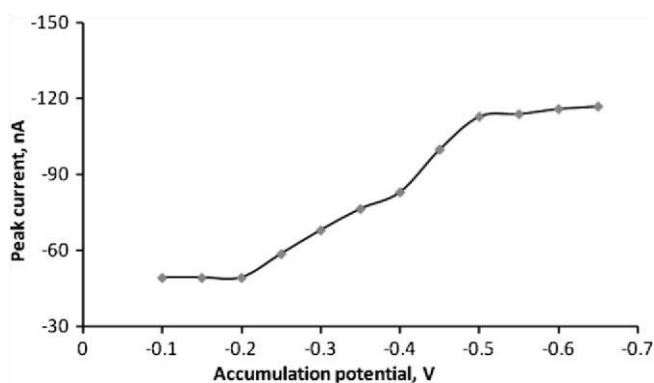
The voltammograms and the peak current, $i_{p,c}$ measured by the developed procedure versus antimony(III) concentration was linear over the range 1 to 12 mg L⁻¹ (Figure 6). The regression equation of the calibration plot, Figure 7, was given by the equation: $i_{p,c} = 0.9971C - 2.3267$ (R² = 0.9971)

$\times 10^{-5}$

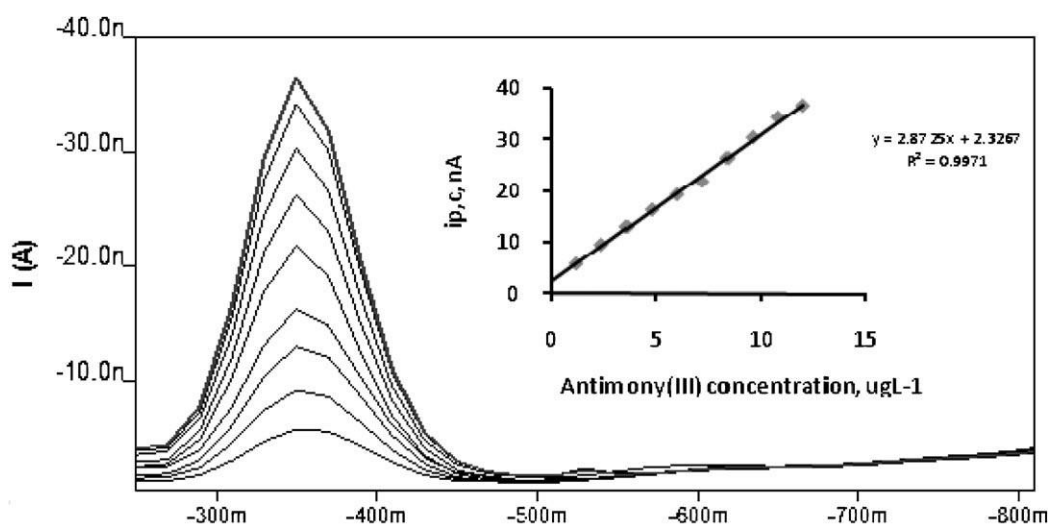
Fig. 5. Effect of accumulation potential on stripping peak current at 0.39 V vs. Ag/AgCl electrode of 2.0 nM antimony(III), 5 nM TAR at a HMDE electrode, pH 5.2 and accumulation time of 120 s.

where C is the antimony(III) concentration in mg L⁻¹. The limits of detection (LOD) and quantitation (LOQ) were calculated using the formula: LOD = 3 s/b and LOQ = 10 s/b, where, s is the standard deviation of the blank and b is the slope of the calibration plot

Fig. 6. DP CSVs and calibration plot of Sb(III)-TAR complex (1.2210^9 – 4.0710^9 mol L⁻¹) at pH 5.2 at 0.39 V at HMDE vs.



[37]. Under the optimum experimental conditions, the values of LOD and LOQ for Sb(III) were found equal to $4.06 \cdot 10^{10}$ (0.05 mg L⁻¹) and 1.3510^9 mol L⁻¹ (1.2 mg L⁻¹), respectively. The plot of the cathodic peak current versus antimony(III) concentration has a linear relationship in the range 1.3510^9 – 9.5310^8 (0.17–12 mg L⁻¹) mol L⁻¹. A relative standard deviation (RSD) of 2.39% (n=5) at 10 mg L⁻¹ antimony(III) was obtained. Antimony(V) was also determined after reduction to antimony(III) with sodium sulfite.



Ag/AgCl electrode.

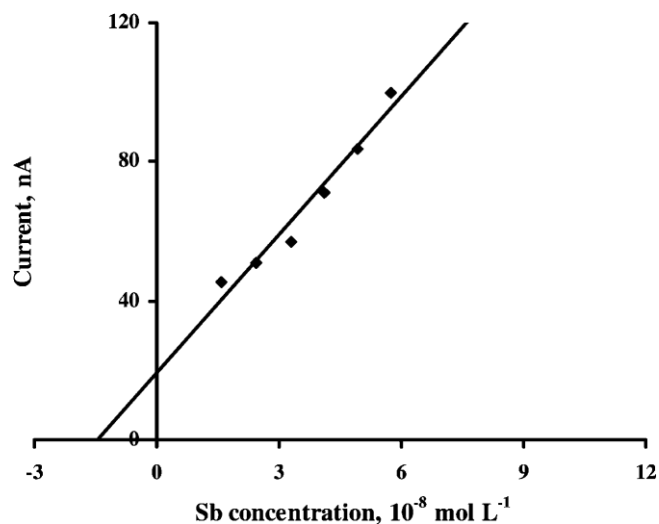


Fig. 7. Standard addition curve for the analysis of total antimony in Red Sea water at HMDE.

U (V)

Table 1. Figure of merits of the developed DP CSV and some of the reported methods for antimony(III) determination. ASV: Anodic stripping voltammetry; SV: spectrophotometry; SP: stripping voltammetry.

Technique	LOD (mg L ⁻¹)	Dynamic range (mg L ⁻¹)	Reference
ASV	0.11	12.04–110	[9]
	1.08	3.65–12.17	[36]
SV	6	10–250	[39]
SP	0.3	0.3–150	[40]
	0.9	0–250	[41]
ASV	0.012	0.012–0.1	[29]
	0.21	0–5	[42]
HPLC	0.07	0.5–200	[15]
UV-Visible	5	10–1500	[44]
ET AAS	0.05	0.05–5	[44]
FIA spectrometry	29	50–2500	[43]

DP CSV	0.05	0.17–12	Present work
--------	------	---------	--------------

The main figures of merits (Table 1) of the proposed method were compared successfully with many of the published electrochemical, chromatographic and spectrometric methods [9,15,29,36,40–44]. The values of LOD and LOQ are lower than those were obtained by some electrochemical methods [9,36,39,42]. The relative standard deviation (RSD) of the developed DP CSV method was 1.054%. The present method has a higher limit of detection (0.05 ng mL^{-1}) than the adsorptive stripping voltammetry for speciation of antimony using pyrogallol at HMDE and Sb-complexes with a lower limit of detection for antimony(III) than that reported antimony determination [29]. However, the reported method [29] suffered from time consuming, selectivity and reproducibility. Moreover, the developed method is more selective and sensitive than most of the reported methods [35–44]. The validation of the DP CSV method for the assay of various concentrations of antimony(III) and (V) species in de ionized water was investigated. The results are summarized in Table 2, where, a satisfactory recovery percentage of antimony species was achieved confirming the precision of the method. The HMDE is safe as the disposal of Hg and storage are undertaken in a safe manner. Both antimony(III) and (V) can be determined with identical sensitivity.

3.4 Interference Study

The analytical utility of the developed method was evaluated by analysis of trace of antimony(III) in matrices of environmental interest, where potentially interfering species can be present. Thus, the analysis of $4.110^8 \text{ mol L}^{-1}$ antimony(III) ions by the developed DP-CSV procedure in the presence of Ni^{2+} , Cu^{2+} , Zn^{2+} , VO_3 , Mn^{2+} , AsO_2 , AsO_3 , Al_3^+ , Fe_2^+ , Fe_3^+ , Bi_3^+ , Pb_2^+ , Sn_2^+ , Cd_2^+ , and Cr^{3+} and the anions: SO_4^{2-} , SCN , SO_4^{2-} , NO_3 , CO_3^{2-} , Cl , Br , and PO_4^{3-} individually at 50–100 fold mass concentration excess over antimony(III) was tested. The tolerance limit was defined as the concentration of the foreign ion added causing a relative deviation within 5% in the magnitude of the peak current i_{BB} at 0.39 V versus Ag/AgCl by complexing with the reagent or by forming peaks that overlap with, or even completely suppress antimony(III) peak. Only the ions Al^{3+} , Fe^{3+} , VO_3 , Bi^{3+} , Pb^{2+} , Sn^{2+} , Cu^{2+} , Zn^{2+} and Cr^{3+} interfered seriously even at 10–20 fold mass excess over antimony(III) by producing a diffusion controlled peaks as shoulders on the cathodic side of the antimony peak (0.39 V). The interference of the ions Al^{3+} , Fe^{3+} eliminated by masking with tri ethanolamine and NaF (0.1% w/v), respectively. The interferences of the ions Bi^{3+} , Pb^{2+} , Sn^{2+} , Cu^{2+} , Zn^{2+} and Cr^{3+} was alleviated by adding few drops of EDTA (0.1% w/v) prior to their measurements to suppress the interfering peak of the diverse ion.

3.5 Applications

Table 2. Analysis of the binary mixture of inorganic antimony(III) and antimony (V) by the developed DP CSV method.

Antimony added (mg L^{-1})		Antimony found (mg L^{-1})		Total Sb recovery (%) [a]
Sb^{3+}	Sb^{5+}	Sb^{3+}	Sb^{5+}	
1.0	10.0	1.16	0.04	98.4
5.0	5.0	5.19	0.08	96.5

[a] Average recovery of five measurements relative standard deviation.

3.5.1 Analysis of CRM (IAEA Soil – 7)

The validation of the developed method is performed by the analysis of antimony content in CRM sample (IAEA Soil-7) after digestion as described. The solution of the CRM sample was analyzed by the direct calibration plot of the developed method (Figure 6). Moreover, analysis of antimony in the CRM sample was also determined by performing the recovery tests in the spiked samples with antimony(III) in the range 2–3 mg via the developed DPCSV method and by the ICP-MS method. Good agreement between the results obtained by the present DPCSV (1.850.05 mg/kg) and the ICP-MS (1.750.03 mg/kg) methods and the recommended value (1.7 mg/kg) and 95% confidence interval (1.4–1.8 mg/kg) confirming the applicability of the developed method.

3.5.2 Antimony Speciation in Marine and Wastewater Samples

The DP CSV procedure was successfully used for the analysis of labile and total antimony ions in Red Sea water and wastewater samples as described in the experimental section at the optimum experimental conditions. The determination of antimony species before and after UV irradiation ($n=5$) are summarized in Table 3. The results were found compatible with ICP-MS method confirming the applicability of the developed for analysis of various water samples containing. An acceptable agreement between the total antimony in water samples determined by the proposed DP CSV and the standard ICP MS methods. The calculated value of the labile and total antimony in Red sea water by the DP CSV method was

4.20.2 mg L⁻¹ and the complexed antimony was 7.4 0.3 mg L⁻¹ confirming the suitability of the method compared the ICP-MS (13.10.2). The t (1.72–2.28) and F (1.2–2.33) tests at 95% confidence did not exceed the theoretical ones 2.31 and 6.388, respectively. The method was also applied for the analysis of total antimony in waste water. An acceptable agreement between the DP CSV (15.81.5 mg L⁻¹) and ICP MS (17.60.4 mg L⁻¹) data was noticed (Table 3).

Table 3. Analysis of total antimony (mg L⁻¹) on water samples by the developed and ICP MS methods (average of four measurements relative standard deviation).

Sample	DP CSV	ICP MS
Red sea water	15.83.521.50.03	17.63.40.0.24
Wastewater [a]		

[a] Wastewater of power plant station

4 Conclusions

The TAR method provides an excellent alternative approach for the speciation of antimony(III, V) at trace levels through prior adsorption of Sb(III)-TAR complex at HMDE because of its

sufficient precision and applicability without sample pretreatment. The TAR reagent appears to be very promising as the basis of a sensitive and clean voltammetric procedure for antimony speciation. The LOD of the method could be improved to lower value by prior preconcentration onto TAR immobilized polyurethane packed column before determination. Work is continuing for on-line speciation of inorganic and organo antimony species in environmental samples.

Acknowledgements

The authors would like to thank the Deanship of Scientific Research, King Abdulaziz University for financial support through Grant Number MX/10/11. Special thanks to the Centre of Excellence in Environmental Studies, King Abdulaziz University, Jeddah, and Kingdom of Saudi Arabia for the financial support.

References

- [1] M. Krachler, J. Zheng, R. Koerner, C. Zdanowitz, D. Fisher, W. Shotyky, *J. Environ. Monitoring* 2005, 7, 1169.
- [2] S. Manahan, *Environmental Chemistry*, 7th ed., Lewis Publishers, London 2001.
- [3] N. J. Wilson, D. Craw, K. Hunter, *Environ. Poll.* 2004, 129, 257.
- [4] P. Smichowski, *Talanta* 2008, 75, 2.
- [5] M. Tighe, P. Ashley, P. Lockwood, S. Wilson, *Sci. Total Environ.* 2005, 347, 175.
- [6] J. Dean, F. Bosqui, V. Lanouette, *Environ. Sci. Technol.* 1972, 6, 518.
- [7] N. Furuta, A. Iijima, A. Kambe, K. Sakai, K. Sato, *J. Environ. Monit.* 2005, 7, 1155.
- [8] F. Quentel, M. Filella, *Anal. Chim. Acta* 2002, 452, 237.
- [9] O. Dominguez Renedo, M. J. Arcos Martinez, *Anal. Chim. Acta* 2007, 589, 255.
- [10] K. A. Francesconi, D. Kuehnelt, *Analyst* 2004, 129, 373.
- [11] K. Pyrzynska, *Talanta* 2001, 55, 657.
- [12] M. Krachler, H. Emons, *Trends Anal. Chem.* 2001, 20, 79.
- [13] C. Dietz, Y. Madrid, C. Camara, P. J. Quevauviller, *Anal. At. Spectrom.* 1999, 14, 1349.
- [14] J. H. Yu, P. Dai, S. G. Ge, Y. Zhu, L. Zhang, X. L. Cheng, *Spectrochim. Acta Part A* 2009, 72, 17.
- [15] H. Pacquette, S. Elwood, M. Ezer, J. Simeonsson, *J. Anal. At. Spectrom.* 2001, 16, 152.
- [16] Y. Ye, J. Sang, H. Ma, G. Tao, *Talanta* 2010, 81, 1502.
- [17] I. Gregori, W. Quiroz, H. Pinochet, F. Pannier, M. J. Gautier, *J. Chromatogr. A* 2005, 1091, 94.
- [18] R. O. Kadara, I. E. Tothill, *Anal. Bioanal. Chem.* 2004, 378, 770.
- [19] P. Smichowski, Y. Madrid, C. Camara, *Fresenius J. Anal. Chem.* 1998, 360, 623.
- [20] T. Tanaka, T. Ishiyama, K. Okamoto, *Anal. Sci., Japan* 2000, 16, 19.
- [21] O. Domnguez Renedo, M. J. Arcos Martinez, *Anal. Chim. Acta* 2007, 589, 255.
- [22] L. Shpigun, V. Lunina, *J. Anal. Chem.* 2003, 58, 983.
- [23] O. Domnguez Renedo, M. J. G. Gonzalez, M. J. Arcos-Martinez, *Sensor* 2009, 9, 219.
- [24] C. Locatelli, G. Torsi, *Microchem. J.* 2004, 78, 175.
- [25] N. N. Lu, I. S. N. Ertas, *Anal. Lett.* 2008, 41, 2621.
- [26] U. Kazumasa, *Bull. Chem. Soc. Japan* 1979, 52, 1215.

- [27] G. Nickless, F. H. Pollard, T. J. Samuelson, *Anal. Chim. Acta* 1967, 39, 37.
- [28] W. Lee, S. E. Lee, M. K. Kim, C. H. Lee, Y. S. Kim, *Bull. Korean Chem. Soc.* 2002, 23, 1067.
- [29] M. J. Gomez Gonzalez, O. Dominguez Renedo, M. J. Arcos Martnez, *Talanta* 2007, 71, 691.
- [30] S. A. Bennett, E. P. Achterberg, D. P. Connelly, P. J. Statham, G. R. Fones, C. R. German, *Earth Planetary Sci. Lett.* 2008, 270, 457.
- [31] C. B. Braungardt, E. P. Achterberg, M. Gledhill, M. Nimmo, F. Elbaz-Poulichet, A. Cruzado, Z. Velasquez, *Environ. Sci. Technol.* 2007, 41, 4214.
- [32] R. Feeney, S. P. Kounaves, *Talanta* 2002, 58, 23.
- [33] A. J. Bard, L. Faulkner, *Electrochemical Methods: Fundamentals and Applications*, Wiley, New York 1980, p. 218.
- [34] R. S. Nicholson, I. Shain, *Anal. Chem.* 1964, 36, 706.
- [35] D. Sawyer, W. R. Heinemann, J. Beebe, *Chemistry Experiments for Instrumental Methods*, Wiley, New York 1984.
- [36] M. Sharp, M. Petersson, K. Edstrom, *J. Electroanal. Chem.* 1979, 95, 123.
- [37] J. Miller, N. Miller, *Statistics for Analytical Chemistry*, 4th ed., Ellis-Horwood, New York 1994, p. 115.
- [38] B. Khoo, J. Zhu, *Analyst* 1996, 121, 1983.
- [39] L. M. Shpigun, V. K. Lunina, *J. Anal. Chem.* 2003, 58, 983. [40] J. M. O. Souza, C. R. T. Tarley, *Anal. Lett.* 2008, 41, 2465.
- [41] S. B. Adeloju, T. M. Young, *Anal. Chim. Acta* 1995, 302, 225.
- [42] W. Wagner, S. Sander, G. Henze, *Fresenius J. Anal. Chem.* 1996, 354, 11.
- [43] I. Gregori, W. Quiroz, H. Pinochet, F. Pannier, M. Gautier, *J. Chromatogr. A* 2005, 1091, 94.
- [44] K. Shrivastava, K. Agrawal, N. Harmukh, *J. Hazard. Mater.* 2008, 155, 173.

Thus, in the case of dithioic acid hydrazides, the orientation of heterocyclization reactions will start from **S** on alkylation or from **N** on condensation (Sadasivan and Alaudeen, 2006, PP. 1145 -1148). The starting materials, dithioic formic acid hydrazide **1** and thiocarbohydrazide **7** possess two donor sites situated at -NH and / or =NH group in addition of sulfur (Sadasivan and Alaudeen, 2006, PP. 1145 -1148).

Recently, a series of cyclic and acyclic systems close to the title compounds has been used extensively in the literature as biocidal reagents (Sadasivan and Alaudeen, 2006, PP. 1145 -1148). Such compounds have been used as complexing agents for pre concentration, and subsequent determination of trace and ultra trace concentrations of toxic ions via both S and N as donor atoms (Hassanien, 2003, PP. 1987 -1997; Shindhu, et al., 2005, PP. 472- 474) as shown below:

<Figure 1>

Considering the biocidal and complexation properties of these compounds and as a part of our search for novel mono- and di-thiocarbohydrazide and alkyl, acyl derivatives, the present article reports the synthesis of heterocyclic nitrogen compounds containing sulfur using dithioic formic acid hydrazide (**1**) and thiocarbohydrazide (**7**) as starting materials via condensation with oxygenated compounds. Moreover, one of the compounds prepared by this methodology was tested as chelating agent for the pre concentration and subsequent determination of mercury (II) ion in water.

2. Experimental

2.1 Reagents and materials

All chemicals and solvents used were of analytical reagent (A.R) grade quality and were used as received. Most of the chemicals were provided by Merck (Darmstadt, Germany). Doubly deionized water was used throughout. Low density polyethylene (LDPE) bottles, Nalgene were used and carefully cleaned first with hot detergent, soaked in 50% HCl (Analar), HNO_3 (2.0 mol L^{-1}), subsequently washed with dilute HCl (0.5 mol L^{-1}) and finally rinsed with distilled water. The sample solution was stored in LDPE bottles and stored at -20°C in a freezer. Stock solutions (0.1 \% w/v) of the steroid reagent were prepared in ethanol. A stock solution of HgCl_2 (1 mg/mL) was prepared by dissolving an accurate weight of the salt in doubly distilled water (100 mL). Britton – Robinson (B –R) buffers of pH 2-11 were prepared from the acid mixture of phosphoric acid, boric acid, acetic acid (0.04 mol L^{-1}) and adjusting the pH to the required value with sodium hydroxide (0.20 mol L^{-1}). A series of standard diluted mercury (II) solutions were then prepared in doubly distilled water.

2.2 Apparatus and measurements

A Perkin Elmer (Lambda EZ-210) double beam spectrophotometer ($190\text{-}1100 \text{ nm}$) with 1 cm (path width) was used for recording the electronic spectra of the compounds. A Perkin Elmer model RXI-FT-IR system 55529 was used for recording the IR spectra of the prepared compounds. A Bruker advance DPX 400 MHz model using TMS as an internal standard was used for recording the ^1H NMR spectra of the compounds on deuterated DMSO. A GC-MS-QP 1000-Ex model was used for recording the mass spectra of the compounds. Melting points were determined with an electro thermal Bibbly Stuart Scientific Melting Point SMPI (US). Molecular weights of the compounds were performed on Micro analytical center, Cairo University, Egypt. Microanalysis (Sulfur %) was performed by microanalytical center Ain-Shams University-Cairo-Egypt. A digital pH-meter (model MP220, Metter Toledo) was used for pH measurements.

2.3 Organic preparation

Mono-hydrazones (2a – d) and bis-hydrazones (5 a and 5b)

A mixture of **1** and the selected aromatic / heteroaldehydes and / or cyclic diketones (1:1) and/ or 1,2-diketones (1:1 molar ratio) and a cyclic diketones (2:1 molar ratio) in ethanol- acetic acid (1:1, 100 mL) was refluxed for 1 h, cooled then poured onto an ice bath. The solid precipitate was collected and crystallized from the appropriate solvent to give **2a-d** and/ or **5a** and **5b**, respectively.

N¹-Arylidene-dithioic formic acid hydrazones (2 a-d):

2 a: This compound was crystallized from ethanol as yellow crystals. Yield = 80%, m.p. $150\text{-}151^\circ\text{C}$. $\text{C}_6\text{H}_7\text{N}_3\text{S}_2$ (185) Calcd.: S, 34.59. Found S, 33.95.

2 b: This compound was crystallized from ethanol as pale yellow crystals. Yield (85.2%), m.p. $105\text{-}106^\circ\text{C}$. IR: $\nu \text{ cm}^{-1}$ = 3500 (OH), 3120 (NH), 1595 (C=N), 1380 (NCSN), 1185 (C-S), 1055 (- C-O-Me). $\text{C}_9\text{H}_{10}\text{N}_2\text{S}_2 \text{ O}_2$ (242) Calcd.: S, 26.44. Found S, 25.58.

2c: This compound was crystallized from ethanol as pale yellowish crystals. Yield (90.05%), m.p. 220-221°C. C₁₁H₁₄N₂S₂O₃ (286) Calcd.: S, 22.37. Found S, 22.18.

2d: This compound was crystallized from ethanol as faint yellow crystals. Yield (60.2%), m.p. 225-226 °C. UV, λ_{nm} (DMF): 380, IR: ν cm⁻¹ = 3315 (NH of indole), 3155 (NH of NHCS), 1686 (C=O), 1551 (C=N), 1432 (NCSN), 1190 (C-S), 826 (phenyl CH). ¹H NMR (DMSO): δ = 4.2 (s, 1H, SH), 6.8-7.2, 7.5-7.8 (each m, 4 H of aromatic CH), 10.2 and 14.5 (each s, 2H, NH of indole and acid hydrazide). MS, m/z (Int. %): 249 (0.0), 203 (M⁺-HCSH, 100), 157 (5.15), 145 (31.91), 131 (15.18), 102 (87.31), 90 (27.13), 77 (5.98). C₉H₇N₃S₂O (237) Calcd.: S, 27.0. Found S, 26.59.

Bis - N-arylidene-dithioic formic acid hydrazones (5a, 5b):

5a: This compound was crystallized from methanol as pale yellow crystals. Yield (65.03%), m.p. 145-146°C. C₆H₁₀N₄S₄ (266) Calcd.: S, 48.12. Found S, 47.95.

5b: This compound was crystallized from methanol as pale yellow crystals. Yield (80.1%), m.p. 190-191 °C. IR: ν cm⁻¹ = 3139 (NH), 1596 (C=N), 1350 (NCSN), 1213(C-S), 793, 763 (phenyl CH). C₁₆H₁₄N₄S₄ (390) Calcd.: S, 32.82. Found S, 32.80.

N¹ - (Phenyl amino carbothia) dithioic formic acid hydrazides (6a)

Phenyl isothiocyanate (0.01 mmol) was added to a solution of **1** (0.01m mol) in DMF (50 mL) and refluxed for 20 min. After cooling, the reaction mixture was poured onto ice. The solid precipitate was collected and crystallized from DMF as deep yellow crystals. Yield (83.2%), m.p. 240-241 °C. IR: ν cm⁻¹ = 3195, 3103 (NH, NH), 1342 (NCSN), 1191 (C-S), 776 (phenyl CH). ¹H NMR (DMSO): δ = 7.2-7.4, 7.5-7.6 (each m, 10H, two phenyl), 8.1 (s, 1H, NH), 9.2 (s, 1H, SH), 10.8, 11.4 (each d, 2H, NH-NH). C₈H₉N₃S₃ (243) Calcd.: S, 39.5. Found S, 38.98.

N¹ - (4- Chlorophenyl amino carbothia) dithioic formic acid hydrazides (6b)

This compound was prepared by mixing 4-chlorophenyl isothiocyanate (0.01 mmol) with a solution of **1** (0.01m mol) in DMF (50 mL) and refluxed for 20 min. After cooling, the reaction mixture was poured onto ice and the solid precipitate was filtered and crystallized from DMF as deep yellow crystals. Yield (63.0%), m.p. 215-216 °C. IR: ν cm⁻¹ = 3180, 3165 (NH, NH), 1355 (NCSN), 1185 (C-S), 777 (phenyl CH), 624 (C-Cl). C₈H₈N₃S₃Cl (277.5) Calcd. S, 34.65. Found S, 34.45.

3-Imino-2--thioxo-4, 5-dihydro-thiazolidin-4-one (3)

An equimolar mixture of **2a** and monochloroacetic acid with anhydrous sodium acetate (5 g) in ethanol (50 mL) was refluxed for 4 h. After cooling, the reaction mixture was poured onto ice and the resulting solid precipitate was collected and crystallized from acetic acid as yellow crystals. Yield (50.12%), m.p. 260-261 °C. IR: ν cm⁻¹ = 3110 (NH), 1710 (C=O), 1603 (C=N), 1356 (NCSN), 1480 (deformation CH₂). MS: m/z (Int.%): 227 (M+2, 5.18), 92 (C₅H₄N₂), 56 (100, C₂H₂NO). C₈H₇N₃S₂O (225.11) Calcd.: S, 28.44 Found S, 28.01.

2-Thioxo-3-(2-oxoindolin-3-imino)-3,4,5,6- tetrahydro-1,3- thiazin-4,6-dione (4)

An equimolar mixture of **2d** and diethylmalonate was added to sodium ethoxide solution in absolute ethanol (0.2 mmol, 100 mL). The reaction mixture was refluxed for 4 h, cooled then poured onto ice-HCl. The produced solid was filtered and crystallized from THF as strong yellow crystals. Yield (70.12%), m.p. 280-281 °C. IR: ν cm⁻¹ = 3353 (OH of thiazine-4, 6 -dione), 3056 (NH of indole), 1667, 1620 (2 C=O), 1607 (C=N), 1362 (NCSN), 1192 (C-S), 738 (phenyl CH). ¹H NMR (DMSO): δ = 3.2 (d, 2H, cyclic O-CH₂-O), 6.2 (s, 1H, OH of 3-indole), 7.3-7.7 (m, 4H, of benzo-protons). MS, m/z (Int. %): 305(0.0), 271 (M-H₂S, 100), 203 (13.11), 157 (51.15), 131 (13.08), 102 (78.34). C₁₂H₇N₃S₂O₃ (305) Calcd.: S, 20.98 Found S, 20.75.

Ketone thiocarbohydrazones (8a-d)

A mixture of compound **7** in hot water (10 mL) and the appropriate heteroaldehydes/ ketone (1:1 molar ratio) in ethanol-acetic acid (1:1, 50 mL) mixture was refluxed for 1 h, cooled and poured onto an ice bath. The produced solid precipitate was filtered and crystallized from ethanol to give **8a-d** as pale – yellow crystals.

8a: Yield (85%), m.p. 182-184 °C. C₆H₈N₄S O (184) Calcd.: S, 17.39. Found S, 17.11.

8b: Yield (90.02%), m.p. 185-186 °C. C₆H₈N₄S₂ (200) Calcd.: S, 32.01. Found S, 31.89.

8c: Yield (95.1%), m.p. 230-231 °C. C₉H₁₂N₄S O (224) Calcd.: S, 14.28 Found S, 13.99.

8d: Yield (80.0%), m.p.260-261^oC. UV, λ_{nm} (DMF): 420. IR: ν cm⁻¹ = 3353 (NH₂), 3150 (NH, NH), 1684 (C=O), 1552 (C=N), 1349 (NCSN), 776 (phenyl CH). The MS, m/z (Int. %): 235(0.0), 203(18.21), 157 (C₈H₅N₃SO), 131 (35.13), 102 (78.11),90 (21.78). C₉H₉N₅SO (235) Calcd.: S,13.61 Found S, 13.41.

Formation of N¹, N³ – di (iminoaryl)thioureas, (9a-e)

In hot ethanol, compound **7** (10 mL) was mixed with the appropriate heteroaldehydes or ketones (1:2 molar ratio) in ethanol-acetic acid (1:1, 50 mL). The reaction mixture was refluxed for 1h, cooled, and poured onto ice. The produced solid was recrystallized from isopropyl alcohol to give yellowish-crystals **9a-e**.

9a. Yield (80%), m.p.230-232 ^oC. C₁₇H₁₈N₄SO₄ (374) Calcd.: S,8.55 Found S,8.15.

9b. Yield (75.2%), m.p.195-196^oC. C₁₁H₁₂N₆S (260) Calcd.: S,12.30 Found S,11,89.

9c. Yield (78.12%), m.p.196-197 ^oC. C₁₁H₁₀N₄SO₂ (262) Calcd.: S,12.21. Found S,11.88..

9d. Yield (75.05%), m.p.140-141 ^oC. C₁₁H₁₀N₄S₃ (294) Calcd.: S,32.65. Found S,32.45.

9e: Yield (80.0%), m.p.260-261^oC. IR: ν cm⁻¹ = 3150, 3099 (NH, NH),1647 (C=O), 1606 (C=N), 1354 (NCSN), 1211 (C-S), 769 (benzo- CH). MS, m/z (Int. %): 364(0.0), 203(17.27), 157 (85.15) , 131 (100), 102 (38.13). 90 (11.18). C₁₇H₁₂N₆SO₂ (364) Calcd.: S,8.79 Found S, 8.65.

1-(1H- 2-oxo-indol-3-hydrazono) thioxo-2,3,4,5-tetrahydropyrazol-3,5-dione (10)

Compound **8d** (0.01 mmol) with dimethyl malonate (0.01 mmol) in solution of sodium ethoxide (0.02 mol, 100 mL) were refluxed for 4 h. After cooling, the reaction mixture was poured onto ice-HCl. The produced solid precipitate was filtered and crystallized from acetic acid as faint yellow crystals. Yield (60.0%), m.p.185 – 186 ^oC. IR: ν cm⁻¹ = 3200-3080 (b, OH \rightleftharpoons NH, NH), 2890 (CH₂), 1693, 1670 (two C=O), 1348 (NCSN), 1185 (C-S), 780 (benzo - CH). MS, m/z (Int. %): 303(0.0), 247(M-56, CN₂O, 21.18), 203 (10.00), 1.47 (8.11) , 111 (12.12), 97 (12.12), 56 (100). C₁₂H₉N₅SO₃ (303) Calcd.: S,10.56; Found S, 9.96.

1,3-Di (1H- 2-oxo-indol-3-imino)-2- thioxobarbituric acid (11)

An accurate of compound **9e** (0.01 mmol) with diethyl malonate (0.01 mmol) in solution of sodium ethoxide (0.02 mol, 100 mL) were refluxed for 4 h. The reaction mixture was cooled, poured onto ice-HCl. The produced solid precipitate was filtered and crystallized from ethanol as deep yellow crystals. Yield (85.12 %), m.p.210-212 ^oC. IR: ν cm⁻¹ = 3090 (NH), 2980 (CH₂), 1720, 1693, 1670 (C=O), 1600, 1595 (C=N), 1350 (NCSN), 1199(C-S), 777 (benzo-CH). C₂₀H₁₂N₆SO₄ (432) Calcd.: S,7.40 Found S, 7.45.

N, N-Di (acyl/thioacyl/amido)thiocarbohydrazides (12a-d)

Carbon disulfide, phenyl isothiocyanate, adipoyl chloride or 4-methoxyphenyl chloride was added by dropwise addition to a solution of compound **7** (0.01 mmol) in DMF (20 mL). The reaction mixtures were refluxed for 1h, cooled and poured onto ice. The formed solids were filtered and crystallized from DMF to give yellowish crystals of **12a-d**, respectively. .

12a. Yield (75%), m.p.155-156 ^oC. C₃H₆N₄S₅ (258) Calcd.: S,62.01 Found S,61.75.

12b. Yield (80%), m.p.195-196^oC. C₁₅H₁₆N₆S₃ (376) Calcd.: S,25.55 Found S,25.27.

12c. Yield (78.1%), m.p.150-151 ^oC. C₂₁H₄₂N₄SO₂ (414) Calcd.: S,7.72. Found S,7.55.

12d. Yield (65.05%), m.p.165-166 ^oC. IR: ν cm⁻¹ = 3350 -3080 (b, NH, NH), 1580 (CONH), 1335 (NCSN), 1189 (C-S), 1080 (-C-O-Me). MS, m/z (Int. %): 374 (1.15), 107 (15.31), 74 (100, CN₂SH₂). C₁₇H₁₈N₄SO₄ (374) Calcd.: S,8.55 Found S, 8.41.

Di (3,5- diaminopyrrolin-1-yl)thioketone, 13

An equimolar mixture of **7** and malononitrile in DMF –EtOH (1:1, 100 mL, 1:1), was refluxed for 4h, cooled then poured onto ice. The solid formed was filtered and crystallized from ethanol to give **13** as deep –yellow crystals. Yield (90.2 %), m.p.110-112 ^oC. UV, λ_{nm} nm (DMF): 375 nm. IR: ν cm⁻¹:3300 (NH₂), 3100 (2 NH), 1580 (C=N), 1180 (C-S). MS, m/z (Int. %): 238 (M⁺,5.0), 203 (25.01), 157 (12.11), 143 (18.18), 56 (100, CN₂O). C₇H₁₀N₈S (238) Calcd.: S,13.44 Found S, 13.21.

2.4 Analytical procedures

2.4.1 Recommended Spectrophotometric determination of mercury (II)

In a series of volumetric flasks (25 mL), an appropriate concentration (0.2-2.0 $\mu\text{g mL}^{-1}$) of mercury (II) solution was allowed to react with the reagent **4** solution (1.50 mL, 0.05 % w/v). To the test solution, an approximate volume (5 mL) of Britton -Robinson buffer of pH 4-5 was added. The reaction mixture was completed with distilled water to the mark of the measuring flask (10 mL) and allowed to stand for 5 min before measuring the absorbance at λ_{max} 505 nm. The results were compared successfully with the concentration of mercury (II) determined with atomic absorption spectrometry.

2.4.2 Preparation of the immobilized reagent **4** polyurethane foams

The reagent **4** (0.1% w/v) in water-ethanol (1:1 v/v) was shaken with the PUFs cubes with efficient stirring for 30 min. The immobilized reagent PUFs cubes were squeezed and dried as reported (El- Shahawi, et al., 200, PP. 221

-228). The retained reagent **4** onto the PUFs cubes was determined employing the equation:

$$a \square (C_o - C) \frac{v}{w} \quad (2)$$

where, C_o and C are the initial and final concentrations (mol L^{-1}) of the reagent **4** in solution, respectively, v = volume of the reagent solution (liter) and w is the mass (g) of the PUFs sorbent.

2.4.3 Analysis of mercury (II) in water samples

Tap - and mineral water samples were collected from the laboratories of Chemistry Department, King AbdulAziz University, and local market of Jeddah city, KSA, respectively. The water samples were filtered through 0.45 μm cellulose membrane filter prior to analysis and stored in LDPE sample bottles (250 mL). The recommended general spectrophotometric procedure used to prepare the standard curve was followed. The concentration of mercury (II) ions was then determined following the recommended spectrophotometric procedure used for the preparation of the standard curve and employing the equation:

$$\text{Mercury (II) concentration} = C_{\text{std}} \times A_{\text{samp}} / A_{\text{std}} \quad (3)$$

where, C_{std} is the standard concentration and A_{samp} and A_{std} are the corrected absorbance of the sample and the standard at λ_{max} 505 nm, respectively.

Alternatively, the standard addition method was employed as follows: transfer known volume (5.0 mL) of the unknown water samples to the volumetric flask (25.0 mL) adjusted to pH.5-6 with B-R buffer (10 mL). An accurate volume (1.5 mL) of the reagent was added to the test solution and the reaction mixture was made up to the mark with distilled water. Repeat the same procedures after adding various concentrations (0.2-1.0 $\mu\text{g mL}^{-1}$) of mercury (II). Measure the true absorbance displayed by the test solutions before and after the addition of the standard (0.2-1.0 $\mu\text{g mL}^{-1}$) mercury (II) solution employing single wave spectrophotometry method. The concentration of mercury (II) was then determined via the calibration curve of the standard addition procedure.

3. Results and Discussion

Heterocyclic systems containing endo- and exocyclic sulfur atom show a wide spectrum of potential applications. Thus, 3-imino - 2- thioxo-4,5-dihydro-thiazolidine-4-one (**3**) and 3-imino-2-thioxo-3,4,5,6-tetrahydro -1,3-thiazine-4,6(2H)dione (**4**) were obtained from condensation of dithioic formic acid hydrazide (**1**) with aldehydes to give the thiohydrazones **2** followed by heterocyclization with chloroacetic acid in ethanol - sodium acetate medium to give **3** or with dimethyl malonate in sodium ethoxide allows the formation of compound **4** [Scheme I].

Formation of compound **3** may be takes place via the nucleophilic attack of sulfide (S^-) to the electropositive carbon of chloroacetic acid ($\text{CH}_2\text{-Cl}$) followed by another nucleophilic attack of more nucleophilic nitrogen of thiohydrazone (N-H) to other electrophilic carbon of acetic acid ($-\text{COOH}$).

Compound **4** may be formed via nucleophilic sulfur atom of dithioic moiety on a more electrophilic carbon dimethyl malonate followed by heterocyclization via second nucleophilic nitrogen on the other electrophilic carbon. On the other hand, condensation of compound **1** with cyclic 1, 2- bicarbonyl compounds as biacetyl & benzil (2:1 by molar ratio) afforded the bis- compounds **5a** and **5b**, respectively. Addition of phenyl / p- chlorophenyl iso thiocyanate in warming DMF yielded N- (arylamino-carbothia) dithioic formic acid hydrazide **6** [Scheme I].

Thiocarbohyrazide (El-Gendy et al, 2001, PP. 376 -383; Rastogi and Yadav, 2005, PP. 448 -451) is one of the most important materials for building heterocyclic compounds containing sulfur and nitrogen (Hassanien, 2003, PP. 1987 - 1997; El-Gendy, et al., 2001, PP. 376 - 383). Thus, condensation of thiocarbohyrazide **7** with cyclic and a cyclic

oxygenated compounds such as heteroaromatic aldehydes: pyrrole/furan/thiophene carboxaldehyde and cyclic hetero ketone e.g. indol-2,3-dione in boiling ethanol – acetic acid gave the mono hydrazone **8** (1:1 by moles) and/or the bis – hydrazone **9** (1:2 by moles) (Scheme II).

Heterocyclization of mono hydrazone **8d** was achieved via refluxing with dimethyl malonate in sodium ethylate furnished 1-[(2-oxoindol-3-ylimino) aminothia]-2,3-dihydro-pyrazol-3,5-dione (**10**). Under the same experimental conditions, refluxing compound **9e** with diethyl malonate afforded 1,

3-di(2-oxoindol-3-ylimino)-2-thioxo-4,5-dihydro-pyrimidin-4,6-dione, **11**. (Scheme II). Addition of CS₂ and phenyl isothiocyanate to **7**, in warming DMF yielded N, N- di (caramido) thioureas **12a** and **12b**, respectively, while compounds **12c** and **12d** were isolated from careful treatment of compound **7** with adipoyl chloride and p-methoxybenzoyl chloride in warming DMF (Scheme II). Heterocyclization of compounds **12** failed because the high acidity with electronic symmetry of molecule in addition to the resonance stabilization of the conjugated anion may be formed (Rastogi and Yadav, 2005, PP. 448 -451). Treatment of acid hydrazide with malononitrile is one of the most important routes for the synthesis of poly functional amino heterocyclic systems (Schachtner, et al., 1999, PP. 335 – 341; El-Gendy, et al., 2001, PP. 376 -383; Hassanien, 2003, PP. 1987 -1997; Rastogi and Yadav, et al., 2005, PP. 448 -451; Burghate et al., 2007, PP. 103 -108). Thus, refluxing thio carbohydrazide **7** with malononitrile in ethanol – DMF afforded di (3, 5-diaminopyrazolin-1-yl) thio ketone, **13** (Scheme II). Compound **13** was also prepared by nucleophilic attack of the first primary NH₂ to the first cyano group followed by ring closing reaction of a second nucleophilic attack of secondary NH₂ to other cyano group.

3.1 Antibacterial activity

Recent literature survey has revealed the need of new compounds endowed with antimicrobial activity. Previous investigation has shown that, some of cyclic sulfur – nitrogen compounds have excellent antimicrobial activity (Burghate, 2007, PP. 103 -108). Therefore, in this study the cyclic sulfur compounds **2**, **5**, **6**, **8**, **9** and **12** were screened as antibacterial active agents using cup – plate diffusion method (Burghate et al., 2007, PP. 103 -108). The used bacterial organisms included both gram positive and gram negative strains: e.g. *Escherichia. coli*; *Bacillus. subtilis*, *Staphylococcus. aureus*, *Pseudomonas .vulgaris* and *Shigella flexneri* in DMF. Streptomycin was used as standard antibiotic. The diameter of the inhibition zone in mm was measured at concentration of 100 µg mL⁻¹. The results are summarized in Table 1, where the compounds **6b** and **12a**, showed high activity, the other compounds presented moderate or low antimicrobial activity compared to streptomycin. The activity of compounds **6b** and **12a** may be attributed to the thiourea and dithioic moieties in their structures, respectively as reported (Abuo-Rahma, et al., 2009, PP. 3879 -3886).

3.2 Analytical application of compound 6-hydroxy-3-(2-oxoindolin-3-ylidene- amino)-2-thioxo-3,4,5,6-tetrahydro -1,3-thiazin-4(3H)-one, **4**

3.2.1 Spectrophotometric determination of trace amounts of mercury (II)

On mixing the compound **4** abbreviated as HOTT with mercury (II) ions in the aqueous media of pH 4-5 and shaking, for 2-3 min, a red colored complex was developed. The absorption spectrum of the reagent showed one well defined absorption peak at 336 nm (λ_2) nm, while the spectrum of the complex **4** at the same pH showed one peak at 505 nm (λ_2) nm (Fig. 1). Thus, in the subsequent work, the absorbance of the aqueous solution was measured at 505 nm against a reagent blank. Maximum absorbance of the produced colored complex was achieved at pH 4–5. In the aqueous solutions of pH < 4, the data revealed no complex formation between compound **4** and mercury (II) ions. In acidic pH, the equilibrium of the reagent moves to left, hence the quantity of the available dissociated species of the chelating agent **4** decreases and not able to form complex with mercury (II). The absorbance of the aqueous phase of pH \geq 6 decreased due to the formation of non- colored complex species of mercury (II) ions e.g. hydroxo-species of mercury (II).

The influence of the concentration of compound **4** revealed that, a 2 mL of 5.1×10^{-4} mol L⁻¹ of the reagent was sufficient to react quantitatively (97–98%) with mercury (II) up to 10 µg mL⁻¹ in the aqueous layer. The molar absorptivity (ϵ) at λ_{max} 505 nm calculated from the absorbance measurement was found equal to 2.5×10^4 L mol⁻¹ cm⁻¹. The chemical structure of the produced mercury (II) complex species was determined by continuous variation method (Sawyer, et al., 1984) at various concentrations of the mercury (II) ions and reagent. The results revealed the formation of complex species of 1:2 molar ratio of mercury (II) to the reagent. Thus, the chemical structure of the developed colored species is most likely Hg (HOTT)₂.

3.2.2 Figure of merits

The values of LOD and LOQ of mercury (II) were determined employing the equations (Miller, 1994):

$$\text{LOD} = 3 \delta / b \quad (4)$$

$$\text{LOQ} = 10 \delta / b \quad (5)$$

where δ , is the standard deviation of the blank reading and b is the slope of the calibration plot. The LOD and LOQ values were found equal to 0.16 and 0.52 $\mu\text{g mL}^{-1}$ mercury (II), respectively. These values could be improved by immobilizing the reagent **4** onto PUFs sorbent in packed column for quantitative collection of trace and ultra trace amounts of mercury. The level of precision is suitable for the routine analysis of the mercury (II) in various types of water samples. The analysis of mercury (II) at the concentration levels of 1.0-15 $\mu\text{g mL}^{-1}$ was achieved with a recovery percentage of $97 \pm 2.9\%$, ($n = 5$). A satisfactory recovery percentage of various mercury (II) species spiked to the tested water samples was also achieved.

3.2.3 Effect of diverse ions

The selectivity of the developed method for the determination of 10 $\mu\text{g mL}^{-1}$ of mercury (II) ions in the presence of a relatively high excess (0.05-0.1 mg mL^{-1}) of some cations e.g. Li^+ , Na^+ , K^+ , Ca^{2+} , PO_4^{3-} , Al^{3+} , Fe^{2+} , Ni^{2+} , Co^{2+} , and Zn^{2+} and the anions MnO_4^- and CrO_4^{2-} , chloride, nitrate, sulfate and fluoride was investigated. The tolerance limit was defined as the concentration of the added foreign ion causing a relative error within $\pm 2\%$ of mercury (II) determination. The results revealed that, all the tested cations does not interfered even at 1:100 tolerable concentration of mercury (II) to the diverse ions, respectively. The interference of MnO_4^- and CrO_4^{2-} was eliminated by the addition of NaN_3 and sodium sulfite in HCl media (1.0 mol L^{-1}), respectively. Thus, the developed method could be extended for the analysis of mercury in various water samples.

3.2.4 Retention profile of mercury (II) onto reagent 6 loaded PUFs

In aqueous solution of pH 4-5, mercury (II) forms an orange – red colored complex species with compound **4**. Thus, the sorption profile of the aqueous solutions containing mercury (II) at pH 4-5 by the reagent **4** loaded PUFs was studied after shaking for 1h at room temperature. The amount of mercury (II) in the aqueous phase after equilibrium was determined spectrophotometrically (Marczenko, 1986). The %E and the D of mercury (II) sorption onto the PUFs decreased markedly at $\text{pH} < 4$ and maximum uptake was achieved at $\text{pH} \sim 4-5$. The high retention of mercury (II) at pH 4-6 is most likely attributed to the deprotonation of the reagent **4** and the available active sites on the reagent loaded PUFs membrane that enhanced the retention of analyte via “solvent extraction and/ or chelation mechanism” (El-Shahawi, et al., 2005, PP. 221 -228). At $\text{pH} > 6$, the sorption performance of the reagent loaded PUFs towards mercury (II) decreased markedly. This behavior is most likely attributed to the instability, hydrolysis, or incomplete extraction of the produced complex of mercury (II) –reagent **4** in the PUFs solid sorbent. These results suggested the use of the reagent **4** treated PUFs in packed column for removal of mercury from wastewater samples after percolation at 5-10 mL min^{-1} flow rate. An acceptable removal percentage (97 ± 2.5) of mercury (II) was achieved.

3.2.5 Validation

The proposed method was validated by the complete removal of the spiked mercury (II) onto tap and wastewater samples at a total concentration $\leq 15.0 \mu\text{g mL}^{-1}$. An acceptable extraction percentage ($95 \pm 3.5\%$, $n = 5$) of mercury was successfully achieved with the aid of the calibration plot and standard addition procedures. The plot of mercury (II) added to the tested water sample versus the amount of mercury (II) retained was linear with a slope of 0.998 and a correlation coefficient of $r = 0.999$ confirming the performance of the developed method for mercury (II) removal from water.

4. Conclusion

New bioactive sulfur compounds bearing heterocyclic moieties were prepared. Only one compound **4** was successfully used as selective chromogenic reagent for single wave spectro- photometric determination of mercury (II) in aqueous media. The presence of different tautomerism in the structure of compound **4** participates effectively on complex formation. The values of LOD and LOQ of the developed spectrophotometric were found equal to 0.16 and 0.52 $\mu\text{g mL}^{-1}$ mercury, respectively. Moreover, the reagent **4** immobilized PUFs could be packed in column for on –line pre concentration and subsequent determination of mercury (II) ions at ultra trace concentrations.

Acknowledgement

The authors would like to thank the Deanship of Scientific Research and the Department of Chemistry, Faculty of Science, King Abdulaziz University, Jeddah, Saudi Arabia for the financial support under the grant number 170/428 and the facilities provided, respectively.

References

- Abdel-Rahman, R.M. (2000). Chemistry of uncondensed 1,2,4-triazines: Part II sulfur containing 5-oxo-1,2,4 – triazin-3-yl moiety. An overview. *Phosphorous, Sulfur, Silicon and the Related Elements*, 166 (1), 315-357.
- Abdel-Rahman, R.M. (2001). Role of Uncondensed 1,2,4-triazine Compounds and Related Heterocyclic systems as Therapeutic Agents. A Review. Part XV. *Pharmazie*, 56(1), 18-22.
- Abdel-Rahman, R.M. (2001). Role of Uncondensed 1,2,4-triazine Derivatives as Biocidal Plant Protection Agents. *Pharmazie*, 56 (3), 195- 204.
- Abdel-Rahman, R.M. (2001). Chemoselective heterocyclization of pharmacological activities of new heterocycles. A Review Part V: Synthesis of biocida sulfur containing 4- thiazolidinones. *Boll. Chim. Farmaceutico*, 140 (6), 401-410.
- Abuo-Rahma, G., Sarhan, H., Gad, G. (2009). Design, synthesis, antibacterial activity and physicochemical parameters of novel N-4-piperazinyl derivatives of norfloxacin. *Biorg.Med.Chem.*, 17, 3879-3886.
- Burghate, M.K., Grandhe, S.V., Ajmire, M.G., Berad, B.N. (2007). Synthesis of (substituted) benzylidenehydrazino-5-arylamino-1,3,4-thiadiazoles and their antimicrobial activity. *J. Indian Chem. Soc.*, 84, 103-108.
- El-Shahawi, M.S., Othman, A.M., Abdel-Fadeel, M.A. (2005). Kinetics, thermodynamic and chromatographic behavior of the uranyl ions sorption from aqueous thiocyanate media onto polyurethane foams. *Anal. Chim. Acta*, 546(7), 221-228.
- El-Gendy Z., Morsy J.M., Allimony H.A., Ali. W.R., Abdel-Rahman, R.M. (2001). Synthesis of heterocyclic nitrogen systems bearing systems 1,2,4- triazine moiety as anti-HIV and anti cancer drugs, Part III. *Pharmazie*, 56, 376 – 383.
- El-Gendy, Z., Morsy, J.M., Allimony, H.A., Abdel-Monem, W.R., Abdel-Rahman, R.M. (2003). Synthesis of some new heterocyclic nitrogen systems bearing 1,2,4-triazine moiety as anti HIV and anti Cancer drugs- Part III. *Phosphorous, Sulfur, Silicon and the Related Elements*, 178 (9), 2055- 2071.
- Gladis, J.M., Rao, T.P. (2004). Determination of trace amounts of gold in acid-attacked environmental samples by atomic absorption spectrometry with electrothermal atomization after preconcentration. *Anal. Bioanal. Chem.*, 379, 60 - 65.
- Hamza, A., Bashammakh A.S., Al-Sibaai, A.A., Al-Saidi, H.M., El-Shahawi, M.S. (2010). Dual-wavelength β -correction spectrophotometric determination of trace concentrations of cyanide ions based on the nucleophilic addition of cyanide to imine group of the new reagent 4-hydroxy-3-(2-oxoindolin-3-ylideneamino)-2-thioxo-2H-1,3-thiazin-6(3H)-one. *Anal. Chim. Acta*, 657, 69-74.
- Hassanien A.A. (2003). Phthalazinone in heterocyclic synthesis: Synthesis of some s-triazole, s-triazolothiadiazine and s- triazolothiadiazole derivatives as pharmaceutical interest. *Phosphorous, Sulfur, Silicon and Related Compounds*, 178, 1987 – 1997.
- Jozlowski, C.A., Ulewicz, M., Walkowiak, W, Girek, T., Tablonska, J. (2002). The effect of tautomeric rearrangement on the separation of Zn(II) and Cd(II) in ion flotation process with 4-thiazolidinone derivatives. *Minerals Engineering*, 15, 677- 682.
- Kadi, M.W., El-Shahawi, M.S. (2009). Differential pulse cathodic stripping voltammetric determination of uranium with arsenazo-III at the hanging mercury dropping electrode. *Radiochim. Acta*, 97, 613 - 620.
- Miller, J.C. Miller, J.N. (1994). *Statistics for Analytical Chemistry* 4th edn. Ellis-Howood, New York, p.115.
- Marczenko, Z. (1986). *Spectrophotometric determination of elements*, 3rd edition, Ellis Horwood Chichester, U.K, PP.68 -70, 203.
- Pandy, J.K., Sengupta, S.K., Pandey, O.P. (2006). Synthesis and spectroscopic studies on oxo vanadium (IV) tetraza macrocyclic complexes derived from substituted β -diketones and 2, 6-diaminopyridine. *J. Indian. Chem. Soc.*, 83, 107-109.
- Piper, J.R., DeGraw, J.I., Colwell, W.T., Johnson, C.A., Smith, R.L., Waud, W.R., Sirotnak, F.M. (1997). Analogues of methotrexate in rheumatoid arthritis. 2. Effects of 5-deazaaminopterin, 5, 10-Dideazaaminopterin, and Analogues on Type II Collagen-Induced Arthritis in Mice. *Eur.J. Med. Chem.*, 40 (3), 377- 384.
- Pulakesh, B. (2007). Synthesis and spectral properties of palladium (II) complexes derived from 5-methyl-3-formyl pyrrole thiosemicarbazone and 5-alkyl/aryl dithiocarbazates. *J. Indian Chem. Soc.*, 84, 544 -547.

- Ramadan, A.T., Abdel-Rahman, R.M., El-Behairy, M. A., Ismail, A.I, Mahmoud, M.M. (1993). The Thermodynamics of complexation of transition and lanthanides metal ions by 3- (α -carboxy - methylaminobenzylidene hydrazine)- 5,6-diphenyl-1,2,4-triazine. *Thermochim. Acta*, 222 (2), 291-303.
- Ramadan, A.T., Abdel-Rahman, R.M., Seada, M. (1992). Studies on complexes of copper (II), nickel (II), cobalt (II) and indium (III) with 3- (α -benzoyl)-benzylidenehydrazine - 5,6-diphenyl-1,2,4-triazine. *Asian J. Chem.*, 4, 569 - 574.
- Rastogi, R.B, Yadav, M. J. (2005). Synthesis of some molybdenum (V) and tungsten (V) complexes of 1- aryl – 2, 5- dithiohydrazodicarbonamides. *J. Indian Chem. Soc.*, 82, 448 – 451
- Sadasivan, V., Alaudeen, M. J. (2007). Synthesis and crystal structure of the zinc (II) complex of 5-(2, 3-dimethyl-1-phenyl-3-pyrazolin-5-one-4-ylhydrazono) hexahydropyrimidine-2-thioxo-4,5,6-trione. *Indian Chem. Soc.*, 46 (12) A, 1959- 1962.
- Sadasivan, V., Alaudeen, M. (2006). A study on the arylazo coupling reaction of bis-(acetyl-acetone) ethylene diaminocopper (II) and bis-(acetyl)acetone)ethylenediaminenickel (II). *J. Indian Chem. Soc.*, 83, 1145- 1148.
- Sawyer, D.T; W. R. Heinemann, W.R., Beebe, J. M. (1984). *Chemistry Experiments for Instrumental Methods*, John Wiley & Sons.
- Sbirna, L.S., Muresan, V, Sbiren, S, Muresani, N. (2005). Complex compounds of nickel (II) with bidentate heterocyclic ligands using both S and N as donor atoms. *J. Indian Chem. Soc.*, 82, 389 – 392.
- Schachtner, J.E., Nienaber, J., Stachel, H.D., Waissner, K. (1999). Fused 1, 2-dithioles, V: Carbenoid anions as intermediates in reactions of pyrrothines and their heteroanalogues. *Die Pharmazie*, 54 (5), 335 - 341.
- Sharma, R.N., Giri, P., Kmari, A., R.N. Pandey, R.N. (2006). Synthesis, spectral and antifungal studies of some iron (II, III) and cobalt (II) complexes of 4-amino-3-ethyl-5-mercapto-5-triazole. *J. Indian Chem. Soc.*, 83, 1139-1143.
- Sindhu S.K., Siddhu D.S., Aqarwal H., Chandra S.J. (2005). Cadmium (II) ion selective electrode based on pyridine-3-carboxaldehyde thiosemicarbazone. *J Indian Chem. Soc.*, 82, 472- 474.
- Yonetoku, Y, Kubta, H, Okamoto, Y., Toyoshima, A., Funatsu, M., Ishikawa, J, Takeuchi, M, Ohta, M, Tsukamoto, S-I. (2006). Novel potent and selective calcium-release-activated calcium (CRAC) channel inhibitors. Part 1: Synthesis and inhibitory activity of 5-(1-methyl-3-trifluoromethyl-1H-pyrazol-5-yl)-2-thiophenecarboxamides. *Bioorg. Med. Chem.*, 14, 4750- 4760.
- Zaki, M.T., Abdel-Rahman, R.M., El-Sayed, A.Y. (1995). Use of arylidenerhodanines for the determination of copper (II), mercury (II) and cyanide ions. *Anal. Chim. Acta*, 307, 127-138.

Table 1. Antibacterial activity of the prepared compounds

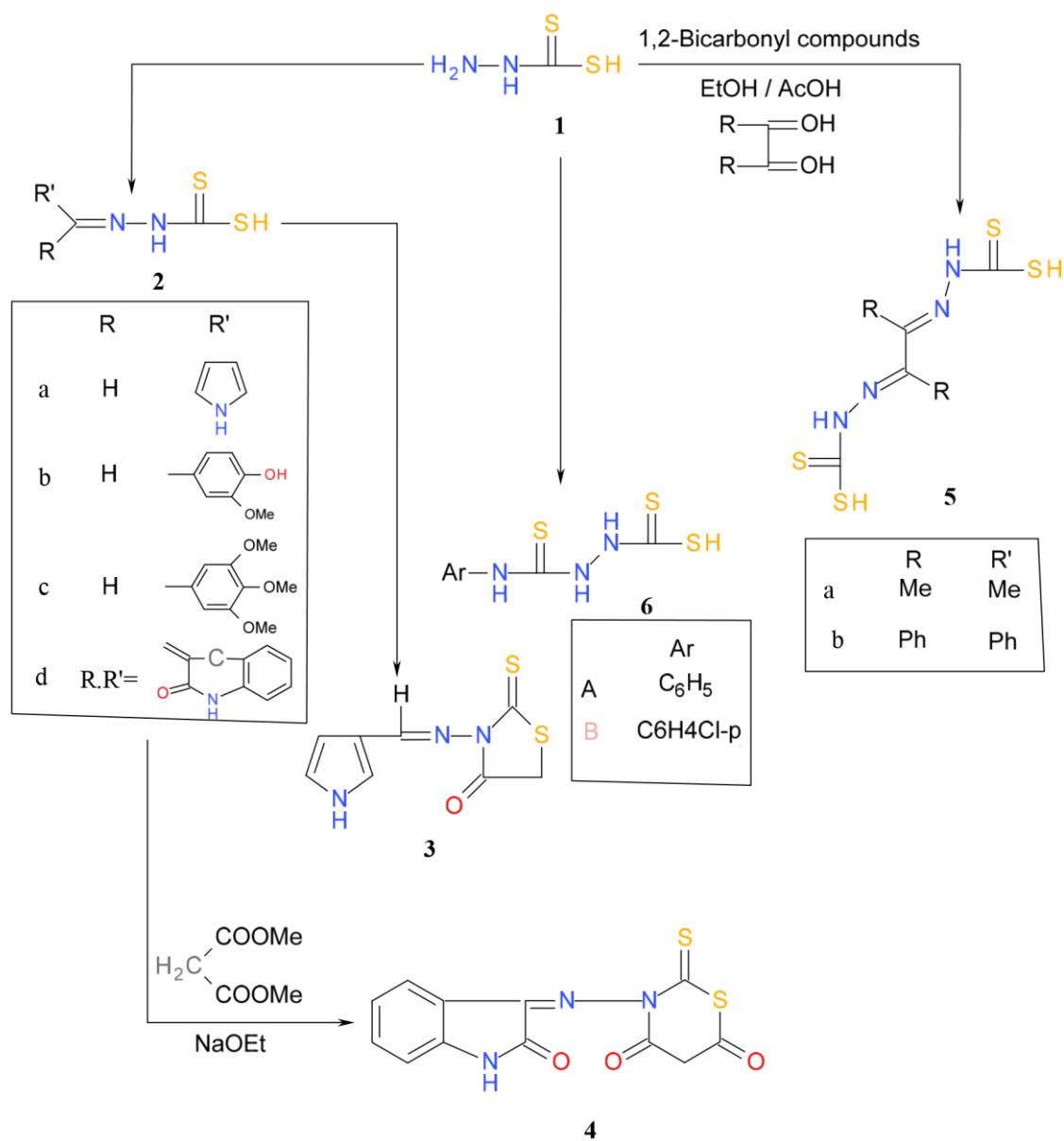
Compound No.	Inhibition zones (mm) ^k				
	E.c	B.s	S.a	P.v	S.f
1	16	15	17	15	18
2e	18	15	16	15	17
5	14	16	15	14	17
6b	23	21	21	22	24
7	15	15	15	15	15
8e	16	15	14	15	15

9e	14	15	14	15	16
12a	26	24	20	21	25
12b	22	21	20	22	24
Streptomycin	25	22	21	21	30

* *E. coli*; *B. subtilis*; *S. aureus*; *P. vulgaris* and *S. flexneri*.

Streptomycin: Reference antibiotics, Bristol-Myers Squibb, Giza, Egypt.

Highly active = inhibition zones > 19 mm; moderately active = inhibition zones 15 -19 mm and lethal active = inhibition zones 11-14 mm.



Scheme I

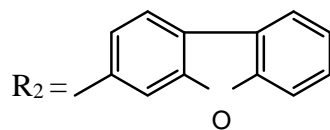
$R_1 = O\text{-substituted heterocyclic}$ 

Figure 1.

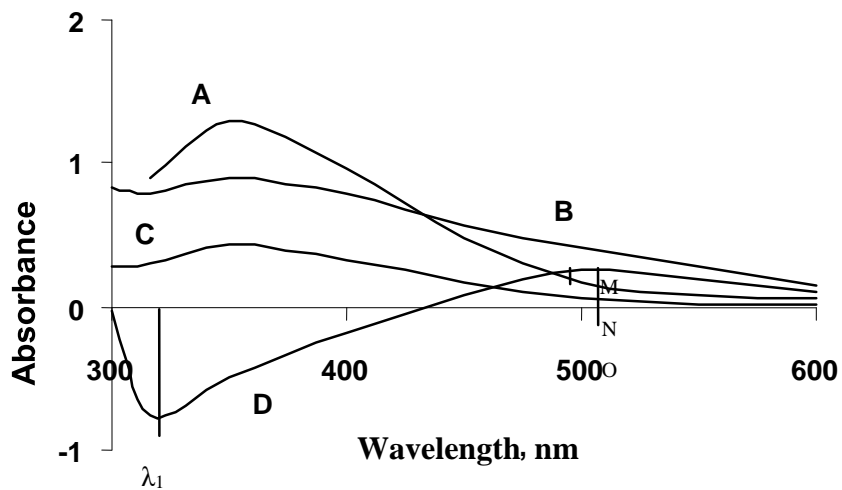


Figure 2. Absorption spectra of reagent 4 and its mercury (II) complex at pH 5-6. Curve A is the spectrum of the reagent blank (reference water); B is mercury (II) complex (reference, water); C is the excess of reagent (reference water) and D is mercury (II) complex (reference, reagent blank).

Synthesis of Polyfunctional Organic Systems Containing 1- Acyl / Aroyl - anilido-butadienes and their uses as Photochemical Probes and Chelating Agents for Removal of Bismuth (III) from Industrial Wastewater

Mohammed Saleh Tawfik Makki^{1*}, Reda Mohammady Abdel-Rahman¹, Mohammad El-Shahawi^{1,2}

¹Department of Chemistry, Faculty of Science, King Abdulaziz University, P. O. Box 80203 Jeddah 21589, Kingdom of Saudi Arabia

²Department of Chemistry, Faculty of Science at Damietta, Mansoura University, Mansoura, Egypt

Abstract

The present article reports the synthesis of a series of some new 1-acyl/ benzoyl -1-anilido-4-methyl /aryl-1, 3-butadiene derivatives (II - IV) by warming primary heteroamines and/or sulfa drugs with pre heated ethyl acetoacetate and / or ethyl benzoylacetate in dry conditions followed by condensation with unsaturated aromatic aldehydes in boiling ethanol-piperidine. The chemical structures of the compounds were characterized via their elemental analysis and spectroscopic measurements (UV Vis., IR, ¹HNMR). Some of the compounds (IIId, e, f, IV d, e,f) were tested as antimicrobial and photochemical probe agents. Compound IVa was physically loaded onto polyurethane solid sorbent and successfully used for the removal and / or pre concentration of bismuth (III) from industrial wastewater. The voltammetric behavior of the two compounds IIa and IVa in N, N-dimethylformamide was investigated.

Keywords: Synthesis; 1, 3-butadiene derivatives; Photochemical probes; Chelating agent; Bismuth (III); Wastewater; Voltammetry

Introduction

Polyfunctionally substituted oxo anilides e.g. azoloazines have received considerable interest in recent years (Hussein et al., 2009). Such class of compounds has diverse physiological activities e.g. acting as central nervous systems depressants and calcium sensitizing agents and possess hypnotic, diuretic, antihistaminic, anti-inflammatory, antimicrobial and hypoglycemic activities (Fathalla et al., 2001). The synthesis and spectroscopic characterization of b-diketones as potential ligands have been reported by Funk et al., 1993; Zheng and Swager, 1994. In this class of compounds, complex formation is conceived by replacement of the enolic proton by chelation with metal ions in a bidentate fashion (Sievers et al., 1993; Knoevenagel and Arnot, 1904).

The b- diketone 3- salicylidene-2, 4- pentanediones and related compounds have been used successfully as proper chelating agents for a series of metal ions (Mishra et al., 1991; Wang et al., 1997). Knoevenagel condensates of substituted benzylidenes with active methylene compounds have been performed efficiently using ultra stable Zeolite as heterogeneous catalyst (Veeraraj et al., 2000). The chelation behavior of a series of dicarbonyl towards some metal ions has been reported (Krishnankutty and Venugopalan, 2001). Metal chelates of b- diones have shown interesting properties in particular in industrial applications (Krishnankutty and Venugopalan, 2001; Cerchiaro et al., 2006; Krishnankutty and Ummathur, 2006). AbdelRahman et al., 1991; Ramadan et al., 1993; Abdel-Rahman, 1988).

A series of benzoyl -acetanilides and their physico organic properties have been reported by (Abdel-Rahman, 1988; AbdelRahman et al., 1991). The starting material prepared has been used for building a series of novel bio- active pyrazoline derivatives. The thermodynamic characteristics and spectroscopic characterization of a series of hydrazone - 1,3- bi carbonyl derivatives and their lanthanide complexes have been investigated (Abdel-Rahman et al., 1991; Ramadan et al., 1993). The dimerized species of 2- diazo-3- methyl-1-phenyl-5- pyrazolone have produced 4- (5-hydroxy-4pyrazolylimino-2-pyrazolin-5- one.

Recent literature survey has indicated that, no work on the Knoevenagel condensate b- ketoanilide and its metal chelates. Therefore, in continuation to our previous work (Bashammakh et al., 2009; Abou-Mesalam et al., 2003; El-Shahawi et al., 2005; El-Shahawi et al., 2008; Farag et al., 2007; Zaki et al.1995), the present study is focused on the synthesis and characterization of a series of some b-diketone derivatives bearing anilido moieties and their unsaturated b-diketone derivatives. In view of their properties, some of the compounds were tested as antimicrobial and photochemical agents. Moreover, one of the prepared compounds for the pre-concentration/separation of bismuth (III) from aqueous as a highly toxic metal ions the industrial waste water. The cyclic voltammetry of two selected compounds were also investigated. **Experimental**

Apparatus & measurements

A Perkin Elmer (Lambda EZ-210) double beam spectrophotometer (190-1100 nm) with 1cm (path width) was used for recording the electronic spectra of the prepared solutions. A Perkin-Elmer (Analyst TM 800, USA) atomic absorption spectrometer (AAS) was used for measuring the concentration of bismuth (III) ions before and after extraction at the optimum operational parameters of the instrument. A Perkins Elmer model RXI-FT-IR system 55529 was used for recording the IR spectra of the prepared compounds. A Bruker advance

*Corresponding author: Mohammed Saleh Tawfik Makki, Department of Chemistry, Faculty of Science, King Abdulaziz University, P. O. Box 80203 Jeddah 21589, Kingdom of Saudi Arabia, Tel: 00-9662-6952000; Fax: 00-9662-6952292; E-mail: mmakki@kau.edu.sa

Received July 06, 2010; Accepted August 21, 2010; Published August 21, 2010

Citation: Makki MST, Abdel-Rahman RM, El-Shahawi MS (2010) Synthesis of Polyfunctional Organic Systems Containing 1- Acyl / Aroyl - anilido-butadienes and their uses as Photochemical Probes and Chelating Agents for Removal of Bismuth (III) from Industrial Wastewater. J Bioanal Biomed 2: 085-090. doi:10.4172/1948593X.1000028

Copyright: © 2010 Makki MST, et al. This is an open-access article distributed under the terms of the Creative Commons Attribution License, which permits unrestricted use, distribution, and reproduction in any medium, provided the original author and source are credited.



DPX 400 MHz model using TMS as an internal standard was used for recording the ¹H NMR spectra of the compounds on deuterated DMSO. A GC-MS-QP 1000-Ex model was used for recording the mass spectra of the compounds. A Metrohm 797 VA trace analyzer and 797 VA stand were used for recording the cyclic voltammetric (CV) experiments. In the CV experiments, a three-compartment (Metrohm) voltammetric cell (10 mL) incorporating Pt wire as working, double junction Ag/AgCl, (3M KCl), as reference and Pt wire (BAS model MW1032) as counter electrodes, respectively. The surface area of the counter electrode was 100 times larger than the area of the working electrode. Digital pH-meter (model MP220, Mettler Toledo) was used for pH measurements. Melting points were determined with an electro thermal Bibby Stuart Scientific Melting Point SMPI (US). Molecular weights and elemental analysis of the compounds were performed on Micro analytical center, Cairo University, Egypt. Microanalysis of nitrogen and sulfur (%) was performed in Microanalytical Center, AinShams University, Cairo, Egypt.

Reagents & materials

Low density polyethylene (LDPE) bottles, Nalgene were carefully cleaned first with hot detergent, soaked in 50% HCl (Analar), HNO₃ (2.0 mol L⁻¹), subsequently washed with dilute HCl (0.5 mol L⁻¹) and finally rinsed with distilled water. N, N-Dimethylformamide (DMF) and the supporting electrolyte tetraethyl ammonium chloride (TMA⁺. Cl⁻) were purchased from BDH chemicals. The sample solution was stored in LDPE bottles and stored at -20°C. Britton – Robinson (B – R) buffers of pH 2-10 were prepared from the acid mixture of phosphoric acid, boric acid, acetic acid (0.04 mol L⁻¹) and adjusting the pH to the required value with sodium hydroxide (0.20 mol L⁻¹). A stock BDH stock solution of bismuth (1000 µg mL⁻¹) in dilute nitric acid was used. A series of standard bismuth (III) solutions in the range 1-100 µg mL⁻¹ was then prepared in doubly distilled water in the presence of few drops of nitric acid (5% m/v). Stock solutions (1x 10⁻² mol L⁻¹) of the compounds –acyl-1-anilido-4- methyl-1,3- butadiene, IIa and 1-benzoyl-1-anilido-4- methyl-1,3- butadiene, IVa in DMF were prepared.

Organic preparation

Preparation of acyl/benzoyl acetanilide derivatives I and III:

To preheated ethyl acetoacetate and/or ethylbenzylacetate (0.01 mol) a selective hetero primary amines and/or sulfa drugs (0.01 mol) were added in dry system then warmed for 10-15 min at 100-110°C, cooled

and finally washed with diethyl ether. The resultant solid was dried and crystallized to give I and III respectively (Table 1).

Preparation of 1-acyl/benzoyl-1-anilido-4-methyl/aryl-1,3butadiene (II and IV): Equimolar mixture of compounds I and/or III and unsaturated aldehydes as crotonaldehyde and/or 4-dimethylaminocinnamaldehyde in absolute ethanol (100 mL), piperidine (0.5 mL) was heated under reflux for 8 h, cooled. The solvent was removed and the obtained solid was crystallized to give II and IV respectively (Table 1).

Preparation of the reagent IVa immobilized PUFs packed column

Polyurethane foam (PUFs) cubes immobilized with the reagent IVa were prepared by mixing the dried foam cubes with the required weight of the reagent (0.05% w/v) in ethanol with efficient stirring for 10 min. The reagent immobilized PUF cubes were then dried to remove the excess reagent with filter papers as reported earlier (Abou-Mesalam et al., 2003; El-Shahawi and El-Sonbati, 2005; ElShahawi et al., 2008). The reagent immobilized PUFs were packed separately in the glass columns by applying the vacuum method of foams packing.

Pre concentration and/ or separation of bismuth (III) by reagent IVa treated PUFs

An accurate weight (0.1±0.01g) of the reagent IVa treated foam cubes was equilibrated with 50 mL of an aqueous solution containing bismuth (III) ions at concentration of 10 µg mL⁻¹. The solutions were then adjusted to the required pH with B-R buffer (pH 2-10). The test solutions were then shaken for 2 h on a mechanical shaker. The aqueous phase was then separated out by decantation and the amount of bismuth (III) remained in the aqueous phase was determined with atomic absorption spectrometry at the optimum wavelength. The amount of bismuth (III) retained on the PUFs cubes was determined from the difference between the concentration of bismuth (III) solution before (C_o) and after (C_a) shaking with the foam cubes.

Results and Discussion

Spectroscopic characterization

Synthesis of 1,3-dicarbonyl anilido and their unsaturated derivatives is very simple and of general applicability. It gives pure compounds with improved yields. Thus, warming some hetero primary amines such as 4-aminoantipyrine, 2-amino-5chloropyridine, 2-amino-5-nitropyridine, 2-amiobenzthiazole and

Compd No.	M.P. (°C)	Yield (%)	Solvent	M. Formula	M. Weight		Nitrogen, %*		Sulfur. %*	
					Found	Calcd	Found	Calcd	Found	Calcd
Ia	130	80	Pet. ether 60-80	C ₁₅ H ₁₇ N ₃ O ₃	285	287	13.10	14.63	-	-
Ib	165	70	Pet. ether 60-80	C ₉ H ₉ N ₂ ClO ₂	210	212	13.42	13.20	-	-
Ic	158	75	Pet. ether 60-80	C ₉ H ₉ N ₃ O ₄	221	223	17.73	18.81		
Id	225	75	Pet. ether 60-80	C ₁₁ H ₁₀ N ₂ SO ₂	231	234	11.52	11.96	13.43	13.40
Ie	135	80	Pet. ether 60-80	C ₁₀ H ₁₂ N ₂ SO ₄	254	256	9.99	10.93	12.35	12.5
If	210	85	Pet. ether 60-80	C ₁₄ H ₁₄ N ₄ SO ₄	333	334	16.64	16.76	9.46	9.58
IIa	150	72	THF	C ₂₀ H ₂₀ N ₄ O ₄	377	380	14.61	14.73	-	-
IIb	170	75	THF	C ₁₅ H ₁₄ N ₂ SO ₂	284	286	8.85	9.79	11.04	11.18
IIIa	140	73	Pet. Ether 100-140	C ₂₀ H ₁₈ N ₃ O ₃	345	349	11.21	12.03		
IIIb	170	78	Pet. Ether 100-140	C ₁₄ H ₁₁ N ₂ ClO ₂	273	275	9.51	10.18		
IIIc	162	80	Pet. Ether 100-140	C ₁₄ H ₁₁ N ₃ O ₄	283	285	13.7	14.73		
IIId	300	90	Pet. Ether 100-140	C ₁₆ H ₁₂ N ₂ SO ₂	296	296	8.55	9.45	10.57	10.81
IIIe	240	85	Pet. Ether 100-140	C ₁₅ H ₁₄ N ₂ SO ₄	314	318	7.90	8.80	9.83	10.06

Citation: Makki MST, Abdel-Rahman RM, El-Shahawi MS (2010) Synthesis of Polyfunctional Organic Systems Containing 1- Acyl / Aroyl - anilidobutadienes and their uses as Photochemical Probes and Chelating Agents for Removal of Bismuth (III) from Industrial Wastewater. J Bioanal Biomed 2: 085-090. doi:10.4172/1948-593X.1000028

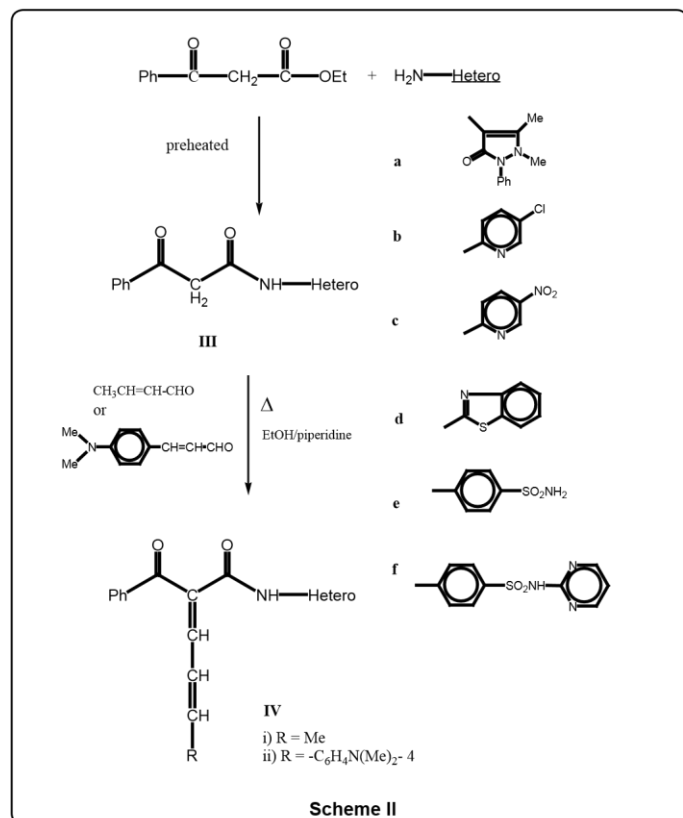
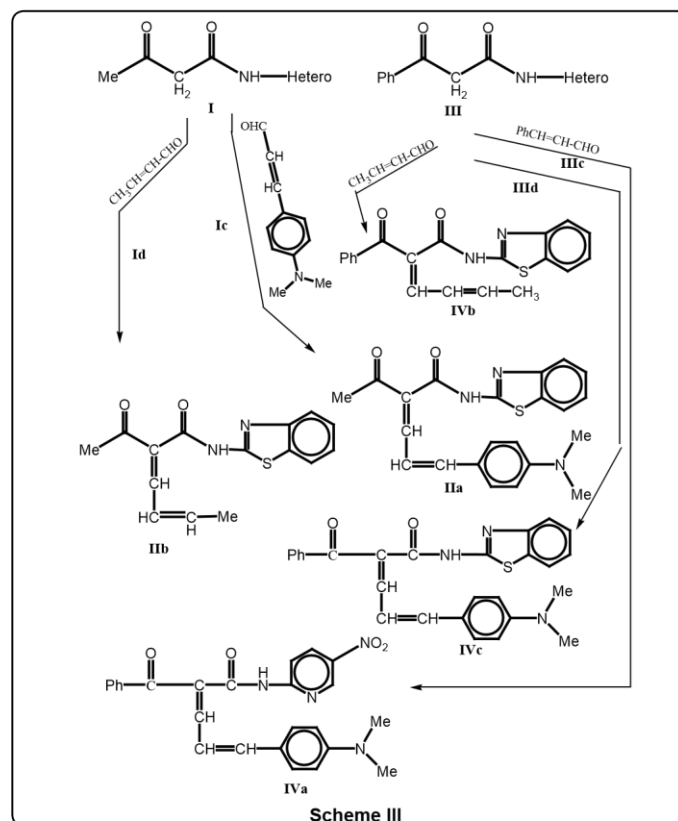
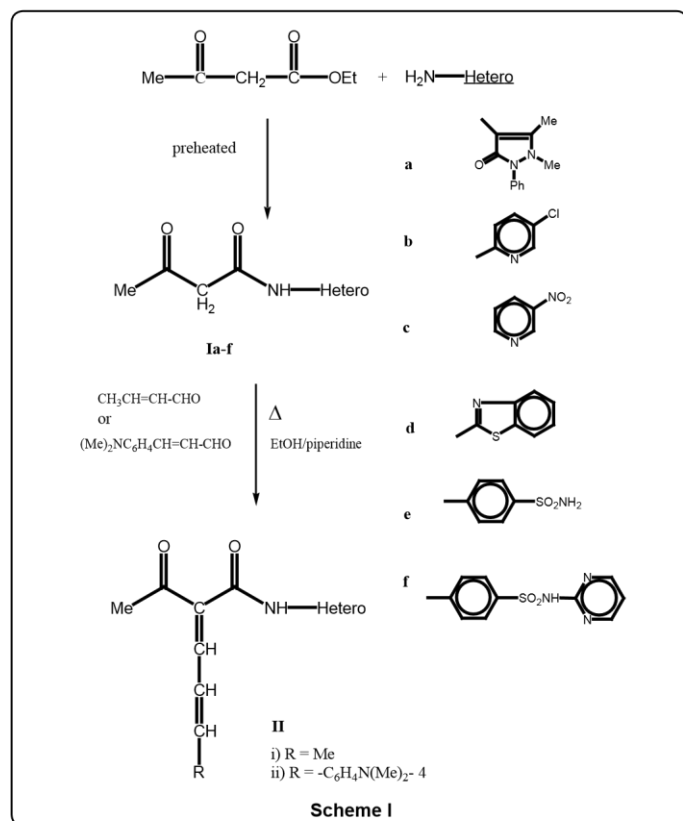
III f	335	82	Pet. Ether 100-140	C ₁₉ H ₁₆ N ₄ O ₄	396	396	12.93	14.14	-	-
IV a	125	70	Diethyl ether	C ₂₅ H ₂₂ N ₄ O ₄	441	442	12.2	12.66	-	-
IV b	280	72	Diethyl ether	C ₂₀ H ₁₆ N ₂ SO ₂	346	348	7.1	8.04	8.88	9.19
IV c	140	60	Diethyl ether	C ₂₇ H ₂₃ N ₃ SO ₂	451	453	8.5	9.27	6.9	7.06

*Analytical data of **C** and **H** for the compounds are within the range ± 0.4 - 0.7% of the theoretical values.

Table 1: Physical properties of prepared compounds I-IVc.

Volume 2(4) : 085-090 (2010) - 086





some sulfa drugs as sulfanilamide and sulfadiazine with preheated ethyl acetoacetate and/or ethyl/benzoyl acetate at 100-110°C for 10-15 min in dry condition led to the formation of acyl/benzoyl acetanilide

derivatives I and III (Scheme I, II). Knoevenagel condensation of compounds I and III with unsaturated aldehydes such as crotonaldehyde and/or 4-dimethylcinnamaldehyde in boiling ethanol with few drops of piperidine as catalyst afforded 1-acyl/benzoyl -1-anilido-4-methyl-1,3-butadiene (II) and 1-acyl/benzoyl -1-anilido-4-(4'-dimethylaminophenyl)-1,3-butadiene (IV), respectively. The compounds prepared are summarized in schemes 1-III. Both carbonyl compounds I-IV having a second carbonyl at β -position, are termed as β diketones. In general hydrogen bonding is possible only in syn form and not in anti form, where the orientation of enolization is towards the aryl or phenyl groups (Mishra et al., 1991) indicating the high enolic content of 4-aryl-1,3-diketones and not in 4-methyl-1,3-diketones.

UV - Visible spectra of compounds II and IV have two strong bands around 360 and 260 nm which characteristics bands of carbonyl chromophore and the conjugated $C=C$ of butadiene ($n \rightarrow \pi^*$ and $\pi \rightarrow \pi^*$ transitions) while that of compounds I and III recorded a low bands at 330 and 240 nm due to a bathochromic shift, indicating the involvement of the two carbonyl groups isolated by methylene group, assigned to the intramolecular charge transfer interaction involving the whole molecule (Sawyer et al., 1984).

IR spectra of compounds I and III show no characteristic $C=O$ absorption band at ν 1725-1710 cm^{-1} which is present in the spectrum of acetylacetone \sim 1680 cm^{-1} while that of II and IV recorded of strong absorption bands at ν 1650 cm^{-1} of true $C=O$ group. Also, intramolecular as well as intermolecular hydrogen bonding are observed in the regions 2700-2500 and 3000-2900 cm^{-1} respectively. The presence of absorption bands at 1610-1480 cm^{-1} ($C=C$) and 960-900 cm^{-1} confirm the presence of trans $-CH=CH-$ moiety of compounds II and IV, respectively. These vibrations indicate that the transformation of the electronic effect is quite apparent through the part comprising the NH, OH and CO groups.



¹HMR spectra of compounds I and III showed a one proton signal at δ~15 ppm confirming the presence of strong intramolecular hydrogen bonded enol proton, in addition, a signal appeared at δ 6.5-6.8 (methine) 6.9-7.9 ppm (aryl)protons. In such systems, the maximum enolization is two especially if containing aryl moieties. On the other hand, ¹HMR spectra of compounds II and IV, showed a resonance signals at 8.0-8.5 ppm (olefinic), 2.5 ppm (methyl protons (due to an allylic coupling between HC=CH and methyl group), in addition of aromatic protons at δ 6.7-7.7 ppm. The tautomeric forms of compounds I and III were confirmed via ¹HMR where, one resonated singlet for proton linked to sp³-carbon at δ 4.66 ppm was noticed. The structures of the compounds Id and IIIId were deduced from ¹³C NMR. The spectrum of compound Id showed δ at 29.9 (CH₃), 202.8 (C=O), 51.7 (CH₂), 164 (b C=O), 174.5 (S-C=N), 153, 130 (C₄ & C₅ of thiazole) and 118 -121.8 ppm (benzocarbons); while compound IIIId revealed δ at 194.2 (C=O), 117 (HO-C=C), 66 (CH=C-OH), 174.5 (S-C=N), 153, 130.8 (C₄ & C₅ of thiazole) and 118.3 -122.8, 136 -128 ppm (benzo and phenyl protons). Based on ¹H and ¹³C NMR data, the acyl/benzoyl anilide derivatives are mainly present in enolic structure with intra molecular hydrogen bonding in solution state. The acyl/benzoyl anilides existed predominantly in the cis- form via some type of interaction.

Mass spectra of compounds I-IV confirmed the degree of stability as indicated from the equilibrium between ketonic and enolic forms. Fragmentation also revealed the loss of Me-CO and Ar-CO from their chemical structures. A good physico chemical evidence for the presence of enolic and or ketonic tautomers of compounds I and III was deduced from free solubility of their Ar-NHCO derivatives in aqueous NaOH which confirm that the enolization forms take place towards aryl and or phenyl groups (Mishra et al., 1991).

Applications of the prepared compounds

Biocidal activity: Some of the synthesized compounds were tested *in-vitro* against microorganisms such as bacteria *Escherichia. Coli* and the fungi *Aspergillums fumigates* in DMF using the agar diffusion disk method (Barry et al., 1981; Winker et al., 1962). The results are compared with piperillin and mycostatine as standard antibiotic. The antimicrobial potentialities of the tested compounds were evaluated by placing pre sterilized filter paper disks (11 mm diameter) impregnated with 50 mg/disk using DMSO as solvent which revealed no zone (IZ) after 5 days incubation at 28°C for fungi (Table 2). Photochemical probe effects of these compounds were determined before and after using UV light at 366 nm as a second test (Table 2). The compounds IIIe,d,f and IVe,d,f showed a highly biocidal effect and only compounds IIIe,d,f were found characterized by photo chemical probe action lower than other prepared compounds. This behavior is most likely attributed to the rich oxygen atoms in their structures with multi excitation states.

Pre concentration and / or separation of bismuth (III) onto reagent IVa immobilized PUFs

In preliminary experiments the use of the reagent IVa immobilized

Compound 50 mg/mL	Before UV irradiation		After UV irradiation at 366 nm	
	Bacteria Escherichia coli	Fungi Asperigillus fumigates	Bacteria Escherichia coli	Fungi Asperigillus fumigates
IIIId	15	17	18	22
e	20	22	25	24
f	25	21	27	27
IVd	13	12	14	14
e	12	10	15	15
f	14	14	17	18

*Highly active >20 mm; moderate (15 - < 20 mm) and weak < 15 mm.

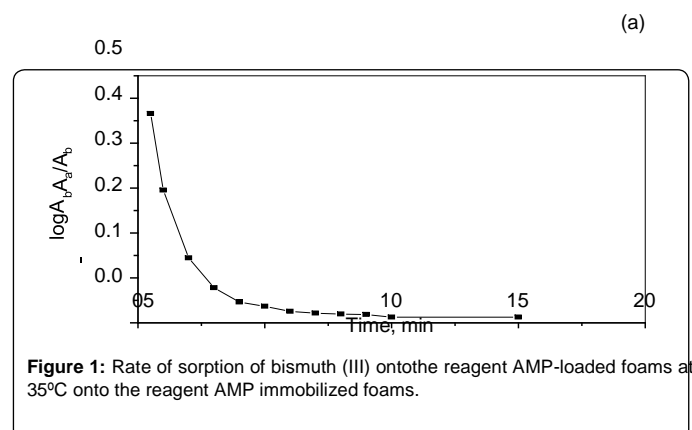
Table 2: The Biocidal and photochemical Effects of Some Compounds*

PUFs for the pre concentration of bismuth (III) from aqueous solution was examined by batch mode of separation. Reasonable amount of bismuth (III) ions are retained onto the reagent immobilized PUFs from the test aqueous solutions. The amount of bismuth (III) retained on the reagent treated PUFs depends on the solution pH. Thus, the sorption profile of bismuth (III) (10.0 µg mL⁻¹) from aqueous solutions (50.0 mL) containing excess of KCl, KBr or KI at different pH (pH 2 -10) onto the reagent loaded foams was examined. After shaking the solutions for 2 h, the amount of bismuth (III) remained in the aqueous solution was determined by. The amount of bismuth (III) retained, the extraction percentage, %E and the distribution ratio, D was then calculated as reported earlier (Abou-Mesalam et al., 2003; El-Shahawi et al., 2005; El-Shahawi et al., 2008). Maximum retention of bismuth (III) by the immobilized reagent PUFs was achieved from the aqueous media of pH 2-3 containing excess iodide ions and the sequence of bismuth (III) uptake followed the order: iodide > bromide > chloride.

On the other hand, the retention of bismuth (III) from the aqueous iodide media decreases on increasing the solution pH. The observed decrease on the bismuth (III) retention at pH >3.5 is most likely attributed to the instability of bismuth-iodide or the ternary complex involving [BiI₄]⁻. IVa⁺] due to the hydrolysis of the species formed between [BiI₄]⁻ and the reagent immobilized polyurethane foams. Similar trends were also reported earlier (Abou-Mesalam et al., 2003; El-Shahawi and El-Sonbati, 2005; El-Shahawi et al., 2008). Thus, a “weak base anion ion exchanger” and a “solvent extraction” mechanism of the [BiI₄]⁻_(aq) may be proposed for the uptake onto the protonated ether (-CH₂-HO⁺-CH₂-) or urethane (-NH⁺₂COO⁻) linkages of the immobilized PUFs.

The effect of contact time and shaking time on the retention of bismuth by the treated AMP- PUFs of bismuth (III) from the aqueous solution containing high excess of KI (5-7% w/v) by AMP-loaded foam was carried out at pH 2.0. The bismuth (II) uptake was fast and reached maximum within ~ 10-15 min contact time. The half-life time (t_{1/2}) of the equilibrium sorption of bismuth (III) as calculated from the plot of -log (C_b- C_a)/C_b versus time onto the reagent immobilized PUFs from the aqueous media to reach 50% saturation of the sorption capacity was in the range 1-1.5 min (Figure 1). The uptake of bismuth (III) ions was fast within the first 10 min and increased up to a constant value in less than 60 min shaking time. Thus, a shaking time of 60 min was adopted in subsequent experiments.

The analytical utility of the reagent IVa treated PUFs solid sorbent was successful assessed using the reagent IVa immobilized PUFs in packed column for complete retention of different concentrations (100 mL, 5-1000 µg L⁻¹) of bismuth (III) in de ionized water. The sample solutions were percolated through the PUFs packed column



Volume 2(4) : 085-090 (2010) - 088

Bismuth (III) species		Recovery, %*
Added, µg/mL	Found, µg/L	
1.0	0.98	96.0± 1.8
5.0	4.7	94.0± 2.7

*Average ± relative standard deviation

Table 3: Retention and recovery of bismuth (III) in wastewater samples by the reagent IVa treated PUFs packed column.

at flow rate of 10 ml min⁻¹. Quantitative retention of bismuth (III) was achieved onto PUFs packed column as noticed from the analysis of bismuth in the effluent solutions by FAAS.

The removal of bismuth (III) from industrial wastewater was also carried out following the same procedures. The water samples of industrial wastewater (0.1 L) of electroplating industry after acidified with phosphoric acid was spiked with various concentrations (1 and 5 µg mL⁻¹) of bismuth (III), acidified with phosphoric acid and filtered through a 0.45 µm cellulose membrane filter. The test water samples were percolated through the reagent packed column at 5 mL min⁻¹ flow rate. The analysis of bismuth in the effluent solution by FAAS revealed complete retention of cadmium from the test solution. The results are summarized in Table 3. Bismuth was quantitatively recovered with acidified solution of nitric acid (10 mL, 3.0 M) and analyzed by FAAS. A satisfactory recovery percentage of total cadmium was achieved in the range 94 – 96 .0±2.7.

Voltammetric study

The cyclic voltammograms (CVs) of the compounds 1-acyl-1-anilido-4-methyl-1,3-butadiene, IIa and 1-benzoyl-1-anilido-4-methyl-1,3-butadiene, IVa in DMF-TMA⁺.Cl⁻ at Pt working electrode versus Ag/AgCl reference electrode at various scan rate were investigated. The results are shown in Figure 2 and Figure 3. The CV of compound IIa (Figure 2) at 100 mVs⁻¹ revealed two well-defined cathodic peaks at 0.1 and -0.75 V versus Ag/AgCl electrode. One well defined anodic peak at -0.15 V was observed on the reverse scan suggesting the irreversible nature of the observed electrochemical process in the employed potential range (-2.0 - 2.0 V). On raising the scan rate (>100 mV s⁻¹), the potential of the two cathodic peaks were shifted cathodically, while the anodic peak shifted anodically confirming the irreversible nature of the observed electrochemical processes (Bashammakh et al., 2009; Bard and Faulkner, 1980). The observed cathodic peaks are most likely assigned to the reduction of the carbonyl group via 2H⁺/2e in two successive one electron / one proton reduction steps (Bard and Faulkner, 1980). Continuous scan of the CV significantly decreased the peak current height indicating passivity of the surface of the Pt electrode via formation of polymeric oxidation product or fouling of the Pt electrode by the produced reduction products suggesting prior adsorption on the surface of the electrode in the potential range (Bard and Faulkner, 1980).

In DMF-TMA⁺.Cl⁻ the CVs of the compound IVa (Figure 3) at the Pt working electrode showed two reduction peaks at 0.1 -0.15 and -0.65- -0.8 V coupled with one broad anodic peak in the potential range 0.3-0.4 V at scan rates of 50-1000 mVs⁻¹ versus Ag/AgCl electrode. The cathodic peaks are safely assigned to the reduction of the carbonyl group in two successive H⁺/e redox steps (Bashammakh et al., 2009). The peak –peak potential difference ($\Delta E_p = (E_{p,a} - E_{p,c})$) between the cathodic (E_{p,c}) and anodic peaks (E_{p,a}) indicated that, the observed redox processes are irreversible. On raising the scan rate both cathodic and anodic peaks are shifted to more negative and positive potential,

respectively confirming the irreversible nature of the observed redox process (Bard and Faulkner, 1980). The plot of the the cathodic peak current (i_{p,c}) versus the square root of the scan rate was linear indicating that the electrochemical processes

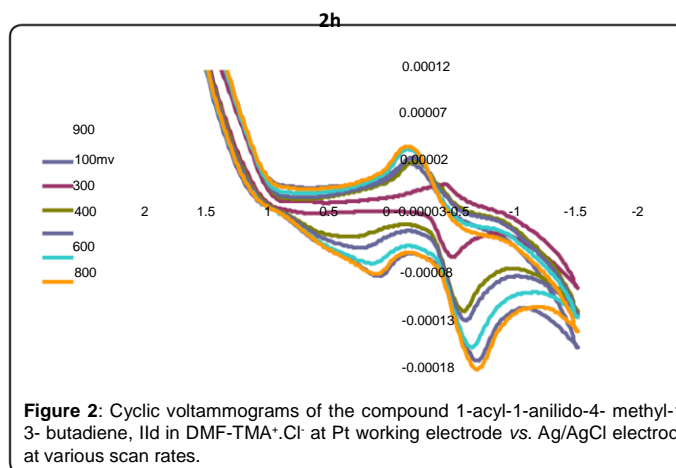


Figure 2: Cyclic voltammograms of the compound 1-acyl-1-anilido-4-methyl-1,3-butadiene, IIa in DMF-TMA⁺.Cl⁻ at Pt working electrode vs. Ag/AgCl electrode at various scan rates.

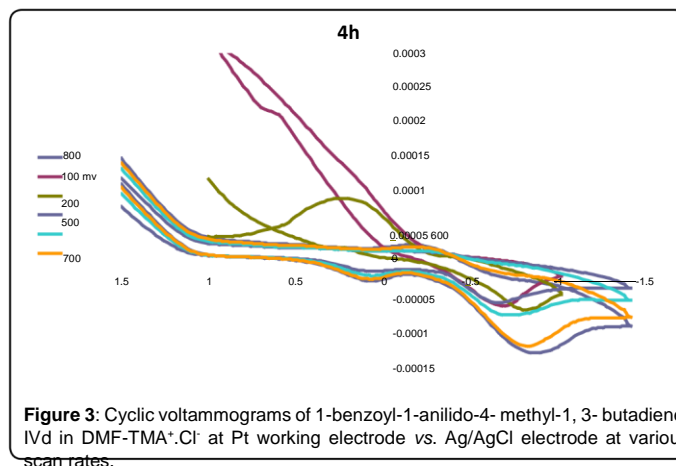


Figure 3: Cyclic voltammograms of 1-benzoyl-1-anilido-4-methyl-1,3-butadiene, IVa in DMF-TMA⁺.Cl⁻ at Pt working electrode vs. Ag/AgCl electrode at various scan rates.

is diffusion controlled processes (Bard and Faulkner, 1980). The plot of E versus log scan rate was found linear at Ag/AgCl. Thus, it can be concluded that, the first reduction processes of the compound precede according to the well known electrode-coupled (EC) chemical reaction mechanism (Bard and Faulkner, 1980). The overall results suggest the possible use of the two compounds as complexing agent in cathodic stripping voltammetry for determination of bismuth (III) ions (II) in water.

Conclusion

The redox behavior of the tested compounds suggest the possible application of the compounds as chelating agent for the determination of ultra trace concentration of heavy metal ions employing differential pulse – adsorptive stripping voltammetry. Moreover, immobilization of one of the prepared compounds on polyurethane foam solid sorbent as trapping agent for minimization and / or separation of bismuth (III) from industrial wastewater was achieved. Work is still continuing for application of the compound in cathodic stripping voltammetric procedures for trace metal analysis in different matrices.



Acknowledgement

The authors would like to thank the Deanship of Scientific Research, King Abdul Aziz University, Saudi Arabia for the financial support under the grant number 428/173. and the Department of Chemistry for the facilities provided in terms of the use of the available equipments, chemicals, technicians and other laboratory facilities.

Volume 2(4) : 085-090 (2010) - 089

References

1. Abdel-Rahman RM, Seada M, Fawzy MM (1991) Synthesis and antimicrobial activity of some new 3,5- disubstituted pyrazolines containing 1,2,4 – triazine moiety. Pak J Sci Ind Res 34: 465-469.
2. Abdel-Rahman RM (1988) Reactions of 3 – hydrazine-5,6 – diphenyl-1,2,4triazine withunsymmetrical 1,3 – bicarbonyl compounds: synthesis of some new 3-(3,3–disubstituted pyrazinol -1-yl-5,6- diphenyl= 1,2,4- triazines and their antimicrobial activities. Indian J Chem 27 B: 548 -553.
3. Abou-Mesalam MM, El-Naggar IM, Abdel-Hai MS, El-Shahawi MS (2003) Use of open-cell resilient polyurethane foam loaded with crown ether for the preconcentration of uranium from aqueous solutions. J Radioanal Nucl Chem 258: 619 -625.
4. Bard AJ, Faulkner LR (1980) Electrochemical Methods, Fundamentals and Applications. Wiley New York pp 218-235.
5. Bashammakh AS, Bahaffi SO, Al-Shareef FM, El-Shahawi MS (2009) Development of an Analytical Method for Trace Gold in Aqueous Solution using Polyurethane Form Sorbents: Kinetic and Thermodynamic Characteristic of Gold (III) Sorption. Anal Sci (Japan) 25: 413-418.
6. Barry AL, Thomsbery C (1981) Susceptibility Testing Diffusion Testes Procedures in Manual of Clinical Microbiology. American Society for Microbiology, Washington, P. 561.
7. Cerchiaro G, Ferreira AMD, Teixeira AB, Magalhães HM, Cunha AC, Ferreira VF, et al. (2006) Synthesis and crystal structure of 2,4-dihydro-4-[(5-hydroxy-3methyl-1-phenyl-1H-pyrazol-4-yl) imino]-5-methyl-2-phenyl-3H-pyrazol-3-one and its copper(II) complex. Polyhedron 25: 2055-2064.
8. Claeson P, Tuchinda P, Reutrakul V (1994) Natural Occurring 1,7-diarylheptanoids. J Indian Chem Soc 71: 509-521.
9. El-Shahawi MS, El-Sonbati MA (2005) Retention profile, kinetics and sequential determination of selenium (IV) and (VI) employing 4,4'-dichlorodithizone immobilized-polyurethane foams. Talanta 67: 806-815.
10. El-Shahawi MS, Hassan SSM, Othman AM, El-Sonbati MA (2008) Retention profile and subsequent chemical speciation of chromium (III) and (VI) in industrial wastewater samples employing some onium cations loaded polyurethane foams. Microchemical J 89: 13-19.
11. El-Shahawi MS, Othman MA, Abdel-Fadeel MA (2005) Kinetics, thermodynamic and chromatographic behavior of the uranyl ions sorption from aqueous thiocyanate media onto polyurethane foams. Anal Chim Acta 546: 221-228.
12. Farag AB, Soliman MH, Abdel-Rasoul OS, El-Shahawi MS (2007) Sorption characteristics and chromatographic separation of gold (I& III) from silver and base Metal ions using polyurethane foams. Anal Chim Acta 601: 218-229.
13. Fathalla WM, Cajan M, Marek J, Pazdera P (2001) One-Pot Quinazolin-4ylidenethiourea Synthesis via N-(2-Cyanophenyl)benzimidoyl isothiocyanate. Molecules 6: 574-587.
14. Funk RL, Fitzgerald JF, Olmstead TA, Para KS, Wos JA (1993) Titaniummediated cyclizations of beta-keto esters with acetals: a convenient route to 2-carbalkoxycyclo- alkenones. J Am Chem Soc 115: 8849-8850.
15. Hussein AHM, El-Gaby MS, Abu-Shanab, Abdel-Raheim MAM (2009) β -Oxo anilides in heterocyclic synthesis: Synthesis of tri- and tetracyclic containing a bridgehead nitrogen atom Org. Commun 2: 66-71.
16. Knoevenagel E, Arnot A (1904) Condensation of salicylaldehyde and cyanoester, benzoyl ester and acetylacetone. Ber 37: 4496-4499.
17. Krishnankutty K, Ummathur MB (2006) Metal complexes of unsaturated diketo anilides. J Indian Chem Soc 83: 639,663,88.
18. Krishnankutty K, Venugopalan P (1998) Metal chelates of curcuminoids. Synth. React. Inorg. Metal- Org. Chem 28: 1313-1325.
19. Krishnankutty K, Venugopalan P (2001) Metal chelates of 6-aryl-5-hexene-2,4diones. J Indian Chem Soc 78: 472 -473.
20. Mishra PK, Chakravorty V, Dash KC (1991) Schiff base complexes of zirconium (IV) derived from Zr (acac) 4. Trans Met Chem 16: 73-75.
21. Ramadan AAT, Abdel- Rahman RM, El-Beahry MA, Ismail AI, Mahmoud MM (1993) Thermodynamics of complexation of transition and lanthanide ions by 3 – (α - carboxymethylaminebenzylidene hydrazino)-5,6-diphenyl-1,2,4- triazine. Thermochim Acta 222: 291-303.
22. Sawyer DT, Heinemann WR, Beebe JM, Reilley CN (1984) Chemistry Experiments for Instrumental Methods. John Wiley & Sons PP 215-221.
23. Sievers RE, Turnispeed SB, Huang L, Laglante AF (1993) Volatile barium β diketones for use as MOCVD precursors. Coord Chem Rev 128: 285-291.
24. Veeraraj A, Sami P, Rahman N (2000) Copper (II) complex of cinnamalideneacetylacetone: Synthesis and Characterization. Proc Indian Acad Sci 112: 515 -521.
25. Wang QL, Yuado M, Bojun Z (1997) Knoevenagel condensation by USY Zeolite. Synth. Commun 27: 4107-4110.
26. Winker CA, Risley EA, Nuss GW (1962) Procedure Society Experimental. Biology Medicinal 111: p544.
27. Zaki MT, Abdel-Rahman RM, El-Syed AY (1995) Use of arylidenerhodanines for the determination of Cu (II), Hg (II) and CN⁻. Anal Chim Acta 307: 127-138.
28. Zheng H, Swager TM (1994) Octahedral Metallomesogens: Liquid Crystallinity in Low Aspect Ratio Materials. J Am Chem Soc 116:761-2.

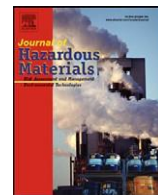
Volume 2(4) : 085-090 (2010) - 090





Contents lists available at ScienceDirect

Journal of Hazardous Materials

journal homepage: www.elsevier.com/locate/jhazmat

Part 1. Spectrophotometric determination of trace mercury (II) in dental-unit wastewater and fertilizer samples using the novel reagent 6-hydroxy-3-(2-oxoindolin-3-ylideneamino)-2-thioxo-2H-1,3-thiazin-4(3H)-one and the dual-wavelength λ -correction spectrophotometry

A. Hamza^a, A.S. Bashammakh^b, A.A. Al-Sibaai^{a,b,c}, H.M. Al-Saidi^c, M.S. El-Shahawi^{a,*}

^aDepartment of Chemistry, Faculty of Science, King Abdulaziz University, P. O. Box 80203, Jeddah 21589, Saudi Arabia ^bThe Centre of Excellence in Environmental Studies, King Abdulaziz University, P. O. Box 80203, Jeddah 21589, Saudi Arabia ^cUniversity College, Department of Chemistry, Umm AL-Qura University, Makkah, Saudi Arabia

article

info

abstract

Article history:

Received 15 October 2009

Received in revised form 13 January 2010

Accepted 14 January 2010 Available online 21 January 2010

Keywords:

Mercury (II)

 λ -Correction spectrophotometry

Water

Fertilizer

ICP-MS

A simple and low cost method was developed and validated for the determination of trace mercury (II) ions in dental-unit wastewater and fertilizer samples. The method was based upon the reaction of mercury (II) ions with the novel reagent 6-hydroxy-3-(2-oxoindolin-3-ylideneamino)-2-thioxo-2H-1,3-thiazin-4(3H)-one, the formed complex shows an absorption maximum at 505nm (λ_{max}) in Britton–Robinson (B–R) buffer (pH 4–6). The corrected absorbance of the formed complex at λ_{max} was obtained employing λ -correction spectrophotometric method. Beer's–Lambert law and Ringbom's plots of the colored Hg–reagent complex were obeyed in the concentration range of 0.2–2.0 and 0.32–0.96gmL⁻¹ mercury (II) ions, respectively with a relative standard deviation in the range of 2.1±1.3%. The limits of detection (LOD) and quantification (LOQ) of the procedure were 0.026 and 0.086gmL⁻¹ Hg²⁺, respectively. The proposed method was applied for the analysis of mercury (II) in dental-unit wastewater and fertilizer samples. The validation of the method was tested by comparison with the data obtained by the inductively coupled plasma-mass spectrometry (ICP-MS). The statistical treatment of data in terms of Student's t-tests and variance ratio f-tests has revealed no significance differences.

E-mail address: mohammad_elshahawi@yahoo.co.uk (M.S. El-Shahawi).

0304-3894/\$ – see front matter © 2010 Elsevier B.V. All rights reserved.
doi:10.1016/j.jhazmat.2010.01.075

1. Introduction

© 2010 Elsevier B.V. All rights reserved.

Mercury is one of the most toxic heavy metal in the earth and it exists in nature at trace and ultratrace amounts in three valence states [1]. Mercury (0, I, II) species and are able to combine with most inorganic and organic ligands to form various complexes, e.g. HgX₄²⁻ (where X=Cl, Br and I) and methyl mercury [1,2]. Mercury can accumulate in animals and plants and also enters into human body through the food chain causing damage to central nervous system [3]. Due to the toxicological effects and potential accumulation of mercury onto human bodies and aquatic organisms, the determination of mercury (II) or organo mercury (II) has seen an upsurge of interest in the last few years [4]. According to WHO, the allowed limits of mercury in drinking water are less than 1.0ngmL⁻¹ [5].

The determination of low concentrations of mercury is a vital task. Therefore, considerable efforts and progress have been carried out to develop accurate, low cost and reliable methods for

mercury determination in contaminated samples without any complicated processing steps [6]. The most common techniques in natural samples are ICP-MS [7,8]; atomic fluorescence [9,10]; cold vapour atomic absorption [11–13]; GC [14]; stripping voltammetry [15,16]; X-ray fluorescence spectrometry [17]; neutron activation analysis [18] and atomic fluorescence spectrometry [19]. The determination and chemical speciation of mercury (II) and/or methyl mercury in a series of complicated matrices, e.g. Mushroom from Tokat-Turkey, water and fish have been reported by Tuzen et al. [20,21]. Moreover, the use of Lichen (*Xanthoparmelia conspersa*) biomass and *Streptococcus pyogenes* loaded Dowex optipore SD-2 has been reported as efficient materials for the removal of mercury (II) and methylmercury from aqueous media [22,23]. Among these techniques, visible absorption spectrophotometry represents the most convenient technique because of the availability of the instrumentation, simplicity, speed, precision, accuracy and low cost.

* Corresponding author. Tel.: +966 0551691130; fax: +966 2 6952292.

A series of chromogenic reagents has been reported for mercury (II) determination in different samples [24–28]. Most of these methods are suffered from the lack of sensitivity due to the significant interference of the excess of chromogenic reagent with the analyte at λ_{max} . This problem was solved by employing the λ_{cor} -correction

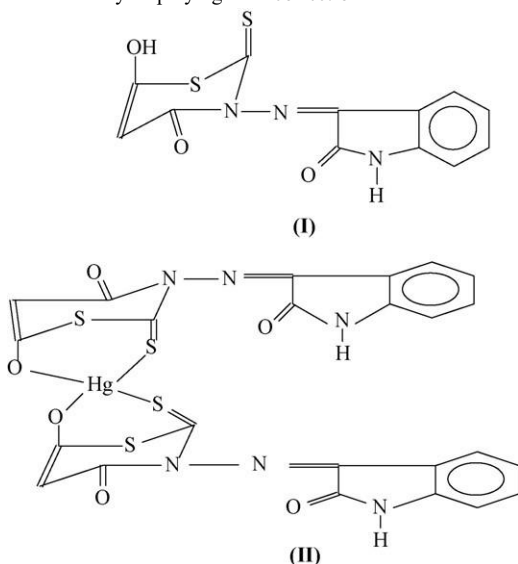


Fig. 1. Chemical structure of the reagent 6-hydroxy-3-(2-oxoindolin-3-ylideneamino)-2-thioxo-2H-1,3-thiazin-4(3H)-one (I) and the proposed structure of its mercury (II) complex (II).

spectrophotometric method to calculate the real absorbance of the complex [29,30].

A recent literature on the analytical applications of the entitled reagent 6-hydroxy-3-(2-oxoindolin-3-ylideneamino)-2-thioxo-2H-1,3-thiazin-4(3H)-one abbreviated as HOTT (Fig. 1) has revealed no study on the use of the reagent for mercury (II) determination and/or other trace metal ions. Therefore, the goals of the present manuscript are focused on the synthesis and spectroscopic characterization (UV–Vis, IR and ^1H NMR) of the HOTT reagent. Moreover, the stoichiometry of the formed mercury (II)HOTT chelate was elucidated in an attempt to develop an accurate method for the analysis of mercury (II) in different water and fertilizer samples. The effect of different parameters that control the absorbance of the formed complex was determined.

2. Experimental

2.1. Reagents and materials

Unless otherwise stated, all chemicals and solvents used were of analytical reagent grade and were used without further purification. A stock solution of mercury (1000mgL^{-1}) was prepared from mercury (II) chloride (BDH, Poole, England). More diluted standard ($0.05\text{--}20\text{mgL}^{-1}$) solutions were then prepared by dilution and were stored in low density polyethylene (LDPE) bottles. An accurate weight (0.05g) of the pure reagent HOTT (Fig. 1) was dissolved in a minimum volume of *N,N*-dimethyl-formamide (DMF), followed by dilution with absolute ethanol (100mL). A series of Britton–Robinson (B–R) buffer (pH 2–11) was prepared by mixing equal proportions of BDH acetic (0.04molL^{-1}), phosphoric (0.04molL^{-1}) and boric (0.04molL^{-1}) acids in deionized water and the pH of the solutions were then adjusted to the required pH by adding various volumes of NaOH (0.2molL^{-1}) solution as reported earlier [31].

2.2. Apparatus

The UV–Vis (190–1100nm) and IR (200–4000 cm^{-1}) spectra were recorded on a Perkin Elmer (Lambda 25, Shelton, CT, USA) and a Perkin Mattson 5000 FTIR spectrophotometers, respectively. The absorbance measurements of the reagent and its mercury (II) complex were also measured with a Perkin Elmer

(Lambda 25, USA) spectrophotometer (190–1100nm) with 10mm (path width) quartz cell. A Bruker NMR (model Vance DPX 400MHz) was used for recording the proton NMR spectra of the reagent and its mercury (II) complex in deuterated DMSO solution using TMS as internal standard. A digital micro-pipette (Volac), an Orion pH-meter (model EA 940) and the scientific melting point SMP1 (UK) were employed for the preparation of the standard and test solutions, pH measurements and melting point, respectively. De-ionized water was obtained from Milli-Q Plus system (Millipore, Bedford, MA, USA) and was used for the preparation of all solutions. Carbon, hydrogen, nitrogen and sulfur content was determined by a Perkin Elmer 2400 C series elemental analyzer, USA. A Perkin Elmer ICP-MS spectrometer (model Elan DRC II, USA) was used under the optimum experimental conditions.

2.3. Synthesis of the chromogenic reagent, HOTT

The reagent 6-hydroxy-3-(2-oxoindolin-3-ylideneamino)-2-thioxo-2H-1,3-thiazin-4(3H)-one was prepared by direct condensation of isatin with dithioic formic acid hydrazide in DMF for 1h. The reaction product was then poured onto an ice bath and the resultant solid precipitate was separated out, washed with ethanol, ether and finally dried. The resultant dried precipitate (10.0mmol) was then refluxed with diethyl malonate (10.0mmol) in ethanol (50.0mL) in presence of sodium ethoxide (20.0mmol) for 4h. The reaction mixture was then cooled, poured onto an ice bath and filtered off. The solid was separated out, washed with ether and acetone, recrystallized from ethanol and finally characterized.

2.4. Recommended procedure

In a series of volumetric flasks (25mL), an appropriate concentration ($0.2\text{--}2.0\text{mgL}^{-1}$) of mercury (II) solution was added to the reagent solution (1.50mL , 0.05% , w/v). To the test solution, an approximate volume (5mL) of B–R buffer of pH 4–5 was added and finally the solution was made up to the mark with distilled water. The solution mixtures were allowed to stand at room temperature for 5min before measuring the absorbance at 336nm (λ_1) and 505nm (λ_2).

2.5. Analytical application

2.5.1. Determination of mercury (II) in tap and mineral water

Tap water collected from the laboratories of Chemistry Department, King AbdulAziz University, Jeddah city, KSA, and mineral water, commercially available in Saudi market, were filtered through 0.45m cellulose membrane filter prior to analysis and stored in LDPE sample bottles (250mL). The recommended general spectrophotometric procedure used to prepare the standard curve was followed and the concentration of mercury (II) ions was then determined from the standard curve using the equation:

$$\text{Mercury(II) concentration} = C_{\text{std}} \times A_{\text{samp}} / A_{\text{std}} \quad (1)$$

where C_{std} is the standard concentration and A_{samp} and A_{std} are the corrected absorbance of the sample and the standard, respectively. Alternatively, the standard addition method was employed as follows: transfer known volume (5.0mL) of the unknown water samples to the volumetric flask (25.0mL) adjusted to pH 5–6 with B–R buffer (10mL). An accurate volume (1.5mL) of the reagent was then added to the test solution and the reaction mixture was then made up to the mark with distilled water. Repeat the same procedures after adding various concentrations ($0.2\text{--}1.0\text{mgL}^{-1}$) of mercury (II). Measure the true absorbance displayed by the test solutions before and after the addition of the standard ($0.2\text{--}1.0\text{mgL}^{-1}$) mercury (II) solution employing

Table 1
Analytical features of some spectrophotometric methods employed for mercury determination.

Reagent/Ref.	max	pH	Linear dynamic range (gmL ⁻¹)	Molar absorptivity (Lmol ⁻¹ cm ⁻¹)	Remarks
Thiobenzoylacetone/[38]	345	4	0.6–12	1.7×10 ^{4a}	Sensitive but interference from Ag ⁺ and excess of chromogenic reagent. Using toxic organic solvents.
Variamine Blue B/[39]	605	2.5–4	0.64–4.4	4×10 ^{4b}	Sensitive but using toxic organic solvents. Time-consuming.
Phenanthroline and eosin/[33]	550	4.5	0.2–1.2	8×10 ⁴	Sensitive, but interference from Al ³⁺ , Co ²⁺ , Ni ²⁺ and excess of dye.
Thiacrown ether and Bromocresol Green/[40]	420	–	0.5–12	–	Less sensitivity and interference from Cu ²⁺ , Cd ²⁺ and Ag ⁺ . Time-consuming.
Diphenylthiocarbazon/[41]	488	Acidic media	0.1–25	2.5×10 ⁴	Low sensitivity
Present work	505	4–6	0.2–2	4×10 ^{4c}	Sensitive, selective and free from the interference of Al ³⁺ , Ag ⁺ , Co ²⁺ , Ni ²⁺ and excess chromogenic reagent. No need for organic solvent.

^a In benzene. ^b In nitrobenzene. ^c With λ -correction spectrophotometry.

λ -correction spectrophotometry method. The concentration of mercury (II) was then determined via the calibration curve of the standard addition procedure.

2.5.2. Analysis of mercury in dental-unit (DU) wastewater

DU wastewater samples were collected from dental chair, King AbdulAziz Hospital, Makkah city, KSA, at the end of working day. An accurate volume of sample was digested by UV-digester in the presence of suitable volumes of both concentrated HNO₃ and H₂O₂ (30%) for 1h. the obtained solution was neutralized by NaOH (5mol L⁻¹) and 10mL of this solution was treated under the conditions of recommended procedure.

2.5.3. Determination of mercury (II) in fertilizer

In a 50mL beaker, an accurate weight (4.50–5.70g) of the local fertilizer (Broxals 1 and 2) was dissolved in de-ionized water after constant stirring for few minutes. The aqueous solution was then completed to 250.0mL with doubled distilled water. An accurate volume of the test solution (5.0mL) was then adjusted to pH 5 with B–R buffer, transferred into the measuring flask (25.0mL) in the presence of the reagent (1.5mL, 0.05%, w/v) and various concentrations (0.2–1.0gmL⁻¹) of mercury (II) were added separately. The solutions were then completed to the mark with doubly de-ionized water and the absorbance of the test solutions was measured by dual-wavelength λ -correction spectrophotometer. The concentration of mercury (II) was finally determined via the standard addition curve. The results were compared with the analytical data obtained from ICP-MS under the conditions described in Table 1. The measurements are the average of three independent measurements and the precision in most cases was $\pm 2\%$.

3. Results and discussion

The characteristics IR vibrations of the solid reagent in KBr disk are observed at 3353, 3147, 1682, 1655, 1585, 1350, 1098, and 977cm⁻¹ and are safely assigned to O–H, N–H, C–O, C–O, C–N, N–C–S, substituted aromatic nucleus [32], respectively.

¹H NMR spectrum of the reagent in d₆-DMSO shows signals at 7.15, 9.5, 10.5 and 10.71 ppm and are safely assigned to (m, 4H, aromatic protons), 9.5 (s, 1H), 10.5 (s, 1H, OH) and 10.71 (s, 1H, NH) protons [32], respectively. The relatively low value of the OH signal is most likely attributed to intramolecular hydrogen bonding. Elemental analysis of the reagent after solvent evaporation and crystallization from ethanol for the structure

[C₁₂H₇N₃O₃S₂] required: 47.2% C, 2.3% H, 13.8% N, and 21% S; Found 47.8% C, 2.5% H, 14.1% N, and

21.6% S. In complex formation, the ligand has numerous coordination sites which gave variable bonding modes and behaves as a mononegative dentate fashion (Fig. 1). A careful comparison of the IR spectrum of the reagent HOTT with the spectrum of its mercury (II) complex in KBr disk revealed that, the ligand is bonded through the thione sulfur as indicated from the observed shift of (C–S) vibration to lower wave number with simultaneous appearance of new band at 395cm⁻¹ due to (Hg–S) [32]. Deprotonation of the enolic OH of the reagent in the complex formation was also confirmed by the disappearance of (OH) and the appearance of (N–O) at 1100cm⁻¹ and (Hg–O) at 549cm⁻¹ and provides an additional support for the oxime oxygen donation. Elemental analysis of the formed mercury (II) complex [Hg(C₁₂H₇N₃O₃S₂)₂] required 35.5% C, 1.73% H, 10.4% N, and 15.8% S, and 24.7% Hg; Found 36.5% C, 1.44% H, 9.2% N, 16.2% S, and 25.1% Hg.

3.1. Absorption spectra of the reagent and its mercury (II) chelate

Preliminary screening investigation on the interaction of the title reagent HOTT (Fig. 1) with mercury (II) ions in the aqueous media and shaking has revealed the formation of a red colored complex. The absorption electronic spectra of the reagent and its mercury (II) complex are shown in Fig. 2. The spectrum of the reagent versus water, showed one well defined peak at 336nm (λ_1), while in the spectrum of its mercury (II) complex against the reagent blank at pH 4–5 a well defined absorption peak (λ_2) at 505nm with a molar absorptivity (ϵ) of 2.5×10⁴ Lmol⁻¹ cm⁻¹ was observed (Fig. 2). These results suggest the possible applica-

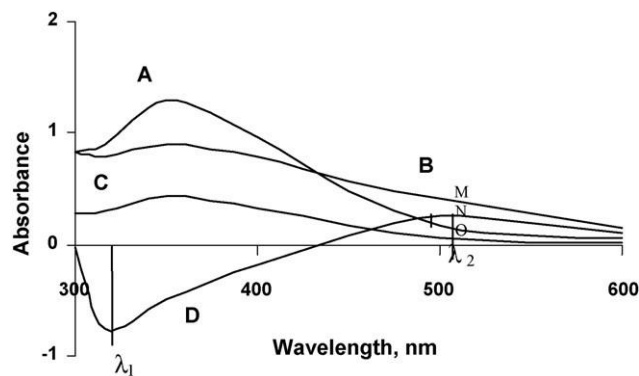


Fig. 2. Absorption spectra of the reagent HOTT and its mercury (II) complex at pH 5. Curve A is the spectrum of the reagent blank (reference water); B is mercury (II) complex (reference, water); C is the excess of reagent (reference water) and D is mercury (II) complex (reference, reagent blank).

tion of the λ -correction spectrophotometric technique to improve the sensitivity of the proposed reaction for the determination of mercury (II) on the subsequent work. Moreover, the interference caused by the excess chromogenic reagent in the reaction mixture will be eliminated. Therefore, the real absorbance (A_c) of the produced mercury (II) complex in solution was calculated using the equation:

$$A_c = \frac{A - A_0}{1 - \alpha\beta} \quad (2)$$

where A and A_0 are the absorbance's of the mercury (II) chelate at λ_2 and λ_1 , respectively versus reagent blank as a reference. The spectrophotometric parameters α and β were calculated employing the equations:

$$\alpha = \frac{A_0 - A_c}{A_0} \quad (3)$$

$$\beta = \frac{A - A_c}{A} \quad (4)$$

where A_0 and A_c are the absorbance's of the blank solution at λ_1 and λ_2 , respectively, against water as a blank; A and A_c are the absorbance's of the complex formed in the solution at λ_2 and λ_1 versus water, respectively. Moreover, it should be noted that, the sensitivity of the developed λ -correction method was improved better than that of the single-wavelength method by selecting the wavelengths λ_1 and λ_2 at the valley and the peak of the electronic spectrum of the chelate versus blank solution [29,30], respectively. Thus, curve C in Fig. 2 demonstrates the theoretical absorption spectrum of the excess reagent. Curve D shows the minimum and maximum absorption of mercury (II)–HOTT complex at pH 4–5 at 336nm (λ_1), and 505nm (λ_2), respectively. Thus, the absorbance of mercury (II) complex formed at λ_2 when blank was used as a reference (single-wavelength method) was found less than the corrected absorbance by λ -correction spectrophotometric technique. Thus, the real absorbance will be equal to the interval MO but not MN. From Fig. 2 (curve A), the calculated parameter β was found equal 0.24 while, the correction coefficient, β_{505} , calculated from Fig. 2 (curve B) was 1.3.

3.2. Influence of different parameters on the determination of mercury (II)

The influence of pH of the aqueous solution employing B–R buffer (pH 2–11) on the developed colored complex was studied by measuring the real absorbance of the solution containing mercury (II) ions at a suitable mercury concentration (1.0gmL⁻¹) in the presence of the reagent HOTT. The results are shown in Fig. 3, where

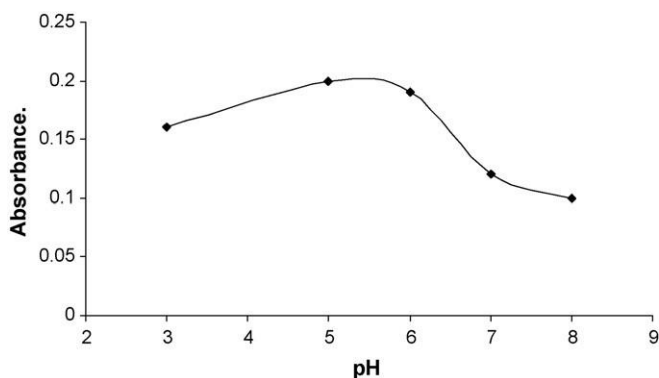


Fig. 3. Influence of pH of the aqueous test solution on the real absorbance of mercury (II)–HOTT complex. Conditions are: reagent concentration=0.003% (w/v) and mercury (II)=1gmL⁻¹.

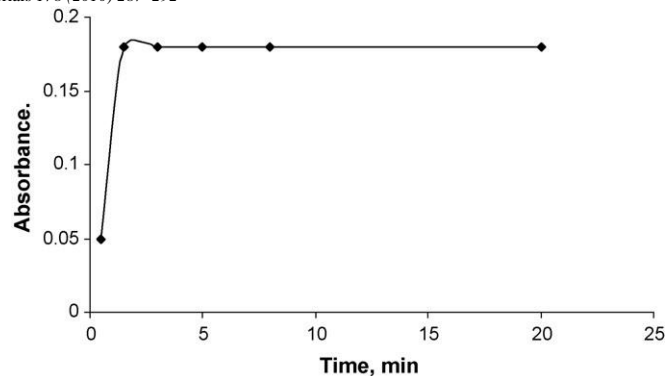


Fig. 4. Plot of the absorbance (stability) of the formed mercury (II)–HOTT complex versus time. Reagent concentration=0.003% (w/v); mercury (II)=1gmL⁻¹ and the aqueous solution pH 5.

it was clearly seen that, maximum absorbance of the produced colored complex was obtained at pH 4–6 and the central value of this range was achieved at pH 5. On the other hand, in the aqueous solution of pH \leq 4, the absorbance was found low since the equilibrium moves to the left and the quantity of the dissociated species of the reagent available to form complex with mercury (II) decreased. In the aqueous solution of pH \geq 5.5, the absorbance of the produced colored complex decreased dramatically. The hydrolysis of the colored complex and the formation of non-colored complex species of mercury (II), e.g. hydroxo complex species of mercury (II) are most likely minimize the colored complex and may account for the observed trend [35]. Thus, in the subsequent work, the aqueous solution was adjusted at pH 5–6 to ensure complete color formation.

The influence of the reagent HOTT concentration on the formation of the complex species of mercury (II) ions (1.0gmL⁻¹) was studied at pH 5–6. Various volumes of the reagent (0.05%, w/v) solution were added to the test solutions. A 1.5mL of the reagent (0.05%, w/v) was found sufficient to quantitatively determine mercury (II) up to 1.0gmL⁻¹ in the aqueous solution. A large excess of the reagent decreased the absorbance possibly owing to the increased acidity of the aqueous phase which minimizes the complex formation.

The stability of the formed complex was examined (Fig. 4) at the optimum conditions. The results showed that, the complex was stable after 0.5min for periods longer than 20min and therefore, this reaction is suitable for quantitative measurements.

3.3. Interference study

The determination of mercury (II) ions at concentration 0.6gmL⁻¹ in the presence of a relatively high excess (0.05–1.0mg) of some diverse ions relevant to water, e.g. alkali and alkaline earth metals, Al³⁺, Ag⁺, Au³⁺, Ni²⁺, Co²⁺, Cd²⁺, Fe³⁺, VO₃⁻, AsO₂⁻, SO₄²⁻, and PO₄³⁻ ions was critically investigated by the developed procedure. The tolerance limit (w/w) was defined as the concentration of the diver's ions added causing a relative error within \pm 3% in the true absorbance of mercury (II)–HOTT complex. The results revealed that the presence of large amounts of the following foreign ions: Ag⁺, Ca²⁺, NH₄⁺, Li⁺ and Mg²⁺ and the anions PO₄³⁻, CH₃COO⁻ and NO₃⁻ did not cause any significant change in the corrected absorbance of the Hg complex even at 1:1000 tolerable concentrations of Hg (II) to the foreign ions, respectively. The ions Co²⁺, Ni²⁺, Cd²⁺, Au³⁺, F⁻ and Cl⁻ at 100-fold excess to the mercury (II) ions also did not interfere. The ions Pb²⁺ and Fe³⁺ at concentrations 50 times higher than those of the analyte interfered seriously. Addition of few drops of NaCl (0.1%, w/v) and NaF (1.0%, w/v) to the aqueous solution eliminates the positive interferences caused by the ions Pb²⁺ and Fe³⁺, respectively. Addition of NaCl and NaF to the aqueous solution

containing mercury (II) and the HOTT reagent forms white precipitate of PbCl₂ and colorless anionic complex species [FeF₆]³⁻ with Fe³⁺. The interference of MnO₄⁻ was also eliminated by the addition of sodium azide to

reduce manganese (VII) to manganese (II). After employing these modifications, the tolerance level of the interfering ions was improved to acceptable limit (98±2%). These results extend the possible use of the method for the determination of mercury (II) ions in various matrices.

3.4. Stoichiometry of the mercury (II) complex

The chemical structure of the produced mercury (II) complex species was determined by the method of continuous variations at various concentrations of the mercury (II) ions and reagent [34]. A plot of the true absorbance of the produced colored solution at 505nm versus the mole fraction of the reagent revealed a graph that indicated the formation of complex having mercury (II) to a reagent molar ratio of 1:2. These data confirmed that, the colored species is most likely fit with the molecular formula of mercury (II)-reagent.

3.5. Analytical performance

Analysis of mercury (II) ions in tap, mineral and DU wastewater samples by the developed (A) and the ICP-MS (B) methods^a.

Water sample	Mercury (II) added (gmL ⁻¹)	Mercury (II) found (gmL ⁻¹) ^a		Recovery (%) ^a	
		A	B	A	B
Tap water	–	ND	ND	–	–
Tap water	1	1.04±0.03	1.06±0.003	104±3.0	106±0.01
Mineral water	0.0	ND	ND	–	–
Mineral water	2	1.98±0.005	2.1±0.002	99±2.5	105±1.57
DU wastewater	0.0	3.83±0.67	3.76±0.56	–	–
DU wastewater	1	4.62±0.52	4.30±0.8	96±2.02	90±1.45

^a Average of three measurements±standard deviation.

Table 3

Analysis of mercury (II) ions in the fertilizer samples by the proposed procedure (A) and ICP-MS (B)^a.

Fertilizer sample	Mercury (II) added (gmL ⁻¹)	Mercury (II) found (gmL ⁻¹)		Recovery (%)	
		A	B	A	B
Broxal 1	0.450	0.452 ± 0.03	0.44 ± 0.03	100.4 ± 6.6	97.8 ± 0.03
Broxal 2	0.250	0.25 ± 0.03	0.26 ± 0.03	100.0 ± 3.3	104 ± 0.03

^a Average of three measurements±standard deviation.

At the optimum experimental conditions of the reaction of the reagent HOTT with mercury (II) in the aqueous solution of pH 4–5, the effective molar absorptivity (ε) calculated from Beer's–Lambert plot and the Sandell's sensitivity index [35] of the mercury (II)-complex with and without the use of ~-correction spectrophotometry were found to be equal to 4.0×10⁴ Lmol⁻¹ cm⁻¹ and 2.5×10⁴ Lmol⁻¹ cm⁻¹ and 0.005gcm⁻² and 0.008gcm⁻², respectively. The plot of the absorbance's of the mercury (II) complex at 505nm versus mercury (II) concentrations employing ~-correction spectrophotometry was obeyed Beer's–Lambert law in the concentration range of 0.2–2.0gmL⁻¹. The regressions of the linear plots without and with the use of ~-correction spectrophotometry were given by Eqs. (5) and (6), respectively:

$$A = 0.101C_x + 0.002 \quad (r^2 = 0.995) \quad (5)$$

$$A_c = 0.183C_x + 0.004 \quad (r^2 = 0.999) \quad (6)$$

The effective concentration range of mercury (II) ions as evaluated by the Ringbom's plot [35] was obeyed in the range 0.2–0.96gmL⁻¹. The precision and accuracy of the developed

Table 2

procedure was evaluated by the recovery studies of four replicate measurements of mercury (II) in distilled water at concentration level of 1.0gmL⁻¹ using ~-correction and the ordinary singlewavelength spectrophotometry methods. The

relative standard deviation and the relative error of the developed ~-correction method were 1.3% and 1.0% while 3.2% and 6.0% for the singlewavelength spectrophotometry, respectively. The level of precision was found suitable for the routine analysis of mercury (II) in various water samples. Under the conditions established for mercury (II) ions, the lower limits of detection (LOD) and quantification (LOQ) of mercury (II) were determined by employing the equations [36]:

$$3\sigma_1$$

$$\text{LOD} = \frac{3\sigma_1}{b} \quad (7) \text{ b}$$

and

$$10\sigma_1$$

$$\text{LOQ} = \frac{10\sigma_1}{b} \quad (8) \text{ b}$$

where σ_1 is the standard deviation ($n = 4$) of the blank and b is the slope of the calibration plot. The values of LOD and LOQ of the developed procedure

without using ~-correction absorbance values were found are 0.16 and 0.52gmL⁻¹ mercury (II), respectively. Such limits were improved to lower detection and quantification limits of 0.026 and 0.086gmL⁻¹ mercury (II), respectively employing the developed ~-correction method at the optimum experimental conditions. Such limits are comparable to most of the spectrophotometric methods involving pre concentration step on solid sorbent [37]. The analytical features of the proposed method were also compared with many of extractive spectrophotometric methods [33,38–41]. The data given in Table 1 revealed that, the developed method is simple, less toxic, reliable and free from interference of the ions Al³⁺, Ag⁺, Co²⁺, and Ni²⁺ and the excess reagent compared to the reported methods [33,38–41].

3.6. Validation and analytical applications of the developed method

The validity of the proposed method was tested by the analysis of mercury (II) in tap, mineral and DU wastewater samples. For this purpose, different concentrations of mercury (II) ions at concentration range 0.2–2.0gmL⁻¹ were spiked onto the tested water samples. The mercury content in each sample was then determined via the developed method and the results are summarized in Table 2. The obtained results were compared with the standard ICP-MS method in terms of Student's t-test (3.03–5.89) and f-test (0.53–0.96). The results summarized in Table 2 revealed that, the percentage recoveries of both methods were in good agreement and always higher than 95% confirming the accuracy of developed procedure and its independence from matrix.

Moreover, the validity of the proposed method was also tested by the analysis of mercury (II) on the Broxal fertilizer under the conditions described in Section 2.5.2. The true absorbance of the test solutions calculated via the proposed dual-wavelength λ -correction spectrometry was plotted versus the concentrations of mercury added. The spiked mercury (II) concentration was determined via the standard addition curve and the results were successfully compared with the value of mercury (II) determined by ICP-MS (Table 3).

4. Conclusions

The method described provides a simple and reliable means of determination of trace amounts of mercury (II) ions in aqueous media by spectrophotometry. The method is sensitive ($\epsilon=4.0\times 10^4 \text{ Lmol}^{-1} \text{ cm}^{-1}$), inexpensive and less toxic than most of the reported extractive spectrophotometric methods [33,38–41]. Moreover, the method also has the advantage of virtual freedom from interference from extraneous ions. Thus, it can act as an alternative approach to the widely used flameless AAS and ICP-OES in rapid and precise determination of trace amounts of mercury in natural water and industrial effluent samples. On the other hand, a calibration matrix constructed with λ -correction spectrophotometric method has been successfully applied for the analysis of mercury (II) ions in real samples. The method requires no complex pretreatment of chromatographic separations and/or preconcentration of the analyte.

Acknowledgements

The authors would like to thank the Centre of Excellence in Environmental Studies, King Abdulaziz University, Jeddah, Saudi Arabia for the funding and support. One of the authors (H.M. Al-Saidi) would like to thank Dr. E. Abdelazeem for his help in providing the dental wastewater samples.

References

- R.A. Gayer, *Toxicological Effects of Methyl Mercury*, National Academy Press, Washington, 2000.
- L.D. Lacerda, W. Salomons, *Mercury from Gold and Silver Mining*, A Chemical Time Bomb, Springer, Berlin, Heidelberg, 1998, p. 146.
- P.J. Craig, *Organometallic Compounds in the Environment*, Longman, Harlow, 1986.
- M.E. Stone, M.E. Cohen, L. Liang, P. Pang, Determination of methyl mercury in dental-unit wastewater, *Dental Materials* 19 (2003) 675–679.
- American Water Works Association, *Water Quality and Treatment*, 4th edn., McGraw Hill Inc., New York, 1990.
- M. Hussein, H. Moghaddam, Sensitized extraction spectrophotometric determination of Hg(II) with dithizone after its flotation as an associate using iodide and ferrioin, *Talanta* 67 (2005) 555–559.
- J. Schmit, M. Youla, Y. Gelin, Multi-element analysis of biological tissues by inductively coupled plasma mass spectrometry, *Anal. Chim. Acta* 249 (1991) 495–501.
- D.E. Nixon, M.F. Burrit, T.P. Moyer, The determination of mercury in whole blood and urine by inductively coupled plasma mass spectrometry, *Spectrochim. Acta: Atom. Spectrosc.* 54 (1999) 1141–1153.
- M. Vijayakumar, T.V. Ramakrishna, G. Aravamudan, Fluorimetric determination of trace quantities of mercury as an ion-association complex with rhodamine 6G in the presence of iodide, *Talanta* 27 (1980) 911–913.
- E. Saouter, B. Blattmann, Analyses of organic and inorganic mercury by atomic fluorescence spectrometry using a semiautomatic analytical system, *Anal. Chim. Acta* 66 (1994) 2031–2037.
- M. Navarro, M.C. Lopez, Microwave dissolution for the determination of mercury in fish by cold vapor atomic absorption spectrometry, *Anal. Chim. Acta* 257 (1992) 155.
- E.M. Martine, P. Berton, R.A. Olsina, J.C. Altamirano, R.G. Wuilloud, Trace mercury determination in drinking and natural water samples by room temperature ionic liquid based d-preconcentration and flow injection-cold vapor atomic absorption spectrometry, *J. Hazard. Mater.* 167 (2009) 475–481.
- J.L. Manzoori, M.H. Sorouraddin, A.M.H. Shabani, Determination of mercury by cold vapor atomic absorption spectrometry after preconcentration with dithizone immobilized on surfactant-coated alumina, *J. Anal. At. Spectrom.* 13 (1998) 305–308.
- J. Nevado, R.C. Marti-Domeadios, F.J. Bernado, M.J. Moreno, Determination of mercury species in fish reference material by gas chromatography-atomic fluorescence detection after closed-vessel microwave-assisted extraction, *J. Chromatogr. A* 1093 (2005) 21–28.
- Z. Zhang, H. Liu, H. Zhang, Y. Li, Simultaneous cathodic stripping voltammetric determination of mercury, cobalt, nickel, and palladium by mixed binder carbon paste electrode containing dimethylglyoxime, *Anal. Chim. Acta* 333 (1996) 119–124.
- C. Faller, N.Y. Stojke, G. Henze, K.Z. Brainina, Stripping voltammetric determination of mercury at modified solid electrode: determination of mercury traces using PDC/Au (III) modified electrode, *Anal. Chim. Acta* 396 (1999) 195–202.
- L. Bunn, J. Gomez, Determination of mercury by total reflection X-ray fluorescence using amalgamation with gold, *Spectrochim. Acta* 52B (1997) 1195–1200.
- P.R. Devi, T. Gangaiah, G.R.K. Naidu, Determination of trace metals in water by neutron activation analysis after preconcentration on poly(acrylamidoxime) resin, *Anal. Chim. Acta* 12 (1991) 533–537.
- A. Shafawi, L. Ebdon, M. Foulkes, P. Stockwell, W. Corns, determination of total mercury in hydrocarbons and natural gas condensate by atomic fluorescence spectrometry, *Analyst* 124 (1999) 185–189.
- M. Tuzen, M. Soylak, Mercury contamination in mushrooms samples from Tokat Turkey, *Bull. Environ. Contam. Toxicol.* 74 (2005) 968–972.
- M. Tuzen, I. Karaman, D. Citak, M. Soylak, Mercury (II) and methylmercury determination in water and fish samples by using solid phase extraction and cold vapor atomic absorption spectrometry combination, *Food. Chem. Toxicol.* 47 (2009) 1648–1652.
- M. Tuzen, A. Sari, D. Mendil, M. soylak, Biosorptive removal of mercury from aqueous solution using Lichen (*Xanthoparmelia Conspersa*) biomass, kinetic and equilibrium studies, *J. Hazard. Mater.* 169 (2009) 263–270.
- M. Tuzen, I. Karaman, D. Citak, M. soylak, Mercury and methylmercury speciation on *Streptococcus pyogenes* loaded Dowex optipore SD-2, *J. Hazard. Mater.* 169 (2009) 345–350.
- S. Suresha, M.F. Silwadi, A.A. Syed, Sensitive and selective spectrophotometric determination of Hg (II), Ni (II), Cu(II), and Co(II) using iminodibenzyl and 3-chloroiminodibenzyl as new reagent and their application to industrial Effluents and soil samples, *Int. J. Environ. Anal. Chem.* 82 (2002) 275–289.
- A.Y. El-Sayed, Zero-crossing derivative spectrophotometric determination of mercury (II) and palladium (II) with 5-(3,4-methoxyhydroxyphenylmethylene)-2-thioxo-1,3-thiazolidine and cetyltrimethylammonium bromide, *Anal. Lett.* 31 (1998) 1905–1916.
- E.B. Sandell, *Colorimetric Method of Analysis*, Wiley Interscience, New York, 1959, pp. 445.
- Xiao-Ling He, Yong-Qiu Wang, K.Q. Ling, Synthesis of a novel bistriazene reagent 4,4-bis[3-(4-phenylthiazol-2-yl)triazenyl]biphenyl and its highly sensitive color reaction with mercury (II), *Talanta* 72 (2007) 747–754.
- S. Chatterjee, A. Pillai, V.K. Gupta, Spectrophotometric determination of mercury in environmental samples and fungicides based on its complex with O-carboxy phenyl diazoamine P-azobenzene, *Talanta* 57 (2002) 461–465.
- A. Abbaspour, L. Baramakeh, Dual-wavelength λ -correction spectrophotometry for selective determination of Zr, *Talanta* 57 (2002) 807–812.
- H. Cao, P.F. Zhang, Determination of antimony in wastewater with chromazurol S by beta-correction spectrophotometry, *Analyst* 119 (1994) 2109–2111.
- A.I. Vogel, *Quantitative inorganic analysis*, 3rd edn., Longmans Group Ltd, England, 1966.
- K. Nakamoto, *Infrared and Raman Spectra of Inorganic and Coordination Compounds*, 3rd edn., Wiley, New York, 1978, p. 305.
- J.R. Mudakavi, Spectrophotometric determination of trace amounts of mercury with phenanthroline and eosin, *Analyst* 109 (1984) 1577–1579.
- D.T. Sawyer, W.R. Heinemann, J.M. Beebe, *Chemistry Experiments for Instrumental Methods*, John Wiley & Sons, 1984;
- A. Ringbom, *Fresen. Z. Anal. Chem.* 155 (1939) 332.
- Z. Marczenko, *Separation and Spectrophotometric Determination of Elements*, 2nd edn., John Wiley and Sons, 1986.
- J.C. Miller, J.N. Miller, *Statistics for Analytical Chemistry*, 4th edn., Ellis-Howood, New York, 1994, p. 115.
- N. Rajesh, M.S. Hari, Spectrophotometric determination of inorganic mercury (II) after preconcentration of its diphenylthiocarbazono complex on a cellulose column, *Spectrochim. Acta A* 70 (2008) 1104–1108.
- M.V.R. Murti, S.M. Khopkar, Extractive spectrophotometric determination of mercury with thiobenzoylacetone: analysis of waste water, *Bull. Chem. Soc. Jpn.* 50 (1977) 738–741.
- M. Tsubouchi, Spectrophotometric determination of mercury (II) by solvent extraction with Variamine Blue B, *Bull. Chem. Soc. Jpn.* 43 (1970) 2812.
- B. Saad, S.M. Sultan, Extraction spectrophotometric determination of mercury (II) using thiocrown ethers and Bromocresol Green, *Talanta* 42 (1994) 1349–1354.
- M.J. Ahmed, M.S. Alam, A rapid spectrophotometric method for the determination of mercury in environmental, biological, soil and plant samples using diphenylthiocarbazono, *Spectroscopy* 17 (2003) 45–52.



Review

An overview on the accumulation, distribution, transformations, toxicity and analytical methods for the monitoring of persistent organic pollutants

M.S. El-Shahawi^{a,*}, A. Hamza^a, A.S. Bashammakh^b, W.T. Al-Saggaf^a

^aDepartment of Chemistry, Faculty of Science, King Abdulaziz University, P.O. Box 80203, Jeddah 21589, Saudi Arabia ^bThe Centre of Excellence in Environmental Studies, King Abdulaziz University, P.O. Box 80203, Jeddah 21589, Saudi Arabia

article info abstract

Article history: Recent years have seen an upsurge of interest in developing low cost and reliable methods for the detection and precise determination of ultra-trace concentrations of persistent organic pollutants (POPs), because of their bioaccumulation, transformation and toxicity. Therefore, a comprehensive review with 25 September 2009

Accepted 25 September 2009 polychlorinated biphenyls (PCBs) and organochlorine pesticides (OCPs) is presented. The review also aims 108 references referring to the distribution, source, accumulation, transformation, types and toxicity of

Available online 2 October 2009 to highlight on the current best practices for the analysis of PCBs and OCPs. Moreover, with the signing of the Stockholm convention on POPs and the development of global monitoring programs, there is an

Keywords:

Persistent organic pollutants increased need for laboratories in developing countries to determine such class of chemicals. A major focus revealed the need for low cost methods that can be implemented easily in developing countries Transformation such as electrochemical techniques.

Chromatographic determination

© 2009 Published by Elsevier B.V.

Contents

1.	Historical overview	1587
2.	Distribution of POPs	1588
3.	Sources of POPs	1588
4.	Type of persistent organic pollutants	1590
4.1.	Intentionally POPs	1590
4.1.1.	Organochlorine pesticides (OCPs)	1590
4.1.2.	Industrial chemicals	1592
4.2.	Unintentionally POPs	1593
4.2.1.	Polycyclic aromatic hydrocarbons (PAHs)	1593
4.2.2.	Dioxins and dibenzofurans	1593
5.	Properties of POPs	1593
6.	Dosage and toxicity of POPs	1594
7.	Extraction and analytical techniques	1595
8.	Removal and/or minimization of POPs	1595
9.	Conclusion	1596
	References	1596

* Corresponding author. Permanent address: Department of Chemistry, Faculty of Science at

Damiatta, Mansoura University, Mansoura, Egypt.

Tel.: +966 2 6952000x64960; fax: +966 2 6952292.

E-mail addresses: mohammad_elshahawi@hotmail.com, malsaeed@kau.edu.sa (M.S. El-Shahawi).

0039-9140/\$ – see front matter © 2009 Published by Elsevier B.V.

[doi:10.1016/j.talanta.2009.09.055](https://doi.org/10.1016/j.talanta.2009.09.055)

1. Historical overview

After the Second World War, scientists began to recognize that, certain chemical pollutants were capable of persistent in the environment for long time, migrating in air, water, soil and sediments and accumulating to levels that could harm wildlife and human health. These chemical pollutants called persistent organic pollutants (POPs) [1]. These pollutants are organic compounds of natural

or anthropogenic origin that possess a particular combination of physical and chemical properties such that, once released into the environment, they remain intact for exceptionally long periods of time as they resist photolytic, chemical and biological degradation [2,3]. Compounds of this nature are highly resistant to degradation by biological photolytic and/or chemical means [3].

Recently, POPs are a matter of concern because of their toxicity and tendency to accumulate in food chains [4]. The environmental impact of a particular species becomes more important than a total metal concentration. Thus, metal speciation is of great importance in environmental science. However, due to their low concentrations, pre-concentration (enrichment) step is needed prior to their determination. The pollution by POPs and determination and chemical speciation of toxic trace metal ions will be discussed more in detail below.

The carbon–chlorine bond is very stable toward hydrolysis and the greater the number of chlorine substitution and/or functional group, the greater the resistant to biological and photolytic degradation. Because POPs break down very slowly, they will present in the environment for long time to come, even if all new sources were immediately eliminated [5]. POPs in the environment are transported at low concentrations by movement of fresh and marine waters and, as they are semi-volatile, are transported over long distances in the atmosphere. The result is widespread distribution of POPs across the globe, including regions where they have never been used [2]. The POP's level found in the Arctic of Alaska is surprising to many people. This is because some of these pollutants have been banned from the United States and Canada for many years. POPs travel toward colder areas like Alaska and then sink due to the colder temperature. The settled contaminants remain in the area for a long period of time because the temperature does not allow them to break down very easily. Because of this, they move from the air and water in to soil and plants, then to animals and humans with ease. The persistence of contaminants in the Arctic from distant sources first came to light in the late 1970 when pesticides were found in polar bear fat tissue, then the reality of atmospheric POPs, their effect on wildlife and human health. A well-known story in the Arctic, researchers have begun to look for evidence of airborne POPs in other cold ecosystems, our mountain environments [6,7].

2. Distribution of POPs

In 1945, a booming industry launched a new, effective tool for dealing with insect pests: DDT. It held great promise, including the hope of saving crops and eradicating disease-carrying insects. Twenty years later, DDT and other similar chemicals had indeed benefited agriculture and relieved some of the problems associated with insects in many areas of the world. However, these gains came at a price, as DDT is toxic to many more organisms than those it was intended to kill. In particular, birds of prey had trouble to reproduce, and their population declined in many polluted parts of the world. Since, the commercial manufacture of anthropogenically synthesized organic chemicals began in the 1920s. Production, use and trade of these substances rose sharply after World War II, driven by a desire to produce more and better food and cash crops, protect public health, and facilitate industrial development [8,9].

The first public warnings about possible dangers came in relation to local environmental effects in the early 1960s, and grew stronger in the 1970s [7]. During 1960 and 1970 they were extensively utilized in order to protect crops and to prevent health diseases. Some of these compounds such as hexachlorobenzene (HCB), hexachlorocyclohexane (HCH) and Dichlorodiphenyltrichloroethane (DDT) were among the most widely used pesticides in the world during 1970–1980. Nowadays they are banned or restricted in the majority of the industrialized countries, but they still used in Africa, South Asia, Central and South America [7–10].

In the late of 1980s, new scientific discoveries resulted in changing perception, highlighting the transboundary nature of the POPs problem. Many of the discoveries were related to the Arctic region. These discoveries were spurred by both qualitative and quantitative improvements in data samples, measurement and analytical techniques. Also, in August 1989, Canada presented a report on hazardous persistent organic chemicals [8].

In the 1990, research found that the largest lake trout in Bow Lake contain high levels of some of these pollutants such as toxaphene. Since, the lake supports only a small population of large lake trout (2.5kg) and people do not consume high amounts of fish from the lake, human health is not at risk. However, predators such as osprey feed exclusively on fish [12]. Also in Taiwan, the Danshui consider the largest river in the north, it receives liquid effluents and atmospheric fallout resulting from industrial and municipal emissions which include multiple forms of POP pollutants associated with these emissions, including polychlorinated biphenyls (PCBs), are transported down-river in association with particulates and deposited in river sediments, as well as those in nearby coastal areas. The presence of these pollutants causes a large toxicity on fish and other living organisms in the river [13].

The persistence in the compounds allows them to accumulate in animals and pass on more. When the pollutants progress in to animals, they accumulate in the fat cells, organs and muscles. In Adriatic sea which is an arm of the Mediterranean sea separating Italy from the Balkan peninsula, there are concentrations so low of some of these pollutants such as PCB, HCB, HCH and organochlorine pesticides (OCPs) in the fish liver collected from the Adriatic sea during 1993–2003 such as DDT in order to estimate the long-term changes in residue levels and the present status of contamination of this aquatic zone [14].

In China, many high-yield grain fields have become high-intense by POPs – especially pesticide – application areas in China. It was shown by sampling surveys from 1985 to 1991 that pesticide consumption ranged from 4.65 to 15.75kg/hm² increasing by threefold and 41.8% annually. Pesticide consumption in southeast regions of China including Zhejiang, Shanghai, Fujian, and Guangzhou provinces accounted for 36.7% of the nationwide consumption, while six provinces in the northwest of China, including Qinghai, Ningxia, Gansu, Xinjiang, Heilongjiang, and Inner Mongolia, only accounted for 3.4%. The consumption of pesticides in Zhejiang was about 9.96kg/hm² and 3.7 times that of the national average (2.71kg/hm²), and 28 times more than that in Inner Mongolia, which was the lowest user of these chemicals. The distribution pattern of pesticide application in China shown in Fig. 1 was as follows: southeast > central > northwest [15].

In 1999, during the so-called dioxin scandal in Belgium, Polish Veterinary Inspectorate ordered an analysis of food samples of Polish and international origin. The Inspectorate tried not to make the results of those analyses publicly available. This can be seen from the Inspectorate's response to the request of world protection agency (WPA) for allowing access to them. They said that in the period in question, no such analyses were made in Poland as seen in Table 1. These data were published in a scientific publication with a limited circulation [16].

3. Sources of POPs

Volcanic activity and vegetation fires are the two possible natural sources of dioxins and dibenzofurans. Some of these volcanoes are located in central Africa. Some attention will be given to sources or uses of particulates in southern and South Africa. One of these sources is fire, both natural, accidental and managed burning of vegetation [17–20]. POPs, as are apparent from their definition, are very

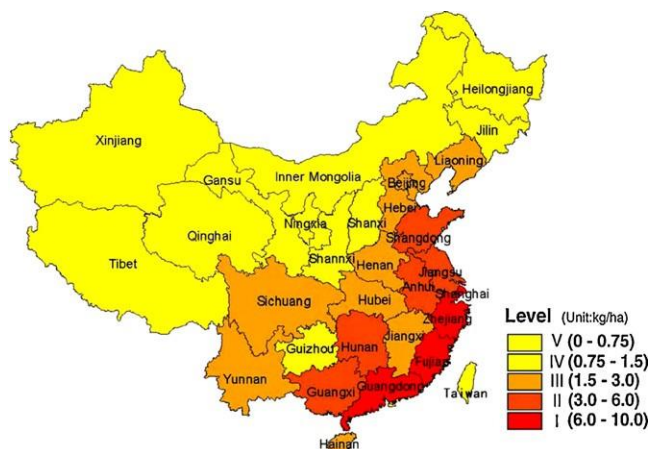


Fig. 1. Distribution of persistent organic pollutants in China in 1996.

They are stored in sediments on the beds of seas, oceans, and large lakes, where they can be released from after a time and then reenter the atmosphere as shown in Fig. 2 [23,24].

During the last 10 years, a lot of sources of POPs were stopped due to the economical changes in the country. Moreover, a lot of new wastewater treatment plants were built during this period. Another reason of the observed decreasing trends in POPs occurrence in waters and sediments is found in the more principal ecological politics of government and local authorities [22]. In Poland, no wide-ranging investigations of dioxin-related environmental contamination, especially the presence of those compounds in human tissues and milk of breastfeeding mothers, have ever been conducted. Any publicly available data is random or based on unreliable estimates. According to the information provided to the Central Statistical Office by the Institute for Environmental Protection, the dioxin and furan emissions in 1998 are estimated at 290.353g TEQ. According to the Institute, the main sources of dioxin emissions in Poland are given in Fig. 3 [25].

stable in all constituents of the environment. They enter the atmosphere from a number of industrial sources such as power stations, heating stations, incinerating plants as well as from household furnaces, transport, use of agricultural sprays, evaporation from water surfaces, soil, or from the landfills. Other sources for POPs compounds such as the unintentional production can be found by incinerations, chemical facilities, diverse combustions, bushfires and putrefaction and wastes containing PCBs. This class of wastes can be found in many areas and stemming from different activities, e.g. the use of obsolete oil, the repairing and maintenance of equipments, demolition of building, evaporation, cement manufacture, animal carcass incinerator, coal combustion, lixiviation of dumps and recycling operations, incineration-municipal, hazardous, medical waste, sewage sludge, industry-chlor-alkali plants, aluminium secondary plants, organ chlorine pesticide plant and cock plant, landfills-hazardous waste/plastic waste, fly ash storage, and organochlorine pesticide storage [21,22].

The sources of access of the substances, oil, fates, liquid fuels, soil, ash and sediment into the water system are wastewaters from plants producing or using POPs, along with runoffs from fields and roads and from the atmospheric deposition. Their largest reservoirs are oceans and seas, where they gather from river sediments, by the atmospheric deposition, by disposing wastes, and by accidents.

Table 1

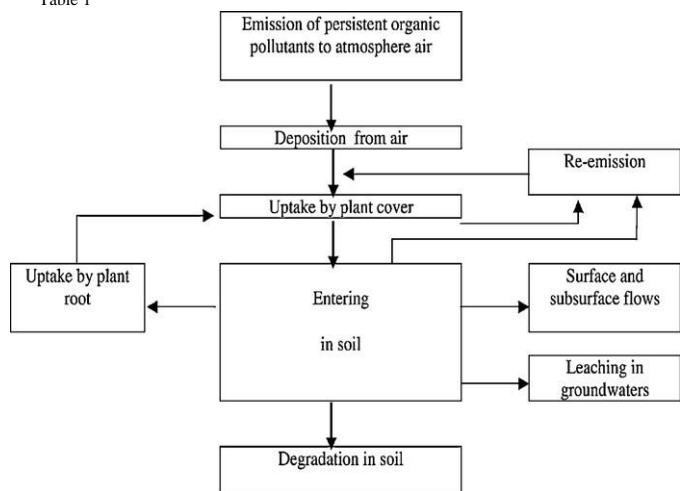


Fig. 2. Conceptual model for the behavior of persistent organic pollutants in the air-plant-soil system.

Recently, the Ministry of Environment has undertaken great efforts to provide a basis for estimating the real emission of dioxins and furans. In different regions of Poland, in urbanized areas as well

Analysis of dioxin scandal in fat of food samples (pg-TEQg⁻¹) of Polish and international origin in 1999 for dioxin scandal with a limited circulation [15–17].

Product	Concentration, pg-TEQg ⁻¹ fat	Reference data, pg-TEQg ⁻¹ fat [15–17]
Fish oil from Baltic fish (imported from Scandinavia)	12.6–50.0	–
Sea Fish (from Baltic Sea)	7.0–40.0	2.4–214.3
Fish oil from Baltic fish	11.2–40.0	–
Pork grilled in open fire	20.0–25.0	–
Fish meal (imported from Scandinavia)	6.5–20.0	–
Poultry	0.6–12.8	0.7–2.2
Freshwater fish	1.2–9.4	2.4
Beef	2.4–8.5	0.1–16.7
Pork	0.05–1.3	0.31
Hard cheese	0.2–7.7	–
Eggs (Yolk)	0.6–7.4	1.2–4.6
Butter	0.6–6.5	0.16–4.8
Powdered milk	0.3–5.0	–
Polish bone meal	0.25–4.25	–
Milk	0.1–4.0	0.5–3.8
Beef fat	3.8	–
Yoghurts with fat content >2%	0.1–1.8	0.18
Used vegetable oil (frying chips)	0.15–0.8	–
Chocolate products	0.05–0.75	–
Fresh vegetable oil	0.02–0.1	0.01–0.2
Low-fat yoghurts	Less than 0.01	–
Meat of Belgian chicken fed on contaminated feed	–	700

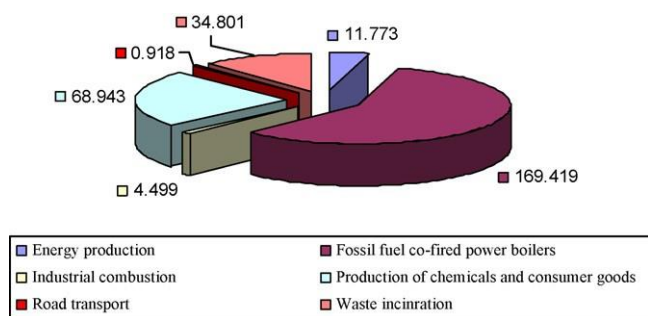


Fig. 3. The main sources of dioxin emissions in Poland.

Table 2

The permissible concentrations (pg-TEQg⁻¹) of PCBs, DDT and gamma-HCH.

Substance	The permissible dose, pg-TEQg ⁻¹ fat
PCBs	2.8
DDT	4.2
Gamma-HCH	13.3

samples fatty tissues of infants

Table 3

Analysis of some selected POPs (mgkg⁻¹) from 10–80 years in one of Warsaw's hospital

Substance	mgkg ⁻¹ of fat		
	Median	Maximum	Mean
PCBs	0.500	36.000	0.856
HCB	0.120	9.020	0.310
Alpha-HCH	0.160		0.016
Beta-HCH	0.120	5.097	0.228
Gamma-HCH	0.030	2.727	0.074
p, p'-DDE	4.382	35.850	5.745 _{p,p}
p, p'-DDT	0.478	9.600	0.537

as those potentially free from dioxin contamination, 118 geological samples have been taken. The analysis thereof will allow for determining the so-called background dioxin level. The reference source for monitoring of that compounds in milk of breastfeeding mothers has been reported by Ludwicki et al. [25] to assign the content of other persistent organic pollutants. The investigation covered a group of 462 women from Warsaw and other localities [26]. The permissible concentrations (pg-TEQg⁻¹) of PCBs, DDT and gammaHCH are summarized in Table 2. The increased level of persistent organic pollutants was found primarily in older women, aged 30 and more, and those who gave birth to more than four children.

In the years 1989–1992, in one of Warsaw's hospitals, samples of fatty tissues have been undertaken from 277 patients aged from 10 to 80 years and were successfully subjected to analysis for a series of PCBs, HCB, alpha-HCH, beta-HCH, gamma-HCH, p,p-DDE and p,p-DDT [25]. The results are summarized in Table 3. Higher concentrations of POPs have been found in tissues of older people [25]. In the case of gamma-HCH, only a higher level was noted in the samples that taken from patients aged below 25 years.

4. Type of persistent organic pollutants

In Stockholm 2001, representatives from 92 countries have agreed to sign the Stockholm Convention on POPs to reduce and/or eliminate the release of 12 original POP substances which are namely the dirty dozen. More contaminants have been discovered; the main concern is over the original 12. These contaminants are the 10 intentionally produced chemicals: aldrin, endrin, chlordane, DDT, dieldrin, heptachlor, mirex, toxaphene, hexachlorobenzene (HCB) and polychlorinated biphenyls (PCBs) and the two unintentionally produced substances polychlorinated dibenzo-p-dioxins (PCDDs) and polychlorinated dibenzofurans (PCDFs) [26,27]. Also, polycyclic aromatic hydrocarbons (PAHs) are also classified as persistent organic compounds, and they are formed as unintentionally substances by combustion and burning of organic compounds. Their occurrences are related to anthropogenic processes, and contamination of PAHs in river sediment is especially serious in high-density industrial areas [26]. The chemical structures of the most common persistent pollutants are given in Fig. 4. Moreover, in general POPs can be divided intentionally and unintentionally into two types of POPs as shown in Fig. 5.

4.1. Intentionally POPs

These compounds will be produced as wanted products by different chemical reactions that include chlorine. These types are organic molecules with linked chlorine atoms, high lipophilicity and, usually, high neurotoxicity, and they are called organochlorine compounds (OCs). Examples of OCs are the chlorinated insecticides, such as dichlorodiphenyltrichloroethane (DDT), and polychlorinated biphenyls (PCBs). They have several compounds which can be divided into two types that are industrial chemicals and organochlorine pesticides [28,29].

4.1.1. Organochlorine pesticides (OCPs)

Pesticides are chemicals or biological substances used to kill or control pests. They fall into three major classes: insecticides, fungicides, and herbicides (or weed killers). There are also rodenticides, nematocides, molluscicides, and acaricides. These chemicals are typically man-made synthetic organic compounds, but there are exceptions which occur naturally that are plant derivatives or naturally occurring inorganic minerals. Since, in the seventeenth century the first naturally occurring insecticide, nicotine from extracts of tobacco leaves, was used to control the plum curculio and the lace bug. In the 1940s, many chlorinated hydrocarbon insecticides were developed though they did not come into widespread use until the 1950s. Common examples include aldrin, dieldrin, heptachlor, and endrin. However, in spite of their early promise, these organochlorine insecticides are now much less used because of their environmental pollution impact [30,31].

Pesticides have been widely used throughout the world since middle of the last century. Around 1000 active ingredients have been employed and are currently formulated in thousands of different commercial products. They include a variety of compounds, mainly insecticides, herbicides and fungicides, with very different physico-chemical characteristics, and large differences in polarity, volatility and persistence. Pesticides are employed for many different purposes. About 80% of the pesticides is used in agriculture and moved in the environment by means of volatilization, runoff, infiltration, transport along the food chain, etc. Although the application of OCPs has been forbidden for a considerable period in many countries, the residues continue to induce a significant impact on the environment and its ecosystems

[32]. Chemicals used in the control of invertebrates include insecticides, molluscicides for the control of snails and slugs, and nematicides for the control of microscopic roundworms. Vertebrates are controlled by rodenticides which kill rodents, avicides used to repel birds, and pesticides used in fish control. Herbicides are used to kill plants. Plant growth regulators, defoliants, and plant desiccants are used for various purposes in the cultivation of plants. Fungicides are used against fungi, bactericides against bacteria, slimicides against slime-causing organisms in water, and algicides against algae. As of the mid-1990s, U.S. agriculture used about 365 million kg of pesticides per year, whereas about 900 million kg of insecticides were used in non-agricultural applications including forestry, landscaping,

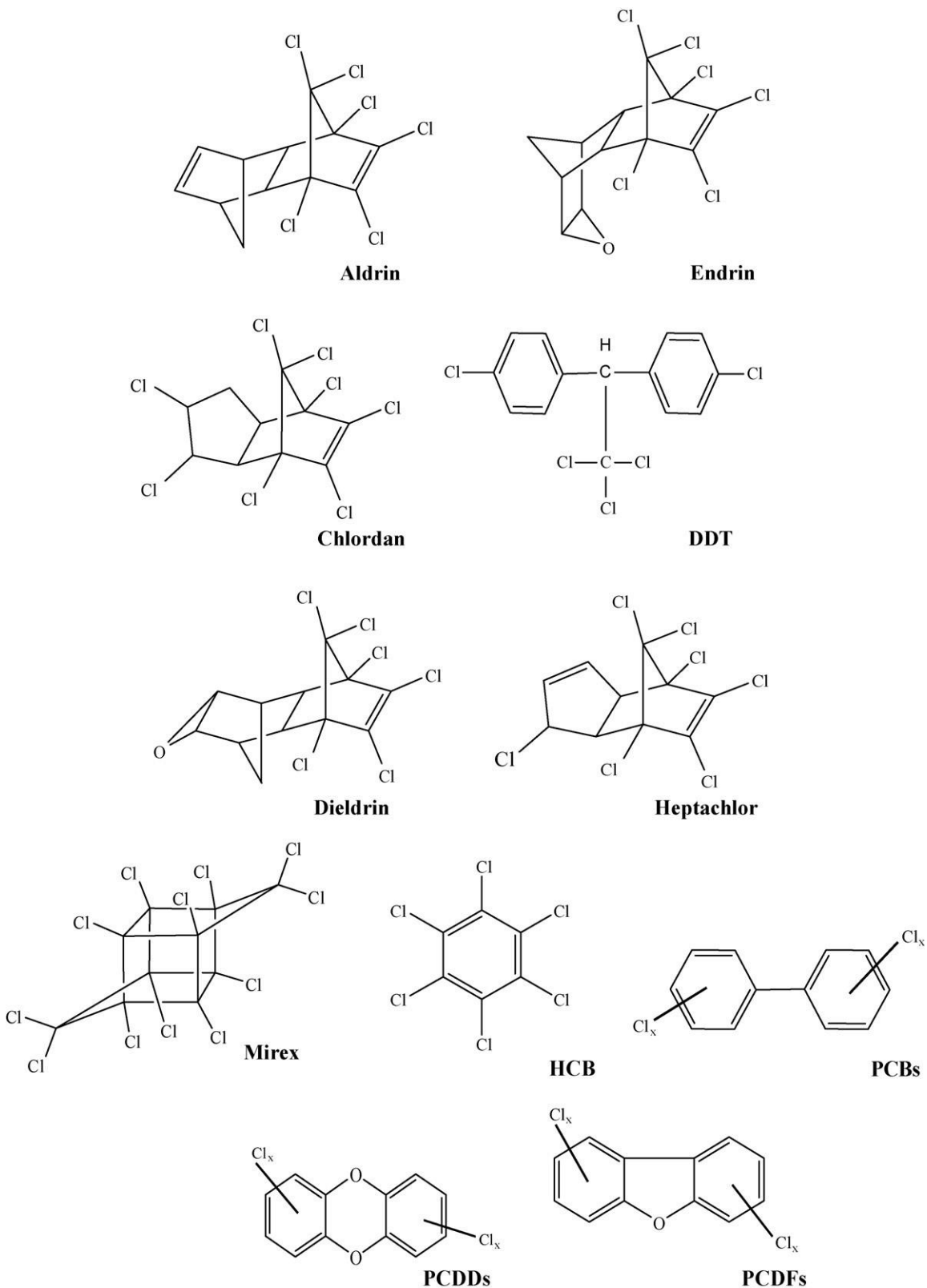


Fig. 4. The chemical structures of the most common persistent pollutants.

gardening, food distribution, and home pest control. Insecticide production has remained about level during the last three or four decades. However, insecticides and fungicides are the most important pesticides with respect to human exposure in food because they are applied shortly before or even after harvesting. Herbicide production has increased as chemicals have increasingly replaced cultivation of land in the control of weeds and now accounts for the majority of agricultural pesticides. The potential exists for large quantities of pesticides to enter water either directly, in applications such as mosquito control or indirectly, primarily from drainage of agricultural lands [33–35].

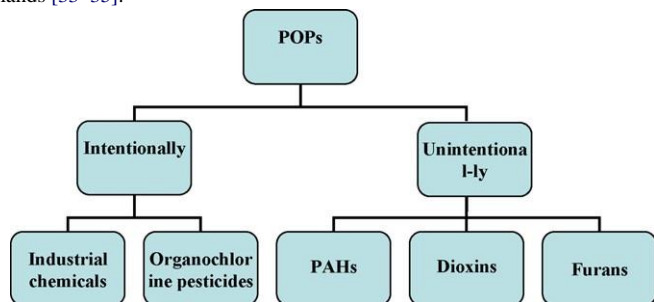


Fig. 5. Classification of POPs.

In the United States in 1993, an approximate percent (75%) of the sold pesticides have been used in agriculture [30]. Government and industry have been used 18%, and home and garden consumption accounts for the remaining 7%. Industrial and commercial users consist of pest control operators, turf and sod producers, floral and scrub nurseries, railroads, highways, utility rights-of-way, and industrial plant site landscape management [31]. The U.S. estimated volume of the conventional pesticides in 1993 is shown in Fig. 6.

Fig. 6.

Many public health benefits have been gained from the use of synthetic pesticides, but in spite of the obvious advantages, the potential adverse impact on the environment and public health can be substantial. Once in the environment, contemporary pesticides are relatively labile and tend not to persist for long periods of time. However, with the widespread use of pesticides, it is virtually impossible to avoid exposure at some level. Due to the general population's exposure to pesticides, it is important to investigate the concentration levels of pesticides and their metabolites in samples from human origin [29,30].

Before the insidious effects of DDT on humans and wildlife were known, this potent nerve poison was widely used to control mosquitoes, black flies and other vectors that carry diseases such as malaria, typhus and yellow fever. Farmers also used it to control insect damage to their crops. In the 1950s and 1960s, DDT was embraced as a cheap, effective, broad spectrum chemical pesticide. It was used worldwide and applied generously and indiscriminately to communities and crops alike. It did the job, reducing the threat of malaria and the loss of income to the agriculture industry [24]. Residues of PCBs were found in all food samples analyzed. However, their concentrations were many times lower than the permissible limits in place in other countries [24].

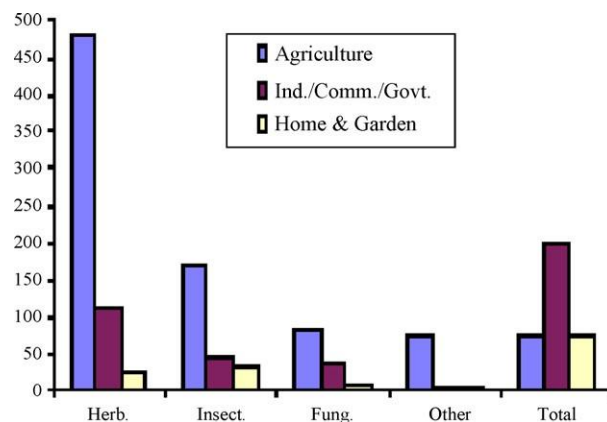


Fig. 6. The U.S. estimated volume for the conventional pesticides in 1993.

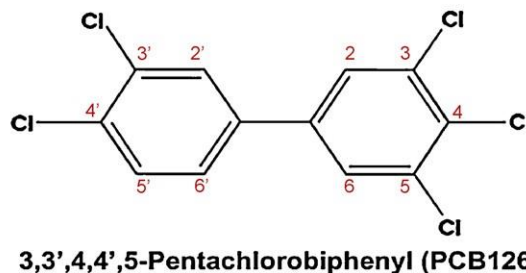
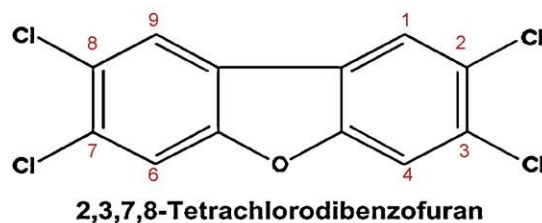
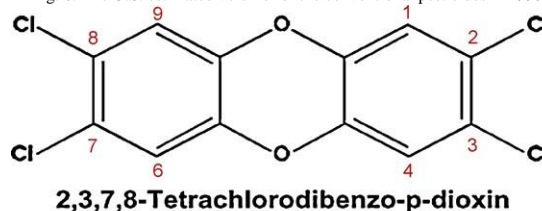


Fig. 7. Basic structures of the chlorinated dibenzo-p-dioxins (dioxins), chlorinated dibenzofurans (furans) and polychlorinated biphenyls (PCBs).

4.1.2. Industrial chemicals

First discovered as environmental pollutants in 1966, polychlorinated biphenyls (PCB compounds) have been found throughout the world in water, sediments, bird tissue, and fish tissue. These compounds constitute an important class of special wastes. PCBs are a class of chemical compounds in which 2–10 chlorine atoms are attached to the biphenyl molecule. Monochlorinated biphenyls (i.e., one chlorine atom attached to the biphenyl molecule) are often included when describing PCBs. The general chemical structure of chlorinated biphenyls is shown in Fig. 7. Theoretically, there are 209 different PCB congeners. Many of them are resistant to degradation, which allows them to persist in the environment for a long time and become widespread via atmospheric and water transport mechanisms [10,36,37].

PCBs are chemicals that were widely used in industrial processes from the 1930s until the late 1970s. Although their production ended in the late 1970s,

the majority of the cumulative world production of PCBs are still in the environment. PCBs were used extensively in many industrial applications, including in fire-resistant transformers and insulating condensers. Prior to 1977, they were used as heat exchanger fluids, and in aluminium, copper, iron and steel manufacturing processing [37]. PCBs were also used as plasticizers, in natural and synthetic rubber products, as adhesives, insulating materials, flame retardant, lubricants in the treatment of wood, clothes, paper and asbestos, chemical stabilizers in paints, pigments and as dispersing agents in formulations of aluminium oxide. PCBs are often found both in the effluent and in the sludge of municipal wastewater. Since PCBs were widely used as dielectric fluids from the 1950s, they are present in transformers in several Brazilian cities, despite its prohibition in the 1980s [38,39].

Every year, over 6000 food samples from all over Poland are being analyzed to determine the contents of residues of pesticides,

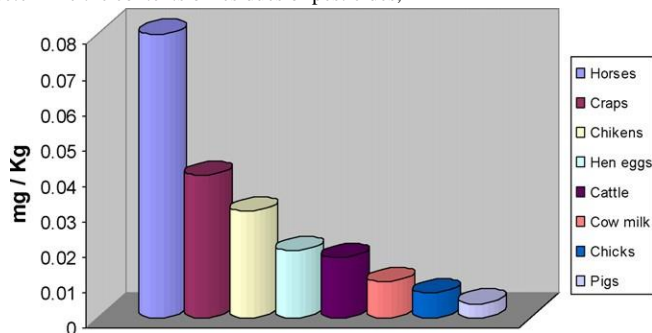


Fig. 8. Distribution of PCBs in food during the years 1995–1999.

polychlorinated biphenyls and other toxic substances in the fatty tissue of various animal species, cow milk and hen eggs. The results are summarized in the diagram given in Fig. 8. This diagram summarizes the results of research in the presence of PCBs in food during the years 1995–1999.

4.2. Unintentionally POPs

They were produced as unwanted by-products of combustion or chemical process that take place in the presence of chlorine compounds. They are divided into three types: polycyclic aromatic hydrocarbons (PAHs), dioxin and furan compounds.

4.2.1. Polycyclic aromatic hydrocarbons (PAHs)

The PAHs consist of two or more fused benzene rings in linear, angular or cluster arrangements, containing only carbon and hydrogen. The central molecular structure is held together by stable carbon-carbon bonds. The United States Environmental Protection Agency (EPA) listed 16 PAHs on a list of priority pollutants since they are considered either possible or probable human carcinogens. Hence, their distribution and the possibility of human exposure to them have been the focus of much attention. The PAHs have been detected in soil, air, and sediments as well as on various consumable products. They can occur naturally in the environment, mainly as a result of synthesis by plants or after forest and prairie fires. However, the greatest amounts of PAHs released into the environment are via anthropogenic processes like fossil fuel combustion and by-products of industrial processing. Agricultural fires as well as cooking may also release PAHs. The distribution of PAHs found in the sediments can give information on precursor sources, that is, if they are pyrogenic or petrogenic [40–42].

4.2.2. Dioxins and dibenzofurans

Chlorinated dibenzo-p-dioxins (dioxins) have been of concern for decades because of their toxic properties, as described below. A structurally similar series of compounds, the chlorinated dibenzofurans (furans), have similar chemical properties and toxic effects, and are generally determined as a group with the dioxins. In recent years there has been a growing trend to include a

specific subgroup of the polychlorinated biphenyls (PCBs): the so-called dioxin-like PCBs (DLPCBs). This has been added to methods along with the dioxins and furans. Fig. 8 shows the structures of 2,3,7,8-TCDD, 2,3,7,8-TCDF and PCB-126. It is commonly recognized that man-made sources and activities are far greater contributors to the environmental burden of polychlorinated dioxins (PCDDs) and dibenzo furans (PCDFs) than natural processes, especially since the 1930s, from which time there had been a steady increase in environmental levels coinciding with the large-scale production and use of chlorinated chemicals [42,43]. Man-made sources of PCDDs and PCDFs can be divided into three main categories: chemical processes, combustion processes and secondary sources [44]. Municipal waste incinerator, coal combustion, chemical waste incineration plant, clinical waste incinerator, landfill gas combustion, crematoria, animal carcass incinerator and cement manufacture are the main sources of PCDDs and PCDFs in Hong Kong [45]. The dioxins and furans, congeners with chlorine substitution at the 2, 3, 7 and 8 positions are considered toxic. Of the 75 possible dioxin and 135 possible furan structures, only 17 have 2,3,7,8-substitution. The carbon numbering system is marked next to each carbon to indicate substitution positions. Dioxin and furan congeners substituted in the 2, 3, 7 or 8 position are toxic, while

PCBs substituted in the 3,3',4,4',5 or 5' position and no or only one

2- or 2'-substitution are considered to be dioxin-like (Table 4). This class of compounds was found able to exhibit dioxin toxicity (see Table 4).

5. Properties of POPs

The behavior and fate of chemicals in the environment are determined by their chemical and physical properties and by the nature of the environment. The chemical and physical properties are determined by the structure of the molecule and the nature of the atoms present in the molecule. The properties of their physico-chemical characteristics that permit these compounds to occur either in vapour phase or adsorbed on atmospheric particles, thereby facilitating their long-range transport through the atmosphere. Some of these properties are: very low solubility, high lipid solubility since these two properties leading to their bioaccumulation in tissues, high toxic compound, and semi-volatile enabling them to move long distance in the atmosphere before deposition [47,48].

POPs can be present as vapours in the atmosphere or are bound to the surface of solid (dust) particles (particles of soil, of water sediments, of ashes). They are transferred to the ground surface from the atmosphere either by the deposition of the flying ashes (dry deposition) or by rain that absorbs substances present in the gas phase and pulls solid particles (wet deposition). The solubility of most POPs in water is minimal. They are, however, easily captured on solid particles (dust, ash, soil, and sediments). They are also fairly soluble in organic fluids (oils, fats, and liquid fuels). This implies that the more solid particles and polluting organic liquids present in the water, the higher the probability of their higher POPs content [49].

In the atmosphere, POPs undergo a slow decomposition due to of the solar radiation (photolysis) in the presence of water humidity and of other organic and inorganic substances. Their persistence in the atmosphere depends on thermal and reaction conditions of the given place. This durability in the tropical atmosphere is a maximum several days for a number of POPs; however, this can stretch up to several years for the occurrence of the same compound in the polar atmosphere [50].

Their stability in the atmosphere results into their long-distance transport of thousands of kilometers. This allows their transport from locations, where a number of them, namely pesticides, are still in use in significant amounts (Africa, South America) to the proximity of the North Pole. This was confirmed by a number of measurements of their presence in the snow and in the ice around the North Pole, as well as in the North Sea organisms. As these substances have never been used in these polar areas, their presence there is a clear proof of their long-distance transport [7,47].

POPs are anthropogenic compounds that are possessing characteristics toxic, persistent, bioaccumulate (build up in fatty tissues in individual organisms). Also, POPs are prone to long-range transboundary atmospheric transport and deposition, are likely to cause significant adverse human health or environmental effects near to and distant from their sources and concentrate further, or biomagnify up food chain. POPs can be divided into three categories: pesticides such as: aldrin, endrin, merix and chlordane, industrial

Table 4

Maximum WHO toxic equivalent factors (TEFs) for humans/mammals, fish and birds [46].

Congener	Humans/mammals	Fish	Birds
2,3,7,8-Tetrachlorodibenzo-p-dioxin (TCDD)	1	1	1
1,2,3,7,8-Pentachlorodibenzo-p-dioxin (PeCDD)	1	1	1
1,2,3,4,7,8-Hexachlorodibenzo-p-dioxin (HxCDD)	0.1	0.5	0.05
1,2,3,6,7,8-Hexachlorodibenzo-p-dioxin (HxCDD)	0.1	0.1	0.01
1,2,3,7,8,9-Hexachlorodibenzo-p-dioxin (HxCDD)	0.1	0.1	0.1
1,2,3,4,6,7,8-Heptachlorodibenzo-p-dioxin (HpCDD)	0.01	0.001	<0.001
1,2,3,4,5,6,7,8-Octachlorodibenzo-p-dioxin (OCDD)	0.0001	<0.0001	0.001
2,3,7,8-Tetrachlorodibenzofuran (TCDF)	0.1	0.05	1
1,2,3,7,8-Pentachlorodibenzofuran (PeCDF)	0.05	0.05	0.1
2,3,4,7,8-Pentachlorodibenzofuran (PeCDF)	0.5	0.5	1
1,2,3,4,7,8-Hexachlorodibenzofuran (HxCDF)	0.1	0.1	0.1
1,2,3,6,7,8-Hexachlorodibenzofuran (HxCDF)	0.1	0.1	0.1
1,2,3,7,8,9-Hexachlorodibenzofuran (HxCDF)	0.1	0.1	0.1
2,3,4,6,7,8-Hexachlorodibenzofuran (HxCDF)	0.1	0.1	0.1
1,2,3,4,6,7,8-Heptachlorodibenzofuran (HpCDF)	0.01	0.01	0.01
1,2,3,4,7,8,9-Heptachlorodibenzofuran (HpCDF)	0.01	0.01	0.01
1,2,3,4,5,6,7,8-Octachlorodibenzofuran (OCDF)	0.0001	<0.0001	0.001
3,4,4',5'-Tetrachlorobiphenyl (PCB 81)	0.0001	0.0005	0.1
3,3',4',4'-Tetrachlorobiphenyl (PCB 77)	0.0001	0.0001	0.05
2',3,4,4',5'-Pentachlorobiphenyl (PCB 123)	0.0001	0.000005	0.00001
2,3',4,4',5'-Pentachlorobiphenyl (PCB 118)	0.0001	<0.000005	0.00001
2,3,4,4',5'-Pentachlorobiphenyl (PCB 114)	0.0005	<0.000005	0.0001
2,3,3',4,4'-Pentachlorobiphenyl (PCB 105)	0.0001	<0.000005	0.0001
3,3',4,4',5'-Pentachlorobiphenyl (PCB 126)	0.1	0.005	0.1
2,3',4,4',5,5'-Hexachlorobiphenyl (PCB 167)	0.00001	<0.000005	0.00001
2,3,3',4,4',5'-Hexachlorobiphenyl (PCB 156)	0.0005	<0.000005	0.0001
2,3,3',4,4',5'-Hexachlorobiphenyl (PCB 157)	0.0005	<0.000005	0.0001
3,3',4,4',5,5'-Hexachlorobiphenyl (PCB 169)	0.01	0.00005	0.001
2,3,3',4,4',5,5'-Heptachlorobiphenyl (PCB 189)	0.0001	<0.000005	0.00001
	0.0001	<0.000005	0.00001

chemicals such as PCB, PCP and HCB, and unintentionally produced by-product like polycyclic aromatic hydrocarbons (PAHs), dioxins and furans compounds. Long-range transport via the atmosphere is the most likely source of these persistent organic pollutants in the Arctic. However, efforts to quantify the amount of POPs transported in this way and to determine source regions are quite limited. POPs have been associated with a number of environmental risks. These risks include oestrogenic effects, disruption of endocrine function with observed impairments of immune system function, generation of functional and physiological effects on reproduction capabilities and reduced survival and growth of offspring [26,51].

6. Dosage and toxicity of POPs

POPs so including are significant concern due to their potential toxicity and prevalence in arrangement of environmental media, even at remote geographical location. The ecotoxicological effects of POPs in the environment have caused much concern in recent years, and this has led to the control or complete ban on the use of these chemicals in many countries. Among the wide range of organic substances contaminating the aquatic environment a major concern has so far focused on PCBs and (OCPs). High persistence and biological degradation resistance of these toxic organic pollutants make them continue to be yet largely present in the marine environment. POPs are found not only in living organism as animals and plants, but also in humans [26,52].

Public concern about contamination by POPs increased recently because several of these compounds are identified as hormone disrupters which can alter normal function of endocrine and reproductive systems in humans and wildlife. There are many risks and effects of having these chemicals in our environment and none of them are a benefit to the earth. After these pollutants are put into the environment, they are able to stay in the system for decades causing problems such as cancer, birth defects, learning disabilities, immunological, behavioral,

neurological and reproductive discrepancies in human and other animal species [52].

POPs contaminate food, water and accumulate in the food chain such as eagles, polar bears, killer whales and human being. There is evidence that many people worldwide may now carry enough POPs in their body fat where POPs accumulate to cause serious health effects, including illness and death. Laboratory investigations and environmental impact studies in the wild have implicated POPs in endocrine disruption, reproductive and immune dysfunction, neurobehavioral and disorder and cancer [53,49].

More recently some POPs have also been implicated in reduced immunity in infants and children, and the concomitant increase in infection, also with developmental abnormalities, neurobehavioral impairment and cancer and tumor induction or promotion. Some POPs are also being considered as potentially important risk factor in the etiology of human breast cancer by some authors [54]. Human exposure to POPs is carried through the food chain. Because the animals are subsisting in water contaminated with these pollutants, they are affected as well when the humans consume these animals, they have also consumed the pollutant which then is accumulated in the body [49].

Because children are still developing, they are much more susceptible to the effects of pollutants. Their developing cells are sensitive to contaminants and are more likely to be affected by exposure of POPs. The brain is

apparently in the greatest concern because some studies have shown that children exposed to POPs during infancy had remarkably lower scores on assessments determining intelligence and ability to shut out distractions [19,55].

At a young POPs can have serious consequences side effects such any of the following: birth defects, certain cancer and tumors at multiple sites, immune system disorders, reproductive problems, reduced ability toward off diseases, stunted growth and permanent impairment of brain function, POPs are a suspected carcinogen, diseases such as endometriosis (a painful, chronic gynecological disorder in which uterine tissues are affected), increased incidence of diabetes and others and Neurobehavioral impairment including learning disorders, reduced performance on standard tests and changes in temperament [55]. Commonly used analytical methods

Table 5

Analytical methods for determination POPs in different matrices.

Methods	Analyte	Environmental matrix	References
GC/ECD	PCBs; OCPs; HCH; HCB; PAHs; DDT	Sediments, soil, liver and fat of birds, water, fungal, human hair, plants, adipose tissue	[56,4,58,61,62,66,69,73,78,81,52,85,5]
GC/MS	PCBs; OCPs; PBDEs; HCH; HCB; PAHs; OPPs; DDT	Dolphins, river water and sediment, livers and fat of birds, human adipose tissue, ice	[57,63,9,72,75,77,60,21,81–83,88–90,11]
HRGC/ECD	HCH; HCB; PCBs	Livers of cod fish, eggs	[4,58]
HRGC/LRMS	Pesticides, PCBs, PAHs	Water, plant	[64,91]
HRGC/MSD	PCBs; OCPs	Water, liver and muscle of tuna	[65]
HPLC-DAD	Pesticides	Ground water	[66]
RH-GC-FPD	OPPs	Fruit and vegetables	[67]
HRGC/HRMS	PCDD/Fs; OCPs; PCBs; HCB; HCH	Flue gas, livers, eggs of birds, river water, sediment, atmosphere, gastropods	[6,68,80,92–94]
GC/NPD	Pesticides	Bananas	[70]
GC-MS-MS	Pesticides	Rain water	[71]
GC-ECNI-MS	Toxaphene	Bird eggs	[74]
LC-MS-MS	Pesticides	Grain sample	[75]
SPE-HPLC	PCBs	Endogenous hormones	[76]
RP-LC-FLD	PAHs	Marin biota	[79]
HPLC/FLD	PAHs	Food sample, soil, air	[21]
PLVI-CC/ECNI-qMS	OCPs; HCB; HCH	Fish tissue	[84]
GC/FID	HCB	Soil	[87]

disposal is not required. SFE behaves significantly differently to classical solvent extraction and recoveries can be reduced or enhanced. Pressurized liquid extraction (PLE), also known as accelerated solvent extraction (ASE) evolved from SFE. Solvents were added to SFE extractions as modifiers in order to mimic classical liquid extractions. SFE without extraction gas and only solvent modifier best matched classical extraction recoveries. This led to the development of PLE. Microwave-assisted extraction (MAE or MASE) uses closed vessels to increase pressure and extraction efficiency. Polar solvents like acetone or water are required to supply heat for extraction. San et al. [95] reported the analysis of wet

Table 6

Extraction techniques of POPs in various matrices at different regions.

Sample matrix	Extraction technique.	Region/country	Analyte	References
Sediment	SE, LSE, LLE, SFE, MASE	Argentina, Singapore, China, Germany, Italy, Canada	PCBs, OCPs, PAHs, HCB, HCH, DDT, PBDEs, PCDD/Fs	[56,60,63,77,82,90,93,97,98]
Soil	SE, SPE, PLE, LLE, sonication	Singapore, Australia, Europe, Brazil, China	PAHs, OCPs, HCB, PCBs	[60,78,21,87,89,99,100]
Fruit and vegetable	GPC, SE, SPE, PLE, passive sampling	Europe, Sweden, China	OPPs, OCPs, DDT, PCBs, PAHs	[67,70,72,73,21,89,91]
Water (marine, fresh, ground rain and wastewater)	Sonication process, SPMD, LLE, filter DOC	Europe, Zambia, Indonesia, Italy, Spain, Turkey	HCH, HCB, PCBs, PAHs, OCPs	[59,64–66,69,71,79,80,85,88]
Fish (liver, tissue, egg and muscle)	SE, LLE	Pakistan, Japan, Philippines, Brazil, China	HCB, HCH, PCBs, OCPs	[4,58,65,84,5]
Dolphin	GPC	India	PBDEs, PCBs, OCPs	[57]
Bird (tissue, egg, liver and fat)	LLE, SE	Greece, USA, Japan	OCPs, PCBs, toxaphene	[62,74,6]
Air	Swipe/biofilms, passive sample	Italy	PCDD/F, HCB	[80,101–103]
Ice and snow core	LLE	Italy	OCPs, PCBs	[9]
Human (hormone, hair, tissue and adipose tissue)	LLE, SPE, SE, LSE, hot SE	China, USA, Romania, Belgium	PCBs, HCH, OCPs, HCB, DDT	[63,76,81,52]

for POPs monitoring and surveillance are summarized in Table 5. Numerous methods have been published over the past 30 years related to specific analytical techniques for the determination of PCBs and OCPs in food and environmental matrices.

7. Extraction and analytical techniques

Classical extraction techniques like liquid/liquid extraction and Soxhlet extraction are described in detail in the methods listed in Table 6. A number of alternative extraction techniques are summarized in Table 3. Supercritical fluid extraction (SFE) uses a gas above the critical point (the combination of temperature and pressure where the gas has liquid-like properties enabling enhanced extraction capability) to extract analytes from the matrix. The main advantage with SFE is that the extracting gas can be evaporated and so solvent

samples by MAE, indicating that significant time was saved by the reduced sample drying requirements. Solid-phase extraction can significantly reduce analysis times and solvent usage for the extraction of water and wastewater samples, even with significant particulate loadings [95]. Particles collected on C18 extraction disks can be extracted quantitatively without Soxhlet or PLE extraction. Watersamples have also been analyzed using semi-permeable membrane devices (SPMDs). SPMD sampling is a form of passive sampling that can be used for water, air or sediments [86,96].

Recently, Namiesnik et al. [97] have reviewed passive sampling techniques in environmental samples. Passive sampling is based on the free flow of analytes from the sampling medium to the collecting medium. This technique eliminates the requirement for power, and is a composite sampling procedure that can reduce analysis cost because of reduced sampling events and analyte loss during shipping and storage as the analyte is on a trapping medium. Swipe tests of

biofilms on surfaces can also be used to monitor ambient conditions, especially after fires or from fugitive emissions.

8. Removal and/or minimization of POPs

Environmentally relevant polar persistent organic pollutants (pharmaceuticals and diagnostic agents) have been chosen according to human consumption and occurrence in the aquatic environment (sewage plant effluents, rivers and groundwater) to investigate their behavior during photocatalytic oxidation. From

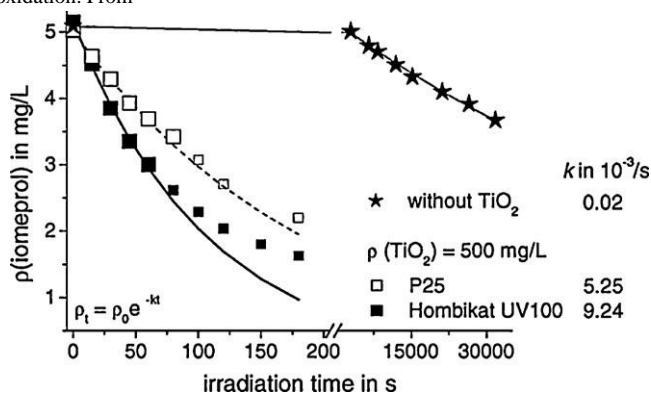


Fig. 9. Changes of iomeprol concentrations (2mgL^{-1} , pH 6.5) during irradiation with and without suspended TiO_2 (Hombikat UV100 or P25 (TiO_2)= 0.5mgL^{-1}).

the data compilation in the literature, the active metabolite clofibrac acid of some lipid lowering agents, the antiepileptic drug carbamazepine and the X-ray contrast media imperils were selected. The degradation of the persistent pollutant was monitored by HPLC/DAD/FLD. The study has been focused also on the identification and quantification of possible degradation products by HPLC/DAD/FLD and HPLC/MS/MS. The degradation process has also been monitored the determination of sum parameters and inorganic ions. Various aromatic and aliphatic degradation products have been identified and quantified [104,105]. Since, the photochemical degradation (irradiation without TiO_2) of the persistent organic pollutants was studied [106]. It turned out to be negligible compared to their photocatalytic degradation. For example the photocatalytic degradation rate constant (k) of iomeprol with Hombikat UV100 was about 500 times higher than the photochemical degradation rate constant of iomeprol (Fig. 9). For the determination of the first order rate constant (k) only the concentration values with $t/r_0=0.5$ (large symbols) were used. The fitting was done by the least squares method [106]. Moreover, the stabilized nanoparticles of FeS have showed excellent degradation (over 94%) of lindane pesticide in its hexane extract to 1,2,4-trichlorobenzene or TCB, a key intermediate of lindane degradation pathway. The non-stabilized FeS could degrade merely 25% lindane in the same period clearly indicated that these nanoparticles catalyzed a rapid reductive dehalogenation reaction [107,108].

9. Conclusion

The determination of POPs in various matrices is characterized by instrumental complexity and highly cost. The electrochemical techniques in particular stripping analysis have no contribution on the analysis of such class of chemicals. Thus, the use of voltammetric techniques for the analysis of such class of compounds will provide an efficient and excellent alternative approach for the determination of POPs in different matrices because of its low cost, sensitively and selectivity for trace and ultra-trace concentration of the POPs in complicated matrices. However, further work is still continuing for the possible application of the on-line voltammetric stripping analysis of the pesticides in serum, routine and various environmental samples.

References

- [1] S. Manahan, Environmental Chemistry, 7th edn, Lewis Publishers/CRC Press LLC, London, 2000.
- [2] J. Buccini, The development of a global treaty on persistent organic pollutants (POPs), in: H. Fiedler (Ed.), The Hand Book of Environmental Chemistry, Persistent Organic Pollutants, 3rd edn, Springer-Verlag, Berlin/Heidelberg, 2003, Chapter 2.
- [3] M. Wang, A. Leung, J. Chan, M. Choi, Chemosphere 60 (2005) 740.
- [4] F. Mason, N. Barak, Chemosphere 21 (1990) 659.
- [5] W. Chu, M. Wong, J. Zhang, Environ. Geochem. Health 28 (2006) 169.
- [6] G. Zhao, Y. Ying, G. Han, B. Ling, Environ. Geochem. Health 28 (2006) 341.
- [7] K. Kumar, K. Watanabe, H. Takemori, N. Iseki, S. Masunaga, T. Takasaga, Arch. Environ. Contam. Toxicol. 48 (2005) 538.
- [8] H. Selin, N. Eckley, Politics Low Econ. 3 (2003) 1.
- [9] J. Krueger, H. Selin, Governance for sound chemicals management: the need for a more comprehensive global strategy, global governance, in press.
- [10] S. Villa, A. Finizio, R. Diazdiaz, N. Vighi, Water Air Soil Pollut. 146 (2003) 335. [11] J. Lyche, J. Skaare, H. Larsen, E. Ropstad, Chemosphere 55 (2004) 621.
- [12] C. Hunge, G. Gang, K. Jiann, K. Yeager, P. Santsch, T. Wade, J. Sericans, H. Hsien, Chemosphere 65 (2006) 1452.
- [13] M. Storelli, R. Addabbo, G. Marcotrigiano, Environ. Int. 30 (2004) 343.
- [14] X. Song, B. Chen, Environ. Prot. 2 (2001) 9.
- [15] A. Grochowalski, B. Oznacznaniem, Polychlorinated Dibenzodioxin, Taylor and Francis, Ltd, Dibenzo-furan, Krakow, 2000.
- [16] Compilation of EU Dioxin Exposure and Health Data, Summary Report, European Commission DG Environment, 1999.
- [17] Exposure and Health Assessment for 2,3,7,8-Tetrachlorobenzop-dioxine (TCDD) and Related Compounds, Part 3 Integrated Summary and Risk Characterization for 2,3,7,8-Tetrachlorobenzop-dioxin (TCDD) and Related Compounds, US EPA, 2000.
- [18] R. Santillo, L. Stringer, P. Johnston, The Global Distribution of PCBs, Organochlorine Pesticides, Polychlorinated Dibenzo-p-dioxins and Polychlorinated Dibenzofurans Using Butter as an Interactive Matrix, Green Peace, 2000.
- [19] H. Bouwman, POPs in Southern Africa, in: H. Fiedler (Ed.), The Hand Book of Environmental Chemistry, Persistent Organic Pollutants, 3rd edn, Springer-Verlag, Berlin/Heidelberg, 2003, Chapter 11.
- [20] M. Wong, B. Poon, Sources, fates and effects of persistent organic pollutants in China, with emphasis on the Pearl River Delta, in: H. Fiedler (Ed.), The Hand Book of Environmental Chemistry, Persistent Organic Pollutants, 3rd edn, Springer-Verlag, Berlin/Heidelberg, 2003, Chapter 13.
- [21] Y. Ying, Y. Yong, R. Dawson, S. Yajuan, H. Zhang, T. Wong, W. Liu, H. Ren, Chemosphere 60 (2005) 731.
- [22] T. Wenzl, R. Simon, J. Kleiner, E. Auklam, Trends Anal. Chem. 25 (2006) 716. [23] R. Galiulin, V. Bashkin, R. Galiulina, Water Air Soil Pollut. 137 (2002) 179.
- [24] J. Petrik, D. Zeme, H. Stiftung, Persistent Organic Pollutants in Poland, Waste Prevention Association "3R", Kraków, 2001.
- [25] J. Ludwicki, K. Goralczyk, K. Czaja, in: H. Marerixach (Ed.), HCH Isomers in Human Tissues in Poland, 4th edn, Forum HCH and Unwanted Pesticides, Poznan, 1999.
- [26] Presented at the ICS, UNIDO Workshop on Contamination of Food and Agro Products, 2000, Croatia.
- [27] H. Fiedler, The Hand Book of Environmental Chemistry, Persistent Organic Pollutants, 3rd edn, Springer-Verlag, Berlin/Heidelberg, 2003, Chapter 1.
- [28] T. Harner, K. Pozo, T. Gouin, A. Macdonald, H. Hung, I. Cieny, A. Peters, Environ. Pollut. 144 (2006) 445.
- [29] Kelce, C. Stone, S. Laws, G. Earl, J. Kempalnen, E. Wilson, Nature 375 (1995) 581.
- [30] Strompl, J. Thiele, Arch. Environ. Contam. Toxicol. 33 (1997) 350.
- [31] A. Aspelin, Pesticide Industry Sales and Usage: 1992 and 1993 Market Estimates, U.S. Environmental Protection Agency, 1994.
- [32] Chen, L. Shi, Z. Shan, Q. Hu, Food Chem. 104 (2007) 1315.
- [33] J. Weinbe, An Overview of POPs Treaty-Public Forum on Persistent Organic Pollutants—the International POPs, Elimination Network, 1998.
- [34] J. Junior, N. Poppi, Talanta 72 (2007) 1833.
- [35] M. Espinosa, A. Granada, J. Carreno, M. Salvatierra, F. Serrano, N. Olea, Placenta 28 (2007) 631.
- [36] O. Panic, T. Gorecki, Anal. Bioanal. Chem. 384 (2006) 1366.
- [37] D. Korytar, P. Leonards, J. Bore, U. Brikmoan, J. Chromatogr. A 958 (2002) 203. [38] D. Amato, J. Torres, Quim 25 (2002) 995.
- [39] A. Amador, Buried pesticides waste hazard to Poland, Waste Manage. Res. 10 (1992).
- [40] T. Aboul-Kassim, B. Simueit, Environ. Sci. Technol. 29 (1995) 247.
- [41] Agency for Toxic Substance and Disease Registry (ATSDR) Toxicology Profile for Polycyclic Aromatic Hydrocarbons US Department of Health and Human Services, Public Health Service, Atlanta, GA, 1995.
- [42] B. Zielinska, S. Samy, Anal. Bioanal. Chem. 384 (2006) 1383.
- [43] C. Fortin, D. Caldbick, Organochlor. Compd. 32 (1997) 417.
- [44] R. Alcock, R. Gemmill, K. Joes, Chemosphere 38 (1998) 759.
- [45] H. Fiedler, Organochlor. Compd. 11 (1993) 221.
- [46] Environmental Protection Department, Assessment of Dioxin Emission in Hong Kong: Final Report, Air Policy and Planning Group, Environmental Protection Department, Hong Kong SAR Government, 2000.

- [47] M. Berg, L. Birnbaum, A. Bosveld, B. Brunstrom, P. Cook, M. Feeley, J. Giesy, A. Hanberg, R. Hasegawa, S. Kennedy, T. Kubiak, J. Larsen, F. Leeuwen, A. Liem, C. Nolt, R. Peterson, L. Poellinger, S. Safe, D. Schrenk, D. Tillit, M. Tysklind, M. Younes, F. Waern, T. Zacharewski, *Environ. Health Perspect.* 106 (1998) 775.
- [48] L. Guzzella, C. Rsciofi, L. Viganò, S. Sarkar, A. Bhattacharya, *Environ. Int.* 31 (2005) 523.
- [49] A. Katsiyannis, C. Samara, *Environ. Res.* 97 (2005) 245.
- [50] X. Huang, L. Lessner, D. Carpenter, *Environ. Res.* 102 (2006) 101.
- [51] B. Wahlstrom, Criteria for additional POPs, in: H. Fiedler (Ed.), *The Hand Book of Environmental Chemistry*, 3rd edn, Springer-Verlag, Berlin/Heidelberg, 2003. [52] A. Sweetman, M. Vall, K. Predouros, K. Tones, *Chemosphere* 60 (2005) 959.
- [53] A. Pauwels, A. Covaci, J. Weyler, L. Delbek, M. Dhont, P. Sutter, T. Haoghe, P. Schepens, *Arch. Environ. Contam. Toxicol.* 49 (2000) 265.
- [54] O. Roots, V. Zitko, A. Roos, *Chemosphere* 60 (2005) 914.
- [55] H. Bolt, G. Degen, *Arch. Environ. Contam. Toxicol.* 76 (2002) 187.
- [56] H. Fiedler, Dioxins and furans (PCDD/PCDF), in: *The Handbook of Environmental Chemistry, Persistent Organic Pollutants*, 3rd edn, Springer-Verlag, Berlin/Heidelberg, 2003.
- [57] M. Menone, J. Moreno, V. Moreno, A. Lanfranchi, T. Metcalfe, C. Metcafe, *Arch. Environ. Contam. Toxicol.* 40 (2001) 335.
- [58] K. Kannan, K. Ramu, N. Kajiwara, R. Sinha, T. Tanabe, *Arch. Environ. Contam. Toxicol.* 49 (2005) 415.
- [59] C. Sanpera, X. Ruiz, L. Jover, G. Liorente, R. Jabeen, A. Muhammad, E. Boncompagni, M. Fasola, *Arch. Environ. Contam. Toxicol.* 44 (2003) 360.
- [60] P. Fernandez, G. Carrera, J. Grimalt, *Aquat. Sci.* 67 (2005) 263.
- [61] C. Basheer, J. Obbard, H. Lee, *Water Air Soil Pollut.* 149 (2003) 315.
- [62] A. Barakat, *Bull. Environ. Contam. Toxicol.* 50 (2003) 174.
- [63] D. Hela, I. Konstantinou, T. Sakellarides, D. Lambropoulou, T. Akriotis, T. Albanis, *Arch. Environ. Contam. Toxicol.* 50 (2006) 603.
- [64] B. Poon, C. Leung, C. Wong, M. Wong, *Arch. Environ. Contam. Toxicol.* 49 (2005) 274.
- [65] L. Norrgren, U. Pettersson, S. Om, P. Beggvist, *Arch. Environ. Contam. Toxicol.* 38 (2000) 334.
- [66] D. Uneo, S. Takahashi, H. Tanaka, A. Subramanian, G. Fillman, H. Nakata, P. Lam, J. Zheng, M. Muchtar, M. Prudente, K. Chung, S. Tanabe, *Arch. Environ. Contam. Toxicol.* 45 (2003) 378.
- [67] M. Cuesta, R. Boque, F. Rius, J. Vidal, A. Frenich, *Chemometr. Intell. Lab. Sys.* 77 (2005) 251.
- [68] K. Patel, R. Fussell, R. Macarthur, D. Goodall, B. Keely, *J. Chromatogr. A* 1046 (2004) 225.
- [69] J. Wang, C. Hung, C. Hsuang, G. Chien, *J. Hazard. Mater.* 161 (2009) 800.
- [70] K. Cailleaud, J. Leray, L. Peluhet, K. Lemenach, S. Souissi, H. Budzinski, *Environ. Pollut.* 157 (2009) 64.
- [71] J. Borges, J. Cabrera, M. Delgado, E. Suarez, V. Saucó, *Food Chem.* 113 (2009) 313.
- [72] A. Scheyer, S. Morville, P. Mirabel, M. Millet, *Atmos. Environ.* 41 (2007) 7241. [73] J. Ramos, R. Otero, L. Ramos, J. Capelo, *J. Chromatogr. A* 1212 (2008) 145.
- [74] H. Gao, X. Jiang, F. Wang, D. Wang, Y. Bian, *Bull. Environ. Contam. Toxicol.* 74 (2005) 673.
- [75] K. Maruya, K. Smalling, M. Mora, *Arch. Environ. Contam. Toxicol.* 48 (2005) 567.
- [76] G. Pang, Y. Liu, C. Fan, J. Zhang, Y. Cao, X. Li, Z. Li, Y. Wa, T. Guo, *Anal. Bioanal. Chem.* 384 (2006) 1366.
- [77] P. Hjelmborg, M. Ghisari, E. Jorgensen, *Anal. Bioanal. Chem.* 385 (2006) 875.
- [78] S. Heim, J. Schwarzbauer, A. Kronimus, R. Littke, A. Herger, *Environ. Chem. Lett.* 1 (2003) 169.
- [79] A. Juhasz, E. Smith, J. Smith, R. Naidu, *Water Air Soil Pollut.: Focus* 3 (2003) 233.
- [80] J. Landaluze, L. Bartolome, O. Zuloaga, L. Gouzalez, C. Dietz, C. Camara, *Anal. Bioanal. Chem.* 384 (2006) 1331.
- [81] C. Bettiol, F. Collavini, S. Guerzoni, E. Molinaroli, D. Rossiui, L. Zaggia, R. Zonta, *Hydrobiologia* 550 (2005) 151.
- [82] A. Covaci, P. Schepens, *Chromatographia* 53 (2001) 366.
- [83] A. Cicero, M. Finoia, M. Gabelini, E. Veschetti, *Environ. Monit. Assess.* 64 (2000) 607.
- [84] I. Corsi, M. Mariottini, A. Badesso, T. Caruso, N. Borghesi, S. Bonacci, A. Iacacca, S. Facardi, *Hydrobiologia* 550 (2005) 237.
- [85] Y. Zhao, L. Yang, Q. Wang, *J. Am. Soc. Mass Spectrom.* 18 (2007) 1375.
- [86] A. Katsiyannis, C. Samara, *Chemosphere* 67 (2007) 1375.
- [87] X. Zhao, M. Zheng, I. Ilang, Q. Zhang, Y. Wang, G. Jiang, *Arch. Environ. Contam. Toxicol.* 49 (2005) 178.
- [88] D. Matheus, V. Bononi, K. Machado, *World J. Microbiol. Biotechnol.* 16 (2000) 415.
- [89] C. Guitart, N. Flor, J. Dachs, J. Bayona, J. Albaiges, *Mar. Pollut. Bull.* 48 (2004) 961.
- [90] Y. Chen, C. Wang, Z. Wang, *Environ. Int.* 31 (2005) 778.
- [91] R. Bettinetti, C. Giarei, A. Provini, *Arch. Environ. Contam. Toxicol.* 45 (2003) 72.
- [92] P. Bergquist, L. Augulyte, V. Jurjaniene, *Water Air Soil Pollut.* 175 (2006) 291.
- [93] M. Ekmekci, *Environ. Geol.* 49 (2005) 19.
- [94] P. Sathe, M. Ikonou, K. Haya, *Aquaculture* 254 (2006) 234.
- [95] Y. San, M. Takaoka, N. Takeda, T. Matsumoto, K. Osnita, *J. Sep. Sci.* 28 (2005) 585.
- [96] K. Taylor, D. Waddell, E. Reiner, K. Macpherson, *Anal. Chem.* 67 (1995) 1186.
- [97] J. Namiesnik, B. Zabigala, A. Kat-Wasik, M. Partyaka, A. Wasik, *Anal. Bioanal. Chem.* 381 (2005) 279.
- [98] M. Mannila, J. Koistinen, T. Vartiainen, *J. Chromatogr. A* 975 (2002) 189.
- [99] A. Vanbeuzekekom, W. Hijman, C. Berkhoff, B. Stoffessen, A. Denboer, G. Groenemeijer, D. Mooibroek, R. Hoogerbrugge, M. Broekman, R. Baumann, E. Hogendoorn, *Talanta* 63 (2003) 1183.
- [100] Method 1668, Revision A, Chlorinated Biphenyl Congeners in Water, Soil, Sediment and Tissue by HRGC/HRMS, US Environmental Protection Agency (1999), Office of Water, Washington, DC.
- [101] International Organization for Standardization Soil Quality Determination of Organochlorine Pesticides and Polychlorinated Biphenyls, in: *Gas Chromatographic Method with Electron Capture Detection*, ISO, Geneva, Switzerland, 2002.
- [102] S. Rayne, M. Ikonou, C. Butt, M. Diamond, J. Troung, *Environ. Sci. Technol.* 39 (2005) 1995.
- [103] C. Lucaciu, L. Faye, E. Reiner, T. Kolic, A. Boden, K. Macpherson, P. Crozier, F. Wania, R. Emerson, *Organohalogen Compd.* 66 (2004) 153.
- [104] N. Hanari, Y. Horii, T. Okazawa, J. Falandysz, I. Bochentin, A. Orlikowska, T. Puzyn, B. Wyrzykowska, N. Yamashita, *J. Environ. Monit.* 6 (2004) 305.
- [105] T. Dol, F. Frimmel, *Catalysis Today* 101 (2005) 195.
- [106] T. Doll, F. Frimmel, *Chemosphere* 52 (2003) 1757.
- [107] N. Assaf-Anid, L. Kun-Yu, *J. Environ. Eng.* 128 (2002) 94.
- [108] K. Paknikar, V. Nagpat, A. Pethkar, J. Rajwade, *Sci. Technol. Adv. Mater.* 6 (2005) 370.



Contents lists available at ScienceDirect

Analytica Chimica Acta

journal homepage: www.elsevier.com/locate/aca

Dual-wavelength λ -correction spectrophotometric determination of trace concentrations of cyanide ions based on the nucleophilic addition of cyanide to imine group of the new reagent 4-hydroxy-3-(2-oxoindolin-3-ylideneamino)-2thioxo-2H-1,3-thiazin-6(3H)-one

A. Hamza^a, A.S. Bashammakh^b, A.A. Al-Sibaai^a, H.M. Al-Saidi^c, M.S. El-Shahawi^{a,*}

^aDepartment of Chemistry, Faculty of Science, King Abdulaziz University, P.O. Box 80203, Jeddah 21589, Saudi Arabia ^bThe Centre of Excellence in Environmental Studies, King Abdulaziz University, P.O. Box 80203, Jeddah 21589, Saudi Arabia ^cDepartment of Chemistry, Teachers College, Umm AL-Qura University, Makkah, Saudi Arabia

article info

Article history:

Received 25 July 2009

Received in revised form 10 October 2009

Accepted 13 October 2009 Available

online 20 October 2009

Keywords:

Cyanide ions

Industrial wastewater

Determination

 λ -Correction spectrophotometry

Nucleophilic addition

abstract

A simple, fast, low cost and sensitive direct λ -correction spectrophotometric assay of cyanide ions based on its reaction with the reagent 4-hydroxy-3-(2-oxoindolin-3-ylideneamino)-2-thioxo-2H-1,3-thiazin-6(3H)-one, abbreviated as HOTT in aqueous media of pH 7–10 is described. The electronic spectrum of the produced brown-red colored species showed well defined and sharp peak at λ_{\max} = 466 nm. The effective molar absorptivity for the produced cyano compound was 2.5×10^4 L mol⁻¹ cm⁻¹. Beer's law and Ringbom's plots were obeyed in the concentration range 0.05–2.0 and 0.30–1.5 mg L⁻¹ cyanide ions, respectively. The proposed method offers 16.0 and 50.3 μ g L⁻¹ lower limits of detection (LOD) and quantification (LOQ) of the cyanide ion, respectively. The analytical utility of the method for the analysis of cyanide ions in tap and drinking water samples was demonstrated and the results were compared successfully with the conventional cyanide ion selective electrode. The short time response and the detection by the naked eye make the method available for the detection and quantitative determination of cyanide in a variety of samples e.g. fresh and drinking water. Moreover, the structure of the produced colored species was determined with the aid of spectroscopic measurements (UV–Vis, IR, ¹H and ¹³C NMR) and elemental analysis.

1. Introduction

Recent years have seen growing interest in anion recognition because of

its importance in a wide range of clinical, chemical and biological applications [1]. Among various anions, cyanide is one of the most concerned anions because it is being widely used in synthetic fibers, resins, herbicides, and the gold-extraction process [2]. Thus, monitoring of cyanide ions in industrial effluents is highly demanded for environmental control, in particular in electroplating, precious metal refining and metal cleaning industries. Cyanide ions either in free or metal-complexed form enter the environment from various human activities e.g. metal finishing, electroplating, steel, petroleum and chemical industries and mining operations [3]. The high toxicity of cyanide ions arises from its complexing ability towards iron (III) in the respiratory enzyme, cytochrome c oxidase. On the other hand, due its acute toxicity, environmental protec-

0003-2670/\$ – see front matter © 2009 Elsevier B.V. All rights reserved.

doi:10.1016/j.aca.2009.10.025

© 2009 Elsevier B.V. All rights reserved.

tion authorities such as Australian and New Zealand Environmental and Conservation Council (ANZECC) issue guidelines allowing a maximum permissible concentration limit of 5.0 μ g L⁻¹ cyanide in fresh and marine waters for protection of aquatic ecosystems [4]. Therefore, considerable attention has been focused on monitoring cyanide concentrations in a variety of samples such as fresh, marine and industrial wastewater by low cost procedures [5,6].

* Corresponding author. Permanent address: Department of chemistry, Faculty of Sciences at Damietta, Mansoura University, Mansoura, Egypt.

E-mail address: mohammad_elshahawi@yahoo.co.uk (M.S. El-Shahawi).

Several methods have been reported for the determination of cyanide ions at low concentration levels, e.g. chromatography [7,8], fluorimetry [9], electro analysis [10–12], indirect determination of cyanide-complexed metal with atomic absorption spectrometry [13]. On the other hand a series of direct and indirect spectrophotometric methods have been reported for the assessment of cyanide ions [13,14]. Most of these methods are based upon the conversion of cyanide ion into cyanogens chloride or bromide followed by the selective chromogenic reactions with pyridine solution of barbituric acid [13,14], pyrazolone [15], isonicotinic acid-barbiturates [16,17], 1,2-phenylenediamine [18], and benzide [19]. The decoloration of some colored complexes such as Cu^{2+} /N,N-diethyl-1,4-phenylenediamine [20], and Ni^{2+} /2-(5-bromopyridylazol)-5-diethylaminephenol [21] has been widely employed as indirect methods for cyanide assessment. A simple indirect simultaneous spectrophotometric

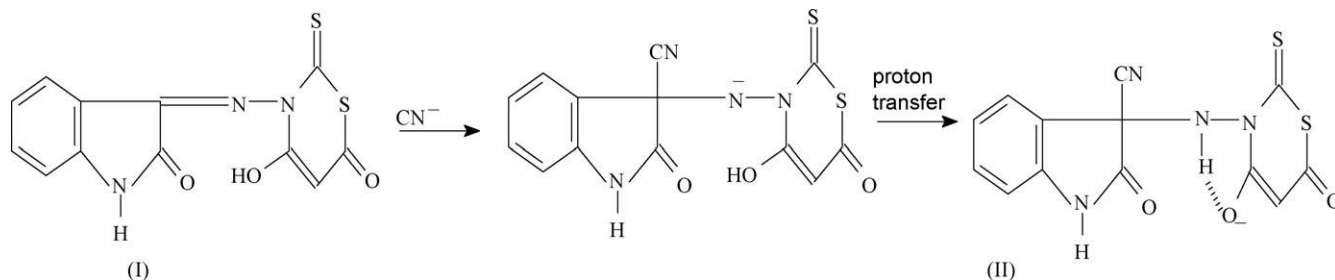


Fig. 1. Nucleophilic addition of cyanide anion to the free reagent HOTT.

determination method for the cyanide and thiocyanate ions after separation on a melamine-formaldehyde resin has been developed by Gumus et al. [22]. However, the low level of cyanide in industrial wastewaters is not compatible with the detection limit of some of these methods [13,14]. Moreover, some of these methods are too expensive [14,18], unselective, considerably suffered from the time consuming of color development [19,22], interferences by most of the common anions [13,15], require careful experimental conditions and the produced colored species of the cyanide ions are unstable and/or the reagent is carcinogenic.

Recently, particular attention has been focused on the utilization of chemosensors based on the strong nucleophilicity of cyanide in aqueous media for the determination of cyanide ions through specific chemical reaction between the guest molecules and the target species. In a routine screening, Drochioiu [23] has reported a specific reaction between cyanide ions and 2,2-di hydroxy-1,3-indanedione in alkaline media. Ren et al. [24] and Sun et al. [25] have also used fused indoline and benzoxazine fragment and nucleophilic addition of cyanide to the imine group of a new type of probe molecule bearing hydrazone functionality for highly selective determination of cyanide ions in water. However, these two methods are suffered from the interference of the excess chromogenic reagent which limits the sensitivity and selectivity. Therefore, in continuation to our previous work on the dual-wavelength λ -correction spectrophotometry [26] on the reagent HOTT containing numerous active sites e.g. C O, C S and C N (Fig. 1), the present article is focused on the use of the title reagent 4-hydroxy-3-(2-oxindolin-3-ylideneamino)-2thioxo-2H-1,3-thiazin-4(3H)-one for the determination of cyanide ions in various water samples. The study was also aimed to fully characterize the structure and mechanism of the produced cyano compound by spectroscopic techniques e.g. IR, ^1H NMR and ^{13}C NMR and elemental analysis.

2. Experimental

2.1. Reagents and materials

Unless otherwise stated, all chemicals and solvents used were of analytical reagent-grade quality and were used without further purification. A stock

solution of cyanide ions (1000gmL^{-1}) was prepared from potassium cyanide (BHD, USA). More diluted standard (0.01 – 20gmL^{-1}) solutions were prepared by dilution of the stock solution and stored in low density poly ethylene (LDPE)

bottles. An accurate weight (0.05g) of the pure reagent HOTT was dissolved in a minimum volume of N, N-dimethylformamide (3 – 5mL , DMF), followed by dilution with absolute ethanol (100mL). A series of Britton–Robinson (B–R) buffer ($\text{pH } 2$ – 11.7) was prepared as reported earlier [27].

2.2. Apparatus

The UV–Vis (190 – 1100nm) and IR (200 – 4000cm^{-1}) spectra were recorded on a PerkinElmer (model Lambda 25, USA) and a Perkin Mattson 5000 FTIR spectrophotometers, respectively. The absorbance of the reagent and its compound with cyanide ions were also measured with a PerkinElmer (Lambda 25, USA) spectrophotometer (190 – 1100nm) with 10mm (path width) quartz cell. A Bruker NMR (model Vance DPX 600MHz) was used for recording the ^1H and ^{13}C NMR spectra of the reagent

and its cyanide compound in deuterated DMSO solution using TMS as an internal standard. A digital-micro-pipette (Volac) and an Orion pH-meter (model EA 940) were employed for the preparation of the standard cyanide and test solutions and pH measurements, respectively. A scientific melting point SMP1 (UK) was used for recording the melting of the reagent and its cyanide compound. Carbon, hydrogen, nitrogen and sulfur contents were determined by a PerkinElmer 2400C series elemental analyzer, USA.

2.3. Synthesis of the reagent, HOTT

The HOTT reagent was prepared by direct condensation of isatin with dithioic formic acid hydrazide in DMF for 1h. The reaction product was then poured onto an ice bath and the resultant solid precipitate was separated out, washed with ethanol and ether and finally dried. The dried precipitate (10.0mmol) was refluxed with diethyl-malonate (10.0mmol) in ethanol (50.0mL) in the presence of sodium ethoxide (20.0mmol) for 4h. The reaction mixture was cooled, poured onto an ice bath and filtered off. The solid was separated out, washed with ether and acetone, recrystallized from ethanol as a yellow powder with an average yield of 63% and melting point of 242°C . Finally elemental analysis of the crystallized compound [$\text{C}_{12}\text{H}_7\text{N}_3\text{O}_3\text{S}_2$] required: 47.2% C, 2.3% H, 13.8% N, and 21% S; found 47.8% C, 2.5% H, 14.1% N, and 21.6% S. The characteristics IR frequencies of the solid reagent in KBr disk were observed at 3353 , 3147 , 1682 , 1655 , 1585 , 1350 , 1098 , 977cm^{-1} and are safely assigned to O–H, N–H, C O, C O (oxindole ring), C N, NC S, C–S, substituted aromatic nucleus [28], respectively. Moreover, ^1H NMR spectrum of the reagent (I) (Fig. 1) in d_6 -DMSO showed the characteristics signals at 110.71 (1H, OH), 10.5 (s, 1H, NH of thioxo-1,3-thiazin-4-one), 9.5 (s, 1H, cyclic H–C–OH) and 7.8 – 8.2ppm (m, 4H, Ar–H). Fine structure of the compound I was also deduced from ^{13}C NMR signals at 163 (1C S), 139 (2C O) of 2,6-tautomeric indole and thiazine, 127 , 126 , 123 , 122 (4C of benzene ring), 117 (C–OH), 110 (C N) and at 66ppm (C_3C) (Fig. 1).

2.4. Preparation of the cyano compound

An accurate amount (0.02mol) of the reagent HOTT was refluxed with an excess of potassium cyanide in methanol (50mL) for 1h. The reaction mixture was then cooled in an ice bath and the produced brown-red colored precipitate was

separated out, filtered off, washed with ether and acetone, and finally recrystallized from ethanol.

2.5. Recommended analytical procedure

An appropriate concentration (0.05–2.0 gmL⁻¹) of the test cyanide solution was transferred to 25 mL measuring flasks containing B–R buffer of pH 7–10 and the reagent HOTT solution (2 mL, 0.05%, w/v). The test solutions were completed to the mark with deionized water and shaken. The solution mixtures were allowed to stand at room temperature for 2–5 min and the absorption spectra were measured from 300 to 600 nm. The absorbance of the produced brown-red colored species at 336 nm (λ_1) and λ_{\max} = 466 nm was finally measured. Calibration plot of the cyanide concentration versus the corrected absorbance of dual-wavelength (λ_1 = 336, and λ_{\max} = 466 nm) λ -correction spectrophotometric method was used for all subsequent measurements of cyanide test and interference test solutions. The spectrophotometric data were measured in triplicate.

2.6. Analytical applications

2.6.1. Determination of cyanide ions in tap and drinking water

Tap water collected from the laboratories of the Chemistry Department, King AbdulAziz University, Jeddah city, KSA, and drinking bottled water, commercially available in Saudi Arabia markets, were filtered through 0.45 m cellulose membrane filter prior to their analysis and stored in LDPE sample bottles (250 mL). The recommended general spectrophotometric procedure used in preparing the standard curve was followed and the concentration of cyanide ions was then determined from the standard curve using the equation:

$$\text{cyanide concentration} = \frac{C_{\text{std}} \times A_{\text{sample}}}{A_{\text{std}}} \quad (1)$$

where, C_{std} is the standard concentration and A_{sample} and A_{std} are the corrected absorbance of the sample and the standard, respectively.

Alternatively, the method of standard addition was carried out as follows: transfer known volume (5.0 mL) of the unknown water samples to the volumetric flask (25.0 mL) adjusted to pH 7–10 with B–R buffer (5 mL). An accurate volume (2 mL) of the reagent was then added to the test solution and the reaction mixture was then made up to the mark with distilled water. Repeat the same procedures after adding various known concentrations (0.1–1.0 gmL⁻¹) of the cyanide ions. Measure the true absorbance displayed by the test solutions before and after addition of the standard cyanide solution employing λ -correction spectrophotometric method. The cyanide concentration was then determined via the calibration curve of the standard addition procedure. The average of five independent measurements was taken and the precision in most cases was $\pm 2\%$.

3. Results and discussion

3.1. Preliminary and spectroscopic studies

In aqueous media, on mixing the reagent HOTT with the cyanide ions, a brown-red colored product was developed immediately. The electronic spectrum of the reagent HOTT against water showed one absorption peak at 366 nm (Fig. 2) assigned to $n \rightarrow \pi^*$ transition [28]. In the reaction with cyanide ions in the pH range of pH 7–10, significant changes in the energies were noticed, where a new absorption band at 466 nm was observed on the electronic spectrum versus water. This band was safely attributed to the nucleophilic addition of the cyanide anion to the imine group of

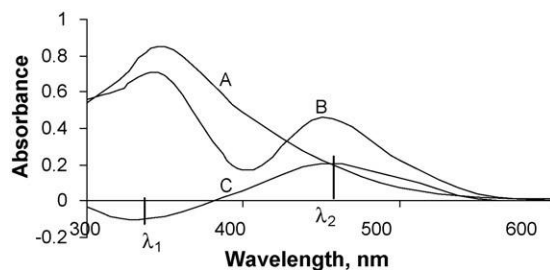


Fig. 2. Electronic spectra of the reagent HOTT and its cyanide compound at pH 9. Curve A is the spectrum of the reagent blank (reference water); curve B is the spectrum of the reagent with cyanide ion (reference, water); and curve C is the spectrum of cyanide-HOTT compound (reference reagent blank).

the reagent HOTT as reported earlier [25] and cleavage of the C–O bond of tautomeric indole and thiazine (Fig. 1) [29,30]. Therefore, solid cyano compound was prepared and isolated as described in the experimental section and subjected to spectroscopic studies to give strong proofs consistent with the proposed structure II (Fig. 1) and to assign the most probable reaction mechanism.

The characteristics IR frequencies of the solid reagent (I) (Fig. 1) in KBr disk changed dramatically after the addition of the cyanide anion. Two new bands were noticed at 3310 and 2088 cm⁻¹ and are safely assigned to NN–H (amine) and C–N [29], respectively. This assignment was also confirmed by the absence of the vibration band at 1585 cm⁻¹ ($\nu_{\text{C=N}}$) in the IR spectrum of the cyano compound

II (Fig. 1). Moreover, the IR spectrum of the cyano compound (II) (Fig. 1) showed also vibration bands at 3353 (OH), 1656 (C=O), 1585 ($\nu_{\text{C=N}}$), 1347 ($\nu_{\text{NC=S}}$), 1096 (C–S) and at 974 cm⁻¹ (substituted aromatic nucleolus) which are observed in the IR spectrum of the free reagent I (Fig. 1) confirming the involvement of the C–N group in the cyanide ion attack.

The ¹H NMR spectrum of compound I after the addition of the cyanide ion was dramatically changed, where the proton of OH group was shifted up field to 2.2 ppm confirming the occurrence of proton transfer of the OH group to the developing cyanide anion. This behavior is most likely close to the nucleophilic addition of cyanide anion to imine group (Fig. 1) as reported earlier [25]. The observed signals at δ 9.2, 7.9–6.8 ppm were noticed and were safely assigned to H–C–OH and benzo protons, respectively. ¹³C NMR spectrum of compound II revealed signals at 164 (1C S), 139 (C O), 129, 124, 123, 122 (4 C of benzene), 118 (C–OH), 110 (C N), 79 (C N) and 40 ppm (N–C–CN) as shown in Fig. 1. The relatively low value of the OH signal is most likely attributed to intra molecular hydrogen bonding. The chemical structure of the produced cyano compound (Fig. 1, II) was also determined by the method of continuous variations at various concentrations of the cyanide ions and reagent [28]. A plot of the true absorbance of the produced colored solution at 466 nm versus the mole fraction of the HOTT reagent revealed the formation of a compound of 1:1 cyanide to reagent molar ratio. These data confirm the presence of numerous active sites in the structure of the HOTT reagent e.g. C O, C S and C N (Fig. 1) and the nucleophilic addition of the cyanide anions to the imine group of the reagent. Elemental analysis of the cyanide-HOTT compound [C₁₃H₆N₄O₂S₂] required 49.68% C, 1.91% H, 17.8% N, and 20.4% S; Found 48.5% C, 1.64% H, 19.2% N, 21.2% S.

3.2. Application of λ -correction spectrophotometry

Most of the reported spectrophotometric methods [15–23] are suffered from the lack of sensitivity due to the significant interference of the excess chromogenic reagent with the analyte at λ_{\max} . This problem can be solved employing λ -correction spectrophotometric method to calculate the real absorbance of the formed colored species [30–32]. Thus, the electronic spectra of the reagent and its compound with cyanide anions were recorded (Fig. 2). The

spectrum of the reagent versus water, showed one well defined peak at 336nm (λ_1), while in the spectrum of cyano compound against the reagent blank at pH 7–10, a well defined absorption peak (λ_2) at 466nm with a molar absorptivity (ϵ) of $7.8 \times 10^3 \text{ Lmol}^{-1} \text{ cm}^{-1}$ was observed (Fig. 2). These results suggest the possible application of the λ -correction spectrophotometric technique to improve the sensitivity of the proposed reaction for the determination of cyanide ions the subsequent work. Moreover, the interference caused by the excess chromogenic reagent in the reaction mixture will be eliminated. Therefore, the real absorbance (A_c) of the produced cyanide-HOTT species in solution was calculated employing the equation [31,32]:

$$A_c = \frac{A - A_1}{1 - \alpha\beta} \quad (2)$$

The spectrophotometric parameters α , β were also calculated employing the equations [31,32]:

$$\alpha = \frac{A_1 - A_2}{A_1 - A_0} = \frac{\epsilon_1 \lambda_1 L - \epsilon_2 \lambda_2 L}{\epsilon_1 \lambda_1 L} \quad (3)$$

$$\beta = \frac{A_2 - A_0}{A_2 - A_1} = \frac{\epsilon_2 \lambda_2 L - \epsilon_1 \lambda_1 L}{\epsilon_2 \lambda_2 L} \quad (4)$$

where, A and A_1 are the absorbance's of the produced cyano compound versus reagent blank at λ_1 and λ_2 , respectively., The values of A_0 and A_2 represent the absorbance's of the blank solution against water at λ_1 and λ_2 , and A_1 and A_2 are the absorbance's of the cyano compound formed in the solution versus water at λ_1 and λ_2 , respectively. Moreover, it should be noted that, the sensitivity of the developed dual-wavelength λ -correction method become better than that of the single wavelength method by selecting the wavelengths λ_1 and λ_2 at the valley and the peak of the electronic spectrum of the cyanide compound versus blank solution [32–34], respectively. Thus, curve C in Fig. 2 shows the minimum and maximum absorption of cyanide-HOTT compound at pH 7–10 at 336nm (λ_1), and 466nm (λ_2), respectively. Thus, the absorbance of cyanide compound formed at λ_2 versus reagent blank (ordinary single wavelength) was found less than the corrected absorbance by λ -correction spectrophotometric technique. Based on the reported equations [33,34], the parameter β was calculated from curve A and was found equal 0.31 while, the value of α_{466} calculated from Fig. 2 (curve B) was 1.1.

3.3. Optimization of chemical variables

The influence of pH on the reaction of the reagent HOTT with cyanide anion can be predicted from the relation: $\text{HCN}/\text{CN} = 10^{9.2}/10^{\text{pH}}$ [35]. The availability of free cyanide ions required completing the addition reaction increases on raising the pH of the aqueous solution. The effect of pH on the real absorbance of the addition product at 466nm was investigated and the results are presented in Fig. 3. Maximum absorbance was achieved on the pH range 7–10. At pH > 10, the absorbance decreased which is most likely attributed to the formation of hydroxo-species that minimizes the formation of cyanide compound. The stability of the produced cyano compound could be low at pH > 10. Thus, in the subsequent work, the pH of the aqueous solution was adjusted at pH 7–10.

The influence of the reagent (HOTT) concentration on the formation of the cyano compound was studied at pH 7–10. Various volumes (1–6mL) of the reagent (0.05%, w/v) solution were added to the test solutions. A 2mL of the reagent (0.05%, w/v) was found sufficient for quantitative determination of cyanide ions up to 2.0 gmL^{-1} in the aqueous solution.

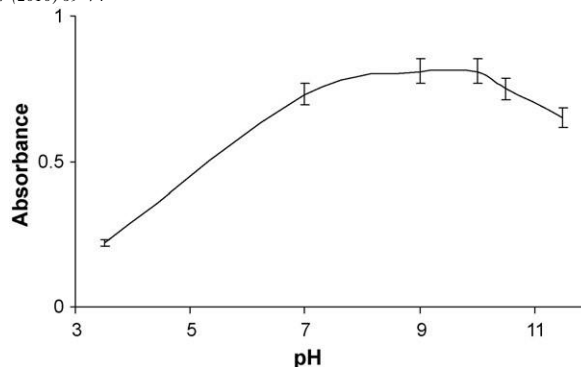


Fig. 3. Plot of the pH of the test aqueous solution versus the true absorbance of the cyanide-HOTT compound. [HOTT]=0.004% (w/v) and cyanide ion=1 gmL⁻¹.

3.4. Interference study

The determination of cyanide ions at concentration 0.6 gmL^{-1} in the presence of a relatively high excess (0.05–1.0mg) of some diverse ions relevant to water e.g. Na^+ , Li^+ , NH_4^+ , K^+ , Ca^{2+} , Mg^{2+} , SO_4^{2-} , Cl^- , I^- , NO_3^- , NO_2^- , PO_4^{3-} , Fe^{3+} , Al^{3+} , Zn^{2+} , and Mn^{2+} and ions was critically investigated by the developed procedure. The tolerance limit (w/w) was defined as the concentration of the diver's ions added causing a relative error within $\pm 3\%$ in the true absorbance of cyanide-HOTT compound. The presence of excess amounts (100-fold) of the foreign ions: Na^+ , K^+ , Ca^{2+} , NH_4^+ , Li^+ and Mg^{2+} , Mn^{2+} , Zn^{2+} and the anions PO_4^{3-} , NO_2^- and NO_3^- to the cyanide ions showed no significant change of the corrected absorbance. The anions SO_4^{2-} , I^- and Cl^- at 100-fold excess to the cyanide ions also did not interfere. The interference of the ions Fe^{3+} and Al^{3+} which probably react with the HTOO and/or cyanide forming stable complexes was eliminated by the addition of sodium fluoride (0.5%, w/v). Thus, the method can tolerate the foreign species tested in satisfactory amounts. Hence, the method is adequately selective for the cyanide determination in water and other matrices.

3.5. Analytical performance of the developed procedure

The analytical utility of the developed procedure was determined in terms the dynamic linear range, LOD, and LOQ, repeatability, recovery and specificity for the determination of the cyanide ions under the established experimental conditions. The effective molar absorptivity (ϵ) and the Sandell's sensitivity index [36] of the cyanide compound with and without the use of the dual-wavelength λ -correction spectrophotometry were found equal $2.5 \times 10^4 \text{ Lmol}^{-1} \text{ cm}^{-1}$ and $7.8 \times 10^3 \text{ Lmol}^{-1} \text{ cm}^{-1}$ and 0.002 gcm^{-2} and 0.0033 gcm^{-2} , respectively. The linear dynamic range was 0.05 – 2.0 gmL^{-1} employing λ -correction spectrophotometry. The regressions of the linear plots without and with the use of λ -correction spectrophotometry were given by the equations:

$$A = 0.269C_x + 0.011 \quad (r^2 = 0.997) \quad (5)$$

$$A_c = 0.454C_x + 0.0097 \quad (r^2 = 0.999) \quad (6)$$

respectively, where, C is the concentration of the cyanide ions in (gmL^{-1}). The effective concentration range of cyanide ions evaluated by the Ringbom's plot [37] was obeyed in the range 0.15 – 1.5 gmL^{-1} . The precision and accuracy of the developed procedure was evaluated by the recovery studies of five replicate measurements of cyanide ions at concentration of 1.0 gmL^{-1} using the developed λ -correction method. The relative standard

Table 1
Analytical features of the developed and some of the reported spectrophotometric methods for the cyanide determination.

Reagent	λ_{\max} (nm)	pH	Linear dynamic range (gmL^{-1})	Limit of detection (gmL^{-1})	Ref.
Hydroxybenzamide/ Ag^+ phenolphthalein.	552	10.3	0.6–4	0.10	[39]
CNBr/pyridinium chloride/sulfanilic acid	460	–	0.5–3	0.50	[40]
Chloramine-T/pyridine barbituric acid	578	6–8	0.3–5	0.10	[41]
Phenolphthalin/ CuS	552	10.3	0.6–4	0.60	[35]
Oxazine	411	7.6	Up to 0.26	0.026	[24]
2,2'-Dipyridyl-2-quinolyldiazone/ Cu^{2+}	353	9.5	0.04–1.2	0.020	[35]
Aquacyanocobyrinic acid heptamethyl ester					
4-Hydroxy-3-(2-oxindolin-3-ylideneamino)-2-thioxo-2H-1,3-thiazin-4(3H)-one	466	7–10	0.05–2	0.016	Present work

Table 2
Analysis of cyanide ions in tap-, bottled- and underground water samples by the proposed (A) and the potentiometric (B) methods^a.

Sample	Cyanide added (gmL^{-1})	Cyanide found (gmL^{-1})		Recovery (%)	
		A	B	A	B
Tap water	0.0	ND	ND	–	–
Tap water	1	1.04±0.13	1.06±0.3	104 ± 3.0	106 ± 0.01
Bottled water	0.0	ND	ND	–	–
Bottled water	2	2 ± 0.06	2.05±0.1	99 ± 2.5	105 ± 1.57
Ground water	0.0	ND	0.008±0.03	–	–
Ground water	1	1.05±0.5	1.09±0.4	105 ± 5.02	109.0±3.2

^a Average of five measurements ± standard deviation.

deviation (RSD) and the relative error of the developed λ -correction method were 2.3% and 1.9%, respectively.

The values of LOD and LOQ were calculated using the formula $\text{LOD} = 3.3/b$ and $\text{LOQ} = 10.3/b$ where b is the standard deviation of the blank and b is the slope of the calibration plot [38]. Employing the ordinary single wavelength spectrophotometry, the values of LOD and LOQ were found 0.16 and 0.52 gmL^{-1} cyanide ions, respectively. Such limits of LOD and LOQ were improved to 0.016 and 0.050 gmL^{-1} , respectively employing the developed λ -correction method. A comparison of the main analytical features of the proposed method was made with many of the previously published spectrophotometric methods [24,35,39–41] is summarized in Table 1. Some of these method exhibited high detection limit (0.1 – 0.6 gmL^{-1}) and serious interferences by halides ions [39–41]. Thus, it can be concluded that, the developed method is more selective and sensitive than the reported methods

3.6. Analytical applications

The validation of the proposed method for the assay of the cyanide ions in tap and drinking bottled water was critically investigated by the direct calibration plot and the standard addition method. The tested water samples (Tap- and drinking water) were processed at the optimum experimental conditions of the developed as mentioned in the experimental section. Moreover, different concentrations of the cyanide ions at concentration range 0.1 – 2.0 gmL^{-1} were also spiked onto the tested water samples. The cyanide content in each sample was then determined via the developed method and the standard solid state cyanide ion selective electrode (ISE) method [42]. The results are summarized in Table 2. The percentage recoveries of both methods were in good agreement and always higher than 95% confirming the accuracy of developed procedure and its independence from matrix interference. The statistical evaluations involving F test revealed no significant differences between the two the variances of the developed and the ISE methods [38].

The calculated value of $F(2.78)$ is less than the tabulated F value (6.39) for five replicate measurements. Therefore, there is no significant difference in the precision of the two methods at the 95% confidence level. The student t test was also applied to the analytical data obtained from the developed and ISE methods [43]. The results revealed no statistical difference between methods. The tabulated t value at 95% confidence limit was found equal 2.306 while the calculated t value of t calculated by applying t test to the results obtained analyzing the bottled water sample was found 0.79 ($n = 5$) at 2 gmL^{-1} concentration of cyanide ions. Moreover, the method was applied for the analysis of cyanide ions in industrial wastewater samples of electroplating baths after prior distillation with HCl (1.0 molL^{-1}). The liberated cyanide ions were absorbed on alkaline KOH (1.0 molL^{-1}). The average recovery (98.6%) of cyanide ions was compared successfully with the data obtained by potentiometry using a solid state cyanide ion selective electrode [42].

4. Conclusions

The reaction of the HTTO reagent with cyanide ion at pH 7–10, develops an intense brown-red color due to the nucleophilic addition of cyanide to imine group. The described method has the advantage of virtual freedom from interference from extraneous ions and can therefore serve as an alternative to the widely used methods for rapid and precise determination of trace amounts of cyanide in natural water and effluent samples. The method requires no complex pretreatment of chromatographic separations and/or preconcentration of the analyte and represents a highly selective and sensitive chemo sensor for the cyanide determination because color change appears rapidly within less than 30s and remains quite stable for up to 1h. The detection limit of the developed method was compared successfully with that of some published spectrophotometric procedures (Table 2). However, work is still continuing for investigating the influence of memory effect, organic material present in the investigated fresh water samples, competitive complexing agents in

addition to the on-line determination of cyanide in industrial wastewater after preconcentration on solid sorbent immobilized with the title reagent.

Acknowledgement

The author H.M. Al-Saidi would like to thank the Department of Chemistry, Teachers College, Umm AL-Qura University, for the scholarship provided. The authors would like also to thank Prof. R. M. Abdel-Rahman for the loan of the HOTT reagent.

References

- [1] V. Amendola, D. Esteban-Gomez, L. Fabbrizzi, M. Licchelli, *ACC. Chem. Res.* 39 (2006) 243.
- [2] G.C. Miller, C.A. Pritsos, *Proc. Symp. Annu. Meet. TMS*, 2001, pp. 73–81.
- [3] B. Sun, B.N. Noller, *Water Res.* 32 (1998) 3698.
- [4] Australian and New Zealand Environmental and Conservation Council (ANZECC), *Australian Water Quality Guidelines for Fresh and Marine Water*, 1992.
- [5] D.L. Duval, J.S. Fritz, D.T. Gjerde, *Anal. Chem.* 54 (1982) 830.
- [6] M. Nonomura, *Met. Finish.* 85 (1987) 15.
- [7] M. Nonomura, *Anal. Chem.* 59 (1987) 2073.
- [8] M. Nonomura, T. Hobo, *J. Chromatogr.* 465 (1989) 395.
- [9] K. Gamoh, S. Imamichi, *Anal. Chim. Acta* 251 (1991) 255.
- [10] R.A. Darst, *Anal. Lett.* 10 (1977) 961;
A. Tanaka, K. Mashiba, T. Deguchi, *Anal. Chim. Acta* 214 (1988) 259.
- [11] A. Amine, M. Alafandy, J.M. Kauffmann, M.N. Pekii, *Anal. Chem.* 67 (1995) 2822. [12] S. Chattaraj, A.K. Das, *Analyst* 116 (1991) 739.
- [13] M.A. Franson (Ed.), *Standard Methods for the Examination of Water and Wastewater*, 15th edn, American Public Health Association, Washington, DC, 1980.
- [14] G.V.L.N. Marty, T.S. Viswanhan, *Anal. Chim. Acta* 25 (1961) 293.
- [15] J. Epstein, *Anal. Chem.* 19 (1947) 272.
- [16] S. Bianting, N.N. Barry, *Water Res.* 32 (1998) 3698.
- [17] E. Nakamura, M. Yagi, *Bunseki-Kagaku* 49 (2000) 55.
- [18] L.S. Bark, H.G. Higson, *Talanta* 11 (1964) 625.
- [19] W.N. Aldridge, *Analyst* 69 (1994) 262.
- [20] M. Drochiou, K. Nagashima, M. Kamaga, N. Nakaro, *Bunsek-Kagaku* 52 (2003) 481.
- [21] M.F. Garcia, M.J. Sanchez, M.A. Rodriguez, *Mikrochim. Acta* II (1989) 259.
- [22] G. Gumus, B. Demirata, R. Apak, *Talanta* 53 (2000) 305.
- [23] G. Drochiou, *Talanta* 56 (2002) 1163.
- [24] J. Ren, W. Zhu, H. Tian, *Talanta* 75 (2008) 760, and references cited there.
- [25] Y. Sun, Y. Liu, W. Guo, *Talanta* (2009).
- [26] A. Hamza, A. S. Bashammakh A. A. Al-Sibaa, H.M. Al-Saidi and M.S. El-Shahawi, Submitted to *J. Hazardous Material* (2009).
- [27] A.I. Vogel, *Quantitative Inorganic Analysis*, 3rd edn, Longmans Group Ltd, England, 1966.
- [28] D.T. Sawyer, W.R. Heinemann, J.M. Beebe, *Chemistry Experiments for Instrumental Methods*, John Wiley & Sons, 1984.
- [29] M. Tomasulo, S. Sortino, A.J.P. White, F.M. Raymo, *J. Org. Chem.* 70 (2005) 8180. [30] M. Tomasulo, S. Sortino, F.M. Raymo, *Org. Lett.* 7 (2005) 1109.
- [31] K. Nakamoto, *Infrared and Raman Spectra of Inorganic and Coordination Compounds*, 3rd edn, Wiley, New York, 1978, p. 305.
- [32] S. Chatterjee, A. Pillai, V.K. Gupta, *Talanta* 57 (2002) 461.
- [33] A. Abbaspour, L. Baramakeh, *Talanta* 57 (2002) 807.
- [34] H. Cao, P.F. Zhang, *Analyst* 119 (1994) 2109.
- [35] S.S.M. Hassan, M.S.A. Hamza, A.E. Kelany, *Talanta* 71 (2007) 1088, and references cited there.
- [36] E.B. Sandell, *Colorimetric Method of Analysis*, Wiley Interscience, New York, 1959, p. 445.
- [37] A. Ringbom, *Z. Fresenius, Anal. Chem.* 155 (1939) 332.
- [38] J.C. Miller, J.N. Miller, *Statistics for Analytical Chemistry*, 4th edn, Ellis Horwood, New York, 1994, p. 115.
- [39] H.A.T. Hussein, *Talanta* 44 (1997) 545.
- [40] C.C. Chien, F.C. Chang, S.C. Wu, *Mikrochim. Acta* II (1980) 9.
- [41] A. Rios, M.D. Luque de Castro, M. Valcarcel, *Talanta* 31 (1984) 673.
- [42] T.S. Ma, S.S.M. Hassan, *Organic Analysis Using Ion Selective Electrodes*, vols. 1–2, Academic Press, London, 1982.
- [43] G.D. Christian, *Analytical Chemistry*, 6th edn, John Wiley & Sons, 2004.

Extraction Equilibrium and Simple Extractive Spectrophotometric Determination of Gold (I& III) in Water Using the Ion - Pairing Amiloride Hydrochloride

A.S. Bashammakh (Corresponding author) & M.S. El-Shahawi

Department of Chemistry, Faculty of Science, King Abdulaziz University

P.O. Box 80203, Jeddah 21589, Saudi Arabia

E-mail: abashammkh@kau.edu.sa

Abstract

The chemical equilibrium of the ternary complex ion associate of the complex anion AuCl_4^- and the ion – pairing reagent 1- (3, 5-diamino-6-chloropyrazinecarboxyl) guanidine hydrochloride monohydrate, $\text{DPG}^+\cdot\text{Cl}^-$ extracted from aqueous solutions of pH 5-6 onto 4-methyl pentan-2-one was demonstrated. The extraction constants (K_{ex} , K_{D} and β) of the chemical equilibrium and the structure of the produced associate were determined. The results have indicated that, the formation of the complex ion associate of the chemical structure $\text{DPG}^+\cdot\text{AuCl}_4^-$ and the extraction mechanism does not involve solvation of the ion associate by the amine and/or water molecules in the organic phase. Beer's law was obeyed in the range 0.01 -2.5 $\mu\text{g mL}^{-1}$ gold (III) in the aqueous solution. The method was applied successfully for the analysis of gold (I) after oxidation to gold (III). The method was also applied for the analysis of gold (I& III) at trace concentrations in industrial wastewater samples. Gold (III) ions at trace level in one liter aqueous solution was concentrated in 10.0 mL by the developed extraction system so an enrichment factor of 100 was achieved. The time taken for the separation and determination of gold ions was in the range of 3-5 min.

Keywords: Chemical equilibria, Speciation of gold (I, III), Ion associate, Wastewater

1. Introduction

Gold is one of the most important noble metals due to its wide application in industry and economic activity. Gold occur on the Earth in very low natural contents and its concentration in natural water is extremely low, in the range of 0.05 - 0.2 ng mL^{-1} . It is well known that gold is one of the most interesting micro amount elements due to its significant role on biology and environment. Thus, simple, sensitive and selective methods for determination of trace gold are of great importance.

Several sophisticated techniques, such as laser induced breakdown spectroscopy, inductively coupled plasma mass spectrometry (ICP –MS), inductively coupled plasma atomic emission spectrometry (ICP-AES), electrochemical, neutron activation analysis, total reflection X-ray fluorescence spectrometry have been applied to the determination of gold (Shoursheinin, 2010, PP. 89 -95; Guanghan, 1992, PP. 51-53; Medved, 2004, PP. 60 – 65; Yu, 2003, PP. 225 -231; Navratilova, 2000, PP. 369-372; Itagaki, 2000, PP. 344-349 and Li, 2006, PP. 841-844) in various matrices including wastewater. However, some of these methods are less often applied in gold analysis due to the complexity and cost of the required instrumentation (Guanghan, 1992, PP. 51-53; Medved, 2004, PP. 60 – 65; Yu, 2003, PP. 225 -231; Navratilova, 2000, PP. 369-372). Thus, spectrophotometric methods still have the advantages in respect of simplicity and low operating costs.

Recently (Zuotao, 1999, PP. 237-241; Pyrzyńska, 2005, PP. 1316-1322; Hu, 2006, PP. 627-630 and Fazli, 2009, PP. 210-212) a wide variety of spectrophotometric methods for the determination of gold have been reported. The ion pairing reagents had widely been applied for the pre concentration and/or determination of noble metal ions (Filatova, 2004, PP. 243-245; El-Shahawi, 2005, PP. 319-326; Hassan, 2005, PP.673- 678; El-Shahawi, 2008, PP.313 - 319). Charged bulky cations e.g. amidine, rhodamine derivatives, basic dyes, 18- crown-6 (18C6) oxonium cation, tetra alkyl ammonium, phosphonium or arsonium halides and tetrazolium salts are often used to form extractable complex ion associates with charged bulky oxoanions or anionic complex species of gold (I) , gold (III) and other metal ions as their halides, cyanides and thiocyanates (Haddad, 1988, PP. 23 – 36; Burns, 1992, PP. 213-215; Burns, 1992, PP. 131-132; El-Shahawi, 1996, PP. 2037-2043; Biswas, 1996, PP. 804-80; Camagong, 2001, PP. 1725-1728; Farag, 2007, PP. 218-228 and Bashammakh, 2009, PP. 413 – 418). Burns, 1988, PP. 185-187 and Burns, 1996, PP.107-109 and other workers (El-Shahawi, 1997, PP. 85-91; AIDhaheri, 1998, PP. 161-1615 and El-Shahawi, 2007, PP.1494-1499) have used the reagent amiloride mono hydrochloride extensively as a

selective ion-pairing reagent for the determination of some oxoanions e.g. perchlorate, perrhenate, periodate and tetra chloroaurate (AuCl_4^-) in different matrices.

Recent literature survey on the title ion – pairing reagent has revealed no study on the chemical equilibrium of the reagent $\text{DPG}^+\cdot\text{Cl}^-$ with AuCl_4^- . Hence, the main objectives of the present article was focused on:

- i. Studying the chemical equilibrium of the reagent $\text{DPG}^+\cdot\text{Cl}^-$ with AuCl_4^- in an attempt to develop a precise extractive spectrophotometric method for the determination and chemical speciation of gold (I, III) species in wastewater samples.
- ii. achieving a better association and a better understanding of the extraction mechanism of the produced ion associate of $\text{DPG}^+\cdot\text{Cl}^-$ with AuCl_4^- in the organic phase.

2. Experimental

2.1 Chemicals and reagents

Analytical reagent grade chemicals and solvents (BDH, Poole, UK) were used as received. Potassium aurate [KAuCl_4] and potassium aurocyanide, [$\text{KAu}(\text{CN})_2$] (Fluka AG, USA) were used for the preparation of stock solutions of gold (III) and gold (I) ions, respectively. The reagent, $\text{DPG}^+\cdot\text{Cl}^-$ (Merck, India) was used without purification. A stock solution (0.01 mol L^{-1} , 100 mL) of the reagent $\text{DPG}^+\cdot\text{Cl}^-$ was prepared by dissolving an accurate weight (0.302g) of it in $\text{H}_2\text{O-HCl}$ (1:1 v/v). Britton - Robinson (B-R) buffer of pH 2.1 - 11 was prepared (Vogel, 1966).

2.2 Apparatus

A double beam Perkin-Elmer (model Lambda EZ-210, USA) spectrophotometer (190-1100 nm) with 1 cm (path width) quartz cell was used for recording the electronic spectra and the absorbance of the organic extracts. Infrared (IR) spectra were recorded on a Broker FT-IR (model IFS 66, USA) spectrophotometer. A Perkin-Elmer (Analyst TM 800, USA) flame atomic absorption spectrometer (FAAS) was used for measuring the concentration of gold ions at 242.8 nm at 0.5 nm slit width before and after extraction with the organic solvent. De-ionized water was obtained from Milli-Q Plus system (Millipore, Bedford, MA, USA) and the pH were recorded on a pH meter (Orion EA940, MA, USA) with absolute accuracy limits being defined by NIST.

2.3 Recommended extraction procedures

2.3.1 Determination of the extraction equilibrium constants (K_D , β , K_{ex})

Aliquot aqueous solutions of gold (III) ions (10 mL , $1-10 \mu\text{g mL}^{-1}$) at pH 5-6 were transferred to separating funnels (50.0 mL). A 2 mL of the reagent $\text{DPG}^+\cdot\text{Cl}^-$ solution ($8.0 \times 10^{-5} \text{ mol L}^{-1}$) was added to each gold solution. The solutions were completed with B-R buffer of pH 5-6 to the mark of measuring flasks (25 mL). Each reaction mixture was mixed well and extracted twice ($2 \times 2.5 \text{ mL}$) with 4-methyl pentan-2-one for 2 min. The two phases were then separated out and the organic extract was collected in a 25 mL beakers containing anhydrous Na_2SO_4 (1.0g). The contents were swirled to mix and transferred to volumetric flask (10 mL). The solid residue was then washed with another 5 mL (2×2.5) of the solvent and the washings were transferred to the measuring flask. The flask was made up to the mark with the solvent. The absorbance of the organic extract was then measured at 362 nm against blank. The extraction procedures were also carried out in separate experiments at pH 5-6 of the aqueous solutions. After extraction, the gold (III) remained in the aqueous phase (C_a) was determined with FAAS. The amount of gold ions of the parallel aqueous solution containing the same amount of gold (III) ions before (C_b) extraction was also measured by FAAS. The amount of gold (III) ions extracted in the organic phase was finally calculated by difference ($C_b - C_a$) between the amount of gold (III) ions before and after extraction. The distribution ratio (D_{Au}) of the extraction step was calculated as reported (Burns, 1996, PP. 107-109 and El-Shahawi, 1997, PP. 85-91). Following these procedures, the effect of the diverse ions on the accuracy of the developed method for gold (III) was investigated.

2.3.2 Determination of gold (I)

An aliquot portion (10 mL) of the aqueous solutions containing gold (I) at concentration $< 5 \mu\text{g mL}^{-1}$ was transferred to conical flask (50 mL) and oxidized to gold (III) with bromine water after boiling for 5 min in a closed system (to avoid the evaporation of gold species) and finally cooled to room temperature ($25 \pm 1^\circ\text{C}$). The gold (III) produced was adjusted to pH 5- 6 and completed to the mark with B-R buffer of pH 5-6. The resulting solution was then analyzed following the recommended procedures for gold (III) determination at 365 nm versus the reagent blank with the aid of standard curve.

2.4 Analytical application

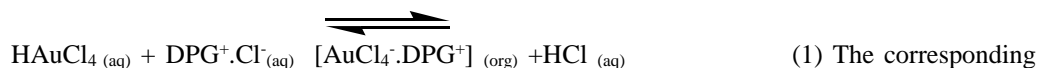
Industrial wastewater samples (100 mL) of fertilizer industry from the boundary side of Jeddah city, Saudi Arabia were collected and filtered through a 0.45 μm membrane filter. The solution pH was then adjusted to pH 5-6 with Britton – Robinson buffer and an accurate amount (0.5 - 10.0 μg) of gold (III) species was added. To the test solution an accurate amount of the reagent $\text{DPG}^+\cdot\text{Cl}^-$ (2.0 mL, $8.0 \times 10^{-5} \text{ mol L}^{-1}$) was added to the sample solution and the solution mixture was then transferred to 100 mL separating funnel. The organic extract was separated out and the absorbance was measured at 362 nm against reagent blank. The concentration of gold (III) in the organic and aqueous phases was also determined with FAAS.

3. Results and discussion

3.1 Extraction equilibrium

On mixing the complex anion AuCl_4^- with the reagent $\text{DPG}^+\cdot\text{Cl}^-$ in aqueous solutions of pH 5-6 containing sodium chloride (10 % m/v) and shaking with the solvent 4-methyl pentan-2-one for about 2 min, a yellow colored complex ion associate was developed in the organic phase. The electronic spectrum of the organic extract in 4-methyl pentan-2-one showed one well defined peak maximum at 362 nm. Thus, the absorbance of the organic extract of AuCl_4^- and $\text{DPG}^+\cdot\text{Cl}^-$ was measured at 362 nm against reagent blank. Assuming no dimerization of the extracted species, the formation of polynuclear complex species is negligible (Alexandrov, 1997, PP. 26-32) and the complex anion AuCl_4^- is only predominant at the given pH, the overall reaction between the reagent $\text{DPG}^+\cdot\text{Cl}^-$ and HAuCl_4 is most likely proceeded as follows (Kamburova, 1992, PP. 997 -1001 and Hiraoka, 1982, PP. 243-245) :

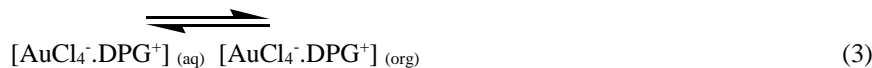
I. Formation of a ternary complex ion associate in the aqueous phase as follows:



equilibrium constant, β is given by the equation:

$$\beta = [\text{DPG}^+\cdot\text{AuCl}_4^-] \text{ (org)} / [\text{AuCl}_4^-] \text{ (aq)} [\text{DPG}^+] \text{ (aq)} \quad (2) \text{ II. Distribution of}$$

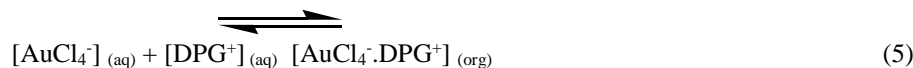
the complex ion associate between the aqueous and organic phases:



with a distribution constant, K_D which is given by the equation:

$$K_D = [\text{DPG}^+\cdot\text{AuCl}_4^-] \text{ (org)} / [\text{DPG}^+\cdot\text{AuCl}_4^-] \text{ (aq)} \quad (4) \text{ III. Extraction}$$

of the complex anion AuCl_4^- as follows:



The corresponding extraction constant, K_{ex} is then given by the equation:

$$K_{\text{ex}} = [\text{DPG}^+\cdot\text{AuCl}_4^-] \text{ (org)} / [\text{DPG}^+] \text{ (aq)} \cdot [\text{AuCl}_4^-] \text{ (aq)} = K_D \beta \quad (6)$$

Assuming the complex species AuCl_4^- is the only predominant species in the aqueous phase at equilibrium at the given pH, the value of the distribution ratio, D_{Au} was then determined at constant concentration of AuCl_4^- and various amounts of the reagent $\text{DPG}^+\cdot\text{Cl}^-$ in the aqueous phase employing the equation (Kamburova, 1992, PP. 997 -1001 and Alexandrov, 1997, PP. 26-32):

$$D_{\text{Au}} = [\text{DPG}^+\cdot\text{AuCl}_4^-] \text{ (org)} / [\text{AuCl}_4^-] \text{ (aq)} + [\text{DPG}^+\cdot\text{AuCl}_4^-] \text{ (aq)} \quad (7)$$

At low $\text{DPG}^+\cdot\text{Cl}^-$ concentration, the term $[\text{DPG}^+\cdot\text{AuCl}_4^-] \text{ (aq)}$ can be neglected and equation (7) takes the form:

$$D_{\text{Au}} = [\text{DPG}^+\cdot\text{AuCl}_4^-] \text{ (org)} / [\text{AuCl}_4^-] \text{ (aq)} \quad (8) \text{ Substituting equation (8)}$$

into equations (2) and (6) and taking the logarithms, equation (9) is obtained:

$$\log D_{Au} = \log K_D + \log \beta + \log [DPG^+.Cl^-] \quad (9)$$

The values of D_{Au} at the initial concentration of $AuCl_4^-$ (1×10^{-6} mol L^{-1}) in the aqueous phase (pH5-6) at various concentrations ($1.0 - 40.0 \times 10^{-5}$ M) of the reagent $DPG^+.Cl^-$ were then calculated. The plot of $\log D_{Au}$ versus $\log [DPG^+.Cl^-]$ was linear (Figure 1) with a slope of 0.91 confirming the formation of 1:1 molar ratio of DPG^+ and $AuCl_4^-$ in the formation of ternary complex ion associate $DPG^+.AuCl_4^-$. The data also have the existence of $AuCl_4^-$ species in the organic solvent and the absence of non-specific interaction between the ion associate and the reagent $DPG^+.Cl^-$ and also between the bulky anion $[AuCl_4^-]_{(aq)}$ and the organic solvent (Hiraoka, 1982, PP.243-245; Alguacil, 1996, PP. 197-208 and El- Shahawi, 1997 PP85 -91). At high concentration of the reagent $DPG^+.Cl^-$, the respective term $[AuCl_4^-]_{(aq)}$ is negligible and equation (7) takes the following form:

$$D_{Au} = [DPG^+. AuCl_4^-]_{(org.)} / [DPG^+. AuCl_4^-]_{(aq)} = K_D \quad (10)$$

Thus, at high $DPG^+.Cl^-$ concentration, the plot of the experimental data in the same coordinates of equation (9) has yielded a straight line slightly parallel to the abscissa with negative slope of -0.04 close to zero (Figure 1) confirming, the proposed chemical model, the proposed ternary complex ion associate, the absence of non-specific interaction between the produced complex associate and the reagent and also between the bulky anion $[AuCl_4^-]_{(aq)}$ and the organic solvent (Hiraoka, 1982, PP. 243-245 and Alguacil, 1996, PP.197-208). The data have also confirmed the non - specific interaction between the extracted species $DPG^+.AuCl_4^-$ and the solvent (Hiraoka, 1982, PP. 243-245 and Alguacil, 1996, PP.197-208). The values of the equilibrium constants (β and K_D) and the extraction constant, ($K_{ex} = \beta \times K_D$) of the formed ion associate computed from the linear plot (Figure 1) are: $\beta = 2.07 \pm 0.2 \times 10^4$, $K_D = 11.97 \pm 0.7$, $K_{ex} = 2.0 \pm 0.3 \times 10^3$. Using these constants, the theoretical correlation of D_{Au} as a function of $DPG^+.Cl^-$ was calculated. The results revealed satisfactory agreement between the experimental and the theoretical data confirming the molar ratio (1:1) of the reagent $DPG^+.Cl^-$ to the complex anion $AuCl_4^-$ in the extracted complex ion associate $DPG^+. AuCl_4^-$. The computed values of the extraction constants β , K_D and K_{ex} are better than the data reported (Patel, 1986, PP. 1547 -1551) using amidine ion pair. The developed extraction procedures also offered lower reaction time, much less toxic option and low cost for the separation and/or determination of gold (III) species.

3.2 Extraction mechanism

Assuming an overall gold (III) extraction in which the reagent amiloride abbreviated by RNH_2 has the general equilibrium equation:



$$K_{ex} = [RNH_3^+.AuCl_4^-]_{(org)} / [AuCl_4^-]_{(aq)} [H^+]_{(aq)} [RNH_2]_{(aq)} \quad (12) \text{ On substituting}$$

equation (1) onto equation (10) equation (13) was obtained:

$$K_{ex} = D_{Au} / [H^+]_{(aq)} \cdot [RNH_2]_{(aq)} \quad (13) \text{ Taking logarithms}$$

and rearranging the equation, the following equation :

$$\log D_{Au} = \log K_{ext} - pH + \log [RNH_2]_{(aq)} \quad (14)$$

was obtained and the corresponding coefficients for the pH and the amiloride concentration was achieved. The plot of pH versus $\log D_{Au}$ at constant reagent concentration and the aqueous phase containing 0.25 mmol L^{-1} gold (III) using aqueous/organic phase volume ratio of 1/1 and shaking for 3 min was linear with a slope 0.965 close to unity confirming the value for the pH coefficient given in equation (14). Based on the work reported earlier (Alguacil, 1996, PP. 197-208) and by definition, when $D_{Au} = 1$ in a solvent extraction system, the pH obtained is known as pH_{50} . Thus, on replacing pH_{50} in equation (11), the following expression was obtained:

$$pH_{50} = \log K_{ext} + \log [RNH_2]_{(aq)} \quad (15)$$

On plotting $\log D_{Au}$ versus $\log [RNH_2]_{(aq)}$ (Figure 1) a slope of 0.956 was obtained. This value close to unity and corresponds to the value of $\log [RNH_2]_{(aq)}$ coefficient given in equations (13) and (14). Elemental analysis of the produced ternary complex ion associate in the solid form after solvent evaporation: $[AuOC_6H_9N_7Cl_5]$ required: 12.6% C, 1.57% H, 17.2% N, 31.1% Cl and 34.7% Au; Found 12.9% C, 1.7% H, 17.7% N, 31.7% Cl and 35.6% Au. The IR spectra of the reagent $DPG^+.Cl^-$ and its solid ion complex associate recorded in KBr disk showed the characteristic frequencies of ν (N-H), ν (N-N), ν (N-H) + (C-N), ν (N-C-S) and ν (Au-Cl) vibrations at 3456 (br.),

1626 (s), 1516 (s) and 450 cm^{-1} (Nakamoto, 1978, PP. 232 -239), respectively confirming the proposed structure. The results also added further conclusive evidence that, the amiloride reagent extracted gold (III) from the aqueous solution containing $[\text{AuCl}_4^-]_{(\text{aq})}$, and the absence of non-specific interaction between the ion associate and the reagent $\text{DPG}^+\cdot\text{Cl}^-$ and also between the bulky anion $[\text{AuCl}_4^-]_{(\text{aq})}$ and the organic solvent (Hiraoka, 1982, PP.243-245 and Alguacil, 1996, PP. 197-208). Thus, the extraction mechanism of the anion AuCl_4^- from the aqueous solution at pH 5- 6 by the reagent $\text{DPG}^+\cdot\text{Cl}^-$ did not involve solvation of the produced ion associate ($\text{DPG}^+\cdot\text{AuCl}_4^-$) in the organic phase by amine and/or water molecules (Hiraoka, 1982, PP.243-245 and Alguacil, 1996, PP. 197-208).

3.3 Analytical performance

The plot of the absorbance of the developed ion associate $\text{DPG}^+\cdot\text{AuCl}_4^-_{(\text{org})}$ in the organic phase at 362 nm vs. gold (III) concentration (C, $\mu\text{g mL}^{-1}$) was linear confirming Beer's -Lambert law (Marczenko, 1986, PP. 68 – 70 and Miller, 1994, PP.115-125) in the concentration range 0.01 -2.5 $\mu\text{g mL}^{-1}$ gold (III) in the aqueous solution with a correlation coefficient of 0.99. The molar absorptivity calculated from Beer's-Lambert plot and the Sandell's sensitivity index (Marczenko, 1986, PP. 69 -70) of the ion associate were found $2.05 \times 10^4 \text{ L mol}^{-1} \text{ cm}^{-1}$, $0.069 \mu\text{g cm}^{-2}$, respectively. The effective concentration range of gold (III) as evaluated by Ringbom's plot (Marczenko, 1986, PP. 69 -70) was found equal 1.5-1.5 $\mu\text{g mL}^{-1}$. A lower limit of detection (LOD) of $0.005 \mu\text{g mL}^{-1}$ was achieved using of the formula $\text{LOD} = 3S_{y/x}/b$ where, $S_{y/x}$ is the standard deviation of y- residual and b is the slope of the calibration plot (Miller, 1994, PP.115-125). The lower limit of quantification (LOQ = $10S_{y/x}/b$) under the established conditions for gold (III) was $0.033 \mu\text{g mL}^{-1}$. The LOD could be improved to lower value by increasing the sample volume of the aqueous phase containing ultra trace concentration of gold and amiloride at the optimum experimental conditions and shaking with the organic solvent. A relative standard deviation (RSD) of 2.96 % (n=5) was obtained for gold (III) at concentration $0.5 \mu\text{g mL}^{-1}$. The figure of merits (LOD, linear range, RSD) of the proposed procedure was compared with many of the reported spectrometric methods and in the literature (Pyrzynska, 2005, PP. 1316-1322; Fazli, 2009, PP. 210-212; Zuotao, 1999, PP. 237-241 and El-Shahawi, 2008, PP. 313 -319). The time consuming on the developed method is comparable with some reported methods (Pyrzynska, 2005, PP. 1316-1322 and Fazli, 2009, PP. 210-212) confirming its precision.

3.4 Interference studies

The selectivity of the developed method for the determination of gold (III) at $1.0 \mu\text{g mL}^{-1}$ was tested in the presence of a relatively high excess ($0.1\text{-}1 \text{ mg mL}^{-1}$) of some diverse ions which are often accompanying gold in water. The tolerance limit was defined as the concentration of the diverse ion added causing a relative error in the absorbance at 362 nm in the range $\pm 3\%$. A recovery percentage of $100 \pm 2.5\%$ gold (III) and a standard deviation of ± 0.12 were achieved in the presence of the ions: Li^+ , Na^+ , K^+ , Ca^{2+} , NH_4^+ , Al^{3+} , Fe^{2+} , Fe^{3+} , Ni^{2+} , Co^{2+} , Pd^{2+} , Pt^{2+} , Cu^{2+} , Zn^{2+} and Ag^+ at 1:100 tolerable concentration of gold(III) to the diverse ions, respectively. The ions Fe^{3+} , MnO_4^- , VO_3^- and NO_3^- interfered seriously even at low concentrations. The positive interference of these ions is most likely assigned to the ability of these anions to form relatively stable complex ion associates with the reagent $\text{DPG}^+\cdot\text{Cl}^-$. Interference of MnO_4^- was eliminated by adding traces of NaN_3 (0.1% w/v) while, the influence of the ions Fe^{3+} and VO_3^- was minimized successfully by the addition of NaF (0.1%) and promotes unambiguous and sensitive determination of gold (III).

3.5 Analytical applications

3.5.1 Analysis of gold (I) and / or gold (III)

The values of the extraction constants (K_D , β and K_{ex}) in the present study and the molar absorptivity suggested the application of the developed extraction equilibria for extractive spectrophotometric determination of gold (III) at trace concentrations of gold ($0.05 - 2.0 \mu\text{g mL}^{-1}$). Different amounts of gold (III) were spiked onto distilled water (100.0 mL) and the solutions were subjected to the pre recommended extraction procedures. A satisfactory recovery percentage in the range $96\text{-}98 \pm 3\%$ was obtained between the amount of gold (III) added and measured confirming the accuracy of the developed procedures. The developed procedure was also applied successfully for the determination of gold (I) species at various concentrations ($0.1\text{-}2.0 \mu\text{g mL}^{-1}$) after oxidation to gold (III) with Br_2 water in the presence of HCl as described earlier (El-Shahawi, 2007, PP.1494-1499). A recovery percentage ($98 \pm 3.4\%$, $n = 5$) of gold (I) was also achieved suggesting the use of the method for the analysis of total inorganic gold and chemical speciation of gold (I & III) species and in aqueous media. Thus, the analysis of the binary mixture of gold (I) and (III) at a total amount ($10\text{-}20 \mu\text{g}/25 \text{ mL}$ aqueous solution) was carried out as follows: an aliquot mixture was first determined according to the described procedure for gold (III). Another aliquot mixture

was oxidized to gold (III) with bromine water-HCl (El-Shahawi, 2007, PP.1494-1499) and determined as described in for gold (I) species. Gold (I) ions in the water samples were then determined by the difference (A_2-A_1) between the absorbance of the aliquots before (A_1) and after (A_2) oxidation. The results are summarized in Table 1. A satisfactory recovery percentage in the range 96.6-103.2% was obtained with good reproducibility. A relative standard deviation in the range of 1.9-2.3 and 2.1-2.2% for gold (I) and (III) was also obtained, respectively. The proposed method was compared favorably with FAAS and the dithizone spectrophotometric methods (Marczenko, 1986, P. 303) for gold (III) determination. The value of the Student's t -test ($t=2.61$ at 95%) was found greater than the theoretical one ($t=2.31$), so there is no significance differences between the two means.

3.5.2 Analysis of gold in wastewater

The extraction procedure was also applied for the separation and subsequent determination of gold (III) by the standard addition of gold (III) species at $5-10 \mu\text{g mL}^{-1}$ onto industrial wastewater samples. A 100.0 mL of water samples was filtered, adjusted to the required pH and extracted as described in the experimental section. The organic extract was analyzed for gold by the developed extractive spectrophotometric method and also by the standard FAAS. The results are given in Table 2. An acceptable recovery percentage of gold (III) in the range of $98-103 \pm 2.42-3.2\%$ was achieved. The decrease in the recovery percentage at $5.0 \mu\text{g mL}^{-1}$ gold was improved by increasing the shaking time of the aqueous test solution with the ion pair reagent to 3-4 min. The t - and F -tests at 95% confidence levels did not exceed the tabulated (theoretical) ones and revealed no significant differences (Table 2) between the averages and the variances of the developed and the standard FAAS methods. At 95% confidence, the calculated value of $t=2.43$ is greater than the theoretical one ($t=2.31$) so there is a difference between the two means.

4. Conclusion

The reaction of the reagent $\text{DPG}^+\cdot\text{Cl}^-$ with AuCl_4^- is rapid (the time taken for the separation and determination of gold ions is at most 3-5 min) and does not involve any stringent conditions. The values of K_D , β , and K_{ex} , of the produced associate $\text{DPG}^+\cdot\text{AuCl}_4^-$ compete favorably with the most ion pair reagents (El-Shahawi, 1996, PP. 2037-2043 and Patel, 1986 and PP. 1547.-1551) and allowed the use of the system for photometric determination of gold (III). Gold (III) ions at trace or ultra trace in one liter aqueous solution was concentrated in 10.0 mL by the developed system so an enrichment factor of 100 was achieved. The extraction system is also suitable for the chemical speciation of gold (I, III) ions.

References

- Aldhaheri, S.M. (1998). Chemical equilibria of the complex ion associate of periodate and the ion pairing reagent 1-(3, 5-diamino-6-chloropyrazinecarboxyl) guanidine hydrochloride monohydrate. *Talanta*, 46, 161-1615.
- Alexandrov, A., Budevsky, O., Dimitrov, A. (1997). Investigation of the extraction equilibrium of ternary ion-association complex of thallium (III) with iodo-nitro-tetrazolium chloride. *Journal of Radioanalytical Chemistry*, 29, 26-32.
- Alguacil, F.J., Caravaca, C. (1996). Synergistic extraction of gold (I) cyanide with the primary amine primene-Jmt and the phosphine oxide cyanex 921. *Hydrometallurgy*, 42, 197-208.
- Bashammakh, A.S., Bahaffi, S.O., Al-Shareef, F.M., El-Shahawi, M.S. (2009). Development of an analytical method for trace gold in aqueous solution using polyurethane form sorbents: kinetic and thermodynamic characteristic of gold (III) sorption. *Anal Sci, (Japan)*, 25, 413 – 418.
- Biswas, S., Mondal, H.K., Basu, S. (1996). Determination of gold by adogen-464 extraction. *Indian J. Chem.*, 35A, 804-805.
- Burns, D.T., Barakat, S.A., Harriott, M., El-Shahawi, M.S. (1992). Flow injection extraction spectrophotometric determination of manganese (VII) with benzyl tributylammonium permanganate. *Anal. Chim. Acta*, 270, 213-215.
- Burns, D.T., Barakat, S.A., El-Shahawi, M.S., Harriott, M. (1992). Flow-injection extraction spectrophotometric determination of permanganate with triphenylsulphonim cations. *Fresenius J. Anal. Chem.*, 344, 131-132.
- Burns, D.T., El-Shahawi, M.S., Kerrigan, M.J., Smyth, P.M.T. (1996). Spectrophotometric determination of rhenium as perrhenate by extraction with amiloride hydrochloride. *Anal. Chim. Acta*, 322, 107-109.
- Burns, D.T., Hanprasopwattana, P. (1988). Extractive spectrophotometric determination of perchlorate using the ion pair amiloride monohydrochloride. *Anal. Chim. Acta*, 118, 185-187.

- Camagong, C.T., Honjo, T. (2001). Separation of gold (III) as its ion –pair complex with 18-crown-6 from hydrochloric acid media by means of solvent extraction. *Anal. Sci.(Japan)*, 17, 1725-1728.
- El-Shahawi, M.S, Al-Hashimi, F.A. (1996). Spectrophotometric determination of periodate or iodate and ions by liquid-liquid extraction as an ion-pair with tetramethylammonium iodide. *Talanta*, 43, 2037-2043.
- El-Shahawi, M.S, Hassan, S.S.M., Othman, A.M., .El-Sonbati, M.A. (2008). Retention profile and subsequent chemical speciation of chromium (III) and (VI) in industrial wastewater samples employing some onium cations loaded polyurethane foams. *Microchemical Journal*, 89, 313 -319.
- El-Shahawi, M.S. (1997). Extraction equilibrium of the ion-associate of periodate with amiloride hydrochloride and simultaneous spectrophotometric determination of periodate and iodate ions by liquid-liquid extraction. *Anal. Chim. Acta*, 356, 85-91.
- El-Shahawi, M.S., Bashammakh, A.S., Bahaffi, S.O. (2007). Chemical speciation and recovery of gold (I & III) from wastewater and silver by liquid-liquid extraction with the ion pair reagent amiloride mono hydrochloride and AAS determination. *Talanta*, 72, 1494-1499.
- El-Shahawi, M.S., Hassan, S.S.M., Othman, A.M., Zyada, M.A., El-Sonbati, M.A. (2005). Chemical speciation of chromium (III&VI) employing extractive spectrophotometry and tetraphenylarsonium chloride or tetraphenylphosphonium bromides as an ion-pair reagent. *Anal. Chim. Acta*, 534, 319-326.
- Farag, A.B., Soliman, M.H., Abdel-Rasoul, O.S., El-Shahawi M.S. (2007). Sorption characteristics and chromatographic separation of gold (I& III) from silver and base metal ions using polyurethane foams. *Anal. Chim. Acta*, 601, 218-228.
- Fazli, Y., Hassan, J., Karbasi, M.H., Sarkouhi M. (2009). A Simple spectrophotometric method for determination of gold (III) in aqueous samples. *Minerals Engineering*, 22, 210-212.
- Filatova, D.G., Ryazanova, L.N., Shiryayeva, O.A., Zorov, N.B., Kaprov, Y. (2004). Atomic absorption determination of gold as complex amines. *J. Anal. Chem.*, 59, 243-245.
- Guanghan, L., Jinya, X. (1992). Determination of trace amounts of gold in wastewater by graphite furnace atomic-absorption spectrophotometry with preconcentration on trioctylphosphine oxide chemically modified tungsten wire matrix. *Talanta*, 39, 51-53.
- Haddad, P.R., Rochester, N.E. (1988). Ion – interaction reversed – phase chromatographic method for the determination of gold (I) cyanide in mine process liquors using automated sample preconcentration, *J. Chromatogr*, 439, 23 – 36.
- Hassan, S.S.M., El-Shahawi, M.S., Othman, A.M., Mosaad, M.A. (2005). A potentiometric rhodamine-B based membrane sensor for the selective determination of chromium ions in wastewater. *Anal. Sci. (Japan)*, 21, 673-678.
- Hiraoka, M. (1982). Crown compounds, their characteristics and applications, El-Sevier, Tokyo, 243-245.
- Hu, Q., Chen, X., Yang, X., Huang, Z., Chen, J., Yang, G. (2006). Solid phase extraction and spectrophotometric determination of Au (III) with 5-(2-hydroxy-5-nitrophenylazo) thiorhodamine. *Anal. Sci (Japan)*, 22, 627-630.
- Itagaki, T., Ashino, T., Takada, K. (2000). Determination of trace amounts of gold and silver in high-purity iron and steel by electrothermal atomic absorption spectrometry after reductive co precipitation. *Fresenius J. Anal. Chem.*, 368, 344-349.
- Kamburova, S.M. (1992). A highly sensitive spectrophotometric method for the determination of iodate using leuco xylene cyanol FF. *Talanta*, 39, 997 -1001.
- Li, J.F., Bai, L.F, Wang, Y.H., Wang, H.Y. (2006). Rapid determination of gold in geological samples using flow injection solid phase chemiluminescences. *Anal. Sci (Japan)*, 22: 841-844.
- Medved, J., Bujdos, M., Matus, P., Kubova, J. (2004). Determination of trace amounts of gold in acid-attacked environmental samples by atomic absorption spectrometry with electrothermal atomization after preconcentration. *Anal. Bioanal. Chem.*, 379, 60 - 65.
- Marczenko, Z. (1986). Spectrophotometric determination of elements, 3rd edition, Ellis Horwood Chichester, U.K, PP.68 -70, 203.
- Marczenko, Z. (1986). Spectrophotometric determination of elements, 3rd edition, Ellis Horwood Chichester, U.K, PP.68 -70, 203.

Miller, J.C., Miller, J.N. (1994). Statistics for analytical chemistry 4th edition, Ellis-Horwood, New York, PP.115-125.

Nakamoto, K. (1978). *Infrared and raman spectra of inorganic and coordination compounds*, 3rd edition, Wiley: New York.

Navratilova, Z., Kula, P. (2000). Determination of gold using clay modified carbon paste electrode. *Fresenius J. Anal. Chem.*, 367, 369-372.

Patel, K.S., Lieser, K.H. (1986). Extraction and spectrophotometric determination of gold (III) by use of amides and amidines. *Anal. Chem.*, 58 (7), 1547 -1551.

Pyrzynska, K. (2005). Recent development in the determination of gold by atomic spectrometry techniques. *Spectrochim. Acta B*, 60, 1316-1322.

Shoursheinin, F., Sajad, B., Parvin, P. (2010). Determination of gold fineness by laser induced breakdown spectroscopy with the simultaneous use of CW-CO₂ and Q-SW Nd: YAG lasers. *Optics and Lasers in Engineering*, 48, 89 -95.

Vogel, A.I. (1966). *A Text Book of Quantitative Inorganic Analysis* 3rd edn., Longmans Group Ltd., England.

Yu, M., Suna, D., Huangb, R., Tian, W., Shen, W., Zhang, H., Xua, N. (2003). Determination of ultra-trace gold in natural water by graphite furnace atomic absorption spectrometry after in situ enrichment with thiol-cotton fiber. *Anal.Chim.Acta*, 479, 225 -231.

Zuotao, Z., Creedy, T.M., Townshend, A. (1999). Flow injection spectrophotometric determination of gold using 5-(4-sulphophenylazo)-8-aminoquinoline, *Anal. Chim. Acta*, 401, 237-241.

Table 1. Analytical data of gold (I) and gold (III) in their binary mixtures in aqueous media (10 mL) by the proposed extractive spectrophotometric method

Gold species,				Recovery, %*	
Taken, µg		Found, µg			
Au ⁺	Au ³⁺	Au ⁺	Au ³⁺	Au ⁺	Au ³⁺
5.0	5.0	4.8	5.1	96.0±2.3	102.0±2.3
10.0	10.0	9.75	10.22	97.5±2.9	102.4 ±2.1
10.0	10.0	9.80	9.90	99.4±2.7	99.0±1.9

* Average (n=5) ± relative standard déviation.

Table 2. Results of the extractive spectrophotometric determination of gold (III) spiked (0.5 – 10 µg) to industrial wastewater samples (100 mL)

Gold species,		Recovery, %*
Gold (III) added, µg	Gold (III) found, µg	

0.0	0.0	0.0 98.±
5.0,	4.9± 0.12	2.42. 5.0±
8.0	8.2± 0.22	2.7
10.0	10.3± 0.32	103.0±3.2

*Average (n=5) ± relative standard déviation.

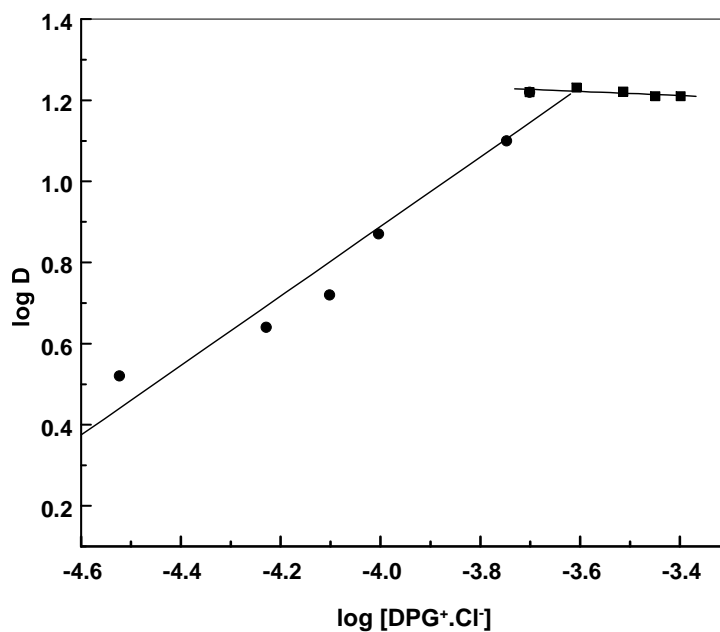


Figure 1. Plot of $\log [DPG^+.Cl^-]$ versus $\log D_{Au}$ of the ion associate $[DPG^+.AuCl_4^-]$ Conditions: Aqueous phase (20 mL) at pH 6-7, organic solvent =5 mL and $[HAuCl_4] = 6.2 \times 10^{-6} \text{ mol L}^{-1}$

Differential pulse cathodic stripping voltammetric determination of uranium with arsenazo-III at the hanging mercury dropping electrode

By M. W. Kadi* and M. S. El-Shahawi

Chemistry Department, Faculty of Science, King Abdulaziz University, Jeddah y, P.O. Box 80203, Jeddah 21589, Saudi Arabia

(Received January 13, 2009; accepted in revised form April 28, 2009)

*Uranium(VI) / Arsenazo-III /
Cathodic stripping voltammetry / HMDE / ICP-MS /
Phosphate fertilizers / Chemical speciation*

Summary. An accurate, inexpensive and less laborious controlled adsorptive accumulation of uranium(VI)-arsenazo-III on a hanging mercury drop electrode (HMDE) has been developed for uranium(VI) determination. The method is based upon the collection of uranium(VI)-arsenazo-III complex at pH 5–6 at the HMDE and subsequent direct stripping measurement of the element in the nanomolar concentration level. The cathodic peak current ($i_{p,c}$) of the adsorbed complex ions of uranium(VI) was measured at -0.35 V vs. Ag/AgCl reference electrode by differential pulse cathodic stripping voltammetry (DP-CSV), preceded by an accumulation period of 150s2.5 in Britton–Robinson buffer of pH 5. The plot of the resulting $i_{p,c}$ vs. uranium(VI) concentration was linear in the range 2.1×10^{-9} to 9.60×10^{-7} mol L $^{-1}$ uranium(VI) and tended to level off at above 9.6×10^{-7} mol L $^{-1}$. The limits of detection and quantification of uranium(VI) were found to be 4.7×10^{-10} and 1.5×10^{-9} mol L $^{-1}$, respectively. A relative standard deviation of $\pm 2.39\%$ ($n = 5$) at 8.5×10^{-7} mol L $^{-1}$ uranium(VI) was obtained. The method was validated by comparing the results with that obtained by ICP-MS method with RSD less than $\pm 3.3\%$. The method was applied successfully for the analysis of uranium in certified reference material (IAEA soil-7), and in phosphate fertilizers.

1. Introduction

Pollution with radioactive elements has been a matter of great concern for the last few decades for human health and animals [1–5]. Uranium is one of the most radioactive elements affecting the environment [6, 7]. The tolerable daily intake of uranium established by the world health organization (WHO) based on Gilman's studies is $0.6 \mu\text{g kg}^{-1}$ of the body weight per day [6–8]. The WHO, Health Canada and Australian drinking water guidelines fixed the maximum uranium concentration to be less than $20 \mu\text{g L}^{-1}$ in drinking waters [7, 8].

Phosphate containing fertilizers have been used worldwide in increasing quantities in order to replenish natural

nutrients. Fertilizers usually employed in agriculture contain traces of heavy metals, K and naturally occurring radionuclides, such as U, Th, and their decay products [9]. In phosphate fertilizers, high uranium concentrations up to hundreds of $\mu\text{g g}^{-1}$ have been reported [10]. Investigations of the uranium pathway from fertilizers to plants and to humans are therefore, very important from the viewpoint of radiological protection of the general population [11]. Naturally occurring uranium consists mainly of the isotopes ^{238}U (99.3%) and ^{235}U (0.7%) [12]. Elevated levels of uranium and daughters are a big health concern because of alpha and gamma activity associated with uranium and members of its decay chain [13]. Radon is an important element in the decay chain of uranium. Because of its gaseous nature radon tends to diffuse and escape the radium containing material to air. Radon is an alpha emitter; inhalation of radon brings up the possibility of decay in the lungs causing higher probability of lung cancer [14, 15].

Spectrophotometry, spectrofluorimetry, flame atomic absorption spectrometry, energy dispersive, total reflectance X-ray fluorescence spectrometric techniques, inductively coupled plasma atomic emission spectrometry (ICP-OES), neutron activation analysis, ICP-mass spectrometry (ICP-MS), and nuclear track detectors are the most common techniques for uranium determination [16, 17]. Most of these methods are too expensive, suffer from several interferences, formation of refractory oxides in the flame region, time-consuming, not precise; require elaborate and cumbersome sample preparation, need complicated instrumentation with time-consuming procedures and/or involve the use of harmful reagents [16].

Determination of trace and ultra trace amounts of uranium and other metal ions such as selenium, mercury, and tungsten in geological, environmental, different waters and biological samples using stripping voltammetric techniques have been reported in the literature [18–24]. Cathodic and anodic stripping voltammetry (SV) at HMDE or modified electrodes reported by Henze *et al.* shown numerous advantages such as speed of analysis, good selectivity and sensitivity with saline matrices like river water and the possibility of simultaneous analysis of mixtures [19–23]. Bismuth-coated carbon fiber and Pb-film plated electrodes have been applied for cathodic stripping voltammetric (CSV) measurements

*Author for correspondence (E-mail: mkadi@kau.edu.sa).

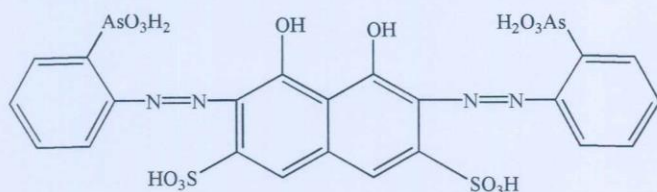


Fig. 1. Chemical structure of arsenazo-III.

of trace uranium in the presence of cupferron [24–26] and other complexing agents [27, 28].

Herein we report, a simple, accurate, convenient and low cost procedure regarding the use of the commonly named reagent arsenazo-III *i.e.* bis-1,6-(*o*-arsonophenylazo)-7,8-dihydroxy naphthalene-2,5-disulphonic acid sodium salt (Fig. 1) for ultra trace determination of uranium(VI) in phosphate fertilizers. The method is based on controlled adsorptive accumulation of uranium(VI)-arsenazo-III complex on a HMDE and subsequent direct stripping from the HMDE and measurement of the element in the nanomolar concentration level. Moreover, the most probable reduction mechanism of UO_2^{2+} chelate will also be discussed.

2. Experimental

2.1 Apparatus

A Perkin Elmer (Lambda EZ-210) double beam spectrophotometer (190–1100 nm) with 1 cm (path width) quartz cell was used for recording the electronic spectra of arsenazo-III and its uranium(VI) complex. ICP-OES (Optima 4100 DV) and ICP-MS (Sciex Elan DRC II, USA) Perkin-Elmer spectrometers were used as reference methods for the analysis of total uranium content in the test aqueous solutions of the certified reference material, and fertilizer samples. The ICP-MS instrument was optimized daily before measurement and operated as recommended by the manufacturers. Digital pH-meter (MP220, Meter Toledo) was used for pH measurements with absolute accuracy limits of ± 0.1 pH unit defined by NIST buffers. De ionized water obtained from Milli-Q Plus system (Millipore, Bedford, MA, USA) was used to prepare all solutions.

Differential pulse cathodic stripping voltammetric (DP-CSV) measurements and cyclic voltammetry were performed on a Metrohm 746 VA trace analyzer and 747 VA stand. A three-compartment borosilicate (Metrohm) voltammetric electrochemical cell (10 mL) was used. The cell configuration includes HMDE (surface area 0.38 mm^2) as working, double-junction Ag/AgCl (3 M KCl), as a reference and platinum wire (BAS model MW-1032) as counter electrodes, respectively. During the electrochemical measurements, the sample solutions were transferred using a digital-micro-pipette (Volac). The data were then recorded at room temperature and the peak current heights were measured by the "tangent fit method" [29].

2.2 Reagents and material

Analytical reagent grade chemicals were used. A stock solution (0.1% w/v) of the reagent arsenazo-III (Aldrich, USA) was prepared by dissolving an accurate weight

($0.1 \pm 0.001 \text{ g}$) of the reagent in 100 mL of deionized water. A stock solution of uranium(VI) (1.0 mg mL^{-1}) was prepared by dissolving an appropriate amount of $\text{UO}_2(\text{NO}_3)_2 \cdot 6\text{H}_2\text{O}$ in deionized water. Concentrated HNO_3 (5.0 mL) was added to a 100 mL of solution to suppress hydrolysis. More diluted uranium(VI) solutions (0.1–1.0 $\mu\text{g mL}^{-1}$) in water were also prepared daily to obtain working solutions. The certified reference material, CRM (IAEA soil-7) was used for quality assurance. Stock solutions ($1000 \mu\text{g mL}^{-1}$) of diverse elements (as chloride or nitrate salts) were prepared from high purity compounds (99.9%, E. Merck, Darmstadt). A series of B–R buffers of pH 2–11 were prepared from the acid mixture H_3PO_4 – H_3BO_3 – CH_3COOH (0.04 mol L^{-1}) adjusting the pH to the required value with NaOH (0.2 mol L^{-1}) as reported earlier [30]. Low density polyethylene (LDPE) were carefully cleaned first with hot detergent, soaked in 50% HCl, HNO_3 (2.0 mol L^{-1}), subsequently washed with dilute HCl (0.5 mol L^{-1}), and finally rinsed with water. Seven fertilizer samples (F_1 – F_7) were collected from the local market of Jeddah City, Saudi Arabia. The aqueous solution of each fertilizer sample was reserved on LDPE bottles. The glassware's were cleaned by soaking them in HNO_3 solution (1.5% w/v) for 24 h before use.

2.3 General DP-CSV procedures

An accurate volume (10 mL) of the B–R buffer as supporting electrolyte at the required pH (2.2–11) was transferred into the electrochemical cell where the electrodes immersed in the test solutions through which pure nitrogen stream was passed for 15 min before recording voltammograms. The scans were initiated in the negative direction of the applied potential from +0.2 V to $-1.3 \text{ V vs. Ag/AgCl}$ reference. After recording the voltammogram, an accurate volume ($10.0 \mu\text{L}$) of arsenazo-III ($1.6 \times 10^{-4} \text{ mol L}^{-1}$) was added. The sample solution was then stirred and purged with nitrogen gas for a period of 5 min. The stirrer was then stopped and after 10 s quiescence time, voltammograms were recorded again. Unless otherwise stated the background voltammogram of the supporting electrolyte and the blank solution was recorded at the required pH under the following parameters: accumulation 5 min; accumulation potential -0.15 V ; starting potential -0.2 V ; pulse amplitude 60 mV and scan rate of 60 mV/s. After recording the voltammogram of the blank solution at the required pH, a $10 \mu\text{L}$ of uranyl(II) solution ($1.0 \times 10^{-6} \text{ g mol L}^{-1}$) was then added. The DP-CASV voltammogram was repeated with a new mercury drop under the same experimental conditions. The peak current of uranium(VI) was measured at about $-0.35 \text{ V vs. Ag/AgCl}$ reference electrode. Following these procedures, the influence of other operational parameters *e.g.* accumulation time, accumulation potential, starting potential, scan rate and pulse amplitude was critically investigated.

The influence of the scan rate ($\nu = 20$ – 500 mV/s) and various uranium concentrations (10 – $100 \mu\text{L}$; $1.0 \times 10^{-4} \text{ mol L}^{-1}$) on cyclic voltammogram was also carried out for uranium(VI)-arsenazo-III ($1.0 \times 10^{-3} \text{ mol L}^{-1}$) at pH 4–5 in the same electrochemical cell under the optimum experimental conditions employing HMDE and Pt working electrodes.

2.4 Analytical applications

2.4.1 Analysis of uranium in certified reference material (IAEA soil-7)

The validity of the developed procedure was investigated by the determination of uranium in CRM (IAEA soil-7) as follows: An accurate weight ($0.20\text{--}0.30 \pm 0.001$ g) of the CRM sample was transferred into a Teflon beaker (50.0 mL) containing HF (7.0 mL), concentrated HCl (2.0 mL), and concentrated HNO₃ (5.0 mL) at room temperature to digest the sample gradually and slowly. The reaction mixture was then heated slowly for 1 h at 100–150 °C on a hot plate. After the evolution of NO₂ fumes had ceased, the reaction mixture was evaporated almost to dryness and mixed again with concentrated HNO₃ (5.0 mL). The process was repeated thrice and the mixture was again evaporated to dryness. After evaporation, the solid residue was then dissolved in dilute nitric acid (10.0 mL, 1.0 mol L⁻¹), transferred to volumetric flask (25.0 mL) and the solution was completed to the mark with deionized water. An accurate volume of the sample solution (5.0 mL) adjusted to pH 5 with B–R buffer (5.0 mL) was then transferred into the volumetric cell containing 10 μL (1.6×10^{-4} mol L⁻¹) of the reagent arsenazo-III. The solution was then analyzed following the recommended experimental procedures for the standard addition method described before. Following the described procedure, the voltammograms were recorded and the change in the current height was measured and used for uranium(VI) determination *via* the linear plot of the standard addition. A blank sample was analyzed following the same digestion and analytical procedures.

2.4.2 Analysis of uranium(VI) in phosphate fertilizer samples

Solutions of the fertilizer samples in water were analyzed according to the recommended electrochemical procedures used for the standard curve of uranium(VI) determination at pH 5. The concentration of uranium was determined from the standard curve employing the equation:

$$U_{\text{concentration}} = C_{\text{istd}} i_{\text{samp}} / A_{\text{istd}} \quad (1)$$

where, C_{istd} is the standard uranium concentration and i_{samp} and A_{istd} are the current heights of the sample and standard in nA, respectively. Voltammograms were then recorded and the change in the current height was measured and used for determining uranium(VI) ions *via* the linear plot of the standard curve. Alternatively, the standard addition (spiking) method was used as follows: transfer known volumes (5.0 mL) of the fertilizer sample solutions adjusted to pH 5–6 into the cell. Measure the current height displayed by the test solution before and after addition of various volumes (0.2–1.0 mL) of the standard uranium(VI) ions ($1.0\text{--}15$ μg mL⁻¹). The uranium content in the test sample was then evaluated with the aid of the calibration curve of the standard addition.

3. Results and discussion

Preliminary investigations have revealed that, on mixing the arsenazo-III with uranium(VI) in aqueous solution and

shaking for few minutes, an intense color change was observed. This change in color is pH dependent. Moreover, in aqueous solutions of pH 4–5, a stable red-purple colored complex was noticed. Complex formation was confirmed from the observed bathochromic shift on the electronic spectrum of the arsenazo-III ($\lambda_{\text{max}} = 350, 500$ nm) compared to the absorption spectrum of uranium(VI)-reagent complex ($\lambda_{\text{max}} = 370, 610$ nm) as shown in Fig. 2. The stoichiometry of the produced complex was determined from continuous variation and molar ratio methods [31]. Both methods have shown that, the molar ratio of uranium(VI) to reagent in the chelate formed is 1 : 3 and that the complex has good stability, in good agreement with the data reported in the literature [32]. These observations suggest the possible use of the complexing agent to develop a simple, and low cost adsorptive cathodic stripping voltammetric method for uranium determination in phosphate fertilizer samples.

The (DP-CSV) of the reagent (4.1×10^{-6} mol L⁻¹) in the absence and the presence of uranium(VI) ions (1×10^{-6} mol L⁻¹) at the HMDE has been critically tested in aqueous B–R buffer solutions over a wide range of pH 2.2–11. Representative data are shown in Fig. 3. In the pH 4–5, the DP-CSVs of uranium(VI)-reagent complex displayed one ill defined peak at -0.27 V and another well defined and sharp reduction waves at -0.38 V vs. Ag/AgCl reference electrode (Fig. 3). The observed peaks belong most likely to the reduction of the azo group ($-\text{N}=\text{N}-$) in the aromatic compound. The observed dependence of the reduction peaks on the pH can be explained by a direct exchange of four electrons in two successive two-electron steps. On increasing the solution pH, the observed cathodic peak at -0.35 was shifted cathodically indicating that, the electrode reaction of the reduction steps involves hydrogen. The plot of the change of the peak potential vs. pH was linear and the

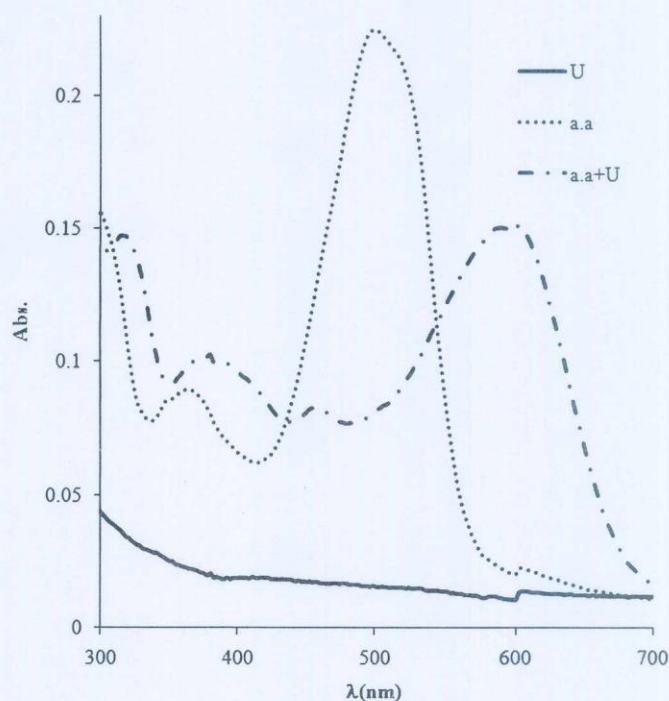


Fig. 2. Electronic spectra of arsenazo-III and its uranium(VI) complex at pH 5.

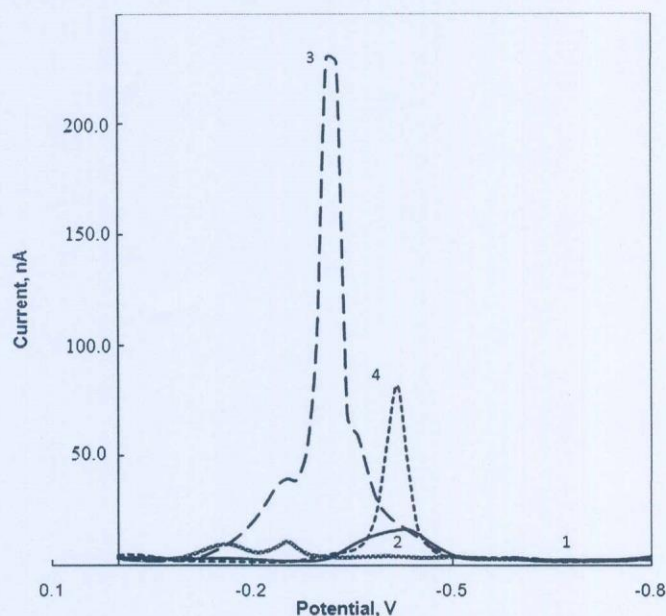


Fig. 3. DP-CSVs of the reagent arsenazo-III (6.1×10^{-6} mol/L) in the presence of uranium(VI) ions (1×10^{-6} mol/L) at pH 4.1 (1); 5 (2), 6.5 (3) and 8.5 (4) at the HMDE, scan rate 50 mV/s; pulse amplitude 50 mV and pulse width 40 ms vs. Ag/AgCl reference electrode.

following regression equation:

$$E_{p,c} = 0.036 - 0.0278 \text{ pH}, \quad (R^2 = 0.988) \quad (2)$$

was obtained with a slope of 27.8 ± 2.7 mV/pH unit. According to these data, the observed shift in the cathodic peak potential to more negative potentials on raising pH denotes that the electrode reaction involves hydrogen ions [33].

Cyclic voltammograms (CVs) of uranium(VI)-reagent complex in B-R buffer of pH 5 at the HMDE was carried out at various scan rates (Fig. 4). At scan rate (ν) less than 40 mV/s, the CV showed ill defined reduction peaks; at moderate scan rates (40–200 mV/s) one well defined reduction peak at -0.32 – -0.35 V (peak I) was observed, while at scan rate higher than 200 mV/s up to 1 V/s two well defined reduction peaks were observed at -0.35 V (peak I) and -1.34 V (peak II) vs. Ag/AgCl reference electrode (Fig. 4). On the reverse scan, no anodic peaks were observed at the investigated scan rate (10–1000 mV s $^{-1}$), confirming

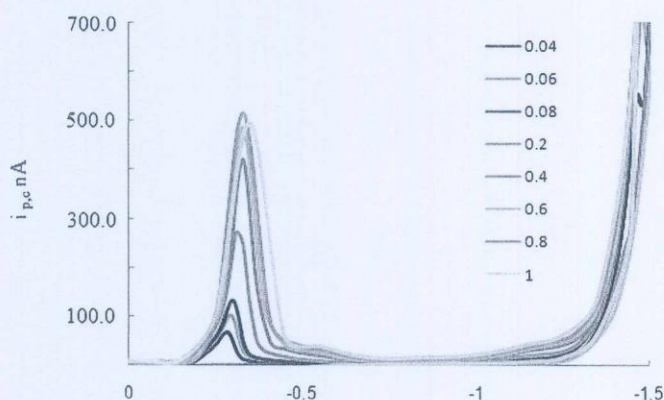


Fig. 4. Cyclic voltammograms of uranium(VI)-arsenazo chelate complex at the HMDE at pH 5 at various scan rates (40–1000.0 mV/s) vs. Ag/AgCl reference electrode.

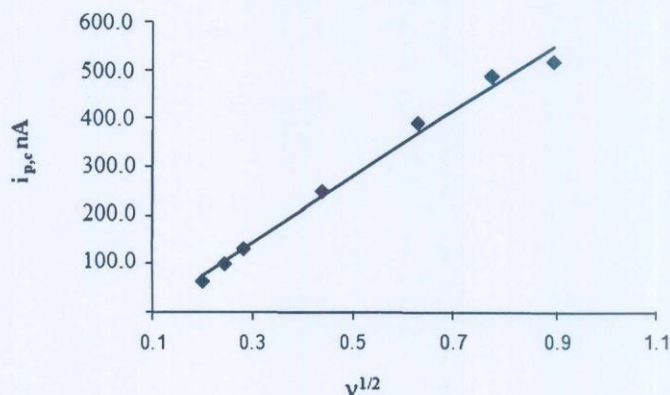


Fig. 5. Plot of the square root of the scan rate vs. the cathodic peak current.

the irreversible nature of the observed reduction process of uranium(VI)-reagent complex in the employed potential window (0.0– -1.0 V).

It is worth mentioning that, the cathodic peak (peak I) is shifted cathodically on raising the ν confirming the irreversible nature of the observed reduction process [34]. Also, the cathodic peak currents, $i_{p,c}$ increased as $\nu^{1/2}$ increases [34] and the plot of $i_{p,c}$ of peak I vs. the $\nu^{1/2}$ (Fig. 5) increased linearly as described by the Randles–Sevcik equation, suggesting that the electrochemical reduction process is a controlled diffusion process [34, 35]. The irreversible nature of this peak was confirmed by the linear dependence of the $E_{p,c}$ of peak I with $\log \nu$ vs. Ag/AgCl. The ratio of $i_{p,c}/\nu^{1/2}$ decreases continuously on raising the scan rate confirming the occurrence of electrode-coupled chemical reaction *i.e.* EC mechanism [34, 35].

Continuous scan of the CV of the uranium(VI)-reagent chelate at 100 mV/s significantly decreased the peak current height and the signal is hardly discernible from the baseline, indicating passivation of the surface of the HMDE electrode *via* formation of polymeric reduction product or fouling of the HMDE electrode by reduction products [34]. This observation suggested possible prior surface adsorption of the electrode in the range 10–500 mV/s at pH 4–5.

The dependence of the CVs response on the depolymerizer *i.e.* uranium(VI) concentration was investigated. The data revealed no significant change in $i_{p,c}$ with the increase of uranium(VI) concentration from 1.6×10^{-4} mol L $^{-1}$ to 9.0×10^{-4} mol L $^{-1}$ confirming the occurrence of electrode coupled chemical reaction. Thus, it can be concluded that, the reduction processes of uranium(VI)-reagent complex at peak I is most likely to proceed according to the well known (EC) chemical reaction mechanism [34, 35].

3.1 Analytical parameters

3.1.1 pH

The influence of pH employing acetate buffer on the peak current height at the peak potential -0.56 V vs. Ag/AgCl reference electrode was studied over a wide range of pH (2.1–11) after pre concentration time of the analyte and arsenazo onto the HMDE for 150 s. The plot of the pH vs. the $i_{p,c}$ at -0.35 V vs. Ag/AgCl reached maximum enhancement at pH 5 (Fig. 6) in accordance with the pKa of the reagent and

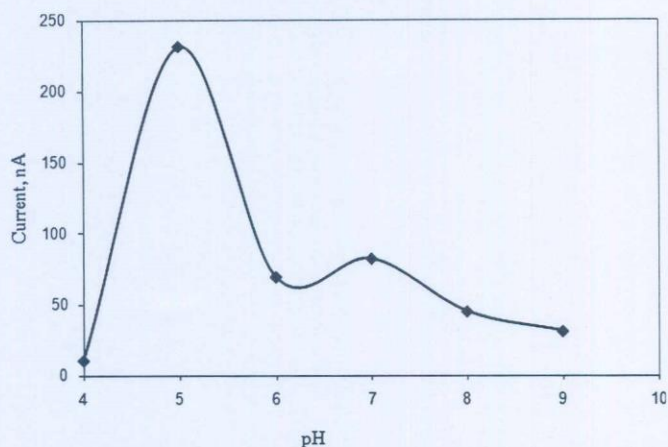


Fig. 6. Plot of pH of the aqueous solution containing uranium(VI)-arsenazo vs. cathodic peak current at the HMDE.

due to formation of stable uranium(VI)-arsenazo-III chelate. A significant decrease in the peak current value at higher pH values was noticed. This behavior is most likely attributed to the development and the stability of the complex formed between the analyte and the ligand at pH 5. At pH higher than pH 5, the formation of hydroxy species of uranium(VI) *e.g.* $\text{UO}_2(\text{OH})_2$ occurred, resulting in a significant decrease in the peak current. Thus, in the subsequent work, the pH of the aqueous solution containing uranium and the reagent, the pH was kept at pH 5.

3.1.2 Accumulation potential

The effect of accumulation potential on the adsorptive cathodic stripping peak current was evaluated over the potential range (-0.15 – -1.0 V) vs. Ag/AgCl after collection of the analyte onto the HMDE for 120 s. The maximum peak current was achieved at -0.15 V and decreased rapidly at lower potentials because the reduction of the uranium(VI)-reagent had already taken place at -0.15 V. Thus, a deposition potential of -0.15 V was selected in the subsequent work.

3.1.3 Accumulation time

The influence of the accumulation time on the solution of pH 5 containing uranium(VI) (4.4×10^{-7} mol L $^{-1}$) and arsenazo-III (7.5×10^{-7} mol L $^{-1}$) at -0.15 V deposition potential was examined. The plot of deposition time vs. the resulting peak current at -0.35 V vs. Ag/AgCl (Fig. 7) displays maximum peak current and a sharp peak at 150 s. At longer adsorption time, the peak current began to decrease suggesting that the electrode surface was saturated with free reagent. Thus, an accumulation time of 150 s at -0.35 V was used for subsequent determinations of uranium(VI) ions. The plot does not pass through the origin because of the strong adsorption of the analyte at the HMDE surface at the equilibrium time which was fixed at 10 s.

3.1.4 Reagent concentration

The effect of the reagent concentrations (1.2×10^{-7} – 2.0×10^{-6} mol L $^{-1}$) on the reduction peak current height

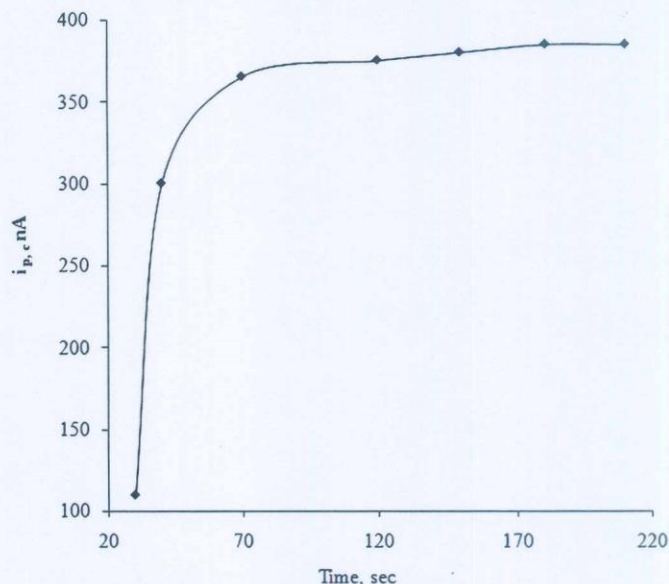


Fig. 7. Plot of deposition time of the aqueous solution containing uranium(VI)-arsenazo-III at pH 5 vs. cathodic peak current at the HMDE.

of the test solution of pH 5 at peak potential -0.35 V vs. Ag/AgCl reference electrode was investigated under the above optimal experimental parameters. The results revealed that, the $i_{p,c}$ increases as arsenazo-III concentration increases to 5.0×10^{-7} mol L $^{-1}$, followed by a constant peak current height at higher ligand concentration. The increased sensitivity is explained by the increased stability of uranium(VI)-reagent chelate similar to uranium(VI)-cupferron methods [25]. The formation of a specific adsorptive uranium-reagent complex at higher reagent concentration may account for the observed trend.

3.1.5 Starting potential

The influence of varying the starting potential (0.1 – -0.6 V) on the DP-CSV peak current at peak potential -0.35 V of uranium(VI)-arsenazo-III complex under the optimum experimental parameters was examined. Maximum enhancement on the peak current was achieved at -0.2 V starting potential followed by gradual decrease at starting potential lower than -0.2 V. Therefore, in the subsequent work, a starting potential of the DP-CASV peak was selected at -0.2 V vs. Ag/AgCl reference electrode.

3.1.6 Scan rate

The influence of the scan rate (20 – 100 mV s $^{-1}$) on the $i_{p,c}$ of arsenazo-III (5.0×10^{-7} mol L $^{-1}$) in the presence of uranium(VI) ions (5×10^{-8} mol L $^{-1}$) at pH 5.0 was investigated at the optimal conditions. The $i_{p,c}$ increased steadily on raising the scan rate up to 60 mV/s. However, to obtain higher accuracy and sensitivity and lower background of the observed sharp and symmetric cathodic peak at -0.35 V, a scan rate of 60 mV/s was adopted in the subsequent work.

3.1.7 Pulse amplitude

The influence of pulse amplitude on the DP-CSV peak of the arsenazo-III in the presence of uranium(VI) at pH 5 over

the range of -20 to -80 mV under the optimal conditions was studied. The results revealed that, the $i_{p,c}$ at -0.35 V increased steadily on increasing the pulse amplitude. However, the observed background and best sensitivity of the D-CSV peak at -0.35 V was achieved at -60 mV pulse amplitude. Therefore, in the subsequent work, -60 mV pulse amplitude was chosen.

3.1.8 Summary of optimized experimental conditions

After these thorough investigations of experimental conditions one can conclude that the optimum parameters for uranium determination are: pH 5, an accumulation potential of -0.15 V, deposition time of 150 s, starting potential of -0.2 V, scan rate of 60 mV/s, pulse amplitude of -60 mV and 5.0×10^{-7} mol L $^{-1}$ arsenazo-III concentration.

3.2 Analytical performance of the developed DP-CASV procedure

Voltammograms and the linear plot of $i_{p,c}$ measured at -0.36 V by the developed DP-CSV procedure vs. uranium(VI) concentration are given in Fig. 7 over the concentration range of 2.1×10^{-9} to 9.60×10^{-7} mol L $^{-1}$. Above 5.0×10^{-8} mol L $^{-1}$ uranium (VI) concentration the calibration curve tended to level off because of adsorption saturation [36, 37] the regression equation of the calibration plot was: $i_{p,c}(nA) = 4.7242C(nM) + 13.465$ with correlation coefficient $R = 0.997$. According to IUPAC [38] the lower limits of detection (LOD) and quantification (LOQ) under the conditions established for uranium(VI) was estimated using Eqs. (3) and (4).

$$\text{LOD} = 3\sigma/k \quad (3)$$

$$\text{LOQ} = 10\sigma/b \quad (4)$$

where σ is the standard deviation of replicate determination values of the blank under the optimal experimental conditions and b is the sensitivity factor *i.e.* the slope of the linear plot of the analyte. The LOD and LOQ for five replicate measurements were found to be 4.7×10^{-10} and 1.5×10^{-9} mol L $^{-1}$, respectively. Such limits could be improved to lower values by increasing the equilibration times at the optimum experimental conditions. Both LOD and LOQ values confirmed the sensitivity of the proposed DP-CSV procedure compared to other reported methods [25, 26]. This level of precision is highly suitable for the routine quality control analysis of uranium(VI) in different matrices. Moreover, a mean recovery percentage of uranium(VI) based on five replicate measurements for 8.0×10^{-8} mol L $^{-1}$ concentrations using calibration curve was $99.47 \pm 1.7\%$. The precision of the DP-CSV procedure for standard solution of uranium(VI) at two different concentrations 6.0×10^{-8} and 4.0×10^{-8} mol L $^{-1}$ by direct determination and standard addition procedures were 2.1 and 1.9% ($n = 5$) expressed as relative standard deviation, respectively.

The validation of the developed DP-CSV method was successfully assessed by comparing the LOD, LOQ and the linear dynamic range with some other voltammetric methods. The results are summarized in Table 1. The performance of the developed method is much better than

Table 1. Comparison between the developed DP-CSV method and other voltammetric methods.

LOD (mol L $^{-1}$)	LOQ (mol L $^{-1}$)	Dynamic range (mol L $^{-1}$)	Reference
2.0×10^{-8}	6.660×10^{-8}	2×10^{-9} – 1.4×10^{-8}	[34]
5.5×10^{-10}	4.2×10^{-9}	Not determined	[32]
2.0×10^{-10}	6.660×10^{-10}	5×10^{-10} – 2×10^{-8}	[31]
4.7×10^{-10}	1.5×10^{-9}	2.1×10^{-9} – 9.6×10^{-7}	Present work

the first two methods. Critical comparison between the developed method and the method reported by Korolczuk *et al.* [25] indicated that the developed method is low in cost, short deposition, selective and quite applicable for routine analysis.

3.3 Interference study

Metal ions and some anions present in most real samples are the most serious interferences in stripping analysis. Thus, the analysis of 5×10^{-8} mol L $^{-1}$ uranium(VI) ions by the developed DP-CSV procedure in the presence of the metal ions Ca^{2+} , Al^{3+} , Fe^{2+} , Fe^{3+} , Cd^{2+} , Ni^{2+} , Cu^{2+} , Zn^{2+} , VO_3^- and Cr^{3+} and the anions: Cl^- , Br^- , SO_4^{2-} , CO_3^{2-} and PO_4^{3-} individually at a 50-fold mass concentration excess over uranium(VI) was tested. The tolerance limit was defined as the concentration of the foreign ion added causing a relative deviation within $\pm 5\%$ in the magnitude of the peak current $i_{p,c}$ at -0.35 V vs. Ag/AgCl by complexing with the reagent or by forming peaks that overlap with, or even completely suppress the uranium(VI) peak. The ions Al^{3+} , Fe^{3+} , VO_3^- and Cr^{3+} interfered even at a 10-fold mass concentration excess over uranium(VI) by producing a diffusion controlled peaks as shoulders on the cathodic side of the analyte peak (-0.35 V). Al^{3+} , Fe^{3+} interference was tolerated after masking with tri ethanolamine and NaF (0.1% w/v), respectively. The interferences of the ions Cu^{2+} , Zn^{2+} and Cr^{3+} was alleviated by adding few drops of EDTA (0.1% w/v) prior to their measurements to suppress the interfering peak of the diverse ions without any affect on the uranium(VI) peak.

3.4 Analytical applications

3.4.1 Analysis of certified reference material

The validation of the presented procedure is performed by the analysis of uranium content in CRM sample (IAEA soil-7) after digestion in concentrated HF-HCl-HNO $_3$ (7 : 2 : 5 v/v) as described in the experimental section. The solution of the CRM sample was analyzed by the direct calibration plot of the developed method (Fig. 8). Moreover, analysis of uranium in the CRM sample was determined by performing the recovery tests in the spiked (standard addition) samples with U(VI) in the range 1–3 μg via the developed DP-CSV method and by the standard ICP-MS method. Observed results are summarized in Table 2. These results are in acceptable agreement with the certified values of the CRM. The relative standard deviation (RSD) for triplicate voltammetric analysis was in the range ± 2.8 – 3.8% , highlighting that good precision was maintained for the real sample. The F- and t-tests at 95% confidence levels showed no significant dif-

ferences between the total uranium content and the labile content. The low content $1.27 \mu\text{g g}^{-1}$ of complexed uranium with the available organic matter in the fertilizer sample is most likely attributed to the occurrence of the phosphate in the original phosphorous sample as inorganic phosphate not organic phosphate sample.

3.4.2 Analysis of uranium content in commercial phosphate fertilizers

The validation of the developed DP-CSV procedure was also achieved by performing the analysis of uranium content in the local phosphate fertilizer samples (F_1 – F_7). Different amounts of uranium were spiked to each sample solution of the tested fertilizer to estimate the accuracy of the procedure. The resulting solutions were analyzed by the pro-

cedure. The results are summarized in Table 2. These results are in acceptable agreement with the certified values of the CRM. The relative standard deviation (RSD) for triplicate voltammetric analysis was in the range ± 2.8 – 3.8% , highlighting that good precision was maintained for the real sample. The F- and t-tests at 95% confidence levels showed no significant dif-

4. Conclusions

The study reveals that uranium can be determined in soils and phosphate fertilizers using the proposed method. The

developed DP-CSV procedure involving the adsorptive accumulation of the uranyl(II)-arsenazo-III complex at the HMDE provides a simple, reliable, fairly rapid and low cost method for measuring the total uranium content in phosphate fertilizers and different types of soil samples. The proposed procedure is able to minimize the limitations related to the sensitivity and selectivity for uranium(VI) determination compared to the other reported methods. The precision of the uranium analysis was found to be better than 5%. The data suggest this method of uranium determination as one of the suitable techniques for uranium determination in phosphate ores and phosphate fertilizers samples on routine basis. However, work is still continuing for investigating the influence of memory effect, organic materials and competitive complexing agents present in the investigated samples. Moreover, the use of the method for determination and chemical speciation of Th and U ions in their matrices will be considered in future works.

Acknowledgment. The authors would like to thank the Deanship of Scientific Research, King Abdul-Aziz University, Saudi Arabia for funding under the grant number 170/428.

References

- Yang, X., Feng, Y., He, Z., Stoffella, P. J., Molecular mechanisms of heavy metal hyperaccumulation and phytoremediation. *J. Trace Elem. Med. Biol.* **18**, 339 (2005).
- Dulski, T. R.: *Trace Elemental Analysis of Metals, Methods and Techniques*. Marcel Dekker Inc., New York (1999).
- Abou-Mesalam, M. M., El-Naggar, I. M., Abdel-Hai, M. S., El-Shahawi, M. S.: Use of open-cell resilient polyurethane foam loaded with crown ether for the preconcentration of uranium from aqueous solutions. *J. Radioanal. Nucl. Chem.* **258**, 619 (2003).
- El-Shahawi, M. S., Othman, M. A., Abdel-Fadeel, M. A.: Kinetics, thermodynamic and chromatographic behaviour of the uranyl ions sorption from aqueous thiocyanate media onto polyurethane foams. *Anal. Chim. Acta* **546**, 221 (2005).
- El-Shahawi, M. S., Othman, M. A., Nassef, H. M., Abdel-Fadeel, M. A.: An investigation into the retention profile and kinetics of sorption of the ternary complex ion associate of uranyl ions with crown ether and picric acid by the polyurethane foams. *Anal. Chim. Acta* **536**, 227 (2005).
- WHO: *Guidelines for Drinking Water Quality*. 2nd Edn., Addendum to Volume 2. Health Criteria and other Supporting Information, WHO/EOS/98.1, Geneva (1998).
- Gilman, A. P., Villencuve, D. C., Seccours, V. E.: Uranyl nitrate: 28-day and 91-day toxicity studies in the Sprague-Dawley rat. *Toxicol. Sci.* **41**, 117 (1998).
- Guidelines for Drinking Water Quality*. 3rd Edn., World Health Organization, Geneva (2003).
- Hamamo, H., Landberger, S., Harbotile, G., Panno, S.: Studies of radioactivity and heavy metals in phosphate fertilizer. *J. Radioanal. Nucl. Chem.* **194**, 331 (1995).
- Qureshi, A. A., Khattak, N. U., Sardar, M., Akram, M., Iqbal, M., Khan, H. A.: Determination of uranium contents in rock samples from Kakul phosphate deposit, Abbotabad (Pakistan), using fission-track technique. *Radiat. Meas.* **34**, 355 (2001).
- Yamazaki, I. M., Geraldo, L. P.: Uranium content in phosphate fertilizers commercially produced in Brazil. *Appl. Radiat. Isotopes* **59**, 133 (2003).
- Kumar, A., Kumar, M., Singh, B., Singh, S.: Natural activities of ^{238}U , ^{232}Th and ^{40}K in some Indian building materials. *Rad. Meas.* **36**, 465 (2003).
- Rehman, S., Imtiaz, N., Faheem, M., Rehman, S., Matiullah, M.: Determination of ^{238}U contents in ore samples using CR-39-based radon dosimeter-disequilibrium case. *Rad. Meas.* **41**, 471 (2006).
- Singh, S., Kumar, A., Singh, B.: Radon level in dwellings and its correlation with uranium and radium content in some areas of Himachal Pradesh, India. *Env. Int.* **28**, 97 (2002).
- Misdaq, M. A., Khajmi, H., Aitnouh, F., Berrazzouk, S., Bourzik, W.: A new method for evaluating uranium and thorium contents in different natural material samples by calculating the CR-39 and LR-115 type II SSNTD detection efficiencies for the emitted α -particles. *Nucl. Instrum. Methods Phys. Res. B* **171**, 350 (2000).
- Rao, T. P., Metilda, P., Gladis, J. M.: Preconcentration techniques for uranium(VI) and thorium(IV) prior to analytical determination – an overview. *Talanta* **68**, 1047 (2006).
- Salama, T. A., Seddik, U., Dosky, T. M., Morsy, A. A., El-asser, R.: Determination of thorium and uranium contents in soil samples using SSNTD's passive method. *Pramana J. Phys.* **67**, 269 (2006).
- Henze, G.: Voltammetric determination of uranium as standard. *Nachrichten Chemie* **56**(12), 1244 (2008).
- De Carvalho, L. M., Schwedt, G., Henze, G., Sander, S.: Redoxspeciation of selenium in water by cathodic stripping using an automated flow system. *Analyst* **124**(12), 1803 (1999).
- Faller, C., Stojko, N. Yu., Henze, G., Brainina, Kh. Z.: Stripping voltammetric determination of mercury at modified solid electrodes: Determination of mercury traces using PDC Au(III) modified electrodes. *Anal. Chim. Acta* **396**(2–3), 195 (1999).
- Zarebski, J., Henze, G.: Analytical aspects of voltammetric and photometric investigations of tungsten(VI)-chloranilic acid complex. *Chem. Anal.* **43**(1), 15 (1998).
- Stojko, N. Y., Brainina, K. Z., Faller, C., Henze, G.: Stripping voltammetric determination of mercury at modified solid electrodes. I. Development of modified electrodes. *Anal. Chim. Acta* **371**(2–3), 145 (1998).
- Nirmaler, H.-P., Lauer, M., Henze, G.: Stripping voltammetry at carbon electrodes with different surface topography – A comparative study. *Electroanalysis* **10** (5) 326 (1998).
- Lin, L., Thongngamdee, S., Wang, J., Lin, Y., Sadik, O. A., Ly, S. Y.: Adsorptive stripping voltammetric measurements of trace uranium at the bismuth film electrode. *Anal. Chim. Acta* **535**, 9 (2005).
- Korolczuk, M., Tyszczyk, K., Grabarczyk, M.: Determination of uranium by adsorptive stripping voltammetry at a lead film electrode. *Talanta* **72**, 957 (2007).
- Monticelli, D., Ciceri, E., Dossi, C.: Optimization and validation of an automated voltammetric stripping technique for ultratrace metal analysis. *Anal. Chim. Acta* **594**, 192 (2007).
- Becker, A., Tobias, H., Porat, Z., Mandler, D.: Detection of uranium(VI) in aqueous solution by a calix[6]arene modified electrode. *J. Electroanal. Chem.* **621**, 214 (2008).
- Farghaly, O. A., Ghandour, M. A.: Cathodic adsorptive stripping voltammetric determination of uranium with potassium hydrogen phthalate. *Talanta* **49**, 31 (1998).
- Delahay, P.: *New Instrumental Methods in Electrochemistry*. Interscience, New York (1966), Chap. 6.
- Britton, H. T. S.: *Hydrogen Ions*. 4th Edn., Chapman & Halls, London (1952), p. 113.
- Sawyer, D. T., Heinemann, W. R., Beebe, J. M.: *Chemistry Experiments for Instrumental Methods*. John Wiley & Sons, New York (1984).
- Marczenko, Z.: *Spectrophotometric Determination of Elements*. 3rd Edn., Ellis Horwood, Chichester, UK (1986), Chap. 23.
- Manjaoui, A., Haladjian, J., Bianco, P.: Electrochemical properties of pyrolytic graphite electrodes modified through adsorbed proteins. *Electrochim. Acta* **35**, 177 (1990).
- Bard, A. J., Faulkner, L. R.: *Electrochemical Methods, Fundamentals and Applications*. Wiley, New York (1980), p. 218.
- Van Benschoten, J. J., Lewis, J. Y., Heinemann, W. R.: Cyclic voltammetry experiment. *J. Chem. Edu.* **60**, 772 (1983).
- Fischer, E., Van Den Berg, C. M. G.: Determination of lead complexation in lake water by cathodic stripping voltammetry and ligand competition. *Anal. Chim. Acta* **432**, 11 (2001).
- Shams, E., Babaei, A., Soltaninezhad, M.: Simultaneous determination of copper, zinc and lead by adsorptive stripping voltammetry in the presence of Morin. *Anal. Chim. Acta* **501**, 119 (2004).
- Miller, J. C., Miller, J. N.: *Statistics for Analytical Chemistry*. 4th Edn., Ellis-Horwood, New York (1994), p. 115.



Spectrofluorimetric method for measuring the activity of the enzyme α -L-fucosidase using the ion associate of 2-chloro-4-nitro phenol–rhodamine-B

M.S. El-Shahawi^{a,*}, A.M. Othman^b, M.E. El-Houseini^c, B. Nashed^d, M.S. Elsofy^d

^aDepartment of Chemistry, Faculty of Science, King Abdulaziz University, P.O. Box 80203, Jeddah 21589, Saudi Arabia ^bGenetic Engineering and Biotechnology Institute, Menofia University, Menofia, Egypt ^cNational Cancer Institute, Cairo University, Egypt ^dModern University for Technology & Information, Egypt

article info

Article history:

Received 10 February 2009
Received in revised form 11 April 2009
Accepted 13 April 2009 Available
online 11 June 2009

Keywords:

α -L-Fucosidase enzyme
Rhodamine-B
2-Chloro-4-nitrophenol
Associate

abstract

A low cost and accurate method for the detection and analytical determination of the activity of the enzyme α -L-fucosidase (AFU) was developed. The method was based upon measuring the fluorescence intensity of the complex ion associate of the ion associate of rhodamine-B and the compound 2-chloro-4-nitrophenol (RB⁺ CNP⁻) at 580nm in phosphate buffer (pH 5) against the reagent blank. The influence of the different parameters, e.g. pH, incubation time, temperature, 2-chloro-4-nitrophenol concentration, foreign ions and surfactants that control the fluorescence intensity of the produced ion associate was critically investigated. The correlation between the fluorescence activity of the enzyme AFU by the developed procedures and the standard method was positive and highly significant in patients and controls ($r^2=0.99$, $p<0.001$). The developed method is simple and proceeds without practical artifacts compared to the standard method.

© 2009 Published by Elsevier B.V.

1. Introduction

Liver cirrhosis is a pre-cancer condition that in many cases can develop into Hepatocellular carcinoma (HCC). Therefore, cirrhotic patients with cirrhosis are usually screened for HCC during their follow-up procedure [1–6]. Tumor markers represent good potential screening tools for the early diagnosis of tumors [7–10]. The primary tumor marker for HCC is a single polypeptide chain glycoprotein namely α -fetoprotein (AFP) [11,12]. The sensitivity and specificity of the AFP as a common tumor marker to detect HCC in all patient samples are insufficient [13,14]. Moreover, it is not secreted in all cases of HCC and may be normal in 40% of patients with early HCC [10,15].

The enzyme α -L-Fucosidase (AFU) can hydrolyze methyl α -L-fucoside and fucosidic linkages of fucoidan and blood-group substances [16]. The AFU enzyme compose of two-enzyme components namely: i, fucosidase which acts on 4-nitrophenyl α -L-fucoside as well as fucosidic linkages of porcine submaxillary mucin at optimal activity at pH 2 and ii, the fucoidanase showed highest activity around pH 5 and acts on the synthetic substrate not on the mucin [17]. The enzyme fucoidanase showed hydrolytic

0039-9140/\$ – see front matter © 2009 Published by Elsevier B.V.
doi:10.1016/j.talanta.2009.04.070

activity towards fucoidan, and not towards 4-nitro phenyl α -L-fucoside and blood group of livers of related species [18]. Clinical studies have demonstrated that, the activity of AFU enzyme represent an excellent test for diagnosis of HCC [19,20]. The AFU enzyme was used for the diagnosis of fucosidosis recognized in born disorder of metabolism and increases the sensitivity of detection to 95.5% in patients with HCC [21,22].

Different spectrometric methods have been reported for the determination of the activity of the enzyme AFU in serum [23–25]. These methods are limited by their long incubation time (30–60min) for the sample and reagent blanks. Moreover, the poor affinity of the enzyme AFU towards the substrate 4-NPF as a colorimetric reagent at pH 4.8, added another disadvantage to these methods. However, the method of Jun and Hua [23] involving the synthesis of 2-chloro-4-nitrophenyl- α -L-fucopyranoside (CNPF) as a substrate has a rapid hydrolytic rate than 4-NPF method [23,24]. The activity of AFU was also determined by spectrofluorescence methods [26,27], affinity chromatography [17], column chromatography packed with *Bacillus cereus* [28] and disc gel electrophoresis technique [17,29]. Most of these methods are unselective, require careful experimental conditions, considerably time consuming and not compatible to detect the activity of AFU at the early stage of diseases. Thus, the present manuscript is focused on the use of the fluorescent ion associate of 2-chloro-4-nitro phenol–rhodamine-B (RB⁺ CNP⁻) for measuring the activity of the AFU enzyme and overcoming the difficulties caused by the previous methods [23–27].

* Corresponding author. Permanent address: Department of Chemistry, Faculty of Sciences at Damietta, Mansoura University, Mansoura, Egypt. Tel.: +966 2 6952000; fax: +966 2 6952292.

E-mail address: mohammad_el-shahawi@yahoo.co.uk (M.S. El-Shahawi).

The developed procedures will be able to control the quality of the final marketed product in both qualitative and quantitative approaches to assure the identity of the disease. The method will be useful in medical applications to detect the different diseases at the very early stage of diseases.

2. Experimental

2.1. Apparatus

A Shimadzu RF5301 PC spectrofluorometer (290–750nm) was used for recording the excitation; emission spectra and measuring the fluorescence intensity of the reagents and the produced complex ion associate. A two matched cuvettes (1.0cm) and an Orion pH meter VWR scientific model (8000) were used for measuring the fluorescence intensity of the ion associate $RB^+ CNP^-$ and other fluorescent species and pH measurements, respectively.

2.2. Reagents and materials and methods

Analytical reagent grade (A.R.) reagents and chemicals (99.9% purity) were used without further purification. Ascorbic acid, bilirubin, hemoglobin, glucose and uric acid, albumin, total protein, total cholesterol and triglyceride were purchased from Fluka (Fluka, AG, Buchs, Switzerland). The substrate 2-chloro-4-nitrophenyl- β -D-fucopyranoside (CNPF) and the enzyme β -D-fucosidase (AFU, EC 3.2.1.51) were laboratory reagent grade from Sigma-Aldrich, Poole, UK. The control enzyme was prepared in bovine serum base and provided in lyophilized powder. The enzyme AFU was also obtained from bovine kidney and the reagents 2-chloro-4-nitro phenol (CNP) and rhodamine-B (RB) were purchased from Sigma Co. Phosphate buffers of various pH (pH 2.5–7) were prepared from phosphoric acid and/or sodium phosphate.

2.3. Preparation of the complex ion associate $RB^+ CNP^-$

In measuring flask (100.0mL), an accurate volume (10mL) of the reagent 2-chloro-4-nitrophenol ($5 \times 10^{-4} \text{ molL}^{-1}$) was allowed to react with 20.0mL of rhodamine-B ($5 \times 10^{-4} \text{ molL}^{-1}$). The solution was then completed to the mark with phosphate buffer of pH 5.0 and the excitation and emission spectra of the reagents 2-chloro-4-nitrophenol and rhodamine-B and the produced complex ion associate ($RB^+ CNP^-$) were then recorded.

2.4. Analytical application

An appropriate amount (450L) of the reagent 2-chloro-4-nitro-phenol fucopyranoside was immediately mixed with 50L of plasma/serum samples of HCC patients (26 persons) and healthy control (7 persons) in incubator at 37 °C for 6min. To the resultant solutions an accurate volume (300L) of rhodamine-B ($5 \times 10^{-4} \text{ molL}^{-1}$) was added and swirled to mix the contents. Each solution was placed in an incubator at 37 °C for 5min. The volume was completed to 3.0mL with phosphate buffer of pH 5 and the emission intensity at 580nm was then measured against the reagent blank. The main characteristics of the patients (male/female) and control groups are given in Table 1.

Table 1
Main characteristics of the patients and control groups.

Status	Number of patients	Males/females		Age (year)	
		No.	%	Median	Range
HCC	20	15/5	75/25	51	24–75
Cirrhosis of chronic hepatitis C and B	4	2/2	50/50	48	37–69
Other neoplasms (gallbladder cancer, colon cancer and others)	2	2/0	100/0	42	28–56
Healthy adults	7	4/3	60/45	36	19–58

3. Result and discussion

3.1. Excitation and emission spectra

Previous studies [26] have shown that, the enzyme AFU reacts with the substrate 2-chloro-4-nitrophenol or 4-nitrophenol at pH 4–5 producing yellow colored product. This reaction has been used for measuring the activity of the enzyme AFU via the absorbance of the produced yellow colored species at pH 5.0 and 37 °C [24]. However, this, method suffered from the interference caused by the yellow color of the serum of patients and of the reagent 2-chloro-4-nitrophenol (or 4-nitro phenol). Another disadvantage was also noticed in many cases of patients of HCC that have high bilirubin [22,23]. Such methods suffered from the lack of sensitivity and accuracy due to the significant interference of the yellow color of the serum. Thus, attempts were made to overcome these disadvantages by testing the interaction of the compound 4-nitro phenol or 2-chloro-4-nitro phenol with rhodamine-B dye in aqueous medium.

In phosphate buffer (pH 5), preliminary investigations showed that, on mixing the reagent CNP with the ion pairing reagent RB and shaking, a green colored complex ion associate was developed and is most likely proceeds according to the following equation:



After equilibrium, the excitation and emission spectra of the produced complex ion associate of rhodamine-2-chloro-4-nitrophenol or rhodamine-4-nitro phenol ($RB^+ CNP^-$) in the aqueous phase at pH 5 were recorded. The excitation and emission spectra (Fig. 1) of the complex associate $RB^+ CNP^-$ showed the characteristic excitation wavelength at 455nm and the characteristic emission wavelength at 580nm. The fluorescence intensity of the rhodamine-B in the emission spectrum at 580nm decreased on adding CNP confirming the associate formation. On the other hand, rhodamine-B showed well defined emission spectrum (Fig. 2) close to the emission spectrum of the complex ion associate $RB^+ CNP^-$ (Fig. 1) while, compound 2-chloro-4-nitrophenol or 4-nitro phenol showed only excitation spectrum and no emission spectrum at 580nm. Thus, in the subsequent work, the activity of the enzyme AFU was determined through measuring the fluorescence intensity of the ion associate $RB^+ CNP^-$ at 580nm against a reagent blank at the optimum experimental conditions.

3.2. Analytical parameters

The influence of the hydrogen ion concentration on the fluorescence intensity of the complex ion associate $RB^+ CNP^-$ was investigated. The emission spectrum of the solution of 2-chloro-4-NP ($5 \times 10^{-5} \text{ molL}^{-1}$) in the presence of rhodamine-B ($5 \times 10^{-5} \text{ molL}^{-1}$) in a wide range of pH 2–8 employing dilute HCl and/or dilute sodium hydroxide was measured. The results shown in Fig. 3 revealed maximum change in the emission intensity in the pH range pH 2.5–6.0. At pH less than pH 2.5, the emission intensity of the produced complex associate $RB^+ CNP^-$ at 580nm

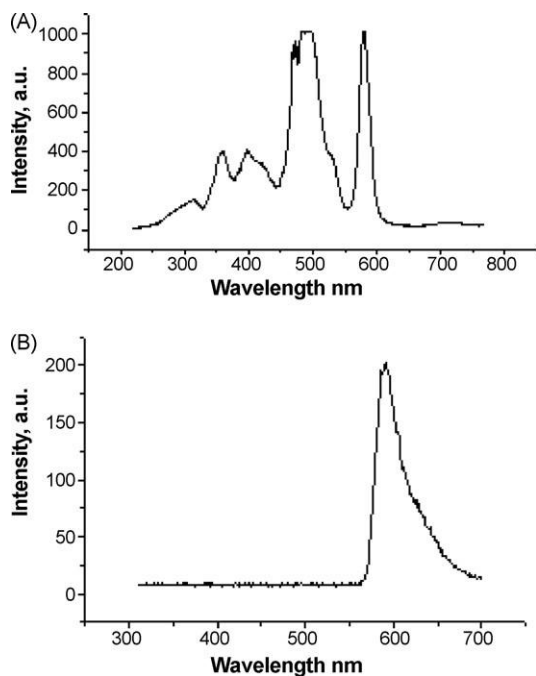


Fig. 1. The excitation (A) and emission (B) spectra of the complex ion associate 2-chloro-4-nitrophenol-rhodamine-B ($2.5 \times 10^{-5} \text{ molL}^{-1}$) in phosphate buffer pH 4–5 at 37 °C.

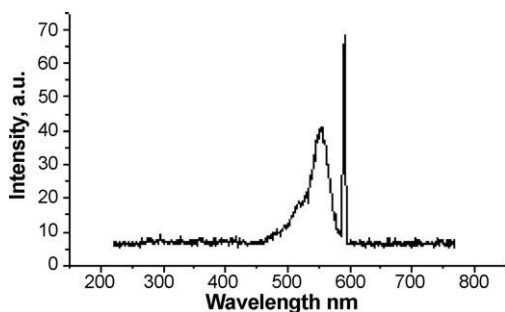


Fig. 2. The emission spectrum of rhodamine-B ($5 \times 10^{-5} \text{ molL}^{-1}$) in phosphate buffer of pH 4–5 at 37 °C.

gradually decreased which is most likely attributed to the instability of the formed ion associate. At pH higher than pH 6.2, the emission intensity at 580 nm was also decreased gradually. Therefore, in the next work, phosphate buffer of pH 5 was selected for recording the enzyme AFU activity through measuring the fluorescence intensity of $\text{RB}^+ \text{CNP}^-$ against reagent blank.

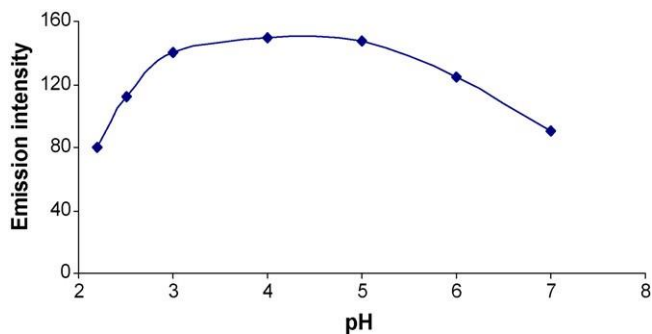


Fig. 3. Effect of pH on the fluorescence intensity on the formation of the complex ion associate 2-chloro-4-nitrophenol-rhodamine-B ($2.5 \times 10^{-5} \text{ molL}^{-1}$) employing phosphate buffer at 37 °C.

The effect of reaction time on the formation of the complex ion associate $\text{RB}^+ \text{CNP}^-$ was critically investigated by mixing the reagent CNP^- (1.0 mL of $5 \times 10^{-4} \text{ molL}^{-1}$) with RB^+ (1.0 mL of $5 \times 10^{-4} \text{ molL}^{-1}$) in phosphate buffer of pH 5 in measuring flask (10 mL). The solutions were completed to the mark with phosphate buffer of pH 5.0 and were left for various time intervals (1.0–30 min) solutions. The fluorescence intensity of the emission spectra of the solutions was then measured at 580 nm. The results revealed that, the fluorescence intensity reached maximum value at 5 min reaction time and slightly decreased at longer time higher than 30 min. Thus, a reaction time of 5–10 min was selected in the subsequent work.

The influence of temperature (15.0–70.0 °C) on the reaction of the reagent CNP^- and rhodamine-B was investigated in phosphate buffer of pH 5 and 5 min reaction time on a water bath. The fluorescence intensity of the emission spectra of the solutions was recorded at 580 nm versus reagent blank. The results showed that, the maximum intensity change was obtained at 35–40 °C and decreased gradually at higher temperature. This behavior may be attributed to the dissociation of the complex ion associate $\text{RB}^+ \text{CNP}^-$.

The influence of sodium dodecyl sulfonate (SDS), cetylpyridinium chloride (CPC) and the non-ionic surfactant Triton X100 on the fluorescence intensity of the produced associate $\text{RB}^+ \text{CNP}^-$ at 580 nm was critically studied. In this experiment, an aliquot solution of phosphate buffer (pH 5) containing 2-chloro-

4-nitrophenol (1.0 mL, $5 \times 10^{-4} \text{ molL}^{-1}$), rhodamine B (1.0 mL, $5 \times 10^{-4} \text{ molL}^{-1}$) and the required surfactant (1.0 mL, 0.1% w/v) was allowed to react for 5 min at 40 °C in an incubator. The fluorescence intensity of the produced associate at 580 nm was then measured and compared with that recorded without addition of surfactant. No significant changes on the fluorescence intensity of the associate $\text{RB}^+ \text{CNP}^-$ were noticed with and without surfactant.

3.3. Interference study

The influence of some interfering species on the selectivity of the developed spectrofluorimetric method was investigated individually. Thus, the developed procedure was applied in the presence of various species commonly associated with the enzyme, e.g. NaCl, KCl ($1 \times 10^{-3} \text{ molL}^{-1}$), albumin (0.5 g), urea (0.005 gL^{-1}), uric acid (0.008 gL^{-1}), total protein (0.001 gL^{-1}) and glucose (0.01 gL^{-1}) in phosphate buffer of pH 5.0 at 5 min contact time at 40 °C. The tolerable limit was defined as the concentration of the added species causing a deviation less than $\pm 3.0\%$ of the fluorescence intensity at the optimum conditions on the fluorescence intensity and emission spectrum of the ion associate $\text{RB}^+ \text{CNP}^-$ ($5 \times 10^{-4} \text{ molL}^{-1}$). The results revealed no significant change on the fluorescence intensity of $\text{RB}^+ \text{CNP}^-$ in the presence of the

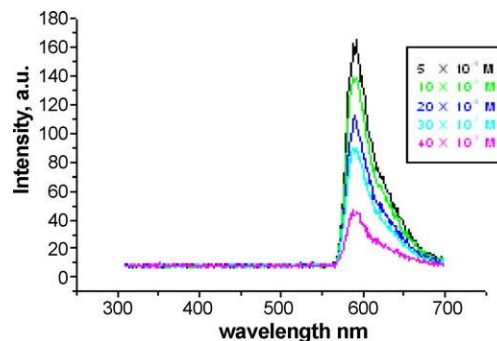
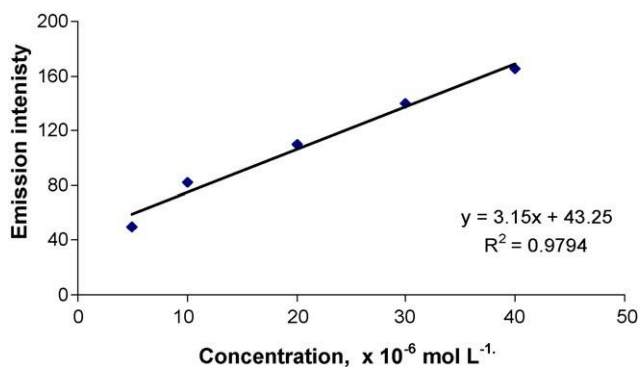


Fig. 4. Emission spectra of various concentrations (5×10^{-6} – 40.0×10^{-6} molL⁻¹) of 2-chloro-4-nitrophenol in the presence of rhodamine-B ($2 \text{ mL}, 5 \times 10^{-5}$ molL⁻¹) in 50-mol L⁻¹ phosphate buffer of pH 4–5 at 37 °C.



22

M.S. El-Shahawi et al. / Talanta 80 (2009) 19–23

Fig. 5. Calibration plot for different concentrations of CNP in aqueous phosphate buffer of pH 4–5 versus emission intensity at 580nm at 37 °C in the presence of rhodamine-B.

tested interfering ions indicating the selectivity of the developed method.

3.4. Dynamic range of the calibration graph and limit of detection

The validation of the proposed spectrofluorimetric procedure for measuring the AFU activity was examined via evaluation of the linear range of the plot of the fluorescence intensity measured versus various concentrations of 2-chloro-4-nitrophenol; lower limit of detection (LOD); limit of quantification (LOQ), repeatability, and specificity. The calibration plot of 2-chloro-4-nitrophenol in phosphate buffer (pH 5.0) was constructed by reacting 2-chloro-4-NP solution at various concentrations (5×10^{-6} – 40.0×10^{-6} molL⁻¹) with rhodamine-B ($2.0 \text{ mL}, 5.0 \times 10^{-5}$ molL⁻¹) and shaking for 5min in an incubator at 37 °C. The emission spectra of the produced associate (RB⁺ CNP⁻) at various concentration of CNP are shown in Fig. 4. The plot of CNP concentration (5×10^{-6} – 40.0×10^{-6} molL⁻¹) versus the fluorescence intensity (at 580nm) was linear (Fig. 5) with good correlation coefficient ($r^2 = 0.979$) and leveled off at concentration higher than 40.0×10^{-6} molL⁻¹ of CNP. This trend is most likely attributed to the shift of the equilibrium (equation (1)) to the left and the quantity of CNP species available to form complex ion associate with $[\text{RB}^+]_{(\text{aq})}$ decreased which minimizes the associate formation [30] may account for the observed effect. A large excess of the reagent slightly decreased the fluorescence intensity possibly owing to the increased acidity of the aqueous phase which minimizes the associate formation [30].

The regression equation of the linear plot (Fig. 5) was: $Y = 3.15C + 43.25$ with a correlation coefficient $r^2 = 0.979$, where Y = emission intensity and C represents the concentration of CNP in M. According to IUPAC [31], the value of the LOD calculated

Table 2

using the formula $\text{LOD} = 3S_{y/x}/b$ where $S_{y/x}$ is the standard deviation of y -residual and b is the slope of the calibration plot was found equal 1.01×10^{-7} molL⁻¹. The value of LOQ where $\text{LOQ} = 10S_{y/x}/b$ under the established conditions for lead (II) was found equal 3.4×10^{-9} molL⁻¹ and a relative standard deviation (RSD) for CNP at concentration of 5×10^{-6} was 2.5% ($n = 3$). Such limits could be improved to lower values by increasing the incubation times at the optimum experimental condition. The values of LOD and LQD confirmed the sensitivity of the proposed procedure compared to the reported methods [23–26]. This precision is suitable for the routine analysis of AFU activity for different patients. Moreover, the repeatability of AFU activity based on five replicate measurements for 5×10^{-6} molL⁻¹ of the reagent CNP calculated from the calibration curve was $97.47 \pm 3.7\%$ indicating good precision of the proposed method.

It was observed that there is no interference from other additives, e.g. interference from trace metal ions in particular Na, K which are commonly present in combination with the AFU enzyme in the serum of HCC patients. No

significant difference could be detected upon comparing the emission intensity of the CNP component alone or in the presence of a high content (1:5) CNP: Na or K ions, respectively. Thus, the developed method is characterized by good specificity.

3.5. Analytical applications

The validation of the proposed spectrofluorimetric method was tested by measuring the activity of the enzyme AFU) for 33 serum samples of male and female patients (26) and healthy (7) in various ages (Table 1). The results obtained are summarized in Table 2. Good agreement between the values obtained by the developed procedure and the standard method [23]. The average value of the AFU enzyme activity obtained by the standard method [23] ($29.28 \pm 2.75 \text{ U/L}$) for the healthy samples (7) was found close to the value achieved by the developed method ($31.14 \pm 3.21 \text{ U/L}$) with an acceptable standard error (3.55–3.90). Also, good correlation between the values of the activity of serum AFU enzyme in some selected control samples measured by the standard and the developed spectrofluorimetric methods ($r^2 = 0.883$, $p = 0.002$) is shown in Fig. 6. The F - and t -tests at 95% confidence levels did not exceed the theoretical ones and no significant differences between the developed and the standard [22] methods were observed confirming the accuracy of the developed procedure. In the HCC patient samples (20), the mean value of the AFU activity achieved by the standard method [23] ($119.55 \pm 74.80 \text{ U/L}$) was found also in good agreement with that obtained by the proposed method ($123.5 \pm 77.8 \text{ U/L}$) with a standard error in the range 13.99–14.08. On the other hand, an excellent correlation between the average values of the activity of the serum AFU enzyme in selected HCC patients

Analytical results of the standard (A) and the developed spectrofluorimetric (B) methods for the healthy and patients' samples.^a

Enzyme activity (U/L)	No	Subject	Methods		
			Standard error (SE)	Mean \pm SD	Range
3.55	29.28 \pm 2.75	16–41	7	Healthy	Standard method (A)
3.9	31.14 \pm 3.21	15–46			Developed spectrofluorimetric method (B)
13.99	119.55 \pm 74.80	54–249	20	HCC	Standard method (A)
14.08	123.5 \pm 77.8	58–255			Developed spectrofluorimetric method (B)
2.81	29.95 \pm 1.68	25–37.8	4	Cirrhosis of Chronic hepatitis C and B	Standard method (A)

2.61	29.25 ± 1.53	24–36.5			Developed pectrofluorimetric method (B)
2.69	29.16 ± 4.67	24–33.1	2	Other Neoplasms (gallbladder cancer, colon cancer and others)	Standard method (A)
1.85	28.33 ± 3.21	26–32			Developed spectrofluorimetric method (B)

^a Average of three measurements ± standard deviation.

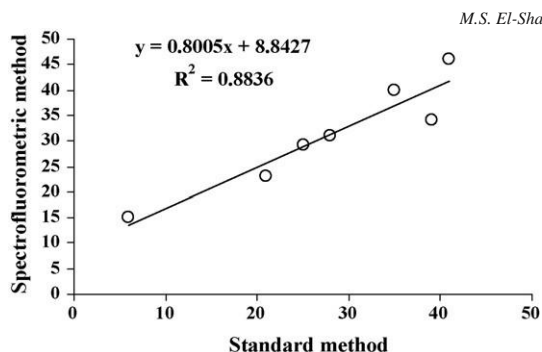


Fig. 6. Correlation between the values of the activity of serum AFU enzyme in some selected control samples as measured by the standard and the developed spectrofluorometric (pH 4–5) methods ($r^2=0.883$, $p=0.002$).

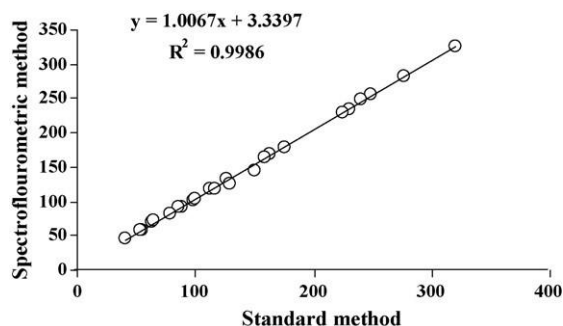


Fig. 7. Correlation between the values of the activity of serum AFU enzyme activity in some selected HCC patients measured by the standard and the developed spectrofluorometric (pH 4–5) methods ($r^2=0.99$, $p=0.001$).

measured by the standard and the developed spectrofluorometric methods ($r^2=0.99$, $p=0.001$) is also shown in Fig. 7 confirming the accuracy of the developed procedure. The correlation is positive and highly significant in patients and controls ($r^2 \approx 0.99$, $p < 0.001$) indicating that the proposed method has more/or less the same accuracy of measurements of AFU activity without its practical artifacts.

Moreover, for Cirrhosis of chronic hepatitis C and B samples (4), the average value obtained by the standard method [24] (29.95 ± 1.68 U/L) was found also quite close to the mean value (29.25 ± 1.53 U/L) obtained by the developed method with a standard error in the range 2.61–2.81 confirming the accuracy of the proposed procedure. In the case of neoplasm's (gallbladder cancer, colon cancer and others) samples (2) the average values obtained by the standard method and the proposed method were found equal 29.16 ± 4.67 and 28.33 ± 3.21 U/L, respectively with a standard error in the range of 1.85–2.69. The *F*- and *t*-tests at 95% confidence levels did not exceed the theoretical ones and no significant differences were observed between the developed and the standard [23] methods confirming the accuracy of the developed procedure.

4. Conclusions

The proposed method is sensitive enough, simple, reliable, fairly rapid and low cost procedure for measuring the activity of the enzyme AFU. This

advantage encourages the application of the proposed method in routine quality control of measuring the activity of AFU in human serum. The method able to minimize the limitations, e.g. the interference caused by the yellow color of these serum of patients and the yellow color of 2-chloro-4-nitrophenol (or 4-nitro phenol) related to the sensitivity and selectivity for AFU activity in patients of Cirrhosis of chronic hepatitis C and B, other neoplasm's, e.g. gallbladder cancer, colon cancer and healthy adults compared to the other reported methods [21–24]. The disadvantage noticed for patients of HCC having high value of bilirubin makes the reported methods [15–18] are not compatible with the detection limit of the proposed method. This behavior is not likely attributed to the suppression effect of the interaction of CNP reagent and rhodamine B under the optimal experimental conditions. Thus, the work is still continuing for studying the effect of various concentrations of bilirubin, memory effect, and competitive complex agents present in the investigated samples.

References

- [1] M.G. Giardina, M. Matarazzo, R. Morante, *Cancer* 83 (1998) 2468.
- [2] K. Okuda, E. Tabor, *Liver Cancer*, Churchill Livingstone, New York, 1997, p. 13. [3] Y. Kubo, K. Okua, H. Musha, T. Nakashima, *Gastroenterology* 74 (1978) 578.
- [4] M. Zoli, D. Magalotti, G. Bianchi, C. Gueli, G. Marchesini, E. Pisi, *Cancer* 78 (1996) 977.
- [5] B. Cobucci-Ponzano, A. Trincone, A. Giordano, M. Rossi, M. Moracci, *J. Biol. Chem.* 278 (2003) 14622.
- [6] L. Aheng-wen, C. Chao-Sheng, C. Shih-Shen, T.M. Kowk-Kong, L. Chun-Hung, C. Cheng-Wen, T.Y. Chuan, I. Yaw-Kuen, *Biochemistry* 48 (2009) 10.
- [7] W.M. El Shemey, O.S. Desouky, M.S. Mohammed, *Phys. Med. Biol.* 48 (2003) N 239.
- [8] C.A. Burtis, E.R. Ashwood, *Tietz Fundamentals of Clinical Chemistry*, 5th edn, W.B. Saunders, PA, Philadelphia, 2001.
- [9] H.J. Shu, T. Saito, H. Watanabe, *Biochem. Biophys. Res. Commun.* 293 (2002) 150.
- [10] T. Nakatsura, Y. Yoshitake, S. Senju, *Biochem. Biophys. Res. Commun.* 306 (2003) 16.
- [11] A. Marenghini, M. Cottone, E. Sciarrino, M.P. Marceno, F. La Seta, G. Fusco, *Dig. Dis. Sci.* 33 (1988) 47.
- [12] H. Oka, A. Tamori, T. Kuroki, K. Kobayashi, S. Yamamoto, *Hepatology* 19 (1994) 61.
- [13] A.K. Sanki, B.J. Voss, S.J. Sucheck, D.R. Ronning, *Anal. Biochem.* 385 (1) (2009) 120.
- [14] Y. Osaki, T. Kimura, A. Arimoto, H. Oka, O. Yamazaki, T. Manabe, H. Chung, M. Kudo, T. Matsunaga, *J. Hepatol.* 49 (2008) 223.
- [15] M.E. El-Houseini, M. El-Sherbiny, M.E. Awad, *J. Egypt. Nat. Cancer Inst.* 4 (2001) 277.
- [16] F. Van Hoof, H.G. Hers, *Eur. J. Biochem.* 7 (1968) 34.
- [17] S. Blumbeig, J. Hildesheim, J. Yarif, K.J. Wilson, *Biochim. Biophys. Acta* 264 (1972) 171.
- [18] G.A. Lewy, A. McAulan, *Biochem. J.* 80 (1961) 433.
- [19] F. Van Hoof, H.G. Hers, *Lancet* 1 (1968) 1198.
- [20] S.W. Johnson, J.A. Alhadeff, *Biochem. Physiol.* 99B (1991) 479.
- [21] Y. Deugnier, *Hepatology* (1984) 4889.
- [22] P. Durand, C. Borrone, C. Della, *J. Pediatr.* 75 (1969) 665.
- [23] K. Zietke, S. Okada, J.S. O'Brien, *J. Lab. Clin. Med.* 79 (1972) 1649.
- [24] J. Troost, M.C. Van der Heijden, G.E. Staal, *Clin. Chim. Acta* 73 (1976) 329.
- [25] W. Ju-Jun, C. En-Hua, *Clin. Chim. Acta* 347 (2004) 103.
- [26] S. Wood, *Clin. Chim. Acta* 58 (1975) 251.
- [27] M. Cuer, A. Barnier, P. de La Salmoniere, G. Durand, N. Seta, *Clin. Chim. Acta* 46 (2000) 560.
- [28] Z.U. Miura, K. Okamoto, H. Yanase, *J. Biosci. Bioeng.* 99 (2005) 629.
- [29] M.W. Ho, J. O'Brien, *F.R. Natl. Acad. Sci. USA* 68 (1971) 2810.
- [30] S. Yamaguchi, K. Uesugi, *Analyst* 109 (1984) 1393.
- [31] J.C. Miller, J.N. Miller, *Statistics for Analytical Chemistry*, 4th edn, Ellis-Howood, New York, 1994, p. 115.

Development of an Analytical Method for Trace Gold in Aqueous Solution Using Polyurethane Foam Sorbents: Kinetic and Thermodynamic Characteristic of Gold(III) Sorption

A. S. BASHAMMAKH, S. O. BAHAFI, F. M. AL-SHAREEF, and M. S. EL-SHAHAWI[†]

*Department of Chemistry, Faculty of Science, King Abdulaziz University,
P. O. Box 80203, Jeddah 21589, Saudi Arabia*

The kinetic parameters of gold(III) sorption by unloaded polyurethane foams (PUFs) and PUFs impregnated with some onium cations *e.g.* tetramethylammonium perchlorate (TMA⁺ClO₄⁻), tetrabutylammonium iodide (TBA⁺I⁻), and tetraheptylammonium bromide (THA⁺Br⁻), have been determined. The retention steps were found to be fast, reached equilibrium in a few minutes and followed a first-order rate equation with an overall rate constant, *k*, of 0.0076 and 0.007 min⁻¹, respectively. The thermodynamic characteristics of gold(III) retention by the unloaded PUFs and THA⁺Br⁻ immobilized PUFs have been critically studied. The negative values of *DH* and *DS* are interpreted as the exothermic and spontaneous reaction of gold(III) sorption onto unloaded PUFs and foams impregnated with THA⁺Br⁻. The cellular structure of the PUFs sorbent offer unique advantages over conventional bulk-type sorbents in the rapid, versatile effective separation and/or preconcentration of gold ions.

(Received January 16, 2008; Accepted May 14, 2008; Published March 10, 2009)

Introduction

Geologically, gold is widely distributed in the crust of the Earth at a background level of 0.03 mg/kg. Hydrothermal ore deposits of gold occur in metamorphic rocks and igneous rocks: alluvial deposits and placer deposits.¹ Gold is mined commercially from two different types of deposits: lode and placer deposits.² Gold is found *in-situ* or at the original location of deposition from mineralizing solutions in lode deposits. On the other hand, the gold concentration is about 4.0 ng g⁻¹ in basic rocks and 1.0 ng g⁻¹ in soils. Values of 0.05 and 0.2 ng mL⁻¹ were found in seawater and river water, respectively.³

A solid-phase extraction of gold by sorption on octadecyl silica membrane disks modified with pentathia-15-crown-5, and subsequent determination by flame atomic absorption spectrometry (FAAS) has been reported by Bagheri *et al.*⁴ A preconcentration method of gold(III), palladium(II) and copper(II) based on the sorption of their ions from various water samples onto a column packed with 3-(2-aminoethylamino)- propyl bonded silica gel has been described by Imamoglu *et al.*⁵ Medved *et al.*⁶ have developed an excellent procedure for the separation and preconcentration of trace metal ions in water using a chelating sorbent Spheron (R) Thiol 1000 at pH < 3 in nitric acid media.

A new method for the simultaneous determination of copper and gold has been developed by derivative spectrophotometry using preconcentration on selected solid sorbent.⁷ A simple and accurate method based on the adsorption of the gold(III)diethyldithiocarbamate complex on Amberlite XAD-2000 resin prior to its determination of gold in environmental samples has

been developed by flame atomic absorption spectrometry after elution with 1 mol L⁻¹ HNO₃ in acetone.⁸ Gold was also determined by electrothermal atomic absorption spectrometry after electrochemical preconcentration on a graphite ridge probe used as a working electrode and sample support.⁹ However, the low level of gold in drinking water is not compatible with the detection limit, and some of these methods are too expensive, unselective and require careful experimental conditions and are considerably time consuming. Thus, preconcentration and separation techniques using liquid-liquid and liquid-solid are frequently required to improve the detection capability and the selectivity of these techniques.¹⁰⁻¹⁵

A novel and low-cost liquid-liquid extraction procedure for the separation of gold(III) at a trace level from an aqueous medium of pH 5 – 9 has been developed by El-Shahawi *et al.*¹⁰ The influence of different parameters on the sorption profiles of trace and ultra traces of gold(I) species from an aqueous cyanide media onto the solid sorbents ion-exchange polyurethane foams (IEPUFs) and commercial unloaded polyurethane foams (PUFs) based polyether type has been investigated.¹¹ The membrane structure and the available surface area of the polyurethane foams make it a very suitable stationary phase, and column filling material.¹¹⁻¹⁶

Herein we report a simple, convenient and low-cost procedure involving liquid-solid extraction procedures employing polyurethane foams as solid sorbents for the preconcentration of gold(III) ions from aqueous media. The kinetic and thermodynamic characteristics of the retention step of gold(III) from the aqueous media by the polyurethane foams were critically determined. The most probable retention mechanism for gold(III) sorption by polyurethane foams will be assigned.

Experimental

Reagents and materials

[†] To whom correspondence should be addressed.
E-mail: mohammad_el_shahawi@yahoo.co.uk

All chemicals used were of analytical reagent-grade quality, and were used without further purification, unless stated otherwise. Most of the chemicals were provided by Merck (Darmstadt, Germany). All of the solutions were made up by doubly demonized distilled water throughout the work. Stock solutions (0.1% w/v) of ion-pairing reagents (TMA⁺ClO₄⁻, TBA⁺I⁻ and THA⁺Br⁻) were prepared by dissolving the required weight of the reagent separately in deionized distilled water. A stock solution (1000 mg mL⁻¹) of gold(III) was used for the preparation of more diluted solutions (1.0 – 100 mg mL⁻¹) in doubly distilled water in the presence of sodium chloride (2% w/v). A stock solution (100 mg mL⁻¹) of potassium gold(I) cyanide, KAu(CN)₂ (Fluka AG, Switzerland) was used in distilled water.

Apparatus

A Perkin–Elmer (Analyst TM 800, USA) graphite furnace atomic absorption spectrometer (GF-AAS) was used for measuring the concentration of Au at a wavelength of 242.8 nm with a 0.5 nm slit width before and after the separation step from the aqueous phase under the optimum settings of the instrument. An Orion pH meter was employed for pH measurements with the absolute accuracy limits at the pH measurements being defined by NIST buffers. A variable mechanical Shaker (Corporation Precision Scientific, Chicago, USA) with a shaking rate in the range of 10 – 250 rpm was used for retention experiments of gold(I) species at different pH. Glass columns (18 cm ¥ 15 mm i.d.) were used for flow experiments.

Preparation of the reagent immobilized polyurethane foam

The reagent foam cubes of TMA⁺ClO₄⁻, TBA⁺I⁻ and THA⁺Br⁻ were prepared by mixing dried foam cubes with water containing ion-pairing reagents (TMA⁺ClO₄⁻, TBA⁺I⁻ and THA⁺Br⁻ (0.1% w/v)) with efficient stirring for 30 min. The immobilized THA⁺Br⁻, TMA⁺ClO₄⁻ or TBA⁺I⁻ reagent foam cubes were then squeezed and dried between two filter papers to remove any excess solution of the ion-pairing reagent, as reported earlier.^{12,13} The reagent unloaded and treated polyurethane foams were used in batch and flow modes operations.

Recommended extraction procedures

An accurate weight (0.1 ± 0.01 g) of the unloaded or reagent, TMA⁺ClO₄⁻, TBA⁺I⁻ and THA⁺Br⁻ loaded foam cubes separately was equilibrated with 50 mL of an aqueous solution containing gold(III) at a concentration level of 50 mg mL⁻¹. The solutions were then adjusted to the required pH with Britton–Robinson buffer (pH 2.2 – 11.4), and also with acetate buffer (pH 2.2 – 5.7). The test solutions were shaken for 1 h on a mechanical shaker, and the aqueous phase was then separated out by decantation. The amount of gold(III) that remained in the aqueous phase was determined by graphite furnace atomic absorption spectrometry (GF-AAS) at 242.8 nm with a 0.5 nm slit width. The amount of gold(III) retained on the PUFs cubes was determined from the difference between the concentration of the gold(III) solution before (*C*₀) and after (*C*_a) shaking with the foam cubes. The amount of gold(III) retained at equilibrium, *q*_e, the extraction percentage (%*E*) and the distribution ratio (*D*) of the gold(III) uptake on the loaded and unloaded foams were calculated, respectively, employing the following equations:

$$q_e = \frac{(C_0 - C_a) \times V}{W} \quad (1)$$

$$\%E = \frac{(C_0 - C_a)}{C_0} \times 100 \quad (2)$$

$$D = \frac{C_0}{100 - \%E} \times \frac{V \text{ (mL)}}{W \text{ (g)}} \quad (3)$$

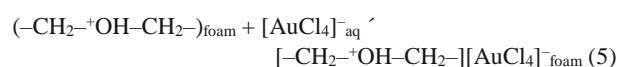
where *V* is the sample volume in mL and *W* is the weight of the reagent foam cubes in grams. Following these procedures, the effect of the shaking time, monovalent cation size (Li⁺, Na⁺, K⁺ and NH₄⁺), solvent polarity, temperature, gold(III) concentration (1.0 ¥ 10⁻⁴ – 20 ¥ 10⁻⁴ mol L⁻¹) and sorbent dose on gold(III) retention was carried out. The %*E* and *D* values are the average of three independent measurements; the precision in most cases was within ±2%.

Results and Discussion

Liquid-solid extraction procedures

The uptake of gold(III) from aqueous media containing acetate buffer is better than that from aqueous media containing B-R buffer. Thus, in subsequent work, the aqueous media containing gold(III) ions was adjusted at pH 3 – 4 in the presence of acetate buffer. The retention of gold(III) onto the unloaded PUFs and PUFs treated THA⁺Br⁻ increased upon increasing the pH of the aqueous solution, and was kept constant between pH 4 – 6, and markedly decreased at a pH of the solution higher than 6 (Fig. 1). This behavior is most likely attributed to an instability or hydrolysis of the produced complex species formed between gold(III) and the reagent immobilized foam of the produced complex ion associate of AuCl₄⁻ with the sorbent site of the THA⁺Br⁻ immobilized PUFs or unloaded PUFs, as reported earlier by El-Shahawi *et al.*^{14,15} and Cordoba *et al.*¹⁶ for HgBr₃⁻ complex species and subsequent hydrolysis. In acidic pH, the observed high retention of gold(III) species by the solid sorbents is most likely attributed to protonation of the chelating sites (ether and/or urethane linkages) in the sorbents that enhanced the retention of the analyte *via* “solvent extraction and/or weak base anion exchange mechanism”. It has been shown that gold(I) and gold(III) can also be extracted by isobutyl methyl ketone and by solvents that possess ether linkages in their structures, *e.g.* diethyl ether, isopropyl ether and polyurethane ether-type foams.^{17–19} A similar retention profile for the extraction of aurocyanide ion-pairs with alkali metal ions into long chain poly ethers has been reported.^{18,19} Based on the obtained results and the data reported earlier,^{17–19} a possible “weak base anion ion exchanger” and a “solvent extraction” mechanism of the [AuCl₄]⁻_{aq} retention onto the protonated ether (–CH₂–HO⁺–CH₂–) oxygen or urethane (–NH₂⁺COO⁻) nitrogen linkages of the immobilized PUFs and unloaded PUFs as a ternary complex ion associate in acidic media most likely proceed, respectively, as follows:

Ether group, PUF:



Urethane group, PUF:

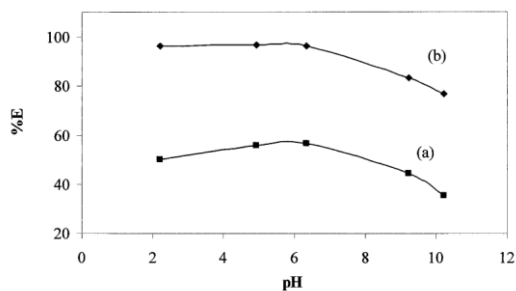
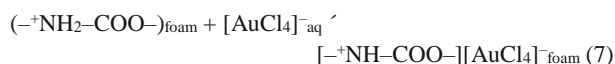
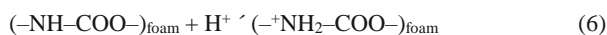


Fig. 1 Effect of pH on the sorption percentage of gold(III) from aqueous solutions onto unloaded (a) and THA⁺Br⁻ (b) immobilized PUFs at 25 ± 0.1 °C.



The pK_a values of the protonated ether oxygen and/or urethane nitrogen ($-^+\text{NH}_2-\text{COO}-$) groups of the solid sorbents PUFs are 3 and 6,^{12,20} respectively. At pH higher than 4 (Fig. 1) the sorption performance of the unloaded PUFs solid sorbent towards AuCl_4^- decreased markedly compared to the THA⁺Br⁻ loaded foams sorbent. This behavior is most likely attributed to deprotonation of the ether oxygen ($-\text{CH}_2-\text{OH}-\text{CH}_2-$) and/or urethane nitrogen ($^+\text{NH}_2-\text{COO}-$) of the unloaded PUFs. Such an effect minimizes the formation of complex ion associate between the anionic complex $[\text{AuCl}_4]_{\text{aq}}^-$ and the protonated unloaded PUFs sorbent. The diffusion of gold(III) as AuCl_4^- through a thin polyurethane film is most likely consistent with its solubility in the PUFs, as reported earlier by Gesser *et al.*²¹ They suggested two alternative mechanisms for the sorption of anionic metal complexes, such as HMCl_4 e.g. HGaCl_4 , by the PUFs. One is based on the close resemblance between sorption and solvent extraction with ether; *i.e.* the PUFs material behaves as a polymeric sorbent for the anionic complex. The other mechanism results from protonation of the ether sites in the polymer when coming into contact with acids in aqueous media; *i.e.* the protonated sites act as anion exchangers in the extraction of HGaCl_4 .²¹

Kinetic behavior of gold(III) sorption onto polyurethane foam sorbents

In batch experiments, the sorption of gold(III) ions onto the unloaded and THA⁺Br⁻ immobilized PUFs sorbents was fast, and equilibrium was attained at a constant value within 60 min of the shaking time. This conclusion was supported by the rate ($t_{1/2} = 1.5 - 2.3$ min) of gold(III) sorption by the unloaded PUFs and THA⁺Br⁻ immobilized PUFs. Thus, gel diffusion is not the only rate-controlling step for both sorbents as in the case of common ion exchange resins.²² Therefore, the kinetic behavior of gold(III) sorption onto the unloaded PUFs and THA⁺Br⁻ immobilized PUFs sorbent depends on the film diffusion and intraparticle diffusion; the more rapid one will control the overall rate of transport. Therefore, the sorbed gold(III) species onto the PUFs sorbent were subjected to Weber–Morris

model:^{23,24}

$$q_t = R_d(t)^{1/2} \quad (8)$$

where R_d is the rate constant of intraparticle transport in mmol g^{-1} and q_t is the sorbed gold(III) concentration (mmol g^{-1}) at

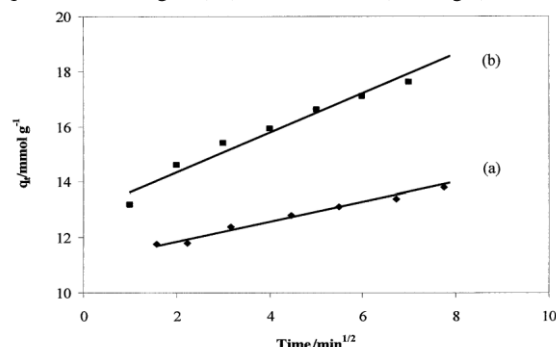


Fig. 2 Weber–Morris plots of the sorbed gold(III) concentration from an aqueous acetate solution versus the shaking time onto unloaded (a) and THA⁺Br⁻ (b) immobilized PUFs at 25 ± 0.1 °C.

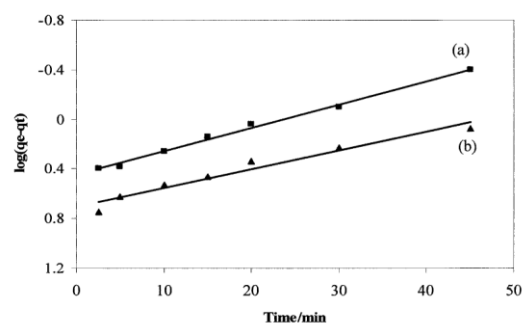


Fig. 3 Lagergren plots of the kinetics of gold(III) sorption from an aqueous acetate solutions onto unloaded (a) and THA⁺Br⁻ (b) immobilized foams at 25 ± 0.1 °C.

time t . The results are shown in Fig. 2. Plots of q_t versus time were found to be linear ($R^2 = 0.975 - 0.980$) in the initial stage for gold(III) retention onto the unloaded- and THA⁺Br⁻ immobilized PUFs sorbents up to 20.3 ± 1.1 min, and deviated upon increasing the shaking time. In the initial stage, the diffusion rate was found to be high, and decreased upon the passage of time, indicating that the rate of the retention step is film diffusion at the early stage of extraction.^{25,26} The values of R_d computed from the two distinct slopes of the Weber–Morris plots for the unloaded PUFs were found to be equal to 0.584 ± 0.01 and 0.34 ± 0.03 mmol g^{-1} , with $R^2 = 0.997$ towards gold(III). In the case of the THA⁺Br⁻ immobilized PUFs (Fig. 3) towards the sorption of AuCl_4^- complex species, the R_d values from the two distinct slope were found to be equal to 1.14 ± 0.04 and 0.64 ± 0.03 $\text{mmol g}^{-1} \text{min}^{-1/2}$, with $R^2 = 0.93 - 0.97$ in the initial stage up to 20.3 min of agitation time, and reduced beyond time longer than 30 min, respectively. The change in the slope for the unloaded PUFs or reagent THA⁺Br⁻ is most likely due to the existence of different pore sizes.^{25,26} The values of R_d indicated that the intraparticle diffusion step can be considered as the rate-controlling step. The lines do not pass through the origin, thus confirming particle film diffusion along with intraparticle diffusion.^{25,26}

Moreover, the rate constant for the retention step of gold(III) onto the tested solid sorbents was also evaluated in light of the Lagergren rate equation:²⁷

$$k_{\text{Lager}}$$

$$\log(q_e - q_t) = \log q_e - \frac{t}{2.303} \quad (9)$$

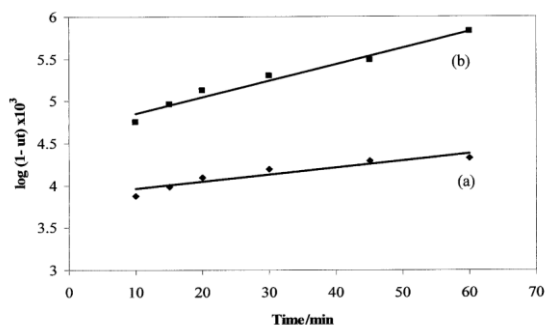


Fig. 4 Bhattacharya–Vénkobachar plots of gold(III) uptake from an aqueous acetate solution onto unloaded (a) and THA⁺Br⁻ (b) immobilized foams at 25 ± 0.1 °C.

where q_e is the amount of gold(III) sorbed at equilibrium, per unite mass of the sorbent (mmol g⁻¹) and k_{Lager} is the first-order overall rate constant for the retention process, s⁻¹ and t = time, s. The plots of $\log(q_e - q_t)$ versus time were found to be linear (Fig. 3) with correlation coefficients (R^2) in the range of 0.95 – 0.99. The values of k_{Lager} calculated from the slopes were found to be 2.49 and 2.07 s⁻¹ for the unloaded PUFs and THA⁺Br⁻ immobilized PUFs towards gold(III) retention. These data suggested first-order kinetics for gold(III) retention towards the two used sorbents. The influence of the adsorbate concentration was investigated, and the results also indicate that the value of k_{Lager} increases upon increasing the adsorbate concentration, thus confirming the formation of a monolayer of gold(III) species onto the surface of the used adsorbent as well as the first-order kinetic nature of the retention processes.²⁷

The results obtained in light of the Lagergren were further confirmed by the Bhattacharya–Vénkobachar kinetic model:²⁸

$$\log_{10}(1 - u_t) = \frac{-k_{Bhatt}}{2.303} t \quad (10)$$

where, $u_t = (C_o - C_t)/(C_o - C_e)$, k_{Bhatt} = over-all rate constant, s⁻¹, t = time, s, C_o = concentration of the metal ion at time t mg L⁻¹, C_e = concentration of gold(III) at equilibrium, mg L⁻¹. Plots of $\log_{10}(1 - u_t)$ versus time for both sorbents are shown in Fig. 4. The values of k_{Bhatt} obtained by this kinetic model at the optimum conditions of gold(III) retention from an aqueous solution (pH 3 – 4) onto the unloaded PUFs and THA⁺Br⁻ treated PUFs were found to be equal to 1.01 ± 0.09 and 2.76 ± 0.1 s⁻¹, respectively. These values are close the data obtained from the Lagergren model, and suggest first-order kinetics for gold(III) retention towards the two used sorbents.

The value of B_t , which is a mathematical function (F) of the ratio of the fraction sorbed (q_t) in mmol g⁻¹ at time t and equilibrium (q_e) in mmol g⁻¹, i.e. $F = q_t/q_e$ calculated for each value of F employing the Reichenburg equation is as follows:²⁹

$$B_t = -0.4977 - 2.303 \log(1 - F) \quad (11)$$

Plots of B_t versus time at 25 °C for both unloaded PUFs and THA⁺Br⁻ sorbents towards gold(III) species were linear up to 40 min (Fig. 5). The straight lines do not pass through the origin, indicating that the particle diffusion mechanism is not solely responsible for the kinetics of AuCl₄⁻ sorption onto the unloaded

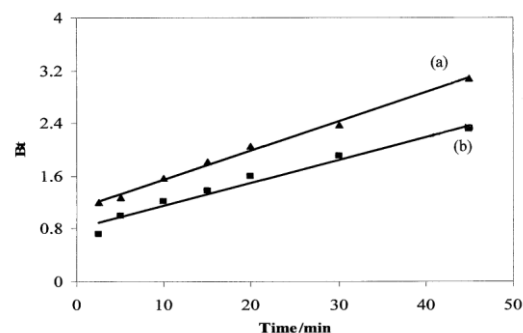


Fig. 5 Reichenburg plots of the kinetics of gold(III) retention from an aqueous acetate solutions onto unloaded (a) and THA⁺Br⁻ (b) impregnated foams at 25 ± 0.1 °C.

PUFs and THA⁺Br⁻ treated PUFs sorbents. Thus, the uptake of AuCl₄⁻ onto the employed sorbents most likely involved three steps: i) bulk transport of AuCl₄⁻ in solution, ii) film transfer involving diffusion of AuCl₄⁻ within the pore volume of unloaded PUFs and THA⁺Br⁻ loaded PUFs and/or along the pore wall surface to the active sorption sites of the sorbent, and finally iii) the formation of a ternary complex ion associate, having the formula $[-CH_2-^+OH-CH_2AuCl_4]^-_{foam}$. Therefore, the actual sorption of AuCl₄⁻ onto the interior surface is rapid, and hence it is not the rate-determining step in the sorption process. Thus, one may conclude that, film and intraparticle transport might be the two main steps that control the sorption step. Thus, “solvent extraction” or a “weak base anion ion exchanger” mechanism is not only the most probable participating mechanisms; most likely, some other processes like specific sites on the PUFs are possibly involved simultaneously in gold(III) retention from the bulk aqueous solution on the tested solid sorbents.^{30–33}

Thermodynamic characteristic of gold(III) retention onto PUFs

The sorption behavior of gold(III) onto unloaded PUFs and THA⁺Br⁻ immobilized PUFs was critically investigated over a wide range of temperature (298 – 353 K) to determine the nature of the retention process of gold(III) by the tested sorbents at pH 3 – 4. The thermodynamic parameters (DH , DS , and DG) of gold(III) uptake onto unloaded PUFs and THA⁺Br⁻ loaded PUFs were evaluated employing the following equations:

$$\ln K_c = \frac{DS}{R} - \frac{DH}{RT} \quad (12)$$

$$DG = DH - TDS \quad (13)$$

$$DG = -RT \ln K_c \quad (14)$$

where DH , DS , DG and T are the enthalpy, entropy, Gibbs free energy changes and temperature in Kelvin, respectively, and R is the gas constant (8.3 j mol⁻¹). K_c is the equilibrium constant depending on the fractional attainment (F_e) of the sorption process. The values of K_c for the retention of gold(III) ions from aqueous media containing NaCl (2% w/v) at equilibrium onto the unloaded PUFs or THA⁺Br⁻ immobilized PUFs were calculated employing:

$$K_c = \frac{F^e}{1 - F_e} \quad (15)$$

The values of the distribution ratio of gold(III) retention onto solid sorbents decreased upon raising temperature of the aqueous media containing gold(III) ions. The plots of the distribution ratio, *i.e.* $\log D$ versus $1/T$ for the gold(III) retention onto the unloaded and reagent immobilized PUFs were linear.

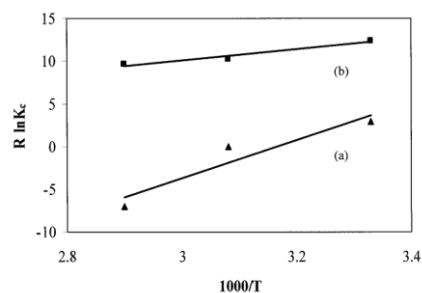


Fig. 6 Plots of the equilibrium constant, $R \ln K_c$ of gold(III) sorption versus $1/T$ (K^{-1}) for gold(III) retention from aqueous acetate solutions onto unloaded (a) and THA^+Br^- (b) immobilized PUFs.

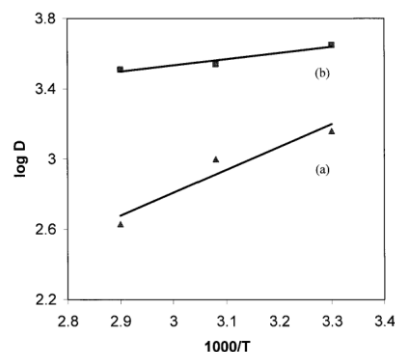


Fig. 7 van't Hoff plots of the distribution ratio ($\log D$) versus $1/T$ (K^{-1}) for gold(III) retention onto unloaded (a) and THA^+Br^- (b) immobilized PUFs.

On the other hand, the value of the equilibrium constant decreased upon increasing the temperature, indicating that the retention process for gold(III) towards the used sorbents is an exothermic reaction. The plots of $\log K_c$ versus $1/T$ (Fig. 6) were linear over the investigated temperature range (300 – 353 K). The numerical values of DH , DS and DG as calculated from the slopes and intercepts of $\log K_c$ versus $1/T$ (Fig. 6) were found to equal $-16.54 \pm 0.1 \text{ kJ mol}^{-1}$, $-9.6 \pm 0.2 \text{ J mol}^{-1} \text{ K}^{-1}$ and $-2.831 \pm 0.05 \text{ kJ mol}^{-1}$ (at 298 K), respectively, for gold(III) sorption onto the unloaded PUFs with a correlation factor of 0.958. On the other hand, the values of DH , DS and DG for gold(III) sorption onto the THA^+Br^- loaded foams are $-22.6 \pm 1.8 \text{ kJ mol}^{-1}$, $-71.4 \pm 2.6 \text{ J mol}^{-1} \text{ K}^{-1}$ and $-2.20 \pm 0.05 \text{ kJ mol}^{-1}$ (at 298 K), respectively, with a correlation factor of 0.976.

Considering the van't Hoff equation, and writing it in terms of the distribution ratio of gold, D , the following expression is obtained:

$$\log D = \frac{-DH}{2.303RT} + C \quad (16)$$

where C is a constant. The plots of $\log D$ versus $1/T$ for gold(III) retention onto the unloaded PUFs and THA^+Br^- loaded PUFs were found to be linear (Fig. 7). The values of DH for gold(III) sorption were then determined from the slopes of the two plots, and were found to equal -18.13 ± 1.5 and $-22.8 \pm 2.1 \text{ kJ mol}^{-1}$ for unloaded and THA^+Br^- loaded PUFs, respectively.

The negative values of DH and the data of D and K_c (Fig. 7) reflected the exothermic behavior of gold(III) uptake by the tested solid sorbents and non-electrostatics bond formation between the adsorbent and the adsorbate. Similarly, the negative values of DS may be indicative of the moderated sorption step of the gold(III) complex ion associate and the ordering of ionic charges without a

compensatory disordering of the sorbed ion associate onto the used sorbents. The negative value of DS of gold(III) sorption indicates that the freedom of motion of gold(III) is more restricted in the foam membrane than in solution. Since the sorption process involves a decrease in the free energy, the DH is expected to also be negative, which was confirmed by the obtained data. Furthermore, as the temperature increases, the physical structure of the membrane may change, which can affect the strength of the intermolecular interactions between the foam membrane and the gold(III) ions. For example, higher temperatures may cause the membrane matrix to become more unstructured, and affect the ability of the polar segments to engage in stable hydrogen bonding with gold(III) ions, which would result in a lower extraction. The negative values of DG at 298 K indicate the spontaneous and physico sorption nature of retention onto PUF. The increase in the DG value with temperature may be due to the spontaneous nature of sorption, and is more favorable at low temperature, thus confirming the exothermic sorption process.

The energy of the urethane nitrogen and/or ether-oxygen sites of the PUFs provided by raising the temperature minimized the possible interactions between the active sites of the PUFs and the complex ion associates of gold(III) ion, resulting a lower sorption percentage of the analyte. Thus, a dual-mode sorption mechanism involves both absorption related to "solvent extraction" and an added component for "surface adsorption", which seems to be a more probable model for gold(III) uptake. These results suggest the use of the reagent loaded foam in flow and pulsating modes for quantitative collection and chemical speciation of gold. The sequential determination of gold(I) and gold(III) after oxidation of the former species with a suitable oxidizing agent to gold(III) could be possible.

Interference study

The effect of some diverse ions relevant to waste water such as alkali and alkaline earth metals (e.g. Cu^{2+} , Hg^{2+} , Pb^{2+} , Bi^{3+} , Co^{2+} , Zn^{2+} , Mn^{2+} , Na^+ , K^+ , Cl^- , SO_4^{2-} , AsO_2^{2-} , SO_4^{2-} , and PO_4^{3-} ions) on the preconcentration of gold(III) ions at 5 mg mL⁻¹ concentration level from the aqueous (100 mL) at pH 4 by the developed reagent loaded PUFs was investigated. The tolerance limits (w/w) less than $\pm 3\%$ change in the percentage uptake of gold ions was taken as being free from interference. The data revealed that the presence of large amounts of foreign ions in the sample had no significant effect on the preconcentration of gold(III) species ($>97 \pm 2\%$). The influence of some other bulky anions, e.g. CrO_4^{2-} , MoO_4^{2-} and PdCl_4^{2-} (10 mg mL⁻¹), on the uptake of gold(III) at 5 mg mL⁻¹ from the aqueous solution at pH 4 by the reagent THA^+Br^- immobilized PUFs sorbents was also investigated. The results revealed complete retention of gold(III) species, and also the retention of a reasonable percentage (25 – 38%) of the other anions under the employed experimental conditions.

Analytical performance

The validation of the developed procedures was successfully used for the removal of gold(III) spiked to wastewater samples at a total concentration of 10 mg mL⁻¹ levels, as follows. The water samples were first acidified with nitric acid (1.0 mol L⁻¹) and filtered through a 0.45 mm cellulose membrane filter. Complete retention of gold(III) was achieved. A satisfactory recovery percentage (95.8 ± 2.1) of gold(III) was achieved, thus confirming the good performance of the developed procedures, and independence from matrix effects.

Conclusion

The use of polyurethane foam solid sorbents for the preconcentration/separation procedures of gold(III) or gold(I) after its oxidation to trivalent gold is able to minimize the limitations related to sensitivity and selectivity for gold determination in different kinds of samples. The kinetic data confirmed the intraparticle diffusion and the first-order model for the retention step. The membrane-like structure of the PUFs is superior compared to other known rigid or granular solid sorbents, and permits rapid separation at a relatively high flow rate. The developed method could be extended for further applications on column-packed PUFs for simple, reliable and low-cost procedures for the quantitative collection and chemical speciation of gold(I) and (III) on-site analysis by graphite furnace-atomic absorption spectrometer or other analytical techniques. Work is continuing to investigate the influence of the most common organic materials present in industrial wastewater samples, competitive complexing agents in addition to the on-line determination of inorganic gold(I) and total inorganic gold(I) and gold(III). The separation of gold(III) from silver(I) and other base metal ions by the developed solid sorbent on a packed-column mode, followed by subsequent onsite analysis by a proper analytical technique will be considered.

References

1. E. Merin, M. Anke, M. Ihnat, and M. Stoeppler, "Elements and Their Compounds in the Environment, Occurrence, Analysis and Biological Relevance", 2nd ed., **2004**, Wiley-VCH Verlag GmbH & KGaA, Weinheim.
2. K. Harold, W. L. Newman, and R. P. Ashley, "Gold", **1996**, U. S. Government Printing Office, 2.
3. J. Medved, M. Bujdos, P. Natus, and J. Kubova, *Anal. Bioanal. Chem.*, **2004**, 379, 60.
4. M. Bagheri, M. H. Mashhadizadeh, and S. Razee, *Talanta*, **2003**, 60, 839.
5. M. Imamoglu, A. O. Aydin, and M. S. Dundar, *Central Eur. J. Chem.*, **2005**, 3, 252.
6. J. Medved, P. Matus, M. Bujdos, and J. Kubova, *Chemical Papers-Chemicke Zvesti*, **2006**, 60, 27.
7. L. Morales and M. I. Toral, *Miner. Eng.*, **2007**, 20, 802.
8. H. B. Senturk, A. Gundogdu, V. N. Bulut, C. Duran, M. S. L. Elci, and M. Tufekci, *J. Hazardous Mater.*, **2007**, 149, 317.
9. M. Konebná and J. Komárek, *Spectrochim. Acta, Part B*,
10. M. S. El-Shahawi, A. S. Bashammakh, and S. O Bahaffi, *Talanta*, **2007**, 72, 1494.
11. A. B. Farag, M. H. Soliman, O. S. Abdel-Rasoul, and M. S. El-Shahawi, *Anal. Chim. Acta*, **2007**, 601, 218.
12. T. Braun, J. D. Navratil, and A. B. Farag, "Polyurethane Foam Sorbents in Separation Science", **1985**, CRC Press, Boca Raton.
13. S. Palagyi, T. Braun, Z. B. Alfassi, and C. M. Wai, in "Preconcentration Techniques for Trace Elements", **1992**, CRC Press, Boca Raton.
14. M. S. El-Shahawi and H. A. Nassif, *Anal. Chim. Acta*, **2003**, 481, 29.
15. M. S. El-Shahawi and M. A. El-Sonbati, *Talanta*, **2005**, 67, 806.
16. M. H. Cordoba, P. N. Navarro, and I. L. Garcia, *Int. J. Environ. Anal. Chem.*, **1988**, 32, 97.
17. K. Rzeszutek and A. Chow, *J. Membr. Sci.*, **2001**, 181, 265.
18. M. H. Mashhadizadeh, R. Mohyaddini, and M. Skamsipur, *Sep. Purif. Technol.*, **2004**, 39, 161.
19. M. Bagheri, M. H. Mashhadizadeh, and S. Razee, *Talanta*, **2003**, 60, 839.
20. G. J. Moody and J. D. R. Thomas, "Chromatographic Separation with Foamed Plastics and Rubbers", **1982**, Dekker, New York.
21. H. D. Gesser and G. A. Horsfall, *J. Chim. Phys.*, **1977**, 74, 1072.
22. S. Palagyi, T. Braun, Z. Homonnay, and A. Vertes, *Analyst*, **1992**, 117, 1537.
23. W. J. Weber Jr and J. C. Morris, *J. Sanit. Eng. Div. Am. Soc. Civ. Eng.*, **1963**, 89 (SA2), 31.
24. W. J. Weber Jr and J. C. Morris, *J. Sanit. Eng. Div. Am. Soc. Civ. Eng.*, **1964**, 90 (SA3), 70.
25. M. M. Saeed and A. Rusheed, *Radiochim. Acta*, **2002**, 90(1), 35.
26. S. L. C. Ferreira, H. C. dos Santos, and M. S. Fernandes, *J. Anal. At. Spectrom.*, **2002**, 17, 115.
27. S. Lagergren and B. K. Sven, *Vatenskapsakad. Handl.*, **1898**, 24.
28. A. K. Bhattacharya and C. Vènkobachar, *J. Gviron. Eng.*, **1984**, 110, 110.
29. D. Reichenburg, *J. Am. Chem. Soc.*, **1972**, 75, 589.
30. P. R. Haddad and N. E. Rochester, *J. Chromatogr.*, **1988**, 439, 23.
31. S. Xu, L. Sun, and Z. Fang, *Anal. Chim. Acta*, **1991**, 245, 7.
32. P. Di and D. E. Davey, *Talanta*, **1994**, 41, 565.
33. S. Zhi-Xing, P. Qiao-Sheng, L. Xing-Yin, C. Xi-Jun, Z. Guang-Yao, and R. Feng-Zhi, *Talanta*, **1995**, 42, 1127.



Sorption profile and chromatographic separation of uranium (VI) ions from aqueous solutions onto date pits solid sorbent

E.M. Saad^a, R.A. Mansour^b, A. El-Asmy^b, M.S. El-Shahawi^{c,*}

^a Chemistry Department, Faculty of Education at Suez, Suez Canal University, Egypt ^b Chemistry Department, Faculty of Science, Mansoura University, Mansoura, Egypt ^c Chemistry Department, Faculty of Science, King Abdulaziz University, Jeddah, P.O. Box 80203, Jeddah 21589, Saudi Arabia

article

info

abstract

Article history:

Received 15 January 2008
Received in revised form 30 April 2008
Accepted 30 April 2008 Available
online 15 May 2008

Keywords:

Uranium (VI)
Retention
Date pits
Separation
Wastewater

The retention profile of uranium (VI) as uranyl ions (UO_2^{2+}) from the aqueous media onto the solid sorbent date pits has been investigated. The sorption of UO_2^{2+} ions onto the date pits was achieved quantitatively ($98 \pm 3.4\%$, $n=5$) after 15 min of shaking at pH 6–7. The sorption of UO_2^{2+} onto the used sorbent was found fast, followed by a first order rate equation with an overall rate constant, k of $4.8 \pm 0.05 \text{ s}^{-1}$. The sorption data were explained in a manner consistent with a “solvent extraction” mechanism. The sorption data were also subjected to Freundlich isotherm model over a wide range of equilibrium concentration ($1\text{--}20 \text{ mg L}^{-1}$) of UO_2^{2+} . The results revealed that, a “dual-mode” of sorption mechanism involving absorption related to “solvent extraction” and an added component for “surface adsorption” is most likely operated simultaneously for uranyl ions uptaking the solid sorbent. The thermodynamic parameters ($-H$, S and G) of the uranyl ions uptake onto the date pits indicated that, the process is endothermic and proceeds spontaneously. The interference of some diverse ions on the sorption UO_2^{2+} from the aqueous media onto the date pits packed column was critically investigated and the data revealed quantitative collection of UO_2^{2+} at 5 mL min^{-1} flow rate. The retained UO_2^{2+} was recovered quantitatively with HCl (3.0 mol L^{-1}) from the column at 5 mL min^{-1} flow rate. The mode of binding of the date pits with UO_2^{2+} was determined from the IR spectral date pits before and after extraction of uranium (VI). The height equivalent (HETP) and the number (N) of theoretical plates of the date pits packed column were determined from the chromatograms. Complete retention and recovery of UO_2^{2+} spiked to wastewater samples by the date pits packed column was successfully achieved. The capacity of the used sorbent towards retention of uranium (VI) from aqueous solutions was much better than the most common sorbents.

Crown Copyright © 2008 Published by Elsevier B.V. All rights reserved.

1. Introduction

elements [3,4]. Low cost and effective biological materials as algae have been also used for the removal of heavy metals in different matrices [8–13].

During the last decade, considerable effort has been directed towards the development of low cost extractive chromatographic resins applicable for the separation and pre-concentration of actinide ions and selected fission products from biodegradable, environmental and nuclear waste samples for subsequent determination [1,2]. Pollution with radioactive elements has been a matter of great concern for the last decades for human health and animals [3–7]. Uranium is one of the most radioactive elements affecting the environment. Therefore, recent years have seen an upsurge of interest in controlling environmental pollution from radioactive

Solid phase extraction (SPE) has been increasingly used for pre-concentration/separation of trace and ultra trace amounts of inorganic and organic species from complex matrices as seen from recent reviews [14–16]. Various researchers have highlighted the advantages of SPE over liquid–liquid extraction most, e.g. AmberliteXAD [14–17], silica [18], octadecyl silica membrane discs [19,20], activated silica gel [21], controlled pore glass [22], polyurethane foam [5–7,23] and cationic or anionic exchange resins [24–31] have been used in batch and flow modes of SPE for the enrichment of UO_2^{2+} from wastewaters and dilute solutions prior determination.

A potential usefulness of date pits as an inexpensive solid sorbent for a number of metal ions has been demonstrated earlier [32]. The uranyl (II) ions are able to form stable complexes with amino acids, hydroxyl and carboxyl

* Corresponding author. Permanent address: Department of Chemistry, Faculty of Science at groups available in the date

Damietta, Mansoura University, Mansoura, Egypt.

E-mail addresses: mohammad_elshahawi@yahoo.co.uk, mohammad elshahawi@hotmail.com (M.S. El-Shahawi).

0039-9140/\$ – see front matter. Crown Copyright © 2008 Published by Elsevier B.V. All rights reserved.

doi:10.1016/j.talanta.2008.04.065

pits [31–38]. Therefore, the present paper reports the salient features of our findings regarding the available function groups, e.g. amino, hydroxyl and carboxyl groups on the date pits and the retention profile of UO_2^{2+} onto this solid sorbent as an effective and low cost solid extractor for the removal and/or minimization of uranyl (II) species from aqueous and wastewater samples. The kinetics, isotherm and thermodynamic characteristics of uranyl ions sorption from the aqueous media onto the date pits will be discussed. Moreover, the most probable retention mechanism of UO_2^{2+} retention onto the used date pits will also be discussed.

2. Experimental

2.1. Apparatus

The electronic spectra and the absorbance measurements of the uranyl ions with arsenazo III [39] were recorded using computercontrolled double beam UV–vis spectrophotometer UV-2401 PC (Shimadzu, Japan) with quartz cell (10mm). The IR spectra were recorded using Mattson (model 5000, MA, USA) FTIR infrared spectrophotometer. The pH values were measured using a pH-meter (Hanna-Instruments 8519, Italy) calibrated against standard buffer solutions (pH 4.0 and 9.2) with absolute accuracy limits at the pH measurements being defined by NIST buffers. Glass columns (18cm×15mm i.d.) and a variable mechanical Shaker (Corporation Precision Scientific, Chicago, USA) with a shaking rate in the range of 10–250rpm were used for the retention experiments of uranium (VI) species at different pH.

2.2. Reagents and materials

The date palm cultivars grown in El-Qassim region, Saudi Arabia, were collected and washed with distilled water to be completely free from dirt and inherent pulp, dried in at 150 °C for 3h and finally crushed to give a dark brown powder (mesh, 5mm). The chemical analyses of the date palm cultivars used in this investigation are summarized in Table 1.

Analytical reagent grade chemicals of metal ions as chlorides and/or nitrates and solvents (BDH, USA) were used. A stock solution of UO_2^{2+} (1000gmL⁻¹) was prepared by dissolving an appropriate amount of uranyl acetate dehydrate (Fluka Chemie AG, Buchs, Switzerland) in double-distilled water. Stock solutions (1000gmL⁻¹) of the metal ions (as chloride or nitrate salts) were prepared in double-distilled water. Arsenazo III (0.1%, w/v) (Fluka Chemie AG) was prepared in ethanol and completed with water. A series of Britton–Robinson buffer solutions of pH 1.8–12.2 were prepared by mixing equimolar

concentrations (0.4molL⁻¹) of the acid mixture: boric, acetic and phosphoric acids in double-distilled water and adjusting the pH of the solution to the required value with NaOH [40]. The other reagents used were of analytical reagent grade.

Table 1

Chemical analysis of date pits from three different locations in Saudi Arabia

Analysis	Component (%)		
	Fard	Khalas	Lulu
Moisture	10.3	7.1	9.9
Crude fat	9.9	13.2	10.5
Crude protein	5.7	6.0	5.2
Ash	1.4	1.8	1.0
Acid detergent fiber	45.6	50.6	49.3
Natural detergent fiber	61.5	64.5	68.8

2.3. Recommended batch procedures

In a low density polyethylene (LDPE) sample bottles, an accurate weight (0.2±0.002g) of the date pits solid sorbent was shaken with an aqueous solution (50mL) at different pH (1.8–12.6) containing uranium (VI) at concentration level of 10gmL⁻¹ UO_2^{2+} for 15min at 25±1 °C. After equilibrium, the amount of UO_2^{2+} ions retained on the solid sorbent was determined from the difference between the absorbance of the uranyl (II) ions–arsenazo III complex before (C_0) and after (C_a) shaking with the date pits sorbent. The sorption percentage (%E) and the distribution ratio (D) were then determined employing the equations: thermostat mechanical shaker,

$$\%E = \left[\frac{C_b - C_a}{C_b} \right] \cdot 100 \quad (1)$$

$$D(\text{mLg}^{-1}) = \frac{\%E}{100 - \%E} \cdot \frac{V}{W} \quad (2)$$

where V and W are the sample volume (mL) and weight of the dried date pits in grams. Following these procedures, the effect of different parameters, e.g. shaking time, temperature (5–60 °C), sorbent doze and UO_2^{2+} concentration on the retention of UO_2^{2+} was carried out. The data are the average of three independent measurements and the precision in most cases was ±2%.

2.4. Column experiment

An aqueous solution of wastewater sample (100mL) spiked with UO_2^{2+} ions (10mgL^{-1}) was percolated through the date pits (2.0g) packed column at a flow rate of 2mLmin^{-1} . Under the same conditions, a blank experiment was also carried out in the absence of UO_2^{2+} ions. Sorption of UO_2^{2+} on the date pits took place as proved from the analysis of uranyl ion in the effluent solution. Elution of the uranyl ion from the date pits packed column was then achieved quantitatively by passing 20mL of HCl (3.0molL^{-1}) at 2mLmin^{-1} flow rate. Equal fractions of the eluate were collected and analyzed spectrophotometrically for uranyl (II) ions. The same procedures were also applied in the blank experiment. The HETP, N and breakthrough capacity were then calculated from the output of the chromatograms.

2.5. Separation and recovery of uranyl ions from various water samples

An aqueous solution of tap or industrial wastewater samples (0.1L) spiked with uranyl ions at a total concentration $\leq 10\text{mgL}^{-1}$ was first filtered through 0.45m cellulose membrane filters and stored in LDPE sample bottles (200mL). The test solution at the optimum experimental conditions of uranyl ions sorption described above was percolated through the date pits ($1.0\pm 0.01\text{g}$) packed columns at 5mLmin^{-1} flow rate using the vacuum method of offpacking [41]. Complete sorption of uranyl ions was achieved quantitatively as indicated from the analysis of uranium (VI) in the effluent solution by the method reported earlier [39]. Complete recovery of the retained uranyl ions was achieved by percolation on aqueous solution of HCl (20mL, 3.0molL^{-1}) at 5mLmin^{-1} flow rate.

3. Results and discussion

3.1. Retention profile of UO_2^{2+} sorption

The pH medium is one of the most important factors that commonly controls and strongly influence the retention of the metal ions by the solid sorbent. The data of the UO_2^{2+} sorption by the date pits from the aqueous solution at different pH are summarized in

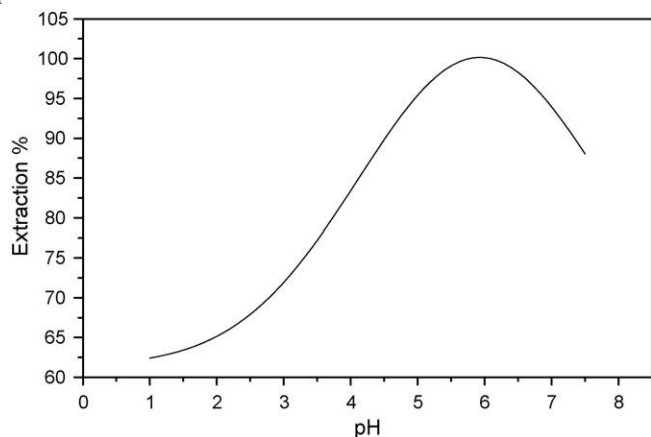


Fig. 1. Influence of the pH of aqueous solution on the uptake (%) of UO_2^{2+} from the aqueous solutions onto the date pits solid sorbent.

Fig. 1. The data revealed that, the uptake of uranyl (II) ions is low at acidic $\text{pH}\leq 5$. The protonation of the available active sites (amino acids, hydroxyl and carboxyl groups) in the date pits most likely inhibit their binding towards the uranyl (II) ions as reported earlier by El-Shahawi et al. [5–7] for the solid sorbent polyurethane foams thus lowering the UO_2^{2+} ions uptake from the aqueous media. The pK_a values of the protonation of the available active sites in the date

pits [42,43] may account for the observed trend (Fig. 1). At $\text{pH} 5.5\text{--}6.5$ range (Fig. 1), the sorption performance of the date pits towards uranyl (II) ions reached maximum (99.7%) and leveled off at pH higher than $\text{pH} 7.5$ (Fig. 1). This behavior is most likely attributed to the instability of the uranyl (II) complexes with the active sites of the date pits sorbent and/or hydrolysis of the produced uranyl (II) complexes with the active sites of the date pits. The diffusion of the uranyl (II) ions through the date pits film is most likely consistent with its solubility in the solid sorbent as reported earlier [32]. Therefore, in the subsequent work, the sorption experiments of uranyl (II) ions by the date pits sorbent were carried out at $\text{pH} 5.5\text{--}6.5$.

The influence of shaking times on the extraction percentage of UO_2^{2+} ions from the aqueous solution of $\text{pH} 5.5\text{--}7$ by the date pits was critically studied. The extraction was fast and the equilibrium reached maximum within 15min of shaking time (Fig. 2) and remains constant. The half-life ($t_{1/2}$) time of the equilibrium sorption of uranyl (II) ions onto the solid sorbent was fast. The value of $t_{1/2}$ calculated from the plots of $-\log(A_b - A_s)/A_b$ was found to

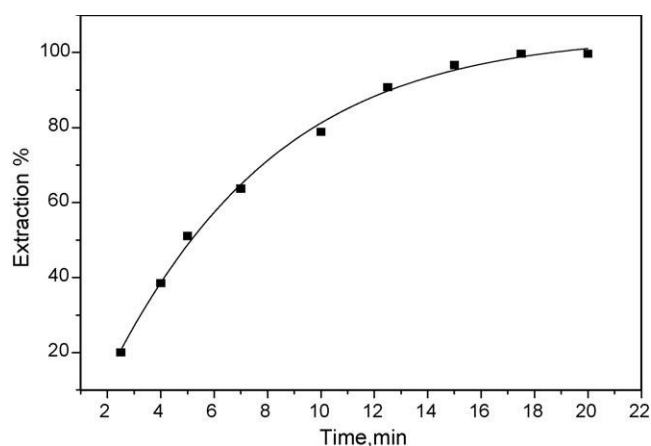


Fig. 2. Effect of shaking time on the retention (%) of UO_2^{2+} from the aqueous solution of $\text{pH} 6\text{--}7$ onto the date pits.

be $1.71\pm 0.02\text{min}$, respectively. Thus, gel diffusion is not the rate controlling step for the solid sorbent as in the case of common ion exchange resins [5,6]. Thus, a 15-min shaking time was adopted in the subsequent experiments.

The effect of the sorbent dose (0.05–0.50g) on the sorption of UO_2^{2+} at $\text{pH} 6.5$ was examined. The uranyl (II) ions sorption increased on increasing the sorbent dose and maximum sorption was achieved at sorbent dose 0.1–0.3g. Therefore, in the subsequent work, a 0.2-g of the solid sorbent was employed. The sorption percentage of uranyl (II) onto the date pits sorbent decreased up to $60\pm 3.5\%$ on increasing the sample volume to 200.0mL.

3.2. Kinetics of UO_2^{2+} uptake onto date pit

The kinetics of UO_2^{2+} sorption onto the date pits was subjected to Lagergren model [43]. The rate constant for the retention step was evaluated in the light of

the Lagergren rate equation [43]:

$$\log(q_e - q_t) = \log q_e - \left(\frac{kt}{2.303} \right) \quad (3)$$

where q_e and q_t are the sorbed concentration of UO_2^{2+} onto date pits at equilibrium and at time t , respectively and k is the overall rate constant. The plot of $\log(q_e - q_t)$ versus time was found linear (Fig. 3) with an overall rate constant of $4.8\pm 0.05\text{s}^{-1}$. The value of k confirmed a first order kinetics for the uranyl (II) ions retention towards the used sorbent. The influence of different sorbent dose

and adsorbate concentration was investigated. The results also indicate that, the value of k increases on increasing the sorbent dose and adsorbate concentration confirming the formation of monolayer of uranyl (II) species onto the surface of the used adsorbent as well as the first order kinetic nature of the process.

The retention of uranyl (II) ions sorption onto the date pits depends on film diffusion and intraparticle diffusion, and the more rapid one will control the overall rate of transport. Thus, the concentration of the sorbed UO_2^{2+} , q_t (mg g^{-1}) was plotted against time applying the Weber–Morris equation [44]:

$$q_t = R_d(t)^{1/2} \quad (4)$$

where R_d is the rate constant of intraparticle transport in $\text{mg g}^{-1} \text{min}^{1/2}$. The diffusion rate was found high in the initial stages and decreased on passage of time up to 18 min, indicating that the rate of the retention step is film diffusion at the early stage

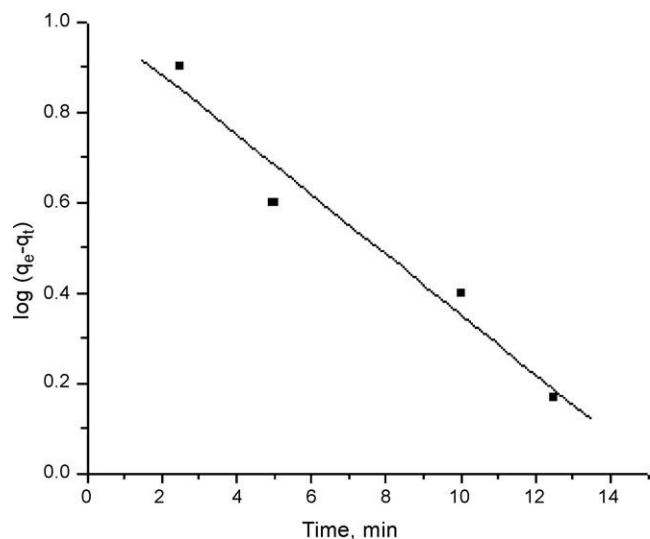


Fig. 3. Plot of $\log(q_e - q_t)$ versus time (min) for the sorbed UO_2^{2+} from the aqueous solution of pH 6–7 onto the date pits at room temperature.

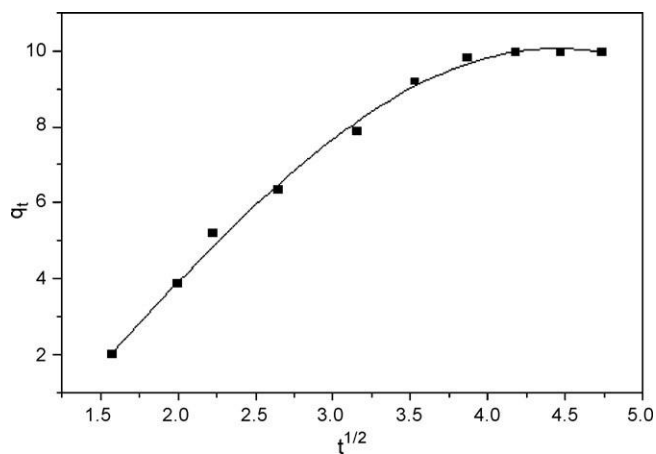


Fig. 4. Weber–Morris plot of sorbed concentration of UO_2^{2+} at 5.0 gmL^{-1} from the aqueous solution of pH 6–7 versus square root of time onto date pits at room temperature.

of extraction. The value of R_d calculated from the slope of the linear plot of q_t versus square root of time (Fig. 4) was found to be $3.8 \text{ mg g}^{-1} \text{ min}^{1/2}$. The values of R_d indicated that intraparticle diffusion step could be a rate-controlling step. The change in the slope may be due to the existence of different pore size [45]. This behavior was also

confirmed from the linear plot of Bt versus time employing Reichenburg equation [46]:

$$Bt = -0.4977 - 2.303 \log(1 - F) \quad (5)$$

where Bt is a mathematical function (F) of q/q_e . The plot was linear up to 12.5 min and does not pass through the origin.

3.3. Thermodynamic studies

The influence of temperature on the UO_2^{2+} retention onto the date pits was investigated in the temperature range of 5–60 °C at pH 6–7 and shaking time of 15 min. The uptake of UO_2^{2+} ions by the date pits increases on raising the temperature up to 25 °C and remains more or less constant confirming the endothermic nature of the retention step. A clear pronounced thermal stability of UO_2^{2+} uptake was also noticed at temperature higher than 25 °C. Thus, in the subsequent work, all experiments were carried out at room temperature. At this temperature, the thermodynamic parameters (H , S , and G) of the uranyl (II) ions sorption from the aqueous media at pH 6–7 onto the date pits were calculated employing the equations:

$$\log K_c = - \frac{H}{2.303RT} + \frac{S}{2.303R} \quad (6)$$

$$G = -RT \log K_c \quad (7)$$

$$G = H - TS \quad (8)$$

The plot of K_c versus $1/T$ (Fig. 5) was linear over the temperature range of 278–293 K. The values of H , S , and G calculated from the slope and intercept of Fig. 6 were found equal to -63.18 J , $27.43 \text{ J mol}^{-1} \text{ K}^{-1}$ and $-3.43 \text{ kJ mol}^{-1}$, respectively. The value of H confirms the exothermic nature of the uranyl uptake. The increase of G with temperature is attributed to the spontaneous nature of the absorption process which is more favorable at low temperature. The data confirm that the compound associate attains the equilibrium within short time suggesting the possible application of the date pits in column operations for the enrichment and separation of UO_2^{2+} species from large sample volume of industrial waste water.

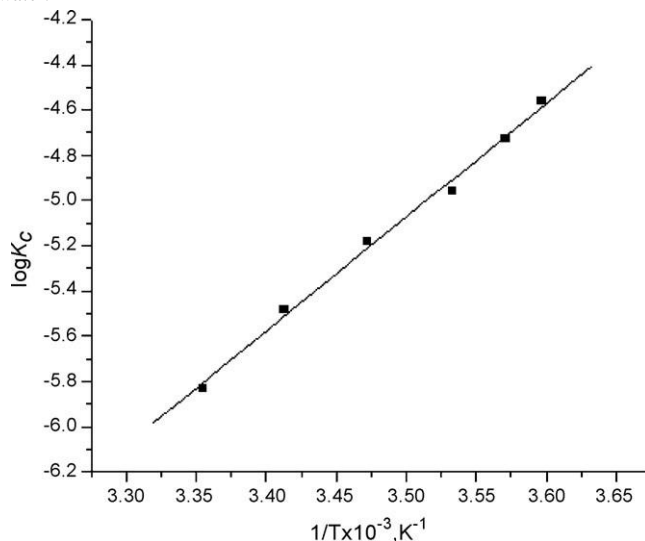


Fig. 5. The plot of equilibrium constant ($\log K_c$) versus $1/T$ of uranyl (II) retention onto the date pits from aqueous solutions of pH 6–7 and 15 min shaking time.

3.4. Sorption isotherms

The uptake of UO_2^{2+} ions from the bulk aqueous solutions at pH 6.5, 15min shaking time and at room temperature onto the date pits was dependent on the initial UO_2^{2+} concentration. Therefore, the sorption profile of UO_2^{2+} was determined over a wide range of equilibrium concentration (1–20 mgL^{-1}). At low and moderate UO_2^{2+} concentrations, the amount of UO_2^{2+} retained onto the solid sorbent varied linearly with that remained in the aqueous solution. Thus, the data was subjected to Freundlich isotherm model [47] over a wide range of equilibrium concentrations. The familiar form of Freundlich [47] isotherm model is expressed in the following linear form:

$$\log C_{\text{ads}} = \log A + \frac{1}{n} \log C_e \quad (9)$$

where A and $1/n$ are Freundlich parameters related to the maximum sorption capacity of solute (mgg^{-1}), C_{ads} is the concentration of the retained uranyl (II) ions onto the date pits per unit mass (mgg^{-1}) at

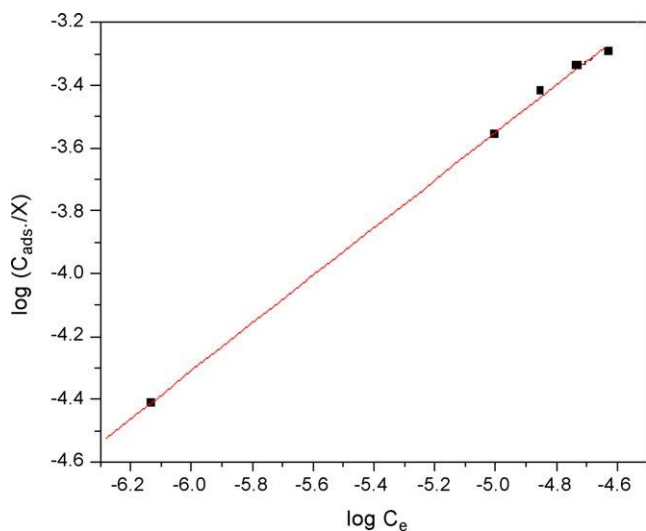


Fig. 6. Freundlich sorption isotherm of uranyl (II) sorption from the aqueous solutions of pH 6–7 onto the date pits at pH 6–7 at room temperature after 15 min shaking time.

equilibrium and C_e is the concentration of UO_2^{2+} left in the aqueous solution (mgL^{-1}). The plot of $\log C_{\text{ads}}$ versus $\log C_e$ (Fig. 6) was found linear ($R^2=0.96–0.97$) over the entire concentration range of uranyl ions indicating a better fit for the experimental data. The values of the Freundlich constants A and $1/n$ computed from the intercepts and slopes of the plots of uranyl (II) ions sorption onto the date pits were found to be $0.6 \pm 0.07 \text{ mgg}^{-1}$ and 0.31 ± 0.01 , respectively. The values of $1/n < 1$ indicated that, the favorable sorption of uranyl ions from the aqueous onto the tested solids sorbent. The value of $1/n (< 1)$ revealed that, the retention capacity is slightly reduced at lower equilibrium concentration and the isotherm does not predict any saturation of the solid surface of the sorbent by the sorbate. Thus, infinite surface coverage is predicted mathematically and physisorption on the surface is expected [37]. The retention capacity of the date pits towards uranyl (II) ions from the aqueous solution was found equal to 10 mgg^{-1} .

3.5. Effect of foreign ions

The influence of a relatively high excess (1mg) of some diverse ions relevant to waste water, e.g. alkali and alkaline earth metals Cu^{2+} , Hg^{2+} , Pb^{2+} , Bi^{3+} , Co^{2+} , Zn^{2+} , Mn^{2+} , Na^+ , K^+ , Cl^- , SO_4^{2-} , AsO_2^{2-} , SO_4^{2-} , and PO_4^{3-} ions on the pre-concentration of uranyl ions at 5 mgL^{-1} uranium (VI) concentration level from the aqueous (50mL) at pH 5–6 by developed date pits was investigated. The tolerance limits (w/w) less than $\pm 3\%$ change in the percentage uptake of uranyl ions was taken as free from interference. The data revealed that, the presence of large amounts of foreign ions in the sample has no significant effect on the pre-

concentration of analyte ($> 98 \pm 2\%$). Thorium (IV) interfered seriously even at 1:1 molar ratio and the uptake of UO_2^{2+} (5 mgL^{-1}) by date pits decreased to 88–90%.

3.6. IR spectral studies

The IR spectrum of the UO_2^{2+} sorbed species was compared with the IR spectrum of date pits alone. The observed shift of some bands in the IR spectra to lower and/or higher wave numbers as well as the appearance of new bands in the low frequency region (600–200 cm^{-1}) are most likely corresponding to the participation of the oxygen and/or nitrogen of the amino acids of the date pits in the complex formation with the uranyl (II) ions [48]. The observed strong band at 935–940 cm^{-1} and the medium intensity band at 6830–835 cm^{-1} are most likely assigned to $\nu_{\text{as}}(\text{O U O})$ and $\nu_{\text{s}}(\text{O U O})$ [48], respectively.

3.7. Chromatographic behavior of uranyl ion on date pits

The kinetics and the sorption data and the available active sites of the date pits towards uranyl (II) in aqueous solutions suggested the use of the sorbent in flow mode. Percolation of an aqueous solution (0.1L) of de-ionized water contained uranyl (II) ions at concentration $\leq 10 \text{ gAumL}^{-1}$ at 2 mLmin^{-1} flow rate. Analysis of uranyl (II) species in the effluent solution against the reagent blank under the same experimental conditions revealed complete sorption of UO_2^{2+} by the date pits packed columns. A series of eluting agents, e.g. HClO_4 (1.0 molL^{-1}), H_2SO_4 (1.0 molL^{-1}) and HCl (1.0 molL^{-1}) was investigated to recover uranyl (II) species from the date pits packed column. Among these reagents, HCl (1 molL^{-1}) was found the most suitable eluting agent. Therefore, the influence of HCl concentration (0.5–5.0 molL^{-1}) on the recovery of uranyl (II) ions from the date pits packed column was critically investigated at 2–3.0 mLmin^{-1} . The results revealed that, the use of HCl at 3.0 molL^{-1} concentrations or higher are suitable as proper eluting agent for complete recovery (97–101 $\pm 2\%$) of uranyl (II) ions from the date pits at 2–3 mLmin^{-1} .

Good recovery of uranyl (II) ions was achieved employing HCl . The retained

species were recovered quantitatively (97–101%) employing HCl as indicated from the analysis of uranium (VI) in the eluate [31]. The performance of the date pits packed column is generally described quantitatively by the number (N) and the height equivalent to the theoretical plates (HETP). The chromatogram of the plot of the volume of the HCl (1.0 molL^{-1}) as eluting agent (12 mL , $6 \times 2 \text{ mL}$) at 2 mLmin^{-1} versus the percent uranyl (II) recovered was used to calculate the column performance employing the Glueckauf equation [4,5]:

$$N = \frac{8V_{\text{max}2}}{W_2} = \frac{L}{\text{HETP}} \quad (10)$$

where N is the number of theoretical plates, V_{max} is the volume of eluate to peak maximum, W is the width of the peak at $1/e$ times the maximum solute concentration and L is the length of the date pits bed column in mm. The values of HETP and N were 0.84mm/plate and 71.1 ± 5 , respectively confirming the good performance of the date pits packed column. The utility of the date pits packed column for the recovery of uranyl (II) ion spiked at 5.0 mgL^{-1} to wastewater samples (100mL) was also investigated at 5 mLmin^{-1} flow rate. Complete sorption of uranyl (II) ions took place and the retained uranyl (II) species in the column were then recovered quantitatively (97–102%) with HCl (25 mL , 1.0 molL^{-1}) at 5 mLmin^{-1} flow rate. The results confirmed the good performance of the proposed date pits solid sorbent in flow mode for the separation of uranyl (II) ions in complicated matrices.

3.8. Analytical performance and application of the proposed method

The validation of the developed method was successfully assessed by comparing the capacity of the used sorbent with the most of other sorbents DCQ-naphthalene [26], PAN-benzophenone [27], Q-AmberliteXAD-4 [28], azo-oxime ion exchanger [29] and DAB-AC [37] towards uranium (VI) uptake. The results are summarized in Table 2. The capacity of the used date pits sorbent ($10 \pm 0.02 \text{ mg g}^{-1}$) towards uranium (VI) is much better than the first four solid sorbent and lower than the solid sorbent DAB-AC ($18.35 \pm 0.2 \text{ mg g}^{-1}$). The developed date pits packed column was successfully used for the removal of uranium (VI) spiked to wastewater samples at a total concentration in the range of $6\text{--}10 \text{ mg L}^{-1}$ levels as follows: the water samples were first acidified with nitric acid (1.0 mol L^{-1}) and filtered through a $0.45\text{-}\mu\text{m}$ cellulose membrane filter. The sample solutions were percolated through the date pits packed columns at 5 mL min^{-1} flow rate. Complete retention of uranium (VI) was achieved. The retained uranium (VI) species was then recovered quantitatively from the date pits packed column with HCl (3.0 mol L^{-1}) at flow rate of 5 mL min^{-1} . A satisfactory recovery percentage (95.8 ± 2.1) of uranium (VI) was achieved con-

Table 2

Retention capacities of the investigated date pits and other solid sorbents towards uranyl (II) ions from aqueous media by batch mode^a

SPE material	Retention/binding capacity (mg g^{-1}) of SPE	Reference
DCQ-naphthalene	1.88 ± 0.02	[26]
PAN-benzophenone	2.34 ± 0.01	[27]
Q-AmberliteXAD-4	2.74 ± 0.02	
Azo-oxime ion exchanger	7.14 ± 0.01	[28] [29] [37]
DAB-AC	18.35 ± 0.2	
Date pits	10 ± 0.02	Present work

^aAverage of five measurements \pm standard deviation.

firming the good performance of the developed procedures and its independence from matrix effects.

4. Conclusions

The date pits solid sorbent offers unique advantage in rapid preconcentration and recovery of UO_2^{2+} in dilute aqueous solution at pH 6–7.5 by flow mode of separation. The interaction between date pits and UO_2^{2+} followed the Freundlich adsorption isotherm models. The dual-mode mechanism involving “complex formation of uranyl (II) ions with the active sites of the sorbent” and an added component for “surface adsorption” of uranyl (II) ions retention offers an excellent description of the observed trend. However, work is still continuing for the chemical separation and recovery of UO_2^{2+} in real samples by on line solid phase spectrophotometry in water.

References

- [1] E.P. Horwitz, R. Chiarizia, M.L. Dietz, Solvent Extr. Ion Exch. 10 (1992) 313.
- [2] E.P. Horwitz, R. Chiarizia, M.L. Dietz, React. Funct. Polym. 33 (1997) 25.
- [3] X. Yang, Y. Feng, Z. He, P.J. Stoffella, J. Trace Elem. Med. Biol. 18 (2005) 339.
- [4] T.R. Dulsk, Trace Elemental Analysis of Metals, Methods and Techniques, Marcel Dekker Inc., 1999.
- [5] M.M. Abou-Mesalam, I.M. El-Naggar, M.S. Abdel-Hai, M.S. El-Shahawi, J. Radioanal. Nucl. Chem. 258 (2003) 619.
- [6] M.S. El-Shahawi, M.A. Othman, M.A. Abdel-Fadeel, Anal. Chim. Acta 546 (2005) 221.
- [7] M.S. El-Shahawi, M.A. Othman, H.M. Nassef, M.A. Abdel-Fadeel, Anal. Chim. Acta 536 (2005) 227.
- [8] B. Volesky, Z.R. Holan, Biotechnol. Prog. 11 (1995) 235.
- [9] J. Matheickal, Q. Yu, G. Woodburn, Water Res. 33 (1999) 335.
- [10] P. Vasudevan, V. Padmavathy, N. Tewari, S.J. Dtingra, Sci. Ind. Res. 60 (2001) 112.

- [11] Y. Ho, J. Porter, G. McKay, Water Air Soil Pollut. 141 (2002) 1.
- [12] P. Kaewsarn, S.P. Padina, Chemosphere 47 (2002) 1081.
- [13] T.P. Rao, J.M. Gladis, Rev. Anal. Chem. 20 (2001) 145.
- [14] T.P. Rao, C.R. Precetha, Sep. Purif. Rev. 32 (2003) 1.
- [15] P. Metilda, K. Sanghamitra, J.M. Gladis, G.R.K. Naidu, T.P. Rao, Talanta 65 (2005) 192, and references cited in.
- [16] F.A. Aydin, M. Soyak, Talanta 72 (2007) 187.
- [17] M.S. Carvalho, M.F. Domingues, J.L. Mantovano, E.Q.S. Filho, Spectrochim. Acta B 53 (1998) 1945.
- [18] M.L. Dietz, E.P. Horwitz, L.R. Sajdak, R. Chiarizia, Talanta 54 (2001) 1173.
- [19] N.L. Misra, S. Dhara, K.D.S. Mudher, Spectrochim. Acta B 61 (2006) 1169.
- [20] M. Merdivan, M.Z. Duz, C. Hamamci, Talanta 55 (2001) 639.
- [21] J.M. Gladis, T.P. Rao, Anal. Bioanal. Chem. 373 (2002) 867.
- [22] S. Hirata, Y. Ishida, M. Aihara, K. Honda, O. Shikino, Anal. Chim. Acta 438 (2001) 205.
- [23] M. Shamsipur, Y. Yamini, P. Shtari, A. Khanchi, M. Ghannadi, Sep. Sci. Technol. 35 (2002) 1011.
- [24] M. Shamsipur, A.R. Ghiasvand, Y. Yamini, Anal. Chem. 71 (1999) 4892.
- [25] T.P. Rao, P. Metilda, J.M. Gladis, Talanta 68 (2006) 1047, and references cited in. [26] S.M. Nnelms, G.M. Greenway, D. Koller, J. Anal. Atom. Spectrom. 11 (1996) 907.
- [27] S. Katragadda, H.D. Gesser, A. Chow, Talanta 44 (1997) 1865.
- [28] C.H. Lee, M.Y. Suh, K.S. Joe, T.Y. Eom, W. Lee, Anal. Chim. Acta 351 (1997) 57.
- [29] C.H. Lee, M.Y. Suh, J.S. Joe, D.Y. Kim, W.H. Kim, Anal. Chim. Acta 382 (1999) 199.
- [30] M.E. Khalifa, Sep. Sci. Technol. 33 (1998) 2123.
- [31] M. Merdivan, M.R. Buchmeiser, G. Bonn, Anal. Chim. Acta 402 (1991) 91.
- [32] S.Y. Bae, G.L. Southard, G.M. Murray, Anal. Chim. Acta 397 (1999) 173.
- [33] J.M. Gladis, T.P. Rao, Anal. Lett. 35 (2002) 501.
- [34] C.R. Preetla, T.P. Rao, Radiochim. Acta 91 (2002) 247.
- [35] J.M. Gladis, T. Prasada Rao, Anal. Lett. 36 (2003) 2107.
- [36] J.S. Hamada, I.B. Hashim, F.A. Sherif, Food Chem. 76 (2002) 136.
- [37] A. Sergeev, G.M. Karshunov, Koord. Khim. 1 (1975) 1654.
- [38] M. Cefola, R.C. Taylor, A.V. Philip, S. Gantile, J. Phys. Chem. 66 (1962) 790.
- [39] Z. Marczenko, Spectrophotometric Determination of Elements, 3rd ed., Ellis Horwood Chichester, UK, 1986, and references cited in Chapter 23.
- [40] H.T.S. Britton, Hydrogen Ions, 4th ed., Chapman & Hall, 1952.
- [41] T. Braun, J.D. Navratil, A.B. Farag, Polyurethane Foam Sorbents in Separation Science, CRC Press Inc., Boca Raton, FL, USA, 1985.
- [42] H.D. Gesser, G.A. Horsfall, J. Chim. Phys. 74 (1977) 1072.
- [43] S. Lagergren, B.K. Sven, Hand 1 (1898) 24.
- [44] W.J. Weber Jr., J.C. Morris, J. Sanit. Eng. Div. Am. Soc. Civ. Eng. 90 (SA3) (1964) 70.
- [45] S.L.C. Ferreira, H.C. dos Santos, M.S. Fernandes, J. Anal. Atom. Spectrom. 17 (2002) 115.
- [46] D. Reichenburg, J. Am. Chem. Soc. 75 (1972) 589.
- [47] G.A. Somorja, Introduction of Surface Chemistry and Catalysis, Wiley, New York, 1994.
- [48] K. Nakamoto, Infrared and Raman Spectra of Inorganic and Coordination Compounds, 3rd ed., Wiley, New York, 1978, p. 305.



Retention profile and subsequent chemical speciation of chromium (III) and (VI) in industrial wastewater samples employing some onium cations loaded polyurethane foams

M.S. El-Shahawi ^{a,*}, S.S.M. Hassan ^b, A.M. Othman ^c, M.A. El-Sonbati ^d

^a Chemistry Department, Faculty of Science, King Abdul-Aziz University, Jeddah, Saudi Arabia

^b Chemistry Department, Faculty of Science, Ain-Shams University, Cairo, Egypt

^c Department of Chemistry, Genetic Engineering and Biotechnology Research Institute, Menoufia University, Menoufia, Egypt

^d Environmental Science Department, Faculty of Science at Damietta, Mansoura University, Mansoura, Egypt

Received 14 August 2007; received in revised form 24 October 2007; accepted 24 October 2007

Available online 1 November 2007

Abstract

The retention of chromium (VI) from aqueous media onto tetraphenylarsonium chloride (TPAs⁺Cl⁻) or tetraphenylphosphonium bromide (TPP⁺Br⁻) immobilized polyurethane foams (PUFs) was fast and followed first order reaction. The kinetic data of the retention step were subjected to Weber-Morris, Lagergren, Bhattacharya and Venkobachar and Bt kinetic models. The results revealed that, film and intraparticle transport might be the two steps controlling the rate of chromium (VI) sorption from the aqueous acid solutions of pH~zero. The positive values of the ΔH of chromium (VI) retention by the reagents loaded PUFs were interpreted as an endothermic process. Under the optimum pH (pH~zero) of the aqueous solution, the proposed TPAs⁺Cl⁻ or TPP⁺Br⁻ immobilized PUFs was successfully used in a series of medical syringe (30, 50 mL capacity) as pulse columns for complete collection of chromium (VI) species present in fresh and industrial wastewater samples at ultra trace low level of chromium (VI) ($\leq 0.05 \mu\text{g mL}^{-1}$). The collected chromium (VI) species onto TPAs⁺Cl⁻ or TPP⁺Br⁻-PUFs was then stripped quantitatively (98–102±2.6%) from the pulse columns with NaOH (2.0 mol L⁻¹) and subsequently analyzed photometrically. The chromium (VI) ions could be pre concentrated up to 100-fold from large volume of water samples. The proposed pulse foam columns were applied successfully for complete collection, recovery (97.5±2.6%, n=5) and subsequent chemical speciation of chromium (III) and (VI) in wastewater samples. The results are in good agreement with the reported and standard methods at 95% confidence. © 2007 Elsevier B.V. All rights reserved.

Keywords: Retention; Chromium (III and VI); PUFs; TPAs⁺Cl⁻; TPP⁺Br⁻; Pulse columns; Chemical speciation

1. Introduction

Chromium (III) is an essential element having an important role in the normal glucose tolerance factor, lipid, protein and fat metabolism in humans with a daily recommended intake of 50–200 $\mu\text{g/day}$ for the adult [1,2]. Chromium (VI) has a definitely adverse impact on living organism. Chromium (VI) can easily penetrate the cell wall and exert its noxious influence in the cell itself, being a source of cancer disease [3,4]. The reference dose

E-mail address: mohammad_el_shahawi@yahoo.co.uk (M.S. El-Shahawi).

0026-265X/\$ - see front matter © 2007 Elsevier B.V. All rights reserved.

doi:10.1016/j.microc.2007.10.006

(RD) for chromium (VI) and chromium (III) are 0.005 mg/kg and

1.0 mg kg^{-1} per day for body weight [3,4], respectively. Thus, chemical speciation of chromium in environmental samples is necessary to accurately assess pollution levels [5–8]. The concentration of chromium in natural water is very low [9–12], in order of a few $5 \mu\text{g L}^{-1}$. Therefore, powerful techniques with sufficient detection power e.g. inert organic solvents are

* Corresponding author. Chemistry Department, Faculty of Science at Damietta, Mansoura University, Egypt.

required.

Inert solvent e.g. chloroform, benzene and dichloromethane have been successfully used for the extraction of the ion associates of chromium (VI) with a series of high molecular weight amines from aqueous acid media [12–15].

The low level of chromium in drinking water is not compatible with the detection limit of most spectrochemical techniques. Thus, preconcentration and separation steps are frequently required in order to improve the detection capability of the employed techniques. Various preconcentration procedures e.g. solvent extraction, strong anion-exchange, activated neutral alumina, chelating resin immobilized with 8-hydroxyquinoline, co-precipitation, precipitation; salt bush biomass and activated carbon have been reported for the chemical speciation of chromium [16–24].

Recent years have seen an upsurge of interest in the applications of PUFs as an excellent support in reversed phase extraction chromatography, gas–solid and gas–liquid partition chromatography [25–32]. The cellular structures, the resilient characteristics and the available surface area of the PUF in both foamed and micro spherical forms make it suitable as an excellent sorbent and as a column filling material with good capacity for firmly retaining various loading and extracting agents [33,34]. This class of sorbent can easily be packed in glass medical syringes of various adequate capacities (30–50.0 mL), compressed and released by moving the plunger of the syringe PUFs [34]. Therefore, in the present manuscript we have tried to use pulse columns packed PUFs sorbent in an attempt to develop a simple, convenient and low cost extraction procedure for the preconcentration, recovery and subsequent chemical speciation of chromium (III) and (VI) species in wastewater. Application of the developed method for the analysis of chromium (VI) in wastewater is also critically considered.

2. Experimental

2.1. Reagents and materials

All chemicals used were of analytical reagent grade. Doubly de-ionized water was used throughout. The reagent diphenylcarbazide, DPC (BDH) solution (0.1% w/v) was prepared by dissolving the required weight in acetone containing sulfuric acid (0.01 mol L⁻¹). Stock solutions of TPAs⁺Cl⁻ (1% w/v),

TPP⁺Br⁻ (1% w/v) and K₂CrO₄ (1 mg mL⁻¹) were prepared in de-ionized water and adjusted to pH zero with HCl (1.0 mol L⁻¹). Foam cubes (10–15 mm edge) of commercial white sheets of polyether-type based PUFs were cut from the foam sheets, purified and finally dried at 80 °C in an oven for 2 h as reported earlier [34] and were used as solid sorbents. The immobilized reagent PUFs

cubes were prepared by mixing the dried foam cubes with an aqueous solution (0.02% w/v) containing TPAs⁺Cl⁻ or TPP⁺Br⁻ (50 mL g⁻¹ dry foam) with efficient stirring for 30 min, squeezed and finally dried [31]. The reagent TPAs⁺Cl⁻ or TPP⁺Br⁻ immobilized PUFs was partially packed (0.3 g) in a series of medical syringe (30 or 50 mL adequate capacity) as pulse columns by applying gentle pressure as reported [34]. All containers used were pre-cleaned by soaking in nitric acid (20% w/v) and rinsed with de-ionized water before use. Low density polyethylene (LDPE) bottles, Nalgene were used for the collection of the different water samples. LDPE bottles were carefully cleaned first with hot

detergent, soaked in 50% HCl (Analar), HNO₃ (2.0 mol L⁻¹),

subsequently washed with dilute HCl (0.5 mol L⁻¹) and finally rinsed with water. Wastewater samples were collected from the industrial liquid waste of electroplating company, Cairo City in LDPE bottles, Nalgene and stored at -20 °C in a refrigerator. Tap- and marine sea water samples were also collected from the boundary side of Ras-El Bar area in the Mediterranean Sea in LDPE bottles. For the chemical speciation measurements of chromium (III) and (VI) in the water samples, the aliquot

samples were acidified with HCl (1.0 mol L⁻¹), stored in LDPE sampling bottles at 4 °C until analysis and finally irradiated with UV for 4 h using 100 W mercury vapor lamp.

2.2. Apparatus

A Varian model AA-875 atomic absorption spectrometer (AAS) was used at the optimum conditions of chromium determination. A series of medical syringe (30 or 50 mL) was used as pulse columns. A Soxhlet extractor and a lab-line Orbital mechanical shaker SO1 (UK) were used for the purification of PUFs cubes and in batch experiments, respectively. The absorbance of the test solutions were measured with a single beam Digital Spectro UV–VIS RS Labomed, spectrophotometer (USA) with quartz cell (10 mm path length). A pH meter model 3305 (JENWAY) was also used for the pH measurements.

2.3. Recommended procedures

2.3.1. Batch experiments

In a dry 100 mL polyethylene bottle, an accurate weight (0.2 ± 0.01 g) of the reagent TPAs⁺Cl⁻ or TPP⁺Br⁻ loaded foam cubes was shaken for 2 h on a mechanical shaker with 50 mL of an aqueous solution containing chromium (VI) ions at 10 µg mL⁻¹ concentration level at 25 ± 0.1 °C at the required pH adjusted by diluted HCl and/or NaOH. After phase separation, a 5 mL of the aliquot solution was transferred to a 10 mL

standard flask containing 1 mL of diphenylcarbazide, DPC. The solution was then diluted with water to the mark, mixed thoroughly and assayed by direct spectrophotometry at 545 nm [19]. Alternatively, the reagent TPAs⁺Cl⁻ were used for the analysis of chromium (VI) at 355 nm in the test solution after extraction into chloroform [20]. At concentrations of chromium (VI) lower than the lower limit of detection (LOD) of DPC [19] or TPAs⁺Cl⁻ [20] method, AAS was used. The amount of chromium (VI) retained at equilibrium, q_e on the foam cubes was then determined from the difference between the absorbance of chromium (VI) solutions before (A_b) and after (A_a) extraction with the reagent foam cubes employing the equation:

$$q_e = \frac{D}{v} (A_b - A_a) P \quad (1)$$

where, v and w are the volume (mL) of the aqueous solution and the weight (g) of the foam cubes, respectively. The extraction percentage (%E) and the distribution ratio (D) of the chromium (VI) sorption onto the reagent-loaded foam were then calculated as reported earlier [33,34]. Following these procedures, the influence of temperature (298–348 K) on the sorption step of chromium (VI) by the loaded PUF sorbents was fully studied. All experiments were performed in triplicate at ambient temperature (25 ± 0.1 °C). The results of %E and D are the average of three independent measurements and the precision in most cases was $\pm 2\%$.

2.3.2. Pulse column-filling operation for chromium (VI)

The extraction efficiency was studied using spiked water samples for the recovery of traces of chromium (VI) species at the optimum acidity of the analyte sorption onto the PUFs. Doubly distilled water and/or industrial wastewater samples (200.0–500.0 mL) were spiked with known chromium (VI) concentrations (0.03–5 $\mu\text{g mL}^{-1}$). The concentrations of chromium (VI) in the spiked water samples were determined as follows: immobilized TPP⁺Br⁻ PUFs cubes (0.3 \pm 0.01 g) were partially packed in a medical syringe (30 and 50 mL) under gentle pressure employing a glass rod. In each medical syringe separation was performed in a manner that allowed the external chromium (VI) solution to enter or leave the syringe at 20–25 mL min⁻¹ by releasing and/or pressing the plunger of the syringe. In this case, separation is performed by repeating the inflow/outflow cycle and each cycle constitutes one pulse. In this arrangement, the %E is related to the distribution ratio, number of pulses (n) and the maximum volume concentration (P) ($P = w_t/v_p$, where w_t is the total sample volume and v_p is the compressed foam volume) by the equation [34]:

$$E_{n,op} = \frac{D}{P} \left(1 - \frac{1}{n} \right) \quad (2)$$

The retained chromium (VI) species onto the PUFs sorbents were then stripped from the foam with NaOH (20 mL,

1.0 mol L⁻¹) by releasing or pressing (pulsing) the glass plunger of the syringe several times (25–30) with the glass tip of the syringe in NaOH solution. The recovery percentage of the retained chromium (VI) onto the TPP⁺Br⁻ immobilized PUFs was then calculated from the original quantity of chromium (VI) species and that determined by AAS after stripping with NaOH from the PUFs sorbents.

2.3.3. Retention and sequential determination of chromium (III)

An aliquot (200 mL) of the aqueous solution containing 0.01–5 $\mu\text{g mL}^{-1}$ of chromium (III) was transferred to a conical flask (50 mL). The test solutions were then oxidized to

chromium (VI) in alkaline media (NaOH, 1.0 mol L⁻¹) after boiling for 10 min with hydrogen peroxide (2 mL, 10% w/v). The test solutions were then cooled adjusted to pH ~ zero by HCl (1.0–2.0 mol L⁻¹) and treated as described for chromium (VI) retention using the pulse column. The retained species were then recovered from the PUFs and quantified as described [20,35] or by AAS standard curve prepared under the same experimental conditions.

2.3.4. Separation and chemical speciation of inorganic chromium (III) and (VI)

Transfer an aliquot portion (200 mL) containing the binary mixture of chromium (III) and (VI) species at a total concentration of chromium species $\leq 0.5 \mu\text{g mL}^{-1}$ to a conical flask. The test solution was adjusted to pH zero with HCl (1.0 mol L⁻¹), treated as described for chromium (VI) retention and stripping as described using the pulse column mode and finally analyzed as reported [30,36] or with AAS. Another aliquot mixture (200 mL) was transferred to the conical flask and treated as described for chromium (III) species before. On the bases of these procedures, the absorbance of the first aliquot (A_1) will be a measure of chromium (VI) ions in the mixture, while the absorbance of the second aliquot (A_2) is a measure of the sum of chromium (III) and (VI) ions. Therefore, the absorbance ($A_2 - A_1$) is a measure of the chromium (III) ions in the binary mixture. At chromium (VI) concentrations lower than the LOD [35,36] AAS was used under the optimum conditions of chromium determination with the aid of standard curve.

2.4. Analytical applications

Industrial wastewater samples (100–500 mL) of electroplating industry were filtered through 0.4 μm cellulose acetate membrane filters immediately upon collection and stored in

LDPE bottles. The sample solutions were then adjusted to pH zero with HCl (1.0 mol L⁻¹) in the laboratory. The water samples were then spiked with chromium (VI) at total concentration level $\leq 0.05\text{--}5 \mu\text{g mL}^{-1}$ chromium (VI) ions. The sample solutions were then retained, stripped and recovered from TPP⁺Br⁻ immobilized PUFs (0.2±0.01 g) using immobilized PUFs packed medical syringes (50 mL) as described for chromium (VI) ions. The recovered chromium (VI) species was then analyzed with AAS and the chromium (VI) present in the wastewater sample was then calculated from the curve of standard addition method using the AAS after stripping from the solid phase with NaOH. The preconcentration procedure was optimized using model solutions containing chromium (VI) ions.

3. Results and discussion

3.1. Retention profile of chromium (VI) onto the PUFs

Screening tests on the application of the PUFs for the retention of chromium (VI) from the aqueous solution have shown that, the amount of the analyte ions extracted from the aqueous solution by the TPAs⁺Cl⁻ or TPP⁺Br⁻ loaded foam depends on the solution pH. Therefore, the sorption profile of an aqueous solution (100 mL, 10 $\mu\text{g mL}^{-1}$) containing chromium (VI) ions at different pH by TPAs⁺Cl⁻ or TPP⁺Br⁻ loaded foams was critically studied after shaking for 1 h at room temperature. The amount of chromium (VI) remaining in the aqueous solution at equilibrium was determined as reported [35,36]. The % E and the D of the chromium (VI) sorption from the aqueous solutions onto the TPAs⁺Cl⁻ or TPP⁺Br⁻ loaded PUFs decreased markedly on increasing the solution pH and maximum uptake was achieved at pH~zero. Representative data are shown in Fig. 1. At high pH, the observed decrease in the chromium (VI) uptake onto the reagent PUFs is most likely attributed to the instability, hydrolysis or the incomplete extraction of the produced complex ion associate of chromium

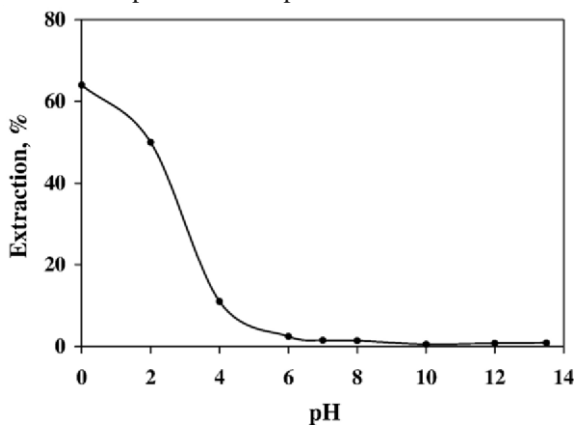


Fig. 1. Effect of pH on the sorption percentage of chromium (VI) from aqueous

solution onto TPP Br immobilized foams at 25±1 °C.

(VI)-TPAs⁺Cl⁻ or chromium (VI)-TPP⁺Br⁻ [37]. Thus, in the subsequent work, the solution was selected at pH zero.

The influence of the nature of the mineral acid (HCl, HNO₃ and H₂SO₄ at 1 M concentration) on the chromium (VI) retention onto the PUFs was also investigated. Of these, HCl was proved satisfactory as the extraction medium of the produced complex ion associate between the halo chromate

(CrO₃Cl)⁻ ions and TPAs or TPP immobilized PUFs. The influence of HCl concentration (1–5 mol L⁻¹) was also examined. A sharp increase in the extraction of chromium (VI) was observed on increasing HCl concentration up to

3.0 mol L⁻¹. Thus, in the subsequent work, HCl (3 M) was selected as a proper extraction medium on the chromium (VI) sorption from the aqueous solution onto TPAs⁺Cl⁻ or TPP⁺Br⁻ loaded PUFs. At HCl concentrations 3 mol L⁻¹, the foam cubes were degraded and a progressive decrease in the chromium (VI) uptake onto the reagent loaded foams was observed in good agreement with the data reported earlier [33,34]. On the bases of these results and the data reported earlier [37,38], a possible “weak base ion exchange” extraction mechanism involving formation of complex ion associate of the general formula CrO₃Cl TPX was retained onto the PUFs, where, X=As⁺ or P⁺.

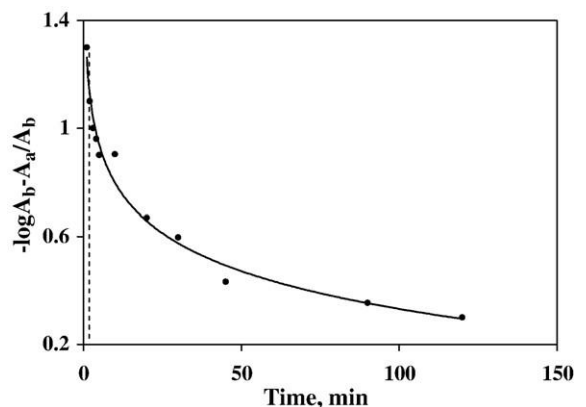


Fig. 2. Rate of chromium (VI) sorption from aqueous solution at 25±1 °C onto TPP Br immobilized foams.

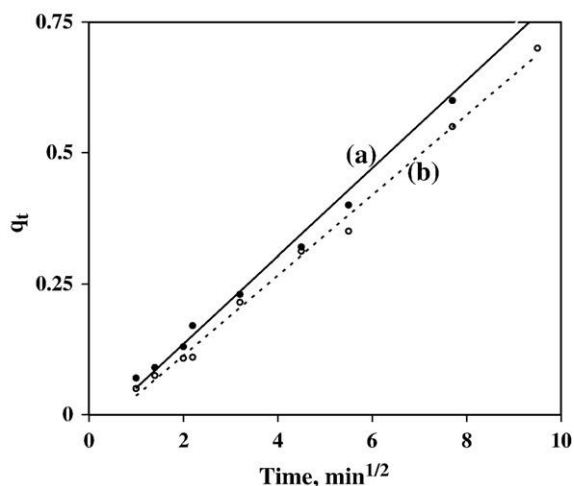


Fig. 3. The sorbed concentration of chromium (VI) at 5 $\mu\text{g}/\text{mL}$ from aqueous Cr^{6+} solutions (50 mL) at pH zero and 25 ± 0.1 $^{\circ}\text{C}$ onto TPP Br immobilized PUFs (0.2 ± 0.01 g) as a function of square root of time.

3.2. Kinetic behavior of chromium (VI) uptake onto the PUFs

The chromium (VI) sorption onto the reagent $\text{TPAs}^{+}\text{Cl}^{-}$ or $\text{TPP}^{+}\text{Br}^{-}$ treated PUFs from the aqueous media containing HCl (3.0 mol L^{-1}) at different time intervals was critically studied. The chromium (VI) ions uptake was found fast and reached equilibrium within ~ 30 min contact time. The half-life time ($t_{1/2}$) of the equilibrium sorption to reach 50% saturation of the sorption capacity is calculated as 2 min (Fig. 2), consequently, 45 min shaking time was adopted in the subsequent experiments.

The sorbed chromium (VI) concentration q_t (mmol g^{-1}) at time t was plotted against time to test the applicability of the Weber-Morris equation [39,40]:

$$q_t \approx R_d \delta t^{1/2}; \quad \delta \approx 3 \text{ min}^{-1/2}$$

where R_d is the rate constant of intraparticle transport in $\text{mmol g}^{-1} \text{min}^{-1/2}$. The diffusion rate is rapid in the initial stages and slows down with passage of time (Fig. 3). The data indicates that, for up to 8 min, the relationship fits well and starts to deviate as the shaking time increases. The values of R_d computed from slopes of the Weber-Morris plot (Fig. 3), in the initial

stage up to 8 min were estimated to be 54 and $64 \text{ mmol g}^{-1} \text{min}^{-1/2}$ for $\text{TPAs}^{+}\text{Cl}^{-}$ and $\text{TPP}^{+}\text{Br}^{-}$, respectively [40,41].

The kinetic data of the chromium (VI) retention onto the reagent immobilized PUFs were also determined employing

Lagergren model [42] over the entire range of agitation time explored using the equation:

$$\log \frac{q_e - q_t}{q_e} \approx \log \frac{q_e - q_t}{q_e} - k t = -2.303 k t$$

where, q_e is the sorbed chromium (VI) concentration onto the PUFs at equilibrium (mmol g^{-1}) and k is the overall first order rate constant.

The plots were linear. The values k calculated from the linear plots of $\log (q_e - q_t)$ versus time up to 60 min (Fig. 4) were found equal 0.0076 ± 0.001 and $0.007 \pm 0.0013 \text{ min}^{-1}$ for $\text{TPAs}^{+}\text{Cl}^{-}$ and $\text{TPP}^{+}\text{Br}^{-}$, respectively. The results obtained in the light of Lagergren were further confirmed

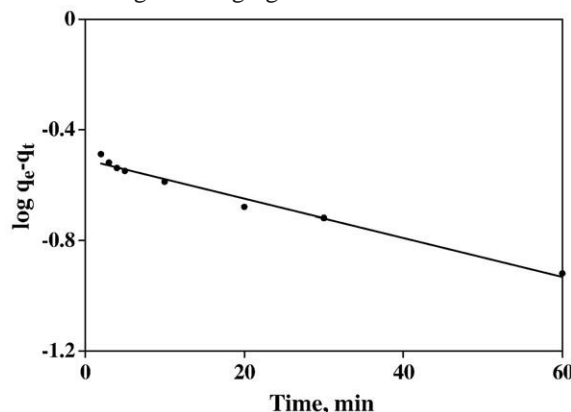


Fig. 4. Lagergren plots of the kinetics of chromium (VI) uptake from aqueous Cr^{6+} solution at pH zero at 25 ± 1 $^{\circ}\text{C}$ onto TPAs Cl (a) and TPP Br (b) immobilized foams.

by Bhattacharya and Venkobachar model [43] confirming the formation of monomolecular layer of chromium (VI) species onto the surface of the adsorbent.

The value of Bt , which is a mathematical function (F) of the ratio of the fraction sorbed (q_t) in mol/g at time t and at equilibrium (q_e) in mol/g i.e. q_t/q_e was calculated for each value of F employing Reichenburg equation [44]:

$$Bt \approx 0.4977 - 2.303 \log \frac{q_t}{q_e} \approx 3 \text{ min}^{-1} F$$

Plots of Bt versus time at 25 ± 1 $^{\circ}\text{C}$ were linear for up to 60 min shaking for chromium (VI) sorption onto $\text{TPAs}^{+}\text{Cl}^{-}$ and $\text{TPP}^{+}\text{Br}^{-}$ loaded foams, respectively. These data confirmed the observed behavior of the Weber-Morris equation test [39,40], where the straight lines (Fig. 3) does not pass through the origin. Thus, particle diffusion is the most probable operating mechanism and does not control the kinetics of chromium (VI) ions sorption onto the $\text{TPAs}^{+}\text{Cl}^{-}$ and $\text{TPP}^{+}\text{Br}^{-}$ immobilized foams. Therefore, the retention of chromium (VI) onto PUF cubes probably involves three steps: bulk transport of chromium (VI) in solution, film transfer involving diffusion of

chromium (VI) species within the pore volume of PUF and/or along the pore wall surface to an active sorption site [33] and finally formation of $[\text{CrO}_3\text{Cl TPX}]_{\text{foam}}$. The actual sorption of the solute on the interior surface site is very fast, and hence it is not the rate-determining step therefore, film and intraparticle transport might be the two steps controlling the rate of sorption from acid solutions (pH~zero).

3.3. Thermodynamic characteristics of chromium (VI) uptake

The thermodynamic parameters (ΔH , ΔS , and ΔG) of chromium (VI) uptake onto TPAs^+Cl^- or TPP^+Br^- immobilized foams have been evaluated [40]. The equilibrium constant K_c of the sorption process of chromium (VI) onto PUFs was calculated employing the equation:

$$K_c = \frac{F_e}{1 - F_e} \quad (5)$$

where F_e is the fractional attainment of the sorption step by the TPAs^+Cl^- or TPP^+Br^- loaded PUFs. The plots of $\log D$ or $\log K_c$ versus $1/T$ (Fig. 5) were found linear over the investigated temperature range (300–353 K). The values of ΔH , ΔS and ΔG calculated from the slopes and intercepts of Fig. 5 were found

equal $5.67 \pm 0.1 \text{ kJ mol}^{-1}$, $17.97 \pm 0.3 \text{ J/(mol K)}$ and $0.31 \pm$

0.04 kJ mol^{-1} (at 298 K), respectively for chromium (VI) sorption onto TPAs^+Cl^- immobilized foam. The values of ΔH , ΔS and ΔG for the chromium (VI) sorption onto the TPP^+Br^-

loaded foams are $13.4 \pm 1.6 \text{ kJ mol}^{-1}$, $43.2 \pm 2.1 \text{ J/(mol K)}$ and

0.6 kJ mol^{-1} , respectively with a correlation factor of 0.998.

The values of ΔH and K_c indicated that, the chromium (VI) sorption onto the TPAs^+Cl^- or TPP^+Br^- loaded PUFs is an endothermic process. The energy of the urethane nitrogen and/or ether-oxygen sites of the PUFs provided by raising the temperature enhanced the possible interaction between the active sites of the PUFs and the complex ion associates of chromium (VI) ions and TPAs^+Cl^- or TPP^+Br^- resulting a higher sorption percentage. Thus, a dual-mode sorption mechanism involves absorption related to "solvent extraction" and an added component for "surface adsorption" seems a more probable model for chromium (VI) uptake. These results suggest the possible use of the reagent loaded foam in flow and pulsating modes for quantitative collection, chemical speciation, sequential determination of chromium (VI) and total inorganic chromium (III).

3.4. Chemical speciation of inorganic chromium (III) species on pulse PUFs column

The analytical utility of the foam pulse column depends mainly on: i—the flexibility of the PUFs; ii—the rate of the reaction between the chromium (VI) ions in the test solution and the reagent TPP^+Cl^- immobilized PUFs and finally iii—the reaction between the eluting agent (NaOH , 1 mol L⁻¹) and the retained chromium (VI) species onto the loaded PUF cubes. Thus, the tip of the syringe packed with the reagent loaded PUFs (0.2±0.01 g) was allowed to pulse with the test solution

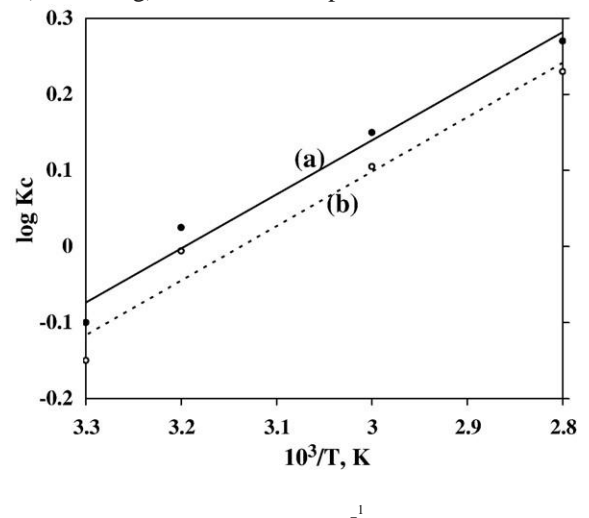


Fig. 5. Variation of $\log K_c$ versus $1000/T$ (K^{-1}) for chromium (VI) uptake at $5 \mu\text{g/mL}$ concentration level from aqueous solution at pH zero onto TPAs^+Cl^- (a) and TPP^+Br^- (b) immobilized PUFs (0.2±0.01 g).

Table 1

Chemical speciation of chromium (III and VI) ions in distilled water (100 mL) by the proposed TPP^+Cl^- pulse foam partially packed syringe (A) and reference AAS (B) methods

Cr(III) added, $\mu\text{g mL}^{-1}$	Cr(VI) added, $\mu\text{g mL}^{-1}$	Total chromium (III and VI), $\mu\text{g mL}^{-1}$	
		A	B
10	–	10.2±0.2	10.1±0.1
5	10	14.8±0.2	15.3±0.2
5	5	9.9±0.3	10.2±0.2

Average (n=5)±standard deviation.

(100 mL, 0.05–5 $\mu\text{g mL}^{-1}$ chromium ions) at pH 3.2 which will go into the pulse column and the PUFs cubes will return back to its original volume. On repeating this process, for several times (30–35), complete (97.4±2.9%) retention of chromium (VI) was only achieved, while chromium (III) does not as detected from AAS measurement of the test solution. The retained chromium (VI) species was then recovered with NaOH

by allowing the tip of the syringe packed with the TPP⁺Cl⁻ PUFs

pulse with the stripping agent (25 mL, 2 mol L⁻¹). The stripping agent will go into the column, and the PUF cubes will return to its original volume. Similarly, on repeating this process for several times the NaOH solution will be exposed to the retained chromium (VI) species on the PUFs. This will result in a reaction between the sorbed chromium (VI) and NaOH. Complete recovery (98.2±3.1%) of the retained chromium (VI) species was achieved after 30–35 pulses (Table 1). These data recommended the use of the pulse column for the separation, recovery and chemical speciation of chromium (III and VI) species from large sample volumes.

proposed reagent immobilized PUFs for the separation and sequential speciation of chromium (III) and (VI).

3.6. Analytical performance of the developed foams packed columns

The performance of the TPP⁺Cl⁻ immobilized PUFs partially packed in the medical syringe (50.0 mL capacity) towards chromium (VI) solution (0.05–5 µg Cr/mL) in the test solution (200.0 mL) was determined. The capacity of the pulse column partially packed with TPP⁺Cl⁻ immobilized PUFs

towards chromium (VI) sorption was found 5.2±0.34 mg g⁻¹. The aliquot solution was allowed to enter or leave the syringe by releasing and/or pressing the plunger of the syringe at 25 mL

min as described before. Complete sorption of chromium (VI) took place as indicated from the AAS analysis of chromium in the effluent solution. The sorbed chromium (VI) species in the column were then stripped quantitatively (98.2–

101.5±1.8%) with NaOH (20.0 mL, 2. mol L⁻¹, 30 pulses). The lower limits of detection (LOD) and quantification (LOQ) of

3.5. Effect of diverse ions on the retention and recovery of chromium (VI) species

The proposed TPP⁺Cl⁻ immobilized PUFs in pulse mode was investigated for the separation of chromium (VI) (5 µg/mL Cr⁶⁺) from aqueous media (50 mL) in the presence of a series of diverse ions under the optimal experimental conditions. A relatively high excess (1 mg) of some diverse ions e.g. Cu²⁺, Al³⁺, Ni²⁺, Co²⁺, Cd²⁺, SO₄²⁻, PO₄³⁻, alkali and alkaline earth metals relevant to waste water and are often accompanying chromium (VI) ions was examined. The amount of foreign ion causing an error ±2% in the uptake of chromium (VI) is considered free from interference ratios (w/w) limit. Good

chromium (VI) sorption under the optimal conditions was computed using the equations [45]:

$$\text{LOD} \approx 11\text{SD} = b \delta 7p \quad \text{LOQ} \approx 10\text{SD} = b \delta 8p$$

where SD is the standard deviation (n=3) of the blank and b is the slope of the calibration plot. The LOD and LOQ of 0.4 and 1.2 µg L⁻¹ were achieved, respectively. For sample volume of 200 mL at pH 3–4, the enrichment factors calculated as the ratio between calibrations graphs with and without preconcentration were up 100 for unloaded and PAR treated PUFs using pulse columns of 50 mL of adequate capacity. The precision of the unloaded-and PAR treated PUFs pulse columns for standard solutions containing 0.5 µg mL⁻¹ of chromium (VI) were 1.8 and 2.3% (n=5), respectively, expressed as relative standard deviation.

3.7. Analytical applications

The retention characteristics of the developed PUFs pulse column suggest its use for the separation and subsequent determination of chromium species at low level (nanomolar) of inorganic chromium (III) and/or (VI) in tap and/or industrial wastewater samples. A first aliquot (100 mL) of water samples

Table 2
Analysis of chromium (III) and (VI) in industrial wastewater (100 mL) by the developed TPP Cl foam partially packed syringe (A) and reference AAS (B) methods

Cr(III) added mL ⁻¹	Cr (VI) added µg mL ⁻¹	Total chromium (III&VI) µg	
		A	B
10	–	13.1±0.2	12.9±0.1
5	10	18.1±0.16	17.9±0.05
5	5	12.9±0.2	12.9±0.2

Average (n=5)±standard deviation.

extraction and recovery efficiency (96.9±2%) for the chromium (VI) ions was achieved successfully in the presence of these diverse ions. In the presence of some other ions e.g. MnO₄⁻, Fe³⁺ and VO₃⁻, 2 mL of NaN₃ (0.1%) and NaF (0.1%) solutions were introduced to the aqueous solution, respectively to obtain unambiguous and selective preconcentration and recovery. The reagent NaN₃ was added to eliminate the interference of permanganate ions via reduction of manganese (VII) to manganese (II) ions. The tolerance limit of these interfering ions was improved to acceptable limit (97.6±2.2%) after employing these modifications. These results and the resilient characteristics of the PUFs also extend the use of the

of an electroplating spiked with (or without) chromium (III) and (VI) at concentration 0.05–5 $\mu\text{g mL}^{-1}$ was treated as described for chromium (VI) in the experimental section. Chromium (VI) species were only retained quantitatively after 30–35 pulse while chromium (III) remained in solution. The retained chromium (VI) species were then recovered with NaOH (25, mol L^{-1}) after 30–35 pulse. Another aliquot (100 mL) of the spiked sample solution was then oxidized to chromate ions with H_2O_2 and treated as described for chromium (VI). The chromium (VI) content before extraction and after recovery in the stripped solutions was finally determined with AAS. The results are summarized in Table 2 using the standard addition methods. The data are in good agreement with the values obtained using direct AAS. On these bases, the amount of chromium in the first aliquot will be equivalent to chromium (VI) in the analyzed sample, while the amount of chromium in the second aliquot will be equivalent to total inorganic chromium (III) and (VI). The concentration of chromium (VI) species present in the industrial wastewater obtained by the developed method is in good agreement with the value obtained by AAS. The retention of chromium (IV) at concentration $\leq 0.01 \mu\text{g mL}^{-1}$ was also tested for one liter of wastewater samples under the optimum experimental conditions was achieved successfully with good extraction and recovery ($98 \pm 2\%$) were achieved.

4. Conclusion

This article demonstrates the utility of PUFs sorbent in pulse mode as a simple, convenient, and low cost solid extractor for the separation, chemical speciation and sequential photometric determination of inorganic chromium (III) and (VI) ions in industrial wastewater. The PUFs packed columns can be re used many times without decrease in its performance. The developed method allows continuous monitoring of chromium (VI) and total inorganic chromium (III and VI) species present in wastewater samples of electroplating industry. The proposed pulse mode of separation does not require transport bulky water samples into the laboratory for analysis, since pre-concentration can easily be made on the spot. The developed method can be optimized for the preconcentration of the analyte for the flow analysis measurements. Future work is continuing for the chemical speciation of organic and inorganic chromium species and some other toxic metal ions in the environmental samples.

References

- [1] E. Merian, *Metals and Their Compounds in The Environment, Occurrence, Analysis and Biological References*, VCH, 1980.
- [2] W. Mertz, *Trace Elements in Human and Animal Nutrition*, Academic Press, London, 1986.
- [3] J.R. Holum, *Elements of General, Organic and Biological Chemistry*, 9th edn., John Wiley and Sons, 1995.
- [4] J.O. Nriagu, E. Nieboer, *Chromium in Natural and Human Environment*, Wiley, New York, 1988 edn.
- [5] J. Threeprom, R. Meelapsom, W. Som-aun, J.M. Lin, *Talanta* 71 (2007) 103.
- [6] Y. Xiang, L. Mei, N. Li, A. Tong, *Anal. Chim. Acta* 581 (2007) 132.
- [7] A. Beni, R. Karosi, J. Posta, *Microchem. J.* 85 (2007) 103.
- [8] V. Comez, M.P. Callao, *Trac* 25 (2006) 1006.
- [9] S.Matsuoka, Y.Tennichi, K.Takehara, K.Yoshimura, *Analyst* 124(1999)787.
- [10] M.J. Marques, A. Salvador, A.M. Rubio, M. de la Guardia, *Fresenius J. Anal. Chem.* 367 (2003) 1386.
- [11] Y. Luo, S. Nakano, D.A. Holman, J. Ruzicka, G.D. Christian, *Talanta* 44 (1977) 1563.
- [12] V.M. Shinde, S.M. Khopkar, *Fresenius Z. Anal. Chem.* 249 (1970) 239.
- [13] J. Adam, *Talanta* 18 (1971) 91.
- [14] M.N. Sastri, D.S. Sundar, *Anal. Chim. Acta* 33 (1965) 340.
- [15] M.S. El-Shahawi, S.S. Hassan, A.M. Othman, M.A. Zyada, M.A. ElSonbati, *Anal. Chim. Acta* 534 (1–2) (2005) 319.
- [16] R. Milacic, J. Scancar, J. Tusek, *Anal. Bioanal. Chem.* 372 (2002) 549.
- [17] A.C. Sahayan, *Anal. Bioanal. Chem.* 372 (2002) 840.
- [18] C.G.B. Bruhn, F.E. Pino, V.H. Campos, J.A. Nobrega, *Anal. Bioanal. Chem.* 374 (2002) 131.
- [19] D.M. Adria Cerezo, M. Lilobat-Esteles, A.R. Mauuri-Aucejo, *Talanta* 51 (2000) 531.
- [20] G.M. Wuilloud, R.G. Wuilloud, J.C.A. de Wuilloud, R.A. Olsina, L.D. Martinez, *J. Pharm. Biomed. Anal.* 31 (2003) 117.
- [21] R.A. Gil, S. Cerutti, J.A. Gasquez, R.A. Olsina, L.D. Martinez, *Talanta* 68 (2006) 1065.
- [22] R. Karosi, V. Andruch, J. Posta, J. Balogh, *Microchem. J.* 82 (2006) 61.
- [23] V. Gomez, A. Pasamontes, M.P. Callao, *Microchem. J.* 83 (2006) 98.
- [24] M.F. Sawalha, J.L. Gardea-Torresedey, G. Parso, J.R. Peralta-Videa, *Microchem. J.* 81 (2005) 122.
- [25] M.S. El-Shahawi, A.M. Othman, H.M. Nassef, M.A. Abdelfadeel, *Anal. Chim. Acta* 536 (1–2) (2005) 227.
- [26] V.A. Lemos, M.S. Santos, E.S. Santos, M.J.S. Santos, W.N.L. dos Santos, A.S. Souza, D.S. de Jesus, C.F. das Virgens, M.S. Carvalho, N. Oleszczuk, M.G.R. Vale, B. Welz, S.L.C. Ferreira, *Spectrochim. Acta B* 62 (2007) 4.
- [27] M.S. El-Shahawi, H.A. Nassif, *Anal. Chim. Acta* 481 (2003) 29.
- [28] M.M. Saeed, M. Ahemd, *Anal. Chim. Acta* 525 (2004) 289.
- [29] S.M. Hasany, M.M. Saeed, M. Ahmed, *Sep. Sci. Technol* 35 (2000) 379.
- [30] P.F. Marchisio, A. Sales, S. Cerutti, E. Marchevski, L.D. Martinez, *J. Hazard. Mater. B* 124 (2005) 113.
- [31] A.N. Anthemidis, G.A. Zachariadis, J. Stratis, *Talanta* 58 (2002) 831.
- [32] S.L. Ferreira, W.N. dos Santos, M.A. Bezerra, V.A. Lemos, J.M. BosqueSendra, *Anal. Bioanal. Chem.* 375 (2003) 443.
- [33] T. Braun, J.D. Navratil, A.B. Farag, *Polyurethane Foam Sorbents in Separation Science*, CRC Press, Inc, FL, Boca Raton, 1985.
- [34] S. Palagyi, T. Braun, *Separation and Preconcentration of Trace Elements and Inorganic Species on Solid Polyurethane Foam Sorbents*, in: Z.B. Alfassi, C.M. Wai (Eds.), *Pre-concentration Techniques for Trace Elements*, CRC Press, Boca Raton, FL, 1992.
- [35] H. Sano, *Anal. Chim. Acta* 27 (1962) 398.
- [36] S. Lacroix, M. Labalade, *Anal. Chim. Acta* 3 (1949) 262.
- [37] I.I. Stewart, A. Chow, *Talanta* 40 (1993) 1345.
- [38] M.N. Sastri, T.S.R. Prasad Rao, *J. Inorg. Nucl. Chem.* 30 (1968) 1727.
- [39] W.J. Weber Jr., J.C. Morris, *J. Sanit. Eng. Div. Am. Soc. Civ. Eng.* 90 (SA3) (1964) 70.
- [40] M. Saeed, S.M. Hasany, M. Ahmed, *Talanta* 50 (1999) 625.
- [41] M. Hasany, M.M. Saeed, M. Ahmed, *Talanta* 54 (2001) 89.
- [42] S. Lagergren, B.K. Sven, *Vatenskapsakad. Handl.* (1898) 24.

- [43] A.K. Bhattacharya, C. Venkobachar, *J. Environ. Eng.* 110 (1984) 110.
- [44] D. Reichenburg, *J. Am. Chem. Soc.* 75 (1972) 589.
- [45] J.C. Miller, J.N. Miller, *Statistics for Analytical Chemistry*, 4th edn., EllisHorwood, New York, 1994, p. 115.



Separation Science and Technology

Publication details, including instructions for authors and subscription information: <http://www.tandfonline.com/loi/lst20>

Adsorption of Polycyclic Aromatic Hydrocarbons onto Activated Carbon from Non-Aqueous Media: 1. The Influence of the Organic

This article was downloaded by: [King Abdulaziz University]

On: 02 February 2014, At: 03:24

Publisher: Taylor & Francis

Informa Ltd Registered in England and Wales Registered Number: 1072954 Registered office: Mortimer House, 37-41 Mortimer Street, London W1T 3JH, UK

Solvent Polarity

A. M. Dowaidar ^a , M. S. El-Shahawi ^b & I. Ashour ^c

^a

Faculty of Engineering, Department of Chemical Engineering , UAE University , Al Ain, United Arab Emirates

^b

Faculty of Sciences, Department of Chemistry , King Abdulaziz University , Jeddah, Kingdom of Saudi Arabia

^c

Department of Petroleum and Chemical Engineering , Sultan Qaboos University , 123, Muscat, Oman Published online: 27 Dec 2007.

To cite this article: A. M. Dowaidar , M. S. El-Shahawi & I. Ashour (2007) Adsorption of Polycyclic Aromatic Hydrocarbons onto Activated Carbon from Non-Aqueous Media: 1. The Influence of the Organic Solvent Polarity, Separation Science and Technology, 42:16, 3609-3622, DOI: [10.1080/01496390701626537](https://doi.org/10.1080/01496390701626537)

To link to this article: <http://dx.doi.org/10.1080/01496390701626537>

PLEASE SCROLL DOWN FOR ARTICLE

Taylor & Francis makes every effort to ensure the accuracy of all the information (the "Content") contained in the publications on our platform. However, Taylor & Francis, our agents, and our licensors make no representations or warranties whatsoever as to the accuracy, completeness, or suitability for any purpose of the Content. Any opinions and views expressed in this publication are the opinions and views of the authors, and are not the views of or endorsed by Taylor & Francis. The accuracy of the Content should not be relied upon and should be independently verified with primary sources of information. Taylor and Francis shall not be liable for any losses, actions, claims, proceedings, demands, costs, expenses, damages, and other liabilities whatsoever or howsoever caused arising directly or indirectly in connection with, in relation to or arising out of the use of the Content.

This article may be used for research, teaching, and private study purposes. Any substantial or systematic reproduction, redistribution, reselling, loan, sub-licensing, systematic supply, or distribution in any form to anyone is expressly forbidden. Terms & Conditions of access and use can be found at

<http://www.tandfonline.com/page/terms->



Taylor & Francis
Taylor & Francis Group

[and-conditions](#)

Separation Science and Technology, 42: 3609–3622, 2007

Copyright # Taylor & Francis Group, LLC

ISSN 0149-6395 print/1520-5754 online

DOI: 10.1080/01496390701626537

Adsorption of Polycyclic Aromatic Hydrocarbons onto Activated Carbon from Non-Aqueous Media: 1. The Influence of the Organic Solvent Polarity

A. M. Dowaidar

Faculty of Engineering, Department of Chemical Engineering, UAE University, Al Ain, United Arab Emirates

M. S. El-Shahawi

Faculty of Sciences, Department of Chemistry, King Abdulaziz
University, Jeddah, Kingdom of Saudi Arabia

I. Ashour

Department of Petroleum and Chemical Engineering, Sultan Qaboos University, Muscat 123, Oman

Abstract: Polycyclic aromatic hydrocarbons (PAHs) can be formed easily during the refinery processes of crude petroleum. Their accumulation poses serious operating problems and their removal is of great importance. In this investigation we tested the ability of activated carbon to remove a number of the PAHs compounds from mixtures of organics solvents, with different chemicals structures and polarities. Batch adsorption tests were used to investigate the effect of chemical structures and polarities of solvents on the adsorption of naphthalene, anthracene, and pyrene on activated carbon. Our investigation revealed that aromatic solvents have high affinity for activated carbon and therefore, inhibit PAHs adsorption, while polar solvents have low affinity for activated carbon and consequently the adsorbent sites are more available for the PAHs molecules. This behavior can be explained by the fact that the PAHs and benzene molecules are able to form π - π complex between π -electrons of benzene rings and active sites on an activated carbon surface. An

Received 23 January 2007, Accepted 13 June 2007

Address correspondence to I. Ashour, Department of Petroleum and Chemical Engineering, Sultan Qaboos University, Box 33 Al-Khod, Muscat 123, Oman.

Tel.: þ 96824141318; Fax: þ96824141354; E-mail: ashour@squ.edu.om

3609

increase in the molecular weight of aliphatic solvents such as hexane and heptane has little effect on adsorption of PAHs to activated carbon. However, cyclic hydrocarbon solvents such as cyclohexane increase the adsorption of small PAHs and decrease the adsorption of heavier PAHs molecules, probably as a result of differences in solubilities.

Keywords: PAHs adsorption, activated carbon, non-aqueous media, equilibrium isotherms

INTRODUCTION

PAHs commonly refer to a large class of organic compounds containing two or more fused aromatic rings made up of carbon and hydrogen atoms. PAHs are chemically inert, soluble in many organic solvents, and are highly lipophilic. Therefore, the behavior and the biological effects of PAHs vary in the environment (1). PAHs with low molecular weights (e.g., naphthalene and phenanthrene) are highly mobile in an aquatic environment and present significant acute toxicity to many organisms. Many PAHs of higher molecular weights (e.g., benzo(a)pyrene) have been shown to be highly carcinogenic and have significant persistence up to many years in the environment (2). On the other hand, some of these PAHs have a certain industrial importance (e.g., in dyes, plastics, pharmaceuticals, and the pesticides industry) (3).

PAHs are found naturally in crude oil, creosote, coal tar, and coal. The release of PAHs have been reported during production and processing, of plasticizers, dyes, and pigments; however, most PAHs enter the environment via the atmosphere from incomplete combustion processes, such as the processing of coal and crude oil during refining, coal gasification, and coking. Crude petroleum oil is also distinguished by the relatively high ratio of compounds with saturated five-membered rings and the presence of highly strained molecules, such as 4,5-methylene phenanthrene (4).

Many techniques (e.g., bioremediation (5–9), ozonation (10–15), photodegradation, and adsorption (16) have been applied successfully for the minimization of PAHs in wastewater of domestic and/or industrial plants and soils. The adsorption techniques are the most frequently used in batch mode for the minimization of such complex species in liquid or gas phases due to its high efficiency and applicability to be used at high temperatures. Activated carbon was considered the most frequent and effective solid adsorbent in this field. Other adsorbents (e.g., alumina, zeolite, fly ash, soils, and clays (17–20) have also been employed successfully to remove PAHs.

The formation of small amounts of PAHs from hydrocracking reactions can build up to concentrations that cause fouling of cooled heat exchanger surfaces, equipment, and fluid lines. The PAHs can build up to the limit of their solubility at temperatures commonly used for the condensation and the

separation of the hydrocracker output products. The fouling problem may also gradually reduce the heat transfer to some extent that conversion and/or feed rate must be reduced. In the light of present trends towards heavier feedstocks, the adsorption, solubility, and precipitation of PAHs are consequently of great interest in the petroleum industry (21, 22). The removal of these compounds from exhausted gases has been studied by Mastral et al. (23–25). However, the studies on the adsorption of PAHs from non-aqueous media are scarce. Therefore, the objective of this work is to investigate the possibility of the minimization of PAHs compounds from organic media using activated carbon. Further, more different factors affecting the adsorption process of PAHs from non-aqueous media will be investigated.

EXPERIMENTAL

Reagents and Materials

A commercial activated carbon (CAC) manufactured by BDH, chemical laboratory supplies (Poole, BH15 1TD, England) was used as a solid adsorbent without further treatment and activated in a vacuum oven at 473.15 K overnight. The BET surface area, the average pore diameter, and other physical parameters of the CAC are summarized in Table 1.

High purity (98–99%) PAHs, namely naphthalene (NA), anthracene (AN), and pyrene (PY) were obtained from Merck. The solid adsorbates were dissolved in the required hydrocarbon solvents to simulate the media of hydrocracker output fluids. BDH (UK) and Fluka (Switzerland) organic solvents, namely hexane, n-heptane, cyclohexane, benzene, and methanol were used without further purification. Benzene was used as the base unit for the PAHs compounds. The non-polar solvents hexane, heptane, and cyclohexane represent the major components in the hydrocracker output fluids. Methanol was used to investigate the influence of solvent polarity on the adsorption of PAHs onto the CAC. The PAHs used in this study and their solubility in mole fraction are listed in Table 2.

Table 1. Physical properties of the CAC adsorbent

Property	Value
BET surface area, m ² /g	734
Total pore volume, cm ³ /g	0.4335
Average pore diameter, °A	23.6
Bulk density, g/L	500

Particle size, mm 850–1700
 Ash content, % (w/w) 5–8

Table 2. Mole fraction solubility for the PAHs in different solvents at 298–299

PAHs/ solvent	Methanol	Hexane	Heptane	Cyclohexane	Benzene	Ref.
Naphthalene	0.0235	0.1168	0.1300	0.1487	0.2946	(27, 28)
Anthracene	0.00024	0.00129	0.00157	0.00157	0.00742	(29)
Pyrene	0.00149	0.00852	0.01101	0.01089	0.06316	(30, 31)

Apparatus

A thermostated water bath shaker (model SB-16, Techni Inc. UK) equipped with a temperature controller (Tempter Junior TE-8J) was used in the batch experiments. A Pye-Unicam double beam UV-Visible spectrophotometer (SP400, UK) was used for measuring the absorbance of each PAH at I_{\max} versus solvent blank. The adsorption of a pure solvent in its gaseous state onto a CAC adsorbent was critically investigated using the apparatus given in Fig. 1. The apparatus is composed of two reservoirs one for the adsorbent (1) and the other one for pure solvent (2). The two reservoirs are connected to each other via two valves (3 and 4) and a manifold was connected to a vacuum pump through a valve (5).

Recommended Batch Sorption Procedures

To investigate the effect of the solvent polarity on the adsorption of the different PAHs onto the CAC adsorbent, the adsorption isotherms of each

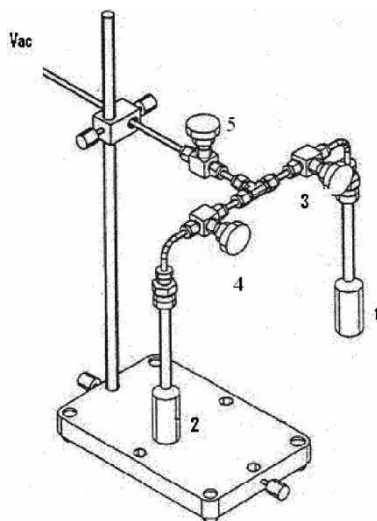


Figure 1. Apparatus for adsorption of pure solvent onto activated carbon.

PAHs were constructed. In a series of Erlenmeyer flasks (100 ml capacity), a known weight ($0.25 \pm .001$ g) of the solid adsorbent was added to 50 ml of the PAHs compound at a concentration ranging from 50 to 1,000 mg/l in the appropriate organic solvent. The flasks were shaken in a thermostated water bath shaker kept at $25 \pm 0.18^\circ\text{C}$ for 48 h. The adsorbent particles were separated from the solution by filtration and the equilibrium concentration of the required PAHs was determined spectrophotometrically at λ_{max} . The amount of the PAH adsorbed on the activated carbon was finally calculated employing the equation:

$$q_e = \frac{V}{W} (C_0 - C_e) \quad (1)$$

where, q_e is the amount of PAHs adsorbed at equilibrium (mg/g); C_0 and C_e are the initial and equilibrium concentrations of PAHs (mg/l), respectively; V is the volume of the sample in liter; and W is the weight of the adsorbent in grams.

Determination of Adsorption Capacity

Semi-quantitative tests were performed separately for the adsorption of each solvent as a single component from a gaseous state. A known mass of activated carbon was placed in a reservoir (1), and a suitable volume of a solvent was

then placed in the other reservoir (2). The apparatus was evacuated for several minutes while the valve on the solvent line was closed, and the evacuation continued in the activated carbon line. After 30 minutes, the valve from the evacuation line to the pump was closed and the activated carbon line went in a vacuum. The adsorption started slowly through the opened valve on the solvent line (4) and left for several days to reach equilibrium. After equilibrium, the activated carbon sample was reweighed and the increase in the adsorbent weight was then calculated.

The amount of solvent adsorbed at room temperature was then calculated.

RESULTS AND DISCUSSION

It is well known that the adsorption of PAHs onto porous solids is complicated by the structure of the PAHs molecule and the energetically heterogeneous nature of the solid surface. Thus, the surface area available in the geometrical sense, to the large molecule may contain a range of adsorption sites of different adsorptive power. The adsorption phenomenon is a manifestation of complicated interactions among the adsorbent, the adsorbate, and the solvent involved. The affinity between the adsorbent and the adsorbate is the main factor controlling the adsorption process (26). Thus, the influence

Table 3. Adsorption capacities of CAC towards pure solvents and pyrene

Solvent	Polarity	Dielectric constant	Solvent adsorbed mg/g	Pyrene adsorbed mg/g
Methanol	Polar (aliphatic)	32.63	234.21	182.84
Hexane	Non-polar (aliphatic)	1.90	240.40	165.93
Cyclohexane	Non-polar (cyclic)	2.00	281.70	151.14
Heptane	Non-polar (aliphatic)	1.90	293.71	149.03
Benzene	Non-polar (aromatic)	2.30	346.97	65.08

of the chemical structure of the adsorbate and the polarity of the non-aqueous solvent has been critically investigated.

A preliminary investigation of the adsorption capacities of the CAC towards pure organic solvents are summarized in Table 3. The data revealed that the aromatic solvent (benzene) adsorbs to CAC better than the polar solvent (methanol). Furthermore, the adsorption of pure solvents with the same number of carbons (i.e. n-hexane, cyclohexane, and benzene) is dependent of the chemical structure of the solvent. The high affinity of CAC towards aromatic solvent can be attributed to its aromatic nature rather than the solvent polarity where the dielectric constant slightly increases from aliphatic to aromatic hydrocarbons.

The adsorption capacities of CAC towards PY from non-aqueous solvents are also, listed in Table 3. The data reveals that the chemical structure of the solvent plays an important role in the adsorption process. It can be seen that the adsorption of PY mixed with polar or non-aromatic solvents is higher than that mixed with the aromatic solvent. The high affinity of a CAC towards an aromatic hydrocarbon solvent creates a competition between the solvent and PAHs molecules as a result of the aromaticity of these molecules. Thus, the aromatic solvent molecules are able to compete with PY molecules and reduce the adsorption uptake to one-third of its uptake from methanol. Due to the aromatic nature of benzene molecule, a p-p complex will be formed between the p- electrons of the benzene rings and the active sites on the carbon surface (27). The small molecular size of the benzene molecule, as compared to PY molecular size, enhances the adsorption of benzene by diffusion to narrow pores which are inaccessible for the large PY molecule. A little competition between the non-aromatic hydrocarbon solvents and PY molecules has been noticed. This explains why activated carbon has lower adsorption capacities for PY in an aromatic solvent than in cyclic and aliphatic hydrocarbon solvents.

Figures 2–4 clearly shows the adsorption capacity of a CAC towards PAHs in organic solvents is a function of PAHs structure and solvent polarity. In other words, PY (four fused aromatic rings) adsorbs to CAC better than NA and AN (two and three fused aromatic rings, respectively). Additionally, the adsorption of PY in methanol is higher than that in

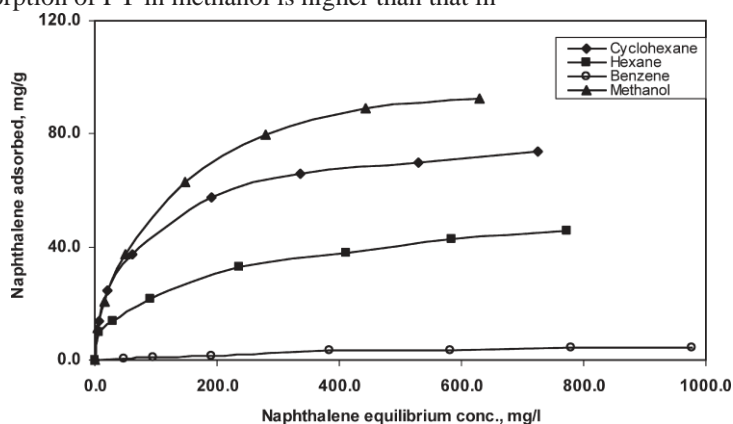


Figure 2. Adsorption isotherms of naphthalene onto CAC from organic solvent at 25 + 0.18C.

non-polar hydrocarbons solvents. This behavior is most likely attributed to the difference in the polarity of methanol and hydrocarbon solvents. The low solubility of PAHs in a polar solvent and their high affinity to the nonpolar

surface of the activated carbon may represent an important parameter for increasing the adsorption capacity from methanol.

The high affinities between PAHs and benzene as a solvent (solubility) restrict the adsorption of PAHs molecules in the aromatic solvent (28). The solubility of a substance decreases as the difference between its polarity and the polarity of the solvent increases. Thus, the adsorbed amount of the PAH molecule increases as its solubility in the solvent decreases.

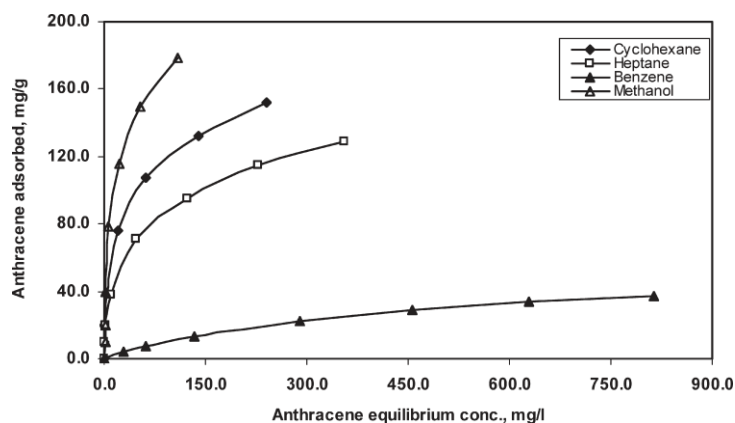


Figure 3. Adsorption isotherms of anthracene onto CAC from organic solvent at 25 + 0.18C.

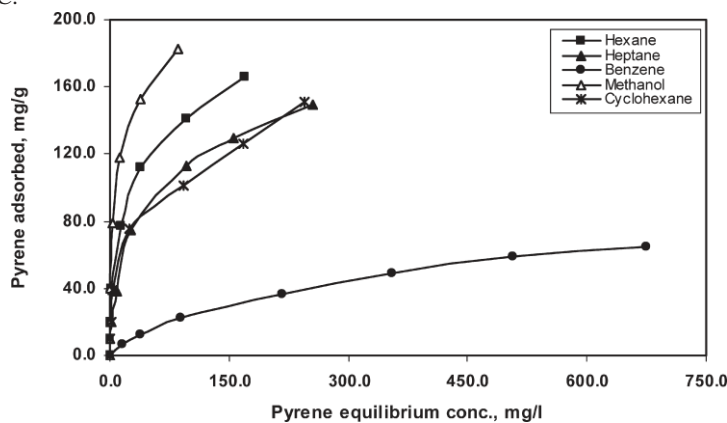


Figure 4. Adsorption isotherms of pyrene onto CAC from organic solvent at 25 + 0.18C.

Figure 5 shows the effect of the PAH's molecular weight on the adsorption process. An increase in the number of aromatic rings in a PAH molecule decreases its solubility and as a result its adsorption ability to activated carbon increases (29–33).

Table 4 reflected the influence of the solubility of the PAHs on their adsorption ability to activated carbon. The maximum adsorption capacity for the tested PAHs was obtained in methanol due to the lowest affinity between the PAHs molecules and the solvent molecules. The PAHs have low solubility in methanol due to incompatible intermolecular forces while the PAHs have a high solubility and great interaction forces towards benzene molecules, yielding a minimum adsorption capacity in an aromatic

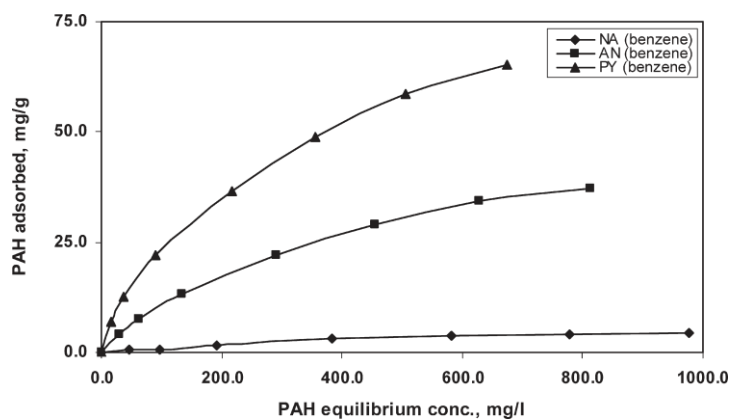


Figure 5. Adsorption isotherms of the tested PAHs in benzene at 25 + 0.18C.

Table 4. Adsorption capacities of CAC towards some PAHs in different solvents

PAHs	Solvent				
	Methanol mg/g	Hexane mg/g	Heptane mg/g	Cyclohexane mg/g	Benzene mg/g
Naphthalene	92.62	45.50	53.47	75.97	4.40
Anthracene	178.15	—	129.04	151.93	37.30
Pyrene	182.84	165.93	149.03	151.14	65.08

solvent. The adsorption uptake follow the order:

Methanol . n-hexane . cyclohexane

Increasing of the molecular weight of the aliphatic solvents (e.g., hexane and heptane) has little effect on the adsorption capacity of NA and PY (Fig. 6). It was noticed that, there is a slight increase in PY uptake in hexane than in heptane which can be attributed to the lower solubility of PY in hexane.

Furthermore, the adsorption of PAH from cyclic hydrocarbon solvents (e.g., cyclohexane) increases is high compared to PAHs from aliphatic hydrocarbon solvents (Fig. 7).

The adsorption isotherms of the tested PAHs in different organic solvents using CAC at $25 + 0.18C$ are demonstrated in Figs. 2–4. The adsorption of PAHs showed isotherms close to type I (34). The initial part of the isotherm represents the micropore filling. The slope of the plateau at higher concentrations is due to multilayer adsorption on the non-microporous surface (mesopores, macropores, and the external surface) (23).

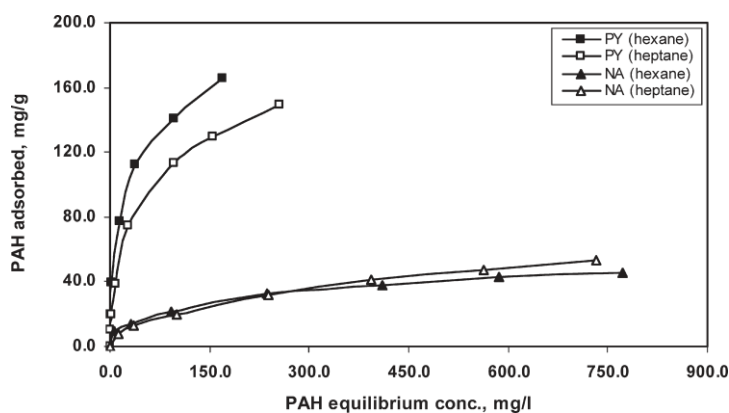


Figure 6. Adsorption of naphthalene and pyrene from hexane and heptane at $25 + 0.18C$.

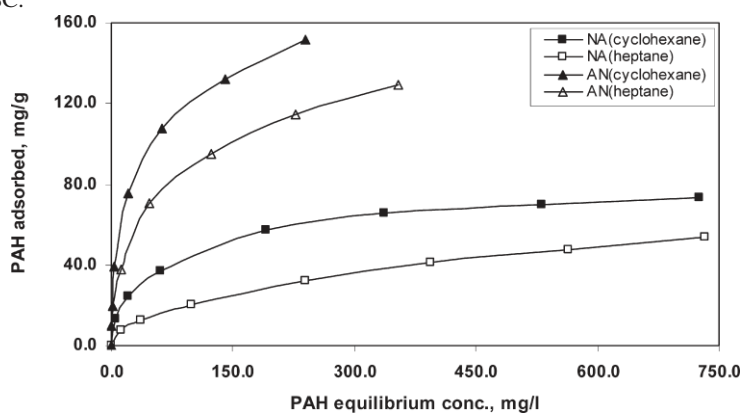


Figure 7. Adsorption of naphthalene and anthracene from cyclohexane and heptane at $25 + 0.18C$.

The Langmuir and Freundlich models were employed for modeling the adsorption isotherms (35). The linear forms for Langmuir and Freundlich models are as shown in Eqs. (2–3), respectively:

$$\frac{C}{q_e} = \frac{1}{K_L} + \frac{a_L}{K_L} C_e \quad (2)$$

$$\frac{1}{\log C_e} = \frac{1}{n} \log K_F + \frac{1}{n} \log q_e \quad (3)$$

where, q_e is the adsorption capacity at equilibrium (mg/g); C_e is the adsorbate equilibrium concentration mg/l, K_L and a_L are the Langmuir constants (l/mg), K_F and n are the Freundlich constants.

The data suggest the applicability of the Langmuir isotherm for the present systems, and formation of monolayer coverage of the adsorbate at the outer surface of the adsorbent. Langmuir constants and correlation coefficient (R^2) in organic solvents are summarized in Table 5. The R_L values for all studied systems were found in the range 0, $R_L, 1$ suggesting favorable adsorption of PAHs onto the investigated adsorbent.

The parameters K_F and n of the linear plots using Freundlich equation are reported in Table 6. The n values for all studied systems, range between 1.320 and 2.892. The minimum value being for adsorption of PAHs from benzene while the maximum value is for adsorption from methanol. The results are in good agreement with the data reported in literature (36). Table 6 shows that the highest K_F values obtained are for adsorption of PAHs from methanol systems while the lowest values are for the adsorption of PAHs from benzene solvent.

Langmuir parameters						
PAHs	Solvent	$K_L \text{ dm}^3 \text{ g}^{-1}$	$a_L \text{ dm}^3 \text{ mg}^{-1}$	$q_{\text{max}}, \text{ mg g}^{-1}$	$R_L (2)$	R_2
Naphthalene	Methanol	1.428	0.014	102.35	0.067	0.99
	Cyclohexane	1.493	0.019	77.630	0.049	0.986
	Hexane	0.573	0.012	48.890	0.079	0.959
	Heptane	0.383	0.006	61.519	0.138	0.970
	Benzene	0.011	0.001	8.047	0.422	0.980
Anthracene	Methanol	14.201	0.072	197.72	0.014	0.983
	Cyclohexane	10.774	0.070	154.830	0.014	0.971
	Heptane	5.041	0.038	132.803	0.0257	0.970
	Benzene	0.139	0.003	54.978	0.284	0.998
Pyrene	Methanol	37.749	0.200	188.90	0.005	0.985
	Cyclohexane	8.889	0.060	149.22	0.017	0.950
	Hexane	16.307	0.097	168.676	0.010	0.964

Heptane	7.055	0.045	155.172	0.022	0.982
Benzene	0.364	0.004	84.988	0.189	0.991

Table 5.
Langmuir parameters for
PAHs adsorption from
Adsorption of PAHs onto Activated Carbon 3619

different solvents

Table 6. Freundlich parameters for PAHs adsorption from different solvents

PAHs	Freundlich parameters			
	Solvent	K_F (dm ³ g ⁻¹)	n	R_2
Naphthalene	Methanol	5.666	2.185	0.962
	Cyclohexane	8.013	2.822	0.965
	Hexane	4.669	2.892	0.994
	Heptane	2.314	2.095	0.999
Anthracene	Benzene	0.028	1.320	0.938
	Methanol	17.675	1.816	0.916
	Cyclohexane	19.905	2.536	0.981
	Heptane	13.830	2.527	0.989
Pyrene	Benzene	0.475	1.502	0.988
	Methanol	31.091	2.174	0.928
	Cyclohexane	18.754	2.579	0.988
	Hexane	26.106	2.649	0.988
	Heptane	14.657	2.278	0.980
	Benzene	1.376	1.657	0.993

CONCLUSION

The adsorption of PAHs onto non-polar adsorbents such as activated carbon depends on the chemical structure of the solvent and the solvent aromaticity. The adsorption capacity of the PAHs on CAC from organic solvents containing aromatic ring decreases due to the competition between the aromatic solvent and PAHs molecules. The polarity of media has a significant effect on the adsorption capacity of the adsorbent. The low solubility of the PAHs in polar solvents increases the adsorption uptake due to the lower affinity between PAHs and polar media. The adsorption isotherms of the tested PAHs can be predicted successfully using Langmuir and Freundlich isotherms with good correlation coefficients.

REFERENCES

1. Casarett, L.J. and Doull, J. (1996) *Toxicology: the Basic Science of Poisons*, 5th Edn.; McGraw-Hill: New York.
 2. Eisler, R. (1987) Polycyclic aromatic hydrocarbon hazards to fish, wildlife, and invertebrates: A Synoptic Review. Biological Report, 85.
 3. Moore, S.W. and Ramamoorthy, S. (1984) *Organic Chemicals in Natural Waters. Applied Monitoring and Impact Assessment*; Desanto, R.S. (ed.); Springer Verlag: New York.
 4. Blumer, M. (1976) Polycyclic aromatic hydrocarbons in nature. *Sci. Am.*, 234: 35.
 5. Wild, S.R. and Jones, K.C. (1989) The effect of sludge treatment on the organic contaminant content of sewage sludge. *Chemosphere.*, 19: 1765.
- Adsorption of PAHs onto Activated Carbon 3621
6. Barr, D.P. and Aust, S.D. (1994) Mechanisms white rot fungi use to degrade pollutants. *Environ. Sci. Technol.*, 28: 78.
 7. Meulenbergh, R., Rijanrnts, H.M., Doddema, H.J., and Field, J.A. (1997) Partially oxidized polycyclic aromatic hydrocarbons show an increased bioavailability and biodegradability. *FEMS Microbiol. Lett.*, 152: 45.
 8. Sepic, E., Bricelj, M., and Leskovsek, H. (1997) Biodegradation studies of polyaromatic hydrocarbons in aqueous media. *J. Appl. Microbiol.*, 83: 561.
 9. Chang, B.V., Chang, S.W., and Yan, S.Y. (2003) Anaerobic degradation of polycyclic aromatic hydrocarbons in sludge. *Adv. Environ. Res.*, 7: 623.
 10. Altschuler, L. and Berliner, E. (1966) Rates of bromination of polynuclear aromatic hydrocarbons. *J. Am. Chem. Soc.*, 88: 5837.
 11. Rivas, F.J., Beltrán, F.J., and Acedo, B. (2000) Chemical and photochemical degradation of acenaphthylene. Intermediate identification. *J. Hazard. Mater.*, B75: 89.
 12. Corless, C.E., Reynolds, G.L., Graham, N.J.D., and Perry, P. (1990) Ozonation of pyrene in aqueous solution. *Water Res.*, 24: 1119.
 13. Sundstrom, D.W., Weir, B.A., and Klei, H.E. (1989) Destruction of aromatic pollutants by UV light catalyzed oxidation with hydrogen peroxide. *Environ. Prog.*, 8: 6.
 14. Sundstrom, D.W., Weir, B.A., Barber, T.A., and Klei, H.E. (1992) Destruction of aromatic pollutants and microorganisms in water by UV light and hydrogen peroxide. *Water Pollut. Res. J. Can.*, 27: 57.
 15. Zevos, N. and Sehensted, K. (1978) Pulse radiolysis of aqueous naphthalene solutions. *J. Phys. Chem.*, 82: 138.
 16. Walters, R.W. and Luthy, R.G. (1984) Equilibrium adsorption of polycyclic aromatic hydrocarbons from water onto activated carbon. *Environ. Sci. Technol.*, 18: 395.
 17. Streuli, C.A. (1971) The interaction of aromatic compounds in alcohol solution with Sephadex LH-20 dextran. *J. Chromatogr.*, 56: 219.
 18. Ake, C.L., Wiles, M.C., Huebner, H.J., McDonald, T.J., Cosgriff, D., Richardson, M.B., Donnelly, K.C., and Phillips, T.D. (2003) Porous organoclay composite for the sorption of polycyclic aromatic hydrocarbons and pentachlorophenol from groundwater. *Chemosphere.*, 51: 835.
 19. Eltekov, Yu.A., Khopina, V.V., and Kiselev, A.V. (1972) Effect of silica surface dehydroxylation on adsorption of aromatic hydrocarbons from solution in n-alkanes. *J. Chem. Soc. Faraday Trans. I.*, 68: 889.
 20. Cavalcante, C.L. Jr. and Ruthven, D.M. (1995) Adsorption of branched and cyclic paraffins in silicalite. 1. equilibrium. *Ind. Eng. Chem. Res.*, 34: 177.

21. Ali, S.H., Al-Mutairi, F.S., and Fahim, M.A. (2005) Solubility of polycyclicaromatics in binary solvent mixtures using activity coefficient models. *Fluid Phase Equilib.*, 230: 176.
22. Al-Sharrah, G.K., Ali, S.H., and Fahim, M.A. (2002) Solubility of anthracene into two binary solvents containing toluene. *Fluid Phase Equilib.*, 193: 191.
23. Mastral, A.M., Garcia, T., Callen, M.S., Murillo, R., Navarro, M.V., and Lopez, J.M. (2002) Sorbent characteristics influence on the adsorption of PAC: I. PAHs adsorption with the same number of rings. *Fuel Proc. Technol.*, 77–78: 373.
24. Mastral, A.M., Garcia, T., Murillo, R., Callen, M.S., Lopez, J.M., and Navarro, M.V. (2003) Measurements of polycyclic aromatic hydrocarbon adsorption on activated carbons at very low concentrations. *Ind. Eng. Chem. Res.*, 42: 155.
25. Mastral, A.M., Garcia, T., Murillo, R., Callen, M.S., Lopez, J.M., Navarro, M.V., and Galban, J. (2003) Study of the adsorption of polyaromatic hydrocarbon binary mixtures on carbon materials by gas-phase fluorescence detection. *Energy and Fuels.*, 17: 669.
26. Furuya, E.G., Chang, H.T., Miura, Y., and Noll, K.E. (1997) A fundamental analysis of the isotherm for the adsorption of phenolic compounds on activated carbon. *Sep. Purif. Technol.*, 11: 69.
27. Radovic, L.R., Moreno-Castilla, C., and Rivera-Utrilla, J. (2000) "Carbon materials as adsorbents in aqueous solutions". In *Chemistry and Physics of Carbon*; Radovic, L.R. (ed.); Marcel Dekker: New York, 27, 227.
28. Marzec, A. (2000) Intermolecular interactions of aromatic hydrocarbons in carbonaceous materials: A molecular and quantum mechanics. *Carbon*, 38: 1863, and references therein.
29. Heric, E.L. and Posey, C.D. (1964) Interaction in nonelectrolyte solutions. solubility of naphthalene in some mixed solvents containing benzene. *J. Chem. Eng. Data.*, 9: 35.
30. Acree, W.E. Jr. (1994) *Polycyclic Aromatic Hydrocarbons in Pure and Binary Solvents*; Oxford University Press: Oxford, United Kingdom, 54.
31. Roy, L.E., Hernandez, C.E., and Acree, W.E. Jr. (1999) Solubility of anthracene in organic non-electrolyte solvents. Comparison of observed versus predicted values based upon Mobile Order Theory, polycyclic aromatic compounds 13: 105.
32. Roy, L.E., Hernandez, C.E., and Acree, W.E. Jr. (1999) Thermodynamics of mobile order theory. Part 3. Comparison of experimental and predicted solubilities for fluoranthene and pyrene. *Polycyclic Aromatic Compounds.*, 13: 205.
33. Judy, C.L., Pontikos, N.M., and Acree, W.E. Jr. (1987) Solubility of pyrene in binary solvent mixtures containing cyclohexane. *J. Chem. Eng. Data.*, 32: 60.
34. Brunauer, S. (1945) *The Physical Adsorption of Gases and Vapors*; Clarendon Press: Oxford, U.K.
35. Walters, R.W. and Luthy, R.G. (1984) Equilibrium adsorption of polycyclic aromatic hydrocarbons from water onto activated carbon. *Environ. Sci. Technol.*, 18: 395.
36. Adamson, A.W. (1990) *Physical Chemistry of Surfaces*, 5th Edn.; Wiley: New York.



available at www.sciencedirect.com



journal homepage: www.elsevier.com/locate/aca



Sorption characteristics and chromatographic separation of gold (I and III) from silver and base metal ions using polyurethane foams

A.B. Farag^{a,12}, M.H. Soliman^a, O.S. Abdel-Rasoul^a, M.S. El-Shahawi^{b,13,14}

^a Chemistry Department, Faculty of Science, Helwan University, Helwan, Egypt

¹² Corresponding author.

E-mail address: mohammad_elshahawi@yahoo.co.uk (M.S. El-Shahawi).

¹³ Present address: Department of Chemistry, Faculty of Science, King Abduaziz University, Jeddah, Saudi Arabia.

¹⁴ -2670/\$ – see front matter © 2007 Elsevier B.V. All rights reserved.

doi:10.1016/j.aca.2007.08.049

^b Chemistry Department, Faculty of Science at Damiatta, Mansoura University, Mansoura, Egypt

article in abstract

o

Article history: The influence of different parameters on the sorption profiles of trace and ultra traces of gold (I) species from the aqueous cyanide media onto the solid sorbents ion exchange polyurethane foams (IEPUFs) and commercial unloaded polyurethane foams (PUFs) based polyether type has been investigated. The retention of gold (I) species on investigated solid sorbents followed a first-order rate equation with an overall rate constant k in the range $2.2\text{--}2.8 \pm 0.2 \text{ s}^{-1}$. The sorption data of gold (I) followed Freundlich and Langmuir isotherm models. Thus, the dual-mode of sorption mechanism involving absorption related to “weak base anion exchanger” and an added component for “adsorption” seems the most likely proposed dual mechanism for retention profile of gold (I) by the IEPUFs and PUFs solid sorbents. The capacity of the IEPUFs and PUFs towards gold (I) sorption calculated from the sorption isotherms was found to be 11.21 ± 1.8 and $5.29 \pm 0.9 \text{ mg g}^{-1}$, respectively. Chromatographic separation of the spiked inorganic gold (I) from deionized water at concentrations $5\text{--}15 \text{ g mL}^{-1}$ onto the developed IEPUFs and PUFs packed columns at 10 mL min^{-1} flow rate was successfully achieved. The retained gold (I) species were then recovered quantitatively from the IEPUFs ($98.4 \pm 2.4\%$, $n=5$) and PUFs ($95.4 \pm 3.4\%$, $n=5$) packed columns using perchloric acid (60 mL , 1.0 mol L^{-1}) as a proper eluting agent. Thiourea (1.0 mol L^{-1})– H_2SO_4 (0.1 mol L^{-1}) system was also used as eluting agent for the recovery of gold (I) from IEPUFs ($95.4 \pm 5.4\%$, $n=3$) and also PUFs ($93.4 \pm 4.4\%$, $n=3$) packed columns. The performance of the IEPUFs and PUFs packed columns in terms of the height equivalent to a theoretical plate (HETP), number of plates (N), and critical and breakthrough capacities towards gold (I) species were evaluated. The developed IEPUFs packed column was applied successfully for complete retention and recovery ($98.5 \pm 2.7\%$) of gold (III) species spiked onto tap and industrial wastewater samples at $<10 \text{ g Au mL}^{-1}$ after reduction to gold (I). The IEPUFs packed column was applied satisfactorily for complete retention and recovery ($98.5 \pm 2.7\%$) of total inorganic gold (I) and/or gold (III) species spiked onto tap- and industrial wastewater samples at $<10 \text{ g mL}^{-1}$ gold. Chromatographic separation of gold (I) from silver (I) and base metal ions (Fe, Ni, Cu and Zn) using IEPUFs and PUFs packed columns was satisfactorily achieved. The proposed method was applied successfully for the pre-concentration and separation from anodic slime and subsequent determination of analyte with satisfactory results (recoveries $>95\%$, relative standard deviations $<4.0\%$).

Keywords:

Polyurethane foam sorbent

Gold (I)

retention

Kinetics

Sorption models

Sorption mechanism

Chromatographic separation

Silver and base metal ions

© 2007 Elsevier B.V. All rights reserved.

1. Introduction

Gold is one of the most important noble metals due to its wide applications in industry and economic activity, yet it is not naturally abundant. Gold is the ultimate refuge from political, economic and financial calamity [1,2]. Gold and silver are commonly found associated with each other and have important applications, but a significant partition of their demand is for jewelry, coinage and decorative arts [2]. The concentration level of gold in basic rocks and soil are about 4.0ngg^{-1} and 1.0ngg^{-1} [3], respectively. The values of 0.05 and 0.2ngmL^{-1} were found in seawater and river water, respectively [3]. Due to the importance and low level of gold in the environmental

samples, a simple, sensitive and selective method for gold separation and determination has been required. Several articles have been published on the pre-concentration of traces of gold in water and other matrixes before their actual determination via solvent extraction, liquid solid and selective transport through liquid membrane [3–16].

Recent years have seen an upsurge interest in the application of a number of solid sorbents e.g. foamed plastics, chelating polymers and silica gel in the reversed phase extraction chromatography, gas–solid and gas–liquid partition chromatography for the pre concentration, separation and subsequent determination of a series of trace metal ions including gold [16–36]. The membrane structure and the available surface area of the polyurethane foams make it very suitable stationary phase and as a column filling material [21–26]. Ion exchange polyurethane foams (IEPUFs), unloaded PUFs and PUFs immobilizing specific reagents have been successfully employed for the separation and determination of metal ions [17–22, 26–36] including gold [17, 18, 23–26] on domestic water; river water, raw sewage and secondary treated sewage.

In contrary to precious group metals (PGM), so far, no papers concerning inorganic gold (I) and gold (III) determination at ultra trace levels in the environmental samples employing polyurethane solid sorbents have been published. Therefore, the goals of the present article are aimed at developing simple, convenient and low cost procedures for the pre-concentration, selective separation and sequential determination of total inorganic gold (I) and gold (III) at ultra trace level in water after reduction of the latter to mono valence gold ions. The salient features regarding the selective separation of inorganic gold (I) and gold (III) in aqueous media from silver (I) and some other base metal ions (Fe, Ni, Cu and Zn) in anodic slime or fresh water samples using IEPUFs packed columns were critically examined.

silver nitrate and sodium hydroxide (BDH Ltd., Poole, England) were used for the preparation of stock solutions of gold (I), gold (III), silver (I) and NaOH in de ionized water, respectively. Other chemicals e.g. HNO_3 , $\text{Na}^{15}\text{SO}_3$, H^{16}O_2 , HCl, HClO_4 , KCN and thiourea (Aldrich Chemical Company, Milwaukee, WC, USA) were used without further purification. Commercial polyurethane foam (PUFs) plugs (30kgm^{-3}) were cut as cubes (10–15mm), washed, dried at 80 ± 0.1 °C in 250mL beaker as described

earlier [17,18] and were stored in low density polyethylene (LDPE) bottle, Nalgene in dark for further work. Stock solutions (1000gmL^{-1}) of iron(III), nickel (II), copper (II) and zinc (II) were obtained from BDH and were used for the preparation of more diluted solutions in de ionized water. A stock solution (1000gmL^{-1}) of gold (I) was prepared by dissolving the required weight of $\text{KAu}(\text{CN})_2$ in alkaline NaOH (0.1molL^{-1}). A series of Britton–Robinson (B–R) buffer (2–11) was prepared by mixing equal proportions of acetic (0.04molL^{-1}), phosphoric (0.04molL^{-1}) and boric (0.04molL^{-1}) acids (BDH) in double distilled water and the pH of the solutions were then adjusted to the required pH by adding various volumes of NaOH (0.2molL^{-1}) solution as reported earlier [37].

2.2. Apparatus

A Perkin-Elmer (model A Analyst TM 800, Norwalk, Ct, USA) atomic absorption spectrometer (AAS) was used for measuring the concentration of Au, Ag, Fe, Ni, and Cu at the wavelengths 242.8, 328.1, 372.0, 232.0 and 324.7nm, respectively at 0.7nm slit width except for iron and nickel at 0.2nm at oxidant (air) flow of 20.0Lmin^{-1} and acetylene flow of 1.5Lmin^{-1} before and after separation step from the aqueous phase under instrument's optimum settings. Flame emission atomic spectrometry (FAES) was also used for the determination of ultra trace of gold at 267.6nm, 0.2nm slit width, oxidant flow of 16.0Lmin^{-1} and 7.8Lmin^{-1} acetylene flow. De-ionized water was obtained from Milli-Q Plus system (Millipore, Bedford, MA, USA) and was used for the preparation of all solutions. A thermo Orion model 720 pH meter (Thermo Fisher Scientific, MA, USA) was employed for the pH measurements with absolute accuracy limits at the pH measurements being defined by NIST buffers. Glass columns (18cm×15mm i.d.) and a variable GFL mechanical Shaker model 1063 (Gesellschaft Fur Laboratechnik, mbH, Burgwedel, Germany) with a shaking rate in the range 10–250rpm were used for the retention experiments of gold (I) species at different pH.

2.3. Synthesis of the ion exchange polyurethane foam (IEPUFs)

IEPUFs sorbent was prepared by mixing the polyether ($20\pm 0.1\text{g}$), de-ionized water ($1.0\pm 0.1\text{g}$), dimethylene ethanolamine ($0.04\pm 0.001\text{g}$), stannous octoate ($0.04\pm 0.001\text{g}$) and polyether polysiloxane ($0.25\pm 0.01\text{g}$). The mixture was stirred to complete homogeneity and an accurate weight of Amberlite IR 400 of pore diameter 9nm and bead size 20–60 mesh was added with continuous stirring for 5min and toluene di-isocyanate ($13.0\pm 0.1\text{g}$) was then added gradually during stirring. The mixture was finally poured in a box for 24h, dried and stored in polyethylene bottles. The prepared IEPUFs were cut into cubes (10–15mm) washed and dried as reported earlier [17,18].

Analytical-reagent grade chemicals and solvents were provided by BDH (BDH Ltd., Poole, England), unless stated otherwise, and were used without further purification. Analytical grade potassium aurocyanide, $\text{KAu}(\text{CN})_2$ (Fluka, AG, Buchs, Switzerland), HAuCl_4 (E. Merck, Darmstadt, Germany),

15. Experimental

16.1. Reagents and materials

2.4. Batch experiments

In a thermo stated mechanical shaker, an accurate weight (0.05 ± 0.001 g) of IEPUFs or PUFs sorbent was shaken at 200rpm shaking rate with 25mL of an aqueous solution containing gold (I) species (5 gmL^{-1} Au) at different pH up to 2h at 25 ± 0.1 °C. After equilibrium, the amount of gold (I) retained on the foam sorbent, the extraction percentage, % *E*, the distribution coefficient, *K_d* and the sorption capacity, *Q* in mmol g^{-1} were then determined from the difference between the concentration of gold (I) determined in the aqueous phase before (*C_b*) and after (*C_a*) shaking with the foam sorbent under instrument's optimum settings. The concentration of the produced gold ions was then determined with the aid of calibration curve of gold (I) ions. Following these procedures, the effect of shaking time, potassium cyanide concentration (3.5×10^{-4} – 1.5×10^{-2} molL^{-1}), monovalent cation size (Na^+ , K^+ and NH_4^+), analyte concentration (1.0×10^{-4} – 20×10^{-4} molL^{-1}) and sorbent doze on the gold (I) retention was carried out. The values of % *E* and *K_d* are the average of three independent measurements and the precision in most cases was $\pm 2\%$.

2.5. Flow experiment

2.5.1. Retention and recovery of inorganic gold (I)

An aqueous solution (0.5L) spiked with gold (I) at concentration $\leq 15 \text{ gAu mL}^{-1}$ at pH 4–5 and in the presence of KCN (2%, w/v) was percolated through the IEPUFs or PUFs (1.0+0.01g) packed columns at 5 mLmin^{-1} flow rate using the vacuum method of foam packing [17,18]. A blank experiment was also carried out in the absence of gold (I) ions. The sample and the blank foam packed columns were then washed with 100mL of an aqueous solution containing potassium cyanide (2%, w/v). Complete retention of gold (I) ions took place as indicated from the determination of gold species in the effluent solution by AAS and/or FAAS as described before. Complete recovery of gold (I) content from the IEPUFs and PUFs packed columns was achieved by percolating HClO_4 (80mL, 1.0 molL^{-1}) or with an aqueous system (100–120.0mL) containing thiourea (1.0 molL^{-1})– H_2SO_4 (0.1 molL^{-1}) at 10 mLmin^{-1} flow rate. Equal fractions of the eluate were then collected for gold determination with FAAS or AAS.

2.5.2. Separation and recovery of inorganic gold (III)

An aqueous solution (0.1L) containing gold (III) species at concentration 1.0 – 5.0 gmL^{-1} was first treated with sodium sulfite (1.0 molL^{-1}) in the presence of HCl (1.0 molL^{-1}) and heated for 10min to reduce gold (III) to the mono valence gold (I) quantitatively. The resultant solutions were then boiled for 10min to release the excess SO_2 . After cooling the reaction mixtures at pH 4–5 and in the presence of KCN (2%, w/v) were then percolated through the IEPUFs (1.0±0.01g) packed columns at 5.0 mLmin^{-1} flow rate at the optimum conditions of gold (I) sorption described above. Complete sorption and recovery of gold (I) ions with perchloric acid (80mL, 1.0 molL^{-1}) was achieved as indicated from the determination of gold (I) with the aid of AAS and calibration curve constructed after reduction of gold (III) to gold (I) using the same experimental procedures.

2.5.3. Separation and recovery of total inorganic gold (I) and gold (III)

An aqueous solution of distilled-, tap- or industrial wastewater samples (0.1L) containing the binary mixture of gold (I) and (III) species at a total concentration $\leq 10 \text{ gmL}^{-1}$ was first treated with sodium sulfite (1.0 molL^{-1}) in

the presence of HCl (1.0 molL^{-1}) and heated for 15min to reduce gold (III) to gold (I) quantitatively. The test solution at the optimum conditions of gold (I) sorption described above was percolated through the IEPUFs (1.0 ± 0.01 g) packed columns at 5 mLmin^{-1} flow rate using the vacuum method of foam packing [16,17]. Complete sorption and recovery of gold (I) ions with perchloric acid (80mL, 1.0 molL^{-1}) was achieved as indicated from the analysis of gold species in the effluent of the test solution and after recovery by FAAS with the aid of AAS calibration curve for gold (I) and (III) constructed after reduction of gold (III) to gold (I) using the same reducing agent following the described procedures above.

2.5.4. Separation of gold (I) from silver (I) ions

An aqueous solution (0.5L) adjusted to pH 4–5 in LDPE bottle, Nalgene was spiked with gold (I) and silver (I) ions at a total concentration $\leq 5 \text{ gmL}^{-1}$ of each ion under the optimum conditions of gold (I) sorption was percolated through the IEPUFs (1.0+0.01g) packed columns at 5 mLmin^{-1} flow rate using the vacuum method of foam packing [17,18]. A blank experiment was also carried out in the absence of gold (I) ions. The sample and the blank IEPUFs packed columns were then washed with 100mL of an aqueous solution containing potassium cyanide (2%, w/v). Quantitative retention of gold (I) and silver (I) ions took place as indicated from their FAAS analysis in the effluent. The retained gold (I) and silver (I) species were then recovered quantitatively from the foam column with HClO_4 (80mL, 1.0 molL^{-1}) and an aqueous mixture of thiourea (120mL, 1.0 molL^{-1})– H_2SO_4 (0.1 molL^{-1}) at 5 mLmin^{-1} flow rate, respectively.

2.5.5. Separation of gold (I) from silver (I) and other base metal (Fe^{3+} , Ni^{2+} , Cu^{2+} , or Zn^{2+}) ions

An aqueous solution (0.5L) spiked with gold (I) and silver (I) and/or base metal (Fe^{3+} , Ni^{2+} , Cu^{2+} or Zn^{2+}) ions at a total concentration of 5 gmL^{-1} of each ion under the optimum conditions of gold (I) sorption was percolated through the IEPUFs columns at 5 mLmin^{-1} flow rate as described in the experimental section. FAAS analysis of the effluent solutions revealed quantitative sorption of gold (I), silver (I) and other base metal ions. The retained base metal ions (Fe^{3+} , Ni^{2+} , Cu^{2+} , or Zn^{2+}), gold (I) and silver (I) were then recovered quantitatively from the foam column by percolating H_2SO_4 (100mL, 0.05 molL^{-1}), HClO_4 (80mL, 1.0 molL^{-1}), thiourea (1.0 molL^{-1})– H_2SO_4 (0.1 molL^{-1}) mixture at 5 mLmin^{-1} flow rate, respectively.

2.5.6. Separation and subsequent determination of gold in anodic slime

The surface of the metallurgical sample (anodic slime) directly after washing was dried at 110 °C for two hrs. An accurate weight (0.2 – 0.25 ± 0.01 g) of the sample was decomposed with aqua regia (10mL) and the solution was evaporated to dryness and cooled. Ten milliliters of concentrated HNO_3 and 2.0mL H_2O_2 (30%, v/v) were added to the residue and the suspension was filtered through filter paper. The insoluble residue was washed with a solution containing dilute nitric acid. The contents of the reaction vessel and the washing solutions were heated on a water bath for 20min and diluted with distilled water in a 50mL calibrated flask. The sample solution was first treated with sodium sulfite (1.0 molL^{-1}) in the presence of HCl (1.0 molL^{-1}) and heated for 15min to reduce gold (III) to gold (I) in the sample. The test solution was then adjusted to pH 4–5 and percolated through the IEPUFs packed column at a reasonable flow rate 5 – 10 mLmin^{-1} then the general procedures were applied. A blank experiment was digested and analyzed following the same digestion and analytical procedures.

3. Results and discussion

3.1. Investigation of the various experimental variables

Preliminary experiments on the retention profile of gold (I) from the aqueous solutions onto the solid sorbents IEPUFs and the commercial unloaded PUFs have shown that the amount of gold (I) ions extracted depends on the solution pH. Therefore, the sorption profiles of gold (I) ions by the employed foam sorbents from the aqueous solutions containing B–R buffer (pH 2–12) were critically investigated after shaking for 2h. The amount of gold (I) retained at equilibrium, q_e , the extraction percentage, %E and the distribution ratio, D were then calculated employing the following equations [17,18]:

$$q_e = (C_b - C_a) \times v \quad (1) \quad w$$

$$\% E = \frac{(C_b - C_a) \times 100}{C_b} \quad (2)$$

$$D = \frac{\% E}{100} \times \frac{v}{\% E \quad w} \quad (3)$$

where C_b and C_a are the gold (I) concentrations determined with AAS in the aqueous phase before and after shaking with the solid sorbents, v and w are the volume (mL) of the aqueous solution and the weight (g) of the foam cubes as solid sorbents, respectively. The data are summarized in Fig. 1. The results revealed that the gold (I) retention by the tested solid sorbents in aqueous acidic solution of pH < 6, reached maximum. On the other hand, the retention of gold (I) onto the IEPUFs and PUFs decreased markedly on raising the solution pH higher than pH 6 (Fig. 1). This behavior is most likely attributed to the instability of the produced ternary complex ion associate of $[\text{Au}(\text{CN})_2]^-$ with the sorbent site of the IEPUFs or PUFs as reported earlier by El-Shahawi and Nassif [29] and Cordoba et al. [38] for $[\text{HgBr}_3]^-$ complex species and subse-

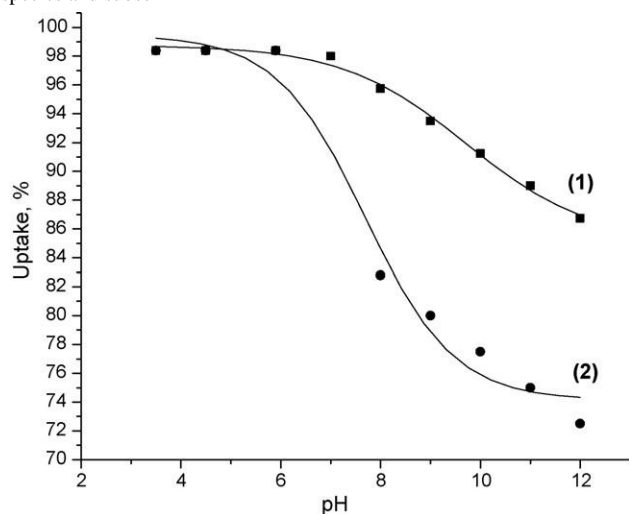
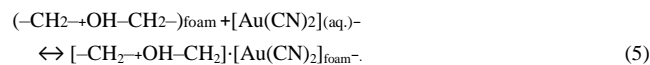
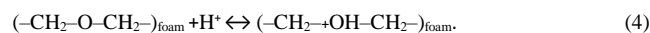


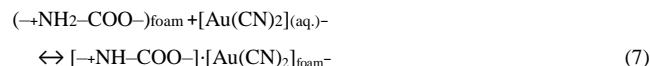
Fig. 1 – Influence of pH on the uptake percentage, % of gold (I) at 5.0 mg L^{-1} from aqueous cyanide media (2%, w/v) onto IEPUFs (1) and PUFs (2) at $25 \pm 0.1 \text{ } ^\circ\text{C}$.

quent hydrolysis. In acidic pH, the observed high retention of gold (I) species by the solid sorbents is most likely attributed to the protonation of the chelating sites (ether and/or urethane linkages) in the sorbents that enhanced the retention of the analyte via “solvent extraction and/or weak base anion exchange mechanism”. It has been shown that gold (I) and gold (III) can be extracted also by methyl isobutyl ketone and by solvents that possess ether linkages in their structures e.g. diethyl ether, isopropyl ether and polyurethane ether-type foams [16,22–28]. A similar retention profile for the extraction of aurocyanide ion-pairs with alkali metal ions into long chain poly ethers has been reported by Chow and co-workers [25,26]. Based on the results obtained and the data reported earlier [17,26,25–28], a possible “weak base anion ion exchanger” and a “solvent extraction” mechanism of the $[\text{Au}(\text{CN})_2]_{(\text{aq})}^-$ retention onto the protonated ether ($-\text{CH}_2-\text{HO}^+-\text{CH}_2-$) oxygen or urethane ($-\text{NH}_2^+\text{COO}-$) nitrogen linkages of the IEPUFs or PUFs as ternary complex ion associates in acidic media is most likely proceeds, respectively as follows:

Ether group, PUF:



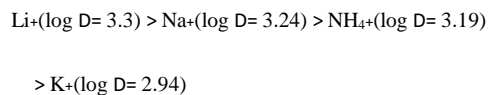
Urethane group, PUF:



The pK_a values of the protonation of the ether oxygen and/or urethane nitrogen ($-\text{NH}_2-\text{CO}-$) groups of the solid sorbents are 3 and 6 form [17,30,33], respectively. At pH higher than pH 6, the sorption of the unloaded PUFs solid sorbent towards $[\text{Au}(\text{CN})_2]^-$ decreased markedly as compared to the IEPUFs sorbent (Fig. 1). This behavior is most likely attributed to the deprotonation of the ether oxygen ($-\text{CH}_2-\text{OH}-\text{CH}_2-$) and/or urethane nitrogen ($-\text{NH}_2-\text{CO}-$) of the unloaded PUFs. Such effect is most likely minimizes the formation of the complex ion associate between the complex anion $[\text{Au}(\text{CN})_2]_{(\text{aq})}^-$ and the unloaded PUFs sorbent. The diffusion of gold (I) as $[\text{Au}(\text{CN})_2]^-$ through thin polyurethane film is most likely consistent with its solubility in the PUFs as reported earlier [39]. In this account, Gesser et al. [39] have suggested two alternative mechanisms for the sorption of the anionic metal complexes such as HMCl_4 e.g. HGaCl_4 by the PUFs. Based on the close resemblance between the obtained sorption data onto the PUFs and the extraction with diethyl ether, PUFs material is most likely behaves as a polymeric sorbent for the anionic complex. The other mechanism results from protonation of the ether sites in the polymer when coming into contact with acids in aqueous media i.e. the protonated sites act as anion exchangers in the extraction of $[\text{Au}(\text{CN})_2]^-$.

The influence of the competitive complexing anion (CN⁻) as potassium cyanide at various concentrations (3.5×10^{-4} – 1.5×10^{-2} molL⁻¹) on the sorption of gold (I) species (3.5×10^{-3} molL⁻¹) by the PUFs and IEPUFs from the aqueous media (pH 5–6) was carried out. The retention percentage (%*E*) of gold (I) species onto the solid sorbents increased on raising the cyanide ion concentration and reached maximum (*E*=83%) at 1:2 Au⁺:CN⁻ molar ratio. At a molar ratio of cyanide ions to gold (I) species higher than 2:1 a leveling off and a slight decrease (*E*=76%) of gold (I) retention onto the solid sorbents were noticed. The competitive extraction of CN⁻ onto the solid sorbents may account for the observed behavior. On the other hand, the gold (I) sorption onto the IEPUFs sorbent was also higher than that of PUFs towards gold (I). The increased number of the available active sites on the IEPUFs compared to that of the unloaded PUFs and the possibility of the former sorbent to act as a “weak anion ion exchanger” may also account for the trend observed.

The influence of the cation size of the ions Li⁺, Na⁺, K⁺ and NH₄⁺ as chloride salts at various concentrations (3.57×10^{-3} – 1.7×10^{-2} molL⁻¹) on the gold (I) retention by IEPUFs and PUFs was studied. On increasing the salt concentration, a significant decrease (~10–21%) in the sorption percentage of [Au(CN)₂]⁻ onto the solid sorbents was noticed and the order of extraction followed the sequence:



This trend is in accordance with the sequence of the hydrated radius of these mono valence ions: NH₄⁺>K⁺>Na⁺>Li⁺ [40]. This effect is most likely attributed to the reduction of the repulsive forces between adjacent sorbed gold (I) as complex anion [Au(CN)₂]⁻ [41]. The competitive extraction of the added anions may also be expected to be somewhat extractable as their neutral species like AuCl [23,26,38] and the ion-dipole interaction of NH₄⁺ with the oxygen sites of the PUFs is not the only predominating factor in the extraction step of gold (I). Thus, “solvent extraction” mechanism with the salt acting as salting-out agent is not only the most probable mechanism. Other processes like specific sites on the sorbent are possibly involved simultaneously in the [Au(CN)₂]⁻ sorption from the bulk aqueous solution [17]. The added Li⁺, Na⁺, K⁺ and NH₄⁺ ions may also reduce the number of water molecules available to solvate the gold (I) ions which would therefore, be forced out of the solvent phase onto the PUFs since some amount of the free water molecules are preferentially used to solvate the cations added. Therefore, it appears also that the water structure enforced ion-pairing (WSEIP) is some what the driving force for the extraction of [Au(CN)₂]⁻ [26,38]. These results are in good agreement with the data reported earlier [17,26].

The effect of the sorbent doze (*w*) and batch factor (*v/w*) on the gold (I) retention at 10gmL⁻¹ onto the IEPUFs and PUFs was investigated. The gold (I) sorption increased on increasing the sorbent doze up to 0.2g of the solid sorbent. Therefore, in the subsequent work, 0.2g of the solid sorbent IEPUFs or PUFs was employed. The sorption percentage of gold (I) onto the IEPUFs and PUFs decreased up to 60±3.5% and 45±2.8%, respectively on increasing the sample volume from 50.0mL to 500mL.

3.2. Kinetic behavior of gold (I) sorption onto IEPUFs and PUFs

In batch experiments, the gold (I) ion sorption onto the IEPUFs and PUFs sorbents was quite fast and the equilibrium was attained more or less a constant value in about 30min shaking and remained constant up to 2h. This conclusion was supported by calculation of the half-life time (*t*_{1/2}) of gold (I) sorption from the aqueous solutions onto the solid sorbents IEPUFs and PUFs. The values of *t*_{1/2} calculated from the plots of log *C/C*₀ versus time (Fig. 2) for gold (I) sorption onto IEPUFs and PUFs where *C*_b=*C*₀ and *C*=*C*_b-*C*_a. The values of *t*_{1/2} were found to be 2.34–2.73±0.05min, for both PUFs and IEPUFs sorbents. Thus, gel diffusion is not the rate-controlling step for IEPUFs as in the case of common ion exchange resins [17].

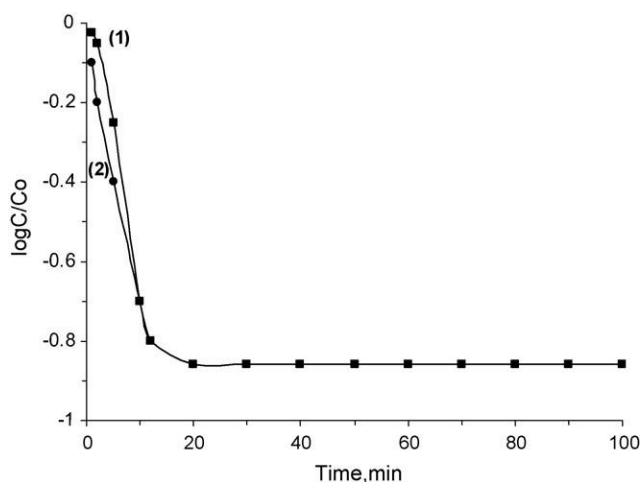


Fig. 2 – Rate of gold (I) sorption at 5.0gmL⁻¹ gold (I) ions from aqueous cyanide media (2%, w/v) onto IEPUFs (1) and PUFs (2) at pH 4–5 and 25±0.1°C.

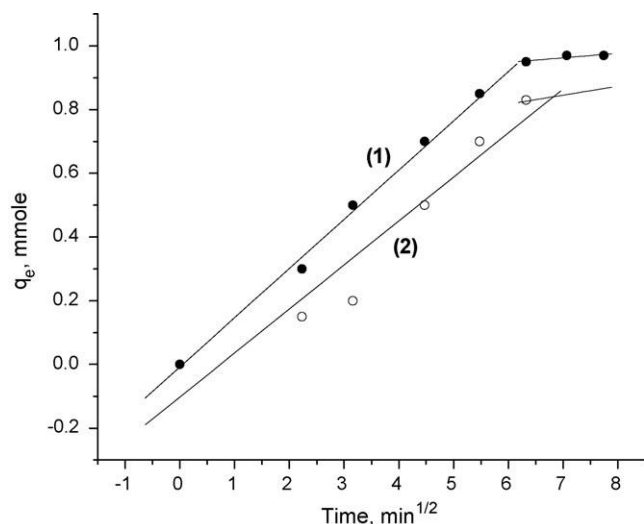


Fig. 3 – The sorbed concentration of gold (I) at 5.0g mL⁻¹ from aqueous cyanide media (2%, w/v) onto IEPUFs (1) and PUFs (2) as a function of time at pH 4–6 and 25±0.1°C.

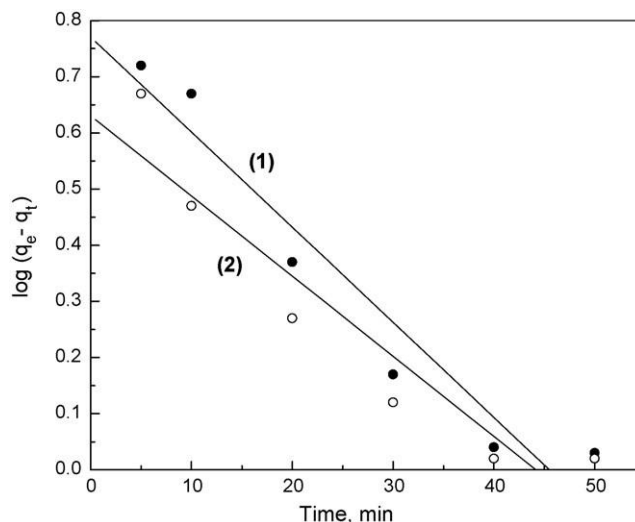


Fig. 4 – Lagergren plots of the kinetics of gold (I) uptake from aqueous cyanide media (2%, w/v) onto IEPUFs (1) and PUFs (2) as a function of time at pH 4–6 and 25±0.1°C.

Thus, a 60min shaking time was adopted in the subsequent work.

The kinetic behavior of gold (I) sorption onto IEPUFs and PUFs sorbents depends on film diffusion and intraparticle diffusion, and the more rapid one will control the overall rate of transport. Thus, the retained gold (I) species onto the used sorbents were subjected to Weber–Morris model [42]:

$$q_t = R_d(t)^{1/2} \quad (8)$$

where R_d is the rate constant of intraparticle transport in mmol g^{-1} and q_t is the sorbed gold (I) concentration (mol g^{-1}) at time t . The plots of q_t versus time were found linear ($R^2 = 0.954–0.979$) up to 40.6 ± 1.1 min for both IEPUFs and PUFs and deviate on increasing the shaking time (Fig. 3). The diffusion rate was found high in the initial stages and decreased on passage of time indicating that the rate of the retention step is film diffusion at the early stage of extraction. The values of R_d computed from the two distinct slopes of the Weber–Morris plots (Fig. 3) for IEPUFs and PUFs sorbent towards $[\text{Au}(\text{CN})_2]^-$ complex species were 154 ± 7 and $142 \pm 2 \text{ mmol g}^{-1} \text{ min}^{-1/2}$ in the initial stage up to 40.0min of agitation time and reduced beyond time higher than 40min, respectively. The change in the slope may be due to the existence of different pore sizes [30,33]. The values of R_d indicated that intra-particle diffusion step can be a rate controlling step.

Moreover, the rate constant for the retention step was evaluated in the light of Lagergren rate equation [43]:

$$\log(q_e - q_t) = \log q_e - \left(\frac{kt}{2.303} \right) \quad (9)$$

where q_e is the amount of gold (I) sorbed at equilibrium, per unit mass of sorbent (mmol g^{-1}) and k is the first-order overall rate constant for the retention process, s^{-1} and $t = \text{time, s}$. The plots of $\log(q_e - q_t)$ versus time were found linear as shown in Fig. 4. The values of k calculated from the slopes were found **Fig. 4 – Lagergren plots of the kinetics of gold (I) uptake**

in the range $2.2–2.8 \pm 0.2 \text{ s}^{-1}$ and suggested first order kinetics for the gold (I) retention towards the two used sorbents. The influence of different sorbent dose and adsorbate concentration was investigated. The results also indicate that the value of k increases on increasing the sorbent dose and adsorbate concentration confirming the formation of monolayer of gold (I) species onto the surface of the used adsorbent as well as the first order kinetic nature of the process.

The value of Bt , which is a mathematical function (F) of the ratio of the fraction sorbed (q_t) in mmol g^{-1} at time t and at equilibrium (q_e) in mmol g^{-1} i.e. $F = q_t/q_e$ was calculated for each value of F employing Reichenburg equation [44]:

$$Bt = -0.4977 - 2.303 \log(1 - F) \quad (10)$$

Plots of Bt versus time at 25 °C for both sorbents towards gold (I) species were found linear (Fig. 5) up to 40min. The straight lines do not pass through the origin indicating that particle diffusion mechanism is not only responsible for the kinetics of $\text{Au}(\text{CN})_2^-$ sorption onto the PUFs and IEPUFs sorbents. Thus, the uptake of $\text{Au}(\text{CN})_2^-$ onto the employed sorbents are most likely involved three steps: (i) bulk transport of $\text{Au}(\text{CN})_2^-$ in solution, (ii) film transfer involving diffusion of $\text{Au}(\text{CN})_2^-$ within the pore volume of IEPUFs or PUF and/or along the pore wall surface to the active sorption sites of the sorbent and finally (iii) formation of the ternary complex ion associate of the formula $[-\text{CH}_2^+\text{OH}-\text{CH}_2]-[\text{Au}(\text{CN})_2]_{\text{foam}}^-$. Therefore, the actual sorption of $\text{Au}(\text{CN})_2^-$ onto the interior surface is rapid and hence it is not the rate determining step in the sorption process. Thus, one may conclude that film and intraparticle transport might be the two main steps controlling the sorption step. Thus, “solvent extraction” or a “weak base anion ion exchanger” mechanism is not only the most probable participating mechanism and most likely, some other processes like specific sites on the PUFs are possibly involved simultaneously in the gold (I) retention from the bulk aqueous solution [16–19] on the solid sorbent.

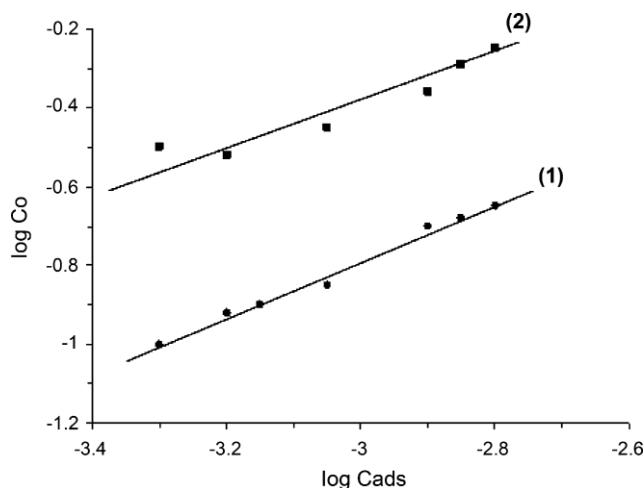


Fig. 5 – Freundlich sorption isotherms of $[\text{Au}(\text{CN})_2]^-$ from aqueous cyanide media (2%, w/v) onto IEPUFs (1) and PUFs (2) at pH 4–5 and $25 \pm 0.1^\circ\text{C}$.

3.3. Sorption isotherms of gold (I) species onto IEPUFs and PUFs sorbents

The retention profile of gold (I) over a wide range of equilibrium concentrations (1.0×10^{-4} – 20×10^{-4} molL $^{-1}$) from the aqueous solution onto the employed sorbents was determined at the optimum concentration of gold (I) retention. The plots of the amount of gold (I) ions retained on the IEPUFs and PUFs sorbents versus their equilibrium concentrations in the bulk aqueous solution revealed that at low or moderate analyte concentration, the amount of $\text{Au}(\text{CN})_2^-$ retained on the foam sorbent varied linearly with the amount remained in the bulk solution. The equilibrium was approached only from the direction that of gold (I) rich aqueous phase confirming the first-order sorption behavior. A relatively reasonable sorption capacity of gold (I) ions towards IEPUFs and PUFs sorbent as predicted from the sorption isotherm was found in the range 11.21 ± 1.8 and 5.29 ± 0.9 mgg $^{-1}$, respectively. The most favorable K_d values were achieved from more diluted solutions. The distribution ratio decreased on raising the gold (I) concentration where, the sorbent membranes became saturated with the retained species $[\text{Au}(\text{CN})_2]^-$ rapidly within 15 min of shaking. Therefore, diffusion of the solute through

a hypothetical film or hydrodynamic boundary layer took place in the sorption step [45,46] and both intraparticle transport and the film diffusion may be the steps controlling the molecular diffusion at the macro pores of the sorbent.

The retention profile of gold (I) from the aqueous solution onto the used sorbents was subjected to Freundlich and Langmuir isotherm models [47] over a wide range of equilibrium concentration through linear regression in a condition of best fit. The Freundlich model [45] is expressed in the following form:

$$\log C_{\text{ads}} = \log A + \frac{1}{n} \log C_e \quad (11)$$

where A and $1/n$ are Freundlich parameters related to the maximum sorption capacity of solute (molg $^{-1}$) and C_{ads} is the sorbed gold (I) concentration onto the IEPUFs and PUFs PUF per unit mass (molg $^{-1}$) at equilibrium. Plots of $\log C_{\text{ads}}$ versus $\log C_e$ (Fig. 6) was linear ($R^2 = 0.96$ – 0.97) over the entire concentration range of gold (I) indicating a better fit for the experimental data. The values of the Freundlich constants A and $1/n$ computed from the intercepts and slopes of the plots for IEPUFs were found to be 0.42 ± 0.07 molg $^{-1}$ and 0.79 ± 0.01 for IEPUFs and 0.33 ± 0.053 molg $^{-1}$ and 0.617 ± 0.023 for PUFs sorbents, respectively. The values of $1/n < 1$ indicate the favorable sorption of gold (I) onto the tested solid sorbents. The sorption capacity is slightly reduced at lower equilibrium concentration and the isotherm does not predict any saturation of the solid surface of the adsorbent by the adsorbate. Thus, infinite surface coverage is predicted mathematically and physico sorption on the surface is expected.

The Langmuir sorption isotherm is expressed in the following linear form [47]:

$$\frac{C_e}{C_{\text{ads}}} = \frac{1}{Qb} + \frac{C_e}{Q} \quad (12)$$

where C_e is the equilibrium concentration (molL $^{-1}$) of gold (I) in solution and Q and b are Langmuir constants related to the maximum adsorption capacity of solute per unit mass of adsorbent required for monolayer coverage of the surface and b is an equilibrium constant related to the binding energy of solute sorption that is independent of temperature. The plots of C_e/C_{ads} versus C_e over the entire concentration range of gold (I) were linear confirming that the adsorption characteristics of the analyte towards

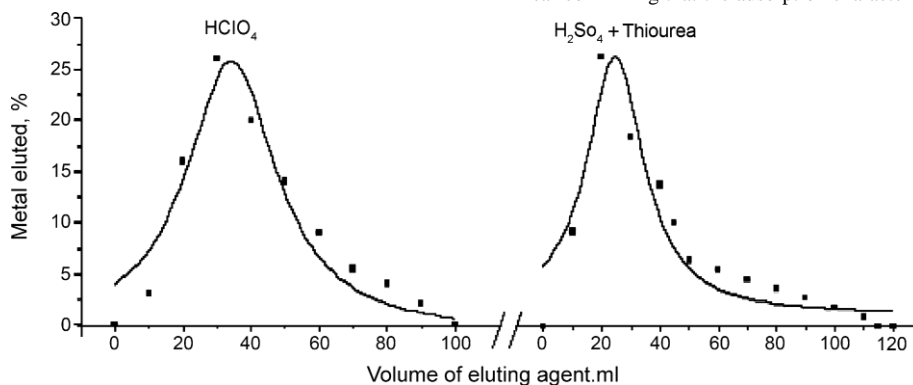


fig. 6 – Chromatographic separation of gold (I) from silver (I) ions from their aqueous media (100mL) containing gold (I) ions at 5gAu mL^{-1} in the presence of KCN (2%, w/v) employing IEPUFs packed column at 10.0mL min^{-1} , pH 4–5 and $25 \pm 0.1^\circ\text{C}$.

IEPUFs and PUFs obey the Langmuir model. The sorption parameters Q and b evaluated from the slopes and intercepts of the Langmuir plots were found to be $9.075 \pm 0.05 \text{ mmol g}^{-1}$ and $20.34 \pm 0.05 \text{ mmol}^{-1}$ of the tested sorbent IEPUFs and $4.67 \pm 0.03 \text{ mmol g}^{-1}$ and $5.9 \pm 0.01 \text{ mmol}^{-1}$ for PUFs sorbent towards gold (I) retention, respectively. These data confirm that an added component for “surface adsorption” participates in the gold (I) uptake.

Based on these results and the data reported earlier [30,33] a dual sorption mechanism involving absorption related to “weak-base anion exchange” and an added component for “surface adsorption” mechanism for gold (I) retention by unloaded PUFs and IEPUFs. Based on the data reported earlier by Chow et al. [23,24], this dual model can be expressed by the following equation:

$$C_r = C_{\text{abs}} + C_{\text{ads}} = \frac{DC_{\text{aq}} + SK_L C_{\text{aq}}}{1 + K_L C_{\text{aq}}} \quad (13)$$

where C_r and C_{aq} are the equilibrium concentrations of gold (I) ions onto the solid sorbent and in aqueous solution, respectively. C_{abs} and C_{ads} are the equilibrium concentrations of gold (I) ions retained onto the used solid sorbents as an absorbed species and adsorbed species, respectively and S and K_L are the saturation values for the Langmuir adsorption model [17].

3.4. Chromatographic behavior of gold (I) on IEPUFs and PUFs packed columns

The membrane structure, the good hydrodynamic and aerodynamic properties of the PUFs [17,18] suggested the use of the IEPUFs and unloaded PUFs in flow mode for the pre concentration of gold (I) species from aqueous solutions. The kinetics and the sorption results of gold (I) onto the IEPUFs and PUFs also recommended the possible application of both sorbents IEPUFs and PUFs separately in packed columns for the chromatographic separation of gold (I) from aqueous solution and silver (I) and base metal ions. Percolation of an aqueous solution (0.5L) of de ionized water containing gold (I) at concentration $\leq 15 \text{ g Au mL}^{-1}$ concentration level through the IEPUFs and PUFs packed columns was carried out as described earlier. Analysis of gold species in the effluent solution against the reagent blank under the same experimental conditions revealed complete sorption of $[\text{Au}(\text{CN})_2]^-$ onto the foam packed columns. A series of eluting agents e.g. HClO_4 (1.0 mol L^{-1}), thiourea (1.0 mol L^{-1})– H_2SO_4 (0.1 mol L^{-1}) and H_2SO_4 (1.0 mol L^{-1}) were investigated to recover gold (I) species. The gold (I) species were recovered quantitatively from the IEPUF ($97.4 \pm 2.4\%$) and PUFs ($95.4 \pm 3.4\%$) packed columns using perchloric acid (80 mL , 1.0 mol L^{-1}). Also an acceptable recovery percentage of gold (I) was achieved from IEPUFs ($95.6 \pm 4.2\%$) and PUFs ($96.4 \pm 4.7\%$) packed columns using thiourea (80 mL , 1.0 mol L^{-1})– H_2SO_4 (0.1 mol L^{-1}) at 5 mL min^{-1} flow rate as a proper eluting system. Representative data employing IEPUFs packed column for gold (I) spiked to distilled water are given in Table 1. Moreover, the performance of the IEPUFs packed column was found better than the PUFs packed column where, the former packed

spiked to distilled water by the proposed IEPUFs packed column at 5 mL min^{-1} employing AAS

Gold species (gmL^{-1})		Recovery (%) ^a
Gold (I) taken	Gold (I) found	

5.0	4.9	98.0 ± 3.4
10.0	9.75	97.5 ± 2.5
15.0	14.7	97.0 ± 2.1

^a Average recovery ($n=5$) \pm relative standard deviation.

column was used more than one time without decrease in the column performance. Also, reproducible recovery percentages of gold (I) was achieved from IEPUFs packed column even at trace concentrations of gold (I) in the test solution. Therefore, IEPUFs packed columns and perchloric acid as a proper eluting agent were used for the pre-concentration, recovery and subsequent determination of gold (I) species at trace concentration were used in the subsequent work.

The proposed IEPUFs packed columns was employed for the collection and recovery of gold (III) species from aqueous solutions after reduction to gold (I) with Na_2SO_3 in acid medium as described earlier. The extraction and recovery of the produced gold (I) at concentration levels $1.0\text{--}5 \text{ gmL}^{-1}$ (0.1L) were determined as described earlier at pH 4–5 for gold (III). Satisfactory recovery percentage ($96.0 \pm 4.5\%$, $n=5$) of gold species was achieved. The extraction, recovery and subsequent determination of the total inorganic gold in the binary mixtures of gold (I) and (III) ions in the aqueous media (0.1L) at a total concentration $\leq 10 \text{ gmL}^{-1}$ by the developed IEPUFs packed columns were attempted as described in the experimental section. The results are summarized in Table 2. Satisfactory recovery percentage of total inorganic gold species was obtained in the range 96.5 ± 3.9 to $98.3 \pm 2.2\%$, $n=4$.

The effect of flow rate ($2\text{--}15 \text{ mL min}^{-1}$) on the uptake and recovery of gold (I) by the IEPUFs packed column was also examined by percolating 100 mL of distilled water spiked with gold (I). Complete retention of gold (I) was achieved ($>96\%$) at flow rate $<10 \text{ mL min}^{-1}$. At higher flow rate, the sorption performance has been decreased and the width of the elution peak increased on increasing the flow rate. On the other hand, the effect of the sample volume ($0.1\text{--}1.0 \text{ L}$) on the gold (I) retention was also investigated at 10 mL min^{-1} flow

Table 2 – The extraction and recovery of total inorganic gold (I) and gold (III) in the binary mixture in the aqueous media by the developed IEPUFs packed columns

Gold species (gmL^{-1})		Average gold found, recovery (%)	
Gold species added			
Au ⁺	Au ³⁺		
1.0	5.0	5.9	98.3 ± 2.2
5.0	5.0	9.6	96.5 ± 3.9

^a Average recovery ($n=5$) \pm relative standard deviation.

rate. Almost complete retention ($96.0 \pm 4.5\%$, $n=5$) has been achieved successfully on the IEPUFs packed columns with good reproducibility.

3.5. Analytical performance of the developed foams packed columns

The performance (HETP & N) of the IEPUFs and PUFs packed columns (1.0g) was determined by passing an aqueous solution (0.5 L) containing gold (I) at 5gmL⁻¹ concentration levels at the optimum condition through the packed column at 5mLmin⁻¹. Complete sorption of gold (I) took place on the IEPUFs packed column. The retained species of gold [Au(CN)₂]- were then eluted with perchloric acid (80.0mL, 1.0molL⁻¹). A series (8×10mL) of fractions of the eluent solution at 5mLmin⁻¹ were then collected and analyzed for gold (I) species by FAAS. The HETP and the number of theoretical plates *N* calculated from the elution curves (Fig. 6) employing the equation [17]:

$$N = 8V_{\max}^2 \frac{L}{W^2 \text{HETP}} \quad (14)$$

where *V*_{max}: volume of eluate at peak maximum, *W*: width of the peak at 1/*e* times the maximum solute concentration and *L* is the length of the foam bed in mm were in the range to 0.96±0.04mm and 95±3, respectively. The *N* and HETP of the foam packed columns were also calculated from the breakthrough capacity curves by percolating 0.5dm³ of the spiked tap water samples with gold (I) at 5.0gmL⁻¹ through the column at 5.0mLmin⁻¹ flow rate. The results are displayed in Fig. 7. The rising portions of the S-shaped curve have large slopes indicating a high transfer rate of [Au(CN)₂]- on/in the foam membranes and rapid attainment of equilibrium between the [Au(CN)₂]- and the foams. The HETP and *N* values of the IEPUFs packed column were calculated employing

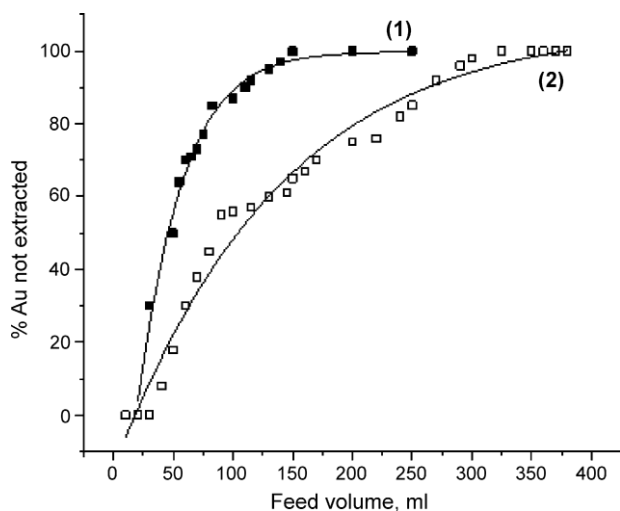


Fig. 7 – Breakthrough curves of [Au(CN)₂]- at 5.0g Au⁺ mL⁻¹ on the IEPUFs (1) and PUFs (2) packed column at 5mLmin⁻¹, pH 4–5 and 25±0.1°C and KCN (2%, w/v).

the equation [17]:

$$N = \frac{V_{50} \times V'}{L} \quad (15)$$

$$\frac{(V_{50} - V')^2}{\text{HETP}}$$

where *V*₅₀: volume of the effluent solution at the center of the breakthrough curve where the concentration is one-half the initial concentration and *V'*: the volume at which the effluent solution has the concentration 0.1578 of the initial concentration. The HETP and *N* were in the range 1.1±0.01mm and 89±3.2, respectively. These values are in good agreement with the results obtained from the chromatogram method. The critical and breakthrough capacities [17,46] of the gold (I) retained onto the IEPUFs and PUFs packed columns calculated from the breakthrough curve (Fig. 7) were found in the 1.75–2.1 and 0.27–0.29mg gold (I) retention per gram of the solid sorbent.

The lower limits of detection (LOD) and limit of quantification (LOQ) of gold (I) retention, recovery and subsequent determination were calculated for the IEPUFs packed column using the equations [48]:

$$3\text{S.D.}$$

$$\text{LOD} = \frac{3\text{S.D.}}{b} \quad (16) \text{ b and}$$

$$10\text{S.D.}$$

$$\text{LOQ} = \frac{10\text{S.D.}}{b} \quad (17) \text{ b}$$

where S.D. is the standard deviation (*n*=3) of the blank and *b* is the slope of the calibration plot. Under the optimal experimental conditions of gold (I) retention and recovery using IEPUFs packed columns, linear calibration curve for gold (I) determination was obtained. For an aliquot sample (50mL), the equation of the calibration curve obtained is as follows: sample volume, 100mL, *A*=0.0011+0.47*C* (*n*=3; *R*²=0.98 and *C*=0–15g⁻¹ gold (I). The LOD and LOQ of 0.01g⁻¹ and 0.033g⁻¹ were achieved, respectively. Such limits could be improved to lower values by collection of gold (I) species from large sample volumes of the aqueous phase at the optimum experimental conditions. The precision of the IEPUFs packed column for the extraction and recovery of standard aqueous solutions (0.1L) containing 1.0 and 5.0g⁻¹ (*n*=3) of gold (I) at 5.0mLmin⁻¹ flow rate were 1.98 and 2.9%, respectively, expressed as relative standard deviations.

3.6. Interference study

The influence of a relatively high excess (1mg) of some diverse ions relevant to waste water e.g., alkali and alkaline earth metals, Cu²⁺, Al³⁺, Ni²⁺, Co²⁺, Cd²⁺, Hg²⁺, Fe³⁺, VO₃⁻, AsO₂²⁻, SO₄²⁻, and PO₄³⁻ ions on the pre-concentration of gold (I) at 5gmL⁻¹ concentration level from aqueous cyanide media (50mL) by developed IEPUFs was investigated. The tolerance limit (w/w) less than ±3% change in the uptake of gold (I) is considered free from interference. The results showed that the presence of large amounts of foreign ions in the sample has no significant effect on the pre-concentration of gold (I). Good extraction efficiency (>98±2%) for the gold (I) ions was achieved successfully in the presence of the investigated diverse ions. In the presence of some other ions such as Fe³⁺ and VO₃⁻, 2mL of NaF (1.0molL⁻¹) solution were introduced

Table 3 – Analytical results for the analysis of total inorganic gold (I) and gold (III) in wastewater by the developed IEPUFs packed column

Gold species (gmL⁻¹)

Gold species added		Average gold found, recovery (%)	
Au ⁺	Au ³⁺		
5.0	5.0	9.70	97.3 ± 2.2
5.0	1.0	5.75	95.8 ± 3.9

*Average recovery (n=5)±relative standard deviation.

to the aqueous solution to obtain unambiguous and selective pre-concentration of gold (I). The fact that NaF solution forms anionic complex species with both Fe³⁺ and VO₃⁻ anions. Also, in the presence of MnO₄⁻, sodium azide is added to reduce manganese (VII) to manganese (II) and to eliminate the interference of permanganate ions. After employing these modifications, the tolerance level of the interfering ions was improved to acceptable limit (98±2%). These results extend the use of the proposed IEPUFs for the separation and sequential determination of gold (I) ions from the industrial effluent of electroplating industry of gold.

3.7. Analytical applications of IEPUFs packed columns

3.7.1. Pre-concentration and separation of gold (I) and/or gold (III) in different water samples

The validation of the developed method was successfully assessed by performing the recovery tests for gold in tap- and industrial wastewater samples. The water samples were first acidified with phosphoric acid and filtered through a 0.45m cellulose membrane filter. An aqueous solution

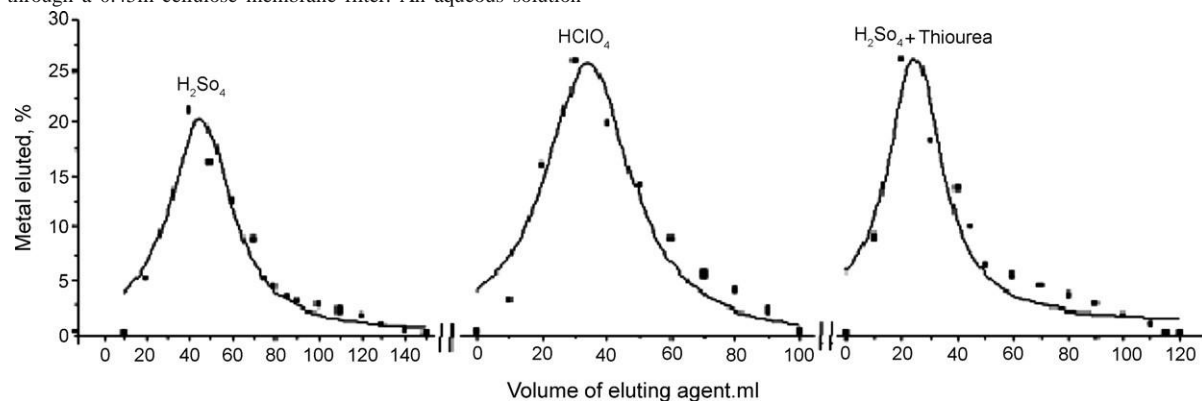


Fig. 8 – Chromatographic separation of gold (I), silver (I) and nickel (II) from their aqueous mixtures (100mL) at 5.0gmL⁻¹ of each metal ion in the presence of KCN (2%, w/v) employing IEPUFs packed column at 5mLmin⁻¹ flow rate at pH 4–5 and 25±0.1°C.

(100mL) of the water sample was then spiked with gold (I) and/or gold (III) species at a total concentration in the range 6–10gmL⁻¹ levels. The sample solution was first reduced and the solutions were percolated through the IEPUFs packed columns at 5–10.0mLmin⁻¹ flow rate as described earlier. The recovered gold species was subsequently determined by FAAS. The results are summarized given in Table 3. A satisfactory recovery percentage of total gold was achieved in the range 95.8±3.9 to 97.3±2.2. The observed agreement (Table 3) between the concentration of gold (I) and/or gold (III) taken and that found revealed the accuracy and the applicability of the proposed method. The IEPUFs packed column was also used for complete collection and recovery of spiked gold (I) onto sea water samples. The aliquots were first collected, filtered through a 0.45m cellulose membrane filter, spiked with gold (I) at concentrations 3–10g/L and analyzed as described before. A reasonable recovery percentage (95.8±2.1) of gold was achieved confirming the

accuracy of the developed procedures and its independence from matrix effects.

3.7.2. Separation of gold (I) from silver (I) and base metal ions

The analytical utility of the IEPUFs packed column for the chromatographic separation of gold (I) from silver (I) in aqueous solution was successfully achieved by the developed procedures. Complete sorption of both metal ions took place. The retained [Au(CN)₂]⁻ and [Ag(CN)₂]⁻ species in the column were then recovered quantitatively with 80mL HClO₄ (1.0molL⁻¹) and 140mL of thiourea (1.0molL⁻¹)–H₂SO₄ (0.1molL⁻¹), respectively. The results shown in Fig. 6 indicated the good performance of the proposed IEPUFs for the separation of both metal ions in their complex mixtures quantitatively.

The chromatographic separation of gold (I) from base metal ions (Fe³⁺, Ni²⁺, Cu²⁺ or Zn²⁺) present in aqueous solutions by the IEPUFs packed column was also investigated as described earlier. Quantitative retention of gold (I) and the base metal ion Fe³⁺, Ni²⁺, Cu²⁺ or Zn²⁺ was achieved as indicated from the FAAS measurements of the effluent solutions. Complete recovery of the base metal ion Fe³⁺, Ni²⁺, Cu²⁺ or Zn²⁺ from gold (I) was achieved quantitatively (97±3.04%) employing the eluting agents H₂SO₄ (0.05molL⁻¹) and perchloric acid (1.0molL⁻¹), respectively.

The applicability of the IEPUFs packed column to separate gold (I) from silver (I) and base metal ions (Fe³⁺, Ni²⁺, Cu²⁺ or Zn²⁺) in their aqueous solution mixtures (100mL) at 5gmL⁻¹ concentration level of each ion was critically investigated as described before. Complete retention of the tested metal ions was achieved as indicated from the analysis of effluent solutions.

Quantitative recovery of the base metal ion was first achieved employing the eluting system H₂SO₄ (0.05molL⁻¹), gold (I) was then eluted by HClO₄ (1.0molL⁻¹) and finally silver (I) was recovered by the system thiourea (1molL⁻¹)–H₂SO₄ (0.1molL⁻¹). The results shown in Fig. 8 confirmed the accuracy of the developed IEPUFs column and suggested the analytical utility of the IEPUFs packed column for gold separation and recovery from dilute aqueous solution samples.

3.7.3. Separation and determination of gold in gold slime

The IEPUFs packed column was applied to the anodic slime samples having a complex matrix for the pre concentration, separation and subsequent AAS determination of gold following the general recommended procedures. The validity of the method was tested by the analysis spiked gold to the anodic slime samples. The recovered gold species by the developed procedures was subsequently determined. Satisfactory results (recoveries

>95%, relative standard deviations <4.0%) more or less close to the value obtained with FAAS (98±2.4%) and the method reported by Hu et al. [14] were obtained. Thus, the developed IEPUFs packed column can find applications for gold separation and/or pre-concentration, recovery from metallurgical samples and ultra diluted aqueous solutions followed by subsequent determination.

4. Conclusion

The developed IEPUFs and PUFs packed columns provides a simple, reliable, fairly rapid and low cost method were successfully used for the pre concentration, separation and subsequent determination of inorganic gold (I) and total inorganic gold (I) and gold (III) from metallurgical sample having a complex matrix such as anodic slime after reduction of the latter to the mono-valence gold. The developed procedures are able to minimize the limitations related to sensitivity and selectivity for gold determination in different kinds of matrices. The kinetic data confirmed that the intra-particle diffusion and the first order model for gold (I) retention onto the tested sorbents. The sorption of gold (I) ions onto the foam sorbents followed Langmuir and Freundlich adsorption isotherms. The IEPUFs packed column was reused many times without loss in the column performance (N, HPTP). The membrane-like structures of the PUFs is superior compared to the known rigid or granular solid sorbents and permit rapid separation at relatively high flow rate. Separation of gold (I) species from silver (I) and base metal ions e.g. Fe³⁺, Ni²⁺, Cu²⁺, and Zn²⁺ was achieved successfully using on IEPUFs packed column. However, work is still continuing for investigating the influence of memory effect, organic material present in the investigated fresh water samples, competitive complexing agents in addition to the on-line determination of inorganic gold (I) and total inorganic gold (I) and gold (III). The effects of some organic species e.g. citrate, oxalate, etc. are currently under investigation. Separation of gold (I) from silver (I) and other base metal ions on IEPUFs packed column followed by subsequent on-site analysis by cold vapor flame atomic absorption or other analytical techniques will be considered.

references

- [1] T.R. Dulski, Trace Elemental Analysis of Metals, Marcel Dekker, Inc., 1999, p. 99.
- [2] N. Pourreza, S. Rastegarzadeh, Anal. Chem. (Warsaw) 50 (2005) 695.
- [3] J. Medved, M. Bujdos, P. Matus, J. Kubova, Anal. Bioanal. Chem. 379 (2004) 60.
- [4] Z. Marczenko, T. Kowalski, Anal. Chim. Acta 156 (1984) 193.
- [5] H.R. Li, Q.X. Rong, X.L. Hou, X.Y. Mao, Talanta 44 (1997) 1313.
- [6] Z.X. Li, J. Anal. At. Spectrom. 21 (2006) 435.
- [7] G. Ertas, O.Y. Ataman, Appl. Spectrosc. 60 (2006) 423.
- [8] J. Medved, P. Matus, M. Bujdos, J. Kubova, Chem. Papers 60 (2006) 27.
- [9] J.S. Zhao, J.S. Li, Z.J. Huang, Q.Y. Wei, J. Chen, G.Y. Yang, Indian J. Chem. A 45A (2006) 1651.
- [10] A. Aworn, A. Thiravetyan, W. Nakbanpote, J. Colloid Interface Sci. 287 (2005) 394.
- [11] Y. Yang, C. Li, K.H. Lee, H.G. Craighead, Electrophoresis 26 (2005) 3622.
- [12] M. Behpour, A.M. Attaran, S.M. Ghoreishi, N. Soltani, Anal. Bioanal. Chem. 382 (2005) 444.
- [13] Z. Marczenko, Spectrophotometric Determination of Elements, third ed., Ellis Horwood, Chichester, UK, 1986.
- [14] Q. Hu, X. Chen, X. Yang, Z. Huang, J. Chen, G. Yang, Anal. Sci. 22 (2006) 627.
- [15] M.S. El-Shahawi, A.S. Bashammakh, S.O. Bahaffi, Talanta 72 (2007) 1492.
- [16] K. Pyrzynska, Spectrochim. Acta Part B 60 (2005) 1316.
- [17] T. Braun, J.D. Navratil, A.B. Farag, Polyurethane Foam Sorbents in Separation Science, CRC Press, Inc., Boca Raton, FL, 1985.
- [18] S. Palagyi, T. Braun, Separation and Preconcentration of Trace Elements and Inorganic Species on Solid Polyurethane Foam Sorbents, in: Z.B. Alfassi, C.M. Wai (Eds.), Preconcentration Techniques for Trace Elements, CRC Press, Boca Raton, 1992.
- [19] M. Behpour, A.M. Attaran, S.M. Ghoreishi, N. Soltani, Anal. Bioanal. Chem. 382 (2005) 447.
- [20] P.F. Marchisio, A. Sales, S. Cerutti, E. Marchevski, L.D. Martinez, J. Hazard. Mater. B 124 (2005) 113.
- [21] P.U. Guang, Y. Yue, Fen Xi 24 (2004) 1270.
- [22] T. Saito, S. Akita, T. Torii, M. Hiraide, J. Chromatogr. B 932 (2001) 159.
- [23] K. Rzeszutek, A. Chow, J. Membr. Sci. 181 (2001) 265.
- [24] R.D. Oleschuk, A. Chow, Talanta 43 (1996) 1545.
- [25] R.D. Oleschuk, The Separation and Isolation of Metals Using Polyurethane Materials, Ph.D. thesis, University of Manitoba, 1998.
- [26] P. Fong, A. Chow, Talanta 39 (1992) 825.
- [27] M.H. Mashhadizadeh, R. Mohyaddini, M. Skamsipur, Sep. Purif. Technol. 39 (2004) 161.
- [28] M. Bagheri, M.H. Mashhadizadeh, S. Razei, Talanta 60 (2003) 839.
- [29] M.S. El-Shahawi, H. Nassif, Anal. Chim. Acta 481 (2003) 29.
- [30] M.S. El-Shahawi, M.A. El-Sonbati, Talanta 67 (2005) 806.
- [31] J. Regas, S. Palagyi, G. Holeczyova, M. Matherny, Chem. Papers-Chemicke zvesti 45 (1991) 509.
- [32] Y. Anjaneyulu, R. Marayya, T.H. Rao, Environ. Pollut. 79 (1993) 283.
- [33] M.A. Saeed, A. Rusheed, Radiochim. Acta 90 (2002) 35.
- [34] S.L.C. Ferreira, H.C. dos Santos, M.S. Fernandes, J. Anal. At. Spectrom. 17 (2002) 115.
- [35] A.M. Kiwan, M.S. El-Shahawi, S.M. Aldaheri, M.H. Saleh, Talanta 45 (1997) 633.
- [36] M.S. El-Shahawi, J. Chromatogr. A 760 (1994) 179.
- [37] A.I. Vogel, Quantitative Inorganic Analysis, third ed., Longmans Group Ltd., England, 1966.
- [38] M.H. Cordoba, P.N. Navarro, I.L. Garcia, Int. J. Environ. Anal. Chem. 32 (1988) 97.
- [39] H.D. Gesser, G.A. Horsfall, J. Chim. Phys. 74 (1977) 1072; H.D. Gesser, G.A. Horsfall, K.M. Gough, B. Krawchuk, Nature 268 (1977) 323.
- [40] K.A. Halhouli, N.A. Darwish, N.M. Al-Dhoon, Sep. Sci. Technol. 30 (1995) 3313.
- [41] M.J. Rosen, Surfactants and Interfacial Phenomena, third ed., Hospitality Industry Publications Services, 2004, p. 140.
- [42] W.J. Weber Jr., J.C. Morris, J. Sanit. Eng. Div. Am. Soc. Civ. Eng. 89 (1963) 31; W.J. Weber Jr., J.C. Morris, J. Sanit. Eng. Div. Am. Soc. Civ. Eng. 90 (1964) 70.
- [43] S. Lagergren, B.K. Sven, Vatenkapskad. Handl. (1898) 24.
- [44] D. Reichenburg, J. Am. Chem. Soc. 75 (1972) 589.
- [45] C.H.R. Nambiar, B. Narayana, B. Rao, R. Mathew, B. Ramachandra, Microchem. J. 53 (1996) 175.
- [46] G.A. Somorjai, Introduction to Surface Chemistry and Catalysis, John Wiley & Sons, Inc., 1994.
- [47] W.X. Ma, F. Liu, K.A. Li, W. Chen, S.Y. Tong, Anal. Chim. Acta 416 (2000) 191.
- [48] J.C. Miller, J.N. Miller, Statistics for Analytical Chemistry, fourth ed., Ellis-Horwood, New York, 1994, p. 115.



Chemical speciation and recovery of gold(I, III) from wastewater and silver by liquid–liquid extraction with the ion-pair reagent amiloride mono hydrochloride and AAS determination

M.S. El-Shahawi*, A.S. Bashammakh, S.O. Bahaffi

Department of Chemistry, Faculty of Science, King Abdulaziz University, P.O. Box 80203, Jeddah 21589, Saudi Arabia

Received 30 October 2006; received in revised form 25 January 2007; accepted 26 January 2007

Available online 9 February 2007

Abstract

A novel and low cost liquid–liquid extraction procedure for the separation of gold(III) at trace level from aqueous medium of pH 5–9 has been developed. The method has been based upon the formation of a yellow colored ternary complex ion associate of tetrachloro gold(III) complex anion, AuCl_4^- with the ion-pair reagent 1-(3,5-diamino-6-chloropyrazinecarboxyl) guanidine hydrochloride monohydrate, namely amiloride, DPG^+Cl^- . The effect of various parameters, e.g. pH, organic solvent, shaking time, etc. on the preconcentration of gold(III) from the aqueous media by the DPG^+Cl^- reagent has been investigated. The colored gold species was quantitatively extracted into 4-methyl pentan-2-one. The chemical composition of the ion associate of DPG^+Cl^- with AuCl_4^- in the organic solvent has been determined by the Job's method. The molar absorptivity ($2.19 \times 10^4 \text{ L mol}^{-1} \text{ cm}^{-1}$) of the associate $\text{DPG}^+\text{AuCl}_4^-$ at 362nm enabled a convenient application of the developed extraction procedure for the separation and AAS determination of traces of aurate ions. Mono-valence gold ions after oxidation to gold(III) with bromine water in HCl (1.0 mol L^{-1}) media have been also extracted quantitatively from the aqueous media by the developed procedure. The chemical speciation of monoand/or tri-valence gold species spiked to fresh and industrial wastewater samples has been achieved. The method has been also applied successfully from the separation of gold(I) and gold(III) species from metallic ions and silver. The developed method has also the advantage of freedom from most diverse ions.

© 2007 Elsevier B.V. All rights reserved.

Keywords: Mono- and tri-valence gold species; Ion-pair reagent DPG^+Cl^- ; Liquid–liquid extraction; Chemical speciation; Wastewater; Silver; Recovery and AAS

1. Introduction

Gold is widely distributed in nature and the chemistry of gold remains an active research area [1]. Some gold(I) compounds are biologically active and used as anti-inflammatory drugs in the treatment of rheumatoid arthritis [1–3]. Due to the low level of gold in the environmental samples and its great importance, many articles have been reported on the separation of traces of gold in water and other matrices containing Cd^{2+} , Zn^{2+} , Cu^{2+} , Ni^{2+} , Mn^{2+} , Co^{2+} , Pd^{2+} , Hg^{2+} , Pb^{2+} , Pt^{4+} , Fe^{3+} , alkaline and

alkaline earth ions before their actual determination [3–9]. The spectrometric methods, e.g. ICP-AES, FAAS, ETAAS, electrophoresis and other spectrophotometric methods involving 2-carboxyl-1-naphthalthiorhodanine (CNTR), Spheron (R) and

* Corresponding author. Tel.: +966 551691130; fax: +966 26952292.

E-mail address: mohammad_el_shahawi@yahoo.co.uk (M.S. El-Shahawi).

0039-9140/\$ – see front matter © 2007 Elsevier B.V. All rights reserved.
doi:10.1016/j.talanta.2007.01.057

(biphenyl) dimethanethiol, etc. are the most used techniques in the analysis of gold at low level [7,9–15]. Few of these methods have sufficient sensitivity and selectivity for the trace levels of mono- and tri-valence gold species in fresh water and industrial wastewater samples [7,11–15]. However, the low level of gold in drinking waters is not compatible with the detection limit and some of these methods are expensive, unselective and require careful experimental conditions and considerable time consuming. Thus, preconcentration and separation techniques using liquid–liquid and liquid–solid are frequently required to improve the detection capability and the selectivity of these techniques [7,12–14].

The ion-pair reagents containing bulky anions are often used to form extractable complex ion associates with charged bulky cationic complex species of neutral ligands, e.g. crown ethers, *o*-phenanthroline derivatives, and metal ions [6–10,16–18]. On the other hand, the bulky cations, e.g. rhodamine derivatives,

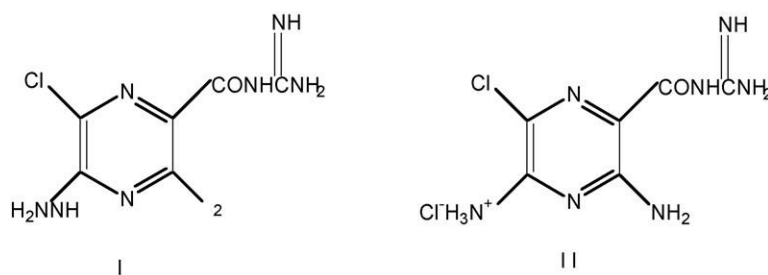


Fig. 1. Chemical structures of the amiloride (I) and amiloride hydrochloride (II).

basic dyes, 18-crown-6 (18C6) oxonium cation, tetra alkyl phosphonium or arsonium halides and tetrazolium salts are also often used to form extractable ion associates with charged bulky oxoanions or bulky anionic complexes of metal [18–30] and gold(III) halides, cyanide and thiocyanate [31–33].

Burns et al. [34,35] and others [36,37] have been successfully used the compound amiloride mono hydrochloride (Fig. 1) as a selective analytical ion-pair reagent for the determination of the oxoanions perchlorate, perrhenate and periodate in different matrixes. The extraction of the produced complex ion associates of amiloride with these oxoanions proceeded rapidly with high recovery factor [27–31].

Recent years [7,10–15] have seen an upsurge of interest for rapid and sensitive analytical methods for the separation and speciation of chemical forms of precious metal ions in environmental samples. A recent literature on the analytical applications of the ion-pair reagent DPG^+Cl^- has revealed no study on the use of the reagent on the liquid–liquid separation of gold(III) from silver and other base metal ions and chemical speciation of chemical forms of mono- and tri-valent gold ions. Thus, the goals of the present article are focused on the use of the title reagent for the separation of gold(III) and speciation of chemical forms of mono- and tri-valence gold species as a ternary complex ion associate of AuCl_4^- and DPG^+Cl^- in non-aqueous media. The extraction mechanism and the chemical separation of gold(I)

and (III) species from silver(I) and other base metal (Fe^{3+} , Co^{2+} , Ni^{2+} , and Cu^{2+}) ions have been also included.

2. Experimental

2.1. Reagents and materials

Analytical reagent grade chemicals nickel(II) sulphate, iron(III) sulphate and copper(II) sulphate and solvents (BDH, USA) were used. Potassium aurocyanide, $\text{KAu}(\text{CN})_2$ (Fluka AG, USA), chloroauric acid, HAuCl_4 (Johnson Matthey & Co., UK), silver nitrate (Fluka, USA) and amiloride mono hydrochloride (E Merck, India) were used for the preparation of stock solutions (1000g mL^{-1}) of gold(I), gold(III) and silver(I) ions, respectively. A stock solution (0.01mol L^{-1}) of amiloride mono hydrochloride (E Merck, India) was prepared by dissolving an accurate weight (0.03g) of the reagent in $100\text{mL H}_2\text{O}-\text{HCl}$ (1:1, v/v). Double distilled de-ionized water was used throughout the work for the preparation of stock solutions (1000g mL^{-1}). A series of

Britton–Robinson buffers (0.04mol L^{-1} in each of acetic, orthophosphoric, and boric acids) adjusted to the required pH with sodium hydroxide (0.2mol L^{-1}) was prepared [38].

2.2. Apparatus

Carbon, hydrogen and nitrogen content were determined on a Perkin-Elmer 2400C series elemental analyzer, USA. A Perkin-Elmer (model Lambda EZ-210, USA) spectrophotometer (190–1100nm) with a 10mm long quartz cell was used for recording the electronic spectra of the reagent and the complex ion associate of gold(III). The absorbance of the organic extract was measured with a single beam Perkin-Elmer (model Lambda EZ-150, USA) UV–vis spectrophotometer with quartz cell (10mm). A Perkin-Elmer (Analyst TM 800, USA) furnace atomic absorption spectrometer (AAS) was used for measuring the concentration of Au, Ag, Fe, Ni, and Cu at the wavelengths 242.8, 328.1, 372.0, 232.0 and 324.7nm, respectively at 0.5nm slit width except for iron and nickel at 0.2nm before and after separation step from the aqueous phase under instrument's optimum settings.

2.3. Recommended extraction procedures

2.3.1. Extraction procedures of gold(III) species

In a separating funnel (50mL), a 2mL aliquot of the ionpairing reagent $\text{DPG}^+\text{-Cl}^-$ ($1.0 \times 10^{-5} \text{ molL}^{-1}$) was mixed with 9.0mL of B–R buffer (pH 6–7) containing various concentrations ($(1.0-6) \times 10^{-5} \text{ molL}^{-1}$) of HAuCl_4 to adjust the pH of the final aqueous solution. The aqueous solution was then diluted to 20.0mL with double distilled water. The aqueous solution was shaken twice, each with 2.5mL of the solvent 4methylpentan-2-one for 2min. After separation of the layers, the organic extract was then collected in a 25mL beaker containing anhydrous sodium sulphate (1.0g) swirled to mix the contents and transferred to a 10mL volumetric flask. The residue was also washed with 5mL (2×2.5) of the same organic solvent, transferred to the measuring flask and finally made up to the mark with the same solvent. The absorbance of the organic extract was then measured at 362nm against a reagent blank. After extraction, the pH of the aqueous phase was determined as equilibrated pH and the amount of gold ions remained in the aqueous phase (C_f) was determined also by AAS. The amount of gold ions of the parallel samples containing the same amount (C_i) of gold(III) ions and

1496

M.S. El-Shahawi et al. / Talanta 72 (2007) 1494–1499

the reagent $\text{DPG}^+\text{-Cl}^-$ was also measured by AAS. The amount of gold(III) ions in the organic phase was finally calculated by the difference ($C_i - C_f$) and the distribution ratio (D_{Au}) was then calculated employing the equation:

$$D_{\text{Au}} = \frac{[\text{DPG}^+ \cdot \text{AuCl}_4^-]_{(\text{org})}}{[\text{AuCl}_4^-]_{(\text{aq})} + [\text{DPG}^+ \cdot \text{AuCl}_4^-]_{(\text{aq})}} \quad (1)$$

2.3.2. Extraction procedures of gold(I) species

An accurate volume (10mL) of the aqueous solution containing gold(I) ions at different concentrations ($1.0-15 \text{ gmL}^{-1}$) was transferred to the conical flask (50mL capacity). Another 10mL of HCl (1 molL^{-1}) and bromine water (2mL) were added to oxidize gold(I) solutions to gold(III) complex species. The solutions were left for 5min and the excess Br_2 and HCl were then removed by boiling the solutions for 10–15min and finally allowed to cool to room temperature ($25 \pm 1^\circ \text{C}$). The solution mixtures were then adjusted to pH 6–7 with B–R buffer, transferred with the washing solutions to a 50mL separating funnels. The resulting solutions were then extracted as described earlier for gold(III) extraction. The concentration of the produced gold ions was then determined with AAS using calibration curves of gold(III) and (I) ions.

2.3.3. Extraction of the binary mixtures of gold(I) and (III)

An aliquot (10mL) of a mixture of mono- and tri-valent gold ions at a total concentration $\leq 25 \text{ gmL}^{-1}$ was transferred to a 50mL separating funnel. The mixture was analyzed with AAS according to the described procedure for the extraction of tri-

valent gold ions. Another aliquot portion (10mL) was transferred and analyzed with AAS as described before for gold(I) determination. On the basis of these procedures, the amount of gold in the organic extract of the first aliquot (C_1) could be a measure of the gold(III) ions in the mixture, while the amount of gold in the organic extract of the second aliquot (C_2) is a measure of the sum of the mono- and tri-valent gold ions. Therefore, the difference ($C_2 - C_1$) is a measure of the gold(I) ions in the binary mixture.

2.4. Analytical applications

2.4.1. Analysis of gold(III) and total gold(I, III) in tap and wastewater samples

Tap and/or industrial wastewater samples (50mL) of fertilizer industry were collected, filtered through a 0.45m membrane filter and the solutions pH were then adjusted to pH 6–7 with B–R buffer. To each of the sample solutions an accurate concentration of gold(I, III) species at a total concentration in the range $5.0-25.0 \text{ gAu mL}^{-1}$ and 2.0mL of the reagent $\text{DPG}^+\text{-Cl}^-$ ($8.0 \times 10^{-5} \text{ molL}^{-1}$) were added. The solution mixtures were then

transferred to 50mL separating funnels. Analyze the mixtures according to the described procedure for gold(III). Another aliquot (50mL) portions were taken exactly and analyzed as described for gold(I) species. On the basis of these procedures, the gold concentration determined by AAS in the first organic extract will be a measure of tri-valent gold ions in the mixture, while the amount of gold in the organic extract of the second aliquot is a measure of the sum of the gold(I) and (III) ions. Therefore, the difference between the two measurements will be a measure of the mono-valent gold ions in the mixture.

2.4.2. Separation of gold(III) from silver(I) and base metal ions in tap water

An aliquot of tap water (10mL) spiked with gold(III) ions in the concentration range $5.0-25.0 \text{ gmL}^{-1}$ Au was accurately transferred into a 50mL separating funnel as described above. To the solution mixture, 2mL containing silver(I) and/or base metal ions (Fe^{3+} , Co^{2+} , Ni^{2+} , Cu^{2+} or Zn^{2+}) at 10.0 gmL^{-1} for each ion and few drops (0.2–0.3mL) of KCl (1%, w/v) were added by the spiking method. The presence of KCl eliminates the possible interference of silver ions by forming AgCl precipitate. The solutions were then analyzed as described for gold(III) ions. The amount of gold(III) and base metal ions in the aqueous phase were determined with AAS from the standard curves of each ion at the optimum wavelength as described before.

3. Results and discussion

On mixing the reagent $\text{DPG}^+\text{-Cl}^-$ with tetrachloro gold anion, AuCl_4^- in aqueous media and shaking with 4-methyl pentan-2-one, a yellow colored complex associate was developed in the organic phase. After equilibrium, the organic phase containing

the complex ion associate of $\text{DPG}^+\cdot\text{Cl}^-$ and AuCl_4^- was separated out and its absorption electronic spectrum was then recorded. The spectrum showed one well-defined peak at 362nm of the organic extracted while, the absorption spectrum of the reagent blank $\text{DPG}^+\cdot\text{Cl}^-$ against pure 4-methyl pentan-2-one showed no absorption peaks in the same wavelength range. On the absence of HAuCl_4 or $\text{DPG}^+\cdot\text{Cl}^-$ in the aqueous phase, no color or extraction of gold ions was detected in the organic layer as indicated from AAS measurement of gold ions in the organic or aqueous layer. Thus, each of $\text{DPG}^+\cdot\text{Cl}^-$ or AuCl_4^- separately did not extract in the organic phase. Therefore, in the subsequent work, the absorbance of the organic extract was measured at 362nm against a reagent blank.

3.1. Investigation of the various experimental variables

Comparative tests of various organic solvents, e.g. *n*-hexane, dichloromethane, carbon tetrachloride, toluene, chloroform, diethyl ether, methyl ethyl ester, aromatic hydrocarbons and 4-methyl pentan-2-one with a wide range of functional group types was investigated for their ability to extract the produced complex associate. The data revealed that, the nature of the solvent contributes substantially to the maximum extraction of the produced complex ion associate of the $\text{DPG}^+\cdot\text{Cl}^-$ and AuCl_4^- ions. Good results were achieved with 4-methyl pentan-2-one and cyclohexanone and the absorbance of the organic phase followed the following order: 4-methyl pentan-2-one > cyclohexanone > ester > ether > dichloromethane > chloroform > toluene > carbon tetrachloride and *n*-hexane, respectively. The relatively high dielectric constant of these two solvents favors extensive ion-pairing formations [39]. Thus, the good extraction percentage (96–98%) with maximum apparent molar absorptivity, and solubility of the produced complex ion associate were achieved. At room temperature, the extraction was complete in less than 2min with better separation of phases in 4-methyl pentan-2-one. The reagent $\text{DPG}^+\cdot\text{Cl}^-$ in this solvent has no extraction and the colored complex ion associate was extracted quantitatively. The ion associate was found also stable for up to 2h in this solvent. Thus, in the subsequent work, the solvent 4-methyl pentan-2-one was selected as a proper solvent. The amount of gold(III) extracted from the aqueous solution into the organic phase versus the amount of gold(III) in the aqueous phase at equilibrium varied linearly at low and moderate trivalent gold(III) concentration ($\leq 10\text{g mL}^{-1}$) followed by a plateau at higher concentration. A solvent capacity of 5g gold(III) ions uptake per milliliter of organic solvent was obtained.

The optimum shaking time was ascertained by measuring the absorbance of the organic extract after 0.5–10min shaking time. Rapid attainment of extraction equilibrium was achieved within 1.5–2min. Thus, a 2min shaking time was taken as the optimum time in the subsequent work to ensure complete extraction. The volume ratio of the aqueous phase (5g mL^{-1} Au) to the organic phase

($V_{\text{(aq)}}/V_{\text{(org)}}$) was also examined for the extraction of gold (5g mL^{-1} Au) species. For a single extraction, it was found that, quantitative extraction of gold was attainable up to 20-fold ($V_{\text{(aq)}}/V_{\text{(org)}}=20:1$).

The effect of pH of the aqueous solution employing B–R buffer on the extraction of the developed colored complex ion associate was studied by measuring the absorbance of the organic extract at 362nm against the reagent blank. Maximum absorbance of the produced ion associate was obtained at pH 5–9 (Fig. 2). In the aqueous solution of $\text{pH} \leq 5$, the ion pair $\text{DPG}^+\cdot\text{Cl}^-$ is less dissociated and gold(III) is most likely exists as chloroauric acid (HAuCl_4) species, which is less dissociated at lower pH as follows:



Thus, in acidic pH, the equilibrium (Eq. (2)) moves to the left and the quantity of $\text{AuCl}_{4(\text{aq})}^-$ ions available to form complex ion associate with $\text{DPG}^+\cdot\text{Cl}^-$ decreased. On the other hand, in aqueous solution of $\text{pH} \geq 9$, the absorbance of the organic extract also decreased. The formation of non-extractable com-

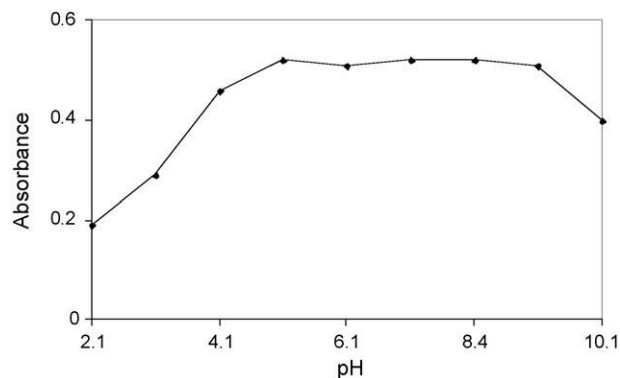
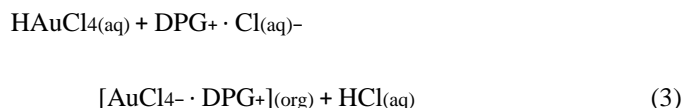


Fig. 2. Influence of pH on the uptake of the ion associate [$\text{DPG}^+\cdot\text{AuCl}_4^-$] onto the solvent 4-methyl pentan-2-one (5mL). Aqueous phase (20mL) at pH 6–7, $\text{Au}=2\text{g mL}^{-1}$ and 0.1mL $\text{DPG}^+\cdot\text{Cl}^-$ (0.01%, w/v).

plex species of gold(III), e.g. hydroxo-species of gold(III) which minimizes the associate formation [40] may account for such trend. Thus, in the subsequent work the pH of the aqueous solution was adjusted at pH 6–7 and the overall reaction between $\text{DPG}^+\cdot\text{Cl}^-$ and $\text{HAuCl}_{4(\text{aq})}$ is most likely be proceeded as follows:



The influence of $\text{DPG}^+\cdot\text{Cl}^-$ concentration on the extraction of the formed ion associate at the optimum experimental conditions

was studied. A 2mL of $8.0 \times 10^{-5} \text{ molL}^{-1}$ of $\text{DPG}^+\cdot\text{Cl}^-$ was found sufficient to extract quantitatively (96–98%) up to 10 mgmL^{-1} of gold(III) from the aqueous by double extraction ($2 \times 2.5 \text{ mL}$) of the organic solvent. The molar absorptivity of the produced ternary complex ion associate $\text{DPG}^+\cdot\text{AuCl}_4^-$ at 362nm calculated from the absorbance measurement was found equal $2.19 \times 10^4 \text{ Lmol}^{-1} \text{ cm}^{-1}$ in 4-methyl pentan-2-one. A large excess of the reagent slightly decreased the absorbance of the organic phase possibly owing to the increased acidity of the aqueous phase which minimizes the associate formation.

3.2. Effect of foreign ions

The selectivity of the developed method for the extraction of 5 mgmL^{-1} of tri-valent gold ions in the presence of a relatively high excess ($0.05\text{--}0.1 \text{ mgmL}^{-1}$) of some cations and anions was investigated. The tolerance limit was defined as the concentration of the foreign ion added causing a relative error within $\pm 2\%$ of the recovery of gold. It was found that, in the extraction of gold(III), the ions: Li^+ , Na^+ , K^+ , Ca^{2+} , NH_4^+ , Al^{3+} , Fe^{2+} , Ni^{2+} , Co^{2+} , Cu^{2+} and Zn^{2+} and the anions: Cl^- , Br^- , SO_4^{2-} ,

1498

CO_3^{2-} , $\text{C}_2\text{O}_4^{2-}$, PO_4^{3-} and $\text{S}_2\text{O}_8^{2-}$ do not interfere at 1:100 tolerable concentration of gold(III) to the diverse ions, respectively. Interference due to Fe^{3+} and VO_3^- and MnO_4^- (1:100, w/w) was eliminated by the addition of few drops of NaF (1%, w/v) and NaN_3 (0.1%, w/v) prior to the extraction, respectively. Interference of Ag^+ ions was removed by adding few drops of KCl (0.1%, w/v) to form AgCl precipitate. In the presence of some other ions, e.g. Pd^{2+} and Pt^{2+} even at low concentrations

(1:10, v/v), positive interference was noticed. The ability of these ions to form extractable stable complex ion associates with the reagent $\text{DPG}^+\cdot\text{Cl}^-$ under the optimum experimental condition is most likely account for such behavior. These ratios do not induce limitations in the matrixes, e.g. salty effluents that could be analyzed by the developed extraction procedure.

3.3. Characterization of the gold(III) ion associates

The composition of the extracted species was determined at two different concentrations of the gold(III) ions and reagent by Job's method [41]. A plot of the absorbance of the organic extract at 362nm versus the mole fraction of $\text{DPG}^+\cdot\text{Cl}^-$ revealed a graph that indicated the formation of an ion-association complex having gold(III) to a reagent molar

M.S. El-Shahawi et al. / Talanta 72 (2007) 1494–1499

Table 1

Analytical results for the extraction of the binary mixture of mono- and tri-valent gold ions in aqueous media by the developed procedure

Gold species (mgmL^{-1})		Average gold (I) and (III) found		Recovery (%) ^a	
Au ⁺	Au ³⁺	Au ⁺	Au ³⁺	Au ⁺	Au ³⁺
5.0	10.0	4.9	10.3	98.0 ± 2.7	103.0 ± 2.7
10.0	15.0	9.7	15.2	97.0 ± 2.2	101.3 ± 2.3
15.0	10.0	14.8	10.2	98.7 ± 2.1	102 ± 1.6

^a Average recovery of five measurements ± relative standard deviation.

ratio of 1:1. The organic extract was also evaporated under vacuum and analyzed for C, H, N and Au. The analytical data of the produced associate was found as follows: $[\text{AuOC}_6\text{H}_9\text{N}_7\text{Cl}_5]$ required 12.62% C, 1.57% H, 17.24% N and 34.7% Au; Found 13.12% C, 1.76% H, 16.96% N and 35.23% Au. These data add further confirmation that, the extracted species are most likely represented as $\text{AuCl}_4^- \cdot \text{DPG}^+$. The stability constant of the produced complex ion associate calculated from the Job's plot from the ratio of the true absorbance (A) to the extrapolated (A_{extp}) absorbance [41] was found equal to 2.46×10^3 .

A series of oxidizing agents such as H_2O_2 , $\text{K}_2\text{S}_2\text{O}_8$ or bromine water has been tested for complete oxidation of monovalence gold species to tri-valent gold species in aqueous media containing dilute acids (1 mol L^{-1}), e.g. CH_3COOH , HCl or H_2SO_4 or KCl (1 mol L^{-1}). Among these oxidizing agents, bromine water in HCl (1 mol L^{-1}) medium and boiling the aliquotaqueoussolutionofmonovalencegoldspeciesfor2min was the most suitable oxidizing agent for gold(I) to gold(III) species. The oxidation performance of mono-valence gold to gold(III) species in the aqueous media followed the sequence: brominewater > $\text{K}_2\text{S}_2\text{O}_8$ > H_2O_2

The variation of HCl concentration (0.1 – 2 mol L^{-1}) in the extraction media on the oxidation of gold(I) to gold(III) by bromine water and boiling was investigated following the same extraction procedure. The results revealed that optimum conditions for complete oxidation of gold(I) to gold(III) is to have an aqueous medium containing HCl (1 mol L^{-1}).

The extraction of gold(I) at concentration levels 1.0 – 15 mg mL^{-1} after oxidation with Br_2 water in HCl (1 mol L^{-1}) and following the recommended extraction procedure for gold(III) was successfully achieved with a recovery percentage of $98 \pm 3.4\%$ ($n=5$). Thus, the analysis of the binary mixtures of gold(I) and (III) ions in the aqueous media by

Table 2

Analytical results of the chemical speciation and recovery of mono- and tri-valent gold ions in wastewater samples by the proposed extraction procedure

Gold species (mg mL^{-1})		Average gold (I) and (III) found		Recovery (%) ^a	
Gold (I) and (III) added				Au^+	Au^{3+}
Au^+	Au^{3+}	Au^+	Au^{3+}		
5.0	10.0	4.8	10.4	96.0 ± 2.4	97.0 ± 2.9
10.0	15.0	9.7	15.2	± 2.8	101.3 ± 2.1
15.0	15.0	14.8	14.8	98.7 ± 3.1	98.7 ± 1.9

^a Average of five measurements \pm relative standard deviation.

the developed extraction procedure was attempted. The results are summarized in Table 1. Satisfactory recovery percentage of various gold(I) and gold(III) species was obtained.

3.4. Analytical applications

3.4.1. Chemical speciation and recovery of gold(I) and (III) from water samples

The validity of the developed extraction procedure was investigated by the determination of the mean percentage recoveries ($n=5$) of gold(III) in distilled water (10 mg mL^{-1} Au) using both the calibration graph and standard addition methods. The average percentage recoveries were found reproducible. The limits of detection (LOD) of gold(III) estimated using the equation: $\text{LOD} = 3S_{y/x}/b$ [42]; where $S_{y/x}$ is the standard deviation of y -residuals and b is the slope of the calibration plot was found equal 6.1×10^{-7} . The value of the lower limit of quantification (LOQ) calculated using the equation: $\text{LOQ} = 10S_{y/x}/b$ [42], was found equal $9.2 \times 10^{-7} \text{ mol L}^{-1}$. This level of precision is suitable for the routine analysis of the gold(III) in water.

The application of the developed extraction procedure for the chemical speciation and recovery of traces of gold(I) and (III) at a total concentration $\leq 25.0 \text{ mg mL}^{-1}$ in tap water was investigated as described in Section 2. A recovery percentage of 97 ± 2.9 was achieved with good reproducibility. Thus, attempts were also applied for the analysis of gold(I, III) in wastewater samples of fertilizer industry following the described experimental procedure. The data are summarized in Table 2. The accuracy of the developed procedure was evaluated by the recovery studies of the gold added. Also, on plotting the amount of gold added versus the amount recovered a regression line with a slope of 0.998 and a correlation coefficient of 0.999 was achieved. The slightly high values of recoveries in the wastewater may be due to the presence of other impurities in the wastewater (Table 2). The F -test at 95% confidence levels did not exceed the tabulated (the-

Table 3

Analytical results of the recovery of Au^{3+ss} (5–15gmL⁻¹) from Ag⁺ and other metal ions, e.g. Fe³⁺, Co²⁺, Ni²⁺, Cu²⁺ or Zn²⁺ at 10.0gmL⁻¹ interfering in tap water samples by the proposed procedure

Gold(III) added (gmL ⁻¹)	Gold(III) found (gmL ⁻¹)	Recovery (%) ^a
5.0	5.15	103 ± 2.1
10.0	10.35	103.5 ± 1.9
15.0	14.8	98.7 ± 2.1

^a Average of three measurements ± relative standard deviation.

oretical) ones and revealed no significant differences between the averages and the variances of the developed procedure and the reported method [30].

3.4.2. Separation of gold(I) and (III) from silver(I) and other base metal ions

The developed extraction procedure was also applied successfully for the separation of gold(III) ions in the concentration range 5–15.0gmL⁻¹ Au from silver(I) and base metal (Fe³⁺, Co²⁺, Ni²⁺, Cu²⁺ and Zn²⁺) ions at 10.0gmL⁻¹ level in tap water samples. The results are summarized in Table 3. More or less complete recovery of gold ions was achieved with good precision (R.S.D. ≤ 2.1%). In terms of *F* (0.075) and Student's *t* tests (1.91), no significant differences in the accuracy and precision [42] between the proposed and the published method [31] were observed.

4. Conclusion

The method provides an excellent alternative approach for the analytical determination of gold because of its low cost, repeatability and sufficient precision. The reaction of the reagent DPG⁺·Cl⁻ with the anion AuCl₄⁻ is rapid, simple, does not involve any stringent conditions and no standing time is needed. The produced ternary complex ion associate DPG⁺·AuCl₄⁻ is stable before determining the ions. Thus, the developed extraction procedure was also applied for the extraction and subsequent AAS determination of inorganic gold(I) and/or (III) ions in fresh and industrial wastewater samples after oxidation of the former ion to gold(III) with bromine water. The procedures have the advantage of virtual freedom from most interfering ions and can serve as a low cost procedure for the separation of gold from silver and base metal ions. However, work is continuing for the recovery of gold species from different matrixes and application of on line procedures for the chemical speciation of inorganic and organic bound gold species in reference and real samples.

References

[1] B. Pal, P.K. Sen, K.K. Sen Gupta, Indian J. Chem. Soc. 83 (2006) 762. [2] N. Pourreza, S. Rastegarzadeh, Chem. Anal. (Warsaw) 50 (2005) 695.

- [3] T.R. Dulski, Trace Elemental Analysis of Metals, Marcel Dekker Inc., 1999, P.99.
- [4] M. Behpour, A.M. Attaran, S.M. Ghoreishi, N. Soltani, Anal. Bioanal. Chem. 382 (2005) 444.
- [5] H.R. Li, Q.X. Rong, X.L. Hou, X.Y. Mao, Talanta 44 (1997) 1313.
- [6] A. Aworn, A. Thiravetyan, W. Nakbanpote, J. Colloid Interf. Sci. 287 (2005) 394.
- [7] Y. Yang, C. Li, K.H. Lee, H.G. Craighead, Electrophoresis 26 (2005) 3622.
- [8] Z. Marczenko, Spectrophotometric Determination of Elements, 3rd ed., Ellis Horwood, Chichester, UK, 1986 (and references cited in Chapter 23).
- [9] Q. Hu, X. Chen, X. Yang, Z. Huang, J. Chen, G. Yang, Anal. Sci. (Jpn.) 22 (2006) 627.
- [10] O. Shima, N. Hirayama, K. Kubono, H. Kokusen, T. Honjo, Anal. Chim. Acta 441 (2001) 157.
- [11] J.-F. Li, Li-F. Bai, Y.-H. Wang, H.-Y. Wang, Anal. Sci. (Jpn.) 22 (2006) 841.
- [12] F. Menegazzo, M. Manzoli, A. Chiorino, F. Boccuzzi, T. Tabakova, M. Signoretto, F. Pinna, N. Pernicone, J. Catal. 237 (2006) 431.
- [13] Z.Y. Chen, Z.J. Huang, J. Chen, J.Y. Yin, Q.D. Su, G.Y. Yang, Anal. Lett. 39 (2006) 579.
- [14] V. Balaran, R. Mathur, V.K. Banakar, J.R. Hein, C.R.M. Rao, T.G. Rao, B. Dasaram, Indian J. Mar. Sci. 35 (2006) 7.
- [15] B. Dasaram, Indian J. Mar. Sci. 35 (1) (2006) 7.
- [16] S. Oshima, N. Hirayama, K. Kubono, H. Kokusen, T. Honjo, Anal. Chim. Acta 441 (2001) 157.
- [17] J. Rydberg, C. Musikas, G.R. Choppin, Principles and Practices of Solvent Extraction, Marcel Dekker, New York, 1992.
- [18] M. Tanaka, H. Akaiwa, Solvent Extraction Chemistry, Shokabo, Tokyo, 2000.
- [19] B. Saad, S.M. Sultan, Talanta 42 (1995) 1349.
- [20] M.S. El-Shahawi, S.M. Al-Dhaheri, Fresen. J. Anal. Chem. 354 (1996) 200.
- [21] M.H. Cordoba, P. Navarro, I.L. Garcia, Int. J. Environ. Anal. Chem. 32 (1988) 97.
- [22] P. Das, H.K. Das, J. Indian Chem. Soc. 70 (1993) 90.
- [23] M.S. El-Shahawi, A.M. Othman, M.A. Abdel-Fadeel, Anal. Chim. Acta 546 (2005) 221.
- [24] M.S. El-Shahawi, S.S.M. Hassan, A.M. Othman, M.A. Zyada, M.A. El-Sonbati, Anal. Chim. Acta 534 (2005) 319.
- [25] P. Padmaja, N. Balasubramanian, T.V. Ramakrishna, Talanta 41 (1994) 255.
- [26] S.S.M. Hassan, M.S. El-Shahawi, A.M. Othman, M.A. Mosaad, Anal. Sci. 21 (2005) 673.
- [27] D.T. Burns, S.A. Barakat, M. Hariott, M.S. El-Shahawi, Anal. Chim. Acta 270 (1992) 213.
- [28] D.T. Burns, S.A. Barakat, M.S. El-Shahawi, M. Hariott, Fresen. J. Anal. Chem. 344 (1992) 131.
- [29] M.S. El-Shahawi, F.A. Al-Hashimi, Talanta 43 (1996) 2037.
- [30] C.T. Camagong, T. Honjo, Anal. Sci. (Jpn.) 17 (2001) 1725.
- [31] K. Gavazov, A. Dimitrov, V. Lekova, Chem. Papers (2007), in press.
- [32] S. Biswas, H.K. Mondal, S. Basu, Indian J. Chem. 35A (1996) 804.
- [33] P.R. Haddad, N.E. Rochester, Anal. Chem. 60 (1998) 536.
- [34] D.T. Burns, P. Hanprasopwattana, Anal. Chim. Acta 118 (1980) 185.
- [35] D.T. Burns, M.S. El-Shahawi, M.J. Kerrigan, P.M.T. Smyth, Anal. Chim. Acta 322 (1996) 107.
- [36] M.S. El-Shahawi, Anal. Chim. Acta 356 (1997) 85.
- [37] S.M. Al-Dhaheri, Talanta 46 (1998) 1613.
- [38] A.I. Vogel, A Text Book of Quantitative Inorganic Analysis, 3rd ed., Longman Group Ltd., England, 1966.
- [39] M. Hiraoka, Crown Compounds, their Characteristics and Applications, Elsevier Science Ltd., Tokyo, 1982.

- [40] S. Yamaguchi, K. Uesugi, Analyst 109 (1984) 1393.
[41] D.T. Sawyer, W.R. Heinemann, J.M. Beebe, Chemistry Experiments for Instrumental Methods, John Wiley & Sons, 1984.
[42] J.C. Miller, J.N. Miller, Statistics for Analytical Chemistry, 4th ed., EllisHorwood, New York, 1994, p. 115.

cigarette smokers, causing an increase in thiocyanate levels in human fluids [1]. The toxicity of thiocyanate is significantly less than that of cyanide; however, chronically elevated levels of thiocyanate can inhibit the uptake of iodine by the thyroid gland

Available online at www.sciencedirect.com



ANALYTICA
CHIMICA
ACTA

Analytica Chimica Acta 592 (2007) 16–23 www.elsevier.com/locate/aca

Extractive liquid–liquid spectrophotometric procedure for the determination of thiocyanate ions employing the ion pair reagent amiloride monohydrochloride

A.S. Bashammakh, S.O. Bahaffi, A.A. Al-Sibai, H.O. Al-Wael, M.S. El-Shahawi*

Department of Chemistry, Faculty of Science, King Abdulaziz University, P.O. Box 80203, Jeddah 21589, Saudi Arabia

Received 22 January 2007; received in revised form 2 April 2007; accepted 4 April 2007

Available online 8 April 2007

Abstract

An accurate, inexpensive and less laborious liquid–liquid extractive spectrophotometric procedure for the determination of thiocyanate ions in aqueous media has been developed. The method has been based upon the formation of a yellow colored complex ion associate of the ion-pairing reagent 1-(3, 5-diamino-6-chloropyrazinecarboxyl) guanidine hydrochloride monohydrate, namely amiloride hydrochloride, DPG^+Cl^- and the thiocyanate ions in aqueous media containing HNO_3 (0.5molL^{-1}) and subsequent extraction with 4-methyl-2-pentanone. The absorption electronic spectrum of the ion associate showed one well-defined peak at λ_{max} 366nm. The stoichiometric mole ratio of DPG^+Cl^- to the thiocyanate ions is 1:1. The effective molar absorptivity (ϵ) of the ion associate at λ_{max} 366nm is $1.1 \pm 0.1 \times 10^4 \text{Lmol}^{-1} \text{cm}^{-1}$. The extraction constants (K_d , K_{ex} , and β) enabled a simple and convenient use of the developed binary ion associate for the extractive spectrophotometric determination of traces of thiocyanate ions in the aqueous media. Beer's law and Ringbom's plots are obeyed in the concentration range 0.05–10 and 0.1–7 gmL^{-1} of the thiocyanate ions, respectively with a relative standard deviation of $\pm 2.3\%$. The calculated lower limits of detection (LOD) and quantitation (LOQ) of the developed procedure for the thiocyanate ions were found equal to 0.02 and 0.066 gmL^{-1} , respectively. The developed method has been applied for the determination of trace amounts of thiocyanate ions in tap-, waste- and natural water samples and compared successfully with the reported methods at the 95% confidence level. The proposed method was also applied successfully for the determination of thiocyanate ions in saliva samples.

© 2007 Elsevier B.V. All rights reserved.

Keywords: Thiocyanate determination; Chemical equilibrium; Amiloride hydrochloride; Solvent extraction; Spectrophotometry; Wastewater and biological samples

1. Introduction

Thiocyanate ions are present in low concentrations in human serum saliva and in urine. If the content of the thiocyanate ions is a little higher in the body than normal, the protein dialysis will be affected and it may even result in coma [1]. The major cyanide sources in daily human activity are the inhaled smoke by

reducing the formation of thyroxin [2]. The concentration of thiocyanate of human saliva is considered as a biomarker

* Corresponding author. Tel.: +96 62 6951214.

E-mail address: mohammad.elshahawi@yahoo.co.uk (M.S. El-Shahawi).

for distinguishing smoking from non-smoking individuals [3]. Saliva thiocyanate may also have an antibacterial role in the mouth, decreasing the corrosion potential of amalgams [3,4]. It is well known that the presence of thiocyanate ions has some relation to local goiter [5–7].

Many spectrophotometric methods based on the formation of the red iron(III)–thiocyanate complex have been reported for the determination of thiocyanate [8,9]. The photometric method for NCS- determination was based upon the formation of yellow colored charge-transfer complex (I_2 NCS-) requires the use of a toxic organic solvent [10]. A method for the determination of trace thiocyanate based on the direct reaction of iodine with 2, 7-dichlorofluorescein in acid medium to produce a weakly fluorescent species has been reported [11]. A rapid, simple and low sensitive solvent extraction flow injection spectrophotometric method for the simultaneous determination of cyanide and thiocyanate ions via formation of colored ($\lambda_{max}=540nm$)

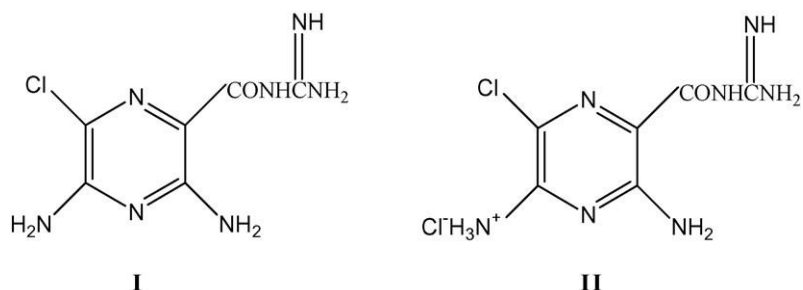


Fig. 1. Chemical structures of amiloride (I) and amiloride hydrochloride (II).

ternary complexes with copper and 2,2-dipyridyl-2-quinolylydrazone in chloroform has been reported [12,13]. However, most of these methods suffer from several interferences and are time-consuming [8–10].

The reported ion selective electrodes [14–20] potentiometric methods for the determination of thiocyanate ions were subjected to interferences. Linear sweep polarography [6], liquid chromatography [21], gas chromatography [22] and ion chromatography [23] methods have also been reported. Most of these methods need complicated instrumentation with time-consuming procedures or involve the use of harmful reagents. Due to the urgent need for selective and low cost extraction procedures for the determination of trace amounts of thiocyanate ions, especially in water samples, the present study reports a simple, low cost and precise liquid–liquid extraction spectrophotometric procedure for the complete extraction and subsequent determination of thiocyanate ions in water employing the ion-pair reagent amiloride hydrochloride (Fig. 1).

The composition, characterization and chemical equilibrium of the formed complex ion associate were also investigated. The developed method not only separates the thiocyanate ions but also preconcentrate them quantitatively. Thus, the method is also potentially useful for the determination of thiocyanate in biological samples e.g. urine and saliva, where evaluated levels of thiocyanate correlate with excessive cigarette smoking.

2. Experimental

2.1. Reagents and materials

Analytical-reagent grade chemicals and solvents were provided by BDH (BDH Ltd., Poole, England), unless stated otherwise, and were used without further purification. All solutions were made up by doubly de-ionized water. Potassium thiocyanate (Fluka, AG, Buchs, Switzerland) was used for the preparation of stock thiocyanate solution. The reagent amiloride monohydrochloride (E. Merck, Darmstadt, Germany) abbreviated as $\text{DPG}^+\text{-Cl}^-$ was used as received. A stock solution of the reagent $\text{DPG}^+\text{-Cl}^-$ (0.01molL^{-1}) was prepared by dissolving an accurate weight of the ion-pairing reagent in 100mL $\text{HCl-H}_2\text{O}$ (1:1, v/v). A series of Britton–Robinson (B–R) buffer (2.1–10.5) was prepared by mixing equal proportions of acetic acid (0.08molL^{-1}), phosphoric acid

(0.08molL^{-1}) and boric acid (0.08molL^{-1}) and adjusting the solution pH to the required value with NaOH (0.02molL^{-1}) as reported earlier

[24].

2.2. Apparatus

A Perkin-Elmer UV/VIS spectrometer (Lambda EZ 150, USA) single beam and a double-beam Perkin-Elmer UV/VIS spectrometer (Lambda EZ 210, USA) with 1cm (path width) quartz cell (10mm) were used for recording the absorbance and electronic spectra of the formed complex ion associate. Deionized water was obtained from Milli-Q Plus system (Milipore, Bedford, MA, USA) was used for preparing all solutions. A pH meter (Orion EA940, MA, USA) was employed for the pH measurements with absolute accuracy limits at the pH measurements being defined by NIST buffers.

2.3. Recommended extraction procedure

In a separating funnel, an aqueous solution (20.0mL) containing thiocyanate ions ($0.05\text{--}10\text{gNCS}^- \text{mL}^{-1}$) and HNO_3 (1.0molL^{-1}) was mixed with 2.0mL of the ion pair reagent $\text{DPG}^+\text{-Cl}^-$ ($2.0 \times 10^{-3} \text{molL}^{-1}$) and swirled to mix the contents. The solution was then completed with distilled water to 25mL and shaken twice with 5mL (2×2.5) of the 4-methyl-2-pentanone for 2min. After shaking, the organic extract was then collected in a 25mL beaker containing anhydrous sodium sulfate (1.0g), swirled, and transferred to a 25mL volumetric flask. The residue was also washed with another 5mL (2×2.5) of the same solvent. The washing solutions and the organic extract were then collected, transferred to the measuring flask (10.0mL) and finally made up to the mark with the same solvent. The absorbance of the organic extract was then measured at 366nm against a reagent blank. The concentration of the thiocyanate ions in the aqueous phase before (C_b) and after (C_a) extraction by the developed method was determined by the method reported earlier [9]. The amount of the thiocyanate ions extracted in the organic phase as $\text{DPG}^+\text{-CNS}^-$ was then calculated from the difference ($C_b - C_a$) between the concentration of the thiocyanate ions in the aqueous phase before and after extraction with the reagent $\text{DPG}^+\text{-Cl}^-$. The distribution ratio

(D_{NCS}) of the thiocyanate ions between the aqueous phase and the organic phase was then calculated employing the equation:

$$D_{\text{NCS}} = \frac{[\text{DPG}^+ \cdot \text{NCS}^-]_{(\text{org})}}{[\text{NCS}^-]_{(\text{aq})} + [\text{DPG}^+ \cdot \text{NCS}^-]_{(\text{aq})}} \quad (1)$$

2.4. Analytical applications

2.4.1. Analysis of thiocyanate in various water samples

2.4.1.1. Direct method. The efficiency of the developed extraction procedure has been studied for the extraction and subsequent

determination of traces of thiocyanate ions in various water samples as follows: pipetted 100 mL of the tap- or water samples from water treatment station of Jeddah city, Saudi Arabia were transferred into a 250 mL beaker. To the sample solutions 0.5 mL of NaOH (1.0 mol L^{-1}) and 0.5 mL of EDTA (0.10 mol L^{-1}) were then pipetted into separating funnels (50.0 mL capacity) and centrifuged to remove any formed precipitate. A 2.0 mL concentrated HNO_3 was added to the water sample, filtered through a 0.45 μm cellulose membrane and the pH was then adjusted to zero with the same acid. The thiocyanate ions in the water samples (20.0 mL) after treatment was extracted and analyzed as described in the recommended procedure with the aid of standard curve against a reagent blank as reported [9].

2.4.1.2. Standard addition method. Alternatively, the standard addition (spiking) method was used as follows: a known volume (10 mL) of the water samples after centrifugation in the presence of NaOH (0.5 mL, 1.0 mol L^{-1}) and EDTA (0.5 mL, 0.10 mol L^{-1}), filtrations through a 0.45 μm cellulose membrane and adjustment of the pH to zero with nitric acid (0.5 mol L^{-1}) was spiked with known concentrations ($0.05\text{--}5 \text{ g mL}^{-1}$) of thiocyanate ions. The solutions (20.0 mL) were then extracted as described before and the absorbance of the organic extract displayed before and after spiking was measured versus a reagent blank. The change in the absorbance was then used for determining the thiocyanate concentration with the aid of standard addition curve.

2.4.2. Analysis of thiocyanate in biological samples

Human saliva was collected from smoker and non-smoker persons ($n=5$) following the reported method of Themelis and Tzanavaras in 2002 [8] according to the following procedures: The mouths of the donors were first washed with saliva stimulator (20.0 mL, citric acid 0.5 g/v) and four times with de-ionized water ($4 \times 10.0 \text{ mL}$) and stored in low density polyethylene (LDPE) bottles, Nalgene. The collected saliva in LDPE bottles was then shaken in a centrifuge at 2000 rpm for 10 min, filtered through a 0.45 μm filter. The resulting solution was then diluted to 10-fold with de-ionized water and finally the concentration of the thiocyanate ions was determined

employing the standard addition method under the optimum experimental conditions of the proposed method.

3. Results and discussion

3.1. Investigation of the various experimental variables

The ion pairing reagent $\text{DPG}^+ \cdot \text{Cl}^-$ reacts with thiocyanate ions in the aqueous solution in the presence of nitric acid (0.5 mol L^{-1}) to form yellow colored complex ion associate. The produced associate was easily soluble in 4-methyl-2-pentanone. After equilibrium, the organic extract was

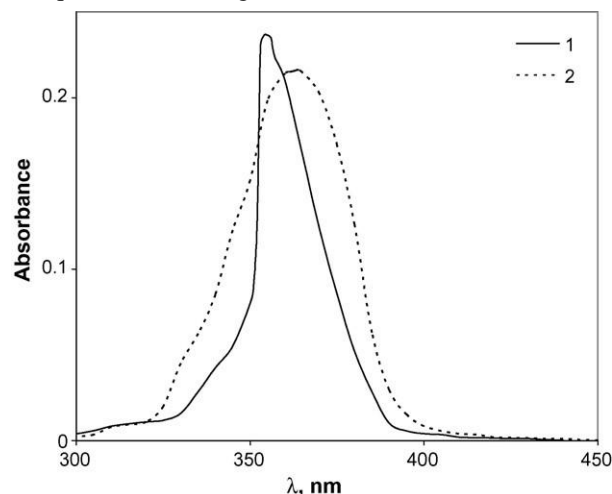
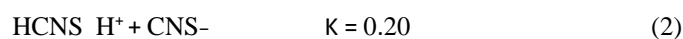


Fig. 2. Electronic spectra of the amiloride hydrochloride (1) in aqueous medium containing nitric acid (0.5 mol L^{-1}) and the produced complex ion associate of the thiocyanate (1.25 g mL^{-1}) and the reagent $\text{DPG}^+ \cdot \text{Cl}^-$ in 4-methyl-2-pentanone (2) against a reagent blank.

separated out and its absorption electronic spectrum (Fig. 2) showed one well defined peak maximum at $\lambda_{\text{max}} 366 \text{ nm}$ ($\epsilon = 1.1 \pm 0.1 \times 10^4 \text{ L mol}^{-1} \text{ cm}^{-1}$) while, in the absence of the thiocyanate ions in the aqueous phase the absorption spectrum of the organic extract of the reagent $\text{DPG}^+ \cdot \text{Cl}^-$ showed no peaks in the range of 250–380 nm. The electronic spectrum of the reagent $\text{DPG}^+ \cdot \text{Cl}^-$ in the aqueous phase showed two well defined peaks at 288 and 354 nm (Fig. 2). In the absence of the potassium thiocyanate or the ion pair reagent $\text{DPG}^+ \cdot \text{Cl}^-$ in the aqueous phase, no color was observed in the organic phase. In the absence of $\text{DPG}^+ \cdot \text{Cl}^-$, this observation was also confirmed from the spectrophotometric measurements of the thiocyanate ions in the aqueous phase [9]. Thus, in the subsequent work, the absorbance of the ion associate in the organic extract at 366 nm was used for the spectrophotometric measurements of thiocyanate ions in the aqueous media.

The chemical composition of the extracted ion associate of $\text{DPG}^+\cdot\text{Cl}^-$ and thiocyanate in 4-methyl-2-pentanone was determined by the Job's continuous variation and molar ratio methods [25]. The data indicated that the ion associate has a thiocyanate to a reagent $\text{DPG}^+\cdot\text{Cl}^-$ molar ratio of exactly 1:1. The chemical composition of the produced complex ion associate is a critical parameter, for the sensitivity, the background absorbance and the determination range of the analyte. Mole ratios of 1:1 resulted in a high sensitivity and acceptable background signals due to the formation of the complex ion associate of the general formula $\text{DPG}^+\cdot\text{NCS}^-$ which is readily extractable into the organic phase [26]. Based on these results in 4-methyl-2-pentanone and the data reported earlier for the complex ion associates of the reagent $\text{DPG}^+\cdot\text{NCS}^-$ with perchlorate [27], perrhenate [28], and periodate [29,30], the overall reaction of thiocyanate ions with $\text{DPG}^+\cdot\text{Cl}^-$ in HNO_3 (0.5molL^{-1}) was most likely proceeded as follows:



The effect of pH (0–10.5) upon the reaction of $\text{DPG}^+\cdot\text{Cl}^-$ with NCS^- ions in the aqueous phase and subsequent solvent extraction of the produced species employing HNO_3 (0.5molL^{-1}) and/or B–R buffer was studied. The concentration of the thiocyanate ions and $\text{DPG}^+\cdot\text{Cl}^-$ was fixed at 1×10^{-5} and $1.2 \times 10^{-5} \text{molL}^{-1}$, respectively. The final pH of the aqueous solution was adjusted before the extraction and the absorbance of the developed colored extract in 4-methyl pentan-2-one was measured at 366nm against reagent blank. In the pH range higher than pH 2.5 no extraction was observed, while on lowering the $\text{pH} \leq 2.1$, the sensitivity and the background absorbance considerably raised and maximum absorbance of the produced complex ion associate was obtained at pH zero. At pH about zero, the thiocyanate ions may exist only as anionic species (NCS^-) depending on the thiocyanate concentration and the ionic strength as reported earlier for periodate anion [29]. Thus, the overall reaction involves formation of the ion associate of the general formula $\text{DPG}^+\cdot\text{NCS}^-$. The decrease in the absorbance of the extracted species on raising the pH is most likely due to the formation of non-extractable forms of thiocyanate ions and/or the instability of the complex species formed in the extraction media.

The extraction performance of the complex ion-associate of thiocyanate ions with $\text{DPG}^+\cdot\text{Cl}^-$ was investigated in a series of organic solvents namely: *n*-hexane, *n*-heptane, diethyl ether, petroleum ether, dichloromethane, carbon tetrachloride, toluene, chloroform, cyclohexane and 4-methyl-2-pentanone. The extraction followed the sequence: 4-methyl pentan-2-one > diethyl ether > petroleum ether > chloroform > toluene > dichloromethane > *n*-hexane > carbon tetrachloride in agreement

to some extent with the order of the dielectric constants of the diluents [32]. Maximum absorbance, apparent molar absorptivity, stability, distribution ratio ($D=22.7$) and solubility of the produced complex ion associate were achieved in 4-methyl-2-pentanone. Thus, 4-methyl-2-pentanone was selected as the proper organic phase in the subsequent work because (i) the extraction is complete in a very short time; (ii) its lower density allows a better separation of the phases and finally (iii) thiocyanate ions or the ion pair reagent $\text{DPG}^+\cdot\text{Cl}^-$ separately are also not extracted into this solvent.

The stability of the produced ion associate depends considerably on the nature of the mineral acid present in the aqueous phase. Thus, the effect of the mineral acids: HCl, H_2SO_4 and HNO_3 at 0.50molL^{-1} concentration upon the extraction of the associate of the thiocyanate with the reagent $\text{DPG}^+\cdot\text{Cl}^-$ was studied. The data revealed that the nature of the mineral acid contributes substantially to the maximum extraction of the complex ion associate and maximum absorbance of the colored species was obtained in HNO_3 (0.5molL^{-1}). In nitric acid (0.5molL^{-1}) an excellent extraction percentage ($98.6 \pm 2.3\%$) of the thiocyanate ions in the organic phase was achieved as indicated from the determination of thiocyanate remained in the aqueous phase [9]. The absorbance value of the colored associate in the organic phase followed the sequence:

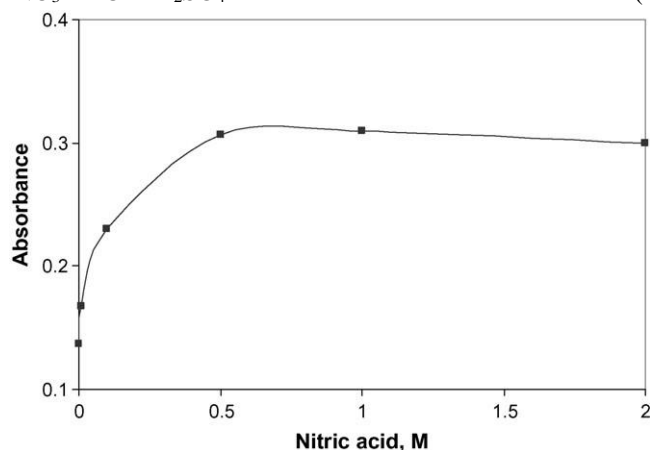
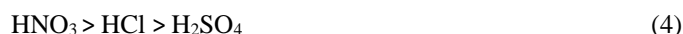


Fig. 3. Influence of HNO_3 concentration (0.1 – 2molL^{-1}) on the extraction of the ion associate of thiocyanate– $\text{DPG}^+\cdot\text{Cl}^-$ into 4-methyl-2-pentanone against a reagent blank.

The data indicated that the stability of the binary ion associate is higher in HNO_3 . Thus, the influence of HNO_3 concentration (0.1 – 4molL^{-1}) on the formation of $\text{DPG}^+\cdot\text{NCS}^-$ and subsequent solvent extraction of the ion associate of thiocyanate was investigated. Maximum extraction was achieved at acid concentration $>0.5\text{molL}^{-1}$ of the aqueous phase (Fig. 3). Thus

in the subsequent work, nitric acid (0.5molL⁻¹) was used as the preferable extraction medium.

The effect of shaking time on the extraction of the complex ion associate DPG⁺·NCS⁻ with 4-methyl-2-pentanone at different time intervals ranging from 30s to 5min was investigated. The extraction was rapid and maximum absorbance was achieved at 2min shaking time or more and hence a 2min shaking time was adopted in the subsequent work. The developed ion associate was stable for up to 3h for samples containing ≤10gmL⁻¹ of thiocyanate in the aqueous solution at pH zero containing HNO₃ (0.50molL⁻¹).

The influence of the reagent DPG⁺·Cl⁻ concentration (1.0×10⁻⁵–2.0×10⁻³ molL⁻¹) on the solvent extraction of the ion associate at the optimum experimental conditions was studied. The use of 2mL of 2.0×10⁻³ molL⁻¹ DPG⁺·Cl⁻ solution was found sufficient for complete extraction of up to 10gmL⁻¹ thiocyanate ions in the aqueous phase (20mL). Accordingly, 2.0mL of 2.0×10⁻³ molL⁻¹ of DPG⁺·Cl⁻ solution was added in all further experiments. The absorbance of the organic extract DPG⁺·NCS⁻ increased linearly on increasing the thiocyanate concentration up to 10gmL⁻¹ in the aqueous phase at the optimum ion-pair concentration (2.0mL, 2.0×10⁻⁴ molL⁻¹ DPG⁺·Cl⁻).

3.2. Interference study

The developed method has been applied for the extraction of 2.5gmL⁻¹ of the thiocyanate ions in the presence of a relatively high excess (0.05–0.1mgmL⁻¹) of the diverse ions: Ca²⁺, NH₄⁺, Al³⁺, Fe²⁺, AuCl₄⁻, the base metal ions e.g. Ni²⁺, Cu²⁺ and Zn²⁺ and the anions: Cl⁻, Br⁻, SO₄²⁻, CO₃²⁻, C₂O₄²⁻, PO₄³⁻ and S₂O₈²⁻. The tolerance limit was defined as the concentration of the foreign ion added causing a relative deviation within ±2% of the recovery of the thiocyanate ions. The ions: Fe³⁺, Co²⁺, VO₃⁻ and MnO₄⁻ interfered seriously even at low concentrations while the other ions did not interfere at 1:100 tolerable concentration of thiocyanate to the diverse ions. The interference of MnO₄⁻ was minimized to 1:25 by the addition of few drops of NaN₃ (0.1%, w/v) prior to their extraction. The interference of the ions VO₃⁻ and MnO₄⁻ is most likely attributed to the ability of these ions to form extractable stable complex ion associates with the reagent DPG⁺·Cl⁻ in the organic phase. On the other hand,

the interference of the ions Co²⁺, VO₃⁻ and Fe³⁺ is possibly attributed to the ability of these ions to form extractable complexes with the thiocyanate ions in the aqueous phase and subsequently extracted onto the organic phase. The interference of the ions VO₃⁻, Co²⁺ and Fe³⁺ was successfully eliminated by the addition of few drops of NaF (1%, w/v) or EDTA (0.5mL, 0.10molL⁻¹). Hence, in the subsequent work of the developed method EDTA (0.5mL, 0.10molL⁻¹) solution was added to mask the possible interference by the ions Fe³⁺, Co²⁺, VO₃⁻, Cr³⁺ on the determination of thiocyanate ions in various water samples.

3.3. Extraction equilibrium in the model system

Assuming that there is no dimerization of the extracted species and the formation of poly anion ion associates is negligible, the equilibrium constants *K*_{ex}, β and *K*_d of the system containing thiocyanate ions and the reagent DPG⁺·Cl⁻ and the solvents (water and 4-methyl-2-pentanone) at pH zero using HNO₃ (0.50molL⁻¹) have been calculated employing the following extraction equilibrium [31,33]:

- (i) Formation of the ion associate proceeded at pH 5–9 according to the equation:



with a corresponding ion associate equilibrium constant, β

$$\beta = \frac{[\text{DPG}^+ \cdot \text{NCS}^-]_{(\text{aq})}}{[\text{NCS}^-]_{(\text{aq})}[\text{DPG}^+]_{(\text{aq})}} \quad (6)$$

- (ii) Distribution of the complex ion associate between the aqueous and the organic phase with a corresponding distribution coefficient, *K*_d



$$K_d = \frac{[\text{DPG}^+ \cdot \text{NCS}^-]_{(\text{org})}}{[\text{DPG}^+ \cdot \text{NCS}^-]_{(\text{aq})}} \quad (8)$$

- (iii) The overall extraction process is then described by the equation:



With the corresponding equilibrium constant, which is often called extraction constant, *K*_{ex}, is given by the equation:

$$K_{\text{ex}} = \frac{[\text{DPG}^+ \cdot \text{NCS}^-]_{(\text{org})}}{[\text{DPG}^+]_{(\text{aq})}[\text{NCS}^-]_{(\text{aq})}} = \frac{\beta}{K_d} \quad (10)$$

$$[\text{DPG}^+]_{(\text{aq})}[\text{NCS}^-]_{(\text{aq})}$$

Taking into consideration that only one complex species of thiocyanate ions is present in the aqueous phase i.e. $\text{NCS}_{(\text{aq})}^-$ is the only predominant species at the given pH. Thus, the distribution ratio, D_{NCS} takes the following:

$$D_{\text{NCS}} = \frac{[\text{NCS}^-]_{(\text{org})}}{(11) [\text{NCS}^-]_{(\text{aq})}} \quad (11)$$

$$= \frac{[\text{DPG}^+ \cdot \text{NCS}^-]_{(\text{org})}}{[\text{NCS}^-]_{(\text{aq})} + [\text{DPG}^+ \cdot \text{NCS}^-]_{(\text{aq})}} \quad (12)$$

Assuming that at low concentrations of the reagent $\text{DPG}^+\text{-Cl}^-$ i.e. $[\text{NCS}^-] \gg [\text{DPG}^+\text{-Cl}^-]$, the association in the aqueous phase $[\text{DPG}^+\text{-NCS}^-]_{(\text{aq})}$ is negligible. Thus, the term $[\text{DPG}^+\text{-NCS}^-]_{(\text{aq})}$ can be neglected in Eq. (12). Therefore, Eq. (12) transforms into:

$$D_{\text{NCS}} = \frac{[\text{DPG}^+ \cdot \text{NCS}^-]_{(\text{org})}}{[\text{NCS}^-]_{(\text{aq})}} \quad (13)$$

After substituting Eq. (13) into Eq. (10) and taking logarithms, the following Eq. (14) is then obtained:

$$\log D_{\text{NCS}} = \log K_d \beta + \log [\text{DPG}^+]_{(\text{aq})} \quad (14)$$

The D values at the initial concentration of NCS^- (2.5 g mL^{-1}) in the aqueous phase of pH zero and various concentrations (1.0×10^{-5} – $40.0 \times 10^{-5} \text{ mol L}^{-1}$) of the reagent $\text{DPG}^+\text{-Cl}^-$ were then calculated. The values of β , K_{ex} and K_d of the extracted ion associate were then determined graphically from the linear plot of $\log D_{\text{NCS}}$ versus $\log [\text{DPG}^+\text{-Cl}^-]$ (Fig. 4). A slope of 0.8 was obtained confirming the formation of complex ion associate of 1:1 molar ratios of thiocyanate ions to the reagent $\text{DPG}^+\text{-Cl}^-$, respectively. The low value of

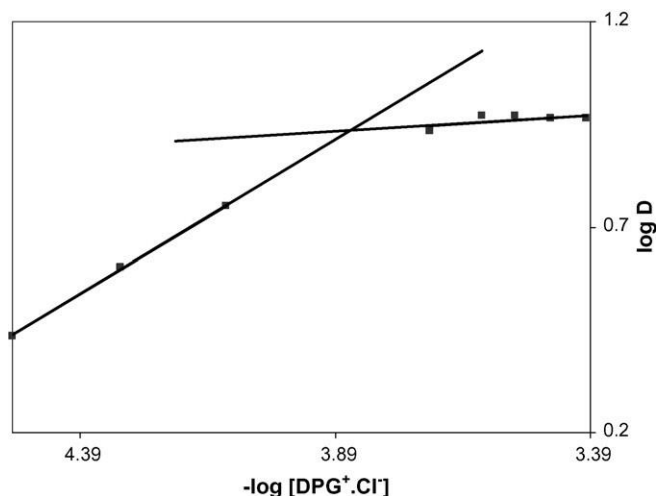


Fig. 4. Plot of $\log \text{DPG}^+ \cdot \text{Cl}^-$ versus $\log D$ of the extracted ion associate

DPG^+ (1.0 mol mL^{-1} NCS^- into 4-methyl-2-pentanone from aqueous media containing HNO) against a reagent blank. The slope than the expected value (1.0) is most likely attributed to the possible interference of HNCS in the extraction step under the experimental conditions employed. However, these data added further support for the existence of the complex ion associate $\text{DPG}^+\text{-NCS}^-$ and the absence of non-specific interaction between the extracted complex ion associate $\text{DPG}^+\text{-NCS}^-$ and the ion-pair reagent $\text{DPG}^+\text{-Cl}^-$ [29]. The data are excellent and are in good agreement with the results obtained from the Job's continuous variation [25]. Therefore, the most probable composition of the extracted species is $\text{DPG}^+\text{-NCS}^-$. At high concentrations of the reagent $\text{DPG}^+ \cdot \text{Cl}^-_{(\text{aq})}$, the respective term $[\text{NCS}^-]_{(\text{aq})}$ be was neglected. Therefore, Eq. (12) takes the form of Eq. (8) i.e. $D_{\text{NCS}} = K_d$. Thus, at high concentration of the $\text{DPG}^+\text{-Cl}^-$, the plot of the experimental data of $\log D$ versus $\log \text{DPG}^+\text{-Cl}^-$ in the same coordinates according to Eq. (8) was linear and slightly parallel to the abscissa with a slope of 0.07 (Fig. 4). The K_d value was then calculated from the intercept of $\log D$ axis of the plot. Thereafter using Eq. (10), the value of β was then calculated. The K_{ex} , K_d and β values calculated from Fig. 4 were found equal to $2.07 \pm 0.2 \times 10^4$, 22.1 ± 0.7 and $1.96 \pm 0.25 \times 10^3$, respectively.

3.4. Photometric characteristics and analytical performance

After adjusting the experimental conditions of the reagent $\text{DPG}^+\text{-Cl}^-$, extraction media and the thiocyanate ions, a linear graph on recording the absorbance at 366nm versus thiocyanate concentration ($0.1\text{--}20\text{gmL}^{-1}$) was obtained. Beer's law is obeyed in the concentration range $0.1\text{--}10\text{gmL}^{-1}$. The molar absorptivity calculated from Beer-Lambert's plot and Sandell's sensitivity index [34,35] of the complex ion associate at 366nm were estimated to be $1.1\pm 0.1\times 10^4\text{Lmol}^{-1}\text{cm}^{-1}$ and 0.08gcm^{-2} , respectively. The effective concentration range of thiocyanate ions as evaluated by Ringbom's plot [36] is obeyed in the range $0.1\text{--}7\text{gmL}^{-1}$. The relative standard deviation (S_r) of five measurements with 5gmL^{-1} of thiocyanate was estimated as 2.2%. The lower limits of detection (LOD) and quantitation (LOQ) under the conditions established for thiocyanate ions were estimated using the equations [37].

$$\text{LOD} = \frac{3}{\delta} \quad (15) \text{ b}$$

and

$$\text{LOQ} = \frac{10}{\delta} \quad (16) \text{ b}$$

where δ is the standard deviation ($n=5$) of the blank and b is the slope of the calibration plot. The lower limits of detection (LOD) and quantitation (LOQ) of the developed procedure are 0.02 and 0.066gmL^{-1} thiocyanate. Such limits could be improved to lower values on increasing the volume of the aqueous phase containing traces of thiocyanate and amiloride at the optimum experimental condition, which will be shaken with the organic solvent. The results were compared successfully with the reported method [9], in terms of the detection limit (3δ), range of linearity and precision. The linear range and the time consumption of the developed method are also better than the reported spectrophotometric methods [8–10].

3.5. Analytical applications

3.5.1. Determination of thiocyanate in various water samples

The values of the effective molar absorptivity (ϵ) of the Beer-Lambert's plot and the values of the extraction constants (K_{ex} , K_d , β and D) of thiocyanate ions of the proposed extraction system have suggested the use of the developed procedure conveniently for thiocyanate determination in various water samples. The water samples were analyzed by the direct method following the recommended extraction procedures described earlier with the aid of calibration curve. The results showed the absence of thiocyanate ions in the tested water samples and are in good agreement with the iron(III)–thiocyanate method [9]. Alternatively, the standard addition method was also applied at

various concentrations of the thiocyanate ($2.5\text{--}10.0\text{gmL}^{-1}$) spiked to water samples. A satisfactory recovery percentage ($97\text{--}104\pm 2.4\%$) of the thiocyanate ions spiked to the seawater samples at the employed concentration was achieved (Table 1) in the presence of EDTA as mentioned in Section 2.4 to prevent the possible interference caused by iron(III), chromium(III) and bismuth(III). The developed extraction procedure was also tested for the separation and spectrophotometric determination of traces of thiocyanate species spiked to the industrial wastewater samples. Thiocyanate ions at a total concentration $\leq 10\text{gmL}^{-1}$ were spiked into the wastewater samples as described in Section 2. The data summarized in Table 2 are in good agreement with the results reported obtained via iron(III)–thiocyanate method [9] with an acceptable recovery percentage ($97\pm 2.5\%$, $n=5$). The F - and t -tests at 95% confidence levels did not exceed the tabulated (theoretical) ones and no significant differences were observed between the developed and the reference methods [9] with respect to precision and accuracy. Thus, statistical analysis revealed that the developed method is good and applicable with the reported method.

3.5.2. Determination of thiocyanate in biological samples

The validity of the developed method was also tested by the determination of the thiocyanate ions in biological samples e.g. human saliva of cigarette smoker and non-smoker members by the standard addition method. The saliva and urine sam-

Table 1
Determination of thiocyanate ions ($2.5\text{--}10\text{gmL}^{-1}$) spiked to seawater samples (20mL) by the developed procedure (A) and reference spectrophotometric [9] method (B)¹⁷

Thiocyanate (gmL ⁻¹) Added	Found		Recovery (%) ^a	
	A	B	A	B
	2.5	2.6	2.5	104.0 ± 2.7
5.0	5.1	5.15	102.0 ± 2.3	103. ± 2.2
10	9.7	10.2	97.0 ± 2.3	102.0 ± 2.2
2.5	2.4	2.4	96.0 ± 2.3	96.0 ± 3.1
5.0	4.9	5.1	98 ± 1.9	102.3 ± 2.6
10	9.8	10.1	98 ± 2.1	101 ± 1.7

^a Average of five measurements ± standard deviation.

¹⁷ Average of five measurements ± standard deviation.

Determination of thiocyanate ions (0.05–10 gmL^{-1}) spiked to wastewater samples (20.0mL) by the developed procedure (A) and reference spectrophotometric [9] method (B)^a

Thiocyanate(gmL^{-1})			Recovery(%) ^a	
Added	Found		A	B
	A	B		
0.05	0.052	0.053	104.0 \pm 1.7	106.0 \pm 1.8
0.5	0.52	0.51	104.0 \pm 2.1	101.0 \pm 2.7

Table 3

Determination of thiocyanate ions (0.05–0.5 gmL^{-1}) spiked to human saliva (20mL) by the developed procedure (A) and standard colorimetric [38] method (B)^a

Thiocyanate, gmL^{-1}			
Added	Found		
	A	B	
Saliva of non-smokers			
0.05			
0.5	0.57 \pm 0.05	1.1	0.60 \pm 0.03
	\pm 0.04		1.2 \pm 0.02
Saliva of smokers			
0.05	2.2 \pm 0.09		2.30 \pm 0.10
0.5	2.9 \pm 0.15		3.1 \pm 0.2

^a Average of five measurements \pm standard deviation.

ples ($n=5$) were prepared and treated as reported earlier [8] in Section 2. The samples were then analyzed by the standard addition method under the optimum experimental conditions. The results (Table 3) are compared with the reference colorimetric method [38]. The data obtained by the developed method for the thiocyanate determination are in good agreement with those obtained via the standard colorimetric method [38] reflecting the utility of the proposed spectrophotometric procedures.

4. Conclusions

The method is simple, rapid, free from systematic errors, low cost and provides reliable procedures for the determination of thiocyanate ions in water samples at low level. The method is less laborious than the conventional method and has a similar precision to that of the conventional ones [9,38,39]. The molar absorptivity of the developed ion associate reaches $1.1 \pm 0.1 \times 10^4 \text{ Lmol}^{-1} \text{ cm}^{-1}$. Most foreign ions do not interfere with the determination of thiocyanate ions. The developed method has been shown to have good operating characteristics (sensitivity, stability, time consuming, detection limit, and a wide linear range). The method can be used for determination of thiocyanate ion in biological samples. The photometric and extractive characteristics make the use of the developed method

attractive and convenient for routine control determination of thiocyanate ions. However, work is continuing for the application of online flow injection analysis for the routine determination of thiocyanate and complexes of metal ions containing thiocyanate.

Acknowledgements

The authors are grateful to the Deanship of the Institute of Research and Consultation, King Abdulaziz University (KAU), Jeddah, Kingdom of Saudi Arabia for providing the financial support for the project work (grant no.178/426). One of the authors (M.E. El-Shahawi) would like to thank the Quality Control Laboratory (QCL), Jeddah for the loan of the reagent amiloride monohydrochloride.

References

- [1] Agency for "Toxic Substances and Disease" Registry Public Health Statement, www.atsdr.cdc.gov/ToxProfiles, 1989.
- [2] Risk Information Web Server, Toxicity Summary for Cyanide, www.Risk.lsd.ornl.gov/tox/profiles/cyanide.
- [3] J.-Y. Gal, Y. Fovet, M. Adib-Yadzi, *Talanta* 53 (2001) 1103.
- [4] WHO Oral Health Country/Area Profile Programs, Department of NonCommunicable Diseases Surveillance/Oral Health WHO Collaborating Centre, Malmo University, Sweden.
- [5] R.F. Maria, M.D. Lopez, H.J. Palomares, *J. Anal. Toxicol.* 12 (1998) 307.
- [6] X.-H. Cai, Z.-F. Zhao, *Anal. Chim. Acta* 212 (1988) 43.
- [7] S. George, J.R. Schenck, *Anal. Biochem.* 130 (1983) 416.
- [8] D.G. Themelis, P.D. Tzanavaras, *Anal. Chim. Acta* 452 (2002) 295.
- [9] J.C. Meeussen, E.J. Timminghoff, M.G. Keizer, *Analyst* 114 (1989) 959.
- [10] S. Ashour, *J. Anal. Chem.* 54 (1999) 538.
- [11] S.-C. Cheng, *Handbook of Inorganic Chemical Reactions*, Publishing House of Shanghai Science and Technology, Shanghai, 1985, p. 1026.
- [12] A.B. Bendtsen, E.H. Hansen, *Analyst* 116 (1991) 647.
- [13] H. Asai, T. Taya, K. Doi, H. Sakamoto, M. Otomo, *Anal. Sci. (Japan)* 7 (1991) 919.
- [14] M. Wojciechowski, J. Balcerzak, *Anal. Chim. Acta* 237 (1990) 127.
- [15] M.M. Ardakani, A. Sadeghi, M. Salavati-Niasari, *Talanta* 66 (2005) 837.
- [16] H.A. Zamani, F. Malekzadegan, M.R. Ganjali, *Anal. Chim. Acta* 555 (2006) 336.
- [17] S. Erden, A. Demirel, S. Memon, M. Yilmaz, E. Canel, E. Kilic, *Sens. Actuators, B* 113 (2006) 290.
- [18] X. Huang, Y. Chai, R. Yuan, X. Wang, Q. Li, *Anal. Sci. (Japan)* 20 (2004) 1185.
- [19] M.R. Ganjali, M. Yousefi, M. Javanbakht, T. Poursaberi, M.S. Niasari, L.H. Babaei, E. Latifi, M. Shamsipur, *Anal. Sci. (Japan)* 18 (2002) 887.
- [20] J.Y. Dai, Y.Q. Chai, R. Yuan, Y.S. Zhang, Y. Liu, X. Zhong, D.P. Tang, *Chem. Lett.* 34 (2005) 62.
- [21] Y. Michigami, K. Fujii, K. Ueda, Y. Yamamoto, *Analyst* 117 (1992) 1855.
- [22] Z.-M. Fu, K.-M. Wu, *J. Environ. Health China* 8 (1991) 271.
- [23] M. Yasuyuki, K. Tomozo, *Anal. Sci.* 9 (1993) 719.
- [24] H.T.S. Britton, *Hydrogen Ions*, fourth ed., Chapman & Halls, London, 1952, p. 113.
- [25] D.T. Sawyer, W.R. Heinemann, J.M. Beebe, *Chemistry Experiments for Instrumental Methods*, John Wiley & Sons, New York, 1984.
- [26] J.J. Cruywagen, J.B.B. Heyns, E.A. Rohwer, *Polyhedron* 17 (1998) 1741.
- [27] D.T. Burns, P. Hanprasopwattana, *Anal. Chim. Acta* 118 (1980) 185.

- [28] D.T. Burns, M.S. El-Shahawi, M.J. Kerrigan, P.M.T. Smyth, *Anal. Chim. Acta* 322 (1996) 107.
- [29] M.S. El-Shahawi, *Anal. Chim. Acta* 356 (1997) 85.
- [30] S.M. AlDhaheri, *Talanta* 46 (1998) 1613.
- [31] A. Alexandrov, O. Budevsky, A. Dimitrov, *J. Radioanal. Chem.* 29 (1976) 2.
- [32] S.M. Kamburova, *Talanta* 39 (1992) 997.
- [33] M. Hiraoka, *Crown Compounds, Their Characteristics and Applications*, Elsevier, 1982.
- [34] E.B. Sandell, *Colorimetric Determination of Trace Metals*, Nescience, New York, 1959.
- [35] IUPAC, Nomenclature, symbol, units and their usages in spectrochemical analysis, *Pure Appl. Chem.* 45 (1976) 105.
- [36] A. Ringbom, *Z. Fresenius, Anal. Chem.* 155 (1939) 332.
- [37] J.C. Miller, J.N. Miller, *Statistics for Analytical Chemistry*, fourth ed., Ellis Horwood, New York, 1994, p. 115.
- [38] T.G. Whiston, G.W. Cherry, *Analyst* 87 (1962) 819.
- [39] G. Gumus, B. Demirata, R. Apak, *Talanta* 53 (2000) 305.

Analysis of domperidone in pharmaceutical formulations and wastewater by differential pulse voltammetry at a glassy-carbon electrode

M. S. El-Shahawi & S. O. Bahaffi & T. El-Mogy

Received: 27 July 2006 / Revised: 21 September 2006 / Accepted: 29 September 2006 / Published online: 9 November 2006
Springer-Verlag 2006

Abstract The redox characteristics of the drug domperidone at a glassy-carbon electrode (GCE) in aqueous media were critically investigated by differential-pulse voltammetry (DPV) and cyclic voltammetry (CV). In Britton–Robinson (BR) buffer of pH 2.6–10.3, an irreversible and diffusion-controlled oxidation wave was developed. The dependence of the CV response of the developed anodic peak on the sweep rate (v) and on depolarizer concentration was typical of an electrode-coupled chemical reaction mechanism (EC) in which an irreversible first-order reaction is interposed between the charges. The values of the electron-transfer coefficient (α) involved in the rate-determining step calculated from the linear plots of $E_{p,a}$ against $\ln(v)$ in the pH range investigated were in the range 0.64 ± 0.05 confirming the irreversible nature of the oxidation peak. In BR buffer of pH 7.6–8.4, a well defined oxidation wave was developed and the plot of peak current height of the DPV against domperidone concentration at

⁻⁶ this peak potential was linear in the range 5.20×10^{-6} to 2.40×10^{-5} mol L⁻¹ with lower limits of detection (LOD) and quantitation (LOQ) of 6.1×10^{-7} and 9.1×10^{-7} mol L⁻¹, respectively. A relative standard deviation of 2.39% ($n=5$) was obtained for 8.5×10^{-6} mol L⁻¹ of the drug. These DPV procedures were successfully used for analysis of domperidone in the pure form ($98.2 \pm 3.1\%$), dosage form ($98.35 \pm 2.9\%$), and in tap ($97.0 \pm 3.6\%$) and wastewater ($95.0 \pm 2.9\%$) samples. The method was validated by comparison with standard titrimetric and HPLC methods. Acceptable error of less than 3.3% was also achieved.

M. S. El-Shahawi (*) : S. O. Bahaffi : T. El-Mogy

Department of Chemistry, Faculty of Science, King Abdulaziz University,

P.O. Box 80203, Jeddah 21589, Saudi Arabia e-mail: mohammad_el_shahawi@yahoo.co.uk

Keywords Electrochemical oxidation · Domperidone ·

Motilium tablets · Wastewater · GCE · DPV

Introduction

Drugs are life-saving compounds but their unnecessary administration to the human body is not desirable. Many drug residues have been found in water and analysis of drug residues is increasing in importance day by day [1]. Drug analysis is undertaken during the different phases of pharmaceutical development, e.g. formulation and stability studies, quality control, toxicology, and pharmacological testing in animals and man [2–4]. Domperidone, 5-chloro-1-(1-[3-(2,3-dihydro-2-oxo-1H-benzimidazol-1-yl)propyl]-4-piperidinyl)-1,3-dihydro-2H-benzimidazol-2-one (Fig. 1), is a dopamine antagonist widely used as an antiemetic compound for short-term treatment of nausea and vomiting of different etiology [5]. It is a dopamine D2 receptor antagonist used for human beings throughout the world for its unique pharmaceutical activity [5–7]. Some pharmaceutical companies and hospitals discharge domperidone in their effluents, resulting in the contamination of our natural water resources.

A complete and excellent survey of the analysis of domperidone was published in two recent reviews [8, 9]. The most common methods for assay of domperidone in tablet dosage forms and in waste water are usually based on spectrophotometry [10–14], colorimetry [15], and liquid chromatography [16–25]. Chromatographic methods have been developed to monitor levels of domperidone in plasma,

tissue fluids, and waste water [21–25]. Most reported methods for analysis of domperidone individually or in the presence of other drugs have not achieved sufficiently low limits of quantitation and/or require sample

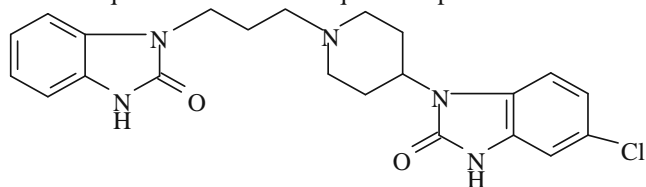


Fig. 1 The structure of domperidone

pretreatment or time-consuming extraction or evaporation steps before analysis of the drug.

The requirements of voltammetric and sensor techniques, in particular, in pharmaceutical and biomedical analysis, clinical chemistry, toxicology, drug-control laboratories, and waste-water analysis increase as more potent compounds are developed, in particular for use as drugs with lower therapeutic concentrations [26, 27]. For this reason we describe herein a detailed electrochemical study of domperidone at a glassy-carbon electrode (GCE) using differential pulse and cyclic voltammetry. It is shown that pH is very important in overall voltammetric behavior. A DPV method was also used for determination of domperidone at a GCE over a wide range of concentrations in the presence of excipients. The proposed method was successfully used for analysis of domperidone in the pure form, Motilium tablets, and in wastewater samples. Results were in agreement with those from standard methods.

Experimental

Apparatus

The cyclic, linear, and differential pulse voltammetric measurements were performed with a PC-controlled AEW2 analytical electrochemical workstation, a Metrohm 746 trace analyzer, and 747 VA stand with ECprog3 electrochemistry software (Sycopel, UK) connected to C-2 stand. A three-compartment electrochemical cell configuration incorporating: a glassy-carbon electrode (BAS model MF-2012, diameter=3 mm) as working electrode, Ag/AgCl–3 mol L⁻¹ KCl (BAS model MF-2063) as reference electrode, and a platinum wire (BAS model MW-1032) as counter-electrode. Origin Pro 7.0 software was used for transformation of the initial signal.

Solid-phase extraction (SPE) was performed with Sep-Pak Vac (1.0 mL) C₁₈ cartridges (Waters, Milford MA, USA). HPLC was performed with a Win Chrom system (GBC) consisting of a solvent delivery pump (GBC, model LC1150), solvent degassing equipment (GBC, model LC1460), and UV-visible. Detector (GBC, model LC-1210). Sample solutions were transferred during electrochemical and chromatographic measurements by a digital-micropipette (Volac). Electrochemical data were then recorded at room temperature and the peak current heights were measured using the “tangent fit method” [28, 29]. A digital pH-meter (Schott Geräte CG 808) with H 61 pH combination electrode (Mainz, Germany) was used for pH measurement.

Reagents and materials

All solutions and reagents were prepared from analytical reagent-grade compounds in double-distilled water. Domperidone and Motilium tablets were obtained from Janssen–Cilag Pharmaceuticals (Beerse, Belgium). BDH acetonitrile, methanol, acetone, and acetic acid were used as received. A standard stock solution (2×10⁻³ mol L⁻¹) of domperidone was prepared by dissolving an accurately weighed amount of the bulk drug in methanol. The solution was stored under refrigeration at 4 °C. More dilute solutions of the drug were prepared daily in volumetric flasks by diluting the stock solution with double-distilled water to the final concentration required. Such solutions were transferred to polyethylene bottles and stored under refrigeration. A series of Britton–Robinson buffers

(0.04 mol L⁻¹ in acetic, orthophosphoric, and boric acids adjusted to the required pH with 0.2 mol L⁻¹ sodium hydroxide) was prepared for use as supporting electrolytes [30].

General DPV procedures

An accurate volume (10 mL) of the BR buffer at the required pH (2.2–11) was transferred to the electrochemical cell and the electrodes were immersed in test solutions through which a stream of pure nitrogen was passed for 15 min before recording the voltammograms. The scans were initiated in the positive direction of the applied potential from +0 V to +1.3 V. After recording the voltammogram of the blank solution, an accurate volume (0.5–2.0 mL) of the drug solution was added. The anodic potential sweep was then recorded under different operating conditions of pH, sweep rate, and pulse amplitude. Before each measurement the GCE was polished manually with a paste of 0.5 mm

alumina in distilled water on a smooth polishing cloth and gently dried with a tissue paper [31, 32].

The effect of scan rate ($v=10\text{--}200\text{ mV s}^{-1}$) on the voltammograms was determined using the same solution. At each scan rate the initial conditions at the electrode surface were restored by polishing manually with 0.5 mm alumina as already described.

Recommended procedures for the analysis of domperidone in tablets:

Direct determination of domperidone

Ten tablets of Motilium (each labeled as containing 10 mg domperidone maleate) were pulverized in a mortar, homogenized, accurately weighed and the average mass per tablet was determined. An appropriate portion of the finally ground material was accurately weighed and dissolved in the minimum volume of methanol by sonication for 10 min. The solution of the drug was shaken for 15 min in a mechanical shaker to achieve complete dissolution of the active material, accurately transferred to 10 mL volumetric flask, and the solution was diluted to volume with methanol. An accurate volume of the clear supernatant liquor was then transferred to the electrochemical cell containing 10 mL of BR buffer, pH 8.4, to yield a final concentration of approximately $2.0 \times 10^{-5}\text{ mol L}^{-1}$ domperidone. The DPV was then recorded under the optimum experimental conditions and the unknown amount of the drug in the test solution was then determined by the developed procedures using the standard curve.

Standard addition method

Alternatively, the standard (spiking) method was used. Known volumes (0.2–1.0 mL) of the test drug solution at pH 8.3 were transferred to the electrochemical cell, with the current height being measured before and after addition of the standard. The change in the current height was recorded and used to determine the drug.

Analysis of the drug in tap and wastewater

Tap and wastewater samples were collected from municipal discharge station in Jeddah city and filtered through Whatman filter paper. An accurate volume (0.5–2 mL) of domperidone solution (0.015 mg mL^{-1} in ethanol) was added to the tap or the industrial wastewater samples (0.5–

1 L) to give a final concentration in the range $0.075\text{--}0.3\text{ }\mu\text{g mL}^{-1}$

mL. The test solutions were then shaken at room temperature for 20 min in a mechanical shaker and left for 2 h. The sample solutions were then percolated through a C_{18} cartridge (previously pre-conditioned with 2 mL of

methanol then 1 mL water) at flow rate of 50.0 mL min⁻¹ as reported elsewhere [25] and the cartridge was finally washed with de-ionized water (5.0 mL). The drug was eluted quantitatively from the C_{18} cartridge with methanol

($2 \times 5.0\text{ mL}$) at a flow rate of 0.50 mL min⁻¹ [25]. The two methanol fractions were combined and the repeatability and percentage recovery of the drug were then determined by HPLC with a C_{18} column, as reported by Ali et al. [25].

The electrochemical procedures developed for domperidone determination at pH 8.4 were then followed and the concentration of drug in the wastewater samples was calculated from the calibration plot for the drug by using the equation:

$$\text{Domperidone concentration} = \frac{C_{\text{std}} i_{\text{sample}} A_{\text{std}}}{i_{\text{std}} A_{\text{sample}}} \quad (1)$$

where C_{std} is the concentration of the standard and i_{sample} and A_{std} are the currents for the sample and standard, respectively, in nA.

Results and discussion

Electrochemical behavior of domperidone

Preliminary studies on the electrochemical oxidation of domperidone in aqueous solution at a GCE by use of DPV have shown that the drug has one well defined oxidation wave in the potential range 0.0–1.3 V relative to the Ag/AgCl reference electrode. Because the pH of the electrolysis medium is one of the variables that often severely affects the shape of voltammograms, the peak potential, and the peak current, the effect of pH was investigated in detail. The DPV voltammograms of domperidone ($7.1 \times 10^{-6}\text{ mol L}^{-1}$) at the GCE over a wide range of pH (2.0–11.3) had a well-defined oxidation peak (Fig. 2). The anodic peak observed is most probably attributed to oxidation of the nitrogen atom of the amide group in the drug [27]. The anodic peak potential was shifted to more negative values on increasing the solution pH, as shown in Fig. 2. The plot of pH against peak potential was found to be linear with a slope of $60 \pm 5\text{ mV/pH}$ unit. The data also revealed that the plot of pH against the anodic peak current was maximum at pH 7.6–8.4 (Fig. 3), in accordance with the pK_a of domperidone. Thus, in subsequent analytical

determination of the drug solution pH was kept in the range 7.6–8.4, with BR buffer as supporting electrolyte.

The cyclic voltammogram obtained for domperidone ($7.0 \times 10^{-4} \text{ mol L}^{-1}$) at the GCE in BR at pH 8.4 had one well-defined anodic peak at 0.70 V (Fig. 4). On reverse scanning no cathodic peak was observed at the scan rates investigated ($10\text{--}200 \text{ mV s}^{-1}$), confirming the irreversible nature of the observed electrochemical oxidation of domperidone in the potential window investigated. Continuous scanning of the CV of the drug significantly reduced the peak current and the signal was hardly discernible from the baseline, indicating passivation of the surface of the GCE electrode by formation of polymeric oxidation products or fouling of the GCE electrode by the oxidation products produced [33, 34].

The effect of sweep rate ($10\text{--}200 \text{ mV s}^{-1}$) on $E_{p,a}$ and $i_{p,a}$ of domperidone ($7.0 \times 10^{-4} \text{ mol L}^{-1}$) at pH 8.4 in cyclic

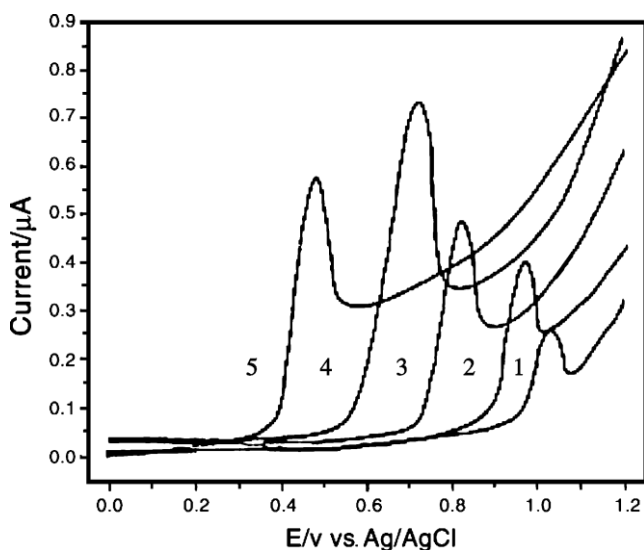


Fig. 2 DPVs of domperidone ($7 \times 10^{-6} \text{ mol L}^{-1}$) at a GCE in BR buffers at pH 2.1 (1), 4.0 (2), 6.0 (3), 8.0 (4), and 10.0 (5). The scan

rate was 10 mV s^{-1} ; the pulse amplitude 50 mV, and the pulse width 30 ms. The reference electrode was Ag/AgCl

voltammetry was critically investigated on freshly polished GCE. In this investigation the GCE was polished thoroughly before each sweep, because decrease in the peak current was observed if the electrode surface was not polished. This observation suggested possible prior adsorption on the surface of the electrode. $E_{p,a}$ was shifted anodically on increasing the scan rate, confirming the

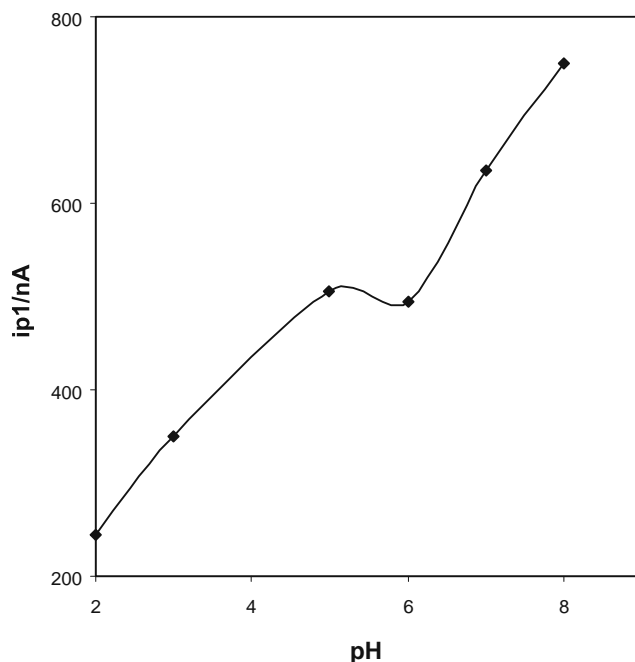


Fig. 3 Plot of $i_{p,a}$ of the oxidation peak potential of domperidone at 0.7 V against pH for DPV at a GCE. The concentration of domperidone was $7.1 \times 10^{-6} \text{ mol L}^{-1}$, the scan rate 20 mV s^{-1} , the pulse amplitude 40 mV, and the pulse width 30 ms. The reference electrode was Ag/AgCl

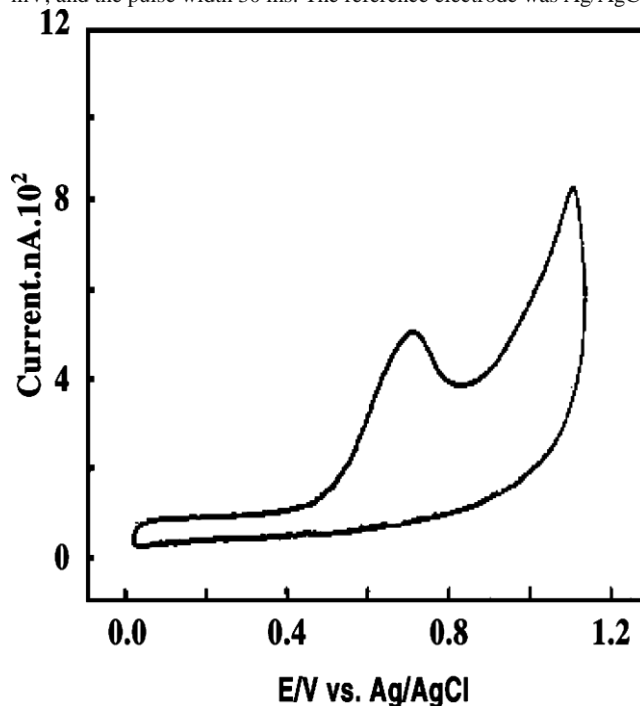


Fig. 4 Cyclic voltammogram obtained for domperidone ($7.0 \times 10^{-4} \text{ mol L}^{-1}$) at a GCE at pH 7.8 and 50 mV s^{-1} scan rate relative to the Ag/AgCl reference electrode

irreversible nature of the oxidation process [35]. The anodic peak current was also increased steadily by raising the scan rate, suggesting the occurrence of slow chemical reactions and limited mass transfer after the electrochemical process

[35, 36]. Finally, the peak current function, $i_p/v^{1/2}$ decreased continuously on increasing the scan rate, indicating the oxidation process followed an electrode-coupled (EC) chemical reaction mechanism [35, 36]. In an EC mechanism with an irreversible electrochemical process, the ratio $i_p/v^{1/2}$ show decreases continuously on increasing the scan rate. The dependence of the voltammetric response of the anodic peak on the scan rate and on depolarizer concentration is also typical of an EC mechanism in which an irreversible first-order chemical reaction is interposed between the charges. This behavior is most probably indicative of kinetic complications in the electrode process involved, or the process comprises several reactions [36].

The plot of $i_{p,a}$ against $v^{1/2}$ (Fig. 5) was linear, indicating that the electrochemical oxidation is a diffusion-controlled electrochemical process [35, 36]. The irreversible nature of the observed anodic peak was suggested from the linear dependence of anodic peak potential, $E_{p,a}$, on $\log v$ at pH 8.4, and other pH. The product of the number of electrons involved in the oxidation process (n) of the ratedetermining step and the corresponding charge-transfer coefficient (α), i.e. αn , was then determined from the slopes of plots of $\log v$ at pH 8.4 and other pH values. Assuming $n=1$, the values of α calculated from the slopes of the

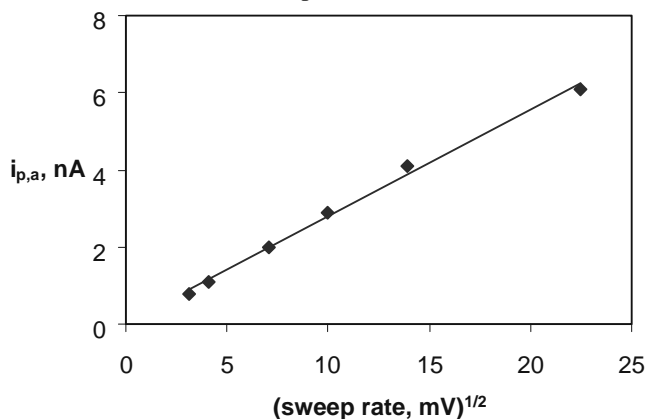


Fig. 5 Variation of $v^{1/2}$ with anodic peak current $i_{p,a}$ at a GCE with Ag/AgCl as reference electrode

straight lines by use of the equation, $\Delta E/\Delta \log v = -30/\alpha n$ were found to be in the range 0.64 ± 0.05 , confirming the irreversible nature of a single, one-electron, oxidation step. At pH 8.4, the plot of $\log i_{p,a}$ against $\log v$ for the anodic peak observed at $E_{p,a} \approx 0.7$ V was found to be linear and could be expressed by the equation:

$$\log i_{p,a} = 0.66 + 0.974 \log v - 0.996$$

These data added further confirmation of the irreversible nature of the oxidation peak. The value of the slope (0.974) was close to the theoretical value (1.0) expected when there is an adsorption process on the electrode surface of the GCE [33, 34]. In subsequent work, therefore, the anodic peak current in the pH range 7.6–8.4 was selected for determination of domperidone in aqueous solution.

The number of protons (p) transferred in the ratedetermining step was also calculated from the linear plot of pH against $E_{p,a}$ by using the equation $\Delta E_p/\Delta pH = 0.059p/\alpha n$. The observed shift is quite close to the theoretical value expected for an electrode reaction involving a 1:1 ratio of electrons/protons [37]. The αn and p values were found to be consistent with a one electron–one proton transfer process involved in the rate-determining step, confirming the above results obtained from CV measurements. It thus seems reasonable to assume that oxidation of the nitrogen atom of the amide group is most probably involved, with one electron and one proton producing a free radical species in the rate-determining step.

Interferences

Commercial domperidone tablets in dosage form are usually coated with diluents, e.g. gelatin, lactose, colloidal silicon dioxide, starch, sodium lauryl sulfate, or talcum powder. It was therefore essential to analyze the uncoated

Table 1 Results from determination of domperidone ($n=5$) in dosage forms (Motilium tablets) by the proposed direct DPV procedure, HPLC [25], and the official titrimetric [39] procedure^a

Function	DPV	HPLC	Official titrimetric method
Average recovery (%)	98.7±3.9	101.35±2.4	98.35±2.9
RSD (%)	2.57	2.10	3.2
t-value	–	1.29 (2.31)	0.16 (2.31)
F-value	–	2.64 (6.388)	1.8 (6.388)

^aThe corresponding theoretical values of t and F at $P=0.05$ are given in parentheses

tablets by the proposed DPV method at a GCE at pH 8.3 to determine whether the coating materials would interfere with the analysis. Each excipient (0.3–0.5 g) was added according to the manufacturer's batch formula to known amounts of domperidone (7×10^{-6} mol L⁻¹). The tolerable limit was defined as the concentration of the excipient causing a deviation of less than $\pm 3\%$ in the anodic peak current of the solution containing the pure active ingredient. The recovery data indicated that the magnitude of the peak

current of domperidone did not deviate by more than $\pm 3\%$ from the peak current of the solution containing no interfering additives, confirming that the developed DPV method is free from serious interferences from the tested excipients. The developed DPV procedure can therefore be regarded as a selective method for determination of the analyte.

Analytical applications

The high adsorption and sensitivity of the developed oxidation peak ($E_{p,a}=0.7$ V) of domperidone at the GCE at pH 8.3 suggests possible application of the developed DPV method for analysis of domperidone in dosage forms.

Under the optimum experimental conditions of pH 8.4, pulse amplitude 50 mV, pulse width 30 ms, and 10 mV s scan rate, DPV of domperidone showed that the peak

Table 2 Results from analysis of domperidone ($0.3 \mu\text{g mL}^{-1}$) in wastewater ($n=5$) by the proposed (standard addition) DPV method, HPLC [25], and the official titrimetric [39] procedure^a

Function	DPV	HPLC	Official titrimetric method
Average recovery (%)	101.40 \pm 2.9	97.35 \pm 1.9	98.35 \pm 2.7
RSD (%)	2.57	2.10	3.2
t-value	–	2.61 (2.31)	1.72 (2.31)
F-value	–	2.33 (6.388)	1.15 (6.388)

^aThe corresponding theoretical values of t and F at $P=0.05$ are given in parentheses

current increased linearly on increasing the drug concentration in the range 5.2×10^{-6} – 2.4×10^{-5} mol L⁻¹. A lower limit of detection (LOD) of 6.1×10^{-7} mol L⁻¹ was obtained by use of the formula $\text{LOD}=3S_{y/x}/b$ [38] (where $S_{y/x}$ is the standard deviation of y -residuals and b is the slope of the

calibration plot). The LOQ was found to be 9.2×10^{-7} mol L⁻¹ and the relative standard deviation (RSD) for domperidone at a concentration of 8.5×10^{-6} mol L⁻¹ was 2.39% ($n=5$).

Analysis of domperidone in dosage forms

The proposed DPV procedure for analysis of Motilium tablets containing domperidone maleate (10 mg) was validated by direct determination and by standard addition procedures. Tablets were processed as described in the

experimental section and analyzed under the optimum experimental conditions. Use of the direct DPV procedure for the quantification of domperidone in five samples furnished results in good agreement with the label claim and with results obtained by HPLC [25] and the official titrimetric procedure [39] at the 99 and 95% probability level (Table 1). The average recovery (Table 1) was $98.7 \pm 3.9\%$, in good agreement with the data obtained by HPLC (101.35 ± 2.4) and the official titrimetric (98.35 ± 2.9) methods [25, 39]. At 99% probability there were no differences between the mean results and RSD values in the range 2.5–3.20% were acceptable. Statistical evaluation involving t and F-tests revealed good agreement between the means and the variances from these methods (Table 1).

The standard addition method was successfully used for analysis of the drug in tablets by the DPV method. Excellent correlation of 0.999 and recovery of $98.9 \pm 2.9\%$ were achieved. These values are in good agreement with the label claim and the results obtained by HPLC [25] and the official titrimetric [39] procedures (Table 1). The accuracy of the DPV method was evaluated by determination of the recovery of added domperidone. On plotting the amount of drug added against the amount recovered, a regression line was obtained with a slope of $0.997 \pm 0.003\%$ and a correlation coefficient of 0.999. The result from an F-test at the 95% confidence level did not exceed the tabulated (theoretical) value, so there were no significant differences between the averages and the variances of the DPV method and the titrimetric procedure [39].

Analysis of domperidone in wastewater

Recoveries of domperidone from tap and wastewater samples by the developed DPV procedure were determined by the standard addition method. An accurately known

volume of the domperidone solution (0.015 mg mL⁻¹ in ethanol) as described in the experimental section was added to the tap and industrial water samples. Recovery of domperidone from tap and wastewater samples was 97.0 ± 3.6 and $101.40 \pm 2.9\%$, respectively, indicating good efficiency of the solid-phase extraction method and the DPV. The slightly higher recoveries in the wastewater may be because of the presence of other impurities in the wastewater (Table 2). Results from t and F-tests at the 99% confidence level did not exceed the tabulated (theoretical) values and revealed no significant differences between the averages and the variances obtained from the DPV, HPLC [25], and titrimetric [39] procedures (Table 2). At the 95% confidence level the calculated value of $t=2.61$ was greater than the theoretical value ($t=2.31$) so there was a difference between the two means.

Conclusion

The proposed DPV method enables simple, inexpensive, rapid, selective, and accurate analysis of domperidone in dosage forms and wastewater. The method compares favorably with reported HPLC and titrimetric methods. The method is therefore an excellent alternative means of analytical determination of domperidone because of its low cost, repeatability, and adequate precision. The sensitivity and selectivity of the procedure could be improved by the preconcentration of the drug from large sample volumes under the optimum experimental condition for retention by SPE. The retained species could be followed by elution with methanol and final determination at the GCE by DPV. The great potential of the GCE is attributed to its low cost and its wide availability; it is commonly used as an electrochemical detector for HPLC and FIA. Work is continuing on possible application for routine on-line voltammetric stripping analysis of the drug in serum and environmental samples.

Acknowledgements One of the authors (M.S. El-Shahawi) would like to thank Dr A.I. Radi for the facilities provided to one of the coauthors (T. El-Mogy). Many thanks are also due to staff in the quality control laboratory, Jeddah, Saudi Arabia, for loan of domperidone and for HPLC measurements.

References

- Kummerer K, Al-Ahamed A, Bertram B, Wiessler M (2000) *Chemosphere* 40:767–773
- Berridge JC (1993) *J Pharm Pharmacol* 45:361–367
- Abo El-Maali N (2004) *Bioelectrochemistry* 64:99–107
- Baselt RC, Carvey RH (1995) *Disposition of toxic drugs and chemicals in man*, 4th edn. Chemical Toxicology Institute, Foster City, CA, USA
- Meuldermans W, Hurkmans R, Swysen J, Hendrickx J, Michiels M, Heykants WJ (1981) *Eur J Drug Metab Pharmacokin* 6:61–70
- Brusa L, Petta F, Pisani A, Miano R, Stanzione P, Moschella V, Galati S, Agro EF (2006) *J Urol* 175:202–207
- Lan H, Du-Rand CJ, Teeter MM, Neve KA (2006) *Mol Pharmacol* 69:185–190
- Gabay PP (2002) *J Hum Lact* 18:274–289
- Henderson A, Whonn A (2003) *Lifelines* 7:54–60
- Mohan YR, Srinivas JS, Avadhanulu AB (1992) *Indian Drugs* 29:281–283
- Rao GR, Kini GR, Avadhanulu AB, Vatsa DK (1990) *East-Pharm* 33:133–138
- Al-Khamis KI, Hagga MEM, Al-Khamees HA (1990) *Anal Lett* 23:451–461
- Baeyens W, De-Moerloose P (1979) *Anal Chim Acta* 110:261–270
- Salem MY, El-Zanfay ES, El-Tarras MF, El-Bardicy MG (2003) *Anal Bioanal Chem* 375:211–216
- Kanumula GV, Raman B (2000) *Indian Drugs* 37:38–41
- Kobylinska M, Kobylinska K (2000) *J Chromatogr B* 744:207–212
- Zarapkar SS, Bhousule NJ, Halker UP (1991) *Indian Drugs* 28:425–427
- Argekar AP, Powar SG (1999) *J Planar Chromatogr* 12:272–379
- Argekar AP, Shah SJ (1999) *J Pharm Biomed Anal* 19:813–817
- Zavitsanos AP, MacDonald C, Bassoo E, Gopaul D (1999) *J Chromatogr B* 730:9–17
- Yamamoto K, Hagino M, Kotaki H, Iga T (1998) *J Chromatogr B* 720:251–276
- Zarapkar SS, Parikh KM, Doshiv J, Sawant SV, Salunkhe UB (1990) *Indian Drugs* 27:353–356
- Reynold JEF (1999) *The complete drug reference*, 32nd edn. Pharmaceutical Press, London
- Royal Pharmaceutical Society (1993) *The British pharmacopoeia*, British Pharmacopoeial Commission. Royal Pharmaceutical Society, London, pp 1768–1774
- Ali I, Gupta VK, Singh P, Pant HV (2006) *Talanta* 68:928–931
- Vire JC, Kaufmann JM, Patriarce GJ (1989) *J Pharm Biomed Anal* 21:1323–1335
- Wahdan T, Abd El-Ghany N (2005) *Il Farmaco* 60:830–833
- Heineman WR, Kissinger PT (1982) *Am Lab* 60:29–34
- Delahay P (1966) *New instrumental methods in electrochemistry*. Interscience, New York, chap 6
- Britton HTS (1952) *Hydrogen ions*, 4th edn. Chapman and Hall, London, pp 113–117
- El-Shahawi MS, Bashammakh AS, El-Mogy T (2006) *Anal Sci (Japan)* 22, in press
- Radi A, El-Shahawi MS, El-Mogy T (2005) *J Pharm Biomed Anal* 37:195–198
- Manjaoui A, Haladjian J, Bianco P (1990) *Electrochim Acta* 35:177–185
- Laviron E, Rouillier L, Degrand CJ (1980) *Electroanal Chem* 12:11–23
- Bard AJ, Faulkner LR (1980) *Electrochemical methods, fundamental and applications*. Wiley, New York, pp 218–227
- Murthy AN, Reddy K (1984) *J Chem Soc Faraday Trans I* 2245–2251
- Nicholson RS, Shain I (1964) *Anal Chem* 36:706–723
- Miller JC, Miller JN (1993) *Statistics for analytical chemistry*. Ellis Horwood Series, PTR Prentice Hall, New York, London, pp 119–121
- Earl CQ, Prozialeck WC, Weiss B (1984) *Life Sci* 35:525–532

Studies on bismuth(III) complexes of ligands containing nitrogen/sulfur and extractive procedure for determination of Bi(III)

Eman M. Saad

Chemistry Department, Faculty of Education, Suez Canal University, Al-Arish, Egypt

Mohammad S. El-Shahwai

Chemistry Department, Faculty of Science, Mansoura University, Demitta, Egypt

Hala Saleh and Ahmed A. El-Asmy*

Chemistry Department, Faculty of Science, Mansoura University, Mansoura, Egypt

Received 18 September 2006; accepted 25 September 2006

Abstract

The coordination behavior of thiosemicarbazide and its thiosemicarbazones towards Bi(III) is the main goal of this investigation. The structure of the isolated complexes has been proved by microanalysis, thermal, spectra (electronic, IR and ms) and voltammetric measurements. The ligands act as neutral or mononegative molecules and the coordination donors were found to be S for HTS; NN for HBTS; NS for HATS and H₂STS and NNS or NSO for H₂DMTS in the complexes. The complexes show thermal decomposition steps ending at 800 C with a stable fragment. The redox properties of the complexes toward oxidation waves are strongly dependent on =N_{thio} substituents. At pH 1.5 and excess of iodide, Bi³⁺ forms an orange–yellow [BiI₄][−] complex which associated with tricapyrylmethylammonium chloride (TCMAC) forming [TCMA]⁺[BiI₄][−] easily extracted into the CHCl₃ layer. The colored organic layer containing the ion pair is determined spectrophotometrically at 490 nm and represents the second goal.

Introduction

Sulfur compounds have great interest due to their ability to form stable chelates with essential metal ions in which the fungus needs its metabolism [1–4]. Some thiosemicarbazones serve as models for enzymes and are used as effective oxidants and catalysts [5, 6]. Bismuth and its compounds have medicinal applications [7] in treatment of a variety of gastrointestinal disorders, including gastric and duodenal ulcers, dyspepsia, diarrhea and colitis [8, 9], and have a direct antibacterial effect on the chronic gastritis and peptic ulcer, causing bacterium, and helicobacter pylori [10–12]. Short half-life α -emitter bismuth isotopes (²¹²Bi, ²¹³Bi) have been used as radio targets for cancer therapy [8, 13, 14]. Bismuth is known for the synthesis of renal metallothionein, MT, forming a very strong complex [Bi₇MT]. Pretreatment with bismuth complexes prevent the toxic side effects of the anticancer drug, cisplatin, without compromising its antitumor activity [15]. It binds preferentially to the human serum transferrin [16]. Bismuth compounds have become attractive candidates for use as reagents in organic synthesis [7, 17],

in semiconductors, cosmetic preparations, alloys and metallurgical additives, and in recycling of uranium nuclear fuels [18]. Bi^(III) ions have been extracted directly as ion-pairs with some cations using different solvents [19].

The present work describes the synthesis, spectroscopic, thermal and electrochemical characterization of Bi^(III) complexes as well as an attempt for extraction Bi^(III) through solvent extraction and direct determination.

Experimental

All chemicals used were of BDH grade and were used as supplied. Oxycarbonate and oxynitrate are the salts of Bi^(III), KI and tricapyrylmethylammonium chloride (TCMAC) are the color and ion pair reagents for Bi^(III) separation and determination, and tetrabutylammonium tetrafluoroborate (TBA⁺ BF₄[−]) is the supporting electrolyte in cyclic voltammetry. Bi^(III) solution was prepared from pure (BiO)₂ CO₃ · 5 H₂O dissolved in a least amount of conc. HCl and

* Author for correspondence: E-mail: aelasma@yahoo.com

Preparation of the ligands

Thiosemicarbazide (HTS) was used as supplied while the thiosemicarbazones, Figure 1, were prepared as reported earlier [20] by condensation of a 1:1 molar ratio of acetophenone, salicylaldehyde, benzophenone or diacetylmonoxime with thiosemi-carbazide in EtOH; a few drops of glacial acetic acid were added. The mixture was heated under reflux on a water bath for 2–3 h. The formed precipitate was separated by filtration, recrystallized from EtOH and dried. The formulae are in good agreement with the stoichiometries concluded from their elemental analysis and confirmed from IR spectra. The $^1\text{H-NMR}$ spectrum of H_2DAMTS in $d_6\text{-DMSO}$ showed signals at δ 11.505 and 10.12 p.p.m. assigned to the OH and NH protons [21]; the relatively high value of the OH signal may be due to intramolecular hydrogen bonding. The spectra of HATS, H_2STS and HBTS showed signals at 10.29, 10.07, 8.70 and 8.09, 8.03, 8.43 p.p.m. assigned to the

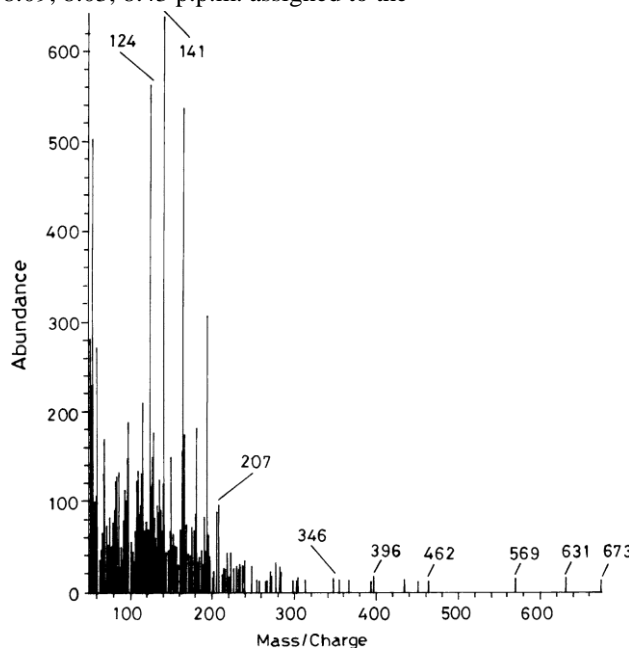
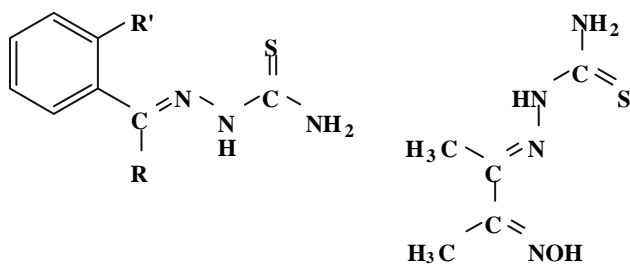


Fig. 1. Mass spectrum of $[\text{Bi}(\text{H}_2\text{DMTS})_2\text{Cl}_3] \cdot 0.5\text{H}_2\text{O}$ (1).



H_2STS : $\text{R} = \text{H}$; $\text{R}' = \text{OH}$

HATS : $\text{R} = \text{CH}_3$; $\text{R}' = \text{H}$

HBTS : $\text{R} = \text{Ph}$; $\text{R}' = \text{H}$

H_2DAMT

standardized complexometrically using xylenol orange indicator.

NH and NH_2 protons, respectively. Moreover, the spectrum of H_2STS showed the OH signal at 10.17 p.p.m. [22].

Preparation of Bi(III) complexes

The complexes were prepared by heating under reflux a 1:2 molar mixture of each ligand (6 mmol) and bismuth salt (3 mmol). $(\text{BiO})_2\text{CO}_3 \cdot \text{H}_2\text{O}$ and/or BiONO_3 were dissolved in HCl and/or HNO_3 , respectively, with drops of redistilled water. The reaction mixture was refluxed on a water bath for 4–6 h. A precipitate directly formed on mixing oxycarbonate and thiosemicarbazide. $[\text{Bi}(\text{HDMTS})_2]\text{NO}_3$ was prepared by direct heating for 15 min and the solution was left to evaporate slowly for 1 day. All the formed precipitates were filtered off, washed with EtOH and Et_2O and finally dried; the yield was found to be 70–80%. Chemical and physical measurements

Structure 1.

C and H contents were determined at the Microanalytical Unit of Cairo University. Bi content was determined according to the standard method [23]. The infrared, electronic, $^1\text{H-NMR}$ ($d_6\text{-DMSO}$, 200 MHz) and mass spectra were recorded on a Mattson 5000 FTIR Spectrophotometer [provided with CsI beam splitter], UV-2100 Unicam UV/Vis, Varian Gemini and Varian MAT 311 Spectrometers, respectively. The thermal analysis was carried out on a Shimadzu Thermogravimetric Analyzer at a heating rate 10 C min^{-1} under nitrogen gas. The pH values were measured using a calibrated pH-meter (Hanna-Instruments, 8519, Italy). The cyclic voltammetry measurements were carried out with a Potentiostat Wave Generator (Oxford press) equipped with a Phillips PM 8043 X-Y recorder. The electrochemical cell consists of platinum wires (0.5 mm diameter) as working and counter electrodes and Ag/AgCl as a reference electrode.

Procedure for extraction and determination of $\text{Bi}^{(\text{III})}$

In a separating funnel, were placed 1 ml of 110^{-4} M of $\text{Bi}^{(\text{III})}$, 0.5 ml of KI (0.1 mol l^{-1}) and dilute to 10 ml with redistilled water. Adjust the pH of the solution at 1.5 using HCl or NaOH (if necessary) and add 3 ml of CHCl_3 solution of TCMAC ($10^{-3}\text{ mol l}^{-1}$). Extract and allow the phases to separate. The absorbance of the separated organic layer was measured at 490 nm against a reagent blank having the same constituents except the analyte and extracted by the same mentioned way.

Results and discussion

The formulae of the complexes together with color, melting points, elemental analysis and formula weights are listed in Table 1. The complexes are stable at room

Table 1. Physical and elemental analysis of Bi^{III} complexes

Compound	Color	L _a	M.P. (C)	Found (calcd.)%				
				C	H	N	Bi	Cl
(1) [Bi(H ₂ DMTS) ₂ Cl ₃] · 0.5H ₂ O 672.8 (673)	Yellow	10.2	>300	18.3 (17.9)	3.2 (3.1)	17.1 (16.7)	31.50 (31.0)	15.9 (15.8)
(2) [Bi(HATS) ₂ Cl ₃] 701.9 (705)	Yellow	17.2	>300	31.4 (30.8)	3.3 (3.2)	12.5 (12.0)	29.0 (29.8)	15.5 (15.2)
(3) [Bi(HTS) ₂ Cl ₃] · 2H ₂ O 533.6	White	10.7	111	4.4 (4.5)	2.4 (2.6)	–	40.0 (39.2)	20.2 (19.9)
(4) [Bi(HBTS) ₃ Cl ₃] 1081.4	Yellow	8.9	191	46.3 (46.7)	3.5(3.6)	11.4 (11.7)	19.5 (19.3)	9.9 (9.8)
(5) [Bi(H ₂ STS) ₃ Cl ₃] 901.1	Orange	20.2	>300	31.5 (31.9)	3.2(3.0)	–	22.7 (23.2)	12.3 (11.8)
(6) [Bi(HDMS) ₂]NO ₃ 617.3	Red	59.2	>300	19.0 (19.5)	3.1(2.9)	–	33.2 (33.9)	–

^a Values of molar conductance in ohm cm² mol⁻¹, the bold values of molecular weights are obtained from mass spectra.

temperature, have non-hygroscopic nature and insoluble in water, except complex (6), and in most organic solvents but are soluble in DMF and DMSO. Most complexes decomposed on heating at >300 C.

Infrared spectral studies

Most important infrared bands of the ligands and their Bi^(III) complexes are given in Table 2. The ligands have numerous coordination sites giving variable bonding modes. All ligands coordinate in the thione form except [Bi(HDMS)₂]NO₃ which formed in the deprotonated form of H₂DMTS. The ligands in [Bi(HATS)₂Cl₃] (2) and [Bi(HBTS)₃Cl₃] (4) behave as neutral bidentate (NS and NN donors). Strong evidence is: the negative shift (ca. 45 cm⁻¹) of m(C=N) [24] and the presence of a new band at

466–521 cm⁻¹ assignable to m(Bi–N) [25]. The coordination via thione sulfur in complex (2) is indicated by the shift of m(C=S) and the appearance of a new band at 395 cm⁻¹ due to m(Bi–S) [26]. In complex (4), the d(NH₂) band is shifted from 1620 to 1588 cm⁻¹ confirming the chelation through the amino group. The appear-

ance of 296 cm⁻¹ band, due to m(Bi–Cl), is consistent with the chloride to be inside the coordination sphere. The ¹H-NMR spectra of [Bi(HBTS)₃Cl₃] (4) shows no changes than the ligand spectrum.

In [Bi(HTS)₂Cl₃] · 2H₂O (3), the ligand interacts as a neutral monodentate via C–SH by the disappearance of m(C=S) and the appearance of m(SH), m(C–S), and m(Bi–S) at 2362, 683 and 365 cm⁻¹, respectively.

In $[\text{Bi}(\text{H}_2\text{DMTS})_2\text{Cl}_3]$ (1) and $[\text{Bi}(\text{HDMTS})_2]\text{NO}_3$ (6), H_2DMTS behaves as a neutral or mononegative tridentate ligand acting as SNO or NNS through $\text{C}=\text{N}_{\text{thio}}$, $\text{C}=\text{NO}$ and $\text{C}=\text{S}$ or $\text{C}=\text{N}_{\text{thio}}$, $\text{C}=\text{N}_{\text{oxime}}$ and $\text{C}=\text{S}$, respectively. The shift to lower frequency ($35\text{--}40\text{ cm}^{-1}$) of $\text{m}(\text{C}=\text{S})$ in the two complexes supports the sulfur participation. Deprotonation of the oxime ($\text{C}=\text{NOH}$) in (6) is confirmed by the disappearance of $\text{m}(\text{OH})$ and the appearance of $\text{m}(\text{N}-\text{O})$ at 1100 and $\text{m}(\text{Bi}-\text{O})$ at 549 cm^{-1} . Also, its $^1\text{H-NMR}$ spectrum shows the disappearance the signal of the OH proton at 11.505 p.p.m. with the downfield shift of the NH_2 signals. The bands due to $\text{m}(\text{C}=\text{N})$ of oxime and thiosemicarbazone are shifted to lower frequency in the spectrum of (1) while the $\text{C}=\text{N}_{\text{thio}}$ band is only shifted by 59 cm^{-1} in (6) with the appearance of a new band at $410\text{--}440\text{ cm}^{-1}$ assignable to $\text{m}(\text{Bi}-\text{N})$ in the spectra of the two complexes. The nitrate bands are in (6) observed at 1690 (m_s), 1413 (m_s^l) and 1028 cm^{-1} (m_{as}) proving that the nitrate ion is ionic and existing outer the sphere [27]. Structure 2 represents $[\text{Bi}(\text{HDMTS})_2]\text{NO}_3$ (6).

In the spectrum of $[\text{Bi}(\text{HSTS})_3\text{Cl}_3]$ (5), a shift of $\text{m}(\text{OH})$ to higher wavelength (3515 cm^{-1}) corresponds to the dissociation of the hydrogen bonding with $\text{C}=\text{N}$ during the complex formation. The lower shifts in the bands of $\text{m}(\text{C}=\text{N})$ and $\text{m}(\text{C}=\text{S})$ by 69 and 16 cm^{-1} with

the appearance of $\text{m}(\text{Bi}-\text{N})$ and $\text{m}(\text{Bi}-\text{S})$ at 514 and 473 cm^{-1} , respectively, indicate chelation through the $\text{C}=\text{N}$ and $\text{C}=\text{S}$ groups. The two bands at 309 and 286 cm^{-1} due to $\text{m}(\text{Bi}-\text{Cl})$ are due to the existence of the complex in trans-form rather than cis-form, and prove the existence of the Cl inside the sphere [28]. Good evidence for this phenomenon comes from the value of its molar conductance (Table 1).

Electronic spectra

The electronic absorption bands of $\text{Bi}^{(\text{III})}$ complexes are given in Table 3. The spectra of the ligands show the p fi p^* band at $37,040\text{--}44,440$ and n fi p^* bands at $29,940\text{--}33,000$ and $26,180\text{--}29,500\text{ cm}^{-1}$ [25]; little change is observed on the spectra of their complexes. The spectra of the complexes show a band at $23.750\text{--}26.180\text{ cm}^{-1}$ due to LMCT [29]. Previous studies on thiosemicarbazone complexes proved that the band at $25,000\text{--}26,040\text{ cm}^{-1}$ should be assigned to O fi M transition [26] where that in the range $21,785\text{--}24,750\text{ cm}^{-1}$ is due to S fi M transition [30]. The CT band of the present complexes lies in the two ranges owing to the greater ability of $\text{Bi}^{(\text{III})}$ to coordinate sulfur and oxygen compounds.

Mass spectra

Compound	m(OH)	m(NH ₂)		m(NH)	m(C=N) _{thio} + d(NH ₂)	m(C=N) _{ox.}	Thioamide bands				m(SH)
		_{mas} (NH ₂)	_{ms} (NH ₂)				I	II	III	IV	
H ₂ DMTS	3415	3254 3231		3146	1615	1550	1485	1285	930	765	–
$[\text{Bi}(\text{HDMTS})_2]\text{NO}_3$	–	3255 3230		3147	1614	1556 ^a	1505	1295	935	730	–
$[\text{Bi}(\text{H}_2\text{DMTS})_2\text{Cl}_3]$	3413	3305 3245		3155	1590	1502	1432	1282	960	725	–
HATS	–	3409 3367		3223	1644 1596	–	1488	1288	962	763	–
$[\text{Bi}(\text{HATS})_2\text{Cl}_3]$	–	3396 3281		3233	1598 1598	–	1485	1273	965	738	–
HTSC	–	3368, 3261 3270		3174	1645, 1620	–	1532	1284	1001	800	–
$[\text{Bi}(\text{HTSC})_2\text{Cl}_3] \cdot 2\text{H}_2\text{O}$	–	3411, 3257		–	1625(br)	–	1547	1306	1076	–	–
HBTS	–	3364 3262		3166	1647 1620	–	1530	1277	1000	767	–
$[\text{Bi}(\text{HBTS})_3\text{Cl}_3]$	–	3379 3265		3161	1603 1588	–	1510	1280	942	773	2362
H ₂ STS	3442	3317 –		3166	1538 1611	–	1489	1270	945	775	–
$[\text{Bi}(\text{H}_2\text{STS})_3\text{Cl}_3]$	3515	3339 –		3170	1607	–	1483	1267	967	759	–

^a Combined with $\text{C}=\text{N}_{\text{thio}}$.

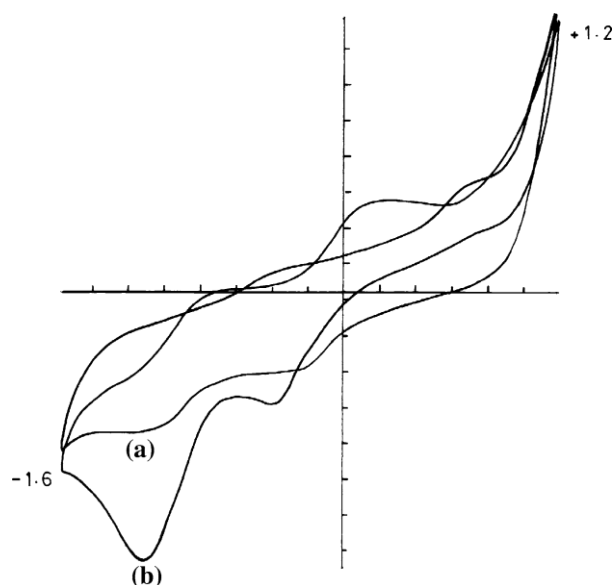


Fig. 2. Cyclic voltammograms of: (a) H_2DMTS and (b) $[\text{Bi}(\text{H}_2\text{DMTS})_2\text{Cl}_3] \cdot 0.5\text{H}_2\text{O}$ (1) at scan rate = 200 mV s^{-1} in $\text{DMSO}/\text{TBA}^+\text{BF}_4^-$ versus Ag/AgCl electrode.

The mass spectra of $[\text{Bi}(\text{H}_2\text{DMTS})_2\text{Cl}_3] \cdot 0.5\text{H}_2\text{O}$ (1) and $[\text{Bi}(\text{HATS})_2\text{Cl}_3]$ (2) are recorded and their molecular ion peaks confirmed the proposed formulae. The calculated and found molecular weights are given in Table 1. The mass spectrum of (1) shows multi peaks corresponding to the successive degradation of the molecule (Figure 1). The first peak at m/e 673 (Calcd. 672.8) represents the molecular ion peak of the complex with 2.35% abundance. The second peak represents the loss of $\text{Cl} + 0.5\text{H}_2\text{O}$. The evolution of $2\text{NH}_2 + 2\text{CH}_3$ is the third peak with $m/e = 569$. The sharp peak (base peak) with m/e 141 represents the stable species ($\text{H}_4\text{N}_4\text{S}_2\text{O}$) after which a series of degradation steps are observed ending with $m/e = 51$.

The mass spectrum of (2) shows multi peaks; the first one at m/e 705 (calcd. 701.9) represents the molecular ion peak of the complex. A series of low abundance peaks were appeared till $m/e = 193$ which represent one molecule of the ligand after the loss of $3\text{Cl} + \text{HATS} + \text{Bi}$. The sharp peaks at $m/e = 77$ and 60 represent the final species, phenyl and 5carbons, respectively.

Table 3. Electronic spectral data of the free ligands and their Bi^{III} complexes (in DMSO)

Compound	Intra ligand band (cm^{-1})	Charge transfer band (cm^{-1})
H_2DMTS	42,920(1.6); 40,485(2.0); 38,168(1.8); 33,003(5.5)	–
$[\text{Bi}(\text{H}_2\text{DMTS})_2\text{Cl}_3] \cdot 0.5\text{H}_2\text{O}$	43,103(5.1); 40,323(3.0); 38,168(3.2); 29,851(5.6)	24,450(0.7)
$[\text{Bi}(\text{HDMTS})_2]\text{NO}_3$	41,152(2.4); 38,168(2.6); 31,850(3.4); 29,940(3.6)	25,640(0.7); 24,940(0.6); 23,750(0.6)
HATS	42,194(1.0); 40,000(0.7); 32,573(2.7)	–
$[\text{Bi}(\text{HATS})_2\text{Cl}_3]$	40,000(2.5); 32,051(5.4); 38,270(2.1)	23,980(0.1)
HTS	43,480(0.06); 40,000(0.03); 37,040(0.16)	–
$[\text{Bi}(\text{HTS})_2\text{Cl}_3] \cdot 2\text{H}_2\text{O}$	41,322(1.4); 38,314(1.1); 32,470(0.8)	26,180(0.2); 24,630(0.1)
HBTS	43,480(2.4); 37,170(1.1); 32,680(3.2); 29,940(2.5)	–
$[\text{Bi}(\text{HBTS})_3\text{Cl}_3]$	41,670(4.5); 38,023(5.2); 32,680(10.2); 29,506(7.6)	–
H_2STS	44,444(0.9); 40,984(2.4); 38,314(1.1); 30,864(2.8); 29,070(2.9)	–
$[\text{Bi}(\text{H}_2\text{STS})_3\text{Cl}_3]$	41,322(2.5); 38,610(2.4); 32,051(3.5); 29,500(4.9)	25,510(0.4); 24,330(0.4)

The values in parentheses are the molar absorptivity (10^4).

Table 4. Electrochemical data of the prepared thiosemicarbazones and its Bi^{III} complexes^a in $\text{DMSO}-\text{TBA}^+\text{BF}_4^-$ versus Ag/AgCl at

200 mV s^{-1} scan rate

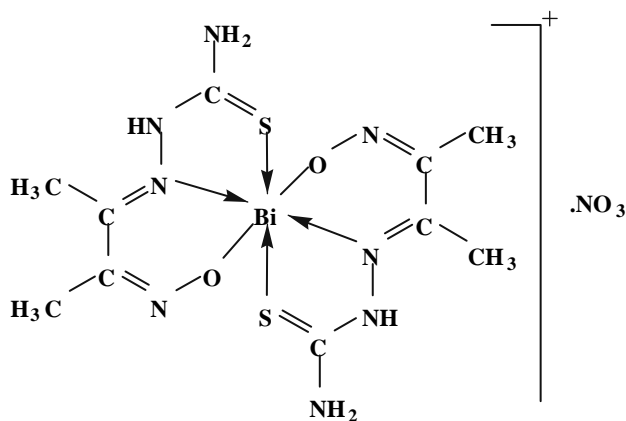
Ligand	First couple				Second couple			
	$E_{p,a}$	$E_{p,c}$	DE_p	$E_{1/2}$	$E_{p,a}$	$E_{p,c}$	DE_p	$E_{1/2}$
HTS	0.40	0.66	1.06	0.13	0.78	0.50	1.28	0.14
$[\text{Bi}(\text{HTS})_2\text{Cl}_3] \cdot 2\text{H}_2\text{O}$	0.26	1.10	0.84	0.68	0.68	0.26	0.94	0.21
H_2DMTS	0.32	1.02	0.70	0.67	0.70	0.16	0.86	0.27
$[\text{Bi}(\text{H}_2\text{DMTS})_2\text{Cl}_3] \cdot 0.5\text{H}_2\text{O}$	0.72	1.12	0.40	0.92	0.16	0.38	0.54	0.11
$[\text{Bi}(\text{HDMTS})_2]\text{NO}_3$	0.78	1.20	0.42	0.99	0.66	0.36	1.02	0.15
HATS	0.66	1.06	1.72	0.20	–	–	–	–
$[\text{Bi}(\text{HATS})_2\text{Cl}_3]$	0.36	1.08	0.72	0.72	0.32	0.36	0.68	0.02
HBTS	0.50	1.10	0.60	0.80	0.74	0.40	1.14	0.17
$[\text{Bi}(\text{HBTS})_3\text{Cl}_3]$	0.40	1.04	0.64	0.72	0.74	0.38	1.12	0.18
H_2STS	0.00	0.60	0.60	0.30	–	–	–	–
$[\text{Bi}(\text{H}_2\text{STS})_3\text{Cl}_3]$	0.44	0.80	0.36	0.62	–	–	–	–

^a $E_{1/2} = (E_{p,c} + E_{p,a})/2$.

The cyclic voltammetry was investigated in $\text{DMSO}[\text{TBA}]^+[\text{BF}_4]^-$ solution at a scan rate of 200 mV s^{-1} for the ligands and $20\text{--}200 \text{ mV s}^{-1}$ for the complexes versus Ag/AgCl reference electrode. The voltammetric data are summarized in Table 4.

The CV's of HTS, H_2DMTS (Figure 2) and HBTS are similar and display two irreversible electrode couples. The first with an anodic peak potential, $E_{p,a}$ at $(0.5)\text{--}(0.4 \text{ V})$ coupled with cathodic wave potential, $E_{p,c}$, at $(1.02)\text{--}(0.66 \text{ V})$. The second electrode couple has an anodic peak potential at $0.70\text{--}0.78 \text{ V}$ and cathodic peak potential at $(0.50)\text{--}(0.16 \text{ V})$. The reagents, H_2STS and HATS, show similar voltammetric behavior in which an irreversible electrode couple is observed in the range $(1.0)\text{--}1.0$ and $(1.5)\text{--}1.0 \text{ V}$, with a cathodic wave in the range $(0.60)\text{--}(1.06 \text{ V})$ coupled with an anodic wave at $0.00\text{--}0.66 \text{ V}$ and $\text{DE}_p = 1.72\text{--}0.60 \text{ V}$.

All complexes, except $[\text{Bi}(\text{H}_2\text{STS})_3\text{Cl}_3]$, show similar features in the investigated potential range $(1.6)\text{--}1.1$, $(1.6)\text{--}1.2$ and $(1.5)\text{--}1.0 \text{ V}$ and displayed two well defined reduction waves in the regions $(1.20)\text{--}(1.04)$ and $(0.38)\text{--}(0.26) \text{ V}$ coupled with two anodic waves in the regions $(0.78)\text{--}(0.26)$ and



Structure 2.

$0.16\text{--}0.74 \text{ V}$ with $E_{1/2} = (0.99\text{--}0.68)$ and $(1.10)\text{--}(0.21) \text{ V}$, respectively. The observed electrode couples are irreversible ($\text{DE}_p > 0.1 \text{ V}$) and are safely assigned to one electron oxidation processes $\text{Bi}^{+3}/\text{Bi}^{+4}$ and $\text{Bi}^{+4}/\text{Bi}^{+5}$, respectively.

The dependence of the cathodic peak current, $i_{p,c}$ of the couple $\text{Bi}^{+4}/\text{Bi}^{+3}$ on the square root of the sweep rate ($m^{1/2}$) suggests a diffusion-controlled electrochemical process [31]. The cathodic peak potential ($E_{p,c}$) of this couple was shifted towards more negative values as m increases indicating irreversible nature of the electrode couple. The irreversibility of this couple was also confirmed from the linear dependence of the cathodic peak potential, $E_{p,c}$ with $\log m$ [32].

A characteristic cyclic voltammogram for $[\text{Bi}(\text{H}_2\text{DMTS})_2\text{Cl}_3] \cdot 0.5\text{H}_2\text{O}$ (1) at $(1.6)\text{--}1.2 \text{ V}$ is shown in Figure 2. A slight displacement of the anodic and cathodic

peaks is observed as the sweep rate increases, the peak current ratios $i_{p,c}/i_{p,a} > 1$; $\text{DE}_p > 60 \text{ mV}$ and the $i_{p,c}$ versus $m^{1/2}$ plot is linear with negative intercept. All these characteristics are of an irreversible one electron process. The dependence of the voltammetric responses of $\text{Bi}^{+4}/\text{Bi}^{+3}$ on the sweep rate, the depolarizer concentration of the analyte as well as the decrease in $i_{p,c}/m^{1/2}$ is typical of an ECE (chemical reaction coupled between two charge processes) type mechanism in which an irreversible first order chemical reaction is interposed between two successive one electron charge transfers. The ECE mechanism of this complex was also confirmed from the observed decrease of cathodic peak current versus the $m^{1/2}$ and from $i_{p,c}/m^{1/2} > 1$ on increasing the scan rate (Figure 3).

The CV of $[\text{Bi}(\text{H}_2\text{STS})_3\text{Cl}_3]$ at 200 mV s^{-1} sweep rate is summarized in Table 4. The complex displayed one well defined electrode couple in the potential range $1.4\text{--}1.0 \text{ V}$. The electrode couple with $E_{1/2} = 0.62 \text{ V}$ and $\text{DE}_p = 0.36 \text{ V}$ is observed and assigned to the irreversible couple $\text{Bi}^{+5}/\text{Bi}^{+3}$. The irreversible nature and the ECE type mechanism of the observed reduction wave were confirmed by the large difference in the potential ($\text{DE}_p > 0.1 \text{ V}$)

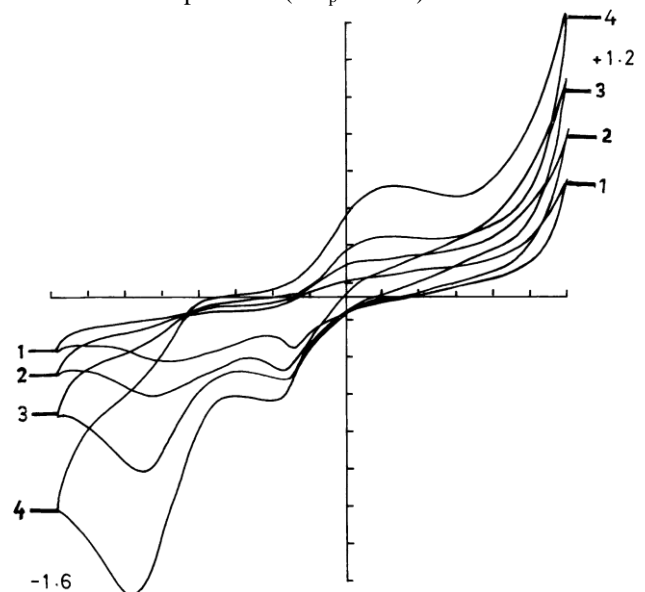


Fig. 3. Cyclic voltammogram of $[\text{Bi}(\text{H}_2\text{DMTS})_2\text{Cl}_3] \cdot 0.5\text{H}_2\text{O}$ (1) at scan rates = $20(1)$, $50(2)$, $100(3)$ and 200 mV s^{-1} (4) in $\text{DMSO}/\text{TBA}^+\text{BF}_4^-$ versus Ag/AgCl electrode.

between the two peak centers of the electrode couple and the linear dependence of the cathodic peak potential, $E_{p,c}$ and the cathodic peak current $i_{p,c}$ with $\log m$ and $m^{1/2}$, respectively (Figure 4).

Thermal studies

The thermograms of $[\text{Bi}(\text{HTS})_2\text{Cl}_3] \cdot 2\text{H}_2\text{O}$ (3) and $[\text{Bi}(\text{HDMTS})_2]\text{NO}_3$ (6) end with bismuth metal. The TG curve of (3) is characterized by steps at $32\text{--}82$, $247\text{--}338$,

340–489 and 490–782 C. Elimination of the two hydrated H_2O is the degradable species in the first step (Calcd. 6.55, found 6.56%). The second step consumed $\text{H}_8\text{N}_4\text{Cl}_3$ radical (Calcd. 29.4, found 31.5%). The third step is consistent with the evolution of C_2N_2

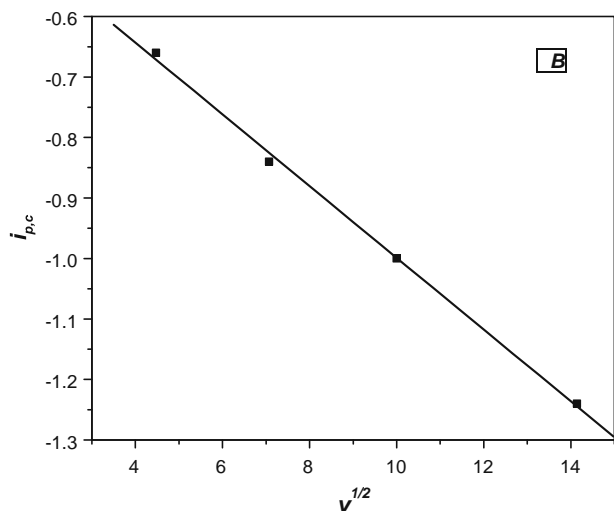


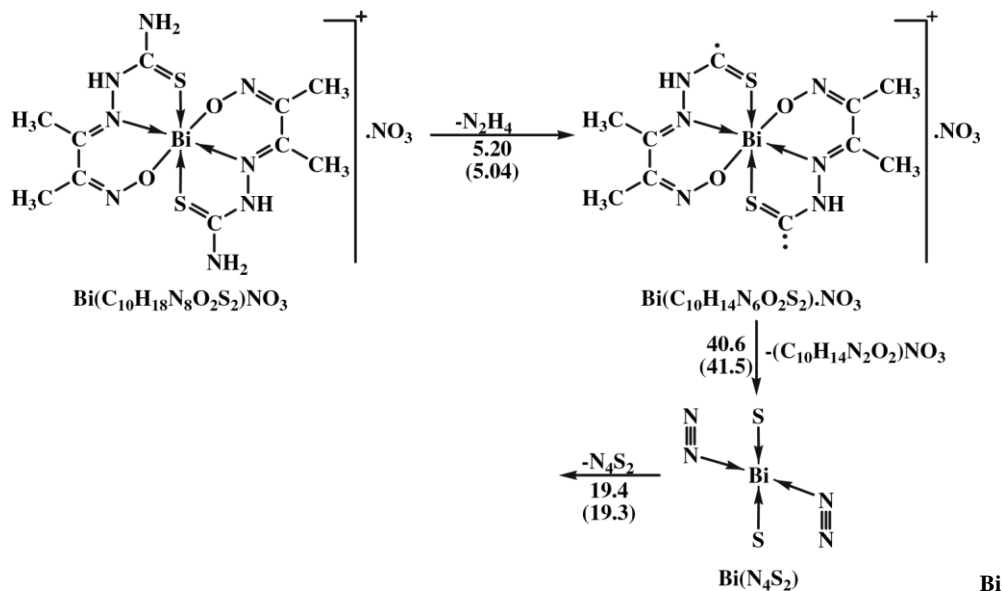
Fig. 4. Influence of the scan rate on $i_{p,c}$ of $[\text{Bi}(\text{H}_2\text{STS})_3\text{Cl}_3]$.

radical (Calcd. 9.7, found 9.9%). The fourth decomposition step corresponds to the evolution of H_2S_2 (Calcd. 14.99, found 14.5%) after which Bi (calcd. 39.4, found 40.5%) was apparently the final residue in agreement with Table 1 data. In the thermogram of

(6), bismuth was also the residua with weight loss of 33.8% (found 35.6). The fragments evolved at 81–150, 151–497 and 498–710 C with 5.2% (found 5.0), 41.5% (found 40.1) and 19.4% (19.3) are N_2H_4 ,

$\text{C}_{10}\text{H}_{14}\text{N}_2\text{O}_2 \cdot \text{NO}_3$ and N_4S_2 respectively (Scheme 1).

The TGA curve of (1) has 219–308 and 309–558 C steps due to the elimination of $[\text{3Cl} + 4\text{CH}_3 + 2\text{NH}_2]$ (29.9, found 31.3) and $[\text{4C} + 2\text{CNH} + 2\text{OH}]$ (20.5, found 20.2) leaving BiS_2N_4 (49.5, found 49.8) as a final product at 560 C. The complex is highly stable till 219 C without weight loss indicating that the half water is removed on drying at room temperature for long time.



Scheme 1.

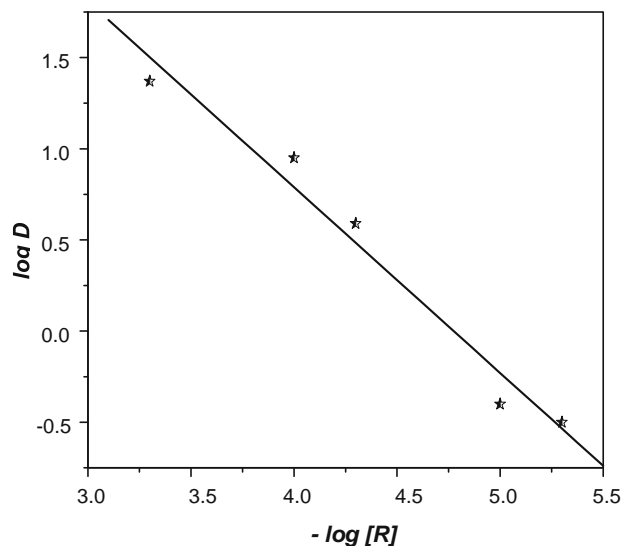


Fig. 5. Variation of the distribution coefficient with the TCMAC concentration in the separation of $110^5 \text{ mol l}^{-1} \text{ Bi}^{\text{III}}$ at $\text{pH} = 1.5$.

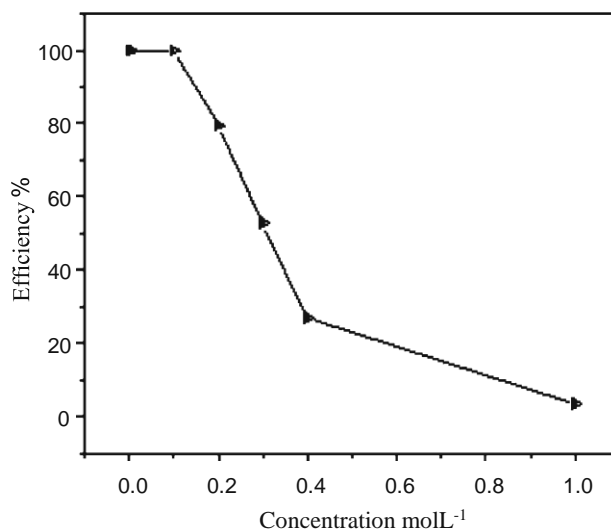


Fig. 6. Effect of KI concentration on the separation of $110^5 \text{ mol l}^{-1} \text{ Bi}^{\text{III}}$ using 110^3 mol l^{-1} of (TCMAC) in chloroform at $\text{pH} = 1.5$.

Table 6. Determination of Bi^{III} spiked to natural water samples by the recommended spectrophotometric procedure after extraction using 510^3 mol l^{-1} of KI and 110^3 mol l^{-1} of TCMAC at $\text{pH} = 1.5$

Type of water (location)	Bi ^{III} added (mg l ⁻¹)	Bi ^{III} found (mg l ⁻¹)	Recovery (%)	0.5 1.0	9.810 ³ 19.7510 ³	9.8810 ³ 19.7610 ³	99.19 99.95
* Weight of wet sample.							

Table 5. Effect of foreign ions on the separation and determination of 110⁵ mol l⁻¹ of Bi^{III} using 110³ mol l⁻¹ of TCMAC and510³ mol l⁻¹ of KI at pH = 1.5 in chloroform

Ion	Concentration (p.p.m.)	Effeciency (%)	Ion	Concentration (p.p.m.)	Effeciency (%)
Fe ^{III}	25	99.8	K ¹⁺	7,800	100.0
	50	113			
Cu ^{III}	350	99.9	Mg ²⁺	240	98.1
	650	100		2400	99.3
Zn ^{III}	65	97.2	Ca ²⁺	400	100.0
	6500	99.8		4000	100.0
Cd ^{III}	500	99.7 ^a	Cl ¹	7000	100.0
	1000	99.9 ^a			
Hg ^{III}	25	100.0 ^a	Br ¹	800	99.3
	50	99.9 ^a			
Pb ^{III}	260	100.0	NO ₃	650	99.7
	300	100.0		25,000	
Na ¹⁺	230	100.0	SO ₄	20,000	99.5
	9200	96.5			

^a The interference eliminated by using 110³ mol l⁻¹ of KI.

Sample	1	2	3	4
Distilled water	1	0.999	99.90	
	2	2.000	100.00	
Tape water (our laboratory)	1	0.997	99.70	
	2	1.996	99.80	
Sahel Sherbin	1	0.970	97.00	
	2	1.991	99.55	
Ground water (Salaka)	1	1.000	100.00	
	2	2.000	100.00	
Sea water (Ras El-Bar)	1	1.000 ^a	100.00	
	2	1.000 ^a	100.00	
Lake water (Manzalah)	1	1.236	123.60	
	2	2.472	123.60	

^a Using 10³ mol l⁻¹ KI.

Table 7. Determination of Bi^{III} in pharmaceutical product (Anusol) using 0.1 mol l⁻¹ of KI and 0.01 mol l⁻¹ of TCMAC at pH 1.5

Sample* (g)	Found (g)	Content (g)	Recovery (%)

An extractive-spectrophotometric determination method for Bi^(III)

Various parameters were studied for the extraction of Bi^(III) as ion pair complex formation. The data reveal that the pH is very important in the extraction of Bi^(III) in chloroform. The extraction efficiency increases with pH having a maximum at 1.5. So, all experiments were carried out at this pH.

To select a suitable counter ion for ion pair formation with [BiL₄]¹, a number of counter ions was examined. Some of the tested cations were found effective but easily emulsified with [BiL₄]¹ and CHCl₃; the difficult arises in the separation of the two phases. [TCMA]⁺ is the cation achieved our goal by forming a very clear separation layer between the two phases and the absorbance is reproducible. The maximum extraction was obtained at 10³-10² mol l⁻¹ range.

The composition of the ion pair was obtained by plotting log D (D = distribution coefficient) versus log C (C = concentration of [TCMA]⁺). As shown in Figure 5, the slope of the straight line is 1.06, revealing that 1:1 is the ratio formed for the ion pair complex. The data is confirmed through molar ratio and continuous variation methods.

The effect of KI concentration was also studied on the extraction of 10^5 mol l⁻¹ of Bi^(III) and the results are shown in Figure 6. A constant extraction efficiency is shown at 0.15 mol l⁻¹ of KI which is suitable for the determination of Bi^(III) in unknown samples.

The effect of solvents (toluene, n-hexane, 1-butanol, ethylacetate and chloroform) on the extraction of Bi^(III) using the formation of ion pair complex is studied. Chloroform and ethylacetate were suitable to give maximum extraction.

Shaking and standing times are also important and examined. It is found that the absorbance of the extract remains constant for shaking time until 3 min at room temperature (25 C). Also, the extract is stable to light over 24 h.

A linear calibration curve was obtained in the 0.0–5 lg Bi^(III) range. The molar absorptivity is found $8.67 \cdot 10^4$ l mol⁻¹ cm⁻¹ at 490 nm and the standard deviation of 2 lg is 0.0054 (n = 10). Also, the regression equation (absorbance = 64750 (n-0.0057) and correlation coefficient (r = 0.9998) were obtained.

The preconcentration procedure for trace metals is strongly affected by diverse ions and the other constituents of the sample. Thus, the reliability of the proposed method was examined in the presence of interfering ions may present in water or pharmaceutical products. The interferences in the determination of Bi^(III) were examined under the general procedure conditions. The results are listed in Tables 5–7.

References

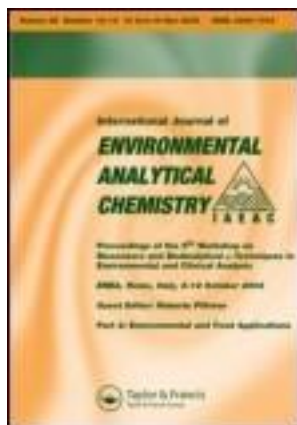
- M. Abram, E.S. Lang and E. Bonfada, *Z. Anorg. Allg. Chem.*, 628, 1419 (2002).
- R. Pogni, M.C. Baratto, A. Diaz and R. Basasi, *J. Inorg. Biochem.*, 79, 333 (2000).
- M.B. Ferrari, F. Bisceglie, G. Pelosi, M. Sassi, P. Tarasconi, M. Cornia, S. Capacchi, R. Albertini and S. Pinelli, *J. Inorg. Biochem.*, 90, 113 (2002).
- S.D. Dhumwad, K.B. Gudasi and T.R. Goudor, *Indian J. Chem.*, 33A, 320 (1994).
- E. Franco, E. Lopez, M.A. Mendiola and M.T. Sevilla, *Polyhedron*, 19, 441 (2000).
- D.W. Maragerum and G.D. Owens, *Metal Ions in Biological Systems*, Marcel Dekker, New York, 1981.
- N.M. Leonard, L.C. Wieland and R.S. Mohan, *Tetrahedron*, 58, 8373 (2002).
- H. Sun and K.Y. Szeto, *Inorg. Biochem.*, 94, 114 (2003).
- J. Pannequin, S. Kovac, J.P. Tantiongco, R.S. Norton, R.S. Shulkes, K.J. Barnham and G.S. Baldwin, *J. Biol. Chem.*, 279, 2453 (2004).
- U. Dittes, E. Vogel and B.K. Keppler, *Coord. Chem. Rev.*, 163, 345 (1997).
- D.Y. Graham, G. Belson, S. Abudayyeh, M.S. Osato, M.P. Dore and H.M.T. El-Zimaity, *Digest. Liver Dis.*, 36, 384 (2004).
- I. Turel, L. Golic, P. Bukovec and M. Gubina, *J. Inorg. Biochem.*, 71, 53 (1998).
- P.J. Sadler, H. Li and H. Sun, *J. Coord. Chem. Rev.*, 185, 689 (1999).
- K. Garmestani, Z. Yao, M. Zhang, K. Wong, C.W. Park, I. Pastan, J.A. Carrasquillo and M.W. Brechbiel, *Nucl. Med. Biol.*, 28, 409 (2001).
- H. Sun, H. Li, I. Harvey and P.J. Sadler, *J. Biol. Chem.*, 274, 29094 (1999).
- M. Zhang, D.R. Gumerov, I.A. Kaltashov and A.B. Mason, *J. Am. Soc. Mass Spectrom.*, 15, 1658 (2004).
- J.N. Arnold, P.D. Hayes, R.L. Kohaus and R.S. Mohan, *Tetrahedron Lett.*, 44, 9173 (2003).
- H. Guo, Y. Li, P. Xiao and N. He, *Analytica Chimica Acta*, 534, 143 (2005).
- D.T. Burns and M.D. Dunford, *Analytica Chimica Acta*, 334, 209 (1996).
- R.M. El-Shazly, G.A.A. Al-Hazmi, S.E. Ghazy, M.S. El-Shahawi and A.A. El-Asmy, *Spectrochim. Acta*, 60A, 3187 (2004).
- D.X. West, Y.H. Yang, T.L. Klein, K.I. Goldberg, A.E. Liberta, J. Aldes-Matinez and S. Hernandez-Ortega, *Polyhedron*, 141, 681 (1995).
- S.I. Mostafa, A.A. El-Asmy and M.S. El-Shahawi, *Transition Met. Chem.*, 25, 470 (2000).
- A.I. Vogel, *A Text Book of Quantitative Inorganic Analysis*, Longmans, London, 1994.
- D.X. West, S.L. Dietrich, I. Thientanavanich and C.A. Brown, *Transition Met. Chem.*, 19, 195 (1994).
- D.X. West, A.K. El-Sawaf and G.A. Bain, *Transition Met. Chem.*, 23, 1 (1998).
- D.X. West, M.M. Salberg, G.A. Bain and A.E. Liberta, *Transition Met. Chem.*, 22, 180 (1997).
- E.A.E. Ahmed, M.Sc. Thesis, Al-Azhar University, Egypt, 2006.
- F.A. El-Saied, A.A. El-Asmy, W. Kaminsky and D.X. West, *Transition Met. Chem.*, 28, 954 (2003).
- A.A. El-Asmy, M.E. Khalifa and M.M. Hassanian, *Synth. React. Inorg. Met.-Org. Chem.*, 31, 1787 (2001).
- S. Mostafa, M.M. Bekheit and M.M. El-Agez, *Synth. React. Inorg. Met.-Org. Chem.*, 30, 2029 (2000).
- L.M. Araya, J.A. Vargas and J.A. Costamana, *Transition Met. Chem.*, 11, 312 (1986).
- B.S. Parajon-Costa, A.C. Gonzalez-Baro and E.J. Baran, *Z. Anorg. Allg. Chem.*, 628, 1628 (1986).

This article was downloaded by: [King Abdulaziz University]

On: 03 February 2014, At: 03:31

Publisher: Taylor & Francis

Informa Ltd Registered in England and Wales Registered Number: 1072954 Registered office: Mortimer House, 37-41 Mortimer Street, London W1T 3JH, UK



International Journal of Environmental Analytical Chemistry

Publication details, including instructions for authors and subscription information:

<http://www.tandfonline.com/loi/geac20>

Chemical equilibria and sequential extractive spectrophotometric determination of selenium(IV) and (VI) using the chromogenic reagent

4,4' dichlorodithizone

Mohammad S. El-Shahawi ^a , Abdelhameed M. Othman ^b ,
Abdulaziz S. Bashammakh ^a & Mervat A. El-Sonbati ^c

^a

Department of Chemistry, Faculty of Science , King Abdulaziz University , Jeddah, Kingdom of Saudi Arabia

^b

Genetic Engineering and Biotechnology Research Institute , Menoufia University , Menoufia, Egypt

^c

Department of Environmental Science, Faculty of Science at Damietta , Mansoura University , Mansoura, Egypt Published online: 25 Jan 2007.

To cite this article: Mohammad S. El-Shahawi , Abdelhameed M. Othman , Abdulaziz S. Bashammakh & Mervat A. El-Sonbati (2006) Chemical equilibria and sequential extractive spectrophotometric determination of selenium(IV) and (VI) using the chromogenic reagent 4,4' dichlorodithizone, International Journal of Environmental Analytical Chemistry, 86:12, 941-954, DOI: [10.1080/03067310600557554](https://doi.org/10.1080/03067310600557554)

To link to this article: <http://dx.doi.org/10.1080/03067310600557554>

PLEASE SCROLL DOWN FOR ARTICLE

Taylor & Francis makes every effort to ensure the accuracy of all the information (the "Content") contained in the publications on our platform. However, Taylor & Francis, our agents, and our licensors make no representations or warranties whatsoever as to the accuracy, completeness, or suitability for any purpose of the Content. Any opinions and views expressed in this publication are the opinions and views of the authors, and are not the views of or endorsed by Taylor & Francis. The accuracy of the Content should not be relied upon and should be independently verified with primary sources of information. Taylor and Francis shall not be liable for any losses, actions, claims, proceedings, demands, costs, expenses, damages, and other liabilities whatsoever

or howsoever caused arising directly or indirectly in connection with, in relation to or arising out of the use of the Content.

This article may be used for research, teaching, and private study purposes. Any substantial or systematic reproduction, redistribution, reselling, loan, sub-licensing, systematic supply, or distribution in any form to anyone is expressly forbidden. Terms & Conditions of access and use can be found at

<http://www.tandfonline.com/page/termsand-conditions>

Chemical equilibria and sequential extractive spectrophotometric determination of selenium(IV) and (VI) using the chromogenic reagent 4,4'-dichlorodithizone

MOHAMMAD S. EL-SHAHAWI^y, ABDELHAMEED M. OTHMAN^z, ABDULAZIZ S. BASHAMMAKH^y and MERVAT A. EL-SONBATI^x

^yDepartment of Chemistry, Faculty of Science, King Abdulaziz University,
Jeddah, Kingdom of Saudi Arabia

^zGenetic Engineering and Biotechnology Research Institute,
Menoufia University, Menoufia, Egypt

^xDepartment of Environmental Science, Faculty of Science at Damietta, Mansoura University,
Mansoura, Egypt

(Received 8 September 2005; in final form 20 December 2005)

The chromogenic reagent 4,4'-dichloro(3-mercapto-1,5-diphenylformazan), $\text{Cl}_2\text{H}_2\text{D}_2$, forms a yellow-red-coloured complex with selenium(IV). The produced complex species was extracted quantitatively into n-hexane, and its absorbance was measured at 416nm. The chemical composition of the extracted selenium(IV)- $\text{Cl}_2\text{H}_2\text{D}_2$ chelate and the molar absorptivity at 416nm were found to be $[\text{SeO}(\text{Cl}_2\text{HD}_2)_2]$ and $910^4 \text{ Lmol}^{-1} \text{ cm}^{-1}$, respectively. The values of the extraction constants (K_D , K_{ex}) enable a convenient application of the proposed system for the liquid-liquid extraction procedure and sequential spectrophotometric determination of traces of inorganic selenium(IV) and/or selenium(VI) after reduction of the later to selenium(IV) with HCl (6M). Beer's law and Ringbom's plots were obeyed in the concentration range 0.01–20 and 0.5–19mgmL⁻¹ of selenium(IV), respectively, with a relative standard deviation of 2.2%. The proposed method has been successfully applied to the determination of selenium(IV) or (VI) and total inorganic selenium(IV) and (VI) in tap and freshwater samples.

Keywords: Chemical equilibria; Speciation; Selenium (IV) and (VI); 4,4'-Dichlorodithizone; Spectrophotometry

1. Introduction

Selenium enters natural waters through seepage from seleniferous soils and industrial waste, and is liberated into the environment (in soil) through a complex biogeochemical reaction forming organoselenium compounds [1]. These compounds are more toxic than inorganic selenium compounds and are absorbed by plants, e.g. cabbage and mustard [2]. However, trace amounts of selenium have been found to be essential

*Corresponding author. Fax: þ20-502230344. Email: mohammad_el_shahawi@yahoo.co.uk

Permanent address: Chemistry Department, Faculty of Science at Damietta, Mansoura University, Mansoura, Egypt.

International Journal of Environmental and Analytical Chemistry
ISSN 0306-7319 print/ISSN 1029-0397 online 2006 Taylor & Francis
DOI: 10.1080/03067310600557554

to maintain normal body metabolism [3]. Selenium can also enhance our ability to protect against certain cancer and heart diseases [4]. The maximum allowed tolerance limit of selenium is 0–50mgL⁻¹ in water, depending on the source, 0.1mgm⁻³ in air, 4–10mgL⁻¹ in tap water, and 0–80mgg⁻¹ in soil [5].

Several methods have been reported for selenium(IV) determination [6–22]. Only a few of the reported spectrophotometric [12] and catalytic [18] methods involving some chromogenic reagents have sufficient sensitivity and selectivity for the trace levels of selenium(IV) in water, polluted water, plant material and steel plant dust. Most of these methods are expensive and unselective, require specific experimental conditions, and are time-consuming [8–11, 15].

Recent years have seen an upsurge of interest in developing novel methods for the chemical speciation of trace amounts of selenium(IV) and (VI) in water [23–27]. The use of the reagent 4,4⁰-dichloro (3-mercapto-1,5-diphenylformazan) for the chemical speciation, determination, and/or preconcentration of selenium(IV) or (VI) employing polyurethane foams has been reported recently by El-Shahawi and El-Sonbati [28]. However, there have been no studies on the application of the title reagent on the liquid–liquid extractive spectrophotometry for the chemical speciation of selenium(IV) and (VI) or other metal ions in aqueous solutions. Thus, the present paper describes the use of the novel title reagent Cl₂H₂D_Z for the chemical speciation and sequential determination of trace amounts of inorganic selenium(IV) and (VI) in water. The chemical equilibria, chemical composition and characterization of the formed selenium(IV)–Cl₂H₂D_Z chelate were also critically investigated. The method developed not only separates the selenium(IV) and (VI) species but also preconcentrates them quantitatively.

2. Experimental

2.1 Reagents and materials

All chemicals used were of analytical reagent grade unless otherwise specified. Solvents (BDH) were used without further purification. Deionized doubly distilled water was used for the preparation of stock solutions of sodium hydrogen selenite (Fluka), sodium selenate (Merck), mineral acids (1M) (BDH), and metal chloride or nitrate salts (BDH). Stock solutions (1mgmL⁻¹) of sodium hydrogen selenite and sodium selenate were prepared by dissolving the appropriate weight of the salts in water. The reagent Cl₂H₂D_Z (structure I) was synthesized by the nitroformazyl method reported by Kiwan and Kassim [29]. The chemical structure of the reagent Cl₂H₂D_Z (Mp 125C) was based on corrected elemental analysis of C, H, N, and Cl and spectral (¹H NMR and IR) data. Elemental analysis of C₁₃H₁₀N₄SCl₂: required C%453.2%, H%43.4%, N%419.1% and Cl%24.2%; found C%453.9%, H%43.5%, N%419.4% and Cl%25.1%.

The significant IR (KBr disk) bands at 3436 (broad), 1636 (strong, s), 1526 (s) and 1487 (s)cm⁻¹ are safely assigned to (N–H), (N–N), (N–H)⋯(C%4N–) and (N–C–S) [12, 29, 30], respectively. The ¹H NMR spectrum of the reagent in d₆-DMSO showed signals at 7.49–7.6 (m 10H, Ar, Hs) and 15.3 (S¹H, NH), confirming the structures proposed in figure 1.

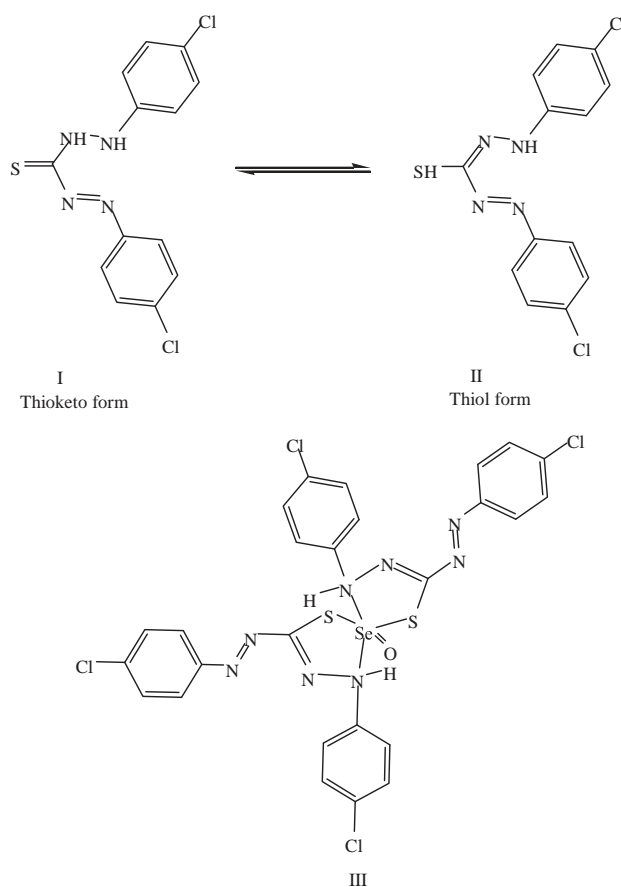


Figure 1. Proposed chemical structures of the reagent $\text{Cl}_2\text{H}_2\text{Dz}$, in thio keto(I) and thiol(II) forms and its selenium(IV) chelate(III).

2.2 Apparatus

Infrared (IR) spectra were recorded on a Bruker FT-IR spectrophotometer model IFS 66. Microanalyses (C, H, N, Cl) were performed on a Perkin-Elmer 240C elemental analyser, Plymouth University, UK. The ^1H NMR spectrum of the reagent $\text{Cl}_2\text{H}_2\text{Dz}$ was recorded on a Jeol 270 FT spectrometer, and values in ppm are relative to TMS for $(\text{CD}_3)_2\text{SO}$. A Shimadzu double beam UV-VIS (UV-160 7pc) spectrophotometer with a 1cm (path width) quartz cell was used for recording the electronic spectra of the reagent and its selenium(IV) chelate. The absorbance of the organic extracts was measured with a single-beam Digital Spectro UV-VIS (RS Labomed) spectrophotometer with glass cells (10mm). A pH meter model 3305 (JENWAY) was used for the pH measurement.

2.3 Recommended procedures

- 2.3.1 Determination of selenium(IV). A 10mL aliquot of an aqueous solution containing selenium(IV) at concentration 10mgmL^{-1} level adjusted to 0pH2 with HCl (1M) was transferred to a 50mL separating funnel. The aqueous solution was extracted twice with 10mL (25) of n-hexane containing the reagent $\text{Cl}_2\text{H}_2\text{D}_Z$ (0.01% w/v) by shaking for 2min. The n-hexane extracts were then collected in a 50mL beaker containing anhydrous sodium sulphate (1g), swirled to mix the contents, and transferred to a 25mL volumetric flask. The residue was also washed with 5mL (22.5) of n-hexane and transferred to the flask. The free $\text{Cl}_2\text{H}_2\text{D}_Z$ was then removed from the combined extracts by shaking with dilute NH_3 solution (two drops of conc. NH_3 solution in 25mL of water). The organic extract was finally made up to the mark with n-hexane, and its absorbance was then measured at 416nm against a reagent blank with the aids of calibration curve prepared under the same experimental conditions.
- 2.3.2 Determination of selenium(VI). An aliquot (10mL) of the aqueous solutions containing $<5\text{mgmL}^{-1}$ of the spiked selenium(VI) was transferred to a 50mL conical flask and reduced to selenium(IV) with HCl (6M) after boiling for 15min in a closed system (to avoid the evaporation of selenium species) and finally cooled to room temperature (251C) as reported earlier [31, 32]. The produced selenium(IV) solution was diluted to 10mL and adjusted to pH'1 with saturated NaOH. The resulting solution was analyzed as described earlier for selenium(IV) determination by the dithizone H_2D_Z method [10, 33] and also by the proposed procedures versus the reagent blank with the aid of standard curves for both methods.
- 2.3.3 Sequential determination of inorganic selenium(IV) and selenium(VI). An aliquot (10mL) of a mixture of selenium(IV) and (VI) at a total concentration 10mgmL^{-1} was transferred to a 50mL separating funnel. The mixture was analyzed according to the described procedure for selenium(IV) determination. Another aliquot (10mL) was transferred and analyzed as described before for selenium(VI) determination. On the basis of these procedures, the absorbance (A_1) of the organic extract of the first aliquot will be a measure of the selenium(IV) ions in the mixture, while the absorbance (A_2) of the organic extract of the second aliquot is a measure of the sum of the selenium(IV) and (VI) ions. Therefore, the absorbance ($A_2 - A_1$) is a measure of the selenium(VI) ions in the binary mixture.

2.4 Applications

2.4.1 Sequential determination of selenium(IV) and total inorganic selenium(IV) and (VI) in freshwater.

. Direct determination method: An aliquot (10mL) of water sample was treated with 0.5mL of NaOH (1M) and 0.5mL of EDTA, and then pipetted into a 50mL separating funnel. The solution was centrifuged to remove any formed precipitate, adjusted to pH zero, and 0.5mL of the reagent $\text{Cl}_2\text{H}_2\text{D}_z$ (0.01% w/v) added. The reaction mixture was then made up with water to a total volume of 25mL and swirled well to mix. The mixture was analyzed according to the described procedure for selenium(IV) determination. Another aliquot sample (10mL) was treated as described earlier for selenium(VI) determination.

The concentrations of selenium(IV) and (VI) and total selenium(IV) and (VI) were then determined from the standard curves of selenium(IV) and (VI).

. Standard addition method: Alternatively, the standard addition (spiking) method was used as follows. A known volume (10mL) of the test solution adjusted to pH zero and 0.5mL of the reagent $\text{Cl}_2\text{H}_2\text{D}_z$ (0.01% w/v) were transferred into a 50mL separating funnel. The absorbance displayed by the test solution was then measured before and after spiking with various concentrations (1–5mgmL⁻¹) of selenium(IV), as described for selenium(IV) determination. The change in the absorbance was then used for determining the selenium(IV) concentration in the aliquot sample. Another aliquot of the test sample (10mL) before and after spiking with various concentrations (1–5mgmL⁻¹) of selenium(VI) was treated as mentioned for selenium(VI) determination. Selenium (IV) and the total inorganic selenium(IV) and (VI) were then determined.

3. Results and discussion

3.1 Absorption spectra

The dithizone analogue $\text{Cl}_2\text{H}_2\text{D}_z$ under study has the thioketo(I) and thiol(II) forms (figure 1). The absorption electronic spectra of the reagent $\text{Cl}_2\text{H}_2\text{D}_z$ and its selenium(IV) chelate in n-hexane are shown in figure 2. The absorption electronic spectra of the two reagents H_2D_z and $\text{Cl}_2\text{H}_2\text{D}_z$ showed two well-defined bands in the region of 429–454 and 615–627nm, whereas their selenium(IV) chelates showed one well-resolved single band in the range 416–435nm (table 1). The two chlorine atoms in the para position of the two phenyl nuclei of $\text{Cl}_2\text{H}_2\text{D}_z$ leads to a slight hypsochromic shift for the observed band at 429nm and a bathochromic shift for the band at 627nm

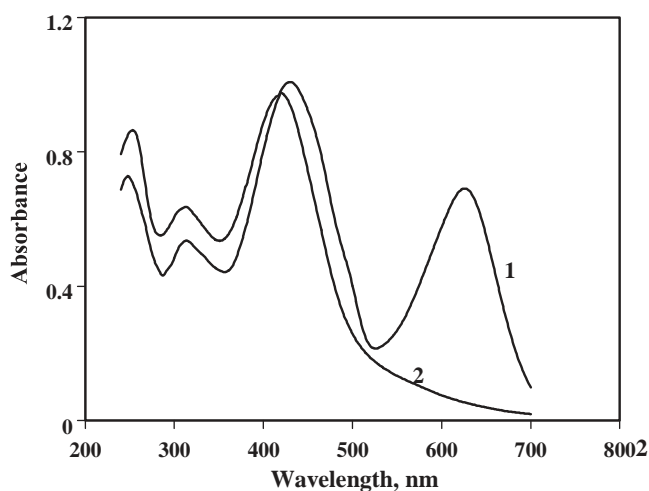


Figure 2. Electronic spectra of the reagent $\text{Cl}_2\text{H}_2\text{Dz}$ (1) and its selenium(IV) chelate (2). Aqueous phase, 10mgmL^{-1} of Se(IV) , 0.2mL of $\text{Cl}_2\text{H}_2\text{Dz}$ (0.01% w/v), and 10mL of n-hexane.

Table 1. Characteristic absorption IR (cm^{-1}) and electronic (nm) spectral data of the reagents H_2Dz and $\text{Cl}_2\text{H}_2\text{Dz}$ and their selenium (IV) chelates in KBr disc and in n-hexane, respectively^a.

Compound	Wavenumber (cm^{-1})				λ_{max} (nm)	$10^4 \text{Lmol}^{-1} \text{cm}^{-1}$
	(N-H)	(N-N)	(N-H) β (-C γ /4N-)	(N-C-S)		
$\text{Cl}_2\text{H}_2\text{Dz}$	2942 (br)	2374 (w)	1504 (s)	1490 (s)	627	2.43
				1450 (s)	429	2.39
H_2Dz	2960 (br)	2365 (w)	1515 (s)	1505 (s)	615	3.53
				1465 (s)	454	1.79
$\text{Se}(\text{Cl}_2\text{HDz})_2\text{Cl}_2$	3436 (m)	1636	1526	1487	416	9.01
	3280 (s)	1580				
$\text{Se}(\text{HDz})_2\text{Cl}_2$	3215 (m)	1610 (s)	1513 (s)	1501 (s)	435	7.01
	3280 (m)	1580 (s)				

^as: strong; m: medium; w: weak; sh: shoulder; br: broad.

compared with H_2Dz (table 1). The value of the molar absorptivity (ϵ) at λ_{max} 627nm decreased to 2.43×10^4 , and that at 429nm increased to $2.39 \times 10^4 \text{Lmol}^{-1} \text{cm}^{-1}$ for the

$\text{Cl}_2\text{H}_2\text{Dz}$ compared with H_2Dz in n-hexane (table 1).

The reagent $\text{Cl}_2\text{H}_2\text{Dz}$ reacts with selenium(IV) in strong acidic medium (2M HCl), to form a yellow-red coloured complex which is insoluble in water and easily soluble in non-polar organic solvents. Based on the electronic spectrum of the produced complex in n-hexane (figure 2), the IR spectral data (table 1), and the results reported earlier for the selenium(IV) chelates of the dithizone [10, 30, 33] and bismuthiol II [34], a structure, III (figure 1), is most

likely proposed for the formed selenium(IV) chelate. Thus, the overall reaction of selenium(IV) with the reagent $\text{Cl}_2\text{H}_2\text{DZ}$ in HCl (2M) most likely proceeds as follows:

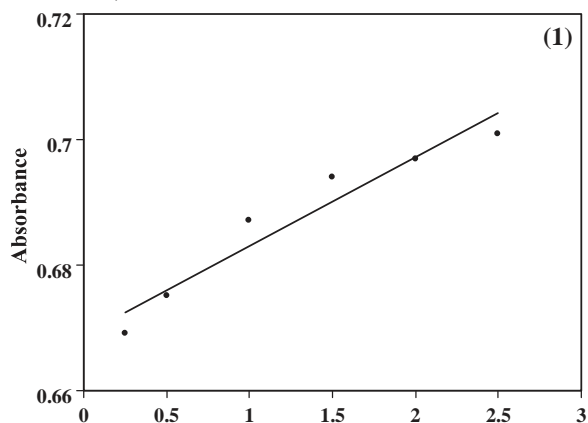


The produced complex has two maxima (figure 2) at 313 ($2.810^3 \text{ Lmol}^{-1} \text{ cm}^{-1}$) and 416nm ($910^4 \text{ Lmol}^{-1} \text{ cm}^{-1}$) in n-hexane which were well resolved and utilized for spectrophotometric determination of selenium(IV). Thus, in the subsequent work, the absorbance data were recorded at 416nm.

The chemical composition of the extracted selenium(IV)– $\text{Cl}_2\text{H}_2\text{DZ}$ chelate in n-hexane was determined by the slope ratio method [35]. The absorbance of n-hexane extracts with a large excess of the reagent and also with a large excess of selenium(IV) solution was finally measured at 416nm against a reagent blank. Plots of the absorbance versus the total concentration of selenium(IV) and also the total concentration of the reagent are shown in figure 3. The slopes of the straight lines obtained on varying selenium(IV) concentrations (S_m) and/or reagent content (S_x) indicated that the selenium(IV) chelate produced has a selenium(IV) to a reagent

$\text{Cl}_2\text{H}_2\text{DZ}$ molar ratio of exactly 1:2 ($S_m/S_x = 1/2$).

To fully characterize the formed selenium(IV) chelate, the n-hexane extract was evaporated under reduced pressure after shaking with ammonia to remove the unreacted reagent $\text{Cl}_2\text{H}_2\text{DZ}$ as reported earlier for selenium(IV) chelate with dithizone [10, 30, 33]. Elemental analysis of the proposed selenium(IV) chelate given in figure 1: $[\text{SeOC}_{26}\text{H}_{18}\text{N}_8\text{S}_2\text{Cl}_4]$ required: 43.6% C, 2.5% H, 15.7% N and 9.6% S; found 42.9%



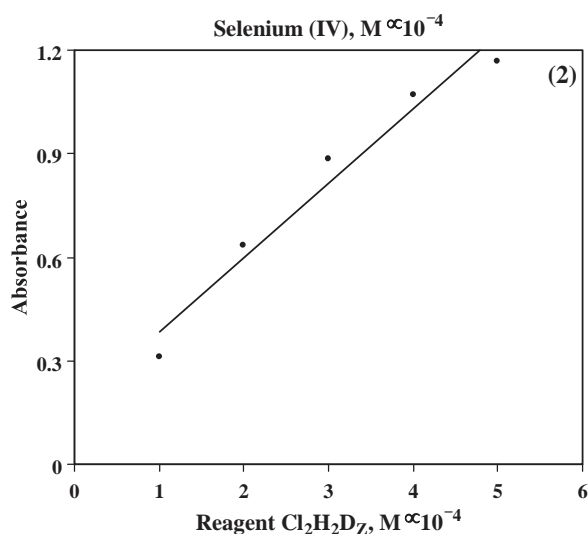


Figure 3. Chemical composition of the selenium(IV) complex by the slope ratio method using excess reagent, 210^4 M (1) and excess selenium(IV), 210^4 M (2).

C, 2.7% H, 15.5% N and 8.9% S. The IR spectra of the isolated solid selenium(IV) chelate recorded separately in KBr discs and as a mechanical mixture of selenium(IV) with $\text{Cl}_2\text{H}_2\text{D}_z$ in a 1:2 molar ratio [28] showed the characteristic frequencies at 3436 (br), 1636 (s), 1526 (s), 1487 (s) and 440cm^{-1} (table 1), which are safely assigned to (N–H), (N–N), (N–H) μ (C–N), (N–C–S), and (Se–Cl) vibrations, respectively [10, 30].

3.2 Optimal experimental conditions for selenium(IV) uptake by liquid–liquid extraction procedure

The effect of pH of the aqueous phase on the extraction of the selenium(IV)– $\text{Cl}_2\text{H}_2\text{D}_z$ complex was studied by measuring the absorbance of the extracted complex in n-hexane at 416 nm. The pH of the aqueous solution was adjusted with dilute HCl and/or NaOH, and directly measured before the extraction. Maximum absorbance of the produced complex was achieved at $\text{pH} < 2$. In acidic solution of $\text{pH} 2$, the protonation of the selenite anions most likely occurred, which enhanced complex formation. In less acidic or alkaline solution, the absorbance decreased, possibly due to the incomplete complex formation, the existence of selenium(IV) as HSeO_3 or SeO_3^{2-} , which minimizes the chelate formation, and finally formation of non-extractable forms of selenium(IV).

The stability of the produced complex species of selenium(VI) was found to depend considerably on the nature and acidity of the aqueous phase. Thus, the effect of a series of mineral acids, e.g. HCl, HNO_3 , H_2SO_4 , and HClO_4 at 1M concentration, was examined. Complete and excellent separation in a short time was achieved using HCl (1M). The influence of HCl concentration (0.5–6M) was then critically investigated. At an HCl

concentration of $>2M$, the extraction of the produced complex decreased due to the possible reduction of selenium(IV) to elemental selenium or selenide [31, 32]. The chromogenic reaction was found to be very fast at room temperature, and the selenium(IV) chelate produced was stable for up to 48h for 2M hydrochloric acid concentration; consequently, HCl (2M) was selected in the subsequent work.

The solubility of the produced selenium(IV) complex was investigated in a series of organic solvents, namely: n-hexane, dichloromethane, carbon tetrachloride, toluene, chloroform, cyclopentanone, and methyl isobutyl ketone. Of these, n-hexane was found to be the best extractant where a maximum apparent molar absorptivity and solubility of the chelate were achieved. Also, the extraction of the developed selenium(IV) chelate in this solvent was completed in a very short time, as a better separation of the layers was obtained. The results also showed that the organic solvents with a low dielectric constant are favoured for the extraction of the chelate produced. However, the extractability of selenium(IV) chelate into $CHCl_3$, which has a dielectric constant higher than n-hexane, was more or less the same as the extractability into n-hexane. This may be due to the solvation of the complex by $CHCl_3$ molecules. The absorbance of the coloured complex in n-hexane was constant for up to 2h for samples containing $10mgmL^{-1}$ selenium(IV) in the aqueous solution containing HCl (2M). Thus, n-hexane was chosen as the preferred organic solvent and a shaking time of 1min was adopted in the subsequent work.

The influence of $Cl_2H_2D_Z$ concentration on the extraction of selenium(IV) complex in n-hexane was investigated with $5mgmL^{-1}$ of selenium(IV). The data are shown in figure 4. The absorbance of the formed complex increased on increasing the reagent $Cl_2H_2D_Z$ concentration for up to $5.110^5 M$ (0.01% w/v). A large excess of the reagent tends to decrease the absorbance of the organic extract, owing to the increased absorbance of the reagent blank.

The effect of NaCl and/or $CaCl_2$ concentration (1–5% w/v) as a measure of water salinity and hardness on the extraction of selenium(IV) complex with the tested reagent from the aqueous solution was studied. No significant effect of these salts was observed in the absorbance of the organic extract of selenium(IV) chelate.

3.3 Extraction equilibria

To calculate the equilibrium constants K_{ex} , , and K_D for the proposed reaction of selenium(IV) with the reagent $Cl_2H_2D_Z$, the following equilibria are considered [36, 37].

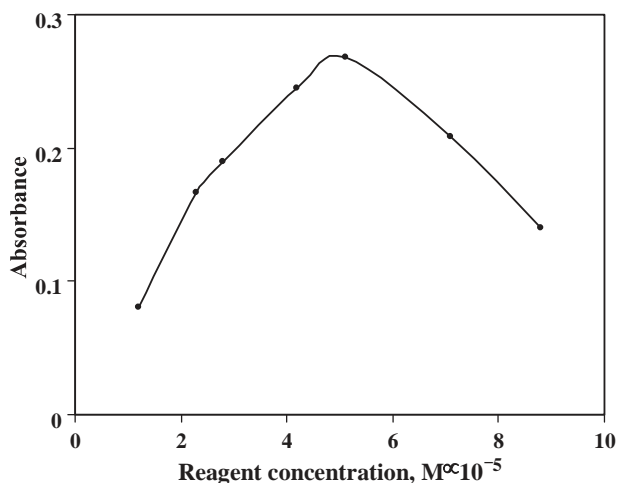


Figure 4. Effect of the reagent Cl₂H₂D_Z concentration [M] on the extraction of selenium(IV) chelate.

Formation of a complex chelate in the aqueous phase containing HCl according to the equation:



with a corresponding equilibrium constant, K_D , where

$$K_D = \frac{[\frac{1}{2}SeO_3Cl_2HDzP_2(aq)]}{[\frac{1}{2}H_2SeO_3(aq)][Cl_2H_2Dz_2(org)]} \quad (4)$$

Distribution of the complex chelate between the aqueous and the organic phase with a distribution constant, K_D

$$K_D = \frac{[\frac{1}{2}SeO_3Cl_2HDzP_2(aq)]}{[\frac{1}{2}SeO_3Cl_2HDzP_2(org)]} \quad (5)$$

$$(6)$$

$$K_D = \frac{[\frac{1}{2}SeO_3Cl_2HDzP_2(org)]}{[\frac{1}{2}SeO_3Cl_2HDzP_2(aq)]}$$

The overall extraction process is then described by the following equation:



with a corresponding extraction constant, K_{ex} .

$$K_{ex} = \frac{[\frac{1}{2}SeO_3Cl_2HDzP_2(org)]}{[\frac{1}{2}H_2SeO_3(aq)][Cl_2H_2Dz_2(org)]} \quad (8)$$

The distribution ratio, D_{Se} , was determined at a constant initial concentration of selenite in the aqueous phase and various concentrations of the reagent Cl₂H₂D_Z in n-hexane. Assuming that one complex species of selenium(IV) is present at equilibrium in the organic phase, the distribution coefficient of the system can be expressed as follows [37]:

$$D_{Se} = \frac{[\frac{1}{2}SeO_3Cl_2HDzP_2(org)]}{[\frac{1}{2}SeO_3Cl_2HDzP_2(aq)] + [\frac{1}{2}H_2SeO_3(aq)]} \quad (9)$$

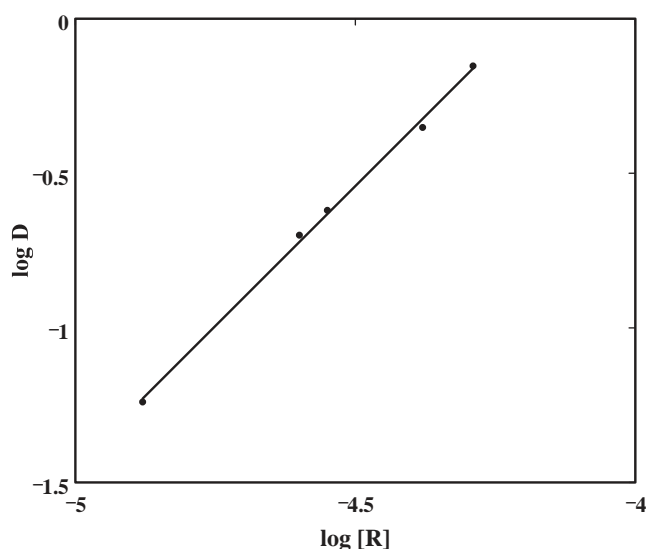


Figure 5. Plot of $\log [\text{Cl}_2\text{H}_2\text{D}_Z]$ vs. $\log D$ of its selenium(IV) chelate in n-hexane.

At a low concentration of $\text{Cl}_2\text{H}_2\text{D}_Z$, the term $[\text{SeO}(\text{Cl}_2\text{HD}_Z)_2]_{(\text{aq})}$ can be neglected, and equation (9) transforms to:

$$D_{\text{Se}} = \frac{1}{4} \frac{1}{2} \text{SeO} \delta \text{Cl}_2\text{HD}_Z \text{P}^{2\delta_{\text{org}}} \frac{1}{2} \text{H}_2\text{SeO}_3 \delta_{\text{aq}} \text{P} \quad \delta_{10} \text{P}$$

After substituting equation (10) into equation (8) and taking the logarithms, equation (11) is obtained as follows:

$$\log D_{\text{Se}} = \frac{1}{4} \log K_D \text{p} \log \frac{1}{2} \text{Cl}_2\text{H}_2\text{D}_Z \delta_{\text{org}} \text{P} \quad \delta_{11} \text{P}$$

The values of K_{ex} , and K_D of the extracted species were then determined graphically from the graph (figure 5) of $\log D_{\text{Se}}$ versus $\log [\text{Cl}_2\text{H}_2\text{D}_Z]_{\text{org}}$. A slope of 2.2 was obtained, indicating the formation of chelate of 1:2 molar ratios of selenite ions to the reagent $\text{Cl}_2\text{H}_2\text{D}_Z$, respectively. These data are in good agreement with the results obtained from the spectral and analytical data. The values of K_{ex} , K_D , and δ were found to be equal to 1.210^4 , 5.6 and 2.110^3 , respectively. These results suggest the possible application of the proposed reagent for extractive sequential spectrophotometric determination of selenium(IV), (VI), and total inorganic selenium(IV) and (VI) in water after reduction of selenate to selenite.

3.4 Spectrophotometric characteristics of selenium(IV) chelate

After adjusting the experimental conditions of the reagent, a linear graph at 416nm was obtained on recording the absorbance of the produced selenium(IV) chelate in n-hexane as a function of the selenium(IV) concentration. Beer's law was obeyed in the concentration range $0.01\text{--}20\text{mgmL}^{-1}$ selenium(IV) in aqueous solution containing HCl (2M). The molar

absorptivity calculated from the Beer–Lambert plot and Sandell's [38] sensitivity index of the selenium(IV)–Cl₂H₂D_Z chelate at 416nm were estimated to be 910⁴ Lmol⁻¹ cm⁻¹ and 0.08mgcm², respectively. The relative standard deviation (S_r) of five measurements with 5mgmL⁻¹ of selenium(IV) is estimated as 2.2%. The detection limit (3) based on three times the SD of the blank [39] was 0.01mgmL⁻¹ of selenium(IV) employing the proposed reagent Cl₂H₂D_Z. Regression analysis of the Beer–Lambert plot of the absorbance at 416nm (A₄₁₆) and the concentration (C, mgmL⁻¹) of selenium(IV) ions in the range 0.01–20mgmL⁻¹ gave the following linear regression equation:

$$A_{416} = 0.0142C + 0.009, \quad r = 0.9992$$

with a slope of 0.0142, intercept of 0.009, and a correlation coefficient of 0.9992 for the complex [SeOC₂₆H₁₈N₈S₂Cl₄]. The effective concentration range of selenium(IV), as evaluated by Ringbom's plot was found to be 0.5–19mgmL⁻¹ [40].

The plot of the amount of selenium(IV) chelate extracted from the bulk aqueous solution into the organic phase versus the amount of selenium(IV) remaining in the bulk aqueous phase varied linearly at low and moderate selenium(IV) concentrations (30mgmL⁻¹), followed by a plateau at a high level of selenite ion concentration, suggesting a first-order behaviour. A solvent capacity of 2mg of selenium(IV) ions uptake/mL n-hexane was achieved successfully with Cl₂H₂D_Z.

3.5 Effect of foreign ions

The influence of a series of diverse ions on the determination of selenium(IV) employing the proposed method was investigated. The tolerance limit was defined as the concentration of the foreign ion added, causing a relative error less than 3%. The selectivity of the developed method at 1mgmL⁻¹ of selenium(IV) was critically examined in the presence of a relatively high excess (0.1–1mgmL⁻¹) of some diverse ions, which often accompany the analyte ion. A percentage recovery of 100±2.5% of selenium(IV) and a standard deviation of 0.38 were achieved in the presence of the ions Li⁺, Na⁺, K⁺, Ca²⁺, NH₄⁺, Al³⁺, Cl⁻, and Br⁻ at 1:100 tolerable concentration of selenium(IV) to the diverse ions, respectively. Positive interferences were observed in the presence of other ions, even at low concentrations, e.g. Cu²⁺, Fe²⁺, MnO₄⁻, V⁵⁺, and NO₃⁻. The reason for these interferences is possibly attributed to the ability of Cl₂H₂D_Z to form relatively stable chelates with such metal ions. Elimination of these interferences from the proposed method was achieved successfully by adding EDTA (0.1%) and other reagents to their aqueous solutions (table 2), which promotes unambiguous and sensitive determination of selenium(IV).

3.6 Sequential determination of selenium(IV) and selenium(VI)

The procedures developed were applied for the analysis of a binary mixture of inorganic selenium(IV) and (VI) ions at a total concentration of 20.0mgmL⁻¹ in the aqueous media. An aliquot mixture was first determined according to the procedure described for selenium(IV) determination. Another aliquot mixture was reduced to selenium(IV) with HCl (6M) and

determined as described in the recommended procedures. The results obtained are summarized in table 3. Satisfactory recoveries (95.6–101.2%) were obtained, with a good reproducibility and a relative standard deviation in the

Table 2. Elimination of the effect of various ions on the determination of selenium (IV).

Foreign ions	Tolerance limit (mgmL ⁻¹)	Note
Cu ₂ p	100	Add 0.5mL of 0.1M EDTA
Fe ₃ p	200	Add 0.5mL of saturated NaF
Mn ₇ p	100	Add a few crystals of NaN ₃
V ₅ p	100	Add 0.5mL of 0.1M EDTA
NO ₃	100	Add a few crystals of NaN ₃

Table 3. Analytical results of determination of binary mixtures of selenium(IV) and (VI).

Selenium species (mgmL ⁻¹) ^a					
Se(IV)		Se(VI)		Recovery (%)	
Taken	Found	Taken	Found	Se(IV)	Se(VI)
10	10.140.21	0	0	101.40.2	–
10	10.160.23	5	4.960.2	101.60.23	99.20.21
10	9.970.19	10	9.90.2	99.70.19	990.22

^a Average (n/45)SD.

range of 1.9–2.3 and 2.1–2.2% for selenium(IV) and (VI), respectively, and compared successfully with the results obtained by dithizone method [10, 12]. These data indicate that the method is applicable with excellent accuracy, even in samples with a high content of dissolved salts, e.g. NaCl and/or CaCl₂.

3.7 Application

The validity of the proposed method for the determination of traces of inorganic selenium(IV) and (VI) in tap and freshwater samples was critically examined. Various amounts (20.0mgmL⁻¹) of selenium(IV) or (VI) and binary mixtures of selenium(IV) and (VI) were spiked to the water samples. Each solution mixture was adjusted to the required acidity, and the selenium(IV) ions were then separated out from the aqueous phase by the reagent Cl₂H₂D_Z in n-hexane. The selenium(IV) in the organic extract was then determined with the aid of the standard curve constructed under the same experimental conditions as described earlier. The total inorganic selenium(IV) and (VI) ions were determined after reduction of selenium(VI) to selenium(IV) ions in the samples. Selenium (VI) ions in the water samples were then determined by the difference (A₂–A₁) between the absorbance of the aliquots before (A₁) and after (A₂) reduction. The data obtained are summarized in table 4. On the basis of these results, tap water samples were found to be free from selenium(IV) and/or (VI). The results obtained by the proposed method were compared favourably to those of the atomic absorption spectrometry (AAS) measurements and the spectrophotometric method involving dithizone

[12] for selenium(IV) ions in tap water samples utilizing certain statistical evaluations. The results of F (0.075) and t (1.91) tests showed no significant differences (table 4) in accuracy and precision between the proposed and the reference method [12]. The low RSD of the developed method evaluated for a series of replicate analysis

Table 4. Analysis of selenium(IV) and (VI) ions spiked to tap water samples (50mL) of selenium(IV) and (VI)^a.

Tap-water sample	Se(IV) added (mgmL ⁻¹)	Se(VI) added (mgmL ⁻¹)	Total Se(IV) and (VI) found (mgmL ⁻¹)
1	10	–	100.2
2	20	–	200.12
3	10	10	20.10.3
4	20	10	30.30.25

^a Average (n=4)SD and t- and F-tests of significance=41.91 and 0.075 at P=0.05, respectively.

of samples containing selenium(IV) at different concentrations reflected a good precision and indicated that the proposed method is applicable with a good accuracy.

4. Conclusion

The proposed method for the determination of inorganic selenium(IV) and/or (VI) ions in aqueous via liquid–liquid extraction is accurate, simple, rapid, and inexpensive; does not involve any stringent reaction conditions; and can be compared favourably in both sensitivity and selectivity with the published methods [13, 16–18]. The formed chelate is very stable, and no standing time is needed before determining the ions. The clear advantage of the method is its applicability for the sequential determination of inorganic selenium(IV) and/or (VI) in freshwater. The method has been applied to the determination of traces of selenium in real matrices as well as in synthetic samples. The use of HCl (5–6M) as a pre-reducing agent permits the quantitative reduction of selenium(VI) to (IV) under relatively simple experimental conditions followed by sequential determination of the produced selenium(IV). Thus, the method can certainly be considered among the most sensitive methods. However, work is still continuing for the sequential determination of total selenium including inorganic and organic bound selenium present in real samples using suitable analytical treatments.

Acknowledgement

The author M. S. El-Shahawi, would like to thank Prof. A. M. Kiwan, for his assistance in the preparation of the reagent Cl₂H₂D₂.

References

- [1] M.I. Sittig. Toxic Metals, Pollution Control and Worker Protection, Noyes Data Corporation, Park Ridge, NJ (1976).
- [2] D.C. Adriano. Biogeochemistry of Trace Metals, Lewis, London (1992). [3] O.A. Levander. Clin. Biochem., 6, 345 (1982).
- [4] L.H. Foster, S. Sumar. Food Chem., 55, 293 (1996).
- [5] G.V. Iyengar, W.E. Kollmer, H.J.M. Bowen. The Elemental Composition of Human Tissues and Body Fluid, Verlag Chemie, Weinheim (1978).
- [6] H. Robberecht, R.V. Grieken. Talanta, 29, 824 (1982).
- [7] W.T. Buckley, J.J. Budac, D.V. Godfrey, K.M. Koenig. Anal. Chem., 64, 724 (1992).
- [8] M.S. Alaejos, D. Romero. Crit. Chem. Rev., 95, 227 (1995).
- [9] R.M. Olivás, O.F.X. Donard, C. Camara, P. Quevauviller. Anal. Chim. Acta, 286, 357 (1994).
- [10] A.D. Campbell, A.H. Yahaya. Anal. Chim. Acta, 119, 171 (1980).
- [11] S.C. Lavale, M. Dave. J. Indian Chem. Soc., 66, 974 (1989).
- [12] H. Afsor, R. Apak, I. Tor. Analyst, 114, 1319 (1989).
- [13] B.L. Osburn, A.D. Shrendrikar, P.W. West. Anal. Chem., 43, 594 (1971).
- [14] K.N. Ramachandran, R. Kaveeshwar, V.K. Gupta. Talanta, 40, 781 (1993).
- [15] A. Safavi, A. Afkhami, A. Massoumi. Anal. Chim. Acta, 232, 351 (1990).
- [16] R. Gurkan, M. Akcay. Microchem. J., 75, 39 (2003).
- [17] A. Afkhami, T. Madrakian. Talanta, 58, 311 (2002).
- [18] K. Pyrzynska. Anal. Sci., 13, 629 (1997).
- [19] H. Khajehsharifi, M.F. Mousavi, J. Ghasemi, M. Shamsipur. Anal. Chim. Acta, 512, 369 (2004).
- [20] H.D. Revanasiddappa, T.N.K. Kumar. Anal. Sci., 17, 1309 (2001).
- [21] A. Afkhami, A. Safavi, A. Massoumi. Talanta, 39, 993 (1992).
- [22] P. Kuban, V. Kuban. Anal. Bioanal. Chem., 378, 378 (2004).
- [23] P. Kuban, P. Kuban, V. Kuban. Electrophoresis, 24, 3725 (2003).
- [24] A. Safavi, M. Mirzaee. Talanta, 51, 225 (2000).
- [25] M. Gallignani, M. Valero, M.R. Brunetto, J.L. Burguera, M. Burguera, Y. Petit de Pena. Talanta, 52, 1015 (2000).
- [26] P. Kuban, P. Kuban, V. Kuban. Electrophoresis, 24, 1397 (2003).
- [27] B.M. Nagabhushara, G.T. Chandroppe, B. Nagappo, N.H. Nagaraj. Anal. Bioanal. Chem., 373, 279 (2002).
- [28] M.S. El-Shahawi, M.A. El-Sonbati. Talanta, 67, 806 (2005).
- [29] A.M. Kiwan, A. Kassim. Anal. Chim. Acta, 88, 177 (1977).
- [30] H. Mabuchi, H. Nakahara. Bull. Chem. Soc., 36, 151 (1963).
- [31] U. Ornemark, A. Olin. Talanta, 41, 67 (1994).
- [32] I.L. Stewart, A. Chow. Talanta, 40, 1345 (1993).
- [33] Z. Marczenko. Separation and Spectrophotometric Determination of Elements, Wiley, New York (1986). [34] J.E. Barmey. Talanta, 14, 1363 (1967).
- [35] D.T. Sawyer, W.R. Heineman, J.M. Beebe. Chemistry Experiments for Instrumental Methods, Wiley, New York (1984).
- [36] A. Alexandrov, O. Budevsky, A. Dimitrov. J. Radioanal. Chem., 29, 243 (1976).
- [37] S.M. Kamburova. Talanta, 39, 997 (1992).
- [38] E.B. Sandell. Colorimetric Determination of Trace Metals, Interscience, New York (1959).
- [39] IUPAC. Pure Appl. Chem., 45, 105 (1976).
- [40] A. Ringbom. Fresenius Z. Anal. Chem., 115, 332 (1939).

Determination of Trace Levels of Diosmin in a Pharmaceutical Preparation by Adsorptive Stripping Voltammetry at a Glassy Carbon Electrode

M. S. EL-SHAHAWI,^{*18} A. S. BASHAMMAKH,^{*} and T. EL-MOGY^{**}

^{*}Department of Chemistry, Faculty of Science, King Abdulaziz University,
P. O. Box 80203, Jeddah 21589, Kingdom of Saudi Arabia

^{**}Department of Chemistry, Faculty of Science at Damietta, Mansoura University, Mansoura 34517, Egypt

A systematic study on the electrochemical behavior of diosmin in Britton–Robinson buffer (pH 2.0 – 10.0) at a glassy carbon electrode (GCE) was made. The oxidation process of the drug was found to be *quasi*-reversible with an adsorption-controlled step. The adsorption stripping response was evaluated with respect to various experimental conditions, such as the pH of the supporting electrolyte, the accumulation potential and the accumulation time. The observed anodic peak current at +0.73 V vs. Ag/AgCl reference electrode increased linearly over two orders of magnitude from 5.0×10^{-8} M to 9.0×10^{-6} M. A limit of detection down to 3.5×10^{-8} M of diosmin at the GCE was achieved with a mean recovery of $97 \pm 2.1\%$. Based on the electrochemical data, an open-circuit accumulation step in a stirred sample solution of BR at pH 3.0 was developed. The proposed method was successfully applied to the determination of the drug in pharmaceutical formulations. The results compared favorably with the data obtained *via* spectrophotometric and HPLC methods.

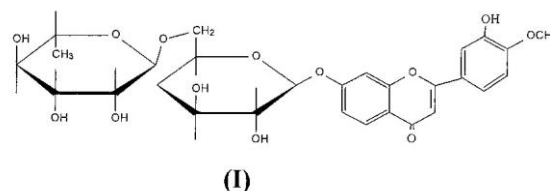
(Received September 4, 2005; Accepted November 21, 2005)

Introduction

Diosmin, which is chemically named 3',5,7-trihydroxy-4'-methoxy flavone 7, rutinoside (I), is a newly developed flavonoid in *Rutaceae* plants. Flavonoids are widely used for their phlebotonic and antioxidant properties, and also as vascular protectors.^{1–8} Recent clinical studies have demonstrated that the diosmin can be used to treat venous leg ulcers and hemorrhoids.³ Diosmin drug has been successfully used as chemopreventive agents in urinary-bladder⁹ and colon carcinogenesis.¹⁰ The drug shows good tolerability and is quite safe and nontoxic.³ Diosmin has certain biological activities, including an anti-inflammatory effect and an inhibition of prostaglandin synthesis.¹¹ In view of increasing interest in these bioflavonoids, especially that used in treating chronic venous, chronic hemorrhoids and as antioxidants, several methods have been reported for the determination of diosmin in plant extracts,^{12,13} biological fluids,^{13,14} and pharmaceutical formulations.¹² A survey of the literature revealed that there are few methods for diosmin determination in pharmaceutical formulations or biological fluids. These methods include: spectrophotometry, spectrodensitometry,¹⁵ and liquid chromatography¹⁶ as well as HPLC methods.¹⁷ Recently, an excellent HPLC method for the simultaneous determination of diosmin in flavonoid extracts and soft gelatin capsules has been published.¹⁷ Currently, no literature data could be found on the electrochemical behavior of diosmin, in general, or its voltammetric determination, in particular.

Therefore, the aim of the present study is to investigate the oxidative behavior of the diosmin at GCE using cyclic

voltammetry (CV) and differential pulse voltammetric (DPV) techniques, and also to optimize the experimental conditions for the determination of this compound in pharmaceutical dosage forms. A methodology for the direct and simple determination of the drug in spiked human serum at a very low level is also included.



Experimental

Reagents and solutions

Diosmin and Dioven[®] tablets were obtained from Amriya Rhone-poulenc Pharmaceutical Industries Co., Alexandria, Egypt. The stated composition of each tablet contains 150 mg diosmin. A diosmin stock solution (1×10^{-3} M) of diosmin was prepared daily by dissolving an appropriate amount in 2 ml of NaOH (0.02 M) and completed to 10 ml with double-distilled water. Dilute solutions were then prepared by diluting the stock solution with water in calibrating measuring flasks, transferred to polyethylene bottles, and were finally kept in a refrigerator. A series of Britton–Robinson (BR) universal buffer solutions of various pH values ranging from pH 2.0 – 10.0 were prepared and used as supporting electrolytes. The BR buffer solutions were prepared by mixing an

¹⁸ To whom correspondence should be addressed.

E-mail: mohammad_el_shahawi@yahoo.co.uk

acid mixture containing acetic (0.04 M), orthophosphoric (0.04 M), and boric acids (0.04 M), and adjusting the pH with an appropriate volume of sodium

1352

hydroxide (0.2 M) solution to the required pH. All solutions were then prepared from Analar-grade reagents in doubledistilled water, and were kept in a refrigerator.

Apparatus

Cyclic, linear sweep and differential pulse voltammetric (DPV) experiments were performed using an AEW2 electrochemical workstation controlled by the EC prog3 electrochemistry software (Sycopel, UK). A thermostated three-compartment electrochemical cell system incorporating a glassy carbon disc electrode (BAS Model MF-2012, $\Phi = 3$ mm) as a working electrode, an Ag/AgCl (3 M KCl) (BAS Model MF-2063) as a reference electrode and a platinum-wire (BAS Model MW-1032) as an auxiliary electrode was used. The solution was deaerated with pure nitrogen before making contact with GCE and the commencement of electrochemical cell. The operating conditions for the DPV were a pulse amplitude of 50 mV, a pulse width of 30 ms, and a scan rate of 10 mV s⁻¹. A Schott Geräte CG 808 digital pH-meter with a H61 pH combination electrode (Mainz, Germany) with an accuracy of ± 0.02 pH was used for pH measurements.

Procedures

Adsorptive stripping differential pulse voltammetry. The transfer of a known volume (5 ml) of the BR buffer electrolyte solution was made into a 10 ml voltammetric cell deaerated under a nitrogen flow for 10 min, and the electrodes were then immersed in the tested solution. All scans were then initiated in the positive direction with an applied potential scan from +0 V to +1.2 V. After measuring the blank solution, an appropriate amount of the standard diosmin solution was introduced into the cell, while the solutions were purged with nitrogen, and then the deposition and stripping steps were repeated. An anodic potential sweep was then carried out under different operational parameters. Before each measurement, the glassy carbon electrode was polished manually with alumina (0.5 mm) dispersed in bidistilled water on a smooth polishing cloth, and gently dried with tissue paper. All measurements were then carried out at room temperature ($25 \pm 1^\circ\text{C}$) under a nitrogen atmosphere. The peak current heights were evaluated by means of the tangent method.^{18,19}

The influence of the scan rate ($v = 10, 20, 50, 100$ and 200 mV s⁻¹) on the cyclic voltammetry of diosmin was investigated using the same solution. At each scan rate, the initial conditions at the electrode surface were restored. The preconcentration step on the analysis of diosmin was critically examined by immersing the polished glassy carbon electrode in a stirred solution (5 ml) of BR buffers containing a known concentration of the drug at a selected period of time. During this period, no potential was applied to the electrode. The stirring was then stopped for an equilibrium time of 15 s and a differential pulse measurement of the surface species was then recorded. The accumulation step was accomplished in the potential range from 0 to +1.2 V. The surface of the glassy carbon electrode was regenerated before each experiment. The electrode was then immersed in a cell solution containing the blank electrolyte until the voltammogram corresponding to the minimum of residual current was obtained. The electrode was then transferred and immersed in the sample solution.

An experimental procedure involving adsorptive stripping voltammetry medium-exchange²⁰ preconcentration was carried out for the analysis of diosmin. The effect of the pH of the

preconcentration solution on the current signal was studied for 5.0×10^{-5} M diosmin at the glassy carbon electrode in BR buffer solutions over the pH range 2.0 – 10.0

ANALYTICAL SCIENCES OCTOBER 2006, VOL.

22

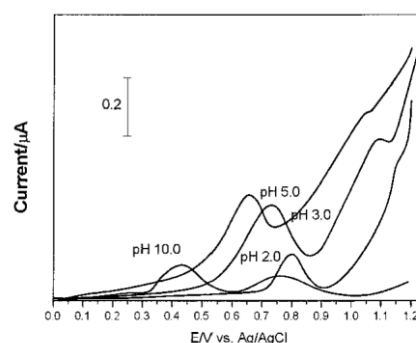


Fig. 1 DPVs for diosmin (5×10^{-5} M) in BR buffers at GCE. Scan rate, 10 mV s⁻¹; pulse amplitude, 50 mV; pulse width, 30 ms.

Tablets assay procedures. In the analysis of diosmin in pharmaceutical dosage, one Dioven tablet was ground to a homogeneous fine powder in a mortar. An amount of this powder corresponding to a 1×10^{-3} M stock solution of diosmin was accurately weighed, transferred into a 10 ml calibrated flask containing 2 ml of NaOH (0.02 M) and finally completed to the mark with distilled water. The contents of the flask were sonicated for 10 min to achieve complete dissolution. The analyzed solutions were then prepared by diluting aliquots of the clear supernatant with the BR buffer at the optimum pH. Voltammograms of the standard solutions of diosmin were also accomplished in a similar way as for the unknown sample solutions of diosmin by adding increasing amounts of the standard diosmin solution to the voltammetric cell. The diosmin content (mg) in the tested sample solution was finally calculated from the prepared standard calibration plot.

Results and Discussion

Electrochemical behavior of diosmin

No previous electrochemical data were available concerning the redox mechanism of diosmin. Thus, preliminary DPV experiments of diosmin (5.0×10^{-5} M) in BR buffer over a wide range of pH 2.0 – 10.0 at GCE were carried out. The DPV showed one well-defined anodic peak accompanied by an illdefined peak at the employed pH range. Therefore, the analytical application in the present study was focused mainly on the first oxidation peak. A representative differential pulse voltammogram recorded for diosmin (5.0×10^{-5} M) at GCE in a BR buffer of pH 3.0 is shown in Fig. 1. Upon increasing the solution pH, the anodic peak potential of diosmin shifted to less-positive values with a slope of 48.8 mV/pH unit (Fig. 2a). This shift is quite close to the theoretical value expected for an electrode reaction involving a 1:1 ratio of electrons/protons.^{21,22} The effect of the solution pH on the peak current is also shown in Fig. 2b. At pH 3, an excellent signal enhancement accompanied by a sharp response was obtained. Thus, in subsequent work, a supporting electrolyte of pH 3.0 was chosen. A typical cyclic voltammogram recorded from 0.0 to +1.2 V versus Ag/AgCl for diosmin (5.8×10^{-4} M) at GCE in BR buffer of pH 3.0 is shown in Fig. 3. In the reverse scan, a cathodic counter

part of the main peak was observed. At various scan rates, the CV showed that the main anodic peak current (i_{p1}) is directly proportional to the sweep rate (v). The dependence of the cathodic and anodic peak currents on the scan rate; v , and $v^{1/2}$ was critically investigated. The relationship between $i_{p,c}$ or $i_{p,a}$ and v is a straight line. The current due to the reduction and

ANALYTICAL SCIENCES OCTOBER 2006, VOL. 22

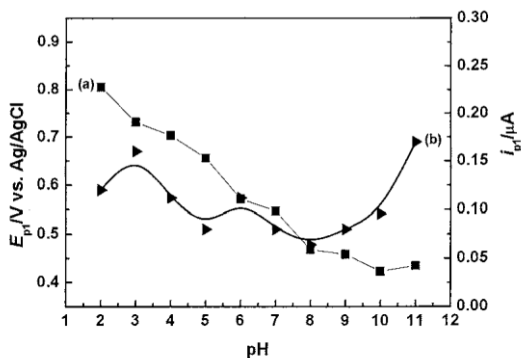


Fig. 2 Effect of the pH on the peak potential (a) and peak current (b) in BR buffers using DPV at GCE diosmin concentration, 5×10^{-5} M; scan rate, 10 mV s^{-1} ; pulse amplitude, 50 mV; pulse width, 30 ms. oxidation is expected to very linearly with v , rather than with $v^{1/2}$. These results indicate that the oxidation of diosmin depends predominately on the adsorbed molecules at the changed interface. This trend is in accord with the adsorption as the rate-limiting step. This wave is *quasi-reversible*; because the peak–peak separation potential ($E_{pa}-E_{pc}$) was found to be 0.1 V, which is greater than $0.059/n$ V, and increased upon increasing the scan rate. Thus, the heterogeneous electron transfer rate is relatively slow and the redox process is *quasireversible*.^{21,23,24} The ratio of the cathodic to the anodic peak currents (i_{pa}/i_{pc}) depends on the sweep rate, and is less than unity, indicating the presence of coupled chemical (CE) reactions.^{22,25} The electrochemical oxidation of diosmin appears to be a complex process, and different reaction pathways are possible. The first oxidation process can be postulated as being an overall one-electron/one proton oxidation of the anisole moiety of the diosmin molecule (peak A), which is reduced in the reverse scan. Upon the reverse scan, the chromone moiety is then reduced (peak B) and reoxidized to the chromone moiety (peak C). The surface coverage attained maximum adsorption obtained for 3.0×10^{-7} mol/l diosmin after a 120 s accumulation period (Fig. 4). Thus, subsequently, an accumulation of 120 s was selected.

The effect of the accumulation potential at the open-circuit potential was investigated. The adsorptive behavior at GCE is independent of the accumulation potential due to the nonelectrochemical nature of the adsorptive process. Considering these data, an open-circuit condition for stripping analysis was selected. The peak current *versus* the accumulation time plots for 5×10^{-4} (a) and 3.0×10^{-7} (b) M diosmin is shown in Fig. 4. The intersections of these graphs with the peak current axis may be attributed to the fact that the adsorption took place during the equilibrium time, which was fixed at 150 s. The breaks at certain stripping times *i.e.* 120 s for 3.0×10^{-7} M and 5.0×10^{-4} M diosmin, mean that the oxidation of the adsorbed diosmin molecules yields a well-defined anodic peak at +0.73 V *versus* Ag/AgCl. The peak height of this peak increased upon increasing the preconcentration time, indicating an enhancement of the concentration of diosmin molecules at the electrode surface, and a linear relationship was observed for a 2-min accumulation time. Also, for a 2-min preconcentration period, an approximately 4-fold enhancement of the peak current was observed over that attained

by the conventional solution-phase pulse voltammetry (0 min). Above 2 min, the accumulation of the peak current started to decrease, suggesting saturation coverage of the electrode surface, although such sensitivity is important. The method also

1353

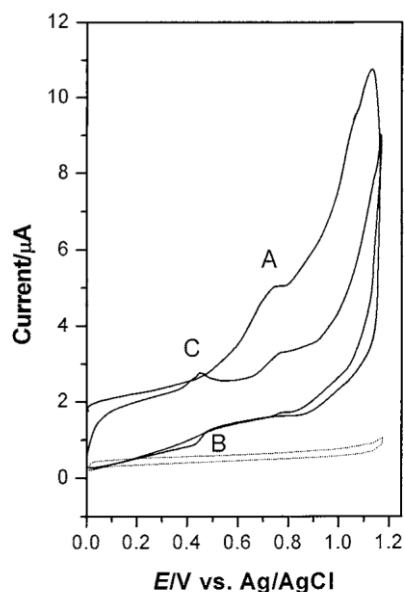


Fig. 3 CVs of diosmin (2.8×10^{-4} M) solution at GCE and 50 mV s^{-1} scan rate. The dotted line represents the blank solution.

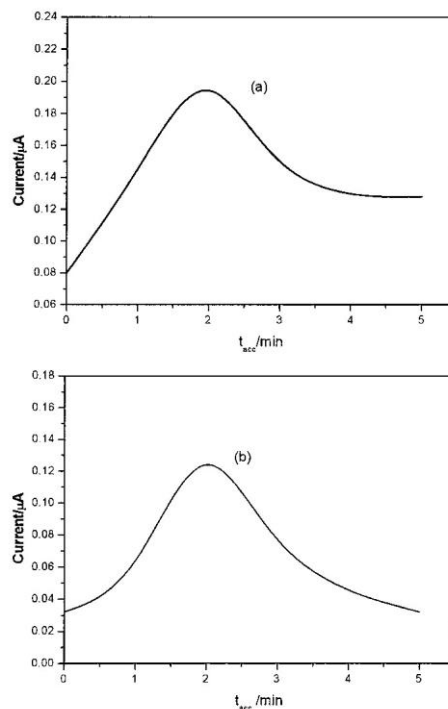


Fig. 4 Effect of the accumulation time (t_{acc}) on the peak current of diosmin at 5×10^{-4} M (a) and 3×10^{-7} M (b) concentration levels.

offers good selectivity based on the medium-exchange steps *i.e.* the electrode was transferred after preconcentration had been finished into another cell at the same pH. Thus, in the subsequent experiments, an open-circuit potential was chosen at a 2-min preconcentration time. Under the optimum experimental

conditions, the peak current at a potential of +0.73 V increased linearly over two orders of magnitude of concentration from 5.0×10^{-8} M to 9.0×10^{-6} M (Fig. 5).

The characteristics of the calibration graph of the peak current versus the concentration calculated from the linear regression, 1354

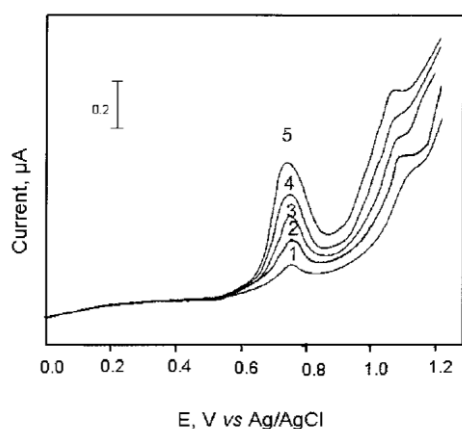


Fig. 5 DPVs of diosmin at various concentrations: 5.8×10^{-8} (1), 1.6×10^{-7} (2), 2.3×10^{-7} (3), 3.3×10^{-7} (4) and 4.4×10^{-7} M (5). Scan rate, 10 mV s^{-1} ; pulse amplitude, 50 mV; pulse width, 30 ms. The dotted lines represent the blank solution.

were: slope, $0.03085 \text{ } \mu\text{A}/\mu\text{M}$; current intercept, $0.1118 \text{ } \mu\text{A}$; and correlation coefficient, 0.9998. At concentrations higher than 1.0×10^{-7} M diosmin, a deviation from linearity was observed due to adsorption saturation of the electrode surface. Shortening the preconcentration period or diluting the sample also extended the linearity. A detection limit of approximately 3.5×10^{-8} M was obtained²⁶ with a 120-s preconcentration time. The reproducibility was determined for 10 replicate experiments with 5.0×10^{-8} M diosmin using DASV; the obtained relative standard deviation was 2.5%.

Analysis of diosmin in dosage forms and in serum

The proposed procedures were successfully applied for the diosmin assay in pharmaceutical formulations. One Dioven tablet (150 mg) was ground to a homogeneous fine powder in a mortar. Voltammograms of the standard solutions of diosmin were then recorded in a similar way as for the unknown sample solutions of diosmin. The concentration was then calculated from a calibration plot of the standard diosmin solution. The diosmin content (mg) in the tested sample solution obtained (4×10^{-6} M) by the proposed method ($98.7 \pm 1.8\%$) was found, and is in accord with the reported ($99.6 \pm 2.1\%$) and the official ($99.2 \pm 2.4\%$) assay methods.^{16,17}

The possibility of applying the preconcentration/medium exchange methodology for the determination of diosmin in human serum was tested. The drug determination in spiked serum samples (100 μl) was critically determined. Three replicate samples containing diosmin at concentrations of 1.0×10^{-6} , 2.0×10^{-6} and 3.0×10^{-6} M were recorded employing the recommended procedures. A recovery percentage in the range $99.2 \pm 1.6\%$ was successfully achieved.

Conclusions

The proposed voltammetric methods at GCE provide the advantages of simplicity, precision and accuracy for the analysis of diosmin in compared with the reported method. The methods are also free from any interference of commonly used excipients and additives in the formulations of the drug. The method was successfully substantially improved for the analysis of diosmin by allowing the drug to accumulate interracially at the GCE. A preconcentration/medium exchange methodology involving the

ANALYTICAL SCIENCES OCTOBER 2006, VOL.

22

transfer of the electrode to a blank solution between the accumulation and measurement steps has been successfully applied for diosmin analysis. The method compares favorably in both sensitivity and selectivity with most of the unpublished methods for the determination of diosmin, and it can thus certainly be placed among the sensitive ones.

Acknowledgements

The author M. S. El-Shahawi would like to thank Dr. A. Radi for the help provided to one of the coauthors (T. El-Mogy) at the early stage of the work.

References

1. P. D. Smith, *J. Vas. Res.*, **1999**, 36, 24.
2. Y. Manuel, B. Keenoy, J. Vertommen, and I. De Leeuw, *Diabetes Nut. Metab.*, **1999**, 12, 256.
3. G. Hitzengerger, *Wein. Med. Wochenschr.*, **1997**, 174, 409.
4. R. Stantus, L. Perdrix, J. Haigle, P. Morliere, C. Maziere, and C. Labrid, *Photodermatol. Photoimmunol. Photomed.*, **1991**, 8, 200.
5. P. Villa, D. Cova, L. De Francesco, A. Guaitani, G. Palladini, and R. Perego, *Toxicology*, **1992**, 73, 179.
6. J. Remacle, A. Houbion, and C. Michiels, *Phlebologie*, **1991**, 44, 881.
7. Y. Tsouderos, Z. Kardiol, and J. Remacle, *Phlebologie*, **1991**, 80, 95.
8. C. Michiels, T. Arnould, A. Houbion, and J. Remacle, *Phlebologie*, **1991**, 45, 779.
9. M. Yang, T. Tanaka, Y. Hirose, T. Deguchi, H. Mori, and Y. Kawada, *Int. J. Cancer*, **1997**, 73, 719.
10. T. Tanaka, H. Makita, K. Kawabata, H. Mori, M. Kakumoto, and K. Satoh, *Carcinogenesis*, **1997**, 18, 957.
11. E. M. Galati, M. T. Monforte, S. Kirjavainen, A. M. Forestieri, and A. Trovato, *Il Farmaco*, **1994**, 49, 709.
12. F. A. El-Yazbi, M. El-Swify, and Y. Hawam, *Bull. Fac. Pharm. Cairo Univ.*, **1999**, 37, 19.
13. C. W. Chang, S. L. Hsiu, P. P. Wu, S. C. Kuo, and P. D. L. Chao, *J. Food Drug Anal.*, **1997**, 5, 111.
14. D. Cova, L. De Angelis, F. Giavarini, G. Palladini, and R. Perego, *Int. J. Clin. Pharm. Therap. Toxicol.*, **1992**, 30, 29.
15. A. El Bayoumi, *Anal. Lett.*, **1999**, 32(2), 383.
16. A. M. El-Shafae and M. M. El-Domiaty, *J. Pharm. Biomed. Anal.*, **2001**, 26(4), 539.
17. F. I. Kanaze, C. Gabriele, E. Kokkalou, M. Georgarakis, and I. Niopas, *J. Pharm. Biomed. Anal.*, **2003**, 33, 243.
18. W. R. Heineman and P. T. Kissinger, *J. Am. Lab.*, **1982**, 60(9), 29.
19. P. Delahay, "New Instrumental Methods in Electrochemistry", **1966**, Chap. 6, Interscience, New York.
20. R. Kalvoda and M. Kopanica, *Pure Appl. Chem.*, **1989**, 61, 97.

21. R. S. Nicholson and I. Shain, *Anal. Chem.*, **1964**, *36*, 706.
22. J. E. B. Randles, *Trans Faraday Soc.*, **1948**, *44*, 327.
23. A. J. Bard and L. R. Faulkner, "*Electrochemical Methods: Fundamentals and Applications*", **1980**, Wiley, New York, 213 – 242.
24. A. M. Bond, "*Modern Polarographic Methods in Analytical Chemistry*", **1980**, Marcel Dekker, New York, 186.
25. A. Sevcik, *Collect. Czech. Chem. Commun.*, **1948**, *13*, 349.
26. J. C. Miller and J. N. Miller, "*Statistics for Analytical Chemistry*", **1993**, Ellis Horwood Series, PTR Prentice Hall, New York, London, 119 – 121.

Spectrophotometric Determination of Copper(II) in Natural Waters, Vitamins and Certified Steel Scrap Samples Using Acetophenone-*p*-chlorophenylthiosemicarbazone

S.E. Ghazy^{a,*}, R.M. El-Shazly^a, M.S. El-Shahawi^b, G.A.A. Al-Hazmi^a and A.A. El-Asmy^a

^a
Chemistry Department, Faculty of Science, Mansoura University, Mansoura, Egypt
Chemistry Department, Faculty of Science, Mansoura University, Damietta, Egypt

^b

(Received 15 May 2005, Accepted 12 February 2006)

A very simple, highly sensitive and selective spectrophotometric procedure was developed for the determination of copper(II). It is based on the reaction at pH 4-9 between the synthesized acetophenone-*p*-chlorophenylthiosemicarbazone (A-*p*-CIPT) and Cu(II) forming a green complex, Cu(II):A-*p*-CIPT (1:2), that floats quantitatively with oleic acid (HOL) surfactant. It exhibits a constant and maximum absorbance at 600 nm in both aqueous and surfactant layers. Beer's law is obeyed over the concentration range 0.25-6.35 mg l⁻¹ with a detection limit of 0.021 mg l⁻¹ for a standard aqueous solution of Cu(II) with a concentration of 3.82 mg l⁻¹ (calculated on the basis of 3σ) and molar absorptivities of 5.5 × 10³ and 1.3 × 10⁴ mol l⁻¹ cm⁻¹ in aqueous and surfactant layers, respectively. Sandell's sensitivity was calculated to be 0.244 μg cm⁻² and the relative standard deviation (n = 9) was 0.19%. The different analytical parameters affecting the flotation and determination processes were examined. The proposed procedure has been successfully applied to the analysis of Cu(II) in natural waters, certified scrap steel samples and vitamin samples. The results obtained agree well with those samples analyzed by atomic absorption spectrometry (AAS). Moreover, the flotation mechanism is suggested based on some physical and chemical studies on the solid complexes isolated from aqueous and surfactant layers.

Key words: Copper, Spectrophotometry, Flotation, Natural waters, Vitamins, Certified samples

INTRODUCTION

Many industrial wastewater streams (such as those used in metal works, semiconductor, and copper industries, mining, etc.) contain heavy metals, which are of great environmental concern and must be removed prior to water discharge or water recycling [1-3]. Copper has received considerable attention

owing to its uses in metallurgy and chemical industries. Moreover, it is an essential constituent of about thirty enzymes and glycoproteins and is required for the synthesis of hemoglobin and for some biological processes. It

*Corresponding author. E-mail: ghazyse@mans.edu.eg

also promotes iron absorption from the gastrointestinal system, is involved in the transport of iron from tissues into plasma, helps to maintain myelin in the nervous system, is important in the formation of bone and brain tissues and is necessary for other many important functions [4,5].

When levels of Cu exceed certain values, however, defense mechanisms to protect against excess Cu are overcome and toxicity results. The reported list of toxic Cu species [6] often includes $\text{Cu}(\text{OH})^+$, $\text{Cu}_2(\text{OH})_2^{2+}$, and CuCO_3 . However, without doubt, Cu^{2+} ions that are present in various aqueous solutions (their presence is a function of pH) are considered to be the most toxic of dissolved copper species [4,6]. Excess copper in water is not only harmful to human beings, but also interferes

with the self-purification of bulk water [7] and exerts an adverse effect on the microbiological treatment of wastewater [8]. Therefore, from the viewpoints of pollution, environmental

of metal ions including evaporation of solvents, electro-deposition, liquid-liquid extraction, surface adsorption, precipitation, ion exchange, ion exchange impregnated materials, immobilized reagents, electro-osmosis and flotation have been reported [9]. Although some of these techniques may be tedious, having limited concentration factors, lengthy and rigid conditions for the separation of solid adsorbents [10], the flotation technique has many advantages that overcome these drawbacks. It has recently received considerable interest owing to its simplicity, rapidity, economy, good separation yields ($R > 95\%$) for small impurity agent concentrations (10^{-6} - 10^{-2} M), a good prospect for application for species having different nature and structure, flexibility and friability of equipment and processing for recovery purpose [11]. It is believed that this process will soon be incorporated as a clean technology to treat water and wastewater [12]. Moreover, flotation is suggested as a method for elimination of interferences [13].

Spectrophotometry still represents an attractive technique for the determination of metal ions in aqueous media because of its simplicity, being inexpensive and is readily available [14]. Therefore, spectrophotometry after selective flotation was chosen for this investigation.

Copper has been removed and/or analyzed in simulated waste solutions, human hair and natural waters by flotation [5,15-24]. Although a vast number of reagents are available for the spectrophotometric determination of copper [5,16,25,32], little

chemistry, geochemistry, marine biology and analytical control in industrial, food, agricultural, pharmaceutical and clinical areas, it is necessary to establish a rapid, simple, sensitive and accurate procedure for the selective concentration of Cu^{2+} prior to its determination.

Numerous techniques for the separation and concentration Cu(II) in the surfactant layer directly after separation by flotation; thus overcoming the problems of elution.

EXPERIMENTAL

Reagents

Unless otherwise stated, all chemicals used were of analytical-reagent grade. Doubly distilled water was used for preparing aqueous solutions. Acetophenone-*p*-chlorophenyl-

thiosemicarbazone, A-*p*-CIPT (Chart 1) was synthesized as work has been done using A-*p*-CIPT and perhaps no trial has been made to float and analyze the analyte with this reagent. Therefore, this work aims to develop a simple and rapid procedure for the selective separation and determination of Cu(II) in natural waters, certified and vitamin samples using HOL as a surfactant and A-*p*-CIPT as a chelating agent. The procedure involves the spectrophotometric determination of has been described elsewhere [33] by condensation of a hot solution of 1:1 4-*p*-chlorophenylthiosemicarbazide with acetophenone. The resulting solution was boiled under reflux for 2h. Then the yellowish-white crystals of A-*p*-CIPT were filtered off, washed with ethanol, recrystallized from absolute ethanol and finally dried in a vacuum desiccator over anhydrous CaCl_2 . The purity was checked by elemental analysis and spectral (mass and infrared) studies. The product is crystalline (m.p.: 192 °C) sparingly soluble in ethanol but easily soluble in acetone, DMF and DMSO; hence its stock solution (1.0×10^{-3} M) was prepared in acetone. Oleic acid (HOL) stock solution (6.36×10^{-2} M) was prepared by dispersing 20 ml of HOL (food grade with sp. gr. 0.895, provided by J.T. Baker Chemical Co.) in 1 l of kerosene. Copper stock solution was prepared by dissolving the requisite amount of $\text{CuCl}_2 \cdot 2\text{H}_2\text{O}$ in doubly distilled water.

CH₃

Spectrophotometric Determination of Copper(II)

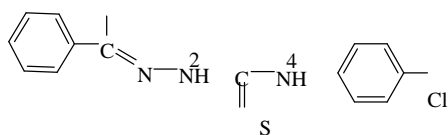


Chart 1

Sample Collection and Pretreatment

One liter of tap, Nile or Seawater samples was filtered, the pH adjusted to 1 with concentrated HCl to prevent losses by sorption or coprecipitation, and preserved in high quality clean plastic containers.

Certified Scrap Steel Sample

The steel sample (#21899), kindly supplied by the Analytical Chemistry Laboratory Service, at the Physikalisch-Technische Bundesanstalt (PTB), Braunschweig, Germany, had the following characteristics: 0.519% copper (by weight); other main components include Cr, Ni, Mn, Zn, with traces of C, P, Si, S, V, Ti, Mo, and Co.

A weighed amount of the sample (200-300 mg) was digested with 10 ml of aqua regia and heated to near dryness. Then the sample was mixed with 5 ml of concentrated sulfuric acid and heated for 30 min. The solution was then diluted and neutralized with NaOH, evaporated, and the remaining solid was ignited at 850 °C (for 5-10 min). Sulfates were converted to the corresponding oxides, cooled, and diluted with doubly distilled water in a 100 ml calibrated flask. After adjusting the pH of the sample solution, Cu(II) was floated and determined spectrophotometrically by the recommended procedure.

ICP Certified Multielement Standard Solution

This solution, also kindly supplied by the Analytical Chemistry Laboratory Service at PTB, contained 1011 $\mu\text{g ml}^{-1}$ Cu(II) in addition to Ag, Al, B, Ba, Bi, Ca, Cd, Co, Cr, Fe, Ga, In, K, Li, Mg, Mn, Na, Ni, Pb, Sr, Tl, and Zn in the same concentration range as copper. Using 50 ml of the sample, after buffering to pH~7, a defined volume of the solution was introduced into the flotation cell to apply the procedure for flotation and determination of copper. Both the steel scrap certified sample and multielement standard solution were used to separate and preconcentrate Mn(II), Ni(II), Cu(II), and Zn(II), as previously described [34].

Theragran Hematinic Sample

Each Theragran-M tablet (Bristol-Myers Squibb Company,

New York) supplies: vitamin A (10000 IU), vitamin D (400 IU), vitamin B1 (10 mg), vitamin B2 (10 mg), vitamin B6 (5 mg), vitamin B12 (5 mg), vitamin C (200 mg), vitamin E (15 IU), niacinamide (100 mg), calcium pantothenate (20 mg), iodine (0.15 mg), iron (12 mg), copper (0.67 mg), manganese (1 mg), magnesium (65 mg) and zinc (1.5 mg). As previously described [5], five tablets were crushed, digested using 5 ml of concentrated of HNO₃ and heated to near dryness. After cooling, the residue was dissolved in another 5 ml of concentrated HNO₃ and the solution was gently evaporated using a water bath. The residue was again heated with 50 ml distilled water, filtered off and diluted to 100 ml in a calibrated flask after adjusting the pH to ~7. A defined volume treated by the recommended procedure for the flotation and determination of copper.

Apparatus

The flotation cell (a cylindrical tube with a 15 mm inner diameter and 290 mm length, a stopcock at the bottom and a stopper at the top) was the same type as previously described [16]. The spectral data were recorded on Unicam UV 2100 UV-Vis and MATSON 5000 FTIR spectrophotometers. The pH was adjusted with HCl and/or NaOH and measured with a digital pH meter (Hanna Instruments, model 8519).

Procedure

Separation. All samples used in this investigation were in the form of aqueous solutions after suitable treatment. Therefore, the following procedure was applied to all samples. A suitable aliquot containing a known amount of Cu(II), specified for each investigation, was mixed with a suitable amount of A-*p*-CIPT followed by the addition of 3 ml of double distilled water. After adjusting with HCl and/or NaOH to the required pH, the solution was transferred to the flotation cell and the total volume was made up to 10 ml with an acetone-water mixture to ensure a final acetone volume fraction of 30%. The cell was shaken well for a few seconds to ensure complexation. To this, 3 ml of HOL (of known concentration) was added. The cell was then inverted upside down twenty times by hand. Bubbles were created inside the cell. Meanwhile, the stopper of the cell was removed to permit air movement. After allowing it to stand for 5 min for complete flotation of the colored complex, the concentration of Cu(II) in the surfactant layer was determined spectrophotometrically.

Determination. The concentration of Cu(II) in the floated layer was determined spectrophotometrically by transferring a suitable volume to the quartz cell and measuring the absorbance at 600 nm against the reagent blank (A-*p*-CIPT). The analyte concentration was calculated from a calibration curve constructed by taking different concentrations of Cu(II).

The flotation efficiency (%F) was calculated from the relation:

$$\%F = C_s/C_i \times 100$$

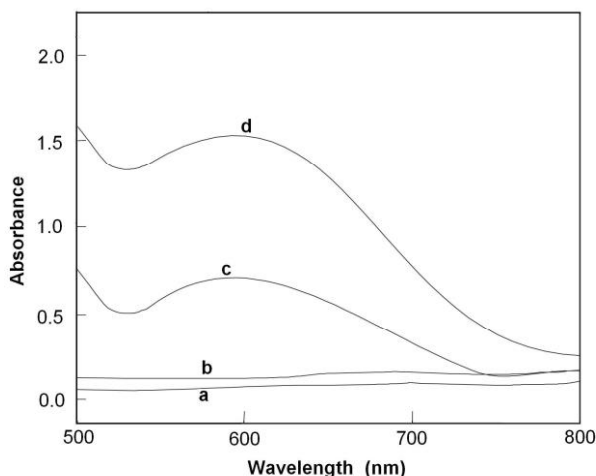


Fig. 1. Absorption spectra of (a) 4×10^{-4} M Cu(II), (b) 8×10^{-4} M A-*p*-CIPT, (c) Cu-A-*p*-CIPT-H₂O complex and (d) Cu-A-*p*-CIPT-HOL complex.

where C_i and C_s denote the initial Cu(II) concentration and its concentration in the surfactant layer, respectively. All the experiments were carried out at room temperature, about 25 °C.

RESULTS AND DISCUSSION

In order to obtain the optimum conditions for the maximum flotation efficiency of Cu(II) with the HOL surfactant, the different factors affecting this process have been studied. It should be noted that the maximum absorbance of the complex Cu-A-*p*-CIPT corresponds to its maximum flotation efficiency. So, the maximum absorbance can be expressed by the maximum floatability of the analyte and the inverse is true, as well [14,35].

Absorption Spectra

The absorption spectra of Cu(II), A-*p*-CIPT reagent and of Cu-A-*p*-CIPT complex formed in aqueous acetone solution (30% v/v) and that floated into the HOL layer are given in Fig. 1. Notice that the absorption spectra of the analyte and the ligand (curves a and b) have no absorption bands in the region that corresponds to that of the complexes Cu-A-*p*-CIPT and Cu-A-*p*-CIPT-HOL, curves

(c) and (d), having their maximum absorbances at 600 nm. Moreover, it is interesting to note that

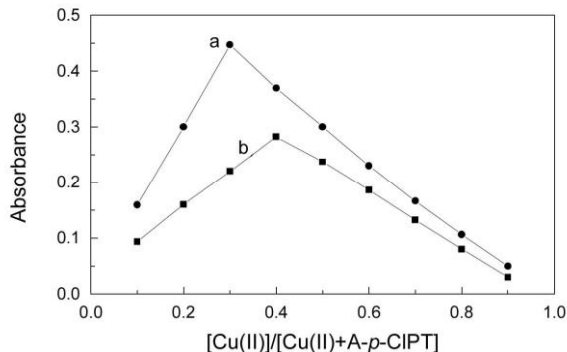


Fig. 2. Composition of Cu(II) complex by the continuous variation methods. (a) Cu(II) complex floated by HOL surfactant. (b) Cu(II) complex in aqueous solution. The measurements were carried out at 600 nm and pH~7, using 1×10^{-4} M A-*p*-CIPT as a blank.

the floated complex has a higher maximum absorbance value in comparison with that formed in the aqueous solution resulting in an enhancement in the sensitivity of the spectrophotometric determination of Cu(II) after flotation. Hence, subsequent analysis of the colored complex was carried out at 600 nm after flotation.

Composition of the Complex

The composition of the copper complex was studied by the continuous variation method. A typical graph obtained (Fig. 2) by the former method showed that 1:2 and 1:1 (Cu:A-*p*-CIPT) complexes are formed in the surfactant and aqueous solutions, respectively (curves a and b). However, the difference in molar ratio between the floated complex and that formed in the aqueous solution may be attributed to the floatability of a small quantity of free reagent in addition to the complex [26]. Moreover, it must be noted from the data in Fig. 2 that the HOL surfactant intensifies the color of the complex (higher absorbance than in the aqueous solution) which confirms the determination of Cu(II) after flotation of its complex [36].

Effect of pH

Since the pH of the medium is a highly significant factor in flotation processes, pH was the first variable to be optimized. A series of experiments was carried out to study the effect of

Spectrophotometric Determination of Copper(II)

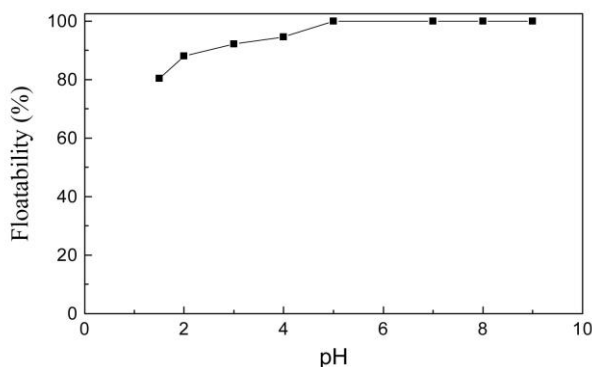


Fig. 3. Floatability of 1.0×10^{-4} M Cu(II) vs. pH using 2.0×10^{-4} M A-*p*-CIPT and 1.0×10^{-3} M HOL.

pH on the flotation efficiency of 1.0×10^{-4} M Cu(II) with 1.0×10^{-3} M HOL in the presence of 2.0×10^{-4} M A-*p*-CIPT. The results presented in Fig. 3 show that the floatability of the Cu- A-*p*-CIPT complex increases with increasing pH, reaching its maximum value (maximum and nearly constant absorbance) in the pH range 5-9. Fortunately, pH~7 was attained by direct addition of reagents and, unless otherwise stated, adjustment of the solution pH was not required. Therefore, pH~7 was used as the optimal pH for other experiments.

Effect of Ligand Concentration

Initial experiments were performed to float Cu(II) with HOL surfactant alone. However, the flotation efficiency did not exceed 40%. Therefore, a trial was made to improve this process using different reagents. It was found that the use of some thiosemicarbazone derivatives as collecting agents in this regard, especially acetophenone-*p*-chlorophenylthiosemicarbazone (A-*p*-CIPT), gave optimistic results. The floatability of a series of solutions containing 1.0×10^{-4} M Cu²⁺, 1.0×10^{-3}

M HOL and various amounts of A-*p*-CIPT at pH~7 was investigated. The results are shown in Fig. 4. As can be seen, the flotation efficiency (equivalent to the maximum absorbance) increases with increasing concentration of the ligands, reaching its maximum value (*ca.* 100%) at a 1:2 (Cu:A-*p*-CIPT) ratio. These results agree well with those obtained in Fig. 2. Moreover, the excess of ligands has no adverse effect on the flotation process and so the procedure be applied to real samples containing Cu(II). Accordingly, a concentration of A-*p*-CIPT which equal to twice that of Cu(II)

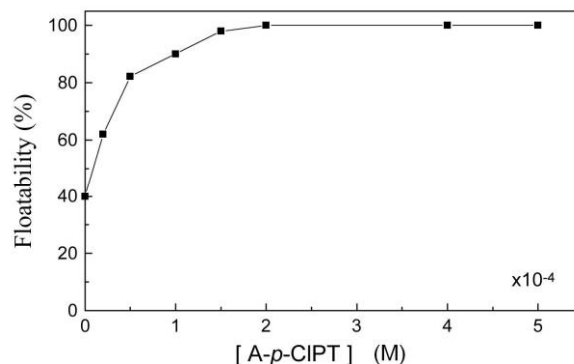


Fig. 4. Floatability of 1.0×10^{-4} M Cu(II) vs. A-*p*-CIPT concentration at pH~7 using 1.0×10^{-3} M HOL.

was used in the recommended procedure.

Effect of Surfactant Concentration

Samples of floated Cu(II) were tested with different concentrations of HOL without ligand (Fig. 5, curve a). The flotation efficiency did not exceed 40%. Therefore the floatability of Cu(II) was tried in the presence of A-*p*-CIPT using various concentrations of HOL. The results, graphically presented in Fig. 5 (curve b), show that the maximum floatability of Cu(II), obtained over a wide concentration, may be due to the formation of a stable envelope of surfactant on the surface of air bubbles or a hydrated micelle coating on the surface of analyte-ligand system [8]. As a result, the hydrophobicity of the resulting surface was not satisfactory for flotation. Accordingly, 1.0×10^{-3} M HOL was used throughout the measurements for Cu(II) determination.

Effect of Cu(II) Concentration

To confirm the data obtained in Fig. 4 another series of experiments were carried out to float various amounts of Cu²⁺ ions in the presence of 2.0×10^{-4} M A-*p*-CIPT using 1.0×10^{-3} M HOL at pH~7 (Fig. 6). As can be seen, the floatability reaches 100% at a Cu(II) concentration of 1.0×10^{-4} M, corresponding to 1:2 molar ratio (Cu:A-*p*-CIPT), which agrees well with the data obtained in Fig. 4. At higher concentrations of the analyte, the flotation efficiency

decreases. This may be attributed to the fact that the amount of A-*p*-CIPT is insufficient to bind all Cu²⁺ ions that exist in the solution.

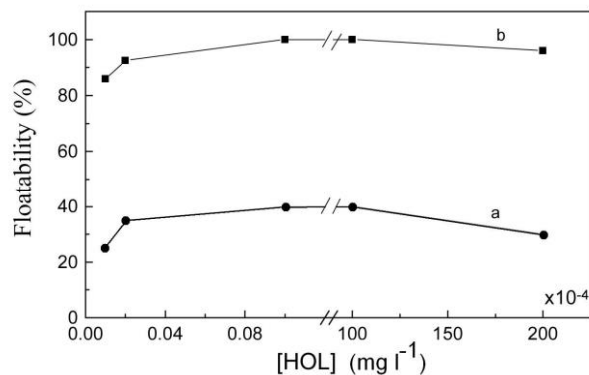


Fig. 5. Floatability of 1.0×10^{-4} M Cu(II) vs. HOL concentration at pH~7. (a) In the absence of A-*p*-CIPT and (b) in the presence of 2.0×10^{-4} M A-*p*-CIPT.

Consequently, in the analysis of copper in its natural unknown samples, excess ligand can be safely used.

Effect of Temperature

To study the effect of temperature on the flotation efficiency of Cu(II), the solution containing Cu(II) and A-*p*-CIPT and that containing the HOL surfactant were either heated or cooled to the same temperature. Then the solution of HOL was quickly poured into the Cu(II) solution. The mixture was introduced into the flotation cell jacketed with 1 cm thick fiberglass insulation. The flotation and determination procedure was then followed. Since the floatability and absorbance of the complex Cu-A-*p*-CIPT were not markedly affected by raising the temperature from 5 to 80 °C, measurements were carried out at room temperature, ~25 °C. However, given that most industrial influents are usually hot, the simple procedure presented here may find its application in the analysis of Cu(II) ions directly in industrial wastewaters.

Effect of Time

The minimum time required for the color development of the Cu-A-*p*-CIPT complex was found to be ~2 min at room temperature. The absorbance of the floated complex, measured at 600 nm, was constant for 20 min., after which the color begins to fade. The total time required for one determination was 6-8 min. Therefore, the use of this simple procedure for analysis of Cu(II) may be considered as time saving compared

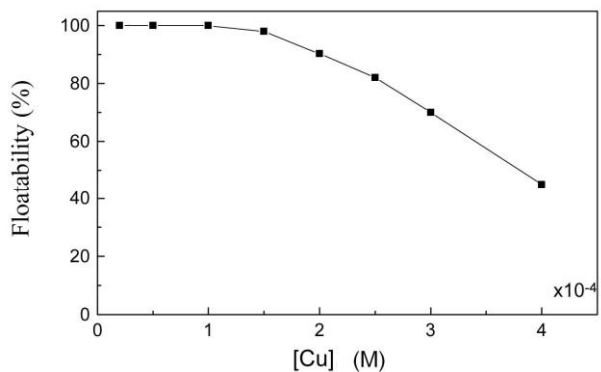


Fig. 6. Floatability of different concentrations of Cu(II) using 2.0×10^{-4} M A-*p*-CIPT and 1.0×10^{-3} M HOL at pH~7.

to some another techniques.

Effect of Foreign Ions

Under the optimized conditions determined as above, analysis of copper(II) ions (1.0×10^{-4} M) using A-*p*-CIPT (2.0×10^{-4} M) as the ligand and oleic acid (1.0×10^{-3} M) as the surfactant was studied in the presence of high concentrations of various cations and anions usually found in some water samples. The tolerable amounts of each ion (presented as ion:Cu ratio) giving a maximum error of $\pm 2\%$ in the flotation efficiency (maximum absorbance) are summarized in Table 1. It can be seen that the ions investigated do not interfere. Thus the recommended procedure is fairly selective and can be safely employed for the determination of Cu(II) in various complex materials.

Effect of Ionic Strength

Table 2 summarizes the effect of varying the ionic strength of different salts on the flotation efficiency of 1.0×10^{-4} M Cu(II) ions with 1.0×10^{-3} M HOL in the presence of 2.0×10^{-4} M A-*p*-

Spectrophotometric Determination of Copper(II)

CIPT at pH~7. The salts used in adjusting the ionic strength generally resemble those present in natural water samples. As can be seen, the ionic strength of the medium has not markedly affected the flotation process nor the determination of Cu(II).

CaCl ₂	0.02	100.0
	0.03	99.3
	0.05	98.5
MgSO ₄	0.02	100.0
	0.03	99.0
	0.05	97.5

Calibration Curve and Sensitivity

Under the optimum conditions described in the

Table 1. Effect of Some Foreign Ions on the Separation and Determination of 1.0×10^{-4} M Cu(II) Using 2.0×10^{-4} M A-*p*-CIPT in the Presence of 1.0×10^{-3} M HOL at pH~7

Foreign ion added	Foreign ion/Cu(II)	Foreign ion added	Foreign ion/Cu(II)
Na ⁺	4786.8	Hg ²⁺	698.0
Mn ²⁺	4000.0	Ni ²⁺	681.4
Zn ²⁺	3975.5	Cd ²⁺	400.0
K ⁺	2813.2	Ba ²⁺	291.3
Mg ²⁺	1646.1	Cl ⁻	15514.8
Al ³⁺	1481.5	SO ₄ ²⁻	2708.3
Ca ²⁺	997.5	NO ₃ ⁻	1774.2
Cr ³⁺ or Cr ⁶⁺	970.7	SiO ₃ ²⁻	526.3
Fe ³⁺	716.8	C ₂ O ₄ ²⁻	430.1

^a 1.0×10^{-4} M Cu(II), 2.0×10^{-4} M A-*p*-CIPT, 1.0×10^{-3} M HOL, pH~7.

Table 2. Effect of Ionic Strength on the Floatability of Cu(II)^a

Salt	Concentration (M)	F (%)
NaCl	0.02	100.0
	0.10	100.0
	0.50	99.5
KCl	0.02	100.0
	0.10	100.0
	0.50	99.2

recommended procedure, the calibration curves (Fig. 7, curves a and b) show good linearity over the range 0.25-6.35 mg l⁻¹ of Cu(II). The molar absorptivities are 5.5×10^3 and 1.3×10^4 l mol⁻¹ cm⁻¹ for the colored complex in the aqueous and scum layers, respectively. The detection limit of a standard aqueous solution of with 3.82 mg l⁻¹ Cu(II), calculated on the basis of

3σ [36], was found to have 0.021 mg l⁻¹ Cu(II), which corresponds to Sandell's sensitivity of 0.244 µg cm⁻² and a

relative standard deviation ($n = 9$) of 0.19%. Moreover, close inspection of the calibration curves reveals that the determination of the analyte after flotation enhances the sensitivity of the spectrophotometric procedure [36].

Flotation Mechanism

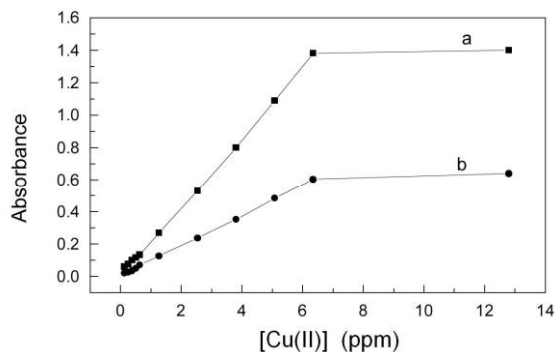
The suggested flotation mechanism of Cu(II) is based on the following points:

Copper(II) reacts with the thiosemicarbazone derivative (A-*p*-CIPT) to form a 1:1 complex in aqueous solution (Chart 2).

The purity of A-*p*-CIPT (Chart 1) was confirmed by elemental analysis [Found (Calcd.); C = 59.4 (59.3); H = 4.5 (4.6)], spectral (mass, electronic and infrared) studies [34]. The most characteristic features of the IR spectrum of A-*p*-CIPT (Fig. 8a) is that it exhibits two bands at 3292 and 3242 cm^{-1} assigned to $\nu(\text{N}^4\text{H})$ and $\nu(\text{N}^2\text{H})$ vibrations, respectively [37]. The bands at 1635 and 797 cm^{-1} are attributed to $\nu(\text{C}=\text{N})$ and $\nu(\text{C}=\text{S})$ vibrations, respectively.

Careful comparison of the IR spectrum of the Cu-A-*p*-CIPT complexes, isolated from the aqueous solution and surfactant layer (Figs. 8b and 8c), with that of A-*p*-CIPT shows that the ligand behaves as a bidentate ligand in the thione form and coordinates through the C=N and C-S groups. These bonding sites are suggested based on the following

Fig. 7. Calibration curves for the determination of Cu(II) at pH~7. (a) in the floated layer and (b) in aqueous solution using 2.0×10^{-4} M A-*p*-CIPT and 1.0×10^{-3} M HOL.



evidence: i) the disappearance of $\nu(\text{N}^2\text{H})$; ii) the shift of $\nu(\text{C}=\text{N})$ to a lower frequency by 41 cm^{-1} ; iii) the appearance of a new band at 443 cm^{-1} , assignable to $\nu(\text{Cu}-\text{N})$ [38,39]; iv) the disappearance of the thioamide band, $\nu(\text{C}=\text{S})$, with the simultaneous appearance of new bands at 607 and 352, ascribed to $\nu(\text{C}-\text{S})$ and $\nu(\text{Cu}-\text{S})$ cm^{-1} vibrations, respectively [40]. The coordinated water gives absorption frequency at 3455, 850, and 550 cm^{-1} due to $\nu(\text{OH})$, rocking and wagging, respectively [41]. Also, the appearance of a new band at 292 cm^{-1} , due to (Cu-Cl) vibration [40], is good evidence for the existence of chloride inside the coordination sphere.

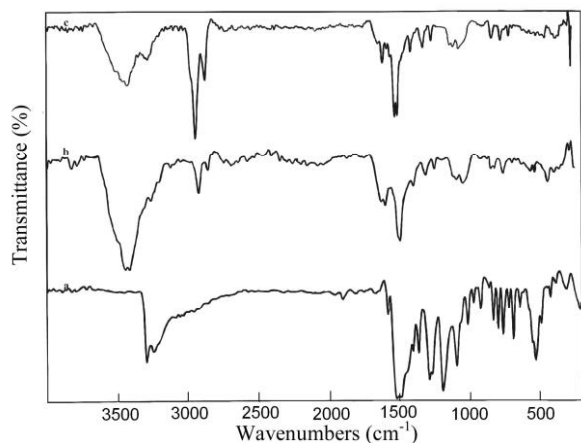
Moreover, the electronic spectra of the complexes (as has been presented elsewhere) [42] exhibits one broad band more or less centered at 16600 cm^{-1} which is assigned to a combination of the transitions ${}^2\text{B}_{1g} \rightarrow {}^2\text{E}_{1g}$ and ${}^2\text{B}_{1g} \rightarrow {}^2\text{A}_{1g}$, associated with a square planar configuration around the Cu(II) ion [41]. In addition to the d-d transition, the band observed at 2197 cm^{-1} is attributed to intraligand charge transfer [41]. All the above observations suggest

a square planar structure for the complex $[\text{Cu}(\text{A-}p\text{-CIPT})(\text{Cl})(\text{H}_2\text{O})]$ as shown in Chart 2.

Oleic acid begins to dissociate at $\text{pH} \geq 5.2$ [42]. Therefore, oleic acid can interact with other systems, through hydrogen bonding, either by its undissociated or dissociated form depending on the pH of the medium.

Spectrophotometric Determination of Copper(II)

The infrared spectra of the complex isolated from the surfactant layer (after thorough washing) has no absorption bands corresponding to the oleic acid surfactant (Fig. 8c). This



added to these samples were examined. To 10 ml aliquots of clear uncontaminated, filtered water samples, 0.5 or 1.5 mg l⁻¹ of Cu(II) were added and the pH was adjusted to ~7. After flotation, the concentration of Cu(II) was determined either spectrophotometrically in the surfactant layer at 600 nm

Fig. 8. Calibration curves for the determination of Cu(II) at pH~7 (a) in the floated layer and (b) in aqueous solution using 2.0×10^{-4} M A-*p*-CIPT and 1.0×10^{-3} M HOL.

means that oleic acid may combine weakly with the complex [Cu(A-*p*-CIPT)(Cl)(H₂O)] perhaps through hydrogen bonds. Oleic acid binds with [Cu(A-*p*-CIPT)(Cl)(H₂O)] giving hydrophobic aggregates that float to the solution surface with aid of air bubbles (created inside the flotation cell by slight shaking) [43].

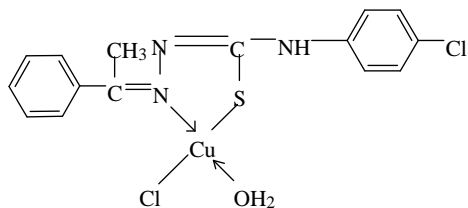


Chart 2

Application

Water samples. To investigate the applicability of the recommended procedure to natural water samples (taken from different locations), the recoveries of known amounts of Cu(II)

Table 3. Determination of Cu(II) Spiked in Natural Water Samples by Spectrophotometric Method

Type of water (location)	Cu(II) added (mg l ⁻¹)	Spectrophotometric Procedure		AAS Procedure	
		Found (mg l ⁻¹)	Recovery (%) ^b	Found (mg l ⁻¹)	Recovery (%) ^b
Distilled water	–	ND	–	ND	–
	0.5	0.499	99.8	0.498	99.6
	1.5	1.5	100.0	1.5	100.0
Tap water (Our laboratory)	–	ND	–	4.5 ± 0.03 ^c	–
	0.5	0.493	98.6	0.495	99.0
	1.5	1.490	99.3	1.495	99.7
Nile water (Mansoura City)	–	ND	–	15.5 ± 0.04 ^c	–
	0.5	0.494	98.8	0.495	99.0
	1.5	1.495	99.7	1.495	99.7
Sea water (Alexandria)	–	ND	–	12.5 ± 0.03 ^c	–
	0.5	0.499	99.8	0.498	99.6
	1.5	1.5	100.0	1.499	99.9
(Ras El-Barr)	–	ND	–	17.5 ± 0.02 ^c	–
	0.5	0.499	99.8	0.499	99.8
	1.5	1.5	100.0	1.5	100.0
Lake water	–	ND	–	10.5 ± 0.03 ^c	–
	0.5	0.499	99.8	0.498	99.6
	1.5	1.5	100.0	1.5	100.0

^a After flotation using 2.0 × 10⁻⁴ M A-*p*-CIPT and 1.0 × 10⁻³ M HOL at pH~7. ND: not detected. Values ^c calculated for the only added amount of Cu(II). Analysis has been carried out by AAS after pre-concentration as reported elsewhere [44] and the values are in ppb.

or by atomic absorption spectrometry (AAS) in the mother liquor at 324.7 nm. The results obtained are given in Table 3. Spectrophotometric determination of Cu(II) after flotation gives satisfactory results compared to those obtained by AAS. Thus the spectrophotometric determination of Cu(II) after flotation makes the procedure highly selective and sensitive. **Certified vitamin and**

simulated samples. The results of the application of the proposed procedure to the recovery and determination of the analyte in two types of certified samples, vitamin tablets and a simulated solution are tabulated in Table

4. The sensitivity of the proposed procedure for the separation and analysis of Cu(II) was investigated by calculating the relative standard deviation for the different samples. The procedure is highly

Spectrophotometric Determination of Copper(II)

sensitive and precise with an RSD that does not exceed 2.95% for the analysis of the vitamin tablets. **REFERENCES**

[1] Y. Göksungur, S. Uren, U. Güvenç, *Bioresource Technol.* 96 (2005) 103.

Table 4. Analysis of Cu(II) in Certified, Vitamin and Simulated Samples ^a

Sample	Certificate (mg l ⁻¹)		Spectrophotometric		AAS		
			Procedure		Procedure		
			Found (mg l ⁻¹)	RSD (%) ^f	Found (mg l ⁻¹)	RSD (%) ^f	
Certified 1 ^b 1011 1005	0.35	1007	0.34	Certified 2 ^c 5.19 5.17	0.98	5.18	0.88
Theragran-M vitamin	0.67 ^e	0.66 ^e	2.95	0.66 ^e	2.25	E Ag 1000 3 ^d	
	1040	1031	1.06	1035	0.99		

^aUsing 1.0 × 10⁻⁴ M A-*p*-CIPT and 1.0 × 10⁻³ M HOL at pH~7. ^bCertified sample 1: multielement standard solution. ^cCertified sample 2: Steel scrap sample. ^dE Ag 1000 3: Simulated sample containing different metals such as Cd, Zn, Pb, Ni, Au, Pt, and Ag in addition Cu(II). ^eValues are given in mg/tablet. ^fCalculated for seven replicate analyses.

- [2] J.S. Kim, S. Akeprathumchia, S. Wickramasinghe, J. Chem. Soc. Jpn. 58 (1985) 1115.
Membr. Sci. 182 (2001) 161. [16] S.E. Ghazy, M.A. Kabil, Bull.Chem. Soc. Jpn. 67 [3] C. Blöcher, J. Dorda, V. Mavrov, H. Chmiel, N.K. (1994) 474.
Lazaridis, K.A. Matis, Water Res. 37 (2003) 4018. [17] N.K. Lazaridis, E.N. Peleka, T.D. Karapantsios, K.A. Matis, Hydrometallurgy 74 (2004) 149.
- [4] M.H. Freemantle, Chemistry in Action, Macmillan Education Ltd., London, 1989. [18] F.M. Doyle, Z. Liu, J. Colloid Interface Sci. 258 (2003) [5] M.E. Khalifa, M.A. Akl, S.E. Ghazy, Chem. Pharm. 396.
Bull. 49 (2001) 664. [19] L. Stoica, C. Constantin, A. Lupu, F.L. Dinu, O.L. Tanase, Environ. Protect. Ecol. 2 (2001) 1009.
- [6] E.M.B. Sorensen, Metal Poisoning in Fish, CRC Press, Boston, MA, USA, 1991. [20] Z. Liu, F.M. Doyle, Colloids and Surfaces A 178 (2001) [7] T. Yubin, C. Fangyan, Z. Honglin, Adsorp. Sci. 79.
Technol. 16 (1998) 595. [21] T. Girek, C.A. Kozlowski, J.J. Koziol, W. Walkowiak, [8] S.E. Ghazy, S.E. Samra, S.M. El-Morsy, Carbohydrate Polymers 59 (2004) 211.
Adsorp.Sci.Technol. 19 (2001) 175. [22] S.E. Ghazy, S.E. Samra, A-F.M. Mahdy, S.M. El[9] S.E. Ghazy, S.E. Samra, A-F.M. Mahdy, S.M. El-Morsy, Environ. Technol. 25 (2004) 1221.
Morsy, Anal. Sci. 19 (2003) 1401. [23] K. Čundeve, T. Stavilov, G. Pavlovska, Microchem. J. [10] D.E. Leyden, W. Wegscheider, Anal. Chem. 53 (1981) 65 (2000) 165.

- 1059A.
- [11] L. Stoica, M. Dinculescu, C.G. Plapcianu, *Water Res.* 32 (1998) 3021.
- [12] J. Rubio, M.L. Souza, R.W. Smith, *Minerals Engineering* 15 (2002) 139.
- [13] D. Zendelovska, G. Pavlovska, K. Cundeva, T. Stafilov, *Talanta* 54 (2001) 139.
- [14] S.E. Ghazy, G.A.E. Mostafa, *Egypt J. Chem.* 45 (2002) 855.
- [15] T. Nagahiro, K. Uesugi, M. Sataki, B.K. Puri, *Bull. Acta* 459 (2002) 323.
- [29] D. Ma, F. Cui, D. Xia, Y. Wang, *Anal. Lett.* 35 (2002) 413.
- [30] V.K. Reddy, S.M. Reddy, P.R. Reddy, T.S. Reddy, *J. Indian Chem. Soc.* 79 (2002) 71.
- [31] J. Cassella Ricardo, *Microchem. J.* 72 (2002) 17.
- [32] R.B. Pawar, S.B. Padgaonkar, A.D. Sawant, *Indian J. Chem.* 40A (2001) 1359.
- [33] R.M. El-Shazly, G.A.A. Al-Hazmi, S.E. Ghazy, M.S. El-Shahawi, A.A. El-Asmy, *Spectrochimica Acta* 60A (2004) 3187.
- [34] K.H. Abou-El-Sherbini, M.M. Hassanien, *Sep. Sci. Tech.* 39 (2004) 1177.
- [35] S.E. Ghazy, *Anal. Sci.* 11 (1995) 33.
- [36] G.A.E. Mostafa, S.E. Ghazy, *Anal. Sci.* 17 (2001) 1189.
- [37] A.A. El-Asmy, Y.M. Shaibi, I.M. Shedaiw, M.A. Khattab, *Synt. React. Inorg. Met. -Org. Chem.* 20 (1990) 461.
- [24] G. Pavlovska, K. Čundeva, T. Stafilov, *Anal. Lett.* 35 (2002) 2347.
- [25] Z. Marczenko, *Separation and Spectrophotometric Determination of Elements*, John Wiley & Sons, York, 1986.
- [26] R.S. Lokhande, S. Nirupa, A.B. Chauhary, *Asian J. of Chemistry.* 14 (2002) 149.
- [27] R.V. Krishna, R.S. Mutta, R.P. Raveendra, R.T. Sreenivasulu, *Chemia Analityczna* 46 (2001) 687.
- [28] E. Prenesti, P.G. Daniele, S. Toso, *Anal. Chem.*
- [38] A.A. El-Asmy, M.E. Khalifa, M.M. Hassanin, *Synth. React. Inorg. Met. -Org. Chem.* 31 (2001) 1787.
- [39] A. Castineras, E. Bermejo, D.X. West, A.K. El-Sawaf, J.K. Swearingen, *Polyhedron* 17 (2001) 2751.
- [40] D.X. West, A.A. Nassar, F.A. El-Saied, M.I. Ayad *Trans. Met. Chem.* 23 (1998) 321.

Spectrophotometric Determination of Copper(II)

- [41] A.H. Osman, A.A.M. Aly, N.A. El-Maali, G.A.A. AlHazmi, *Synth. React. Inorg. Met. -Org. Chem.* 32 (2002) 1293.
- [42] G.A.A. Al-Hazmi, *Ph.D. Thesis*, Chem. Dep., Fac. Sci., Mansoura Univ., 2004.
- [43] S.E. Ghazy, *Sep. Sci. Technol.* 30 (1995) 933.
- [44] I.M.M. Kenawy, M.A.H. Hafez, M.A. Akl, *Anal. Sci.* 16 (2000) 493.

Synthesis and spectroscopic characterization of cobalt(II) thiosemicarbazone complexes

RAFAT M. EL-SHAZLY, G. A. A. AL-HAZMI, S. E. GHAZY, M. S. EL-SHAHAWI and A. A. EL-ASMY*

Chemistry Department, Faculty of Science, Mansoura University, Mansoura, Egypt

(Received 7 March 2005; in final form 20 June 2005)

Thiosemicarbazone derivatives are formed on reaction between acetophenone, salicylaldehyde, benzophenone and/or 2-hydroxy-4-methoxybenzophenone and thiosemicarbazide or its N⁴H substituents (ethyl-, phenyl-, and p-chlorophenyl-). The ligands were investigated by elemental analysis and spectral (IR, ¹HNMR and MS) studies. The formulas of the prepared complexes have been suggested by elemental analyses and confirmed by mass spectra. The coordination sites of each ligand were elucidated using IR spectra revealing bidentate and tridentate coordination. Different geometries for the complexes were proposed on the basis of electronic spectra and magnetic measurements. The complexes have been analyzed thermally (TG and DTG) and the kinetic parameters for some of their degradation steps were calculated.

Keywords: Cobalt(II) complexes; Thiosemicarbazones; Spectra; Thermal studies

1. Introduction

Thiosemicarbazones and their complexes have been extensively studied owing to their pharmaceutical and biological properties such as antitumor [1–3], fungicidal [4], bactericidal and antiviral activities. They have also been used for analysis of metals, for device applications relative to telecommunications, optical computing, optical storage and optical information processing [1]. There has been considerable interest in thiosemicarbazones derived from salicylaldehyde [5], 2-hydroxyacetophenone [6], 2-aminobenzaldehyde, 2-aminoacetophenone [7], acetophenone [8] and in particular, those with substitution at the N(4) position of the thiosemicarbazone moiety [9]. The stoichiometry and stereochemistry of the metal complexes were found to be different for unsubstituted thiosemicarbazones compared to the N(4) substituted [10–13]. Transition metal complexes for several of these compounds

have also been screened for their medicinal properties and possess cytotoxic activity [14]. In this work, we focus our interest on compounds having N(1) and N(4) substituted thiosemicarbazones

*Corresponding author. Tel.: þ20101645966. Email: aelasma@yahoo.com

Journal of Coordination Chemistry
 ISSN 0095-8972 print: ISSN 1029-0389 online 2006 Taylor & Francis
 DOI: 10.1080/00958970500412099

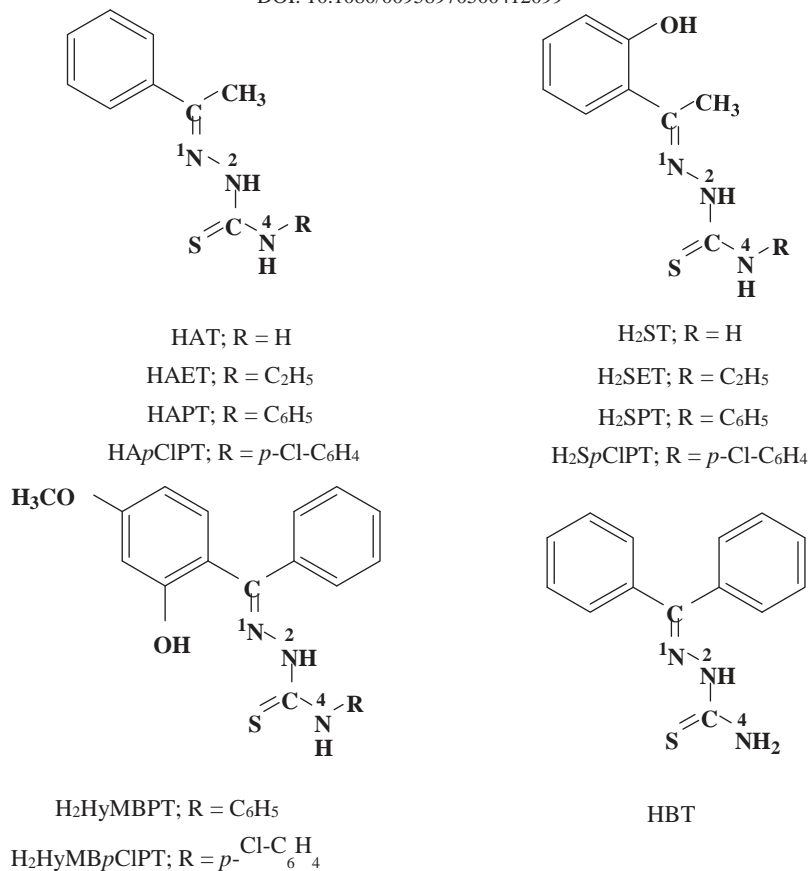


Figure 1. Structures of ligands.

(figure 1) and their Co(II) complexes. In addition, the decomposition steps of the complexes were studied thermally.

2. Experimental

Reagent grade (BDH) precursors to ligands and solvents were purified by the usual methods [15]. Cobalt acetate was purchased from Merck and used as received. All other chemicals were purchased from commercial sources and used without further purification. The abbreviations, full names, melting points and formula weights of the investigated ligands are listed in table 1.

2.1. Preparation of ligands

The ligands under investigation were prepared by the same procedure. The preparation of 1-acetophenone thiosemicarbazones (HAT) is explained in detail as an example. Equimolar amounts of acetophenone (12mL, 0.1mol) and ethanolic solution (50mL)

19058.8(59.3)4.2(4.6)304.0303.8

Table 1. Abbreviations, full names, melting points, elemental analyses and formulae weights of the ligands.

Abbreviated name	Full name	Color	M.P. (°C)	Found (Calcd) %	
				F	W
HATI-Acetophenone	thiosemicarbazone	White	132.55	8(65.9)	5.7(5.7)–193.3
HAETI-Acetophenone	4-ethylthiosemicarbazone	White	145.60	0(59.7)	6.4(6.8)221.0221.3
HAPT1-Acetophenone	4-phenylthiosemicarbazone	White	198.67	0(66.9)	5.9(5.6)–269.4
HApCIPT1-Acetophenone	4-phenylthiosemicarbazone	Yellow	245.49	3(49.2)	5.0(4.6)–195.2
H ₂ SET1-Salicylaldehyde	4-ethylthiosemicarbazone	White	184.53	3(53.8)	5.4(5.9)223.0223.3
H ₂ SPT1-Salicylaldehyde	4-phenylthiosemicarbazone	Yellowish white	205.61	0(61.9)	4.8(4.8)–271.3
H ₂ SpCIPT1-Salicylaldehyde	4-phenylthiosemicarbazone	Yellow	106.60	(66.8)	4.8(5.1)377.0377.5
H ₂ H ₂ MBpCIPT1-(2-Hydroxy-4-methoxybenzophenone)	4-p-chloro-phenylthiosemicarbazone	Yellow	135.61	2(61.2)	4.3(4.4)412.0411.9
HBT1-Benzophenone	thiosemicarbazone	White	191.66	6(65.8)	4.6(5.1)255.9255.3

*Values obtained from mass spectra.

chlorophenylthiosemicarbazone Yellowish white

chlorophenylthiosemicarbazone Yellow

of thiosemicarbazide (9.1g, 0.1mol) were heated at reflux on a water bath for 2h. A few drops of glacial acetic acid were added at the onset of the reflux. The precipitate thus formed was removed by filtration, recrystallized from absolute ethanol and dried.

The yield of the prepared ligands was found in the range 65–80%. Identification of the ligands was confirmed by elemental analysis and mass spectra (table 1) as well as IR spectra (table 2).

2.2. Preparation of complexes

The preparation of $[\text{Co}_2(\text{AT})_3(\text{OH})(\text{H}_2\text{O})]_2 \cdot 5\text{H}_2\text{O}$ is taken as a representative example. A solution of $\text{Co}(\text{OAc})_2 \cdot 4\text{H}_2\text{O}$ (0.746g, 3mmol) in 30mL aqueous-ethanol (1:1) solution was added dropwise with stirring to a solution of HAT (0.579g, 3mmol). The mixture was heated under reflux on a water bath for 4h. The precipitate was filtered off, washed several times with hot water, hot ethanol and diethyl ether and finally dried in a vacuum desiccator.

All the other complexes were prepared by the same procedure.

2.3. Physical measurements

Carbon and hydrogen content was determined by the Microanalytical Unit at Cairo University. Analysis of cobalt ions carried out complexometrically using standard methods [16].

The infrared spectra in the region 200–4000 cm^{-1} were recorded, as KBr discs, on a Mattson 5000 FTIR spectrophotometer with a CsI beam splitter. The electronic spectra

(Nujol mull and DMF solution) were recorded on a UV₂ Unicam UV/VIS Spectrophotometer. ¹HNMR spectra were recorded in DMSO-d₆ on a Varian

Gemini Spectrophotometer (200MHz). The mass spectra were recorded on a Varian

MAT 311 instrument. The effective magnetic moments were evaluated using a
pffffffffffffffffffffffffffffi

Johnson Matthey magnetic susceptibility balance by applying: $\mu_{\text{eff}}^2 / 4.828 \mu_{\text{B}}^2 T$, where μ_{M} is the molar susceptibility corrected using Pascal's constants for the diamagnetism of all atoms in the complexes and T is the absolute temperature. The thermal studies were carried out on a Shimadzu thermogravimetric analyzer with a heating rate of 10 Cmin^{-1} .

3. Results and discussion

The Co(II) complexes of HAT, HAET, HAPT, HApCIPT, H₂ST, H₂SET, H₂SPT, H₂SpCIPT, H₂HyMBPT, H₂HyMBpCIPT and HBT (see table 1 for abbreviations) are readily obtained by mixing aqueous-ethanol solutions of the ligands (figure 1) with $\text{Co}(\text{OAc})_2 \cdot 4\text{H}_2\text{O}$. All the formed complexes are stable in atmospheric conditions, insoluble in water and common organic solvents, but completely soluble in dimethyl formamide (DMF) and dimethylsulphoxide (DMSO) except for $[\text{Co}(\text{BT})(\text{OAc})] \cdot 2\text{H}_2\text{O}$ which is insoluble and $[\text{Co}_2(\text{AT})_3(\text{OH})-(\text{H}_2\text{O})]_2 \cdot 5\text{H}_2\text{O}$, $[\text{Co}(\text{APT})_2(\text{H}_2\text{O})_2]$, $[\text{Co}_2(\text{ST})_2(\text{H}_2\text{O})_2] \cdot 0.5\text{H}_2\text{O}$,

[Co(SPT)(H₂O)] and [Co(SpCIPT)(H₂O)₂]H₂O which are partially soluble. The analytical data and some physical properties of the complexes are presented in table 2.

Table 2. Physical properties, elemental analysis and formula weights of the complexes.

Complex/Formula	Formula weight		Color	Yield (%)	M.P. (°C)	Found (Calcd %)		
	Found*	Calcd				C	H	Co
[Co ₂ (AT) ₃ (OAc)(H ₂ O)] · H ₂ O C ₂₉ H ₃₉ Co ₂ N ₆ O ₂ S ₃	774.0	775.8	Dark brown	78	>300	45.2 (44.9)	5.2 (5.1)	15.6 (15.2)
[Co(AET) ₂ (H ₂ O) ₂] C ₂₂ H ₃₂ CoN ₆ O ₂ S ₂	—	535.6	Brownish green	80	>300	49.7 (49.4)	5.6 (6.0)	10.7 (11.0)
[Co(APT) ₂ (H ₂ O) ₂] C ₃₀ H ₃₂ CoN ₆ O ₂ S ₂	—	631.7	Dark brown	83	221	57.4 (57.0)	4.9 (5.1)	9.7 (9.3)
[Co ₂ (ApCIPT)(OAc)(OH) ₂ (H ₂ O)] · H ₂ O C ₁₇ H ₂₂ ClCo ₂ N ₃ O ₆ S	548.0	549.8	Dark brown	81	>300	37.6 (37.1)	3.8 (4.0)	21.9 (21.4)
[Co ₂ (ST) ₂ (H ₂ O) ₂] · 0.5H ₂ O C ₁₆ H ₁₉ Co ₂ N ₆ O _{4.5} S ₂	548.0	548.8	Brown	71	>300	35.5 (34.9)	4.0 (3.5)	21.6 (21.5)
[Co ₂ (SET) ₂ C ₂ H ₅ OH C ₂₂ H ₂₈ Co ₂ N ₆ O ₃ S ₂	606.0	606.5	Dark brown	86	>300	43.0 (43.6)	4.4 (4.6)	18.9 (19.4)
[Co(SPT)(H ₂ O)] C ₁₄ H ₁₃ CoN ₃ O ₂ S	345.0	346.3	Yellowish brown	81	>300	47.9 (48.5)	3.8 (3.8)	16.6 (17.0)
[Co(SpCIPT)(H ₂ O) ₂] · H ₂ O C ₁₄ H ₁₆ ClCoN ₃ O ₄ S	415.0	416.8	Brown	78	>300	40.5 (40.3)	4.1 (3.9)	14.7 (14.1)
[Co(HyMBPT)(H ₂ O) ₃] · H ₂ O C ₂₁ H ₂₅ CoN ₃ O ₆ S	—	506.4	Brown	75	>300	49.7 (49.8)	4.5 (4.9)	12.0 (11.6)
[Co ₂ (HyMBpCIPT)(OH) ₂ (H ₂ O) ₃] C ₂₁ H ₂₄ ClCo ₂ N ₃ O ₇ S	615.0	615.9	Dark brown	76	>300	40.8 (40.9)	3.9 (3.9)	19.1 (19.1)
[Co(BT)(OAc)] · 2H ₂ O C ₁₆ H ₁₉ CoN ₃ O ₄ S	408.0	408.3	Dark brown	79	>300	46.7 (47.1)	4.3 (4.7)	13.7 (14.4)

*Values obtained from ms.

3.1. ^1H NMR spectra of ligands

The ^1H NMR spectra of HAET, HAPT and H_2HyMPT in d_6 -DMSO show signals at 12.08–11.40 and 9.92–8.51ppm, which are assigned to the N^2H and N^4H protons, respectively [8]. The ^1H NMR spectra of HAT and H_2ST show signals at 10.30, 10.07 and 8.09, 8.03ppm which are assignable to the NH_2 and NH protons, respectively. However, the spectrum of H_2ST shows the OH signal [10] at 10.17 and the NH_2 at 10.07ppm. The higher value of NH_2 signals may be due to intramolecular hydrogen bonding.

3.2. IR spectra of ligands and their complexes

The important IR bands of the ligands and their complexes are summarized in table 3. The mode of bonding of ligands to Co(II) was investigated. The data show the formation of two modes of chelation. The ligands in the first mode are mononegative bidentate and coordinate through the azomethine (C^1N) and thiol (C-S) groups. This type of coordination was found in $[\text{Co}_2(\text{AT})_3(\text{OAc})(\text{H}_2\text{O})]\text{H}_2\text{O}$, $[\text{Co}(\text{AET})_2(\text{H}_2\text{O})_2]$, $[\text{Co}(\text{APT})_2(\text{H}_2\text{O})_2]$, $[\text{Co}_2(\text{ApCIPT})(\text{OAc})(\text{OH})_2(\text{H}_2\text{O})]\text{H}_2\text{O}$ and $[\text{Co}(\text{BT})(\text{OAc})] 2\text{H}_2\text{O}$. The bonding sites are assigned based on the following evidence: (i) the disappearance of (N^2H), (ii) the shift of (C^1N) to lower frequency by 11–66 cm^{-1} [16], (iii) the appearance of a new band due to (C^1N)* at the same spectral region as for (C^1N) of the thiosemicarbazone moiety, (iv) coordination of the azomethine nitrogen is also consistent with the presence of a new band at 402–470 cm^{-1} , assignable to (Co-N) vibration [17] and (v) the thioamide band (IV) is absent with the simultaneous appearance of new bands in the 606–662 and 346–383 cm^{-1} regions due to (C-S) [18] and (Co-S) vibrations [19], respectively. To confirm the coordination through the thiolato sulfur, the reduction of thioamide band(III) is possible if coordination occurs both through N and S atoms. The acetate ligand in $[\text{Co}_2(\text{ApCIPT})(\text{OAc})(\text{OH})_2(\text{H}_2\text{O})]\text{H}_2\text{O}$ and $[\text{Co}(\text{BT})(\text{OAc})]2\text{H}_2\text{O}$ is bidentate as indicated by the appearance of two new bands at 1348–1374 and 1417–1526 cm^{-1} due to symmetric and asymmetric stretching vibrations [20], respectively. In $[\text{Co}_2(\text{AT})_3(\text{OAc})(\text{H}_2\text{O})]\text{H}_2\text{O}$, the acetate group is monodentate (two new bands with the difference of 157 cm^{-1} between the two bands). The bands observed at 485 and 506 cm^{-1} in the spectra of $[\text{Co}_2(\text{AT})_3(\text{OAc})(\text{H}_2\text{O})]\text{H}_2\text{O}$ and $[\text{Co}_2(\text{ApCIPT})(\text{OAc})(\text{OH})_2(\text{H}_2\text{O})]\text{H}_2\text{O}$ are assigned to (M-O) of coordinated water or OH.

A second mode of chelation was found through the C^1N , C-S and phenolic oxygen groups in which the ligand is binegative tridentate. This behavior is found in the complexes $[\text{Co}_2(\text{ST})_2(\text{H}_2\text{O})_2]0.5\text{H}_2\text{O}$, $[\text{Co}_2(\text{SET})_2]\text{C}_2\text{H}_5\text{OH}$, $[\text{Co}(\text{SPT})(\text{H}_2\text{O})]$, $[\text{Co}(\text{SpCIPT})-(\text{H}_2\text{O})]\text{H}_2\text{O}$, $[\text{Co}(\text{HyMBPT})(\text{H}_2\text{O})_3]\text{H}_2\text{O}$ and $[\text{Co}_2(\text{HyMBpCIPT})(\text{OH})_2(\text{H}_2\text{O})_3]$. Elucidation of this mode is proposed by: (i) the disappearance of (N^2H); (ii) the shift of (C^1N) to lower frequency by 9–83 cm^{-1} ; (iii) the phenolic oxygen of these ligands, on loss of the OH proton, occupies the third (through bridging) coordination site (disappearance of one of the OH band); (iv) a band at 486–505 cm^{-1} in the spectra of the complexes is assignable to (M-O) for the bridging phenolato oxygen; (v) the disappearance of (C^1S) at 778–835 cm^{-1} in the complex spectra with the appearance of a new band at 606–638 cm^{-1} due to (C-S) vibrations, and new bands appeared in the low frequency region for (M-S) at 345–370 cm^{-1} and (M-N) at 405–453 cm^{-1} , evidence for S, N and O donors.

Table 3. IR spectral bands of the ligands and their complexes (cm⁻¹).

Compound	$\nu(\text{NH}_2)$	$\nu(\text{OH})$	$\nu(\text{N}^4\text{H})$	$\nu(\text{N}^2\text{H})$	$\nu(\text{C}=\text{N})$	$\nu(\text{C}=\text{S})$	$\nu(\text{C}-\text{S})$	$\delta(\text{OH})$	$\nu(\text{M}-\text{O})$	$\nu(\text{M}-\text{N})$	$\nu(\text{M}-\text{S})$
HAT	3409 3367 3415 3368	—	—	3223	1628	790	—	—	—	—	—
[Co ₂ (AT) ₃ (OH)(H ₂ O)] · 2.5H ₂ O	—	3441	—	—	1611	—	606	1330	485	402	351
HAET	—	—	3319	3225	1630	788	—	—	—	—	—
[Co(AET) ₂ (H ₂ O) ₂]	—	—	3316	—	1586	—	624	—	513	462	370
HAPT	—	—	3299	3250	1605	794	—	—	—	—	—
[Co(APT) ₂ (H ₂ O) ₂]	—	—	3306	—	1594	—	610	—	—	405	352
HapCIPT	—	—	3292	3242	1635	797	—	—	—	—	—
[Co ₂ (ApCIPT)(OAc)(OH) ₂ (H ₂ O)] · H ₂ O	—	3387 3442	3290	—	1616	—	656	1390	506	446	346
H ₂ ST	3371 3317 3377 3304	—	—	—	1611	778	—	1366	—	—	—
[Co ₂ (ST) ₂ (H ₂ O) ₂] · 0.5H ₂ O	—	3426	—	—	1601	—	618	1327	486	430	350
H ₂ SET	—	3405	3353	3250	1607	791	—	1375	—	—	—
[Co ₂ (SET) ₂ C ₂ H ₅ OH]	—	3420	3365	—	1598	—	606	—	492	405	345
H ₂ SPT	—	3420	3381	3146	1621	835	—	1389	—	—	—
[Co(SPT)(H ₂ O)]	—	3417	3381	—	1610	—	638	1373	492	412	346
H ₂ S _p CIPT	—	3333	3236	3154	1610	830	—	1331	—	—	—
[Co(S _p CIPT)(H ₂ O) ₂] · H ₂ O	—	3314	3205	—	1608	625	625	1328	489	453	345
H ₂ HyMBPT	—	3470	3302	3162	1634	809	—	1327	—	—	—
[Co(HyMBPT)(H ₂ O) ₃] · H ₂ O	—	—	3305	—	1596	—	609	1319	502	405	350
H ₂ HyMB _p CIPT	—	3439	3290	3181	1634	788	—	1348	—	—	—
[Co ₂ (HyMB _p CIPT)(OH) ₂ (H ₂ O) ₃]	—	—	3253	—	1597	—	623	1316	505	423	370
HBT	3364 3262 3329 3256	—	—	3175	1620	800	—	—	—	—	—
[Co(BT)(OAc)] · 2H ₂ O	—	—	—	—	1554	—	662	—	525	470	383

3.3. Magnetic and electronic spectral studies

The investigated thiosemicarbazones have a ring $n \rightarrow \pi^*$ band at 32790–40820 cm^{-1} and $n \rightarrow \pi^*$ band at 28570–30960 cm^{-1} ; little change in energies is seen for their complexes. Another $n \rightarrow \pi^*$ band in the spectra of the free thiosemicarbazones is also found in the spectra of the cobalt(II) complexes at 27000–28250 cm^{-1} . The band at 22680–24040 cm^{-1} in the spectra of the complexes may be due to LMCT. Previous studies on thiosemicarbazone complexes proved that a band in the region 25000–26040 cm^{-1} should be assigned to an O \rightarrow M(II) transition [21] whereas a band in the range 21790–24750 cm^{-1} is due to S \rightarrow M(II) transition [22]. All spectral measurements were carried out in Nujol and DMF; the medium has little effect.

The magnetic moments and the electronic spectral bands of the complexes are listed in table 4. The complexes $[\text{Co}(\text{AET})_2(\text{H}_2\text{O})_2]$, $[\text{Co}(\text{APT})_2(\text{H}_2\text{O})_2]$ and $[\text{Co}(\text{HyMBPT})(\text{H}_2\text{O})_3]\text{H}_2\text{O}$ have magnetic moments of 4.82, 5.04 and 5.20 BM, respectively, which lie in the range reported for an octahedral geometry around the Co(II) [17]. Electronic spectra of the complexes recorded in Nujol and DMF are similar, characterized by two bands at 14290–16950 and 17360–20280 cm^{-1} attributed to the ${}^4\text{T}_{1g} \rightarrow {}^4\text{A}_{2g}(\text{e})$ and ${}^4\text{T}_{1g} \rightarrow {}^4\text{T}_{1g}(\text{P})(\text{e})$ transitions, respectively. The observed bands are similar to those reported for octahedral complexes of Co(II) [23]. The ligand field parameters (B , Δ , 10Dq) are calculated by the equations used for the d^7 system [24] and are listed in table 4. The values agree fairly well with those reported for octahedral Co(II) complexes. Considerable reduction in the B value from 971 to 697–896 cm^{-1} and Δ (from unity to 0.718–0.922) indicates the covalent character of the L–M bond [8]. The color of these complexes is in good agreement with those reported for octahedral geometry.

The complexes $[\text{Co}_2(\text{AT})_3(\text{OAc})(\text{H}_2\text{O})]\text{H}_2\text{O}$, $[\text{Co}_2(\text{ApCIPT})(\text{OAc})(\text{OH})_2(\text{H}_2\text{O})]\text{H}_2\text{O}$ and $[\text{Co}(\text{SPT})(\text{H}_2\text{O})]$, have 4.02, 4.46 and 4.70 BM magnetic moments, respectively, which lie within the values reported for tetrahedral Co(II) complexes [25]. Other evidence is their electronic spectra which show one band at 15625–16050 cm^{-1} due to the ${}^4\text{A}_2 \rightarrow {}^4\text{T}_1$ transition in a tetrahedral structure [25]. The ligand field parameters of these complexes are also presented in table 4. The values of 10Dq may be taken as good criteria for the strength of the ligands based on crystal field. It is found that in the octahedral complexes, the order of ligands is: $\text{H}_2\text{HyMBPT} > \text{H}_2\text{ST} > \text{HAET} > \text{HAPT}$. The order of ligands in tetrahedral complexes is: $\text{HApCIPT} > \text{HAT} > \text{H}_2\text{SPT}$.

The magnetic moment values of the complexes $[\text{Co}_2(\text{SET})_2]\text{C}_2\text{H}_5\text{OH}$ (3.01 BM) and $[\text{Co}(\text{BT})(\text{OAc})]2\text{H}_2\text{O}$ (2.80 BM) agree with the electronic spectra which showed one d-d transition at 18900–19100 cm^{-1} suggesting a square planar geometry around

Co(II).

The 3.28 and 3.40 BM values measured for $[\text{Co}(\text{ST})(\text{H}_2\text{O})]_2 \cdot 0.5\text{H}_2\text{O}$ and $[\text{Co}_2(\text{HyMBpCIPT})(\text{OH})_2(\text{H}_2\text{O})_3]$ are less than reported for octahedral complexes (4.8–5.2 BM). The anomalous values may be due to cobalt–cobalt interaction or to high-spin–low-spin equilibrium. Their electronic spectra showed three bands at 16000, 12990 and 20410 cm^{-1} attributed to the ${}^4\text{A}_2 \rightarrow {}^4\text{A}_2(\text{P})$, ${}^4\text{A}_2 \rightarrow {}^4\text{E}$ and

${}^4\text{E} \rightarrow {}^4\text{E}(\text{P})$ transitions, respectively,

perhaps a trigonal bipyramidal structure [26]. Figure 3 represents the geometry of $[\text{Co}(\text{ST})(\text{H}_2\text{O})]_2 \cdot 0.5\text{H}_2\text{O}$ in which sulphur bridged two cobalt atoms.

Table 4. Magnetic moments, electronic spectral bands and ligand field parameters of Co(II) complexes.

Complex	μ_{eff} (BM)	State	ν_{max} (cm^{-1})	Ligand field parameters			Supposed structure
				B (cm^{-1})	β	10Dq (cm^{-1})	
[Co ₂ (AT) ₃ (OH)(H ₂ O)] · 2.5H ₂ O	4.02	DMF	15 873	793	0.817	3172	Tetrahedral
		Nujol	15 847	757	0.780	3406	
[Co(AET) ₂ (H ₂ O) ₂]	4.82	DMF	18 796, 16 000	836	0.860	8360	Octahedral
		Nujol	18 248, 15 923	795	0.818	8750	
[Co(APT) ₂ (H ₂ O) ₂]	5.04	DMF	19 305, 16 000	859	0.884	8590	Octahedral
		Nujol	18 552, 16 000	795	0.819	8745	
[Co ₂ (ApCIPT)(OAc)(OH) ₂ (H ₂ O)] · H ₂ O	4.46	DMF	16 050	666	0.686	4670	Tetrahedral
		Nujol	15 847	652	0.671	4670	
[Co ₂ (ST) ₂ (H ₂ O) ₂] · 0.5H ₂ O	3.20	DMF	19 305, 16 949	828	0.852	9108	Octahedral
		Nujol	20 150, 16 949	896	0.922	8967	
[Co ₂ (SET) ₂]C ₃ H ₅ OH	3.01	DMF	19 047	—	—	—	Square planar
		Nujol	18 932	—	—	—	
[Co(SPT)(H ₂ O)]	4.70	DMF	15 625	763	0.785	3433	Tetrahedral
		Nujol	16 000	789	0.813	3156	
[Co(SpCIPT)(H ₂ O) ₂] · H ₂ O	4.16	DMF	17 667	—	—	—	Trigonal bipyramidal
		Nujol	20 610, 16 050, 13 050	—	—	—	
[Co(HyMBPT)(H ₂ O) ₃] · H ₂ O	5.20	DMF	17 361, 16 863	697	0.718	8940	Octahedral
		Nujol	20 283, 14 285	880	0.906	9213	
[Co ₂ (HMBpCIPT)(OH) ₂ (H ₂ O) ₃]	3.40	DMF	16 666	—	—	—	—
		Nujol	20 405, 16 000, 12 990	—	—	—	Trigonal bipyramidal
[Co(BT)(OAc)] · 2H ₂ O	2.80	Nujol	18 903	—	—	—	Square planar

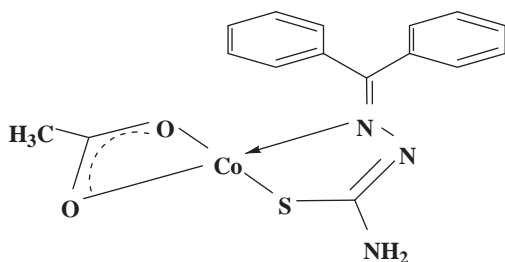


Figure 2. Structure of $[\text{Co}(\text{BT})(\text{OAc})]2\text{H}_2\text{O}$.

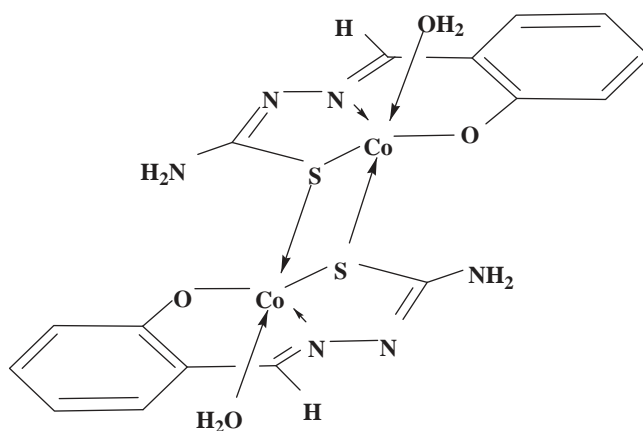


Figure 3. Structure of $[\text{Co}_2(\text{ST})_2(\text{H}_2\text{O})_2] 0.5\text{H}_2\text{O}$.

In the electronic spectrum of $[\text{Co}(\text{SpClIPT})(\text{H}_2\text{O})_2]\text{H}_2\text{O}$, the d–d band is observed at 16610cm^{-1} and LMCT transition at 25000cm^{-1} . The spectrum of this complex resembles five-coordinate cobalt(II) complexes [5, 27]. A square-pyramidal structure may be assigned for this complex, supported by its magnetic moment.

3.4. Mass spectral studies

The mass spectra of most complexes show molecular ion peaks in good agreement with the suggested formulas. The found and calculated molecular weights are presented in table 2. One spectrum is described in detail for $[\text{Co}(\text{ST})(\text{H}_2\text{O})_2] 0.5\text{H}_2\text{O}$ (figure 4) showing multi peaks representing successive degradation of the molecule. The first peak at $m/e/4548.0$ (Calcd 549.3) represents the molecular ion peak of the complex with 90.59% abundance; this formula contains half water molecule. Scheme 1 demonstrates the proposed decomposition path for the complex. One of the strongest peaks (base peak) at $m/e/4370$, represents the stable species, $\text{C}_9\text{H}_{11}\text{Co}_2\text{N}_5\text{O}_2\text{S}$, after which many peaks are observed ending with Co at $m/e/460$.

3.5. Thermal studies

The thermal decomposition steps for some complexes were analyzed applying Coats–Redfern [27] and Horowitz–Metzger [28] equations. The energy of activation (E),

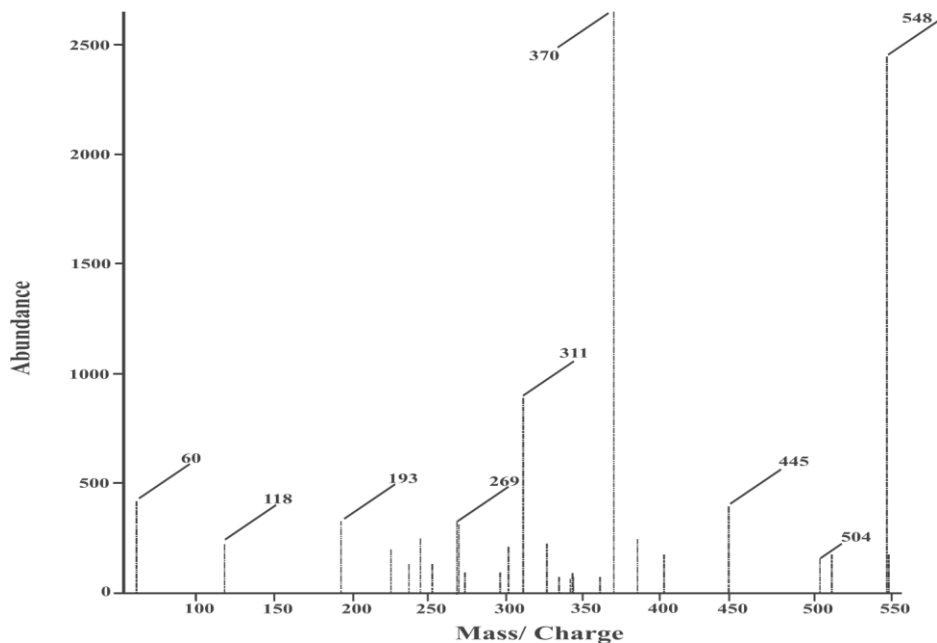


Figure 4. Mass spectrum of $[\text{Co}_2(\text{ST})_2(\text{H}_2\text{O})_2]0.5\text{H}_2\text{O}$.

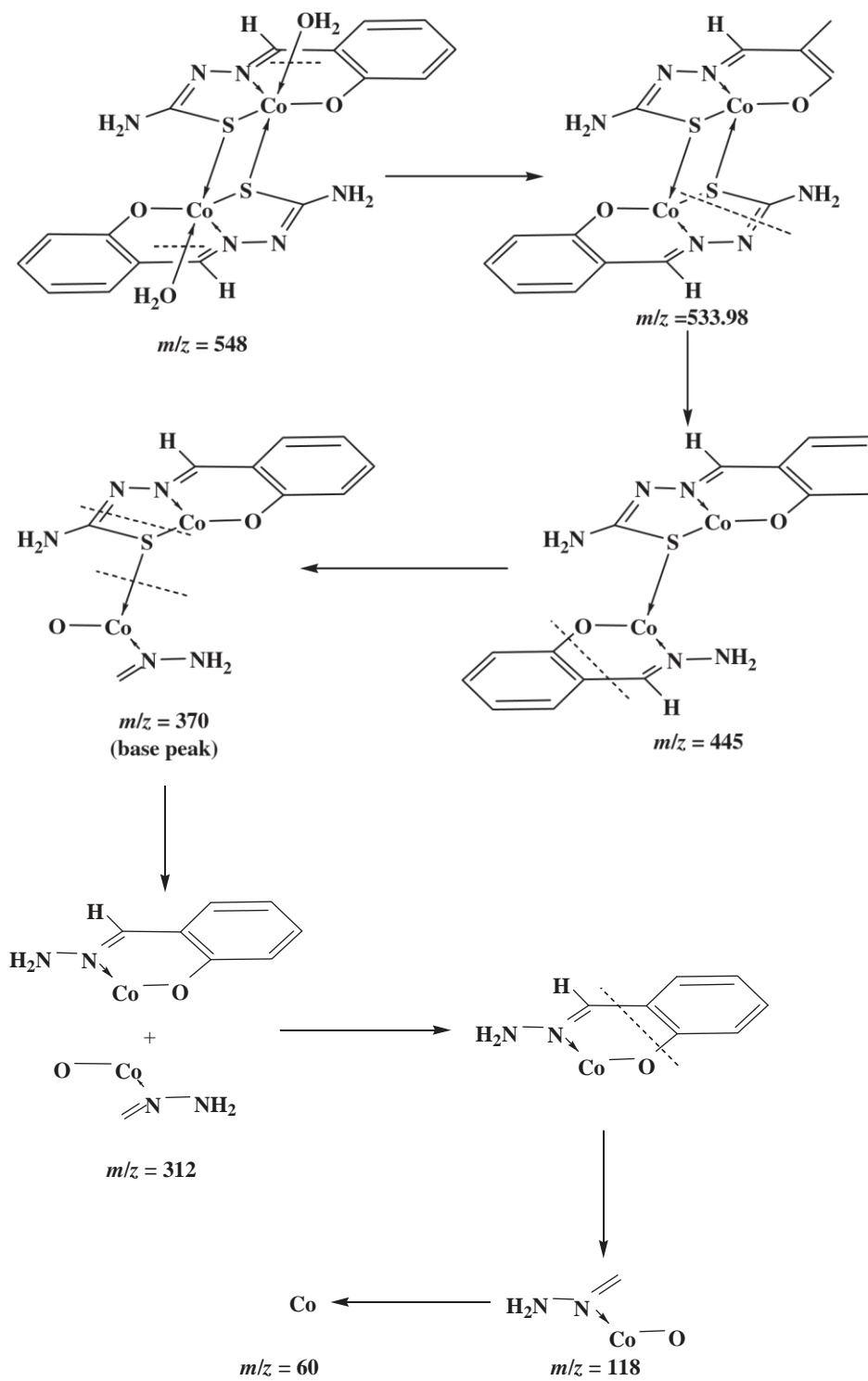
enthalpy (H^*), entropy (S^*) and the free energy (G^*) were calculated (table 5). The relatively high E values ($41.5\text{--}151.3\text{kJmol}^{-1}$) indicate strong bonds to Co(II) ions while the negative S^* values indicate that the activated complexes have more ordered structure than the reactants.

The TG thermograms of the complexes were studied in the temperature range $30\text{--}800\text{C}$.

As a representative example for the decomposition of these complexes, the TG of $[\text{Co}(\text{AET})_2(\text{H}_2\text{O})_2]$, shown in figure 5, is described. Its thermogram reveals four decomposition stages (scheme 2). The two coordinated water molecules may be eliminated in the first step which is major together with another decomposition product (Calcd 50.9%, Found 50.3%) with an activation energy of 78.2kJmol^{-1} and a first-order reaction. The third step suggests the expulsion of two HNC_2H_5 (Calcd 16.5%, Found 17.4%) which may dimerize or abstract hydrogen before decomposition (this step is second order with activation energy of 76.3kJmol^{-1}). A continuous decomposition takes place until 800C . The residue is CoS (Calcd 16.9%, Found 16.1%).

4. Conclusion

Although the same preparative technique was used, isolation of different Co(II) complexes of some N^4H thiosemicarbazone derivatives was surprising. Different geometries were proposed for these complexes based on electronic and magnetic data. All complexes have thermal stability. The existence of ligand tautomers



Scheme 1. Fragmentation pattern of $[\text{Co}(\text{ST})(\text{H}_2\text{O})_2] \cdot 0.5\text{H}_2\text{O}$ using mass spectra.

Table 5. Kinetic parameters of the thermal decomposition of the complexes

Complex Step	RNErNE	S*	H*	G*
[Co ₂ (AT ₃ OH)(H ₂ O)] _{2,5} ^H	2O2nd1261.70.9989271.5	237.156.9194.7		
	3rd11206.511220.9	76.4200.3260.6		
Co(AET ₂ H ₂ O) ₂]st0.99931178.20.9967185.1		197.973.7176.6		
	3rd0.9997276.30.9995291.2	243.370.1252.5		
[Co(APT ₂ H ₂ O) ₂]st0.99991151.30.99971166.9		48.8147172.4		
	2nd0.99980.3330.30.99840.3344.7	328.623.2304.1		
[Co ₂ ST ₂ H ₂ O] _{1,5} ^H	2O1st0.98492177.30.98492188.6	96.1172.7164.6		
	4th0.99790.66125.60.99820.66139	151.8120.6220		
Co(HyMBPT)(H ₂ O) ₃] H ₂ O2nd0.9994151.10.9993158.8		240.847.2160.8		
	3rd0.9968139.70.9941154.2	297.633.7233		
Co(BT)(OAc ₂ H ₂ O)1st0.9993259.30.9982263.5		154.456.5108.5		
	3rd10.33109.50.99960.33131	206.2102.9264.9		

^a r² correlation coefficient, n^{1/4} order of the decomposition reaction; E, H* and G* are in kJ/mol⁻¹, S* in K/mol⁻¹.

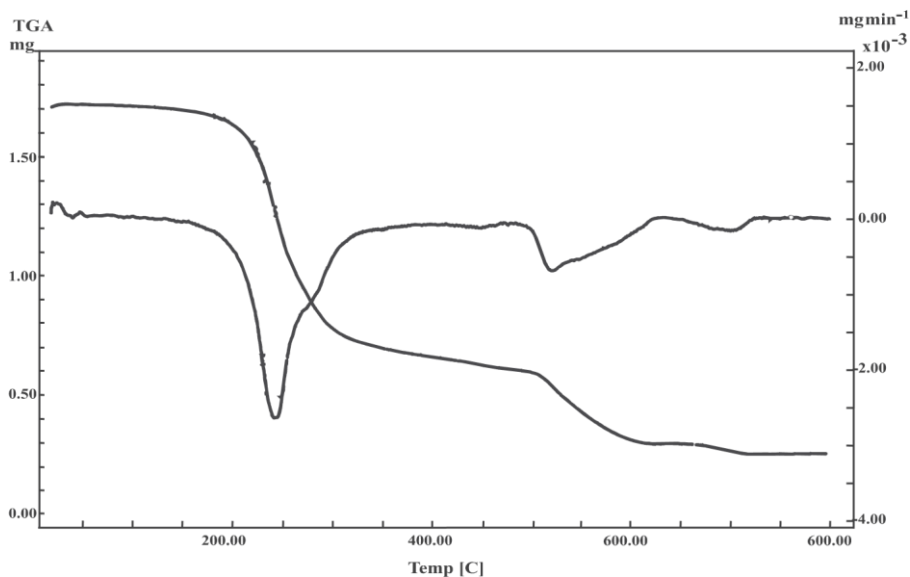
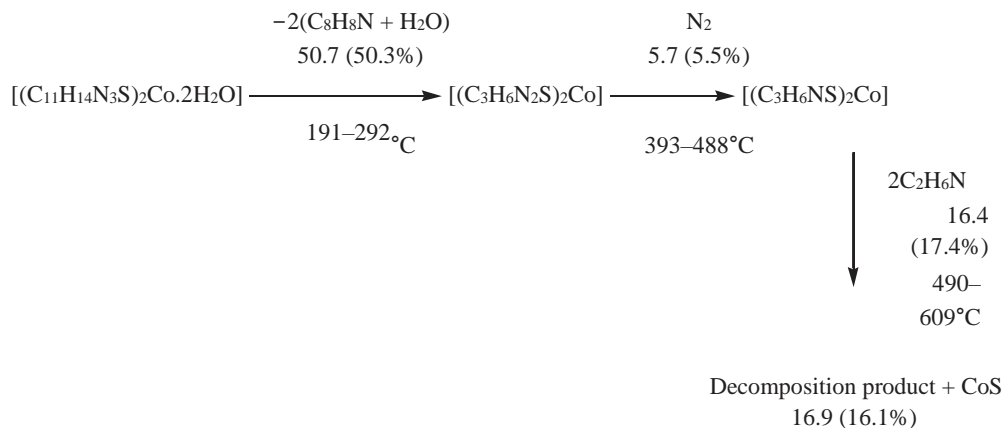


Figure 5. TG and DTG thermograms of $[\text{Co}(\text{AET})_2(\text{H}_2\text{O})_2]$.



Scheme 2. Thermal decomposition of $[\text{Co}(\text{AET})_2(\text{H}_2\text{O})_2]$.

may be significant. The ligands function as mononegative bidentate and binegative tridentate depending on the substituent group of the ligands.

References

- [1] E. Jouad, A. Riou, M. Allain, M.A. Khan, G.M. Bouet. *Polyhedron*, 20, 67 (2001).

- [2] D.X. West, J.K. Swearingen, J.V. Martinez, S.H. Ortega, A.K. El-Sawaf, A. Meurs, A. Castineiras, I. Garcia, A. Bermejo. *Polyhedron*, 18, 2919 (1999).
- [3] L.J. Ackerman, P.E. Franwick, M.A. Green, E. John, W.E. Running, J.K. Swearingen, J.W. Webb, D.X. West. *Polyhedron*, 18, 2759 (1999).
- [4] E. Bermejo, R. Carballo, A. Castineiras, R. Dominguez, C. Maichle-Mossmer, J. Strahle, D.X. West. *Polyhedron*, 18, 3695 (1999).
- [5] P. Bindu, M.R.P. Kurup. *Ind. J. Chem.*, 38, 388 (1999).
- [6] R.P. John, A. Sreekanth, M.R.P. Kurup, S.M. Mobin. *Polyhedron*, 21, 2515 (2002).
- [7] A.A. Nassar, F.A. El-Saied, M.I. Ayad, D.X. West. *Transition Met. Chem.*, 24, 617 (1999).
- [8] A.A. El-Asmy, Y.M. Shaibi, I.M. Shedaiwa, M.A. Khattab. *Synth. React. Inorg. Met.-Org. Chem.*, 20(4), 461 (1990).
- [9] D.X. West, Y.-H. Yang, T.L. Klein, K.I. Goldberg, A.E. Liberta, J. Valdes-Martinez, S. HernandezOrtega. *Polyhedron*, 14, 1681 (1995).
- [10] D.X. West, H. Gebremedin, R.J. Butcher, J.P. Jasinski, A.E. Liberta. *Polyhedron*, 12, 2489 (1993).
- [11] X. West, J.S. Ives, J. Krecji, M.M. Salberg, T.L. Zumbahlen, G.A. Bain, A.E. Liberta, J. ValdesMartinez, S. Hernandez-Ortega, R.A. Toscano. *Polyhedron*, 14, 2189 (1995).
- [12] G.A. Bain, D.X. West, J. Krecji, J. Valdes-Martinez, S. Hernandez-Ortega, R.A. Toscano. *Polyhedron*, 16, 855 (1997).
- [13] D.X. West, A.A. Nassar, F.A. El-Saied, M.A. Ayad. *Transition Met. Chem.*, 23, 321 (1998).
- [14] A.A. El-Asmy, Y.M. Shaibi, I.M. Shedaiwa, M.A. Khattab. *Synth. React. Inorg. Met.-Org. Chem.*, 18(4), 331 (1988).
- [15] D.D. Perrin, W.L.F. Armorego. *Purification of Laboratory Chemicals*, 3rd Edn, Pergamon Press, New York (1988).
- [16] A.I. Vogel. *A Text Book of Quantitative Inorganic Analysis*, Longmans, London (1994).
- [17] M.M. Mostafa, A.A. El-Asmy, G.M. Ibrahim. *Transition Met. Chem.*, 8, 54 (1983).
- [18] A.A. El-Asmy, M.A. Morsi, A.A. El-Shafei. *Transition Met. Chem.*, 11, 494 (1986).
- [19] S.D. Dhumwad, K.B. Gudasi, T.R. Goudar. *Ind. J. Chem.*, 33(A), 320 (1994).
- [20] K. Nakamoto. *Infrared and Raman Spectra of Inorganic and Coordination Compounds*, 3rd Edn, Vol. 305, Wiley, New York 305 (1978).
- [21] D.X. West, M.M. Salberg, G.A. Bain, A.E. Liberta. *Transition Met. Chem.*, 22, 180 (1997).
- [22] S. Mostafa, M.M. Bekheit, M.M. El-Agez. *Synth. React. Inorg. Met.-Org. Chem.*, 30, 2029 (2000).
- [23] A.A.M. Aly, M.S. El-Meligy, A.S. Zidan, M. El-Shabasy. *An. Quim.*, 86, 19 (1990).
- [24] A.B.P. Lever. *Inorganic Electronic Spectroscopy*, Elsevier, Amsterdam (1986).
- [25] A.A. El-Asmy, A.Z. El-Sonbati, A.A. Ba-Issa. *Transition Met. Chem.*, 15, 222 (1990).
- [26] A.A. El-Asmy. *Bull. Chim. Soc. Fr.*, 2, 171 (1989).
- [27] A.W. Coats, J.P. Redfern. *Nature*, 20, 68 (1964).
- [28] H.H. Horowitz, G. Metzger. *Anal. Chem.*, 25, 1464 (1963).

Copyright of Journal of Coordination Chemistry is the property of Taylor & Francis Ltd and its content may not be copied or emailed to multiple sites or posted to a listserv without the copyright holder's express written permission. However, users may print, download, or email articles for individual use.



A novel barium polymeric membrane sensor for selective determination of barium and sulphate ions based on the complex ion associate barium(II)–Rose Bengal as neutral ionophore

A.M. Othman^b, M.S. El-Shahawi^{a,*}, M. Abdel-Azeem^a

^a Chemistry Department, Faculty of Science at Damietta, Mansoura University, Damietta, Dumyat 34517, Egypt

^b Genetic Engineering and Biotechnology Research Institute (GEBRI), Minufiya University, Sadat City, Egypt

Received 27 May 2005; received in revised form 3 September 2005; accepted 10 September 2005

Available online 13 October 2005

Abstract

A simple, long life, rapid response and sensitive barium(II)–PVC membrane sensor that typically follows Nernstian behavior has been developed for the assay of barium(II) ions. The developed sensor has been made by incorporating the complex ion associate of barium(II)–Rose Bengal (Ba–RB) as an ionophore into a plasticized PVC matrix. The sensor is stable and exhibited fast potential response of 20s and gave a good linear response with a Nernstian slope of 28.5 ± 0.4 mV/decade of activity within the concentration range 5×10^{-5} to 10^{-1} M over a wide range of pH 4.5–10.0 for barium(II) ions. The developed sensor showed comparatively good selectivity for barium(II) ions with respect to other alkali, alkaline earth, transition and heavy metal ions. The plasticizer *o*-nitrophenyloctyl ether controlled significantly the calibration slope and the lifetime of the fabricated sensor. The proposed sensor was used successfully for the analysis of barium(II) ions in wastewater samples and in lithophone pigment with excellent recovery percentages in the range 98.9–99.8 \pm 1.6%. The determination of sulphate in fresh and potable water samples with the developed sensor has been also achieved successfully. The described sensor provides a reliable means with good correlation with the data obtained by atomic absorption spectrometry (AAS) and other spectrophotometric methods for the analysis of trace amounts of barium(II) and/or sulphate ions in different matrices.

© 2005 Published by Elsevier B.V.

Keywords: Barium(II) ions; Sulphate ions; PVC membrane sensor; Wastewater; Pigment

1. Introduction

The utility of ion selective electrodes (ISE) is being increasingly realized by analytical chemists in view of the rapid growth of industry and technology all over the world as they represent rapid, accurate and low cost procedures for trace metal analysis [1–5].

Recently, a series of novel membrane sensors based on polyethers [6,7], organophosphine [8] as neutral carrier and dimethyl 4,4-dimethoxy-5,6,5,6-dimethylene dioxy biphenyl-2,2-dicarboxylate liver drug [9] as ionophore in plasticized PVC matrix have been prepared and successfully used for the analy-

E-mail address: mohammad_elshahawi@yahoo.co.uk (M.S. El-Shahawi).

0003-2670/\$ – see front matter © 2005 Published by Elsevier B.V.

doi:10.1016/j.aca.2005.09.016

sis of barium(II) and/or sulphate ions in wastewater samples. A series of barium ion selective electrodes have been used for barium(II) ions determination [10–20], besides using them for indirect titration of sulfate [16–18] and for the analysis of non-ionic surfactants [19,20]. Most of the existing sensors are unsatisfactory for quality control routine analysis and unattractive for direct potentiometric monitoring because of their strict pH, low stability and lack of reproducible response with time.

Recently, the anionic dyestuff Rose Bengal (RB) (Fig. 1) was successfully used as an ion pair reagent for the extractive spectrophotometric determination of barium(II) in water [21].

* Corresponding author. Tel.: +20 403906.

Thus, in the present investigation, the complex ion associate of barium(II)–Rose Bengal was used as a novel ionophore in a PVC membrane sensor for the determination of barium(II) and/or sulphate ions. The developed sensor showed good sen-

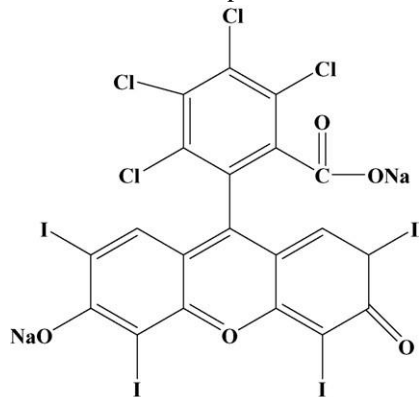


Fig. 1. Chemical structure of Rose Bengal.

sitivity, stability and significant selectivity for the analysis of barium(II) ions in wastewater and lithophone pigment.

2. Experimental

2.1. Reagents and materials

All chemicals used were of analytical reagent grade and were used without further purification unless otherwise stated. Doubly distilled water was used throughout the work for the preparation of the stock solutions of barium(II) chloride and metal chloride or nitrate of the metal ions: Na^+ , K^+ , Rb^+ , NH_4^+ , Mg^{2+} , Ca^{2+} , Sr^{2+} , Ba^{2+} , Mn^{2+} , Co^{2+} , Ni^{2+} , Cd^{2+} , Zn^{2+} and Al^{3+} . Standard aqueous solutions of barium chloride (10^{-5} to 10^{-1} M) were accurately prepared by gradual dilution of the stock solution of the salt. These solutions (10 ml) were then stirred in a water bath at 25 ± 1 °C and transferred to 50 ml beakers. The reagents Rose Bengal dye, high molecular weight poly(vinyl chloride) powder (PVC), *o*-nitrophenyloctyl ether (*o*-NPOE), potassium tetrakis (4-chlorophenyl) borate (KTpCIPB) and tetrahydrofuran (THF) were purchased from Fluka. Dibutyl sebacate (DBS) and dioctyl phthalate (DOP) were obtained from Aldrich.

2.2. Apparatus

The potentiometric measurements were made at 25 ± 1 °C with an Orion model SA 720 digital pH/mV meter microprocessor ionanalyser. The sensor based on the complex ion associate of barium(II)–Rose Bengal and PVC membrane was used with an Orion double junction Ag/AgCl reference electrode (model 90-02) containing potassium chloride solution (10%, w/v) in the outer compartment. A combination Ross glass pH electrode (Orion model 81-02) was used for all pH

measurements. The absorbance and the absorption spectra were recorded on a Varian 634s spectrophotometer.

2.3. Preparation of Ba–RB ionophore

The complex ion associate of barium–Rose Bengal (Ba–RB) was prepared by mixing 10 ml of barium chloride (1×10^{-2} M) with another 10 ml of 10^{-2} M of Rose Bengal. The mixture was then shaken well for 10 min and the produced precipitate was filtered through a Whatman filter paper (no. 42), washed with deionized water, dried at room temperature and finally grounded to a fine powder.

2.4. Fabrication of PVC barium(II)–Rose Bengal membrane sensor

The polymeric membrane was prepared by mixing the ion pair reagent Ba–RB (10 mg) with PVC (180 mg), the plasticizer *o*-NPOE (370 mg) and of the anion excluder KTpCIPB (5 mg) in 5 ml of freshly prepared THF. The resulting homogeneous syrup cocktail was poured into a petri dish (8 mm diameter), covered with filter paper and left to stand overnight to allow slow evaporation of the solvent at room temperature. A semi-transparent master flexible PVC membrane with an average thickness of 0.1 mm was obtained. A disc (8 mm diameter) was cut using a cork borer and glued to polyethylene tubing, to an interchangeable PVC tip, which was dipped onto the end of the electrode glass body as previously described [22–24]. The electrode was filled with the internal solution that was prepared from a mixture of an equal volume of an aqueous solution of barium chloride (1×10^{-2} M) and potassium chloride (1×10^{-2} M) and Ag/AgCl-coated wire electrode (1 mm diameter) was used as an internal reference electrode. The sensor was finally pre-conditioned after preparations by soaking in barium chloride solution (10^{-2} M) for 1 h and stored in the same solution when not in use. The sensor was washed with doubly distilled water and blotted with tissue-paper measurements. The external reference electrode was a double junction of Ag/AgCl. The electrochemical cell used was: Ag/AgCl || 10^{-2} M KCl – test solution || PVC membrane || internal filling solution – 10^{-2} M KCl || Ag/AgCl reference electrode. The developed sensor was conditioned by soaking in barium(II) chloride solution (10^{-2} M) for 2 h and was stored in the same solution when not in use.

2.5. Sensor calibration

The sensor Ba–RB in conjunction with a double junction Ag/AgCl reference electrode was immersed in the test solution of standard barium chloride (1×10^{-5} to 1×10^{-2} M). The potential readings were recorded starting from the low to the high concentrations when stabilized to ± 0.2 mV and plotted versus

logarithmic barium(II) ions concentration. The calibration graph was used on the subsequent determination of the unknown barium ion. The detection limit was taken at the point of intersection of the extrapolated linear segments of the standard curve of barium(II) ions. Repeatability was measured by immersing the sensor alternatively into 10^{-2} and 10^{-3} M BaCl_2 solutions at 25 ± 1 °C. Sensor life span was examined by repeated monitoring of the slope of the calibration curve of barium(II) ions periodically.

2.6. Sensor selectivity

The potentiometric selectivity coefficients ($K_{\text{Ba},\text{B}}^{\text{pot}}$) of the developed sensor were determined using the separate solution method [23,25] and calculated employing the rearranged Nikolsky equation:

$$\log K_{\text{Ba}^{2+},\text{B}}^{\text{pot}} = \frac{[E_{\text{Ba}^{2+}} - E_{\text{B}}]}{S} + \left[\frac{1 - Z_{\text{Ba}^{2+}}}{Z_{\text{B}}} \right] \log \text{Ba}^{2+} \quad (1)$$

where $E_{\text{Ba}^{2+}}$ is the potential measured in 10^{-2} M for Ba^{2+} , E_{B} is the potential measured in 10^{-2} M of the interfering anion, $Z_{\text{Ba}^{2+}}$, Z_{B} are the charges of the Ba^{2+} and the interfering species, respectively, and S is the slope of the electrode calibration curve plot [26]. Aliquots (10 ml) of barium(II) chloride solution (10^{-2} M) were adjusted to pH 6. The proposed sensor was immersed in the solution and the potential reading of 10^{-2} M solution of the interfering ions: Li^+ , Na^+ , K^+ , NH_4^+ , Mg^{2+} , Ca^{2+} , Sr^{2+} , Fe^{2+} , Co^{2+} , Ni^{2+} , Zn^{2+} , Pb^{2+} , Mn^{2+} , Cd^{2+} , or Al^{3+} adjusted to pH 6 was measured.

2.7. Analytical applications

2.7.1. Analysis of barium(II) in wastewater

Industrial wastewater samples containing various amounts of Ni^{2+} , Cu^{2+} and Cr^{6+} collected from electroplating plants were tested for the analysis of barium(II) content as follows. An aliquot (10 ml) of the water samples was acidified by adding 1 ml of concentrated nitric acid and filtered to remove suspended particles. The solutions were then adjusted to pH 6 with dilute NaOH and/or HCl, transferred to 50 ml calibrated flask and completed to the mark with doubly distilled water and finally shaken well. The developed sensor in conjunction with an Ag/AgCl reference electrode was immersed in the test solutions as described earlier. The potential readings were then measured and the barium(II) content was finally determined from the standard calibration curve (direct method).

Alternatively, the standard addition method was used for the analysis of barium(II) in wastewater samples as follows. Transfer a known volume of the industrial wastewater samples after filtration adjusted to pH 6 into 100 ml flask. Measure the potentials displayed by the test solution of the wastewater samples before and after addition of 2.0 ml aliquot of the standard barium(II) solution (10^{-2} M). The change in the electrode potential was then recorded and used for determining the barium(II) ions.

2.7.2. Analysis of barium(II) in lithophone pigment

An accurate weight (0.5 ± 0.01 g) of the lithophone pigment CIS was dissolved in 10 ml of hot concentrated nitric acid. The solution was then heated for 30 min and filtered through Whatman filter G.42. The filtrate and the washing solutions were adjusted to pH 6 and transferred to 50.0 ml calibrated flask and completed to the mark with double distilled water. The potential of the test solution was then measured and the barium(II) content was determined with aid of the standard curve prepared under the same experimental conditions. Alternatively, the standard addition method was also employed for barium(II) determination in lithophone pigment.

2.7.3. Analysis of sulphate in tap water

The potable water samples (5 ml) spiked with various concentrations of sodium sulphate (10^{-1} to 10^{-2} M) adjusted to pH 5–6 with dilute HCl and/or NaOH were placed in the electrochemical titration cell. A known volume of the titrant BaCl_2 (10^{-2} M) was added gradually to the same titration cell by means of micro burette till the equivalence point. After each addition, the mixture was left for 2 min and the potential readings and the volume of the titrant added were recorded gradually. The potential readings were then plotted versus the titrant volume. Experiments were repeated several times for concordance.

3. Results and discussion

3.1. Performance characteristics of Ba–RB sensor

Electrically neutral, lipophilic ion complexing agents are known to behave as an ionophore or ion carrier [26]. Such neutral carriers are able to extract some ions with excellent selectivity from the aqueous solutions into hydrophobic membrane phase and transporting them across barriers by carrier translocation [26]. When the neutral carriers are incorporated into a waterimmiscible membrane, it functions as an ion selective sensor and exhibits a nearly Nernstian response to the primary ion.

Preliminary experiments have shown that Rose Bengal is not suitable as an ionophore in PVC membrane for barium(II) ions. On the other hand, barium(II) ions in aqueous media react with Rose Bengal to form an insoluble colored complex ion associate (Ba–RB). The formula of the complex ion associate was determined by Job's method and the results showed a mole ratio

response to barium ions in terms of calibration slope of 28.5 ± 0.5 mV/decade over a concentration range of 1×10^{-5} to 1×10^{-1} M and detection limit of 2.5×10^{-6} M. The plasticizer *o*-NPOE enhances the extraction capability, revealing high sensitivity. The *o*-NPOE plasticized sensor containing the anion excluder KTpCIPB also gave a better recovery percentage, precision and less standard deviation than the sensors plasticized with DOP and DSB under the same experimental conditions. The anion excluder KTpCIPB improved the selectivity for barium(II) ions because it enhanced the response characteristics of the sensor by reducing the membrane resistance and decreasing the activation barrier of the membrane–solution interface [14,27].

3.3. Effect of pH

The dependence of the potential response of the *o*-NPOE plasticized Ba–RB membrane sensor on the solution pH over a wide range of pH 2.0–11 using dilute HCl and/or NaOH was critically investigated at different concentrations of standard barium(II) chloride. The electrochemical cell of the type Ag/AgCl/ 10^{-2} M BaCl₂ solution— 10^{-2} M KCl (inner solution)/plastic membrane/ 10^{-3} M BaCl₂ solution (outer solution)/Orion double junction reference electrode with KCl (10%) in the outer compartment with varying acidity was used successfully. The potential pH profiles for 10^{-2} and 10^{-3} M increased (Fig. 3) and became progressively sensitive to the interference caused by the hydrogen ions. The instability of the complex ion pair Ba–RB at pH <4.5 and the presence of the additive upon the membranes are also important issues and may control the membrane response and stability [30,31]. At pH >10.5, the potential response of the sensor slightly decreased, probably due to the hydrolysis of Ba²⁺ ions and the formation of insoluble poly hydroxy complex species of barium(II) in the solution which causes a decrease in the activity of barium(II) ions [20]. Thus, a pH of 4.5–10.0 is used in the next work for barium(II) ion determination.

3.4. Effect of foreign ions

The potentiometric selectivity coefficient ($K_{Ba,B}^{pot}$) of the developed Ba–RB membrane sensor depends on the selectivity

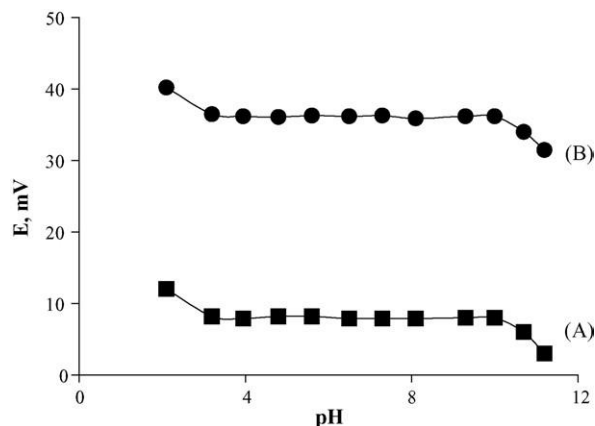


Fig. 3. Effect of pH on the potential response of barium(II)–Rose Bengal sensor 10^{-3} M (A) and 10^{-2} M (B).

of the ion-exchange process at the membrane–sample interface, the mobility of the respective ions in the membrane and the hydrophobic interactions between the primary ions and the organic membrane [18,25]. The free energy of transfer of the barium(II) ions between the aqueous and the organic phases also controls the selectivity of the proposed sensor. The separate solution and mixed solution methods are usually used to determine the potentiometric selectivity of the sensor towards different cations [23,28]. The separate solution method was preferred and successfully applied as it usually corresponds more closely to the situation of the sample. The results of the potentiometric selectivity of BaCl₂ solution (10^{-2} M) and the foreign ion (10^{-2} M) at pH 6 are summarized in Table 3. The data indicated that the sensor exhibited a good selectivity towards Ba²⁺ with respect to the tested ions: Li⁺, Na⁺, Rb⁺, NH₄⁺, Mg²⁺, Ca²⁺, Fe²⁺, Co²⁺, Cu²⁺, Ni²⁺, Zn²⁺, Pb²⁺, Mn²⁺, Cd²⁺, and Ce³⁺. For Al³⁺ ions, good selectivity (Table 3) was achieved by adjusting the solution pH to 4.5–5.0 to enhance the solubility of aluminum species in the tested media. On the other hand,

Table 3

Selectivity coefficient ($K_{Ba,B}^{pot}$) of the developed Ba–RB PVC membrane sensor

Interferent, B	$K_{Ba,B}^{pot}$
Li	1.9×10^{-3}
Na	5.4×10^{-4}
K ⁺	2.03

Rb ⁺	5.4×10 ⁻⁴	
NH ₄ ⁺		
Mg ²⁺		
Ca ²⁺		
Sr ²⁺	5.0 ^{xx} ×10 ^{10⁻³³}	
Co ²⁺	³	
Ni ²⁺	1.9	
Cu ²⁺	5.7	10
Mn ²⁺	8.1×10 ⁻⁴	
Fe ²⁺		
Pb ²⁺	1.2 ^x ×10 ⁻³⁴	
Zn ²⁺	1.85	10
Cd ²⁺		
Al ³⁺	3.5 ^x ×10 ⁻³⁴	
Ce ³⁺	1.2	10
	2.0×10 ⁻²	
	2.5×10 ⁻⁵	
	2.8 ^{xx} ×10 ⁻⁵⁴⁴	
	2.7	10
	6.3	10
	1.9×10	

Table 4
Analysis of barium(II) ions in wastewater (A) and lithophone pigment (B) samples by the developed sensor^a

Sample	Recovery %±standard deviation			
	(A)		(B)	
	Ba–RB	AAS	Ba–RB	AAS
1	100.3 ± 0.7	99.4 ± 0.6	99.5 ±	99.2±0.6
2	0.6	100.0 ± 0.8	98.6±0.7	99.6 ± 0.5
3	99.6 ± 0.5	99.2 ± 0.7	98.9±0.6	100.2 ± 0.6

^a Average of five measurements±standard deviations.

K⁺ and Sr²⁺ interfered seriously and the order of the response of the proposed sensor for the alkaline metal ions: Mg²⁺, Ca²⁺, and Sr²⁺ followed the sequence: Ba²⁺ > Sr²⁺ > Ca²⁺ > Mg²⁺ as shown in Fig. 2. No improvement of the sensor selectivity for Ba²⁺ over K⁺, Sr²⁺ and CrO₄²⁻ was noticed. On the contrary, the response of the sensor for Ba²⁺ over H₂PO₄⁻, NO₃⁻ or I⁻ ions was observed, probably due to the strong interaction of these species with the anion excluder KTpCIPB. Measurements of the electronic absorption spectra of the reagent RB and RB in the presence of Ba²⁺, Mg²⁺, Ca²⁺, H₂PO₄⁻, NO₃⁻ and I⁻ ions showed absorption maxima at 553, 565, 552, 548, 557, 557, 556 nm, respectively. Significant red shift in the visible spectrum of RB (553 nm) and great change of the molar absorptivity were noticed with Ba²⁺

(565 nm) confirming the selectivity coefficient data (Table 3) and are inconsistent with the published results [21].

3.5. Analytical applications

3.5.1. Analysis of barium(II) ions in wastewater

The analytical utility, sensitivity and selectivity of the proposed membrane sensor was verified by the analysis of barium(II) ions in industrial wastewater samples containing Ni²⁺, Cu²⁺ and Cr⁶⁺ metal ions using direct and standard addition (spiking) techniques. The results for barium determination in wastewater samples are given in Table 4. Recovery experiments were performed by repeated measurements (*n* = 5) of wastewater samples containing various amounts of barium(II) ions in the range 1 × 10⁻³ to 1 × 10⁻⁴ M. A recovery percentage in the range 99.2–100.0 ± 0.8 with a relative standard deviation of ±1.6% was achieved. These results are compared successfully with the data obtained employing the standard atomic absorption spectrometry (AAS), where an average recovery of 99.5% and a mean standard deviation of ±1.6% were obtained. The *F*-test revealed no significant difference between the means and vari-

Table 5
Analysis of sulphate(II) ions in potable water by the developed sensor^a

Sample	Recovery %±standard deviation	
	Ba–RB sensor	Titration method
1	98.3±0.7	99.2±0.6
2	99.4±0.5	97.8±0.8
3		99.2±0.7

^a Average of five measurements±standard deviations.

Table 6
The performance characteristics of Ba–RB membrane sensor compared with other barium sensors

Parameter	Reported sensors					Present work
	[17]	[11]	[12]	[13]	EDT ^c	
Slope (mV/decade)	30.0	26.6	28.0	32.0		28.5
LLLR ^a (M)	3×10^{-6}	1×10^{-5}	9×10^{-6}	8×10^{-6}	7×10^{-5}	1×10^{-5}
LLD ^b (M)	2×10^{-6}	3×10^{-6}			5×10^{-5}	2.5×10^{-6}
pH range	1.6–8.1	2–10	1.5–10	2–8	5–9	4.5–10

^a LLLR (M): lower limit of linear range. ^b LLD (M): lower limit of detection. ^c Commercial electrode from EDT Analytical (London).

ances of the two sets of results. The good agreement between the proposed sensor and the standard spectrometric method provides an alternative approach to AAS since, the developed sensor is low cost, simple and rapid for routine analysis of barium(II) content in real samples without a prior pretreatment in the presence of some other metal ions.

3.5.2. Analysis of barium(II) ions in lithophone pigment

The developed sensor was also tested for the analysis of barium(II) ions in lithophone pigment (chemical composition ZnS, 28–30% and BaSO₄, 68–70%). The results obtained for the analysis of barium(II) ions by the proposed sensor and AAS are given in Table 4. An average recovery of $98.9 \pm 1.2\%$ with a mean standard deviation of $\pm 0.9\%$ were achieved by the developed method and are in good agreement with the results obtained by AAS (Table 4).

3.5.3. Analysis of sulphate(II) ions in potable water

The potentiometric titration curve of sodium sulphate solution (1×10^{-2} M) against barium chloride solution (10^{-2} M) employing the developed sensor was constructed with potential break of ~ 40 mV (Fig. 4). The results of sulphate ions analysis in potable water spiked with different concentrations of sulphate ions by the proposed sensor are summarized in Table 5. The data obtained are in good agreement with the results obtained by the standard titration method employing barium perchlorate and thorin indicator [29]. The average recov-

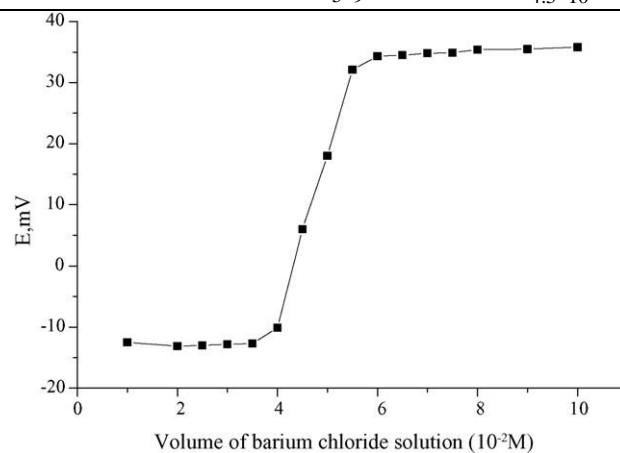


Fig. 4. Typical potentiometric titration curve for 15.0 ml of sodium sulphate (10^{-2} M) with barium chloride (10^{-2} M) employing Ba–RB sensor.

eries 98.9; 98.4% and mean standard deviation of 0.6% and 0.7% were obtained by the proposed Ba–RB sensor and the reported method [29], respectively. These data are compared favorably in both sensitivity and selectivity with the reported method [29] for the analysis of sulphate ions. Thus, the proposed sensor can certainly be placed among the most sensitive ones.

3.5.4. Comparison with other sensors and reported methods

The response characteristics of the proposed Ba–RB membrane sensor for the analysis of barium(II) ions is compared with some of the reported sensors for barium(II) determination (Table 6). The present sensor exhibits better or comparable wider lower linear range (5×10^{-5} M), lower limit of detection (2.5×10^{-5} M), wide range of pH 4.5–10 and much shorter response time in comparison to most of the reported sensors. The developed sensor is also more convenient than methods based on solvent extraction prior to spectrophotometric measurements [21]. The commercial availability of Ba–RB ionophore at a considerably cheap price compared to ionophore based sensors [10,14,30,31] add further advantage to the present sensor. The selectivity coefficients of the present sensor are in the order of 1×10^{-3} or smaller, indicating that the metal ions used have negligible disturbance of the functioning of the barium sensor. The results obtained by the proposed sensor are in satisfactory agreement with those obtained by AAS and its lifetime is long compared to other sensors [30,31]. The present sensor was found to work well under laboratory conditions and was applied

successfully for direct titration of sulphate in pure water and in also in synthetic mixtures.

4. Conclusion

The developed sensor is simple, rapid, low cost and provides reliable procedures for the analysis of barium(II) ions in lithophone pigment and in industrial wastewater samples at level 2.5 g/ml. The sensor can be used directly, as there is no need for long or tedious separation procedures and no need for expensive and sophisticated instrument. The proposed sensor was found also suitable for direct analysis of sulphate ions in potable water. These characteristics make the use of the developed sensor attractive and convenient tool for routine control analysis of barium(II) and/or sulphate ions determinations in different matrices. The proposed sensor can certainly be placed among the most sensitive ones for analysis of barium.

Acknowledgement

The authors would like to thank Mr. H.M. Nassef for his assistance in figure preparations.

References

- [1] S.S.M. Hassan, M.M. Ali, A.M.Y. Attawiya, *Talanta* 54 (2001) 1153.
- [2] S.S.M. Hassan, M.B. Saleh, A.A. Abdel Gaber, R.A.H. Mekheimer, N.A. Abdel-Kream, *Talanta* 53 (2000) 285.
- [3] R.K. Mahajan, I. Kaur, T.S.A. Lobana, *Talanta* 59 (2003) 101.
- [4] M.H. Mashhadizadeh, I. Sheikhshoae, *Talanta* 60 (2003) 73.
- [5] M. Shamsipur, M.R. Ganjali, A. Rauhollahi, A.M. Maghimi, *Anal. Acta Chim.* 434 (2001) 27.
- [6] G.J. Moody, J.D.R. Thomas, *Nonionic Surfactants Chemical Analysis*, Marcel Dekker, New York, 1986.
- [7] E.Y. Khmel'nitskaya, B.N. Kolokolov, *Zh. Anal. Khim.* 50 (1995) 1108. [8] M.B. Saleh, J. Fresenius, *Anal. Chem.* 367 (6) (2000) 530. [9] S.S.M. Hassan, M.B. Saleh, A.A. Abdel Gaber, N.A. Abdel Kaream, *Talanta* 59 (2003) 161.
- [10] M. Guggi, E. Pretsch, W. Simon, *Anal. Chim. Acta* 91 (1977) 107.
- [11] M.W. Laubli, O. Dinten, E. Pretsch, W. Simon, F. Vogtle, F. Bongardt, T. Kleiner, *Anal. Chem.* 57 (14) (1985) 2756.
- [12] M.B. Chandra, M.C.J. Chattopadhyaya, *Indian Chem. Soc.* 67 (1990) 229.
- [13] K. Nagashima, T. Hobo, G.J. Moody, J.D.R. Thomas, *Anal. Chim. Acta* 222 (1) (1989) 211.
- [14] A.A. Bonklouze, J.C. Vire, V. Cool, *Anal. Chim. Acta* 273 (1–2) (1993) 153.
- [15] Y.P. Feng, G. Goodlet, N.K. Harris, M.M. Islam, G.J. Moody, J.D.R. Thomas, *Analyst* 116 (5) (1991) 469.
- [16] G.J. Moody, J.D.R. Thomas, *Analyst* 113 (7) (1988) 1023.
- [17] D.L. Jones, G.J. Moody, J.D.R. Thomas, R.M. Hangos, *Analyst* 104 (1979) 973.
- [18] G.J. Moody, J.D.R. Thomas, *Lab. Pract.* 28 (1979) 125.
- [19] D.L. Jones, G.J. Moody, J.D.R. Thomas, *Analyst* 106 (1981) 439.
- [20] D.L. Jones, G.J. Moody, J.D.R. Thomas, B.J. Birch, *Analyst* 106 (1981) 974.
- [21] H. Parham, A.G. Fazeli, *Anal. Sci. (Jpn.)* 16 (2000) 575.
- [22] A. Graggs, G.J. Moody, G.D.R. Thomas, *J. Chem. Educ.* 51 (1974) 451.
- [23] T.S. Ma, S.S.M. Hassan, *Organic Analysis Using Ion Selective Electrodes*, Academic Press, London, 1982.
- [24] S.S.M. Hassan, W.H. Mahmoud, A.M. Othman, *Talanta* 44 (1997) 1087, and references cited therein.
- [25] IUPAC Analytical Chemistry Division, Commission on Analytical Nomenclature, *Pure Appl. Chem.* 67 (1995) 507.
- [26] Y.A. Ovchinnikov, V.T. Ivanov, A.M. Shkrob, *Membrane Active Complexes*, BBA Library, Elsevier, Amsterdam, Netherlands, 1974.
- [27] G.K.J. Budnikov, *Anal. Chem.* 55 (2000) 1014.
- [28] Y. Umezawa, K. Umezawa, H. Sato, *Pure Appl. Chem.* 67 (1995) 507.
- [29] S.K. Menon, A. Sathyaplan, Y.K. Agrawal, *Rev. Anal. Chem.* 16 (1997) 333.
- [30] R.J. Levins, *Anal. Chem.* 43 (1971) 1045.
- [31] A.M.Y. Jaber, G.J. Moody, J.D.R. Thomas, *Analyst* 101 (1976) 179.



Retention profile, kinetics and sequential determination of selenium(IV) and (VI) employing 4,4-dichlorodithizone immobilized-polyurethane foams

M.S. El-Shahawi*, M.A. El-Sonbati

Chemistry and Environmental Science Department, Faculty of Science at Damietta, Mansoura University, Mansoura, Egypt

Received 1 December 2004; received in revised form 2 April 2005; accepted 4 April 2005

Available online 23 May 2005

Abstract

Polyurethane foams (PUFs) loaded with the chromogenic reagent 4,4-dichlorodithizone ($\text{Cl}_2\text{H}_2\text{Dz}$) have been investigated for the quantitative retention, chemical speciation and sequential determination of traces of inorganic selenium(IV) and (VI) from aqueous media containing bromide ions. The retention profile of selenium(IV) onto the reagent loaded foam followed a dual-mode sorption mechanism involving both absorption related to “solvent extraction” and an added component for surface adsorption. The kinetics and thermodynamic characteristics of selenium(IV) uptake onto PUFs have been studied. The kinetics of selenium(IV) sorption onto PUFs was found fast, reached equilibrium in few minutes and followed a first-order rate constant in presence of bromide ions in the extraction media. The thermodynamic parameters, H , S and G , indicated the exothermic and spontaneous nature of the sorption process. The sorption and the recovery percentages of inorganic selenium(IV) from fresh water by the proposed loaded foam columns were achieved quantitatively. The height equivalent to theoretical plate (HETP), the number of layers (N), breakthrough capacity and the critical capacity for selenium(IV) uptake onto $\text{Cl}_2\text{H}_2\text{Dz}$ loaded foams columns were found to be 1.3, 103, 8.6 and 7.2mg/g, respectively. The method was successfully applied for the chemical speciation and sequential determination of inorganic selenium(IV) and/or (VI) species spiked to fresh and industrial wastewaters. © 2005 Published by Elsevier B.V.

Keywords: Selenium(IV) and (VI); $\text{Cl}_2\text{H}_2\text{Dz}$; Kinetics; Sorption isotherms; Sorption mechanism; Thermodynamics; PUFs

1. Introduction

Selenium enters into natural waters through seepage from seleniferous soils and industrial waste and liberated into the environment (in soil) through complex biogeochemical reaction forming organoselenium compounds [1]. These compounds are more toxic than inorganic selenium compounds and absorbed by plants such as cabbage and mustard [2,3]. However, trace amounts of selenium have been found to be essential to maintain normal body metabolism [4], since it takes part in the glutathione peroxidase enzyme [4,5]. Selenium(IV) species can also enhance our ability to protect

*Corresponding author.

E-mail address: mohammad-el-shahawi@hotmail.com (M.S. El-Shahawi).

0039-9140/\$ – see front matter © 2005 Published by Elsevier B.V.
doi:10.1016/j.talanta.2005.04.012

against certain cancer and heart diseases [6,7]. The maximum allowed tolerance limit of selenium is $<0.1 \text{ mg/m}^3$ in air, $<0.05 \text{ g/ml}$ in water and $\leq 80 \text{ g/kg}$ in soil [8].

Polyurethane foam (PUF) sorbent represents a cheap and efficient separation and preconcentration media with steadily

increasing versatile application in inorganic species analysis [9,10]. Applications of PUFs are of great importance in overcoming many pollution hazards of inorganic pollutants by bringing them to an acceptable concentration in water and other media [9]. Selenium and tellurium have been sorbed from HCl and HBr media by polyether and polyester-based polyurethane foam [11].

Recently, a number of solid sorbents involving untreated and treated foamed plastics have been tested as supports in the reversed-phase extraction chromatography [12–22]. The broad range of surface functional groups present in the basic unit of PUF influences its retention properties and reactivity. PUF unloaded or immobilizing specific chromogenic reagents have been successfully employed on-line for the preconcentration, separation and determination of different inorganic species in natural and fresh waters and biological samples [15–19].

The present work is aimed at developing simple, convenient and low cost procedures for the preconcentration, chemical speciation and sequential spectrophotometric determination of inorganic selenium(IV) and (VI) ions in water employing the reagent 4,4-dichlorodithizone ($\text{Cl}_2\text{H}_2\text{D}_Z$) immobilized PUFs. The kinetics and thermodynamic characteristics of the sorption step onto PUF are critically discussed. Several adsorption models will be used for the retention of randomly distribution sites of equal energy in which Freundlich and Langmuir adsorption isotherms are most commonly used. The mechanism of selenium(IV) sorption employing dithizone or dithizone analogues is a subject of contradictory opinions [23,24].

2. Experimental

2.1. Reagents and materials

All chemicals used were of analytical reagent grade and acids were used without further purification. A stock solution (1000 g/ml) of NaHSeO_3 was prepared in double distilled water. A stock solution of the reagent $\text{Cl}_2\text{H}_2\text{D}_Z$ (0.1%, w/v) was prepared in 10 ml chloroform. The solution was kept refrigerated prior to use under acidified aqueous solution containing sulphuric acid (0.2 M) and sodium sulphate (0.1 M). Commercial white sheets of open cell polyether type PUFs (25 kg/m^3) were used. The foam cubes (10–15 mm edge) were cut from the foam sheets, washed, dried at 80°C for 2 h [22] and finally stored in plastic bottles for further use. The reagent $\text{Cl}_2\text{H}_2\text{D}_Z$ loaded foam cubes were prepared by mixing the dried foam cubes with chloroform containing $\text{Cl}_2\text{H}_2\text{D}_Z$ at 0.02% (w/v) (50 ml/g dry foam) with efficient stirring in the presence of sulphur dioxide for 30 min and were dried as reported earlier [22]. The reagent $\text{Cl}_2\text{H}_2\text{D}_Z$ immobilized PUFs was found stable for up to 20 h. The

$\text{Cl}_2\text{H}_2\text{D}_Z$ immobilized PUFs ($\approx 4.0 \pm 0.01 \text{ g}$) were packed in a glass column as reported earlier [22].

2.2. Synthesis of 1,5-di-(4-chlorophenyl)-3-mercaptopformazan ($\text{Cl}_2\text{H}_2\text{D}_Z$)

The reagent $\text{Cl}_2\text{H}_2\text{D}_Z$ was prepared by the nitroformazyl method [25]. The nitroformazan was recrystallized from ethanol, converted to 1,5-di-(4-chlorophenyl)-3-mercaptopformazan and finally purified by dissolution in chloroform. The chloroform extract was stripped with dilute sodium hydroxide solution (2%, w/v) and finally pouring the extract into sulphuric acid (0.5 M). The solid reagent was washed with ethanol until it became acid free, dried, dissolved in chloroform, precipitated with cyclohexane and finally dried in vacuum (mp 125°C). Elemental analysis of $\text{C}_{13}\text{H}_{10}\text{N}_4\text{SCl}_2$ —required: C = 53.2%, H = 3.4%, N = 19.1% and Cl = 24.2%; found: C = 53.9%, H = 3.5%, N = 19.4% and Cl = 25.1%.

2.3. Apparatus

A Soxhlet extractor and a lab-line Orbital mechanical shaker SO1 (UK) were used for the foam purification and batch retention experiments. Glass columns (18 cm \times 15 mm i.d.) were used in the flow experiments. A single beam Digital Spectro UV–VIS RS Labomed, spectrophotometer with quartz cell (10 mm path length) and a pH meter model 3305 (JENWAY) were used for the absorbance and pH measurements of the test solutions, respectively.

2.4. General extraction procedures

2.4.1. Batch experiments

In a dry 100 ml polyethylene bottle, an accurate weight ($0.5 \pm 0.01 \text{ g}$) of the reagent $\text{Cl}_2\text{H}_2\text{D}_Z$ loaded foam cubes was shaken on a mechanical shaker for 2 h with 50 ml of an aqueous solution containing selenium(IV) ions at 5 g/ml concentration level at $20 \pm 0.1^\circ\text{C}$ and at the required pH adjusted by diluted HCl or NaOH. After phase separation, a 10 ml aliquot was assayed spectrophotometrically at 435 nm [23]. The amount of selenium(IV) retained on the foam cubes was determined from the difference between the absorbance of selenium(IV) solutions before (A_b) and after (A_f) shaking with the reagent $\text{Cl}_2\text{H}_2\text{D}_Z$ foam cubes. The extraction percentage (%E) and the distribution ratio (D) of the selenium(IV) uptake on the loaded foam were calculated employing the equations:

$$\%E = \left(\frac{A_b - A_f}{A_b} \right) \times 100 \quad (1)$$

%E v (ml)

$$D = \frac{v}{100} \times \frac{\%E}{w \text{ (g)}} \quad (2)$$

where v is the sample volume in milliliters and w is the weight of the reagent foam cubes in grams. Following these procedures, the kinetics, retention and thermodynamic studies were adopted. All experiments were performed in triplicate at ambient temperature (20 ± 0.1 °C). The results are the average of three independent measurements and the precision in most cases was $\pm 2\%$. The expected statistical error in the $\%E$ and D calculations is within the range of ± 2.4 .

2.4.2. Column experiments

An aqueous solution (2–3 l) of tap, deionized or industrial wastewater samples spiked with selenium(IV) at 0.05–1 g/ml level at the optimum experimental conditions was percolated through the foam (4.0 ± 0.01 g) packed column at 2.5 ml/min flow rate. Under these conditions sorption of selenium(IV) took place. The selenium(IV) content before percolation and in the effluent solution was measured at 435 nm against a reagent blank [23]. The sorbed selenium(VI) species on the foam column were then eluted with 20 ml chloroform at 3 ml/min flow rate and measured [23].

2.5. Sequential determination of selenium(VI)

Transfer an aliquot (10 ml) of the aqueous solutions containing 0.5–10 g/ml of selenium(VI). The solutions were then reduced to selenium(IV) with HCl (6 M) by boiling for 15 min in a closed system (to avoid the evaporation of selenium species) and cooled as reported earlier [11]. The pH of the test solution was then adjusted to pH 0–1 by few drops of saturated NaOH. The produced selenium(IV) solutions were diluted to 10 ml and analyzed as reported [23] via their standard curves prepared under the same experimental conditions.

3. Results and discussion

3.1. Absorption spectra

The electronic spectra of the reagents H_2D_Z , $Cl_2H_2D_Z$ and their selenium(IV) chelates in $CHCl_3$ are summarized in Table 1. The characteristic infrared (IR) frequencies of the solid reagents and their selenium(IV) chelates in chloroform and in parallelepiped PUFs are also included in Table 1. The electronic spectra of the reagents showed two well resolved absorption bands in the region of 454–429 and 615–627 nm, whereas their selenium(IV) chelates showed one well defined single band in the range 416–435 nm with a slight basochromic shift in the PUFs (420–440 nm). The introduction of chlorine atoms into the *para* positions of the

two phenyl nuclei of dithizone analogue ($Cl_2H_2D_Z$) leads to a slight hypsochromic shift for the band at 429 nm and basochromic shift for the band at 627 nm compared to dithizone (Table 1). The molar absorptivity (ϵ) value at λ_{max} 627 nm decreased to 2.43×10^4 l mol⁻¹ cm⁻¹ and at 429 nm increased to 2.39×10^4 l mol⁻¹ cm⁻¹ for the reagent

$Cl_2H_2D_Z$ compared to H_2D_Z in $CHCl_3$ (Table 1). Since the geometry of the complex $Se[(HD_Z)_2] Cl_2$ was found tetrahedral [23,24], the corresponding complex of $Cl_2H_2D_Z$ is most likely tetrahedral. This suggestion was also confirmed from the analytical data of the chelate $[SeC_{26}H_{18}S_2Cl_4]Cl_2$ given in Table 1 (required: C = 42.9, H = 2.5, N = 15.4 and S = 8.8;

Table 1

found: C = 42.8, H = 2.7, N = 15.5 and S = 8.04). The IR spectrum of the isolated solid complex was compared with the IR spectra of the selenium(IV) salt and the free reagent $Cl_2H_2D_Z$ recorded separately in KBr discs and as a mechanical mixture of selenium(IV) with the $Cl_2H_2D_Z$ in 1:2 molar ratio. The characteristic IR frequencies observed at 3436 (br), 1636 (s), 1487 (s) and 440 cm⁻¹ are safely assigned to $\nu(N-H)$, $\nu(N-N)$, $\sigma(N-H) + (-C-N-)$, $\nu(N-C-S)$ and $\nu(Se-Cl)$ [24], respectively.

Preliminary investigation has shown that the reagent $Cl_2H_2D_Z$ immobilized PUF forms a red colored complex with selenium(IV) in the aqueous solution containing HCl (4 M) and NaBr (2 M). The produced complex was easily retained from the aqueous solution onto the PUF cubes. The reagent foam combines both the selectivity of the chelating agent and/or the advantageous rapidity of kinetic process between trace metal ions in the aqueous phase and the chromofoam in the foam membranes. Thus, the analytical utility of this reaction for the separation, chemical speciation and sequential determination of inorganic selenium(IV) and (VI) was found possible in both static and dynamic modes.

3.2. Retention profiles of selenium(IV) sorption onto $Cl_2H_2D_Z$ loaded PUF

In the aqueous solution containing NaBr (2 M), the amount of selenium(IV) ions sorbed onto the reagent $Cl_2H_2D_Z$ loaded foams was found to depend on the solution pH. Therefore, the sorption profiles of selenium(IV) ions from the aqueous solution onto the reagent loaded foams were investigated at various pH 0–12. The sorption percentage of selenium(IV) decreased with increasing the solution pH and maximum uptake was achieved in the range of pH 0–2 indicating that the protonated active sites of PUF are more compatible sites for the sorption of the complex species of selenium(IV). The decrease in the selenium(IV) uptake by the reagent loaded foams at pH > 2 is attributed to the instability

of the complex formed between selenium(IV) and the reagent $\text{Cl}_2\text{H}_2\text{D}_z$ and subsequent hydrolysis at higher pH. Thus, in the subsequent work, the solution pH was kept at pH 0–2.

In acidic medium (2 M HCl), the nitrogen atom of the amide ($-\text{NH}-\text{CO}-\text{O}-$) and/or oxygen atom of ether ($-\text{CH}_2-\text{O}-\text{CH}_2-$) groups of the PUF have strong tendency either to donate the lone pair of electrons to the central metal atom or to take the hydroxonium (H^+) ions to form ammonium and hydroxyl ions, respectively, to neutralize the

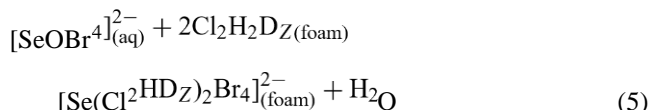
The pK_a values of protonation of ether oxygen and amide nitrogen are -3 and -6 [26], respectively. Thus, the ether groups of the PUFs in HCl (2 M) media are easily protonated as compared to the amide nitrogen and the interaction of $[\text{Se}(\text{Cl}_2\text{H}_2\text{D}_z)_2\text{Br}_4]^{2-}$ species appears to be more stronger.

The influence of mineral acid, e.g., HCl, HNO_3 , HClO_4 or H_2SO_4 (1 M), on the selenium(IV) uptake onto $\text{Cl}_2\text{H}_2\text{D}_z$ immobilized PUFs indicated that the sorption is quantitative in HCl. The sorption percentage of selenium(IV) increases

Characteristic absorption IR (cm^{-1}) and electronic (nm) spectral data for the reagents H_2D_z and $\text{Cl}_2\text{H}_2\text{D}_z$ and their selenium(IV) chelate in KBr disc and chloroform, respectively¹⁹

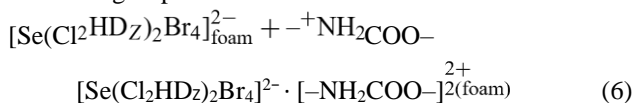
Compound	Wavenumber(cm^{-1})		λ_{max} (nm)		$\epsilon \times 10^{-4} \text{ l mol}^{-1} \text{ cm}^{-1}$	
	$\nu(\text{N}-\text{H})$	$\nu(\text{N}-\text{N})$	$\delta(\text{N}-\text{H})+(\text{-C}=\text{N}-)$	$\nu(\text{N}-\text{C}-\text{S})$		
$\text{Cl}_2\text{H}_2\text{D}_z$	2942 (br)	2374 (w)	1504 (s)	1490 (s), 1450 (s)	627, 429	2.43, 2.39
H_2D_z	2960 (br)	2365 (w)	1515 (s)	1505 (s), 1465 (s)	615, 454	3.58, 1.79
$\text{Se}(\text{Cl}_2\text{HD}_z)_2\text{Cl}_2$	3436 (m), 3280 (s)	1636, 1580	1526	1487	416	9.01
$\text{Se}(\text{HD}_z)_2\text{Cl}_2$	3215 (m), 3280 (m)	1610 (s), 1580 (s)	1513 (s)	1501 (s)	435	7.01

charge of the produced complex anion in the retention process [26]. The selenium(IV) ion in its complex is most likely not bonded directly to the active sites of the PUFs but it exists as an entity like quaternary ammonium salt. Thus, the most probable sorption mechanism of selenium(IV) from aqueous bromide media at $\text{pH} < 2$ onto $\text{Cl}_2\text{H}_2\text{D}_z$ immobilized PUFs could be proceeded as follows [9,26]:

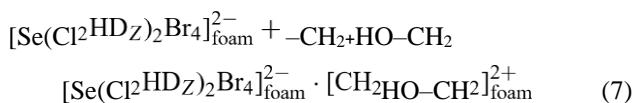


The produced anionic complex of selenium $[\text{Se}(\text{Cl}_2\text{H}_2\text{D}_z)_2\text{Br}_4]^{2-}$ on the PUFs is further interacted with the protonated urethane nitrogen ($-\text{NH}_2\text{COO}-$) and/or ether oxygen ($-\text{CH}_2\text{HO}-\text{CH}_2-$) linkages of the PUFs to form a complex ion associate with PUFs as follows:

Urethane group:



Ether group:



with increasing HCl concentration up to 4 M and in the presence of NaBr (2 M). Increasing the acidity (HCl) higher than 4 M has a negative effect due to the degradation of the foam and the possible reduction of selenium(IV) to elemental selenium. Therefore, in the subsequent experiments, a solution containing HCl (4 M) and NaBr (2 M) was selected as a sorptive medium for further extraction studies of selenium(IV). The results obtained are in a good agreement with the data reported elsewhere [11]. Thus, “solvent extraction” is the most probable mechanism for selenium(IV) uptake by the reagent $\text{Cl}_2\text{H}_2\text{D}_z$ immobilized foams.

The effect of shaking time on the uptake of selenium(IV) at 10 g/ml concentration from aqueous media by $\text{Cl}_2\text{H}_2\text{D}_z$ loaded foams was carried out. The retention of selenite ions

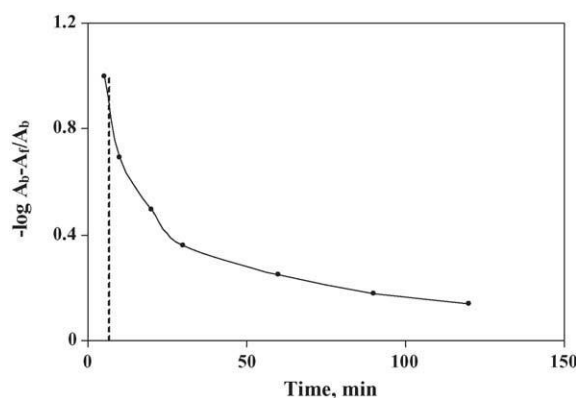


Fig. 1. Rate of sorption of selenium(IV) at 10g/ml concentration level onto $\text{Cl}_2\text{H}_2\text{D}_z$ immobilized foams ($0.5 \pm 0.01\text{g}$).

¹⁹ s: strong, m: medium, w: weak, sh: shoulder and br: broad.

by $\text{Cl}_2\text{H}_2\text{D}_z$ loaded foams was approximately slow and maximum equilibrium has reached a constant value in 2 h shaking time with the PUF and then leveled off with increasing time >2 h. Consequently, 2 h shaking time was adopted in the subsequent experiments. This conclusion was supported by the rate of selenium(IV) sorption by $\text{Cl}_2\text{H}_2\text{D}_z$ loaded foams and the average half-life time ($t^{1/2}$) of equilibrium sorption as calculated from Fig. 1 was in the range 7.8 min.

The effect of the reagent $\text{Cl}_2\text{H}_2\text{D}_z$ concentration (0.01–0.05%, w/v) immobilized onto the PUF on the extraction of selenium(IV) at concentration level 5 g/ml was investigated. No significance effect on the sorption of selenium(IV) was observed. Thus, immobilized $\text{Cl}_2\text{H}_2\text{D}_z$ -PUFs of 0.02% (w/v) was selected in the subsequent retention experiments.

The effect of foam dose (w) and batch factor (v/m) on the retention of selenium(IV) at 10 g/ml concentration level onto $\text{Cl}_2\text{H}_2\text{D}_z$ loaded foams was also investigated. The sorption of selenium(IV) increased on increasing the foam dose up to 0.5 g of the reagent foam. Thus, in the subsequent work, 0.5 g loaded foam was employed. The extraction percentage of Se(IV) uptake by the reagent loaded foam decreased up to 45% extraction with increasing the sample volume from 25 to 500 ml.

The influence of cation (Li^+ , Na^+ , Ca^{2+} , Cs^+ , K^+ and NH_4^+) size as metal chlorides and their concentrations on the sorption profile of selenium(IV) at 10 g/ml concentration level onto the immobilized $\text{Cl}_2\text{H}_2\text{D}_z$ foam was studied. The results showed no significance effect on the extraction of selenium(IV) in the presence of different concentrations of the salts. Thus, in the subsequent work, the sorption procedures were carried out without salt addition.

3.3. Kinetic behavior of selenium(IV) sorption onto $\text{Cl}_2\text{H}_2\text{D}_z$ loaded foams

The kinetic behavior of selenium(IV) sorption onto $\text{Cl}_2\text{H}_2\text{D}_z$ immobilized foams depends on two transport act in parallel, i.e., film diffusion and intraparticle diffusion, and the more rapid one will control the overall rate of transport. Thus,

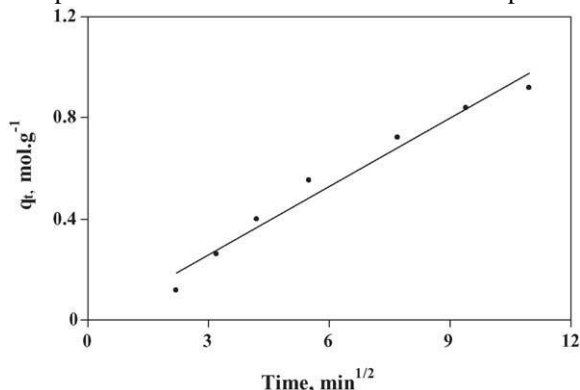


Fig. 2. The sorbed concentration of selenium(IV) onto $\text{Cl}_2\text{H}_2\text{D}_z$ loaded foams vs. $t^{1/2}$ at 25 ± 0.1 °C.

the sorbed selenium(IV) concentration q_t (mol g^{-1}) at time t was plotted, versus $t^{1/2}$ to test the Weber–Morris equation [27]:

$$q_t = R_d(t)^{1/2} \quad (8)$$

where R_d is the rate constant of intraparticle transport in $\text{mmol g}^{-1} \text{min}^{-1/2}$. The plot of q_t versus $t^{1/2}$ was found linear (Fig. 2) up to 100 min and deviates as the shaking time increases. In the initial stage, the diffusion rate was slow and decreased with passage of time indicating that the adsorption rate is film diffusion controlled at the early stage of sorption in batch reactor. The value of R_d was computed from the slope of the Weber–Morris plot (Fig. 2). The line does not pass through the origin confirming particle film diffusion along with intraparticle diffusion [26]. The value of R_d was estimated to be $90 \text{ mmol g}^{-1} \text{min}^{-1/2}$ in good agreement with the data reported by Saeed et al. [28,29].

Moreover, the kinetic data were also determined from the mass action process, which assumes that the movement of selenium(IV) complex into the pores of PUFs is a diffusion process regardless of the mechanism used. This is achieved employing the Lagergren equation [29,30]:

$$\log(q_e - q_t) = \log q_e - \left(k \frac{t}{2.303} \right) \quad (9)$$

where q_e is the sorbed concentration of selenium(IV) onto PUF at equilibrium (mol g^{-1}) and k is the overall rate constant of the sorption process. The plot of $\log(q_e - q_t)$ versus time is shown in Fig. 3. The graph indicated that the process of adsorption is first-order reaction with respect to the adsorbed concentration [31] and the numerical value of the overall rate constant k was found equal to 0.012 min^{-1} .

The value of Bt , which is a mathematical function (F) of q_t/q_e , can be calculated for each value of F employing Reichenburg equation [32]:

$$Bt = -0.4977 - 2.303 \log(1 - F) \quad (10)$$

A plot of Bt versus time (Fig. 4) at 25 ± 1 °C was found linear up to 60 min and the line does not pass through the origin as observed earlier [22]. This behavior was observed in

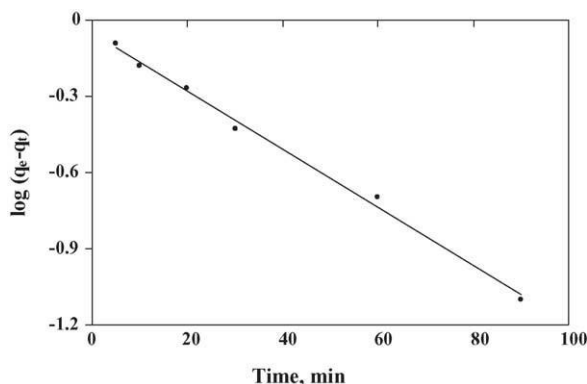


Fig. 3. Lagergren plot of the kinetics of the sorption of selenium(IV) at 10g/ml concentration level onto $\text{Cl}_2\text{H}_2\text{D}_z$ loaded foams ($0.5 \pm 0.01\text{g}$) at 25 ± 0.1 °C.

the case of the Morris–Weber equation [27] test and indicated that a “particle diffusion” mechanism is not only operative for the kinetics of $[\text{Se}(\text{Cl}_2\text{HD}_z)_2]\text{Cl}_2$ retention onto PUF. Therefore, the retention profile of the selenium(IV) chelate involves three steps: bulk transport of SeOCl_2 and/or $[\text{SeOBr}_4]^{2-}$ in solution, film transfer involving diffusion of these species within the pore volume of the PUFs and/or along the pore wall surface to an active sorption sites and finally formation of $[\text{Se}(\text{Cl}_2\text{HD}_z)_2]\text{Cl}_2$. The actual sorption of SeOCl_2 on the interior surface site is slow; hence, it is the rate determining step. Thus, film and intraparticle transport are the main predominating factors controlling the sorption rate.

3.4. Sorption isotherm of selenium(IV)

The sorption profile of selenium(IV) from the bulk aqueous solution containing HCl (4 M) and NaBr (2 M) onto the $\text{Cl}_2\text{H}_2\text{D}_z$ loaded foam was determined over a wide range of equilibrium concentration (5–100 g/ml). The amount of selenium(IV) ions retained on the loaded foams is plotted versus their corresponding remaining concentration in the bulk aqueous phase. The data revealed that, at low or moderate

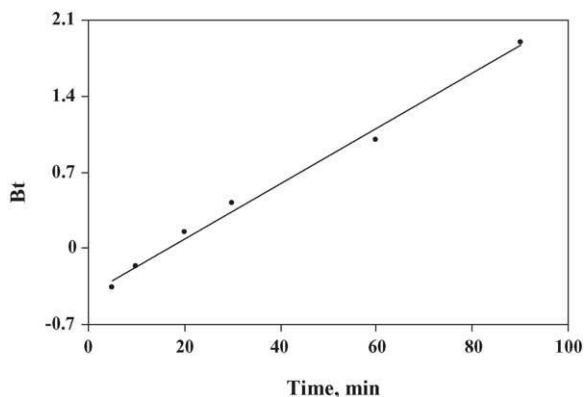


Fig. 4. Reichenburg plot of the kinetics of selenium(IV) uptake at 10g/ml concentration level onto $\text{Cl}_2\text{H}_2\text{D}_z$ loaded foams ($0.5 \pm 0.01\text{g}$) at 25 ± 0.1 °C.

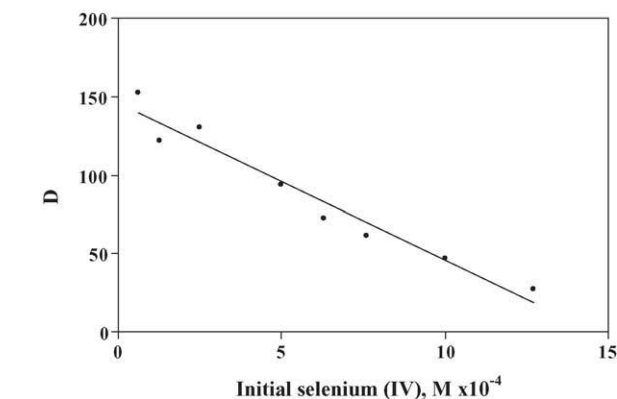


Fig. 5. Plot of the distribution ratio of selenium(IV) uptake onto $\text{Cl}_2\text{H}_2\text{D}_z$ loaded foams ($0.5 \pm 0.01\text{g}$) vs. the initial concentration of selenium(IV).

selenium(IV) concentration, the amount of selenite ion retained on the $\text{Cl}_2\text{H}_2\text{D}_z$ loaded foams varied linearly with the corresponding selenium(IV) concentration remaining in the aqueous solution. The equilibrium was approached from the direction that selenium(IV) rich reagent foams suggesting a first-order behavior. These results are in good agreement with data reported [28,29,31]. The extraction capacity of selenium(IV) from the sorption isotherm is relatively low (4.4 mg/g loaded foam) and the equilibrium is approached at low analyte concentration. The distribution ratio (D) decreased with increasing selenium(IV) concentration and the foam membranes became saturated with the retained species (Fig. 5). Thus, the D fell off as the saturation was approached and the diffusion of the solute through the hydrodynamic boundary layer took place in the sorption step. The most favorable D values were found for more dilute solutions. Thus, intraparticle transport and film diffusion may be the steps controlling molecular diffusion at the macropores of the PUF sorbent [29,30]. Therefore, “solvent extraction” is the most probable mechanism for selenium(IV) sorption from the aqueous solution by the reagent loaded foams.

Several models, e.g., Langmuir, Freundlich and Dubinin–Radushkevich (D – R) isotherms [33–35], were used to describe the variation of the sorption data of selenite ions over a wide range of equilibrium concentrations onto PUFs. Based on the kinetic consideration, the familiar form of Langmuir sorption isotherm can be expressed in the linear form [33]:

$$\frac{C_e}{C_{\text{ads}}} = \frac{1}{Q_b} + \frac{C_e}{Q} \quad (11)$$

where C_e is the equilibrium concentration (M) of selenium(IV) in solution, C_{ads} the adsorbed selenium(IV) concentration onto the reagent loaded foams per unit mass of

sorbent at equilibrium (mol g^{-1}), Q a constant related to the maximum sorption capacity of solute per unit mass of adsorbent required for monolayer coverage of the surface and b is an equilibrium constant related to the binding energy of solute sorption that is independent of temperatures. The plot of C_e/C_{ads} versus C_e shown in Fig. 6 strictly follows the ad-

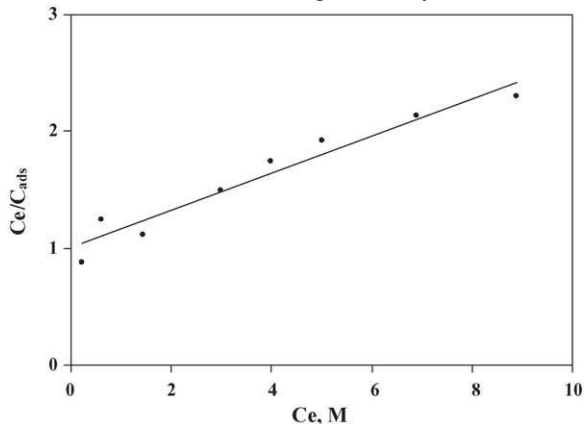


Fig. 6. Langmuir sorption isotherm of selenium(IV) uptake at various concentration levels onto $\text{Cl}_2\text{H}_2\text{D}_2$ loaded foams ($0.5 \pm 0.01\text{g}$) at $25 \pm 0.1^\circ\text{C}$.

sorption model and is a linear graph throughout the entire concentration range of selenium(IV). The sorption parameters Q and b for the system evaluated from the slope and intercept of Fig. 6 were found equal to $0.013 \pm 0.003 \text{ mol g}^{-1}$ and $16 \pm 1.0 \text{ dm}^3/\text{mol}$, respectively. The values of Q and b showed good retention of selenium(IV) ions onto the PUF.

The sorption data were also subjected to Freundlich sorption isotherm [34] in the following form:

$$\log C_{\text{ads}} = \log A + \frac{1}{n} \log C_e \quad (12)$$

where A and $1/n$ are Freundlich parameters related to the maximum sorption capacity of solute (mol g^{-1}). These parameters encompass maximum sorption capacity of solute (mol g^{-1}), the surface heterogeneity and the exponential distribution of active sites and their energies. The values of A and $1/n$ computed from the intercept and slope of the linear plot of $\log C_{\text{ads}}$ versus $\log C_e$ (Fig. 7) over the entire concentration of selenium(IV), were found equal to $0.024 \text{ mmol g}^{-1}$ and 0.6 , respectively. The value $1/n < 1$ indicates favored adsorption and that the sorption capacity is slightly reduced at lower equilibrium concentration. The isotherm does predict

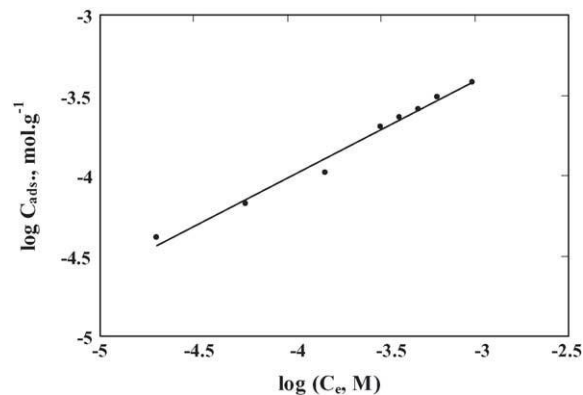


Fig. 7. Freundlich sorption isotherm of selenium(IV) uptake at various concentration levels onto $\text{Cl}_2\text{H}_2\text{D}_2$ loaded foams ($0.5 \pm 0.01\text{g}$) at $\text{pH} \sim 1$ and $25 \pm 0.1^\circ\text{C}$.

saturation of selenium(IV) onto the solid surface of the reagent immobilized PUF and the infinite surface coverage is predicted mathematically indicating a multilayer sorption of the surface.

The Dubinin–Radushkevich isotherm model [35] is postulated within adsorption space close to adsorbent surface to evaluate the sorption free energy and to get some information about the nature of bonding, i.e., either physisorption or chemisorption. The D–R isotherm can be linearized as follows:

$$\ln C_{\text{ads}} = \ln K_{\text{DR}} - \beta \epsilon^2 \quad (13)$$

where K_{DR} is the maximum sorption capacity of selenium(IV) retained, β the activity coefficient constant related to the sorption free energy of the transfer of the solute from the bulk solution to the solid sorbent ($\text{mol}^2 \text{kJ}^2$) and ϵ is polanyi potential which is given by the equation:

$$\epsilon = RT \ln \left(1 + \frac{1}{C_e} \right) \quad (14)$$

where R is the gas constant ($0.0834 \text{ kJ mol}^{-1} \text{K}^{-1}$) and T is the absolute temperature in Kelvin. The plot of $\ln C_{\text{ads}}$ versus ϵ^2 shown in Fig. 7 is linear indicating that the D–R isotherm is obeyed for selenium(IV) sorption over the entire concentration range. The numerical values of K_{DR} and β calculated from the slope and the intercept were found equal to $25.32 \pm 0.23 \text{ mol g}^{-1}$ and $-0.0062 \pm 0.0005 \text{ mmol}^2 \text{kJ}^2$, respectively. Assuming the surface of the reagent foam is heterogeneous and an approximation to a Langmuir isotherm model is chosen as a local isotherm for all sites that are energetically equivalent, the quantity β related to the mean free energy (E) of the transfer of 1 mol of solute from infinity to the surface of PUF can be expressed by the equation:

$$E = \frac{1}{\sqrt{-2\beta}} \quad (15)$$

The value of E was found within the range of 2.9 ± 0.1 kJ/mol confirming solvent extraction and physical sorption of selenium(IV) complex onto PUF (Fig. 8).

3.5. Thermodynamic characteristics of selenium(IV)

The sorption behavior of selenium(IV) onto the reagent $\text{Cl}_2\text{H}_2\text{D}_z$ immobilized foams was critically investigated at 22, 40 and 60 °C to determine the nature of the retention step of selenium(IV) by the PUF at 10 g/ml level aqueous sample (100 ml) and the optimum experimental conditions. The thermodynamic parameters of selenium(IV) uptake have been evaluated employing the equations:

$$\ln K_c = \frac{-\Delta H}{RT} + \frac{\Delta S}{R} \quad (16)$$

$$\Delta G = \Delta H - T \Delta S \quad (17)$$

$$\Delta G = -RT \ln K_c \quad (18)$$

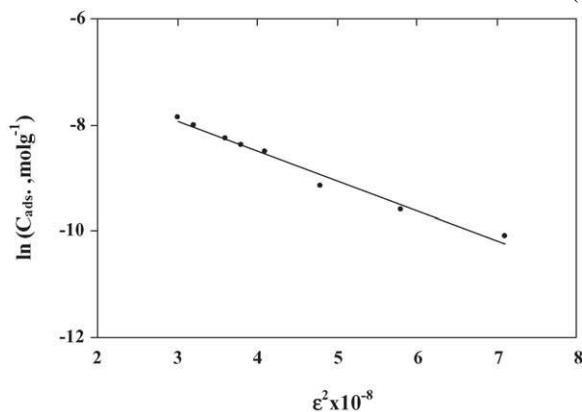


Fig. 8. Dubinin–Radushkevich (D–R) sorption isotherm of selenium(IV) uptake at various concentration level onto $\text{Cl}_2\text{H}_2\text{D}_z$ loaded foams (0.5 ± 0.01 g) at $\text{pH} \sim 1$ and 25 ± 0.1 °C.

where ΔH , ΔS and G are the enthalpy, entropy and Gibbs free energy changes, respectively, and K_c is the equilibrium constant depending on the fractional attainment (F_c) of the sorption process of selenium(IV) onto the $\text{Cl}_2\text{H}_2\text{D}_z$ immobilized PUFs at equilibrium. The plots of $\log K_c$ and $\log D$ versus $1/T$ were found linear (Fig. 9) over the entire range of temperature (295–333 K). The numerical values of H and S as calculated from the slope and intercept of $\log K_c$ versus

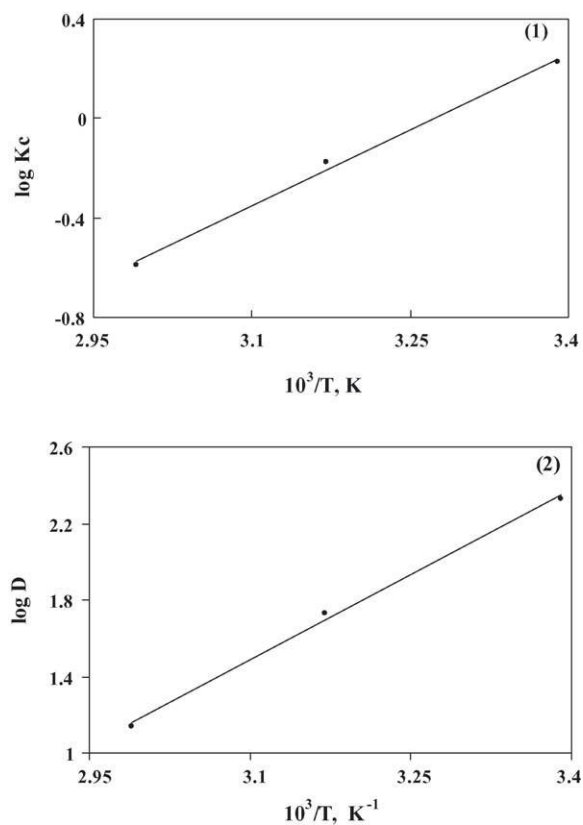


Fig. 9. Plots of equilibrium constant, K_c (1), and distribution coefficient, D (2), vs. $1/T$ (K^{-1}) for the sorption of selenium(IV) at 10g/ml concentration level from aqueous solution onto $\text{Cl}_2\text{H}_2\text{D}_z$ loaded foams (0.5 ± 0.01 g).

$1/T$ (Fig. 9) were found equal to -17.1 and -55.8 kJ/mol, respectively. The negative value of H and the data of K_c and D given in Fig. 9 reflect the exothermic behavior of selenium(IV) uptake from the aqueous solution by the PUFs and non-electrostatic bond formation between the adsorbent and the adsorbate. Similarly, the negative value of S may be indicative of the slow sorption of $\text{Se}(\text{Cl}_2\text{HD}_z)_2\text{Cl}_2$ chelate and ordering of ionic charges without a compensatory disordering of the complex sorbed onto the active sites of the PUF [13]. The negative value of S of selenium(IV) sorption indicates that the freedom of motion of selenium(IV) is more restricted in the foam membrane than in solution. Since the sorption process involves a decrease in free energy, the H is expected to be also negative, which is confirmed by the data obtained. Furthermore, as the temperature increases, the physical structure of membrane may be changing which can affect the strength of the intermolecular interactions between the foam membrane and selenite ions. For example, the higher temperature may cause the membrane matrix to become more unstructured and affect the ability of the polar segments to engage in stable hydrogen bonding with selenite ions, which would result in a lower extraction. The negative value of ΔG (-566 kJ/mol) at 295 K, with a correlation factor of 0.9956, indicates spontaneous and physisorption nature of

retention onto PUF. The increase in the G value with temperature may be due to the spontaneous nature of sorption and is more favorable at low temperature confirming the exothermic sorption process. These results and the flow characteristics of the PUF suggest the possible use of the reagent loaded PUFs in column operations for the enrichment and separation of inorganic selenium(IV) and (VI) species from large sample volumes of water.

3.6. Chromatographic behavior of selenium(IV) retention onto $\text{Cl}_2\text{H}_2\text{D}_Z$ loaded PUFs

Columns packed with $\text{Cl}_2\text{H}_2\text{D}_Z$ loaded foams were successfully employed for the separation of selenium(IV). In these experiments, aqueous solutions (2–3 l) of double distilled water containing selenium(IV) at 0.05–1 g/ml concentration level, HCl (4 M) and NaBr (2 M) were percolated through the foam packed column at 2.5 ml/min flow rate. A separate blank experiment was also carried out. Analysis of selenium(IV) in the effluent solution of the loaded foam packed column after shaking with CHCl_3 [24] against a reagent blank indicated complete sorption of selenium(IV). The sorbed selenium(IV) chelate on the foam membrane was then recovered from the foam column with chloroform (20 ml) at 3 ml/min flow rate. Satisfactorily recovery percentages ($\geq 95\%$) of the tested selenium(IV) ions were obtained by the proposed loaded foam columns.

The column performance was calculated from the values of height equivalent to theoretical plate (HETP) and N estimated from the breakthrough capacity curve. Thus, aqueous feed solution (5 l) containing selenium(IV) at 0.05 g/ml concentration level in HCl (4 M)/NaBr (2 M) was perco-

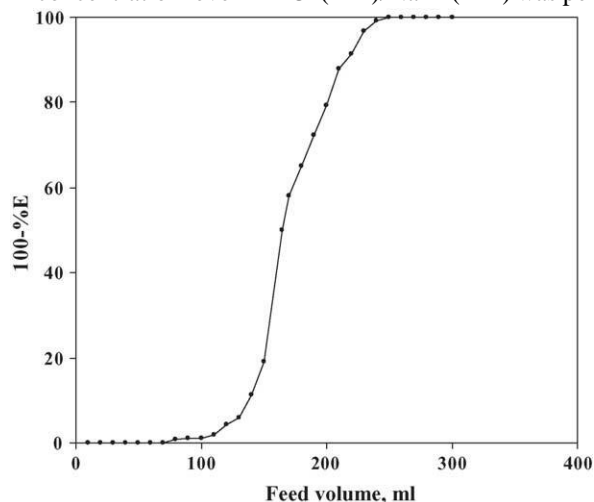


Fig. 10. Breakthrough curve of selenium(IV) uptake at 0.05 g/ml concentration level from aqueous solution onto $\text{Cl}_2\text{H}_2\text{D}_Z$ immobilized foam (4 ± 0.01 g) packed column at 5 ml/min.

lated through the loaded foam column at 5 ml/min. The S-shaped curve (Fig. 10) represents: (i) the breakthrough volume and (ii) the volume needed to reach bed saturation of selenium(IV). It is clear that the raising position in the curves has a large shape, indicating a high transfer rate of selenium(IV) sorption in the membrane forming the skeleton of the foam material and a high rate of equilibrium attainment between the analyte and the reagent immobilized foams. The HETP and N values for selenium(IV) uptake onto $\text{Cl}_2\text{H}_2\text{D}_Z$ loaded foams were calculated from the breakthrough curve (Fig. 10) employing equation [19]:

$$N \frac{V_{50} - V'}{(V_{50} - V')^2} \text{HETP} = \frac{V_{50} V'}{L} = \frac{L}{V_{50} - V'} \quad (19)$$

where N is the number of theoretical plates, V_{50} the volume of the effluent solution at center of the S-shaped of the breakthrough curve where the concentration is one-half the initial concentration, V' the volume at which the effluent solution has a concentration of 0.1578 of the initial concentration and L is the length of the foam bed in millimeters. The values of HETP and N were found equal to 1.3 ± 0.1 mm and 103 ± 4 , respectively.

The analytical performance of the $\text{Cl}_2\text{H}_2\text{D}_Z$ loaded foam column was also determined from the values of N , HETP, critical and breakthrough (BC) capacities [9,36]. The critical capacity of selenium(IV) ions onto $\text{Cl}_2\text{H}_2\text{D}_Z$ loaded foam column was found equal to 7.2 mg/g at 2.5 ml/min flow rate. The BC of selenium(IV) onto $\text{Cl}_2\text{H}_2\text{D}_Z$ loaded foam was calculated employing the equation [35]:

$$\text{BC} = \frac{V_{50} C_0}{m} \quad \left(\frac{\text{mg}}{\text{g}} \right) \quad (20)$$

where C_0 is the initial concentration (g/l) of selenium(IV), V_{50} the feed volume (ml) at 50% extraction and m is the mass (g) of the dry foam beds in foam column which was found equal to 8 mg/g for selenium(IV) sorption onto loaded foams at 2.5 ml/min (Fig. 10). This value is quite good as compared to other solid support like Voltalef, silica gel and solid inorganic ion exchanger column [36,37].

3.7. Effect of diverse ions

To assess the selectivity of the proposed reagent $\text{Cl}_2\text{H}_2\text{D}_Z$ immobilized PUFs, the uptake of selenium(IV) at 5–20 g/ml concentration level from an aqueous solution (50 ml) under the optimum experimental conditions was critically investigated in the presence of some diverse ions. It was found possible to preconcentrate accurately 5–20 g/ml of selenium(IV) in the presence of up to 500 mg/l of the following ions: PO_4^{3-} , N_3^- , Mg^{2+} , Ca^{2+} , Cr^{6+} , Na^+ , K^+ , Li^+ , NH_4^+ , F^- , Cl^- , Br^- , Al^{3+} , Te^{6+} , Se^{6+} , WO_4^{2-} , Cr^{3+} and Te^{4+} .

In the presence of the ions Cu^{2+} , V^{4+} , Fe^{3+} , MnO_4^- and NO_3^- at 100 g/ml concentration level, the uptake of selenium(IV)

was not complete. In case of the ions Cu^{2+} , V^{4+} and Fe^{3+} , simple modifications of the sample solutions involving addition of 0.50 ml of EDTA (0.1 M) and NaF (0.1 M) were introduced to obtain complete sorption of selenium(IV). The addition of NaN_3 removed completely the interference of KMnO_4 .

3.8. Applications

3.8.1. Removal of inorganic selenium(IV) and/or (VI) in water

The feasibility of the proposed foam method for the collection and recovery of selenium(IV) and/or (VI) and total inorganic selenium(IV) and (VI) after prior reduction of Se(IV) to (VI) from natural and tap water was investigated on five different fresh, natural and wastewater samples. A 1 l of natural water sample spiked with selenium(IV) and/or selenium(VI) at various concentrations (5–10 g/l) was percolated through the reagent PUF packed column at 2.5 ml/min flow rate at the optimum conditions. Selenium(IV) was quantitatively retained while selenium(VI) was passed through the column without sorption. The retained selenium(IV) species on the foam column were then recovered with 25 ml chloroform at 3 ml/min flow rate and measured [24]. Selenium(VI) was also retained after its prior reduction to selenium(IV) with HCl (6 M) as described [24], recovered with chloroform and determined [11]. In the preconcentration of total inorganic selenium(IV) and (VI), the spiked water samples were initially reduced to selenium(IV) by HCl (6 M). The produced selenium(IV) solution was quantitatively retained on the reagent foam column at 3 ml/min. Good recovery (95–98%) of the retained selenium(IV) species was then obtained. The method is possible to achieve excellent accuracy even in samples with high content of dissolved solids.

3.8.2. Sequential spectrophotometric determination of selenium(IV) and/or (VI)

The validity of the proposed method for the sequential determination of selenium(IV) and (VI) in water was also investigated. An aqueous sample solution (100 ml) spiked with selenite and/or selenate ions at a total concentration of 1–10 g/ml, HCl (4 M) and NaBr (2 M) was percolated through $\text{Cl}_2\text{H}_2\text{D}_z$ immobilized foams packed column at 2.5 ml/min. Only selenium(IV) was quantitatively retained as indicated from the analysis of selenium(IV) in the effluent versus reagent blank [23]. The retained selenium(IV) species were quantitatively recovered with chloroform (20 ml) at 2–3 ml/min. The recovered extract was transferred to a 50 ml conical flask containing anhydrous sodium sulphate (1 g). The flask was swirled to mix the contents and the free $\text{Cl}_2\text{H}_2\text{D}_z$ was then removed from the combined extracts by shaking with dilute solution (10 ml) of NH_3 (two drops of

concentrated NH_3 solution in 25 ml of water). The organic extract was then shaken with dilute acetic acid (0.2%) and the chloroform extract was transferred to a 50 ml volumetric flask. The solution was made up to the mark with chloroform. The absorbance of the organic extract was then measured at 435 nm against a reagent blank with the aid of standard curve. Satisfactory results with average recoveries in the range $98 \pm 3.2\%$ were obtained for the spiked selenium(IV). Selenium(VI) was also determined by the proposed reagent $\text{Cl}_2\text{H}_2\text{D}_z$ after prior reduction to selenium(IV) by HCl (6 M). The results ($99.6 \pm 1.2\%$) revealed good agreement with the data obtained by the standard dithizone method [23,24].

4. Conclusion

PUF sorbent immobilized with $\text{Cl}_2\text{H}_2\text{D}_z$ offers unique advantage over granular sorbent in rapid separation and sequential determination of inorganic selenium(IV) and (VI) after reduction to selenium(IV) in extremely dilute aqueous solution (ppb level) by flow mode from fluid water samples. The thermodynamic data confirmed the exothermic nature of selenium(IV) sorption onto the $\text{Cl}_2\text{H}_2\text{D}_z$ immobilized PUFs. The kinetic data confirmed the intraparticle diffusion process and the first-order model for the sorption step. The results provided a deeper insight into the kinetics and sorption mechanism of selenium(IV) by PUFs. The great potentialities of PUF membranes are attributed to their inexpensiveness and large scale of availability all over the world in many industrial applications. However, work is still continuing for the chemical separation and determination of inorganic and organoselenium(IV) and (VI) species in real samples by solid-phase spectrophotometry. Other study will involve the possible application of on-line preconcentration and determination of selenium(IV or VI) by AAS.

Acknowledgement

The author M.S. El-Shahawi would like to thank Prof. A.M. Kiwan for the loan of the reagent 4,4-dichlorodithizone.

References

- [1] M.I. Sittig, Toxic Metals, Pollution Control and Worker Protection, Noyes Data Corporation, Park Ridge, USA, 1976. [2] D.C. Adriano, Biogeochemistry of Trace Metals, Lewis, London, 1992.
- [3] D.V. Frost, Critical Review in Toxicology, CRC Press, 1972.
- [4] J.M.M. Neal, L.S. Balistrieri, in: L.W. Jacobs (Ed.), Selenium in Agriculture and the Environment, Soil Science Society of America (SSSA), American Society of Agronomy, Madison, WI, 1989.
- [5] O.A. Levander, Clin. Biochem. 6 (1982) 345.
- [6] L.H. Foster, S. Sumar, Food Chem. 55 (1996) 293.
- [7] American Chemical Health Association, Standard Methods for the Examination of Water and Wastewater, 19th ed., American Health and

- American Water Association and Water Environment Federation, Washington, DC, 1992, pp. 3–85.
- [8] G.V. Iyengar, W.E. Kollmer, H.J.M. Bowen, *The Elemental Composition of Human Tissues and Body Fluid*, Verlag Chemie, Weinheim, 1978.
- [9] T. Braun, J.D. Navratil, A.B. Farag, *Polyurethane Foam Sorbents in Separation Science*, CRC Press, Boca Raton, FL, USA, 1985.
- [10] T. Braun, A.B. Farag, *Talanta* 22 (1975) 699.
- [11] I.I. Stewart, A. Chow, *Talanta* 40 (1993) 1345.
- [12] R.J. Cassella, *J. Environ. Monit.* 4 (4) (2002) 522.
- [13] M.S. El-Shahawi, H.A. Nassif, *Anal. Chim. Acta* 481 (2003) 29.
- [14] S.G. Dmitrienko, L.N. Pyatkova, Y.A. Zolotov, *J. Anal. Chem.* 57 (2002) 875.
- [15] S.G. Dmitrienko, O.A. Sviridova, L.N. Pyatkova, V.M. Senyavin, *Anal. Bioanal. Chem.* 374 (2002) 361.
- [16] M.N. Abbas, G.A. Mostafa, *Anal. Chim. Acta* 410 (2000) 185.
- [17] O.D. Sant'Ana, L.G. Oliveira, L.S. Jesuino, M.S. deCarvalho, M.L.F. Domingues, R.J. Cassella, R.E. Santelli, *J. Anal. At. Spectrom.* 17 (2002) 258.
- [18] R.J. Cassella, R.E. Santelli, A.G. Branco, V.A. Lemos, S.L.C. Ferreira, M.S. deCarvalho, *Analyst* 124 (1999) 805.
- [19] M. Nagase, M. Toba, H. Kondo, K. Hasebe, *Analyst* 123 (1998) 1091.
- [20] D.S. deJesus, R.J. Cassella, S.L.C. Ferreira, A.C.S. Costa, M.S. de Carvalho, R.E. Santelli, *Anal. Chim. Acta* 366 (1998) 263.
- [21] R.J. Cassella, D.T. Bitencourt, A.G. Branco, S.L.C. Ferreira, D.S. de Jesus, M.S. deCarvalho, R.E. Santelli, *J. Anal. At. Spectrom.* 14 (1999) 1749.
- [22] T. Braun, A.B. Farag, *Anal. Chim. Acta* 71 (1974) 133.
- [23] Z. Marzenko, *Separation and Spectrophotometric Determination of Elements*, third ed., John Wiley & Sons Inc., New York, 1986.
- [24] H. Mabuchi, H. Nakahara, *Bull. Chem. Soc. (Jpn.)* 36 (1963) 151.
- [25] A.M. Kiwan, A.Y. Kassim, *Anal. Chim. Acta* 88 (1977) 177.
- [26] M.M. Saeed, M. Ahmed, *Anal. Chim. Acta* 525 (2004) 289.
- [27] W.J. Weber Jr., J.C. Morris, *J. Sanit. Eng. Div. Am. Soc. Civ. Eng.* 89 (SA2) (1963) 31;
W.J. Weber Jr., J.C. Morris, *J. Sanit. Eng. Div. Am. Soc. Civ. Eng.* 90 (SA3) (1964) 79.
- [28] M.M. Saeed, S.M. Hasany, M. Ahmed, *Talanta* 50 (1999) 625.
- [29] S.M. Hasany, M.M. Saeed, M. Ahmed, *Sep. Sci. Technol.* 35 (2000) 379.
- [30] S. Lagergren, B.K. Sven, *Vatenskapsakad. Handl.* (1898) 24.
- [31] S.M. Hasany, M.M. Saeed, M. Ahmed, *Talanta* 54 (2001) 89, and references cited therein.
- [32] D. Reichenburg, *J. Am. Chem. Soc.* 75 (1972) 589.
- [33] L. Langmuir, *J. Am. Chem. Soc.* 40 (1918) 136.
- [34] H. Freundlich, *Colloidal Capillary Chemistry*, Methuen, London, 1926.
- [35] M.M. Dubinin, L.V. Radushkevich, *Proc. Acad. Sci. USSR Phys. Chem. Soc.* 55 (1974) 331.
- [36] I.M. El-Naggar, E.S. Zakaria, M.M. Abou-Mesalam, H.F. Aly, *Caech. J. Phys.* 48 (1998) 29.
- [37] W.X. Ma, F. Liu, K.A. Li, W. Chen, S.Y. Tong, *Anal. Chim. Acta* 416 (2000) 191.



Kinetics, thermodynamic and chromatographic behaviour of the uranyl ions sorption from aqueous thiocyanate media onto polyurethane foams

M.S. El-Shahawi ^{a,*}, M.A. Othman ^b, M.A. Abdel-Fadeel ^a

^a Chemistry Department, Faculty of Science at Damietta, Mansoura University, Mansoura, Egypt

^b Genetic Engineering and Biotechnology Research Institute (GEBRI), Minufiya University, Sadat City, Egypt

Received 31 January 2005; received in revised form 7 May 2005; accepted 10 May 2005

Available online 22 June 2005

Abstract

The retention profile of uranyl ions from aqueous thiocyanate media by polyether-type based polyurethane foams (PUFs) has been studied to gain more information regarding the mechanism of extraction. The effect of pH, shaking time, surfactant type, extraction media, temperature and analyte concentration on the retention of uranyl ions onto PUFs has been studied. It has been found that, the sorption of uranyl ions involved in the formation of a ternary complex ion associate of uranyl ion, thiocyanate and PUFs is highly dependent on these parameters. The kinetics and thermodynamics of the uranyl ions sorption have been studied in more detail. The dependency of the extraction on the parameters can be explained via a “solvent extraction,” mechanism. However, owing to the complex nature of the PUFs a dual-mode sorption mechanism involving both absorptions related to “solvent extraction” and an added component for “surface adsorption” may be operated simultaneously. Attempts for quantitative retention and recovery of the uranyl ions in tap and industrial waste water samples by the proposed PUFs columns has been carried out and satisfactory results have been obtained. The cellular structure of the PUF sorbent offer unique advantages over a conventional bulk type sorbents in rapid, versatile effective separation and/or preconcentration of uranyl ions.

© 2005 Elsevier B.V. All rights reserved.

Keywords: Uranyl ions; PUFs; Sorption; Thiocyanate media; Kinetics and thermodynamics

1. Introduction

In the past decades, a number of solid sorbents, e.g. the inorganic ion exchanger stannic phosphate, organic ion exchanger and hydrous titanium oxide dispersed in polyacrylamide gel particles, have been reported for uranium recovery from seawater [1–7]. On-line determination and enrichment of uranium at trace levels in the industrial processing of nuclear fuel employing Dowex-50X8, exchanger, have been reported [8,9]. Also column chromatographic separation of uranium(VI) and other elements using the

0003-2670/\$ – see front matter © 2005 Elsevier B.V. All rights reserved.
doi:10.1016/j.aca.2005.05.018

crown polymer poly (dibenzo-18-crown-6) and ascorbic acid medium have been successfully achieved [8–10]. In addition, Amberlite XAD-4 functionalized with 5-aminoquinoline-8ol, chelating resin containing bicine ligands and crown ethers have been used for preconcentrating uranyl ions prior its spectrophotometric determination [11–14].

Recently, the pre-concentration of uranium(VI) ions from aqueous solutions onto open cell PUFs impregnated with organic extractants, e.g. crown ethers and long chain tertiary amines (Adogen) have been reported [15–19]. PUFs immobilizing salicylate ions and crown ethers have been successfully employed for the preconcentration of uranyl ions as salicylate or crown ether complex in water, waste water, mine drainage and sea water at pH 4 [16–18]. Also, the photometric determination and separation of uranium(VI)

* Corresponding author. Tel.: +20 50370324. E-mail address: mohammad el shahawi@yahoo.co.uk (M.S. El-Shahawi).

with 1-phenyl-3-(2-thiazolyl) thiourea and cadmium(II) as tetra iodide complex using polyurethane foam as sorbent have been reported [20–22].

Trace uranyl ions even at low concentration exhibit toxic effects in biological systems [23]. Thus, there is a need for simple and convenient techniques for the separation and determination of uranyl(II) ions in water at low concentration levels employing solvent extraction and/or liquid–solid sorption techniques [24–26]. Polyurethane foams have been used as an inexpensive solid extractor and effective sorbent for the removal of trace metal ions from water [22,24,27]. The foam sorbent gives unique advantage over conventional granular support in rapid, versatile and effective separation of different species from fluid samples [27].

In this article, we report the sorption of uranyl ions present in aqueous thiocyanate media employing PUFs sorbent. The factors control the retention profile and the sorption mechanism of uranyl ions uptake from aqueous thiocyanate media onto the PUFs have been also critically investigated. In addition, the study helps in promoting the use of PUFs for the separation and determination of the uranyl ions in various segments of industry. Moreover, the kinetics, thermodynamics and chromatographic characteristics of the sorption step by the PUFs have been also discussed.

2. Experimental

2.1. Reagents and materials

All chemicals and solvents used were of analytical reagent grade and were used without further purification. Doubly deionized water was used throughout. A stock solution (1000 g/ml) of uranyl ions was prepared by dissolving an accurate weight (0.1787 g) of uranyl acetate monohydrate in dilute nitric acid (2 M) and the solution was completed to 100 ml with distilled water. Also a series of standard uranyl ion solutions in water, stock solutions of potassium thiocyanate (40% w/v) in water, tertiary butyl phosphate (TBP) in toluene (0.1% v/v) and Britton Robinson (BR) buffers were prepared.

Commercial white sheets of open cell polyether based polyurethane foam (30 Kg/m³) were used. Foam cubes (10–15 mm edge) were cut from the foam sheets, washed and finally dried at 80 °C as reported [27]. The TBP loaded foam cubes were prepared by mixing the dried foam cubes with TBP in toluene (0.1% w/v, 10 ml g⁻¹ dry foam) with efficient stirring for 20 min. The TBP loaded foam cubes were then squeezed and dried as reported [27].

2.2. Apparatus

Glass columns (18 cm length × 15 mm i.d.) and a Soxhlet extractor were used in the retention experiments and for the foam purification, respectively. The absorbance measurements were recorded on a single beam digital spectro-

UV–vis RS labomed, INC with a glass cell (10 mm path length). An Orion pH meter VWR scientific model (8000) and a Lab-line orbit Environ-Shaker model (35271-1) were used for the pH measurements and shaking experiments, respectively.

2.3. Batch experiments

In separate 100 ml stoppered flasks, an accurate weight (0.3 ± 0.01 g) of the un-loaded or TBP loaded foam cubes was mixed with 50 ml of an aqueous solution containing uranyl ions (10 g/ml) and ammonium thiocyanate (0.5 M) at various pH (2–10) employing BR buffer. The solutions were shaken for 60 min in a mechanical shaker at 20 ± 0.1 °C. After shaking, the aqueous phase was separated out and the amount of the remaining uranyl ions in the aqueous phase was determined at 655 nm [26]. The amount of uranyl(II) ions retained onto the PUFs cubes was then determined from the difference between the absorbance of uranyl ions solution before, compound retained on the foam cubes was then calculated from the difference between the absorbance of the aqueous phase before (A_b) and after (A_f) shaking with the reagent foam cubes. The sorption percentage (% E) and the distribution ratio K_d have been determined as reported employing the equations:

$$\begin{aligned} \%E &= \frac{A_b - A_a \times}{A_b} \times 100 \quad (1) \\ &= \%E \times v = \frac{K_d}{100 - \%E} \times w \quad (2) \end{aligned}$$

where v is the volume of the solution in ml equilibrated with w g weight of the PUF sorbent. All experiments were carried out at least in triplicate and the results are the average of three independent measurements and precision in most cases was ±2%. Similarly, the influence of shaking time, surfactant, cation size, ionic strength, foam doze, thiocyanate concentration and temperature on the retention of uranyl ions onto the PUFs have been carried out.

2.4. Chromatographic behaviour of uranyl ions onto unloaded and TBP loaded foam packed column

Tap, distilled or industrial waste water samples (5 l) containing potassium thiocyanate (1% w/v) ions spiked with uranyl ions (10 g/ml) were percolated through the un-loaded and TBP reagent loaded foams (3.0 ± 0.01 g) packed columns at a reasonable flow rate (10 ml/min). Blank experiments were also carried out for the unloaded and TBP treated PUFs under the same experimental conditions of flow rate. The columns were then washed with 50 ml HCl (1 M) and the effluent and the washing solutions were then collected. The

uranyl content before and after percolation in the effluent and washing solutions was then measured [26]. The retained uranyl species in the foam columns were quantitatively eluted from the unloaded and the TBP loaded foam columns with 50 ml of NaOH (1 M) at 5 ml/min flow rate. Then the uranyl(II) content in the eluate was measured against a blank reagent [26].

3. Results and discussion

The solid PUFs sorbent concentrate traces of inorganic species from the aqueous media by the phase distribution rather than adsorption mechanism [23,27,28]. Therefore, a detailed investigation on the retention profile, mechanism of pre-concentration and determination of uranyl ions from the thiocyanate media employing unloaded and PUFs with some plasticizers is under taken below.

3.1. Retention profile of uranyl from aqueous thiocyanate media onto PUFs

The amount of uranyl ions retained onto the unloaded and TBP-loaded foams from the aqueous thiocyanate solution was found to be pH dependent. Thus, the sorption profile of uranyl ions at 10 g/ml concentration level from aqueous thiocyanate solutions onto PUFs at different pH was investigated. The aqueous solutions were shaken for 1 h with un-loaded and TBP loaded PUFs. The results of uranyl sorption onto the PUFs are shown in Fig. 1. Similar behaviour was also obtained on replacing the universal BR buffer by acetate buffer. The uptake of uranyl onto the foam cubes increases with increasing the solution pH up to pH ~ 3 and shows the lowest sorption at pH > 3. The observed behaviour at pH ≤ 3 is most likely attributed to the formation of anionic thiocyanate complex species of uranyl in solution which is retained onto the protonated ether (–CH₂–OH–CH₂–)⁺ oxygen or urethane (–NH₂COO–)⁺ nitrogen linkage of the PUFs as a ternary complex ion associate in acidic media as follows:

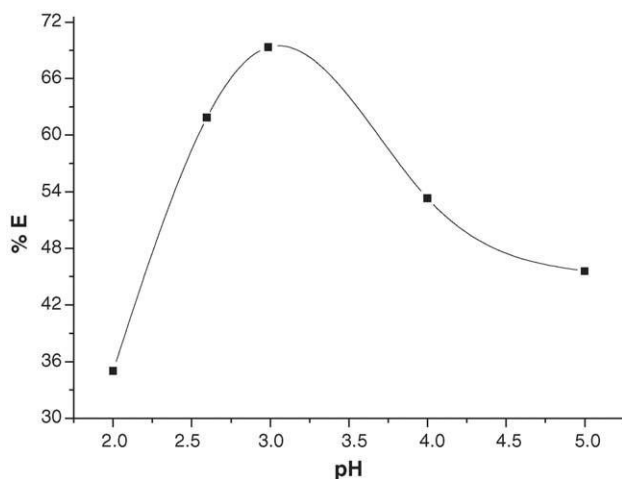
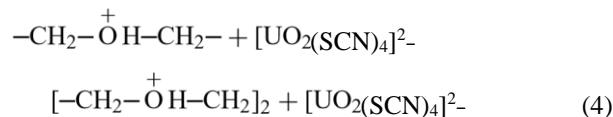
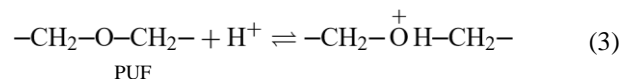
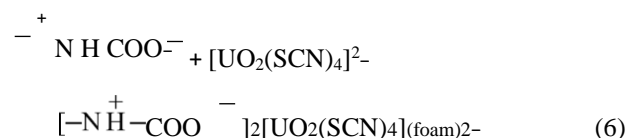
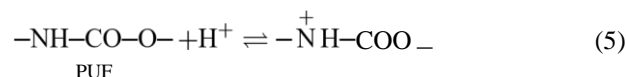


Fig. 1. Effect of pH on the sorption percentage of uranyl(II) ions at 10g/ml level from aqueous thiocyanate media (0.5M) onto unloaded PUFs (0.3±0.019).

- Ether group:



- Urethane group:



The pK_a values of the protonation of the oxygen atom of ether group and nitrogen atom of amide groups are 3 and 6, respectively. Therefore, in acidic media the ether group can easily be protonated at pH ≤ 3 and the interaction of [UO₂(SCN)₄]²⁻ species appears to be stronger than that with the urethane group. However, the sorption performance of the PUFs is also dependent on the nature of the species to be sorbed onto PUFs. The sorption of uranyl thiocyanate complex species could be due to the anion exchange properties of PUF, which may act as a weak or strong anion ion exchanger. The existence of anion exchanger sites arises from the tendency of both the nitrogen atom of the urethane linkage and/or ether oxygen atom to accept protons at pH ≤ 3.

The decrease in the uranium(VI) uptake by the foam cubes at pH > 3 is most likely attributed to the hydrolysis of the uranyl(II) thiocyanate complex or the instability of the produced ternary complex ion associate of complex species of uranyl(II) ions, thiocyanate and the unloaded or the TBP immobilized PUFs. Hence incomplete extraction of the uranyl ions onto the PUFs is achieved [29].

The influence of shaking time on the uranyl ions uptake from the aqueous media by the unloaded and TBP-loaded foam cubes was studied. The sorption of uranyl ions was found fast onto TBP immobilized foams and maximum equilibrium was reached within ~30 min contact time (Fig. 2) and remains constant. Consequently, 45 min shaking time was adopted in the subsequent experiments. This conclusion was also supported by the rate of uranium(VI) sorption by the unloaded and TBP-immobilized foams. The half-life time

($t_{1/2}$) of the equilibrium sorption for un-loaded and TBP-loaded foams was found equal 3.6 and 2.4 min, respectively.

The influence of a series of surfactants, e.g. neutral, cationic or anionic surfactants on the sorption of uranium(VI) onto the un-loaded and TBP-loaded foams was investigated. In the presence of the anionic surfactant sodium dodecylsulphate (SDS), a significance enhancement on the sorption of uranyl ions onto the unloaded PUFs was noticed. The sorption of uranyl ions onto the unloaded PUFs increased

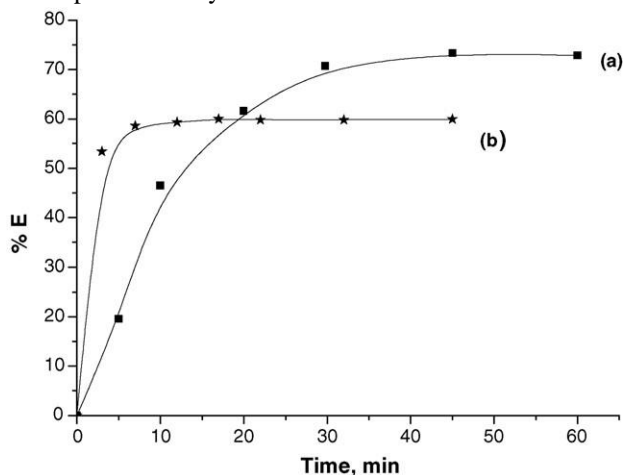


Fig. 2. Effect of shaking time on the extraction percentage of uranyl(II) ions (10g/ml) from aqueous thiocyanate media (0.5M) at pH<3 onto unloaded (a) and TBP-loaded (b) PUFs (0.3±0.019).

in the presence of SDS up to 0.1% (w/v) in the aqueous extraction media and levels off at higher surfactant concentrations >0.1% (w/v). This behaviour may be attributed to the increase of the solution viscosity leading to progressive change in the physical properties of the micro environment of the complex ion associate of uranium(VI). The increased solution viscosity enhances the dissociation and/or the formation of aggregate complexes with low diffusion constants [30]. The competition between the surfactant and the uranium(VI) thiocyanate complex may also predominate in the observed behaviour. Also, the surfactant may react directly with the anionic thiocyanate complex of uranyl ions and this may retard the extraction process [28].

The effect of various cations (Li^+ , Na^+ , K^+ and NH_4^+) at different concentrations (1×10^{-4} to 1×10^{-2} M) on the uptake of uranyl(II) ions at (10 g/ml) from the aqueous thiocyanate medium onto PUFs was studied. In the presence of LiCl, NaCl, KCl and NH_4Cl , a slight increase ($6.7 \pm 1.2\%$) in the uranyl sorption was observed and the sorption percentage followed the sequence:



This behaviour is attributed to the reduction of the repulsive forces between adjacent sorbed uranium(VI) complex ion associates [31]. These data are consistent with a “solvent extraction” mechanism with a salt acts as salting-out agent. The added electrolytes required water for their hydration, thereby reducing the amount of water available for solution of the uranyl thiocyanate complex species. However, “solvent extraction” mechanism is not only the most probable mechanism and other processes like surface area and specific sites on the PUFs are possibly involved simultaneously in the uranyl(II) sorption from the bulk solution [21,26].

The influence of the sorbent dose ($0.1\text{--}0.5 \pm 0.01$ g) on the distribution ratio of uranyl ions uptake from aqueous thiocyanate media at the optimum pH was investigated. The sorption of uranyl onto the PUFs increases with increasing the foam dose up to 0.3 g and remains constant. Thus, in the subsequent work, 0.3 g of the PUFs was used in the batch experiment. The influence of sample volume (0.1–1 l) on the uranyl ions sorption onto the PUFs was investigated. The distribution ratio of the uranyl ions onto the PUFs dose decreases gradually by increasing the batch factor (v/w).

The effect of potassium thiocyanate concentration on the extraction of uranyl ion onto the PUFs was investigated. The uptake of uranyl ions onto the un-loaded PUFs increases sharply with increasing the thiocyanate concentration up to uranyl: CNS- molar ratio >1:4. Thiocyanate and uranyl ions in acid medium form a stepwise series of yellow complexes such as $[\text{UO}_2(\text{SCN})_4]^+$, $[\text{UO}_2(\text{SCN})_4]$ and $[\text{UO}_2(\text{SCN})_4]^{2-}$. Higher concentrations of thiocyanate displace the equilibrium towards the last mentioned reported [26]. Thus, the observed behaviour is possibly attributed to the formation of anionic complex species $[\text{UO}_2(\text{SCN})_4]^{2-}$ which are highly extractable by the protonated ether and/or urethane linkage of the unloaded or TBP-immobilized foam at pH < 3. Similar trends involving “solvent extraction” mechanism for UO_2^{2+} , MoO_2^{2+} and Al^{3+} uptake by diethylether and polyether type based polyurethane foams have been reported [32,33]. Therefore, “Solvent extraction” is the most probable mechanism for the sorption of the complex species $[\text{UO}_2(\text{SCN})_4]^{2-}$ by the unloaded and TBP treated foams and proceeds as follows:



3.2. Kinetic behaviour of uranyl ions sorption from aqueous thiocyanate by PUFs

The sorbed uranium(VI) concentrations q_t (mol g^{-1}) at time t (min) onto the PUFs was plotted against time to test the Weber–Morris equation [34,35]:

$$q_t = R_d(t)^{1/2} \quad (8)$$

where R_d is the rate constant of intraparticle transport in $\text{mmol g}^{-1} \text{min}^{-1/2}$. It was found that, the diffusion rate is found fast at the initial stages and slows down with passage of time. The R_d values computed from the observed distinct slopes of the Weber–Morris [34,35] plots at the initial stage were estimated to be 4.15 ± 0.04 and $0.4355 \pm 0.06 \text{ mmol g}^{-1} \text{min}^{-1/2}$ for the unloaded and TBP immobilized PUFs, respectively. Also, the data indicates that, for up to $t^{1/2}$ equal 6 and 9 min, the relationship holds good for unloaded and TBP-loaded foams, respectively and deviates as the shaking time increases.

Moreover, the variation of the sorption of uranyl ions from aqueous thiocyanate media onto the un-loaded and TBP loaded foams was subjected to the Lagergren equation [36]:

$$\log(q_e - q_t) = \log q_e - kt/2.3 \quad (9)$$

where q_e is the sorbed uranyl ions concentration onto the PUFs at equilibrium in mmol g^{-1} and k is the overall first-

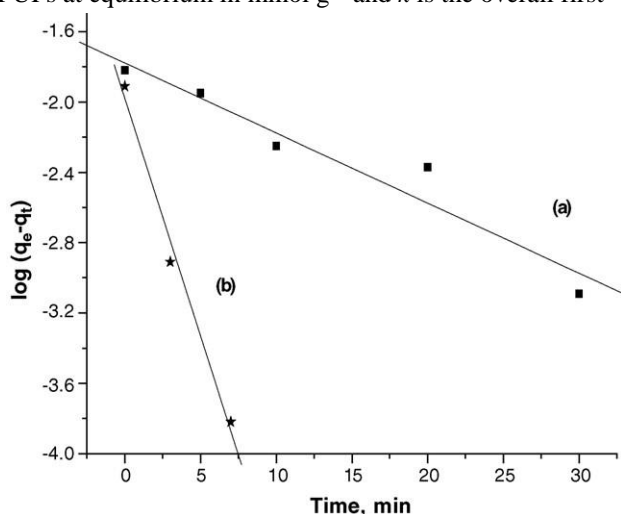


Fig. 3. Lagergren plots of the kinetics of uranyl(II) ions (10g/ml) sorption from aqueous thiocyanate media (0.5M) at pH<3 onto unloaded (a) and TBP-loaded (b) PUFs (0.3±0.019).

order rate constant. The plots of $\log(q_e - q_t)$ versus time up to 60 min were found linear (Fig. 3). The k values for the uranyl ions sorption from the aqueous solution onto the unloaded and reagent loaded foams were estimated to be 0.1 ± 0.02 and $0.62 \pm 0.04 \text{ s}^{-1}$, respectively.

The BT which is a mathematical function (F) of q_t/q_e for each value of F is given by Reichenburg equation [37]:

$$BT = -0.4977 - 2.303 \log(1 - F) \quad (10)$$

The plots of BT versus time at $25 \pm 1 \text{ }^\circ\text{C}$ were found linear up to 30 and 10 min (Fig. 4) for uranyl sorption from the aqueous solution onto the unloaded and TBP loaded foams, respectively. The two straight lines do not start from the origin confirming the observed behaviour of the Weber–Morris equation [34,35]. Thus, the particle diffusion is not the most probable operating mechanism and does not properly control

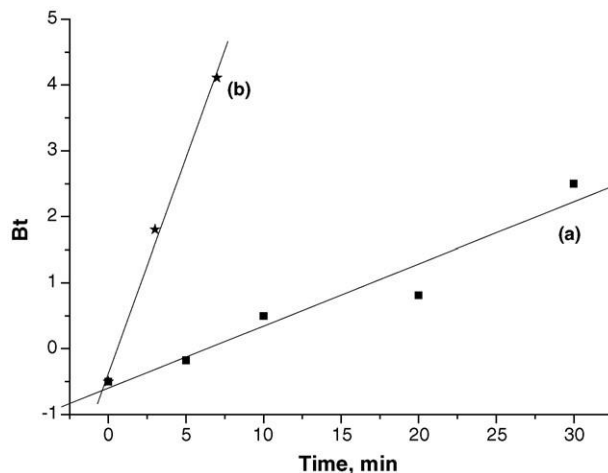


Fig. 4. Reichenburg plot of the kinetics of uranyl(II) ions (10g/ml) sorption from aqueous thiocyanate media (0.5M) at pH<3 onto unloaded (a) and TBP-loaded (b) PUFs (0.3±0.019).

the kinetics of uranyl ions sorption onto the unloaded and TBP-loaded foams. Thus, the actual sorption of the solute onto the interior surface site is fast, and hence it is not the rate determining step. Therefore, either film or intraparticle transport may be the rate limiting steps controlling the rate of uranyl ions sorption from the acid solutions at $\text{pH} < 3$ containing thiocyanate ions.

3.3. Thermodynamic characteristics of uranyl ions uptake onto PUFs

The distribution of uranyl ions between the aqueous phase and the PUFs changes with temperature because the solubility

of the analyte in the two phases changes with temperature.

Thus, the thermodynamic parameters (ΔH , ΔS , ΔG) of uranium(VI) sorption onto the un-loaded and TBP-loaded foams were evaluated using the following equations:

$$\ln K_C = \Delta S/R - \Delta H/RT \quad (11)$$

$$\Delta G = \Delta H - T\Delta S \quad (12)$$

$$\Delta G = -RT \ln K_C \quad (13)$$

where ΔH , ΔS , ΔG , T , R and K_C are the enthalpy, entropy, Gibbs free energy changes, absolute temperature in Kelvin, the gas constant ($\sim 8.3 \text{ J mol}^{-1}$) and the equilibrium constant of uranyl ions sorption by PUFs, respectively. The equilibrium constant depends on the fractional attainment

(F_e) of the sorption process of uranyl ions at equilibrium onto the unloaded and TBP-loaded foams [17,18]. The plots of $\log K_d$ and/or $\log K_C$ versus $1/T$ are shown in Figs. 5 and 6. The plots were linear over the entire range of temperature (298–345 K). The values of H and S were then calculated from the slope and intercept of Fig. 7, whereas; G values were computed employing Eq. (12).

The H and S values for the sorption of uranyl ions onto the unloaded foams were estimated to be $-24.24 \pm$

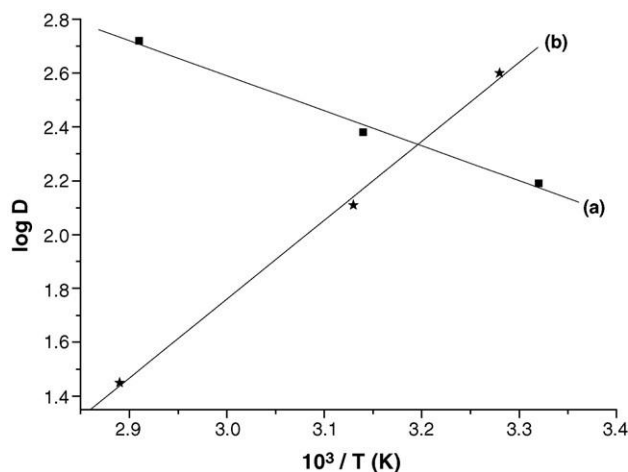


Fig. 5. Variation of $\log D$ vs. $1/T$ (K^{-1}) for the uranyl(II) ions (10g/ml) sorption from aqueous thiocyanate (0.5M) media at $pH < 3$ complex onto unloaded (a) and TBP-loaded (b) PUFs (0.3 ± 0.019).

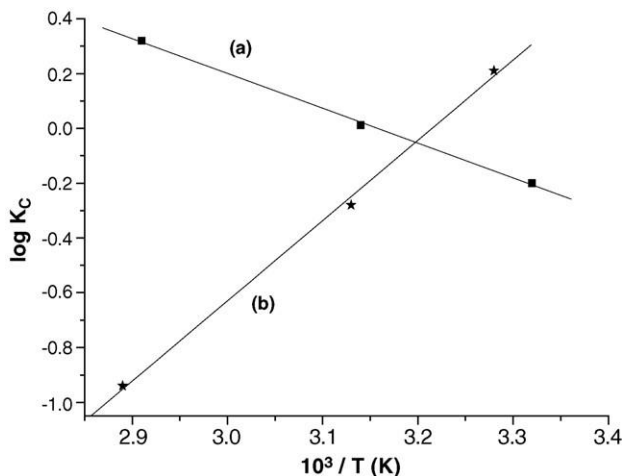


Fig. 6. Variation of $\log K_C$ vs. $1/T$ (K^{-1}) for the uranyl(II) ions (10g/ml) sorption from aqueous thiocyanate (0.5M) media at $pH < 3$ complex onto unloaded (a) and TBP-loaded (b) PUFs (0.3 ± 0.019).

2.4 J mol^{-1} and $3.89 \pm 0.63 \text{ J mol}^{-1} \text{ K}^{-1}$, respectively, while

$\Delta H = 55.2 \pm 3.6 \text{ kJ mol}^{-1}$ and $\Delta S = 4 \pm 0.7 \text{ J mol}^{-1} \text{ K}^{-1}$ for uranyl ions extraction onto TBP-loaded foams, respectively. The negative and positive values of H confirm the exothermic and endothermic nature for the uranyl ions uptake onto the un-loaded and TBP-loaded PUFs, respectively. One explanation is that, in the unloaded PUFs, the ether

membranes groups interact less strongly with each other and therefore they are largely available for intermolecular interactions with uranyl ions. As the temperature increases some of the interactions among the polar groups may be strengthened due to the decreased energy of the individual segments. As a result, the polar groups are more available for interactions with uranyl ions in the test solution.

The positive entropy obtained for the extraction of uranyl(II) ions onto the PUFs membrane indicates that, the freedom of motion of uranyl is less restricted in the PUFs membrane than in solution. Since the sorption process involves an increase in the free energy, we would expect H to be also positive which was confirmed from the data obtained for the TBP loaded PUFs, where the sorption of the uranyl ions by the ether-type PUFs membrane is an endothermic process. By applying Le Chatelier's principle we would expect that, the sorption of the uranyl ions by the unloaded PUFs at equilibrium to increase on increasing temperature. Thus, the uranyl ions sorption onto the unloaded and TBPloaded PUFs is more favorable at low and high temperature confirming the exothermic and endothermic chemi-sorption processes, respectively and excellent performance of the uranyl ions retention onto the PUFs. The high energy of the urethane nitrogen or ether-oxygen sites of the TBP-loaded PUFs provided by raising temperature, enhances the possible interaction between the active sites of the unloaded PUFs and the anionic complex of uranyl ions thiocyanate ions which results a higher sorption at high temperature. The bond formation between the uranyl thiocyanate complex ion and the unloaded PUFs, based on H – bonding and/or ionic bonding comprising the interaction through the chemi-sorption, may account for the endothermic nature of uranyl ions uptake. Thus, “solvent extraction” is the most probable mechanism for uranyl ions sorption onto the unloaded and TBP-loaded PUFs. These results suggest the possible use of the PUFs in flow mode for quantitative collection and chemical enrichment of uranyl ions from large sample volumes of various water samples.

3.4. Chromatographic behaviour of uranyl ions retention onto the PUFs: packed column

The performance of unloaded and TBP-loaded foams packed column for the quantitative retention of uranyl ions from aqueous thiocyanate media was carried out by percolating 200 ml of an aqueous solution containing uranyl ions at 5 g/ml concentration level at $pH \leq 3$ through the foam columns at 10 ml/min flow rate. Analysis of the uranyl ions in the effluent solution against a reagent blank indicates the complete sorption of UO_2^{2+} onto the unloaded and TBPloaded foams columns. Thus, the retained species were eluted successfully from the foam columns with 20 ml acetone at 5 ml/min flow rate.

The performance of the packed foam column is generally described quantitatively by the number of theoretical plates (N) and the height equivalent to the theoretical plate (HETP). The HETP is defined as the length of column foam bed necessary for the rapid attainment of solute equilibrium between the mobile phase and the stationary phase. The HETP and N values were evaluated from the breakthrough capacity curve at 10 g/ml uranyl ions concentration level and 10 ml/min flow rate (Fig. 7) using the following equation [27]:

$$N = \frac{V_{50} V'}{(V_{50} - V')^2} \quad \text{HETP} = \frac{L}{N} \quad (14)$$

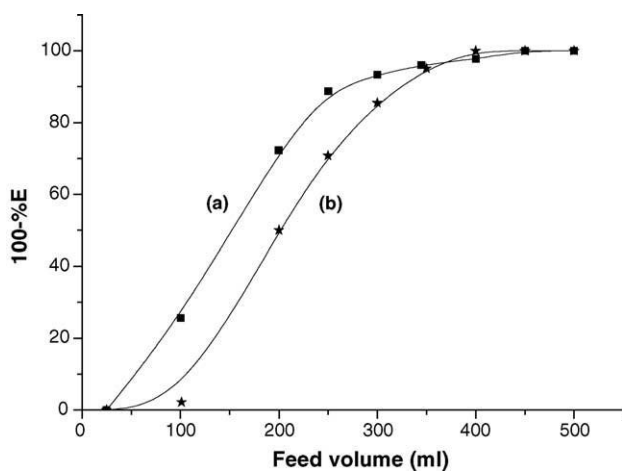


Fig. 7. Breakthrough capacity curves for uranyl(II) ions (10g/ml) sorption from aqueous thiocyanate media (0.5M) onto the unloaded (a) and TBPloaded (b) PUFs (0.3 ± 0.019).

where V_{50} is the volume of the effluent solution at the center of the S-shaped of the breakthrough curve where the concentration is one-half the initial concentration and V is the volume at which the effluent solution has a concentration of 0.1578 of the initial concentration. The HETP and N values were estimated to be 1.22 ± 0.1 and 82 ± 2 and 0.99 ± 0.15 and 101 ± 2 , for uranium(VI) retention onto the unloaded and TBP-loaded foams, respectively.

The critical capacity of the uranium(VI) species retained on the un-loaded and TBP-loaded foams column calculated from Fig. 7, was determined as 1.1 ± 0.1 and 1.8 ± 0.1 mg/g at 10 ml/min flow rate, respectively. The raising portions of the S-shaped curve (Fig. 7) have large slopes indicating a high transfer rate of uranium(VI) on/in the foam membranes and a rapid attainment of equilibrium between the complex ions associate of uranium(VI) thiocyanate in aqueous phase and on/in the foam membranes. The breakthrough capacity (BC) of uranium(VI) onto the unloaded and TBP-loaded foam was calculated employing the equation [38]:

$$BC = \frac{V_{50}C_0}{m} (\text{mg/g}) \quad (15)$$

where C_0 is the initial concentration of uranium(VI) in g/ml, V_{50} the effluent volume (ml) at 50% breakthrough curve of the respective initial concentration in the feed solution and m is the mass (g) of the dry foam beds. The values of BC at 5 ml/min flow rate were determined as 2.51 ± 1.5 and 4 ± 1 mg/g for uranium(VI) sorption onto the unloaded and TBP-loaded foams, respectively. These values are quite good as compared to other solid support such as Voltalef, silica gel and solid inorganic ion exchanger column in rapid, versatile and effective separation for uranyl ions in fluid samples via static and flow mode [15,27].

3.5. Effect of diverse ions

The retention profile of uranyl(II) ions from aqueous thiocyanate by the proposed unloaded PUFs columns was considered to be a prime important. Thus, the sorption of uranyl ions at ≤ 10 g/ml concentration level in the presence of a large excess (1 mg/ml) of diverse ions were critically examined. The results revealed that, it is possible to preconcentrate the tested concentration of uranyl ions quantitatively ($99.5 \pm 2.6\%$) in the presence of up to 1 mg/ml of the following anions: nitrate, phosphate, tartrate, citrate, bromate, sulphite, vanadate, bromide and sulphate. Also, in the presence of the following metal ions: Cu^{2+} , Mn^{2+} , Co^{2+} , Ni^{2+} , Zn^{2+} , Ca^{2+} , and Li^+ at 0.1 mg/ml concentration level, complete extraction of uranyl ions was achieved successfully. Then, the retained uranyl ions were recovered and finally determined [26]. The data revealed that, the uranyl ions are

recovered quantitatively from the foam packed columns with NaOH at a reasonable flow rate (10 ml/min). These results also extend the use of the proposed foam method for the complete separation of traces of uranyl ions in different matrices.

3.6. Applications

The feasibility of the proposed TBP-immobilized foam packed column for the quantitative collection and recovery of uranium(VI) spiked into tap, sea water and/or industrial waste water samples containing excess thiocyanate ions (5% w/v) was examined. Five different water samples were spiked with uranyl(II) ions at concentrations range 1–10 g/ml at $\text{pH} \leq 3$ was allowed to pass through 0.45 m Millipore. The samples were percolated through the TBP-loaded PUF column at 10 ml/min flow rate. Complete retention of uranyl(II) ions ($99.6 \pm 2.1\%$) was achieved as indicated from the analysis of uranyl(II) ions in the effluent solution [26]. The sorbed uranium(VI) species were then recovered from the foam column by percolating 50 ml of NaOH (1 M) at 5 ml/min flow rate. The uranyl ions in the recovered solutions were then determined as described earlier [27]. A reasonable average percentage recovery of (98.4 ± 1.6) was obtained. The data also showed that the method is excellent, sensitive, selective and even possible for water samples with high content of dissolved solids.

4. Conclusion

The excellent performance of the PUFs sorbent towards uranyl(II) ions retention was explained using “solvent extraction” model or a dual-mode sorption model involving both “solvent extraction” and “surface adsorption” mechanism. The proposed dual-mode of sorption offered an excellent description of the observed behaviour and seems to be the most plausible mechanism. According to this model, when the analyte concentration is high, “solvent extraction” became the most predominant mechanism because of higher capacity. However, when the analyte concentration was low an added component of adsorption was responsible for the majority of the sorption. The proposed method permits rapid and effective separation at a relatively high flow rate without loss in column performance. The method lends feasibility for on-site analysis of uranyl(II) ions by AAS or neutron activation analysis. Further studies will be continued to easily estimate the extraction constants of both adsorption and absorption and the stability constants of binding sites of PUFs with $[\text{UO}_2(\text{SCN})_4]^{2-}$ species.

References

- [1] V.K. Jain, S.G. Pillai, R.A. Pandya, Y.K. Agrawal, P.S. Shrivastav, *Talanta* 65 (2005) 466.
- [2] P. Metilda, K. Sanghamitra, J. Mary Gladis, G.R.K. Naidu, T. Prasada Rao, *Talanta* 65 (2005) 192.
- [3] M.A. Maheswari, M.S. Subramanian, *React. Funct. Polym.* 62 (2005) 105.
- [4] P. Metilda, J. Mary Gladis, T. Prasada Rao, *Anal. Chim. Acta* 512 (2004) 63.
- [5] P.C. Mayankutty, M.W. Nadkarni, Bhabha, Atomic Research Center, Report, BARC (1977), 914.
- [6] E. Kluge, K.H. Lieser, *Radiochim. Acta* 27 (1980) 161.
- [7] R.K. Rastogi, M.A. Mahajan, N.K. Chaudhuri, *Sep. Sci. Technol.* 32 (1997) 1711.
- [8] H. De-Beer, P.P. Coetzee, *Radiochim. Acta* 57 (1992) 113. [9] J.L. Perez, C.G. Gorica, E. Gorica, B. Cardero, *Anal. Chim. Acta* 246 (1992) 291.
- [10] B.S. Mohite, A.S. Jadhav, *J. Chromatogr. A* 983 (2003) 277.
- [11] J.M. Gladis, T.P. Rao, *Anal. Bioanal. Chem.* 373 (2002) 867.
- [12] V.K. Jain, A. Handa, S.S. Sait, P. Shrivastav, Y.K. Agrawal, *Anal. Chim. Acta* 429 (2001) 237.
- [13] K. Dev, R. Pathak, G.N. Rao, *Talanta* 48 (1999) 579.
- [14] P.K. Mohapatra, V.K. Manchanda, *Talanta* 47 (1998) 1271.
- [15] M.M. Abou-Mesalam, I.M. El-Nagar, M.S. Abdel-Hai, M.S. ElShahawi, *J. Radioanal. Nucl. Chem.* 258 (2003) 619.
- [16] M.S. Carvalho, *Spectrochim. Acta* 53 (1998) 1945.
- [17] M.M. Saeed, S.M. Hasany, M. Ahmed, *Talanta* 50 (1999) 625.
- [18] S.M. Hasany, M.M. Saeed, M. Ahmed, *Sep. Sci. Technol.* 35 (2000) 379.
- [19] H.D. Gesser, S. Ahmed, *J. Radioanal. Nucl. Chem.* 140 (1990) 395.
- [20] P. Chandak, *Indian J. Chem.* 35 (1996) 809.
- [21] S. Katragadda, H.D. Gesser, A. Chow, *Talanta* 44 (1997) 1865.
- [22] M.M. Saeed, M. Ahmed, *Anal. Chim. Acta* 525 (2004) 289.
- [23] L.G.A. Vande Water, W.L. Driessen, J. Reedijk, D.C. Sherrington, *Eur. J. Inorg. Chem.* (2002) 221.
- [24] M.S. El-Shahawi, A.M. Othman, H.M. Nassef, M.A. Abdel-Fadeel, *Anal. Chim. Acta* 536 (2005) 227.
- [25] I. Kubrakova, T. Kudinova, A. Formanovsky, N. Kuzmin, *Analyst* 119 (1994) 2477.
- [26] Z. Marczenko "Separation and Spectrophotometric Determination of Elements" Ellis Hozwood Limited, 1986 Chapter 59 and references cited in.
- [27] T. Braun, J.D. Navratil, A.B. Farag, *Polyurethane Foam Sorbents in Separation Science*, CRC Press Inc, Boca Rotan, FL, 1985.
- [28] V.K. Gupta, S.K. Srivastava, R. Tyagi, *Water Res.* 34 (2000) 1543.
- [29] I.I. Stewart, A. Chow, *Talanta* 40 (1993) 1345.
- [30] N. Condamines, C. Musikas, *Sol. Ext. Ion. Exch.* 10 (1992) 69.
- [31] K.A. Halhouli, N.A. Darwish, N.M. Al-Dhoun, *Sep. Sci. Technol.* 30 (1995) 3313.
- [32] J.J. Oren, K.M. Gough, H.D. Gesser, *Can. J. Chem.* 57 (1979) 2032.
- [33] A.B. Farag, M.S. Elshahwi, S. Farag, *Talanta* 41 (1994) 617.
- [34] W.J. Weber Jr., J.C. Morris, *J. Sanit. Eng. Div. Am. Soc. Civ. Eng.* 89 SA2 (1963) 31.
- [35] W.J. Weber Jr., J.C. Morris, *J. Sanit. Eng. Div. Am. Soc. Civ. Eng.* 90 SA3 (1964) 79.
- [36] S. Lagergren, B.K. Sven, *Vatenskapsakad. Handl.* (1898) 24.
- [37] D. Reichenburg, *J. Am. Chem. Soc.* 75 (1972) 589.
- [38] W.X. Ma, F. Liu, K.A. Li, W. Chen, S.Y. Tong, *Anal. Chim. Acta* 416 (2000) 191.

A Potentiometric Rhodamine-B Based Membrane Sensor for the Selective Determination of Chromium Ions in Wastewater

Saad S. M. HASSAN,^{*20} M. S. EL-SHAHAWI,^{**} A. M. OTHMAN,^{***} and M. A. MOSAAD^{**}

**Chemistry Department, Faculty of Science, Ain Shams University, Cairo, Egypt*

***Chemistry Department, Faculty of Science at Damietta, Mansoura University, Egypt*

****Genetic Engineering and Biotechnology Research Institute (GEBRI), Minufiya University, Sadat City, Egypt*

The construction and performance characteristics of a novel chromate ion-selective membrane sensor are described and used for determining chromium(III) and chromium(VI) ions. The sensor is based on the use of a rhodamine-B chromate ion-associate complex as an electroactive material in a poly(vinyl chloride) membrane plasticized with *o*-nitrophenyloctyl ether as a solvent mediator. In a phosphate buffer solution of pH 6–7, the sensor displays a stable, reproducible and linear potential response over the concentration range of $1 \times 10^{-1} - 5 \times 10^{-6} \text{ mol l}^{-1}$ with an anionic Nernstian slope of $30.8 \pm 0.5 \text{ mV decade}^{-1}$ and a detection limit of $1 \times 10^{-6} \text{ mol l}^{-1} \text{ Cr(VI)}$. High selectivity for Cr(VI) is offered over many common anions (*e.g.*, F^- , Br^- , Cl^- , IO_4^- , CN^- , acetate, oxalate, citrate, sulfate, phosphate, thiosulfate, selenite, nitrate) and cations (*e.g.*, Ag^+ , Ca^{2+} , Sr^{2+} , Co^{2+} , Ni^{2+} , Cu^{2+} , Mn^{2+} , Fe^{2+} , Zn^{2+} , Cd^{2+} , Al^{3+} , Cr^{3+}). The sensor is used for determining Cr(VI) and/or Cr(III) ions in separate or mixed solutions after the oxidation of Cr(III) into Cr(VI) with H_2O_2 . As low as $0.2 \mu\text{g ml}^{-1}$ of chromium is determined with a precision of $\pm 1.2\%$. The chromium contents of some wastewater samples were accurately assessed, and the results agreed fairly well with data obtained by atomic absorption spectrometry.

(Received November 16, 2004; Accepted February 9, 2005)

Introduction

Although chromium ions exist in several oxidation states, Cr(III) and Cr(VI) predominate in the ambient environment. Chromium(III) is essential to humans and other animals due to its role in glucose and cholesterol metabolism, whereas Cr(VI) has many industrial applications and is very toxic.^{1,2} Occupational exposure to chromium occurs from chromate processing, stainless-steel production, chrome plating and tanning industries.³ Due to the severe toxicity of Cr(VI), a total chromium measurement cannot be used to determine the actual environmental impact.^{4,5} Thus, the chemical speciation of chromium in environmental samples is necessary for accurate assessments of pollution levels.

The methods cited in the literature for the determination of both Cr(VI) and Cr(III) include spectrophotometry,^{6–8} fluorometry,^{9,10} inductively coupled plasma,¹¹ atomic emission spectrometry,¹² atomic absorption spectrometry,^{13,14} X-ray fluorescence spectrometry,¹⁵ differential pulse polarography,¹⁶ adsorptive stripping voltammetry,^{17,18} and high-pressure liquid chromatography.¹⁹ Many of these methods, however, involve several time-consuming manipulation and extraction steps, derivatization reactions and are liable to various interference, not applicable to colored and turbid solutions and require sophisticated instruments.

Potentiometric sensors for the determination of Cr(VI) have been suggested as an alternative simple technique. These are based on the use of chromate complexes with bathophenanthroline,²⁰ quaternary ammonium ions,^{21–25} quaternary phosphonium ions,^{26,27} and crystal violet²⁸ as electroactive materials dispersed in

polymeric membranes. Some of these sensors, are not applicable for determining chromium at concentration levels $< 10^{-3}$ or $10^{-4} \text{ mol l}^{-1}$, display a non-Nernstian response, suffer from the interference by many cations and anions and require a long time for stable response.^{20,21,27}

The present paper describes the preparation and characterization of a novel potentiometric sensor for Cr(VI). This is based on the use of an ion-associate complex of rhodamine-B cation with the chromate anion in a poly(vinyl chloride) matrix membrane plasticized with *o*-nitrophenyloctyl ether. The proposed sensor has some significant advantages over many previously reported chromium sensors,^{20,21} since it offers a lower detection limit ($1 \times 10^{-6} \text{ mol l}^{-1}$), covers a wider working concentration range ($1 \times 10^{-1} - 5 \times 10^{-6} \text{ mol l}^{-1}$), displays a faster response time (10–20 s) and exhibits a higher selectivity in the presence of many common interfering ions. The sensor is satisfactory used for the accurate determination of Cr(III) and Cr(VI) ions in industrial wastewater, either singly or sequentially.

Experimental

Apparatus

Potentiometric measurements were carried out at $25 \pm 1^\circ\text{C}$ with an Orion pH/mV meter microprocessor Ionalyzer (Model 720). The developed rhodamine-B chromate PVC membrane sensor was used in conjunction with an Orion double junction Ag/AgCl reference electrode (Model 90-02) containing 10% (w/v) potassium

²⁰ To whom correspondence should be addressed. E-mail: saadsmhassan@yahoo.com

chloride solution in the outer compartment. The type of electrochemical cell used for e.m.f. measurements was: Ag/AgCl | $1 \times 10^{-2} \text{ mol l}^{-1} \text{ CrO}_4^{2-}$ - $1 \times 10^{-2} \text{ mol l}^{-1} \text{ KCl}$ (inner solution) || plastic membrane || $1 \times 10^{-3} \text{ mol l}^{-1} \text{ CrO}_4^{2-}$ (outer solution) || Orion double junction reference electrode with 10% w/v KCl. The pH measurements were performed with an Orion combination Ross glass electrode (Model 81-02). A Perkin-Elmer Lambda 15 UV/VIS spectrophotometer was used for absorbance measurements using 1.00 cm quartz cuvettes. Atomic absorption spectrometric measurements were made with a Perkin-Elmer 3100 at 357.9 nm using the recommended method.²⁹

Reagents and materials

All chemicals and reagents used were of analytical reagent grade unless otherwise stated, and doubly distilled water was used throughout. High-molecular-weight poly(vinyl chloride) (PVC), *o*-nitrophenyloctyl ether (*o*-NPOE), dioctylphthalate (DOP), dibutylsebacate (DBS) and potassium chromate were supplied from Fluka. Rhodamine-B (RB) and tetrahydrofuran (THF) were obtained from Riedel-De-Haen. A standard stock solution ($1 \times 10^{-1} \text{ mol l}^{-1}$) of potassium chromate was prepared by dissolving 1.942 g in 100 ml of a phosphate buffer of pH ~ 7 . Dilute chromate solutions (1×10^{-2} – $1 \times 10^{-7} \text{ mol l}^{-1}$) at pH ~ 7 were freshly prepared by diluting the stock solution with the phosphate buffer. A $1 \times 10^{-2} \text{ mol l}^{-1}$ stock solution of rhodamine-B was prepared by dissolving 0.479 g of the reagent in a minimum volume of distilled water, followed by filtration and dilution to 100 ml with distilled water.

Rhodamine-B chromate ion pair complex

Rhodamine-B chromate complex was prepared by mixing 20 ml of $1 \times 10^{-2} \text{ mol l}^{-1}$ potassium chromate with 40 ml of $1 \times 10^{-2} \text{ mol l}^{-1}$ rhodamine-B. The mixture was shaken for 10 min and the produced precipitate was filtered off through a Whatman filter paper No. 42, washed with deionized water, dried at room temperature and ground to a fine powder.

Rhodamine-B chromate membrane sensor

A 10 mg portion of the rhodamine-B chromate ion-associate complex was thoroughly mixed with 190 mg of PVC powder and 360 mg of *o*-nitrophenyloctyl ether plasticizer in a glass Petri dish (5 cm diameter). The mixture was dissolved in ~ 5 ml of freshly distilled THF, covered with filter paper and left to stand overnight to allow slow evaporation of the solvent at room temperature. A transparent PVC master membrane with an average thickness of ~ 0.1 mm was obtained, sectioned with a cork borer (10 mm i.d.), glued to polyethylene tubing (7 mm i.d.) and used to prepare the sensor, as previously described.^{30,31}

Sensor calibration

Aliquots (10 ml) of standard Cr(VI) solutions (1×10^{-1} – $1 \times 10^{-7} \text{ mol l}^{-1}$) in phosphate buffer of pH ~ 7 were transferred to 50 ml beakers, stirred and thermostated at $25 \pm 1^\circ\text{C}$. The chromium membrane sensor in conjunction with a double junction Ag/AgCl reference electrode were immersed in the test solution. The potential readings were recorded after stabilization to ± 0.2 mV and the e.m.f. was plotted versus logarithm [Cr(VI)]. The calibration plot was used for subsequent measurements of Cr(VI) in unknown test solutions. The detection limit was taken at the point of intersection of the extrapolated linear segments of the calibration curve.

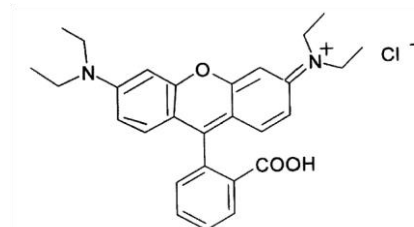


Fig. 1 Chemical structure of rhodamine-B reagent.

Sensor selectivity

The potentiometric selectivities of the sensor towards different inorganic cations in the nitrate form and several anions in the form of potassium or sodium salts were determined by the separate solutions technique.^{30,32} The potential responses of $1 \times 10^{-3} \text{ mol l}^{-1}$ of both Cr(VI) and the interfering ions in separate aliquots in phosphate buffer of pH ~ 7 were measured. The selectivity coefficients were calculated from the rearranged Niclosky equation,^{30,33}

$$\log K_{\text{CrO}_4/\text{Z}_B} = \frac{E_{\text{CrO}_4} - E_B}{S} + \left[1 + \frac{Z_{\text{CrO}_4}}{Z_B} \right] \log [\text{CrO}_4^{2-}]$$

where E_{CrO_4} and E_B are the potential readings observed after 1 min of exposing the sensor to the chromate and the interfering ions, Z_{CrO_4} and Z_B are the charges of the chromate and interfering species B, respectively, and S is the slope of the calibration plot (mV per concentration decade).

Determination of chromium(III)

A 10 ml portion of solutions containing 10 – 100 μg Cr(III) was transferred into a 50 ml Erlenmeyer flask, followed by the addition of 10 ml of 20% v/v hydrogen peroxide. The solution was adjusted to pH 7 – 9 with a dilute NaOH solution. The reaction mixture was boiled for 5 min, left to cool, quantitatively transferred to a 50 ml volumetric flask and completed to the mark with phosphate buffer of pH ~ 7 . The produced Cr(VI) was determined as described above. A blank experiment was run to correct for the reagent effect.

Sequential determination of Cr(III) and Cr(VI)

A 10 ml aliquot of Cr(III)/Cr(VI) mixtures was transferred to a 50 ml beaker, and Cr(VI) was directly determined as described above. To a separate 10 ml aliquot of the test solution, a 10 ml hydrogen peroxide (20% v/v) was added and the pH was adjusted to pH 7 – 9. The mixture was boiled for 5 min. After cooling, the solution was transferred to a 50 ml volumetric flask and completed to the mark with a phosphate buffer of pH ~ 7 . The total contents of Cr(VI) equivalent to those originally present and Cr(III) after conversion into Cr(VI) were determined as described above and Cr(III) was calculated based on the difference.

Sequential determination of Cr(III) and Cr(VI) in wastewater

Wastewater samples from electroplating and aluminum painting plants were collected in polyethylene containers, and adjusted to pH ~ 7 with phosphate buffer. A 1 – 25 ml aliquot of the samples was transferred to a 50 ml volumetric flask and completed to the mark with phosphate buffer of pH ~ 7 . The potential of a 10 ml aliquot of the solution was measured as a function of the Cr(VI) content. The total chromium [(Cr(III) + Cr(VI))] was measured in

a second 10 ml aliquot of the sample test solution after boiling with 10 ml H₂O₂ (20% v/v) for 5 min in a slightly alkaline solution (pH 7–9), as described above.

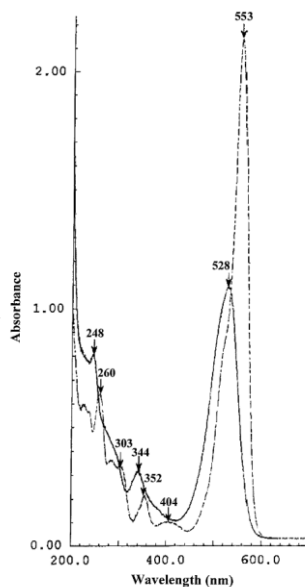


Fig. 2 Electronic spectra of rhodamine-B (—) and rhodamine-B chromate ion-pair complex (---).

Results and Discussion

Characterization of rhodamine-chromate ion-associate complex

A preliminary investigation showed that chromate ions were selectively extracted with rhodamine-B (Fig. 1) at pH ~7 in organic solvents (e.g., benzene, toluene and chloroform). The electronic spectrum of the extract displayed three absorption maxima at 248, 344 and 528 nm, compared to those exhibited at 260, 352, 404 and 553 nm by rhodamine-B reagent (Fig. 2). No change in the absorption spectra of the reagent in the presence of NO₃⁻, PO₄³⁻, SO₄²⁻ and Cl⁻ ions was noticed. The composition of the red purple rhodamine-B chromate ion-associate complex in solution was determined by the continuous variation method.³⁴ A plot of the absorbance of the organic extract versus Cr(VI)/[Cr(VI) + RB] revealed the formation of the 2:1 [RB:Cr(VI)] complex. These results are consistent with an elemental analysis data obtained for the solid complex, which agreed fairly well with the formula C₅₆H₆₂N₄O₁₀Cr (calculated, C: 67.1%, H: 6.2%, N: 5.6%, Cr: 5.2%, found, C: 67.9%, H: 6.2%, N: 5.9%, Cr: 5.1%). The infrared spectrum of the solid complex in KBr disc showed vibrations for symmetric and asymmetric stretching modes of the Cr=O group at 995 and 901 cm⁻¹, respectively.

Performance characteristics of chromium membrane sensor

Rhodamine-B chromate ion-associate complex was incorporated in PVC membranes plasticized with *o*-NPOE, DBS and DOP solvent mediators, and used as membrane sensors for the potentiometric determination of Cr(VI) in aqueous solutions. The sensors were evaluated at ambient temperature according to the IUPAC recommendations.³² The data showed that the composition of the membrane constituents affected both the potentiometric response and the selectivity of the sensor. A membrane with the composition 2:63:35 wt% chromium complex, *o*-NPOE and PVC,

respectively, exhibited the best response characteristics for Cr(VI) with a Nernstian anionic slope of 30.8 ± 0.5 mV decade⁻¹ over the concentration range 1 × 10⁻¹ – 5 × 10⁻⁶ mol l⁻¹ (correlation coefficient 0.998, *n* = 5). The limit of detection, evaluated according to the standard

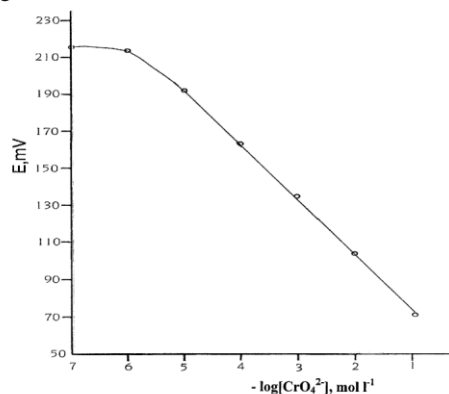


Fig. 3 Potentiometric response of the rhodamine-B chromate PVC membrane sensor.

methods³² from the intersection of the two extrapolated segments of the calibration graph, was found to be 1 × 10⁻⁶ mol l⁻¹ (i.e., 0.2 µg ml⁻¹) Cr(VI). The general performance characteristics remained constant when evaluated with different sensor membranes with the same composition and at different times of the membrane operative life. The main analytical features of the developed Cr(VI) sensor are summarized in Table 1, and a typical calibration plot is shown in Fig. 3.

The response time (*t*₉₅) of the chromium sensor was tested by measuring the time required to achieve 95% of the steady potential response at pH ~7 for 10⁻³ and 10⁻² mol l⁻¹ after successive immersion in a series of Cr(VI) solutions with one decade difference, starting from low to high concentration. The response time required for the sensor to reach values within ±0.5 mV of the final equilibrium potential ranged from 30–40 s in solutions ≤ 1 × 10⁻³ mol l⁻¹ to 10–20 s at concentrations ≥ 1 × 10⁻³ mol l⁻¹. The sensor displayed constant-potential readings within ±1 mV from day-to-day, and the calibration slope remained constant within ±1 mV decade⁻¹ over a period of 8 weeks without any hysteresis phenomenon. After 9 weeks, the calibration slope declined by -5 mV decade⁻¹, the linear range gradually decreased and the response time increased to 1–1.5 min. This behavior is attributed to a possible leaching of the ion-associate complex from the membrane matrix.

Effect of pH

Chromium(VI) ions in aqueous solution exist as chromate (CrO₄²⁻), dichromate (Cr₂O₇²⁻), hydrogen chromate (HCrO₄⁻), hydrogen dichromate (HCr₂O₇⁻), trichromate (Cr₃O₁₀²⁻) and tetrachromate (Cr₄O₁₃²⁻) anions, depending on the pH of the solution.³⁵ The last three ions have been detected in solutions of pH < 0 or at Cr(VI) concentration greater than 1 mol l⁻¹. At pH ≤ 0, H₂CrO₄ is a significant species; at pH = 2–6, HCrO₄⁻ and Cr₂O₇²⁻ species occur together; and at pH > 6, CrO₄²⁻ ions predominate. The dependence of the potential response of the sensor over a wide range of pH 2–10 was investigated with different concentrations of standard Cr(VI) solutions. The pH of the test solutions was adjusted with dilute HCl and/or NaOH.

The potential–pH profiles of the sensor for 10^{-2} and 10^{-3} mol l $^{-1}$ Cr(VI) are shown in Fig. 4. A steady potential was obtained over the pH range 5.5 – 8. At pH < 5.5, the e.m.f. of the sensor sharply decreased and the calibration slope approached the Nernstian slope of mono-charged anion due to the formation of monovalent hydrogen chromate HCrO_4^- and/or hydrogen dichromate HCr_2O_7^- anions via the following reactions:^{20,35}

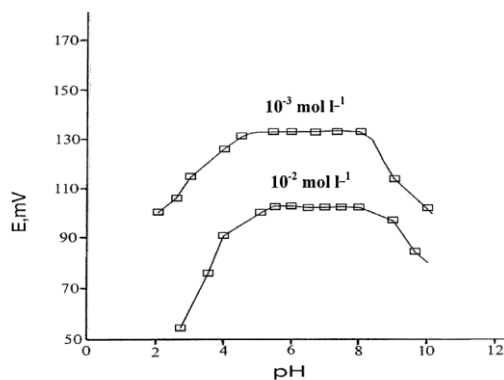


Fig. 4 Effect of the pH on the potentiometric response of the rhodamine-B chromate PVC membrane sensor.

Table 3 Sequential potentiometric determination of Cr(III) and Cr(VI) ions in some synthetic binary mixtures using the rhodamine-B chromate PVC membrane sensor

Cr(III)/ $\mu\text{g ml}^{-1}$		Recovery, % _a	Cr(VI)/ $\mu\text{g ml}^{-1}$		Recovery, % _a
Added	Found ^a		Added	Found	
$\text{H}^+ + \text{CrO}_4^{2-} = \text{HCrO}_4^-$; $\text{H}^+ + \text{Cr}_2\text{O}_7^{2-} = \text{HCr}_2\text{O}_7^-$.					

Under these conditions, both HCrO_4^- and HCr_2O_7^- displayed a slope of 45 mV decade $^{-1}$. At pH > 8, the potential readings of the sensor decreased due to interference caused by the hydroxyl ions and a decrease of the activity of CrO_4^{2-} ions. All subsequent measurements were performed in a phosphate buffer solution of pH ~7.

Effect of a membrane solvent mediator

Three PVC membrane sensors containing rhodamine-B chromate ion-pair complex with DOP, DBS and *o*-NPOE plasticizers were prepared and tested for a Cr(VI) assessment by measuring the calibration slope, sensitivity and lower limit of detection. The performance characteristics of a sensor incorporating *o*-NPOE plasticizer showed a good response for as low as 2×10^{-6} mol l $^{-1}$ for Cr(VI). In addition, the repeatability of the sensor response at room temperature was much better, faster and stable than other sensors with membranes plasticized with DOP or DBS, which showed a narrower linear response range (1×10^{-4} – 1×10^{-1} mol l $^{-1}$), a smaller calibration slope (-26.0 ± 0.5 , -22.5 ± 0.5 mV decade $^{-1}$) and a higher limit of detection (1×10^{-5} – 8×10^{-4} mol l $^{-1}$).

Sensor selectivity

The potentiometric selectivity coefficients, $K_{\text{CrO}_4^{2-}, \text{B}}^{\text{pot}}$, of the developed chromate membrane sensor depend on the selectivity of the ion-exchange process at the membrane–sample interface, the mobility of the test ions in the membrane and the free energy for the transfer of chromate ions between the aqueous and organic phases. The hydrophobic interaction between the primary ions and the organic membrane controlled the sensor selectivity.³⁶

Table 2 depicts the obtained selectivity coefficients data. It can be seen that for the anions (chloride, bromide, nitrate, selenite, sulfite, thiosulfate, sulfate, citrate, acetate, phosphate and oxalate), the selectivity coefficients are on the order of 10^{-3} – 10^{-4} , indicating no significant interference. This was confirmed by measuring the electronic spectra of the extract of rhodamine-B in the presence of

these ions where no change of the RB spectrum was observed due to the presence of any of these ions. The selectivity coefficients measured for Ca^{2+} , Sr^{2+} , Co^{2+} , Ni^{2+} , Cu^{2+} , Mn^{2+} , Fe^{2+} , Zn^{2+} , Cd^{2+} , Al^{3+} , Cr^{3+} and Ag^+ cations (Table 2) indicated negligible interference.

20.0	20.2 \pm 0.2	101.0	30.0	30.5 \pm 0.3	101.7
30.0	30.3 \pm 0.3	100.9	20.0	20.5 \pm 0.3	102.5
20.0	19.6 \pm 0.2	98.0	10.0	20.4 \pm 0.2	102.0
10.0	9.8 \pm 0.2	98.0		10.1 \pm 0.3	101.0

a. Average of 5 measurements.

Table 1 General performance characteristics of the rhodamine-B chromate PVC membrane sensor

Parameter	Chromate sensor
Slope/mV decade $^{-1}$	30.8 \pm 0.5
Intercept/mV	43 \pm 0.4
Correlation coefficient ($n = 5$)	0.998
Lower limit of linear range/mol l $^{-1}$	5×10^{-6}
Lower limit of detection/mol l $^{-1}$	1×10^{-6}
Response time for $> 1 \times 10^{-3}$ mol l $^{-1}$ /s	10 – 20
Working range/pH	5.5 – 8

Table 2 Potentiometric selectivity coefficients ($K_{\text{CrO}_4^{2-}, \text{B}}^{\text{pot}}$) of the rhodamine-B chromate PVC membrane sensors

Interferent, B	$K_{\text{CrO}_4^{2-}, \text{B}}^{\text{pot}}$	Interferent, B	$K_{\text{CrO}_4^{2-}, \text{B}}^{\text{pot}}$
----------------	--	----------------	--

Cl ⁻	7.9×10^{-3}	Ca ²⁺	1.4×10^{-4}
Br ⁻	1.2×10^{-3}	Sr ²⁺	1.2×10^{-4}
IO ₃ ⁻	1.9×10^{-2}	Co ²⁺	6.3×10^{-3}
NO ₃ ⁻	7.9×10^{-4}	Ni ²⁺	3.4×10^{-3}
SO ₄ ²⁻	5.4×10^{-4}	Cu ²⁺	1.6×10^{-3}
S ₂ O ₃ ²⁻	2.9×10^{-3}	Mn ²⁺	1.2×10^{-4}
Acetate	6.9×10^{-3}	Fe ²⁺	2.0×10^{-3}
Oxalate	3.9×10^{-4}	Cd ²⁺	4.2×10^{-4}
Citrate	4.4×10^{-4}	Al ³⁺	2.7×10^{-4}
Selenite	4.4×10^{-4}	Cr ³⁺	7.0×10^{-3}
Phosphate	1.4×10^{-3}	Ag ⁺	8.5×10^{-3}
	3.5×10^{-4}		1.6×10^{-2}

Analytical applications

A rhodamine-B chromate PVC membrane sensor was tested for the determination of a 10 – 50 µg ml⁻¹ certified reference Cr(VI) solution. The average recovery ranged from 96.7 to 98.1% and the mean standard deviation was ±0.3% ($n = 10$).

Certified reference Cr(III) solutions (10 – 50 µg ml⁻¹) were also determined after prior oxidation to Cr(VI) with alkaline H₂O₂. Hydrogen peroxide in an aqueous alkaline solution was found to be the most suitable oxidizing agent for quantitative conversion of Cr(III) into Cr(VI). Excess H₂O₂ was easily decomposed by boiling, and the produced Cr(VI) was determined under the optimized experimental conditions. An average recovery of 98.7% and a mean standard deviation of ±0.3% were obtained ($n = 10$).

Binary synthetic mixtures of Cr(III) and Cr(VI) ions were next determined by a direct measurement of Cr(VI) in one aliquot, followed by the oxidation of Cr(III) to Cr(VI) in a second aliquot with H₂O₂ and assay of the total chromium ions. The results given in Table 3 show average recoveries of 98 ± 2.0 –

Table 4 Sequential determination of Cr(III) and Cr(VI) ions in wastewater samples using the rhodamine-B chromate PVC membrane sensor and atomic absorption spectrometry (AAS)

Wastewater sample	Cr(III) found/µg ml ^{-1a}		Recovery, % ^a	Cr(VI) found/µg ml ^{-1a}		Recovery, % ^a
	AAS	Chromate sensor		AAS	Chromate sensor	
Electroplating exhaust bath	—	—	—	3.1 ± 0.1	3.0 ± 0.2	96.8
	—	—	—	6.3 ± 0.2	6.3 ± 0.3	100.0
Chromate plating bath	—	—	—	23.2 ± 0.2	23.4 ± 0.2	100.8
	—	—	—	68.3 ± 0.2	68.2 ± 0.2	99.9
Aluminum painting	2.7 ± 0.2	2.6 ± 0.1	96.3	16.4 ± 0.3	16.1 ± 0.2	98.2
	9.1 ± 0.3	8.9 ± 0.2	97.8	18.9 ± 0.3	18.4 ± 0.3	97.4

a. Average of 5 measurements.

101 ± 1.0 and $101 \pm 1.0 - 102.5 \pm 2.5\%$ for Cr(III) and Cr(VI) ions, respectively.

The analytical usefulness of the developed sensor was examined for the determination of hexavalent and trivalent chromium ions in some industrial wastewater samples collected from the effluents of electroplating exhaust baths, chromate baths and aluminum painting wastewater effluents; the results are given in Table 4. Most of the tested samples from electroplating wastes contained

different concentrations of Au³⁺, Cu²⁺, Ni²⁺ and Ag⁺ ions beside the chromium species. The data indicated that cyanide ions, if present in the electroplating effluent, reduces Cr(VI) to Cr(III), but the treatment step with H₂O₂ destroys the excess CN⁻ and converts all Cr(III) to Cr(VI). In aluminum painting wastewater, both Cr(III) and Cr(VI) are detected in the range of 2.7 – 9.1 µg ml⁻¹ and 16.1 – 18.4 µg ml⁻¹, respectively. A comparison of these data with results obtained using the AAS method showed a close agreement within $\pm 0.1 - 0.5$ µg ml⁻¹ ($\pm 0.8 - 3.7\%$). An *F*-test revealed that there was no significant difference between the mean and variances of the two sets of results. The inherent advantages of the proposed potentiometric assay method are the excellent selectivity, applicability to a wide concentration range of Cr(VI) in turbid and colored solutions, fast response, simple assembly, high accuracy, good precision and low cost.

Conclusions

A chromium PVC membrane sensor has been developed based on the use of rhodamine-B chromate as a novel electroactive material. The sensor is used for the sequential determination of Cr(III) and Cr(VI) ions. It provides a simple, fast, cost effective and reliable technique for the precise, reproducible and accurate determination of chromium ions. The sensor exhibits an anionic Nernstian response of 30.8 ± 0.5 mV decade⁻¹ at pH 5.5 – 8 and a high selectivity towards Cr(VI) with respect to many anions and cations. The detection limit is 1×10^{-6} mol l⁻¹ and the linear range is $1 \times 10^{-1} - 5 \times 10^{-6}$ mol l⁻¹. Results obtained for the assay of chromium ions in the wastewater of some industries compared favorable well with data obtained by atomic absorption spectrometry.

References

1. A. Kabata-Pendias and H. Pendias, "Trace Elements in Soils and Plants", **1984**, CRC Press, Boca Raton, FL, 1 – 68, 193 – 199.
2. H. A. Schroeder, J. J. Balassa, and I. H. Tipton, *J. Chron. Dis.*, **1962**, *15*, 941.
3. Agency for Toxic Substances and Disease Registry(ATSDR), "Toxicological Profile for Chromium", **1993**, U.S. Public Health Service, U.S. Department of Health and Human Services, Atlanta, GA.

4. E. Merian, "Metals and Their Compounds in the Environment, Occurrence, Analysis and Biological References", **1980**, VCH, New York.
5. E. J. Arar, S. E. Long, T. D. Martin, and S. Gold, *Environ. Sci. Technol.*, **1992**, *26*, 1944.
6. D. T. Burns and M. D. Dunford, *Anal. Chim. Acta*, **1996**, *319*, 205.
7. M. Shiro, T. Yoshika, T. Ko, and Y. Kzauhisa, *Analyst*, **1999**, *124*, 789.
8. M. Bittner and J. A. C. Broekaert, *Anal. Chim. Acta*, **1998**, *364*, 31.
9. T. M. A. Razek, S. Spear, S. S. M. Hassan, and M. A. Arnold, *Talanta*, **1999**, *48*, 269.
10. L. Wang, L. Wang, T. Xia, L. Dong, G. Bian, and H. Chen, *Anal. Sci.*, **2004**, *20*, 1013.
11. L. Shen-Kay and B. Harald, *Fresenius, J. Anal. Chem.*, **1998**, *360*, 545.
12. J. E. T. Anderson, *Anal. Chim. Acta*, **1998**, *361*, 125.
13. K. S. Subramanian, *Anal. Chem.*, **1988**, *60*, 11.
14. R. M. Milacic and J. Stupar, *Analyst*, **1994**, *119*, 627.
15. C. K. Mann and J. C. White, *Anal. Chem.*, **1958**, *30*, 989.
16. C. Harzdorf and G. Janser, *Anal. Chim. Acta*, **1984**, *165*, 201.
17. X. Zhu, B. Hu, Z. Jiang, Y. Wu, and S. Xiong, *Anal. Chim. Acta*, **2002**, *471*, 121.
18. O. Dom Nguéz and M. J. Arcos, *Anal. Chim. Acta*, **2002**, *470*, 241.
19. S. Cathum, C. E. Brown, and W. Wong, *Anal. Bioanal. Chem.*, **2002**, *373*, 103.
20. S. S. M. Hassan, M. N. Abass, and G. A. E. Moustafa, *Talanta*, **1996**, *43*, 797.
21. D. Guo, C. Ji, P. He, and H. Gao, *Anal. Proc.* [London], **1987**, *24*, 343.
22. D. Feng and Ch. Chen, *Huaxue Xuebao*, **1983**, *41*, 371.
23. P. C. Gritzapis, C. E. Efststhiou, and T. P. Hadjiioannou, *Anal. Chim. Acta*, **1985**, *171*, 165.
24. T. Limori, M. Sugawara, and T. Kambara, *Denki Kagaku Oyobi Kogyo Butsuri Kagaku*, **1979**, *47*, 549.
25. Yu. I. Urusov, V. V. Sergievskii, A. F. Zhukov, and A. V. Gordievskii, *Zh. Anal. Khim.*, **1979**, *34*, 156.
26. A. M. Tsygankov, V. V. Kuznetsov, N. P. Tarasova, G. A. Yagdin, A. F. Zhukov, and Yu. I. Urusov, *Zh. Anal. Khim.*, **1986**, *41*, 2228.
27. K. Wang and R. Yu, *Fenxi Huaxue*, **1986**, *14*, 599.
28. E. Hopirtean, C. Lifeanu, and F. Kormos, *Rev. Chim.* [Bucharest], **1977**, *28*, 378.
29. S. S. M. Hassan, "Organic Analysis Using Atomic Absorption Spectrometry", **1984**, Ellis Horwood, Chichester, England.
30. T. S. Ma and S. S. M. Hassan, "Organic Analysis Using Ion Selective Electrodes", **1982**, Vol. I, Academic Press, London.
31. S. S. M. Hassan, W. H. Mahmoud, and A. M. Othman,
32. IUPAC Analytical Chemistry Division, Commission on Analytical Nomenclature, *Pure Appl. Chem.*, **1995**, *67*, 507.
33. S. S. M. Hassan, M. B. Saleh, A. A. Abdel Gaber, and N. A. Abdel Kreem, *Talanta*, **2003**, *59*, 161.
34. P. Job, *Ann. Chim. Phys.*, **1939**, *6*, 97.
35. R. K. Tandon, P. T. Crisp, J. Ellis, and R. S. Baker, *Talanta*, **1984**, *31*, 227.
36. R. D. Armstrong, A. K. Covington, and W. G. Proud, *J. Electroanal. Chem.*, **1988**, *257*, 155.
Talanta, **1997**, *44*, 1087.

Spectral, magnetic, thermal and electrochemical studies on new copper(II) thiosemicarbazone complexes

GAMIL A. A. AL-HAZMI^y, M. S. EL-SHAHAWI^z, I. M. GABRY and A. A. EL-ASMY^{*y}

^yChemistry Department, Faculty of Science, Mansoura University, Mansoura, Egypt

^zChemistry Department, Faculty of Science, Mansoura University, Damietta, Egypt

(Received 19 July 2004; revised 22 September 2004; in final form 28 February 2005)

The chelation behavior of some $\text{N}(1)$ and $\text{NH}(4)$ thiosemicarbazones towards copper(II) ions has been investigated. The isolated complexes are characterized by elemental analysis, magnetic moment, electronic, IR, ESR and ms spectra, and by thermal and voltammetric measurements. The substituents on $\text{N}(1)$ and/or $\text{NH}(4)$ thiosemicarbazones and the log K values of the ligands play an important role in complex formation. The IR spectra showed that the reagents HAT, HAET, HAPT, HApCIPT, H_2ST and HBT are deprotonated in the complexes and act as mononegative SN donors; H_2SET , H_2SpCIPT , H_2HyMBPT and $\text{H}_2\text{HyMBpCIPT}$, as binegative NSO donors while H_2SPT is a mononegative NSO donor. The ESR spectra of the complexes are quite similar and exhibit axially symmetric g -tensor parameters with $g_{\parallel} > g_{\perp} > 2.0023$. The loss of thiol and/or hydroxyl hydrogen was confirmed from potentiometric titrations of the ligands and their copper(II) complexes. The protonation constants of the ligands as well as the stability constants of their Cu(II) complexes were calculated. Thermogravimetric analysis of the complexes suggests different decomposition steps. The Coats–Redfern and Horowitz–Metzger equations have been used to calculate the kinetic and thermodynamic parameters for the different thermal decomposition steps of some complexes. The redox properties, nature of the electroactive species and the stability of the complexes towards oxidation are strongly dependent on the substituents on the precursor $\text{NH}(4)$ thiosemicarbazone. The redox data are discussed in terms of the kinetic parameters and the reaction mechanism.

Keywords: Copper(II) complexes; Thiosemicarbazones; Spectra; Thermal; Redox behavior

1. Introduction

Thiosemicarbazones have remarkable properties and have been the subject of numerous coordination chemical studies [1]. They have anticarcinogenic and antimicrobial activities [2, 3]. The fungicidal activity of these compounds is due to their ability to form stable chelates with essential metal ions, which the fungus needs in its

metabolism [4]. In addition, some mono- or polynuclear Schiff-base copper(II) complexes based on thiosemicarbazone serve as models for enzymes such as galectose oxidase and may be used as effective oxidants and redox catalysts [5, 6]. Copper(II) complexes of salicylaldehyde [7, 8], 2-hydroxyacetophenone, 2-aminoaceto-phenone [9] and 2-acetylpyridine [10] NH(4)-substituted thiosemicarbazones have been extensively studied. The redox behavior of copper(II) model compounds is of special interest since the metal is involved in electron-transfer processes in some biological systems [5, 6]. Thus, the work reported herein is focused on the synthesis, spectroscopic and electrochemical characterization of copper(II) complexes of this class of ligands. The electrochemical behavior of some of these complexes was investigated by cyclic voltammetry because of their possible applications as superoxide dismutase mimetic complexes and as copper sensors. In addition, the decomposition kinetics and thermodynamic characteristics of the decomposition steps of some of the complexes have been studied employing Coats–Redfern and Horowitz–Metzger equations.

2. Experimental

All chemicals used were of analytical reagent grade (BDH) and were used as supplied. The formulae, abbreviations and the names of the ligands are listed in table 1. Tetrabutylammonium tetrafluoroborate ($\text{TBA}^{\text{b}}\text{BF}_4$) was used as a supporting electrolyte.

2.1. Synthesis of ligands

The thiosemicarbazones, figure 1, (see table 1 for full and abbreviated names) were prepared as reported earlier [11] by condensing 1:1 molar ratios of acetophenone, salicylaldehyde, benzophenone or 2-hydroxy-4-methoxybenzophenone in ethanol with ethanolic solutions of some nitrogen compounds, thiosemicarbazide, ethyl-, phenyl or p-chlorophenyl-thiosemicarbazides. The reaction mixtures were refluxed in a water bath for 2–3h in the presence of few drops of glacial acetic acid. The formed precipitates were separated by filtration, recrystallized from ethanol and dried. The proposed formulae of the ligands are in good agreement with the stoichiometries concluded from their analytical data and mass spectra and confirmed from the IR spectral data (table 3). The ^1H NMR spectra of HAET, HAPT and H_2HyMPT in d_6 -DMSO showed signals at 12.08–11.40 and 9.92–8.51 assigned to the NH(2) and NH(4) protons, respectively [12]. The spectra of HAT and H_2ST showed

signals at 10.29, 10.07 and 8.09, 8.03 assigned to the NH(2) and NH₂ protons, respectively. Moreover, the spectrum of H₂ST showed the OH proton signal at 10.17ppm [13].

2.2. Synthesis of copper(II) complexes

The complexes were prepared by refluxing a 1:1 molar mixture of each ligand (3mmol) with copper acetate (3mmol). The reaction mixture was refluxed on a water bath for 4–6h. The precipitate was filtered off, washed with hot water, hot ethanol and diethyl ether and finally dried in a vacuum desiccator over anhydrous CaCl₂.

Table 1. Abbreviated and full names, melting points, elemental analyses and formulas weights (FW) of the ligands.

Abbreviated name	Full name	Color	M.P., C	Found (Calcd. %)		FW	
				C	H	Found*	Calcd.
HAT	1-Acetophenonethiosemicarbazone	White	132	55.8 (55.9)	5.7 (5.7)	–	193.3
HAET	1-Acetophenone-4-ethylthiosemicarbazone	White	145	60.0 (59.7)	6.4 (6.8)	221.0	221.3
HAPT	1-Acetophenone-4-phenylthiosemicarbazone	White	198	67.0 (66.9)	5.9 (5.6)	–	269.4
HApCIPT	1-Acetophenone-4-p-chlorophenylthiosemicarbazone	Yellowish white	190	58.8 (59.3)	4.2 (4.6)	304.0	303.8
H ₂ ST	1-Salicylaldehydethiosemicarbazone	Yellow	245	49.3 (49.2)	5.0 (4.6)	–	195.2
H ₂ SET	1-Salicylaldehyde-4-ethylthiosemicarbazone	White	184	53.3 (53.8)	5.4 (5.9)	223.0	223.3
H ₂ SPT	1-Salicylaldehyde-4-phenylthiosemicarbazone	Yellowish white	205	61.0 (61.9)	4.8 (4.8)	–	271.3
H ₂ SpCIPT	1-Salicylaldehyde-4-p-chlorophenylthiosemicarbazone	Yellow	212	54.3 (54.9)	4.0 (3.9)	304.0	305.9
H ₂ HyMBPT	1-(2-Hydroxy-4-methoxybenzophenone) 4-phenylthio-semicarbazone	Yellow	110	66.0 (66.8)	4.8 (5.1)	377.0	377.5
H ₂ HyMBpCIPT	1-(2-Hydroxy-4-methoxybenzophenone) 4-p-chloro-phenylthiosemicarbazone	Yellow	135	61.2 (61.2)	4.3 (4.4)	412.0	411.9
HBT	1-Benzophenonethiosimecarbazone	White	191	66.6 (65.8)	4.6 (5.1)	255.9	255.3

*Values obtained from mass spectra.

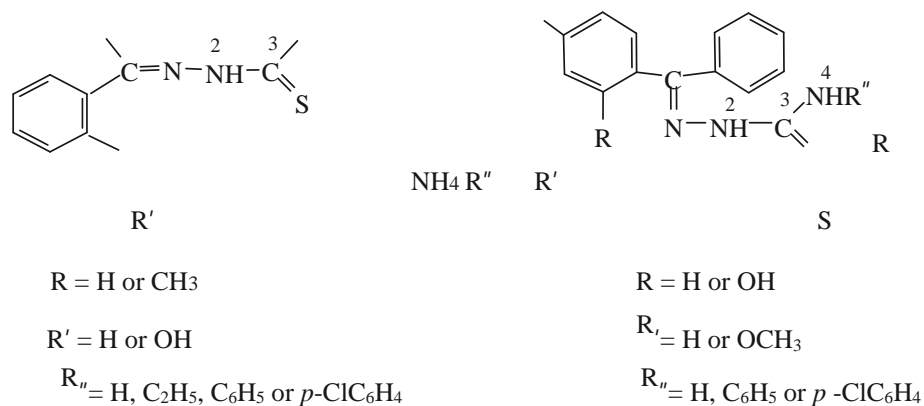


Figure 1. Chemical formulae of the thiosemicarbazone ligands.

2.3. Chemical and physical measurements

Carbon and H contents were determined at the Microanalytical Unit of Cairo University. Copper analysis was carried out according to the standard method [14]. The infrared spectra (KBr discs), electronic spectra (Nujol mulls and DMF solutions),

¹H NMR in *d*₆-DMSO (200MHz) and mass spectra were recorded on a Mattson 5000 FTIR spectrophotometer, UV₂ Unicam UV/Vis, Varian Gemini and Varian MAT 311 spectrometers, respectively. Magnetic moment values were evaluated at room temperature (251C) using a Johnson Matthey magnetic susceptibility balance. ESR spectra were obtained on a Bruker EMX Spectrometer working in the X-band (9.78GHz) with 100kHz modulation frequency. The microwave power and the modulation amplitude were set at 1mW and 4 Gauss, respectively. The low-field signal was obtained after four scans with a tenfold increase in receiver gain. Powder ESR spectra were obtained in 2mm quartz capillaries at room temperature. Thermal studies were carried out on a Shimadzu thermogravimetric analyzer at a heating rate of 10Cmin⁻¹ under nitrogen. Cyclic voltammetry measurements were carried out with a Potentiostat wave generator (Oxford Press) equipped with a Phillips PM 8043 X-Y recorder. The electrochemical cell assembly consisted of platinum wires of 0.5mm diameter as working and counter electrodes and Ag/AgCl as a reference electrode. The protonation constants of the ligands and the formation constants of their complexes at 298.05K were determined potentiometrically by the Irving–Rossotti method [15].

3. Results and discussion

The formulae of the complexes are listed in table 2 together with their physical properties, elemental analyses and formula weights obtained from mass spectra. The isolated solid complexes are stable at room temperature, non-hygroscopic in nature and almost insoluble in water and in most organic solvents but are very soluble in DMF and DMSO. Most decomposed on heating at >300C.

3.1. IR spectral studies

The most important infrared bands of the ligands and their copper(II) complexes with their probable assignments are given in table 3. The existence of numerous

Table 2. Physical properties, analytical data and formula weights (FW) of the copper(II) complexes.

No.	Complex	Color	M.P., C	Found (Calcd. %)			FW	
				C	H	Cu	Found*	Calcd.
1	[Cu(AT)(OH)(H ₂ O) ₃]	Olive green	>300	33.0 (33.1)	4.8 (5.2)	19.3 (19.4)	327.0	326.8
2	[Cu(AET)(OH)(H ₂ O)]	Brown	>300	41.0 (41.4)	5.2 (5.4)	19.5 (19.9)	321.0	318.9
3	[Cu ₂ (APT) ₃ (OAc)]	Olive green	200	56.1 (56.9)	4.5 (4.6)	12.8 (12.8)	–	991.2
4	[Cu(ApCIPT)(OAc)(C ₂ H ₅ OH)]	Green	>300	47.9 (48.4)	4.5 (4.7)	13.5 (13.5)	470.0	471.5
5	[Cu(HST) ₂]H ₂ O	Dark brown	>300	40.5 (40.9)	3.9 (3.8)	13.4 (13.5)	468.3	470.0
6	[Cu ₂ (SET)(Oac) ₂ (H ₂ O) ₂]H ₂ O	Brown	248	32.0 (32.3)	4.3 (4.6)	24.0 (24.4)	519.2	520.5
7	[[Cu(HSPT)(OAc)(H ₂ O) ₂]H ₂ O	Yellowish green	>300	42.4 (43.0)	4.4 (4.7)	13.8 (14.2)	–	446.9
8	[Cu ₂ (SpCIPT)(OH) ₂ (H ₂ O) ₂]	Yellowish brown	>300	32.8 (33.6)	3.5 (3.2)	25.4 (25.4)	500.7	500.9
9	[Cu(HyMBPT)(H ₂ O) ₃]0.5H ₂ O	Olive green	>300	49.4 (50.2)	4.6 (4.8)	12.8 (12.6)	502.5	502.0
10	[Cu(HyMBpCIPT)(H ₂ O)]	Greenish brown	>300	50.8 (51.3)	3.4 (3.7)	13.5 (12.9)	491.2	491.4
11	[Cu ₂ (BT)(OAc)(OH) ₂ (H ₂ O)]H ₂ O	Olive green	>300	38.0 (37.6)	4.3 (4.1)	25.2 (24.9)	508.0	510.5

*Values obtained from mass spectra.

Table 3. Most significant most IR spectral data (cm⁻¹)^a of the copper(II) complexes and corresponding bands of the free ligands in parentheses.

Complex	(NH ₂)	(OH)	(N ⁴ H)	(N ² H)	(C ¹ /4N)	(C ¹ /4S)	(C–S)	(OH)	(Cu–O)	(Cu–N)	(Cu–S)
1	3380, sh (3410, s) 3335, w (3370, w)	3415, m	–	(3220, w)	1590, s (1630, s)	(790, m)	615, m	1345, w	–	445, w	370, w
2	–	3570, vs	3260, sh (3320, s)	(3225, s)	1565, m (1630, m)	(790, m)	615, s	1345, m	495, m	445, w	365, w
3	–	–	3325, s, br (3300, m)	(3250, m)	1590, m (1605, m)	(795, m)	615, w	–	500, w	410, w	340, w
4	–	–	3290, w (3290, s)	(3240, m)	1625, w (1635, w)	(795, m)	690, w	–	500, w	445, w	350, w
5	3365, w (3370, w) 3275, w (3315, s)	3440, w (3440, w)	–	(3165, m)	1595, s (1610, s)	(780, w)	630, w	1365, s (1365, s)	–	430, w	340, w
6	–	(3405, w)	3355, m, br (3355, s)	(3250, s)	1600, vs (1605, m)	(790, m)	640, w	(1375, m)	485, w	400, w	330, w
7	–	3405, w	3345, m, br	(3145, m)	1600, vs	(835, w)	650, w	1370, m	500, m	430, w	355, w

G. A. A. Al-Hazmi
et al.

		(3405, w)	(3380, w)		(1620, s)			(1389, m)			
8	–	3350, m, br (3335, m)	3225, sh (3235, m)	(3154, m)	1600, vs (1610, s)	(830, w)	610, w	1315, s (1330, m)	500, w	440, w	355, w
9	–	(3470, w)	3280, w (3300, s)	(3160, m)	1595, m (1635, m)	(810, w)	660, w	(1325, m)	490, w	425, w	365, w
10	–	(3440, w)	3280, m (3290, s)	(3180, s)	1625, m (1635, s)	(790, w)	615, w	1315, m (1350, m)	495, w	430, w	340, w
11	3340, w (3365, m) 3265, w (3260, m)	3410, w	–	(3175, s)	1600, m (1620, m)	(800, m)	610, w	1380, s	470, w	425, w	340, w

s^aStrong, m¹medium, w¹weak, v¹very, br¹broad and sh¹shoulder.

coordination sites in the ligands gives variable bonding modes. Comparison of the IR spectra of ligands and their copper(II) complexes revealed that the ligands are bonded to the Cu(II) ions in their thiol form with several coordination modes. In the complexes [Cu(AT)(OH)(H₂O)₃] (1), [Cu(AET)(OH)(H₂O)] (2), [Cu₂(APT)₃(OAc)] (3), [Cu(ApCIPT)(OAc)(C₂H₅OH)] (4), [Cu(HST)₂](H₂O) (5) and [Cu₂(BT)(OAc)(OH)₂(H₂O)](H₂O) (11), the ligands are mononegative, bidentate, and the spectra prove that the ¹/₄N and S atoms are the coordination centers. Strong evidence arises from: (i) the disappearance of (N²H); (ii) the negative shift (10–65cm⁻¹) of (C¹/₄N) [16]; (iii) the appearance of a new band, attributed to (C¹/₄N*), at the same position as for the (C¹/₄N) of the thiosemicarbazone; (iv) coordination of the azomethine nitrogen is also consistent with the presence of a new band at 410–445cm⁻¹ assignable to the (Cu–N) vibration [17] and finally (v) coordination via thiolate sulfur is indicated by the absence of the characteristic thioamide (C¹/₄S) vibration with the simultaneous appearance of new bands in the regions 610–690 and 325–370cm⁻¹ due to (C–S) and (Cu–S) vibrations [17, 18], respectively. In the complexes [Cu₂(SET)(OAc)₂(H₂O)₂](H₂O) (6), [Cu₂(SpCIPT)(OH)₂(H₂O)₂] (8), [Cu(HyMBPT)(H₂O)₃].0.5H₂O (9) and [Cu(HyMBpCIPT)(H₂O)] (10), the ligands are binegative, tridentate, and interact with the Cu(II) ions via N (azomethine), S and phenolic oxygen atoms by releasing the hydrogen ions from both thioamide, through thioenolization, and OH groups. This mode of chelation was confirmed by: (i) the disappearance of (N²H) and (C¹/₄S) conjugated with the appearance of (C–S) at 610–640cm⁻¹ and (Cu–S) at 330–365cm⁻¹; (ii) the phenolate group acts as the third coordination site to the metal ion indicated by disappearance of the stretching [(OH)] and bending [(OH)] vibrations; (iii) the band arising from (C¹/₄N) in the free ligand is shifted (10–40cm⁻¹) upon coordination towards a lower frequency region in the complex spectra and finally (iv) the observation of new bands in the regions 485–500 and 400–425cm⁻¹ attributed to (Cu–O) [18] and (Cu–N) vibrations, respectively, confirming bonding through oxygen and nitrogen. In the complex [Cu(HSPT)(OAc)(H₂O)₂](H₂O) (7), the ligand is mononegative, tridentate by deprotonation of the thioamide (NHCS) group upon thioenolization and coordination to copper(II) through the C¹/₄N, OH and C–S groups. The shift to lower frequency (15cm⁻¹) of the (OH) vibration lends support OH participation. Thioenolization is confirmed by the disappearance of (C¹/₄S) and (N²H) with the appearance of (C–S) at 650 and (Cu–S) at 355cm⁻¹. Also, the new band observed at 500cm⁻¹ assigned to (Cu–O) provides additional support for oxygen donation from the hydroxyl group. The bands due to (C¹/₄N) are shifted to lower frequency in the spectrum of the complex with the appearance of a new band at 430cm⁻¹ assignable to (Cu–N). All the data support the mononegative tridentate (SNO) behavior of H₂SPT (figure 2).

In the complexes, [Cu(ApCIPT)(OAc)(C₂H₅OH)] (4), [Cu₂(SET)(OAc)₂(H₂O)₂](H₂O) (6) and [Cu(HSPT)(OAc)(H₂O)₂](H₂O) (7), the acetate group coordinates in a monodentate manner as indicated by the frequency difference (190cm⁻¹) between _s and _{as} vibrations [19, 20] whereas, in the complexes [Cu₂(APT)₃(OAc)] (3) and [Cu₂(BT)(OAc)(OH)₂(H₂O)](H₂O) (11), the acetate group coordinates to the copper(II) ions in a bridging bidentate fashion as indicated by the difference (180cm⁻¹) between the two acetate bands. Finally, the bands

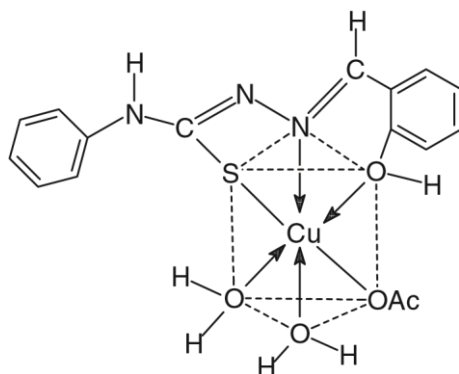


Figure 2. The proposed structure of $[\text{Cu}(\text{HSPT})(\text{OAc})(\text{H}_2\text{O})_2]\cdot\text{H}_2\text{O}$ (7).

Table 4. Formation constants of the complexes and deprotonation constants of ligands (in parentheses).

System	Half method			Least-squares method				
	$\log K_1$	$\log K_2$	$\log K_3$ log	$\log K_1$	$\log K_2$	$\log K_3$ log		
Cu(II)–HAT	9.87 (11.29)	4.29	–	14.16	9.85 (11.30)	4.29	–	14.14
Cu(II)–HAET	9.33 (9.88)	4.74	–	14.07	9.40 (9.88)	4.75	–	14.15
Cu(II)–HAPT	6.42 (6.47)	5.92	4.50	16.84	(6.46)	5.70	4.55	10.25
Cu(II)–ApCIPT	(8.72)	8.53	6.10	14.63	(8.65)	8.42	–	8.42
Cu(II)–H ₂ ST	13.71 (12.39)	7.82 (10.00)	–	21.53	13.83 (12.36)	7.91 (10.00)	–	21.74
Cu(II)–H ₂ SET	15.31 (10.80)	5.94 (6.00)	–	21.25	15.35 (10.80)	6.20 (6.10)	–	21.55
Cu(II)–H ₂ SPT	(10.25)	7.96 (7.92)	–	7.96	13.21 (10.24)	8.10 (7.79)	–	21.31
Cu(II)–H ₂ SpCIPT	(11.29)	7.25 (8.32)	–	7.25	(11.30)	7.30 (8.30)	–	7.30
Cu(II)–H ₂ HyMBPT	13.08 (11.48)	8.08 (4.82)	–	21.16	13.00 (11.48)	8.10 (4.92)	–	21.10
Cu(II)–H ₂ HyMBpCIPT	(11.36)	8.13 (9.27)	–	8.13	(11.42)	8.15 (9.35)	–	8.15
Cu(II)–HBT	10.38 (11.20)	–	–	10.38	10.40 (11.00)	–	–	10.40

$\log K_1$ Overall formation constant.

of coordinated water observed at 810–860 and 530–595 cm^{-1} , are assigned to $\nu(\text{H}_2\text{O})$ and $\omega(\text{H}_2\text{O})$, respectively [21].

Strong evidence for the loss of hydrogen ion(s) is supported by the potentiometric studies.

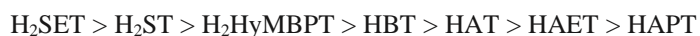
3.2. Potentiometric studies

Potentiometric (pH-metric) titrations of the ligands and their copper(II) complexes against 0.01M NaOH, in the absence or in the presence of HCl (0.01M) in ethanol–water (50% v/v) at 0.1M were carried out [22]. The values of the average number of protons δn_{AP} , the average number of ligand molecules attached per metal ion (n) and the free ligand exponent

(pL) were calculated at different pH values. Plotting of $\delta n_{\lambda p}$ versus pH gives the proton-ligand formation constant ($\log K_1$ and/or $\log K_2$). The data calculated from the half- and least-square methods [15] are summarized in table 4. The $\log K$ values of the investigated ligands depend not only on the chemical structure but also on the inductive effect of the substituents. Careful inspection of the data (table 4) reveals that:

- (a) The following observations may be considered concerning the substituents on the N^4H group: (i) the ligands containing NH_2 group ($R^{00}H$ in figure 1) have high $\log K_1$ values which decrease, for each category, in the following order: $H > Et > pClPh > Ph$; (ii) the presence of H or Et (electron-donating) increases the electron density on the azomethine group which hinders the deprotonation and increases the basicity of the ligands and (iii) the presence of an electron-withdrawing group (Ph or $pClPh$) decreases the electron density on the azomethine moiety and enhances deprotonation. Thus, the latter ligands are less basic (lower $\log K$) than the former ones.
- (b) The substituents on the $C^1/4N$ group have a great effect on the basicity of the ligands. The order of the ligands is: $H_2ST > HAT > HBT$. The two phenyl groups of the benzophenone moiety decrease the electron density on the azomethine group facilitating proton withdrawal by the inductive effect.

The metal–ligand stability constants were determined by applying the curve-fitting method to the data of n versus pL and the results are summarized in table 4. The data revealed that the values of $\log K_1$ are higher than those of $\log K_2$ or $\log K_3$ for the same complex because all available sites for binding the first ligand are free which is not the case for binding the second or third. According to the values of $\log K_1$ & $\log K_2$, the stability of the complexes varied with the substituents on the thiosemicarbazone moiety in the following sequence for the ligands:



The bulky 2-hydroxy-4-methoxybenzophenone decreases the stability of its complex more than the salicylaldehyde moiety. Also, the increase in the volume of the $NH(4)$ substituents showed the same trend of stability, $H > Et > Ph$.

3.3. Electronic spectra and magnetic studies

The magnetic moments and the significant electronic absorption bands of the copper(II) complexes, recorded in DMF solution and in Nujol mull, are given in table 5. Thiosemicarbazones have a ring π^* band at $32785\text{--}40815\text{cm}^{-1}$ and n^* band at $28570\text{--}30960\text{cm}^{-1}$ [17]; little change in their energies are recorded for their complexes. Another n^* band in the spectra of the free thiosemicarbazones is also found in the spectra of the copper(II) complexes at $27000\text{--}28250\text{cm}^{-1}$.

The band at $22,220\text{--}26,040\text{cm}^{-1}$ in the spectra (DMF) of the complexes may be due to LMCT [23]. Previous studies on copper(II)-thiosemicarbazones indicated that a band in the region $25000\text{--}26040\text{cm}^{-1}$ could be assigned to an $O \rightarrow Cu(II)$ transition [24] whereas a band in the range $21785\text{--}24750\text{cm}^{-1}$ is due to a $S \rightarrow Cu(II)$ transition [25]. The CT band of the complexes

is therefore due to S!Cu CT owing to the greater reducibility of copper(II) in the presence of sulfur compounds than with oxygen compounds.

The electronic spectra of [Cu(AT)(OH)(H₂O)₃] (1), [Cu(HSPT)(OAc)-(H₂O)₂]H₂O (7) and [Cu(HyMBPT)(H₂O)₃]0.5H₂O (9) in Nujol and DMF are similar indicating

Table 5. Magnetic moments, electronic spectra (cm⁻¹) in DMF (Nujol) and ESR data for the copper(II) complexes.

Complex	μ_{eff} (BM)	d-d Transition bands	Charge-transfer bands	Spin Hamiltonian parameters					
				$A_k 10^4$ (cm ⁻¹)					
				g_k	g_z		G	a	b
1	2.20	13 335 (14 285)	23 210 (23 200)	2.38	2.06	170	6.30	0.91	0.89
2	1.90	17 480 (17 545)	24 440 (22 575)	–	–	–	–	–	–
3	1.72	17 450 (20 000)	22 470 (21 980)	2.15	2.04	165	3.75	0.66	0.67
4	2.32	16 665 (16 975)	22 220 (22 470)	–	–	–	–	–	–
5	1.53	16 805 (17 230)	25 380 (22 505)	2.27	2.08	160	3.37	0.78	0.89
6	1.86	17 095 (17 100)	25 000 (22 125)	–	–	–	–	–	–
7	2.06	15 600 (14 245)	24 750 (25 510)	–	–	–	–	–	–
8	1.48	17 480 (17 795)	24 690	–	–	–	–	–	–
9	1.80	13 175 (14 365)	23 750 (24 510)	–	–	–	–	–	–
10	1.91	12 880 (18 115)	26 040 (21 785)	–	–	–	–	–	–
11	1.20	16 585 (15 890)	–	–	–	–	–	–	–

that DMF has no effect on complex formation. The broad band centered at 13175–15600cm⁻¹ (DMF) and 14300cm⁻¹ (Nujol) is assigned to the ²E_{2g} ! ²T_{2g} transition in an octahedral geometry [25]. The broadness of the observed band may be due to the Jahn–Teller effect, which enhances the distortion of the octahedral geometry. The green color of these complexes supports the proposed geometry. The magnetic-moment values were found within the range reported for d⁹ systems containing one unpaired electron and suggest Cu–L covalent bonds.

The electronic spectra of [Cu(AET)(OH)(H₂O)] (2), [Cu₂(APT)₃(OAc)] (3), [Cu(ApCIPT)(OAc)(C₂H₅OH)] (4), [Cu₂(SET)(OAc)₂(H₂O)₂]H₂O (6) and [Cu₂(BT)(OAc)(OH)₂(H₂O)]H₂O (11) show one band at 15890–20000cm⁻¹ (Nujol) and 16585–17480cm⁻¹ (DMF), indicating a square-planar geometry. For square-planar complexes, three spin-allowed transitions are possible, assigned to ²B₁ ! ²A₁ $\ddot{d}_{x^2-y^2}$! d_{z^2} , ²B₁ ! ²B₂ \ddot{d}_{xy} ! d_{xy} and ²B₁ ! ²E_v $\ddot{d}_{x^2-y^2}$! d_{xz}, d_{yz} but the band could not be resolved into three bands [26]. This geometry is further supported by the values of their magnetic moments [26]. The lowest value (1.20BM) for [Cu₂(BT)(OAc)(OH)₂(H₂O)]H₂O (11) indicates a significant interaction between the copper(II) centers [27]. Moreover, the complex [Cu(ApCIPT)(OAc)(C₂H₅OH)] (4) has a magnetic moment (2.32BM) higher than the calculated value for one unpaired electron and may be due to spin-orbit coupling [27].

The electronic spectra of the complexes [Cu(HST)₂]H₂O (5), [Cu₂(SpCIPT)(OH)₂(H₂O)₂] (8) and [Cu(HyMBpCIPT)(H₂O)] (10) show a band at 17,230–18115cm⁻¹ (Nujol) and 12880–17480cm⁻¹ (DMF), which is safely assigned to the

$T_2 ! E$ transition in a tetrahedral symmetry [28]. The magnetic moments (table 5) of the complexes [Cu(HST)₂]H₂O (5) and [Cu₂(SpCIPT)(OH)₂(H₂O)₂] (8) are below the expected

value (1.70–2.20BM) for a tetrahedral geometry which may be attributed to copper–copper interaction [29].

The band positions in the spectrum of $[\text{Cu}(\text{HyMBpClPT})(\text{H}_2\text{O})]$ (10) in DMF are very different from that recorded in Nujol (table 5) showing that the complex is significantly affected by solvolysis or hydrogen bonding. In DMF solution, some complexes have d–d transitions larger or smaller (table 5) than those recorded for solid complexes suggesting that the same species are present both in the solids and the solutions.

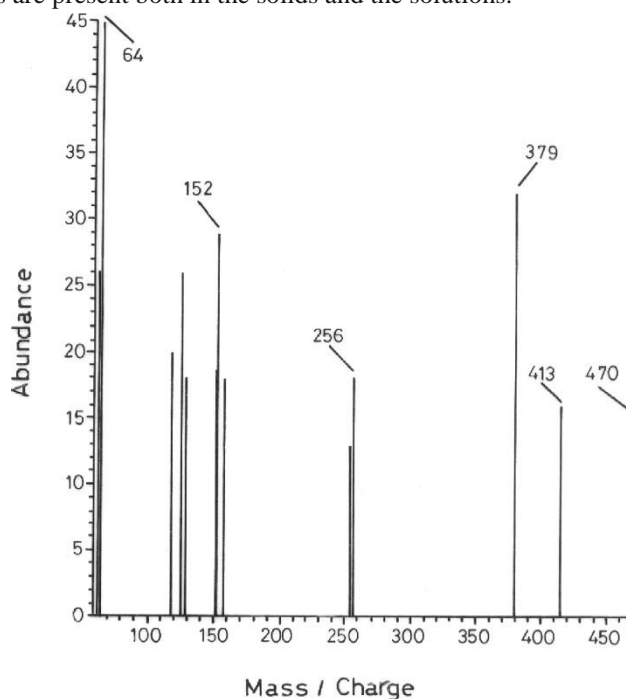


Figure 3. Mass spectrum of $[\text{Cu}(\text{ApClPT})(\text{OAc})(\text{C}_2\text{H}_5\text{OH})]$ (4).

3.4. Mass spectra

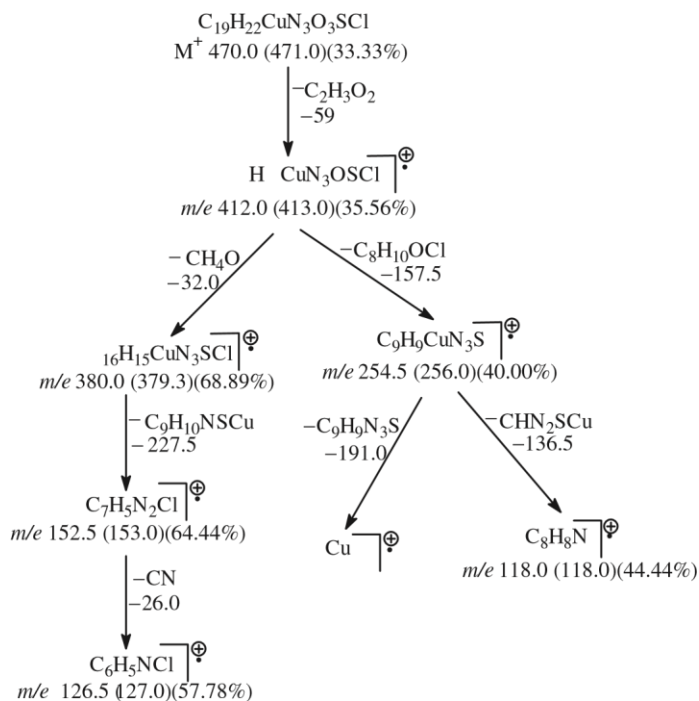
The mass spectra for most of the complexes and the molecular ion peaks confirmed the proposed formulae. Calculated and found molecular weights are given in table 2. As a typical example, the mass spectrum (figure 3) of $[\text{Cu}(\text{ApClPT})(\text{OAc})(\text{C}_2\text{H}_5\text{OH})]$ (4) shows peaks corresponding to the successive degradation of the molecule. The first peak at m/e 470 (Calcd. 471) represents the molecular ion peak of the complex (M^{p1}) with 33.33% abundance. The sharp peak (base peak) with m/e 64 represents the stable and final residue (Cu). Scheme 1 demonstrates the proposed degradation steps for the investigated complex.

3.5. ESR spectra

The spin Hamiltonian parameters and the G values of some of the solid Cu(II) complexes ($S=1/2$, $I=3/2$) are given in table 5. The ESR spectra of the complexes are quite similar and display axially symmetric g-tensor parameters with $g_k > g_{\perp} > 2.0023$ indicating that the copper site has a $d_{x^2-y^2}$ ground state, characteristic of square-planar or octahedral geometry [30].

In axial
the g-
related to
by the

symmetry,
values are
the G-factor
expression,



$G^{1/4}(g_k^2)/(g_{\perp}^2)$. According to Hathaway [31], if the value of G is greater than 4, the exchange interaction between copper(II) centers in the solid state is negligible, whereas when it is less than 4, a considerable exchange interaction exists in the solid complex. Analysis of the ESR spectrum of the complex

C17 19

C

$m/e 63.5 (64.0)$
base peak

Scheme 1. Fragmentation pattern of [Cu(ApCIPT)(OAc)(C₂H₅OH)] (4).

[Cu(AT)(OH)(H₂O)₃] (1) indicates that $g_k > g_r > 2.0023$ and $A_k \approx 17010^4 \text{ cm}^{-1}$. This observation suggests an elongated octahedral geometry [31]. The powder ESR spectral profile of [Cu₂(APT)₃(OAc)] (3) is typical of square-planar copper(II) and agrees well with the reported data [32, 33]. Also, the spectrum showed an additional weak ESR absorption at 1500G near $g \approx 4$ for a spin-coupled Cu(II) dimer which is not observed in the other two complexes (table 4). The small g_k values indicate strong interaction between the ligand and the metal ion. The ESR spectrum of [Cu(HST)₂]₂H₂O (5) reveals that the Cu(II) center is axial with simulated spin Hamiltonian parameters $g_k \approx 2.27$, $g_r \approx 2.08$ and $A_k \approx 160 \cdot 10^4 \text{ cm}^{-1}$. These values are most closely correlated with copper(II) ions with a tetrahedral structure ($g_k \approx 2.25$ and $A_k (150-250) \cdot 10^4 \text{ cm}^{-1}$ [34]. The G factor in [Cu(AT)(OH)(H₂O)₃] (1) is higher than 4 suggesting the absence of exchange coupling between copper(II) centers in the solid state [30], while in [Cu₂(APT)₃(OAc)] (3) and [Cu(HST)₂]₂H₂O (5), G is less than 4 suggesting copper-copper exchange interactions.

The molecular-orbital coefficients, δ^2 (a measure of the covalency of the in-plane π -bonding between the 3d orbital and the ligand orbitals) and δ^2 (the covalent in-plane π -bonding) were calculated employing the following equations [35]:

$$\delta^2 \approx \frac{A_k - 0.036 \delta g_k}{2 \cdot 0023 \delta g_r - 3 \cdot 7 \delta g_r - 2 \cdot 0023 \delta g_r - 0.04}$$

$$\delta^2 \approx \frac{\delta g_k - 2 \cdot 0023 \delta E}{8 I^2},$$

where $I \approx 4828 \text{ cm}^{-1}$ for the free copper(II) ion and E is the electronic transition energy. The lower value of δ^2 compared to δ^2 indicates that the π -bonding in plane is more covalent than the in-plane π -bonding. These data are in good agreement with the data reported earlier [31, 35]. The δ^2 value (0.91) in the complex [Cu(HST)₂]₂H₂O (5) indicates the existence of slight ionic character for the metal-ligand π -bonding, where the value of δ^2 (0.89) indicates the presence of considerable contribution of metal-ligand π -bonding in the plane.

3.6. Thermal studies

Non-isothermal calculations have been extensively used to evaluate the kinetic and thermodynamic parameters for the different thermal decomposition steps in the complexes employing the Coats-Redfern [36] and the Horowitz-Metzger [37] equations. Activation enthalpies ($H^\ddagger \approx ERT$), activation entropies ($S^\ddagger \approx 2.303 [\log (Zh/KT)]R$) and free energies of activation ($G^\ddagger \approx H^\ddagger - TS^\ddagger$) are given in table 6, where Z, K and h are the pre-exponential factor, Boltzman and Plank constants, respectively [38]. The kinetic parameters calculated by the Horowitz-Metzger method revealed no significant difference from those evaluated by the Coats-Redfern method. The activation energies could not be calculated for unsuitable or overlapped steps. The high value of E for the complex [Cu(HSPT)(OAc)(H₂O)₂]₂H₂O (7) indicates that the ligand is strongly bonded to the Cu(II) ion. The E value observed for the second decomposition stage of [Cu(AT)(OH)(H₂O)₃] (1) was found to be higher than that of

the first indicating a low rate of decomposition. In the complex $[\text{Cu}(\text{HSPT})(\text{OAc})(\text{H}_2\text{O})_2]\text{H}_2\text{O}$ (7), the E value for the second step is lower than that of the first one explaining why its rate of decomposition is high [12]. During the decomposition reactions, a reverse effect was observed where the rate of removal of the remaining ligand was smaller after the expulsion of one or two ligands except for $[\text{Cu}(\text{AT})(\text{OH})(\text{H}_2\text{O})_3]$ (1).

The negative S^\ddagger values for all decomposition steps in all complexes indicate that the complexes, with the exception of $[\text{Cu}(\text{HSPT})(\text{OAc})(\text{H}_2\text{O})_2]\text{H}_2\text{O}$ (7), are more ordered [39]. The activation energy of the first step (table 6) shows the following sequence: $[\text{Cu}(\text{HSPT})(\text{OAc})(\text{H}_2\text{O})_2]\text{H}_2\text{O}$ (7) > $[\text{Cu}_2(\text{APT})_3(\text{OAc})]$ (3) > $[\text{Cu}(\text{ApClPT})-(\text{OAc})(\text{C}_2\text{H}_5\text{OH})]$ (4) > $[\text{Cu}_2(\text{BT})(\text{OAc})(\text{OH})_2(\text{H}_2\text{O})]\text{H}_2\text{O}$ (11) > $[\text{Cu}(\text{AT})(\text{OH})-(\text{H}_2\text{O})_3]$ (1).

In the thermograms (30–1000C) of some complexes, the first step corresponds to the evolution of water of crystallization and/or coordinated water and the end products may be CuS , CuO or Cu .

The thermogram (figure 4) of the complex $[\text{Cu}_2(\text{SpClPT})(\text{OH})_2(\text{H}_2\text{O})_2]$ (8) is taken as a representative example for the decomposition of these complexes. It is characterized by four degradation steps in the range 188–234, 234–269, 498–673 and 673–877C (scheme 2). Elimination of two H_2O and two OH (Calcd. 13.9%, found 14.5%) is the first step. The second step consumes a $\text{C}_6\text{H}_4\text{O}$ radical (Calcd. 18.4%, found 19.0%). The first, second and fourth steps are not suitable for kinetic analysis. The third step is slow with an activation energy of 107.2kJmol^{-1} (Coats–Redfern eqn.) and first order. The radical $\text{C}_6\text{H}_4\text{Cl}$ is assumed to be evolved in the third and fourth steps (Calcd. 22.6%, found 23.3%). Moreover, the thermogram shows a progressive decomposition up to 900C after which a constant weight was observed and the $(\text{CuS})_2\text{Cu}$ product (Calcd. 31.7%, found 30.6%) was the final residue.

Table 6. Kinetic and thermodynamic parameters for the thermal decomposition of some of the complexes.*

Compound	Step	Coats–Redfern eqn.			Horowitz–Metzger eqn.			S [#]	H [#]	G [#]
		r	n	E	r	n	E			
[Cu(AT)(OH)(H ₂ O) ₃] (1)	1st	0.9917	0.33	36.0	0.9959	0.33	43.6	268.5	32.1	157.5
	3rd	1.0000	2.00	91.6	0.9995	2.00	101.7	206.3	86.0	224.2
[Cu(AET)(OH)(H ₂ O)] (2)	2nd	1.0000	2.00	73.8	0.9995	2.00	84.2	172.4	70.0	148.9
	4th	0.9999	0.66	267.1	0.9998	0.66	282.7	56.5	259.3	312.6
[Cu ₂ (APT) ₃ (OAc)] (3)	1st	0.9950	1.00	92.6	0.9932	1.00	100.7	149.7	88.6	159.5
[Cu(ApCIPT)(OAc)(C ₂ H ₅ OH)] (4)	1st	0.9948	1.00	59.9	0.9939	1.00	65.3	226.1	55.9	162.4
[Cu(HSPT)(OAc)(H ₂ O) ₂] H ₂ O (7)	1st	0.9988	2.00	373.3	0.9984	2.00	374.9	391.4	368.9	163.8
	2nd	1.0000	2.00	275.3	0.9999	2.00	285.3	16.8	268.6	266.6
	3rd	0.9944	1.00	107.2	0.9940	1.00	117.4	233.8	100.1	299.1
	1st	0.9941	1.00	39.0	0.9931	1.00	42.8	274.0	34.9	169.4
	2nd	1.0000	0.33	73.4	0.9999	0.33	87.7	242.8	67.7	234.0
[Cu ₂ (SpCIPT)(OH) ₂ (H ₂ O) ₂] (8)										
[Cu ₂ (BT)(OAc)(OH) ₂ (H ₂ O)]H ₂ O (11)										

*r^{1/4}Correlation coefficient, n^{1/4}order of the decomposition reaction; E, H[#] and G[#] are in kJmol⁻¹, S[#] in JKmol⁻¹.

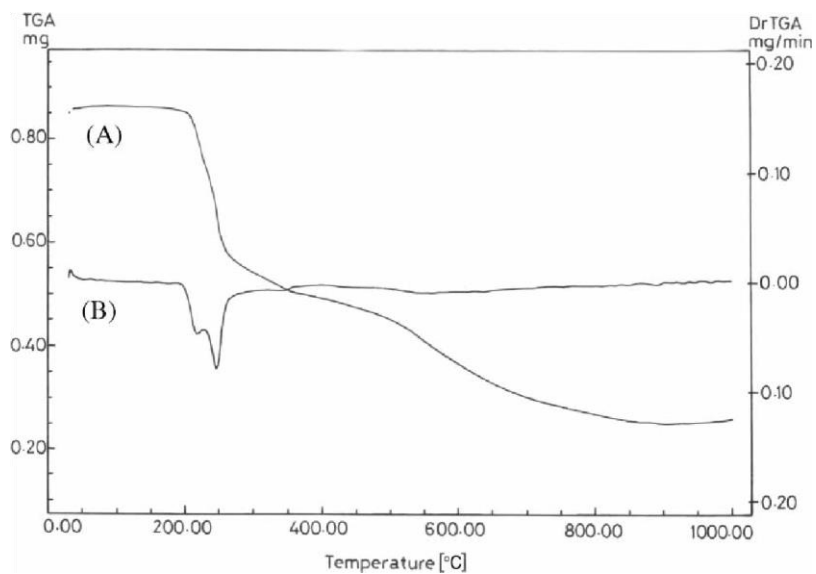
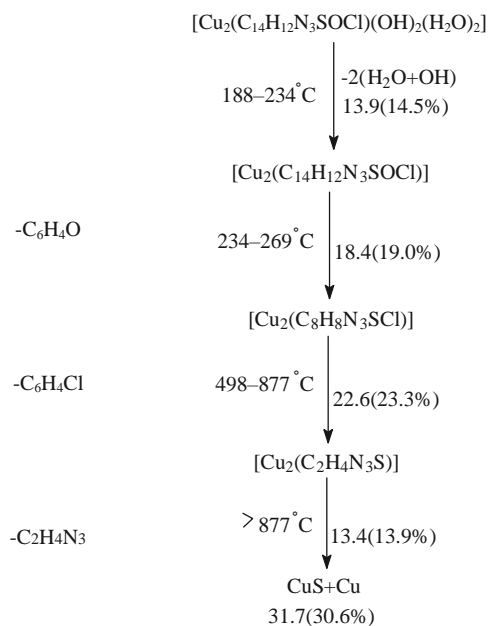


Figure 4. TG (A) and DTG (B) thermograms of $[\text{Cu}_2(\text{SpCIPT})(\text{OH})_2(\text{H}_2\text{O})_2]$ (8).



Scheme 2. Proposed thermal decomposition pattern of $[\text{Cu}_2(\text{SpCIPT})(\text{OH})_2(\text{H}_2\text{O})_2]$ (8).

3.7. Redox properties

Electrochemical responses of the mononuclear complexes (1), (2) and (4) were investigated in DMF $\text{TBA}^+\text{BF}_4^-$ solutions by cyclic voltammetry at incremental scan rates ($10\text{--}200\text{mVs}^{-1}$) versus Ag/AgCl reference electrode. The voltammetric data are summarized in table 7. The complexes showed similar features in the investigated

Table 7. Electrochemical data of some of the copper(II) complexes in DMF TBA^bBF₄ vs Ag/AgCl at 100Vs¹.*

Complex	First electrode		: couple		Second electrode		≥ couple		Third electrode couple					
	E _p		E _p		E _p		E _p		E _p					
	E _{p,a}	E _{p,c}	E _{1/2}	E _{p,a}	E _{p,c}	E _{1/2}	E _{p,a}	E _{p,c}	E _p	E _{1/2}	E _{p,a}	E _{p,c}	E _p	E _{1/2}
[Cu(AT)(OH)(H ₂ O) ₃] (1)	0.25	0.60	0.35	0.43	0.24	0.04	0.20	0.14	0.80	0.68	0.12	0.74		
[Cu(AET)(OH)(H ₂ O)] (2)	0.26	0.64	0.38	0.45	0.17	0.05	0.12	0.11	0.78	0.68	0.10	0.73		
[Cu ₂ (APT) ₃ (OAc)] (3)	0.04	0.36	0.40	0.16	0.27	0.05	0.32	0.11	0.81	0.69	0.12	0.75		
[Cu(ApCIPT)(Oac)(C ₂ H ₅ OH)] (4)	0.25	0.56	0.31	0.40	0.33	0.16	0.17	0.25	0.94	0.73	0.21	0.83		

* E_{1/2} = 1/4(E_{p,c} + 3E_{p,a})/2.

potential range 1.2–1.4V and displayed three well-defined reduction waves in the regions 0.64 to 0.36, 0.04–0.16 and 0.68–0.73V coupled with three anodic waves in the regions 0.26–0.04, 0.17–0.33 and 0.78–0.94V with $E_{1/2}$ ¼0.40 to 0.16; 0.11–0.25 and 0.73–0.83, respectively. Comparison with analogous copper(II) complexes [7, 40], for the nearly irreversible (E_p 0.1V) electrode couples allow assignment to one-electron oxidation processes Cu^0/Cu^I , $\text{Cu}^I/\text{Cu}^{II}$ and $\text{Cu}^{II}/\text{Cu}^{III}$, respectively. The one-electron nature of these irreversible electrode couples has also been established by comparing its current height with similar couples displayed by analogous copper(II) complexes [40].

The electron-withdrawing (*p*-ClC₆H₄) group in the complex [Cu(ApCIPT)(OAc)(C₂H₅OH)] (4) shifts the oxidation potential of the electrode couples $\text{Cu}^I/\text{Cu}^{II}$ and $\text{Cu}^{II}/\text{Cu}^{III}$ to more positive values and makes their reduction processes more difficult compared with [Cu(AT)(OH)(H₂O)₃] (1) and [Cu(AET)(OH)(H₂O)] (2) (table 7). The electron-attracting *p*-ClC₆H₄ group lowers the electron density at the reduction center, which becomes more positive and more easily reduced. The presence of the C₂H₅ (electron-donating) group has an opposite effect to that

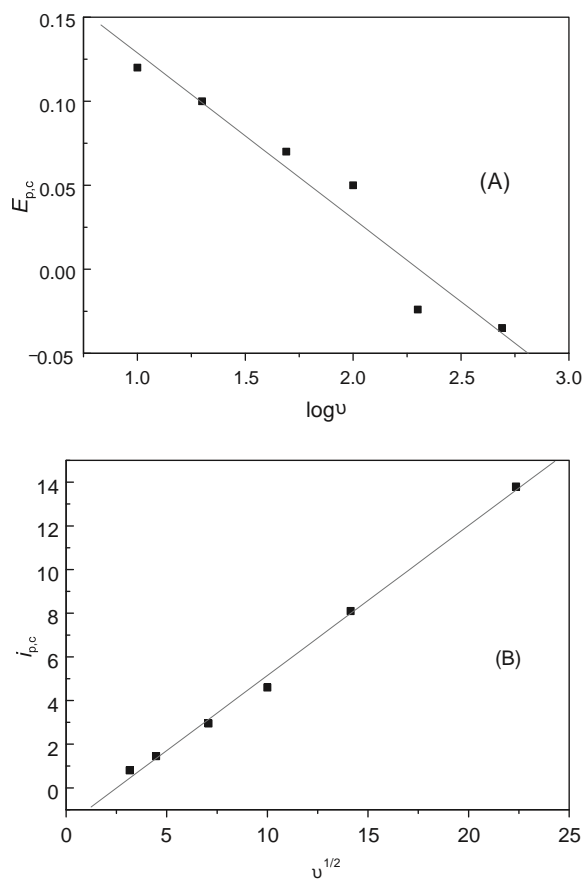


Figure 5. Dependence of the cathodic peak potential, $E_{p,c}$ (A) and the cathodic peak current, $i_{p,c}$ (B) on the scan rate of the electrode couple $\text{Cu}^{III}/\text{Cu}^{II}$ of [Cu(AT)(OH)(H₂O)₃] (1).

reported for the reduction of similar compounds [5, 6]. The ethyl group makes both oxidation and reduction processes more difficult than for $[\text{Cu}(\text{AT})(\text{OH})(\text{H}_2\text{O})_3]$ (1). This may be explained by the steric effect of the ethyl group at the reduction center, which would hinder the approach of the reduction center to the electrode surface [41].

The dependence of the cathodic peak current, $i_{p,c}$, of the electrode couple $\text{Cu}^{\text{III}}/\text{Cu}^{\text{II}}$ on the square root of the sweep rate ($v^{1/2}$) for (1) suggests a diffusion-controlled electrochemical process [42] (figure 5). The cathodic peak potential ($E_{p,c}$) of this couple shifts towards more negative values as v increases indicating an irreversible electrode couple, which was also confirmed from the linear dependence of the cathodic peak potential, $E_{p,c}$, with $\log v$ [43] (figure 5). The product of the number of electrons involved in the reduction process (n) and the corresponding charge-transfer coefficient (α) can be determined from the slope of this line. Assuming $n\alpha/4$, $1/40.62$, which is in the expected range for a single one-electron transfer step [42]. A similar feature was observed for the couples of H and NH_2 derivatives.

Characteristic cyclic voltammograms for (1) at 1.2–0.0V are shown in figure 6. A slight displacement of the anodic and cathodic peaks is observed as the sweep rate increases, the peak current ratios $i_{p,c}/i_{p,a} > 1$; $E_p > 60\text{mV}$ and the $i_{p,c}$

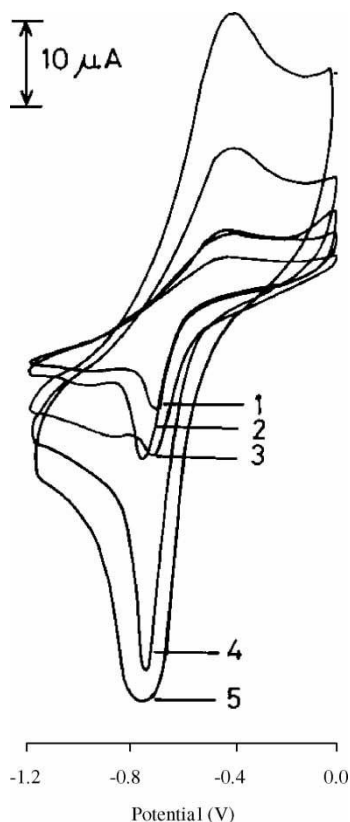


Figure 6. Influence of scan rate (mVs^{-1}) on the electrode couple $\text{Cu}^{\text{II}}/\text{Cu}^{\text{I}}$ of $[\text{Cu}(\text{AT})(\text{OH})(\text{H}_2\text{O})_3]$ (1). 10 (1), 20 (2), 50 (3), 100 (4) and 200 (5) mVs^{-1} .

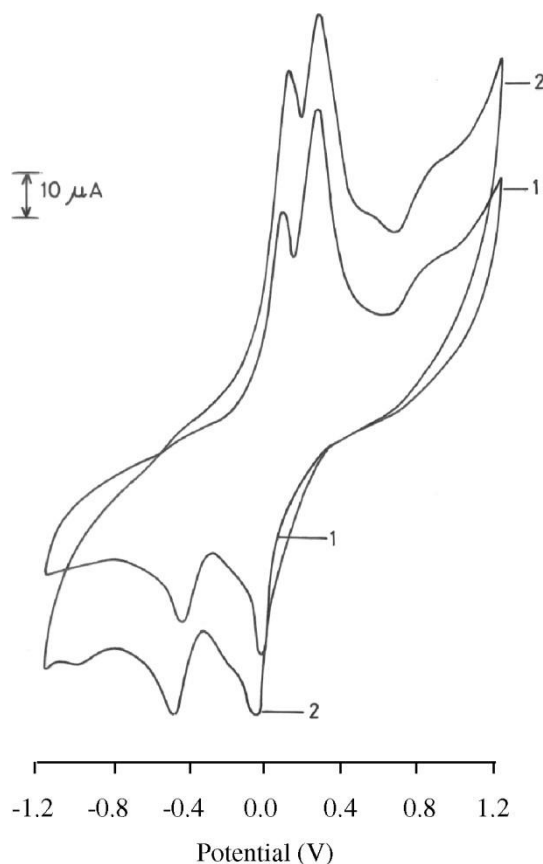
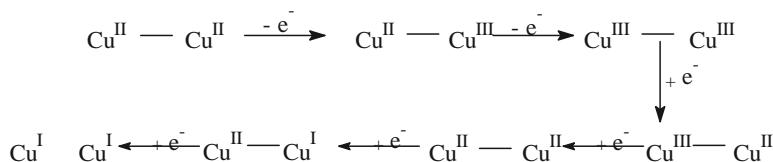


Figure 7. Cyclic voltammograms of $[\text{Cu}_2(\text{APT})_3(\text{OAc})]$ (3) at 100 (1) and at 200 (2) mVs^{-1} in DMF TBA^bBF_4 vs the Ag/AgCl reference electrode.

versus $i^{1/2}$ plot is linear with a positive intercept. All these characteristics indicate an irreversible, one-electron process. The dependence of the voltammetric response of $\text{Cu}^{\text{I}}/\text{Cu}^0$ on the sweep rate, the depolarizer concentration of the analyte as well as the decrease in $i_{p,c}^{1/2}$ is typical of an ECE (electrochemical reaction coupled between two charge processes) type mechanism in which an irreversible first-order chemical reaction is interposed between two successive one-electron charge transfers. The ECE mechanism of this complex was also confirmed by the observed decrease of cathodic peak current vs. the $i^{1/2}$ and from $i_{p,c}^{1/2} > 1$ on increasing the scan rate.

The CV of binuclear complex (3) at 100mVs^{-1} sweep rate is shown in figure 7 and summarized in table 7. The irreversible nature and the ECE-type mechanism of the observed reduction peaks were confirmed by the large difference in the potential ($E_p > 0.1\text{V}$) between the two peak centers of the couples $\text{Cu}^{\text{I}}/\text{Cu}^0$ and $\text{Cu}^{\text{II}}/\text{Cu}^{\text{I}}$ and the linear dependence of the cathodic peak potential, $E_{p,c}$, of each electrode process with \log . At 200mVs^{-1} the CV showed two irreversible reduction peaks coupled with two irreversible oxidation waves in the potential range 1.2–1.2V. At the highest scan rate ($>200\text{mVs}^{-1}$) such behavior is prevented.

Scheme 3. Proposed electrochemical behavior of $[\text{Cu}_2(\text{APT})_3(\text{OAc})]$.

These observations may be attributed to the sequential one-electron transfer reactions as shown in scheme 3.

Similar sequential one-electron transfer for a number of binuclear $\text{Cu}^{2\text{b}}$ complexes has been reported [44, 45]. These data confirm the proposed binuclear structure.

The $E_{1/2}$ values for the electrode couple $\text{Cu}^{\text{I}}/\text{Cu}^0$ of the mononuclear complexes are more negative compared with the binuclear complex. This difference may be due to the binuclear complex accepting an electron more easily due to electrostatic effects compared to mononuclear complexes. The E_p of the $\text{Cu}^{\text{I}}/\text{Cu}^0$ couple for mononuclear complexes is also smaller than the binuclear one. This difference may be due to the binuclear $\text{Cu}(\text{II})$ complexes undergoing Cu-N or Cu-S bond rupture as soon as Cu^{I} reduces to Cu^0 [46].

References

- [1] M. Abram, E.S. Lang, E. Bonfada, Z. Anorg. Allg. Chem., 628, 1419 (2002).
- [2] R. Pogni, M.C. Baratto, A. Diaz, R. Basasi, J. Inorg. Biochem., 79, 333 (2000).
- [3] M.B. Ferrari, F. Bisceglie, G. Pelosi, M. Sassi, P. Tarasconi, M. Cornia, S. Capacchi, R. Albertini, S. Pinelli, J. Inorg. Biochem., 90, 113 (2002).
- [4] S.D. Dhumwad, K.B. Gudasi, T.R. Goudor, Indian J. Chem., 33A, 320 (1994).
- [5] E. Franco, E. Lopez-Torres, M.A. Mendiola, M.T. Sevilla, Polyhedron, 19, 441 (2000) and references therein.
- [6] D.W. Maragerum, G.D. Owens, In Metal Ions in Biological Systems, H. Sigel (Ed.), Marcel Dekker, New York (1981).
- [7] P. Bindu, M.R.P. Kurup, T.R. Salyakeerty, Polyhedron, 18, 321 (1999).
- [8] M.B. Ferrari, S. Capacchi, G. Pelosi, G. Reffo, P. Tarasconi, R. Albertini, S. Pinell, P. Lunghi, Inorg. Chim. Acta, 286, 134 (1999).
- [9] D.X. West, A.A. Nassar, F.A. El-Saied, M.A. Ayad, Transition Met. Chem., 23, 321 (1998).
- [10] D.X. West, H. Gebremedhin, R.J. Butcher, J.P. Jasinski, A.E. Liberta, Polyhedron, 12, 2489 (1993).
- [11] R.M. El-Shazly, G.A.A. Al-Hazmi, S.E. Ghazy, M.S. El-Shahawi, A. El-Asmy, Spectrochim. Acta A, 60, 3187 (2004).
- [12] D.X. West, Y.-H. Yang, T.L. Klein, K.I. Goldberg, A.E. Liberta, J. Valdes-Matinez, S. HernandezOrtega, Polyhedron, 14, 1681 (1995).
- [13] S.I. Mostafa, A.A. El-Asmy, M.S. El-Shahawi, Transition Met. Chem., 25, 470 (2000).
- [14] A.I. Vogel, A Text Book of Quantitative Inorganic Analysis, Longman, London (1972).
- [15] H.M. Irving, H.S. Rossotti, J. Chem. Soc., 2904 (1954).
- [16] D.X. West, S.L. Dietrich, I. Thiantanavanich, C.A. Brown, Transition Met. Chem., 19, 195 (1994).
- [17] D.X. West, A.K. El-Sawaf, G.A. Bain, Transition Met. Chem., 23, 1 (1998).
- [18] D.X. West, M.M. Salberg, G.A. Bain, A.E. Liberta, Transition Met. Chem., 22, 180 (1997).
- [19] K. Nakamoto, Infrared and Raman Spectra of Inorganic and Coordination Compounds, 3rd Edn, p. 305, Wiley, New York (1978).
- [20] A.H. Osman, A.A.M. Aly, N.A. El-Maali, G.A.A. Al-Hazmi, Synth. React. Inorg. Met.-Org. Chem., 32, 1293 (2002).

- [21] A.H. Osman, A.A.M. Aly, N.A. El-Maali, G.A.A. Al-Hazmi, *Synth. React. Inorg. Met.-Org. Chem.*, 32, 663 (2002).
- [22] H. Irving, H. Rossotti, *Acta Chem. Scand.*, 10, 72 (2002).
- [23] A.A. El-Asmy, M.E. Khalifa, M.M. Hassanian, *Synth. React. Inorg. Met.-Org. Chem.*, 31, 1787 (2001). [24] L.M. Fostak, I. Garcí'a, J.K. Swearingen, E. Bermejo, A. Castin'eiras, D.X. West, *Polyhedron*, 22, 83 (2003).
- [25] S. Mostafa, M.M. Bekheit, M.M. El-Agez, *Synth. React. Inorg. Met.-Org. Chem.*, 30, 2029 (2000).
- [26] A. Sreekan, M.R.P. Kurup, *Polyhedron*, 22, 3321 (2003).
- [27] D.X. West, M.A. Lockwood, M.D. Owens, A.E. Liberta, *Transition Met. Chem.*, 22, 366 (1997).
- [28] R.M. El-Shazly, A.A. El-Asmy, A. El-Shekil, *Synth. React. Inorg. Met.-Org. Chem.*, 21, 385 (1991).
- [29] N.T. Akinchan, D.X. West, Y.H. Yang, M.M. Salberg, T.L. Klein, *Transition Met. Chem.*, 20, 481 (1995).
- [30] G. Speie, J. Csihony, A.M. Whalen, C.G. Pie-Pont, *Inorg. Chem.*, 35, 3519 (1996).
- [31] B.J. Hathaway, *Struct. Bonding (Berlin)*, 57, 55 (1984).
- [32] M.L. Miller, S.A. Ibrahim, M.L. Golden, M.Y. Daresbourg, *Inorg. Chem.*, 42, 2999 (2003).
- [33] A. Diaz, A. Fragosa, R. Cao, V. Ve'rez, *J. Carbohydrate Chem.*, 17, 293 (1998).
- [34] P. Comba, T.W. Hambley, M.A. Hitchman, H. Stratemeier, *Inorg. Chem.*, 34, 3903 (1995).
- [35] K. Jayasubramanian, S.A. Samath, S. Thambidurai, R. Murugesan, S.K. Ramalingam, *Transition Met. Chem.*, 20, 76 (1995).
- [36] A.W. Coats, J.P. Redfern, *Nature*, 20, 68 (1964).
- [37] H.H. Horowitz, G. Metzger, *Anal. Chem.*, 25, 1464 (1963).
- [38] R.M. Mahfouz, M.A. Monshi, S.M. Alshehri, N.A. El-Salam, A.M.A. Zaid, *Synth. React. Inorg. Met.-Org. Chem.*, 31, 1873 (2001).
- [39] A.A. Aly, A.S.A. Zidan, A.I. El-Said, *J. Thermal Analysis*, 37, 627 (1991).
- [40] E. Franco, E. Lopez-Torres, M.A. Mendiola, M.T. Sevilla, *Polyhedron*, 19, 441 (2000).
- [41] G.M. Abdou-Elenien, N.A. Ismail, M.M. Hassanin, A.A. Fahmy, *Can. J. Chem.*, 70, 2704 (1992) and references therein.
- [42] L.M. Araya, J.A. Vargas, J.A. Costamana, *Transition Met. Chem.*, 11, 312 (1986).
- [43] B.S. Parajon-Costa, A.C. Gonzalez-Baro, E.J. Baran, *Z. Anorg. Allg. Chem.*, 628, 1628 (2002).
- [44] B. Adhikary, S.K. Mandal, K. Nag, *J. Chem. Soc. Dalton Trans.*, 935 (1988).
- [45] R.C. Long, D.N. Hendrickson, *J. Am. Chem. Soc.*, 105, 1513 (1983). [46] C. Parter, *Coord. Chem.*, 28, 297 (1997).

Copyright of Journal of Coordination Chemistry is the property of Taylor & Francis and its content may not be copied or emailed to multiple sites or posted to a listserver without the copyright holder's express written permission. However, users may print, download, or email articles for individual use.

Ligand influence on the electrochemical behavior of some copper(II) thiosemicarbazone complexes

Gamil A. Al-Hazmi

Chemistry Department, Faculty of Science, Taiz University, Taiz, Yemen

Mohammed S. El-Shahawi*

Chemistry Department, Faculty of Science, Mansoura University, Damietta, Egypt

Ahmed A. El-Asmy

Chemistry Department, Faculty of science, Mansoura University, Mansoura, Egypt

Received 25 November 2004; accepted 20 January 2005

Abstract

The redox properties of the title mono- and binuclear copper(II) chelates have been investigated by cyclic voltammetry in DMF at a working platinum electrode. The cathodic reduction and anodic oxidation of the investigated chelates produced the corresponding electrochemical Cu^{I} and Cu^{III} species stable only in the voltammetric time scale. The effects of substituents on $E_{1/2}$, redox properties and stability towards oxidation of the complexes were related to the electron-withdrawing or releasing ability of the substituents on the $\text{C}@\text{N}^{\text{I}}$ [H , CH_3 or C_6H_5] and/or $\text{N}^{\text{II}}\text{H}$ [H , C_2H_5 , C_6H_5 or $p\text{ClC}_6\text{H}_4$] groups. The electron attracting substituents stabilize the $\text{Cu}(\text{II})$ complexes while electron-donating groups favor oxidation to $\text{Cu}(\text{III})$. Changes in the $E_{1/2}$ for the complexes due to remote substituent effects could be related to changes in basicity of $\text{N}^{\text{II}}\text{H}$. Thus, variation in $\text{N}^{\text{II}}\text{H}$ has more influence on $E_{1/2}$ than changes in $\text{C}@\text{N}^{\text{I}}$. The correlation between $E_{1/2}$ of the complexes and pK_a of the ligands has been attributed to the spherical potential generated by the electron density of the donor atoms at the antibonding d orbitals.

Introduction

Thiosemicarbazones have been a subject of interest in recent decades due to their variable applications in industry and analytical chemistry [1, 2]. Some derivatives of thiosemicarbazones have shown antiparasitic, antimicrobial, antineoplastic, and biological activity [1–5]. In many cases, the biological activities of thiosemicarbazones are related to their chelating properties to metal ions in vivo [4, 5]. The introduction of transition metal ions into molecules containing a chromophore, which is based on the thiosemicarbazone moiety has resulted in increasing the light fastness, but in many cases produced lower color strength. The redox properties include various oxidation and reduction reactions of the central metal ion, ligand, and processes which involve both the central atom and the ligand [6, 7]. The redox potentials of the $\text{Cu}^{\text{III}}/\text{Cu}^{\text{II}}$ and $\text{Cu}^{\text{II}}/\text{Cu}^{\text{I}}$ couples have been shown to be markedly affected by the nature of the solvent, background electrolyte and by the structure of the ligand and of the complex as a whole. The redox potentials of the $\text{Cu}^{\text{II}}/\text{Cu}^{\text{I}}$ systems also depend on the relative thermodynamic stabilities of the two oxidation states in a given ligand environment. The

influence of various structural features e.g., ring size, degree and arrangement of unsaturation and alkyl substitution [6, 8] on the redox properties of the copper systems has been assessed. The changes in the coordination sphere are connected to the half wave potential values for the electrode couple $\text{Cu}^{\text{II}}/\text{Cu}^{\text{I}}$ and the superoxide dismutase (SOD) mimetic activity [6, 9]. Since the electrochemistry of the title complexes has not been previously considered, the aim of the present study is focused on the redox behavior of thiosemicarbazone $\text{Cu}(\text{II})$ chelates. One purpose of the study of these chelates in non-aqueous electrolytes was to see whether the increased brightness and associated increases in light stability and electron-acceptor properties of the ligands was reflected in the electrochemical properties. The influence of the substituent in the thiosemicarbazone moiety on the stability of $\text{Cu}(\text{II})$, was also investigated. The nature, kinetics and mechanism of the electrode couples are critically discussed.

Experimental

Reagents and materials

* Author for correspondence

borate ($\text{TBA}^+\text{BF}_4^-$) and the solvent DMF were BDH chemicals and were used without further purification. DMF was chosen as an appropriate solvent since it is more readily purified; the reagents and the title Cu(II) chelates have significant solubility in this solvent. Also, DMF has a suitable electrochemical window and it is a better Lewis base, a property which seems to be very important for the tested chelates.

Preparation of ligands and their complexes

The thiosemicarbazone ligands and a representative structure of one of the complexes [10] are given in Figures 1 and 2. The copper(II) complexes were prepared and characterized as described earlier [11]. The formulae, abbreviations and the IUPAC names of the ligands are given in Table 1.

All chemicals used were of analytical reagent grade. The supporting electrolyte tetrabutylammonium tetrafluoro-

borate ($\text{TBA}^+\text{BF}_4^-$) and the solvent DMF were BDH chemicals and were used without further purification. DMF was chosen as an appropriate solvent since it is more readily purified; the reagents and the title Cu(II) chelates have significant solubility in this solvent. Also, DMF has a suitable electrochemical window and it is a better Lewis base, a property which seems to be very important for the tested chelates.

0.04 to 0.16 and 0.68 to 0.73 V coupled with three anodic waves in the regions 0.26 to 0.04, 0.17 to 0.33 and 0.78 to 0.94 V, respectively. Typical cyclic voltammogram behavior of the complex $[\text{Cu}(\text{AT})(\text{OH})(\text{H}_2\text{O})_3]$ is shown in Figure 2. Based on comparison with other Cu(II) [6, 12] analogues, the observed couples are safely assigned to the irreversible (DE_p 0.1 V) one-electron oxidation processes $\text{Cu}^0/\text{Cu}^{\text{I}}$, $\text{Cu}^{\text{I}}/\text{Cu}^{\text{II}}$ and $\text{Cu}^{\text{II}}/\text{Cu}^{\text{III}}$ respectively. The one-electron nature of these couples has been established by comparing its current height with similar couples displayed by other analogues of Cu(II) complexes [6, 12]. On the basis of the structure given in Figure 3, one can explain the electrochemical oxidation and reduction processes of the complexes. The reduction may take place by the addition of a hydrogen atom to the thiol group, while the oxidation by the removal of the OH hydrogen is as shown in the following two equations:



Apparatus

The cyclic voltammetry measurements were carried out with a Potentiostat Wave Generator (Oxford electrode) equipped with a Phillips PM 8043 X-Y recorder. The electrochemical cell assembly consists of Pt wires of 0.5 mm diameter as working and counter electrodes and Ag/AgCl as a reference electrode. The CV measurements at different scan rates (10 – 500 mV s^{-1}) were measured at 25 C and the concentration of the supporting electrolyte (100 mmol) was ca. 10 times higher than the tested solution. The surface area of the working electrode was ca. 30 times smaller than that of the counter electrode.

Results and discussion

The electrochemical data of the prepared Cu(II) complexes in DMF– $\text{TBA}^+\text{BF}_4^-$ in the potential range 1.2 to $+1.4$ V versus a Ag/AgCl reference electrode are summarized in

Table 2. The mononuclear complexes: $[\text{Cu}(\text{AT})(\text{OH})(\text{H}_2\text{O})_3]$, $[\text{Cu}(\text{AET})(\text{OH})(\text{H}_2\text{O})_3]$ and $[\text{Cu}(\text{pCIPT})(\text{OAc})(\text{C}_2\text{H}_5\text{OH})_3]$ displayed three well defined reduction waves in the regions 0.64 to 0.60 , 0.54 to 0.50 and 0.44 to 0.40 V, respectively. The electron-withdrawing, $p\text{-ClC}_6\text{H}_4$, group in the complex $[\text{Cu}(\text{pCIPT})(\text{OAc})(\text{C}_2\text{H}_5\text{OH})_3]$ shifts the oxidation potential of the electrode couples $\text{Cu}^{\text{I}}/\text{Cu}^{\text{II}}$ and $\text{Cu}^{\text{II}}/\text{Cu}^{\text{III}}$ to more positive values (Table 2) and makes their reduction processes more difficult when compared with the complexes $[\text{Cu}(\text{AT})(\text{OH})(\text{H}_2\text{O})_3]$ and $[\text{Cu}(\text{AET})(\text{OH})(\text{H}_2\text{O})_3]$. This is in good agreement with the fact that the electron-attracting property of the $p\text{-ClC}_6\text{H}_4$ group lowers the electron density at the reduction center and becomes more positive and more easily reduced. Also, the presence of the electron-donating ethyl group has an opposite effect and makes both oxidation and reduction processes more difficult than that of $[\text{Cu}(\text{AT})(\text{OH})(\text{H}_2\text{O})_3]$. This may be due to the ethyl group hindering the approach of the reduction center to the electrode surface [13].

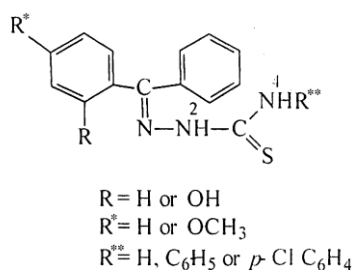
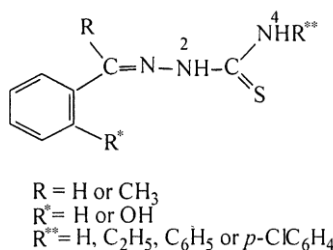


Fig. 1. General structural formulae of the ligands.

The dependence of the cathodic peak current, $i_{p,c}$ of the electrode couple $\text{Cu}^{\text{III}}/\text{Cu}^{\text{II}}$ on the square root of the sweep rate ($v^{1/2}$) for the complex $[\text{Cu}(\text{AT})(\text{OH})(\text{H}_2\text{O})_3]$ suggests a diffusion-controlled electrochemical process [14] (Figure 4A). The cathodic peak potential ($E_{p,c}$) of this couple was shifted towards more negative values as v increases, indicating the irreversible nature of the electrode couple. The irreversibility of this couple was also confirmed from the linear dependence of the

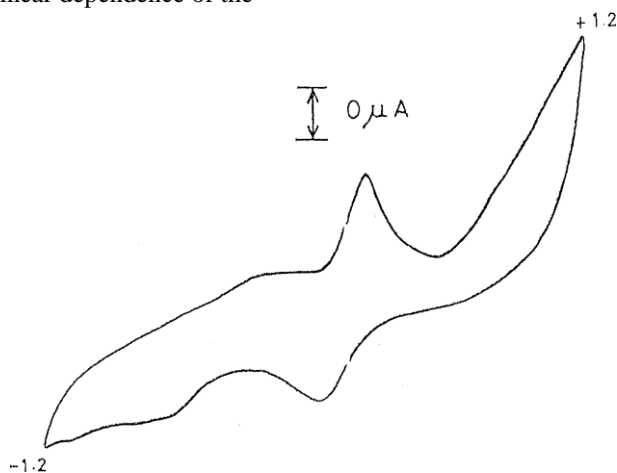


Fig. 2. Cyclic voltammogram of $[\text{Cu}(\text{AT})(\text{OH})(\text{H}_2\text{O})_3]$ in $\text{DMFTBA}^+\text{BF}_4^-$ versus Ag/AgCl reference electrode at 100 mV s^{-1} scan rate.

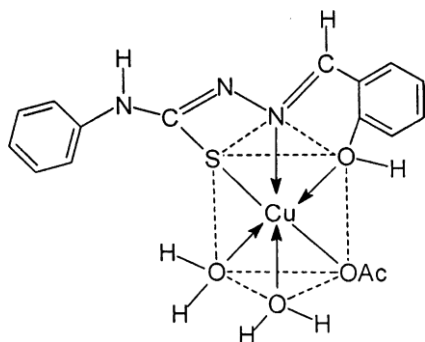


Fig. 3. Structure of $[\text{Cu}(\text{HSPT})(\text{OAc})(\text{H}_2\text{O})_2] \cdot 2\text{H}_2\text{O}$.

cathodic peak potential, $E_{p,c}$ with $\log v$ [15] (Figure 4B). The number of electrons involved in the reduction process (n) and the corresponding charge transfer coefficient (a) can be determined from the slope of this line and by employing the equation [16]: $E_{p,c} - E_{p,c}^{1/2} \approx 1.857 (RT/anF)$ where $E_{p,c}/2$ is the cathodic peak potential at half height, R is the gas constant, T is the absolute temperature (Kelvin) and F is the Faraday. Assuming $n \approx 1$, an a value (0.62) is obtained which is in the expected range for a single one-electron transfer step

Table 1. Abbreviation, name and pK_a of the prepared ligands^a

Abbreviation	Name	pK_a
HAT	1-Acetophenonethiosemicarbazone	11.29
HAET	1-Acetophenone-4-ethylthiosemicarbazone	9.90

HAPT	1-Acetophenone-4-phenylthiosemicarbazone	6.50
HApCIPT	1-Acetophenone-4-p-chlorophenylthiosemi-carbazone	8.72
H_2ST	1-Salicylaldehydethiosemicarbazone.	12.39
H_2SET	1-Salicylaldehyde-4-ethylthiosemicarbazone	10.80
H_2SPT	1-Salicylaldehyde-4-phenylthiosemicarbazone	10.25
H_2SpCIPT	1-Salicylaldehyde-4-p-chlorophenylthiosemi-carbazone	11.29
H_2HyMBPT	1-(2-Hydroxy-4-methoxybenzophenone) 4-phenylthio-semicarbazone	11.48
$\text{H}_2\text{HyMBpCIPT}$	1-(2-Hydroxy-4-methoxybenzophenone) 4-p-chloro-phenylthiosemicarbazone	11.36
HBT	1-Benzophenonethiosemicarbazone	11.20

^a pK_a of the ligands are taken from Ref [10].

[14]. Similar features were observed for the same couples of $\text{Cu}(\text{II})$ complexes with HAET and HApCIPT. Moreover, the $i_{p,a}/v^{1/2}$ ratio remains approximately constant along the whole range of the sweep rate indicating that a coupled chemical reaction takes place after the charge transfer process and characteristics for the ECE (electrochemical reaction coupled between two charge processes) mechanism [16].

Characteristic cyclic voltammograms for the complex [Cu(AT)(OH)(H₂O)₃] in the potential limit)1.2 to 0.0 V versus v are shown in Figure 5. A slight displacement of the anodic and cathodic peaks is observed as the sweep rate increases; the peak current ratios $i_{p,c}/i_{p,a} > 1$; $DE_p > 60$ mV and $i_{p,c}$ versus $v^{1/2}$ plot was found to be linear with a positive intercept. All these characteristics are assigned to an irreversible one electron process [17], The dependence of the voltammetric response of Cu^I/Cu⁰ on the sweep rate, the decrease in $i_{p,c}/v^{1/2}$ and on the depolarizes concentration of the complex is typical of an ECE mechanism in which an irreversible first order chemical reaction is interposed between two successive one electron charge transfers. The ECE mechanism of the electrode couple of this complex was also confirmed from the observed decrease

Table 2. Electrochemical data of the prepared copper(II) complexes in DMF-TBA⁺BF₄ versus Ag/AgCl at 100 V s^{1/2}

Complex	First electrode couple				Second electrode couple				Third electrode couple			
	E _{p,a}	E _{p,c}	DE _p	E _{1/2}	E _{p,a}	E _{p,c}	DE _p	E _{1/2}	E _{p,a}	E _{p,c}	DE _p	E _{1/2}
[Cu(AT)(OH)(H ₂ O) ₃])0.25)0.60	0.35)0.43	0.24	0.04	0.20	0.14	0.80	0.68	0.12	0.74
[Cu(AET)(OH)(H ₂ O)])0.26)0.64)0.38	0.45	0.17	0.05	0.12	0.11	0.78	0.68	0.10	0.73
[Cu ₂ (APT) ₃ (OAc)]	0.04)0.36	0.40)0.16	0.27)0.05	0.32	0.11	0.81	0.69	0.12	0.75
[Cu(ApCIPT)(OAc)(C ₂ H ₅ OH)])0.25)0.56	0.31)0.40	0.33	0.16	0.17	0.25	0.94	0.73	0.21	0.83
[Cu(HST) ₂] ₂ H ₂ O)0.17)0.61	0.44)0.39	0.38	0.14	0.24	0.26	0.87	0.76	0.11	0.82
[Cu ₂ (SET)(OAc) ₂ (H ₂ O) ₂] ₂ H ₂ O)0.19)0.65	0.46)0.42	0.29	0.02	0.27	0.16	0.65	0.55	0.10	0.60
[Cu(HSPT)(OAc)(H ₂ O) ₂] ₂ H ₂ O)0.31)0.55	0.42)0.43	0.86	0.21	0.65	0.54	1.10	0.74	0.36	0.92
[Cu ₂ (SpCIPT)(OH) ₂ (H ₂ O) ₂])0.25)0.70	0.45)0.47	0.21	0.15	0.06	0.18	0.85	0.62	0.23	0.74
[Cu(HyMBPT)(H ₂ O) ₃] ₂ 0.5H ₂ O)0.22)0.70	0.48)0.46	0.33	0.03	0.30	0.18	0.91	0.74	0.17	0.83
Cu(HyMBpCIPT)(H ₂ O)]	0.32)0.14	0.46	0.09	0.54	0.50	0.04	0.52	–	–	–	–
[Cu ₂ (BT)(OAc)(OH) ₂ (H ₂ O)] ₂ H ₂ O)0.40)0.74	0.34)0.57	0.12	0.08	0.20	0.02	0.78	0.56	0.22	0.67

^a E_{1/2} = (E_{p,c} + E_{p,a})/2.

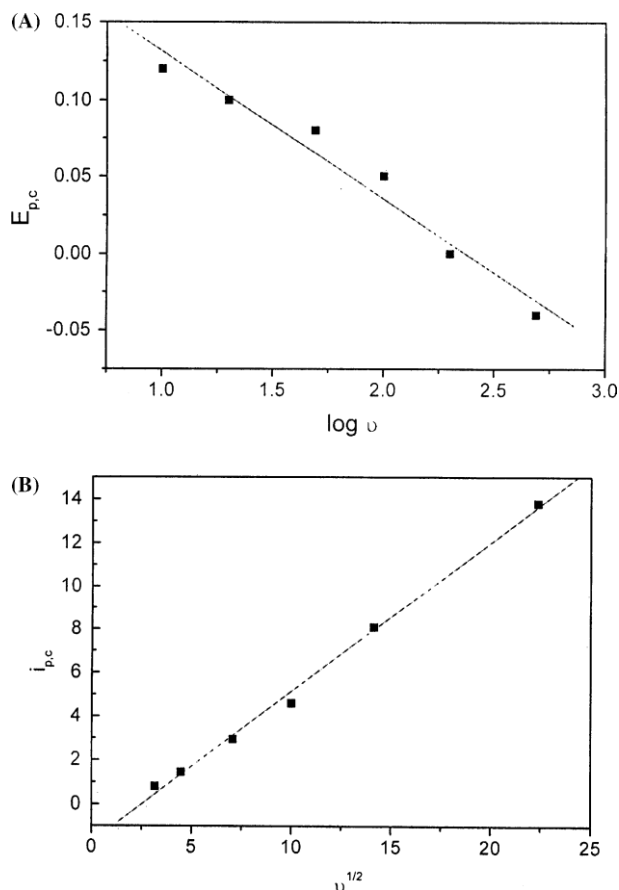


Fig. 4. The dependence of the $E_{p,c}$ (A) and $i_{p,c}$ (B) of the electrode couple $\text{Cu}^{\text{III}}/\text{Cu}^{\text{II}}$ on the scan rate for $[\text{Cu}(\text{AT})(\text{OH})(\text{H}_2\text{O})_3]$.

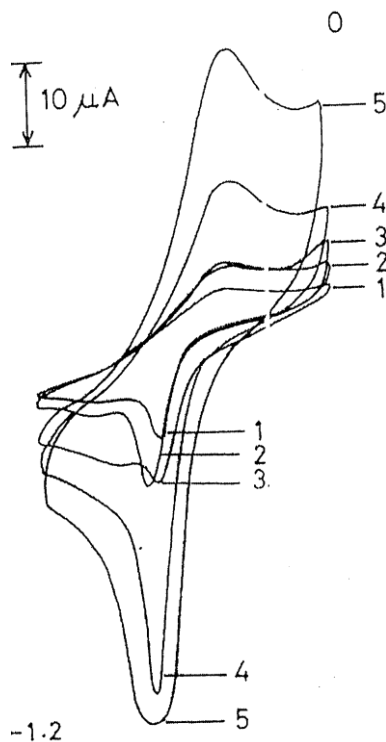


Fig. 5. Influence of the scan rate on the couple $\text{Cu}^{\text{II}}/\text{Cu}^{\text{I}}$ of $[\text{Cu}(\text{AT})(\text{OH})(\text{H}_2\text{O})_3]$ versus Ag/AgCl at 10 (1), 20 (2), 50 (3), 100 (4) and 200 (5) mV s^{-1} .

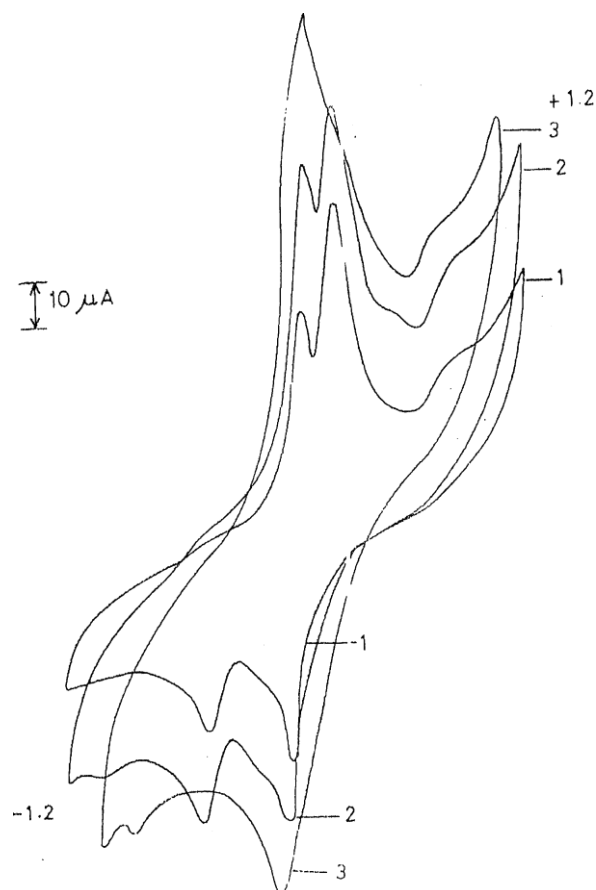
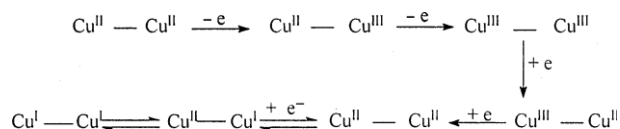


Fig. 6. Cyclic voltammograms of $[\text{Cu}_2(\text{APT})_3(\text{OAc})]$ versus Ag/AgCl electrode at 100 (1), 200 (2) and 500 (3) mV s^{-1} in $\text{DMF-TBA}^+\text{BF}_4^-$.

in the cathodic peak current versus $v^{1/2}$ and $i_{p,c}/v^{1/2} > 1$ on increasing the scan rate.

The CV of the binuclear complex $[\text{Cu}_2(\text{APT})_3(\text{OAc})]$ at 100 mV s^{-1} sweep rate is shown in Figure 6. The irreversible nature and the ECE mechanism of the observed reduction peaks were confirmed by the large difference in the potential ($\Delta E_p > 0.1 \text{ V}$) between the two peak centers of the couples $\text{Cu}^{\text{I}}/\text{Cu}^0$ and $\text{Cu}^{\text{II}}/\text{Cu}^{\text{I}}$ and the linear dependence of the cathodic peak potential, $E_{p,c}$ of each electrode process with $\log v$. At $v \leq 200 \text{ mV s}^{-1}$, the CV showed two irreversible reduction peaks coupled with two irreversible oxidation waves in the potential range 1.2 to 1.2 V . At high scan rate $> 200 \text{ mV s}^{-1}$, such behavior is prevented. These observations may be attributed to the sequential one-electron transfer reactions as shown in Scheme 1.

Similar sequential one electron transfer M^{2+}/M^+ , $\text{M}^{2+}/\text{M}^{3+}$ redox couples has also been observed for a number of binuclear $\text{Cu}(\text{II})$ complexes [18–20]. The data confirm the proposed binuclear structure of the prepared complex.



Scheme 1.

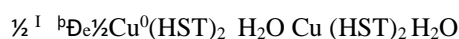
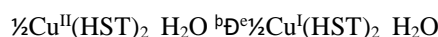
The $E_{1/2}$ values for the couple $\text{Cu}^{\text{I}}, \text{Cu}^0$ of the mononuclear complexes are more negative compared with the binuclear one (Table 2). This difference may be due to the molecular charge of the dicationic species accepting electrons more easily due to the electrostatic effect compared to the mononuclear one. The DE_p values of the couple $\text{Cu}^{\text{I}}/\text{Cu}^0$ for the mononuclear complexes were found to be smaller than that of the binuclear one. This difference may be due to the fact that the binuclear complexes undergo CuAN or CuAS bond rupture as soon as Cu^{I} reduction occurs [20].

The CV of $[\text{Cu}(\text{AT})(\text{OH})(\text{H}_2\text{O})_3]$, $[\text{Cu}(\text{AET})(\text{OH})(\text{H}_2\text{O})]$, $[\text{Cu}_2(\text{APT})_3(\text{OAc})]$ and $[\text{Cu}(\text{ApCIPT})(\text{OAc})(\text{C}_2\text{H}_5\text{OH})]$ showed the current weak ratios $i_{p,c}/i_{p,a} > 1$, $DE_p > \text{mV}$ and $i_{p,c}$ versus $t^{1/2}$ decreasing to a constant value for $t \geq 0.5$ couple $\text{V s}^{1/2}$ for the couple $\text{Cu}^{\text{II}}/\text{Cu}^{\text{III}}$. These data are characteristic of an irreversible one electron process and a diffusion-controlled electrochemical process [14, 16]. The resulting responses are typical of an uncomplicated one-electron charge transfer whose nature appeared perfectly irreversible from the CV at the highest scan rates explored. The CV's of these complexes shift cathodically as t increases, confirming the irreversible nature of the couple $\text{Cu}^{\text{II}}/\text{Cu}^{\text{III}}$ [16]. On the basis of these data, the overall cathodic process can be identified as an ECE mechanism in which the homogeneous process is a multistep one.

The linear dependence of the cathodic peak current, $i_{p,c}$, of the electrode couple $\text{Cu}^{\text{I}}/\text{Cu}^{\text{II}}$ on $t^{1/2}$ for $[\text{Cu}(\text{HST})_2]\text{H}_2\text{O}$ suggests a diffusion-controlled electrochemical process. The cathodic peak potential ($E_{p,c}$) of this couple shifted towards more negative values as t increases, indicating the irreversible nature of the couple. This irreversible nature was also confirmed from the linear dependence of the cathodic peak potential, $E_{p,c}$ with $\log t$. The $i_{p,c}/i_{p,a}$ ratio of this couple < 1 , at a slow scan rate, gradually tends to unity with increasing scan rate. Moreover, the $i_{p,c}/m^{1/2}$ ratio decreased along the whole t analyzed. All these trends indicate that a coupled chemical reaction takes place after the charge transfer process and is typical of an ECE-type mechanism in which the former one electron charge transfer occurs at a more negative potential than the latter. Assuming $n = 1$, a value of $a = 0.4$, is obtained in the range expected for a single irreversible one-electron transfer step ($a < 0.5$) [16].

The CV's of $[\text{Cu}(\text{HST})_2]\text{H}_2\text{O}$, $[\text{Cu}(\text{HSPT})(\text{OAc})(\text{H}_2\text{O})_2]\text{H}_2\text{O}$ and $[\text{Cu}(\text{HyMBPT})(\text{H}_2\text{O})_3]0.5\text{H}_2\text{O}$ are similar and display three well-defined electrode couples. The observed electrode couples at $E_{p,c} = 0.61$ to 0.55 V, $E_{p,a} = 0.31$ to 0.17 with $E_{1/2} = 0.46$ to 0.39 V, $E_{p,c} = 0.03$ to 0.21 , $E_{p,a} = 0.33$ to 0.86 with $E_{1/2} = 0.18$ to 0.54 V and $E_{p,c} = 0.74$ to 0.76 V, $E_{p,a} = 0.87$ to 1.10 and $E_{1/2} = 0.82$ to 0.92 V versus Ag/AgCl are safely assigned to the irreversible one electron oxidation processes $\text{Cu}^0/\text{Cu}^{\text{I}}$, $\text{Cu}^{\text{I}}/\text{Cu}^{\text{II}}$ and

$\text{Cu}^{\text{II}}/\text{Cu}^{\text{III}}$, respectively. The one-electron nature of these irreversible couples was indicated by the large difference in potentials ($DE_p > 0.1$ V) between each of the two counter peaks in the subsequent anodic scans. Thus, these two electrochemical processes are most likely to proceed as follows:



The peak current ratio ($i_{p,c}/i_{p,a}$) for these electrode couples was found, < 1 , (Figure 7A) and DE_p increased with increasing the scan rate, confirming the occurrence of a slow chemical reaction following the electrode processes and the mass transfer is limited [16]. The dependence of the $i_{p,c}$ of the electrode couple $\text{Cu}^{\text{II}}/\text{Cu}^{\text{III}}$ on $t^{1/2}$ for $[\text{Cu}(\text{HST})_2]\text{H}_2\text{O}$. (Figure 7b) suggested a diffusion controlled electrochemical process. A similar trend was also observed for $[\text{Cu}(\text{SPT})(\text{OAc})(\text{H}_2\text{O})_2]\text{H}_2\text{O}$.

The oxidation potentials of the observed electrode couples of the prepared complexes were found to depend on the substituent effects. The electron-withdrawing ($p\text{-ClC}_6\text{H}_4$) group in $[\text{Cu}(\text{ApCIPT})(\text{OAc})(\text{C}_2\text{H}_5\text{OH})]$, $[\text{Cu}_2(\text{SpCIPT})(\text{OH})_2(\text{H}_2\text{O})_2]$ and $[\text{Cu}(\text{HyMBpCIPT})(\text{H}_2\text{O})]$ shift the oxidation potential of the $\text{Cu}^{\text{I}}/\text{Cu}^{\text{II}}$ and $\text{Cu}^{\text{II}}/\text{Cu}^{\text{III}}$ couples to more positive values and makes their reduction easier when compared with the unsubstituted and/or ethyl-substituted complex (Table 2). These data

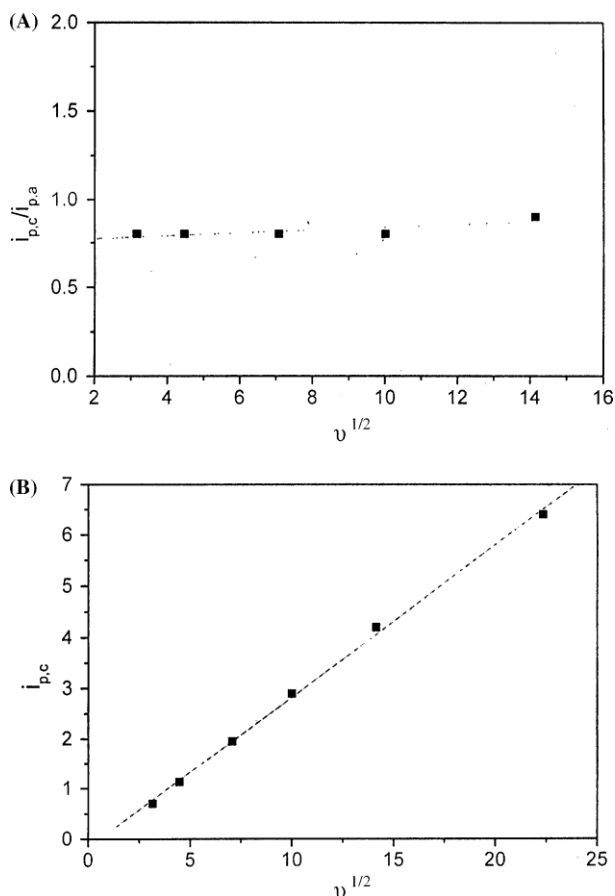


Fig. 7. Plots of $t^{1/2}$ versus the peak current ratio ($i_{p,c}/i_{p,a}$) (A) and the peak current $i_{p,c}$ (B) for the couple $\text{Cu}^{\text{II}}/\text{Cu}^{\text{I}}$ of $[\text{Cu}(\text{HST})_2]\text{H}_2\text{O}$.

are in good agreement with the fact that the electron-withdrawing property of the $p\text{-ClC}_6\text{H}_4$ group lowers the electron density at the reduction center, becomes more positive and thereby more easily reduced.

The CV of the binuclear complexes $[\text{Cu}_2(\text{SET})(\text{OAc})_2(\text{H}_2\text{O})_2]\text{H}_2\text{O}$ and $[\text{Cu}_2(\text{SpCIPT})(\text{OH})_2(\text{H}_2\text{O})_2]$ at 100 mV s^{-1} scan rate showed a similar trend. Three well-defined electrode couples were observed and are safely assigned to $\text{Cu}^0/\text{Cu}^{\text{I}}$, $\text{Cu}^{\text{I}}/\text{Cu}^{\text{II}}$ and $\text{Cu}^{\text{II}}/\text{Cu}^{\text{III}}$ in the direction of increasing potential (Table 2). The irreversible nature and the ECE mechanism for the couples $\text{Cu}^0/\text{Cu}^{\text{I}}$ and $\text{Cu}^{\text{II}}/\text{Cu}^{\text{III}}$ were confirmed by the large differences in the DE_p , and the linear dependence of the cathodic peak potential, $E_{p,c}$ with $\log t$ except for $[\text{Cu}_2(\text{SpCIPT})(\text{OH})_2(\text{H}_2\text{O})_2]$ where a reversible couple $\text{Cu}^{\text{I}}/\text{Cu}^{\text{II}}$ with $\text{DE}_p \approx 60 \text{ mV}$ was observed. At $m \approx 200 \text{ mV s}^{-1}$, the CV's of these two complexes showed two irreversible reduction peaks potential coupled with two irreversible oxidation peaks in the potential range 1.2 to 1.2 V assigned to the couples $\text{Cu}^{\text{I}}/\text{Cu}^{\text{II}}$ and $\text{Cu}^{\text{I}}/\text{Cu}^{\text{III}}$. At a scan rate $>200 \text{ mV s}^{-1}$, such behavior is prevented due to the sequential oneelectron transfer reactions in both complexes, as described.

A comparison of the redox potentials ($E_{1/2}$) of the two complexes $[\text{Cu}(\text{HST})_2]\text{H}_2\text{O}$ and $[\text{Cu}_2(\text{SET})(\text{OAc})_2$

$(\text{H}_2\text{O})_2]\text{H}_2\text{O}$ for the observed electrode couples (Table 2) indicated that, the ability of these complexes to be reduced decreases with electron donation (C_2H_5). Similarly, a comparison between the $E_{1/2}$ of the electrode couples of the two complexes $[\text{Cu}(\text{HSPT})(\text{OAc})(\text{H}_2\text{O})_2] \text{H}_2\text{O}$ and $[\text{Cu}_2(\text{SpCIPT})(\text{OH})_2(\text{H}_2\text{O})_2]$ (Table 2) revealed that the electron-withdrawing $p\text{-ClC}_6\text{H}_5$ group makes the latter couple more positively charged and hence causes it to be more easily reduced. The $i_{p,c}/t^{1/2}$ values for these two complexes slowly increased with increasing the t ($20\text{--}500 \text{ mV s}^{-1}$), indicating that the observed behavior does not favor the ECE mechanism, and the species initially formed in the electrode may also react further to give products that reoxidize at the same potential [21, 22].

The peak current ratios ($i_{p,c}/i_{p,a}$) of the electrode couple $\text{Cu}^{\text{I}}/\text{Cu}^{\text{II}}$ for $[\text{Cu}_2(\text{SET})(\text{OAc})_2(\text{H}_2\text{O})_2]\text{H}_2\text{O}$ and $[\text{Cu}_2(\text{BT})(\text{OAc})(\text{OH})_2(\text{H}_2\text{O})]\text{H}_2\text{O}$ are almost constant (Figure 8). This is most probably indicative of some kinetic complication of the electrode process involved, or it comprises several reactions [23, 24].

The $[\text{Cu}(\text{HyMBpCIPT})(\text{H}_2\text{O})]$ complex showed two oxidation waves at $E_{p,a} \approx 0.32$ and 0.54 V coupled with two cathodic peaks with $E_{p,c} \approx 0.14$ and 0.50 V with $\text{DE}_p \approx 0.46$ and 0.04 V . The first irreversible electrode couple is assigned to the couple $\text{Cu}^{\text{I}}/\text{Cu}^{\text{II}}$. The second reversible ($\text{DE}_p < 60 \text{ mV}$) electrode couple is assigned to the couple $\text{Cu}^{\text{II}}/\text{Cu}^{\text{III}}$ oxidation. The cyclic voltammetric responses at different potential scan rates revealed that at the slowest scan rate, a chemical reaction follows a one electron quasi-reversible charge transfer, while at the highest scan rate the chemical reaction is prevented.

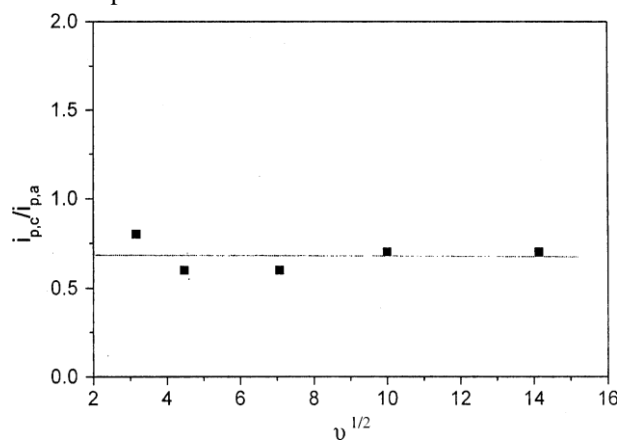


Fig. 8. Plot of $t^{1/2}$ versus peak current ratio ($i_{p,c}/i_{p,a}$) for the couple $\text{Cu}^{\text{II}}/\text{Cu}^{\text{I}}$ of $[\text{Cu}_2(\text{SET})(\text{OAc})_2(\text{H}_2\text{O})_2]\text{H}_2\text{O}$.

Another electrode couple with $E_{p,c} \approx 1.03 \text{ V}$ coupled with an anodic wave at $+1.05 \text{ V}$ was observed and assigned to the redox reaction of the azomethine group [25].

A comparison between the redox behavior of the two complexes $[\text{Cu}(\text{HyBPT})(\text{H}_2\text{O})_3]0.5\text{H}_2\text{O}$ and $[\text{Cu}(\text{HyMBpCIPT})(\text{H}_2\text{O})]$ revealed that the ability of the latter complex to be reduced is easier than the former one. The irreversibility of the coupling of these two complexes was indicated by the linear dependence of the $E_{p,c}$ with $\log t$. The values of $i_{p,c}/t^{1/2}$ increased with increases in the t , confirming that the observed behavior favors the ECE mechanism. The rate of $i_{p,a}/i_{p,c}$ is more or less equal to unity, suggesting a one electron-transfer process.

The substitution on the C@N^1 and N^4H groups has a significant effect on the $E_{1/2}$ of the complexes (Table 2). The electron-withdrawing groups stabilize the copper(II) complexes, while the electron-donating groups favor copper(III) oxidation. These effects can be evaluated from the plots of $E_{1/2}$ for the electrode couple $\text{Cu}^{\text{I}}/\text{Cu}^{\text{II}}$ and $\text{Cu}^{\text{II}}/\text{Cu}^{\text{III}}$ of the complexes versus the corresponding pK_a of the ligands. Representative data are given in Figure 9. The data reveal that, the changes in $E_{1/2}$ for the copper (II) complexes are strongly related to changes in the nucleophilic properties of substituents on C@N^1 and N^4H (Table 2). Furthermore, the values of $E_{1/2}$ for the couples $\text{Cu}^{\text{I}}/\text{Cu}^{\text{II}}$ and $\text{Cu}^{\text{II}}/\text{Cu}^{\text{III}}$ suggest that these couples are more sensitive to changes in the nucleophilic parameters of the N^4H substituents than the changes in C@N^1 derivatives. Within the context of ligand field theory, the correlation between $E_{1/2}$ of the complexes and the pK_a of the ligands involved has been attributed to the spherical potential generated by the electron density of the donor atoms in the antibonding d orbitals as reported by Lintvedt and Fenton [26]. Thus, complexes formed with ligands possessing a high electron density on their atoms (high pK_a) will show lower $E_{1/2}$ values than those formed with weaker bases.

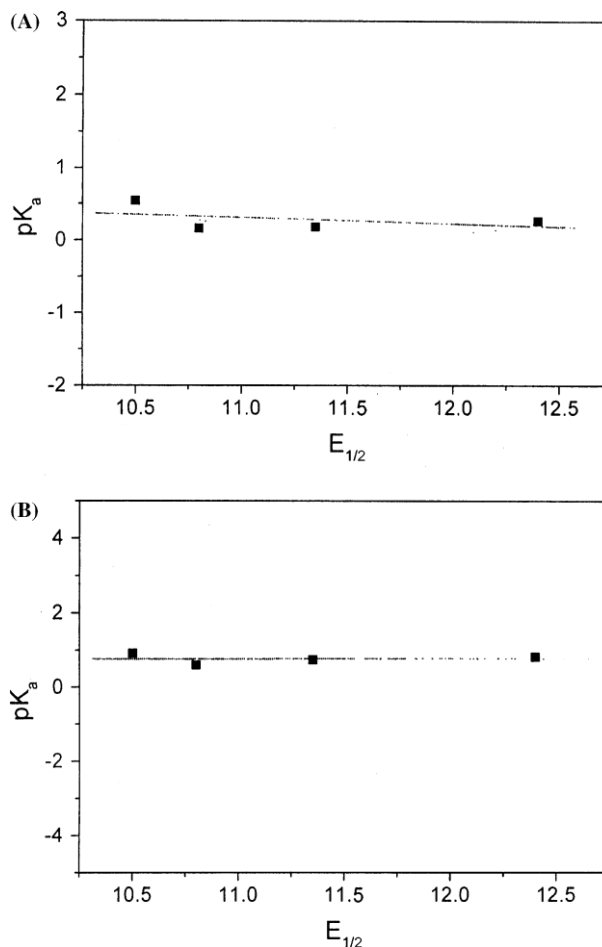


Fig. 9. Plots of pK_a for the couples $\text{Cu}^{\text{I}}/\text{Cu}^{\text{II}}$ (A) and $\text{Cu}^{\text{II}}/\text{Cu}^{\text{III}}$ (B) versus $E_{1/2}$ for the complexes $[\text{Cu}(\text{HST})_2]\text{H}_2\text{O}$, $[\text{Cu}_2(\text{SET})(\text{OAc})_2(\text{H}_2\text{O})_2]\text{H}_2\text{O}$, $[\text{Cu}(\text{HSPT})(\text{OAc})(\text{H}_2\text{O})_2]\text{H}_2\text{O}$ and $[\text{Cu}_2(\text{SpCIPT})(\text{OH})_2(\text{H}_2\text{O})_2]$.

Conclusion

In the present investigation, the ligand influence on the redox properties and the stability of a series of thiosemicarbazone-Cu(II) complexes has been studied. The $E_{1/2}$ for the couple $\text{Cu}^{\text{II}}/\text{Cu}^{\text{III}}$ is very sensitive to electron-withdrawing or donating-properties of the substituent. These facts allow us to predict the tendency towards oxidation of the complexes on pK_a of the ligands. The Cu^{I} and Cu^{II} compounds may be found being used as one-electron redox reagents since the former is a strong reducing agent and the latter a strong oxidizing agent.

References

1. M.M.B. Pessoa, G.F.S. Andrade, M.R. dos Santos and M.L.A. Temperin, *J. Electroanal. Chem.*, 545, 117 (2003).
2. F.A. French, E.J. Blanz, Jr., S.C. Shaddix and R.W. Brockman, *J. Med. Chem.*, 17, 172 (1974).
3. F.A. French, E.J. Blanz, Jr., *Cancer Res.*, 26, 1638 (1966).
4. D.X. West, S.B. Padhye and P.B. Sonawane, *Struct. Bond.*, 76, 76 (1991).
5. M.F. Iskander, L. El-Sayed and N.M.H. Salem, *Polyhedron*, 23, 23

- (2004).
6. E. Franco, E. Lopez-Torres, M.A. Mendiola and M.T. Sevilla, *Polyhedron*, 19, 441 (2000).
 7. J.A. Streeky, D.G. Pillsburg and D.H. Busch, *Inorg. Chem.*, 19, 3148 (1980).
 8. A.A. Isse, A. Gennaro and E. Vianello, *J. Chem. Soc., Dalton Trans.*, 2091 (1993).
 9. Z. Durackova, M.A. Mendiola, M.T. Sevilla and A. Valent, *Bioelectro-Chem. Bioenerg.*, 48, 109 (1999).
 10. R.M. El-Shazly, G.A.A. Al-Hazmi, S.E. Ghazy, M.S. El-Shahawi and A.A. El-Asmy, *Spectrochim. Acta Part A*, 60, 3187 (2004).
 11. G.A.A. Al-Hazmi, M.S. El-Shahawi, I.M. Gabr and A.A. El-Asmy, *J. Coord. Chem.*, accepted for publication.
 12. G.F. de Sousa, V.M. DeFlona and E. Niquet, *J. Molecular Structure*, 687, 17 (2004).
 13. G.M. Abdou-Elenien, N.A. Ismail, M.M. Hassanin and A.A. Fahmy, *Can. J. Chem.*, 70, 2704 (1992) and refs therein.
 14. L.M. Araya, J.A. Vargos and J.A. Costamana, *Transition Met. Chem.*, 11, 312 (1986).
 15. B.S. Parajon-Costa, A.C. Gonzalez-Baro and E.J. Baran, *Z. Anorg. Allg. Chem.*, 628, 1628 (2002).
 16. B.S. Parajoan-Costa, A.C. Gonzalez-Baro and E.J. Baran, *Z. Anorg. Allg. Chem.*, 628, 1419 (2002).
 17. B. Adhikary, S.K. Mandal and K. Nag, *J. Chem. Soc., Dalton Trans.*, 935 (1988).
 18. R.C. Long and D.N. Hendrickson, *J. Am. Chem. Soc.*, 105, 1513 (1983).
 19. C. Pater, *J. Coord. Chem.*, 28, 297 (1992).
 20. A.J. Bard and L.R. Faulkner, *Electrochemical Methods Fundamental and Applications* John Wiley, New York, 1980. p. 218.
 21. M.S. El-Shahawi and W.E. Smith, *Analyst*, 119, 327 (1994).
 22. N.C. Paramanik and S. Bhattacharya, *Polyhedron*, 16, 1761 (1997).
 23. A.N. Murthy and K. Reddy, *J. Chem. Soc., Faraday Trans. I*, 80, 2745 (1984) and refs therein.
 24. I. Tabakovic, M. Lacan and S. Damoni, *Electrochim. Acta*, 21, 241 (1974).
 25. J. Zhang and F.C. Anson, *J. Electroanal. Chem.*, 348, 81 (1993).
 26. R.L. Lintvedt and D.E. Fenton, *Inorg. Chem.*, 19, 569 (1980).

TMCH 6153



An investigation into the retention profile and kinetics of sorption of the ternary complex ion associate of uranyl ions with crown ether and picric acid by the polyurethane foams

M.S. El-Shahawi ^{a,*}, A.M. Othman ^b, H.M. Nassef ^a, M.A. Abdel-Fadeel ^a

^a Chemistry Department, Faculty of Science at Damietta, Mansoura University, Mansoura, Egypt

^b Chemistry Department, Genetic Engineering and Biotechnology Research Institute, Menoufia University, Menoufia, Egypt

Received 18 August 2004; received in revised form 23 December 2004; accepted 23 December 2004

Available online 11 February 2005

Abstract

The retention profile of uranyl ions from aqueous media by polyether-type-based polyurethane foams (PUFs) was studied to gain more information regarding the mechanism of uranyl ions extraction. The influence of pH, extraction time, picric acid (PC), crown ether (CE) and uranyl ions concentration on the sorption step by the PUFs was studied. The data revealed that the sorption of uranyl (II) ions involved formation of a ternary complex ion associate between uranyl (II) ions with crown ether and picric acid and its retention is highly dependent on the parameters studied. The dependency of the sorption percentage on the parameters was explained in a manner consistent with a “solvent extraction” mechanism. The kinetics of uranyl ions sorption onto crown-ether-loaded PUFs was found fast and followed a firstorder rate constant in the presence of picric acid in the aqueous phase. The sorption data were also followed Langmuir, Freundlich and Dubinin–Radushkevich (D–R) isotherms over the entire concentration range of uranyl ions employed. Thus, a dual-mode sorption mechanism involves absorption related to “solvent extraction” and an added component for surface adsorption may be operated simultaneously. The proposed retention procedures were applied successfully for the determination of uranyl (II) ions and picric acid in aqueous media. © 2005 Elsevier B.V. All rights reserved.

Keywords: Uranyl ions; Crown ether; Picric acid; Kinetics; Sorption isotherms; Polyurethane foams

1. Introduction

In the past decade, a number of solid sorbents, e.g. organic ion exchanger and hydrous titanium oxide, dispersed in polyacrylamide gel particles have been reported for uranium recovery from seawater [1–4]. The inorganic ion exchanger stannic phosphate and solvent extraction have been reported [5–7]. Column chromatographic separation methods of uranium (VI) and other elements using poly(dibenzo-18-crown-6) and ascorbic acid medium have been successfully achieved [8]. Amberlite XAD-4 functionalized with 5-aminoquinoline-8-ol, chelating resin

0003-2670/\$ – see front matter © 2005 Elsevier B.V. All rights reserved.
doi:10.1016/j.aca.2004.12.078

containing bicine ligands and crown ethers have been used for the preconcentration of uranyl ions prior its spectrophotometric determination [9–12].

The preconcentration of uranium (VI) ions from aqueous solution onto open cell polyurethane foams (PUFs) impregnated with crown ether and long-chain tertiary amines (Adogen) organic extractant has been reported [13,14]. A sensitive method for the preconcentration of uranium as salicylate complex in waste water, mine drainage and seawater at pH 4 on powdered polyurethane foam has been developed by Carvalho [15]. The photometric determination and separation of uranium (VI) employing 1-phenyl-3-(2-thiazoly)thiourea immobilized PUFs as sorbent have been reported by Chan-

* Corresponding author. Tel.: +20 50370324.

E-mail addresses: mohammad-el-shahawi@yahoo.co.uk, mohammad-el-shahawi@hotmail.com (M.S. El-Shahawi).

dak [16]. Phosphonic acid-immobilized PUFs has been used for the preconcentration of uranyl ions from aqueous media at $\text{pH} = 7 + 1.5$ over a wide range of temperature [17,18].

Herein we report the uptake of uranyl ions from aqueous media employing solvent extraction and PUF membranes. For the purpose of better defining the factors affecting the sorption behavior of the uranyl ions from the aqueous media by the foam membranes, the parameters control the retention profile and mechanism of uranyl ions uptake from the aqueous media are studied. The investigation also helps in promoting the use of PUFs for the separation and for determination of the uranyl ions and picric acid in various segments of industry. The kinetics and sorption isotherms characteristics of uranyl ions uptake by the PUFs are also considered.

2. Experimental

2.1. Reagents and materials

All chemicals and solvents were of analytical reagent grade and were used without further purification. Doubly deionized water was used throughout. A stock solution (1 g/ml) of uranium (VI) was prepared by dissolving an accurate weight of uranyl acetate monohydrate in nitric acid (2 ml). The solution was then completed to 100 ml with distilled water and a series of standard uranyl ion solutions in water were then prepared. Stock solutions of crown ether (0.5%, w/v), picric acid (0.5%, w/v), bromo-cresol (0.1%, w/v), and chromo-azoral S (0.1%, w/v) in water and tributyl phosphate in toluene (TBP, 0.1%, w/v) were prepared.

Commercial white sheets of open cell polyether-based PUFs (30 kg/m^3) were used. Foam cubes (10–15 mm edge) were cut from the foam sheets, washed and finally dried at $80 \text{ }^\circ\text{C}$ [19]. The reagent CE-PUF cubes were prepared by mixing the dried foam cubes with an aqueous solution of crown ether (0.1%, w/v, 10 ml g^{-1} dry foam). Also the plasticized reagent CE-PUF cubes were prepared by mixing the CE-loaded PUFs with TBP in toluene (0.4 g/10 ml) with efficient stirring for 20 min. The reagent CE or CE-TBP-loaded foam cubes were then squeezed and dried as reported [19].

2.2. Apparatus

Glass columns (18 cm length \times 15 mm ID) and a Soxhlet extractor were used in retention experiments and for the foam purification. The absorbance measurements were recorded with a single beam digital spectro UV–vis RS labomed, Inc. with a glass cell (10 mm path length). An Orion pH meter VWR scientific model (8000) and a Lab-

Line Orbit EnvironShaker model (35271-1) were used for the pH measurements and shaking experiments.

2.3. Liquid–liquid extraction procedures

2.3.1. Effect of pH

The effect of pH (2–10) adjusted with dilute NaOH and/or HCl on the uranyl ions sorption from the aqueous media was investigated by shaking 50 ml of each aqueous solution containing uranyl ions ($3.2 \times 10^{-5} \text{ M}$), picric acid ($9.7 \times 10^{-5} \text{ M}$) and crown ether ($3.3 \times 10^{-4} \text{ M}$) at the required pH adjusted with dilute HCl and/or NaOH (0.1 M). The solutions were then shaken with 10 ml of chloroform for 10 min. After equilibrium, the amount of uranyl ions remained in the aqueous phase was determined spectrophotometrically at 655 nm [20] against a reagent blank. The extraction percentage (%*E*) and the distribution ratio (*D*) were then determined as reported earlier [13]. Following these procedures, the influence of shaking time, organic solvent, ion pair reagents, picric acid, crown ether and uranyl (II) ions concentrations on the extraction of uranium (IV) in liquid–liquid extraction was carried out.

2.4. Liquid–solid extraction procedures

2.4.1. Effect of pH

In separate 100 ml stoppered flasks, an accurate weight ($0.2 \pm 0.002 \text{ g}$) of the unloaded or CE-loaded foam cubes was mixed with 50 ml of an aqueous solution containing $1.85 \times 10^{-5} \text{ M}$ of uranyl (II) ions and picric acid (0.5%, w/v) at different pH (2–10). The solutions were shaken for 60 min in a mechanical shaker at $20 \pm 0.1 \text{ }^\circ\text{C}$. After shaking, the aqueous phase was then separated out and the amount of uranyl ions remained in the aqueous phase was finally determined spectrophotometrically using arsenazo III [20]. The amount of uranyl (II) ions retained on the foam cubes, the %*E* and the distribution ratio (*D*) were then determined. Similarly, the influence of shaking time, sample volume ($0.1\text{--}2 \text{ dm}^3$), batch factor (*v/m*) where *v* is the sample volume and *m* is the mass of the CE-loaded PUFs, foam doze and uranyl (II) ions concentration on the retention percentage of the analyte onto the CE-loaded PUFs was carried out.

2.5. Chromatographic behavior of uranyl (II) ions onto the reagent CE-loaded foam packed column

Tap, distilled or industrial wastewater samples (5 dm^3) spiked with uranyl (II) ions at 5–50 ppm concentration level were percolated through the CE-loaded foams ($3 \pm 0.01 \text{ g}$) packed column at 10 ml/min flow rate. A blank experiment under the same experimental conditions of flow rate and reagent CE-loaded foams was also carried out. The columns

were then washed with 50 ml of HCl (1 M) and the effluent and washing solutions were then collected. The uranyl ions in the aqueous solutions before and after percolation through the foam column were then measured [20]. The retained uranyl (II) species in the foam packed column were then quantitatively eluted with 25 ml NaOH (1 M) at 5 ml/min flow rate and finally measured in the eluate [20] against a reagent blank.

3. Results and discussion

Trace metal ions including uranium (VI) and picric acid exhibit toxic effects in biological systems, even at low concentration levels [21]. Thus, there is a need for reliable and rapid procedures for the chemical separation and determination of uranyl ions and picric acid in water. Low uranium (VI) levels are usually determined by selective separation employing solvent extraction and/or liquid–solid sorption techniques [22].

3.1. Liquid–liquid extraction

Crown ethers are a unique class of compounds with hydrophilic interior and lipophilic exterior capable of metal ion transport across non-aqueous barriers [23,24]. These compounds have gained great importance as specific “cation”binding agents, because of their cavity size and lipophilic structure which are capable of promoting ion extraction and transport in biological and liquid membranes [24]. Takeda [25] have reported “size-selective extraction” of some alkali metal ions employing crown ethers and picrate ion as an organophilic counter anion. Thus, in the present investigation, crown ether and picric acid were successfully used for the uptake of uranium (VI) employing liquid–liquid and liquid–solid PUFs extraction procedures. Preliminary investigations have shown that CE and PC are able to form a ternary complex ion associate with uranium (VI) in good agreement with the data reported earlier [26]. The high solubility of uranium (VI) and the reagents in the aqueous phase seem to rule out the formation of complex ion associate. Thus, organic solvents immiscible with water and PUFs were used successfully for the uptake of the produced ternary complex ion-associate of uranium (VI).

The influence of pH of the aqueous phase on the extraction of the ternary complex ion associate of uranium (VI) with the reagent CE and PC was studied. The final pH of the aqueous solution was adjusted before the extraction step. The results are shown in Fig. 1. Maximum extraction of the produced ternary complex ion associate of uranium (VI) was achieved at pH 5–6. Thus, in the subsequent work, the solution pH

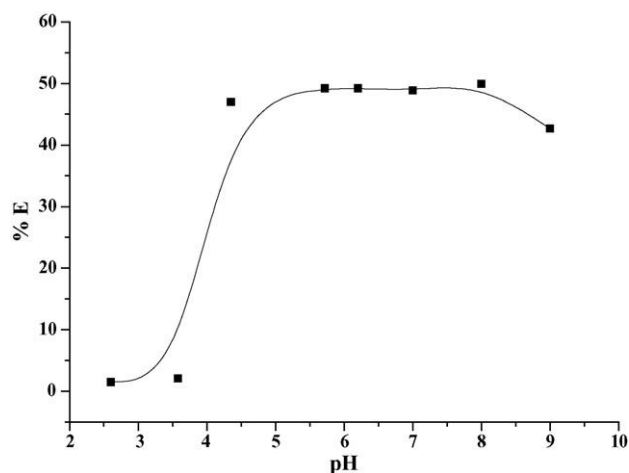


Fig. 1. Effect of pH of the aqueous media on the extraction percentage of uranyl (II) ions onto CHCl_3 .

was kept at pH 5–6 to avoid the possible hydrolysis of the produced ternary complex and to ensure that picric acid exists in ionized form.

The influence of shaking time (1–30 min) on the extraction of the produced ternary complex ion associate of uranium (VI) onto chloroform at pH 5 of the aqueous phase was measured. The extraction was found slow and reached maximum after 20 min shaking time. Thus, a shaking time of 30 min was adopted for maximum extraction in the subsequent work.

The extraction percentage and D of the produced ternary complex ion-associate of uranium (VI) with CE and picrate anion was investigated in the following solvents: *n*-hexane, carbon tetrachloride, diethylether, petroleum ether, chloroform, toluene and kerosene. The extraction percentage of the uranyl ions followed the order: diethylether > chloroform > carbon tetrachloride > toluene > kerosene > *n*-hexane > petroleum ether. Chloroform was chosen as the preferred organic solvent in the subsequent work because its greater density allows a better separation of the phases, the extraction was complete ($E = 98 \pm 2\%$) in a very short time and a better separation of the layers was also obtained. Uranium (VI) and the reagent PC or CE separately are also not extracted into this solvent.

The uptake of the cationic complex of uranium (VI)–crown ether was critically investigated employing a series of counterions, namely picric acid, bromo-cresol and chromo-azoral S at pH 5–6. The extraction percentage of the uranyl ions followed the order: picric acid > bromo cresol > chromo-azoral S in good agreement with the order of their pK_a . Thus, picric acid was successfully used in the subsequent work.

The influence of picric acid concentration at a fixed CE content on the solvent extraction of the produced ternary complex ion associate of uranium (VI) at the optimum experimental conditions was studied. The results are

summarized in Fig. 2. It has been found that 0.4 ml of 0.5% (w/v) of PC is sufficient to extract uranyl (II) ions at level ≤ 20 g/ml

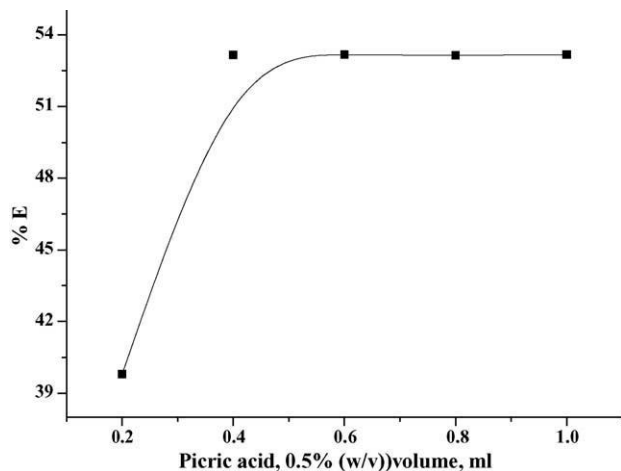


Fig. 2. Effect of picric acid concentration (0.5%, w/v) on the extraction percentage of uranyl (II) ions onto CHCl_3 .

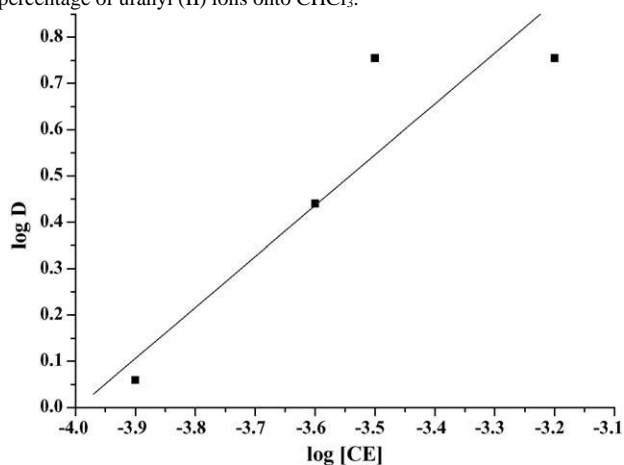


Fig. 3. Plot of log CE concentration (M) in the aqueous phase vs. log D of uranyl (II) ions in CHCl_3 layer.

quantitatively in a single extraction using chloroform. A large excess of the reagent concentration does not improve the extraction performance of the uranyl ions. Amounts of the reagent smaller than the recommended values gave incomplete ternary complex ion associate formation. Plot of log D of the chloroform extract versus log [PC] at pH 5–6 was found linear with a slope of 1.8 ± 0.1 suggesting the extraction of two picrate anions and the stoichiometry of the uranyl ions:picric acid is 1:2 molar ratio.

The influence of crown ether concentration at a fixed PC content on the solvent extraction of the ternary complex ion associate at the optimum experimental conditions was studied. The results indicated that 1 ml of 0.5% (w/v) of CE is sufficient to extract uranium (VI) ≤ 20 g/ml in a single extraction using chloroform. Amount of the CE smaller than

the recommended value gave incomplete complex formation. Plot of log [CE] concentration versus log D of the chloroform extract was found linear (Fig. 3) indicating 1:1 uranium (VI):crown ether molar ratio. Thus, the overall structure $[\text{UO}_2\text{-CE}]^{2+} \cdot [(\text{PC})_2]^{2-}$ is the most probable chemical formula of the produced ternary complex ion associate.

After adjusting the experimental conditions of pH of the extraction media, shaking time, extracting solvent, PC and crown ether concentrations, a linear graph was obtained on plotting the absorbance of uranium (VI) stripped from CHCl_3 layer with nitric acid (1 M) as arsenazo (III)–uranium (VI) complex [20] versus the initial uranyl ions concentration (5–25 g/ml) in the aqueous solution. The influence of uranyl ions concentrations in the aqueous solution at pH 5–6 on the uptake of uranium (VI) by the organic solvent (10 ml) was also investigated. The results indicated that, the percent extraction of uranium (VI) decreased gradually on increasing the uranyl ion concentrations > 25 ppm.

3.2. Liquid–solid extraction involving PUFs

Recently, polyurethane foam sorbent has been used as an inexpensive solid and effective extractor for the removal

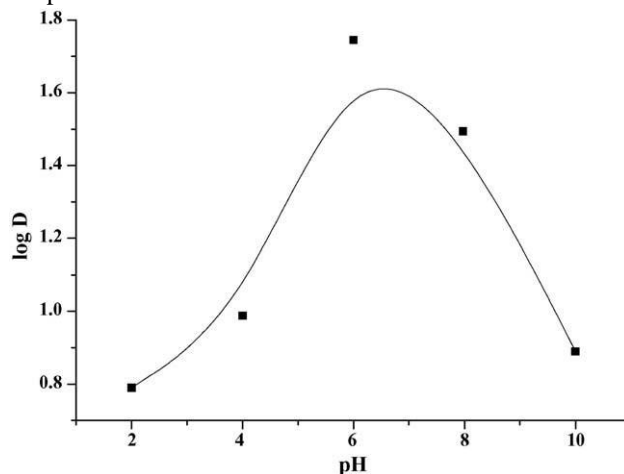


Fig. 4. Plot of pH vs. log D of uranyl (II) ions sorbed onto PUFs.

of trace metal ions and organic contaminants from water [27–29]. The data reported earlier [19,29] have indicated that the solid foam membranes concentrate inorganic species from aqueous media by the phase distribution rather than adsorption mechanism. However, owing to the complex nature of the PUFs, a detailed investigation on the preconcentration and determination of uranium (VI) and picric acid employing crown ether was critically investigated below.

3.2.1. Retention profile of uranyl ions onto crown ether immobilized PUFs

Preliminary investigations have shown that the amount of uranyl ions extracted from the aqueous solution containing picric acid onto the CE-loaded foams depends on the solution pH. Therefore, the sorption profile of uranyl ions (10 g/ml) onto the CE-loaded PUFs from the aqueous solutions was investigated at various pH. After shaking for 1 h, the amount of uranyl ions retained on the loaded foam cubes was then calculated from the difference between the absorbance of the uranyl ions in the aqueous phase before (A_b) and after (A_f) PUFs extraction. The sorption of uranyl ions onto the loaded foams increased markedly with increasing the solution pH up to $\text{pH} \approx 6$ and displayed the lowest sorption at $\text{pH} > 7$ (Fig. 4). The formation of the cationic complex species of uranyl ions with crown ether at $5 < \text{pH} < 7$ which are in turn form a ternary complex ion associate with picrate anion may account for such behavior. Similar trends involving “solvent extraction” mechanism for UO_2^{2+} and MoO_2^{2+} uptake by ether and PUFs have been reported [30,31]. Based on the data reported earlier [30,31] and the results of the solvent extraction investigations, the overall chemical equilibrium between the aqueous solution containing uranyl ions and picrate anions and the CE-loaded PUFs may be proceeded as follows:

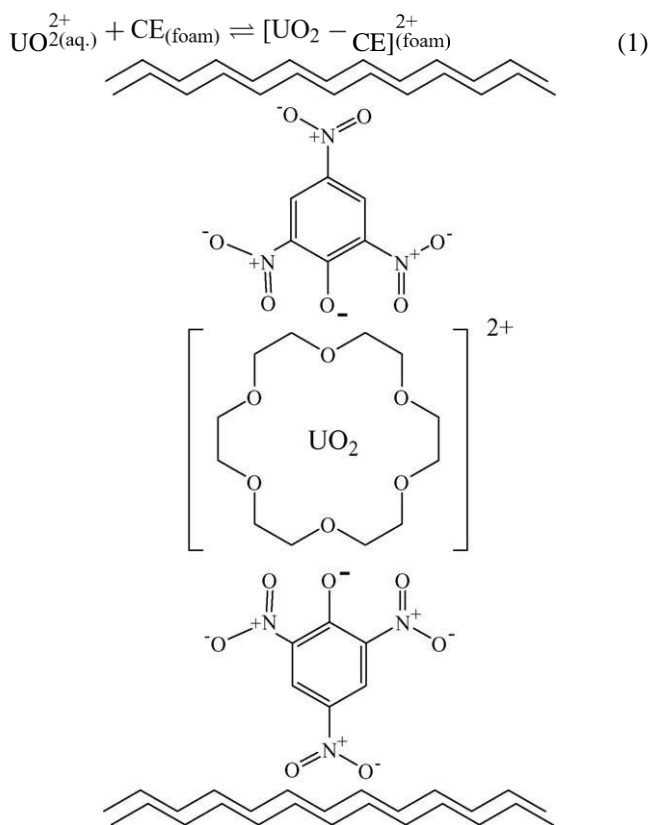
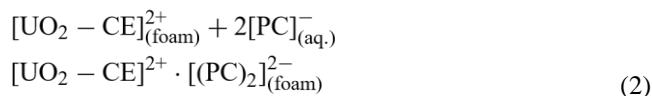


Fig. 5. The proposed chemical structure of the sorbed ternary complex ion associate of picric acid anion, crown ether and uranyl ion onto the PUFs.



Therefore, the sorption of uranyl ions by CE-loaded foams is consistent with the “solvent extraction” mechanism [19,29]. The similarity between these results and the solvent extraction data [30,31] suggested that the extraction of uranyl ions from the aqueous solution in the presence of the picrate anions onto CE-loaded PUFs can be proceeded by an ion pair “solvent extraction” mechanism via an organic solvent of moderate dielectric constant like PUFs [28]. The decrease in the uranyl ion uptake by the loaded foams at $\text{pH} > 6$ is possibly attributed to the instability of the produced complex ion associate $[\text{UO}_2 - \text{CE}]_{(\text{foam})}^{2+} \cdot [(\text{PC})_2]_{(\text{foam})}^{2-}$ and subsequent hydrolysis to $[\text{UO}_2 - \text{CE}]_{(\text{foam})}^{2+}$. These data suggest that the organophilicity of the picric acid anions is the determining factor in the sorption of uranyl ions by the CE-loaded foams and the water structure enforced ion pairing (WSEIP) is the most likely driving force in the extraction step. Based on the solvent extraction data and Eqs. (1) and (2), a proposed chemical structure of the retained ternary complex ion associate of UO_2^{2+} , CE and PC onto the PUFs is given in Fig. 5.

The effect of shaking time on the uranium (VI) sorption by the CE or CE-TBP immobilized PUFs from the aqueous solution containing an excess of picric acid was also investigated. The results revealed that the uranyl ion sorption onto the CE-loaded foams was found fast, followed a first-order rate constant in the presence of picric acid and maximum equilibrium was attained within 50 min shaking time. Thus, 1-h shaking time was adopted for the entire extraction studies in the subsequent experiments. The half-life time ($t_{1/2}$) of the equilibrium sorption of uranyl (II) ions on the CE-loaded PUFs was found equal 4 ± 0.1 min.

The sorption profile of uranyl ions by the CE-loaded foams and TBP plasticized CE-foams was investigated. The extraction percentage followed the sequence: $\text{CE} \geq \text{CE} + \text{TBP}$ PUFs. Thus, the uranyl ion uptake by the CE-loaded foams occurs in one fast step and gel diffusion was not the ratecontrolling step as in the case of common ion exchange resins [18,19]. Thus, in the subsequent work the CE-loaded PUFs was used.

The influence of sample volume ($0.1\text{--}2 \text{ dm}^3$) and batch factor (v/m) on the sorption of uranium (VI) ions from the aqueous solution of pH 6 containing picric acid anions was investigated at the optimum experimental conditions. The sorption percentage and the distribution ratio of uranyl ions onto the loaded PUFs decreased gradually on increasing the batch factor, in good agreement with the data reported earlier [18,29]. Similarly, the influence of the dosage of the CE-loaded PUFs ($0.1\text{--}0.5 \text{ g}$) on the retention of uranyl ions ($1.3 \times 10^{-4} \text{ M}$) was investigated from aqueous solution of pH 5–

6. The distribution ratio increases with an increase in the foam dose, attains a maximum value around 0.2 ± 0.01 g of the sorbent and the sorption percentage remained almost constant $>98\%$ from 0.2 to 0.4 g. The D starts decreasing with an increase in the amount of the sorbent ≥ 0.5 g indicating that, the sorption sites and the pore volume available in the CE-loaded PUFs are sufficient to accommodate all uranyl ions in aqueous solution at foam dose 0.2–0.4 g. Therefore, in further experiments the PUFs dose (0.2 g) was used.

3.2.2. Kinetic behavior of uranyl ions sorption onto CE-loaded PUFs

The kinetics of uranyl (II) ions sorption by CE-loaded PUFs under the optimum experimental conditions of pH, CE and PC counterion was studied in the range of 1–60 min shaking time. The data revealed that maximum extraction of uranyl (II) ions was obtained after 45-min shaking. The results were subjected to the Weber–Morris equation [32]:

$$q_t = R_d t^{1/2} \quad (3)$$

where R_d is the rate constant of intraparticle transport in $\text{mmol g}^{-1} \text{min}^{-1/2}$ and q_t the sorbed uranyl (II) ions concentration in mol g^{-1} at time t in min onto the CE-loaded PUFs. The linear plot of the sorbed uranyl (II) ions concentration onto CE-loaded PUFs at time t , q_t (mmol/g) versus the square root of time is given in Fig. 6. The diffusion rate was found rapid in the initial stage and slows down with passage of time. The R_d value computed from the observed distinct slope of the Weber–Morris plot (Fig. 6) was found equal $0.28 \pm 0.02 \text{ mmol g}^{-1} \text{min}^{-1/2}$ onto the CE-loaded PUFs.

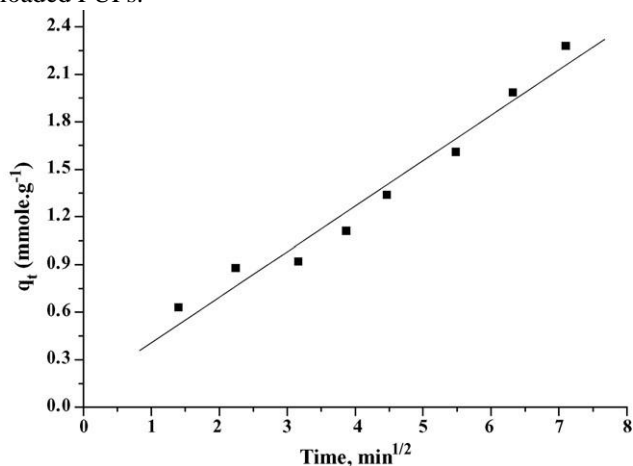


Fig. 6. The sorbed concentration of uranyl (II) ions onto CE-loaded PUFs from aqueous solution of pH 5 as a function of shaking time.

The data also indicated that, for up to $t^{1/2}$ equal 3.25 min, the relationship holds good and deviates as the shaking time increases.

Moreover, the dependence of the uranyl (II) ions sorption onto the CE-loaded foams on the agitation time was subjected to the Lagergren equation [33]. The familiar form of Lagergren equation [33,34] is given by the equation:

$$\log(q_e - q_t) = \log q_e - \left(\frac{kt}{2.303} \right) \quad (4)$$

where q_e is the sorbed concentration of uranyl (II) ions onto the PUFs at equilibrium (mmol g^{-1}) and k the overall rate constant. The plot of $\log(q_e - q_t)$ versus time up to 30 min was found linear (Fig. 7). The value of the first-order overall rate constant (k) for the uranyl (II) ions sorption from the aqueous solution onto the CE-loaded foams was found equal $0.024 \pm 0.001 \text{ min}^{-1}$.

The value of Bt , which is a mathematical function (F) of the ratio of the fraction sorbed (q_t) in mol/g at time t and that

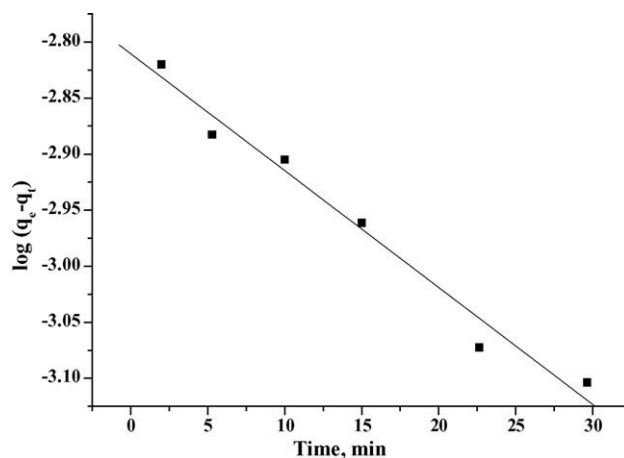


Fig. 7. Lagergren plots of the kinetics of uranyl (II) ions sorption onto CE-loaded PUFs.

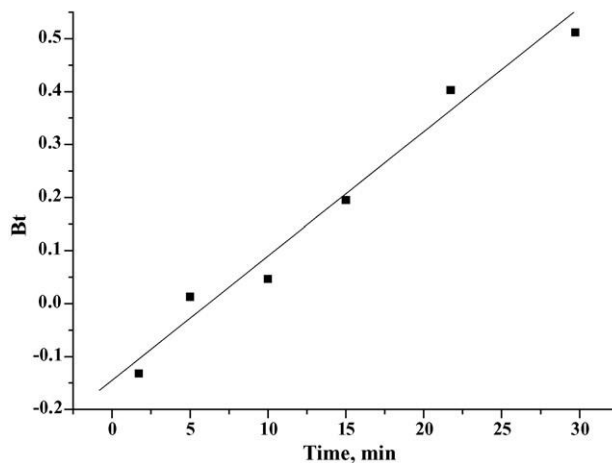


Fig. 8. Reichenburg plot of the kinetics of uranyl (II) ions sorption onto CE-loaded PUFs.

at equilibrium (q_e) in mol/g, i.e. $F = q_t/q_e$ was calculated for each value of F employing Reichenburg equation [35]:

$$Bt = -0.4977 - 2.303 \log(1 - F) \quad (5)$$

A plot of Bt versus time at 25 ± 1 °C is given in Fig. 8. The plot was found linear up to 30 min for uranyl (II) ions sorption from the aqueous solution onto the CE-loaded foams. The straight line with a slope of 0.023 ± 0.002 (Fig. 8) does not pass through the origin confirming the observed behavior of the Weber–Morris equation [32]. Thus, particle diffusion is the most probable operating mechanism and does not control the kinetics of uranyl (II) ions sorption onto the CE-loaded foams. Therefore, the retention of the uranyl (II) ions onto the PUF cubes is most likely involves three steps: (i) bulk transport of uranyl (II) ions from the aqueous solution, (ii) diffusion of uranium (VI) species within the pore volume of PUF and/or along the pore wall surface to an active sorption site [36] and finally (iii) formation of the ternary complex ion associate of uranyl (II) ions onto the CE-loaded PUFs. Thus, the actual sorption of the solute onto the interior surface site is rapid, and hence it is not the rate-determining step. Therefore, intraparticle transport may be the one step controlling the rate of sorption of uranyl (II) ions from the aqueous picrate solution of pH 5–6.

3.2.3. Sorption isotherm of uranyl (II) ions onto CE-loaded foams

The sorption profile of uranyl (II) ions from the aqueous solutions containing an excess of picric acid at pH 5–6 onto CE-loaded foams was determined over the equilibrium concentrations (5×10^{-5} to 3×10^{-4} M) of uranyl (II) ions. The pH of the aqueous solution was adjusted at pH ≈ 6 with dilute HCl and/or NaOH. The amount of uranyl (II) ions retained on/in the CE-loaded PUFs at low concentration varied linearly with the corresponding equilibrium concentration of uranyl ions in the bulk solution (Fig. 9). Thus, “solvent

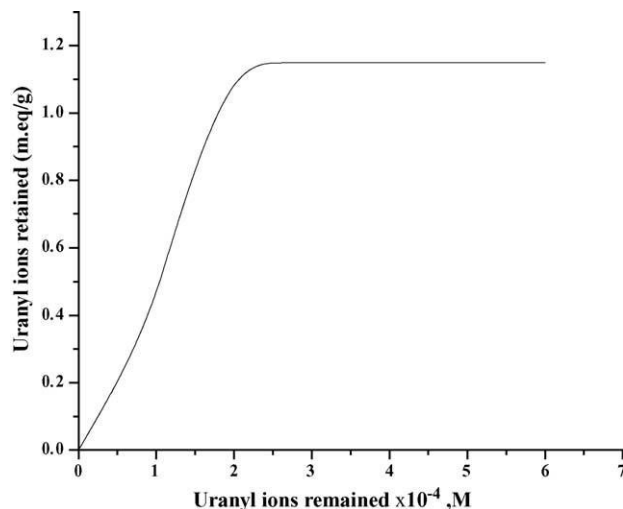


Fig. 9. Sorption isotherms of uranyl (II) ions onto CE-loaded PUFs from aqueous solution of pH 5.

extraction” is the most probable mechanism for the sorption of uranyl ions from the aqueous solution by the CE-loaded foams [19,29]. However, in view of the complex nature of the PUF membranes, several mechanisms of uranyl (II) ions sorption could be involved simultaneously [19]. Diffusion of the solute through a hydrodynamic boundary layer also possibly takes place in the sorption phenomena. Thus, the diffusion of uranyl (II) ions is governed by molecular diffusion and is rapid and generally occurs at the macropores of the sorbent. Thus, the CE-loaded PUFs have good sorption efficiency towards uranyl (II) ions in the aqueous phase containing PC anions.

The retention profile of uranyl ions in the aqueous solution onto CE-loaded PUFs was subjected to Langmuir, Freundlich and Dubinin–Radushkevich [37–39] over a wide range of equilibrium concentrations. The familiar form of Langmuir sorption isotherm is expressed in the linear form as follows:

$$\frac{C_e}{C_{ads}} = \frac{1}{Q} + \frac{C_e}{Qb} \quad (6)$$

where C_e is the uranyl (II) ions concentration (M) in aqueous solution at equilibrium, C_{ads} the sorbed uranyl (II) ions concentration (mmol g^{-1}) onto the reagent CE-loaded foams per unit mass of sorbent at equilibrium, Q and b are constants related to the maximum sorption capacity and the binding energy of the solute sorption that is independent of temperature, respectively. Plot of C_e/C_{ads} versus C_e was found linear throughout the entire concentration range of uranyl (II) ions. The sorption parameters Q and b for the adsorption process evaluated from the slope and intercept of

the plot were found equal $2.8 \pm 0.1 \text{ mmol g}^{-1}$ and $0.21 \pm 0.1 \times 10^3 \text{ dm}^3 \text{ mol}^{-1}$ for uranyl (II) ions sorption onto CE-loaded foams.

Freundlich sorption isotherm [38] fits the experimental data over a wide range of concentration. The Freundlich model is expressed in the following form:

$$\log C_{\text{ads}} = \log A + \frac{1}{n \log C_e} \quad (7)$$

where A and $1/n$ are Freundlich parameters related to the maximum sorption capacity of the solute in mmol g^{-1} and energy of the sorption process, respectively. These parameters encompass the surface heterogeneity and the exponential distribution of active sites and their energies. The numerical values of A and $1/n$ computed from the intercept and the slope of the linear plot of $\log C_{\text{ads}}$ versus $\log C_e$ over the entire concentration of uranyl (II) ions in the aqueous phase were found equal to $0.34 \pm 0.01 \text{ mmol g}^{-1}$ and 1.1 ± 0.02 of uranyl (II) ions retained onto the CE-loaded PUFs. The value of $1/n > 1$ indicates that the sorption capacity is slightly unfavoured at lower equilibrium concentrations. The Freundlich isotherm does not predict the saturation of the PUFs sorbent by the uranyl (II) ions. Therefore, infinite surface coverage is predicted mathematically and physico-multi-layer sorption of the sorbent surface.

The Dubinin–Radushkevich (D–R) isotherm model [39] is postulated within the adsorption space close to the adsorbent surface. The D–R isotherm can be linearized as follows:

$$\ln C_{\text{ads}} = \ln K_{\text{DR}} - \beta \epsilon^2 \quad (8)$$

where K_{DR} is the maximum sorption capacity of uranyl (II) ions (mmol g^{-1}), β is a constant related to the energy ($\text{kJ}^2 \text{ mol}^{-2}$) of the transfer of the solute from the bulk solution to the solid sorbent and is Polanyi potential which is given by the equation

$$\epsilon = RT \ln \left(1 + \frac{1}{C_e} \right) \quad (9)$$

where R is the gas constant ($R = 0.082 \text{ kJ mol}^{-1} \text{ K}^{-1}$) and T the absolute temperature in Kelvin. The plot of $\ln C_{\text{ads}}$ versus ϵ^2 was found linear and obeyed D–R isotherm for the uranyl (II) ions sorption onto the CE-loaded PUFs over the entire concentration range tested. The numerical values of β and K_{DR} have been calculated from the slope and intercept and were found in the range $-0.0042 \pm 0.0004 \text{ kJ}^2 \text{ mol}^{-2}$ and $0.134 \pm 0.0002 \text{ mmol g}^{-1}$, respectively. Thus, a dual sorption mechanism for uranyl (II) ions uptake involves both absorption related to “solvent extraction” and an added

component for “surface adsorption” of the CE-loaded PUFs could be proceeded. This model is mathematically expressed as follows:

$$C_r = C_{\text{abs}} + C_{\text{ads}} = K_D C_{\text{aq}} + \frac{SK_L C_{\text{aq}}}{1 + K_L C_{\text{aq}}} \quad (10)$$

where C_r and C_{aq} are the equilibrium concentrations of uranyl (II) ions onto the CE-loaded PUFs and in solution, respectively, C_{abs} and C_{ads} are the equilibrium uranyl (II) ions onto the CE-loaded foams as an absorbed and adsorbed species, respectively, S is the saturation value for the Langmuir adsorption, K_D the distribution coefficient and K_L the Langmuir constant. This equation can be solved for the distribution ratio D as follows:

$$D = K_D + \frac{SK_L}{1 + K_L C_{\text{aq}}} \quad (11)$$

It obvious that D is dependent on the uranyl (II) ions concentration. Therefore, Eq. (10) fitted well with the extraction data shown in Fig. 9. The above data and the favourable flow and hydrodynamic characteristic [19] of the PUFs sorbent suggested the possible use of the CE-loaded PUFs for the enrichment of traces of uranyl (II) ions present in the radioactive liquid waste employing flow mode of separation and subsequent determination of uranyl (II) ions and picric acid in water.

3.2.4. Applications

3.2.4.1. Preconcentration and analysis of uranyl (II) ions in water. The feasibility of the proposed CE-loaded PUFs method in column mode for the determination of uranyl (II) ions in tap, distilled and/or industrial wastewater samples was examined. A 5-dm^3 water sample at $\text{pH} \sim 5\text{--}6$ spiked with uranyl (II) ions ($5\text{--}50 \text{ ppm}$) concentration level and at a total concentration $\leq 1 \text{ ppm}$ uranyl (II) ions was percolated through CE-loaded PUFs column at 10 ml/min flow rate. Uranyl (II) ions were retained quantitatively for the concentrations tested as indicated from the analysis of the uranyl (II) ions in the effluent solution. The sorbed uranyl (II) species onto the CE-treated foam column were then recovered quantitatively by percolating a 50-ml of NaOH (1 M) at 5 ml/min flow rate. The uranyl (II) ions in the recovered solution were then determined as described earlier [20]. A reasonable recovery percentage of $97.6 \pm 1.6\%$ was obtained. The data showed that the method is simple, convenient and applicable for routine work involving removal and determination of uranyl (II) ions even in water samples with high content of dissolved salts like NaCl , CaCl_2 , MgCl_2 or MgSO_4 .

3.2.4.2. Analysis of picric acid in water. The validity of the proposed solvent extraction procedures for the determination of picric acid in water samples was tested as follows: various water samples of tap water ($0.05\text{--}5\text{ dm}^3$) containing excess amounts of crown ether (0.1%, w/v) and uranyl (II) ions ($1 \times 10^{-4}\text{ M}$) were spiked with different concentrations (25–50 ppm) of picric acid and at a total picric acid concentration level ≤ 1 ppm. Each reaction mixture was adjusted to $\text{pH} \sim 5\text{--}6$ and shaken with chloroform (10 ml) for 30 min. After equilibrium the organic phase was separated out, stripped with nitric acid (1 M) and finally analyzed for uranium (VI) as arsenazo–uranyl (II) ion complex by the reported method [20] with the aid of standard curve. Picric acid was then determined indirectly from the amount of uranyl (II) ions in the organic phase and with the aid of standard curve for uranyl (II) ions. Satisfactory results were obtained for picric acid with an average recovery of $97.6 \pm 2.3\%$. On the basis of the obtained results, tap water samples are free from picric acid.

4. Conclusion

The study of the extraction of the uranyl (II) ions showed that these ions are extracted as a ternary complex ion associate $[\text{UO}_2\text{--CE}]^{2+}\cdot[(\text{PC})_2]^{2-}$. The retention of these species involved a number of mechanisms. The dual-mode of sorption offers an excellent description of the observed behavior and the two models presented seem the most plausible. According to this model, when the analyte concentration is high, “solvent extraction” becomes the predominant mechanism because of higher capacity, while when the analyte concentration is low “surface” adsorption is responsible for the majority of the sorption. The great potentialities of open cell type resilient PUFs membranes are attributed to their inexpensiveness and the large-scale availability all over the world for many industrial applications. However, further studies are continued to easily estimate the extraction constants of both adsorption and absorption steps.

References

- [1] A.D. Kelmer, *Sep. Sci. Technol.* 16 (1981) 1019.
- [2] H. Yamashita, F. Nakajima, *Bull. Chem. Soc. Jpn.* 53 (1980) 3050.
- [3] H.S. Mahal, B. Venkataramani, K.S. Venkateswarlu, *J. Inorg. Nucl. Chem.* 43 (1981) 3335.
- [4] S. Nakamura, S. Mori, H. Yoshimuta, Y. Ito, M. Kanno, *Sep. Sci. Technol.* 23 (1988) 731, and references therein.
- [5] R.K. Rastogi, *Sep. Sci. Technol.* 32 (1997) 1711.
- [6] H. De-Beer, P.P. Coetzee, *Radiochim. Acta* 57 (1992) 113. [7] J.L. Perez, C.G. Gorica, E. Gorica, B. Cardero, *Anal. Chim. Acta* 246 (1992) 291.
- [8] B.S. Mohite, A.S. Jadhav, *J. Chromatogr. A* 983 (2003) 277.
- [9] J.M. Gladis, T.P. Rao, *Anal. Bioanal. Chem.* 373 (2002) 867.
- [10] V.K. Jain, A. Handa, S.S. Sait, P. Shrivastav, Y.K. Agrawal, *Anal. Chim. Acta* 429 (2001) 237.
- [11] K. Dev, R. Pathak, G.N. Rao, *Talanta* 48 (1999) 579.
- [12] P.K. Mohapatra, V.K. Manchanda, *Talanta* 47 (1998) 1271.
- [13] M.M. Abou-Mesalam, I.M. El-Nagar, M.S. Abdel-Hai, M.S. ElShahawi, *J. Radioanal. Nucl. Chem.* 258 (2003) 619.
- [14] H.D. Gesser, S. Ahmed, *J. Radioanal. Nucl. Chem.* 140 (1990) 395.
- [15] M.S. Carvalho, *Spectrochim. Acta* 53 (1998) 1945.
- [16] M. Chandak, *Indian J. Chem.* 35 (1996) 809.
- [17] S. Katragadda, H.D. Gesser, A. Chow, *Talanta* 44 (1997) 1865.
- [18] M.M. Saeed, M. Ahmed, *Anal. Chim. Acta* 525 (2004) 289.
- [19] T. Braun, J.D. Navratil, A.B. Farag, *Polyurethane Foam Sorbents in Separation Science*, CRC Press, Boca Rotan, FL, 1985.
- [20] S.B. Savvin, *Talanta* 8 (1961) 673; S.B. Savvin, *Talanta* 11 (1964) 1.
- [21] L.G.A. Vande Water, W.L. Driessen, J. Reedijk, D.C. Sherrington, *Eur. J. Inorg. Chem.* (2002) 221.
- [22] I. Kubrakova, T. Kudinova, A. Formanovsky, N. Kuzmin, *Analyst* 119 (1994) 2477.
- [23] I.M. Kothoff, *Anal. Chem.* 51 (1979) 1.
- [24] G.W. Gokel, *Crown Ether and Compounds*, RSC, London, 1992.
- [25] Y. Takeda, *Bull. Chem. Soc. Jpn.* 54 (1981) 526.
- [26] P.K. Mohapatra, V.K. Manchanda, *Talanta* 47 (1998) 1271.
- [27] V.K. Gupta, S.K. Srivastava, R. Tyagi, *Water Res.* 34 (2000) 1543.
- [28] A.S. Khan, W.G. Baldwin, A. Chow, *Can. J. Chem.* 59 (1981) 1490.
- [29] M.S. El-Shahawi, H.A. Nassef, *Anal. Chim. Acta* 481 (2003) 29.
- [30] J.J. Oren, K.M. Gough, H.D. Gesser, *Can. J. Chem.* 57 (1979) 2032.
- [31] A.B. Farag, M.S. El-Shahawi, S. Farrag, *Talanta* 41 (1994) 617.

- [32] W.J. Weber Jr., J.C. Morris, J. Sanit. Eng. Div. Am. Soc. Civ. Eng. 89 (SA2) (1963) 31;
W.J. Weber Jr., J.C. Morris, J. Sanit. Eng. Div. Am. Soc. Civ. Eng. 90 (SA3) (1964) 79.
- [33] S. Lagergren, B.K. Sven, Vatenkapsakad. Handl. (1898) 24.
- [34] S.M. Hasany, M.M. Saeed, M. Ahmed, Talanta 54 (2001) 89, and references cited in.
- [35] D. Reichenburg, J. Am. Chem. Soc. 75 (1972) 589.
- [36] S. Aksoyoglu, J. Radioanal. Nucl. Chem. 134 (1989) 393.
- [37] L. Langmuir, J. Am. Chem. Soc. 40 (1918) 136.
- [38] H. Freundlich, Colloidal Capillary Chemistry, Methuen, London, 1926.
- [39] M.M. Dubinin, L.V. Radushkevich, Proc. Acad. Sci. USSR Phys. Chem. Soc. 55 (1974) 331.



ELSEVIER

SCIENCE @ DIRECT®

ANALYTICA
CHIMICA
ACTA

Analytica Chimica Acta 534 (2005) 319–326 www.elsevier.com/locate/aca

Chemical speciation of chromium(III,VI) employing extractive spectrophotometry and tetraphenylarsonium chloride or tetraphenylphosphonium bromide as ion-pair reagent

M.S. El-Shahawi^{a,*}, S.S.M. Hassan^b, A.M. Othman^c, M.A. Zyada^a, M.A. El-Sonbati^a^a Chemistry and Environmental Science Department, Faculty of Science at Damietta, Mansoura University, Mansoura, Egypt^b Chemistry Department, Faculty of Science, Ain Shams University, Cairo, Egypt^c Chemistry Department, Genetic Engineering and Biotechnology Research Institute, Menoufia University, Menoufia, Egypt

Received 23 April 2004; received in revised form 18 November 2004; accepted 18 November 2004

Available online 12 February 2005

Abstract

A simple and accurate extractive spectrophotometric procedure for the chemical speciation of chromium(III,VI) species in aqueous media has been developed. The method is based upon the extraction of the complex ion-associate formed between the chloro chromate (CrO_3Cl^-) anion and the ion-pair reagent tetraphenylarsonium chloride (TPAs^+Cl^-) or tetraphenylphosphonium bromide (TPP^+Br^-) at $\text{pH} \leq 0$ in chloroform followed by direct spectrophotometric measurement at 355 nm. The optimum concentration range evaluated by Beer–Lambert's law, Ringbom's plot, the molar absorptivity, the Sandell's sensitivity, the extraction and stability constants (K_D , K_{ex} and β), the stoichiometry and the extraction equilibria of the produced complex ion-associates have been determined and gave a convenient applications of the investigated system for analytical purposes. Chromium(III) was also determined by the proposed procedure after prior oxidation to chromate with H_2O_2 in alkaline solution. The method has been applied successfully for the analysis of chromium(VI) and total chromium(III,VI) in industrial wastewater of electroplating plant.

© 2004 Published by Elsevier B.V.

Keywords: Chemical speciation; Chromium(III,VI); Ion-pairs; Extraction equilibria and spectrophotometry

1. Introduction

Chromium occurs in the environment in two major valence states(III,VI). Chromium(III) compounds are sparingly soluble in water, while chromium(VI) species are readily soluble, which may result in enhancing chromium(VI) level in water sources [1,2]. Chromium(VI) is more toxic than chromium(III) and is known to be a carcinogen [1]. Chromium(III) is an essential element to normal glucose tolerance factor, protein and fat metabolism in humans with a daily recommended intake of 50–200 g/day for the adult [2,3]. The reference dose (RD) for chromium(VI,III) are 0.005 mg/kg and 1 mg/kg/day for body weight, respectively.

0003-2670/\$ – see front matter © 2004 Published by Elsevier B.V.
doi:10.1016/j.aca.2004.11.085

Due to the widely different toxicity of chromium(VI), total chromium measurement cannot be used to determine the actual environmental impact [1,4]. Thus, chemical speciation of chromium in environmental samples is necessary to accurately assess pollution levels. Inert solvents (e.g. chloroform, benzene and dichloroethane) have been successfully used for the extraction of the ion-associates of chromium(VI) with high molecular weight amines e.g., trioctylamine, tribenzylamine and tetrabutyl-ammonium hydroxide and TBP from aqueous acid media [5–12].

Novel methods for the chemical speciation of chromium(III,VI) employing adsorptive stripping voltammetry and in situ separation and sequential determination with electrothermal vaporization-inductively coupled

* Corresponding author. Tel.: +20 50370324.

E-mail address: mohammad@hotmail.com (M.S. El-Shahawi).

plasma-atomic emission spectrometry have been reported [13,14]. The determination of the total chromium content in industrial effluents and wastewaters by FI-FAAS and on-line blank correction have been reported [15,16].

A high-performance liquid chromatographic method with diode array detection based on the chelating agent ammonium pyrrolidine dithiocarbamate has been developed for the analysis of chromium species (Cr^{3+} , CrO_4^{2-} and $\text{Cr}_2\text{O}_7^{2-}$) [17]. The method was found capable for discriminating not only between chromium(III,VI), but also between the chemical forms of chromium(VI): CrO_4^{2-} and $\text{Cr}_2\text{O}_7^{2-}$.

Recent years have seen an upsurge of interest for rapid and sensitive analytical methods for the determination and speciation of chemical forms of toxic metal ions in environmental samples. Thus, the present paper describes a simultaneous, convenient and low cost solvent extraction spectrophotometric procedures for the chemical speciation of chromium(III,VI) in water samples employing TPAs^+Cl^- and/or TPP^+Br^- as ion-pair reagents. The script also discusses the extraction mechanism, equilibria and thermodynamic stability of the produced complex ion-associates.

2. Experimental

2.1. Reagents and materials

All chemicals and solvents used were of analytical reagent grade quality and were used without further purification. Doubly deionized distilled water was used throughout. Stock solutions (1%, w/v) of TPAs^+Cl^- and TPP^+Br^- were prepared separately by dissolving an accurate weight of the compound in water adjusted to pH 0 with hydrochloric acid (1 M). A stock solution of chromium(VI) (1 mg/ml) was prepared by dissolving an accurate weight of K_2CrO_4 in water (100 ml) at pH \sim 0. A series of standard chromium(VI) solutions were then prepared in water at pH \sim 0.

2.2. Apparatus

Infrared (IR) spectra were measured on FT-IR spectrophotometer model IFS 66. Microanalyses (C, H, Cl) were performed on a Perkin-Elmer, 240 C elemental analyzer, Plymouth University, UK. A Shimadzu double beam UV-vis (UV-1607pc) and a single beam Digital Spectro UV-vis RS Labomed, spectrophotometers with quartz cell (10 mm path length) were used for recording the solution electronic spectra and the absorbance of the produced complex ion-associates in the organic solvent. A pH meter model 3305 (JENWAY) was used for the pH measurements. 2.3. Recommended procedures

2.3.1. Determination of chromium(VI)

An aqueous solution of chromium(VI) ions (10 ml, 20 g/ml) at pH 0 employing HCl (1 M) was transferred to a 100 ml separating funnel. To this solution, a 2 ml of the reagent TPAs^+Cl^- or TPP^+Br^- and water were then added to give a total volume of 25 ml of the aqueous solution. The reaction mixture was mixed well and extracted twice (2×2.5 ml) with chloroform. The extracts were then collected in a dry 25 ml beaker containing anhydrous sodium sulphate (\sim 1 g), swirled to mix and transferred to a 10 ml volumetric flask. The residue was washed twice with another 5 ml (2×2.5) of chloroform and the washings were then transferred to the flask and completed to the mark with the same solvent. The absorbance of the organic phase was then measured at 355 nm with reference to the extract of reagent blank test.

2.3.2. Determination of chromium(III)

To a known volume (10 ml) of an aqueous solution containing ≤ 20 ppm chromium(III) in 50 ml conical flask, hydrogen peroxide (0.5 ml, 30%, w/v) solution was added and the pH of the solution was adjusted to pH \sim 9 with few drops of saturated NaOH. The reaction mixture was boiled for few minutes, allowed to cool and the pH of the reaction mixture was then adjusted to pH 0 with few drops of concentrated HCl. The solution mixture was transferred with the water washing solutions to a 50 ml separating funnel. To the mixture, 2 ml of the reagent TPAs^+Cl^- or TPP^+Br^- and 10 ml (2×5) of chloroform were then added. The absorbance of the produced ion-pair in chloroform layer was measured as described for chromium(VI) determination versus a reagent blank test in the presence of hydrogen peroxide.

2.3.3. Analysis of binary mixtures of chromium(III,VI)

Transfer an aliquot (10 ml) of a mixture containing chromium(III,VI) at a total concentration ≤ 20 g/ml to a 50 ml separating funnel. Analyze the mixture according to the described procedure for chromium(VI). Treat another aliquot as described for chromium(III) determination. On the basis of the proposed procedures, the absorbance (A_1) of the organic extract of the first aliquot will be a measure of the chromium(VI) in the mixture, while the absorbance (A_2) of the chloroform extract of the second aliquot is a measure of the sum of the chromium(VI) and (III) ions. Therefore, the absorbance ($A_2 - A_1$) is a measure of the chromium(III) ions.

2.3.4. Analysis of chromium(VI) and total chromium(III,VI) in wastewater samples

2.3.4.1. Direct determination. Industrial wastewater samples were first filtered with 0.22 m nuclepore filter. An aliquot of 10 ml of the sample is pipetted into a 50 ml separating funnel, adjusted to pH 0 with HCl (1 M) and a 2 ml of the reagent TPAs^+Cl^- or TPP^+Br^- were then added. The reaction mixture was then completed with water to a total volume of 25 ml in

the presence of few drops of saturated NaF and EDTA and mixed well. Analyze the mixture according to the described procedure for chromium(VI) determination. Treat another aliquot sample (10 ml) as described earlier for chromium(III) determination. The concentration of chromium(VI) and total chromium(III,VI) were then determined from the standard curves of chromium(III,VI).

2.3.4.2. Standard addition. Alternatively, the standard addition (spiking) method was used as follows: transfer a known volume (10 ml) of the test solution at pH 0 and 2 ml of the reagent TPAs⁺Cl⁻ or TPP⁺Br⁻ into a 50 ml separating funnel. Measure the absorbance displayed by the test solution as described for chromium(VI) determination before and after addition of various concentration (5–20 g/ml) of chromium(VI). The change in the absorbance was then recorded and used for determining the chromium(VI). Treat another aliquot of the test sample (10 ml) as described earlier for chromium(III) before and after addition of various concentrations (5–20 g/ml) of chromium(III). Chromium(III) and the total chromium(III,VI) were then determined as described.

3. Results and discussion

3.1. Extraction spectrophotometry

On mixing chromium(VI) with the reagent TPAs⁺Cl⁻ or TPP⁺Br⁻ in aqueous solution containing HCl (1 M) and shaking with chloroform, yellow-colored complex ion-associates were developed in the organic phase. The absorption spectra of the produced complex ion-associates in chloroform are given in Fig. 1. In the spectra of the ion-associates, only one well-defined absorption maximum at 355 nm was observed. The absorption spectrum of the reagent blank TPAs⁺Cl⁻ or TPP⁺Br⁻ against pure CHCl₃ indicated that the two reagents practically do not absorb in the tested region (300–600 nm). Therefore, in the subsequent work the absorbance measurements were carried out at 355 nm against reagent blank in chloroform.

To optimize the reaction conditions, the influence of pH of the aqueous phase on the formation and solvent extraction of the complex ion-associate of chromium(VI) with the reagent TPAs⁺Cl⁻ or TPP⁺Br⁻ was studied by measuring the absorbance in chloroform extract at 355 nm. The final pH of each aqueous solution was adjusted with dilute HCl and/or NaOH before the extraction. Maximum absorbance

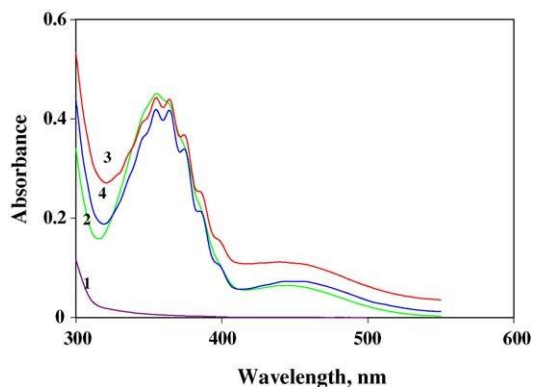


Fig. 1. Absorption spectra of the reagent (1), the chromium(VI) ions (2) in aqueous phase and the complex ion-associate of chromium(VI) with TPAs⁺Cl⁻ (3) and TPP⁺Br⁻ (4) in chloroform.

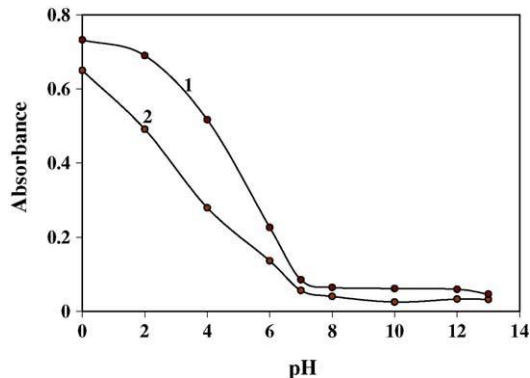
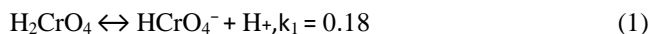
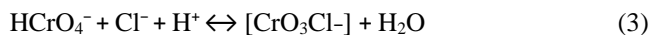


Fig. 2. Effect of pH on the extraction of the developed complex ion-associate of chromium(VI) with TPAs⁺Cl⁻ (1) and TPP⁺Br⁻ (2).

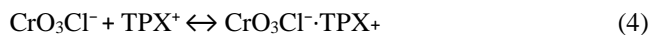
of the produced complex ion-associates was obtained at pH 0 (Fig. 2). At pH ≤ 0, chromium(VI) exists only as oxospecies, which are rapidly hydrolyzed in the aqueous solution generating neutral, anionic or oxoanions species depending on the pH, chromium(VI) concentration and ionic strength [18]. The most studied chemical equilibria [19] involving chromium(VI) are:



Thus, at low pH, the second equilibrium (Eq. (2)) moves to the left and the quantity of HCrO₄⁻ ions increases. According to Balogh et al. [20] postulation, the produced HCrO₄⁻ species in HCl ≥ 1 M are converted to chloro chromate anion (CrO₃Cl⁻) according to the equation:



which are directly proportional to the quantity of the produced complex ion-associate in the organic layer as follows:



where, X = As or P. The absorbance of the extracted species decreased with increasing pH possibly due to the formation of non-extracted forms of chromium(VI) or because of the hydrolysis of the formed complex ion-associate [21].

The stability of the produced ion-associates was found to depend considerably on the acidity of the aqueous phase. Thus, the effect of mineral acids HCl, H₂SO₄, HNO₃ and

HClO₄ at 1 M concentration upon the extraction of the complex ion-associate of chromium(VI) with the ion-pair reagent TPAs⁺Cl⁻ or TPP⁺Br⁻ was studied. The data revealed that, the nature of the mineral acid contributes substantially to the maximum extraction of the produced complex ion-associate of chromium(VI) and good results were easily achieved with HCl.

The influence of HCl concentration on the formation and solvent extraction of the complex ion-associates of chromium(VI) was investigated. Maximum extraction was obtained at 1 M HCl concentration. At high HCl acidity (>1 M) of the aqueous phase, the extraction of the formed ion-associates decreased due to the possible reduction of chromium(VI) to the more stable lower valent state chromium(III), which has no ability to form complex ion-associate with the tested reagents. The observed behavior could also be due to the decrease of the reaction rate of formation the complex ion-associate and transition of chromium(VI) to non-ionic forms which are less or not extractable in chloroform.

The extraction performance of the produced complex ion-associates CrO₃Cl⁻·TPX⁺ in: *n*-hexane, dichloromethane, carbon tetrachloride, toluene, chloroform and methyl isobutyl ketone was investigated. The extraction percentage followed the order: dichloromethane ≥ chloroform > toluene ≥ methyl isobutyl ketone > *n*-hexane ≈ carbon tetrachloride in good agreement with the order of the dielectric constants of the diluents. Good extraction with maximum apparent molar absorptivity, stability and solubility were achieved in dichloromethane and chloroform. Chloroform was chosen in the subsequent work as the preferred organic solvent because (i) the extraction is complete in a very short time; (ii) its greater density allows a better separation of phases and finally, (iii) chromium(VI) and the tested reagents are also do not extract into this solvent.

The extraction performance of the complex ion-associate CrO₃Cl⁻·TPX⁺ after shaking with chloroform for different time intervals ranging from 30 s to 5 min was measured. The extraction is rapid, maximum and constant absorbance was achieved at shaking time of 1 min or more. Thus, in the subsequent work a 2-min shaking time was adopted for maximum extraction. The developed yellow-colored complex ion-associates in chloroform were found stable for up to 3 h for samples containing ≤20 ppm chromium(IV) in the aqueous solution at pH 0 (1 M HCl).

The influence of the surfactants sodium dodecyl sulphate (anionic), tetramethyl ammonium chloride (cationic) and Toctylphenoxy polyether (neutral) on the development of the colored complex ion-associate CrO₃Cl⁻·TPX⁺ has been investigated. Sodium dodecyl sulphate (SDS) caused turbidity with emulsion formation and the absorbance value of the organic extract decreased. Therefore, SDS was omitted from the investigation. The distribution ratios of the complex ion-associate CrO₃Cl⁻·TPX⁺ decreased gradually with

increasing the cationic or neutral surfactant concentration. The increase of the solution viscosity leading to a progressive change in the physical properties of the microenvironment of the formed complex ion-associate may account for such behavior. This effect also enhances the dissociation of the complex ion-associate and increases the formation of aggregate complexes with low diffusion constants [22]. The competition of the surfactant and the ion-pair reagent TPAs⁺Cl⁻ or TPP⁺Br⁻ towards CrO₃Cl⁻ anion may also account for such behavior.

The influence of the ion-pair reagent TPAs⁺Cl⁻ or TPP⁺Br⁻ concentration on the solvent extraction of the produced complex ion-associate at the optimum experimental

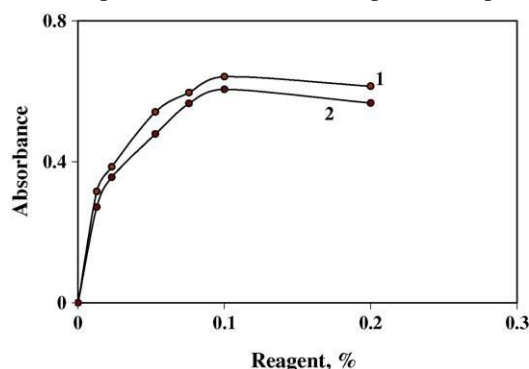


Fig. 3. Effect of the reagent TPAs⁺Cl⁻ (1) and TPP⁺Br⁻ (2) concentration (% w/v) on the solvent extraction of the developed chromium(VI) ion-associate.

conditions was studied. The results are shown in Fig. 3. The absorbance of the organic extract (CrO₃Cl⁻·TPX⁺) of aqueous solutions containing ≤20 g/ml of chromium(VI) and various amounts of the ion-pair reagent was measured in chloroform. It has been found that, 2 ml of 0.1% (w/v) of both TPAs⁺Cl⁻ and TPP⁺Br⁻ are sufficient to extract up to 200 g of chromium(VI) in a double extraction with chloroform (2 × 5 ml). A large excess of the reagent concentration tends to decrease the absorbance possibly owing to the increased absorbance of the reagent blank. Amounts of the reagents smaller than the recommended value gave incomplete complex formation. Therefore, in the subsequent work extractions are carried out using 2 ml of 0.1% (w/v) of the reagent TPA⁺Cl⁻ or TPP⁺Br⁻.

3.2. Spectrophotometric characteristics of chromium(VI) associates

After adjusting the experimental conditions, linear graphs at 355 nm were obtained on plotting the absorbance of the produced ion-associates CrO₃Cl⁻·TPX⁺ in chloroform versus chromium(VI) ions concentration. Beer–Lambert's law was obeyed between 1 and 50 ppm chromium(VI) in aqueous solution of pH 0. The molar absorptivities calculated from

Beer's law and Sandell's sensitivity indexes [23] of the $\text{CrO}_3\text{Cl}^- \cdot \text{TPAs}^+$ and $\text{CrO}_3\text{Cl}^- \cdot \text{TPP}^+$ at 355 nm in chloroform were found equal to $1.7 \pm 0.1 \times 10^4$, $1.4 \pm 0.12 \times 10^4 \text{ l mol}^{-1} \text{ cm}^{-1}$ and 0.003, 0.0038 g cm^{-2} , respectively. The relative standard deviation of five measurements with 20 ppm of chromium(VI) employing the reagent TPAs^+Cl^- and TPP^+Br^- was found equal to 0.31 and 0.61%, respectively. A detection limit (3) [24] of 0.01 ppm chromium(VI) was also achieved. Regression analysis of the complex ion-associates $\text{CrO}_3\text{Cl}^- \cdot \text{TPAs}^+$ and $\text{CrO}_3\text{Cl}^- \cdot \text{TPP}^+$ at 355 nm (A_{355}) in the range of 1–50 ppm of chromium(VI) gave the following linear regression equations:

$$A_{355} = 0.0135C + 0.0359 \quad (5)$$

and

$$A_{355} = 0.0125C + 0.026 \quad (6)$$

respectively, where A_{355} is the absorbance of the complex ion-associate at 355 nm and C is the molar concentration of chromium(VI) ions. Correlation coefficients of 0.997 and 0.999 for the complex ion-associates were obtained, respectively. The effective concentration range of chromium(VI) measured by Ringbom's plot (transmittance, % versus log chromium(VI)) [25] at 355 nm was found 5–40 ppm.

The extracted amount of chromium(VI) from the bulk aqueous solution into the organic phase as $\text{CrO}_3\text{Cl}^- \cdot \text{TPX}^+$ versus the amount of chromium(VI) in the aqueous phase was relatively high followed by a plateau. At low or moderate chromium(VI) concentration, the amount of chromium(VI) ions extracted into the organic phase varied linearly with that remained in the bulk aqueous solution suggesting the first-order behavior. A solvent capacity of 3.2 and 2.61 g chromium(VI) ions uptake/ml chloroform was successfully achieved with TPAs^+Cl^- and TPP^+Br^- , respectively.

3.3. Characterization of the chromium(VI) ion-associates

The chemical composition of the developed complex ion-associate M^+X_n^- in chloroform was determined by Job's method [26]. A plot of the absorbance of the organic extract at 355 nm versus the mole fraction of the reagent TPAs^+Cl^- or TPP^+Br^- produced a graph that indicated the formation of an ion-association complex having a chromium(VI) to a reagent ratio of exactly 1:1. The chemical compositions of the ion-associates $\text{CrO}_3\text{Cl}^- \cdot \text{TPX}^+$ were also confirmed from the mole ratio method [27].

With a 1:1 complex ion-associate, for which the Job's method is applicable and assuming only one complex species is formed, the ratio of the true absorbance (A) to the extrapolated (A_{extp}) absorbance is a measure of the mole fraction of the complex ion-associate M^+X_n^- actually formed [27] via

the reaction:



Thus,

$$[\text{MX}] = \frac{A}{A_{\text{extp}}} C \quad (8)$$

The stability constant (K) of the complex ion-associate was

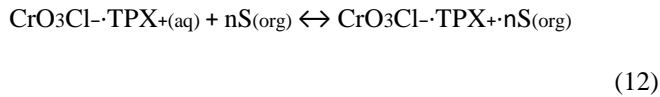
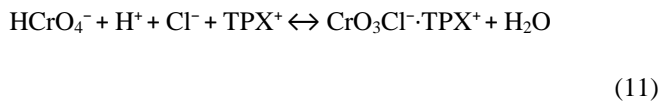
then calculated employing the equation:

$$k = \frac{(A/A_{\text{extp}})C}{[C_m (A/A_{\text{extp}})C][C_x (A/A_{\text{extp}})C]} \quad (9)$$

where C is the total analytical concentration of the metal (C_m) or ligand (C_x), whichever is the limiting concentration at the point in question. The values of the stability constants of the produced complex ion-associates of chromium(VI) with the reagents TPAs^+Cl^- and TPP^+Br^- were found equal to 5.6×10^4 and 5.7×10^4 , respectively.

The solid complex ion-associates were isolated from the organic phase after solvent evaporation under reduced pressure. The produced ion-associates were then characterized from their elemental analysis: $\text{CrO}_3\text{Cl}^- \cdot \text{TPAs}^+$ required 55.54% C, 3.86% H, 6.83% Cl; found 56.69% C, 4.13% H, 6.94% Cl; $\text{CrO}_3\text{Cl}^- \cdot \text{TPP}^+$ required 60.7% C, 4.2% H, 7.81% Cl; found 62.1% C, 4.17% H and 7.7% Cl). The characteristics infrared frequencies (IR) of the isolated complex ion-associates in KBr discs were compared with those of chromium(VI) and the ion-pair reagent, TPAs^+Cl^- or TPP^+Br^- recorded separately in KBr discs and as a mechanical mixture of chromium(VI) with the extractants in 1:1 mole ratio. The IR spectra of the isolated compounds showed the absorption bands characteristic of both chromium(VI) and the tested reagents but with some differences ascribed to the formation of the complex ion-associates. A common feature in the IR spectra of the produced complex ion-associates is the presence of symmetric and antisymmetric stretching modes of the $\nu \text{Cr}=\text{O}$ at 995 and 907 cm^{-1} [28]. Another band at 430 cm^{-1} is observed, which is assigned to $\nu \text{Cr Cl}$ stretching vibration [28]. This band is not observed in the IR spectra of chromium(VI) and the ion-pair reagents. Thus, the proposed chemical structures of the ion-associates are different from that suggested by Burns et al [29]. Therefore, the most

probable overall reaction mechanism for the formation of the complex ion-associate is most likely proceeds as follows:



where S is the extractant, (aq) the aqueous phase and (org) the organic phase.

3.4. Extraction equilibria

To calculate the formation constants K_{ex} , D and β of the produced complex ion-associates of chromium(VI) with the ion-pair reagents TPAs^+Cl^- and TPP^+Br^- in HCl (1 M), the following extraction equilibria were considered [30].

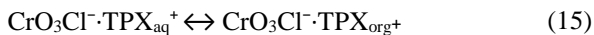
- (i) Formation of a complex ion-associate in the aqueous phase according to the reaction:



with an ion-associate constant, β

$$\beta = \frac{[\text{CrO}_3\text{Cl}^- \cdot \text{TPX}^+]_{\text{aq}}}{[\text{CrO}_3\text{Cl}^-]_{\text{aq}}[\text{TPX}^+]_{\text{aq}}} \quad (14)$$

- (ii) Distribution of the complex ion-associate between the aqueous and the organic phase:



with a distribution constant, D

$$D = \frac{[\text{CrO}_3\text{Cl}^- \cdot \text{TPX}^+]_{\text{org}}}{[\text{CrO}_3\text{Cl}^- \cdot \text{TPX}^+]_{\text{aq}}} \quad (16)$$

Chromium species, ppm				Recovery, % ^a	
Cr(III)		Cr(VI)		Cr(III)	Cr(VI)
Taken	Found	Taken	Found		
5	5.1	5	5	102 ± 2.3	100 ± 2.4
10	10.4	5	5	104 ± 1.5	100 ± 3.1

- (iii) The overall extraction process can be expressed as:



with a corresponding extraction constant, K_{ex}

$$K_{\text{ex}} = \frac{[\text{CrO}_3\text{Cl}^- \cdot \text{TPX}^+]_{\text{org}}}{[\text{TPX}^+]} D\beta \quad (18)$$

Assuming the species CrO_3Cl^- is present only in the organic phase at equilibrium, the distribution ratio $D_{\text{CrO}_3\text{Cl}^-}$ can then be determined at a constant total CrO_3Cl^- concentration in the aqueous phase and various amounts of the reagent $[\text{TPX}^+]$ employing the equation:

$$D_{\text{CrO}_3\text{Cl}^-} = \frac{[\text{CrO}_3\text{Cl}^- \cdot \text{TPX}^+]_{\text{org}}}{[\text{CrO}_3\text{Cl}^- \cdot \text{TPX}^+]_{\text{aq}} + [\text{CrO}_3\text{Cl}^-]_{\text{aq}}} \quad (19)$$

At low concentration of TPX^+Y^- ($\text{Y} = \text{Cl}$ or Br), the term $[\text{CrO}_3\text{Cl}^- \cdot \text{TPX}^+]_{\text{aq}}$ can be neglected and Eq. (19) transforms into the following equation [31]:

$$D_{\text{CrO}_3\text{Cl}^-} = \frac{[\text{CrO}_3\text{Cl}^- \cdot \text{TPX}^+]_{\text{org}}}{[\text{CrO}_3\text{Cl}^-]_{\text{aq}}} \quad (20)$$

After substituting Eq. (20) into Eq. (13) and taking the logarithms, the following equation:

$$\log D_{\text{CrO}_3\text{Cl}^-} = \log D\beta + \log [\text{TPX}]_{\text{f}} \quad (21)$$

is then obtained. The β , K_{ex} and D values were then determined graphically from the plots of the distribution ratio, $\log D_{\text{CrO}_3\text{Cl}^-}$ versus $\log [\text{TPX}^+]$ for both reagents (Fig. 4). The values of K_{ex} , D and β were found equal to $2.5 \pm 0.1 \times 10^4$, $2.29 \pm 0.2 \times 10^4 \text{ l mol}^{-1}$, 26.2 ± 0.3 ,

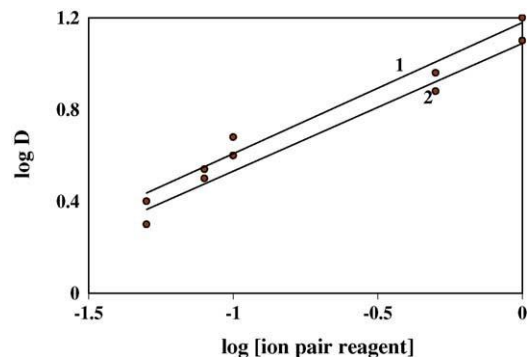


Fig. 4. Plot of the $\log D$ of the developed chromium(VI) ion-associate vs. \log of the reagent TPAs^+Cl^- (1) and TPP^+Br^- (2) concentration at 1M of HCl.

Table 1

Analytical results for the binary mixtures of chromium(III,VI)

10	10	10^a	9.9	100 ± 2.1	99 ± 2.6
Average ($n=5$) ± S.D.					

23.8 ± 0.26 and $1.0 \pm 0.1 \times 10^3$, $8.9 \pm 0.1 \times 10^2$ mol⁻¹ for both TPAs⁺Cl⁻ and TPP⁺Br⁻, respectively. The linear plots of log *D* versus log [TPX⁺Y⁻] at pH 0 (Fig. 4) gave

slopes of 1.0 ± 0.1 confirming the existence of monovalent chromium(VI) as CrO₃Cl⁻ ion and the absence of non-specific interaction between the extracted complex ionassociates and the ion-pair reagents TPAs⁺Cl⁻ or TPP⁺Br⁻ [32]. Therefore, the most probable composition of the extracted species is 1:1 (CrO₃Cl⁻:TPX⁺). These results confirm the data obtained from continuous variation and mole ratio methods.

3.5. Analysis of the binary mixtures of chromium(III,VI)

Analysis of binary mixtures of chromium(III,VI) ions in the aqueous media was carried out by the developed method. The results are summarized in Table 1. Satisfactory results for the determination of various amounts of chromium(III,VI) were obtained with recovery percentages in the range $(100-104) \pm 2.3$ and $(99-100) \pm 3.1$, respectively.

3.6. Effect of diverse ions

The influence of a series of diverse ions on the extraction and determination of chromium(VI) with the reagents TPAs⁺Cl⁻ and TPP⁺Br⁻ was investigated. The tolerance limit was defined as the concentration of the foreign ion added causing a relative error less than $\pm 3\%$. The selectivity of the developed method at 5 g/ml of chromium(VI) was critically examined in the presence of a relatively high excess (10 mg) of some diverse ions, which are often accompanying with the analyte ion. A percentage recovery of $100 \pm 1.5\%$ with a standard deviation of ± 0.3 was achieved in the presence of the ions: Li⁺, Na⁺, K⁺, Ca²⁺, NH₄⁺, Co²⁺, Ni²⁺, Al³⁺, Cd²⁺, Hg²⁺, Zn²⁺, Cr³⁺, Cl⁻, Br⁻, I⁻, NO₂⁻, PO₄³⁻, SO₄²⁻ and N₃⁻. Positive interferences were observed in the presence of some other ions, e.g. Cu²⁺, Fe²⁺, Pb²⁺, Mn⁷⁺, V⁵⁺ and NO₃⁻. For removal of these interferences from the proposed method, simple modifications were introduced in the aqueous solution (Table 2). After employing these modifications, the tolerance level of the interfering ions was improved to a great extent.

Table 2

Effect of some diverse ions on the determination of 5g/ml chromium(VI)

Foreign ions	Tolerance limit, ppm (weight of interfering ions/weight of Cr ⁶⁺)	Note
Cu ²⁺	200	Add one crystal of KI and Na ₂ S ₂ O ₃
Fe ³⁺	200	Add 1ml of NaF (1M)
Pb ²⁺	200	Add one crystal of NaF
Mn ⁷⁺	500	Add one crystal of NaN ₃
V ⁵⁺	500	Add H ₂ O ₂ +NaOH and boil
NO ₃ ⁻	100	Add few crystals of NaN ₃

3.7. Applications

The validity of the proposed method for the determination of chromium(III,VI) in tap and wastewater samples was critically examined. Various amounts of chromium(VI) or binary mixture of chromium(III,VI) were spiked to the tap water samples. Each reaction mixture was adjusted to pH ~0 and the chromium(VI) ions were first determined as described earlier with the aid of the standard curve constructed for CrO₃Cl⁻·TPX⁺ complex ion-associate under the same experimental conditions. The total chromium(III,VI) ions were then determined after prior oxidation of chromium(III) ions present in the tap water samples with H₂O₂ as described earlier for chromium(III) ions determination. Chromium(III) ions in the water samples were then determined by the difference (A₂ - A₁) between the absorbance of the first (A₁) and second (A₂) aliquots. The data obtained for the tap water samples are summarized in Table 3. On the basis of these results, tap water samples were found free from chromium(III) and/or (VI). These results were also confirmed from the atomic absorption spectrometry (AAS) measurements of chromium ions in tap water samples with good reproducibility.

The developed method was also applied successfully for the analysis of chromium(VI) and total chromium(III,VI) in wastewater samples of electroplating plant employing direct calibration and standard addition procedures (Fig. 5). The results obtained for the total chromium by direct calibration graph (2.9 ± 0.1 ppm) and standard addition (3.1 ± 0.12 ppm) are in excellent agreement with the certified values determined by AAS (3.11 ± 0.1 ppm). The results of the developed method also indicated the ab-

Table 3

Analytical results of tap water samples (50ml)

Cr(VI) added, ppm	Cr(III) added, ppm	Total Cr(III,VI) found, ppm ^a
20	—	20.1 ± 0.15
30	—	30 ± 0.18
20	20	39.8 ± 0.12
30	30	60 ± 0.3

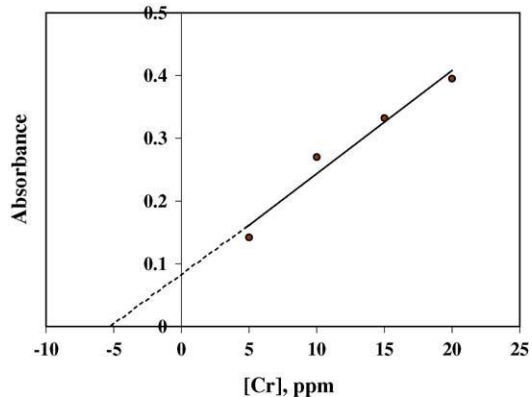
^a Average (n=5)±S.D.

Fig. 5. Determination of chromium(VI) in industrial wastewater by the standard addition method.

sence of chromium(III) in the tested industrial wastewater samples.

References

- [1] E. Merian, Metals and Their Compounds in the Environment, Occurrence, Analysis and Biological References, VCH, 1980.
- [2] W. Mertz, Trace Elements in Human and Animal Nutrition, Academic Press, London, 1986.
- [3] J.R. Holum, Elements of General Organic and Biological Chemistry, 9th ed., Wiley, 1995.
- [4] USEPA Method 7196A, Chromium, Hexavalent (Colorimetric), 1992.
- [5] V.M. Shinde, S.M. Khopkar, Fresen. Z. Anal. Chem. 249 (1970) 239.
- [6] J. Adam, Talanta 18 (1971) 91.
- [7] G.B. Fasolo, R. Malvano, A. Massaglia, Anal. Chim. Acta 29 (1963) 569.
- [8] W.J. Maeck, M.E. Kussy, J.E. Rein, Anal. Chem. 34 (1962) 1602.
- [9] C.K. Mann, J.C. White, Anal. Chem. 30 (1958) 989.
- [10] R.K. Brookshier, H. Freund, Anal. Chem. 23 (1951) 1110.
- [11] M.N. Sastri, D.S. Sundar, Fresen. Z. Anal. Chem. 195 (1963) 343.
- [12] M.N. Sastri, D.S. Sundar, Anal. Chim. Acta 33 (1965) 340.
- [13] X. Zhu, B. Hu, Z. Jiang, Y. Wu, S. Xiong, Anal. Chim. Acta 471 (2002) 121.
- [14] O. Dom'nguez, M.J. Arcos, Anal. Chim. Acta 470 (2002) 241.
- [15] I. Lopez-Garcia, B.M. Merono, N. Campillo, M. HernandezCordoba, Anal. Bioanal. Chem. 373 (2002) 98.
- [16] I.P.A. Morais, M.R.S. Souto, A.O.S.S. Rangel, Anal. Bioanal. Chem. 373 (2002) 119.
- [17] S. Cathum, C.E. Brown, W. Wong, Anal. Bioanal. Chem. 373 (2002) 103.
- [18] J.J. Cruywagen, J.B.B. Heyns, E.A. Rohwer, Polyhedron 17 (1998) 1741.
- [19] T.C. Huang, C.C. Huang, D.H. Chen, Solvent Extr. Ion Exch. 15 (1997) 837.

- [20] I.S. Balogh, I.M. Maga, A. Hargitai-Toth, V. Andruch, *Talanta* 53 (2000) 543.
- [21] S. Yamaguchi, K. Uesugi, *Analyst* (London) 109 (1984) 1393.
- [22] J. Babcock, *J. Memb. Sci.* 7 (1980) 71.
- [23] E.B. Sandell, *Colorimetric Determination of Trace Metals*, Interscience, New York, 1959.
- [24] J.E. Barmey, *Talanta* 14 (1967) 1363.
- [25] A. Ringbom, *Fresen. Z. Anal. Chem.* 115 (1939) 332.
- [26] P. Job, *Anal. Chim.* 11 (6) (1936) 97.
- [27] D.T. Sawyer, W.R. Heineman, J.M. Beebe, *Chemistry Experiments for Instrumental Methods*, Wiley, 1984.
- [28] M.N. Sastri, T.S.R. Prasada Rao, *J. Inorg. Nucl. Chem.* 30 (1968) 1727.
- [29] D.T. Burns, S.A. Barakat, M. Horriott, *Anal. Chim. Acta* 265 (1991) 126.
- [30] A. Alexandrov, O. Budevsky, A. Dimitrov, *J. Radioanal. Chem.* 29 (1976) 243.
- [31] S.M. Kamurova, *Talanta* 39 (1992) 997.
- [32] N. Condamines, C. Musikas, *Solvent Extr. Ion. Exch.* 10 (1992) 69.



Short communication

Differential pulse voltammetric determination of the dopaminergic agonist bromocriptine at glassy carbon electrode

A. Radi*, M.S. El-Shahawi, T. Elmogy

Department of Chemistry, Faculty of Science, Mansoura University, 34517 Dumyat, Egypt

Received 2 May 2004; received in revised form 6 October 2004; accepted 10 October 2004

Available online 23 November 2004

Abstract

The electrochemical oxidation of bromocriptine at glassy carbon electrode has been carried out in Britton–Robinson (B–R) buffer solutions in the pH range 2.0–11.0 employing cyclic, linear sweep and differential pulse voltammetry (DPV). Bromocriptine showed one well-defined oxidation peak accompanied by a smaller one. The oxidation process was found irreversible. For analytical purposes, the well-resolved diffusion controlled voltammetric peak at pH 5 was critically investigated. The linear relationship between peak current height and bromocriptine concentration allowed the differential pulse voltammetric determination of the drug over a wide concentration range, from 0.04 to 5.00 gml⁻¹ with a detection limit of 0.01 gml⁻¹. A relative standard deviation of 1.44% at 0.1 gml⁻¹ level was obtained. The proposed DPV method was successfully applied for the individual tablet assay to verify the uniformity content of bromocriptine in commercial tablets. © 2004 Published by Elsevier B.V.

Keywords: Bromocriptine; Differential pulse voltammetry; Glassy carbon electrode; Electrochemical oxidation; Pharmaceutical analysis

1. Introduction

The semi-synthetic ergot alkaloid bromocriptine [1] exhibits several therapeutic effects [2–6]: (i) it has a beneficial effect in severely disabled patients suffering from Parkinson's disease, (ii) it is used, like other ergot alkaloids, in the treatment of migraine, and (iii) it is a strong inhibitor of prolactin formation and have therapeutic potency in the treatment of hyperprolactinaemia. These effects have been related to its ability to block dopamine receptors and to its interaction with calmodulin-induced activation of phosphodiesterases in human brain [7,8].

Several analytical procedures have been published for quantification of bromocriptine levels in biological fluids. Radioimmunoassay methods have been used to measure bromocriptine in rat tissue and in human plasma [9,10].

* Corresponding author. Tel.: +20 57 403 866; fax: +20 57 403 868. E-mail address: abdradi@yahoo.com (A. Radi).

0731-7085/\$ – see front matter © 2004 Published by Elsevier B.V.
doi:10.1016/j.jpba.2004.10.013

Gas chromatographic, mass spectrometric and liquid chromatographic techniques have been described for the determinations of bromocriptine in human plasma [11–14]. High-performance liquid chromatographic (HPLC) methods with UV or MS detector have also been reported [15–16]. Few reports for the determination of the drug in formulations including X-ray fluorescence spectroscopic analysis [17] and high-performance liquid chromatography [18] have been published.

So far, it seems that, no report has been appeared in the literature on the electrochemical redox properties of bromocriptine. Electroanalytical techniques, especially

modern pulse techniques, such as differential pulse have been used for the determination of a wide range of pharmaceuticals [19]. Thus, the present paper describes the electrochemical behavior of bromocriptine at a glassy carbon electrode using cyclic, linear sweep and differential pulse voltammetry and the analytical

determination of the title drug in tablets by differential pulse voltammetry.

A. Radi et al. / Journal of Pharmaceutical and Biomedical Analysis 37 (2005) 195–198

2. Experimental

2.1. Apparatus

The voltammetric measurements were performed using a PC controlled AEW2 analytical electrochemical workstation with ECprog3 electrochemistry software (Sycopel, UK) connected to C-2 stand with a three-electrode configuration: a glassy carbon (BAS model MF-2012, $\varnothing = 3$ mm) working electrode, an Ag–AgCl–3 M KCl (BAS model MF-2063) reference electrode and a platinum wire (BAS model MW-1032) counter electrode. OriginPro 7.0 software was used for the transformation of the initial signal. A Schott Gerate CG 808^o digital pH meter with H 61 pH combination electrode (Mainz, Germany) was used for the pH measurements.

2.2. Reagents

Bromocriptine mesylate and Lactodel[®] tablets were obtained from (Amoun Phar., Cairo, Egypt). Stock solution of bromocriptine was prepared by dissolving the drug in methanol. Stock solution was stored under refrigeration and was stable for at least eight weeks. Working solutions of bromocriptine were obtained by serial dilution of the stock solution into methanol. Britton–Robinson buffers (0.04 M in each of acetic, orthophosphoric, and boric acids, adjusted to the required pH with 0.2 M sodium hydroxide) were used as supporting electrolytes. All solutions were prepared from AnalaR-grade reagents in double distilled water.

2.3. Procedure

A 10 ml of the electrolyte solution was transferred into the voltammetric cell. After measurement of the blank solution, the appropriate amount of bromocriptine solution was added and the anodic potential sweep was carried under different operational parameters. All measurements were carried out at room temperature. The peak heights were evaluated by means of the tangent method. The glassy carbon electrode was polished manually with alumina ($\varnothing = 0.01$ m) in the presence of bidistilled water on a smooth polishing cloth prior to each measurement.

2.3.1. Tablets assay procedure

One finely ground tablet of Lactodel[®] (amount declared 2.5 mg bromocriptine mesylate per tablet) was dissolved in 5 ml methanol. The contents were sonicated for 10 min to insure complete dissolution. A suitable amount of the supernatant liquor was diluted to 10 ml with 0.04 M B–R buffer solution at pH 5.0 to obtain a bromocriptine concentration of 0.10 g ml⁻¹. The sample solution was transferred to a voltammetric cell and recorded at least twice

following the optimized experimental conditions. The amount of bromocriptine (mg) in the sample solution was calculated from the prepared standard calibration plot.

3. Results and discussion

Preliminary differential pulse voltammetry experiments of 1.0 g ml⁻¹ bromocriptine in B–R buffer over the pH range 2.0–11.0 at glassy carbon electrode were carried out. Representative differential pulse voltammograms are shown in Fig. 1. At the investigated pH, one well-defined peak was observed accompanied by a smaller one. Thus, in the subsequent work the study was focused mainly on the first oxidation peak because of its analytical interest. The plot of E_{p1} versus pH showed two straight lines (Fig. 2a), which can be expressed by the following equations in differential pulse voltammetry in B–R buffer: E_{p1} (V) = 1.011 + 0.070 pH, $r = 0.996$ and E_{p1} (V) = 0.070 + 0.025 pH, $r = 0.997$. The intersection observed in the plot at pH 7 is most likely attributed to a change in protonation–deprotonation process of the electroactive indolic moiety in the molecular structure of bromocriptine. The best results with respect to signal enhancement (Fig. 2b) accompanied by sharper response was obtained with B–R buffer at pH 5.0. Thus, this supporting electrolyte was chosen for subsequent measurement experiments.

Cyclic voltammetry was also used to investigate the anodic oxidation of bromocriptine. A typical cyclic

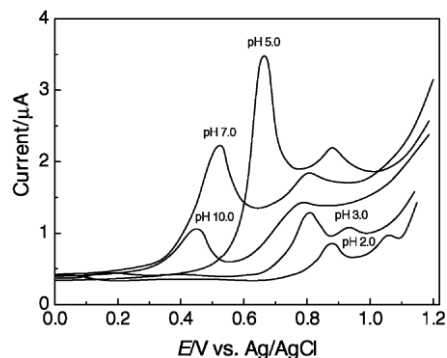


Fig. 1. Differential pulse voltammograms for 1.0 g ml⁻¹ bromocriptine in B–R buffers of different pH values, at glassy carbon electrode. Scan rate, 10 mVs⁻¹; pulse amplitude, 50 mV; pulse width, 30 ms.

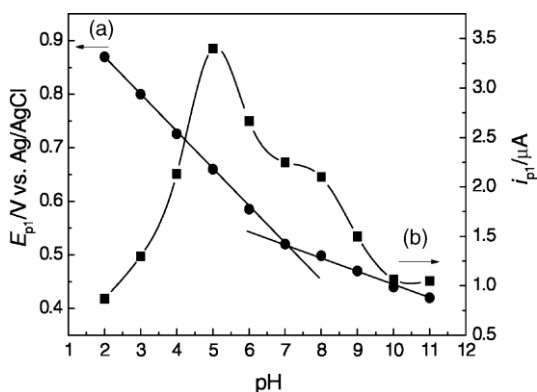


Fig. 2. Effect of pH on (a) peak potential and (b) peak current in B-R buffer using differential pulse voltammetry at glassy carbon electrode. Bromocriptine concentration, 1.0gml⁻¹; scan rate, 10mVs⁻¹; pulse amplitude, 50mV; pulse width, 30s.

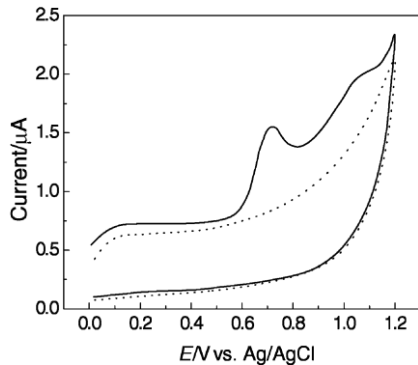


Fig. 3. Cyclic voltammograms of 10.0gml⁻¹ bromocriptine solution on glassy carbon electrode in B-R buffer at pH 5.0. Scan rate, 100mVs⁻¹. The dotted lines represent blank solution.

voltammogram of 10.0 g ml⁻¹ bromocriptine at glassy carbon electrode in Britton–Robinson buffer at pH 5.0 is shown in Fig. 3. Bromocriptine showed a main anodic peak followed by a smaller one. No reduction peaks were obtained in the reverse scans at any scan rate used (until 500 mV s⁻¹), suggesting the irreversible character of the overall process involved at the glassy carbon electrode.

Cyclic voltammograms recorded at different potential scan rates showed a positive shift in the peak potential, which confirms the irreversibility of the process, with a simultaneous increase in the peak current height when the scan rate was increased. The linear relationship existing between peak current and the square root of the scan rate (correlation coefficient 0.999) gave a slope of 0.90. The plot of logarithm of peak current versus logarithm of scan rate (v) also gave a straight line (correlation coefficient $r = 0.998$) with a slope of 0.55, close to the theoretical value of 0.5, which is expected for an ideal reaction of solution species [20], indicating that the oxidation process is predominantly diffusion-controlled in the whole range of scan rate studied.

The plot of the anodic peak potential (E_p) versus the logarithm of scan rate (v) was found linear, with a slope value $b = 2.303RT/\alpha n_a F$ of 0.082, where α is the charge transfer coefficient and n_a the number of electrons involved in the rate-determining step. The dependence of E_p on pH is $\partial E_p/\partial \text{pH} = mb$ [21], where m is the electrochemical reaction order with respect to the H⁺ ion. The experimental value was found around 0.070 V per pH unit, meaning that $m = 1$. These data are actually as expected for a one proton, one electron transfer process from the nitrogen atom of the indolic moiety in the rate-determining step.

3.1. Analytical application

In order to develop a voltammetric method for the determination the drug, we selected the differential pulse mode. Differential pulse mode yielded voltammogram in which the peak currents were greater than those obtained by cyclic and linear sweep voltammetry. The DP voltammograms (pulse amplitude, 50 mV; pulse width 50 ms; scan rate, 20 mV s⁻¹) showed successive enhancement of peak current on increasing bromocriptine concentration. An excellent calibration curve over a wide range 0.04–5.00 g ml⁻¹ was obtained. The calibration graph fitted the equation:

$$i_{p1} (\mu\text{A}) = (0.0289 \pm 0.0151) + (3.3997 \pm 0.0306) C (\text{g ml}^{-1}),$$

with a correlation coefficient $r = 0.9995$. The limit of

detection (LOD) of the developed procedure was calculated to be 0.01 g ml⁻¹, based upon the definition: $\text{LOD} = 3S_{y/x}/b$ [22], where $S_{y/x}$ is the standard deviation of y -residuals and b is the slope of the calibration plot. The reproducibility of the measurement was calculated for five independent runs of 1.0 g ml⁻¹ bromocriptine solution. The relative standard deviations were calculated to be 0.72 and 1.44% for peak potential and peak current, respectively.

The effect of various inactive ingredients (colloidal silicon dioxide, gelatin, lactose, magnesium stearate, silicon dioxide, sodium lauryl sulfate, starch, titanium dioxide, yellow iron oxide) in the bromocriptine tablets was examined carrying out the determination of 1.0 g ml⁻¹ bromocriptine by the developed method in the presence of each inactive ingredient at concentrations that can be found in the tablet dosage form. A deviation of more than 2% from the peak current of the solution containing no inactive ingredients was taken as a sign of interference. The results showed that the inactive ingredients in the bromocriptine tablets do not cause positive or negative error in the measurements, indicating that there was no interference to the method.

The proposed DP voltammetry method was applied for the individual tablet assay in order to verify the uniformity content of bromocriptine in tablets. The bromocriptine was commercially provided by Amoun Phar. (Cairo, Egypt)

presentation named Lactodel® tablets containing 2.5 mg of bromocriptine. High-performance liquid chromatography (HPLC) with UV [18] detector was chosen as a comparison method to evaluate the validity of the proposed voltammetric procedure. The results obtained by the proposed DPV were compared to those of the HPLC method utilizing certain statistical evaluations. The results of the statistical evaluations are demonstrated in Table 1. The results of *F*- and *t*-tests showed that there were insignificant differences between the two techniques. Moreover, The content for all assayed tablets falls within the claimed amount, fulfilling the

Table 1

Application of the proposed voltammetric method to the determination of bromocriptine analysis in single Lactodel® tablets

	Proposed voltammetric method	Reference HPLC method [18]
Labeled amount (mg)	2.50	2.25
<i>n</i>	6	6
\bar{x}	2.48	2.51
<i>s</i>	0.040	0.011
CL	±0.042 1.91	±0.012
<i>t</i> -test of significance	(2.23 ^a)	
<i>F</i> -test of significance	0.075 (5.05 ^a)	

^a The tabulated *t*- and *F*-values, respectively, at *P*=0.05.

198

A. Radi et al. / Journal of Pharmaceutical and Biomedical Analysis 37 (2005) 195–198

criteria of acceptance set according to the USP23 Uniformity of the Dosage Units [23]. Content uniformity test allows not a single one of the assayed tablets to deviate more than 10%.

4. Conclusions

The developed voltammetric method provides the advantage of simplicity, precision and reliability. It allows direct determination of bromocriptine by skipping several tedious sample preparation steps. The proposed method is free from the interferences of inactive ingredients used in the drug formulation. In this study, the glassy carbon electrode was selected, as it is very commonly used as electrochemical detector for HPLC and FIA techniques.

References

[1] US Pharmacopoeia, twenty seventh ed., US Convention, Rockville, MD, 2004, p. 266.
 [2] D. Parkes, in: N.J. Harper, A.B. Simmonds (Eds.), *Advances in Drug Research*, Academic Press, New York, 1977, pp. 247–344.
 [3] H.P. Weber, in: M. Goldstein (Ed.), *Ergot Compounds and Brain Function: Neuroendocrine and Neuropsychiatric Aspects*, Raven Press, New York, 1980, pp. 25–34.
 [4] K.Y. Ho, M.O. Thomer, *Drugs* 36 (1988) 67–82.

[5] F. Marzatico, C. Cafe, M. Taborelli, G. Benzi, *Neurochem. Res.* 18 (1993) 1101–1111.
 [6] E. Del Pozo, L. Varga, H. Wyss, G. Tolis, H. Friesen, R. Wenner, L. Vetter, A. Uettwiler, *J. Clin. Endocrinol. Metab.* 39 (1974) 18–26.
 [7] C.Q. Earl, W.C. Prozialeck, B. Weiss, *Life Sci.* 35 (1984) 525–534.
 [8] B. Weiss, W.C. Prozialeck, T.L. Wallace, *Biochem. Pharmacol.* 31 (1982) 2217–2226.
 [9] J.S. Bevan, D. Baldwin, C.W. Burke, *Ann. Clin. Biochem.* 23 (1986) 686–693.
 [10] D. Valente, E. Ezan, C. Creminon, M. Delaforge, H. Benech, P. Pradelles, J.M. Grognet, *J. Immunoassay* 17 (1996) 297–320.
 [11] N-E. Larsen, R. Ohman, M. Larsson, E.F. Hvidberg, *J. Chromatogr.* 174 (1979) 341–349.
 [12] K.H. Schellenberg, M. Linder, A. Groeppelin, F. Erni, *J. Chromatogr.* 394 (1987) 239–251.
 [13] N. Haering, Z. Salama, H. Jaeger, *Arzneim. Forsch.* 38 (1988) 1529–1532.
 [14] L.M. Nyholm, P.J.R. Sjoberg, K.E. Markides, *J. Chromatogr. A.* 755 (1996) 153–164.
 [15] D.G. Phelan, N.H. Greig, S.I. Rapoport, T.T. Soncrant, *J. Chromatogr.* 533 (1990) 264–270.
 [16] Y.J. Choi, M.K. Seo, I.C. Kim, Y.H. Lee, *J. Chromatogr. B* 694 (1997) 415–420.
 [17] M.A. Raggi, F. Lucchini, P. Da-Re, *Collect. Czech. Chem. Commun.* 56 (1991) 2229–2233.
 [18] N.H. Foda, F. El-Shafie, *J. Liq. Chromatogr. Relat. Technol.* 19 (1996) 3201–3209.
 [19] M.A. Brooks, in: P.T. Kissinger, W.R. Heineman (Eds.), *Laboratory Techniques in Electroanalytical Chemistry*, second ed., MarcelDekker, New York, 1996.
 [20] D.K. Gosser Jr., *Cyclic Voltammetry. Simulation and Analysis of Reaction Mechanisms*, VCH, New York, 1993, p. 43.
 [21] J.M. Rodriguez-Mellado, M. Blazquez, M. Dominguez, J.J. Ruiz, *J. Electroanal. Chem.* 195 (1985) 263–270.
 [22] J.C. Miller, J.N. Miller, *Statistics for Analytical Chemistry*, Ellis Horwood Series, PTR Prentice Hall, New York, London, 1993, p. 119.
 [23] US Pharmacopoeia, twenty-seventh ed., US Convention, Rockville, MD, 2004, p. 2396.



ELSEVIER

Spectroscopic, thermal and electrochemical studies on some nickel(II) thiosemicarbazone complexes

R.M. El-Shazly^a, G.A.A. Al-Hazmi^{a,*}, S.E. Ghazy^a,
M.S. El-Shahawi^b, A.A. El-Asmy^a

^a Chemistry Department, Faculty of Science, Mansoura University, Mansoura, Egypt

^b Chemistry Department, Faculty of Science, Mansoura University, Damietta, Egypt

Received 24 November 2003; received in revised form 18 February 2004; accepted 18 February 2004

Abstract

Several complexes of thiosemicarbazone derivatives with Ni(II) have been prepared. Structural investigation of the ligands and their complexes has been made based on elemental analysis, magnetic moment, spectral (UV–Vis, i.r., ¹H NMR, ms), and thermal studies. The i.r. spectra suggest the bidentate mononegative and tridentate (neutral, mono-, and binate) behavior of the ligands. Different stereochemistries were suggested for the isolated complexes. The thermogravimetry (TG) and derivative thermogravimetry (DTG) have been used to study the thermal decomposition and kinetic parameters of some ligands and complexes using the Coats-Redfern and Horowitz-Metzger equations. The redox properties and stability of the complexes toward oxidation waves explored by cyclic voltammetry are related to the electron withdrawing or releasing ability of the substituent of thiosemicarbazone moiety. The samples displayed Ni^{II}/Ni^I couples irreversible waves associated with Ni^{III}/Ni^{II} process.

© 2004 Elsevier B.V. All rights reserved.

Keywords: Nickel(II) complexes; Mass spectra; Thiosemicarbazone complexes; IR spectroscopy; Redox properties

1. Introduction

Macrocyclic Schiff bases of thiosemicarbazones and their metal complexes are well known to be biologically important and interesting because of their anticarcinogenic, antibacterial, and antifungal properties [1,2]. Also, they have been screened for their medicinal properties because they possess some degree of cytotoxic activity [3].

The biological activity of certain thiosemicarbazones is due to their ability to form chelates with transition metal ions [4]. Crystal structures for salicylaldehyde thiosemicarbazone and 2-hydroxyacetophenone-thiosemicarbazone have been reported [5], and both mainly exist in the *E*-conformation with respect to the thiosemicarbazone azomethine bond. Biological activities may also be related to the redox properties of the complexes [6]. The redox properties include oxidation and reduction of the central metal ion and various oxidation and reduction of

the ligands, and the processes involve both the central atom and the ligand [6]. The redox potential of

* Corresponding author. Tel.: +22-50-2340100; fax: +22-50-2246781. E-mail address: gamilalHazmi@hotmail.com (G.A.A. Al-Hazmi).

1386-1425/\$ – see front matter © 2004 Elsevier B.V. All rights reserved.
doi:10.1016/j.saa.2004.02.035

the Ni^I/Ni^{II} and Ni^{II}/Ni^{III} couples have been shown to be markedly affected by the nature of the solvent, background electrolyte, and the structure of the chelating ligand and the complex [7].

Ni(II) complexes of acetophenone, 4-aminoacetophenone, and 4-acetylacetophenone thiosemicarbazones containing the neutral or anionic forms of these ligands were prepared and fully characterized [8]. As a part of our work involving thiosemicarbazone derivatives and their complexes [9–11],

this paper gives an insight about the preparation, spectral, characterization, and cyclic voltammetric studies of some Ni(II) complexes. The kinetics and thermodynamic parameters for some thermal decomposition steps as well as the mechanisms and kinetics of the electron transfer of the observed electrode couples for some complexes have been critically studied.

2. Experimental

All chemicals used were of analytical reagent grade (BDH) and used as supplied.

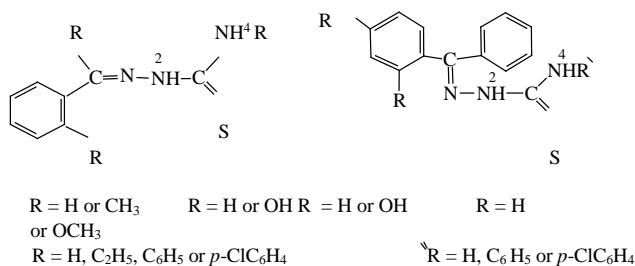


Fig. 1. General formulas of the ligands.

2.1. Preparation of ligands

The thiosemicarbazone ligands (Fig. 1) were prepared by mixing equimolar amounts of acetophenone (12 ml, 0.1 mol), salicylaldehyde (12.2 ml, 0.1 mol), benzophenone (18.2 g, 0.1 mol), and/or *o*-hydroxymethoxybenzophenone (22.8 g, 0.1 mol) in 30 ml ethanol, with an ethanolic solution (20 ml) of thiosemicarbazide (9.1 g, 0.1 mol), ethyl- (11.9 g, 0.1 mol), phenyl- (16.7 g, 0.1 mol), and/or *p*-chlorophenyl (20.1 g, 0.1 mol) thiosemicarbazides. The reaction mixture

Table 1

were then refluxed on a water bath for 2–3 h. Few drops of glacial acetic acid being added at the onset of the reflux. The precipitates formed were separated out, filtered off, recrystallized from ethanol, and dried in a desiccator over anhydrous CaCl₂. The proposed chemical structures of the prepared thiosemicarbazone ligands are in good agreement with the stoichiometries concluded from their analytical data and mass spectra (Table 1) and confirmed from the IR spectral data (Table 2). Most of these ligands are white or pale yellow and have melting point below 245 °C (Table 1). The ¹H NMR spectra of the reagents HAET, HAPT, and H₂HyMPT in d₆-DMSO show signals at δ = 12.08–11.40 and 9.92–8.51 ppm assigned to the N²H and N⁴H protons, respectively [12]. The spectra of HAT and H₂ST show signals at δ = 10.29, 10.07, and 8.09, 8.03 ppm safely assigned to the NH₂ and NH protons, respectively. Moreover, the spectrum of H₂ST shows the OH and NH₂ proton signals at 10.17 and 10.07 ppm [9], respectively. The general structure of the ligands is given in Fig. 1, where the abbreviations and their names are listed in Table 1.

Abbreviation, name, melting point, elemental analysis and formula weight (F.W.) of the prepared ligands

Abbreviation	Name	m.p. (°C)	Found (Calcd. %)		F.W.	
			C	H	Found ^a	Calcd.
HAT	1-Acetophenonethiosemicarbazone	132	55.8 (55.9)	5.7 (5.7)	–	193.3
HAET	1-Acetophenone-4-ethylthiosemicarbazone	145	60.0 (59.7)	6.4 (6.8)	221.0	221.3
HAPT	1-Acetophenone-4-phenylthiosemicarbazone	198	67.0 (66.9)	5.9 (5.6)	–	269.4
HA _p CIPT	1-Acetophenone-4- <i>p</i> -chlorophenylthiosemicarbazone	190	58.8 (59.3)	4.2 (4.6)	304.0	303.8
H ₂ ST	1-Salicylaldehydethiosemicarbazone	245	49.3 (49.2)	5.0 (4.6)	–	195.2
H ₂ SET	1-Salicylaldehyde-4-ethylthiosemicarbazone	184	53.3 (53.8)	5.4 (5.9)	223.0	223.3
H ₂ SPT	1-Salicylaldehyde-4-phenylthiosemicarbazone	205	61.0 (61.9)	4.8 (4.8)	–	271.3
H ₂ S _p CIPT	1-Salicylaldehyde-4- <i>p</i> -chlorophenylthiosemicarbazone	212	54.3 (54.9)	4.0 (3.9)	304.0	305.9
H ₂ HyMBPT	1-(2-Hydroxy-4-methoxybenzophenone) 4-phenylthio-semicarbazone	110	66.0 (66.8)	4.8 (5.1)	377.0	377.5
H ₂ HyMB _p CIPT	1-(2-Hydroxy-4-methoxybenzophenone) 4- <i>p</i> -chloro-phenylthiosemicarbazone	135	61.2 (61.2)	4.3 (4.4)	412.0	411.9
HBT	1-Benzophenonethiosimecarbazone	191	66.6 (65.8)	4.6 (5.1)	255.9	255.3

^a Values obtained from mass spectra.

Table 2

Physical properties, analytical data and formula weight (F.W.) of the prepared n complexes

No.	Complex	Color	m.p. (°C)	Found (Calcd. %)			F.W.	
				C	H	Ni	Found ^a	Calcd.
1	[Ni(AT) ₂](H ₂ O)	Dark brown	268	47.5 (46.8)	4.4 (4.7)	12.3 (12.7)	–	461.1
2	[Ni(AET) ₂]	Dark brown	234	52.3 (52.9)	5.1 (5.6)	11.4 (11.7)	499.0	499.3
3	[Ni ₂ (APT) ₃ (OH)(H ₂ O)]H ₂ O	Yellowish green	>300	55.0 (55.4)	4.0 (4.8)	11.9 (12.0)	–	975.5
4	[Ni(A _p CIPT) ₂]	Yellowish brown	>300	54.8 (54.2)	4.2 (3.9)	8.6 (8.8)	664.0	664.3
5	[Ni(HST)(OAc)]	Pale brown	>300	38.1 (38.5)	3.5 (3.5)	19.2 (18.8)	312.0	311.9
6	[Ni(HST)(H ₂ O)] ₂ ·2C ₂ H ₅ OH	Reddish brown	>300	38.8 (38.8)	5.7 (5.9)	16.0 (15.8)	369.0	371.1
7	[Ni(HSPT)(OAc)(H ₂ O) ₂]	Brown	>300	44.9 (45.3)	4.5 (4.5)	13.8 (13.8)	422.0	424.1
8	[Ni(H ₂ S _p CIPT)(OAc) ₂ (H ₂ O)]	Brown	>300	43.2 (43.0)	4.0 (4.3)	11.7 (11.3)	498.0	500.7
9	[Ni(HHyMBPT)(OH)(H ₂ O)]	Yellow	223	53.0 (53.6)	3.9 (4.5)	12.5 (12.5)	470.0	470.2
10	[Ni ₂ (H ₂ HyMB _p CIPT)(OAc) ₄ (H ₂ O) ₃]	Reddish brown	>300	42.1 (42.5)	4.4 (4.4)	14.1 (14.3)	820.0	819.5
11	[Ni(BT)(OAc)(H ₂ O) ₂](H ₂ O)	Greenish brown	>300	46.6 (47.1)	4.1 (4.7)	14.4 (14.4)	–	426.1

^a Values obtained from mass spectra.

2.2. Preparation of complexes

All complexes were prepared by adding stoichiometric quantities of the ligands (3 mmol) in ethanol and nickel acetate (3 mmol) in bidistilled water. The reaction mixtures were then refluxed on a water bath for 4–6 h. The precipitates formed were filtered off, washed with hot water, hot ethanol, and diethylether, and finally dried in a vacuum desiccator over anhydrous CaCl_2 .

2.3. Physical measurements

C and H content was determined at the Microanalytical Unit of Cairo University. The analysis of metal ions was carried out according to the standard methods [13].

The infrared spectra, as KBr discs, were recorded on a Mattson 5000 FTIR Spectrophotometer. The electronic and ^1H NMR (200 MHz) spectra were recorded on UV_{2–100} Unicam UV–Vis and a Varian Gemini Spectrophotometers, respectively. The mass spectra were recorded on a Varian MAT 311 instrument. The thermal studies were carried out on a Shimadzu thermogravimetric analyzer at a heating rate of $10\text{ }^\circ\text{C min}^{-1}$. The cyclic voltammetry measurements were carried out with a Potentiostat wave generator (Oxford Press) equipped with a Phillips PM 8043 X-Y recorder. The electrode assembly consists of platinum wires of 0.5 diameter as working and counter electrodes and Ag/AgCl as a reference electrode. Tetrabutylammonium tetrafluoroborate ($\text{TBA}^+\text{BF}_4^-$) was used as supporting electrolyte.

3. Results and discussion

The isolated complexes are stable in air, insoluble in water and common organic solvents, but completely soluble in DMF and DMSO except for $[\text{Ni}(\text{AT})_2]\text{H}_2\text{O}$, $[\text{Ni}(\text{HHyMBPT})(\text{OH})(\text{H}_2\text{O})]$, $[\text{Ni}(\text{AET})_2]$, and $[\text{Ni}_2(\text{H}_2\text{HyMBpCIPT})(\text{OAc})_4(\text{H}_2\text{O})_3]$, which are partially soluble in DMF and DMSO.

The elemental analysis, color, and melting point together with the formula weight obtained from the ms spectra for the complexes are listed in Table 2. Attempts to propose the structure of the isolated complexes come from full investigation using the following studies.

3.1. IR spectral studies

The most characteristic bands of the ligands and their complexes are summarized in Table 3. Representative example for their spectra is given in Fig. 2.

The coordination sites of ligands under investigation with Ni(II) ions were elucidated using IR spectra. The data obtained suggest that the ligands bind to the metal ions by several manners. Firstly, HAT, HAET, HAPT, HA p CIPT, and HBT behave as mononegative bidentate and coordinate through the C=N and C–S groups with displacement of one hydrogen atom upon enethiolization. The mode of coordination was found in $[\text{Ni}(\text{AT})_2]\text{H}_2\text{O}$, $[\text{Ni}(\text{AET})_2]$, $[\text{Ni}_2(\text{APT})_3(\text{OH})(\text{H}_2\text{O})]\text{H}_2\text{O}$, $[\text{Ni}(\text{ApCIPT})_2]$, and $[\text{Ni}(\text{BT})(\text{OAc})(\text{H}_2\text{O})_2]\text{H}_2\text{O}$, and was suggested by the following evidence: (i) the disappearance of $\nu(\text{N}^2\text{H})$, (ii) the shift of $\nu(\text{C}=\text{N})$ to lower frequency by $10\text{--}65\text{ cm}^{-1}$ [14], (iii) the appearance of a new band attributed to $\nu(\text{C}=\text{N}^*)$ at the same spectral region for the $\nu(\text{C}=\text{N})$ of the thiosemicarbazone moiety, (iv) coordination of the azomethine nitrogen is also consistent with the presence of a new band at $440\text{--}460\text{ cm}^{-1}$ assignable to the $\nu(\text{Ni}-\text{N})$ vibration [15], and (v) the thioamide band (IV) is absent with the simultaneous appearance of new bands in the $610\text{--}680$ and $345\text{--}370\text{ cm}^{-1}$ regions due to the $\nu(\text{C}-\text{S})$ [16] and $\nu(\text{Ni}-\text{S})$ vibrations [17], respectively.

Secondly, H_2SpCIPT and $\text{H}_2\text{HyMBpCIPT}$ appear to be in the thioketo form, neutral, and tridentate, coordinating via the C=S, C=N, and phenolic oxygen groups. This behavior is observed in $[\text{Ni}(\text{H}_2\text{SpCIPT})(\text{OAc})_2(\text{H}_2\text{O})]$ and $[\text{Ni}_2(\text{H}_2\text{HyMBpCIPT})(\text{OAc})_4(\text{H}_2\text{O})_3]$ and supported by the following evidence: (i) the $\nu(\text{C}=\text{S})$ and $\nu(\text{C}=\text{N})$ bands are shifted to lower frequency by $5\text{--}45\text{ cm}^{-1}$, and (ii) the

Table 3

Significant IR spectral bands (cm^{-1}) of the nickel(II) complexes with relevant bands of the free ligand in parenthesis

Complex	$\nu(\text{NH}_2)$	$\nu(\text{OH})$	$\nu(\text{N}^4\text{H})$	$\nu(\text{N}^2\text{H})$	$\nu(\text{C}=\text{N})$	$\nu(\text{C}=\text{S})$	$\nu(\text{C}-\text{S})$	$\delta(\text{OH})$	$\nu(\text{Ni}-\text{O})$	$\nu(\text{Ni}-\text{N})$	$\nu(\text{Ni}-\text{S})$
1	3395 (3410) 3345 (3370)	–	–	(3220)	1620 (1630)	(790)	645	–	–	454	355
2	–	–	3210(3320)	(3225)	1565 (1630)	(790)	610	–	–	445	365
3	–	3435	3290(3300)	(3250)	1575 (1605)	(795)	615	1340	–	460	345
4	–	–	3280(3290)	(3240)	1590 (1635)	(795)	610	–	–	450	370
5	3325 (3370) 3260 (3315)	3405 (3440)	–	(3165)	1605 (1610)	(780)	650	1330 (1365)	505	425	350
6	–	(3405)	3330 (3355)	(3250)	1595 (1605)	(790)	620	1330 (1375)	500	440	340
7	–	3420 (3405)	3385 (3380)	(3145)	1600 (1620)	(835)	655	1375 (1389)	500	450	350

8	–	3320 (3335)	3230 (3235)	3130 (3154)	1605 (1610)	820 (830)	–	1305(1330)	505	420
9	–	3460 (3470)	3295 (3300)	3160 (3160)	1590 (1635)	810 (810)	–	1320(1327)	505	440
10	–	3430 (3440)	3230 (3290)	3110 (3180)	1590(1635)	745 (790)	–	1310(1350)	505	410
11	3365 (3365) 3280 (3260)	–	–	(3175)	1590 (1620)	(800)	680	–	490	440

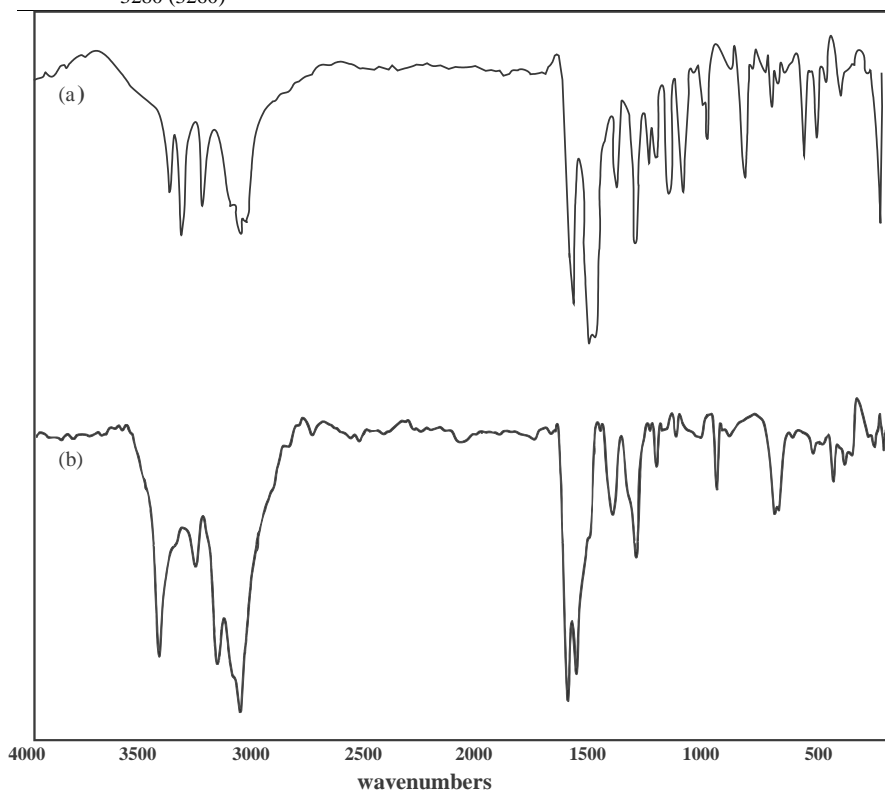


Fig. 2. IR spectra of: (a) $[\text{Ni}_2(\text{H}_2\text{HyMBpCIPT})(\text{OAc})_4(\text{H}_2\text{O})_3]$ and (b) $[\text{Ni}(\text{BT})(\text{OAc})(\text{H}_2\text{O})_2]\cdot\text{H}_2\text{O}$.

phenolic oxygen of these ligands occupy the third coordination site with the shift of $\nu(\text{OH})$ band by 10–15 cm^{-1} to lower frequency. The band at 505 cm^{-1} is assignable to $\nu(\text{Ni}-\text{O})$ of the bridging phenolate oxygen, and (iii) the appearance of new bands in the low frequency region at 345–385 and 410–420 cm^{-1} , which are assigned to the $\nu(\text{Ni}-\text{S})$ and $(\text{Ni}-\text{N})$ [18] vibrations, respectively.

The third mode of chelation was found through the C=N, C–S, and phenolic oxygen groups in which H_2ST and H_2SPT act as mononegative tridentates. This behavior is found in $[\text{Ni}(\text{HST})(\text{OAc})]$ and $[\text{Ni}(\text{HSPT})(\text{OAc})(\text{H}_2\text{O})_2]$. Elucidation of this mode is proposed by: (i) the disappearance of $\nu(\text{N}^2\text{H})$, (ii) the shift of $\nu(\text{C}=\text{N})$ bands to lower frequency by 50–20 cm^{-1} , (iii) the disappearance of $\nu(\text{C}=\text{S})$ with the appearance of a new band at 650–655 cm^{-1} , (iv) the shift (15–35 cm^{-1}) of $\nu(\text{OH})$ and (15–35 cm^{-1}) of $\delta(\text{OH})$ to lower frequency, and (v) new bands appeared in the low frequency region for $\nu(\text{Ni}-\text{S})$ at 350 cm^{-1} , $\nu(\text{Ni}-\text{N})$ at 425–450 cm^{-1} , and $\nu(\text{Ni}-\text{O})$ at 500–505 cm^{-1} gave a good evidence for the participation of S, N, and O donors.

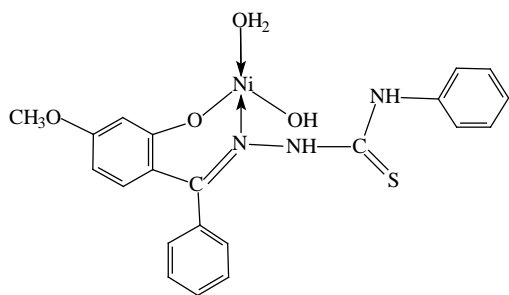
In $[\text{Ni}(\text{SET})(\text{H}_2\text{O})]1.5\text{H}_2\text{O}\cdot\text{C}_2\text{H}_5\text{OH}$, the ligand releases the hydrogen ions from both the thio keto, through

thioenolization, and the OH groups and behaves as a binegative tridentate. This behavior was confirmed based on the following evidence: (i) the disappearance of $\nu(\text{N}^2\text{H})$ and $\nu(\text{C}=\text{S})$ conjugated with the appearance of $\nu(\text{C}-\text{S})$ at 620 cm^{-1} and $\nu(\text{Ni}-\text{S})$ at 340 cm^{-1} , (ii) the deprotonated OH group occupies the third (through bridging) coordination site, (iii) the shift of $\nu(\text{C}=\text{N})$ band from 1605 to 1595 cm^{-1} , and (iv) the new bands observed at 440 and 500 cm^{-1} attributed to the $\nu(\text{Ni}-\text{N})$ and $\nu(\text{Ni}-\text{O})$ vibrations, respectively, gave a good evidence for the participation of N and O donors.

In $[\text{Ni}(\text{HHyMBPT})(\text{OH})(\text{H}_2\text{O})]$, H_2HyMBPT behaves as a mononegative, bidentate ligand coordinating via the deprotonated OH and C=N groups as shown in Scheme 1. The mode of complexation is suggested by the clear change in the position of $\nu(\text{C}=\text{N})$ band by 44 cm^{-1} , the shift of $\nu(\text{OH})$ and $\delta(\text{OH})$ to lower frequency, the appearance of new bands at 440 and 505 cm^{-1} assigned to $\nu(\text{Ni}-\text{N})$ and $\nu(\text{Ni}-\text{O})$. Also, the $\nu(\text{C}=\text{S})$ and $\nu(\text{N}^2\text{H})$ bands remain unshifted, suggesting that the C=S group is out of coordination.

The acetate group coordinates in a monodentate or bidentate manner [19]. The monodentate in $[\text{Ni}(\text{HST})(\text{OAc})]$,

[Ni(HSPT)(OAc)(H₂O)₂], and [Ni(H₂SpCIPT)(OAc)₂(H₂O)] is



Scheme 1.

deduced from the frequency difference (ν) between ν_s and ν_{as} (more than 185 cm^{-1}) [20]. The bidentate behavior of the acetate group in [Ni(BT)(OAc)(H₂O)₂]₂H₂O is supported by the appearance of two new bands at 1420 and 1525 cm^{-1} due to symmetric and asymmetric stretching vibrations, respectively. [Ni₂(H₂HyMBpCIPT)(OAc)₄(H₂O)₃] displays three bands in its spectrum at 1525 , 1395 , and 1337 cm^{-1} , which are assigned to the existence of bidentate and monodentate coordinations of the acetate group [21]. The monodentate behavior is deduced from the frequency difference ($\Delta\nu = 188\text{ cm}^{-1}$) between the 1525 and 1337 cm^{-1} bands, and the difference between the 1525 and 1395 cm^{-1} ($\Delta\nu = 88\text{ cm}^{-1}$) bands is correlated to the bidentate behavior.

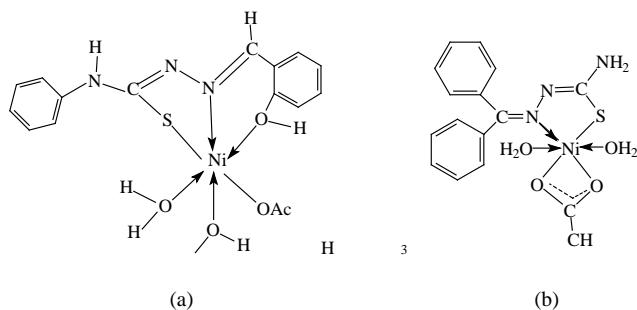
3.2. Magnetic and electronic spectral studies

The magnetic moments and electronic spectral bands of the complexes are summarized in Table 4.

The magnetic moment values of [Ni(HSPT)(OAc)(H₂O)₂], [Ni(H₂SpCIPT)(OAc)₂(H₂O)], [Ni₂(H₂HyMBpCIPT)(OAc)₄(H₂O)₃], and [Ni(BT)(OAc)(H₂O)₂]₂H₂O are found within the range reported for the octahedral geometry around the Ni(II) ion [22]. The value (1.8 B.M.) measured for each nickel atom in [Ni₂(H₂HyMBpCIPT)(OAc)₄(H₂O)₃] is less than that reported for systems containing two unpaired electrons, which may be attributed to the existence of nickel–nickel interaction [23].

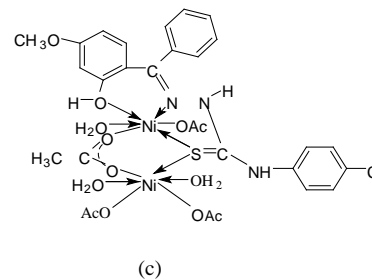
The electronic spectra of these complexes, recorded in Nujol mull and DMF solutions, have a great similarity and show two main broad bands centered at $16,665$ – $18,050$ and $23,255$ – $24,510\text{ cm}^{-1}$ assigning to the $3A_{2g} \rightarrow 3T_{1g}(F)$ and $3A_{2g} \rightarrow 3T_{1g}(P)$ transitions, respectively, in an octahedral geometry [24]. The proposed structures for [Ni(HSPT)(OAc)(H₂O)₂], [Ni(BT)(OAc)(H₂O)₂]₂H₂O, and [Ni₂(H₂HyMBpCIPT)(OAc)₄(H₂O)₃] are shown in Scheme 2 (a, b, and c, respectively). The spectrochemical

Table 4



(a)

(b)



(c)

Scheme 2.

parameters Dq , B , and β of some of the complexes are given in Table 4. The Dq values are found in the range $(9.80$ – $10.3) \times 10^3\text{ cm}^{-1}$ close to that observed for NiO_4N_2 and reasonable for most complexes containing oxygen, nitrogen, and/or sulphur. The observed Dq values ordered the ligands in the middle range of the spectrochemical series and provides that the $\text{C}=\text{N}$, OH , and $\text{C}=\text{S}$ of the ligands are complexed to the Ni(II) ion in an octahedral geometry.

The B values of the prepared octahedral complexes (Table 4) were found in the range 69.9–72.0% that of the free ion ($B^0 = 1030 \text{ cm}^{-1}$) [25], indicating considerable overlap with strongly covalent nickel-ligand bond character [23]. The decrease in B values is most likely associated with the reduction in the nuclear charge of the cation.

The nephelauxetic parameter, β is in the range 0.66–0.74, indicating that these ligands are in the middle of the

Magnetic moment, electronic spectral data in DMF and nujol (in parentheses) of the nickel(II) complexes with some ligand field parameters

Complex	μ_{eff} (B.M.)	ν_{max} (cm^{-1})	Ligand field parameters			Supposed structure
			B (cm^{-1})	β	$10Dq$ (cm^{-1})	
1	0.90	22575 (20875), 18380 (17575)	–	–	–	Tetrahedral + square planar (nujol)
2	3.51	16865 (17300)	–	–	–	Tetrahedral
3	3.21	24690, 17950 (17390)–	–	–	–	Tetrahedral
4	2.16	24570 (20705), 16665 (17855)	–	–	–	Tetrahedral + square planar (nujol)
5	0.95	24440 (20240), 17390 (17665)	–	–	–	Tetrahedral + square planar (nujol)
6	1.26	20245 (20450), 16475 (17210)	–	–	–	Tetrahedral + square planar
7	3.05	23925 (23925), 17545 (18050)	750 (7640)	0.72 (0.74)	100060 (10170)	Octahedral
8	2.80	23585 (23585), 16950 (17730)	720 (750)	0.66 (0.72)	9900 (10000)	Octahedral
9	3.80	17450 (17270)	–	–	–	Tetrahedral
10	1.80	23925 (23255), 17240 (17220)	700 (730)	0.68 (0.71)	10395 (9830)	Octahedral
11	2.90	23420 (24510), 17360 (16665)	740 (710)	0.71 (0.68)	9905 (10180)	Octahedral

nephelauxetic of other nitrogen, sulphur, and oxygen donor series. The values are higher than that observed for NiN_6 or NiO_6 , confirming the coordination via N, O, and/or S. Thus, it seems reasonable to presume that most of the chelates formed in this series involve NiO_4NS or NiO_4N_2 chromophores.

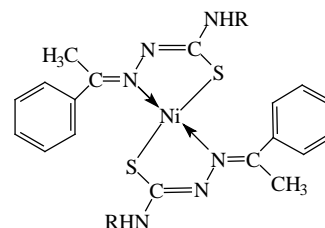
The magnetic moment values (3.51, 3.21, and 3.80 B.M.) measured for the complexes $[\text{Ni}(\text{AET})_2]$, $[\text{Ni}_2(\text{APT})_3(\text{OH})(\text{H}_2\text{O})]\text{H}_2\text{O}$, and $[\text{Ni}(\text{HHyMBPT})(\text{OH})(\text{H}_2\text{O})]$ lie in the range reported for a tetrahedral structure [26]. The lower value measured per one nickel atom for the binuclear complex may be due to nickel–nickel interaction [23]. This geometry is further evidenced by the electronic spectral data, which show one d–d transition band at $16,865\text{--}17,950 \text{ cm}^{-1}$, which is assigned to the ${}^3\text{T}_1 \rightarrow {}^3\text{T}_1(\text{P})$ transition.

The complexes $[\text{Ni}(\text{AT})_2]\text{H}_2\text{O}$, $[\text{Ni}(\text{ApCIPT})_2]$, $[\text{Ni}(\text{HST})(\text{OAc})]$, and $[\text{Ni}(\text{SET})(\text{H}_2\text{O})]1.5\text{H}_2\text{O} \cdot \text{C}_2\text{H}_5\text{OH}$ have 0.90, 2.16, 0.95, and 1.26 B.M. magnetic moments, respectively, which are less than that reported for the d^8 –octahedral and/or tetrahedral complexes and higher than diamagnetic square-planar complexes. The values may suggest the existence of the complexes in a mixed stereochemistry [27]. Such supposition is also confirmed from the analysis of their electronic spectra, which show two bands. The band observed at $16,475\text{--}18,380 \text{ cm}^{-1}$ is in accordance with a tetrahedral

configuration and assigned to the ${}^3\text{T}_1 \rightarrow {}^3\text{T}_1(\text{P})$ d–d transition. The other band at $20,240\text{--}22,575 \text{ cm}^{-1}$ is referring to a square-planar geometry [11]. The DMF has a large effect in the spectra of $[\text{Ni}(\text{ApCIPT})_2]$, $[\text{Ni}(\text{AT})_2]\text{H}_2\text{O}$, and $[\text{Ni}(\text{HST})(\text{OAc})]$ and no effect in the spectrum of $[\text{Ni}(\text{SET})(\text{H}_2\text{O})]1.5\text{H}_2\text{O} \cdot \text{C}_2\text{H}_5\text{OH}$, indicating that the DMF acts as a ligand in such complexes. Scheme 3 (a–c) represents the structure of $[\text{Ni}(\text{AT})_2]\text{H}_2\text{O}$, $[\text{Ni}(\text{AET})_2]$, and

$[\text{Ni}(\text{ApCIPT})_2]$, respectively.

The spectra and the position of the bands of some complexes in DMF are found to be different from the corresponding ones recorded in nujol (Table 4), showing that these complexes are significantly unstable, commencement of solvolysis or presence of low symmetry components of crystal field [23]. These complexes could also undergo chemical dissolution in DMF and hence the composition of the chromophores may become different in solution than in solid.



R = H (a), C_2H_5 (b) or $p\text{-ClC}_6\text{H}_4$ (c)

Scheme 3.

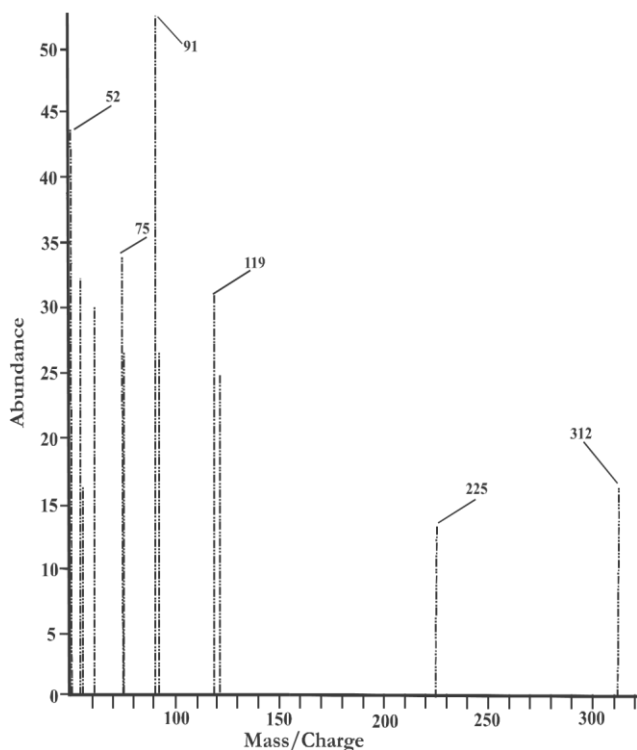


Fig. 3. Mass spectrum of the complex [Ni(HST)(OAc)].

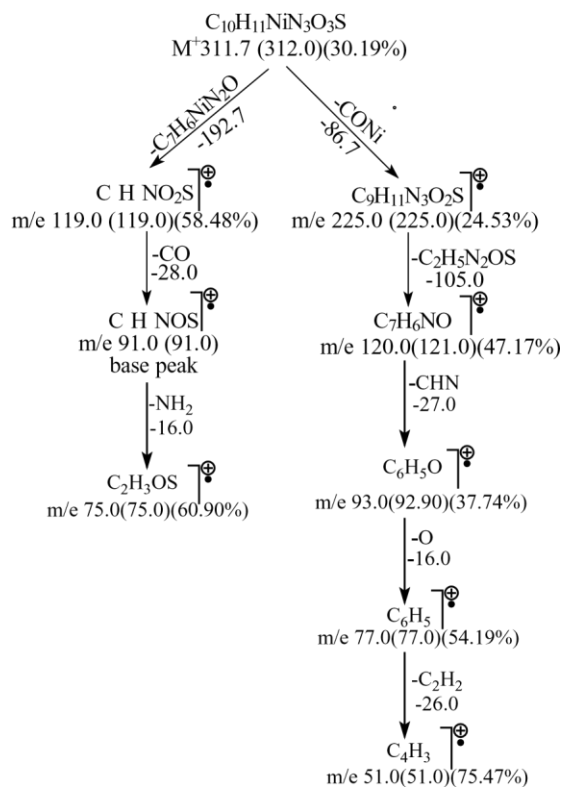
3.3. Mass spectra

The mass spectra of most complexes were recorded and their molecular ion peaks confirm the suggested formula of these complexes. The calculated and found values of the molecular weights of some of the complexes are given in Table 2. Representative mass spectrum of the complex [Ni(HST)(OAc)] is shown in Fig. 3. The spectrum shows numerous peaks representing successive degradation of the molecule. The observed peak at m/e 312.0 (Calcd. 311.7) represents the molecular ion peak of the complex with 30.19% abundance. Scheme 4 demonstrates the proposed paths of the decomposition steps for the investigated complex. One of the strongest peaks (base peak) at m/e 91.0 represents the stable species C_2H_5NOS .

3.4. Thermal studies

3.4.1. Kinetic analysis

Non-isothermal kinetic analyses for the decomposition of HAET, HAPT, and $H_2HyMBPT$ and some Ni(II) complexes were carried out by the application of two different procedures: the Coats-Redfern [28] and the Horowitz-Metzger [29] methods. The kinetic parameters (E and n) were calculated according to the above two methods, where the thermodynamic parameters (ΔH^* , ΔS^* and ΔG^*) were calculated according to the Coats-Redfern equation and their



values are tabulated in Table 5. The activation enthalpy (ΔH^*), the activation entropy (ΔS^*), and the free energy of activation

35

25

Scheme 4. Proposed fragmentation pattern of [Ni(HST)(OAc)].

(ΔG^*) were calculated using the following equations:

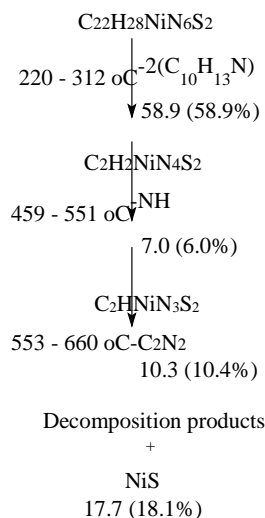
$$\Delta S^* = 2.303 \left[\log \left(\frac{Zh}{KT} \right) \right] R$$

$$\Delta H^* = E - RT$$

$$\Delta G^* = \Delta H^* - T_s \Delta S^*$$

where Z , K , and h are the pre-exponential factor, Boltzman, and Plank constants, respectively [30]. Comparison of the two sets of kinetic parameters shows no significant difference between them considering the approximations

Table 5

Scheme 5. Proposed thermal decomposition pattern of $[Ni(AET)_2]$.

involved in the Horowitz-Metzger method. The activation energies could not be calculated for the overlapping or unsuitable steps. The relatively high E values indicate that the ligand is strongly bonded to the Ni(II) ions. The negative $\Delta^* S$ values in $[Ni_2(APT)_3(OH)(H_2O)]H_2O$ (third step) and $[Ni_2(H_2HyMBpCIPT)-(OAc)_4(H_2O)_3]$ (first and second steps) indicate that the activated complexes have more ordered structure than the reactants and the reactants are slower than the normal [30,31].

The thermal decomposition of some ligands and complexes was recorded at temperature 30–1000 °C. The thermograms exhibit several thermal events. The first step in the TG thermogram of some complexes corresponds to the expulsion of water of crystallization and/or coordination. The end products for most complexes were NiS or NiO. The activation energies calculated for the first step in the TG thermograms of the ligands and complexes lie in the ranges 83.9–127.7 and 164.0–304.0 kJ mol⁻¹, respectively (Coats-Redfern equation).

The thermal decomposition of $[Ni(AET)_2]$ (Fig. 4) as an example for the decomposition of these compounds shows three steps at 220–312, 459–551, and 553–660 °C (Scheme 5). The first step due to elimination of $2(C_{10}H_{13}N)$

Kinetic parameters of the thermal decomposition of some of ligands and their complexes^a

Compound	Step	Coats-Redfernequation			Horowitz-Metzgerequation			S^*	H^*
		r	n	E	r	n	E		
HAET	1st	0.99891	0.00100	90.99980	1.00107	1			
HAPT	1st	0.99990	0.66	83.90	0.99980	0.66	89.6		
H ₂ HyMBPT	1st	0.99822	0.00127	70.99732	0.00138	3			
	2nd	0.99872	0.00140	10.99772	0.00145	7			
$[Ni(AET)_2]$	1st	1.00002	0.00296	21.00002	0.00309	5	119.6232.4		
$[Ni_2(APT)_3(OH)(H_2O)]H_2O$	3rd	0.99220	0.33183	60.99400	0.33191	3			
	6th	0.99951	0.00284	50.99951	0.00295	3	2.4253.0		
$[Ni(ApCIPT)_2]$	1st	0.97071	0.00304	20.97071	0.00311	2	2255.7299.7		
$[Ni(HhyMBPT)(OH)(H_2O)]$	2nd	0.99621	0.00304	70.99581	0.00315	1	1178.2299.8		
$[Ni_2(H_2HyMBpCIPT)(Oac)_4(H_2O)_3]$	1st	0.99931	0.00164	00.99921	0.00173	4			

2nd0.99991.00 46.50.99851.00 60.5

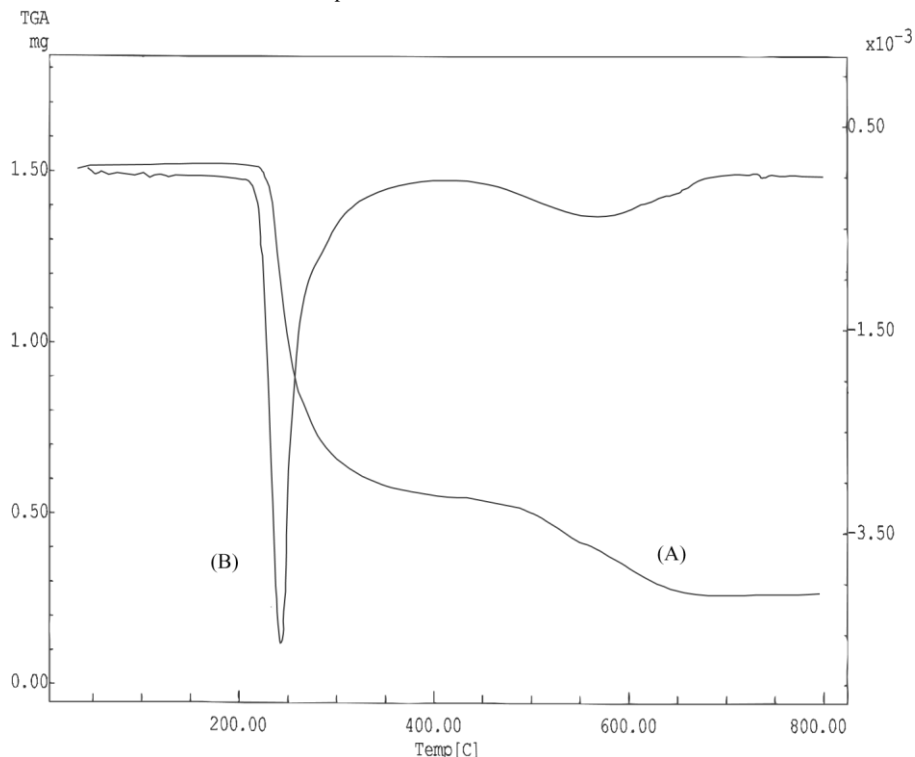
^a r = correlation coefficient, n = order of the decomposition reaction; E , ΔH^* , and ΔG^* are in kJmol^{-1} , ΔS^* in JKmol^{-1} .Fig. 4. TG (A) and DTG (B) thermograms of the complex $[\text{Ni}(\text{AET})_2]$.

Table 6

Electrochemical data of some of the prepared nickel(II) complexes in DMF-TBA+BF_4^- ^a

Complex	First electrode couple	
	$E_{p,a}$	$E_{p,c}$
$[\text{Ni}(\text{AT})_2]\text{H}_2\text{O}$		1.39
$[\text{Ni}(\text{AET})_2]$		1.20
$[\text{Ni}_2(\text{APT})_3(\text{OH})(\text{H}_2\text{O})]\text{H}_2\text{O}$	-1.12	—
	-0.80	—
	-0.20	—
	-0.72	—
$[\text{Ni}(\text{ApCIPT})_2]$		1.08

^a Scan rate = 100mVsec^{-1} ; $E_{1/2} = (E_{p,c} + E_{p,a})/2$.

(Calcd. 58.9%, found 58.9%) has activation energy of 296.2 kJ mol^{-1} and second order reaction. Elimination of 2NH (Calcd. 6.0%, found 7.0%) takes place in the second step. The second and third steps are not suitable for kinetic analysis. The final stable residue as identified from the mass loss consideration is NiS (Calcd. 18.1%, found 17.7%).

3.5. Cyclic voltammetry

The cyclic voltammetric behavior of the complexes $[\text{Ni}(\text{AT})_2]\text{H}_2\text{O}$, $[\text{Ni}(\text{AET})_2]$, $[\text{Ni}_2(\text{APT})_3(\text{OH})(\text{H}_2\text{O})]\text{H}_2\text{O}$, and $[\text{Ni}(\text{ApCIPT})_2]$ in DMF-TBA+BF_4^- are found similar and displayed two well-defined electrode couples. The results are summarized in Table 6. Representative data are also shown in Fig. 5. The complexes showed two successive one electron processes. The first electrode couple of these complexes is safely assigned to the irreversible couple $\text{Ni}^{\text{II}}/\text{Ni}^{\text{I}}$ with $E_{1/2}$ of -0.49 to -1.25 V ($\Delta E_p = 0.27\text{--}0.58\text{ V}$) and represented as follows:

+1.5 V

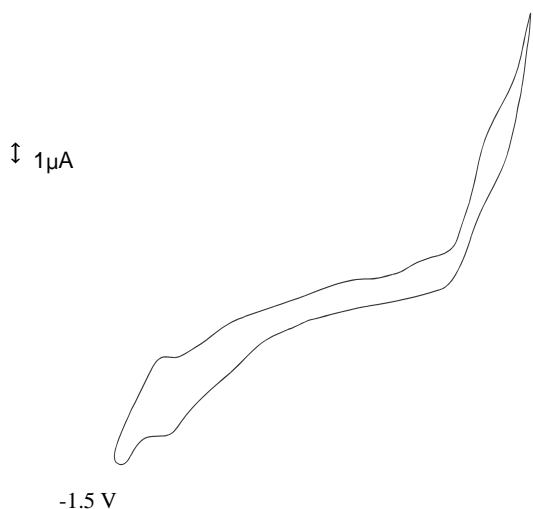
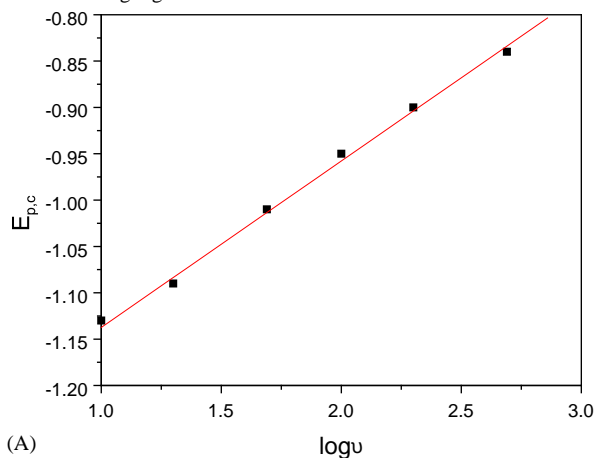
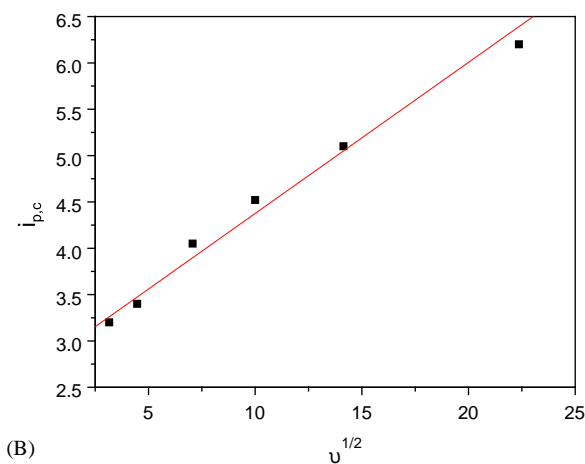


Fig. 5. Cyclic voltammogram of the complex $[\text{Ni}(\text{AT})_2]\text{H}_2\text{O}$ in DMF-TBA+BF₄⁻ vs. Ag/AgCl electrode.



(A)



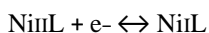
(B)

Fig. 6. The dependence of the cathodic peak potential $E_{p,c}$ (A) and the cathodic peak current $i_{p,c}$ (B) of the electrode couple Ni^{II}/Ni^I of the complex $[\text{Ni}(\text{AT})_2]\text{H}_2\text{O}$.

The second electrode couple with $E_{1/2} = 0.82\text{--}1.11$ V is assigned to the irreversible electrode couple Ni^{II}/Ni^{III} by comparison with analogous Ni(II) complexes [7]. The irreversible nature of the observed electrode couples has been established by comparing its peak current height ($i_{p,c}/i_{p,a} > 1$) with other similar complexes [7]. The irreversible nature of this couple is also confirmed by the linear dependence of the cathodic peak potential ($E_{p,c}$) with logarithm sweep rate ($\log u$) as shown in Fig. 6A. From the slope of this line and assuming the number of electrons (n) involved in the oxidation step equals one, the value of the electron transfer coefficient (α) is 0.59. The peak-to-peak potential separation (ΔE_p) of the electrode couple Ni^{II}/Ni^{III} increased with increasing the scan rate confirming the occurrence of a slow chemical reaction and a limited mass transfer following the electrode process [32]. Thus, the electron transfer process is irreversible and the species that initially formed in the electrode process may also react further to give products that are not reoxidized at the same potential as in the first formed species [33].

The dependence of the voltammetric responses of the Ni^{II}/Ni^{III} couple on the scan rate and on the depolarizer concentration is that typical of an ECE (chemical reaction coupled between two charge transfer processes) mechanism in which an irreversible first order chemical reaction is interposed between two successive one-electron transfers [34]. For an ECE process with an irreversible chemical reaction, $i_{p,c}/u^{1/2}$ showed decrease with increasing scan rate. The ratio $i_{p,c}/u^{1/2}$ slowly decreases with scan rate (20–200 mV/sec) for all complexes, confirming that the observed behavior favors the ECE mechanism. The dependence of the cathodic peak current $i_{p,c}$ of the electrode couple Ni^{II}/Ni^{III} on the square rate of the sweep rate ($u^{1/2}$) suggests diffusion-controlled electrochemical process (Fig. 6B).

As may be observed in Table 6, substitution on thiosemicarbazone moiety has a significant effect on $E_{1/2}$ for the complexes; electron-withdrawing groups stabilize the Ni(II) in the complexes $[\text{Ni}_2(\text{APT})_3(\text{OH})(\text{H}_2\text{O})]\text{H}_2\text{O}$ and $[\text{Ni}(\text{ApCIPT})_2]$ while the electron-donating group favor oxidation to Ni(III). This is possibly because the electron-withdrawing chlorine or phenyl ring makes the complex more positively charged and hence causes it to be more easily reduced. Similarly the electron-donating groups make the complexes $[\text{Ni}(\text{AT})_2]\text{H}_2\text{O}$ and $[\text{Ni}(\text{AET})_2]$ less positively charged and hence less easily reduced. The oxidation potential of this couple does not correlate linearly with the Hammett constant (σ), and the E° of the couple is sensitive to the nature of the substituent in the thiosemicarbazone moiety with Ni^{II}/Ni^{III}.



4. Conclusion

A series of Ni(II) complexes of some thiosemicarbazones have been prepared and fully characterized. The kinetic and thermodynamic characteristics of some of the prepared complexes are discussed. Proposed fragmentation and thermal decomposition patterns for some of the complexes are also given. The cyclic voltammetric of the complexes showed that the Ni(II) compounds undergo one-electron reduction and oxidation to form the corresponding Ni(I) and Ni(III) compounds. The Ni(I) and Ni(III) compounds may be found being used as one-electron redox reagents since the former is a strong reducing agent and the latter is strong oxidizing agent.

References

- [1] A.A. El-Asmy, T.Y. Al-Ansi, Y.M. Shaibi, *Transition Met. Chem.* 14 (1989) 446.
- [2] P. Bindu, M.R.P. Kurup, T.R. Satyakeerty, *Polyhedron* 18 (1998) 321.
- [3] E. Franco, E.P. Torres, M.A. Mendiola, M.T. Sevilla, *Polyhedron* 19 (2000) 441.
- [4] R.P. John, A. Sreekanth, R. Maliyckal, P. Kurup, *Chemica Acta Part A* 59 (2003) 1349.
- [5] D.X. West, Y-H. Yang, T.L. Klein, K.I. Goldbery, A.E. Liberta, *Polyhedron* 14 (1995) 3051.
- [6] J.A. Streeky, D.G. Pillsburg, D.H. Busch, *Inorg. Chem.* 19 (1984) 3148.
- [7] M.S. El-Shahawi, W.E. Smith, *Analyst* 119 (1994) 327.
- [8] A.A. El-Asmy, Y.M. Shaibi, I.M. Shedaiwa, M.A. Khattab, *Synth. React. Inorg. Met. Org. Chem.* 20 (1990) 461.
- [9] S.I. Mostafa, A.A. El-Asmy, M.S. El-Shahawi, *Transition Met. Chem.* 25 (2000) 470.
- [10] J.P. Jasinski, J.R. Bianchani, J. Cueva, F.A. El-Saied, A.A. El-Asmy, D.X. West, *Z. Anorg. Allg. Chem.* 629 (2003) 202.
- [11] F.A. El-Saied, A.A. El-Asmy, W. Kaminstry, D.X. West, *Transition Met. Chem.* 28 (2003) 954.
- [12] D.X. West, Y-H. Yang, T.L. Klein, K.I. Goldberg, A.E. Liberta, J. Valdes-Matinez, S. Hernandez-Ortega, *Polyhedron* 14 (1995) 1681.
- [13] A.I. Vogel, "A Text Book of Quantitative Inorganic Analysis", Longmans, London, 1961.
- [14] D.X. West, M.M. Salberg, G.A. Bain, A.E. Liberta, *Transition Met. Chem.* 22 (1997) 180.
- [15] D.X. West, A.K. El-Sawaf, G.A. Bain, *Transition Met. Chem.* 23 (1998) 1.
- [16] A.A. El-Asmy, M.A. Morsi, A.A. El-Shafei, *Transition Met. Chem.* 11 (1986) 494.
- [17] D.X. West, M.A. Lockwood, A.E. Liberta, X. Chen, R.D. Willett, *Transition Met. Chem.* 18 (1993) 221.
- [18] N.C. Saha, R.J. Butcer, S. Chaudhuri, N. Saha, *Polyhedron* 22 (2003) 383.
- [19] K. Nakamoto, "Infrared and Raman Spectra of Inorganic and Coordination Compounds", 3rd Edn., Wiley, New York, 305, 1978.
- [20] A.H. Osman, A.A.M. Aly, N.A. El-Maali, G.A.A. Al-Hazmi, *Synth. React. Inorg. Met. Org. Chem.* 32 (2002) 1293.
- [21] A. El-Shekeil, A.Z. El-Sonbati, *Transition Met. Chem.* 17 (1992) 420.
- [22] A.A. El-Asmy, Y.M. Shaibi, I.M. Shedaiwa, M.A. Khattab, *Synth. React. Inorg. Met. Org. Chem.* 18 (1988) 331.
- [23] A.B.P. Lever, "Inorganic Electronic Spectroscopy", Elsevier, Amsterdam, 1986.
- [24] A.A. El-Asmy, M. Mounir, *Transition Met. Chem.* 13 (1988) 143.
- [25] J.E. Huhely "Inorganic Chemistry, Principles of Structure and Reactivity" 3rd Edn., Haper Collins publishers, 1983.
- [26] A.A. El-Asmy, K.M. Ibrahim, M.M. Bekheit, M.M. Mostafa, *Synth. React. Inorg. Met. Org. Chem.* 15 (1985) 287.
- [27] A.A. El-Asmy, T.Y. Al-Ansi, R.R. Amin, M. Mounir, *Polyhedron* 9 (1990) 2029.
- [28] A.W. Coats, J.P. Redfern, *Nature* 20 (1964) 68.
- [29] H.H. Horowitz, G. Metzger, *Anal. Chem.* 25 (1963) 1464.
- [30] R.M. Mahfouz, M.A. Monshi, S.M. Alshehri, N.A. El-Salam, A.M.A. Zaid, *Synth. React. Inorg. Met. Org. Chem.* 31 (2001) 1873.
- [31] A.A. Aly, A.S.A. Zidan, A.I. El-Said, *J. Thermal Anal.* 37 (1991) 627.
- [32] N.C. Paramanik, S. Bhattacharya, *Polyhedron* 16 (1997) 1761.
- [33] M.C. Huges, D.J. Macero, *Inorg. Chem.* 3 (1974) 2739.
- [34] A.J. Bard, L.R. Faulkner, "Electrochemical Methods Fundamental and Applications", John Wiley, New York, 1980, p. 218.



Polymer membrane sensors for sildenafil citrate (Viagra) determination in pharmaceutical preparations

A.M. Othman^a, N.M.H. Rizk^a, M.S. El-Shahawi^{b,*}

^a Genetic Engineering and Biotechnology Research Institute (GEBRI) Minufiya University, Sadat City, Egypt

^b Department of Chemistry, Faculty of Science at Damietta, Mansoura University, New Damietta, Egypt

Received 10 September 2003; received in revised form 7 January 2004; accepted 19 January 2004

Abstract

The construction and performance characteristics of ion selective membrane electrodes for sildenafil citrate (SC) drug (the active component of Viagra) are described. The proposed sensors are based on the formation of the complex ion associates of SC with sodium tetraphenylborate (SC–TPB) and phosphomolybdic acid (SC–PMA) as ionophores in poly vinyl chloride membrane (PVC). Both electrodes SC–PMA and SC–TPB showed a linear and stable potential response with near-Nernstian slope of 55.5 ± 0.35 and 53.5 ± 0.3 mV per decade over a wide range of concentration 10^{-2} to 10^{-5} M sildenafil with good reproducibility, respectively. The electrodes showed a fast response time of 30 and 40 s. and were used over a wide range of pH 3–6. The selectivity coefficients indicated good selectivity for SC drug over a large number of nitrogenous compounds and some inorganic cations. The proposed sensors are tested for the analysis of SC in pure form, pharmaceutical preparations and blood serum. An average recovery of $98.9\text{--}99.5 \pm 0.6\%$ and correlation to the existing methods of 0.998 were achieved. © 2004 Published by Elsevier B.V.

Keywords: Sildenafil citrate; Potentiometry; Pharmaceutical preparations; PVC matrix

1. Introduction

A reliable and specific assay is of great importance for characterization of a drug's disposition, tolerance and safety. Sildenafil citrate (SC) is known chemically as: 1-[4-ethoxy-3-(6,7-dihydro-1-methyl-7-oxo-3-propyl-1H-pyrazolo-[4,3d]pyrimidin-5-yl) phenyl sulphonyl]-4-methylpiperazine citrate (structural formula is given in Fig. 1) [1]. This drug is a potent and a selective inhibitor of cyclic guanosine mono phosphate (cGMP) specific phosphodiesterase type 5 (PED5) [1,2]. The mode of action of sildenafil in the erection of the penis involves the release of nitric oxide (NO) in the corpus cavernosum during sexual stimulation. The produced NO activates the enzyme guanylate cyclase, which results in increased levels of cGMP, producing smooth muscle relaxation of the penile in the corpus cavernosum and therefore having the potential to improve penile erectile function by allowing inflow of blood [2,3].

* Corresponding author. Tel.: +20-50370344. E-mail

address: mohammad el shahawi@hotmail.com (M.S. El-Shahawi).

0003-2670/\$ – see front matter © 2004 Published by Elsevier B.V.
doi:10.1016/j.aca.2004.01.016

Sildenafil citrate dysfunction is rapidly becoming one of the most popular and widely used drug [4]. Few reports have been appeared describing accurate spectrochemical, chromatographic and electroanalytical techniques for quantification and stability assay of sildenafil citrate [5–14]. Most of these methods are expensive, suffer from lack of selectivity and require careful control of conditions and considerable time for routine control analysis [10,11]. Therefore, precise and simple methods for the quantification of sildenafil citrate in pharmaceutical preparations are required.

Recent years have seen an upsurge of interest in the application of ion sensors in the field of medicinal analysis. This provides fast, accurate, reproducible and selective determination of various species [15–18]. The present communication describes the application of two developed sensors for SC determination in pharmaceutical preparations using the ion-association complex of SC with the electroactive phase sodium tetraphenylborate (NaTPB) or phosphomolybdic acid (PMA) in a poly vinyl chloride (PVC) matrix over a wide concentration range. The proposed methods are successfully applied for the determination of SC in the presence of other components (excipients) in four different products of Viagra (50 and 100 mg per tablet).

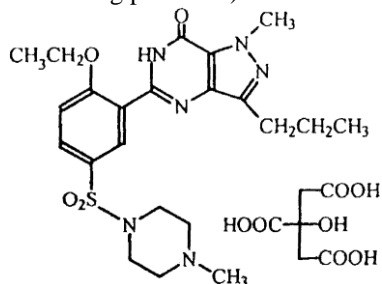


Fig. 1. Structural formula of sildenafil citrate.

2. Experimental

2.1. Reagents and materials

All chemicals were of analytical reagent grade unless otherwise specified. Doubly distilled water was used for the preparation of stock solutions of sildenafil citrate, excipients, diluents and metal chloride or nitrate salts. Pure SC was obtained from (Ranbaxy Labs., India). Tetrahydrofuran (THF), NaTPB and PMA were obtained from Sigma (St. Louis, MO). Dioctylphthalate (DOP), *o*-nitrophenyloctyl ether (*o*-NPOE), potassium tetra-*p*-chlorophenylborate (KTPCIPB) and high molecular mass PVC were purchased from Aldrich. A stock solution (10^{-2} M) of sildenafil citrate at pH 4.5–5 was prepared by dissolving 0.667 g of the salt in 100 ml water adjusted with acetate buffer (pH = 4.5) or with dilute NaOH and/or HCl. Dilute solutions (1×10^{-3} to 1×10^{-6} M) of SC were freshly prepared by diluting the stock solution with doubly distilled water and acetate of pH 5. Stock solution (1×10^{-2} M) of NaTPB and PMA were prepared by dissolving an accurate weight of the reagent in a minimum volume of distilled water followed by filtration and dilution to 100 ml. Stock solutions of the metal chlorides or nitrates (0.1 M) were freshly prepared in water before use.

2.2. Apparatus

Potentiometric measurements were made at 25 ± 1 °C using an Orion microprocessor ion analyzer 420A pH/mV with the proposed SC–PMA or SC–TPB membrane sensor in conjunction with a double-junction Ag/AgCl reference electrode (Orion 90-02) containing 10% (w/w) potassium chloride solution in the outer compartment. A combination Ross glass pH (Orion 81-82) glass electrode was used for the pH measurements.

2.3. Preparation of sildenafil drug ion pairs

The complex ion associates SC–PMA and SC–TPB ion pairs were prepared by mixing 10 ml (10^{-2} M) of an aqueous solution of SC with 20 ml (10^{-2} M) of PMA or NaTPB reagent, respectively. The mixtures were then shaken for 10 min and the formed precipitates were filtered off through a Wattman filter papers 42, washed with deionized distilled water, dried at room temperature and finally grounded to a fine powder.

2.4. Preparation of sildenafil citrate-PVC membrane sensors

A 10 mg portion of SC–PMA or SC–TPB was thoroughly mixed with 0.19 g PVC powder, 0.35 g of the plasticizer DOP or *o*-NPOE and 1 mg of the anion excluder KTPCIPB in a glass petridish (5 cm diameter). The cocktail was dissolved in 7 ml of freshly distilled THF, covered with a filter paper and left to stand overnight to allow slow evaporation of the solvent at room temperature. A transparent master PVC membrane with an average thickness of ~ 0.1 mm thick) was sectioned with a cork borer (10 mm diameter) and glued to polyethylene tubing as previously described [18,19]. The electrochemical system used was as follows: Ag/AgCl sat. KCl/test solution/membrane/internal filling solution of pH ~ 5 /sat. KCl/Ag/AgCl. The internal solution was a mixture of an equal volume of SC and potassium chloride solutions (1×10^{-2} M). The prepared sensors were conditioned by soaking in sildenafil citrate solution (1×10^{-2} M) for 2 h and were stored in the same solution when not in use.

2.5. Sensor calibrations

The developed sensors were calibrated by transferring aliquots (10 ml) of SC citrate (1×10^{-2} to 1×10^{-6} M) to 50 ml beaker at pH ~ 5 using acetate buffer at constant ionic strength of KCl (1.30 M). The pH of the test solution was adjusted with few drops of dilute HCl or NaOH (1×10^{-3} M). Each sensor was immersed in the test solution of SC in conjunction with a double junction Ag/AgCl reference

electrode. The potential readings were then recorded when stabilized to ± 0.2 mV and plotted versus logarithmic SC concentration. The calibration graphs obtained from direct potentiometry were then used in the subsequent determination of the unknown sildenafil concentrations in the tested samples.

2.6. Selectivity of the developed sensors

Aliquots (10 ml) of 1×10^{-3} M SC solution were adjusted to pH 5.0 with acetate buffer and the SC-TPB or SC-PMA sensor was immersed in the test solution and the potential was measured. The potentials of 1×10^{-3} M solution of the interferent adjusted to pH 5.0 were measured. The selectiv-

ity coefficients $K_{SC,B}^{pot}$ were determined employing separate solution method (SSM) with the rearranged Nicolsky equation [14,20]:

$$\log K_{SC,B}^{pot} = \left(\frac{E_1 - E_2}{S} \right) + \left(1 + \frac{z_1}{z_2} \right) \times \log(a) \quad (1)$$

where, E_1 is the potential measured in 1×10^{-3} M SC, E_2 the potential measured in 1×10^{-3} M of the interfering compound, z_1 and z_2 are the charges of the SC and interfering species B, respectively and S is slope of the electrode calibration plot.

2.7. Analysis of sildenafil in pharmaceutical preparations

2.7.1. Direct determination of sildenafil citrate

Three tablets of each pharmaceutical product (Viagra 50 or 100 mg) were weighed, pulverized and an appropriate portion (equivalent to 50 mg) was then dissolved in the minimum volume of distilled water by sonication for 10 min. The solution mixture was shaken in a mechanical shaker and accurately transferred to 50 ml measuring flask. The pH of the solution was then adjusted to pH 5 with dilute HCl and/or NaOH, completed to the mark with water, shaken and finally determined by the proposed sensor.

2.7.2. Standard addition method

Alternatively, the standard addition (spiking) method was used as follows: transfer a known volume of the test solution (1–8 ml) of the drug at pH 5 into a 25 ml measuring flask. Measure the potentials displayed by the test solution of the drug before and after addition of 1 ml aliquot of standard sildenafil citrate solution (1×10^{-2} M). The change in the

electrode potential (ΔE) was then recorded and used for determining the drug.

2.8. Analysis of sildenafil citrate in human serum

The serum samples were first processed and diluted with an aqueous solution of acetate buffer of pH 5 in a ratio of 1:9 serum to buffer to minimize fouling due to the serum. Aliquots of SC solution (1×10^{-2} to 1×10^{-4} M) were then spiked to the serum samples. The sensor SC-PMA or SC-TPB and an Orion double junction Ag/AgCl reference electrode were then immersed in 50 ml beaker containing the solution of the serum sample and SC. The potential of each solution was then measured before and after adding SC. The potential difference (ΔE) between the two measurements was then used for determining SC concentration in the unknown test solutions using standard addition method [14].

3. Result and discussion

3.1. Potentiometric measurements

In preliminary experiments, the complex ion associates SC-TPB and SC-PMA were used as ionophores in the preparation of a series of plasticized *o*-NPOE or DOP-PVC matrix membrane sensor. The composition of the membrane plays a crucial role in the sensor response. In the absence of the plasticizer NPOE or DOP and the anion excluder KTp-Table 1

Response characteristics of *o*-NPOE plasticized SC-PMA and SC-TPB PVC membrane sensors^a

Paramet	SC-PMA	SC-TPB
Slope (mV per decade)	55.5	
Intercept (mV)	287.2	282.5
Correlation coefficient (r) ($n = 5$)		± 0.35 0.996
Lower limit of linear range (M)		$\times 10^{-5}$ $\times 10^{-6}$
Response time for 1×10^{-3} M (s)	0.997 5	30 4–6
Working pH range		40 3–6

Detection limit
(M)

^a Average (n = 5) ± standard deviation of values recorded during 1 month.

CIPB on the PVC membrane sensor based on the ionophores SC-TPB or SC-PMA no response is obtained. Incorporation of the plasticizer NPOE or DOP in the membrane gives near-Nernstian to SC with cationic slope of 54.5 ± 0.43 and $48.0 \pm$

detections of approximately 6×10^{-6} and 5×10^{-6} M for SC-TPB and SC-PMA were achieved, respectively. The data also confirm that the ion pairs of the extracting agents NaTPB and PMA with SC seem to have the same solubility in the PVC membrane.

The response time of the two *o*-NPOE plasticized SC-PMA and SC-TPB sensors was tested at 1×10^{-3} and 1×10^{-2} M of sildenafil citrate and the sequence of the measurements are recorded from low to high concentrations. The response time for the two sensors to reach values within ± 0.2 mV of the final equilibrium potential at 1×10^{-2} M sildenafil citrate

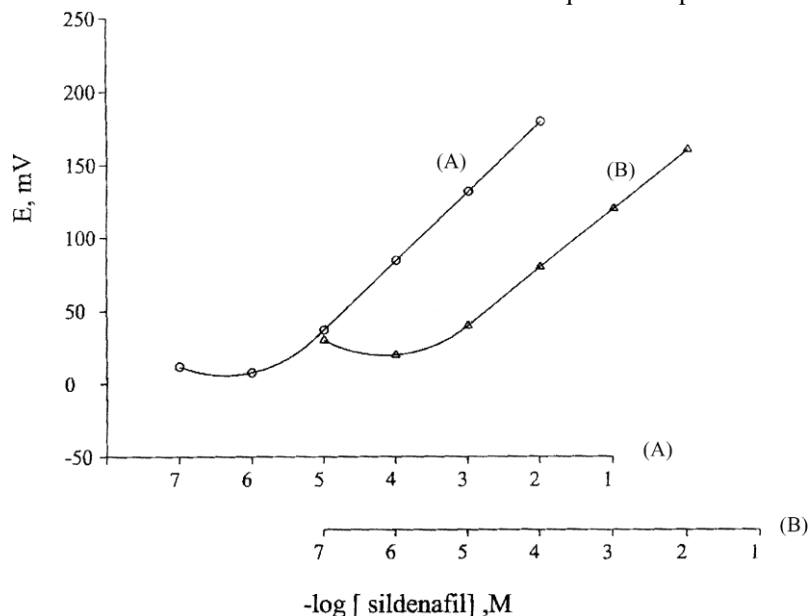


Fig. 2. Potentiometric response of the *o*-NPOE plasticized SC-PMA; (A) and SC-TPB; (B) PVC membrane sensors. 0.2 mV per decade for the SC analyte, respectively.

3.1.1. Performance characteristics of the sildenafil sensors

Good results are obtained with plasticized (DOP or *o*-NPOE)-PVC membrane sensors incorporating SC-TPB or SC-PMA ion pair prepared from the cast solutions of composition 2:69.8:28:0.2 wt.% of SC-PMA or SC-TPB, *o*-NPOE or DOP, PVC and KTpCIPB, respectively. The data on the performance characteristics were calculated according to IUPAC recommendation [21,22]. The critical response characteristics of the *o*-NPOE plasticized membrane electrodes based on SC-TPB or SC-PMA ion pair incorporating the anion excluder KTpCIPB are summarized in Table 1. Representative results are also shown in Fig. 2. The data indicated that, the two sensors are almost identical in terms of calibration slopes, near-Nernstian response over a relatively wide range of concentrations and the detection limit. The sensors SC-TPB and SC-PMA plasticized with *o*-NPOE exhibited near-Nernstian response in the range 10^{-2} to 10^{-5} M of sildenafil with cationic slope of 53.5 ± 0.5 and 55.5 ± 0.6 mV per decade, respectively. The lower limit of

were found equal 30 and 40 s for the SC-PMA and SC-TPB sensors, respectively. Both sensors have a potential stability and fluctuation of the calibration slope not exceeding 0.6 mV per decade over a period of 5 weeks. After that, the calibration slope and the linear range of response gradually decreased and the response time increased to 2–2.5 min for both sensors probably due to the leaching of the ion-pair from the PVC membrane. The detection limit for the SC-PMA sensor was found lower than that obtained for the sensor SC-TPB. This behavior is most likely attributed to the increased solubility of the SC-TPB compared to the SC-PMA complex ion associates. The calibration graphs for the two electrodes were found reproducible from day-to-day provided that the electrodes were stored in the appropriate sildenafil drug solution before use.

3.1.2. Effect of pH

The dependence of the potential response of the *o*-NPOE plasticized SC-TPB and SC-PMA based sensors for different concentration of SC (1×10^{-2} , 1×10^{-3} and 1×10^{-4} M) over various pH (2–10) using dilute HCl and/or NaOH was

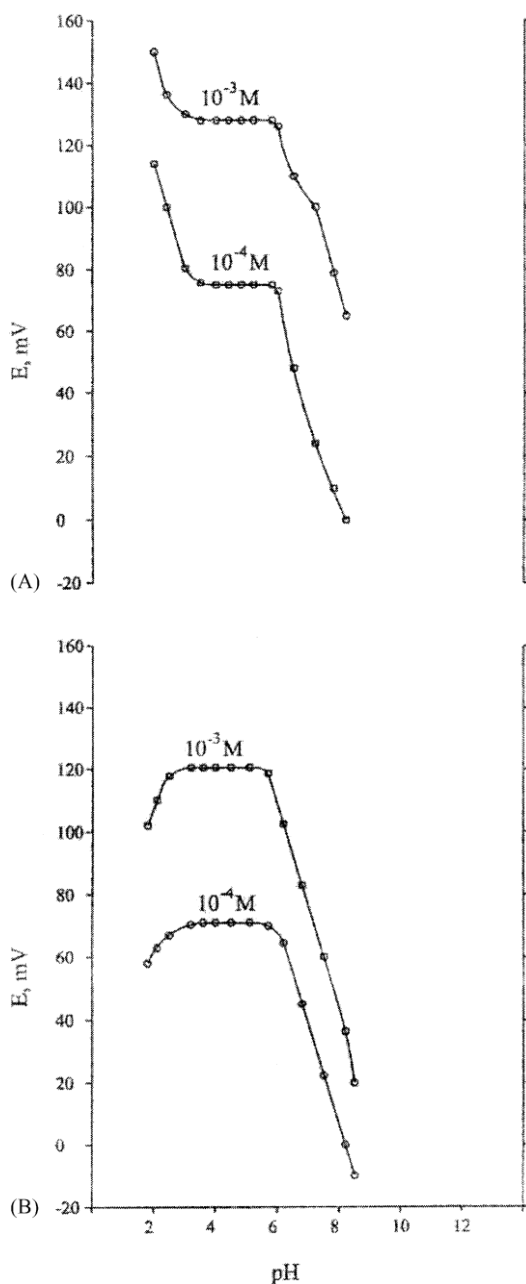


Fig. 3. Influence of pH on the potentiometric response of the *o*-NPOE plasticized SC-PMA; (A) and SC-TPB; (B) PVC membrane sensors.

sildenafil in the presence of many nitrogenous compounds such as amines, amino acid, and some inorganic cations was observed. The results showed no serious interference by a number of pharmaceutical excipients, diluents and active ingredients commonly used in the drug formulations (e.g. glucose, lactose, maltose, mannitol, starch, talc powder and magnesium stearate) at concentration as high as a 10–100-fold molar excess over sildenafil. The selectivity studies of the *o*-NPOE plasticized SC-PMA sensor containing the excluder KTpCIPB in its chemical composition showed a

better results over the SC-TPB sensor under the same conditions of operation (Table 2).

The plasticized PVC membrane sensors behave differently from liquid membrane sensors. Effectively, the ion exchange sites are poorly mobile and the coefficient $K_{SC,B}^{pot}$ of such system is given by the equation:

$$K_{SC,B}^{pot} = \frac{U_{BK} K_{SC}}{U_{SC} K_B} \quad (2)$$

where U_{SC} and U_B are the mobilities of the SC and the interfering species in the membrane phase and K_{SC} and K_B are the molar distribution coefficients of SC and the interfering ions between the aqueous phase and the PVC membrane. The fact that, in the PVC membrane, the ions are subjected to restricted mobility which are approximately the same for all counter ions when they complexed with long chain complexing agents [24]. Thus, the selectivity was related to the partition coefficients of the SC and the interfering ion between the membrane and the aqueous phase.

3.1.4. Effect of solvent mediators

Sildenafil PVC matrix membranes containing the plasticizer *o*-NPOE or DOP were prepared separately and tested for the calibration slope, lower limit of detection and sensitivity. A narrow linear response range from 5×10^{-4} to 5×10^{-2} M and a slope of 48 ± 0.2 mV per decade were achieved with the membrane sensors SC-TPB and SC-PMA plasticized with DOP. The two SC-TPB and SC-PMA sensors plasticized with *o*-NPOE showed high sensitivity, a wide range of linear response from 5×10^{-5} to 5×10^{-2} M and an average near-Nernstian of cationic slope of 53.5 ± 0.5 and 55.5 ± 0.35 mV per decade, respectively (Table 1). The sensor SC-PMA plasticized with *o*-NPOE containing KTpCIPB showed a good recovery percentage, precision response time and less standard deviation than the sensor SC-TPB under the same conditions of solvent mediator and anion excluder. Incorporation of the KTpCIPB (0.2% (w/v)) in the sensor cocktail containing SC-TPB or SC-PMA, PVC and *o*-NPOE enhanced the potentiometric working characteristics (response time and cationic slope) of the two sensors. The reagent KTpCIPB reduces the membrane resistance by reducing the activation barrier of the membrane–solution interface [15], and increase the mobility of the respective SC between the membrane and the aqueous phase [14].

3.2. Application of the proposed sensors

3.2.1. Analysis of sildenafil citrate in pharmaceutical preparations

The proposed sensors SC–TPB and SC–PMA are successfully applied for the determination of SC in pure form and in pharmaceutical preparations. Since the commercial SC tablets are coated with some diluents it was essential to analyze uncoated tablets to verify whether the coating materials would interfere with the analysis. The results indicated no interference from the coating materials, excipients or additives. On the other hand, when the membrane sensor is exposed

Table 3

Potentiometric determination of sildenafil citrate in tablets using SC–TPB and SC–PMA membrane sensors

Pharmaceutical products	Claimed values		Recovery ^a (%)			Ref. [10]
	SC–TPB	SC–PMA				
Viagra (Pfizer, USA)	10098.6					
Caverta 100 (Ranbaxy Laboratories, India)	10099.1		± 0.62	98.6 ± 0.62	99.7 ± 0.63	
			± 0.54	99.8 ± 0.36	99.7 ± 0.82	
			± 0.83	99.5 ± 0.43	98.6 ± 0.73	
			± 0.64	99.6 ± 0.45	100 ± 0.64	
Vega (Asia Co., Sorya)	50	99.3				
Kamagra (Ajanta Pharma, India)	10098.9					
		$F = 1.47^1$				$F = 0.86^1$
		$t = 0.65^2$	$F = 1.52^1, t = 0.62^2$			$t = 0.82^2$

^a Average (n = 5) ± standard deviation.

to high concentration of Ca²⁺ or Mg²⁺ ions interference occurred which was successfully eliminated by adding few drops of diethylenetriamine pentaacetic acid (5%). The results (Table 3) for the analysis of sildenafil in the pharmaceutical preparations by the developed SC–PMA and SC–TPB sensors, are in good agreement with the claimed values and the data obtained from spectrophotometry [10]. The average recovery was 98.97 ± 0.63% with a relative standard deviation (R.S.D.) of ±0.6% for the sensor SC–TPB and 99.4 ± 0.43%, and R.S.D. of ±0.43% for the sensor SC–PMA, respectively. The *F*-test revealed that no significant differences between the means and the variances of the two sets of results of the two sensors. The detection limit and the linear range by the developed SC sensors are also better than the data reported by the spectrophotometric methods [10,11]. The developed sensors were found suitable for routine control analysis of sildenafil citrate in tablets without prior pretreatment.

Alternatively, the standard addition method was also successfully employed for the analyses of the drug in tablet

by the developed sensors. Good correlation of 0.998 and recovery percentage of 99.6 ± 0.9% between the results obtained and the claimed values were achieved. The accuracy of the proposed sensors was estimated by the recovery studies of SC added to its tablet. On plotting the amount of SC added versus the amount recovered a regression line was obtained with a slope of 0.998 ± 0.006%, an intercept of near zero (0.033 ± 0.02%) and a correlation coefficient of near unity (0.999). The *F*- and *t*-tests at 95% confidence levels did not exceed the tabulated (theoretical) ones and no significant

differences observed between the developed sensors and the method reported [10] with respect to precision and accuracy (Table 3). Thus, statistical analysis revealed that the proposed sensors are good and comparable with the reported methods.

3.2.2. Analysis of human serum

Potentiometric measurements of SC in human serumacetate buffer of pH 5 before and after spiking known concentrations (10⁻² to 10⁻⁴ M) of SC were carried as described employing the sensors SC–PMA and SC–TPB. The results yielded an average recovery of 98.7% with a relative standard deviation of ±0.6% for the sensor SC–PMA and 98.5, and ±0.8% for the sensor SC–TPB, respectively.

4. Conclusions

The two proposed sensors offer simple, rapid, low cost, accurate and selective procedures for the determination of Viagra in pure form and in pharmaceutical preparations. The limit of detection (6 × 10⁻⁶ M) of the proposed sensor for SC compared favorably with some of the reported methods for SC determination [10,11]. The proposed sensors are faster and more convenient than those based on solvent extraction prior to the chromogenic complex formation and

spectrophotometric measurements [10,11]. The sensors were successfully employed for the determination of SC in dosage form and human serum without pretreatment or separation. The tolerance limits (5% errors maximum) for the tested diluents are experimentally adequate in real samples of complex matrices such as pharmaceutical preparation and biological fluids. Thus, the method can be used in routine control analyses for SC.

References

- [1] J. Henion, E. Brewer, G. Rule, *Anal. Chem.* 70 (1998) 20:650 A-6A.
- [2] S.A. Ballord, C.J. Gingeli, K. Tang, L.A. Turner, M.T. Price, A.M. Naylor, *J. Urol.* 159 (1998) 2164.
- [3] F. Montorsi, T.E.D. McDermott, R. Morgan, A. Olsson, A. Schuitz, H.J. Kirkeby, I.H. Osterloh, *Urology* 53 (1999) 1011.
- [4] R.A. Kloner, R.M. Zusman, *Am. J. Cardiol.* 84 (1999) 5B:11N.
- [5] J.D.H. Cooper, D.C. Muirhead, J.E. Taylor, P.R. Baker, *J. Chromatogr. B* 701 (1997) 87.
- [6] Y.M. Liu, H.C. Yang, J.R. Miao, *Yaowu-Fenxi-Zazhi* 20 (2000) 161.
- [7] M.E.S. Metwally, *Mansoura J. Pharm. Sci.* 16 (2000) 1.
- [8] J.J. Berzas, J. Rodriguez, G. Castaneda, M.J. Villasenor, *Anal. Chim. Acta* 417 (2000) 143.
- [9] R.J. Lewis, R.D. Johanson, C.L. Blank, Final Report No.: Dot/Faa/AM-00120, US Department of Transportation, Federal Aviation Administration, 2000, p. 1.
- [10] N.D. Dinesh, P. Nagaraja, N.M. Made Gowda, K.S. Ranappa, *Talanta* 57 (2002) 757.
- [11] A.S. Amin, A. El-Beshbeshy, *Mikrochim. Acta* 137 (2001) 63.
- [12] F.T. Dong, J. Liaa, Z. Yuan, Y. Liangg, X. Zhang, *Fenxi-Ceshi Xuebaq* 19 (2000) 353.
- [13] A.I. Segall, M.T. Vitzle, V.L. Perez, M.L. Palacios, M.T. Pizzorno, *J. Liq. Chromatogr. A* 23 (2000) 1377.
- [14] T.S. Ma, S.S.M. Hassan, *Organic Analysis Using Ion Selective Electrodes*, Academic Press, London, 1982.
- [15] G.K. Budnikov, *J. Anal. Chem.* 55 (2000) 1014.
- [16] R.I. Stefan, G.E. Bailulescu, H.Y. Aboul-Enein, *Crit. Rev. Anal. Chem.* 27 (1997) 307.
- [17] S.K. Menon, A. Sathyapalan, Y.K. Agrawal, *Rev. Anal. Chem.* 16 (1997) 333.
- [18] S.S.M. Hassan, W.H. Mahmoud, A.M. Othman, *Talanta* 47 (1998) 377.
- [19] A. Graggs, G.J. Moody, G.D.R. Thomas, *J. Chem. Educ.* 51 (1974) 451.
- [20] S.S.M. Hassan, W.H. Mahmoud, A.M. Othman, *Talanta* 44 (1997) 1087 (and references cited therein).
- [21] IUPAC Analytical Chemistry Division, Commission on Analytical Nomenclature, *Pure Appl. Chem.*, 67 (1995) 507.
- [22] A.J. Bard, L.R. Faulkner, *Electrochemical Methods Fundamentals and Applications*, Wiley, New York, 1980.
- [23] S.S.M. Hassan, S.A. Marzouk, *Talanta* 41 (1994) 891.
- [24] G. Eiseman, *Anal. Chem.* 40 (1968) 310.

2004 © The Japan Society for Analytical Chemistry

Potentiometric Determination of Dopamine in Pharmaceutical Preparations by Crown Ether-PVC Membrane Sensors

A. M. OTHMAN,* N. M. H. RIZKA,* and M. S. EL-SHAHAWI**²²

*Engineering and Biotechnology Research Institute (GEBRI), Minufiya University, Sadat City, Egypt

**Chemistry Department, Faculty of Science at Damietta, Mansoura University, Damietta, Egypt

Two simple, rapid and sensitive sensors for the assay of dopamine hydrochloride have been developed. The methods are based upon the formation of the membrane sensors 12-crown-4-phosphotungestic acid (crown ether-PTA)-dopamine and 12-crown-4-tetraphenylborate (crown ether-TPB)-dopamine as neutral carriers. The sensors were stable and showed fast potential responses of 10 s, and near-Nernstian cationic slopes of 53.3 – 56.2 mV/decade of activity between pH 2.2 – 6 for the monovalent dopamine cation over a wide range concentrations 1×10^{-5} – 1×10^{-1} M. The selectivity coefficients of the developed sensors indicated excellent selectivity for dopamine over a large number of organic and inorganic species and pharmaceutical excipients. The mediator *o*-nitrophenyloctyl ether significantly affected the lifetime of the fabricated sensors of dopamine. Satisfactory results were obtained for the determination of dopamine in dosage form by the proposed sensors with an average recovery of 99.85% for the nominal concentration.

(Received June 2, 2003; Accepted November 25, 2003)

Dopamine (DA) is one of the naturally occurring catecholamines, 4-(2-aminoethyl)benzene-1,2-diol hydrochloride (Fig. 1). It is an important chemical transmitter and an adrenal modular hormone at the terminals of sympathetic nerve.¹ Dopamine also acts as a biogenic amine, which functions as a neurotransmitter in the brain and nervous system of mammals.² Dopamine hydrochloride salt is widely used in the treatment of bronchial asthma, hypertension, heart failure, cardiac surgery and renal failures associated with shock episodes.^{3,4}

The detection and quantification of dopamine are of practical importance in chemical, biological, clinical, environmental and many other fields. A large number of procedures, *e.g.* spectrophotometric,^{5–8} gas, liquid and high-performance liquid chromatography,^{9–13} potentiometry and voltammetric methods^{14–16} have been developed. A number of biosensors at carbon-paste electrode modified with polyphenol oxidase have been fabricated for dopamine assay in the presence of metabolically related compounds.¹⁶ The present paper describes the use of two novel sensors for the analysis of dopamine hydrochloride in pharmaceutical products. The two sensors are based upon the use of an ion-association complex of 12-crown-4-tetraphenylborate or 12-crown-4-phosphotungestic acid as a neutral carrier in a plasticized PVC-matrix with a solvent mediator, *o*-nitrophenyloctyl ether. The two sensors display stable, fast and linear response over a wide range of concentrations and pH values.

hydrochloride, excipients, diluents and metal chloride or nitrate salts. Low-molecular-weight polyvinyl chloride (PVC), *o*-nitrophenyloctyl ether (*o*-NPOE), sodium tetraphenyl borate (NaTPB), phosphotungestic acid (PTA) and dopamine hydrochloride (DA) were supplied from Sigma. The crown ether (CE) 12-crown-4-ether, namely 1,4,7,10,13-pentaoxacyclopentadecane, and tetrahydrofuran (THF) were obtained from Fluka. Pharmaceutical preparations of dopamine

Experimental

Chemicals and materials

All of the chemicals and reagents were of analytical reagent grade unless otherwise stated. Doubly distilled water was used to prepare stock (0.1 M) and dilute solutions of dopamine

²² To whom correspondence should be addressed.

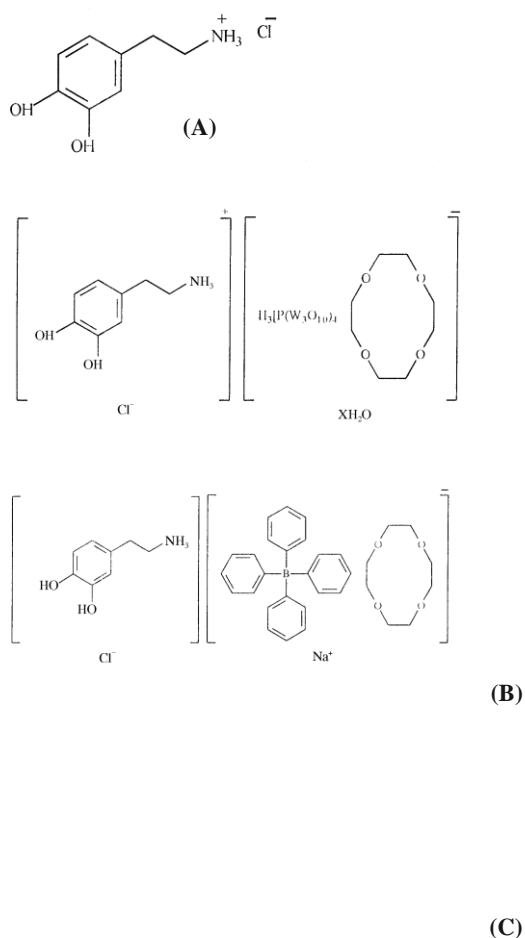


Fig. 1 Chemical structures of dopamine (A), CE-PTA (B) and CETPB (C).

652

hydrochloride were purchased from local drug stores and were of USP quality. A standard stock solution (1×10^{-1} M) of dopamine hydrochloride was prepared by dissolving 0.474 g of the salt in 25 ml acetate buffer (pH 4). Dilute solutions of the drug 10^{-2} – 10^{-6} M were freshly prepared by diluting the stock solution with doubly distilled water.

Apparatus

Potentiometric measurements were carried out at $25 \pm 1^\circ\text{C}$ with an Orion pH/mV meter (Model 720) microprocessor Ionalyzer. Two sensors, dopamine-12-crown-4-tetraphenylborate and dopamine-12-crown-4-phosphotungstic acid-PVC membrane sensors, were used with a double-junction Ag/AgCl reference electrode (Orion Model 90-02) containing a 10% (w/v) sodium nitrate solution in the outer compartment. The pH measurements were performed with a combination Ross glass electrode (Orion Model 81-02). A Perkin-Elmer Lambda 15 UV/VIS spectrophotometer was used for absorbance measurements.

Procedures

Preparation of ionophores. The ion-association complexes (ionophores), 12-crown-4-phosphotungstic acid (CE-PTA) and 12-crown-4-tetraphenylborate (CE-TPB), were prepared by mixing 10 ml of 1×10^{-2} M of PMA or NaTPB with 10 ml of 10^{-2} M of 12-crown-4, respectively. The mixtures were then shaken well for 10 min and the produced precipitates were filtered off through Whatman filter paper (No. 42), washed with deionized

water, dried at room temperature and finally ground to a fine powder.

Fabrication of PVC dopamine membrane sensors. A 10 mg portion of the complex ion associate CE-PTA or CE-TPB was mixed in a glass petri dish (5 cm diameter) with 170 mg of PVC powder and 380 mg of the plasticizer *o*-nitrophenyloctyl ether. The cocktail was dissolved in 5 ml of freshly distilled THF; and the petri dish was covered with filter paper and left overnight to allow slow evaporation of the solvent at room temperature. A transparent master PVC membrane with an average thickness of ≈ 0.1 mm was obtained, sectioned with a cork borer (10 mm diameter) and glued to polyethylene tubing as previously described.^{18,19} The electrode was filled with an internal solution prepared from a mixture of an equal volume of an aqueous Ag/AgCl/ 10^{-2} M KCl– 10^{-2} M dopamine solution || PVC membrane || 10^{-2} M solution (10^{-2} M) dopamine at pH 4.0 and potassium chloride. The prepared sensors were finally preconditioned by soaking them in a dopamine hydrochloride solution (1×10^{-2} M) for 1 h and stored in this solution when not in use. A reference Ag/AgCl wire electrode (1 mm diameter) was immersed in the internal solution.

Sensors calibrations

The developed sensors were calibrated by transferring 10 ml aliquots of an aqueous solution (10^{-1} – 10^{-6} M) of dopamine hydrochloride to 50 ml beakers, followed by immersing the dopamine-PVC membrane sensor in conjunction with a doublejunction Ag/AgCl reference electrode in the test solution. The potential readings were recorded after stabilization to 0.2 mV, and the e.m.f was plotted as a function of the logarithmic of the dopamine concentration. The calibration graphs were used for subsequent determinations of the unknown dopamine concentrations.

Sensor selectivity

The potentiometric selectivity coefficients ($K^{\text{pot}}_{\text{DA,B}}$) of the two sensors were determined by a separate solution technique using 1

ANALYTICAL SCIENCES APRIL 2004, VOL. 20
 $\times 10^{-2}$ M of the drug and the interferent¹⁸ as follows. The proposed sensor, CE-PTA or CE-PMA, was immersed in a 10 ml portion of 10^{-2} M of a dopamine solution adjusted to pH 4.0 and a potential reading was then made. The potential of a 10^{-2} M solution of the interferent species adjusted to pH 4 was measured. The potentiometric selectivity coefficients ($K_{\text{Ba},\text{B}^{\text{pot}}}$) is determined by employing the rearranged Niclosky equation,^{18,19} $\log K^{\text{pot}}_{\text{DA,B}} = [E_{\text{DA}} - E_{\text{B}}/S] + [1 + Z_{\text{DA}}/Z_{\text{B}}]\log DA$

where E_{DA} is the potential measured in 10^{-2} M for dopamine, E_{B} is the potential measured in 10^{-2} M of the interfering anion, Z_{DA} and Z_{B} are the charges of dopamine and the interfering ions, respectively, and S is the slope of the electrode calibration curve plot.¹⁸

Determination of dopamine in a pharmaceutical preparation

Direct determination of dopamine hydrochloride. Four ampoules of each pharmaceutical product were well mixed by shaking and an appropriate volume (5.0 ml) of an aliquot solution containing 1–10 mg was accurately transferred to a 100 ml calibrated flask and completed to the mark with acetate buffer (pH 4). The content was determined by measuring the e.m.f of the resulting solution by the proposed potentiometric method.

Standard addition method for the analysis of dopamine hydrochloride. Alternatively, the standard addition (spiking) technique was used as follows. A known volume of the test solution (50 ml) of the drug at pH 4.0 was transferred into a calibrated measuring flask (100 ml). The potentials displayed by

the test solution of the drug was measured before and after the addition of 0.5 ml of the standard dopamine hydrochloride solution (10^{-2} M). The change in the electrode potential was then recorded and used for determining the drug. The proposed methods were then compared with the reported spectrophotometric method for dopamine determination in pharmaceutical preparations at room temperature.²⁰

Results and Discussion

Performance characteristics of dopamine sensors

Macroyclic crown ethers are well-known as selective ligands for various ions.²⁰⁻²³ The compound 12-crown-4 reacted with phosphotungstic acid or tetraphenylborate, and the produced species were successfully used as neutral electrical carriers for the cationic response of some alkaline ions.^{22,23} These precipitates are easily prepared and have lower solubility than mono (crown ethers), and have similar characteristics as a crown ether.²³ Dopamine reacts with phosphotungstic acid and tetraphenylborate, forming soluble ion-associate complexes in an aqueous medium. Thus, the precipitate CE-PTA or CE-TPB in a PVC membrane containing *o*-NPOE plasticizer was used as electrical carriers for the determination of dopamine hydrochloride after soaking in 10^{-2} M DA solution. These membranes were electrochemically evaluated under a static mode of operation according to the IUPAC recommendation.²⁴ The membranes were prepared using casting solutions of 30:2:68 wt% of polyvinyl chloride, neutral carrier complex and solvent mediator, respectively. Table 1 summarizes the response characteristics, *e.g.* calibration slopes, response time, detection limits and intervals the linearity, over a period of three months for different assemblies of each sensor at the optimum pH and room temperature using the IUPAC recommendations.²⁴ The sensors showed good behavior regarding the response time

Table 1 Performance characteristics of dopamine PVC membrane sensors

Parameter ^a	PVC membrane sensor	
	CE-PTA	CE-TPB
Slope (mV/decade)	56.2 ± 0.5	53.3 ± 0.54
Intercept (mV)	-99 ± 0.4	-70 ± 0.3
Correlation coefficient (<i>r</i>) (<i>n</i> = 5)	0.997	0.998
Lower limit of linear range (M)	6×10^{-4}	8×10^{-4}
Lower limit of detection (M)	5×10^{-5}	6×10^{-5}
Response time for 1×10^{-3} M (s)	10	10
Working pH range	3.5 – 6.0	2.5 – 6.0

a. Average of 5 measurements.

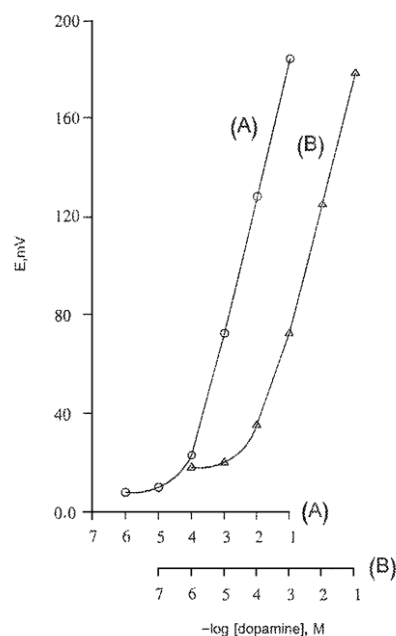


Fig. 2 Potentiometric responses of dopamine sensors CE-TPB (A) and CE-PTA (B).

Table 2 Selectivity coefficient ($K_{DA,B}^{pot}$) of dopamine PVC membrane sensors

Interferent, B	$K_{DA,B}^{pot}$	
	CE-PTA	CE-TPB
L-Dopa	3.16×10^{-2}	5.81×10^{-2}
Na ⁺	8.62×10^{-2}	1.39×10^{-3}
K ⁺	1.00×10^{-3}	2.65×10^{-3}
Mg ²⁺	5.26×10^{-3}	2.34×10^{-3}
Ca ²⁺	1.26×10^{-2}	4.28×10^{-2}
Urea	2.18×10^{-3}	1.03×10^{-2}
Triethanol amine	1.95×10^{-2}	1.07×10^{-2}
Glycine	1.96×10^{-3}	1.15×10^{-2}
Glucose	5.38×10^{-2}	1.18×10^{-2}
Maltose	1.34×10^{-3}	4.86×10^{-2}
Catechol	2.31×10^{-3}	3.26×10^{-3}
Pyrogallol	6.02×10^{-3}	7.46×10^{-3}
Resorcinol	1.19×10^{-3}	3.26×10^{-3}
Hydroquinone	4.75×10^{-3}	1.32×10^{-2}
<i>p</i> -Aminophenol	8.18×10^{-2}	1.11×10^{-2}

<i>p</i> -Aminobenzoic	1.19×10^{-3}	2.51×10^{-2}
Adrenaline	8.12×10^{-2}	7.11×10^{-2}
Noradrenaline	7.13×10^{-3}	6.51×10^{-2}

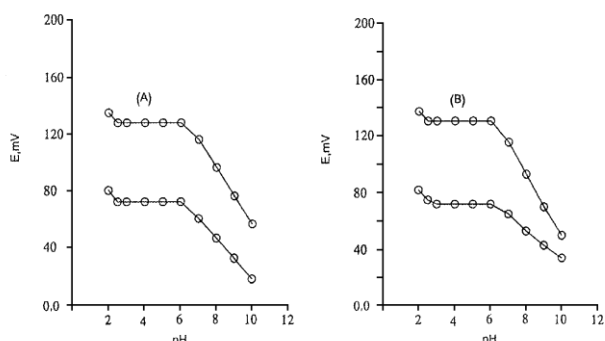


Fig. 3 Effect of the pH on the potential responses of dopamine sensors with CE-TPB (A) and CE-PTA (B).

and reproducibility of the e.m.f values of the electrodes. A typical calibration graph and the response characteristics of dopamine sensors based on CE-PTA or CE-TPB are shown in Fig. 2. At room temperature the two sensors displayed a linear response for dopamine hydrochloride over the concentration range $10^{-1} - 10^{-6}$ M and calibration slopes of 56.3 mV/decade and 53.3 mV/decade for the CE-PTA and CE-TPB sensors, respectively. The response time (t_{95}) of dopamine sensors was tested by measuring the time

membranes, an anion response can be observed that results in a reduction of the cation response. Thus, upon using 12-crown-4, the Nernstian slope response seems to demonstrate that the mobility of the cation complex is much higher than that of the free anion in the membrane phase. The sensor CE-PTA was found to be better than the sensor CE-TPB in terms of calibration slope, the near-Nernstian response over a wide range of concentrations and the detection limit under the

ANALYTICAL SCIENCES APRIL 2004, VOL. 20

Table 3 Determination of dopamine in some pharmaceutical formulations using direct potentiometry (A), spectrophotometry (B) and non-aqueous titrimetry (C)

Pharmaceutical product	Recovery, % ^a		
	A		B
	CE-PTA	CE-TPB	C
required to achieve a 95% steady potential for 10^{-4} and 10^{-3} M dopamine hydrochloride solutions when their concentrations were rapidly increased by one decade. Short response times of 10 s for DA > 10^{-3} M and 30 s for DA > 10^{-4} M, were obtained. The sensors displayed constant potential readings within 1 mV from day to day and the calibration slopes did not change by more than 1 mV per decade over a period of two weeks for PVC sensors. All of the sensors exhibited constant-slope values during at least 6 weeks, followed by a gradual decrease in their sensitivity as time passed. The calibration graphs for the two electrodes were found to be reproducible from day to day, provided that the sensors were stored in appropriate dopamine before use.	condition of solvent mediator <i>o</i> -NPOE. This behavior is most likely attributed to the high solubility of the complex ion associate CE-PTA, as compared to CE-TPB.		
It is well-known that crown ethers are very sensitive to the cation size of the tested anions. Thus, dopamine hydrochloride can be shifted very well into the cavity of CE-PTA; this complex may be stronger than that of CE-TPB with dopamine. This effect leads to a higher concentration of complex species	<i>Effect of the pH</i> Measurements of the pH dependence of dopamine sensors were performed over a wide range of pH 2 – 10. The pH was adjusted using dilute sodium hydroxide and/or hydrochloric acid. The potential–pH profile for 10^{-2} and 10^{-3} M drug Intropin, 200 mg/5 ml, Amp. Dupont, Co., UK Dopamine hydrochloride 200 mg/5 mL, Amp. DBL, Co., UK Dopamine hydrochloride 100 mg/5 mL, Amp. DBL, Co., UK Dopamine Fresenius 200 mg/5 ml, Amp. Fresenius Co., Germany		
in the membrane with CE-PTA. Boles and Buck ²⁵ have reported that, at a high concentration of complex species in solutions using the two sensors are summarized in Fig. 3. The data revealed a linear potential <i>versus</i> the pH in the range of pH 3 – 6 from the point of view of sensor functions. It is apparent that, at pH < 3, the dopamine sensors became progressively more sensitive to the protonated dopamine species. In addition, the e.m.f readings sharply increased. In a test at pH > 6, precipitation of the free dopamine base occurred with a gradual increase in the	a. Average of three measurements ± standard deviation. 100.3 ± 0.7 99.4 ± 0.6 98.3 ± 0.8 98.2 ± 0.7 99.5 ± 0.6 100.0 ± 0.8 98.1 ± 0.7 98.4 ± 0.8 99.9 ± 1.2 98.6 ± 1.2 99.3 ± 0.9 98.21 ± 1.4 99.6 ± 0.5 99.2 ± 0.7 97.9 ± 0.9 98.7 ± 0.5		

concentration of the unprotonated species.¹⁸ It has been shown that more than 50% of dopamine hydrochloride doubles the charge and, consequently, the concentration of the unprotonated species gradually increases, and therefore the drug cations become sensible.

Effect of foreign ions

The potentiometric selectivity coefficient ($K^{\text{pot}}_{\text{DA,B}}$) of the CEPTA and the CE-TPB PVC dopamine membrane-based sensors depends on the selectivity of the ion-exchange process at the membrane-sample interface and the mobility of the respective ions in the membrane, as well as the hydrophobic interactions between the primary ions and the organic membrane. The selectivity of the dopamine membrane electrodes is also related to the free energy of transfer of the dopamine hydrochloride drug cation between the aqueous and organic phases. The potentiometric selectivity of the two sensors towards different substances was determined with 10^{-3} M aqueous solutions of dopamine hydrochloride and foreign compounds using a separate solution method^{26,27} at pH 4.0. The obtained results are summarized in Table 2. Good selectivity towards dopamine was achieved in the presence of many inorganic and organic cations, amines, quinons and phenols, pharmaceutical excipients and diluents commonly used in drug formulations (e.g. glucose, lactose, maltose) at concentrations as high as a 10 – 100 fold molar excess over the dopamine concentration. The CE-PTA sensor was found to be more selective than the CE-TPB sensor. The other substances listed in Table 2 were chosen as representative of potentially low-level contaminants in pharmaceutical preparations or in biological fluids.

Potentiometric determination of dopamine in dosage forms

The proposed CE-PTA and CE-TPB sensors were successfully applied for the analysis of dopamine in pure form and in pharmaceutical preparations. The results for the analysis of dopamine in pharmaceutical preparations by the developed sensors are summarized Table 3. The data obtained by the proposed sensors are in good agreement with the claimed values, and compare favorably with the standard method of British Pharmacopoeia.²⁸ Average recoveries of 99.8 and 99.6% with mean standard deviations of $\pm 0.6\%$ and $\pm 0.7\%$, were obtained employing the CE-TPB and CE-PTA sensors, respectively. The data are also in good agreement with the certified values obtained by the reported spectrophotometric method²⁰ (average recovery of 98.1%, and standard deviation of $\pm 0.8\%$) and British Pharmacopoeia non-aqueous titrimetry²⁹ (89.4 and standard deviation ± 0.6). It is obvious from the results given in Table 3 that the proposed sensors can be successfully used for the selective determination of dopamine hydrochloride in the presence of its degradations.

Alternatively, the standard addition method was also applied to the analysis of dopamine in tablets by the proposed sensors. Good correlations of 0.998 and a recovery percentage of $99.7 \pm 0.6\%$ were obtained between the experimental results and the claimed values. The two sensors are also suitable for the quality-control analysis of dopamine in tablets without any prior pretreatment.

The prepared sensors were successfully used for the analysis of dopamine hydrochloride in pharmaceutical preparations at levels

$>1.9 \mu\text{g ml}^{-1}$. The developed sensors are selective, sensitive and attractive in terms of low cost for routine control analysis. The proposed sensors exhibit favorable performance characteristics of pH, low detection limit, calibration slope, and fast response; also the drug does not need any pretreatment or separation step and yields highly selective measurements in a synthetic mixture of electroactive substances. The sensors can be produced simply and reliably on a large scale and for these reasons may be regarded as being disposable.

References

1. T. Stabler, *J. Med. Tech.*, **1986**, 3, 351.
2. J. Axelord, *J. Neurosurg.*, **1981**, 55, 669.
3. C. L. Guan, J. Ouyang, Q. L. Li, B. H. Liu, and W. R. G. Baeyens, *Talanta*, **2000**, 50, 1197.
4. J. Liu, Z. H. Wang, G. A. Luo, Q. W. Li, and H. W. Sun, *Anal. Sci.*, **2002**, 18, 751.
5. P. Nagaraja, K. C. S. Murthy, K. S. Rangappa, and N. M. M. Gowda, *Talanta*, **1998**, 46(8), 39.
6. C. L. Hrynczewicz, M. Koberda, and M. S. Konkowski, *Electroanalysis*, **1998**, 7, 477.
7. V. A. Cardon, A. M. Mauri, E. M. Llobat, M. C. Pascual, and M. J. Simeon, *Fresenius, J. Anal. Chem.*, **1994**, 350(12), 706.
8. M. E. El-Kommos, F. A. Mohamed, and A. S. Kheder, *J. Assoc. Anal. Chem.*, **1990**, 73, 516.
9. R. M. V. Camanas, J. M. S. Mallois, J. R. T. Lapasio, and G. Ramisramos, *Analyst*, **1995**, 120, 1767.
10. E. Hollenbach, C. Schultz, and H. Lehnert, *Life Sci.*, **1998**, 63, 737.
11. O. Niwa and M. Morita, *Anal. Chem.*, **1996**, 68, 737.
12. M. Takahashi, M. Morita, O. Niwa, and H. Tabei, *Sens. Actuators*, **1993**, B13, 336.
13. L. R. Junior, J. C. B. Fernandes, G. De Oliveira Neto, and L. T. Kubota, *J. Electroanal. Chem.*, **2000**, 481, 34.
14. M. Chen and H. L. Li, *Electroanalysis*, **1998**, 7, 477.
15. O. Niwa, M. Morita, and H. Tabei, *Sens. Actuators*, **1993**, B14, 558.
16. K. Odashima, K. Yagi, K. Tohda, and Y. Umezawa, *Bioinorg. Med. Chem. Lett.*, **1999**, 9, 2375.
17. E. S. Forzani, G. A. Rivas, and V. M. Solis, *J. Electroanal. Chem.*, **1997**, 435, 77.
18. T. S. Ma and S. S. M. Hassan, "Organic Analysis Using Ion Selective Electrodes", **1982**, Vols. 1 and 2, Academic Press, London.
19. A. Craggs, G. J. Moody, and J. D. R. Thomas, *J. Chem. Educ.*, **1974**, 51, 451.
20. M. E. El-Kommos, *J. Pharm. Belg.*, **1987**, 42, 371.
21. C. J. Pederson, *J. Am. Chem. Soc.*, **1967**, 89, 7017.
22. D. DaWang and J. S. Shih, *Analyst*, **1985**, 110, 635.
23. J. Jeng and J. S. Shih, *Analyst*, **1984**, 109, 641.
24. IUPAC Analytical Chemistry Division, *Pure and Appl. Chem.*, **1995**, 67, 507.
25. J. H. Boles and R. P. Buck, *Anal. Chem.*, **1972**, 45, 2057.
25. S. S. M. Hassan and N. M. H. Rizk, *Anal. Lett.*, **2000**, 33, 1037.
26. N. M. H. Rizk, *Mikrochim. Acta*, **2002**, 138, 53.
27. British Pharmacopoeia, **2000**, Vol. 1, Version 4.0 Crown Copyright.
28. H. Zhoo, Y. Zha, and Z. Yuan, *Anal. Chim. Acta*, **2001**, 441, 117.



Synthesis, spectroscopic characterization, redox properties and catalytic activity of some ruthenium(II) complexes containing aromatic aldehyde and triphenylphosphine or triphenylarsine

M.S. El-Shahawi*, A.F. Shoair

Chemistry Department, Faculty of Science at Damietta, Mansoura University, Mansoura, Egypt

Received 6 January 2003; received in revised form 11 April 2003; accepted 14 April 2003

Abstract

A series of new mixed ligand penta-coordinated square pyramidal ruthenium(II) complexes containing benzaldehyde or its substituents and triphenylphosphine or triphenylarsine have been synthesized and characterized. In the electronic spectra, three well-defined peaks in the visible region were observed and assigned to d–d transitions in D_{4h} and low spin axially distorted from O_h symmetry. The spectrochemical parameters of the complexes were calculated and placed the ligands in the middle of the spectrochemical series. The redox properties and stability of the complexes toward oxidation were related to the electron-withdrawing or releasing ability of the substituent in the phenyl ring of the benzaldehyde. The electron-withdrawing substituents stabilized Ru^{2+} complexes, while electron-donating groups favored oxidation to Ru^{3+} . The mechanism and kinetics of the catalytic oxidation of benzyl alcohol by the complex $[RuCl_2(PPh_3)(C_6H_5CHO)_2]$ in the presence of *N*-methylmorpholine-*N*-oxide have also been studied.

© 2003 Elsevier B.V. All rights reserved.

Keywords: Synthesis; Ruthenium(II); Spectroscopic characterization; Redox properties; Reactivity

1. Introduction

Transition metal complexes with some ligand systems containing N- and N,O-donors have been recognized as inorganic catalysts for olefin epoxidation, alcohols and aliphatic and aromatic hydroxylations [1–8]. The ruthenium(II or III) complexes containing weak donor ligands are lacking in comparison to other donor ligands [9–12]. Ruthenium(II) complexes have been characterized by their high stability mainly when ligands with donor atoms such as N, P, S, As or O are present in the coordination sphere [13,14].

Recent years have seen an upsurge of interest in finding versatile ruthenium(II) complexes that allow both catalytic and electrochemical behavior. In view of that and as a part of our continuing work on O,O-donor ligands we report herein the synthesis and characterization of some novel ruthenium(II) complexes containing triphenylphosphine (or

* Corresponding author. Tel.: +20-5-740-3867; fax: +20-5-740-3868.

E-mail address: mohammad-el-shahawi@hotmail.com (M.S. El-Shahawi).

1386-1425/\$ – see front matter © 2003 Elsevier B.V. All rights reserved.
doi:10.1016/S1386-1425(03)00191-4

triphenylarsine) and acceptor aromatic aldehyde (Fig. 1). The nature of the electrode reactions of the prepared complexes and the oxidative behavior of one of the complexes were discussed.

2. Experimental

2.1. Reagents and materials

All the chemicals used are of analytical reagent grade. The reagent *N*-methylmorpholine-*N*-oxide (NMO), $RuCl_3 \cdot 3H_2O$, benzaldehyde, 4-Br-benzaldehyde, anisaldehyde, *o*-phthaldehyde, triphenylphosphine (PPh_3) and triphenylarsine

(Asph₃) were obtained from Aldrich. The complex [RuCl₂(Pph₃)₂] was prepared as reported [15]. The supporting electrolyte tetrabutylammonium-hexafluorophosphate (TBA)⁺PF₆⁻ was dried in vacuum before use. The solvents used were degassed and the ruthenium percentage in the complexes was determined by the reported methods [16,17]. The electrochemical measurements were carried out at 30 °C.

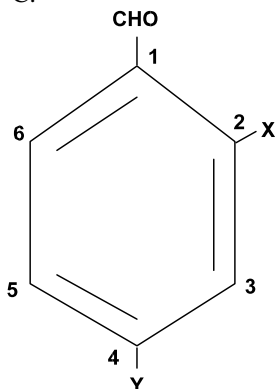


Fig. 1. Atom numbering scheme of the aldehyde molecules. X=H, Y=CH₃O; X=H, Y=Br and X=CHO, Y=H.

2.2. Physical measurements

Infrared (IR) spectra (200–4000 cm⁻¹) as KBr discs were measured on a Matson 500 FT-IR spectrometer at room temperature. ¹H NMR in DMSO-d₆ and electronic spectra in CH₂Cl₂ (~5×10⁻⁴ M) were recorded on a Varian Gemini VM-200 and a Unicam UV₂₋₁₀₀ UV-visible spectrometers, respectively. Cyclic voltammograms (CVs) were recorded on a potentiostat/wave generator (Oxford Electrodes) equipped with a 7000 AM X-Y recorder. A conventional three-electrode electrochemical cell was used comprising a platinum micro-cylinder working electrode, a spiral platinum wire (0.5 mm diam) as a counter electrode and Ag/AgCl reference electrode to which all potentials are referred. The electrochemical experiments were performed using a concentration of 1×10⁻³ mol dm⁻³ of the complex and 1×10⁻² mol dm⁻³ of the supporting electrolyte in CH₂Cl₂. The solutions of the complexes were bubbled with dry N₂ for 20 min before CV measurements. All microanalyses (C, H, Cl) analyses were performed on a Perkin–Elmer, 240 C elemental analyzer at Plymouth University, UK.

2.3. Recommended procedures

2.3.1. Synthesis of ruthenium(II) complexes

2.3.1.1. [RuCl₂(Pph₃)₂], L=HC₆H₄CHO, 4-CH₃OC₆H₄CHO or 4Br-C₆H₅CHO. A suspension of L (2 mmol) and

RuCl₂(Pph₃)₃ (0.95 g, 1 mmol) in degassed ethanol (40 cm³) was refluxed for 3 h during which the complex RuCl₂(Pph₃)₃ was dissolved and the reaction mixture was turned to brownish (or green) color. A brown or green precipitate appeared after slow evaporation of the solvent, filtered off, washed with ethanol, diethylether and finally dried in vacuum.

2.3.1.2. [RuCl₂(Asph₃)L₂], L=HC₆H₄CHO or 4-CH₃OC₆H₄CHO. An accurate weight (0.104 g; 0.5 mmol) of hydrated RuCl₃ in ethanol (10 cm³) was mixed with benzaldehyde or anisaldehyde (1 mmol) and triphenylarsine (0.15 g, 0.5 mmol) in 10 cm³ ethanol under constant stirring. The reaction mixture was refluxed for 2 h. Green precipitate was separated out, filtered off, washed with ethanol and finally dried in vacuum.

2.3.1.3. [RuCl₂(MPh₃)L₂], M=P or As, L'=2-CHO C₆H₄CHO. To a solution of RuCl₃·3H₂O (0.21 g, 1 mmol) in degassed methanol (20 cm³), the reagent *o*-phthaldehyde (0.27 g, 2 mmol) in 10 cm³ methanol was added and the reaction mixture was refluxed for 1 h. A solution of triphenylphosphine (0.25 g, 1 mmol) or triphenylarsine (0.29 g, 1 mmol) in methanol (10 cm³) was then added slowly to the hot solution with constant stirring. The resulting reaction mixture was refluxed for 2 h. On concentrating and cooling the solution, a brown or purple precipitate was separated out, filtered off, washed with diethylether and finally dried in vacuum.

2.3.2. Catalytic oxidation

The catalytic activity of the prepared complexes for the oxidation of benzyl alcohol (phCH₂OH) to benzaldehyde (phCHO) was tested in the presence of NMO as a co-oxidant. A typical reaction using the complex [RuCl₂(Pph₃)(C₆H₅CHO)₂] as a catalyst and BA as a substrate at 1:200 molar ratio is described as follows: A solution of [RuCl₂(Pph₃)(C₆H₅CHO)₂] (0.001 g, 0.01 mmol) in 10 cm³ CH₂Cl₂ was added to a solution of benzyl alcohol (2 mmol) and NMO (20 cm³, 3 mmol) with constant stirring. The solution mixture was refluxed for 2 h and the solvent was then evaporated from the mother liquor under reduced pressure. The solid residue was then extracted with diethylether (3×10 cm³) and the ethereal extract was then filtered off and quantified as 2,4-dinitrophenylhydrazone derivative. The catalytic activity of the complex was determined from the percent yield (Y%) and the turnover (T.O) conversion of BA to benzaldehyde as follows:

$$Y (\%) = \frac{\text{Weight of BA oxidized to benzaldehyde}}{\text{Weight of BA}} \times 100 \quad (1)$$

$$\text{T.O} = \frac{\text{Total weight of BA}}{\text{mmoles of product}} \quad (2) \text{ mmoles of catalyst}$$

3. Results and discussion

The prepared complexes are listed in Table 1 together with their elemental analyses and colors. The complexes are green/brown, dark green and purple in color. Two types of complexes having the general formulae $[\text{RuCl}_2(\text{MPh}_3)\text{L}_2]$ and $[\text{Ru}_2\text{Cl}_4(\text{H}_2\text{O})_2(\text{MPh}_3)_2\text{L}'_2]$ where $\text{M}=\text{P}$ or As , $\text{L}=\text{H}-\text{C}_6\text{H}_4\text{CHO}$, $p\text{-Br}-\text{C}_6\text{H}_4\text{CHO}$ or $p\text{-CH}_3\text{O}-\text{C}_6\text{H}_4\text{CHO}$ and $\text{L}'=o\text{-CHO}-\text{C}_6\text{H}_4\text{CHO}$ are formed. The proposed chemical structures of the complexes are in good agreement with the stoichiometries concluded from their analytical data (Table 1). During the course of these synthetic reactions, ruthenium(III) undergoes a

Table 1
Analytical data and color of the prepared ruthenium(II) complexes

Complex	Color	Calculated (found) %			
		C	H	Ru	Cl
$[\text{RuCl}_2(\text{Pph}_3)(\text{C}_6\text{H}_5\text{CHO})_2]$	Brown	59.4 (60.2)	4.1 (4.2)	15.6 (15.34)	10.9 (11.2)
$[\text{RuCl}_2(\text{Pph}_3)(p\text{-CH}_3\text{OC}_6\text{H}_4\text{CHO})_2]$	Brown	57.7 (58.4)	4.3 (4.1)	14.3 (14.0)	10.0 (10.3)
$[\text{RuCl}_2(\text{Pph}_3)(p\text{-BrC}_6\text{H}_4\text{CHO})_2]$	Green	47.7 (48.8)	3.1 (3.4)	12.5 (12.1)	8.8 (8.6)
$[\text{RuCl}_2(\text{Asph}_3)(p\text{-CH}_3\text{OC}_6\text{H}_4\text{CHO})_2]$	Brown	54.4 (55.8)	4.1 (4.3)	13.4 (12.9)	9.4 (9.8)
$[\text{RuCl}_2(\text{Asph}_3)(\text{C}_6\text{H}_5\text{CHO})_2]$	Green	55.6 (55.1)	3.9 (3.6)	14.6 (14.1)	10.2 (9.7)
$[\text{Ru}_2\text{Cl}_4(\text{Pph}_3)_2(\text{H}_2\text{O})_2(o\text{-CHOC}_6\text{H}_4\text{CHO})_2]$	Brown	54.9 (54.2)	3.6 (3.9)	17.1 (17.4)	12.5 (12.1)
$[\text{Ru}_2\text{Cl}_4(\text{Asph}_3)_2(\text{H}_2\text{O})_2(o\text{-CHOC}_6\text{H}_4\text{CHO})_2]$	Brown	66.6 (66.1)	3.4 (3.2)	16.5 (15.8)	11.6 (11.2)
$[\text{RuCl}_2(\text{Pph}_3)_3]$	Green	49.7 (48.9)	3.4 (3.2)	23.2 (24.1)	16.3 (15.7)

one-electron reduction and the solvent may serve as the reductant. The isolated solid complexes are stable in air at room temperature, non-hygroscopic in nature and almost insoluble in common organic solvents. The complexes are easily soluble in dichloromethane, DMF and DMSO. The conductivity measurements of the complexes fall in the range for non-electrolytes [18]. Magnetic susceptibility measurements showed that, all the complexes are diamagnetic at room temperature as expected for ruthenium(II) (low spin d^6 , $S=0$) complexes.

3.1. Spectroscopic studies

The IR spectra of the complexes (Table 1) displayed the characteristic bands due to triphenylphosphine at $440\text{--}455\text{ cm}^{-1}$ or triphenylarsine at $272\text{--}295\text{ cm}^{-1}$ [19]. The free aldehydes showed their characteristic strong carbonyl frequency $\nu(\text{C}=\text{O})$ in the region $1675\text{--}1710\text{ cm}^{-1}$ [13,19]. In the IR spectra of the complexes, the νCO vibrational mode was shifted ($\sim 30\text{--}40\text{ cm}^{-1}$) towards the lower frequency region from that observed for the free ligands confirming

participation of the oxygen atom of the aldehyde ($-\text{CHO}$) group in the complex formation [13,19]. The medium IR bands between 450 and 520 cm^{-1} in the spectra of the complexes are assigned to $\nu(\text{Ru}-\text{O})$ vibration [13,19]. The observed bands in the regions $430\text{--}470$ and $320\text{--}330\text{ cm}^{-1}$ in the mononuclear complexes (1–5) are tentatively assigned to the $\nu_{\text{Ru}-\text{Cl}}$ vibrations [19]. The two bands located in the region $320\text{--}330\text{ cm}^{-1}$ are consistent with $\nu_{\text{Ru}-\text{Cl}}$ vibrations of the dichloro ligands in *cis*- geometry as previously reported for *cis*- $[\text{RuCl}_2(\text{Pph}_3)_2(\text{RCN})_2]$ [20]. In the *o*-phthaldehyde complexes the presence of coordinated water molecules in the complexes (6 and 7) was confirmed by the appearance of a sharp band around $3440\text{--}3445\text{ cm}^{-1}$ and two weaker bands around 700 and 850 cm^{-1} . The latter two bands are safely assigned to wagging and/or rock vibrations of aqua ligands [21,22]. Therefore, in the *o*-phthaldehyde complexes we postulated that, the two *o*-phthaldehyde molecules (or the two chlorine atoms) bridge the two ruthenium(II) atoms as shown

Fig. 2. This structure was also confirmed on the basis of the spectroscopic data and by the analogy with related complexes [12–14].

The ^1H NMR spectra of the free aldehydes and their ruthenium(II) complexes (Table 2) showed a similar pattern and are in accordance with the reported data [12,13]. The $-\text{CHO}$ proton signal in the free aldehydes was appeared as a sharp singlet in the region δ 9.8–10.2 ppm. In the ruthenium(II) complexes, the aldehyde proton signal was shifted down field as a singlet at δ 10.0–10.25 and 10.10–10.3 ppm for mono- and *o*-dialdehyde, respectively. These data confirm participation of the $-\text{CHO}$ group upon complex formation [17,18] and the structure (Fig. 2) proposed for the *o*-phthaldehyde complexes. Similar features have been observed for the 2-hydroxy-1-naphthaldehyde ruthenium complexes [12,23]. The de-shielding caused by the donation of the lone pair of electrons of the aldehyde oxygen atom to the central metal ion could account for the observed chemical shift in the ^1H NMR spectra [22,24]. The observed signal

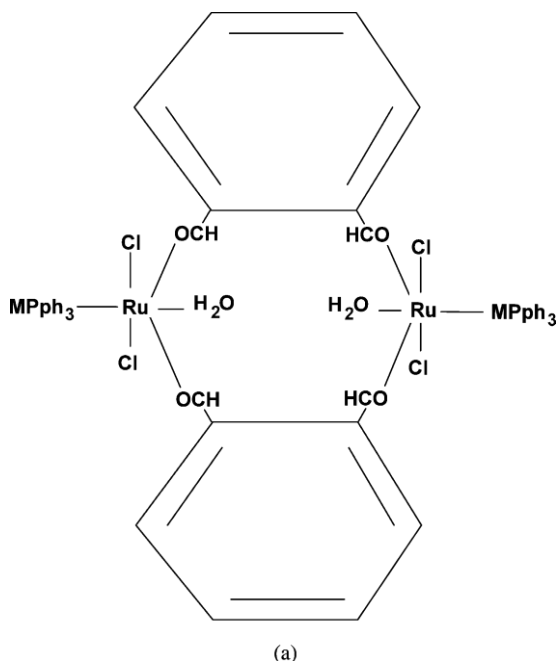


Fig. 2. Proposed chemical structure of the binuclear *O*-phthalaldehyde ruthenium(II) complex $[\text{RuCl}_2(\text{MPPh}_3)(o\text{-CHO-C}_6\text{H}_4\text{CHO})_2]$, $\text{M}=\text{P}$ or As .

Table 2

Significant IR-vibrational frequencies (cm^{-1}) and ^1H NMR (δ ppm) of the ruthenium(II) complexes with relevant bands of the free aldehyde in parentheses

Complex	$\nu_{\text{C=O}}$	$\nu_{\text{Ru-O}}$	$\nu_{\text{Ru-Cl}}$	$\nu_{\text{Ru-P}}$	$\nu_{\text{Ru-As}}$	Complexed H_2O	δ (ppm)
1	1685(s), (1715)	480(m)	460(s)	445			10.12, 7.2, 7.58, 7.5
2	1675(s), (1710)	450(m)	430(s)	451			10.20, 6.90, 7.36, 7.3, 3.9, (10.1), (7.12), (7.4), (3.92)
3	1700(s), (1730)	505(m)	450(s)	455			10.20, 6.98, 7.5, 7.46
4	1795, (1735)	520(m)	445(s)	440			10.25, 7.38, 7.4, 7.3, 3.8
5	1690, (1730)	490(m)	465(s)		272		10.2, 7.25, 7.52, 7.5
6	1710(s), (1745)	510(m)	470		285	3440(s), 850(w), 700(w)	10.16, 7.28, 7.6, 7.6, (9.85), (7.10), 7.56, 7.50
7	1710(s), (1745)	510(m)	470(s)		295	3445(m, br), 860(w), 705(w)	10.3, 7.01, 7.6, 7.5
8			475	455	295		

* s, strong; m, medium; br, broad and w, weak.

at δ 3.8–3.94 ppm in the anisaldehyde and its complexes is attributed to the methoxy proton [22,25]. This proton undergoes deshielding to a magnitude of 0.45 ppm in the complexes supporting the involvement of the $-\text{CHO}$ group in the complex formation. The resonance arising from H_3 and H_5 (see Fig. 1 for atom numbering scheme) in the mono aldehydes were shifted as double–doublet (7.1–7.6 ppm) to high field to a greater extent than H_2 and H_6 (7.4–7.9 ppm). A sharp multiplet signal in the range δ 6.90–7.29 ppm was observed and was attributed to the pPh_3 or AsPh_3 protons. In

the free benzaldehyde and *O*-phthalaldehyde ligands, the H_3 , H_4 and H_5 protons appeared as doublets at 7.3, 8.1 and 7.9 ppm. In the complexes, the signals arising from H_3 , H_5 and H_6 protons were observed at high field similar to that reported for Sb^{3+} and Zn^{2+} complexes with similar ligands [23]. This behavior is most likely due to the decreasing in the electronic density of the aromatic ring of the coordination. The multiple peaks of the substituted aromatic protons resonate in the region δ 7.15–7.20 ppm due to one bound triphenylphosphine (or triphenylarsine) and two inequivalent aldehyde ligands. These data confirmed that the PPh_3 or AsPh_3 and chloride ligands are mutually *cis*- as reported for similar geometry of ruthenium(II) complexes [26,27].

The UV–visible spectra of the complexes are similar to those observed for other analogous of low spin penta-coordinated square pyramidal ruthenium(II) complexes [26,27]. The spectral of the complexes with their ligand field parameters ($10D_q$, B) in CH_2Cl_2 are summarized in Table 3. The spectra of these complexes are similar and displayed three well bands in the range $(16.9\text{--}17.8)\times 10^3$,

Table 3

$(19.4\text{--}23.6)\times 10^3$ and $(24.9\text{--}27.6)\times 10^3 \text{ cm}^{-1}$. The molar extinction coefficients of these bands are low relative to those of metal to ligand charge transfer (MLCT) transition [27]. Assuming that, the complexes belong to D_4 or low spin axially distortion from octahedral symmetry, the first two bands (Table 3) are safely assigned to the ν_1 ($^1A_{1g} \rightarrow ^1E_{2g}$) and ν_2 ($^1A_{1g} \rightarrow ^1A_{2g}$) d–d transitions in the range corresponding to the spin allowed transitions from the lower frequency side [26,28]. The third peak is possibly assigned to a contribution

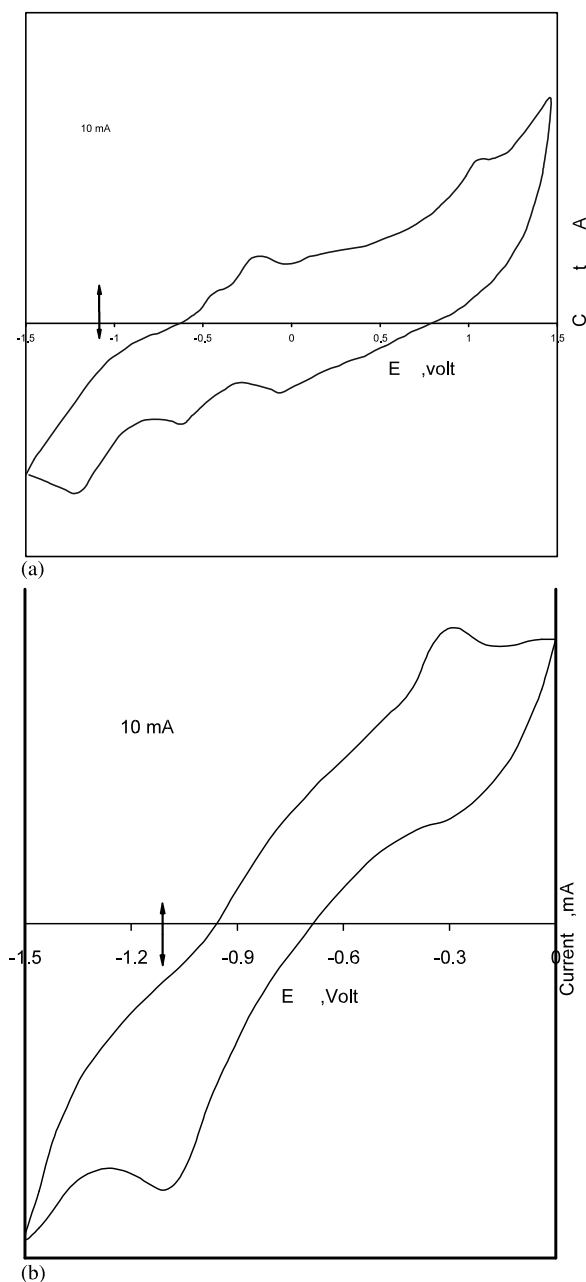
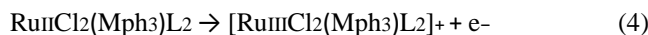


Fig. 3. CVs of $[\text{RuCl}_2(\text{Pph}_3)(p\text{-BrC}_6\text{H}_4\text{CHO})_2]$, (a) and $\text{RuCl}_2(\text{Asph}_3)(p\text{-CH}_3\text{OC}_6\text{H}_4\text{CHO})_2$, (b) in dichloromethane–(TBA)PF₆ solution vs. Ag/AgCl electrode.

complexes. Thus, this electrode couple is safely assigned to Ru^{II}/Ru^{III} oxidation as follows:



The potential of this couple was found not sensitive to the nature of the substituent in the *para*-position of the aldehyde ligand. The electrode potential (E^\ominus) slightly increased with increasing electron-withdrawing character. The plot of E^\ominus

versus Hammett constant (2δ) [32] of the *para*-substituent in the aldehyde was found linear.

The irreversible one electron metal-centered oxidation in the potential range 0.52–0.98 V is safely assigned to the Ru^{III}/Ru^{IV} oxidation [30] as follows:

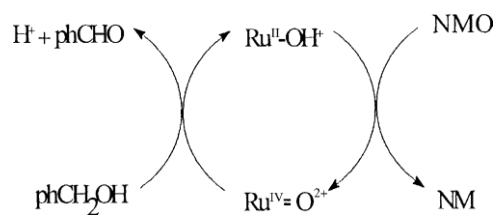


The oxidation potential of this couple correlates linearly with the Hammett constant (δ) of *p*-substituent and the E^\ominus of this couple is sensitive to the nature of *p*-substituent compared with Ru^I/Ru^{III}. The data also confirm that the electron-withdrawing groups attached to the aldehyde moiety stabilize the Ru^{II} complexes while electron-donating groups favor oxidation of Ru^{III}.

3.3. Catalytic oxidation

The applications of ruthenium(II) complexes as an inexpensive and easy to handle co-oxidant for selective oxidation of alcohols are well known in the literature [12,33]. No oxidation of benzyl alcohol to benzaldehyde was achieved employing NMO only. Thus, the catalytic oxidation of benzyl alcohol to phCHO by the precursor catalyst $[\text{RuCl}_2(\text{Pph}_3)(\text{C}_6\text{H}_5\text{CHO})_2]$ in the presence of NMO (1:200 molar ratio of catalyst to substrate) at room temperature in dry CH₂Cl₂ was carried out. Excellent experimental yield (70±5%) with good turnover (140±2) of BA to BCHO was successfully achieved. These results are better as compared with the data reported for $[\text{Ru}^{\text{II}}(\text{bpy})_2\text{acac}]\text{PF}_6$, $[\text{Ru}^{\text{II}}(\text{bpy})_2\text{Cl}_2]\text{IO}_4$, $[\text{Ru}^{\text{II}}\text{Cl}_2(\text{Pph}_3)_3]$ and Ru^{II} complexes of 1,1-bis isoquinoline (BIQN) [32,33]. The formation of benzaldehyde was confirmed by the formation of 2,4-dinitrophenylhydrazone.

The mechanism of oxidation of benzyl alcohol to benzaldehyde by the catalyst $[\text{RuCl}_2(\text{Pph}_3)(\text{C}_6\text{H}_5\text{CHO})_2]$ in the presence of the co-oxidant could be proceeded via the formation of π -peroxoruthenium(IV) intermediate species which are capable to abstract hydrogen atom from the OH group in benzyl alcohol (Scheme 1). This mechanism is similar to that reported for $[\text{RuBr}_2(\text{Pph}_3)(\text{C}_6\text{H}_5\text{CHO})_2]$, $[\text{Ru}^{\text{II}}\text{Cl}_2(\text{Pph}_3)_3]$, $[\text{Ru}^{\text{II}}(\text{terpy})(\text{BIQN})\text{Cl}]\text{ClO}_4$ and $[\text{R}(\text{trPy})(\text{R}_2\text{dppi})\text{O}]^{2+}$ complexes [34,35], where terpy=2,2,6,2-terpyridine; H₂dppi=3,6-bis(pyridin-2-yl)pyridazine and trpy=2,2,2-terpyridine. The reaction velocity of this type of reactions always shows first-order kinetics in terms of the amount of unconsumed benzyl alcohol [36].



Scheme 1.

4. Conclusions

The weak O-donor aromatic aldehydes coordinate to ruthenium(II) ions. The mono- and di-aldehydes tend to impose penta-coordinated square-based pyramidal and octahedral coordination sphere, respectively, at the metal centers as a consequence of the reduced conformational flexibility caused by the presence of PPh₃ (or AsPh₃). Substitution of the hard O- or Br-donor atom in the *para*-position of the benzaldehyde facilitates the redox properties. The catalytic reactivity of the complex [RuCl₂(PPh₃)(C₆H₅CHO)₂] towards oxidation of benzyl alcohol was found higher than that reported for N,N- and some N,O-neutral ligands under similar conditions [33]. Further experiments are currently in progress to explore the mechanism and kinetics of the catalytic activity of some other complexes of this series.

Acknowledgements

The author M.S. El-Shahawi wishes to thank Dr E.P. Achterberg, Plymouth University, UK and the British Council, for time and support in the form of chemicals (RuCl₃·3H₂O and *o*-phthaldehyde) and ¹H NMR and elemental analysis.

References

- [1] J. Bartis, Y. Kunina, M. Blumenstein, L.C. Francesconi, *Inorg. Chem.* 35 (1996) 1497.
- [2] R. Neumann, *Prog. Inorg. Chem.* 47 (1998) 317.
- [3] C.W. Royers, B.O. Patrick, S.J. Retting, M.O. Wolf, *J. Chem. Soc. Dalton Trans.* (2001) 1278.
- [4] D.F. Field, B.A. Messerle, L. Soler, I.E. Buys, T.W. Hambley, *J. Chem. Soc. Dalton Trans.* (2001) 1319.
- [5] V. Aranyos, J. Hjelm, A. Hagfeldt, H. Greenberg, *J. Chem. Soc. Dalton Trans.* (2001) 1319.
- [6] K. Sui, S. Peng, S. Bhattacharya, *Polyhedron* 18 (1999) 631, references therein.
- [7] W.P. Griffith, S.I. Mostafa, *Polyhedron* 11 (1992) 2997.
- [8] A.M. El-Hendawy, M.S. El-Shahawi, *Polyhedron* 8 (1989) 2813.
- [9] S.I. Mostafa, A.A. El-Asmy, M.S. El-Shahawi, *Trans. Met. Chem.* 25 (2000) 470.
- [10] W.P. Griffith, A.F. Shoair, M. Suriaatmaga, *Synth. Commun.* 30 (2000) 3091.
- [11] W.P. Griffith, B. Reddy, A.F. Shoair, M. Suriaatmaga, A.J.P. White, D.J. Williams, *J. Chem. Soc. Dalton Trans.* (1998) 2819.
- [12] B.C. Paul, H.K. Das, *Polyhedron* 15 (1996) 2433, references therein.
- [13] B.C. Paul, K.P. Sarma, R.K. Poddar, *Polyhedron* 12 (1993) 285. [14] A.B.P. Lever, *Inorg. Chem.* 29 (1990) 1271, references therein.
- [15] T.A. Stephenson, G.J. Wilkinson, *J. Inorg. Nucl. Chem.* 28 (1966) 945.
- [16] M.S. El-Shahawi, S.A. Barakat, *Talanta* 42 (1995) 1641.
- [17] M.S. El-Shahawi, M. Almehdi, *J. Chromatogr. A* 697 (1995) 185.
- [18] W.J. Geary, *Coord. Chem. Rev.* 7 (1971) 81.
- [19] J.R. Ferraro, *Low Frequency Vibrations of Inorganic and Coordination Compounds*, Plenum Press, New York, 1971.
- [20] J.D. Gilbert, G. Wilkinson, *J. Chem. Soc. (A)* (1969) 1749.
- [21] R.M. Silverstein, C.G. Bassler, J.C. Morrill, *Spectrophotometric Identification of Organic Compounds*, Wiley Interscience, New York, 1967.
- [22] K. Nakamoto, *Infrared and Raman Spectra of Inorganic and Coordination Compounds*, Wiley Interscience, New York, 1971.
- [23] S.I. Mostafa, *Trans. Met. Chem.* 23 (1998) 397, references therein.
- [24] J.V. McArdle, S.R. Sofen, S.R. Cooper, K.N. Raymond, *Inorg. Chem.* 17 (1978) 3075.
- [25] J.R. Dyer, *Application of Absorption Spectroscopy of Organic Compounds*, Prentice-Hall, New Jersey, 1978.
- [26] R.K. Poddar, K.P. Sarma, M.C. Sarma, *Polyhedron* 4 (1985) 1419.
- [27] L.D. Field, B.A. Messerle, L. Soler, I.E. Buys, T. Hambley, *J. Chem. Soc. Dalton Trans.* (2001) 1959, and references therein.
- [28] A.B.P. Lever, *Inorganic Electronic Spectroscopy, Theory and Applications* (1984) Elsevier Amsterdam.
- [29] R. Abu-Eittah, M.M. Hammed, *Bull. Chem. Soc. Jpn.* 57 (1984) 844.
- [30] N.C. Pramanik, S. Bhattacharya, *Polyhedron* 16 (1997) 1755, references therein.
- [31] M.C. Huges, D.J. Macero, *Inorg. Chem.* 3 (1974) 2739.
- [32] L.P. Hammett, *Physical Organic Chemistry*, second ed., McGraw Hill, New York, 1970.
- [33] W.P. Griffith, *Chem. Soc. Rev.* (1992) 179, and references therein. [34] S.I. Murahashi, S.I. Oda, T. Naota, T. Kuwabara, *Tetrahedron Lett.* 34 (1993) 1299; M.E. Marmion, K.J. Takeuchi, *J. Am. Chem. Soc.*, 110 (1988) 142.
- [35] R.A. Heck, C.E. Immoos, A. Ohman, M.G. Hill, *Inorg. Chem.* 37 (1998) 2150.
- [36] M.M. Taquiklan, R.S. Shukla, *J. Mol. Catal.* 34 (1986) 19.

Use of open-cell resilient polyurethane foam loaded with crown ether for the preconcentration of uranium from aqueous solutions

M. M. Abou-Mesalam,^{1*} I. M. El-Naggar,¹ M. S. Abdel-Hai,¹ M. S. El-Shahawi²

¹ Atomic Energy Authority, Hot Labs. Centre, P.Code 13759, Cairo, Egypt

² Chemistry Department, Faculty of Science at Damietta, Mansoura University, Egypt

(Received May 27, 2003)

The preconcentration of uranium from aqueous solutions on open-cell resilient polyurethane foams (PUF) impregnated with crown ether as an organic extractant in different conditions was investigated. The data showed that 50 minutes is a sufficient time to attain equilibrium with a maximum extraction percentage for uranium ion on polyurethane foams loaded with crown ether. Also the extraction percentage of uranium is increased markedly with increasing the pH values up to pH ~ 6 and displayed the lowest extraction at 8 > pH > 6. The different isotherms of uranium sorption have shown that the sorption followed a Freundlich isotherm. Column studies have been carried out in order to extend these studies to the plant scale. From the data of column sorption and breakthrough curves, the height equivalent of theoretical plates (HETP), and breakthrough capacity which affect the efficiency of the column have been calculated and found to be 1.03 mm/plate, 64–5 and 58.3 mg uranium/gram polyurethane foam impregnated with crown ether, respectively.

Introduction

The potential usefulness of open-cell resilient polyurethane foams (PUF) as an extractant from aqueous waste solutions has been demonstrated for a number of chemical inorganic and organic substances.^{1–3} Considerable efforts have been made to use polyurethane foam as sorbent for the separation and preconcentration of metal ions.^{4–6} The foam acts as a weak anion exchanger with low capacity since these foams contain amido- and amino-groups.¹ The hydrodynamic properties of polyurethane foams are excellent due to their quasi-spherical membrane structure.⁷ Polyurethane foams can be used as effective and inert supports for various extractants and are used for the preconcentration of metal ions in analytical and water treatment processes.^{8,9} Polyurethane foams containing different functional groups can be prepared by immobilizing various organic extractants or chelating agents.¹⁰

This paper reports the salient features of our findings regarding the sorption of uranium by polyurethane foams loaded with crown ether as an organic extractant. The selection of uranium was made on the basis of its industrial and technological importance. Experimental

Reagents and materials

All chemical reagents used were of analytical grade and used without further purification.

Commercial white sheets of open cell polyether type polyurethane foams were used. Foam cubes of approximately 10–15 mm edge were cut from the foam

sheets. The foam was washed with 1M HCl followed by distilled water until the foams were free from Cl ions.¹¹ The foam cubes were then washed with acetone for 6 hours to open their pores, washed with deionized water and dried at 80 °C in an oven.

A stock solution of crown ether (0.2% w/v) was prepared by dissolving 0.2 g of the reagent in 100 ml double distilled water.

A Britton-Robinson (BR) buffer (pH 2–10) solutions were prepared by mixing equimolar concentrations (0.06M) of boric acid, acetic acid and phosphoric acid in double distilled water and adjusting the pH of the solution with NaOH (0.04M) solution.¹²

Polyurethane foam loaded with crown ether was prepared by mixing dried foam cubes with an aqueous solution containing crown ether (25 ml/g dry foam) with efficient stirring for 20 minute. The reagent loaded foam cubes were squeezed and dried as reported.¹¹

Batch extraction procedure

The effect of shaking time on the extraction of uranium by unloaded and loaded polyurethane foams with crown ether and/or TBP was carried out in a mechanical shaker at 20 °C. A weight of foam (0.25–0.002 g) was mixed with 60 ml aqueous solution containing 10 ppm uranium, 0.01 g picric acid and Britton-Robinson buffer pH 6. After different time intervals the amount of uranium remaining in the aqueous phase was determined spectrophotometrically by Arsenazo-III.¹² The extraction percentage (%E) was calculated as:

$$\% E = \{(A_b - A_a)/A_b\} \cdot 100 \quad (1)$$

where A_b and A_a are the absorbance equivalent to uranyl ion in the aqueous phase before and after extraction, respectively.

* E-mail: mabumesalam@yahoo.com

The effect of pH of the medium on the extraction of uranium was carried out by equilibrating of 0.2 g of polyurethane foam cubes loaded with crown ether with 20 ml of an aqueous solution containing 10 ppm uranium and 0.01 g picric acid. The solutions were adjusted to the required pH by adding 20 ml Britton-Robinson buffer (pH 2–10). The solutions were shaken for 60 minutes in a mechanical shaker at 20–1 C and the aqueous phase was then separated. The amount of uranium remaining in the aqueous phase was determined spectrophotometrically and the extraction percentage (%E) and the distribution coefficient (K_d) were calculated using the relation:

$$K_d = \{ \%E / (100 - \%E) \} \cdot V / m \text{ ml/g} \quad (2)$$

where V is the solution volume and m is the weight of the foam.

The weight of polyurethane foam loaded with crown ether required to obtain maximum extraction percentage was determined by measuring the extraction percentage of 20 ml (10 ppm) uranium on different weights of polyurethane foam loaded with crown ether from aqueous solution containing 0.01 picric acid and 20 ml Britton-Robinson buffer (pH 6). The mixture was shaken in a mechanical shaker for 60 minutes at 20–1 C. After equilibrium the aqueous solution was separated and the amount of remained uranyl ion in the aqueous phase was determined spectrophotometrically.

The effect of uranium ion concentration on the amount adsorbed per unit weight of adsorbent was tested by shaking 0.17–0.002 g of polyurethane foam cubes loaded with crown ether with 25 ml of different uranium concentrations (2–12 ppm) and 0.01 g picric acid at optimum pH in a thermostat shaker at 20–1 C. After one hour the foam cubes were separated by decantation and the amount of uranium in the aqueous phase was measured spectrophotometrically.

Column extraction studies

Column studies have been carried out in order to extend the measurements to the plant scale. An accurate weight (0.52–0.002 g) of polyurethane foam loaded with crown ether was packed in a column using the vacuum method of foam packing.¹³ A 100 ml of the feed solution containing 10 ppm uranium and 0.02 g picric acid at the optimum pH was percolated through the foam column at 1.5 ml/min flow rate. Sorption of uranium ion on the foam column took place as proved from the analysis of uranium ion in the effluent solution. Elution of the uranyl ion from the crown ether loaded foam column was achieved quantitatively by passing 50 ml acetone at a flow rate 2 ml/min. Equal fractions of the eluate were collected and analyzed spectrophotometrically for uranium.

The same procedures were also applied for the blank preparation by percolating the aqueous solution without uranyl ion through a fresh foam column at the same experimental conditions.

Results and discussion

In batch experiments, the effect of shaking time on the extraction percentage of uranyl ion from aqueous solution containing an excess of picric acid by the crown ether (CE)-, tri-butyl phosphate (TBP)-, and CE-TBP loaded foams and unloaded foams were carried out. The results obtained are summarized in Fig. 1. The data revealed that the extraction of the uranyl ion by polyurethane foam loaded with crown ether was fast and the equilibrium was attained within 50-minute shaking time and remained constant on increasing the extraction time. Thus, 50-minute shaking time was adopted in the subsequent experiments.

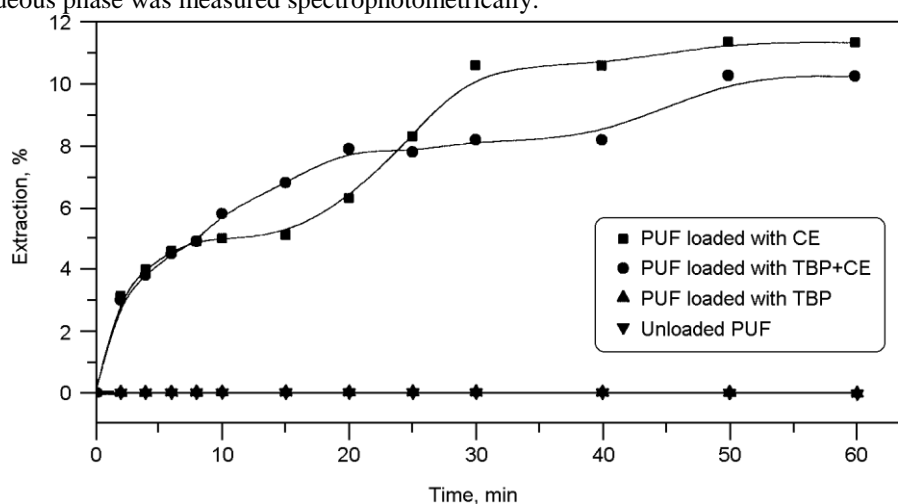


Fig. 1. Effect of shaking time on the extraction of uranium on unloaded and loaded PUF

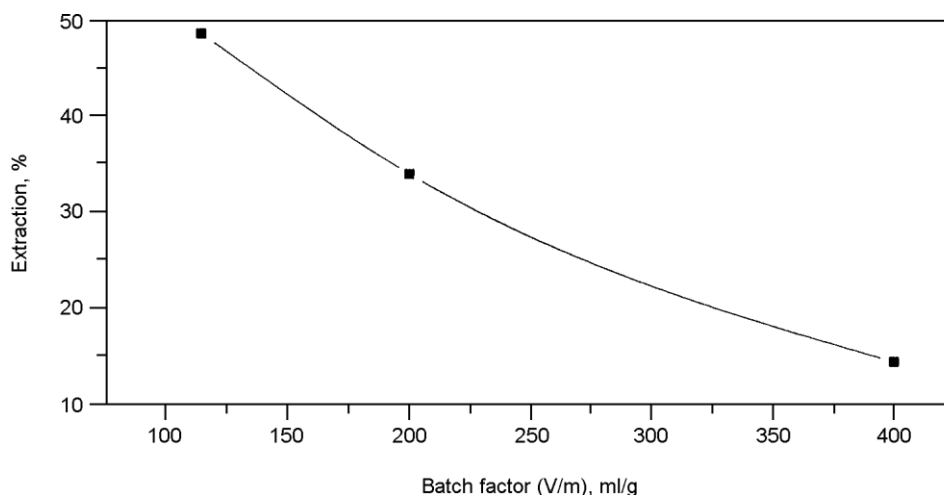


Fig. 2. Batch factor vs. extraction percentage of uranium on PUF loaded with crown ether at 25–1 C

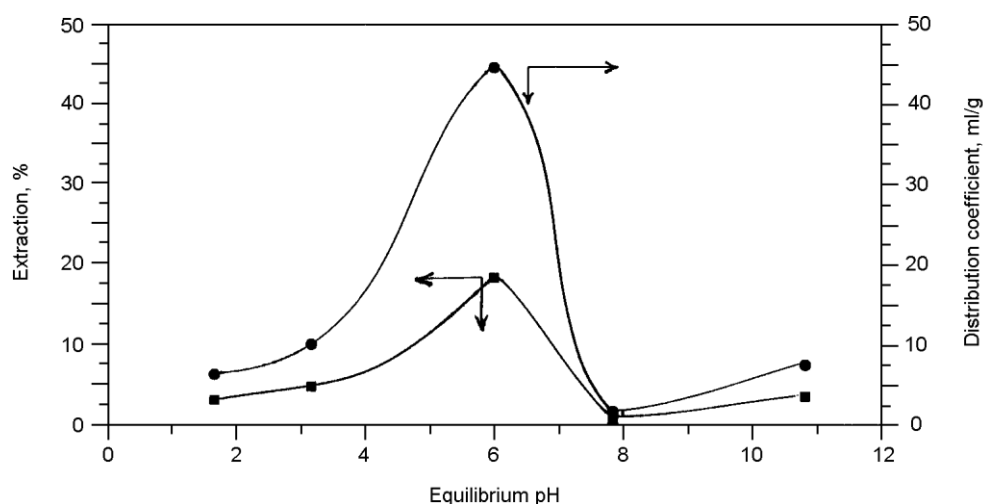


Fig. 3. Effect of pH on the extraction and the distribution coefficient of uranium on PUF loaded with crown ether at 25–1 C

The sorption profile of uranium ions by the unloaded foams and foams loaded with CE-, TBP and CE-TBP followed the sequence:

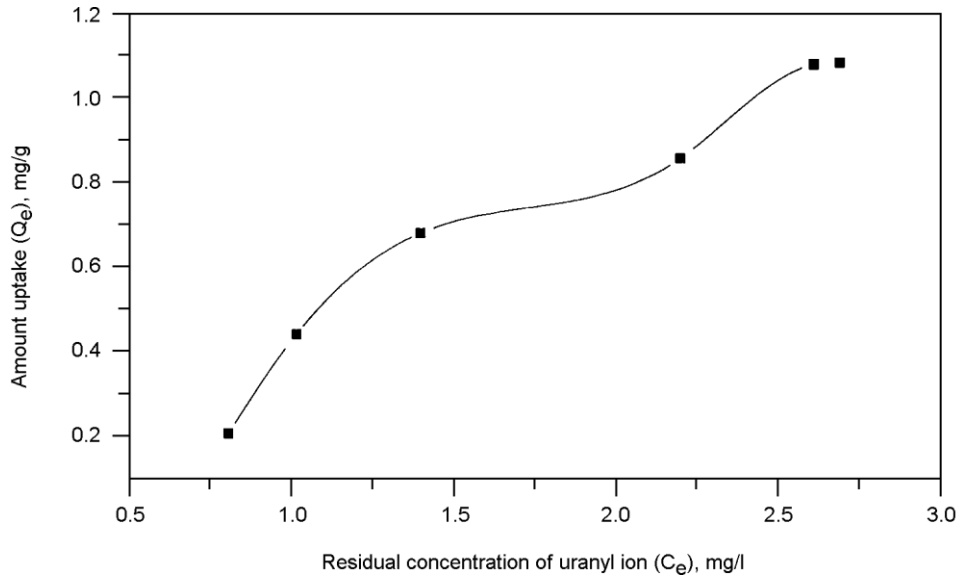
CE CE+TBP > TBP ~ unloaded foam

Thus, the uranium ion uptake by the loaded foams occurs in one fast step, i.e., gel diffusion was not the rate-controlling step as in the case of the common ion exchange resins. The data suggest the possible use of crown ether loaded foam in the next work for a detailed investigation involving sorption of uranium ions from aqueous solution.

The variation of batch factor (V/m) with the extraction percentage is shown in Fig. 2. The data indicated that the extraction ion decreased gradually on increasing of the batch factor (V/m). The maximum extraction percentage was obtained with a V/m value of 100 ml/g and weight of loaded polyurethane foam 0.4 g. A similar trend was also observed by EL-SHAHAWI et al.⁴ on increasing of the batch factor.

Effect of pH on the extraction of uranium ion by crown ether loaded polyurethane foams

The amount of uranium ion extracted from the aqueous solution was found to depend on the pH of the solution. Therefore, the sorption profiles of 10 ppm uranium ion onto 0.2–0.01 g loaded foams from aqueous solutions (100 ml) containing 0.01 g picric acid at various pH were critically investigated. After shaking for 50 minutes, the amount of uranyl ion remained in the aqueous solution was determined spectrophotometrically using Arsenazo III.¹² The amount of uranyl ions retained on the foam was then calculated by difference between the absorbance of the uranyl ion before (A_b) and after (A_a) extraction. The variation of the extraction percentage and the distribution coefficient of uranium with the pH are shown in Fig. 3. The extraction of uranium ion on the loaded foams increased markedly with increasing the solution pH up to pH ~ 6 and displayed the lowest sorption at pH > 6. The increase of uranyl ion



Scheme 1. Proposed structure of the ion associate picric acid anion and the cationic complex species of crown ether uranyl ion Fig. 4. Relation between the amount uptake and the residual concentration of uranium ion retention on PUF loaded with crown ether at 25–1 C

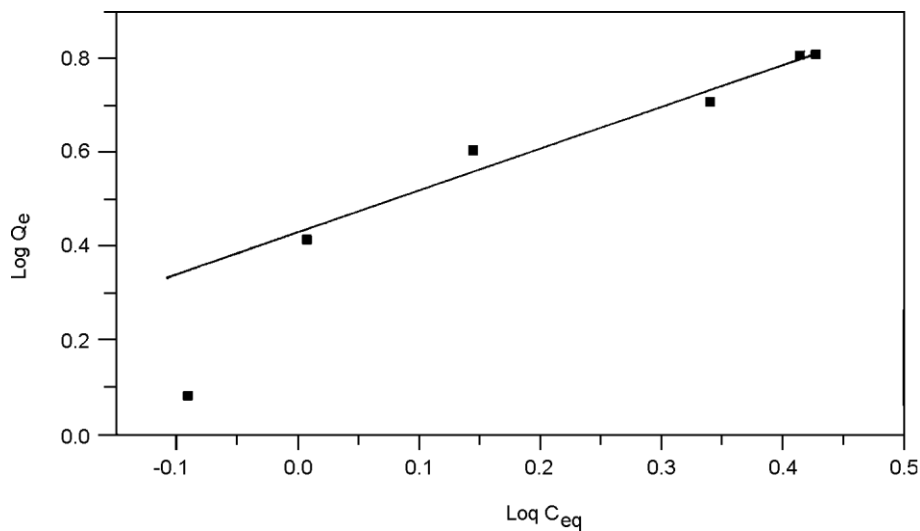


Fig. 5. Freundlich isotherm for the adsorption of uranium ion on PUF loaded with crown ether at 25–1 C

The Freundlich model is shown in Fig. 5. The plot of applicability of the Freundlich isotherm for physical $\log Q_e$ versus $\log C_{eq}$ is a straight line over the entire adsorption. Thus, a dual mechanism involves both concentration of uranium ion. The values of K and $1/n$ absorption related to solvent extraction and an added computed from the intercept and slope of this plot were component for surface adsorption of the polyurethane found to be 1.95 mol/g and 0.33, respectively. The value foam.

of $1/n$ suggests that the sorption capacity is reduced at The above data and the favorable flow, and lower equilibrium concentration and the isotherm does hydrodynamic characteristics¹⁵ of polyurethane foam not predict any saturation of the PUF by the uranium sorbents suggest their possible use for enrichment of ion. These data confirm that infinite surface coverage is traces of uranium ions present in radioactive waste predicted and physicosorption on the PUF surface

is employing flow mode of separation and subsequent expected. The linear plot also supports the validity and determination of the analyte.

Chromatographic behavior of uranium ion on polyurethane foams loaded with crown ether

The performance of a packed column is concerned with the broadening of an initially compact band of solute as it passes through the column. The broadening results from the column design and its operating conditions.¹⁵ This efficiency is generally described quantitatively by the number of theoretical plates (N) and the height equivalent to the theoretical plate (HETP). The performance of crown ether polyurethane foam packed column for quantitative retention of uranyl ion was carried out by percolating 20 ml of an aqueous solution containing 10 ppm of uranium ion on an excess of picric acid at the optimum pH through the column at 1.5 ml/min. Analysis of uranyl ion in the effluent solution against reagent blank indicated complete sorption of UO_2^{2+} onto the loaded foam column. The retained species were then eluted successfully with (20 ml) acetone at 2 ml/min. A typical chromatogram is shown in Fig. 6. The HETP was calculated from the elution curve employing the Glueckauf equation:¹⁷

$$N = \{8 (V_{\max.})^2\} / W^2 = L / \text{HETP} \quad (4)$$

where N is the number of theoretical plates, V_{\max} is the volume of eluate to peak maximum, W is the width of the peak at 1/e times the maximum solute concentration, and L is the length of the foam bed column in mm.

The values of the HETP and N were 1.23 mm/plate and 64–5, respectively.

The N and HETP values of the column were also calculated from the breakthrough curve (S-shaped). The results of percolating 5 ml of an aqueous solution at 5 ppm concentration level of uranium are displayed in Fig. 7. The N and HETP values of the foam packed column were calculated by:

$$N = (V \cdot \bar{V}) / (V \cdot \bar{V})^2 = L / \text{HETP} \quad (5)$$

where V is the volume of the effluent solution at the center of the S-shaped breakthrough curve where the concentration is one-half the initial concentration and \bar{V} is the volume at which the effluent solution has a concentration of 0.1578 of the initial concentration. The HETP and N values obtained by this method were found to be 1.03 mm/plate and 68–4, respectively, in good agreement with the values of HETP and N values calculated from the elution curve (Fig. 6).

The S-shaped curve in Fig. 7 represents the breakthrough volume and the volume needed to reach bed saturation. In the S-shaped curve, the rising portions has a large slope indicating a high transfer rate of uranium in the foam membranes and a rapid attainment of equilibrium between the picrate anions and crown ether-uranyl cations.

The breakthrough capacity of uranium uptake per gram of the loaded sorbent was calculated by:¹⁸

$$\text{Uptake} = \{(V_{50\%}) \cdot C_0\} / m \text{ mg/g} \quad (6)$$

where C_0 is the initial concentration of uranium, $V_{50\%}$ is the effluent volume (ml) at 50% breakthrough and m is

the weight of the loaded foam in column bed. The uptake of uranium was found to be 58.3 mg/g at a flow rate of 1.5 ml/min. This value is quite good as compared to other

solid supports like silica gel and solid inorganic ion exchangers in column mode.¹⁵

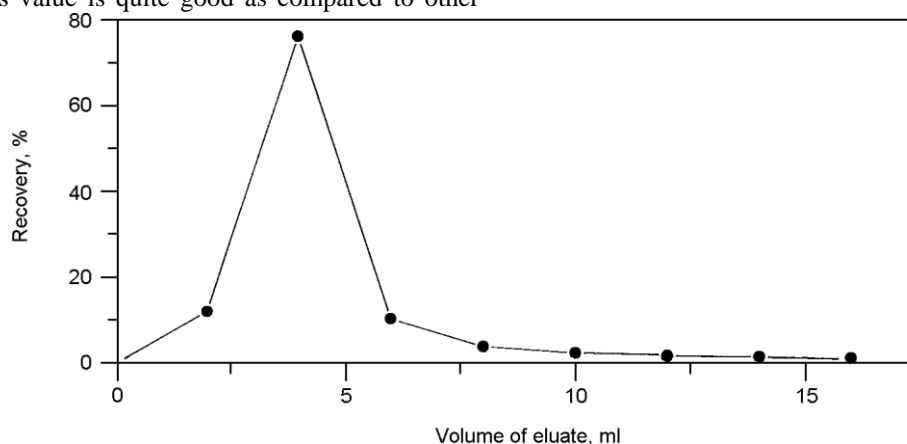


Fig. 6. Elution curve of uranyl ion from PUF loaded with crown ether column at 1.5 ml/min flow rate, column height = 7.85 cm and loaded foam weight = 0.52 g

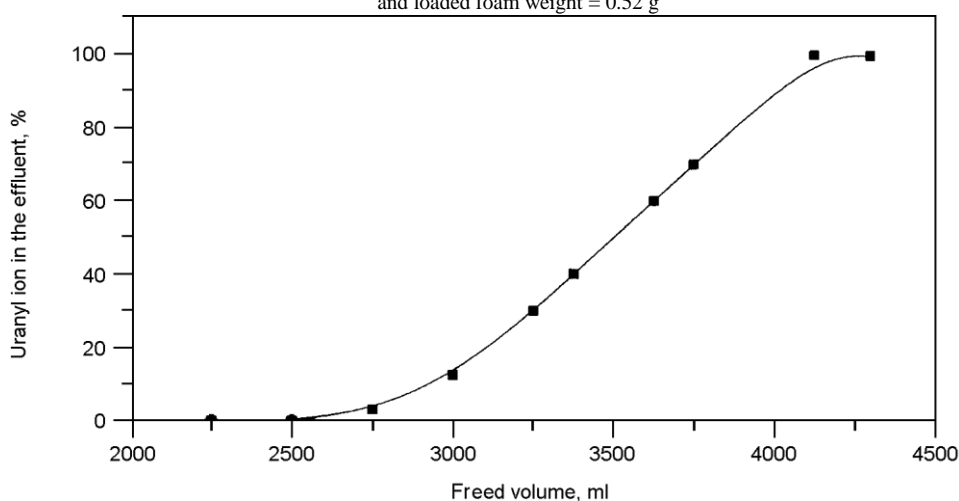


Fig. 7. Breakthrough curve for uranyl ion on a column of PUF loaded with CE at 5 ml/min flow rate, column height = 7 cm and foam weight = 0.6 g

Conclusions

The results are providing a deeper insight into the mechanism of the retention of uranium from aqueous solution by membrane-like polyurethane foams (PUF), being superior compared to other known sorbents e.g. chelating polymers, immobilized rigid or granular solids in reversed phase extraction chromatography. The proposed methods permit rapid and effective separations at relatively high flow rate without loss in column performance.

References

1. H. J. M. BOWEN, *J. Chem. Soc.*, A1082 (1970).
2. T. BRAUN, *Fresenius Z. Anal. Chem.*, 314 (1983) 592.
3. S. PALAGYI, T. BRAUN, *Preconcentration Techniques for trace Elements*, S. B. ALFASSI and C. N. WAI (Eds), CRC Press, Boca Raton, Florida, USA, 1992, p. 363.
4. K. KATRAGADDA, H. D. GESSER, A. CHOW, *Talanta*, 44 (1997) 1865.
5. G. A. HAMZA, A. B. FARAG, A. AMERH, *Anal. Sci.*, 6 (1990) 8894.
6. D. S. DE JESUS, R. J. CASSELLA, S. L. C. FERRIERA, A. C. S. COSTA, M. S. CARVALHO, R. E. SANTELLI, *Anal. Chim. Acta*, 366 (1998) 263.
7. T. C. HUANG, D. H. CHEN, S. D. HUANG, *J. Chem. Eng. Japan*, 61 (1992) 371.
8. H. D. GESSER, S. AHMED, *J. Radioanal. Nucl. Chem.*, 140 (1990) 396.
9. K. SHAKIR, G. BEHEIR, M. AZIZ, *J. Radioanal. Nucl. Chem.*, 61 (1992) 371.
10. T. BRAUN, J. D. NAVRATIL, A. B. FARAG, *Polyurethane Foam Sorbents in Separation Science*, CRC Press Inc., Boca Raton, Florida, USA, 1985.
11. M. S. EL-SHAHAWI, M. A. ALMEHDI, *J. Chromatogr.*, A697 (1995) 185.
12. A. I. VOGEL, *Quantitative Inorganic Analysis*, 3rd ed., Longmans Group Ltd., England, 1966.
13. Y. ANJANEYULU, R. MARAYA, T. H. RAO, *Environ. Pollut.*, 79 (1993) 283.
14. M. S. EL-SHAHAWI, H. A. NASSIF, *Anal. Chim. Acta*, in press.
15. T. BRAUN, A. B. FARAG, *Talanta*, 22 (1975) 699.
16. T. BRAUN, A. B. FARAG, *Talanta*, 19 (1972) 828.
17. G. A. SOMORJA, *Introduction of Surface Chemistry and Catalysis*, Wiley, 1994.
18. E. GLUECKAUF, *Trans. Faraday Soc.*, 51 (1955) 34.

Copyright of Journal of Radioanalytical & Nuclear Chemistry is the property of Kluwer Academic Publishing / Academic and its content may not be copied or emailed to multiple sites or posted to a listserv without the copyright holder's express written permission. However, users may print, download, or email articles for individual use.

Chemical and Thermodynamic Characteristics of the Isotopic Exchange Reaction between Radioiodine and Iodohippuric Acid Isomers

M. S. EL-SHAHAWI,**²⁴ G. EL-SHABOURY,* M. A. M. ALY,* and M. EL-TAWOOSY*

*Radioisotope Production Division, Hot Labs. Center, Atomic Energy Authority, Code No. 13759, Cairo, Egypt

**Chemistry Department, Faculty of Science at Damietta, Mansoura University, Damietta, Egypt

The parameters affecting the absolute radiochemical yield of the isotopic exchange reaction between radioiodine ($^{125}\text{I}^-$) and iodohippuric acid isomers on molten ammonium acetate as a medium exchange at 120°C without any carrier added (radioiodine, $^{125}\text{I}^-$) was determined. The isotopic exchange reactions of radioiodine as $^{125}\text{I}^-$ for iodine-127 of *o*- and *p*-iodohippuric acid isomers occur more rapidly than *m*-iodohippuric acid isomer. These reactions proceed by nucleophilic second order substitution reaction. The kinetics and thermodynamic parameters of these isotopic exchange reactions were determined. The absolute radiochemical yield and radio pharmaceutical purity were determined by HPLC and TLC techniques.

(Received December 16, 2002; Accepted April 28, 2003)

Introduction

Recently, radioiodinated compounds labeled with iodine radionuclides have been developed as clinical radiopharmaceuticals.¹ Such compounds are intended for the incorporation of highly toxic effects associated with the auger electrons emitted from radionuclides onto the DNA or close to the tumor cell membrane.^{1,2} Radioiodinated sodium iodohippurate is a diagnostic radiopharmaceutical currently used in nuclear medicine for the non-invasive determination of renal function, renal blood flow and urinary tract obstruction.³⁻⁷

The properties of radioiodine are reviewed in relation to its use in labeled compounds.^{3,8} Iodine is characterized by a varied spectrum of oxidation states and can form a variety of complex ions and multivalent complex species.⁹ The picture of exchange reaction mechanisms is complex, but can be rationalized in terms of the stabilization of intermediate complexes formed with different (negative, neutral or positive) iodine species.¹⁰

The radioiodination of sodium iodohippurate, or hippuric acid isomers, by the isotopic exchange reaction between the substrate and Na^*I exchange isotopes leads to the formation of other labeling products *e.g.*, glycylo-iodohippurate (*g-o*-IHA) and *o*-iodobenzoic acid (*o*-IBA).¹¹⁻¹⁹ Thus the mechanism of the isotopic exchange reaction between the iodohippurate isomers and radioiodine (as iodide, $^*\text{I}^-$) in the molten state ($160 - 170^\circ\text{C}$) with no-carrier added (nca) is of great importance.¹⁹⁻²¹

The goal of the present study was focused on the application of the no-carrier added (nca) radioiodine, $^{125}\text{I}^-$ in molten ammonium acetate (m.p. 114°C) for an isotopic exchange reaction between *o*-, *m*- or *p*-iodohippuric acid isomers and radioiodine as iodide ion, $^{125}\text{I}^-$. Ammonium acetate melt controls the formation of other labeling products rather than iodohippuric acid isomers.

Experimental

Reagents and chemicals

All chemicals used were of analytical reagent grade. Sodium iodide [$^{125}\text{I}^-$] solution was purchased from Amersham (England) of radiochemical grade carrier free and reductant free. A sodium iodide concentration of $(0.8 - 1.0) \times 10^9 \text{ Bq}/\mu\text{l}$ was diluted with 0.1 M NaOH up to 20 μl to keep the specific activity constant $(0.8 - 1.0) \times 10^9 \text{ Bq}/\text{mg}$ iodohippuric acid isomer, during the experiment. Thin-layer chromatography was performed on aluminum backed TL sheets coated with silica gel 60 (Merck). Solvents of HPLC grade were delivered from Sigma. Water used throughout the experiments was obtained from a Milli-Q (MQ) water purification system (Millipore). All glassware were cleaned by soaking in an aqueous 1% Decon100 for at least 24 h, followed by rinsing with MQ water, and then acetonitrile prior to use.

Apparatus

A Shimadzu a high-performance liquid chromatography (HPLC) equipped with a LC-dual pump, U6K injector, M 441 spectrophotometric detector, RP-C₁₈ column ($250 \times 4 \text{ mm i.d.}$) and M 740 recorder was used for the analysis of the radioiodinated iodohippuric acid isomer. A Scalar rate meter (SR 7), scintillation counter and a Metrohm pH-meter were used for radioactivity and pH measurements, respectively.

Synthesis of [^{125}I] iodohippuric isomers

In a quick-fit glass vessel described earlier^{21,22} 6 mg amount of the iodohippuric acid isomer, 20 μl of Na^{125}I $(0.8 - 1.0) \times 10^9 \text{ Bq}/\text{mg}$ IHA in 0.1 M NaOH and 0.2 - 0.25 ml ammonium solution (10% w/v) were mixed in a V-shaped bottom tube. The mixture was gently swirled to dissolve the contents and to insure complete homogeneity. After a gentle stream of dry nitrogen gas was applied

1332 To whom correspondence should be addressed.
E-mail: Mohammad_el_shahawi@hotmail.com

to evaporate the solvents, the closed reaction vessel was then kept in an oil bath at $120 \pm 1^\circ\text{C}$ for 10 min under a vacuum. The reaction mixture was cooled in an ice bath and the solidified melt was then redissolved in 50.0 μl ethanol, and finally submitted for TLC. The reaction products were characterized and determined after developing with benzene–acetic acid–water–*n*-butanol (5:5:2:1 v/v) on silica-gel plates and drying. The radiochemical yield (*Y*) was calculated by cut and count of the integrated chromatogram peaks as follows:

$$Y, \% = \frac{\text{Radioactivity of the isotopic exchange product}}{\text{Total activity of the TLC plate}} \times 100 \quad (1)$$

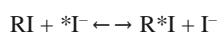
The retention factors (*R_t*) of the IHA isomers, *g*-*o*-IHA, *o*-IBA and Na^{125}I were found to equal 0.5 ± 0.02 , 0.25 ± 0.02 , 0.81 ± 0.05 and 0 ± 0.05 , respectively, in good agreement with the data reported by Saeed and Gaffar.²³

HPLC analysis of the radioiodinated iodohippuric acid isomers

Two aliquots (10 – 20 μl) were withdrawn from the reaction vessel solution at various time intervals. The first aliquot was pipetted into a test tube for an analysis of the total activity. The second aliquot was injected onto an RP-C₁₈ column with trace amounts of inactive *o*-, *m*- and *p*-iodohippuric acid. The mobile phase, methanol:water:acetic acid (300:700:1 v/v), was passed through C₁₈ column with a flow rate of 1.0 ml/min until the absorbance appeared to be constant at 254 nm. The temperature of the column was controlled by a temperature controller, and was kept at $25 \pm 1^\circ\text{C}$. A frontal chromatogram was recorded while the mobile phase was eluted and collected discontinuously under the optimum conditions. The radioactivity of the fractions and the aliquot were determined by a γ -counter. The absolute radiochemical yield was calculated by collecting the radioactive peaks and comparing their activities with that of a sample of the same volume that was not HPLC chromatographed. The HPLC peak of each radioactive iodohippuric isomer has the same retention time (*t_R*) as the inactive sample. The *t_R* of *o*-, *m*- and *p*-IHA isomers were found to equal 3.48 ± 0.1 , 10.6 ± 0.08 and 11.32 ± 0.05 min, respectively.

Results and Discussion

Consider that the thermodynamics of the exchange labeling is a degenerate substitution reaction, where the reaction products are chemically identical to the starting materials. Therefore, the energy of the products will be the same as the reactants and the equilibrium constant will be equal to unity. Thus, the mechanism of the isotopic exchange reaction could be proceeded as follows:⁶



$$K = \frac{[\text{R}^*\text{I}][\text{I}^-]}{[\text{RI}][{}^*\text{I}]} = 1 \quad (2)$$

$$\frac{[\text{R}^*\text{I}]}{[\text{RI}]} = \frac{[\text{I}^-]}{[{}^*\text{I}]} = 1 \quad (3)$$

$$\% \text{ Exchange} = \frac{[\text{R}^*\text{I}]}{[\text{R}^*\text{I}] + [{}^*\text{I}]} \times 100 = 100 \frac{[\text{I}^-]}{[\text{I}^-] + [\text{RI}]} \quad (4)$$

At equilibrium, the proportion of the incorporated radioiodine *i.e.* the labeling yield, is an inverse function of the ratio of the carrier iodine to the substrate. The yield drops dramatically above a ratio of about 0.1 iodide to the substrate ratio. For no carrier added radioiodine, the exchange yield based on the equilibrium considerations should be greater than 99.9% for the displacement of halogen or other leaving groups from iodohippuric acid isomers.

The parameters affecting the isotopic exchange reaction of ${}^*\text{I}^-$ with IHA isomers

A preliminary investigation showed the importance of the parameters: pH, temperature, exchange medium and substrate concentration on the rate of the isotopic exchange reaction of radioiodine as ${}^*\text{I}^-$ and iodohippuric acid isomers in a molten ammonium acetate. Three components (Fig. 1) were formed corresponding to *g*-*o*-IHA, IHA isomer and *o*-IBA when the isotopic exchange was performed in molten medium of the substrate, itself, at 160 – 170 $^\circ\text{C}$. These data are not in good agreement with the known principles of nucleophilic substitution.^{6,21}

The influence of sodium hydroxide concentration (0.02 – 0.1 M) containing most of the dispensed radioactive iodine on the radioiodination of iodohippuric acid was studied. An excess of sodium hydroxide concentration up to 0.1 M inhibited the yield of the isotopic exchange reaction to less than 75%. A good radiochemical yield was obtained at 0.03 M sodium hydroxide concentration. The isotopic exchange reactions proceed very rapidly close to the neutralization equivalent point.⁶ Thus, in subsequent work, neutralization of the radioactive sodium iodide solution was carried out before performing the experimental procedures and the isotopic radiodination exchange reaction of IHA isomers was also performed at 0.03 M NaOH.

The influence of the iodohippuric acid isomer content on the radiochemical yield in a molten medium of ammonium acetate at 120 $^\circ\text{C}$ was investigated. The radiochemical yield gradually increased up to 98.2, 97.2 and 98.5% for *o*-, *m*- and *p*-¹²⁵IHA isomers, respectively at 6 mg of each IHA isomer. Thus, a 6 mg portion of the iodohippuric acid isomer was used in the subsequent work.

The influence of ammonium acetate (0 – 50 mg) as a molten medium on the isotopic exchange reaction of the IHA isomers and radioiodine (${}^*\text{I}^-$) at 120 $^\circ\text{C}$ for 10 min reaction time was investigated. The radiochemical yield of *o*-, *m*- and *p*-¹²⁵IHA isomers increased linearly from ~82, 79.4 and 86 to 98.2, 97.3 and 98.3 upon increasing ammonium acetate from 5 to 25 mg, respectively. The observed increase in the radiochemical yield is most likely attributed to the *in situ* thermal decomposition of ammonium acetate rendering the final pH of the reaction mixture on the acidic side required to perform the isotopic exchange reaction.⁶

The effect of the temperature (25 – 120 $^\circ\text{C}$) and reaction time (0 – 30 min) on the radiochemical yield of the radioiodinated IHA isomer was studied with 6 mg IHA isomer, 25 mg ammonium acetate and 20 μl Na^{125}I in dry state in a thermostat glycol path. A radiochemical yield of 98.2, 97.2 and 98.5% was obtained for *o*-, *m*- and *p*-¹²⁵IHA, respectively, at 120 $^\circ\text{C}$ within 10 min. Thus, in subsequent experiments, the temperature was selected to be 120 $^\circ\text{C}$.

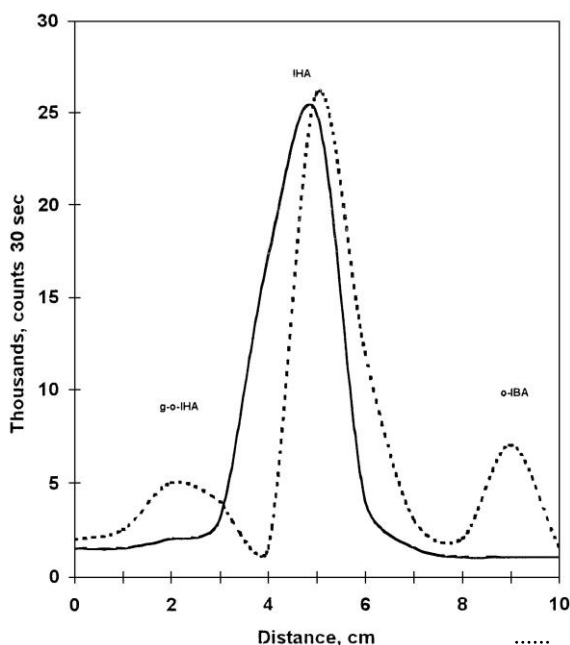
Kinetics and thermodynamic studies

The isotopic-exchange radioiodination reaction of the IHA isomer and the radioactive iodine as ${}^*\text{I}^-$ can be expressed as



This reaction can be considered as a simple homogeneous
ANALYTICAL SCIENCES SEPTEMBER 2003, VOL.

19



radioisotope exchange reaction, and its kinetics follows the exponential exchange law:^{6,20}

$$-\ln(1 - F) = \frac{[A] + [B]}{[A] \cdot [B]} R t \quad (5)$$

where F is the fraction of the exchange, $[A]$ for the concentration of IHA in g mol^{-1} , $[B]$ the concentration of Na^{125}I (nca), R for isotopic exchange rate and t for time in min. The fraction of the exchange was calculated employing

$$F = \frac{X}{X_{\infty}} \quad (6)$$

where X and X_{∞} are the radiochemical yields (% labeling) at time t and at the equilibrium time, $t = \infty$, respectively. Upon plotting $\log(1 - F)$ versus time, a straight line with a negative slope passing through the origin was obtained at the reaction temperatures employed for o -, m - and p -IHA isomers (Fig. 2). These data suggest that the kinetics of the reaction depend on the concentration of both IHA isomer and the radioiodine as iodide ion. These results strongly suggest a simple secondorder isotopic exchange reaction of radioactive iodine as I^- with each of the iodohippuric acid isomer.^{19,20}

The values of the specific rate constant (k) of the proposed isotopic exchange were calculated from the slope (p) of the corresponding straight line of the plot of $\log(1 - F)$ versus time (Fig.2) employing the following equations.¹⁹

$$-2.303 \log(1 - F) = P t \quad (7)$$

$$k = \frac{2.303 P}{a} \quad (8)$$

Fig. 1 Radiochromatograms of the nucleogenic isotopic exchange radioiodination reaction of o -IHA with () and without () ammonium acetate.

1333

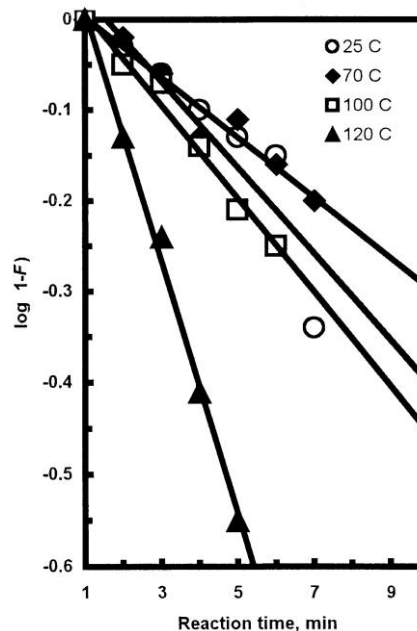


Fig. 2 Variation of $\log(1 - F)$ versus time at different temperatures in 25 mg molten ammonium acetate, 6 mg o -IHA isomers and radioactive iodine.

where $a = [^{125}\text{I}] + \text{IHA}$. The amount of the radioactivity of the no carrier added [^{125}I] iodide tracer (20 μl , 20×10^3 Bq) used in each run was negligible compared to the total chemical quantity of each IHA isomer. Thus, the amount of [^{125}I] + IHA \approx IHA = $0.39334 \text{ g mol}^{-1}$. The values of the specific rate constant for o -, m - and p -IHA isomers were found equal to 0.8034, 0.698 and $0.933 \text{ mol}^{-1} \text{ min}^{-1}$ at 120°C , respectively. The average k values at all temperatures for the radioiodination of iodohippuric acid isomers follows the sequence p -IHA $>$ o -IHA $>$ m -IHA.

The activation energy (E) of the isotopic exchange reaction of radioactive iodide ions with each isomer of IHA was obtained, employing the Arrhenius equation

$$\ln k = \frac{-E}{RT} + \text{constant} \quad (11)$$

where R is the universal gas constant ($1.987 \text{ cal mol}^{-1}$) and T is the absolute temperature. Upon plotting $\log k$ versus $1/T$ straight line with a slope of $-E/2.303R$ is obtained. The results obtained for o -, m - and p -IHA isomers are summarized in Fig.

3. The E values (Table 1) were found to equal 10.01, 10.11 and $9.92 \text{ kcal mol}^{-1}$ for o -, m - and p -IHA, respectively at 120°C in molten ammonium acetate. These data are in good agreement with the sequence of the specific rate constant of the radioiodination reaction of p - $>$ o - $>$ m -IHA isomer. These results can further be based on the electronegativity (*i.e.* electron withdrawing character) of the iodine atom in p - and o positions compared to the m -position of the IHA isomer.

The dependence of the radioiodination reaction of the IHA isomers on the temperature have also been evaluated from a thermodynamic point of view. The numerical values of ΔG , ΔH and ΔS were obtained from the slopes and intercepts in Fig. 3. The results are summarized in Table. 1. The values were estimated with a correlation factor of 0.9919. The numerical value of E evaluated

from equation 10 is $9.92 \pm 0.21 - 10.11 \pm 0.12$, which reflects the non-spontaneous nature of the proposed isotopic exchange reaction. The positive values of ΔG and ΔH and the fact that the reaction proceeds more favorably at high temperatures confirm the endothermic and non-spontaneous nature of the reaction, respectively. It is worth noting that the

1334

Acknowledgements

The authors are grateful to Prof. Y. M. Moustafa for his kindly help in manuscript preparation and Profs. M. T. El-Kolaly, K. Farah and Dr. A. A. El-Mohty for the facilities provided.

References

ANALYTICAL SCIENCES SEPTEMBER 2003, VOL. 19

Table 1 Kinetic and thermodynamic parameters of the isotopic exchange reactions of *o*-, *m*-, and *p*-IHA with radioactive iodine as $^{125}\text{I}^{\text{a}}$

Activation parameters	<i>o</i> -IHA	<i>m</i> -IHA	<i>p</i> -IHA
E , kcal mol $^{-1}$	10.01 ± 0.1	10.11 ± 0.12	9.92 ± 0.021
K_{120} , L kcal mol $^{-1}$ min $^{-1}$	0.8034 ± 0.06	0.698 ± 0.05	0.933 ± 0.07
ΔH , kcal mol $^{-1}$	9.23 ± 0.09	9.33 ± 0.08	9.14 ± 0.06
ΔG , kcal mol $^{-1}$	23.397 ± 1.2	23.505 ± 1.2	23.271 ± 1.4
ΔS , kcal mol $^{-1}$ deg $^{-1}$	$(-3.605 \pm 0.2) \times 10^{-2}$	$(-3.607 \pm 0.16) \times 10^{-2}$	$(-3.5 \pm 0.18) \times 10^{-2}$

a. Average \pm standard deviation.

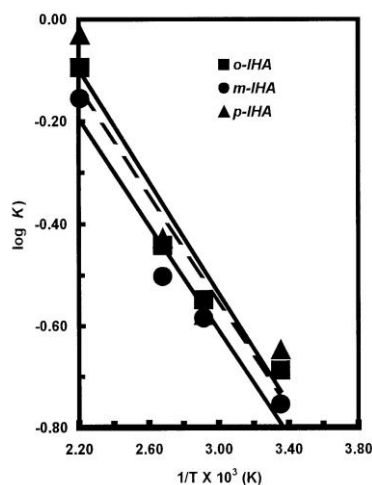


Fig. 3 Rate constant ($\log k$) versus $1/T$ of the radioiodination of IHA isomers with radioactive iodine in 25 mg molten ammonium acetate.

pK_a of the *o*-, *m*- and *p*-IHA, the possible intermolecular Hbonding formation in the *o*-IHA isomer and the intermolecular H-bonding formation in the *m*- and *p*-IHA isomers¹⁷ are participating factors in the thermodynamic values (Table 1) and could account for the sequence of the radioiodination of IHA isomers.

Conclusion

This article has demonstrated the use of ammonium acetate as a molten medium for the nucleophilic isotopic exchange reaction of radioiodine (as iodide) with iodohippuric acid isomers to enhance the radiochemical yield of each isomer without the formation of bi-products e.g., *g-o*-IHA and *o*-IBA. The method is simple and reliable for routine use with an excellent radiochemical yield and purity of the radioactive IHA isomers. Adjusting the pH of radioiodinated NaI before performing the isotopic exchange reaction restored the quantitative substitution reaction with a high radiochemical purity > 99%. The positive values of ΔH and ΔG indicate exothermic and non-spontaneous nature of the isotopic exchange reaction, respectively.

1. T. M. Behr, M. Loehr, C. Angerstein, E. Wehrmann, and W. Becker, *Eur. J. Nucl. Med.*, **2000**, 27(7), 153.
2. J. P. Slabert, J. H. Langerhoven, and B. S. Smit, *J. Radioanal. Nucl. Chem.*, **1999**, 240, 505.
3. L. A. Hawkins "Radiopharmacy and Radiopharmaceuticals", **1985**, London, 221; A. R. Wafelman, C. A. Hoefnagel, H. J. M. Maesseni, R. A. A. Maes, and J. H. Beijnen, *Eur. J. Nucl. Med.*, **1997**, 24, 544.
4. E. S. Marcus and J. H. Kuperus, *J. Nucl. Med.*, **1985**, 26(5), 62.
5. L. M. Thorson, J. C. Hung, and B. S. Hollar, *Nucl. Med. Commun.*, **1992**, 13, 832.
6. H. N. Wagner, "Principle of Nuclear Medicine", **1968**, Dekker, New York, 628.
7. R. M. Baldwin, *J. Appl. Radiat. Isotopes*, **1986**, 37, 817.
8. F. A. Cotton, G. Wilkinson, and P. I. Gaus, "Basic Inorganic Chemistry", 3rd ed., **1995**, John Wiley, New York.
9. M. P. Moon and J. F. Wolfe, *J. Org. Chem.*, **1979**, 44, 4081.
10. D. L. Fotman, P. J. Robbins, and V. J. Sodd, *Int. J. Appl. Radiat. Isot.*, **1978**, 29, 449.
11. E. Hallaba and G. El-Shaboury, *Isotope Npraxis*, **1977**, 13(1), 27.
12. T. J. Mangner, J. Wu, and D. M. Wieland, *J. Org. Chem.*, **1982**, 47, 1484.
13. M. T. El-Kolaly, S. ElBayoumy, M. Raiehand, and A. A. El-Mohty, *J. Radioanal. Nucl. Chem.*, **1993**, 174(1), 3.
14. L. Kronald, P. Hardilek, and K. Kopicka, *J. Radioanal. Nucl. Chem.*, **1990**, 139, 8911.
15. M. Zhaoxing, Li-Taihua, and Li-Boij, *J. Nucl. Radioanal. Chem.*, **1989**, 11(24), 108.
16. A. El-Wetery, N. Belacy, M. T. El-Kolaly, and M. Raieh, *Arab. J. Nucl. Sci. Appl.*, **1993**, 26, 44.
17. J. March, "Advanced Organic Chemistry, Reaction Mechanisms and Structures", **1968**, McGraw Hill, Inc., New York.
18. A. S. El-Wetery and G. El-Shaboury, *Arab. J. Nucl. Sci. Appl.*, **1998**, 31(1) 75.
19. H. Elias, Ch. Arnold, and G. Kloss, *J. Radiat. Isot.*, **1973**, 24, 463.
20. G. H. Hinkle, G. P. Basamadjin, A. S. Krischner, and R. D. Ice, *J. Pharm. Sci.*, **1981**, 70, 312.
21. G. El-Shaboury and K. Farah, *Appl. Radiat. Isot.*, **1991**, 42, 1091.
22. J. H. Bijl, F. M. Kaspersen, and L. Linder, *Radioanal. Chem.*, **1977**, 35, 55.
23. M. M. Saeed and A. Ghaffar, *J. Radioanal. Nucl. Chem. Art*, **1998**, 232, 171.



ELSEVIER Analytica Chimica

Available online at www.sciencedirect.com

SCIENCE @ DIRECT®

Acta 487 (2003) 249–259

ANALYTICA
CHIMICA
ACTA

www.elsevier.com/locate/aca

Kinetics and retention characteristics of some nitrophenols onto polyurethane foams

M.S. El-Shahawi*, H.A. Nassif

Department of Chemistry, Faculty of Science at Damietta, Mansoura University, Mansoura, Egypt

Received 19 August 2002; received in revised form 20 March 2003; accepted 5 May 2003

Abstract

The kinetics of sorption of the nitrophenols by the unloaded polyurethane foams (PUFs) were found fast, reached equilibrium in few minutes and followed a first-order rate equation with an overall rate constant k in the range $(0.16–0.21) \pm 0.01 \text{ min}^{-1}$. The retention of the tested nitrophenols by the unloaded foams is consistent with the “solvent extraction” mechanism. However, the sorption also followed Langmuir, Freundlich and Dubinin–Radushkevich (D–R) isotherms. The mean free sorption energy of the nitrophenols onto the PUF was found equal to $7.5 \pm 0.4 \text{ kJ/mol}$, which reflects physical sorption. Thus, a dual-mode involves both absorption related to solvent extraction and an added component for surface adsorption seems a more likely sorption mechanism model. While a dual-mode sorption model explains the observed retention behavior, the data suggest that, solvent extraction plays a much larger role than the added component for surface adsorption. The sorption and recovery percentages of the nitrophenols from fresh, natural and industrial wastewater by the proposed unloaded foam columns were quantitatively achieved. The height equivalent to theoretical plates (HETP), N , the breakthrough capacity and the critical capacity for the unloaded foam columns were found in the range of $(0.8–1.1) \pm 0.6 \text{ mm}$, $(94–132) \pm 3$, $3.2–4.02$ and $1.5–2.67 \text{ mg/g}$, respectively. The method was successfully applied for the retention and recovery of the tested nitrophenols spiked to fresh and industrial wastewaters.

© 2003 Elsevier Science B.V. All rights reserved.

Keywords: Kinetics and retention characteristics; Nitrophenols; Polyurethane foams

1. Introduction

Polyurethane foams (PUFs) have been proposed for the preconcentration, separation and determination of phenols and other pollutants in water and air [1–8]. Preconcentration of aerosols onto porous polyurethane foam plugs have been reported by Kenny et al. [9]. The

membrane-like structure of the foams together with the efficient sorption properties offers many advantages

* Corresponding author. Tel.: +20-2-057-403867; fax:

+20-2-057-403868.

E-mail address: [mohammad el shahawi@hotmail.com](mailto:mohammad_el_shahawi@hotmail.com) (M.S. El-Shahawi).

over other solid collectors with other solid materials [10,11].

Our earlier work on the sorption mechanism of phenols and other organic contaminants from aqueous media by PUFs have showed that the foams are capable of sorbing organic compounds by solvent extraction mechanism [12,13]. Herein we report the transport of some nitrophenols onto PUF for the purpose of better defining the factors affecting the sorption mechanism of these compounds from water by the foam membranes. This study also helps in promoting the use of PUFs for the separation and determination of nitrophenols in various segments of industry.

2. Experimental

003-2670/03/\$ – see front matter © 2003 Elsevier Science B.V. All rights reserved.

doi:10.1016/S0003-2670(03)00558-0

2.1. Reagents and materials

All chemicals and reagents used were of analytical reagents grade. The compounds tested are *o*-nitrophenol ($pK_a = 7.17$), *m*-nitrophenol ($pK_a = 8.28$) and *p*-nitrophenol ($pK_a = 7.15$). Milli-Q water was used to prepare the required solutions. A stock solution (100 ppm) of each nitrophenol was prepared in water in the presence of traces of sodium hydroxide. A series of standard solutions of these compounds was prepared by diluting their stock solutions with water and stored in low density polyethylene bottles (LDPE-Nalgene). Commercial polyether type based PUF cubes (3–5 mm edge) were purified as reported earlier [4].

2.2. Apparatus

A single beam Digital Spectro UV-Vis RS Labomed Inc., spectrophotometer with 10 mm path length quartz cells and glass columns (18 cm × 15 mm i.d.) were used. An Orion pH meter (8000) and a Lab-Line Orbit Environ-Shaker were used.

2.3. General procedures

2.3.1. Immobilization of the unloaded foams with $Al(OH)_3$ or $Fe(OH)_3$

An accurate amount (0.3 ± 0.01 g) of the dried PUF cubes was stirred with 20 cm³ suspension of the modifying agent finely precipitate $Fe(OH)_3$ or $Al(OH)_3$ at pH = 3.5 and 6, respectively, for 30 min. The foam

cubes were then separated out, washed with water and pressed between two sheets of filter papers to remove any traces of $Fe(OH)_3$ or $Al(OH)_3$. The amount of $Fe(OH)_3$ and $Al(OH)_3$ remained in solution were determined with EDTA [14] after dissolving with few drops of HNO_3 (5%). The amount of $Fe(OH)_3$ or $Al(OH)_3$ retained (a) on the foam cubes was then calculated by employing the equation [9]:

$$a = (C_0 - C) \frac{v}{m} \quad (1)$$

where C_0 and C are the initial and equilibrium modifying agent concentrations (mol/l) in solutions,

respectively, v is the volume of solution in liters and m is the mass (g) of sorbent.

2.3.2. Batch experiments

In 250 cm³ polyethylene bottles, the unloaded or immobilized foam cubes (0.3 ± 0.002 g) were equilibrated with 80 cm³ of an aqueous solution of each compound (15 g/cm³) separately. The solution pH was adjusted with Britton–Robinson buffer (pH = 2–10) and shaken in a shaker at 25 ± 0.1 °C for 1 h. The aqueous phase was then separated out and the amount of the tested nitrophenol remaining in it was determined from its absorbance measurements at λ_{max} against a reagent blank. The amount of the compound retained on the foam cubes was then calculated from the difference between the absorbance of the aqueous phase before (A_b) and after extraction (A_f). Following these procedures, the effect of salt effect, shaking time and nitrophenol concentration on the sorption behavior by the foam cubes were determined. The sorption percentage (% E), the amount of phenol retained at equilibrium (q_e) per unit mass of solid sorbent (mol/g) and the distribution coefficient (K_d) of the sorbed nitrophenols onto the foam cubes were computed using the equations:

$$\% E = \frac{A_b - A_f}{A_b} \times \frac{100}{\quad} \quad (2)$$

$$q_e = (A_b - A_f) \frac{v}{w} \quad (3)$$

$$K_d (\text{cm}^3 \text{g}^{-1}) = \frac{\%E}{100 - \%E} v \quad (4)$$

where v is the volume of the solution in cm^3 equilibrated with w the weight in g of the PUF sorbent. All experiments were carried out at least in triplicate and the results are the average of three independent measurements and precision in most cases was $\pm 2\%$.

2.3.3. Column experiments

In column experiment, 100 cm^3 of distilled, natural and industrial wastewater samples containing the tested nitrophenol (10 ppm) at $\text{pH} \leq 2$ were percolated through the column packed with $3 \pm 0.002 \text{ g}$ of the unloaded foams at $5 \text{ cm}^3/\text{min}$ flow rate using the vacuum method of foam packing [4]. The retained nitrophenol was successfully recovered with 20 cm^3 acetone at $2 \text{ cm}^3/\text{min}$. The absorbance of the effluent and the fractions of the eluate were measured at λ_{max} against a reagent blank.

3. Results and discussion

3.1. Kinetics and retention profiles of the nitrophenols onto the PUF

Previous work [15,16] on the immobilization of finely precipitate like $\text{Fe}(\text{OH})_3$ or $\text{Al}(\text{OH})_3$ as modifying agents onto solid support, e.g. PUF have showed that, the diffusion of the solute through the hypothetical film or hydrodynamic layer during the sorption step increased. Thus, retention of tested nitrophenols from the aqueous media by the unloaded foams and foams immobilized with finely distributed $\text{Al}(\text{OH})_3$ or $\text{Fe}(\text{OH})_3$ precipitate was critically investigated at different pH values. The pH value significantly influences the sorption of the tested species and the maximum uptake of the nitrophenols occurred at $\text{pH} < 5$. Representative sorption profiles of the investigated compounds by the unloaded and immobilized foams after 1 h shaking are summarized in Fig. 1. Thus, the pH of the aqueous solutions was selected at $\text{pH} \sim 2$ in the subsequent work. The average

nitrophenols uptake by the unloaded and loaded foams followed the sequence: m -nitrophenol $>$ p -nitrophenol $>$ o -nitrophenol

No significant differences on the uptake of the nitrophenols on the loaded and unloaded foams were observed. These data suggest that, the modifying agent possibly did not cause any consistent improvement in the surface area of the foam. Therefore, the subsequent work, the unloaded foams were only used in the sorption step. Two regions are apparent from the graph (Fig. 1). These are the plateau of approximately zero slope below $\text{pH} \leq 4$ and the linear segment with respective slopes in the range -0.65 to -0.75 at $\text{pH} \geq$

6 for the loaded and unloaded foams. In the retention of an acid like o -, m - and p -nitrophenol of which the molecular species are extractable, slopes of 0.0 and -1.0 below and above the $\text{p}K_a$ of the extracted species, respectively, are expected [14]. The slopes of the straight lines are approximately equal to 0 and -1 for $\text{pH} \leq 2$ and above 6, respectively. The deviation of the values of the slopes from the theoretical values probably occurred because the pH of the data points

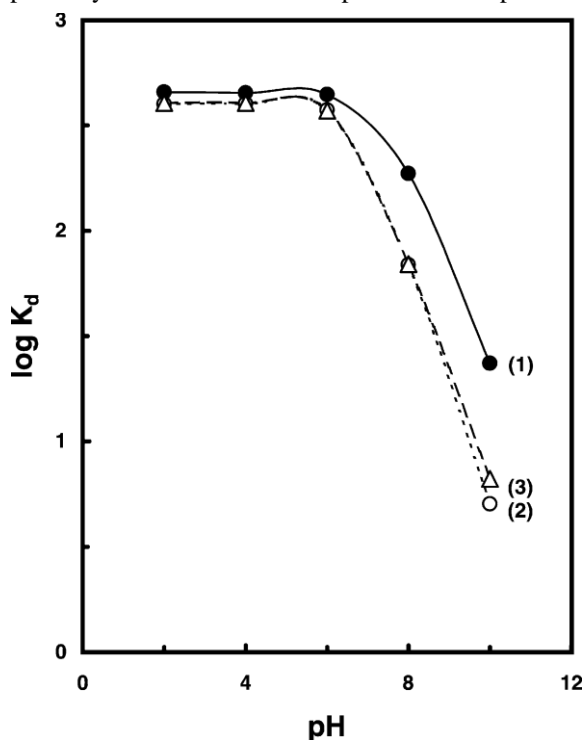


Fig. 1. Plot of $\log K_d$ vs. pH for the distribution of *m*-nitrophenol between the unloaded (1) PUF, (2) $\text{Fe}(\text{OH})_3$ and (3) $\text{Al}(\text{OH})_3$ —immobilized foams and aqueous solution.

is close to the $\text{p}K_a$ of the nitrophenols. These results suggest that, the nitrophenols are extracted by a simple “solvent extraction” mechanism [7,8] in which only the neutral molecular species are extractable. These data are in good agreement with the explanation advanced by Cooney and Wijaya [17] on the sorption of nitrophenols by solid support. According to the authors [17], nitrophenols will be retained to a lesser extent at higher pH values due to the repulsive forces prevailing at higher pH values between the adsorbate ions. Moreover, Cooney’s explanation predicts that, the pH of the solution will have a sound adverse effect on the adsorbability of the adsorbent at values greater than the $\text{p}K_a$ of the adsorbate, which is around 8.5 in this case. Thus, the nitrophenols poorly extracted by the unloaded foams at $\text{pH} \geq 4$.

The kinetic of the uptake of *o*-, *m*- and *p*-nitrophenols from the aqueous solution at $\text{pH} < 2$ on the unloaded polyurethane foams was rapid and the equilibrium was attained within 10 min followed by a plateau. Hence,

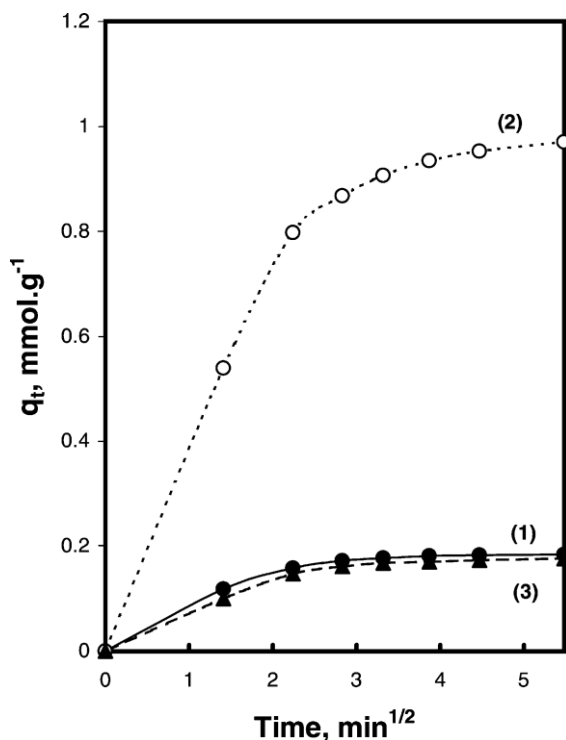


Fig. 2. The sorbed concentration of *o*-nitrophenol (1), *m*-nitrophenol (2) and *p*-nitrophenol (3) from an aqueous solution at $\text{pH} = 2$ onto the PUF as a function of time, $t_{1/2}$ at 25 ± 0.1 °C.

a 30 min shaking time was adopted in the subsequent experiments. The average half-life time ($t_{1/2}$) of the equilibrium sorption of *o*-, *m*- and *p*-nitrophenols were in the range 3–4 min. The sorbed nitrophenol concentration at time t , q_t (mol/g) was plotted against t (Fig. 2) to test the Morris–Weber equation [18].

$$q_t = R_d(t)^{1/2} \quad (5)$$

where R_d is the rate constant of intraparticle transport in $\text{mol}/(\text{g min}^{1/2})$. The data indicated that, for up to 4 min, the relationship holds good and deviates as the shaking time increase. The R_d values were computed from the two distinct steps of the Morris–Weber plot (Fig. 2). The values of R_d in the initial stage up to 4 min were in the range $(0.07\text{--}0.38) \pm 0.005$ $\text{mmol}/(\text{g min}^{1/2})$ and became $(0.01\text{--}0.067) \pm 0.005$ $\text{mmol}/(\text{g min}^{1/2})$ beyond 10 min shaking time. The diffusion rate was rapid in the initial stage and slow with the passage of

time. The change in the slope may be due to the existence of different sized pores. Moreover, the kinetic data were

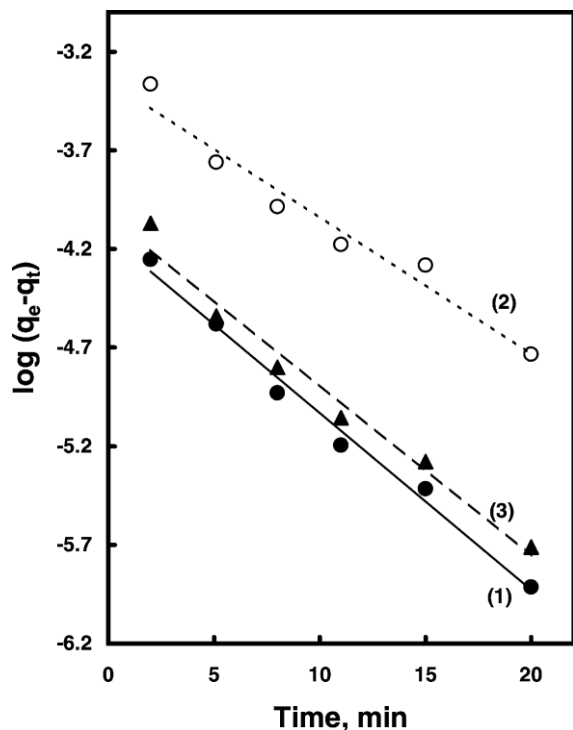


Fig. 3. Lagergren plot of the kinetics of *o*-nitrophenol (1), *m*-nitrophenol, (2) and *p*-nitrophenol (3) sorption onto the PUF at 25 ± 0.1 °C.

also evaluated over the entire range of agitation time explored using the Lagergren equation [19].

$$\log(q_e - q_t) = \log q_e - \left(\frac{kt}{2.303} \right) \quad (6)$$

The plots of $\log(q_e - q_t)$ versus time up to 20 min are linear (Fig. 3). The values of the first order overall rate constant (k) are 0.21 ± 0.005 , 0.16 ± 0.001 and $0.2 \pm 0.01 \text{ min}^{-1}$ for *o*-, *m*- and *p*-nitrophenols, respectively. The value of B_t which is a mathematical function of the ratio of fraction sorbed q_t in mol/g at time t and at equilibrium (q_e) in mol/g was calculated for each value of F employing Reichenburg equations [20]:

$$F = \frac{q_t}{q_e} \quad (7)$$

$$F = 1 - \frac{6}{\pi^2} e^{-B_t}$$

or

$$B_t = -0.4977 - 2.303 \log(1 - F) \quad (8)$$

A plot of B_t versus time at 25 °C for each nitrophenol was found linear up to 8 min and passed through the origin. These data indicate that, particle diffusion is the most probable operating mechanism and does control the kinetics of compounds sorption on the unloaded foam. Therefore, the uptake of nitrophenol on PUF may involve three steps: bulk transport of nitrophenol in solution, film transfer involving diffusion of nitrophenols within the pore volume of PUF and/or along the pore wall surfaces to an active sorption site [21]. The actual sorption of the solute on the interior surface sites is very rapid, and hence it is not a rate determining step. Therefore, film and intraparticle transport may be the two steps controlling the rate of sorption from acid solutions.

The effect of CaCl_2 concentrations (0.05–0.2 M) on the uptake of the nitrophenols from the aqueous solution by the PUFs was carried out. A minor effect of CaCl_2 on the retention profiles of the nitrophenols onto the unloaded foams was observed, indicating no partial nullification of repulsion forces between the adjacent sorbed nitrophenolate anions and no mutual interaction between the solution pH and the presence of CaCl_2 [22]. This suggests that the phenols must present in a non-ionized form in aqueous solution and extract as neutral species [7]. Calcium chloride also reduces the equilibrium concentration of nitrophenols. The data were found in good agreement with the data reported by Darwish et al. [22] therefore; “solvent extraction” mechanism plays a major role on the sorption of the nitrophenols. However, this mechanism is ruled out since small amount of the sorbate could not be accounted on using the available dipole moment of the substrate [23].

The effect of alkali metal (Na^+ , K^+ and NH_4^+) chlorides at concentration levels <0.2 M on the nitrophenols (20 g/ml) uptake onto the PUF was studied. The data demonstrated a slight increase in the nitrophenols sorption onto the PUF and the order of the extraction followed the sequence:



This effect is also attributed to partially nullifying the repulsive forces between adjacent sorbed $\text{NO}_2\text{C}_6\text{H}_5\text{O}^-$ ions [22]. The ion–dipole interaction of NH_4^+ with the oxygen sites of the polyurethane foams was not predominating factor in the extraction of the nitrophenols. This effect is consistent with a “solvent extraction” mechanism with the salt acting as salting-out agent. The added alkali metal ions reduced the numbers of water molecules available to solvate onto the nitrophenols which would therefore, be forced out of the solvent phase onto the foam because some of free water molecules are preferentially used to solvate the cations added. The cations added with high charge density ($\text{Na}^+ > \text{NH}_4^+ > \text{K}^+$) are expected to exert a greater salting-out effect. Thus, the influence of the salts can be explained by the salting-out effect on a “solvent extraction” mechanism. These results are in good agreement with the data reported by Palagyi et al. [24,25].

3.2. Sorption isotherms of the nitrophenols on unloaded PUF

The sorption behavior of *o*-, *m*- and *p*-nitrophenols from the aqueous solution by the unloaded foams was found to depend on its own concentration in the range of 20–500 mg/l. Therefore, in separate experiment, the retention of each nitrophenol onto the unloaded foams was measured at $\text{pH} < 2$ and at 25 ± 0.1 °C. At this pH compounds are predominantly in neutral or protonated form [14]. The results are given in Fig. 4. The distribution ratio decreased sharply with increasing the nitrophenol concentration because the foam became almost saturated with the retained species. Thus, film diffusion and intraparticle transport does not control the rate of sorption of the nitrophenols onto PUF at $\text{pH} < 2$ and the most favorable distribution ratios are observed for more diluted solutions. The isotherms of nitrophenols showed a first-order behavior, where a good linear correlation between the amount of compound retained onto the PUF and that remained in the aqueous solution was achieved over a wide range of equilibrium concentrations. The isotherms of the three compounds followed the sequence:

m-nitrophenol > *p*-nitrophenol > *o*-nitrophenol

The data are consistent with a “solvent extraction” mechanism and in good agreements with the results previously reported [8,12]. The equilibrium was not approached for all nitrophenols, i.e. the unloaded foams have good sorption efficiency towards the tested nitrophenols. Obviously, this behavior could not be matched by any other known rigid or granular solid sorbents [4]. The sorption was very rapid and over

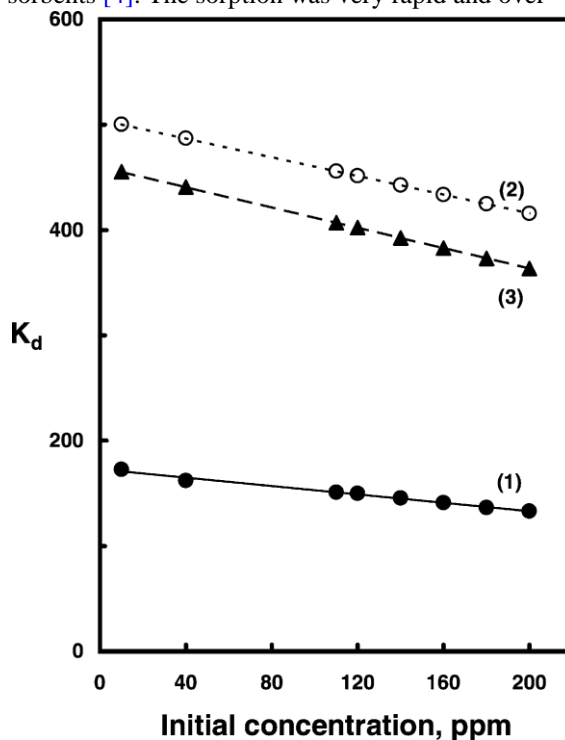


Fig. 4. Variation of the distribution ratio of *o*-nitrophenol (1), *m*-nitrophenol (2) and *p*-nitrophenol (3) onto PUF as a function of their own concentrations.

90% of the nitrophenols were sorbed within 10 min shaking time as described earlier. This indicates that the mass transfer of the nitrophenols from the bulk aqueous solution onto the PUF can be expressed in the form of its diffusion behavior. The diffusion of the solute through a hypothetical ‘film’ or hydrodynamic boundary layer takes place in the sorption phenomena [26]. The film diffusion is governed by molecular diffusion and considered to be rapid and generally occurs at the macropores of the PUF sorbent [27].

The variation of the sorption of the nitrophenols onto PUF was subjected to Langmuir [28], Freundlich [29],

and Dubinin and Radushkevich [30] sorption isotherms over a wide range of concentrations. The familiar form of Langmuir sorption isotherm based on the kinetic consideration was expressed in the following linear form [28]:

$$\frac{C_e}{C_{\text{ads}}} = \frac{1}{Qb} + \frac{C_e}{Q} \quad (9)$$

Table 1
Adsorption data of nitrophenol by different isotherms models

Sorbate	Langmuir			Freundlich		D-R	
	Q	b	R_L	A	$1/n$	K_{DR}	β
<i>o</i> -Nitrophenol	0.029 ± 0.001	101 ± 0.4	$(0.87 \pm 0.003) - (0.1 \pm 0.01)$	0.1 ± 0.01	0.85 ± 0.005	0.06 ± 0.01	0.01 ± 0.001
<i>m</i> -Nitrophenol	0.034 ± 0.001	281 ± 0.2	$(0.71 \pm 0.002) - (0.98 \pm 0.001)$	0.6 ± 0.02	0.63 ± 0.01	0.09 ± 0.001	0.008 ± 0.001
<i>p</i> -Nitrophenol	0.029 ± 0.001	260 ± 0.4	$(0.72 \pm 0.08) - (0.98 \pm 0.002)$	0.4 ± 0.02	0.6 ± 0.01	0.07 ± 0.001	0.008 ± 0.001

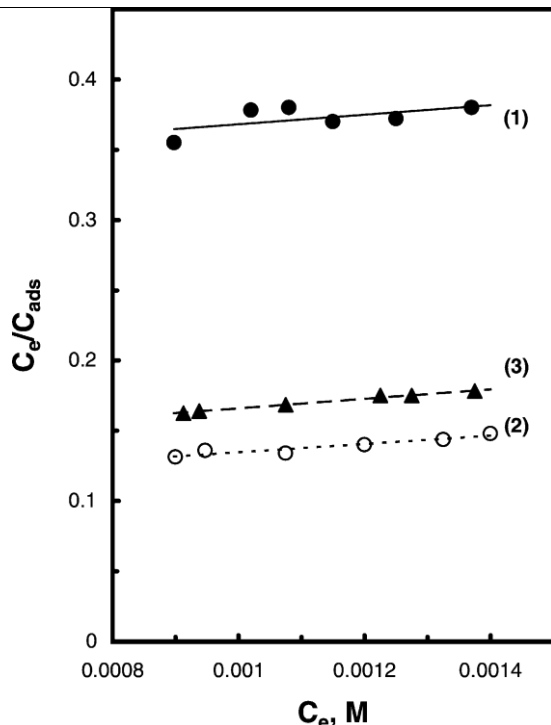


Fig. 5. Langmuir sorption isotherm of *o*-nitrophenol (1), *m*-nitrophenol (2) and *p*-nitrophenol (3) in aqueous solution at pH = 2 onto PUF.

where C_e is the equilibrium concentration of the tested nitrophenol (M) in solution, C_{ads} the amount of nitrophenol sorbed per unit weight of the PUF (mol/g). The parameters Q and b are constants related to the maximum amount of solute adsorbed and the binding energy of solute, respectively, that are independent of temperature. A plot of C_e/C_{ads} versus C_e , is linear (Fig. 5) throughout the entire concentration range for each

nitrophenol. The sorption parameters Q and b for each nitrophenol have been evaluated from the slope and the intercept of Fig. 5. The data are summarized in Table 1. The value of saturation capacity, Q corresponding to the monolayer coverage and should, therefore, be substantially independent of temperature. However, the adsorption coefficient, b is related to the enthalpy of the adsorption and should vary with temperature.

Another dimensionless equilibrium parameter, R_L can be estimated using the equation:

$$R_L = \frac{1}{1 + bC_i} \quad (10)$$

where C_i is the initial concentration of nitrophenol in solution. The values of R_L (Table 1) indicate high sorption of nitrophenol onto PUF.

The sorption data were also subjected to Freundlich sorption isotherm [29] over a wide range of concentration. The Freundlich model [29] is expressed in the following form:

$$\log C_{\text{ads}} = \log A + \frac{1}{n} \log C_e \quad (11)$$

where A and $1/n$ are Freundlich parameters related to the maximum sorption capacity of solute (mol/g) and intensity of sorption, respectively. The values of these parameters A and $1/n$ can be taken as a relative indicator of adsorption capacity of PUF for a narrow sub-region having equally distributed energy sites towards nitrophenols. These constants also encompass the surface heterogeneity and the exponential distribution of active sites and their energies. The plot of $\log C_{\text{ads}}$ versus $\log C_e$ (Fig. 6) is linear over the entire concentration of each nitrophenol. The numerical values of A and $1/n$ of each nitrophenol were computed from the intercept and slope of Fig. 6 and are summarized in Table 1. The values of $1/n$ and A are in the range $(0.6\text{--}0.85) \pm 0.01$; $(0.1\text{--}0.6) \pm 0.02$ mol/g, respectively, with correlation factor of 0.972. The numerical values of $1/n$ reflect that 60–85% active sites have equal energy where adsorption takes places. Thus, the Freundlich isotherms of the adsorbed nitrophenols does not predict any saturation of the solid surface of the sorbent by the sorbate. Thus, infinite surface coverage is predicted mathematically and physico-sorption on the surface is expected with the correlation factor.

The Dubinin–Radushkevich (D–R) isotherm model [30] is postulated within adsorption “space” close to adsorbent surface. The D–R isotherm can be linearized as follows:

$\ln C_{\text{ads}} = \ln K_{\text{D-R}} - \beta \epsilon^2$ (12) where $K_{\text{D-R}}$ is the maximum amount of nitrophenol that can be retained onto PUF, β a constant related to dimensions of energy and ϵ Polanyi potential which is given by the equation:

$$\epsilon = RT \ln \left(1 + \frac{1}{C_e} \right) \quad (13)$$

where R is the gas constant in kJ/(mol K), T the temperature in kelvin and C_e the equilibrium concentration of nitrophenol of in solution. The plots of $\ln C_{\text{ads}}$ versus ϵ^2 are shown in Fig. 7 for each nitrophenol. The D–R isotherms of the nitrophenols sorption onto

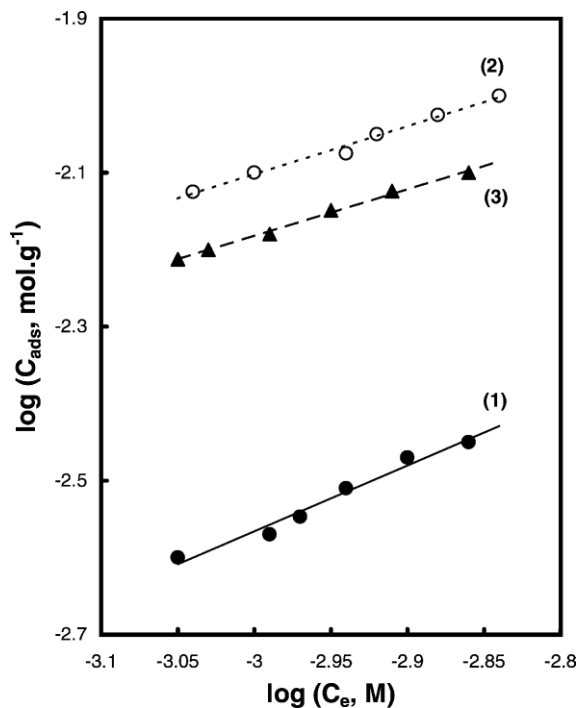


Fig. 6. Freundlich sorption isotherm of *o*-nitrophenol (1), *m*-nitrophenol (2) and *p*-nitrophenol (3) in aqueous solution at pH = 2 onto PUF.

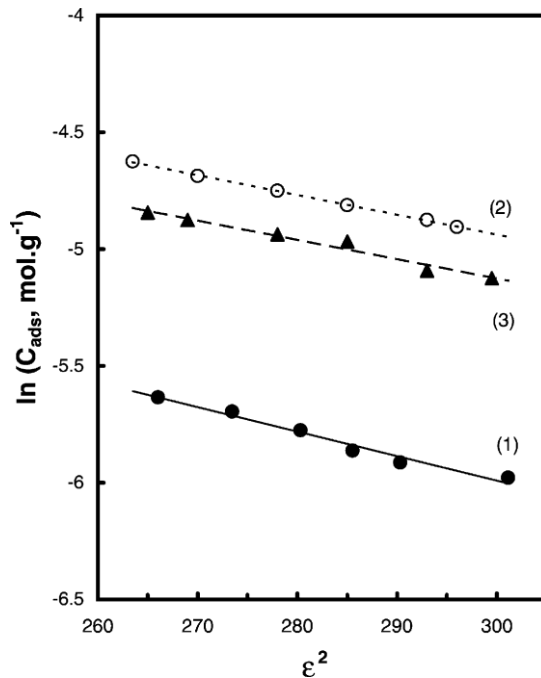


Fig. 7. Dubinin–Radushkevich (D–R) sorption isotherm of *o*-nitrophenol (1), *m*-nitrophenol (2) and *p*-nitrophenol (3) in aqueous solution at pH = 2 onto PUF.

PUF are linear over their entire concentrations tested. The numerical values of β and K_{DR} are calculated from the slopes and intercept (Fig. 7) using linear regression curve fitting method. The data are given in Table 1. The values of K_{DR} and β were found in the range $(0.06–0.09) \pm 0.01$ mol/g and $(0.008–0.01) \pm 0.001$ mol²/kJ², respectively. Assuming the surface is heterogeneous and an approximation to a Langmuir isotherm model is chosen as a local isotherm for all sites that are energetically equivalent, then the quantity $\beta^{1/2}$ can be related to the mean free energy (E) of the transfer of 1 mol of solute from infinity in solution to the surface of PUF foam as follows:

$$E = \frac{1}{\sqrt{-2\beta}} \quad (14)$$

The numerical values of E evaluated from Eq. (14) using the value of β from Eq. (12) does not reflect the chemical sorption based on ion exchange mechanism [31]. The E values lie within the range of 7.5 ± 0.4 kJ/mol envisaged from solvent extraction. These data suggest an added component for surface adsorption of nitrophenols onto PUFs. Thus, a dual-mode sorption mechanism seems a more likely model and the solvent extraction plays a major role than the added component for surface adsorption. These results and the flow characteristics of the PUFs suggest the possible application of the foam sorbent in column mode for the quantitative retention and recovery of the tested nitrophenols from more diluted aqueous solutions of fresh and industrial wastewater.

3.3. Chromatographic behavior of nitrophenol onto unloaded PUFs

Preliminary investigation on the sorption profiles of *o*-, *m*- and *p*-nitrophenols from the aqueous solution onto PUF suggested the possible application of the foam in column mode for the quantitative collection and recovery of the tested nitrophenols from large volume water samples. Thus, a 100 cm³ of tap, natural and industrial wastewater samples at pH < 2 spiked with 1–10 g of each of the three nitrophenols were

percolated through the PUF column at 5 cm³/min flow rate. Complete sorption ($98.2 \pm 3\%$) of the tested nitrophenol was achieved. The proposed method was also applied for the retention and recovery of *o*- and *p*-nitrophenols present in fresh and industrial wastewater. Fresh water samples were collected from Nile river near thermal power station at Damietta city and ground water samples from Mansoura city, Egypt. A 1 l of water sample at pH < 2 spiked with 30–40 ppb of *o*- or *p*-nitrophenol was percolated through the foam columns (15 mm i.d.) at 10 cm³/min flow rate. Satisfactory results ($98.7–103.0 \pm 1.3\%$, $n = 5$) on the retention of the tested nitrophenols were achieved. The retained species of the *ortho*-nitrophenol were then eluted from the foam columns with 25 cm³ acetone at 2–3 cm³/min flow rate and accurately determined by measuring the absorbance of the effluent solution against a reagent blank [32]. The results are summarized in Table 2. The data revealed good extraction and recovery of the tested nitrophenol by the proposed foam columns.

The performance of the foam column was determined from the number of theoretical plates (N) and the height equivalent to theoretical plates (HETP). Thus, a 100 cm³ of distilled water at pH < 2 spiked with 30–40 ppb *o*-nitrophenol were percolated through the foam column at 5 cm³/min. The retained species

Table 2

Preconcentration and recovery of *o*-nitrophenol in simulated fresh and industrial wastewater

Sampl e ^a	Concentr ation ^b added (ng/cm ³)	Concentration found (ng/cm ³)	Reco very (%)
Nile water	30	31	± 2 ± 1
Groun d water	30	30.6	
Indus tria l wa ter	30 40 1	31.3 ± 1.8 39.5 ± 1.6	103.6 ± 1.4 98.7 ± 2.1

^a At 95% confidence level. ^b

Sample volume = 1.0dm³.

were then eluted from the foam column with 20 cm³ acetone at 2 cm³/min. A 2 cm³ fractions of the effluent solution were then collected in order and its absorbance were then measured against a reagent blank at λ_{\max} . The values of N and the HETP of the foam column were then determined employing Glueckauf equation [33]:

$$N = \frac{8V_{\max}^2}{W^2} = \frac{L}{\text{HETP}} \quad (15)$$

where V_{\max} is the volume of eluate to peak maximum, W the width of the peak at 1/e times the maximum solute concentration and L the length of the foam column bed in mm. The N and HETP values as calculated from the chromatograms were found equal 132 ± 3 and 0.8 ± 0.02 mm, respectively, at 2–3 cm³/min flow rate.

The HETP and N values were also determined from the breakthrough capacity curve. An aqueous solution (0.5 dm³) of *o*-, *m*- or *p*-nitrophenol at 5 ppm level was percolated separately through the foam column at 5 cm³/min flow rate. The results are shown in Fig. 8. The values of N and HETP were then calculated by employing the equation [18]:

$$N = \frac{V_{50}V'}{(V_{50} - V')^2} = \frac{L}{\text{HETP}} \quad (16)$$

where V_{50} is the volume of the effluent solution at the center of the S-shaped curve (Fig. 8) and V' the value at which the effluent solution has a value of 15.78% extraction of the initial concentration. found equal 94 ± 2 and 1 ± 0.1 mm, respectively, for the foam column of 15 mm i.d.

The effect of the foam column internal diameter (i.d.) on the sorption of the *o*-nitrophenol was examined. The values of N slightly increased from 94 ± 2

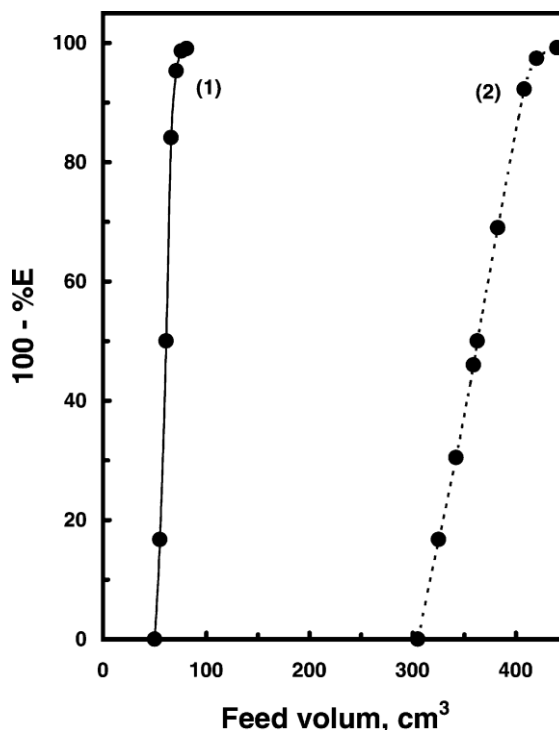


Fig. 8. Breakthrough capacity curves of *o*-nitrophenol (10ppm) sorption onto PUF columns of (1) 5mm and (2) 15mm i.d., at 2–3 cm³/min flow rate and 25 ± 0.1 °C.

to 95 ± 2 and the HETP decreased from 1 ± 0.1 to 0.85 ± 0.01 mm, on increasing the internal diameter from 5 to 15 mm, respectively. Similar results were also obtained for *p*-nitrophenol. The effect of the sample volume on the nitrophenol retention was also investigated by passing 50 and 500 cm³ (10 g/cm³) through the foam column at 5 cm³/min flow rate. In all cases, the retention obtained was found higher than 97%.

The analytical utility of the foam columns (5 and 15 mm i.d.) for the separation of the nitrophenols from the aqueous solution was determined from their breakthrough capacity curves of *o*-nitrophenol at 10 ppm concentration level. The two curves in Fig. 8 present both (i) the breakthrough volume and (ii) the volume needed to reach bed saturation for *o*-nitrophenol. It is clear that, the raising portion in the curve have a large shape which indicates both a high diffusion rate of *o*-nitrophenol onto the membrane

forming the skeleton of the foam material and a high rate of equilibrium attainment between the analyte and the sorbent. Similar behavior was achieved for *p*-nitrophenol. The critical capacities of the foam columns of 5 and 15 mm i.d. packed with 0.5 ± 0.01 and 3.0 ± 0.02 g dry foam for *o*-nitrophenol were found equal 1.5 ± 0.01 and 2.7 ± 0.02 mg/g foam, respectively. The breakthrough capacities of *o*-nitrophenol calculated by the method of Ma et al. [34] were found equal 3.2 and 4.03 mg/g dry foam for 15 and 5 mm i.d., respectively.

3.4. Interference study

The retention of the tested nitrophenol from the aqueous solution in the presence of some interfering ions that commonly was critically carried out by the proposed foam method. Thus, the uptake of *o*-nitrophenol at 20–50 ppb concentration level was investigated in the presence of up to 1 mg of the following ions: oxalate, formate, acetate, nitrate, sulphate, phosphate, selenate, chloride, and bromate and the metal ions Zn, Mg, Cu, Ba, Na, Ca and Li. Good retention and recovery (97.8–101.9%) of the tested nitrophenols were achieved successfully employing the foam column at 5 ml/min flow rate.

4. Conclusion

The study of the sorption of nitrophenols by the PUFs membrane shows that these compounds are extracted in their neutral form. The PUF sorbent offers unique advantages in rapid separation of complex species from fluid water samples. The kinetic data and the sorption isotherms of *o*-, *m*- and *p*-nitrophenols onto PUF are controlled by the solution pH. A minor effect on the sorbate uptake was observed in the presence of CaCl₂. The results also provide a deeper insight into the mechanism of sorption of nitrophenols by the PUF. However, work is still continuing in our laboratory for increasing the number of phenols that can be retained, separated out and simultaneously determined by the proposed method. Further studies will involve investigation of these extractions for a wider range of organic compounds in order to obtain a clearer view of the extraction mechanism taking place.

Acknowledgements

The authors would like to thank Prof. Y.M. Moustafa, Physics Department, Mansoura University, for his assistance in the preparation of figures.

References

- [1] M.S. El-Shahawi, *J. Chromatogr. A* 760 (1997) 179.
- [2] M.S. El-Shahawi, M.H. Abdel-kader, R.S. Al-mehrezi, *Anal. Sci. (Jpn.)* 13 (1997) 633.
- [3] M.S. El-Shahawi, S.M. Aldhaheeri, *Anal. Chim. Acta* 320 (1996) 277.
- [4] T. Braun, J.D. Navratil, A.B. Farag, *Polyurethane Foam Sorbents in Separation Science*, CRC Press, Boca Raton, FL, 1985.
- [5] A.B. Farag, M.S. El-Shahawi, *J. Chromatogr.* 552 (1991) 371.
- [6] J.W. Marlin, D.C.G. Muir, C.A. Moody, *Anal. Chem.* 74 (2002) 584; H.B. Park, Y.M. Lee, *J. Membr. Sci.* 197 (2002) 283.
- [7] K. Rzeszutek, A. Chow, *Talanta* 46 (1998) 507; F. Fong, A. Chow, *Talanta* 39 (1992) 497.
- [8] K. Rzeszutek, A. Chow, *Talanta* 49 (1999) 757. [9] L.C. Kenny, R.J. Atiken, G. Beaumont, P. Gerner, *J. Aerosol Sci.* 32 (2001) 271.
- [10] H. Oda, C. Yokokawa, *Carbon* 21 (1983) 485.
- [11] V.K. Gupta, S.K. Srivastava, R. Tyagi, *Water Res.* 34 (2000) 1543.
- [12] M.S. El-Shahawi, *Talanta* 41 (1994) 1481.
- [13] M.S. El-Shahawi, A.B. Farag, M.R. Mostafa, *Sep. Sci. Technol.* 29 (1994) 289.
- [14] R. Werbowesky, A. Chow, *Talanta* 43 (1996) 263; G.D. Christian, *Analytical Chemistry*, fifth ed., Wiley, New York, 1994, p. 486.
- [15] W.J. Weber, in: F.L.K. Iojke (Ed.), *Principles of Adsorption Process*, vol. 19, Marcel Dekker, New York, 1988, p. 16.
- [16] D. Lal, J.R. Arnold, B.L.K. Somayajulu, *Geochim. Cosmochim. Acta* 28 (1964) 1111.
- [17] D.O. Cooney, J. Wijaya, in: A.I. Liapis (Ed.), *Proceedings of the Second Conference of Engineering Foundation on Fundamentals of Adsorption*, New York, 1987.
- [18] S. Weber, J. Morris, *J. San. Eng. Div. ASEC* 899SA₂ (1963) 31.
- [19] S. Lagergren, B.K. Sven, *Vatenskapsakad. Handl.* (1898) 24.
- [20] D. Reichenburg, *J. Am. Chem. Soc.* 75 (1953) 589.
- [21] S. Aksoyoglu, *J. Radioanal. Nucl. Chem.* 134 (1989) 393.
- [22] N.A. Darwish, K.A. Halhouli, N.M. Al-Dhoon, *Sep. Sci. Technol.* 31 (1996) 705.
- [23] M. Kotake, *Constants of Organic Compounds*, Asakura, Tokyo, 1963, p. 500.
- [24] S. Palagyi, T. Braun, *J. Radioanal. Nucl. Chem.* 163 (1992) 1377.

- [25] S. Palagyi, T. Braun, Z. Homonnay, A. Vertes, *Analyst* 117 (1992) 1537.
- [26] W.J. Weber, in: F.L. Slejko (Ed.), *Principles of Adsorption and Desorption Process*, vol. 19, Marcel Dekker, New York, 1985, p. 16.
- [27] S.D. Faust, O. Aly, *Adsorption Process of Water Treatment*, Butterworths, Boston, 1986.
- [28] I. Langmuir, *J. Am. Chem. Soc.* 40 (1918) 136.
- [29] H. Freundlich, *Colloid and Capillary Chemistry*, Methuen, London, 1926.
- [30] M.M. Dubinin, L.V. Radushkevich, *Proc. Acad. Sci. USSR, Phys. Chem. Soc.* 55 (1947) 331.
- [31] F. Helfferich, *Ion-Exchange*, Mc-Graw Hill, New York, 1962, p. 166.
- [32] J.P. Rawat, K.P.S. Muktawat, *Microchem. J.* 30 (1984) 289.
- [33] E. Glueckauf, *Trans. Faraday Soc.* 51 (1955) 34.
- [34] W.X. Ma, F. Liu, K.A. Li, W. Chen, S.Y. Tong, *Anal. Chim. Acta* 416 (2000) 191, and references cited therein.



ELSEVIER Analytica Chimica

Available online at www.sciencedirect.com

SCIENCE @ DIRECT®

Acta 481 (2003) 29–39

ANALYTICA
CHIMICA
ACTA

www.elsevier.com/locate/aca

Retention and thermodynamic characteristics of mercury(II) complexes onto polyurethane foams

M.S. El-Shahawi*, H.A. Nassif

Department of Chemistry, Faculty of Science at Damietta, Mansoura University, Mansoura, Egypt

Received 6 May 2002; received in revised form 7 January 2003; accepted 16 January 2003

Abstract

Polyurethane foams (PUF) loaded with crystal violet and some onium cations were successfully employed for the retention of mercury(II) traces present in aqueous media. The kinetics and thermodynamics of the sorption of mercury(II) ions onto PUFs have been studied. The sorption of mercury(II) ions onto PUF follows a first-order rate equation which results as $k = 0.25 \pm 0.01 \text{ min}^{-1}$. The sorption data followed Langmuir, Freundlich and Dubinin–Radushkevich (D–R)-type sorption isotherms. The D–R parameters were $\beta = -0.0123 \pm 0.0002 \text{ mol}^2/\text{kJ}^2$, $K_{DR} = 90 \pm 5 \text{ mol/g}$ and $E = 6.38 \text{ kJ/mol}$.

The negative values of H and S may be interpreted as the exothermic chemisorption process and indicative of the faster chemisorption of the HgBr_3^- complex sorbed onto the active sites of the sorbent. Quantitative retention and recovery (99.5 ± 2.1) of mercury(II) ions in water at $\leq 5 \text{ ppb}$ level by the foam columns were achieved. The HETP, the number (N) of the theoretical plates, the breakthrough and the critical capacity of the mercury(II) uptake by the foam column were found to be 0.65 ± 0.01 , $155 \pm 4.1 \text{ mm}$, 10.8 and 8.1 mg/g , respectively, at $5 \text{ cm}^3/\text{min}$ flow rate. A retention mechanism based on the sorption data has been proposed. This mechanism involves both absorption related to solvent extraction and an added component for surface adsorption.

© 2003 Elsevier Science B.V. All rights reserved.

Keywords: Polyurethane foams; Thermodynamic; Polyurethane

1. Introduction

Owing to the toxicity and the low level of mercury in environmental and biological samples many articles have been published on the preconcentration of mercury traces in water before their actual

determination [1–5]. Dithizone (H_2Dz) reagent forms an orange–yellow dithizonate complex, $\text{Hg}(\text{HDz})_2$. The produced complex is easily extracted in CCl_4 or CHCl_3 [6]. Mercury(II) ions was also extracted and de-

*Corresponding author. Tel.: +20-50-403867/403980. E-mail

addresses: mohammad el shahawi@hotmail.com,
sinfac@mum.mans.eun.eg (M.S. El-Shahawi).

terminated as tetraiodomercury(II)-Cd-phenanthroline ion-pair into benzene and selectively stripped into EDTA solution [7].

During the past decades, a number of solid sorbents, e.g., foamed plastics, chelating polymers and immobilized silica gel have been tested as supports in the reversed phase extraction chromatography, gas–solid and gas–liquid partition chromatography [8–12]. The available surface area and cellular structures of polyurethane foam makes it very suitable stationary phase and as a column filling material [9–11]. Polyurethane foams (PUF) immobilizing specific chromogenic organic reagents have been successfully employed for the sensitive detection, semiquantitative

003-2670/03/\$ – see front matter © 2003 Elsevier Science B.V. All rights reserved.
doi:10.1016/S0003-2670(03)00074-6

determination, selective collection and recovery of several metal ions including mercury(II) species on domestic water; river water, raw sewage and secondary treated sewage [13–22].

This paper reports the preconcentration and determination of mercury(II) traces in aqueous bromide solution onto PUFs after retention onto a column containing PUF loaded with crystal violet and other onium cations. Crystal violet and other onium cation reagents react with mercury(II) ion forming stable complex ion associates [23]. The kinetics and thermodynamics of the sorption step are also considered.

2. Experimental

2.1. Reagents and materials

All chemicals used were of analytical reagent grade. The onium cations (OC⁺): crystal violet (CV), cetyltrimethylammonium bromide (CTMA) and tetramethylammonium bromide (TMA) were used without further purification. BDH polyvinyl alcohol (PVA) and sodium dodecyl sulphate (SDS) were used as received. Foam cubes of 15 mm edge of commercial white sheets of open-pore polyether-type polyurethane

foam (30 kg/m³) were washed and dried at 80 °C for 2 h. [9]. Solutions of PVA (1% (v/v)) and CV, CTMA, SDS and TMA of concentration (0.005% (w/v)) were freshly prepared in deionized water. A stock solution of (0.1% (w/v)) dithizone (H₂Dz) was prepared in chloroform. A standard solution of mercuric chloride (1000 ppm) was prepared in deionized water acidified with nitric acid (0.5% (v/v)) and standardized against EDTA [24].

2.2. Apparatus

A Shimadzu double beam UV-Vis (UV-160 7PC) spectrophotometer with quartz cells (10 mm) was used for recording the electronic spectra and the absorbance measurements of H₂Dz and its mercury(II) complex, Hg(HDz)₂. An Orion pH meter; glass columns (18 cm

× 15 mm i.d) and a Lab-Line Orbit Environ-Shaker (35271-1) were used for the retention experiments of mercury(II).

2.3. Preparation of the immobilized reagent (CV, CTMA, TMA or SDS) foams

In separate experiment, the reagent foam cubes were prepared by mixing an aqueous solution of each reagent 0.005% (w/v) with the dried foam cubes (10 cm³/g dry foam) separately with efficient stirring for 20 min. The immobilized foam cubes were then pressed between filter paper sheets to remove the excess acetone present in the foam cubes, dried at 80 °C and stored in dark in a plastic bottle for further work [22].

2.4. Recommended procedures

2.4.1. Batch experiments

An accurate weight (0.3 ± 0.002 g) of the reagent foam cubes was shaken with 100 cm³ aqueous solution containing mercury chloride (100 ppm) and sodium bromide (4 × 10⁻⁴ M) for various time intervals up to 30 min at 20 ± 1 °C. After equilibrium, the amount of mercury(II) retained on the foam cubes was

determined from the difference between the mercury(II) concentration as $\text{Hg}(\text{HDz})_2$ before (C_i) and after (C_a) shaking with PUF. The sorption percentage (% E) and distribution coefficient (K_d) (cm^3/g) were calculated using the equations:

$$E = \frac{C_i - C_a}{C_i} \times 100 \quad (1)$$

$$E = \frac{K_d + v/w}{K_d} \times 100 \quad (2)$$

$$K_d = \frac{E v}{100 - \%E} \times \frac{1}{w} \quad (3)$$

where v is the volume of sample solution in cm^3 and w the weight of the reagent foam cubes in grams. Following these procedures, the effect of different parameters on the mercury(II) uptake was carried out. The data are the average of at least three independent measurements and precision in most cases was $\pm 4\%$.

2.4.2. Flow experiments

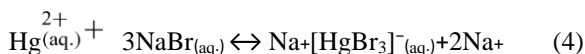
Tap or distilled water samples (1 dm^3) spiked with mercury(II) at concentration (5–10 ppb) were percolated at $5 \text{ cm}^3/\text{min}$ flow rate through column packed with $3.5 \pm 0.002 \text{ g}$ reagent (CV or TMA)-foams using the vacuum method of foam packing [9]. A blank experiment was also carried out in the absence of the mercury(II) ions. The mercury(II) content in the effluent solution was then measured spectrophotometrically at 485 nm after solvent extraction of its $\text{Hg}(\text{HDz})_2$ complex in chloroform [24] against a reagent blank. Elution of mercury(II) content in foam column was achieved quantitatively by percolating 100 cm^3 acetone at $5 \text{ cm}^3/\text{min}$ flow rate. The HETP and N were then calculated from the output of the chromatograms and breakthrough capacity experiments.

3. Results and discussion

3.1. Retention profiles of mercury(II) ions on PUF

The onium cations employed in this investigation are most likely able to form ion associates with the bulky anions of mercury(II). The amount of mercury(II) ions sorbed onto the reagent foams from the aqueous solution containing sodium bromide was found to depend on the solution pH. Therefore, the sorption profiles of mercury(II) ions by the loaded foam cubes from the aqueous solutions containing Britton–Robinson buffer (pH 2–10) and an excess of NaBr were investigated after shaking for 30 min. The uptake of mercury(II) on the loaded foams increased markedly with an increase in the solution pH up to pH ~ 6 and displayed the lowest sorption greater than pH 8 (Fig. 1). The increase in the sorption of mercury(II) at moderate pH ($5 < \text{pH} \leq 6$) is most likely attributed to the formation of the anionic complex species $[\text{HgBr}_3]^-$ in the solution as reported by Cordoba et al. [25]. The decrease in the mercury(II) uptake at pH > 7 are possibly attributed to the unstability of the complex ion $[\text{HgBr}_3]^-$ and subsequent hydrolysis at higher pH [17]. In acetate buffer, the mercury(II) uptake by the reagent-PUF was found low at the examined pH. This is possibly due to the formation of the binuclear mercury(II) acetate complex, which in turn reduce the formation of $[\text{HgBr}_3]^-$ in the aqueous media [21]. Thus, the solution pH was kept at pH ~ 6 in the subsequent work.

Based on Cordoba et al. [25] work, a possible “solvent extraction” mechanism of the mercury(II) uptake by the loaded foams may be operating as follows:



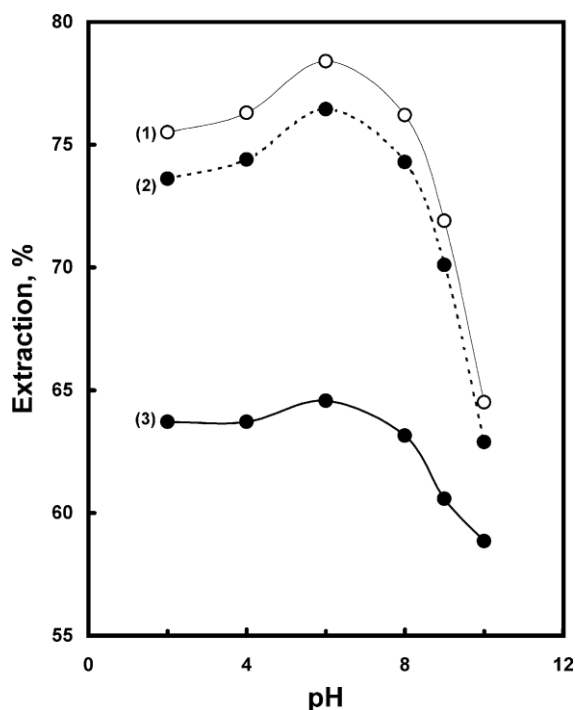
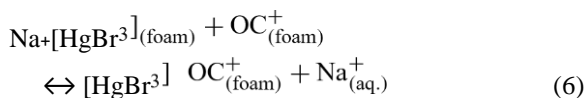


Fig. 1. Effect of pH on the sorption efficiency (%) of mercury(II) bromide complex onto CV (1), TMA (2) and CTMA (3) loaded foams.



A similar retention mechanism was reported by Fong and Chow [26] for the extraction of aurocyanide ion-pairs with alkali metal ions into long chain polyethers.

The influence of the type of the onium cation- and SDS-loaded foams on the mercury(II) uptake from the aqueous media pH 5–6 containing an excess of bromide ions at was carried out. The sorption profile of mercury(II) ions followed the sequence:

CV- > TMA- > SDS- CTMA-loaded foams

The hydrophobicity of the onium cations is a determining factor in the extraction of the anionic complex $[\text{HgBr}_3]^-$ from water by the loaded polyether foams. It appears also that the water structure enforced

ion-pairing (WSEIP) is the driving force for the extraction of $[\text{HgBr}_3]^-$ [26].

The mercury(II) ions uptake by the loaded foams was found fast and the sorption increased with shaking time. The equilibrium has attained a constant value in 15 min shaking with the PUF and remains constant up to 30 min and then leveled off with increasing time >30 min. Consequently, a 30 min shaking time was adopted in the next experiments. This conclusion was supported by the rate of mercury(II) sorption by the CV-loaded foams (Fig. 2). The mercury(II) uptake by the loaded foams occurs in one fast step and gel diffusion is not the rate-controlling step as in the case of common ion exchange resins [9]. The half-life of equilibrium sorption as calculated from Fig. 2 was found equal 1.1 ± 0.01 min.

The sorbed mercury(II) concentration q_t (mol/g) at time t was also plotted against time (Fig. 3) to test the Morris–Weber equation [27]:

$$q_t = R_d(t)^{1/2} \quad (7)$$

where R_d , the rate constant of intraparticle transport. The relationship holds good for up to 10.2 min

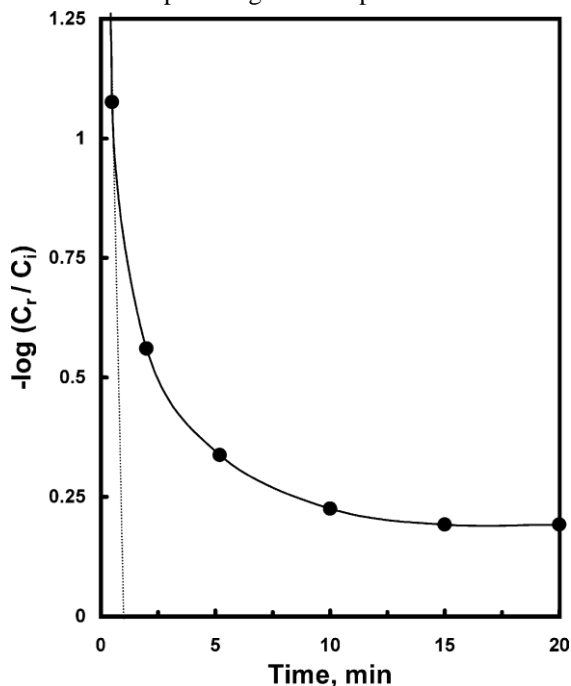


Fig. 2. Rate of sorption of mercury(II) bromide complex onto the CV-loaded foams at 25 ± 0.1 °C.

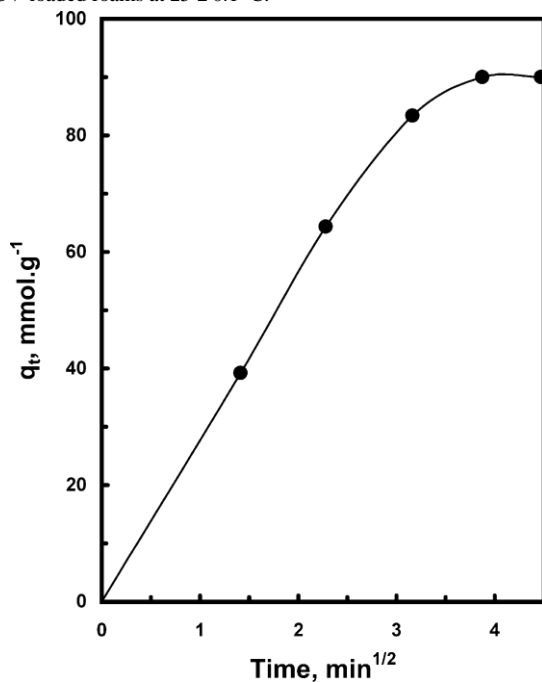


Fig. 3. The sorbed concentration of mercury(II) bromide complex onto CV-loaded foams as a function of time at pH 6 and 25 ± 0.1 °C.

and deviates as the shaking time increases. The diffusion rate was high in the initial stages and decreased with the passage of time. The values of R_d were computed from two distinct slopes of the Morris–Weber plot (Fig. 3). The value of R_d was estimated to be 27.3 ± 0.05 mmol/(g min^{1/2}) in the initial stage up to 10.2 min agitation time, and reduced to 3.8 ± 0.05 mmol/(g min^{1/2}) beyond this time. The change in the slope may be due to the existence of different pore sizes [17]. Moreover, the kinetic data were also evaluated using the Lagergren equation [17]:

$$\log(q_e - q_t) = \log q_e - \frac{kt}{2.303} \quad (8)$$

where q_e is the sorbed mercury(II) onto the PUF at equilibrium (mol/g) and k the over all rate constant. The sorption of the mercury(II) complex follows the

Lagergren equation up to 10 min. The plot shown in Fig. 4 is linear and the slope gives a value of the first-order overall rate constant $k = 0.25 \pm 0.01$ min⁻¹.

The value of Bt , which is a mathematical function (F) of q/q_e can be calculated for each value of F as

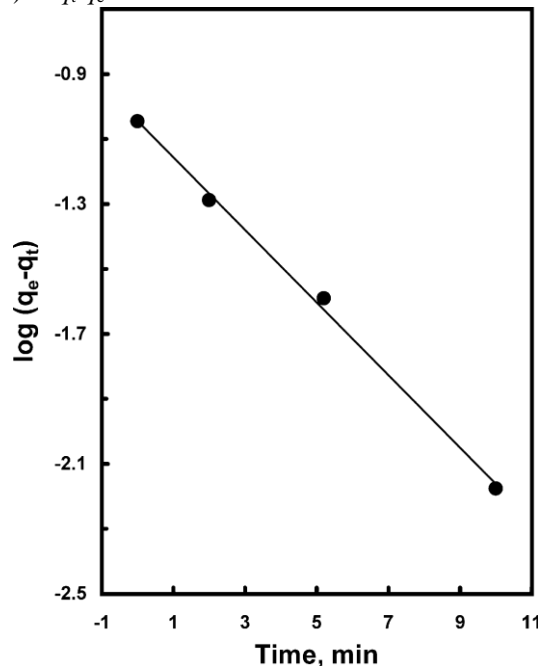


Fig. 4. Lagergren plot of the kinetics of [HgBr₃]⁻ onto CV-loaded foams at 25 ± 0.1 °C.

shown by Reichenburg equation [28]:

$$F = \frac{1}{\pi^2} e^{-\frac{6}{Bt}} \quad \text{or} \quad (9)$$

$$Bt = -0.4977 - 2.303 \log(1 - F)$$

A linear plot of Bt versus time at 25 °C was found linear up to 10 min. The straight line does not pass through the origin as observed earlier [27]. This behavior indicates that a particle diffusion mechanism is not responsible for the kinetics of HgBr₃⁻ sorption onto loaded foams. Therefore, the uptake of HgBr₃⁻ onto PUF involves three steps: bulk transport of HgBr₃⁻ in solution, film transfer involving diffusion of HgBr₃⁻ within the pore volume of PUF and/or along the pore wall surface to an active sorption sites. The

actual sorption of HgBr_3^- on the interior surface is very rapid and hence it is not a rate determining step. One may therefore conclude that, film and intraparticle transport may be the main factors controlling the rate of sorption.

The influence of the complexing anions (Cl^- , Br^- , I^- or CNS^-) at various concentrations (3.57×10^{-3} to 1.7×10^{-2} M) on the sorption of mercury(II) ions (3.6×10^{-3} M) ions onto the CV-loaded foams from the aqueous solution was studied. Significant increases in the sorption percentage of mercury(II) was observed at 1:3 Hg^{2+} :bromide molar ratio, and shows leveling off at a higher concentration level. The produced species $[\text{HgBr}_3]^-$ are then able to form an ion associate with the crystal violet-loaded PUF forming the complex ion associate $[\text{HgBr}_3]^- \cdot \text{CV}^+$ on the foam membranes. The decrease in the sorption of Hg^{2+} with increasing complexing anions (Cl^- , Br^- and CNS^-) concentration is possibly attributed to the competitive extraction of these ions which may be expected to be somewhat extractable as their complexing anions with mercury(II) or as neutral species like $\text{Hg}(\text{CNS})_2$ [17]. The sorption profiles of mercury(II) ions in aqueous solution by the CV-loaded foams at various concentrations of the complexing anions followed the order:

$\text{Br}^- > \text{Cl}^- > \text{CNS}^-$

In the aqueous iodide solution maximum sorption of mercury(II) on the CV-loaded foams was achieved at 1:4 Hg^{2+} : I^- molar ratio, suggesting the formation of the complex ion $[\text{HgI}_4]^{2-}$ which was then extracted onto the PUF as an ion-pair $[\text{HgI}_4]^{2-} \cdot (\text{CV})_2^{2+}$. At iodide concentrations lower (or higher) than 1:4 Hg^{2+} : I^- molar ratios, a sharp decrease in the mercury(II) uptake was observed. This behavior is attributed to the formation of the precipitate HgI_2 or the competitive extraction of I^- onto the PUF as $[\text{HgI}_4]^{2-}$, respectively [29]. Thus, “solvent extraction” mechanism is not alone the most probable mechanism and other processes like specific sites on the PUFs are possibly involved simultaneously in the mercury(II) uptake from the bulk aqueous solution [10,11].

The protective colloid PVA plays an important role as a stabilizing and retarding agent for the precipitation of the ion associate $[\text{HgBr}_3]^- \cdot \text{CV}^+$ on

standing overnight [25]. Thus, the influence of various concentrations (0.03–0.3% (w/v)) of PVA on the uptake of the ternary complex $[\text{HgBr}_3]^- \cdot \text{CV}^+$ onto the loaded foams was examined. Addition of PVA to the sorptive media of mercury(II) ions may change the environment around the central metal ion and subsequently its solution chemistry and sorption behavior. However, no significant changes on the mercury(II) uptake were observed. Thus, the reagent PVA was not used on the mercury(II) uptake by the loaded foams in the subsequent work. The effect of sample volume (0.1–1 dm^3) on the mercury(II) sorption onto the reagent-foams was also investigated at the optimum conditions. The sorption percentage of mercury(II) in the aqueous solution onto the CV-loaded foam decreased to 16% level on increasing the sample volume from 0.1 to 1 dm^3 .

3.2. Sorption isotherm of mercury(II) on CV-loaded foams:

The amount of mercury(II) retained onto the CV-loaded PUFs from the bulk aqueous solution was found to depend on its initial concentration. Therefore, the sorption profile of mercury(II) over a wide range of equilibrium concentrations (1.78×10^{-3} to 1.6×10^{-2} M) onto PUFs was determined. At low or moderate mercury(II) concentration, the amount of metal ion retained on the CV-loaded foams varied linearly with that remained in the bulk solution. The equilibrium was approached only from one direction, that of mercury(II) rich aqueous phase suggesting first-order behavior. The sorption capacity of mercury(II) ions as predicted from the sorption isotherm is relatively high and the equilibrium is not approached. The most favorable K_d values were found for more diluted solutions. The distribution ratio decreased with increasing mercury(II) concentration and the foam membranes became saturated with the retained species rapidly. The sorption of $[\text{HgBr}_3]^-$ was rapid and >85% of mercury(II) ions are sorbed within 5 min shaking indicating that, diffusion of the solute through a hypothetical film or hydrodynamic boundary layer takes place in the sorption step [23]. The intraparticle transport and the film diffusion may be the steps

controlling the molecular diffusion at the macropores of the sorbent [9,30].

The retention profile of mercury(II) in the aqueous solution was subjected to Langmuir, Freundlich and Dubinin–Radushkevich isotherms [17,31] over a wide range of equilibrium concentrations. The familiar form of Langmuir sorption isotherm is expressed in the following linear form [17]:

$$\frac{C_e}{C_{\text{ads}}} = \frac{1}{Qb} + \frac{C_e}{Q} \quad (10)$$

where C_e is the equilibrium concentration (M) of mercury(II) in solution; C_{ads} the sorbed mercury(II) con-

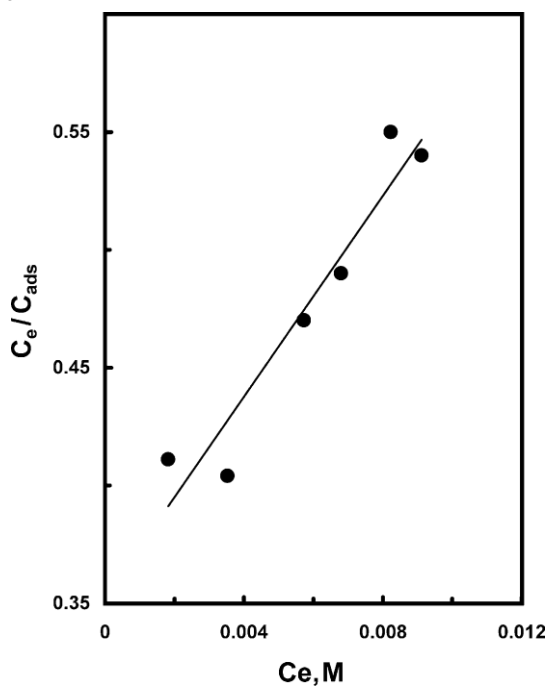


Fig. 5. Langmuir sorption isotherm of $[\text{HgBr}_3]^-$ onto CV-loaded PUF at 298K.

centration onto PUF per unit mass of sorbent (mol g) at equilibrium. Q and b are constants related to the maximum sorption capacity and the binding energy of solute sorption that is independent of temperature. A plot of C_e/C_{ads} versus C_e , shown in Fig. 5 is linear throughout the entire concentration range of mercury(II). The sorption parameters Q and b

evaluated from the slope and intercept of Fig. 5 were found equal 0.047 ± 0.0005 mol/g and 59.6 ± 0.05 dm^3/mol , respectively. The dimensionless equilibrium parameters, R_L was also estimated using the equation:

$$R_L = \frac{1}{1 + bC_i} \quad (11)$$

The values of R_L were found in the range $(1.1 \text{ to } 4.7 \pm 0.03) \times 10^{-3}$ indicating good retention of mercury(II) ions onto the PUF. The Freundlich model [17] is expressed in the following form:

$$\log C_{\text{ads}} = \log A + \frac{1}{n} \log C \quad (12)$$

where A and $1/n$ are Freundlich parameters related to the maximum sorption capacity of solute (mol/g). The plot of $\log C_{\text{ads}}$ versus $\log C_e$ (Fig. 6) is a straight line

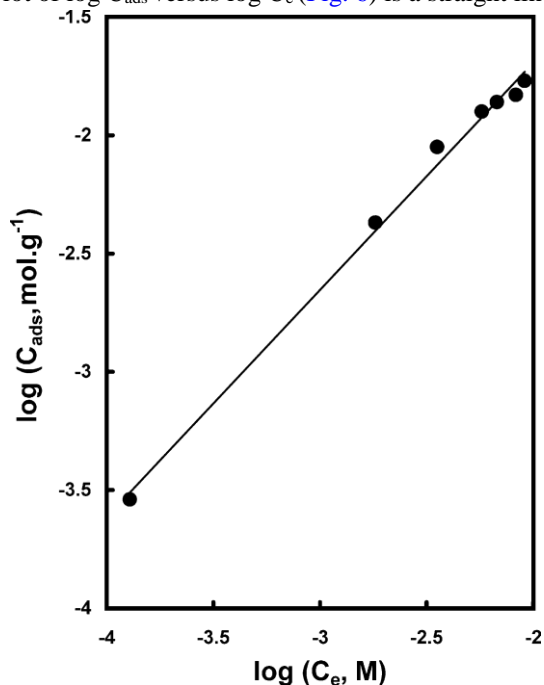


Fig. 6. Freundlich sorption isotherm of $[\text{HgBr}_3]^-$ onto CV-loaded PUF at 298K.

over the entire concentration of mercury(II). The values of A and $1/n$ computed from the intercept and slope of this plot were found equal to 1.7 ± 0.1 mol/g and 0.96 ± 0.01 , respectively. The value of $1/n$ (<1)

indicates that the sorption capacity is slightly reduced at lower equilibrium concentration and the isotherm does not predict any saturation of the solid surface of the sorbent by the sorbate. Thus, infinite surface coverage is predicted mathematically and physicosorption on the surface is expected. The Dubinin–Radushkevich (D–R) isotherm model [31,32] is postulated within adsorption “space” close to the adsorbent surface. The D–R isotherm can be linearized as follows:

$$\ln C_{\text{ads}} = \ln K_{\text{DR}} - \beta \epsilon^2 \quad (13)$$

where K_{DR} is the maximum amount of mercury(II) retained, β is a constant related to the energy of the transfer of the solute from the bulk solution to the solid sorbent and ϵ^2 is the Polanyi potential which is equal to

$$\epsilon^2 = RT \ln \left(1 + \frac{1}{C_e} \right) \quad (14)$$

where R is the gas constant (kJ/(mol K)) and T the absolute temperature (K). The plot of $\ln C_{\text{ads}}$ versus ϵ^2 is linear indicating that, the D–R isotherm is obeyed for mercury(II) sorption over the entire concentration range. The values of K_{DR} and β were found equal to 90 ± 0.5 mol/g and -0.0123 ± 0.002 mol²/kJ², respectively.

Assuming the surface is heterogeneous and an approximation to a Langmuir isotherm model is chosen as a local isotherm for all sites that are energetically equivalent. Then the quantity $(\beta)^{1/2}$ can then be related to the mean free energy (E) of the transfer of one mole of solute from infinity to the surface of PUF foam. This quantity can be obtained by the equation:

$$E = \frac{1}{\sqrt{2\beta}} \quad (15)$$

The value of E was found within the range of 6.38 kJ/mol envisaged for solvent extraction and far close to the values $E = 12.9 \pm 0.4$, 12.4 ± 0.3 , 24.7 ± 1.1 and 12.3 ± 0.35 kJ/mol reported for mercury(II), cobalt(II), silver(I) and palladium(II) onto PUF from aqueous solution, respectively [17]. The correlation factors for the three isotherms using linear regression analysis were found in the range of 0.9847–0.9931. The values of the sorption capacity of mercury(II) ions onto the PUF by the different tested sorption isotherms are of the same order of magnitude. This difference in

the sorption capacity can be interpreted in terms of the assumptions taken into consideration in deriving these sorption models.

The thermodynamic parameters of the mercury(II) uptake onto the TMA-loaded PUF have been evaluated using the equations:

$$\ln K_c = \frac{\Delta H}{RT} + \frac{\Delta S}{R} \quad (16)$$

$$\Delta G^\circ = \Delta H - T \Delta S \quad (17)$$

$$\Delta G^\circ = -RT \ln K_c \quad (18)$$

where ΔH , ΔS , ΔG and T are the enthalpy, entropy, Gibbs free energy and temperature in kelvin, respectively, R is the gas constant (8.3143 J/mol) and K_c the equilibrium constant depending upon the fractional attainment (F_e) of the sorption of mercury(II) complex at equilibrium onto PUF [17]. The plots of $\log K_d$

(or K_c) versus $1/T$ (Fig. 7) was found linear over

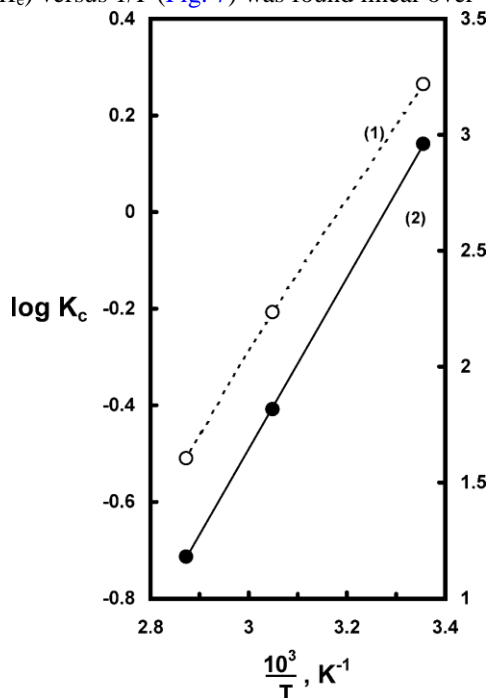


Fig. 7. Variation of equilibrium constant (1) and distribution coefficient (2) vs. $1/T$ (K^{-1}) of $[\text{HgBr}_3]$ -complex sorbed onto CV-loaded PUF.

the entire range of temperatures (298–343 K). The values of H and S are estimated from the slope and the intercept of Fig. 7, respectively, whereas G was evaluated using Eq. (18). The values of ΔH , S and G were found equal to -13.28 ± 0.5 kJ/mol, -49.3 ± 1.2 J/(mol K) and -1.51 ± 0.12 kJ/mol at 298 K, respectively, with a correlation factor of 0.9919. The values of K_d and K_c given in Fig. 7 confirm the exothermic nature of the mercury(II) uptake from the aqueous solution onto the PUF.

The increase in the numerical value of G with temperature may be due to the spontaneous nature of sorption and is more favorable at low temperatures confirming the exothermic chemisorption process. Similarly, the negative value of entropy change may be indicative of the faster sorption of the HgBr_3^- ion and the ordering of ionic charges without a compensatory disordering of the complex sorbed onto the active sites of the PUF [33]. These data are in good agreement with the values of $t_{1/2}$ and the observation that, the complex ion associate attained the equilibrium within short time. The high energy of the urethane nitrogen or ether–oxygen sorption sites of the PUF provided by increasing temperature help in preventing the interaction between the active sites of the PUF and the HgBr_3^- ion resulting a lower sorption at higher temperature. The bond formation between HgBr_3^- and PUF based on H- and/or ionic bonding comprising ion exchange or ion association interaction through chemisorption may account for the exothermic nature of mercury(II) uptake [34]. These data suggested that, “solvent extraction” mechanism plays a major role in the sorption step than added component for surface adsorption. These results and the flow characteristics of the PUF suggest the possible applications of the reagent foams in column operations for the enrichment and separation of mercury(II) species from large sample volumes of fresh and industrial waste waters.

3.3. Chromatographic behavior of mercury(II) on CV- or TMA-foams columns

On the basis of the above data, an aqueous solution (3–5 dm³) of tap, de ionized or industrial waste waters spiked with 1–5 g mercury(II) at pH 5–6 was percolated through the foam packed columns at 20

cm³/min flow rate. Analysis of mercury in the effluent solution against the reagent blank indicated complete sorption of $[\text{HgBr}_3]^-$ onto the loaded CV- or TMA-foam columns. The sorbed mercury(II) ion associate was then recovered quantitatively ($98.1 \pm 3.4\%$) from the foam column with 20 cm³ acetone at 2 cm³/min flow rate.

The effect of flow rate (5–25 cm³/min) on the mercury(II) uptake by the TMA-loaded foam columns was examined by percolating 1 dm³ of distilled water spiked with 1 g mercury(II). Complete retention of mercury(II) was achieved quantitatively (>96%) at flow rate ≤ 20 cm³/min. The effect of the sample volume (0.1–3 dm³) on the mercury(II) sorption was also investigated by passing these solutions through the column at 20 cm³/min flow rate. In all cases, almost complete sorption of the spiked mercury(II) was successfully achieved the results obtained on the mercury(II) sorption with the onium cations loaded foams were found much better than those obtained with other solid sorbents [11,13]. The cellular membrane structures and the aerodynamic properties of the foams [8,9] enhanced the mercury(II) uptake on the foam columns at high flow rates.

The performance (HETP) of the packed column was determined by passing an aqueous solution (1 dm³) spiked with 10 g mercury(II) through the TMA-foam packed column at 5 cm³/min. Complete sorption of mercury(II) took place and the retained $[\text{HgBr}_3]^-$ species in the column were then eluted with 20 cm³ (5 × 4 cm³ fractions) acetone at 2 cm³/min. Mercury(II) in the eluent solution was then determined and the HETP was calculated from the elution curve employing Glueckauf [35] equation:

$$N = \frac{8 V_{\max}^2}{W^2} = \frac{L}{\text{HETP}} \quad (19)$$

where V_{\max} is the volume of eluate to peak maximum, W the width of the peak at $1/e$ times the maximum solute concentration and L the length of the foam bed in mm. The HETP and N values were found equal to 0.66 ± 0.01 mm and 150 ± 5 , respectively.

The N and HETP of the reused TMA-loaded foam columns were also calculated from the breakthrough capacity curve. The results of percolating 5 dm³ of the

spiked tap water through the column at 5 cm³/min are displayed in Fig. 8. The rising portions of the S-shaped

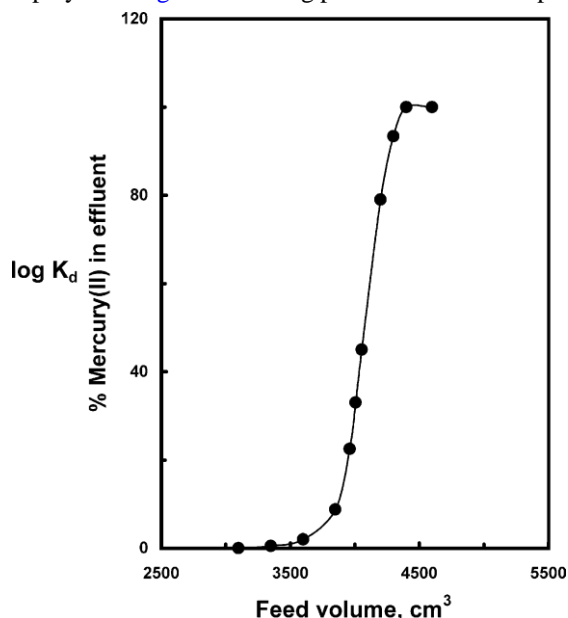


Fig. 8. Breakthrough curve of [HgBr₃]⁻ on the reused TMA-loaded foams packed column at 5cm³/min.

curve have large slopes indicating a high transfer rate of Hg(II) on/in the foam membranes and rapid attainment of equilibrium between the [HgBr₃]⁻ and the onium cation loaded foams. The HETP and *N* values of the foam packed column were calculated from the equation:

$$N = \frac{V_{50} V'}{\text{HETP}} = \frac{L}{(V_{50} V')^2} \quad (20)$$

where *V*₅₀ is the volume of the effluent solution at the center (50% extraction) of the S-shaped and *V* the volume at which the effluent solution has a value of 0.1578 of the initial concentration. The HETP and *N* values were found equal to 0.64 ± 0.01 mm and 160 ± 3.2, respectively in good agreement with the values obtained from the chromatogram method.

The critical capacity of the Hg(II) species onto TMA-loaded foam column was calculated from the S-shaped curve (Fig. 8) and was found equal to 8.1 mg/g at 5 cm³/min flow rate. The breakthrough capacity of mercury(II) uptake per one gram (mg/g) of the onium

cation-loaded sorbent was also calculated from the equation [36]

$$\text{Uptake} = \frac{V_{50} C_0}{m} \quad (21)$$

where *m* is the mass (g) of the column foam bed. The uptake of mercury(II) was found equal to 10.8 mg/g at 5 cm³/min. The value is good as compared to Voltalef, silica gel and solid inorganic ion exchanger column [10,35].

The TMA-loaded foam column was successfully employed for the analysis of mercury(II) traces. In this method, a spiked mercury(II) (≤5 ppb) sample solution (1 dm³) was percolated through the TMA-foam column at 2–3 cm³/min flow rate at pH 5–6. Mercury(II) retained on the column as Hg(HDz)₂ was then eluted with acetone at a 2 cm³/min and analyzed at 610 nm via the amount of unreacted dithizone in acetone. The absorbance of the acetone containing H₂Dz before (*A*_b) and after (*A*_f) extraction (or recovery) of mercury(II) in the effluent (or eluent) solution is equivalent to the initial [H₂Dz]₀ and the unreacted dithizone concentrations, respectively. The sorption (or recovery) percentage of mercury(II) (g mol/l) in the effluent (or eluent) solution was determined using the equation:

$$[\text{Hg}_{2+}] = \frac{[\text{H}^2\text{Dz}]_0 \times [A_b - A_f]}{2 A_b} \quad (22)$$

3.4. Sorption and recovery of mercury from water samples

The applicability of the proposed method for the quantitative collection and recovery of mercury(II) from natural water was tested on five different samples that were spiked with mercury(II) at concentrations between 20 and 60 g/l. Good recoveries (94.9–102%) were reached for the analyzed samples. These data proved that the method is possible to achieve excellent accuracy even in samples with high content of dissolved solids.

3.5. Interference study

The preconcentration of mercury(II) from the aqueous by the proposed foam column was considered to be a prime important. Thus, the uptake of mercury(II) at 10–100 ppb concentration level in the presence of some diverse ions were critically investigated. It was found possible to preconcentrate the tested concentrations of mercury in the presence of up to 1mg of the following ions: acetate, citrate, tartrate, ascorbate, phosphate, nitrate, perchlorate, selenite, selenate, nitrite, bromate, sulfite, vanadate, chloride, bromide and sulfate and the metal ions: Zn, Cu, Mn, Ba, Mg, Ca, Li and ammonium. The retained mercury(II) was then recovered quantitatively from the foam column with acetone at reasonable flow rate.

4. Conclusion

The retention profile of HgBr_3^- complex onto the loaded PUF follows Langmuir, Freundlich and D–R adsorption isotherms. The sorption energy, E , gives an idea of the nature on sorption and the uptake mechanism. The onium cation loaded foams column was reused many times without loss in the column performance (N, HPTP). The membrane-like structure of the PUFs is superior to any other known rigid or granular solid sorbents and permit rapid separation at relatively high flow rate. The proposed method lends feasibility to using the foam column for on-site analysis of mercury by cold vapour atomic absorption or other analytical techniques.

References

- [1] D. Rosales, J.L.G. Ariazo, *Anal. Chem.* 57 (1985) 1411. [2] A.K. Shrivastava, S.G. Tandon, *Toxicol. Environ. Chem.* 5 (1982) 311.
- [3] W.J. Stratton, S.E. Lindberg, C.J. Perry, *Environ. Sci. Technol.* 35 (2001) 170.
- [4] S.S.M. Hassan, M.B. Saleh, A.A. Abdel Gaber, R.A.H. Mekheimer, N.A. Abdel Kream, *Talanta* 53 (2000) 285.
- [5] A. Gotzl, W. Riepe, *Talanta* 54 (2001) 821.
- [6] Z. Marczenko, *Spectrophotometric Determination of Elements*, 3rd ed., Ellis Horwood, Chichester, 1986. [7] P. Padmja, N. Balasubramanian, T.V. Ramakrishna, *Talanta* 41 (1994) 255.
- [8] G.J. Moody, J.D.R. Tomas, *Chromatographic Separation and Extraction with Foamed Plastics and Rubbers*, Marcel Dekker, New York, 1982.
- [9] T. Braun, J.D. Navrati, A.B. Farag, *Polyurethane Foam Sorbents in Separation Science*, CRC Press, Boca Raton, FL, 1985.
- [10] T. Braun, *Fresenius Z. Anal. Chem.* 333 (1989) 785.
- [11] S. Palagyi, T. Braun, in: Z.B. Alfassi, C.M. Wai (Eds.), *Preconcentration Techniques for Trace Elements*, CRC Press, Boca Raton, FL, 1992.
- [12] R. Singh, A.R. Khwaja, B. Gupta, S.N. Tandon, *Talanta* 48 (1999) 527; M. Hafez, I.M.M. Kenawy, M.A. Akl, R.R. Lashein, *Talanta* 53 (2001) 749.
- [13] S. Palagyi, T. Braun, *J. Radioanal. Nucl. Chem.* 163 (1992) 69.
- [14] A.B. Farag, M.E. Attia, H.N.A. Hassan, *Anal. Chem.* 52 (1980) 2153.
- [15] I. Valente, H.J.M. Bowen, *Anal. Chim. Acta* 90 (1977) 315. [16] J. Regas, S. Palagyi, G. Holeczyova, M. Matherny, *Chem. Papers* 45 (1991) 509.
- [17] M.M. Saeed, S.M. Hasany, M. Ahmed, *Talanta* 50 (1999) 625, and references there in; S.M. Hasany, M.M. Saeed, M. Ahmed, *Sep. Sci. Technol.* 35 (2000) 379.
- [18] Y. Anjaneyulu, R. Marayya, T.H. Rao, *Environ. Poll.* 79 (1993) 283.
- [19] M.M. Saeed, A. Rusheed, *Radiochim. Acta* 90 (1) (2002) 35. [20] S.L.C. Ferreira, H.C. dos Santos, M.S. Fernandes, *J. Anal. Atom. Spectrom.* 17 (2002) 115.
- [21] A.M. Kiwan, M.S. El-Shahawi, S.M. Aldhaheri, M.H. Saleh, *Talanta* 45 (1997) 633, and references cited in.
- [22] M.S. El-Shahawi, *J. Chromatogr. A* 760 (1994) 179.
- [23] C.H.R. Nambiar, B. Narayana, B. Rao, R. Mathew, B. Ramachandra, *Microchem. J.* 53 (1996) 175.
- [24] R. Litman, E.T. Williams, H.L. Finston, *Anal. Chem.* 49 (1977) 983.
- [25] M.H. Cordoba, P.N. Navarro, I.L. Garcia, *Intern. J. Environ. Anal. Chem.* 32 (1988) 97.
- [26] P. Fong, A. Chow, *Talanta* 39 (1992) 825, and references cited in.
- [27] S. Weber, J.C. Morris, *J. San. Eng. Div. ASEC* 89 SA2 (1963) 31.
- [28] D. Reichenburg, *J. Am. Chem. Soc.* 75 (1972) 589.
- [29] S.J. Al-Bazi, A. Chow, *Anal. Chem.* 55 (1982) 1094.
- [30] W.J. Weber, S. Lang, *Environ. Progr.* 2 (1983) 167.
- [31] G.A. Somorjai, *Introduction to Surface Chemistry and Catalysis*, Wiley, 1994.
- [32] M.M. Dubinin, L.V. Radushkevich, *Proc. Acad. Sci. USSR Phys. Chem. Soc.* 55 (1974) 331.
- [33] C. Luo, S. Huang, *Sep. Sci. Technol.* 28 (1993) 1253.
- [34] L.G. Sillen, A.E. Martell, *Stability Constants of Metal Ion Complexes, Suppl. I*, vol. 1471, Chemical Society, London, p. 179.
- [35] E. Glueckauf, *Trans. Faraday Soc.* 51 (1955) 34.
- [36] W.X. Ma, F. Liu, K.A. Li, W. Chen, S.Y. Tong, *Anal. Chim. Acta* 416 (2000) 191.

Extraction and recovery of Au, Sb and Sn from electrorefined solid waste

S.M. Saleh^a, S.A. Said^a, M.S. El-Shahawi^{b,*}

^a Department of Chemistry, Faculty of Science, Helwan University, Helwan, Cairo, Egypt

^b Department of Chemistry, Faculty of Science at Damietta, Mansoura University, Damietta, Egypt

Received 22 June 2000; received in revised form 29 January 2001; accepted 29 January 2001

Abstract

Acid leaching of gold, antimony, and tin from the electrorefined solid waste was investigated. The parameters affecting the leaching process such as, acid concentration, shaking time, temperature, chlorine gas and pulp density were evaluated. Quantitative extraction of Au from the leaching liquor containing Sb and Sn species in HCl (2M) employing Aliquat-336 in kerosene (10% (v/v)) was achieved. Maximum recovery (99.2±3.4%) of Au from the organic phase was obtained quantitatively using thiourea–hydrochloric acid (2% (w/v), 0.2M) stripping system. Quinol solution at 6% (w/v) concentration was found able to reduce Au(III) in the striped aqueous solution to Au. Extraction of Sb species from the leachant liquor at HCl (6M) was quantitatively obtained using Aliquat-336 (10% (v/v)) in kerosene after oxidation with 8% (w/v) sodium periodate. The Sb(V)-Aliquat-336 ion associate in the organic phase was then stripped as Sb(III) by reduction with oxalic acid (1M), precipitated as Sb₂S₃ by sodium sulfide (2% (w/v)) and finally reduced to Sb with hydrogen. Sn(IV) species in the leachant liquor containing HCl (6M) was reduced to Sn(II) with zinc granules (6.5% (w/v)) and extracted with Aliquat-336 (10% (v/v)) in kerosene as an ion associate. The produced complex ion associate was then stripped from the organic phase using sodium hydroxide (1M), precipitated as Sn(II) oxide and finally reduced to Sn with hydrogen. © 2001 Elsevier Science B.V. All rights reserved.

Keywords: Gold; Antimony; Tin; Leaching; Extraction

1. Introduction

Due to the importance of gold (Au), and its extremely low level in various matrices, sensitive methods for reliable leaching, extraction, recovery and determination are required [1]. However, most of these methods are very laborious, not practicable, require high acidity and suffer from some constraints on their wide applications in routine analysis [2].

In a major advance in Au refining technology, modern hydrometallurgical techniques have been adopted

* Corresponding author. Tel.: +2-050-370344.

E-mail address: sinfac@mum.mans.eun.eg (M.S. El-Shahawi).
to produce high-purity Au from feeds containing silver (Ag) and platinum (Pt) group metals with a wide range of Au contents [3–5]. In this intermediate process, impure Au feed material was leached by HCl media under oxidizing conditions. Au in the leach solution was selectively extracted into the organic solvent,

while the other soluble metal ions retained in the raffinate [4,5]. Au was then recovered as a metal powder by direct reduction from the loaded strip liquor.

Recently, methods for the leaching, preconcentration and determination of total antimony (Sb) and its speciation in many environmental samples have been reviewed [6–8]. Some of these methods are practically impossible because of the lack of sufficient

also used for the determination of Sb and Sn at 217.6 and 224.6nm, respectively. The analysis of the input waste materials of the total Au, Sb and Sn from the oxidized samples was critically carried out on Jopin Yvon-24 sequential inductively coupled plasma-atomic emission spectrometry employing a high resolution monochromator. The calibration of the instrument was done using standard BDH solutions (10ppm) under the condition described in the

0003-2670/01/\$ – see front matter © 2001 Elsevier Science B.V. All rights reserved. PII: S0003-2670(01)00866-2

sensitivity and selectivity and also require the addition of oxidizing or reducing agents [9] to ensure that all Sb is present in the sample either as Sb(V) or Sb(III) species. Organotin compounds are known to be potent toxins and are widely used in different industries, e.g. stabilizers, pesticides and fungicides [10]. The introduction of such compounds into the environment could cause serious problems due to their high toxicity and tendency to bioaccumulation [10,11].

The dissolution of Au, Sb and Sn in the solid waste was achieved by a number of techniques [12]. The usual leaching agent for Au was hydrochloric acid in chlorine gas media followed by separation using Amberlite-120 [13–15]. Solvent extraction of Au, Sb and Sn as their chloride complexes employing long chain amines as liquid ion-exchangers have been reported by Lanher et al. [16]. Numerous studies on the electrochemical dissolution of Au in chloride media have also been reported [17,18].

This paper describes a simple, rapid, inexpensive and possibly versatile technique for the preparation of solid slime samples conveniently analyzable by the flame AAS methods. The study was also concerned with the isolation and recovery of Au, Sb and Sn from the leachant liquor of the solid slime.

2. Experimental

2.1. Apparatus and chemical analysis

A Pye-Unicam PU-9100X atomic absorption spectrometer was used for the analysis of Au, Sb, and Sn from the leaching liquor. An air-acetylene flame was employed for the analysis of Au at 242.8nm, after passing through concentrated H₂SO₄ for purification. A hydride generator Model Unicam VP 90/F 190 was

manufacture recommendation. A thermostat water bath (Model Haake SWB 20) with 200rpm and a Metrohm pH-meter (Model 691) were used for the hydrometallurgical processes and pH measurements.

2.2. Reagents

The samples of electrorefined solid waste were kindly provided from the General Metal Co. Cairo, Egypt. The composition data of the entitled trace metals in the electrorefined solid waste were obtained using a quantometer Model 34000 (Applied Research, Ecublens, Switzerland) and standard chemical methods [19]. All reagents used were of analytical reagent grade and Merck. Standard stock solutions (100ppm) of Au, Sb and Sn were prepared from BDH chemicals. All glasswares were cleaned with hot nitric acid followed by rinsing with distilled water. The technical product methyl tri-capryltertiaryammonium chloride (Aliquat-336) was obtained from Henkel Co., and was used without further purification. Other chemicals and solvents were of analytical reagent grade. SX-1 100% aliphatic commercial kerosene was obtained through the courtesy of Philips Chemicals and was used as diluent. Doubly distilled water was used through out this work.

2.3. Recommended procedures

2.3.1. Leaching of Au, Sb and Sn

An accurate weight (10–15g) of the solid slime was placed in a 250ml conical flask containing 100ml of hydrochloric acid (2M) and subjected to a fixed rate (10ml/min) of chlorine gas for 1h. The solution mixture was then shaken at 60°C for 6h and filtered. The leaching liquor and the washing solutions of HCl (2M) were collected and made up to 200ml with

hydrochloric acid (0.5M) for the subsequent work. Cover the flask with aluminum foil to protect the contents from the daylight.

2.3.2. Recovery of Au from the leachant liquor

A 50ml of the leaching liquor containing 5% (w/v) sodium tartarate and 10ml (2 × 5ml) of 10% (v/v) aliquat-336 in kerosene were taken in a 250ml separating funnel. The funnel was swirled to mix the contents for 10min. The two phases were then separated out and the organic extract was then transferred to a dry 25ml volumetric flask. The solid residue of the leaching liquor was washed with 5ml kerosene and the organic extract and the washings were then swirled to mix, collected in the volumetric flask, dehydrated with anhydrous Na₂SO₄ (1g) and finally made up to the mark with kerosene. The Au(III) in the organic extract was then stripped with 50ml aqueous solution of thiourea– [33] HCl (2% (w/v), 0.2M) stripping system and analyzed for Au. The aqueous solution of Au(III) was shaken for 10min with 10ml of 6% (v/v) quinol solution in the presence of 2% (w/v) sodium tartarate solution to reduce the Au(III) species to Au(II).

2.3.3. Recovery of Sb from the leachant liquor

The acidity of the aqueous leachant liquor (free from Au) was adjusted to 6M with concentrated HCl and shaken for 30min with 8% (w/v) NaIO₄ at 60°C. After cooling the reaction mixture was then shaken with 10ml (2 × 5ml) kerosene containing 10% (w/v) aliquat-336 and anhydrous Na₂SO₄ (1g) for 10min. The produced Sb(V)-Aliquat-336 ion associate in the organic phase was then stripped with 50ml aqueous solution of oxalic acid (1M), precipitated as Sb₂S₃ with 2% (w/v) sodium sulfide. The precipitate Sb₂S₃ was then collected, washed with hot H₂O and finally reduced to Sb employing hydrogen.

2.3.4. Recovery of Sn from the leachant liquor

The leachant liquor (free from Au, and Sb) containing 6M HCl and Sn(IV) was shaken with 6.5% (w/v) zinc granules for 2h at 60°C. The reaction mixture was then filtered to remove the unreacted zinc granules. The filtrate containing Sn(II) was then shaken with 10ml (2×5ml) of 10% (w/v) Aliquat-336 in kerosene containing anhydrous Na₂SO₄ (1g) for 15min. The produced ion associate of Sn(II)-aliquat-

336 in the organic phase was stripped with 10ml NaOH (1M) under bubbling nitrogen gas. The produced precipitate of Sn(II) oxide was then separated out, washed with hot water, dried at 120°C and finally reduced to Sn with hydrogen.

3. Results and discussion

The preliminary investigation of the electrorefined solid waste samples revealed that the slime is rich with the following metal ions: Au, 0.21; Sb, 3.1; and Sn, 21.0kg/t. The extraction and recovery procedures employed in this investigation were also applied to standard solutions (the quality control samples) of Au, Sb and Sn at various concentrations. The results showed no losses of Au, Sb and Sn under the used experimental conditions and the recovery percentages were in the range 99.2 ± 3.4%.

The technique suggested for the leaching of the Au slime was based upon its interaction with hydrochloric acid solution containing an excess of chlorine. Thus, an accurate weight of the Au slime was shaken with 100ml hydrochloric acid at different concentrations (0.01–9M) and at a fixed flow rate (10ml/min) of passing chlorine, at room temperature for 30min. Chlorine species in the aqueous solution were distributed according to the following equations [20]:



$$K = 4.5 \times 10^{-4} \quad (1)$$



In HCl media, the concentration of ClO⁻ species as strong base is negligible. Therefore, the mass balance equations for the total chlorine and chloride ions, respectively can be written as follows:

$$C_{\text{Cl}} = 2[\text{Cl}_2] + 3[\text{Cl}_3^-] + [\text{HClO}] \quad (4)$$

$$C_{\text{Cl}^-} = [\text{Cl}^-] + [\text{HClO}] - [\text{Cl}_3^-] \quad (5)$$

where C_{Cl} is the total chlorine concentration that was determined by iodide/thiosulphate method [21] and C_{Cl^-} is the total chloride concentration added to the solution as HCl.

Fig. 1 shows the leaching percent of Au from the solid slime at different hydrochloric acid concentrations at 10ml/min flow rate of chlorine gas passing through the leaching solution for 1h. The maximum leaching percentage of Au was achieved at 0.5M acid concentration or more. On the other hand, the maximum leaching percentage of Sb and Sn was obtained at HCl concentration ≥ 2 M. No significant dissolution of the solid slime was taken place at acid concentration < 0.5 M and at a flow rate of chlorine gas < 10 ml/min through the leaching liquor for 1h. This behavior is possibly attributed to the change in the distribution of chlorine species through the leaching liquor [22]. Thus, in the subsequent work the acid concentration

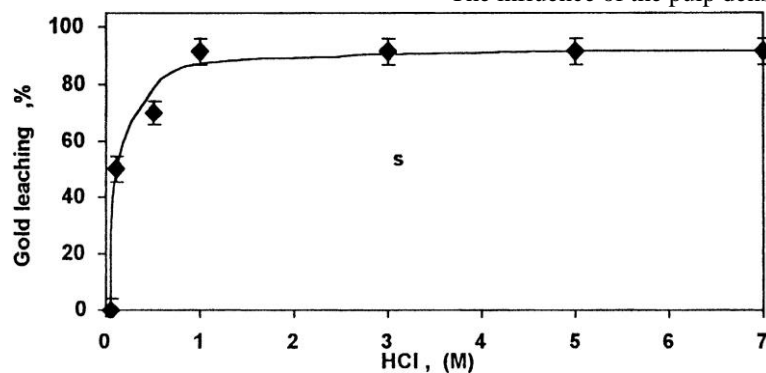


Fig. 1. Effect of HCl concentration (M) on the Au leaching (%) from the solid waste at 25°C, 5h shaking time and 10ml/min chlorine gas. and the flow rate of chlorine gas were adjusted at 2M and 10ml/min, respectively.

The influence of temperature on the metal leaching from the solid slime was found critical. Thus, 5g of the solid slime were shaken with 100ml HCl (2M) for 1h at 10ml/min chlorine gas at various temperature ranging from 25 to 120°C. The data are summarized in

Fig. 2. The leaching percent increased with increasing temperature up to 60°C after which the leaching percent reached a constant value. Thus, the temperature was chosen at 60°C in the next work.

The choice of shaking time on the metal leaching from the solid slime was found critical. Thus, the concentrations of Au, Sb and Sn in the leach liquor were determined at different shaking times at the optimum experimental conditions of HCl concentration, flow rate of chlorine gas and temperature. The results are summarized in Fig. 3. The leaching percent of Au, Sb and Sn was increased with increasing shaking time up to 5h and reached a constant value.

The influence of the pulp density (the amount of the

electrorefined solid waste:volume of the leaching acid liquor) on the Au leaching was found critical. Thus, the amount of Au in the leachant liquor was determined at various pulp density of the Au slime under the optimum experimental conditions. The leaching

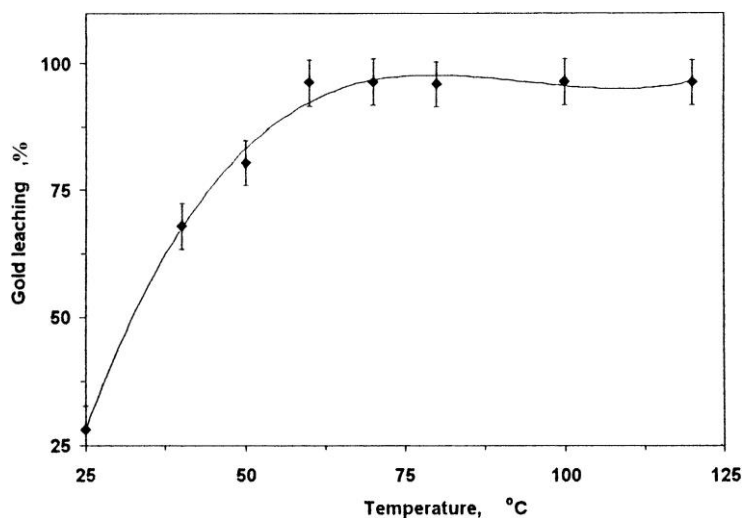


Fig. 2. Effect of temperature on the Au leaching (%) from the solid waste, 5h shaking time and 10ml/min chlorine gas.

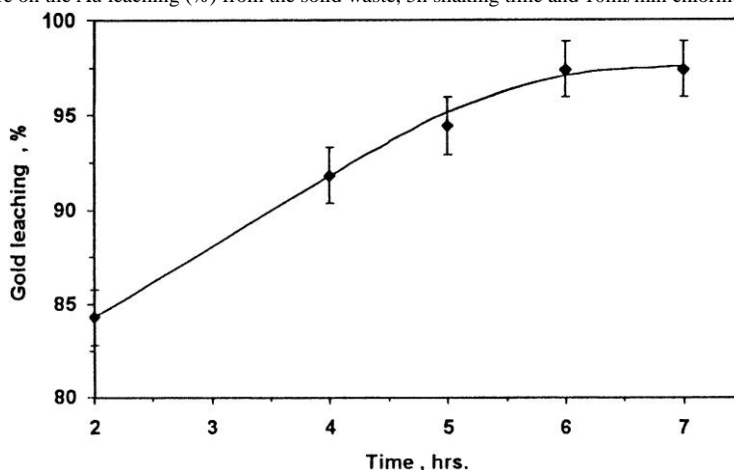
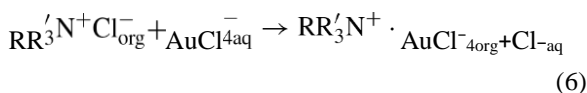


Fig. 3. Effect of shaking time (h) on the Au leaching (%) from the solid waste at 60°C, 1M HCl concentration and 10ml/min chlorine gas.

percent of Au (Fig. 4) was increased by shaking the Au slime for 5h with the leachant up to 15g:100ml pulp density and reached an approximate constant value.

Extraction of Au(III) from the leached solution containing Sb and Sn species at different HCl concentration was critically investigated employing various concentrations of Aliquat-336 in kerosene. Fig. 5 shows that Au(III) was extracted rapidly and achieved maximum extraction at ~1M acid concentration.

Thus, the mechanism proposed for the Au(III) extraction could be proceeded as follows:



where R = CH₃ and R' = [(CH₂)₇CH₃]₃.

The observed decrease in the Au(III) extraction at acid concentration >3M is possibly attributed to the

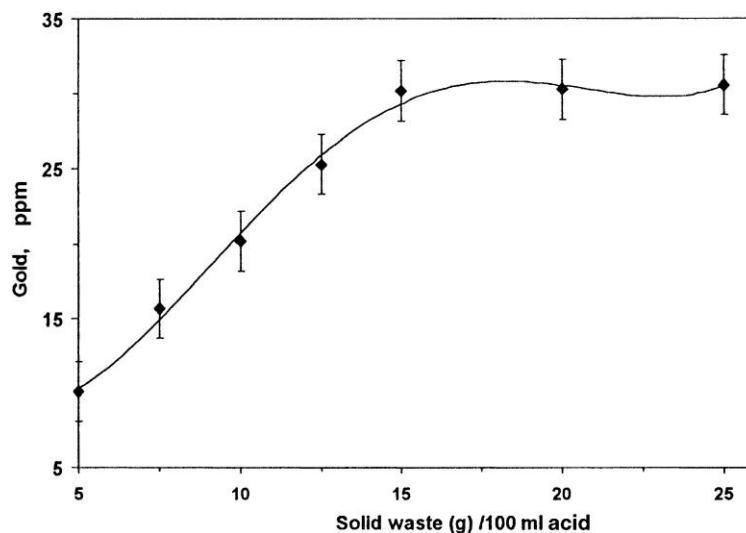


Fig. 4. Effect of pulp density (solid waste, g/100ml acid) on the Au leaching (ppm) from the solid slime at 60°C, 1M HCl concentration and 5h shaking time at 10ml/min chlorine gas.

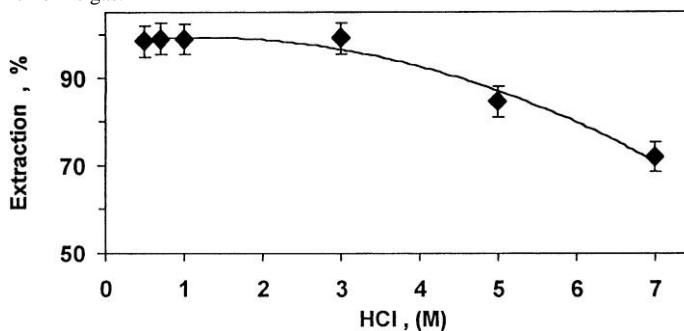


Fig. 5. Effect of HCl concentration (M) on the Au extraction (%) from the leaching with aliquat-336 (10% (w/v)) in kerosene. competition between the chloroaurate ion (AuCl_4^-) and the hydrochloric acid to form complex ion associate with the amine as reported by Caracava [23]. At HCl concentration $\leq 2\text{M}$ Sb and Sn species were not detected in the organic phase during the extraction of Au(III) with aliquat-336 in kerosene from the leaching liquor. This observation was also confirmed by the absence of Sb and Sn species in the solid residues of the organic extract after evaporation of kerosene. This observation is in good agreement with the reported data [24,25].

The influence of Aliquat-336 concentration on the Au(III) extraction at 15g:100ml pulp density was investigated. Maximum extraction (Fig. 6) of the produced ion-pair was obtained at 10% (v/v) aliquat-336 concentration. Over this concentration the extraction efficiency of Au(III) decreased. These results are in accordance with the results obtained by Algert [26]. Addition of 5% (w/v) tartarate solution to the leaching liquor enhances the extraction efficiency of Au(III) and prevents any traces of Sb and Sn species to be extracted in the organic phase.

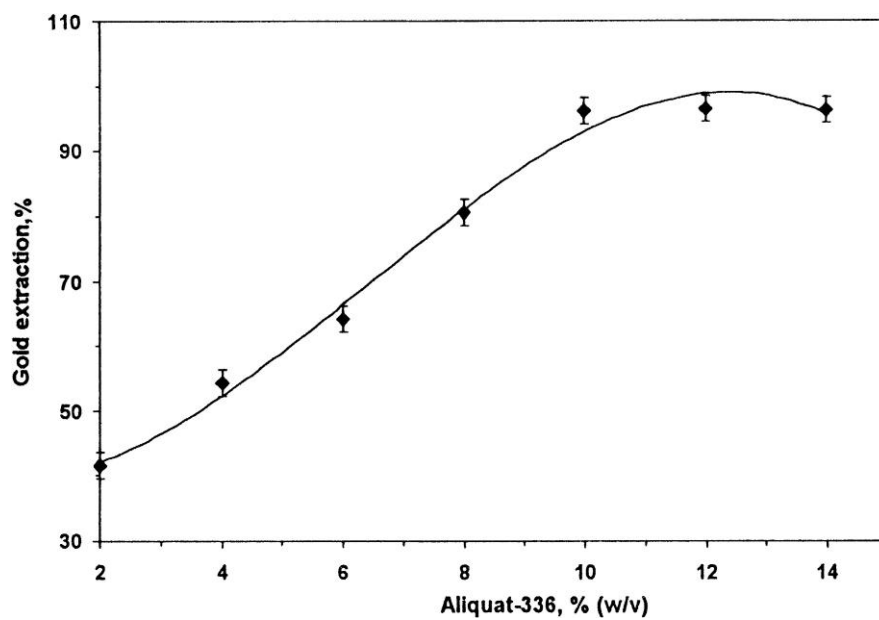


Fig. 6. Effect of aliquat-336 (% w/v) on the Au extraction from the leaching liquor at 1M HCl concentration.

Chloroform, benzene, toluene, dichloromethane, nitrobenzene and kerosene were used as possible extractant for the complex ion associate of chloroaurate-Aliquat-336. Fast separation, highest absorbance and good stability of the produced complex ion associate were obtained in chloroform and kerosene. No significant changes in the degree of extraction was occurred in these solvents when the shaking time varied from 10 to 30min. Therefore, kerosene was selected as a proper solvent since it is inexpensive, readily available, less toxic, allows a better separation of the layers and was used without purification.

The effect of various stripping agents on the Au(III) recovery from the organic phase containing Aliquat-336 was investigated. The organic phase was shaken with different concentrations of the stripping systems: thiourea–HCl and thiourea–HClO₄. Thiourea–HCl system at concentration 2% (w/v), 0.2M was found capable to strip Au(III) quantitatively (99.2%) from the organic phase. The fact that, HCl–thiourea system able to convert the complex ion associate of AuCl₄–Aliquat-336 to a cationic complex species of Au(thiourea)+Cl₂ similar to the data reported for Au–dithizone complex in chloride media [27]. The produced cationic species of Au(III)–dithizone can be striped easily from the organic phase.

The effect of quinol concentration on the reduction of Au(III) ions to Au on the stripped solwas invest. The Au species in the stripped solution were boiled for 20min with various concentrations of quinol solution as a reducing agent in the presence of 5% (w/v) tartarate solution. The results are summarized in Fig. 7.

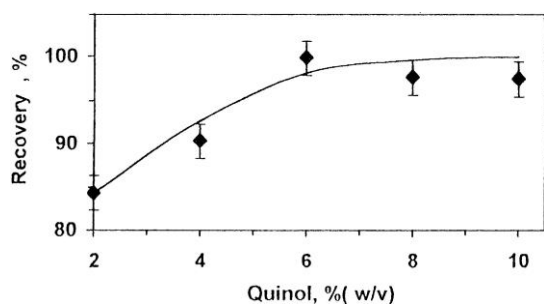
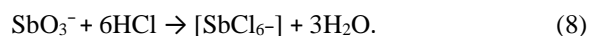
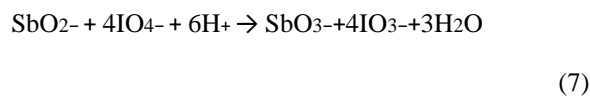


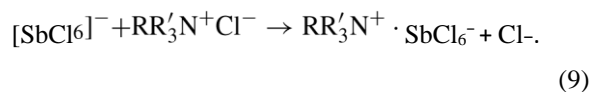
Fig. 7. Effect of quinol concentration (% (w/v)) on the Au recovery (%) from the stripped aqueous solution.

The precipitation of Au was increased with increasing quinol concentration up to 6% (3ml for every 0.025g of Au). These data are in accordance with the results reported by Basset et al. [21].

The separation efficiency of Sb from the leachant liquor (free from Au ions) employing aliquat-336 (10% (v/v)) in kerosene at 6M HCl concentration was investigated in the presence of sodium periodate as an oxidant. Thus, 20ml of various concentrations 2, 4, 6, 8 and 10% (w/v) of sodium periodate were added to the leached liquor and the acidity of the solution mixture was adjusted to 6M HCl. The solution mixture was then heated for 1h and shaken with 6% (v/v) Aliquat-336 in kerosene. The produced chloro complex species of Sb formed a complex ion associate with the aliquat-336 [24]. Maximum Sb extraction in 6M HCl was achieved at 8% (w/v) sodium periodate (Fig. 8). The mechanism of Sb extraction in kerosene layer is more likely based upon the oxidation of antimonite species (SbO₂⁻) to antimonate (SbO₃⁻) with NaIO₄ according to the following equations [28–30]:



The chloro complex of Sb [SbCl₆⁻] was then reacted with the aliquat-336 to form the Sb(V)-Aliquat-336 ion associate that was extracted quantitatively in the organic phase as follows:



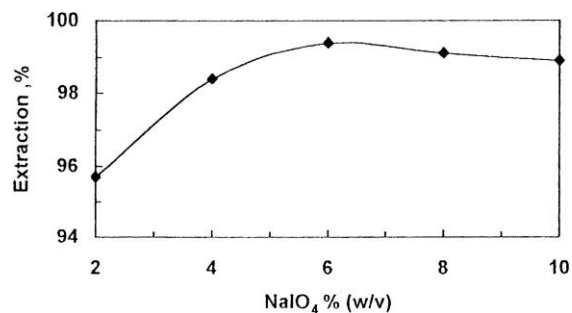


Fig. 8. Effect of NaIO₄ concentration (% (w/v)) on the Sb extraction (%) from the leaching liquor.

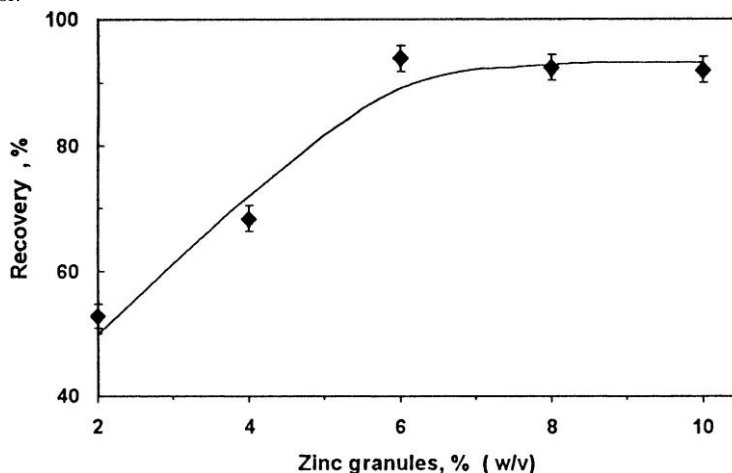


Fig. 9. Effect of zinc granules (% (w/v)) on the Sn(II) recovery (%) from the leaching liquor.

In this step, aliquat-336 must be added rapidly to the solution after the addition of sodium periodate because the complex species [SbCl₆]⁻ slowly hydrolyses to [Sb(OH)Cl₅]⁻ as reported by Nielsch and Boltz [24]. These complex species were not extracted quantitatively in the organic phase with Aliquat-336 [31]. The complex associate of Sb(V)-Aliquat-336 in the organic phase was then stripped by the reduction with 1M oxalic acid solution and precipitated as Sb₂S₃ with sodium sulfide 2% (w/v). The produced Sb(III) sulfide was then reduced to Sb employing hydrogen.

Sn species in HCl media were detected in the organic phase under the above conditions. According to the following equation [10]:



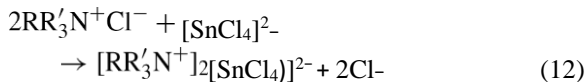
and



the produced SnCl₄ species are neutral. Therefore, such species were not able to form an ion associate with the aliquat in the organic phase.

The extraction of Sn(IV) species from the remaining leachant (free from Au and Sb ions) liquor was achieved employing zinc granules as a reducing agent. Various amounts of 2, 4, 6, 8 and 10% (w/v) of zinc granules were added to equal amounts of the leached liquor and the solutions were gently evaporated to

dryness and analyzed for Sn. The Sn residues were redissolved in 6M HCl solution and shaken with 10% (v/v) Aliquat-336 in kerosene. Good extraction percentage of Sn(II) was achieved employing 6.5% (w/v) of zinc granules (Fig. 9). The extraction of Sn(II) in the organic phase is more likely proceeded as follows:



The produced complex ion associate Sn(II) in the organic phase was then stripped by shaking with 50ml sodium hydroxide (1M) solution. The formed precipitate of Sn(II) oxide was then reduced to Sn with hydrogen as reported by Rabah [32].

4. Conclusions

The present study demonstrates reliable, low cost and applicable procedures in routine analysis for Au, Sb and Sn recovery from their solid slimes and leachate liquor. The reagents Aliquat-336, quinol, sodium periodate and zinc granules are inexpensive and readily available. The components of the organic phase are extremely stable and no deterioration in performance was noticed during the working procedures. Such procedures could also be improved using polyurethane foam column [1] to recover the title metals from large sample volumes of the leachate of liquid or solid waste. The cost of the processes could be competitive due to the low-energy consumption and the high selectivity of Au recovery of from its secondary resources.

References

- [1] M.S. El-Shahawi, A.B. Farag, *Anal. Chim. Acta* 307 (1995) 139.
- [2] A.Z. Abu-Zuhouri, M.S. El-Shahawi, M.M. Kamal, *Anal. Chim. Acta* 282 (1993) 133.
- [3] M.J. Nical, M.D. Adams, *J. S. Afr. Inst. Min. Metall.* 97 (6) (1997) 281.
- [4] A. Feather, K.C. Sole, I.J. Bryson, in: *Proceedings of the Randol Gold Forum 97*, Monterey, CA, 18–21 May, 1997.
- [5] A. Feather, K.C. Sole, I.J. Bryson, *J. S. Afr. Inst. Min. Metall.* 97 (4) (1997) 169.
- [6] S. Garbos, E. Bulska, A. Hulanicki, N.L. Shcherbinina, E.M. Sedykh, *Anal. Chim. Acta* 342 (1997) 167.
- [7] U. Forstner, in: R. Leehsher, R.D. Davis, P.L. Hermit, *Chemical Methods for Assessing Bioavailable Metals in Sludge and Soils*, Elsevier, London, 1985, pp. 1–30. [8] D. Purves, *Trace Elements Contamination of the Environment*, Elsevier, Amsterdam, 1985, pp. 6–16.
- [9] M.B. de la Calle-Guntinas, Y. Madrid, C. Camara, *Anal. Chim. Acta* 247 (1991) 7.
- [10] M.S. El-Shahawi, A.Z. Abu-zuhouri, *Bull. Chem. Soc. Jpn.* 71 (1998) 71, and references therein.
- [11] H. Vrijhof, *Sci. Total Environ.* 43 (1985) 221.
- [12] A.R. Udupa, S.K. Kawatra, M.S. Prasad, *Min. Process. Ext. Met. Rev.* 7 (1990) 115.
- [13] J. Rydberg, C. Musikas, G.R. Choppin, *Principles and Solvent Extraction*, Marcel Dekker, New York, 1992.
- [14] F. Habashi, *Principles of Extractive Metallurgy*, 2nd Edition, Gordon and Breach, New York, 1980, pp. 39–51.
- [15] Z.X. Chen, P.J. Pryer, H.P. Ongerith, S.E. Jackson, *J. Anal. At. Spectrom.* 11 (1996) 805.
- [16] V. Lanher, C.H. Kao, *J. Phys. Chem.* 30 (1926) 126.
- [17] T. Honkoshi, S. Yoshimura, N. Kubota, M.N. Sato, *Nippon Kagaku Kaishi* 8 (1983) 1118.
- [18] A.M. Diaz, G.H. Kelsall, N.J. Welham, *Electroanal. Chem.* 361 (1993) 25.
- [19] American Society for Testing and Materials (ASTM), in: *Annual Book of Standards — Chemicals Analysis of Metals and Metal-Bearing Ores*, Vols. 3 and 5, ASTM, Philadelphia, PA, 1983, pp. 18–21.
- [20] H. Majiama, E. Peters, Y. Awakura, K. Tsgui, in: S.E. Manahan (Ed.), *Environmental Chemistry*, 6th Edition, *Met. Trans. B* 21 (1990) 735, Lewis Publishers, CRC Press, Boca Raton, FL, 1994.
- [21] J. Basset, R.C. Denny, G.H. Jeffrey, J. Mendham, *Text Book of Quantitative Inorganic Analysis*, 4th Edition, 1986.
- [22] J. Vinals, C. Nunez, J. Crrosecos, *Hydrometallurgy* 38 (1995) 125.
- [23] C. Caracava, *Hydrometallurgy* 35 (1994) 27.
- [24] W. Nielsch, G. Boltz, *Microchim. Acta* (1954) 313.
- [25] R.T. Arnesen, A.R. Selmer-Olsen, *Anal. Chim. Acta* 33 (1965) 335.
- [26] S. Alpert, *Developments in Solvent Extraction*, Ellis Horwood, England, 1988.
- [27] Y.A. Zolotov, L.A. Demina, O.M. Petrukhin, *Zh. Analit. Khim* 25 (1970) 2315.
- [28] A.B. Farag, M.S. El-Shahawi, E.M. El-Nemma Fres, *J. Anal. Chem.* 346 (1993) 455.
- [29] J.A. Edwards, D.R. Slim, *J. Chem. Soc., Chem. Commun.* (1974) 178.
- [30] K. Yamamoto, T. Shimakawa, *Anal. Sci. Jpn.* 16 (2000) 641, and references therein.
- [31] F.A. Cotton, G. Wilkinson, P.L. Gaus, *Basic Inorganic Chemistry*, 3rd Edition, Wiley, New York, 1995.
- [32] M.A. Rabah, *Hydrometallurgy* 47 (1998) 281.
- [33] A. Poma, S. Bianchini, M. Miranda, Thiourea is listed on the California list of suspected carcinogens, *Mutat. Res.* 446 (1999) 143.

Ruthenium(II) 2-hydroxybenzophenone N(4)-substituted thiosemicarbazone complexes

Sahar I. Mostafa* and Ahmed A. El-Asmy

Chemistry Department, Faculty of Science, Mansoura University, Mansoura, Egypt

Mohamed S. El-Shahawi

Chemistry Department, Faculty of Science (Damietta), Mansoura University, Mansoura, Egypt

Received 21 September 1999; accepted 30 November 1999

Abstract

New ruthenium(II) complexes with 2-hydroxybenzophenone N(4)-substituted (Me, Ph and/or piperidyl) thiosemicarbazones have been prepared and characterised by elemental analysis, molar conductivity, thermal analysis, spectroscopy (i.r., ¹H-n.m.r. and u.v.±vis.) and by cyclic voltammetry. The thiosemicarbazones coordinate to ruthenium(II) as mononegative tridentate ligands via the deprotonated hydroxyl group, N¹ nitrogen and thione sulphur centres. The redox properties, nature of the electrode processes and the stability of the complexes towards oxidation in CH₂Cl₂ are discussed. The change in the E_{1/2} values of the complexes can be related to the basicity of the N(4)-substituents. All the complexes display an irreversible one-electron charge-transfer couple in the potential range studied.

Introduction

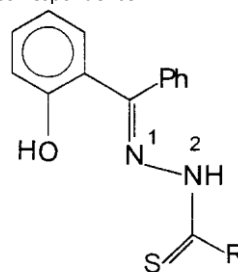
Thiosemicarbazones and their complexes are of considerable interest because of their antimicrobial activity, especially as virus growth inhibitors [1]. 2-Hydroxyacetophenone N(4)-substituted thiosemicarbazones coordinate with cobalt(II), nickel(II) and copper(II) ions as either mononuclear neutral [2, 3] or binuclear charged [4, 5] chelating agents. The binuclear nickel(II) and copper(II) complexes of 5-methylsalicylaldehyde N(3)substituted thiosemicarbazones have also been reported [6], as has the X-ray crystal structure of [Cu(5-NO₂Sapip)DMF] (5-NO₂Sapip = 5-nitrosalicylaldehyde piperidylthiosemicarbazone) [7]. The mixed ligand complexes of salicylaldehyde thiosemicarbazone (saltsc) with [M(PPh₃)₂Br₂] (M = Ru, Os) have been isolated and characterised. Also, the X-ray crystal structure of [Ru(PPh₃)₂(saltsc)₂] complex has been discussed [8].

We now describe the preparation, spectral characterisation and electrochemical behavior of ruthenium(II) complexes of 2-hydroxybenzophenone N(4)-substituted thiosemicarbazones (H₂HBPM, H₂HBPPH and H₂HBPpip). Figure 1 shows the structure of the thiosemicarbazones under investigation.

Experimental

2-Hydroxybenzophenone-4-methylthiosemicarbazone(H₂HBPM), 2-hydroxybenzophenone-4-phenylthiosemi-

* Author for correspondence



R = N⁴Me (H₂HBPM)

R = N⁴Ph (H₂HBPPH)

R = N⁴(CH₂)₅ (H₂HBPpip)

Fig. 1. 2-Hydroxybenzophenone N(4)-substituted thiosemicarbazones.

carbazone (H₂HBPPH) and 2-hydroxybenzophenone piperidylthiosemicarbazone (H₂HBPpip) were prepared by the literature method [6].

[Ru(HL)₂] á nH₂O (H₂L = H₂HBPM, H₂HBPPip, n = 0; HL = H₂HBPPH, n = 1)

Hydrated RuCl_3 (0.104 g, 0.5 mmol) in EtOH (5 cm^3) was added to H_2HBPM (0.43 g, 1.5 mmol), H_2HBPPH (0.52 g, 1.5 mmol) or H_2HBPIP (0.51 g, 1.5 mmol) in EtOH (20 cm^3). The reaction mixture was boiled under reflux for 2 h and, upon addition of 5 M AcONa (5 cm^3), a brown precipitate formed. This was removed by filtration, washed with H_2O , EtOH, finally with Et_2O , then dried in vacuo.

Spectroscopic data of the isolated complexes

$[\text{Ru}(\text{HHBPM})_2]$

I.r.: $\nu(\text{N}^4\text{H})$ 3055; $\nu(\text{N}^2\text{H})$ 2926; $\nu(\text{C@C}) + \nu(\text{CAC})$ 1528, 1410; $\nu(\text{C@N})$ 1592; $\nu(\text{NAN})$ 1020; $\nu(\text{C@S}) + \nu(\text{CN})$ & $\nu(\text{C@S})$ 1319, 755; $\nu(\text{CAO})$ 1233; $\nu(\text{RuAO})$ 440; $\nu(\text{RuAN})$ 465; $\nu(\text{RuAS})$ 370 cm^{-1} . U.v.-vis. (DMF): $k_{\text{max}} \cdot \epsilon_0 = \text{dm}^3 \text{mol}^{-1} \text{cm}^{-1}$: 600 (480), 400 (5100), 314 (6980), 260 nm (7140). $^1\text{H-n.m.r.}$ (d) 8.77 (s, N^2H), 8.56 (s, N^4H), 3.45 (s, Me), 7.25±7.45 p.p.m. (m, Ph).

$[\text{Ru}(\text{HHBPPH})_2] \cdot \text{H}_2\text{O}$

I.r.: $\nu(\text{N}^4\text{H})$ 3053; $\nu(\text{N}^2\text{H})$ 2922; $\nu(\text{C@C}) + \nu(\text{CAC})$ 1547, 1383; $\nu(\text{C@N})$ 1587; $\nu(\text{NAN})$ 1020; $\nu(\text{C@S}) + \nu(\text{CN})$ & $\nu(\text{C@S})$ 1314, 750; $\nu(\text{CAO})$ 1232; $\nu(\text{RuAO})$ 450; $\nu(\text{RuAN})$ 475; $\nu(\text{RuAS})$ 360 cm^{-1} . U.v.-vis. (DMF): $k_{\text{max}} \cdot \epsilon_0 = \text{dm}^3 \text{mol}^{-1} \text{cm}^{-1}$: 614 (670), 370 (5590), 315 (6985), 290 nm (7060), 258 (12500). $^1\text{H-n.m.r.}$ (d) 8.79 (s, N^2H), 10.31 (s, N^4H), 7.30±7.64 p.p.m. (m, Ph).

$[\text{Ru}(\text{HHBPPIP})_2]$

I.r.: $\nu(\text{N}^4\text{H})$ 2930; $\nu(\text{N}^2\text{H})$ 2853; $\nu(\text{C@C}) + \nu(\text{CAC})$ 1546, 1401; $\nu(\text{C@N})$ 1590; $\nu(\text{NAN})$ 1019; $\nu(\text{C@S}) + \nu(\text{CN})$ & $\nu(\text{C@S})$ 1332, 751; $\nu(\text{CAO})$ 1238; $\nu(\text{RuAO})$ 440; $\nu(\text{RuAN})$ 470; $\nu(\text{RuAS})$ 375 cm^{-1} . U.v.-vis. (DMF): $k_{\text{max}} \cdot \epsilon_0 = \text{dm}^3 \text{mol}^{-1} \text{cm}^{-1}$: 595 (636), 403 (2175), 317 (2960), 261 nm (5350). $^1\text{H-n.m.r.}$ (d) 8.35 (s, N^2H), 3.89±3.97 (mt, CH_2 of piperidine), 7.21±7.62 p.p.m. (m, Ph).

Instrumentation

Microanalyses were determined by the Microanalytical Unit of Cairo University. Magnetic moments at 25 °C were recorded using a Johnson Matthey magnetic susceptibility balance with $\text{Hg}[\text{Co}(\text{SCN})_4]$ as calibrant. Electronic spectra in DMF were recorded using a

Unicam UV₂₋₁₀₀ u.v.-vis. spectrometer. I.r. spectra were measured as KBr discs on a Matson 5000 FT-IR spectrometer. $^1\text{H-n.m.r.}$ spectra were measured on a Varian Gemini WM-200 spectrometer at the National Research Centre, Cairo. T.g. measurements were made in the 20±800 °C range at the heating rate of 10 °C min^{-1} , using $\alpha\text{-Al}_2\text{O}_3$ as a reference, on a Shimadzu Thermogravimetric

Analyzer TGA-50 (Analytical Unit, Mansoura University). Conductometric measurements were carried out at room temperature on a YSI Model 32 conductivity bridge. Cyclic voltammetry was performed on a potentiostat wave generator (Oxford press) equipped with a 7000 AM X-Y recorder. The electrochemical cell assembly consists of a spiral Pt wire (0.5 mm diam) as auxiliary electrode, with glassy carbon and Ag/AgCl as working and reference electrodes, respectively. The constant potential electrolysis was 471

carried out on a Princeton Applied research model 173/179 potentiostat/digital/coulometer equipped with a 175 universal programmer. Diagnostic criteria for the reversibility of the electron-transfer process were employed in the usual manner as described by Nicholson and Shain [9]. The voltammetric measurements were performed using ca. 10^{-3} M $[\text{Ru}(\text{HL})_2]$ and 0.5 M $(\text{nBu}_4\text{N})\text{PF}_6$ as supporting electrolyte at room temperature in CH_2Cl_2 .

Results and discussion

The analytical data of the complexes are in agreement with the empirical formulae shown in Table 1. Their molar conductivities (L_m) in DMF at room temperature showed them to be non-electrolytes [10].

Vibrational spectra

The i.r. spectral data for 2-hydroxyacetophenone N(4)-substituted thiosemicarbazones, 5-substituted salicylaldehyde thiosemicarbazones, 2-aminoacetophenone N(4)-unsubstituted and substituted thiosemicarbazones and their complexes have been reported [2±7, 11]. In the i.r. spectra of H_2HBPM , H_2HBPPH , H_2HBPIP and their ruthenium(II) complexes, as expected, the $\nu(\text{OH})$ stretching vibration, observed at ca. 3340 cm^{-1} in the free ligands, is missing in the spectra of the complexes [12, 13]. The bands at ca. 3290 and 3200 cm^{-1} in the free ligands, arising from $\nu(\text{N}^4\text{H})$ and $\nu(\text{N}^2\text{H})$, respectively, are shifted to lower wave numbers in the complexes, indicating involvement of N^1 and the deprotonated hydroxy oxygen centres in coordination [14]. This view is further supported by the band shifts at ca. 1610 and 990 cm^{-1} in the free ligands, due to $\nu(\text{C@N})$ and $\nu(\text{NAN})$ vibrations, respectively [14], which are sensitive to metal coordination. The band at ca. 800 cm^{-1} in the free ligands arising from $\nu(\text{C@S})$ of the thioamide, is shifted upon coordination and shifted to lower wave numbers. This is to be expected since the thione sulphur is taking part in complexation [15]. The isolated complexes show extra i.r. bands at ca. 440, 470 and 370 cm^{-1} which may be due to $\nu(\text{RuAO})$ [16, 17], $\nu(\text{RuAN})$ [16, 17] and $\nu(\text{RuAS})$ [18] stretchings, respectively.

Electronic spectra

The electronic spectra of the free ligands, in DMF, showed that each thiosemicarbazone under investigation Table 1. Analytical data of ruthenium(II) complexes

Compound	Found (Calcd.) (%)			K _{Mn}
	C	H	N	
[Ru(HHBPM) ₂]	54.1 (53.8)	4.1 (4.2)	12.5 (12.5)	12
[Ru(HHBPPH) ₂] · 2 H ₂ O	59.0 (59.2)	4.1 (4.2)	10.4 (10.4)	6
[Ru(HHBPPip) ₂]	58.4 (58.7)	5.2 (5.2)	10.7 (10.8)	8

^ain DMF (X¹ cm² mol⁻¹).

472

has a n → p* transition in the 300±325 nm region assignable to the phenyl rings [19]. The energies are raised by ca. 10 nm in the complexes [6]. The 391±396 nm region bands are assignable to the n → p* transition of the thiosemicarbazone thioamide moiety, and are shifted to higher energies in the complexes [15]. The ground state of ruthenium(II) in an octahedral environment is ¹A_{1g} and only two spin allowed transitions, ¹A_{1g} → ¹T_{1g} and ¹A_{1g} → ¹T_{2g} are expected [20]. The electronic spectra of the [Ru(HL)₂] (H₂L = H₂HBPM, H₂HBPPH, H₂HBPpip), complexes in DMF, show three bands in the 614±595, 403±370 and 317±314 nm regions which may arise from ¹A_{1g} → ¹T_{1g}, ¹A_{1g} → ¹T_{2g} and ligand (p±dp) transitions, respectively

^{1g}

[17]. This result may be attributed to low-spin octahedral geometries around the ruthenium(II) ions [20].

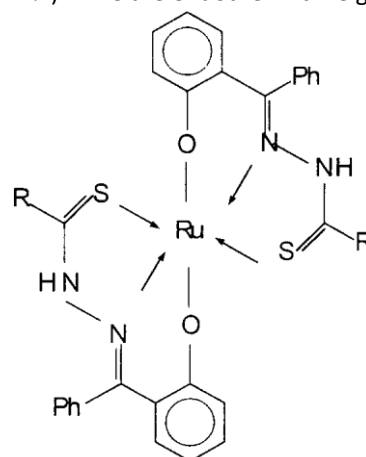
H-n.m.r. spectra

The ¹H-n.m.r. data for H₂HBPM, H₂HBPPH and H₂HBPpip and their ruthenium(II) complexes in CDCl₃ have been analysed. For the free ligands, the aromatic protons appear at δ 7.0±7.5 p.p.m., the CH₃ protons (H₂HBPM) give a singlet at δ 3.23 p.p.m. while the CH₂ protons of piperidine appear as triplets in the δ 3.67±3.70 p.p.m. region. The OH, N²H and N⁴H protons appear as singlets at δ 10.59, 8.62, 8.41 (H₂HBPM), 10.38, 8.67, 10.22 (H₂HBPPH) and 12.02, 8.24, ± (H₂HBPpip), respectively. In H₂HBPpip, the OH proton resonance at δ 12.02 p.p.m., suggests considerable intramolecular hydrogen bonding (N¹¼¼¼HAO) [7]. For the complexes, the broad resonance arising from the hydroxy proton disappears, whereas that arising from the N²H and N⁴H protons are shifted downfield, indicating a decrease in the electron density caused by electron withdrawal by ruthenium(II) from the thione sulphur, the N(2) and the deprotonated hydroxy oxygen centres [16, 21]. As expected, for these complexes, cis and trans isomers are possible, the presence of one resonance for each signal suggesting trans configurations [8, 13] as shown in Figure 2.

Thermal studies

The thermal decomposition of the investigated complexes was studied using the t.g. technique.

The thermogram of [Ru(HHBPM)₂] shows the first weight loss endotherm between 214 and 314 °C, which may correspond to the release of two MeNHCS fragments [14, 22] (Found 22.4; Calcd., 22.1%). The second weight loss (Found, 49.2; Calcd., 49.3%) between 314 and 378 °C may be attributed to the elimination of two (Ph)₂C fragments. The last step, at 400 °C, may be due to the formation of mixed Ru₂O₃±RuO₂ (Found, 26.9; Calcd., 28.6%). The t.g. curve of [Ru(HHBPPH)₂] · 2 H₂O, shows the first weight loss between 85 and 170 °C, which may be due to the release of a hydrated water molecule (Found, 2.9; Calcd., 2.2%) while the endothermic weight loss



R = N⁴Me (H₂HBPM)

R = N⁴Ph (H₂HBPPH)

R = N⁴(CH₂)₅ (H₂HBPpip)

Fig. 2. Trans configuration of [Ru(HL)₂] (H₂L = H₂HBPM, H₂HBPPH, H₂HBPpip).

between 211 and 357 °C, may be due to the release of two PhNHCS fragments (Found, 32.1; Calcd., 33.5%). The next t.g. inflection lies in the 359±616 °C range and may arise from the release of two (Ph)₂C fragments (Found, 41.1; Calcd., 40.6%), leaving a mixed Ru₂O₃±RuO₂ residue at 620 °C (Found, 24.8; Calcd., 23.6%).

The thermogram of [Ru(HHBPPip)₂] shows two t.g. inflections in the 212±323 and 323±387 °C ranges. The first weight loss may be attributed to the release of two C₅H₁₀NCS fragments (Found, 31.8; Calcd., 32.8%) while the second step is due to the removal of two (Ph)₂C fragments (Found, 42.1; Calcd., 42.3%) followed by mixed Ru₂O₃±RuO₂ residue at 405 °C (Found, 23.5; Calcd., 24.6%).

Electrochemistry

The electrochemical behavior of the reported ruthenium(II) complexes in CH₂Cl₂ was investigated by cyclic voltammetry versus Ag/AgCl electrode and the data are summarised in

Table 2. The $E_{1/2}$ values of the complexes are similar. A representative voltammogram of $[Ru(HHBP_{pip})_2]$ at 100 mV s^{-1} shows one irreversible electrode couple in the potential range $+1$ to $+1.5 \text{ V}$ at potential scan rates $0.02 \pm 0.2 \text{ V s}^{-1}$ at $25 \text{ }^\circ\text{C}$ (Figure 3). On the basis of $E_{1/2}$ values and comparison with similar ruthenium(II) complexes [23, 24], the observed couples can be assigned to $Ru^{II/III}$. The analysis of the cathodic, i_c , and anodic, i_a , pair of peaks shows that the product $i_{pa} (m)^{1/2}$ for the anodic peak is constant within 3%. The diffusion coefficient of the reduced species obtained from the i_{pa} versus $m^{1/2}$ plot and the coulometric data (0.98 F mol^{-1}) at $E_{1/2}$ for the observed electrode couple indicates that the anodic peak corresponds to a one-

Table 2. Half wave potential for the ruthenium(II) complexes

Compound	$E_{1/2}(V)_a$
$[Ru(HHBPM)_2]$	0.51
$[Ru(HHBPh)_2]$	0.41
$[Ru(HHBP_{pip})_2]$	0.46

^a $E_{1/2}$ (V) versus Ag/AgCl in $10^{-3} \text{ mol dm}^{-3}$ in CH_2Cl_2 . All potentials measured at scan rate 100 mV s^{-1} using $(n\text{-Bu}_4\text{N})\text{PF}_6$ (0.5 mol dm^{-3}) as a supporting electrolyte.

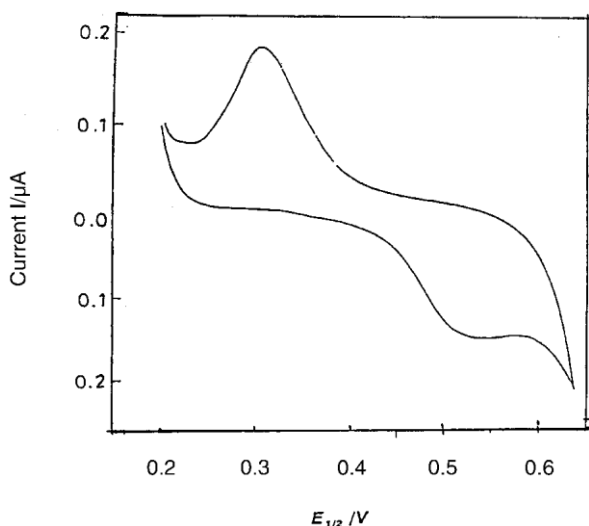


Fig. 3. Cyclic voltammogram of $[Ru(HHBP_{pip})_2]$ in CH_2Cl_2 with $(n\text{-Bu}_4\text{N})\text{PF}_6$ (0.5 mol dm^{-3}) at 100 mV s^{-1} .

electron oxidation of the starting complex. This conclusion further supports the assignment of the anodic oxidation $Ru^{II/III}$ peak [25].

The substituted group $[R = \text{NMe}, \text{NPh}, \text{N}(\text{CH}_2)_5]$ may have a significant effect on the $E_{1/2}$ of the complexes, since the electron-withdrawing Ph group stabilizes the ruthenium(II) complexes, whereas the electron-donating groups $[\text{Me}, (\text{CH}_2)_5]$ favour oxidation of ruthenium(II) to ruthenium(III). Thus, the observed small influence of R on the $E_{1/2}$ (Table 2) should be due to the large distance from the metallic centre changing the ruthenium charge density slightly. This behavior is consistent with the absence of conjugation between R and N(4)-substituted thiosemicarbazones.

Nature of the electrode process

At low scan rates ($m \leq 50 \text{ mV s}^{-1}$), the electrode process at the anodic peak can be better described as an $E_{c,irr}$ type. On increasing the scan rate ($\geq 100 \text{ mV s}^{-1}$), the cathodic peak potential shifts to more negative values [47]

while the anodic one shifts to a less negative potential. This behavior demonstrates the irreversible nature of the electrode process [26]. Furthermore, the irreversibility is revealed by the difference between E_{pa} and E_{pc} .

References

- D.X. West, S.B. Padhye, P.B. Sonawane and R.C. Chikate, Asian J. Chem. Rev., 1, 125 (1990); D.X. West, A.E. Liberta, S.B. Padhye, R.C. Chikate, P.B. Sonawane, A.S. Kumbhar and R.G. Yerande, Coord. Chem. Rev., 123, 49 (1993).
- M. Soriano-Garcia, R.A. Toscano, J. Valdes-Martinez and J.M.Fernandez, Acta Crystallogr., C41, 498 (1985).
- L.H. Reddy, K.G. Reddy and D.V. Reddy, Proc. Ind. Sci. Acad., 55, 517 (1989).
- B. Singh and U. Srivastava, Synth. React. Inorg. Met.-Org. Chem., 19, 279 (1989).
- S. Laly and G. Parameswaran, Thermochim. Acta, 168, 43 (1990).
- D.X. West, M.M. Salberg, G.A. Bain and A.E. Liberta, Transition Met. Chem., 22, 180 (1997).
- D.X. West, M.M. Salberg, G.A. Bain and A.E. Liberta, J. Valdes-Martinez and S. Hernandez-Ortega, Transition Met. Chem., 21, 206 (1996).
- F. Basuli, S.M. Peng and S. Bhattacharya, Inorg. Chem., 36, 5645 (1997).
- R.S. Nicholson and I. Shain, Anal. Chem., 36, 706 (1964).
- W.J. Geary, Coord. Chem. Rev., 7, 81 (1981).
- D.X. West, A.A. Nassar, F.A. El-Saied and M.I. Ayad, Transition Met. Chem., 23, 321 (1998).
- J. Valdes-Martinez and R.A. Toscano, Polyhedron, 14, 1681 (1995).
- S.I. Mostafa, Transition Met. Chem., 23, 397 (1998).
- S.I. Mostafa and M.M. Bekheit, Chem. Pharm. Bull. Jpn, in press.
- D.X. West, A.K. El-Sawaf and G.A. Bain, Transition Met. Chem., 23, 1 (1998).
- S.I. Mostafa and S.A. Abd El-Maksoud, Monatsh. Chem., 129, 455 (1998).
- A.M. Ramadan, I.M. El-Mehasseb and R.M. Issa, Transition Met. Chem., 22, 529 (1997).
- S.K. Sengupta, S.K. Sahni and R.N. Kapoor, Indian J. Chem., 19A, 810 (1980).
- H.H. Jalil and M. Orchin, Theory and Applications of Ultraviolet Spectroscopy, Wiley, New York, 1962.
- V. Chauhan and S.K. Dikshit, Synth. React. Inorg. Met.-Org. Chem. 9, 1037 (1989).
- W.P. Grieth and S. Mostafa, Polyhedron, 11, 2997 (1992).
- M.A. Zayed and F.A. Nour El-Dein, Thermochim. Acta, 114, 53 (1987).
- Z. Naal, E. Tfouni and A.V. Bemedetti, Polyhedron, 13, 133 (1994).
- M. Armando, R. Lena, M. Rafael and D.R.J. Federice, J. Coord. Chem., 29, 359 (1993).
- Z.N. Rocha and E. Tfouni, Polyhedron, 11, 2375 (1992).
- P. Dalhy, New Instrumental Methods in Electrochemistry, Interscience, New York, 1953.

TMCH4643



ELSEVIER

The Science of the Total Environment 256 (2000) 87–194

**the Science of the
Total Environment**

An International Journal for Scientific Research
Into the Environment and its Relationship with Man

www.elsevier.com/locate/scitotenv

Trace metals in liver, skin and muscle of *Lethrinus lentjan* fish species in relation to body length and sex

M.H. Al-Yousuf^a, M.S. El-Shahawi^{1,b,U}, S.M. Al-Ghais^c

^a

Desert and Marine Environment Research Center, UAE University, P.O. Box: 17777, Al-Ain, United Arab Emirates

^b

Department of Chemistry, Faculty of Science, UAE University, P.O. Box: 17551, Al-Ain, United Arab Emirates

^c

Department of Biology, Faculty of Science, UAE University, P.O. Box: 17551, Al-Ain, United Arab Emirates

Received 3 February 1998; accepted 30 August 1999

Abstract

A post-Gulf sea water pollution assessment program was carried out in the liver, skin and muscle tissues of the localized *Lethrinus lentjan* fish species Family: Lethrinidae Teleost. Monitoring the concentration of the major heavy metals at different sites along the western coast of the United Arab Emirates UAE on the Arabian Gulf was studied. The concentrations of Zn, Cu and Mn were found to follow the order: liver>skin>muscle while the cadmium level follows the sequence: liver>muscle>skin. The influence of fish sex and body length on the metal accumulation of those metals in the tested fish organs was critically investigated. The average metal concentrations in liver, skin and muscle of female fish were found to be higher than those found in the male fish. The detected metal levels were generally similar to previous pre-war, 1991 levels. The study concludes that the marine fish from the Arabian Gulf are comparatively clean and do not constitute a risk for human health. © 2000 Elsevier Science B.V. All rights reserved.

Keywords: Trace metals; Fish; Organs; Bodylength; Sex

1. Introduction

Trace elements occur in minute concentration in biological systems. They may exert beneficial or harmful effects on plant, animal, and human life depending upon the concentration (Forstner and

This work was done while Dr M.S. El-Shahawi was on leave at the Department of Chemistry, Faculty of Science, UAE University, Al-Ain, P.O. Box 17551 UAE.

^U

Corresponding author. Tel.: +971-3-2050-346781; fax: +971-3-2050370344. Wittman, 1981. These elements are introduced into the environment through various routes, smelting processes, fuel combustion and industrialization (Forstner and Wittman, 1981). They get their way into aquatic systems, rivers, lakes or oceans

through atmospheric fallout, dumping wastes, accidental leaks, runoff of terrestrial systems industrial and domestic effluents and geological weathering (Eisler, 1981).

Some metals and organochlorine pesticides became a matter of concern because of their toxicity and tendency to accumulate in food chains (Friligos, 1985;

0048-9697/00/\$ - see front matter © 2000 Elsevier Science B.V. All rights reserved.

PII: S0048-9697(99)00363-0

Mason and Barak, 1990; Barlas, 1999; Parlak et al., 1999). Fish are located at the end of the aquatic food chain and may accumulate metals and pass them to human beings through food causing chronic or acute diseases (Forstner and Wittman, 1981; Fowler et al., 1991; Khan and Weis, 1993; Jørgensen and Pedersen, 1994; Adeyeye et al., 1996).

The age, size and feeding habits of fish or aquatic animals, beside their retention time in polluted waters affect the heavy metals accumulation in these organisms (Mitra, 1986; Schuhmacher et al., 1992). The marine environment in the Arabian Gulf region has been the subject of study in recent years due to accidental oil spills, discharge of Ballast water, dredging and burial for coastal development, uncontrolled discharge of the sewage and industrial waste water (Abu-Hilal and Khordagui, 1992; Kureishy, 1993; Jørgensen and Pedersen, 1994). Added to this, waters in this area have been exposed to the effects of many environmental pollutants from desalination, power generation and wastewater

treatment plants. All these stresses and activities are posing a serious threat to the marine environment.

The United Arab Emirates (UAE) is one of the Arabian Gulf countries; its shores extend a distance of 700 km. Chemical pollution with hydrocarbons and heavy metals is the most serious problem that has been aggravated by the deliberate release of crude oil during

the 1991 Gulf War. Fish is important for the UAE economy and it can be considered a major food in the region. Added to this, little information is available about the physical and chemical properties of Gulf water. Therefore, this study has focused on monitoring the accumulation behavior of some heavy metals after the Gulf war. The tissues of *Lethrinus lentjan* species family: Lethrinidae (Teleost) have been frequently used as means of evaluating heavy metal pollution in coastal waters. This fish is one of the most popular fish in the Gulf countries and has a commercial importance for over 75% of the population.

2. Materials and methods

2.1. Sample preparation

Samples of *Lethrinus lentjan* fish (Family: Lethrinidae Teleost) of both sexes were collected

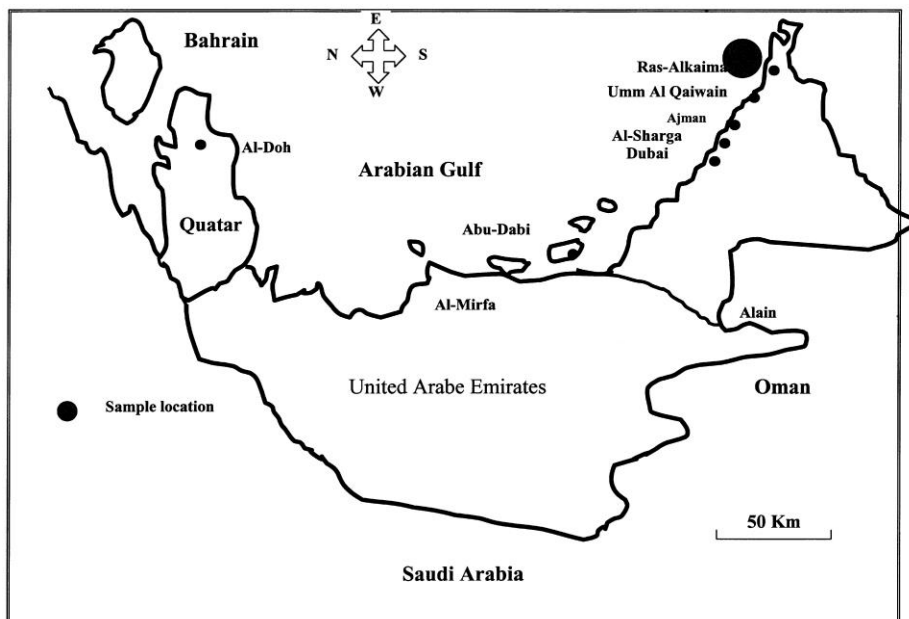


Fig. 1. Sampling locations along western coast of United Arab Emirates.

from the western coast of the UAE (Fig. 1) on more than one occasion during the year, 1994. Each time approximately 50 samples of different sizes were collected, placed in an ice box, transported to the laboratory and kept in a freezer (-15°C) prior to the analysis. The fish samples were then defrosted and their standard length and weight were recorded. Whole fish were dissected on a clean bench shortly after thawing with the aid of a stainless steel knife which had been cleaned with acetone and hot distilled water prior to use. Sex was determined by inspection of gonads after opening the body cavity. The fish samples were finally preserved in clean dry polyethene bottles prior to analysis.

2.2. Chemical analysis

Wet tissues of muscle, skin and liver were processed for analysis as described earlier Barak and Mason, 1990. An accurate sample weight (5 g) of fish tissues was gently digested for 2 h. in 10 ml concentrated nitric acid (70% v/v) followed by 10 ml of acid mixture HNO₃/HClO₄ (4:1 v/v) in a Pyrex vessel. The solution was gently heated for 24 h at 80°C until the digestion was completed. The solution mixture was then heated to dryness. After cooling, 25 ml distilled water was added to the solid residue and the resulting solution was further heated at 100°C for 10 min. The solution was then transferred to a 25-ml measuring flask and completed with distilled water. For each series of 10 samples, two analytical blanks were prepared in a similar manner without samples to check the possible contamination. The digestion procedures were applied to standards the quality control samples of Zn, Cu, Mn and Cd concentrations. The results showed that no losses of metals occurred and the recovery percentage was in the range of 99.6–2.8%.

All reagents used were of analytical reagent grade (BDH, England and Merck, Germany). Standard stock solutions (100 ppm) of Cu, Mn, Zn and Cd were prepared from BDH Chemicals, England. Deionized water was used throughout the study. All glassware

was carefully cleaned with hot nitric acid followed by thorough rinsing with distilled water before use.

The aqueous digest was analyzed for copper, zinc, manganese and cadmium in triplicate using a GBC-906 double beam atomic absorption spectrometer and GBC graphite furnace with fuel-rich equipped with background corrector, autosampler, recorder and air acetylene flames.

3. Results and discussion

Trace metal concentrations tested in stationary fish was used as an environmental indicator in water areas affected by human activities and as a monitoring technique for assessing the efficiency of control measures (Jørgensen and Pedersen, 1994). Thus, the levels of zinc, copper, manganese and cadmium in *Lethrinus lentjan* fish were critically examined in different fish organs. These elements are known to have a great ability to form stable chelates with the available active sites in the immobile protein molecules in the investigated fish tissues (Kendrick et al., 1992).

The concentrations of Zn, Cu, Mn and Cd are expressed in mg/kg wet tissues in liver, skin and muscle of female, male and not determined sex *Lethrinus lentjan* fish are summarized in Table 1. The distribution pattern of Zn, Cu and Mn follows the order: liver>skin>muscle; while cadmium follows the sequence: liver>muscle>skin. Thus, the liver tissues in fish are more often recommended as an environmental indicator organism of water pollution than any other fish organs. This is possibly attributed to the tendency of liver to accumulate pollutants of various kinds at higher levels from their environment as previously reported by Galindo et al. (Galindo et al., 1986). The specific metabolism process, and the enzyme-catalyzed reaction taking place in liver involving Zn, Cu, Mn and Cd may also account for this behavior (Jaffar and Pervais Shahid, 1989). In liver (Table 1) the data are in good agreement with the results reported by Harrison and Kalverkamp (1990). Similar results for copper concentration were obtained in the liver of *Lethrinus nebulosus* (4.79–0.15 ppm) around the State of Qatar before, during and after the Gulf

War & Kureishy, 1993. The accumulation of the tested metals in liver could be based on the

family in the Arabian Gulf region following the Gulf War, 1991 & Abdulmoneim and El-Deek, 1992 ..

Table 1

Mean \pm S.D. and one-way Anova of heavy metal concentration in liver, skin and muscle of *Lethrinus lentjan* female, male and not determined sex N fish tissues ppm collected from Ras Al-Khaima UAE coast water.

Tissue	Sex	No. ^b	Cu		P %	Zn		P %	Mn		Cd		P %	
Liver	Female	140	5.61	1.97	0.05	70.08	36.62	0.05	1.35	0.2	0.05	0.78	0.33	0.05
	Male	22	3.52	0.25		34.1	4.7		0.97	0.21		0.63	0.12	
	N	29	4.43	0.58		39.54	2.78		1.15	0.05		0.51	0.2	
		191	4.88	1.71 ^a	0.05	1.22	0.23	0.05	1.22	0.23	0.05	0.66	0.28	0.05
Skin	Female	139	0.28	0.08	0.05	42.28	8.51	0.05	0.12	0.03	0.05	0.08	0.03	0.05
	Male	22	0.4	0.18		31.42	2.95		0.11	0.2		0.06	0.07	
	N	39	0.35	0.14		37.75	8.1		0.27	0.12		0.11	0.08	
		200	0.33	0.13 ^a	0.05	318.39	8.35	0.05	0.16	0.11	0.05	0.08	0.06	0.05
Muscle	Female	150	0.17	0.06	0.05	3.3	0.28	0.05	0.1	0.02	0.05	0.12	0.02	0.05
	Male	21	0.16	0.02		2.82	0.15	0.05	0.08	0.02	0.05	0.09	0.01	0.05
	N	43	0.18	0.11		3.61	0.45		0.13	0.02		0.11	0.04	
		214	0.17	0.06 ^a		3.31	0.39		0.11	0.02		0.11	0.02	

^a x is the average concentrations of the element in female, male and N tissues.

^b Number of fish samples.

greater tendency of the elements to react with the oxygen carboxylate, amino group, nitrogen and/or sulphur of the mercapto group in the metallothionein protein which is at highest concentration in the liver Kendrick et al., 1992; El-Shahawi, 1996. These complexes are slowly redistributed to the renal cortex. Liver has also an important role in contaminant storage, redistribution, detoxification or transformation and also acts as an active site of pathological effects induced by contaminants (Evans et al., 1993). The average copper concentration in the muscle tissues of *Lethrinus lentjan* fish (0.17–0.06 ppm) were found to be lower than the data reported for the *Lethrinus mahsenoides* (0.34–0.13 ppm) and *Lethrinus nebulosus* (0.45–0.17 ppm) species of the same

In liver and skin of female and male fish the average concentration (Table 1) of the tested elements follows the sequence: Zn>Cu>Mn>Cd; while in muscle the distribution follows the order: Zn>Cu>Mn>Cd, respectively. The highest accumulation was observed also for zinc and copper in the tested organs. The fact that copper is stored in the liver to form tetrahedral metallothionein and metallo-enzymes complex species through the mercapto and the disulphide groups present in the protein (Vinikour et al., 1980; Schuhmacher et al., 1992). Copper granules in the cellular organelles may also be sequestered in the lysosomes as reported by Abu Damir et al. (1993). The accumulation of Zn can also be caused by the zinc metalloenzymes and Zn²⁺-protonated enzymes Kendrick et al., 1992 to form stable five- or six-membered ring chelates (Cotton and Wilkinson, 1988; Schriver et al., 1994).

The average zinc concentration in liver and skin (Table 1) was found to be high in female compared to male fish and the difference is significant ($P < 0.05$). Similar accumulation of zinc was reported by Khan and Weis (1993). The nature of hormones and the available number of active sites in the protein and cytochrome P-450 in female and male fish may account for this behavior (Jørgensen and Pedersen, 1994). The average copper level (Table 1) in liver, skin and muscle were found to be 5.61, 1.97, 0.28, 0.08 and 0.17, 0.06 ppm in female species and 3.52, 0.25, 0.4, 0.18 and 0.16, 0.02 ppm in male fish, respectively. A significant ($P < 0.05$) relationship between copper levels in female and male in fish liver was found ($P < 0.05$) while in skin and muscle no significant differences were observed ($P > 0.05$). Manganese in female and male fish liver (Fig. 3) showed a significant ($P < 0.05$) difference while no significant ($P > 0.05$) difference was observed in the skin and muscle. The distribution of cadmium in the three organs in female and male fish was found to be insignificant ($P > 0.05$). The accumulation of manganese in liver, skin and muscle tissues is possibly attributed to the ability of the element to coordinate with the binding sites available in mitochondria (Kendrick et al., 1992). The specific metabolism process and the enzyme-catalyzed reaction involving manganese taking place in the liver could also account for this behavior (Jaffar and Pervais Shahid, 1989).

The average levels (Table 1) of the tested metals in muscle tissues do not reveal any significant ($P > 0.05$) increases as a result of the 1991 oil spill in the Gulf area. The levels found are comparable to those noted for biota in other areas of the world (Eisler, 1981) and in good agreement with the earlier data reported by Kureishy (1991). The accumulation behavior of Zn, Cu, Mn and Cd in the liver, skin and muscle with the fish size was examined in terms of correlation coefficient (r). In liver, good correlation coefficients for zinc ($r = 0.92$) and cadmium ($r = 0.85$) were found, while copper ($r = 0.636$) and manganese ($r = 0.592$) showed poor correlation with fish length, respectively. Representative data for Zn and Cd in liver are represented in Fig. 2. These data are in good agreement with that reported by Evans (Evans et al., 1993). The excretion rate of Zn, Cu, and Cd could be

very slow with an accumulation rate greater than the rate of tissue growth during much of the life time. The manganese content was found to be high at small fish size because of the increased uptake of the element with early growth (Evans et al., 1993).

In skin, copper ($r = 0.92$) and zinc ($r = 0.49$) levels increased with increasing fish size while manganese ($r = 0.72$) and cadmium ($r = 0.896$) levels decreased. Representative data are summarized in Fig. 3. Similar finding on *Lethrinus nebulosus* and other fish species were reported (Kureishy, 1993; Vas and Gordon, 1993). The growth rate of the new tissues being incorporated at a greater rate than metals transported into the tissues to establish steady state concentration (dilution by growth), the changes in the composition and the relative size of the target organ with

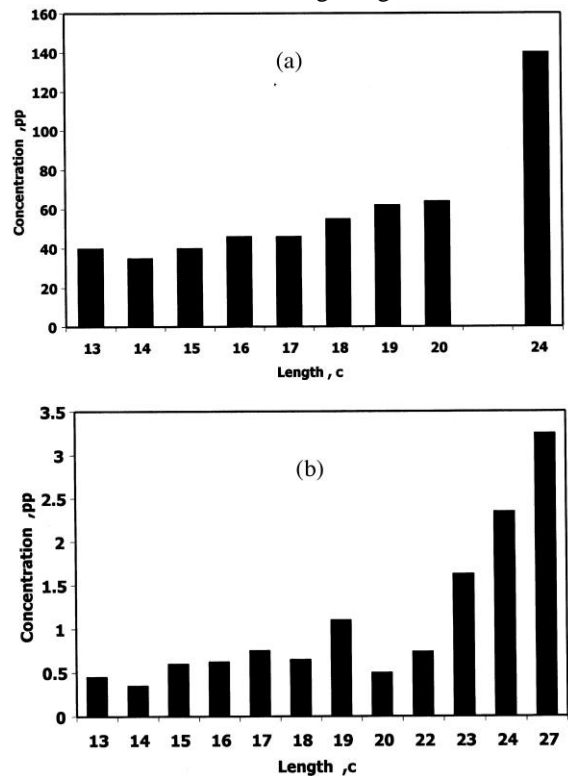


Fig. 2. Mean zinc (a) and cadmium (b) concentrations in liver (ppm) of *Lethrinus lentjan* fish vs. standard length.

growth, e.g. lipid content and translocation of the elements among tissues may account for this behavior (Vinikour et al., 1980; Nicholson et al., 1991).

In muscle no clear relationship between the zinc content and fish size was observed. Zinc seemed to accumulate up to a certain level and then remains constant in tissues due to several mechanisms (Marcovecchio and Moreno, 1993). The interdependency of the uptake and diminution rates when sufficient levels of the essential elements for metabolism are sequestered in the body and equilibrium is established between the body burden of zinc and the environment concentration (Marcovecchio and Moreno, 1993). The copper concentration slightly decreased with increasing fish size. The muscle tissues are not considered to be specific physiological sites for copper (Zia and Khan, 1989). The cross-correlation

coefficient calculated for trace metals in muscle tissues were significant ($P < 0.01$) for the following pairs of metals, Cd/Mn, Mn/Cu and Cd/Cu. Fig. 4 shows the distribution behaviour of manganese and cadmium in muscle with fish size. A strong correlation ($r = 0.96$) between manganese content and fish size was observed. Similar behavior was also observed for cadmium ($r = 0.896$), suggesting metabolic regulation at older fish age. The new tissues also could be formed at a greater rate than metals transported into the tissues to establish a steady state concentration (Vinikour et al., 1980).

4. Conclusion

The accumulation of zinc, copper, manganese and cadmium in liver tissues of *Lethrinus lentjan* fish were found high compared to skin and muscle tissues. The concentration levels of the elements as reported in this study do not constitute a risk factor for human health and appear to be below the permissible limits for human consumption ($Cu < 10$, $Zn < 150$, and $Cd < 0.2$ mg/kg wet weight set by the Australian National Health and Medical Research Council (Sharif et al., 1991). Attention therefore, has to be focused by local authorities on keeping the pollution levels under control in this valuable recreational and commercial water body and by international bodies to ensure forbidding reoccurrence of previous and further pollution tragedies in the Gulf region. In addition, the concentrations of the elements are generally amongst the lowest values reported in the literature and reflect a comparatively clean and pollution-free environment on the *Lethrinus lentjan* fish after Gulf War, 1991. The levels of the metals in liver and muscle tissues differed

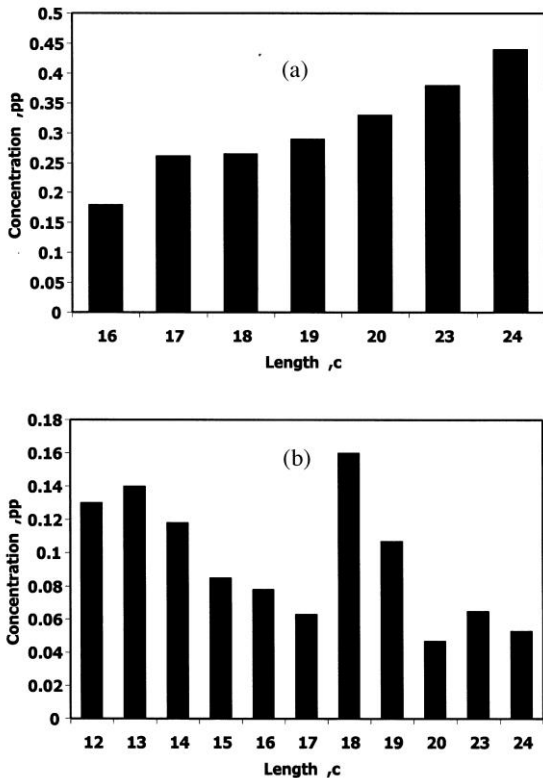


Fig. 3. Mean copper (a) and cadmium (b) concentrations in skin of *Lethrinus lentjan* fish vs. standard length.

tion coefficient calculated for trace metals in muscle tissues were significant ($P < 0.01$) for the following pairs of metals, Cd/Mn, Mn/Cu and Cd/Cu.

Fig. 4 shows the distribution behaviour of manganese and cadmium in muscle with fish size. A

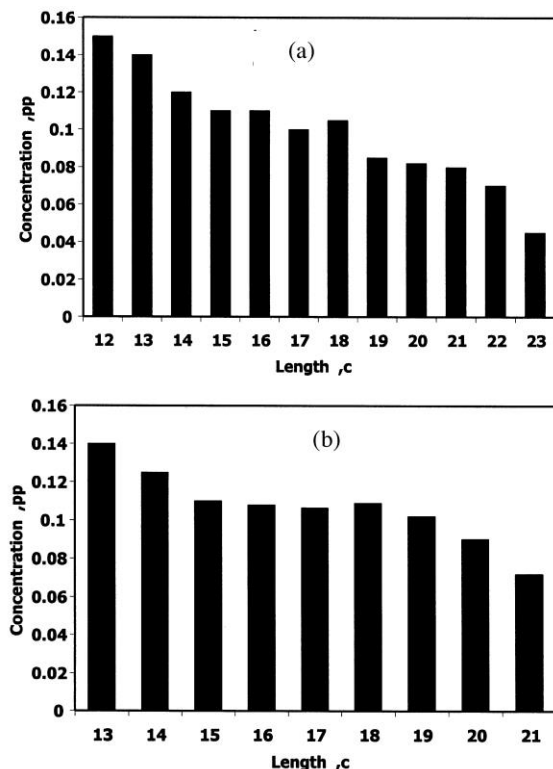


Fig. 4. Mean manganese a and cadmium b concentrations of *Lethrinus lentjan* fish vs. standard length.

little or remained constant before and after the Gulf War. The provincial tolerable intake of cadmium by human beings is 1.2 mg/kg^{yl} body weight/day. To reach this limit the person will be required to consume 800 g of *Lethrinus lentjan* fish per day, which is far more than the average consumption of fish by a normal person per day.

Acknowledgements

The authors would like to thank Professor A.S. Al-Sharhan, Dean of the Faculty of Science and Desert and Marine Environment Research Center, UAE University for his support to research project.

References

Abdulmoneim MA, El-Deek MS. Lethrinus family: a model of edible Red Sea fishes with low heavy metals accumulation.

- National Institute of Oceanography and Fisheries, Alexandria, Egypt, 2nd Alex Conference. Science and Technology 1992;439–448.
- Abu-Hilal A, Khordagui HK. Heavy metals in creeks and nearshore sediments of the United Arab Emirates, The Arabian Gulf and Gulf of Oman. Annual Report, Desert and Marine Research Center, UAE, Al-Ain, 1992.
- Abu Damir H, Eldirdiri I, Adam SEI, Howarth JA, Salih YM, Idris OS. Experimental copper poisoning in the camel *Camelus dromedarius*. J Comp Path 1993;108:191–208.
- Adeyeye ET, Akingugha NJ, Fesobi ME, Tenabe VO. Determination of some metals in *Clarias gariepinus* Cuvier and Valenciennes, *Cyprinus-Carpio* L and *Oreochromis Niloticus* L fishes in a polyculture fresh water pond and their environments. Aquaculture 1996;147–34:205–214.
- Barak NAE, Mason CF. Mercury, cadmium and lead in eels and roach: the effects of size, season and locality on metal concentration in flesh and liver. Sci Total Environ 1990;92:249–256.
- Barlas ME. Determination of organochlorine pesticides residues in aquatic systems and organisms in upper sakarya Basin, Turkey. Bull Environ Contam Toxicol 1999;62:278–285 and references therein.
- Cotton FA, Wilkinson GJ. Advanced inorganic chemistry, 4th ed. John Wiley, 1988.
- Eisler R. Trace Metal concentrations in marine organisms. London: Pergamon Press, 1981.
- El-Shahawi MS. Spectroscopic and electrochemical studies of chromium(III) complexes with some naturally occurring ligands containing sulphur. Spectrochim Acta 1996;52A:139–148.
- Evans DW, Doo DKDo, Hanson P. Trace element concentration in fish livers: implication of variations with fish size in pollution monitoring. Mar Pollut Bull 1993;26:329–354.
- Forstner U, Wittman GTW. Metal pollution in the aquatic environment. Berlin, Heidelberg, Germany: Springer-Verlag, 1981:272,486.
- Fowler SW, Readman JW, Oregioni B, Villeneuve JP, McKay K. Petroleum hydrocarbons and trace metals in near shore Gulf sediments and biota before and after the 1991 War: an assessment of temporal and spatial trends. Mar Pollut Bull 1991;27:171–182.
- Friligos N. Nutrient conditions in the Euboikos Gulf (west Aegean). Mar Pollut Bull 1985;16:435–442.
- Galindo L, Hardisson A, Montelongo FG. Correlation between lead, cadmium, copper, zinc and iron concentrations in frozen tuna fish. Bull Environ Contam Toxicol 1986;36:595–599.
- Harrison SE, Kalverkamp JF. Metal contamination in liver and muscle of Northern Pike *Esox lucius* and White Sucker *Catostomus commersoni* and in sediments from lakes near the Smelter at Fin Flon, Manitoba. Environ Toxicol Chem 1990;9:941–956.
- Jaffar M, Pervais Shahid S. Investigation on multi-organ heavy trace metal content of meat of selected dairy, poultry, fowl and fish species. Pak J Sci Ind Res 1989;32:175–177.

- Jørgensen LA, Pedersen S. Trace metals in fish used for time trend analysis and as environmental indicators. *Mar Pollut Bull* 1994;28:24–32.
- Jørgensen LA, Pedersen B. Trace metals in fish used for time trend analysis and on environmental indicators. *Mar Pollut Bull* 1994;26:235–243.
- Kendrick MH, May MT, Plishka MJ, Robinson KD. Metals in biological systems. England: Ellis Horwood Ltd, 1992.
- Khan T, Weis JS. Bioaccumulation of heavy metals in two populations of Mummichog *Fundulus heteroclitus*. *Bull Environ Contam Toxicol* 1993;51:1–5.
- Kureishy TW. Heavy metals in algae around the coast of Qatar. *Mar Pollut Bull* 1991;27:414–416.
- Kureishy TW. Contamination of heavy metals in marine organisms around Qatar before and after the Gulf War oil spill. *Mar Pollut Bull* 1993;27:183–186.
- Marcovecchio TD, Moreno VJ. Cadmium, zinc and total mercury levels in the tissues of several fish species from La Plata river Estuary, Argentina. *Environ Monit Assess* 1993;25:119–130.
- Mason CF, Barak NAE. A catchment survey for heavy metals using the eel *Anguilla Anguilla*. *Chemosphere* 1990; 21:43–69. 5:699.
- Mitra B. Mercury in the ecosystem. Switzerland: Transtech. Publications, 1986:377.
- Nicholson MD, Green NW, Whsot SJ. Regression models for assisting trends in cadmium and PCBs in cod livers from Oslofjord. *Mar Pollut Bull* 1991;22:77–82.
- Parlak H, Katalay B, Buylakisik B. Accumulation and loss of chromium by mussels *M. galloprovincialis*. *Bull Environ Contam Toxicol* 1999; 62:286–292 and references cited in.
- Schriver DF, Atkins PW, Longford CH. Inorganic chemistry, 2nd ed. Oxford University Press, 1994.
- Schuhmacher M, Domingo JL, Corbella J, Bosque MA. Heavy metals in marine species from the Terragona Coast, Spain. *J Environ Sci Health A* 1992; 27:7:1939–1948, and references therein.
- Sharif AKM, Mustafa AL, Minrza AM, Saifullah S. Trace metals in tropical marine fish from the Bay of Bengal. *Sci Total Environ* 1991;107:135–192.
- Vas P, Gordon JDM. Trace metals in deep-sea sharks from the rockall trough. *Mar Pollut Bull* 1993;26:7:400–402.
- Vinikour WS, Goldstein RM, Anderson ARV. Bioconcentration patterns of zinc, copper, cadmium and lead in selected fish species from the Fox River, Illinois. *Bull Environ Contam Toxicol* 1980;25:727–734.
- Zia S, Khan MAA. Copper uptake and regulation in a copper-tolerant Decapod *Cambarus bartoni* Fabricius. *Decapoda, Crustacea*. *Bull Environ Contam Toxicol* 1989;. 42:103–110.

Trace Metals in *Lethrinus lentjan* Fish from the Arabian Gulf (Ras Al-Khaimah, United Arab Emirates): Metal Accumulation in Kidney and Heart Tissues

M. H. Al-Yousuf,¹ M. S. El-Shahawi²

¹ Desert and Marine Environment Research Center, United Arab Emirates University, Post Office Box 17777, Al-Ain, United Arab Emirates

² Department of Chemistry, Faculty of Science at Damietta, Mansoura University, New Damietta, Damietta, Egypt

Received: 17 March 1998/Accepted: 21 December 1998

The environment of the Arabian Gulf region has been a subject of study in recent years due to the accidental oil spills in 1991, the uncontrolled discharge of the sewage and industrial waste waters as well as human activities. Thus, several papers have indicated the possible extent of heavy metal build up or accumulation in marine organisms taken from Red Sea and Arabian Gulf (Kureishy 1993 and Al-Ghais 1995). Monitoring systems are essential to track longexisting pollution processes (Dassenakis *et al.* 1996) but the lack of them in many regions (Arabian Gulf region) make it difficult to draw certain conclusions about the long term results of human activities.

The Arabian Gulf is set in an extremely arid region of the world where the circular pattern of the water is counter-clockwise and it 2-4 years to turnover. Thus, in the present communication, the levels of the nonessential elements Pb and Cd in the kidney and heart tissues of *Lethrinus lentjan* fish was examined after the long term environmental effects of the 1991 Gulf War to determine whether these levels constitute a health hazard to consumers. The contents of these elements in marine fishes are often used as indicators of marine pollutants in addition to monitor the source points and site of dumping ground (Kendrick *et al.* 1992).

MATERIALS AND METHODS

Fish samples of both sex of *Lethrinus lentjan* fish were collected from the Arabian Gulf at Ras Al-Khaimah District (Western Coast) of the United Arab Emirates (Figure 1). The fish samples were collected randomly in the months of April, May and June 1993 at an interval of two weeks. Each time about 25-30 fishes of varying sizes were collected, placed in an ice box, transported to the

laboratory and kept in a freezer at -20°C prior to the analysis. At the time of metal analysis

Correspondence to: M. S. El-Shahawi

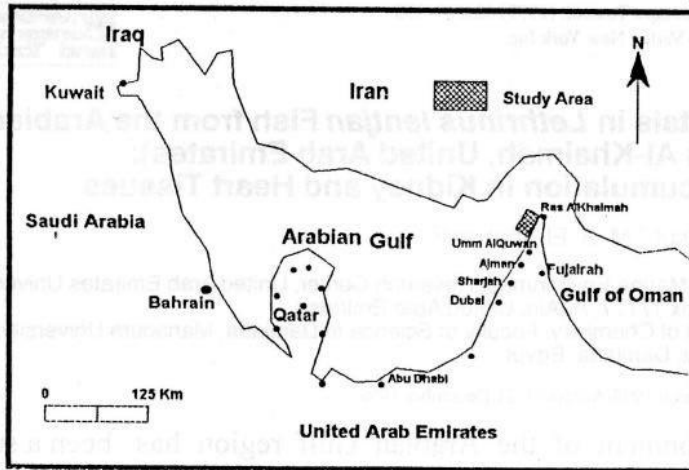


Figure 1. Sample stations where *Lethrinus lentjan* fish were collected along the United Arab Emirates coast on the Arabian Gulf.

the fish samples were defrosted and their standard length and weight were recorded. The tissues (kidney or heart) to be analyzed were separated and grounded with stainless steel kits and glass equipment. Each sample analyzed was composed of several individuals at least 6-8 of fish tissues (kidney or heart) pooled together.

Destruction of organic matter of samples was carried out by wet digestion (Mason and Barak 1990). The procedure supplied was as follows: exactly 4-5 gm of lyophilized (defrosted) sample weights were placed in 50 ml Erlenmeyer flask and 10 ml of concentrated HNO₃ added. After 15 min predigestion at room temperature, 10 ml mixture of concentrated HNO₃-HClO₄ (4:1 v/v) was added and the reaction was maintained on a hot plate stabilized at 70±5°C for 24 hrs with gentle shaking until the digestion was completed. The resulting solid residue was finally redissolved with deionized distilled water and transferred to 25 ml measuring flask and diluted with deionized water to the mark. For each series of 10 samples two blanks were run to check the possible contamination. The digestion procedures were applied to standards (the quality control samples) of Cu, Zn, Mn, Co, Ni, Pb and Cd concentrations. The results obtained showed no losses of any metal occurred and the recovery percentage of the tested metals were found 99±2.62% under the experimental conditions. A double beam GBC 906 flame atomic absorption and GBC Graphite furnace

spectrometers with fuel-rich equipped with background corrector, autosampler, recorder and air-acetylene flames were used. Air was supplied through Pu 9003 air compressor fitted with filter and regulator, moisture trap and oil free pump. Acetylene was delivered after passing through concentrated H₂S O₄ for purification.

RESULTS AND DISCUSSION

The results of trace metal analysis (mean ppm wet weight) in kidney tissues of *Lethrinus lentjan* fish are summarized in Table (1). The data indicated that, the accumulation pattern of the tested elements follows the order : Zn > Cu > Pb > Ni > Co > Mn > Cd. The high accumulation of Zn (43.26 ± 16.87 ppm) wet weight could certainly be based on specific metabolism process and coenzyme catalyzed reactions involving zinc taking place in kidney (Jaffar and Pervaiz, 1989). Zinc also acts as a catalyst in metal biomolecules bound to amino acid side chains containing N, O and/or sulfur donor legends (Vinikour *et al.* , 1980 and Kendrick *et al.* , 1992) to form tetrahedral zinc metalloproteins and metalloenzymes in kidney tissues (Shiver *et al.*, 1994). These data do not differ significantly with *Lethrinus nebuloses* and *Lethrinus mahsenoids* fish species of the same family in the same organ as reported (Kureishy, 1993).

The mean Cd (0.30±0.14 ppm) concentration was low in kidney tissues (Table 1). Cadmium species have low tendency towards the available active sites (N and/or O donor atoms) in kidney tissues to form tetrahedral or square planer cadmium(II) complex species (Schriver *et al.*, 1994). The complex species of Cd are kinetically inert to ligand substitution and therefore its accumulation as metalloprotein complexes is expected to low. However, the binding rate of sulphurhydryl groups, feeding habits, excretion rate, solubility of Cd species, the restricted relocations of different elements and the available number of coordinating sites in the fish kidney to form stable cadmium chelates are possible participating factors accounting for such behavior (Jaffar and Pervaiz, 1989 and Kendrick *et al.*, 1992).

Cadmium levels reported in this study (Table 1) were found within the ranges reported by other investigators (Sharif *et al.*, 1993 and Wood and Van Vleet , 1996). The mean concentration of lead (2.48±1.45 ppm) in kidney was found high as compared to cadmium (0.30 ± 0.14 ppm). Kidney cadmium and lead concentrations were positively

Table 1. Total heavy metal concentrations (mean ppm wet weight) in pooled kidney and heart tissues of *Lethrinus lentjan* fish of the Arabian Gulf region. (x) represents the average of five measurements.

Element	Kidney (x)	Std. Dev.	Std. Error	Heart (x)	Std. Dev.	Std. Error
C u	3.25	1.53	0.22	3.87	1.26	0.18
Zn	43.26	16.87	2.46	32.38	10.19	1.47
M n	0.64	0.24	0.04	0.31	0.17	0.03
Co	1.23	0.22	0.08	1.67	0.50	0.12
Ni	1.58	0.47	0.13	1.58	0.45	0.12
Pb	2.48	1.45	0.3 1	3.22	1.94	0.35
Cd	0.30	0.14	0.02	0.34	0.23	0.04

correlated with liver cadmium and lead concentrations indicating that both organs act as storage sites for both metals. Many explanations have been offered for this trend in kidney (Table 1). The metallothionein protein is ubiquitous and is in highest concentration in fish kidney (Amdur, 1991), and it is able to form stable chelates with lead as compared to cadmium. The solubility of lead species in natural water in the area of fish catching is also a factor in the observed trend. The excretion rate of lead is rapid and it has greater tendency to bioaccumulate in the nucleus at an early stage of fish growth as reported by Sharif *et al.* (1993); this behaviour is not common for cadmium. In fish, cadmium is also less regulated and it can enter fish through food chains as solid granules (organometallic) which are then stored or excreted. Translocations of metal among tissues and fish habitats may also account for such behavior (Amdur, 1991).

Lead and cadmium levels in kidney of the examined samples were ranged from 2.28 ppm to 2.62 ppm and 0.28 ppm to 0.34 ppm, respectively on wet weight basis. Concentrations close to this value have been reported for tropical species from other areas of the world (Babji *et al.*, 1979). Considering the conversion factor of 4.8-5.0 for fresh weight and taking 6-10 g of fish as the maximum consumption per person per day in coastal areas of United Arab Emirates, the average intakes of lead and cadmium through fish will be in the range 10.98 - 18.30 mg g⁻¹ and 1.80-3.00 mg g⁻¹, respectively. These values of lead and cadmium are well below the provincial tolerable intake by human beings of total lead (7

mg Kg⁻¹ body wt. day⁻¹) and cadmium (1-1.2 mg Kg⁻¹) (FAO/WHO, 1972-1987). Thus, the results positively indicate that the marine fishes from the Arabian Gulf are comparatively clean and unpolluted.

Copper, manganese, cobalt, nickel levels in kidney tissues (Table 1) reported in this study were significantly lower or within the ranges reported by other researchers (Sharif *et al.*, 1991, 1993 and Kureishy, 1993) and followed previously reported trends: Zn>Cu>Ni>Co>Mn. Significantly higher copper concentrations 13.25±1.53 ppm, have also been observed. This appears to be a result of fish kidney contain a cystine rich copper binding protein, which in thought to have either a detoxifying or storage function (Luckey and Venugopal, 1977).

Table 1 summarizes data on trace metals Zn, Cu, Mn, Ni, Co, Cd and Pb in the heart tissues of *Lethrinus lentjan* fish. The data indicated that the mean concentration of the tested elements in the heart tissues followed the order : Zn > Cu > Pb > Co > Ni > Cd > Mn. The higher accumulation of Zn (32.38±10.19 ppm) is possibly attributed to the fact that zinc is a bioessential element, so the fish tissues maintain the concentration within a specific range by homeostasis (Falconer *et al.*,

1983). These data are in good agreement with the results reported by Law *et al.*, (1991) for Zn (22.19-42.49 ppm) in the heart tissues in common fish. The reason for this behaviour in the heart tissues could be based on specific metabolism process, a cystine-rich copper binding protein and enzyme catalyzed reactions involving Zn and Cu taking place in the heart tissues of *Lethrinus lentjan* fish.

In the heart tissues the distribution of Pb (3.22±1.44 ppm) was found high as compared to Cd (0.34±0.23 ppm). Thus, the heart of *Lethrinus lentjan* fish accumulated more Pb than Cd. The prevalence of lead as compared to cadmium in the heart tissues is attributed to the ability of lead to form stable chelates with the available binding sites than cadmium. The potential surface of lead contamination to *Lethrinus lentjan* fish is also diet. Manganese contents showed a minimum level in the heart. This content was found to be lower than the corresponding value reported by Kureishy, 1993. The zinc, cobalt, nickel and copper content agreed well with the data reported by Kureishy, 1993 for *Lethrinus lentjan* fish in the same region. These data again positively indicate that the marine fishes from the Arabian Gulf are comparatively clean and unpolluted.

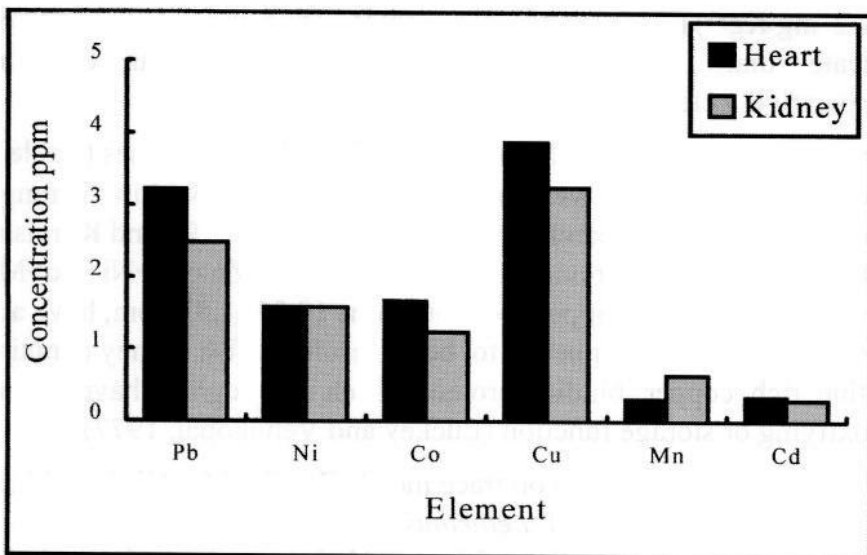


Figure 2. Uptake (mean ppm wet weight) of the trace metals Pb, Ni, Co, Cu, Mn and Cd by the heart and kidney tissues of *Lethrinus lentjan* fish. Data represent an average of five experiments of 25-30 fish pooled in each experiments.

Figure 2 and Table 1 show a comparison of the mean concentrations of the tested elements in kidney and heart tissues. The average lead (3.22 ± 1.94 ppm), nickel (1.58 ± 0.45 ppm), cobalt (1.67 ± 0.50 ppm), copper (3.87 ± 1.26 ppm) and cadmium (0.34 ± 0.23 ppm) concentrations were found high in the heart tissues whereas zinc and manganese levels were found high in kidney (Table 1). The prevalence of Pb as compared to Cd in both fish organs appears to be a result of the initial increase in lead during the first year of life followed by maintenance of a fairly constant concentration throughout the life span of the fish (Vinikour *et al.*; 1980 and Windson *et al.*; 1987). Similarly, significant increase in zinc (43.26 ± 16.83 ppm) and manganese (0.64 ± 0.24 ppm) in kidney were found high as compared to zinc (32.38 ± 10.19 ppm) and manganese (0.31 ± 0.17 ppm) in heart tissues, respectively. Similar distribution patterns of heavy metal accumulation have been reported in marine mammals and sea-birds reported by other researchers and followed previously reported trends with mean metal concentrations decreasing in the order heart > kidney for all elements except zinc and manganese (Sharif *et al.*, 1991, 1993 and Wood and Van Vleet, 1996).

Acknowledgments. We thank Prof. A. S. Al-Sharhan, Dean of the Faculty of Science, UAE University, for the facilities provided and Dr. S. Ahamed for his help in analyzing the samples.

REFERENCES

- Al-Ghais SM (1995) Heavy metal concentrations in the tissues of *sparm sarba forskal*, 1775 from the United Arab Emirates. Bull Environ Contam Toxicol 55 : 581-587.
- Amdur MO, Doull J, Klaassen CD (1991) The basic science of poisons, 4th ed. Pergamon press.
- Babji AS, Embong MS, Wood WW (1979) Heavy metals contents in coastal water fishes of west, Malaysia Bull Environ Contam Toxicol 23 : 830-837.
- Dassenakis MI, Kloukinotou MA, Paylidou AS (1996) The influence of long existing pollution on trace metal levels in a small tidal Mediterranean Bay. Mar Pollut Bull 32 : 275-282.
- Falconer CR, Davies IM, Topping G (1983) Trace metals in the common porpoise phocoena. Mar Environ Res 8 : 119-127.
- FAO/WHO. Joint FAO/WHO Expert Committee on Food Additives 1972-1987, Reports 505, 631, 683, 696 and 751, World Health Organization, Geneva.
- Jaffar J, Pervaiz S (1989) Investigation of multiorgan heavy trace metal content of meat of selected dairy, poultry, fowl and fish species. Pakistan J Sci Indust Res 32 : 175-177.
- Kendrick MH, Moy MT, Plishka MJ, Robinson KD (1992) Metals and biological systems. Ellis Horwood Ltd., England.
- Kureishy TW (1993) Contamination of heavy metals in marine organisms around Qatar before and after the Gulf War oil spill. Mar Pollut Bull 27 : 183-186.
- Law RJ, Fileman CF, Hopkins AD, Baker JR, Harwood J, Jackson DB, Kennedy S, Martin AR, Morris RJ (1991) Concentrations of trace metals in the livers of marine mammals (seals, porpoises and dolphins) from water around the British Isles. Mar Pollut Bull 22 : 183-191.

- Luckey TD, Venugopal IB (1977) Metal toxicity in mammals. Volume 1: Physiologic and chemical basis for metal toxicity. Plenum Press, New York, USA.
- Mason CF, Barak NA (1990) A catchment survey for heavy metals using the eel (*Anguilla Anguilla*). Chemosphere 21 : 695-699.
- Sharif AKM, Mustafa AI, Hossain MA, Amin MN, Saifullah S (1993) Lead and cadmium contents in ten species of tropical marine fish from the bay of Bengal. Sci Tot Environ 133 : 193-199.
- Shriver DF, Atkins PW, Longford CH (1994) Inorganic chemistry. Second edition, Oxford University Press.
- Vinikour WS, Goldstein RM, Anderson RV (1980) Bioconcentration patterns of zinc, copper, cadmium and lead in selected fish species from the Fox river, Illinois. Bull Environ Contam Toxicol 25 : 727734.
- Wood CM, Van Vleet ES (1996) Copper, cadmium and zinc in liver, kidney and muscle tissues of Bottlenose Dolphins (*Tursiops truncatus*) stranded in Florida. Mar Pollut Bull 32 : 886-889.

Differential Pulse Polarographic Analysis of Chlorpyrifos Insecticide

A.S.R. Al-Meqbali,^b M.S. El-Shahawi,^b and M.M. Kamal^{a,*b,bb}

Chemistry Department, Faculty of Science, UAE University, P.O. Box 17551, Al-Ain, United Arab Emirates ^{pp}

Permanent address: Chemistry Department, Faculty of Science, Assiut University, Assiut, Egypt

Received: January 16, 1998

Final version: April 28, 1998

Abstract

The differential pulse polarographic (DPP) behavior of chlorpyrifos (CP) was investigated over a wider range of pH (pH 1.8–pH 10.1). CP compound displays a well-resolved cathodic reduction peak at 1.2 V (vs. Ag/AgCl) (pH 3.2). This peak probably corresponds to the reduction of the C=N-centre of the pyridyl moiety. The effect of solution and operational parameters on the sensitivity of the DPP peak was carefully examined in order to select the optimum conditions for determination of the CP compound. Under the optimum conditions the reduction response gives a linear calibration plot over a concentration range of 9.70×10^{-7} – 6.92×10^{-6} M and the detection limit was found to be 8.7×10^{-7} M. The effects of some diverse metal ions, anions and some other organophosphorus insecticides on the determination of CP compound were studied. The applicability of DPP for determination of the CP insecticide in commercial samples as well as in some irrigation water (treated wastewater and underground water) was detected.

Keywords: Differential pulse polarography, Chlorpyrifos, Irrigation water

1. Introduction

Chlorpyrifos is a member of the organophosphorus class of insecticides. This class of insecticides has become one of the most widely used groups of pest control chemicals. Early organophosphorus compounds were found to be efficacious for insect control and thus brought into widespread use, e.g., chlorpyrifos, parathion and malathion. Spectrophotometric, GC, HPLC and polarographic techniques have been used for determination of a number of organophosphorus pesticides [1–6]. Spectrophotometric and enzymatic methods have been used for determination of chlorpyrifos in apples [7]. Also, first derivative and kinetic spectrophotometric methods were applied for determination of chlorpyrifos and some other organophosphorus pesticides [8]. Electrochemical methods, e.g., polarography and voltammetry have been applied for determination of some pesticides in soil and water [9–11]. But no work has been reported in the literature dealing with polarographic behavior as well as the polarographic determination of the title compound.

This article includes the differential pulse polarographic behavior of CP insecticide and its reduction mechanism at the DME. A differential pulse polarographic procedure for determination of the CP compound in pure and commercial samples as well as in some irrigation waters is included.

2. Experimental

2.1. Reagent and Materials

All reagents and chemicals used were of analytical reagent grade. Universal Britton-Robinson buffer solutions prepared by neutralization of equal molar mixture (0.04 M) of phosphoric, boric, and acetic acids with 0.2 M NaOH to provide 1.8–12 pH range.

1×10^{-2} M solution of metal ions were prepared by dissolving the appropriate amount of metal nitrate in double distilled water. Also, 1×10^{-2} M solution of various anions were prepared by dissolving the required weight of sodium salts in a definite volume of double distilled water. Series of the dilute solutions were prepared diluting a specific volume of the stock solution with water.

1×10^{-3} M solution of the chlorpyrifos [*o,o*-diethyl-*o*-(3,5,6-trichloro-2-pyridyl)phosphorothioate] was prepared by dissolving an appropriate amount of the solid pure reagent in absolute ethanol. 1×10^{-3} M solutions of the organophosphorus malathion and diazinon insecticides were prepared in ethanol.

2.2. Instrumentation

Differential pulse polarograms were obtained with a PAR 264A polarographic and voltammetric analyzer connected with a PAR 303A mercury electrode. The three electrode assembly consisted of a DME as a working electrode, a saturated Ag/AgCl reference electrode, and a platinum wire auxiliary electrode. All experiments were performed at 22.618°C, pulse amplitude of 50 mV, 1 s drop time, and 5 mV/s scan rate (unless otherwise stated). pH measurements were made with a Metrohm 632 digital pH-meter.

2.3. Procedures

10 mL of the blank solution (buffer solution containing 25% ethanol) was placed in the polarographic cell. The solution was purged with nitrogen for 16 min. The differential pulse polarogram for the blank solution was recorded at 1 s drop time, 50 mV pulse amplitude, 0.4 V starting potential, and 5 mV/s scan rate (unless otherwise stated). The 0.50 or 0.05 mL of the stock solution of the tested compound was added, 60–120 s deoxygenation was carried out using purified nitrogen gas, then the differential pulse polarogram of the tested compound was recorded under the above mentioned conditions.

3. Results and Discussion

The differential pulse polarographic behavior of the investigated compound was recorded in solutions of varying pH (Fig. 1). It shows a cathodic peak located at relatively high negative electrode potential. The cathodic peak is due to the electroreduction of the azomethine centre ($\text{C}=\text{N}$) of the pyridine ring. This was confirmed by the low temperature coefficient (0.02 mA deg^{-1}) which is typical

of this type of the process. Moreover, the possibility that the peak represents a hydrogen-evolution catalytic process was ruled out based on the same argument [12, 13]. Similar behavior has been reported for quinoline [14], pyrimidine [15], and purine [16] compounds. According to the general mechanism established for Differential Pulse Polarographic Analysis of Chlorpyrifos Insecticide

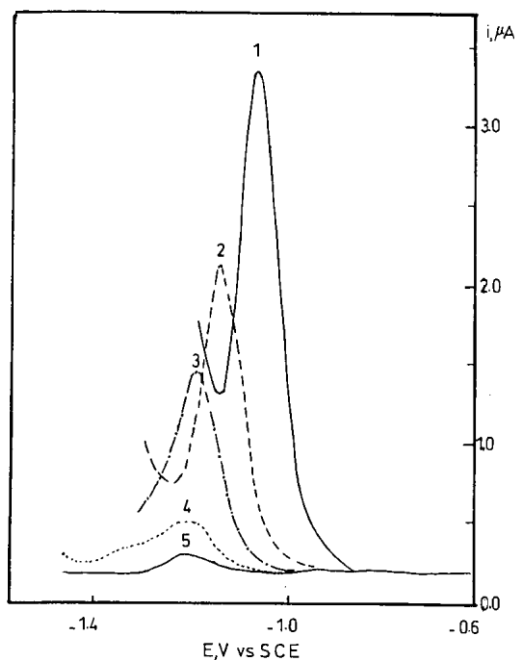


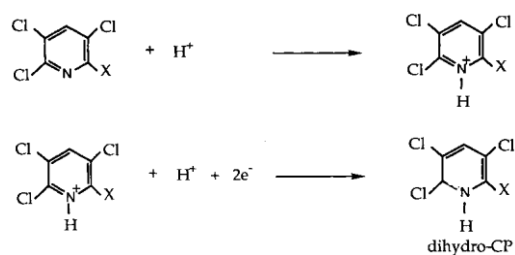
Fig. 1. Effect of pH on the DPP behavior of 5×10^{-5} mol/L CP. 1) pH 2.2, 2) pH 3.2, 3) pH 4.1, 4) pH 5.1 and 5) pH 7.2.

such *N*-heterocyclic compounds [17, 18], the $\text{C}=\text{N}$ of the heterocyclic system undergoes in acid to neutral media a totally irreversible electrode reaction with a total uptake of $2e^-/2H^+$.

The determination of a compound characterized with a DPP peak very close to the background discharge is difficult. It is important to select operational and solution conditions to give a well-resolved cathodic reduction peak from the background discharge as well as giving most sensitive DPP peak. Under the optimum operational conditions (pulse amplitude, scan rate, and drop time) and solution conditions (pH, ionic strength, nature of supporting electrolyte, and percentage of ethanol) CP compound will be determined to very low concentrations. Also, the application of the DPP technique for determination of CP in some environmental samples may be possible under the optimum selected experimental conditions.

3.1. Dependence of the DPP Peak of Chlorpyrifos on the Solution and Operational Conditions

In universal buffer solution containing 25% (v/v) ethanol the differential pulse currents of CP recorded as a function of potential are shown in Figure 1. DPP current voltage curves of the investigated compound in acid and neutral media (pH#7.2) show a well-developed reduction peak corresponding to the reduction of $\text{C}=\text{N}$ centre of the pyridine ring via $2e^-/2H^+$ mechanisms (Scheme 1). Under various conditions the pyridine moiety was found polarographically inactive. However, in the investigated compound (CP) the mesomeric effect of the three



Scheme 1.

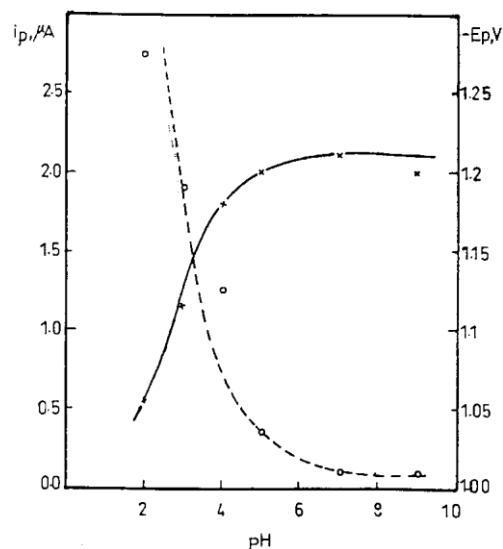


Fig. 2. Dependence of the peak height (a) and peak potential (b) of the DPP peak of 5×10^{-5} mol/L CP on the pH.

chlorine atoms attached to the pyridine moiety increases the localization of the electrons in the pyridine system and consequently enhance the reducibility of the $\text{C}=\text{N}$ centre.

Figure 2 shows the dependence of peak height and peak potential of the DPP peak of the CP compound on the pH of the blank solution. The DPP shifts to more negative potentials with increasing the pH showing a remarkable change at around pH 5, the reported pK_a of the CP compound was 5.1 [19]. The maximum sensitivity and response peak current was found at pH 2.2 compared to other pH's. The inconsistency of the reduction peak current in the more acidic buffer solutions (pH < 2.2) is explained by the effect of strong hydrogen evolution and the peak being completely overlapped by the background discharge. As the pH approaches the moderately acidic and neutral range the reduction response decreases analogously to an acid dissociation curve (Fig. 2) because the protonation kinetics under these circumstances contribute progressively to the control of the overall rate of the reduction [17, 18]. Therefore, it can be concluded that pH 2.2 is the optimum pH for the determination of the investigated compound using DPP at the DME.

The effect of many solution parameters on the DPP peak of CP compound were studied at pH 2.2. It was found that the buffered pH 2.2 solution containing 0.025M NaNO_3 and 25% ethanol is the optimum media for CP determination. However, the unbuffered media, e.g., H_2SO_4 , HNO_3 and CH_3COOH (1×10^{-2} mol/L) containing Na_2SO_4 or CH_3COOH gave a less sensitive reduction peak. Also, at a lower or higher percentage of ethanol than 25% lowering of the peak response was observed.

At the optimum solution conditions for CP determination, the effects of pulse amplitude, scan rate, and the drop time on the DPP response of the CP compound were carefully examined. It was found

that a pulse amplitude of 50mV, scan rate of 2mV/s and 1.0s drop time were the optimum conditions for CP determination.

3.2. Quantitative Determination of Chlorpyrifos Insecticide by DPP

The optimum conditions for the analytical determination of the investigated compound by DPP were found to be pH 2.2 in the presence of (0.025M) NaNO₃ and 25% (v/v) ethanol, 258C, 50mV pulse amplitude, 2mV s⁻¹ scan rate and drop time 1s. The DP polarograms of various concentrations (9.7×10¹⁷–6.92×10¹⁶M) of CP under the above-mentioned condition were recorded and the

Electroanalysis **1998**, 10, No. 11

786

variation of the peak height of DPP response with the concentration of CP was linear. The result of the calibration straight line was subjected to the least square refinement. It was found that the straight line had regression coefficient (*r*²) 0.995, slope 9.4×10¹⁴mA/M and an intercept of 0.00560.002mA. The results of five replicated measurements of the peak height of the DPP peak corresponding to 2.5×10¹⁶M concentration of chlorpyrifos revealed that the relative standard deviation (RSD) was 4.7%. It should be mentioned that, under the optimum conditions for determination of CP using DPP the detection limit was found to be 8.7×10¹⁷M.

3.3. Influence of Diverse Species on the DPP Determination of Chlorpyrifos

Determination of CP compound in irrigation water was one of our interesting goals. Therefore, the influence of some cationic and anionic species which are commonly present in irrigation water on the DPP determination of CP was carefully examined. The effects of some other pesticides were considered.

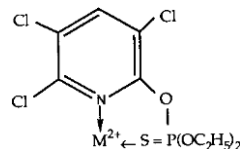
Interference studies were carried out with various cations, some are polarographically active, e.g., Cu(II), Cd(II), Pb(II), Zn(II) and Cr(VI) and some polarographically inactive, e.g., Ca^{2b}, and Mg^{2b}. The effect of different anions which are more likely present in irrigation water, e.g., NO₃⁻, SO₄⁻, CO₃⁻, Cl⁻, Cr₂O₇⁻, I⁻ and F⁻ were also investigated.

Under the optimum conditions for CP determination Cu(II), Pb(II) and Cd(II) exhibited a cathodic reduction DPP peaks located at less negative potentials compared to the peak potential of CP peak. These results indicate that the DPP peak of the abovementioned metal ions did not overlap the CP peak. The degree of recovery of 5×10¹⁵M/L of CP, in presence of 1×10¹⁵M of these metal ions was 92.664.1%, however, the degree of recovery markedly decreased in the presence of 1×10¹⁴M/L of these metal ions (83.565%). The DPP behavior of Zn(II) and Cr(VI) displayed a cathodic reduction peaks at potentials very close to the DP peak and overlapped to some extent with the DPP response of the CP compound. The degree of recovery of 5×10¹⁵M of CP, in presence of 1×10¹⁵M Zn(II) and Cr(VI) was 87.362.7%.

The decrease in the peak height of the CP compound in the presence of the tested metal ions could be explained by the tendency of CP compound to form six membered ring chelates via the nitrogen and sulfur atom. The metal ion complex has a lower diffusion coefficient relative to the free CP compound and consequently it exhibits a less DPP current (Scheme 2). Ca^{2b} and Mg^{2b} are not polarographically active and they have no tendency to form a metal ion CP complexes. Therefore, both of these metal ions slightly affect the peak height of the CP peak. The degree of recovery of

5×10¹⁵mol/L of CP, in presence of both of these metal ions was almost 100%.

The effect of various interfering anions (CO₃⁻, NO₃⁻, SO₄⁻, Cr₂O₇⁻, I⁻, Cl⁻ and F⁻) on the DPP behavior of 5×10¹⁵M of CP compound under the optimum conditions was checked. Some of these anions, e.g., NO₃⁻, CO₃⁻ and SO₄⁻ had no effect on the DPP current of CP and the height of the DPP peak was almost constant. In presence of relatively higher concentration of I⁻, Cl⁻ and F⁻



Scheme2. Structure of the possible CP-metal ion complex.

Electroanalysis **1998**, 10, No. 11

A.S.R. Al-Meqbali et al.

(1×10¹⁴M) the peak height decreased to some extent and consequently the degree of recoveries of CP compound were found to be 92.164.5%. However, in presence of Cr₂O₇⁻ the peak of the CP compound height increases markedly. It was found that dichromate ion, Cr₂O₇⁻, displayed a DPP peak at the same potential limits of the CP peak.

3.4. Influence of Malathion and Diazinon Pesticides on the DPP Behaviour of Chlorpyrifos

The DPP behavior of 5×10¹⁵M of CP was investigated in the presence of various concentrations (1×10¹⁴–5×10¹⁵M) malathion and diazinon. The latter compounds were polarographically inactive and consequently did not show any differential pulse current. It was found that neither of the compounds interfered with the DPP behavior of CP and the degree of recovery of the DPP current of 5×10¹⁶M of CP was 100% in presence of malathion and/or diazinon pesticides.

3.5. Applications of the DPP for Trace Determination of Chlorpyrifos

The DPP method was applied for analytical determination of the CP compound in a commercial formulation. The data sheet of the commercial sample stated that the stock liquid solution contains 48% w/w of chlorpyrifos. A 1×10¹³M solution of the commercial sample was prepared by dissolving the appropriate weight of the commercial liquid in absolute ethanol. A 5×10¹⁶M solution from the latter solution gave a well-defined DPP peak. Comparison of the peak height with the calibration plot indicated that the degree of recovery of the CP in the commercial concentration was 96.60 60.12%.

The analytical determination of CP compound in some water samples, e.g., tap, treated waste, and underground water was also examined. The degree of recoveries of the 1×10¹⁵mol/L of the pure CP compound prepared in the various water types containing 25% ethanol were 99.760.4%, 97.360.6% and 101.060.1% for tap water, underground water, and treated waste water, respectively.

4. References

- [1] E.R. Clark, I.A. Quazi, *Analyst* **1990**, 105, 564.

-
- [2] S. Derek Farrington, F.J. Lovett, P.V. Lynch, *Analyst* **1993**, 108, 353.
- [3] F.A. Gunther, Y. Iwater, B. Berck, G.V. Smith, *Bull. Environ. Cont. Toxicology* **1986**, 24, 903.
- [4] S. Josephi, *Anal. Chem.* **1991**, 63, 118 R.
- [5] S. Josephi, *Anal. Chem.* **1995**, 67, 1 R.
- [6] N.Y. Sreedhar, P. Rajendra Kumar Reddy, G.V. Subba Reddy, S.J. Reddy, *Talanta* **1997**, 44, 1859.
- [7] A.N. Diaz, F.G. Sanchez, V.B. Derlrio, *Anal. Lett.* **1995**, 26, 1071.
- [8] M.M. Galera, J.L.M. Vidal, A.G. Frenich, *Anal. Lett.* **1994**, 27, 807.
- [9] P. Carrai, L. Nucci, F. Pergola, *Anal. Lett.* **1992**, 25, 63.
- [10] A. Galvez, M. Pedrero, F.J.M. de Villena, J.M. Pingarron, L.M. Polo, *Anal. Chim. Acta* **1993**, 273, 349.
- [11] F. Mezzzi, F. Botre, G. Lorenti, G. Simonetti, F. Porcelli, G. Scibona, C. Botre, *Anal. Chim. Acta* **1995**, 316, 79.
- [12] S.G. Mairanouskii, *Catalytic and Kinetic Wave Polarography*, Plenum Press, New York **1968**.
- [13] M.S. Ibrahim, *Collect. Czech. Chem. Commun.* **1994**, 59, 1472.
- [14] M.M. Kamal, A.A.M. Aly, Y.M. Temerk, *Annal. Chim.* **1989**, 79, 97.
- [15] Y.M. Temerk, P. Valenta, H.W. Nurnberg, *J. Electroanal. Chem.* **1979**, 100, 77.
- [16] M.M. Kamal, *Electroanalysis* **1992**, 4, 553.
- [17] B. Janik, P.J. Elving, *J. Electrochem. Soc.* **1969**, 116, 1087.
- [18] B. Janik, P.J. Elving, *Chem. Rev.* **1968**, 68, 295.
- [19] M.H. Saleh, *M.Sc. Thesis*, University of The United Arab Emirates, Environmental Science Programme **1996**.

M. S. El-Shahawi · M. M. Kamal

Determination of the pesticide Chlorpyrifos by cathodic adsorptive stripping voltammetry

Received: 10 July 1997 / Revised: 1 April 1998 / Accepted: 6 April 1998

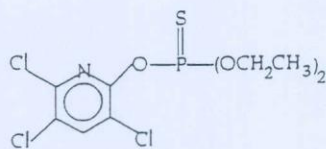
Abstract The adsorption behavior and differential pulse cathodic adsorptive stripping voltammetry of the pesticide Chlorpyrifos (CP) were investigated at the hanging mercury drop electrode (HMDE). The pesticide was accumulated at the HMDE and a well-defined stripping peak was obtained at -1.2 V vs Ag/AgCl electrode at pH 7.50. A voltammetric procedure was developed for the trace determination of Chlorpyrifos using differential pulse cathodic adsorptive stripping voltammetry (DP-CASV). The optimum working conditions for the determination of the compound were established. The peak current was linear over the concentration range 9.90×10^{-8} – 5.96×10^{-7} mol/L of Chlorpyrifos. The influence of diverse ions and some other pesticides was investigated. The analysis of Chlorpyrifos in commercial formulations and treated waste water was carried out satisfactorily

Introduction

By the activities of modern industries and agriculture many anthropogenic organic pollutants have found their way into the environment. Therefore, the distribution of insecticides in marine water samples deserves great interest [1]. Organophosphorous pesticides are very important from a toxicological point of view due to their bioaccumulation ability. Chlorpyrifos, *o,o*-diethyl-*o*-(3,5,6-trichloro-2-pyridyl) phosphorothioate (Fig. 1), can be readily absorbed by the mammalian skin, and can cause health risks [2]. Various chromatographic [3–5], spectrometric [6] and electrochemical [7–10] techniques have been used for the determination of insecticides.

Chlorpyrifos was determined in natural waters and soil samples by magnetic particle-based ELISA [11], differential degradation using diode-array spectrophotometry optimized by partial least squares [12], multivariate spectral analysis [13], derivative spectrometry [14], partial least squares (PLS) [15] and ratio spectra methods [16]. The simultaneous determination of

Fig. 1 Structure of the pesticide Chlorpyrifos



M. S. El-Shahawi (✉)
Department of Chemistry, Faculty of Science at Damietta,
Mansoura University, Damietta, Egypt

M. M. Kamal
Department of Chemistry, Faculty of Science,
Assiut University, Assiut, Egypt

the carbamate pesticide carbaryl and a group of organophosphate pesticides including Chlorpyrifos was developed using reversed phase HPLC [17].

To our knowledge there has been no study on the use of adsorptive stripping voltammetric determination of Chlorpyrifos in a commercial formulation [18]. Thus the voltammetric reduction behavior of Chlorpyrifos and the differential pulse cathodic adsorptive stripping voltammetric determination of the aforementioned pesticide in a pesticide formulation, treated waste water and underground water samples were investigated.

Experimental

Apparatus

Differential pulse cathodic adsorptive and cyclic voltammetric measurements were carried out with an EG & G Princeton Applied Research, Model 264A Polarographic Analyzer/Stripping Voltammeter coupled with EG & G PAR model 303A electrode and XY-recorder model MF 8050. A three-electrode electrochemical cell consisting of an Ag/AgCl and platinum wire as reference and counter electrode, respectively, were used. A hanging mercury drop electrode (HMDE) with a surface area of 1.2×10^{-2} cm² was used as working electrode. A pulse amplitude of 50 mV with a scan rate of 10 mV/s for different pulse and a scan rate 100 mV/s for cyclic voltammetry measurements were applied. pH measurements were carried out with a pH meter Metrohm Model 632.

Reagents and chemicals

All chemicals used were of analytical reagent grade. Britton-Robinson (BR) universal buffer solutions containing a mixture of equal amounts (0.08 mol/L) of phosphoric, boric and acetic acids with sodium hydroxide (0.02 mol/L) were applied as supporting electrolyte and to provide the various pH values. The constant final ionic strength ($m = 0.1$) of the test solution was maintained with sodium nitrate solution. A stock solution (1×10^{-4} mol/L) of Chlorpyrifos (technical grade, 98% w/w) abbreviated as CP was made up in ethanol. A series of standard solutions of CP was prepared by diluting the stock solution with distilled water in presence of few drops of ethanol to prevent turbidity.

Recommended procedure

A solution (1–2 mL) of the pesticide (1.00×10^{-6} mol/L) was placed into the voltammetric cell containing 10 mL of the Britton-Robinson buffer (pH = 7.5) as supporting electrolyte containing 30% ethanol (v/v). A stream of purified nitrogen was purged through the cell for 15 min under constant stirring. Differential-pulse cathodic adsorptive stripping voltammetry (DP-CASV) was carried out at an accumulation potential of -0.2 V and an accumulation period of 120 s. After the collection time, the stirring was stopped and after 15 s equilibrium time the voltammogram was recorded by applying a negative potential (-0.20 to 1.70 V) with 10 mV/s scan rate and 50 mV pulse amplitude after recording the background voltammogram of the supporting electrolyte. The CASV was repeated with a new mercury drop after addition of a new sample with a differing concentration of CP.

scan rate 100 mV/s to allocate the Faradaic response and the redox voltammetric behavior of the adsorbed CP species. In CV, the first cycle initiated at -0.2 V showed a dominant small pair of redox peaks at -1.2 V vs Ag/AgCl electrode where the anodic peak is the mirror image of the cathodic one across the potential axis. Subsequent repetitive scans significantly enhanced the growth of redox peaks as sharp and narrow peaks (Fig. 3). After cycling the potential for 5 min the peaks reached a stable state as the cathodic and anodic peak heights became constant. This behavior indicates that the adsorption of the pesticide on the HMDE is not caused by reactant adsorption [23] which agrees with normal pulse polarographic data. The results also reflect the stability of the adsorption layer and the high accumulation of the CP species on the mercury electrode made the pH conditions proposed.

Quantitative trace determination of CP

The applicability of the DP-CASV technique as an analytical method for the trace determination of CP was optimized carefully concerning adsorption starting potential (E_s), pH, pulse amplitude, scan rate, accumulation potential. The optimum conditions for the CP determination were found to be pH 7.56, pulse amplitude 50 mV, scan rate 10 mV/s, accumulation time 120 s and -0.2 V starting accumulation potential.

The effect of replacing the nitrate anion (NO_3^-) as a supporting electrolyte solution (pH 7.5) by various anions such as Cl^- , SO_4^{2-} and ClO_4^- on the DP-CASV voltammogram of 5×10^{-7} mol/L of CP was also examined. A more sensitive and reproducible peak was recorded in the presence of NO_3^- , while in the presence of chloride or sulfate ions the height of peak (II) slightly decreased. This reflected the role of anions of indifferent supporting electrolytes on the degree of adsorption and accumulation of the CP compound at the mercury charged surface.

The height of peak (II) (i_p , mA) increased linearly with the concentration of the CP compound over the concentration range (9.9×10^{-8} – 5.96×10^{-7} mol/L). The variation of i_p (μA) with C ($\mu\text{mol/L}$) was based on the regression equation of the calibration line ($i_p = aC + b$), where a and b are the slope and the intercept of the straight line, respectively. The calibration curve has a slope of ($0.886 \pm 0.042 \mu\text{A}/\mu\text{mol/L}$) and an intercept of $0.047 \pm 0.006 \mu\text{A}$. Chlorpyrifos can therefore be determined using a calibration graph or by standard addition. The validity of the method was supported by the value of the regression coefficient of 0.99. Moreover, the relative standard deviation ($n = 5$) with 4×10^{-7} mol/L Chlorpyrifos at a 95% confidence limit was 1.8%. The lowest measurable concentration under the conditions chosen was found to be $9.90 \times 10^{-8} \mu\text{mol/L}$.

Influence of foreign species

The selectivity of the proposed method for CP was tested in the presence of relatively high concentrations (8×10^{-3} mol/L) of Cr(III), Cd(II), Zn(II), Ni(II), Co(II), Cr(VI), Cu(II), Pb(II), F^- , Br^- and I^- . Only chromium (VI) and copper (II) ions interfered seriously with the procedure proposed. The reduction of chromium (VI) to intermediate oxidation states between V and III at -1.2 V vs Ag/AgCl may be responsible for the interference of chromium (VI) [24]. Interference of copper (II) and lead (II) is attributed to a possible complex formation of these ions with the CP compound via the phosphorothioate group $\text{P}=\text{S}$ and the pyridine nitrogen forming six-membered ring chaletes which are then accumulated at the HMDE surface. Several pesticides present in commercial formulations together with CP has been tested as interferents. Dimethoate and endosulfan were tolerated at a 25:1 (interference: analyte) mol/L: mol/L

and satisfactory recovery percentage (92–102%) of CP was achieved.

Application of the proposed method

The analysis of CP in absence and in presence of other pesticides, e.g. endosulfan and/or carbaryl at concentration 1.0×10^{-5} mol/L in treated waste waters (0.01–0.1 L), have been carried out employing standard addition method (1.0×10^{-7} – 5.96×10^{-7} mol/L). The reduction peak of Chlorpyrifos ($E_p = -1.2$ V vs Ag/AgCl) was not affected by these pesticides because the reduction peak of endosulfan proceeded at a less negative potential ($E_p = -0.42$ vs Ag/AgCl) and carbaryl is electrochemically inactive. A sample of 20 mL of treated waste water was analyzed by the proposed method, no Chlorpyrifos could be detected in the tested samples. To establish the possible matrix effect of water samples, in separate experiments treated waste water samples were spiked with Chlorpyrifos to a final concentration of 2×10^{-7} mol/L and were analyzed employing the procedure recommended. Average recoveries of 90–97% with a precision (RSD) of 4.92% were obtained for the spiked samples. The method was also applied for the determination of CP in commercial formulations after adding 5 mL of ethanol to 10 mL of sample and dilution to 100 mL with distilled water. The recovery of CP was in the range 86–97%.

Conclusion

The feasibility of the proposed method for the trace determination of CP in treated waste water samples by DP-CASV was achieved successfully at the HMDE. The sensitivity of the method can be improved by prior preconcentration of trace amounts of CP from large sample volumes on a polyurethane foam column followed by elution with acetone in a Soxhlet extractor [25] and subsequent determination by the procedure proposed. The method is simple, sensitive and relatively rapid and can be adopted for environmental control. Further work is done to determine CP in plants and in presence of some other pesticides, surfactants and phenolic compounds which can be present in water.

Acknowledgement The authors would like to thank Mr. Ali S. Al-Maqbali for his assistance.

References

- Malisse JRH (1990) Egypt J Anal Chem 1: 49
- Hellawell JM (1988) Environ Pollut 50: 61, Abdo MSE, Al-Ameeri RS (1987) J Environ Sci Health Part A 22: 27
- Sharma J (1988) J Liq Chromatogr 11: 2121
- Marzouk MA, Salem R, El-Ahraf R, Willis VV (1986) Vet Med J 34: 5
- Stan MS (1989) J Chromatogr 467: 85
- Bondoli A, Pala F, Magalini SI (1980) Cah Anesthesiol 28: 595
- Jehring H, Dela Chavellerie-Haaf V, Meyer A, Henze G (1989) Fresenius Z Anal Chem 332: 890
- Pingarron AJ, Pingarron JM, Polo LM (1992) Talanta 39: 899; Reviejo AJ, Santos A, Pingarron JM, Polo LM (1992) Electroanalysis 4: 111
- Kalvoda R, Kopanica M (1989) Pure Appl Chem 61: 97
- Prabu HG, Manisankar P (1994) Analyst 119: 1867; Coomber DC, Tucker DJ, Bond AM (1996) Anal Chem 68: 1267

11. Oubina A, Gascon J, Ferrer I, Barcelo D (1996) *Environ Sci Techn* 30: 509
12. Espinosa-Mansilla A, Salinas F, Zamoro A (1994) *Analyst* 119: 1183
13. Espinosa-Mansilla A, de la Pena AM, Salinas F, Zamoro A (1992) *Anal Chim Acta* 258: 47
14. Martinez-Galera M, Vidal JLM, Frenich AG (1994) *Anal Lett* 47: 807
15. Martinez-Galera M, Vidal JLM, Frenich AG, Vazquez PP (1995) *J Aqac Intern* 78: 423
16. Espinosa-Mansilla A, Salinas F, Zamoro A (1995) *J Agric Food Chem* 43: 146
17. Brayan JC, Haddad PR, Sharp GJ, Dilli S, Demarchelier JM (1988) *J Chromatogr* 447: 249
18. Florence TM (1979) *J Electroanal Chem* 97: 219
19. Ahmed ZA, Ahmed ME, Ibrahim MS, Kamal MM, Temerk YM (1994) *Talanta* 41: 659
20. Nürnberg HW (1960) In: Langmuir IS (ed) *Advances in Polarography*, Vol. 2 Pergamon, London, p 694
21. Kamal MM (1992) *J Electroanalysis Chem* 4: 453
22. Chau ASY, Afghan BK, Robinson JW (1981) *Analysis of Pesticides in Water Vol. II*, CRC press
23. Dong S (1984) *Fenxi Yigi* 1: 1
24. El-Shahawi MS (1986) PhD Thesis, Strathclyde University, Glasgow, U.K.
25. El-Shahawi MS, Kiwan AM, Aldhaheer SM, Saleh MH (1995) *Talanta* 42: 1471

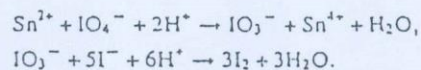
BULLETIN
OF THE
CHEMICAL SOCIETY OF JAPAN

Volume 71, Number 2, February 1998

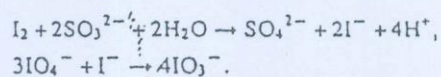
Sequential Titrimetric and Spectrophotometric Determinations of Trace Amounts of Tin(II) and Tin(IV) by Amplification Reactions

M. S. El-Shahawi* and A. Z. A. Zuhri

In an aqueous acidic solution (pH 2.2—3.5) per iodate ions reacted with tin(II), and the released iodate reacted with I^- as follows:



Alternatively, the released iodine was extracted into chloroform and reduced with sodium sulfite and the produced I^- was reacted with IO_4^- as follow:



Bull. Chem. Soc. Jpn., 71 (1998)
1—0000

These reactions were used for titrimetric and spectrophotometric determinations of tin(II).

Sequential Titrimetric and Spectrophotometric Determinations of Trace Amounts of Tin(II) and Tin(IV) by Amplification Reactions

Mohammed S. El-Shahawi,* and Ali Z. Abu Zuhri†

Department of Chemistry, Faculty of Science at Damiatta, Mansoura University, Damiatta, Egypt

†Department of Chemistry, Faculty of Science, Al-Najah National University, Nablus, West Bank, Jordan

(Received July 7, 1997)

Two simple and accurate titrimetric and spectrophotometric methods have been developed for the determination of tin. The methods were based upon the oxidation of tin to tetravalent tin with sodium periodate at pH 2.2–3.5; excess periodate ions were then masked with 5% sodium molybdate at the same pH. The released iodate ions were determined spectrophotometry (at 350 nm) as triiodide after the addition of KI. This proposed procedure offered a six-fold amplification for each tin(II) ion. Alternatively, the released iodine was extracted with chloroform and shaken with an aqueous solution of 1% (w/v) sodium sulfite. The iodide ions produced in the aqueous phase were then oxidized with sodium periodate after removing the unreacted sodium sulfite by boiling with H₂SO₄ (2 M). The released iodate was finally determined by iodometry or spectrophotometry. This procedure offered 144-fold amplification per tin(II) ion. The determination of tin(IV) after prior reduction to tin(II) with sulfur dioxide was also found to be suitable. Analyses of the binary mixtures of tin(II)–tin(IV) in an aqueous solution, tin in organotin compounds and tin(II) and tin(IV) in artificial sea-waters were successfully carried out.

Interest in the determination of tin compounds has risen dramatically over recent years as a result of increased awareness of their toxicity in the environment. The increased worldwide production and consumption of tin are primarily due to the wide range of industrial applications discovered for organotin chemicals.¹⁾

Organotin compounds are known to be potent toxins, and are widely used in different industries, specifically as poly(vinyl chloride) stabilizers, pesticides, and fungicides as well as industrial and agricultural biocides.^{2,3)} Large trialkyl or triaryltin compounds are directly introduced in the environment as agricultural pesticides, or result from the degradation of such metals as poly(vinyl chloride).⁴⁾ The introduction of such compounds into the environment could cause serious problems, mainly due to their high toxicity and tendency to bioaccumulation.⁵⁾

The determination of tin compounds in the environment is becoming increasingly more important.⁶⁾ Several techniques have already been employed to determine tin and/or its organic derivatives, including gas chromatography,^{4,7)} flow-injection using solid-phase spectrophotometry,⁸⁾ voltammetry,⁹⁾ and atomic spectrometry.^{10,11)}

Tin ion in inorganic compounds is probably best determined titrimetrically with iodate after reduction to tin(II) with aluminum metal under a protective atmosphere.¹²⁾ This oxidimetric method took time, and was thus not tried on the micro scale. The obvious interferences are all those ions which undergo similar redox reactions.

Iodometric chemical amplification procedures with their simplicity and sensitivity are still of special interest.^{13–15)}

Thus, the present study reports on an evaluation of several digestion methods with the aim to obtain simple, rapid, and accurate iodometric and spectrophotometric amplification procedures for the determination of tin(II) and (IV) and organotin compounds.

Experimental

Apparatus: A Pye Unicam double-beam UV-visible spectrophotometer (model SP 8-400) with 10 mm quartz cells was used for absorbance measurements. A Philips digital pH meter (model 9418) with glass and saturated calomel electrodes was also used for pH measurements.

Reagents and Materials: Unless otherwise specified, all of the chemicals used were of analytical reagent grade. The reagents sodium molybdate (5% w/v), sodium periodate solution (0.35% w/v), sodium thiosulfate (5×10^{-3} M, 1 M = 1 mol dm⁻³), aqueous solution of starch (1% w/v) and solution of sodium sulfite (2 M) were freshly prepared in distilled water and 8-hydroxyquinoline (Merk) in isobutylmethyl-ketone (IBMK) (0.5% w/v). Buffer solutions of pH 2.2–4.7 were prepared by mixing 150 cm³ of glacial acetic acid with an appropriate amount of saturated sodium acetate and diluting with water whenever is required. All glassware was kept in 10% nitric acid for at least 20 h, and subsequently washed three times with ultrapure water before use.

Standard solutions of tin (Sn²⁺ and Sn⁴⁺) were prepared by dissolving SnCl₂·2H₂O (supplied by Prolabo) and SnCl₄ (supplied by GVL Apioda) in 100 cm³ of double-distilled water in the presence of 10 cm³ of concentrated hydrochloric acid in order to prevent the hydrolysis of tin(IV).¹⁷⁾ The tin(II) solution was kept under nitrogen and in the presence of metallic Al in order to prevent aerial oxidation and stabilizing the tin(II) species.^{18,19)} Butyltin(II) chloride and dibutyltin(IV) dichloride (95–96.5% purity) were obtained from

Alfa product. Standard butyltin solutions ($50 \mu\text{g cm}^{-3}$ as Sn) were prepared separately by dissolving appropriate amount of each butyltin compound in water. These solutions were then stored at 4°C , and dilute ones were prepared daily.

Synthetic marine water²⁰ with a salinity of about 36 g kg^{-1} was prepared from demineralized water and salts in the following molar concentration: NaCl, 0.41; MgCl_2 , 0.029; MgSO_4 , 0.028, and KCl, 0.009 M.

Determination of Tin(II): Aliquot portions ($1\text{--}5 \text{ cm}^3$) of tin(II) solutions containing $1\text{--}50 \mu\text{g}$ of the element were transferred into a 100 cm^3 conical flask. Then 10 cm^3 of acetate buffer of pH 2.5–3.4 and 5 cm^3 of periodate solution were added. The reaction mixture was heated on a boiling water bath under N_2 for 30 min. to attain complete oxidation. The reaction mixture was cooled to room temperature and 5 cm^3 of 5% sodium molybdate solution added. Then crystalline KI (20–40 mg) was added and the solution was treated by one of the following methods: (i) 6-fold amplification. The released iodine spectrophotometry was determined as triiodide at 350 nm after the addition of KI (0.1 g). A blank determination was run and the necessary correction applied. (ii) 144-fold amplification. Alternatively, the released iodine was extracted with 10 cm^3 (2×5) portions of chloroform, and the extracts collected in a separating funnel and then shaken with two 5 cm^3 portions of sodium sulfite to reduce the released iodine to iodide. After the aqueous (upper) layer was transferred to a 100 ml Erlenmeyer flask, 5 cm^3 of 2 M H_2SO_4 was added and heated until dryness to remove SO_2 . To the produced solid residue of iodide, 20 cm^3 of water was added and the pH of the solution adjusted to pH 3 with acetate buffer; finally, 5 ml of NaIO_4 was added. The flask was stoppered and the reaction mixture allowed to stand for 10 min at room temperature; it was then placed in a boiling water bath for 20 min. After the solution was cooled 5 cm^3 of sodium molybdate, 10 cm^3 of acetate buffer (pH \approx 3), and 20–40 mg of KI were added and the released iodine determined by iodometry or spectrophotometry. A blank was run to correct the reagent error and any error caused by the possible aerial oxidation of tin(II).

Determination of Tin(IV): A known volume ($1\text{--}5 \text{ cm}^3$) of a tin(IV) solution containing various amounts of the tetravalent element ($1\text{--}50 \mu\text{g}$) was transferred into 100 cm^3 Erlenmeyer flasks, and $2\text{--}5 \text{ cm}^3$ of a saturated sodium sulfite solution added to each flask followed by 5 cm^3 of 2 M H_2SO_4 . The reaction was left to stand for 3 min and then gently evaporated on a hot plate until excess SO_2 had been completely removed. Then, ca. 5 cm^3 of water was added, and the pH of the water solution adjusted to pH 3; then 10 cm^3 of acetate buffer of pH 3 was added and the released tin(II) determined using the recommended procedure. A blank was run to correct the reagent error.

Analysis of Binary Mixtures of Tin(II) and Tin(IV): Different aliquot portions of the mixture were transferred to a 100 cm^3 conical flask containing various amounts of tin(II) and (IV). The tin(II) in the aliquot was determined titrimetrically or spectrophotometrically as in the procedure employing 144-fold amplification. The tetravalent element was reduced to the divalent state with sodium sulfite in an acid solution, and the total content of the element determined following the procedure of tin(IV) determination. The difference between the two values of the thiosulfate solutions or the absorbance of I_3^- ions was equivalent to tin(IV).

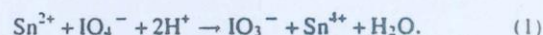
Determination of Tin(II) or (IV) in Marine Water: Marine water samples (100 cm^3) acidified to pH 2 with hydrochloric acid (0.1 M) were filtered through a $0.45 \mu\text{m}$ Millipore filter followed by adding 10 cm^3 of tartaric acid (1 M) and 10 cm^3 of sodium salt of EDTA (1×10^{-3} M). Various amounts ($5\text{--}25 \mu\text{g}$) of the tin(II) or

tin(IV) were added to aliquots of water samples, followed by adding ca. 10 cm^3 of bromine water and 10 cm^3 of 1 M sodium fluoride. After the reaction mixture was allowed to stand for 10 min. and excess bromine boiled off, 5 cm^3 oxine (0.5%) in IBMK was added and shaken for 1 min. The extraction was then repeated three times and the extracts were combined and evaporated to dryness. The residue was then redissolved in 10 cm^3 of water–HCl (4:1 v/v); finally, the total tin content was determined following the above recommended procedure of tin(IV) determination after adjusting the pH to 3. A blank was then run to correct the reagent error.

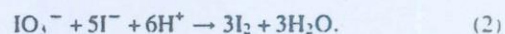
Analysis of Tin in Organotin Compounds: An accurate weight of organotin compounds was digested in a 250 cm^3 combustion flask with 10 cm^3 of concentrated H_2SO_4 and 5 cm^3 of 30% H_2O_2 , as reported by Marr.²¹ The tin content according to the recommended procedure of tin(IV) were then determined.

Results and Discussion

Sodium or potassium periodate in acid medium was found to oxidize tin(II) to tin(IV) as follows:



The released iodate and tin(IV) ions react with KI in acid media according to the following equations:



It was reported²² that reaction (2) take place rapidly and quantitatively in an acidic medium at $\text{pH} \leq 3.5$. Reaction (3) takes place and proceeds forward in a strong acidic medium (4 M H_2SO_4). This statement is criticized here since preliminary experiments showed that the tin(IV)-iodide reaction is a function of the solution pH, and that the reaction is difficult to take place and is quite negligible in a moderate acidic medium ($\text{pH} \geq 3$).

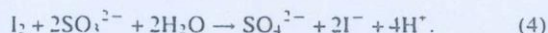
The oxidation of tin(II) with potassium periodate was found to depend on the pH, the reaction time and the temperature. Thus, fixed amounts ($100 \mu\text{g}$) of tin(II) adjusted to pH 2.5–6.5 were allowed to react with sodium periodate (5 cm^3) for different time intervals (5–30 min) and different temperatures (ambient or 100°C) on a boiling water bath. The solutions were then adjusted to $\text{pH} \approx 3$ with 5 cm^3 of the acetate buffer; the unreacted periodate ions were then masked with sodium molybdate, forming heteropoly acid $\text{H}_5[\text{I}(\text{MoO}_4)_6]$.^{23,24} The released iodate was then allowed to react with KI. The complete oxidation of tin(II) with periodate was found in the pH range 2.2–3.2 after heating the reaction mixture on a boiling water bath for 20 min. Fortunately, the pH values suitable for the quantitative oxidation of tin(II) element with periodate are quite appropriate for masking the excess periodate with molybdate.^{25,26} Thus, the acetate buffer solution (pH=3) was added at the beginning of the experiment and before the addition of KI.

At $\text{pH} > 3.6$ reactions (1–3) were very slow, while at $\text{pH} < 2.2$ the reactions proceeded rapidly with 6-fold amplification of tin(II). The molybdate did not mask the unreacted periodate quantitatively at $\text{pH} < 2.2$, since the molybdate-periodate was partially decomposed,²³ and aerial oxidation

of iodide can also occurred under these conditions in the absence of bubbling N_2 . Therefore, at pH 3 each original tin(II) element liberated six equivalents of iodine, i.e. the proposed method afforded a six-fold amplification for each tin(II) ion. The released iodine (Eq. 2) was then determined spectrophotometry as I_3^- at 350 nm. The developed procedures were employed for the determination of varying amounts (10–50 μg) of tin(II). Satisfactory results were obtained with recovery percentage of determination being 96.40–102.5% and with the standard deviation in the range 0.15–0.26 (Table 1). The lowest measurable concentration (3σ) under the prementioned conditions was found to be 0.20 ppm tin(II) or tin(IV).

Tin(IV) was determined by a prior reduction to tin(II) followed by a determination of the produced tin(II) element by the proposed procedure. Sodium sulfite in an acidic media was found to be the most suitable reducing agent, where the unreacted sulfite ion could be easily removed by boiling off the formed sulfur dioxide. The spectrophotometric determination of various levels (10–50 μg) of tin(IV) in aqueous media by the proposed 6-fold amplification is given in Table 2 with the standard deviation in the range 0.15–0.26.

Alternatively, the proposed 6-fold amplification procedure of tin(II) determination was further improved where after masking the unreacted periodate the released iodine from Eq. 2 at pH 3 was extracted quantitatively on shaking with two 10 cm^3 portions of CHCl_3 . The extracted iodine was then shaken with sodium sulfite solution in order to reduce the iodine to iodide according to the equation²⁵⁾



The released iodide in the aqueous (upper) layer was then allowed to react with sodium periodate to produce iodate according to the following equation:²¹⁾



The released iodate produced from Eq. 5 was determined

Table 1. Spectrophotometric Determination of Various Amounts of Sn(II) in Aqueous Media

Sn(II) ion present (μg)	Sn(II) found (μg) ^{a)}	% Error ^{b)}
50	48.30 \pm 0.22	-2.60
20	20.40 \pm 0.26	02.00
10	10.25 \pm 0.15	02.50

a) Average of 5 determinations \pm standard deviation.

b) % Error = $\frac{\text{Average of tin found} \times 100}{\text{tin added}}$

Table 2. Spectrophotometric Determination of Various Amounts of Sn(IV) in Aqueous Media

Sn(IV) ion present (μg)	Sn(IV) found (μg) ^{a)}	% Error
50	50.40 \pm 0.26	0.80
20	20.20 \pm 0.15	1.00
10	10.20 \pm 0.22	2.00

a) Average of 5 determinations \pm standard deviation.

iodometrically, and also by spectrophotometry (at 350 nm) after the addition of potassium iodide, as described. Thus, according to Eq. 5, the overall amplification employing oxidation of iodide by sodium periodate would be a 144-fold amplification of the iodine per each tin(II) element originally present. The proposed 144-fold amplification procedure was successfully employed for the analysis of tin(II). The results of the analysis of tin(II) iodometry and spectrophotometry are summarized in Table 3 with standard deviation and error percentage in the range 0.12–0.32 and 0.52–2.2%, respectively. Moreover, a spectrophotometric procedure employing 144-fold amplification can be extended to lower concentrations of tin(II) by the extraction of the released iodine in CHCl_3 containing alcoholic KI, and measuring the absorbance of the triiodide ion formed at 360 nm.²⁶⁾ If a reasonably large amount of tin(II) ion > 1 ppm is present it is preferable to dilute the solution of the released iodate produced from the 144-fold method to 100 cm^3 , and to measure the concentration of the released iodine by either iodometry or spectrophotometry. The detection limit ($3 \times$ noise) and the correlation coefficient were found to be 0.2 ppm and 0.99, respectively.

The absorbance–concentration relationship was found to be linear over the concentration range 0.05–10 $\mu\text{g cm}^{-3}$ employing 144-fold amplification for a tin(II) determination. The optimum concentration range for the effective spectrophotometric determination, evaluated by Ringbom's method,²⁷⁾ was found in the range 0.15–5 ppm for 144 amplification. The standard deviation calculated for five measurements at 3 ppm of tin(II) was 0.6. The detection limit ($3 \times$ noise) and the correlation coefficient were found to be 0.01 ppm and 0.992, respectively.

An analysis of a binary mixture of tin(II) and (IV) ions in aqueous media was employed by the proposed procedure. An aliquot mixture was first allowed to react with sodium periodate employing the procedure described for a tin(II) determination. Another aliquot mixture was then reduced to tin(II), as described in the above recommended procedure. On the basis of these procedures the volume ($V_1 \text{ cm}^3$) of sodium thiosulfate or the absorbance (A_1) of the released iodine of the first aliquot would be equivalent to tin(II). The volume ($V_2 \text{ cm}^3$) of sodium thiosulfate or the absorbance (A_2) of the released iodine for the aliquot would be equivalent to the sum of Sn(II) and Sn(IV). Thus, the volume ($V_2 - V_1 \text{ cm}^3$) or the absorbance ($A_2 - A_1$) is equivalent to tin(IV).

Table 3. Determination of Various Amounts of Tin(II). Iodometry (a) and Spectrophotometry (b) Using 144-fold Amplification Procedure^{a)}

Tin(II) taken (μg)	Tin(II) found (μg)		Error (%)	
	a	b	a	b
10	10.20 \pm 0.21	10.1 \pm 0.12	2.00	1.00
20	20.30 \pm 0.20	20.1 \pm 0.20	1.50	0.50
50	51.10 \pm 0.32	50.5 \pm 0.26	2.20	1.00

a) Average of 5 determination \pm standard deviation.

Satisfactory results were obtained with standard deviations in the range 0.40–0.52 and 0.26–0.36 for the iodometry and spectrophotometry of the released iodine, respectively. The volume of sodium thiosulfate (0.005 M) equivalent to the blank taken through the whole procedure using freshly prepared NaIO_4 was in the range 0.2–0.25 cm^3 .

Effect of Diverse Ions: The interference of various ions Tl^+ , Zn^{2+} , Pt^{2+} , Mn^{2+} , Cr^{3+} , Cr^{6+} , Ni^{2+} , Ru^{3+} , Al^{3+} , Li^+ , Co^{2+} , Fe^{3+} , Pd^{2+} , Ca^{2+} , Mg^{2+} , Ba^{2+} , and La^{3+} at a concentration (10 μg) approximately exceeding those normally found in sea water was investigated employing a 6-fold amplification procedure. The selectivity of the proposed method was tested by the determination of a fixed concentration (5 μg) of tin(II). Satisfactory results were obtained with a percentage recovery of 97.2–103.5. Mn^{2+} , Tl^+ , Cr^{6+} , Pt^{2+} , Fe^{3+} , and Ru^{3+} seriously interfered. The interference of Fe^{3+} was masked by the addition of 2 cm^3 of NaF (1 M). The selectivity of the 6-fold procedure was examined by the relatively high excess (0.1 mg) of the following ions: WO_4^{2-} , HCO_3^- , Br^- , PO_3^{3-} , SO_3^{2-} , SbO_3^{2-} , and CO_3^{2-} . The percentage recovery of tin(II) was $100 \pm 5\%$.

Application of the Proposed Method: The applicability of the proposed procedures for the analysis of tin(II) and tin(IV) in 0.1 dm^3 artificial sea and marine water were carried out employing the standard addition method. In separate experiments aliquot samples spiked with various amounts (5–25 μg) of tin(II) were added to the water samples, and were analyzed spectrophotometry employing the 144-fold amplification procedure as described. A blank was run for a correction. Satisfactory results (Table 4) were obtained for the spiked samples with the help of a concurrently standard curve prepared under the same instrumental setting. A percentage error of 2–4.8% ($n=5$) and a correlation coefficient of 0.988 were obtained. The total tin in the unspiked water samples (blank) employing the recommended procedure of the extraction with oxine in IBMK were found in the range $5-7 \pm 1.2$ ppm, in agreement with the results obtained by a method reported by Bermejo-Barrera.¹⁰⁾ The values are quite high, possibly due to the characteristics of the places where the samples were collected. In estuaries the water is more static than that in open seas; also, in small harbors (sport and fishing) antifouling paints containing butyltin compounds are used more than in bigger harbors. The analysis of a low concentration of tin (<0.1 ppm) in water is also possible by

Table 4. Analysis of Various Amounts of Tin(II) Spiked to Marine Water Iodometry (a) and Spectrophotometry (b) Employing 144-fold Amplification Procedure^{a)}

Tin(II) taken (μg) ^{a)}	Tin(II) found (μg) ^{b)}		Error (%)	
	a	b	a	b
05	05.20 \pm 0.32	05.10 \pm 0.26	4.00	2.00
20	20.50 \pm 0.41	20.40 \pm 0.23	2.50	2.00
25	26.20 \pm 0.31	25.41 \pm 0.29	4.80	2.20

a) Total volume of aqueous sea water was 0.1 dm^3 . b) Average of 5 determinations \pm standard deviation.

Table 5. Determination of Tin in Organic Compounds Using 144-fold Amplification Reaction Procedure

Compound	% Tin calcd	% Tin found ^{a)}	% Error
Monobutyltin(II) chloride	56.20	57.70 \pm 0.21	+2.27
Tributyltin chloride	36.50	37.44 \pm 0.31	+2.57
Diethyltin chloride	39.08	40.30 \pm 0.38	+3.12

a) Average of 5 determination \pm standard deviation.

the proposed procedure after preconcentration and elution of tin employing a polyurethane foam column,^{28,29)} followed by the determination of the tin(II) according to the above described procedure.

The proposed 144-fold amplification titrimetric procedure was successfully employed for the analysis of tin in organotin compounds. A survey of the literature indicates that an acid mixture of H_2SO_4 – H_2O_2 digestion and Oxygen flask techniques is the most favorite digestion system for the decomposition of tested organotin compounds. Therefore, an accurate weight of the organotin compound was digested with 10 cm^3 of concentrated sulfuric acid and 5 cm^3 of hydrogen peroxide (30%). After digestion, tin was usually present in the di- and tetravalent states, and was determined according to the described procedure for tin(IV). The results concerning the analysis of different organotin compounds are summarized in Table 5 along with the average error percentage in the range 2.27–3.12%.

Conclusion

The present article demonstrates the applicability of amplification the reactions involving periodate in the analysis of organotin compounds. Although the 6-fold amplification procedure for tin(II) determination is faster, 144-fold amplification procedures are more sensitive for lower concentrations. The two methods provide a simple, inexpensive, reliable and precise approach in the routine analysis of tin. The spectrophotometric method provides an attractive alternative to atomic absorption for the determination of tin. A clear advantage of the method is that it is applicable for tin(II) or (IV) speciation in their mixture.

The authors would like to thank Prof. A. B. Farag for the helpful discussions.

References

- 1) N. Nakashima, *Bull. Chem. Soc. Jpn.*, **52**, 1844 (1979), and references therein.
- 2) J. A. J. Thompson, R. C. Pierce, M. G. Shaffer, Y. K. Chau, J. J. Cooney, W. R. Cullen, and R. J. Maguire, "Organotin Compounds in the Aquatic Environment: Scientific Criteria for Assessing Their Effects on Environmental Quality," National Research Council of Canada, Ottawa (1985), NRCC Publ. No. 22494.
- 3) R. J. Maguire, *Appl. Organomet. Chem.*, **1**, 475 (1987).
- 4) B. Lalere, H. Budzinski, O. F. X. Donard, and P. Garrigues, "19th International Symp. on Chromatography," Aix-en-Provence, France, 13–18, September, 1992.
- 5) H. Vrijhof, *Sci. Total Environ.*, **43**, 221 (1985).

- 6) P. M. Sarradin, A. Astruc, R. Sabrier, and M. Astruc, *Mar. Pollut. Bull.*, **28**, 621 (1994).
- 7) G. Lespes, C. Carlier-Pinasseau, M. Potin-Guatier, and M. Astruc, *Analyst*, **121**, (1996), and references cited in.
- 8) L. F. Captian-Vallvey, M. C. Valencia, and G. Miron, *Anal. Chim. Acta*, **289**, 365 (1994); S. Nalini, N. Balasubramanian, and T. V. Ramakrishna, *Bull. Chem. Soc. Jpn.*, **68**, 1145 (1995).
- 9) S. B. O. Adeloju and F. Pablo, *Anal. Chim. Acta*, **270**, 143 (1992).
- 10) P. Bermejo-Barrera, M. C. Tubio-Franco, J. M. A. Guir-Paz, R. M. Soto-Ferreiro, and A. Bermejo-Barrera, *Microchem. J.*, **53**, 395 (1996).
- 11) Y. K. Chau, S. Zhang, and R. J. Maguire, *Analyst*, **117**, 1161 (1992).
- 12) M. Farnsworth and J. Pekola, *Anal. Chem.*, **31**, 410 (1959).
- 13) M. S. El-Shahawi and A. B. Farag, *Anal. Chim. Acta*, **307**, 1161 (1995).
- 14) M. S. El-Shahawi and S. A. Barakat, *Talanta*, **42**, 1641 (1995).
- 15) M. S. El-Shahawi and M. M. Kamal, *Anal. Sci. (Jpn.)*, **11**, 323 (1995).
- 16) J. K. Sircar, S. Bhattacharjee, J. Konar, K. C. Ghosh, A. C. Basak, S. N. Jha, and L. P. Pandey, *Microchem. J.*, **54**, 163 (1996).
- 17) C. F. Baes, Jr., and R. E. Mesmer, "The Hydrolysis of Cations," John Wiley & Sons, New York (1976).
- 18) F. D. Snell, "Photometric and Fluorometric Methods of Analysis, Metal," Part I, John Wiley & Sons, New York (1978).
- 19) H. Onishi, "Photometric Determination of Trace Metals," Part IIB, 4th ed, John Wiley & Sons, New York (1989).
- 20) G. Weber, *Anal. Chim. Acta*, **186**, 49 (1986).
- 21) I. L. Marr, *Talanta*, **22**, 387 (1975).
- 22) A. I. Vogel, "Textbook of Quantitative Inorganic Analysis," 3rd ed. Longman, London (1972).
- 23) D. Burnel, *Compt. Rend.*, **261**, 1982 (1965).
- 24) A. Townshend and D. T. Burns, *Talanta*, **39**, 715 (1992), and references therein.
- 25) D. Amin, K. Y. Saleem, and W. A. Bashir, *Talanta*, **29**, 694 (1982), and references cited in.
- 26) T. C. Ovenston and W. T. Rees, *Anal. Chim. Acta*, **5**, 123 (1951).
- 27) A. Ringbom, *Z. Anal. Chem.*, **21**, 332 (1938); G. H. Ayres, *Anal. Chem.*, **21**, 652 (1949).
- 28) L. O. Vsk and A. Chow, *Talanta*, **27**, 157 (1981).
- 29) R. Caletka, R. Hausheck, and V. Krivan, *Anal. Chim. Acta*, **229**, 127 (1990).

Heavy metal (Ni, Co, Cr and Pb) contamination in liver and skin tissues of *lethrinus lentjan* fish family: lethrinidae (toelost) from the Arabian Gulf

M.S. El-Shahawi^{1*} and M.H. Al-Yousuf²

¹Department of Chemistry, Faculty of Science at Damietta, Mansoura University, Damietta, Egypt and

²Desert and Marine Environment Research Center, UAE University, PO Box 17777, Al-Ain, United Arab Emirates

Concentrations of nickel, cobalt, chromium and lead in liver and skin tissues were measured in *Lethrinus lentjan* fish collected from coastal waters of the United Arab Emirates (UAE). The levels of Ni, Co, Pb and Cr were found to follow the order: liver > skin. Metal levels found in liver and skin fish organs followed the sequence: Cr > Pb > Ni > Co. The data suggest future comparison for trace metals as a function of sex and fish size be made. The data also positively indicate that the tested fish from the Arabian Gulf have metal concentrations well below the permissible levels reported by WHO.

Introduction

As a consequence of the activities of modern industries and agriculture many man-made organic and inorganic pollutants have found their way into the environment (Clark & Anlikar, 1980, Vinikour *et al.*, 1980). Heavy metals that are of particular relevance to fresh water are Pb, Cr, Cu, Ni, Co, Mn, Hg and Zn (Dassenakis *et al.*, 1996). The danger involved for human health because of the presence of heavy metals in the marine environment derive not only from their persistence and toxicity, but also from the remarkable degree of concentration they undergo through the tropic chain (Hernandez *et al.*, 1990). These elements also accumulate in bottom sediments from which they may be released by various processes of remobilization and can move up to food chain causing chronic and acute ailments to man (Currey *et al.*, 1992). These elements can attach to the gastrointestinal or renal tubular cells

which are particularly susceptible to toxicity (Amdur *et al.*, 1991).

Recently many investigations have reported the accumulation of heavy metals in marine organisms occupying high tropic levels in the marine food fish and showed the utility of these species as biological indicators of heavy metal pollution (Lock *et al.*, 1992; Sharif *et al.*, 1993; Bou-Olayan *et al.*, 1995; Bruschiweiler *et al.*, 1996). However, only limited studies are available on heavy metal accumulations in tissue(s) or organ(s) of *Lethrinus lentjan* fish (Kureishy, 1993). In recent years the marine environment in the Arabian Gulf region has been a subject of study due to the accidental oil spills, the uncontrolled discharge of the sewage and industrial waste waters as well as human activities. Thus, several papers have indicated the possible extent of heavy metal accumulation in marine organisms taken from the Arabian

Correspondence to: M.S. El-Shahawi. *This work was done while Dr El-Shahawi was on leave at Department of Chemistry, Faculty of Science, UAE University, PO Box 17551, UAE.

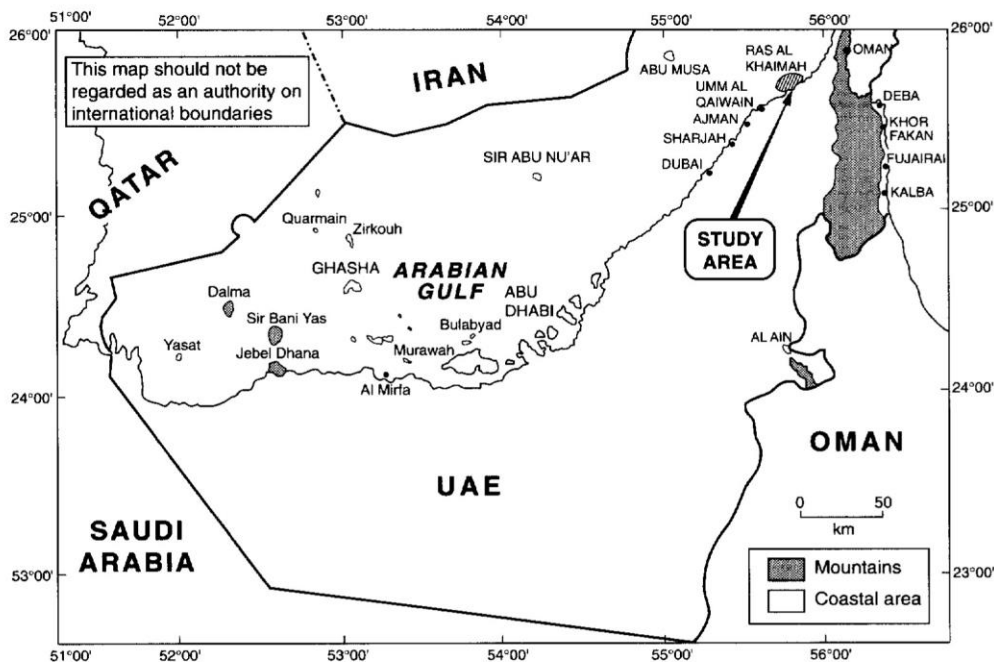


Figure 1. Sampling locations along western coast of the UAE.

Gulf and Red Sea (Abdulmoneim & El-Deck, 1992; Kureishy, 1993; Hassan *et al.*, 1996). Monitoring systems are essential to track long-existing pollution process (Waldman & Shevah, 1993) but absence of these systems in the Arabian Gulf region makes it very difficult for researchers to draw certain conclusions about the long-term effects of human activities. Thus, the present study was conducted to assess the trace metal (Ni, Co, Cr and Pb) accumulation in liver and skin tissues of *Lethrinus lentjan* fish consumed by the population of the United Arab Emirates and to clarify whether these levels constitute a health hazard to the consumer. These elements were selected because most studies on heavy-metal pollution in fish have examined one or more of these elements as natural impurities.

Materials and methods

Sampling and preparation

Fish samples (20–30) of both sexes of *Lethrinus lentjan* fish were collected from the Arabian Gulf at Ras Al-Khaimah district (western coast) of the UAE (Figure 1). The fish

samples were taken randomly every 2 weeks during the period from May to June 1993. The fish samples were placed in an ice box transported to the laboratory and finally frozen at -20°C prior to analysis. At the time of metals analysis the fish were defrosted and their standard length were recorded. Tissues (liver and skin) to be analyzed were then separated and grounded with stainless steel kits and glass equipment.

General digestion procedure

Destruction of the fish tissues was carried out by wet digestion (Mason & Barak, 1990). The procedure applied as follows: an accurate sample weight of wet tissues liver and skin (3–5 g) were placed in 50 ml erlenmeyer flask and 10 ml of concentrated HNO_3 were added. After 15 min predigestion at room temperature, 10 ml mixture of concentrated HNO_3 – HClO_4 (4 : 1 v/v) were added and the reaction mixture was maintained on a hot plate stabilized at $70 \pm 5^{\circ}\text{C}$ for about 24 h. The solution was finally transferred to a 25 ml measuring flask and diluted with deionized water to the mark. For each series of samples a blank was made to

check the possible contamination. The digestion procedure was applied to standards of each tested element (Ni, Co, Cr and Pb) and the results obtained showed no losses of any metal occurred in the experimental conditions.

Apparatus

Analyses of Ni, Co, Cr and Pb in liver and skin tissues were carried out with a GBC 206 flame atomic absorption spectrometer equipped with fuel-rich and stoichiometric air-acetylene flames. Air was supplied through Pu 9003 air compressor fitted with filter and regulator, moisture trap and oil-free pump. Acetylene was delivered after passing through concentrated H₂SO₄ for purification.

Results and discussions

Differential accumulation of trace metals in liver

Elements existing most probably as cationic species in sea water (Ni, Cu, Zn, Cr, Mn, etc.) and which tend to form strong ionic complexes tend to accumulate in the internal organs (Mears & Eister, 1977). The occurrence of trace metals Ni, Cr, Co and Pb has been well documented to concentrate in fish organs to various degrees (Rowe & Massaro, 1974). Thus, trace metal concentrations in stationery fish were used as a bioindicator in water area affected by human activities and as a monitoring technique for assessing inefficiency of control measures (Jargensen & Pederson, 1994). The concentrations of Ni, Co, Cr and Pb in liver tissues of *Lethrinus lentjan* fish are summarized in Table 1. These elements are known to have great ability to form stable chalets with the available active sites in the immobile protein molecules in the fish tissues (Jaffar & Pervaiz, 1989; Kendrik *et al.*, 1992).

The listed results are averaged for triplicate parallel measurements conducted for each metal in each fish organ. The data indicated that the order of the trace metal distribution followed the concentration pattern: Cr > Pb > Ni > Co. The significant increase of Cr and Pb concentrations in 1993 may be due to a contribution from the 1991 Gulf War oil spill to environmental contamination in Gulf water. This is due to the ability of bivalves to accumulate metals to detectable levels. Significant amounts of crude oil (Al-Yakoob *et al.*, 1993) and incomplete comusion products (Readman *et al.*, 1992) were introduced into the marine environment during the Gulf War. Petroleum and petrochemical industry wastes contribute significantly to metal enrichment of the Arabian Gulf marine environment (Sadiq & Zaidi, 1985) and thus may have accounted for the increased metal levels in post-war survey. The reason for the high accumulation of chromium (2.336 ± 1.036 ppm) and lead (1.608 ± 0.868 ppm) wet weight by liver could certainly be based in specific metabolism process and enzyme catalyzed reaction involving Cr and Pb taking place in the liver. The sulfur legends in liver also have a great tendency to co-ordinate with the tested elements in particular lead via oxygen carboxylate, amino group nitrogen and/or sulfur of the mercapto group in the metallothionein protein which is in highest concentrations in liver (Kendrick *et al.*, 1992; El-Shahawi, 1996). The produced complexes are slowly redistributed to the renal cortex. Liver has also an important role in contaminants storage, redistribution, detoxification or transformation and also acts as an active site of pathological effects induced by contaminants (Evans *et al.*, 1993).

The data of the tested metals in liver (Table 1) are in good agreement with the results reported by Harrison and Klaverkamp (1990)

Table 1. Total heavy metal concentrations (mean ppm wet weight) in pooled liver and skin tissues of *Lethrinus lentjan* fish of the Arabian Gulf region*

Element	Liverx	SD	SE	Skinx	SD	SE
Co	1.067	0.150	0.061	0.985	0.153	0.076
Ni	1.181	0.182	0.074	1.190	0.467	0.165
Pb	1.608	0.868	0.181	1.539	0.482	0.086
Cr	2.336	1.036	0.328	2.420	1.929	0.860

*x represents the average of five measurements ($n = 50$).

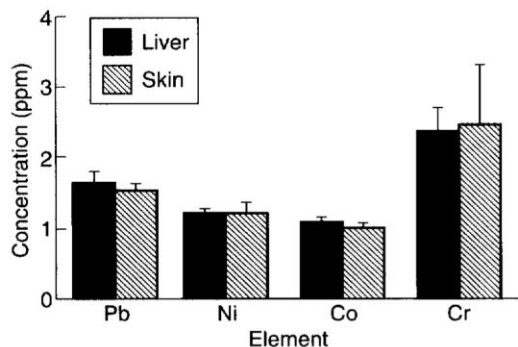


Figure 2. Uptake (mean ppm wet weight) of the trace metals Ni, Co, Cr and Pb by the liver and skin tissues of *Lethrinus lentjan* fish ($n = 50$).

and Jaffar and Pervais (1989). Similar results of nickel and cobalt except chromium and lead were also obtained in the liver of *Lethrinus nebulosus* around Qatar State before, during and after the oil spill in the Gulf War, 1991 (Kureishy, 1993). The produced metal complexes are slowly redistributed to the renal cortex. Liver also has an important role in contaminant storage, redistribution, detoxification or transformation and also acts as an active site of pathological effects induced by contaminants (Evans *et al.*, 1993).

Differential accumulation of trace metals in skin tissues

In skin (Table 1) the average concentration of the tested elements followed the sequence: Cr > Pb > Ni > Co. Most of chromium and lead are stored in the skin to form octahedral and tetrahedral metallothionein and metalloenzymes complex species, respectively, through the mercapto and the disulphide groups present in the protein (Vinikour *et al.*, 1980; Schumacher *et al.*, 1992). The accumulation of chromium(III) is also attributed to the formation of stable five- or six-membered ring chalets with the available metalloenzymes (Schrivver *et al.*, 1994). Similar accumulation of nickel and cobalt were reported by Kureishy (1993). The types of hormones and the number of available active sites in the protein and cytochrome P-450 in the tested fish organ may account for this behaviour (Kendrick *et al.*, 1992). The specific metabolism process and the enzyme catalyzed reactions taking place in skin could also account for this behaviour (Jaffar & Pervais, 1989).

Comparison on the uptake of the tested elements by liver and skin

Figure 2 and Table 1 shows a comparison of the mean concentration of the tested elements Ni, Co, Cr and Pb in liver and skin tissues. The average chromium (2.420 ± 1.923 ppm) and nickel (1.190 ± 0.467 ppm) concentration in skin tissue were found high in skin tissues as compared to liver, whereas lead (1.608 ± 0.868 ppm) and cobalt (1.067 ± 0.150 ppm) were highest in liver (Table 1). The prevalence of lead in liver as compared to skin appears to be a result of the increased amount of metallothionein protein in liver and its greater tendency to co-ordinate with lead. Similar accumulation patterns of Ni, Co, Cr and Pb in liver and skin have been reported in marine mammals as in sea-birds reported by other researchers and followed previously reported trends with mean metal concentrations decreasing in the order: liver > skin for the tested elements (Sharif *et al.*, 1991, 1993; Kureishy, 1993).

Conclusion

The accumulation of Ni, Co, Cr and Pb in liver tissues of *Lethrinus lentjan* fish (Table 1) were found high as compared to skin. Taking 6–10 g of fish as the maximum consumption per person per day for coastal areas of the UAE, it is estimated that the average level of the tested elements are below the provisional tolerable weekly intake (PTWI) by human beings of total metal concentration ($\mu\text{g kg}^{-1}$ body weight at week^{-1}) (WHO, 1973 National Research Council, 1989; Sharif *et al.*, 1991). The concentration of the tested elements are among the lower side of the reported values and reflect a comparatively clear and pollution-free environment on the *Lethrinus lentjan* fish after the Gulf War. The concentrations of the tested metals in liver and skin tissues differed little or remained constant before and after the Gulf War. The data may be taken also as a convenient base line against which any further pollution could be measured.

Acknowledgement—The authors would like to thank Professor A.S. Al-Sharhan, Dean of the Faculty of Science and Desert and Marine Environment Research Center, UAE University, for the facilities provided and Dr Shakeel Ahmed for his assistance in analysing the samples.

References

- Abdulmoneim MA & El-Deck MS (1992): *Lethrinus* family: a model of edible Red Sea fishes with low heavy metals accumulation, *National Institute of Oceanography and Fisheries*. **19**, 589–596.
- Al-Yakoob S, Sneed T & Al-Hashash H (1993): Polycyclic aromatic hydrocarbons in edible tissue of fish from the Gulf after the 1991 oil spill. *Mar. Pollut. Bull.* **27**, 297–301.
- Amdur MO, Doull J & Klaassen CD (1991): *The Basic Science of Poisons*. 4th edn. England: Pergamon Press.
- Bou-Olayan AH, Al-Mattar S, Al-Yakoob S & Al-Hazeem S (1995): Accumulation of lead, cadmium, copper and nickel by Pearl Oyster, *pinctada radiata*, from Kuwait Marine Environment, *Mar. Pollut. Bull.* **30**, 211–214.
- Bruschweiler BJ, Wurgler PE & Fent K (1996): Inhibitory effects of heavy metals on cytochrome PHSO: an induction in permanent fish hepatoma cells. *Arch. Environ. Contam. Toxicol.* **31**(4), 475–482.
- Clark E & Anlikar R (1980): In *The Handbook of Environmental Chemistry*, vol. 3, part A, ed. O Hutzinger, p. 181. Berlin: Springer Verlag.
- Currey NA, Benko WI, Yaru BT & Kabi R (1992): Determination of heavy metals, arsenic and selenium in barramundi (*Lates calcorifer*) from Lake Murray, Papua New Guinea, *Sci. Total Environ.* **128**, 305–320.
- Dassenakis MI, Kloukinotou MA & Paylidou (1996): The influence of long existing pollution on trace metal levels in a small tidal Mediterranean Bay, *Mar. Pollut. Bull.* **32**, 275–282.
- El-Shahawi MS (1996): Spectroscopic and electrochemical studies of chromium(III) complexes with some naturally occurring ligands containing sulfur. *Spectrochimica Acta*. **52A**, 139–149.
- Evans DW, Doo DK & Hanson P (1993): Trace element concentration in fish livers: implications of variations with fish size in pollution monitoring. *Mar. Pollut. Bull.* **26**(6), 329–334.
- Harrison SE & Klaverkamp JF (1990): Metal contamination in liver and muscle of Northern Pike (*Esox lucius*) and white sucker (*Catostomus commersoni*) and in sediments from lakes near the smelter at Fin Flon, Manitoba. *Environ. Toxicol. Chem.* **9**, 941–956.
- Hassan ES, Banat IM, El-Shahawi MS & Abu-Hilal AH (1996): Bacterial nutrients and heavy metal ions pollution assessment along the eastern coastal area of the United Arab Emirates. *J. Aquatic Ecosystem Health* **5**, 73–81.
- Hernandez FH, Median J, Ansuategui J & Conesa M (1990): Heavy metal concentrations in some marine organisms from the Mediterranean Sea (Castellon, Spain): metal accumulation in different tissues. *Sci. Mar.* **54**(2), 113–129.
- Jaffar M & Pervaiz S (1989): Investigation of multiorgan heavy trace metal content of meat of selected diary, poultry, fowl and fish species. *Pak. J. Sci. Ind. Res.* **32**, 175–177.
- Jargensen TA & Pederson B (1994): Trace metals in fish used for time trend analysis and as environmental indicator. *Mar. Pollut. Bull.* **28**, 24–32.
- Kendrick MH, Moy MT, Plishka MJ & Robinson KD (1992): *Metals and Biological Systems*, England: Ellis Horwood.
- Kureishy TW (1993): Contamination of heavy metals in marine organisms around Qatar before and after the Gulf War oil spill. *Mar. Pollut. Bull.* **27**, 183–186.
- Lock JW, Thompson DR, Furness RW & Bartle JA (1992): Metal concentrations in seabirds of the New Zealand region. *Environ. Pollut.* **75**, 289–300.
- Mason CF & Barak NAE (1990): A catchment survey for heavy metals using the eel (*Anguilla Anguilla*). *Chemosphere* **21**(4–5), 695–699.
- Mears HC & Eister R (1977): Trace metals in liver from Bluefish, Tautog and Tilefish in relation to body length. *Chesapeake Science* **18**, 315–318.
- National Research Council (1989): *Recommended Dietary Allowances*, 10th edn. Washington, DC: National Research Council.
- Readman JW, Fowler SW, Villeneuve JP, Cattini C, Oregioni B & Mee LD (1992): Oil and combustion contamination of the Gulf marine environment following the war. *Nature*, **358**, 662–665.
- Rowe DW & Massaro EJ (1974): Cadmium uptake and time dependent alterations in tissues levels in the White Catfish *Loctalurus catus*. *Bull Environ. Contam. Toxicol.* **11**, 244–249.
- Sadiq M & Zaidi TH (1985): Metal concentration in the sediments from the Arabian Gulf Coast of Saudi Arabia. *Bull. Environ. Contam. Toxic.* **34**, 565–571.
- Sharif AKM, Mustafa AI, Hossian MA, Amin MN & Saifullah S (1993): Lead and cadmium contents in ten species of tropical marine fish from the Bay of Bengal. *Sci. Total Environ.* **133**, 193–199 and references therein.
- Sharif AKM, Mustafa AI & Saifullah S (1991): Trace metals in tropics marine fish from the Bay of Bengal. *Sci. Environ.* **197**, 135–192.
- Schriner DF, Atkins PW & Longford CH (1994): *Inorganic Chemistry*, 2nd edn. Oxford: Oxford University Press.
- Schumacher M, Domingo JL, Corbella J & Bosque MA (1992): Heavy metals in marine species from the Tarragona Coast, Spain. *J. Environ. Sci. Health* **A27**, 1939–1948.
- Vinikour WS, Goldstein RM & Anderson RV (1980): Bioconcentration patterns of zinc, copper, cadmium and lead in selected fish species from the Fox River, Illinois. *Bull. Environ. Contam. Toxicol.* **25**, 727–734.
- Waldman M & Shevah Y (1993): Biodegradation and leaching of pollution: monitoring aspects. *Pure Appl. Chem.* **65**, 1565–1603.
- WHO (1973): *Trace Elements in Human Nutrition*, Technical Report Series 230. Geneva: World Health Organization.

PII S0160-4120(97)00127-X

POST-GULF-WAR ASSESSMENT OF NUTRIENTS, HEAVY METAL IONS, HYDROCARBONS, AND BACTERIAL POLLUTION LEVELS IN THE UNITED ARAB EMIRATES COASTAL WATERS

I.M. Banat* and E.S. Hassan

Department of Biology, University of the UAE, Al-Ain, Abu-Dhabi, UAE

M.S. El-Shahawi

Department of Chemistry, University of the UAE, Al-Ain, Abu-Dhabi, UAE

A.H. Abu-Hilal

Desert and Marine Environment Research Center, UAE University, Al-Ain, UAE

EI 9609-200 M (Received 12 September 1996; accepted 24 July 1997)

A post-Gulf War coastal sea water pollution assessment program was carried out through monitoring the concentrations of major nutrients, heavy metal ions, selected hydrocarbons, and selected bacterial communities counts at different sites along the coasts of the United Arab Emirates on the Arabian Gulf. Abu-Dhabi and Dubai coastal waters had occasional high nutrient levels with some fluctuations and wide spatial and temporal variations, suggesting the presence of anthropogenic sources of pollution creating these conditions near the sampling sites. Sharjah and Ajman Creeks had lower nutrient levels. Bacterial counts had distinct patterns peaking in spring and autumn, and diminishing during summer and winter. Total and faecal coliform counts fluctuated depending on the presence of nearby recreation and commercial areas, and were at no time consistently high. *Bacillus*, *Pseudomonas*, *Staphylococcus*, *Micrococcus*, and *Alteromonas* were the predominant bacterial genera in these waters. Slightly higher hydrocarbon concentrations were detected both in surface waters and sediments, most likely a result of the deliberate release of crude oil into the Gulf waters during the Gulf War. ©1998 Elsevier Science Ltd

INTRODUCTION

Beaches and coastal areas the world over have been, in the past few decades, continuously exposed to numerous environmental pollutants among which the most potentially hazardous are toxic chlorinated compounds, heavy metals, residual chemicals and nuclear wastes, radioactive compounds and hydrocarbons from

oil spill accidents. In addition, discharges from desalination, power generation, sewage and wastewater treatment plants are also detrimental to the aquatic environment.

The Arabian Gulf (otherwise known as the Persian Gulf) is a shallow basin with an average depth of 35-40 m and a total area of around 240 km². It is connected to the Gulf of Oman and the Arabian Sea through a narrow bottleneck of the Straits of Hormuz.

*Present address: School of Applied Biological and Chemical Sciences, University of Ulster, Coleraine BT52 1SA, Northern Ireland, UK.

The UAE is located near the Straits of Hormuz at the lower part of the Gulf and its eastern borders run along the Gulf of Oman. The Gulf waters have been exposed to the effects of many environmental pollutants. Some information is available about the water physical and chemical properties, which are of primary importance for determining and/or limiting the occurrence and distribution of biological life in the Gulf (Hassan et al. 1996). The pH values in the eastern and northern coastal waters of the UAE were mainly in the alkaline range of 7.5-8.5 (Hassan et al. 1993, 1996; Abu-Hilal et al. 1994). Salinity levels reported for different parts of the Gulf waters were as follows in g/L: Kuwait 39-41, Qatar 40-43, Saudi Arabia 40-42 (Dorgham et al. 1987; Dorgham 1991), and for close-by northern coastal waters of the UAE 38-42 (Banat et al. 1993). In an assessment for tar pollution levels carried out post-Gulf War, Abu-Hilal and Khordagui (1993) concluded that tar ball levels on the beaches of the UAE were higher than pre-Gulf War levels.

More information is available on the microbial sanitary conditions in selected areas of the UAE coastal waters including the prevailing microbial communities and pollution indicator bacterial population counts and assessments (Hassan 1993; Banat et al. 1993; Abu-Hilal et al. 1994). Wastewater discharge was identified by these reports as a major pollution source for these waters. Some upwelling activities were also reported in part of the Gulf waters (Thangaraja 1990) and occasional red tide blooms were also observed in these sites during February to April as a result of the high total dissolved nitrogen (TDN) levels.

Among the components of wastewater most likely to have an impact on marine ecosystems are nutrients, organic matter, and microorganisms. Although eutrophication has been long recognized as one of the problems in freshwater environments, several reports have described marine eutrophication (Cederwall and Elmgren 1980). Eutrophication is defined as an increase in nutrients which usually leads to increased growth of algae and plants. A review by Rosenberg (1984) concluded that it is becoming increasingly apparent that nutrient enrichment has already brought about eutrophication in some local coastal waters and even in entire sea areas. He also predicted (Rosenberg 1985) eutrophication to be the future marine coastal nuisance, a predicament that was substantiated by Degobbi (1989), who reported increased eutrophication of the North Adriatic Sea. There are, therefore, reasons to believe that eutrophication can, in the near

future, become a common hazard in marine coastal areas in many parts of the world. Such a process would have damaging effects on both inshore fisheries and recreational facilities.

Monitoring major nutrient levels is an important task to assess the pollution degree and/or the quality of water resources (Friligos 1985; Rosenberg 1985). Monitoring pollution along the coasts of Alicante in Spain, Zoffmann et al. (1989) concluded that nutrient evaluation is critical in determining the level of wastewater discharge and suitability of some coastal structural configurations in handling such discharges. Satsmadjis and co-workers (1985) reported nutrient concentrations in the Mediterranean water around Navarin, Greece, as follows ($\mu\text{g L}^{-1}$): nitrate, 0.2-5; phosphate, 0.2-2; ammonia, 0.3-10; and, nitrite, 0.1-2. Riley (1978), in comparison, reported that the ranges of nutrient concentrations in marine water under normal environmental conditions are as follows ($\mu\text{g L}^{-1}$): nitrate, 1.0 to 120; phosphate, 1.0 to 160; ammonia, 0.0 to 50; and, nitrite, 0.2 to 30.

Monitoring pathogenic and/or opportunistic microbes such as bacteria, fungi, and parasites has also been frequently used as a means of evaluating contamination of coastal waters. To that end, standard plate counts, total and faecal coliform, and faecal streptococci counts remain the main indicators of pollution levels (Pipes et al. 1987). Rees (1993), reporting on health implementation of coastal waters in Britain, emphasized that monitoring water sanitary conditions using standard plate counts, total and faecal coliform, and faecal streptococci counts are essential indicators of pollution levels. Other bacterial populations, particularly those for saprophytic bacteria, are also considered by many investigators to be good bio-indicators for water quality (Mood 1977; Muller 1977; Ptak and Grinsbury 1977; Hassan 1993). Elevated numbers of such bacteria are considered a clear indicator for potential health risks posed by opportunistic pathogens (LeChevallier et al. 1980).

In assessing levels of pollution, Zoffmann et al. (1989) concluded that the counts of *Escherichia coli*, corresponding to a period of 30 consecutive days, should not exceed $10^3/100$ mL in more than 10% of the samples, or $200/100$ mL in more than 50% of the samples obtained from the tested waterbody. They also classified marine beach contamination with faecal coliform as follows: beaches with cell counts of less than 100/L, free from contamination; 100 to 1000/L, slightly contaminated; 2000 to 10 000/L, highly contaminated; and more than 10 000/L, dangerously contaminated. They therefore suggested the numbers of total and

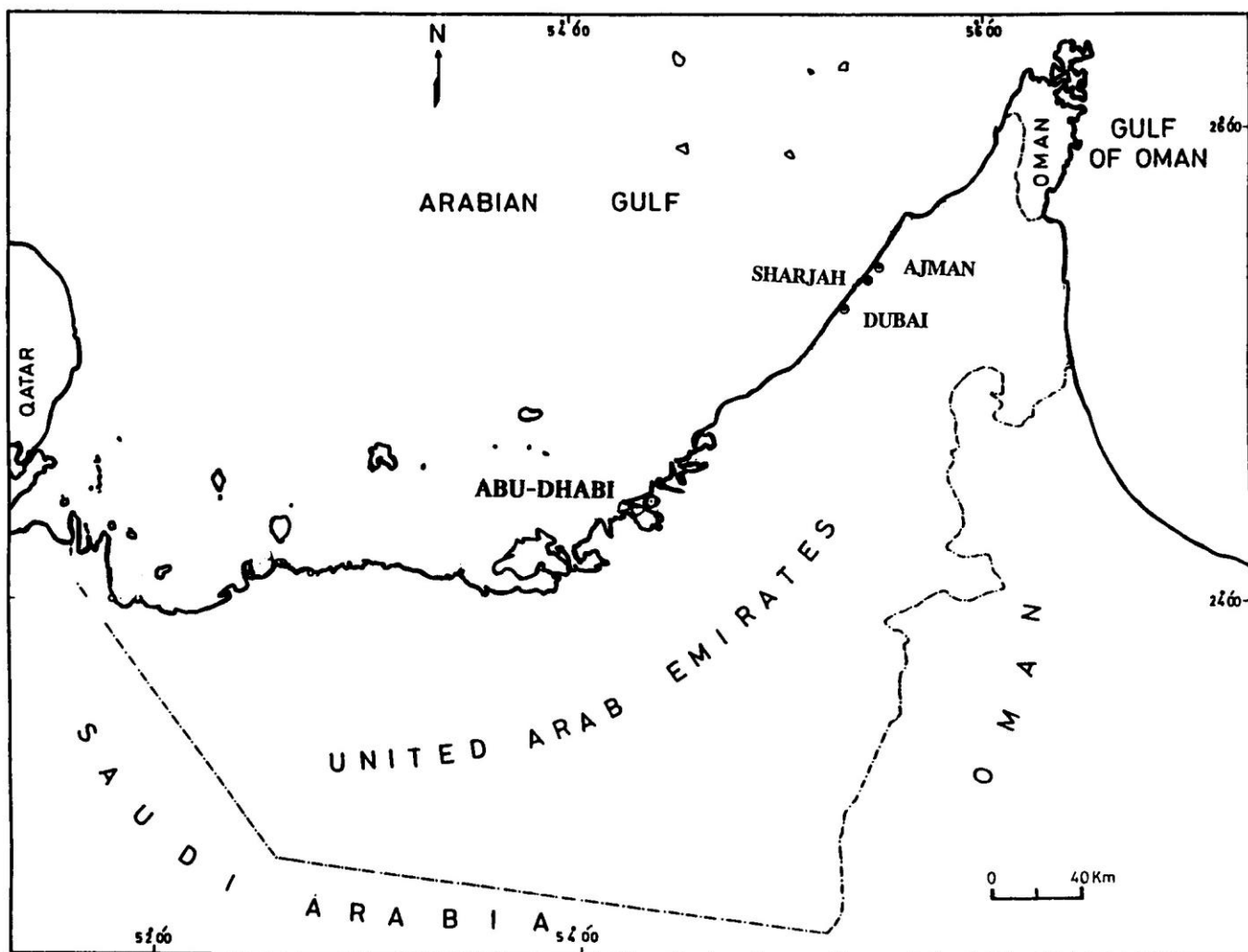


Fig. 1. A map showing the location of the sampling sites, Abu-Dhabi, Dubai, Sharjah, and Ajman in Arabian Gulf coast of the UAE.

faecal coliform in good quality beach waters should be $\leq 5000/L$ and $1000/L$, respectively, monitored every two months, while the imperative levels that warrant immediate action are $\geq 100\,000/L$ and $20\,000/L$, respectively. Waters are considered suitable for bathing when 95% of the samples taken at the same site have values lower than the suggested guideline level and when 80% have values under those of the imperative level.

Taking into consideration all of the above factors which influence pollution of marine waters, carrying out a systematic and continuous long-term monitoring of pollution in places under use as recreational beaches becomes highly desirable. Such an exercise helps determine their state/quality and develop rational programs for improvements when required. In this paper, the nutrient chemicals, microbial, heavy metal ions, and total hydrocarbons in the Gulf coastal waters of the UAE, an important recreational and commercial area in the Gulf, are reported.

MATERIALS AND METHODS

Sampling area and sampling

Several sampling sites were selected within or adjacent to the creeks of Abu-Dhabi, Dubai, Sharjah, and Ajman, which are four Emirates along the northern coast of the UAE (Fig. 1), covering a coastline of about 150 km length. The water depth in these sites ranged between 50-60 cm at high tide and 10-20 cm at low tide. Well-developed mangrove forests are scattered on the coastal waters of all four sites and intensive commercial and recreational activities are located near the sites in Abu-Dhabi and Dubai. Samples were collected in sterile plastic bottles at monthly intervals as described previously (Hassan et al. 1996). Sampling was carried out during the period between March 1991 and February 1992 unless otherwise specified.

Chemical analysis, bacterial enumeration and identification

Water chemical analysis. Temperature and pH were measured in the field. Salinity was measured *in situ* using a Lab Comp Analyzer (Model SCT-100). Dissolved oxygen was determined by the Winkler titration method (Strickland and Parsons 1972). The concentration of ammonia was determined spectrophotometrically as described by Strickland and Parsons (1972). The nitrite and phosphate were determined according to Parsons et al. (1984), while nitrate was estimated according to Grasshoff (1976).

Bacterial enumeration and identification. Enumeration of colony forming units (CFU) of different bacterial communities was carried out using the standard plate count. Total saprophytic bacteria (TSB) and salt tolerant saprophytic bacteria (STSB) were counted using the method described in Banat et al. (1993). Gram negative bacteria (GNB) were counted on MacConkey agar while total coliforms (TC) and faecal coliforms (FC) were counted using the most probable number (MPN) technique. Morphologically distinct colonies were isolated from the counting plates and were identified to the genus level while coliform isolates were identified to the species level using morphological, physiological, and biochemical standard methods (Holt 1984, 1986; Balows et al. 1992). The identification of the Gram-negative isolates was checked using API-20E (France) system.

Heavy metal analysis

Heavy metals analyses were carried out by atomic absorption spectrometry using a Phillips Pu-9100 x atomic absorption spectrometer equipped with a Phillips P.312 microprocessor according to Lo et al. (1991). Water samples used for heavy metal analysis were collected during 1993.

Hydrocarbon analysis

A 20 mL Mercuric Chloride solution (10 g/L^{-1}) was immediately added to the samples used for hydrocarbons determination to inhibit all biological activities. Samples were then extracted with dichloromethane, dried, reconstituted, and analyzed using a Hitachi model F-2000 spectrofluorimeter at 360 nm and excitation at 310 nm for recording the intensity of fluorescence against standards of chrysene and Kuwaiti crude oil as described by IOC (1976) and Dedomenico et al. (1994).

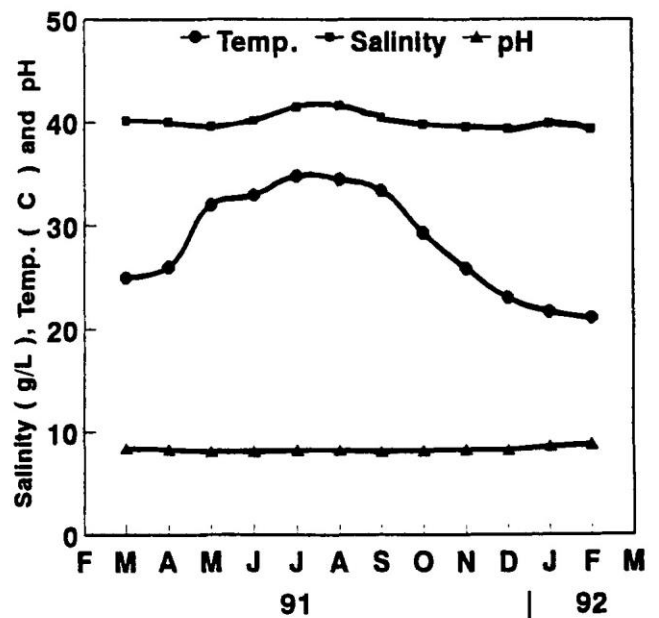


Fig. 2. Mean values of *in situ* water temperature, pH, and salinity.

RESULTS AND DISCUSSION

The pH, temperature, and salinity profiles are shown in Fig. 2. The pH values were slightly alkaline in nature but were mainly within the expected range for surface marine water reported earlier for other parts of the Gulf region and fluctuated within the range 7.6-8.3. Some of the sites within each Emirate showed occasional relatively lower pH values (data not shown). This might be due to close proximity of these sites to the mangrove forests where, at low tide, the water currents leaving this area have low pH and oxygen levels due to the activities of the benthic marine mangrove ecosystem.

The temperature profile reflected expected seasonal ambient temperature variations for this area, with lower values $21.5\text{-}24^\circ\text{C}$ in the winter months and a highest value of 34°C in mid-summer (July). Salinity, on the other hand, had a slight fluctuation within the range 38 g/L to 43 g/L (Fig. 2), which characterizes other neighboring areas in the Gulf with the higher values during the hot summer months.

Nutrients levels

The levels detected for ammonium, nitrate, and nitrite ions (Table 1) fluctuated widely. Their mean values, however, were within the expected levels reported for surface sea waters but were higher than that reported for Greek coastal waters in the Mediterranean. The monthly TDN for the four investigated areas ranged between $0.1\text{-}55.0 \mu\text{g N L}^{-1}$, had no parti-

Table 1. Range and mean of dissolved oxygen, ammonia, nitrite, and nitrate concentrations in the surface waters of Abu-Dhabi, Dubai, Sharjah, and Ajman.

Station	DO (mg/L)	PO ₄ (µgP/L)	NH ₃ (µgN/L)	NO ₃ (µgN/L)	NO ₂ (µgN/L)	TDN(µgN/L)
Abu-Dhabi	6.1 - 6.7 (6.4)	0.2 - 23.1 (5.65)	<0.1 - 43.0 (19.5)	<0.1 - 10.8 (5.9)	<0.1 - 4.7 (1.5)	0.1 - 55.0 (27.0)
Dubai	5.4 - 6.7 (6.2)	0.2 - 10.2 (2.3)	<0.1 - 14.0 (2.4)	<0.1 - 30.0 (3.6)	<0.1 - 1.5 (0.3)	0.1 - 45.0 (6.3)
Sharjah	6.1 - 6.7 (6.5)	0.1 - 1.9 (0.5)	<0.1 - 2.9 (1.2)	<0.1 - 2.9 (0.5)	<0.1 - 0.3 (0.1)	0.1 - 5.6 (1.9)
Ajman	6.7 - 6.9 (6.8)	0.1 - 0.5 (0.2)	<0.1 - 2.1 (1.1)	<0.1 - 3.8 (0.6)	<0.1 - 0.2 (<0.1)	0.1 - 6.1 (1.7)

DO = Dissolved oxygen; TDN = Total dissolved nitrogen.

cular spatial or temporal trends and was generally lower in Sharjah and Ajman waters compared to those for Abu-Dhabi and Dubai waters. Occasional high concentrations are probably a reflection of a recent pollution input at the time of sampling as some sampling sites are near fishing and commercial marine routes or anchorage zones for boats, ships, and tankers. In addition, the upwelling activities observed in part of the Gulf, as described earlier, may account for the high levels of TDN occasionally observed.

Phosphate levels in the different sites also had a wide concentration range, 0.1-23.1 µg P L⁻¹ (Table 1). Relatively high phosphate was observed during the months of March and April in most sites. Most of these values, however, were within expected levels for surface marine waters (Riley et al. 1978). It is probably at this time of the year that most of the microbial degradation and release of such compounds in the water might take place, particularly in shallow waters where microbial activity thrives in bottom sediments. No apparent correlation was noticed between phosphate levels and microbial counts detected.

Dissolved oxygen (DO) levels (Table 1) fluctuated between 5.4 to 6.9 mg L⁻¹. Few samples had DO levels lower than 5.0 mg L⁻¹. Factors that may contribute to this low DO are the presence of a nearby mangrove forest and continuous pollutants' input from the intensive commercial activities and also the occasional oil pollution observed in the form of minor oil slicks. The maintenance of appropriate levels of DO is essential for a healthy marine environment and recommended levels of DO are ≈6 mg L⁻¹ and not less than 5 mg L⁻¹.

Heavy metals and hydrocarbons

The mean ranges of metal ions in water samples from all the sites are shown in Table 2. The heavy

Table 2. Ranges and mean values of heavy metal ions (µg/L) in the UAE coastal waters on the Arabian Gulf.

Element	Ranges	Mean ± SD
Manganese	0.70 - 1.30	0.93 ± 0.34
Iron	1.50 - 4.35	3.13 ± 1.29
Lead	0.84 - 1.25	1.00 ± 0.18
Cadmium	0.20 - 0.30	0.26 ± 0.04
Zinc	8.60 - 11.9	9.96 ± 1.45
Chromium	0.20 - 0.29	0.25 ± 0.04
Nickel	0.49 - 0.67	0.58 ± 0.08
Cobalt	0.51 - 0.65	0.58 ± 0.06
Copper	2.60 - 3.40	2.95 ± 0.33

metal ion levels were variable in the various locations. Manganese and iron in Ottawa coastal sea water, in comparison, ranged between 1.08 to 1.74 and 0.88 to 1.12 µg L⁻¹, respectively (Sturgeon et al. 1980). Copper levels in Lake Michigan, the English Channel, the Baltic Sea, and the Mediterranean Sea ranged between 3 to 5, ≤ 0.2 and 1 to 5 µg L⁻¹, respectively (Wiener 1979; Moore and Ramamourthy 1984). Copper and zinc levels in the Red Sea were in the ranges 3.3 to 3.9 and 6.9 to 14.3 µg L⁻¹, respectively (Hamza and Amireh 1992); while in Australian sea water, were 0.17 to 0.65 µg L⁻¹, respectively (Florence and Batley 1975). Copper and zinc levels in polluted water generally range between 0.5-1.0 and 0.5-15 µg L⁻¹, respectively (Moore and Ramamourthy 1984). The greater values observed in the samples in this study might be the result of high redox potentials of the adjoining paddy soils resulting in both ions being sequestered and chelated with organic molecules, which might have aided transportation of the heavy metals (Govardham 1990).

The levels of cadmium, lead, chromium, and nickel in polluted water were reported to vary as follows: cadmium, 0.29 to 0.55; lead, ≤ 3.0 ; chromium, 1.0 to 2.0; and nickel, 1.0 to 3.0 $\mu\text{g L}^{-1}$ (Moore and Ramamourthy 1984). Both chromium and nickel levels in uncontaminated sea water are 0.05 to 0.5 and $\leq 1.8 \mu\text{g L}^{-1}$, respectively. Higher levels of lead often occur in water bodies near highways and large cities due to high gasoline combustion. The slightly higher levels of some of these elements in this study are an indication of disturbance to the ecosystem by various anthropogenic factors such as various industrial water discharges or the occasional and often deliberate release of oil in the Gulf waters.

The polyaromatic hydrocarbon concentrations in surface sea water were found in the range of 0.065 - 0.41 $\mu\text{g L}^{-1}$ as chrysene equivalents and from 1.47 to 6.6 $\mu\text{g L}^{-1}$ as Kuwait crude oil equivalents. Sediment hydrocarbons were found in the range of 0.89 - 1.2 $\mu\text{g kg}^{-1}$ as chrysene equivalents and from 19.2 to 26.4 $\mu\text{g kg}^{-1}$ as Kuwait crude oil equivalents. These values are higher than levels reported for the English Channel waters (Law et al. 1987) or the Mediterranean Sea (Dedomenico et al. 1994). Intense industrial activities in this part of the Gulf, in addition to reduced motion of water and wind and the high crude oil input into the waters during the Gulf War may account for these relatively high concentrations.

Bacterial communities enumeration

The trends observed for the overall means of bacterial populations' counts in the tested sites are shown in Fig. 3. TSB fluctuated between 3×10^4 to 4×10^5 CFU/mL, while the STSB counts ranged between 2×10^4 to 2.4×10^5 CFU/mL and the GNB ranged between 1×10^4 and 1.3×10^5 CFU/mL.

The three bacterial communities had the same fluctuation patterns, with relatively low counts during both the summer months (June and July) and the winter months (January to April), and two peaks, a relatively small one in mid-spring (May) and a high one in autumn (October). Both of these peaks were at times when the temperature was around 30°C and decreased at higher or lower temperatures. Similar observations were reported for other coastal waters around the UAE (Hassan et al. 1993; 1996). Only limited inter-site differences were observed, which could be due to localized effects.

TC and FC counts (Fig. 4) followed the same pattern described earlier for the other bacterial populations.

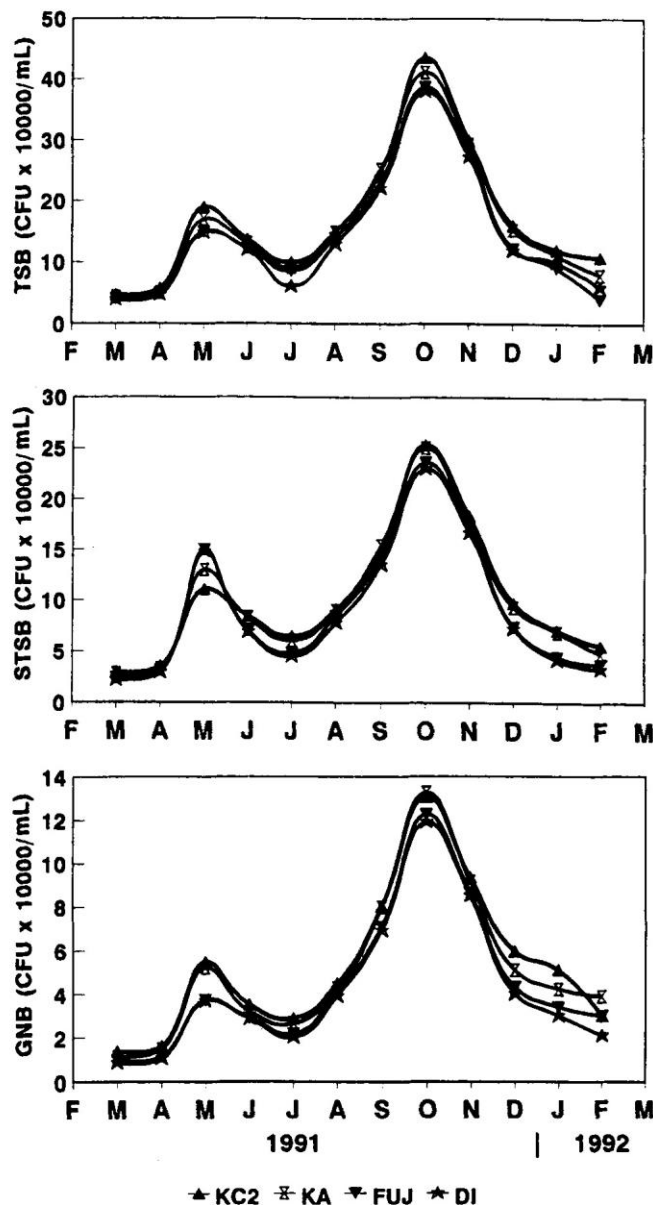


Fig. 3. Mean counts of TSB, STSB, and GNB in all the sites tested

The two high peaks were observed in May and October. Their ranges fluctuated between 0-650 and 0-190 CFU/100 mL, respectively. The main species detected were *Escherichia coli*, *Citrobacter freundii*, and *Enterobacter agglomerans*. The main Gram positive and Gram negative bacterial species identified are listed in Table 3. The predominant Gram-positive bacterial genera detected were *Bacillus*, *Staphylococcus*, and *Micrococcus*, while the predominant Gram-negative genera were *Alteromonas*, *Pseudomonas*, and *Alcaligenes*. A comparison of the total numbers for the different bacterial communities after and before the Gulf War was carried out (Table 4). Only the Abu-Dhabi area showed generally higher

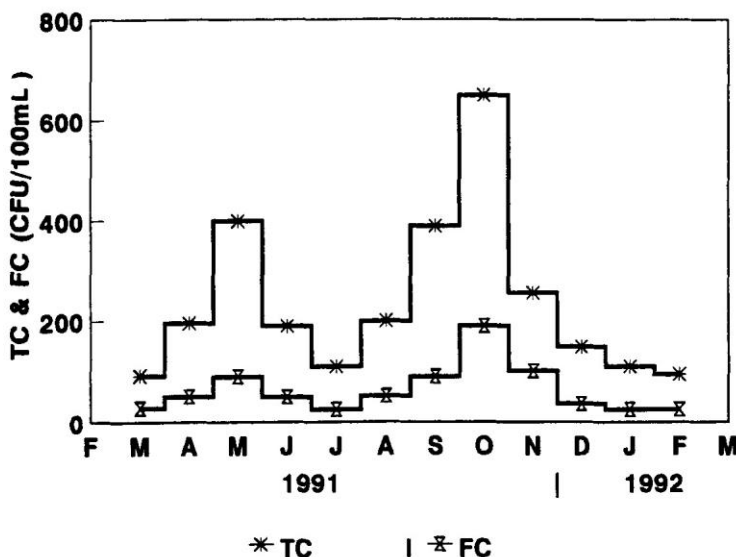


Fig. 4. Mean counts of total and faecal coliform bacteria in all the sites tested.

Table 3. The most common species of bacteria identified in coastal waters of UAE.

Gram positive	Gram negative
<i>Bacillus licheniformis</i>	<i>Alteromonas haloplanktis</i>
<i>B. firmus</i>	<i>A. citrea</i>
<i>B. megaterium</i>	<i>A. communis</i>
<i>B. cereus</i>	<i>A. ruba</i>
<i>B. pumilus</i>	
<i>Staphylococcus sciuri</i>	<i>Pseudomonas marina</i>
<i>S. xylosus</i>	<i>P. doudehoffii</i>
<i>S. epidermidis</i>	<i>P. nautica</i>
<i>Micrococcus varians</i>	
<i>M. luteus</i>	
<i>M. roseus</i>	

Table 4. The difference of bacterial counts (counts post-war/counts pre-war x 100).

Station	% difference of bacterial counts (post/pre-Gulf War)				
	TSB	STSB	GNB	TC	FC
Abu-Dhabi	1.60	1.10	2.00	1.30	2.00
Dubai	0.71	0.34	0.40	0.63	1.10
Sharjah	0.48	0.44	0.54	0.33	0.64
Ajman	0.94	0.63	0.50	0.38	0.50

TSB = total saprophytic bacteria; STSB = salt tolerant saprophytic bacteria; GNB = gram negative bacteria; TC = total coliform; FC = faecal coliform.

counts post-war compared to pre-war results. All other sites had lower post-war counts.

CONCLUSION

Post-Gulf War nutrients, dissolved oxygen, and bacterial levels were all within normal ranges with occasional increases mainly due to local discharges or pollution sources. Most heavy metal levels were within expected ranges for sea waters while a few were slightly higher than expected. Hydrocarbon levels were high compared to levels in other sea water. There appears to be a slight degree of microbial pollution in UAE coastal waters. Chemical pollution with hydrocarbons, however, is the more serious problem that has been aggravated by the deliberate release of crude oil during the Gulf War. Attention, therefore, has to be focused by local authorities to keep pollution sources under control by international bodies to ensure avoidance of any reoccurrence of previous pollution tragedies in this valuable recreational and commercial water body.

REFERENCES

Abu-Hilal, A.H.; Khordagui, H.K. Assessment of tar pollution on the United Arab Emirates beaches. *Environ. Int.* 19: 589-596; 1993.

Abu-Hilal, A.H.; Banat, I.M.; Hassan, E.S.; Adam, A.B. Sanitary conditions in three creeks in Dubai, Sharjah and Ajman Emirates on the Arabian Gulf (UAE). *Environ. Monit. Assess.* 32: 21-36; 1994.

Balows, A.; Truper, H.G.; Dworkin, M.; Harder, W.; Schleifer, K. *The prokaryotes: A handbook on the biology of bacteria:*

- Ecophysiology, isolation, identification, applications. Second ed. Vol.II-IV. New York, NY: Springer Verlag; 1992: 1300-3338.
- Banat, I.M.; Hassan, E.S.; Abu-Hilal, A.H.; Adam, A.B. Microbial and nutrient pollution assessment of coastal and creek waters of northern UAE. *Environ. Int.* 19: 669-678; 1993.
- Cederwall, H.; Elmgren, R. Biomass increase of benthic macrofauna demonstrates eutrophication of the Baltic Sea. *Ophelia Suppl.* 1: 287-304; 1980.
- Dedomenico, L.; Crisafi, E.; Magazzu, G.; Puglisi, A.; Larosa, A. Monitoring of petroleum hydrocarbon pollution in surface waters by a direct comparison of fluorescence spectroscopy and remote sensing techniques. *Mar. Pollut. Bull.* 28: 587-591; 1994.
- Degobbis, D. Increased eutrophication of the northern Adriatic Sea: Second Act. *Mar. Pollut. Bull.* 20: 452-457; 1989.
- Dorgham, M.M.; Muftah, A.; El-Deeb, K.Z. Plankton studies in the Arabian Gulf II. The autumn phytoplankton in the northwestern area. *Arab Gulf J. Sci. Res. Agric. Biol. Sci.* B5: 215-235; 1987.
- Dorgham, M.M. Temporal and spatial variations of the phytoplankton in Quatari waters, Arabian Gulf. *J. Fac. Sci. UAE Univ.* 3: 105-128; 1991.
- Florence, T.M.; Batley, G.E. Removal of trace metals from seawater by chelating resin. *Talanta* 22: 201-204; 1975.
- Friligos, N. Nutrient conditions in the Euboikos Gulf (west Aegean). *Mar. Pollut. Bull.* 16: 435-439; 1985.
- Govardham, V. Ground water pollution hazardous to human life. A case study of Nalgonda district. *Ind. J. Environ. Protect.* 10: 54-61; 1990.
- Grasshoff, K. Methods of seawater analysis. New York, NY, and Weinheim, Germany: Verlag Chemie; 1976.
- Hamza, A.G.; Amireh T.A. Determination of Pb, Cd, Cu and Zn ions in Red Sea water along Jeddah coast by differential pulse anodic stripping voltammetry. *J. Fac. Sci. UAE Univ.* 4: 80-90; 1992.
- Hassan, E.S. Monitoring of microbial water quality and saprophytic bacterial genera of the Abu-Dhabi coastal area, UAE. *Mar. Biol.* 116: 489-495; 1993.
- Hassan, E.S.; Banat, I.M.; Shair, S.A.; Abu-Hilal, A.H. Microbial assessment of coastal waters in three northern Emirates in the UAE. *J. Fac. Sci. UAE Univ.* 5: 91-103; 1993.
- Hassan, E.S.; Banat, I.M.; El-Shahawi, M.S.; Abu-Hilal, A.H. Bacterial, nutrients and heavy metal ions pollution assessment along the eastern coastal area of the United Arab Emirates. *J. Aqu. Ecosys. Health* 5: 73-81; 1996.
- Holt, J.D. Bergeys manual of systematic bacteriology. Vol. I. Baltimore, MD: Williams and Wilkins; 1984: 140-601.
- Holt, J.D. Bergeys manual of systematic bacteriology. Vol. II. Baltimore, MD: Williams and Wilkins; 1986: 999-1372.
- IOC (Intergovernmental Oceanographic Commission). Manuals and Guides, No. 7: Guide to operational procedures for the IGOSS pilot project on marine pollution (petroleum) monitoring. Paris: UNESCO; 1976: 50.
- Law, R.J.; Marchand, M.; Dahlmann, G.; Fileman, T.W. Results of two bilateral comparison of the determination of hydrocarbon concentrations in coastal sea water by fluorescence spectroscopy. *Mar. Pollut. Bull.* 12: 153-157; 1987.
- LeChevallier, M.W.; Seidler, R.J.; Evans, T.M. Enumeration and characterization of standard plate count bacteria in chlorinated and raw water supplies. *Appl. Environ. Microbiol.* 40: 922-930; 1980.
- Lo, J.M.; Lin, Y.P.; Lin, K.S. Preconcentration of trace metals in sea water matrix for inductively coupled plasma atomic absorption spectrometry. *Analyt. Sci. (Japan)* 7: 455-460; 1991.
- Mood, E.W. Bacterial indicators of water quality in swimming pools and their role. In: Hoadley, A.W.; Dutka, B.J., eds. Bacterial indicators/hazards associated with water. Philadelphia, PA: American Society for Testing and Materials; 1977: 239-246.
- Moore, J.W.; Ramamourthy, S. Heavy metals in natural waters. New York, NY: Springer Verlag; 1984.
- Muller, G. Bacterial indicators and standards for water quality in the Federal Republic of Germany. In: Hoadley, A.W.; Dutka, B.J., eds. Bacterial indicators/hazards associated with water. Philadelphia, PA: American Society for Testing and Materials; 1977: 159-167.
- Parsons, T.R.; Maita, Y.; Lalli, C.M. A manual of chemical and biological methods for seawater analysis. New York, NY: Pergamon Press; 1984.
- Pipes, W.O.; Mueller, K.; Troy, M.; Minnigh, H. Frequency-of-occurrence monitoring for coliform bacteria in small water systems. *J. Amer. Water Work. Assoc.* 79: 59-63; 1987.
- Ptak, D.J.; Ginsburg, W. Bacterial indicator of drinking water quality. In: Hoadley, A.W.; Dutka, B.J., eds. Bacterial indicators/hazards associated with water. Philadelphia, PA: American Society for Testing and Materials; 1977: 218-221.
- Rees, G. Health implementation of sewage in coastal waters: The British case. *Mar. Pollut. Bull.* 26: 14-19; 1993.
- Riley, J.P. Nutrient chemicals (including those derived detergents and agricultural chemicals). In: Goldberg, E.D., ed. A guide to marine pollution. New York, London, Paris: Gordon and Breach Science Publishers; 1978.
- Rosenberg, R., ed. Eutrophication in marine waters surrounding Sweden-A review. Swedish National Environment Protection Board. Report 1808. 1984: 140.
- Rosenberg, R. Eutrophication-The future marine coastal nuisance. *Mar. Pollut. Bull.* 16: 227-231; 1985.
- Satsmadjis, J.; Nakopoulou, C.; Hadjigeorgiou, E. Distribution of nutrients in the Bay of Navarin, Greece. *Mar. Pollut. Bull.* 16: 120-123; 1985.
- Strickland, J.D.H.; Parsons T.R. A practical handbook of seawater analyses. Canada: Bull. Fish. Res. Bd.; 1972.
- Sturgeon, T.E.; Berman, S.S.; Desaulniers, A.; Russell, D.S. Preconcentration of trace metals from sea water for determination by graphite furnace atomic absorption spectrometry. *Talanta* 27: 85-94; 1980.
- Thangaraja, M. Studies on red tides of Oman. Marine Science and Fisheries Center (MSFC) Research Report No. 90-2. Muscat, Sultanate of Oman: Ministry of Agriculture and Fisheries; 1990: 18.
- Wiener, J.R. Aerial inputs of cadmium, copper lead and manganese into a freshwater pond in the vicinity of coal fired power plant. *Water Air Soil Pollut.* 12: 343-353; 1979.
- Zoffmann, C.; Rodriguez-Valera, F.; Perez-Fillol, M.; Ruia-Bevia, F.; Torreblanca, M.; Colom, F. Microbial and nutrient pollution along the coasts of Alicante, Spain. *Mar. Pollut. Bull.* 20: 74-81; 1989.

Sensitive detection and semiquantitative determination of mercury(II) and lead(II) in aqueous media using polyurethane foam immobilized 1,5-di-(2-fluorophenyl)-3-mercaptoformazan

A.M. Kiwan^a, M.S. El-Shahawi^{a,*}, S.M. Aldhaheri^a, M.H. Saleh^b

^a Department of Chemistry, Faculty of Science, UAE University, P.O. Box: 17551, Al-Ain, United Arab Emirates

^b Ministry of Health, P.O. Box: 841, Abu Dhabi, United Arab Emirates

Received 31 January 1997; received in revised form 8 April 1997; accepted 15 April 1997

Abstract

1,5-Di-(2-fluorophenyl)-3-mercaptoformazan (F_2H_2Dz) immobilized and plasticized with tri-*n*-butylphosphate (TBP) polyurethane foam (PUF) were found suitable for the detection of mercury(II) and lead(II) in extremely dilute aqueous solutions. In batch mode of extraction with immobilized F_2H_2Dz -foam as low as 0.05 and 0.15 $\mu\text{g ml}^{-1}$ of mercury(II) and lead(II), respectively were detected and the colored chelates were found more stable over 72 h. Lower concentrations of these metal ions (≤ 1 ppb) were detected by plasticized F_2H_2Dz -TBP foam packed in column extraction mode. Semiquantitative determination of these metals was also possible using a suitable standard color scale. The effect of diverse ions on the detection of 1 μg mercury(II) and lead(II) by the proposed F_2H_2Dz -foam test was critically investigated. The method was satisfactorily applied for the detection of mercury(II) or lead(II) in natural water samples. © 1997 Elsevier Science B.V.

Keywords: Polyurethane foam; 1,5-Di-(2-fluorophenyl)-3-mercaptoformazan; Mercury(II); Lead(II) detection

1. Introduction

The toxicity of mercury and lead is attributed to their harmful effects on the central nervous system disturbing haem synthesis as well as for causing neuropsychiatric disorders [1,2]. Lead and its compounds have an important role in many industries where small amounts of it are ingested and/or inhaled regularly with food and drink

[3,4]. Mercury is a toxic element sparsely distributed in the lithosphere and water where its average concentrations range from 0.08 and 0.80 ppm in igneous and sedimentary rocks, respectively [5]. Natural soils have been found to contain mercury in the range 0.01–0.50 ppm [5].

Dithizone (H_2Dz) reacts with many metals and organometallic ions to form highly colored complexes which are insoluble in water but can be extracted into organic solvents [6–8]. Although this reagent is a sensitive analytical reagent for many metal ions, it is not selective in neutral or

* Corresponding author. Department of Chemistry, Faculty of Science at Damietta, Mansoura University, Damietta, Egypt.

alkaline media. However, its selectivity is enhanced by controlling the pH values, and/or by adding suitable complex forming agents (masking agents) to the aqueous solution [6] and by introducing various substituents in its phenyl rings [7].

The pioneering studies of Braun and Farag [9] on the application of PUF sorbents to trace elements led to the revealing of the potentialities of their special geometrical form: spherical membrane-shaped geometry and to the proposal of their general use in column operations as a substitute for the traditional granular supports in extraction chromatography [9,10]. Open cell PUF immobilizing or anchoring specific chromogenic organic reagents (chromofoams) have been successfully employed for the sensitive detection and semiquantitative determination and collection of several metal ions including Pb^{2+} and Hg^{2+} ions [10–16]. No work has been yet reported on the application of polyurethane foam immobilizing 1,5-di-(2-fluorophenyl)-3-mercaptoformazan, ($\text{F}_2\text{H}_2\text{Dz}$) for the detection and quantitative collection of mercury(II) and lead(II) in aqueous media. Accordingly, the use of immobilized-polyurethane foam is described here for simple, rapid, and sensitive detection of trace concentrations of mercury and lead.

2. Experimental

2.1. Reagents and materials

All chemicals used were of Analytical Reagent Grade. Open cell polyether based polyurethane foam was supplied by K.G. Schaum (Stoffwerk, Kremsmunster, Austria). Foam cubes of approximately 1 cm^3 were cut from polyurethane foam sheet. The foam material (cubes of ca. 5 mm edge) was washed and dried as previously reported [10]. Stock solutions containing 1.00 mg ml^{-1} of mercury and lead were prepared by dissolving the appropriate amounts of mercury(II) chloride and lead(II) nitrate in deionized water slightly acidified with nitric acid and standardized by EDTA titration. BDH tributylphosphate (TBP) was used without further purification. Series of standard mercury and lead solutions were prepared by

dilution with water acidified with few drops of 1 M nitric acid solution.

2.2. Synthesis of

1,5-di-(2-fluorophenyl)-3-mercaptoformazan, ($\text{F}_2\text{H}_2\text{Dz}$)

The reagent 1,5-di(2-fluorophenyl)-3-mercaptoformazan was prepared by the nitroformazyl method as described elsewhere [7]. The reagents $\text{F}_2\text{H}_2\text{Dz}$ and H_2Dz solutions were prepared separately by dissolving 0.02 g of each reagent in 100 ml dichloromethane. These solutions were kept refrigerated prior to use under acidified aqueous solutions containing 0.2 M sulphuric acid and 0.1 M sodium sulphite. The foam cubes were loaded with $\text{F}_2\text{H}_2\text{Dz}$ or H_2Dz in the presence of sulphur dioxide and were dried as reported by Braun and Farag [11]. The plasticized $\text{F}_2\text{H}_2\text{Dz}$ -TBP or H_2Dz -TBP foams were prepared by mixing the dried foam cubes with the reagents in TBP (0.1% w/v) with efficient stirring for 15 min and dried as reported [11].

2.3. Apparatus

A Shimadzu double beam UV-visible scanning spectrophotometer model UV-2101 PC with 1 cm stoppered quartz cells and a Shimadzu FTIR-8101 Fourier Transform infrared spectrophotometer were used. An Orion pH-meter and glass columns (15 cm height \times 10 mm I.D.) were also used.

2.4. General procedures

2.4.1. Batch experiments

To examine the uptake of mercury(II) and lead(II) on 1,5-di(2-fluorophenyl)-3-mercaptoformazan-loaded or plasticized $\text{F}_2\text{H}_2\text{Dz}$ -TBP treated foam, one reagent-loaded foam cube is mixed and shaken with 2–3 ml of the test solution for 2–3 min. A color change of the foam from green to orange-red or pink in the presence of mercury and lead was observed, respectively. For the semiquantitative determination of mercury and lead, a foam color scale is prepared from a series of standard solutions with different concentration of

Table 1

Characteristic absorption i.r. (cm^{-1}) and electronic (nm) spectral data for the reagents $\text{F}_2\text{H}_2\text{Dz}$ and H_2Dz and their mercury(II) and lead(II) chelates in KBr for discs^a

Compound	Wave number, cm^{-1}					
	$\nu(\text{N-H})$	$\nu(\text{N=N})$	$\delta(\text{N-H})+(\text{C=N})$	$\nu(\text{N-C-S})$	λ_{max} (nm)	$\epsilon \times 10^{-3} \text{ l mol}^{-1} \text{ cm}^{-1}$
$\text{F}_2\text{H}_2\text{Dz}$	2950 (br)	2380 (w)	1510 (s)	1485 (s)	632	25.3
				1450 (s)	454	23.7
H_2Dz	2960 (br)	2365 (w)	1515 (s)	1505 (s)	615	35.8
				1465 (s)	454	17.9
$\text{Hg}(\text{F}_2\text{HDz})_2$	3300 (m)	1620 (s)	1510 (m)	1490 (s)	484	64.8
		1590 (m)		1470 (cm)		
		3100 (w)	1540 (s)			
$\text{Pb}(\text{F}_2\text{HDz})_2$	3340 cm					
	3290 (s)	1615 (s)				
	3085 (w)	1600 (s)	1520 (s)	1495 (s)	521	65.1
		1540 (s)		1475 (s)		
$\text{Hg}(\text{HDz})_2$	3210 (cm)					
	3170 (br)	1600 (s)	1510 (s)	1505 (s)	485	71.0
$\text{Pb}(\text{HDz})_2$		1570 (s)				
	3280 (m)	1610 (s)	1515 (s)	1510 (s)	518	69.05
	3180 (s)	1564 (vw)				

^a s = strong, m = medium, w = weak, vw = very weak, sh = shoulder and br = broad.

each metal and the reagent $\text{F}_2\text{H}_2\text{Dz}$ loaded-foam. The concentration of the unknown sample solution was determined by comparison to this scale under the same conditions.

2.4.2. Column experiments

One gram of the $\text{F}_2\text{H}_2\text{Dz}$ -loaded or plasticized $\text{F}_2\text{H}_2\text{Dz}$ -TBP foam in the presence of a acidified aqueous solution of sodium sulphate was homogeneously packed in a glass column by the vacuum method [9,12]. $\text{F}_2\text{H}_2\text{Dz}$ -foam bed in the column was then covered with an acidified aqueous solution of sodium sulphite. A standard series of the metal ion (Hg^{2+} or Pb^{2+}) in 100 ml aqueous solutions at the optimum pH of complex formation was percolated through $\text{F}_2\text{H}_2\text{Dz}$ loaded foam columns at flow rates of 2–3 ml min^{-1} . The aqueous solution of the unknown sample (100 ml) is then passed through the reagent foam column under identical experimental conditions. For the semiquantitative determination of Hg^{2+} or Pb^{2+} , the length of the resulting colored zone foam bed was compared to that of the standard series.

3. Results and discussion

Table 1 summarizes the characteristic infrared frequencies of the solid reagents $\text{F}_2\text{H}_2\text{Dz}$ and H_2Dz along with their mercury(II) and lead(II) complexes. The electronic spectra of the reagents and their complexes with mercury(II) and lead(II) in dichloromethane and in parallelepiped polyurethane foams are also included in Table 1. The electronic spectra of the reagents in dichloromethane showed two well resolved absorption bands in the region of 445–448 and 609–615 nm, whereas their mercury(II) and lead(II) complexes showed well defined single bands in the range 484–521 with slight hypsochromic shift in polyurethane foams. In dichloromethane and polyurethane foams, the introduction of fluorine atoms into the ortho positions of the phenyl nuclei of dithizone leads to small bathochromic shifts in both its bands and also on the values of their relative molar absorptivities compared to dithizone (Table 1). The $\log \epsilon_1$, max decreased to 25.3×10^3 and the $\log \epsilon_2$

max is increased to $23.7 \times 10^3 \text{ l mol}^{-1} \text{ cm}^{-1}$ of $\text{F}_2\text{H}_2\text{Dz}$ compared to H_2Dz in dichloromethane. Since $\text{Hg}(\text{HDz})_2$ was found to be tetrahedral [17], the corresponding complex of $\text{F}_2\text{H}_2\text{Dz}$ is most likely tetrahedral.

Considerable interest has been focused on the use of the chromofoam test in batch and dynamic modes for the separation and preconcentration of different metal ions including Hg^{2+} and Pb^{2+} species from aqueous media [9–16]. The immobilization of water insoluble chelating agent within the solid foam combines the advantages of both liquid–liquid and liquid–solid extraction techniques [10]. The immobilized reagent foam combines both the selectivity of the chelating agent and the advantageous rapidity of kinetic process between metal ions in the aqueous solution and the reagent immobilized in the foam membranes [11].

3.1. Detection and semiquantitative determination of mercury(II) with 1,5-di-(2-fluorophenyl)-3-mercaptoformazan

In a weakly acidic solution ($\text{pH} < 5$), 1,5-di-(2-fluorophenyl)-3-mercaptoformazan forms an insoluble orange-red chelate with mercury(II) ions. The complex formed is readily extracted by organic solvents [7] without change in color. This reaction was employed with unloaded foam, $\text{F}_2\text{H}_2\text{Dz}$ -loaded foam and $\text{F}_2\text{H}_2\text{Dz}$ -TBP plasticized foams to detect mercury(II) in the aqueous solution. The reagent $\text{F}_2\text{H}_2\text{Dz}$ is uniformly distributed within the foam cubes and acts as an efficient collector for the mercury(II) present in the aqueous media. The developed colored complex on the foam was easily observed.

On shaking one cube of the unloaded foam with the test solution mixture of the orange-red $\text{Hg}(\text{F}_2\text{HDz})_2$ complex in a test tube, it was possible to detect as low as 0.15 ppm mercury. The sensitivity of the test was slightly improved to (0.10 ppm) and the color development was achieved in less than 1 min of shaking in the presence of acetate ions. This may be attributed to the ability of acetate ions to act as a coordinating ligand and form a quasi octahedral adduct in the large surface area and the bulk of the

polyurethane foam as postulated in Fig. 1. Acetate anion is known to coordinate with the mercury(II) ions and form stable complexes [18,19] as indicated by the values of their stability constants ($\log k_1 = 5.55$ and $\log \beta_2 = 9.30$). Such unusual octahedral coordination of $\text{Hg}(\text{II})$ is known for a number of O-donor ligands [20]. The nitrogen of the urethane or oxygen of the ether linkage of the polyurethane foam under these conditions may also acts as a coordinating ligand towards mercury(II) ions producing a mixed ligand complex [21].

The detection of mercury(II) ions was improved further to 0.05 and 0.01 ppm by employing immobilizing $\text{F}_2\text{H}_2\text{Dz}$ on polyurethane foam and plasticized $\text{F}_2\text{H}_2\text{Dz}$ -TBP foam ion batch extraction mode, respectively. The color of the mercury complex was developed on the plasticized foam faster than in the case of the unplasticized foam where the tri-n-butylphosphate may act as a plasticizer on the foam. The color was also stable for more than 48 h. The plasticizer has a dual purpose [11,12], i.e. it acts as an efficient non-volatile solvent as well as a plasticizer for the foam itself.

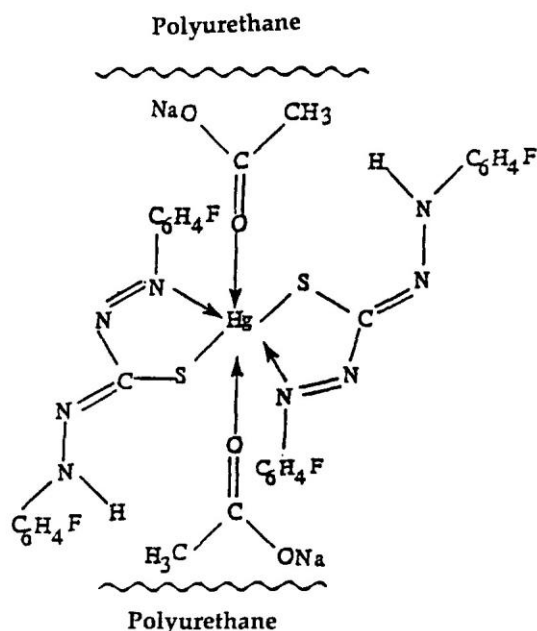


Fig. 1. A postulated structure of the mixed acetate F_2HDz -mercury(II) quasi complex on the polyurethane foam.

Table 2

Comparative sensitivity of batch F₂H₂Dz (a) and H₂Dz (b) for the detection of mercury(II) ions employing polyurethane foams

Method	Amount of Hg ²⁺ detected (ppm)		Reference
	(a)	(b)	
Spot test on spot plate	—	5.0	Feigl and Anger, 1972
Unloaded foam in the absence of acetate ions	0.15 ^a	0.25 ^a	
Unloaded foams in the presence of acetate ions	0.10 ^a	0.20	Farag et al., 1987
Immobilized reagent foam in the presence of acetate ions	0.05 ^a	0.10	Abou-Elmaty, 1990
Plasticized TBP-reagent foam	0.01 ^a	0.10	Abou-Elmaty, 1990

^a Present work.

This modification increases the mobility of the molecular segments and decreasing the glass transition temperature (T_g) of the system [11]. The mobility of plasticizer molecules within the polymeric network above the T_g is quite high and the individual plasticizer molecules have varying degrees of mobility within the foam matrix [11]. Therefore, the preconcentration and the diffusion rates of chemical species through the micropores and the quasi-spherical membrane structures of the plasticized foam material were found higher than with the unplasticized foams. Obviously, these results (Table 2) are much better than those reported with dithizone [22,23] and the conventional spot test [24].

In aqueous media, the diffusion of mercury(II) species into the micropores of the foam membranes is possibly consistent with the solubility of the Hg(F₂HDz) complex as previously reported for HFeX₄ and HAuX₄ [25]. The retention of mercury(II) ions on F₂H₂Dz-TBP loaded foams may involve three steps: bulk transport of solute in solution, film transfer involving diffusion of solute through a hypothetical film boundary and diffusion of the solute with the pore volumes of the adsorbent and along pore-wall surfaces to active adsorption sites as reported for cobalt(II) retained on 2-thenoyltrifluoroacetone impregnated on polyurethane foam [26]. Thus, in the TBP-foam, the film and the intraparticle transport are the major factors controlling rates of retention of mercury(II) from solutions by porous sorbents.

The color intensity on the F₂H₂Dz-foam was found to depend on the concentration of mer-

cury(II) in the aqueous solution. Thus a semiquantitative determination of mercury(II) was found possible by comparing the color of the test solution with a standard color scale of the foam cubes prepared with 0.1, 0.5, 1, 5, 10 and 15 ppm mercury(II) in aqueous solution. The proposed foam method was examined for the detection of mercury(II) in natural water spiked with mercury(II) ions and satisfactory results were obtained.

Moreover, the proposed F₂H₂Dz-foam reagent was easily packed in a column for quantitative collection and semiquantitative determination of mercury(II) in extremely dilute aqueous solution. This was achieved by percolating 100 ml of the test solution through the foam column at 2–3 ml min⁻¹ flow rate. It was found possible to detect as low as 1 ppb of mercury in of the aqueous solution. This result is much better than that reported (100 ppb) for the detection of mercury(II) ions in aqueous solution with a column packed with jel beads containing dithizone [27]. The length of the colored foam bed was found proportional to the amount of mercury(II) ions present in the aqueous solution. At flow rate > 5 ml/min the colored zone boundary became diffuse. Thus, semi-quantitative determination of mercury(II) in 100 ml aqueous solution was successfully carried out at 2–3 ml/min using a standard color scale covering the range 1–20 ppb of mercury(II) where a linear relationship between the length (cm) of the colored foam zone on the foam column and the mercury(II) concentration was achieved (Fig. 2¹).

¹ Each point in the figure represents an average of three measurements ± standard deviation.

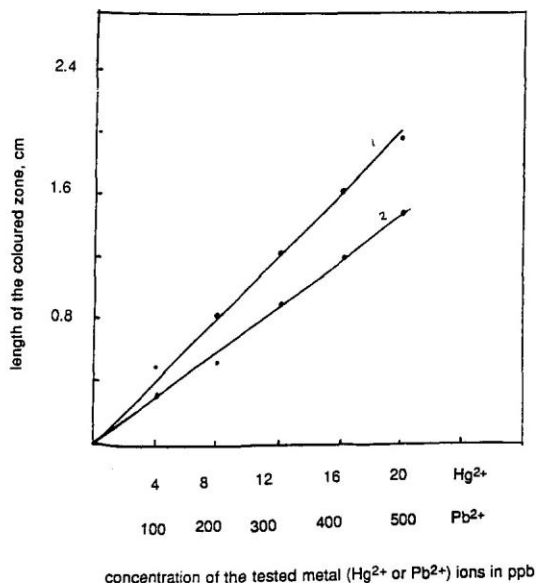


Fig. 2. Relationship between the length of the colored zone foam-bed (mm) on the foam column and the concentrations of mercury(II), 1 or lead(II), 2. Each point in the curve represents an average of three measurements \pm SD.

The results obtained with immobilized or plasticized-TBP foam with F_2H_2Dz were found better than those obtained for dithizone (Table 2). The high distribution ratio, $\log D = 4.45$ of $Hg(F_2HDz)_2$ chelate compared to $\log D = 3.92$ of $Hg(HDz)_2$ may account for the higher sensitivity of F_2H_2Dz as compared to H_2Dz towards mercury(II). The values of the D for the complexes $Hg(F_2HDz)_2$ and $Hg(HDz)_2$ retained on the polyurethane foams were calculated employing the equation:

$$D = \frac{\%E}{100 - \%} \times \frac{Vs (ml)}{w (g)}$$

where E , V_s and W are the percentage of the Hg^{2+} ions extracted from the bulk solution, volume of the tested solution and weight of polyurethane foams, respectively.

The higher molecular weight and the diffusion rates of the chelate $Hg(F_2HDz)_2$ through the thin membrane of the polyurethane foams may be also responsible for enhancing the sensitivity of the F_2H_2Dz towards metal ions as compared to H_2Dz . This behavior is consistent with the general understanding that, the larger the molecular weight of the sorbate the larger the amount of the chelate retained on the non-polar phase when the substances concerned are similar in nature [28]. These findings are parallel to the relevant liquid-liquid extraction data reported by Kiwan and Kassim [7,8] for the higher distribution ratio of F_2H_2Dz and its metal chelates compared to dithizone and its complexes [29,30].

3.2. Detection and semiquantitative determination of lead(II) with 1,5-di(2-fluorophenyl)-3-mercaptoformazan

Lead(II) in aqueous solutions at a concentration as low as 0.10 ppm was easily detected by shaking the test solution with a cube of plasticized F_2H_2Dz -TBP foam, in a batch extraction mode. A comparison between this result (Table 3) and the reported data employing dithizone and other chelating agents [3,15,22–24] shows that the proposed method is more sensitive for the detection of lead(II) than dithizone. Semiquantitative determination of lead(II) was also possible by F_2H_2Dz -

Table 3
Comparative sensitivity of batch F_2H_2Dz (a) and H_2Dz (b) for the detection of lead(II) ions employing polyurethane foams

Method	Amount of Pb^{2+} detected (ppm)		Reference
	(a)	(b)	
Spot test	—	0.80	Feigl and Anger, 1972
Unloaded foam	0.30	0.30	Present work
Immobilized reagent foam	0.15 ^a	0.20	Farag et al., 1986
Plasticized TBP-reagent foams	0.01	0.10	Present work

^a Present work.

Table 4

Detection of 1 μg of mercury and lead with 1,5-di-(2-fluorophenyl)-3-mercaptopformazan immobilized polyurethane foams in the presence of some interfering ions

Ion	Compound added	Tolerance limit ^a		Note
		(a)	(b)	
MnO_4^-	KMnO_4	$1:1 \times 10^3$	$1:1 \times 10^3$	Add one crystal (~ 0.5 g) of sodium azide
Formate	Formic acid	$1:1 \times 10^4$	$1:1 \times 10^4$	Add bromine water and boil the solution
Bi^{3+}	$\text{Bi}(\text{NO}_3)_3 \cdot 7\text{H}_2\text{O}$	$1:1 \times 10^3$	$1:1 \times 10^3$	Add few crystals (~ 0.5 g) of thiourea
Zn^{2+}	ZnSO_4	$1:1 \times 10^4$	$1:1 \times 10^3$	Add 1 ml of HNO_3 (0.01)
Mn^{2+}	$\text{MnSO}_4 \cdot 4\text{H}_2\text{O}$	$1:4 \times 10^3$	$1:1 \times 10^4$	Add 1 ml of bromine water and boil the solution
Fe^{2+}	FeSO_4	$1:5 \times 10^3$	$1:1 \times 10^4$	Add one crystal (~ 0.5 g) of NaF
Fe^{3+}	FeCl_3	$1:1 \times 10^3$	$1:1 \times 10^3$	Add 1 ml of saturated NaF
Cd^{2+}	$\text{Cd}(\text{NO}_3)_2$	$1:1 \times 10^3$	$1:1 \times 10^2$	Add one crystal (~ 0.5 g) of thiourea
Cr^{3+}	$\text{Cr}(\text{NO}_3)_3 \cdot 6\text{H}_2\text{O}$	$1:1 \times 10^3$	$1:1 \times 10^4$	Add bromine water and boil the solution
Ni^{2+}	NiCl_2	$1:1 \times 10^3$	$1:1 \times 10^3$	Add one crystal (~ 0.5 g) of thiourea
NO_2^-	NaNO_2	$1:1 \times 10^3$	$1:1 \times 10^3$	Add 1–2 ml of NaF (1 M)
VO_3^-	$(\text{NH}_4)_2\text{VO}_3$	$1:1 \times 10^3$	$1:1 \times 10^3$	Add one crystal (~ 0.5 g) of NaF

(a) Tolerance limit of the interfering ions towards 1 μg mercury(II) ions.

(b) Tolerance limit of the interfering ions towards 1 μg lead(II) ions.

TBP foam in batch extraction mode using the standard color scale 0.1, 0.5, 1, 5 and 10.0 ppm under the same experimental conditions.

The proposed plasticized $\text{F}_2\text{H}_2\text{Dz}$ foam was employed in column for the quantitative collection of lead(II) in extremely dilute aqueous solution by passing 1 l of the test solution (at pH 4.5–6) through the foam column at 2–5 ml min^{-1} flow rate. As low as 50 ng ml^{-1} of lead(II) ions was easily detected by the proposed procedures. The length of the orange-red colored foam bed was found stable for more than 48 h and proportional to the concentration of lead(II) in the aqueous solution (Fig. 2). These results extend the use of the foam column for the semiquantitative determination of lead(II) ions at the concentration level 50–500 ppb in aqueous media.

3.3. Interference studies

To assess the selectivity of the proposed reagent $\text{F}_2\text{H}_2\text{Dz}$ immobilized polyurethane foam, the detection of mercury(II) or lead(II) by the proposed batch mode was investigated in the presence of various ions. It was found possible to detect as low as 1 μg of Hg^{2+} or Pb^{2+} in the aqueous media in the presence of up to 10 mg of NO_2^- ,

NO_3^- , SeO_3^{2-} , SeO_4^{2-} , acetate, SO_4^{2-} , F^- , $\text{C}_2\text{O}_4^{2-}$, IO_3^- , BrO_3^- , $\text{B}_4\text{O}_7^{2-}$, Ba^{2+} , Ca^{2+} , Mg^{2+} , Mn^{2+} , MoO_4^{2-} , NH_4^+ , PO_4^{3-} , WO_4^{2-} , BrO_3^- , IO_4^- , and Li^+ . In the presence of some other ions e.g. Cd^{2+} , Fe^{2+} , Fe^{3+} , Pd^{2+} , Cr^{3+} , Bi^{3+} , Mn^{2+} , Cd^{2+} , Zn^{2+} , $\text{S}_2\text{O}_3^{2-}$, MnO_4^- , NO_2^- , Zn^{2+} and formate, simple modifications of the sample solution were introduced to obtain unambiguous and sensitive detection of Hg and Pb (Table 4). These results also extend the use of the proposed foam test for the detection of Hg and Pb in the different matrices.

3.4. Application of the proposed method

The validity of the proposed method for the detection, semiquantitative and quantitative collection of mercury(II) or lead(II) in natural water was also investigated. A water sample 1 dm^3 acidified to 0.1 mol dm^{-3} sulphuric acid was deaerated by nitrogen gas for at least 15 min and mixed with 10 ml of sodium sulphite (0.1 M). The solution mixture was spiked with 1–10 μg mercury(II) or 50–80 μg lead(II) and was allowed to pass through 0.45 μm Millipore filter. Sodium fluoride (10 ml, 0.1 M) solution was added, and the pH of the final solution was then adjusted to

pH 2.5–3. The solution mixture was percolated through F_2H_2Dz -loaded foam column at 3–5 ml min^{-1} . The length (mm) of the produced red-orange color due to mercury(II) complex or the pink color in the case of lead(II) complex on the foam bed was compared with standard color scales of both metal ions prepared under the same experimental conditions (Fig. 2). Satisfactory results were obtained for the spiked metal ions.

The practical utility of the method for the removal of mercury(II) or lead(II) from water sample was attempted at $2 \leq pH \leq 3$ with F_2H_2Dz -foam packed column (15 cm height \times 1.5 cm I.D.). A 0.5 dm³ aqueous solution containing 1–10 μg of mercury(II) or lead(II) at pH 3–5 were percolated through the F_2H_2Dz -foam column at 3–5 ml min^{-1} flow rate. Analysis of mercury(II) or lead(II) in the effluent solution indicated the absence of mercury(II) or lead(II) and quantitative retention of both metal ions on the foam column.

4. Conclusions

The resilient open cell polyurethane foams plasticized and/or immobilized with some F_2H_2Dz represent an efficient separation and preconcentration medium for mercury(II) and lead(II) in extremely dilute aqueous solutions (ppb level). Foams loaded with 1,5-di-(2-fluorophenyl)-3-mercaptoformazan were found more suitable as compared to dithizone and other chelating agents in the detection, semiquantitative determination and quantitative collection of mercury(II) and lead(II) ions in aqueous media. Further work still remains for improving the selectivity and the utility of the proposed method for the direct spectrophotometric determination of Hg^{2+} or Pb^{2+} on parallelepiped polyurethane foams or by preconcentration of these species from natural and wastewaters on columns packed with F_2H_2Dz -foam followed by elution with selective eluting agent e.g. acetone-HCl (1:3 v/v). The foam sorbents give unique advantage over granular sorbents in rapid, versatile and effective separation of different species from fluid samples. The great potentialities of open cell type resilient

polyurethane foam membranes is attributed to their inexpensiveness and the large scale availability all over the world for many industrial applications.

Acknowledgements

The authors would like to thank the UAE University Scientific Council for a research grant provided to one of us (A.M. Kiwan) and the Ministry of Health, U.A.E. for the assistance provided to Mr M.H. Saleh.

References

- [1] R. Chakraborty, S.S. Bhattacharya, A.K. Das, *Bull. Chem. Soc. Jpn.* 66 (1993) 2233.
- [2] J.F. de Silva, R.J.P. Williams, *The Biological Chemistry of the Elements*, Clarendon Press, Oxford, 1993, p. 539.
- [3] A.B. Farag, A. El-Waseef, M.H. Abdel Rahman, *Acta Chimica Hungarica* 122 (1986) 273 and references therein.
- [4] G. Somar, H. Aydin, *Analyst* 110 (1985) 631; S. Landi, F. Fagioli, *Anal. Chim. Acta* 298 (1994) 363.
- [5] H.J.M. Bowen, *Environmental Chemistry Academic Press*, London, 1979.
- [6] Z. Marczenko, *Separation and Spectrophotometric Determination of Elements*, Ellis Horwood, Chichester, UK, 1986, p. 88.
- [7] A.M. Kiwan, A.Y. Kassim, *Anal. Chim. Acta* 88 (1977) 177.
- [8] A.Y. Kassim, Ph.D. Thesis, Kuwait University, Kuwait, 1975.
- [9] T. Braun, A.B. Farag, *Talanta* 22 (1975) 699; T. Braun, A.B. Farag, *Anal. Chim. Acta* 99 (1978) 1.
- [10] S. Palagyi, T. Braun, *Radioanal. J. Nucl. Chem.* 163 (1992) 69; A. Chow, D. Buksak, *Can. J. Chem.* 53 (1975) 1373.
- [11] T. Braun, A.B. Farag, *Anal. Chim. Acta* 73 (1974) 301 and references therein; T. Braun, M.N. Abbas, L. Bakos, A. Elet, *Anal. Chim. Acta* 131 (1981) 311.
- [12] T. Braun, J.D. Navratil, A.B. Farag, *Polyurethane Foam Sorbents in Separation Science*, CRC Press, Boca Raton, FL, 1985.
- [13] A.M. El-Wakil, M.S. El-Shahawi, A.B. Farag, *Anal. Lett.* 23 (1990) 703.
- [14] A.B. Farag, E.M. El-Nemma, *Int. J. Chem.* 3 (1992) 81.
- [15] P. Rychlovsky, J. Bily, P. Denkova, *Chem. Papers* 47 (1993) 233.
- [16] Y. Anjaneyulu, R. Maraya, T.H. Rao, *Environ. Pollut.* 79 (1993) 283.
- [17] M. Harding, *J. Chem. Soc.* (1958) 4136.
- [18] D. Panerjea, T.P. Singh, *Z. Anorg. Chem.* 331 (1964) 225.

- [19] Stability Constants Supplement No. 1. Special Publication 25, Chemical Society, London, 1971, p. 114.
- [20] N.N. Greenwood, A. Earnshaw, Chemistry of the Elements, Pergamon, London, 1985, p. 1413 and references therein.
- [21] A.B. Farag, M.S. El-Shahawi, S. Farrag, *Talanta* 41 (1994) 617.
- [22] A.B. Farag, M.E.M. Hassouna, M.H. Abdel-Rahman, *Bull. Chem. Soc. Belg.* 96 (1987) 147.
- [23] W.M. Abou-Elmaty, M.Sc. Thesis, Mansoura University, Mansoura, Egypt, 1990.
- [24] F. Feigl, V. Anger, *Spot Tests in Inorganic Analysis*, 6th ed., Elsevier, Amsterdam, 1972.
- [25] R.D. Oleschuk, A. Chow, 42 (1995) 957; 433 (1996) 1545.
- [26] M.M. Saeed, A. Rasheed, N. Ahamed, J. Tolgyessy, *Sep. Sci. Technol.* 29 (1994) 2143.
- [27] Y.K. Lee, K.Ja. Whang, K. Ueno, *Talanta* 22 (1975) 535.
- [28] A.D. Adamson, *Physical Chemistry of Surfaces*, 2nd ed., Academic Press, New York, 1967.
- [29] Calculated from the Stability Constants Data, in: G. Iwantscheff, *Das Dithizon und Seine, Anwendung in der Mikro und Spurenanalyse*, 2nd ed., Verlag Chemie, Weinheim, 1972.
- [30] I.M. Kolthoff, E.B.S. Sandell, E.J. Meehan, S. Bruckenstein, *Quantitative Chemical Analysis*, Macmillan, London, 1969, p. 352.

Extraction equilibrium of the ion-associate of periodate with amiloride hydrochloride and simultaneous spectrophotometric determination of periodate and iodate by liquid±liquid extraction

M.S. El-Shahawi

Chemistry Department, Faculty of Science, New Damietta, Damietta, Egypt

Received 18 November 1996; received in revised form 30 January 1997; accepted 30 January 1997

Abstract

The extraction equilibrium of the ion-associate of periodate with amiloride hydrochloride was investigated spectrophotometrically. The ion-association constants, K_D and K_{ex} were determined. A convenient and simple spectrophotometric method was developed for periodate determination at 354 nm after extraction into 4-methyl-2-pentanone as an 1 : 1 ion-pair with amiloride at pH 4.0±5.5. Beer's law was obeyed between 0.01±10 mg ml⁻¹ periodate in aqueous solution of pH 4.0 and the optimum concentration range evaluated by Ringbom's plot was found to be 0.09±8 mg ml⁻¹. The Sandell sensitivity, the molar absorptivity and the relative standard deviation ($n=5$) for 5 mg of periodate were found to be 510⁻⁴ mg cm⁻², 4.10.2210⁻⁴ l mol⁻¹ cm⁻¹ and 1.1% respectively. Iodate was also determined by the proposed procedure after prior oxidation to periodate with potassium peroxodisulphate. Binary mixtures of iodate and periodate in aqueous solution were successfully determined by the proposed procedure. The effects of pH, reagent concentration and diverse ions are reported. The method was applied successfully for the determination of iodate and periodate in artificial fresh water. © 1997 Elsevier Science B.V.

Keywords: Extraction equilibrium; Periodate; Iodate determination; Amiloride hydrochloride; Ion-associate

1. Introduction

Relatively few spectrophotometric methods have been reported for the determination of iodate and periodate ions. The spectrophotometric methods can be classified into three main categories: (i) indirect removal of a reagent by precipitation, (ii) extraction of ion pairs and (iii) redox reactions following co-precipitation of periodate with hydrated iron(III)

oxide [1] or hydrated aluminium oxide [2]. Suitable counterions for ion-pair extraction include triphenyltetrazolium chloride [3] and tetramethylammonium iodide [4]. Periodate can be determined spectrophotometrically by its redox reactions with o-dianisidine [5], benzhydrazide [6], 2,2-azinedi(3-ethylbenzothiazolesulphonic acid) [7] or cyclohexane-1,3-dione bithiosemicarbazone [8].

The existing methods [4,9±11] for the spectrophotometric determination of periodate and iodate ions are, to some degree, unsatisfactory for routine analysis as the procedures require careful maintenance of the experimental conditions, suffer from some lack of selectivity and sensitivity, and require a laborious enrichment step. This paper deals

0003-2670/97/\$17.00 # 1997 Elsevier Science B.V. All rights reserved. PII S0003-2670(97)00103-7

with the develop-

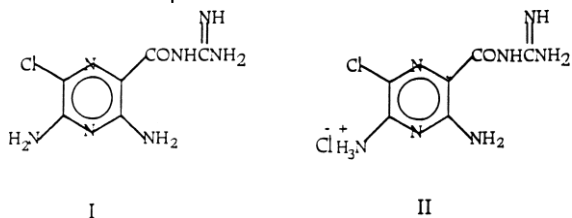


Fig. 1. Structures of amiloride (I) and amiloride hydrochloride (II).

ment of a simple method for the selective reaction of periodate with amiloride hydrochloride (3,5-diaminoN-(aminoiminomethyl)-6-chloropyrazinecarboxamide hydro-chloride) (Fig. 1). The protonated amiloride-periodate ion-associate could be extracted into 4-methyl-2-pentanone, which formed the basis of the developed spectrophotometric procedure for periodate.

2. Experimental

2.1. Apparatus

A Shimadzu model UV-2101 PC double beam UV± visible scanning spectrophotometer was used for recording the absorption spectra and making absorbance measurements, with matched quartz cells of 10 mm path length. A Phillips 9418 digital pH meter with glass and saturated calomel electrodes was used for the pH measurements.

2.2. Reagents and materials

All chemicals and solvents used were of analytical reagent grade. Double distilled water was used

throughout. Britton±Robinson (BR) buffer (pH 2.2± 11.5) was prepared from boric, acetic and phosphoric acids and sodium hydroxide in water. Stock solutions of potassium periodate and potassium iodate (1 mg ml⁻¹, both BDH) were prepared separately by dissolving the exact weight of the corresponding salt in hot water. More dilute solutions were prepared as

required. Amiloride hydrochloride (Am[®]Cl[⊖]) dihydrate (Merck, Sharp and Dohme International) was used as supplied. A 0.01 M stock solution was made by dissolving 0.3021 g of the compound in 100 ml of water.

2.3. Recommended procedures

2.3.1. Determination of periodate

Transfer an aliquot (1±5 ml) of the aqueous solution of potassium periodate containing 1±30 mg of periodate to a 100 ml separating funnel. Add 10 ml of buffer (pH 4.0), 5 ml of amiloride hydrochloride (0.01 M) and water to give a total 25 ml of aqueous solution and mix. Extract twice (22.5 ml) with 4-methyl-2-pentanone and collect the extracts in a dry 50 ml beaker containing anhydrous sodium sulphate (1 g) and swirl to mix. Transfer the extract to a 10 ml volumetric flask, wash the residue with 5 ml of solvent, transfer the washings to the volumetric flask and make up the solution to the mark with the solvent. Measure the absorbance of the organic phase at 354 nm against a reagent blank prepared under the same experimental condition.

2.3.2. Determination of iodate ion

Transfer a known volume (1±5 ml) of sodium iodate solution (containing 1±50 mg of iodate ions) to a 100 ml conical flask. Add 10 ml of potassium peroxydisulphate (2% w/v) solution and 10 ml of water to the flask, boil the solution for 10 min and allow the reaction mixture to cool. Add 10 ml of BR buffer (pH 4.6) followed by 5 ml of 0.01 M amiloride hydrochloride. Transfer the mixture and the water washing solution of the flask to a 100 ml separating funnel. Extract the formed ion-pair with 5 ml of 4-

methyl-2-pentanone and follow the recommended procedure for periodate determination. Run a blank prepared under the same experimental conditions in the presence of potassium peroxodisulphate.

2.3.3. Analysis of binary mixtures of periodate and iodate

Transfer an aliquot (1 ± 5 ml) of a mixture of iodate and periodate (50 mg total) to a 100 ml separating funnel. Analyse the mixture according to the described procedure for periodate. Treat another aliquot as for iodate determination. On the basis of the proposed procedure, the absorbance (A_1) of the organic extract of the first aliquot will be a measure of the periodate ions in the mixture while the absorbance (A_2) of the extracted solution of the second aliquot is a measure of the sum of the periodate and iodate ions. Therefore, the absorbance (A_2/A_1) is a measure of the iodate ions in the binary mixture.

3. Results and discussion

3.1. Absorption spectra and choice of extracting solvent

On mixing an aqueous solution of amiloride hydrochloride and potassium periodate, an ion-associate was formed. The absorbance of this aqueous solution of the ion-associate corresponds to the sum of the absorbances of the individual components periodate and amiloride hydrochloride which is an indication that the resulting compound is an ion-associate. The solubility of the ion-associate was investigated in the following solvents: n-hexane, dichloromethane, 1,2-dichloroethane, carbon tetrachloride, toluene, 4-methyl-2-pentanone, benzene, iso-butylether and nitrobenzene. Of these 4-methyl-2-pentanone was the best extractant, and maximum apparent molar absorptivity and solubility was achieved. In that solvent the extraction was also complete in a very short time and a better separation of layers was obtained. Hence, 4-methyl-2-pentanone

was chosen as the preferred solvent because its greater density allows a better separation of phases. $\text{Am}^{\oplus}\text{Cl}^{\ominus}$ and KIO_4 do not extract into this liquid.

The absorption spectrum of the yellow ion-associate in 4-methyl-2-pentanone extracted from aqueous solution at pH 4.0 is given in Fig. 2. The spectrum of amiloride hydrochloride in the aqueous solution at pH 4.0 is also given. The yellow ion-associate has three absorption maxima, at 354, 280 and 222 nm, while no peaks were found in this range for a solution of amiloride hydrochloride extracted by 4-methyl-2-pentanone. Therefore, the absorbance data for the formed ion-associate complex in the organic phase was measured at 354 nm.

3.2. Effect of shaking time and stability of the ion-associate

The extraction of the ion pair into 4-methyl-2-pentanone was rapid, so 2 min shaking time was adopted in subsequent work. The absorbance of the coloured ion-associate in 4-methyl-2-pentanone was

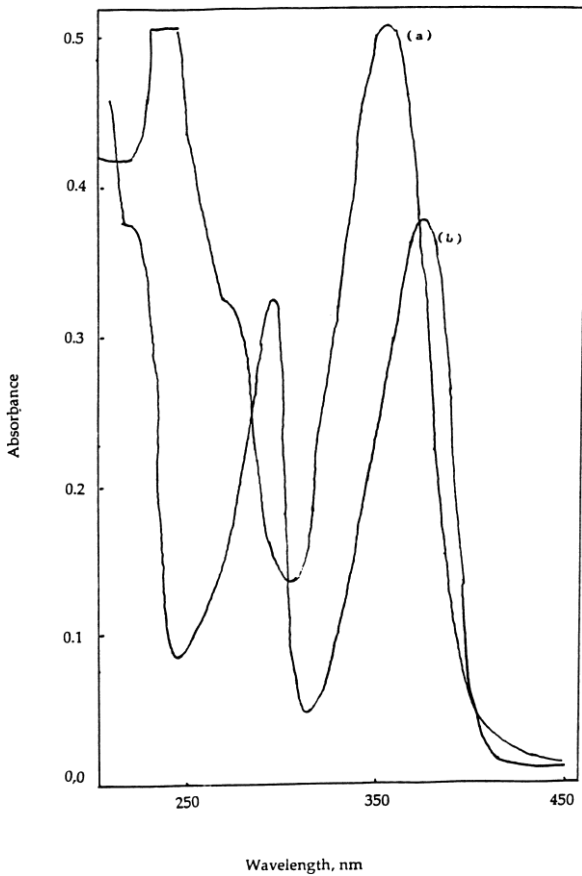


Fig. 2. Absorption spectra of the extracted ion-associate $\text{Am}^{\text{III}} \text{IO}_4^-$ in 4-methyl-2-pentanone (a) and amiloride hydrochloride (b) at pH 4.0 in the aqueous phase.

constant for up to 3 h for samples containing $0.01 \pm 15 \text{ mg ml}^{-1}$ periodate in the aqueous solution at pH 4.0. The addition of sodium chloride ($0.01 \pm 0.05 \text{ M}$) did not improve the amount of ion-associate extracted at $0.1 \pm 10 \text{ mg ml}^{-1}$ periodate suggesting that the periodate species is quantitatively extracted without a salt effect.

3.3. Effect of pH

The effect of the pH of the aqueous phase was studied by measuring the absorbance of the extracted ion-associate in 4-methyl-2-pentanone. The natural pH of each aqueous solution was measured before the extraction. The experimental data (Fig. 3) showed that the maximum absorption of the produced ion-pair was

Fig. 3. Influence of pH of the aqueous phase on the absorbance of the extracted ion-associate in 4-methyl-2-pentanone at 354 nm. Each point is the mean of 5 determinations.

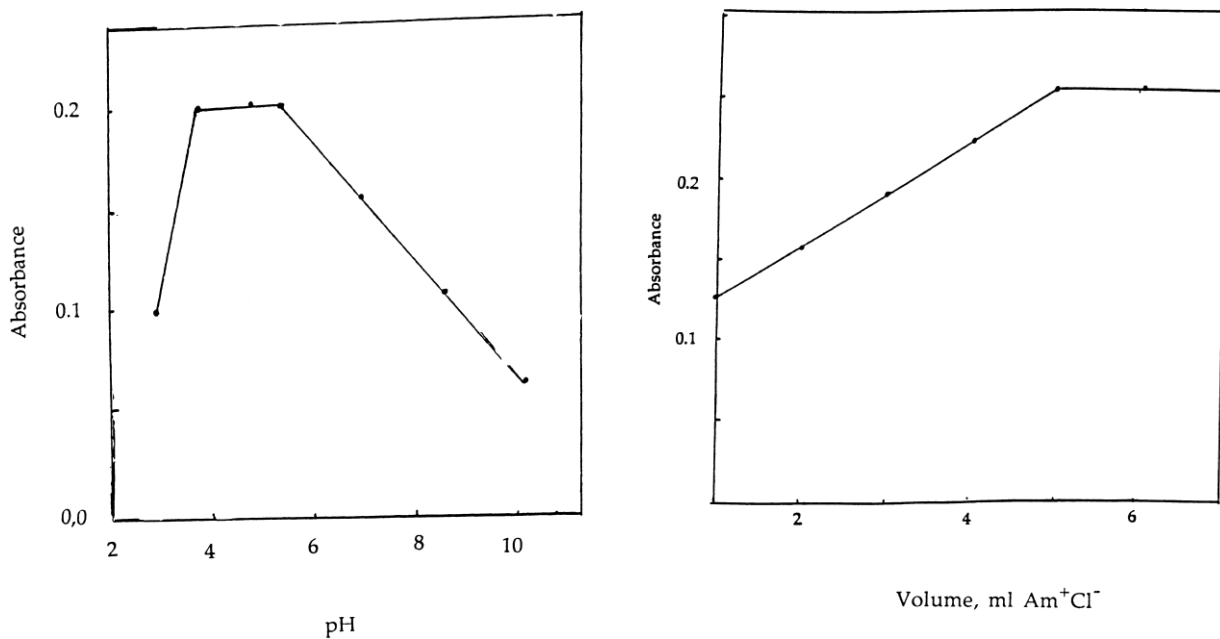


Fig. 4. Dependence of the absorbance (at 354 nm) of the ionassociate in 4-methyl-2-pentanone with amiloride hydrochloride concentration (0.01 M) in the aqueous solution.

instead of BR buffer no significant differences in the absorbance values were observed. Thus a BR buffer solution of pH 4.0 was normally selected and employed as described in the recommended procedures.

obtained at pH 4.0 ± 5.5 . In an aqueous solution of $\text{pH} < 4.0$ or $\text{pH} > 5.5$, the absorbance of the extracted species was decreased possibly due to the protonation of the periodate or the hydrolysis of the ion-associate [12], respectively. When HCl was used

3.4. Effect of amiloride hydrochloride concentration

The superiority of amiloride hydrochloride as a counter-ion for ion-association extraction systems has been demonstrated previously [13,14]. Therefore, the use of other counter-ions was not investigated in this study. The influence of amiloride hydrochloride concentration on the determination of periodate for a series of solutions ($0.05 \pm 10 \text{ mg ml}^{-1}$) of periodate in the aqueous solution was investigated. The addition of 5 ml of amiloride hydrochloride solution at a concentration $2.10 \times 10^{-3} \text{ M}$ in a total 25 ml of aqueous solution was found sufficient completely to form the ion-associate with 10 mg ml^{-1} periodate (Fig. 4) at pH 4.0.

3.5. Characterization of the extracted ion-associate

The composition of the extracted ion-associate in 4-methyl-2-pentanone was determined by means of the continuous variation (Fig. 5) and mole ratio methods. Equimolar $1.10 \times 10^{-3} \text{ M}$ solutions of potassium periodate and amiloride hydrochloride were mixed in complementary proportions to give a fixed total volume and the pH of the solutions adjusted to pH 4.0. The mixtures were allowed to equilibrate for 5 min. The ion-associate was extracted into 4-methyl-2-pentanone and the absorbance was measured against a reagent blank. A plot of the absorbance of the extract versus $\frac{[\text{IO}_4^-]}{[\text{IO}_4^-] + [\text{Am}^+\text{Cl}^-]}$ produced a graph (Fig. 5) that indicated the formation of an ion-association complex having a periodate to a reagent ratio of exactly 1 : 1.

The ion-associate was isolated in the solid state from the organic phase by evaporation under reduced pressure and was characterized by elemental analysis (Calculated, C 17.8, H 2.2, N 24.2, Cl 8.8%,

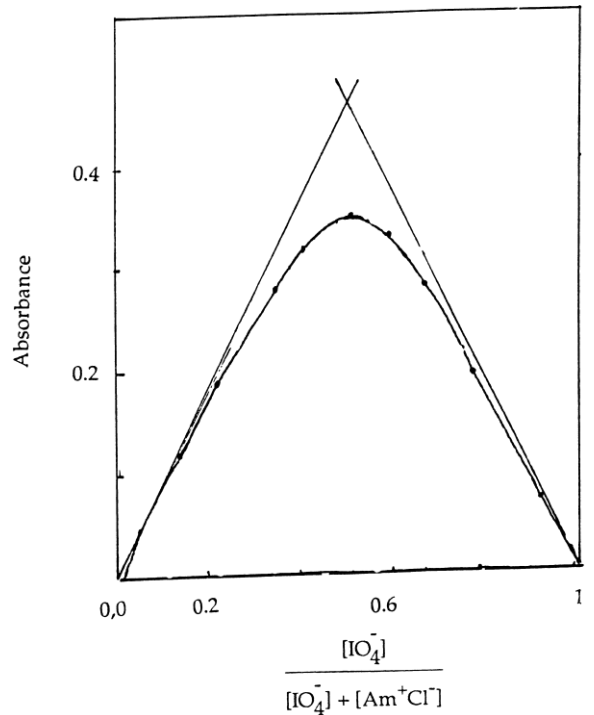


Fig. 5. Determination of the composition of the extracted ion-associate in 4-methyl-2-pentanone by Job's method; $[\text{IO}_4^-] = 0.002 \text{ M}$ (1 ml) and $[\text{amiloride hydrochloride}] = 0.001 \text{ M}$ at 354 nm.

found C 17.7, H 2.2, N 24.7 and Cl 9.1%) and UV-visible spectrum. The spectrum of the isolated ion-associate dissolved in 4-methyl-2-pentanone was identical with that of the organic phase obtained by extraction of the periodate with amiloride at pH 4.0. Moreover, the IR spectrum of the isolated compound dissolved in 4-methyl-2-pentanone was identical with that of the amiloride-periodate extraction into 4-methyl-2-pentanone phase indicating the extracted and isolated species to be identical. The IR spectrum of the isolated compound in a KBr disc was compared with those of KIO_4 and amiloride hydrochloride recorded separately in KBr discs and as a mechanical mixture of KIO_4 with the extractant in a 1 : 1 mole ratio. The spectrum of the isolated compound

showed the absorption bands characteristic of both KIO_4 and amiloride hydrochloride but with some differences ascribed to the formation of the ion-associate.

3.6. Extraction equilibria

The extraction equilibrium was investigated according to the chemical model reported by Alexandrov et al. [15]. The following equilibria were considered:

(i) Formation of an ion-associate in the aqueous phase according to the reaction:



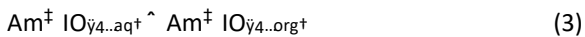
with an ion-association constant, b

$$b = \frac{[Am^{2+}IO_4^-]}{[Am^{2+}][IO_4^-]} \quad (2)$$

:



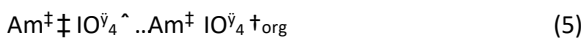
(ii) Distribution of the ion-associate between the aqueous and organic phases:



with a distribution constant, K_D

$$K_D = \frac{[Am^{2+}IO_4^-.org]}{[Am^{2+}IO_4^-.aq]} \quad (4)$$

(iii) The overall extraction process can be then expressed as



with a corresponding equilibrium constant K_{ex}

$$K_{ex} = \frac{[Am^{2+}IO_4^-.org]}{[Am^{2+}][IO_4^-]} \quad (6)$$



The K_{ex} and K_D values can be determined graphically from the plot of the distribution ratio, $\log D$, vs. $\log[Am^{2+}]$ (Fig. 6). The distribution ratio $D = \frac{[Am^{2+}IO_4^-.org]}{[Am^{2+}][IO_4^-]}$ was determined at a constant total IO_4^- concentration in the aqueous phase and various concentrations of amiloride hydrochloride, according to the formula:

$$D = \frac{[Am^{2+}IO_4^-.org]}{[Am^{2+}][IO_4^-]} \quad (7)$$

assuming only one species of periodate is present in the organic phase at equilibrium.

The values of K_{ex} , K_D and b were found to be $(3.20.49)10^4 \text{ l mol}^{-1}$, 2.80.41 and $(1.20.28) 10^4 \text{ l mol}^{-1}$ respectively (n=5). These values were also obtained by employing the method of Likussar and Boltz [16] with $[Am^{2+}] = 1.110^{-4} \text{ M}$ and

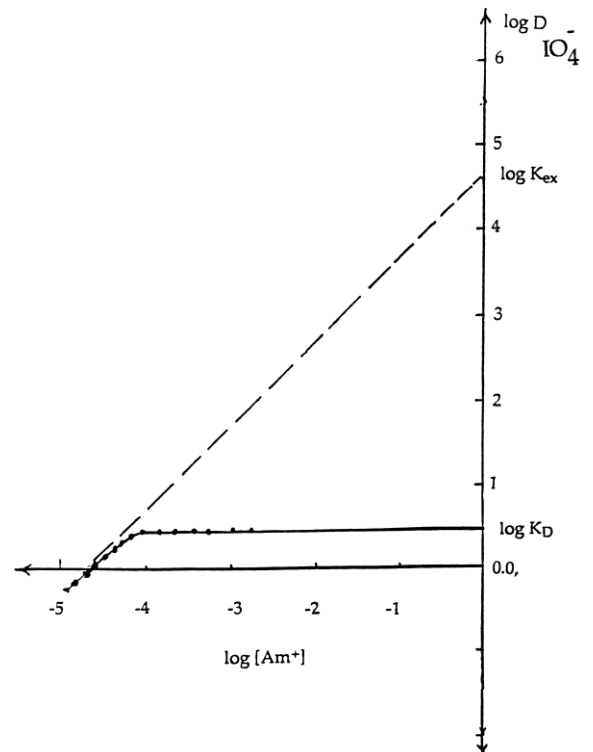


Fig. 6. Plot of $\log [Am^{2+}]$ vs. $\log D = \frac{[Am^{2+}IO_4^-.org]}{[Am^{2+}][IO_4^-]}$ ($[IO_4^-] = 1.910^{-5} \text{ M}$).

confirmed the data obtained according to the chemical model reported by Alexandrov et al. [15]. The composition of the extracted ion-associate was also calculated from the slope of the plot in Fig. 6; the mole ratio of amiloride to periodate ion was found to be exactly 1 : 1, confirming the value obtained from the continuous variation and mole ratio methods.

3.7. Spectrophotometric characteristics

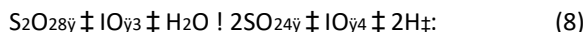
The most suitable extraction conditions normally adopted were as follows: amiloride concentration (0.05 w/v, 2.10×10^{-3} M), buffer pH 4.0, shaking time (120 s) and 4-methyl-2-pentanone as extracting solvent. A linear calibration graph ($r=0.98$) was obtained by recording the absorbance of the ion-associate in the organic phase as a function of the periodate ion concentration. Beer's law was obeyed between 0.01 ± 10 mg ml⁻¹ periodate in aqueous solution of pH 4.0. The effective concentration of periodate evaluated by Ringbom's plot [17] was found to be 0.09 ± 8 mg ml⁻¹. The molar absorptivity calculated from the Beer's law plot and the Sandell sensitivity index [18] at 354 nm were found to be (4.10.22)

10^4 l mol⁻¹ cm⁻¹ and 510^4 mg cm⁻², respectively. The sensitivity of this reaction is far better than the recent spectrophotometric procedures reported by Kamburova [3], El-Shahawi and Al-Hashimi [4] and Fernandez-Gutierrez et al. [19]. The relative standard deviation of five measurements of 5 mg of periodate was 1.1%. The detection limit (3s) was 0.01 mg ml⁻¹ periodate.

3.8. Determination of iodate

A series of oxidising agent K₂S₂O₈, H₂O₂ and KMnO₄ was used for the possible oxidation of IO₃⁻ to IO₄⁻ without interference in the proposed procedure for the periodate determination. Boiling for 10 min with potassium peroxodisulphate (2% w/v) in water was found to be the most convenient procedure for the oxidation of the iodate to periodate, without

interference of unreacted peroxodisulphate. The reaction probably proceeds as follows:



The determination of 0.01 ± 10 mg ml⁻¹ iodate in aqueous solution was carried out. Satisfactory results were obtained with relative standard deviation of 1.2% for 5 measurements.

Moreover, the proposed procedures were also employed successfully for the analysis of binary mixtures of periodate and iodate (both 1 ± 10 mg) in 25 ml of aqueous media. An aliquot of the mixture was analysed for periodate employing the procedure described in Section 2.3.1. Another aliquot was then treated with potassium peroxodisulphate as described in Section 2.3.2 giving the total periodate and iodate. The iodate concentration was obtained by difference. A relative standard deviation in the range of $1.2 \pm 1.3\%$ ($n=5$) was obtained.

3.9. Effect of diverse ions

The selectivity of the developed procedure in the presence of a relatively large excess (5 mg) of some anions: NO₃⁻, Br⁻, SO₄²⁻, CO₃²⁻, HCO₃⁻, IO₃⁻, CrO₄²⁻, MnO₄⁻, S₂O₈²⁻, AsO₄³⁻, AsO₃³⁻, SbO₃⁻, SbO₄³⁻, EDTA²⁻, C₂O₄²⁻, S₂O₃²⁻, SCN⁻, PO₄³⁻, BiO₃⁻, Cl⁻, WO₄²⁻, SeO₃²⁻, BrO₃⁻, formate, citrate, acetate, oxalate, tartrate and MoO₄²⁻ in the determination of 5 mg of periodate (or iodate) was studied. Good recoveries (99.41.6%) were obtained in the presence of all ions except S₂O₃²⁻, I⁻, CNS⁻ and NO₃⁻. The interference of various cations: NH₄⁺, Cu²⁺, Tl⁺, Al³⁺, Cd²⁺, Zn²⁺, Pt²⁺, Au⁺, Pb²⁺, Co²⁺, Fe³⁺, Bi³⁺, Sn²⁺, Ni²⁺, Mg²⁺, Ba²⁺ and Li⁺ at 5 mg level was also examined. None of these ions interfered in the proposed method, and a good recovery (100.01.1%) was achieved. Mn²⁺, Cu²⁺, Cr³⁺, Cu²⁺, Hg²⁺ and Ru³⁺ interfered negatively even at very low concentrations. All interference effects probably arose by reactions with periodate in the aqueous phase [20] under the experimental conditions of the

developed procedures. Also, the produced species might interact with amiloride to form ion pairs which can be extracted into the organic layer. The interferences of mercury(II) and copper(II) were removed with EDTA at pH 4±6.

The determination of 5 mg of periodate or iodate added to artificial fresh water containing 10 mg l⁻¹ each of sodium, calcium, chloride, sulphate and carbonate was carried out against a blank. The relative standard deviation was 0.5% and the error was ca 1.1± 1.2% in each case.

Acknowledgements

The author would like to thank Professor D.T. Burns, The Queen's University of Belfast, for valuable discussions and for the amiloride hydrochloride.

References

- [1] A.I. Novikov, E.I. Finkel'shtein, *Zh. Analit. Khim.* 19 (1964) 541.
- [2] S.N. Bhattacharyya, P.K. Chetia, *Anal. Chem.* 19 (1967) 369.
- [3] M. Kamburova, *Talanta* 39 (1992) 987.
- [4] M.S. El-Shahawi, F.A. Al-Hashimi, *Talanta* 43 (1996) 2037 and references therein.
- [5] M. Guernet, *Bull. Soc. Chim. (France)* (1964) 478.
- [6] A.M. Escarilla, P.F. Maloney, P.M. Maloney, *Anal. Chim. Acta* 45 (1969) 199.
- [7] G. Mahuzier, B.S. Kirkacharian, C. Harfouche-Obeika, *Anal. Chim. Acta* 76 (1975) 79.
- [8] M.C. Mochon, J.A. Munozleyva, *Analyst* 109 (1984) 951.
- [9] A. Hareez, W. Bashir, *Microchem. J.* 31 (1985) 375. [10] M. Callejon, J. Munoz, *Microchem. J.* 34 (1986) 83.
- [11] M. Roman Ceba, J.C. Sanchez, T. Galeano Diaz, *Microchem. J.* 31 (1985) 256.
- [12] S. Yamaguchi, K. Uesugi, *Analyst (London)* 109 (1984) 1393.
- [13] D.T. Burns, P. Hanprasopwattana, *Anal. Chim. Acta* 118 (1980) 185.
- [14] D.T. Burns, M.S. El-Shahawi, M.J. Kerrigan, P.M.T. Smyth, *Anal. Chim. Acta* 323 (1996) 107.
- [15] A. Alexandrov, O. Budevsky, A. Dimitrov, *J. Radioanal. Chem.* 29 (1976) 243.
- [16] W. Iikisar, D. Boltz, *Anal. Chem.* 43 (1971) 1265.
- [17] A. Ringbom, *Fresenius' Z. Anal. Chem.* 115 (1939) 332.
- [18] E.B. Sandell, *Colorimetric Determination of Trace Metals*, Interscience, New York, 1959.
- [19] A. Fernandez - Gutierrez, A. Munoz de La Pena, J.A. Murillo, *Anal. Lett.* 16 (1983) 759.
- [20] M.S. El-Shahawi, S.A. Barakat, *Talanta* 42 (1995) 1641; and references therein.

Retention and Separation Behavior of Some Organophosphorus and Pyrethroid Insecticides on Polyurethane Foams

M. S. EL-SHAHAWI*†, M. H. Abdel KADER** and R. S. Al-MEHREZI***

*Department of Chemistry, Faculty of Science, UAE University, Al-Ain, P. O. Box 17551, United Arab Emirates

**National Institute of Laser Research, Cairo University, Cairo, Egypt

***Ministry of Agriculture and Fisheries, Central Laboratory, Al-Ain, P. O. Box 16054, United Arab Emirates

The application of polyurethane foam for the preconcentration of Cypermethrin, Malathion and Parathion insecticides was examined by the static mode of extraction. The retention of the tested species from aqueous media with the polyether polyurethane foam suggests that the solvent extraction and the cation chelation mechanism might be operative. Quantitative retention and recovery of the tested insecticides by the foam column mode of separation were carried out and satisfactory recovery percentages (up to $99.10 \pm 3.12\%$) were obtained. The number and the height equivalent of the theoretical plate of the foam columns were found in the range of $165 - 170 \pm 4$ and $1.85 - 1.93 \pm 0.26$ mm, respectively at $10 \text{ cm}^3/\text{min}$ flow rate. Separation of the binary mixtures of Malathion-Cypermethrin and Parathion-Cypermethrin insecticides from the aqueous media was achieved successfully. The helical structure of the foam sorbents offers rapid, versatile and effective separations and preconcentration of different compounds from fluid samples over conventional bulk-type granular sorbents.

Keywords Polyurethane foam, organophosphorous insecticide, pyrethroid insecticide, Parathion, Malathion

As a consequence of the activities of modern industries and agriculture many man-made pollutants have found their way into the environment, without the availability of much knowledge on their possible harmful effect on the environment.^{1,2} The insecticides can enter water systems from agriculture land, direct entry from crop spraying, industrial and sewage effluent, dust and rain fall. The presence of these compounds in the aquatic environment has been known to cause severe health problems to animals and humans.³

The most common reported extraction procedures for the removal or reduction of these pollutants are limited and are too expensive for routine analysis where many large volume samples are concentrated on site prior to quantitative analysis.⁴⁻⁹ The classical paper of Bowen¹⁰ and the pioneering studies of Braun and Farag^{11,12} on the application of polyurethane foam (PuF) sorbents to trace elements led to revealing the potentialities of their geometrical form: spherical membrane-shaped geometry in extraction chromatography.¹⁰⁻²² In this paper, the extraction of some insecticides by polyether based polyurethane foam from large volume water samples is reported. The influence of various parameters on the retention of the tested species was carried out to determine whether the sorption on the polyurethane

foams takes place by solvent extraction mechanism or by other mechanisms.

Experimental

Reagents and materials

All of the chemicals used were of analytical reagent grade. Open-cell polyether based polyurethane foam was supplied by Greiner K. G. Schaum (Stoffwerk, Kremsmunster, Austria). Foam cubes of approximately 1 cm^3 were cut from a polyurethane foam sheet. The foam cubes were washed with HCl (10%v/v) and distilled water. The acid-free foam cubes were then washed with acetone in a Soxhlet extractor for 6 h and dried in an oven at 80°C for 2 h.¹¹ Stock solutions (1 M) of lithium, sodium, ammonium and potassium chlorides were prepared in distilled water. A Britton-Robinson buffer (pH 2-11) was used. The compounds tested were Parathion, *o,o*-diethyl-4-nitrophenyl phosphorothioate; Cypermethrin, cyano(3-phenoxyphenyl)methyl 3-(2,2-dichloroethyl)-2,2-dimethylcyclopropanecarboxylate and Malathion, diethyl[(dimethoxyphosphinothionyl)thio]butanedioate. A stock solution of each compound ($200 \mu\text{g}/\text{cm}^3$) was prepared in a 100 cm^3 measuring flask by dissolving the exact weight of the compound in ethanol. Standard solutions of these compounds were then prepared by diluting their stock solutions with distilled (or tap) water in the presence of few cm^3 of

† To whom correspondence should be addressed. Present address: Chemistry Department, Faculty of Science at Damiatta, Mansoura University, Damiatta, Egypt.

ethanol whenever required. The pyrethroid Cypermethrin is extremely lipophilic and adsorbs strongly to glassware; therefore, a freshly prepared stock solution and diluted solutions were prepared directly before the experiment.

Apparatus

A Pye Unicam SP8-100 spectrophotometer was used for recording the absorption spectra and for routine absorbance measurements, with matched 2 mm and 10 mm quartz cells. An Orion pH meter and glass columns (12 cm height \times 10 mm i.d.) and Lab-Line Orbit Environ-Shaker Model 35271-I were also used.

General procedure

Batch experiments. To examine the effect of the shaking time on the uptake of the tested compounds by the polyurethane foam, the foam cubes (0.3 \pm 0.004 g) were equilibrated with a freshly prepared 100 cm³ aqueous solution at pH 5–6 of each compound at 80 μ g/cm³ in ethanol–water (5% v/v) in 250 cm³ conical flasks and shaken in a thermostated shaker at 20 \pm 0.1 $^{\circ}$ C for various time intervals of up to 1 h. The aqueous phase was then separated and the amount of the compound remaining in it was determined from absorbance measurements at suitable wavelength against a reagent blank. The insecticide retained on the foam was calculated by the difference of absorbance. Following these procedures, the influence of the compound concentration (10–100 μ g/cm³), solution pH, temperature, ethanol/concentration and increasing salt concentration (\leq 0.1 M) of the different metal (Li, Na, K) chlorides and NH₄Cl on the extraction efficiency of the tested species by the polyurethane foam was determined. The % extraction (*E*) and the distribution coefficient (*D*) were calculated employing the equations:

$$\% \text{Extraction} = \left(\frac{A_0 - A}{A_0} \right) \times 100, \quad (1)$$

$$D = \frac{\% \text{Extraction}}{100 - \% \text{Extraction}} \times \frac{\text{Volume of solution (cm}^3\text{)}}{\text{Weight of dry foam (g)}}. \quad (2)$$

Here, *A*₀ and *A* are the concentrations of the tested compounds in aqueous solutions before and after extraction, respectively.

Column experiments. One gram of the dry foam was packed into a column using the vacuum method of foam packing.^{11,12} A tap or distilled water (0.1–6 dm³) sample containing 0.01 mg of the compound tested at pH 5–7 was passed through the foam column at 10 cm³/min flow rate. After squeezing water from the foam material, the compound was then recovered from the foam with 100 cm³ acetone in a Soxhlet extractor for 1 h. The sample quantity was then determined by measuring the absorbance of the solution against a reagent blank after being concentrated to 25 cm³ with a rotary evaporator.

The effect of the sample volume and flow rate on the extraction efficiency of the compounds by the foam were also determined.

Results and Discussion

Batch experiments

Batch experiments using polyurethane foams have shown that the retention of the investigated insecticides (Parathion (I); Malathion (II) and Cypermethrin (III)) (Fig. 1) from an aqueous solution at 5 < pH < 7 was rapid, and equilibrium was reached in less than 50 min followed by a plateau (Fig. 2; each point in the figure represents the mathematical average of five measurements). Hence, a minimum shaking time of 1 h was adopted in the subsequent work. The average values of the half-life time (*t*_{1/2}) of the equilibrium sorption of the tested compounds on the unloaded foams were found in the range of 3–5 min for Malathion and Cypermethrin and 2–2.5 min for Parathion. These results can be attributed to the high mobilities and diffusion rate of Parathion through the quasi-spherical membrane structure of the foams.

The sorption of the tested insecticides (I, II and III) from the aqueous solution by the polyurethane foam was found to depend on their concentrations. Thus, the sorption isotherms of the tested compounds on the PuF were developed over a wide range of equilibrium concentrations (10–100 μ g/cm³) for each species at 20 $^{\circ}$ C. The pH values of the aqueous solution were adjusted to pH 5–7. The sorption isotherm of the tested insecticides exhibited a first-order behavior in the low-concentration range and tended to a plateau at high bulk-solution concentration. The sorption profiles of the different species (Fig. 3) increased in the order



Similar results were also obtained in diethylether. Thus, a solvent-extraction mechanism might be involved in the sorption of the tested species by the polyether foam.¹⁶ These results do not agree with the general understanding that the larger is the molecular weight (MW) of the adsorbate Parathion (MW=291.0), Malathion (MW=362), and Cypermethrin (MW=416) the larger is the amount retained on the foams when the substances concerned are similar in nature.²³ However, the complex nature of the membrane of the polyether foam implies that several mechanisms could be involved simultaneously.^{17–21}

The influence of the pH on the excitation of the tested compounds (80 μ g/cm³) by the foams was examined over the pH range 2–11. Sorption profiles of the compounds by the foams are given in Fig. 4. The percentage removal of the compounds by the foams increased markedly in the pH range 5–7. Lowering the pH (<4) tends to protonate the nitrogen atoms of the urethane linkage and/or the ether oxygen atoms of the polyurethane foam as follows:¹⁶

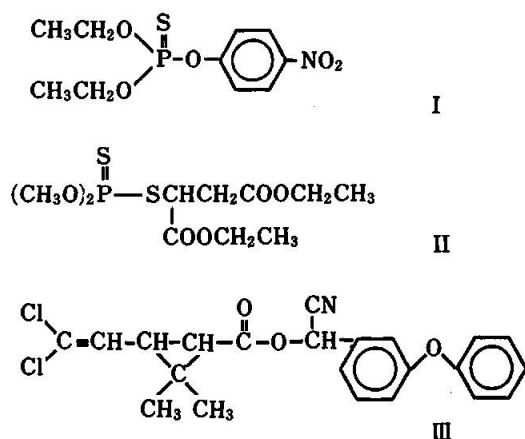


Fig. 1 Structures of the organophosphorus insecticides Parathion (I), Malathion (II) and the pyrethroid Cypermethrin (III).

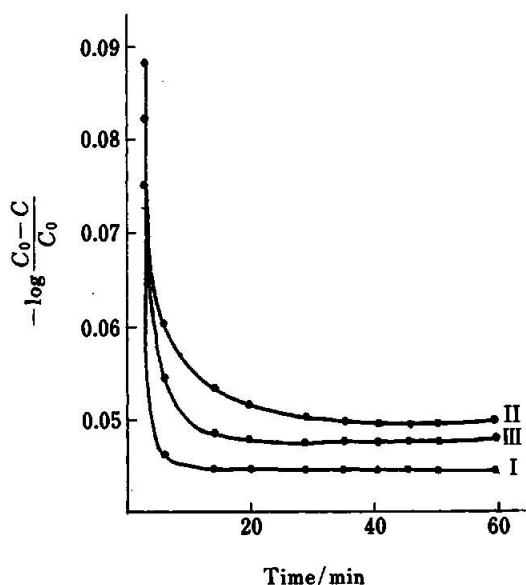


Fig. 2 Effect of the shaking time on the sorption profiles of the tested insecticides (I, II, III) at $80 \mu\text{g}/\text{cm}^3$ in aqueous solution (100 cm^3) at pH 5–7 and $20 \pm 0.1^\circ\text{C}$ by the polyether foams ($0.30 \pm 0.01 \text{ g}$).



or



Thus, sorption of the compounds decreased. On the other hand, the insecticides uptake was also reduced at elevated pH (>7). This is possibly attributed to the increased polarity of the tested species. These data clearly show that the pH values significantly influence the sorption of the tested species.

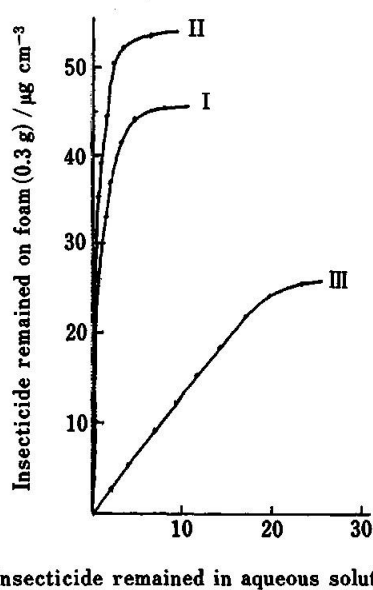


Fig. 3 Extraction isotherm of Parathion (I), Malathion (II) and Cypermethrin (III) at a concentration of $10 - 100 \mu\text{g}/\text{cm}^3$ by foams ($0.30 \pm 0.01 \text{ g}$) from a 100 cm^3 aqueous solution sample at pH 5–7 and $20 \pm 0.1^\circ\text{C}$ and 1 h extraction time.

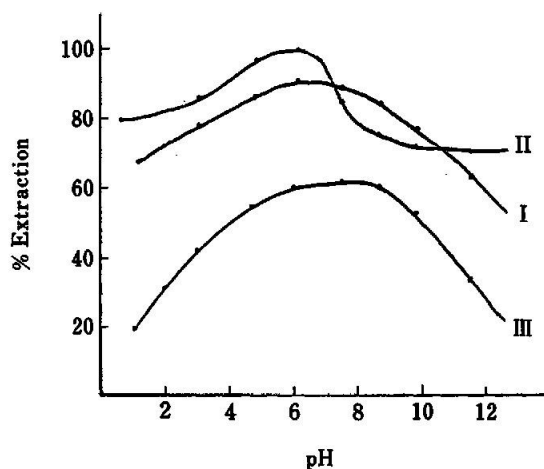


Fig. 4 Effect of the pH on the extraction percentage of Parathion (I), Malathion (II) and Cypermethrin (III) at $80 \mu\text{g}/\text{cm}^3$ by the foam ($0.30 \pm 0.01 \text{ g}$) from 100 cm^3 aqueous sample. Other conditions as in Fig. 2.

The influence of various concentrations of alkali metal (Li, Na, K) chlorides and NH_4Cl at concentrations $\leq 0.1 \text{ M}$ on the sorption percentage of the tested compounds at $80 \mu\text{g}/\text{cm}^3$ by the polyether foam was studied at pH 5–7; the results are summarized in Table 1. Significant increases in the distribution ratios of Malathion and Parathion were observed with increasing concentrations from 0.01 to 0.1 M and the following orders of extraction were achieved:



Table 1 The logarithm distribution coefficient (D) data for the sorption of the tested insecticides by the polyurethane foams in the presence of different univalent cations

Cation/M	Logarithm distribution coefficient, D			
	Parathion	Cypermethrin	Malathion	
Li ⁺	0.01	3.52±0.16	2.38±0.12	2.42±0.12
	0.05	3.46±0.12	2.52±0.17	2.58±0.12
	0.10	3.42±0.10	32.42±0.12	3.05±0.16
Na ⁺	0.01	3.42±0.13	2.82±0.16	2.28±0.10
	0.05	3.41±0.13	2.39±0.16	2.55±0.12
	0.10	3.40±0.12	2.50±0.17	2.68±0.18
K ⁺	0.01	3.39±0.10	3.75±0.08	2.05±0.14
	0.05	3.36±0.16	3.49±0.19	1.85±0.15
	0.10	3.2 ±0.20	1.79±0.16	3.62±0.12
NH ₄ ⁺	0.01	3.35±0.16	3.50±0.13	2.15±0.16
	0.05	3.31±0.12	2.61±0.12	1.96±0.15
	0.10	3.22±0.16	2.72±0.14	1.84±0.15

Cations: extraction from aqueous solution (100 cm³) at pH of maximum extractibility of each insecticide (80 µg cm⁻³). Average of five measurements±standard deviation (SD) at room temperature.

The distribution ratio of Malathion increased along with the amount of LiCl and NaCl added from log $D=2.42$ and 2.28 to 3.05 and 2.68 for Li⁺ and Na⁺ ions at 0.01 and 0.1 M, respectively. This behavior is characteristic of a solvent-extraction mechanism with the salt acting as a salting-out medium and the cation-chelation mechanism is excluded.^{15,16} The added salts increased the sorption profiles of the tested compounds into the polyether foams by reducing the number of water molecules available to solvate the organic compounds, which would therefore be forced out of the solvent phase into the foam. In such a case some amount of free water molecules are preferentially used to solvate the ions.

To confirm the salting out of the added salts on the sorption profiles of Malathion and Parathion by the foams, the extraction of a 200 cm³ ethanolic aqueous solution (5%v/v) of the former species (80 µg/cm³) in (v/v) at pH 2 and pH 6 was investigated after 1 h shaking. The added LiCl (0.1 M) to the aqueous media enhanced the distribution ratio of Malathion in a solution of pH 6 (log $D=3.05$) than at a lower pH of 1 (log $D=1.9$). These results confirm that both Malathion and Parathion are highly extractable in the neutral form and the solvent-extraction mechanism is the more predominant mechanism.

The sorption profiles of Cypermethrin by the unloaded foams decreased with increasing the concentration (0.001–0.1 M) of the alkali metal (Li⁺, Na⁺, K⁺) and NH₄⁺ chlorides and the following order of sorption was achieved at 0.1 M salt concentration:



Therefore the ion-dipole interaction of NH₄⁺ with the

oxygen sites of the polyurethane foam might be highly predominant in the sorption of Cypermethrin, and the cation chelation mechanism may be operative in the sorption process by the polyurethane foams.^{18–22}

The influence of the temperature on the sorption profiles of the tested insecticides by the polyether foams were determined at 25, 35, 45 and 55°C. The distribution ratios of the tested compounds increased slightly with increasing temperature. Assuming no precipitation or chelation and that the tested insecticides exist in the neutral form at pH 5–7, the equilibrium constant (K) for the equation



is equivalent to the distribution ratio, D .^{22,24} Employing

$$\ln K = \frac{\Delta H^\circ}{RT} + \frac{\Delta S^\circ}{R}, \quad (9)$$

the values of the standard enthalpy change ΔH° and the standard entropy change ΔS° for the sorption of the tested compounds on polyurethane foams were calculated. The ΔS° for Malathion and Parathion were found to be -20 ± 2 and -38 ± 4 J/mol deg., respectively while for Cypermethrin the ΔS° was found to be -16 ± 1.8 J/mol deg. The high molecular weight of Cypermethrin (MW=416.6) may account for its higher value of ΔS° . The observed decrease in the ΔS° of Malathion and Parathion is possibly due to the presence of a P=S group, which could reduce the ion-dipole interaction with the oxygen sites of the polyurethane foam. This would therefore reduce the degrees of freedom of movement of the tested organic compound in the polyurethane foam, as previously reported.^{24,25} The results are consistent with the solvent-extraction mechanism. The ΔH° for the tested compounds were found to be in the range 32 ± 3.92 kJ mol⁻¹. Raising the temperature slightly enhanced the retention of the tested species by the foams. Increasing the temperature may facilitate the partition of the compounds through the urethane linkage and/or ether oxygen atoms of the foams. However, the polymeric nature and/or different functional groups of hetero atoms in the foam may also take a part in the sorption process.

The influence of the total ethanol (5–15%v/v) concentration on the preconcentration of the tested compounds by the foam were examined at pH 5–7. The sorption percentage of Malathion (80 µg/cm³) and Parathion decreased by the addition of ethanol to the aqueous solution. This is probably due to the formation of lipophilic association in an aqueous solution.²⁶ Thus, since the species present in an aqueous solution are well solvated it is difficult for these species to form ion pairs in an aqueous solution. These data are also consistent with the fact that with a pair of low dielectric constant, the degree of extraction should increase along with increasing the polarity of the polar process.^{24,25}

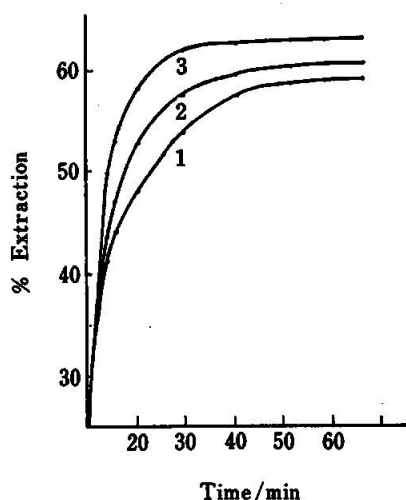


Fig. 5 Effect of the extraction media on the sorption profiles of Cypermethrin by a polyether foam at pH 6–7 and 1 h extraction time: 5% (1), 10% (2) and 15% (3)(v/v) ethanol. Other conditions as in Fig. 2.

Thus the solvent-extraction mechanism is the most probable mechanism for the sorption of Malathion and Parathion. In contrast, the sorption profile of Cypermethrin increased along with the increasing ethanol concentration (Fig. 5). Therefore, the nature of the media has a marked effect on the sorption characteristics of the tested compounds.

Flow experiments

Batch experiments on the sorption behavior of the tested compounds from an aqueous sample solution by the polyether foams suggest the possible application of the foam in a column mode for the preconcentration and recovery of the tested insecticides at the optimum pH of sorption for each insecticides. Tap or distilled water samples (0.1–6 dm³) containing 0.01 mg of each insecticide were percolated separately through the polyurethane foam columns, as describes. More or less complete retention of the investigated compounds was achieved by a foam column at 10 cm³/min. The insecticides were then recovered from the foam column up to 99.10±3.10% with 100 cm³ acetone in a Soxhlet extractor. The recovery percentage of the tested insecticides from by the proposed foam column are summarized in Table 2.

The dependence of the sorption profiles of the tested insecticides by the foam column on flow rate (5–25 cm³/min) and sample volume (0.1–6 dm³) were investigated. Aqueous sample (2 dm³) containing 0.01 mg of Parathion were percolated through the foam column at various flow-rates up to 25 cm³/min. Complete retention of Parathion was obtained at flow rates up to 15 cm³/min and decreased significantly up to 85% at a flow rate of 20–25 cm³/min. No significant decrease in the retention percentage was observed upon increasing

Table 2 Extraction and recovery of the tested compounds separately (0.01 mg) from 3 dm³ distilled (a) and tap (b) water by the proposed unloaded foam column

Compound	% Recovery		Wavelength/nm
	(a)	(b)	
Parathion	95.60±2.12	95.91±1.92	273
Malathion	93.50±2.44	99.10±3.12	206
Cypermethrin	94.22±1.80	95.71±1.71	273

Average±RSD for five measurements.

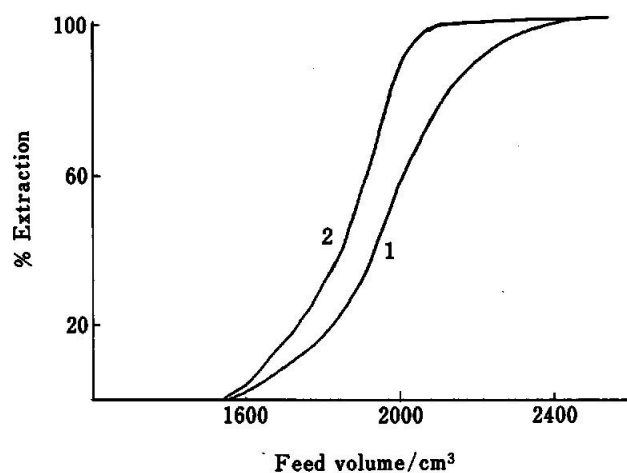


Fig. 6 Breakthrough capacity curves of the sorption profiles on Parathion at 50 µg/cm³ by the polyether foams at flow rate 10 (1) and 20 (2) cm³/min.

the sample volume from 2 to 6 dm³ at a flow rate of <15 cm³/min.

The foam column performance was calculated from the breakthrough capacity curve of Parathion (50 µg/cm³) at 10 cm³/min flow rate (Fig. 6). The height equivalent to the theoretical plates (HETP) was calculated employing Eq. (10),

$$N = \frac{V_1 \cdot V_2}{(V_1 - V_2)^2} = \frac{L}{[\text{HETP}]}, \quad (10)$$

where L =length of the column foam bed, mm; N =number of the theoretical plates; V_1 =volume (cm³) of the effluent at the center of the S-shaped of the breakthrough curve where the concentration is one half the initial concentration and V_2 is the volume (cm³) at which the effluent has a concentration of 0.1578 of the initial concentration. The value of N and HETP obtained by this method were found in the range 165–170±4 and 1.93±0.22 mm, respectively. The HETP values for Malathion were also calculated from its elution curves with acetone at a 10 and 20 cm³/min flow rate and were found to be 1.85±0.26 mm in agreement with the data obtained from the breakthrough capacity curve.

The proposed foam column method has been successfully employed for the separation of binary mixtures of Malathion-Cypermethrin, and Parathion-Cypermethrin insecticides from different volumes (0.1 – 2 dm³) of the aqueous media. A mixture containing 0.05 mg of Malathion (or Parathion) was separated from 0.01 mg of Cypermethrin at pH 1.5 and 0.1 M lithium chloride employing polyether foam column at a 3–5 cm³/min flow rate. The sorption of Malathion (or Parathion) took place while Cypermethrin was not retained on the foam column and collected quantitatively in the effluent. Malathion (or Parathion) was then recovered from the foam column by 100 cm³ acetone in a Soxhlet extractor as described.

Polyether foam in the batch and column modes can be applied to trapping trace amounts of pyrethroid and phosphorous insecticides from a large sample volume of aqueous media. The sorption profiles of Malathion and Parathion in the presence of alkali metal ions were consistent with the "solvent-extraction mechanism", while the extraction profile of Cypermethrin was indicative of a "cation-chelation mechanism." Studies on the extraction of the tested compounds illustrated the importance of the extraction media and the molecular weight of the sorbate. Open-cell-type resilient polyurethane foams exhibit excellent hydrodynamic properties which permit their utilization in rapid separation in the column mode operations at a relatively high flow rate without any significant impairment of the separation efficiency.

The authors would like to thank Professor A. S. Al-Sharhan, Dean of the Faculty of Science and Desert and Marine Environment Research Center, UAE University and the Ministry of Agriculture and Fisheries, UAE, for the studentship provided to one of us, R. S. Al-Mehrezi.

References

1. J. R. H. Malisse, *Egypt J. Anal. Chem.*, **1**, 49 (1990).
2. C. A. Edward, "Persistent Pesticides in the Environment", 2nd ed., CRC Press, Boca Raton, 1973.
3. C. A. Edward, "Environmental Pollution by Pesticides", p. 409, Plenum Press, New York, 1973.

4. B. A. Ahling and S. Jenson, *Anal. Chem.*, **36**, 134 (1964).
5. B. K. Afgan, R. J. Wilinon, A. Chow, T. W. Findley, H. D. Gesser and K. I. Srikameswaran, *Water Res.*, **18**, 9 (1984).
6. H. Oda, M. Kishida and C. Yokokawa, *Carbon*, **21**, 243 (1981).
7. H. Oda and C. Yokokawa, *Carbon*, **21**, 485 (1983).
8. J. F. Uthe, J. Reinke and H. D. Gesser, *Environ. Lett.*, **3**, 117 (1972).
9. A. H. Romanto and R. S. Sofferan, *J. Am. Water Works Assoc.*, **1963**, 55, and references therein.
10. H. J. M. Bowen, *J. Chem. Soc. A*, **1970**, 1082.
11. H. S. Rathore, I. Ali and T. Begum, *Microchem. J.*, **51**, 293 (1995); M. S. El-Shahawi, *J. Chromatogr.*, (1997), in press.
12. T. Braun and A. B. Farag, *Anal. Chim. Acta*, **99**, 1 (1978).
13. A. B. Farag, M. S. El-Shahawi and S. Farag, *Talanta*, **41**, 617 (1994).
14. A. B. Farag, A. M. El-Wakil, M. S. El-Shahawi and M. Mashaly, *Anal. Sci.*, **5**, 415 (1989).
15. S. Palagyi and T. Braun, *Analyst* [London], **117**, 1537 (1992).
16. S. Palagyi and T. Braun, *J. Radioanal. Nucl. Chem.*, **69**, 163 (1992).
17. T. Braun, *Fresenius' Z. Anal. Chem.*, **314**, 652 (1983); **333**, 785 (1989).
18. M. S. El-Shahawi, A. M. Kiwan, S. M. Aldhaheeri and M. H. Saleh, *Talanta*, **42**, 147 (1995).
19. S. Palagyi and T. Braun in "Preconcentration Techniques for Trace Elements", ed. Z. B. Alfassi and C. M. Wai, CRC Press, Boca Raton, 1992.
20. G. J. Moody and J. D. R. Thomas, "Chromatographic Separation and Extraction with Foamed Plastics and Rubbers", Dekker, New York, 1982.
21. T. Braun, J. D. Navratil and A. B. Farag, "Polyurethane Foam Sorbents in Separation Science", CRC Press, Boca Raton, 1985.
22. M. S. El-Shahawi, *Talanta*, **41**, 1481 (1994).
23. A. D. Adamson, "Physical Chemistry of Surfaces", 2nd ed., Academic Press, New York, 1967.
24. L. Schafer and T. A. Wildman, *Can. J. Chem.*, **57**, 450 (1979).
25. T. Schafer, R. Sebastian, R. Laatikainen and S. R. Salman, *Can. J. Chem.*, **62**, 326 (1983).
26. R. C. West, "Handbook of Chemistry and Physics", 54th ed., CRC Press, Boca Raton, 1973.

(Received April 11, 1997)

(Accepted May 15, 1997)

Short communication

Detection and semiquantitative determination of bismuth(III) in water on immobilized and plasticized polyurethane foams with some chromogenic reagents

M.S. El-Shahawi*¹, R.S. Al-Mehrezi

Department of Chemistry, Faculty of Science, UAE University, P.O. Box 17551, Al-Ain, United Arab Emirates

Received 7 November 1995; revised 16 April 1996; re-revised 17 May 1996; accepted 22 May 1996

Abstract

Polyurethane foams immobilizing 1,2-di-(2-fluorophenyl)-3-mercaptoformazan (F_2H_2Dz) and dithizone (H_2Dz) have been used for the detection of bismuth(III) in water via batch, dynamic and pulsed column modes of extraction. The detection limits of bismuth(III) with the F_2H_2Dz - and H_2Dz -immobilized foams were found to be 0.01 and 0.02 $\mu g ml^{-1}$ respectively. Lower concentrations (≤ 1 ppb) of bismuth(III) were also detected by employing dynamic and pulsed columns packed with plasticized tri-*n*-butylphosphate and F_2H_2Dz -immobilized reagent foams. The electronic spectra and partition coefficients of the reagents H_2Dz and F_2H_2Dz and their bismuth(III) chelates in chloroform and in polyurethane foams have been determined. Bismuth (V) was also detected by the proposed procedure after prior reduction to bismuth(III) with sulphur dioxide at $pH < 1$. The effect of diverse ions on the detection of 1 μg of bismuth(III) was critically investigated using F_2H_2Dz -immobilized foam. © 1997 Elsevier Science B.V.

Keywords: Bismuth(III); Chromogenic reagents; Polyurethane foams

1. Introduction

Various reagents have been used for the detection, extraction and spectrophotometric determination of bismuth(III) [1]. Most of these reagents suffer from limitations, e.g. long extraction period, low stability of the compounds formed, low tolerance limit, critical pH and interferences [1,2].

Open cell polyurethane foams have been suc-

cessfully used for the extraction and collection of various species in aqueous media [3]. Foams loaded with dithizone and other chromogenic reagents (chromofoams) have been reported for the sensitive detection and semiquantitative determination of some metal ions, including bismuth(III), employing batch and column extraction modes [4–9].

There has been no study of the use of 1,5-di(2-fluorophenyl)-3-mercaptoformazan agent in the detection and preconcentration of bismuth(III)

* Corresponding author. Fax: (+971) 3-671-291.

Table 1

Characteristic absorption (cm^{-1}) in KBr discs^a and electronic (nm) spectral data for the reagents $\text{F}_2\text{H}_2\text{Dz}$ and H_2Dz and their bismuth(III) chelates in chloroform and in polyurethane foams (values in parentheses)

Compound	Wave number (cm^{-1})				λ_{max} (nm)	$\epsilon(10^{-3} \text{ l mol}^{-1} \text{ cm}^{-1})$	$\log k_{\text{ex}}$ l
	$\nu(\text{N-H})$	$\nu(\text{N}=\text{H})$	$\delta(\text{N-H}) + (\text{C}=\text{N})$	$\nu(\text{N-C-S})$			
$\text{F}_2\text{H}_2\text{Dz}$	3320 (br)	2380 (w)	1510 (s)	1485 (s)	632 (614.5)	25.3	
		1598 (s)		1450 (s)	545 (460.5)	23.7	
H_2Dz	3340 (br)	2365 (w)	1515 (s)	1505 (s)	615 (614)	35.8	
				1465 (s)	448 (480)	17.9	
$\text{Bi}(\text{F}_2\text{HDz})_3$	3440 (m)	1615 (s)	1535 (s)	1485 (s)	490 (487)	91.4	9.75
	3245 (m)	1595 (m)		1460 (s)	(605)		
	3090 (br)			1440 (m)			
$\text{Bi}(\text{HDz})_3$	3420 (m)	1610 (s)					11.49
	3190 (m)	1590 (m)	1530 (s)	1490 (s)	489 (478)	80	
	3060 (m)			1480 (sh)	(616)		

^a s = strong, m = medium, w = weak, sh = shoulder, br = broad.

and other metal ions in aqueous solution employing polyurethane foams. Thus, the present paper describes the use of the immobilized and plasticized 1,5-di-(2-fluorophenyl)-3-mercaptopformazan ($\text{F}_2\text{H}_2\text{Dz}$) and dithizone (H_2Dz) polyurethane foams for the sensitive and selective detection and the semiquantitative determination of traces of bismuth(III) in aqueous media.

2. Experimental

2.1. Reagents and materials

All the reagents used were of analytical-reagent-grade unless otherwise specified. An open cell polyether type polyurethane foams (bulk density 30 kg m^{-3}) was supplied by Greiner K.G. Schaumstoffwerk (Kremsmunster, Austria). The foam material (cubes with 0.5 cm sides) was washed and dried as previously described [10]. A stock solution containing 1 mg ml^{-1} of bismuth(III) was prepared by dissolving the appropriate amount of bismuth(III) nitrate pentahydrate in deionized water acidified with a few drops of 0.5 M nitric acid and standardized by EDTA titration. A bismuth(III) solution ($100 \mu\text{g ml}^{-1}$) was also prepared by dissolving 0.123 g of bismuthic acid in 100 ml of 0.5 M KOH [11].

Tri-*N*-butylphosphate (TBP; BDH) was used without further purification. A series of standard bismuth(III) and (V) solutions was prepared by dilution with water acidified with a few drops of nitric acid.

The reagent $\text{F}_2\text{H}_2\text{Dz}$ was prepared by the nitroformazyl method [12,13]. This reagent and the H_2Dz (Merck) solutions were prepared by dissolving 10 mg of each reagent separately in 50 ml of chloroform. The $\text{F}_2\text{H}_2\text{Dz}$ - and H_2Dz -loaded foams were prepared by mixing the dried foam cubes with $\text{F}_2\text{H}_2\text{Dz}$ and H_2Dz solutions (10 ml g^{-1} dry foam) respectively and stirring for 10 min. The reagent-loaded foam cubes were then squeezed and dried as reported [10]. Plasticized $\text{F}_2\text{H}_2\text{Dz}$ and H_2Dz foams were prepared by mixing the dried foam cubes with $\text{F}_2\text{H}_2\text{Dz}$ and H_2Dz (0.1% w/v) in TBP respectively, stirring for 15 min and then drying [10].

2.2. Apparatus

A Shimadzu UV 2101 PC UV-visible scanning spectrophotometer and a Shimadzu FTIR-8101 Fourier transform infrared spectrophotometer were used for recording the IR and electronic spectra of the reagents and their bismuth(III) complexes in chloroform and in parallelepiped polyurethane foam. An Orion pH-meter, glass

Table 2

Comparative sensitivity of batch and dynamic modes of extraction for the detection of bismuth(III) ions (ppb) using F₂H₂Dz and H₂Dz immobilized or plasticized TBP foams

Method	Amount of bismuth(III) detected (ppb)			
	F ₂ H ₂ Dz		H ₂ Dz	
	Batch	Dynamic	Batch	Dynamic
Unloaded foam	100	—	100	—
Immobilized reagent foam	10	5	20 ^a	10 ^a
Plasticized TBP reagent foam	5	1	20	10

^a Data were obtained from Ref. [4].

columns (16 cm height × 5 mm i.d.) and medical syringes (100 ml capacity) as pulsating columns were used.

2.3. General procedures

2.3.1. Batch experiment

One of the immobilized reagent or plasticized TBP–reagent foam cubes was shaken with 3–5 ml of the bismuth(III) aqueous solution (pH < 4) for 2 min. The colour of the reagent foam changed from green to orange–brown and to orange with H₂Dz and F₂H₂Dz respectively. The colour that developed on the foam cube was taken as evidence for the detection of bismuth(III).

2.3.2. Column experiments

1 g of the F₂H₂Dz or H₂Dz-loaded or plasticized reagent–TBP foams was packed in a glass column by the vacuum method of foam column packing [14]. 250 ml of the bismuth(III) solution of optimum pH was allowed to pass through the foam column at a flow rate of 2–3 ml min⁻¹. The coloured foam bed produced was used for the detection of bismuth(III) ions.

2.3.3. Pulsating column experiments

50 ml of the bismuth(III) solution of suitable pH was transferred to a 100 ml medical syringe. The solution was then compressed and released with one cube of F₂H₂Dz-immobilized or plasticized F₂H₂Dz–TBP foam. An orange colour on the foam cube was then observed after 25 successive pulses.

3. Results and discussion

Table 1 summarizes the IR data for the regions of interest in the spectra of the solid reagents H₂Dz and F₂H₂Dz and their solid complexes of bismuth(III) in a potassium bromide disc. The reagents F₂H₂Dz and H₂Dz and their bismuth(III) complexes were characterized by IR spectral [15–17] (Table 1) and elemental analysis. The electronic spectra of the reagents and bismuth(III) complexes in chloroform and in parallelepiped polyurethane foams are also given in Table 1 and Fig. 1. The electronic spectra of the bismuth(III) complexes in chloroform (Fig. 1A) and in polyurethane foams (Fig. 1B) have well-defined bands at 489–490 and 478–487 nm respectively and a broad shoulder of low intensity at 270–360 nm. The introduction of fluorine atoms at the C-2 position of the phenyl radicals of H₂Dz leads to small bathochromic shifts of both of its bands (632 and 454 nm → 615 and 448 nm respectively) for H₂Dz. The position of λ_{\max} for the bismuth(III) complex of F₂H₂Dz in chloroform underwent similar shifts (Table 1) as compared with the bismuth(III) complex of H₂Dz. The relative molar absorptivities in chloroform of the two absorption bands of F₂H₂Dz and its bismuth(III) complex were similarly affected by the introduction of fluorine atoms compared with H₂Dz and its bismuth(III) complex (Table 1).

3.1. Detection and semiquantitative determination of bismuth(III) with F₂H₂Dz

Bismuth(III) forms orange–red and orange–

Table 3

Detection of 1 μg of bismuth(III) with $\text{F}_2\text{H}_2\text{Dz}$ -immobilized polyurethane foams in the presence of some interfering ions

Foreign ions	Compound added	Tolerance limit	Note
Cd^{2+}	CdBr_2	$1:1 \times 10^4$	Add a few crystals of sodium sulphite
Fe^{2+}	FeSO_4	$1:1 \times 10^4$	Add 1 ml of NaF (1 M)
Fe^{3+}	FeCl_3	$1:1 \times 10^4$	Add 1 ml of NaF (1 M)
Ni^{2+}	$\text{NiCl}_2 \cdot 4\text{H}_2\text{O}$	$1:1 \times 10^3$	Add a few drops of KCN (1 M)
Au^{3+}	AuCl_3	$1:1 \times 10^3$	Add a few crystals of sodium sulphite and adjust pH to ≈ 1
MnO_4^-	KMnO_4	$1:1 \times 10^3$	Add one crystal of sodium azide
Mn^{2+}	MnSO_4	$1:1 \times 10^4$	Add bromine water and boil the solution
Hg^{2+}	HgCl_2	$1:1 \times 10^4$	Add one crystal of ascorbic acid
Pd^{2+}	$\text{Pd}(\text{NO}_3)_2$	$1:1 \times 10^3$	Add one crystal of NaF or thiourea
Cr^{3+}	$\text{CrCl}_3 \cdot 6\text{H}_2\text{O}$	$1:1 \times 10^3$	Add H_2O_2 and boil the solution
Ag^+	AgNO_3	$1:1 \times 10^3$	Add a few crystals of KCNS
Zn^{2+}	ZnSO_4	$1:1 \times 10^3$	Adjust the pH of the aqueous solution to < 2 with HNO_3 (1 M)
Oxalate	$\text{H}_2\text{C}_2\text{O}_4 \cdot 2\text{H}_2\text{O}$	$1:1 \times 10^3$	Add bromine water and boil the solution
VO_3^-	NH_4VO_3	$1:1 \times 10^3$	Add 1 ml of NaF (1 M)

brown complexes [12, 18] with $\text{F}_2\text{H}_2\text{Dz}$ and H_2Dz in acidic aqueous solution ($\text{pH} < 5.2$) respectively. These reactions were tried with foam immobilized with $\text{F}_2\text{H}_2\text{Dz}$ and H_2Dz and plasticized reagent-TBP foam for the detection and semiquantitative determination of bismuth(III) in aqueous solution.

On shaking one cube of the unloaded foam with the mixed test solution of $\text{Bi}(\text{F}_2\text{HDz})_3$ in a test tube at $\text{pH} < 4$ for 2–3 min as little as 0.10 ppm bismuth(III) was easily detected. The sensitivity of the test was significantly improved by immobilizing or plasticizing the foam cubes with the reagent $\text{F}_2\text{H}_2\text{Dz}$. On shaking one cube of the immobilized $\text{F}_2\text{H}_2\text{Dz}$ foam and one cube of the plasticized $\text{F}_2\text{H}_2\text{Dz}$ -TBP with 2–3 ml of the test aqueous solution of bismuth(III) concentrations as low as 0.01 and 0.005 ppm were easily detected respectively. The relatively high available surface area of the foam cube acts as an efficient collector for the bismuth(III) ions present in the aqueous solution at low concentration. In addition, it is easy to observe the characteristic red colour of the reaction product on/in the thin membranes of the foam material. The TBP plays a dual purpose [5] as it acts as an efficient non-volatile solvent for the reagent

$\text{F}_2\text{H}_2\text{Dz}$ and as a plasticizer for the plastic foam itself. This enhances the permeability of the foam material and the rate of sorption of bismuth(III) ions from the aqueous solution on the plasticized reagent foam. A comparison between these results (Table 2), those reported with the usual spot test [19] and those of Hamza et al. [4] employing H_2Dz -loaded foam shows that the $\text{F}_2\text{H}_2\text{Dz}$ -immobilized foam and plasticized $\text{F}_2\text{H}_2\text{Dz}$ -TBP foam methods are much more sensitive for the detection of bismuth(III) than H_2Dz and other chelating agents [4, 19].

The colour density on the foam cubes was found to depend on the concentration of the bismuth(III) ions. Thus, semiquantitative determination of bismuth(III) was achieved by comparison of the colour of the plasticized $\text{F}_2\text{H}_2\text{Dz}$ -TBP foam cube with a standard colour scale prepared from 0.01, 0.05, 0.1, 0.5, 1 and 10 ppm bismuth(III) solutions under the same experimental conditions.

The proposed $\text{F}_2\text{H}_2\text{Dz}$ -loaded and plasticized $\text{F}_2\text{H}_2\text{Dz}$ -TBP foams were easily packed in the column mode producing a foam bed suitable for the detection of bismuth(III) present in an extremely dilute aqueous solution. Concentrations

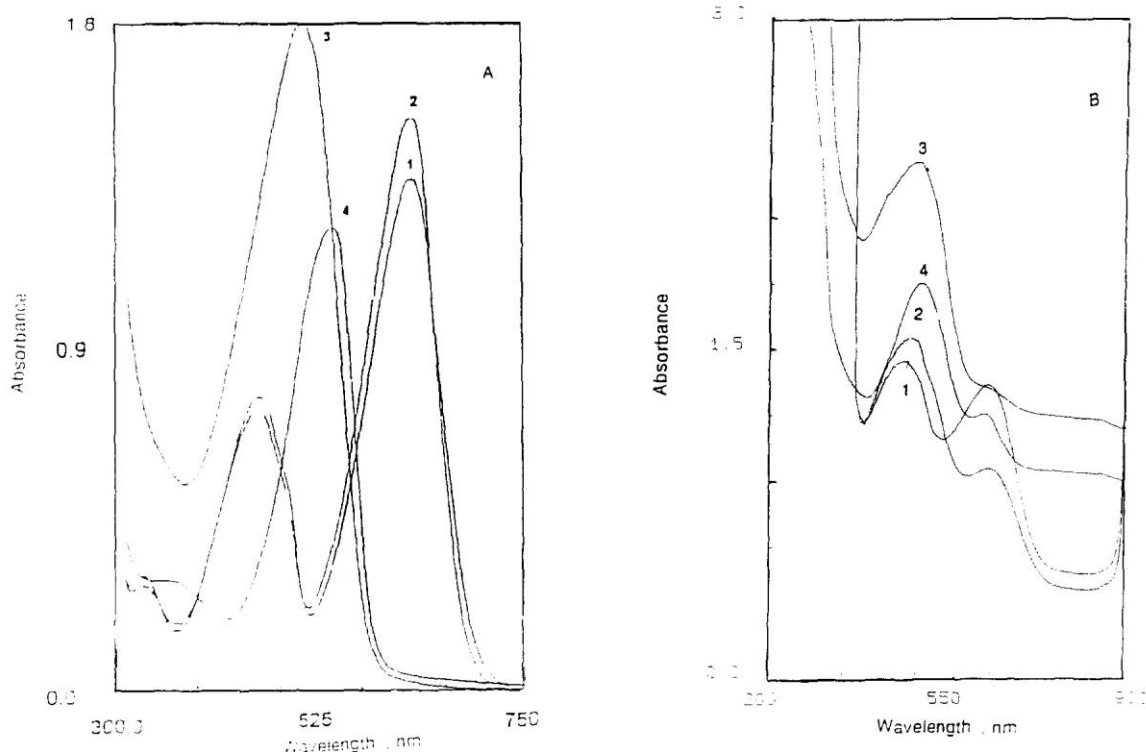


Fig. 1. Electronic spectra of (1) F₂H₂Dz, (2) H₂Dz, (3) Bi(F₂HDz)₃ and (4) Bi(HDz)₃ in chloroform (A) and in polyurethane foam (B).

as low as 5 and 1 ppb of bismuth(III) in aqueous solution were easily detected with F₂H₂Dz-loaded and plasticized F₂H₂Dz–TBP foams respectively. The length of the coloured zone was found to be proportional to the bismuth(III) concentration in the aqueous phase (Fig. 2). Thus, semiquantitative determination of bismuth(III) in extremely dilute solutions was found to be possible using a standard colour covering the range 5–80 ppb and employing F₂H₂Dz-loaded foam.

The proposed F₂H₂Dz-loaded and plasticized F₂H₂Dz–TBP foam cubes were used in a medical syringe for the detection of bismuth(III). As little as 5 ppb of bismuth(III) was easily detected after 25 successive pulses with F₂H₂Dz-loaded and plasticized F₂H₂Dz–TBP foams. Semiquantitative determination was also found to be possible with standards of 5, 10, 15, 20 and 25 ppb bismuth(III) solution by comparison of the colour of the foam cubes at a constant number of pulses ≥ 25 .

3.2. Determination and semiquantitative determination of bismuth(III) with H₂Dz foam

The use of H₂Dz allows the detection of as little as 0.02 ppm bismuth(III) in aqueous solution by shaking one cube of H₂Dz-loaded foam or plasticized H₂Dz–TBP foam with the test solution. These data are in good agreement with the data reported by Hamza et al. [4]. As little as 5 ppb of bismuth(III) was easily detected in aqueous solution by H₂Dz-loaded and plasticized H₂Dz–TBP foam columns at a flow rate of 2–3 ml min⁻¹. The semiquantitative determination of bismuth(III) with immobilized foams was found to be possible in the concentration range 1–30 ng ml⁻¹ (Fig. 2).

The results obtained with F₂H₂Dz were much better than those obtained with H₂Dz. The higher acidity of F₂H₂Dz ($pK_a = 4.05$) and the higher extraction constant of its bismuth(III) complex ($\log K_{ex} = 11.41$) compared to the values

for H_2Dz ($pK_a = 4.7$) [20] and its $Bi(HDz)_3$ complex ($\log K_{ex} = 9.8$) may partially account for this behaviour. The distribution ratios of $Bi(F_2HDz)_3$, ($\log D = 4.1$) and $Bi(HDz)_3$ ($\log D = 3.8$) in the thin membrane of the polyurethane foam may also play significant roles in the preconcentration. Similarly, the fluorine atom at the ortho position of the phenyl moiety of H_2Dz was found to increase the partition coefficient of F_2H_2Dz between CCl_4 and H_2O to 2.1×10^4 compared to 1.1×10^4 for H_2Dz [21,22] in the same two-phase system. The partition coefficient of $Cu(F_2HDz)_2$ between CCl_4 and H_2O was found to be 1.53×10^5 [21], compared to 7.3×10^4 for $Cu(HDz)_3$ (calculated from the stability constants data of Ref. [23]).

Bismuth (V) was also detected by the proposed method after prior reduction to bismuth(III).

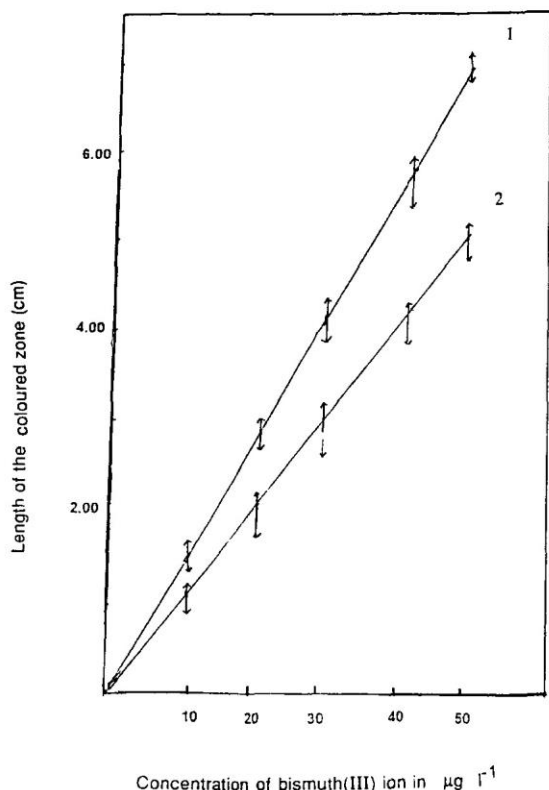


Fig. 2. Relationship between the length of the coloured zone (cm) on the immobilized (1) F_2H_2Dz , (2) H_2Dz , foam columns and the concentration of bismuth(III) in ppb.

Sodium sulphite (1%) in acid media was found to be the most convenient reducing agent, where the unreacted sulphur dioxide was easily removed by boiling. As little as 0.02 ppm of bismuth (V) was easily detected in batch mode after reduction to bismuth(III) followed by shaking this solution with plasticized F_2H_2Dz -TBP foams.

3.3. Interference study

Elimination of interferences in the detection of bismuth(III) in water employing the F_2H_2Dz -loaded foam was considered to be a prime importance. Thus, the selectivity of the proposed batch F_2H_2Dz -loaded foam method for the detection of bismuth(III) in the presence of diverse ions was critically investigated. It was possible to detect $1\ \mu g$ of bismuth(III) in the presence of up to 1 mg of the following ions: Li^+ , Ca^{2+} , Ba^{2+} , Mg^{2+} , Sr^{2+} , Al^{3+} , NH_4^+ , Mn^{2+} , Zn^{2+} , SO_4^{2-} , NO_3^- , Br^- , Cl^- , VO_3^- , WO_4^{2-} , SO_3^{2-} , BrO_3^- , NO_2^- , NO_3^- , ClO_4^- , SeO_3^{2-} , SeO_4^{2-} , SbO_2^- , AsO_2^- , acetate, citrate, tartrate, ascorbate, phosphate and chromate. In the presence of some other ions (≤ 0.01 mg) which interfered seriously with the proposed method, simple modifications were made to the aqueous sample solution to eliminate their interferences, affording unambiguous and sensitive detection of bismuth(III) as given in Table 3.

3.4. Application of the proposed method

The feasibility of the method for the detection of bismuth in sea and waste water samples was also examined. A water sample (0.2 l) acidified with $0.1\ mol\ l^{-1}$ nitric acid was allowed to pass through a $0.45\ \mu m$ Millipore filter, and then 10 ml of $1 \times 10^{-3}\ mol\ l^{-1}$ disodium salt of EDTA and 10 ml of $1 \times 10^{-3}\ mol\ l^{-1}$ NaF were added. The reaction mixture was allowed to stand for 15 min and then 1 ml of sodium sulphite solution and 5 ml of concentrated HCl were added. The solution was boiled to dryness, diluted with 20 ml of distilled water and the pH was then adjusted to 9–10 with ammonia followed by the addition of 10 ml of 2% (w/v) sodium diethyldithiocarbamate (NaDDC). The $Bi(DDC)_3$ complex produced was

then extracted by shaking with 10 ml of xylene [24]. Back extraction of bismuth(III) was achieved with 5 ml of concentrated HNO_3 and finally the pH of the solution was adjusted to 3–5. Negative results for the detection of bismuth in sea and waste water with batch immobilized- $\text{F}_2\text{H}_2\text{Dz}$ foam were obtained while with a column packed with $\text{F}_2\text{H}_2\text{Dz}$ foam it was possible to detect bismuth(III) in the concentration range 10–20 ppb in seawater. This concentration range was detected by flameless atomic absorption spectrometry to be 12 ± 2 ppb bismuth.

An attempt was made to demonstrate the utility of the method for the quantitative collection of bismuth(III) at $3 < \text{pH} < 5$ with a column packed with $\text{F}_2\text{H}_2\text{Dz}$ foam. 100 ml of a $10 \mu\text{g ml}^{-1}$ aqueous solution of bismuth(III) was precolated through a foam column (12 cm height \times 1.5 i.d.) packed with $\text{F}_2\text{H}_2\text{Dz}$ foam at $1\text{--}2 \text{ min}^{-1}$. Analysis of the effluent solution by atomic absorption spectrometry showed quantitative collection (95–98%) of bismuth(III) on the foam column with a standard deviation σ of 1.30.

4. Conclusion

This article has demonstrated the possible use of plasticized or immobilized polyurethane foams for the sensitive and selective detection and quantitative collection of bismuth(III) in water at extremely low concentrations. Elimination of the interference of diverse ions in the detection of bismuth in water by the proposed procedure is of prime importance. Much work still remains to be done on improving the selectivity and utility of the method for the direct determination of bismuth(III), or bismuth (V) after prior reduction, either by direct solid phase spectrometry on parallelpiped polyurethane foams or by elution of the $\text{Bi}(\text{F}_2\text{HDz})_3$ chelate from the packed foam column with a selective eluting agent.

Acknowledgements

The authors thank Professor A.M. Kiwan for

valuable discussions and for the loan of the reagent $\text{F}_2\text{H}_2\text{Dz}$.

References

- [1] A.P. Argekar and A.K. Shetty, *Analyst*, 120 (1995) 1819 (and references cited therein).
- [2] M.S. El-Shakawi and S.M. Al-Dhaheri, *Fresenius' J. Anal. Chem.*, 320 (1995) 279.
- [3] M.S. El-Shawawi, A.M. Kiwan, S.M. Al-Dhaheri and M.H. Saleh, *Talanta*, 42 (1995) 1471.
- [4] A.G. Hamza, A.B. Farag, T.A. Amireh, Z.E. El-Bassyouni and F.M. Al-Nowaiser, *Anal. Sci.*, 6 (1990) 889.
- [5] T. Braun, J.D. Navartil and A.B. Farag, *Polyurethane Foam Sorbents in Separation Science*, CRC Press, Boca Raton, FL, 1985.
- [6] A.B. Farag, A.M.A. Helmy, M.S. El-Shahawi and S. Farrag, *Analysis*, 17 (1989) 478.
- [7] A.G. Hamza, A.B. Farag and A. Al-Herthani, *Microchem. J.*, 32 (1985) 13.
- [8] A.B. Farag, A.M. El-Wakil, M.E.M. Hassouna and M.H. Abdel-Rahman, *Anal. Sci.*, 3 (1987) 541.
- [9] A.B. Farag, A. El-Waseef and M.H. Abdel-Rahman, *Acta. Chim. Hung.*, 122 (1986) 273.
- [10] M.S. El-Shahawi, *Talanta*, 41 (1994) 1481.
- [11] D.R. Lide, *Handbook of Chemistry and Physics*, 2nd edn., CRC Press, Boca Raton, FL, 1991.
- [12] A.M. Kiwan and A. Y. Kassim, *Anal. Chim. Acta*, 88 (1977) 177 (and references cited therein).
- [13] D.M. Hubbard and E.W. Scott, *J. Am. Chem. Soc.*, 65 (1943) 2390.
- [14] T. Braun and A.B. Farag, *Anal. Chim. Acta*, 73 (1974) 301.
- [15] S. Taki and T. Kato, *Tech. Rep. Tohoku Univ.*, 21 (1957) 319, 26 (1962) 35.
- [16] L.G. Bellamy, *Advances in Infrared Group Frequencies*, Methuen, London 1968, p. 357.
- [17] A. Mawby and H.M. N.H. Irving, *Anal. Chim. Acta*, 55 (1971) 269.
- [18] Z. Marczenko, *Separation and Spectrophotometric Determination of Elements*, Ellis Horwood, New York, 1986, p. 169.
- [19] F. Feigl and V. Anger, *Spot Tests in Inorganic Analysis*, 6th edn., Elsevier, Amsterdam, 1972.
- [20] H. Irving and C.F. Bell, *J. Chem. Soc.*, (1952) 1716; (1953) 3538.
- [21] A.Y. Kassim, Ph.D. Thesis, University of Kuwait, Kuwait, 1975.
- [22] I.M. Kolthoff, E.B. Sandell, E.J. Meehan and S. Bruckenstein, *Quantitative Chemical Analysis*, Macmillan, London, 1969, p. 352.
- [23] G. Iwantscheff, *Das Dithizone and Seine Anwendung in der Mikro-und Spurenanalyse*, 2nd edn., Verlag Chemie, Weinheim, Germany, 1972.
- [24] Y. Shijo, M. Mitsuhashi, T. Shimizu and S. Sakurai, *Analyst*, 117 (1992) 1929.

Retention profiles of some commercial pesticides, pyrethroid and acaricide residues and their application to tomato and parsley plants¹

M.S. El-Shahawi²

Chemistry Department, Faculty of Science, UAE University, P.O. Box 17551, Al-Ain, United Arab Emirates

Received 9 March 1996; revised 1 October 1996; accepted 9 October 1996

Abstract

This work deals with the preconcentration of some water soluble pesticides, pyrethroids and acaricides by polyurethane foams. The retention profiles of the tested species were found quickly and reached equilibrium in a few min. Various parameters – e.g. pH, extraction media, shaking time, salt effect, temperature and sample volume – affecting the preconcentration of the tested species by the unloaded foams and tri-*n*-octylamine and tri-*n*-methylphosphate treated foams were optimized. The unloaded foams were employed in a column mode to study the quantitative retention and recovery of the tested species. The sorption efficiency and recovery of the compounds by the unloaded foam column were found to be up to 99.5%±2.1. The height equivalent of a theoretical plate for the unloaded foam column was found to be in the range 1.9–2±0.2 mm. The sorption mechanisms of the tested compounds by the foams are discussed. Analysis of N, P, Na, K, Cu, Zn, Mn, Fe, humidity, wet and dry mass of tomato and parsley untreated and sprayed for different time intervals – i.e. 24, 72 and 120 h – with Chlorpyrifos, was carried out .

Keywords: Polyurethane foam; Sample preparation; Tomato; Parsley; Environmental analysis; Stationary phases, LC; Thermodynamic parameters; Water analysis; Pesticides; Pyrethroids; Acaricides

1. Introduction

In recent years industrial growth and the need to increase agriculture productivity have resulted in the presence of pollutants in water and air. Since these compounds are present at levels lower than ppb their determination causes problems [1]. Among these substances, pesticides, pyrethroids and acaricides must be watched with particular attention because of

their very low limits of tolerability. These compounds are deliberately directed against living organisms and show strong bioaccumulation [1,2].

The most common reported extraction procedures for the water pollutants are liquid–liquid extraction [3], adsorption on activated charcoal [4] and/or cellulose triacetate membrane filters [5], Tenax, Chromosorb 101 and Porapak as trapping materials [6]. Such preconcentration methods are not satisfactory with respect to their capacity for trapping pollutants present at very small amounts and their recovery, and they are also too extensive for routine analysis where many large sample volumes are concentrated on site prior to quantitative analysis [7].

¹ Paper originally submitted for the thematic issue on Pesticide Residues [J. Chromatogr. A, 754 (1996)].

² On leave from the Chemistry Department, Faculty of Science, at Damiatta, Mansoura University, Damiatta, Egypt.

Recently, porous polyurethane foam has been used as an inexpensive solid extractor and effective sorbent for the removal of water pollutants [8,9]. The membrane-like structure of the foam together with its efficient sorption properties offered higher concentrating ability and flow-rates compared with other solid granular supports [10]. The present study was aimed at investigating the retention profiles of some pesticides, pyrethroids and acaricides in water at low levels (ppb) by polyether-based polyurethane foams. The influence of Chlorpyrifos on the uptake of some essential elements, e.g. N, K, P, Na, Fe, Zn, Mn and Cu, and on the wet and dry mass and humidity percentage of tomato and parsley plants after different times of spraying was also studied.

2. Experimental

2.1. Reagents and materials

All chemicals used were of analytical reagent grade. Open pore polyether-type-based polyurethane foams were supplied by K.G. Schaum (Stoffwerk, Kremsmunster, Austria). Foam cubes of approximately 1 cm³ were cut from polyurethane foam sheets. The foam cubes were dried as reported previously [11]. The foam cubes were loaded with tri-*n*-octylamine (TOA) and tri-*n*-methylphosphate (TMP) by mixing the dried foam cubes with 5% TOA and 5% TMP separately in *n*-hexane (20 cm³/g dry foam) with stirring for 10 min, respectively, and drying as reported [11]. Stock solutions (1 M) of lithium, sodium, ammonium and potassium chlorides were prepared separately in distilled water. Britton–Robinson buffer (pH 2–12) solutions were prepared by mixing equimolar concentration (0.08 M) of boric, acetic and phosphoric acid in distilled water and adjusting the pH with sodium hydroxide (0.04 M).

The tested pesticides are Chlorpyrifos, *o,o*-diethyl-*o*-(3,5,6-trichloro-2-pyridyl) phosphorothioate (I); Parathion, *o,o*-diethyl-4-nitrophenyl phosphorothioate (II); Malathion, diethyl-[(dimethoxyphosphinothioyl)thio]butanedioate (III); the pyrethroid Cypermethrin, cyano(3-phenoxyphenyl)methyl-3-(2,2-dichloroethyl)-2,2-dimethylcyclopropanecarboxylate (IV); and the acaricides Dicofol, 2,2,2-trichloro-

1-bis(4-chlorophenyl)ethanol (V) and Bromopropylate, isopropyl-4,4-dibromobenzilate (VI). The structures of these compounds are given in Fig. 1.

A stock solution of each compound (100 µg/cm³) was prepared by dissolving the exact mass of the compound in ethanol. A series of various concentrations of these compounds was then freshly prepared by diluting their stock solutions with distilled or tap water and a few drops of ethanol whenever it was required to provide a clear solution. The solutions were stored in polyethylene bottles.

2.2. Apparatus

UV absorbance of the tested insecticides was obtained with a Pye Unicam UV-Vis SP8-400 spectrometer with 0.2- and 1-cm quartz cells. An Orion pH meter and glass columns (15 cm×15 mm I.D.) and a Lab-Line Orbit Environ-Shaker Model 35271-1 were also used. A Corning flame photometer (410) and a Pye Unicam SP-9 atomic absorption spectrometer were used to measure the concentration of Na, K, Fe, Mn, Zn and Cu. Calcium was determined by EDTA titration. The Kjeldahl method was used for the determination of the nitrogen content in plant (tomato and parsley) tissues. Hot Box oven Honda spray machine with high pressure and stoppered flasks (50 cm³ capacity) were used.

2.3. General procedures

2.3.1. Batch experiments

Influence of shaking time on the retention profiles of the tested compounds on the unloaded and loaded polyurethane foams

The unloaded and loaded (TOA or TMP) polyurethane foam cubes (0.3+0.004 g) were equilibrated with 100 cm³ aqueous solution at pH 4–6 of each compound at concentrations of 100 µg/cm³ in polyethylene bottles and shaken in a thermostated mechanical shaker at 20±0.1°C for various time intervals up to 2 h. After shaking, the foam cubes were separated and the amount of the compound remaining in the aqueous phase was determined from its absorbance measurements at the wavelength of maximum absorbance against a blank; the amount of the insecticide retained on the foam was calculated

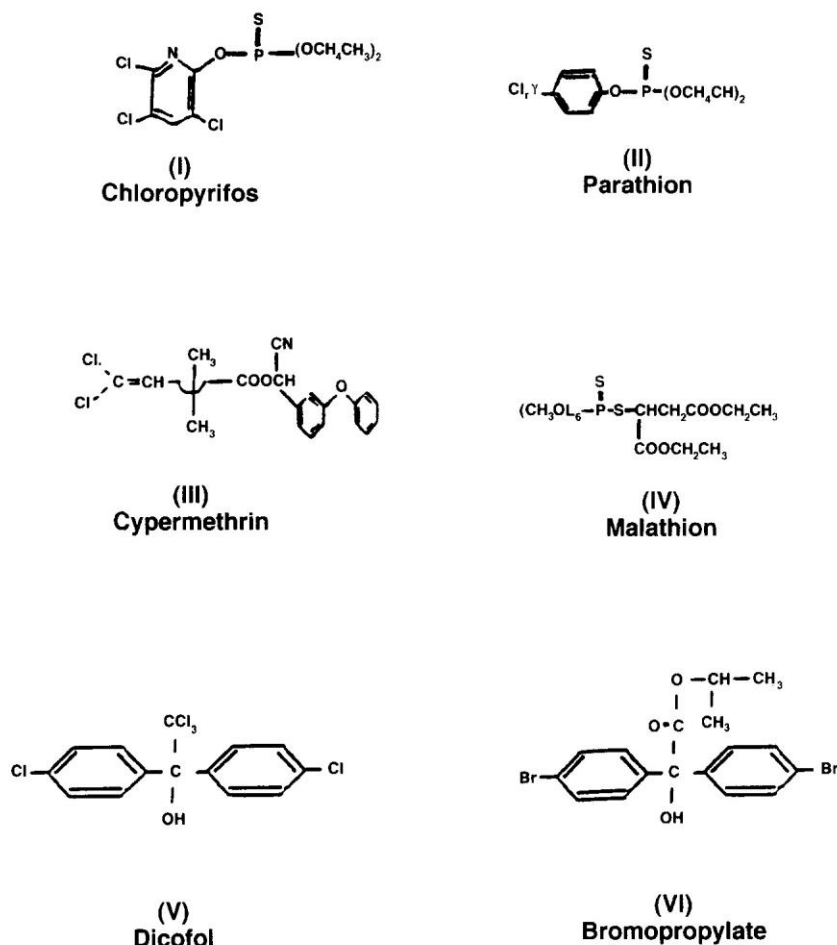


Fig. 1. The structure of the tested organophosphorous insecticides, pyrethroid and acaricides.

using this difference. The extraction efficiency (%*E*) and the distribution coefficient (*D*) of the tested species by the unloaded foams were determined employing the equations:

$$\% \text{Extraction } (E) = \frac{a_0 - a}{a} \times 100 \quad (1)$$

and

$$D = \frac{\%E}{100 - \%E} \times \frac{\text{Volume of solution (l)}}{\text{Mass of foam (kg)}} \quad (2)$$

or

$$D = \frac{\%E}{100 - \%E} \times \frac{\text{Volume of solution (cm}^3\text{)}}{\text{Mass of foam (g)}} \quad (3)$$

where a_0 = concentration of the tested compound in

solution before extraction and a = concentration of the solute in solution after extraction.

Following these procedures, the influence of solution pH, nature of extraction media, temperature, compound concentration and salt concentration ($\leq 0.1 M$) of different chloride salts (Li, Na, K and NH_4) on the retention profiles of the tested compounds by the unloaded, TOA- and TMP-loaded polyurethane foams were critically determined.

2.3.2. Column experiments

Chromatographic behaviour of the tested insecticides on a column packed with the unloaded foam

Quantitative retention and elution of the tested compounds on the unloaded foam columns were

carried out using the vacuum method of foam packing [11]. Tap or distilled water (0.1–6 dm³) samples containing 0.05 mg of the tested compound at the pH of maximum retention on the unloaded foams was percolated through the column packed with 3±0.006 g of the unloaded foam at 10 cm³/min. After squeezing water from the foam material, the compound was recovered from the foam with 100 cm³ acetone in a Soxhlet extractor for 6 h. The sample quantity was then determined from a pre-constructed calibration curve by measuring the absorbance of the extracted acetone solution against a blank.

2.3.3. Plant analysis

Sample preparation

Plant sample (leaves) of tomato and parsley were sprayed with 20 g of commercial Chlorpyrifos (40%, w/w) mixed with 20 dm³ water (4:1×10⁴, w/v) in the open field using a high-pressure sprayer. The treated plant samples were left for periods of 24, 72 and 120 h. Five samples each of untreated and treated leaves were then collected, washed with distilled water until all dust and sand were removed completely and finally dried with a napkin. The leaves were cut into small pieces, washed with water and spread for 24 h at room temperature for drying and grinding into powder form.

Determination of the total nitrogen content

A mass of the dry leaves (0.2–0.3 g) was accurately weighed and placed in a 800 cm³ Kjeldahl flask; 50 cm³ of concentrated sulphuric acid containing 1.65 g of salicylic acid were added. Five grams of sodium thiosulphate were added, the mixture was heated for 30 min, cooled and 10 g of a sodium hydrogensulphate–selenium mixture (100:1, w/w) were added and the mixture was digested in the Kjeldahl apparatus. After complete digestion, the mixture was cooled and 300 cm³ of water and 100 cm³ of concentrated sodium hydroxide were added. Then the distillate standard sulphuric acid was distilled and titrated and the nitrogen content was determined employing the equation:

$$\%N = \frac{14NV}{10W} \quad (4)$$

where N and V are the normality and volume in cm³ of sulphuric acid consumed in the titration and W is the mass of the dry leaves in g.

Determination of P, Na, K, Cu, Zn, Mn and Fe by wet ashing

An accurate mass (2–3 g) of the ground plant material was placed in 20 cm³ of a concentrated sulphuric–perchloric acid mixture (1:1, v/v). The reaction mixture was heated on a hot plate until the acid fumes were completely evolved; the volume of the reaction mixture was reduced to 3–5 cm³ by evaporation on a hot plate and 50 cm³ of distilled water were added to the mark. Calibration graphs for phosphorous and molybdenum were made by UV-visible spectrophotometry; for sodium and potassium flame photometry was used, and for copper, zinc, manganese and iron atomic absorption spectrometry was employed. The unknown sample concentration was then obtained from a calibration graph of each element employing the following equation:

$$\%M = \frac{C \text{ (ppm)} \times \text{solution volume (cm}^3\text{)}}{10^4 \times \text{sample mass (g)}} \quad (5)$$

where $M = P, Na, K, Cu, Zn, Mn$ or Fe and C is the concentration of the element to be determined in ppm.

Determination of the moisture or humidity content

The sample was spread in the container, rapidly weighed, dried in a circulation oven at 70–80°C to a constant mass, cooled in a desiccator, weighed. The humidity and dry matter percentages of the plant leaves were obtained by employing the equations:

$$\text{Moisture (\%)} = \frac{\text{Loss in mass on drying (g)}}{\text{Initial sample mass (g)}} \times 100 \quad (6)$$

$$\text{Dry matter (\%)} = \frac{\text{Oven dry mass (g)}}{\text{Initial sample mass (g)}} \times 100 \quad (7)$$

Ash content

The crucible in a muffle furnace was heated to about 500°C, cooled in a desiccator, weighed and an accurate mass of 1 g of oven-dried sample was transferred into the crucible. The crucible containing the dry sample was placed into a cool muffle furnace

and the temperature was increased to 500°C. After 3 h at 500°C the crucible was removed, allowed to cool in a desiccator, weighed and the ash content was determined by employing the equation:

$$\text{Ash (\%)} = \frac{\text{Ash mass (g)}}{\text{Oven dry mass (g)}} \times 100 \quad (8)$$

Dry ashing

A 0.2-g amount of air-dried ground sample was weighed into an acid-washed porcelain basin, ignited to 500°C for 3 h in a muffle furnace (refer to ashing procedure) and cooled; 5 cm³ of HCl (1:1, v/v) were added and the sample was covered with a watch glass and heated on a steam bath for 15 min. Then 1 cm³ of concentrated HNO₃ was added, the sample evaporated to dryness, and heating continued for 1 h; 2 cm³ of HCl (1:1, v/v) were added, the sample swirled to dissolve the residue, diluted to 20 cm³ with water and warmed to complete dissolution. Then the sample was filtered through a No. 44 filter paper into a 100 cm³ volumetric flask and diluted with distilled water to the mark. Blank determination was carried out in the same way.

3. Results and discussion

The use of unloaded polyurethane foams (PuF) in the separation and preconcentration processes led to observation of the potential of their spherical geometrical form (spherical membrane-shaped geometry) and to the proposal of their general use in column operations as a substitute for the traditional granular supports in extraction chromatography. The membrane-like structure of the foams together with the efficient sorption and mass-transfer properties offer higher concentrating abilities and flow-rate compared with other solid supports. Thus, in recent years, considerable progress has been made in the use of polyurethane foam as an inexpensive solid extractor and effective sorbent for the removal of water pollutants.

3.1. Retention behaviour of the tested compounds on the unloaded and loaded foams by batch experiments

Batch experiments using unloaded foams have

shown that the retention of Parathion, Malathion, Chlorpyrifos and Cypermethrin was rapid and the equilibrium was reached in less than 50 min, followed by a plateau. Hence, a minimum shaking time of 1 h was adopted in the subsequent work. The results obtained are summarized in Fig. 2. The average values of the half-life ($t_{1/2}$) of the sorption equilibrium calculated from Fig. 2 were found to be in the range 2–3 min.

Similarly, batch experiments using unloaded, TMP- and TOA-loaded polyurethane foams have shown that the extraction of the investigated acaricides Dicofol and Bromopropylate from aqueous solution at pH ≤ 3 is rapid and the equilibrium is reached in less than 1 h, followed by a plateau. A good extraction efficiency and rapid preconcentration of the tested acaricides from aqueous media were obtained with TOA-treated foam as compared to the unloaded and TMP-loaded foams. The average values of the half-life ($t_{1/2}$) of equilibrium sorption on the unloaded, TOA- and TMP-loaded foams were found to be in the range 3–5, 2.5–3 and 3–4 min, respectively. The tri-*n*-octylamine acts as a plasticizer on the polyether foam. Thus, the collection

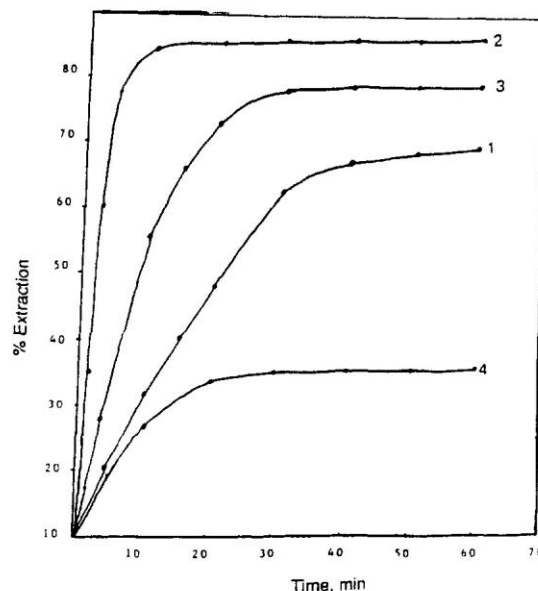


Fig. 2. Effect of shaking time on the sorption profiles of (1) Parathion, (2) Malathion, (3) Chlorpyrifos and (4) Cypermethrin at 100 mg/cm³ in aqueous solution (100 cm³) at pH 5–7 and 20 ± 0.1°C using the unloaded foam (0.3 ± 0.004 g).

rates of the compounds with plasticized TOA foams are generally better than with unplasticized ones. This can be attributed to the high mobilities and diffusion rates of the tested acaricides through the open pores and the quasi-spherical membrane structure of the plasticized TOA foam [11,12]. The plasticizer acts as an efficient nonvolatile solvent for the foam plastic itself. These results are in good agreement with the data reported by Braun et al. [13]. The foam membrane acts as a true sorbent where the diffusion rates of the chemical species in the membrane structure are considerably higher than those in bulky solids [14,15].

The influence of the pH on the extraction of each of the tested compounds by the unloaded foams at $100 \mu\text{g}/\text{cm}^3$ concentration was examined over the pH range 2–12. The sorption profiles of the investigated compounds by the unloaded foams increased markedly in the pH range 5–7 except for Chlorpyrifos which reached a maximum retention in the pH range 2–4. Malathion displays the lowest removal at pH 9 and the percentage removal slightly increased at higher pH. Lowering the pH tends to protonate the nitrogen atoms of the urethane linkage of the polyurethane foam, Fig. 3, as reported by El-Shahawi [16]. The percentage removal of Dicofol and bromopropylate by the unloaded foams decreased at moderate pH (5–7) and reaches a maximum at $\text{pH} < 3$ at which the compounds exist in the neutral form. Thus, the sorption of these compounds involves neutral species and this is consistent with a solvent extraction mechanism [16].

3.2. Sorption isotherms

The extraction isotherms of the tested compounds (I–IV) on the unloaded foams were developed over a wide range of equilibrium concentrations (10–100

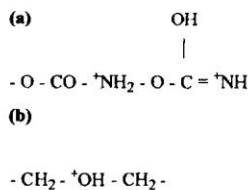
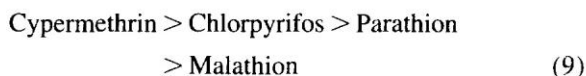


Fig. 3. (a) Protonated urethane, and/or (b) ether oxygen atoms of the polyurethane foam.

$\mu\text{g}/\text{cm}^3$) for each species at 100°C . The pH values of the aqueous solution were adjusted to a pH in the range 4–7, so that the compounds were predominately in the undissociated form. At low concentration the sorption isotherms exhibited a first-order behaviour and tended to plateau at higher bulk solution concentrations. Fig. 4 shows plots of the remaining concentration of the tested insecticides in the aqueous phase versus their concentration retained on the foam material. The sorption of the different species by the unloaded foams increased in the order:



Similar trends for the extraction of the tested

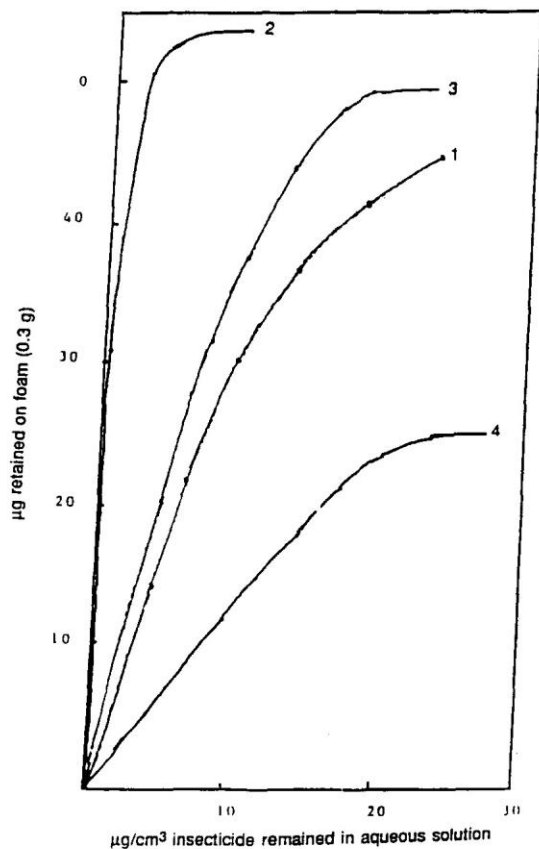


Fig. 4. Extraction isotherm of (1) Parathion, (2) Cypermethrin, (3) Chlorpyrifos and (4) Malathion at concentrations of 10–100 $\mu\text{g}/\text{cm}^3$ using the unloaded foams (0.3 ± 0.004 g) from a 100 cm^3 aqueous sample at pH 5–7 and $20 \pm 0.1^\circ\text{C}$ and 1 h extraction time.

compounds were obtained with diethyl ether and for other similar species retained on the polyurethane foams [16]. Therefore, 'solvent extraction' is the most probable mechanism for the sorption of the tested species by the unloaded polyurethane foam [7]. However, it is worth noting that the molecular masses (M_r) of Chlorpyrifos ($M_r=345.5$), Malathion ($M_r=230.3$), Parathion ($M_r=291.0$) and Cypermethrin ($M_r=419.6$) are also participating factors in the extraction step by the foam. These data are also consistent with the general understanding that the larger the molecular mass of the sorbate the larger the amount of the tested insecticides retained on the foam when the substances concerned are similar in nature [17].

The sorption behaviour of the investigated acaricides (Dicofol and Bromopropylate) from aqueous solution by the unloaded and TMP- and TOA-loaded foams was found also to depend on the concentration. Thus, the extraction isotherms were developed over a wide range of equilibrium concentrations ($10\text{--}200\ \mu\text{g}/\text{cm}^3$) for each compound at $20\pm 0.1^\circ\text{C}$. The pH values of the aqueous solution in these experiments were adjusted at $\text{pH}\leq 3$. A good linear correlation between the concentration of each compound extracted on the unloaded and TMP- and

TOA-loaded foams was achieved. The sorption profiles obtained using the unloaded and loaded foam increased in the order:

$$\text{TOA - foam} > \text{TMP - foam} > \text{unloaded foam} \quad (10)$$

The influence of various concentrations of alkali metal (Li^+ , Na^+ , NH_4^+ and K^+) chlorides at concentrations $\leq 0.1\ \text{M}$ on the sorption percentage of the tested compounds at $80\ \mu\text{g}/\text{cm}^3$ was studied at the optimum pH extraction. The results obtained on the sorption by the unloaded foams are summarized in Table 1. A significant increase in the distribution ratios of Malathion, Dicofol and Bromopropylate was observed with increasing LiCl or NaCl concentrations from 0.01 to 0.1 M and the following order of extraction was noted:

$$\text{Li}^+ > \text{Na}^+ > \text{NH}_4^+ > \text{K}^+ \quad (11)$$

This behaviour is characteristic of the 'solvent extraction mechanism' with the salt acting as salting out and the cation-chelation mechanism excluded [9,16]. The distribution ratios of Malathion increased with the amount of salt added from $\log D=3.43$ and 3.41 to 3.52 and 3.42 for Na^+ and Li^+ ions at 0.05 and 0.1 M (Fig. 5). The added salts (Li^+ , Na^+)

Table 1

Logarithm distribution coefficient (D) data for the sorption profiles of the tested compounds using the unloaded foams in the presence of different univalent cations

Cation concentration (M)	Insecticides			Pyrethroid	Acaricides	
	Malathion	Parathion	Cypermethrin	Chlorpyrifos	Dicofol	Bromopropylate
Li^+						
0.01	3.43	2.94	2.70	3.79	3.84	3.61
0.05	3.49	2.58	2.55	3.71	3.60	3.66
0.10	3.52	2.42	2.41	3.59	3.38	3.69
Na^+						
0.01	3.41	2.65	2.91	3.92	3.54	3.50
0.05	3.44	2.40	2.76	3.90	3.37	3.53
0.10	3.42	2.28	2.64	3.90	3.37	3.53
				3.88	3.30	3.55
K^+						
0.01	3.37	2.05	3.60	4.60	2.58	3.92
0.05	3.30	2.02	3.52	4.72	2.62	3.45
0.10	3.19					
NH_4^+						
0.01	3.35	2.03	2.61	4.40	3.37	3.62
0.05	3.32	1.98	2.50	4.45	3.35	3.58
0.10	3.23	1.92	2.42	4.52	3.40	3.54

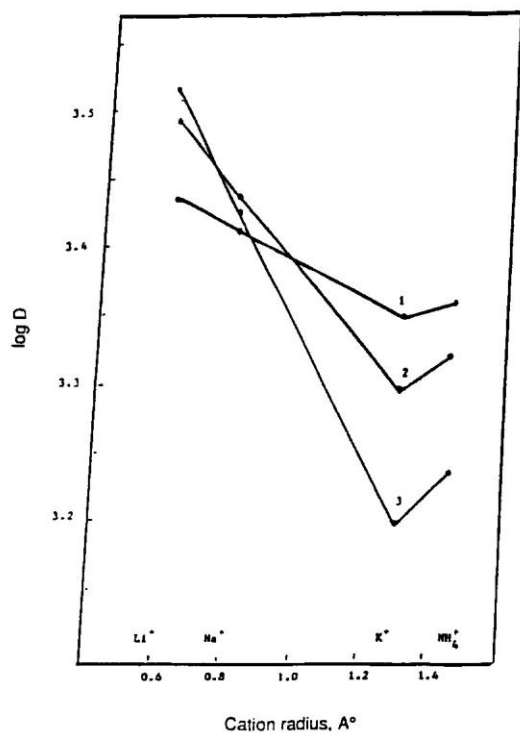


Fig. 5. Effect of extraction media on the sorption profile of Malathion using unloaded foam at 1 h shaking time, with (1) 0%, (2) 5% and (3) 10% of ethanol–water (v/v). Other conditions are as in Fig. 2.

increased the sorption profiles of the tested compound into the polyether foams by reducing the number of water molecules available to solvate the organic compound which would, therefore, be forced out of the solvent phase into the foam. In such cases some amount of the free water molecules are preferentially used to solvate the ions added [18]. Hence, the influence of these salts can be explained by the salting-out effect and 'solvent extraction' is the most probable mechanism [9].

The retention behaviour of Cypermethrin and Chlorpyrifos by the unloaded foams (Table 1) decreased with increasing concentration of the alkali metal Li^+ , Na^+ , K^+ and NH_4^+ chlorides, and the following order of sorption

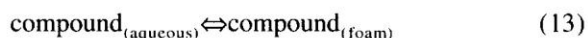
$$\text{K}^+ > \text{Na}^+ > \text{NH}_4^+ > \text{Li}^+ \quad (12)$$

was achieved at 0.1 M salt concentration. Therefore, the ion dipole interaction of NH_4^+ with the oxygen

sites of polyurethane foam might highly predominate in the sorption profiles of Cypermethrin and Chlorpyrifos.

According to the 'cation-chelation mechanism' the presence of K^+ ions should facilitate the extraction of Cypermethrin and Chlorpyrifos by the foam more than the other alkali metal ions (NH_4^+ , Na^+ or Li^+) because of the better fit of this ion into the central cavity of the oxygen-rich helix in the polyurethane foam. The sorption profiles of Cypermethrin and Chlorpyrifos are in good agreement with the data recently reported by Palagyi et al. [15]. Therefore, the 'cation-chelation mechanism' is the most probable mechanism for the sorption of these species. In accordance with this mechanism, the polyalkenoxy chains of the PuF sorbent form a clathrate with suitable simple cations [16].

In batch experiments the influence of temperature (35, 45 and 55°C) on the sorption profiles of the tested species (I–IV) by unloaded foams was determined at the pH of maximum extraction of each compound. The percentage extractions and the distribution ratios of the tested compounds increased slightly with increasing temperature and similar trends to that obtained at 20°C were achieved. Assuming no precipitation or chelation and the extracted species to be neutral, then the equilibrium constant K for the equation



is equivalent to the distribution ratio, D . Thus by plotting $\ln D$ vs. T and employing the equation:

$$\ln K = \frac{\Delta H^0}{RT} + \frac{\Delta S^0}{R}, \quad (14)$$

the values of the standard enthalpy change ΔH^0 and the standard entropy change ΔS^0 were obtained (Table 2). The ΔS^0 for Malathion and Parathion were found to be -20 ± 2 and -38 ± 4 J/mol deg, while for the Cypermethrin and Chlorpyrifos the ΔS^0 values were found to be -16 ± 1.8 and -19 ± 2 J/mol deg, respectively, for the sorption into the unloaded foam. The high molecular mass of the Cypermethrin ($M_r = 416.6$) may account for its higher value of ΔS^0 . The observed decrease in the ΔS^0 of Malathion and Parathion is possibly due to the presence of the P=S group which could reduce the

Table 2
Thermodynamic data for the sorption of the tested insecticides and acaricides by (a) unloaded, and (b) TOA-loaded foams

	ΔH^0 (kJ/mol)		ΔS^0 (J/mol deg ⁻¹)	
	a	b	a	b
Malathion	24±2		20±2	
Parathion	26±1.2		38±4	
Cypermethrin	28±1.8		16±1.8	
Chlorpyrifos	25±2.1		19±2	
Dicofol	20.12±2	22.7±2.3	27.9±2.9	33±2
Bromopropylate	23.2±2.6	27.2±3	30±3	42±3

Conditions: extraction from aqueous solution (100 cm³) at pH 3 and temperature range 20–55°C.

ion-dipole interaction with the oxygen sites of the polyurethane foam. This also would reduce the degrees of freedom of movement of the tested organic compounds in the polyurethane foam, as previously reported [18–20].

The polymeric nature and/or the different functional groups or heteroatoms in the foam may also take a part in the sorption process of both Malathion and Parathion. These data are also consistent with the solvent extraction mechanism and are in good agreement with the data previously reported by Schumack and Chow [19]. The values of ΔH^0 were found in the range 24–28±2.1 kJ/mol. Raising the temperature may facilitate the partition of the tested species through the polyurethane foam via urethane linkage and/or ether oxygen atoms.

The values of the standard entropy change ΔS^0 and the standard enthalpy change ΔH^0 for the tested acaricides on the unloaded and TOA-treated foams are also summarized in Table 2. The ΔS^0 for the Dicofol and Bromopropylate were found to be in the range –27–30±3 J/mol deg, for extraction into the unloaded foams and –33–42±3 J/mol deg, for sorption into the TOA foams. The decrease in the entropy change with the use of the TOA foam is believed to be due to the hydrogen bonding reducing the degree of freedom of movement of the organic compound in the polyether foam, as reported [20]. These results are consistent with the solvent-extraction mechanism. The bonding of the organic compound with the foam was estimated to be about 10 kJ/mol, which is lower than the intermolecular H-bonding (30 kJ/mol) [16,19]. Raising the temperature may facilitate the formation of intermolecu-

lar H-bonding between the hydrogen group of the tested acaricide and the polyurethane foam via nitrogen and/or oxygen atoms.

The influence of the sorption media on the pre-concentration of the tested compounds by the foams was examined at the optimum pH by the addition of various proportions of ethanol (0–10%). The sorption percentages of Malathion and Parathion were decreased by the addition of ethanol up to 10%. Representative results are summarized in Fig. 6. This behaviour is probably due to the formation of different association in the aqueous solution [20]. These data are also consistent with the fact that with a compound of low dielectric constant, the degree of extraction should increase with increasing polarity of the polar phase [16]. Thus the 'solvent extraction mechanism' is the most probable mechanism for the sorption of Malathion and Parathion. In contrast, the sorption profiles of Cypermethrin and Chlorpyrifos increased with increasing ethanol concentration.

The effect of ethanol (0–10%) on the sorption percentage of the tested acaricide by the unloaded and TMP-loaded foams was determined. The sorption profiles of compounds V and VI by the unloaded foams are given in Fig. 7. The extraction of the compounds by the unloaded foams increased by the addition of ethanol (up to 10%) to the aqueous solution. Similar trends were also obtained with TMP-loaded foams. Dicofol and Bromopropylate species in the aqueous solution are well solvated in the presence of ethanol and so it is difficult for these ions to form ion-pairs in the aqueous solution. Thus, the solvent extraction mechanism is the most probable mechanism.

3.3. Chromatographic behaviour of the tested insecticides on polyurethane foam columns

Static experiments on the sorption behaviour of the tested pesticides, pyrethroid and acaricides (I–VI) from the aqueous solution with the unloaded foams suggest the possible application of the foam in the column extraction mode. Distilled or tap-water samples (0.1–6 dm³) containing 0.05 mg of each compound were percolated separately through the foam columns at a flow-rate of 10–15 cm³/min at the pH of maximum extractibility. More or less complete retention of the tested compounds was

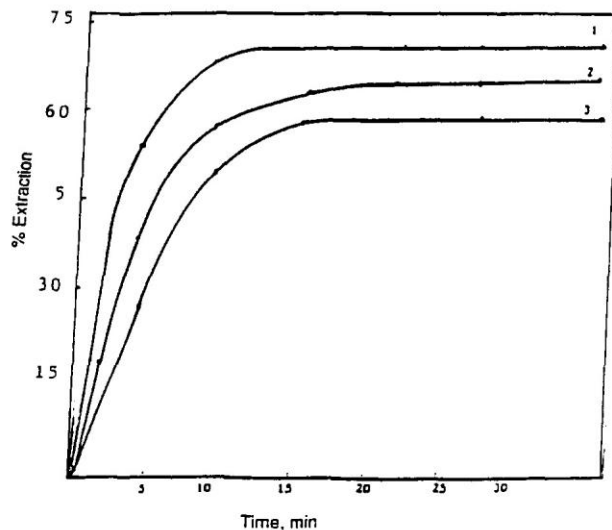


Fig. 6. Effect of extraction media on the sorption profile of Malathion using the unloaded foam at 1 h shaking time, with (1) 0%, (2) 5% and (3) 10% of ethanol. Other conditions are as in Fig. 2.

achieved by the foam column. After squeezing water from the foam, the retained compounds were recovered quantitatively from the foam material with 100 cm³ acetone in a Soxhlet extractor and determined spectrophotometrically at the optimum wavelength. Satisfactory recovery percentages (99.5% ± 2.1) of the tested compounds from the aqueous media by the proposed foam column method are summarized in Table 3.

The dependence of the sorption profiles of the tested species by the proposed unloaded foam column on the flow-rate (2–25 cm³/min) and sample volume (0.1–6 cm³) was investigated. An aqueous sample (2 dm³) containing 0.05 mg Parathion was percolated through the foam column at various flow-rates up to 25 cm³/min. Complete retention of Parathion was obtained at a flow-rate up to 15 cm³/min. The extraction efficiency decreased significantly to 76% at a flow-rate of 20–25 cm³/min from a 6 dm³ aqueous sample solution. On the other hand, on increasing the sample volume from 2 to 6 dm³ at a flow-rate < 15 cm³/min, no significant decrease on the retention percentage was observed.

To determine the performance of the untreated foam column by the chromatogram method a quantitative retention of Dicofol (0.01 mg) in 0.5 dm³ aqueous solution at optimum pH of extraction was

achieved followed by elution with 200 cm³ acetone–HCl (1:1, v/v) from the unloaded foam column at a flow-rate of 5 cm³/min. The height equivalent to a theoretical plate (HETP) was obtained from the elution curves using the equation [9]

$$N + \frac{L}{\text{HETP}} = \frac{8V_{\max}^2}{w_e}, \quad (15)$$

where N = number of theoretical plates, V_{\max} = volume of elute at the peak maximum, w_e = width of the peak at $1/e$ of the maximum solute concentration and L = length of the column foam bed in mm. The HETP values were found to be equal to 1.9 ± 0.2 and 2 ± 0.2 mm at flow-rates of 15 and 20 cm³/min, respectively.

The unloaded foam column performance was also calculated from the breakthrough capacity curve method for Parathion (Fig. 8). An aqueous solution (5 dm³) of Parathion (50 µg/cm³) was percolated through the column at 10 and 20 cm³/min and the height equivalent to the theoretical plates was calculated by employing the equation:

$$N = \frac{V_1 V_2}{(V_1 - V_2)^2} = \frac{L}{\text{HETP}}, \quad (16)$$

where V_1 = volume of the effluent at the centre of the

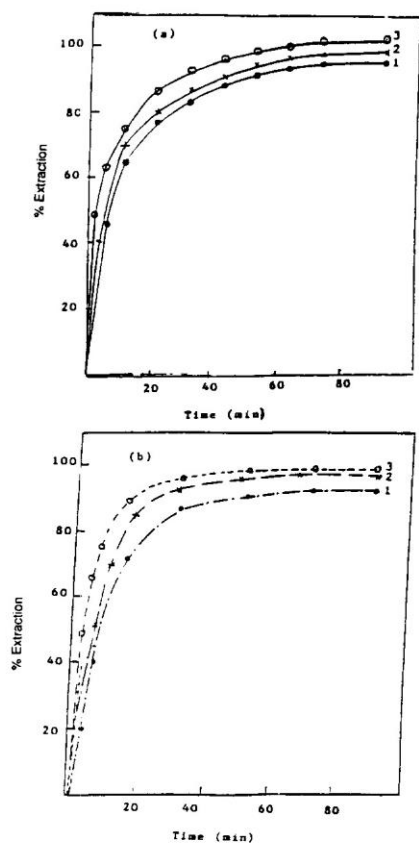


Fig. 7. Effect of extraction media on the sorption profile of (a) Dicofol and (b) Bromopropylate using unloaded foams at pH < 3 and 1 h extraction time. Ethanol concentrations are: (1) 0%, (2) 5% and (3) 10%. Other conditions are as in Fig. 2.

Table 3

Extraction and recovery of the tested compounds from 3 dm³ distilled and tap water by the proposed unloaded foam column^a

Compound	Recovery (%)		Wavelength (nm)
	Distilled water	Tap water	
Parathion	95.6 ± 0.4	95.9 ± 0.4	274
Malathion	93.5 ± 0.5	99.5 ± 2.1	206
Cypermethrin	94.2 ± 0.4	95.7 ± 0.7	273
Chlorpyrifos	96.5 ± 0.6	97.2 ± 0.4	206
Dicofol	97 ± 1.2	94.9 ± 2.1	248
Bromopropylate	97.2 ± 2.2	95.1 ± 1.7	242

^a Average ± S.D. for five measurements.

S-shaped part of the breakthrough capacity curve where the concentration is one-half of the initial concentration and V_2 is the volume at which the effluent has a concentration of 0.1578 of the initial concentration. The volume of HETP obtained by this method was found to be in the range 2.1 ± 0.2 mm at flow-rates of 10 and 20 cm³/min. These values are in good agreement with the data obtained from the chromatogram methods at a flow-rate of 10 cm³/min.

The proposed foam column method has been successfully employed for the separation of the binary mixtures Malathion–Cypermethrin and Parathion–Cypermethrin insecticides from different volumes (0.1–2 dm³) of the aqueous media. A mixture containing 0.05 mg Malathion (or Parathion) was separated from 0.05 mg of Cypermethrin at pH 1.5 and 0.1 M lithium chloride. Sorption of Malathion (or Parathion) took place while Cypermethrin was not retained on the foam column and collected quantitatively in the eluent. Malathion (or Parathion) was then recovered from the column by 100 cm³ acetone in a Soxhlet extractor, as described before.

3.4. Capacity

Break-through capacity was defined as the amount of the compound that could be retained on the column when the solution of the tested compound was allowed to pass through it at a reasonable flow-rate (5–10 cm³/min) until the compound was first detected in the effluent solution. Practically, this capacity was determined from the actual volume that was collected just before the appearance of the compound in the effluent solution minus the free-column volume. The resulting value was multiplied by the concentration of the marginal solution. After reaching the break-through volume, percolation of the test solution was continued until the effluent solution concentration reached that of the feed aliquot. The curves of Fig. 8 present the break-through volume and the volume needed to reach feed saturation for Parathion (50 µg/cm³) at the optimum pH at flow-rates of 10 and 20 cm³/min. The break-through and the overall capacities of the proposed column packed with 1 g dry foam for the retention of Parathion were 0.4 and 0.35 mg insecticide per g of

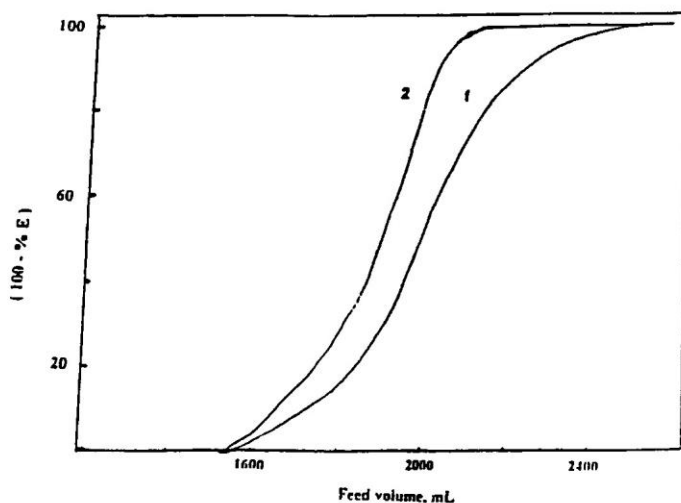


Fig. 8. Breakthrough capacity curves of the sorption profiles for Parathion at flow-rates of (1) 10 cm³/min and (2) 20 cm³/min using the unloaded foam column.

the unloaded foam at 10 and 20 cm³/min, respectively.

3.5. Effect of Chlorpyrifos treatment on tomato and parsley plants

Total trace-element analysis of tomato and parsley

plants was performed before (1) and after spraying with Chlorpyrifos in water for 24 (2), 72 (3) and 120 (4) h. The results are summarized in Tables 4 and 5 for tomato and parsley, respectively. The overall average concentration pattern of the essential elements N, K, P, Na, Fe, Zn, Mn and Copper in tomato is summarized in Table 4.

Table 4

Total trace element of tomato before and after spraying with Chlorpyrifos in water (0.04%, w/v)^a

S. No.	Type	Content (%)				Concentration (ppm)			
		N	K	P	Na	Fe	Zn	Mn	Cu
1	Tomato before spray	3.45±0.52	0.80±0.08	0.43±0.10	0.31±0.04	100.±3.40	12.0±2.40	55.5±2.80	41.0±3.10
2	Tomato after spray 24 h	3.16±0.60	0.86±0.12	0.46±0.26	0.36±0.05	110.±2.80	11.5±1.80	61.0±2.90	26.0±2.20
3	Tomato after spray 72 h	3.22±0.32	0.87±0.22	0.45±0.14	0.29±0.09	080.±4.00	12.0±1.20	45.0±2.10	30.0±2.80
4	Tomato after spray 120 h	3.36±0.40	0.75±0.11	0.46±0.10	0.32±0.07	055.±3.20	12.0±1.30	40.0±2.60	16.0±1.20

^a Average of three measurements.

Table 5

Total trace element of plant parsley before and after spraying with Chlorpyrifos in water (0.04%, w/v)^a

S. No.	Type	Content (%)				Concentration (ppm)			
		N	K	P	Na	Fe	Zn	Mn	Cu
1	Parsley before spray	3.10±0.29	1.90±0.07	0.39±0.20	1.50±0.10	72.5±3.20	30.5±2.90	31.0±2.40	07.0±1.20
2	Parsley after spray 24 h	3.67±0.29	1.97±0.07	0.43±0.34	1.48±0.07	70.0±2.80	32.5±1.60	33.5±1.90	07.0±1.10
3	Parsley after spray 72 h	3.81±0.30	2.60±0.08	0.43±0.50	0.92±0.08	60.0±2.10	34.0±3.00	35.0±1.80	08.0±1.10
4	Parsley after spray 120 h	3.75±0.24	2.52±0.10	0.50±0.60	1.05±0.06	65.0±1.80	34.0±2.20	35.0±2.10	08.0±0.90

^a Average of three measurements.

Table 6
Wet mass, dry mass and humidity of tomato before and after spraying with Chlorpyrifos in water (0.04%)^a

S. No.	Sample	Wet mass (g)	Dry mass (g)	Humidity (%)
1	Tomato before spray	11.78±0.70	02.13±0.11	81.90±6.22
2	Tomato after 24 h spray	14.81±0.90	02.08±0.07	86.10±4.90
3	Tomato after 72 h spray	17.78±0.40	07.53±0.60	81.00±5.20
4	Tomato after 120 h spray	17.57±0.42	03.43±0.10	78.40±3.20

^a Average of five measurements.

For iron (55–110±4 ppm), manganese (40–61±2.9 ppm) and copper (16–41±3.1 ppm), the concentration pattern follows the sequences 2>1>3>4, 2>1>3>4 and 1>3>2>4, respectively. The observed decrease of these elements is possibly attributed to the great ability of Chlorpyrifos and its modes of action [21] to penetrate through tomato plant tissues and complexing with these metal ions. Accumulation of Chlorpyrifos complex species may also decrease the uptake of these metal ions. No significant changes in the uptake of zinc (12±0.4 ppm) and nitrogen (3.2–3.4±0.6%) were observed.

In plant parsley (Table 5) the distribution of phosphorous (0.39–0.50±0.2%) and copper (7–9±1.2 ppm) before and after spray follows the sequence 4>3>2>1, while for nitrogen (3.1–3.8±0.3%) and potassium (1.9–2.6±0.1%) the uptake follows the order 3>4>2>1.

In the case of sodium (0.9–1.5±0.1%) and iron (60–72.5±3.9 ppm) the distribution follows the sequence 1>2>4>3, while for zinc (30.5–34±3 ppm) and manganese (31–35±2.4 ppm), the uptake follows the sequences 4>3>2>1 and 3>4>2>1, respectively. The uptake of phosphorous and copper increased with increasing spray time of Chlorpyrifos, while the uptake of sodium and iron decreased. These results may be attributed to the influence of Chlorpyrifos on the plant tissues.

Tables 6 and 7 show the effect of Chlorpyrifos on the percentages of humidity, wet mass and dry mass for tomato and parsley plants. In tomato (Table 6) the percentages of humidity (78.4–86.1%), dry mass (2.1–7.5%) and wet mass (11.8–17.8%) distribution patterns follow the sequences 2>1>3>4, 3>4>1>2 and 3>4>2>1.

In parsley plant (Table 7), a more or less similar observation on the humidity (78.4–81%), dry mass (2.3–3.8%) and wet mass (12.3–17.6%) was observed. The distribution patterns follow the sequences 2>3>1>4, 4>2>1>3 and 4>2>3>1.

These results suggest a similar mode of action of Chlorpyrifos on the humidity percentages of plant tomato and parsley. A more or less similar mode of action of Chlorpyrifos on the dry and wet mass was found for tomato and parsley tissues untreated and treated with Chlorpyrifos for different periods of time (0–120 h).

4. Conclusion

Loaded and unloaded foams in batch and column modes can be applied to trap trace amounts of insecticides, pyrethroids and acaricides from water. The retained species can be separated with an appropriate eluent, provided that there is a suffi-

Table 7
Wet mass, dry mass and humidity of parsley before and after spraying with Chlorpyrifos in water (0.04%)^a

S. No.	Sample	Wet mass (g)	Dry mass (g)	Humidity (%)
1	Parsley before spray	12.29±0.20	2.55±0.40	79.00±5.20
2	Parsley after 24 h spray	15.61±0.30	2.97±0.40	81.00±2.90
3	Parsley after 72 h spray	14.32±0.62	2.34±0.12	79.00±3.40
4	Parsley after 120 h spray	17.57±0.75	3.80±0.25	78.00±4.20

^a Average of five measurements.

ciently large difference in the optimum condition of extraction of each compound. The study of the tested compounds shows that Parathion, Malathion and acaricides are extracted in their neutral form by a simple solvent extraction mechanism. This conclusion is supported by the short time required for the extraction equilibrium and the salting-out phenomenon. The molecular mass of the sorbate and the strong hydrogen bonding between the tested acaricides with the polyether foam have also a great influence on the extraction process. Moreover, the plasticization of the foam with TOA offers a wider range of modifications than normal granular solids. The good hydrodynamic properties of the foam sorbents give unique advantages in rapidity, versatility and preconcentration of the tested compounds. The foam provides advantages because it is low cost, easily separable and non-polluting. The foam membrane offers unique advantages because of its high flow-rates, effective separations and preconcentrations of different species from fluid systems when large sample volumes are analyzed.

References

- [1] A.S.Y. Chan, B.K. Afghan and J.W. Robinson, *Analysis of Pesticides in Water, Significance, Principles, Techniques and Chemistry of Pesticides*, CRC Press, Boca Raton, FL, Vol. 1, 1982.
- [2] C.A. Edward, *Persistent Pesticides in Environment*, CRC Press, Boca Raton, FL, 2nd ed., 1973.
- [3] C.A. Edward, *Environmental Pollution by Pesticides*, Plenum Press, New York, 1981, p. 409.
- [4] J.P. Mieux and M.W. Dietrich, *J. Chromatogr. Sci.*, 11 (1973) 559.
- [5] B. Versino, M. DeGroot and F. Geiss, *Chromatographia*, 7 (1974) 302.
- [6] D.S. Walker, *Analyst*, 103 (1978) 397.
- [7] M.S. El-Shahawi, A.B. Farag and M.R. Mostafa, *Sep. Sci. Technology*, 29 (1994) 289.
- [8] S. Palagyi and T. Braun, in Z.B. Al-Fassi and C.M. Wai (Editors), *Preconcentration Techniques for Trace Elements*, CRC Press, Boca Raton, FL, 1992.
- [9] T. Braun, J.D. Navratil and A.B. Farag, *Polyurethane Foam Sorbents in Separation Science*, CRC Press, Boca Raton, FL, 1985.
- [10] M.S. El-Shahawi and S.M. Aldhaheeri, *Anal. Chim. Acta* 320 (1996) 277; I.L. Stewart and A. Chow, *Talanta*, 40 (1993) 1345.
- [11] T. Braun and A.B. Farag, *Anal. Chim. Acta*, 73 (1974) 301.
- [12] G.J. Moody and J.D.R. Thomas, *Chromatographic Separation with Foamed Plastics and Rubbers*, Marcel Dekker, New York, 1982.
- [13] T. Braun, *Z. Anal. Chem.*, 333 (1989) 85; T. Braun and A.B. Farag, *Anal. Chim. Acta*, 99 (1978) 1; and references cited in these.
- [14] S. Palagyi and T. Braun, *J. Radanal. Nucl. Chem.*, 163 (1992) 69.
- [15] S. Palagyi, T. Braun, Z. Homony and A. Vertes, *Analyst*, 117 (1992) 1537.
- [16] M.S. El-Shahawi, *Talanta*, 41 (1994) 1481, and references cited therein.
- [17] A.W. Adamson, *Physical Chemistry of Surfaces*, Academic Press, New York, 2nd ed., 1967.
- [18] P. Fong and A. Chow, *Talanta*, 39 (1992) 497.
- [19] L. Schumack and A. Chow, *Talanta*, 34 (1987) 957; A.B. Farag, A.M. El-Wakil and M.S. El-Shahawi, *Fresenius Z. Anal. Chem.*, 324 (1986) 59.
- [20] T. Schafer, R. Sebastian, R. Laatikainen and S.R. Salman, *Can. J. Chem.*, 62 (1983) 326.
- [21] R.S. Al-Mehrezi, M. Sc. Thesis, UAE University, United Arab Emirates (1996).

Bacterial, nutrients and heavy metal ions pollution assessment along the eastern coastal area of the United Arab Emirates

E. S. Hassan¹, I. M. Banat¹, M. S. El-Shahawi² & A. H. Abu-Hilal³

¹Department of Biology, ²Department of Chemistry² and ³Desert and Marine Environment Research Center, UAE University, Al-Ain, UAE

Received 29 March 1995; accepted in revised form 19 December 1995

Keywords: bacterial pollution, sea water pollution, Arabian Gulf, UAE coast, Gulf of Oman

Abstract

A program to monitor nutrients and heavy metal ions concentrations in addition to selected bacterial communities counts was carried out at three sites along the eastern coast of the United Arab Emirates on the Gulf of Oman. Total saprophytic bacteria (TSB), salt tolerant saprophytic bacteria (STSB), Gram-negative bacteria (GNB), total coliform (TC), and faecal coliform bacteria (FC) were enumerated. The concentrations of heavy metal ions including Mn, Fe, Pb, Cd, Zn, Cr, Ni, Co and Cu were determined by atomic absorption spectrometry. Bacterial counts had a distinct pattern with peaks in mid spring (May) and in autumn (October). The TSB, STSB and the GNB ranges fluctuated between, 3.3×10^4 to 4×10^5 , 1.8×10^4 to 2.5×10^5 and 0.7×10^4 to 1.3×10^5 colony forming units (CFU) ml⁻¹, respectively. Total and faecal coliform bacteria fluctuated depending on several factors including the presence of nearby recreation and commercial areas, but were at no time consistently high. *Bacillus*, *Pseudomonas*, *Staphylococcus*, *Micrococcus* and *Alteromonas*, were the predominant bacterial genera in these waters. Major nutrients and trace heavy metal ions concentrations were within the normal ranges for sea water with occasional sharp fluctuations in some sites. It was generally concluded that the area is slightly polluted.

1. Introduction

In the last few decades marine beaches all over the world have been exposed to many environmental pollutants such as toxic chlorinated compounds, heavy metals, residual chemicals and nuclear wastes, radioactive compounds and hydrocarbons from oil spill accidents. Discharges from desalination, power generation, sewage and wastewater treatment plants are also detrimental to the environment. Among the component of wastewater, most likely to have an impact on marine ecosystems, are nutrients, organic matter, trace heavy metals and microorganisms.

It has been reported that the high concentration of nutrients in the coastal waters can cause its eutrophication (Rosenberg, 1985; Degobbi, 1989). This process has hazardous effects on marine ecosystems as well as fishing and recreational facilities. Monitoring major nutrient levels is important to assess the pollution degree and/or the quality state of water resources

(Frigilos, 1985; Rosenberg, 1985; Zoffmann *et al.*, 1989). Riley (1978) reported that, the range of nutrient concentrations in marine water under normal environmental conditions are as follows (in $\mu\text{g l}^{-1}$): nitrate, 1.0 to 120; phosphate, 1.0 to 160; ammonia, 0.0 to 50 and nitrite, 0.2 to 30.

Pathogenic and/or opportunistic pathogenic microbes such as viruses, bacteria, fungi and parasites can also cause contamination of coastal areas. Monitoring water sanitary conditions using standard plate counts, total or faecal coliform and faecal streptococci counts therefore, are very important indicators of pollution levels (Rees, 1993). Zoffmann *et al.* (1989) reported that the counts of *Escherichia coli* corresponding to a period of 30 consecutive days should not exceed $10^3/100$ ml in more than 10% of the samples, or $200/100$ ml in more than 50% of the samples. They classified marine beaches contamination with faecal coliform as follows: beaches with counts (cells/100 ml) less than 10, free from contamination; 10 to 200,

slightly contaminated; 200 to 1000 highly contaminated; and more than 1000, dangerously contaminated. They also mentioned that the guideline for the numbers of total and faecal coliform (per 100 ml) in good quality beach waters is ≤ 500 and 100, respectively, monitored every two months, while the imperative levels are ≥ 10000 and 2000, respectively. Waters are considered suitable for bathing when 95% of the samples taken at the same site have values lower than the guide level and when 80% have values under those of the imperative level.

Long-term studies of pollution in marine coastlines is highly desirable to assess their state and quality and to develop rational environmental protection programs or pollution remediation when necessary. This work therefore, was an attempt to comprehensively evaluate pollution levels in the eastern coast waters of the UAE which is an important recreational and commercial area. This was carried out from three different angles, namely monitoring selected bacterial counts, measurements of both nutrients and heavy metal ions concentrations. Consequently, we report on utilizing the standard plate counts, total coliform, faecal coliform, nutrients, heavy metals and physico-chemical properties as overall parameters indicative of sanitary conditions.

2. Materials and methods

2.1. Description of the sampling area

The sampling area extended along the eastern coast shore lines of the UAE on the Gulf of Oman (the eastern part occupies the entrance of the Arabian Gulf). Three sampling sites (Figure 1) were selected covering a coastline of about 75-km length as follows:-

- Site 1** Kalba (KA); is located directly on the Gulf of Oman at about 4-km to the North of Kalba creek which would have less currents and more chance for water stagnation.
- Site 2** Between Fujairah and Khor-Fakkan (FUJ); is located on the open Gulf in the area between the Emirate of Fujairah and Khor-Fakkan Port.
- Site 3** Diba (DI); is located on the most northern part of Oman Gulf.

Stretches of paddy soils are common in the areas of these three sites.

2.2. Sampling

Sampling was carried out during the period between March 1990 and February 1991. Duplicate samples were collected in sterile plastic bottles from the surface water layer of each site at monthly intervals. Samples were placed on ice and transported back to the laboratory for immediate analysis or stored frozen until chemically analyzed.

2.3. Water chemical analysis

Temperature and pH were measured in the field. Salinity was measured *in situ* using a Lab Comp Analyzer (Model SCT-100). Dissolved oxygen (D.O.) was determined by the Winkler titration method (Strickland & Parsons, 1972). The concentration of ammonia was determined spectrophotometrically as described by Strickland & Parsons (1972). The nitrite and phosphate were determined according to Parsons *et al.* (1984), while nitrate was estimated according to Grasshoff (1976). Heavy metal analysis was carried out by atomic absorption spectrometry according to Lo *et al.* (1991).

2.4. Bacterial enumeration

Enumeration of colony forming units (CFU) of different bacterial communities were carried out using the standard plate count (SPC) (APHA *et al.*, 1980). Total saprophytic bacteria (TSB) and salt tolerant saprophytic bacteria (STSB) were counted using the method described in Banat *et al.* (1993). Gram negative bacteria (GNB) were counted on MacConkey agar while total coliforms (TC) and faecal coliforms (FC) were counted using the most probable number (MPN) technique (Hassan *et al.*, 1995). Samples containing high numbers of TC and FC were also stored at both room temperature and under refrigeration and were periodically reexamined to determine the survival rate of these two populations.

2.5. Identification of the isolated colonies

A total of 696 morphologically distinct colonies were isolated randomly from the counting plates and were identified to the genus level while 294 coliform isolates were identified to the species level using morphological, physiological and biochemical standard methods (Cowan, 1974; MacFaddin, 1980; Starr *et al.*, 1981a, b; Holt, 1984, 1986; Gordon, 1987; Balows *et al.*, 1992). The identification of the Gram-negative isolates were double checked using API-20E (France) systems.

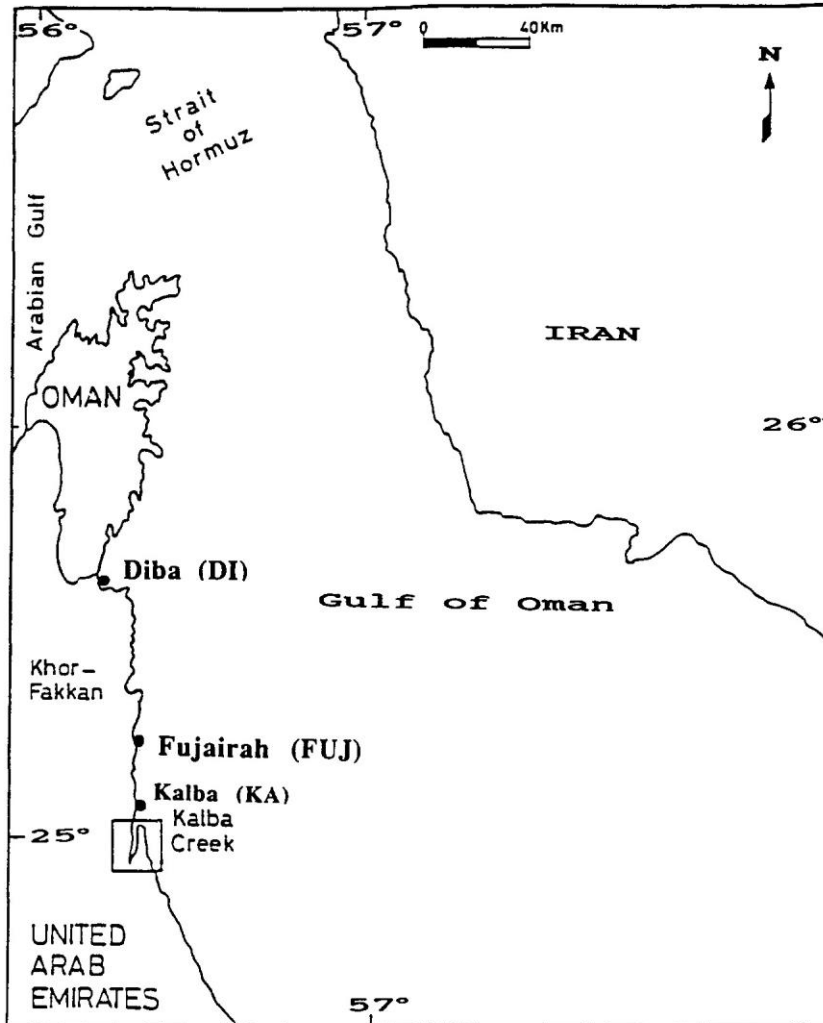


Figure 1. A map showing the location of the sampling sites Kalba, Fujairah and Diba in Eastern coastal area of the UAE.

3. Results

Water temperature, salinity, pH and dissolved oxygen results are shown in Figures 2 and 3. Temperature had a distinctive trend reflecting typical local seasonal variations with lower values between 23.5 to 26 °C in the winter months and a highest value of 35 °C in mid summer (June and July). The pH values recorded from March to May were relatively lower than those recorded during September through to December, however the pH values recorded throughout the study period fluctuated within the range 7.67 to 8.26. Salinity fluctuated within the range 3.6 to 4.5% (w/v) expected for the Gulf water. Dissolved oxygen fluctuated between 3.7 to 6.8 mg l^{-1} . Very few (<5%) of the samples had DO concentrations less than 5.0 mg l^{-1}

mainly in Kalba site. Most (>50%) of the samples had values above 6.0 mg l^{-1} .

The monthly total dissolved inorganic nitrogen concentrations (TDIN) for the three sites investigated are shown in Figure 4. Wide variations between 8.0 to 256 $\mu g l^{-1}$ were recorded for TDIN with no particular trends. However, TDIN concentrations were generally lower in the Kalba site compared to the other two sites along the northern part of the Gulf of Oman. The results of ammonia, nitrate and nitrite ions are shown in Figure 5. The values detected for ammonia, nitrate and nitrite ions were mostly within the predominant range of concentration present in sea water as described by Riley (1978).

Phosphate concentrations in the different sites also had a wide varying range between 8.0 to 399 $\mu g l^{-1}$

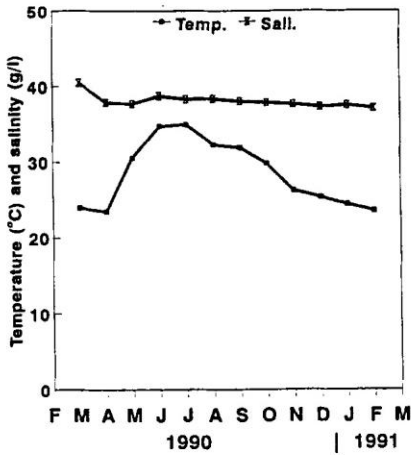


Figure 2. Mean values of *in situ* water temperature and salinity. (Mar. 1990–Feb. 1991).

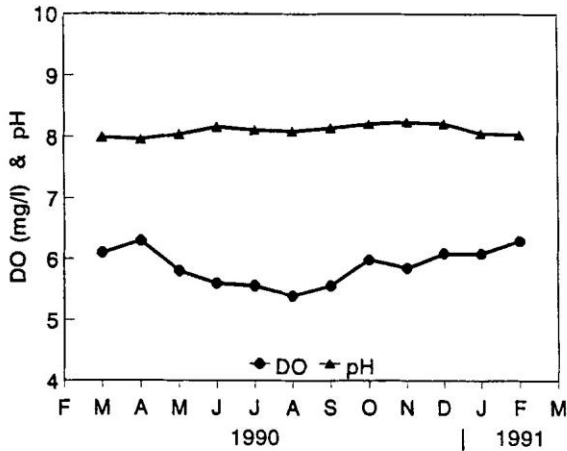


Figure 3. Mean values of dissolved oxygen concentration and pH values for the duration of the study.

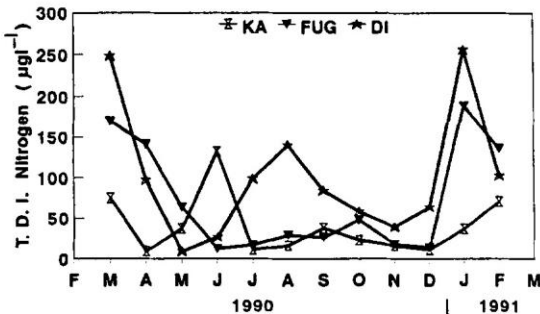


Figure 4. Total dissolved inorganic nitrogen in the coastal water of KA, FUJ and DI sites for the duration of the study.

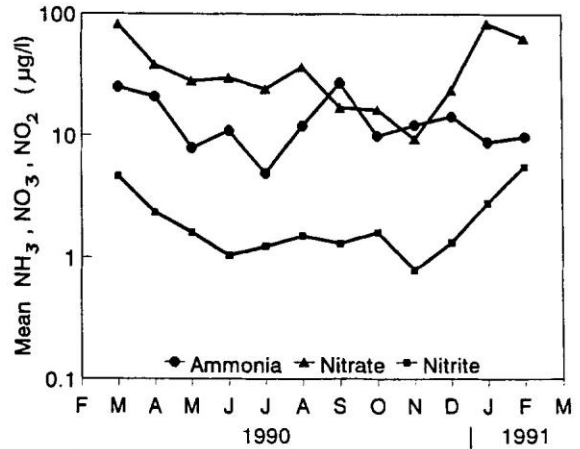


Figure 5. Mean concentrations of ammonia, nitrate and nitrite for the duration of the study.

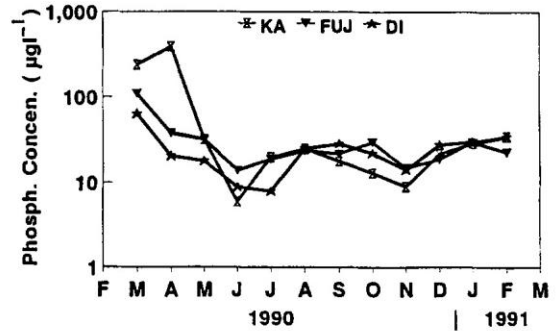


Figure 6. Phosphate concentrations in the coastal water of KA, FUJ and DI sites for the duration of the study.

(Figure 6). Lower phosphate concentrations were detected in the northern sites of the Gulf of Oman in comparison to those in Kalba site. However, relatively high concentrations of phosphate were observed during March and April in most sites. Only two samples throughout the investigation had values $>200 \mu\text{g l}^{-1}$, which were above the expected levels for surface marine waters (1 to $160 \mu\text{g l}^{-1}$).

Heavy metal ions concentrations in water samples from the three sites are shown in Table 1. Note that the Fujairah site samples consistently had the highest concentrations compared to those of Diba and Kalba sites.

The numbers of CFUs/ml of the various bacterial populations are shown in Figure 7. The TSB fluctuated between 3.3×10^4 to 4.0×10^5 , while the STSB counts ranged between 1.8×10^4 to 2.5×10^5 and the GNB ranged between 0.7×10^4 to 1.3×10^5 . The three bacterial communities had the same fluctu-

Table 1. Ranges of heavy metals concentrations in water samples collected from the three studied sites ($\mu\text{g l}^{-1}$)

Element	Sites		
	DI	FUJ	KA
Manganese	0.70–0.72	1.28–1.30	0.58–0.60
Iron	3.50–3.60	4.30–4.35	1.50–1.55
Lead	0.94–0.95	1.20–1.25	0.84–0.88
Cadmium	0.29–0.30	0.27–0.28	0.20–0.21
Zinc	9.30–9.40	11.7–11.9	8.60–8.90
Chromium	0.24–0.25	0.29–0.29	0.20–0.21
Nickel	0.58–0.60	0.66–0.67	0.49–0.50
Cobalt	0.60–0.61	0.64–0.65	0.51–0.52
Copper	2.60–2.70	3.30–3.40	2.80–2.90

ation patterns, with relatively low counts during both the summer months (minimum in July) and the winter months (January to April). They had two peaks, a relatively small one in mid Spring (May) and a high one in Autumn (October).

The counts of TC and FC (Figure 8) also followed the same pattern described earlier for the other bacterial populations. The two high peaks were observed in May and October. Their ranges fluctuated between 0 to 700 and 0 to 200 CFU/100 ml, respectively. Confirmatory tests showed 57 out of 72 samples contained verified TC, whereas, 48 samples out of 72 contained verified FC. Kalba site had the highest numbers of both TC and FC throughout the investigation. Table 2 shows the percentage of TC and FC in the different count ranges, while Table 3 shows the counts of all the bacterial communities in those samples containing high numbers of TC and FC ($\geq 500/100$ ml and $100/100$ ml, respectively). Out of a total of 294 coliform isolates the following were identified; 180 *Escherichia coli*, 54 *Citrobacter freundii*, 27 *Enterobacter agglomerans* and 33 unidentified spp. Three dominant Gram-positive and 16 Gram-negative genera were common in the surveyed beaches (Table 4). Most frequent were the genera *Bacillus* and *Pseudomonas*.

Survival rates experiment conducted on samples with the highest total and faecal coliform counts under both room temperature and refrigeration (4°C) are shown in Figure 9. More than 50% of both communities perished after a period of 10 days at room temperature, while it took longer time in the refrigerated samples. Nevertheless, complete removal occurred for both TC and FC at a maximum of 75 days in room temperature and 100 days in the refrigerated samples.

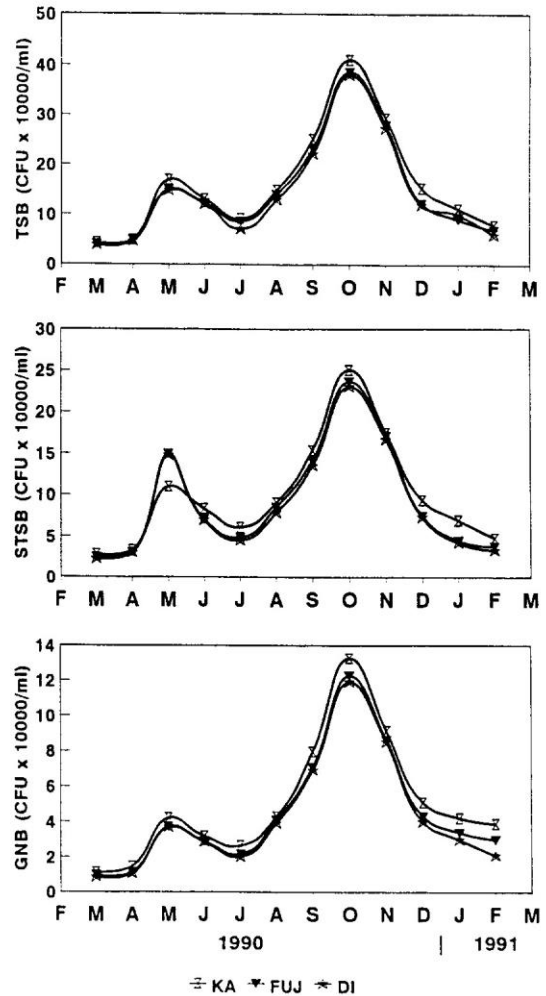


Figure 7. Mean counts of total saprophytic bacteria (TSB), salt tolerant saprophytic bacteria (STSB) and Gram negative bacteria (GNB).

4. Discussion

Water temperature profile had a wide range (18 to 37°C) and reflected the air temperature at time of sampling. It clearly showed the seasonal variations and the long summer season in this subtropical geographical area and was similar to the profile of close by coastal waters in the Abu-Dhabi area (Hassan, 1993).

Seasonal variation of pH values between samples of different sites were insignificant. The values were slightly alkaline but remained within the range that is typical for surface marine water (Dietrich & Kalle, 1957). The pH values in our Kalba site were relatively lower than those for the other sites located along the northern Gulf of Oman. This might be due to the close proximity of this site to the mangrove forests where at

Table 2. Percentage of samples containing faecal (FC) and Total (TC) coliform/100 ml in the ranges shown below

Sampling site	Faecal coliform			Total coliform		
	0-10	10-100	100-200	0-100	100-500	>500
KA	0.0	83.3	16.7	16.7	75.0	8.3
FUJ	25.0	66.7	8.0	33.3	58.3	8.3
DI	41.7	50.0	8.0	25.0	66.7	8.3

Table 3. CFU of the various bacterial communities in samples with FC and/or TC exceeding the guideline

Sampling site	Month of collection	CFU/100 ml		CFU $\times 10^4$ ml ⁻¹		
		FC	TC	TSB	STSB	GNB
DI	Oct	100	500	38.0	23.0	12.0
FUJ	Oct	160	510	38.7	23.6	12.3
KA	Oct	190	700	41.1	25.1	13.3
	Nov	101	256	29.4	17.5	9.2

Table 4. Bacterial genera frequently present and their % appearance

Genera	% appearance
<i>Gram-Negative</i>	
<i>Pseudomonas</i>	12.1
<i>Alteromonas</i>	6.5
<i>Vibrio</i>	6.5
<i>Acinetobacter</i>	3.4
<i>Moraxella</i>	3.0
<i>Alcaligenes</i>	2.6
<i>Escherichia</i>	2.6
<i>Achromobacter</i>	2.2
<i>Enterobacter</i>	2.2
<i>Aeromonas</i>	1.7
<i>Azotobacter</i>	1.7
<i>Chromobacterium</i>	1.7
<i>Citrobacter</i>	1.3
<i>Rhizobium</i>	1.3
<i>Flavobacterium</i>	0.9
<i>Serratia</i>	0.9
<i>Unidentified</i>	6.0
<i>Gram-Positive</i>	
<i>Bacillus</i>	24.1
<i>Staphylococcus</i>	7.3
<i>Micrococcus</i>	6.9
<i>Unidentified</i>	5.2

due to the activities of the benthic marine mangrove ecosystem.

Salinity values in general showed slight seasonal and temporal changes and it ranged from 3.6 to 4.5‰ (w/v) which is wider than ranges reported for neighboring Kuwait (3.9 to 4.1‰), Qatar (4.0 to 4.3‰), Saudi Arabia (4.0 to 4.2‰) (Dorgham *et al.*, 1987; Dorgham, 1991) and other coastal waters of the UAE (3.8 to 4.2‰) (Banat *et al.*, 1993; Abu-Hilal *et al.*, 1994; Hassan *et al.*, 1995).

Lower DO concentrations in Kalba site compared to those along the Gulf of Oman are probably due to the proximity of the Kalba site to Kalba creek. The latter is a shallow creek with a narrow opening and with a topography that does not allow rapid flow of water currents in and out. In addition to this, other factors may have contributed to lower DO such as the presence of a nearby mangrove forest, continuous pollutants' input from the intensive commercial activities and occasional oil pollution observed in the form of minor oil slicks in the creek. The maintenance of appropriate levels of DO is essential for a healthy marine environment and recommended levels of DO should be maintained at around 6 mg l⁻¹ and not less than 5 mg l⁻¹.

Ammonia, nitrate and nitrite concentrations showed wide fluctuations, however most values were within the expected levels for surface sea waters. Consequently, TDIN content also fluctuated extensively (8.0 to 256 μ g l⁻¹) with no distinct pattern and seemed to reflect the fluctuating levels of contamination at the

low tide the water leaving this area have a slightly low pH values (about 7.0) and oxygen values (<5.5 mg l⁻¹)

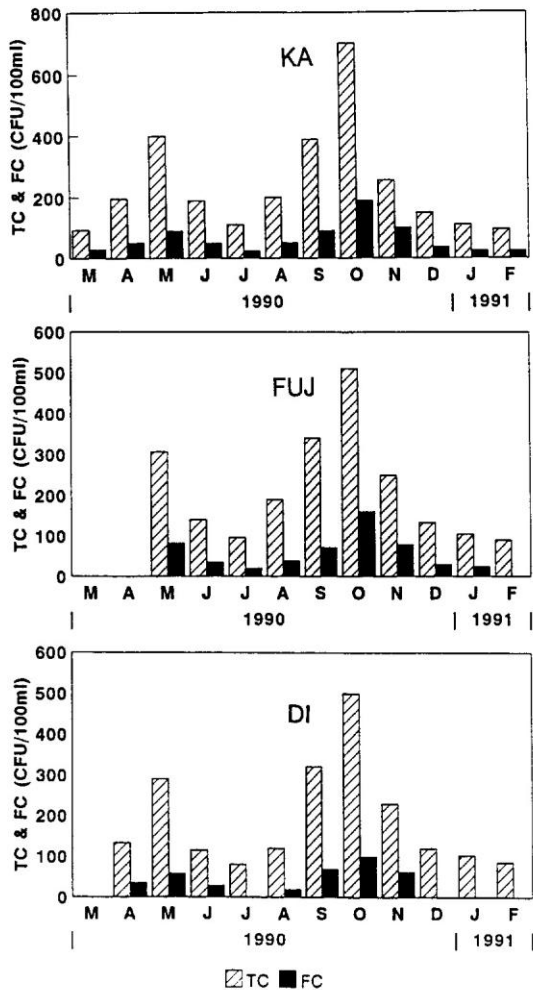


Figure 8. Total and faecal coliform bacteria counts.

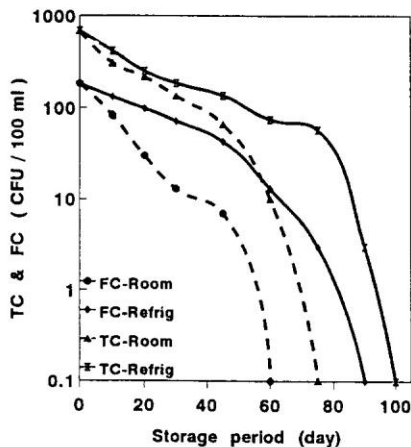


Figure 9. Disappearance of total (TC) and faecal (FC) coliform bacteria at both room temperature and refrigeration (from a composite sample selected from samples with high coliform counts).

time of sampling. The occasional peaks are probably a reflection of recent pollution input. Some of the sampling sites are near fishing and commercial marine routes or anchorage zone for boats, ships and tankers. In addition the DI and FUJ sites in the Gulf of Oman had particularly high levels of TDIN which is probably due to the upwelling activities observed in that part of the Gulf (Thangaraja, 1990). Note that red tide blooms have also been observed in these sites between February and April probably due to high TDIN levels. In addition, both DO and nitrate levels had an inverse relationship with bacterial counts. Both nutrients were at their lowest when bacterial counts peaked suggesting bacterial uptake.

Phosphate ranges in marine water are 1.0 to 160 $\mu\text{g l}^{-1}$ (Riley, 1978), yet markedly higher levels were detected during the spring season in KA site. It is probable that most of the microbial degradation and release of phosphate might take place at this time of the year particularly in shallow waters where bottom sediments usually thrives with microbial activity. However, no apparent correlations were noticed between phosphate levels and microbial counts detected in water samples from these sites. The role of upwelling activities and/or eutrophication on phosphate concentration fluctuations in KA are not known.

The heavy metal ion concentrations were variable in the three sites. Iron, Copper, Zinc and Manganese were in the ranges 1.5 to 4.35, 2.6 to 3.4, 8.6 to 11.9 and 0.58 to 1.30 $\mu\text{g l}^{-1}$, respectively. Manganese and Iron in Ottawa coastal sea water in comparison, ranged between 1.08 to 1.74 and 0.88 to 1.12 $\mu\text{g l}^{-1}$, respectively (Sturgeon *et al.*, 1980). Copper levels in lake Michigan, the English Channel, the Baltic sea and the Mediterranean sea are 3 to 5, ≤ 0.2 , ≤ 0.2 and 1 to 5 $\mu\text{g l}^{-1}$, respectively (Wiener, 1979; Moore & Ramamourthy, 1984). Copper and Zinc levels in the Red Sea were in the ranges 3.3 to 3.9 and 6.9 to 14.3 $\mu\text{g l}^{-1}$, respectively (Hamza & Amireh, 1992); while in Australian sea water were 0.17 to 0.65 $\mu\text{g l}^{-1}$, respectively (Florence & Batley, 1975). Copper and Zinc levels in polluted water generally range between 0.5 to 1.0 and 0.5 to 15 $\mu\text{g l}^{-1}$, respectively (Moore & Ramamourthy, 1984). The greater values observed in our samples might be the result of high redox potentials of the adjoining paddy soils hence both ions are sequestered and chelated with organic molecules which might have aided transportation of the heavy metals (Govardham, 1990).

The levels of Cadmium, Lead, Chromium, Nickel and Cobalt in our water were in the ranged 0.2 to 0.3,

0.84 to 1.25, 0.2 to 0.29, 0.49 to 0.67 and 0.51 to $0.65 \mu\text{gl}^{-1}$, respectively. The levels of these metals in polluted water were reported to vary as follows; Cadmium, 0.29 to 0.55; Lead, ≤ 3.0 ; Chromium, 1.0 to 2.0 and Nickel, 1.0 to $3.0 \mu\text{gl}^{-1}$ (Moore & Ramamourthy, 1984). Both Chromium and Nickel levels in uncontaminated sea water vary between 0.05 to 0.5 and $\leq 1.8 \mu\text{gl}^{-1}$, respectively. Higher concentrations of lead often occurs in water bodies near highways and large cities due to the combustion of gasoline (Moore & Ramamourthy, 1984). The slightly higher levels of some of these elements in the study sites is an indication of disturbance to the ecosystem by various anthropogenic factors such as various industrial water discharge and occasional minor oil slicks pollution in the area.

Monitoring the microbial communities' counts particularly those for saprophytic bacteria, has attracted much attention and is considered by many investigators to be a better bio-indicator for water quality (Geldreich *et al.*, 1972; Mood, 1977; Muller, 1977; Ptak & Ginsburg, 1977; Hassan, 1993). Elevated counts of such bacteria are considered a clear indicator for potential health risks posed by opportunistic pathogens (Le Chevallier *et al.*, 1980). The present bacterial communities' counts had close correlation and followed the same general pattern. The TSB counts were continuously highest followed by the STSB and the GNB. Two high peaks were observed, a relatively small one in May and a relatively broad higher one between the months of August and December. A variety of physical, chemical and biological factors could affect the increase and decrease of bacterial numbers. However, temperature seem to be the main contributing factor to these peaks as both occurred at times when the temperature was about 30°C and decreased at both higher and lower temperatures. A similar pattern was reported in northern UAE coastal waters (Hassan *et al.*, 1993). Only limited inter-site differences were observed which could be due to localized effects.

The TC and FC counts, which are more of a direct measure of faecal contamination and human activities (Schiemann, 1985; Pipes *et al.*, 1987), also closely correlated to the counts of other bacterial communities and therefore, supporting the validity of monitoring such communities. Most bacterial water quality guidelines, utilizes either maximum numbers of coliform and/or a threshold mean sample count throughout a specified period of time (USEPA, 1986). Applying the guidelines specified by Zoffmann *et al.* (1989), the sanitary quality of the studied coastal waters is as

follows: 33% of the samples collected were free of contamination and the remainder 67% of the samples had a slight one (FC = 10 to 200 CFU/100 ml). Only 3 samples were observed to contain FC counts $\geq 100/100$ ml and/or TC ≥ 500 CFU/100 ml which exceeded recommended levels (Zoffmann *et al.*, 1989). Interestingly these samples had also high numbers of all the other communities well above $(2.0, 1.0, \text{ and } 0.5) \times 10^5$ CFU ml^{-1} , for TSB, STSB and GNB, respectively. Subsequently, the following guidelines for bacterial communities' counts are proposed for monitoring the sanitary quality of surface waters in the studied and nearby Gulf coastal areas; counts should not exceed the following: the conventional 500/100 ml and 100/100 ml for TC and FC, respectively, and/or 2.0, 1.0, and 0.5×10^5 CFU ml^{-1} , for TSB, STSB and GNB, respectively.

Kalba site showed the highest count of TC and FC in spite of the absence of known wastewater discharges in the area. Nevertheless, numerous human activities are noticeable in the area such as the presence of a nearby boating activities, recreational facilities in addition to the degree of pollution facilitated by the winds and currents. With slight attention to these sites microbial pollution could be eliminated in a relatively short period of time as indicated by the rate of survival monitored for TC and FC (Figure 9).

In this study we undertook a program for monitoring all of the above parameters to decrease the inadequacies inherent in any single technique and to minimize the degree of infallibility of using the usual coliform counts as a sole appropriate pollution indicator. Taking all into consideration it was concluded that there are indications of a slight degree of chemical and bacterial pollution in the UAE eastern coastal waters. Attention therefore, has to be focused by local authority to keep the pollution under control in this valuable recreational and commercially water body for the region.

References

- Abu-Hilal, A. H., I. M. Banat, E. S. Hassan & A. B. Adam, 1994. Sanitary conditions in three creeks in Dubai, Sharjah and Ajman Emirates on the Arabian Gulf (UAE). *Environmental Monitoring and Assessment* 32: 21–36.
- APHA (American Public Health Association), 1980. *Standard Methods for the Examination of Water and Wastewater*, 5th edn. American Public Health Association, Inc., Washington, D.C., 1200 pp.
- Balows, A., H. G. Trüper, M. Dworkin, W. Harder & K. Schleifer, 1992. *The Prokaryotes a Handbook on the Biology of Bacteria*:

- Ecophysiology, Isolation, Identification, Applications*, section edition, Vol. II-IV. Springer Verlag, New York, pp. 1300-3338.
- Banat, I. M., E. S. Hassan, A. H. Abu-Hilal & A. B. Adam, 1993. Microbial and nutrient pollution assessment of coastal and creek waters of northern UAE. *Environment International* 19: 669-678.
- Cowan, S. T., 1974. *Manual for the Identification of Medical Bacteria*, second edition. Cambridge University Press, Cambridge, U.K., pp. 45-186.
- Degobbi, D., 1989. Increase eutrophication of the Northern Adriatic Sea; second act. *Marine Pollution Bulletin* 20: 452-457.
- Dietrich, G. & K. Kalle, 1957. *Allgemeine Meereskunde*. Berlin, Gerbrüder Bornträger, 492 pp.
- Dorgham, M. M., 1991. Temporal and spatial variations of the phytoplankton in Qatari waters, Arabian Gulf. *Journal Faculty of Science, UAE University* 3: 105-128.
- Dorgham, M. M., A. Muftah & K. Z. El-Deeb, 1987. Plankton studies in the Arabian Gulf II. The autumn phytoplankton in the Northwestern area. *Arab Gulf Journal of Scientific Research Agriculture & Biological Sciences* B5: 215-235.
- Florence, T. M. & G. E. Batley, 1975. Removal of trace metals from seawater by chelating resin. *Talanta* 22: 201-204.
- Friligos, N., 1985. Nutrient conditions in the Euboikos Gulf (west Aegean). *Marine Pollution Bulletin* 16: 435-439.
- Geldreich, E. E., H. D. Nash, D. J. Reasoner & R. H. Taylor, 1972. The necessity of controlling bacterial populations in potable water: Community water supply. *Journal of American Water Works Association* 67: 596-602.
- Gordon, R. E., 1987. The Genus *Bacillus*. In: A. I. Laskin & H. A. Le Chevalier (eds), *CRC Handbook of Microbiology*, second edition, Volume I. Bacteria. pp. 319-336. CRC Press, Boca Raton, Florida.
- Govardham, V., 1990. Ground water pollution hazardous to human life. A case study of Nalgonda district. *Indian Journal of Environmental Protection* 10: 54-61.
- Grasshoff, K., 1976. *Methods of Seawater Analysis*. Verlag Chemie, Weinheim. New York, 317 pp.
- Hamza, A. G. & T. A. Amireh, 1992. Determination of Pb, Cd, Cu and Zn ions in Red Sea water along Jeddah coast by differential pulse anodic stripping voltammetry. *Journal Faculty of Science, UAE University* 4: 80-90.
- Hassan, E. S., 1993. Monitoring of microbial water quality and saprophytic bacterial genera of the Abu-Dhabi coastal area, UAE. *Marine Biology* 116: 489-495.
- Hassan, E. S., I. M. Banat & A. H. Abu-Hilal, 1995. Post-Gulf War nutrients and microbial assessments for coastal waters of Dubai, Sharjah and Ajman Emirates (UAE). *Environment International* 1: 23-32.
- Hassan, E. S., I. M. Banat, S. A. Shair & A. H. Abu-Hilal, 1993. Microbial assessment of coastal waters in three northern Emirates in the UAE. *Journal of the Faculty of Science UAE University* 5: 91-103.
- Holt, J. D., 1984. *Bergeys Manual of Systematic Bacteriology* Vol. I. Williams and Wilkins, Baltimore, pp. 140-601.
- Holt, J. D., 1986. *Bergeys Manual of Systematic Bacteriology*, Vol. II. Williams and Wilkins, Baltimore, pp. 999-1372.
- Le Chevallier, M. W., R. J. Seidler & T. M. Evans, 1980. Enumeration and characterization of standard plate count bacteria in chlorinated and raw water supplies. *Applied and Environmental Microbiology* 40: 922-930.
- Lo, J. M., Y. P. Lin & K. S. Lin, 1991. Re-concentration of trace metals in sea water matrix for inductively coupled plasma atomic absorption spectrometry. *Analytical Science (Japan)* 7: 455-460.
- MacFaddin, J. F., 1980. *Biochemical Tests for Identification of Medical Bacteria*, second edition. Williams and Wilkins, Baltimore, London, pp. 345-466.
- Mood, E. W., 1977. Bacterial indicators of water quality in swimming pools and their role. In: A. W. Hoadley & B. J. Dutka (eds), *Bacterial Indicators/Hazards Associated with Water*. pp. 239-246. American Society for Testing & Materials, Philadelphia.
- Moore, J. W. & S. Ramamourthy, 1984. *Heavy Metals in Natural Waters*. Springer-Verlag, New York, 268 pp.
- Muller, G., 1977. Bacterial indicators and standards for water quality in the Federal Republic of Germany. In: A. W. Hoadley & B. J. Dutka (eds), *Bacterial Indicators/Hazards Associated with Water*. pp. 159-167. American Society for Testing & Materials, Philadelphia.
- Parsons, T. R., Y. Maita & C. M. Lalli, 1984. *A Manual of Chemical and Biological Methods for Seawater Analysis*. Pergamon Press, New York, 173 pp.
- Pipes, W. O., K. Mueller, M. Troy & H. Minnigh, 1987. Frequency-of-occurrence monitoring for coliform bacteria in small water systems. *Journal of American Water Workers Association* 79: 59-63.
- Ptak, D. J. & W. Ginsburg, 1977. Bacterial indicator of drinking water quality. In: A. W. Hoadley & B. J. Dutka (eds), *Bacterial Indicators/Hazards Associated with Water*. pp. 218-221. American Society for Testing & Materials, Philadelphia.
- Rees, G., 1993. Health implementation of sewage in coastal waters; the British case. *Marine Pollution Bulletin* 26: 14-19.
- Riley, J. P., 1978. Nutrient chemicals (including those derived detergents and agricultural chemicals). In: E. D. Goldberg (ed), *A Guide to Marine Pollution*. Gordon and Breach Science Publishers, New York/London/Paris, 168 pp.
- Rosenberg, R., 1985. Eutrophication - the future marine coastal nuisance. *Marine Pollution Bulletin* 16: 227-231.
- Schiemann, D. A., 1985. Experiences with bacteriological monitoring of pool water. *Infection Control* 6: 413-418.
- Starr, M. P., H. Stolp, H. G. Trüper, A. Balows & H. G. Schlegel, 1981a. *The Prokaryotes: A Handbook on Habitats, Isolation and Identification of Bacteria*. Vol. I. Springer-Verlag, Berlin, pp. 653-862.
- Starr, M. P., H. Stolp, H. G. Trüper, A. Balows & H. G. Schlegel, 1981b. *The Prokaryotes: A Handbook on Habitats, Isolation and Identification of Bacteria*. Vol. II. Springer-Verlag, Berlin, pp. 1105-1912.
- Strickland, J. D. H. & T. R. Parsons, 1972. *A Practical Handbook of Seawater Analyses*. Bulletin of Fisheries Research Bd., Canada, pp. 167, 310.
- Sturgeon, T. E., S. S. Berman, A. Desaulniers & D. S. Russell, 1980. Preconcentration of trace metals from sea water for determination by graphite furnace atomic absorption spectrometry. *Talanta* 27: 85-94.
- Thangaraja, M., 1990. *Studies on Red Tides of Oman. Marine Science and Fisheries Center (MSFC) Research Report No. 90-2*. Ministry of Agriculture and Fisheries. Muscat, Sultanate of Oman, 18 pp.
- USEPA (U.S. Environmental Protection Agency), 1986. Office of Drinking Water, National interim primary drinking water regulations, EPA-440/5-84-002.
- Wiener, J. R., 1979. Aerial inputs of cadmium, copper lead and manganese into a freshwater pond in the vicinity of coal fired power plant. *Water, Air and Soil Pollution* 12: 343-353.
- Zoffmann, C., F. Rodriguez-Valera, M. Perez-Fillol, F. Ruia-Bevia, M. Torreblanca & F. Colom, 1989. Microbial and nutrient pollution along the coasts of Alicante, Spain. *Marine Pollution Bulletin* 20: 74-81.



Spectrophotometric determination of periodate or iodate ions by liquid–liquid extraction as an ion-pair using tetramethylammonium iodide

M.S. El-Shahawi*¹, F.A. Al-Hashemi

Chemistry Department, Faculty of Science, UAE University, Al-Ain, P.O. Box 17551, United Arab Emirates

Received 19 June 1995; revised 13 September 1995; revised 2 October 1995; revised 3 November 1995;
revised 1 December 1995; accepted 4 December 1995

Abstract

A simple and accurate extractive spectrophotometric procedure was developed for the microdetermination of periodate and iodate in aqueous media. The determination of periodate was based upon the extraction of the ion-pair formed between the periodate and tetramethylammonium iodide at pH 4 in chloroform followed by direct spectrophotometric measurements at 509, 358 and 288 nm. The optimum concentration range evaluated by Ringbom's plot, the molar absorptivity, the Sandell's sensitivity and the stoichiometry of the formed ion-pair were critically determined. Iodate could be determined quantitatively by the proposed procedure after oxidation to periodate with potassium persulphate. The effect of the diverse ions on the determination of the periodate and/or iodate by the proposed procedures was also investigated. The application of the method for the analysis of iodate or periodate in the artificial fresh water was successfully carried out.

Keywords: Determination; Iodate; Ion-pair; Periodate

1. Introduction

Because iodate and periodate exclusively associate with oxidation of metal ions [1–6], polyhydroxylated compounds [6,7] and catalytic applications [8] at trace levels, sensitive methods are required for their reliable quantification. Several

spectrophotometric methods for the determination of both ions have been reported [9–13]. The existing methods for spectrophotometric determination of these ions were unsatisfactory for routine analysis as the procedures required direct maintenance of the experimental conditions (e.g. a strictly fixed pH, standing of the samples before the determination and low stability of the compound formed) and suffer from the lack of selectivity, sensitivity, the requirement of a laborious enrichment step and a low tolerance limit [12,13].

* Corresponding author.

¹Permanent address: Chemistry Department, Faculty of Science at Damietta, Mansoura University, Mansoura, Egypt.

The oxoanions are the least investigated species that form a liquid–liquid extractable ion-pair with onium cations [14–18]. The aim of the present study was to develop a simple and sensitive extraction spectrophotometric analytical procedure for the determination of periodate or iodate ions in aqueous matrices. The method we suggest is superior to some of the reported methods in sensitivity, and stability of the associate obtained [11–13].

2. Experimental

2.1. Reagents and materials

All the chemicals and solvents used were of analytical reagent grade. Britton–Robinson (B–R) buffer (pH 2.2–11.5) was prepared from boric, acetic and phosphoric acids and sodium hydroxide in double distilled water. Stock solutions of potassium periodate (BDH) and potassium iodate (1 mg ml^{-1}) were prepared separately by dissolving the exact weight of the corresponding salt in hot distilled water. The reagent tetramethylammonium iodide (Fluka, Purum > 98%) was used without further purification. Tetramethylammonium iodide (TMA^+I^-) (0.5% w/v) and potassium persulphate (2% w/v) were prepared in distilled water.

2.2. Apparatus

A Pye-Unicam Sp 8-400 double beam UV-visible spectrophotometer was used for recording the absorption spectra and the absorbance measurements with a quartz cell of 10 mm path length. A Phillips 9418 digital pH-meter was used for the pH measurements.

2.3. Recommended procedures

2.3.1. Determination of periodate ion

An aliquot (1–5 ml) of the aqueous solution of potassium periodate containing 1–50 μg of periodate ion was transferred to a 100 ml separating funnel. A volume of 10 ml of Britton–Robinson buffer (pH 4), 5 ml of water and 5 ml of te-

tramethylammonium iodide (0.5% w/v) were added and mixed. This was extracted twice with 5 ml of chloroform (2×2.5) and the extracts were collected in a 50 ml beaker containing anhydrous sodium sulphate (1 g). The beaker was swirled to mix the contents. The extract was transferred to a 10 ml volumetric flask, the residue was washed with 5 ml CHCl_3 and transferred to the volumetric flask. The solution was made up to the mark with the solvent. The absorbance of the organic phase was measured at 509, 358 and 288 nm against a reagent blank prepared under the same experimental condition.

2.3.2. Determination of iodate ion

A known volume (1–10 ml) of sodium iodate solution (containing 1–50 μg of iodate ions) was transferred to a 100 ml Erlenmeyer conical flask. A volume of 10 ml of potassium persulphate (2% w/v) and 10 ml of water were added to each flask, the solution was boiled for 10 min and the reaction mixture was allowed to cool. The pH of the solution was adjusted (pH 4) with 10 ml buffer followed by the addition of 5 ml of the reagent (TMA^+I^-). The reaction mixture and the washing solution of the flask were transferred to a 100 ml separating funnel. The formed ion-pair was extracted with 5 ml chloroform (2×2.5) and the recommended procedure for periodate determination was followed. A blank prepared under the same experimental conditions in the presence of potassium persulphate was run.

3. Results and discussion

The technique suggested for the determination of the periodate ions was based on its interaction in acidic medium with an excess of tetramethylammonium iodide. The solubility of the produced ion associate of the periodate with (TMA^+I^-) was investigated in the following solvents: dichloromethane, *n*-hexane, dichloroethane, isobutylether, benzene, nitrobenzene, tetrachloromethane, chloroform and toluene. The highest absorbance of the produced ion-associate was obtained in chloroform and toluene in a very short time. In chloroform the extraction was com-

plete and a better separation of phases was obtained. Therefore, chloroform was selected as a proper solvent for these reasons and because its greater density allows a better separation of the layers. The absorption spectrum of the formed yellow-violet ion-pair in chloroform extracted from the aqueous solution at pH 4 is given in Fig. 1(a). The coloured ion associate formed has three absorption maxima at 509, 358 and 288 nm in the UV-visible region whilst no peaks were found in this range in the spectra of (TMA^+I^-) and the periodate in chloroform. Therefore, the absorbance measurements for the ion-associate formed from the reaction of (TMA^+I^-) and IO_4^- were measured at 509, 358 and 288 nm. In Fig. 1(b) the absorption spectrum of iodine in chloroform is also given which differs from the spectrum of the postulated ion-pair.

The extraction of the formed ion-associate into chloroform was rapid and a shaking time of 2 min was selected in the subsequent work. The absorbance of the pink-coloured associate in chloro-

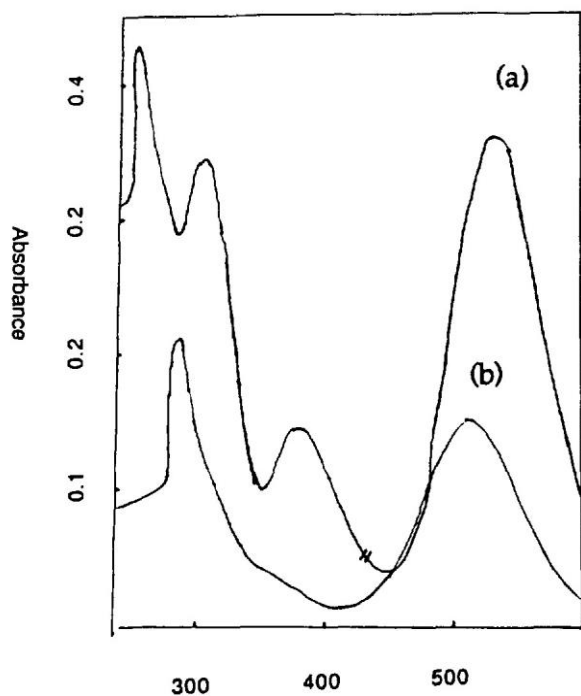


Fig. 1. Absorption spectra of the extracted ion-pair formed between (TMA^+I^-) and periodate ions (a) at pH 4 or the aqueous phase and iodine (b) in chloroform.

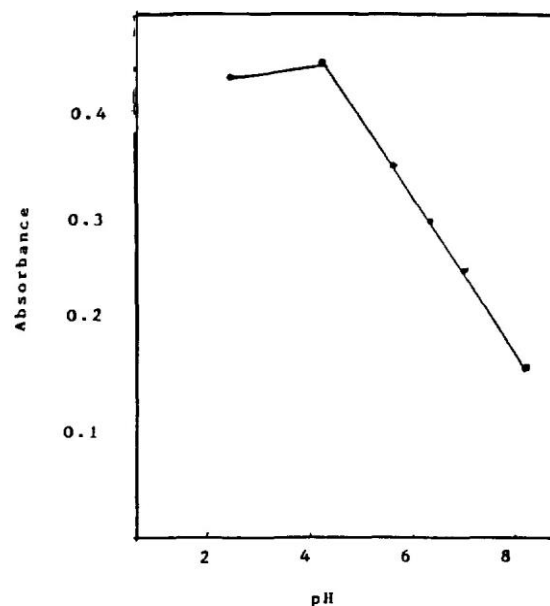


Fig. 2. Influence of pH of the aqueous phase on the absorbance of the extracted ion-pair in chloroform at 509 nm.

form was found to be constant up to 2 h for samples containing $0.05\text{--}10\ \mu\text{g ml}^{-1}$ periodate in aqueous solution at pH 4 and $\lambda = 509$ and 358 nm. The addition of sodium chloride in the concentration range $0.01\text{--}0.5\ \text{mol l}^{-1}$ did not improve the amount of the ion-associate extracted at $5\ \mu\text{g ml}^{-1}$ periodate aqueous phase at pH 4 suggesting that the reaction is quantitative without salt effect.

To optimize the reaction conditions we studied the effect of the pH of the aqueous phase upon the interaction of the periodate with (TMA^+I^-) by measuring the absorbance of the produced ion-associate in chloroform. The final pH of each aqueous solution was measured before the extraction. The experimental data (Fig. 2)¹ showed that the maximum absorption of the produced ion-pair was obtained at pH 4. In strong ($\text{pH} < 4$) or weak acidic solution ($4 < \text{pH}$) the absorbance of the extracted species decreased owing to the incomplete dissociation of the periodate salt or the hydrolysis of the ion-associate formed. When HCl

¹ Each point in the figures represents an average of five measurements.

or HClO_4 was used instead of Britton–Robinson buffer (pH 3–4) no significant differences in the absorbance values were observed. Thus a B–R buffer solution of pH 4 was finally chosen and employed as described in the recommended procedures.

Tetramethylammonium hexafluorophosphate, tetraphenylphosphonium chloride, tetramethylammonium iodide, tetramethylammonium bromide, tetramethylammonium chloride and tetraphenylarsonium chloride were investigated at the optimum pH. Good results were obtained with tetramethylammonium iodide and the highest absorbance of the coloured associate was obtained in chloroform from an aqueous solution of pH 4. The effect of (TMA^+I^-) concentration upon the determination of periodate was studied. The absorbances of the extracted species in chloroform for a series of solutions containing 10–20 μg of periodate and various amounts of the reagent (TMA^+I^-) up to 1.2% (w/v) in water at pH 4 was examined. It was found that 5 ml of (TMA^+I^-) at a concentration of $\leq 0.5\%$ (w/v) was sufficient to form the ion-associate for 20 μg or less of periodate ion (Fig. 3).

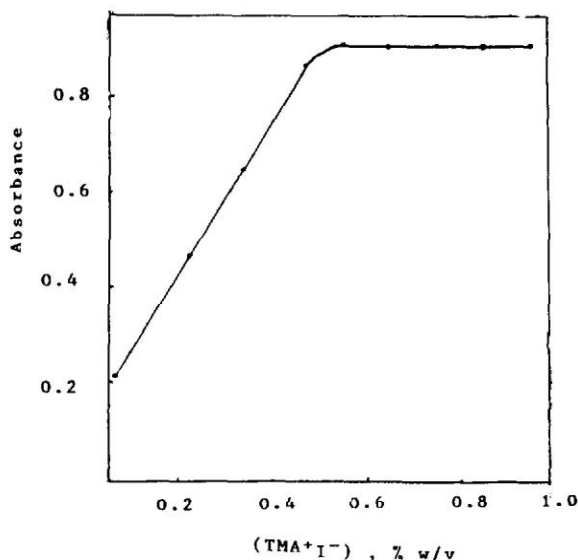
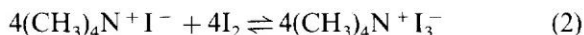
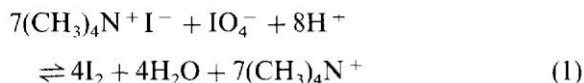
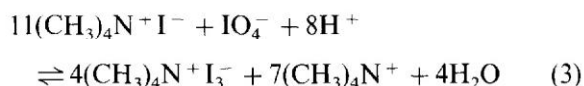


Fig. 3. Dependence of the absorbance (at $\lambda = 509$ nm) of the formed ion-pair in chloroform with (TMA^+I^-) concentration (% w/v) in aqueous solution.

The mechanism of the produced ion-associate was critically investigated. It appears from Fig. 1 that the extracted product is not iodine nor an ion-pair between periodate ion and TMA^+ . Actually, the reaction of (TMA^+I^-) with periodate ions gave quasi-immediately a red-orange precipitate which was readily extracted in chloroform (in yellow-violet colour). This reaction appears to proceed in two successive steps: (1) a rapid one involving the liberation of some iodine and subsequently (2) formation of the precipitate. These results suggest the possible formation of the complex ion I_3^- which subsequently may interact with the tetramethylammonium cation. These results were also confirmed by reacting the triiodide ion I_3^- (prepared from $\text{I}_2 + \text{KI}$) with the tetramethylammonium cation followed by extracting the produced species in chloroform. The electronic spectrum of this species was exactly similar to the spectrum of the produced ion associate from the reaction of (TMA^+I^-) with periodate ions. Thus a possible mechanism of the produced ion-associate $(\text{CH}_3)_4\text{N}^+\text{I}_3^-$ is proposed as follows:



and the overall reaction is



These results also explain why only $(\text{CH}_3)_4\text{N}^+\text{I}_3^-$ gives good results since there is a need to have an excess of iodide ion in solution to form the complex ion I_3^- , as indicated in Eqs. (1)–(3). For instance, with tetramethylammonium chloride periodate gives iodine at a slow rate but there is no iodide to form the complex ion I_3^- . However, on reacting periodate ions with tetramethylammonium bromide no colour is formed.

3.1. Photometric characteristics

The composition of the ion-pair $(\text{CH}_3)_4\text{N}^+\text{I}_3^-$ was established spectrophotometrically by the Job's method. Equimolar solutions of potassium

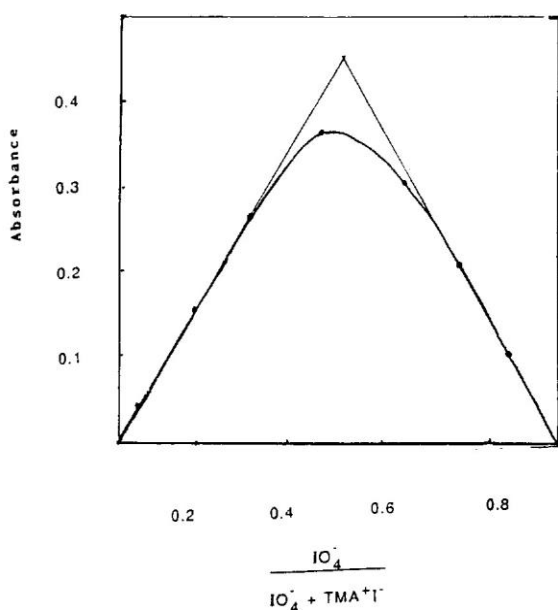


Fig. 4. Determination of the composition of the extracted ion-associate by the Job's method: $[\text{IO}_4^-] = 0.002$ (1 ml) and $[(\text{TMA}^+\text{I}^-)] = 0.001$ at 509 nm.

periodate and the (TMA^+I^-) reagent of a concentration of 0.001 M were mixed in complementary proportions to a fixed total volume and the pH of the solutions was adjusted to pH 4. The mixture was allowed to stand for 5 min for completion of the reaction. The ion-associate was then extracted with 5 ml chloroform and the absorbance was measured against a blank obtained by extraction of the reagent containing no periodate. A plot of absorbance of the extracted ion-associate in chloroform versus $[\text{IO}_4^-]/([\text{IO}_4^-] + [\text{TMA}^+\text{I}^-])$ produced a graph (Fig. 4) that indicated the formation of an associate having a periodate to a reagent ratio of 1:1.

Linear graphs at 509, 358 and 288 nm were obtained by recording the absorbance of the associate $(\text{CH}_3)_4\text{N}^+\text{I}_3^-$ in organic phase as a function of periodate ion concentration. Beer's law was obeyed between 0.05–10 mg l⁻¹ periodate in aqueous solution of pH 4. The effective concentration of periodate as evaluated by Ringbom's plot [19] was found to be 0.2–7 mg l⁻¹. The molar absorptivity calculated from Beer's law and

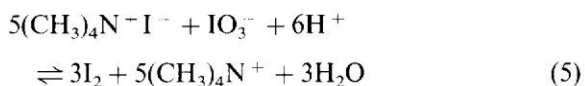
the Sandell [20] sensitivity index of the associate $(\text{CH}_3)_4\text{N}^+\text{I}_3^-$ at 509 and 358 nm was found to be 6.4×10^4 and 1.2×10^5 l mol⁻¹ cm⁻¹ and 0.0003 and 0.0006 $\mu\text{g cm}^{-2}$, respectively. The selectivity and sensitivity of the spectrophotometric measurement is far better than the recent spectrophotometric procedure developed by Kamburova [13] and Fernandez-Gutierrez et al. [21] since in the present work the measurements were carried out in the visible region while in the reported method [13] all the absorbance data were recorded in the UV region. The relative standard deviations of five measurements with 10 μg periodate, (at 95% confidence limit) of the method were 0.8% and 1.2% at 509 and 358 nm, respectively. Detection limits [22] of 0.016 and 0.03 $\mu\text{g ml}^{-1}$ of periodate and regression coefficients of 0.996 and 0.942 were achieved by the proposed procedure at 358 and 509 nm, respectively. Regression analysis of the Beer–Lambert plot of the absorbance at 358 nm (A_{358}) and the concentration of periodate (C) in mg ml⁻¹ in the range of 1–10 $\mu\text{g ml}^{-1}$ gave the following linear regression equation:

$$A_{358} = 0.026 + 0.035C \quad (n = 5) \quad (4)$$

This equation has a slope of 0.035 with an intercept of 0.021.

3.2. Determination of iodate ions

Preliminary experiments showed interference of iodate with the proposed procedure of periodate determination. The reaction of the iodate ions with the reagent $(\text{CH}_3)_4\text{N}^+\text{I}_3^-$ is slow and possibly proceeds to produce the ion-associate $(\text{CH}_3)_4\text{N}^+\text{I}_3^-$ as follows:



The produced iodine may react with the iodide ion of the excess reagent $(\text{CH}_3)_4\text{N}^+\text{I}^-$ to form the complex ion I_3^- which subsequently reacts with the tetramethylammonium cation to form the ion-associate $(\text{CH}_3)_4\text{N}^+\text{I}_3^-$. Therefore different attempts involving oxidation of iodate to periodate were carried out. A series of oxidizing agents, e.g. $\text{K}_2\text{S}_2\text{O}_8$, H_2O_2 and KMnO_4 were used

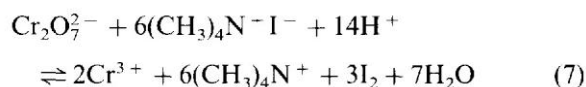
for the possible oxidation of $\text{IO}_3^- \rightarrow \text{IO}_4^-$. Boiling the iodate ions for 10 min with potassium persulphate (2% w/v) in water was found to be the most convenient procedure for the oxidation of the iodate to periodate without interference of the unreacted persulphate. The determination of various levels ($1\text{--}50 \mu\text{g ml}^{-1}$) of iodate in aqueous solution was carried out and satisfactory results with absolute standard deviations ($n = 5$) in the range 0.2–0.35 were achieved. A linear correlation ($r = 0.967$) was found between the absorbance at 509 nm (A_{509}) and concentration of iodate (C) in $\mu\text{g ml}^{-1}$ in the range $1\text{--}20 \mu\text{g ml}^{-1}$. Regression analysis of Beer's plot gave the following linear regression equation:

$$A_{509} = 0.035 + 0.039C \quad (n = 5) \quad (6)$$

3.3. Effect of diverse ions

The selectivity of the proposed method in the presence of a relatively high excess (2 mg) of some ions, e.g. NO_3^- , Br^- , SO_4^{2-} , CO_3^{2-} , HCO_3^- , $\text{S}_2\text{O}_8^{2-}$, AsO_2^- , SbO_2^- , EDTA^{2-} , $\text{C}_2\text{O}_4^{2-}$, $\text{S}_2\text{O}_3^{2-}$, SCN^- , SeO_3^{2-} , TeO_4^{2-} , PO_4^{3-} , BiO_3^- , WO_4^{2-} , SeO_3^{2-} , BrO_3^- and MoO_4^{2-} upon the extraction equilibrium in the determination of $10 \mu\text{g}$ of periodate (or iodate) by the proposed procedure was studied. Good recoveries in the range $100 \pm 2\%$ were obtained with all the ions except $\text{S}_2\text{O}_3^{2-}$, and BiO_3^- ions interfered seriously. The tolerance limits of various cations (0.1 mg), e.g. NH_4^+ , Al^{3+} , Cd^{2+} , Zn^{2+} , Pt^{2+} , Au^+ , Pb^{2+} , Co^{2+} , Fe^{3+} , Bi^{3+} , Sn^{2+} , Ni^{2+} , Mg^{2+} , Ba^{2+} and Li^+ , were also examined. All these ions did not interfere with the proposed method and a good recovery percentage ($100 \pm 1.5\%$) was achieved. The ions Mn^{2+} , Cr^{6+} , Cr^{3+} , Mn^{7+} and Ru^{3+} interfered seriously even at very low concentrations. The reason for these interferences is possibly attributed to the ability of periodate ions in the aqueous media to oxidize Mn^{2+} , Cr^{3+} , Ru^{3+} and $\text{S}_2\text{O}_3^{2-}$ producing MnO_4^- , $\text{Cr}_2\text{O}_7^{2-}$, RuO_4 and IO_3^- ions, respectively, at the developed experimental conditions as previously reported [4–6,23]. The produced species and the trioxobismuthate BiO_3^- are possibly able to oxidize the iodide ion in the reagent (TMA^+I^-)

producing iodine. A representative reaction possibly proceeds as follows:



The produced iodine subsequently reacts with the iodide ion in the reagent (TMA^+I^-) forming the ion-associate $(\text{CH}_3)_4\text{N}^+\text{I}_3^-$ as given in Eq. (2). On the other hand, the $\text{S}_2\text{O}_3^{2-}$ ions were found able to reduce the produced ion-associate $(\text{CH}_3)_4\text{N}^+\text{I}_3^-$ to the iodide ion.

The determination of $10 \mu\text{g}$ of periodate or iodate by the proposed procedure in artificial fresh water containing 10 mg l^{-1} of sodium, calcium, chloride, sulphate and bicarbonate together was carried out against a blank. The periodate or iodate concentrations were determined by the preconstructed standard curves. The precision was 0.7% and the percentage error was in the range -1.1% – 1.3% .

4. Conclusion

The proposed procedure for periodate or iodate determination is superior as compared to most of the reported procedures. It offers many advantages, e.g. good precision, accuracy, the obtained associate is very stable and no standing time is needed before determining the ions. The clear advantages of the method are that it is applicable for IO_4^- (or IO_3^-) determination in artificial sea water. The determination of IO_4^- besides IO_3^- or iodate besides IO_4^- is not possible.

References

- [1] M.S. El-Shahawi and A.B. Farag, *Anal. Chim. Acta*, 307 (1995) 139.
- [2] A.B. Farag, M.S. El-Shahawi and E.M. El-Nemman, *Fresenius Z. Anal. Chem.*, 346 (1993) 455.
- [3] A.M. El-Wakil, A.B. Farag, M.S. El-Shahawi, *Talanta* 36 (1989) 783.
- [4] A.M. El-Wakil, A.B. Farag, M.S. El-Nahas, *Talanta* 40 (1993) 841, and references cited within.
- [5] A.M. El-Wakil, A.B. Farag, M.S. El-Shahawi, *Fresenius Z. Anal. Chem.*, 337 (1990) 886.
- [6] A. Townshend and D.T. Burns, *Talanta*, 39 (1992) 715.

- [7] A. Gaikwad, M. Silva and D. Perez-Bendito, *Analyst*, 119 (1994) 1819.
- [8] P.S. Radhakrishnamurti and H.P. Panda, *React. Kinet. Catal. Lett.*, 14 (1980) 193.
- [9] Z. Marczenko, *Separation and Spectrophotometric Determination of Elements*, Ellis Horwood Limited, Chichester, 1986, p. 319.
- [10] M. Román Ceba, J.C. Jiménez Sánchez Sánchez and T. Galeano Diaz, *Microchem. J.*, 31 (1985) 256.
- [11] A. Hareez and W. Bashir, *Microchem. J.*, 31 (1985) 375.
- [12] M. Callejon Mochon and J.A. Munoz Leyva, *Microchem. J.*, 34 (1986) 83.
- [13] M. Kamburova, *Talanta*, 39 (1992) 997.
- [14] D.T. Burns, M. Harriott and S.A. Barakat, *Anal. Chim.*, 258 (1992) 325.
- [15] M.S. El-Shahawi, A.Z. Abu Zuhri and S.M. Al-Daheri, *Fresenius Z. Anal. Chem.*, 350 (1994) 874.
- [16] D.T. Burns, S.A. Barakat, M. Harriott and M.S. El-Shahawi, *Anal. Chim. Acta*, 270 (1992) 213.
- [17] D.T. Burns, S.A. Barakat, M. Harriott and M.S. El-Shahawi, *Fresenius Z. Anal. Chem.*, 344 (1992) 131, and references cited within.
- [18] D.T. Burns, M. Harriott and S.A. Barakat, *Anal. Chim. Acta*, 259 (1992) 33.
- [19] A. Ringbom, *Fresenius Z. Anal. Chem.*, 115 (1939) 332.
- [20] E.B. Sandell, *Colorimetric Determination of Trace Metals*, Interscience, New York, 1959.
- [21] A. Fernandez-Gutierrez, A. Munoz de la Pena and J.A. Murillo, *Anal. Lett.*, 16 (1983) 759.
- [22] J.E. Barmey, *Talanta*, 14 (1967) 1363.
- [23] M.S. El-Shahawi and S.A. Barakat, *Talanta*, 42 (1996) 277, and references cited within.

Spectrophotometric determination of bismuth(III and V) in water after ion-pair liquid–liquid extraction using tetramethylammonium cation as counter ion

M.S. El-Shahawi*, S.M. Aldhaheri

Chemistry Department, Faculty of Science, UAE University, Al-Ain, P.O. Box 17551, United Arab Emirates

Received: 25 January 1995/Revised: 20 March 1995/Accepted: 23 March 1995

Abstract. A simple extractive spectrophotometric method for the determination of bismuth has been developed. It is based upon oxidation of bismuth(III) to bismuthate with potassium periodate at pH 7–8. The resulting species is then extracted with tetramethylammonium iodide in chloroform followed by direct spectrophotometric measurement at 513 nm. The optimum concentration range evaluated by Ringbom's method was found to be 0.05–10 mg l⁻¹. The molar absorptivity and Sandell's sensitivity for the formed ion-pair at 513 nm have been found to be 4.2·10⁴ mol⁻¹ cm⁻¹ and 0.09 lg/cm², respectively.

* *Permanent address:* Chemistry Department, Faculty of Science at Damietta, Mansoura University, Damietta, Egypt

Correspondence to: M.S. El-Shahawi

(BR) buffer solutions (pH 2–12) which contained sodium hydroxide, orthophosphoric acid, boric acid and glacial acetic acid were prepared with distilled water. Bismuth(III) stock solution (100 lg/ml) was prepared by dissolving an accurately weighed amount of Bi(NO₃)₃·9H₂O in 10% HNO₃ and standardized by photometric

titration with standard Na EDTA at 530 nm using

2

xylenol orange [9].

Bismuth(V) stock solution (100 lg/ml) was prepared by dissolving the exact weight of bismuthic acid [10] in 100 ml of 0.5 mol/l KOH and diluting to 500 ml with doubly distilled water and diluting to the necessary concentration whenever required. Tetramethylammonium iodide (TMAI) was used as supplied. A 1% (w/v) stock solution of TMAI was prepared in water. A 2% (w/v) solution of potassium periodate (BDH) was prepared by dissolving 2.3 g of the salt in a mixture of 2 ml conc. HNO₃ and 25 ml of water, gently warming to complete the dissolution, cooling and diluting to 100 ml with water. For the interference studies, stock solutions of the other metal ions (1 mg/ml) were prepared from analytical reagent grade chloride or nitrate salts.

A Pye — Unicam double beam UV-visible spectrometer model SP-8-400 with 10 mm quartz cells was used for all the absorbance measurements. A Philips digital pHmeter (model 9418) with glass and saturated calomel electrodes was used for the pH-measurements.

Recommended procedures

1. *Determination of bismuth(III).* Transfer aliquot portions (5 ml) containing various amounts (0.1–100 lg) bismuth(III) to a 100 ml conical flask. Add 10 ml of Britton-Robinson buffer (pH 7), 20 ml of water and 5 ml of 2% (w/v) potassium periodate solution and boil for 10 min. Cool the

Introduction

The most common reported spectrophotometric procedures for bismuth determination involve chelation with mucic acid [1], dithizone [2], xylenol orange [3] and tetra-n-butylammonium tetraiodobismuthate [4]. However, most of these methods are expensive, not practicable in routine analysis, suffer from lack of selectivity and require a laborious enrichment step e.g. precipitation, flotation, etc.

The oxo anions are amongst the least studied group of species which form liquid–liquid extractable ion pairs with onium cations [5–8]. The present communication reports the use of tetramethylammonium iodide as an ion-pairing extractant for bismuthate and the application of the system to the spectrophotometric determination of bismuth in water after oxidation of bismuth(III) to bismuth(V) with potassium periodate at pH 7–8.

Experimental

Reagents and solutions

Analytical-reagent grade chemicals and doubly distilled water were used throughout the work. Britton-Robinson

reaction mixture, add 5 ml of 1% (w/v) tetramethylammonium iodide solution and mix. Extract the resulting ion pair twice with 5 ml (2)2.5 of chloroform and collect the extracts in a dry 50 ml beaker containing anhydrous sodium sulphate (0.5 g), swirl to mix.

Transfer the extract into a 10 ml flask, wash the residue into the beaker with 5 ml chloroform transfer into the flask, make up the volume to the mark with chloroform and cover the flask. Measure the absorbance of the organic phases at 513 nm against a reagent blank. Establish the concentration by reference to the calibration graph.

2. *Determination of bismuth(V)*. Transfer aliquot portions (5 ml) of the bismuth(V) solution containing 1–100 µg of the element into 100 ml Erlenmeyer flasks and add 10 ml of Britton-Robinson buffer (pH 7) solution to each flask followed by adding 5 ml of TMAI and follow the recommended procedure 1 of extraction and determination. Establish the concentration of bismuth(V) by reference to the calibration curve.

3. *Determination of the binary mixtures of bismuth(III) and (V)*. Transfer aliquots (5 ml) of the mixture to a series of 100 ml conical flasks containing various amounts of bismuth(III) and (V). Add 5 ml of KIO₃ solution, 10 ml of 4 Britton-Robinson buffer (pH 7), boil the solution mixture for 10 min and follow the recommended procedure 1. To another aliquot portion add 10 ml of buffer (pH 7), 5 ml of reagent TMAI and follow the recommended procedure 2 of bismuth(V) determination. On the basis of the proposed procedure, the absorbance (A₁) of the extracted ion-pair (BiO⁻~TMA⁺) in the first aliquot is equivalent to $\frac{1}{3}$

bismuth(III) plus (V) and the absorbance A₂ of the ion₂

pair in the second aliquot is equivalent to bismuth(V). Therefore the absorbance A₁—A₂ is equivalent to bismuth(III) in the sample.

Results and discussion

Methylene chloride, 1,2-dichloroethane, nitrobenzene, hexane, chloro-benzene, toluene, carbon tetrachloride, benzene and chloroform were used as possible extracting solvents for the bismuthate-TMA species formed. The extraction of the BiO⁻~3-TMA⁺ into chloroform was fast and no significant change in the degree of extraction occurred when the shaking time was varied from 2 to 30 min. The absorption spectra of the bismuthate-TMA ion pair tetramethylammonium iodide in chloroform and bismuth(III) in aqueous solution at pH 7 are given in Fig. 1. Therefore, the absorbance measurements of the formed ion pair were measured at 513 nm.

Stability of the coloured BiO⁻~3-TMA⁺ ion pair and effect of electrolytes

After the extraction of the coloured BiO⁻~TMA⁺ ion pair 3 in chloroform as described under the recommended procedure 1, the absorbance was found to be constant up to 1 h for samples containing 0.05–30 µg/ml when stored in stoppered tubes at room temperature. The addition of sodium chloride or sodium nitrate up to 0.1 mol/l did not improve the amount of the ion pair BiO⁻~TMA⁺ extrac-

3

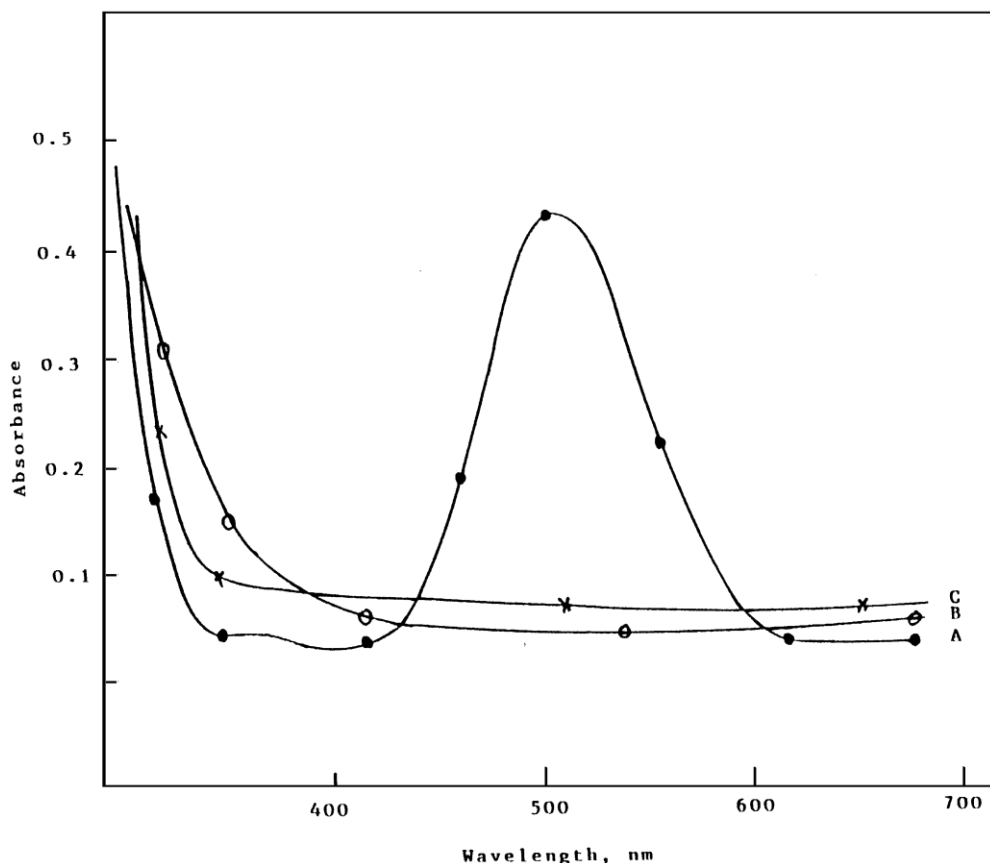


Fig. 1. Absorption spectra of extracted bismuth tetramethylammonium ion pair in chloroform (A), bismuth nitrate (B) and tetramethylammonium iodide (C) aqueous solution at pH 7 against blank

ted at a concentration of 20 $\mu\text{g/ml}$ bismuth(III), indicating that the bismuth species are extracted quantitatively without salt effect. In the presence of NaCl at concentration

0.1 mol/l, the absorbance of the extracted species decreased, which is possibly due to the ability of the bismuth(III) species to form chloro complexes which are less oxidized by potassium periodate and are also less extractable by the organic phase under the experimental conditions [11].

The influence of the pH of the aqueous phase on the extraction of bismuth(III) or (V) was examined by measuring the absorbance of the organic phase for $\text{BiO} \sim \text{TMA}^+$ species in chloroform. The final pH of each aqueous solution was measured before the extraction and other conditions were kept constant. The obtainable results are summarized in Fig. 2. Therefore, a BrittonRobinson buffer of pH 7 was finally selected and employed as described in the experimental procedure.

Effect of reagent and potassium periodate concentration

Tetramethylammonium iodide, tetrabutylammonium iodide, tetraphenylphosphonium bromide, tetraphenylammonium chloride, benzyltributylammonium chloride and tetraphenylarsonium chloride were used as ion-pair extracting agents for bismuthate at pH 6.5–8 under optimal experimental conditions. Only tetramethylammonium iodide extracted bismuthate and the highest absorbance was obtained in chloroform. The effect of the ion-pair TMA^+I^- concentration on the extraction of the bismuthate was critically examined. It was found that 5 ml of 0.1% (w/v) of TMA^+ solution was sufficient to

form $\text{BiO} \sim \text{TMA}^+$ ion pair for 10 μg or less of bismuth(III).

The influence of potassium periodate concentration (0.1–1% w/v) on the oxidation of bismuth(III) was investigated. The absorbance of the extracted $\text{BiO} \sim \text{TMA}^+$ species increased rapidly with the periodate concentration up to 0.5% and decreased slowly thereafter. A periodate concentration of 0.5% (w/v) was therefore chosen in the subsequent work.

Various sequences of addition of bismuth(III), reagent (TMAI) periodate solutions and chloroform have been tested to select the optimum experimental conditions for the maximum absorbance of the $\text{BiO} \sim \text{TMA}^+$ ion pair.

Addition of KIO₃ to the test solution of bismuth(III), 4 boiling at pH 7, then adding TMAI and chloroform followed by shaking vigorously for 2 min, showed maximum absorbance at 513 nm. Different trials employing various additions of chloroform (5 ml) to the test aqueous solution (10 μg) of bismuth have also been carried out. A double extraction with 2.5 ml of chloroform was finally chosen and used as described in the recommended procedure.

Using the optimum experimental conditions described above, calibration curves at 513 nm of the $\text{BiO} \sim \text{TMA}^+$ ion-pair were constructed. A linear graph was obtained by

measuring the absorbance of the organic phase as a function of the bismuth(III) concentration. Beer's law was obeyed up to 20 $\mu\text{g}/\text{l}$ bismuth in the organic phase. The optimum concentration range for the effective spectrophotometric determination of bismuth(III) evaluated by Ringbom's plots [12] has been found to be 0.05–10 $\mu\text{g}/\text{l}$ metal ion. The molar absorptivity calculated from Beer's

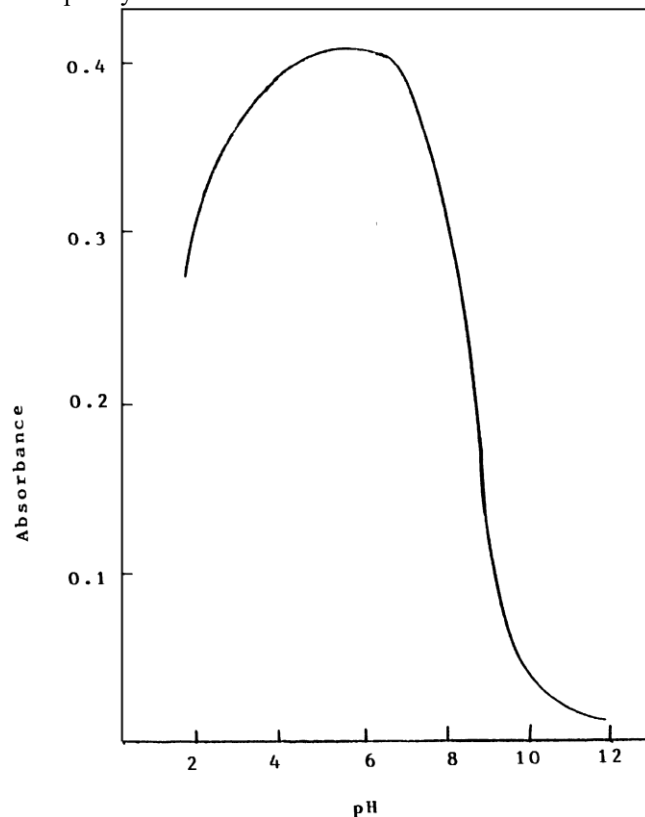


Fig. 2. Effect of pH on the absorbance of the extracted bismuthate-tetramethylammonium ion pair in chloroform. Other conditions are kept constant

law and Sandell's [13] sensitivity for the $\text{BiO} \sim \text{TMA}^+$

ion-pair at 513 nm have been found to be $4.2 \times 10^4 \text{ l mol}^{-1} \text{ cm}^{-1}$ and $0.09 \text{ } \mu\text{g}/\text{cm}^2$, respectively. The sensitivity of this reaction is far better than those of many well known methods for bismuth(III) determination [1–3]. Reproducibility tests for five measurements of 5 $\mu\text{g}/\text{ml}$ of bismuth in the organic phase showed a standard deviation of $\pm 0.2 \text{ } \mu\text{g}/\text{ml}$, a relative standard deviation of 1.9% and a regression coefficient of 0.98. A detection limit of 0.01 $\mu\text{g}/\text{ml}$ bismuth(III) in the aqueous phase was found.

Effect of diverse ions

The influence of some diverse ions on the proposed method was checked for the determination of 10 μg of bismuth(III) in 50 ml aqueous solution under the conditions of the general

procedure. The selectivity of the proposed method in the presence of a relatively high excess (0.1 mg) of the following anions was investigated: NO⁻, CO₂⁻, HCO⁻, Br⁻, Cl⁻, PO₃⁻, HPO₂⁻, S O₂⁻,

3 3 3 4 4 2 8
 SO₂⁻, F⁻, IO₃⁻, MoO₄⁻, S₂O₈⁻, AsO₂⁻, SbO₂⁻, WO₄⁻, acetate, tartrate, oxalate, formate and EDTA. The percentage recovery was 100±2% and the relative standard deviation was 1.3%.

The tolerance limits for various cations (e.g. Na⁺, NH⁺, Al³⁺, Cd²⁺, Mg²⁺, Ba²⁺, Co²⁺, Pb²⁺ and Li⁺) at 4

3. Trojanowicz M, Angustyniak W, Hulanicki A (1984) Mikrochim Acta II : 17
4. Hasebe K, Taga M (1982) Talanta 29 : 1135
5. El-Shahawi MS, Abu-Zuhri AZ, Aldhaheiri SM (1994) Fresenius J Anal Chem 350 : 674
6. Burns DT, Barakat SA, Hariott M, El-Shahawi MS (1992) Anal Chim Acta 270 : 213
7. Burns DT, Barakat SA, El-Shahawi MS, Hariott M (1992) Fresenius J Anal Chem 344 : 131
8. Burns DT, Harriot M, Barakat SA (1993) Anal Chim Acta 259 : 135
9. Vogel AI (1972) Text book of quantitative inorganic analysis, 3rd edn Longman, London

Table 1. Effect of foreign ions on the determination of 10 lg bismuth(III) in 50 ml aqueous solution

Foreign ion	Added as	Amount added (mg)	Found lg	Masking agent
Cu(II)	CuSO	0.01	10.2	
Fe(II)	4 FeCl	0.2	10.3	one crystal of KI and Na S O
Ni(II)	3 NiCl	0.1	9.9	2 2 3
V(V)	2	0.01	9.8	one crystal of KF few drops of 1% KCN solution
Mn(VII)	NH VO	0.2	10.3	one crystal of NaF
	4 4			few drops of 1% NaN
	KMnO			
	4			3

10 mg level were examined by the proposed procedure with 20 lg bismuth(III) concentration in 50 ml aqueous solutions. The percentage recovery of bismuth was found in the range 100±3% in each case. In the presence of some other ions (e.g. Mn(VII), Fe(III), Cu(II) V(V) and Ni(III)) simple modifications (Table 1) were introduced in the aqueous solution to eliminate their interferences.

10. Lide DR (1991) Handbook of chemistry and physics, 2nd edn. Chemical Rubber Company
11. McDonald CW, Bedenbaugh JH (1970) Mikrochim Acta (Wien)
12. Ringbom A (1938/39) Fresenius Z Anal Chem 115 : 332
13. Sandell EB (1959) Colorimetric determination of trace metals, Interscience, New York 14. Braun T, Farag AB (1972) Anal Chim Acta 61 : 265

Conclusion

The present study demonstrates that the liquid—liquid extraction involving ion-pair formation represents the basis of the determination of bismuth. The method is simple and accurate for trace analysis of bismuth. The clear advantage of the method that is not only applicable for bismuth(III) or (V) speciation in their mixtures, but can also be used for their determination in sea water. The sensitivity of the proposed method can be improved employing a polyurethane foam column [14] to preconcentrate trace amounts of bismuth from large sample volumes, followed by determination by the proposed procedure after elution of bismuth with a selective eluting agent. The determination of Bi(III) besides Bi(V) or Bi(V) besides Bi(III) is also possible.

Acknowledgement. The authors would like to thank Miss S. Al-Marhoon and Professor A.Z. Abu Zuhri for their help.

References

1. Gonzalez Portal A, Baluja-Santos C, Bermejo-Maslinez F (1986) Analyst, III : 547
2. Kasterke B (1974) Chem Anal (Warsaw) 19 : 63

Spectrophotometric determination of rhenium as perrhenate by extraction with amiloride hydrochloride

D. Thorburn Burns ^{a,*}, M.S. El-Shahawi ^b, M.J. Kerrigan ^a, P.M.T. Smyth ^a

^a Department of Analytical Chemistry, The Queen's University of Belfast, Belfast BT9 5AG, Northern Ireland, UK

^b U.A.E. University, Al-Ain, United Arab Emirates

Received 7 September 1995; accepted 27 October 1995

Abstract

Rhenium (0–20 μg) may be determined as perrhenate spectrophotometrically at 362 nm after its extraction at pH 4 with amiloride hydrochloride into 4-methyl-2-pentanone. The relative standard deviation for 7 determinations of 10 μg of perrhenate is 1.5%. The effects of pH and diverse ions are reported. Only perchlorate, periodate and iodide interfere seriously. The system has been applied to the determination of rhenium on alumina and on carbon catalysts.

Keywords: Catalytic methods; Spectrophotometry; Rhenium; Amiloride hydrochloride

1. Introduction

The most commonly used methods for the determination of rhenium are those based on the reduction of rhenium(VII) with tin(II) prior to reaction with thiocyanate or α -furildioxime to give extractable coloured products [1–3]. Both methods require careful control of conditions and considerable time to achieve maximum colour development. Such delays can be avoided by direct extraction of rhenium(VII) as perrhenate with onium cations [4] or basic dyes [5] such as Brilliant Green [6,7]. The present communication describes the application of the extraction of the protonated amiloride–perrhenate ion pair into 4-methyl-2-pentanone for the analysis of rhenium-

based catalysts. The only prior use of amiloride as an analytical reagent is for the determination of the perchlorate ion [8].

2. Experimental

2.1. Apparatus

A Pye-Unicam SP8-400 and a Philips PU8675 UV–visible spectrophotometer were used for recording spectra and for routine absorbance measurements, respectively, with matched 1 cm quartz cells.

2.2. Reagents and solutions

2.2.1. Amiloride hydrochloride

The reagent 3,5-diamino-*N*-(aminoiminomethyl)-6-chloropyrazinecarboxamide hydrochloride dihy-

* Corresponding author.

drate (amiloride, Merck, Sharp and Dohme) was used as supplied. A 0.01 M stock solution was made by dissolving 0.3021 g of the reagent in 100 ml of water.

2.2.2. Stock solution of perrhenate ion

A stock $5 \mu\text{g ml}^{-1}$ perrhenate (Johnson Matthey) solution was prepared by dissolving 0.1157 g of potassium perrhenate in exactly 1 l of water and diluting 5.00 ml of this solution to 100 ml in a volumetric flask.

2.2.3. Universal buffer [9]

Citric acid (6.008 g), potassium dihydrogenphosphate (3.893 g), boric acid (1.769 g) and diethylbarbituric acid (5.266 g) were dissolved in 1 l of distilled water. Aliquots (100 ml) were titrated with 0.2 M sodium hydroxide to produce buffer solutions of the desired pH within the range 2.6–12.

All reagents were of analytical grade and doubly distilled water was used throughout.

2.3. General procedure

Place a 1–8 ml aliquot of sample solution containing 4–20 μg of rhenium(VII) in a separating funnel, add 10 ml of pH 4.0 buffer and 5 ml of amiloride solution. Extract with 10.0 ml of 4-methyl-2-pentanone. Discard the lower aqueous layer. Filter the organic layer through a Whatman No. 1 paper into a 10-ml volumetric flask. Make up to volume with the same solvent and mix. Measure the absorbance at 362 nm against a reagent blank prepared in the same way.

2.4. Procedure for catalyst dissolution

2.4.1. Rhenium on alumina pellets

Weigh one pellet, crush to a fine powder in an agate mortar and transfer to a platinum dish. Add 1.0 g of sodium peroxide and 1.0 g of sodium hydroxide, mix and fuse carefully over a Bunsen flame until reaction is complete (about 20 min). Cool, add 30 ml of water and heat gently to dissolve all the material. Cool, filter through a Whatman No. 40 filter paper into a 250 ml volumetric flask and dilute to volume with water. Prepare a blank using the same weight of pure alumina (Anderman) as the catalyst pellet.

2.4.2. Rhenium on carbon

This sample is pyrophoric and must be handled as follows. Open the sample container in a dry nitrogen purged glove box. Transfer a sample (5–10 μg) to a preweighed aluminium sample pan (as supplied by Perkin-Elmer for use with CHN analysers and for differential calorimeters) and seal with a small press [10]. Reweigh, place in a platinum dish and take into solution as described above, fusing until colourless (about 30 min). Prepare a blank with use of an empty sample pan and lid.

2.5. Extraction

Transfer a 5.00 ml aliquot of catalyst solution into a separating funnel and add 5 ml of 5% (w/w) citric acid solution. The pH should be in the range 3–5. Adjust to pH 4.0 by adding 0.2 M hydrochloric acid or sodium hydroxide as necessary. Continue as in the general procedure but omit addition of buffer.

2.6. Examination of the main experimental variables

A variety of solvents including alcohols, ketones, esters, ethers, chlorinated and aromatic solvents were examined for extraction efficiency by mixing 10 ml aliquots of $1 \mu\text{g ml}^{-1}$ perrhenate solution with 10 ml of pH 4.0 buffer, 5 ml of reagent solution, and extracting with 10 ml solvent. The organic phase was separated and filtered to remove water and the absorbance of the extract measured at 362 nm against a solvent blank. 4-Methyl-2-pentanone was the most efficient extractant and gave a low blank in the absence of perrhenate.

The pH of the aqueous solutions was adjusted by addition of 10 ml of buffer solution of defined pH prior to extraction. The reagent blank was constant in the range pH 3–7 whilst the apparent extraction of perrhenate increased by 5% from pH 3–5 and decreased rapidly with further increase in pH. Solutions were buffered at pH 4.0 in all subsequent work.

3. Results and discussion

Linear calibration graphs were obtained over the range 0–15 μg of perrhenate ion (in 5 ml of aqueous solution). For 10 μg of perrhenate the coefficient of

Table 1
Effect of interfering anions on the determination of perrhenate

Ion ^a	Change in absorbance (%)
ClO ₄ ⁻	452
I ⁻	108
IO ₄ ⁻	420

^a Net ratio to perrhenate = 100:1.

variation, estimated from 7 replicates, was 1.5%. The apparent molar absorptivity based on extraction at pH 4.0 was $1.06 \times 10^4 \text{ l mol}^{-1} \text{ cm}^{-1}$ which is comparable with that found using the perchlorate ion [8], namely $1.29 \times 10^4 \text{ l mol}^{-1} \text{ cm}^{-1}$.

The possible interferences of diverse ions on the solvent extraction of 10 μg of perrhenate were examined at a 100:1 (w/w) ion–perrhenate ratio. The only serious interferences are those listed in Table 1. The other ions tested did not interfere.

Results for the determination of rhenium in the catalyst materials (Table 2) are in good agreement with the expected values. The method is faster and

Table 2
Analysis of rhenium-based catalysts

Sample	Rhenium content (%)	
	Specified	Found
Rhenium on 1/8 in. alumina pellets	0.5	0.49 \pm 0.07
Rhenium on carbon	5.0	5.01 \pm 0.05

Sample obtained from Aldrich.

Mean \pm 95% confidence intervals for 5 replicates.

more convenient than those based on the reduction of rhenium(VII) prior to chromogenic complex formation and that using solid phase extraction of Brilliant Green perrhenate with microcrystalline benzophenone [7].

Acknowledgements

We wish to record our thanks to Merck, Sharp and Dohme for the gift of amiloride hydrochloride used herein.

References

- [1] F.D. Snell, *Photometric and Fluorometric Methods of Analysis: Metals*, Wiley, New York, 1978.
- [2] Z. Marczenko, *Separation and Spectrophotometric Determination of Elements*, Ellis Horwood, Chichester, 1986.
- [3] H. Onishi, *Photometric Determination of Traces of Metals, Park IIB: Individual Metals Magnesium to Zirconium*, 4th edn., Wiley, New York, 1989.
- [4] A.J. Bowd, D.T. Burns and A.G. Fogg, *Talanta*, 16 (1969) 719.
- [5] A.J. Bowd, D.T. Burns and A.G. Fogg, *Talanta*, 18 (1971) 1175.
- [6] A.G. Fogg, C. Burgess and D.T. Burns, *Analyst*, 95 (1970) 1012.
- [7] D.T. Burns and N. Tungkananuruk, *Anal. Chim. Acta*, 204 (1988) 359.
- [8] D.T. Burns and P. Hanprasopwattana, *Anal. Chim. Acta*, 118 (1980) 185.
- [9] W.C. Johnson and A.J. Lindsey, *Analyst*, 64 (1939) 490.
- [10] R. Belcher (Ed.), *Instrumental Organic Elemental Analysis*, Academic Press, London, 1977.

Preconcentration and separation of acaricides by polyether based polyurethane foam

M.S. El-Shahawi *, S.M. Aldhaheeri

Chemistry Department, Faculty of Science, UAE University, Al-Ain, P.O. Box 17551, United Arab Emirates

Received 30 January 1995; revised 1 September 1995; accepted 8 September 1995

Abstract

This paper reports the preconcentration of some dissolved organic phosphorous and chlorinated acaricides in water by porous polyether based polyurethane foam. Preliminary screening tests on the retention of the tested compounds, i.e., dicofol and bromopropylate, by polyether foams indicated that a very high percent removal of the tested species was obtained. The retention rate was found fast and reaches equilibrium in a few minutes. The various parameters, e.g., pH, extraction media, shaking time, salt effect, temperature and sample volumes affecting the preconcentration of the tested species by the unloaded foam, trioctylamine and trimethylphosphate treated foam have been optimized via batch modes of separation. The unloaded foams were employed in column modes for the retention and recovery of the tested species. The sorption efficiency and recovery of the compounds by the unloaded foams column were found to be up to 97.5%. The height equivalent to a theoretical plate (HETP) obtained by the unloaded foam was found to be in the range $1.1\text{--}1.3 \pm 0.2$ mm. The sorption mechanism of the tested compounds by the foams was discussed.

Keywords: Acaricides; Polyurethane foam; Preconcentration; Environmental analysis; Water pollutants

1. Introduction

As a consequence of the activities of modern industries and agriculture many manmade organic pollutants have found their way into the environment, without the availability of much knowledge on their possible harmful effects on the environment [1]. The range of potential toxic substances is extensive and includes heavy metals and organic pollutants such as pesticides and acaricides [2]. The acaricides

are toxic agents and are widely and regularly applied over large areas accessible to the public [3,4].

Pesticides and acaricides have great potential for bioaccumulation, however there is still a lack of effective means of the treatment and removal or minimizing of these species to an acceptable concentration [5]. The most common reported extraction procedures are steam distillation, liquid–liquid extraction, adsorption on active carbon, oxidation reaction, reversed liquid-liquid partition filter chromatography and cellulose triacetate membrane filters [6–11]. Such preconcentration methods are limited by low flow rates and are too expensive for routine analysis where many large volume samples are concentrated on site prior to quantitative analysis [10,11].

* Corresponding author. On leave from the Chemistry Department, Faculty of Science at Damietta, Mansoura University, Damietta, Egypt.

The introduction of porous polyurethane foam as an inexpensive solid extractor and effective sorbent has been made for the removal of water pollutants [12–23]. The membrane like structure of the foams together with efficient sorption properties offered higher concentrating ability and flow rate compared with other solid supports [21–23]. The work described herein was to evaluate the use of polyether-based polyurethane foam for the removal of two acaricides from large volume water samples. These compounds were chosen because they are hydrophobic common water pollutants and are likely to be extracted by the foam. The study was also aimed to determine whether the extraction takes place by solvent extraction, cation chelation, anion exchange or by other mechanisms.

2. Experimental

2.1. Reagents and materials

All chemicals used were of analytical reagent grade except otherwise specified. Open pore polyether-based polyurethane foam was supplied by Schaumstoffwerke (Kremsmunster, Austria). Foam cubes of approximately 1 cm³ were cut from polyurethane foam sheets. These foam cubes were soaked in 1 M hydrochloric acid for 24 h with occasional squeezing and washed with water until they were acid free. They were then washed with acetone (BDH) in a Soxhlet extractor for 8 h. [18,19]. The foam cubes loaded with tri-*n*-octylamine (TOA) and trimethylphosphate (TMP) (both from BDH) were prepared by mixing the dried foam cubes with 5% TOA and 3% TMP in *n*-hexane (20 cm³/g dry foam) with stirring for 10 min, respectively and dried as previously reported [12]. The structures of the tested acaricides: 2,2,2-trichloro-1,1-bis(4-chlorophenyl)ethanol (dicofol, I) and isopropyl-4,4'-dibromobenzylate (bromopropylate, II), are given in Fig. 1. A stock solution of each compound (1 mg/cm³) was prepared in a 100 cm³ measuring flask by dissolving an exact weight of the compound in ethanol. A series of standard solutions of these compounds were prepared by diluting their stock solutions with water and few drops of ethanol when-

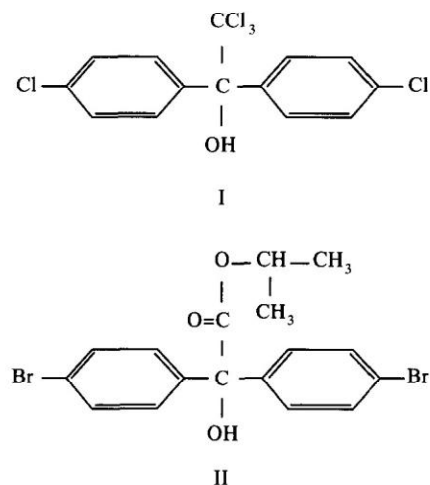


Fig. 1. Structure of the tested acaricides.

ever is required to provide a clear solution in the polyethylene bottles.

2.2. Apparatus

The absorbance measurements of the acaricides were obtained with a Pye Unicam SP 8-400 double beam UV–visible spectrophotometer with a 1 cm pathlength quartz cell. An Orion pH meter and glass columns (12 cm × 10 mm i.d.) together with a Lab-Line Orbit Environ-Shaker Model 35271-1 were also used.

2.3. General procedures

2.3.1. Batch experiments

To examine the effect of shaking time on the uptake of dicofol and bromopropylate on unloaded, TOA- and TMP-loaded polyurethane foam, the foam cubes (0.3 ± 0.004 g) were equilibrated with 100 cm³ aqueous solutions at pH < 3 of each compound (60 μg/cm³) in separate polyethylene bottles and shaken in a thermostated shaker at 20 ± 0.1°C for various time intervals up to ca. 2 h. The aqueous phase was then separated and the remaining compound was determined from its absorbance at the suitable wavelength against the blank. The acaricide amount retained on the foam was calculated by difference. Following these procedures, the effect of

the compound concentration ($10\text{--}200\ \mu\text{g}/\text{cm}^3$), solution pH, temperature extraction media and increasing salt concentration ($\leq 0.1\ \text{M}$) of different alkali

metal (Li^+ , Na^+ , K^+ , NH_4^+) chlorides on the extraction efficiency of the tested species by the unloaded, TOA- and TMP-loaded polyurethane foam were de-

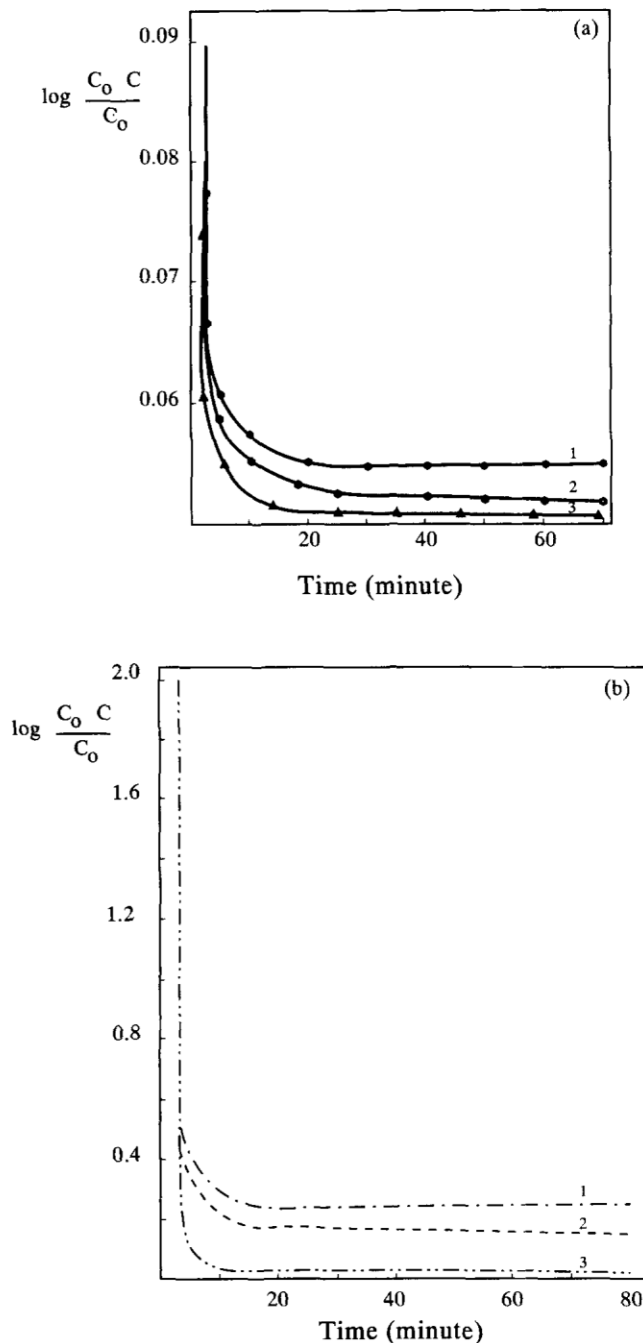


Fig. 2. Effect of shaking time on the sorption profiles of dicofol (a) and bromopropylate (b) by unloaded (1), TMP-loaded (2) and TOA-loaded (3) foams (0.3 g) at $100\ \mu\text{g}/\text{cm}^3$ at pH 3 and $20 \pm 0.1^\circ\text{C}$.

terminated. The extraction percentage (E) and distribution coefficient (D) were calculated as follows:

$$E = [(C_0 - C)/C_0] \times 100$$

where C_0 is the concentration of the tested compound in solution before extraction and C the concentration in solution after extraction, and

$$D = \frac{E}{(100 - E)} \times \frac{\text{Volume of solution (l)}}{\text{Weight of foam (kg)}}$$

2.3.2. Column experiments

For the column experiments 3 g of dry unloaded foam were packed into the column using the vacuum method of foam packing [12]. Tap or distilled water (0.1–3 dm³) sample containing 0.1 mg of the compound tested at $2 < \text{pH} < 3$ was passed through the foam column at 10 cm³/min. After squeezing water from the foam material, the compound was then recovered from the foam with 100 cm³ acetone in a Soxhlet extractor for 6 h. The acaricide quantity was then determined by measuring the absorbance of the solution against reagent blank after being concentrated to 25 cm³ with a rotary evaporator. The effect of sample volume and flow rate on the extraction efficiency of the tested compounds by the unloaded foams were also determined.

3. Results and discussion

Batch experiments using unloaded, TMP- and TOA-loaded polyurethane foams have shown that the extraction of the investigated dicofol and bromopropylate from aqueous solution at $\text{pH} \geq 3$ is rapid and the equilibrium is reached in experimental sorption times < 1 h followed by a plateau. The results are given in Fig. 2. A good extraction efficiency and rapid preconcentration of the tested compounds from aqueous media were obtained with the TOA-treated foam (Fig. 2) as compared to the unloaded and TMP-loaded foams. The average values of the half-time ($t_{1/2}$) of equilibrium sorption calculated from Fig. 2 on the unloaded, TOA- and TMP-loaded foams were found in the range 3–5 and 2.5–3 and 3–4 min, respectively. The tri-*n*-octylamine acts as a plasticizer on the polyether foam. Thus, the collec-

tion rates of the compounds with the plasticized TOA-foams are generally better than with the un-plasticized ones. This can be attributed to the high mobilities and diffusion rates of the tested acaricides through the open pores and the quasi-spherical membrane structure of the plasticized TOA-foam [13,16]. The plasticizer has a dual purpose [13], i.e., it acts as an efficient non-volatile solvent as well as a plasticizer for the foam plastic itself. These results are in good agreement with the data reported by Braun et al. [20]. The foam membrane acts as a true sorbent where the diffusion rates of the chemical species in the membrane structure are considerably higher than those in bulky solids [21,22]. Moreover, the plasticization of the foam membrane with TOA offers a wider range of modifications than normal (granular) solids [21].

3.1. Sorption isotherm

The sorption behaviour of the investigated compounds from aqueous solution by the unloaded and TOA-loaded foams was found to depend on the concentration. Thus, the extraction isotherms were developed over a wide range of equilibrium concentrations (10–200 $\mu\text{g}/\text{cm}^3$) for each compound at $20 \pm 0.1^\circ\text{C}$. The pH values of the aqueous solutions in these experiments were adjusted at pH 2. The isotherms of the tested compounds exhibited a first order behaviour in the low concentration range and tended to plateau at high bulk solution concentrations as shown in Fig. 3. The sorption of the different compounds by the unloaded and loaded foams increases in the order: unloaded foam $<$ TMP-foam $<$ TOA foam.

Similar trends of the sorption profiles of the tested species were obtained with diethyl ether. Therefore, solvent extraction is the most probable mechanism for the extraction of these compounds by the foam from the aqueous solution.

It is worth to note that the molecular weight (MW) of dicofol and bromopropylate is a participating factor in the extraction by the polyether foam, where the extraction percentage of bromopropylate (MW = 426) $>$ dicofol (MW = 353.5). These results are consistent with the general understanding that the larger the molecular weight of the sorbate, the larger the amount of the tested acaricides re-

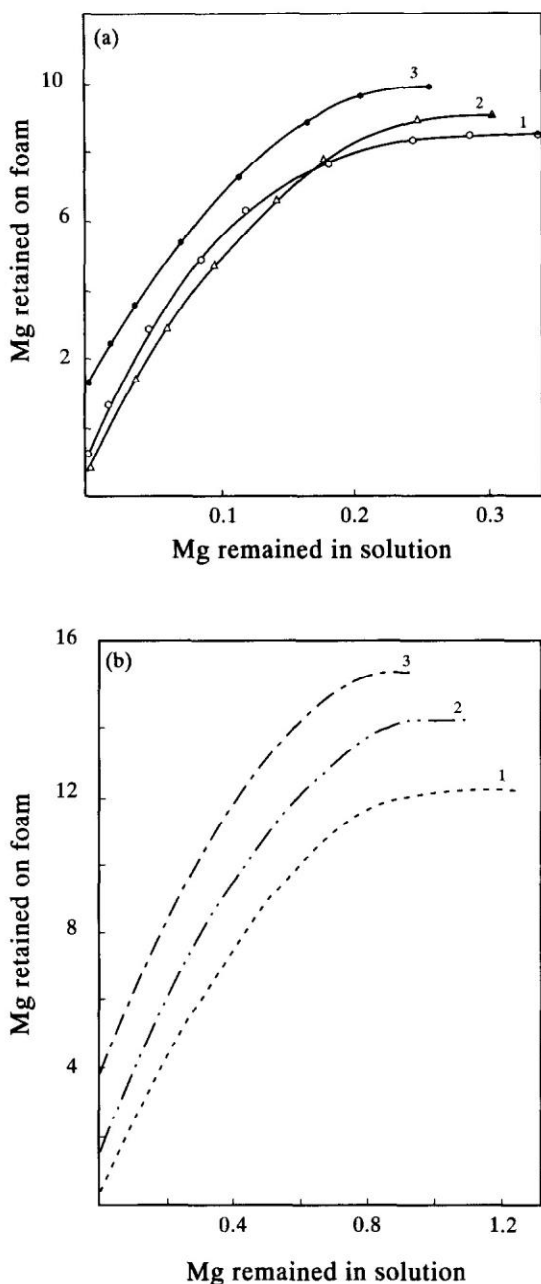


Fig. 3. Extraction isotherms of dicofol (a) and bromopropylate (b) at concentration of $10\text{--}200\ \mu\text{g}/\text{cm}^3$ by unloaded (1), TMP-loaded (2) and TOA-loaded foams (3) from aqueous solution at pH 3 at $20 \pm 0.1^\circ\text{C}$ and 1 h shaking time.

tained on the foam when the compounds concerned are similar in nature [18].

The effect of the pH of the aqueous phase on the

extraction of the tested compounds ($80\ \text{g}/\text{cm}^3$) by the unloaded foams was investigated over a wide pH range (pH 2–11). The percentage removal of the compounds by the unloaded foams decreased at moderate pH (5–7) and reaches maximum at pH < 3 at which the compounds exist in the neutral form. Thus the extraction mechanism involves extraction of neutral species. This observation is also consistent with a solvent-extraction mechanism and is in good agreements with the data previously reported [18,23].

3.2. Effect of electrolyte and temperature

The influence of various concentrations of alkali metal chlorides (concentrations < 0.10 M) on the sorption profile of dicofol and bromopropylate at $80\ \mu\text{g}/\text{cm}^3$ was studied at pH < 3 employing unloaded foams. The data obtained are given in Fig. 4. Significant increases in the sorption profiles of compounds I and II by the unloaded foam were observed in the presence of NH_4Cl , KCl , NaCl and LiCl and the following order of extraction: $\text{K}^+ < \text{NH}_4^+ < \text{Na}^+ < \text{Li}^+$ was found. These data confirm that the salting out effect follows the hydration order of the tested cations. The distribution ratios of dicofol increased with the amount of the salt added from $D = 15.84 \times 10^2$ and 23.44×10^2 to 19.95×10^2 and $69.8 \times 10^2\ \text{l}/\text{kg}$ for Na^+ and Li^+ at 0.05 and 0.1 M (Fig. 4a), respectively. This fact is characteristic of a solvent-extraction mechanism with the salts acting as salting-out and excluded the cation chelation mechanism in the extraction systems involved [21–23]. The added salts increased the sorption profiles of the tested species into the foams by reducing the number of water molecules available to solvate the organic compound which would therefore be forced out of the solvent phase into the foam since some amount of “free” water molecules are preferentially used to solvate the ions added. The charge density for the ions studied is in the order: $\text{K}^+ < \text{NH}_4^+ < \text{Na}^+ < \text{Li}^+$ for the sorption of dicofol and bromopropylate. Hence the influence of the salts can be explained by the salting out effect on a solvent-extraction mechanism.

To confirm the salting out of the salts on the sorption profiles of the tested species by the polyether foam, an extraction of $100\ \text{cm}^3$ of dicofol ($60\ \mu\text{g}/\text{cm}^3$) solution containing 0.1 M hydrochloric

acid was investigated after 30 min of shaking. The added LiCl (< 0.10 M) to the extraction media enhanced the distribution ratio of dicofol more in a solution of pH 1 ($D = 50.12 \times 10^2$ l/kg) than at higher pH 4 ($D = 6.31 \times 10^2$ l/kg). This is possibly attributed to the increased amount of neutral species present at pH 1 as compared to that at pH 4. The sorption profile of dicofol by unloaded foam at pH 1

in the presence of the above alkali metal chlorides also increased in the same order: $K^+ < NH_4^+ < Na^+ < Li^+$.

These results confirm that the tested compounds are highly extractable in the neutral form and the solvent-extraction mechanism is the most probable mechanism.

Hydrogen bonding between the hydroxyl group of

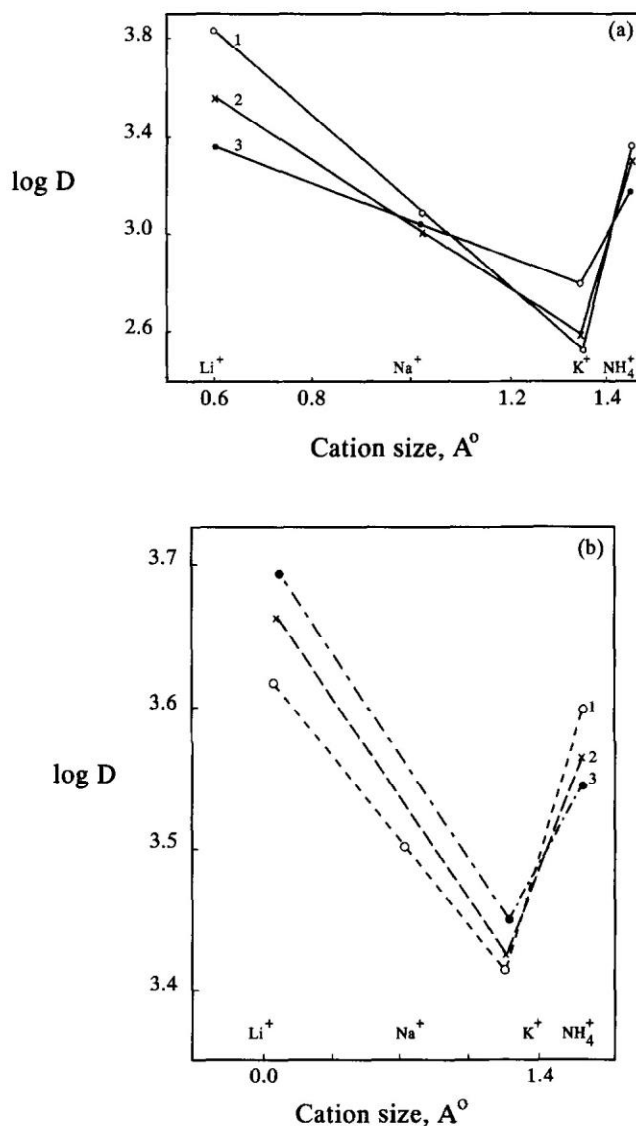
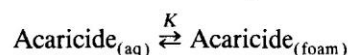


Fig. 4. Effect of cation size and concentration (0.1 M) of various univalent (Li^+ , Na^+ , K^+ and NH_4^+) cations on the sorption profiles of dicofol (a) and bromopropylate (b) by unloaded foams. Salt concentrations are: 0.1 M (\circ); 0.05 M (\times) and 0.01 M (\bullet). Other conditions as in Fig. 2 and 1 h extraction time.

the acaricides and polyurethane foam can account for the sorption profiles of the tested species. Overall, the results (Fig. 5) obtained are consistent with the solvent-extraction mechanism as previously reported in Refs.[17,18,23].

The degree of extraction of the tested acaricides by the unloaded and TOA-loaded foams were measured at 35, 45 and 55°C. Similar trends to that obtained at 20°C were obtained and the percentage sorption profile increases slightly with increasing temperature. Assuming no chelation or precipitation took place and that the tested compounds exist as neutral species at pH < 3 then the equilibrium constant K for the equilibrium:



is equivalent to the distribution ratio, D [18,23]. The equilibrium constant, K , with standard enthalpy change, ΔH° , and standard entropy change, ΔS° , is given by the equation:

$$\ln K = -\Delta H^\circ/RT + \Delta S^\circ/R$$

Thus, the values of the ΔS° and ΔH° can be obtained by plotting $\ln D$ vs. $1/T$ (Table 1). The ΔS° values for the compounds were found in the range $27\text{--}39 \pm 4 \text{ J mol}^{-1} \text{ deg}^{-1}$ for extraction into the unloaded foams and $33\text{--}42 \pm 3 \text{ J mol}^{-1} \text{ deg}^{-1}$ for sorption into TOA-foams, respectively. The decrease in entropy change in the use of TOA-foam is believed to be due to hydrogen bonding reducing the freedom of movement of the acaricide in the polyether foam as previously reported [23]. These results are consistent with the solvent-extraction

Table 1

Thermodynamic data for the sorption of the tested acaricides by unloaded (a) and TOA loaded (b) foams

	ΔH° (kJ/mol)		ΔS° (J mol ⁻¹ deg ⁻¹)	
	a	b	a	b
Dicofol	20.12 ± 2	22.7 ± 2.3	27.9 ± 2.9	33 ± 2
Bromopropylate	23.2 ± 2.6	27.2 ± 3	30 ± 3	42 ± 3

Conditions: extraction from aqueous solution (100 cm³) at pH 3, and temperature range 20–55°C.

mechanism. The bonding of the organic compound with the foam was estimated as about 10 kJ mol^{-1} which is lower than the intramolecular H-bonding (30 kJ mol^{-1}) [21]. Raising the temperature may facilitate the formation of intermolecular H-bonding between the acaricide (I or II) and the polyurethane foam via nitrogen and/or oxygen as shown in Fig. 5.

The influence of ethanol (0–10%) on the sorption percentage of the compound tested was carried out by the unloaded, TMP- and TOA-loaded foams. The sorption profiles of compounds I and II by the unloaded foams are given in Fig. 6. The extraction of the compounds by the unloaded foams increased by the addition of ethanol (up to 10%) to the aqueous solution. Similar trends were also obtained with TMP-loaded foams. Dicofol and bromopropylate species in the aqueous solution are well solvated in the presence of ethanol and so it is difficult for these ions to form ion pairs in aqueous solution [24]. Thus, the solvent extraction mechanism is the most probable mechanism and the nature of the media has therefore a marked effect on the sorption characteristics of the compounds tested.

The sorption profiles of the tested species by the TOA foam are given in Fig. 7. The extraction percentage of bromopropylate decreased as compared to the unloaded foams (Fig. 6) and TMP-loaded foams by the addition of ethanol to the aqueous solution. This is probably due to the formation of lipophilic association in the aqueous solution [18]. These data are also consistent with the fact that when a compound of low dielectric constant is distributed between a phase which has a low dielectric constant and another which has a high dielectric constant, the degree of extraction should increase with increase in the polarity of the polar phase. These observations

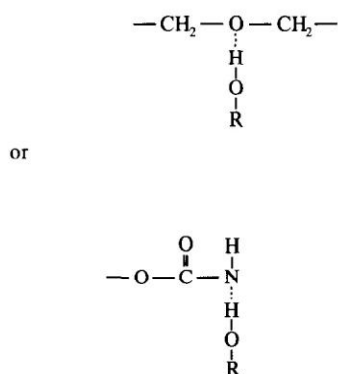


Fig. 5. R = Acaricide (I or II) structure without hydroxyl group.

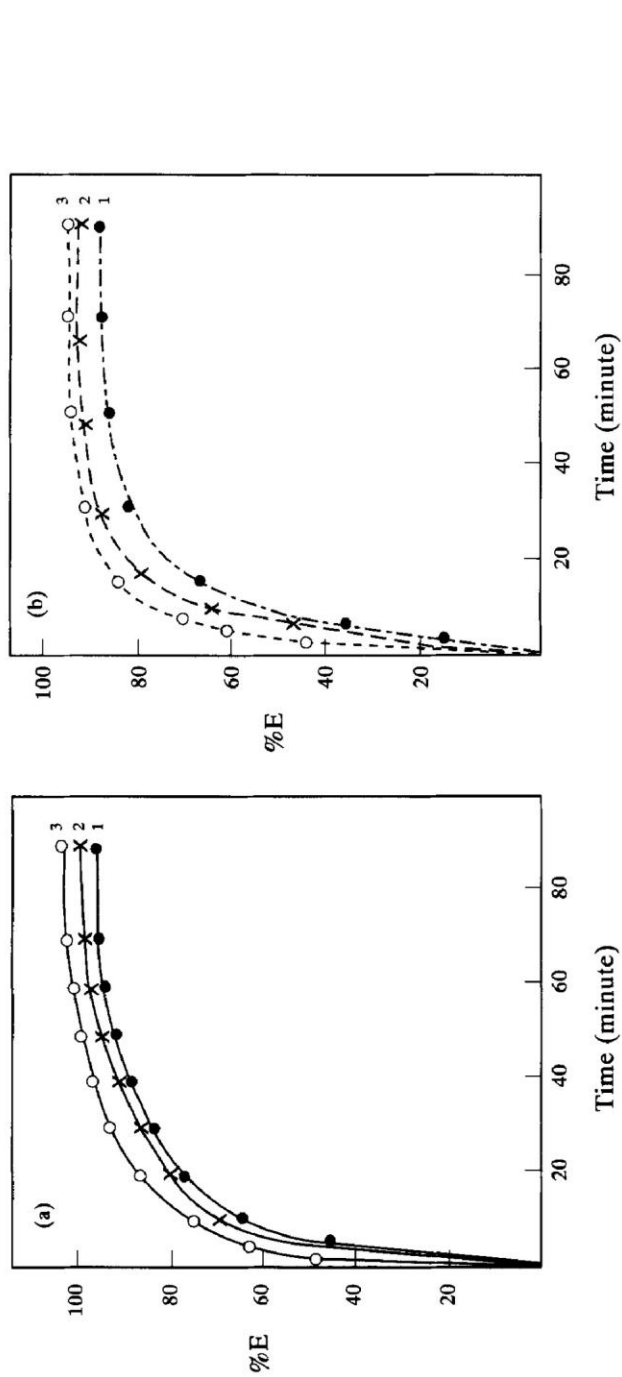


Fig. 6. Effect of ethanol on the sorption profile of dicofol (a) and bromopropylate (b) by unloaded foams, at pH 3 and 1 h extraction time. Ethanol concentrations are: 0% (1), 5% (2) and 10% (3). Other conditions as in Fig. 2.

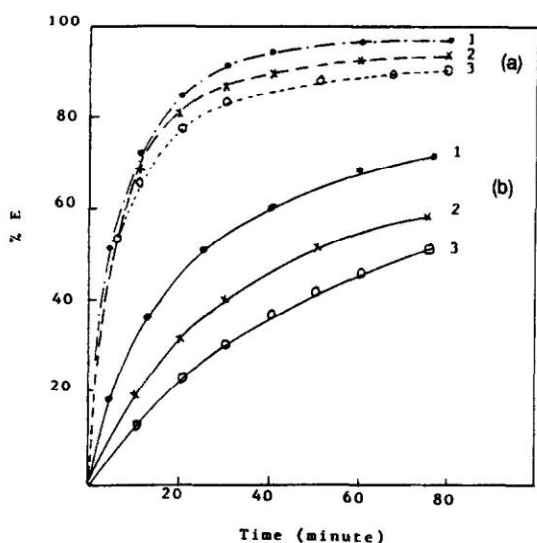


Fig. 7. Effect of ethanol on the sorption profiles of dicofol (a) and bromopropylate (b) by TOA-loaded foams, at pH 3 and 1 h extraction time. Ethanol concentrations are: 0% (1), 5% (2) and 10% (3). Other conditions as in Fig. 2.

are also consistent with a solvent-extraction mechanism.

3.3. Flow experiments

In batch experiments, the sorption behaviour of the tested acaricides from aqueous solution with the unloaded polyurethane foam suggest the possible application of the foam in the column extraction mode for quantitative collection and recovery of the tested compounds from aqueous media at $2 < \text{pH} < 3$. Distilled or tap water samples ($0.1\text{--}3 \text{ dm}^3$) con-

taining $0.01\text{--}0.1 \text{ mg}$ of each compound were percolated separately through the foam columns at a flow-rate of $15 \text{ cm}^3/\text{min}$. Complete retention (97–100%) of the tested compounds was achieved by the foam column. The compounds were then recovered from the foam with acetone in a Soxhlet apparatus. The percentage recovery of the tested compounds from the aqueous media and tap water sample by the proposed foam column method are summarized in Table 2. Satisfactory recovery percentages ($(94.2\text{--}98.4) \pm 1.8$) were obtained with standard deviations in the range $0.1\text{--}0.5$ and a correlation coefficient of 0.94 was also achieved. The proposed procedures were also employed at $0.01\text{--}0.1 \text{ mg}$ of each acaricide spiked in natural water samples ($1\text{--}3 \text{ dm}^3$) and a satisfactory recovery percentage was achieved (Table 2). The effect of flow rate and sample volume on the retention of the compounds by the unloaded foams was examined by percolating 100 cm^3 of dicofol (0.05 mg) through the column at various flow-rates ($5\text{--}25 \text{ cm}^3/\text{min}$) and sample volumes ($0.1\text{--}5 \text{ dm}^3$). Complete retention of the compound was obtained up to a flow rate of $15 \text{ cm}^3/\text{min}$ from 5 dm^3 aqueous solution. The extraction efficiency decreased significantly up to 76% at $20 \text{ cm}^3/\text{min}$ from 5 dm^3 aqueous solution. To determine the performance of the foam column by the chromatographic method [25], quantitative retention and elution of dicofol (0.01 mg) with 100 cm^3 acetone–HCl ($3:1, \text{ v/v}$) through the foam column at flow rates of $3\text{--}5 \text{ cm}^3/\text{min}$ was carried out. The height equivalent to a theoretical plate (HETP) values were found equal, 1.2 ± 0.2 and $1.3 \pm 0.2 \text{ mm}$, at flow rates of 10 and $15 \text{ cm}^3/\text{min}$, respectively. The HETP value for

Table 2

Extraction and recovery of spiked amount of the tested acaricides ($0.01\text{--}0.1 \text{ mg}$) from 3 dm^3 aqueous solution by the proposed unloaded foam column

Compound	Spiked amount (mg)	Recovery (%)			Wavelength (nm)
		a	b	c	
Dicofol	0.01	97.5 ± 1.5	95.9 ± 2	93.2 ± 1.8	248
	0.05	97.5 ± 1.6	95.1 ± 1.5	91.0 ± 1.7	
	0.1	96.5 ± 1.8	98.4 ± 1.1	93.0 ± 1.4	
Bromopropylate	0.01	97.0 ± 1.7	95 ± 2.3	95.0 ± 1.2	242
	0.05	97.6 ± 1.4	94.2 ± 1.7	96.3 ± 1.4	
	0.1	98.0 ± 1.2	93.2 ± 1.5	97.2 ± 1.7	

Average of five measurements from (a) distilled, (b) tap and (c) sea water.

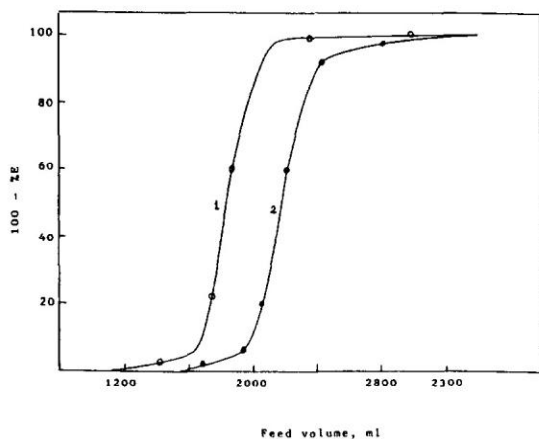


Fig. 8. Break through capacity curves of the sorption profiles of dicofol (1) and bromopropylate (2) at $10 \text{ cm}^3/\text{min}$ flow rate by unloaded foam column at $20 \pm 0.1^\circ\text{C}$.

the unloaded foam column was also calculated from the breakthrough capacity curve (Fig. 8) of dicofol and bromopropylate at $10 \text{ cm}^3 \text{ min}^{-1}$ employing the following equation [13]:

$$N = \left(\frac{V_1 V_2}{(V_1 - V_2)^2} \right) = \left(\frac{L}{\text{HETP}} \right)$$

where V_1 is the volume of effluent at the center of the S-shaped breakthrough capacity curve where the concentration is one half of the initial concentration, and V_2 is the volume at which the effluent has a concentration of 0.1578 of the initial concentration. The values of HETP obtained by this method was $1.3 \pm 0.2 \text{ mm}$, confirming the values obtained from the elution curves.

4. Conclusion

Unloaded foams in batch and column modes can be applied to trap trace amounts of acaricides from water, and the retained species can be separated with an appropriate eluent, provided that there is a sufficiently large difference in the optimum conditions of extraction of each compound. The study of the tested compounds shows that the acaricides are extracted in their neutral form by a simple solvent-extraction mechanism. This conclusion is supported by the short time required to reach extraction equilibrium

and the salting-out phenomenon. Although a simple-solvent extraction mechanism is involved, the molecular weight of the sorbate and the strong hydrogen bonding between the tested acaricides with the polyether foam have great influence on the extraction process. Moreover, the plasticization of the foam with TOA offers a wider range of modifications than normal granular solids. The foam membrane offers unique advantages in offering high flow rates, effective separations and preconcentrations of different species from fluid systems when large sample volumes are analyzed.

References

- [1] J.R.H. Malisse, *Egypt. J. Anal. Chem.*, 1 (1990) 49.
- [2] J.M. Hellowell, *Environ. Pollut.*, 50 (1988) 61; M.S.E. Abdo and R.S. Al-Ameeri, *J. Environ. Sci. Health, Part A*, 22 (1987) 27.
- [3] A.S.Y. Chan, B.K. Afghan and J.W. Robinson, *Analysis of Pesticides in Water: Significance, Principles, Techniques and Chemistry of Pesticides*, Vol. 1, CRC Press, Boca Raton, FL, 1982.
- [4] A. Agostiano, M. Caselli and M.R. Prevezano, *Water, Air, Soil Pollut.*, 19 (1983) 309; H. Konig and W. Strabel, *Fresenius' J. Anal. Chem.*, 315 (1983) 205.
- [5] C.A. Edwards, *Environmental Pollution by Pesticides*, Plenum Press, New York, 1973.
- [6] A.H. Romano and R.S. Safferman, *J. Am. Water Works Assoc.*, 55 (1963) 169, and references cited therein.
- [7] H. Oda and C. Yokoawa, *Carbon*, 21 (1983) 485.
- [8] H. Oda, M. Kishida and C. Yokokawa, *Carbon*, 19 (1981) 243.
- [9] J.F. Uthe, J. Reinke and H.D. Gesser, *Environ. Lett.*, 3 (1972) 117.
- [10] B. Ahling and S. Jensen, *Anal. Chem.*, 36 (1964) 134.
- [11] B.K. Afghan, R.J. Wilinon, A. Chow, T.W. Findley, H.D. Gesser and K.I. Srikameswaran, *Water Res.*, 18 (1984) 9.
- [12] G.J. Moody and J.D.R. Thomas, *Chromatographic Separation with Foamed Plastics and Rubbers*, Marcel Dekker, New York, 1982.
- [13] T. Braun, J.D. Navratil and A.B. Farag, *Polyurethane Foam Sorbents in Separation Science*, CRC Press, Boca Raton, FL, 1985; M.A. Ahsan, B.C. Varma, M.H. George and J.A. Barrie, *Polym. Commun.*, 32 (1991) 509.
- [14] A.B. Farag and M.S. El-Shahawi, *J. Chromatogr.*, 552 (1991) 371.
- [15] A.B. Farag, A.M. El-Wakil, M.S. El-Shahawi and M. Mashaly, *Anal. Sci.*, 5 (1989) 415.
- [16] T. Braun and A.B. Farag, *Anal. Chim. Acta*, 73 (1974) 301; L. Stewart and A. Chow, *Talanta*, 40 (1993) 1345.
- [17] M.S. El-Shahawi, A.B. Farag and M.R. Mostafa, *Sep. Sci. Technol.*, 29 (1994) 289; A.B. Farag, A.M. El-Wakil and

- M.S. El-Shahawi, *Fresenius' Z. Anal. Chem.*, 324 (1986) 59;
M.S. El-Shahawi, *Talanta*, 41 (1994) 1481, and references
cited therein.
- [18] A.W. Adamson, *Physical Chemistry of Surfaces*, 2nd edn.,
CRC press, Boca raton, FL, 1973.
- [19] A.B. Farag, M.S. Ei-Shahawi and S. Farrag, *Talanta*, 41
(1994) 617.
- [20] T. Braun, *Z. Anal. Chem.*, 333 (1989) 785; T. Braun and
A.B. Farag, *Anal. Chim. Acta*, 99 (1978) 1, and references
cited therein.
- [21] S. Palagyi and T. Braun, *J. Radioanal. Nucl. Chem.*, 163
(1992) 69.
- [22] S. Palagyi, T. Braun, Z. Homonnay and A. Vertes, *Analyst*,
117 (1992) 1537.
- [23] L. Schumack and A. Chow, *Talanta*, 34 (1987) 957; T.
Schafer and T.A. Wildman, *Can. J. Chem.*, 57 (1979) 450; T.
Schafer, R. Sebastian, R. Laatikainen and S.R. Salman, *Can.*
J. Chem., 62 (1983) 326.
- [24] T. Hayashita and M. Takagi, *Talanta*, 32 (1985) 399.
- [25] E. Glueckauf, *Trans. Faraday Soc.*, 16 (1955) 34.

Spectroscopic and electrochemical studies of chromium(III) complexes with some naturally occurring ligands containing sulphur

M.S. El-Shahawi¹

Chemistry Department, Faculty of Science, U.A.E. University, Al-Ain, P.O. Box 17551, United Arab Emirates

Received 20 March 1995; accepted in final form 24 July 1995

Abstract

Several Cr(III) complexes of L(-)cystine, L(-)cysteine, dibenzyldisulphide, α -mercaptosuccinic acid and 5,5'-dithiobisnitrobenzoic acid were prepared and characterized by their vibrational, electronic and circular dichroism measurements. The coordination of sulphur-containing amino acids involved amino and carboxylate groups. In the visible spectra, two peaks were observed at 15 900–18 700 and 23 000–25 300 cm^{-1} and were assigned to ${}^4A_{2g} \rightarrow {}^4T_{2g}$ and ${}^4A_{2g} \rightarrow {}^4T_{1g}$ (f) d–d transitions, respectively in octahedral (O_h) or pseudo-octahedral (D_3) symmetry. Three sharp Cotton effects were observed in the circular dichroism spectra of cysteine and cystine chelates and were assigned to the ${}^2E({}^2E_g)$, ${}^2A_2({}^2T_{1g})$, and ${}^2E({}^2T_{1g})$ d–d transitions. The observed Cotton effects in the allowed band arise from the splitting of ${}^4A_{2g} \rightarrow {}^4T_{2g}$ to ${}^4A_1({}^4T_{2g})$ and ${}^4E({}^4T_{2g})$ transition. The parameters D_q , B , β_{35} and the variation of interelectronic repulsion value with ionic charge, Z^* for the complexes were calculated. The magnetic moments (3.6–3.9 B.M) are close to the spin-only value for a d^3 Cr(III) ion in octahedral symmetry. Cyclic voltammetry experiments on some of the complexes revealed a reversible Cr(III)/Cr(II) redox couple and pronounced solvent and scan rate effects on the peak potentials and peak currents.

Keywords: Chromium(III) complex; Optically active ligand; Spectroscopic and electrochemical studies

1. Introduction

The interactions of sulphur-containing naturally occurring ligands and their derivatives, with transition metal ions have been the subject of great interest in recent years because of the poten-

tial use of these compounds in therapy [1,2]. Thus, a knowledge of the nature and the extent of the bonding between a metal ion and sulphur ligands is of significant importance [3]. Cr(III) or Cr(VI) reacts with many naturally occurring ligands forming several isomeric complexes due to the high affinity of Cr(III) for N, O and/or S donor atoms [3]. Therefore, the chemistry of chromium with such ligands is obviously of great importance [1,4].

¹ Permanent address: Chemistry Department, Faculty of Science, Mansoura University, Damietta, Egypt.

A chromium-containing insulin-potentiating factor was isolated and found to contain Cr(III), cysteine and glutamic acid [5]. Also, the title ligands and their coordination compounds seem to be implied in the therapeutic activity displayed by drugs containing transition metal ions or the ligand itself [6–8]. The present paper deals with the preparation and characterization of the Cr(III) complexes of some naturally occurring ligands containing sulphur. The interactions between Cr(III) and these ligands are of great importance in view of the presumed role of the Cr–S bond in the biochemical processes. These compounds are also interesting for their role as unique models in studying complex formation with various substrates.

2. Experimental

2.1. Reagents and materials

The ligands L(–)cysteine, (Cys), L(–)cystine, (Cyst); 5,5'-dithiobisnitrobenzoic acid, (Dtnb); dibenzylidysulphide, (Dbs) and α -mercaptosuccinic acid, (Msa) were of reagent grade. The complex CrCl_3Py_3 and anhydrous CrCl_3 were prepared by the methods of Taft et al. [9] and Ray [10], respectively. Cyclic voltammetric measurements were made at 10^{-3} M of the complex tested in CH_3OH or CH_2Cl_2 using tetrabutylammonium tetrafluoroborate TBA (BF_4) as supporting electrolyte.

2.2. Preparation of the complexes

To a solution of CrCl_3Py_3 (2 mmol) in dry MeOH, the appropriate weight of the ligand was added to obtain 1:1 and 1:3 chromium–ligand molar ratios. The solutions were refluxed for 4 h and the resulting coloured solutions were filtered off and reduced to 10 cm³ using a rotary evaporator. Each solid complex was redissolved in methanol and chromatographed twice on sephadex sp-25 with KI (0.1 M). The Cr(III) complex eluted as a single band and the final eluate was concentrated to a small volume and 10 cm³ ether were added. Solid precipitates were separated out

with all ligands except α -mercaptosuccinic acid and 5,5'-dithiobisnitrobenzoic acid. The precipitates were then washed with ether, cold methanol and finally dried over CaCl_2 . On adding ≈ 0.2 g of solid NH_4Cl to the cold concentrated solution of CrCl_3Py_3 with Dtnb or Msa, a green–purple precipitate separated out which was washed with ether and finally dried at 100°C. The complexes were redissolved in methanol and the purities were checked by thin layer chromatography (TLC) employing CHCl_3 – $\text{C}_2\text{H}_5\text{OH}$ (1:3 v/v) as a mobile phase and transient iodine as a detection method.

2.3. Physical measurements

The IR spectra in a KBr disk were measured with a Perkin–Elmer 487 spectrometer. The UV-visible and circular dichroism (CD) spectra were recorded with a Varian 634S spectrometer and an instrument described elsewhere [11], respectively. Magnetic measurements were made on a Johnson Matthey magnetic balance. Silica gel TLC plates (Merck 60 F₂₅₄) 10 × 20 cm were employed to check the purity of the complexes formed. Electrochemical measurements were performed with a Hi-Tek Di 2101 potentiostat in combination with a Hi-Tek digital integrator that recorded the total current.

3. Results and discussion

Interaction of Cr(III) with the title ligands was extensively investigated in view of either the role of these compounds in the reduction of toxic Cr(VI) to Cr(III)–thiol bond in the initiation of insulin action and the effectiveness of these species in the removal of chromium bound to hemoglobin [12]. The prepared complexes, their elemental analyses and their physical and chemical properties are listed in Table 1. The complexes are stable and have fairly low melting points (<190°C) which inhibited their thermal analysis. The complexes are purple, green or green-violet in colour. The magnetic moments (3.6–3.90 B.M.) are close to the calculated spin-only value (3.87 B.M.) for a d^3 octahedral Cr(III) complex with a substantially

Table 1
Analytical data, room temperature, magnetic moments (BM) and physical properties of the complexes

Complex	Calcd (found) %				Colour	M.P. (°C)	μ_{eff} (BM)
	C	H	N	Cl			
1 Cr(Cys) ₃	26.2	4.3 (25.8)	10.1 (4.4)	– (10.0)	deep violet	135	3.9
2 (Cr(Cys) ₂ Cl) ₂	21.9 (21.5)	3.6 (3.8)	8.5 (8.2)	10.8 (10.4)	violet	146	3.6
3 Cr(Cyst) ₃	28.0 (27.7)	3.9 (4.1)	10.9 (10.8)	–	green–violet	130	3.8
4 (Cr(Cyst) ₂ Cl) ₂	25.5 (25.4)	3.5 (3.7)	9.9 (9.6)	6.2 –	green–violet	136	3.75
5 Cr(Dtnb)(Cys) ₂	(34.6)	(3.1)	(7.9)	–	dark green	149	3.7
6 CrCl ₃ (Dbs) ₃	28.0 (28.3)	4.68 (4.6)	–	11.87	green	167	3.6
7 (NH ₄) ₃ [CrCl ₃ (MSa) ₃]	21.8 (21.6)	4.50 (4.6)	6.3 (6.1)	16.1 (15.7)	green	160	3.7
8 (NH ₄) ₂ [CrCl ₂ (Dtnb) ₂]	35.9 (35.4)	2.4 (2.0)	6.1 (5.7)	7.1 (7.4)	green–violet	189	3.6

⁴A₂ ground state [13]. The higher value of the magnetic moment observed for the complex Cr (Pen-H)₂Cl suggests mixing of ⁴A_{2g} with the terms derived from the excited state ⁴T_{2g}. The observed difference in the magnetic moment of such complexes was probably due to the hygroscopic nature of the complex. Nevertheless, the value is indicative of octahedral Cr(III). Antiferromagnetic exchange interactions between the Cr atoms of dinuclear complexes were lower in value [13].

The significant IR frequencies of the complexes with relevant bands of the free ligands (in brackets) are given in Table 2. The bands were assigned by comparison to those of the free ligands and related complexes [3,14]. Displacements of the COO[–] antisymmetric stretches to higher wavenumbers (20–70 cm^{–1}) were observed, indicating that the carboxylate groups of the ligands were involved in the coordination [9]. The absorption bands corresponding to the antisymmetric NH₂ stretches of the tested amino acids, L(–)cystine and L(–)cysteine, were shifted to lower wave numbers on forming a coordinated bond with Cr(III). Therefore, in the amino acid complexes, the amino group participates in the formation of Cr–N bond. The coordination of the amino group was also confirmed via the bending $\delta(\text{NH}_2)$

and the twisting $\rho_t(\text{NH}_2)$ vibrations of the complexes. The $\delta(\text{NH}_2)$ and the $\rho_t(\text{NH}_2)$ vibrations were shifted from 1505–1540 and 1120 cm^{–1} to 1570–1580 and 1200 cm^{–1} respectively, confirming the participation of the nitrogen atom of the amino group of the ligand in the coordination with Cr(III) [15].

The stretching vibration mode expected for SH (usually seen at 2500 cm^{–1}) was not observed, however, a well-resolved peak was observed at 523 cm^{–1}, the region in which the S–S stretch might be expected [15]. In the complex Cr(Dtnb)(Cys)₂, prepared by refluxing Cr(III)–Dtnb–Cys in 1:1:1 molar ratios, the coordination of Dtnb was difficult to determine with certainty. However, the two observed bands at 1670 (as) and 1390 (s) cm^{–1} and the band found at 1270 cm^{–1} suggest possible coordination of Dtnb via carboxylate and sulphur [3,16]. Also, in the Cr(III)–Dtnb complex eight similar shifts were observed in the IR spectra indicating coordination of Dtnb to Cr(III) via carboxylate and sulphur [16]. In the free dibenzylsulphide (Dbs) ligand, the observed band at 1275 cm^{–1} was shifted to 1370 cm^{–1} in the Cr(III) complex confirming coordination of Dbs via sulphur. In the complexes 6–8, the chlorine atoms were possibly located in

Table 2
Significant IR frequencies (cm^{-1}) of the complexes with relevant bands of the free ligands in brackets

Complex	$\nu_{\text{as}}(\text{COO}^-)$	$\nu_{\text{s}}(\text{COO}^-)$	$\Delta\nu$	$\nu(\text{NH}_2)$	$\nu(\text{SH})$	$\nu(\text{Cr-Cl})$
1	1640 (1590)	1380 (1450)	260 (140)	3160 (3180)	not visible (2550)	
2	1650	1390	280	3240	2555	390, 350, 270
3	1640 (1600)	1410 (1380)	230 (220)	not visible (3450)		
4	1650	1400	250	3420		370, 340, 300
5	1640, 1670 (1610)	1410, 1390 (1450, 1420)	230 (240)	3240	2560 (2550)	
6	–	–	–	–	–	380, 320
7	1640 (1610)	1400 (1360)	240 (250)	–	not visible	360, 290
8	1680 (1590)	1390 (1350)	290 (240)	–		410, 340

the remaining coordinating sites of chromium and no suggestion can be made from the IR spectra concerning the chloride position, because the two Cr–Cl vibrations split differently in these complexes. However, it seems reasonable to assume that the trans disposition of the ligands is a steric requirement for such vibrations. In the region 270–410 cm^{-1} two $\nu(\text{Cr-Cl})$ vibrational modes were observed for the complexes 6–8, while three $\nu(\text{Cr-Cl})$ modes of vibration were found in the spectra of the complexes 2 and 4 suggesting C_{3v} and D_{2v} local symmetry of the ligand atoms around Cr(III) [17], respectively. The observed bands in the far IR region 570–200 cm^{-1} were tentatively assigned to mixed $\nu(\text{Cr-Cl})$, $\nu(\text{Cr-O})$, $\nu(\text{Cr-S})$ and/or $\nu(\text{Cr-Cl})$ vibrations [18].

It is not clear from the elemental analysis and the IR spectra of the complexes (2, 4 and 8) whether these data arise from one complex species or a mixture of different complex species in methanol. Therefore TLC plates with transient iodine as detector were used and confirmed that only one complex species is present in each solution of these complexes in methanol. The lability of the pyridine ligands and the ease of formation of chloride bridges leads to aggregation [2]. Thus, it seems reasonable to presume a structure such as **I** for the complexes 2 and 4 and **II** or **III** for the complex 8 as shown in Fig. 1.

The electronic spectra of the complexes are summarized in Table 3. Two peaks were observed

in the ranges 15 900–18 700 and 23 000–25 300 cm^{-1} and were assigned to $\nu_1: {}^4A_{2g} \rightarrow {}^4T_{2g}$ and $\nu_2: {}^4A_{2g} \rightarrow {}^4T_{1g}(f)$ d–d transitions in octahedral symmetry [19], respectively. The ν_2/ν_1 data were consistent with those of other trivalent Cr(III) complexes containing N, O and/or chlorine [3,19]. A charge transfer band overlaps the $\nu_2({}^4A_{2g} \rightarrow {}^4T_{1g}(f))$ band and totally obscures the $\nu_3({}^4A_{2g} \rightarrow {}^4T_{1g}(p))$ band in the UV spectra of Dtnb– and Dbs–Cr(III) complexes. In the complexes 1, 3, 4, the forbidden transition ν_2 at 23 000–23 500 cm^{-1} gave a higher absorption coefficient than the allowed band transition ν_1 at 16 400–17 300 cm^{-1} (Fig. 2) suggesting symmetry reduction of these complex species [19,20]. This also led one to assume that the coordination of these complexes is not trans with respect to nitrogen or oxygen of the ligand. The formation of a S–Cr(III) bond is usually characterized by an intense S–Cr charge transfer transition at ≈ 250 nm [19], such an absorption band was not observed in the electronic spectra of the prepared complexes suggesting no coordination via a sulphur site of the tested ligands.

The parameters, D_q , B, and β_{35} are given in Table 3. The D_q values were observed in the range 1587–1869 cm^{-1} and were far closer to the chloride ion value ($D_q = 1318$ cm^{-1} for CrCl_6 and $D_q = 2190$ cm^{-1} for CrN_6 [19]) and place the ligands in the central range of the spectrochemical series. These data also provide strong evidence

Table 3

Electronic spectra (cm^{-1}) and circular dichroism (nm) data of the prepared complexes in methanol with ligand field parameters^a

Complex No.	${}^4A_{2g} - {}^4T_{2g}$ $\nu_1 \times 10^3$ (log ϵ)	${}^4A_{2g} - {}^4T_{1g(f)}$ $\nu_2 \times 10^3$ (log ϵ)	${}^4A_{2g} - {}^4T_{1g(p)}$ $\nu_3 \times 10^3$ (log ϵ)	D_q	B	β_{35}	CD(nm)
1	17.3 (1.60)	23.5 (1.70)	31.3 (2.1)	1733	600	0.65	350(+), 459(-), 536(+), 522(+), 590(-)
2	18.7 (1.57)	25.3 (1.53)	31.30 (1.9)	1869	639	0.69	360(+), 480(-), 498(-), 570(-), 590(-, s)
3	16.4 (1.64)	23.0 (1.66)	28.6 (1.94)	1639	660	0.71	380(+), 435(-), 540(+), 550(+), 595(-)
4	17.1 (1.57)	23.5 (1.73)	–	1709	631	0.68	380(+), 450(-), 460(-), 580(+)
5	16.70 (1.65)	23.8 (1.62)	31.3 (1.92)	1666	732	0.80	480(-), 520(+), 620(-)
6	16.1 (1.52)	23.3 (1.49)	–	1612	740	0.79	
7	17.2 (1.73)	23.0 (1.71)	31.4 (2.10)	1724	547	0.59	
8	15.9 (1.79)	23.3 (1.72)	–	1587	786	0.85	

^a Logarithm extinction coefficient ($1 \text{ mol}^{-1} \text{ cm}^{-1}$) of the complexes is given in parentheses. (B for Cr(III) ion is 918 cm^{-1} .)

transient iodine detection confirmed the occurrence of only one complex species in solution. Thus, the observed splitting is primarily due to the two ions present with symmetry splitting superimposed. The optically active complexes formed are likely to be *fac* since stronger and better defined Cotton effects were observed in the CD spectra of the amino acid Cr(III) chelate [19].

The CD spectral patterns of the complexes (1–3) are similar to those of Λ -tris (ethylenediamine) chromium(III) complexes in the spin forbidden transition region in O_h symmetry [19,24] where three CD bands were observed. The lowest and the highest frequency CD bands are of opposite sign to the central one (Fig. 3). On the basis of the CD dominance in the first spin-allowed band region of the O_h complexes (1–3), one may conclude that the absolute configuration of these complexes is similar to those of bis(oxalato) complexes with the (Δ - Δ) configuration enforced by stereospecificity [24]. Therefore, the evident similarity of the CD patterns of the complexes (1–3), Cr(en)_3 [24] and $[\text{Cr}(\text{OX})(\text{Phen})_2]^+$ is possibly due to a kind of configurational dissymmetry rather than the vicinal effect of the coordinated amino acid ligand.

Assuming that the prepared complexes belong to O_h , or pseudo D_3 symmetry, the three sharp peaks observed at 350–380(+), 425–480(-), and 498–540(+) nm are safely assigned to the ${}^2E({}^2E_g)$, ${}^2A_2({}^2T_{1g})$ and ${}^2E({}^2T_{1g})$ in the region corresponding to the spin-forbidden transitions from the lower frequency side [19,24]. The two CD bands on the higher-frequency side (Table 3) are ascribed to the ${}^4A_2({}^2T_1)$ and are of opposite signs which precludes assigning them to the ($2\bar{A}$, \bar{E}_b) and E_a components of the 2T_1 state for which the rotational strengths are proportional to the net rotational strength for the first spin allowed ${}^4A_2({}^4T_{2g})$ transitions [2,24]. The assignment to (\bar{E}_a, \bar{E}_b) and $2\bar{A}$ or to \bar{E}_b and ($2\bar{A}$, \bar{E}_a) accounts for the CD signs of the observed bands. This assignment is made because the rotational strengths of the (\bar{E}_a, \bar{E}_b) and $2\bar{A}$ or the \bar{E}_b and ($2\bar{A}$, \bar{E}_a) components are expected to be of opposite signs since $R({}^4A_1)$ contributes to $R(\bar{E}_a, \bar{E}_b)$ and $R(\bar{E}_b)$ and also because the rotational strength for the ${}^4A_2({}^4E)$ transition, which contributes largely to $R(2\bar{A})$ and $R(\bar{E}_a)$ should have a sign opposite to that of $R({}^4A_1)$ as given in Table 3 [19,24]. The transition energy of the lowest frequency CD peak agrees well with those of the absorption spectra (Table 3). The lowest frequency CD band of

positive sign in the spin-forbidden transition region is safely assigned to the 2E components (\bar{E} , $2\bar{A}$). Thus the CD band due to the ${}^4A_2({}^2E)$ transition should be of same sign as the major CD band in the first spin-allowed ${}^4A_{2g}({}^4T_{2g})$. The

observed Cotton effects at 552–580 (+) and 590–630 (–) nm were safely assigned to the splitting of the ${}^4A_{2g}({}^4T_{2g})$ to ${}^4A_1({}^4T_{2g})$ and ${}^4E({}^4T_{2g})$ d–d transitions in trigonal symmetry [19,24]. An energy splitting pattern for these transitions in d^3 in O_h , D_3 and D_3' symmetry is previously reported by Lever [19] and Kaizaki et al. [24].

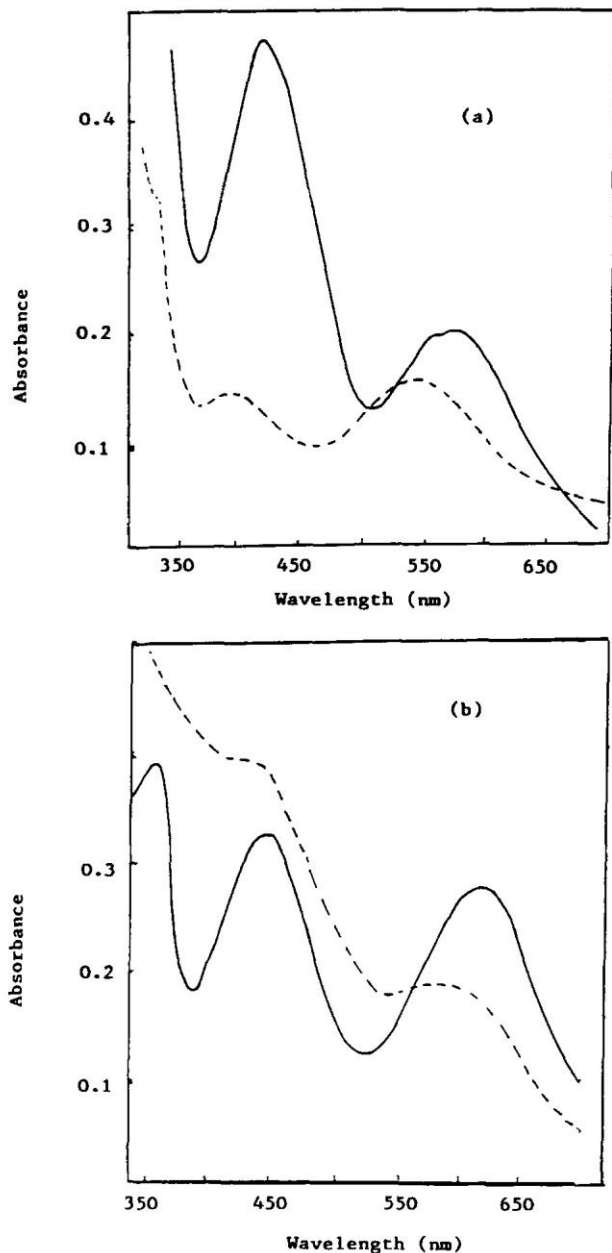
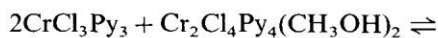
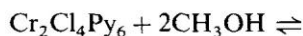


Fig. 2. Electronic spectra of (a) $\text{Cr}(\text{Cys})_3$, — and $[\text{Cr}(\text{Cys})_2\text{Cl}]_2$, ---- and (b) $\text{Cr}(\text{Cyst})_3$, — and $[\text{Cr}(\text{Cyst})_2\text{Cl}]_2$, ----.

4. Cyclic voltammetry

The CVs of the complex CrCl_3Py_3 in $\text{CH}_3\text{OH}-\text{TBA}(\text{BF}_4)$ and in $\text{CH}_2\text{Cl}_2-\text{TBA}(\text{BF}_4)$ are shown in Fig. 4. In $\text{CH}_3\text{OH}-\text{TBA}(\text{BF}_4)$ the voltammogram shows two electrode couples with $E^0 = 0.770$ and -0.460 V (average of the anodic and cathodic potential peaks) and $\Delta E_p = 0.062$ and 0.820 V vs SCE, respectively. Controlled potential electrolysis (CPE) at 0.9 and -0.55 V vs SCE showed an indication of one electron transfer for each electrode couple. Thus, these two electrode couples were tentatively assigned to $\text{Cr}(\text{III}) \rightleftharpoons \text{Cr}(\text{II})$ and $\text{Cr}(\text{II}) \rightarrow \text{Cr}(\text{I})$, respectively. The ratio of the peak currents i_c/i_a which should be 1.0 at all scan rates used and peak separation ΔE_p were decreased with decreasing scan rate from 1000 to 10 mV s^{-1} . The results suggest the occurrence of a slow chemical reaction similar to that found for related complexes [25], following the electrode process which removes the electrode reaction products before they can be reduced on the reverse scan or the species that initially formed in the electrode processes react further to give products that were not reoxidized at the same potential as the first formed species [25]. A reaction mechanism which would account for this behaviour in methanol has been proposed previously for the tris(phen) chromium(III) complex [25]. A possible mechanism is



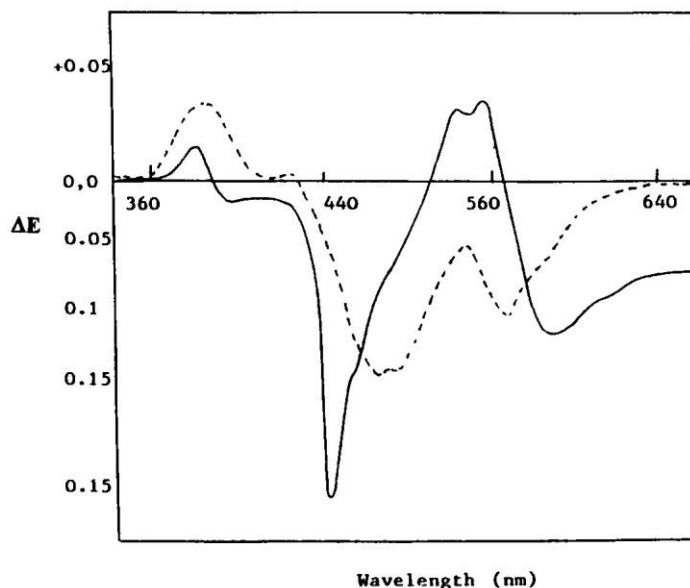


Fig. 3. CD spectra of $\text{Cr}(\text{Cyst})_3$, —, and $[\text{Cr}(\text{Cyst})_2\text{Cl}]_2$, ----.

In $\text{CH}_2\text{Cl}_2\text{-TBA}(\text{BF}_4)$, two irreversible electrode couples were observed with $E^0 = 0.48$ and $+0.8$ V and an ill-defined electrode couple with $E^0 = -0.66$ V vs SCE at 50 mV s^{-1} for the complex CrCl_3Py_3 . CPE at 0.85, 0.52 and -0.7 V vs SCE was not successful because of the low solubility of the complex in this solvent. The results emphasise the different substitution reactions of CrCl_3Py_3 in the two solvents. The donor-acceptor properties of both solvents, liquid-junction potentials and the extent of ionpairing of the BF_4^- in both solvents [26] or a combination of all of these to a different degree may account for this behaviour. The ion-pairing decreases with an increase in the dielectric constant and is quite significant for the Cr(I) state [27].

The CV of the complex $\text{Cr}(\text{Cys})_3$ in $\text{CH}_3\text{OH}-(\text{BF}_4)$ showed three electrode couples with $E^0 = 0.86$, -0.07 and -0.7 V vs SCE and $\Delta E_p = 0.06$, 1.06 and 0.6 V at 20 mV s^{-1} . CPE at E^0 for each electrode couple showed an evidence of one electron transfer for each couple. Thus, these electrode couples are assigned to Cr(III)/Cr(II), Cr(II)/Cr(I) and Cr(I)/Cr⁰, respectively. A slight decrease in E^0 for the couple Cr(III)/Cr(II) was found at 50 mV s^{-1} ($E^0 = 0.83$ V vs SCE),

possibly due to the increase of the influence of the ion-pairing effects with increasing charge [27].

5. Conclusions

According to the reported data, it can be concluded that all sides of the sulphur containing ligands can be potential σ -donor bases in the reaction conditions described here. However, all the tested amino acids showed no coordination of sulphur sites. The stable coordination of sulphur sites requires both σ donor and d_π acceptor behaviour of sulphur. Hence it can be suggested that the Cr-S bond needs a high electron density on the metal to be stable. The two bulky phenyl groups in the Dbs and Dtnb ligands increase the back donor effect of sulphur, making chromium able to supply the electron density required for the back-donation to sulphur. Therefore, the coordinating behaviour of Dbs and Dtnb was different from that of cysteine, cystine and α -mercaptosuccinic acid. In the cysteine, cystine and mercaptosuccinic acid derivatives, chlorine successfully competes with sulphur for the coordination to Cr(III) in the non-aqueous media. The

toxicity of most Cr(III) complexes appears to be low and chromium in this oxidation state may be required as a trace nutrient [28]. Cr(III) complexes of the title ligands may be important in the excretion of chromium by animals treated with chromate.

Acknowledgements

The author thanks Professors D.H. Brown and W.E. Smith for the helpful discussions and the facilities provided for carrying out the CD spectra.

References

- [1] H. Sigel, *Metal Ions in Biological Systems*, Dekker, New York, 1979; P. O'Brien and G. Wang, *Polyhedron*, 12 (1993) 1409; P. O'Brien and G. Wang, *Environ. Geochem.*, 11 (1989) 75; P. O'Brien and Z. Ozolins, *Inorg. Chim. Acta*, 161 (1989) 261.
- [2] M.S. El-Shahawi, *Trans. Metal Chem.*, 18 (1993) 385.
- [3] M. Freni, A. Gervasini, P. Romiti, T. Beringhelli and F. Morazzoni, *Spectrochim. Acta Part A*, 39 (1983) 85; P. O'Brien, Z. Ozolins and G. Wang, *Inorg. Chim. Acta*, 166 (1989) 301.
- [4] M.S. El-Shahawi and S.E. Ghazy, *Trans. Metal Chem.*, 17 (1992) 541; M.S. El-Shahawi and A.A. El-Bindary, *Z. Naturforsch.*, 48b (1993) 282; P. O'Brien, J. Pratt, F.J. Swanson, P. Thornton and G. Wang, *Inorg. Chim. Acta*, 169 (1990) 265.
- [5] W. Mertz and K. Schwarz, *Am. J. Physiol.*, 196 (1959) 614.
- [6] C.A. Green, N. Koline, J.I. Legg and R.D. Willett, *Inorg. Chim. Acta* 176 (1990) 82.
- [7] D.H. Brown, G.C. Mckinley and W.E. Smith, *J. Chem. Soc. Dalton Trans.*, (1978) 199.
- [8] J. Peisach and W.E. Blumberg, *Molec. Pharmacol.*, 5 (1969) 200.
- [9] J.C. Taft and M.M. Jones, *Inorg. Synth.*, 7 (1963) 132.
- [10] A.R. Ray, *Inorg. Synth.*, 5 (1957) 154.
- [11] D.H. Brown, G.C. Mchlnay and W.E. Smith, *J. Chem. Soc. Dalton Trans.*, (1978) 1874.
- [12] R.A. Anderson and W. Mertz, *Trends Biochem. Sci.*, 2 (1977) 277.
- [13] C. Preti and G. Tosi, *J. Inorg. Nucl. Chem.*, 38 (1976) 1125, D.J. Hodgson, in R. D. Willet, D. Gatteschi and O. Kahn (Eds.), *Magneto-structural Corrections in Exchange Coupled Systems*, Reidel, Dordrecht, 1985, p. 497.
- [14] P.E. Hoggard, *Inorg. Chem.*, 20 (1981) 415.
- [15] J.R. Kincaid and K. Nakamoto, *Spectrochim. Acta Part A*, 32 (1976) 277; G. Socrates, *Infrared Characteristic Group Frequencies*, Wiley, Chichester, 1980.
- [16] M.C. Baird, C. Hartwell and G. Wilkinson, *J. Chem. Soc. A*, (1967) 2037; J.D. Gilbert, M.C. Baird and G. Wilkinson, *J. Chem. Soc. A*, (1968) 2198.
- [17] R.J.H. Clark and C.S. Williams, *Inorg. Chem.*, 4 (1965) 350.
- [18] L.J. Bellamy, *The Infrared Spectra of Complex Molecules*, Chapman and Hall, London, 1975.

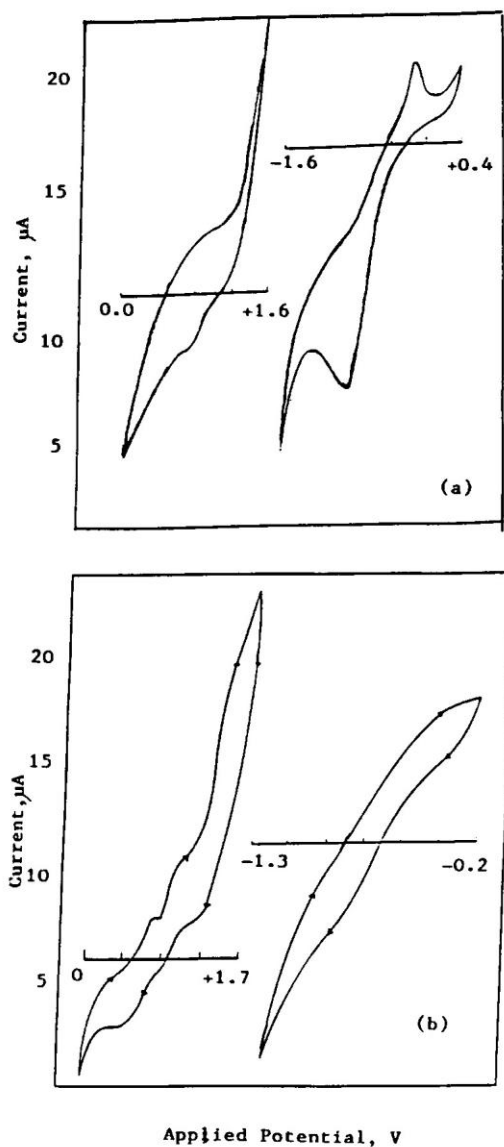


Fig. 4. Cyclic voltammogram of CrCl_3Py_3 in (a) $\text{CH}_3\text{OH}-\text{TBA}(\text{BF}_4)$ and (b) CrCl_3Py_3 in $\text{CH}_2\text{Cl}_2-\text{TBA}(\text{BF}_4)$.

- [19] A.B.P. Lever, *Inorganic Electronic Spectroscopy*, Elsevier, New York, 1968; M. Abdullah, J. Barrett and P. O'Brien, *J. Chem. Soc. Dalton Trans.*, (1985) 2085.
- [20] T. Bruer, *Helv. Chim. Acta*, 46 (1963) 2389.
- [21] D. Sutton, *Electronic Spectra of Transition Metal Complexes*, McGraw-Hill, London, 1968.
- [22] C.K. Jorgenson, *Acta Chim. Scand.*, 10 (1956) 500.
- [23] H. Oki and K. Otsuks, *Bull. Chem. Soc. Jpn*, 49 (1976) 1841; J.A. Cooper, L.F. Blackwell and P.D. Buckley, *Inorg. Chim. Acta*, 92 (1984) 23.
- [24] S. Kaizaki, J. Hidaka and Y. Shimura, *Inorg. Chem.*, 12 (1973) 142; S. Kaizaki, M. Ito, M. Nishimura and Y. Matsushita, *Inorg. Chem.*, 24 (1985) 2080; S. Sugano, *J. Chem. Phys.*, 33 (1960) 1883.
- [25] M.C. Huges and D.J. Macero, *Inorg. Chem.* 3 (1974) 2739.
- [26] D.A. Bohling, J.F. Evans, and K.R. Mann, *Inorg. Chem.*, 21 (1982) 3547.
- [27] V. Gutman, *The Donor–Acceptor to Molecular Interaction*, Plenum Press, New York, 1978.
- [28] L. Marincic, J.S. Soeldner, C.K. Cotton, J. Giner and S. Morris, *J. Electrochem. Soc.*, 126 (1979) 43.

Chemical amplification methods for the sequential determination of trace amounts of ruthenium by titrimetric and spectrophotometric procedures

M.S. El-Shahawi ^{a,*}, S.A. Barakat ^b

^a Department of Chemistry, Faculty of Science, UAE University, Al-Ain, P.O. Box 17551, United Arab Emirates

^b Department of Chemistry, Jordan University of Science and Technology, Irbid, P.O. Box 3030, Jordan

Received 13 May 1994; revised 13 March 1995; accepted 19 April 1995

Abstract

Two simple, inexpensive and rapid iodometric and spectrophotometric procedures were developed for trace amount determination of ruthenium. The proposed methods were based on the oxidation of ruthenium(II or III) with sodium periodate at pH 2.4–3.6, masking the excess periodate with sodium molybdate. The released iodate was then allowed to react with KI at pH 3, with subsequent determination of the released iodine spectrophotometry as triiodide at 350 nm or iodometry with 0.005 M sodium thiosulphate. This procedure offers an 18- and 15-fold amplification per Ru(II) or Ru(III) ion, respectively. Alternatively, the produced iodine was extracted with CHCl_3 , shaken with an aqueous solution of sodium sulphite and the produced iodide ion was then allowed to react with bromine (or sodium periodate). The released iodate was subsequently determined by iodometry or spectrophotometry after addition of KI. The bromine and sodium periodate oxidation procedures offered 90- and 360-fold amplification per ruthenium(III) ion, and 108- and 432-fold amplification per ruthenium(II) ion. Ruthenium(IV) content was determined by these procedures after prior reduction to Ru(III) with sulphurous acid. The binary mixtures Ru(II)–Ru(III); Ru(III)–Ru(IV) and Ru(II)–Ru(IV) in aqueous solution at concentration $0.05 \mu\text{g ml}^{-1}$ were successfully analyzed by the developed procedures. The utility of the proposed methods for the analysis of ruthenium in its complexes was demonstrated. Natural seawater and seawater spiked with ruthenium were analyzed satisfactorily.

Keywords: Ruthenium; Iodometry; Spectrophotometry; Trace analysis; Natural water

1. Introduction

Compared to most other elements, ruthenium has a limited influence on the biosphere because only small quantities ever reach living organisms [1]. The amount of ruthenium readily introduced into rivers, lakes and oceans through industrial wastes is minute [1]. Thus, sensitive, reliable and practicable methods are required for the quantitation of ruthenium at trace levels.

The most common reported spectrophotometric procedures for ruthenium determination require laborious enrichment steps [2–6], e.g. flotation, precipitation and solvent extraction. However, most of these methods suffer from lack of selectivity and sensitivity [3–5].

Recently, several polarographic and voltammetric methods have been developed for the determination of ruthenium [7–10]. These methods were based on adsorptive collection of ruthenium(III) chelates on HMDE, but neither their sensitivity nor selectivity are very satisfactory and they are not practicable in routine analysis of ruthenium.

* Corresponding author. On leave from the Chemistry Department, Faculty of Science at Damiatta, Mansoura University, Mansoura, Egypt.

Recently, the application of the so-called Leipert amplification reaction [11] was reported, in which potassium periodate solution in aqueous acidic media was used for the oxidation of various metal ions [12–15] and the produced iodate was subsequently determined by iodometry. The present paper describes two simple and accurate amplification procedures for the measurement of trace levels of ruthenium in aqueous solution.

2. Experimental

2.1. Reagents and materials

Unless otherwise specified, all reagents were of analytical reagent grade. All solutions were prepared from doubly-distilled water. Stock solutions (1 mg ml^{-1}) of ruthenium(III) (atomic absorption standard, BDH) and 100 mg ml^{-1} of Ru(V) were prepared from ruthenium dioxide [16] and diluted with water for standard addition whenever required. Ruthenium(II) solution ($100 \text{ } \mu\text{g ml}^{-1}$) was prepared by the reduction of a measured solution of $\text{RuCl}_3 \cdot 6\text{H}_2\text{O}$ (Johnson Mathey, London) in $\text{HCl-H}_2\text{O}$ (1:20, v/v) as previously reported [17]. Buffer solutions of pH 2.4–4.6 were prepared by mixing about 200 ml of glacial acetic acid with approximately 200 ml of water and the pH adjusted with a saturated solution of sodium acetate. Sodium thiosulphate (0.005–0.01 M) was prepared and standardized against KIO_3 (0.01 M) of the same normality. Sodium periodate (0.35% w/v), sodium molybdate (10% w/v) and sodium sulphite (5% w/v) solutions were prepared in doubly-distilled water.

2.2. Apparatus

A Pye-Unicam double beam UV/visible spectrometer model Sp-8-400 with 10 mm quartz cells was used for the absorbance measurements. A Philips digital pH-meter (model 9418) with glass and saturated calomel electrodes, and a 250 ml oxygen-flask with fused silica sample holder were used.

2.3. Recommended procedure

I. Determination of ruthenium(II) or (III)

To a 100 ml conical flask (or 100 ml separating funnel) was transferred 1–5 ml of sample

solution containing 5–200 mg of Ru(II) or Ru(III) solution and 10 ml of water. The pH (2.4–3.6) of the solution was adjusted with 10 ml acetate buffer, 5 ml of sodium periodate added and the reaction mixture left for 5 min. Na_2MoO_4 (5 ml) was added to mask the unreacted periodate and the solution shaken twice with 10 ml (2×5) of CCl_4 . The aqueous layer was separated and then treated by one of the following procedures.

(a) 18- or 15-fold amplification. To the aqueous solution of the produced iodate was added a few crystals of KI at $\text{pH} \approx 3$, and the released iodine was determined by spectrophotometry as triiodide at 350 nm or by iodometry with 0.005 M $\text{Na}_2\text{S}_2\text{O}_3$. These procedures offer 18- and 15-fold amplification of Ru(II) and Ru(III), respectively. A blank was run for correction.

(b) 108- or 90-fold amplification. The aqueous solution of the released iodate was allowed to react with KI (50–70 mg) at pH 3 and the released iodine twice extracted with 10 ml (2×5) of CHCl_3 in a separating funnel. The chloroform solution was shaken with 25 ml of water containing 2 ml of sodium sulphite to reduce the iodine to iodide. The aqueous (upper) layer was transferred to a 100 ml Erlenmeyer flask, 5 ml of bromine added, and the solution left for 3–5 min. The excess bromine was removed by boiling off the solution or by drop-wise addition of formic acid. Five millilitres of 2N H_2SO_4 , and three to four crystals of KI were added and the released iodine determined by spectrophotometry or iodometry, as described earlier. A blank was run to correct the reagent error. This procedure offers 108- and 90-fold amplification of Ru(II) and Ru(III), respectively.

(c) 432- or 360-fold amplification. To the aqueous solution of the produced iodide was added 5 ml of NaIO_4 , the flask stoppered, and the reaction mixture allowed to stand for 5 min at room temperature. The flask was placed in a boiling water bath for about 15 min, allowed to cool and then 10 ml of acetate buffer, 5 ml of Na_2MoO_4 , three to four crystals of KI ($\approx 0.1 \text{ g}$) were added and the released iodine determined by spectrophotometry or by iodometry; a blank was run for correction.

II. Determination of ruthenium(IV)

Aliquot portions (1–100 μg) of the ruthenium(IV) element were transferred to a 100 ml conical flask. Five millilitres of Na_2SO_3 and 5 ml of HCl (20% w/v) were added and the reaction mixture left to stand for 5 min.

The solution was evaporated gently on a hot plate until the excess SO_2 was completely removed, and then 20 ml of H_2O and 0.5 g of Na_2CO_3 were added to neutralize the unreacted acid; the produced ruthenium(III) was determined using the recommended procedure I. A blank was run for correction. Quantitative reduction of Ru(IV) to Ru(III) was confirmed by determining the content of the ruthenium(III) produced colorimetrically [18].

III. Analysis of the binary mixtures ruthenium(II) and (III)

Aliquots of the mixture were transferred into a 100 ml flask and the recommended procedure I-a followed. Another aliquot of sample mixture was reduced to the divalent ruthenium as previously reported [17] and procedure I-a followed. On the basis of the proposed procedure, if the volume of the sodium thiosulphate consumed in the first solution is V_1 ml and for the second solution is V_2 ml, the concentration of Ru(II) and Ru(III) can be obtained.

IV. Analysis of binary mixture ruthenium(III) and (IV)

Aliquots containing various amounts of ruthenium(III) and (IV) were transferred into a 100 ml conical flask and the described procedure I-a followed. Another aliquot sample was then reduced to the trivalent ruthenium as described in procedure II and the solution determined according to procedure I-a. According to the proposed procedure, if the volume of thiosulphate solution consumed for the first aliquot mixture is V_1 ml and that used for titration of the second aliquot mixture is V_2 ml, the concentration of Ru(III) and Ru(IV) can be obtained.

V. Analysis of ruthenium(II) or (III) in their complexes

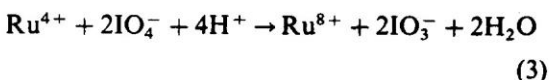
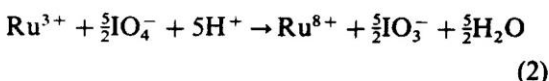
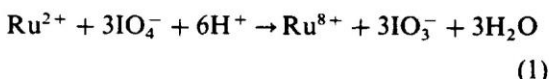
The ruthenium complexes used in this work were prepared by the previously reported [19,20] procedures. Exactly 2–3 mg of the organoruthenium complexes was weighted and wrapped as usual by the Schoniger technique [21] in a 250 ml oxygen-flask filled with a fused silica spiral. Ten millilitres of aquaregia was

placed in a 250 ml oxygen-flask, the flask filled with oxygen and the sample combusted. When the combustion was complete, the flask was shaken for 2–3 min, opened and the stopper and the sample holder rinsed down with 5 ml of HNO_3 (5% v/v). The solution was heated to dryness and 10 ml of H_2O , 2 ml of conc. HCl and 10 ml of Na_2SO_3 added. The solution was left for 2 min at room temperature. It was then boiled to remove SO_2 , and reduced with hydroxylamine as previously reported [17], finally the recommended procedure I-a was followed for ruthenium(II) determination. A blank was run for corrections.

3. Results and discussion

Amplification reactions proved to be very efficient for the determination of analytes at low levels [12–15]. Thus iodometric amplification procedures with their simplicity and sensitivity are still of special attraction. This motivated us to search for new procedures for the determination and speciation of microamounts of various ruthenium species with the use of iodine–starch end point or spectrophotometry of the released iodine as triiodide at 350 nm.

Amplification procedures based on oxidation with sodium periodate are extendable to any species possessing two oxidation states with sufficiently low standard redox potential. Thus, the proposed procedures for ruthenium(II), (III) or (IV) determination were principally based on oxidation of these ions in acid media to octavalent ruthenium with sodium periodate according to the following equations:



The released iodate and ruthenium(VIII) can oxidize potassium iodide according to the equations

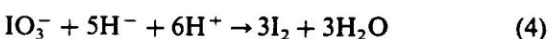


Table 1

Determination of various amounts of Ru²⁺ (or Ru³⁺) by iodometry (a) and spectrometry (b) using the 18-fold (or 15-fold) amplification procedures ^a

Metal ion taken (μg)	Metal ion found (μg)		Error (%) ^b	
	a	b	a	b
5	5.2 ± 0.2	5.1 ± 0.2	4	2
10	10.1 ± 0.3	10.1 ± 0.3	1	1
20	20.3 ± 0.3	20.2 ± 0.2	1.5	1
50	51.1 ± 0.3	50.3 ± 0.3	2.2	0.6
75	76.1 ± 0.5	75.6 ± 0.3	2.1	0.8
100	101.4 ± 0.5	101 ± 0.3	1.5	1
150	152 ± 0.3	152 ± 0.2	1.3	1.3
200	203 ± 0.2	202 ± 0.3	1.5	1.0

^a Average ± standard deviation ($n = 5$).

^b Error % = [(metal taken - metal found) × 100] / (metal taken).

Reactions (1)–(4) proceeded rapidly and quantitatively in acidic media (pH < 4) as can be predicted from the redox potential concerned [15]. Moreover, reaction (5) took place and proceeded forwards in acidic medium, i.e. ruthenium(VIII) liberated iodine from KI. This statement is criticized in this work, where preliminary experiments showed that the Ru(VIII)–I reaction was a function of the solution pH and the reaction was quite negligible in the solution of pH > 2.4, while in 2N H₂SO₄ it took place faster and proceeded quantitatively.

Further preliminary experiments showed that the oxidation of ruthenium(II), (III) or (IV) with sodium periodate was pH and reaction time dependent. Therefore, the effects of these factors were studied for a fixed concentration (60 mg) of each of these ions in the pH range 2.4–6. The solutions were then allowed to react with NaIO₄ for different time intervals (2–30 min). The pH of the solutions was adjusted to pH ≈ 3 using acetate buffer and the excess unreacted NaIO₄ was masked with sodium molybdate at the same pH. The released iodate and ruthenium(VIII) were then allowed to react with KI and the liberated iodine was determined by iodometry (with 0.005 M Na₂S₂O₃) and by spectrophotometry of the triiodide species formed at 350 nm against a reagent blank. The results indicated that the optimum pH of the complete oxidation of the ruthenium species was in the range 2.5–4 after 5 min. Under these conditions, each original ruthenium(II), (III) and (IV) released 18, 15 and 12 equivalent iodines, i.e. the proposed method afforded 18-, 15 and 12-fold amplification per ruthenium(II), (III) and (IV) ion, respectively. At pH < 2, reactions from

(5)–(9) proceeded rapidly with 23-, 20- and 17-fold amplification of Ru(II), (III) and (IV) respectively, but under these conditions sodium molybdate did not mask the unreacted periodate quantitatively since the molybdate–periodate complex was partially decomposed [22] and also aerial oxidation of iodide could occur. Thus, the percentage recovery of the tested ruthenium ion and blank values were erroneously high owing to reaction of the released periodate with iodide. At pH > 5, reactions (5)–(7) proceeded slowly to form perruthenate (RuO₄⁻) ions [2] of lower amplification, and the iodide–iodate reaction was slow under these conditions. Fortunately, the pH values suitable for the quantitative oxidation of ruthenium(II), (III) or (IV) ions were quite appropriate for masking the excess unreacted periodate with molybdate. The developed method was employed for the determination of various amounts (5–200 mg) of ruthenium(II) or (III) by iodometry and spectrophotometry. The results are summarized in Table 1. Satisfactory results with standard deviations ($n = 5$) in the range 0.2–0.5 and 0.2–0.3 were obtained employing the iodometry and spectrophotometry procedures for Ru(II) or (III) respectively. It is worth mentioning that before addition of KI it was advisable to shake the solution with 10 ml CCl₄ (2 × 5) to remove the produced RuO₄ and to prevent any possibility of reaction between RuO₄ and KI at the optimum pH.

Moreover, the sensitivity of the proposed method for ruthenium(IV) determination can be increased by prior reduction to Ru(III) using sodium sulphite, hydroxylamine or zinc/HCl followed by determination according to procedure I. Sodium sulphite in acidic media

Table 2

Determination of various amounts of ruthenium(IV) by iodometry (a) and spectrometry (b) using the 15-fold amplification procedure^a

Ruthenium(IV) taken (μg)	Ruthenium(IV) found (μg)		Error (%)	
	a	b	a	b
10	10.1 \pm 0.3	10.1 \pm 0.2	1	1
20	20.2 \pm 0.4	20.2 \pm 0.2	1	1
50	51.3 \pm 0.4	50.7 \pm 0.2	2.5	1.4
75	76 \pm 0.5	75.3 \pm 0.4	1.3	0.4
100	103 \pm 0.5	101.3 \pm 0.2	3	1.3

^a Average \pm standard deviation ($n = 5$).

was found to be the most suitable reagent, where the unreacted sulphite ion could be easily removed by boiling off the formed sulphur dioxide. The determination of various amounts (10–100 μg) of ruthenium(IV) in aqueous media by the proposed method is given in Table 2. Satisfactory results were obtained by iodometry and spectrophotometry with relative standard deviations in the range 0.5–2.9 and 0.2–1.9%, respectively.

The proposed method was also employed for the analysis of the binary mixture Ru(II) and (III) in aqueous media. An aliquot mixture was first allowed to react with sodium periodate employing procedure I-a. Another aliquot mixture was then reduced to ruthenium(II) as previously reported [16], followed by determination of the total Ru(II) by the proposed procedure I-a. On this basis, if V_1 and V_2 ml were the volumes of the sodium thiosulphate equivalent to the aliquot mixture in the first and second steps, respectively, then we obtain

$$C_1(\mu\text{g}) = (6V_1 - 5V_2)M(\text{A.W.})10^3/18 \quad (6)$$

$$C_2(\mu\text{g}) = (V_2 - V_1)M(\text{A.W.})10^3/3 \quad (7)$$

where C_1 and C_2 are the concentrations of Ru(II) and Ru(III), in μg , respectively, A.W. is the atomic weight of ruthenium and M is the molarity of sodium thiosulphate. Satisfactory results were obtained (Table 3) employing iodometric procedures with 18- and 15-fold amplifications. The absolute standard deviation was found in the range 0.3–0.4.

Moreover, the analysis of the binary mixture Ru(II) and (IV) was also employed by the proposed 15- and 12-fold amplification procedure. An aliquot mixture was first reacted with sodium periodate employing procedure I-a. Another aliquot mixture was then reduced with sulphite ions in acidic media to reduce ruthenium(IV) to Ru(III) as described in procedure

II, followed by determination of the total Ru(III) by the described procedure I-a. According to these procedures, if V_1 and V_2 ml were the volumes of the sodium thiosulphate consumed for the first and second aliquot, then we obtain

$$C_1(\mu\text{g}) = (5V_1 - 4V_2)M(\text{A.W.})10^3/15 \quad (8)$$

$$C_2(\mu\text{g}) = (V_2 - V_1)M(\text{A.W.})10^3/3 \quad (9)$$

where C_1 and C_2 are the concentration of Ru(II) and Ru(IV), in μg , respectively. The results obtained are summarized in Table 4, with a relative absolute error in the range 0.5–3.4%. In separate experiments, aliquot samples containing various amounts of Ru(III) and (IV) in a concentration range of 0.05–1 $\mu\text{g ml}^{-1}$ ($n = 5$) were analyzed by the developed spectrophotometric procedure. Satisfactory results were obtained with $99 \pm 2\%$ recovery and absolute standard deviations in the range 0.12–0.28.

The proposed iodometric procedure for the analysis of various amounts of the binary mixture Ru(II) and Ru(IV) was also carried out. An aliquot mixture was first allowed to react with NaIO_4 employing procedure I-a. Another aliquot mixture was reduced with sulphite ions in acidic media from Ru(IV) to Ru(III) and the reaction mixture was then allowed to react with sodium periodate as described in procedure II. On this basis, if V_1 and V_2 ml were the volumes of the sodium thiosulphate consumed in the first and second aliquot mixture, then we obtain

$$C_1(\mu\text{g}) = \frac{(5V_1 - 4V_2)M(\text{A.W.})10^3}{18} \quad (10)$$

$$C_2(\mu\text{g}) = \frac{(V_2 - V_1)M(\text{A.W.})10^3}{3} \quad (11)$$

Table 3

Simultaneous determination of various amounts of ruthenium(II) and (III) in their binary mixtures by iodometry employing the 18- and 15-fold amplification procedure^a

Metal ion taken (μg)		Metal ion found (μg)	
Ru ²⁺	Ru ³⁺	Ru ²⁺	Ru ³⁺
20	50	20.1 \pm 0.3	51.1 \pm 0.3
40	50	40.2 \pm 0.4	51.2 \pm 0.4
100	50	101.3 \pm 0.4	51.2 \pm 0.4
150	100	153.3 \pm 0.4	101.9 \pm 0.5
200	100	202 \pm 0.3	101.6 \pm 0.3

^a Average \pm standard deviation ($n = 3$).

where C_1 and C_2 are the concentrations of Ru(II) and Ru(IV), in μg , respectively in the binary mixture. Satisfactory results were obtained with good accuracy and reproducibility in the concentration range 5–100 μg of Ru(II) or Ru(IV) ions.

Moreover, the proposed 18-, 15- and 12-fold amplification procedures of Ru(II), Ru(III) and Ru(IV), respectively could be increased by employing further oxidation by bromine water and sodium periodate [23]. The released iodine from Eqs. (1)–(3) after addition of potassium iodide was quantitatively extracted twice with 10 ml portions (2×5) of CHCl_3 or CCl_4 and shaken with sodium sulphite solution to reduce the iodine to iodide. The released iodide in the aqueous (upper) layer was then allowed to react with bromine as well as with sodium periodate to produce iodate ions. The produced iodate was quantitatively determined iodometrically or spectrophotometrically after adjusting the pH and addition of KI as described earlier. The overall fold amplifications of ruthenium(II) determination were 108- and 432-fold employing oxidation of the produced iodide by bromine and sodium periodate, respectively. Similarly, the overall amplifications of ruthenium(III) determination involving oxidation of the produced 15I^- by bromine and sodium periodate were 90- and 360-fold, respectively. The two proposed amplification procedures, 90- and 360-fold have been employed iodometrically for the analysis of various amounts (2–50 μg) of ruthenium(III). The results obtained are summarized in Table 5 with an average absolute error of 0.2–2.5%. The blank values taken through the whole procedure using freshly prepared periodate, doubly-distilled water and molybdate solutions ranged between 0.10 and 0.15 ml of 0.005 M $\text{Na}_2\text{S}_2\text{O}_3$. The sensitivity of the proposed pro-

cedures could be improved by the addition of traces of ascorbic acid after addition of iodide to prevent the oxidation of iodide by atmospheric oxygen [24].

In addition, the spectrophotometric procedure employing 90-fold amplification of ruthenium(III) determination was carried out. The absorbance–concentration relationship was found to be linear in the concentration range from 0.1 to 5 mg l^{-1} of ruthenium(III). A linear calibration curve was also obtained in the concentration range 0.05–5 mg l^{-1} at 360-fold amplification and $\lambda = 350\text{ nm}$ for ruthenium(III) determination. Moreover, the sensitivity of these amplification procedures could be extended to lower concentrations ($< 0.1\text{ mg l}^{-1}$) of ruthenium(III), by extraction of the released iodine in $\text{CHCl}_3\text{-C}_2\text{H}_5\text{OH-KI}$ and measuring the absorbance of the triiodide at 360 nm [24]. The standard deviation ($n = 3$) for a solution of 5 mg l^{-1} Ru(III) was 0.4 and 0.22 at 90- and 360-fold amplification, respectively. The detection limit ($3 \times \text{noise}$) was 0.03 mg l^{-1} . It is worth mentioning that, for a reasonably large amount of ruthenium(II) or (III) ($> 50\text{ mg}$) present, it is advisable to dilute the solution of the released iodate from oxidation of iodide ions by bromine or sodium periodate and follow the previously recommended procedure.

3.1. Interference studies

The interference of various cations, e.g. Cd^{2+} , Ni^{2+} , Sn^{2+} , Pd^{2+} , Ir(III) , Os(III) , Au^+ , Ca^{2+} , Mg^{2+} , Al^{3+} , UO_2^{2+} , Pt^{2+} , Pt^{4+} , Zn^{2+} , and Li^+ , at 0.5 mg and pH 3 on the selectivity of the proposed method were examined by the determination of a fixed concentration (30 mg) of ruthenium(II) or (III) in aqueous solution. The percentage recovery of ruthenium(II) or (III) was found to be $100 \pm 2.4\%$. The toler-

Table 4

Simultaneous determination of various amounts of ruthenium(III) and (IV) in their binary mixtures by iodometry employing the 15- and 12-fold amplification procedure^a

Metal ion taken (μg)		Metal ion found (μg)	
Ru ³⁺	Ru ⁴⁺	Ru ³⁺	Ru ⁴⁺
20	50	20.1 \pm 0.3	51.1 \pm 0.2
40	50	40.3 \pm 0.4	51.2 \pm 0.3
100	50	101.3 \pm 0.2	51.2 \pm 0.2
150	100	153.3 \pm 0.5	101.6 \pm 0.5
200	100	202 \pm 0.3	103.4 \pm 0.3

^a Average \pm standard deviation ($n = 4$).

ance limits of various anions at 30 μg ruthenium(II) or (III) in the presence of a relatively high excess (1 mg) of the anions AsO_2^- , AsO_3^- , SbO_2^- , SbO_3^- , SeO_3^- , SeO_4^- , TeO_4^- , NO_3^- , SO_4^- , PO_4^- , HPO_4^- , Cl^- , Br^- , SCN^- , formate, WO_4^- and SiO_3^- have been critically investigated. The percentage recovery of ruthenium(III) was $100 \pm 2.6\%$ and the standard deviation was found in the range 0.2–0.7. In the presence of some other ions which are commonly found associated with ruthenium, e.g. V^{5+} and Pb^{2+} at 100-fold excess of ruthenium(III) at 30 μg concentration, simple modifications involving addition of 10 ml of NaF (1 M) to the aqueous solution were introduced. The percentage recovery of ruthenium(III) was $100 \pm 3\%$. Interference of cobalt(II), iron(III) and bismuth(III) at 100-fold excess of ruthenium(III) was eliminated by adding 5 ml of EDTA (0.01 M). Bismuth(III) was also eliminated by shaking the aqueous solution at pH 9–10 with 10 ml xylene in the presence of sodium diethyldithiocarbamate (2% v/v). Copper(II) interfered seriously with the proposed procedure.

Under the optimum conditions of the pro-

Table 5

Determination of various amounts of ruthenium(III) by iodometry using 90-fold and 360-fold amplification procedures^a

Ruthenium(III) taken (μg)	Metal ion found (μg)	
	90-fold	360-fold
2	2.05 \pm 0.1	2.0 \pm 0.1
5	5.1 \pm 0.1	5.1 \pm 0.1
10	10.1 \pm 0.1	10.1 \pm 0.1
20	20.2 \pm 0.1	20.1 \pm 0.1
50	50.2 \pm 0.1	50.1 \pm 0.2
100	100.4 \pm 0.2	100.5 \pm 0.3

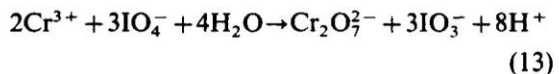
^a Average \pm standard deviation ($n = 3$).

posed procedures ($2.5 < \text{pH} < 3.6$), chromium(VI) did not interfere owing to the reaction

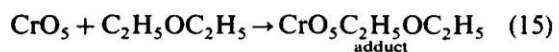
$$\text{Cr}_2\text{O}_7^{2-} + 6\text{I}^- + 14\text{H}^+ \rightarrow 2\text{Cr}^{3+} + 3\text{I}_2 + 7\text{H}_2\text{O} \quad (12)$$

This reaction was pH dependent and did not occur at $\text{pH} > 2.3$. These results are in good agreement with the published work by El-Wakil et al. [13] on chromium(VI) determination.

Chromium(III) interfered seriously with the proposed method, since the reaction



proceeded at $\text{pH} < 4$. However, this interference from chromium(III) could be removed easily by oxidizing the aliquot solution of chromium(III) with H_2O_2 in 2N H_2SO_4 , and the produced blue perchromic acid extracted quantitatively with diethylether as previously reported [25] according to



Thus, chromium(III) interference could be removed completely. The excess hydrogen period was eliminated by adding tin(II), and the ruthenium species was then determined by the proposed procedure II.

3.2. Applications of the proposed methods

3.2.1. Analysis of ruthenium(II) and (III) in their complexes

The proposed procedure I-a for the analysis of ruthenium(II) or (III) in their complexes [19] was carried out successfully after combustion of the sample as described earlier. Ruthenium usually present in the di-, tri- and tetravalent

Table 6
Results of the extractive spectrophotometric determination of Ru in various ruthenium(III) complexes^a

Complex	Ru present ^b (%)	Ru found ^c (%)
RuCl ₂ (PPh ₃) ₂ (Koj)	24.52	24.5 ± 0.2
RuCl ₂ (PPh ₃) ₂ (Malt)	24.46	24.40 ± 0.3
RuCl ₂ (PPh ₃) ₂ (trop)	24.7	24.9 ± 0.3
RuCl ₂ (PPh ₃) ₂ (acac)	25.32	24.9 ± 0.2
Ru(5-Cl-Sal ₂ en)(PPh ₃) ₂	10.43	10.78 ± 0.3

^a Abbreviations: Kojic acid (Koj); maltol (malt); tropolone (trop); acetylacetonone (acac); and *N,N*-ethylenebis(5-chlorosalicylideneiminato)bis(triphenylphosphine(5-Cl-Sal₂en)(PPh₃)₂).

^b Certified value.

^c Average ± standard deviation (*n* = 5).

state was reduced to ruthenium(II) [17], and determined by iodometry and spectrophotometry with the help of the concurrently proposed standard curve under the same experimental conditions as the described procedure I-a. The results are summarized in Table 6 with an average absolute error of 0.2–0.3. The blank values taken throughout the whole procedure using freshly prepared reagents ranged between 0.2 and 0.25 ml of 0.005 M Na₂S₂O₃. Evidently, for ruthenium complexes containing a large percentage of ruthenium, it was advisable to dilute the solution of the produced iodate in the first procedure I-a to 25 ml with distilled water and treat 5 ml of this solution as described earlier.

3.2.2. Determination of ruthenium in natural waters

The applicability of the proposed method for the determination of low concentrations of spiked ruthenium(III) ions to tap-, mineral and seawater (0.1–1 l) is possible by the standard addition procedure. In separate experiments, aliquot samples were allowed to react with 5 ml of bromine water for 10 min, and the excess bromine was removed by boiling off the solution. The samples were then spiked with various amounts (5–40 µg) of Ru(III). Filtration of the sample solution through a 0.45 µm membrane was carried out, followed by addition of 10 ml of EDTA (0.001 M) and 10 ml of NaF (1 M); the sample was then analyzed employing procedure II. The concentration of the tested ruthenium species in such water was under the detection limit and recovery of the spiked Ru(III) was achieved. The results of the analysis of various amounts of ruthenium(III) spiked tapwater and seawater are summarized in Table 7. Good reproducibility with relative

standard deviations in the range 1–2.9% (*n* = 5) was obtained. The analysis of very low concentrations (less than nanomolar levels) of Ru(III) in water is also possible using the proposed procedure by prior preconcentration of the element from a large sample volume on polyurethane foam column, followed by elution of the extracted Ru(III) species from the foam as reported earlier [26] and subsequent determination of the ruthenium(III) in the effluent according to the described procedure I-a with the help of a concurrently prepared standard curve at the same instrumental setting.

4. Conclusion

The present work presents accurate, precise, inexpensive, reliable methods in routine analysis for the trace determination of ruthenium ions in their matrix. Therefore, the method provides an attractive alternative approach to determination of the atomic absorption of ruthenium. The advantages of the method are that it is not only applicable to Ru(II), (III) and (IV) speciation in their solutions, but it can also be used for the analysis of ruthenium in its complexes and natural water samples. The sensitivity and selectivity of the developed methods can be improved by prior preconcentration of the trace amounts of ruthenium species from large sample volumes on polyurethane foam column. Elution of ruthenium from the column is possible with selective eluting agent followed by determination with the proposed procedure. The 15-fold amplification procedure for Ru(III) determination was faster, but the 90- and 360-fold amplification procedures were more sensitive and applicable at very low concentrations of the tested element. The determi-

Table 7

Analysis of various amounts of ruthenium(III) spiked seawater by iodometry (a) and spectrophotometry (b) employing the 90-fold amplification procedure ^a

ruthenium(III) added (μg)	Ruthenium(III) found (μg) ^b		Error (%)	
	a	b	a	b
5	5.1 ± 0.1	5.10 ± 0.1	2	2
10	10.30 ± 0.3	10.1 ± 0.2	3	1
20	20.3 ± 0.3	20.2 ± 0.3	1.5	1
25	25.7 ± 0.4	25.2 ± 0.3	2.8	0.8
40	40.7 ± 0.5	40.65 ± 0.4	1.8	1.25

^a Average \pm standard deviation ($n = 5$).

^b Total volume of aqueous seawater was 0.1 dm^3 .

nation of Ru(II) besides Ru(III) or Ru(IV) besides Ru(II) is also possible with good accuracy.

References

- [1] E. Merian, *Metals and their Compounds in the Environment, Occurrence, Analysis and Biological Relevance*, VCH, Weinheim, 1981, p. 1143.
- [2] M.S. El-Shahawi, A.Z. Abu Zuhri and S.M. Al-Daheri, *Fresenius' Z. Anal. Chem.*, 350 (1994) 874.
- [3] R.K. Sharma, *Bull. Chem. Soc. Jpn.*, 66 (1933) 1084, and references cited therein.
- [4] Z. Marczenko, *Separation and Spectrophotometric Determination of Elements*, Ellis Horwood, New York, 1986, p. 492.
- [5] A.M. Almuaided and A. Townshend, *Microchem. J.*, 48 (1933) 21.
- [6] M.S. El-Shahawi and M. Al-Mahdy, *J. Chromatogr.*, 697 (1995) 185.
- [7] M.S. El-Shahawi, A.Z. Abu Zuhri and M.M. Kamal, *Fresenius' Z. Anal. Chem.*, 348 (1994) 730.
- [8] R. Palaniappan and T.A. Kummar, *Analyst*, 118 (1993) 293.
- [9] R. Palaniappan and V. Revathy, *Analyst*, 114 (1989) 517.
- [10] R. Palaniappan, *Bull. Electrochem. Soc., India*, 39 (1991) 367.
- [11] T. Leipert, *Mikrochemie*, (1992) 226.
- [12] A.M. El-Wakil, A.B. Farag and M.S. El-Shahawi, *Talanta*, 36 (1989) 783.
- [13] J.W. Hamaya and A. Townshend, *Talanta*, 19 (1972) 141.
A.M. El-Wakil, A.B. Farag and M.S. El-Shahawi, *Fresenius' Z. Anal. Chem.*, 337 (1990) 886.
- [14] A.M. El-Wakil, A.B. Farag and M.S. El-Nahas, *Talanta*, 40 (1993) 841.
- [15] A.B. Farag, M.S. El-Shahawi and E.M. El-Nemma, *Fresenius' Z. Anal. Chem.*, 346 (1993) 455.
- [16] D.R. Lide, *Handbook of Chemistry and Physics*, 72nd edn., CRC Press, Boca Raton, FL, 1991/1992, p. 493.
- [17] G. Ciantelli, P. Legithimo and F. Pantani, *Anal. Chim. Acta.*, 52 (1971) 303.
- [18] C.W. McDonald and J.H. Bedenbaugh, *Mikrochim Acta (Wien)*, (1970) 612.
- [19] A.M. El-Hindawy and M.S. El-Shahawi, *Polyhedron*, 118 (1993) 293.
- [20] M. Armando, R. Lena, M. Rafael and D.J. Federico, *J. Coord. Chem.*, 29 (1993) 359.
- [21] T.S. Ma and R.C. Rinter, *Modern Organic Elemental Analysis*, Dekker, New York, 1979.
- [22] D. Brunel, *CR. Acad. Sci., Paris*, 261 (1965) 1982.
- [23] D. Amin, K.Y. Saleem and W.A. Bashir, *Talanta*, 29 (1982) 694, and references cited therein.
- [24] T.C. Ovenston and W.T. Rees, *Anal. Chim. Acta*, 5 (1951) 123.
- [25] A.M. El-Wakil, M.S. El-Shahawi and A.B. Farag, *Anal. Lett.*, 23 (1990) 103.
- [26] S.J. Al-Bazi and A. Chow, *Talanta*, 31 (1984) 189.

The retention behaviour and separation of some water-soluble organophosphorus insecticides on polyester-based polyurethane foams

M.S. El-Shahawi ^{a,*}, A.M. Kiwan ^a, S.M. Al-Daheri ^a, M.H. Saleh ^b

^a Department of Chemistry, Faculty of Science, UAE University, Al-Ain, P.O. Box: 17551, United Arab Emirates

^b Ministry of Health, Abu Dhabi, P.O. Box: 848, United Arab Emirates

Received 28 October 1994; revised 16 March 1995; accepted 20 March 1995

Abstract

This paper reports the concentration of some dissolved organic phosphorus insecticides in water by open-cell polyurethane foam. The results of preliminary screening tests on the retention of the tested insecticides (Diazinon, Malathion and Chlorpyrifos) by polyester foams indicated that a very high percent removal of the insecticides was obtained. The retention rate was fast and reaches equilibrium in a few minutes. The various parameters affecting the preconcentration of the tested insecticides by unloaded foam, e.g. pH, extraction media, shaking time, salt effect, flow rate, temperature and sample volumes have been optimized via the static mode of separation. The unloaded foams were employed in columns for the retention and recovery of the tested species. The sorption efficiency and the recovery of the tested compounds by the unloaded foam column were found to be up to 95.5%. The equivalent to a theoretical plate by the unloaded foam was found in the range $1.12\text{--}1.32 \pm 0.2$ mm. The sorption mechanism of the tested species by the foam is discussed. The separation of some of the tested species in a mixture was achieved. The foam membrane offers unique advantages over conventional bulk-type granular sorbents and solvent extraction in offering high flow rates, rapid, versatile, effective separation and preconcentration of different species from aqueous samples. The foam provides the advantages of being, insoluble, easily separable and non-polluting, as well as inexpensive.

1. Introduction

The classes of compounds responsible for the pollution of potable water resources include polyaromatic hydrocarbons, detergents, phenols, polychlorinated biphenyls and pesticides [1]. The pesticides are not toxic agents and are widely and regularly applied over large areas accessible to the public [2]. The compounds can enter water systems from various sources, e.g. run-off from agricultural land, direct entry from crop spraying, industrials and sewage effluent,

cattle spraying, dust and rainfall [3,4]. These species are deliberately directed against living organisms and applications almost occur without control [5].

The removal or reduction of these water pollutants to an acceptable concentration by extraction with cellulose triacetate membrane filters, steam distillation, oxidation reactions, reversed liquid-liquid partition filter chromatography and adsorption on active carbon has been reported [6–9]. Such preconcentration methods are often slow or cumbersome and are too expensive for routine analysis where large volume samples are concentrated on-site prior to quantitative analysis [8,9].

The use of unloaded polyurethane foams (PuF) in separation and preconcentration pro-

* Corresponding author. Permanent address: Chemistry Department, Faculty of Science at Damietta, Mansoura University, Mansoura, Egypt.

cesses led to the revealing of the potential of their spherical geometric form: a spherical membrane-shaped geometry and the proposal of their general use in column operations as a substitute for the traditional granular supports in extraction chromatography [10]. Thus, in recent years considerable progress has been made in the use of polyurethane foam as an inexpensive solid extractor and effective sorbent for the removal of water pollutants [11–23]. The membrane-like structure of the foams together with efficient sorption and mass-transfer properties offer a higher concentrating ability and flow rate compared with other solid supports. The solid foam concentrates various species in solution by a phase distribution mechanism rather than adsorption.

The object of the work described herein was to evaluate the applicability of polyurethane foam for the extraction and separation of some insecticides from large volume samples of aqueous media. Conclusions concerning the most probable sorption mechanism by the foam have also been drawn.

2. Experimental

2.1. Reagents and materials

All reagents and chemicals used were of analytical reagent grade. Universal Britton-Robinson (B-R) buffer solutions containing a mixture of equal amounts (0.04 mol l^{-1}) of phosphoric acid, boric acid and acetic acid with sodium hydroxide (0.01 mol l^{-1}) were used to provide different pH ranges. Polyurethane foam, an open-cell polyester-type (bulk density, 30 kg m^{-3}) was supplied by Greiner K.G. Schaum (Stoffwerk, Kremsmunster, Austria). Foam cubes of volume approximately 1 cm^3 were cut from polyurethane foam sheet. These foam cubes were soaked in 1 M hydrochloric acid for 10 h with occasional squeezing to remove any possible inorganic species, and were washed with water until they were acid-free. They were then washed with acetone in a Soxhlet extractor for 24 h to remove organic contaminants and finally dried as previously reported [18].

The insecticides tested were Chlorpyrifos, *o,o*-diethyl-*o*-(3,5,6-trichloro-2-pyridyl)phosphorothioate; Malathion; diethyl [(dimethoxyphosphinothioyl)thio]butanedioate and Diazinon, *o,o*-diethyl-*o*-(3-isopropyl-6-methyl-pyrim-

idine)phosphorothioate. Stock solutions ($200 \mu\text{g cm}^{-3}$) of each compound were prepared in 10 cm^3 ethanol and were diluted with distilled water. A series of standard solutions of these compounds was prepared by diluting their stock solutions with distilled water. The solutions were stored in polyethylene bottles.

2.2. Apparatus

A Pye– Unicam double-beam UV-Visible spectrophotometer model Sp 8-400 with 10 mm quartz cells was used for all the absorbance measurements. An Orion pH meter, a mechanical shaker type G10 Gyrotary (New Brunswick, Scientific Co.) and glass columns ($15 \text{ cm} \times 1.5 \text{ cm i.d.}$) were also employed.

2.3. General procedures

Batch experiments

To investigate the effect of shaking time on the sorption of the tested insecticides on polyurethane foam, the foam cubes (0.2 g) were equilibrated with 100 cm^3 of each compound ($100 \mu\text{g cm}^{-3}$) in separate polyethylene bottles, and were shaken for time intervals up to 2 h. The foam cubes were then separated by decantation. The amount of compound remaining in the solution was measured spectrophotometrically at the wavelength of maximum absorption. The sorption behaviour of the compounds as evaluated from the degree of sorption (E) and the distribution ratio (D)

$$E = \frac{[C]_i - [C]_f}{[C]_i} 100 \quad (1)$$

$$D = \frac{[C]_i - [C]_f}{[C]_f} \frac{V}{W} \quad (2)$$

where $[C]_i$, and $[C]_f$ are the initial and final insecticide concentrations, respectively, in the solution, V is the volume of the solution (cm^3) and W is the weight of dry foam (g). Following these procedures, the effects of solution pH employing Britton-Robinson buffer, acidity, temperature, compound concentration, extraction medium and increasing salt concentration ($\leq 0.1 \text{ M}$) of different alkali metal (Li^+ , Na^+ , K^+ , NH_4^+) chlorides on the sorption efficiency of the tested species by the polyester-based polyurethane foam were critically examined.

Table 1
The logarithm distribution coefficient (D) data for the sorption of the tested insecticides by unloaded foams in the presence of different univalent cations^a

Cation concentration (M)	Logarithm distribution coefficient, D		
	Chlorpyrifos	Malathion	Diazinon
LiCl			
0.01	3.8 ± 0.1	2.9 ± 0.2	2.3 ± 0.2
0.05	3.8 ± 0.1	3.2 ± 0.1	2.50 ± 0.07
0.1	3.70 ± 0.09	3.6 ± 0.1	2.8 ± 0.1
NaCl			
0.01	4.1 ± 0.1	1.70 ± 0.05	1.9 ± 0.1
0.05	4.1 ± 0.1	1.8 ± 0.1	1.6 ± 0.1
0.1	4.0 ± 0.1	1.9 ± 0.1	0.40 ± 0.07
KCl			
0.01	4.3 ± 0.1	1.5 ± 0.1	1.75 ± 0.07
0.05	4.4 ± 0.1	1.6 ± 0.1	1.55 ± 0.09
0.1	4.5 ± 0.1	1.5 ± 0.1	0.90 ± 0.05
NH ₄ Cl			
0.01	4.3 ± 0.1	1.3 ± 0.1	1.50 ± 0.08
0.05	4.3 ± 0.1	1.4 ± 0.1	1.28 ± 0.07
0.1	4.2 ± 0.1	1.3 ± 0.1	0.76 ± 0.09

^a Extraction from aqueous solution (100 cm³) at the pH of maximum extractibility of each insecticide (80 µg cm⁻³). Average of five measurements ± standard deviation (S.D.) at room temperature.

Flow experiments

In the column experiments, 3 g of dry foam were homogeneously packed into the column using the vacuum method of foam column packing [12]. Tap or distilled water (0.1–5 dm³) samples containing 0.1 mg of the insecticide tested were passed through the foam column at 10–15 cm³ min⁻¹. After squeezing water from the foam, the compound was then recovered quantitatively from the foam with 200 cm³ of

acetone in a Soxhlet extractor for 8 h. The analyte was determined by measuring the absorbance of the solution against a reagent blank after being concentrated to a volume of 25 cm³ with a rotary evaporator. The effect of sample volume, flow rate and column foam bed on the extraction efficiency of the compounds by the foam were also determined. The chromatographic separation of Malathion and Chlorpyrifos were carried out employing the foam packed column procedures.

3. Results and discussion

Preliminary experiments using unloaded polyester-type-based polyurethane foam have shown that the extraction of the investigated compounds (I, II, III in Fig. 1) is rapid and equilibrium is reached in less than 50 min, followed by a plateau. The results obtained are summarized in Fig. 2. (Each point in the figure represents an average of five measurements ($n = 5$) with relative standard deviations in the range 1.8–2.1%.) Rapid preconcentration and good extraction efficiency of the tested compounds from aqueous media were obtained. The average values of the half-life ($t_{1/2}$) of equilibrium sorption calculated from Fig. 2 are in the range 2–3 min.

3.1. Extraction isotherm

The uptake of the tested compounds from aqueous solution by the unloaded foam was dependent on the initial concentration. There-

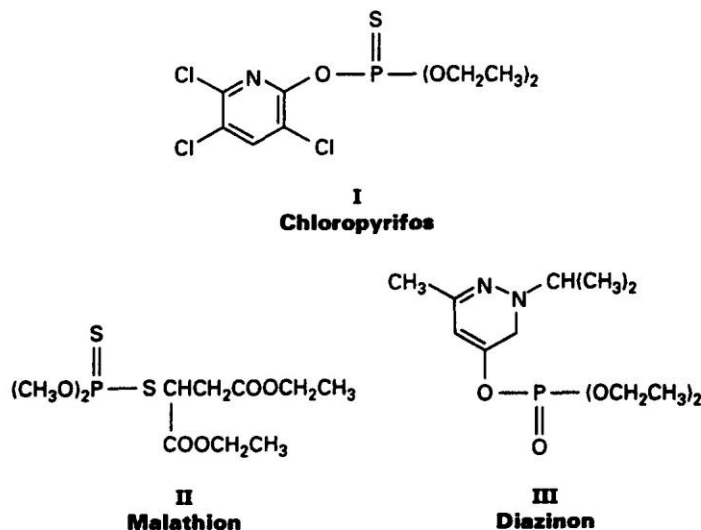


Fig. 1. Structure of the tested insecticides.

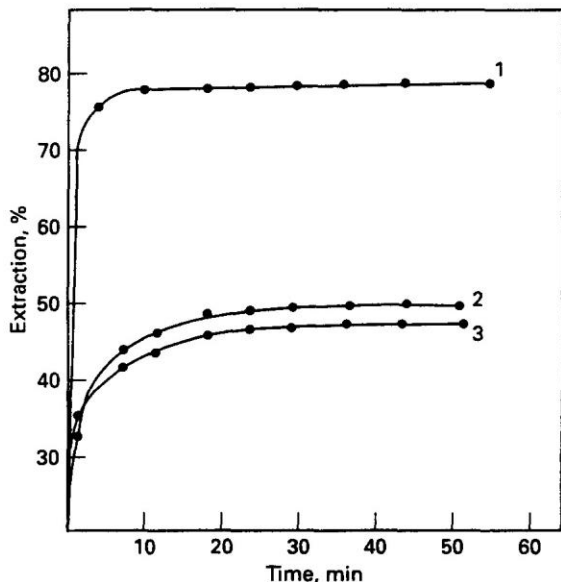


Fig. 2. Effect of shaking time on the sorption profiles of (curve 1) Chloropyrifos, (curve 2) Malathion, and (curve 3) Diazinon at $100 \mu\text{g cm}^{-3}$ in aqueous solution (100 cm^3) at pH 5–6 and $20 \pm 0.1^\circ\text{C}$ by unloaded foams (0.3 g).

fore, the sorption isotherms were determined over a wide range of equilibrium concentrations ($10\text{--}200 \mu\text{g cm}^{-3}$) for each insecticide at 20°C . The pH values of the aqueous media in these experiments were adjusted with Britton-Robinson buffer to pH 5–6, so that the compounds were predominantly in the undissociated form. At low concentration of the compounds, the sorption isotherms exhibited first-order behaviour and tended to plateau at higher bulk solution concentration as shown in Fig. 3. The sorption of the different species by the unloaded foam increases in the order

Chloropyrifos > Malathion > Diazinon

Similar trends for the sorption of the tested compounds were obtained with diethyl ether and for other similar species retained on polyurethane foams [14,15]. Therefore solvent extraction is the most probable mechanism for the sorption of the tested species by the polyester foam from aqueous media at the tested pH [15]. However, it is worth noting that the molecular weight (M_w) of Chloropyrifos ($M_w = 345.5$), Diazinon ($M_w = 268$) and Malathion ($M_w = 330.5$) are also participating factors in the extraction step by the polyester foam. These data are consistent with the general understanding that the higher the molecular weight of the sorbate, the larger the amount of the tested insecticides retained on the foam

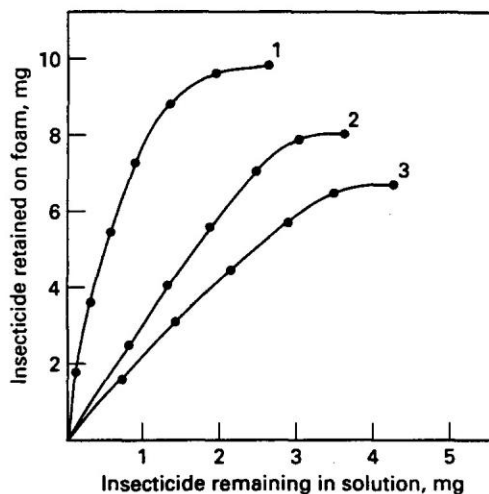


Fig. 3. Extraction isotherms of (curve 1) Chloropyrifos, (curve 2) Malathion and, (curve 3) Diazinon at concentrations $10\text{--}200 \mu\text{g cm}^{-3}$ by unloaded foams from a 100 cm^3 aqueous solution sample at pH 5–6 and $20.0 \pm 0.1^\circ\text{C}$ and 1 h extraction time.

when the substances concerned are similar in nature [24,25].

The influence of the pH of the aqueous solution on the sorption profile of the compounds at concentration $100 \mu\text{g cm}^{-3}$ by the unloaded foams was determined over a pH range of 1–12 employing 0.1 mol l^{-1} hydrochloric acid solution and Britton-Robinson buffer. The sorption profiles of the compounds by the unloaded foams are summarized in Fig.

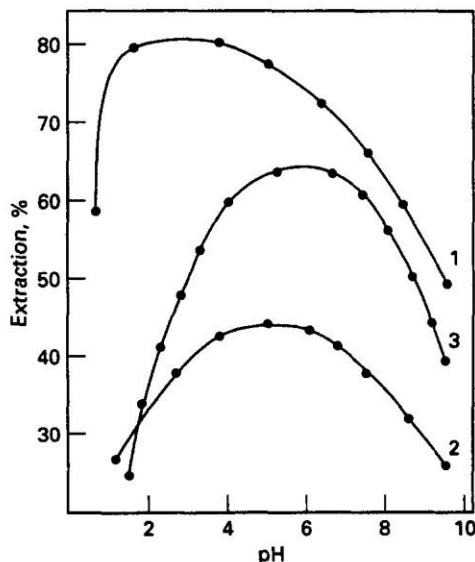


Fig. 4. Effect of pH on the extraction percentage of (curve 1) Chloropyrifos, (curve 2) Malathion and, (curve 3) Diazinon by unloaded foam (0.3 g) from a 100 cm^3 aqueous sample ($80 \mu\text{g cm}^{-3}$). Other conditions in Fig. 2.

4. The extraction percentage of Chloropyrifos reached a maximum in the pH range 2–4 and decreased at moderate and higher pH. Diazinon and Malathion display maximum retention at pH 6–8, at which the compounds exist in the neutral form. Thus the sorption mechanism involves neutral species and this is consistent with a solvent-extraction mechanism as previously reported [14,20].

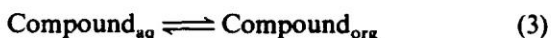
The effect of different concentrations of alkali metal chlorides, e.g. LiCl, NaCl, KCl and NH_4Cl , at concentrations ≤ 0.1 M on the sorption profiles of the tested compounds ($80 \mu\text{g cm}^{-3}$) was investigated. The results obtained are summarized in Table 1. A significant increase in the sorption profiles of Diazinon and Malathion by the polyester foam was observed in the presence of the salts LiCl, NaCl, KCl and NH_4Cl at concentrations ≤ 0.1 M and the order of sorption $\text{Li}^+ > \text{Na}^+ > \text{K}^+ > \text{NH}_4^+$ was observed for Diazinon and Malathion (Table 1). The distribution ratio of Malathion increased with the amount of salt added from $\log D = 2.9$ and 1.7 to $\log D = 3.6$ and 1.9 (Table 1) while for Diazinon it changed from $\log D = 2.3$ and 1.9 to $\log D = 2.8$ and 0.4 for Li^+ and Na^+ ions at 0.01 M and 0.1 M, respectively. The added salts (Li^+ , Na^+) increased the sorption profiles of the Diazinon and Malathion into the foams by reducing the number of water molecules available to solvate the sorbed species which would therefore be forced out of the solvent phase into the foam, since some amount of “free” water molecules are preferentially used to solvate the ions added [17,18]. Hence the influence of these salts can be explained by the salting out effect and “solvent extraction” is the most probable mechanism [21,26].

The sorption profiles of Chloropyrifos by the foam increased in the presence of the alkali salts in the following order of cations: $\text{K}^+ > \text{NH}_4^+ > \text{Na}^+ > \text{Li}^+$ (Table 1). Therefore, the ion–dipole interactions of NH_4^+ ions with oxygen atom sites of the polyurethane foam are possibly highly predominating in the sorption of Chloropyrifos. According to the “cation-chelation mechanism”, the presence of K^+ ions should facilitate the extraction of the Chloropyrifos by the foam more than the other alkali metal ions (NH_4^+ , Na^+ or Li^+) because of the better fit of this ion into the central cavity of the oxygen-rich helix in the polyurethane foam. Therefore, the obtainable results of the sorption profiles of Chloropyrifos

are in good agreement with the data recently reported by Palagyi et al. [26,27]. Therefore the “cation-chelation mechanism” is the most probable mechanism for the sorption of Chloropyrifos. In accordance with this mechanism, the polyalkenoxy chains of the PuF sorbent form a helical structure [28]. This helical structure of the polyurethane foam sorbent forms a clathrate with suitable simple cations.

To confirm the salting out of the salts added on the sorption profiles of Diazinon and Malathion by the foams, an extraction of 200 cm^3 of the former compound at $80 \mu\text{g cm}^{-3}$ was investigated at pH 4 and 9 after shaking for 30 min. The added Li^+ ions (0.01 M) to the sorption media enhanced the distribution ratio of Diazinon more in a solution of pH 4 ($\log D = 3.6$) than at pH 9 ($\log D = 2.4$). This behaviour is possibly attributed to the increased amount of neutral species at pH 4 as compared to pH 9 and the compound is highly extractable in the neutral form. Thus a “solvent-extraction mechanism” with the salts acting as salting out agents is the most probable mechanism for the preconcentration of Diazinon and Malathion by the polyurethane foam [14].

The influence of temperatures of 35, 45 and 55°C on the sorption profiles of the tested species by the foam were determined at the pH of maximum extraction of each insecticide. Similar trends to that obtained at 20°C were found and the percentage retention increases slightly with increasing temperature. Assuming no precipitation or chelation and that the extracted compounds exist as neutral species, then the equilibrium constant K for the equation



is equivalent to the partition ratio, D . Employing the equation

$$\ln K = -\Delta H^\circ/RT + \Delta S^\circ/R \quad (4)$$

the values of the standard entropy change, ΔS° for the sorption of the Diazinon and Malathion by the unloaded foams were found to be in the range -32 – $-36 \pm 2 \text{ J mol}^{-1} \text{ deg}^{-1}$. The value of ΔS° for the sorption of Chloropyrifos by the foam was found to be $-19 \pm 2 \text{ J mol}^{-1} \text{ deg}^{-1}$. The low values of the entropy change for Diazinon and Malathion are possibly attributed to the decrease in the freedom of movement of the organic compound in the polyurethane foam as previously

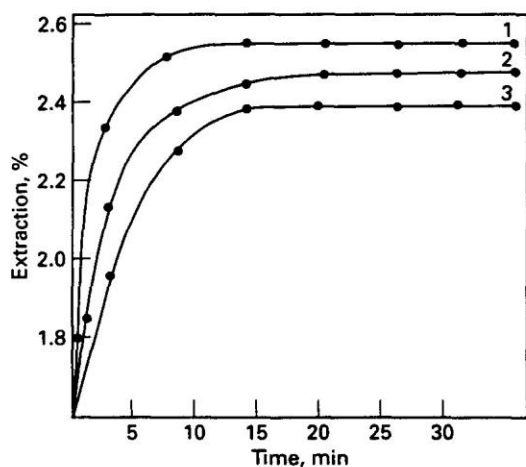
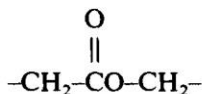
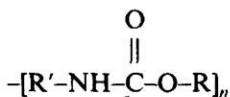


Fig. 5. Effect of extraction media on the sorption profile of Malathion by unloaded foam at pH 6–7 and a 1 h extraction time. Ethanol additions: curve 1, 0%; curve 2, 10%; curve 3, 15%. Other conditions as in Fig. 2.

reported [14]. These results are consistent with the solvent-extraction mechanism. The values of the standard enthalpy change, ΔH° were found to be in the range $26 \pm 4 \text{ kJ mol}^{-1}$. Raising the temperature may facilitate the partition of the tested species through the polyurethane foam via the urethane linkage and/or ester oxygen atoms.



or



The influence of the extraction media on the sorption percentage of the tested species by the polyurethane foam was examined by the addition of ethanol (0–15%). The sorption profiles of Diazinon and malathion by the unloaded foams decreased on the addition of ethanol to the aqueous media up to 15%. Representative results are summarized in Fig. 5. This behaviour is possibly due to the formation of a lipophilic association in the aqueous solution [29]. Water is a solvent with a high dielectric constant; therefore, ions in the aqueous solution are well solvated and so it is difficult for these species to form ion pairs in the aqueous solution. These data are consistent with the fact that with a compound of low dielectric constant and another which has a high dielectric constant, the retention percentage should

increase with increase in the solvent polarity of the polar phase. These results are also consistent with the solvent-extraction mechanism in the sorption of these species by the unloaded foam. The nature of the media has therefore a marked effect on the sorption characteristics of the compounds.

3.2. Flow experiments

The sorption behaviour of the tested compounds from aqueous solution with the unloaded polyurethane foam suggests a possible application of the foam in the column extraction mode for the quantitative collection and recovery of the tested compounds from aqueous media at the pH of maximum extractability for each compound. Distilled or tap water samples ($0.1\text{--}5 \text{ dm}^3$) containing 0.1 mg of each compound were percolated separately through the foam columns at a flow rate of $10\text{--}15 \text{ cm}^3 \text{ min}^{-1}$. Complete retention of the tested compounds was achieved by the foam column. After squeezing water from the foam the compounds were then recovered from the foam with acetone in a Soxhlet extractor. Satisfactory recovery percentages (91.5–95.5%) of the tested compounds from the aqueous media by the proposed foam column method are obtained (Table 2). The effects of flow rate and sample volume on the retention of the compounds by the unloaded foams were also examined by percolating aqueous sample volumes ($0.1\text{--}5 \text{ dm}^3$) of Diazinon (0.1 mg) through the column at various flow rates between 5 and $25 \text{ cm}^3 \text{ min}^{-1}$. Complete retention of the compound was obtained from 5 dm^3 of aqueous

Table 2

Extraction and recovery of the tested insecticides (0.1 mg) from 3 dm^3 of aqueous solution at a $10 \text{ cm}^3 \text{ min}^{-1}$ flow rate by the proposed unloaded foam column^a

Compound	Recovery %		Wavelength ^b (nm)	pKa
	(a)	(b)		
Chloropyrifos	93 ± 2	95 ± 2	206 (4.4)	4.55
Malathion	92 ± 1	93 ± 3	280 (3.13)	5.21
Diazinon	95 ± 2	96 ± 2	290 (2.94)	4.97

^a Conditions: Extraction from aqueous solution (200 cm^3) at the pH of maximum sorption of each insecticide. Average of five measurements from (a) distilled water and (b) tap water ± SD at room temperature.

^b The logarithm of the extinction coefficient (ϵ , $1 \text{ mol}^{-1} \text{ cm}^{-1}$) of the tested insecticides is given in parentheses.

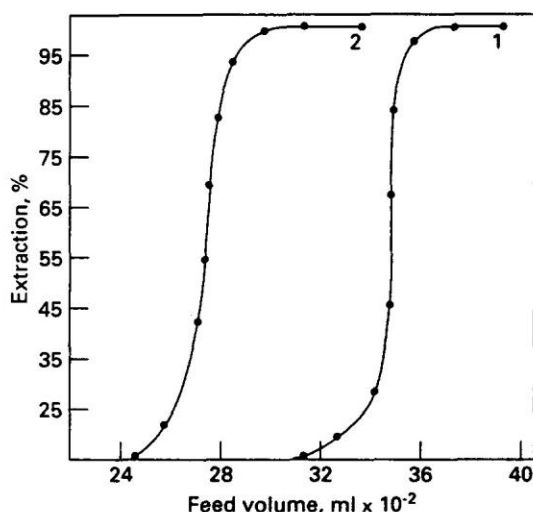


Fig. 6. Break through capacity curves of the sorption profiles of Diazinon by unloaded foam at flow rates of (curve 1) $15 \text{ cm}^3 \text{ min}^{-1}$ and (curve 2) $25 \text{ cm}^3 \text{ min}^{-1}$ by unloaded foam column.

solution and the extraction efficiency decreased significantly to 76% at $25 \text{ cm}^3 \text{ min}^{-1}$ from a 5 dm^3 aqueous volume. To determine the performance of the foam column by the chromatogram method, quantitative retention of Diazinon (0.01 mg) followed by elution with 200 cm^3 of acetone–HCl (3:1 (v/v)) through the foam column at a $5 \text{ cm}^3 \text{ min}^{-1}$ flow rate was carried out. The height equivalent to a theoretical plate (*HETP*) was obtained from the elution curves using the equation [11]

$$N = \frac{8V_{\max}^2}{W_e} = \frac{L}{HETP}$$

where N is the number of theoretical plates, V_{\max} is the volume of eluate at the peak maximum, W is the width of the peak at $1/e$ the maximum solute concentration and L is the length of the column foam bed. The *HETP* values were found to be equal to $1.1 \pm 0.2 \text{ mm}$ and $1.3 \pm 0.2 \text{ mm}$ at flow rates of $15 \text{ cm}^3 \text{ min}^{-1}$ and $20 \text{ cm}^3 \text{ min}^{-1}$, respectively.

The *HETP* value for the unloaded foam column was also calculated from the break-through capacity curve (Fig. 6) of Diazinon at $15 \text{ cm}^3 \text{ min}^{-1}$ and $25 \text{ cm}^3 \text{ min}^{-1}$ employing the equation [11]

$$N = \frac{V\bar{V}}{(V\bar{V})^2} = \frac{L}{HETP}$$

where V is the volume of effluent at the center of the S-shaped section of the breakthrough capacity curve where the concentration is one-

half of the initial concentration, and \bar{V} is the volume at which the effluent has a concentration of 0.1578 of the initial concentration. The value of the *HETP* obtained by this method was $1.2 \pm 0.2 \text{ mm}$, confirming the values obtained from the elution curves.

The separation of Malathion (0.1 mg) from Chlorpyrifos (0.05 mg) in aqueous solution at pH 2 and in the presence of sodium chloride (0.1 M) for Chlorpyrifos has been successfully carried out on the polyurethane foam. The solution mixture was percolated through the foam column at $15 \text{ cm}^3 \text{ min}^{-1}$. The sorption of Chlorpyrifos took place while Malathion was not retained on the foam column and collected quantitatively in the effluent. Chlorpyrifos was then recovered from the foam with 100 cm^3 of acetone at $2\text{--}3 \text{ cm}^3 \text{ min}^{-1}$ and was determined spectrophotometrically at 206 nm.

4. Conclusion

Unloaded foams in the batch and the column modes can be applied to trap trace amounts of insecticides from water, and the retained species can be recovered with an appropriate eluent. The separation of the tested species can be achieved provided that there is a sufficiently large difference in the optimum condition of extraction of each compound. A study of the rested compounds shows that the insecticides are extracted in their neutral form by a simple solvent-extraction mechanism. This conclusion is supported by the short time required for extraction equilibrium and the slating out phenomenon. The nature of the sorption media has a marked effect on the extraction performance of the tested species by the foam. Moreover, the foam offers a wider range of modifications than normal granular solids. The good hydrodynamic properties of the foam sorbent give the unique advantage of rapid, and versatile preconcentration of the tested compounds.

Acknowledgment

The authors wish to thank Professor Salah Elnahwy, Dean of the Faculty of Science for his excellent support and help during this work.

References

- [1] J.R.H. Malissa, *Egypt J. Anal. Chem.*, 1 (1990) 49.
- [2] A.S.Y. Chau, B.K. Afghan and J.W. Robinson, *Analysis of Pesticides in Water, Significance, Principles, Techniques and Chemistry of Pesticides*, Vol. 1, CRC Press, Boca Raton, FL, 1982.
- [3] C.A. Edward, *Persistent Pesticides in the Environment*, 2nd edn., CRC Press, Boca Raton, FL, 1973.
- [4] C.A. Edward, *Environmental Pollution by Pesticides*, Plenum Press, New York, 1981, p. 409.
- [5] L.T. Kurkland, S. Shibko, A. Kolbye and R. Shapiro, *Environ. Res.*, 4 (1971) 9.
- [6] A.H. Romano and R.S. Safferman, *J. Am. Water Works Assoc.*, 55 (1963) 169.
- [7] J.F. Uthe, J. Reinke and H.D. Gesser, *Environ. Lett.*, 3 (1972) 117.
- [8] B. Ahling and S. Jensen, *Anal. Chem.*, 36 (1964) 134.
- [9] H. Oda and C. Yokokawa, *Carbon*, 21 (1983) 483.
H. Oda, M. Kishida and C. Yokokawa, *Carbon*, 19 (1981) 243.
- [10] T. Brawn, J.D. Navratil and A.B. Farag, *Polyurethane Foam Sorbents in Separation Science*, CRC Press, Boca Raton, FL, 1985.
- [11] S. Palagyi and T. Brawn, *Separation and Preconcentration of Trace Elements and Inorganic Species on Solid Polyurethane Foam Sorbents*, in Z.B. Alfassi and C.M. Wai (Eds.), *Preconcentration Technique for Trace Elements*, CRC Press, Boca Raton, FL, 1992.
- [12] A.B. Farag, A.M. El-Wakil, M.S. El-Shahawi and M. Mashaly, *Anal. Sci. (Jpn.)*, 5 (1989) 415.
- [13] A.B. Farag and M.S. El-Shahawi, *J. Chromatogr.*, 552 (1991) 371.
- [14] M.S. El-Shahawi, *Talanta*, 41 (1994) 1481.
- [15] M.S. El-Shahawi, A.B. Farag and M.R. Mostafa, *Sep. Sci. Technol.*, 29 (1994) 289.
- [16] A.B. Farag, A.M. El-Wakil and M.S. El-Shahawi, *Fresenius' Z. Anal. Chem.*, 324 (1986) 59.
- [17] P. Fong and A. Chow, *Talanta*, 39 (1992) 497–825.
- [18] I.I. Stewart and A. Chow, *Talanta*, 40 (1993) 1345.
- [19] L. Schumack and A. Chow, *Talanta*, 34 (1987) 957.
- [20] T. Braun, *Fresenius, Z. Anal. Chem.*, 333 (1989) 785.
- [21] B.K. Afghan, R.J. Wilinon, A. Chow, T.W. Findley, H.S. Gesser and K.I. Srikameswaran, *Water Res.*, 18 (1984) 9.
- [22] T. Braun and A.B. Farag, *Anal. Chim. Acta*, 99 (1978) 1.
- [23] G.J. Moody and J.D.R. Thomas, *Chromatographic Separation with Foamed Plastics and Rubbers*, Dekker, New York, 1982.
- [24] K.G. Kirkwood, *J. Chem. Phys.*, 2 (1934) 351.
- [25] A.W. Adamson, *Physical Chemistry of Surfaces*, 2nd edn., Academic Press, New York, 1967.
- [26] S. Palagyi and T. Braun, *J. Ration. Nucl. Chem.*, 163 (1992) 69 and references therein.
- [27] S. Palagyi and T. Braun, *Z. Homonnay and A. Vertes, Analyst*, 117 (1992) 1537 and references therein.
- [28] A. Roychaudhuri, S.K. Roy and A.K. Chakraburty, *Talanta*, 39 (1992) 1377.
- [29] R.C. West, *Handbook of Chemistry and Physics*, 54th edn., CRC Press, Boca Raton, FL, 1973.

Iodometric determination of gold and platinum by 168- and 126-fold chemical amplification reactions

M.S. El-Shahawi^{a,*}, A.B. Farag^b

^a Chemistry Department, Faculty of Science, UAE University, P.O. Box 17551, Al-Ain, United Arab Emirates

^b Chemistry Department, University of Qatar, P.O. Box 2713, Doha, Qatar

Received 25 April 1994; revised 16 September 1994; accepted 16 December 1994

Abstract

A simple, low cost method is described for the determination of gold(I) and platinum(II) at the μg level with 8- and 6-fold amplification, respectively. The method is based on oxidation in a solution (pH 2.4–4.3) of gold(I) or platinum(II) with aqueous potassium periodate, masking the unreacted periodate with molybdate and iodometric determination of the produced iodate and gold(III) or platinum(IV). The sensitivity of the proposed method can be enhanced by separation of the liberated iodine on a polyurethane foam column, and oxidizing the collected iodine with an excess of periodate. The iodate produced in the effluent and washing solution is then titrated iodometrically after masking the excess periodate. This procedure offers a 168- and 126-fold amplification for gold(I) and platinum(II), respectively. Analysis of the binary mixtures of gold(I) and (III) or platinum(II) and (IV) in aqueous solution has been carried out successfully.

Keywords: Gold; Platinum; Iodometry

1. Introduction

Because of the importance of gold and platinum and their extremely low levels in various matrices, sensitive methods are required for reliable quantitation [1,2]. Neutron activation analysis, spectrophotometric and electro-analytical techniques are the most frequently used techniques [3–5]. However, there are constraints on their wide applications in routine analysis; because of the specialised nature of some of these techniques, some of these methods are very laborious, and not very practicable, and the reactions sometimes require high acidities.

Recently, the application of an amplification reaction was reported in which potassium periodate in aqueous acidic solution was used for oxidation of various metal ions [6–10], masking of the excess periodate with molybdate and the iodate produced determined by reaction with iodide. This paper describes an accurate iodometric amplification procedure for the microgram determination of gold(I) and -(III) and platinum(II) and -(IV) in aqueous solution, based on this reaction.

2. Experimental

2.1. Reagents

All reagents were of analytical reagent grade. All solutions were prepared from doubly distilled water.

* Corresponding author.

¹ Permanent address: Chemistry Department, Faculty of Science at Damietta, Mansoura University, Mansoura, Egypt.

Polyurethane foam, an open-cell type polyether (bulk density 30 kg m^{-3}) was supplied by K.G. Greiner Schaum (Stoffwerk, Kremsmunster, Austria). The foam material was washed and treated as previously described [11]. A strong ion exchanger Amberlite 400 was used to preconcentrate gold(I). Stock solutions of 1 mg ml^{-1} gold(III) and platinum(II) (atomic absorption standard, BDH) were used and diluted with water just before use. Gold(I) stock solution (0.1 mg ml^{-1}) was prepared by adding 3 ml of saturated sodium sulphite to a standard solution of gold(III), acidifying with 5 ml H_2SO_4 (2 M), and removing the excess sulphurous acid by boiling the solution for 5 min. The pH of the solution was adjusted to 3 with sodium hydroxide and the solution was diluted with water to the mark of a calibrated flask. A stock solution of platinum(IV), 1 mg ml^{-1} was prepared by dissolving the exact weight of K_2PtCl_6 in distilled water and the volume was made up to 100 ml with water in a calibrated flask. A 10% ammonium molybdate solution was prepared by dissolving 10 g of the salt in water. Potassium periodate solution was prepared by dissolving 0.35 g of KIO_4 in 100 ml of distilled water containing a few drops of saturated borax solution. Sodium thiosulphate solution (0.01–0.005 M) was prepared and standardized against potassium iodate. Buffer solutions of pH 2.4–3.4 were prepared by mixing 200 ml of glacial acetic acid with water and adjusting the pH with sodium acetate solution (0.1 M).

2.2. Apparatus

Water-jacketed glass columns, $18 \text{ cm} \times 15 \text{ mm}$, were used in column experiments. An Orion Research Model 601 digital iolyzer/pH meter and a 250 ml oxygen flask with fused-silica sample holder of conventional specifications were used.

2.3. Recommended procedure

Determination of gold(I) or platinum(II)

In a 100 ml conical flask, mix 1–5 ml of sample solution containing 10–200 mg gold(I) or 20–500 mg platinum(II) and 10 ml water. Adjust the pH to 2.4–3.4 with acetate buffer, then add 5 ml of KIO_4 solution and heat the reaction mixture on a water bath for 20 min. After cooling add 5 ml buffer of pH

3 and 10 ml of molybdate solution, and treat by one of the following methods

8- or 6-fold amplification. To the aqueous solution of the iodate and Au(III) or Pt(IV) produced, add a few crystals of KI (30–60 mg) and titrate the liberated iodine with 0.005 M $\text{Na}_2\text{S}_2\text{O}_3$. Run a blank determination and apply the necessary corrections.

168- or 126-fold amplification. The aqueous solution of the produced iodate and Au(III) or Pt(IV) is allowed to react with KI (70–60 mg) at pH 3 to liberate iodine and gold(I). To the aqueous solution of the iodine and gold(I), add 20 ml of HCl (1 M) and percolate the solution through an Amberlite IRA-400 column at 5 ml/min to preconcentrate gold(I) quantitatively on the resin. After washing the column with 20 ml of HCl (1 M) at the same flow rate, collect the iodine in the washing solution and the effluent. The iodine produced is retained quantitatively from the aqueous solution on a polyurethane foam column at 5 ml min^{-1} . A 50 ml portion of distilled water is then passed through the foam column at 5 ml min^{-1} to wash out the excess KI. 10 ml of potassium periodate solution and 5 ml of borate buffer (pH 7) are then added to the upper separating funnel of the column while its tap is closed. Water, thermostated at 80°C , is then circulated through the external jacket of the column for 10 min and the KIO_4 solution is then allowed to pass through the foam column at 3 ml min^{-1} . Another 5 ml of periodate–borate buffer are passed through the column at the same flow-rate followed by 50 ml of distilled water at a flow-rate of 5 ml min^{-1} to wash out the iodate produced. The effluent and washings are collected in a conical flask and 25 ml of acetate buffer is then added after cooling. The iodate produced is then titrated iodometrically after masking the unreacted periodate with molybdate, as described above. Run a blank determination.

Determination of gold(III) or platinum(IV)

Transfer a portion of gold(III) or platinum(IV) solution (1–5 ml) containing up to 200 μg of Pt(IV) and add 3–5 ml of saturated sodium sulphite and 10 ml of water followed by 2 ml of concentrated H_2SO_4 . Allow the reaction mixture to stand for 3 min then evaporate the solution gently on a hot-plate until the

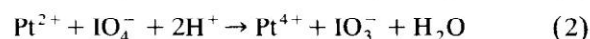
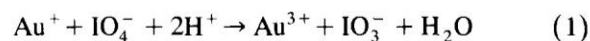
excess SO_2 has been completely removed. Add 10 ml of distilled water and adjust the pH (2.6–3.6) with acetate buffer. Determine the total content of the element by the procedure described above.

Analysis of gold or platinum in organic compounds

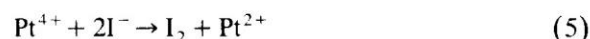
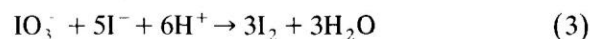
Weigh exactly 1–2 mg of the organo-gold (or -platinum) compound and wrap the sample as usual for the oxygen-flask technique [12,13]. Add 10 ml of aqua regia and 5 ml of KClO_3 , fill the flask with oxygen and combust the sample. Shake the flask for 2–3 min, open it and rinse the stopper and sample holder with 10 ml of doubly distilled water. Boil the solution on a hot plate until the volume has been reduced to ca. 10 ml and follow the described procedure for gold(III) or platinum(IV) determination after neutralizing the solution with Na_2CO_3 . Run a blank for correction.

3. Results and discussion

In acidic media potassium periodate was found to oxidize gold(I) and platinum(II) to gold(III) and platinum(IV), respectively, as follows:



The released iodate and gold(III) or platinum(IV) can oxidize potassium iodide according to the following equations:



Reaction 3 takes place rapidly and proceeds quantitatively in acidic media at $\text{pH} \leq 3.6$. Preliminary experiments showed that reaction 4 proceeds quantitatively at $\text{pH} \leq 3.4$ while reaction 5 does not take place in moderate acidic medium ($\text{pH} \geq 2.4$).

Moreover, oxidation of gold(I) and platinum(II) with periodate depends on the pH, reaction time and temperature. Thus fixed amounts (100 μg) of gold(I) and platinum(II) adjusted to pH 2.2–6, were allowed to react with potassium periodate (5 ml) for different time intervals (5–60 min) and at different tempera-

tures (ambient or 100° C) on a boiling water bath. The solutions were then adjusted to the required pH by adding 10 ml of acetate buffer and the excess periodate was masked with molybdate. The results showed that a suitable pH for the quantitative oxidation of gold(I) and platinum(II) with periodate is in the range 2.4–3.4 after heating the reaction mixture on a boiling water bath for 15 min. Fortunately, the pH values suitable for the quantitative oxidation of gold(I) and platinum(II) with periodate ions are quite appropriate for masking the unreacted periodate with molybdate. The released iodate and gold(III) were then allowed to react with potassium iodide. Thus, the acetate buffer solution of pH 3 was added at the beginning of the experiment and before addition of KI. At $\text{pH} < 2.4$ reaction 5 proceeds rapidly with 8-fold amplification of platinum(II), but under these pH conditions the molybdate does not mask the excess periodate quantitatively [14]. Thus erroneously high results and blank values were obtained due to the reaction of the unmasked periodate with iodide. At pH 2.4–3.4 each original gold(I) or platinum(II) ion releases eight or six atoms of iodine, respectively, i.e., the proposed method affords an eight- or six-fold amplification for gold(I) or platinum(II), respectively. The proposed procedure was employed for the determination of 100–200 μg of gold(I) and 20–500 μg of platinum(II). The results are summarized in Table 1. The regression coefficients and the relative standard deviation ($n = 5$) at 100 μg Au(I) or Pt(II) were found to be 0.944 and 1.6%.

The proposed method can be employed for the determination of gold(III) or platinum(IV) after reduction to the mono and the divalent state, respec-

Table 1
Determination of various amounts of gold(I) and platinum(II) in aqueous media^a

Gold(I)		Platinum(II)	
Taken, μg	Found, μg	Taken, μg	Found, μg
10.0	10.1 \pm 0.2	20.0	20.8 \pm 0.3
20.0	20.1 \pm 0.4	50.0	51.1 \pm 0.6
50.0	49.9 \pm 0.5	100	101 \pm 0.3
100	101.4 \pm 0.5	150	150 \pm 0.7
200	201 \pm 0.6	200	01 \pm 0.8
		500	502 \pm 0.6

^a Average \pm S.D. of 5 measurements.

tively. A search was made for a suitable reducing agent. Sodium sulphite in acidic media was found to be most suitable for the prior reduction of gold(III) or platinum(IV) to gold(I) or platinum(II), respectively, without interfering with the proposed iodometric method. The unreacted sulphite can be removed by boiling off sulphur dioxide. Satisfactory results for the determination of various amounts of gold(III) or platinum were obtained with a standard deviation in the range 0.2–0.3, in the 100–500 μg range ($n = 5$).

Analysis of a binary mixture of gold(I) and (III) or platinum(II) and (IV) in aqueous media was carried out by the proposed procedure. An aliquot of each mixture was allowed first to react with potassium periodate employing the recommended procedure as described above. The released iodine in the gold mixture is equivalent to the gold(I) and (III) present, while that released from the platinum mixture is equivalent to platinum(II) ions only, and is titrated with $\text{Na}_2\text{S}_2\text{O}_3$ (0.005 M). Another aliquot of the gold mixture is allowed to react with KI at $\text{pH} < 3$; the released iodine is equivalent to gold(III) only. Another aliquot of platinum mixture was then reduced to platinum(II) with sodium sulphite as described above followed by determination of the released iodate by the proposed procedure. The volume of thiosulphate solution used in the first titration (A ml) of the gold mixture is equivalent to the sum of Au(I) and Au(III) while for the platinum mixture it is equivalent to Pt(II) only. If the volume of the thiosulphate solution required in the second titration procedure is B ml, the difference, $B - A$ ml, is equivalent to the gold(I) or platinum(IV) in their mixtures. The results obtained are summarized in Table 2, and good reproducibility is achieved.

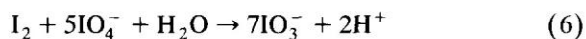
The degree of amplification of gold(I) and platinum(II) can be increased by employing polyurethane foam. Polyether-based polyurethane foam sorbents have proved to be very efficient for the rapid absorption and separation of iodine in aqueous and gaseous media [10,15]. The presence of a relatively large excess of iodide ions in aqueous solution has no effect on the absorption of iodine [10,15]. Thus, on passing the aqueous solution of the released iodine and gold(I) (Eqs. 3 and 4) containing HCl (1 M) through the Amberlite IRA-400 column, the gold(I) species only is preconcentrated quantitatively from

Table 2
Determination of binary mixtures of Au(I) + (III) and Pt(II) + (IV) in aqueous media^a

Gold taken (found), μg		Platinum taken (found), μg	
Au(I)	Au(III)	Pt(II)	Pt(IV)
20.0	50.	50.0	50.0
(20.2)	(51 \pm 0.2)	(50.6 \pm 0.4)	(51.2 \pm 0.3)
50.0	100	100	50
(50.9 \pm 0.3)	(101 \pm 0.4)	(101 \pm 0.6)	(51 \pm 0.1)
100	50.0	150	100
(101 \pm 0.5)	(50.7 \pm 0.4)	(151 \pm 0.4)	(101 \pm 0.4)
150	50.0	200	150
(151 \pm 0.2)	(50.9 \pm 0.3)	(202 \pm 0.3)	(151 \pm 0.31)

^a Average \pm S.D. ($n = 3$).

the solution in the column [16] at 5 ml min^{-1} . Gold(I) as its chloro complex is strongly adsorbed on the anion exchanger and is very difficult to elute into the solution as previously reported [17]. Released iodine in the effluent and washing solution from the gold(I) system or iodine and platinum(IV) (Eqs. 3 and 5) produced from the platinum(II) system is allowed to percolate through the foam column at 5 ml min^{-1} at room temperature. The retained iodine on the foam column is determined by oxidation with KIO_4 at $\text{pH} 7$ and 80°C to produce iodate which is quantitatively eluted from the column with distilled water. This step produces a 21-fold amplification according to the equation [18]:



The iodate and gold(III) or iodate and platinum(IV) released by Eqs. 1 and 2 produced an 8- or 6-fold amplification of the iodine equivalent to each gold(I) or platinum(II) ion, respectively, under the optimal conditions. Thus, overall a 168- and 126-fold amplification with respect to the gold(I), or platinum(II) originally present is obtained, respectively.

3.1. Interference studies

The determination of a fixed amount (40 μg) of gold(I) or platinum(II) in the presence of a relatively large excess (1 mg) of AsO_3^{3-} , SbO_3^{3-} , SO_4^{2-} , PO_4^{3-} , Cl^- , Br^- , CO_3^{2-} , HCO_3^- , NO_3^- , $\text{B}_4\text{O}_7^{2-}$, SiO_3^{2-} , or WO_4^{2-} was examined by the proposed procedure. The percentage recovery of gold or platinum was

always $100 \pm 2.5\%$. Interference of Fe^{3+} , Pb^{2+} , VO_2^+ , or MoO_4^{2-} at 100-fold excess with respect to $50 \mu\text{g}$ of gold(I) or platinum(II) was removed by adding NaF to the aqueous solution to give a concentration of 1 M. Bismuth(III) was eliminated by shaking the aqueous solution with 10 ml xylene at pH 9–11 in the presence of 10 ml sodium diethyldithiocarbamate solution. manganese(II) and ruthenium(II) or -(III) chloride interfered seriously.

3.2. Application of the proposed method

Analysis of gold and platinum in their complexes

The developed procedure for the analysis of gold(I) (8- or 168- fold) and platinum(II) (6- or 126-fold) has been successfully employed for the determination of gold or platinum in their organocompounds [19,20] after combustion as described earlier. Gold is usually present in solution as gold(III) while platinum is present as Pt(II) or -(IV). The residual solutions were diluted with water and determined according to the procedure described above. Representative results are given in Table 3, with an average absolute error of 1.2–1.8%. The blank values taken through the whole procedure using freshly prepared periodate, distilled water and molybdate solutions ranged between 0.15–0.2 ml of 0.01 M thiosulphate solution.

It is worth mentioning that if a reasonably large amount of gold or platinum is present, it is advisable to dilute the solution of iodate produced in the first step to 25 ml with distilled water and treat only 5 ml of this solution by the foam amplification procedure.

Organic compounds containing a lower percentage of gold or platinum can be analyzed by running the proposed procedure on the whole absorption solution after the oxygen flask combustion.

3.3. Determination of gold or platinum added to natural water samples

The determination of very low concentrations of gold or platinum (less than nanomolar levels) in tap, mineral, polluted portable or sea water (0.1 l) is also possible by the proposed method. Filtration of the samples solution through a $0.45 \mu\text{m}$ membrane was followed by adding 10 ml of 1×10^{-3} M Na_2EDTA and 10 ml of 1 M NaF. Preconcentration of gold(III) or platinum(II) from the acidic aqueous solution of the sample onto a porous polyurethane foam column was then carried out [21,22]. Elution of the extracted gold or platinum species from the foam column is carried out as described earlier [21,22]. To the effluent solution, 10 ml of conc. $\text{H}_2\text{SO}_4\text{--HNO}_3$ (1:3, v/v) were added in a fume cupboard, heated on a hot plate until white fumes of SO_3 were evolved and cooled to room temperature. The residue was then heated with 10 ml deionised water so as to dissolve the salts followed by the determination according to the above procedure. The concentration of the tested metal ions in such water samples was below the detection limit, so only the recovery of the spiked Au(III) or Pt(II) was determined. Satisfactory results were obtained with a relative standard deviation in the range 1.7–2.1%. If the waste water is highly coloured or contains a significant concentration of

Table 3

Determination of gold and platinum in some compounds by the proposed amplification procedures ^a

Compound ^b	Metal (%)		
	Calculated	Found	
		a	b
$(\text{C}_2\text{H}_5)_3\text{PAuCl}$	55.9	56.4 ± 0.3	56.9 ± 0.4
$(\text{C}_2\text{H}_5)_3\text{PAuCl}(\text{Sc}_6\text{H}_4\text{COOH})$	41.8	42.2 ± 0.3	42.5 ± 0.4
$(\text{C}_2\text{H}_5)_3\text{PAuCl}(\text{Sc}_6\text{H}_4\text{COOH})$	31.9	32.2 ± 0.2	32.6 ± 0.4
H_2PtCl_6	47.6	47.6 ± 0.5	48 ± 0.3
$\text{Pt}(\text{MEA})_2\text{Cl}_4$	42.5	42.9 ± 0.4	41.8 ± 0.6
$\text{Pt}(\text{DEA})_2\text{Cl}_4$	37.8	38.2 ± 0.4	40.6 ± 0.4

^a With (a) and without (b) foam amplification, mean \pm S.D. ($n = 3$).

^b MEA and DEA are mono- and diethanolamine, respectively.

organic matter, the sample should be evaporated and the volume reduced to 20 ml. Add 5 ml of concentrated HNO_3 and 1 ml of 30% H_2O_2 . Heat and evaporate the solution to dryness. After cooling, dissolve the residue with 5 ml dilute acid, transfer the solution to a 250 ml flask and follow the general procedure as described above.

4. Conclusion

The proposed method provides a possible alternative approach to flame atomic absorption spectrometry for the determination of gold or platinum. The advantages of the method are that it is not only applicable for the simultaneous determination of metals in various oxidation states in the mixture but it can also be used for their determination in complexes. The sensitivity of the proposed procedure can be improved by employing a polyurethane foam column for trace preconcentration of the tested metal ions from large sample volumes followed by iodometric microdetermination by the proposed procedure after elution from the foam [10]. The determination of gold in the presence of platinum or vice versa is not possible by the proposed procedure.

Acknowledgements

The authors would like to thank Miss. K. El Taqiz for her excellent assistance during this work.

References

- [1] A.Z. Abu Zuhri, M.S. El-Shahawi and M.M. Kamal, *Anal. Chim. Acta*, 282 (1993) 133.
- [2] M.S. El-Shahawi, A.Z. Abu Zuhri and M.M. Kamal, *Fresenius' J. Anal. Chem.*, 348 (1994) 730.
- [3] S.B. Adeloju, A.M. Bond, S.N. Tan and G. Wei, *Analyst*, 115 (1990) 1569; V.O. Oturba, M. Strnadova and B. Skalnikova, *Talanta*, 40 (1993) 221.
- [4] P.S. Tjioc, K.J. Volkers, J.J. Kroom and J.J.M. Goeij, *Int. J. Environ. Anal. Chem.*, 17 (1984) 13.
- [5] E.D. Ehman and D.E. Vance, *CRC, Crit. Rev. Anal. Chem.*, 20 (1989) 405.
- [6] A.M. El-Wakil, A.B. Farag and M.S. El-Shahawi, *Talanta*, 36 (1989) 783.
- [7] A.M. El-Wakil, A.B. Farag and M.S. El-Shahawi, *Fresenius' J. Anal. Chem.*, 337 (1990) 886.
- [8] A.B. Farag, M.S. El-Shahawi and E.M. El-Nemma, *Fresenius' J. Anal. Chem.*, 346 (1993) 455.
- [9] A.M. El-Wakil, A.B. Farag and M.S. El-Nahas, *Talanta*, 40 (1993) 841.
- [10] A.B. Farag, H.N.A. Hassan, A.M. Khalil and A.F. Abdel-Azis, *Analyst*, 110 (1985) 1265; and references cited therein.
- [11] M.S. El-Shahawi, A.B. Farag and M.R. Mostafa, *Sep. Sci.*, 29 (1994) 289.
- [12] A.M.G. Macdonald, *Analyst*, 86 (1961) 4.
- [13] T.S. Ma and R.C. Riittner, *Modern Organic Elemental Analysis*, Marcel Dekker, New York, 1979.
- [14] D. Burnel, *C.R. Acad. Sci., Paris*, 261 (1965) 1982.
- [15] A.B. Farag, M.E. Attia and H.N.A. Hassan, *Indian J. Chem.*, 20B (1981) 683.
- [16] A. Mizuike, Y. Lida, K. Yamada and S. Hirano, *Anal. Chim. Acta*, 32 (1965) 428; W. Koch and J. Korkisch, *Mikrochim. Acta*, (1973) 117.
- [17] W. Qi, X. Wu, C. Zhou, H. Wu and Y. Gao, *Anal. Chim. Acta*, 270 (1992) 205.
- [18] R. Belcher, J.W. Hamya and A. Townshend, *Anal. Chim. Acta*, 49 (1970) 57.
- [19] P.D. Cookson and E.R.T. Ticknic, *J. Coord. Chem. Rev.*, 26 (1992) 313.
- [20] M.S. Masoud and S. Abou-El-Enein, 2nd Chemistry Conference, Faculty of Science, Alex. Univ., Alexandria, Egypt, June 1988.
- [21] T. Braun and A.B. Farag, *Anal. Chim. Acta*, 99 (1978) 1; S. Sukiman, *Radiochem. Radionol. Lett.*, 18 (1974) 129.
- [22] A.S. Khan and A. Chow, *Talanta*, 31 (1984) 692; S.J. Al-Bazi, and A. Chow, *Anal. Chem.*, 52 (1983) 1094.



Spectral and electrochemical studies of D-tartaric and DL-mandelic acids with different chromium ions

M. S. EL-SHAHAWI†§ and S. A. BARAKAT‡

† Chemistry Department, Faculty of Science, United Arab Emirates University, P.O. Box 17551, Al-Ain, United Arab Emirates

‡ Chemistry Department, Faculty of Science, Jordan University of Science and Technology, Irbid 3030, Jordan

(Received 18 January 1994; in revised form 11 March 1994; accepted 18 March 1994)

Abstract—The UV–vis, circular dichroism (CD) and cyclic voltammetry (CV) measurements of the binary systems chromium(III), chromium(VI) or peroxochromium(VI)–D-tartaric or DL-mandelic acid have been studied in aqueous media at different pH. The electronic spectra of the binary mixtures chromium(III) or peroxochromium(VI)–ligand contained the expected *d–d* transition for a d^3 chromium(III) ion in octahedral symmetry. Strong Cotton effects were observed for the solutions of chromium(III) or peroxochromium(VI) D-tartaric acid. The parameters D_q , B , β_{35} and the interelectronic repulsion parameter with the ionic charge, Z^* , for the species formed provide reassurance that the hydroxyacid oxygen was complexed to chromium(III) ion. Equilibrium quotients for some of the chromium(III) complex species were calculated at pH \approx 6.5.

INTRODUCTION

UNTIL recently chromium was not regarded as an essential micronutrient, however some renewed interest in the chromium(III) complexes of naturally occurring ligands has resulted [1–4]. In a number of foodstuffs a significant relationship was found between the extractable chromium and biological activity [5]. This raises the possibility that chromium could be complexed with naturally occurring ligands, therefore attention has been paid in recent years to the investigation of chromium importance in many biological systems *in vivo* [6, 7]. In this paper we present, an investigation of the UV–vis, circular dichroism and cyclic voltammetry of some of the binary systems of chromium(III), chromium(VI) and peroxochromium(VI) with the title α -hydroxyacids.

EXPERIMENTAL

The α -hydroxyacids, DL-mandelic and D-tartaric were of reagent grade. Chromium(III) trichloride hexahydrate, potassium dichromate and hydrogen peroxide were BDH chemicals. Chromium(III) 26.6 g (100 mmol) and chromium(VI) 29.4 g (100 mmol) were prepared in distilled water. These solutions were diluted whenever required to give 1:1 and 1:3 molar ratios of chromium: α -hydroxy acid. The solution spectra and cyclic voltammetry measurements were recorded at room temperature at different pH. The solutions were allowed to equilibrate for 1 h before measurements. Sodium sulphate was used as supporting electrolyte in the cyclic voltammetric measurements and its concentration was ten times that of the chromium ion.

PHYSICAL MEASUREMENTS

Electronic spectra were recorded on a Beckman Acta MIV spectrometer. Circular dichroism measurements were recorded on an instrument described elsewhere [8]. Cyclic voltammetry was carried out on a P.A.R. 175 Universal programmer, a Wenking PGS potentiostat and 7000 AM X–Y recorder. The working and secondary electrodes were platinum wires of 0.5 mm diameter. A SCE served as reference electrode and an Orion pH meter was used for the pH measurements. Silica gel TLC plates (Merck 60 F₂₅₄) 10 × 20 cm were employed.

§ Author to whom all correspondence should be addressed.

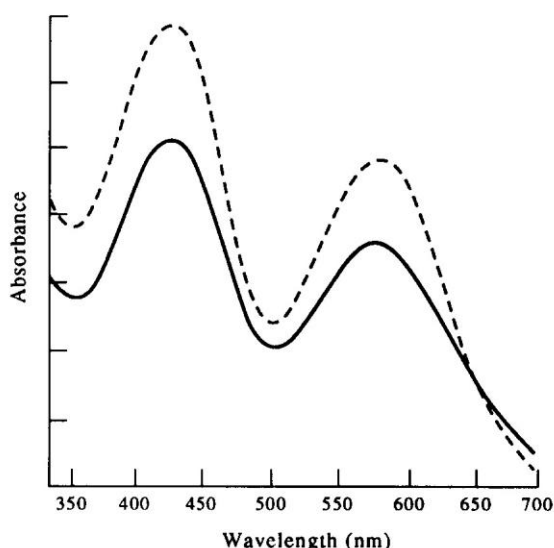


Fig. 1. Electronic UV-vis solution spectra of the chromium(III)-D-tartaric acid complexes at pH 6: — (1:1); (1:3).

RESULTS AND DISCUSSION

In the spectra of chromium(III)-D-tartaric acid systems, the ${}^4A_{2g} \rightarrow {}^4T_{2g}$ transitions in octahedral or pseudo octahedral symmetry [9] were shifted to shorter wave numbers with increasing pH except at pH 6 for the 1:3 ratio, it is increased to $17,600\text{ cm}^{-1}$ with a modest increase in intensity (Fig. 1). The ${}^4A_{2g} \rightarrow {}^4T_{1g}$ $d-d$ transitions were smoothly shifted to longer wave numbers. These shifts could be due to change in the environment of the chromium(III) resulting from amongst other things, the deprotonation of the hydroxyl and carboxylic acid groups [10–12] (Fig. 2) and the complexed water molecules as shown in Fig. 2.

The spectral data of chromium(III)-DL-mandelic acid solutions in 1:1 and 1:3 ratios are similar suggesting formation of similar complex species. A study of how the electronic spectra evolve with changing chromium-ligand ratio with excess ligand concentration showed no significant changes in the position of the absorption bands suggesting unique composition with that of the 1:3 chromium-ligand ratio. The ${}^4A_{2g} \rightarrow {}^4T_{1g(p)}$ $d-d$ transitions [9] were shifted to shorter wave numbers, whereas the changes in the ${}^4A_{2g} \rightarrow {}^4T_{2g}$ $d-d$ transitions are not regular with increasing pH.

In the spectra of chromium(VI)-D-tartaric or DL-mandelic acid systems prepared in 1:1 and 1:3 ratio, two peaks were observed at $35,700$ and $28,600\text{ cm}^{-1}$. These bands were altered to $37,000$ and $25,300\text{ cm}^{-1}$, respectively, with increasing pH from 2 to 7.6, suggesting weak interaction of chromium(VI) ions with these ligands. In the case of chromium(VI)-D-tartaric acid solutions prepared in 1:3 ratios, weak Cotton effects at $310\text{--}320$ (+, w), $385\text{--}450$ (+, v, w) and $520\text{--}560$ (+, w) nm at $2 \leq \text{pH} < 5.5$ were observed. The intensity of the CD bands was increased with increasing time, suggesting formation of chromium(VI) or chromium(III) complex species with the ligand [13].

The colour of the peroxochromium(VI) with D-tartaric or DL-mandelic acid solutions prepared in 1:1 and 1:3 ratios were changed from yellow to deep blue at $2 \leq \text{pH} < 3$, purple at $3 < \text{pH} < 7.6$ and orange-violet at $7.6 < \text{pH} < 9$. The spectra of the solutions contained the $d-d$ bands for octahedral chromium(III)- α -hydroxyacid complexes [9]. Benzaldehyde odour was detected in the peroxochromium(VI)-mandelic acid systems, suggesting oxidation of mandelic acid by the chromium(VI) species [14]. The ability of HCrO_4^- ion to form esters with electron pair donors, particularly with OH groups is known [15, 16]. The oxygen bonded chromate esters have been identified as intermediate in the oxidation of organic substrates by chromium(VI) [17]. The oxidation of optically active hydroxyacids by chromium(VI) could be an important biological process, and the

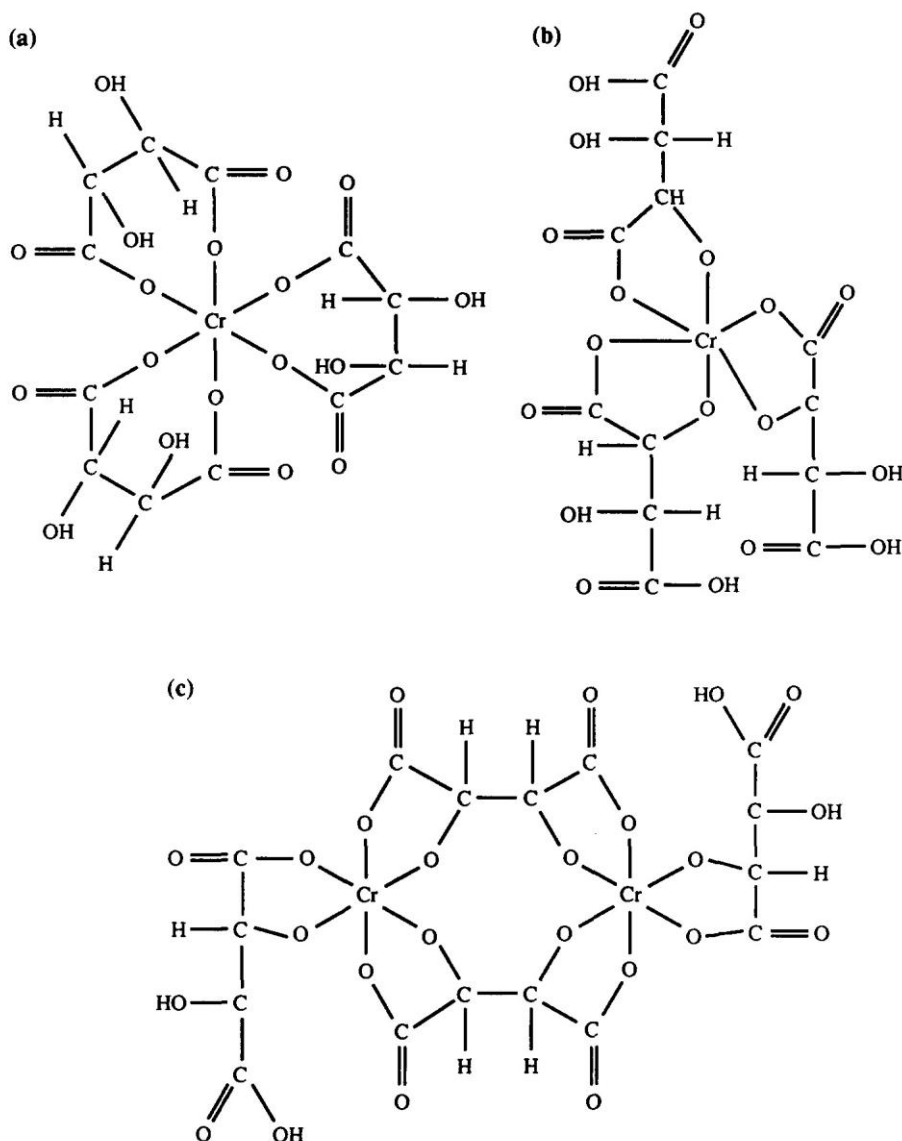


Fig. 2.

role of the metal ion in the reactions with these ligands is of significance in view of the nature of electron transport enzymes which often incorporate carboxy and hydroxyl groups [15].

The D_q values [9] were observed in the range 1666–1786 and 1709–1818 cm^{-1} for the 1:1 and 1:3 chromium(III)–D-tartaric or DL-mandelic acid, respectively. The values of B for tartaric acid chelates were observed lower than those for DL-mandelic acid. This is probably due to the fact that tartaric acid is potentially capable to coordinate as bi-, tri- or tetradentate species while mandelic acid can only function as mono- or bidentate complexing agents. The bulky phenyl group in mandelic acid also stabilizes the conformation of the complexes. The values of nephelauxetic β_{35} are slightly lower than the range observed for CrN_3X_3 (β_{35} : 0.58–0.65) [18] and higher than the values for CrS_6 (β_{35} : 0.44–0.45). Thus, it seems reasonable to presume that most of these chelates contain oxygen and/or chlorine from the original salt $\text{CrCl}_3 \cdot 6\text{H}_2\text{O}$. The variation of the interelectronic repulsion parameter with the ionic charge, Z^* values for $3d^3$ chromium(III) ion in these complex species were found in the range 0.72–0.82 which is considerably below the formal value for +3 [9].

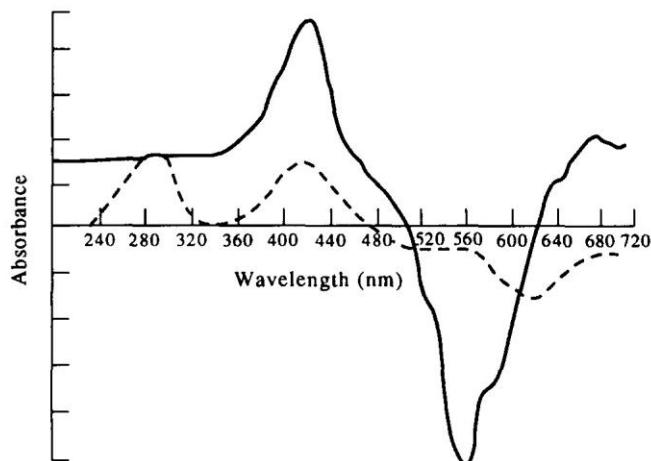


Fig. 3. Circular dichroism solution spectra of the chromium(III)-D-tartaric acid (1:3) at pH 6: — (1:1); (1:3).

The equilibrium was achieved after 1 h upon mixing of chromium(III), and D-(-)-tartaric or DL(-)-mandelic acid solution at pH 6.5 as no subsequent spectral changes were observed. Thus, equilibrium quotients, Q , of these solutions were calculated employing the equation [19]:

$$\frac{1}{A - A_0} = \frac{1}{A_\infty - A_0} + \frac{1}{A_\infty - A_0} \frac{1}{Q[L^-]}$$

where L^- = deprotonated acid. Equilibrium quotients measured at pH 6.5 for chromium(III) chelates with tartaric and mandelic acid were found equal to 3.3 and 4.1 M^{-1} , respectively.

The CD curves of the solutions of the binary mixture chromium(III) and peroxochromium(VI)-D-tartaric acid at different pH confirmed the formation of octahedral chromium(III)-D-tartaric acid complexes. The splitting in the CD spectra showed marked variation corresponding to the shifts obtained in the electronic UV-vis spectra. Two well-defined Cotton effects in the range 390–416(+) and 540–575(-) (Fig. 3) nm were observed for most complexes and were assigned to ${}^4A_{2g} \rightarrow T_{1g}(p)$ and ${}^4T_{2g} d-d$ transitions, respectively, in octahedral symmetry [9]. In addition to these bands, both solutions at pH 6 of 1:1 and 1:3 exhibit another strong positive Cotton effect in the range 586–620 (+) of spin allowed transition. The observed splitting in the forbidden band transition was safely assigned to the splitting of the ${}^4A_{2g} \rightarrow {}^4T_{1g(p)}$ to ${}^2E({}^2E_g)$, ${}^2A_2({}^2T_{1g})$ and ${}^2E({}^2T_{1g})$ ($d-d$) transitions from the lower frequency side [9, 11]. A weak CD band was observed at 275–282(+) nm and was assigned to the charge transfer peak (LMCT) observed for most chromium(III)-hydroxyacid complexes [10, 11].

In the cyclic voltammograms of the chromium(III) with D-tartaric or DL-mandelic acid solutions at pH 2–6 three electrode processes were observed and were assigned to $Cr(III) \rightarrow Cr(II)$, $Cr(II) \rightarrow Cr(I)$ and $Cr(I) \rightarrow Cr(0)$, based on controlled potential electrolysis at E° for each electrode couple vs SCE, respectively. A comparison of the first redox potential E° [$Cr(III) \rightarrow Cr(II)$] of $Cr(III)$ -D-tartaric acid ($E^\circ = -0.26$ V) and $Cr(III)$ -DL-mandelic acid ($E^\circ = -0.23$ V) systems at pH 6 indicate that the former are more easily reduced than the latter. This is possibly because the bulky phenyl group in mandelic acid stabilizes the conformation of the complex species obtained.

CONCLUSION

The results suggest that some care must be exercised in the use of metal-solubilizing drugs such as α -hydroxyacids on patients who have undergone joint replacement.

Although the reaction is slow it could be significant. The oxidation of optically active α -hydroxyacids by chromium(VI) or peroxochromium(VI) is of great importance in the biological process and the role of the metal ion in the reactions with the title ligands is significant in view of the nature of the electron transport enzymes which incorporate carboxy and hydroxyl groups. Another problem that could arise is the *in vivo* effect of the metal complexes formed, particularly if the patient is allergic to certain metals. Stainless steels often contain a range of transition-metal ions, including chromium which is known to cause allergic responses.

The effect of pH and molar ratio on the UV-vis (cm^{-1}), circular dichroism (nm) with ligand field spectral parameters and cyclic voltammetry of some of the binary systems D-tartaric and DL-mandelic acids with different chromium ions have been deposited with the British Library Document Supply Centre at Boston Spa, Wetherby, West Yorks, LS23 7BQ, U.K. as supplementary publication No. Sup. 13086 (5 pages).

Acknowledgement—Thanks to Professor D. H. Brown, for helpful discussions and the facilities provided for carrying out the CD spectra.

REFERENCES

- [1] M. S. El-Shahawi and S. E. Ghazy, *Transition Met. Chem.* **17**, 543 (1992).
- [2] M. S. El-Shahawi and A. A. El-Bindary, *Z. Naturforsch.* **48b**, 282 (1993).
- [3] W. Mertz, *Physiol. Rev.* **49**, 163 (1969).
- [4] D. H. Brown, W. E. Smith, M. S. El-Shahawi and M. F. K. Wazir, *Inorg. Chem. Acta* **124**, L25 (1986) and references therein.
- [5] E. W. Toepfer, W. Mertz, E. E. Roginsky and M. M. Polansky, *J. Agric. Fd Chem.* **21**, 69 (1973).
- [6] M. S. El-Shahawi, Ph.D. Thesis, Strathclyde University, Glasgow, U.K. (1986).
- [7] L. E. Gerdomey and H. M. Goff, *Inorg. Chem.* **21**, 3847 (1982).
- [8] D. H. Brown, G. C. Mckeinlay and W. E. Smith, *J. Chem. Soc. Dalton* 1874 (1977).
- [9] A. B. P. Lever, *Inorganic Electronic Spectroscopy*. Elsevier, Amsterdam (1968).
- [10] S. Kaizaki, J. Hidaka and Y. Shimura, *Bull. Chem. Soc. Jpn* **42**, 988 (1969).
- [11] S. Kaizaki, J. Hidaka and Y. Shimura, *Bull. Chem. Soc. Jpn* **4**, 2207 (1967).
- [12] H. Oki and K. Otsuka, *Bull. Chem. Soc. Jpn* **49**, 1841 (1976).
- [13] R. H. Izquierdo, J. L. Peral-Fernandez and R. Gellego-Andreu, *Anal. Chim. Acta* **142**, 325 (1982).
- [14] S. N. Mahapatro, A. K. Panigrahi, R. Panda and D. M. Patro, *Inorg. Chem.* **23**, 2294 (1984).
- [15] D. Benson, *Mechanism of Oxidation by Metal Ions*. Elsevier, Amsterdam (1976).
- [16] J. K. Beattie and G. P. Haight, *Prog. Inorg. Chem.* **17**, 93 (1972).
- [17] J. H. Espenson, *Acc. Chem. Res.* **3**, 347 (1970).
- [18] C. Pretio and G. Tosi, *Can. J. Chem.* **53**, 2545 (1974).
- [19] R. W. Ramette, *J. Chem. Educ.* **44**, 647 (1967).



Chromium(III) complexes of naturally occurring ligands

M. S. EL-SHAHAWI

Chemistry Department, Faculty of Science, U.A.E. University, Al-Ain, P.O. Box 17551,
United Arab Emirates

(Received 22 December 1993; in revised form 14 March 1994; accepted 16 March 1994)

Abstract—Chromium(III) complexes prepared from CrCl_3Py_3 and anhydrous CrCl_3 with $\text{L}(-)$ -threonine, nicotinic acid, glycine, $\text{D}(-)$ -penicillamine, $\text{L}(-)$ -cysteine and $\text{L}(-)$ -cystine have been characterized. The magnetic moments (3.4–4.05 B.M.) are close to the spin only value for a d^3 chromium(III) ion in octahedral or pseudo octahedral symmetry. In the electronic spectra two sharp peaks are observed at $(15.9\text{--}19.8) \times 10^3$ and $(22.0\text{--}26.7) \times 10^3 \text{ cm}^{-1}$ and are assigned to $d\text{--}d$ transitions in the pseudo octahedral configuration. The parameters (D_q , B , β_{35}) and the interelectronic repulsion parameter with the ionic charge, Z^* , are calculated and place the ligand in the middle of the spectrochemical series. In the circular dichroism spectra three Cotton effects are observed in the forbidden band of the optically active chelates and are assigned to the ${}^2E({}^2E_g)$, ${}^2A_2({}^2T_{1g})$ and ${}^2E({}^2T_{1g})$ while that in the spin allowed band are a result of the splitting of the ${}^4A_{2g}({}^4T_{2g})$ to ${}^4A_1({}^4T_{2g})$ and ${}^4E({}^4T_{2g})$ transitions. The structure of threonine, cystine and cysteine chelates are likely to be *fac* since strong and well defined Cotton effects are observed. The Cotton effects of penicillamine chelates are weak suggesting formation of the *mer* structure. Prolonged heating or bubbling air through the solution of CrCl_3Py_3 containing $\text{L}(-)$ -threonine, glycine or nicotinic acid for several hours enhances chromium(VI) formation.

INTRODUCTION

THE BIO-COMPATIBILITIES of metals have been tested *in vivo* and *in vitro* with naturally occurring compounds. However, with patients in particular those with rheumatoid arthritis, drug therapy continues [1]. Therefore, metal complexes of naturally occurring ligands have long been of interest as models for interactions which may occur in nature [2]. The interactions of sulphur-containing amino acids in particular D -penicillamine and their derivatives with transition metal ions have been the subject of great interest in recent years because of the potential use of these ligands in metal therapy [2–4]. Thus a knowledge of the nature of the bonding between metal ion and these ligands is of great importance.

The nutritional role of chromium(III) has been well established for mammals for the maintenance of normal glucose, lipid and protein metabolism [5–7], but chromium(VI) is reported to be toxic [8, 9]. The carcinogenicity of chromium(VI) is considered in terms of the uptake/reduction model [9]. Analysis of chromium containing brewers yeast fractions implied that various amino acids and nicotinic acid served as structural components of the active complexes [10]. The structure of the Glucose Tolerance Factor (GTF) molecule is unknown but has been suggested to possess two nicotinic acid molecules in a *trans* coordination to Cr(III) through the N atom of the pyridine ring. Ligation to Cr(III) through the carboxylate oxygen of nicotinic acid is reported [11]. Chromium containing an insulin potentiating factor has been isolated and found to contain chromium(III), glycine, cysteine and glutamic acid [11]. A significant relationship was found also between the alcohol-extractable chromium content of foodstuffs and biological activity [12]. These facts raise the possibility that the active chromium(III) could be complexed with naturally occurring ligands in a non-aqueous environment *in vivo* [13, 14].

Chromium reacts with naturally occurring ligands forming several isomeric complex species due to the high affinity of chromium(III) for N, O and/or S donor atoms [15]. Therefore, both chromium and many of its likely complexed species are thought to vary in disease states [1, 16]. However, little work has been carried out on the non-aqueous preparations of chromium(III) complexes with naturally occurring ligands [13, 14]. The title ligands and their coordination compounds seem to be implied in the therapeutic activity displayed by drugs of transition metal ions [16, 17]. The present paper deals with

the preparation and characterization of chromium(III) complexes which contain naturally occurring ligands in their coordination sphere. These species are kinetically inert and are interesting for their role as unique models in studying complex formation with various substrates.

EXPERIMENTAL

Reagents and materials

Nicotinic acid (nic), glycine (gly), L(-)-cystine (cyst), L(-)-threonine (thr) and D(-)-penicillamine (pen) were of reagent grade BDH pyridine (py) and methanol were used without further purification. Anhydrous CrCl_3 was obtained by the standard method from green $\text{CrCl}_3 \cdot 6 \text{H}_2\text{O}$ [18]. The complex $\text{CrCl}_3 \cdot \text{py}_3$ was prepared by the method of TAFT and JONES [19] and was stored in a vacuum desiccator over CaCl_2 .

Preparation of the complexes

To a solution of $\text{CrCl}_3 \cdot \text{py}_3$ or anhydrous CrCl_3 (2 mmol) in methanol, the appropriate weights of the ligand were added to generate 1:3 molar ratios of chromium(III)-ligand. The solutions were refluxed with constant stirring. A number of complexes appeared to be formed in less than 1 h, however all solutions were refluxed for 4 h and the resulting coloured solutions were filtered, reduced in volume using a rotary evaporator and 50 cm^3 of ether was added. The desired precipitate which began to separate out was filtered off, washed with ether and finally dried over anhydrous CaCl_2 . The solid complexes were then redissolved in methanol and the absorption spectra were measured at room temperature. Chromium content was determined as Cr_2O_3 by the method reported elsewhere [20].

Physical measurements

The IR, UV-vis and circular dichroism spectra were measured on a Perkin-Elmer 457 spectrometer, a Varian 634-S spectrometer and an instrument described elsewhere [21]. Magnetic measurements were made on a Johnson Matthey magnetic balance. Silica gel TLC plates (Merck 60 F₂₅₄) $10 \times 20 \times 0.2 \text{ cm}$ were employed.

RESULTS AND DISCUSSION

The biological role of chromium is of great importance in view of either the role of the Cr-O, Cr-N and/or Cr-S bond in the initiation of insulin action and the effectiveness of some naturally occurring ligands for the removal of chromium bound to haemoglobin or the role of these species in the reduction of toxic chromium(V) or (VI) to chromium(III) [1, 2]. The prepared complexes are listed in Table 1 together with their elemental analysis as well as with other physical and chemical properties. The complexes are green/violet, purple, and wine red in colour and have fairly low melting points ($\leq 250^\circ\text{C}$). The elemental analysis indicates that the complexes obtained from $\text{CrCl}_3 \cdot \text{py}_3$ have the general formula $[\text{Cr}(\text{L}-\text{H})_3]$ where L = gly, cys, cyst or thr, while for D(-)-penicillamine and nicotinic acid, the complexes $\text{Cr}(\text{pen})_2\text{Cl}$ and $\text{Cr}(\text{nic})_3\text{py}_3$ were formed. The complexes formed from anhydrous CrCl_3 have the general formula $\text{Cr}_2(\text{L}-\text{H})_4\text{Cl}_2$ except for nicotinic acid which forms the complex $\text{Cr}_2(\text{nic})_4\text{Cl}_6$. Some of the complexes are intensely hygroscopic which accounts for deviations between the observed and calculated elemental analysis (Table 1). The effective magnetic moments (3.4–4.05 B.M.) are exactly as expected for chromium(III) complexes except nicotinic acid chelates. Therefore, the ligand field of these complex species is interpretable and close to the spin only value for a d^3 chromium(III) system in octahedral or pseudo octahedral symmetry with symmetry with substantially 4A_2 ground state [14]. Higher value of the magnetic moments ($> 4.05 \text{ B.M.}$) was observed for the complexes $\text{Cr}(\text{pen}-\text{H})_2\text{Cl}$. Mixing of the A_2 state with the terms derived from the excited state T_2 in chromium(III) complex species could

Table 1. Analytical data; room temperature magnetic moments, μ (B.M.) and physical properties of the complexes^a

Complex	Colour	C	Found (Calcd) (%)			Cr	μ_{eff} (B.M.)	m.p. (°C)
			H	N	Cl			
1. Cr(thr) ₃ H ^b	Wine red	36.6 (36.0)	7.0 (6.7)	10.1 (10.5)		13.0 (12.7)	3.9	
2. Cr(cys-H) ₃	Green-violet	26.3 (26.2)	4.5 (4.4)	9.7 (10.1)		12.2 (12.6)	3.9	130
3. Cr(cys-H) ₃	Purple	28.0 (27.7)	3.9 (4.1)	10.9 (10.8)		6.6 (6.8)	3.8	170
4. Cr(gly-H) ₃	Green-violet	25.6 (25.2)	4.50 (4.2)	14.9 (14.7)		18.7 (18.2)	3.8	210
5. Cr(pen-H) ₂ Cl	Violet	31.6 (31.3)	5.4 (5.2)	7.4 (7.3)	9.5 (9.3)	13.4 (13.6)	4.05	190
6. Cr(nic-H) ₃ Py ₃	Green	59.8 (60.2)	4.4 (4.9)	13.2 (12.8)		7.6 (7.9)	3.4	206
7. Cr ₂ (thr-H) ₄ Cl ₂	Purple violet	32.7 (32.3)	5.7 (5.4)	10.8 (10.6)	12.2 (11.9)	8.9 (8.7)	3.7	216
8. Cr ₂ (cys-H) ₄ Cl ₂	Purple	21.7 (22.0)	3.6 (3.7)	8.8 (8.5)	10.4 (10.8)	15.6 (15.9)	3.6	208
9. Cr ₂ (cyst-H) ₄	Violet	25.7 (25.5)	3.7 (3.9)	9.6 (9.9)	6.5 (6.3)	9.5 (9.2)	3.6	217
10. Cr ₂ (gly-H) ₄ Cl ₂	Green	20.6 (20.4)	3.6 (3.4)	11.6 (11.9)	15.4 (15.1)	21.8 (22.1)	3.8	196
11. Cr ₂ (pen-H) ₄ Cl ₂	Purple	31.7 (31.3)	5.9 (5.7)	7.6 (7.3)	9.5 (9.2)	13.2 (13.5)	3.7	230
12. Cl ₂ (nic) ₄ Cl ₆	Green	43.6 (43.2)	3.4 (3.0)	8.6 (8.4)	10.7 (10.6)	15.2 (15.6)	3.5	242
13. CrCl ₃ py ₃		45.2 (45.5)	3.7 (3.8)	10.5 (10.6)	26.7 (26.9)	13.3 (13.1)	3.8	

^a The first six complexes were prepared from CrCl₃py₃ and the last seven complexes were obtained from anhydrous CrCl₃-ligand in 1:3 molar ratio in methanol.

^b Complex decomposes without melting.

account for the higher volume of magnetic moment of complex Cr(pen-H)₂Cl as previously reported for chromium(III) complex species [4, 14]. The difference in the field strength of the environment could facilitate the mixing of ⁴A₂ state with the excited state T₂ terms in chromium(III) species. The observed difference in the magnetic moment of the complex is also probably due to the hygroscopicity of the complex but the values nevertheless are indicative of octahedral chromium(III). The μ_{eff} values of the nicotinic acid complex species (3.4–3.5 B.M.) are less than the spin-only value for a d³ chromium(III) ion in octahedral symmetry. Thus, the non-bonding electron pair on the pyridine nitrogen of the nicotinic acid ligand is not directly involved in the d-orbital of the high spin chromium(III) species as reported [22]. The lower values of μ_{eff} of the complex Cr₂(nic)₄Cl₆ as well as the molecular weight (809) determined by the Rast method for the complex Cr₂(nic)₄Cl₆ confirm the formation of dimeric structures [23].

The major absorption IR frequencies of the prepared complexes are given in Table 2 with relevant bands of the free ligands and their probable assignments. Displacement of the δ (NH₂) vibrational modes to higher wave number (25–40 cm⁻¹) and another mode probably ρ_t (NH₂) twisting vibrations also suffers from bathochromic shift (30–70 cm⁻¹) in the complexes on forming a coordinate bond compared with the free NH₂ [24]. The absorption bands corresponding to the symmetric vibration (1650–1690 cm⁻¹) and the antisymmetric stretching mode (3020–30245 cm⁻¹) of the amino groups in the amino acid ligands are also shifted to lower wave numbers on complex formation, confirming that, the nitrogen atom of the amino group participates in the coordination [24, 25]. Displacement of the COO⁻ symmetric stretches to lower wave numbers (20–30 cm⁻¹) and of the antisymmetric stretches (35–50 cm⁻¹) to higher wave numbers is observed for all complexes showing that the carboxylate groups of the tested ligands are involved in the coordination [25].

Table 2. Significant vibrational frequencies (cm^{-1}) of the prepared complexes with relevant bands of the free ligand in parentheses

Complex	$\nu_{\text{as}}\text{COO}^-$	$\nu_{\text{s}}\text{COO}^-$	$\Delta\nu$	νNH_2	νNH_2	$\nu(\text{C}_5\text{H}_5\text{-N})$	$\nu\text{Cr-Cl}$
1	1600 (1625)	1410 (1375)	190 (250)	1477 (1416)	1135 (1107)		
2	1650 (1590)	1340 (1330)	300 (220)	1560 (1510)	1135 (1120)		
3	1640 (1600)	1410 (1380)	230 (220)	not visible (3450)			
4	1615 (1595)	1370 (1400)	245 (195)	1480 (1470)	1110 (1095)		
5	1635 (1610)	1360 (1400)	275 (210)	1465 (1440)	1050 (1025)		
6	1740 (1720)	1400 (1428)	340 (292)	—	630, 470		
7	1730	1410	320	1485	11450	—	370, 305
8	1660	1355	305	1545	1150	—	390, 310, 285
9	1630	1365	275	1515	1130	—	380, 310
10	1610	1360	250	1490	1120	—	380, 330, 295
11	1640	1385	255	1460	1115	—	370, 315, 290
12	1735	1410	325	—	—	635, 410	390, 340, 280
13	—	—	—	—	—	640, 420	330, 330, 280

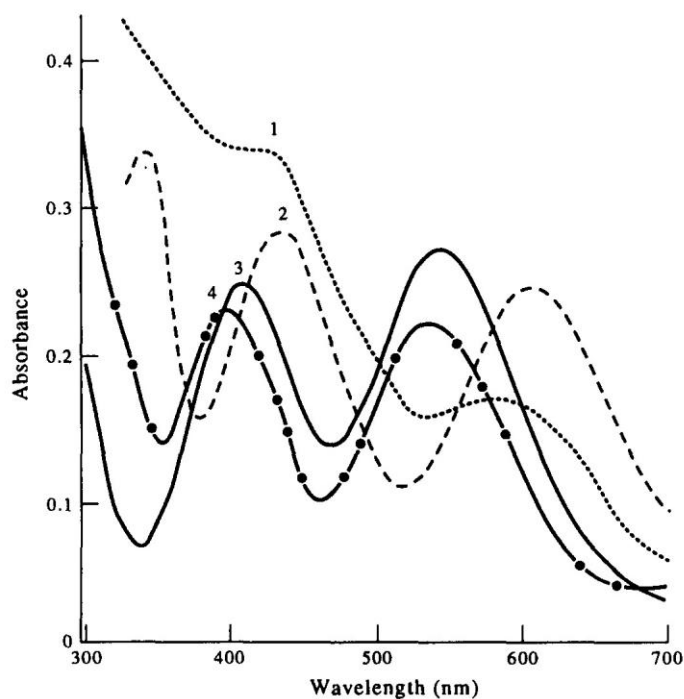
In the IR spectra of the L(-)-threonine complexes, the OH stretching vibration mode at 3160 cm^{-1} and the in-plane δ (OH) deformation at 1340 cm^{-1} coincides with that of the free ligand. This band also arises in the same region as that of the OH stretching for the 4-hydroxy-L-proline cadmium(II) complex in which the hydroxyl groups have not coordinated with the metal ion [26]. Therefore, the band assignments of nicotinic acid complexes have been made by comparison with the 3-substituted pyridine ligands and their chromium(III) complexes [27]. These results suggest the oxygen atom of the hydroxyl group does not participate in the formation of the Cr-O bond [26]. The IR spectra of the L(-)-cysteine and D(-)-penicillamine complexes were compared with that of the free ligand. The data show the presence of a free SH group ($\nu_{\text{SH}} 2380\text{--}2400\text{ cm}^{-1}$) as was found in the free ligand [26] and does not complex easily in a non-aqueous solvent. The IR spectra (Table 2) of the nicotinic acid complexes represent the superposition and the most striking feature of these chelates is the appearance of additional bands of various wave numbers. In the nicotinic acid complexes (6, 12), an absorption band at 1520 cm^{-1} and a moderately intense band in-plane deformation component at 1015 cm^{-1} are found in the spectra. This peak most likely results from the nitrogen atom of the pyridine ring bound to chromium(III) as found in 3-substituted pyridine ligands and their chromium(III) complexes [27].

The pyridine ring vibrations at 605 and 405 cm^{-1} [28] are not observed in the IR spectra upon complex formation, confirming the absence of $\text{C}_5\text{H}_5\text{N-Cr}$. In the anhydrous CrCl_3 complexes of the tested ligands, vibration modes are observed in the region $390\text{--}280\text{ cm}^{-1}$ and are assigned to ν (Cr-Cl) [28]. Three ν (Cr-Cl) stretching modes are observed between 390 and 280 cm^{-1} for some of the complexes and are absent in the corresponding free ligand region indicating C_{2v} local symmetry of ligand atoms around the chromium(III) rather than C_{3v} which would allow two modes [14, 28]. The chlorine atoms are located around chromium(III) rather than C_{3v} which would allow two modes [14, 28]. The chlorine atoms are located around chromium(III) in the remaining coordinating sites. However, no suggestion can be made from the IR spectra for the chloride position because the two ν (Cr-Cl) vibrations differentially split are present in the CrCl_3 complexes.

The UV-vis solution spectra of the complexes in MeOH are given in Table 3. Representative spectra are shown in Fig. 1. The electronic spectra are similar with two main bands at $(15.9\text{--}19.8) \times 10^3$ and $(22.0\text{--}26.7) \times 10^3\text{ cm}^{-1}$ with lower molar extinction coefficients relative to those of charge transfer transition. These bands are assigned to

Table 3. Electronic spectral data (cm^{-1}) of the prepared complexes with ligand field parameters in methanol^a

Complex	${}^4A_{2g} \rightarrow {}^4T_{2g}$	${}^4A_{2g} \rightarrow {}^4T_{1g(F)}$	${}^4A_{2g} \rightarrow {}^4T_{1g(P)}$	ν_1/ν_2	D_q	B	β_{35}	Z^*
	$\nu_1 \times 10^3$ (log ϵ)	$\nu_2 \times 10^3$ (log ϵ)	$\nu_3 \times 10^3$ (log ϵ)					
1	19.80 (1.8)	26.7 (1.7)	31.65 (2.1)	1.34	1980	659	0.72	0.74
2	16.4 (1.7)	22.9 (1.82)		1.40	1640	659	0.72	0.84
3	16.4	23.0	28.6		1639	660	0.71	0.74
4	15.8 (1.45)	22.9 (1.60)	20.30	1.45	1587	743	0.81	0.85
5	17.21 (1.62)	23.8 (1.68)		1.38	1724	647	0.70	0.78
6	16.3 (1.55)	23.8 (1.74)	31.25	1.45	1639	779	0.85	0.82
7	18.5 (1.9)	24.5 (1.70)		1.32	1852	567	0.62	0.73
8	18.6 (1.56)	25.3 (1.72)		1.35	1869	639	0.70	0.75
9	17.2	23.8		1.28	1720	647	0.70	0.72
10	18.50 (1.6)	25.31 (1.9)	31.25	1.36	1850	664	0.72	
11	18.3 (1.8)	25.6 (1.9)	30.76	1.39	1835	727	0.79	0.72
12	16.9 (1.62)	24.3 (1.52)	30.30	1.4	1694	772	0.84	0.82
13	16.1 (1.6)	22.5 (1.64)	—	1.39	1613	637	0.70	0.79

^a B for chromium(III) ion = 918 cm^{-1} .Fig. 1. Absorption electronic spectra of $\text{Cr}_2(\text{cyst-H})_4\text{Cl}_2$, 1; $\text{Cr}(\text{cyst-H})_3$, 2; $\text{Cr}_2(\text{thr-H})_4\text{Cl}_2$, 3 and $\text{Cr}_2(\text{gly-H})_4\text{Cl}_2$, 4, in methanol.

the $\nu_1(^4A_{2g} \rightarrow ^4T_{2g})$ and $\nu_2(^4A_{2g} \rightarrow ^4T_{1g(F)})$ $d-d$ transitions, respectively in octahedral and pseudo octahedral symmetry [4, 14]. ν_2/ν_1 data are consistent with those of other trivalent chromium(III) complexes containing N, O and/or chlorine. A strong charge transfer band overlaps the ν_2 and totally obscures the $\nu_3(^4A_{2g} \rightarrow ^4T_{1g(F)})$ band in the UV region of the spectra of some of the complexes. The forbidden transition band, ν_2 , $^4A_{2g} \rightarrow ^4T_{1g(F)}$ in the cystine complexes (Fig. 1) shows a higher absorption coefficient than the spin-allowed ν_1 , $^4A_{2g} \rightarrow ^4T_{2g}$ which is possibly because of the symmetry reduction [29]. Thus the coordination of the complex is not *trans* with respect to N, O or Cl atoms.

The visible spectra (Fig. 1) of cystine chelates are seen to be unsymmetrical showing the presence of a very weak band under the envelope on the high energy side [29]. The apparent splitting observed may be taken as evidence of the *trans* pyridine nitrogen or the amino group nitrogen of both complexes, respectively. The ν_2 splitting in a *cis* CrN_3Cl_3 and $CrN_2O_2Cl_2$ chromophore would be expected to be less than that in the *trans* isomer [30] which is totally different from that observed for cysteine complexes confirming formation of *trans* N isomers. The *trans* isomer may also show splitting of the $^4A_{2g} \rightarrow ^4T_{2g}$ band which is used as further support of the structural assignment of these complex species.

The visible spectra and the positions of the absorption bands of the complexes $Cr(thr)_3$, $Cr(cys)_3$ and $Cr_2(nic)_4Cl_6$ in MeOH are found different from the corresponding ones recorded in KBr discs, showing that the complexes are significantly unstable, commencement of solvolysis or presence of low symmetry components of crystal field [30]. These complexes could also undergo chemical dissolution in methanol and hence the composition of the chromophores became different in solution and in solid [25].

The parameters D_q , B and β_{35} of the complexes are given in Table 3. The D_g values are found in the range $1590-1870\text{ cm}^{-1}$ and are far closer to the range observed for $CrCl_6$ [3], CrN_6 and CrS_6 [31] and slightly closer to the D_q values of CrN_3Cl_3 or CrN_3O_3 chromophores [32]. Thus it seems reasonable to presume that most of these complex species contain oxygen, nitrogen and/or chlorine. The observed D_q values place the ligands in the middle range of the spectrochemical series and provides reassurance that the NH_2 or C_5H_5N nitrogen of the ligands is complexed to chromium(III) ion. The D_q value of the complex $Cr(thr-H)_4Cl_2$ is quite close to the reported values ($D_q = 1970\text{ cm}^{-1}$) for *fac* tris(amino acidato) chromium(III) [31].

The B values of the complexes are calculated by [31]:

$$B = \frac{2\nu_1^2 + \nu_2^2 - 3\nu_1\nu_2}{15\nu_2 - 27\nu_1}$$

The B values of the complexes prepared from $CrCl_3py_3$ are observed higher than that obtained from $CrCl_3$ except for glycine complexes (Table 3). It could be due to the formation of different configuration dissymmetry and the vicinal effect of the coordinated ligand. The B values of the tris threonine complex is observed higher than that of $D(-)$ -penicillamine or $L(-)$ -cysteine chelates. The fact that, the hydroxyl group of $L(-)$ -threonine stabilizes the conformation of threonine chelate as compared to the mercapto and the two methyl groups present in $D(-)$ -penicillamine and cysteine. Also, the B values of the complexes 6, 11 and 12 are observed higher than that for all complexes. The fact that the electron repulsion effect of C_5H_5N in nicotinic acid and the two methyl groups of $D(-)$ -penicillamine increase the basic donor effect of carboxylate and amino and carboxylate groups of both ligands, respectively making chromium able to supply the electron density required for the back donation and stabilize the formation of chelates [4]. The B -values of the complexes are *ca.* 56–74% of that of the free ion (918 cm^{-1}) indicating considerable orbital overlap with strongly covalent metal–ligand bond. According to JORGENSEN [33], the decrease in B^- values is associated with a reduction in the nuclear charge on the cation and an increased tendency to be reduced.

The nephelauxetic parameter, β_{35} , is in the range 0.72–0.85 indicating that these ligands are in the middle of the nephelauxetic of other nitrogen and oxygen donor series.

Table 4. Circular dichroism (CD) spectral data (nm) of the prepared complexes in methanol

Complex	CD (nm)
1	300(-), 420(-), 466(+), 480(+), 590(-), 614(-)
2	275(-), 350(+), 450(-), 536(+), 552(+), 590(-)
3	380(-), 435(+), 510(+), 630(-)
4	270(-), 320(-), 350(+), 380(-), 430(+), 510(+), 570(+)
5	300(-), 350(+), 430(-), 490(+), 504(+), 580(-)
6	310(-), 335(+), 410(+), 470(-), 550(+), 624(-), 610(-)
7	290(+), 335(-), 408(+), 430(+), 575(+), 665(-)
8	275(-), 420(+), 480(+), 520(+), 580(+)

These values are higher than the range observed for CrN_6 (0.4–0.65), CrO_6 (0.65–0.67), CrN_3O_3 (0.65–0.66) [25], CrS_3Cl_3 (0.54–0.65) [31] and CrN_3X_3 (0.58–0.65) [23] confirming coordination via nitrogen, oxygen and/or chlorine. Thus, it seems reasonable to presume that most of the chelates formed in this series involve CrO_3N_3 or $\text{CrN}_2\text{O}_2\text{X}_2$ chromophores. The variation of the interelectronic repulsion parameter with the ionic charge, z^* values for $3d^3$ chromium(III) ion in the complexes lie in the 0.72–0.84 range which is considerable below the formal value of 3.

The circular dichroism spectral data are given in Table 4 with representative spectra in Fig. 2. Well defined Cotton effects are observed for all complexes except that formed with nicotinic acid and glycine. The observed splitting in the CD spectra of the complexes is primarily due to the occurrence of two ions with symmetry splitting superimposed [31] or as a result of the mixture of complex species. Thus, TLC plates with mixed solvent $\text{C}_2\text{H}_5\text{OH}-\text{CHCl}_3$ (1:4 v/v) and transient iodine were employed and confirmed that only one complex species is present in solution. However, the complexes were purified with silica gel column (20 × 2 cm i.d.). The complexes are likely to be *fac* since stronger and better defined Cotton effects are observed [31].

Assuming that the complexes belong to D_3 symmetry, the observed Cotton effects at 504–590 and 550–665 nm are safely assigned to the splitting of the allowed band ${}^4A_{2g} \rightarrow {}^4T_{2g}$ to ${}^4A_1({}^4T_{2g})$ and ${}^4E({}^4T_{2g})$ $d-d$ transitions [31]. In the spin forbidden band transition, three well defined peaks at 335–420, 380–480, and 430–536 nm are observed. These bands are tentatively assigned to the $2A({}^2E_g)$, ${}^2A_2({}^2T_{1g})$ and ${}^2E({}^2T_{1g})$ from the

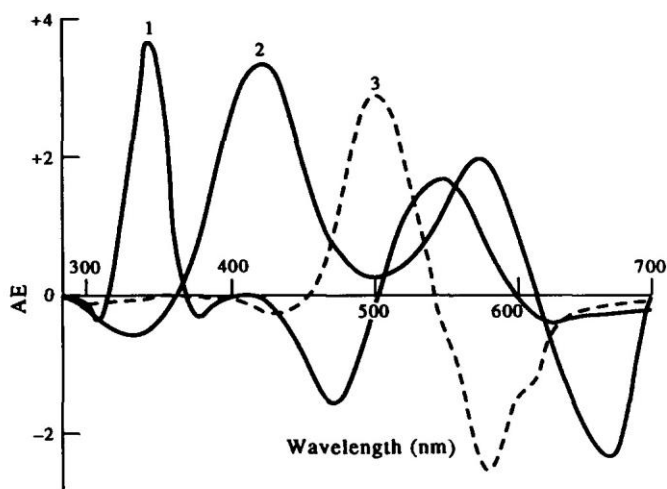


Fig. 2. Circular dichroism spectra of $\text{Cr}(\text{cys})_3$, 1; $\text{Cr}_2(\text{cyst-H})_4\text{Cl}_2$, 2 in methanol and $\text{Cr}_2(\text{thr-H})_4\text{Cl}_2$, in KBr disk.

lower frequency side, respectively [23, 31]. The two CD patterns at the higher frequency side in the spin forbidden for some of the complexes (Table 4) are of opposite sign precludes assigning them to the $[2A, E_b]$ and E_a components of the 2T_1 state for which the rotational strengths are proportional to the net rotational strength for the first spin allowed ${}^4A_1({}^4T_{2g})$ transition [34]. The assignment to $[E_a, E_b]$ and $2A$ or to E_b and $[2A, E_a]$ accounts for the CD signs of the observed bands. The assignment is made because $R({}^4A_1)$ contributes largely to $R[E_a, E_b]$ and $R(E_b)$ and also because the rotational strength for the ${}^4E \leftarrow {}^4A_2$ transition contributes to $R(2A)$ and $R(2A, E_a)$ should have opposite sign to $R({}^4A_1)$ [35]. The weak CD band at 280–300(–) nm is possibly due to the charge transfer peak found at 310–280 nm in the UV spectra of most chromium(III) complexes [23].

The observed Cotton effects of D(–)-penicillamine complexes have greater strength compared to L(–)-cystine chelates, possibly due to the additional stability of D(–)-penicillamine complex species in non-aqueous media via the two bulky methyl groups. The CD pattern of complexes 1–3 are similar to that of tris(en) [23] indicating that the optical activity of the compounds is due to a kind of configurational dissymmetry rather than the vicinal effect of the coordinated acid. The absolute configuration determined on the basis of the CD dominance in the spin allowed band region is in accordance with that based on comparison between the CD spectra of bis(oxalato) complexes with the $[\Delta-\Delta]$ configuration enforced by stereospecificity [23]. The sign of the Cotton effects of L(–)-threonine complexes are different indicating formation of complex species of opposite configuration. The sign of the Cotton effects of L(–)-cysteine, L(–)-cysteine and L(–)-penicillamine chelates are different suggesting formation of similar species but with ligands of opposite configuration.

Chromium(VI) formation

Experiments involving CrCl_3py_3 with L(–)-threonine, glycine, or nicotinic acid (1:3 molar ratio) in MeOH showed that, bubbling air or prolonged reflux under stirring through these solutions for several hours (7–10 h) leads to the oxidation of chromium(III) to chromium(IV, V or VI), while L(–)-cysteine and L(–)-penicillamine did not. The oxidation process is confirmed by the fact that, upon addition of KI and CCl_4 to the acidified (2 M H_2SO_4) solution of reaction products of CrCl_3py_3 -threonine, glycine, or nicotinic acid, iodine was liberated to the CCl_4 layer. Blank solution of CrCl_3py_3 gave no iodine. Electronic spectra of these solution mixtures in acid media showed well-defined peaks at 257–265, 350–355 (s) and 560–580 nm. An ill defined shoulder at 410–440 nm (v,w) obscured by an intense band at 350 nm is also found in the spectra.

The electronic spectra of the species formed in the reaction mixture are found different from the spectra of chromium(IV) or (V) [36] and are quite similar to that of chromium(VI) species [37]. Thus the high lying two energy bands in the electronic spectra of the solution mixture are assigned to charge transfer $\text{O} \rightarrow \text{Cr}$ [37] in chromium(VI) species. The other two low lying energy bands at 410–440 (sh) and 564–580 nm are assigned to ${}^4A_{2g} \rightarrow {}^4T_{1g(f)}$ and ${}^4A_{2g} \rightarrow {}^4T_{2g}$ $d-d$ transitions, respectively for chromium(III) species in D_3 symmetry remained without oxidation in the reaction mixture. The absorbance of the formed species at 278 and 352 nm are found to increase while that at 560 nm decreased by prolonged heating or aeration of the solution mixture confirming chromium(VI) formation. Iodometric microgram determination of chromium(VI) [38] released from these solutions after bubbling air or reflux under stirring (8–10 h) showed the presence of up to 5–7.5% Cr(VI). Thus, chromium(III) species appear to be oxidized to chromium(VI) by air or reflux to some extent in methanol unless a reducing agent, e.g. cysteine, penicillamine, etc. is present in solution which would cause a reduction of chromium(VI). This raises the possibility that the active chromium(III) complexes of some naturally occurring ligands could in non-aqueous environment *in vivo* produce chromium(VI). These results suggest that if similar complexes are formed *in vivo* they would have time to reach many intracellular compartments and could hence be active in the toxicity of chromate [39]. Hence, if chromium(VI) is found

oxidation of thiol and sulphhydryl groups present in biological substrates could be undertaken. This also shows the effectiveness of various chelating agents for the removal of chromium bound to haemoglobin. Another problem could arise *in vivo* if the patient is allergic to certain metals, and also, it is known that chromium causes allergic response [1].

Acknowledgement—The author would like to thank Professor D. H. Brown and W. E. Smith for helpful discussion and the facilities provided in the circular dichroism measurements.

REFERENCES

- [1] D. H. Brown and W. E. Smith, *Inorg. Chim. Acta* **93**, L29 (1984); H. Sigel, *Metal Ions in Biological Systems*. Dekker, New York (1979).
- [2] J. J. Chisholm, *J. Pediatr.* **73**, 1 (1986).
- [3] R. A. P. Kark, D. C. Poskanzer and J. Bullock, *Engl. J. Med.* **285**, 10 (1971).
- [4] M. Freni, A. Gervasini and P. Rumiti, *Spectrochim. Acta* **39A**, 85 (1983).
- [5] K. G. Stollenwerk and D. B. Grove, *J. Environ. Analysis* **14**, 396 (1985).
- [6] R. A. Anderson and W. Mertz, *Trends Biochem. Sci.* **2**, 277 (1977).
- [7] R. A. Anderson, *Sci. Total Environ.* **17**, 13 (1981).
- [8] S. Langard and T. Norseth, *Handbook on the Toxicology of Metals* (Edited by L. Friberg), p. 338. Elsevier/North-Holland Biomedical Press, Amsterdam (1974).
- [9] K. E. Wetterhahn and P. H. Connert, *Struct. Bonding (Berlin)* **54**, 93 (1983).
- [10] E. W. Toepfer, W. Mertz, M. M. Polansky, E. E. Roginski and W. R. Wolf, *J. Agric. Fd Chem.* **25**, 162 (1977).
- [11] W. Mertz and K. Schwarz, *Am. J. Physiol.* **196**, 614 (1959); J. Barrett, M. K. Kormoh and P. O. Brien, *Inorg. Chim. Acta* **107**, 269 (1985) and references therein.
- [12] E. W. Toepfer, W. Mertz, E. E. Roginski and M. M. Polansky, *J. Agric. Fd Chem.* **21**, 69 (1973).
- [13] D. H. Brown, W. E. Smith, M. S. El-Shahawi and M. F. K. Wazir, *Inorg. Chim. Acta* **124**, L25 (1985) and references therein.
- [14] M. S. El-Shahawi and A. A. El-Bindary, *Z. Naturforsch.* **48b**, 282 (1993); M. S. El-Shahawi and S. G. Ghezy, *Trans. Med. Chem.* **7**, 543 (1992).
- [15] J. M. Tsangaris, *J. Am. Leather Ass.* **65**, 78 (1970).
- [16] G. K. Friman, *Inorganic Biochemistry* (Edited by G. L. Eicharn). Translated into Russian, izd Mir, Moscow (1978).
- [17] D. H. Brown, G. C. Mckinlay and W. E. Smith, *J. Chem. Soc. Dalton* 199 (1978).
- [18] A. R. Ray, *Inorg. Synth.* **5**, 154 (1957).
- [19] J. C. Taft and M. M. Jones, *Inorg. Synth.* **7**, 132 (1963).
- [20] R. C. Marya, *Indian J. Chem.* **22A**, 529 (1983).
- [21] D. H. Brown, G. C. Mckinlay and W. E. Smith, *J. Chem. Soc. Dalton* 1874 (1977).
- [22] R. M. Ramadan, W. H. Mahmoud, A. S. Attia and M. F. El-Shahat, *Spectrochim. Acta* **49A**, 117 (1993).
- [23] S. Kizaki, J. Hidaka and Y. Shimura, *Bull. Chem. Soc. Jpn* **40**, 2207 (1967); S. Kaizaki, J. Hidaka and Y. Shimura, *Inorg. Chem.* **12**, 142 (1973).
- [24] J. R. Kincaid and K. Nakamoto, *Spectrochim. Acta* **32A**, 277 (1976); H. Oki, *Bull. Chem. Soc. Jpn* **50**, 680 (1972); H. Oki and E. Otsuke, *Bull. Chem. Soc. Jpn* **49**, 1841 (1976); K. Nakamoto, Y. Marimoto and A. E. Martell, *J. Am. Chem. Soc.* **83**, 4528 (1961).
- [25] N. K. Davidenko, V. A. Raspopina, Yu. N. Shewchenko and O. I. Gordienko, *Russ. J. Inorg. Chem.* **28**, 523 (1987).
- [26] Y. Inomata, T. Takeuchi and T. Moziwaki, *Spectrochim. Acta* **110A** (1984) and references therein; A. K. Das and J. Das, *J. Ind. Chem. Soc.* **60**, 67 (1983).
- [27] I. Barrett, M. K. Kormoh and P. O. Brien, *Inorg. Chim. Acta* **107**, 269 (1985); J. C. Change, M. A. Haile and G. R. Keith, *J. Inorg. Nucl. Chem.* **34**, 360 (1972).
- [28] R. J. H. Clark and C. S. Williams, *Inorg. Chem.* **14**, 358 (1965).
- [29] T. Bruer, *Helv. Chem. Acta* **56**, 2888 (1963); J. R. Perumareddi, *Coord. Chem. Rev.* **4**, 73 (1969).
- [30] E. S. Raper, S. Redshaw and J. R. Creighton, *Inorg. Chim. Acta* **87**, 21 (1984).
- [31] A. B. Lever, *Inorganic Electronic Spectroscopy*. Elsevier, Amsterdam (1968); D. Sutton, *Electronic Spectra of Transition Metal Complexes*. McGraw-Hill, London (1988); S. Kaizaki, M. Ito, N. Nishimura and Y. Matushita, *Inorg. Chem.* **24**, 2080 (1985).
- [32] C. Preti and G. Tosi, *Can. J. Chem.* **6**, 2545 (1974).
- [33] C. K. Jorgensen, *Acta Chim. Scand.* **10**, 500 (1956).
- [34] S. Keizoki, J. Kidaka and Y. Shimura, *Inorg. Chem.* **12**, 142 (1973); S. Sugaro, *J. Chem. Phys.* **33**, 1883 (1960).
- [35] E. S. Raper, S. Redshaw and J. R. Creighton, *Inorg. Chim. Acta* **87**, 21 (1984).

- [36] E. G. Hope, P. J. Jones, W. Levason, J. S. Ogden, M. Tajik and J. W. Turff, *J. Chem. Soc. Dalton Trans.* 2445 (1984).
- [37] M. Wolfsherg and L. Helmolz, *Chem. Phys.* **20**, 837 (1952).
- [38] A. M. El-Wakil, A. B. Farag and M. S. El-Nahas, *Talanta* **40**, 841 (1993).
- [39] D. M. Whitfield, S. Stojkovski and B. Sarker, *Coord. Chem. Rev.* **122**, 171 (1993); P. O. Brien, J. Barrett and F. Swanson, *Inorg. Chim. Acta* **108**, L19 (1985); A. M. Aulry and M. A. Olatunji, *Can. J. Chem.* **55**, 3335 (1977).



ELSEVIER

Journal of Chromatography A, 697 (1995) 185–190

JOURNAL OF
CHROMATOGRAPHY A

Qualitative, semi-quantitative and spectrophotometric determination of ruthenium(III) by solid-phase extraction with 3-hydroxy-2-methyl-1,4-naphthoquinone-4-oxime-loaded polyurethane foam columns

M.S. El-Shahawi*, M. Almehdi

Chemistry Department, Faculty of Science, UAE University, P.O. Box 17551, Al-Ain, United Arab Emirates

Abstract

A sensitive and selective extraction method was developed for the detection, semi-quantitative and spectrophotometric determination of ruthenium(III) in aqueous media. The method is based on the sorption of the ruthenium(III) complex of 3-hydroxy-2-methyl-1,4-naphthoquinone-4-oxime on a porous polyurethane foam membrane. In batch experiments, it was possible to detect as low as 0.1 and 0.02 ppm of ruthenium(III) with unloaded foam and foam loaded with reagent, respectively. The method was also employed for the detection of 10 ppb of ruthenium using the reagent foam column mode. The selectivity of the method for the detection of 1 ppm of ruthenium(III) in the presence of high concentrations of diverse ions was achieved. Preconcentration of ruthenium(III) from large sample volumes was carried out on a loaded foam column at pH 5–7, eluted with acetone and determined spectrophotometrically at 450 nm. The sorbed complex species on the foam showed an absorption maximum at 460 nm with a molar absorptivity of $2.8 \times 10^4 \text{ dm}^3 \text{ mol}^{-1} \text{ cm}^{-1}$. On this basis, a method for the direct spectrophotometric determination of ruthenium(III) based on liquid–solid extraction of the Ru(III)–reagent complex on thin-layer parallelepiped foam was developed. The proposed methods were applied for the determination of ruthenium(III) in water and in its complexes.

1. Introduction

Compared with most other elements, ruthenium has a limited influence on the biosphere [1]. The amount of ruthenium readily introduced into rivers, lake and oceans through industrial wastes, catalyst application and materi-

al sciences [2–4] is minute. Sensitive, reliable and practicable methods are required for the determination of the element at trace levels [5].

The most common reported spectrophotometric procedures include the use of thioridazine hydrochloride [6], 9,10-phenanthrenequinone monoxime [7], sulphochlorophenolazorhodamine [8], *o*-mercaptoacetanilide in the presence of picaline [9], a catalytic method with periodate oxidation [10], ion-pair formation [11] and 3-hydroxy-2-methyl-1,4-naphthoquinone 4-oxime [12]. However, most of these reagents suffer from the lack of selectivity and sensitivity and

* Corresponding author. Permanent address: Chemistry Department, Faculty of Science at Damiatta, Damiatta, Egypt.

usually require laborious enrichment steps. Several polarographic and voltammetric methods have been developed for the determination of ruthenium [13–16], but neither their sensitivity nor selectivity is very satisfactory.

Recently, several workers have proposed open-cell polyurethane foam as an inexpensive solid extractor for many organic and inorganic species [17–19]. Direct spectrophotometric measurements of the absorbance of a thin layer of solid polyurethane foam, reported as a new trend [20,21], have markedly improved the sensitivity of determination and avoided the tedious preconcentration step that is necessary in trace analysis. This paper reports the application of polyurethane foam loaded with 3-hydroxy-2-methyl-1,4-naphthoquinone-4-oxime reagent for the detection and semi-quantitative and direct spectrophotometric determination of trace levels of ruthenium in aqueous solution.

2. Experimental

2.1. Reagents and materials

Analytical-reagent grade chemicals and doubly distilled water were used throughout. Britton–Robinson (BR) buffer solution (pH 2.5–12) containing sodium hydroxide, glacial acetic acid, orthophosphoric acid and boric acid was prepared with distilled water. A stock standard solution (1 mg ml^{-1}) of ruthenium(III) (atomic absorption standard, BDH) was used and diluted with water for standard addition whenever required. Tributyl phosphate (TBP) (pure grade) was used without further purification. Polyurethane foam (PUF), an open-cell, polyether type (bulk density 30 kg m^{-3}), was supplied by Greiner (Schaumstoff-Werk-Kremsmunster, Austria). The foam materials (cubes of 5-mm edge and a parallelepiped of $10 \times 35 \times 2 \text{ mm}$ dimensions) were washed as reported previously [22]. 3-Hydroxy-2-methyl-1,4-naphthoquinone-4-oxime (HMNQO) was prepared by the method of Sharma [12]. A $1 \cdot 10^{-3} \text{ M}$ solution of HMNQO was prepared by dissolving the required mass of HMNQO in 100 ml of ethanol.

2.2. Reagent foam preparation

About 1 g of the dried white foam cubes and parallelepiped foam were equilibrated with 10 ml of HMNQO in ethanol followed by the addition of 1 ml of TBP with efficient stirring. The foam material was then allowed to remain in contact with the solution for 1 h and dried as reported previously [22].

2.3. Apparatus

A Pye Unicam SP8-400 double-beam UV–Vis spectrometer with a quartz cell of 10-mm path length and a Philips Model 9418 pH meter were used for absorbance and pH measurements, respectively. Glass columns of length 10 and 15 cm and I.D. 20 and 5 mm were used in the dynamic experiments.

2.4. Detection and semi-quantitative determination of ruthenium(III)

Batch experiments

To 3–5 ml of the aqueous solution of ruthenium(III) at 60°C and pH 7 in a normal test-tube was added one cube of unloaded, HMNQO-loaded or HMNQO–TBP-treated foam and the mixture was shaken for 3–5 min. The change in the colour of the foam cube from white to red-violet due to the coloured Ru(III)–HMNQO complex collected on the reagent foam is evidence for the detection of ruthenium(III).

Column experiments

A foam column detection test was carried out by percolating 100 ml of the aqueous solution of ruthenium(III) at 60°C and pH 5–7 through the HMNQO–TBP-loaded foam bed in the column ($10 \text{ cm} \times 5 \text{ mm}$ I.D.) at 5 ml min^{-1} . The developed red-violet colour on the foam bed is evidence for the detection of ruthenium(III).

2.5. Direct spectrophotometric determination of ruthenium by liquid–solid extraction on thin-layer parallelepiped polyurethane foam

Standard ruthenium(III) solutions (1–10 ml) containing 1–50 μg of ruthenium(III) were

pipetted into a 100-ml erlenmeyer flask, followed by 10 ml of buffer (pH 7) and 10 ml of 0.001 M HMNQO solution and the solution was heated at 60°C for 0.5 h. The volume of each solution was made up to 50 ml with distilled water, a piece of thin-layer parallelepiped foam was added and the solution was shaken for 10 min. The parallelepiped foam was then removed from the solution by decantation, washed thoroughly by squeezing twice with water, placed in a 10-mm quartz cell containing ethanol and set in the light path of the spectrometer. The absorbance of the coloured complex sorbed into the foam was measured at 460 nm against the HMNQO–thin-layer parallelepiped foam in ethanol. The net absorbance of the Ru–HMNQO chelate in the foam, A_F^* , was calculated from the equation

$$A_F^* = A_{F(Ru)} - A_{F(B)}$$

where $A_{F(Ru)}$ and $A_{F(B)}$ are the absorbances of the ruthenium complex on foam and blank, respectively.

2.6. Determination of Ru(III) in its complexes

The ruthenium(III) complexes were prepared as described previously [4] and digested employing the oxygen flask method as reported [11]. The resultant solution was reduced with 10 ml of 5% sodium sulphite solution followed by adding 5 ml of concentrated HCl. After boiling to remove the excess of SO₂ and transfer into a 50-ml volumetric flask, the solution was diluted to volume with water and the procedure in Section 2.5 was followed. The concentration was determined by reference to a calibration graph prepared under the same experimental conditions.

3. Results and discussion

The reaction of ruthenium(III) with HMNQO represents one of the most recent sensitive and selective approaches to the spectrophotometric determination of ruthenium after solid-phase extraction into microcrystalline *p*-dichlorobenzene [12]. The coloured product is formed rapid-

ly and the equilibrium between the two phases is attained in a few seconds.

3.1. Qualitative and semi-quantitative determination of ruthenium(III)

The solution of ruthenium(III) was coloured (red-violet) by the addition of HMNQO at pH 5–7 [12]. This colour reaction was tested for the detection of ruthenium(III) with unloaded, HMNQO-loaded and HMNQO–TBP-treated foams. The surface area of the foam cube acts as an efficient collector for Ru(III)–HMNQO from aqueous solution at low concentration. The characteristic colour of the reaction product on the thin membranes of the foam material also allowed the detection of ruthenium(III) in extremely dilute aqueous solution.

On shaking one cube of the unloaded foam with 3–5 ml of hot Ru(III)–HMNQO at pH 7, it was possible to detect as little as 0.1 ppm of ruthenium(III). On shaking one cube of each HMNQO-loaded and HMNQO–TBP-treated foam with 3–5 ml of a hot aqueous solution of ruthenium, it was possible to detect as little as 0.05 and 0.02 ppm of ruthenium, respectively. The colour density on the foam cubes was found to depend on the concentration of Ru(III) in the aqueous solution. Hence it was possible to determine Ru(III) semi-quantitatively by comparison of the colour of the foam cubes with a standard colour scale (0.1–10 ppm) of ruthenium(III) employing HMNQO–TBP-treated foams under the same experimental conditions. The results obtained with HMNQO–TBP-treated foams are far better than those obtained with unloaded foams and HMNQO-loaded foams. The added TBP acts as a plasticizer of the foam material and enhances the diffusion of the species through the solid membrane and allows the collection of ruthenium(III) on the foam matrix [17,18,22].

The proposed HMNQO-loaded foam cubes can be easily packed in columns, producing a foam bed suitable for the detection and semi-quantitative determination of ruthenium in extremely dilute aqueous solutions. This was achieved by percolating 100 ml of the test ruthenium(III) solution through the foam col-

umn at a reasonable flow-rate (5 ml min^{-1}). The detection limit was found to be 10 ppb. The length of the coloured zone is proportional to the concentration of ruthenium. Semi-quantitative determination was possible using a colour scale covering concentrations from 5 to 50 ppb ruthenium(III).

Effect of diverse ions

The selectivity of the proposed HMNQO-loaded foam method was examined by detecting $1 \mu\text{g}$ of Ru(III) in the presence of a relatively high excess (10 mg) of each of Ba^{2+} , Cd^{2+} , La^{3+} , Zn(II) , Al(III) , Cr(III) , Hg(II) , Pt(IV) , Ca^{2+} , Sr^{2+} , HPO_4^{2-} , $\text{C}_2\text{O}_4^{2-}$, NO_3^- , VO_3^- , SeO_3^{2-} , SeO_4^{2-} , acetate and formate ions. No interferences were observed using the straightforward procedures; V^{4+} , Pd^{2+} , Pt^{2+} and Os^{3+} interfered seriously. In the presence of some other ions, e.g., permanganate, copper(II), nickel(II), cobalt(II) and iron(III), simple modifications to the aqueous solution were introduced to eliminate their interferences in the proposed method. The results obtained are summarized in Table 1.

3.2. Quantitative determination of ruthenium(III)

Colourless polyurethane foam showed that the absorbance of the foam matrix is consistently lower than the absorbance of the corresponding thin layer of ion-exchange resin and has no absorption peaks in the range 400–800 nm [20].

The electronic spectrum of the parallelepiped thin-layer HMNQO-loaded foams showed no bands and the absorbance was negligible in the visible region, whereas the spectrum of Ru(III)–HMNQO sorbed on a thin layer of foam showed a well defined absorption peak at 460 nm (Fig. 1). This peak was tentatively assigned to ligand (π) \rightarrow metal (d) charge transfer [23]. The electronic spectrum of the reagent HMNQO showed no absorption in the visible region (Fig. 1). Preliminary experiments showed that Ru(III) is quantitatively extracted by the HMNQO-loaded foam and a 3–5-min shaking time is sufficient to reach equilibrium for 100 ml of aqueous Ru(III) solution at pH 7 and 60°C . Lower or higher acidity gives incomplete extraction, as indicated by the decrease in the absorbance at 460 nm.

Validity of Beer's law

The absorbance of the HMNQO-loaded foam was measured against the concentration of Ru(III). A good linear relationship between the absorbance of the Ru(III) complex species in the foam and ruthenium(III) concentration was obtained under the experimental conditions used. Beer's law was obeyed up to 20 ppm of ruthenium. The molar absorptivity obtained from Beer's law and the Sandell sensitivity [23] for Ru(III)–HMNQO sorbed on the foam at 460 nm were found to be $2.8 \cdot 10^4 \text{ dm}^3 \text{ mol}^{-1} \text{ cm}^{-1}$ and $0.0022 \mu\text{g cm}^{-2}$, respectively. A detection limit of 0.02 ppm of ruthenium was found. Reproducibility tests with five measurements of 10 ppm of ruthenium in the thin-layer foam showed a standard deviation of $0.2 \mu\text{g cm}^{-3}$.

Table 1
Effect of foreign ions on the detection of $1 \mu\text{g}$ of ruthenium(III)

Foreign ion	Added as	Amount added (mg)	Masking agent
Fe^{3+}	FeCl_3	0.05	Add one crystal of KF
Ni^{2+}	NiCl_2	0.05	Add a few drops of 1% KCN solution
V^{5+}	NH_4VO_3	0.05	Add one crystal of NaF
MnO_4^-	KMnO_4	0.01	Add a few drops of 1% NaN_3 solution
MoO_4^{2-}	Na_2MoO_4	0.01	Shake the solution with diethyl ether–carbon tetrachloride (1:1, v/v) followed by addition of Ag_2SO_4

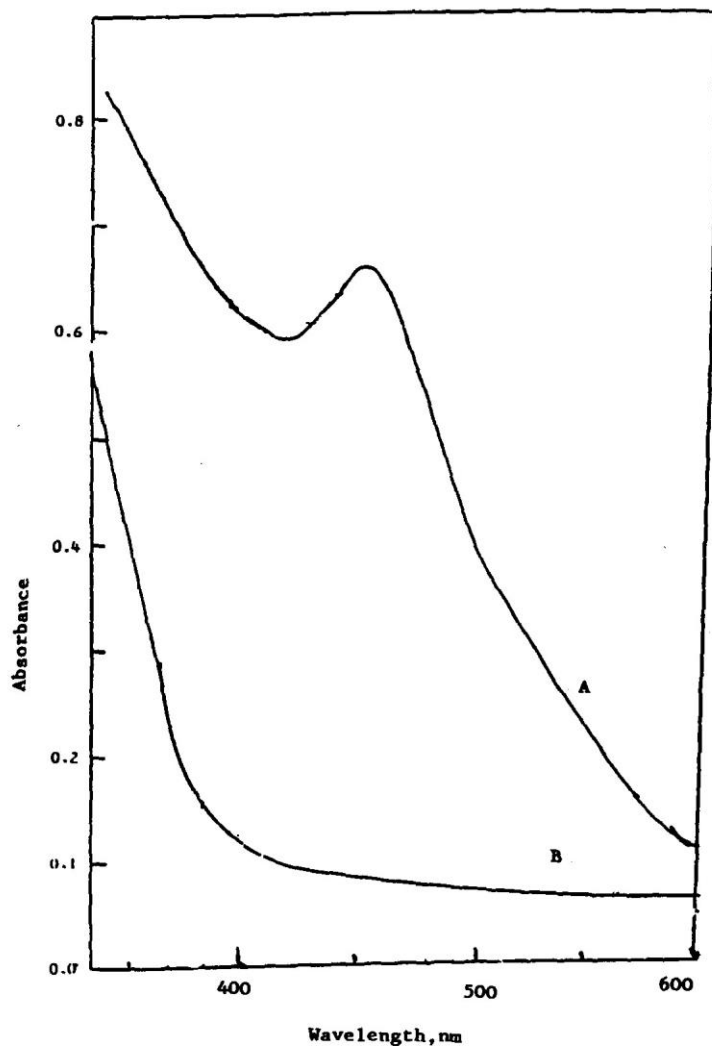


Fig. 1. Absorption spectra of ruthenium-HMNQO complex on thin-layer foam (A) against reagent blank HMNQO-loaded foam and (B) in aqueous solution at pH 7.

These results are better than those reported by Sharma [12].

The sensitivity of the method is better than or comparable to those of well known methods for ruthenium determination [12,13,24].

3.3. Analytical applications of the method

Determination of ruthenium(III) in water

The proposed extraction procedure was been applied for the determination of ruthenium in

tap and sea waters employing the procedure in Section 2.5. Negative results were obtained, indicating the absence of ruthenium. Tap water (0.5 dm^3) samples containing various amounts of Ru(III) were added to the natural water and analysed by the proposed method; a 98–99% recovery of the added Ru(III) was obtained. The applicability of the method to the determination of lower than nanomolar levels of Ru(III) in water is also possible by filtration of the sample solution through a $0.45\text{-}\mu\text{m}$ membrane followed

Table 2
Results for the foam extractive spectrophotometric determination of Ru in its complexes

Complex ^a	Ru calculated (%)	Ru found (%) ^b	Standard deviation (%)
RuCl ₂ (PPh ₃) ₂ (koj)	24.52	24.8	0.26
RuCl ₂ (PPh ₃) ₂ (malt)	24.46	24.60	0.20
RuCl ₂ (PPh ₃) ₂ (trop)	24.7	24.4	0.20
RuCl ₂ (PPh ₃) ₂ (acac)	25.32	24.7	0.20

^a Abbreviations: kojic acid (koj), maltol (malt), tropolone (trop) and acetylacetonone (acac).

^b Average of three determinations.

by extraction of the element with the HMNQO-loaded foam column (15 cm × 2 cm I.D.) at 5 ml min⁻¹. The sorbed complex is then eluted with acetone as reported [25] and analysed either by the procedure in Section 2.5 at 460 nm or by measuring the absorbance of the effluent solution of acetone containing the Ru(III)–HMNQO complex at 350 nm.

Determination of ruthenium(III) in its complexes

The microdetermination of ruthenium(III) in its complexes employing the proposed spectrophotometric procedures after digestion of the complexes was carried out. The results of these determinations are given in Table 2. The results obtained are in good agreement with the calculated values.

References

- [1] E. Merian, *Metals and Their Compounds in the Environment, Occurrence, Analysis and Biological Relevance*, VCH, Weinheim, 1981.
- [2] M.M. Taquikhan and R.S. Shukla, *J. Mol. Catal.*, 34 (1986) 19.
- [3] R. Palaniappan and T.A. Kumar, *Analyst*, 118 (1993) 293, and references cited therein.
- [4] A.M. El-Hendawy and M.S. El-Shahawi, *Polyhedron*, 8 (1989) 2813.
- [5] Z. Marczenko, *Separation and Spectrophotometric Determination of Elements*, Ellis Horwood, Chichester, 1986.
- [6] H.S. Gowda, J.B. Raji and S.A. Ahmed, *Indian J. Chem.*, 23A (1984) 621.
- [7] A. Wasey, R.K. Bansal, M. Sataka and B.K. Puri, *Bull. Chem. Soc. Jpn.*, 56 (1983) 3603.
- [8] R.F. Gurive, L.M. Trutneva, S.B. Savvin and N.N. Chalisova, *Zh. Anal. Khim.*, 39 (1984) 1653.
- [9] A.K. Das and J. Das, *Indian J. Chem.*, 23A (1984) 359.
- [10] A.M. Almuaided and A. Townshend, *Microchem. J.*, 48 (1993) 210.
- [11] M.S. El-Shahawi, A.Z. Abu-Zuhri and S.M. Aldaheri, *Fresenius' J. Anal. Chem.*, in press.
- [12] R.K. Sharma, *Bull. Chem. Soc. Jpn.*, 66 (1993) 1084.
- [13] M.S. El-Shahawi, A.Z. Abu-Zuhri and M.M. Kamal, *Fresenius' J. Anal. Chem.* (1994) 348.
- [14] R. Palaniappan and V. Revathy, *Analyst*, 114 (1989) 517.
- [15] R. Palaniappan, *Bull. Electrochem. Soc. India*, 39 (1991) 367.
- [16] E.P. Medyansteva, G.K. Budinkov, O.N. Romanova and I.V. Zhivolup, *Zh. Anal. Khim.*, 42 (1989) 639.
- [17] M.S. El-Shahawi, *Talanta*, in press, and references cited therein.
- [18] M.S. El-Shahawi, A.B. Farag and M.R. Mostafa, *Sep. Sci. Technol.*, 29 (1994) 289.
- [19] A.B. Farag, M.S. El-Shahawi and S. Farrag, *Talanta*, in press.
- [20] A.M. El-Wakil, M.S. El-Shahawi and A.B. Farag, *Anal. Lett.*, 23 (1990) 703.
- [21] Y.A. Gawargious, M.N. Abbas and H.N.A. Hassan, *Anal. Lett.*, 21 (1988) 1477.
- [22] A.B. Farag, A.M. El-Wakil and M.S. El-Shahawi, *Analyst*, 106 (1981) 809.
- [23] E.B. Sandell, *Colorimetric Determination of Trace Metals*, Interscience, New York, 1959.
- [24] G. Dinst and F. Hecht, *Mikrochim. Acta*, (1963) 895.
- [25] S.J. Al-Bazi and A. Chow, *Talanta*, 31 (1984) 189.

Microgram Determination of Bismuth by Sequential High-Fold Chemical-Amplification Reactions

M. S. EL-SHAHAWI and M. M. KAMAL

Chemistry Department, Faculty of Science, UAE University,
Al-Ain, P. O. Box: 17551, United Arab Emirates

Keywords Bismuth(III, IV) determination, amplification reaction, iodometry, spectrophotometry, natural water

Iodometric chemical-amplification procedures with their simplicity and sensitivity are still of special attraction.¹⁻⁶ The extraction of BiI₃ with benzene from an H₂SO₄-KI solution, followed by the reoxidation of BiI₃ with bromine, forms the basis of a very sensitive indirect starch-iodine amplification method for bismuth(III) determination.⁶ In this paper, two simple titrimetric and spectrometric methods are described for the determination of bismuth(III) and (V) in aqueous media. The methods are based on the use of sodium periodate to oxidize the bismuth(III) ions to the pentavalent state and a subsequent titrimetric or spectrophotometric determination of the released iodine after the addition of KI.

Experimental

Apparatus

A Pye-Unicam double-beam UV-visible spectrophotometer (Model Sp-8-400) with 10-mm quartz cells and a Philips digital pH meter (Model 9418) were used for absorbance and pH measurements, respectively.

Reagents and materials

Analytical reagent-grade chemicals were used without further purification. A bismuth(III) solution (100 µg/ml) was prepared by accurately dissolving a weighed amount of Bi(NO₃)₃ in 10% HNO₃ and standardized with Na₂EDTA.⁷ A bismuth(V) solution (100 µg/ml) was prepared by dissolving 0.1234 g of bismuthic acid in 100 ml of 0.5 mol dm⁻³ KOH⁸, and diluted with distilled water whenever required. A 2.5% (m/v) sodium diethyldithiocarbamate (NaDDC) was freshly prepared in water before use. Sodium thiosulfate solutions (0.005–0.01 mol dm⁻³) and sodium molybdate solution (5% m/v) were prepared in distilled water. Buffer solutions of pH 2.3–4.7 were prepared by mixing 200 ml of glacial acetic acid with 100 ml of water, and adjusting the pH with a saturated solution of sodium acetate. Sodium periodate (0.35 m/v) sodium and sulfite (1% m/v) solutions were freshly prepared in distilled water.

Artificial seawater⁹ with a salinity of about 36 g/kg was prepared from demineralized water and salts in the following molar concentrations: NaCl, 0.4; MgCl₂, 0.029; MgSO₄, 0.028 and KCl, 0.009 mol dm⁻³.

Recommended procedures

I. Determination of bismuth(III). Transfer aliquot portions of a bismuth(III) solution containing 10–200 µg of the element into a 100-ml conical flask. Add 10 ml of an acetate buffer (pH 2.3–3.5) and 5-ml of sodium periodate solution. Heat the solution mixture on a boiling-water bath for 15 min. Let the reaction mixture cool, and then add 5-ml of sodium molybdate to mask the unreacted sodium periodate, followed by adding a few crystals of KI at pH 3. Extract the liberated iodine with two 10-ml portions of CCl₄. Collect the extracts in a separating funnel and shake with 10-ml of water containing 1-ml of sodium sulfite to reduce the iodine to iodide. Transfer the aqueous (upper) layer to a 100-ml Erlenmeyer flask, and determine the iodide by one of the following methods:

[48-fold amplification] To the iodide solution add 5-ml of bromine and stir for 3 min. Destroy any excess bromine by dropwise addition of formic acid, add 5-ml of 1 mol dm⁻³ sulfuric acid and 3–4 crystals of KI and determine the released iodine as triiodide by measuring the absorbance of the solution at 350 nm (ref. 10) against a blank or by titration with 2.5×10⁻³ mol dm⁻³ thiosulfate using starch as an indicator. Run a blank to correct any reagent error.

[192-fold amplification] To the iodide solution, add 5-ml of NaIO₄, stopper and allow the reaction mixture to stand for 10 min at room temperature, then place the flask in a boiling-water bath for 20 min. Cool the solution, add 5 ml of sodium molybdate, 10 ml of acetate buffer (pH≈3) and 2–3 crystals of KI and determine the released iodine as triiodide in the usual manner.

II. Determination of bismuth(V). Transfer aliquot portions of bismuth(V) containing 10–100 µg of the element into 100 ml Erlenmeyer flasks, add 2 ml of a sodium sulfite solution to each flask followed by adding

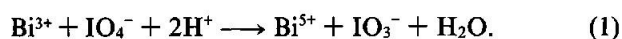
5 ml of HNO₃ (1 : 1). Allow the reaction to stand for 3 min and evaporate the solution gently on a hot plate until any excess SO₂ is completely removed. Add 5 ml of water, and determine the released bismuth(III) using procedure I.

III. Determination of bismuth in seawater. A seawater sample (400 µl) acidified to 0.1 mol dm⁻³ in hydrochloric acid is filtered through a 0.45 µm Millipore filter followed by adding 10 ml of 1 mol dm⁻³ tartaric acid, 10 ml of 1×10⁻³ mol dm⁻³ of disodium salt of EDTA and 10 ml of 1×10⁻³ mol dm⁻³ NaF. Allow the reaction mixture to stand for 10 min, and add 1 ml of sodium sulfite solution, and 2 ml of conc. HCl. Then boil the solution, and finally leave it to cool. The pH of the solution is adjusted to between 9–10 by the addition of ammonia, and then transferred into a separating funnel containing 10 ml of 2% (m/v) NaDDC. The produced Bi-DDC complex is extracted into 10-ml of xylene by shaking for 2 min, as previously reported.¹¹ The back extraction of bismuth is then carried out with 5 ml of conc. HNO₃, and the contents shaken for 5 min. The aqueous phase is then collected in a 10 ml measuring flask after washing the organic phase with another 5 ml (2×2.5) of conc. HNO₃. Finally, determine the total bismuth content following procedure II.

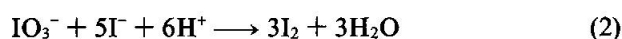
IV. Analysis of bismuth in real samples. Transfer different aliquot volumes (1–5 ml) of a laboratory-synthesized aluminum-bismuth alloy (prepared as described earlier)¹⁰ to 100-ml conical flask. Add 2 ml of saturated Na₂SO₃, 10 ml of nitric acid (1 : 1) and follow the recommended procedure II.

Results and Discussion

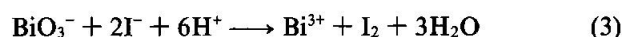
The proposed method for bismuth(III) determination is based principally on its oxidation to the pentavalent state in acid media with sodium periodate according to the following equation:



The released iodate and bismuth(V) can oxidize potassium iodide according to



and



Reaction (2) takes place rapidly and proceeds quantitatively in an acidic medium at pH≤3.5. Moreover, reaction (3) is a function of the solution pH, as can be predicted from the redox potential concerned.⁹ Preliminary experiments showed that bismuth(V)-KI reacts and proceeds forward quantitatively at pH<4 *i.e.* bismuth(V) ions release iodine upon a reaction with KI; the released iodine can be determined iodometry or

Table 1 Determination of various amounts of bismuth(III), iodometry (a) and spectrophotometry (b) using 8-fold amplification procedure

Bismuth(III) taken/µg	Bismuth(III) found/µg		Error, %	
	a	b	a	b
10	10.2±0.2	10.1±0.1	1	2
20	20.3±0.3	20.2±0.2	1.5	1
50	51.2±0.3	50.6±0.28	2.4	1.2
100	101.2±0.35	101 ±0.1	1.2	1
150	153 ±0.3	151 ±0.20	2	0.7
200	202 ±0.20	201 ±0.25	1	0.5

Average±standard deviation (*n*=5).

Error=(average bismuth found/bismuth added)×100.

spectrophotometrically as triiodide at 350 nm against reagent blank.

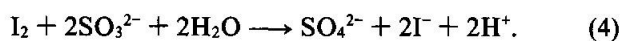
Moreover, the oxidation of bismuth(III) with sodium periodate is pH, temperature and reaction time dependent. Therefore, the effects of these factors were studied on a fixed concentration (80 µg) of bismuth(III) in the pH range 2.2–5.4. These solutions were then allowed to react with 5 ml of NaIO₄ for different time intervals (5–60 min) and different temperatures (ambient or 100°C) on a boiling-water bath. After cooling, the solutions were adjusted to pH 3 by adding 10 ml of acetate buffer; the excess sodium periodate was masked with molybdate ions at the same pH. The released iodate and bismuth(V) (reaction (1)) were then allowed to react with KI (≈40 mg), and the liberated iodine was determined by both iodometry and spectrophotometry. The results indicated that, the optimum pH range for complete oxidation of bismuth(III) with periodate was obtained in the pH range 2.3–4.0 after boiling the solution on a water bath for 15 min. At pH≥4 reactions (1)–(3) proceeded slowly. A pH<2.2 it proceeded rapidly, but the molybdate did not mask the unreacted periodate ions quantitatively, since the molybdate-periodate complex was partially decomposed. Thus, the blank values are erroneously high due to the reaction of the released periodate with iodide.¹² Fortunately, the pH values suitable for the quantitative oxidation of bismuth(III) with periodate ions (pH 2.3–3.5) are quite appropriate for masking any excess unreacted periodate. Thus, an acetate buffer solution (pH 3) was added at the beginning of the experiments. Each original bismuth(III) ion release eight equivalents of iodine; *i.e.* the proposed method affords 8-fold amplification for each one bismuth(III) ion. The developed method was employed for the determination of various amounts of bismuth (10–200 µg) iodometrically as well as spectrophotometrically at 350 nm. The results are summarized in Table 1. Satisfactory results were obtained employing iodometric and spectrophotometric procedures with standard deviations in the 0.2–0.35 and 0.15–0.28, ranges respectively.

Bismuth(V) can be determined either iodometrically or

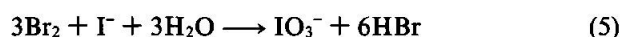
spectrophotometrically employing Eq. (3). The sensitivity and the detection limit of this method can be improved by a prior reduction of bismuth(V) to bismuth(III), followed by the determination of the produced bismuth(III) element by the 8-fold amplification procedure described earlier. A series of reducing agents was used to reduce Bi(V)→Bi(III) quantitatively without interfering with the proposed procedure. Sodium sulfite (1%) in acid media was found to be the most convenient reducing agent, where the unreacted sulfite ion can be removed by boiling off sulfur dioxide formed. The determination of various levels (10–100 µg) of bismuth(V) in aqueous media was carried out and satisfactory results were obtained with a standard deviation in the 0.2–0.5 range.

An analysis of a binary mixture of bismuth(III) and (V) in an aqueous media was carried out using the proposed procedure. An aliquot mixture was allowed first to react with sodium periodate employing the procedure described for bismuth(III) determination. Another aliquot mixture was allowed to react with KI at pH<3, followed by a determination of the released iodine. On the basis of these procedures, the volume (V_1 ml) of sodium thiosulfate or the absorbance (A_1) of the released iodine for the first aliquot was equivalent to the sum of bismuth(III)+(V). The volume (V_2 ml) of sodium thiosulfate or the absorbance of the released iodine (A_2) for the second aliquot was equivalent to bismuth(V). Thus the volume (V_1-V_2 ml) or the absorbance (A_1-A_2) was equivalent to bismuth(III). Satisfactory results were obtained with an absolute error in the 0.5–2.4 range.

Moreover, the sensity of the proposed 8-fold amplification procedure of bismuth(III) determination could be increased employing the oxidation with bromine water and sodium periodate. The released iodine from Eqs. (2) and (3) is extracted quantitatively upon shaking with two 10-ml portions of CCl_4 and shaken with sodium sulfite solution to reduce the iodine to iodide according to the equation¹³



The released iodide in the aqueous (upper) layer is allowed to react with bromine or sodium periodate to produce iodate according to the following equations:¹³



The released iodate produced from Eq. (5) or (6) is quantitatively determined iodometrically and also spectrophotometry after the addition of KI (50–70 mg). Thus, according to Eq. (5), the overall amplification employing the oxidation of iodide by bromine is 48-fold while Eq. (6) produces an overall 192-fold amplification of the iodine equivalent to each bismuth(III) element originally present. The proposed two amplification procedures have been successfully for an analysis of

Table 2 Determination of various amounts of bismuth(III) by iodometry (a) and spectrophotometry (b) using 48-fold and 192-fold amplification procedures

Bismuth(III) taken/µg	Bismuth(III) found/µg			
	48-fold		192-fold	
	a	b	a	b
5	5.1±0.2	5.0±0.1	5.0±0.1	5.0±0.1
10	10.1±0.2	10.1±0.1	10.1±0.1	10 ±0.2
20	20.1±0.2	20.2±0.1	20.1±0.1	20.1±0.3
50	50.2±0.3	50.2±0.1	50.1±0.2	50.6±0.2
100	100.6±0.4	100.4±0.2	100.5±0.3	100.4±0.3

Average±standard deviation ($n=3$).

5–100 µg bismuth(III). The obtained results are summarized in Table 2 with good accuracy. The spectrophotometric procedure employing 192-fold amplification can be extended to a lower concentration (≤ 0.1 µg) of bismuth by the extraction of the released iodine in $CHCl_3$ containing alcoholic KI, and measuring the absorbance of the triiodide at 360 nm, as previously reported.¹⁴

The absorbance–concentration relationship was found to be linear for 0.3–20 µg ml⁻¹ of bismuth(III) or (V) employing 48-fold amplification. A linear calibration graph was also obtained over a concentration range of 0.1–12 µg ml⁻¹ at 192-fold amplification for Bi(III) determination. The optimum concentration range for the effective spectrophotometric determination evaluated by the Ringbom's method¹⁵ is 5–16 ppm for 48-fold amplification and 1.2–10 ppm for 192 amplification. The relative standard deviation ($n=5$) was in the range 1.3–1.7%. The detection limit ($3\times$ noise) and correlation coefficient were found to be 0.1 ppm and 0.987 for 1–20 ppm, respectively.

Application of the proposed method

The applicability of the proposed procedures for the analysis of bismuth(III) or (V) in tap, polluted potable or seawater and artificial seawater (0.1–1 l) has been examined employing the recommended procedure (IV) using the standard addition method. Negative results were obtained, indicating the absence of bismuth. In separate experiments water samples spiked with various amounts (5–50 µg) of bismuth were analyzed employing procedure (III). Satisfactory results with a relative standard deviation in the range 1.3–1.7% ($n=3$) and a correlation coefficient of 0.96 were obtained. The analysis of a very low concentration of bismuth (as low as <0.1 µg/ml) in seawater is also possible by the proposed procedure after preconcentration and recovery of bismuth from large sample volume on polyurethane foam column¹⁶ and a determination of the produced bismuth according to the described procedure II.

A spectrophotometric analysis ($n=3$) of two weighed samples of bismuth in laboratory synthesized Al-Bi alloy by the proposed 192-fold amplification procedure

($\text{Bi}_2\text{O}_3\%$ =5.7) was in good agreement with the values obtained by the standard method ($\text{Bi}_2\text{O}_3\%$ =5.82).¹⁷ A relative standard deviation in the 1.7–2.2% range was obtained.

Effect of foreign ions

The interference of various ions (Zn^{2+} , Pt^{2+} , Sn^{4+} , K^+ , Ni^{2+} , Al^{3+} , Na^+ , Li^+ , Co^{2+} , Fe^{3+} , Pd^{2+} , Mo^{6+} , Cd^{2+} , Ca^{2+} , Mg^{2+} , Ba^{2+} and La^{3+}) which are commonly in association with bismuth, was investigated at a concentration (50 μg) approximately exceeding those normally found in seawater employing the recommended procedure (III). The selectivity of the proposed 8-fold procedure was tested by a determination of a fixed concentration (10 μg) of bismuth(III). Satisfactory results were obtained with a percentage recovery of 99.2 ± 1.2 . Mn(II), Au(I), Ti(I) and Ru(III) seriously interfered. The determination of a fixed concentration (40 μg) of bismuth(III) in the presence of a relatively high excess (0.5 mg) of various ions: (WO_4^{2-} , HCO_3^- , Br^- , Cl^- , PO_4^{3-} , SO_4^{2-} , AsO_3^- , SbO_3^- and CO_3^{2-}) was examined. The percentage recovery of bismuth(III) was $100 \pm 3\%$.

References

1. A. M. El-Wakil, A. B. Farag and M. S. El-Nahas, *Talanta*, **40**, 841 (1993).
2. A. B. Farag, M. S. El-Shahawi and E. M. El-Nemma, *Fresenius' J. Anal. Chem.*, **346**, 455 (1993).
3. A. M. El-Wakil, A. B. Farag and M. S. El-Shahawi, *Talanta*, **36**, 783 (1989).
4. A. B. Farag, H. N. Hassan, A. M. Khalil and A. F. Abdel Aziz, *Analyst* [London], **110**, 1265 (1985).
5. A. Townshend and D. T. Burns, *Talanta*, **39**, 715 (1992); J. W. Hamaya and A. Townshend, *ibid.*, **19**, 141 (1972).
6. Z. Marczenko, "Separation and Spectrophotometric Determination of Elements", Ellis-Horwood, Chichester, 1986; Z. Marczenko, I. Zotadek and A. Limbach, *Chem. Anal.* [Warsaw], **14**, 741 (1969).
7. A. I. Vogel, "Textbook of Quantitative Inorganic Analysis", 3rd ed., Longman, London, 1972.
8. D. R. Lide, "Handbook of Chemistry and Physics", 2nd ed. Chemical Rubber, 1991.
9. G. Weber, *Anal. Chim. Acta*, **186**, 49 (1986).
10. A. Richard, "Sample Pretreatment and Separation", p. 60, Wiley, New York, 1987; T. Ozawa, *Nippon Kagaku Zasshi*, **87**, 573 (1966).
11. Y. Shijo, M. Mitsuhashi, T. Shimizu and S. Sakurai, *Analyst* [London], **117**, 1929 (1992).
12. D. Burnel, *C. R. Acad. Sci., Paris*, **261**, 1982 (1965).
13. D. Amin, K. Y. Saleem and W. A. Bashir, *Talanta*, **29**, 694 (1982) and references therein.
14. T. C. Ovenston and W. T. Rees, *Anal. Chim. Acta*, **5**, 123 (1951).
15. A. Ringbom, *Z. Analyt. Chem.*, **21** (1938) 332; G. H. Ayres, *Analyt. Chem.*, **21**, 652 (1949).
16. Y. A. Gawargious, M. N. Abbas and H. N. A. Hassan, *Anal. Lett.*, **21**, 1477 (1988); T. Braun and A. B. Farag, *Anal. Chim. Acta*, **61**, 265 (1972).
17. B. Kasterke, *Chem. Anal.* [Warsaw], **19**, 63 (1974).

(Received December 21, 1994)

(Accepted February 6, 1995)

Spectroelectrochemistry of Nickel(II) Complexes of *N,N'*-Bis(salicylaldehyde)-*o*-Phenylenediamine and *N,N'*-Bis(2-hydroxy-1-naphthaldehyde)-*o*-Phenylenediamine Using an Optically Transparent Thin-layer Electrode*

M. S. El-Shahawi

Chemistry Department, Faculty of Science, UAE University, Al-Ain, P.O. Box 17551, United Arab Emirates

W. E. Smith

Pure and Applied Chemistry, Strathclyde University, Glasgow, UK G1 1XL

The Schiff base nickel(II) complexes of *N,N'*-bis(salicylaldehyde)-*o*-phenylenediamine and *N,N'*-bis(2-hydroxy-1-naphthaldehyde)-*o*-phenylenediamine provide an opportunity for the spectroelectrochemical investigation of the azomethazine and transition-metal chromophores using a gold-mesh optically-transparent thin-layer electrode (OTTLE) in protic solvents. Cyclic voltammetry of these compounds showed a well ordered electrochemical behaviour with reductions in both the metal and ligand. All complexes showed two well defined electrode couples, Ni^{II}/Ni^I and Ni^{II}/Ni^{III}. The dependence of the electrochemical parameters on the solvent, supporting electrolyte, scan rate and the nature of the ligands is discussed. Application of the OTTLE cell technique to the study of the redox chemistry of the nickel(II) pigments tested proved efficient for the spectral and electrochemical characterization of the various oxidation states. The spectropotentiostatic experiments provided redox potentials, *n* values, close to those obtained by controlled potential coulometry and in agreement with those values predicted from the bulk cyclic voltammetry. The estimated standard electrode potential (*E*⁰) values agreed well with those obtained by Nernstian analysis, and facilitated the acquisition of *E* and *n* values, which are not readily obtained by conventional techniques. This was possible even for quasi-reversible reactions where the peak separation does not yield accurate *n* values. Exhaustive electrolysis of the small volume of solution in the OTTLE ensured the quantitative generation of a particular redox state without interference from extraneous redox reactions. The effect of an additional aromatic ring is to provide an additional redox couple. The electrochemical and spectral behaviours were in good agreement, which suggests that the phenomenon of colour fading in the complex and electrochemical changes produce similar trends.

Keywords: Spectroelectrochemistry; nickel(II) complexes; gold mesh electrode

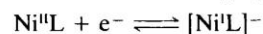
Introduction

The introduction of a substantial amount of transition metal ion character to the molecular orbitals involved in the chromophore of dyes and pigments has been shown to result in

high lightfastness and, in many instances, to produce low colour strength.¹ The electronic absorption bands associated with transition-metal Schiff-base complexes arise from various sources with a wide range of intensities.^{1,2} The ligand field transitions of the metal ion are relatively weak, although they have a significant effect on the shade and brightness of the complex.²

Bis(azomethazine) Schiff base nickel(II) complexes have been the subject of interest as pigments for the past few years.^{2,3} The low symmetry (C_{2v}) of these molecules produces more intense d-d transitions.⁴ To increase the brightness, the d-d absorption must be eliminated and planarity of the molecule retained. Substitution of an *o*-phenylenediamine bridge and a naphthalene aromatic ring results in a shift of the intense charge-transfer band to lower energy, which masks the d-d transition.³⁻⁵ This increase in the π-delocalization within the complex occurs without loss of planarity or a change in symmetry of the molecule.

The chemical behaviour of nickel(II) complexes very often depends on the facile redox properties of the complexes. However, few studies of the redox behaviour of nickel(II) complexes have combined electrochemical and spectroscopic techniques;⁶⁻⁹ the species produced were found to be either d⁹ nickel(I) complexes or nickel(II)-stabilized radical anions.^{8,9} These two sets of species were distinguished from their electron spin resonance (ESR) spectra, with the former having anisotropic *g* values greater than 2, and the latter, isotropic *g* values close to 2. Change *et al.*,¹⁰ and Pletcher and co-workers^{11,12} investigated the electron-transfer mechanism of a series of nickel(II) complexes using optically transparent electrodes, ultraviolet-visible and ESR spectroscopy. Some of the complexes were reduced to nickel(I) species,



whereas for the other complexes,



where L is the ligand.

Recently, spectroelectrochemistry has become a popular technique for studying redox reactions such as those of blue copper proteins,¹³ hexachlorometallates [MCl₆]²⁻ (M = Re, Os, Ir and Ru),¹⁴ gold(I),¹⁵ pyrrole pigments¹⁶ and a series of tetrakis(2-pyridylmethyl)-ethylenediamine complexes of nickel, copper and chromium.¹⁷⁻¹⁹ This paper correlates the electrochemical and spectral properties of nickel Schiff base complexes of *N,N'*-bis(salicylaldehyde)-*o*-phenylenediamine (1) and *N,N'*-bis(2-hydroxy-1-naphthaldehyde)-*o*-phenylenediamine (2) with the electronic structure of variously substi-

* Presented at the International Symposium on Electroanalysis in Biomedical, Environmental and Industrial Sciences, Loughborough, Leicestershire, UK, April 20-23, 1993.

tuted Schiff-base ligands. The optically transparent thin-layer electrode (OTTLE) cell was used for measuring the redox potentials, n values, and spectral changes of the electrogenerated redox states.

Experimental

Materials and Solvents

The salicylaldehyde, 2-hydroxy-1-naphthaldehyde, *o*-phenylenediamine, solvents and nickel nitrate used were of analytical-reagent grade. Tetraethylammonium hexafluorophosphate [(TEA)PF₆] and tetrabutylammonium hexafluorophosphate [(TBA)PF₆] were obtained from Aldrich and were used as supporting electrolytes without further purification. *N,N*-Dimethylformamide (DMF) solvent was purified by repeated distillation from KOH and P₂O₅, and was stored over molecular sieves (0.4 mm) under nitrogen. Most experiments used DMF as solvent for the following reasons: it is relatively easy to purify; it functions as a good Lewis base (a property that appears to be very important for these Schiff-base complexes²⁰); it has suitable electrochemical and optical properties for the OTTLE²¹ technique; and most Schiff-base complexes and ligands have significant solubility in this solvent. The Schiff-base ligands and their nickel(II) pigments were prepared by the reported procedures,^{4,5} and were re-dissolved (10⁻³ mol l⁻¹) in DMF and also in dimethyl sulfoxide (DMSO).

Apparatus and Procedures

Electronic absorption spectra were recorded using a Beckman Acta MIV spectrophotometer. Infrared spectra were obtained in KBr discs on a Perkin-Elmer 457 grating spectrophotometer. The OTTLE cell was constructed as described by Rohrbach *et al.*²⁰ A single minigrad (100 wires per inch), electroformed, gold mesh (Buckbee-Mears) was sandwiched between two 0.1 mm Teflon tape spacers to an optical pathlength of 0.3 mm, and then a copper wire was connected to the gold minigrad to provide an external contact for the working electrode. A platinum wire served as auxiliary electrode and Ag–AgCl as reference electrode. Cyclic voltammetry and controlled potential coulometry were performed with a Hi-Tek D1 2101 potentiostat in combination with a Hi-Tek digital integrator that recorded the total current passed.

Results and Discussion

To check the suitability of the constructed OTTLE cell for spectroelectrochemistry, the cyclic voltammetry of 0.01 mol l⁻¹ K₃[Fe(CN)₆] in aqueous 0.1 mol l⁻¹ KCl solution was initiated at -0.6 V *versus* a saturated calomel electrode in the negative direction. A one-electron reduction peak corresponding to the reduction of Fe(CN)₆³⁻ to Fe(CN)₆⁴⁻ was observed at 0.17 V. Switching the potential scan to the positive direction, resulted in an anodic peak at 0.27 V corresponding to the reoxidation of Fe(CN)₆⁴⁻ to Fe(CN)₆³⁻. The peak separation, ΔE_p , was 0.10 V and the formal redox potential, E^0 , 0.22 V *versus* Ag–AgCl. The peaks are skewed due to the IR drop, which is rather large in the thin-layer cell, and the

high solution resistance. However, these peaks are in good agreement with earlier data recorded at 5 mV s⁻¹.²¹

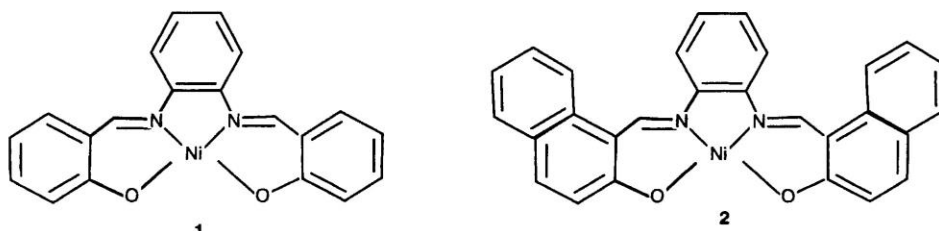
Bis(salicylaldehyde)-o-Phenylenediamine Nickel(II)

The cyclic voltammogram of *N,N*-bis(salicylaldehyde)-*o*-phenylenediamine nickel(II) (Nisalop) in DMF using (TBA)PF₆ as supporting electrolyte (Fig. 1) revealed three oxidation waves at -0.710, 1.08 and 1.38 V, two well defined cathodic peaks at -1.24 and 0.9 V, and an ill defined wave at 1.30 V *versus* Ag–AgCl. Controlled potential electrolysis of the solution in the thin-layer cell at -0.80 and 1.2 V *versus* Ag–AgCl indicated that 1 mol mol⁻¹ of the complex had been transferred. The third electrode couple was assigned to oxidation and reduction of the Nisalop complex. Therefore, the first two electrode couples are possibly nickel(I)/nickel(II), and nickel(II)/nickel(III). Controlled potential electrolysis at -1.2 V *versus* Ag–AgCl was accompanied by characteristic colour changes (from red to brown). The Nisalop species has a low-spin planar d⁸ configuration and is highly coloured, but on reduction the anion is even more intensely coloured, and the visible absorption bands have molar absorption coefficients in the range 3–4 × 10⁴ m² mol⁻¹.

The redox potentials nickel(II)/nickel(III) of Nisalop in DMF–(TBA)PF₆ and DMSO–(TBA)PF₆ are given in Table 1. The standard electrode potentials obtained in DMSO are smaller than those obtained in DMF, possibly because these solvents have appreciably different relative permittivities for the donor–acceptor interaction between the ions and solvent junction potentials.^{22,23} The effect of the scan rate (50–1000 mV s⁻¹) on the electrode potentials of Nisalop can also be seen in Table 1; representative voltammograms for the electrode couple nickel(II)/nickel(III) are shown in Fig. 2. Increasing the scan rate on the bulk cyclic voltammetry of the complex from 50 to 1000 mV s⁻¹ increased the cathodic–anodic peak separation, and the ratio of the peak currents of the reverse scan (i_p^r) to those of the forward scan (i_p^f) varied from 0.90 to 0.98. This behaviour suggested that different species formed with different scan rates or that the species that initially formed during the reduction process changed to some other form or decomposed to products that were not reoxidized at the same potential as the first species formed.⁸ Surprisingly, at scan rates ≤ 50 mV s⁻¹ a new anodic peak was observed at 1.56 V *versus* Ag–AgCl; this was coupled with an ill defined cathodic peak at 1.48 V *versus* Ag–AgCl. This anodic peak is possibly due to the nickel(III)/nickel(IV) couple, such complexes having been confirmed by controlled potential coulometry at 1.50 V *versus* Ag–AgCl.

Comparison of the redox potentials of Nisalop in DMSO–(TBA)PF₆ (E^0 , -0.94, 0.85 and 0.35 V) and in DMSO–(TEA)PF₆ (E^0 , -1.025, 0.78 and -0.4 V) *versus* Ag–AgCl indicates that the ease with which the electrode reactions nickel(II) to nickel(I), and nickel(III) to nickel(II) proceed depends on the supporting electrolyte. This is probably due to ion pairing of the anions, which is a function of the relative permittivity of the solvent.^{22,23}

Spectropotentiostatic experiments in the OTTLE cell were used to obtain the absorption spectra of the air-sensitive



Scheme 1

nickel(II) and nickel(III) electrogenerated species of the Nisalop complex. The spectra (Fig. 3) were recorded from +0.55 to +1.0 V versus Ag–AgCl in 0.05 and 0.3 V steps with a 3 min equilibration period for the electrogenerated species. At a given wavelength, the absorbance changes observed in these experiments can be related to the ratio of the concentrations of the reduced (R) and oxidized (O) species:

$$\frac{[R]}{[O]} = \frac{A_3 - A_2}{A_2 - A_1}$$

where A_1 is the absorbance of the completely reduced form, A_3 , the absorbance of the completely oxidized form, and A_2 , the absorbance of the mixtures of oxidized and reduced forms. The absorption was found to decrease as the applied voltage increased; finally, at 1.2 V no reading was obtained. This suggests that the oxidation was followed by bleaching of the colour, possibly due to the disappearance of the compound from the solution; the oxidation was probably that of Ni^{II} to Ni^{III}. Fig. 4 shows the effect of time on the absorption spectra of the electrogenerated species at 0.9 V versus Ag–AgCl in

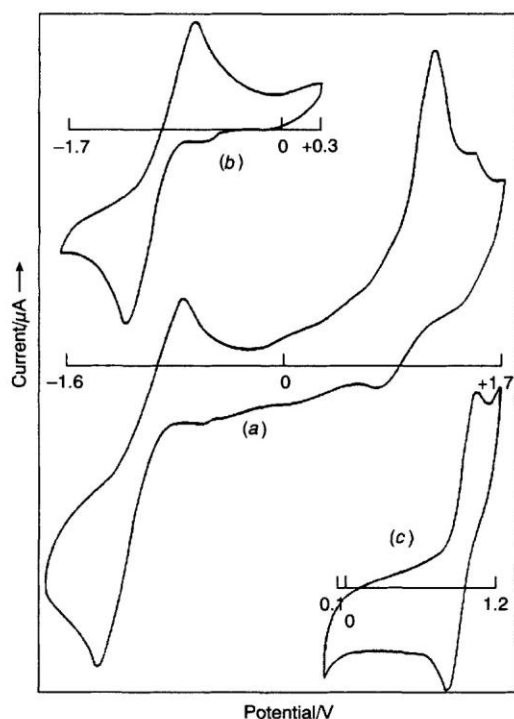


Fig. 1 Cyclic voltammograms of 3.0 mmol l⁻¹ *N,N*-bis(salicylaldehyde)-*o*-phenylenediamine nickel(II) in DMF-(TBA)PF₆ obtained using the OTTL cell at a scan rate of 5 mV s⁻¹. Potential limits: A, -1.6–+1.7; B, -1.7–+0.3; and C, 0.1–1.2 V versus Ag–AgCl

Table 1 Effects of scan rate and solvent on the redox potential of the nickel(II)/nickel(III) couple of the Nisalop complex versus Ag–AgCl. E^0 , standard electrode potential; $E_{p,a}$, anodic peak potential; $E_{p,c}$, cathodic peak potential; and ΔE_p , anodic–cathodic peak separation

Scan rate/ mV s ⁻¹	DMSO-(TBA)PF ₆				DMF-(TBA)PF ₆			
	$E_{p,a}$	$E_{p,c}$	ΔE_p	E^0	$E_{p,a}$	$E_{p,c}$	ΔE_p	E^0
50	1.0	0.860	0.140	0.93	0.840	0.717	0.123	0.778
100	1.020	0.845	0.175	0.932	0.840	0.707	0.133	0.773
200	1.060	0.820	0.240	0.940	0.845	0.697	0.157	0.775
500	1.080	0.820	0.260	0.95	0.871	0.686	0.185	0.778
1000	1.080	0.800	0.280	0.94	0.902	0.686	0.216	0.794

DMF. The graphs of absorbance versus applied potential at wavelengths of (a) 375 and (b) 475 nm are shown in Fig. 5. These illustrate the spectral changes that accompany the variation in the redox state of Nisalop. The Nernst plots,

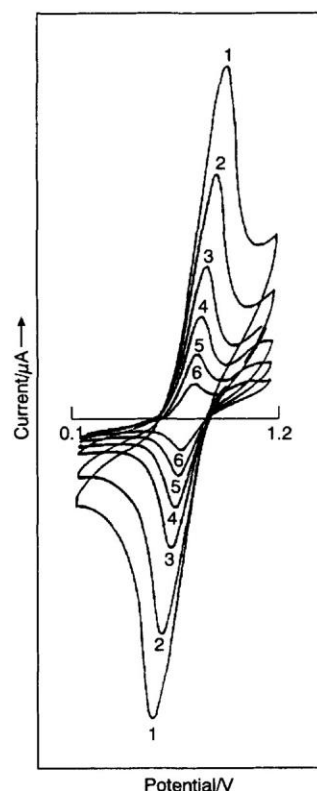


Fig. 2 Effect of scan rate on the electrode couple nickel(II)/nickel(III) of the Nisalop complex in DMF-(TBA)PF₆. Scan rate: 1, 10; 2, 20; 3, 50; 4, 100; 5, 200; and 6, 500 mV s⁻¹ (versus Ag–AgCl)

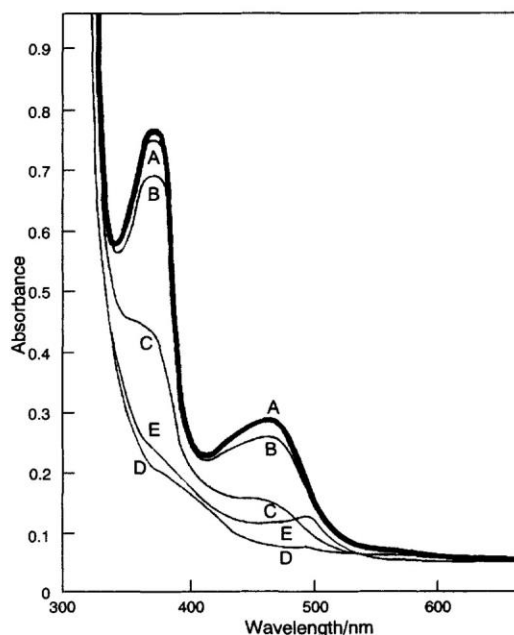


Fig. 3 Absorption spectra of 3.0 mmol l⁻¹ *N,N*-bis(salicylaldehyde)-*o*-phenylenediamine nickel(II) in DMF-(TBA)PF₆. Applied potential: A, +0.55; B, +0.6; C, +0.65; D, +0.7; and E, +1.0 V versus Ag–AgCl

E_{applied} versus $\log [O]/[R]$, at these wavelengths were linear, giving n values of 0.98 at 375 nm and 1.4 at 475 nm. The intercepts gave E^0 values of 0.789 and 0.84 V versus Ag–AgCl.

The spectra of the nickel(II) and nickel(III) species (Fig. 3) also demonstrate one significant advantage of the OTTLE technique over more conventional procedures for obtaining spectra of air-sensitive nickel(III) species. In the OTTLE technique, exhaustive electrolysis ensures that only Ni(III) species are present in the light beam, whereas with conventional techniques it is very difficult to manipulate nickel(III) solutions without suffering some extraneous interference from nickel(II).

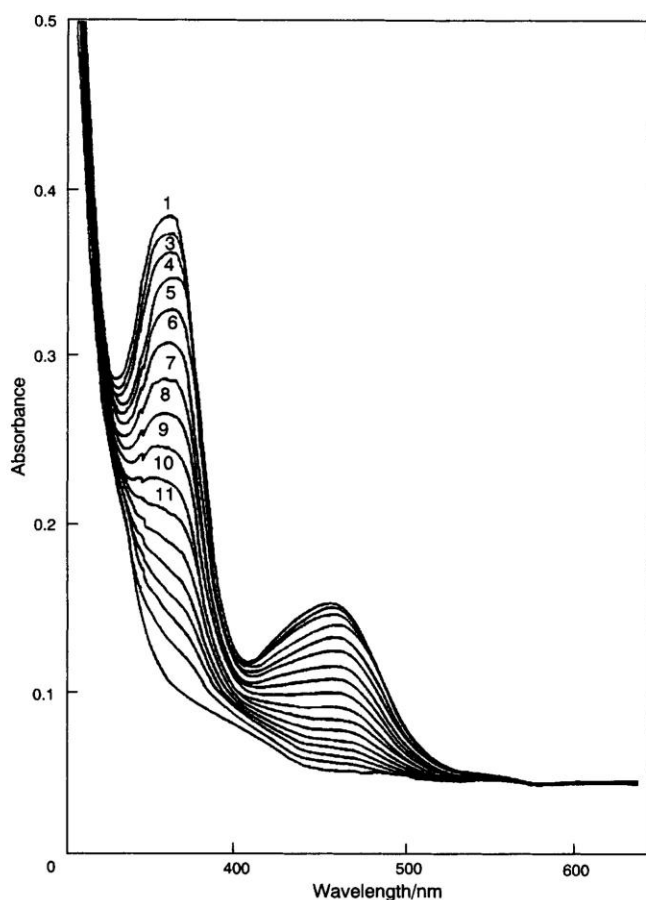


Fig. 4 Absorption spectra of 3.0 mmol l^{-1} *N,N*-bis(salicylaldehyde)-*o*-phenylenediamine nickel(II) in DMF-(TBA)PF₆ at +0.6 V versus Ag–AgCl. Spectra were recorded every 3 min and increasing time from curves I–II

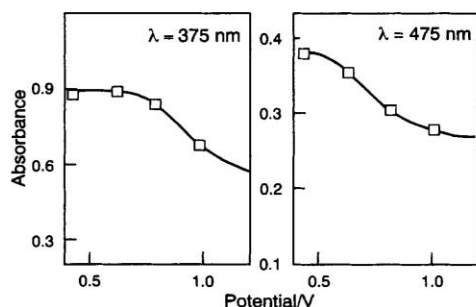


Fig. 5 Plots of absorbance of Nisalop versus applied potentials in DMF-(TBA)PF₆ (Ag–AgCl electrode). (a) $\lambda = 375 \text{ nm}$; and (b) $\lambda = 475 \text{ nm}$

Bis(2-hydroxy-1-naphthaldehyde)-*o*-Phenylenediamine Nickel(II)

The results of the cyclic voltammetry of bis(2-hydroxy-1-naphthaldehyde)-*o*-phenylenediamine nickel(II) (NiNap₂OP) were generally similar to those of Nisalop. Three electrode couples were observed at scan rates of 5 mV s^{-1} . The first electrode couple was assigned as Ni^{II}/Ni^{III} with $E^0 = -0.93 \text{ V}$, and the second as Ni^{II}/Ni^I with $E^0 = -0.84 \text{ V}$ versus AgCl. An electrode couple with $E^0 = 1.4 \text{ V}$ versus Ag–AgCl was perhaps due to the redox behaviour of the NiNap₂OP ligand. The voltammograms of the complex in DMF-(TBA)PF₆ and DMSO-(TBA)PF₆ showed no significant differences in electrode potentials. These results suggest that little or no ligand interaction occurred between DMF or DMSO molecules and the neutral or electrogenerated species.²⁴

Conclusion

The nickel(II) complexes studied in DMF-(TBA)PF₆ showed well ordered electrochemical behaviour with reduction in both metal and ligand. The effect of an additional aromatic ring, such as in naphthaldehyde, in a complex is that it traps an extra electron and thus provides an additional redox couple. The electrochemical and spectral behaviours are in good agreement, suggesting that the initial concept that fading and electrochemical changes in light produce similar trends is justified. It has also been shown that all the complexes form nickel(I) and (II). Application of the OTTLE technique to non-aqueous solvents has proved efficient for the spectral and electrochemical characterization of the various oxidation states. The OTTLE spectropotentiostatic technique facilitates the acquisition of E^0 and n values, which are not readily provided by more conventional techniques. Exhaustive electrolysis of the small volume of solution contained in the OTTLE cell ensures the quantitative generation of a particular redox state without interference from extraneous redox reactions.

References

- Macdonald, L. G., Ph.D. Thesis, Strathclyde University, 1980.
- Brown, D. H., Morris, J. H., Oates, G., and Smith, W. E., *Spectrochim. Acta, Part A*, 1982, **38**, 333, and references cited therein.
- El-Shahawi, M. S., Ph.D. Thesis, Strathclyde University, 1986.
- Holm, R. H., Everett, G. W., and Chakravorty, A., *Prog. Inorg. Chem.*, 1966, **7**, 83.
- Casellato, U., Vigoto, P. A., Fenton, D. A., and Vidici, M., *Chem. Soc. Rev.*, 1979, **8**, 199.
- Lovecchio, F. V., and Gore, E. S., *J. Am. Chem. Soc.*, 1974, **96**, 3109.
- Gagne, R. R., and Ingle, D. M., *J. Am. Chem. Soc.*, 1980, **102**, 1444.
- Bowmaker, G. A., Boyd, P. D. W., Campbell, G. K., Hope, J. M., and Martin, R. L., *Inorg. Chem.*, 1982, **21**, 1152.
- Bowmaker, G. A., Boyd, P. D. W., and Campbell, G. K., *Inorg. Chem.*, 1982, **21**, 2403.
- Change, D., Malinski, T., Ulman, A., and Kadish, K. M., *Inorg. Chem.*, 1984, **23**, 817.
- Gosden, C., Kerr, J. B., Pletcher, D., and Rosas, R., *J. Electroanal. Chem. Interfacial Electrochem.*, 1981, **117**, 101.
- Beckerr, J. Y., Kerr, J. B., Pletcher, D., and Rosas, R., *J. Electroanal. Chem. Interfacial Electrochem.*, 1981, **117**, 87.
- St. Clair, C. S., Ellis, W. R., Jr., and Gray, H. B., *Inorg. Chim. Acta*, 1992, **191**, 149.
- Kennedy, B. J., and Heath, G. A., *Inorg. Chim. Acta*, 1992, **195**, 101.
- Anderson, J. E., and Sawtelle, S. M., *Inorg. Chim. Acta*, 1992, **194**, 171.
- Ribo, J. M., Farrera, J. A., Claret, J., and Grubmayr, K., *Bioelectrochem. Bioenerg.*, 1992, **29**, 1.

- 17 Daluz, D., Franco, C. V., Vancato, L., and Neves, A., *J. Coord. Chem.*, **1992**, **26**, 269.
- 18 Kuneaka, A., Iuati, A., Gross, M., and Frens, Y., *J. Electroanal. Chem.*, **1992**, **338**, 213.
- 19 Cinquantin, A., Seeber, R., Cini, R., and Zanillo, P., *J. Electroanal. Chem.*, **1982**, **134**, 65.
- 20 Rohrbach, D. F., Deutsch, E., and Heineman, W. R., in *Characterization of Solutes in Non-aqueous Solvents*, ed. Mamentov, G., Plenum, New York, **1978**, p. 177.
- 21 DeAngiles, T. P., and Heineman, W. R., *J. Chem. Educ.*, **1976**, **53**, 594.
- 22 Cinquantin, A., Seeber, R., Cini, R., and Zanillo, P., *J. Electroanal. Chem.*, **1982**, **134**, 65.
- 23 Gutman, V., *The Donor Acceptor Approach to Molecular Interactions*, Plenum, New York, **1978**.
- 24 Kadish, K. M., Coccolios, B. B., Simonet, B., Chang, D., Ledon, H., and Coccolios, P., *Inorg. Chem.*, **1985**, **24**, 2148.

Paper 3/003088B

Received June 9, 1993

Accepted October 6, 1993

Spectrophotometric determination of ruthenium after extraction of perruthenate with benzyltributylammonium chloride

M.S. El-Shahawi*, A.Z. Abu Zuhri, S.M. Al-Daheri

Chemistry Department, Faculty of Science, UAE University, P.O. Box 17551, Al-Ain, U.A.E.

Received: January 1994/Accepted: 16 May 1994

Abstract. A simple and convenient extractive spectrophotometric method for the determination of ruthenium has been developed. It is based on the oxidation of the different ruthenium (II, III or IV) species to perruthenate with potassium periodate at pH 7.8. The perruthenate is then extracted with benzyltributylammonium chloride in chloroform followed by direct spectrophotometric measurements at 342 and 380 nm. The optimum concentration range was found to be 0.1–5 mg l⁻¹, the standard deviation \pm 2.1%. The method has been successfully applied to the determination of ruthenium in organoruthenium compounds.

Introduction

The quantification of ruthenium at trace levels is required for geological surveys, catalytic applications of many organic compounds and material sciences [1–3]. Its spectrophotometric determination using organic reagents has been reported [4–7]. However, most of these reagents suffer from lack of selectivity and sensitivity, and require laborious enrichment steps, e.g. flotation, precipitation etc.

The oxoanions are the least investigated group forming liquid-liquid extractable ion pairs with onium cations [8–11]. Ruthenate [12,13] and perruthenate [14], have been used to determine large amounts of ruthenium. These methods are based on the formation of an orange ruthenate ion (RuO₄²⁻) or perruthenate ion (RuO₄⁻) in alkaline solutions containing hypochlorite or periodate [14,15]. They require much time for the extraction procedure and the tolerance limit for ruthenium(III) is low. This paper reports the use of benzyltributylammonium (BTA) cations as an ion-pairing extractant for perruthenate from aqueous media and its application to the determination of ruthenium in or-

ganoruthenium compounds, synthetic samples and natural water.

Experimental

Britton–Robinson (BR) buffer solutions (pH 3.2–11.5) containing sodium hydroxide, orthophosphoric acid, boric acid and acetic acid were prepared in distilled water. Ruthenium(III) chloride hexahydrate (500 μ g ml⁻¹) (Johnson Matthey, London) was dissolved in hydrochloric acid (1:20) and the filtrate diluted to a known volume with distilled water. The ruthenium content was determined colorimetrically [6]. Ruthenium dioxide [BDH] was fused with sodium hydroxide and then dissolved in distilled water. The ruthenium(IV) content was determined colorimetrically after its reduction to ruthenium(III) with sulphur dioxide. Benzyltributylammonium chloride (BTA) (Fluka, purum > 98% Cl) was used as supplied. A 1% (w/v) stock solution of BTA was prepared in water. A 2% (w/v) solution of potassium periodate [BDH] was prepared by dissolving 2.3 g of KIO₄ in a mixture of 2 ml conc. nitric acid and 25 ml of water, and diluting to 100 ml with water.

A Phillips 9418 digital pH-meter was used for pH measurements. A Pye-Unicam SP 8-4 00 double beam UV-visible spectrophotometer was used for the absorbance measurements with a 10 mm quartz cell.

Recommended procedures

1. *Determination of Ru(III) and (IV).* Transfer aliquot portions (5 ml) containing various amounts (0.1–100 μ g) of ruthenium(III) or (IV) into a 100 ml separating funnel. Add 10 ml of Britton–Robinson buffer (pH 7.8), 20 ml of water, 5 ml of 2% (w/v) potassium periodate solution and 5 ml of 1% (w/v) benzyltributylammonium chloride solution and mix. Extract twice with 5 ml (2 \times 2.5 ml) of chloroform and collect the extracts in a dry 50 ml beaker containing anhydrous sodium sulphate (1 g) and swirl to mix. Transfer the extract into a 10 ml volumetric flask, wash the residue with 5 ml chloroform and transfer into the volumetric flask; make up to the mark with chloroform. Measure the absorbance of the organic phase at 380 and 342 nm against a reagent blank.

* Permanent address: Chemistry Department, Faculty of Science, Mansoura University, Damietta Egypt

Correspondence to: M.S. El-Shahawi

2. *Determination of ruthenium in its complexes.* The ruthenium complex used in this work were prepared by the previously reported procedure [2]. Weigh accurately 2–3 mg of the sample and wrap it as usual with the Schöniger technique [17]. Place about 10 ml of aqua regia in a 250 ml oxygen combustion flask, fill the flask with oxygen and light the paper fuse. When the combustion is complete, shake the flask for 10 min, open it and rinse down the stopper and gauze with about 10 ml of dilute nitric acid. Place the flask on a hot plate and boil gently until the volume of the solution has been reduced to about 5 ml. Add 2 ml of saturated Na_2SO_3 solution followed by 5 ml conc. nitric acid. Evaporate the solution gently to dryness. Take up the salt in 5 ml of distilled water and transfer it into 50 ml volumetric flask, make up the solution to the mark with distilled water and follow the recommended procedure described for ruthenium(III) determination.

Results and discussion

Methylene chloride, 1,2 dichloroethane, nitrobenzene, tetrachloromethane, chlorobenzene, toluene, carbon tetrachloride, benzene and chloroform were tested as possible extracting solvents for the perruthenate-BTA species formed. The highest absorbance was obtained in chloroform, the extraction also being complete. Therefore, chloroform was selected as a proper solvent for these reasons and because its greater density allows a better separation of the phases.

The absorption spectra of the RuO_4 -BTA ion pair and BAT^+Cl^- in chloroform and RuCl_3 at pH 7.8 are given in Fig. 1. Two well resolved bands at 342 and 380 nm were observed in the spectrum of the perruthenate-BTA, while no bands were found in the spectrum of BTA in chloroform. In the spectrum of ruthenium(III) chloride in aqueous media at pH 7.8, one band was found at 314 nm. Therefore, the absorbance measurements for the perruthenate-BTA were measured at 342 and 380 nm.

The extraction of the RuO_4 -BTA into chloroform was rapid and 2 min stirring time was adopted in the subsequent work. The absorbance of the coloured RuO_4 -BTA ion pair in chloroform was found to be constant up to 1 h for samples containing 0.1–20 $\mu\text{g}/\text{ml}$. The addition of sodium chloride or sodium nitrate up to 0.01 mol/l did not improve the amount of RuO_4 -BTA extracted at a concentration of 10 $\mu\text{g}/\text{ml}$ ruthenium, indicating that the perruthenate species is extracted quantitatively without salt effect. In the presence of a salt effect at concentrations > 0.01 mol/l, the absorbance of the extracted perruthenate-BTA species decreased, which is possibly due to the ability of the ruthenium species to form chloro complexes which are less extractable by the organic phase and are less oxidized by potassium periodate at the experimental conditions [16, 18].

The influence of the pH of the aqueous phase on the extraction of ruthenium(III) or (IV) was examined by measuring the absorbance of the organic phase for the perruthenate-BTA species in chloroform. The results are

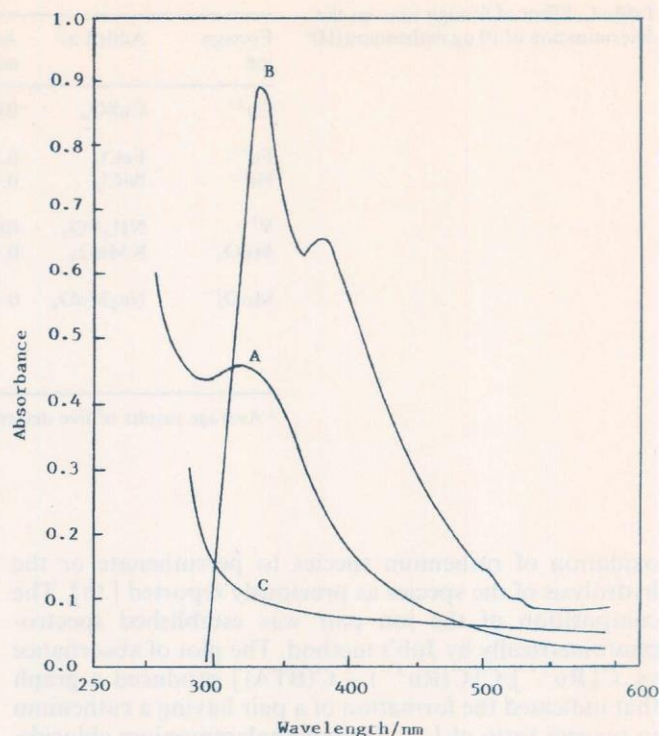


Fig. 1. Absorption spectra of ruthenium in aqueous media at pH 7.8 (A), extracted RuO_4 -BTA ion-pair (B) against reagent blank and benzyltributylammonium chloride (C) in chloroform

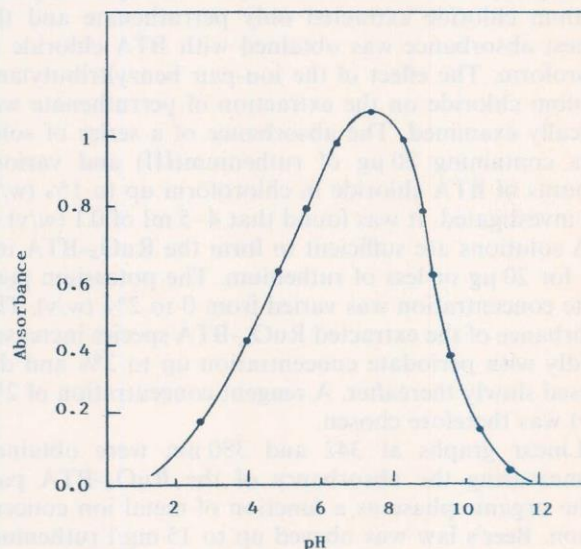


Fig. 2. Effect of pH on the absorbance measurements of the extracted RuO_4 -BTA (40 μg) ion pair against reagent blank in chloroform. Other conditions are kept constant

summarized in Fig. 2, from which it can be seen that a maximum and constant absorbance of the organic phase can be obtained in the pH range 6.5–7.8. In more acidic or alkaline solutions, the absorbance of the extracted species decreased, possibly due to the incomplete

Table 2. Results of the extractive spectrophotometric determination of Ru in various ruthenium(III) complexes^a

Complex	Ru present ^b (%)	Ru found ^c (%)	Standard deviation
RuCl ₂ (PPh ₃) ₂ (Koj)	24.52	24.5	0.2
RuCl ₂ (PPh ₃) ₂ (malt)	24.46	24.40	0.26
RuCl ₂ (PPh ₃) ₂ (trop)	24.7	24.9	0.3
RuCl ₂ (PPh ₃) ₂ (acac)	25.32	24.9	0.22

^a Abbreviations: Kojic acid (Koj); maltol (malt); tropolone (trop) and acetylacetonone (acac)

^b Certified value

^c Average of five determinations

Acknowledgement. The authors would like to thank Miss M.A. Mostafa for her assistance.

References

1. Taquikhan MM, Shukla RS (1986) *J Mol Catalysis* 34: 19
2. El-Hendawy AM, El-Shahawi MS (1989) *Polyhedron* 8: 2813 and references therein
3. Palaniappan R, Kumar TA (1983) *Analyst* 118: 293 and references therein
4. Gowda MS, Raj JB, Ahmed SA (1984) *Indian J Chemistry* 23A: 62
5. Das AK, Das J (1984) *Indian J Chemistry* 23A: 359
6. Gurva RF, Trutneua LM, Savvin SB, Chalisova NN (1984) *Zh Anal Khim* 39: 1653
7. Wasey A, Bansal RK, Stake M, Puri BK (1983) *Bull Chem Soc Jpn* 56: 3603
8. Burns DT, Harriott M, Barakat SA (1992) *Fresenius J Anal Chem* 343: 488
9. Burns DT, Harriott M, Barakat SA (1992) *Anal Chim Acta* 258: 135
10. Burns DT, Harriott M, Barakat SA (1992) *Anal Chim Acta* 259: 33
11. Burns DT, Harriott M, Barakat SA (1993) *Anal Chim Acta* 259: 135
12. Marczenko Z, Balcerzak M, Kun S (1980) *Talanta* 27: 1087
13. Norkus PK, Yankankas Yu Yu (1972) *Zh Analit Khim* 27: 2014
14. Dinstl G, Hecht F (1963) *Mikrochim Acta* 895
15. Marczenko Z (1986) *Separation and spectrophotometric determination of elements*. Horwood, Chichester
16. McDonald CW, Bedenbaugh JH (1970) *Microchim Acta (Wien)* 612
17. MacDonald AMG (1961) *Analyst* 86: 3
18. Yamaguchi S, Uesugi K (1984) *Analyst (Lond)* 109: 1393
19. Ringbom A (1939) *Fresenius Z Anal Chem* 115: 332
20. Sandell EB (1959) *Colorimetric determination of trace metals*. Interscience, New York
21. Larsen RP, Ross LE (1957) *Anal Chem* 29: 1412

Adsorptive stripping voltammetric measurements of trace amounts of platinum(II) and ruthenium(III) in the presence of 1-(2-pyridylazo)-2-naphthol

M. S. El-Shahawi¹, A. Z. Abu Zuhri¹, M. M. Kamal²

¹Department of Chemistry, Faculty of Science, UAE University, Al-Ain, P.O. Box 17551, United Arab Emirates

²Department of Chemistry, Faculty of Science, Assiut University, Assiut, Egypt

Received: 3 June 1993/Accepted: 27 September 1993

Abstract. An extremely sensitive stripping voltammetric procedure for low level measurements of platinum (II, IV) or ruthenium (III, IV) is reported. The method is based on the interfacial accumulation of the platinum (II) or ruthenium (III)-1-(2-pyridylazo)-2-naphthol complex on the surface of a hanging mercury drop electrode, followed by the reduction of the adsorbed complex during the cathodic scan. The peak potential was found to be -0.8 V vs. Ag/AgCl electrode and the reduction current of the adsorbed complex ions of platinum (II) or ruthenium (III) was measured by differential pulse cathodic stripping voltammetry. The optimum experimental conditions were: 1.5×10^{-7} mol/l of 1-(2-pyridylazo)-2-naphthol solution of pH 9.3, preconcentration potential of -0.2 V, accumulation time of 3 min and pulse amplitude of 50 mV with 4 mV s^{-1} scan rate in the presence of ethanol-water (30% v/v) – sodium sulphate (0.5 mol/l). Linear response up to 6.4×10^{-8} and 5.1×10^{-8} mol/l and a relative standard deviation (at 1.2×10^{-8} mol/l) of 2.4 and 1.6% ($n = 5$) for platinum (II) and ruthenium (III) respectively were obtained. The detection limits of platinum and ruthenium were 3.2×10^{-10} and 4.1×10^{-10} mol/l, respectively. The electronic spectra of the Pt(II) – PAN and Ru(III) – PAN complexes were measured at pH 9.3 and the stoichiometric ratios of the complexes formed were obtained by the molar ratio method. The effects of some interfering ions on the proposed procedure were critically investigated. The method was found suitable for the sub-microdetermination of ruthenium (IV) and platinum (IV) after their reduction to ruthenium (III) and platinum (II) with sulphur dioxide in acid media. The applicability of the method for the analysis of binary mixtures of ruthenium (III) and (IV) or platinum (II) and (IV) has also been carried out successfully. The method is simple, rapid, precise, and promising for the determination of the tested metal ions at micromolar concentration level.

Introduction

Because of the importance of platinum and ruthenium and its extremely low levels in various matrices, sensitive methods are required for their reliable quantitation [1]. In particular, the quantification of ruthenium at trace levels is desired for geological surveys, catalytic applications and material sciences. Therefore, the most common reported spectrophotometric procedures for ruthenium and platinum usually require laborious enrichment steps (co-precipitation, solvent extraction, flotation, etc.) [1]. Many organic reagents have been proposed for the spectrophotometric determination of platinum [2–5] and ruthenium [6–10].

Recently procedures have been developed for determining metal ions by adsorptive collection of their complexes on a carbon paste electrode [11] and a modified carbon electrode [12]. Adsorptive voltammetric measurements based on complexing of different metal ions with various heterocyclic azo derivatives as complexing agents were investigated [13–17]. In addition to their inherent sensitivity, such adsorptive stripping voltammetric schemes possess a great potential for in-situ field screening or on-line monitoring of the tested metal ion.

Several polarographic methods have been reported for the determination of trace amounts of ruthenium [18–20] with salicylaldehyde thiosemicarbazone (SAT). These methods are based on the adsorption of the Ru(III)-SAT complex on mercury electrodes, after undergoing single-electron reduction; but neither their sensitivity nor selectivity are very satisfactory. The present study describes an adsorptive voltammetric stripping procedure for the measurements of trace levels of platinum (II or IV) or ruthenium (III or IV). The method relies on the effective interfacial cathodic stripping differential pulse voltammetry (CS-DPV) of the accumulated platinum(II)-PAN or ruthenium (III)-PAN complex on a hanging mercury drop electrode (HMDE). The PAN-based procedure offers higher sensitivity for the simultaneous microdeterminations of the binary mixtures of Ru(III) + Ru (IV) or Pt(II) + Pt (IV).

Experimental

Apparatus

Adsorptive voltammetric measurements were carried out by means of a Metrohm (Herisau, Switzerland) E-506 polarograph coupled with an 663 VA polarographic stand. A three-electrode combination was used, consisting of an Ag/AgCl electrode as the reference and platinum wire as the counter electrode. The working electrode is a hanging mercury drop electrode (HMDE). A Metrohm Model E_A-87620 cell, flushed with high-purity nitrogen, was used throughout. A pulse amplitude of 50 mV was used with a scan rate of 4 mV s⁻¹, a drop time of 2 s and a mercury height of 45 cm. The pH-measurements were made with a Metrohm 632 pH-meter. The electronic spectra of the solutions were recorded on a Pye-Unicam 8100 spectrophotometer using 1 cm quartz cells. All experiments were performed at room temperature 22 ± 0.5 °C.

Reagents

Unless otherwise specified all chemicals used were of analytical reagent grade. Universal Britton-Robinson (BR) buffer solutions containing a mixture of equal amounts (0.04 mol/l) of phosphoric, boric and acetic acids with sodium hydroxide (0.01 mol/l) were used to provide different pH ranges (3.4–11.5). A constant ionic strength ($\mu = 0.5$) was maintained with sodium sulphate solution. A stock solution of 10⁻³ mol/l of 1-(2-pyridylazo)-2-naphthol (PAN) was prepared in ethanol. Stock solutions of 1 mg/ml of ruthenium(III), and platinum(II) (atomic absorption standard, BDH) were used and diluted with water for standard addition whenever required. Solutions of 100 µg/ml of Ru (IV) were prepared from ruthenium dioxide using the recommended procedure [21]. Platinum(IV) stock solution (1 mg/ml) was obtained from Tanaka Kikinzoku Kogyo K.K. as hydrochloric acid solution.

Recommended procedures

1. Determination of platinum(II) or ruthenium(III). The supporting electrolyte solution (10 ml) containing 1.5 × 10⁻⁷ mol/l of PAN and 30% ethanol (v/v) at pH 9.30 in the polarographic cell was purged with nitrogen for 10 min. The preconcentration potential (usually -0.2 V) was applied to a fresh mercury drop while the solution was stirred for an accumulation period of 3 min. Following the preconcentration period, the stirring was stopped and after 15 s the voltammogram was recorded by applying a negative-going differential pulse scan with 4 mV s⁻¹ scan rate and an amplitude of 50 mV. The scan was terminated at -1.5 V and aliquots of the ruthenium(III) or platinum(II) standard solutions were introduced after recording the background voltammograms. Throughout this operation, nitrogen was passed over the solution. The adsorptive stripping was repeated with a new mercury drop with the addition of the ruthenium(III) or platinum(II) sample.

2. Determination of platinum(IV) or ruthenium(IV). Transfer a liquid portion containing various amounts of platinum(IV) or ruthenium(IV) into a 100-ml conical flask and add 3-ml of conc. H₂SO₄ followed by adding 10-ml of sodium sulphite (1 mol/l). Allow the reaction mixture to stand for 5 min and evaporate the solution gently on a hot plate until the excess SO₂ is completely recovered. Add 10 ml of doubly distilled water to the produced platinum(II) or ruthenium(III) solutions and follow the recommended procedure 1. Satisfactory results confirming complete reduction of Pt(IV) → Pt(II) and Ru(IV) → Ru(III) species were obtained. Similar reduction reactions of metal ions are well known in the literature [22, 23].

3. Analysis of binary mixtures of platinum(II) and (IV). Transfer an aliquot portion of the mixture into the cell and determine the platinum(II) ions following the recommended procedure 1. Another aliquot sample mixture is then reduced to the divalent platinum as described in procedure 2. Determine the total content of the platinum employing the procedure recommended for platinum(II). On the basis of the proposed method the difference between the stripping peak height current in the first and second step is equivalent to the platinum(IV) species in the mixture.

4. Analysis of binary mixtures of ruthenium(III) and (IV). Determine ruthenium(III) in the aliquot mixture as described in procedure 1. Another aliquot sample is then reduced to trivalent ruthenium as described in the recommended procedure 2 and the total content of the ruthenium is determined by measuring the peak current employing the recommended procedure for ruthenium(III). The difference between the stripping peak height in the first and second step is equivalent to ruthenium(IV).

Results and discussion

The reagent 1-(2-pyridylazo)-2-naphthol was found to be electrochemically active in the ethanol-water system in the presence of sodium sulphate at various pH-values. Therefore, many attempts employing different reduction media have been used to select the optimum experimental conditions for the peak height (µA) and for the resolution of the reduction wave of the reagent. In a solution of 30% ethanol-water (v/v) at pH 9.3 and 0.5 mol/l sodium sulphate supporting electrolyte a well defined reduction wave was observed at -0.82 V vs. Ag/AgCl electrode (Fig. 1) and the peak current was found to be high at the optimum experimental conditions. Also the solubility of the reagent PAN in ethanol was quite good as compared to water or any other common organic solvents. The observed reduction peak is attributed to the reduction of the azo group N = N in the molecule as reported by Zhao et al. [24].

In the presence of platinum(II) or ruthenium(III) ions, under the same experimental conditions of PAN, a well defined and largely enhanced reduction peak is observed at the same potential of the reduction wave of

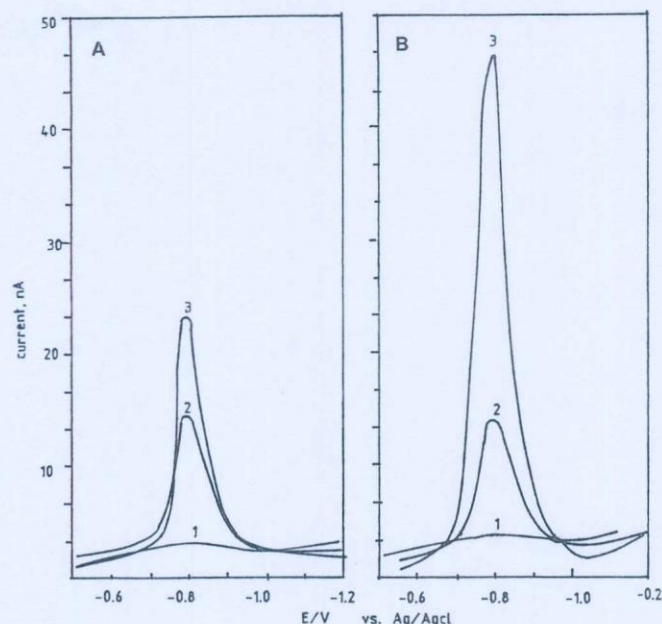
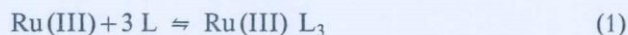


Fig. 1 A, B. Cathodic stripping voltammograms of: A 5×10^{-8} mol/l Ru(III) (1); 1.5×10^{-7} mol/l PAN (2); 3.7×10^{-9} mol/l Ru(III) + 1.5×10^{-7} mol/l PAN (3) and B 5×10^{-8} mol/l Pt(II) (1); 1.5×10^{-7} mol/l PAN, (2) and 9.7×10^{-9} mol/l Pt(II) + 1.5×10^{-7} mol/l PAN, (3) in 30% ethanol-water and 0.5 mol/l Na_2SO_4 at pH 9.35; $\sigma_p = -0.2$ V, $t_s = 3$ min; $4 \text{ mV} \cdot \text{s}^{-1}$; 50 mV amplitude

PAN as is given in Fig. 1. The peak current increased markedly in relation to the platinum(II) or ruthenium(III) concentration and accumulation time. The enhancement of this reduction peak possibly results from the adsorption of platinum(II)-PAN or ruthenium(III)-PAN complex on the electrode surface.

The molecular structures of the Ru(III)-PAN and Pt(II)-PAN complex species at pH 9.3 were elucidated by the spectrophotometric molar ratio method and were found equal to 1 : 3 and 1 : 2 mole ratios, respectively. The stability constants determined by the method of Harvey, et al. [25] were found equal to 3.9×10^7 and 8.4×10^6 for Ru(III)-PAN and Pt(II)-PAN chelates, respectively. These results suggest the formation of stable octahedral Ru(III)-PAN and tetrahedral Pt(II)-PAN complex species [26] and the most important reactions in the bulk of the solution involved the equilibrium:



where L is PAN.

The electrocapillary curves of the solutions of 1.5×10^{-7} mol/l PAN, 1.5×10^{-7} mol/l PAN + 5×10^{-8} mol/l Ru(III) and 1.5×10^{-7} mol/l PAN + 5×10^{-8} mol/l Pt(II) at pH 9.3 were obtained by measuring the drop times of the DME. The results are summarised in Fig. 2. A substantial change in the drop time was observed, suggesting strong adsorption of PAN and its Ru(III) and Pt(II) chelates on the surface of the DME, causing changes in the surface tension of the mercury drop [20]. The curves of Ru(III)-PAN and Pt(II)-PAN were similar

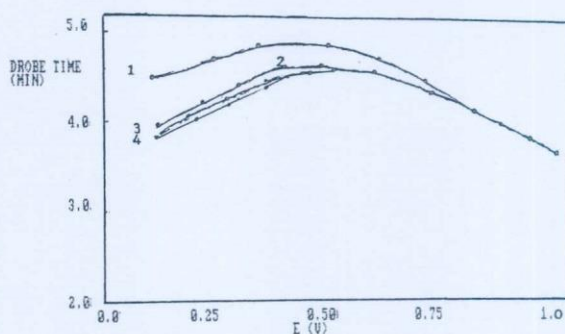
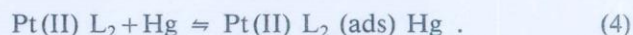
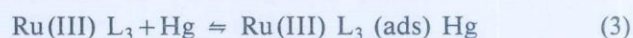


Fig. 2. Electrocapillary curves of the solutions: (1) Britton-Robinson buffer; (2) 1.5×10^{-7} mol/l PAN; (3) 1.5×10^{-7} mol/l PAN + 5×10^{-8} mol/l Ru(III) and (4) 1.5×10^{-7} mol/l PAN + 5×10^{-8} mol/l Pt(II) at pH 9.3

to those of PAN, indicating adsorption of both ruthenium(III) and platinum(II) complex species as PAN or Pt(II) at the electrode surface. Using the method of Zhao et al. [27], the composition of the electroactive species Ru(III)-PAN and Pt(II)-PAN on the electrode surface were obtained employing the equation [28, 29]:

$$\frac{I}{i_p} = \frac{I}{i_{p \cdot \max}} + \frac{1}{\beta i_{p \cdot \max} C_A^m}$$

where i_p is the measured peak current, $i_{p \cdot \max}$ is the peak current when all the metal ions form the complex, C_A is the concentration of the ligand, β is the conditional stability constant and m is the coordination number of the complex adsorbed on the electrode surface. Plots of $\frac{I}{i_p}$ vs. $\frac{1}{C_A^m}$ showed a straight line when $m = 3$ for Ru(III)-PAN and $m = 2$ for Pt(II)-PAN. This indicates that the composition of the electroactive complex species Ru(III)-PAN and Pt(II)-PAN on the surface of the mercury electrode is the same as in the bulk solution. Hence the adsorption process can be expressed as follows:



The applicability of the adsorptive stripping voltammetric behaviour of Ru(III)-PAN and Pt(II)-PAN complex species for the microdetermination of trace amounts of Ru(III) and Pt(II) in water by cathodic stripping differential pulse voltammetry was attempted. Therefore, the effects of varying pH, collection time, accumulation potential, concentration of PAN and voltage scan rates as well as the effects of other elements on the peak reduction current were critically investigated.

The influence of varying pH of the aqueous solution on the peak height current and peak potential on the adsorption preconcentration of the Ru(III)-PAN and Pt(II)-PAN complex species was examined at the HMDE. For this purpose, 5×10^{-8} mol/l of each metal ion (Ru or Pt) separately was allowed to react with 1.5×10^{-7} mol/l of PAN at different pH-values. Other conditions of the recommended general procedure were kept constant. A lowering of the pH < 8 caused an anodic shift of the ca-

thodic stripping peak potential and a decrease in the peak height current. At $\text{pH} > 10$ no significant adsorption of both complex species on the HMDE was observed. The current was at a maximum in the pH -range 8–10 in universal buffer containing ethanol-water (30% v/v) and 0.5 mol/l sodium sulphate. Large peak enhancement (~ 3 fold at 3 min collection time), best signal/background characteristics and reproducibility was obtained at pH 9.3. At this pH the sensitivities of the peaks are excellent for both ruthenium and platinum. Therefore, the different effects of pH on the Ru(III)-PAN and Pt(II)-PAN complex species at the HMDE provide no way to distinguish between the two metal ions by CS-DPV. Large peak current enhancement of Pt(II)-PAN was observed, much greater than that of Ru(III)-PAN at the HMDE in this pH -range, i.e. the platinum(II) complex species is more strongly adsorbed than ruthenium(III) complex species.

The interfacial behaviour of the Ru(III)-PAN and Pt(II)-PAN complex species can be exploited for effective preconcentration, prior to voltammetric measurement. By performing the accumulation at a potential region in the "valley" between the ligand and complex species, only a single complex peak was observed. For example, the effect of convection mass dependent on the accumulation of the Ru(III)-PAN and Pt(II)-PAN species from a stirred solution gave rise to an ADP peak current 2 times as large as that obtained with the quiescent solution in the same accumulation period ≤ 180 s. In the stirred solutions, the voltammetric curves were recorded after 15 s rest period.

The influence of the accumulation potential on the stripping peak current of Ru(III)-PAN and Pt(II)-PAN was examined over the potential range 0.1 to -0.5 V against the Ag/AgCl electrode under the optimal experimental conditions. The largest peak current was obtained at a deposition potential of 0 to -0.3 and -0.2 V for ru-

thenium(III) and platinum(II) complex species, respectively, as shown in Fig. 3. Therefore, -0.2 V was selected as a proper accumulation potential throughout the microdetermination of ruthenium and platinum species. Also, this potential provides the best signal to background characteristics.

The dependence of the stripping peak current of Ru(III)- and Pt(II)-PAN complex species on the collection time was examined at HMDE. Other conditions were kept constant as in the general procedure. Figure 4 shows plots of peak current vs. preconcentration times of one level of ruthenium (3.7×10^{-9} mol/l) concentration and two levels of platinum concentrations (6.4×10^{-8} mol/l, 9.7×10^{-9} mol/l). In all three instances, the current increases rapidly with increasing preconcentration time up to 3 min and then levelled off at longer time reflecting the enhancement and complete coverage of the complex species on the electrode surface. A preconcentration period of 120 and 180 s yielded ~ 9 - and 12-fold enhancement of the peak current of both complex species, respectively, as against that observed without preconcentration. If these processes are diffusion-controlled with no adsorptive accumulation, the peak height will be independent of the collection time before scanning [30]. But, the larger the preconcentration time, the more metal chelates are adsorbed and the larger is the peak current. This proves that the DP curves are based on adsorptive processes. From the symmetrical shape of the reduction peak current of both complex species formed and the fact that the peak potential does not change significantly with the scan rate, it can be concluded that the electro-chemical reduction of the formed chelates is a reversible process [31].

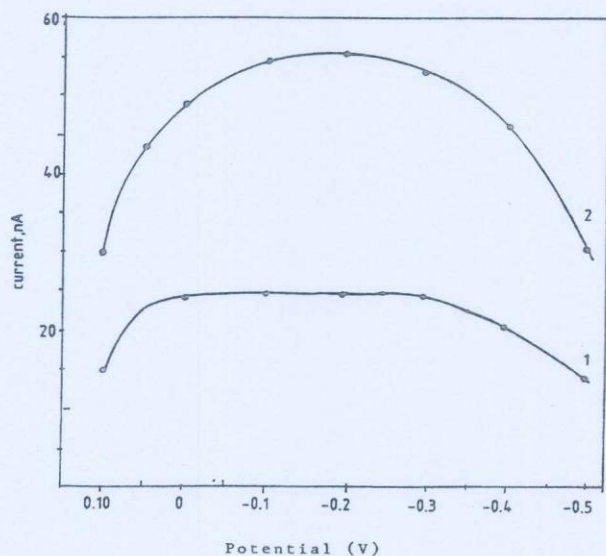


Fig. 3. Dependence of the reduction peak current of the adsorbed Ru(III)-PAN or Pt(II)-PAN complex on the accumulation potential. 3.7×10^{-9} mol/l Ru(III) + 1.5×10^{-7} mol/l PAN (1) and 4.2×10^{-8} mol/l Pt(II) + 1.5×10^{-7} mol/l PAN, (2). Other conditions as in Fig. 1

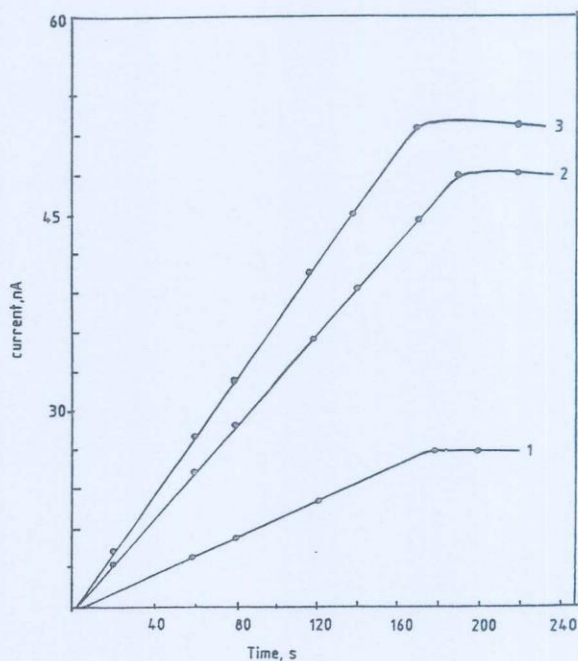


Fig. 4. Peak current vs. accumulation periods plots of: 3.7×10^{-9} mol/l Ru(III) + 1.5×10^{-7} mol/l PAN (1); 9.7×10^{-9} mol/l Pt(II) + 1.5×10^{-7} mol/l PAN (2) and 6.4×10^{-8} mol/l Pt(II) + 1.5×10^{-7} mol/l PAN, (3). Other conditions as in Fig. 1

The effect of an excess of the reagent PAN concentration was examined. The peak heights of a series of solutions containing 4×10^{-8} mol/l of ruthenium(III) or platinum(II) and various amounts of the reagent was investigated. It was found that the peak height increases linearly with the PAN concentration up to 1.5×10^{-7} mol/l and tend to remain constant at a large excess of the reagent. Therefore, in the subsequent work 1.5×10^{-7} mol/l PAN was selected as a proper ligand concentration.

Quantitative determination of ruthenium(III) and platinum(II)

The greatest advantage of the ruthenium(III) or platinum(II) determination by the proposed adsorptive voltammetric method is the inherent sensitivity. Under the optimum conditions of pH 9.3 in 30% ethanol, collection time 3 min, accumulation potential -0.2 V, reagent concentration of 1.5×10^{-7} mol/l, pulse scan of $4 \text{ mV} \cdot \text{s}^{-1}$ and 50 mV amplitude, linear relationships were obtained between the peak height currents ($I_F - I_B$) and ruthenium(III) or platinum(II) concentration, as shown in Fig. 5. I_F and I_B are the peak height currents of Ru(III) or Pt(II)-PAN chelates and PAN, respectively under the same experimental conditions. Linear responses up to 6.4×10^{-8} and 5.1×10^{-8} mol/l, regression coefficients of 0.94 and 0.96 and detection limits of 3.2×10^{-10} and 4.1×10^{-10} mol/l of ruthenium(III) and platinum(II) respectively, were obtained. Reproducibility tests of 5 results of ruthenium(III) or platinum(II) at 1.2×10^{-8} mol/l showed standard deviations of +0.8 and 0.2 and relative standard deviations of 2.4 and 1.6%, respectively.

Moreover, the method has been applied for the determination of ruthenium(IV) or platinum(IV) by prior reduction of these solutions to the trivalent or divalent species by sodium sulphite in acid media. The metal content (Ru or Pt) was then determined following the recommended procedure 1 described above. Satisfactory results and linear calibration curves were obtained for both metal ions on plotting metal concentration vs. peak height current.

It is worth mentioning that the proposed method was also employed for the simultaneous microdetermination of the binary mixtures Ru(III) + (IV) and Pt(II) + (IV) in aqueous media. An aliquot sample of the mixture was first determined employing the recommended procedure described for ruthenium(III) or platinum(II). Another aliquot sample of each binary mixture Ru(III) + (IV) or Pt(II) + (IV) was allowed to react with sulphur dioxide for 5 min in acidic solution (1 mol/l H_2SO_4). The excess SO_2 gas was then removed by boiling and the resultant Ru(III) or Pt(II) species were measured by measuring the peak height current by the recommended procedure 1. The peak current in the first step is equivalent to ruthenium(III) or platinum(II), while the difference between the stripping height currents in the second and first steps is equivalent to ruthenium(IV) or platinum(IV) in the mixture, whatever binary mixture was used. Satisfactory results were obtained for a series of binary mixtures in the

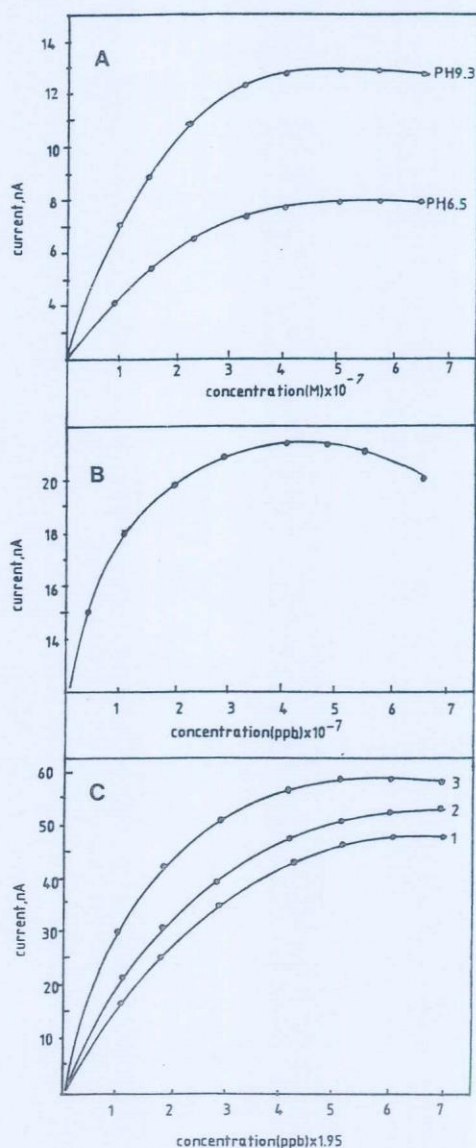


Fig. 5 A-C. Calibration plots of the reduction peak current with the concentration of PAN; pH 9.3; A $1-8 \times 10^{-8}$ mol/l Ru(III) + 1.5×10^{-7} mol/l PAN, B $1-9 \times 10^{-8}$ mol/l Pt(II) + 1.5×10^{-7} mol/l PAN, C. Other conditions as in Fig. 1. (1) 30 s; (2) 120 s; (3) 180 s

concentration range of linearity for both ruthenium(III) or platinum(II).

Tap water samples spiked with known quantities of Ru(III) or Pt(II) were analysed by the proposed method. The recoveries of spiked Ru(III) or Pt(II) were 98–101%. The applicability of the method for the determination of very low concentrations (less than nanomolar levels) in tap water (0.1–1 l) is also possible by the proposed method. Filtration of the sample solution through a $0.45 \mu\text{m}$ membrane was followed by extraction of ruthenium(III) or platinum(II) from the acidic aqueous solution of large volume by a porous polyurethane foam column [32, 33]. Elution of the extracted ruthenium(III) or platinum(II) with a selective eluting agent from the foam column is possible as described earlier by Chow et al. [32, 33], followed by the de-

termination of Ru(III) or Pt(II) according to the proposed procedure. The determination of platinum(II) and/or ruthenium(III) in tap water samples in the presence of an excess of interfering ions ($>100 \mu\text{g}$ of Cu^{2+} , Fe^{3+} and Ni^{2+}) was found to be difficult even after a pre-separation step of Pt(II) or Ru(III) with polyurethane foam.

Effect of diverse ions

The influence of different ions, which are commonly in association with the tested metal ions and form complexes with the reagent 1-(pyridylazo)2-naphthol, was examined. No interference was found in the presence of a relatively high excess ($6.0 \times 10^{-5} \text{ mol/l}$) of Ca(II), Mg(II), Ba(II), Sr(II), Cd(II), Ce(III), La(III), Zn(II), Bi(III), and Pb(II). Ni(II), Cr(III), Zn(II) and molybdate at $1.0 \times 10^{-7} \text{ mol/l}$ reduced the peak current by about 30%, while Au(III), Cu(II), Fe(III), Pd(II), Rh(III), Ir(III) and Co(II) at $1.0 \times 10^{-7} \text{ mol/l}$ interfered seriously. Ions such as molybdate may form mercury(I) salts covering the HMDE which in turn reduced the peak current height. The possible formation of a mercury(I) molybdate complex [34, 35] could account for the decrease in the reduction of the peak current height of the Ru(III)-PAN or Pt(II)-PAN chelates. Nevertheless, the determination of the Ru(III)+(IV) or Pt(II)+(IV) was not affected by the presence of up to $20 \mu\text{g l}^{-1}$ of molybdenum(VI). The selectivity of the proposed method was tested by determinations of a fixed concentration ($2 \times 10^{-8} \text{ mol/l}$) of ruthenium(III) and platinum(II), separately under the optimum conditions.

Conclusion

The present study demonstrates that the adsorptive accumulation of 1-(pyridylazo)2-naphthol can be the basis of an ultrasensitive stripping procedure for ruthenium and platinum. The method provides a simple, precise, sensitive and selective approach to the trace analysis determination of ruthenium and platinum. The detection limits obtained for Ru(III) and Pt(II) are comparable to those obtained by other techniques currently used. The lower detection limits of the tested species are in agreement with the large degree of adsorption of the Ru(III) and Pt(II)-PAN chelates. The peak potentials (E_p) of the CSV peak of Ru(III)-PAN and Pt(II)-PAN systems coin-

cide. Thus, the determination of platinum(II) besides ruthenium(III) or ruthenium(III) besides platinum(II) is not possible by the proposed method.

References

1. Marczenko Z (1986) Separation and spectrophotometric determination of elements. Ellis Horwood
2. Marczenko Z, Kalinowski K (1983) *Anal Chim Acta* 153:219
3. Ivanov VM, Figurovskaya VN, Busev AI (1972) *Zavod Lab* 38:1311
4. Ivanov VM, Gorbunova GN (1980) *Zh Anal Khim* 35:2365
5. Gorbunova GN, Ivanu VM (1980) *Zh Anal Khim* 35:705
6. Ivanov VM, Busev AI, Popova LV, Bogdanovich LI (1969) *Zh Anal Khim* 24:1064
7. Gur'eva RF, Trutneva LM, Sauvin SB, Chalisova NN (1984) *Zh Anal Khim* 39:1653
8. Sindhwani SK, Singh RP (1971) *Anal Chim Acta* 55:409
9. Wasey A, Bansal RK, Staka M, Puri BK (1983) *Bull Chem Soc Jpn* 56:3603
10. Koelble G, Kalcher K, Voulgaropoulos A (1992) *Fresenius J Anal Chem* 342:83
11. Shi Q, Hong J, Lu R, Gaodeng ZY (1990) *Xuexiao Huaxue Xuebac* 11:414
12. Farias PAM, Ferreeira SLC, Ohara AK, Bastos MB, Goulart MS (1992) *Talanta* 39:1245
13. Wang J, Lu J (1992) *Analyst* 117:1913
14. Farias PAM, Ferreeira SLC, Ohara AK (1992) *Electroanalysis* 3:985
15. Wang J, Tian B, Lu J (1992) *Talanta* 39:1273
16. Palaniappan R (1991) *Bull Electrochem* 7:367
17. Palaniappan R (1990) *J Electrochem Soc India* 39:21
18. Palaniappan R (1989) *Analyst* 114:1043
19. Palaniappan R, Revathy V (1989) *Analyst* 114:517
20. Palaniappan R, Kumar TA (1993) *Analyst* 118:293
21. Lide DR (1991) *Handbook of chemistry and physics*, 72nd edn. Chemical Rubber
22. El-Wakil AM, Farag AB, El-Shahawi MS (1990) *Fresenius J Anal Chem* 337:886
23. El-Wakil AM, Farag AB, El-Shahawi MS (1989) *Talanta* 36:383
24. Zhao V, Jin W (1989) *J Electroanal Chem* 267:271
25. Harvey AE, Manning DL (1950) *J Am Chem Soc* 72:4488
26. Griffith WP (1967) *The chemistry of the rare platinum metals*. Wiley
27. Zhao J, Jin WR (1989) *J Electroanal Chem* 267:271
28. Li NQ, Gao X (1973) *Fenxi Huaxue* 1:40
29. Gao X (1986) *Handbook on the physics and chemistry of rare earth element*. Elsevier, Amsterdam, p 163
30. Li Q, Li S (1989) *Fenxi Tonybao* 3:45
31. Zhao J, Sun D, Jin W (1990) *Anal Chim Acta* 268:293
32. Khan AS, Chow A (1984) *Talanta* 31:692
33. Albazi SJ, Chow A (1983) *Anal Chem* 55:1094
34. Laviron E (1974) *J Electroanal Chem* 52:355
35. Khan CH, van den Berg CMG (1989) *Mar Chem* 27:31

Properties and structure of ZnO–PbO–B₂O₃ glasses

H. Doweidar, A. A. Megahed & S. Abd Al-Maksoud

Physics Department, Faculty of Science, Mansoura University, Mansoura 35516, Egypt

M. S. El-Shahawi

Chemistry Department, Faculty of Science, Mansoura University, Domiate, Egypt

Y. El-Fol

Al-Azhar Education Institute, Mansoura, Egypt

Manuscript received 2 June 1993

Revision received 28 January 1994

DC conductivity, density and infrared investigations have been carried out on ZnO–PbO–B₂O₃ glasses. The activation energy for conduction shows a maximum value at a specific ZnO concentration, depending on the glass composition. Both the conductivity and the density increase with an increase in the oxygen to boron ratio in a common dependence regardless of glass composition. The molar volume decreases with increasing ZnO for all compositions. The results are discussed considering the dual role of ZnO and its effect on glass structure. It is concluded that these properties are controlled by the structure of the zinc lead borate network. The infrared spectra for all the glasses have the same features indicating the presence of the same structural groupings.

Zinc lead borate glasses belong to the so called group of soft glasses. Such glasses are used in different applied fields such as glass discharge tubes, solder for sealing colour television bulbs, integrated circuit packages, etc.^(1–3) The electrical conduction in Na₂O–PbO–B₂O₃ and CdO–PbO–B₂O₃ glasses has been investigated previously.⁽⁴⁾ Due to the dual structural role of CdO (as both network modifier and network former), different conductivity–composition dependences were observed for the two glass systems. The present investigation is concerned with the structural role of ZnO in ZnO–PbO–B₂O₃ glasses and its effect on some of the physical properties.

Experimental

Glass preparation

Glasses were prepared in 100 g batches by mixing appropriate amounts of reagent grade ZnCO₃, Pb₃O₄ and H₃BO₃ (Table 1). The components were melted using porcelain crucibles in an electric furnace at a temperature ranging between 900 and 1050°C, depending on the glass

composition. The crucible and its contents were kept in the furnace about 1 h and the melt was swirled frequently before being poured into preheated steel moulds. All glasses were annealed at 350°C and allowed to cool normally to room temperature.

DC resistance measurements

For the electrical measurements samples were prepared in the form of discs of 10 mm radius and about 2–3 mm thickness. The flat surfaces of the sample were coated with graphite in the form of discs of 5 mm radius. An insulation tester (Levell Tester TM 14) was used to measure the resistance of the samples.

Over a temperature range from about 230–420°C, depending on the glass composition the calculated resistivity, ρ , obeyed the Arrhenius equation

$$\rho = \rho_0 \exp(E/KT) \quad (1)$$

where ρ_0 is the pre-exponential factor, E is the activation energy for conduction, K is Boltzmann's constant and T is the absolute temperature. In the temperature region used, Equation (1) gives straight lines when plotting $\ln \rho$ versus $1/T$. A relative error of $\pm 5\%$ is estimated for the resistivity values, whereas the experimental error in determining the activation energies is estimated to be less than 2 kJ/mol. The limits of error were computed from the average deviation among the resistivities of at least three samples of each glass. They also represent the error involved in the comparison of the sample resistance with that of a standard resistance of the same order.

Table 1. Formulae of the investigated glass groups

Group number	Molar formula	x (mol%)
1	xZnO.(60-x)PbO.40B ₂ O ₃	0, 5, 10, 15, 20, 25, 30, 32.5
2	xZnO.40PbO.(60-x)B ₂ O ₃	0, 5, 10, 15, 17.5, 20, 22.5, 25
3	xZnO.50PbO.(50-x)B ₂ O ₃	0, 5, 10, 15, 20, 25
4	xZnO.60PbO.(40-x)B ₂ O ₃	0, 5, 10, 15, 20, 22.5, 25

Dedicated to Professor W. Müller-Warmuth, Institut für Physikalische Chemie, Münster, Germany on the occasion of his 65th birthday

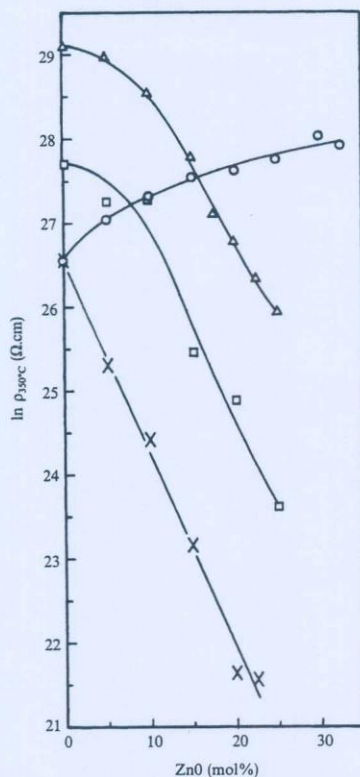


Figure 1. Dependence of $\ln \rho_{350^\circ\text{C}}$ on the ZnO content of the glasses 1 (o), 2 (Δ), 3 (\square) and 4 (\times)

Density determination

Density was determined at room temperature using the Archimedes method with xylene as an immersing medium. As a rule, at least three samples of each glass were used to determine the density. The measured densities were reproducible to $\pm 0.02 \text{ g/cm}^3$.

Infrared spectroscopy

The infrared spectra of the glasses were investigated between 200 and 4000 cm^{-1} by the KBr technique using a Perkin-Elmer infrared spectrophotometer model PE 1340.

Results and discussion

DC conductivity

The resistivity at 350°C and the activation energy are represented as functions of ZnO content in Figures 1 and 2 respectively. The resistivity increases with ZnO in the glasses of group 1, where PbO is replaced by ZnO. For groups 2–4, where ZnO replaces B₂O₃, the resistivity decreases with the increase of ZnO. Activation energy E (Figure 2) increases with ZnO to a maximum value E_{max} and then decreases. The same behaviour was also found for the dependence of the microhardness H_v of $x\text{ZnO} \cdot (50-x)\text{PbO} \cdot 50\text{B}_2\text{O}_3$ glasses on the ZnO content.⁽⁵⁾ For groups 2–4, E_{max} shifts to lower ZnO concentrations as PbO increases.

PbO is known to enter the glass network both as a network modifier and a network former. NMR⁽⁶⁾ and Raman⁽⁷⁾ spectra studies indicate that, for up to about 20 mol% PbO, all the PbO is used for the boron coordina-

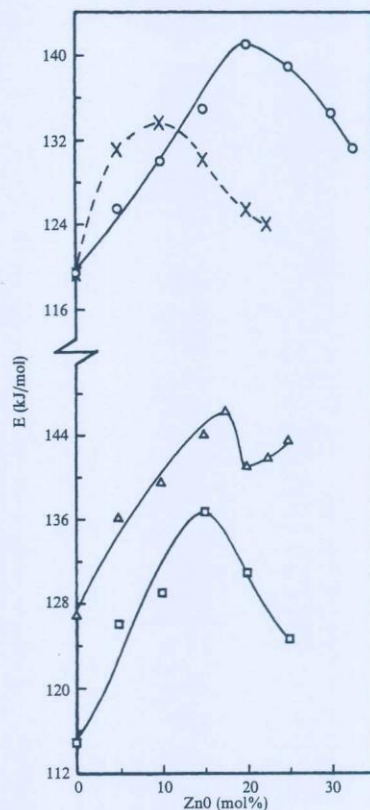


Figure 2. Change of activation energy with ZnO content of the glasses 1 (o), 2 (Δ), 3 (\square) and 4 (\times)

tion conversion, i.e. as a modifier oxide. Above 20 mol% PbO, some lead is used to form PbO₄ pyramids (network former oxide). The fraction of the network former PbO increases with the increase of PbO content, whereas the fraction of the modifier PbO increases to a maximum value at about 45 mol% PbO and then decreases.⁽⁸⁾

ZnO also acts as both glass modifier and as glass former.⁽⁹⁾ As far as the authors know, the change in concentration of the two types of ZnO in ZnO-B₂O₃ glasses has not yet been studied. However, some general lines can be obtained when compared with CdO in borate glasses. Mulkern *et al.*⁽¹⁰⁾ indicated that the fraction of network former CdO increases linearly with the molar content of CdO in CdO-B₂O₃-SiO₂ and CdO-B₂O₃-GeO₂ glasses.

In binary PbO-B₂O₃ glasses, modifying Pb²⁺ cations are assumed to be the charge carriers.^(8,11) ¹¹B wide line NMR investigations on $x\text{ZnO} \cdot (50-x)\text{PbO} \cdot 50\text{B}_2\text{O}_3$ glasses⁽⁵⁾ indicated that nonbridging oxygen ions, NBOs, form in the borate network upon adding ZnO. This indicates that the total concentration of the glass modifier oxides (PbO+ZnO) increases with increasing ZnO. Because ZnO can act as both a glass modifier and a glass former, the increase in NBO concentration can be due to one or two or both of the explanations. The first, which is more probable, is that the modifier fraction in the added ZnO is higher than that in the PbO. The second is that some of the modifier ZnO can replace PbO₄ pyramids (the network former PbO).

The molar volume, V_m (Figure 7), of the studied glasses decreases upon increasing ZnO and this should lower the mobility of Zn²⁺ ions. On the other hand formation

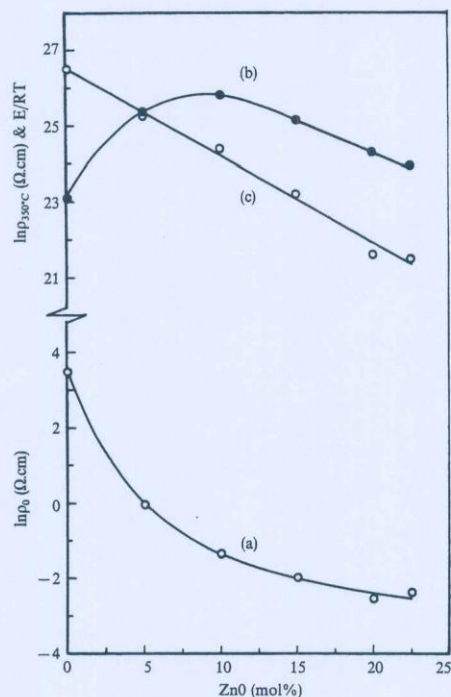


Figure 3. Dependence of (a) $\ln \rho_0$, (b) E/KT and (c) $\ln \rho_{350^\circ\text{C}}$ on ZnO content for the group 4 glasses

of NBOs causes a rupture of the bonds in the borate network, which increases the mobility of Zn^{2+} and lowers E . It can be deduced that the effect of the V_m decrease predominates in the region of $E < E_{\text{max}}$ and the effect of NBOs is predominant for $E > E_{\text{max}}$. The shift of E_{max} towards lower ZnO concentration when PbO is increased (groups 2–4) is in agreement with this assumption. As PbO increases, the B_2O_3 content decreases and therefore a lower ZnO quantity is needed to form the concentration of NBOs sufficient to predominate the change of E with ZnO.

Comparing Figures 1 and 2, it can be seen that (except for group 1) the resistivity decreases even when E increases. It appears that there is some discrepancy between the behaviour of $\ln \rho$ and that of E in the regions of increasing E values. Equation (1) can be rewritten as

$$\ln \rho = \ln \rho_0 + E/KT \quad (2)$$

This relation indicates that the resistivity is characterised (at a given temperature) by two parameters; namely ρ_0 and E . Although ρ_0 is calculated using the determined values of ρ and E , Equation (2) shows that the value of $\ln \rho$ is the resultant of $\ln \rho_0$ and E/KT , which are related to the composition and structure of glass. The form and rate of change of $\ln \rho$ should be controlled by the rates of change of both $\ln \rho_0$ and E/KT . The dependence of $\ln \rho_0$, E/KT and $\ln \rho_{350^\circ\text{C}}$ on the ZnO content is represented in Figure 3 for the glasses of group 4. The resistivity of this group decreases with the increasing ZnO because the rate of decrease of $\ln \rho_0$ is higher than the rate of increase of E/KT in the region of $E < E_{\text{max}}$. In the region of $E > E_{\text{max}}$, both $\ln \rho_0$ and E/KT decrease and produce decreasing values of $\ln \rho_{350^\circ\text{C}}$. Therefore, the resistivity is expected to increase with ZnO when the rate of increase of E/RT exceeds that of the decrease of $\ln \rho_0$,

which is the case for group 1.

Stevens⁽¹²⁾ investigated the ionic conduction in oxide glasses. The model presented considers an ion with a charge q in a potential well which is separated by a potential barrier of height E from another potential well at a distance a . From the jump probabilities in an electric field, the following equation could be obtained

$$\rho = (6KT/Nq^2a^2fs) \exp(E/KT) \quad (3)$$

where N is the concentration of the mobile ions, f is the vibration frequency of the ion and s is the number of interstices (holes) directly surrounding the mobile ion. From Equation (3), the pre-exponential factor ρ_0 can be taken as

$$\rho_0 = 6KT/Nq^2a^2fs \quad (4)$$

Due to the change of a ⁽¹²⁾ and probably of s and f with temperature, ρ_0 is a temperature independent constant.

Considering similar assumptions as those leading to Equation (3), ρ_0 is given⁽⁹⁾ in another form as

$$\rho_0 = 2KT/Nq^2a^2f \quad (5)$$

where s is ignored. Anyway, Equations (4) and (5) indicate that ρ_0 should decrease with increasing N and a values. The increase of ZnO content causes an increase of both N and the concentration of NBOs (number of holes). In the light of the V_m decrease (Figure 7), it is to deduce that there should be a decrease of a and an increase of s upon increasing ZnO. The resultant effect of these factors appears as a decrease of $\ln \rho_0$.

Figure 4 shows that ρ_0 decreases rapidly as ZnO is increased and reaches a limiting value for ZnO > 10 mol%. This may indicate that up to about 10 mol% ZnO, the decrease of resistivity is due to the increase of the mobile Zn^{2+} ions concentration. The increase of Zn^{2+} ions mobility can be responsible for the decrease of resistivity for ZnO > 10 mol%. Similar effects were found for $\text{Na}_2\text{O-PbO-B}_2\text{O}_3$ and $\text{CdO-PbO-B}_2\text{O}_3$ glasses.⁽⁴⁾

The dependence of conductivity at 350°C ($\ln \sigma_{350^\circ\text{C}}$)

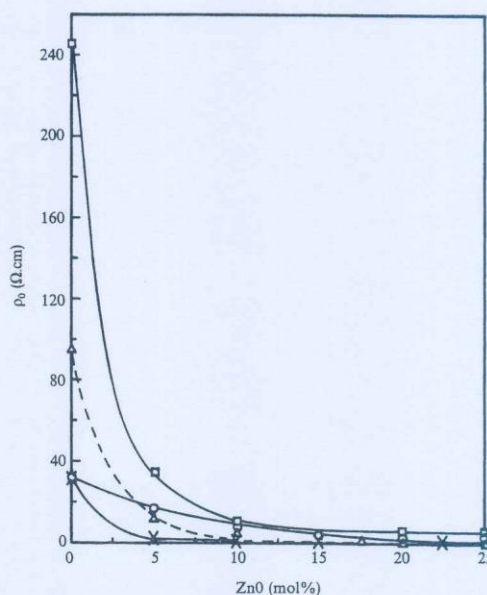


Figure 4. Change of the pre-exponential factor ρ_0 with ZnO content of the glasses: 1 (O), 2 (Δ), 3 (\square) and 4 (\times)

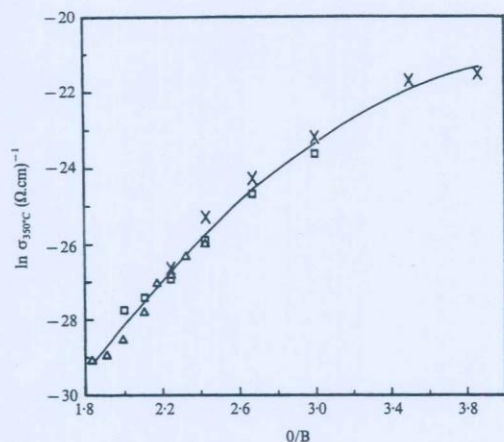


Figure 5. The natural logarithm of conductivity, $\ln \sigma_{350^\circ\text{C}}$, as a function of the oxygen to boron ratio of the glasses 2 (Δ), 3 (\square) and 4 (\times)

on the oxygen to boron ratio O/B is given in Figure 5. It is shown that the conductivity generally increases with the increase of O/B (which relates to the glass composition as a whole) regardless of the glass composition. The dependence represents a common behaviour for all glass groups. In Na₂O-PbO-B₂O₃ glasses,⁽⁴⁾ where Na₂O is a network modifier, the conductivity increases with the O/B ratio but there is a distinct behaviour for each glass group, depending on the PbO content. This is because Na₂O associates itself with B₂O₃ and the conductivity is characterised by the composition of the sodium borate matrix. The dependence shown in Figure 5 indicates that the conductivity of the studied glasses depends mainly on the structure of the zinc lead borate matrix, where ZnO can partly play the role of a network former. Similar effects were observed for CdO-PbO-B₂O₃,⁽⁴⁾ PbO-B₂O₃ and V₂O₅-PbO-B₂O₃ glasses,⁽⁸⁾ i.e. for glasses in which the network modifying oxides can be network former too.

Density and molar volume

Figure 6 represents the change of density of the studied glasses with ZnO. The density of the glasses in group 1 decreases when ZnO is increased. Such a behaviour can be due to the mass decrease per mole of glass as PbO is substituted by ZnO (the relative molecular mass of PbO is 2.74 times that of ZnO). In groups 2-4 where ZnO substitutes B₂O₃, the density increases with the increase of ZnO. In these groups, additions of ZnO convert BO₃³⁻ triangles into BO₄ tetrahedra (group 2) and/or BO₄ tetrahedra into asymmetric BO₃³⁻ units (NBOs). Both the two types of structural units are denser than the symmetric BO₃³⁻ units in vitreous B₂O₃.⁽¹³⁾ In addition, the relative molecular mass of the glass increases upon substituting B₂O₃ with ZnO and this causes a density increase.

Figure 7 shows that the molar volume V_m of all glass groups decreases upon increasing the ZnO content. The molar volume is calculated using the relation

$$V_m = M_g/D \quad (6)$$

where M_g is the relative molecular mass of the glass and D is the glass density. A decrease of V_m is generally ex-

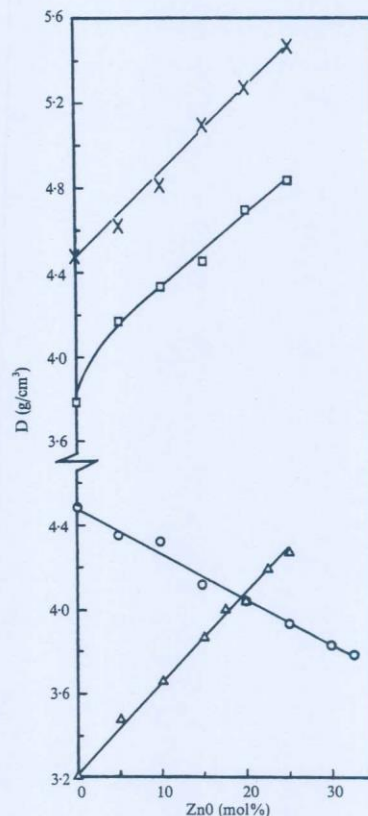


Figure 6. Dependence of density on the ZnO content of the glasses 1 (o), 2 (Δ), 3 (\square) and 4 (\times)

pected when the density increases. However, also in this case, the change of V_m depends on the rates of change of both M_g and D . In the present study, there are two conditions leading to the V_m decrease. The first is that when M_g and D decrease with the increase of ZnO (group 1), where M_g decreases with a higher rate than that for the D decrease. Secondly V_m decreases when both M_g and D increase with ZnO (groups 2-4) but M_g increases with a lower rate compared with that of the D increase.

The density is found to be controlled with the O/B ratio. Figure 8 shows that D increases with the increase of O/B regardless of the glass composition. This behaviour may reflect the presence of a zinc lead borate net-

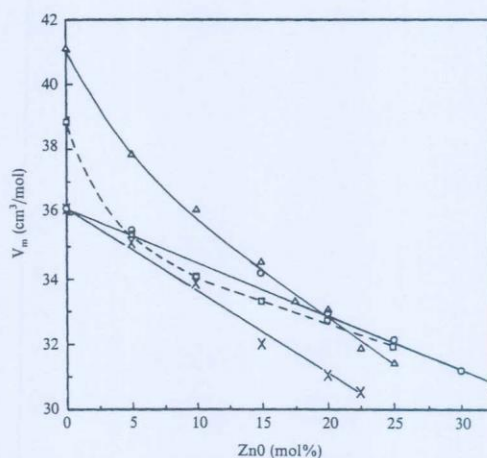


Figure 7. Molar volume as a function of ZnO content of the glasses 1 (o), 2 (Δ), 3 (\square) and 4 (\times)

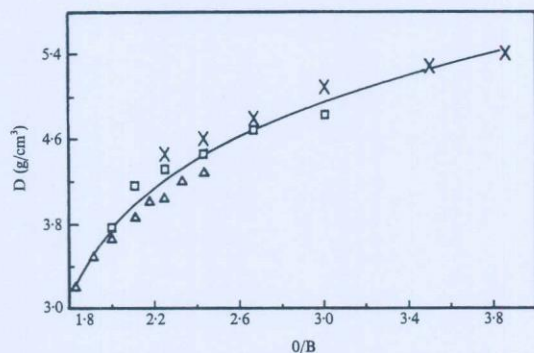


Figure 8. Density dependence on the O/B ratio for the glass samples 2 (Δ), 3 (\square) and 4 (\times)

work, as previously deduced. The similarity between the dependence of both the conductivity (Figure 5) and the density (Figure 8) on the O/B ratio may suggest some correlation between the two properties. Figure 9 indicates that there is a unique dependence for all glasses, where $\ln \sigma_{350^\circ\text{C}}$ increases with the increase of D . As previously deduced, the increase of D is associated with increasing concentrations of the mobile Zn^{2+} cations (glass modifier ZnO) and NBOs. This means that both N and s (Equation (3)) increase and this leads to higher conductivities in spite of the V_m decrease.

Infrared spectra

The infrared spectra of some selected ZnO–PbO– B_2O_3 glasses are given in Figure 10. The spectrum of a 60PbO.40 B_2O_3 glass is also presented (plot 3). All the spectra contain three prominent absorption bands around 690, 960 and 1340 cm^{-1} . Shoulders are observed at about 450, 830, 1050 and 1220 cm^{-1} . Bands and shoulders at the same frequencies are recorded for PbO– B_2O_3 glasses having PbO content between 30 and 60 mol%.⁽⁸⁾ Similar spectra are also observed for Na_2O –PbO– B_2O_3 and CdO–PbO– B_2O_3 glasses.⁽¹⁴⁾ The similarity of the spectra of all these glasses indicates that the absorption bands are related to the structural groupings in the borate network, regardless of the cations of the other oxides in the glass.

The absorption band at 690 cm^{-1} is attributed to bending vibrations of pentaborates.^(15–16) The 960 cm^{-1} band referred to B–O stretching vibrations of tetrahedral BO_4^-

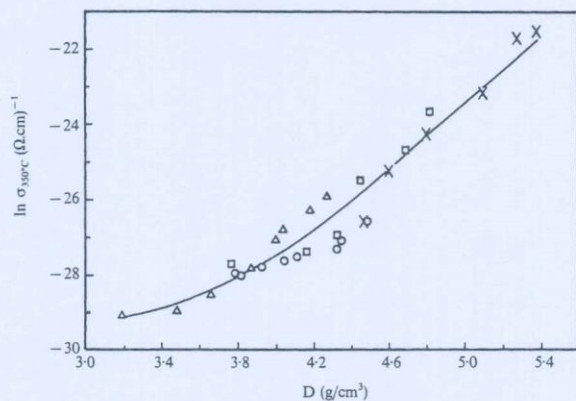


Figure 9. Change of $\ln \sigma_{350^\circ\text{C}}$ with density of the glasses 1 (\circ), 2 (Δ), 3 (\square) and 4 (\times)

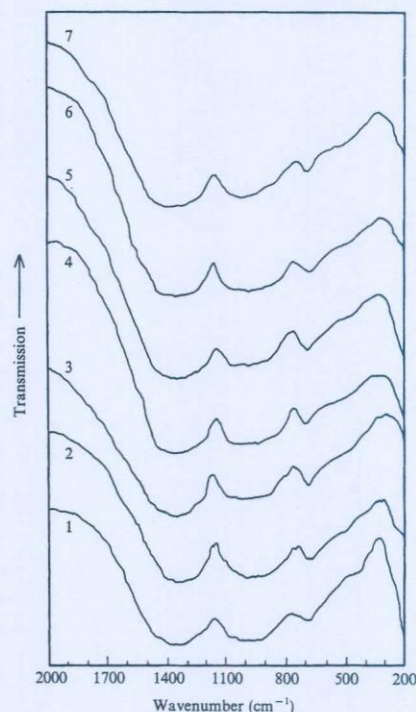


Figure 10. Infrared spectra of the glass samples (1) 10ZnO.40PbO.50 B_2O_3 , (2) 10ZnO.50PbO.40 B_2O_3 , (3) 60PbO.40 B_2O_3 , (4) 5ZnO.60PbO.35 B_2O_3 , (5) 10ZnO.60PbO.30 B_2O_3 , (6) 15ZnO.60PbO.25 B_2O_3 and (7) 20ZnO.60PbO.20 B_2O_3

whereas that at 1340 cm^{-1} is assigned to B–O stretching vibrations of trigonal BO_3^- units in metaborates, pyroborates and orthoborates.⁽¹⁵⁾

Low frequency bands (239, 410 and 475 cm^{-1}), in the infrared spectra of lithium borate glasses, are assigned to vibrations of Li^+ cations against their network sites.^(15,17) In comparison, the shoulder at 450 cm^{-1} in the spectra of the glasses investigated can be attributed to vibrations of metal cations such as Pb^{2+} or Zn^{2+} . Because this shoulder appears in the spectra of PbO– B_2O_3 glasses,^(5,8) it is preferred to attribute it to vibrations of Pb^{2+} cations. The shoulder at 830 cm^{-1} can be compared with that at 870 cm^{-1} in the spectra of Li_2O – B_2O_3 glasses, which is attributed to vibrations of borate arrangements containing BO_4^- tetrahedra. The shoulder at 1050 cm^{-1} can be referred to stretching vibrations of BO_4^- tetrahedra and that at 1220 cm^{-1} can arise from B–O stretching vibrations of BO_3^- units in metaborate chains and orthoborates.⁽¹⁵⁾

It is worth mentioning that there is an absorption band around 3500 cm^{-1} in the spectra of all glasses studied (not indicated in Figure 10). This band is attributed to O–H stretching vibrations.⁽¹⁸⁾ The OH⁻ groups form NBO sites and should contribute to those formed upon introducing ZnO into the glass.

Comparing the spectra shown in Figure 10 it can be deduced that there is no effect of the composition on the types of the structural groupings in the studied glasses. This can be due to the presence of symmetric BO_3^- triangles, BO_4^- tetrahedra and asymmetric BO_3^- units (NBOs) in each of the studied glasses.

Conclusion

In ZnO-PbO-B₂O₃ glass system, ZnO enters the structure as both a glass modifier and a glass former. In these glasses a zinc lead borate network is proposed to be responsible for the change in both the conductivity and the density. Both the two quantities increase with the increase of the O/B ratio. The increase of conductivity with the increasing density is correlated with the structural changes in the zinc lead borate network upon increasing ZnO. The similarity of the infrared spectra indicates that the investigated glasses contain the same structural groupings.

References

- Gallup, J. & Dingwall, A. F. *Bull. Am. Ceram. Soc.*, 1957, **36**, 47.
- Fummala, R. R. In *Borate glasses: structure, properties and applications*. Edited by L. D. Pye, V. D. Frechette & N. J. Kreidl. 1978, Plenum Press, New York.
- Shenkai, N., Bradt, R. C. & Rindone, G. E. *J. Am. Ceram. Soc.*, 1982, **65**, 123.
- Doweidar, H., Megahead, A. A., Abd Al-Maksoud, S. & El-Fol, Y. *Phys. Chem. Glasses*, 1994, **35** (2), 84-88.
- Doweidar, H., Abou Zeid, M. A. & El-Damrawi, G. M. *J. Phys. D: Appl. Phys.*, 1991, **24**, 2222.
- Bray, P. J., Leventhal, M. & Hooper, H. O. *Phys. Chem. Glasses*, 1963, **4** (2), 47-66.
- Meera, B. N., Sood, A. K., Chandrabhas, N. & Ramakrishna, J. *J. Non-Cryst. Solids*, 1990, **126**, 224.
- Doweidar, H., Gohar, I. A., Megahed, A. A. & El-Damrawi, G. *Solid State Ionics*, 1991, **46**, 275.
- Scholze, H. *Glass: nature, structure and properties*. 1991. Springer Verlag, New York.
- Mulkern, R. V., Chung, S. J., Bray, P. J., Chryssikos, G. D., Turcotte, D. E. & Risen, W. M. *J. Non-Cryst. Solids*, 1986, **85**, 69.
- Cheny Chang-Yin. *Chem. Abs.*, 1980, **93**, 52428.
- Stevels, J. M. *Handbuch der Physik*. Vol. 20. 1957. Springer Verlag, Berlin.
- Feil, D. & Feller, S. *J. Non-Cryst. Solids*, 1990, **119**, 103.
- El-Fol, Y. *MSc Thesis*, Mansoura University, Egypt. 1993.
- Kamitsos, E. I., Patsis, A.P., Karakassides, M. A. & Chryssikos, G. D. *J. Non-Cryst. Solids*, 1990, **126**, 52.
- Kamitsos, E. I., Karakassides, M. A. & Chryssikos, G. D. *J. Phys. Chem.*, 1987, **91**, 1073.
- Exarhos, G. J. & Risen Jr, W. M. *Solid State Commun.*, 1972, **11**, 755.
- Bray, P. J. *Interaction of radiation with solids*, 1967. Plenum, New York.

Electrochemical synthesis, magnetic, spectral and cyclic voltammetric studies on lactic acid complexes

Ahmed A. El-Asmy* and Eman M. Saad

Chemistry Department, Faculty of Science, Mansoura University, Egypt

Mohamed S. El-Shahawi

Chemistry Department, UAE University, Al-Ain 17551, United Arab Emirates

Summary

Complexes of iron, cobalt, nickel and copper with lactic acid (H_2LA) were prepared by electrochemical oxidation of the metal in non-aqueous solution; this new method gives a high yield (73–87%). The reaction mechanism and the electrochemical efficiency show that cobalt, nickel and copper give divalent complexes and the iron complex is trivalent. The isolated complexes were characterized by physicochemical techniques. C.v.s of the complexes indicate the irreversibility of the electrode processes and confirm the oxidation state of the metals.

Introduction

The hydroxy acid molecules constitute some of the most important sites for the binding of metal ions in biosystems⁽¹⁾ and their coordination compounds are frequently considered in the therapeutic activity displayed by various drugs⁽²⁾. Banait and Pahil⁽³⁾ synthesized a number of copper(II) carboxylates by anodic oxidation of copper in the presence of some carboxylic acids. They found that the reaction proceeded with current efficiencies in the 0.95–1.00 mol F^{-1} range and all the products were conducting compounds. Other authors⁽⁴⁾ have prepared metal carboxylates, $M(O_2CR)_n$, by the electrochemical oxidation of first row transition metals in the presence of carboxylic acids in acetonitrile. The present paper describes the isolation and characterization of lactic acid complexes prepared by electrochemical oxidation of the metals in the presence of an acetone solution of lactic acid.

Experimental

Iron, nickel and copper were used as sheets ($2 \times 2 \times 0.02$ cm), cobalt was used as a rod (m5N5). Acetone (BDH) was dried over anhydrous $MgSO_4$. Lactic acid was used as supplied (Sigma). Other chemicals were of BDH quality.

The electrochemical technique was the same as reported previously^(5,6) with a cell consisting of a 100 ml tall-form beaker containing 50 ml of an acetone solution of lactic acid (10 ml) with the platinum cathode and the sacrificial anode immersed in the solution. The solution compositions, electrochemical conditions and yields are given in Table 1.

Cobalt(II), nickel(II), iron(III) and copper(II) were determined complexometrically using semi-xylenol orange (SXO) as indicator⁽⁷⁾. Carbon and hydrogen analyses were carried out at the Microanalytical Unit of Cairo University. I.r. spectra in the 200–4000 cm^{-1} range were recorded on a Perkin–Elmer 1430 spectrometer as Nujol

mulls or KBr discs. Solution optical spectra were recorded on a Pye-Unicam SP 8800 spectrometer. Conductivity measurements were made using a Tacussel conductivity bridge type CD6NG and 10^{-3} M solutions in DMSO. Magnetic measurements were made on a Johnson-Matthey magnetic susceptibility balance.

C.v. measurements were carried out with a potentiostat wave generator (Oxford electrodes) equipped with a Philips PM 8043 X–Y recorder. The electrode assembly consisted of platinum wires of 0.5 diameter as working and counter electrodes and a SCE as a reference. $NaClO_4$ or tetraethylammonium hexafluorophosphate (TEAPF₆) were used as supporting electrolytes.

Results and discussion

The electrochemical oxidation of iron, cobalt, nickel and copper in the presence of lactic acid (H_2LA) in acetone solution yields complexes of formulae $[Fe(HLA)_2 \cdot OH \cdot (Me_2CO)]2H_2O$, $[Co(HLA)OH(Me_2CO)_2]_2 \cdot 2(Me_2CO)$, $[Ni(HLA)_2(Me_2CO)H_2O]3H_2O$ and $[Cu(LA)(Me_2CO)_2]_2$ in high yield.

All of the complexes are stable to atmospheric exposure except for the iron(II) complex, which is easily oxidized to iron(III). The molar conductivity values (Table 1) measured in H_2O indicate that the complexes are nonelectrolytes⁽⁸⁾, except for the copper(II) complex, whose value of $79 \Omega^{-1} cm^2 mol^{-1}$ may be due to solvolysis or partial dissociation. The analytical results, molar conductance values and electrochemical data are listed in Table 1.

Comparing the i.r. spectra of H_2LA with its metal complexes suggests that the ligand behaves in a mononegative bidentate manner, coordinating through the hydroxyl and carboxylic groups with the liberation of a proton from the latter. The band observed at $2560 cm^{-1}$ in the free ligand suggests intramolecular hydrogen bonding⁽⁹⁾. In the spectra of the metal complexes, this band disappears and another band instead is observed at $3560 cm^{-1}$, indicating the disruption of the hydrogen bond and coordination of the hydroxide to the metal. Further evidence for hydroxide coordination is the lower shift ($30 cm^{-1}$) of the band at $1340 cm^{-1}$ due to $\delta(OH)$. The $\nu_{as}(COO)$ of the free ligand would be expected to shift if the carboxylate group is involved in coordination. The observed frequency at $1720 cm^{-1}$ in the free ligand spectrum is shifted to ca. $1580 cm^{-1}$. The $\nu_{symm}(COO)$ mode is observed at $1360 cm^{-1}$ in the complexes. The difference ($200 cm^{-1}$) between the ν_{asym} and $\nu_{symm}(COO)$ vibrations indicates monodentate coordination of the carboxylate. Finally, we assigned bands at $300 cm^{-1}$ in the spectra of the cobalt(II), copper(II) and nickel(II) complexes, respectively, to the M–O stretching vibration⁽¹¹⁾.

The reflectance spectrum (Nujol) of the copper(II) complex is characterized by a broad main band centred

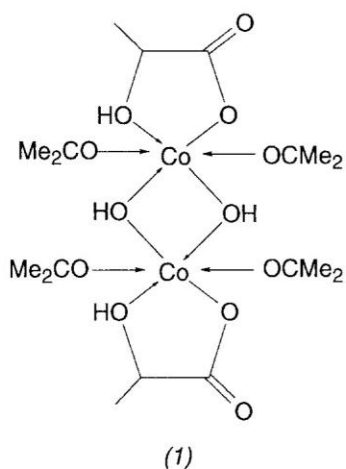
* Author to whom all correspondence should be directed.

Table 1. Analytical and preparative electrochemical data for the complexes.

Compound	Colour	M.p. (°C)	μ_{eff} (B.M.)	Found (Calcd.)(%)			i (mA)	V	Metal dissolved (g)	E_f	Λ_m
				C	H	M					
[Fe(HLA) ₂ OH(Me ₂ CO)]·2H ₂ O	Pale brown	> 300	–	31.5 (31.3)	5.9 (6.1)	16.1 (16.2)	40	30	0.075	0.45	11.7
[Co(HLA)OH(Me ₂ CO) ₂] ₂ ·2(Me ₂ CO)	Pink	> 300	5.14	40.4 (40.3)	7.1 (7.3)	17.1 (16.5)	40	35	0.082	0.45	6.9
[Ni(HLA) ₂ (Me ₂ CO)H ₂ O]·3H ₂ O	Pale blue	> 300	3.5	29.0 (29.5)	6.4 (6.6)	16.5 (16.0)	20	20	0.055	0.42	12.4
[Cu(LA)(Me ₂ CO) ₂] ₂	Pale blue	> 300	2.14	40.2 (40.4)	6.1 (6.0)	23.7 (23.7)	20	20	0.046	0.48	79.0

at 13 500 cm⁻¹ and a well-defined shoulder near 12 500 cm⁻¹, which may be assigned to the ²B_{1g} → ²E_g and ²B_{1g} → ²A_{1g} transitions, respectively, in D_{4h} symmetry⁽¹²⁾. The broadness of the 13 500 cm⁻¹ band suggests that the copper(II) complex has a tetragonal geometry as a result of lowering of symmetry due to the Jahn-Teller effect⁽¹³⁾. The magnetic moment value (2.14 B.M.) lies within the permissible range for one unpaired electron in compounds with bonds which are strongly covalent.

The pink cobalt(II) complex, [Co(HLA)(OH)(Me₂CO)₂]₂·2(Me₂CO) has two absorption bands at 18 900 and 20 400 cm⁻¹ which are assigned to the ⁴T_{1g} → ⁴A_{2g} and ⁴T_{1g} → ⁴T_{2g}(P) transitions, respectively. The B, β, 10Dq and ν₂/ν₁ values are calculated to be 820.8 cm⁻¹, 0.85, 10 020 cm⁻¹ and 2.13, respectively; together with the magnetic moment (5.14 B.M.), these are typical of octahedral geometry^(14,15), as shown in structure (1). The i.r. spectrum of this complex suggests the *cis*-form rather than *trans*.



The i.r. spectrum shows a band at 1005 cm⁻¹ assigned to Co—O—H bending; Ferraro and Walker⁽¹⁶⁾ identified this mode at 955 cm⁻¹ in [(bipy)Cu(OH)₂(bipy)]SO₄·5H₂O. Three spin-allowed transitions are expected for octahedral nickel(II) complexes⁽¹⁷⁾. Although only two were observed for our complex, the third is probably above our instrument's frequency limit. Bands at 15 900 and 23 500 cm⁻¹ are assigned to the ³A_{2g} → ³A_{1g}(F) and ³A_{2g} → ³T_{1g}(P) transitions, respectively, while a band at 30 200 cm⁻¹ is due to a charge transfer (CT) transition⁽¹⁸⁾. The magnetic moment value (3.5 B.M.) is slightly higher than the spin only value (2.8–3.2 B.M.) for octahedral geometry; this may be due to the presence of a tetrahedral

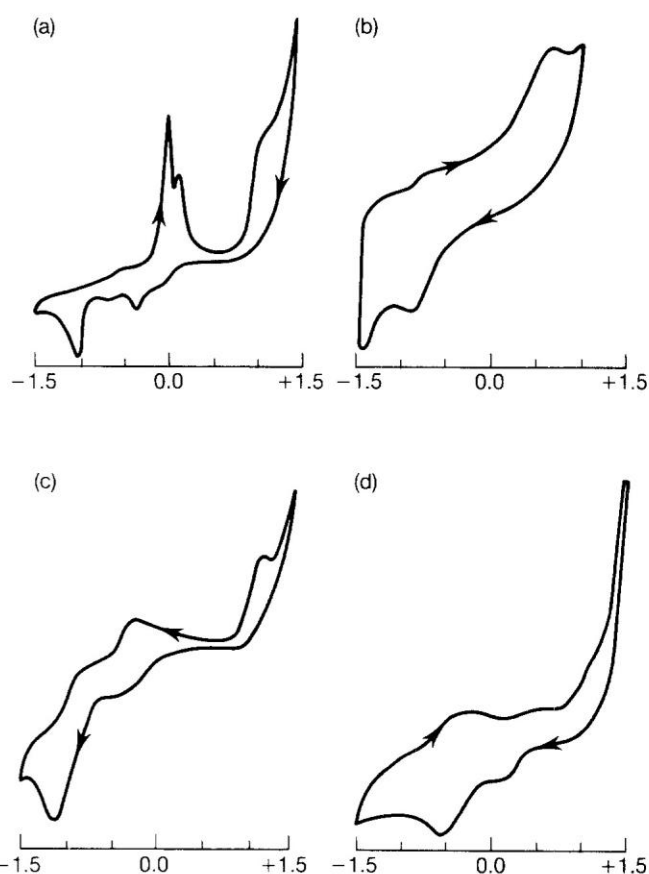


Figure 1. Cyclic voltammograms in DMSO; (a) copper(II) complex in NaClO₄ at 100 mV s⁻¹; (b) cobalt(II) complex in NaClO₄ at 100 mV s⁻¹; (c) nickel(II) complex in TEAPF₆ at 100 mV s⁻¹; (d) iron(III) complex in NaClO₄ at 200 mV s⁻¹.

species mixed with the octahedral complex in the same crystal.

The c.v. for [Cu(LA)·(Me₂CO)₂]₂ (Figure 1) shows three cathodic peaks at 0.05, -0.3 and -1.02 V, coupled with two smaller anodic peaks at 1.15 and 0.19 V and a broad anodic peak at 0.05 V versus SCE. The latter anodic peak is characteristic of an electrochemically active species adsorbed on the electrode surface^(19,20). The presence of an anodic peak at 1.15 V could be assigned to a one electron oxidation of the complex followed by decomposition⁽¹⁹⁾. A similar voltammogram was observed for Cu(ClO₄)₂ in DMF⁽²⁰⁾. Moreover, the two cathodic peaks at -0.30 and -1.02 V suggest reduction of the complex in two steps. Hence the oxidation state of the complex varies from copper(0) to copper(III) in the c.v. experiment. For [Co(HLA)OH(Me₂CO)₂]₂·2(Me₂CO), the voltam-

mograms show two well-defined cathodic waves at -0.87 and 0.36 V coupled with two anodic waves at -0.59 and 0.83 V, similar to the pattern reported for $[\text{CoSal}_2 \cdot \text{en}]^{(21)}$. These two electrode couples are tentatively assigned to $\text{Co}^{\text{III/II}}$ and $\text{Co}^{\text{II/I}}$ with $E^0 = 0.595$ and -0.736 V versus SCE, respectively. In the case of $[\text{Ni}(\text{HLA})_2(\text{Me}_2\text{CO})\text{H}_2\text{O}] \cdot 3\text{H}_2\text{O}$, three irreversible electrode couples are observed and may be assigned as $\text{Ni}^{\text{III/II}}$, $\text{Ni}^{\text{II/I}}$ and $\text{Ni}^{\text{I/0}}$ with $E^0 = 1.073$, -0.38 and -0.91 V, respectively. Two well-defined cathodic waves at -0.55 and 0.18 V are observed in the voltammogram of the iron(III) complex, plus an ill-defined cathodic peak at -1.25 V. These cathodic peaks are coupled with two oxidation peaks at -0.30 and 0.6 V and ill-defined anodic peaks at 0.93 and 1.12 V. The two reduction waves at 0.18 and 0.55 V are metal centred, since lactic acid is electrochemically inactive in the potential range used. These waves may be assigned to $\text{Fe}^{\text{III/II}}$ and $\text{Fe}^{\text{II/I}}$ with $E^0 = 0.39$ and -0.42 V. The assignments of the redox states for all the complexes were confirmed by controlled potential coulometry at the standard electrode potential of each couple.

Nature of the electrode processes

On increasing the scan rate (20 – 500 mV s^{-1}), the cathodic peak potentials ($E_{\text{p,c}}$) of the copper, nickel, cobalt and iron complexes shifted to more negative values, whereas the anodic peak potentials were shifted to less negative values (Figure 1). This behaviour shows the irreversible nature of the electrode process⁽²²⁾. The irreversibility is also revealed by the difference between $E_{\text{p,c}}$ and $E_{\text{p,a}}$, since for one electron and two electron reversible processes ΔE_{p} should be 60 and 30 mV, respectively (in our case $\Delta E_{\text{p}} > 90$ mV).

In conclusion, the formal redox potentials indicate that the cobalt(II) and iron(III) complexes are strong oxidants, the copper(II) complex is a mild oxidant and the nickel(II) complex is a strong reductant.

References

- ⁽¹⁾ G. K. Friman in G. L. Erchorn (Ed.), *Inorganic Biochemistry*, Izd. Mir, Moscow, 1978, Russian translation.

- ⁽²⁾ A. Gercely and I. Ssvago, *Metal Ions in Biological Systems*, Interscience, New York, 1978, Vol. 9.
⁽³⁾ J. S. Banait and P. K. Pahil, *Polyhedron*, **4**, 1031 (1985).
⁽⁴⁾ N. Kumer, D. G. Tuck and K. D. Watson, *Can. J. Chem.*, **65**, 4 (1987).
⁽⁵⁾ H. E. Mabrouk, A. A. El-Asmy, T. Al-Ansi and M. Mounir, *Bull. Soc. Chem., Fr.*, 127 (1991).
⁽⁶⁾ H. E. Mabrouk, A. A. El-Asmy and M. Mounir, *Transition Met. Chem.*, in press.
⁽⁷⁾ A. I. Vogel, *A Text Book of Quantitative Inorganic Analysis*, 2nd Edit., Longmans, London, 1951.
⁽⁸⁾ W. J. Geary, *Coord. Chem. Rev.*, **7**, 81 (1971).
⁽⁹⁾ J. I. Bullock and H. A. Tajmir-Riahi, *J. Chem. Soc., Dalton Trans.*, 36 (1978).
⁽¹⁰⁾ I. M. Procter, B. J. Hathaway and P. Nicholls, *J. Chem. Soc., A*, 1678 (1968).
⁽¹¹⁾ B. V. Murdula, G. Venkatanarayana and P. Lingaiah, *Ind. J. Chem.*, **28A**, 1011 (1989).
⁽¹²⁾ M. S. M. Campell and R. Grzeskowiak, *J. Chem. Soc. A*, 396 (1967).
⁽¹³⁾ A. A. El-Asmy, T. Y. Al-Ansi, R. R. Amin and M. Mounir, *Polyhedron*, **9**, 2029 (1990).
⁽¹⁴⁾ A. A. El-Asmy and M. Mounir, *Transition. Met. Chem.*, **13**, 143 (1988).
⁽¹⁵⁾ A. B. P. Lever, *Inorganic Electronic Spectroscopy*, Elsevier, Amsterdam, 1968.
⁽¹⁶⁾ J. R. Ferraro and W. R. Walker, *Inorg. Chem.*, **4**, 1382 (1965).
⁽¹⁷⁾ L. L. Martin, R. L. Martin, K. S. Murray and A. Sargeson, *Inorg. Chem.*, **29**, 1389 (1990).
⁽¹⁸⁾ K. K. Yusuff and R. Sereekata, *Synth. React. Inorg. Met.-Org. Chem.*, **21**, 553 (1991).
⁽¹⁹⁾ C. Dendrinou-Samara, P. D. Jannakoudakis, D. P. Kessissoglou, G. E. Manoussakis, D. Mentzafos and A. Terzis, *J. Chem. Soc., Dalton Trans.*, 3259 (1992).
⁽²⁰⁾ G. Christou, S. P. Perlepes, E. Libby, K. Falting, J. C. Huffman, R. J. Webb and D. N. Hendrickson, *Inorg. Chem.*, **29**, 3657 (1990).
⁽²¹⁾ D. F. Rohrbach, E. Deutsch and W. R. Heineman in G. Mamentav (Ed.), *Characterization of Solutes in Non Aqueous Solvents*, Plenum Press, New York, 1978, p. 177.
⁽²²⁾ P. Dalhay, *New Instrumental Methods in Electrochemistry*, Interscience, New York, 1953.

(Received 10 May 1993)

TMC 3043



THE SORPTION BEHAVIOUR AND SEPARATION OF SOME METAL THIOCYANATE COMPLEXES ON POLYETHER-BASED POLYURETHANE FOAM

A. B. FARAG,² M. S. EL-SHAHAWI^{1*} and S. FARRAG¹

¹Chemistry Department, Faculty of Science, UAE University, Al-Ain, P.O. Box 17551, United Arab Emirates

²Chemistry Department, Faculty of Science, Qatar University, Doha-2713, State of Qatar

(Received 15 April 1993. Revised 18 November 1993. Accepted 18 November 1993)

Summary—The preliminary screening tests on the preconcentration of lanthanum(III), aluminium(III), molybdenum(VI), gallium(III) and tungsten(VI) thiocyanate complexes in aqueous media by unloaded foam indicated a reasonable percentage of metal ions were retained on the foam. The influence of various parameters affecting the retention of these complex species from the aqueous media by the foam were critically studied and the possible mechanisms of the sorption of the compounds were suggested. However, owing to the complex chemical nature of the polyether-polyurethane foam, several mechanisms may be involved simultaneously. Attempts for the quantitative retention and recovery of the tested complexes by the foam columns were also made and satisfactory results were obtained. The height equivalent to theoretical plates (HETP) of the foam columns were calculated from the chromatograms and break through capacity curve and were found in the range 1.8–2.3 mm at flow rates up to 15 cm³/min. The proposed foam column method has been successfully used for the separation of a series of complex mixtures of the tested metal thiocyanate complexes in aqueous media. The membrane properties of the foam sorbents offer unique advantages over conventional bulk type granular sorbents in rapid, versatile effective separations and preconcentrations of different complexes from fluid samples.

It is known that metal thiocyanate complexes are effectively extracted in the form of ion-association complexes into oxygen-containing organic solvents^{1,2} and this has been widely used for the separation of metals.³ However, the volatility and toxicity of organic solvents sometimes pose problems in the practical operation of the process, and multiple extraction must be used.³ Concentration of the resulting volume of solvent down to a volume required for an appropriate concentration of the species to be measured often results in interference from material present in low concentration in the organic solvent.^{4,5}

Systematic studies on the metal-selective separation by solid polymer membrane technologies under hydraulic pressure have been made.^{6–10} The sorption of ion-association complexes is assumed to be important in the development of solid membranes which selectively rejects metal species or are permeated by

them.¹⁰ The sorption behaviour of the metal thiocyanate complexes by solid polymer membrane followed a Langmuir-type adsorption isotherm.¹⁰

Recently, after the pioneering work of Bowen,^{11,12} Braun and Farag,^{13–15} and Chow *et al.*,^{16,17} the use of polyurethane foam (PUF) has been established and found wide application in different separation procedures from aqueous thiocyanate media.^{16–20} The retention behaviour of Au, Fe, Ga, Hf, In, Mo, W, Tc, Nb, Pa, Sb (V), Sn (IV), Ta and Zn on polyether-based polyurethane foam in HCl-KSCN medium have been reported by Caletka *et al.*^{21,22}

The application of polyurethane foams sorbents in trace elements led to the revealing of the potentialities of their special geometrical form: spherical membrane-shaped geometry and to the proposal of their general use in column operations as a substitute for the traditional granular supports in extraction chromatography.^{23–26} The resilient property and quasi-spherical membrane geometry combined with the high retention capacity due to large surface area has made polyurethane foam the preferred

*Author for correspondence. Permanent Address: Chemistry Department, Faculty of Science at Damiatta, Damiatta, Egypt.

sorbent over conventional solvents and other extraction techniques for the separation of elements by selective sorption on the foam.^{25,26}

This paper reports the effect of various parameters on the extraction and separation of some metal ions from aqueous thiocyanate media by unloaded foams and conclusions concerning the most probable sorption mechanism by the polyurethane foam have been drawn.

EXPERIMENTAL

Reagents and materials

All reagents and chemicals were of analytical reagent grade. Polyurethane foam, an open cell polyether type (bulk density 30 kg/m³) was supplied by Greiner K.G. Schaum (Stoffwerk Kremsmunster, Austria). The foam cubes were cut, washed and finally dried as previously described.¹⁴ Stock solutions (1 mg/cm³) of lanthanum(III), aluminium(III), molybdenum(VI), gallium(III) and tungsten(VI) were prepared in distilled water. Stock solutions (1M) of lithium, ammonium, sodium, potassium and rubidium chlorides were also prepared in distilled water. A universal buffer solutions series of Britton-Robinson were used. The average standard deviation of the weight of the foam was 1.6%.

Apparatus

A Unicam Sp-90A series atomic absorption spectrometer with a conventional 10-cm slit burner head for an air-acetylene flame and an inductively coupled plasma (ICP) Jobin Yvon (JY 38) were used. Mechanical shaker type G10 Gyrotary (New Brunswick, Scientific Co.), and an Orion pH meter and glass columns of 12 cm height and internal diameter 1.5 cm were also employed.

General procedures

Batch experiments. To investigate the effect of shaking time on the uptake of the tested metal ions (La, Al, Mo, Ga and W) by the unloaded foam, the foam cubes (0.2 g) were equilibrated with 25 cm³ of ammonium thiocyanate (0.1M) solution containing 5 mg of the tested metal ions in separate polyethylene bottles. These solutions were shaken for various time intervals and the foam cubes were then separated by decantation. The amount of the metal ion remaining in the

aqueous solution was measured by atomic absorption spectrometry. The sorption behaviour of the complexes were evaluated from the degree of sorption (*E*) and the distribution ratio (*D*):

$$E = \frac{[M]_i - [M]_F}{[M]_i} \times 100 \quad (1)$$

$$D = \frac{[M]_i - [M]_F}{[M]_F} \times \frac{V_s}{W} \quad (2)$$

where $[M]_i$ and $[M]_F$ are the initial and final metal concentrations, respectively in the solution; V_s is the volume of solution (cm³) and W is the weight of dry foam (g). Following these procedures, the effect of pH, acidity, thiocyanate concentration and ionic strength on the sorption behaviour of the tested metal ions were critically examined.

Column experiments. In the column experiments, 1 g of dry foam was packed into the column using the vacuum method of foam column packing.¹⁴ Aqueous thiocyanate solution (0.1–0.5 dm³) sample containing 1 mg of the tested metal ions (La, Al, Ga, Mo or W) were passed through the foam column at 1–5 cm³/min flow rate at the optimum conditions of each metal ion. The columns were then washed with 100 cm³ of ammonium thiocyanate solution. The tested metal ions were quantitatively extracted. Elution of the retained species from the foam column were quantitatively obtained by percolating selective eluting agents for each metal ion. The effluent and washing solutions were collected in a 100-cm³ measuring flask and measured by ICP. Chromatographic separation of the mixtures Mo-La-Al; Al-W-Ga; W-La (or Al), La-Ga (or W) and Ga-Al (or La) were carried out employing the foam packed column procedures.

RESULTS AND DISCUSSION

Static experiments

Preliminary batch experiments have shown that the uptake of the investigated metal ions (La, Al, Ga, Mo and W) from aqueous thiocyanate solutions by the unloaded foam is rapid and equilibrium is reached in less than 1 hr followed by a plateau. A better extraction percentage (>90%) was obtained within a short period of time (~20 min) for tungsten(VI). Representative results are given in Fig. 1.* It was shown that the maximum extractibility of Ga and Al are reached at shorter times (4–6 min) than that for Mo and La.

*Each point in figures represent average of 5 measurements, $n = 5$ with relative standard deviations in the range 1.6–1.8%.

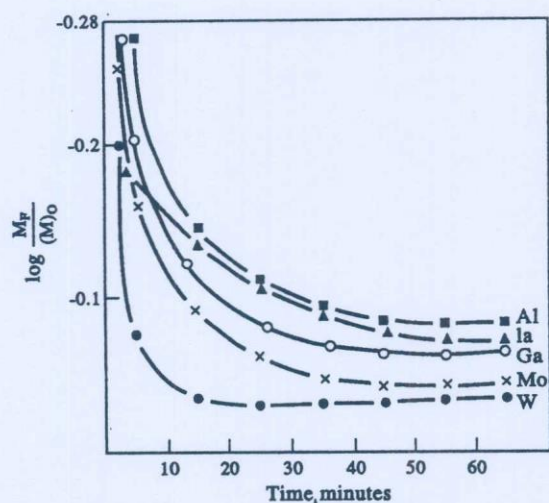


Fig. 1. Effect of shaking time on the sorption profiles of tungsten(VI), molybdenum(VI), gallium(III), lanthanum(III) and aluminium(III) by the foam from aqueous thiocyanate media.

The effect of pH and acidity (HCl or HClO₄) up to 6M on the extraction of the tested metal ions from aqueous thiocyanate media by the unloaded foam were carried out. The sorption profiles of the investigated species are summarized in Figs 2 and 3. The extraction percentage of W, La and Mo (Fig. 2) increased by increasing the hydrochloric acid concentration while for gallium and aluminium (Fig. 3) the extraction efficiency increased as the acidity decreased. The increased acidity could initiate the decomposition and polymerization of thiocyanate or isothiocyanic acid in aqueous solution.²⁵

The effect of acidity on the distribution ratio of the tested species from the thiocyanate media by the unloaded PUF is given in Fig. 4. The *D* values of Mo, W and La increased sharply while for Al and Ga the extraction decreased with

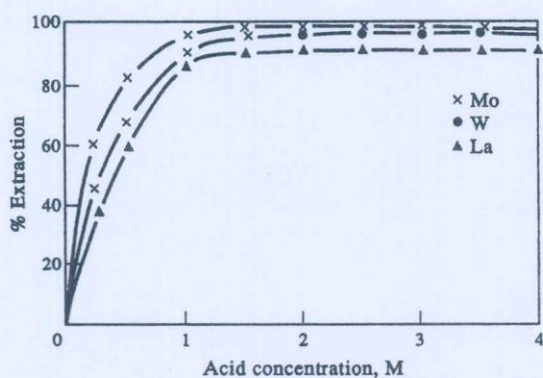


Fig. 2. Effect of acid concentration on the sorption profiles of molybdenum(VI), tungsten(VI) and lanthanum(III) by the foam.

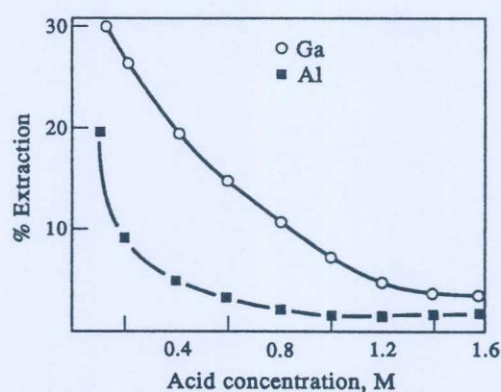


Fig. 3. Effect of acid concentration on the sorption profiles of gallium(III) and aluminium by the foam.

increasing initial acid concentration. The sorption behaviour of aluminium and gallium may be attributed to the competitive extraction of hydrochloric or perchloric acid and complex species of thiocyanate in aqueous solution.¹⁷⁻¹⁹ Solvent extraction mechanism and other processes are possibly involved in the uptake of these metal complexes. The specific sites on the foam membrane presumably are capable of absorbing lanthanum(III), molybdenum(VI) and tungsten(VI), via an ion exchange mechanism.

Figure 5 shows the effect of thiocyanate concentration on the sorption profiles of the tested metal complexes. The degree of sorption of metal thiocyanate complexes by the unloaded foams decreases in the order

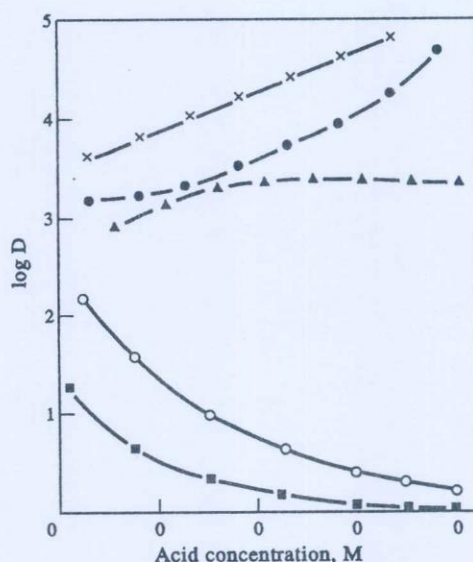


Fig. 4. Effect of acid concentration on the distribution coefficients of the tested metal ions between the aqueous thiocyanate media and polyurethane foams. La (▲); Al (■); Ga (○); W (●) and Mo (×).

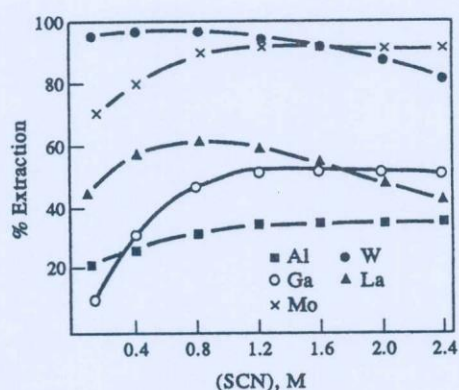
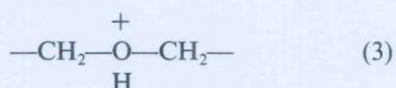


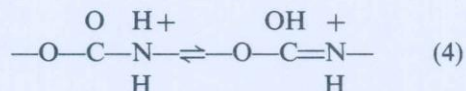
Fig. 5. Effect of thiocyanate concentration on the sorption of the tested metal ions by the unloaded foams.

$W > Mo > La > Ga > Al$. It is reported that polyether-type polyurethane foam successfully sorbs these complexes^{14,15} and the chemical structure of the PUF material has such a subtle effect on the sorptivity of metal complexes analogous to that in metal extraction by organic solvents of various structure and polarity.^{10,14}

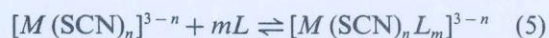
The sorption profiles of La, Ga and Al thiocyanate complexes by the unloaded foam increased sharply with increasing the thiocyanate concentration, possibly due to the formation of anionic octahedral complexes such as $(NH_4)_{3-n}M(SCN)_n$,²⁷ where $M = La, Ga$ or Al . The sorption of these complex species could be due to the anion exchange properties of PUF which may act as a weak or strong anion exchanger. The existence of anion exchange sites arise from the tendency of both the nitrogen atoms of the urethane linkage and or the ether oxygen atoms to accept protons at higher acid concentration to give:



or



and hence the polyether-type foam will have anion-exchange sites of various strengths.^{14,15} Sorption of these three thiocyanate complexes could also be through a ligand addition mechanism since polyurethane foam contains large numbers of lone electron pairs on its nitrogen or oxygen atoms which are supposedly involved in the coordination of interaction with the anionic complex species.^{16-18,26}



where L represents the lone pair of electron and its associated atom in the polyurethane and $m + n = 6$ in all cases. Higher concentrations of ammonium thiocyanate and acid decreased the sorption profiles of molybdenum and tungsten (Fig. 5). This may be attributed to the increased influence of thiocyanic acid and 5-amino-1,2,4-dithiazole-3-thione formed during sorption of these complex species by PUF.²³⁻²⁸ This behaviour also could be due to the competitive extraction of ammonium thiocyanate which may be expected to be somewhat extractable as the neutral octahedral $Mo(SCN)_6$ and $W(SCN)_6$ complex species.²⁷⁻²⁹

The sorption of a neutral thiocyanate metal complex could occur, depending on experimental conditions as reported elsewhere.^{19,29} Tungsten(VI) at high acidity is present as WO^{4+} which reacts with SCN^- to form anionic species $[WO(SCN)_n]^{4-n}$. These are possibly sorbed on PUF through a cation chelation mechanism.^{17,23} According to this mechanism complexation of cations, *e.g.*, K^+ , NH_4^+ or H_3O^+ , takes place in the PUF cavities through ion-dipole interaction and/or hydrogen bonding.¹⁸ The anionic species formed, *i.e.*, $[WO(SCN)_n]^{4-n}$, are then extracted as counter ions to the captured cations in the PUF cavities.^{25,26}

The effect of thiocyanate concentration on the distribution ratio of the tested metal ions Al, Ga, La, Mo and W by the unloaded foams are summarized in Fig. 6. The D values for La, Ga and Al increased with increasing thiocyanate concentration possibly due to the ability of these metal ions to form anionic octahedral complexes $[M(SCN)_6]^{3-}$ which are highly extractable by the unloaded foams. The D values of molybdenum(VI) and tungsten(VI) decreased with increasing thiocyanate concentration. For molybdenum(VI), D increases with C_{SCN^-} with a small maximum at $\sim 0.4M$ thiocyanate concentration and remains almost constant.

The effect of various concentrations of lithium, sodium, potassium and ammonium chlorides on the sorption profiles of the tested metal ions by the unloaded foam at the optimum conditions of concentration of thiocyanate and acidity of each tested ion were carried out. Representative results are given in Fig. 7. The sorption profiles of La(III), Al(III) and MO(VI) thiocyanate complexes increased with the increase of the cation size in the following order of cations: $NH_4^+ > K^+ > Na^+ > Li^+$ [Fig. 7(a)] while for tungsten(VI) and gallium(III) [Fig. 7(b)], the sorption percentage increased in the

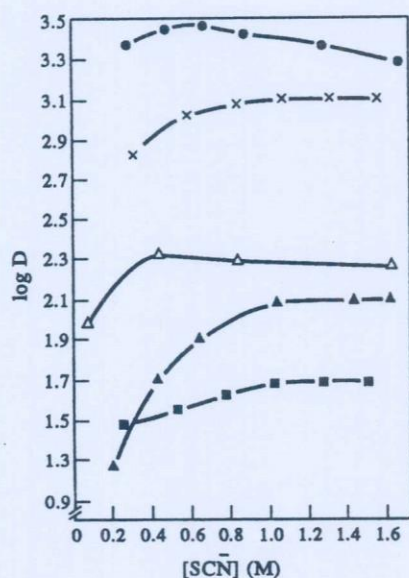
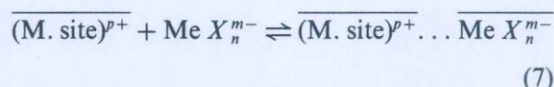
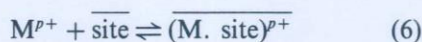


Fig. 6. Effect of thiocyanate concentrations on the distribution ratios of the tested metal ions between the aqueous thiocyanate media and polyurethane foams. W (O); La (x); Mo (Δ); Ga (\triangle) and Al (\blacksquare).

following order: $\text{Li}^+ > \text{Na}^+ > \text{K}^+ > \text{NH}_4^+$. Therefore, the ion-dipole interaction of NH_4^+ with oxygen sites of PUF are possibly highly predominating in the extraction of Al^{3+} , La^{3+} and Mo^{6+} ions. The ability of the anionic thiocyanate complexes of these metal ions to form ion-pairs increases with increasing cation size ($\text{NH}_4^+ > \text{K}^+ > \text{Na}^+ > \text{Li}^+$) and possesses a

maximum in the presence of NH_4^+ . These results are in agreement with the data recently reported by Palagyi and Braun *et al.*^{24,25} Therefore "cation chelation mechanism" is the most probable mechanism for the sorption of these complex species. In accordance with this mechanism, the polyalkenoxy chains of the PUF sorbent form a helical structure.²³ The helical structure of the foam sorbent forms a clathrate with suitable simple cations and the anionic metal complex is then sorbed on these cationic sites.²⁴ Many cations, M^{p+} (e.g., Na^+ , K^+ , Li^+ , NH_4^+ or H_3O^+) are capable of being multiply complexed by the PUF at specific sites giving a solid phase (or matrix) species which can be required as equivalent to an ion exchange matrix or to a solvated cations in solid solutions as follows:



The chelated cation $(\text{M. site})^{p+}$ and the accompanying anions $\text{Me } X_n^{m-}$ are possibly associated within the PUF matrix. If considerable sorption of another ion association complex containing M^{p+} and some moderately extracted anion, A^- occurs before or concurrently with the sorption of $\text{Me } X_n^{m-}$, then the latter may be more conveniently regarded as sorbed by an anion exchange process in which it is exchanged for

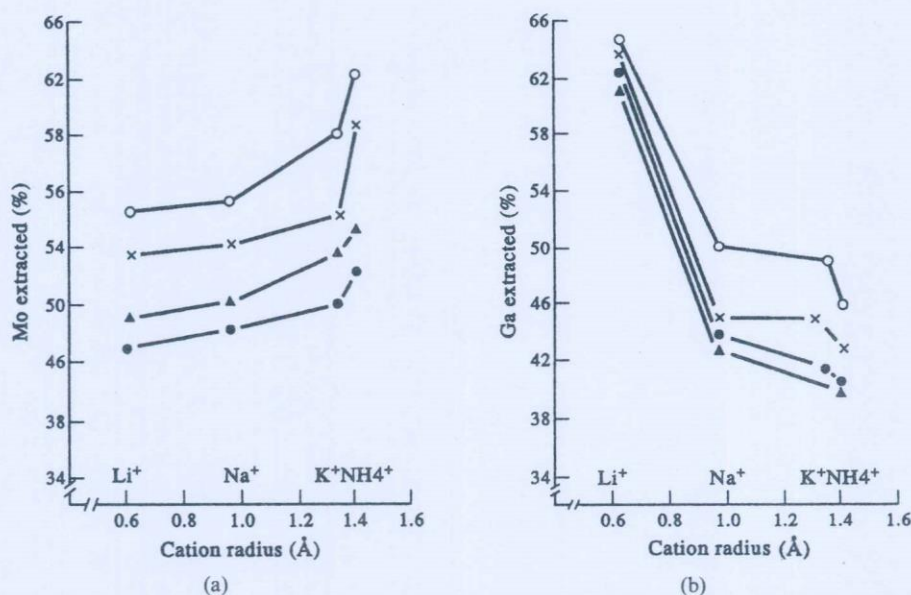
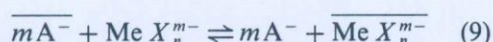
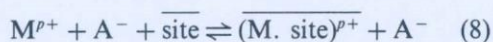
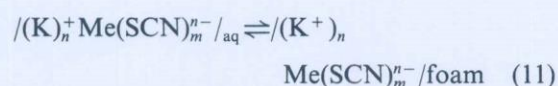
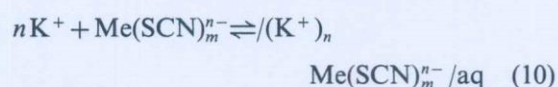


Fig. 7. Effect of the size of various univalent cations on the sorption profiles of molybdenum (a) and gallium (b) thiocyanate complexes by polyurethane foam. Salt concentrations are 0.2M (O); 0.4M (x); 0.6M (\blacktriangle); 0.8M (\bullet).

A^- at the positive sites that result from chelation of M^{p+} by the polymer. A matrix similar to anion-exchanger results at which exchange of the anionic counter-ions can occur and the sorption mechanism of $Me X_n^{m-}$ may then be:



The sorption profiles of Ga(III) and W(VI) by the PUF from acid thiocyanate increases in the order: $Li^+ > Na^+, K^+$ [Fig. 7(b)]. Similar trends were obtained in the solvent extraction of uranium(VI) by ethers and polyether foams.²⁹ Solvent extraction is therefore the most probable mechanism for the sorption of the complex species of Ga and W by the unloaded foams as follows:²⁹



Mossbauer spectroscopy studies on the sorption of Fe(III) from acid thiocyanate media also supported the above mentioned approach. The sorbed species by PuF was $Fe(SCN)_3$, similar to diethyl ether extraction.³⁰ In the thiocyanate-containing system, the difference between aqueous and etheric solution is almost negligible and $Ga(SCN)_3$ species are probably present in both solvents with the PUF-sorbed species. A six-coordinated complex $Ga(SCN)_3 \cdot 3D$ is probably formed with some of the donor groups (D) of the polyurethane foam in agreement with an earlier observation.³¹

Column experiments

In these experiments distilled water samples containing 1 mg of each metal ion at the optimum thiocyanate and acid concentrations of maximum sorption were percolated through separate PUF columns as described in the experimental procedure. Complete sorption and recovery of the metal ions were achieved from the foam column. Molybdenum(VI) and lanthanum(III) ions were eluted from the foam column with acetone while aluminium(III), gallium(III), and tungsten(VI) were recovered with HCl (1M), NH_4OH (2M) and HCl-acetone (1:1), respectively and determined by ICP.

The dependence of the sorption profile of molybdenum(VI) on the flow rate was investi-

gated by percolating 1 mg of Mo(VI) through the foam column at various flow rates up to 15 cm^3/min . Complete retention was obtained up to 10 cm^3/min and it decreased significantly at a higher flow rate. The height equivalent to theoretical plates (HETP) were calculated from the elution curves and found to be in the range $1.8-2.3 \pm 0.1$ mm at 5-15 cm^3/min flow rate. The HETP were also obtained from the breakthrough capacity curve and were found in the range $2.0-2.2 \pm 0.15$ mm (average of 5 determinations). The average standard deviations for the HETP was found in the range 1.6-1.8%.

Separation of the tested metal thiocyanate complexes from each other is possible from different volumes (0.1-1 dm^3) of the aqueous thiocyanate solution. A mixture containing 1 mg of molybdenum was separated from 1 mg of lanthanum (or aluminium) at the optimum conditions of pH and thiocyanate concentration for molybdenum sorption by PUF at 1-5 cm^3/min . Sorption of molybdenum took place while La or Al complexes were not retained on the foam columns and collected quantitatively in the effluent. Molybdenum(VI) was then recovered from the column by 100 cm^3 of acetone at 3-5 cm^3/min flow rate. Separation of the ternary mixture Al-W and Ga (or Mo) were also carried out. A mixture containing 1 mg of each of these ions in aqueous thiocyanate solution (0.1-0.5 dm^3) at pH 7.5 was percolated through the foam column at 1-2 ml/min. Sorption of aluminium only took place and eluted with HCl 200 cm^3 of (1M), while W and Ga (or Mo) were passed through the column without retention. Separation of 1 mg of W from La or Al (1 mg) in aqueous solution containing NH_4CNS (1M) and HCl (4M) was also carried out on the unloaded foam column. Sorption of W took place at 0.5-1 ml/min while Al or La was passed through the column without extraction.

Separation of 1 mg of La from Ga or W (1 mg) were also carried out from aqueous thiocyanate (1M) solution at pH ≈ 8 . Lanthanum(III) was only retained on the foam column and eluted with 200 cm^3 acetone at 0.5 ml/min while gallium(III) or tungsten was passed through the column without sorption. Separation of 1 mg of Ga from Al (or La) mixture from aqueous NH_4CNS (1M) at pH 4 in the presence of LiCl was also obtained on the PUF column. Gallium was only retained and eluted with 100 ml of ammonia solution (2M) at 1-2 ml/min while the other metal ions were passed through the foam column without sorption.

REFERENCES

1. R. Bock, *Z. Anal. Chem.*, 1951, **133**, 110.
2. C. Rozycki, *Chem. Anal.*, 1969, **14**, 755.
3. T. Sekine and Y. Hasegawa, *Solvent Extraction Chemistry*, Dekker, New York, 1977.
4. T. Saito and K. Hagiwara, *Z. Anal. Chem.*, 1983, **315**, 201.
5. S. Voerman, *Bull. Environ. Cont. Toxic.*, 1969, **4**, 64.
6. Q. T. Ngugen, P. Aptel and J. Neel, *J. Membr. Sci.*, 1980, **6**, 71.
7. T. Hayashita, M. Takagi and K. Ueno, *Sepr. Sci. Techn.*, 1983, **18**, 461.
8. *Idem, ibid.*, 1984, **19**, 315.
9. M. Igawa, A. Saito, N. Sasamura, M. Tanaka and M. Seno, *J. Membr. Sci.*, 1983, **14**, 59.
10. T. Hayashita and M. Takagi, *Talanta*, 1985, **32**, 399.
11. H. J. M. Bowen, *J. Chem. Soc. A.*, 1970, 1082.
12. H. J. M. Bowen, *British Patent 1*, 1973, **305**, 375.
13. T. Braun and A. B. Farag, *Anal. Chim. Acta*, 1972, **61**, 265.
14. T. Braun, J. D. Navratil and A. B. Farag, *Polyurethane Foam Sorbents in Separation Science*, CRC Press, Boca Raton, Florida, 1985.
15. T. Braun, *Z. Anal. Chem.*, 1989, **333**, 785, and references therein.
16. A. Chow and D. Buksak, *Can. J. Chem.*, 1975, **53**, 1373.
17. R. F. Hamon, A. S. Khan and A. Chow, *Talanta*, 1982, **29**, 313.
18. S. J. Al-Bazi and A. Chow, *ibid.*, 1982, **29**, 507.
19. *Idem, ibid.*, 1983, **30**, 487.
20. G. J. Moody and J. D. R. Thomas, *Chromatographic Separation and Extraction with Foamed Plastics and Rubbers*, Marcel Dekker, New York, 1982.
21. R. Caletka, R. Hausbeck and V. Krivan, *Talanta*, 1986, **33**, 315.
22. *Idem, Anal. Chim. Acta*, 1990, **229**, 127.
23. A. Roychaudhuri, S. K. Roy and A. K. Chakraborty, *Talanta*, 1992, **39**, 1377.
24. S. Palagyi and T. Braun, *J. Radioanal. Nucl. Chem.*, 1992, **163**, 69, and references therein.
25. S. Palagyi, T. Braun, Z. Homonnay and A. Vertes, *Analyst*, 1992, **117**, 1537, and references therein.
26. S. Palagyi and T. Braun, *Separation and Preconcentration of Trace Elements and Inorganic Species on Solid Polyurethane Foam Sorbents* in Z. B. Alfassi and C. M. Wai (eds.), *Preconcentration Techniques for Trace Elements*, CRC Press, Boca Raton, Florida, 1992.
27. S. J. Al-Bazi and A. Chow, *Anal. Chem.*, 1983, **55**, 1094.
28. *Idem, Talanta*, 1984, **31**, 189.
29. J. J. Oren, K. M. Gough and H. D. Gesser, *Can. J. Chem.*, 1979, **57**, 2032.
30. F. E. Beamish, *The Analytical Chemistry of the Noble Metals*, Pergamon Press, Oxford, 1972.
31. M. N. Abbas, A. Vertas and T. Braun, *Radiochem. Radioanal. Lett.*, 1982, **54**, 17.



RETENTION AND SEPARATION OF SOME ORGANIC WATER POLLUTANTS WITH UNLOADED AND TRI-n-OCTYLAMINE LOADED POLYESTER-BASED POLYURETHANE FOAMS

M. S. EL-SHAHAWI

Chemistry Department, Faculty of Science, U.A.E. University, P.O. Box 17551, Al-Ain, United Arab Emirates

(Received 16 November 1993. Revised 1 February 1994. Accepted 10 February 1994)

Summary—The analytical utility of unloaded and polyester-based polyurethane loaded foams with tri-n-octylamine (TOA) in the removal of some phenols from water were carried out. In static mode, the TOA-loaded foams showed a good affinity of extraction towards the tested compounds as compared to the untreated foams. The various parameters affecting the retention efficiency of the tested compounds from aqueous media by the foam were examined via batch technique. The TOA-loaded foams were employed in column modes for the extraction and recovery of the tested phenols. The retention efficiency and the recovery of the tested compounds from the loaded foam column were up to 98.5%. Sorption of the compounds by the foam were brought by solvent extraction mechanism. The molecular weight and the pK_a of the compounds play an important role in the extraction process. The height equivalent to a theoretical plate (HETP) of the TOA-foam column was found in the range $1.8-2.05 \pm 0.1$ mm at flow-rates up to $10 \text{ cm}^3/\text{min}$. Separation of some of the tested phenols was also carried out by the TOA-foam columns. The membrane properties of the polyester foam sorbents give unique advantages over conventional granular sorbents in rapid, versatile and effective separations and preconcentrations of the tested compounds.

Phenols are common water pollutants because these compounds are the product of many industrial process, e.g. manufacture of dyes, plastics, drugs and antioxidants.¹ The presence of these compounds in the waste water of chemical factories often represents a risk to the environment.^{2,3} Although some phenols are used in medicine and as detergents and disinfectants, they are very toxic to most aquatic organisms, humans and can do much damage, especially to the urinogenital organs, liver and kidney.⁴ It has also an adverse effect on the taste and odour of fish, even at low concentrations.^{5,6} The reduction of such water pollutants to an acceptable concentration by extraction with organic solvents, steam distillation, oxidation reaction, adsorption on active carbon, reversed liquid-liquid partition filter chromatography and cellulose triacetate membrane filters has been investigated.^{7,10}

Recently, considerable progress has been made in the use of polyurethane foam as an inexpensive solid extractor and effective sorbent for the removal of water pollutants.¹¹⁻²² The

solid foam concentrates inorganic and organic substances from different media by the phase distribution mechanism rather than adsorption.^{12,13} The membrane like structure of the foams, together with efficient sorption properties offer higher concentrating ability and flow-rate compared with other solid supports.^{22,23} The present work deals with the use of polyester polyurethane foam for the removal of some phenols from high volume water samples. These compounds were chosen because they are quite hydrophobic and are likely to be extracted by the foam. The objective of the study was also to determine whether the extraction takes place by solvent extraction, cation chelation, anion exchange or by other mechanisms.

EXPERIMENTAL

Reagents and materials

All chemicals used were of analytical reagent grade. Open pores cell polyester-based polyurethane foam, was supplied by K. G. Schaum (Stoffwerk, Kremsmunster, Austria). Foam

cubes of approximately 1 cm³ were cut from polyurethane foam sheet. These foam cubes were soaked in 1M hydrochloric acid for 24 hr with occasional squeezing to remove any possible inorganic species and washed with water until they were acid free. They were then washed with acetone in a Soxhlet extractor for 8 hr to remove organic contaminants and finally dried in an oven at 60°C for 3 hr.¹¹ The foam cubes loaded with tri-n-octylamine (TOA) were prepared by mixing the dried foam cubes with 2% TOA in chloroform (10 cm³/g dry foam) with stirring for 15 min and dried as previously reported.¹² The compounds tested were: *o*-chlorophenol, phenol, *o*-nitrophenol, *m*-cresol, *o*-cresol and salicylaldehyde. A stock solution of each compound (100 μg/cm³) was prepared in 100 cm³ measuring flask by dissolving the exact weight of the compound in distilled and/or tap water. A series of standard solutions of these compounds were prepared by diluting their stock solutions with water.

Apparatus

UV absorbance measurements for the determination of the organic compounds were obtained with a Varian DMS 634-S spectrophotometer with 1 cm quartz cell. An Orion pH meter and glass columns (12 cm height × 10 mm I.D.) and Lab-Line Orbit Environ-Shaker model 35271-1 were also used.

General procedures

Batch experiments. To examine the effect of shaking time on the uptake of the tested compounds on unloaded and TOA loaded polyurethane foam, the foam cubes (0.3 ± 0.004 g) were equilibrated with 100 cm³ aqueous solution at pH ~ 2 of each compound (60 μg/cm³) in separate polyethylene bottles and shaken in a thermostated shaker at 20°C for various time intervals up to 2 hr. The aqueous phase was then separated and the amount of the compound remaining in it was determined from its absorbance at a suitable wavelength (Table 1)²⁴ against blank. The compound amount retained on the foam was calculated by difference. Following these procedures, the effect of compound concentration (10–80 μg/cm³), solution pH, temperature extraction media, secbutylamine (≤ 5 × 10⁻⁴M) and increasing salt concentration (≤ 0.15M) of different alkali metal (Li⁺, Na⁺, K⁺, NH₄⁺) chlorides on the extraction efficiency of the tested species by the polyester-based

Table 1. Extraction and recovery of the compounds tested (0.1 mg) from 3 dm³ aqueous solution (2 ≤ pH ≤ 3) at 20 ± 0.1°C by the proposed loaded TOA-foam column (1 g) mode at 5–10 cm³/min*

Compound	pK _a ²⁸	% recovery		Wavelength (nm)
		(a)	(b)	
Phenol	9.9	97.5	96	265
<i>o</i> -Chlorophenol	8.5	98	95	274
<i>o</i> -Nitrophenol	7.17	97	95	346
<i>m</i> -Cresol	10.1	98.5	97	272
<i>o</i> -Cresol	10.2	97.5	97	280
Salicylaldehyde	10	96	97	257

*Average of three measurements from distilled water (a) and tap water (b).

polyurethane foam were determined. The % extraction (*E*) and distribution coefficient (*D*) were calculated from

$$\% \text{ extraction } (E) = \left(\frac{C_0 - C}{C_0} \right) \times 100,$$

where *C*₀ = concentration of the tested compound in solution before extraction, *C* = concentration in solution after extraction, and

$$D = \frac{\% \text{ extraction}}{(100 - \% \text{ extraction})} \times \frac{\text{volume of solution (l)}}{\text{weight of foam (kg)}}$$

Column experiments. In the column experiment, 1 g of dry TOA-loaded foam was packed into the column using the vacuum method of foam packing.¹² Tap or distilled water (0.1–3 dm³) sample containing 0.1 mg of the compound tested at 2 ≤ pH ≤ 3 was passed through the foam column at 5–10 cm³/min. After squeezing water from the foam material, the compound was then recovered from the foam with 100 cm³ acetone in a Soxhlet extractor for 6 hr. The sample was then determined by measuring the absorbance of the solution against reagent blank after being concentrated to 10 cm³ with a rotary evaporator. The effect of sample volume and flow rate on the extraction efficiency of the compounds by the TOA-foams were also determined.

RESULTS AND DISCUSSION

Static experiments

Preliminary experiments using unloaded and TOA-loaded polyurethane foams have shown that the extraction of the investigated compounds is rapid and the equilibrium is reached in less than 1 hr, followed by plateau. Represent-

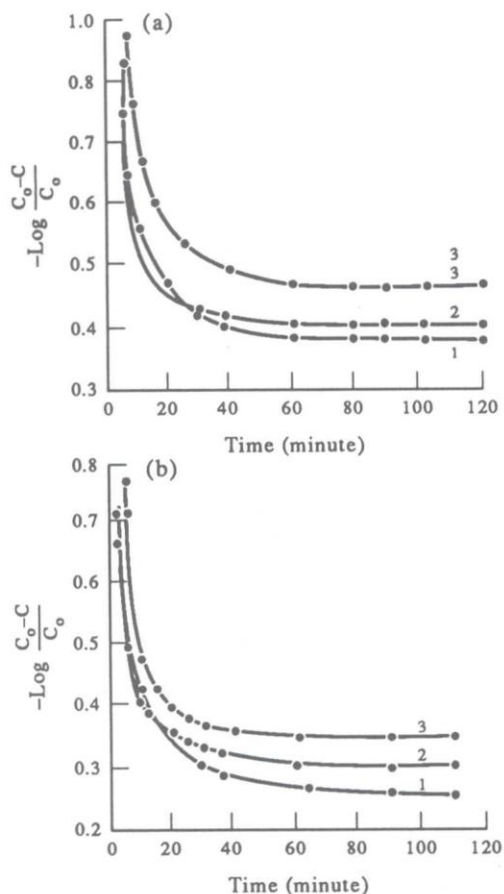


Fig. 1. Effect of shaking time on the sorption profiles of the tested compounds ($60 \mu\text{g cm}^{-3}$) in aqueous solution (100 cm^3) at pH 3 and $20 \pm 0.1^\circ\text{C}$ by unloaded (a) and TOA-loaded polyester foam (b). *o*-Chlorophenol (1), *o*-nitrophenol (2) and *o*-cresol (3).

tative results are given in Fig. 1. A good extraction efficiency and rapid preconcentration of the tested compounds from aqueous media were obtained with the TOA-treated foam (Fig. 1b) as compared to the unloaded polyester foam (Fig. 1a). The average values of the half-life ($t_{1/2}$) of equilibrium sorption calculated from the curves of the effect of shaking time on the extraction percentage of the compounds tested on the unloaded and TOA-loaded foams are in the range 4–5 and 2.5–3 min, respectively. The tri-*n*-octylamine possibly acts as a plasticizer on the polyester foam. The plasticizer has a dual purpose,¹² *i.e.* it acts as an efficient non-volatile solvent as well as a plasticizer for the foam plastic itself. Thus the collection rates of the phenolic compounds with the plasticized TOA-foams are generally better than with the unplasticized ones. This can be attributed to the high mobilities and diffusion rates of the phenolic compounds through the open pores and the

quasi-spherical membrane structure of the plasticized TOA-foam.^{12,19,20} These results are also in good agreement with the data reported by Braun *et al.*²¹ The polyester foam membrane also acts as a true sorbent where the diffusion rates of the chemical species in the membrane structure are considerably higher than those in bulky solids.^{22,23} Moreover, the plasticization of the polyester based polyurethane foam membrane with TOA offer a wider range of modifications than normal (granular) solids,²² *e.g.* Voltalef which is considered one of the best

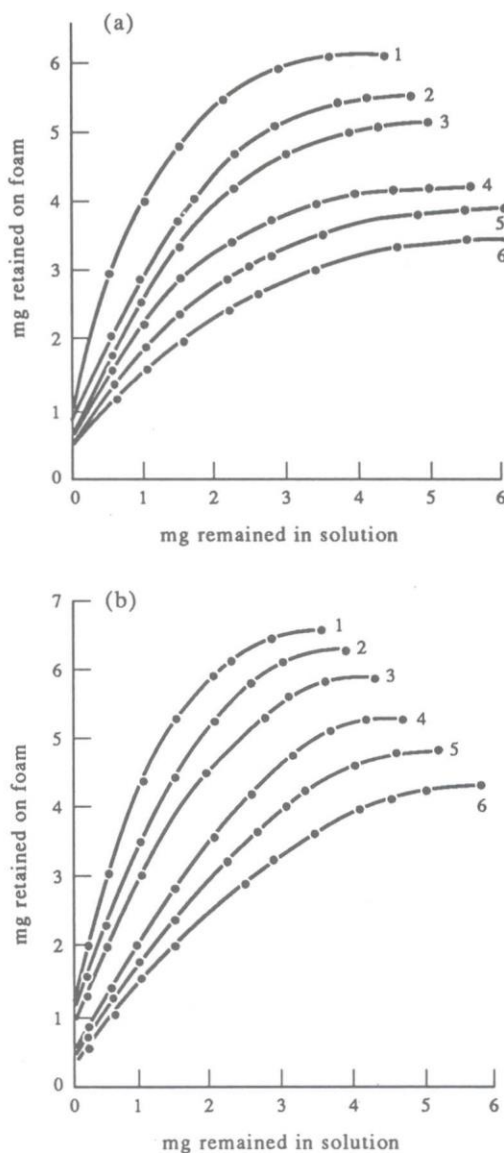


Fig. 2. Extraction isotherm of the tested compounds ($10\text{--}80 \mu\text{g/cm}^3$) by unloaded (a) and TOA-loaded foams (b) at from 100 cm^3 aqueous solution sample at pH 3 and $20 \pm 0.1^\circ\text{C}$ and 1 hr extraction time phenol (1), *m*-cresol (2), *o*-cresol (3), *o*-nitrophenol (4), *o*-chlorophenol (5) and salicylaldehyde (6).

granular supports in extraction chromatography.

Extraction isotherm

The uptake of the investigated compounds from aqueous solution by the unloaded and TOA-loaded polyester foams was found to depend on the concentration. Thus, the extraction isotherms were developed over a wide range of equilibrium concentrations ($10\text{--}80\ \mu\text{g}/\text{cm}^3$) for each compound at 20°C . The pH values of the aqueous solutions in these experiments were adjusted at pH 3 so that the compounds were predominately in undissociated form. The isotherms of the tested compounds exhibited a first order behaviour in the low concentration range and tended to plateau at high bulk solution concentration as shown in Fig. 2. A good linear correlation between the concentration of each phenolic compound extracted on the TOA-foam and in aqueous solution over a relatively wide range of concentrations was observed. It was also found that the extraction profiles of the compound tested by TOA-foam (Fig. 2b) were generally higher than that obtained with the unloaded polyester foam (Fig. 2a). The sorption of the different phenolic compounds by the unloaded and TOA-loaded foams (Fig. 2) increased in order: phenol > *m*-cresol > *o*-cresol > *o*-nitrophenol > *o*-chlorophenol > salicylaldehyde. Similar trends for the sorption profiles of tested compounds were obtained with diethylether and with polyether based polyurethane foams.^{17,18} Therefore, solvent-extraction is the most probable mechanism for the

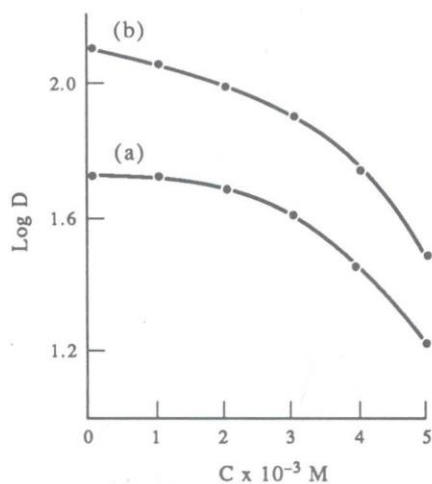


Fig. 3. Effect of sec-butylamine concentration ($\leq 5 \times 10^{-4} M$) on the distribution coefficient of *o*-nitrophenol (a) and *o*-cresol (b) by polyester foam from $100\ \text{cm}^3$ aqueous sample ($60\ \mu\text{g}/\text{cm}^3$) at $2.5 \leq \text{pH} < 3$.

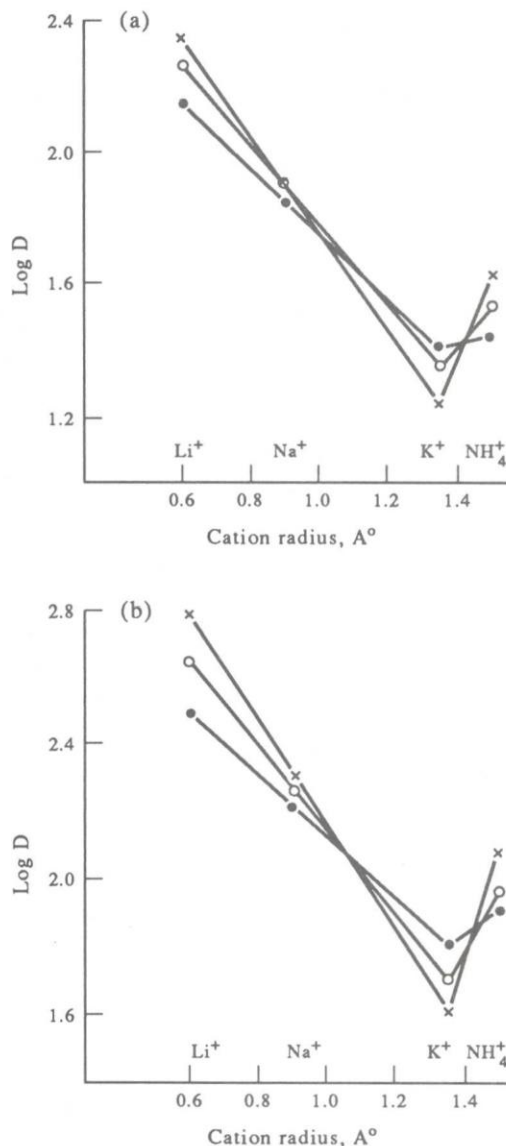


Fig. 4. Effect of the size and concentrations ($0.1\text{--}0.15 M$) of various univalent (Li^+ , Na^+ , K^+ , NH_4^+) cations on the sorption profiles of *o*-nitrophenol (a) and *o*-cresol (b) by loaded polyester foam. Salts concentrations are $0.05 M$ (●); $0.1 M$ (○) and $0.15 M$ (x). Other conditions as in Fig. 1 and 1 hr extraction time.

extraction of these compounds by the polyester foam from aqueous solution.

Hydrogen bonding between the hydroxyl group on the organic compound and polyester foam can account for the sorption profile sequence of the tested species. When the hydrogen bonding is prevented by placing a strongly intramolecular hydrogen bonding adjacent to hydroxyl as in the case of *o*-nitrophenol, *o*-chlorophenol and salicylaldehyde, the extraction profiles by the polyester foam decreased. The fact that intramolecular hydrogen bonding

Table 2. Thermodynamic data for extraction of the tested phenolic compounds by unloaded (a) and ToA-loaded polyester foam (b)*

Compound	$-\Delta H^\circ$ (kJ/mol)		$-\Delta S^\circ$ (J . mol ⁻¹ . deg ⁻¹)	
	a	b	a	b
Phenol	27 ± 2	26 ± 3	30.0 ± 1.5	35.0 ± 2
<i>m</i> -Cresol	25 ± 2.5	26 ± 2	28 ± 3	33 ± 3
<i>o</i> -Cresol	22 ± 3	24 ± 2	25 ± 3	30 ± 2
<i>o</i> -Nitrophenol	21.5 ± 2.5	23 ± 3	24.0 ± 2	29.3 ± 3
<i>o</i> -Chlorophenol	21 ± 2	22 ± 2	23.0 ± 3	27 ± 3
Salicylaldehyde	20 ± 3	21 ± 3	20 ± 2	26 ± 2

*Conditions: Extraction from aqueous solution (100 cm³) at pH ≤ 3, all values ± SD calculated from slope, temperature range 25–65°C.

takes place in *o*-nitrophenol, *o*-chlorophenol and salicylaldehyde may prevent the hydrogen bonding between it and the foam. Overall, the results (Fig. 2) obtained are consistent with solvent-extraction mechanism as previously reported by El-Shahawi *et al.*¹⁷ and Schumack *et al.*^{25–27} and does not agree with the general understanding that the larger the molecular weight of the absorbate, the larger the amount extracted when the substances concerned are similar in nature.²⁸ However, it is worth of note that the p*K*_a (Table 1)²⁴ and the molecular weight (MW) of *o*-chlorophenol, *o*-nitrophenol and salicylaldehyde are also participating factors in the extraction by the polyester foam where the extraction percentage of *o*-nitrophenol (p*K*_a 7.7, MW 121) > *o*-chlorophenol (p*K*_a 8.5, MW 112.5) > salicylaldehyde (p*K*_a 10, MW 106).

The extraction of *o*-nitrophenol and *o*-cresol (60 μg/cm³) from aqueous solution (2.5 ≤ pH ≤ 3) by polyester foam was carried out in the presence of different concentrations (≤ 5 × 10⁻⁴ M) of *sec*-butylamine with a shaking time of 1 hr. The compounds tested are extractable and the results are summarized in Fig. 3. These results suggest that no ion-pair formation occurs between the tested phenolic compound anions and the protonated amines. As the concentration of the amine increased, the extraction percentage and the distribution ratio of the compounds tested decreased. These results also confirmed that the tested compounds are extracted by a simple solvent-extraction mechanism in which only the neutral molecular species is extractable and the cation chelation mechanism is completely excluded.^{11,12} The protonated *sec*-butylamine cations are too hydrophilic to affect the extraction of the phenolic compound anions from the aqueous solution by the polyester foam.

According to the cation chelation mechanism, the presence of the K⁺ should facilitate the

extraction of the phenoxy anions by the foam more than the other alkali metal ions (Li⁺, Na⁺ or NH₄⁺) because of the better fit of this ion into the central cavity of the oxygen-rich helix in the polyurethane foam. Thus, the influence of various concentrations of alkali metal chlorides (≤ 0.15 M) on the sorption profiles of *o*-nitrophenol and *o*-cresol (60 μg/cm³) was studied at pH ≈ 3. The results obtained are summarized in Fig. 4. Significant increase in the sorption profiles of the compound tested by the TOA-foam was observed in the presence of LiCl, NaCl, KCl, and NH₄Cl and the following order of extraction: K⁺ < NH₄⁺ < Na⁺ < Li⁺, was achieved. The distribution ratio of the tested compounds also increased with the amount

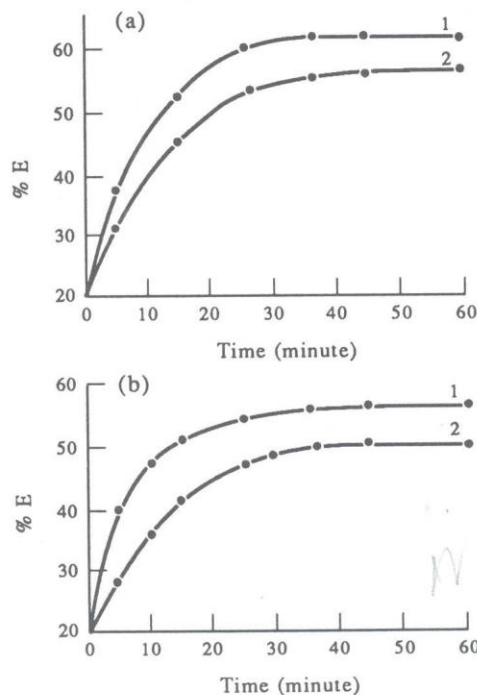


Fig. 5. Effect of extraction media on the sorption profile of phenol (a) and *o*-nitrophenol (b) by TOA-loaded foam at pH 2.5 and 1 hr extraction time. Ethanol 0% (1) and 5% (2). Other conditions as in Fig. 1.

of salt added from $\log D = 1.23$ and 2.14 to 1.6 and 2.35 for NH_4^+ and Li^+ ions at 0.1 and $0.15M$ (Fig. 4), respectively. This fact is characteristic of a solvent-extraction mechanism with the salts acting as salting-out and excluded the cation chelation mechanism in the extraction systems involved.^{22,23} The added salts increased the sorption profiles of the tested phenols into the polyester foams by reducing the number of water molecules available to solvate the organic compound which would, therefore, be forced out of the solvent phase into the foam since some amount of 'free' water molecules are preferentially used to solvate the ions added. The charge density for the ions studied is in the order $\text{K}^+ < \text{NH}_4^+ < \text{Na}^+ < \text{Li}^+$. Hence, the influence of the salts can be explained by the salting out effect on a solvent-extraction mechanism.

To confirm the salting out of the salts on the sorption profiles of the tested species by the polyester foam, an extraction of 100 cm^3 of *o*-nitrophenol ($60 \mu\text{g}/\text{cm}^3$) solution containing $0.1M$ hydrochloric acid was investigated after 30 min shaking time. The added salts of alkali metal chlorides ($\leq 0.15M$) to the extraction media enhanced the distribution ratio of *o*-nitrophenol more in a solution of pH 1 ($\log D = 2.7$) than at higher pH ≈ 4 ($\log D = 1.1$). This is possibly attributed to the increased amount of neutral *o*-nitrophenol present at pH 1 as compared to that at pH 4. The sorption profile of *o*-nitrophenol by unloaded polyester foam at pH 1 in the presence of the above alkali metal chlorides also increased in the same order: $\text{K}^+ < \text{NH}_4^+ < \text{Na}^+ < \text{Li}^+$. These results confirm that the phenolic compounds tested are highly extractable in the neutral form and the solvent-extraction mechanism is the most probable mechanism.

The effect of temperature on the extraction efficiency of the unloaded and TOA-loaded foams determined at 35 , 45 and 55°C . Similar trends to that obtained at 20°C were observed

and the percentage sorption profile increases slightly with increasing temperature. Discrepancies were observed in the case of *o*-nitrophenol where the extraction is significantly increased as compared to the other phenols. The lower $\text{p}K_a$ and the higher molecular weight of *o*-nitrophenol as compared to the other phenols could account for this behaviour.²⁸ Assuming no chelation or precipitation and that the tested compounds exist as neutral species at $\text{pH} \leq 3$ then the equilibrium constant K for the equation

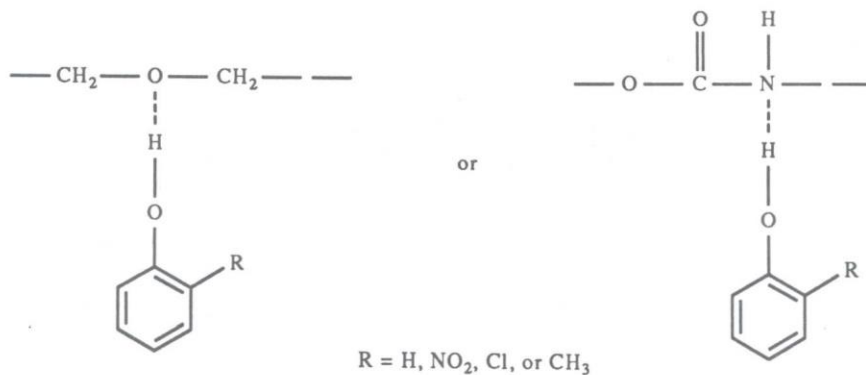


is equivalent to distribution ratio, D . Employing the equation:

$$\ln K = -\Delta H^\circ/RT + \Delta S^\circ/R,$$

the values of the standard entropy change, ΔS° and standard enthalpy change, ΔH° are obtained (Table 2). The ΔS° for the compounds were found in the range -20 to $-30 \pm 3 \text{ J} \cdot \text{mol}^{-1} \cdot \text{deg}^{-1}$ for extraction into the unloaded foams and -25 to $-35 \pm 2 \text{ J} \cdot \text{mol}^{-1} \cdot \text{deg}^{-1}$ for sorption into TOA-foams, respectively. The decrease in entropy change in the use of TOA-foam is believed to be due to hydrogen bonding reducing the degree of freedom of movement of the organic compound in the polymer as previously reported.²⁵⁻²⁷ These results are consistent with solvent-extraction mechanism. The bonding of the organic compound with the foam was estimated as about 10 kJ/mol^{-1} which is lower than the intramolecular H-bonding in *o*-nitrophenol and salicylaldehyde (30 kJ/mol).²⁵⁻²⁷

Raising the temperature may prevent the formation of intramolecular hydrogen bonding in *o*-nitrophenol and facilitate the formation of intermolecular H-bonding between *o*-nitrophenol and the polyurethane foam via nitrogen and/or oxygen as shown in the structures.



The influence of the pH of the aqueous phase on the extraction of the compound tested ($60 \mu\text{g}/\text{cm}^3$) by the TOA-loaded foams was examined over a wide range of pH (3–11) by measuring the absorbance of the aqueous phase after extraction. The percentage removal of the compounds increased markedly with decreasing pH and reaches a plateau at $\text{pH} \approx 3$ at which the compounds exist in the neutral form. Thus the extraction mechanism involves neutral species and there is no evidence for a mechanism requiring ionic species. This observation is also consistent with a solvent-extraction mechanism and is in good agreement with the data previously reported.^{25–27} The pH values were adjusted with HCl and/or NaOH.

The influence of the ethanol (0–5%) on the extraction efficiency of the compounds tested was examined for two selected compounds, namely phenol and *o*-nitrophenol by the loaded foams at $\text{pH} \sim 2.5$. The sorption profiles of the compounds tested are given in Fig. 5. The extraction of the compounds by the foams decreased by the addition of ethanol to the aqueous solution. This is probably due to formation of lipophilic association in the aqueous solution.²⁹ Water is a solvent with a high dielectric constant. Thus ions in aqueous solution are well solvated and so it is difficult for ions to form ion-pairs in aqueous solution. These data are also consistent with the fact that with a compound of low dielectric constant and another which has a high dielectric constant, the degree of extraction should increase with increase in the polarity of the polar phase. Thus solvent-extraction mechanism is the most probable mechanism and the nature of media has, therefore, a marked effect on the sorption characteristics of the compounds.

Column experiments

The extraction behaviour of the tested compounds from aqueous solution with TOA-loaded polyurethane foam suggests the possible application of the foam in column extraction mode for quantitative collection and recovery of the tested compounds from aqueous media at $2 \leq \text{pH} \leq 3$. Distilled or tap water samples ($0.1\text{--}3 \text{ dm}^3$) containing 0.1 mg of each compound were percolated separately through the foam columns at a flow-rate of $5\text{--}10 \text{ cm}^3/\text{min}$. More or less complete retention of the tested compounds was achieved by the foam column (Table 1). The compounds were then recovered from the foam up to 98.5% with acetone in a

Soxhlet apparatus. The percentage recovery of the tested compounds from the aqueous media by the proposed foam column method are also summarized in Table 1. The dependence of retention of the tested compounds on flow-rate and sample volume was examined by percolating 100 cm^3 of *o*-nitrophenol (0.1 mg) through the column at various flow-rates ($1\text{--}15 \text{ cm}^3/\text{min}$) and sample volumes ($0.1\text{--}3 \text{ dm}^3$). Complete retention of the compound was obtained up to $10 \text{ cm}^3/\text{min}$ flow-rate from 3 dm^3 aqueous solution and the extraction efficiency decreased significantly up to 70% at $15 \text{ cm}^3/\text{min}$ from 3 dm^3 aqueous volume solution. To determine the TOA foam column performance by the chromatogram method the quantitative retention and elution of *o*-nitrophenol (0.05 mg) with 100 cm^3 sodium hydroxide ($0.05M$) through the foam column at $3\text{--}5 \text{ cm}^3/\text{min}$ flow-rate was carried out. The height equivalent to a theoretical plate (HETP) was obtained from the elution curves using the equation:³⁰

$$N = \left(\frac{8V_{\text{max}}^2}{W^2} \right) = \left(\frac{L}{\text{HETP}} \right),$$

where N = number of theoretical plates, V_{max} = volume of eluate at peak maximum, W = width of the peak at $\frac{1}{2}$ the maximum solute concentration and L = length of the foam bed. The HETP values were found equal 1.8 ± 0.1 and $2.05 \pm 0.2 \text{ mm}$ at flow rates of $2\text{--}5$ and $10 \text{ cm}^3/\text{min}$, respectively. The HETP value was also calculated from the break through capacity curve at $10 \text{ cm}^3/\text{min}$ using the equation.¹²

$$N = \left(\frac{V \bar{V}}{(V - \bar{V})^2} \right) = \frac{L}{\text{HETP}},$$

where V is the volume of effluent at the center of the S-shaped break through curve where the concentration is one half the initial concentration, and \bar{V} is the volume at which the effluent has a concentration of 0.1578 of the initial concentration. The value of HETP obtained by this method was $1.9 \pm 0.2 \text{ mm}$, confirming the values obtained from the elution curves.

The method has been successfully employed in the separation of *o*-nitrophenol from salicylaldehyde in aqueous media at $\text{pH} \approx 2$. An aqueous solution mixture (100 cm^3) containing 0.1 mg of each phenol was passed through a column of TOA-loaded polyester foam (3 g) at $5 \text{ cm}^3/\text{min}$ flow-rate. The phenols retained successfully on the column and *o*-nitrophenol was then sequentially displaced by passing through

the column 100 cm³ solution of NaOH (0.01M) at 2 cm³/min flow-rate. Salicylaldehyde was finally recovered from the column with 50 cm³ of NaOH (0.05M) at 3–5 cm³/min flow-rate. The phenols obtained by this stepwise elution were determined spectrophotometrically in successive 5 cm³ fractions of eluate after acidification with 0.01M HCl against blank.

CONCLUSIONS

Polyester foam in batch and column techniques can be applied to trap trace amounts of phenolic compounds from water, and the retained phenols can be separated with an appropriate eluent, provided that there is a sufficiently large difference in the pK_a of the compounds. Based on the distribution coefficient of the phenols between the polyester foam and the eluent, it is possible to predict the course of the separation and the optimum conditions. Thus separation of some of the tested phenols from each other are possible from different sample volumes (0.1–3 dm³) of the aqueous solution at pH ≤ 3. The study of the tested compounds shows that the phenols are extracted in their neutral form by a simple solvent-extraction mechanism. This conclusion is supported by the short time required for extraction equilibrium to be achieved, the evidence of the salting-out phenomenon and the pH effect. Although a simple-solvent extraction mechanism is involved, phenol, *o*-cresol and *m*-cresol are more extractable by polyester foam than *o*-chlorophenol, *o*-nitrophenol and salicylaldehyde. This result can be attributed to the stronger hydrogen bonding between the former compounds with polyester foam, since all these compounds contain a hydroxyl group which is capable of forming hydrogen bonds with the foam. The possible intramolecular hydrogen bonding in the latter compounds prevents the intermolecular hydrogen bonding with the foam resulting in a decrease in its sorption profiles by the foam.

REFERENCES

- J. Trocewicz, *19th Int. Symp. Chromatogr.*, Aix-en-provence, France, September, 1992.
- U.S. Environmental Protection Agency, *Methods of Chemical Analysis of Water and Wastes*. Cincinnati, Ohio, 45268, 1983.
- C. A. Edwards, *Persistent Pesticides in the Environment*, 2nd Edn. CRC Press, Boca Raton, FL, 1973.
- L. Campanella, T. Beone, M. P. Sammartino and M. Tomassetti, *Analyst*, 1973, **118**, 979.
- C. A. Edwards, *Environmental Pollution by Pesticides*, p. 409. Plenum Press, 1973.
- P. A. Pfeifer, G. K. Bonn and O. Bobleter, *Fresenius Z. Anal. Chem.*, 1983, **315**, 205.
- H. Oda, M. Kishida and C. Yokokawa, *Carbon*, 1981, **19**, 243.
- H. Oda and C. Yokokawa, *Carbon*, 1983, **21**, 485.
- J. F. Uthe, J. Reinke and H. D. Gesser, *Environ. Lett.*, 1972, **3**, 117 (and Refs therein).
- A. H. Romano and R. S. Safferman, *J. Am. Water Works Assoc.*, 1963, **55**, 169.
- P. Fong and A. Chow, *Talanta*, 1992, **39**, 497, 825.
- T. Braun, J. D. Navratil and A. B. Farag, *Polyurethane Foam Sorbents in Separation Science*. CRC Press, Boca Raton, FL, 1985.
- M. A. Ahsan, B. C. Varma, M. H. George and J. A. Barrie, *Polym. Commun.*, 1991, **32**, 509.
- G. J. Moody and J. D. R. Thomas, *Chromatographic Separation with Foamed Plastics and Rubbers*. Marcel Dekker, N.Y. 1982.
- A. B. Farag and M. S. El-Shahawi, *J. Chromatogr.*, 1991, **552**, 371.
- A. B. Farag, A. M. El-Wakil, M. S. El-Shahawi and M. Mashaly, *Anal. Sci.*, 1989, **5**, 415.
- M. S. El-Shahawi, A. B. Farag and M. R. Mostafa, *Sepr Sci*, 1994, **29**, 289.
- A. B. Farag, A. M. El-Wakil and M. S. El-Shahawi, *Fresenius Z. Anal. Chem.*, 1986, **324**, 59.
- T. Braun and A. B. Farag, *Anal. Chim. Acta.*, 1974, **73**, 301.
- I. I. Stewart and A. Chow, *Talanta*, 1993, **40**, 1345.
- T. Braun, *Z. Anal. Chem.*, 1989, **333**, 785.
- T. Braun and A. B. Farag, *Anal. Chim. Acta*, 1978, **99**, 1 (and Refs therein).
- S. Palagyi and T. Braun, *J. Rational. Nucl. Chem.*, 1992, **163**, 69.
- S. Palagyi and T. Braun, *Analyst*, 1992, **117**, 1537.
- L. Schumack and A. Chow, *Talanta*, 1987, **34**, 957.
- T. Schafer and T. A. Wildman, *Can. J. Chem.*, 1979, **57**, 450.
- T. Schafer, R. Sebastian, R. Laatikainen and S. R. Salman, *Can. J. Chem.*, 1983, **62**, 326.
- A. W. Adamson, *Physical Chemistry of Surface*, 2nd Edn. Academic Press, New York, 1967.
- R. C. Weast, *Handbook of Chemistry and Physics*, 54th Edn, CRC Press, 1973.
- T. Hayashita and M. Takagi, *Talanta*, 1985, **32**, 399.
- E. Gluenkauf, *Trans. Faraday., Soc.*, 1955, **15**, 34.

66

TECHNICAL NOTE

**Preconcentration and Separation of Phenols
from Water by Polyurethane Foams**

M. S. EL-SHAHAWI*

CHEMISTRY DEPARTMENT
FACULTY OF SCIENCE
U.A.E. UNIVERSITY
P.O. BOX 17551, AL-AIN, UNITED ARAB EMIRATES

A. B. FARAG

CHEMISTRY DEPARTMENT
QATAR UNIVERSITY
DOHA, QATAR

M. R. MOSTAFA

CHEMISTRY DEPARTMENT
FACULTY OF SCIENCE
DAMIATTA, EGYPT

ABSTRACT

The application of untreated and polyurethane foams treated with tributylphosphate (TBP) in the preconcentration of some phenols from water via static and flow experiments was carried out. Batch experiments with the TBP-loaded foams showed a good affinity toward extraction of the tested compounds as compared to the untreated foams. The use of the unloaded and TBP loaded foams was also employed in column modes for the preconcentration of the phenols used. The effect of extraction media, phenol concentration, time of shaking, temperature, sample volume, ionic strength, eluting solvent, and flow rate on the retention efficiency of the compounds by the foam were investigated. The extraction efficiency and the recovery of the compounds from the foam material by the column were obtained up to 100%. Sorption of the compounds by the foam was brought by a solvent extraction mechanism. The pK_a and the molecular weight of the absorbates play an important role in the sorption process. The height equivalent to

* To whom correspondence should be addressed.

theoretical plates (HETP) for the foam column were obtained from the Glueckauf equation and the breakthrough capacity curve, and were found to equal 1.8–2.05 mm at flow rates up to $10 \text{ cm}^3 \cdot \text{min}^{-1}$. Attempts were also made to separate some of the tested phenols by dynamic techniques.

Key Words. Polyurethane foam; Phenols; Preconcentration; Recovery; Tributylphosphate

INTRODUCTION

Phenol and phenol-like compounds represent a class of man-made environmental pollutants which also occur naturally in the environment (1). The presence of these compounds in the wastewater of chemical factories often represents a risk to the environment (2, 3). The main sources of these species are combustion processes, chemical factories, and industrial and sewage effluents (3, 4). The occurrence of such compounds in the aquatic environment has been known to cause severe health problems to animals, birds, and humans (5, 6). The removal or reduction of these pollutants to an acceptable concentration by extraction with organic solvents, steam distillation, oxidation reaction, adsorption on carbon, reversed liquid–liquid partition filter chromatography, or the use of cellulose triacetate membrane filters has been investigated (7–11). Such preconcentration techniques are often slow or cumbersome, limited by a relatively low flow rate ($0.65 \text{ cm}^3 \cdot \text{min}^{-1}$), and too expensive for routine work where many large volume samples are concentrated on-site prior to quantitative analysis (10).

Recently, several authors have proposed open cell polyurethane foam as an inexpensive solid extractor and effective sorbent for the removal of water pollutants (12–18). The solid foam concentrates various species in solution by the phase distribution mechanism rather than adsorption (12, 13). The membrane-like structure of the foams together with the efficient sorption properties offer many advantages over other solid collectors as they allow a higher concentrating ability compared with other solid materials which depend only on adsorption (19, 20).

The present work deals with the use of polyurethane foam for the extraction of some phenols from high volume samples of aqueous media in an attempt to establish the conditions where good extraction and recoveries of these compounds could be obtained.

EXPERIMENTAL

Reagents and Materials

All chemicals used were of analytical reagent grade. Polyurethane foam, an open polyether type (bulk density $30 \text{ kg}\cdot\text{m}^{-3}$), was supplied by K.g. Schaum (Stoffwerk, Kremsmunster, Austria). The foam, loaded with tributylphosphate (TBP), was prepared by mixing the dried foam cubes with 2% TBP in benzene ($10 \text{ cm}^3\cdot\text{g}^{-1}$ dry foam) with stirring for 15 minutes. The reagent foam was then dried (12). The compounds tested were phenol, *o*-chlorophenol, *o*-nitrophenol, *m*-cresol, *p*-cresol, resorcinol, and salicylaldehyde. A stock solution of each compound containing $100 \mu\text{g}\cdot\text{cm}^{-3}$ was prepared in a 100-cm^3 measuring flask by dissolving the exact weight of the compound in distilled and/or tap water. A series of standard solutions of these compounds was prepared by diluting their stock solutions with water. All solutions were stored in polyethylene bottles.

Apparatus

A double-beam spectrophotometer, Varian DMS 634 with a 1-cm quartz cell, was used for the absorbance measurements. An Orion pH meter and glass columns, $12 \text{ cm} \times 10 \text{ mm}$ i.d., were also used.

GENERAL PROCEDURES

Batch Experiments

To investigate the effect of shaking time on the uptake of the compounds on polyurethane foam, the foam cubes (0.3 g) were equilibrated with a 100-cm^3 solution of each compound ($60 \mu\text{g}\cdot\text{cm}^{-3}$) in separate polyethylene bottles and shaken for various time intervals up to 1 hour. The foam cubes were then separated by decantation, and the amount of the compound remaining in solution was measured spectrophotometrically at the wavelength of maximum absorption. The amount of compound retained on the foam was calculated by difference. Following these procedures, the effects of extraction media, phenol concentration ($10\text{--}80 \mu\text{g}\cdot\text{cm}^{-3}$), ionic strength, pH, and temperature on the extraction efficiency were determined.

Flow Experiments

In the flow of experiments, 1 g of dry foam was packed into the column using the vacuum method of foam packing (12). Tap or distilled water

(1–3 dm³) samples containing 0.2 mg of each compound were passed through the foam column at 10–15 cm³·min⁻¹. After squeezing water from the foam material, the compound was recovered from the foam with 100 cm³ ethanol in a Soxhlet extractor. The sample was determined by measuring the absorbance of the solution against a reagent blank. Following these procedures, the effect of eluting solvent and flow rate on the extraction were also determined.

RESULTS AND DISCUSSION

The introduction of porous polyurethane foam as a cellular solid extractant for high volume water samples has been proven advantageous due to its easy handling and clean-up and its high ability to sorb many different organic and inorganic species (12, 13). The polyurethane foam method allows the isolation of the analyte from the matrix and yields an appropriate enrichment factor. The excellent hydrodynamic properties of the foam column allow the application of quite high flow rates without the need to use vacuum, while the rapid attainment of sorption equilibrium in the thin membranes forming the foam material reduces the time required for analysis.

Preliminary experiments using unloaded and TBP-loaded polyurethane foam have shown that the extraction of the investigated compounds is rapid and equilibrium is reached in less than 1 hour, followed by a plateau. Hence, a minimum of 1 hour was used in obtaining the extraction isotherms. The results obtained are summarized in Fig. 1. A good extraction efficiency was obtained with the TBP-treated foam (Fig. 1a) as compared to the unloaded foam (Fig. 1b).

Extraction Isotherm

The uptake of the investigated compounds from aqueous solution by the unloaded and TBP-loaded foams was found to depend on its concentration. Thus, in separate experiments the extraction isotherms were developed over a wide range of equilibrium concentrations (10–80 µg·cm³) for each compound. The pH values of the aqueous solutions in these experiments were selected (>5, Ref. 6) so that the compounds are predominantly in undissociated forms. The isotherms of the tested compounds exhibited a first-order behavior in the low concentration range and tended to plateau at high bulk solution concentrations, as shown in Fig. 2. The sorption of the different phenolic compounds by the unloaded foams (Fig. 2a) increases in the order *o*-nitrophenol < *o*-chlorophenol < phenol < *m*-cresol < *p*-cresol < resorcinol < salicylaldehyde. Similar trends were

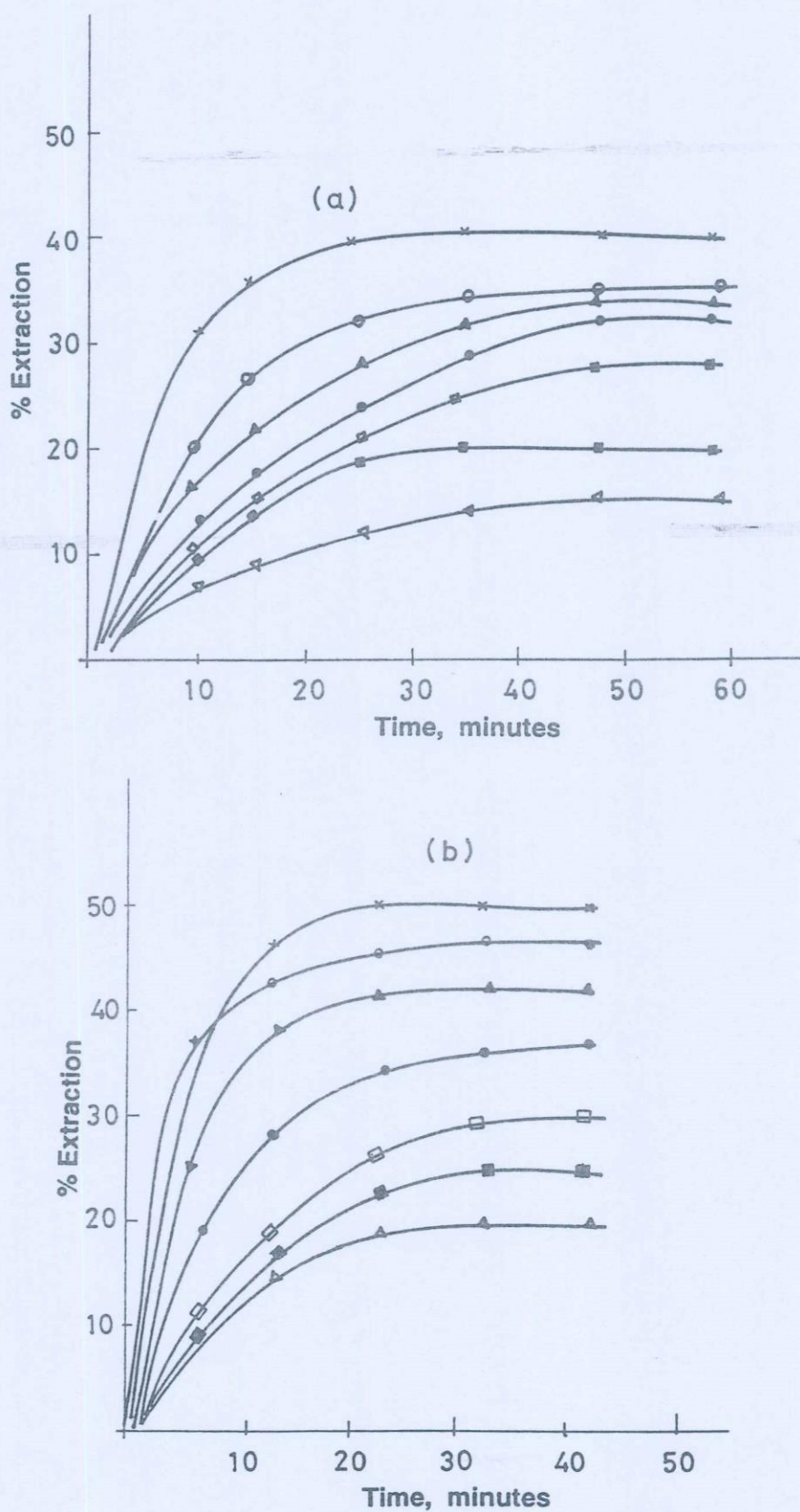


FIG. 1 Effect of shaking time on the extraction of the compound tested with unloaded (a) and TBP-loaded foams (b). (x) Resorcinol, (O) salicylaldehyde, (▲) *p*-cresol, (●) *m*-cresol, (□) phenol; (■) *o*-chlorophenol, and (Δ) *o*-nitrophenol.

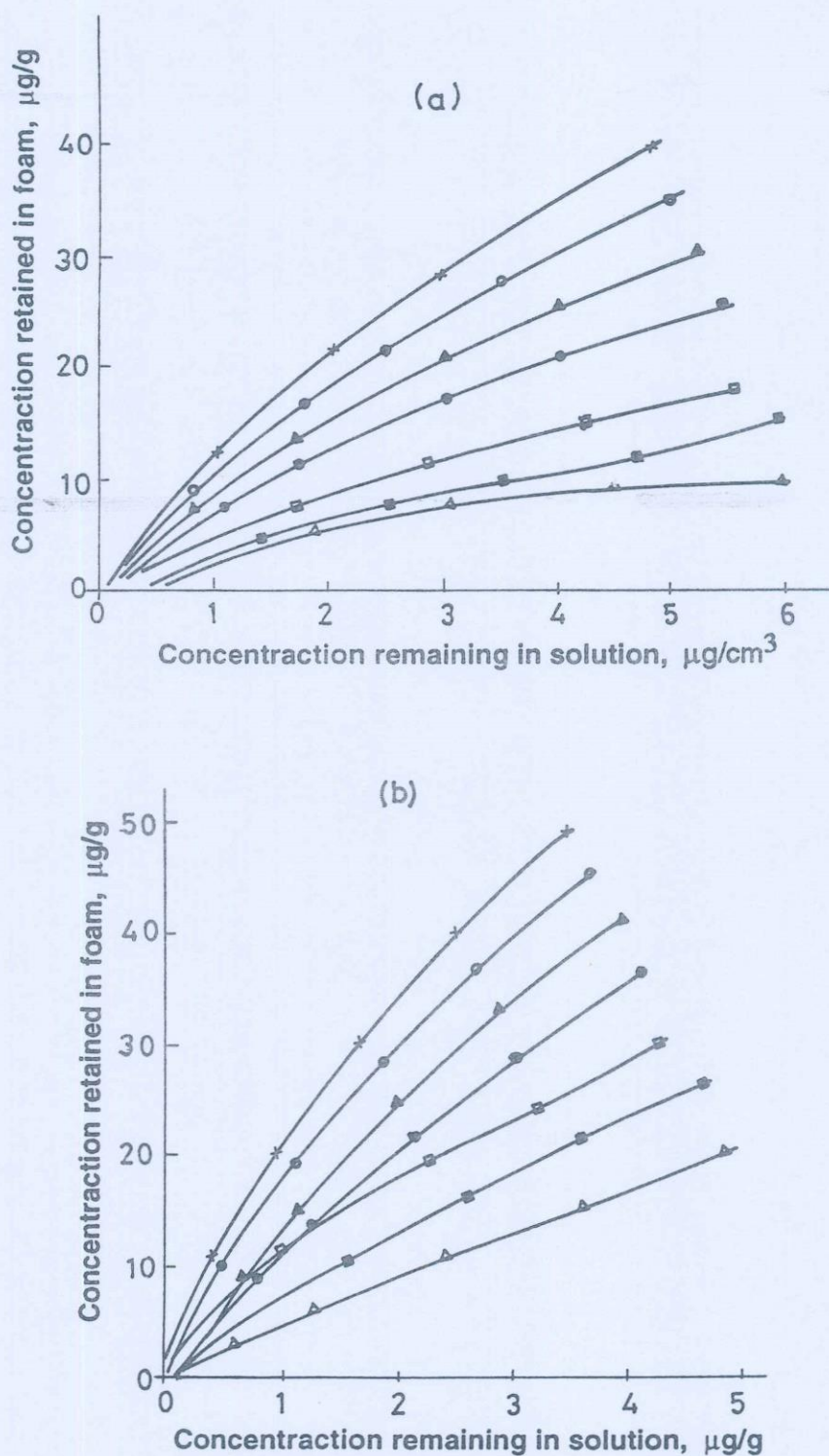


FIG. 2 Extraction isotherms of the compound tested with unloaded (a) and TBP-loaded foams (b). (x) Resorcinol, (o) salicylaldehyde, (▲) *p*-cresol, (●) *m*-cresol, (□) phenol, (■) *o*-chlorophenol, and (△) *o*-nitrophenol.

obtained with TBP-loaded foams (Fig. 2b). Therefore, a solvent extraction mechanism is the most probable for the extraction of these compounds by the untreated foams, and an anion-exchange mechanism is completely excluded. This was confirmed by investigating the extraction of these compounds with ether. The sequence of the extraction efficiency was found to be similar to that obtained by unloaded and TBP-loaded foams. It is worth noting that the extraction percentage depends on the pK_a (Table 1) of the absorbate. The molecular weight of the absorbate and hydrogen bonding are also participating factors in the extraction. However, these results do not agree with the general understanding that the larger the molecular weight of the absorbate, the larger the amount extracted when the substances concerned are similar in nature (21).

The effect of temperature on the extraction efficiency of the unloaded and TBP-loaded foams were determined at 35, 45, and 55°C. Similar trends of TBP-loaded and unloaded foams were obtained, and the percentage sorption increased slightly with increasing temperature. Discrepancies were observed in the case of *o*-nitrophenol, which has a higher acidity and molecular weight, where the percentage extraction is highly increased as compared to the other phenols.

The influence of the pH of the aqueous phase on the extraction of each of the compounds tested ($60 \mu\text{g}\cdot\text{cm}^3$) by the unloaded foams was examined over the pH range 3–11 by measuring the absorbance of the aqueous phase after extraction. The sorption profiles of the investigated compounds are given in Fig. 3, from which it can be seen that the percentage removal of

TABLE 1
Extraction and Recovery of the Compound Tested (0.2 mg) from 3 L
Aqueous Solutions by the Proposed Unloaded Foam Column at 8–10
 $\text{cm}^3\cdot\text{min}^{-1a}$

Compound	pK_a	% Recovery ^b		Wavelength
		a	b	
Phenol	9.9	100	102.1	265
Resorcinol	9.8	98	95	276
<i>o</i> -Chlorophenol	8.5	97	99	274
<i>o</i> -Nitrophenol	7.17	99	93	346
<i>m</i> -Cresol	10.1	96	98	272
<i>p</i> -Cresol	10.2	98	99	280
Salicylaldehyde	10	99	102.1	257

^a Average of three data from distilled water (a) and from Nile river water (b).

^b Poor recoveries were obtained with ethanol.

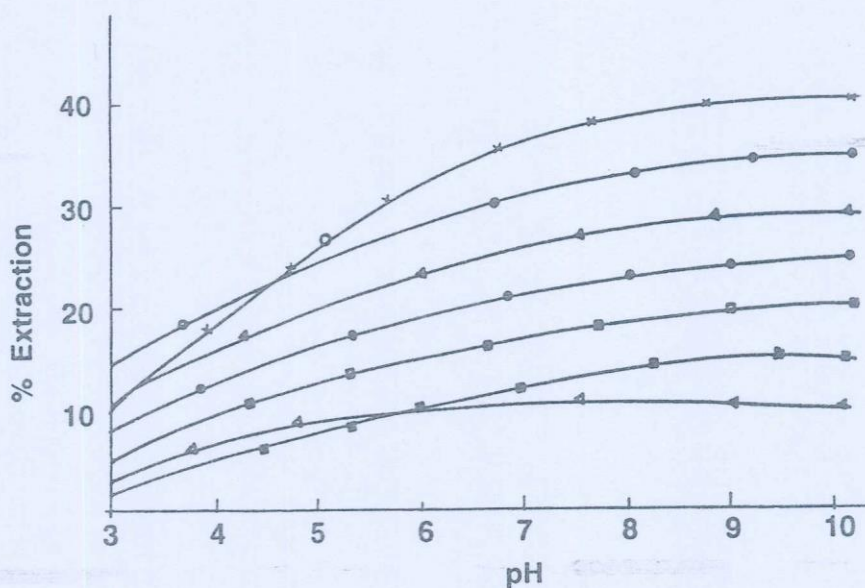


FIG. 3 Effect of pH on the extraction of the compound tested with unloaded foams. (×) Resorcinol, (○) salicylaldehyde, (▲) *p*-cresol, (●) *m*-cresol, (□) phenol, (■) *o*-chlorophenol, and (△) *o*-nitrophenol.

the compounds increases markedly with increasing pH and reaches a plateau at $\text{pH} \approx 10$. The pH values were adjusted with HCl or NaOH. The addition of sodium chloride (0.01–0.1 M) did not increase the amount of compound extracted in any system.

The influence of ethanol (0–10%) on the extraction efficiency of the compounds tested was examined with two selected compounds, phenol and resorcinol, by the unloaded foams. The sorption profiles of the compounds tested are given in Fig. 4. It has been found that extraction of the compounds by the foams is generally decreased by the addition of ethanol to the aqueous phenolic compound solution. This is probably due to formation of a lipophilic association in the aqueous solution (22). These data are in agreement with the suggestion of Kirkwood (19) that the smaller the dielectric constant, the larger the amount extracted. Thus, the nature of the media has a marked effect on sorption characteristics.

Dynamic Experiments

The results obtained for the extraction properties of the compounds tested in aqueous solution with unloaded polyurethane foam suggest the possible application of polyurethane foam in the column extraction mode for the quantitative collection and recovery of these compounds from aqueous media. Distilled or tap water samples (0.1–3 dm³) containing 0.3 mg of each compound were percolated through separate foam columns at a flow rate of 5–10 cm³·min⁻¹. More or less complete retention of the compounds tested was achieved in the foam column. After squeezing

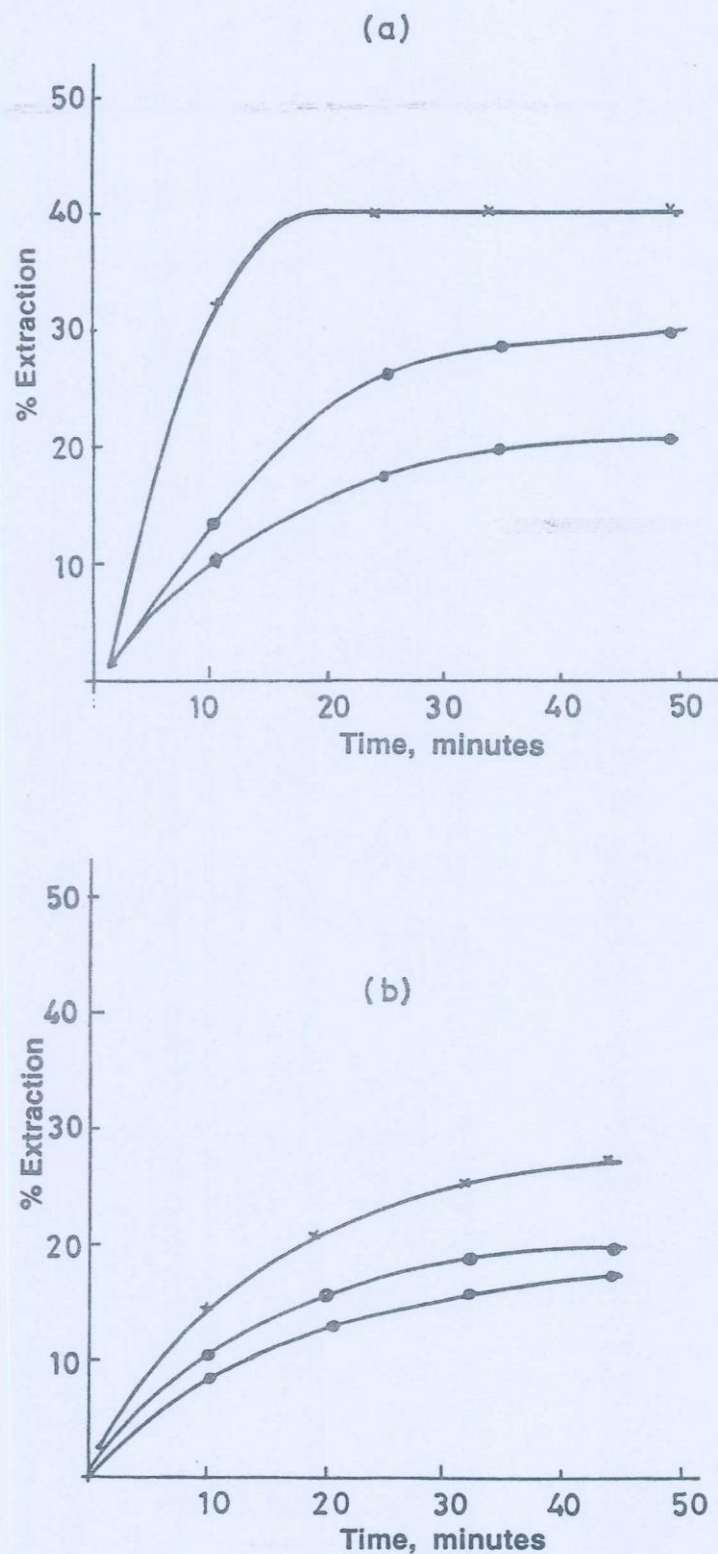


FIG. 4 Effect of ethanol percentage on the extraction of resorcinol (a) and phenol (b):
(\times) 0%, (\circ) 5%, (\bullet) 10% ethanol.

water from the foam column, the compounds were then recovered from the foam column with 100 cm³ acetone in a Soxhlet extractor and determined spectrophotometrically at the maximum absorption wavelength for each species after being concentrated to 25 cm³. The percentage recoveries of the tested compounds from the aqueous media using the proposed foam column are summarized in Table 1. The dependence of retention of the compounds tested on the flow rate and volume of sample was examined by percolating resorcinol (0.2 mg) through the column at various flow rates and sample volumes. Complete retention of the compound was obtained up to 10 cm³·min⁻¹ and 3 dm³ aqueous solution. The extraction efficiency decreased significantly to 70% at 15 cm³·min⁻¹. The quantitative retention and elution of resorcinol (0.050 mg) were carried out, and the height equivalent to a theoretical plate (HETP) was obtained from the elution curves by using the equation (23):

$$N = \left(\frac{8V_{\max}^2}{w^2} \right) = \left(\frac{L}{\text{HETP}} \right)$$

where N is the number of plates, V_{\max} is the volume of eluate at peak maximum, w is the width of the peak at $1/e$ (the maximum solute concentration), and L is the length of the foam bed. The HETP values were 1.8 and 2.05 mm at flow rates of 2–5 and 10 cm³·min⁻¹, respectively. The HETP value was also calculated for resorcinol from the breakthrough capacity curve at 10 cm³·min⁻¹ by using the equation (12):

$$N = \left(\frac{VV'}{(V - V')^2} \right) = \frac{L}{\text{HETP}}$$

where V is the volume of effluent at the center of the S-shaped breakthrough curve where the concentration is one-half the initial concentration, and V' is the volume at which the effluent has a concentration of 0.1578 of the initial concentration. The value of HETP obtained by this method was 1.9 mm, confirming the values obtained from the elution curves. The method has been tested for the separation of *o*-nitrophenol and resorcinol. *o*-Nitrophenol was first eluted with 0.05 M NaOH and resorcinol was then recovered with acetone at a flow rate of 2 cm³·min⁻¹.

REFERENCES

1. H. König and W. Strabel, *Fresenius' Z. Anal. Chem.*, 315, 205 (1983).
2. U.S. Environmental Protection Agency, *Methods of Chemical Analysis of Water and Wastes*, Cincinnati, Ohio, 1983.
3. C. A. Edwards, *Persistent Pesticides in the Environment*, 2nd ed., CRC Press, Boca Raton, Florida, 1973.

4. C. A. Edwards, *Environmental Pollution by Pesticides*, Plenum Press, 1973, p. 409.
5. L. T. Kurkland, S. Shibko, A. Kolbye, and R. Shapiro, *Haz. Mercury Environ. Res.*, 4, 9 (1971).
6. P. A. Pfeifer, G. K. Bonn, and O. Bobleter, *Fresenius' Z. Anal. Chem.*, 315, 205 (1983).
7. H. Oda, M. Kishida, and C. Yokokawa, *Carbon*, 19, 243 (1981).
8. H. Oda and C. Yokokawa, *Ibid.*, 21, 485 (1983).
9. J. F. Uthe, J. Reinke, and H. D. Gesser, *Environ. Lett.*, 3, 117 (1972).
10. A. H. Romano and R. S. Safferman, *J. Am. Water Works Assoc.*, 55, 169 (1963).
11. M. M. Mostafa, S. E. Samra, and A. M. Youssef, *2nd Chemistry Conference, Faculty of Science, Alexandria University, Alexandria, Egypt, June 1988*, p. 32.
12. T. Braun, J. D. Navratil, and A. B. Farag, *Polyurethane Foam Sorbents in Separation Science*, CRC Press, Boca Raton, Florida, 1985.
13. G. J. Moody and J. D. R. Thomas, *Chromatographic Separation with Foamed Plastics and Rubbers*, Dekker, New York, 1982.
14. A. B. Farag and M. S. El-Shahawi, *J. Chromatogr.*, 552, 371 (1991).
15. A. B. Farag, A. M. El-Wakil, M. S. El-Shahawi, and M. Mashaly, *Anal. Sci.*, 5, 415 (1989).
16. A. B. Farag, A. M. El-Wakil, and M. S. El-Shahawi, *Fresenius' Z. Anal. Chem.*, 324, 59 (1986).
17. A. B. Farag, M. S. El-Shahawi, A. M. El-Wakil, and M. N. Abbas, *Bull. NRC, Egypt*, 14, 39 (1989).
18. A. B. Farag, A. M. El-Wakil, M. S. El-Shahawi, and M. N. Abbas, *Ibid.*, 14, 29 (1989).
19. K. G. Kirkwood, *J. Chem. Phys.*, 2, 351 (1934).
20. R. C. Weast, *Handbook of Chemistry and Physics*, 54th ed., CRC Press, 1973.
21. A. W. Adamson, *Physical Chemistry of Surfaces*, 2nd ed., Academic Press, New York, 1967.
22. T. Hayashita and M. Takagi, *Talanta*, 32, 399 (1985).
23. E. Glueckauf, *Trans. Faraday. Soc.*, 15, 34 (1955).

Received by editor January 20, 1993

Spectrophotometric Determination of Ampicillin by Ternary Complex Formation with 1,10-Phenanthroline and Copper(II)

ALI Z. ABU ZUHRI,¹ ADEL H. RADY, MOHAMED S. EL-SHAHAWI, AND SALEM M. AL-DHAHERI

Department of Chemistry, Faculty of Science, United Arab Emirates University, P.O. Box 17551 Al Ain, United Arab Emirates

Received August 12, 1993; accepted October 22, 1993

A simple and convenient spectrophotometric procedure is described for the determination of ampicillin. The method is based on the formation of a yellow ternary complex with 1,10-phenanthroline and copper(II) in acetate-buffer solution (pH \approx 5.0) and measurement at 446 nm. The stoichiometry and stability constant of the ternary complex were determined. Beer's law is obeyed in the concentration range 2.5–100 $\mu\text{g cm}^{-3}$. The optimum concentration range evaluated by Ringbom's method, the molar absorptivity, and the Sandell sensitivity of the ternary complex were determined. A variety of pharmaceutical dosage forms containing ampicillin were successfully analyzed by the proposed procedure, giving a relative standard deviation of 1.0%. Comparison of results with those of an official method shows good agreement and indicates no significant difference in the precision of the two methods. © 1994 Academic Press, Inc.

INTRODUCTION

Lactam antibiotics, such as ampicillin, represent the most important class of drugs against infectious diseases caused by bacteria (1, 2). Therefore ampicillin is widely used in current therapy as an antibiotic drug. Spectrophotometric methods are the most popular methods for determination of ampicillin in bulk and pharmaceutical formulations using different types of reagents (3–6), but they require much time and the tolerance limit of ampicillin is low. The reported titrimetric procedures for the estimation of ampicillin are not satisfactory for microgram quantities (7, 8). Some attention has been given to the study of the metal complexes of ampicillin. El-Wahed and Ayad (9) potentiometrically determined the composition and stability constants of the ampicillin–Cu(II) complexes. According to these authors the ampicillin reacts with Cu(II) at low pH (2.0–3.5) and has a low stability constant. The ampicillin–Cu(II) complexes have been investigated spectrophotometrically by Veselinovic and Kapetanovic (5). They found that the absorption band of ampicillin–Cu(II) mixtures is observed at 316 nm and the complex undergoes hydrolysis. Tawakol *et al.* (10) reported a method for complexometric determination of ampicillin, based on the formation of a chelates with Cu(II). They found that the color of the chelates is unstable and changes with time.

Comparison of all results cited above indicates that the binary complex formed

¹ To whom correspondence should be addressed.

between ampicillin and Cu(II) is unstable and undergoes hydrolysis with time. The method described here utilizes the color reaction of ampicillin with 1,10-phenanthroline (1,10-phen) and Cu(II) in acetate buffer solution (pH 5.0) for microgram amounts of ampicillin. The method has been applied to the determination of ampicillin in various pharmaceutical preparations.

EXPERIMENTAL

Reagents

All chemicals used were of analytical grade. Stock solutions of $5.0 \times 10^{-3} M$, 1,10-phenanthroline and $5 \times 10^{-3} M$ copper(II) nitrate were prepared in distilled water. Ampicillin (85.5%) was obtained from Julfar Pharmaceutical Co. (Ras El-Khaimah, U.A.E.), and its solution (1 mg cm^{-3}) was prepared daily in dilute nitric acid. Acetate buffer solution of pH 5.0 was prepared as described by Britton (11). All solutions were prepared in demineralized water.

Apparatus

The absorption spectra of solutions were recorded on a Pye Unicam Model SP8-400 UV/VIS spectrophotometer with 1-cm silica cells. pH measurements were carried out using a Metrohm 632 pH meter. All measurements were performed at $20 \pm 0.1^\circ\text{C}$.

Recommended Procedure

Solutions of $5.0 \times 10^{-4} M$ 1,10-phenanthroline, 2.0 ml, and $1.0 \times 10^{-3} M$ copper(II), 1.0 ml, were added to suitable volumes of standard drug solutions in a 10-ml volumetric flask, and the solution was diluted to volume with acetate buffer solution (pH 5.0) and mixed. The reaction mixture was placed in a water bath at 40°C for 10 min and then cooled. The absorbance was measured at 446 nm against a 1,10-phenanthroline-copper(II) solution reagent blank.

RESULTS AND DISCUSSION

Binary mixtures of Cu(II)-ampicillin, Cu(II)-1,10-phenanthroline, and ampicillin-1,10-phenanthroline have been used to select the optimum conditions for color developing. A significant yellow color was formed only after the addition of ampicillin to a mixture of Cu(II) and 1,10-phen. The absorption spectrum of the final solution exhibits a well-defined absorption peak at 446 nm. This behavior may be considered as evidence for the formation of a mixed ligand complex (12).

Effect of Time and Temperature and the Salt Effect

It was found that the time required to reach the maximum color intensity of the reaction mixture is temperature dependent. At room temperature (20°C) the time is 40 min, but if the reaction mixture is placed in a water bath at 40°C for 10 min, the maximum intensity is attained immediately after cooling the mixture as shown in Fig. 1. The color remains constant for about 2 days. The reaction time was established by increasing it in increments of 2 min and it was found that 10 min is sufficient to yield maximum absorbance. The addition of sodium chloride (0.01-

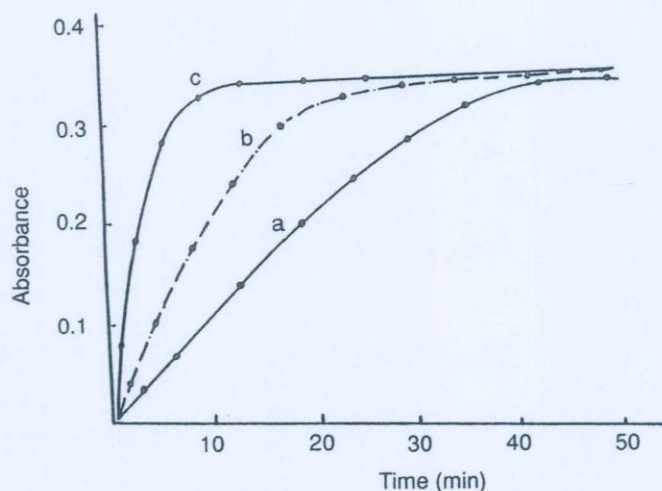


FIG. 1. The effect of temperature on the time required to attain the maximum color intensity of the complex (ampicillin = 40 μg , $[\text{Cu(II)}] = 1 \times 10^{-3} \text{ M}$, $[\text{phen}] = 5 \times 10^{-4} \text{ M}$, pH 5.0). (a) 20°C, (b) 30°C, and (c) 40°C against reagent blank.

0.1 M) did not improve the color intensity, indicating that the ternary complex is formed with or without the salt effects.

Effect of pH and Reagent Concentration

The influence of the aqueous phase pH on the color developing of ampicillin ($10 \mu\text{g cm}^{-3}$) was examined by measuring the absorbance of the solution after cooling the solution. The results are summarized in Fig. 2. The ternary complex is formed within the pH range 3.0–5.5, and the maximum color development was attained at pH 5.0. The effects of increasing copper(II) concentration (at constant $[\text{phen}]$) and the effects of increasing 1,10-phenanthroline concentration (at constant $[\text{Cu(II)}]$) on the intensity of the ternary complex have been examined. In the presence of ampicillin ($\leq 86 \mu\text{g}$) the optimum concentration of phen and copper(II) for attaining a maximum intensity is found to be 5×10^{-4} and $1 \times 10^{-3} \text{ M}$, respectively. Acetate buffer solution was chosen and used in the subsequent work as described in the recommended procedure.

Stoichiometry and Stability of the Complex

The stoichiometry of the ternary complex was determined by Job's method of continuous variations and the mole ratio method. The results indicate that the mole ratio of ampicillin:phen:Cu(II) is 1:2:1. The formation constant ($\log B$) of the ternary complex has been calculated from the data obtained by a potentiometric method previously reported (12), and it was found to be 8.34. Hence the ternary complex is more stable than the binary complex formed between ampicillin and copper(II) which was obtained spectrophotometrically ($\log B = 5.31$) (5). So, the

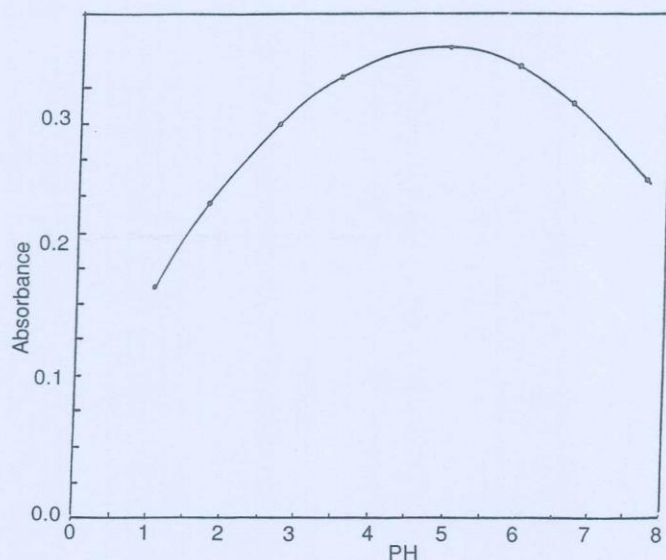


FIG. 2. Effect of pH on the absorbance of the ternary complex Ampicillin-Cu(II)-phen following the recommended procedure for other conditions against reagent blank.

proposed method for the determination of ampicillin is superior as compared to the earlier methods (1-5) with respect to the stability of the ternary complex formed.

Beer's Law and Sensitivity

Under the optimum experimental conditions described above a calibration curve was made of a series of standard solutions of ampicillin complexed with phen and copper(II). The absorbance was measured at 446 nm against a blank prepared similarly without the ampicillin following the recommended procedure. A linear graph was obtained by measuring the absorbance of the solution as a function of ampicillin concentration which passed through the origin. The points on the standard calibration curve each represent the outcome of five determinations. The calibration curve was used for subsequent determination of unknown ampicillin samples. Beer's law was valid over the concentration range $2.5\text{--}86\ \mu\text{g cm}^{-3}$, and the detection limit was $2.5\ \mu\text{g cm}^{-3}$. The precision of the method was studied with a series of 10 determinations for $40.0\ \mu\text{g cm}^{-3}$ ampicillin. The mean absorbance was 0.33 with a relative standard deviation of 1.0%. The optimum concentration range evaluated by Ringbom's plot (13) has been found to be $3.5\text{--}70\ \mu\text{g cm}^{-3}$ ampicillin. The molar absorptivity calculated from Beer's Law was $3.3 \times 10^4\ \text{liter mol}^{-1}\ \text{cm}^{-1}$ at 466 nm, and the Sandell (14) sensitivity was found to be $0.12\ \mu\text{g cm}^{-2}$.

Application to Dosage Forms

Results of the analysis of the ampicillin in different dosage forms using the proposed method are listed in Table 1. Values obtained by the official method (15)

TABLE 1
Analysis of Ampicillin by the Proposed and Official Methods

Sample	Amount taken (mg)	Recovery ^a ± SD (%)	
		Proposed method	Official method (15)
Ampicillin capsules (500 mg/cap)	50	99.6 ± 0.6	99.9 ± 0.3
Ampicillin capsules (250 mg/cap)	50	98.8 ± 0.6	98.4 ± 0.5
Ampicillin suspension (250 mg/5 ml)	50	101.1 ± 0.7	99.8 ± 0.8
Ampicillin injection (500 mg/vial)	50	97.6 ± 0.9	97.9 ± 0.6
Ampicillin injection (250 mg/vial)	50	99.5 ± 0.3	100.7 ± 1.0

^a Average ± standard deviation of five determinations.

are presented for comparative purposes and are in good agreement with values obtained by the proposed method.

REFERENCES

1. Jung, F. A.; Pigrim, W. R.; Poyser, J. P.; Siret, P. J. *Top. Antibiol. Chem.*, 1980, 4, 1.
2. Page, M. I. *Acc. Chem. Res.*, 1984, 17, 144.
3. Devani, M. B.; Patel, L. T.; Patel, T. M. *Talanta*, 1992, 39, 1391.
4. Rizk, M.; Walash, M. I.; Abu-Ouf, A. A.; Belal, F. *Anal. Lett.*, 1981, 14, 1407.
5. Veselinovic, D.; Kapetanovic, V. J. *Serb. Chem. Soc.*, 1985, 50, 401.
6. Korany, M. A.; Abdel-Hay, M. H. *Talanta*, 1989, 36, 1253.
7. Talegaonkar, J.; Bopari, K. S. *Indian Drugs*, 1981, 487, 410.
8. Leo, S. D.; Pitrolo, G. *Bull. Chim. Soc. Jpn.*, 1973, 112, 487.
9. Abd El-Wahed, M. G.; Ayad, M. *Anal. Lett.*, 1984, 17, 205.
10. Tawakol, M. S.; Ismail, S. A.; Amer, M. M. *Pharmazie*, 1975, 30, 542.
11. Britton, H. T. S. *Hydrogen Ions*, Fourth ed. Chapman and Hall, London, 1952.
12. Shoukry, M. M. *Talanta*, 1992, 39, 1629.
13. Ringbom, A. *Fresenius Z. Anal. Chem.*, 1939, 115, 332.
14. Sandell, E. B. *Chlorimetric Determination of Trace Metals*. Interscience, New York, 1959.
15. *British Pharmacopia*. H.M. Stationary Office, London, 1988.

Spectrophotometric and Polarographic Studies of
Di-2-pyridyl ketone 2-thienoylhydrazone.

Keywords : Di-2-pyridyl ketone 2-thienoylhydrazone, spectrophotometry,
differential-pulse polarography.

Ali Z. Abu Zuhri*, Mohamad S. El-Shahawi, Mostafa M. Kamal,
Mohamad Al-Nuri** and Mohamed Hannoun**

Department of Chemistry, Faculty of Science, UAE. University, Al-Ain,
P.O.Box 17551, United Arab Emirates.

ABSTRACT

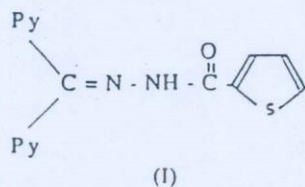
The spectral and differential pulse polarographic (DPP) behaviour of di-2-pyridyl ketone 2-thienoylhydrazone (DPKTH) has been investigated in 30% (v/v) ethanol-buffer mixtures over a wide range of pH (2.0-12.0). The spectral bands located at 325, 276, 230 and 208 nm of the DPKTH in ethanol are assigned to the possible electronic transitions of the molecule. The spectral data at various pH values indicates that the molecule characterized by the keto = enol tautomerization and the pK_a value for the enolic form of the compound is determined in aqueous ethanol and was found to be 10.6. The effect of various operational parameters on the reduction current and the mechanism of the electrode reaction of DPKTH at the DME are discussed. The main reduction peaks are attributed to the reduction of C=N centre of both the keto and enol forms. This behaviour is compared with the DPP behaviour of the other related acid hydrazone compounds. The applicability of DPP technique for the trace determination of DPKTH was tested under the optimum experimental conditions and the detection limit is found to be 0.09 μM .

-
- * To whom correspondence should be addressed
 - ** Chem. Dept., Al-Najah National Univ., Nablus, West Bank.

INTRODUCTION

The polarographic behaviour of hydrazone compounds has been subject of many investigations¹⁻⁴, but only a few reports are available on the electroreduction of nitrogen-containing heterocyclic hydrazones⁵⁻⁷. The mechanism of reduction has been discussed in Kitaev and Buzykin's review⁸. A four electron reduction mechanism is observed in acidic and alkaline solutions involving cleavage of the N-N bond with the formation of the corresponding amino compounds⁹⁻¹¹. A 2- electron mechanism followed by hydrolysis resulting in the formation of the corresponding carbonyl compound has been reported^{5,12}. Most of hydrazones suffer from the hydrolytic decomposition in acidic and alkaline solutions^{13,14}. It was reported that¹⁵, the hydrazones which contain a di-2-pyridyl group attached to the carbon of the hydrazone centre exhibit a higher stability against hydrolysis. The polarographic behaviour of hydrazone compounds related to nitrogen-containing heterocyclic hydrazones are scarce.

In this work, we synthesized a new hydrazone compound, a di-2-pyridyl ketone 2-thienoylhydrazone, DPKTH (I), which is N and S containing heterocyclic hydrazone. Stability of this compound enhances the study of the spectrophotometric and polarographic behaviour and of the mechanism of reduction over wide pH and potential ranges. The tautomer equilibrium and the proton dissociation behaviour of enolic form are investigated spectrophotometrically. The DPP behaviour of this compound and the influence of pyridine and/or thiophene rings on the reduction mechanism is considered.



EXPERIMENTAL

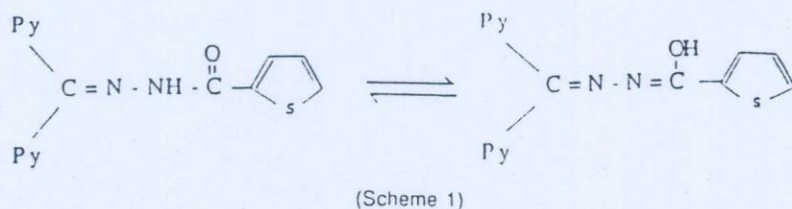
- (a) Chemical solutions : All reagents and solvents used were of analytical reagents grade. Di-2-pyridyl ketone 2-thienoyl-hydrazone (DPKTH) was prepared according to the reported method¹⁶.

A 10^{-2} M DPKTH solution in ethanol served as the stock solution. A universal buffer solutions series of Britton-Robinson (0.08 M) were used as supporting electrolytes. A constant ionic strength, $\mu=0.10$ was maintained using Na_2SO_4 solution (0.5 M).

(b) Apparatus : DPP was carried out using a Metrohm 506 polarecord with an 505 mercury drop electrode (Metrohm). The three electrode system was completed by means of a platinum wire auxiliary electrode and an Ag-AgCl reference electrode. A pulse amplitude of 100 mV was used with a scan rate of $\pm 4 \text{ mV s}^{-1}$ and a forced drop time of 1.4 s. The solutions were deaerated by passing through it a slow stream of pure nitrogen. Spectroscopic data were obtained with a Pye Unicam Sp 8-100 spectrophotometer using 1 cm quartz cell. A Metrohm 632 pH-meter was used for the pH measurements. All measurements were performed at room temperature ($22 \text{ }^\circ\text{C} \pm 0.5$).

RESULTS AND DISCUSSION

Mechanism of hydrolysis of hydrazone compounds was investigated spectrophotometrically and polarographically^{13,14,17,18}. It was found that, the aldimine linkage undergoes a shift from the rate limiting decomposition of the carbinolamine intermediate in strong acidic medium to the rate limiting formations of the carbinolamine in mild acidic or basic medium¹⁷⁻¹⁹. However, the di-2-pyridyl ketone acid hydrazones of various acid hydrazide exhibit a higher degree of stability against hydrolysis over a wide pH range (2.1-11.6)²⁰. The stability of DPKTH is most likely due to the higher conjugation structure of its enolic form, since the donating character of the di-pyridyl system may enhance the formation and stability of the enol form as well as decreases the possibility of the protonation of the nitrogen atom of the aldimine linkage (scheme 1). The protonation step is the prerequisite step for the hydrolytic decomposition process. The stability of DPKTH allows the investigation of its spectrophotometric and polarographic behaviour in the pH range 2.0-12.0 and comparing these data with other similar di-pyridyl hydrazone compounds¹⁵.



Spectrophotometric behaviour of DPKTH :

In ethanol the electronic spectrum (Fig. 1) of the DPKTH showed four well resolved bands with λ_{\max} at 325, 276, 230 and 208 nm. The first two bands are assigned to $n \rightarrow \pi^*$ of the azomethene of the ketoamine tautomer (I) which absorbs at higher wavelength than the corresponding enolimine tautomer(II)²¹ (Scheme 2). However, the intramolecular hydrogen bonding plays in hydroxylic solvents negligible role. The latter two bands are due to ${}^1L_a \pi \rightarrow \pi^*$ and ${}^2L_b \pi \rightarrow \pi^*$ transitions characteristics of pyridyl heterocyclic electronic systems²². The proton dissociation behaviour of the ligand has been studied spectrophotometrically in ethanol - water medium (30:70, v/v) at different pH in presence of 0.1 M Na_2SO_4 . The spectra of the ligand (Fig. 1) are affected by the pH leading to a change in the band positions and/or their intensities. The low energy band $n \rightarrow \pi^*$ (325 nm) transition induced a pronounced pH spectral shift where at pH 5.4 and 11.7 it is shifted to sharp band at 320 and broad band at 365 nm, respectively. The broadening of the $n \rightarrow \pi^*$ transition at pH 11.7 is probably due to the mixing of the ground state of the different electronic state resulting from the charge transfer of the donor atom^{22,23}. The values of the lowest energy band $\pi \rightarrow \pi^*$ and $n \rightarrow \pi^*$ transitions are in the order: enol > anion \approx conjugated acid \gg zwitter ion. The longest wavelength bands observed at pH 11.7 is possibly attributed to the zwitter ions present in equilibrium with the enol form. At pH 7.1 the band at 230 nm (Fig. 1B) is strongly enhanced due to the stabilization caused by the media and the specific interaction of the hydrogen bonding properties of the species formed at this pH. Also, the higher ratio of the keto to enol form at pH 7.1 as compared to pH 7.5 may account for this behaviour. Thus, it gives rise to keto-enol tautomerism with shifting to the enol form (II) as is indicated by the intensity of the 230 nm band (Fig. 1). At pH 7.5, the band at 320 nm suffers a noticeable hypsochromic shift which is characteristic of dipolar species formation (III) due to the stabilization of the ground state by the media²⁴. The pK_a of the ligand was estimated from the absorbance - pH curve (Fig.2) at 276 and 230 nm using the recommended procedures²³ and it was found that, $\text{pK}_a = 10.6$.

Differential pulse polarographic behaviour of DPKTH :

The differential pulse polarograms of $5 \times 10^{-5}\text{M}$ of DPKTH were recorded at various pH values as a function of the potential in universal buffer solutions containing 30% ethanol. Representative polarograms are given in Fig.3. In acidic or neutral media two consecutive peaks (I and II) and an ill-defined peak (III), close to the H^+ discharge are observed in the polarograms. The height of

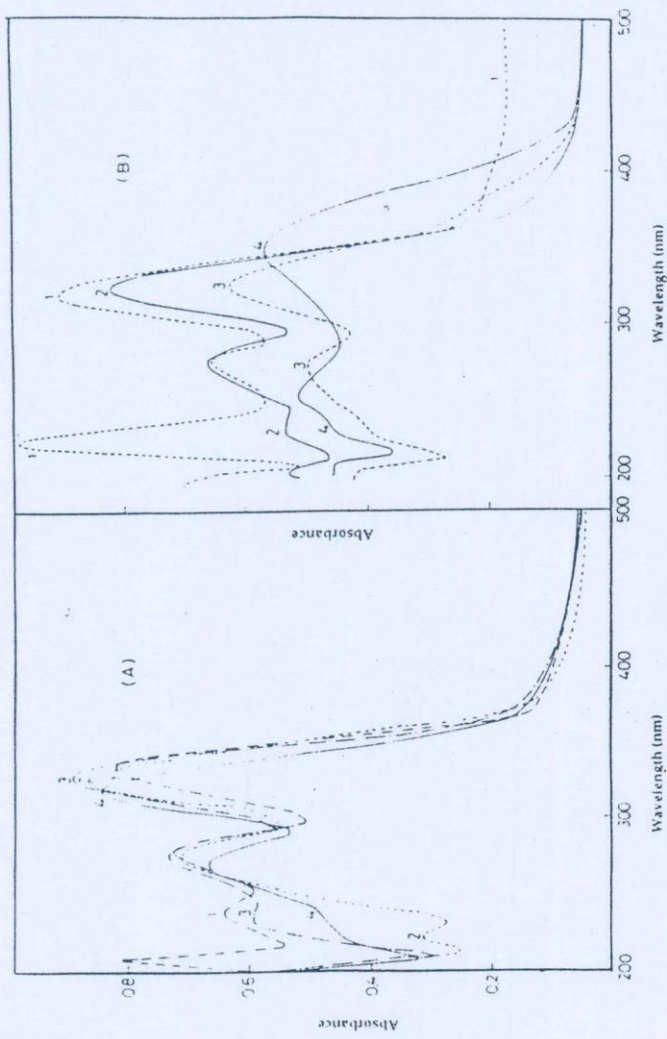


Fig. 1. Absorption spectra of 5×10^{-4} M of DPKTH at various pH values. A) (1) Pure ethanol; (2) pH 3.9; (3) pH 5.4; (4) 7.5B) (1) pH 7.1; (2) pH 9.5; (3) 10.7; (4) 11.58.

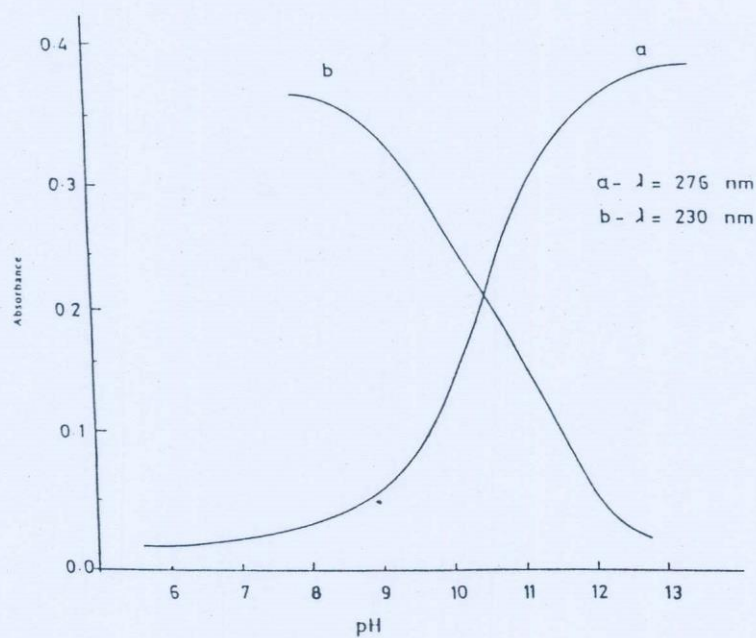
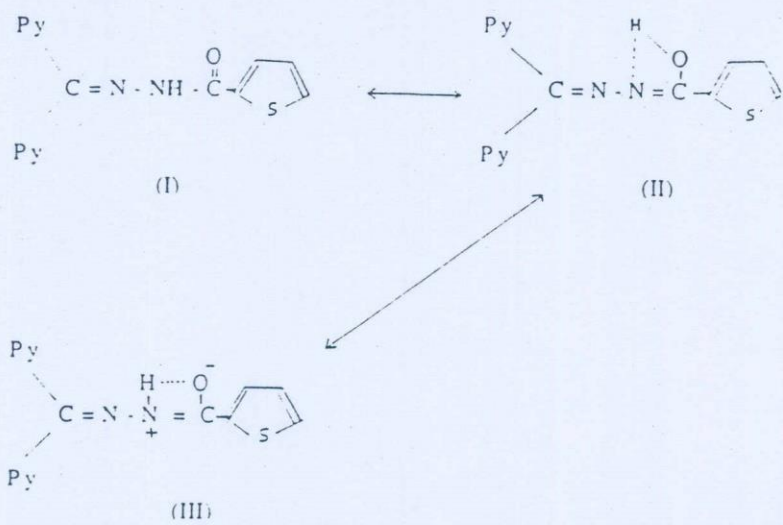


Fig. 2. pH absorbance curve of DPKTII ($5 \times 10^{-4} \text{M}$) at 276 and 230 nm.

peak II increases gradually with increasing the pH until 7.1 where at this pH the height of peaks I and II are almost the same (Fig.3) indicating equilibrium between the keto and enol form species. In alkaline solution, a well developed peak (Peak IV) is observed and the peak height is almost constant at $\text{pH} \geq 10.6$, whereas at $\text{pH}'s > 7.1$, the enolic form is the more predominant species in solution. The height of peak IV is found to be more or less twice that of peak I or II indicating that the number of electrons consumed in alkaline solutions (peak IV) is double of that in acidic or slightly acidic solutions (peak I or II).

The effect of pH on the potential of the reduction peaks I and IV are also investigated. The E_p values is shifted to more negative potential with increasing pH, indicating that the H^+ ions are involved in the electrode reaction. The $\Delta E_p/\Delta \text{pH}$ relation of the peak I and IV were straight lines with slope equal to 0.063 and 0.058 V within the pH ranges 2.1 - 7.1 and 7.1 - 11.4 for peak I and IV, respectively.

These facts are confirmed by studying the controlled potential electrolysis (CPC) of the DPKTH solution at mercury pool cathode at $\text{pH} = 4.1$ at -0.8 V; $\text{pH} 7.1$ at -0.1 V and at $\text{pH} = 10.2$ at -1.3 V vs. Ag/AgCl . It was found that at $\text{pH} 4.1$, (peak I) and $\text{pH} 7.1$ (peak II) corresponds to 2.2. electron while at $\text{pH} 10.2$, 4 electrons are found correspond to peak IV. In the electronic spectrum of the compound after CPC at 4.1 and -0.8 V vs Ag/AgCl the two observed bands at 325 nm and 230 nm are vanished while the band at 276 nm is shifted to 260 nm indicating reduction of $\text{C} = \text{N}$, centre. When the CPC is carried out at $\text{pH} = 10.4$ and -1.3 V vs. Ag/AgCl , three bands are obtained at 260, 240 and 210 nm possibly due to the reduction of $\text{C} = \text{N}$ followed by cleavage of the $\text{N}-\text{N}$ bond¹⁵. These results are in agreement with that reported by Issa et al²⁴ for some other pyridylazo dyes.

According to the aforementioned results and the general mechanism reported for the reduction of similar hydrazones^(1,3,9,10,15), the reduction mechanism of DPKTH is represented as follows :

- (1) Peaks I and II observed at $\text{pH} \leq 7.1$ are probably assigned to the reduction of the $\text{C} = \text{N}$ centres of both ketonic and enolic species, respectively. Peak II corresponds to the reduction of $\text{C} = \text{N}$ centre of the enolic form, since the higher conjugation in the structure of the enolic species enhances the delocalization of the π - electron system at the azomethine centre making the reduction more difficult in comparing with the ketonic structure. These results are confirmed from the electronic spectra of the ligand (Fig. 1A) where the $n \rightarrow \pi^*$ transition at 325 nm is shifted to higher wavelength and

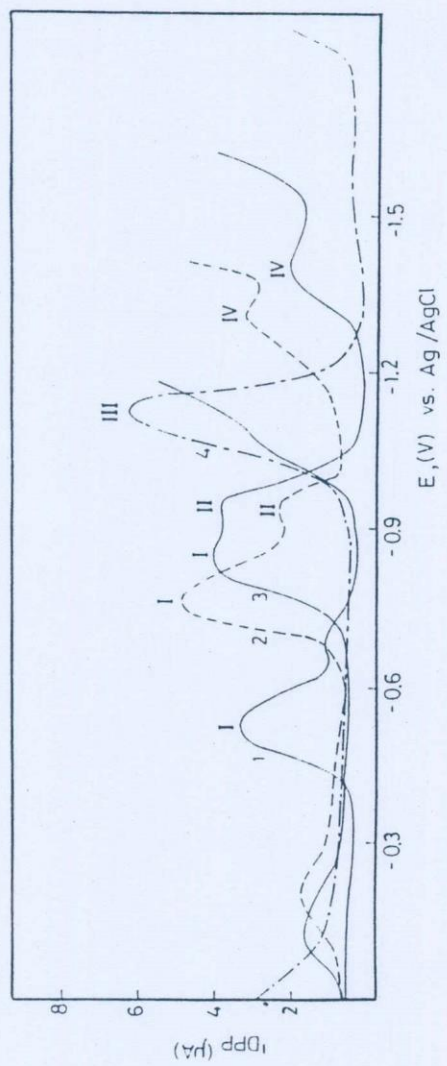


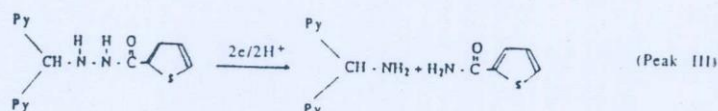
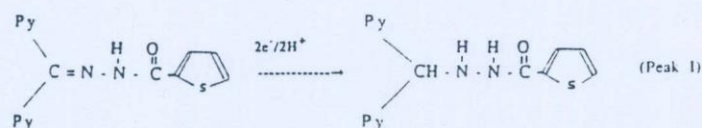
Fig. 3. pH - dependence of the differential pulse polarograms of 5×10^{-5} M DPKTH . (1) pH 2.1 ; (2) 6.1 ; (3) pH 7.1 and (4) pH 10.4.

the ${}^1L_a \pi \rightarrow \pi^*$ transition at 230 nm is strongly enhanced, with increasing pH showing stabilization of the enol form, and the keto form become less predominant.

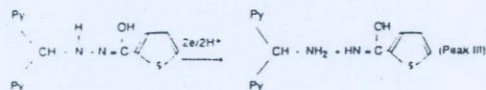
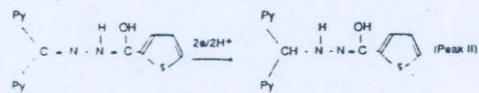
- (2) The coincide of the value of E_p of peak III at pH's < 7.1 with the reported value for the reduction of $\begin{matrix} \text{H} & \text{H} \\ | & | \\ \text{N} & - & \text{N} \end{matrix}$ bond in similar hydrazones^{7,10} indicates that peak III is probably due to the cleavage of the hydrazo group $\text{HN} - \text{NH}$ following the first reduction step and the overall process involves uptake of $4e/4\text{H}^+$ in two consecutive steps.
- (3) In alkaline solutions a well defined reduction peak (peak IV) is observed. The height of this peak is double that of peak I or II recorded in acidic medium. Therefore peak IV is attributed to the reduction of $\text{C} = \text{N}$ centre of the enolic $\begin{matrix} \text{H} & \text{H} \\ | & | \\ \text{N} & - & \text{N} \end{matrix}$ bond. The fact that the E_p of peak IV is pH independent at pH's $> \text{p}K_a$ of the compound. This fact is also confirmed from the electronic spectra of the compound DPKTH (Fig.1B) at pH 10.7 and 11.7 where, the two bands at 230 and 276 nm are shifted to 220 and 253 nm, respectively and became less intense and obscured nearly in one broad band. The low lying energy band at 325 nm is also shifted to 365 nm showing that the enol species became highly predominant (Scheme II).

According to these results and the general mechanism of the polarographic reduction of some other hydrazones^{6,15}, the reduction pathway of the ketonic and enolic forms of DPKTH in acidic and neutral solutions can be represented by the following equations.

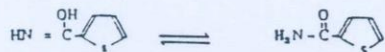
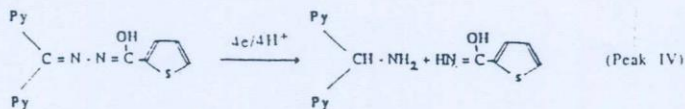
(A) Reduction of the ketonic form



(B) Reduction of the enolic form



However, in alkaline solutions, the enolic form is the more predominant species and the reduction pathway can be represented as follows :



In acidic solutions ($\text{pH} \leq 5$) a very small peak is observed at less negative potential in comparison to the main reduction peak. This peak is probably a pre-adsorption peak due to the interaction of the π -electron system of the enolic and/or the ketonic form of the compound with the relative positively charged electrode surface¹⁵.

Therefore, it is evident that, the DPKTH is reduced via a 4 electron mechanism with cleavage of the -N-N-bond similar to that proposed by Lund¹⁴ and recently by Mathur, *et al*²⁵. The DPP behaviour of the investigated di-2-pyridyl ketone 2-thiophenylhydrazon \bar{c} (DPKTH) compound is compared with that of di-2-pyridyl ketone benzoylhydrazon \bar{c} (DPKBH)¹⁵ it is found that :

- (1) In acidic solutions, peaks I and II of DPKTH are well resolved while a very broad peak is observed in case of di-2-pyridyl ketone 2-benzoylhydrazon \bar{c}

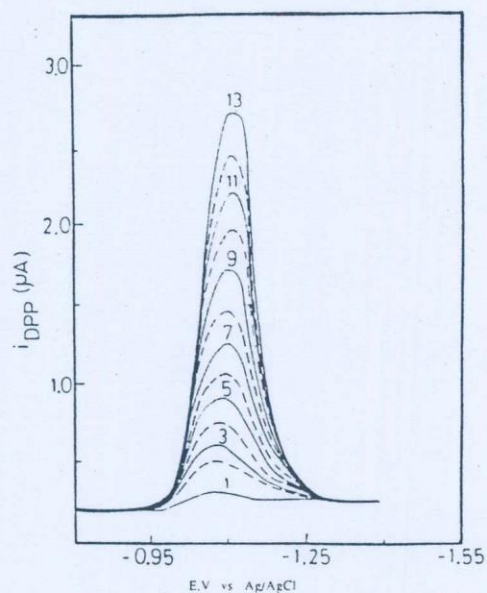


Fig. 4. Concentration dependence of the differential pulse polarograms of DPKTH at pH 9.35. (1) 0.96 ; (2) 2.3 ; (3) 4.49 ; (4) 4.90 ; (5) 6.30 ; (6) 7.75 ; (7) 9.60 ; (8) 11.90 ; (9) 14.15 ; (10) 16.36 ; (11) 18.52 ; (12) 20.64 ; (13) 22.73 μM of DPKTH.

(DPKBH) ¹⁵ showing that a low contribution of the enolic form in the reduction process of DPKBH is found.

- (2) Over all investigated pH range the peak potential of the reduction peaks of DPKTH has a less negative value as compared to that of DPKBH. This may be explained by the inductive effect of the thiophenyl group in DPKTH, which enhances the delocalization of the electron densities through the hydrazone rest making the reduction of DPKTH more easier.

The determination of acid hydrazone derivatives by the differential pulse polarographic technique was reported ^{15,17,26}. The compound tested DPKTH shows a very high degree of stability over the investigated pH-range and

exhibits a very sensitive DPP peak at pH 9.35. Thus pH 9.35 was used for the trace determination of the tested compound by DPP. The influence of some other parameters (scan rate, drop time and amplitude) on the maximum Faradaic response and higher resolution of the DPP peak of the compound DPKTH at pH 9.33 has been considered. The maximum Faradaic response and higher resolution were obtained at 4 mV.S^{-1} scan rate, 100 mv pulse amplitude and 1.4-2 s drop time. Also, it was found that, the height and the peak potential of the concentration sensitive peak is pH independent at higher pH values.

The applicability of DPP technique as an analytical method for the determination of DPKTH was tested at pH 9.35 as a function of concentration of the depolarizer under the optimum conditions. The height of the peak increases gradually with increasing concentrations of DPKTH (Fig.4) and the response of the peak height (i_p , μA) as a function of concentration (C , μM) is linear. The variation of the i_p , μA with concentration is based on the straight line equation $i_p = aC + b$, where a and b are slope and intercept of the straight line, respectively. The calibration curve, generated over the concentration range $0.097 - 22.73 \mu\text{M}$, has a slope of $0.1 \pm 0.004 \mu\text{A}/\mu\text{M}$ an intercept of $0.02 \pm 0.008 \mu\text{A}$ and a regression coefficient of the fit 0.989. The practical detection limit, arbitrarily expressed as three times the overall background value, was found to be 0.09 arbitrarily μM ($n=5$). The validity of the method is supported by the constancy of the peak height-concentration ratio.

References

1. H. Lund. Acta Chem. Scand. , 1959, 13, 249
2. H. Lund. Electrochim. Acta, 1983, 28, 395.
3. H.M. Fahmy, A.M. Helmy and M.A. Azzem, J. Electroanal. Chem., 1986, 201, 101.
4. Yu. P. Kitaev, I.M. Skrekova and L.I. Maslova, Izv Akad Nauk SSSR Ser Khim, 1970, 10, 2194.
5. A.Z. Abu Zuhri and A. El-Dissouky, Mikrochim. Acta, 1991, 111.
6. A.Z. Abu Zuhri and J.S. Shalabi, J. Chem. Soc., Perkin Trans. II, 1985, 499 and references therein.
7. M.A. Gomez Nieto , M.D. Luque De Castro and M. Valcarcel, Electrochim. Acta, 1983, 28, 1725.
8. Yu. P. Kitaev and B.I. Buzzakin, "Hydrazones", Izad Mauku, Moscow, 1974.

9. H. Lund, *Tetrahedron Lett.*, 1968, 3651.
10. R.N. Goyal, J.R. Bushan and A. Agarwal, *J. Electroanal. Chem. Interfacial Electrochem.*, 1981, 171, 281.
11. A.Z. Abu Zuhri, M.A. Abu-Eid and J.S. Shalabi, *Mikrochim. Acta.*, 1987, 153.
12. A.Z. Abu Zuhri and J.S. Shalabi, *Monatsh. Chem.* 1987, 118, 1335.
13. M.A. Abu-Eid, F. Mahmoud, M. El-Nuri and A.Z. Abu Zuhri, *Monatsh. Chem.*, 1989, 120, 323.
14. Y.M. Temerk, M.M. Kamal and M.E. Ahmed, *J. Chem. Soc. Perkin Trans. II.* 1984, 337.
15. M.M. Kamal, A.Z. Abu Zuhri and M. Hannoun, *Fresenius. Z. Anal. Chem.* 1992, 344, 275 and references therein.
16. M.A. Al-Nuri, M. Abu-Eid, N.A. Zatar, S. Khalaf, M. Hannoun and M. Khamis, *Anal. Chim. Acta* 1992, 259, 175.
17. M.M. Kamal, Y.M. Temerk, M.E. Ahmed and Z.A. Ahmed, *J. Prakt. Chem.*, 1986, 328, 841.
18. N.J. Less-Gayed, M.A. Abou Taleb, A. El-Bitash and M.F. Iskander, *J. Chem. Soc. Perkin Trans. II.* 1992, 213.
19. R.K. Chaturved and E.H. Cordes, *J. Am. Chem. Soc.*, 1967, 89, 1230.
20. T. Nakanishi and M. Otomo, *Microchem. J.* 1986, 33, 172.
21. P.W. Alexander and R.J. Sleet, *Aust. J. Chem.* 1970, 23, 1183.
22. M.S. Masoud, A.A. Hasanein and A.M. Heiba, *Spectroscopy Lett.*, 1984, 17, 441.
23. J.C. Colleter, *Ann. Chim. (Paris)*, 1960, 450.
24. Y.M. Issa, B.E. El-Anadouli and B.A. El-Shetary, *Ind. J. Chem.*, 23A, 1984, 183.
25. N.C. Mathur, R.N. Goyal and W.V. Malik, *Indian J. Chem.*, 1990, 29A, 76.
26. Y.M. Temerk and A.Z. Abu Zuhri, *electrochim Acta*, 1980, 25, 1287; Y.M. Temerk, I.M. Issa and A.Z. Abu Zuhri, *J. Chem. Soc. Perkin Trans II* 11: 1465.

Received December 7, 1993
Accepted February 5, 1994

Chromium(III) complexes of naturally occurring amino acids

Mohamed S. El-Shahawi

Chemistry Department, Faculty of Science, UAE University, PO Box 17551, Al-Ain, United Arab Emirates

Summary

Amino acid complexes of CrCl₃Py₃ have been prepared and studied by elemental analysis, magnetic susceptibility, vibrational (i.r.), electronic and circular dichroism spectroscopy. Two peaks in the visible spectra are assigned to a d–d transition in pseudo octahedral symmetry. The spectrochemical parameters (Dq, B and β₃₅) for the complexes were calculated which confirm that pyridine nitrogen and/or chlorine are not removed. Prolonged heating or bubbling of air through the solution of CrCl₃·Py₃ containing L-(–)-histidine or L-(–)-threonine for several hours enhanced formation of chromium (VI).

Introduction

Amino acids provide important sites for binding of metal ions in biosystems. Coordination compounds are frequently implicated in the therapeutic activity displayed by drugs containing transition metal ions⁽¹⁾ or by the ligand itself⁽²⁾. The composition, stability and structure of selected amino acid metal chelates have been studied⁽³⁾.

The biological role of chromium as an essential trace element was proposed when it was found that rats fed a chromium-deficient diet developed an impaired tolerance towards intravenous glucose⁽⁴⁾. Recently, chromium containing an insulin potentiating factor has been isolated and found to contain chromium(III), glycine, cysteine and glutamic acid⁽⁵⁾. A significant relationship was found between the alcohol-extractable chromium content of foodstuffs and biological activity⁽⁵⁾. These facts raise the possibility that chromium(III) could be complexed with naturally occurring ligands. Therefore, we have investigated the importance of chromium in many biological systems *in vivo* in a non-aqueous environment^(6,7). It is of interest to discover whether chromium(III) will complex with the naturally occurring amino acids in non-aqueous media. This paper deals with the preparation and spectroscopic characterization of some chromium(III)–amino acid complexes. The additivity and separability of the configurational and vicinal c.d. curves in the spin-forbidden and the first spin-allowed transitions are substantiated.

Experimental

L-(–)-threonine (Thr), L-(–)-histidine (His), L-(–)-cysteine (Cys), and DL-alanine (Ala) were reagent grade. BDH pyridine (Py) and dry MeOH were used without further purification. CrCl₃Py₃ was obtained by the method of Taft *et al.*⁽⁸⁾.

Preparation of the complexes

To a solution of CrCl₃Py₃ (1 mmol) in MeOH (50 cm³), weights of the amino acid were added commensurate with 1:1 and 1:3 chromium(III)–ligand ratios. The mixture was heated under reflux with constant stirring and a colour change was observed in less than 1 h. The colour of the complexes depends on the type and the molar ratio

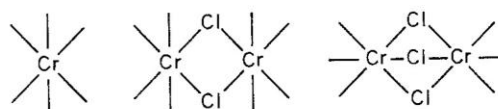
of the amino acid added relative to chromium(III). All solutions were heated under reflux for ca. 4 h, then reduced in volume (ca. 20 cm³). On cooling to room temperature and adding Et₂O (10–15 cm³), solid compounds were obtained. These were redissolved in MeOH and the solution was passed through a 40 mm diameter jacketed column, filled with Cos-Sephadex C₂₅ cation exchange resin to a depth of ca. 30 cm, at 3 ml min⁻¹. The complexes were eluted with dry warm MeOH over 20 min and the purity of the complexes was checked by t.l.c. (EtOH–H₂O, 1:5 v/v). Each eluent was concentrated on a rotary evaporator and the resulting crystalline solids, which were formed at room temperature, were dried *in vacuo*.

Physical measurements

I.r. spectra were recorded on a Perkin-Elmer 457 spectrophotometer using KBr discs. U.v.-vis. and c.d. spectra were measured respectively on a Beckman Acta MIV spectrometer and an instrument that uses a photoelastic modulator to change the polarization of the light beam as described elsewhere⁽⁹⁾. Magnetic measurements were made on a Johnson Matthey magnetic susceptibility balance. Merck 60 F₂₅₄ silica gel t.l.c. plates were employed.

Results and discussion

Interaction of chromium(III) with amino acids is of great importance in view of the role of Cr–O, Cr–N and/or Cr–S bonds in the initiation of insulin action, the effectiveness of these ligands in the removal of chromium bound to haemoglobin, or the role of these ligands in the reduction of toxic chromium(VI) to chromium(III). The analytical results for the complexes formed seem, at first sight, difficult to rationalize. However, if chloride bridges are considered, a pattern emerges: the monomer has six coordinating sites, the dimer with double chloride bridges ten coordinating sites and the dimer with three chloride bridges nine sites, as is shown in Scheme 1. Further complicating factors are the possible multidentate nature of the ligands and the possibility that the chloride ion is present either as the anion or complexed to the chromium. This latter conjecture can be tested by adding an aqueous solution of AgNO₃ to the complex solution in methanol. If a white precipitate is formed, the chloride ions are ionic in character, while if they are not then chloride ions are directly bonded to the chromium(III) ion.



Scheme 1

The complexes prepared, together with elemental analyses and other physical and chemical properties, are listed in Table 1. The complexes are purple, green-violet, deep wine red or red-pink and have melting points < 180°C. Owing to their inherent stability, thermal

Table 1. Analytical data, magnetic moment (BM) and some physical properties of the complexes^a.

Complex	Found (Calcd.) (%)					Colour	μ_{eff} (BM)	M.p. (°C)
	C	H	N	Cl	Cr			
(1) Cr(Thr) ₃	36.6 (36)	7.0 (6.7)	10.1 (10.5)	–	13 (12.7)			
(2) Cr(His) ₃	41.7 (42.0)	4.4 (4.1)	24.1 (24.5)	–	9.8 (10.1)	Violet	3.6	160
(3) Cr(Cys) ₃ ^b	26.3 (26.2)	4.5 (4.4)	9.7 (10.1)	–	12.2 (12.6)	Green-violet	3.7	–
(4) Cr(Ala) ₃	34.6 (34.5)	5.9 (5.7)	13.0 (13.3)	–	16.11 (16.5)	Pink	3.8	130
(5) Cr(Thr) ₂ PyCl	38.4 (38.7)	5.4 (5.2)	10.0 (10.4)	8.6 (8.8)	12.6 (13.1)	Purple	3.6	170
(6) Cr(His) ₂ Cl	36.2 (36.4)	3.6 (3.5)	15.4 (15.9)	21.0 (21.2)	14.2 (14.7)	Green-purple	3.45	196
(7) [Cr(Cys)PyCl ₂] ₂	30.0 (29.8)	3.5 (3.4)	8.4 (8.7)	21.7 (22.0)	16.2 (16.4)	Pale blue	3.3	–
(8) [Cr(Ala)PyCl ₂] ₂	27.1 (27.6)	4.4 (4.1)	9.1 (9.7)	24.7 (24.5)	17.4 (17.9)	Green-violet	3.36	150

^aThe last four complexes were prepared from 1:1 molar ratios. ^bComplex (3) decomposes without melting above 160°C.

analysis is inhibited. Some of the complexes are intensely hygroscopic, which accounts for deviations between calculated and observed elemental analyses. The magnetic susceptibility data (3.4–3.95 BM) are close to the spin-only value for a d³ chromium(III) system in octahedral or pseudo octahedral coordination with substantially ⁴A₂ ground state⁽⁷⁾. The higher magnetic susceptibility values ($\mu > 3.7$ BM) for some of the complexes suggest mixing of ⁴A₂ with terms derived from the excited state ⁴T₂. The mixing is possibly due to the difference in field strength of the environment⁽¹⁰⁾. The lower magnetic susceptibility value ($\mu > 3.75$ BM) suggest formation of a dimeric or polymeric structure⁽⁷⁾.

The significant i.r. frequencies of the complexes (with relevant bands of the free ligands in parentheses) and their probable assignments are summarized in Table 2. Displacements of the COO— symmetric stretches to lower wavenumbers (20–35 cm⁻¹) and of the antisymmetric stretches to higher wavenumber (15–60 cm⁻¹) are observed, showing that the amino acid carboxylate groups are involved in the coordination^(11,12). The $\delta(\text{NH}_2)$ vibrational mode is shifted to higher wavenumbers (40–70 cm⁻¹) and another mode, probably a $\rho_1(\text{NH}_2)$ twisting vibration, is also shifted to higher wavenumbers (30–80 cm⁻¹)

in the complexes on forming a coordinate bond compared with the free NH₂ group⁽¹³⁾. The absorption bands corresponding to the antisymmetric (3030–3250 cm⁻¹) and symmetric (1640–1680 cm⁻¹) vibrations of the amino groups are also shifted to lower wavenumbers compared to the usual range for such vibrations on complex formation, showing that the nitrogen atom of the amino group participates in the coordination^(12,13).

In the L-(–)-threonine complexes, the absorption band positions corresponding to the $\nu(\text{OH})$ stretching vibration at 3160 cm⁻¹ and the in-plane $\delta(\text{OH})$ deformation at 1340 cm⁻¹ agree with the absorption bands of the OH stretching vibration for 4-hydroxy-L-proline cadmium(II) complex in which the hydroxyl groups have not coordinated with the metal ion⁽¹¹⁾. These results suggest that in the OH group the oxygen atom does not participate in Cr—O bond formation⁽¹¹⁾. However, the hydrogen bonding in the L-(–)-threonine metal chelates could shift the stretching OH group vibration to higher frequencies by the formation of a chelate without participation in the formation of a Cr—O bond⁽¹¹⁾.

The i.r. spectra (Table 2) of the histidine complexes (2) and (6) are extremely complex and represent the super-

Table 2. Significant i.r. frequencies (cm⁻¹) of the complexes, with relevant bands of the free ligand in brackets.

Complex	$\nu_{\text{as}}(\text{COO—})$	$\nu_{\text{s}}(\text{COO—})$	$\Delta\nu$	$\delta(\text{NH}_2)$	$\rho(\text{NH}_2)$	C ₅ H ₅ N vibration	$\nu(\text{Cr—Cl})$
(1)	1600 (1625)	1410 (1375)	190 (250)	1477 (1416)	1135 (1107)		
(2)	1625 (1600)	1390 (1410)	235 (190)	1562 (1505)	1190 (1110)		
(3)	1650 (1590)	1340 (1370)	310 (220)	1560 (1510)	1135 (1120)		
(4)	1590 (1575)	1408 (1415)	182 (1601)	1570 (1520)	1140 (1108)		
(5)	1610	1390	220	1485	1140	650, 420	360, 330, 295
(6)	1615	1380	235	1568	1180	625, 425	390, 315
(7)	1640	1350	290	1575	1150	645, 410	400, 340
(8)	1608	1400	208	1570	1130	635, 420	390, 320

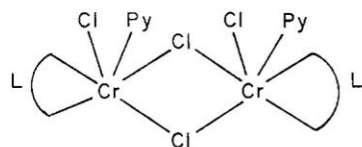
Table 3. Electronic and c.d. solution (solid) spectral with ligand field parameters^a.

Complex	${}^4A_{2g} \rightarrow {}^4T_{2g}$ (ν_1)	${}^4A_{2g} \rightarrow {}^4T_{1g}(f)$ (ν_2)	${}^4A_{2g} \rightarrow {}^4T_{1g}(p)$ (ν_3)	Dq	B	β_{35}	C.d.
(1)	19 802 (18 518)	26 666 (24 272)	31 645(5,54)	1980 (1852)	659 540	0.72 (0.59)	420(-), 466(+), 480(+), 590(-), 614(-) [490(+), 497(+), 570(+), 605(-)]
(2)	19 700 (19 607)	25 189 (25 974)		1980 (1961)	520 (603)	0.57 (0.63)	360(-), 390(+), 490(-), 560(+), 580(+) [450(-), 520(+), 550(+)]
(3)	16 386 (17 331)	22 970 (23 529)		1639 (17 331)	1659 600	0.72 (0.65)	350(+), 450(-), 536(+), 552(+), 590(-)
(4)	19 230 (18 690)	25 100 (24 961)	30 674	1923 (18 696)	550 (622)	0.60 (0.67)	
(5)	17 544	24 213	31 547	1754	656	0.71	420(-), 490(+), 550(+), 590(+), 620(+)
(6)	20 470	26 709		2047	589	0.64	420(-), 464(-), 516(+), 570(-), 590(-)
(7)	16 129	22 988		1613	665	0.70	340(+), 425(-), 520(+), 590(-)
(8)	18 248	23 255		1825	461	0.50	

^aB = 918 cm⁻¹ for chromium(III).

position of various wavenumbers. In complex (6) an absorption band at 1490 cm⁻¹ (absent from the spectrum of histidine itself) and also a moderately intense in-plane deformation component at 980 cm⁻¹ and thus ring breathing at 1030 cm⁻¹, are observed, suggesting nitrogen coordination of the imidazole ring^(12,14). Thus, the i.r. spectra (Table 2) suggest coordination of L(-)-histidine in the 1:1 derivative via amino, carboxylate and the nitrogen atom of the imidazole ring, while in the 1:3 derivative coordination via amino and carboxylate is proposed.

The i.r. spectra of complexes (3), (4), (7) and (8) (Table 2) suggest possible coordination of carboxylate and the amino group of L(-)-cysteine and DL-alanine to chromium(III). The SH band in cysteine is very weak and may be masked in the complex, and does not complex easily in non-aqueous solvents. Thus a structure such as shown in Scheme 1, could be formed for the complexes (7) and (8).

**Scheme 2.** L = L(-)-cysteine or DL-alanine.

The pyridine ring vibrations at 605 and 405 cm⁻¹^(15,16) are shifted to 625–650 and 420–425 cm⁻¹, respectively, upon complex formation, confirming the C₅H₅N → Cr coordination mode. In the 1:1 derivatives, vibrations in the 370–290 cm⁻¹ range are assigned to $\nu(\text{Cr}-\text{Cl})$ ^(15,16). Two $\nu(\text{Cr}-\text{Cl})$ vibrations are observed at 330–370 and 290–340 cm⁻¹ for the complexes (5)–(7) and are absent in the corresponding free ligand region, suggesting C_{3v} local symmetry for ligand atoms around the chromium, rather than C_{2v}, which would allow three vibrational modes⁽¹⁶⁾. Three $\nu(\text{Cr}-\text{Cl})$ vibrational modes are observed at 360, 340 and 310 cm⁻¹ for (7), confirming C_{2v} local symmetry. However, no suggestion can be made for the chloride positions from the i.r. spectra because the two differentially split $\nu(\text{Cr}-\text{Cl})$ vibrations are present in most of the 1:1 derivatives. Moreover, the *trans* position is a steric requirement of such vibrations⁽¹⁰⁾.

Visible spectral data in methanol and in solid KBr are given in Table 3, with representative spectra in Figures 1

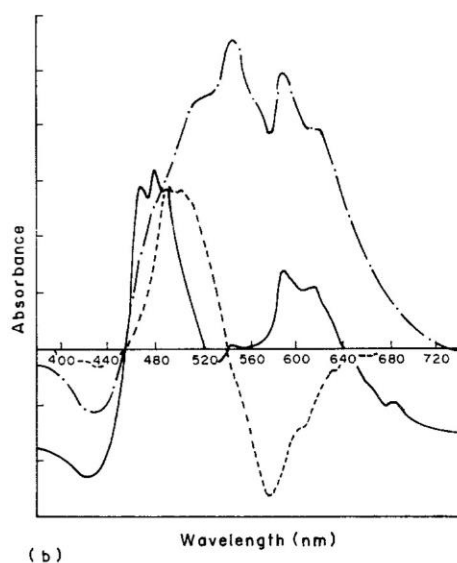
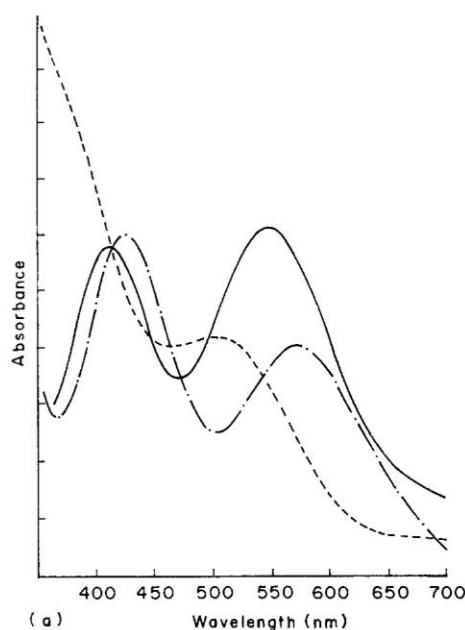
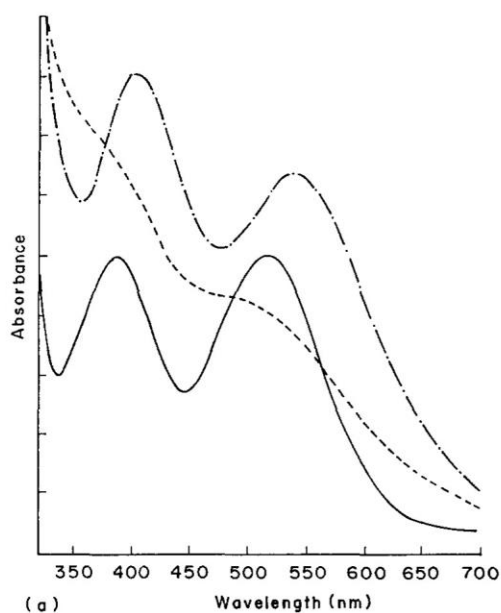
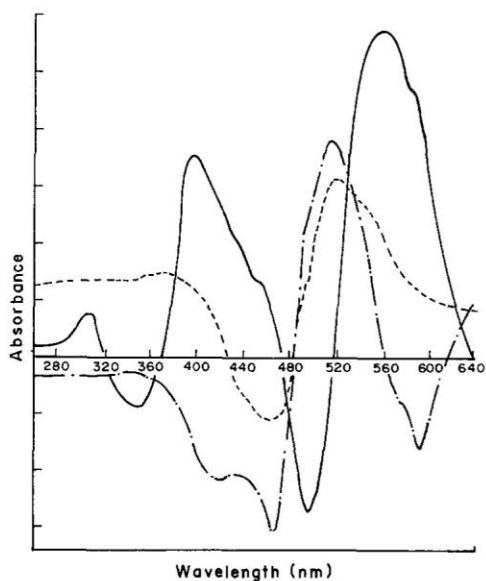


Figure 1. (a) Electronic spectra of Cr(Thr)₃ (—, solution; ····, solid) and solution spectrum of Cr(Thr)₂PyCl (— · — ·). (b) C.d. spectra of Cr(Thr)₃ (—, solution; ····, solid) and solution c.d. spectrum of Cr(Thr)₂PyCl (— · — ·).



(a)

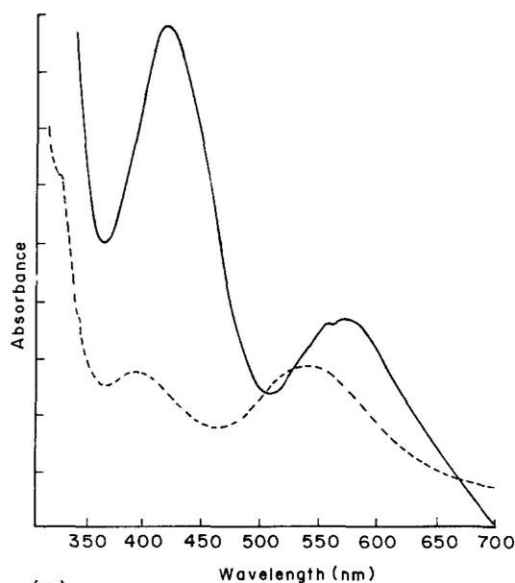


(b)

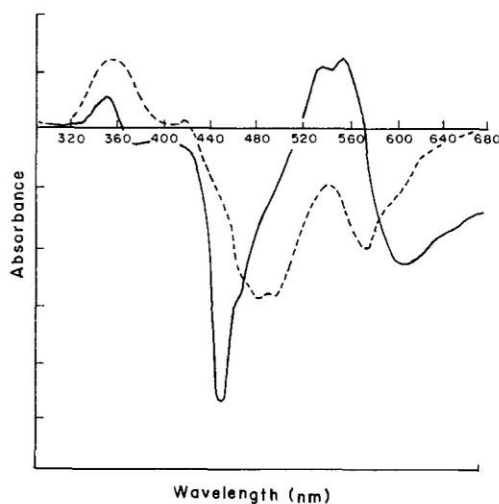
Figure 2. (a) Electronic spectra of $\text{Cr}(\text{His})_3$ (—, solution;, solid) and solution spectrum of $\text{Cr}(\text{His})_2\text{Cl}$ (-·-·-). (b) C.d. spectra of $\text{Cr}(\text{His})_3$ (—, solution;, solid) and solution c.d. spectrum of $\text{Cr}(\text{His})_2\text{Cl}$ (-·-·-).

and 3. Two defined peaks are observed at $16\,129$ – $16\,07$ and $22\,988$ – $26\,66\text{ cm}^{-1}$ and are assigned to the $\nu_1(^4A_{2g} \rightarrow ^4T_{2g})$ and $\nu_2(^4A_{2g} \rightarrow ^4T_{1g}(f))$ d–d transitions respectively in octahedral or pseudo octahedral symmetry⁽¹⁷⁾. A charge transfer band overlaps the ν_2 band and totally obscures the $\nu_3(^4A_{2g} \rightarrow ^4T_{1g}(p))$ band in the u.v. spectra of some of the complexes. The spin-forbidden transition band $\nu_2(23\,529\text{ cm}^{-1})$ in complex (3) (Figure 3) gives a higher absorption coefficient than the allowed band $\nu_1(17\,331\text{ cm}^{-1})$, which is possibly because of the symmetry reduction^(17,18). This leads also to the presumption that the coordination of the complex is not *trans* with respect to nitrogen or oxygen atoms.

The visible spectrum of complex (6) is seen to be unsymmetrical, indicating the presence of small peak under the envelope on the high-energy side⁽¹⁹⁾. Also, the apparently greater splitting observed may be taken as evidence of



(a)



(b)

Figure 3. (a) Electronic solution spectra of $\text{Cr}(\text{Cys})_2$ (—) and $[\text{Cr}(\text{Cys})\text{PyCl}_2]_2$ (---). (b) c.d. spectra of $\text{Cr}(\text{Cys})_3$ (—) and $[\text{Cr}(\text{Cys})\text{PyCl}_2]_2$.

trans-(carboxylate) histidine geometry⁽¹⁹⁾. Angular overlap model analysis of the electronic absorption spectra of *trans*-(carboxylate), *trans*-(imidazole) and *trans*-(amine) chromium(III) complexes of histidine have been reported⁽²⁰⁾ ($\Delta_{N_o} = 17.1 \times 10^3$, $\Delta_{N(i)} = 21.7 \times 10^3$ and $\Delta_{N(a)} = 22.7 \times 10^3\text{ cm}^{-1}$). The value $\Delta_o = 17.1 \times 10^3\text{ cm}^{-1}$ is in agreement with the data of complex (6) ($\Delta_o = 17.5 \times 10^3\text{ cm}^{-1}$), confirming formation of *trans*-(carboxylate) histidine geometry⁽¹⁹⁾. The bis-complex with tridentate histidine coordinate facially in octahedral field. The ν_2 splitting in a *cis*- CrN_4O_2 chromophore would be expected to be about half of that in the *trans* isomer⁽²¹⁾, which is totally different from that observed for complex (6), confirming formation of a *trans*-carboxylate isomer. The coordination of the four N atoms is inferred from the positions of the maxima in the visible spectra. The structural assignments can be made easily since the *cis*-O isomer usually has maxima at higher energy than the *trans*-O isomer. In addition, the *trans*-O isomer may show

a splitting of the ${}^4A_{2g} \rightarrow {}^4T_{2g}$ band which is used as further support for the structural assignment of complex (6). The similarity of the spectra of complex (6) to those of *trans*-carboxylate $[\text{Cr}(\text{His})_2]^+$ (λ_{max} 382 and 536 nm) and *trans*-O $[\text{Cr}(\text{en})_2(\text{OAC})_2]^+$ (λ_{max} 373 and 535 nm⁽²¹⁾) is further support for structural assignment of complex (6).

The spectra and the positions of the absorption bands of complexes (1) and (2) in MeOH are different from the corresponding ones recorded in KBr discs (Figures 1 and 2) showing that the complexes are significantly unstable, commencement of solvolysis, or the presence of low-symmetry components of the crystal field⁽²¹⁾. The complexes could also undergo chemical dissolution in methanol and hence the composition of the chromophores become different in solution and in solid^(12,22).

The parameters Dq , B and β_{35} have been calculated by Tanabe–Sugano procedures^(17,23) and are summarized in Table 3. The Dq values are in the range 1613–1961 cm^{-1} and close to the chloride ion (Dq for $\text{CrCl}_6^{-3} = 1318 \text{ cm}^{-1}$)⁽¹⁷⁾. These values place the ligands in the higher end of the spectrochemical series and provide reassurance that the amino acid is complexed to chromium(III) ion. The complexes in methanol can be arranged in the order (7) < (3) < (5) < (8) < (6) = (1) < (4) < (2) in terms of field strength. The Dq of complex IV ($Dq = 1869 \text{ cm}^{-1}$) is close to the value reported for tris-(alaninato)chromium(III) complex ($Dq = 1870 \text{ cm}^{-1}$)⁽²²⁾. $Dq = 2190 \text{ cm}^{-1}$ for CrN_6 and $Dq = 17500 \text{ cm}^{-1}$ for CrO_6 systems, while $Dq = 1970 \text{ cm}^{-1}$ for *fac*- CrN_3O_3 ^(21,23). These data indicate that *fac*-tris(amino acidato) compounds are formed in 1:3 ratio; however, the absorption maxima of tris(histidinato), (cysteinato) or (threoninato) are different from those predicted by Matsuola⁽²⁴⁾.

The B values for the complexes are calculated from the equation⁽²⁷⁾

$$B = 2v_1^2 + v_2^2 - 3v_1v_2 / (15v_2 - 27v_1)$$

The B values of the 1:3 derivatives are observed to be lower than that of 1:1 molar ratio, except for alanine and histidine (Table 3). This is probably due to the fact that the electron repulsion effect of methyl group in alanine and the bulky imidazole ring of histidine increase the basic donor effect of carboxylate and amino groups, making chromium able to supply the electron density required for back donation and stabilizing the conformation of chelates⁽¹⁰⁾. It could also be due to formation of different configuration dissymmetry and vicinal effect of the coordinated ligand⁽²⁴⁾. The B value of the tris(histidine) complex (2) is observed to be higher than that of complexes (1) and (3). This is possibly because the imidazole ring of histidine stabilizes the conformation of histidine chelates as compared to the hydroxyl on the mercapto group present in threonine or cysteine, respectively. The β_{35} values (0.50–0.72) are higher than the range observed for CrS_6 (0.44–0.45)⁽¹⁷⁾ and are somewhat close to the range observed for CrN_6 (0.64–0.65), CrO_6 (0.65–0.67), CrN_3O_3 (0.65–0.66)⁽²²⁾, CrS_3Cl_3 (0.54–0.65)⁽²¹⁾ and CrN_3Cl_3 (0.58–0.65)⁽²⁵⁾, confirming coordination via nitrogen, oxygen and/or chlorine. It therefore seems reasonable to presume that most of the chelates formed in this series involve CrO_3N_3 , or $\text{CrN}_2\text{O}_2\text{X}_2$ chromophores. The field parameters for complex (4) ($Dq = 1869 \text{ cm}^{-1}$, $B = 620$, $\beta_{35} = 0.67$) and complex (6) ($Dq = 2047 \text{ cm}^{-1}$, $B = 589$, $\beta_{35} = 0.64$) are close to the values reported for *fac*- $\text{Cr}(\text{Ala})_3$, $Dq = 1870 \text{ cm}^{-1}$, $B = 613$,

$\beta_{35} = 0.67$ ⁽²²⁾ and *fac-trans*-carboxylate $[\text{Cr}(\text{His})_2]^+$, $Dq = 2049 \text{ cm}^{-1}$, $B = 590$, $\beta_{35} = 0.64$ ⁽²⁰⁾, respectively, confirming the structures proposed.

The c.d. spectra are summarized in Table 3 and representative spectra are given in Figures 1 to 3. Strong Cotton effects are observed for all complexes except with that formed with DL-alanine, which is optically inactive. The Cotton effects confirm that the tested ligands are complexed to chromium(III) to produce optically active octahedral or pseudo octahedral chromium(III) complexes^(17,18). The complexes are likely to be *fac* since stronger and better defined Cotton effects are observed⁽¹⁷⁾. It is not clear from the c.d. curves whether the observed Cotton effects arise from one complex species or a mixture of different complex species in methanol. Therefore, t.l.c. plates with the mixed solvent $\text{C}_2\text{H}_5\text{OH}-\text{CHCl}_3$ (1:5 v/v) and transient iodine were used and confirmed that only one complex species is present in solution. Thus, the observed splitting is primarily due to the two ions present with symmetry splitting superimposed. The c.d. pattern of the complexes are similar to that of the tris(ethylenediamine) complex⁽²⁶⁾ in the spin-forbidden transition region; that is, three c.d. peaks are observed and the lowest and the highest frequency c.d. bands are of opposite sign to the central one (Table 3). Assuming that the complexes belong to D_3 symmetry, the three sharp peaks at 340–420, 390–466 and 470–516(+) nm in the spin-forbidden transitions are safely assigned to the ${}^2E_g({}^2E_g)$, ${}^2A_2({}^2T_{1g})$ and ${}^2E(T_{1g})$ d–d transitions⁽¹⁷⁾. The two c.d. bands at the higher-frequency side in the spin-forbidden transition are of opposite signs, which precludes assigning them to the $[2A, E_b]$ and E_a components of the 2T_1 state for which the rotational strengths are proportional to the net rotational strength for the first spin-allowed transitions⁽²⁶⁾. The assignment to $[E_a, E_b]$ and $2A$ or to E_b and $[2A, E_a]$ accounts for the c.d. signs of the observed bands. That is, the rotational strengths of the $[E_a, E_b]$ and $2A$ or of the E_b and $[2A, E_a]$ components are expected to be of opposite signs, because $R({}^4A_1)$ contributes largely to $R[E_a, E_b]$ and $R(E_b)$ and because the rotational strength for the ${}^4E \leftarrow {}^4A_2$ transition, which contributes largely to $R(2A)$ and $R[2A, E_a]$, should have opposite sign to $R({}^4A_1)$ ⁽²¹⁾. The Cotton effects at 520–595 and 550–610 nm are due to splitting of the allowed band ${}^4A_{2g} \rightarrow {}^4T_{2g}$ to ${}^4A_1({}^4T_{2g})$ and ${}^4E({}^4T_{2g})$ d–d transition^(7,17).

The signs of the Cotton effects of L(–)-threonine complexes (1) and (5) are the same, suggesting formation of complex species of similar configuration, while the sign of the Cotton effects of histidine (2), (6) and cysteine (3), (7) complexes are different, indicating formation of similar species but with ligands of opposite configuration. The c.d. spectra of histidine complexes (2) and (6) have greater strength compared to cysteine or threonine complexes, possibly owing to the ability of histidine to coordinate as a tridentate ligand in such media and the additional stability of histidine complexes via imidazole nitrogen, while L(–)-cysteine and L(–)-threonine are more likely coordinated as bidentate ligands via carboxylate and amino groups in non-aqueous media. The evident similarity of the c.d. patterns of the complexes (1)–(3), tris(en)⁽²⁶⁾ and $[\text{Cr}(\text{OX})\text{phen}]^+$ is possibly due to the optical activity being due to a kind of configurational dissymmetry rather than the vicinal effect of the coordinated amino acid. The absolute configuration determined on the basis of the c.d. dominance in the first spin-allowed band region is in accordance with that based

on comparison between the c.d. spectra of bis(oxalato) complexes and of the binuclear L-tartrato complexes with the $[\Delta-\Delta]$ configuration enforced by stereospecificity⁽²⁶⁾.

Chromium(VI) formation

Further experiments using CrCl_3Py_3 with L-(–)-threonine and L-(–)-histidine in 1:3 molar ratio in dry MeOH showed that bubbling of air or prolonged heating under reflux through these solutions for several (8–10) hours leads to oxidation of chromium(III) species, while cysteine and alanine do not. The oxidation process is confirmed by the fact that, upon addition of KI and CCl_4 to the acidified ($2 \text{ mol dm}^{-3} \text{ H}_2\text{SO}_4$) solution mixture, iodine was liberated in the CCl_4 layer while a blank solution of CrCl_3Py_3 gave no reaction. The electronic spectra of the solution mixture showed two defined peaks at 257 and 352 nm and a weak shoulder at ca. 410 nm. The absorbances at these peaks are found to be increased by aeration or prolonged heating of the solution, suggesting formation of chromium(VI) species. The spectra of the species formed are different from the spectra of chromium(IV) or chromium(V)⁽²⁷⁾. Thus chromium(III) species appear to be oxidized by air to some extent in MeOH unless a reducing agent is present in solution which would cause a reduction of chromium(VI). The reason for chromium(VI) formation is not yet clear; however, this raises the possibility that the active chromium(III)–amino acid complexes of some naturally occurring ligands in non-aqueous environment could produce chromium(VI) *in vivo*. The substantial stability of chromium(VI) species formed in solution suggests that if similar complexes are formed *in vivo* they would have time to reach many intracellular compartments and could hence be active in the toxicity of chromate⁽²⁸⁾. Thus if chromium(VI) is found, oxidation of thiol and sulphhydryl groups present in biological substrates could be undertaken⁽²⁸⁾. This also shows the effectiveness of various chelating agents for the removal of chromium bound to haemoglobin.

References

- ⁽¹⁾ G. K. Friman in G. L. Eicharn (Ed.), *Inorganic Biochemistry* (Russ. trans), IZd Mir, Moscow, 1978.
⁽²⁾ A. P. Gercely and I. Suvago, *Metal Ions in Biological Systems*, 9 (1978).

- ⁽³⁾ K. Blomquist and E. R. Still, *Inorg. Chem.*, 23, 3730 (1984).
⁽⁴⁾ K. Blomquist and E. R. Still, *Inorg. Chim. Acta*, 82, 141 (1984).
⁽⁵⁾ W. Mertz and K. Schwarz, *Am. J. Physiol.*, 196, 614 (1959).
⁽⁶⁾ D. H. Brown, W. E. Smith, M. S. El-Shahawi and M. F. K. Wazir, *Inorg. Chim. Acta*, 124, L25 (1986).
⁽⁷⁾ M. S. El-Shahawi and S. E. Ghazy, *Transition Met. Chem.*, in press.
⁽⁸⁾ J. C. Taft and M. M. Johnes, *Inorg. Synth.*, 7, 132 (1963).
⁽⁹⁾ D. H. Brown, G. C. McKinlay and W. E. Smith, *J. Chem. Soc., Dalton Trans.*, 199 (1978).
⁽¹⁰⁾ M. Freni, A. Gervasini and P. Romiti, *Spectrochim. Acta*, 39A, 85 (1983).
⁽¹¹⁾ Y. Inomata, T. Takeuchi and T. Moriwaki, *Spectrochim. Acta*, 110A, 179 (1984) and refs therein.
⁽¹²⁾ N. K. Davidenko, V. A. Raspopina, Yu. N. Shewchenko and O. I. Gordienko, *Russ. J. Inorg. Chem.*, 28, 523 (1987).
⁽¹³⁾ J. R. Kincaid and K. Nakamoto, *Spectrochim. Acta*, 32A, 277 (1976); H. Oki, *Bull. Chem. Soc. Jpn*, 50, 680 (1972).
⁽¹⁴⁾ R. H. Carlson and T. L. Brown, *Inorg. Chem.*, 5, 268 (1966).
⁽¹⁵⁾ R. J. H. Clark and C. S. Williams, *Inorg. Chem.*, 4, 358 (1965).
⁽¹⁶⁾ N. S. Gill, R. H. Nuttal, D. E. Scaife and D. W. A. Sharp, *J. Inorg. Nucl. Chem.*, 18, 79 (1961).
⁽¹⁷⁾ A. B. P. Lever, *Inorganic Electronics Spectroscopy*, Elsevier, Amsterdam, 1968.
⁽¹⁸⁾ T. Bruer, *Helv. Chim. Acta*, 56, 2388 (1963).
⁽¹⁹⁾ J. R. Perumareddi, *Coord. Chem. Rev.*, 4, 73 (1969).
⁽²⁰⁾ P. E. Hoggard, *Inorg. Chem.*, 20, 417 (1981).
⁽²¹⁾ E. S. Raper, S. Redshaw and J. R. Creighton, *Inorg. Chim. Acta*, 87, 21 (1984).
⁽²²⁾ H. Oki and E. Otsuke, *Bull. Chem. Soc. Jpn*, 49, 1841 (1976).
⁽²³⁾ D. Shotton, *Electronic Spectra of Transition Metal Complexes*, McGraw-Hill, London, 1968.
⁽²⁴⁾ N. Matsuoka, J. Hidaka and Y. Shimura, *Bull. Chem. Soc. Jpn*, 40, 1868 (1967).
⁽²⁵⁾ S. Kaizaki, J. Hidaka and Y. Shimura, *Bull. Chem. Soc. Jpn*, 42, 2207 (1967).
⁽²⁶⁾ S. Kaizaki, J. Hidaka and Y. Shimura, *Inorg. Chem.*, 12, 142 (1973); S. Sugaro, *J. Chem. Phys.*, 33, 1883 (1960); *Russ. J. Chem.*, 28, 523 (1981).
⁽²⁷⁾ E. G. Hope, P. J. Jones, W. Levason, J. S. Ogden, M. Tajik and J. W. Turff, *J. Chem. Soc., Dalton Trans.*, 2445 (1984).
⁽²⁸⁾ P. O. Brien, J. Barrett and F. Swanson, *Inorg. Chim. Acta*, 108 (1985) L19; A. McAuley and M. A. Olatunji, *Can. J. Chem.*, 55, 3335 (1977).

(Received 7 July 1992)

TMC 2828

Iodometric microdetermination of arsenic and antimony in organic compounds by use of amplification reactions

A. B. Farag¹, M. S. El-Shahawi² and E. M. El-Nemra¹

¹ Chemistry Department, Qatar University, Doha-2713, Qatar

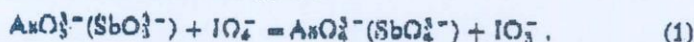
² Chemistry Department, United Arab Emirates University, UAE

Received September 26, 1992; revised December 11, 1992

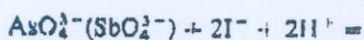
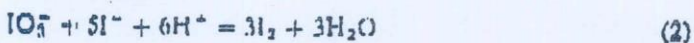
Summary. A six-fold iodometric amplification method is described for the determination of arsenic and antimony in organic compounds. It is based on the oxidation of arsenite (antimonite) with periodate and subsequent reaction of arsenate (antimonate) and iodate with iodide. Average recoveries were 99.8 and 99.5%, average standard deviations 0.22 and 0.34% for As and Sb, respectively.

Several methods have been described for the determination of arsenic and antimony in organic compounds [1] and in aqueous media [2]. A simple titrimetric method, based on iodometric amplification reactions, has been attractive as it affords sufficient accuracy for the determination of arsenic and antimony at the trace level. A three-fold iodometric amplification method for the determination of arsenic in organic compounds has been developed [3], but unfortunately, this method cannot be applied in the presence of other acid forming elements. An iodometric procedure suitable only for the determination of triphenyl arsine has been suggested [4]. The determination of some organo-antimony compounds by direct reaction with periodate has also been described [5]; however, a previous knowledge of the structure of the analyzed samples is necessary.

The oxidation of arsenite and antimonite ions with periodate can be illustrated as follows:



The released iodate and arsenate (antimonate) can oxidize iodide as follows



Correspondence to: A. B. Farag

It is well known that in strong acid media reaction (3) proceeds forward. However this reaction was found to be negligible in solutions having pH > 2.5. The oxidation of arsenite or antimonite with periodate (reaction 1) was found to be quantitative in the pH-range of 2.8–3.6 upon heating the reaction mixture on a boiling water bath for 20 min. This pH-range is quite suitable for masking the excess of unreacted periodate. Subsequently, an acetate buffer solution of pH ca. 3 was added at the beginning of the experiment. As is evident, each analyzed element will liberate six equivalents of iodine.

This six-fold amplification method was applied to the determination of varying concentrations (20–200 µg) of trivalent arsenic or antimony and satisfactory results were obtained. The average recoveries of arsenic and antimony were 99.4 and 100.7, respectively. Also, the quinquivalent element can be determined by the proposed method after quantitative reduction to the trivalent form. Saturated sodium sulphite solution (1 ml) in sulphuric acid medium (1 ml, 5 mol/l) has proven to be the most suitable reducing agent as the excess of sulphur dioxide is completely eliminated by gentle heating. The pH is then adjusted to ca. 3 and the trivalent element is oxidized as described above.

The proposed method was also successfully employed for the analysis of binary mixtures of the two oxidation forms of arsenic or antimony. The procedure is based on the direct determination of the trivalent element in an aliquot of the mixture by the periodate oxidation method. Another aliquot is then treated with sodium sulphite for the reduction of the quinquivalent element, and the total trivalent element is eventually determined. The thiosulphate solution which is equivalent to the quinquivalent element in the mixture is then calculated by difference.

Finally, the proposed six-fold amplification method has been examined for the microdetermination of arsenic or antimony in organic compounds. A mixture of nitric and sulphuric acids is employed to mineralize the organic compound in a micro-Kjeldahl flask. Arsenic or antimony produced is then reduced to the trivalent form prior to the treatment with periodate as described above. Application of this method to the analysis of *o*-hydroxybenzene-arsonic acid, *o*- and *p*-arsanilic acid, antimony potassium tartrate, stibophen and triphenylstibine revealed a satisfactory accuracy. The average recoveries for arsenic and antimony were 99.8% and 99.5%, the average standard deviations 0.22 and 0.34%, respectively.

References

1. Ma TS, Rittner RC (1979) Modern organic elemental analysis. Dekker, New York
2. Wilson CL, Wilson DK (1962) Comprehensive analytical chemistry vol. IC. Elsevier, Amsterdam
3. Gawargious YA, Boulos LS, Hammad BN (1976) Talanta 22:513
4. Gawargious YA, Bareda A, Hassouna MEM (1986) Microchem J 33:116
5. Gawargious YA, Boulos A, Bareda A (1976) Analyst 101:458

Adsorptive stripping voltammetric behaviour of gold(III) at a hanging mercury drop electrode in the presence of 1-(2'-pyridylazo)-2-naphthol

A.Z. Abu Zuhri and M.S. El-Shahawi

Department of Chemistry, Faculty of Science, UAE University, P.O. Box 17551, Al-Ain (United Arab Emirates)

M.M. Kamal

Department of Chemistry, Faculty of Science, Assiut University, Assiut (Egypt)

(Received 18th January 1993; revised manuscript received 23rd April 1993)

Abstract

The stripping voltammetric determination of gold(III) based on the adsorptive accumulation of the Au(III)-1-(2'-pyridylazo)-2-naphthol complex on a hanging mercury drop electrode is reported. The reduction current of the adsorbed gold complex ions is measured by differential-pulse cathodic stripping voltammetry. The peak potential is at -0.8 V vs. Ag/AgCl. The effects of various parameters (pH, ligand concentration, accumulation potential and collection time) on the response in the presence of ethanol-water (30%, v/v) and 0.5 M sodium sulphate are discussed. A linear response up to 5.0×10^{-8} M and a relative standard deviation of 2.9% at 3.0×10^{-8} M were obtained. The UV-visible spectrum of the complex formed was also measured. The applicability of the method to the determination of gold(I) and mixtures of gold(I) and (III) compounds was also successfully carried out. Possible interferences by trace metals on the proposed method were examined.

Keywords: Stripping voltammetry; Gold; Waters

Several electrochemical techniques have been applied to the trace determination of gold. Jacobs [1] and Monien [2] reported the determination of gold using carbon and carbon paste electrodes, respectively. Yoshimori et al. [3] determined gold by anodic stripping voltammetry at a glassy carbon electrode. Recently, procedures have been developed for determining gold by adsorptive collection on a Rhodamine B-modified carbon paste electrode [4] and a trioctylamine-modified carbon electrode [5]. Adsorptive voltammetric measurements based on the complexing of different metal ions with various pyridylazo derivatives as complexing agents have also been investigated [6–10].

Correspondence to: A.Z. Abu Zuhri, Department of Chemistry, Faculty of Science, UAE University, P.O. Box 17551, Al-Ain (United Arab Emirates).

This paper describes an adsorptive voltammetric method for the determination of traces of gold based on differential-pulse cathodic stripping voltammetry (DPCSV) of the accumulated Au(III) complex with 1-(2'-pyridylazo)-2-naphthol (PAN) at a hanging mercury drop electrode. The optimum analytical conditions for gold determination are reported.

EXPERIMENTAL

Reagents and materials

Unless specified otherwise, all reagents were of analytical-reagent grade. All solutions were prepared from doubly distilled water and/or ethanol. A stock solution of 1 mg ml^{-1} gold (atomic absorption standard; BDH) was used and

diluted with water for standard addition whenever required. A 10^{-3} M stock solution of PAN was prepared in ethanol. Britton–Robinson buffer solutions of various pH were prepared and served as the supporting electrolyte in 0.5 M sodium sulphate. Gold(I) was prepared by reducing gold(III) by sulphur dioxide, the excess of sulphur dioxide being removed by boiling the solution for 10 min. The gold content was assayed by oxidation of the gold (I) solution with bromine water; the excess of bromine removed by boiling. The final gold(III) solution was then treated with excess of potassium iodide at pH 2 and the liberated iodine was determined by titration with 0.005 M sodium thiosulphate.

Apparatus

The voltammograms were recorded on a Metrohm 506 Polarecord with a Metrohm 663 VA stand. The working electrode was a hanging mercury drop electrode (HMDE) and Ag/AgCl and platinum wire served as reference and auxiliary electrodes, respectively. pH measurements were made with a Metrohm Model 632 pH meter. The UV–visible spectra of the solutions were recorded on a Pye-Unicam SP 8-100 spectrophotometer using a 1 cm quartz cell. All experiments were performed at room temperature ($22 \pm 0.5^\circ\text{C}$).

Recommended procedure for gold determination

Determination of gold(III). Transfer 10 ml of the supporting electrolyte containing 1×10^{-7} – 5×10^{-7} M PAN and 30% ethanol at pH 9.3 into the voltammetric cell. Purge cell with nitrogen for 10 min and apply an accumulation potential of -0.2 V to a fresh mercury drop for an accumulation period of 3 min with stirring. Stop the stirring and after 15 s record the voltammogram by applying a negative scan from 0.0 to -1.2 V using the differential-pulse mode. After the ground voltammogram has been obtained, repeat the adsorptive stripping with a new drop with the addition of gold sample. After each sample addition, pass nitrogen through for about 2 min.

Determination of gold(I). Transfer aliquot portions of gold(I) solution into a 100-cm^3 conical flask and add 5 cm^3 of bromine water. Allow the

reaction mixture to stand for 3 min, then evaporate the solution gently on a hot-plate until the excess of bromine has been completely removed. Determine the total content of the element by following the procedure for the determination of gold(III).

Analysis of mixtures of gold(I) and (III). Determine gold(III) in an aliquot of the mixture as described for the determination of gold(III). Then oxidize another aliquot sample with bromine water to form gold(III) as described for the determination of gold(I) and determine the total content of the element by measuring the peak current employing the procedure described for gold(III). On the basis of the proposed method, the difference between the stripping peak height in the first and second steps is equivalent to the gold(I), while the peak current in the first step is equivalent to gold(III).

RESULTS AND DISCUSSION

PAN was found to be electrochemically active in the presence of 30% ethanol–water. Therefore, different attempts employing different reduction media were used to select the optimum experimental conditions for measurement of the peak current and for the resolution of the reduction peak of PAN. In 30% (v/v) ethanol–water and with 0.05 M Na_2SO_4 as supporting electrolyte at pH 9.3, a well resolved reduction peak was observed at -0.82 V vs. Ag/AgCl and the peak current was high under the optimum experimental conditions. The solubility of PAN in ethanol is better than that in water and other common solvents. The observed reduction peak is attributed to the reduction of the azo group in the molecule [9]. In the presence of gold(III) ions, a well defined, much enhanced reduction peak is observed at the same potential of PAN reduction wave, as shown in Fig. 1. The peak current increased markedly in proportion to the Au(III) concentration and accumulation time. The enhanced peak possibly results from the adsorption of an Au(III)–PAN complex on the electrode surface.

To verify the adsorption behaviour of PAN

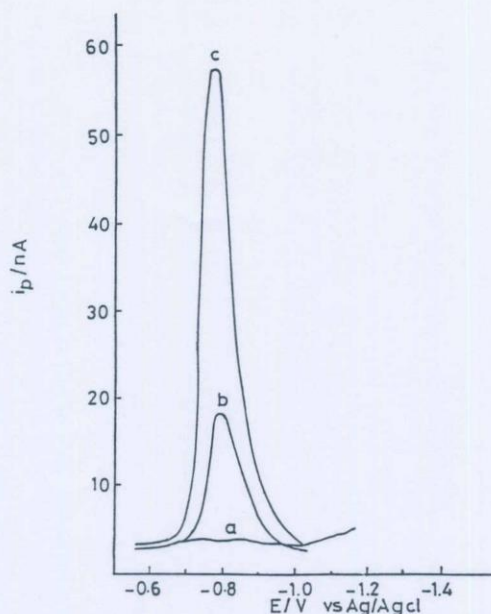


Fig. 1. Cathodic stripping voltammograms of (a) 4.0×10^{-8} M Au(III), (b) 1.5×10^{-7} M PAN and (c) 4.0×10^{-8} M Au(III) + 1.5×10^{-7} M PAN at pH 9.35 with deposition at -0.2 V and a collection time of 3 min in the presence of 30% ethanol.

and its Au(III) complex at the electrode, electrocapillary curves were recorded. The curve of a solution containing PAN and Au(III) was similar to that of PAN itself, indicating adsorption of both the Au(III) complex and the reagent at the electrode. Using the method proposed by Gao [11], the composition of the electroactive complex formed on the electrode surface is 1:2 [Au(III):PAN molar ratio].

The formation of an Au(III)–PAN chelate was confirmed from the UV–visible spectral measurements. The absorption spectrum of PAN in 30% ethanol at pH 9.3 exhibits four bands at 468, 415 (sh), 295 and 220 nm. The first three bands are assigned to $\pi \rightarrow \pi^*$ electronic transitions in the azo group, the hydrogen chelate ring and the 2-naphthol moiety [12]. The last band is due to a ${}^1L_a \pi \rightarrow \pi^*$ transition characteristic of the pyridyl heterocyclic electronic system [13]. The UV–visible spectrum of gold(III) solution under the same conditions showed three well resolved bands at 316, 230 and 205 nm. On mixing gold(III) and PAN solution at pH 9.3 in 30% ethanol, the

two Au(III) bands at higher wavelength disappear and the band at 468 nm of PAN becomes poorly resolved and is replaced with a shoulder at 450–470 nm, suggesting complex formation of gold(III) with PAN.

To elucidate the composition of the complex, solutions of gold(III) and reagent of 0.002 and 0.004 M were used. A series of solutions was prepared, keeping the concentration of Au(III) constant while varying the concentration of PAN and the pH values of the solutions were adjusted to 9.3 with Britton–Robinson buffer. The mixtures were allowed to stand for 20 min for completion of the reaction and the absorbance at 450 nm was measured against a blank containing no gold(III) under the same experimental conditions. The absorbance increased with up to a fourfold excess of the reagent, but increased steeply in the presence of up to a twofold excess of reagent, indicating the formation of a 1:2 gold(III)–PAN chelate [14].

To check the applicability of the adsorptive preconcentration behaviour of the Au(III)–PAN complex at the HMDE for the determination of trace amounts of gold(III) in water by DPCSV, different parameters, pH, collection time, accumulation potential and PAN and gold(III) concentrations, were investigated.

The influence of the pH of the aqueous solution on the peak height and peak potential on the adsorptive preconcentration of the Au(III)–PAN complex was examined at the HMDE. Other conditions were kept constant. The greatest peak enhancement (threefold at 3 min) and the best signal-to-background characteristics and reproducibility were obtained at pH 9.35. Therefore, pH 9.3 was adopted in subsequent work.

The dependence of the maximum stripping peak current on the collection time was examined for a sample containing 4.0×10^{-8} M Au(III) at pH 9.3 over the range 0–10 min. The maximum peak height was obtained at 3 min and was constant at longer times (Fig. 2). From the symmetrical shape of the reduction peak of the complex formed and the fact that the peak potential does not change with variation in the scan rate, it can be concluded that the electrochemical reduction of the Au(III)–PAN chelate is reversible.

The effect of the accumulation potential on the stripping peak current of the gold complex was examined over the potential range 0.0 to -0.5 V in 30% ethanol and 0.5 M Na_2SO_4 with the optimum pH and collection time. The largest peak current was obtained at a deposition potential of -0.2 V (Fig. 3). Therefore, -0.2 V was selected as the accumulation potential in the recommended procedure.

The effect of excess of the reagent was examined. The peak heights of a series of solutions containing 4.0×10^{-8} M gold(III) and various concentrations of the reagent were measured. It was found that the peak height increased linearly with increasing PAN concentration up to 5×10^{-7} M. The peak height tended to remain constant at larger excesses of the reagent. Under the optimum experimental conditions used, the maximum peak height was obtained at a ligand concentration of 5.0×10^{-7} M.

Determination of gold(III)

The greatest advantage of the determination of gold by the proposed adsorptive voltammetric

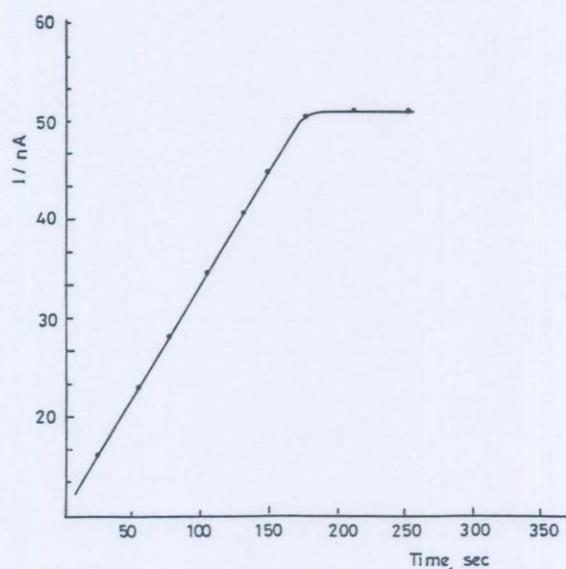


Fig. 2. Dependence of the reduction peak current on accumulation time for 4.0×10^{-8} M Au(III) with 1.5×10^{-7} M PAN at pH 9.35 with deposition at -0.2 V in the presence of 30% ethanol.

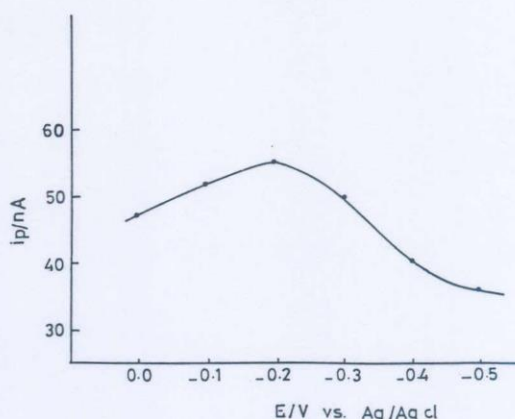


Fig. 3. Variation of peak current as a function of accumulation potential. Other conditions as in Fig. 1c.

method is the inherent sensitivity. Under the optimum conditions of pH 9.3 (Britton-Robinson buffer) in 30% ethanol, collection time 3 min, accumulation potential -0.2 V, negative differential-pulse scan (scan rate and amplitude) and reagent concentration 5.0×10^{-7} M, a linear relationship was obtained between the peak-height current ($I_F - I_B$) and the gold(III) concentration in the range $0-5.0 \times 10^{-8}$ M, where I_F and I_B are the peak-height currents of the gold(III)-PAN complex and PAN, respectively, under the same optimum experimental conditions. The regression coefficient and detection limit were found to be 0.996 and 1.0×10^{-9} M, respectively. Reproducibility tests on ten results at 4.0×10^{-8} M Au(III) showed a relative standard deviation of 2.9%.

The method was applied to the determination of gold(I), by prior oxidation to gold(III) by bromine water followed by the procedure described for the determination of gold(III). Satisfactory results were obtained and a linear calibration graph of gold concentration versus peak height was obtained.

The proposed method was also employed for the simultaneous determination of the gold(I) and gold(III) in a binary mixture in aqueous media. An aliquot of the mixture was first analysed employing the recommended procedure described for gold(III). Another aliquot was oxidized with bromine water, the unreacted bromine

was removed by boiling the solution and the peak current was measured by the procedure described for gold(III) determination. The difference between the stripping peak height was equivalent to the gold(I) concentration and the peak current in the first step was equivalent to the gold(III) concentration.

The method is also applicable to the determination of very low concentrations (less than nanomolar levels) in environmental samples. The sample is filtered through a 0.45- μm membrane followed by preconcentration of gold from a large sample volume of an acidic aqueous solution using porous polyurethane foam [15]. Elution of the sorbed gold by acetone from the foam column is possible, as reported previously [15], followed by determination using the proposed procedure.

Effect of diverse ions

The effects of diverse ions that are often present together with gold and form complexes with PAN were studied. The selectivity of the proposed method was examined by the determination of 4.0×10^{-8} M of gold(III) under the optimum experimental conditions. No interference was obtained in the presence of a relatively high excess (6.0×10^{-5} M) of Cd(II), Sr(II), Ba(II), Ca(II), Mg(II), Pd(II), Bi(III), Ni(II), Pb(II), Zn(II), La(II) and Ce(III). Bi(III), Ni(II), Pb(II), Zn(II), La(III), Cr(III) and molybdate at 1.0×10^{-7} M decreased the peak current of gold(III) by about 20–30%, while Cu(II), Fe(II) and Co(II) at 1.0×10^{-7} M interfered seriously. Ions such as molybdate may form mercury(I) salts covering the

HMDE. The possible formation of mercury(I) molybdate [16,17] could explain the decrease in the reduction peak height of the Au(III)–PAN chelate. Nevertheless, the determination of gold was not affected by the presence of up to 20 g l^{-1} of Mo(VI).

REFERENCES

- 1 E.A. Jacobs, *Anal. Chem.*, 35 (1963) 2112.
- 2 H. Monien, *Fresenius' Z. Anal. Chem.*, 237 (1968) 409.
- 3 T. Yoshimori, M. Arakawa and T. Takeuchi, *Talanta*, 12 (1965) 147.
- 4 G. Koelbi, K. Kalcher and A. Voulgaropoulos, *Fresenius' Z. Anal. Chem.*, 342 (1992) 83.
- 5 Q. Shi, J. Hong, R. Lu, G. Ma and Y. Zhou, *Gaodeng Xuexiao Huaxue Xuebao*, 11 (1990) 414; *Anal. Abstr.*, 54 (1991) 2D21.
- 6 P.A.M. Farias, S.L.C. Ferreira, A.K. Ohara, M.B. Bastos and M.S. Goulart, *Talanta*, 39 (1992) 1245.
- 7 J. Zhao and W. Jin, *J. Electroanal. Chem.*, 256 (1988) 181.
- 8 J. Lu, W. Jin and S. Wang, *Anal. Chim. Acta*, 238 (1990) 375.
- 9 J. Zhao and W. Jin, *J. Electroanal. Chem.*, 267 (1989) 271.
- 10 P.A.M. Farias and A.K. Ohara, *Electroanalysis*, 3 (1991) 985.
- 11 X. Gao, *Handbook on the Physics and the Chemistry of Rare Earths*, Elsevier, Amsterdam, 1986, p. 163.
- 12 P.W. Alexander and R.J. Sleet, *Aust. J. Chem.*, 23 (1970) 1183.
- 13 M.S. Masoud, A.A. Hasanein and A.M. Heiba, *Spectrosc. Lett.*, 17 (1984) 441.
- 14 J.H. Yoe and A.L. Jones, *Ind. Eng. Chem., Anal. Ed.*, 16 (1944) 111.
- 15 T. Braun and A.B. Farag, *Anal. Chim. Acta*, 99 (1978) 1.
- 16 E. Laviron, *J. Electroanal. Chem.*, 52 (1974) 355.
- 17 C.H. Khan and C.M.G. van den Berg, *Mar. Chem.*, 27 (1989) 31.

Preconcentration and Separation of Some Organic Water Pollutants with Polyurethane Foam and Activated Carbon

M. S. El-Shahawi

Chemistry Department, Faculty of Science, U.A.E. University, P. O. Box 17551, Al-Ain, United Arab Emirates

Key Words

Preconcentration
Polyurethane foam
Insecticides
Phenols
Separation

Summary

Although pesticides and phenols, cause reproductive failure in many areas of the world, there is a no effective means of treating waste water containing these compounds. This work deals with the adsorption of insecticides and phenols from aqueous solution by untreated porous polyurethane foam and activated carbon. Static experiments showed that in comparison with activated carbon a reasonable percentage of the compounds was adsorbed by the foam. Attempts were therefore made to extract these species from aqueous solution by foam column chromatography.

The results showed that the adsorption of the compounds was brought about by a mechanism similar to that of solvent extraction. The effect of various experimental conditions such as temperature, extracting medium, pH, contact time, volume of sample flow rate, compound concentration, and eluting solvents on the retention and separation of the compounds has been determined. The height equivalent to a theoretical plate (HETP) was calculated from breakthrough capacity curves and from chromatograms obtained from polyurethane foam columns for the insecticide Dyfonate; values were in the range 2.1–2.3 mm at 10–15 ml min⁻¹. Extraction of the compounds from natural water, and subsequent recovery, were both found to be complete. The high capacity of polyurethane provides advantages over activated carbon; in particular, large sample volumes can be analyzed at high flow rates.

Introduction

The compound classes responsible for pollution of potable water resources include polyaromatic hydro-

carbons, polychlorinated biphenyls, detergents, phenols, and pesticides [1]. The pesticides are toxic agents and are widely and regularly applied over large areas accessible to the public [2, 3]. These compounds are deliberately directed against living organisms and application occurs almost without control [4].

The removal of these organic pollutants, or their reduction to an acceptable concentration, can be performed by extraction with organic solvents, steam distillation, adsorption on active carbon and other solid supports, or the use of reversed liquid – liquid partition filter chromatography [5–9]. Such preconcentration methods are limited by low flow rate; they are often slow and are too expensive for routine analysis where many large volume samples are concentrated on site prior to quantitative analysis [5].

Gesser et al. [7] recently suggested the application of polyurethane foam for the collection of trace organic contaminants from water, using a batch technique: several investigations have since been published describing the application of foam as a collector for separating and concentrating various pesticides, phenols, and other organic substances [10–12].

The object of the work described herein was to evaluate the applicability of polyurethane foam and activated carbon for the preconcentration of insecticides and phenols, and to establish conditions furnishing good recoveries and high precision.

Experimental

Reagents and Materials

Prolabo steam-activated carbon was ground in a household-type blender to provide a range of smaller particle sizes; a uniform fraction was then separated, dried in an oven at 150 °C for 4 h, and stored over calcium chloride. Polyurethane foam, polyether type (bulk density 30 kg m⁻³), supplied by Schaumstoffwerk, Kremsmünster, Austria, was cut as previously described [12]. Tributyl phosphate (TBP)-loaded foams were prepared by mixing the dry foam cubes with TBP (5 cm³ per gram dry foam) for ten min, followed by drying [12]. The insecticides tested were Dursban, O, O-diethyl-O-(3,5,6-trichloro-2-pyridyl) phosphorothio-

ate, I; Karphos, O, O-diethyl-O-(S-phenyl-3-isoxazolyl) phosphorothioate, II; and Dyfonate, O-ethyl-S-phenylethyl phosphonodithiooate, III. The phenolic compounds used were O-chlorophenol, O-nitrophenol, and salicylaldehyde.

A stock solution of each compound ($100 \mu\text{g cm}^{-3}$) was prepared in a measuring flask (100 cm^3) by dissolving the exact weight of the tested species in 5 cm^3 acetone and diluting with distilled water. A series of standard solutions of these compounds was prepared by diluting the stock solutions with deionized distilled water and/or tap water. The solutions were then stored in polyethylene bottles.

Apparatus

Absorbance was measured with a Pye Unicam double-beam SP 8100 spectrophotometer, pH with a Metrohm 632 pH meter. All measurements were performed at room temperature.

General Procedures

Batchwise experiments. a) Adsorption experiments: Carbon samples (0.3 g) were shaken with solutions of each insecticide (50 cm^3 ; $20\text{--}80 \mu\text{g cm}^{-3}$) for various intervals up to 6 h. After vigorous agitation each solution was kept at 25°C until adsorption equilibrium was achieved. The amount of the compound remaining in solution was measured spectrophotometrically at the wavelength of maximum absorption; the amount retained by the carbon was calculated by difference. b) Sorption experiments: The effect of the length of the shaking period on the uptake of each compound was performed for both TBP foam and untreated polyurethane foam. The foam cubes (0.3 g) were equilibrated with a solution of each compound (100 cm^3 ; $60 \mu\text{g cm}^{-3}$) in Erlenmyer flasks and shaken for various periods up to 1 h. The foam cubes were then removed and the amount of the compound remaining in solution measured spectrophotometrically at the wavelength of maximum absorption. Following these procedures, other experiments were performed to determine the effects of other factors on the efficiency of extraction of the compounds by the foams.

Flow experiments. In order to determine the effect of eluting solvent and flow rates on the extraction efficiency of the foam and on the separation of some of the tested compounds, dry foam (1 g) was packed into glass columns ($12 \text{ cm} \times 10 \text{ mm I.D.}$) as previously reported [11] and samples of tap or distilled water ($0.5\text{--}3 \text{ dm}^3$) containing each compound ($200 \mu\text{g}$) were percolated through the foam column at $5\text{--}10 \text{ cm}^3 \text{ min}^{-1}$. After squeezing water from the foam, each compound was then extracted from the foam column with acetone (100 cm^3) in a Soxhlet extractor and the quantity determined by measuring the absorbance of the solution against a reagent blank.

Results and Discussion

The structures of the insecticides tested are given in Figure 1. Preliminary experiments using a batch technique have shown that collection of the investigated compounds is possible using both activated carbon and unloaded foam. Extraction efficiency was higher and equilibrium reached more rapidly (less than 1 h) with the polyurethane foam.

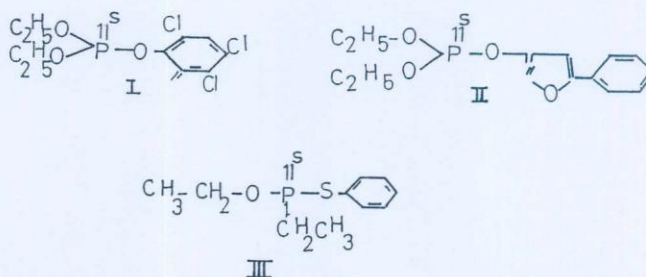


Figure 1
The structures of the insecticides tested.

Adsorption isotherms on Activated Carbon

In order to determine equilibrium characteristics for activated carbon, adsorption isotherms of the three insecticides were determined over a wide range of equilibrium concentrations ($20\text{--}80 \mu\text{g cm}^{-3}$) for six h. The pH of the solutions were adjusted to below 6 so that the adsorbates were predominately in the undissociated form. The adsorption isotherms are presented in Figure 2. It is evident that, at any equilibrium concentration the amount adsorbed follows the order: Dursban > Karphos > Dyfonate: the amount adsorbed is dependent on the molecular weight of the adsorbate where Dursban, Karphos, and Dyfonate have the molecular weights 349.5, 312, and 246, respectively. It

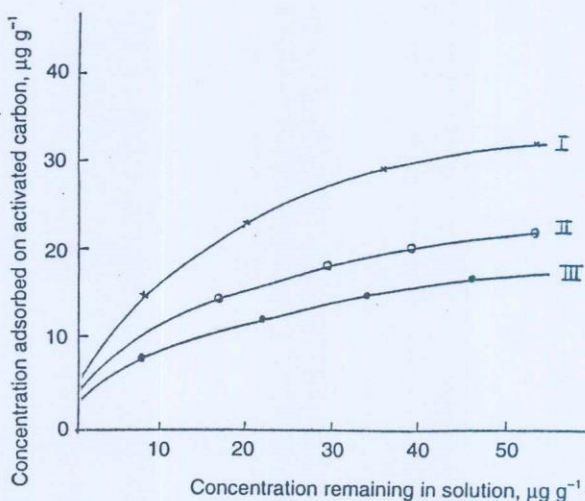


Figure 2
Adsorption isotherms of the insecticides on activated carbon (X) Dursban; (o) Karphos; and (•) Dyfonate

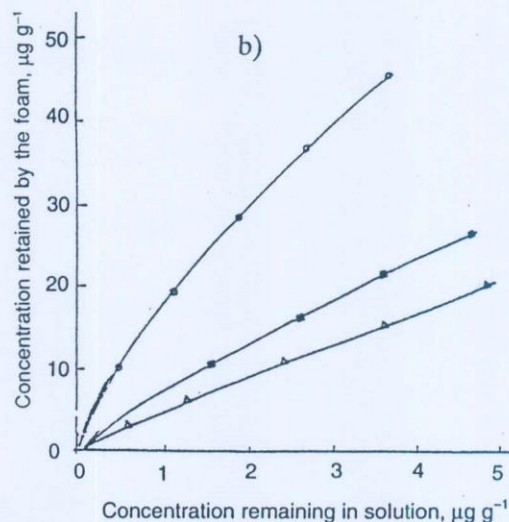
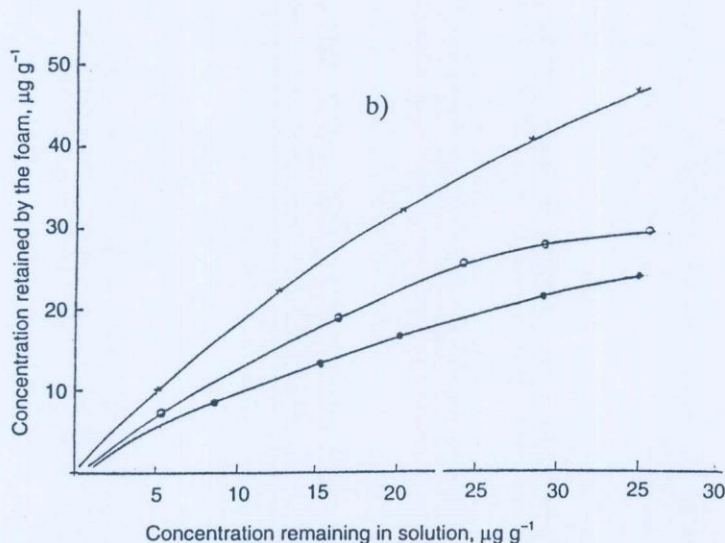
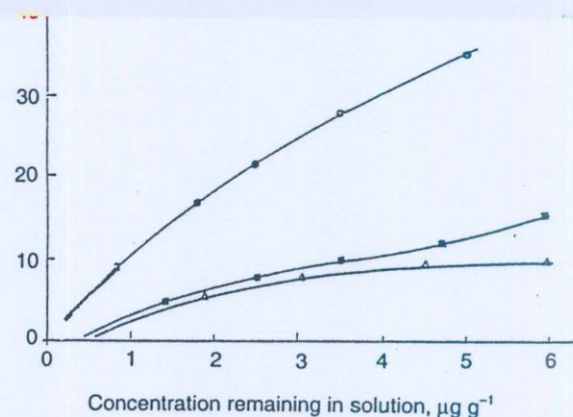
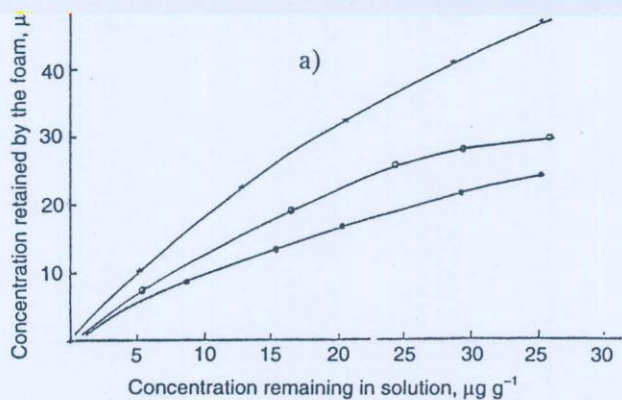


Figure 3

Extraction isotherms of the insecticides on unloaded (a) and TBP-foam (b); (X) Dursban; (o) Karphos; and (*) Dyfonate

Figure 4

Extraction isotherms of the phenolic compounds on unloaded (a) and TBP-foams (b). (Δ) *o*-nitrophenol; (■) *o*-chlorophenol; and (o) salicylaldehyde.

seems, therefore that Traube's rule [13] is applicable in the systems investigated and the results conform with the general understanding that, the larger the molecular weight of the adsorbate, the larger the amount adsorbed when the substances concerned are similar in nature. This order is also in accord with the suggestion of Kirkwood [14] that the smaller the dielectric constant of the adsorbate the larger the amount adsorbed.

Extraction Isotherms on Polyurethane Foams

The use of unloaded and TBP-loaded polyurethane foams as sorbent material enables simple isolation of the analyte from the matrix and yields an appropriate enrichment factor. This, together with the rapid attainment of the sorption equilibrium in the thin membrane forming the foam material, reduces the time required for analysis.

The uptake of the tested compounds from aqueous solution by the unloaded TBP-foams was found to

depend on their concentrations. The extraction isotherms of each insecticide were, therefore, determined for unloaded foams over a wide range of equilibrium concentrations ($20\text{--}80\ \mu\text{g cm}^{-3}$) for 1 h. The results are presented in Figure 3; the isotherm of the compounds exhibited first order behaviour at low concentrations. The sorption percentage increased in the order Dursban > Karphos > Dyfonate: the sequences are similar to those obtained from the activated carbon.

The extraction of the phenolic compounds from the aqueous solution by unloaded and TBP-loaded foam was found to depend on their concentration. The pH of the aqueous solutions was maintained between 5 and 6. The isotherms of the compounds tested ($10\text{--}80\ \mu\text{g cm}^{-3}$) exhibited first order behaviour at low concentrations and tended to plateau at high concentrations in the bulk solution, as shown in Figure 4. The sorption of the compounds by the unloaded and TBP-loaded foams increased in the order *o*-nitrophenol < *o*-chlorophenol < salicylaldehyde.

To investigate the mechanism of extraction of these compounds by the unloaded polyurethane foam, the extraction of the compounds from aqueous solution by diethyl ether was determined under the same experimental conditions. The extraction sequence of the compounds was exactly the same as that obtained with unloaded foams. Solvent extraction is, therefore, the most probable mechanism for the extraction of these pollutants by the unloaded foams; an anion-exchange mechanism is excluded. The molecular weight of the sorbate, the pK_a , and hydrogen bonding obviously play an important role in determining the efficiency of extraction by the untreated foam. These results agree with the general understanding that the larger the molecular weight of the sorbate the larger the amount extracted when the substances concerned are similar in nature [13, 14].

The influence of temperature on the sorption of the tested compounds ($60 \mu\text{g cm}^{-3}$) by the unloaded and TBP-loaded foams was determined at 35, 45, and 55 °C via batch experiments. The sorption profiles increased slightly with increasing temperature and the trends were similar to those obtained at room temperature.

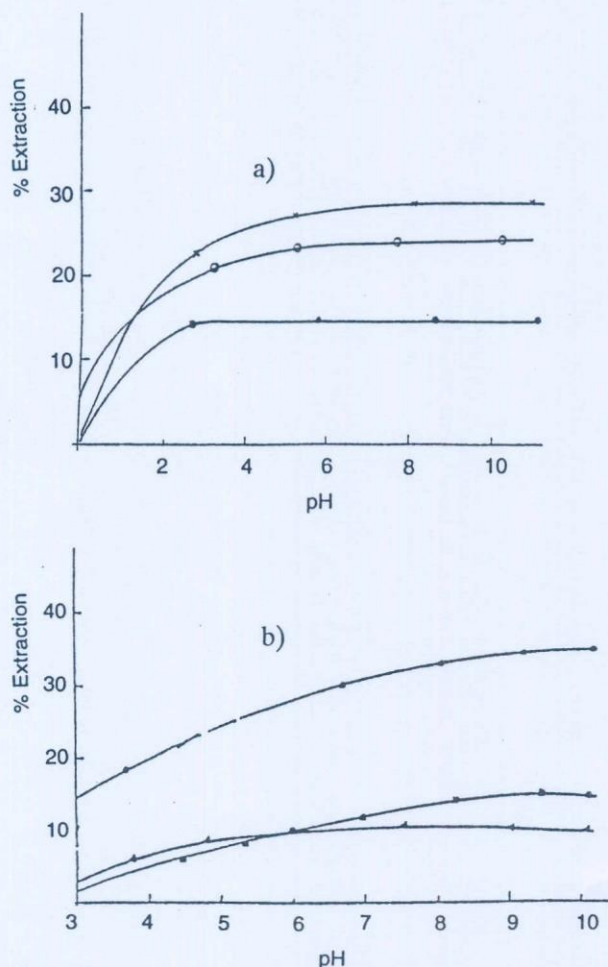


Figure 5
Effect of pH on the extraction of the insecticides (a) and phenolic compounds (b) by unloaded foam.
a. (X) Dursban; (o) Karphos; and (•) Dyfonate
b. (Δ) *o*-nitrophenol; (■) *o*-chlorophenol; and (o) salicylaldehyde.

Addition of sodium chloride (0.01–0.1 M) to the aqueous test solution did not improve the amount of the compound extracted by the unloaded foams in any system.

The effect of the pH of the aqueous solution on the extraction of the compounds (60 g cm^{-3}) by the unloaded foams was performed over a pH range of 3–9. The sorption profiles of the compounds by the unloaded foams are summarized in Figure 5. The degree of sorption of the compounds by the unloaded foam increased markedly with increasing pH and reached a plateau at pH ~ 10. The pH values were adjusted with hydrochloric acid (HCl) or sodium hydroxide (NaOH).

The influence of the medium on the sorption profile was studied for Dursban ($60 \mu\text{g cm}^{-3}$) with the unloaded foams. Addition of ethanol (0–20 %) to the bulk aqueous solution caused the sorption percentage to decrease. The results are summarized in Figure 6. Additional of ethanol is considered to reduce the formation of sorption-active species (lipophilic ion association) in aqueous solution [15]. It is also expected that ethanol causes swelling, which increases the effective surface area of the foam for the sorption of such compounds. Excess ethanol, however, reduces the dielectric constant of the solution bringing the polarities (or environments) of the bulk aqueous solution and the polyurethane foam matrix closer to each other. This, in effect, reduces the extent of sorption on to the foam by ion-association [13]. The nature of the media thus has a marked effect on sorption characteristics.

Flow Experiments

The extraction of the tested compounds by the unloaded foams via batch experiments, suggested the possible application of polyurethane foam in a column for

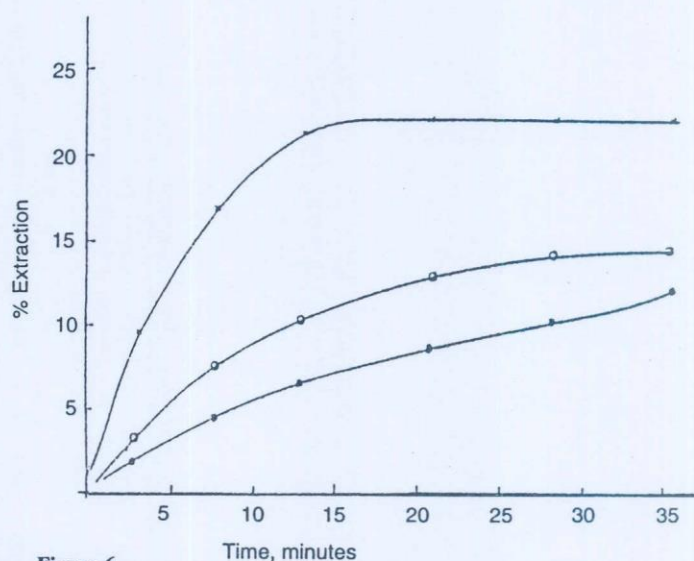


Figure 6
Effect of percentage ethanol (0–20 %) on the extraction of Dursban by unloaded polyurethane foam.
(X) %; (o) 10 %; and (•) 20 % ethanol.

collection and recovery of the insecticides. The excellent hydrodynamic properties of the foam columns enable the application of quite a high flow rate without the need for a vacuum. Tap and/or distilled water samples (0.2–3 dm³) containing 0.2–0.3 mg of each compound were passed through the foam column at 5–10 cm³ min⁻¹. Quantitative extraction of the compounds was achieved. After the water had been squeezed from the foam, the compounds were then eluted from the column with acetone (100 cm³) in a Soxhlet extractor, and determined spectrophotometrically at the maximum wavelength. The results are summarized in Table I. The dependence of the retention of the compounds by the unloaded foams on the flow rate (5–20 cm³ min⁻¹) and sample volumes (0.2–4 dm³) were also studied. Complete retention of the compound was achieved at flow rates up to 10 cm³ min⁻¹ and volumes of aqueous sample up to 3 dm³. At a higher flow rate (20 cm³ min⁻¹) and sample volume (4 dm³) the extraction percentage decreased significantly to 70–80 %.

The chromatograms obtained from retention of Dyfonate (0.1 mg) from aqueous solution and its elution using acetone were used to calculate the height equivalent to a theoretical plate (HETP) of the unloaded polyurethane foam column using the equation [16]:

$$N = \frac{8 V_{\max}^2}{W} = \frac{L}{\text{HETP}}$$

where N is number of plates, L the length of the foam bed, V_{max} the volume of eluate at peak maximum, and W the width of the peak at $\frac{1}{e}$ the maximum solute concentration.

The HETP values were found to be 2.1 and 2.3 mm at flow rates of 8–10, and 15 cm³ min⁻¹, respectively. The

Table I. Extraction of the compound tested (200 µg) from 3 dm aqueous solution by unloaded polyurethane foam columns, and recovery at a flow rate of 8–10 cm³ min⁻¹.*

Compound	% Recovery		Wavelength (nm)
	(a)	(b)	
Dursban	98	101	290
Karphos	97	95	280
Dyfonate	96	99	285
<i>o</i> -Chlorophenol	97	99	274
<i>o</i> -Nitrophenol	99	93	346
Salicylaldehyde	99	102	257

(a) Average of five determinations from distilled water

(b) Average of five determination from tap water

* Poor recoveries (20–25 %) were obtained for the compounds tested on employing an activated carbon column at 2–5 cm³ min⁻¹.

HETP for Dyfonate at 10 cm³ min⁻¹ on the unloaded foam column was also obtained by using the breakthrough capacity curve and employing the equation:

$$N = \frac{V' \cdot V}{(V' - V)^2} = \frac{L}{\text{HETP}}$$

where V' is the volume of eluate at the centre of the S-shaped breakthrough capacity curve, where the concentration is one-half the initial concentration, and V is the volume at which the effluent has a concentration of 0.1578 of the initial concentration. The HETP value obtained by this method was 1.8 mm, quite close to the value obtained from the elution curves. The capacity of the unloaded foam obtained from the breakthrough capacity curve was found to be 10.5 mg Dyfonate per gram of dry unloaded foam. The method has been used for the separation of Dyfonate (0.1 mg) and Dursban (0.05 mg) from aqueous solution on an unloaded polyurethane foam column. Dursban was eluted first with acetone at 2–5 cm³ min⁻¹ and Dyfonate by increasing the flow to 10 cm³ min⁻¹. The method has been applied for the extraction of Dyfonate from various samples of waste water and the degree of retention found to be 80 %.

References

- [1] J. R. H. Malissa, Egypt. J. Anal. Chem. **1**, 49 (1990).
- [2] A. S. Y. Chau, B. K. Afghan, J. W. Robinson, „Analysis of Pesticides in Water, Significance, Principles, Techniques and Chemistry of pesticides“, CRC Press, Inc. Boca Raton, Vol. 1 (1982).
- [3] H. Konig, W. Strabel, Fresenius Z. Anal. Chem. **315**, 205 (1983).
- [4] L. T. Kurkland, S. Shibko, A. Kolbye, R. Shapiro, Haz. Mercury Environ. Res., **4**, 9 (1971).
- [5] A. H. Romano, R. S. Safferman, J. Amer. Water, Works Assoc. **55**, 169 (1963) and references therein.
- [6] H. Oda, C. Yokokawa, Carbon **21**, 483 (1983).
- [7] J. F. Uthe, J. Reinke, H. D. Gesser, Environ. Lett. **3**, 117 (1972).
- [8] B. Ahling, S. Jensen, Anal. Chem. **36**, 134 (1964).
- [9] B. K. Afghan, R. J. Wilinon, A. Chow, T. W. Findley, H. D. Gesser, K. I. Srikameswaran, Water Res. **18**, 9 (1984).
- [10] G. J. Moody, J. D. R. Thomas, „Chromatographic Separation with Foamed Plastics and Rubbers“ Marcel Dekker, 1982.
- [11] T. Braun, J. D. Naveratil, A. F. Farag, „Polyurethane Sorbents in Separation Science“, CRC Press, Boca Raton, FL, 1985.
- [12] A. B. Farag, M. S. El-Shahawi, J. Chromatogr. **552**, 371 (1991) and references therein.
- [13] A. W. Adamson, „Physical Chemistry of Surface“ 2nd edn., Academic Press, N.Y. 1967.
- [14] K. G. Kirkwood, J. Chem. Phys. **2**, 351 (1934).
- [15] T. Hayashita, M. Takagi, Talanta, **32**, 399 (1985).
- [16] E. Gluenkauf, Trans. Faraday. Soc. **15**, 34 (1955).

Received: Sep 14, 1992

Revised manuscript

received: Oct 30, 1992

Accepted: Nov 20, 1992

Chromium(III) Complexes with Some Optically Active α -Hydroxy Acids

M. S. El-Shahawi* and A. A. El-Bindary

Chemistry Department, Faculty of Science at Damietta, Mansoura University, Damietta, Egypt

Z. Naturforsch. **48b**, 282–286 (1993); received September 9/November 23, 1992

Chromium Complexes, α -Hydroxy Acids, IR Spectra, CD Spectra

Complexes obtained from CrCl_3Py_3 with some optically active α -hydroxy acids have been characterized by elemental analysis, magnetic susceptibility, vibrational (IR), electronic and circular dichroism (CD) spectra. The magnetic susceptibility data are close to the spin-only value for a d^3 chromium(III) ion in octahedral or distorted octahedral symmetry. Three (Cr–Cl) vibrational modes in the region $410\text{--}290\text{ cm}^{-1}$ are observed for some of the complexes indicating C_{2v} local symmetry of ligand atoms around the chromium(III). In the electronic spectra two peaks are observed in the range $16949\text{--}18018$ and $22986\text{--}24570\text{ cm}^{-1}$. They are assigned to d–d transitions in pseudo octahedral symmetry. The structure of the complexes is likely to be facial since strong and well defined Cotton effects are observed. The parameters (D_q, B, β_{35}) for the complexes provide reassurance that pyridine nitrogen is preserved.

Introduction

The chemistry of chromium is of considerable interest [1]. Chromium(III) is considered to be essential to mammals for the maintenance of glucose, lipid and protein metabolism, but chromium(VI) is reported to be toxic [2]. The carcinogenicity of chromium(VI) is considered in terms of the uptake/reduction model [3].

Little work has been carried out on the non-aqueous preparations of chromium(III) compounds with naturally occurring ligands [4, 5]. However, for aqueous media a large number of chromium(III) complexes with α -hydroxy acids have been reported [6–11]. The coordinating properties of the title ligands and their coordination compounds seem to be implied in the therapeutic activity displayed by drugs of transition metal ions [12, 13]. The present investigation deals with the characterization of the complexes of chromium(III) with some optically active α -hydroxy acids in methanol.

Experimental

Reagents and materials

D-tartaric (Tar), L-malic (Mal), L-mandelic (Man) and L-lactic (Lac) acids were of reagent grade. BDH pyridine (Py) and methanol were

* Reprint requests to Dr. M. El-Shahawi.

Present address: Chemistry Department, Faculty of Science, UAE University, Al-Ain 17551 United Arab Emirates.

Verlag der Zeitschrift für Naturforschung,
D-W-7400 Tübingen
0932-0776/93/0300-0282/\$ 01.00/0

used without further purification. The complex CrCl_3Py_3 was prepared by the method of Taft *et al.* [14] and was stored in a vacuum desiccator over CaCl_2 .

Preparation of the complexes

To a solution of CrCl_3Py_3 (1 mmol) in dry methanol, the appropriate weights of the α -hydroxy acid are added to obtain 1:1 and 1:3 chromium(III) ligand molar ratios. The mixture was then refluxed with constant stirring. A number of complexes appeared to be formed in less than one hour, however, all solutions were refluxed for 4 h. The solutions were then reduced in volume cooled to room temperature, and 50 cm^3 ether were added. Crystalline solids separated out. They were washed with ether and finally dried in a desiccator. The solid complexes were then redissolved in methanol and the absorption spectra were measured at room temperature. Chromium was determined as oxide by the method reported [15].

Physical measurements

The IR, UV-visible and circular dichroism spectra were measured from KBr disks with a Perkin Elmer 457 spectrometer, a Varian 634 S spectrometer and an instrument described elsewhere [16], respectively. Magnetic measurements were made on a Johnson Matthey magnetic balance. Silica gel TLC plates (Merck 60 F 254) $10 \times 20\text{ cm}$ were employed.

Results and Discussion

The prepared complexes are listed in Table I together with their elemental analyses as well as with

Table I. Analytical data; room temperature magnetic moments μ (B. M.) and physical properties of the complexes.

Compound	Percentage calculated (found)			N	Cl	Colour	μ_{eff}	$M_{\beta, \mu}$	M. p. [$^{\circ}$ C]
	Cr	C	H						
Cr(Tar) ₃ Py ₃	7.0 (6.8)	43.7 (43.9)	4.0 (3.7)	5.7 (5.4)	—	purple	3.9	189	
Cr(Mal) ₃ Py ₃	7.6 (7.3)	47.0 (47.4)	4.4 (4.2)	6.1 (5.9)	—	violet	4.05	142	
Cr(Man) ₃ Py ₃	7.0 (6.8)	63.0 (62.7)	4.9 (5.1)	5.7 (5.5)	—	green	4.0	170	
Cr(Lac) ₃ Py ₃	9.4 (9.6)	49.6 (50.0)	5.4 (5.7)	7.6 (7.8)	—	green violet	3.87	140	
Cr ₂ (Tar) ₂ Py ₄	14.6 (14.4)	47.2 (46.8)	3.4 (3.2)	7.9 (8.1)	—	purple	3.4	187	
Cr ₂ (Man) ₂ Py ₄ Cl ₂	13.1 (12.8)	54.6 (54.1)	4.0 (3.9)	7.0 (7.2)	9.0 (8.7)	green	3.42	197	
Cr ₂ (Lac) ₂ Py ₄ Cl ₂	15.6 (15.9)	46.8 (47.0)	4.1 (4.3)	8.4 (8.1)	15.6 (15.7)	green	3.45	160	
Cr ₂ (Mal) ₂ Py ₄ Cl ₂	13.7 (13.9)	44.4 (44.6)	3.7 (3.5)	7.3 (7.6)	9.3 (9.6)	purple	3.4	176	

other physical and chemical properties. The elemental analyses indicate that the complexes obtained from the 1:3 ratio of reagents have the formula $[\text{Cr}(\text{L}-\text{H})_3\text{Py}_3]$, where L = Tar, Mal, Man or Lac. The complexes formed from the 1:1 ratio have the formula $[\text{Cr}_2(\text{L}-2\text{H})_2\text{Py}_4\text{Cl}_2]$ except for D-tartaric acid which forms the complex $\text{Cr}(\text{Tar}-3\text{H})_2\text{Py}_4$. The complexes are purple or green violet in colour and have fairly low melting points ($< 200^{\circ}\text{C}$). The magnetic susceptibility data (3.4–4.05 B.M.) are close to the spin-only value for a d^3 chromium(III) ion in octahedral or slightly distorted octahedral ligand field with a $^4\text{A}_2$ ground state. The higher values of the magnetic susceptibilities observed for the complexes $\text{Cr}(\text{L}-\text{H})_3\text{Py}_3$ suggest a mixing of $^4\text{A}_2$ with the terms derived from the excited state $^4\text{T}_2$. The mixing is possibly due to the difference in the field strength of the environment [17]. The lower values of the magnetic moment for the complexes prepared in 1:1 ratio suggest the formation of dimeric structures [10].

The significant IR frequencies of the complexes with relevant bands of the free ligands and their probable assignments are given in Table II. The strong broad bands in the ranges 3290–3460 and 3020–3100 cm^{-1} observed in the hydroxy acids are tentatively assigned to OH stretching vibrations, because there are no bands in these ranges in

DL-amino-*n*-butyric acid which has no hydroxyl group [18, 19]. The largest bathochromic shift (35–90 cm^{-1}) for the OH group upon coordination is expected for the complexes prepared in 1:1 ratio [18, 19]. In these complexes, the oxygen atom of the hydroxyl group may participate in the formation of a Cr–O bond, and the hydrogen bond which is present in the free ligand may break or become weaker for these compounds. However, for the complexes prepared in 1:3 ratio, the position of the absorption bands corresponding to the OH stretching vibration mode agree with the absorption bands of the free ligand, showing that the oxygen atom of the OH group does not participate in the formation of Cr–O.

Displacements of the COO^- symmetric stretches by 20–25 cm^{-1} to lower wavenumbers and of the antisymmetric stretches by 20–60 cm^{-1} to higher wavenumbers are observed, showing that the carboxylate groups of the hydroxy acids are probably involved in the coordination [19]. Three (Cr–Cl) vibrational modes in the region 410–290 cm^{-1} for the complexes $[\text{Cr}_2(\text{L}-2\text{H})_2\text{Py}_4\text{Cl}_2]$. L = Mal, Man or Lac are observed, indicating C_{2v} local symmetry of ligand atoms around the chromium rather than C_{3v} which would allow two bands [20]. Cr–N stretching vibrations were also observed in the range 365–310 cm^{-1} for most of the prepared complexes.

Table II. Significant IR frequencies (cm^{-1}) of the complexes, with relevant bands of free ligand in brackets, and band assignments.

Compound	νOH	$\nu_{\text{as}}\text{COO}^-$	$\nu_{\text{s}}\text{COO}^-$	$\Delta\nu$	$\nu(\text{Cr}-\text{N})$	$\nu(\text{Cr}-\text{Cl})$
$\text{Cr}(\text{Tar})_3\text{Py}_3$	3450 (3450)	1620 (1590)	1350, 1360 (1380)	270	370, 320, 300	—
$\text{Cr}(\text{Mal})_3\text{Py}_3$	3455 (3460)	1625 (1595)	1360 (1400)	265	360, 316, 290	—
$\text{Cr}(\text{Man})_3\text{Py}_3$	3460 (3460)	1650 (1610)	1350 (1390)	300	370, 316, 290	—
$\text{Cr}(\text{Lac})_3\text{Py}_3$	3295 (3290)	1640 (1620)	1360 (1380)	240	375, 310, 295	—
$\text{Cr}_2(\text{Tar})_2\text{Py}_4$	3470	1650	1360	295	360, 340, 300	—
$\text{Cr}_2(\text{Mal})_2\text{Py}_4\text{Cl}_2$	3480	1625	1350	275	380, 335, 295	370, 330, 285
$\text{Cr}_2(\text{Man})_2\text{Py}_4\text{Cl}_2$	3485	1630	1355	275	365, 340, 316	290, 310, 290
$\text{Cr}_2(\text{Lac})_2\text{Py}_4\text{Cl}_2$	3340	1645	1355	290	360, 340, 310	370, 320, 295

The electronic spectra of the complexes are summarized in Table III, and representative spectra are given in Fig. 1. Two peaks are observed in the ranges 16949–18018 and 22986–24570 cm^{-1} and are assigned to ${}^4\text{A}_{2g} \rightarrow {}^4\text{T}_{2g}$ and ${}^4\text{A}_{2g} \rightarrow {}^4\text{T}_{1g(f)}$ d-d transitions, respectively, in the octahedral and pseudooctahedral symmetry [21]. Another strong peak is observed in the range 29411–32258 cm^{-1} for some of the complexes and is assigned to ${}^4\text{A}_{2g} \rightarrow {}^4\text{T}_{1g(p)}$ d-d transitions. The spectra of the complexes $\text{Cr}_2(\text{Mal})_2\text{Py}_4\text{Cl}_2$; $\text{Cr}_2(\text{Lac})_2\text{Py}_4\text{Cl}_2$ and $\text{Cr}(\text{Lac})_3\text{Py}_3$ reveal that the spin forbidden transition at 22988–24390 cm^{-1} gives higher absorption coefficients than the spin allowed band at 16948–17794 cm^{-1} (Fig. 1) sug-

gesting symmetry reduction of these compounds [7].

The spectra of the complexes formed in 1:1 ratio are different from those prepared in 1:3 ratio confirming the formation of different types of structures involving more extensive replacement of the initial ligands by hydroxy acid ligands. Bonding of the tartrate ligand to chromium(III) could be either through two carboxyl groups; or one hydroxy and one carboxyl group [22], or dimers could be formed by tartrate bridges [10].

The parameters D_q , B, and β_{35} have been calculated by Tanabe-Sugano procedures [21, 23] and are summarized in Table III. The D_q values of the complexes are close to that of the chloride ion (D_q

Table III. Electronic spectra (cm^{-1}) and circular dichorism (nm) data of the complexes with ligand field parameters in methanol.

Complex	${}^4\text{A}_{2g} \rightarrow {}^4\text{T}_{2g}$ ν_1	${}^4\text{A}_{2g} \rightarrow {}^4\text{T}_{1g(f)}$ ν_2	${}^4\text{A}_{2g} \rightarrow {}^4\text{T}_{1g(p)}$ ν_3	D_q	B	β_{35}	CD (nm)
$\text{Cr}(\text{Tar})_3\text{Py}_3$	17921	23809	—	1792	559	0.61	445(-), 490(+), 570(+), 590(+), 620(+, sh)
$\text{Cr}(\text{Mal})_3\text{Py}_3$	18018	24570	—	1802	638	0.70	384(+), 440(+), 486(+), 550(-), 594(+), 640(-), 654(-)
$\text{Cr}(\text{Lac})_3\text{Py}_3$	17094	23255	—	1709	597	0.65	400(-), 470(-), 530(-), 580(+), 630(-)
$\text{Cr}(\text{Man})_3\text{Py}_3$	17544	23809	—	1754	606	0.66	290(+), 400(-), 526(-), 590(+), 655(-), 670(-)
$\text{Cr}_2(\text{Tar})_2\text{Py}_4$	17794	24390	34482	1779	645	0.70	410(-), 520(+), 550(+), 590(+), 650(-), 640(-), 654(-)
$\text{Cr}_2(\text{Mal})_2\text{Py}_4\text{Cl}_2$	17921	24096	29411	1792	592	0.65	386(+), 440(+), 480(-), 550(+), 590(-), 640(-), 650(-)
$\text{Cr}_2(\text{Lac})_2\text{Py}_4\text{Cl}_2$	16949	22986	30303	1695	584	0.64	405(-), 475(-), 534(-), 580(+), 630(-)
$\text{Cr}_2(\text{Man})_2\text{Py}_4\text{Cl}_2$	17391	23255	31250	1739	560	0.61	300(+), 410(+), 545(+), 595(-, w), 650(-)

* (B for the Cr(III) ion is 918 cm^{-1}).

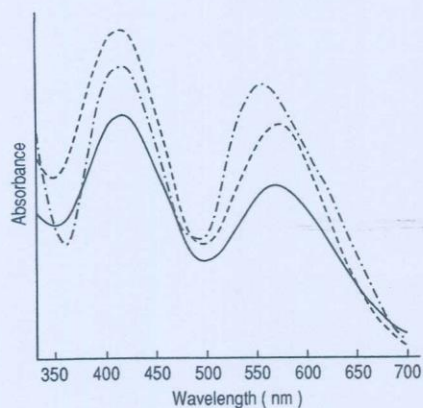


Fig. 1a. Electronic spectra of the complexes, $\text{Cr}_2(\text{Lac})_2\text{Py}_4\text{Cl}_2$, —; $\text{Cr}_2(\text{Lac})_3\text{Py}_3$, ---- and $\text{Cr}_2(\text{Mal})_2\text{Py}_4\text{Cl}_2$, - · - · in methanol.

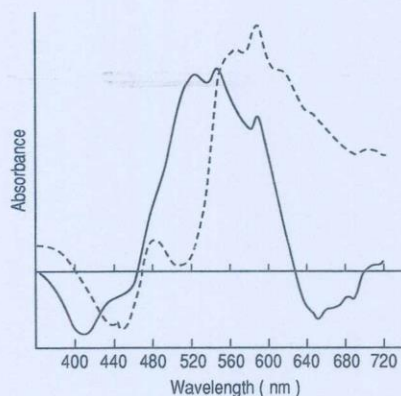


Fig. 1b. Circular dichroism spectra of the complexes, $\text{Cr}_2(\text{Tar})_2\text{Py}_4$, — and $\text{Cr}(\text{Tar})_3\text{Py}_3$, ---- in methanol.

for CrCl_6^{3-} is 1318 cm^{-1}) and provide reassurance that pyridine nitrogen rather than chlorine binding is preserved [24, 25]. The ligand field strengths of the complexes can be arranged in the order: $\text{Cr}(\text{Mal})_3\text{Py}_3 > \text{Cr}_2(\text{Mal})_2\text{Py}_4\text{Cl}_2 = \text{Cr}(\text{Tar})_3\text{Py}_3 > \text{Cr}_2(\text{Tar})_2\text{Py}_4 > \text{Cr}(\text{Man})_3\text{Py}_3 > \text{Cr}_2(\text{Man})_2\text{Py}_4\text{Cl}_2 > \text{Cr}(\text{Lac})_3\text{Py}_3 > \text{Cr}_2(\text{Lac})_2\text{Py}_4\text{Cl}_2$. The same information regarding the coordinating capacity of the α -hydroxy acids arranged in the above order is also confirmed from the values of β_{35} for these complexes. The β_{35} values are slightly higher compared to the range observed for CrN_3X_3 chromophores (β_{35} : 0.58–0.65) [26] or CrS_6 systems (β_{35} : 0.44–

0.45). Hence the chelates appear to involve CrN_3O_3 and/or $\text{CrN}_2\text{O}_2\text{Cl}_2$ chromophores. The β values for most of the 1:3 complexes are higher than those of the 1:1 complexes. This is probably due to the fact that not all chlorine ligands in CrCl_3Py_3 have been replaced by the α -hydroxyacid ligand in the 1:1 ratio, or it could be due to configurational dissymmetry and vicinal effects of the coordinated α -hydroxy acid [10].

The results of the CD spectra are summarized in Table III, and representative spectra are given in Fig. 1b. The observed Cotton effects confirm that the α -hydroxy acids are complexed with Chromium(III) ion to produce optically active octahedral chromium(III) complexes. The complexes are likely to be fac in terms of α -hydroxy acid carboxylate and/or hydroxy groups since strong and well defined Cotton effects are observed [19, 21]. The CD spectra of D-tartaric or L-malic acid complexes have greater strengths than those prepared from L-lactic or L-mandelic acid. This is possibly due to the ability of tartaric or malic acid to coordinate as tridentate species through the oxygens of carboxyl and primary hydroxyl groups, while L-lactic or L-mandelic acid can only function as bidentate complexing agents.

The different signs of the Cotton effects of $\text{Cr}(\text{Tar})_3\text{Py}_3$, [445(-), 490(+), 570(+), 590(+), 620(+), 640(+), 654(-) nm] and $\text{Cr}(\text{Mal})_3\text{Py}_3$, [384(+), 440(+), 486(+), 550(-), 594(+), 640(-), 654(-) nm] in methanol suggest similar complexes but with ligands of opposite configuration. On the other hand, the signs of the Cotton effects of $\text{Cr}(\text{Lac})_3\text{Py}_3$, [400(-), 470(-), 530(-), 580(+), 630(-) nm] $\text{Cr}(\text{Man})_3\text{Py}_3$, [290(+), 400(-), 526(-), 590(+), 655(-), 670(-) nm] are analogous, suggesting formation of similar complex species.

It is not clear from the CD curves whether the Cotton effects arise from one species or a mixture of different complex species in methanol. Therefore, TLC using ethanol-water 8:3 (v/v) was used, and it confirmed only one complex species is present in solution. Hence, the observed Cotton effects [360–380(+), 439–460(-) nm] in the spin forbidden transition are assigned to ${}^2\text{E}({}^2\text{E})$, ${}^2\text{A}_2({}^2\text{T}_{1g})$ and ${}^2\text{E}({}^2\text{T}_{1g})$ in octahedral symmetry. The Cotton effects observed in the range 510–650 (nm) arise from the splitting of the spin allowed ${}^4\text{A}_{2g} \rightarrow {}^4\text{T}_{2g}$ to ${}^4\text{A}(\text{T}_{2g})$ and ${}^4\text{E}({}^4\text{T}_{2g})$ transitions. The band observed at 285–290(+) nm could

arise from the charge transfer peak observed at 260–270 nm in the UV-spectra of most chromium(III) complexes [16, 17].

We thank Professors D. H. Brown and W. E. Smith for helpful discussions and the facilities provided for number the CD spectra.

-
- [1] K. G. Stollenwerk and D. B. Grove, *J. Environ. Anal.* **14**, 396 (1985).
- [2] S. Langard and T. Norseth, in L. Friberg (ed.): *Handbook on the Toxicology of Metals*, p. 338, Elsevier/North Holland Biomedical Press, Amsterdam (1979).
- [3] K. E. Wetterhahn and P. H. Connett, *Struct. Bonding (Berlin)* **54**, 93 (1983).
- [4] D. H. Brown, W. E. Smith, M. S. El-Shahawi, and M. F. K. Wazir, *Inorg. Chim. Acta.* **124**, 125 (1986).
- [5] M. S. El-Shahawi, Ph. D. Thesis, Strathclyde University, U. K. (1986).
- [6] A. J. McCaffery and S. F. Mason, *Trans. Farad. Soc.* **59**, 1 (1963).
- [7] T. Bruer, *Helv. Chim. Acta* **46**, 2389 (1963).
- [8] H. Benar, E. Viona, and T. Lupu, *Rev. Fiz. Chim. Ser. 5*, 371 (1969).
- [9] R. E. Tapscott and R. L. Belford, *Inorg. Chem.* **6**, 735 (1967).
- [10] S. Kizaki, J. Hidaka, and Y. Shimura, *Bull. Chem. Soc. Jpn.* **40**, 2207 (1967).
- [11] P. Vieles, A. Bonmiol, and B. Lissorguges, *C. R. Acad. Sci. Paris, Ser. C* **266**, 1482 (1968).
- [12] A. Gercely and I. Sovago, *Metal Ions in Biological Systems*, Vol. 9, p. 77 (1978).
- [13] D. H. Brown, G. C. McKinlay, and W. E. Smith, *J. Chem. Soc. Dalton* **1978**, 199.
- [14] J. C. Taft and M. M. Jones, *Inorg. Synth.* **7**, 132 (1963).
- [15] R. C. Marya, *Indian J. Chem.* **22A**, 529 (1983).
- [16] D. H. Brown, G. C. McKinlay, and W. E. Smith, *J. Chem. Soc. Dalton* **1977**, 1874.
- [17] M. Freni, A. Gervasini, and P. Romiti, *Spectrochim. Acta* **39A**, 85 (1983).
- [18] Y. Inomata, T. Takeuchi, and T. Moriwaki, *Spectrochim. Acta* **40**, 179 (1984).
- [19] Y. Inomata, T. Takeuchi, and T. Moriwaki, *Inorg. Chim. Acta* **68**, 186 (1983).
- [20] R. J. H. Clark and C. S. Williams, *Inorg. Chem.* **4**, 350 (1965).
- [21] A. B. P. Lever, *Inorganic Electronic Spectroscopy*, Elsevier, New York (1968).
- [22] S. Kaizaki, J. Hidaka, and Y. Shimura, *Bull. Chem. Soc. Jpn.* **42**, 988 (1969).
- [23] D. Sutton, *Electronic Spectra of Transition Metal Complexes*, McGraw-Hill, London (1968).
- [24] J. A. Copper, B. F. Anderson, P. D. Puckley, and L. F. Blackwell, *Inorg. Chim. Acta* **91**, 1 (1984).
- [25] L. E. Gerdon and H. M. Goff, *Inorg. Chem.* **21**, 3847 (1982).
- [26] C. Preti and G. Tosi, *Can. J. Chem.* **53**, 2545 (1974).

Flow-injection extraction–spectrophotometric determination of manganese(VII) with benzyltributylammonium cations

D. Thorburn Burns, S.A. Barakat, M. Harriott and M.S. El-Shahawi¹

Department of Analytical Chemistry, The Queen's University of Belfast, Belfast BT9 5AG (UK)

(Received 14th April 1992)

Abstract

A flow-injection manifold has been developed for the spectrophotometric determination of manganese(VII) at 548 nm after extraction into chloroform of the ion-associate, benzyltributylammonium permanganate. The carrier stream was a pH 6 buffer containing 10% (w/v) ammonium fluoride and the reagent stream was 0.10% (w/v) benzyltributylammonium chloride. The injection rate was 20 h⁻¹. The calibration graph is linear up to 25 µg ml⁻¹ and the detection limit (3 × baseline noise) is 0.91 µg ml⁻¹ Mn(VII), based on 250-µl injection volumes. The system has been applied to the determination of manganese in steels and a cupro-nickel alloy.

Keywords: Flow injection; Spectrophotometry; Benzyltributylammonium cations; Cupro-nickel alloy; Extraction; Liquid–liquid extraction; Manganese

The oxo anions are amongst the least studied group of species which form liquid–liquid extractable ion-pairs with onium cations [1–2]. Permanganate has been monitored to determine manganese in high-quality calcium carbonate [3] and in iron, steel and non-ferrous metals [4] after extraction with the tetraphenylarsonium cation. Extraction with the tetraphenylphosphonium cation has been applied similarly in the analysis of ferrous alloys [5], as has the ethylenebis(triphenylphosphonium) cation to steels using both liquid–liquid [6] and adsorptive ion-pair extraction with microcrystalline naphthalene [7].

The present communication reports the development of a flow-injection manifold using benzyl-

tributylammonium chloride as an ion-pairing extractant for permanganate, and the application of the system to the spectrophotometric determination of manganese in steels etc., after oxidation of manganese(II) to manganese(VII) by potassium periodate.

EXPERIMENTAL

Apparatus

Absorbances were measured at 548 nm with a Pye Unicam SP-6550 ultraviolet–visible spectrophotometer fitted with a 30-µl 10 mm path length optical quartz flow cell (Hellma) and recorded with a Philips 825 chart recorder. Solutions were pumped using a fixed proportioning pump (Technicon) fitted with Acidflex pump tubes for the organic phase and Tygon pump tubes for the aqueous phases. Samples were injected using a four-way Rheodyne valve fitted

Correspondence to: D.T. Burns, Department of Analytical Chemistry, The Queen's University of Belfast, Belfast BT9 5AG (UK).

¹ Department of Chemistry, UAE University, Al-Ain P.O. Box 17551 (United Arab Emirates).

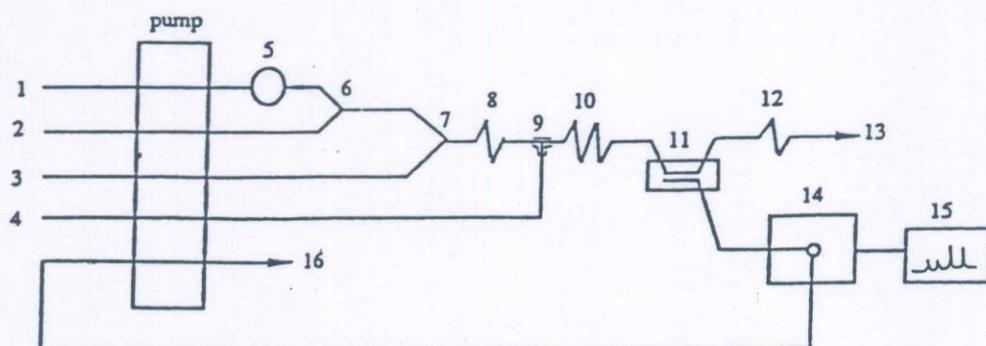


Fig. 1. Schematic diagram of the flow-injection system: (1) buffer solution pH 6 at 0.70 ml min^{-1} ; (2) aqueous 10% (w/v) ammonium fluoride solution at 0.70 ml min^{-1} ; (3) aqueous 0.10% (w/v) benzyltributylammonium chloride solution at 0.67 ml min^{-1} ; (4) chloroform at 0.70 ml min^{-1} ; (5, 7) mixing points ("Hex"); (6) sample solution ($250 \mu\text{l}$); (8) mixing coil (25 cm, 0.5 mm i.d.); (9) segmenter ("Tee"); (10) extraction coil (150 cm, 0.5 mm i.d.); (11) phase separator; (12) restrictor coil; (13) aqueous waste; (14) spectrophotometer; (15) recorder; (16) organic waste pumped at 0.68 ml min^{-1} .

with a by-pass coil, Flow lines were PTFE tubing (0.5 or 0.8 mm i.d.). The flow system is shown diagrammatically in Fig. 1. Omnifit three-way connectors were used at the mixing points "Hex" for mixing aqueous phases and "Tee" for mixing organic and aqueous phase (segmenter). The phase separator was constructed following the design reported by Al-Wehaid [8] and fitted with a $1\text{-}\mu\text{m}$ pore size PTFE membrane (Zefluor, Gelman Sciences).

Reagents and solutions

All reagents, unless otherwise specified, were of analytical grade; twice distilled water was used throughout.

Benzyltributylammonium chloride 0.10% (w/v) solution was prepared by dissolving the salt (Fluka, purum > 98%Cl) in water.

A stock solution of $500 \mu\text{g ml}^{-1}$ manganese (VII) was prepared by dissolving 1.438 g of potas-

sium permanganate (AnalaR, BDH) in 500 ml of water, boiling the solution gently for 1 h, cooling, filtering through a sintered glass filter (porosity G2) to remove any manganese(IV) oxide formed, and diluting to exactly 1 l [9]. This solution was standardised against sodium oxalate and stored in a dark brown bottle.

A stock solution of $500 \mu\text{g ml}^{-1}$ manganese(II) was prepared by dissolving 1.438 g of potassium permanganate (AnalaR, BDH) in water and carefully adding to it a saturated solution of sulphur dioxide until the permanganate colour was just discharged; the solution was then diluted to exactly 1 l [10]. More of the dilute solutions were prepared daily as required.

A pH 6 buffer solution was prepared by mixing 61.5 ml of 0.2 M disodium hydrogenphosphate with 438.5 ml of 0.2 M sodium dihydrogenphosphate and diluting to 1 l with water. A sulphuric-phosphoric acid solution was prepared by mixing

TABLE 1

Determination of manganese in steels

Sample	Sample weight (g)	Manganese content (% w/w)	
		Certified ^a	Found ^b
BCS 459 "Mild" Steel	1.5	0.088 (0.085-0.090)	0.087 ± 0.005
E.C.R.M. 081-1 unalloyed steel	0.30	$0.769 (s = 0.008)^c$	0.766 ± 0.006
BCS 457 mild steel	1.0	0.28 (0.28-0.29)	0.28 ± 0.002
BCS 180/1 cupro-nickel	0.50	0.81 (0.79-0.81)	0.808 ± 0.005

^a Certified range in parantheses. ^b Mean \pm 95% confidence limits for 4 replicates. ^c Standard deviation of 10 samples.

150 ml of concentrated sulphuric acid and 150 ml of 85% (w/w) orthophosphoric acid, and carefully adding the mixture to 600 ml of water, cooling, and then diluting to 1 l.

Ammonium fluoride solution 10% (w/v) solution was made by dissolving 10 g of ammonium fluoride (AnalaR BDH) in 100 ml of water. A 0.5% (w/w) potassium periodate solution was made by dissolving 2.5 g potassium periodate in a mixture of 500 ml of water and 100 ml of concentrated nitric acid by gentle warming; after cooling, the solution was diluted to 500 ml with water.

Procedure for steel samples

Dissolve accurately weighed samples (see Table 1, to contain 500 to 2000 μg Mn) in 35 ml sulphuric/phosphoric acid mixture in 250-ml conical flasks. Oxidise with 2 ml of concentrated nitric acid and boil to expel nitrous fumes. If any carbides remain evaporate to fumes and cool. Add 50 ml of water and 5 ml of concentrated nitric acid. Boil for 2 min, add 10 ml of 0.5% (w/v) potassium periodate solution and boil for a further 4 min. Cool, transfer to a 100-ml volumetric flask and make up to volume with distilled water [10]. Measure the peak-height absorbance using the flow system and the conditions given in Fig. 1. Evaluate the amount of manganese present from a calibration graph prepared from the results obtained from aliquots of manganese(II) solution proceeding as for the steel samples.

RESULTS AND DISCUSSION

The peak heights were found to be independent of the length of the extraction coil from 0.5 to 4.0 m; 1.5 m was chosen for routine use because this gave a convenient resistance to flow and reduced the risk of leakages in the phase-separator block. The effect of pH was investigated and the peak heights were found to be independent of pH over the range 2-12. A pH 6

buffer solution was used for the rest of the experiments.

The interferences of diverse ions were also investigated and were as for the manual method [11], chromium(VI) being the only ion which interfered significantly. In ratios up to 30:1, there was no significant effect at 548 nm provided that the extracts were protected from daylight, in which the absorbance slowly decreased.

A linear calibration graph was obtained over the range 0-25 $\mu\text{g ml}^{-1}$ Mn(VII) at 548 nm. The detection limit ($3 \times$ base line noise) was 0.91 $\mu\text{g ml}^{-1}$ Mn. The results for the determination of manganese in metallurgical samples (Table 1) are in good agreement with certificate values. The method is simple in its operation and faster (20 injections h^{-1}) than conventional manual liquid-liquid extractions [11]. It was also noticed that this method works well over a wider range of pH values using benzyl-tributyl-ammonium chloride as an ion-pairing reagent than for other methods, which is an extra advantage.

REFERENCES

- 1 A.J. Bowd, D.T. Burns and A.G. Fogg, *Talanta*, 16 (1969) 719.
- 2 D.T. Burns, *Anal. Proc.*, 19 (1982) 355.
- 3 M.L. Richardson, *Analyst*, 87 (1962) 435.
- 4 H. Goto and Y. Kakita, *Fresenius' Z. Anal. Chem.*, 254 (1971) 18.
- 5 Deputy Minister of the Romanian Ministry of Petroleum Industry and Chemistry, *Brit. Pat.*, 1,094,778, 23.65. See *Anal. Abstr.*, 15 (1968) 4681.
- 6 D.T. Burns and D. Chimpalee, *Anal. Chim. Acta*, 199 (1987) 241.
- 7 D.T. Burns, D. Chimpalee and N. Chimpalee, *Fresenius' Z. Anal. Chem.*, 332 (1988) 453.
- 8 A. Al-Wehaid, Ph.D. Thesis, University of Hull, (1987).
- 9 H.A. Laitinen, *Chemical Analysis*, McGraw Hill, New York, 1960, pp. 359-377.
- 10 *Methods of thermal analysis of steel*, British Steel Corporation, Sheffield, 1974, pp. 82-85.
- 11 D.T. Burns, M. Harriott and S.A. Barakat, *Anal. Chim. Acta*, 258 (1992) 325.

Chromium(III) complexes of D(-)tartaric and L(-) mandelic acids

Mohamed S. El-Shahawi

Chemistry Department, Faculty of Science at Damietta, Mansoura University, Damietta, Egypt

Shaban E. Ghazy*

Chemistry Department, Faculty of Science, Mansoura University, Mansoura, Egypt

Summary

The binary complexes of anhydrous chromium(III) chloride with D(-) tartaric acid L(-) mandelic acids have been characterized by elemental analyses, magnetic susceptibility, vibrational, electronic and circular dichroism spectra. The magnetic susceptibility data are close to the spin only value for a d³ chromium(III) ion. Three (Cr—Cl) vibrational modes in the region 420–290 cm⁻¹ are observed for the formed complexes indicating C₂ local symmetry of ligand atoms around the chromium(III) rather than C₃, which would allow two modes. In the visible spectra, two peaks in the 21052–22222 and 15384–16129 cm⁻¹ range are observed and are assigned to the ⁴A_{2g} → ⁴T_{1g}(F) and ⁴A_{2g} → ⁴T_{2g} transitions. The parameters (Dq, B, β₃₅) place the ligands in the higher end of the spectrochemical series and provide reassurance that the hydroxy acid oxygen complexes to chromium(III) ion. The Cotton effects observed in the spin-forbidden band are assigned to the ²E(²E_g), ²A₂(²T_{1g}) and ²E(²T_{1g}), while that in the spin-allowed band are a results of the splitting of the ⁴A_{2g}(⁴T_{2g}) to ⁴A₁(⁴T_{2g}) and ⁴E(⁴T_{2g}) transitions. The tartaric acid chelates are likely to be *fac* in terms of ligand carboxylate and/or hydroxy groups since stronger and better defined Cotton effects are observed while mandelic acid chelates are weak suggesting formation of the *mer* structure.

Introduction

The nutritional role of chromium(III) has been well established for the maintenance of normal glucose metabolism^(1–3). Analysis of chromium containing brewers yeast fractions implied that various amino acids, hydroxy acids and nicotinic acid served as structural components of the active complexes^(4,5). A significant relationship was found between the alcohol-extractable chromium and biological activity in a number of food stuffs^(6,7). Hence an alcohol extraction is often the first step in the isolation of the glucose tolerance factor. This raises the possibility that the active chromium could be in a non-aqueous environment *in vivo*⁽⁷⁾. Little is known of the complexing ability of chromium(III) with naturally occurring ligands in non-aqueous media^(7–12).

The hydroxy acid molecules constitute some of the most important sites for the binding of metal ions in biosystems⁽¹³⁾ and their coordination compounds are frequently considered in the therapeutic activity displayed by various drugs^(13,14). The composition, stability and structure of the metal hydroxy acid complexes have been studied^(15–17), however, chromium(III) complexes containing these ligands have been studied comparatively little^(9–11). The aim of this paper is to investigate chromium(III) complexes which contain hydroxy acid in the coordination sphere. These compounds are kinetically

inert and are interesting for their role as unique models in studying complex formation with various substrates.

Experimental

Reagents and materials

The organic compounds, D(-) tartaric (Tar.) and L(-) mandelic (Man.) acids, were of reagent grade. Anhydrous CrCl₃ was obtained by the standard method from green CrCl₃·6H₂O. All complexes were prepared from anhydrous CrCl₃ in dry MeOH⁽¹⁸⁾.

Preparation of the complexes

To anhydrous CrCl₃ (0.32 g, 2.0 mmol) in dry MeOH, the appropriate weights of the ligand were added to generate 1:1 and 1:3 molar ratios of chromium(III)-hydroxy acid. The solutions were refluxed for 11 h and the resulting coloured solutions were filtered, reduced in vol. using a rotary evaporator and NH₄Cl (0.5 g) was added. The desired precipitate which began to separate was filtered off, washed with Et₂O and finally dried over anhydrous CaCl₂. Attempts to prepare chromium(III) complexes of L(-) lactic and L(-) malic acids were not successful. The chromium content was determined as Cr₂O₃ by the method reported elsewhere⁽¹⁹⁾. For measuring the electronic and circular dichroism solution spectra, at room temperature, the solid complexes were dissolved in MeOH.

Physical measurements

The u.v.-vis. and i.r. spectra of the complexes were measured with a Varian 634 and a Perkin-Elmer spectrometers, respectively. The c.d. spectra were measured as described elsewhere⁽²⁰⁾. Magnetic measurements were made on a Johnson Matthey magnetic susceptibility balance. Silica Gel TLC plates (Merck 60F 254) 10 × 20 × 0.2 cm were employed.

Results and discussion

Interactions of chromium(III) with the title ligands were extensively investigated in view of either the role of Cr—O bond in the initiation of insulin action and the effectiveness of these ligands for the removal of chromium bound to haemoglobin, or the role of these acids in the reduction of toxic chromium(IV) to chromium(III). The elemental analyses as well as other physical and chemical properties of the prepared complexes are given in Table 1. The 1:1 complexes have the formula (NH₄)₄[Cr₂(Tar-3H)₂Cl₄] and (NH₄)₃[Cr(Man-2H)₂Cl₂] while the 1:3 complexes have the formula (NH₄)₃[Cr(Tar-H)₃Cl₃] and (NH₄)₃[Cr(Man-H)₃Cl₃]. The complexes are purple or dark violet and have fairly low m.p.s (<210°C). The magnetic susceptibility data (3.3–3.9 B.M.) reveal that the

* Author to whom all correspondence should be directed.

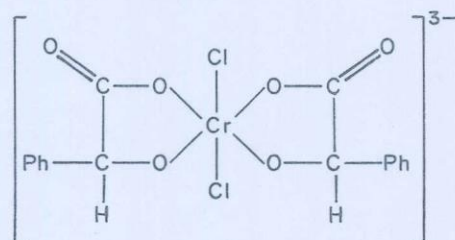
Table 1. Analytical data, magnetic moments^a (B.M.) and melting points for the complexes.

Complex	Colour	Cr	Found (Calcd.)%				μ_{eff} (B.M.)	M.p., (°C)
			H	N	C	Cl		
(1) $(\text{NH}_4)_4[\text{Cr}_2(\text{C}_4\text{H}_3\text{O}_6)_2\text{Cl}_4]$	purple	16.5 (17.0)	3.7 (3.6)	9.4 (9.2)	15.4 (15.7)	23.5 (23.2)	3.3	204
(2) $(\text{NH}_4)_3[\text{Cr}(\text{C}_4\text{H}_5\text{O}_6)_3\text{Cl}_3]$	purple	7.6 (7.8)	4.5 (4.1)	6.6 (6.4)	21.6 (21.8)	15.6 (16.0)	3.9	186
(3) $(\text{NH}_4)_3[\text{Cr}(\text{C}_8\text{H}_6\text{O}_3)_2\text{Cl}_2]$	green-violet	10.7 (10.9)	5.3 (5.0)	8.4 (8.8)	40.5 (40.2)	14.9 (14.8)	3.8	208
(4) $(\text{NH}_4)_3[\text{Cr}(\text{C}_8\text{H}_7\text{O}_3)_3\text{Cl}_3]$	violet	7.9 (7.8)	4.7 (4.9)	6.4 (6.3)	43.0 (43.3)	15.6 (15.8)	3.7	190

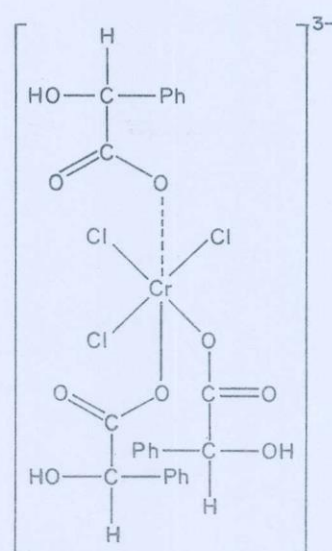
^aRoom temperature.

ligand field of the complexes is interpretable for a d^3 chromium(III) ion in octahedral or slightly distorted octahedral with substantially 4A_2 ground state. The lower magnetic moment as well as the molecular weight (609) determined by the Rast method for the complex $(\text{NH}_4)_4[\text{Cr}_2(\text{Tar-3H})_2\text{Cl}_4]$, confirm the dimeric structure (4).

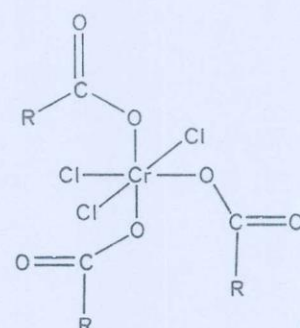
The i.r. spectral data of the complexes are summarized in Table 2. Displacement of the COO^- symmetric stretches to lower wavenumbers ($25\text{--}40\text{ cm}^{-1}$) and of the antisymmetric stretches to higher wavenumbers ($30\text{--}50\text{ cm}^{-1}$) are observed for all complexes, showing that the carboxylate groups of the hydroxyacids are involved in the coordination⁽²¹⁾. In the 1:3 complexes, the OH stretching vibration mode coincides with that of the free ligands showing that the oxygen atom of the hydroxyl group does not participate in the formation of the Cr—O bond. Also, the three chlorines are located in the remaining coordination sites and no suggestion can be made from the i.r. spectra for the chloride position, because the two Cr—Cl vibrations differently split in both complexes. However, it seems to us that *trans* disposition of ligand is a steric requirement for both derivatives. On the other hand, the OH band in the 1:1 complexes is shifted to a higher wavenumber ($30\text{--}40\text{ cm}^{-1}$) indicating that this group participates in coordination. The binding of the mandelate ligand to chromium could be either through two carboxyl groups or through one carboxyl and one hydroxy group as shown in structures (1) and (2). The tartrate ligand coordinates to chromium either through one carboxyl group or through one carboxyl and one hydroxyl group^(9,12). Dimers could also be formed by tartrate bridges as shown previously by Shimura *et al.*⁽¹¹⁾. The complexes exhibit three (Cr—Cl) vibrational modes in the region $420\text{--}285\text{ cm}^{-1}$ indicating

 $(\text{NH}_4)_3[\text{Cr}(\text{C}_8\text{H}_6\text{O}_3)_2\text{Cl}_2]$

(1)



(2)

 $(\text{NH}_4)_3[\text{Cr}(\text{C}_8\text{H}_7\text{O}_3)_3\text{Cl}_3]$ R = $\text{CH}(\text{OH})\text{C}(\text{OH})\text{CO}_2\text{H}$ $(\text{NH}_4)_3[\text{Cr}(\text{C}_4\text{H}_5\text{O}_6)_3\text{Cl}_3]$

(3)

C_{2v} local symmetry of ligand atoms around the chromium rather than C_{3v} which would allow two modes⁽²²⁾.

The u.v.-vis. spectra of the complexes are summarized in Table 3. Two peaks in the 21052–22222 and 15384–

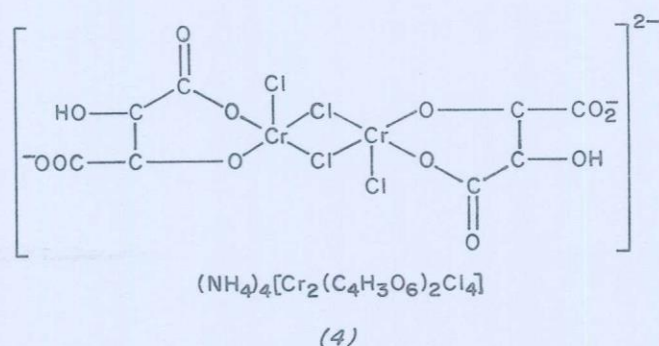


Table 2. Significant vibrational frequencies (cm⁻¹) of the complexes with relevant bands of the free ligand in brackets.

Complex	$\nu(\text{OH})$	$\nu_{\text{as}}(\text{COO}^-)$	$\nu_{\text{s}}(\text{COO}^-)$	$\nu(\text{Cr}-\text{Cl})$
(1)	3480 (3450)	1640 (1590)	1355 (1380)	285 420, 316, 240
(2)	3450	1635	1360	275 400, 330, 295
(3)	3485 (3460)	1645 (1610)	1370 (1390)	275 410, 340, 300
(4)	3460	1640	1365	285 405, 335, 294

16129 cm⁻¹ ranges are observed and assigned to the ${}^4A_{2g} \rightarrow {}^4T_{1g}(\text{F})$ and ${}^4A_{2g} \rightarrow {}^4T_{2g}$ transitions, respectively, in octahedral or pseudo-octahedral symmetry⁽²³⁾. Another strong peak is observed in the 27397–33500 cm⁻¹ range which is assigned to the ${}^4A_{2g} \rightarrow {}^4T_{1g}(\text{P})$ transition. The spin-forbidden transition in the 21052–21978 cm⁻¹ range gives a higher absorption coefficient than the spin-allowed band at 15384–15625 cm⁻¹ for the mandelic acid chromium(III) complexes which is possible because of the symmetry reduction^(23,24).

The parameters (Dq, B, β_{35}) have been calculated by Tanabe–Sugano procedures^(23,25) and are summarized in Table 3. The Dq values of the complexes place the ligands in the higher end of the spectrochemical series and far closer to the chloride ion (Dq for CrCl₆³⁻ = 1318 cm⁻¹). These values provide reassurance that the hydroxy acid oxygen is complexed to chromium(III) ion and the complexes can be arranged in the order: (4) < (3) < (2) < (1) in the ligand field strength. The B values for the complexes are calculated from the equation⁽²⁶⁾.

$$B = 2\nu_1^2 + \nu_2^2 - 3\nu_1\nu_2 / (15\nu_2 - 27\nu_1)$$

Table 3. Electronic and circular dichroism solution spectra with ligand field parameters.

Complex	${}^4A_{2g} \rightarrow {}^4T_{2g}$	${}^4A_{2g} \rightarrow {}^4T_{1g}(\text{F})$	${}^4A_{2g} \rightarrow {}^4T_{2g}(\text{P})$	Dq	B	β_{35}	c.d.
(1)	16129	22222	—	1613	598.6	0.65	285(+), 380(+), 450(-), 550(+), 650(-)
(2)	15748	21978	27397	1575	620	0.67	290(+), 360(+), 439(-), 520(-), 580(+), 680(+)
(3)	15625	21978	27777	1563	638.8	0.69	290(+), 345(+), 400(-), 525(-), 590(+), 655(-)
(4)	15384	21052	29850	1538	552	0.6	Peaks unresolved

(B for the Cr^{III} ion is 918 cm⁻¹)

^a See Table 1.

On the basis of B values the complexes are arranged in the order: (4) < (1) < (2) < (3) which is probably due to the fact that tartaric acid is potentially capable to coordinate as a bi-, tri- or tetradentate species while mandelic acid can only function as a mono- or bidentate complexing agent. The coordinating capacity of the ligands are also confirmed from the β_{35} values of the complexes. The calculated values are higher than the range observed for CrS₆ systems (β_{35} : 0.44–0.45) and slightly close to that observed for CrN₃X₃ chromophores (β_{35} : 0.58–0.65)^(27,28). It seems reasonable to presume that most of the complexes in this series contain oxygen and chlorine.

The c.d. spectral data of the complexes are presented in Table 3. The observed Cotton effects confirm that the ligands are complexed with a chromium(III) ion to produce optically active chromium(III) compounds. The spectra of tartaric acid chelates have greater strength than those of mandelic acid. Hence the tartaric acid chelates are likely to be *fac* in terms of ligand carboxylate and/or hydroxy groups since stronger and better defined Cotton effects are observed which could give rise to the structure compared to those which could not⁽²⁴⁾. The Cotton effects of the mandelic acid chelates are weak suggesting formation of *mer* structure⁽²⁴⁾.

Stereospecificity of the D-tartrate complexes

The similarity of the c.d. spectrum of the complex (NH₄)₄[Cr₂(Tar-3H)₂Cl₄] and the [Cr(OX)₂dip] complexes^(24,29) (dip = 2,2-dipyridyl, OX = C₂O₄²⁻) are evident, possibly because the optical activity is due to the configurational dissymmetry rather than vicinal effect of the coordinated D-tartrate ions, for the following reasons: (i) a D-tartrate ion cannot span four coordination sites around one metal ion⁽¹²⁾, (ii) the c.d. spectrum of the D-tartrate complex in the visible region of calculated per chromium(III) ion is more intense than those of the corresponding oxalate complexes and (iii) according to the construction of molecular models, the most probable structure for the experimental formula obtained is the binuclear one in which two chromium(III) ions are bridged by two tetradentate D-tartrate ions as proposed for many tartrate systems^(12,30). In the structure formed, the stereospecificity due to the two dissymmetric ligands is perfect and as far as the D-tartrate is used, the binuclear complex has an absolute configuration $\Delta(\text{C}_2) - \Delta(\text{C}_2)$ about the two tris chelate type octahedra is the only one possible to be constructed as is previously reported⁽¹²⁾. In this complex, it seems likely that one proton remains undissociated per two tetranegative D-

tartrates. Nevertheless, all the D-tartrates seem to be acting as tetradentate ligands. It is known that the oxalato complexes easily racemize in aqueous solutions with half-lives of *ca.* 50 min., while the L-tartrato complexes do not racemize at all^(12,29).

The sign of the Cotton effects of the D(-) tartrate complexes are analogous, suggesting formation of species with similar structure. It is not clear from the c.d. curves whether the Cotton effects arise from one species or a mixture of different species, hence TLC using EtOH-water (5:7 v/v) was used and confirmed that only one complex species is present in MeOH solution.

Band assignments

Assuming that the complexes belong to D_3 symmetry, the observed Cotton effects, 360–380 (+), 439–450 (–) and 520 (–) nm in the spin-forbidden transitions are assigned to the ${}^2E({}^2E_g)$, ${}^2A_2({}^2T_{1g})$ and ${}^2E({}^2T_{1g})$ d–d transitions⁽¹⁰⁾. The Cotton effects found in the 550–580 (+) and 650–680 (+) range in the spin-allowed band result from the splitting of the ${}^4A_{2g} \rightarrow {}^4T_{2g}$ to ${}^4A_1({}^4T_{2g})$ and ${}^4E({}^4T_{2g})$ transitions. A weak band observed at 285–290 (+) nm due to the charge transfer peak is shown at 260–270 nm in the u.v. spectra of most chromium complexes⁽¹⁰⁾.

References

- (1) W. Mertz, *Physiol. Rev.*, **49**, 163 (1969).
- (2) R. A. Anderson, *Sci. Total Environ.*, **17**, 13 (1981).
- (3) R. A. Anderson and W. Mertz, *Trends Biochem. Sci.*, **2**, 277 (1977).
- (4) W. Mertz, E. W. Toepfer, E. E. Roginski and M. M. Polansky, *Fed. Proc. Fed. Am. Soc. Exp. Biol.*, **33**, 2275 (1974).
- (5) E. W. Toepfer, W. Mertz, M. M. Polansky, E. E. Roginski and W. R. Wolf, *J. Agric. Food Chem.*, **25**, 162 (1977).
- (6) E. W. Toepfer, W. Mertz, E. E. Roginski and M. M. Polansky, *J. Agric. Food Chem.*, **21**, 69 (1973).
- (7) D. H. Brown, W. E. Smith, M. S. El-Shahawi, and M. F. K. Wazir, *Inorg. Chim. Acta*, **124**, L25 (1986).
- (8) M. Freni, A. Gervasini, P. Romiti, T. Beringhell and F. Marazzoni, *Spectrochim. Acta*, **39A**, 85 (1983).
- (9) A. J. McCaffery and S. F. Mason, *Trans. Farad. Soc.*, **59**, 1 (1963).
- (10) S. Kaizaki, J. Hidaka and Y. Shimura, *Inorg. Chem.*, **12**, 142 (1973).
- (11) S. Kaizaki, J. Hidaka and Y. Shimura, *Bull. Chem. Soc. Jpn.*, **40**, 2207 (1967).
- (12) S. Kaizaki, J. Hidaka and Y. Shimura, *Bull. Chem. Soc. Jpn.*, **42**, 988 (1969).
- (13) G. K. Friman in G. L. Eicharn (Ed.), *Inorganic Biochemistry* (Trans. into Russ.), Izd. Mir, Moscow, 1978.
- (14) A. Gercely and I. Svago, *Metal Ions in Biological Systems*, **9** (1978).
- (15) K. Blomqvist and E. R. Still, *Inorg. Chem.*, **23**, 3730 (1984) and refs therein.
- (16) K. Blomqvist and E. R. Still, *Inorg. Chim. Acta*, **82**, 141 (1984).
- (17) L. Johansson, *Acta Chem. Scand., Sec. A*, **34**, 495 (1980).
- (18) A. R. Ray, *Inorg. Synth.*, **5**, 154 (1957).
- (19) R. C. Maurya, *Indian J. Chem.*, **22A**, 524 (1982).
- (20) D. H. Brown, G. C. McKinlay and W. E. Smith, *J. Chem. Soc., Dalton Trans.*, 1874 (1977).
- (21) Y. Inomata, T. Takeuchi and T. Moriwaki, *Inorg. Chim. Acta*, **68**, 186 (1983).
- (22) R. J. H. Clark and C. S. Williams, *Inorg. Chem.*, **4**, 350 (1965).
- (23) A. B. P. Lever, *Inorganic Electronic Spectroscopy*, Elsevier, Amsterdam, 1968.
- (24) T. Bruer, *Helv. Chem. Acta*, **56**, 2388 (1963).
- (25) D. Sutton, *Electronic Spectra of Transition Metal Complexes*, McGraw-Hill, London (1968).
- (26) C. L. Sharma, P. K. Jain and T. K. De., *J. Inorg. Nucl. Chem.*, **42**, 1681 (1980).
- (27) C. Preti and G. Tosi, *Can. J. Chem.*, **53**, 2545 (1974).
- (28) C. Preti and G. Tosi, *J. Inorg. Nucl. Chem.*, **38**, 2545 (1974).
- (29) J. A. Broomhead, *Aust. J. Chem.*, **15**, 228 (1962).
- (30) R. E. Tapscott and R. L. Belford, *Inorg. Chem.*, **6**, 735 (1967).

(Received 23 September 1991)

TMC 2633

Flow-injection extraction-spectrophotometric determination of permanganate with the triphenylsulphonium cation

D. Thorburn Burns¹, S. A. Barakat¹, M. S. El-Shahawi², and M. Harriott¹

¹ Department of Analytical Chemistry, The Queen's University of Belfast, Belfast BT9 5AG, Great Britain

² Department of Chemistry, UAE University, P. O. Box 17551, Al-Ain, United Arab Emirates

Received April 13, 1992

Summary. Permanganate can be determined spectrophotometrically at 548 nm after flow-injection extraction into chloroform of the ion-associate triphenylsulphonium permanganate. The carrier stream was a pH 6 buffer containing 10% (w/v) ammonium fluoride and the reagent stream was 0.10% (w/v) triphenylsulphonium chloride. The injection rate was 20 h⁻¹. The calibration graph is linear up to 40 µg ml⁻¹ and the detection limit is 1.10 µg ml⁻¹ Mn(VII), based on injection volumes of 250 µl. The system has been applied to the determination of manganese in steels and a cupro-nickel alloy.

Introduction

Some onium salts have become cheaply and readily available due to their application by organic chemists as "naked anions" in phase-transfer reactions and related synthetic methods [1]. Triphenylsulphonium chloride, first prepared by Courtot and Tung in 1933 [2], has recently been used as a phase transfer catalyst in organic oxidations [3–5], as a stabilizer in polyester polymers [6], for the control of chlorosis in plants [7], and for soil conditioning [8]. Very little analytical work has been reported. Although Portratz and Rosen noted that triphenylsulphonium tetrathiocyanatoctacobaltate (II) could be extracted into chloroform [9], the reagent's quantitative applications have only recently been described [10, 11]. Precipitation reactions with the triphenylsulphonium cation have been followed polarographically, those with mercury and bismuth were said to be quantitative [9].

The present communication, based on an earlier manual method [11], reports the use of the triphenylsulphonium cation as an ion-pairing extractant for permanganate using the flow injection technique and the application of the system for the determination of manganese in steels and in a cupro-nickel alloy.

Experimental

Equipment. Absorbances were measured at 548 nm with a Pye Unicam SP6-550 ultraviolet-visible spectrometer fitted with a 30 µl 10 mm special optical quartz flow cell (Hellma) and recorded with a Phillips 8251 recorder.

Solutions were pumped by using a fixed-speed proportioning pump (Technicon) fitted with Acidflex pump tubes for the organic phase and Tygon tubes for the aqueous phases. Samples (250 µl) were injected using a four-way Rheodyne valve fitted with a by-pass coil. Flow lines were PTFE tubing (0.5 and

Correspondence to: D. T. Burns

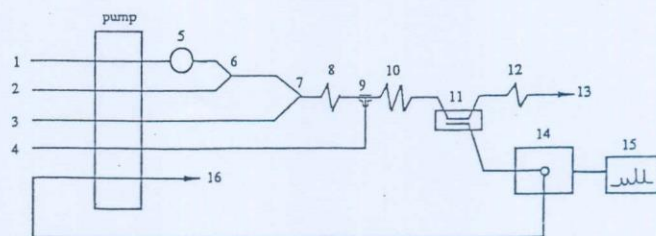


Fig. 1. Schematic diagram of the flow-injection system: 1 buffer solution pH 6 at 0.70 ml min⁻¹; 2 aqueous 10% (w/v) ammonium fluoride solution at 0.70 ml min⁻¹; 3 aqueous 0.10% (w/v) triphenylsulphonium chloride at 0.69 ml min⁻¹; 4 chloroform at 0.70 ml min⁻¹; 5, 7 mixing points ("Hex"); 6 sample solution (250 µl); 8 mixing coil (25 cm, 0.5 mm i.d.); 9 segmenter ("Tee"); 10 extraction coil (150 cm, 0.5 mm i.d.); 11 phase separator; 12 restrictor coil; 13 aqueous waste; 14 spectrophotometer; 15 recorder; 16 organic waste pumped at 0.68 ml min⁻¹

0.8 mm i.d.). The flow system is shown diagrammatically in Fig. 1. Omnifit three-way connectors were used at the mixing points, "Hex" for mixing aqueous phases and "Tee" for mixing organic and aqueous phases. The phase separator was constructed following the design reported by Al-Wehaid [12] and fitted with a 1 µm pore size PTFE membrane (Zefluor; Gelman Sciences).

Reagents. A stock 500 µg ml⁻¹ manganese(VII) solution was prepared by dissolving 1.438 g of potassium permanganate (AnalaR, BDH) in 500 ml of distilled water, boiling the solution for 1 h, cooling, filtering through a sintered glass (porosity G2) to remove any manganese(IV) oxide formed, and diluting to 1.0 l. This solution was stored in a dark brown glass bottle. A stock 500 µg l⁻¹ manganese(II) solution was prepared by dissolving 1.438 g of potassium permanganate (AnalaR, BDH) in distilled water and carefully adding to it a saturated solution of sulphur dioxide until the permanganate colour just disappeared, this solution was diluted to 1 l.

A pH 6 buffer solution was prepared by mixing 61.5 ml of 0.2 mol/l disodium hydrogenphosphate with 438.5 ml of 0.2 mol/l sodium dihydrogenphosphate and diluting to 1.0 l with distilled water. A sulphuric/phosphoric acid solution was prepared by mixing 150 ml of conc. sulphuric acid and 150 ml of 85% orthophosphoric acid and carefully adding this mixture to 600 ml of water, cooling and diluting to 1.0 l. The 0.5% (w/w) potassium periodate solution was made by dissolving 2.5 g potassium periodate in a mixture of 300 ml of water and 100 ml of conc. nitric acid by gentle warming; after cooling, the solution was diluted to 500 ml with water.

All other reagents were of analytical grade and double-distilled water was used throughout.

General procedure. Samples and standards were examined by using the flow system outlined in Fig. 1 under the specified conditions. Peak heights were measured.

Procedure for steel samples. An accurately weighed sample containing 1000–3000 µg Mn was dissolved in 35 ml of the sulphuric/phosphoric acid mixture in a 250 ml conical flask and oxidised with 2 ml of conc. nitric acid. After boiling to expel nitrous fumes (and if any carbides remained, evaporating to fumes), the solution was cooled, and 50 ml of water and 10 ml

Table 1. Determination of manganese

Sample	Sample wt. (g)	Manganese content (% w/w)	
		Certified ^a	Found ^b
BCS 459 Mild steel	1.5	0.088 (0.085–0.090)	0.0860 ± 0.0005
E.C.R.M. 081-1 Unalloyed steel	0.30	0.769 (s = 0.008) for 10 samples	0.765 ± 0.007
BCS 457 Mild steel	1.0	0.28 (0.28–0.29)	0.285 ± 0.002
BCS 180/1 Cupro nickel	0.50	0.81 (0.79–0.81)	0.808 ± 0.004

^a With certified range in parentheses

^b Mean ± 95% confidence limits for 4 replicates

of conc. nitric acid were added. The solution was boiled for 2 min, and 10 ml of 0.5% (w/v) potassium periodate solution were added. After boiling for a further 4 min, the solution was cooled, transferred to a 100 ml volumetric flask and made up to volume with distilled water [13].

The peak-height absorbances were measured for triplicate 250 µl injections of each sample using the flow system (Fig. 1). The amount of manganese present was evaluated from a calibration graph (0–40 µg ml⁻¹ Mn) prepared with aliquots of manganese(II) solution, treated as for the steel samples.

Results and discussion

The peak heights were found to be independent of the length of the extraction coil from 0.5 to 4.0 m; 1.5 m was chosen for routine use because this gave a convenient resistance to flow and reduced the risk of leakages in the phase-separator block. The effect of pH was investigated by varying the pH of the buffer solutions from pH 2 to 12 by varying the volume of 0.2 mol/l sodium hydroxide or hydrochloric acid solution added to a stock buffer solution. The peak heights were found to be constant over the pH range 5 to 8. A pH 6 buffer solution was used for the rest of the experiments.

The interferences from diverse ions were found to be the same as those for a manual procedure [11], chromium(VI) being the only ion which interfered significantly. In ratios up to 30:1, there was no significant effect at 548 nm provided that the system was protected from daylight.

A linear calibration was obtained over the range 0–40 µg ml⁻¹ Mn(VII) at 548 nm. For the determination of 15 µg ml⁻¹, the relative standard deviation was 1.0% (10 results) and the detection limit (3 × baseline noise) was 1.10 µg ml⁻¹. The results

for the determination of manganese in metallurgical samples are in good agreement with certificate values (Table 1). The method is simple to operate and faster (20 injections h⁻¹) than conventional manual liquid/liquid extractions [11, 14].

References

1. Keller WE (1979) Compendium of phase-transfer reactions and related synthetic methods. Fluka, Buchs, Switzerland
2. Courtot C, Tung TY (1933) Compt Rend 197:1226
3. Kartsutoshi O, Tokio Y, Fukio K (1969) Bull Chem Soc Japan 42:1800
4. Fuki K, Kanai K, Takezono T, Kitana H (1964) Kogyo Kagaku Zass 67:1131
5. Kanai K, Okubo K, Katano H, Fukui K (1965) Bull Japan Pet Inst 7:52
6. Abrahams IM, Benezera LL, Goold RD (1962) US Patent 3, 028-361, April 3, 1962. Chem Abstr 57:2411f
7. Antogonini J, Curtis R, Day HM (1956) 'Symposium on metal chelates in plant nutrition', Seattle, p 61. Chem Abstr 52:5565f
8. Pugh AL, Vomocil JA, Nielson TR (1960) Agron J 52:399
9. Portratz HA, Rosen JM (1949) Anal Chem 21:1276
10. Thorburn Burns D, Kheawpintong S (1984) Anal Chim Acta 162:437
11. Burns DT, Harriott M, Barakat SA (1992) Fresenius J Anal Chem 343:488
12. Al-Wehaid A, Thesis PD (1987) University of Hull
13. Analytical Panel, Methods of Chemical Analysis of Iron and Steel, British Steel Corporation, Sheffield (1974) pp 82–83
14. Burns DT, Chimpalee D (1987) Anal Chim Acta 199:241

REMOVAL OF HETEROPOLYANIONS INTERFERENCE IN THE ATOMIC ABSORPTION DETERMINATION OF SILVER AND GOLD

Amin M. ABDALLAH¹, Mohamed S. EL-SHAHAWI²,
Mohamed M. EL-DEFRAWY¹ and Eman E. ASKAR¹

¹*Department of Chemistry, Faculty of Science, University of Mansoura, Egypt*

²*Department of Chemistry, Faculty of Science at Damietta, University of Mansoura,
Damietta, Egypt*

The harmful effect of heteropolyanion (HPA) formation on the atom population of the coinage metals, Ag and Au in the flame has been investigated. The ultraviolet spectra and thin layer chromatography were used to assess the phenomenon and to elucidate the mechanism of heteropolyanion interaction with the analyte. The effect can completely be eliminated by adding an excess of cyanide, resorcinol, ethylenediamine or EDTA or preparing the aspirated solution at low hydrogen ion concentration. Digestion, solvent extraction, thin layer chromatography and UV-visible measurements revealed that the HPA entities are packed together to form crystals with irregular surfaces and large cavities which permit the insertion of the analyte in these cavities. The mechanism of the insertion of the analyte to the HPA was discussed.

Badano niekorzystny wpływ tworzenia heteropolianionów (HPA) na populację atomów Ag i Au w płomieniu. Do wykrycia i zbadania mechanizm oddziaływań heteropolianionów z analitem zastosowano spektrofotometrię UV-Vis i chromatografię cienkowarstwową. Te oddziaływania można wyeliminować przez dodanie nadmiaru cyjanków, rezorcynolu, etylenodiaminy lub EDTA albo też przez przygotowanie do analizy roztworu o małym stężeniu jonów wodorowych. Metodami ekstrakcji, TLC oraz spektrofotometrii UV-Vis wykazano, że HPA tworzą skupiska o nieregularnych powierzchniach z dużymi zagłębieniami, które umożliwiają insercję analitu. Przedyskutowano mechanizm insercji analitu do HPA.

In cool flames, sensitivity of the absorption method is indirectly hindered by inhibitory effects as compound formation with the analyte in the flame [1, 2] or the solution [3-6]. The literature reveals that some of the interferences are gener-

ally found by all investigators [7], while some others are found occasionally under particular circumstances [8, 9]. This observation suggests to put forward a classification of interferences encountered in the atomic absorption procedures as resulting from:

a) property of the analyte itself to interact or not with concomitant and/or flame species to give particles of compounds which have variable thermochemical stabilities [10–12]; the term "inherent interference" is assigned for this type of interference;

b) sample pretreatment, percentage and type of concomitants which impart some characteristics to the medium and consequently on the analyte atom population in the flame, affecting the occurrence and magnitude of an interference. This type of interference takes place almost due to formation of some entities (the analyte is not one of their components) that may affect the analyte atom population in the flame; such interference can be termed "phenomenal interference". This interference takes place essentially due to polymeric formations, complex compounds, selective association, ... etc.

The majority of the published work on HPAs concerned the determination of non-metals [13–17]. The stability of the HPA depends on the acidity of the solution in which it exists and on the size and charge of the heteroatom [18–20].

This paper substantiates the phenomenal interference caused by some heteropolyanions, viz: 12-phosphomolybdate or 12-silicomolybdate on the atomic absorption determination of silver and gold in fuel-rich air-acetylene flame. Reasons to study such effect are: the need to determine traces of silver and gold for their subsequent extraction from solutions of very complex nature as laboratory wastes; in addition it was desired to ascertain the phenomenon which has been investigated before [4]. The way to eliminate the effect of formation of these structures has also been investigated.

EXPERIMENTAL

Reagents, materials and apparatus

All reagents used were of analytical reagent grade unless otherwise stated. BDII phosphomolybdic acid $H_3PO_4 \cdot 12MoO_3 \cdot 24H_2O$, (M.wt. 2257.26) was used. Other preparations of HPAs were carried out using the recommended procedures [21]. Solutions of silver(I) and gold(III) were prepared from stock spectrosol solutions ($1mg\ l^{-1}$) for atomic absorption spectrometry by diluting to the requisite volume using doubly distilled water. Thin layer chromatography developing chamber and thin layer chromatographic (TLC) plates 10 cm \times 10 cm silica gel (activated at 100°C for 30 min) were prepared.

A Unicam SP-90 A series 2 atomic absorption spectrometer was used with Unicam silver or gold hollow-cathode lamp and a conventional 10 cm slot burner head for an air-acetylene flame. The instrumental parameters used are given in Table I. The ultraviolet spectra of solutions were recorded on a Varian DMS 6345 double beam spectrometer using 1 cm quartz cuvettes.

Table 1. The optimum instrumental conditions for the determination of silver or gold by AAS

Instrumental parameter	Silver	Gold
Lamp current, mA	4.0	10.0
Wavelength, nm	328.07	242.79
Slit width, mm	1.0	1.0
Observation height*, mm	8.0	8.0
Air flow-rate, l min ⁻¹	5.0	5.0
Acetylene flow-rate, l min ⁻¹	1.1	1.1

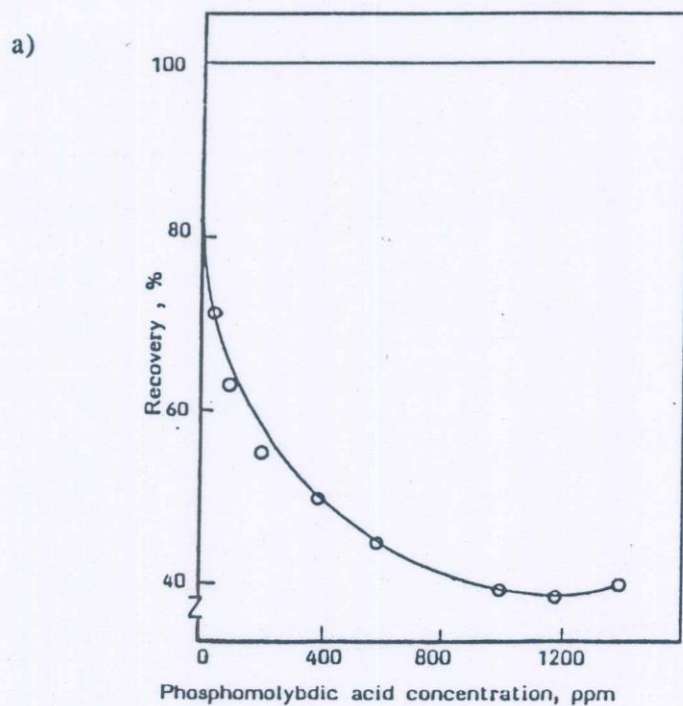
*The distance from the top of the burner to "grazing incidence position".

Procedure

One ml of the analyte stock solution corresponding to 50 or 200 µg of Ag or Au was placed in a 10 ml volumetric flask. The interfering species solution(s) plus nitric, hydrochloric or perchloric acid were added in appropriate amounts to reach pH between 1.0–1.5 and diluted to the mark with water. The absorbance of the mixture was compared with that of the analyte standard solution.

RESULTS AND DISCUSSION

The aim to rejuvenate investigation on the interference effects in the atomic absorption determination of Ag and Au stems from the observation that almost all investigators assure the freedom of measurements of these elements from interference [22–24]. Figure 1a indicates the effect of variable concentration of the heteropoly phosphomolybdic acid on the recovery of 5 ppm silver from nitric acid solution.



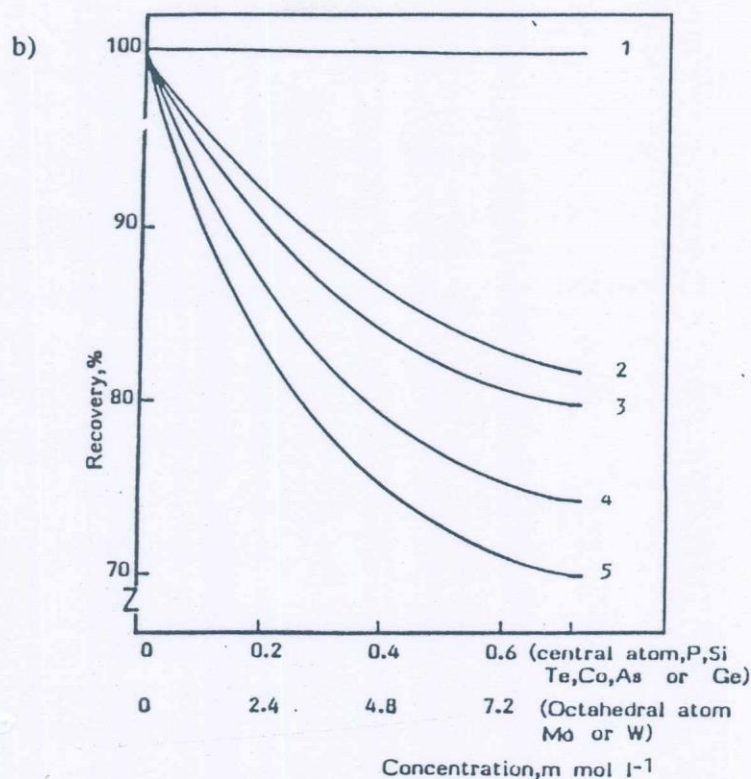


Fig. 1. a) Effect of phosphomolybdic acid, $H_3PO_4 \cdot 12 MoO_3 \cdot 24 H_2O$, in 0.3 mol l^{-1} nitric acid solution on the recovery of 5 ppm of Ag. b) Effect of heteropoly anion formation on the recovery of 5 ppm of Ag; 1 – recovery of 5 ppm of Ag as silver nitrate in 0.3 mol l^{-1} nitric acid solution was considered 100; all other recoveries were related to this value; 2 – telluro- or arsenomolybdate, 3 – arseno- or tellurotungstate, 4 – silico- or germanotungstate and 5 – cobaltotungstate

It is clear that the effect is conspicuous and may suppress the recovery to minimum. Figures 1b and 2 substantiate the phenomenon. Heteropoly species of variable central and octahedral atoms (laboratory prepared) were added to the analyte in nitric acid solution. Aspiration was carried out as usual.

The graphs in Fig. 1b are built up as the average results for the effects that coincide with 5% difference to show practically the harmful depressive interference of the heteropoly formations on the absorbance of Ag. To ascertain the persistence of the phenomenon, the flame profiles as a proof on the analyte atom population at different observation heights of the flame and at variable fuel rates have been constructed. Figure 3 indicates that the effect is suppressive and consistent through the different flame heights. Figure 4 b shows that the increase in fuel up to 1.25 l min^{-1} does not significantly improve the absorbance signal of

silver, but eliminates the interfering effect of the heteropoly formation and almost levels the signals to reliable magnitude. It can be concluded that such interference is specific and depends mainly on the properties of the heteropolyanions which may be affected by the reductant acetylene as the absorbances increase at the lower parts of the flame as well as by the increase of the fuel ratio.

Narrow changes in the hydrogen ion concentration of the analyte solution (pH 1–4) have no clear improvement on the absorbance signal of Ag or Au. However, when similar preparations were subject to extraction with ether [4] and aspiration of the aqueous layer revealed the restoring of the analyte absorbance signal to that of the reference. Furthermore, digesting the analyte solution on a steam bath for 24 h, adjusting the volume and aspirating the digested solution improved the analyte absorbance signal without levelling it to that of the standard.

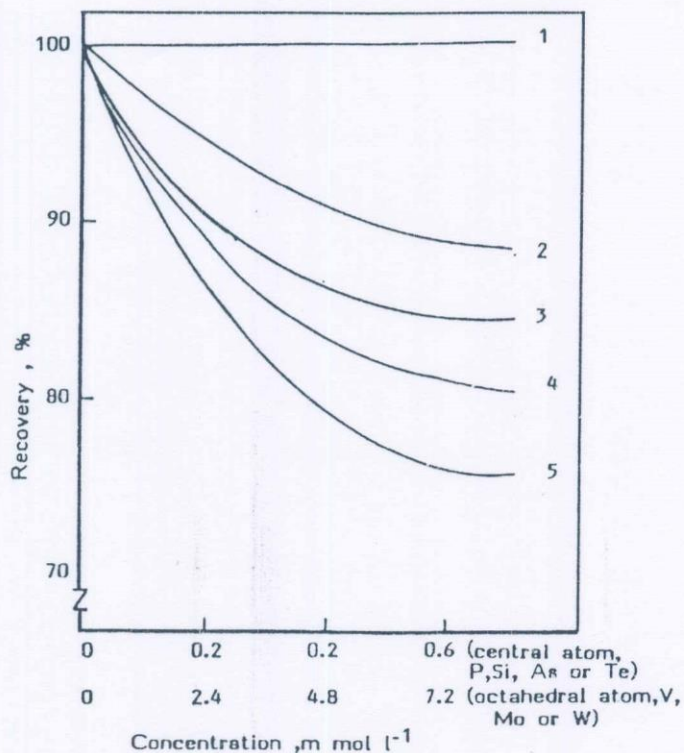


Fig. 2. Effect of heteropoly formation on the recovery of 20 ppm of Au; 1 – recovery of 20 ppm of Au as sodium aurate in 0.3 mol l^{-1} nitric acid solution was considered 100, all other recoveries were related to this value; 2 – phospho-, silico- or tellurovanadate, 3 – arseno-, telluro- or phosphomolybdate, 4 – phosphotungstate and 5 – silico- or tellurovanadate

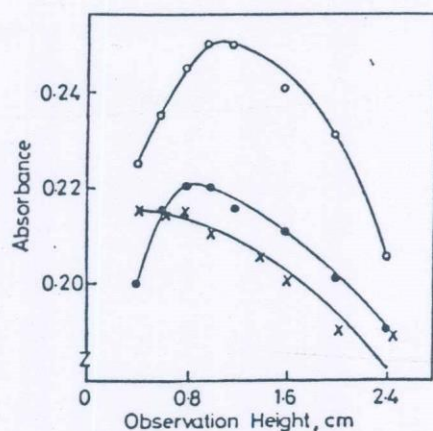


Fig. 3. Effect of change of burner-height on the distribution of Ag atoms in the flame; (o) solution as in 1) in Fig. 1b, (●) solution (o) plus phospho- or silicomolybdate and (x) solution (o) plus phospho- or silicotungstate in 0.3 mol l^{-1} nitric acid solution

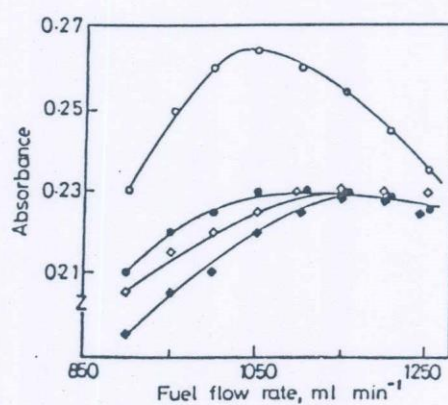


Fig. 4. Effect of change of fuel rate on the distribution of Ag atoms in the flame; (o) solution as in 1) in Fig. 1b, (●) solution (o) plus silicomolybdate, (□) solution (o) plus phosphomolybdate and (■) solution (o) plus telluromolybdate in 0.3 mol l^{-1} nitric acid solution

Investigation on the nature of the heteropoly anion formation interference

Molecular spectrophotometry

The UV spectra in nitric acid solution of Ag, Au, silicate (soluble), phosphate or molybdate were recorded individually and indicated maximum absorption bands at 200, 225, 245, 205 and 203 nm respectively. An insignificant shifts in the wavelengths has been observed when mixtures of Ag or Au with phosphate, silicate or molybdate were carried out in 0.3 mol l^{-1} nitric acid solutions (against reagent blank prepared under the same conditions). These results suggest compound

formations between Ag or Au with these species. Such compounds are easily decomposed in the flame without apparent effect on the absorbance signals of the analyte Ag or Au. On measuring the spectra of Ag or Au in the presence of heteropoly species in nitric acid solution (Figs. 5-7) complete disappearance of the analytes absorption maxima and persistent existence of the maximum absorption bands of the heteropoly species were observed.

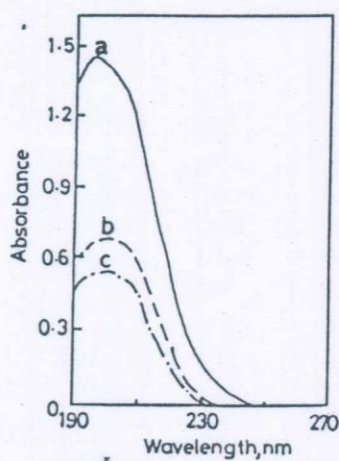


Fig. 5. Ultraviolet spectra of: a) silver nitrate solution, b) phospho- or silicomolybdate and c) solution (a) plus solution (b)

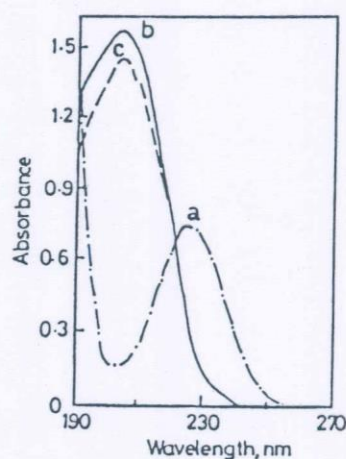


Fig. 6. Ultraviolet spectra of: a) sodium aurate solution, b) phosphomolybdate and c) solution (a) plus solution (b)

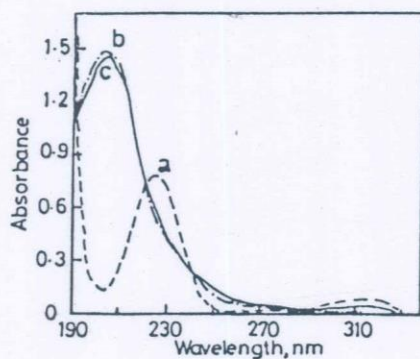


Fig. 7. Ultraviolet spectra of: a) sodium aurate solution, b) silicomolybdate and c) solution (a) plus solution (b)

These results assure the non-existence of compounds between the analyte and the heteropoly species. It is possible that Ag or Au is being inserted to the cavities of the HPA. If the case is similar to that taking place in the flame, the interpretation of such harmful interfering effect will be plausible particularly if the flame profiles (Figs. 3 and 4) are considered as criteria on the incomplete disintegration of the internally loaded HPA with the analyte during its instant transient in the flame.

Thin layer chromatography

To ascertain the findings obtained from UV-visible measurements, solutions of Ag, Au, phosphomolybdate or silicomolybdate only or in mixtures were spotted on TLC plates. In the developing chamber, the plates were presaturated with the solvent system [chloroform-ethanol-acetic acid 10:3:1 (V/V)] for about 2 h and were dried and left in sublimed iodine or dithizone [0.1 % (m/V)] in carbon tetrachloride and sprayed separately. The HPA entity appears as purple-violet, Ag or Au appears as pale yellow spots in case of using sublimed iodine as a marker. In case of dithizone, Ag appears as red coloured while the HPA entity appears as pale green coloured spots on the plates. The values of R_f in case of Ag, Au, phosphomolybdate and silicomolybdate alone are 0.48, 0.42, 0.30 and 0.33, respectively. While in case of Ag-phosphomolybdate, Ag-silicomolybdate, Au-phosphomolybdate and Au-silicomolybdate mixtures the values are 0.28, 0.31, 0.27 and 0.30 respectively. These values are close to that obtained for the HPA entity alone. The complete disappearance of Ag or Au characteristic spot on the TLC plates has also been observed when increasing the time of equilibrium with the HPA with insignificant change in the R_f values of the HPA entities. These results confirm that the interference of the HPA entity in the flame on the atomic absorption determination of Ag or Au is of physical nature. In other words such phenomenon means that Ag or Au has been included in the structure of the HPA without any chemical reaction.

Control of heteropolyanion formation

Now, it is possible to propose a simple way to get rid of the interference of the HPA formation on the absorbance signals of Ag or Au determined by atomic spectrometry. Such proposal stems from the understanding of the mechanism of the HPA formation interference. Basically, controlling of such type of interference may take place through spoiling the HPA formation in the aspirated solution or enlarging the coordination sphere around the analyte to forbid its insertion in the cavities of the HPA. Figure 8 shows the effect of $1 \text{ mol l}^{-1} \text{ NH}_3$ or NaOH solution as levelling agent for Ag from different HPA interference effect. The coincidence of the graphs indicates that raising the pH of the aspirated solution affects the deformation of the HPA entity in solution before reaching the flame. Hence it will not affect the absorbance signal of the analyte because of its non-existence.

A series of chelating agents *viz*: potassium cyanide, resorcinol, ethylenediamine or EDTA has been added to the solution of Ag or Au including the HPA entity.

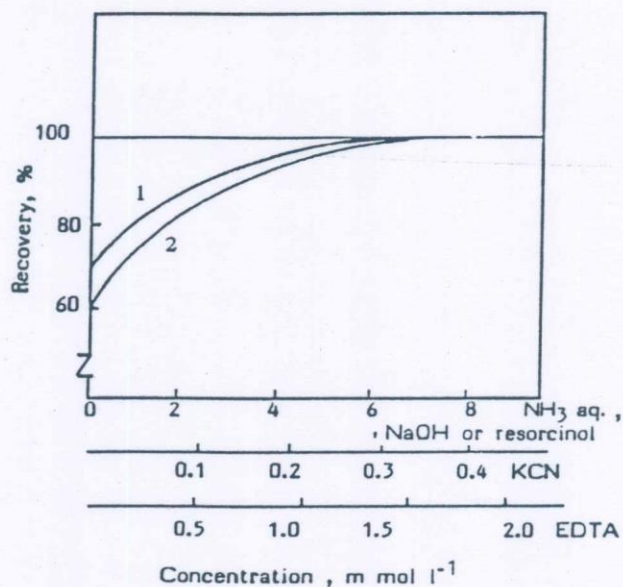


Fig. 8. Recovery of 5 ppm of Ag from heteropoly anion formations interference using: aqueous ammonia, sodium hydroxide, potassium cyanide, resorcinol or EDTA solution, from: 1) 0.01 mol l⁻¹ phospho-, silico-, arseno- or telluromolybdate and 2) 0.002 mol l⁻¹ phospho-, silico- or tellurotungstate

Figure 8 indicates the levelling effect of such chelating agents where 100 % recoveries of Ag or Au has been obtained. Potassium cyanide is the best in levelling the Ag or Au absorbance signal where complete recovery has been obtained at low concentration. The effect of potassium cyanide can be attributed to the complex formation of the cyanide ion with silver which is not easily occluded on the HPA entity.

REFERENCES

1. Rubéska T. and Moldan B., *Anal. Chim. Acta*, **37**, 421 (1967).
2. Sastri V. S., Chahrabarti C. L. and Willis D. E., *Can. J. Chem.*, **47**, 578 (1969).
3. Thomas P. E. and Pickering W. F., *Talanta*, **18**, 127 (1971).
4. Abdallah A. M., Kabil M. A. and Mostafa M. M., *Chem. Anal.*, **31**, 3 (1986).
5. El-De'rawy M. M., Khalifa M. E., Abdallah A. M. and Akl M. A., *J. Anal. Atomic Spectr.*, **2**, 333 (1987).
6. Abdallah A. M. and Kabil M. A., *Chem. Anal.*, **33**, 75 (1988).
7. Gilbert Jr. P. T., *Analysis Instrumentation*, Proc. Xth Nat. Anal. Inst. Symp., San Francisco 1964.
8. Kirkbright G. F. and Sargent M., *Atomic Absorption and Fluorescence Spectroscopy*, Academic Press, London 1974.
9. Belcher C. B. and Kinson K., *Anal. Chim. Acta*, **30**, 483 (1964).
10. David D. J., *Analyst*, **83**, 655 (1958).
11. Andrew T. R. and Nichols P. N. R., *Analyst*, **87**, 25 (1962).
12. Janousek I. and Malat M., *Anal. Chim. Acta*, **58**, 448 (1972).
13. Khan A. S. and Chaw A., *Anal. Lett.*, **16**, 265 (1983).
14. Brooks R. R., Royn D. E. and Zhany H. F., *Anal. Chim. Acta*, **3**, 1 (1981).

15. Smith J. D. and Milne P. S., *Anal. Chim. Acta*, **123**, 263 (1981).
16. Fishman M. and Spencer R., *Anal. Chem.*, **49**, 1589 (1977).
17. Marczenko Z., *Spectrophotometric Determination of Elements*, Ellis Horwood, Chichester 1976.
18. Bimal M., Khanand M. A. and Novman A. A., *Water Sci. Techn.*, **19**, 9 (1967).
19. Atwell M. G. and Herbert J. Y., *Appl. Spectr.*, **23**, 480 (1969).
20. Thomerson D. R. and Price W. J., *Analyst*, **96**, 321 (1971).
21. Bailer J. C., Emeleus H. J., Nyholm R. and Trotman D. A. F., *A Comprehensive Inorganic Chemistry*, Pergamon Press, London 1: 73.
22. Apolitskii V. N., Galanova A. P., Kudryavina A. K., Latysheva Y. P. and Pronin V. A., *Zh. Prikl. Spectr.*, **17**, 759 (1972).
23. Halls D. J. and Townshend A., *Anal. Chim. Acta*, **36**, 278 (1966).
24. Dean J. A., *Flame Emission and Atomic Absorption Spectrometry*, **3**, 73 (1974).

Received October 1991

Accepted April 1992

PG3. FLOW INJECTION CHEMILUMINOMETRIC DETERMINATION OF SODIUM CYCLAMATE

A. C. Calokerinos, J. M. Psarelis and E. G. Sarantonis, *Laboratory of Analytical Chemistry, University of Athens, Panepistimiopolis, Zografou, 157 71 Athens, Greece*

The oxidation of sulfite by potassium permanganate or cerium(IV) in acidic solution is a well known chemiluminescent reaction. The emission intensity is greatly enhanced by the presence of a variety of sensitizers in the reaction mixture. A group of sensitizers for this reaction includes compounds with cyclohexyl-groups, such as 3-cyclohexylaminopropanesulfonic acid (CAPS),¹ compounds with structure similar to CAPS² and steroid hormones.³

Sodium cyclamate is an artificial sweetener with a limited number of analytical methods for its quantification. Nevertheless, it increases the emission intensity from the cerium(IV)-sulfite reaction by an action similar to that of CAPS. This observation allowed the development of a simple method for the determination of sodium cyclamate in the region 1.00–50.0 $\mu\text{g ml}^{-1}$. The effect of other sweeteners will be discussed together with the potential application of chemiluminescence in this area of analytical research.

References

- 1 Koukli, I. I., Sarantonis, E. G., and Calokerinos, A. C., *Analyst*, 1988, **113**, 603.
- 2 Koukli, I. I., Sarantonis, E. G., and Calokerinos, A. C., *Anal. Lett.*, 1990, **23**, 1167.
- 3 Syropoulos, A. B., Sarantonis, E. G., and Calokerinos, A. C., *Anal. Chim. Acta*, 1990, **239**, 195.

PG4. CONTINUOUS FLOW CHEMILUMINOMETRIC DETERMINATION OF TETRACYCLINES BY OXIDATION WITH N-BROMOSUCCINIMIDE IN PHARMACEUTICAL PREPARATIONS

A. C. Calokerinos, S. A. Halvatzis and M. Timotheou-Potamia, *Laboratory of Analytical Chemistry, University of Athens, Panepistimiopolis, Zografou, 157 71 Athens, Greece*

Chemiluminescence (CL) has been successfully extended to reactions involving compounds of pharmaceutical and biological interest.¹ N-Bromosuccinimide (NBS) is an oxidizing reagent that has been found to participate in a plethora of CL reactions. In aqueous solutions the oxidizing properties of NBS are attributed to hypobromous acid generated by hydrolysis of the reagent.²

A simple continuous flow procedure will be described for the determination of tetracycline·HCl (0.050–3.00 $\mu\text{g ml}^{-1}$), oxytetracycline·HCl (0.50–5.00 $\mu\text{g ml}^{-1}$), doxycycline·HCl (0.50–7.00 $\mu\text{g ml}^{-1}$) and demethylchlorotetracycline·HCl (0.30–3.00 $\mu\text{g ml}^{-1}$). The method is based on the CL generated during the oxidation of the analytes by NBS in alkaline media. The emission intensity is greatly enhanced by the synergistic effect of ammonia, when present in the solution. All measurements were made by using the continuous flow CL analyser described recently.³ The analysis is automated and samples can be analysed at a rate of about 130 solutions h^{-1} with a relative error of about 1.5%. The detection limits for tetracycline·HCl and demethylchlorotetracycline·HCl were of the order of ng ml^{-1} . The results obtained for the assay of commercial preparations compared well with those obtained by the official methods and demonstrated good accuracy and precision.

References

- 1 Abbott, R. W., Townshend, A., and Gill, R., *Analyst*, 1986, **111**, 635.
- 2 *The Determination of Organic Compounds with N-Bromosuccinimide and Allied Reagents*, eds. Mathour, N. K., and Narang, C. K., Academic Press, London, 1975.
- 3 Halvatzis, S. A., Timotheou-Potamia, M. M., and Calokerinos, A. C., *Analyst*, 1990, **115**, 1229.

PG5. FLOW INJECTION EXTRACTION SPECTROPHOTOMETRIC DETERMINATION OF MANGANESE IN STEEL AS TRIPHENYLSULFONIUM OR BENZYLTRIPHENYLAMMONIUM PERMANGANATE

D. Thorburn Burns and M. Harriott, *Department of Analytical Chemistry, The Queen's University of Belfast, Belfast BT9 5AG, UK*, and S. A. Barakat and M. S. El-Shahawi, *Department of Chemistry, United Emirates University, Al-Ain, United Arab Emirates*

Manganese(VII) can be determined spectrophotometrically at 548 nm after flow injection extraction into chloroform of the ion-pairs triphenylsulfonium permanganate or benzyltributylammo-

nium permanganate. The manifolds have a carrier stream of a pH 6 buffer containing 10% m/m ammonium fluoride; the reagent streams were 0.1% m/v or m/m, respectively of triphenylsulfonium or benzyltributylammonium chloride. Calibration graphs were linear up to 25 $\mu\text{g ml}^{-1}$ manganese and detection limits were 1.1 and 0.91 $\mu\text{g ml}^{-1}$ (3 \times baseline noise) respectively based on 250 μl injections. The injection rate was 20 h^{-1} . The systems have been applied to the determination of manganese in a range of steels.

PG6. FLOW INJECTION EXTRACTION SPECTROPHOTOMETRIC DETERMINATION OF MOLYBDENUM AND OF ALUMINIUM WITH QUINOLIN-8-OL

D. Thorburn Burns, M. Harriott, D. Boland and P. Pornsinlapitip, *Queen's University, Belfast, UK*

PG7. FLOW INJECTION ANALYSIS: CHEMILUMINESCENCE METHOD FOR SELECTIVE DETERMINATION OF CHROMIUM(III)

R. Escobar, Lin Qingxiong and A. Giraúm, *Departamento de Química Analítica, and F. F. de la Rosa, Departamento de Bioquímica Vegetal y B.M., Universidad de Sevilla, Seville, Spain*

'Flow injection analysis' (FIA) has been applied to the determination of Cr^{III} in water and food samples. The method is based on the measuring of Cr^{III} -catalysed light emission from luminol oxidation by hydrogen peroxide. The apparatus is constituted by a 'flow injection analysis' system, a flow cell and a photodetector connected to a recorder. The flow cell, situated near the photodetector, is a spiral tube made with transparent Teflon. The typical signal is a narrow peak, in which the height is proportional to the light emitted and, consequently, to the concentration of Cr^{III} . The detection limit is 0.01 ppb and the linear range extends up to 5 ppb. The optimal experimental conditions have been studied. Thus, the best concentrations for the reagents, the optimum pH value and the best injection speed have been determined. Interferences by several metal ions have been examined, and the proposed system shows a high selectivity. The method has been successfully applied to the determination of Cr^{III} in water and the conditions for the application to ashing foods are in the process of being investigated.

PG8. SINGLE BOUNDARY MEASUREMENTS AND SANDWICH TECHNIQUES IN FLOW INJECTION ANALYSIS

Alan E. Davies and Arnold G. Fogg, *Chemistry Department, Loughborough University of Technology, Loughborough, Leicestershire LE11 3TU, UK*

When a sufficiently large-volume injection is made in flow injection (FI) analysis in a single-channel manifold, signals due to on-line reactions are observed at each of the two boundaries formed. This situation can be represented as $B > A > B$, where B is the carrier stream and A is the injectate. By stream switching, or by using combinations of valves and valve types, situations represented by $C > B > A$ can be produced. This arrangement and others have been used by several groups to produce so-called sandwich methods. When B is a reagent and A and C different standard solutions, double standardizations can be made. With C and A different reagents and B the sample, different determinations can be made at the two boundaries.

Previously we reported amperometric and visible spectrophotometric FI methods in which a reagent (the monitorand) is formed on-line, and reacted on-line with the determinand. With small-volume injections two separate injections are made to obtain the full monitorand signal and the reduced signal in the presence of determinand. We report here the use of the $C > B > A$ configuration to obtain the two signals with a single injection, and other aspects of single-boundary spectrophotometric measurements are discussed.

PG9. SIMULTANEOUS DETERMINATIONS OF METAL IONS BASED ON THE ESTABLISHMENT OF pH AND LIGAND CONCENTRATION GRADIENTS IN FLOW SYSTEMS

Angel Rios, Miguel Valcárcel and Juliana Marcos, *Department of Analytical Chemistry, Faculty of Sciences, University of Córdoba, E-14004 Córdoba, Spain*

Unsegmented flow methods are normally applied at constant flow rates. However, some methods reported in the past few years involve variable flow rate. One of the most interesting aspects of this new operational approach is that it can be used to establish concentration gradients in the flow system. Thus, pH

Your order details**Our Order Ref:** 00699427-001**Your Ref:** 79**Despatched on:** 1/5/2014**Your item details**

UIN: BLL01011734447
Title: Bulletin de la Société chimique de France.
Publisher:
ISSN: 0037-8968
Year: 1991
Pages: 641-643
Author name(s): Farag A.B.; El Shahawi M.S.; Helmy A.; Fa
Article title words: The extraction and recovery of some organic insecticides from aqueous media with cellular polyurethanes

Your shipping address

King Abdul Aziz University
Library Deanship
Al-Jamh st
Jeddah
21589
SAUDI ARABIA

Comments

Thank you for using Document Supply Services!

King Abdul Aziz University
Library Deanship
Al-Jamh st
Jeddah
21589
SAUDI ARABIA



Copyright Statement

Unless out of copyright, the contents of the document(s) attached to or accompanying this page are protected by copyright. They are supplied on condition that, except to enable a single paper copy to be printed out by or for the individual who originally requested the document(s), you may not copy (even for internal purposes), store or retain any electronic medium, retransmit, resell, or hire the contents (including the single paper copy referred to above). However these rules do not apply where:

1. you have written permission of the copyright owner to do otherwise;
2. you have the permission of The Copyright Licensing Agency Ltd, or similar licensing body;
3. the document benefits from a free and open licence issued with the consent of the copyright owner;
4. the intended usage is covered by statute.

Breach of the terms of this notice is enforceable against you by the copyright owner or their representative.

This document has been supplied under our Copyright Fee Paid service. You are therefore agreeing to the terms of supply for our Copyright Fee Paid service, available at:

<http://www.bl.uk/reshelp/atyourdesk/docsupply/help/terms/index.html>

The extraction and recovery of some organic insecticides from aqueous media with cellular polyurethanes

AB Farag², MS El-Shahawi¹, AMA Helmy², S Farrag²

¹ Chemistry Department, Faculty of Science, Mansoura University
Damietta, Egypt

² Chemistry Department, Faculty of Science, Mansoura University
Mansoura, Egypt

(received December 10 1990, accepted March 27 1991)

The results of preliminary screening tests involving the removal of some organic insecticides from aqueous media with polyurethane foam are described. The foam material was found to have a good affinity towards the absorption of the insecticides tested (Somigold, Dimilin and Trifluoron). The possibility of using polyurethane foam in column dynamic extraction mode for the recovery of these insecticides from aqueous solutions were examined. The insecticides tested have successfully been extracted onto the foam column when 100-300 cm³ aliquots of their dilute solutions were percolated through the column at reasonable flow rates (2-5 cm³min⁻¹). The collected insecticides were then recovered from the foam with 100 cm³ acetone in Soxhlet extractor. After the reduction of volume to 5 cm³ in a rotary evaporator, the concentration of the insecticides were then determined spectrophotometrically. The application of the developed method for the extraction and recovery of the above mentioned insecticides in the Nile river water has been evaluated. Obviously the use of polyurethane foam provides advantages over other solid absorbents particularly where large samples have to be handled. Polyurethane foam offers a good capacity and low cost solid extractor in comparison with other known sorbents.

extraction isotherm / recovery / insecticides / natural water / polyurethane foam

Résumé - L'extraction et la récupération de quelques insecticides organiques à partir de milieux aqueux par polyuréthanes cellulaires. La mousse de polyuréthane possède une bonne affinité pour l'absorption des insecticides testés (Somigold, Dimilin et Trifluoron). Ces insecticides ont été extraits avec succès d'une colonne de mousse, quand 100 à 300 cm³ de leurs solutions diluées furent percolées à une vitesse raisonnable 2-5 cm³min⁻¹. Les insecticides collectés ont été extraits par 100 cm³ d'acétone puis réduit à 5 cm³ par évaporation et dosés spectrophotométriquement. Cette méthode sera testée pour la récupération de ces insecticides dans les eaux du Nil.

isotherme d'extraction / récupération / insecticides / mousse de polyuréthane

Introduction

With the recent growth of the chemical industries all over the world, there has been a corresponding increase in the uses of hazardous chemicals and insecticides. Because of the application of some of these insecticides in the agricultural field, there has been greater concern over the public health and environmental risks involved in the accidental release of these chemicals (1).

The presence of pesticides and polychlorinated biphenyls (PCBs) in the air, industrial building and water has been well documented (2, 3). The analysis of chlorinated pesticide residues and PCBs in water continue to present problems (4). The extraction of chlorinated pesticides from water with organic solvents is time consuming and can only be done with 95-100%

efficiency (5). The adsorption of PCB on activated carbon is complete but its recovery is variable, inefficient (25-30%) and the recovered material is significantly different from the initial PCB (6). The reversed liquid-liquid partition filter chromatography developed by Ahling *et al* (7) gave excellent recovery for PCB but requires continuous supervision and was limited by relatively low flow rate (0.65 cm³min⁻¹).

Use of porous polyurethane foam (PPF) as an absorbent for high volumes of aqueous or gaseous media has proven advantageous due to its ease of handling and cleanup and its ability to capture many different organic compounds (8, 9). These foams allowed reasonable flow rates of the mobile phase without the aid of a pump. These properties have resulted in extensive use of PPF for collecting airborne pollutants (10-12).

The present article deals with the use of polyurethane foam as trapping medium for the extraction and recovery of some organic insecticides from high volume samples of aqueous media.

Experimental

Reagent and materials

The reagents used were of analytical grade and the solvents were of spectroscopic grade polyurethane foam, a polyether of open cell type was supplied by Greiner KG, Schaumstoffwerk-Kremsmunster, Austria. The volume weight of the foam was 30 kg m^{-3} . The foam cubes (10 mm edge) were washed by 1 M hydrochloric acid followed by distilled water and acetone and were finally dried at 80°C . The insecticides tested were: Trifluoron, [2-chloro-N-[4-trifluoromethoxy]-phenylamino]-carbonylbenzamide; Dimilin, [N-[(4-chlorophenyl)-amino]carbonyl]-2,6-difluorobenzamide and Somigold which is a derivative of [phosphoric acid-(7-chloro-bis-cyclo-3,2,0-hepta-2,6-diene-6-yl)-1-dimethylester]. These insecticides were used as received.

Stock solutions containing 4 mg cm^{-3} of each insecticide were prepared by dissolving the exact weight of the insecticide in 100 cm^3 of acetone. A series of standard solutions of these compounds were prepared by diluting their stock solutions with water so as to obtain, 20, 40, 60, 80, 90 and $100 \mu\text{g cm}^{-3}$ solutions. All the solutions were stored in polyethylene bottles.

Apparatus

A Varian 634 DMS double-beam Spectrophotometer with 1 cm quartz cell was used for determining the concentration of the compounds employing a wavelength suitable for each insecticide. Glass columns of 15 mm diameter and 18 cm length were employed.

General procedure

In separate batch experiments, 0.4 g foam was mixed with 100 cm^3 solutions of each compound containing 20 to $100 \mu\text{g cm}^{-3}$. These solutions contained in a series of stoppered polyethylene bottles were shaken for 3 hours in a mechanical shaker. The compound remaining in the aqueous solutions was determined by the UV-visible spectrophotometer, and the amount of compound retained on the foam was calculated by difference.

In the dynamic experiments 0.5 g dry foam was packed in the column using the vacuum method of column packing (9). 5 mg of each compound in 3000 cm^3 water (distilled or Nile river water) were percolated through the foam column at $5\text{--}10 \text{ cm}^3 \text{ min}^{-1}$. After squeezing water from the foam material, the insecticide is recovered from the foam with $100\text{--}120 \text{ cm}^3$ acetone in a soxhlet apparatus. The eluate is then concentrated in a rotary evaporator, to 30 cm^3 and the sample is analysed by measuring the absorbance of the solution at a suitable wavelength.

Results and discussion

The application of porous polyurethane foams as cellular solid extractants is considered as a useful addition to the field of chemical separation and preconcentration. The polyurethane foam method allows the isolation of the analyte from the matrix and yields an appropriate enrichment factor. Also the hydrodynamic properties

of foam column allow the application of quite high flow rates without the aid of vacuum. This together with the rapid attainment of the absorption equilibrium on the membranes forming the foam material reduces the time required for analysis.

In order to examine the suitability of the foam for the extraction of the insecticides tested in aqueous media, the rate of extraction of the compounds was determined by varying the time of contact between the foam and the test samples using batch experiments. The foam matrix was found to have a good affinity towards the extraction of the compounds examined and the extraction is increased by increasing shaking time up to 2 hours after which time remained constant. Hence a minimum of 2 hours was used in obtaining the extraction isotherms.

Extraction isotherms

The uptake of the compounds in aqueous media by the foam was found to depend on its concentration. Thus in separate experiments, absorption isotherms were developed over a wide range of equilibrium concentration ($20\text{--}100 \mu\text{g cm}^{-3}$) for each compound. The pH values of the aqueous insecticide solutions in these experiments were usually 6 so that the insecticide species are predominately in undissociated forms. The absorption isotherms of the three insecticides tested exhibited a first order behaviour in the low concentration range and then tended to plateau at high bulk solution concentration as shown in figure 1. These results suggested the possibility of using polyurethane foam in dynamic column experiment for the extraction of these insecticides from aqueous solution.

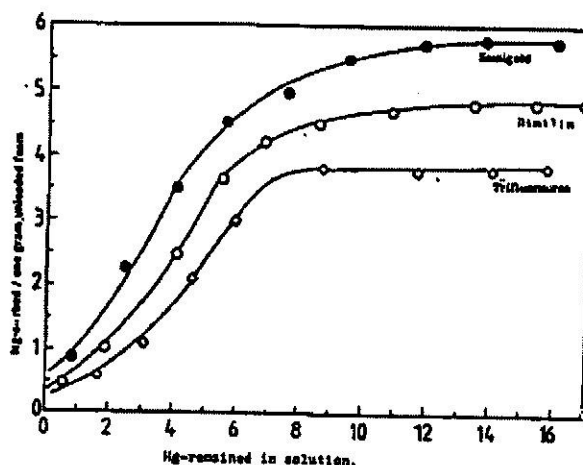


Fig 1. Extraction isotherm of the insecticides tested.

Dynamic experiment

Three liters of each insecticide solution (in distilled or Nile river water) were passed through the foam column at a flow rate $5\text{--}10 \text{ cm}^3 \text{ min}^{-1}$ which was chosen on the basis of preliminary tests. The results of the extraction and recovery of the compounds are summarized in

Table I. Extraction and recovery of the insecticides tested from 3 L aqueous solutions by the proposed foam column at 5-10 cm³ min⁻¹.

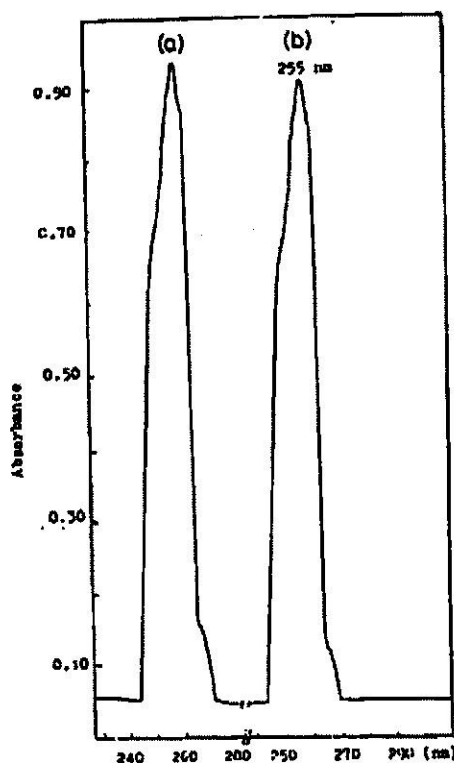
Insecticide	Amount (mg)	% Recovery		Wavelength (λ) (nm)
		a	b	
Dimilin	5	95	92	262
Trifluoron	5	96	97	270
Somigold	5	85	87	255

a - Average of three data from distilled water

b - Average of three data from Nile river water.

Table I. Recoveries of the insecticides were more than 90% except Somigold. Better results were obtained for the separation and recovery of Somigold when the flow-rate was reduced to 2-5 cm³ min⁻¹. A representative example of the separation of Dimilin is shown in figure 2. The absorption spectra of Dimilin solution with and without the foam concentration step, indicate the efficiency of the proposed foam columns.

Fig 2. UV absorption spectra of Somigold :
a - Before percolation through the foam column.
b - After recovery from the foam column.



References

- (1) Charlton J, Chow A, Gesser HD *Hazard Assessment of Chemicals*, (1983) 2, 245
- (2) Lewis RG, Lee Jr RE in *Air Pollution from Pesticides and Agricultural Processes*, Lee Jr RE Ed, CRC Press: Cleveland, 1976, Chapter 2
- (3) Giam CS, Chan HS, Neff GS *Anal Chem* (1975) 47, 2319
- (4) Veith GD, Lee GF *Water Res* (1970) 4, 265
- (5) Kahs L, Wayman CH *Anal Chem* (1964) 36, 1340
- (6) Rosen AA, Moddleton FM *Anal Chem* (1959) 31, 1729
- (7) Ahling B, Jensen S *Anal Chem* (1970) 42, 1483
- (8) Moddy GJ, Thomas JDR *Chromatographic Separation and Extraction with Foamed Plastics and Rubbers*. Dekker, New York, 1982
- (9) Braun T, Navartil JD, Farag AB *Polyurethane Foam Sorbents in Separation Science*, CRC Press, Florida, 1985
- (10) Burdick NF, Bidleman TF *Anal Chem* (1981) 53, 1926
- (11) Farag AB, El-Wakil AM, El-Shahawi MS, *Fres Z Anal Chem* (1986) 324, 59
- (12) Farag AB, El-Wakil AM, El-Shahawi MS, Mashaly M *Anal Sci* (1989) 5, 449

Spectrophotometric Determination of Nickel(II) with Some Schiff Base Ligands

M. S. El-SHAHAWI

*Chemistry Department, Faculty of Science at Damietta, Mansoura University,
Damietta, Egypt*

Sensitive and convenient methods for the spectrophotometric determination of nickel(II) with *N,N'*-bis(salicylaldehyde)ethylenediamine, *N,N'*-bis(salicylaldehyde)*O*-phenylenediamine and *N,N'*-bis(2-hydroxy-1-naphthaldehyde)*O*-phenylenediamine have been developed. The optimum concentration range evaluated by Ringbom's method and the effect of diverse ions on the determination were also investigated. The molar absorptivity and the Sandell sensitivity of the complexes were obtained. The present methods have been applied for the analysis of standard samples of nickel(II) in tap water and in industrial wastewater.

Keywords Nickel(II) determination, Schiff base, spectrophotometry, natural water

The Schiff base compounds have been extensively studied because of their biological and structural importance.¹⁻⁴ Several Schiff base ligands have been proposed as spectrophotometric reagents for metal ions.⁵ The importance of these compounds lies mainly in their specific and selective reactions with metal ions. There are many effective spectrophotometric methods for the determination of trace amounts of nickel(II)⁶⁻⁸ but they require much time for the extraction procedure and the tolerance limit for nickel(II) is low. Work done on bisazomethazine Schiff base ligands involving salicylaldehydediamine and its derivatives^{9,10} revealed that, these compounds behaved as promising reagents for a number of metal ions, because they react with these metal ions to give complexes that are insoluble in water. This paper describes the conditions for the extraction spectrophotometric determination of microgram amounts of nickel(II) with some Schiff base ligands.

Experimental

Apparatus

An Orion pH meter was used for pH measurements. A Varian 634S double beam UV-Visible spectrophotometer was also used for the absorption spectra and the absorbance measurements, with a quartz cell of 10 mm path length.

Synthesis of the reagents

The reagents *N,N'*-bis(salicylaldehyde)ethylenediamine (Salen), *N,N'*-bis(salicylaldehyde)*O*-phenylenediamine (Salop) and *N,N'*-bis(2-hydroxy-1-naphthaldehyde)*O*-phenylenediamine (Napop) were prepared by a

method similar to those described previously^{10,11} using the following general procedure. To 50 mmol salicylaldehyde or 2-hydroxy-1-naphthaldehyde in ethanol, 25 mmol ethylenediamine or *O*-phenylenediamine were added. The reaction mixture was refluxed for one hour with constant stirring; the resulting precipitates were cooled and filtered off, washed with methanol and dried over silica gel. The Schiff bases and their nickel(II) complexes were characterized on the basis of their electronic spectra, characteristic IR frequencies and elemental analysis. Analysis for hydrogen, nitrogen and carbon of the compounds prepared gave acceptable results, with carbon values within 0.4% of the theoretical values.

Reagents

All reagents used were of analytical reagent grade unless stated otherwise. A stock solution of nickel (1 mg cm^{-3}) was prepared by dissolving an accurate weight of nickel sulfate in doubly distilled water and standardized by EDTA.¹² Solutions (0.02%(g/v)) of Salen, Salop and Napop were prepared in chloroform.

Recommended procedures

Into a 100 cm³ separating funnel, transfer 20 cm³ of sample solution containing up to 70 mg of nickel(II). Add 5 cm³ of pH 4.5–5 acetate buffer solution and 5 cm³ of the reagent in chloroform followed by 5 cm³ of chloroform. Shake the mixture vigorously for 5 min and allow the layers to separate. Transfer the organic phase to a 10 cm³ volumetric flask after drying it over anhydrous sodium sulfate. Measure the absorbance of the organic phase at the maximum wavelength for each complex against a reagent blank prepared in the same

manner. Calibration curves are obtained under similar conditions. Establish the concentration by reference to the calibration graph with solutions containing 20–70 μg of nickel.

Results and Discussion

Chloroform, toluene, carbon tetrachloride, methyl-

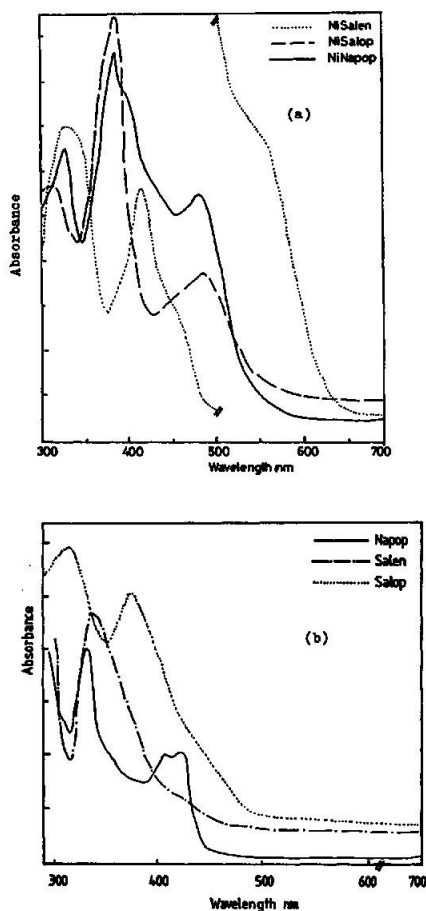


Fig. 1a Absorption UV-visible spectra of the nickel(II) complexes (1.2×10^{-4} M) against reagent blank in chloroform.

Fig. 1b Absorption UV-visible spectra of the Schiff base reagents (2.0×10^{-4} M) against chloroform.

enechloride and chlorobenzene were used as possible extracting agents for the tested complexes. All solvents used extract the complexes, but the highest absorbance is obtained in chloroform, the extraction also being more clean and complete in this solvent. Chloroform was selected as a proper solvent for these reasons and because its greater density allows a better separation of phases.

Absorption spectra

Some important infrared absorption frequencies of the solid reagents and their solid nickel(II) complexes are given in Table 1 with their probable assignments. The electronic absorption of the ligands and their complexes in chloroform is also given in Table 1. Representative spectra are shown in Fig. 1. The electronic spectra of the complexes have three bands in the UV-visible region, which are partially resolved, and a broad shoulder of low intensity. The absorption maxima of the complexes were found in the range 310–330, 380–415 and 450–480 nm. The reagents form 1:1 complexes with nickel(II).^{4,10} In the subsequent work, the absorbance measurements for the complexes NiSalen, NiSalop and NiNapop were carried out at 415, 377 and 380 nm, respectively.

Effect of shaking time

The effect of shaking time on the absorbance of the tested complexes was checked from 2–30 min. It was observed that the extraction of the chelates into chloroform was fast and rapid. No change in the degree of extraction occurred when the stirring time was varied from 5–30 min. Therefore, a 5 min shaking time was adopted in the subsequent work.

Stability of the color complexes and effect of electrolytes

After the extraction of each color complex as described under the recommended procedure, the absorbances were found constant up to 20 h for samples containing 20–60 μg . Samples were stored in stoppered tubes at room temperature; the absorbance values remained constant over this time period. The addition of sodium chloride (0.01–0.1 M) did not improve the amount of complex extracted in any system, indicating that the complexes are extracted quantitatively without or with salt effect.

Table 1 Infrared spectra and band assignments of the solid compounds and details of their electronic spectra in chloroform

Compound	Wavenumber/ cm^{-1}			Peak position in nm with intensity in $1 \text{ mol}^{-1} \text{ cm}^{-1}$ parentheses
	$\nu\text{C}=\text{N}$	$\nu\text{M}-\text{O}$	$\nu\text{M}-\text{N}$	
Salen	1620	—	—	330, 405 (w)
Salop	1612	—	—	340, 385
Napop	1620	—	—	335, 40, 415 (w)
NiSalen	1625	520	430	334 (1.8×10^4), 415 (1.26×10^4), 480 (sh), 560 (sh)
NiSalop	1610	550	460	310 (2.5×10^4), 377 (3.9×10^4), 480 (1.3×10^4)
NiNapop	1620	560	430	330 (2.2×10^4), 380 (3.0×10^4), 475 (1.8×10^4)

Effect of reagent concentration

The effect of an excess of the chromogenic reagents was examined. The absorbance of a series of solutions containing 60 μg of nickel(II) and various amounts of the Schiff base ligand in chloroform was examined. It was found that 3–5 cm^3 of 0.02% g/v of each ligand solution sufficed to complex 60 μg or less of nickel. A large excess of the reagent tends to decrease the absorbance, possibly owing to the increased absorbance of the reagent blank.¹³ Amounts of the reagents smaller than the recommended values gave incomplete complex formation.

Effect of pH

The influence of the pH of the aqueous phase on the extraction of nickel (50 μg) was examined by measuring the absorbance of the organic phase for each nickel complex in chloroform. The final pH of each aqueous solution was measured before the extraction. Other conditions were kept constant. The results are summarized in Fig. 2, from which it can be seen that a maximum and constant absorbance of the organic phase for NiSalen, NiSalop and NiNapop can be obtained over the pH range 4.5–7, 4.8–7.5 and 5–7.5, respectively. The pH values were adjusted with HCl and NaOH. When HClO_4 is used instead of HCl in the preparation of the samples, no significant differences in the range of constancy absorbance of the tested complexes were observed. In more acidic or alkaline solution, the absorbance decreased, possibly because of the incomplete complex formation or the hydrolysis of the complexes, respectively.¹⁴ An acetate buffer solution was finally chosen and used as described under the recommended procedure.

Beer's law and sensitivity

Under the optimum experimental conditions described above, calibration curves of the nickel complexes were constructed. A linear graph was obtained for each complex by measuring the absorbance of the organic

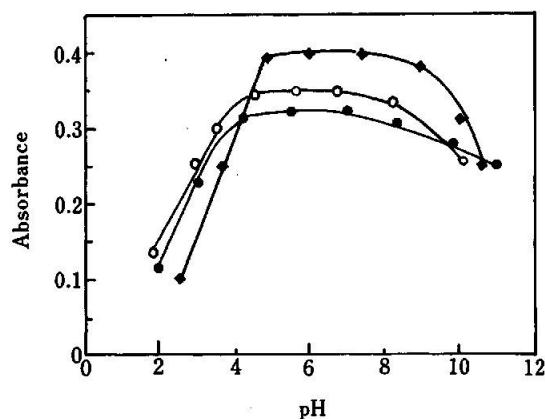


Fig. 2 Effect of pH on the absorbance of the extracted nickel(II) complexes: Salen, ●; Salop, ○ and Napop, ◆ against reagent blank in chloroform.

phase as a function of metal ion concentration. For the Salen reagent, Beer's law was obeyed up to 7 $\mu\text{g cm}^{-3}$ nickel in the organic phase. The optimum concentration range evaluated by Ringbom's plots^{15,16} has been found to be 14–52.2 μg metal ion. The molar absorptivity calculated from Beer's law and the Sandell¹⁷ sensitivity for the NiSalen complex have been found to be $1.26 \times 10^4 \text{ l mol}^{-1} \text{ cm}^{-1}$ and $0.049 \mu\text{g cm}^{-2}$, respectively at 415 nm. In the case of NiSalop and NiNapop complexes, calibration graphs showed good linearity. Beer's law was obeyed over the concentration range up to 6.5 and up to 5.5 $\mu\text{g cm}^{-3}$ for these two complexes in the organic phase. The molar absorptivity and the Sandell sensitivity have been found to be $3.9 \times 10^4 \text{ l mol}^{-1} \text{ cm}^{-1}$ and $0.076 \mu\text{g cm}^{-2}$ for NiSalop and $3.0 \times 10^4 \text{ l mol}^{-1} \text{ cm}^{-1}$ and $0.006 \mu\text{g cm}^{-2}$ for NiNapop in chloroform at 377 and 380 nm, respectively. The sensitivities of these reactions are comparable to those of many well known methods for nickel.^{6,7} Reproducibility tests for five results at 4 $\mu\text{g cm}^{-3}$ of nickel showed a standard deviation of ± 0.12 .

Effect of diverse ions

The effects of some of the diverse ions which are often in association with the tested metal ion were studied. The selectivity of the proposed method using the reagent Salen was examined by the determination of a fixed concentration (40 μg) of nickel in the presence of a relatively high excess (10 mg) of: NO_3^- , CO_3^{2-} , HCO_3^- , SO_4^{2-} , Cl^- , Br^- , PO_4^{3-} , TeO_4^{2-} , SeO_4^{2-} , AsO_3^{3-} , AsO_4^{3-} , WO_4^{2-} , tartrate, EDTA and citrate. The percentage recovery was $100 \pm 1.5\%$ and the standard deviation was ± 0.27 .

The tolerance limits of various cations at 50 μg nickel were also tested in the presence of up to 1 mg of the following ions: Li^+ , Na^+ , K^+ , NH_4^+ , Ca^{2+} , Mg^{2+} , Ba^{2+} , Al^{3+} , Sb^{3+} , Ag^+ , Ce^{3+} . The percentage recovery of nickel(II) was $100 \pm 0.7\%$. In the presence of some other ions, simple modifications were introduced in the aqueous solution to eliminate their interferences in the determination by the proposed method. The results obtained are summarized in Table 2.

Application to natural water

The proposed extraction method involving formation of NiSalen has been applied to the determination of nickel(II) in tap water and in industrial wastewater. The determination of nickel(II) in 20–50 cm^3 of tap water was carried out. The results were all negative, indicating the absence of nickel(II). When various amounts of nickel(II) (20–50 mg) were added to the tested samples, satisfactory results for the spiked nickel(II) recovery were obtained. In analysis of 50–100 cm^3 samples of industrial wastewater by the present method, 0.4 mg cm^{-3} nickel(II) content was determined. This was in agreement with the results obtained by the standard methods.¹⁸ Traces of potassium iodide followed by 2 cm^3 of sodium thiosulfate (0.2%) in water were added to eliminate any interference due to the presence of copper(II). Results for standard additions

Table 2 Effect of foreign ions on the determination of 40 µg of nickel^a

Foreign ion	added as	Amount added/mg	Found/µg	Error, %	Masking agent
Fe ³⁺	FeCl ₃	1.0	40.2	+0.50	add one crystal of KF (5 mg).
MnO ₄ ⁻	KMnO ₄	2.0	39.8	-0.50	add one crystal of NaN ₃ .
Co ²⁺	CoBr ₂	0.2	40.4	+1.00	add 0.1 cm ³ of EDTA (0.01 M).
Cu ²⁺	CuSO ₄	0.1	40.3	+0.75	add one crystal of KI and of Na ₂ S ₂ O ₃ (5 mg).
VO ₃ ⁻	NH ₄ VO ₃	1.0	40.2	+0.50	add one crystal of NaF (5 mg).
Pb ²⁺	Pb(NO ₃) ₂	1.0	39.8	-0.50	add one crystal of NaF (5 mg) and of KCNS (5 mg).

a. Results were only obtained from NiSalen.

Table 3 Results for nickel in natural water

Nickel taken/µg	Nickel found ^a /µg	Recovery, %
Tap water		
20	20.20±0.3	101.0
50	50.30±0.4	100.6
Industrial water		
20	21.00±0.3	105.0
50	53.00±0.2	106.0

a. Average of 5 determinations.

of nickel(II) in industrial water samples gave fairly satisfactory results. The results of these determinations are given in Table 3.

References

1. A. Frust, "Chemistry of Chelation of Cancer", p. 105, CC Thomas, Illinois, 1963.
2. E. J. Blanz and F. A. French, *Cancer Res.*, **28**, 2419 (1968).
3. M. S. Masoud and L. S. Refaat, *Trans. Met. Chem.*, **7**, 315 (1982).
4. M. S. Masoud, A. Akelah and S. S. Kandil, *Indian J. Chem.*, **24A**, 885 (1982).
5. K. Burger, "Organic Reagents in Metal Analysis", Pergamon Press, New York, 1973.
6. A. L. J. Rao and C. Shekhar, *Microchem. J.*, **30**, 283 (1984).
7. K. Kudo and N. Hishinuma, *J. Radioanal. Chem.*, **5**, 331 (1970).
8. Z. K. Doctor and B. C. Halder, *Radiochem. Radioanal. Lett.*, **7**, 339 (1971).
9. G. Mamentov, "Characterization of Solutes in Nonaqueous Solvents", pp. 178-195, Plenum Press, New York, 1978.
10. M. S. El-Shahawi, Ph. D. Thesis, Strathclyde University, U. K., 1986.
11. R. S. Dowing and F. L. Urbach, *J. Am. Chem. Soc.*, **92**, 5861 (1970).
12. A. I. Vogel, "Quantitative Inorganic Analysis", 3rd ed., Longman, Oxford, 1969.
13. Y. K. Agrawal and K. T. John, *Anal. Lett.*, **17**, 2349 (1984).
14. S. Yamaguchi and K. Uesugi, *Analyst [London]*, **109**, 1393 (1984).
15. A. Ringbom, *Fresenius' Z. Anal. Chem.*, **115**, 332 (1939).
16. G. H. Agres, *Anal. Chem.*, **21**, 652 (1949).
17. E. B. Sandell, "Colorimetric Determination of Traces of Metals", Interscience, New York, 1959.
18. H. S. Gowda, K. N. Thimmaiah and S. M. Ahamed, *Indian J. Chem.*, **21A**, 327 (1982).

(Received December 3, 1990)

(Accepted February 27, 1991)

Removal of organic pollutants from aqueous solution

V. Comparative study of the extraction, recovery and chromatographic separation of some organic insecticides using unloaded polyurethane foam columns

A. B. FARAG

Chemistry Department, Faculty of Science, Mansoura University, Mansoura (Egypt)
and

M. S. EL-SHAHAWI*

Chemistry Department, Faculty of Science at Damietta, Mansoura University, Damietta (Egypt)

ABSTRACT

The concentration of dissolved insecticides in aqueous media was determined by chromatographic separation on polyurethane foam columns. The results of preliminary screening tests on the removal of insecticides by the unloaded polyurethane foam indicated that a reasonable percentage of the insecticides was retained on the foam. Therefore attempts were made to extract these compounds from aqueous media using foam columns. Various parameters affecting the retention and separation of these compounds were studied, including temperature, flow-rate, pH, insecticide concentration, shaking time, sample volume and eluting solvent. The complete separation and quantitative recovery of these compounds from the foam with acetone in a Soxhlet extractor were achieved. The method can be used to preconcentrate insecticides in tap water and modified to determine dissolved insecticides in industrial and natural waters. Polyurethane foam has a good capacity for use when large volume samples need to be handled and is an inexpensive sorbent compared to other known solid sorbents.

INTRODUCTION

Insecticides can enter water systems from various sources. Edward [1,2] has reported sources of insecticides to include run-off from agricultural land, direct entry from crop spraying, industrial and sewage effluent, cattle spraying, dust and rainfall. The presence of insecticides in the aquatic environment has been known to cause severe health problems to animals, birds and humans [3]. The removal or reduction of these organic pollutants to an acceptable concentration by extraction with steam distillation, solvent extraction, oxidation, or adsorption on carbon or other solid supports has been investigated [4-7]. Such preconcentration techniques are often slow or cumbersome and too expensive for routine use where many large volume samples are concentrated on-site prior to quantitative analysis [7].

Polyurethane foam has recently been used as an inexpensive solid extractor and effective sorbent for the removal of water pollutants [8–13]. The solid foam concentrates various species in solution by a phase distribution mechanism rather than by adsorption [12,13].

This paper reports the effect of various parameters on the extraction of some organic insecticides from aqueous solution by polyurethane foam and attempts to establish the mechanism of extraction by the unloaded foam.

EXPERIMENTAL

Reagents and materials

All chemicals used were of analytical-reagent grade. Polyurethane foam, an open cell polyether (bulk density 30 kg m^{-3}) was supplied by K.G., Schaum (Stoffwerk, Kremsmunster, Austria). The foam was cut and washed as previously described [9]. Foam loaded with tributyl phosphate (TBP) was prepared by mixing the dried foam cubes with 5% TBP in benzene ($5 \text{ cm}^3 \text{ g}^{-1}$ dry foam) with stirring for 10 min. The reagent foams were then dried [9].

The insecticides studied were: Dimethoate, O,O-dimethyl-SCN (methyl carbamoyl methyl) phosphorodithioate (I); Azodrine (Nuvacron), 3-hydroxy-*N*-methyl-*cis*-crotonamide dimethyl phosphate (II); and Lannate (methomyl), 5-methyl-*N*-(methyl carbamoyl) oxythioacetamide (III). Stock solutions ($100 \mu\text{g cm}^{-3}$) of each compound were prepared in a 100-cm^3 measuring flask by dissolving the exact weight of the insecticide in 5 cm^3 of acetone and diluting with distilled water. A series of standard solutions of these compounds was prepared by diluting their stock solutions with water; the solutions were stored in polyethylene bottles.

Apparatus

A Varian 634 S double-beam UV-visible spectrophotometer with 1-cm quartz cells was used for the absorbance measurements. An Orion pH meter and glass columns, $12 \text{ cm} \times 10 \text{ mm}$ I.D., were also used.

General procedures

Batch experiments. To investigate the effect of shaking time on the uptake of the compounds on polyurethane foam, the foam cubes (0.3 g) were equilibrated with a 100-cm^3 solution of each compound ($60 \mu\text{g cm}^{-3}$) in separate polyethylene bottles and shaken for various time intervals up to 30 min. The foam cubes were then separated by decantation and the amount of the compound remaining in solution was measured spectrophotometrically at the wavelength of maximum absorption. The amount of compound retained on the foam was then calculated by difference. Following these procedures, the effect of pH, extraction media and temperature were determined. An extraction isotherm was determined for each compound ($20\text{--}100 \mu\text{g cm}^{-3}$).

Flow experiments. In the flow experiments, 1 g of dry foam was packed into the column using the vacuum method of foam column packing [14]. Tap or distilled water ($0.5\text{--}3 \text{ dm}^3$) samples containing 0.3 mg of each compound were passed through the foam column at $5\text{--}10 \text{ cm}^3 \text{ min}^{-1}$. All the compounds were retained quantitatively. After squeezing water from the foam, the compound was then recovered from the foam

in a Soxhlet extractor with 50 cm³ of acetone. The analyte was determined by measuring the absorbance of the solution.

The mixture containing Dimethoate (0.1 mg) and Lannate (0.1 mg) was passed through the foam column at 2–3 cm³ min⁻¹. Dimethoate was washed out first with 100 cm³ of acetone and Lannate was then recovered with 50 cm³ of 0.3 M sodium chloride at pH 5.

RESULTS AND DISCUSSION

Preliminary experiments have shown that the extraction of the investigated compounds (I, II and III, Fig. 1) by the unloaded and the TBP-loaded polyurethane foam using batch experiments is rapid and equilibrium is reached in less than 30 min, followed by a plateau. The results obtained are summarized in Fig. 2. A better percentage extraction was obtained with the TBP-loaded foam and a shaking time of 30 min was used in subsequent work.

Extraction isotherm

The uptake of the investigated insecticides from aqueous solution by the unloaded and TBP-loaded foam was dependent on their initial concentrations. Therefore, the extraction isotherms were determined over a wide range of equilibrium concentrations (20–100 µg cm⁻³) for each compound. The results are presented in Fig. 3. The extraction isotherms of the insecticides tested exhibited a first-order behaviour at low concentrations. The adsorption of the different species by the unloaded foam increases in the order: Azodrine > Dimethoate > Lannate. Similar trends were obtained with the TBP-loaded foams. Solvent extraction is therefore the most probable mechanism for the adsorption of these compounds by the unloaded foams. The acidity of the absorbate (pK_a) and the molecular weight obviously play an important role in determining the adsorption efficiency in the TBP-loaded foam; this is also the case with the unloaded foam. The effect of temperature on the extraction efficiency of the unloaded foam was determined at 35 and 45°C. The percentage adsorption increases slightly with increasing temperature.

The effect of pH on the total insecticide removal was carried out over the pH range 3–9. The adsorption profiles of the investigated compounds are given in Fig. 4. It can be seen that the extraction of compounds I and II increases with increasing pH and reaches a plateau at about pH 6. In contrast, compound III displays a minimum removal at pH 5 by the unloaded foam and the percentage removal increases markedly at higher pH.

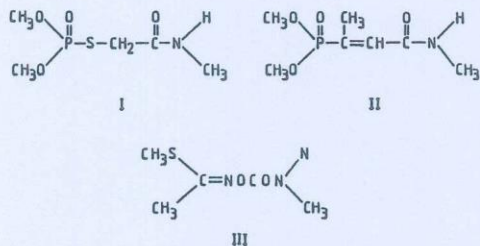


Fig. 1. Structures of I, II and III.

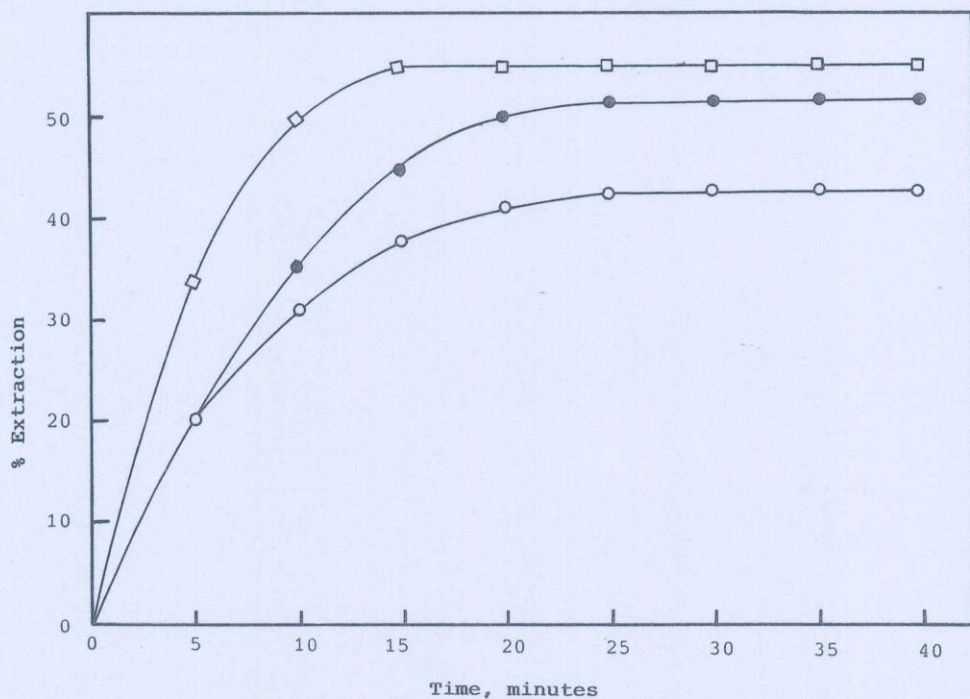


Fig. 2. Effect of shaking time on the extraction of the insecticides by unloaded foam. (□) Azodrine; (●) Dimethoate; and (○) Lannate.

The efficiency and rate of extraction of Lannate by the unloaded foam was generally decreased by the addition of ethanol (0–10%) to the aqueous solution. This is probably due to the formation of inactive species (liophilic association) which are not adsorbed from the aqueous solution [15]. The results are summarized in Fig. 5. The amount of Lannate adsorbed at equilibrium for each ethanol concentration is in the order 0% > 5% > 10% ethanol content. This order agrees with the suggestion of Kirkwood [16] that the smaller the dielectric constant, the larger the amount extracted. Thus, the nature of the media has a marked effect on the adsorption characteristics.

Dynamic experiments

On the basis of the batch experiments, the quantitative retention and recovery of these compounds were investigated using the foam column mode. Distilled or tap water samples (0.5–3 dm³) containing 0.3 mg of each compound were percolated through separate foam columns at a flow-rate of 5–10 cm³ min⁻¹. Complete retention of the compounds was achieved. The insecticides were then recovered from the foam columns with 50 cm³ of acetone in a Soxhlet extractor and determined spectrophotometrically at the maximum absorption wavelength for each species. The results are summarized in Table I. The dependence of recovery on flow-rate through the foam column was investigated by percolating Lannate (0.1 mg) through the column at

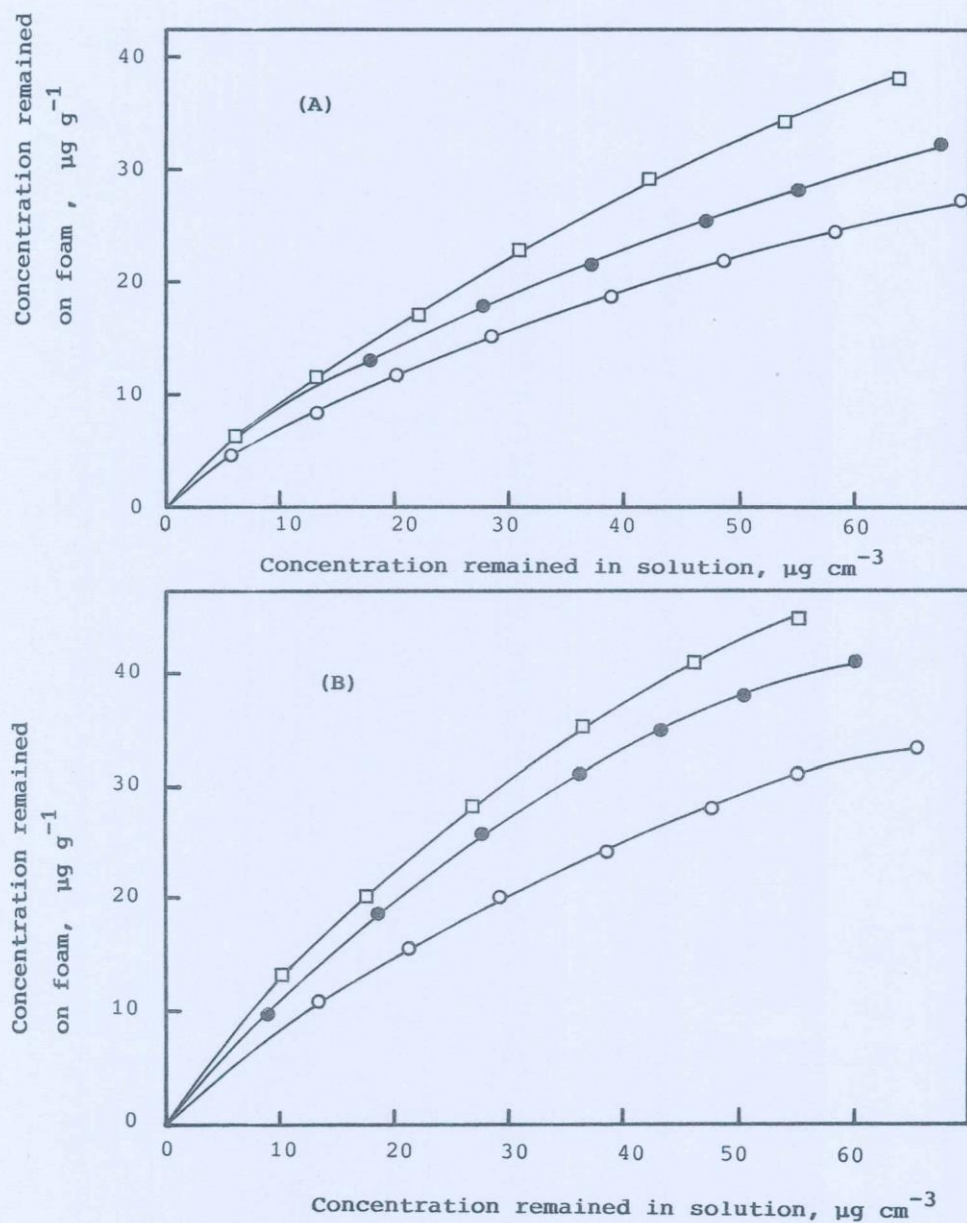


Fig. 3. Extraction isotherms of the insecticides with (A) unloaded foam and (B) TBP-loaded foam. (\square) Azodrine; (\bullet) Dimethoate; and (\circ) Lannate.

various flow-rates. Complete retention of Lannate was obtained up to $10 \text{ cm}^3 \text{ min}^{-1}$ and the efficiency of extraction decreased significantly to 64% at $15 \text{ cm}^3 \text{ min}^{-1}$.

The quantitative retention and elution of Dimethoate was determined. Fig. 6 shows the chromatograms for eluting Dimethoate at flow-rates of 1–3, 5 and 8–10 cm^3

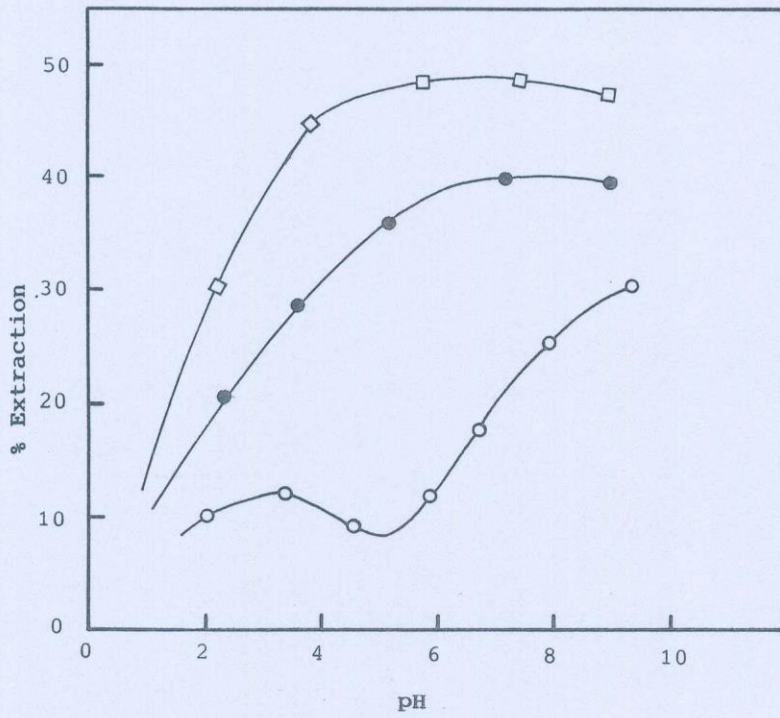


Fig. 4. Effect of pH on the extraction of the insecticides tested with unloaded foam. (□) Azodrine; (●) Dimethoate; and (○) Lannate.

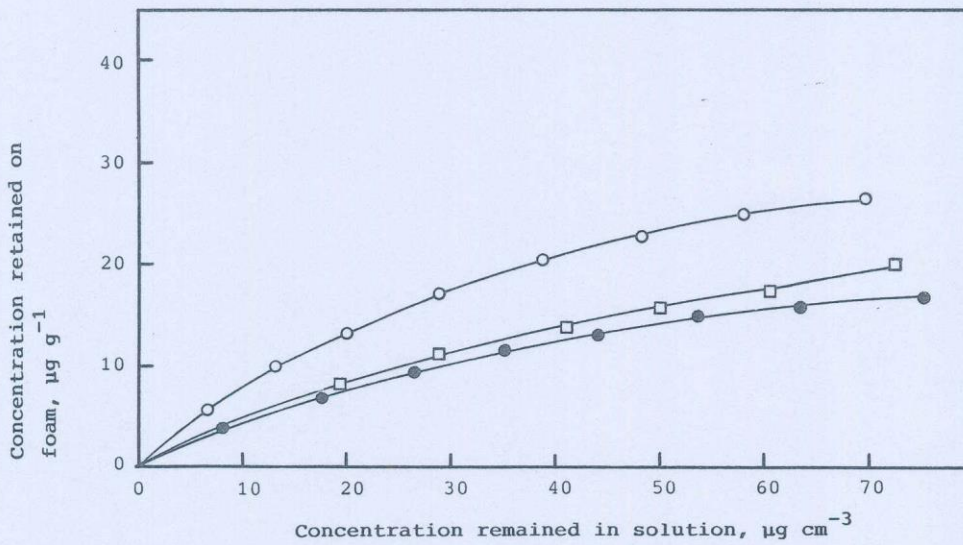


Fig. 5. Effect of ethanol percentage on the extraction of Lannate. (○) 0%; (□) 5%; and (●) 10% ethanol.

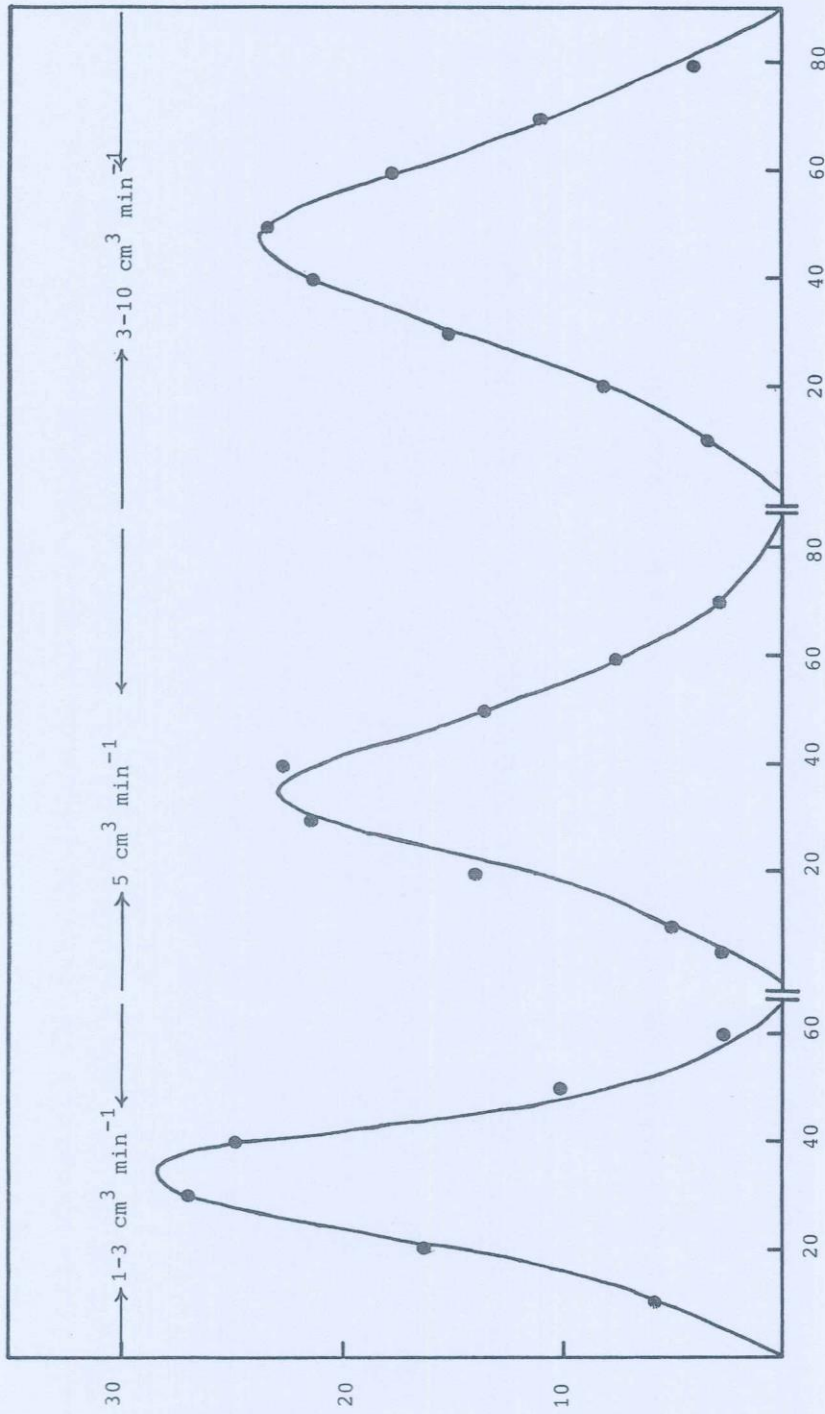


Fig. 6. Effect of flow-rate on the elution of Dimethoate (0.1 mg) with acetone.

TABLE I
EXTRACTION AND RECOVERY OF THE INSECTICIDES

A 0.3-mg mass was extracted from 2 dm³ of aqueous solution by the unloaded foam columns at 3–5 cm³ min⁻¹. (a) Average of duplicate determinations from distilled water; (b) average of duplicate determinations from tap water.

Insecticide	Recovery (%)		Wavelength (nm)
	a	b	
Dimethoate	97	94	320
Azodrine	95	98	306
Lannate	93	90	570

min⁻¹. The height equivalent to a theoretical plate (HETP) was calculated from the elution curves using the equation [17]

$$N = 8 \left(\frac{V_{\max}^2}{W^2} \right) = \left(\frac{L}{\text{HETP}} \right)$$

where N = number of plates, V_{\max} = volume of eluate at peak maximum, W = width of the peak at 1/e the maximum solute concentration and L = length of the foam bed. The HETP values were 2.1, 2.4 and 2.6 mm at flow-rates of 1–3, 5 and 8–10 cm³ min⁻¹, respectively. The value of HETP was also calculated from the break-through capacity curve using the equation [11]

$$N = \left(\frac{\bar{V} \cdot V'}{(\bar{V} - V')^2} \right) = \left(\frac{L}{\text{HETP}} \right)$$

where \bar{V} is the volume of effluent at the centre of the S-shaped break-through curve where the concentration is one half the initial concentration, and V' is the volume at which the effluent has a concentration of 0.1578 of the initial concentration. The value of HETP obtained by this method was 2.3 mm, confirming the values obtained from the elution curves. The proposed column method has been tested for the separation of Dimethoate and Lannate. Dimethoate was eluted first with acetone and Lannate was then recovered with 0.3 M sodium chloride at pH 5 at a flow-rate of 1–2 cm³ min⁻¹.

REFERENCES

- 1 C. A. Edward, *Persistent Pesticides in the Environment*, CRC Press, Boca Raton, FL, 2nd ed., 1973.
- 2 C. A. Edward, *Environmental Pollution by Pesticides*, Plenum Press, New York, p. 409.
- 3 L. T. Kurkland, S. Shibko, A. Kolbye and R. Shapiro, *Haz. Mercury Environ. Res.*, 4 (1971) 9.
- 4 A. H. Romano and R. S. Safferman, *J. Am. Water Works Assoc.*, 55 (1963) 169.
- 5 H. Oda, M. Kishida and C. Yokokawa, *Carbon*, 19 (1981) 243.
- 6 H. Oda and C. Yokokawa, *Carbon*, 21 (1983) 485.
- 7 J. F. Uthe, J. Reinke and H. D. Gesser, *Environ. Lett.*, 3 (1972) 117.
- 8 A. B. Farag, A. M. El-Wakil, M. S. El-Shahawi and M. Mashaly, *Anal. Sci.*, 5 (1989) 415.
- 9 A. B. Farag, A. M. El-Wakil and M. S. El-Shahawi, *Fresenius Z. Anal. Chem.*, 324 (1986) 59.

- 10 G. J. Moody and J. D. R. Thomas, *Chromatographic Separation and Extraction with Foamed Plastics and Rubbers*, Marcel Dekker, New York, 1982.
- 11 T. Braun, J. D. Naveratil and A. B. Farag, *Polyurethane Foam Sorbents in Separation Science*, CRC Press, Boca Raton, FL, 1985.
- 12 H. J. Bowen, *J. Chem. Soc. A*, (1970) 1082.
- 13 K. M. Gough and H. D. Gesser, *J. Chromatogr.*, 115 (1975) 383.
- 14 T. Braun and A. B. Farag, *Anal. Chim. Acta*, 62 (1972) 476.
- 15 T. Hayashita and M. Takagi, *Talanta*, 32 (1985) 399.
- 16 K. G. Kirkwood, *J. Chem. Phys.*, 2 (1934) 351.
- 17 E. Glueckauf, *Trans. Faraday Soc.*, 51 (1955) 34.

14. Peverill, K.I., "Results of the interlaboratory Quality Assurance Programme". In: Report by State Chemistry Laboratory, Victoria, Australia, 21 pps, (1983).
15. Hutton, J.T., and Norrish, K., X-Ray Spectrom., 5, 6, (1977).
16. Van Staden, J.F., Water, South Afr., 12, 43, (1986).
17. Bassett, L.G., Bunce, S.C., Carter, A.E., Clark, H.M., and Hollinger, H.B., "Principles of Chemistry", Prentice Hall Inc., Sydney, 223, (1966).

Received August 22, 1989
Accepted January 28, 1990

TRACE ANALYSIS BY DIRECT SPECTROPHOTOMETRIC
MEASUREMENTS ON POLYURETHANE FOAM. DETERMINATION
OF CHROMIUM (VI) AS BLUE PERCHROMIC ACID WITH
UNLOADED & TRI-n-BUTYLPHOSPHATE LOADED FOAM

KEY WORDS: Chromium (VI) determination, perchromic acid,
tributylphosphate, polyurethane foam

A. M. El-Wakil, M. S. El-Shahawi* and A. B. Farag
Chemistry Department, Faculty of Science, Mansoura
University, Mansoura, Egypt
* Chemistry Dept., Faculty of Sci., Mansoura
University, Damietta, Egypt

ABSTRACT

The formation of blue perchromic acid represents one of the most sensitive and selective tests for the identification of chromium. The sorption of perchromic acid on TBP loaded foam has been investigated for the detection, semiquantitative and quantitative determinations of chromium (VI). In foam batch method, it was possible to detect as low as 0.6, 0.4 and 0.2 ppm of chromium (VI) with unloaded or tricaprylylamine loaded foams, TBP-amine-loaded foams and TBP loaded foams, respectively.

The selectivity of the proposed TBP loaded foam test for the detection of chromium (VI) in the presence of diverse interfering ions was also investigated. In addition, it was possible to determine chromium (VI) semiquantitatively by comparing the colour of the foam cube with a prepared standard colour scale. The proposed method has been employed for the determination of chromium (VI) in tap water. A method for the direct and quantitative spectrophotometric determination of chromium (VI) TBP-loaded foam parallelepipeds has been developed. The TBP-perchromic acid has a maximum absorbance at 580 nm which is quite identical to the absorption maxima in TBP solution. The present method was applied for the analysis of chromium (VI) in natural water and satisfactory results were obtained.

INTRODUCTION

The determination of chromium in environmental and biological systems is currently of considerable interest because the toxicity of this metal to aquatic and terrestrial organisms, including humans, depends on its oxidation state¹. Chromium (III) is considered to be essential to mammals for the maintenance of glucose, lipid and protein metabolism, but chromium (VI) is reported to be toxic because of its ability to oxidise other species and its adverse impact on lung, liver and kidney².

Chromium enters water ways primarily as a result of effluent discharge from coating towers, electroplating and tanning industries, oxidative dyeing and leaching from sanitary landfills^{3,4}. Chromium (VI) may also enter the drinking water distribution system from the corrosion inhibitors used in water pipes³.

Solvent extraction, co-precipitation⁵, graphite furnace atomic absorption spectrometry⁶ and sorption of chromium-diphenylcarbazone with XAD-2 resin⁷ are usually used for the determination of chromium (III) and chromium (VI) in natural waters. The application of direct absorption spectrophotometry to trace element determination in natural water is quite difficult and an additional preconcentration step is usually required which may affect the simplicity and sensitivity of this technique^{8,9}. A reasonable solution to this problem has been recently suggested¹⁰⁻¹², utilizing a method for directly measuring the absorbance of the ion exchanger after concentrating the required trace species in the resin phase. This method has improved the sensitivity of analysis and avoids the tedious preconcentration step.

The analytical utility of polyurethane foam as an unusual sorbent efficient for separation and preconcentration of various organic and inorganic species from aqueous media suggested the application of this foam material as a preconcentration matrix^{13,14}. Polyurethane foam thin layer spectrometry^{15,16} provides a simple and sensitive technique. The foam material can be used loaded with a chromogenic reagent where the interesting coloured species is developed in the foam matrix.

As a continuation to our previous work on the semiquantitative determination of chromium (VI) by diphenylcarbazide-loaded foam¹⁷, the possible application of unloaded polyurethane foam, and several reagent loaded foams for the extraction of chromium (VI) as a blue perchromic acid, has been examined. Visual and direct spectrophotometric determination methods are described for the semiquantitative and quantitative determination of chromium (VI) in aqueous media.

EXPERIMENTALReagents and Materials

All chemicals used were of Analytical Grade. A stock solution of chromium (VI) (1mg. cm^{-3}) was prepared by dissolving the exact weight of potassium dichromate in distilled water and standardizing iodometrically¹⁸. Hydrogen peroxide (20 volumes) were assayed by titration with a standard permanganate solution shortly before use. Tributylphosphate, Aldrich Chemical was used without further purification.

Polyurethane foam, polyether type (bulk density 30 kg. m^{-3}) was supplied by K.G., Schaumstoffwerk, Kremsmunster, Austria. The foam material was cut as regular parallelepipeds of $20 \times 10 \times 1\text{ mm}$ dimensions for quantitative analysis and as cubes of 5 mm edge for the semiquantitative method. The foam pieces were then washed and dried at 80°C as described previously¹⁹.

Tributylphosphate (TBP) stock solution, 5% (v/v) was prepared by mixing the dried foam pieces with 5% TBP solution in benzene ($5\text{ cm}^3 \cdot \text{g}^{-1}$ dry foam) with efficient stirring for 15 min. Also, the reagent foams were prepared either by mixing the foam cubes or parallelepipeds with TBP solution in benzene, TBP solution mixed with tricaprilyltertiaryamine (1:5 v/v) or undiluted TBP. The reagent foams were then dried between sheets of filter papers to remove the excess reagent solutions.

Apparatus

An Orion pH meter was used for pH measurements and a Varian 634 double beam UV-Visible Spectrometer (1 cm cell) was used for the absorbance measurements (slit width = 1 mm).

Recommended procedures1. Batch foam experiments

To detect chromium (VI) by the static method, $2\text{-}3\text{ cm}^3$ of previously cooled chromium (VI) solution ($<5^\circ\text{C}$) was mixed with one cube of the reagent foam in a test tube. To this solution, 1 cm^3 of cold hydrogen peroxide ($<5^\circ\text{C}$) was added and the test tube was shaken for 2-3 min.

To examine the selectivity of the proposed reagent foam, the detection of $1\text{ }\mu\text{g}$ chromium (VI) in the presence of varying amounts of diverse cations and anions was carried out by the static method.

2. Liquid-liquid extraction

An aqueous cold solution (90 cm^3) containing known quantities of chromium (VI) ($50\text{ - }200\text{ }\mu\text{g}$) acidified with sulphuric acid ($0.05\text{-}1\text{ N}$) was cooled to below 5°C in a refrigerator, and 20 cm^3 TBP in benzene were mixed with 10 cm^3 of cold hydrogen peroxide and shaken for 15 min in a separatory funnel. The two phases were then separated and the absorbance of the organic phase was measured at 560 nm against a blank TBP solution in benzene.

3. Liquid-solid static extraction for quantitative analysis

In 250 cm^3 polyethylene bottles, 90 cm^3 of an aqueous solution containing varying amounts of chromium (VI) ($20\text{-}200\text{ }\mu\text{g}$) and cooled to below 10°C in a refrigerator were mixed with one TBP-loaded polyurethane foam parallelepiped. To this solution, 10 cm^3 of cold hydrogen peroxide were added and shaken in a mechanical shaker for 15 min. After equilibration, the foam thin sheet is separated, rinsed with a few milliliters of deionized water, and placed in a 1 cm spectrophotometer cell

for the direct measurement of the absorbance of the blue coloured species sorbed into the foam. The net absorbance of the perchromic acid-TBP in the foam A_F^* is calculated from the equation

$$A_F^* = A_F(\text{Cr}) - A_F(\text{B})$$

where $A_F(\text{Cr})$ and $A_F(\text{B})$ are the absorbances of the perchromic acid-TBP foam in the presence of chromium (VI) and in its absence, respectively.

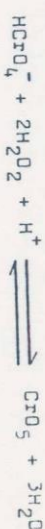
4. Analysis of water samples

To 90 cm³ of water sample, containing chromium (VI) (20 or 40 µg) acidified with sulphuric acid (0.075N), one TBP-foam parallelepiped was added, the solution was then cooled below 5°C and 10 cm³ of cold hydrogen peroxide were added. The solution was shaken for 15 min and the foam sheet was separated and washed with deionized water and placed in the spectrophotometer cell for the direct measurements.

RESULTS AND DISCUSSION

The attraction of using foamed cellular materials for the extraction and separation of various species lies in their favourable hydrodynamic and aerodynamic properties. In addition to the hydrodynamic consideration, the mechanical properties of open cell polyurethane foam facilitate its direct use in analysis. The immobilization of hydrophobic organic extractants on solid foams combines the advantages of both liquid-liquid and liquid-solid extraction techniques¹⁴. Polyurethane foam loaded with specific reagents allows the isolation and concentration of the analyte from the matrix and yields an appropriate enrichment.

The formation of blue perchromic acid represents one of the most sensitive and selective tests for the identification of chromium¹⁹. The coloured product is formed when hydrogen peroxide is added to acidified solutions of dichromate. The predominant equilibrium in dilute aqueous solution is



This species decomposes rapidly in aqueous media in a complex manner to chromium (III) species²⁰. It may be stabilized, however, by the extraction into a variety of organic solvents such as hexane²¹, ethyl acetate^{22,23}, ether¹⁹, but the colour is stable only for short periods. Tributylphosphate was found to extract the blue perchromic acid and the colour remains stable for 48 hours^{24,25}. TBP extraction was employed for the detection of chromium (VI) in aqueous solution using a normal spot test method and the detection limit was found to be 2.5 ppm²⁵.

Qualitative and semiquantitative

determination of chromium (VI)

In the present work, cubes of unloaded polyurethane foam, tricaprylyltertiaryamine loaded foam, TBP-tertiaryamine loaded foam and TBP-foam were examined for the extraction of the blue perchromic acid. The relatively large available surface area of the foam cubes acts as an efficient collector for the perchromic acid present in the aqueous solution at low concentration.

On shaking one cube of the unloaded foam or of the loaded foam with 1-2 cm³ of the acidic aqueous cold solution of chromium (VI) and adding one cm³ of cold hydrogen peroxide, it was possible to detect as low as 0.6, 0.4 and 0.2 ppm of chromium (VI) with unloaded or tricaprylylamine loaded foams, TBP-amine loaded and TBP

loaded foams, respectively. The colour density on the foam cube was found to depend on the concentration of the metal ion in aqueous solution. A comparison between the results obtained and those reported in literature, from the normal spot test method shows that the foam methods are generally much more advantageous. TBP-loaded foam gave the most sensitive results.

The selectivity of the proposed foam test was examined by the detection of 1 μ g of chromium (VI) in the presence of a relatively high excess of each of La^{3+} , Ca^{2+} , Mg^{2+} , Sr^{2+} , Al^{3+} , Cd^{2+} , Ce^{3+} , K^+ , Tl^+ , As^{3+} , Sb^{3+} , NH_4^+ , Ag^+ , Hg^{2+} , Ru^{3+} , Ce^{4+} , U^{6+} , Ni^{2+} , Zn^{2+} , Co^{2+} , La^{3+} , Sn^{2+} , Cl^- , Br^- , F^- , I^- , VO_3^- , $\text{C}_2\text{O}_4^{2-}$, citrate, formate and acetate. The results obtained were successful, using the straight forward method. In the presence of some other ions, simple modifications were introduced in the aqueous solution in order to eliminate their interference and to obtain sensitive detection of chromium (VI) using the proposed foam test (Table 1).

Using the TBP-loaded foam, it was possible to determine chromium (VI) semiquantitatively by comparing the colour of the foam cube with a standard colour scale (1,5,10 and 20 ppm) chromium (VI) prepared under the same experimental conditions. The proposed method was examined for the detection of chromium (VI) in tap water spiked with dichromate, and satisfactory results were obtained.

Quantitative determination of chromium (VI)

Experience with polyurethane foam showed that the absorbance of the foam matrix and those of a Dowex-1x8 resin packed in a micro-cell of 1 mm light-path¹⁵ are consistently lower than the corresponding absorbance of the resin layer and have

DETERMINATION OF CHROMIUM (VI)

Table 1. Effect of various ions on the detection of chromium (VI) in 2.3 cm^3 aqueous solution.

Foreign Ion	Added Compound	Tolerance Limit	Note
Fe (II)	$\text{Fe}(\text{NH}_4)_2(\text{SO}_4)_2$	1: 1×10^4	Add one crystal of KF.
Fe (III)	$\text{Fe}_2(\text{SO}_4)_3$	1: 1×10^4	Add 1 ml of saturated KI solution.
Cu (II)	CuCl_2	1: 1×10^4	Add traces of solid KI and $\text{Na}_2\text{S}_2\text{O}_3$.
MnCl_4^-	KMnO_4	1: 1×10^4	Add few crystals of solid NaNO_3 .
Pb (II)	$\text{Pb}(\text{NO}_3)_2$	1: 2×10^4	Add few drops of conc. HNO_3 to adjust pH to 1.5.
WO_4^{2-}	Na_2WO_4	1: 2×10^4	Add few drops of conc. HNO_3 to adjust pH to 1.5.

no absorption peaks in the range 400-800 nm¹⁶. The absorption spectra of the reagent TBP in benzene, TBP loaded foam and of perchromic acid are shown in Fig. 1. It can be seen that the adduct formed has three absorption peaks at 375 (s), 580 (v,s) and 720 (w) nm. The absorbance of the reagent TBP in benzene or TBP-foam is negligible in the visible region. Throughout this work, the absorption readings were taken at 580 nm (molar absorptivity $455 \text{ mol}^{-1} \text{cm}^{-1}$).

It was reported^{24,25} that TBP solution in benzene does extract chromium (VI) quantitatively from acidic aqueous hydrogen peroxide solution. In the present work, chromium (VI) was quantitatively extracted by TBP-loaded foam from sulphuric acid or hydrochloric acid media. In the presence of sulphuric acid, the proper acidity is in the range of 0.05 - 0.1 N, while

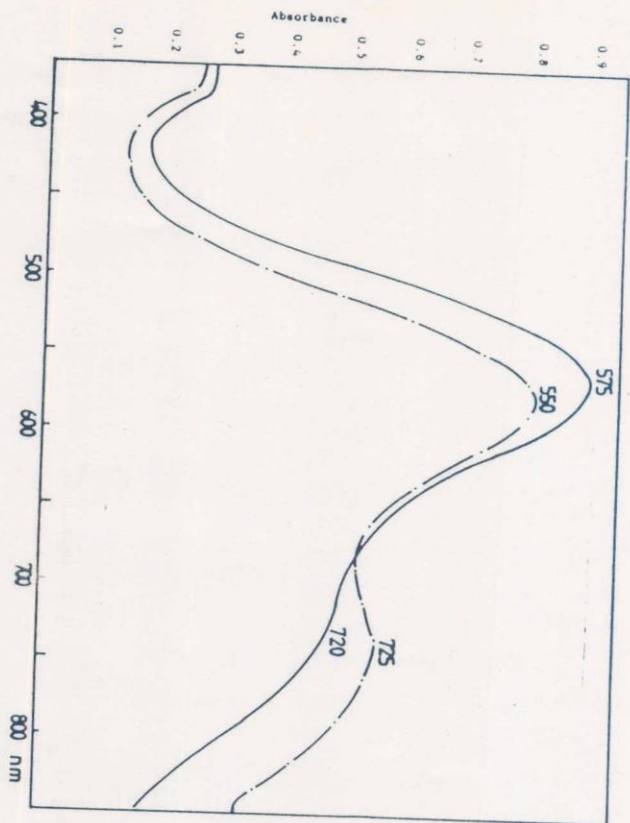


Figure 1. Absorption spectra of the reagent perchromic acid-TBP in benzene (a) and perchromic acid-TBP loaded foam.

In the presence of hydrochloric acid the range is between 0.01 and 0.5 N. Lower or higher acidity gives incomplete extraction as observed by the decrease in the absorbance at 580 nm. Optimum time for shaking was found to be 15 min, though more shaking time does not have any adverse effects on the absorbance of the sorbed species.

Validity of Beer's Law

The absorbance of the perchromic acid-TBP foam was measured after immersing the foam parallelepiped in various

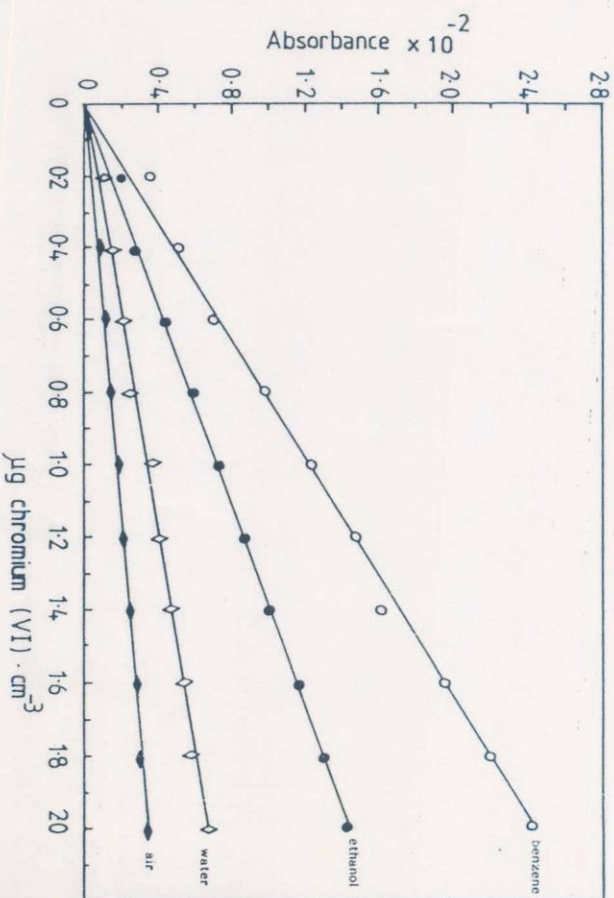


Figure 2. Calibration curves of perchromic acid at 580 nm in polyurethane foam in various measuring media (a = benzene, b = ethanol, c = water, d = air).

media (water, benzene, ethanol and air) in the spectrometer cell. A good linear relationship was obtained between the absorbance of chromium species in the foam phase and chromium in dilute aqueous solution (Fig. 2). Considerable improvement in the absorbance values was noticed in benzene as compared with other media and solvents, which agrees with previous results¹⁶ and is attributed to the high refractive index of benzene. Samples were stored in stoppered polyethylene bottles in a refrigerator for more than 24 hours. The absorbance values

Table 2. Effect of foreign ions on the determination of 50 µg of chromium (VI) as perchromic acid.

Foreign Ion	Concentration (mg)	Chromium(VI) Found (µg)	Error, %	Note
VO ₃ ⁻	0.5	49.6	-0.8	
F ⁻	1	50.0	Nil	
Cd ²⁺	1	50.2	+0.4	
Na ⁺	1	50.1	+0.2	
Cu ²⁺	0.8	50.4	+0.8	Traces of solid KI and Na ₂ S ₂ O ₃ added.
Mo (VI)	1	50.0	Nil	
Al (III)	1	50.0	Nil	
Mg ²⁺	1	49.6	-0.8	
MnO ₄ ⁻	1	50.7	+1.4	Crystal of sodium azide added.
NH ₄ ⁺	1	50.0	Nil	
PO ₄ ³⁻	1	50.2	+0.4	

were found to remain constant over this time period. Evidently, the foam material allows a good concentration factor, which renders the proposed direct foam spectrometric method quite sensitive and selective.

Effect of diverse ions

The interference due to diverse ions in the determination of chromium (VI) with TBP-foam was studied. 50 µg chromium (VI) can be determined in the presence of up to 1 mg of the following ions: vanadate, cadmium (II), copper (II), molybdate,

Table 3. Chromium (VI) determination of five simulated samples for each concentration.

Chromium (VI) added (µg)	Chromium (VI) found (µg)	Confidence Limit	Error %
20	20.3	20.3 ± 0.23	+1.5
40	40.4	40.4 ± 0.20	+1.0

aluminum (III), mercury (II), phosphate or sodium (I). Per-manganate ion interferes in the determination and its effect can be easily eliminated by adding one crystal of sodium azide to the test solution before adding hydrogen peroxide and the foam. The results obtained are provided in Table 2.

The determination of chromium (VI) in water from the river Nile was carried out, and all results were negative. Nile water samples spiked with known amounts of chromium (VI) (20, 40 µg) were analysed and the results are given in Table 3. The average yields were 98-102%. Although it is usually difficult to determine chromium (VI) accurately in natural waters, the presently developed method proved to be quite suitable for this purpose.

REFERENCES

1. K. G. Stollenwerk and D. B. Grove, J. Environ. Qual. 14, 396 (1985).
2. S. Langard, T. Norseth "Handbook on the Toxicology of Metals", L. Friberg at al. (Eds.), Elsevier/North-Holland Biomedical Press: Amsterdam, pp 363-397 (1979).

3. E. Orvini, T. Zerliss, M. Gallorini and M. Spezial, *Radiochem. Radioanal. Lett.* **43**, 173 (1980).
4. D. A. Brown, W. K. Glass, M. R. Jan and R. M. W. *Environ. Technol. Lett.* **7**, 283 (1986).
5. S. Osaki, T. Osaki, N. Hiraehima and Y. Takashima, *Talanta* **30**, 523 (1983).
6. K. S. Subramanian, *Anal. Chem.* **60**, 11 (1988).
7. S. Osaki, T. Osaki and Y. Takashima, *Talanta* **30**, 683 (1983).
8. S. Motomizu, T. Wakimoto and K. Hoei, *Anal. Chim. Acta* **138**, 329 (1982).
9. T. Kiriyama and K. Kuroda, *Talanta* **31**, 472 (1984).
10. K. Yoshimura, H. Waki and S. Ohashi, *Talanta* **23**, 449 (1976).
11. K. Yoshimura and H. Waki, *Talanta* **32**, 345 (1985).
12. Y. Takagi and M. Oshida, *Anal. Chim. Acta* **165**, 195 (1984).
13. G. J. Moody and J. D. R. Thomas "Chromatographic Separation and Extraction with Foamed Plastics and Rubbers", Dekker, New York (1982).
14. T. Braun, J. D. Navratil and A. B. Farag "Polyurethane Foam Sorbents in Separation", Science, CRC Press, Inc., Boca Raton, Florida (1985).
15. M. N. Abbas, H. N. A. Hassan and A. B. Farag, *Proc. 1st Chem. Conf., Fac. Sci. Mansoura Univ., Mansoura, Egypt*, **1** (1986).
16. Y. A. Gawargios, M. N. Abbas and H. N. A. Hassan, *Anal. Lett.* **21** (1988).
17. A. B. Farag, A. M. El-Wakil and M. S. El-Shahawi, *Analyst (London)* **106**, 809 (1983).
18. A. I. Vogel "Quantitative Inorganic Analysis" Longman London, 3rd Ed. (1961).

19. P. E. Wenger and R. Dukker "Reagents for Qualitative Analysis", Amsterdam, 122 pp. (1948).
20. P. Moore, S. F. Kettle and R. G. Wilkins, *Inorg. Chem.* **5**, 467 (1966).
21. P. D. Blundy, *Analyst (London)* **63**, 555 (1958).
22. A. Glaesner and M. Steindberg, *Z. Analyt. Chem.* **153**, 215 (1956).
23. R. K. Brookshier and H. Freund, *Anal. Chem.* **23**, 1110 (1951).
24. M. N. Sastri and D. S. Sundar, *Chemist-Analyst* **50**, 101 (1961).
25. M. N. Sastri and D. S. Sundar, *Z. Analyt. Chemie* **112**, 443 (1963).

Iodometric microdetermination of thallium in aqueous media and in organic compounds by chemical amplification reactions

A. M. El-Wakil, A. B. Farag, and M. S. El-Shahawi

Department of Chemistry, Faculty of Science, Mansoura-University, Mansoura, Egypt

In an earlier paper [1], an iodometric amplification method for the determination of either Mn(II) or a mixture of Mn(II) and Mn(VII) has been described. When applying the same principle for the determination of Tl(I) or a mixture of it with Tl(III) ions, the developed method has proved to be rapid, simple and accurate. The method is based on the oxidation of various concentrations of Tl(I) solution (0.5–5 ml) containing (10–200 µg) Tl with 5 ml-KIO₄ solution (0.35 g/100 ml + 0.5 ml saturated borax solution) in the presence of 2 ml acetate buffer (pH 2.8–3). The reaction mixture is heated on a water bath for 15 min. After cooling, 2 ml of a freshly prepared ammonium molybdate solution are added to mask the excess unreacted periodate. The produced (IO₃⁻ + Tl³⁺) ions



are then titrated with standard thiosulphate solution in the presence of a few crystals of KI (20–40 mg), giving ultimately rise to eight iodine atoms for each Tl(I) ion originally present, according to:



i.e., it is an 8-fold iodometric amplification reaction (Table 1).

If thallium is present solely as Tl(III), it would lead to a 2-fold amplification (Eq. 3) when titrated directly with iodide ion, while it is possible by our proposed method to reduce it firstly with saturated sulphite (0.5 ml) in the presence of H₂SO₄ and then to eliminate the excess H₂SO₃ by heating. Application of the periodate oxidation mentioned above extends the method to 8-fold amplification.

Moreover, the method can be applied for the determination of a mixture of Tl(I) and Tl(III) ions. An aliquot is oxidized directly, leading to the determination of Tl(I) in the presence of the indifferent Tl(III) ion. Another aliquot should be reduced first with sulphite; then on applying the periodate oxidation, total thallium is determined and the difference in thiosulphate volume between the 2nd and 1st steps would be equivalent to Tl(III) ion. This enables us to apply the method to redox systems in which both ions are present (Table 2). In addition, this method is successfully employed for the determination of thallium in some organic compounds after digestion with conc. HNO₃ (Table 3).

Offprint requests to: A. M. El-Wakil

Table 1. Determination of various amounts of Tl(I) in aqueous media

Tl(I)-ion present (µg)	Average ^a Tl(I) found (µg) ($\bar{X} = \Sigma X/n$)	Standard deviation (s)
200	199.6	0.14
150	149.76	0.13
100	100.2	0.10
50	49.6	0.16
20	20.24	0.12
10	10.32	0.16

^a Average of 5 determinations

Table 2. Determination of various amounts of Tl(III) in aqueous media

Tl(III)-ion present (µg)	Average ^a Tl(III) found (µg) ($\bar{X} = \Sigma X/n$)	Standard deviation
200	200.25	0.13
150	149.20	0.17
100	100.28	0.16
50	50.48	0.20
25	25.30	0.15
10	9.60	0.21

^a Average of 5 determinations

Table 3. Determination of thallium in organic compounds after acid digestion

Compound	%Thallium calc.	%Thallium ^a found	Standard deviation
Thallos acetate	77.59	77.89	0.30
Thallos formate	81.95	82.09	0.45

^a Average of 5 determinations

Reference

1. El-Wakil AM, Farag AB, El-Shahawi MS (1989) Talanta 36:783

Received January 4, 1990; revised February 20, 1990

Phase separation and physical properties of sodium borosilicate glasses with intermediate silica content

This content has been downloaded from IOPscience. Please scroll down to see the full text.

1990 J. Phys. D: Appl. Phys. 23 1441

(<http://iopscience.iop.org/0022-3727/23/11/014>)

View the table of contents for this issue, or go to the journal homepage for more

Download details:

IP Address: 136.206.1.12

This content was downloaded on 10/12/2013 at 19:56

Please note that terms and conditions apply.

Phase separation and physical properties of sodium borosilicate glasses with intermediate silica content

H Doweidar†, M S El-Shahawi‡, F M Reicha†, H A Silim† and K El-Egaly†

† Physics Department, Faculty of Science, Mansoura University, Mansoura, 35516, Egypt

‡ Chemistry Department, Faculty of Science, Domiate, Mansoura University, Mansoura, 35516, Egypt

Received 19 June 1989, in final form 25 June 1990

Abstract. Microstructures of sodium borosilicate glasses with intermediate silica content, doped with CuO, were examined. Electron micrographs of heat-treated glasses show two randomly distributed phases. DC conductivity measurements indicate that alkali oxide is associated with B_2O_3 . CuO is assumed to act as a network modifier in the borate matrix and does not affect the phase separation process. Optical absorption in the UV and visible regions was also examined. Phase separation causes a shift of the UV edge towards longer wavelengths, which is considered to be a result of light scattering on SiO_2 -rich particles produced by heat treatment.

1. Introduction

In the immiscibility region of the $Na_2O-B_2O_3-SiO_2$ system, glasses are characterized which have a great tendency to phase separation (Vogel 1971). Electron microscope investigations show microstructural changes when such glasses are treated thermally (Elmer *et al* 1970, Vogel 1971). A homogeneous glass can be separated to a silica-rich phase and an alkali borate-rich phase. The interconnection of the two phases depends on the glass composition. In $Na_2O-B_2O_3-SiO_2$ glasses with intermediate SiO_2 content, the latter phase is indicated (Vogel 1971) to be the continuous one and should therefore be the electrically conducting phase. However, phase separation is suggested to start on a very fine scale during cooling the glass from the melt (Elmer *et al* 1970). The separated phases increase in size with time, at a constant temperature, and with temperature for a specific time, but the relative amounts of the microphases remain essentially unchanged.

The present work discusses the effect of phase separation in sodium borosilicate glasses, with intermediate silica content, on the DC conduction and the optical absorption.

2. Experimental details

The studied glasses have the general formula x

$Na_2O \cdot (54.5 - x) B_2O_3 \cdot 45 SiO_2 \cdot 0.5 CuO$, where x is the molar percentage of Na_2O . The value of x ranges between 4.5 mol% (G1) and 19.5 mol% (G6) as indicated in table 1. The glasses were prepared using reagent grade chemicals. Na_2O was introduced as Na_2CO_3 , B_2O_3 as crystalline H_3BO_3 , CuO as $CuCO_3 \cdot Cu(OH)_2 \cdot H_2O$ and SiO_2 was introduced in the form of acid-washed quartz sand. The glasses were melted in platinum crucibles in an electric furnace for about two hours at a temperature ranging between 1250 and 1350 °C, depending on the glass composition. Homogenized melts were poured into preheated steel moulds. The glasses were annealed at about 450 °C and allowed to cool to room temperature with a rate of 60 °C h⁻¹. The glasses were then reheated for the desired time interval at the desired temperature and allowed to cool normally.

Freshly fractured surfaces of the glasses were leached at room temperature for 40 s with diluted HCl. The rinsed and dried surface was preshadowed with Pt-C at an angle of incidence ranging from 17.5 to 20°. The sample was then coated with a carbon layer evaporated normal to the surface. The replica was separated from the glass and used for electron microscope photography.

For the electrical measurements, samples were prepared in the form of plates of parallel faces with the

Table 1. Compositions of the glasses studied (in mol%).

Glass	SiO ₂	B ₂ O ₃	Na ₂ O	CuO	R(= Na ₂ O/B ₂ O ₃)	K(= SiO ₂ /B ₂ O ₃)
G1	45	50	4.5	0.5	0.10	0.90
G2	45	48	6.5	0.5	0.15	0.94
G3	45	46	8.5	0.5	0.20	0.98
G3A	40	50	10.0	—	0.20	0.80
G4	45	44	10.5	0.5	0.25	1.02
G5	45	40	14.5	0.5	0.38	1.13
G6	45	35	19.5	0.5	0.57	1.29

dimensions 30, 15 and 2 mm. The flat surfaces of the sample were coated with graphite, using specpure graphite rod, in the form of discs of radius 5 mm. An insulation tester (Levell Tester TM 14) was used to measure the resistance of the samples in the temperature range from about 160 to 400 °C. The experimental error in determining the activation energies for conduction is estimated to be less than 0.02 eV, whereas a relative error of conductivities is expected to be $\pm 5\%$. The limits of error were computed from the average deviation among the resistivities of at least three samples of each glass. They also represent the error involved in the comparison of the sample resistance with that of a standard resistance of the same order.

Optical measurements were performed using a Varian 63 UV-Visible spectrophotometer with a range of 200–900 nm. The measurements were carried out at room temperature. Different samples of the same glass show identical transmission curves. Five samples of G6 were used to determine the limits of error of the absorption parameters. Values of λ_{abs} (the wavelength

corresponding to maximum absorption in the range of 777–794 nm) are given directly by the instrument with an estimated error of ± 1 nm.

3. Results and discussions

The temperature dependence of resistivity of the studied glasses is shown in figure 1. The linear dependence indicates that the resistivity ρ obeys the wellknown relation

$$\rho = \rho_0 \exp(E/R_0T) \quad (1)$$

where ρ_0 is a constant depending on the glass composition, E is the activation energy for conduction and R_0 is the universal gas constant.

As generally known (Hakim and Uhlmann 1971), the activation energy for conduction E decreases with increase in alkali oxide content. This is shown in figure 2, in which R_2O is the concentration of Na₂O + CuO in the glass. Similar dependence is also found for the resistivity. The decrease of E indicates that the height of the potential barrier becomes smaller with the increase of R_2O .

In alkali borosilicate glasses, alkali oxide is proposed to associate itself either with B₂O₃ only (Milberg *et al* 1972, Konijnendijk 1975, Yun and Bray 1978, Bray 1985) or with both of B₂O₃ and SiO₂ (Doweidar

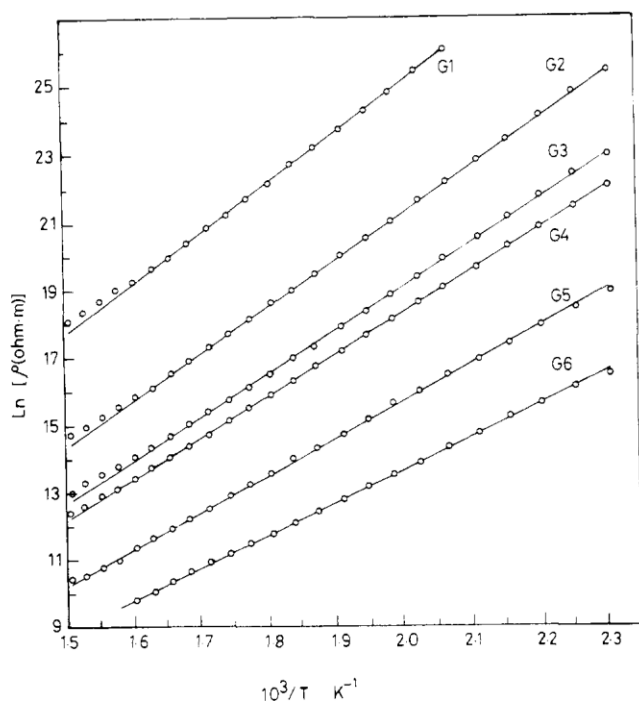


Figure 1. Resistivity–temperature dependence for glasses G1–G6.

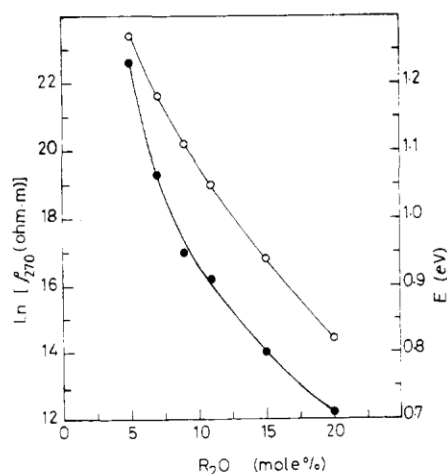


Figure 2. Dependence of both the resistivity (●) and the activation energy for conduction (○) on R_2O ($R_2O = \text{Na}_2\text{O} + \text{CuO}$).

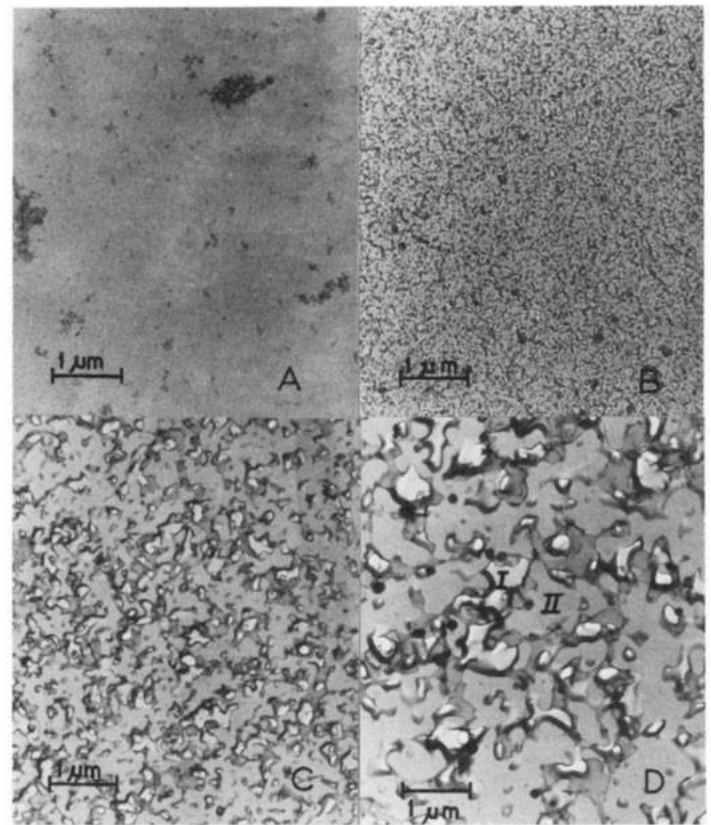


Figure 3. Electron micrographs of G2: A, as obtained after annealing; B, after 1 h at 560 °C; C, after 4 h at 560 °C; D, after 8 h at 560 °C.

Table 2. Change of R_{\max} with K values for sodium borosilicate glasses (after Bray 1985).

K	R_{\max}
0	~0.5
0.5	~0.57
1	~0.63
2	~0.68
3	~0.79

et al 1988), to form alkali borate and alkali silicate networks. The result depends on the factors K (mol% SiO_2 /mol% B_2O_3) and R (mol% Na_2O /mol% B_2O_3). When alkali oxide is introduced into B_2O_3 matrix, BO_3 triangles convert into BO_4 tetrahedra. The fraction of BO_4 groups (N_4) increases, with the increase of alkali oxide, to a maximum at a specific value of R known as R_{max} . R_{max} is defined as the R value corresponding to the maximum value of N_4 . R_{max} is found to increase with the increase of K (Bray 1985) (table 2). In glasses with $R < K$, which is the present case, regardless of the value of K , there are no non-bridging oxygen ions either in the borate or in the silicate network for $R < R_{\text{max}}$ (Doweidar *et al* 1988). In the studied glasses K ranges between 0.9 and 1.286 (table 1) and R is clearly less than the corresponding R_{max} of G1–G6 (table 2). It is, therefore, assumed that the alkali oxide content is associated in such glasses with B_2O_3 .

Investigations of heat-treated samples of G1–G6 indicated that the resistivity and also the activation energy do not change with the temperature or the time of heat treatment, although the highest heat-treatment temperature (580 °C) is close to the transformation region T_g of some of the studied glasses. Mostly there is tolerance of resistivity, around an intermediate value, with less than a half order. Similarly, a tolerance of the activation energy is found to be ± 0.023 eV.

Except for G5 and G6, the compositions studied lay in the immiscibility region of the Na_2O – B_2O_3 – SiO_2 system (Vogel 1971). The constancy of resistivity and the activation energy with the time and temperature of heat treatment suggests that the nature and the relative amount of the conducting phase (the alkali borate phase) remain the same. The activation energy was found to change markedly, 0.22–0.39 eV, with the temperature of heat treatment for Na_2O – B_2O_3 – SiO_2 glasses with low SiO_2 content (25 mol%) (Doweidar and Silim 1979). The effect is explained by considering a distribution of Na_2O between the silicate and borate networks. Heat treatment would cause redistribution of alkali oxide in glass. Recent (Doweidar *et al* 1988) NMR results indicate that this distribution of Na_2O in such glasses is to be considered. This leads one to conclude that, in the studied glasses, Na_2O would associate itself with B_2O_3 only (in the melt as well as in the solid glass). Phase separation on a very fine scale may take place in these glasses without heat treatment, since their resistivities and activation energies are the same as the corresponding heat-treated glasses.

To investigate the effect of Cu^{2+} on the phase separation process in the studied glasses, glass G3A was investigated. This glass is free of CuO and lies in the immiscibility region of the Na_2O – B_2O_3 – SiO_2 system. Conductivity measurements indicated that this glass behaves similarly to the glasses containing copper ions. This means that doping with CuO does not affect the phase separation process, i.e. CuO may play the role of a network modifier.

Electron micrographs of the investigated glasses (figures 3 and 4) show similar effects of heat treatment. Glasses G1–G4 contain two phases. Phase I (figure 3) which is the insoluble one, referred to as the silica-rich phase, increases in size with the heat-treatment time (figure 3A–D). This phase seems to be distributed randomly in the alkali borate phase (phase II, figure 3E). As shown in figure 4, the tendency to phase separation rapidly decreases in glasses with $R_2\text{O} > 9$ mol%, i.e. for $R > 0.2$ (G4–G6). Similar results were obtained (Vogel 1971) for binary Na_2O – B_2O_3 glasses. It should be mentioned that the composition of glass G5 lies on the boundary of the immiscibility region of the Na_2O – B_2O_3 – SiO_2 system, whereas that of G6 lies outside the immiscibility region. This may be a reason for the weak response to heat treatment of G5 and G6.

In Na_2O – B_2O_3 – SiO_2 glasses with intermediate SiO_2 content, Vogel (1971) indicated that the silica-rich phase separates in the form of isolated droplets and the alkali borate phase separates into two subphases: an alkali-rich borate phase in the form of isolated droplets distributed within a continuous B_2O_3 -rich phase.

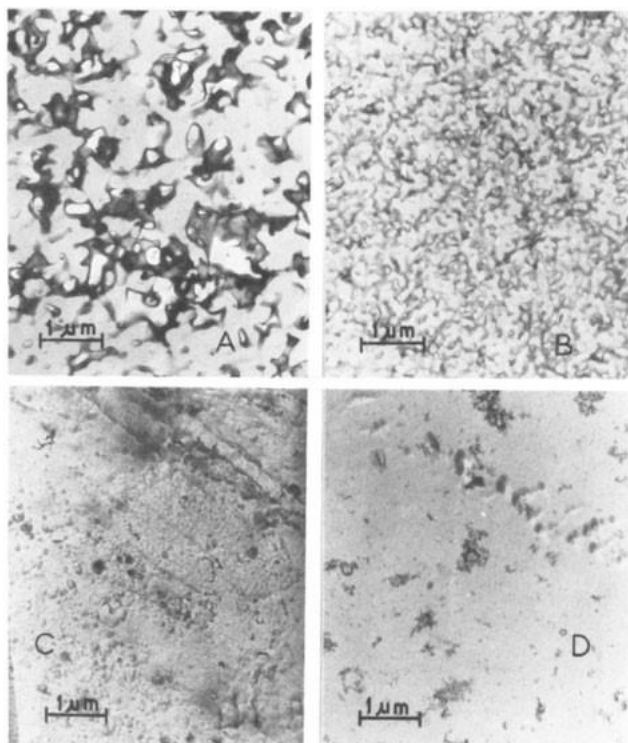


Figure 4. Electron micrographs of glasses treated thermally for 8 h at 560 °C: A, G3; B, G4; C, G5; D, G6.

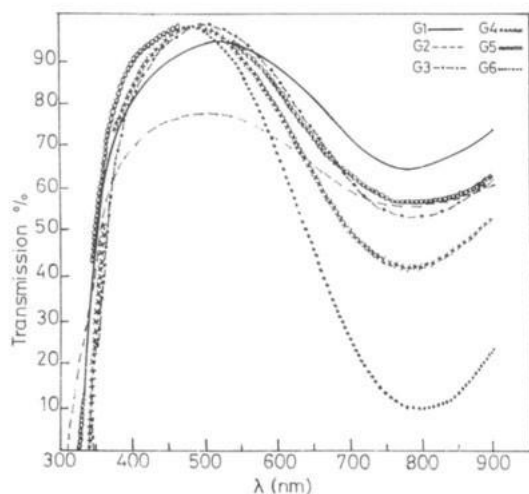


Figure 5. Spectral transmission of G1–G6, in uv and visible regions.

Such processes are not observed in the present study. Formation of silica-rich droplets is shown (Elmer *et al* 1970) to take place in glasses treated thermally for a prolonged time and at a sufficiently high temperature (100 h at 650 °C for a glass of the composition 10.29 Na₂O, 36.64 B₂O₃ and 53.07 SiO₂ in mol%). This is in accordance with the rules of thermodynamic equilibrium for which a minimum interfacial area of the separated phases is required (Haller 1965).

The colour of the glasses, which are perfectly transparent, changes from a faint green (G1) to faint blue

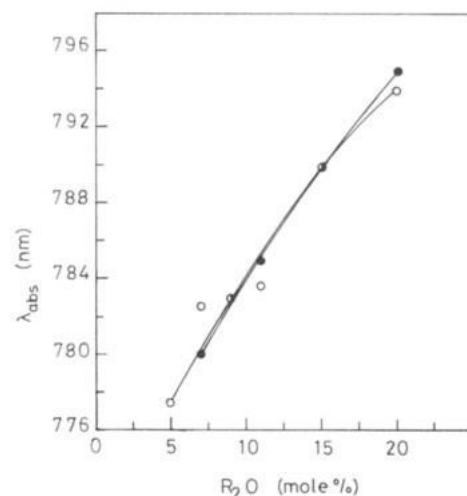


Figure 6. λ_{abs} , the wavelength of the absorption band, as a function of R₂O content for untreated glasses (○) and glasses treated for 4 h at 560 °C (●).

(G3) and deep blue (G6). The electronic absorption spectra of G1–G6 reveal a unique broad absorption band in the range 777–794 nm (figure 5). This band is possibly assigned to the B_{1g} → B_{2g} d–d transition for the 3d¹ hole in octahedral and pseudo-octahedral symmetry with a strong tetragonal distortion (Hecht 1968, Imagawa 1968, Bowmaker *et al* 1975, Laurie *et al* 1975, Shen *et al* 1982).

In figure 6, it is shown that the wavelength of the absorption band (λ_{abs}) increases with the increase of R₂O. This is to be expected, since CuO is assumed to be incorporated in the borate network as a modifying oxide in the studied glasses. The change of λ_{abs} should be, therefore, connected with the structural changes in the alkali borate network.

The average B–O distance increases from 0.137 nm in vitreous B₂O₃ to 0.145 nm in a sodium borate glass containing 33.3 mol% Na₂O (Oh *et al* 1985). This causes an increase of the average distance between a Cu²⁺ ion and its surrounding ions and may reduce the probability for a Cu²⁺ ion to attract the non-bonding electron on P_z of the intervening oxygen ion. The energy for an electron in the Cu²⁺ ion to be excited from the B_{2g} back-bonding orbital to the B_{1g} back-bonding orbital should decrease with the increase of R₂O. It appears, however, that λ_{abs} increases linearly, rather than exponentially, as the alkali oxide increases up to $R = 0.8$ (figure 7). The rate of increase of λ_{abs} rapidly decreases for $R > 0.8$, which can be attributed to the destruction of the structure due to formation of non-bridging oxygen ions in both the borate and the silicate networks at such R values ($R > R_{\text{max}}$ for glasses with $R > 0.8$ in figure 7).

The position of the absorption band is not affected by the heat treatment (time and temperature) (figure 6). This may indicate that the ionic distributions surrounding Cu²⁺ in these glasses do not change with the applied thermal treatment. The similarity of the ligand field strength (10 D_q) for Cu²⁺ in all the studied glasses

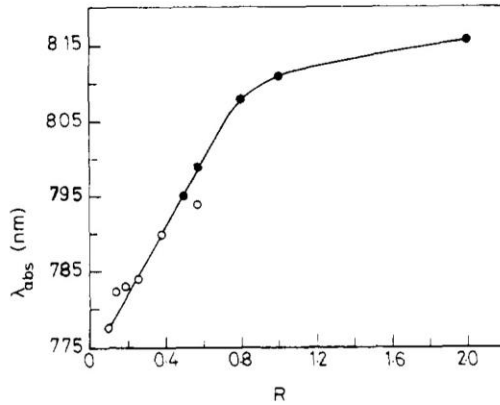


Figure 7. Change of λ_{abs} with R value of sodium borosilicate glasses; (○) the present results and (●) data taken from Shen *et al* (1982).

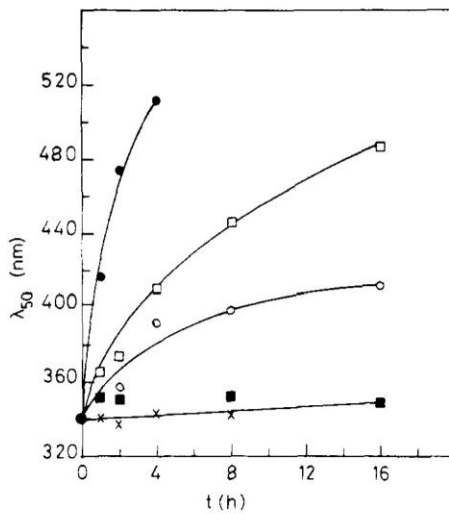


Figure 8. Effect of the heat-treatment time, at different temperatures, on λ_{50} of G2 (×, 500 °C; ■, 520 °C; ○, 540 °C; □, 560 °C; ●, 580 °C).

($1.25\text{--}1.28 \times 10^{-3} \text{ cm}^{-1}$) also suggests an identical coordination environment of copper (II) in these glasses. However, when the temperature or the time of heat treatment is increased, the prominent ligand field band is shifted to lower energy.

The transmission of glass in the ultraviolet region is characterized by a sharp decline known as the absorption edge (McSwain *et al* 1963). The position of the absorption edge depends on the alkali oxide content and the concentration of non-bridging oxygen ions. It is generally proposed (Stevens 1947, Scholtze 1959) that the UV edge is due to the transition of an electron belonging to a non-bridging oxygen ion which needs, to be excited, less energy than the energy needed for the electrons in bridging oxygen ions.

To analyse the absorption in the UV region, λ_{50} has been taken as a parameter, where λ_{50} is the wavelength at which the transmission becomes 50% of the maximum transmission in the visible region (Rötger and Basen 1963). McSwain *et al* (1963) indicated that the

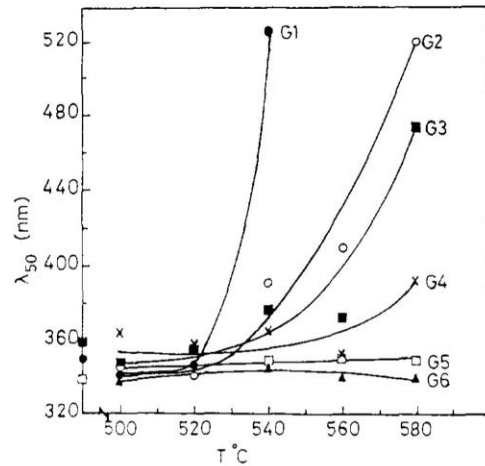


Figure 9. Effect of the heat-treatment temperature on λ_{50} of samples of G1–G6 treated for 4 h.

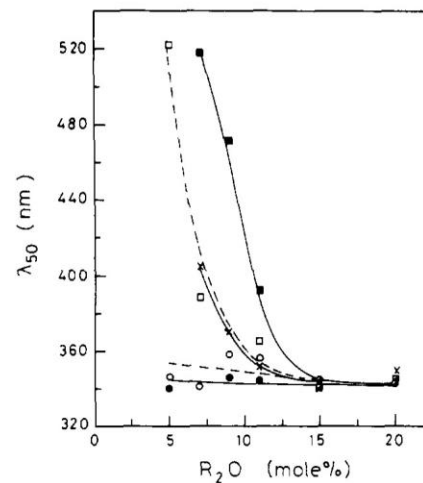


Figure 10. Dependence of λ_{50} on R_2O content for samples treated thermally for 4 h at different temperatures (●, 500 °C; ○, 520 °C; ×, 540 °C; □, 560 °C; ■, 580 °C).

position of the absorption edge moves to longer wavelengths for $R > 0.2$ in $\text{Na}_2\text{O-B}_2\text{O}_3$ glasses. Between $R = 0.2$ and $R = 0.43$, λ_{50} increases from 255 to 278 nm respectively. In the present case, where R ranges between 0.10 and 0.57, λ_{50} has a nearly constant value, 353 ± 6 nm. This indicates that the presence of SiO_2 in the studied glasses shifts λ_{50} to much longer wavelengths. This shift of λ_{50} cannot be attributed to interaction between the photons and the oxygen ions in the Si–O–Si network, because glassy SiO_2 has high transparency in the UV region. Also, it cannot be considered a result of higher concentration of non-bridging oxygen ions in the borate network, because $R < R_{\text{max}}$ in the studied glasses. However, the reason for such a great shift of λ_{50} , between $\text{Na}_2\text{O-B}_2\text{O}_3$ glasses and the studied $\text{Na}_2\text{O-B}_2\text{O}_3\text{-SiO}_2$ glasses, may become clear when studying the effect of heat treatment on λ_{50} .

Figure 8 shows the dependence of λ_{50} on the time of heat treatment at different temperatures for G2 (values of λ_{50} are determined with an error of ± 5 nm).

It is shown that λ_{50} increases with higher rates at higher temperatures and remains nearly around its initial value when treating the glass at relatively low temperatures. Similar dependence is also found for the other glasses. The glasses become translucent to opaque on tempering. The effect decreases from G1 to G4. Glasses G5 and G6 remain transparent and do not show any change of λ_{50} or of colour. Although there should be some diffusion processes during the heat treatment, through which non-bridging oxygen ions may form, especially when an alkali-rich borate subphase forms, the great shift of λ_{50} towards longer wavelengths in figure 8 cannot be attributed to such a process. We are more likely to assume that this increase of λ_{50} , which is in direct proportion to the turbidity of the sample, is due to light scattering through the particles of SiO_2 phase precipitated during the heat treatment. As the time increases, the particle size increases (figure 3A–D), and we therefore expect a shift of λ_{50} to longer wavelengths.

The effect of heat-treatment temperature on λ_{50} is shown in figure 9. There is no effect of the temperature, or the time, of heat treatment on λ_{50} of the glasses G5 and G6, which lie outside the immiscibility region of the $\text{Na}_2\text{O}-\text{B}_2\text{O}_3-\text{SiO}_2$ system. The absence of any effect of heat treatment on G5 and G6 indicates that CuO, at the concentration used, does not activate phase separation processes. In figure 9, λ_{50} remains nearly constant up to a specific temperature, depending on the glass composition and the time of heat treatment, and then starts to increase. However, for a specific heat-treatment time, the temperature at which λ_{50} starts to increase decreases with the decrease of R_2O content in the glass. This should indicate that the tendency to phase separation decreases, in the studied glasses, as the alkali oxide increases, i.e. with the increase of BO_4 concentration. The same conclusion can also be obtained from figure 10, in which λ_{50} is

represented as a function of R_2O concentration for glasses treated thermally for 4 h at different temperatures.

The obtained results indicate the possibility of controlling the optical properties of such glasses, to obtain glasses with specific UV absorption, through heat treatment.

References

- Bowmaker G A, Waters T N and Wright P E 1975 *J. Chem. Soc.* 867
 Bray P J 1985 *J. Non-Cryst. Solids* **73** 19
 Doweidar H, Meikhail M S and Holland D 1988 *J. Non-Cryst. Solids* **101** 280
 Doweidar H and Silim H A 1979 *Bull. Fac. Sci. Mansoura Univ.* **7** 269
 Elmer T H, Nordberg M E, Carrier G B and Korda E J 1970 *J. Am. Ceram. Soc.* **53** 171
 Hakim R M and Uhlmann D R 1971 *Phys. Chem. Glasses* **12** 132
 Haller W 1965 *J. Chem. Phys.* **42** 686
 Hecht H G 1968 *Phys. Chem. Glasses* **9** 179
 Imagawa H 1968 *Phys. Status Solidi* **30** 469
 Konijnendijk W L 1975 *PhD Thesis (Philips Res. Suppl. No 1)*
 Laurie S H, Lund T and Raynor J B 1975 *J. Chem. Soc.* 1389
 McSwain B D, Borrelli N F and Goug-Jen Su 1963 *Phys. Chem. Glasses* **4** 1
 Milberg M E, O'Keefe J G, Verhelst R A and Hooper H O 1972 *Phys. Chem. Glasses* **13** 79
 Oh K D, Miyaka M, Morikawa H and Marumo F 1985 *Rep. Res. Lab. Eng. Mater. Tokyo Inst. Technol.* **10** 1
 Rötger H and Basen H 1963 *Silikattechn.* **14** 166
 Scholtze H 1959 *Glastechn. Ber.* **32** 81
 Shen D, Wang K, Huang X, Chen Y and Bai J 1982 *J. Non-Cryst. Solids* **52** 151
 Stevels J M 1947 *Proc. 11th. Int. Congr. Pure and App. Chem.* **5** 519
 Vogel W 1971 *Struktur und Kristallization der Gläser* (Leipzig: VEB Deutscher Verlag Für Grundstoffindustrie) p 98
 Yun Y H and Bray P J 1978 *J. Non-Cryst. Solids* **27** 363

ISSN 0970-7077

ASIAN JOURNAL OF CHEMISTRY

(An International Quarterly Research Journal of Chemistry)
11/100, Rajendra Nagar, Sector-3, SAHIBABAD-201 005 (Ghaziabad) INDIA

Editor in Chief
Dr. R. K. AGARWAL

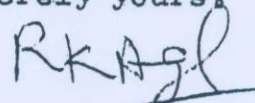
Dated...19.6.1989.

Dr. M. Mashaly
Department of Chemistry
Faculty of Science at Damietta
Mansoura University
Damietta, Egypt.

Dear Dr. Mashaly,

We are pleased to inform you that your research paper entitled, " Domestic indoor pollution: CGC and CGC/MS investigation of the exhaust of Kerosene lamp, " (Index No.108/89) has been finally accepted for publication in Asian Journal of Chemistry.

Sincerely yours,



Dr. R. K. Agarwal
Editor-in-Chief,
Asian Journal of Chemistry.

Note : Subscription must be sent either by M. O. or by D.D. drawn on any bank at Delhi or Ghaziabad, in favour of ASIAN JOURNAL OF CHEMISTRY. SAHIBABAD



Mansoura University
Faculty of Science

DOMESTIC INDOOR POLLUTION: CGC AND CGC/MS INVESTIGATION OF
THE EXHAUST PARTICULATE MATTER DEPOSITED ON THE INSIDE WALL
OF KEROSENE LAMP

M. Mashaly^{1*}, M.S. Elshahawi¹ and P. Sandra²
Chemistry Department, Damietta Faculty of Science, Mansoura
University and Research Institute for Chromatography,
Wevelgem, Belgium

Reprinted from the Bulletin of the Faculty of Science,
Mansoura University, vol. 17(1), 1990

1990

Mans. Sci. Bull. vol. 17(1): 45-56

DOMESTIC INDOOR POLLUTION: CGC AND CGC/MS INVESTIGATION OF THE EXHAUST PARTICULATE MATTER DEPOSITED ON THE INSIDE WALL OF KEROSENE LAMP

M. Mashaly^{1*}, M.S. Elshahawi¹ and P. Sandra²

Chemistry Department, Damietta Faculty of Science, Mansoura University and Research Institute for Chromatography, Wevelgem, Belgium.

(Received 13/3/1989)

ABSTRACT

The kerosene lamp which is commonly used in Egyptian villages for indoor lightening exhausts air pollutants. An exhaust portion in the form of particulate matter deposited on the inside wall of the kerosene lamp was extracted by refluxing with cyclohexane. The concentrated extract was chromatographed over a silica gel column and eluted with cyclohexane to isolate the hydrocarbons. The kerosene fuel and its exhaust were analyzed by Capillary Gas Chromatography (CGC) and the exhaust was also analyzed by CGC/Mass Spectrometry (CGC/MS). n-Alkanes were major chemical class in both the fuel and its exhaust. Some aromatics were also present in the exhaust.

INTRODUCTION

Kerosene lamp is still of common use among the Egyptians for lightening in case of electricity cut-off which happens frequently. Not all the villages are yet supplied with electricity, so, the kerosene lamp is more common there. Many Egyptian families, especially those of low income, used to prepare baked fava beans (a very popular food called Fool Medammes) by overnight hanging the cooking vessel over the top of a gentle flamed kerosene lamp. With closed doors and windows of mostly narrow houses or flats, the emitted kerosene exhaust for an overnight period would possibly causes measurable indoor pollution. Breathed air is waisted and property is badly affected. The exhaust of the burned kerosene diffuses into the atmosphere as well as deposits on any nearby cold surface in the form of a thin black layer of kerosene-smelling fine particulate matter.

Unfortunately, no technical equipments were available to monitor polluted air. Therefore, the present work deals with the particulate matter deposited on the inside wall of the glass top of the kerosene lamp. The study deals with this exhaust portion for being a pollution factor and also as a representative indication of some types of the exhaust pollutants emitted into air. It aims at getting qualitative and quantitative information about some pollutants to which people using these lamps are exposed. CGC and CGC/MS were used in the course of this study.

EXPERIMENTAL

Collection of the exhaust particulates:

Two kerosene lamps of the standard size number 10, with about 400 ml kerosene-tank capacity were used. Each lamp was fueled with 2x250 ml kerosene^{1,7-9}. At the end of the experiment, the kerosene left in the tanks was

measured to obtain the burned volume. To obtain the weight of the particulates, the glass top of each lamp was weighed before and after sampling. Non smoky flame was used (about 1 cm height) for a total period of 7 h for each lamp. At the end of the experiments, the first and second lamps gave 3.8 mg and 4.3 mg particulate matter from a total of 447 ml and 468 ml kerosene, respectively. The collected particulate matter was of a mean value 0.0089 mg/ml kerosene.

Temperature detection:

In separate experiments on the same lamps, after one hour burning, the temperature at the higher edge (exhaust outlet) of the kerosene lamp was in the range 245-255°C. On removing the glass top, allowing the flame to be in the open air, its temperature was in the range 345-355°C.

Extraction of the nonpolar organic soluble content of the exhaust particulates:

The part of the glass top of the lamp on which a black layer was deposited, was crushed into very small pieces. The crushed glass from the two lamps was combined, refluxed with 3x300 ml cyclohexane (tested by GC for its purity) for three hours each. The cyclohexane extracts were combined and concentrated under reduced pressure. The light yellowish concentrated extract was adjusted to 10 ml.

A rough estimation of the weight percentage of the organic soluble content was done by open air evaporation of 2x100 µl cyclohexane extract dropped on the pan of a sensitive electric balance. The values were 5.12%, wt/wt, relative to the sample weight and 0.00045 mg/ml, wt/v, relative to the volume of consumed fuel.

Fractionation of the cyclohexane extract:

The concentrated extract was further concentrated to about 0.4 ml under a very slow stream of dry nitrogen. The sample was next placed on the top of a silica gel column, the nonpolar fraction was eluted with cyclohexane and the eluate was concentrated to 1.5 ml.

CGC analysis:

Kerosene and the non polar fraction of the exhaust sample were analyzed by CGC using a Carlo Erba HRGC 4130 instrument equipped with a flame ionization detector (FID). The column and operating conditions were as follows: fused silica SE-52 (25 m x 0.25 mm I.D, 0.25 μm d_f), temperature programme 60°/2 min. iso/5° min^{-1} /310°C/5 min.iso., FID (330°C, H_2 : 0.5 kg cm^{-2} , air: 1 kg cm^{-2}), carrier gas (H_2) inlet pressure 0.5 kg cm^{-2} and chart speed 0.5 cm min^{-1} . Integration was done using Spectra Physics SP42900 Integrator.

Kerosene and the exhaust sample were also spiked with a standard mixture of the n-alkanes n- C_9H_{20} -to-n- $\text{C}_{16}\text{H}_{34}$, n- $\text{C}_{18}\text{H}_{38}$ -to-n- $\text{C}_{20}\text{H}_{42}$ and the even n- $\text{C}_{22}\text{H}_{46}$ -to-n- $\text{C}_{28}\text{H}_{58}$ and analyzed by CGC under the above conditions to assist peak identification.

CGC/MS analysis:

The sample was analyzed by CGC/MS in the electron impact mode (70 eV). To obtain comparable results, the column and conditions used for the CGC analysis were applied, except that helium was used as a carrier gas; max. temp. 290°C.

In addition, separate injections were done for selective ion monitoring of the possible presence of certain aromatic compounds in the exhaust sample.

RESULTS AND DISCUSSION

Fig. 1 shows the CGC chromatogram of the nonpolar fraction of the exhaust particulates of the kerosene lamp. Some identified compounds are marked in Fig. 1 with their carbon numbers (the n-alkanes) or names. Qualitative and quantitative comparison between the identified n-alkanes in both kerosene and the kerosene exhaust are listed in Table 1. Peak identification was based on: (i) standard analysis with reference n-alkanes, (ii) CGC/MS computer data feed system (iii) CGC/MS: selective ion monitoring to search for the possible presence of certain aromatics and (iv) comparison with our previous work in the field of environmental pollution²⁻⁶.

In perfect combustion reactions, excess air (O_2) and high temperature or flame are required for the conversion of hydrocarbons into carbon dioxide, water and heat. The design of the kerosene lamp is not ideal for a hydrocarbon combustion process. Air entry into the flame is limited through a few number of small narrow openings. After one hour lightening, the temperature at the exhaust outlet at the top edge of the lamp (about 20 cm high over the flame) was 245-255°C. On removing the glass top of the lamp, allowing burning to occur in an open air, the flame area was increased due to the presence of excess air (O_2); at this step (flame height about 1.2 cm), the flame temperature was in the range 345-355°C. On placing the glass top on the lamp again, the flame area was reduced due to reduced O_2 amount entering into the flame; expected reduction in the flame temperature may consequently occur. Under these conditions, one may expect that in the kerosene lamp,

fuel components may undergo partial combustion and partial evaporation (by heat).

The exhaust of the kerosene lamp causes domestic indoor air pollution. The health impacts of the exhaust will mostly be due to its content of CO_2 (and possibly CO , due to incomplete combustion), hazardous vapours (fuel components and burning products) and particulates of respirable size. The main routes of entry of the exhaust into the body are through inhalation and skin absorption.

The cyclohexane organic soluble content, i.e., the nonpolar fraction, represented only 5.12% w/w of the collected particulate matter. This means that most of the deposited exhaust (>94%) was nonextractable matter such as carbon black and/or strongly polar compounds. The nonpolar fraction was expected to be, mostly, aliphatic and aromatic hydrocarbons.

Fuel consumption was about 65.4 ml/h and the collected sample was 0.579 mg/h. On the other hand, the collected exhaust particulates represented about 0.0089 mg/ml fuel. This low value means that: (i) a larger fraction of the exhausted particulate matter did not deposit on the inner wall of the glass top of the lamp, but instead, was emitted directly into air, possibly because of being of finer particle size; (ii) another probability is that most of the exhaust was emitted into air in the gas (e.g., CO_2 and CO) or vapour forms (e.g., b.p. range of n- C_8H_{18} to n- $\text{C}_{19}\text{H}_{40}$ is 126-320°C). A situation combining the above mentioned probabilities (i and ii) was also possible.

It is logic that in the whole emitted exhaust (i.e., the collected portion plus the uncollected one which dispersed into air) the number, type and concentration of

Fig. 1. CGC chromatogram of the nonpolar fraction of the exhaust particulates of the kerosene lamp.

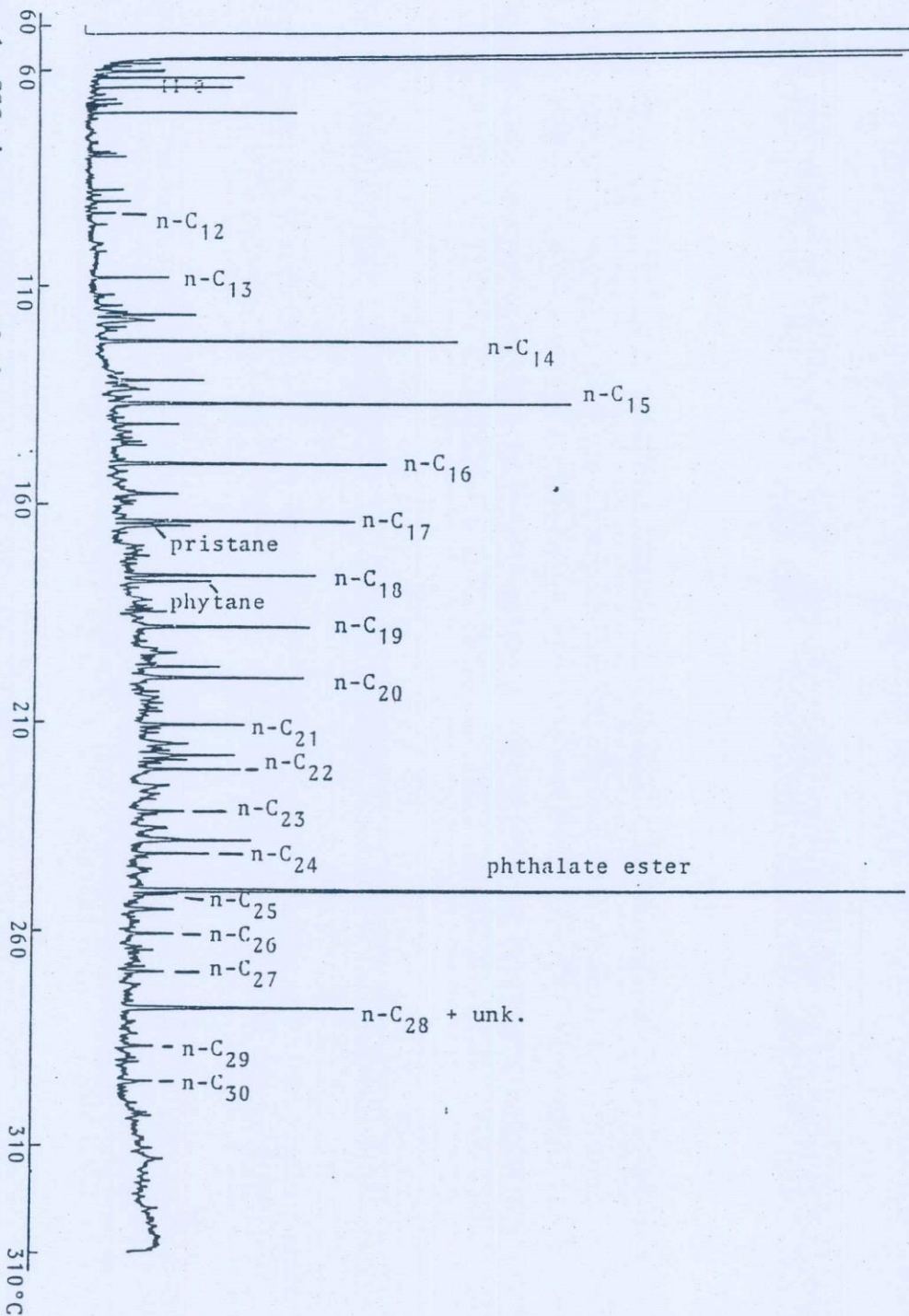


Table 1. Compounds identified in the fuel and exhaust particulates deposited on the inside wall of the kerosene lamp.

Compound	% in fuel	% in exhaust
n-C ₈ H ₁₈	0.715	
n-C ₉ H ₂₀	2.628	
n-C ₁₀ H ₂₂	5.352	
n-C ₁₁ H ₂₄	6.294	
n-C ₁₂ H ₂₆	5.118	0.25
n-C ₁₃ H ₂₈	4.850	0.69
n-C ₁₄ H ₃₀	4.208	3.62
n-C ₁₅ H ₃₂	2.048	4.85
n-C ₁₆ H ₃₄	0.608	2.96
n-C ₁₇ H ₃₆	0.231	2.75
Pristane	0.096	1.45
n-C ₁₈ H ₃₈	0.079	1.92
Phytane	traces	1.07
n-C ₁₉ H ₄₀	0.029	1.70
n-C ₂₀ H ₄₂	traces	1.40
n-C ₂₁ H ₄₄	traces	1.27
n-C ₂₂ H ₄₆		0.97
n-C ₂₃ H ₄₈		0.73
n-C ₂₄ H ₅₀ (+unk.)		1.16
Phthalate		12.26
n-C ₂₅ H ₅₂		0.69
n-C ₂₆ H ₅₄		0.51
n-C ₂₇ H ₅₆		0.54
n-C ₂₈ H ₅₈ (+unk.)		2.79
n-C ₂₉ H ₆₀		0.39
n-C ₃₀ H ₆₂		0.35

pollutants should be more than that detected in the investigated exhaust portion.

In all cases, the probability of inhaling (all forms) or absorbing through the skin (condensed vapours) of the exhaust was increased. Particulate matter will deposit in the lungs and chemical components will next go to the blood resulting in bad health effects, the simplest of which is having headache or feeling dizzy after long exposure to the exhaust (e.g., overnight period).

In the exhaust sample, (Fig. 1), more than 200 compounds were detected by CGC, most of them were present in small or trace concentration making their identification by CGC/MS difficult. From Table 1, it is clear that the n-alkanes were major chemical class in the kerosene fuel (ca.32%) and its exhaust (ca.29%). The highest n-alkane concentration was moved from n-C₁₁H₂₄ in the fuel to n-C₁₅H₃₂ in the exhaust. n-Alkanes from n-C₈H₁₈ to n-C₁₃H₂₈ (b.p. 126-234°C) which showed concentrations up to the highest (n-C₁₁H₂₄) in the fuel were not detected (n-C₈H₁₈ to n-C₁₁H₂₄) or were present in small concentrations in the exhaust due to combustion and/or emission of their vapours into air. n-Alkanes higher than n-C₁₄H₃₀ (b.p. > 266°C) which showed small-to-trace concentrations or could not be detected in the fuel (concentrations smaller than the lower detection limit) were enriched in the exhaust, mostly because of accumulative adsorption or condensation of their vapours on the exhaust particulates.

Different independent CGC/MS runs were carried out on the exhaust sample for selective ion monitoring of trace concentrations of certain aromatic compounds which are commonly present in the exhaust of combusted fossil fuels²⁻⁵. Because of being present in trace concentrations,

the positions of the identified aromatics could not be located in the CGC chromatogram (Fig. 1). Depending on peak abundance, relative retention times and comparing with previous work²⁻⁵, the following ion masses could be detected: 128 for naphthalene, $C_{10}H_8$, (region of n- C_{12}); 142 for methylnaphthalenes, $C_{11}H_{10}$, (region of n- C_{13}); 184 for C_4 -naphthalenes, $C_{14}H_{16}$, (region of n- C_{17}); 184 for dibenzothiophene, $C_{12}H_8S$, (region before phenanthrene); 178 for phenanthrene and anthracene, $C_{14}H_{10}$ (region of n- C_{17} -to-n- C_{18}); 192 for methylphenanthrenes or methylanthracenes, $C_{15}H_{12}$, (region before n- C_{19}) and 202 for fluoranthene and pyrene, $C_{16}H_{10}$, (region of n- C_{20} -to-n- C_{21}). The presence of aromatic compounds in such a small number and trace concentrations in the exhaust of the kerosene lamp is logic, where the production of polycyclic aromatic compounds from fossil fuels is favoured by several factors amongst which is a temperature much higher than that of the flame of the kerosene lamp².

Domestic indoor pollution by the exhaust of the kerosene lamp will disappear if the standard of living is raised and electricity cut-off is stopped.

REFERENCES

1. Hatch L.F. and Matter S., "From Hydrocarbons to Petrochemicals", Gulf Publishing Company, Houston, Texas (1981) p. 9.
2. Mashaly M., Ph.D. thesis, Organic Chemistry Department, Faculty of Science, State University of Ghent, Ghent, Belgium (Feb. 1985).
3. Mashaly M., The II Conference on Chemistry and its Applications, Mansoura University, Faculty of Science, chemistry Department Mansoura, Egypt. September, 27-29 (1988), presented, Proceeding book pp. 416-424.

4. Mashaly M., Nevejans F., Sandra P. and Verzele M., Six Inter. Symp. on Capillary Chromatography. Riva del Garda, Italy, May 14-16, (1985), pp. 340-351.
5. Mashaly M. and Sandra P., 8th Inter. Symp. on Capillary Chromatography. Riva del Garda, Italy, May 19-21, (1987) pp. 476-481.
6. Mashaly M., Sandra P., Sofan M. and El-Shahawi M.S., The 1st National Conf. on Environmental Studies and Research, Cairo, Egypt, Jan. 31-Feb. 4, (1988) pp. 405-413.
7. Morrison R.H. and Boyd R.N. "Organic Chemistry" 4th ed., Allyn and Bacon, INC., Boston, U.S.A., (1973) p. 86 .
8. Nelson W.L., "Petroleum Refinery Engineering", 4th ed., McGraw-Hill Book Company, INC., New York (1958).
9. Waddams A.L., "Chemicals from Petroleum" 2nd ed., The English Language Book Society and John Murray, London (1968) p. 15.

COMPLEXES OF RUTHENIUM(III) DERIVED FROM O,O-DONOR LIGANDS

AHMED M. EL-HENDAWY† and MOHAMED S. EL-SHAHAWI

Chemistry Department, Faculty of Science, Damietta, Egypt

(Received 28 April 1989; accepted 24 July 1989)

Abstract—The complexes $[\text{Ru}^{\text{III}}\text{Cl}_2(\text{PPh}_3)_2\text{L}]$ (L = monoanions of maltol, kojic acid, tropolone and acetylacetonone) were prepared and characterized by spectroscopic and electrochemical measurements. The catalytic oxidation of alcohols in the presence of excess N-methylmorpholine-N-oxide by $[\text{Ru}^{\text{III}}\text{Cl}_2(\text{PPh}_3)_2(\text{acac})]$ has also been reported.

It has been recently noted¹ that reaction of $\text{RuCl}_2(\text{Ph}_3\text{P})_3$ with Schiff bases ($\text{OC}_6\text{H}_4\text{CH}=\text{N}-\text{R}$, where R = Ph, *o*- or *p*- ClC_6H_4), in warm benzene under aerobic conditions, gives the green paramagnetic ruthenium(III) products *trans*- $[\text{RuCl}_2(\text{OC}_6\text{H}_4\text{CH}=\text{NR})(\text{Ph}_3\text{P})_2]$, which in turn form $[\text{Ru}^{\text{II}}(\text{OC}_6\text{H}_4\text{CH}=\text{NR})_2(\text{Ph}_3\text{P})_2]$ in the presence of triethylamine under anaerobic conditions.² The brown complexes $[\text{RuX}_2(\text{EPh}_3)_2(3\text{-bromotropolonato})]$ (E = P or As; X = Cl or Br) have been synthesized by refluxing $[\text{Ru}^{\text{III}}\text{X}_3(\text{EPh}_3)_3]$ and 3-bromotropolone in benzene.³

We now report the preparation of the new complexes $[\text{Ru}^{\text{III}}\text{Cl}_2(\text{PPh}_3)_2\text{L}]$ [L = monoanions of maltol (malt), 3-hydroxy-2-methyl-4-pyrone; kojic acid (koj), 5-hydroxy-2-(hydroxymethyl)-4-H-pyran-4-one; tropolone (trop), 2-hydroxy-2,4,6-cycloheptatrienone, acetylacetonone (acac)], starting with $[\text{Ru}^{\text{II}}(\text{PPh}_3)_3\text{Cl}_2]$. We also discuss their spectroscopic and electrochemical behaviour, together with the application of $[\text{Ru}^{\text{III}}\text{Cl}_2(\text{PPh}_3)_2(\text{acac})]$ to the catalytic oxidations of alcohols in the presence of N-methylmorpholine-N-oxide (NMO) as co-oxidant, since the $\text{Ru}^{\text{II}}\text{Cl}_2(\text{PPh}_3)_2/\text{NMO}$ system has been reported before.^{4,5}

RESULTS AND DISCUSSION

Elemental analyses indicate that the complexes have the formula $[\text{RuCl}_2(\text{PPh}_3)_2\text{L}]$ (L = koj, I; malt, II; trop, III; or acac, IV). Most of the complexes are only soluble in CH_2Cl_2 and their molar conductivities are very low.

† Author to whom correspondence should be addressed.

The IR spectra of the complexes showed all the bands due to triphenylphosphine and coordinated L. The band at 1555 cm^{-1} , observed in both kojato and maltolato complexes, is tentatively assigned to the $\nu(\text{C}=\text{O})$ vibration. The largest bathochromic shift ($75\text{--}105\text{ cm}^{-1}$) for the carbonyl group upon coordination is expected.⁶ Tropolonato and acetylacetonato complexes showed strong bands near 1360 and 1375 cm^{-1} , respectively, arising from $\nu(\text{C}-\text{O})$ vibrations, as observed for $\text{W}_2\text{O}_5(\text{trop})_2$ ⁷ at 1360 cm^{-1} ; also, distinct bands were found at 1510 and 1520 cm^{-1} similar to those reported for $[\text{RuCl}_2(\text{PPh}_3)_2\text{L}]$ ³ (L' = 3-bromotropolonato), and these are characteristic of coordinated diketones.⁸ The *trans*-arrangement of chloro ligands in $[\text{RuCl}_2(\text{PPh}_3)_2\text{L}]$ is suggested by the appearance of only one band near 335 cm^{-1} which is due to (Ru—Cl) vibrations.^{9,10} Some of these IR bands are also observed in the Raman spectra (see Table 1).

The magnetic moments of the complexes at room temperature (in Table 1) are near the spin-only value corresponding to one unpaired electron, suggesting the low spin $d^5(t_{2g})^5$ configuration for the ruthenium(III) ion in an octahedral environment.

Electronic spectra and electron spin resonance

The electronic spectra of complexes II, III and IV in CH_2Cl_2 show a broad intense band around 600 nm which could be assigned to a $d-d$ electronic transition, whereas the intense band near 375 nm is tentatively assigned to a $M \rightarrow L \pi^*$ -transition.³ The bands near or below 300 nm may arise from either an intraligand or from $M \rightarrow L$ charge-transfer

Table 1. Spectroscopic, electrochemical and magnetic data for complexes

Compound	IR and Raman data ^a (cm ⁻¹)			UV-vis data, λ_{\max} (nm) (ϵ , M ⁻¹ cm ⁻¹)	$E_{1/2}$ (V) ^b	ΔE	μ_{eff} (BM)
	$\nu(\text{C}=\text{O})$	$\nu(\text{C}-\text{O})$	$\nu(\text{Ru}-\text{Cl})$				
I	1555s <u>1552w</u>		337m	540(393), 369(3383) 273(11,717)			1.84
II	1555s <u>1551w</u>		340m	625(284), 378(5950) 297(25,150), 267sh (23,617)	-0.55	0.08	1.92
III	1510s	1360s <u>1356m</u>	340m	577(168), 375(10,750) 300(28,367)	-0.34	0.06	1.82
IV	1520s	1375s	330m <u>323m</u>	605(276), 388(3333) 299(22,667), 283(20,167) 272(19,800), 265(20,167)	-0.29	0.07	1.73

^a Raman data are underlined.

^b Scan rate: 50 mV s⁻¹.

bands. Similar but shifted bands are assigned for complex I which is soluble only in DMF.

The spin Hamiltonian parameters for complexes II and IV were sufficiently resolved to allow more than the facile deduction that the unpaired electron is delocalized onto the ligand. The observed lines were similar to each other. The g_{\parallel} values were 1.88 and 1.92, while g_{\perp} values were 2.30 and 2.38 for complexes II and IV, respectively, with respect to DPPH. These values are in good agreement with the g values reported for analogous ruthenium(III) species.³ The spectra are typical of a large axial distortion of an elongated octahedral ruthenium(III) ion environment^{3,11} (a representative example is given in Fig. 1).

Cyclic voltammetric studies

The cyclic voltammogram (CV) of the complexes for $\sim 10^{-3}$ M concentration in CH₂Cl₂ using

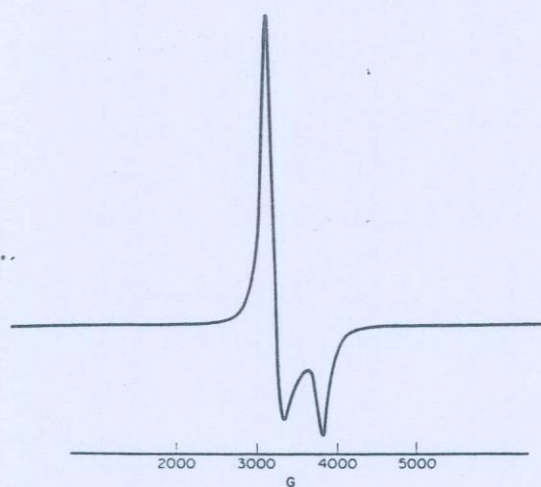


Fig. 1. ESR spectra of *trans*-[RuCl₂(PPh₃)₂(acac)].

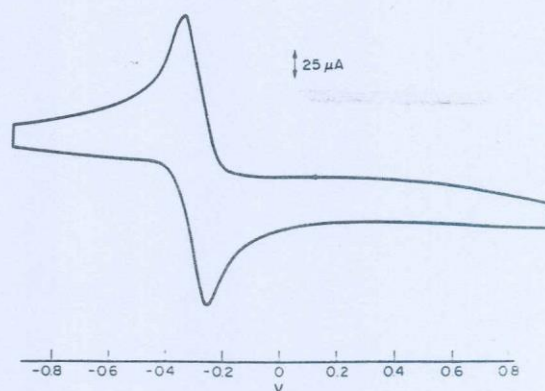


Fig. 2. Cyclic voltammogram of *trans*-[RuCl₂(PPh₃)₂(acac)] (10^{-3} M) in CH₂Cl₂ with 0.1 M (Bu₄N)PF₆ as supporting electrolyte; scan rate 50 mV s⁻¹; volts vs Ag/AgCl electrode.

0.1 M Bu₄NPF₆ as the supporting electrolyte. shows only one reversible (or quasi-reversible, $\Delta E = 70$ –80 mV) reduction wave at a negative potential (data in Table 1 and Fig. 2 as a typical example). This corresponds to Ru^{III}/Ru^{II} reduction vs Ag/AgCl electrode. We also prepared Ru(acac)₃¹² and found that its CV was the same as that previously reported,¹³ for both reversible redox reduction and oxidation waves at $E_{1/2} = -0.71$ and $+1.13$ V corresponding to Ru^{III/II} and Ru^{III/IV}, respectively. The redox potential values for our complexes compared with those for Ru(acac)₃ (for the couple Ru^{III}-Ru^{II}) reflect the order of increasing electron-donating nature, i.e. compound IV < III < II < Ru(acac)₃. This decrease of electron donating character in our complexes could explain why they only display one reduction wave.

Table 2. Catalytic oxidations of alcohols by *trans*-[RuCl₂(PPh₃)₂acac]/NMO

Alcohol	Product ^a	Yield	Time (h)	Turnover ^b
Benzyl	A	99	2	77
<i>p</i> -Methoxybenzyl	A	98	1.5	75
Cinnamyl	A	60	2	50
Benzohydrol	K	94	2	50
Benzoin	K	55	3	50
Cyclohexanol	K	74	3	50

^a A = corresponding aldehyde. K = corresponding ketone.

^b Turnover = moles of product/moles of catalyst.

Catalytic oxidation of alcohols

Ru^{II}Cl₂(PPh₃)₃ has been used in the presence of excess NMO, for catalytic oxidation of alcohols to give the corresponding aldehydes or ketones.^{4,5} Thus [RuCl₂(PPh₃)₂(acac)] was found to give such catalytic oxidations in the presence of excess NMO. Primary alcohols are oxidized to the corresponding aldehydes, and secondary alcohols to ketones (Table 2). There is no oxidation by NMO in the absence of the catalyst and no reaction between [RuCl₂(PPh₃)₂(acac)] (IV) and the alcohols in the absence of NMO as shown by electronic spectroscopy. On mixing IV (10⁻³ M) and NMO (0.15 M) in CH₂Cl₂ and shaking, the green colour changes to yellowish and the bands at 605 and 388 nm for compound IV are replaced by bands at 525 and 375 nm. The intensity of the former band was found to increase with time: at 1, 2, 4 and 5 h, the corresponding absorbances were 0.37, 0.43, 0.54 and 0.75, respectively, whereas the intensity of the band at 375 nm remained nearly constant. The appearance of these two bands is similar to those observed for high oxidation state ruthenium complexes.^{5,10} This could explain the continuation of the catalytic cycle of oxidation.

EXPERIMENTAL

Preparation of complexes

All preparations use RuCl₂(PPh₃)₃ which was synthesized by the literature method.¹⁴

trans-[RuCl₂(PPh₃)₂L] (L = koj or malt) (I, II). To kojic acid (0.21 g, 1.5 mmol) dissolved in hot methanol (10 cm³) was added RuCl₂(PPh₃)₃ (0.48 g, 0.5 mmol). The mixture gave a green solution on reflux, and after 1 h a yellow precipitate formed, which was filtered off, washed with hot methanol

and then ether, and dried *in vacuo* (Found: C, 60.1; H, 4.2; Cl, 8.4. [RuCl₂(PPh₃)₂(koj)] (I) requires: C, 60.2; H, 4.2; Cl, 8.5%).

Similar procedures were used in which maltol replaced kojic acid and a green precipitate was obtained (Found: C, 61.4; H, 4.3; Cl, 8.8. [Ru(PPh₃)₂Cl₂(malt)] (II) requires: C, 61.4; H, 4.3; Cl, 8.6%).

trans-[RuCl₂(PPh₃)₂(trop)] (III). Tropolone (0.18 g, 1.5 mmol) was dissolved in benzene (25 cm³) and RuCl₂(PPh₃)₃ (0.96 g, 1 mmol) added. After refluxing the mixture for 0.5 h, a reddish-brown solution resulted. A yellow precipitate formed on continued heating; this was filtered off, washed with methanol and then ether, and dried *in vacuo* (Found: C, 63.1; H, 4.2; Cl, 9.0. [RuCl₂(PPh₃)₂(trop)] requires: C, 63.2; H, 4.3; Cl, 8.7%).

trans-[RuCl₂(PPh₃)₂(acac)] (IV). To RuCl₂(PPh₃)₃ (0.24 g, 0.25 mmol) was added excess acetylacetate (10 cm³) and the mixture was refluxed on a steam bath for 2 h. Green microcrystals were isolated, filtered off and washed with ether and dried *in vacuo* (Found: C, 62.1; H, 4.6; Cl, 8.9. [RuCl₂(PPh₃)₂(acac)] requires: C, 61.9; H, 4.7; Cl, 8.9%). Yields of 60–75% of the above complexes were obtained.

Catalytic oxidations by *trans*-[RuCl₂(PPh₃)₂(acac)] (IV)

The oxidation of benzohydrol is typical. To benzohydrol (1 mmol) was added NMO (3 mmol) in 25 cm³ of CH₂Cl₂ and 2 × 10⁻² mmol of compound IV. The solution was stirred for 2 h during which time the colour changed from green to brown. The mixture was evaporated to dryness and extracted with ether (2 × 25 cm³); the combined ethereal extracts were filtered and evaporated to give benzophenone which was characterized as its 2,4-dinitrophenylhydrazone derivative.

IR spectra were measured on a Perkin-Elmer 683 spectrophotometer as liquid paraffin mulls between CsI plates and as KBr discs. Raman spectra were measured on a Spex Ramalog 5 instrument with a CRL Innova Krypton ion laser with excitation at 6471 or 5682 Å as KBr discs. ESR spectra were recorded with a Varian E-12 spectrometer equipped with 100 kHz modulation. Cyclic voltammetric studies were carried out on a potentiostat/wave generator (Oxford Electrodes) using platinum working electrode. Magnetic measurements were made on a Johnson Matthey magnetic susceptibility balance.

Acknowledgements—We thank Zahar Hussein for carrying out the ESR spectra. Dr W. P. Griffith for helpful advice and also Johnson Matthey Ltd for the loan of ruthenium trichloride.

REFERENCES

1. V. Alteparmakian and S. D. Robinson, *Inorg. Chem. Acta* 1986, **116**, L37.
2. J. R. Thornback and G. Wilkinson, *J. Chem. Soc., Dalton Trans.* 1978, 110 and refs therein.
3. O. K. Medhi and U. Agarwala, *J. Inorg. Nucl. Chem.* 1980, **42**, 1413.
4. K. B. Sharpless, K. Akashi and K. Oshima, *Tetrahedron Lett.* 1976, 2503.
5. K. Vijayasri, J. Rajaram and J. C. Kuriacose, *Proc. Indian Acad. Sci.* 1986, **97**, 125.
6. K. Yamada, *Bull. Chem. Soc. Jpn* 1962, **35**, 1323.
7. W. P. Griffith, C. A. Pumphrey and A. C. Skapski, *Polyhedron* 1987, **6**, 891.
8. K. Nakamoto, *IR Spectra of Inorganic and Coordination Compounds*. Wiley, New York (1964).
9. D. W. Raichart and H. Taube, *Inorg. Chem.* 1972, **11**, 999.
10. A. El-Hendawy, W. P. Griffith, M. N. Moussa and F. I. Taha, *J. Chem. Soc., Dalton Trans.* 1989, 901.
11. W. West, *Techniques of Chemistry, Theory and Application of Electron Spin Resonance* (Vol. XV). John Wiley, New York (1979).
12. A. Endo, K. Shimizu, G. P. Sato and M. Mukaida, *Chem. Lett.* 1984, **437**.
13. J. H. Tocher and J. P. Fackler, *Inorg. Chim. Acta* 1985, **102**, 211.
14. T. A. Stephenson and G. Wilkinson, *J. Inorg. Nucl. Chem.* 1966, **28**, 945.

IODOMETRIC MICROGRAM DETERMINATION OF Mn(II) IN AQUEOUS MEDIA BY AN INDIRECT CHEMICAL AMPLIFICATION REACTION

A. M. EL-WAKIL, A. B. FARAG and M. S. EL-SHAHAWI

Department of Chemistry, Faculty of Science, Mansoura University, Mansoura, Egypt

(Received 3 March 1988. Revised 27 December 1988. Accepted 19 January 1989)

Summary—A rapid, simple and highly sensitive iodometric amplification method is described for the determination of microgram amounts of Mn(II). The method is based on oxidation of Mn(II) with an excess of periodate in acetate buffer (pH 2.8–3.0), masking of the unreacted periodate with molybdate, and after addition of iodide, titration of the liberated iodine is with thiosulphate. The proposed method offers 20-fold amplification for Mn(II) and was found suitable for the determination of Mn(II) in the presence of permanganate ions. Mn(II) in tap water and an industrial waste water has been successfully determined by the proposed method.

Amplification reactions have been defined¹ as reactions in which the normal equivalence is altered in some way so that a more favourable measurement can be made. Iodometric amplification reactions have been extensively applied.²⁻⁹

The application of suitable iodometric amplification methods to the determination of trace amounts of Mn(II) and/or permanganate in aqueous solution was the aim of the present work.

EXPERIMENTAL

Reagents

Unless otherwise specified all reagents were of analytical-reagent grade.

Ammonium molybdate solution. Ten g of ammonium heptamolybdate tetrahydrate per 100 ml, freshly prepared.

Buffer solution, pH 2.8–3.0. Dilute 150 ml of glacial acetic acid to 500 ml with 0.15M sodium acetate.

Potassium periodate solution. Dissolve 1.75 g of the recrystallized solid reagent in 500 ml of distilled water containing 3 ml of saturated disodium tetraborate solution.

Sodium thiosulphate solution, 0.005M. Standardized against potassium iodate solution.

Saturated sodium sulphite solution.

Manganese sulphate solution, Mn 1 mg/ml. Prepare from any convenient hydrate, acidify with two drops of concentrated sulphuric acid to prevent hydrolysis, and standardize by any convenient method. Dilute further as required.

Potassium permanganate solution, Mn 1 mg/ml. Standardize against arsenious oxide¹⁰ or by any other reliable method.

Procedure

Determination of manganese(II). Transfer a known volume of Mn(II) solution containing 1–150 µg of manganese to a 100-ml conical flask, add 1.5–2.0 ml of acetate buffer and 5 ml of periodate solution, and let stand for 15 min at room temperature. Then add 2 ml of ammonium molybdate solution to mask the unreacted periodate. Add 20–50 mg of potassium iodide and titrate the liberated iodine with sodium thiosulphate (starch as indicator).

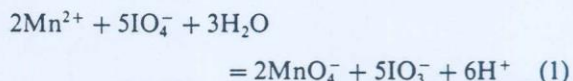
Determination of permanganate. Transfer a known volume of permanganate solution containing up to 100 µg of manganese to a 100-ml conical flask, and add 0.5 ml of saturated sodium sulphite solution followed by 1 ml of concentrated nitric acid. Evaporate the solution to dryness, dissolve the white residue in about 5 ml of water and determine the manganese as above.

Determination of manganese(II) in the presence of permanganate. Transfer a known volume of the mixture to a 100-ml conical flask, and add 1.5–2.0 ml of acetate buffer followed by a few crystals of potassium iodide. Titrate the liberated iodine with sodium thiosulphate (*A* ml). Analyse an equal volume of the mixture as described for the determination of Mn(II) (*B* ml).

The volume *A* of thiosulphate solution is equivalent to the permanganate present. The volume *B* is equivalent to the sum of the Mn(II) and the permanganate, and the net volume equivalent to Mn(II) is (*B* – *A*).

RESULTS AND DISCUSSIONS

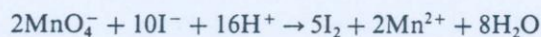
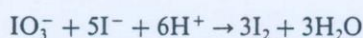
Potassium periodate in acid medium oxidizes Mn(II) to permanganate.¹⁰⁻¹⁴



The degree of oxidation of Mn(II) is reported¹¹⁻¹⁴ to depend on the presence of a mineral acid (nitric, sulphuric or phosphoric), which it is suggested prevents the precipitation of manganese periodate or oxide. Hamaya and Townshend¹³ reported it necessary to heat Mn(II) with periodate in a boiling water-bath for 30 min for the oxidation to be complete. Gawargious *et al.*¹⁵ claimed that the addition of a small amount of sodium oxalate reduces the oxidation time. In the present work complete oxidation of small amounts (1–150 µg) of Mn(II) with periodate was achieved at room temperature in acetate buffer (pH 2.8–3.0). The proposed method is based on this oxidation followed by masking the unreacted

periodate with molybdate, and determination of the iodate and permanganate thus produced. This is done by adding potassium iodide and titrating the liberated iodine with sodium thiosulphate. Molybdate does not interact with the permanganate produced from the manganese(II) range recommended, but recoveries are slightly low when the amount of Mn(II) is higher than 150 μg . This appears to be due to interaction between larger amounts of permanganate and the molybdate added in excess. This was examined by adding molybdate to a solution of permanganate equivalent to 250 μg of manganese, and monitoring the permanganate concentration photometrically. The absorbance was lowered by the presence of molybdate. However, this does not matter if the amount of manganese in the test sample is restricted to 150 μg or less.

The final reaction is the determination of the iodate and permanganate:



Hence one Mn(II) ion will give rise to 10 molecules of iodine, and 1 ml of 0.005M thiosulphate is equivalent to 13.73 μg of Mn. The procedure gives good results for 5–150 μg of manganese (Table 1), and can be extended down to 1 μg if a larger uncertainty can be accepted. The blank values are quite reasonable (0.1–0.15 ml of 0.005M thiosulphate).

The method has been applied to the determination of Mn(II) in tap water and an industrial waste water. In analysis of 50 ml of the tap water the volume of thiosulphate solution consumed was equivalent to that of the blank, indicating the absence of Mn(II) ions. When various amounts of Mn(II) (10–50 μg) were added to the test samples, highly reproducible results for the added Mn(II) were obtained, and when a 10-ml sample of an industrial waste water from an iron metallurgical project was examined, the 0.35 $\mu\text{g}/\text{ml}$ Mn(II) content was easily determined and was in good agreement with the results obtained by standard methods. Fluoride was added to eliminate any interference due to the

Table 1. Determination of various amounts of Mn(II) in aqueous media

Mn(II) taken, μg	Mn(II) found,* μg
150	149.0 \pm 0.4
100	100.7 \pm 0.2
50	50.5 \pm 0.2
20	20.5 \pm 0.2
10	10.14 \pm 0.05
5	5.04 \pm 0.01

*Average standard deviation (10 determinations).

Table 2. Determination of Mn(II) ion in the presence of KMnO_4 , mean \pm standard deviation of 5 replicates

Mn ²⁺ , μg		MnO ₄ ⁻ , μg	
Taken	Found	Taken	Found
5	5.07 \pm 0.03	43.1	42.4 \pm 0.4
10	10.00 \pm 0.0	43.1	42.4 \pm 0.4
20	19.6 \pm 0.2	43.1	42.1 \pm 0.6
50	49.6 \pm 0.2	43.1	43.0 \pm 0.2
100	99.5 \pm 0.3	43.1	43.9 \pm 0.2

presence of Fe(III). Analysis for standard additions of Mn(II) gave precise and accurate results.

Permanganate can readily be determined iodometrically.¹⁰ The sensitivity of the method can be increased considerably by reduction of the permanganate to Mn(II), followed by determination of this by the method described above. A variety of reducing agents have been examined for this purpose, and sodium sulphite has been found to be the most suitable in acid medium.

Selection of the most suitable acid (nitric, sulphuric or perchloric) for eliminating the excess of sulphite and destroying any manganese sulphite complexes¹⁶ formed, was a matter of several trials. With sulphuric or perchloric acid the re-oxidation to permanganate with periodate is very slow, especially with larger amounts (\sim 100 μg) of manganese. Use of a mixture of nitric and perchloric acids leads to intermediate higher oxidation states of manganese, e.g., MnO_2 , which are not amenable to complete oxidation to permanganate, thus leading to low results.

Nitric acid is the most suitable mineral acid for the purpose, manganese-sulphite complexes and excess of sulphite being readily eliminated by evaporation of the nitric acid solution. Satisfactory results are obtained for up to 100 μg of manganese.

The proposed method can also easily be employed for the determination of Mn(II) in the presence of permanganate. An aliquot of the mixture is first allowed to react with iodide in acid medium and the iodine released, which is equivalent to the permanganate present, is titrated with a standard thiosulphate solution. Another aliquot is then treated with periodate, by the procedure described for the determination of Mn(II). The difference between the volumes of thiosulphate consumed is equivalent to the Mn(II). The results presented in Table 2 show the suitability of the proposed method for the determination of Mn(II) in the presence of permanganate.

REFERENCES

1. R. Belcher, *Talanta*, 1968, **15**, 357.
2. S. K. Tobia, Y. A. Gawargious and M. F. El-Shahat, *Z. Anal. Chem.*, 1973, **265**, 23.
3. A. Besada, *ibid.*, 1974, **271**, 368.
4. Y. A. Gawargious, L. S. Boulos and A. Besada, *Analyst*, 1976, **101**, 458.

5. A. Besada, Y. A. Gawargious and S. Y. Kareem, *Talanta*, 1976, **23**, 392.
6. A. B. Farag, A. M. El-Wakil, H. N. A. Hassan and A. F. Abdel-Aziz, *Indian J. Chem.*, 1985, **24A**, 896.
7. A. B. Farag, H. N. A. Hassan, A. M. Khalil and A. F. Abdel-Aziz, *Analyst*, 1985, **110**, 1265.
8. Y. A. Gawargious, L. S. Boulos and B. N. Faltaoos, *Talanta*, 1976, **23**, 513.
9. A. M. El-Wakil and A. B. Farag, *Z. Anal. Chem.*, 1981, **307**, 207.
10. A. I. Vogel, *Quantitative Inorganic Analysis*, 3rd Ed., Longmans, London, 1975.
11. M. B. Richards, *Analyst*, 1930, **55**, 554.
12. J. P. Mehlig, *Ind. Eng. Chem., Anal. Ed.*, 1939, **11**, 274.
13. J. W. Hamaya and A. Townshend, *Talanta*, 1972, **19**, 141.
14. N. A. Clark, *Ind. Eng. Chem., Anal. Ed.*, 1933, **5**, 241.
15. Y. A. Gawargious, A. Besada and I. H. Habib, *Proc. 1st Chem. Conf., Fac. Sci., Mansoura Univ.*, 24-26 Sept. 1986, Egypt.
16. A. M. El-Wakil, *Ph.D. Thesis*, Czechoslovak Academy of Sciences, Prague, 1975.

additions

es.
ned iodo-
d can be
perman-
on of this
reducing
dose, and
the most

sulphuric
sulphite
mplexes¹⁶
sulphuric
perman-
ally with
Use of
leads to
nganese,
complete
to low

d for the
d excess
oration
ults are

nployed
ence of
is first
im and
he per-
standard
s then
bed for
between
ivalent
able 2
od for
nce of

Shahat,

Analyst,

Extraction and Recovery of Some Organic Insecticides on Polyurethane Foam Columns

A. B. FARAG*, A. M. EL-WAKIL*, M. S. EL-SHAHAWI** and M. MASHALY**

**Department of Chemistry, Faculty of Science, Mansoura University, Mansoura, Egypt*

***Department of Chemistry, Faculty of Science, Mansoura University, Damietta, Egypt*

Polyurethane foam, polyether type, has been recommended as an efficient collector in separating and concentrating some selected chlorinated insecticides and polychlorinated biphenyls from aqueous media. In the present work, the collection and recovery of Baythroid, CME-134 and the ethyl derivative of Sumicidine insecticides from water were examined using static and columns foam extraction modes. The extraction isotherm of the three insecticides tested exhibited a first order behavior in the low concentration. Insecticides were successfully retained on the foam column at reasonable flow rates. The collected insecticides were recovered from the foam material with 100 cm³ acetone in a Soxhlet extractor, and their concentrations were then measured spectrophotometrically. The application of the developed method for the extraction of the above mentioned insecticides in Nile river water has been evaluated.

Keywords Polyurethane foam extractant, preconcentration technique, insecticides, organic pollutants, foam separation

Low concentrations of organochlorine pesticides have been found in waters from most areas of the world, higher levels being detected in streams draining watersheds in which pesticides have been applied.¹ Because of the application of some of these insecticides in agriculture, there has been great concern over the public health and environmental risks involved in the accidental release of these chemicals.²

Various methods have been employed for the determination of organochlorine pesticides at low concentration levels in water. The extraction of pesticides with organic solvents³ is usually recommended for their preconcentration. Unfortunately, multiple extractions must be used, followed by a concentration step to reduce the volume of the solvent down to the volume required for an appropriate concentration of pesticides to be measured. The latter step will lead to a concentration of the impurities originally present in organic solvent as well, which causes a serious interference.⁴ Also, owing to the very low levels of pesticides present in most waters, it becomes necessary to handle large volumes of water. The reversed liquid-liquid partition filter chromatography developed by Ahling *et al.*⁵ gave excellent recovery for PCB, but requires continuous supervision and was limited by relatively low flow rate (0.65 cm³ min⁻¹). Chemical enrichment of organic insecticides in water has also been carried out using activated carbon, but its recovery is variable, inefficient (25–30%) and the recovered material is significantly

different from the initial PCB.^{6,7}

Recently, a number of publications have appeared describing the possibility of using polyurethane foams as efficient cellular solid collectors useful for application in aqueous and gaseous media.^{8,9} The quasispherical membrane structure of these foams has offered special advantages over other solid collectors. Since then, several investigations have been published^{10,11} describing the application of untreated polyurethane foams as collectors in separating and concentrating various chlorinated insecticides and other organic substances in water.

In this paper, we report the use of polyurethane foam as a collector suitable for the extraction and recovery of some chlorinated and fluorinated organic insecticides from aqueous media.

Experimental

Reagents and materials

The reagents used were of analytical grade and the solvents were of spectroscopic grade. Polyurethane foam, a polyether of open cell type (bulk density 30 kg m⁻³) was supplied by Greiner KG, Schaumstoffwerk-Kremsmunster, Austria. The foam cubes (5 mm edge) were washed with 1 M hydrochloric acid solution, followed by distilled water and acetone, and dried at 80°C. The insecticides used were: Baythroid 3-(O-

fluorophenoxy)cyanobenzyl- α -isopropyl- β,β' -dichloroacrylate (I); CME-134 [1-(2,4-difluoro-3,5-dichlorophenyl-3-(2,6-difluorobenzoyl)]urea (II); and α -cyano-*m*-phenoxybenzylethyl-*p*-chlorophenyl acetate (III) which is a derivative of Somicidine. These insecticides were used as received.

Stock solutions containing 2 mg cm^{-3} of each insecticide were prepared by dissolving the exact weight of the insecticide in 50 cm^3 of acetone. A series of standard solutions of these compounds were prepared by diluting their stock solutions with water so as to obtain 10, 20, 30, 40, 50 and $60 \text{ }\mu\text{g cm}^{-3}$ solutions. All these solutions were stored in polyethylene bottles.

Glass columns, 15 mm in diameter and 15 cm in length, were employed. A half grams of unloaded dry foam was packed in the glass column using the vacuum method of foam column packing.¹

Apparatus

A Varian 634 double-beam spectrophotometer with 1 cm quartz cuvettes and gas chromatograph (Pye Unicam 104 series) were used for the determination of the insecticides tested. A polyethylene glycol column (SE 52) was employed at 120°C .

General procedure

Batch experiment. In separate batch experiments, 0.3 g dry foam (10 mm edge) was mixed with 100 cm^3 solutions of each compound containing 10 to $70 \text{ }\mu\text{g cm}^{-3}$. These solutions contained in a series of stoppered polyethylene bottles were shaken for 2 h by a mechanical shaker. The compound which remained in the aqueous solution was determined by UV-visible spectrophotometer, and the amount of compound retained on the foam was calculated as the difference.

Flow experiments. In the flow experiments, 0.5 g dry foam was packed in the column using the vacuum method of foam column packing.¹² Four milligrams of each insecticide in 3 dm^3 of water (distilled or tap water) are passed through the foam column at $5 - 10 \text{ cm}^3 \text{ min}^{-1}$. It was found that all the insecticides were retained almost quantitatively by the first run, except for α -cyano-*m*-phenoxybenzyl-ethyl-*p*-chlorophenyl acetate, which required either a second run or decreasing the flow rate to about $2 \text{ cm}^3 \text{ min}^{-1}$ for complete extraction. After squeezing water from the foam material, the insecticide is recovered from the foam with 100 cm^3 acetone by a Soxhlet apparatus. The eluate is concentrated in a rotary evaporator to 30 cm^3 and the analyte in 2 cm^3 sample is determined by measuring the absorbance of the solution in a 1 cm cell at the absorption maximum.

Results and Discussion

One of the attractive topics in the field of chemical separation has been the application of polyurethane foam columns. This method allows the isolation of the

analyte from the matrix and yields an appropriate enrichment factor. Also, the advantageous hydrodynamic properties of foam columns allow the application of a quite high flow rate without the aid of vacuum. This, together with the rapid attainment of the absorption equilibrium on the surface of the polyurethane foam, reduces the time required for analysis.

In order to investigate the suitability of the foam for the extraction of the insecticides tested in aqueous solution, batch experiments were carried out to collect the insecticides. The foam matrix was found to have a good affinity towards the extraction of the insecticides tested. The extraction ratio is increased by increasing shaking time up to 2 h. After 2 h it remained constant, so a shaking time of 2 h was used in extraction isotherm.

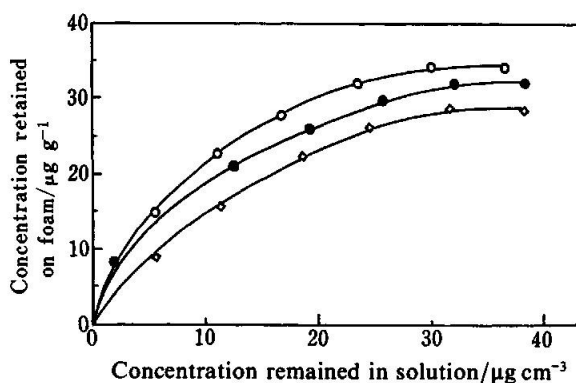
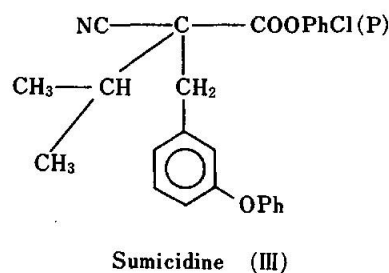
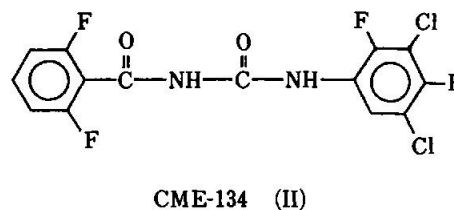
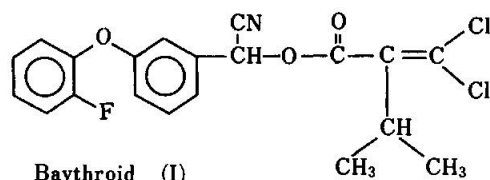


Fig. 1 Extraction isotherm of the insecticides tested. O, Baythroid; ●, CME-134; ◇, Somicidine.

Table 1 Extraction and recovery of the insecticides tested from 3 dm³ aqueous solutions by polyurethane foam columns at 5–10 cm³ min⁻¹ flow rates

Insecticide	Amount/ mg	Recovery, %		Wavelength/ nm
		a	b	
Baythroid	4.0	96	90	270
CME-134	4.0	90	94	245
Derivative of Somicidine	4.0	92	95	262

a. Average of three determinations from distilled water.
b. Average of three determinations from Nile river water.

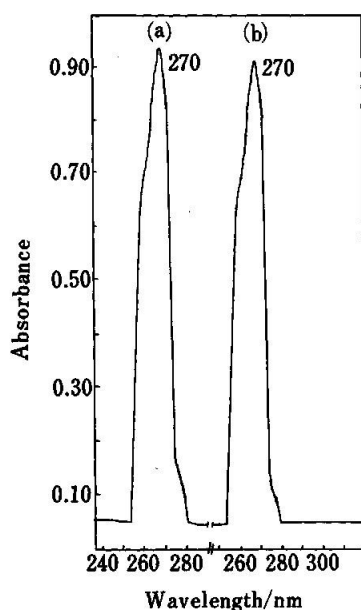


Fig. 2 U.V. absorption spectra of Baythroid in acetone: (a), before percolation through the foam column; (b), after recovery from the foam column.

Extraction isotherm

The uptake of the insecticides tested in aqueous media by the foam was found to depend on their concentrations. Therefore, in separate experiments, adsorption isotherms were carried out over a wide range of equilibrium concentration from 10 to 60 $\mu\text{g cm}^{-3}$ for each compound. The extraction isotherms of the three insecticides tested exhibited a first order behavior in the low concentrations, as indicated in Fig. 1. Therefore, a simple and more efficient method was developed using the untreated polyurethane foam in column dynamic experiments for the extraction of these insecticides from

aqueous solution.

Flow experiment

Three liters of sample solution containing each insecticide, prepared by distilled water or the Nile river water, were passed through the foam column at a flow rate of 5–10 cm³ min⁻¹ which was chosen on the basis of a preliminary tests. The insecticides were then recovered from the foam material with acetone by a Soxhlet apparatus, and their concentrations were measured by UV-visible spectrophotometric technique. The results of the extraction and recovery of the insecticides tested in 3 dm³ aqueous solutions by the proposed foam columns are summarized in Table 1. A representative example of the separation of Baythroid is shown in Fig. 2. The UV-visible spectra of Baythroid in acetone with and without the foam at the concentration step illustrate the efficiency of the proposed foam columns.

References

1. M. G. Wolmen, *Science*, **174**, 905 (1971).
2. J. Charlton, A. Chow and H. D. Gesser, *Hazard Assessment of Chemicals*, **2**, 245 (1983).
3. L. Kahn and C. H. Wayman, *Anal. Chem.*, **36**, 1340 (1964).
4. A. Bevenue, T. W. Kelley and J. W. Hylin, *J. Chromatogr.*, **54**, 71 (1971).
5. B. Ahling and S. Jensen, *Anal. Chem.*, **42**, 1483 (1970).
6. A. A. Rosen and F. M. Meddleton, *Anal. Chem.*, **31**, 1729 (1959).
7. J. F. Uthe, J. Reinke and H. D. Gesser, *Environ. Lett.*, **3**, 117 (1972).
8. G. J. Moody and J. D. R. Thomas, *Chromatographic Separation and Extraction with Foamed Plastics and Rubbers*, Dekker, New York, 1982.
9. T. Braun, J. D. Navratil and A. B. Farag, *Polyurethane Foam Sorbents in Separation Science*, CRC Press, Florida, 1985.
10. A. B. Farag, A. M. El-Wakil and M. S. El-Shahawi, *Fresenius' Z. Anal. Chem.*, **324**, 59 (1986).
11. A. B. Farag, M. S. El-Shahawi and A. M. El-Wakil, "A Comparative Study of the Concentration of Some Phenols by Loaded and Un-loaded Open Cell Polyurethane Foam", 2nd Chem. Conf., Fac. of Science, Mansoura Univ., Sept., 27–29, 1988.
12. T. Braun and A. B. Farag, *Anal. Chim. Acta*, **62**, 476 (1972).

(Received February 25, 1989)

(Accepted June 20, 1989)

Sensitive detection and semiquantitative determination of molybdenum(VI) using unloaded and specially treated polyurethane foams

A.B. FARAG, A.M.A. HELMY, M.S. ELSHAHAWI and S. FARRAG

Chemistry Department, Faculty of Science, Mansoura University, Mansoura, Egypt.

RÉSUMÉ

Détection sensible et détermination semi-quantitative du molybdène(VI) au moyen de mousses de polyuréthane spécialement traitées.

Des mousses de polyuréthane chargées de solution de phénylhydrazine dans le tétrachlorure de carbone en absence et en présence de tricapriline (plastifiant) ont été étudiées du point de vue de la détermination du molybdène dans des solutions aqueuses acides (pH voisin de 2). Dans des expériences de simple équilibre des quantités de molybdène aussi faibles que 0,05 et 0,1 ppm sont aisément détectées qu'il s'agisse de mousses avec ou sans plastifiant. En mode dynamique on détecte, avec percolation sur une colonne, des concentrations de molybdène aussi faibles que 0,002 et 0,025 ppm. L'intérêt des mousses de polyuréthane traitées ou non par la tricapriline pour l'extraction de Mo(VI) en milieu thiocyanate a été évalué. La détection du molybdène à des teneurs de 0,01 et 0,05 ppm est réalisée aisément avec des mousses chargées ou non, par simple équilibre. Dans les expériences en colonne, des teneurs aussi faibles que 0,003 et 0,005 ppm de molybdène sont aisément détectées. Des mesures semiquantitatives sont également possible. L'influence de divers ions éventuellement présents en solution est discutée.

Mots-clés : Molybdène (VI). Analyse de traces. Mousses de polyuréthane.

INTRODUCTION

Because of low abundance of molybdenum in natural waters, preliminary isolation methods have usually been employed in its determination. Solvent extraction [1, 2] sorption on modified cellulose [3], cation-exchange sorption on Zeokarb 225 [4] and on charcoal [5] are the most common methods for this purpose.

In recent years, polyurethane foams have been successfully employed to absorb many organic and inorganic species from aqueous, nonaqueous and gaseous media [6]. This method has been tested for the detection and semiquantitative determination of chromium (VI) [7], iron (II) [8], cobalt (II) [9], nickel (II) [10], lead (II) [11], silver (I) [12], copper (II) [13, 14], palladium (II) [14], mercury (II) [15], tin (II) [15] and cadmium (II) [15] in aqueous solution using polyurethane foam loaded with selective organic reagents. Squeezing

SUMMARY

Polyurethane foams loaded with phenylhydrazine solution in carbon tetrachloride in the absence or presence of tricapriline tertiary amine (plasticizer) have been examined for the determination of molybdenum in aqueous acidic solution (pH ca. 2). In static experiments as low as 0.05 and 0.1 ppm molybdenum were readily detected with phenylhydrazine plasticized and unplasticized foams, respectively. However, in the dynamic column extraction mode concentrations of 0.002 and 0.025 ppm molybdenum were easily detected with the plasticized and unplasticized foams, respectively. The analytical utility of untreated polyurethane foam and foam loaded with tricapriline tertiary amine solution for the selective detection of molybdenum (VI) in aqueous thiocyanate media have also been evaluated. The detection of 0.01 and 0.05 ppm of molybdenum is easily carried out using the loaded and unloaded foam, respectively, in batch extraction mode. In dynamic column experiment as low as 0.003 and 0.005 ppm of molybdenum were easily detected. The semi-quantitative determinations of molybdenum by the proposed foam detection methods have also been achieved. The effect of diverse ions present in aqueous solution together with molybdenum on the proposed foam tests have also been investigated.

Key-words : Molybdenum (VI). Trace analysis. Polyurethane foams.

and pulsating foam column methods have also been used [8, 15] to detect some metal ions. The detection and semiquantitative determination of alkylbenzene sulphonate from aqueous media containing crystal violet or methylene blue has been achieved with unloaded polyurethane foam [16].

In this work unloaded polyurethane foam and foam loaded with phenyl hydrazine and/or tricapriline tertiary amine were used for the selective and sensitive detection of very low concentrations of molybdenum (VI) in aqueous solutions.

EXPERIMENTAL

Reagents and materials

All reagents were of analytical-grade unless otherwise specified. An open-cell polyether-type polyurethane foam (bulk density 30 kg·m⁻³) was supplied by Greiner KG

Manuscrit reçu le 21 novembre 1988; accepté le 16 janvier 1989.

0.1 g of the solid reagent in 100 cm³ of carbon tetrachloride. Solution of 10% potassium thiocyanate was prepared in water. The reagent foam cubes were prepared by mixing the dried foam cubes with phenylhydrazine and/or tricaprylyl tertiary amine (3 cm³·g⁻¹ dry foam) with efficient stirring for 5 min. The loaded foam material is then dried between sheets of filter papers to remove the excess of the reagent solution and stored in stoppered bottles.

In the batch (static) experiments, one cube unloaded or loaded foam cube is mixed with 1-2 cm³ of the test solution for 2-3 min. The colour of the foam cube is changed from white to red-orange in the presence of molybdenum. The colour intensity is matched with the colour developed with a standard molybdenum solution.

In the column (dynamic) experiments, 0.4 g of the unloaded foam and/or 0.5 g of the loaded foam cubes were packed in a glass column 5 mm in diameter and 10 cm in length by the vacuum method of foam column packing [9]. The test solution is allowed to pass through the foam column at a flow rate of 5 cm³·min⁻¹. The length of the red coloured zone on the foam bed is then compared with those of standard series.

RESULTS AND DISCUSSION

Qualitative and semiquantitative determination of molybdenum in aqueous potassium thiocyanate media

Solutions of molybdates are coloured yellow by the addition of potassium thiocyanate and hydrochloric acid. If a small amount of stannous chloride solution is added, trivalent molybdenum will be obtained which combines with CNS⁻ ions to produce red, water-soluble complex H₂[Mo(CNS)₆] [17]. This colour reaction has been used for the detection of molybdenum in aqueous solution employing the usual spot test method. The detection limit of molybdenum by this spot reaction is 2 µg·cm⁻³ (i.e. 2 ppm). This reaction was tried with unloaded and tricaprylyl tertiary amine loaded foam to detect molybdenum. The relatively high available surface area of the foam cube, acts as an efficient collector for molybdenum present in the aqueous solution at low concentration. This together with the ease of observing the characteristic red colour of the reaction products on the thin membranes of the foam material allowed the detection of molybdenum ion in dilute aqueous solutions.

On shaking one cube of foam loaded with tricaprylyl tertiary amine or the unloaded foam with 1-2 cm³ of acidic aqueous thiocyanate solution containing stannous chloride, it was possible to detect as low as 0.01 and 0.05 ppm of molybdenum, respectively. In agreement with the previous studies [7-9], these results are better than that reported by the conventional spot test method (2 ppm) [17].

To examine the selectivity of the proposed foam test, the detection of 1 µg of molybdenum in the presence of a relatively high excess (10 mg) of each Ba²⁺, Mg²⁺, Cd²⁺, La³⁺, Ca²⁺, Sr²⁺, HPO₄²⁻, C₂O₄²⁻, Br⁻, VO₃⁻, I⁻, F⁻, NO₃⁻, tartrate, formate and acetate was successfully carried out as in the usual spot test. In the presence of

Foreign ion	Compound added	Tolerance limit*	Note
Pb(II)	Pb(NO ₃) ₂	1 : 2 × 10 ¹	Drops of conc HNO ₃ were added
Fe(II)	FeSO ₄ (NH ₄) ₂ SO ₄	1 : 1 × 10 ⁴	One crystal of KF was added
Fe(III)	Fe ₂ (SO ₄) ₃	1 : 1 × 10 ⁴	One crystal of KF was added
Cu(II)	CuSO ₄ ·5H ₂ O	1 : 1 × 10 ⁴	Crystals of KI were added, Followed by the addition of Na ₂ S ₂ O ₃ crystals.
Cr(III)	CrCl ₃ ·6H ₂ O	1 : 1 × 10 ⁴	Oxidation by bromine water was carried out and excess eliminated by heating
MnO ₄ ⁻	KMnO ₄	1 : 1 × 10 ⁴	Crystal of sodium azide was added

also allows the simple determination of the amount of molybdenum (Table 1).

Using the loaded and unloaded foam tests, it was possible to determine molybdenum semiquantitatively by comparison of the colour of the foam cube with standards 0.05, 1, 5, 10 and 20 ppm molybdenum solution prepared under the same experimental conditions. The proposed foam test was examined for the detection of molybdenum in the Nile water spiked with molybdates and satisfactory results were obtained.

The proposed loaded foam cubes can be easily packed in columns producing foam bed suitable for the detection and semiquantitative determination of molybdenum in extremely dilute aqueous solution. This was achieved by percolating 100 cm³ of the test solution through the foam column at a reasonable flow rate (5 cm³·min⁻¹). The detection limit of molybdenum in this column method was found to be 5 ppb. The length of the red coloured zone is proportional of the concentration of molybdenum. Semiquantitative determination was possible using a colour scale covering the concentration from 5 to 50 ppb.

Qualitative and semiquantitative determination of molybdenum in aqueous solution with phenylhydrazine loaded foam

Molybdate in acid solution give a blood-red colour at very low concentration or red precipitate with phenylhydrazine [17]. The chemistry of the reaction has not been fully explained, probably the phenylhydrazine is oxidized by molybdic acid to the diazonium salt which undergoes coupling with the excess phenylhydrazine. The latter may bind the molybdenum present in the aqueous solution [17]. This reaction was carried out to detect molybdenum in aqueous solution using spot plate and spot paper with detection limits 6.4 and 2.6 ppm, respectively [17]. Polyurethane foam loaded with phenylhydrazine solution in carbon tetrachloride or tricaprylyl amine have been tested for detecting molybdenum. As low as 0.01 and 0.1 ppm molybdenum were easily detected from aqueous solution using

henylhydrazine plasticized and unplasticized foam cubes, respectively.

The proposed phenylhydrazine chromofoam test was successfully employed to detect 1 µg molybdenum in the presence of up to 10 mg of Li⁺, Al³⁺, As³⁺, Cd²⁺, CNS⁻, Ba²⁺, Mg²⁺, Ca²⁺, Sr²⁺, HP₄²⁻, CO₃²⁻, Br⁻, I⁻, F⁻, NO₃⁻, tartrate, formate, acetate and vanadate. For some other ions, only slight modification of the aqueous solution is needed before the addition of the

reagent foam cube (Table I).

Semiquantitative determination of molybdenum was also possible using colour scale 0.05, 0.1, 1, 10 and 20 ppm. Smaller amounts of molybdenum (2 ppb) were easily detected by passing 100 cm³ of the aqueous solution through a column packed with 0.4 g of the reagent foam. Semiquantitative determination of molybdenum was also possible using the colour scale 2, 10, 20, 30 and 40 ppb at a flow rate of 5 cm³·min⁻¹.

REFERENCES

- [1] CHAN (K.M.), RILEY (J.P.). — *Anal. Chim. Acta*, 1966, 36, 220.
- [2] BUTLER (L.R.P.), MATTHEWS (P.M.). — *Anal. Chim. Acta*, 1966, 36, 319.
- [3] MUZZARELLI (R.A.A.), ROCCHETTI (R.). — *Anal. Chim. Acta*, 1973, 64, 371.
- [4] FICKLIN (W.H.). — *Anal. Lett.*, 1982, 15, 865.
- [5] KIRIYAMA (T.), KURODA (R.). — *Talanta*, 1984, 31, 472.
- [6] BRAUN (T.), NAVRATIL (J.D.), FARAG (A.B.). — *In Polyurethane Foam Sorbents in Separation Science*, CRC, Florida, 1985.
- [7] FARAG (A.B.), ELWAKIL (A.M.), ELSHAHAWI (M.S.). — *Analyst* (London), 1981, 106, 809.
- [8] FARAG (A.B.), ELWAKIL (A.M.), ELSHAHAWI (M.S.). — *Ann. Chim. (Rome)*, 1982, 72, 103.
- [9] BRAUN (T.), FARAG (A.B.). — *Anal. Chim. Acta*, 1974, 73, 301.
- [10] FARAG (A.B.), ELWAKIL (A.M.), ELSHAHAWI (M.S.). — *Talanta*, 1982, 29, 789.
- [11] FARAG (A.B.), ELWASEEF (A.), ABDEL-RAHMAN (M.H.). — *Acta Chim. Hung.*, 1986, 122, 273.
- [12] FARAG (A.B.), ELWAKIL (A.M.), HASSOUNA (M.E.M.), ABDEL-RAHMAN (M.H.). — *Anal. Sci.*, 1987, 3, 541.
- [13] BRAUN (T.), FARAG (A.B.). — *Anal. Chim. Acta*, 1974, 73, 301.
- [14] FARAG (A.B.), MORSI (M.A.), IBRAHIM (S.A.). — *Ind. J. Chem.*, 1986, 25A, 882.
- [15] SRIKAMESWARAN (K.), GESSER (H.D.). — *J. Envi. Sci. Health*, Part A, 1978, 13, 415.
- [16] TANAKA (T.), HIRO (K.), KAWAHARA (A.). — *Bunseki Kagaku*, 1973, 22, 320.
- [17] FEIGL (F.). — *Spot Tests in Inorganic Analysis*, 5th ed. Elsevier, Amsterdam, 1958.

The Extraction and Recovery of Some Organic Amines from Aqueous Solution by Polyurethane Foam

A.B. Farag, M.S. EL-Shahawi, A.M. EL-Wakil and M.N. Abbas *

Chemistry Department, Faculty of Science, Mansoura University, Mansoura, and * National Research Centre, Dokki, Cairo, Egypt.

Polyurethane foams (1-3) which are recently introduced as solid polymeric extractants apparently concentrate various species in solution by the phase distribution mechanism rather than adsorption (4,5). Other concentration techniques are either slow or cumbersome and / or expensive for routine usage where many large volume samples are concentrated at the site prior to quantitative analysis (6).

The object of the present work was to evaluate the potential of polyurethane foam as an extractor for the concentration of some aromatic amines and to establish the mechanism of extraction by the unloaded foam and the conditions where optimum recoveries and precision could be obtained at room temperature. The effect of some important factors such as contact time, pH, aromatic amine concentration, extraction media, flow rate and eluting solvent were also investigated.

Experimental

Reagents and materials : All chemical used were of analytical grade and the solvents were of spectroscopic grade.

Polyurethane foam, polyether type (bulk density 30 kg / m^3) was supplied by Greiner KG, Schaumstoffwerk, Kremsmunster, Austria. The foam was cut into cubes (5 mm edge), washed and dried as previously described (7). Tributyl phosphate (TBP) - loaded foam was prepared by mixing the dried foam pieces with 5% TBP solution in benzene ($3 \text{ cm}^3 / \text{g}$ dry foam) with efficient stirring for 10 min. The reagent foams were then dried between some sheets of filter paper to remove the excess reagent solution. The aromatic amines tested were : aniline; 2-chloroaniline; 3-chloroaniline; 4-chloroaniline, 4-nitroaniline; 4-bromoaniline; o-phenylenediamine; m-phenylenediamine and p-phenylenediamine. A stock solution of each compound containing 1 mg / cm^3 was prepared in 250 cm^3 measuring flask by dissolving the exact weight of the aromatic amine in 5 cm^3 hot ethanol and diluting with distilled water to the mark. A series of standard solutions of these compounds were prepared by diluting their stock solutions with water. All the solutions were stored in polyethylene bottles.

Apparatus : A double - beam spectrophotometer, Varian DMS 634 with 1 cm quartz cell was used for the absorbance measurements. Glass columns of 15 mm diameter and 15 cm length were used .

Recommended Procedures

Batch experiments : The effect of shaking time on the uptake of the compounds tested on polyurethane foam was studied.

In these experiments, 0.4g of dry foam was shaken with 100 cm³ aqueous solution of each compound (100 µg/cm³) in a mechanical shaker for different time intervals. After shaking the concentration of the compound remaining in the aqueous solution was measured spectrophotometrically at the wavelength of maximum absorption .

Following this procedure, the effect of pH and extracting media on the extraction efficiency was also studied .

Extraction isotherm. : In separate batch experiments, 0.4 g of dry foam was mixed with 100 cm³ solution of each aromatic amine (20-100 mg/cm³) in a series of stoppered polyethylene bottles of 250 cm³ capacity which were shaken for 2 hr in a mechanical shaker. The compound that remained in the aqueous solution was determined spectrophotometrically and the amount of the compound retained on the foam was calculated by difference.

Flow experiments : Tap or distilled water (0.5-3 dm³) containing 2 mg of each aromatic amine was percolated separately through the foam column (containing 2 g dry foam) prepared by the vacuum method of packing (8) , at different flow rates (5-10cm³ / min). After passing the solution through the foam column water was squeezed from the foam material and the organic compound was recovered with 100cm³ acetone in a soxhlet extractor. The elute is then analysed by measuring the absorbance of the solution at the wave maximum against ethanol solvent as a blank.

Results and Discussion

A study of the effect of shaking time on the extraction of the aromatic amines tested was carried out using unloaded polyurethane foam in batch extraction experiments . 10 mg of each aromatic amine in 100 cm³ aqueous medium were shaken with 0.4 g unloaded foam for different time intervals. The results obtained are summarized in Fig. 1. As it is evident from the curves of this figure, the uptake of the compounds tested by the foam has increased sharply in a period of 10 min ; and then reaches a plateau indicating that the extraction of these compounds with the foam is quite rapid suggesting the possible application of polyurethane foam in column extraction mode for the extraction of these amines at reasonable flow-rates.

The effect of pH on the extraction of the amines tested has been studied . Hydrochloric acid or sodium hydroxide solutions were used to adjust the pH to the required values. 100 cm³ of sample solution of each compound containing 10 mg of the amine tested was shaken for 30 min. The results obtained for some of the aromatic amines are summarized in Fig. 2. Generally, the extraction of 4-bromoaniline, p-phenylenediamine, p-nitroaniline and o-phenylenediamine is slightly increased with pH up to pH 9. At pH values higher than 9 the extraction of p-phenylenediamine and p-nitroaniline is drastically decreased, while that of o - phenylenediamine is only slightly decreased. In contrary the extraction of 4-bromoaniline is increased at pH values higher than 9.

Regarding the effect of the presence of ethanol in aqueous solution, it has been found that the efficiency and rate of extraction of the amine examined by the unloaded polyurethane foam are generally decreased by the addition of ethanol to the aqueous amine solution. This is probably due to formation of sorption inactive (lipophile association) in the aqueous solution⁽⁹⁾. It has been also found that the uptake of the compounds in aqueous solution (pH 6.3 -7.8) on the unloaded foam depends on the concentration of the tested species. Thus, in separate experiments, extraction isotherms were followed over a wide range of equilibrium concentrations (20-100 mg. cm³) for each compound. The results obtained are presented in Fig.3. Obviously, the extraction isotherms are quite linear over a wide range of amine concentration.

For phenylenediamines tested, Fig. 3A shows that the extraction efficiency is decreased in the order of p-phenylenediamine > m-phenylenediamine > o-phenylenediamine. Note mentioning is that the extraction efficiency is decreased with the decrease in the dielectric constant of the amine examined.

The extraction isotherms of aniline and of the other five aniline derivatives from aqueous solution are illustrated in Fig. 3B. As it is clear from the curves of this figure the extraction efficiency is increased in the order: aniline < 3-chloroaniline < 2-chloroaniline < 4-nitroaniline < 4-bromoaniline; that is the larger the molecular weight of the absorbate, the better is the extraction efficiency of the aniline derivative.

To investigate the mechanism of extraction of these compounds by unloaded polyurethane foam, the extraction isotherms of these amines in aqueous solution on TBP-loaded polyurethane foam were determined under otherwise the same experimental condition. The results obtained are exactly the same as those obtained with unloaded foam, suggesting that the solvent extraction mechanism is the most probable mechanism for the removal of the amines tested with unloaded polyurethane foam.

The results obtained for the extraction properties of the aromatic amines tested in aqueous solution with unloaded polyurethane foam suggest the possible application of polyurethane foam in column extraction mode for quantitative collection and recovery of these compounds from aqueous media. Distilled or tap water samples of 0.5-3dm³ of each compound (2mg) is percolated through separate foam column at a flow rate of 5-10 cm/min which was chosen on the bases of preliminary tests. All the compounds are more or less completely retained on the foam column except in the case of aniline, o-phenylenediamine and m-phenylenediamine, where it was necessary to use lower flow rates (2-3 cm³ / min) for complete extraction. After squeezing water from the foam the amine retained in the foam was recovered with 100 cm³ ethanol by soxhlet extraction for 2 hr. The effluent was then analysed spectrophotometrically. The results obtained for the extraction and recovery of the compounds tested from 3 litres of aqueous solution using the proposed foam column are summarized in Table 1.

TABLE 1. Extraction and recovery of the aromatic amines tested from three litres aqueous solution by unloaded polyurethane foam column.

Absorbance	% Recovery		Wavelength (mm)
	A	B	
4 - Bromoaniline	85.6	89.7	296
4 - Nitroaniline	80.7	87.6	375
p - Phenylenediamine	92.6	95.6	315
4 - Chloroaniline	79.6	68.4	295
3 - Chloroaniline	82.7	80	292
m - Phenylenediamine	90	84.7	293
2 - Chloroaniline	92.6	90	291
Aniline	95.6	90	287.5
o - Phenylenediamine	92.6	90.6	289

A - Average of duplicate determination from distilled water .

B - Average of duplicate determination from tap water .

References

- 1- Moody, G.J. and Thomas, J.D.R. " *Chromatographic Separation and Extraction with Foamed Plastics and Rubbers*", Dekker, New York (1982).
- 2- Braun, T., Navratil, J.D. and Farag, A.B. " *Polyurethane Foam Sorbents in Separation Science* ", CRC Press, Inc., Boca Rotan, Florida (1985).
- 3- Afghan, B.K., Wilkenson, R.J., Chow, A., Findly, T.W., Gesser, H.D. and Srikameswaran, K.I., *Water Res.*, 18,9 (1984) .
- 4- Bown, H.J.M., *J.Chem. Sec. A*, 1082 (1970) .
- 5- Ough, K.M.G. and Gesser, H.D., *J. Chromatogr.* 115 , 383 (1975) .
- 6- Uthe, J.F., Reinke, J. and Gesser, H.D., *Environ. Lett.*3, 117 (1972) .
- 7- Farag, A.B., EL-Wakil, A.M. and EL-Shahawi, M.S., *Analyst* (London) 106, 809 (1981).
- 8- Braun, T. and Farag, A.B., *Anal. Chem. Acta.* 62, 476 (1972) .
- 9- Hayashita, T. and Takagi, M., *Talanta*, 32 , 399 (1985) .

(Received 16 / 8 / 1989) .

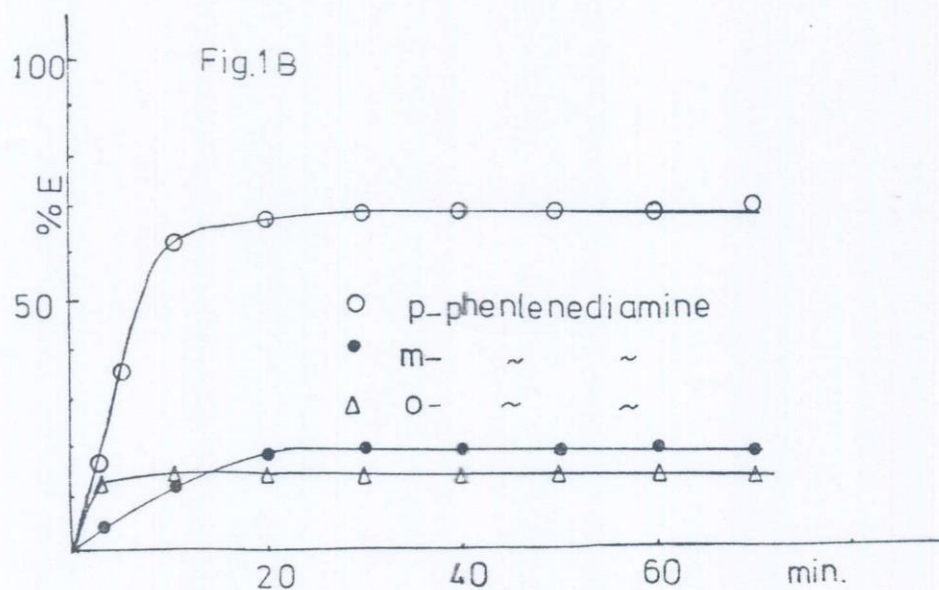
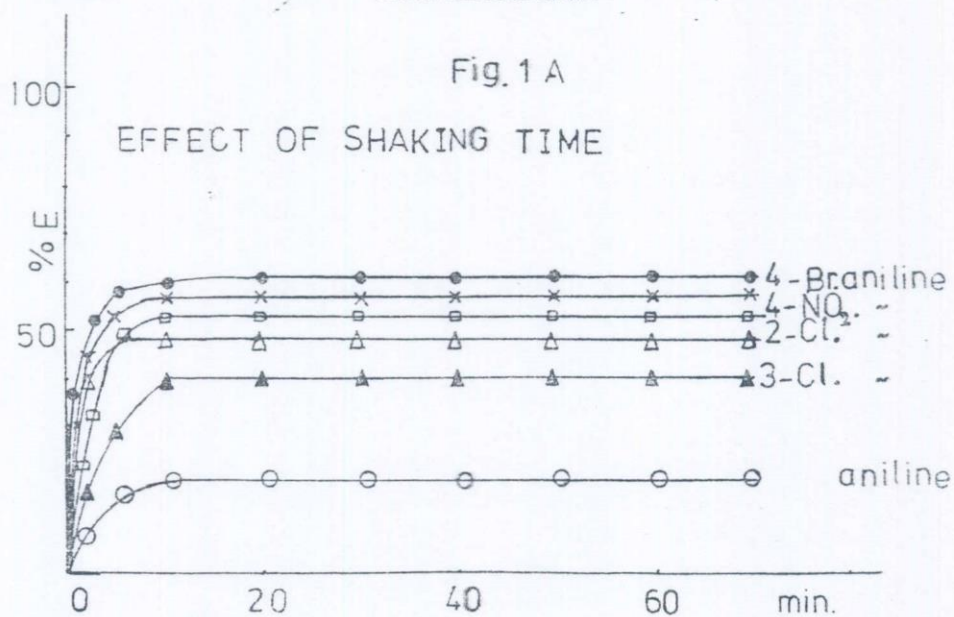


Fig. 1. Effect of shaking time
 A. Phenylenediamine derivatives
 B. Aniline derivatives
 Sample volume 100 cm³
 Weight of dry foam 0.4 g

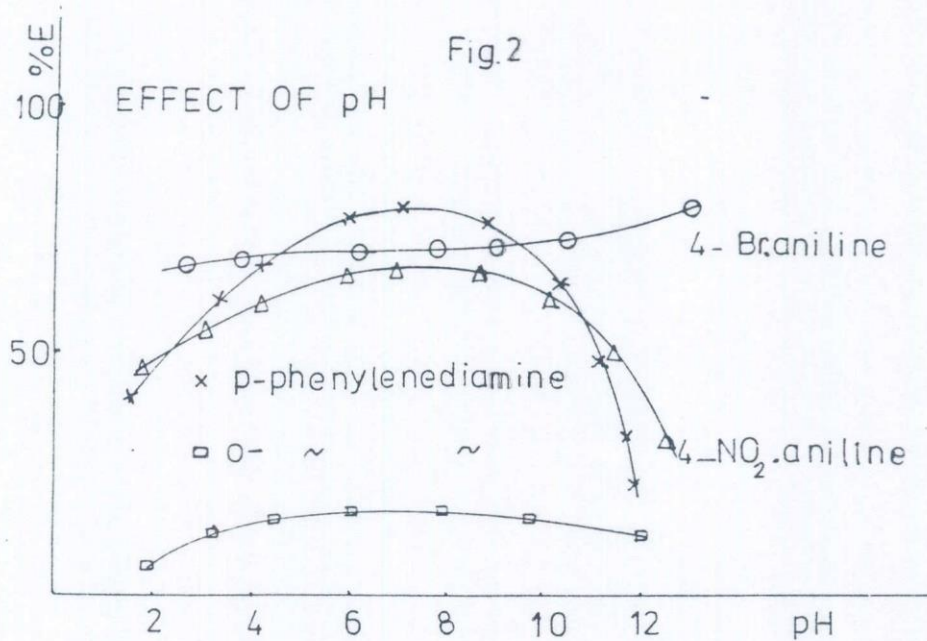


Fig. 2. Effect of pH
Sample volume 100 cm³
Weight of dry foam 0.4 g
Shaking time 2 hr

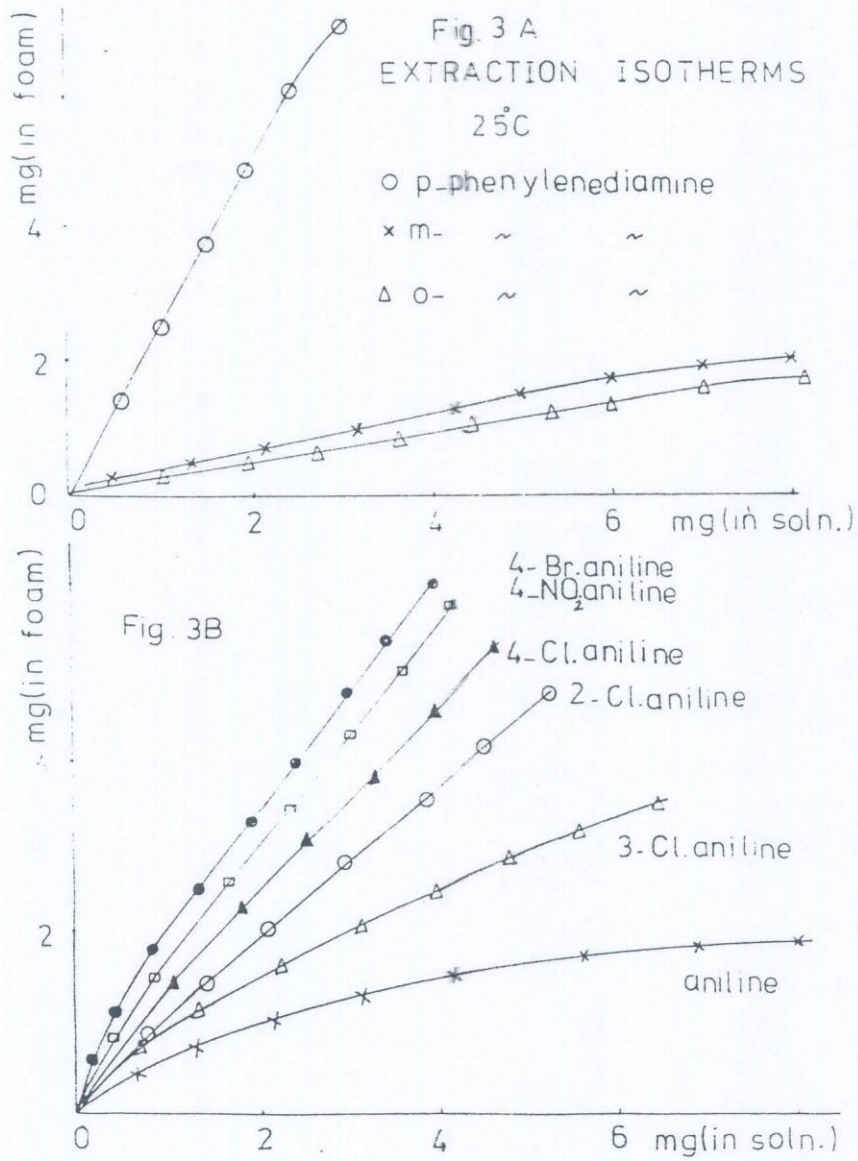


Fig. 3. Extraction isotherms
A. Phenylenediamine derivatives
B. Aniline derivatives
Sample volume 100 cm³
Weight of dry Foam 0.4 g
Shaking time 2 hr
Temp. 25 °C.

Collection and Recovery of Some Mono- and Di - Carboxylic Acids on Polyurethane Foam

A.B. Farag, A.M. El-Wakil, M.S. El-Shahawi, and M.N. Abbas*

*Chemistry Department, Faculty of Science, Mansoura University and *National Research Centre, Dokki, Cairo, Egypt.*

The removal or reduction of organic pollutants to an acceptable concentration either by extraction with organic solvents, steam distillation, oxidation reaction or adsorption on carbon has been investigated (1-3).

Recently, several authors have proposed open cell polyurethane foam as an inexpensive solid extractor and effective sorbent for the removal of water pollutants (4-8).

The membrane like structure of these foams together with efficient sorption properties offered many advantages over other solid collectors as they allow higher concentrating ability compared with the other solid materials which depend only on adsorption (9,10).

The present work is devoted to investigate the sorption of some mono- and dicarboxylic acids at very low concentration from aqueous solution on polyurethane foam and establish the conditions where good recoveries and increased precision could be obtained at room temperature.

Experimental

Reagents and Materials

All chemicals used were of analytical grade. Polyurethane foam of polyether type (bulk density 30kg/m^3) was supplied by K.G. Schaumstoffwerk-Kremsmunster, Austria.

The foam material was cut as cubes of 5mm edge and then washed and dried at 80° as described previously (6). Tertiary amine and tributyl phosphate loaded foams were prepared by mixing the dry foam cubes with tricaptyl tertiary amine solution or 5% solution of TBP in benzene, 5cm^3 per each gram of dry foam, respectively, for 10 min.

The excess reagents were removed by drying the foam cubes between two sheets of filter paper. The organic acids tested were gallic, lactic, mandelic, oxalic, succinic, tartaric, acetic, aminoacetic (glycine), iodoacetic, and trichloroacetic acids. Stock solutions containing 1mg/cm^3 of each compound were prepared in distilled water. A series of standard solutions of these compounds were prepared by diluting their stock solution with water. All solutions were stored in polyethylene bottles.

Apparatus

An Orion pH meter was used for pH measurements.

A Varian DMS 634 double beam spectrophotometer was used for measuring the absorbance.

Glass columns of 15 mm diameter and 15 cm length were used for dynamic experiments.

Recommended Procedure

1 - Batchwise experiments

To investigate the effect of shaking time, polyurethane foam cubes (0.4 g) were equilibrated with 100 cm³ of the aqueous solution of each acid (100 µg/cm³) in separate polyethylene bottles and shaken with a mechanical shaker for different time intervals up to 2 hr, then the foam cubes were separated by decantation and the organic acid remained in solution was measured spectrophotometrically at the optimum wavelength. The carboxylic acid collected on the foam was calculated by difference.

The effect of pH of solution on the extraction efficiency of the carboxylic acids tested was investigated, hydrochloric acid or sodium hydroxide solutions were used to adjust the pH of sample solution to the desired value.

The effect of ethanol / water ratio on the extraction efficiency has also been studied.

2 - Extraction isotherm

In separate batch experiments, polyurethane foam cubes (0.4 g) were shaken with 100 cm³ of each compound (20-100 µg/cm³) in aqueous solution at the optimum pH in stoppered flasks for 2 hr.

The organic acid remained in solution after separating the foam cubes was measured spectrophotometrically and the amount retained in the foam was calculated by difference.

3 - Flow experiments

Tap or distilled water (2-3 dm³) samples containing 250 µg of each compound was percolated through the foam column (containing 0.4 g of dry foam) prepared by the vacuum method of foam column packing, at a flow rate of 5-10 cm³/min.

After squeezing water from the foam material, the compound was recovered from the foam with 100 cm³ acetone or ethanol in a soxhlet extractor and the sample was measured spectrophotometrically after being concentrated in a rotary evaporator to 10 cm³.

Results and Discussion

The introduction of porous polyurethane foam as a cellular sorbent for high volume water or air samples has been proven advantageous due to its easy handling and clean up and its high ability to sorb many different organic and inorganic species. The use of polyurethane foam as sorbent material allow the simple isolation of the analyte from the matrix and yields an appropriate enrichment factor. The excellent hydrodynamic properties of the foam column allow the application of a quite high flow rates without the need to use vacuum, while the rapid attainment of the sorption equilibrium in the thin membranes forming the foam material reduces the time required for analysis.

In this study the use of unloaded, TBP-loaded and tricaprlyl amine-loaded polyurethane foam for the extraction of some mono-and dicarboxylic acids has been investigated, ten acids were used in this study namely, acetic, aminoacetic (glycine), iodoacetic, trichloroacetic, gallic, lactic, mandelic, succinic, oxalic and tartaric acids.

The effect of shaking time on the extraction of the compounds tested was carried out with unloaded foam using batch experiments.

The results are shown in Fig. 1, where it can be seen that the percentage extraction of almost all the tested compounds increases with time and reaches a plateau after about 2 hr.

Extraction isotherm

The uptake of the compounds tested from aqueous media by the foam was found to depend on the concentration of the examined compound. Fig. 2 and Fig. 3 show that sorption isotherms of the tested compounds using unloaded and amine loaded foams are linear over a wide concentration range. The sorption of the different acids by unloaded foam increases in the order tartaric > oxalic > succinic for dicarboxylic acids, while for the monocarboxylic acids the sequence is mandelic > glycine > gallic > iodoacetic > trichloroacetic > lactic. It is worth to note that the extraction efficiency increases with the increase in pKa and molecular weight of the absorbate .

Discrepancies was observed in the case of oxalic acid which has higher acidity and lower molecular weight as compared with succinic acid.

In the case of the amine loaded foam, the sequence of extraction efficiency is found to be : oxalic > tartaric > succinic for dicarboxylic acids, while that for monocarboxylic acids is trichloroacetic > iodoacetic > mandelic > lactic > gallic > acetic > glycine .

Obviously the acidity of the absorbate (pKa) play an important role in determining the absorption efficiency in the amine - loaded foam, while this is not the case with unloaded foam where the extraction efficiencies decrease with increasing the acidity .

These results suggest that the mechanism of sorption of these acids by unloaded polyurethane foam is most probably solvent extraction, and the anion exchange mechanism is completely excluded.

This was confirmed by investigating the extraction of some of these acids with TBP-loaded foam. The sequence of the extraction efficiency is found to be : mandelic > glycine > gallic > iodoacetic > trichloroacetic > lactic, which is similar to that of unloaded foam.

The effect of pH on the extraction efficiency of some of the tested acids with unloaded foam was carried out over the pH range 2-9. The sorption profiles of these acids from aqueous media by the unloaded foam are shown in Fig. 4.

The percentage extraction of almost all the tested compounds was found to increase with increasing the pH and reaches a plateau at about pH=7.

In establishing the effect of organic solvents on the extraction of some carboxylic acids from aqueous media with unloaded foam, various proportions of ethanol-water were used as mixed solvent, and mandelic acid was used as example .

The results are shown in Fig .5, where increasing the ethanol proportion is found to increase the extraction efficiency .

Flow experiments

The extraction of the carboxylic acids via batch experiments showed that the unloaded foam extracts efficiently these compounds from water. On this basis, the possible application of unloaded polyurethane foam in column extraction mode for the quantitative collection and recovery of the tested compounds was attempted. Three litres solution of each compound (two samples were prepared for each compound, in distilled and tap water) were percolated through the foam column at a flow rate of $3-5 \text{ cm}^3 \cdot \text{min}^{-1}$. More or less complete retention of the compounds tested are observed in the foam column .

The compounds were then recovered from the foam column with 100 cm^3 of ethanol or acetone in a soxhlet extractor and their concentrations were measured spectrophotometrically after being concentrated to 10 cm^3 .

The percentage recoveries of the tested compounds from aqueous media using the proposed foam column method are summarised in Table 1 .

References

- 1 - Romano, A. H. and Safferman, R. S., *J. Amer. Water, Works Assoc.* 55, 169 (1963).
- 2 - Oda, H., Kishida, M. and Yokokawa, C., *Carbon* 19 ,243 (1981).
- 3 - Ode, H., Yokokawa, C. ,*Carbon* 21 ,485 (1983) .
- 4 - Braun, T., Navratil, T. D. and Farag, A. B. " *Polyurethane Foam Sorbents in Separation Science* ," CRC Press, Inc., Boca Raton, Florida (1985) .
- 5 - Moody, G. J., Thomas ,J. D. R. " *Chromatographic Separation and Extraction with Foamed Plastics and Rubbers* ," Dekker, New York (1982) .
- 6 - Farag, A. B., Elwakil, A. M. and El - Shahawi, M. S., *Fres. Z. Anal. Chem.*, 324, 59 (1986) .
- 7 - Farag, A. B., Elwakil, A. M., El - Shahawi, M. S. and Mashaly, M., *Anal. Sci. Japan*. (*accepted for publication*).
- 8 - Farag, A. B., El - Shahawi, M. S. and Elwakil, A. M., A paper presented in *The 2nd National Conference*, Faculty of Science, Mansura University 27 - 29 Sep.(1988).
- 9 - Kirkwood, K. G., *J. Chem. Phys.* 2 , 351 (1934).
- 10 - Weast, R. C. " *Hand Book of Chemistry and Physics* " 54 th ed., CRC press (1973).

(Received 10 / 8 / 1989) .

TABLE 1. Extraction and recovery of the compounds tested (250 μ g)from 3 dm aqueous solution by unloaded polyurethane foam columns at 3-5 cm / min flow rates .

Compound	% Recovery		Wavelength Eluting	
	a	b	(nm)	Solvent
Mandelic acid	92	84	252	Ethanol
Tartaric acid	94	89	208	Acetone
Succinic acid	86	87	208	Acetone
Oxalic acid	90	83	250	Ethanol
Lactic acid	94	90	210	Ethanol
Gallic acid	80	76	272	Ethanol
Trichloroacetic acid	92	90	256	Ethanol
Iodoacetic acid	74	84	270	Ethanol
Acetic acid	70	76	208	Acetone
Glycine	89	84	285	Ethanol

a - Average of duplicate determinations from distilled water .

b - Average of duplicate determination from tap water .

Fig. 1a

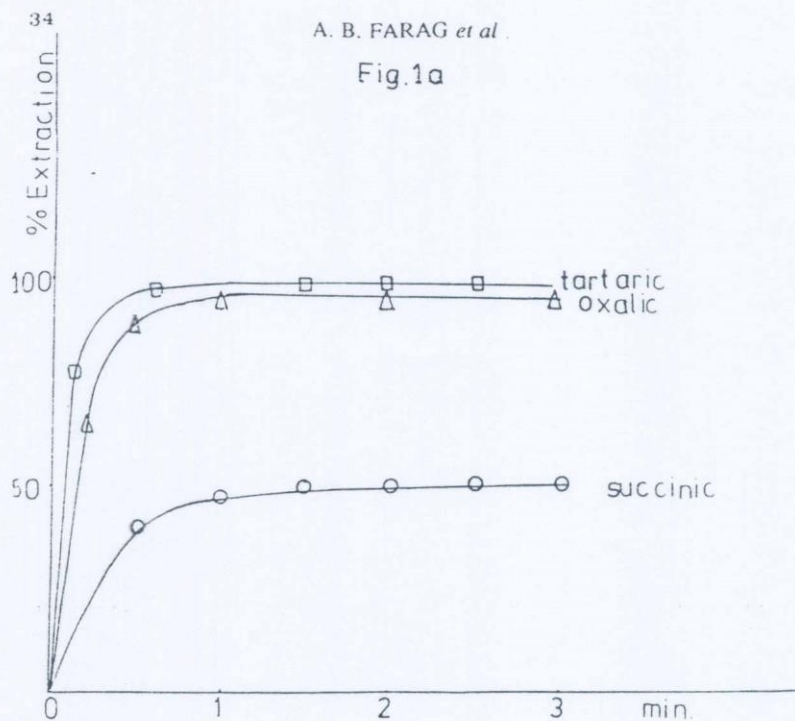


Fig. 1b

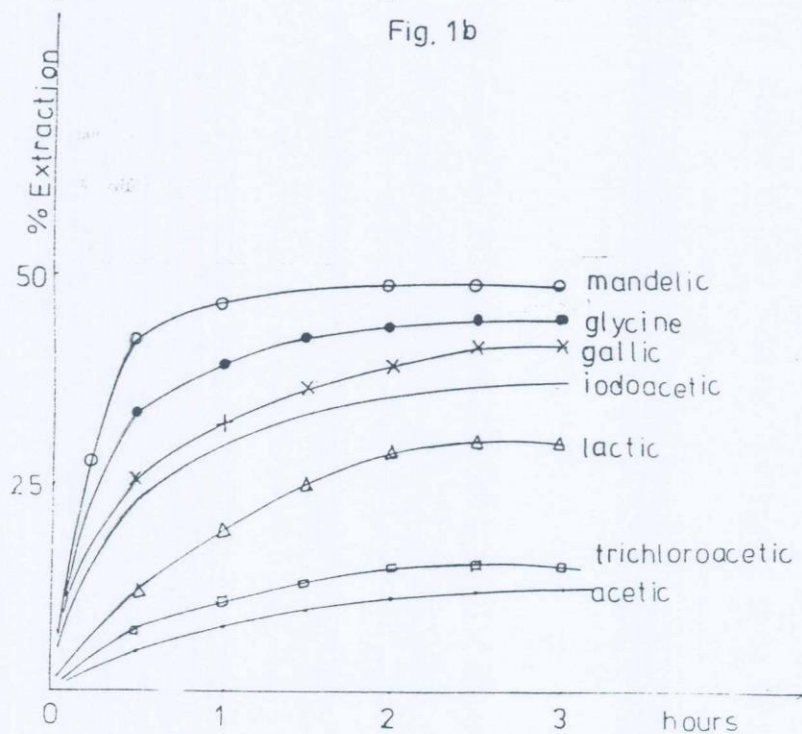


Fig. 1. Effect of shaking time
 A. Dicarboxylic acids
 B. Monocarboxylic acids
 Sample volume 100 cm³
 Weight of dry foam 0.4 g.

COLLECTION AND RECOVERY OF SOME MONO-AND DI-CARBOXYLIC ACIDS ...

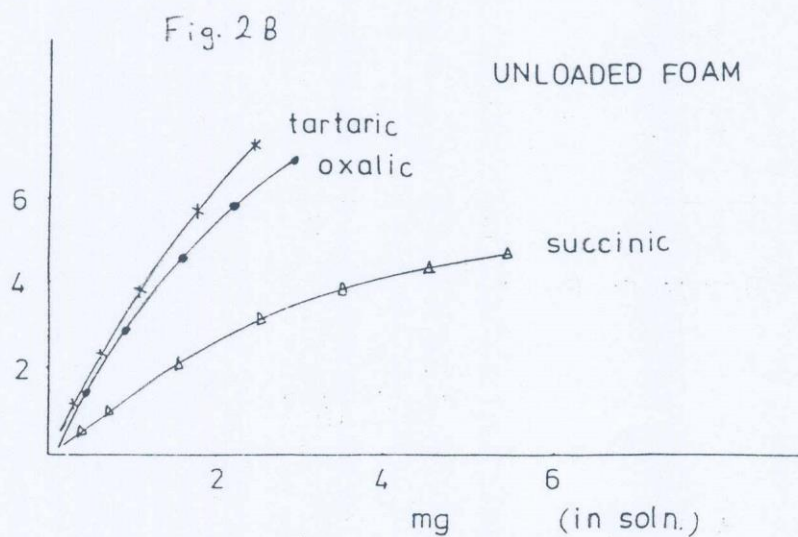
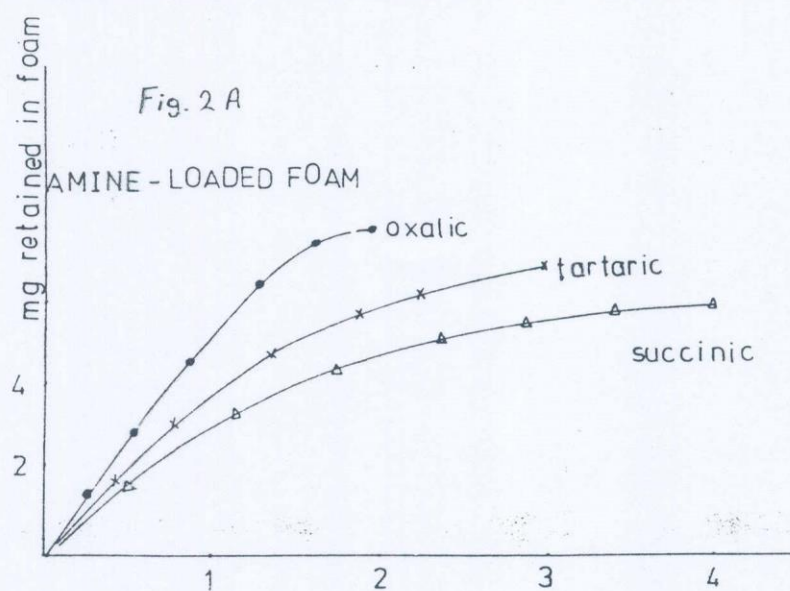


Fig. 2. Extraction isotherms / Dicarboxylic acids

A. Amine loaded foam

B. Unloaded foam

Sample volume 100 cm³

Weight of foam 0.4 g

Shaking time 2 hr.

Temp. 25 °C

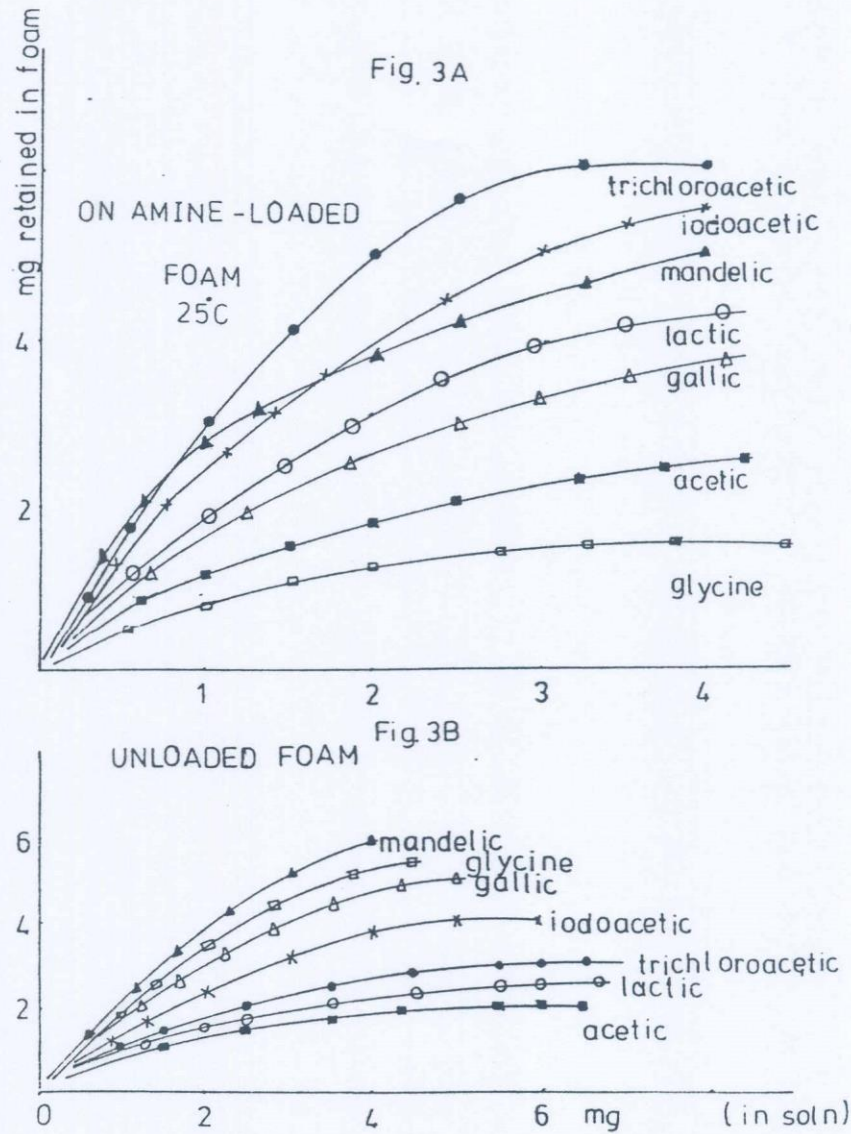


Fig. 3. Extraction isotherms/ Monocarboxylic acids

A. Amine-Loaded foam

B. Unloaded foam

Sample volume 100 cm³

Weight of foam 0.4 g

Shaking time 2 hr

Temp. 25 °C

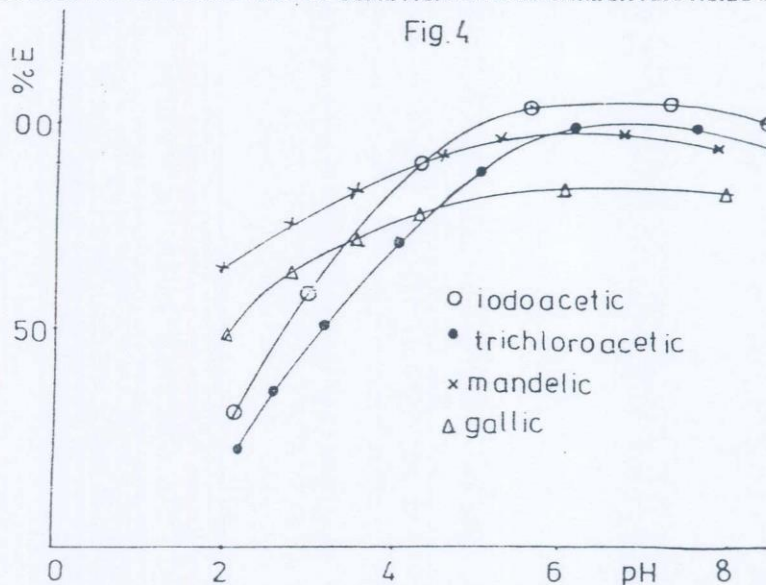


Fig. 4. Effect of pH
Sample volume 100 cm³
Weight of foam 0.4 g.
Shaking time 2 hr.

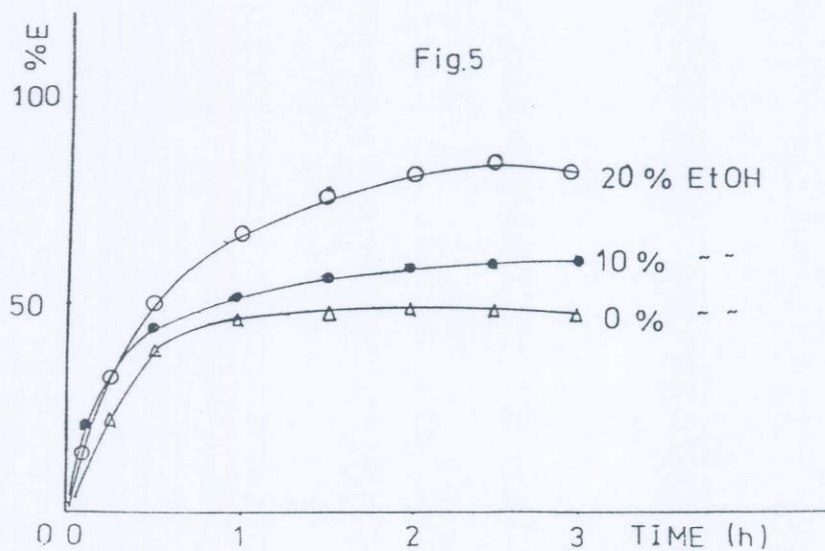


Fig. 5. Effect of ethanol
Sample volume 100 cm³
weight of foam 0.4 g.

REMOVAL OF ORGANIC POLLUTANTS FROM AQUEOUS SOLUTION.
Part II: A COMPARATIVE STUDY OF THE CONCENTRATION OF SOME
PHENOLS BY LOADED AND UNLOADED OPEN CELL POLYURETHANE FOAMS

A.B. Farag, M.S. El-Shahawi* and A.M. El-Wakil

Chemistry Department, Faculty of Science, Mansoura
University, Mansoura, Egypt

*Chemistry Department, Faculty of Science, Mansoura
University, Domiatt, Egypt

ABSTRACT

The attraction of using foamed cellular materials in batch and column techniques for the extraction and separation lies in their good absorption characteristics and favourable hydrodynamic and aerodynamic properties. Thus, in this investigation, the concentration of some dissolved phenols in aqueous media was carried out by unloaded open cell polyurethane and loaded foams. The results of preliminary batch screening test comparing the total phenols removed by the foam indicated that, a reasonable percent of phenols were retained on the foam. Therefore, attempts were made to extract these compounds from aqueous media using foam columns. Various parameters affecting the separation of these compounds have been investigated including the flow rate, volume of the sample and the eluting solvent. Complete extraction and recovery of these compounds from the foam material with organic solvents in a Soxhlet extractor were obtained. The extraction of phenols from natural waters was also carried out and the method can be adapted to analyse the dissolved phenols in environmental samples.

INTRODUCTION

Phenol and phenol-like compounds represent a class of manmade environmental pollutants which also occur naturally in the environment. The main source of these are the combustion processes and chemical factories. So, regulations concerning waste water containing phenols have been issued in many countries¹⁻³. Therefore any excess of phenols in waste water must be removed, either by extraction, steam distillation, adsorption method or oxidation reactions.

by diluting their stock solutions with water. All the solutions were stored in polyethylene bottles.

Procedure

Extraction isotherm. In separate experiments polyurethane foam (0.3 g) was shaken with 50 cm³ of each phenol (20–100 µg.cm⁻³) in polyethylene flasks (100 cm³ capacity). After 3-hrs shaking in a mechanical shaker, the aqueous solution is separated and the unextracted phenol was determined spectrophotometrically at the optimum wavelength. The concentration of the compound retained on the foam was obtained by difference.

Dynamic flow experiment. Tap or distilled water (3 dm³) containing 200 µg of each phenolic compound is percolated through the foam column (containing 0.4 g foam) prepared by the vacuum method foam packing¹² at a flow rate of 5–10 cm³ min⁻¹. After squeezing water from the foam material, the compound is recovered from the foam with 120 acetone in a Soxhlet extractor. *β*-naphthol and resorcinol were recovered from the foam with 100 cm³ ethyl alcohol. The eluate is then concentrated in a rotary evaporator to 20 cm³ and the sample is measured spectrophotometrically.

RESULTS AND DISCUSSION

Use of porous polyurethane foam as an absorbent for high volume water and air sampling has proven advantageous due to its ease of handling and clean up and its ability to capture many different organic compounds^{7,8,13}. Also, the hydrodynamic properties of foam column allow the application of quite high flow rates without the aid of vacuum. This together with the rapid attainment of the absorption equilibrium on the thin membranes forming the foam material reduces the time required for analysis.

In order to investigate the analytical utility of the unloaded foam and the foam loaded with tricaprylyl tertiary amine for the extraction of some phenolic compounds. Seven compounds were investigated namely: picric acid, pyrocatechol, *α*-naphthol, *β*-naphthol, resorcinol, *o*-nitrophenol and *p*-nitrophenol. To study the effect of time on the uptake of these compounds by polyurethane foam, batch experiments were carried out in a series of polyethylene flasks containing 0.4 g foam and 100 µg of each phenolic compound in 50 cm³. pH values 6 are selected to ensure that the extracted species present predominantly in the undissociated form. The amount of phenolic compound remained in solution after shaking for different times was then determined spectrophotometrically and the percentage extracted by the foam was calculated by difference. Generally, the absorption of the tested compounds on the foam are quite rapid.

4. H. Oda, M. Kishida and C. Yokokawa; Carbon: 19 (1981) 243.
5. H. Oda and C. Yokokawa; Carbon: 21 (1982) 485.
6. R.G. Will and J.F. Grutsch; U.S. Patent: 3 (1971) 552.
7. A.B. Farag, A.M. El-Wakil and M.S. El-Shahawi; Fres. Z. Anal. Chem.: 324 (1986) 59.
8. T. Braun, J.D. Navratil and A.B. Farag; Polyurethane Foam Sorbents In Separation Science, CRC Press, Inc., Boca Raton, Florida (1985).
9. B.K. Afghan, R.J. Wilkinson, A. Chow, T.W. Findley, H.D. Gesser and K.I. Srikameswaran; Water Res.: 18 (1984) 9.
10. H.J.M. Bowen; J. Chem. Soc.: A (1970) 1082.
11. K.M. Gough and H.D. Gesser; J. Chromat.: 115 (1975) 383.
12. G.J. Moody and J.D.R. Thomas; Chromatographic Separation and Extraction with Foamed Plastics and Rubbers, Dekker, New York (1982).
13. N.F. Burdick and T.F. Bidleman; Anal. Chem.: 53 (1981) 1926.

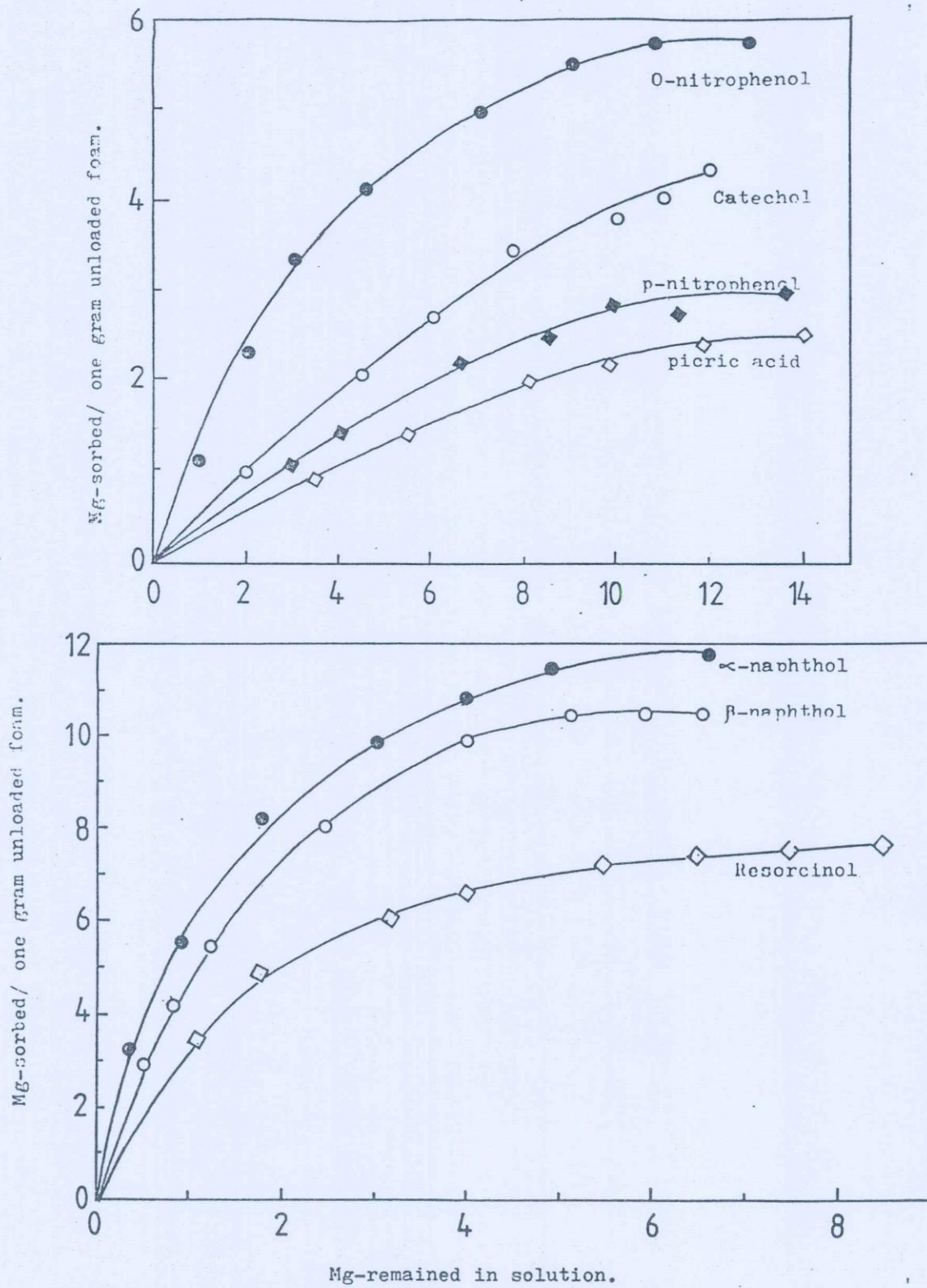


Fig. 1- Extraction isotherm of the phenolic compounds tested.

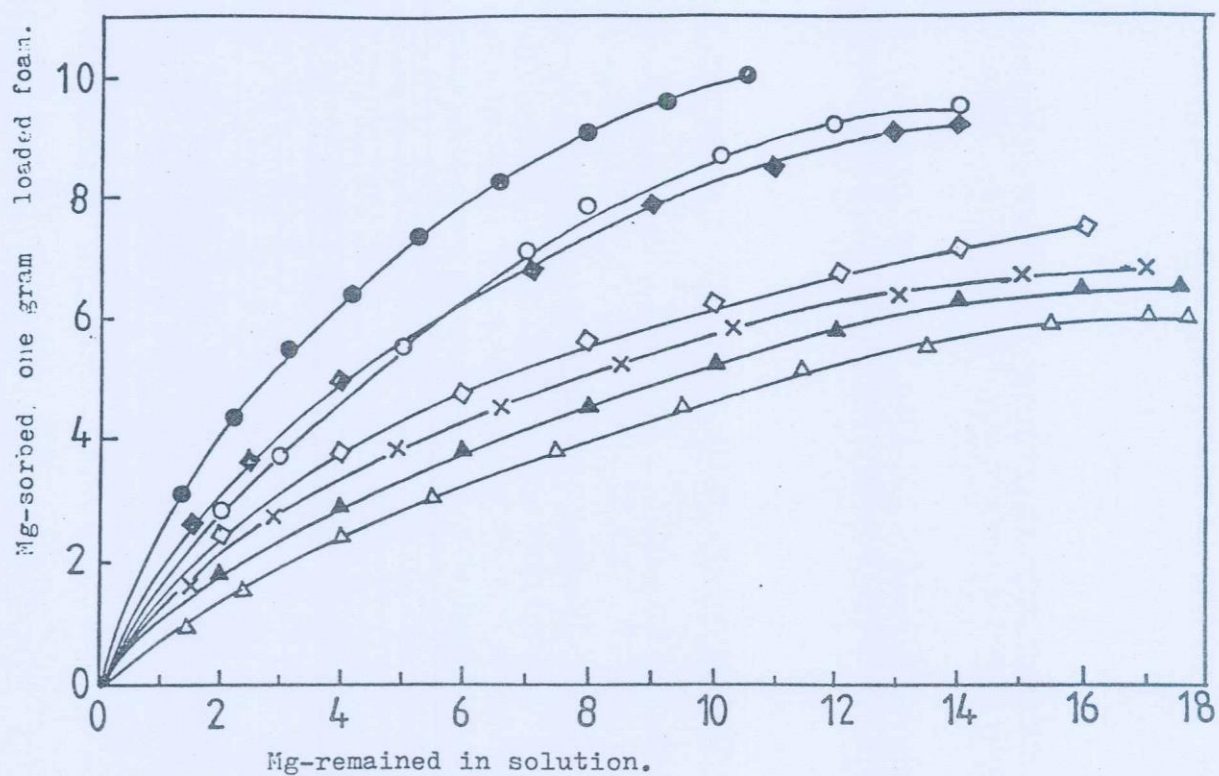


Fig. 2- Extraction isotherm of different phenolic compounds.

picric acid	;	p-nitrophenol
0-nitrophenol	;	Resorcinol
β-naphthol	;	∞-naphthol
catechol		

Table 1. The absorption of the different phenolic compounds at three different initial concentrations in aqueous solution.

Absorbate	pKa	initial amounts of phenols in water ($\mu\text{g.cm}^{-3}$)		
		(40 μg) % Recovery	(60 μg) % Recovery	(100 μg) % Recovery
Picric acid	0.38	22.0	20.0	15.0
p-Nitrophenol	7.15	32.5	23.3	16.0
o-Nitrophenol	7.17	55.0	46.0	33.8
α -Naphthol	9.34	87.0	82.5	70.0
β -Naphthol	9.51	82.5	65.7	64.0
Resorcinol	9.81	74.3	61.7	47.0
Pyrocatechol	9.85	62.3	26.0	21.5

Temp. 25°C

Shaking time = 3 hrs.

pH = 6-7.

Table 2. The extraction and recovery of phenols from 3 dm³ of water using polyurethane foam columns at 5-10 cm³ min⁻¹ flow-rate.

Phenolic compound	Amount added (μg)	Amount measured (μg)	% Recovery	Wavelength (nm)
Picric acid	200	190	95.0	360
α -Naphthol	200	187	93.5	308
β -Naphthol	200	193	96.5	285
Resorcinol	200	191	95.5	276
o-Nitrophenol	200	191	95.5	346
p-Nitrophenol	200	192	96.0	310
Pyrocatechol	200	180	90.0	270

Average of three determinations.

Extraction isotherm. The uptake of the different phenolic compounds by the foam was found to depend on the concentration of the examined compound in aqueous solution. Thus, sorption isotherms are developed over a wide range of equilibrium concentration (20-100 µg) for each compound. Figs. 1 and 2 show the sorption isotherms of the tested compounds on unloaded and amine-loaded foam, respectively. The isotherms show linear relations on relatively wide range of concentrations. The percent absorption of the different phenolic compounds tested by polyurethane foam at three different initial concentrations in the aqueous solution are given in Table 1. The percentage extraction by the unloaded foam decreases in the order: picric acid < p-nitrophenol < catechol < pyrogallol < o-nitrophenol < resorcinol < p-aminophenol < β-naphthol < α-naphthol; while for the amine-loaded foam, the sequence is: picric acid > p-nitrophenol > o-nitrophenol > α-naphthol > β-naphthol > resorcinol > pyrocatechol. The acidity, PKa, of the absorbate plays an important role in determining the absorption capacity on the amine-loaded foam. However, this is not the case with unloaded foam where the absorption efficiencies are generally decreased with increasing the acidity. In the latter case, the molecular weight of the absorbate has a clear effect. Also, the hydrogen bonding in o-nitrophenol and probably in pyrocatechol is a participating factor.

Dynamic (column) extraction: The extraction of phenolic compounds in batch experiments showed that the unloaded foam extracts efficiently the different phenolic compounds from water. This suggests the possible application of polyurethane foam in column extraction mode for the quantitative collection and separation of the tested phenolic compounds. On percolating one or two liters of dilute aqueous solution containing 200 µg of each phenolic compound through foam columns containing 2 g foam at 5-10 cm³ min⁻¹ flow rate, more or less complete retention of the phenolic compounds are retained on the foam columns. The compounds retained by the foam are then recovered with 100-120 cm³ acetone in a Soxhlet extractor. However, β-naphthol and resorcinol are recovered with 100 cm³ ethanol. The effluent is concentrated on a rotatory evaporator to 20 cm³ and the sample is analysed spectrophotometrically.

The results of the extraction and recovery of phenols tested from water (3 dm³) by the foam column method are summarized in Table 2.

REFERENCES

1. G.W. Strohl; Mikrochim. Acta: 1 (1969) 103.
2. U.S. Environmental Protection Agency; Methods for Chemical Analysis of Water and Wastes: Cincinnati, Ohio 45268, (1983).
3. P.A. Pfeifer, G.K. Bonn and O. Bobleter; Fresenius Z. Anal. Chem.: 315 (1983) 205.

Because most phenols are present in extremely low concentration levels, they have been concentrated prior to their quantitative analysis by various methods including adsorption on carbon⁴⁻⁵ and flexible polyurethane foams⁶.

Recently, several authors have proposed open cell polyurethane foam as an inexpensive solid extractor⁷⁻⁸. The membrane like structure of these foams together with the efficient absorption properties offered many advantages over other solid collectors as they allow higher concentrating ability compared with other solid materials which depend on adsorption route alone³⁻⁹. Polyurethane foams apparently concentrate by the phase distribution mechanism rather than adsorption^{10,11}. Furthermore, other concentration techniques are either slow or cumbersome and/or expensive for routine usage where many large volume samples are concentrated at the site prior to quantitative analysis.

It would be of interest to explore the potentiality of polyurethane foam for the extraction of some phenols at very low concentration in aqueous media and to establish the conditions where good recoveries and increased precision could be obtained at room temperature. This paper describes the results of such study and the conditions for the separation of these phenols in aqueous solutions. Phenols were selected in this study as they are similar in structure to the common insecticides and herbicides which resist biodegradation and they are considered to be one of the most important causes of taste and odour in water supplies.

EXPERIMENTAL

Apparatus. A double-beam spectrophotometer, Varian DMS 634, with 1 cm quartz cuvette was used for the quantitative determination of the phenols tested. Glass columns of 15 mm diameter and 15 cm length were employed.

Reagents and Materials. The reagents used were of analytical grade and the solvents were of spectroscopic grade. Polyurethane foam, a polyether of open cell type was supplied by Greiner, KG, Schaumstoffwerk-Kremsmünster, Austria. The volume weight of the foam was 30 kg.m^{-3} . The foam cubes (5 mm edge) were washed by 1 M-hydrochloric acid followed by distilled water, then acetone and finally dried at 80°C . The loaded foams were prepared by mixing the dry foam with tricaprylyl tertiary amine for 10 minutes and the excess amine was removed by drying the foam between sheets of filter paper. The phenols tested were: picric acid, pyrocatechol, α -naphthol, β -naphthol, resorcinol, o-nitrophenol and p-nitrophenol. These solutions were of laboratory grade and used without further purification. Stock solutions containing $100 \text{ } \mu\text{g. cm}^{-3}$ of each phenolic compound in hot distilled water were prepared. A series of standard solutions of these compounds were prepared

التلوث داخل المنازل : فحص عادم مصباح الكيروسين باستخدام كروماتوجرافيا
الغاز ذو الأعمدة الشعرية منفردا ومتكاملا مع مطياف الكتلة

محمد محمد مشالى ، محمد سرور الشهاوى ، وبات سندرا *
قسم الكيمياء - كلية العلوم بدمياط - جامعة المنصورة - مصر
* معهد أبحاث الكروماتوجرافى - ويفلجـم - بلجيكا

يستخدم مصباح الكيروسين للأنفاة داخل المنازل ويكثر استخدامه فى الريف المصرى
بسبب عدم اكتمال توصيل الكهرباء ، ويستخدم فى المدن عند انقطاع الكهرباء . كما أن
قطعا كبيرا من الأسر محدود الدخل يستخدم المصباح أيضا فى طهى غذاء الفول المدمس
وذلك بتعليق اناء الطهى فوق فوهة المصباح لفترة لتقل عن ثمانى ساعات وفى جميع الاحوال يتصاعد
من المصباح عادم فى صورة غازات وأبخرة ومواد صلبة دقيقة الحجم وذلك نتيجة للاحتراق الغير
تام للوقود (الكيروسين) . هذا العادم يلوث الوسط المحيط وخاصة الهواء اللازم للتنفس وبالتالي
يضر بصحة الانسان .

وتهدف هذه الدراسة الى التعرف النوعى والكمى على بعض مكونات التلوث وذلك باستخدام
المطوئات الصلبة كموسر . تم استخلاص المواد العضوية غير القطبية من العادم الصلب
بالغليان مع الكهسان الحلقي وتلى ذلك عمل كروماتوجرافى للعينة المستخلصة باستخدام عمود
من السيلكاجل للتنقية والتركيز وفصل مجموعة الهيدروكربون . وتم التعرف الكمي والنوعى
لمكونات العادم باستخدام كروماتوجرافيا الغاز ذو الأعمدة الشعرية منفردا وأيضًا متكاملًا مع
مطياف الكتلة .

وأوضحت الدراسة أن البرافينات تشكل مجموعة رئيسية من حيث النوع والعدد والتركيز
فى كل من الوقود (الكيروسين) والعادم . كما تم أيضا تعيين بعض مركبات الهيدروكربون
الارومانية البسيطة وعديدة الحلقة فى العادم .

CGC AND CGC/MS INVESTIGATION OF THE ALIPHATIC HYDROCARBON FRACTION OF STREET DUST OF GIZA SQUARE, EGYPT.

M. MASHALY¹, P. SANDRA², M. SOFAN¹ and M.S. EISHAHAWI¹

¹Chemistry Department, Faculty of Science, Damietta, Egypt.

²Research Institute for Chromatography, P.O.Box 91, B-8610 Wevelgem-Belgium.

SUMMARY

A street dust sample was extracted by sonication with cyclohexane. The extract, was chromatographed over a silica gel column by elution with cyclohexane to isolate the total hydrocarbons. The concentrated eluate was partitioned with nitromethane. The HC retained in the cyclohexane and the polycyclic aromatics moved to the nitromethane. The HC fraction was analysed by CGC and CGC/MS. Twenty nine HC were identified, They are present in a Gaussian distribution ranging from $n-C_{14}H_{30}$ to $n-C_{40}H_{82}$, with a maximum at $n-C_{21}H_{44}$. The two biological markers, pristane and phytane were also present. The sample profile and composition have a strong relation to fuel and combustion source emissions.

INTRODUCTION

Aliphatic hydrocarbons (HC) are important environmental pollutants. More than 200 HC (alkanes, alkenes and alkynes) have been detected in air [1]. A large fraction of this

chemical class of pollutants originates from combustion of fossil fuels amongst which car and industrial exhausts.

Recently, Egypt began to take care of the problem of environmental pollution. Still much has to be done in this respect especially with regard to the health impacts of the problem.

This work contributes to better understanding of the problem. The first part dealt with the aromatic fraction[2]. This part deals with the qualitative chromatographic investigation of the HC fraction of street dust of Giza Square as one of the heaviest polluted zones in Egypt.

EXPERIMENTAL

Solvents

The solvents used in this work were either spectroscopic grade or distilled in all glass apparatus. They were tested by CGC for their impurities.

Sample and sample extraction

A representative sample of street dust (dry, 10.0 g, particle size < 500 μm) swept from different zones of Giza Square, Giza, Egypt was extracted with cyclohexane (4x30ml) by sonication [3-5] (4x15 min) in an ultrasonic bath (100 watt, operating frequency: 41 kHz) at 15-25°C. The extracts were filtered through a pre-extracted filter paper. The volume of the combined cyclohexane extracts was then reduced

to ca. 10 ml at 40°C using a vacuum rotary evaporator. The extract was further concentrated to ca. 0.5 ml under a slow stream of dry nitrogen at room temperature.

Isolation of the total hydrocarbon fraction

The concentrated extract (0.5 ml) was chromatographed on a silica gel (Merck) column (15x1.0 cm i.d., 150 µm) by eluting the total hydrocarbon fraction (aliphatics, HC and polycyclic aromatics) with 60 ml cyclohexane.

Isolation of the HC fraction

The cyclohexane eluate was evaporated to ca. 5 ml under a slow stream of dry nitrogen, then partitioned with nitromethane (5x5 ml). The HC fraction retained in the cyclohexane and the aromatic fraction moved to the nitromethane [2,6,7]. After back extraction, the cyclohexane solution (HC) was concentrated to ca. 2 ml under a slow stream of dry nitrogen, then analysed by CGC and CGC/MS.

CGC analysis of the HC fraction

CGC was performed on an SE-52 column (21 m x 0.32 mm I.D, $d_f = 0.32 \mu\text{m}$) installed in a Carlo Erba 4160 instrument equipped with cold on-column injector. Operating conditions were injection temperature 35°C, column temperature ballistically programmed to 80°C, then to 315°C at 5°C min⁻¹ followed by 15 min isothermal, detector (FID) at 350°C, carrier gas (H₂) flow rate = 0.35 kg cm⁻², attenuation = 16 and chart speed 0.5 cm min⁻¹.

CGC/MS analysis of the HC fraction

Electron impact (70 ev) spectra were obtained on a Finnigan 4000 system equipped with a Data General Nova 3 computer. The column and conditions as reported for the CGC analysis were used to obtain comparable results except that helium was used as a carrier gas.

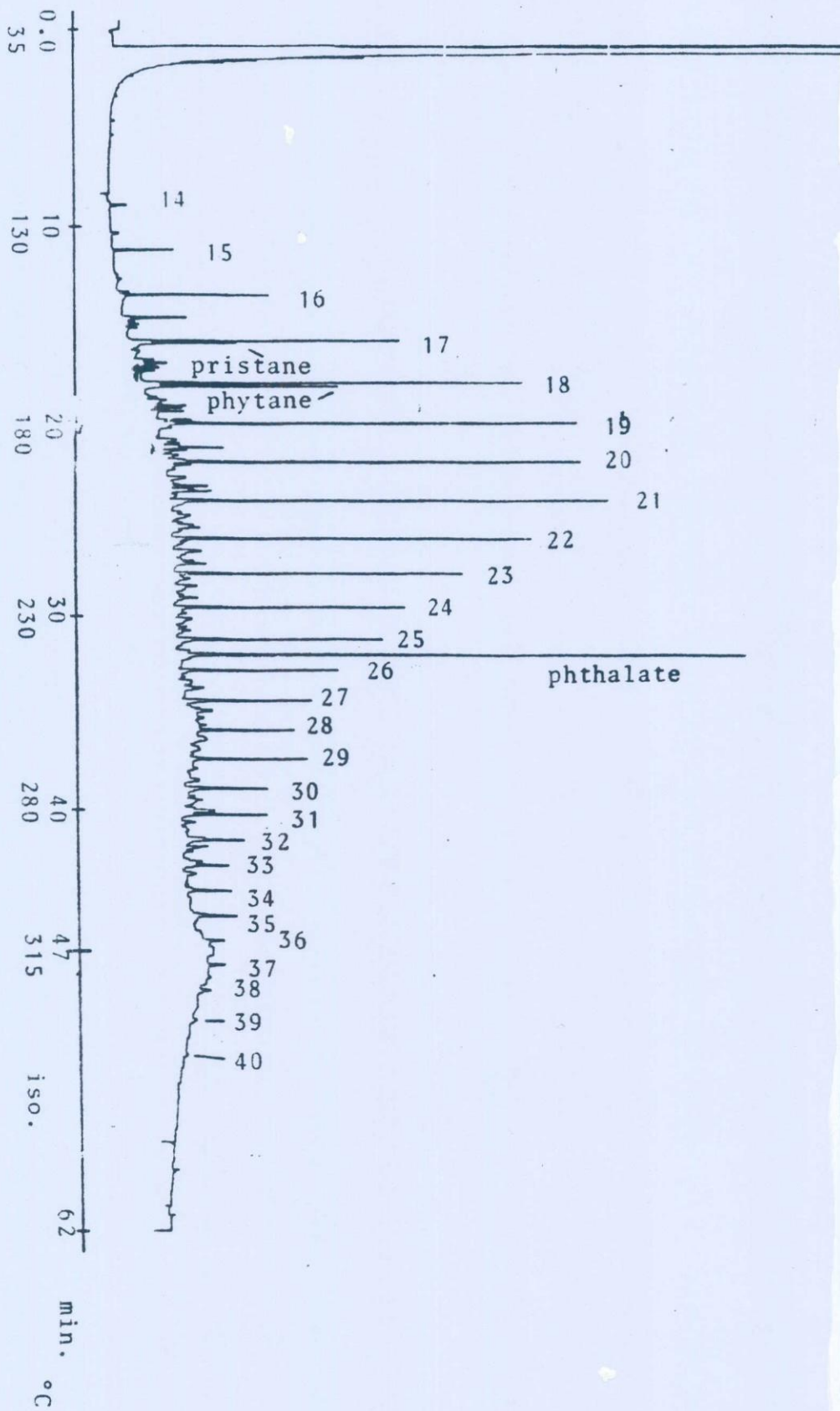
RESULTS AND DISCUSSION

Figure 1 shows the chromatogram of the CGC analysis of the HC fraction isolated from the representative street dust sample collected from Giza Square, Giza, Egypt. More than 60 compounds were detected in the sample; most of them were present in trace concentrations making their identification difficult.

The identified compounds are assigned in Fig. 1 with their carbon numbers or names. Identification was based on CGC/MS analysis and cochromatography with a standard mixture of the n-alkanes with carbon numbers: 14, 15, 17-22, 25, 26, 28, 30, 32, 34, 36, 38 and 40. Twenty nine HC were identified including the n-alkanes with carbon numbers: C₁₄ to C₄₀.

The two biological markers pristane and phytane were also identified. Other saturated and unsaturated HC were expected to be present in the sample. Their identification was difficult because of their presence in trace concentrations or lack of reference compounds.

Fig. 1: Chromatogram of the HC fraction of street dust, Giza square, Egypt. For details: see text.



The chromatographic profile and sample composition is characteristic for environmental pollution samples of combusted fossil fuels. The identified compounds were present in a Gaussian distribution ranging from $n\text{-C}_{14}\text{H}_{30}$ to $n\text{-C}_{40}\text{H}_{82}$, with a maximum at $n\text{-C}_{21}\text{H}_{44}$.

The source of HC pollutants can be expected. Giza Square, is one of the most heaviest traffic zones in Egypt. It is also part of "Big Cairo", one of the worst polluted cities in the world. Tenth of thousands of different types and qualities of cars and buses cross, fuel or station in the square all long the day. All types of motor fuels used in Egypt (gasoline, diesel and solar) contain HC in different percentages. Incomplete fuel combustion due to inefficient engine systems results in the emission of exhaust with unburned or partially combusted fuel containing many types of pollutants, including HC components [2,7]. Most cars and buses have to run slowly or to stop 5-15 minutes in some controlling light spots which cause fuel to be exhausted unburned or partially combusted. The majority of cars and buses are old and run without engine control. It is known that old cars contribute more to pollution than new cars [8]. Moreover, Giza Square is centered in a region with nearby several fuel stations and many industrial sites. These represent another source of unburned or partially combusted fuel. The danger of these pollution sources is that their emissions (unburned or partially combusted

fuels, gases or particulate matter) are very close to human beings. Moreover, the pollutants easily migrate [9] and are transferred in air, water and soil. They, therefore, harm all living systems.

The presence of the HC pollutants in the street dust of Giza Square is due to the fall on the ground of particulate matter (emitted from the combustion sources mentioned earlier or suspended in air) with HC adsorped on its surface and deposition and adsorption on the street dust particles of the HC components of the unburned or partially combusted fuels.

Some suggestions to reduce the problem of environmental pollution are:

- Providing sufficient public transport ways with limiting the rapid increase in the number of private cars.
- Controlling the engine quality by regular testing and providing exhaust systems with filters.
- Using fuels of high octane number to increase combustion efficiency and reduce exhaust emissions.
- Increasing the number of roads to reduce traffic density.
- Providing factories with suitable filters or purifiers to reduce exposure of pollutants into the environment.
- Increase in population results in an increase in using transport ways, leading to consumption of larger fuel amounts which on incomplete combustion emit into the

environment, especially air, larger amounts of pollutants. Preventing migration from the country side into Cairo and giving more and sufficient authority to the local governments may improve this situation with about 20% reduction of pollution in Big Cairo.

CONCLUSION

Both fuel and combustion source emissions participate in polluting the area of the Giza Square. This conclusion is confirmed by the fact that Giza Square is centered in a very heavy motor traffic region with nearby several fuel stations and many industrial sites. Effective efforts can and have to be done to reduce pollution in Egypt.

ACKNOWLEDGEMENT:

The authors are grateful to Mr. M. Schelfaut (State University of Ghent, Belgium) for performing the CGC/MS analysis.

REFERENCES

- [1] T. Graedel, "Chemical Compounds in the Atmosphere", Academic Press, New York (1978) pp. 50-67 and pp. 71-84.
- [2] M. Mashaly and P. Sandra, proceeding of the Eighth International Symposium on Capillary Chromatography, Riva del Garda, Italy, May 19-21 (1987) v. 1, pp. 467-481.
- [3] D. Grosjean, Anal. Chem. 47 (1975) 797.

- [4] C. Golden and E. Sawicki, *Int. J. Environ. Anal. Chem.* 4 (1975) 9.
- [5] National Institute of Occupational Safety and Health, in "NIOSH Manual of Analytical Methods", HEW Publication no. NIOSH 77-157 (1977).
- [6] D. Hoffmann and E. Wynder, *Anal. Chem.*, 32 (1960) 295.
- [7] M. Mashaly, Ph.D. thesis (1985) pp. 28-31.
- [8] T. Jensen and R. Hites, *Anal. Chem.*, 55 (1983) 594.
- [9] R. Gerinke and I. Lewis, *Anal. Chem.*, 47 (1975) 2151.

Chromium(III) Complexes with Sugars

D. H. BROWN, W. E. SMITH, M. S. EL-SHAHAWI and M. F. K. WAZIR

Department of Pure and Applied Chemistry, University of Strathclyde, Cathedral Street, Glasgow G1 1XL, U.K.

(Received March 4, 1986)

The biological role of chromium as an essential trace element was suggested when it was found that rats on a chromium deficient diet developed an impaired tolerance for intravenous glucose [1]. More recently an insulin potentiating factor containing chromium has been isolated [2]. This so-called glucose tolerance factor (GTF) was found to contain chromium(III) and nicotinic acid as well as glycine, cysteine and glutamic acid [3] - the latter three being the constituents of the tripeptide glutathione. The mechanism by which glucose tolerance is improved is unknown but evidence suggests that GTF somehow potentiates insulin activity. In all the samples of GTF isolated, nicotinic acid has been present, thus considerable research effort has been directed towards examining the reactions of chromium(III) with nicotinic acid. This has resulted in the isolation of a number of both nitrogen and oxygen donor complexes [4].

The chromium content of a number of foodstuffs has been determined [5] and a significant relationship was found between the alcohol extractable chromium and biological activity. It is of interest that an alcohol extraction is often the first step in the isolation of GTF. This raises the possibility that the active chromium could be in a non-aqueous environment *in vivo*. Little is known of the complexing ability of chromium(III) with naturally occurring ligands in non-aqueous media. In particular it is of interest

to see if such chromium(III) will complex with sugars in such media as no stable complexes are found in aqueous solution.

Experimental

The starting complex chromium(III) trichloride tripyridine was prepared by the method of Taft *et al.* [6]. The complexes were prepared in solution by refluxing for four hours a 1:3 mixture of the chromium(III) trichloride tripyridine and the required ligand in dried methanol. In every case colour changes were observed within a few minutes of the start of the refluxing. Complex formation was detected in solution by changes in UV-Vis spectra and the appearance of Cotton effects corresponding to the transition of chromium(III). All the ligands used - glucose, galactose, mannose, ribose, arabinose, xylose, sorbose, sucrose, lactose - were optically active.

Results

All the ligands reacted to give chromium(III) complexes with UV-Vis absorption peaks around 440 and 605 corresponding to the ${}^4A_{2g} \rightarrow {}^4T_{1g}$ and ${}^4A_{1g} \rightarrow {}^4T_{1g}$ transitions of octahedral chromium(III). The results are shown in Table I.

Discussion

The above results show that all of the sugars examined reacted fairly rapidly with chromium(III) to produce optically active complexes. The smell of pyridine (confirmed by HPLC) suggested that the pyridine was being replaced rather than the chloride. None of the complexes prepared were likely to be *fac* in terms of sugar hydroxy groups since, if this was the case, stronger and better defined Cotton effects would have been expected for those sugars which could give rise to this structure com-

TABLE I. UV-Vis and CD Spectra of Chromium(III) Sugar Complexes

Sugar	UV-Vis (${}^4A_{2g}(F) \rightarrow$)			CD (nm)				
	${}^4T_{1g}(P)$	${}^4T_{1g}(F)$	${}^4T_{2g}(F)$					
Glucose	350	440	615	-430	+580	-700		
Ribose	380	445	620	-420	-534	-700		
Arabinose	350	440	605	+440	+580	+670		
Xylose	340	430	600	-400	+470	-551	+646	
Galactose	350	440	610	-385	-444	-577	+665	
Mannose	350	440	605	+404	+470	-560	+650	+670
Sorbose	360	450	608	+368		+550		
Sucrose	370	430	601	-414	-490	-540	-680	
Lactose	310	440	620	-400	+454	-570	+660	

complexing seems likely. However, no solid complexes were isolated to confirm this suggestion. Thus if the nicotinic acid found in GTF is bound to chromium through the nitrogen of the pyridine, then given suitable conditions, replacement by glucose may facilitate either glucose transport or metabolism.

References

1 W. Mertz and K. Schwarz, *Arch. Biochem. Biophys.*, 58, 504 (1955).

- 2 W. Mertz and K. Schwarz, *Am. J. Physiol.*, 196, 614 (1959).
- 3 K. Schwarz and W. Mertz, *Arch. Biochem. Biophys.*, 72, 515 (1957).
- 4 J. V. McArdle, E. deLaubenfels, A. L. Shorter and M. I. Ammon, *Polyhedron*, 1, 471 (1982); E. Gonzalez-Vergara, J. Hegenauer, P. Saltman, M. Sabat and J. A. Ibers, *Inorg. Chim. Acta*, 66, 115 (1982); L. E. Gordon and H. M. Boff, *Inorg. Chem.*, 21, 2881 (1982).
- 5 E. W. Toepfer, W. Mertz, E. E. Roginsky and M. M. Polansky, *J. Agric. Food. Chem.*, 21, 69 (1973).
- 6 J. C. Taft and M. M. James, *Inorg. Synth.*, 7, 132 (1963).
- 7 E. Voelter, E. Bayer, R. Records, E. Bunnenberg and C. Djerassi, *Annalen*, 718, 238 (1968); D. H. Brown and J. MacPherson, *J. Inorg. Nucl. Chem.*, 32, 3309 (1970).

Table 2. Results on the four-factor test function

C (%)	Experiments								Steps							
	$i_{\max} = 1$		$i_{\max} = 2$		$i_{\max} = 3$		$i_{\max} = 4$		$i_{\max} = 1$		$i_{\max} = 2$		$i_{\max} = 3$		$i_{\max} = 4$	
	X	SD														
Termination procedure: (a)																
0	76	16	86	21	98	26	113	36	72	16	48	13	39	11	38	14
			(-13%)		(-28%)		(-49%)				(34%)		(46%)		(47%)	
optimal 40	76	17	74	20	69	18	65	15	72	17	57	16	45	14	38	12
			(2%)		(9%)		(14%)				(20%)		(37%)		(47%)	
Termination procedure: (b)																
0	49	14	50	15	52	17	53	18	45	14	24	8	17	6	14	5
			(-2%)		(-6%)		(-9%)				(47%)		(63%)		(70%)	
optimal 40	48	14	45	15	44	15	42	15	44	14	31	12	24	11	19	10
			(5%)		(9%)		(13%)				(28%)		(46%)		(56%)	

For meaning of the symbols: see Table 1

The simulations were performed on a HP 9845 B micro-computer.

Results and discussion

The simulations on the two-factor test functions show that repeated reflection of two vertices ($C = 0\%$) and parallel processing of the experiments gives about 50% reduction of time compared to the normal procedure; in that case only the first three experiments can be done parallel (Table 1). There is an increase of the number of experiments and steps going from the Gauss response surface to Brooks 3 and 4. This is because of increase of irregularity of the response surfaces.

On Brooks 1, 2, 3 and 4 a reduction of the number of experiments takes place by repeated reflection of 2 vertices. On Gauss, Brooks 1 and Brooks 2 further reduction of the number of experiments is possible by using the decision rule upon which one or two vertices are reflected. This does not reduce the number of steps.

On Brooks 2 ca. 3% of the runs failed to reach the optimum; on Brooks 3 ca. 5% failed.

The simulations on the four-factor test function (Table 2) reveal, too, that continuous reflection of more than one vertex gives a reduction in time but now there is the additional effect that the more experiments can be done parallel the higher the saving in time (up to 56% or 70%, depending on the termination procedure chosen). The number of experiments increases with the number of vertices reflected at the same time. Variation of the criterion C shows that 40% is an optimal value in respect

to the number of experiments. In that case 13 or 14% can be saved but this does not reduce the number of steps.

Only at $i_{\max} = 1$ ca. 8% of the runs failed to reach the optimum.

The gains given in Tables 1 and 2 are tested by a Students' *t*-test on paired results, $\alpha = 0.01$. In Table 2 the gains are significant when they exceed ca. 6%.

Reflecting more than one vertex at a time may be useful when the experiments can be done parallel: time will be saved. If parallel processing of the experiments is impossible it may be safer to reflect one vertex per simplex.

References

1. Spendley W, Hext GB, Himsworth FR (1962) *Technometrics* 4:441
2. Wiel PFA van der (1980) *Anal Chim Acta* 122:421
3. Wiel PFA van der, Maassen R, Kateman G (1983) *Anal Chim Acta* 153:83
4. Hendrix C (1980) *Chemtech* 10:448
5. Brooks SH (1959) *Operation Res* 7:430
6. Powell MJD (1962) *Comput J* 5:147
7. Long DE (1969) *Anal Chim Acta* 46:193

Received August 28, 1985

Fresenius Z Anal Chem (1986) 324:58-59
© Springer-Verlag 1986

Collection and separation of some organic insecticides on polyurethane foam columns

A. B. Farag, A. M. El-Wakil, and M. S. El-Shahawi

Department of Chemistry, Faculty of Science,
Mansoura-University, Mansoura, Egypt

Anreicherung und Trennung organischer Insecticide
mit Hilfe von Polyurethanschaum-Säulen

Introduction

Polyurethane foams comprise a new class of collectors useful for application in aqueous and gaseous media [1, 2]. The quasi-

Offprint requests to: A. B. Farag

spherical membrane structure of these foams has offered special advantages over other solid collectors. These foams allowed reasonable flow-rates of the mobile phase without the aid of a pump.

Gesser et al. [3] suggested the application of polyurethane foams for the collection of trace organic contaminants from water using a batch technique. Since then several investigations have been published describing the application of untreated polyurethane foams as collectors in separating and concentrating various chlorinated insecticides and other organic substances.

The work reported here was aimed at evaluating the use of polyurethane foam as a collector suitable for the extraction and recovery of some phosphorus and sulphur-containing organic insecticides from aqueous media.

Short communications ... was supplied by Stenier K.G., Schaumstoffwerk-Kremsmunster, Austria. The volume weight of the foam was 30 kg m^{-3} . The foam cubes (5 mm edge) were washed by 1 M hydrochloric acid followed by distilled water and acetone and finally dried at 80°C . The insecticides tested were: Summicidin [α -cyano-m-phenoxy-benzyl- α -isopropyl-p-chlorophenyl acetate], Thiodane 35 emulsifiable, which is a cyclic sulphurous acid ester of active ingredient, endosulphur; Hostaquick SOEC [phosphoric acid-(7-chlore-bis-cyclo-3,2-0-hepta-2,6-diene-6-yl-1-di-methylester)] and Hostathion HOEC (Triazophos) which is a derivative of Hostaquick. These insecticides were used as received.

Apparatus. Glass columns of 15 mm diameter and 15 cm length were employed. Gas-liquid chromatographic instrument (PYE Unicam 104 series) was used for the determination of the insecticides tested. A polyethylene glycol column was employed at 120°C .

Column preparation. 0.3 g unloaded dry foam cubes was packed in the glass column using the vacuum method of foam column packing [2].

Procedure. 30 mg of each insecticide in 2 l of water is percolated through the foam column at $10\text{--}15 \text{ ml min}^{-1}$. After squeezing water from the foam material, the insecticide is recovered from the foam with 120 ml acetone in a Soxhlet apparatus. The eluate is then concentrated in a rotary evaporator to 10 ml and 5 μl sample is analysed using a gas chromatographic method.

Results and discussion

One of the promising separation and preconcentration techniques is by foam column collectors. This method allows the isolation of the analyte from the matrix and yields an appropriate enrichment factor. Also, the advantageous hydrodynamic properties of foam columns allow the application of a quite high flow-rate without the aid of vacuum. This together with the rapid attainment of the absorption equilibrium on the thin membranes forming the foam material reduces the time required for analysis.

In preliminary batch experiments, attempts were made to collect some sulphur and phosphorus containing organic insecticides on polyurethane foam. The foam material was found to have a good affinity towards the absorption of the insecticides tested (Hostathion HOEC, Hostaquick SOEC, Thiodan 35 and Summicidin). These results suggested the possibility of using polyurethane foam in column dynamic experiments for the extraction of these insecticides from aqueous solutions.

Two liters of each insecticide solution were passed through the foam column at a flow-rate of $10\text{--}15 \text{ ml min}^{-1}$, which was chosen on the basis of a preliminary test. The insecticides were then recovered from the foam material with acetone in a Soxhlet apparatus and their concentrations were measured by a gas chromatographic technique. The results of the extraction and recovery of the insecticides examined from 2 l aqueous solutions by the proposed foam column are summarized in Table 1. Better results were obtained for the separation and recovery of Summicidin when the flow-rate was reduced to 5 ml min^{-1} . A typical example of the separation of Hostathion is shown in Fig. 1. The chromatograms of Hostathion with and without the foam concentration step illustrate the efficiency of the proposed foam columns.

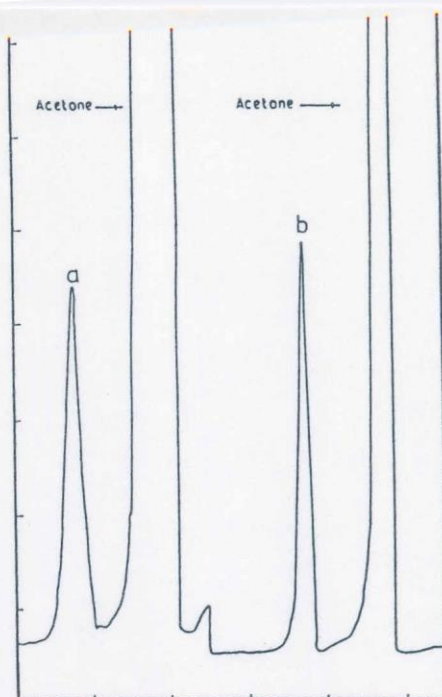


Fig. 1. Chromatogram of Hostathion 40 EC. *a* Hostathion (30 mg/10 ml) in acetone (5 μl sample is injected). *b* Hostathion (30 mg/2 l) in aqueous sample after using the foam pre-concentration step

Table 1. Extraction and recovery of the insecticides tested from 2 l aqueous solutions by polyurethane foam columns at $10\text{--}15 \text{ ml min}^{-1}$ flow rate

Insecticide	Amount (mg)	% Recovery
Hostathion HOEC	30	93.4
Hostaquick SOEC	30	100.0
Thiodan 35	30	98.3
Summicidin	20	90.3

The present work has demonstrated the capabilities of polyurethane for the collection and recovery of sulphur and phosphorus insecticides from dilute aqueous solution.

References

- Braun T, Navartil JD, Farag AB (1985) Polyurethane foam sorbents in separation science. CRC Press, Florida
- Moody GJ, Thomas JDR (1982) Chromatographic separation and extraction with foamed plastics and rubbers. Dekker, New York
- Gesser HD, Chow A, Davis FC, Uthe JF, Reinke J (1971) Anal Lett 4:883

Received December 10, 1985

Fresenius Z Anal Chem (1986) 324:59–60
© Springer-Verlag 1986

Table 2. Results on the four-factor test function

C (%)	Experiments								Steps							
	$i_{\max} = 1$		$i_{\max} = 2$		$i_{\max} = 3$		$i_{\max} = 4$		$i_{\max} = 1$		$i_{\max} = 2$		$i_{\max} = 3$		$i_{\max} = 4$	
	X	SD														
Termination procedure: (a)																
0	76	16	86	21	98	26	113	36	72	16	48	13	39	11	38	14
			(-13%)		(-28%)		(-49%)				(34%)		(46%)		(47%)	
optimal 40	76	17	74	20	69	18	65	15	72	17	57	16	45	14	38	12
			(2%)		(9%)		(14%)				(20%)		(37%)		(47%)	
Termination procedure: (b)																
0	49	14	50	15	52	17	53	18	45	14	24	8	17	6	14	5
			(-2%)		(-6%)		(-9%)				(47%)		(63%)		(70%)	
optimal 40	48	14	45	15	44	15	42	15	44	14	31	12	24	11	19	10
			(5%)		(9%)		(13%)				(28%)		(46%)		(56%)	

For meaning of the symbols: see Table 1

The simulations were performed on a HP 9845 B micro-computer.

Results and discussion

The simulations on the two-factor test functions show that repeated reflection of two vertices ($C = 0\%$) and parallel processing of the experiments gives about 50% reduction of time compared to the normal procedure; in that case only the first three experiments can be done parallel (Table 1). There is an increase of the number of experiments and steps going from the Gauss response surface to Brooks 3 and 4. This is because of increase of irregularity of the response surfaces.

On Brooks 1, 2, 3 and 4 a reduction of the number of experiments takes place by repeated reflection of 2 vertices. On Gauss, Brooks 1 and Brooks 2 further reduction of the number of experiments is possible by using the decision rule upon which one or two vertices are reflected. This does not reduce the number of steps.

On Brooks 2 ca. 3% of the runs failed to reach the optimum; on Brooks 3 ca. 5% failed.

The simulations on the four-factor test function (Table 2) reveal, too, that continuous reflection of more than one vertex gives a reduction in time but now there is the additional effect that the more experiments can be done parallel the higher the saving in time (up to 56% or 70%, depending on the termination procedure chosen). The number of experiments increases with the number of vertices reflected at the same time. Variation of the criterion C shows that 40% is an optimal value in respect

to the number of experiments. In that case 13 or 14% can be saved but this does not reduce the number of steps.

Only at $i_{\max} = 1$ ca. 8% of the runs failed to reach the optimum.

The gains given in Tables 1 and 2 are tested by a Students' *t*-test on paired results, $\alpha = 0.01$. In Table 2 the gains are significant when they exceed ca. 6%.

Reflecting more than one vertex at a time may be useful when the experiments can be done parallel: time will be saved. If parallel processing of the experiments is impossible it may be safer to reflect one vertex per simplex.

References

1. Spendley W, Hext GB, Himsworth FR (1962) *Technometrics* 4:441
2. Wiel PFA van der (1980) *Anal Chim Acta* 122:421
3. Wiel PFA van der, Maassen R, Kateman G (1983) *Anal Chim Acta* 153:83
4. Hendrix C (1980) *Chemtech* 10:448
5. Brooks SH (1959) *Operation Res* 7:430
6. Powell MJD (1962) *Comput J* 5:147
7. Long DE (1969) *Anal Chim Acta* 46:193

Received August 28, 1985

Fresenius Z Anal Chem (1986) 324:58-59
© Springer-Verlag 1986

Collection and separation of some organic insecticides on polyurethane foam columns

A. B. Farag, A. M. El-Wakil, and M. S. El-Shahawi

Department of Chemistry, Faculty of Science,
Mansoura-University, Mansoura, Egypt

Anreicherung und Trennung organischer Insecticide
mit Hilfe von Polyurethanschaum-Säulen

Introduction

Polyurethane foams comprise a new class of collectors useful for application in aqueous and gaseous media [1, 2]. The quasi-

Offprint requests to: A. B. Farag

spherical membrane structure of these foams has offered special advantages over other solid collectors. These foams allowed reasonable flow-rates of the mobile phase without the aid of a pump.

Gesser et al. [3] suggested the application of polyurethane foams for the collection of trace organic contaminants from water using a batch technique. Since then several investigations have been published describing the application of untreated polyurethane foams as collectors in separating and concentrating various chlorinated insecticides and other organic substances.

The work reported here was aimed at evaluating the use of polyurethane foam as a collector suitable for the extraction and recovery of some phosphorus and sulphur-containing organic insecticides from aqueous media.

Short communications was supplied by Stenier K.G., Schaumstoffwerk-Kremsmunster, Austria. The volume weight of the foam was 30 kg m^{-3} . The foam cubes (5 mm edge) were washed by 1 M hydrochloric acid followed by distilled water and acetone and finally dried at 80°C . The insecticides tested were: Summicidin [α -cyano-m-phenoxy-benzyl- α -isopropyl-p-chlorophenyl acetate], Thiodane 35 emulsifiable, which is a cyclic sulphurous acid ester of active ingredient, endosulphur; Hostaquick SOEC [phosphoric acid-(7-chloro-bis-cyclo-3,2-0-hepta-2,6-diene-6-yl-1-di-methylester)] and Hostathion HOEC (Triazophos) which is a derivative of Hostaquick. These insecticides were used as received.

Apparatus. Glass columns of 15 mm diameter and 15 cm length were employed. Gas-liquid chromatographic instrument (PYE Unicam 104 series) was used for the determination of the insecticides tested. A polyethylene glycol column was employed at 120°C .

Column preparation. 0.3 g unloaded dry foam cubes was packed in the glass column using the vacuum method of foam column packing [2].

Procedure. 30 mg of each insecticide in 2 l of water is percolated through the foam column at $10\text{--}15 \text{ ml min}^{-1}$. After squeezing water from the foam material, the insecticide is recovered from the foam with 120 ml acetone in a Soxhlet apparatus. The eluate is then concentrated in a rotary evaporator to 10 ml and 5 μl sample is analysed using a gas chromatographic method.

Results and discussion

One of the promising separation and preconcentration techniques is by foam column collectors. This method allows the isolation of the analyte from the matrix and yields an appropriate enrichment factor. Also, the advantageous hydrodynamic properties of foam columns allow the application of a quite high flow-rate without the aid of vacuum. This together with the rapid attainment of the absorption equilibrium on the thin membranes forming the foam material reduces the time required for analysis.

In preliminary batch experiments, attempts were made to collect some sulphur and phosphorus containing organic insecticides on polyurethane foam. The foam material was found to have a good affinity towards the absorption of the insecticides tested (Hostathion HOEC, Hostaquick SOEC, Thiodan 35 and Summicidin). These results suggested the possibility of using polyurethane foam in column dynamic experiments for the extraction of these insecticides from aqueous solutions.

Two liters of each insecticide solution were passed through the foam column at a flow-rate of $10\text{--}15 \text{ ml min}^{-1}$, which was chosen on the basis of a preliminary test. The insecticides were then recovered from the foam material with acetone in a Soxhlet apparatus and their concentrations were measured by a gas chromatographic technique. The results of the extraction and recovery of the insecticides examined from 2 l aqueous solutions by the proposed foam column are summarized in Table 1. Better results were obtained for the separation and recovery of Summicidin when the flow-rate was reduced to 5 ml min^{-1} . A typical example of the separation of Hostathion is shown in Fig. 1. The chromatograms of Hostathion with and without the foam concentration step illustrate the efficiency of the proposed foam columns.

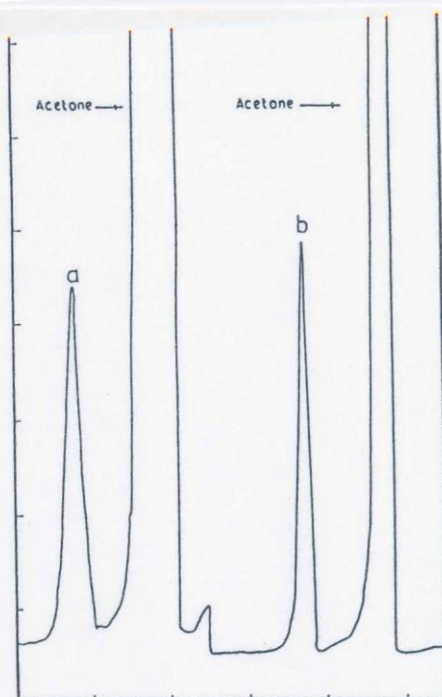


Fig. 1. Chromatogram of Hostathion 40 EC. *a* Hostathion (30 mg/10 ml) in acetone (5 μl sample is injected). *b* Hostathion (30 mg/2 l) in aqueous sample after using the foam preconcentration step

Table 1. Extraction and recovery of the insecticides tested from 2 l aqueous solutions by polyurethane foam columns at $10\text{--}15 \text{ ml min}^{-1}$ flow rate

Insecticide	Amount (mg)	% Recovery
Hostathion HOEC	30	93.4
Hostaquick SOEC	30	100.0
Thiodan 35	30	98.3
Summicidin	20	90.3

The present work has demonstrated the capabilities of polyurethane for the collection and recovery of sulphur and phosphorus insecticides from dilute aqueous solution.

References

- Braun T, Navartil JD, Farag AB (1985) Polyurethane foam sorbents in separation science. CRC Press, Florida
- Moody GJ, Thomas JDR (1982) Chromatographic separation and extraction with foamed plastics and rubbers. Dekker, New York
- Gesser HD, Chow A, Davis FC, Uthe JF, Reinke J (1971) Anal Lett 4:883

Received December 10, 1985

Fresenius Z Anal Chem (1986) 324:59–60
© Springer-Verlag 1986

SEPARATION OF CADMIUM(II), IRON(III), NICKEL(II) AND COPPER(II)
IN AQUEOUS SOLUTIONS USING ADOGEN-FOAM COLUMNS

A.B. Farag, A.M. El-Wakil and M.S. El-Shahawi

Department of Chemistry, Faculty of Science, Mansoura University,
Mansoura, Egypt

Received : 01/04/1985 - Accepted : 30/09/1985

SUMMARY

Polyurethane foam, polyether of open-cell type, immobilizing Adogen-364 (trialkyl tertiary amine) has been prepared and its capability for the separation of some metal ions in aqueous solution was examined. Adogen-loaded foam columns have successfully been used in the separation of cadmium(II), iron(III), nickel(II) and copper(II). Typical examples of separations are given.

INTRODUCTION

In the last few years, a number of publications have appeared describing the possibility of using cellular plastics (mainly polyurethane foams) as a quasispherical matrix for immobilizing and supporting a wide variety of inorganic and organic reagents. A current status of the application of these reagent foams for the retention, separation and preconcentration of many organic and inorganic species in aqueous and gaseous media, has recently been reviewed¹⁻⁵.

The preparation and application of an open-cell type polyurethane foam loaded with a liquid anion exchanger was first described by Braun et al⁶. They used tri-n-octyl amine(TOA)-foam for the separation of cobalt from nickel in a hydrochloric acid system. Polyurethane foams treated with Amberlite LA-2 and Aliquat-336 have also been suggested^{7,8} for the separation of some metal ions in acidic aqueous solutions.

The present work is a further extension to the subject with the purpose of immobilizing Adogen on polyurethane foam and examining the analytical utility of this anion exchange foam for the separation of cadmium(II), iron(III), nickel(II) and copper(II) in aqueous hydrochloric acid solution.

EXPERIMENTAL

Reagents and Materials :

Except otherwise mentioned, all reagents used were of analytical -reagent grade. Adogen-364 was obtained from Archer-Daniels-Midland Co., Minneapolis. It is a water - insoluble trialkyl tertiary amine mixture of C₈ and C₁₀ chains with C₈ predominating. Average molecular weight 390, sp.gr. 0.802. This reagent was used as received. Solutions of Adogen-364 were prepared by dilution with xylene. Polyurethane foam, polyether of open-cell type (bulk density 30 kg.m⁻³), was supplied by Greiner KG, Schaumstoffwerk, Kremsmunster, Austria. The foam material (cubes of 5 mm edge) was washed with 1M-hydrochloric acid followed by distilled water. The foam cubes were then washed with acetone and dried at 80°C.

Stock solutions containing 10 mg ml⁻¹ of iron(III), cadmium(II), nickel(II) and copper(II) ions were prepared by dissolving the corresponding metal salt in 1M hydrochloric acid.

Adogen-loaded foam was prepared by equilibrating the clean dried foam with Adogen solution (3 ml g⁻¹ dry foam) with efficient stirring for 10 min. The

Adogen foam columns were prepared by the drawing procedure reported earlier⁹.

Apparatus :

Glass columns 15 mm diameter and 15 cm length were used in the dynamic experiments. In the batch extraction experiments, stoppered flasks were employed. Atomic absorption spectrophotometer of the type Unicam SP 90 A series 2 was used for determining the concentration of cadmium, iron, nickel and copper employing the suitable hollow cathod lamp.

Procedure :

In the case of separating a mixture containing 2 mg of each of cadmium(II), iron(III), and nickel(II) in 2M hydrochloric acid using the Amine-loaded foam columns; the feed mixture (5-15 ml) was allowed to percolate through the foam column at 2-4 ml⁻¹. Nickel was removed from column by 1M hydrochloric acid. Iron was then eluted from the column by 1M sodium fluoride solution and finally cadmium was recovered with 1M nitric acid solution.

In the separation of cadmium(II), iron(III) and copper(II); the mixture (containing 2 mg of each metal ion) was passed through the foam column at 2-4 ml min⁻¹. Copper(II) was washed out firstly with 50 ml of 0.3M Hydrochloric acid saturated with sodium chloride. Iron(III) was then eluted with 1M sodium fluoride solution and finally cadmium(II) was recovered with 1M nitric acid solution.

RESULTS AND DISCUSSION

One of the attractive topics in the field of extraction chromatography has been the application of polyurethane foam columns, because they have higher ability to retain various stationary liquid phases and better hydrodynamic properties than conventional columns.

In order to investigate the suitability of the proposed Adogen-foam for the separation of different inorganic species in aqueous solution, a detailed study of several parameters has been carried out.

The effect of amine concentration on the extraction efficiency of, e.g., cadmium(II) on Adogen-foam has been carried out in batch experiments. For this reason, 0.2 g of foam cubes loaded with a solution of different concentrations of Adogen in xylene is mixed with 1M hydrochloric acid solution (10 ml) containing 2 mg of cadmium. The mixture is shaken for 2 hr. in a mechanical shaker and then cadmium was determined in the aqueous solution employing atomic absorption spectrophotometric method. Cadmium retained on the foam was calculated by difference. The results indicate that the extraction of cadmium increases on increasing the amine concentration in the loading solution. For this reason, the original amine solution was employed in the subsequent experiments.

The effect of hydrochloric acid concentration on the extraction of cadmium (II), iron(III), nickel(II) and copper(II) has been investigated in the batch extraction system. Nickel(II) and copper(II) show no extraction in hydrochloric acid concentration in the range 0.1-5M. The extraction of cadmium(II) and iron(III) was found to be quite complete at acid concentrations higher than 0.5M and 2M, respectively.

Quantitative retention and elution of cadmium(II) and iron(III) have been investigated in column extraction mode. Columns packed with 5 g Adogen-foam were employed for this purpose. The results of the current study show that both ions are completely retained on the foam column from 2M hydrochloric acid solution at a flow rate of 2-4 ml min⁻¹. Iron(III) and cadmium(II) were recovered from the Adogen-foam column with 1M sodium fluoride and 1M nitric acid solutions, respectively. The elution curves were found to be quite sharp and symmetric using elution flow rates up to 7 ml min⁻¹.

The capacity of the Adogen-loaded foam toward the extraction of cadmium(II) in aqueous hydrochloric acid solution was measured in batch and column systems¹⁰ and found to be 50 mg and 53 mg cadmium(II) per gram loaded foam, with standard deviations, 1.18 and 0.96, respectively.

As a consequence of the above characterization of the Adogen foam column performance, the proposed foam columns have been tested for the separation of cadmium(II)-iron(III)-nickel(II); and cadmium(II)-iron(III)-copper(II) mixtures. The separations of these mixtures were successfully carried out using a feeding solution of 5-15 ml containing 0.1-5 mg of each ion dissolved in 2 M hydrochloric acid solution. At this acidity, both cadmium(II) and iron(III) were retained quantitatively on the foam column. Nickel(II) and copper(II) were washed out with 1 M hydrochloric acid and 0.3M hydrochloric acid saturated with sodium chloride, respectively. Iron(III) was eluted with 1M sodium fluoride solution and cadmium was then recovered with 1M nitric acid solution.

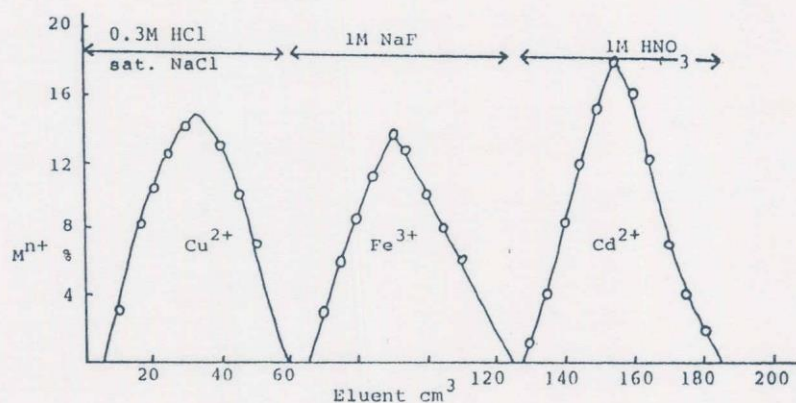


FIG. 1. Separation of Cu-Fe-Cd in 1M hydrochloric acid solution using Adogen-foam column.

FIG. 1, shows, for instance, a chromatogram illustrating the efficiency of the proposed Adogen-foam column in the separation of copper(II), iron(III) and cadmium(II) ions in aqueous solution.

REFERENCES

1. T. Braun and A.B. Farag, *Talanta*, 22, 699-705 (1975).
2. T. Braun and A.B. Farag, *Analyt. Chim. Acta*, 99, 1-36 (1978).
3. G.J. Moody and J.D.R. Thomas, *Analyst*, 104, 1-15 (1979).
4. G.J. Moody and J.D.R. Thomas, *Chromatographic Separation and Extraction with Foamed Plastics and Rubbers*, Marcel Dekker, New York, 1982.
5. T. Braun, *Z. Anal. Chem.*, 314, 652 (1983).
6. T. Braun, E. Huszar and L. Bakos, *Analyt. Chim. Acta*, 64, 77-84 (1973).
7. M.P. Maloney, G.J. Moody and J.D.R. Thomas, *Proc. Anal. Div. Chem. Soc.*, 14, 244-250 (1977).
8. A.M. El-Wakil, A.B. Farag and A. Kh. Ez-Eldin, *Sep. Sci. Technol.*, 17, 1058-1089 (1982).
9. T. Braun and A.B. Farag, *Analyt. Chim. Acta*, 62, 476-480 (1972).
10. T. Braun and A.B. Farag, *Analyt. Chim. Acta*, 61, 265-276 (1972).

DETECTION AND SEMIQUANTITATIVE DETERMINATION OF NICKEL WITH DIMETHYLGLYOXIME-LOADED FOAM

A. B. FARAG, A. M. EL-WAKIL and M. S. EL-SHAHAWI

Chemistry Department, Faculty of Science, Mansoura University, Mansoura, Egypt

(Received 19 December 1981. Accepted 24 March 1982)

Summary—Rapid, sensitive and selective detection and semiquantitative determination of nickel in aqueous solution can be obtained by using dimethylglyoxime loaded on polyurethane foam, either by batch or column extractions, the detection limits being 0.05 and 0.01 ppm respectively.

Polyurethane foam loaded with water-insoluble reagents which yield coloured reaction products seems very attractive for raising the sensitivity of spot-tests. This method has been tested for the detection of cobalt(II),¹ chromium(VI)² and iron(III)³ with polyurethane foam loaded with Amberlite LA-1, 1,5-diphenylcarbazine and tricapriline, respectively. These tests were more sensitive than the normal spot-tests on a spot-plate,⁴ on paper impregnated with reagent⁴ or with the resin spot-test,⁵ and had good selectivity.

They could also be used for semiquantitative determination.

In the present work polyurethane foam loaded with dimethylglyoxime was evaluated as a reagent for detection and semiquantitative determination of nickel.

EXPERIMENTAL

Reagents

All reagents were of analytical-reagent grade unless otherwise specified. Tricaprylamine (Alamine 336), pure grade, was kindly provided by General Mills, Kankakee, Illinois, U.S.A. An open-cell, polyether type polyurethane foam (bulk density 30 kg/m³) was supplied by Greiner KG, Schaumstoffwerk-Kremsmunster, Austria. The foam material (cubes of 5 mm edge) was washed and dried as previously described.^{1,2}

The dimethylglyoxime solution was prepared by dissolving about 0.2 g in 10 ml of Alamine 336. The reagent-foam was prepared by immobilizing the dimethylglyoxime-amine solution on the polyurethane foam by a procedure similar to that described previously.⁶

In the flow experiment, 0.5 g of the loaded foam was packed in a glass tube 5 mm in diameter and 10 cm long, by the vacuum method.⁷

RESULTS AND DISCUSSION

The colour reaction of dimethylglyoxime with nickel is well known. Experience with reagent-loaded polyurethane foam has shown that metal ions at very low concentration in aqueous solution can be collected on the reagent-foam simply by shaking, or by percolating the solution through a foam column at a reasonable flow-rate.

In preliminary experiments, an alcohol solution of dimethylglyoxime was tried for loading the foam, but the results were not satisfactory. A saturated solution of dimethylglyoxime in Alamine 336 proved suitable, however, the reagent not being leached from the foam on shaking vigorously with aqueous solution or on elution at relatively high flow-rates. Evidently, the amine serves a dual purpose, as a suitable solvent for the dimethylglyoxime and as a plasticizer for the foam material.

Shaking one cube (5 mm edge) of the foam for 1–2 min with 2 ml of aqueous nickel solution (pH 7–9), allowed detection of the nickel at relatively very low concentrations (0.05 ppm) by means of the red colour formed on the foam. The sensitivity was superior to that of the normal spot-test on a spot-plate (3.2 ppm) or impregnated paper (0.5 ppm).

It was found possible to detect 1 µg of nickel in the presence of 20 mg of Ti⁴⁺, In³⁺, Hg(I), Cd²⁺, Zn²⁺, Ca²⁺, Ba²⁺, Rb⁺, Mg²⁺, NH₄⁺, PO₄³⁻, S₂O₃²⁻, SO₄²⁻, SCN⁻, CH₃COO⁻, CO₃²⁻, HCO₃⁻, Cl⁻, Br⁻, I⁻, SO₃²⁻, B₄O₇²⁻, ascorbate or tartrate. Bi³⁺, Au³⁺, Pd²⁺ and Pt⁴⁺ interfere in the same way as in the usual spot-test.

In the presence of some other ions simple modifications of the aqueous solution are needed for the clear and sensitive detection of nickel (Table 1). Iron(II) must be oxidized to iron(III) before addition of fluoride.

Semiquantitative determination is possible by comparison of the colour of the foam cube with standards prepared with 0.05, 0.1, 1, 10 and 50 ppm nickel solutions under the same conditions.

A still lower concentration of nickel (0.01 ppm) can be detected by percolating 100 ml of the nickel solution through 0.5 g of reagent-foam (packed in a column) at a flow-rate of 3–5 ml min. The length of the coloured zone is proportional to the concentration of nickel, which can be estimated by using standards covering the concentration range 10–50 ng/ml.

Table 1. Effect of various ions on the detection of 1 μg of nickel(II) in 2-ml of aqueous solution

Foreign ion	Compound added	Colour of the foam*	Tolerance limit,† μg	Notes
Cu(II)	CuCl ₂	White	1:10 ⁴	Crystals of KI added, followed by Na ₂ S ₂ O ₃ crystals.
Co(II)	Co(NO ₃) ₂	White	1:10 ²	
Ce(IV)	Ce(SO ₄) ₂	White	1:10 ³	
Fe(III)	FeCl ₃	Yellow	1:10 ⁴	One drop of saturated KF solution added
Lu(III)	Lu(NO ₃) ₃	White	2:10 ³	
Mn(II)	MnSO ₄	White	1:10 ⁴	Oxidation with Br ₂ water, excess of bromine eliminated by heating
Pb(II)	Pb(NO ₃) ₂	White	1:10 ²	
Oxalate	Na ₂ C ₂ O ₄	White	1:10 ⁴	Crystals of CaCl ₂ added
CrO ₄ ²⁻	K ₂ CrO ₄	Pale yellow	1:10 ²	
NO ₂ ⁻	NaNO ₂	White	2:10 ³	
VO ₃ ⁻	NH ₄ VO ₃	Pale yellow	1:10 ²	
MoO ₄ ²⁻	(NH ₄) ₆ Mo ₇ O ₂₄	White	1:10 ⁴	Saturated solution of H ₂ C ₂ O ₄ added, followed by a few crystals of CaCl ₂ ; values obtained by comparison with a blank.
MnO ₄ ⁻	KMnO ₄	White	2:10 ³	Few drops of 1M H ₂ SO ₄ and 1 ml of Na ₂ C ₂ O ₄ added, then heating to ca. 80°; after cooling, nickel detected as usual.
Formate	HCOONa	White		Oxidation with Br ₂ water, excess of bromine eliminated by heating

*The colour in the absence of nickel.

†The amount of the foreign ion below which 1 μg of nickel can easily be detected.

REFERENCES

1. T. Braun and A. B. Farag, *Anal. Chim. Acta*, 1974, **73**, 301.
2. A. B. Farag, A. M. El-Wakil and M. S. El-Shahawi, *Analyst*, 1981, **106**, 809.
3. *Idem*, *Ann. Chim. Soc. Chim. Ital.*, in the press.
4. F. Feigl and V. Anger, *Spot Tests in Inorganic Analysis*, 6th Ed., Elsevier, Amsterdam, 1972.
5. M. Fujimoto, *Chemist-Analyst*, 1965, **54**, 58, 92.
6. T. Braun and A. B. Farag, *Talanta*, 1975, **22**, 699.
7. *Idem*, *Anal. Chim. Acta*, 1972, **62**, 476.

QUALITATIVE AND SEMIQUANTITATIVE DETERMINATION OF
IRON (III) IN AQUEOUS THIOCYANATE SOLUTION USING
TRICAPRYLYL AMINE FOAM

Abdel-Fattah Bastawi FARAG^(O); Ahmed Mohamad EL-WAKIL
and Mohamad Sorour El-SHAHAWI

Chemistry Department, Faculty of Science, Mansoura
University, Mansoura, Egypt.

INTRODUCTION

One of the common methods for the detection of small amounts of iron (III) in aqueous solution is that based on its reaction with thiocyanate ion¹. Iron gives several red-blood coloured compounds, depending on the thiocyanate ion concentration and present in equilibrium with each other^{2,3}.

In previous work^{4,5}, it was emphasized that the application of polyurethane foam loaded with some reagents increased the sensitivity of the spot colour reactions of cobalt (II) and chromium (VI) ions.

The present work is a further extension of the subject so as to cover the detection and semiquantitative determination of very low concentrations of iron in thiocyanate medium. Polyurethane foam previously treated with tricaprylyl amine was examined for this purpose.

EXPERIMENTAL.

General reagents and materials- All reagents used were of analytical reagent grade, except otherwise mentioned. Tri-caprylyl tertiary amine (Alamine 336), pure grade, was used without further purification. Polyurethane foam, an open-cell, polyether type (bulk density 10 kg/m³) was supplied by Greiner KG. Schaumstoff-Werk-Kremsmunster, Austria. The foam material (cubes of 5 mm edge) was washed with 1 M hydrochloric acid followed by distilled water until the washings were free from chloride ion. The foam material was then washed with acetone and dried at 80 °C. The reagent foam was prepared as previously described⁴.

Apparatus-Glass columns of 5 mm diameter and 10 cm length were used in the column experiments. The columns were packed by the vacuum method⁶. About 0.5 g of the loaded foam was employed.

5ml all-glass syringes (i.e. without any metal connection)

FARAG and coworkers

was used in the pulsed column method.

RESULTS AND DISCUSSION

The sensitivity of the iron colour reaction in thiocyanate medium could be increased by extracting the anionic complex formed, in a liquid anion exchanger immobilized on polyurethane foam. In this case the anion exchanger which is homogeneously distributed on the relatively high available surface area of the foam membranes, functions as a good collector for the coloured iron-thiocyanate complex.

On shaking one cube (5 mm edge) of the amine-foam with 2 ml of aqueous acidic solution (pH 2-4) of iron (III) in the presence of excess thiocyanate ions (1%), it was possible to detect iron in relatively very low concentrations (0.1 ppm) after 1-2 min. This result was found to be better than that obtained with spot test methods using a normal spot plate (5ppm)¹ or modified spot test (0.5 ppm)².

The detection of 1 µg iron in the presence of relatively high excess (20 mg) of each Pb^{2+} , Mn^{2+} , Cd^{2+} , Ni^{2+} , Zn^{2+} , In^{3+} , Ti^{4+} , $S_2O_3^{2-}$, SO_4^{2-} , Cl^- , Br^- and formate ions, was successfully carried out straight forwardly using the method recommended. In the presence of some other ions, simple modifications were introduced in order to obtain clear and sensitive detection for iron using the proposed foam method (see Table 1).

Also, the semiquantitative determination of iron (III) in thiocyanate medium using the proposed amine foam was found to be possible. The colour density on the reagent foam cube was found to be proportional to the concentration of iron (III) in the aqueous solution. A standard colour scale 0.1, 0.5, 1.0, 10.0 and 20 ppm proved to be quite stable. The colour developed on the foam cube after shaking with the unknown solution is successfully matched with that obtained in the proposed standard colour scale and so the concentration of the unknown solution could simply be determined semiquantitatively.

The resilient character of polyurethane foam used, allowed the possibility of using the amine foam in what is called pulsed column. The reagent foam material is packed into a medical syringe. By pressing the glass plunger, the foam compresses. When the tip of the column is kept in the thiocyanate solution of iron and the plunger is gradually released, the aqueous solution penetrates into the column and the foam material returns to its original volume. Repetition of this process allows the external solution to come into contact with the reagent several times which results in complete extraction of the iron (III) thiocyanate complex on the foam.

Using one foam cube (2 cm edge) in a 5 ml capacity syringe, it was possible to detect 5 ppb iron (III) after repetitive pulsations in aqueous acidic solution (100 ml).

Smaller amounts of iron (1.0 ppb) could be collected and detected from 100 ml aqueous thiocyanate solution by passing it through a reagent foam column (packed with 0.5 g foam) at a reasonable flow rate (3-5 ml/min). The length of the coloured zone was found to be proportional to the concentration of iron in aqueous solution. Therefore semiquantitative determination of Fe^{3+} at the ppb concentration level could be possible. The following colour scale proved to be satisfactory: 1, 5, 10, 20 and 30 ppb.

TABLE 1- Effect of various ions on the detection of 1 μ g of iron (III) in 2 ml aqueous solution.

Foreign ion	Added compound	Colour of the foam*	Iron: Foreign ion**	Note
Cu(II)	CuCl ₂	White	1:2.10 ⁴	Crystals of KI were added, followed by the addition of Na ₂ S ₂ O ₃ crystals.
Hg(II)	HgCl ₂	White	1:2.10 ⁴	Crystals of KSCN were added.
Bi(III)	Bi ₂ (SO ₄) ₃	White	1:2.10 ⁴	The bismuth salt was dissolved in 1 N H ₂ SO ₄ .
Co(II)	Co(NO ₃) ₂	Blue	1:2.10 ³	Concentration of KSCN was decreased and the value was obtained by comparison with a blank test.
Acetate	CH ₃ COONa	White	1:2.10 ⁴	Drops of 0.1 N H ₂ SO ₄ were added.
Tartrate	KNaC ₄ H ₄ O ₆	White	1:2.10 ⁴	Oxidation by bromine water, followed by addition of 0.1 N H ₂ SO ₄ drops to adjust pH ~ 2.
PO ₄ ³⁻	Na ₃ PO ₄	White	1:2.10 ⁴	Drops of 0.1 N H ₂ SO ₄ were added to adjust pH ~ 2.
C ₂ O ₄ ²⁻	Na ₂ C ₂ O ₄	White	1:2.10 ⁴	CaCl ₂ crystals were added.
Li(I)	Li ₂ SO ₄	Pale white	1:2.10 ⁴	The value is obtained by comparison with a blank test.
Ca(II)	CaCl ₂	White	1:2.10 ⁴	Adjust the pH to ~ 2.
Mg(II)	MgCl ₂	Pale pink	1:2.10 ⁴	0.1 N H ₂ SO ₄ drops were added.
B ₄ O ₇ ²⁻	Na ₂ B ₄ O ₇ · 10 H ₂ O	White	1:2.10 ⁴	A few drops 0.1 N H ₂ SO ₄ were added.
NO ₂ ⁻	NaNO ₂	White	1:2.10 ⁴	Oxidation by Br ₂ water and excess bromine was eliminated by heating.
VO ₃ ⁻	NH ₄ VO ₃	pale yellow	1:2.10 ⁴	Values obtained by comparison with a blank test.
MnO ₄ ⁻	KMnO ₄	Pink	1:2.10 ³	Add Na ₂ SO ₃ crystals followed by 2 N H ₂ SO ₄ .

* The foam colour of the blank test (i.e. in the absence of iron(III)).

** The amount of the foreign ion below which the detection of 1 μ g of iron (III) can easily be achieved.

Received June 29th, 1981.

REFERENCES

- 1) F.FEIGL, A.ANGER; "Spot Tests in Inorganic Analysis, Elsevier, Amsterdam, 6th. ed., 1972.
- 2) H.J.SCHLESINGER, H.B. VON VALKENBURGH: J.Am. Chem. Soc., 53, 1212 (1931); S.Z. LEWIN, R.SEIDEN: J.Chem. Education, 30, 445 (1953).
- 3) A.I.VOGEL: "Quantitative Inorganic Analysis, Longmans, 3rd. ed., (1966).
- 4) T.BRAUN A.B. FARAG; Anal. Chim. Acta, 73, 301 (1974).
- 5) A.P.FARAG, A.M. EL-WAKIL, M.S. EL-SHAHAWI: Analyst (London), 106, 809 (1981).
- 6) T.BRAUN, A.B.FARAG: Anal. Chim. Acta, 62, 476 (1972).
- 7) M.ZEIGLER, O.GLEMSEK, N.PETRI: Z.Anal.Chem., 153, 241 (1956).
- 8) T.BRAUN, A.B.FARAG: Anal.Chim. Acta, 65, 139 (1973).

Qualitative and Semiquantitative Determination of Chromium(VI) in Aqueous Solution Using 1,5-Diphenylcarbazide Based Foam

A. B. Farag, A. M. El-Wakil and M. S. El-Shahawi

Chemistry Department, Faculty of Science, Mansoura University, Mansoura, Egypt

Keywords: Chromium detection; 1,5-Diphenylcarbazide foam test

The detection and determination of low concentrations of chromium in aqueous solution are important for many purposes, particularly in environmental pollution analyses. Many spot-test reagents have been suggested for this purpose. 1,5-Diphenylcarbazide appears to

be one of the most sensitive and satisfactory of the reagents available. Chromium(VI) gives a violet colour with this reagent.²⁻⁴

The sensitivity and selectivity of spot reactions have been greatly improved by impregnating the reagents on filter-paper,¹ by the ring oven technique,⁵ and by the resin spot-test method.⁶ The introduction of polyurethane foam^{7,8} as a separatory medium in gas and liquid chromatography seemed to be very attractive. Polyurethane foam loaded with Amberlite LA-1 has been employed for the qualitative and semi-quantitative determination of cobalt(II) in aqueous thiocyanate solution.⁹

In this work the application of polyurethane foam, previously treated with 1,5-diphenylcarbazide reagent, for the detection and semi-quantitative determination of chromium(VI) in batch and flow experiments has been investigated.

Experimental

Reagents and Materials

Unless otherwise specified all reagents were of analytical-reagent grade. Tricaprylylamine (Alamine-336), pure grade, was used without further purification. Polyurethane foam, an open-cell, polyether type (bulk density 30 kg m⁻³), was supplied by Greiner KG, Schaumstoff-Werk-Kremsmunster, Austria. The foam material (cubes of 5-mm edge) was washed with 1 M hydrochloric acid followed by distilled water until the washings were free from chloride ion. The foam was then washed with acetone and dried at 80 °C.

A stock solution containing 1 mg ml⁻¹ of chromium(VI) was prepared by dissolving potassium dichromate in 0.01 M perchloric acid. 1,5-Diphenylcarbazide solution was prepared by dissolving 0.1 g of the solid material in 10 ml of benzene followed by the addition of 10 ml of the amine.

Caution—Benzene is highly toxic and appropriate precautions should be taken.

Reagent foam preparation

One gram of the dried foam cubes (white) was equilibrated with 3 ml of the 1,5-diphenylcarbazide solution with efficient stirring and was then allowed to remain in contact with the solution for about 1 h to ensure complete equilibration. The loaded foam material (pale yellow) was then dried between two sheets of filter-paper to remove the excess of reagent solution.

Apparatus

Glass columns of 5-mm diameter and 10-cm length were used in the dynamic experiments.

TABLE I
EFFECT OF DIFFERENT CATIONS ON THE DETECTION OF 1 μg OF CHROMIUM(VI)

Foreign ion	Compound added	Maximum tolerable amount of the foreign ion/mg*	Maximum tolerable concentration of interfering ion relative to Cr(VI)
La(III)	La(NO ₃) ₃	10	10 ⁴
Ce(IV)	Ce(SO ₄) ₂	10	10 ⁴
Co(II)	Co(NO ₃) ₂ ·5H ₂ O	1	10 ³
Fe(III)	FeCl ₃ †	10	10 ⁴
Ni(II)	NiSO ₄ ·7H ₂ O	10	10 ⁴
Tl(I)	TlNO ₃	1	10 ³
In(III)	InCl ₃ ·7H ₂ O	1	10 ³
Ba(II)	BaCl ₂	10	10 ⁴
Ca(II)	CaCl ₂ ‡	10	10 ⁴
Sr(II)	SrCl ₂	10	10 ⁴
Rb(I)	RbNO ₃	10	10 ⁴
Mg(II)	MgCl ₂	10	10 ⁴
NH ₄ ⁺	NH ₄ Cl	10	10 ⁴

* The amount of foreign ion below which the determination of 1 μg of chromium(VI) in 2 ml of aqueous solution can be easily achieved.

† The foam colour in the blank test [*i.e.*, in the absence of chromium(VI)] was yellow.

‡ A few drops of 1 N perchloric acid were added to the CaCl₂ solution.

The foam columns were prepared using the vacuum method of foam column packing described previously.^{10,11} About 0.3 g of the loaded foam was employed.

Results and Discussion

The application of polyurethane foam to the detection and semi-quantitative determination of lead, copper and cobalt in aqueous solution has been reported previously.⁹ Fundamental data and the application to the detection of 1 μg of cobalt in the presence of relatively high concentrations of various other elements showed the usefulness of the method in trace element analysis. The use of this method for the determination of chromium(VI) was the subject of the present investigation.

1,5-Diphenylcarbazide was dissolved in benzene, an equal volume of tricaprylylamine was then added. The added amine has two functions: it acts as a plasticiser to the foam material and as an anion exchanger, which allows the collection of chromate ion on the foam matrix.

The colour reaction of chromium(VI) and 1,5-diphenylcarbazide could be carried out on the foam material simply by mixing one cube of the plasticised 1,5-diphenylcarbazide foam

TABLE II
EFFECT OF VARIOUS ANIONS ON THE DETECTION OF 1 μg OF CHROMIUM(VI)

Foreign ion*	Compound added	Maximum tolerable amount of the foreign ion/mg \dagger	Maximum tolerable concentration of interfering ion relative to Cr(VI)	Notes
Acetate ..	CH ₃ COONa	10	10 ⁴	Drops of 0.1 N perchloric acid were added
Oxalate ..	Na ₂ C ₂ O ₄	10	10 ⁴	Oxidation by bromine water was carried out followed by addition of drops of 0.1 N perchloric acid
Tartrate ..	KNaC ₄ H ₄ O ₆	10	10 ⁴	Conditions as mentioned for oxalate
S ₂ O ₃ ²⁻ ..	Na ₂ S ₂ O ₃	0.1	10 ²	Oxidation by bromine water was carried out and the excess of bromine was eliminated by heating
Cl ⁻ ..	NaCl	10	10 ⁴	
Br ⁻ ..	NaBr	10	10 ⁴	
CNS ⁻ ..	KCNS	10	10 ⁴	Drops of 0.1 N perchloric acid were added
PO ₄ ³⁻ ..	Na ₃ PO ₄	10	10 ⁴	pH adjusted to about 2
HPO ₄ ²⁻ ..	Na ₂ HPO ₄	10	10 ⁴	pH adjusted to about 2
H ₂ PO ₄ ⁻ ..	NaH ₂ PO ₄	10	10 ⁴	
HCO ₃ ⁻ ..	KHCO ₃	10	10 ⁴	pH adjusted to about 2
B ₄ O ₇ ²⁻ ..	Na ₂ B ₄ O ₇ ·10H ₂ O	10	10 ⁴	pH adjusted to about 2
NO ₂ ⁻ ..	NaNO ₂	10	10 ⁴	Oxidation by Br ₂ was carried out followed by adjusting pH to about 2
I ⁻ ..	NaI	10	10 ⁴	
Formate ..	HCOONa	10	10 ⁴	Oxidation by Br ₂ was carried out followed by adjusting pH to about 2
SO ₃ ²⁻ ..	Na ₂ SO ₃	0.1	10 ²	
SO ₄ ²⁻ ..	Na ₂ SO ₄	0.1	10 ²	
VO ₃ ⁻ ..	NH ₄ VO ₃ \dagger	0.1	10 ²	
MoO ₄ ²⁻ ..	(NH ₄) ₂ MoO ₄ \dagger	10	10 ⁴	Drops of a saturated solution of oxalic acid were added
MnO ₄ ⁻ ..	KMnO ₄	0.5	2 × 10 ²	
L-Ascorbate ..	L-Ascorbic acid	0.1	10 ²	Oxidation by bromine water was carried out followed by removal of excess of bromine

* With metal ions that interfere due to their own colour in solution, it was found better to take out the foam cube (after shaking with the test solution) and to shake it with a few millilitres of water. The red-violet colour that appears in the presence of chromium(VI) was then better observed.

\dagger The amount of the foreign ion below which the detection of 1 μg of chromium(VI) in 2 ml of aqueous solution can be easily achieved.

\ddagger The foam colour in the blank test [*i.e.*, in the absence of chromium(VI)] was yellow.

with 1–2 ml of an aqueous, acidic solution of chromium (pH 2–4). Using this method, as little as 0.1 μg of chromium(VI) could be detected, a red-violet colour appearing on the foam cube after shaking for 1–2 min.

The detection limits for chromium using the 1,5-diphenylcarbazide reagent in a normal spot test,¹ on impregnated filter-paper¹ and in the proposed foam test were found to be 5.0, 0.5 and 0.1 p.p.m., respectively. These results indicate clearly that the proposed foam test is by far the most sensitive.

Initial results for the semi-quantitative determination of chromium(VI) using the proposed method were satisfactory. The colour density on the reagent foam cube was found to be proportional to the concentration of chromium(VI) in the aqueous solution. A standard colour scale for 0.1, 0.5, 1 and 5 p.p.m. of chromium(VI) was found to be suitable.

The 1,5-diphenylcarbazide foam was examined for the detection of 1 μg of chromium(VI) in the presence of relatively high concentrations of a wide range of different cations and anions in aqueous solutions. It was shown that the foam test for chromium is selective. The ratios of the concentrations of chromium(VI) detected to the concentrations of the accompanying ions are shown in Tables I and II.

The 1,5-diphenylcarbazide-loaded foam was next applied in column operations. The fact that polyurethane foam is easily packed in a column having good hydrodynamic properties suggests the possibility that even lower concentrations of chromium(VI) could be detected using 1,5-diphenylcarbazide foam columns. Small amounts of chromium could be collected from 100 ml of aqueous solution (pH 2–4) by passing it through the foam column at reasonable flow-rates (3–5 ml min⁻¹). The change in colour of the foam bed due to the coloured products of the collected chromate ion on the reagent foam is a test for chromium(VI). It was further observed that the length of the coloured zone is approximately proportional to the concentration of chromium in the aqueous solution. Semi-quantitative determination of chromium(VI) at the parts per 10⁹ (p.p.b.) level could, therefore, be achieved. The following colour scale proved to be satisfactory: 10, 20, 30, 40 and 50 p.p.b. The lengths of the coloured zones formed were found to be 2, 4.5, 10, 12 and 15 mm, respectively, at the specified flow-rate. These results offered further evidence of the advantages of the proposed foam test.

Conclusion

The semi-quantitative determination of as little as 0.1 p.p.m. and the detection of 10 p.p.b. of chromium(VI) in aqueous solution was achieved in batch and column experiments, respectively. The semi-quantitative determination of chromium(VI) was also carried out using a suitable colour scale. The detection of chromium was successful in the presence of relatively high concentrations of various other elements.

References

1. Feigl, F., and Anger, V., "Spot Tests in Inorganic Analysis," Sixth Edition, Elsevier, Amsterdam, 1972.
2. Cazeneuve, P., *C.R. Acad. Sci.*, 1900, **131**, 346.
3. Cazeneuve, P., *Bull. Soc. Chim. Fr.*, 1900, **23**, 701.
4. Cazeneuve, P., *Bull. Soc. Chim. Fr.*, 1901, **25**, 761.
5. Weisz, H., *Mikrochim. Acta*, 1954, 140.
6. Fujimoto, M., *Chemist Analyst*, 1965, **54**, 58 and 92.
7. Braun, T., and Farag, A. B., *Anal. Chim. Acta*, 1978, **99**, 1.
8. Moody, G. J., and Thomas, J. D. R., *Analyst*, 1979, **104**, 1.
9. Braun, T., and Farag, A. B., *Anal. Chim. Acta*, 1974, **73**, 301.
10. Braun, T., and Farag, A. B., *Anal. Chim. Acta*, 1972, **61**, 265.
11. Braun, T., and Farag, A. B., *Anal. Chim. Acta*, 1972, **62**, 476.

Received October 22nd, 1980
Accepted February 10th, 1981